Virchows Arch (2005) 447: 1–8
DOI 10.1007/s00428-005-1274-7

REVIEW ARTICLE

Tibor Tot

DCIS, cytokeratins, and the theory of the sick lobe

Received: 24 February 2005 / Accepted: 12 April 2005 / Published online: 31 May 2005
© Springer-Verlag 2005

Abstract We postulate that ductal carcinoma in situ (DCIS), and consequently breast carcinoma in general, is a lobar disease, as the simultaneously or asynchronously appearing, often multiple, in situ tumor foci are localized within a single lobe. Although the whole lobe is sick, carrying some form of genetic instability, the malignant transformation of the epithelial cells may appear localized to a part or different parts of the sick lobe at the same time or with varying time difference. It may be confined to terminal ductal lobular units (TDLUs), to ducts or both. The malignant transformation is often associated with aberrant branching and/or aberrant lobularization within the sick lobe. Involvement of a single individual TDLU or of a group of adjacent TDLUs generates a unifocal lesion. Multifocal lesions appear if distant TDLUs are involved. Diffuse growth pattern in DCIS indicates involvement of the larger ducts. The extent of the involved area in multifocal or diffuse cases varies considerably. Diffuse growth pattern with or without evidence of aberrant arborisation within the sick lobe seems to characterize a subgroup of DCIS with unfavourable prognosis. In this paper, we discuss the anatomical, embryological and pathological background of the theory of the sick lobe and present supporting evidence from modern radiological breast imaging, long-term follow-up studies and from our own series of 108 DCIS cases.

Keywords Breast · Ductal carcinoma in situ · Cytokeratins · Neoplasia · Hypothesis

Introduction

Breast carcinoma is a heterogeneous and progressive disease with many variations in morphological appearance, which has always made attempts of classification of breast tumors very difficult. Mammography screening during the last decades has changed the panorama of breast carcinoma, detecting small invasive tumors in asymptomatic women and also detecting malignant lesions in their non-invasive state [3, 16]. Under the circumstances of adequate surgical removal of the lesions, proper histopathologic work-up and systematic mammographic-pathologic correlation, this evolution offers the opportunity of studying breast carcinoma at the earliest stages in its natural history, which in turn may offer a key to better understanding the many variations of breast cancer morphology.

Classical whole organ studies had long ago demonstrated that the vast majority of in situ and invasive breast carcinomas are multifocal/multicentric/diffuse [10, 12]. However, the traditional technique used routinely in most breast pathology laboratories today does not allow repetition of the results of whole organ studies in most cases. The "modern" approach of focusing on histological, immunohistological and molecular analysis of the dominant invasive lesion may lead to underestimation of the importance of the alterations in the tissue adjacent to the dominant mass. In our laboratory, the diagnostic routine is specially adapted to the work-up of quadrantectomy specimens (the method of choice in breast conserving surgery in Scandinavia). This method of two- and three-dimensional large (up to 10×8 cm) histological sections gives the contiguous piece of tissue necessary for proper analysis of the extent and distribution of the lesions belonging to a breast carcinoma and represents an ideal background for detailed and systematic radiopathologic correlation [13, 31, 33]. Based on our 20 years experience and more than 5000 consecutive breast cases documented and analysed this way, we have become more and more convinced that the multiple malignant lesions exhibit a lobar distribution within the breast. Thus, we postulate that ductal carcinoma in situ, and consequently breast carcinoma in general, is a lobar disease, which means that the simultaneously or asynchronously appearing, often multiple, in situ (and invasive) tumor foci belong to a single lobe in one breast [34]. While in situ carcinomas keep their lobar distribution

T. Tot (✉)
Department of Pathology, Central Hospital,
791 82 Falun, Sweden
e-mail: tibor.tot@ltdalarna.se
Tel.: +46-23-492696
Fax: +46-23-492389

during their entire development, invasive carcinomas may step out from this frame and grow beyond the borders of the sick lobe, especially in their advance phase.

The diagnosis of breast carcinoma always reflects the actual status of the process of malignant transformation within the sick lobe in the moment of perception. Prolonged time of evolution of the neoplastic process may lead to development of new tumor foci and/or to growth of the already existing foci. Thus, the morphology of breast carcinoma is clearly time-related, which means that the malignant transformation of the cells within the sick lobe may depend on complex genetic-biological timing.

Complex lobar anatomy of the breast

The breast is a glandular organ with lobar morphology [5]. A typical lobe consists of one lactiferous duct opening on the nipple, branching into segmental, subsegmental and terminal ducts and ending up in thousands of lobules. The terminal duct and the corresponding lobule represent the so-called terminal ductal-lobular unit (TDLU), which is considered to be the most important morphologic-functional unit in the breast [32, 36]. Although rare anastomoses between the lobes have been described in one study [22], the breast lobes are considered to be well-defined individual units in the related literature [11, 18]. However, the lobar division of the breast parenchyma is complex, with considerable variation in origin, size and shape of the lobes [5, 11, 18, 31].

A normal lobe of the breast is a complex dynamically evolving and involuting structure during the woman's entire lifetime [31]. There are relatively few TDLUs before puberty [35]. During the reproductive period the numerous TDLUs undergo cyclical changes following the menstrual cycle [17]. The number of the TDLUs is highest during the period of late pregnancy and lactation and is substantially reduced after the menopause [33]. Thus, TDLUs may appear and disappear, the number of them being dependent on the woman's age, constitution and hormonal status. This is probably correct for the smaller ducts, too. The number of the lactiferous ducts and the number of the openings on the nipple is, however, independent of hormonal influences and age. Thus, the number of the breast lobes is constant during the woman's lifetime, but their size and shape and the number of their ducts and lobules varies and depends on anatomical variations, hormonal and age related influences [31]. The actual morphology of the lobe is maintained by the finely regulated equilibrium of development and involution of the ducts (arborisation) and lobules (lobularization).

In one study [11], the breast lobes varied in size, representing between 2% and 23% of the breast volume. Although a malignant transformation may lead to considerable enlargement of the sick lobe, the original size of the lobe may be crucial in determining the extent of the eventually developing disease and the chances for successful breast-conserving surgery. The surgical method of quadrantectomy (segmentectomy) represents an attempt to radically excise the sick lobe and not only the radiologically and/or clinically evident lesion(s). As the lobar morphology of the breast is complex, the surgical intervention is often inaccurate (with local recurrence rate up to 30% in cases without radiotherapy) [24].

Embryological background

The lobes of the breast (the epithelium and the myoepithelium of their ducts and lobules) are of ectodermal origin. During the 21st week of the intrauterine life, buds from the embryonal ectoderm are formed as non-luminated, solid protrusions into the embryonal mesenchyme [2]. All the buds represent an initiation of one potential breast lobe, but some of them probably are abortive. Some of the buds (at least those in the accessory breasts developing along the embryonal mammary line) disappear during intrauterine life. Luminalization begins during the 26th week [2]. The next steps are ramification (branching of the luminated buds, forming smaller and smaller ducts) and lobularization (forming the lobules as groups of blindly ending vesicles on the terminal ducts) [15]. The ramification process is almost completed during intrauterine life, while lobularization mainly characterizes the postpubertal period [33].

Luminalization of the buds, ramification and lobularization represent a complex process related to changes of the expression of different genes and to consequent changes in the phenotype of the epithelial cells. This process can be successfully monitored, determining the cytokeratin (CK) phenotype of the structures of the breast at different stages of intrauterine development. The buds in the initial stage have the same immunophenotype as the basal cells in the embryonal ectoderm and express CK14, vimentin, S-100-beta and p63 [2]. During the period between weeks 21–26 of intrauterine life, expression of CK17, CD10 and alpha-smooth muscle actin appears [2, 15]. Luminarization of the buds is associated with the appearance of cells expressing CK19, while ramification is related to cells not expressing CK19. Lobularization, in turn, seems to be associated with expression of CKs 8 and 18 in the epithelial cells [2, 15]. As demonstrated in several studies, the hyperplastic breast epithelium exhibits "basal cell type" CKs, but DCIS does not [23].

The embryonal development of CK phenotype within the breast lobe may reflect a complex and sensitive genetic regulatory mechanism behind the processes of initialisation, arborisation and lobularization. The similarity of the neoplasia-related and embryonic phenotypic variations may indicate that the malignant transformation is somehow related to lobularization and/or arborisation within the sick lobe, targeting and altering these processes. According to our observations on two- and three-dimensional large histologic sections and to the experience from radiopathologic correlative studies, low-grade DCIS targets most often the process of lobularization while the high-grade DCIS may also alter the process of arborisation.

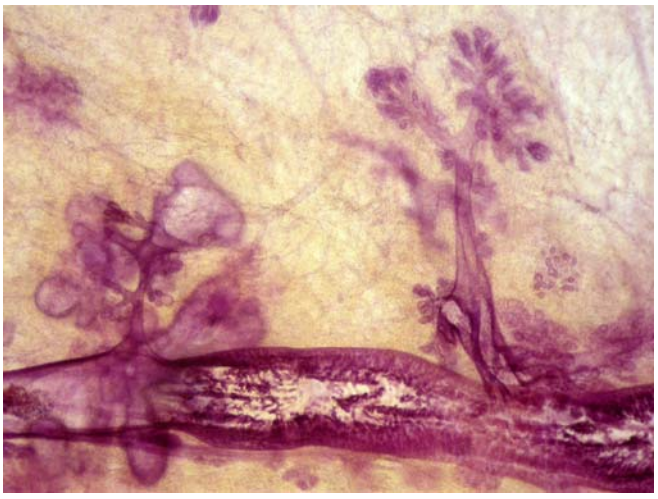


Fig. 1 DCIS involving a segmental duct, but not the related terminal ducts and TDLUs (thick section image, 20×) Note the regular branching into relatively long, narrower ducts

In addition to changes related to the epithelial cells, the embryonal mesenchyme surrounding the mammary buds, and partly the newly formed ducts also exhibits some changes. Overexpression of tenascin C, as demonstrated by immunohistochemistry, is considered to be a sensitive indicator of remodelling of the mesenchyme into a specific periductal stroma [28]. Thus, tenascin C overexpression may represent an indirect indicator of initialisation of a breast lobe during the embryonal period and a sign of arborisation within the lobe. Tenascin C overexpression can also be demonstrated surrounding some duct-like structures in a proportion of cases of (often high-grade) DCIS [14, 28], which may additionally prove the involvement of this type of malignancy in the process of arborisation within the sick lobe. This phenomenon is sometimes designated as "duct neogenesis" [30].

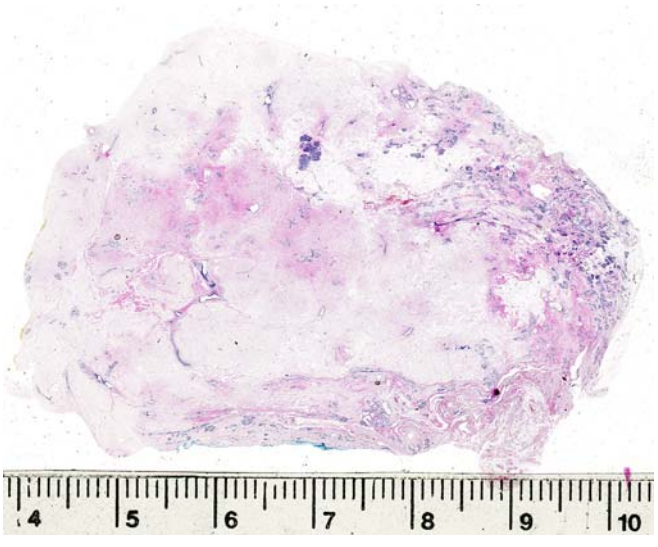


Fig. 2 Unifocal lesion in DCIS. Large histologic section

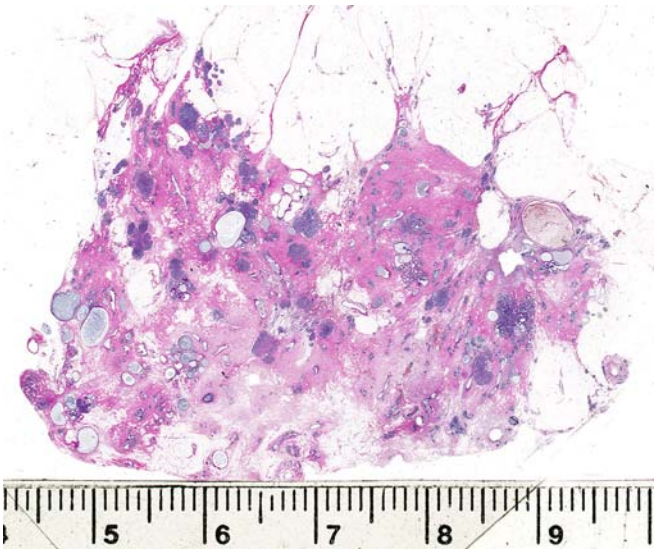


Fig. 3 Multifocal DCIS involving many distant TDLUs, leaving uninvolved tissue in between

Subgross morphology of ductal carcinoma in situ

Our observation based on examination of the large histologic sections and stereomicroscopic analysis of three-dimensional large thick sections, in concordance with the results of previous published similar studies [8, 9] can be briefly summarized in the following. Structures of carcinoma in situ may be demonstrated in TDLUs as well as in ducts. The ductal epithelium may be involved without demonstrable DCIS in the related TDLUs (Fig. 1). The ductal epithelium may be discontinuously involved with "gaps" exhibiting seemingly normal epithelium [9].

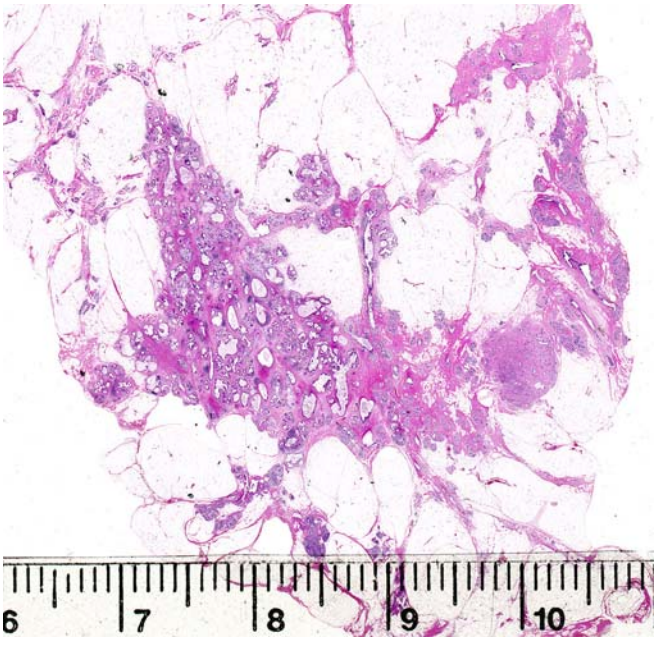


Fig. 4 Diffuse growth pattern in DCIS: the lesion involves the ducts system without well-outlined TDLUs in the left half of the image. The round structure to the right is a fibroadenoma

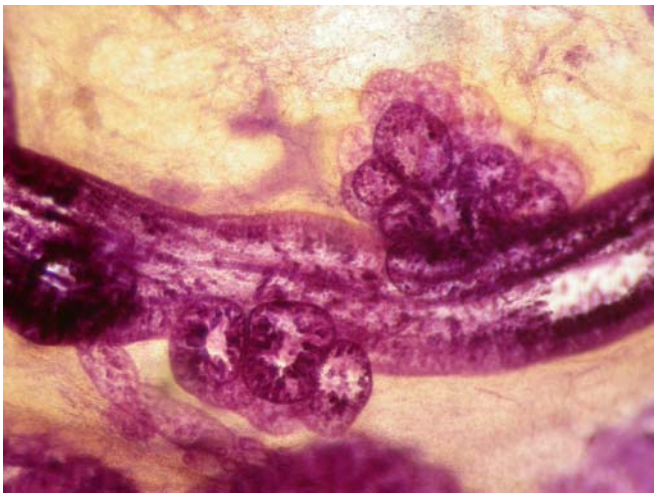


Fig. 5 Aberrant arborisation in DCIS. Note the absence of narrower branches as compared with previous image in Fig. 1 (thick section image, 20×)

The presence of the structures of an in situ carcinoma in a TDLU leads to considerable enlargement and distortion of this structure. The size of the involved individual TDLUs may vary between 1–2 mm to 20 mm or even more. The enlarged TDLU is regularly perceived as a round (spherical) or oval, well outlined structure (Fig. 2). If there are several distant TDLUs containing structures of in situ carcinoma, they are also seen as individual, well-delineated lesions, giving the impression of multifocality of the malignant process (Fig. 3). Involved TDLUs adjacent to each other may form a conglomerate, where the units are no longer separable as individual on radiology or gross examination. In addition to an enlarged single TDLU, this conglomerate is another example of the unifocal lesions. Involvement of the larger ducts may lead to their dilatation, but the long, branching tree of the involved duct system is perceived rather as a diffuse network of tubes than a well-outlined individual structure (Fig. 4). In conclusion, DCIS may manifest as a unifocal, multifocal or diffuse lesion (as well as a combination of multifocal and diffuse lesions) indicating involvement of one individual TDLU or a conglomerate of adjacent TDLUs (unifocal DCIS), simultaneous involvement of several distant TDLUs (multifocal DCIS) or involvement of the larger ducts (diffuse DCIS).

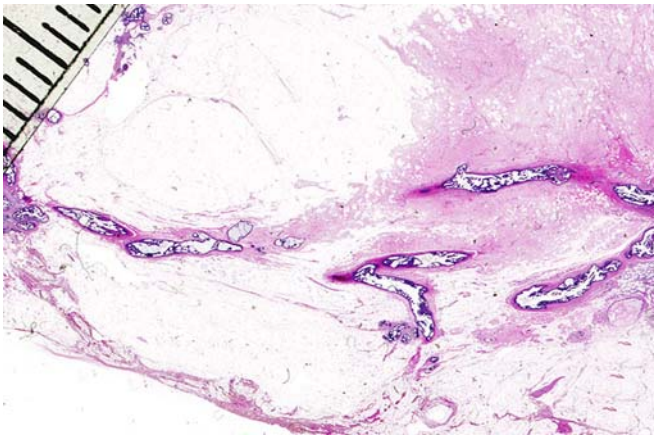


Fig. 6 Duct involvement in DCIS without evidence of altered arborisation. The number of the involved ducts corresponds to normal anatomy and the branching is regular

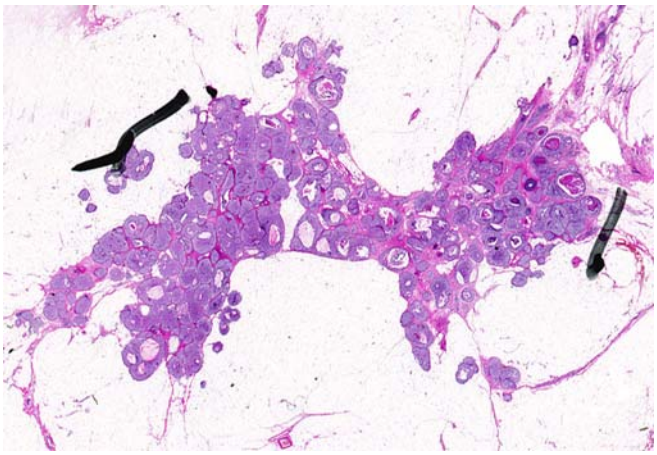


Fig. 7 DCIS with evident disturbance in arborisation as the number of the duct-like structures exceed the anatomically expected number (duct-neogenesis)

While involvement of the TDLUs alters these structures on a relatively uniform way, distending and distorting them similarly, involvement of the ducts may or may not be associated with different changes in ramification of the duct system. In the normal situation, the ducts give raise to smaller and smaller branches, which end up in TDLUs. If this process is altered, the ducts may give abortive branches (Fig. 5) without narrower ducts and TDLUs. In more severe cases, an abnormally large number of duct-like structures are seen in the area of the in situ carcinoma, regularly lacking smaller branches and TDLUs. Already, the tightness of the ducts indicates that they are newly formed, "neogenetic" and cannot represent a part of an anatomically normal lobe (Figs. 6 and 7). As these duct-like structures are often surrounded by a remodelled stroma overexpressing tenascin C (and regularly associated with periductal lymphoid cell infiltration), we assume that this phenomenon corresponds to an aberration in the process of arborisation within the sick lobe.

Theory of the sick lobe

Based on the anatomical, embryological and pathological data discussed above, we postulate that ductal carcinoma in situ, and consequently breast carcinoma in general, is a lobar disease. This means that the simultaneously or asynchronously appearing, often multiple, in situ tumor foci are localised in a single lobe of one breast. We assume that this sick lobe is genetically malconstructed from birth, carrying some kind of genetic instability from its initiation during fetal life. Further accumulation of genetic changes during the decades of the postnatal period may lead to malignant transformation of the epithelial cells in any part of the sick lobe. We believe, that this is a life-long process initiated

during the fetal period of life, which can be influenced or even interrupted by radical excision of the sick lobe and, possibly, with other therapeutic interventions. In addition to malignant transformation at the cellular level, there are two sensitive points in morphogenesis of the sick lobe, which are also regular targets of the neoplastic events: the process of lobularization and the process of arborisation. Altered lobularization is regularly seen in the majority of cases of DCIS, while different alterations in arborisation represent the hallmark of high-grade DCIS.

The biological timing of the malignant transformation of the cells within the sick lobe may be very variable [4, 6, 7]. Simultaneous involvement of most of the epithelial cells within the sick lobe leads to rapid development of extensive, diffuse, usually high-grade, DCIS. The malignant transformation may also be microfocal and localized to one or more individual TDLUs (as in low-grade DCIS, lobular carcinoma in situ or in atypical ductal or lobular hyperplasia). In these cases, the transformation may involve very distant TDLUs within the sick lobe with time difference varying up to several years or decades.

Supporting evidence

Radiological observations on individual extensive DCIS cases support the theory of lobar distribution of multiple and diffuse lesions. Cases with nipple discharge in extensive micropapillary DCIS may manifest such a distribution of the individual filling defects in a lobe filled with contrast on galactography (Fig. 8a and b). The microcalcifications on the mammogram in high-grade DCIS may also exhibit a distribution resembling the anatomy of the duct system of a single lobe. Magnetic resonance images in cases of high-grade DCIS often outline a whole involved breast lobe, including the lactiferous ducts (Fig. 9), [20].

We studied a series of 108 consecutive DCIS cases diagnosed in period 1996–2001 on our department. The so-called “special type DCIS” such as intracystic papillary carcinomas and papillomas with DCIS were excluded, as their growth pattern depends on the morphology of pre-existent lesions. Most of the cases were initially treated with breast conserving surgery and radiotherapy. In 30 cases, based on close or dirty margins (less than 10 mm circumferential margin), the surgical intervention was completed with re-resection or mastectomy. The cases were reviewed by the author and followed up to 31 December 2004. The cases were grouped according to their distribution as unifocal, multifocal and diffuse (as defined above), according to their extent (the area including all the structures corresponding to DCIS within a large histologic section) as extensive (more than 20 mm in largest diameter) and non-extensive. They were also graded as low-grade (low nuclear grade without central necrosis), intermediate (low nuclear grade with central necrosis or intermediate nuclear grade with or without necrosis) and high-grade (high nuclear grade with or without necrosis). The diffuse cases were further divided into a neogenetic group (with evidence of alterations in arborisation of the lobe often

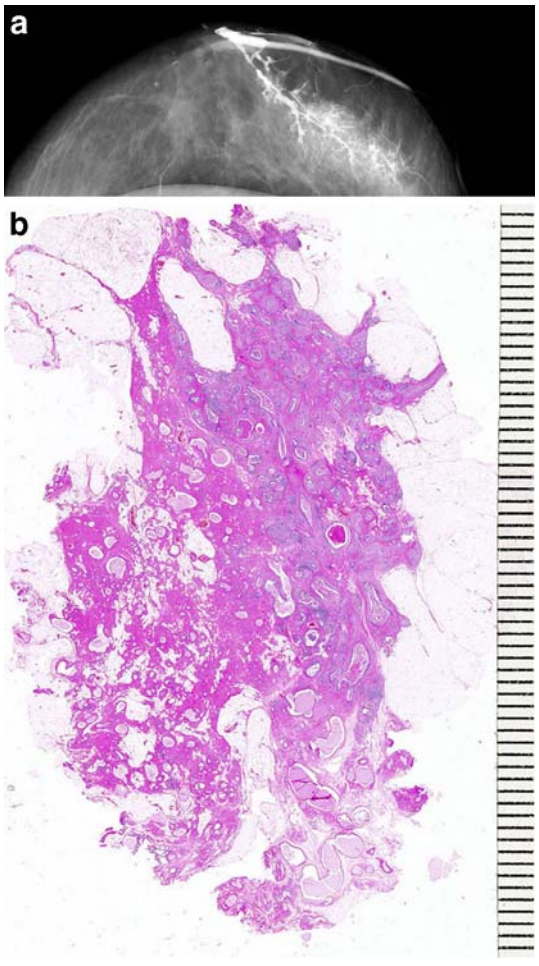


Fig. 8 **a** Galactogram showing a lobe-like distribution of filling defects and parenchymal lesions surrounding the duct system. **b** The corresponding large histologic section showing extensive, diffuse DCIS

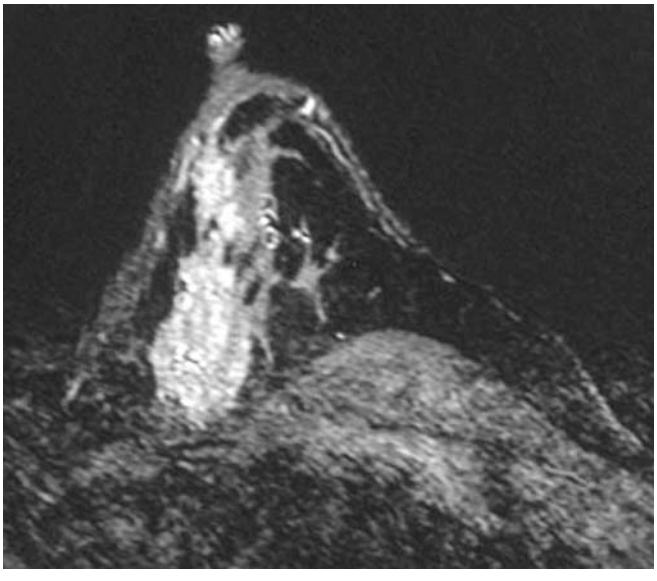


Fig. 9 Lobar distribution of the lesions in a case of high-grade DCIS indicated on a magnetic resonance image

Table 1 Local recurrences by extent and distribution of the lesions in 108 consecutive cases of ductal carcinoma in situ

Extent	Unifocal	Multifocal	Diffuse, non-neogenetic	Diffuse neogenetic	Mixed	Sum
Extensive	0/0	4/24	3/18	4/14	0/2	19% (11/58)
Non-extensive	1/41	0/5	0/3	0/1	0/0	2% (1/50)
Sum	2% (1/41)	14% (4/29)	14% (3/21)	27% (4/15)	0% (0/2)	11% (12/108)

manifesting in tightly packed ductal structures without TDLUs) and a non-neogenetic group. The results are presented in Table 1 and in the diagram in Fig. 10 and indicate that the extensive cases recurred significantly more often compared to non-extensive ones, the diffuse neogenetic subgroup being the prognostically most unfavourable. The same study also demonstrated that low-grade DCIS tends to be multifocal, the cases with intermediate grade tend to be unifocal, while the diffuse cases are mostly of high grade. In fact, the duct-neogenetic subgroup contained exclusively high-grade DCIS cases. One patient with extensive high-grade DCIS without demonstrable invasion, but with evident alterations in arborisation of the duct system developed metastases and died later on of the disease, as was verified on autopsy.

Several long-term follow-up studies have demonstrated that mammographially detected casting-type microcalcification are associated with higher risk of local recurrence of DCIS and with associated invasive carcinoma than the other types of microcalcifications. [21, 26]. As the casting-type microcalcifications most often indicate presence of duct-neogenetic high-grade DCIS, these studies represent an indirect evidence for unfavourable prognosis of this DCIS subtype. Further, small invasive breast carcinomas (less than 15 mm in size) have a more unfavourable outcome in overall survival if associated with casting type microcalcifications [29, 30]. The other types of microcalcifications indicating presence of intermediate or low-grade DCIS, were not associated with increased mortality in the cited studies.

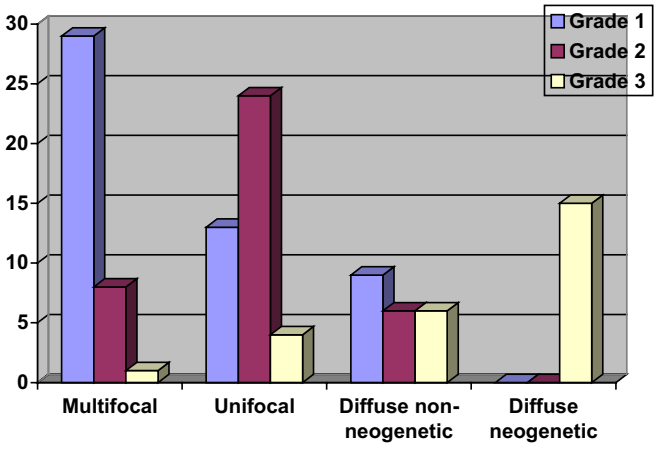


Fig. 10 Grade distribution by growth pattern in 108 consecutive cases of ductal carcinoma in situ

The presented evidence indicates that diffuse involvement of large areas of the sick lobe in DCIS, with altered arborization of the duct system is a characteristics of the unfavourable subgroup of DCIS. Extensive and/or multifocal involvement of the sick lobe with altered lobularization, but with normal arborization is typical of grade I, less often grade II DCIS and is associated with higher local recurrence rate compared to the unifocal cases. The unifocal DCIS cases seem to represent the prognostically most favourable subgroup.

Discussion

Several investigators have previously assessed the extent and the distribution of carcinoma in situ within the breast, however, multicentricity and multifocality in breast carcinoma in situ remains a debated topic in the literature. The reported incidence of multicentricity ranges from 0 to 78%, depending on the used criteria and methods [9, 27]. The group of Holland and Faverly, using the technique of whole organ sectioning and thick section images, demonstrated that ductal carcinoma in situ may exhibit either a continuous or a discontinuous growth; they divided the cases with discontinuous growth into multifocal (less than 4 cm gaps between the foci) and multicentric (larger gaps) and concluded that most of the in situ carcinomas are unicentric (showing a segmental distribution) [9]. Page believe that "multicentricity is a misconception" and that the majority of in situ carcinomas are limited to a single focus with continuous growth pattern, which may be perceived in histological preparations as discontinuous after artificial fragmentation [25]. Andersen et al. divided the cases of ductal carcinoma in situ into microfocal, tumor forming, diffuse and mixed. Their microfocal cases correspond to the low-grade lesions targeting the terminal ductal-lobular units of the sick lobe. The diffuse cases in their series mostly correspond to the diffuse extensive high-grade cases in our concept [1]. Analysing the three-dimensional distribution of in situ and invasive breast carcinomas, Mai et al. concluded that the in situ component is often located in a single duct, the small invasive carcinomas appear adjacent to the in situ and the whole tumor may form a pyramid with the summit towards the nipple [19]. Thus, the suspicion that DCIS and invasive breast carcinoma may have a segmental (lobar) distribution has been expressed previously. The theory of the sick lobe adds the dimension of time to morphological findings and connects the malignant transformation to an anatomically well-defined

structure of the breast lobe and to disturbances in the dynamically maintained processes of arborisation and lobularization within it.

The most widely accepted concept of breast cancer development, the Wellings concept, connects the initiation of the malignant transformation to changes in the TDLUs [36]. According to this concept, breast carcinoma develops from the individual TDLUs with secondary involvement of the ducts by spread of the tumor cells as well as invasion of the tumor cells through the basement membrane. This concept is considered valid in many benign breast lesions, too, with only a small minority of the lesions developing primarily in the ductal system (e.g. papillomas). Although many in situ carcinomas exhibit the distribution corresponding to the terminal units, the continuous "spread" of the in situ cancer along the ducts in a several cm large area, seen not rarely in cases of DCIS, is difficult if not impossible to explain by the origin of the process in a few individual 1–2 mm large units; the signs of migration of the tumor tissue are seldom evident. Studying the three-dimensional morphology of the early stage breast carcinomas, however, evidenced involvement of large areas of the ductal tree in addition to lobular involvement or, at least partially, without lobular involvement. As discussed above, new insight into this process gave the recent anatomical and embryological studies, and first of all, the new radiological imaging methods enabling the definition of a new concept, the theory of the sick lobe, challenging the classical concept of Wellings. The theory of the sick lobe, in contrast to the concept of Wellings, is based on a hypothesis that the malignant transformation may appear in any part(s) of the sick lobe, not only in the TDLUs. The so-called "pagetoid spread" or other forms of tumor spread in DCIS may be explained as malignant transformation of the cells of the ducts distant to the TDLU, rather than spreading of the malignant cells from the involved TDLU. Thus, the biological timing of the malignant transformation, the involved structures of the lobe and the involved morphogenetic processes (lobularization and arborisation) determine the morphology and the natural history of DCIS subtypes.

Consequences/future perspectives

Provided that the theory of the sick lobe is correct, the extent of the disease in breast cancer in situ can no longer be defined as the area including all the detected lesions, but becomes equal to the area delineated by the borders of the sick lobe. Radical interventions have to shift their target from the detected lesion(s) to aiming to excise or otherwise destroy the entire sick lobe. Multicentricity of breast carcinoma may be redefined as the presence of two or more sick lobes within a single breast, the large majority of cases remaining unicentric. Multifocality, in turn, may be defined as presence of more than one individual tumor foci within the sick lobe.

As the sick lobe is formed already during intrauterine life, this theory assumes that prenatal influences of different noxious factors may play a role in predisposing the individual to breast cancer. On the other hand, decades of postnatal life are necessary for the development of breast carcinoma. The surgical intervention itself interrupts this otherwise life-long process only if it leads to excision or destruction of the entire sick lobe. Involvement of different structures and processes into the morphogenesis of breast carcinoma may indicate different pathways of malignant transformation in various categories of breast carcinoma.

Further development of modern imaging methods may play a crucial role in proving or questioning this theory, as methods effectively outlining the sick lobe and the lesions within it at the same time may become routinely used. If proved as correct, in general or in a substantial proportion of cases, the theory of the sick lobe may represent a real challenge in diagnostic breast pathology in the near future.

References

1. Andersen JA, Blichert-Toft M, Dyreborg U (1987) In situ carcinomas of the breast. Types, growth pattern, diagnosis, and treatment. Eur J Surg Oncol 13:105–111
2. Bartek J, Bartkova J, Taylor-Papadimitriou J (1990) Keratin 19 expression in the adult and developing mammary gland. Histochem J 22:537–544
3. Cady B, Michaelson JS (2001) The life-sparing potential of mammographic screening. Cancer 91:1724–1731
4. Chen HH, Thurfjell E, Duffy SW, Tabar L (1998) Evaluation by Markov chain model of a non-randomised breast cancer screening programme in women aged under 50 years in Sweden. J Epidemiol Community Health 52:329–335
5. Cooper AP (1840) On the anatomy of the breast. Longmans, London
6. Duffy SW, Chen HH, Tabar L, Day NE (1995) Estimation of mean sojourn time in breast cancer screening using Markov chain model of both entry to and exit from the preclinical detectable phase. Stat Med 14:1531–1543
7. Duffy SW, Chen HH, Tabar L, Fagerberg G, Paci E (1996) Sojourn time, sensitivity and positive predictive value of mammographic screening for breast cancer in women aged 40–49. Int J Epidemiol 25:1139–1145
8. Egan RI (1982) Multicentric breast carcinomas: clinical-radiographic-pathologic whole organ studies and 10-year survival. Cancer 49:1123–1130
9. Faverly DRG, Burgers L, Bult P, Holland R (1994) Three dimensional imaging of mammary ductal carcinoma in situ: clinical implications. Semin Diagn Pathol 11:193–198
10. Gallager HS, Martin JE (1969) The study of mammary carcinoma by mammography and whole organ sectioning. Cancer 23:855–873
11. Going JJ, Moffat DF (2004) Escaping from Flatland: clinical and biological aspects of human mammary duct anatomy in three dimensions. J Pathol 203:538–544
12. Holland R, Velling SH, Mravunac M, Hendricks JH (1985) Histologic multifocality of Tis, T1-2 breast carcinomas: implications for clinical trials of breast conserving surgery. Cancer 56:979–990
13. Jackson PA, Merchant W, McCormick CJ, Cook MG (1994) A comparison of large block macrosectioning and conventional techniques in breast pathology. Virchows Arch 425:243–248
14. Jahkola T, Toivonen T, Nordling S, von Snitten K, Virtanen I (1998) Expression of Tenascin C in intraductal carcinoma of human breast: relationship to invasion. Eur J Cancer 34:1687–1692
15. Jolicoeur F, Gaboury LA, Oligny LL (2003) Basal cells of second trimester fetal breasts: immunohistochemical study of myoepithelial precursors. Pediatr Dev Pathol 6:398–413

16. Lindgren A, Holmberg L, Thurfjell E (1997) The influence of mammography screening on the pathological panorama of breast cancer. APMIS 105:62–70
17. Longacre TA, Bartow SA (1986) A correlative morphologic study of human breast and endometrium in menstrual cycle. Am J Surg Pathol 10(6):382–393
18. Love SM, Barsky SH (2004) Anatomy of the nipple and breast ducts revisited. Cancer 1001:1947–1957
19. Mai, KT, Yazdi HM, Burns BF, Perkins DG (2000) Pattern of distribution of intraductal and infiltrating ductal carcinoma: a three-dimensional study using serial coronal giant sections of the breast. Hum Pathol 31:464–474
20. Neubauer H, Li M, Kuehne-Heid R, Schneider A, Kaiser WA (2003) High grade and non-high grade ductal carcinoma in situ on dynamic MR mammography: characteristic findings for signal increase and morphological pattern of enhancement. Br J Radiol 76:3–12
21. Nishimura S, Takahashi K, Gomi N, Tada K, Makita M, Tada T, Iwase T, Yoshimoto M, Akiyma F, Sakamoto G, Kasumi F (2004) What is the predictor for invasion in non-palpable breast cancer with microcalcifications? Breast Cancer 11:49–54
22. Ohtake T, Abe R, Kimijima I, Fukushima T, Tsuchiya A, Hoshi K, Wahasa H (1995) Intraductal extension of primary invasive breast carcinoma treated by breast-conservative surgery. Computer graphic three-dimensional reconstruction of the mammary duct-lobular systems. Cancer 76:32–45
23. Otterbach F, Bankfalvi A, Bergner S, Decker T, Kreck R, Boecker W (2000) Cytokeratin 5/6 immunohistochemistry assists the differential diagnosis of atypical proliferations of the breast. Histopathology 37:232–240
24. Ottesen GL, Graversen HP, Blichert-Toft M, Christensen IJ, Andersen JA (2000) Carcinoma in situ of the female breast. 10 year follow-up results of a prospective nationwide study. Breast Cancer Res Treat 62:192–210
25. Page DL, Rogers LW, Schuyler PA, Dupont WD, Jensen RA (2002) The natural history of ductal carcinoma in situ of the breast. In: Silverstein MJ (ed) Ductal carcinoma in situ of the breast. Lippincott, Philadelphia, pp 17–21
26. Ringberg A, Idvall I, Fernö M et al (2000) Ipsilateral local recurrence in relation to therapy and morphological characteristics in patients with ductal carcinoma in situ of the breast. Eur J Surg Oncol 26:444–451
27. Rosen PP (2001) Rosens's breast pathology. Lippincott, Philadelphia, pp 300–301
28. Sakakura T, Ishihara A, Yatani R (1991) Tenascin in mammary gland development: from embryogenesis till carcinogenesis. Cancer Treat Res 53:383–400
29. Tabár L, Chen HH, Duffy SW, Yen MF, Chiang CF, Dean PB, Smith RA (2000) A novel method for prediction of long-term outcome of women with T1a, T1b, and 10–14 mm invasive breast cancers: a prospective study. Lancet 355:429–433
30. Tabár L, Chen HT, Yen MFA, Tot T, Tung TH, Chen LS, Chiu YH, Duffy SW, Smith RA (2004) Mammographic tumor features can predict long-term outcomes reliably in women with 1–14-mm invasive carcinoma. Cancer 101:1745–1759
31. Tabár L, Tot T, Dean PB (2005) Breast cancer: the art and science of early detection with mammography. Perception, interpretation, histopathologic correlation. Thieme, Stuttgart, pp 405–438
32. Tot T, Tabár L, Dean PB (2000) The pressing need for better mammographic-pathologic correlation of many variations in normal breast anatomy. Virchows Arch 437:338–344
33. Tot T, Tabár L, Dean PB (2002) Practical breast pathology. Thieme, Stuttgart, pp 116–123
34. Tot T (2005) Correlating the ground truth of mammographic histology with the success or failure of imaging. Technol Cancer Res Treat 4(1):23–28
35. Vogel PM, Georgiade NG, Fetter BF, Vogel FS, McCarty KS Jr (1981) The correlation of histologic changes in the human breast with the menstrual cycle. Am J Pathol 104:23–34
36. Wellings SR, Jensen HM, Marcum RG (1975) An atlas of subgross pathology of the human breast with special reference to possible precancerous lesions. J Natl Cancer Inst 55:231–273

Virchows Arch (2005) 447: 9–11
DOI 10.1007/s00428-005-1227-1

ORIGINAL ARTICLE

Andreas Kreft · Torsten Hansen · Charles James Kirkpatrick

Thyroid transcription factor 1 expression in cystic lesions of the neck: an immunohistochemical investigation of thyroglossal duct cysts, branchial cleft cysts and metastatic papillary thyroid cancer

Received: 21 December 2004 / Accepted: 6 February 2005 / Published online: 10 June 2005
© Springer-Verlag 2005

Abstract Cervical metastases of papillary thyroid cancer (PTC) are of particular diagnostic importance, because they can mimic branchiogenic cysts clinically and histopathologically when undergoing cystic change. Immunohistochemical stains for thyroid transcription factor 1 (TTF-1), which are positive in thyroid cancers, are reported to be valuable in establishing diagnosis. However, TTF-1 may also be expressed in dysontogenetic cysts of the neck. Therefore, immunohistochemical stains for TTF-1 and thyroglobulin (TG) were performed on each of the ten thyroglossal duct cysts, branchial cleft cyst and lymph node metastasis of PTC. Five in ten cases of thyroglossal duct cysts were positive for TTF-1, but all were negative for TG. One of the ten branchial cleft cysts stained for TTF-1, while all cases were negative for TG. All ten cases of lymph node metastases of PTC showed positive for TTF-1, nine of which were positive for TG. Since a positive immunostaining for TTF-1 in cystic lesions of the neck was not only found in metastases of PTC, but also in non-malignant branchiogenic cysts, additional investigations, e.g. an immunostaining for TG, should be added in difficult cases.

Keywords Thyroid transcription factor 1 · Thyroglossal duct cysts · Branchial cleft cysts · Papillary thyroid cancer

A. Kreft (✉) · T. Hansen · C. J. Kirkpatrick
Institut für Pathologie,
Klinikum der Johannes Gutenberg Universität,
Langenbeckstr. 1,
55101 Mainz, Germany
e-mail: kreft@pathologie.klinik.uni-mainz.de
Tel.: +49-613-1173136
Fax: +49-613-1176604

Introduction

Thyroid transcription factor 1 (TTF-1) is a DNA-binding protein that plays an important role in the development of the thyroid, lung and brain of the fetus [8]. In the adult it can be detected immunohistochemically in the epithelia of the thyroid, including parafollicular C cells, and the lung as well as in primary tumours and metastases deriving from these tissues [6, 11]. Therefore, immunostaining for TTF-1 is recommended in metastases of unknown primary, in which adenocarcinoma [2] or neuroendocrine tumour of the lung [4], or thyroid carcinoma [1] are considered as a possible origin.

Cervical metastases of papillary thyroid cancer (PTC) are of particular diagnostic importance, because they can mimic branchiogenic cysts clinically and histopathologically when undergoing cystic change [5, 10]. Metastases may be the first item that would draw medical attention, before the tumour in the thyroid is suspected [9]. Immunohistochemical reactions, including TTF-1, are recommended for a thorough diagnosis [11, 12]. So far, however, dysontogenetic cervical cysts have not been tested for their expression of TTF-1.

Thus, we performed immunohistochemical stains of TTF-1 including branchial cleft cysts, thyroglossal duct cysts and metastases of PTC, and added immunoreaction for thyroglobulin (TG).

Materials and methods

From the laboratory file of the Institut für Pathologie, Uniklinikum Mainz, we recruited ten patients each with thyroglossal duct cysts, branchial cleft cyst, with columnar epithelium and cystic lymph node metastasis of PTC

Table 1 Clinical data of the patients

	Patients	Male/ Female	Median age (range)
Thyroglossal duct cysts	10	5/5	57 years (29–75 years)
Branchial cleft cysts	10	4/6	39 years (16–68 years)
Metastases of papillary thyroid cancer	10	6/4	38 years (20–84 years)

(Table 1). The primary tumour was identified within the thyroid of all patients with metastases of PTC. No evidence of malignancy was found in patients with thyroglossal duct- and branchial cleft cysts.

All specimens were fixed in buffered formalin (4%) and embedded in paraffin wax. Immunohistochemistry was carried out using the DAB method after deparaffination. Staining reactions were performed with the antibody against TTF-1, clone 8G7G3/1 (NeoMarkers, California, USA), at a dilution of 1:50 with microwave pre-treatment, using citrate buffer adjusted at pH 6, and the antibody against TG, clone 2H11 (BioGenix, San Ramon, CA, USA), as ready-to-use kit with no pre-treatment.

Results

In thyroglossal duct cysts, a positive immunostaining for TTF-1 was detected in the nuclei of the lining epithelia in five of ten cases. The positivity was found to be focal and less marked than in PTC. It was focused in the basal part of the columnar epithelia (Fig. 1). TG was not detected in the duct epithelia, but in the adjacent thyroid tissue.

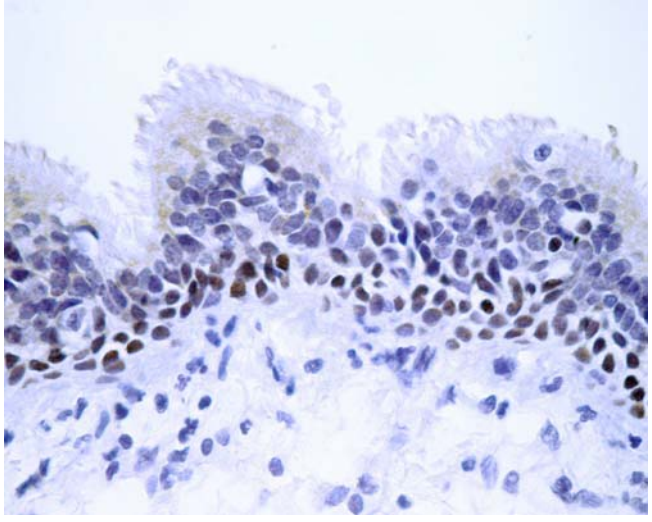


Fig. 1 Weak nuclear staining for thyroid transcription factor 1 (TTF-1) in a thyroglossal duct cyst, accentuated in the basal part of the epithelia

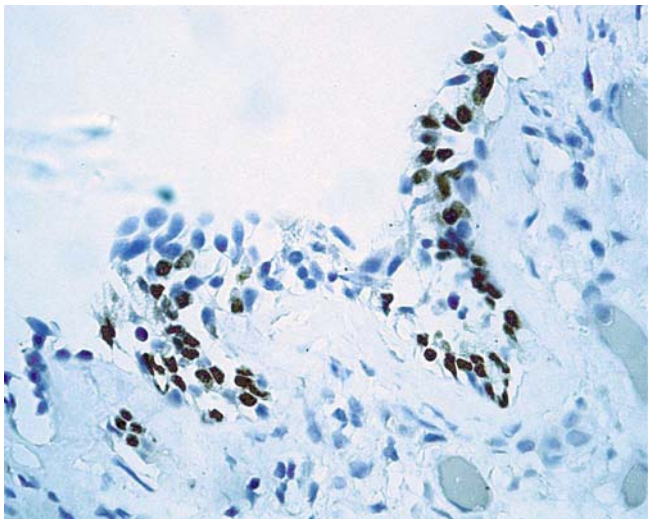


Fig. 2 Focal, but marked nuclear staining of TTF_1 in one of ten branchial cleft cysts

One of the ten branchial cleft cysts revealed a weak but distinct nuclear positivity of TTF-1 (Fig. 2). The other nine cases were negative for TTF-1. All these tissue specimens, including the one that tested positive for TTF-1, were negative for TG.

All ten cases with lymph node metastases of PTC showed an intense nuclear immunostaining for TTF-1 (Fig. 3). Cytoplasmatic staining for TG revealed varying results—ranging from intense and extensive reactions to weak and focal positivity in nine of the ten cases. One case was completely negative.

Discussion

Immunohistochemically, we were able to demonstrate the expression of TTF-1 in five of ten cases of thyroglossal

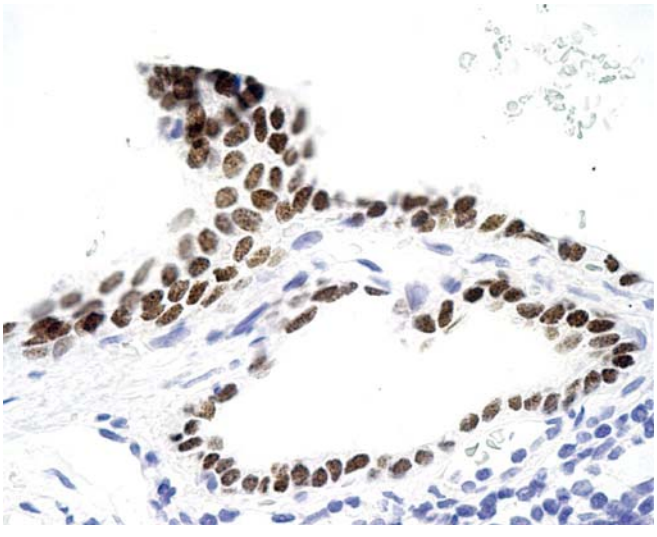


Fig. 3 Strong nuclear staining for TTF_1 in PTC, a constant finding in these lesions

duct cysts and one branchial cleft cyst, as well as in all metastases of PTC investigated. The former, to the authors' knowledge, is the first report of positivity for TTF-1 in these lesions. The latter finding corresponds to results in previous studies, which demonstrated TTF-1 positivity in the adult in normal epithelia and tumours of the thyroid and the lung [6, 11]. Only two tumours unrelated to these organs were also positive for TTF-1: small cell cancer of other-than-lung origin [3] and ependymoma [14]. Thus TTF-1 is a rather specific immunohistochemical marker of lung and thyroid tissue.

Since the thyroglossal duct gives rise to the thyroid gland, its epithelia may already express TTF-1. Therefore, an immunohistochemical positivity for TTF-1 in the thyroglossal duct cyst indicates its relation to the thyroid. A comparable phenomenon is described in tracheobronchial fistulas, where the expression of TTF-1 indicates their origin from the lung [13].

In the branchial cleft cysts, which derive from the branchial clefts and not from the pharyngeal pouch like the thyroid epithelia and C cells [7], there is no developmental relation to the thyroid or the lung. Of these lesions, only one of ten cases stained positively for TTF-1. This may be explained by the respiratory-like metaplasia of the epithelia.

Most of the cases of PTC stained positively for TG. However, we could not demonstrate a positive staining in one case. This may be explained by the relatively inconstant staining for this antibody, which we observed in our reactions and which has also been reported for metastases of thyroid cancer [1]. However, in our study the staining was specific, thereby adding valuable diagnostic information.

The practical implication of our finding is that immunohistochemical reactions for TTF-1 do not reliably distinguish between cystic metastases of PTC and thyroglossal duct cysts or branchial cleft cysts. Therefore, in cases with differential diagnosis of a benign cystic lesion and metastasis of PTC, additional investigations, e.g. an immunostaining for TG, should be performed.

References

1. Bejarano PA, Nikiforov YE, Swenson ES, Biddinger PW (2000) Thyroid transcription factor-1, thyreoglobuline, cytokeratin 7, cytoceratin 20 in thyroid neoplasms. Appl Immunohistochem Mol Morphol 8:189–194
2. Chang YL, Lee YC, Liao WY, Wu CT (2004) The utility and limitations of thyroid transcription factor-1 protein in primary and metastatic pulmonary neoplasms. Lung Cancer 44:149–157
3. Cheurk W, Kwan MY, Suster S, Chan JKC (2001) Immunostaining for thyroid transcription factor 1 and cytoceratin 20 aids the distinction of small cell carcinoma from Merkel Cell Carcinoma, but not pulmonary from extrapulmonary small cell carcinomas. Arch Pathol Lab Med 125:228–231
4. Du EZ, Goldstraw P, Zacharias J, Tiffet O, Craig PJ, Nicholson AG, Weidner N, Yi ES (2004) TTF-1 expression is specific for lung primary in typical and atypical carcinoids: TTF-1 positive carcinoids are predominantly in peripheral location. Hum Pathol 35:823–825
5. Fernandez MP, Ismail S, Ro JY (2001) Pathologic quiz case: cystic lesion in the neck of a 51-year-old woman. Arch Pathol Lab Med 125:833–834
6. Katoh R, Miyagi E, Nakamura N, Li X, Suzuki K, Kakudo K, Kobayashi M, Kawaoi A (2000) Expression of thyroid transcription factor-1 (TTF-1) in human c cells and medullary thyroid carcinomas. Hum Pathol 31:386–393
7. Kellman RM, Freije JE (2001) Clinical considerations for non-neoplastic lesions of the neck. 762–770
8. Lazzaro D, Price M, de Felice M, Di Lauro R (1991) The thyroid transcription factor TTF-1 is expressed at the onset of thyroid and lung morphogenesis and in restricted regions of the foetal brain. Development 113:1093–1104
9. Monchik JM, De Petris G, De Crrea C (2001) Occult papillary carcinoma of the thyroid presenting as a cervical cyst. Surgery 129:429–432
10. Nakagawa T, Takashima T, Tomiyama K (2001) Differential diagnosis of a lateral cervical cyst and solitary cystic lymph node metastasis of occult thyroid papillary carcinoma. J Laryngol Otol 115:240–242
11. Ordonez NG (2000) Thyroid transcription factor-1 is a marker of lung and thyroid carcinomas. Adv Anatom Pathol 7:123–127
12. Roh MS, Hong SH (2002) Utility of thyroid transcription factor-1 and Cytokeratin 20 in identifying the origin of metastatic carcinomas of cervical lymph nodes. J Korean Med Sci 17:512–517
13. Spilde TL, Bhatai AM, Miller KA, Ostlie DJ, Chaignaud BE, Holcomb GW, Snyder CL, Gittes GK (2002) Thyroid transcription factor-1 expression in the human neonatal tracheoesophageal fistula. J Pediatr Surg 37:1065–1067
14. Zamecnik J, Chanova M, Kodet R (2004) Expression of thyroid transcription factor 1 in primary brain tumors. J Clin Pathol 57:1111–1113

Virchows Arch (2005) 447: 12–17
DOI 10.1007/s00428-005-1235-1

ORIGINAL ARTICLE

Miguel García-González · Ihab Abdulkader · Angel Vázquez Boquete · Xosé Manuel Lens Neo · Jerónimo Forteza · José Cameselle-Teijeiro

Cyclooxygenase-2 in normal, hyperplastic and neoplastic follicular cells of the human thyroid gland

Received: 5 November 2004 / Accepted: 16 February 2005 / Published online: 10 June 2005
© Springer-Verlag 2005

Abstract This study was undertaken to investigate cyclooxygenase-2 (COX-2) expression in follicular cells of the human thyroid. COX-2 expression was studied immunohistochemically in a total of 174 samples. COX-2 immunoreactivity was confined to the cell cytoplasm with the nuclei remaining unlabelled. COX-2 expression was observed in five cases (17.2%) of normal follicular cells and in one case (16.6%) of solid cell nests. Follicular carcinoma expressed COX-2 more frequently than follicular adenoma (93.4% vs 21.1%) ($p \leq 0.001$). A higher percentage of cases of papillary microcarcinomas up-regulated COX-2 in comparison with all papillary carcinomas ($p \leq 0.05$). However, we could not establish any relationships among COX-2, patients' ages or lymph node metastases in papillary carcinomas. COX-2 expression was found in 12 (92.3%) poorly differentiated carcinomas and in 13 (92.8%) undifferentiated carcinomas. We found that COX-2 is not always useful as a marker of malignancy. Our results suggest that COX-2 plays a role in progression of all thyroid carcinomas, but in papillary carcinomas, seems more important only in the early stages. COX-2 expression in the undifferentiated carcinoma deserves special consideration due to its prognosis and to the fact that selective COX-2 inhibitors were found to enhance tumour response to radiation in some studies.

M. García-González · X. M. L. Neo
Department of Nephrology,
Hospital Clínico Universitario,
Choupana s/n,
15706 Santiago de Compostela, Spain

I. Abdulkader · A. V. Boquete · J. Forteza · J. Cameselle-Teijeiro (✉)
Department of Pathology,
Hospital Clínico Universitario,
Universidad de Santiago de Compostela,
Choupana s/n,
15706 Santiago de Compostela, Spain
e-mail: apjocame@usc.es
Tel.: +34-981-950858
Fax: +34-981-950889

Keywords Cyclooxygenase-2 · Thyroid cancer · Papillary carcinoma · Undifferentiated carcinoma · Immunohistochemistry · In situ hybridisation

Introduction

There are two isoforms of cyclooxygenase (COX), COX-1 and COX-2, involved in the synthesis of prostaglandins from arachidonic acid [29]. The COX-1 enzyme is expressed constitutively in most mammalian tissues where, although often undetected, it can be rapidly induced. The COX-2 gene is an early-response gene that is up-regulated by proinflammatory stimuli, growth factors, oncogenes and tumour-promoting phorbol esters [10, 13, 22].

COX-2 seems to play a role in carcinogenesis as well as in carcinoma progression; COX-2 is up-regulated in transformed cells [24], in colorectal cancers [20, 22], ulcerative colitis-associated neoplasia [1], hepatocellular carcinoma [14], oesophageal and gastric carcinomas [25, 34], pulmonary and mammary tumours [22], pancreatic cancer [27], renal cell carcinoma [11], prostate carcinoma [33] and pituitary tumours [30]. COX-2 knockout mice also have a lower incidence of several tumour types including skin papillomas and intestinal polyps [2, 18, 26]. Epidemiological studies have also shown that chronic intake of non-steroidal anti-inflammatory drugs, which function as COX inhibitors, reduces the incidence of gastrointestinal cancer [8, 9, 32].

Enhanced expression of COX-2 in lymphocytic thyroiditis and Hashimoto's thyroiditis suggests an important role of this enzyme in these inflammatory thyroid processes [5, 17]. Thyroid cancer of follicular cells includes several histological types of tumours with various molecular alterations and different clinical behaviours. Papillary carcinoma is the most common malignant tumour of the thyroid and has a relatively indolent clinical course in contrast to the rapidly fatal course of anaplastic (undifferentiated) carcinoma [6]. Poorly differentiated carcinomas fall between well-differentiated (papillary and follicular) carcinomas and undifferentiated carcinomas in terms of

both morphologic appearance and behaviour [6]. Specht et al. [23] reported that COX-2 mRNA level was higher in malignant nodules than in adjacent normal tissue or in benign nodules. Most recently, Ito et al. [12] concluded that the up-regulation of COX-2 may contribute predominantly in the early phase of papillary carcinoma progression while playing a more adjuvant role in follicular carcinoma progression. On the other hand, Siironen et al. [21] showed that COX-2 expression increases with age in papillary thyroid cancer.

In the present study, we examine the expression of COX-2 in a series of normal and hyperplastic follicular cells as well as in well-differentiated (papillary and follicular), poorly differentiated and anaplastic (undifferentiated) carcinomas.

Materials and methods

Tissue specimens

One hundred seventy-four thyroid tissue specimens were obtained from the files of the Department of Pathology, Hospital Clínico Universitario, Santiago de Compostela, Spain. This study was approved by the ethical committee of our institution. Tissue slices had been fixed in 10% formalin and embedded in paraffin wax for histological, immunohistochemical and in situ hybridisation studies. Each case was classified according to the Chan criteria [6]. Specimens were normal thyroid tissue, 29; solid cell nests, 6; Graves' disease, 10; nodular hyperplasia, 15; follicular adenoma, 33; papillary carcinoma, 39 (13 cases of microcarcinomas, 8 cases of classical type, 6 cases of follicular variant, 1 case of solid variant, 4 cases of cribriform-morular variant, 2 cases of Whartin-tumour-like variant and 5 lymph node metastasis); follicular carcinoma, 8; Hürthle cell follicular carcinoma, 7; poorly differentiated carcinoma, 13 (11 cases of insular carcinoma and 2 cases of columnar cell carcinomas); and undifferentiated carcinoma, 14. Of the normal specimens, 16 were from the autopsy specimens, and the other 13 were "normal" tissue taken from non-tumoural areas of the other specimens.

Immunohistochemistry and in situ hybridisation

Immunohistochemical studies were performed on tissue sections 4 μm thick using a COX-2 monoclonal antibody (Cayman Chemical, Ann Arbor, MI, USA, microwaved, 1:50). The reaction was detected using a universal second antibody kit that utilized a peroxidase-conjugated labelled-dextran polymer (Dako EnVision Peroxidase/DAB; Dako, Glostrup, Denmark) in order to avoid misinterpreting endogenous biotin or biotin-like activity in cell cytoplasms [7] or nuclei [3] as positive staining. Paraffin blocks of colorectal cancer known to be positive for COX-2 were used as positive controls. Sections for each negative control were incubated with PBS instead of the primary antibody. Scoring of the immunohistochemical results was performed according to the methods described by Ito et al. [12], with minor modifications. We selected at least five representative fields. Based on the percentages of immunopositive cells, three subdivisions were made as follows: diffusely positive (++), greater than 50% of cells were positive; heterogeneously positive (+), 10–49% of cells were positive; and negative (−), less than 10% of the cells were positive. Equivocal immunointensity was considered to be negative.

As representative cases, in situ hybridisation was performed on 4-μm sections in four cases of normal thyroid tissue, two cases of solid cell nests, one case of Graves' disease, four cases of papillary carcinoma, one case of follicular carcinoma, one case of Hürthle cell follicular carcinoma, two cases of insular carcinoma, one case of columnar cell carcinoma and three cases of undifferentiated carcinoma to confirm immunohistochemical results. Before hybridisation, tissue sections were deparaffinized, rehydrated and washed in TE buffer (Tris 10 mM, EDTA 1 mM). Thereafter, the tissues were treated with proteinase K (4 μg/ml), washed in TE buffer and 2×SSC buffer and dehydrated with 96% and 100% ethanol. Hybridisation was carried out using a 3′FITC-labelled oligoprobe (5′-TCATCAACACTGCCTCAATTCAGTCTCTCATCTGC AATAA-3′) directed against the human COX-2 mRNA. Sections were hybridised at 37°C overnight. After hybridisation, stringent washes were performed in 2×SSC, 1× SSC and 0.5×SSC at room temperature. The oligoprobes were detected using an alkaline phosphatase-labelled anti-FITC antibody (Dako) and visualized with nitroblue tetrazolium (NBT)/BCIP until desired stain intensity was achieved. Sections were counterstained with methylene green and mounted in an aqueous media. We used sections of colon cancer as positive controls for COX-2 mRNA. For negative control, we have substituted the oligoprobe hybridisation mix with hybridisation buffer. Estimation of immunohistochemical and in situ hybridisation scores for each case was performed by different observers (MAGG, JC-T and IA), independently, and determined after discussion when scores were discrepant.

Statistical analysis

χ^2 analysis and Fisher's exact probability test were adopted to examine the relationship between variables. Two results were considered significant when $p<0.05$.

Results

Table 1 summarises the immunohistochemical findings. COX-2 immunoreactivity was confined to the cell cytoplasm with the nuclei remaining unlabelled. Epithelial cells of solid cell nests were negative in five cases and diffusely positive in one case. Although the percentage of immunopositive cells was higher in malignant tumours than in

Table 1 COX-2 expression in neoplastic and non-neoplastic cells of the thyroid gland

	Age, mean (range)	COX-2 immunoexpression			
		−, *n* (%)	+, *n* (%)	++, *n* (%)	Total
Normal thyroid tissue	56.5 (28–89)	24 (82.7)	4 (13.8)	1 (3.4)	29
Solid cell nests	53.2 (34–76)	5 (83.3)		1 (16.7)	6
Graves' disease	37.2 (30–47)	10 (100)			10
Nodular hyperplasia	48 (32–73)	15 (100)			15
Follicular adenoma	48.7 (22–69)	26 (78.8)	2 (6)	5 (15.1)	33
Papillary carcinoma	25.5 (12–84)	12 (30.8)	12 (30.8)	15 (38.5)	39
Follicular carcinoma	63.1 (33–84)	1 (6.7)	1 (6.7)	13 (86.7)	15
Poorly differentiated carcinoma	67.4 (39–75)	1 (7.7)	1 (7.7)	11 (84.6)	13
Undifferentiated carcinoma	67.7 (47–82)	1 (7.1)		13 (92.8)	14

Age is expressed in years
Stain: diffusely positive (++), greater than 50% of cells were positive; heterogeneously positive (+), 10–49% of cells were positive; and negative (−), less than 10% of the cells were positive

benign ones ($p \leq 0.001$), the distribution of COX-2 reactivity was not restricted to tumour cells (Table 1) (Fig. 1). COX-2 expression was observed in five (17.2%) cases of normal thyroid tissue adjacent to three Hürthle cell follicular carcinomas, one follicular carcinoma and one follicular adenoma (Fig. 1a). On the other hand, follicular

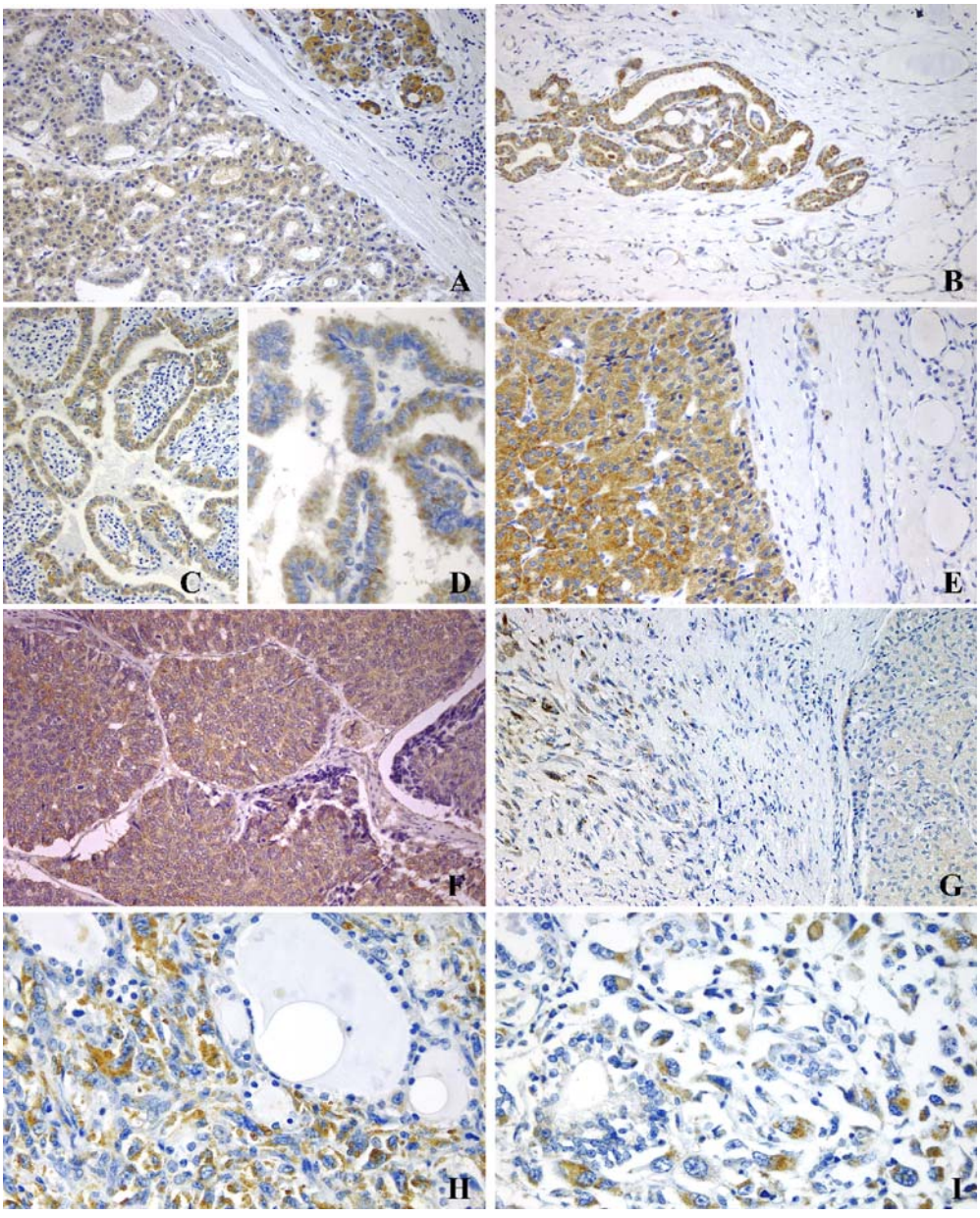


Fig. 1 **a**–**i** Immunoexpression of cyclooxygenase-2 (COX-2) in follicular adenoma (×200) (**a**), papillary microcarcinoma (×200) (**b**), Whartin-tumour-like variant of papillary carcinoma (×200) (**c**), classical variant of papillary carcinoma (×400) (**d**), follicular carcinoma (×200) (**e**), insular carcinoma (×200) (**f**) and undifferentiated carcinomas (**g**–**i**). A cluster of normal follicular cells adjacent to a follicular adenoma is positive for COX-2 (**a**). No COX-2 expression is seen in normal thyroid epithelial cell adjacent to a papillary microcarcinoma (**b**), and follicular carcinoma (**e**). **g** Stronger intensity of staining in undifferentiated carcinoma cells in comparison with residual poorly differentiated areas in the same tumour (×200). **h** and **i**, Undifferentiated carcinomas showing neoplastic cells positively stained for COX-2 while the entrapped normal follicles are negative (×400)

Table 2 COX-2 expression in well-differentiated carcinomas of the thyroid gland

	COX-2 immunoexpression			
	−, *n* (%)	+, *n* (%)	++, *n* (%)	Total
Papillary carcinoma				39
Microcarcinoma	1 (7.7)	5 (38.5)	7 (53.8)	13
Classical variant	4 (50)	2 (25)	2 (25)	8
Follicular variant	3 (50)	3 (50)		6
Solid variant			1 (100)	1
Cribriform-morular variant	3 (75)		1 (25)	4
Whartin-tumour-like variant		1 (50)	1 (50)	2
Lymph node metastasis	1 (20)	1 (20)	3 (60)	5
Follicular carcinoma				15
NOS	1 (12.5)	1 (12.5)	6 (75)	8
Hürthle cell			7 (100)	7

Stain: diffusely positive (++), greater than 50% of cells were positive; heterogeneously positive (+), 10–49% of cells were positive; and negative (−), less than 10% of the cells were positive
NOS not-otherwise-specified

carcinoma expressed COX-2 more frequently than follicular adenoma ($p \leq 0.001$) (Fig. 1e). Twenty-seven (68.8%) of the papillary carcinomas showed COX-2 immunoexpression (Fig. 1b–d). A higher percentage of cases (92.3%) of papillary microcarcinomas up-regulated COX-2 in contrast to all papillary carcinomas ($p \leq 0.05$) (Table 2). The mean age in the 23 COX-2-positive papillary carcinomas was 49.9±17.3 in comparison with 42.15±19.6 in the COX-2-negative papillary carcinomas. We could not establish any relationship between COX-2 expression and patients' age or lymph node metastases.

COX-2 expression was found in 12 (92.3%) poorly differentiated carcinomas and in 13 (92.8%) undifferentiated carcinomas (Fig. 1f–i). In two cases of undifferentiated carcinoma, residual areas of poorly differentiated carcinoma and mucoepidermoid carcinoma were identified showing less immunointensity for COX-2 than the anaplastic areas (Fig. 1g).

In situ hybridisation analysis showed no staining in solid cell nests. A staining pattern supported the immunohistochemical findings in the other types of samples examined (Fig. 2).

Discussion

In this study, we found that COX-2 expression was frequently up-regulated in thyroid carcinomas as previously reported [12, 17, 21, 23], whereas COX-2 expression was limited in normal follicular cells. Solid cell nests of the thyroid, usually considered as normal embryonic remnants of the ultimobranchial body, were recently proposed as thyroid stem cells [19]; in situ hybridisation was negative in epithelial cells of these structures, and weak immunostaining was found in only one case of our series. COX-2 expression in some normal follicular cells was observed in our study and also observed by Ito et al. [12]. We think that this fact, together with negative expression of COX-2 in 30.8% of papillary carcinomas tested, indicates that COX-2 is not always useful as a marker of malignancy.

At least some follicular carcinomas are believed to arise from preexisting adenomas, although this has not yet been confirmed [6]. In our series, the percentage of COX-2 expression in follicular carcinomas was higher than that reported by Ito et al. [12] (93.3% vs 40.9%), but the percentages were similar in follicular adenomas. We cannot discard the possibility that some follicular adenomas up-regulating COX-2 could in fact be "malignant" tumours that have not yet revealed morphologic criteria of malignancy. Papillary carcinomas frequently over-express COX-2 [12, 17, 21]; but this expression is significantly reduced in tumours related to old age, large size, satellite tumours and the presence of a solid, scirrhous or trabecular growth pattern [12], thus, suggesting that the activation of this enzyme is required in the early phase of papillary carcinoma progression [12]. In our study, a significant higher percentage of papillary microcarcinomas up-regulated COX-2 in comparison with all papillary carcinomas. We think that in papillary carcinomas, COX-2 expression seems more important only in the early stages. At the same time, the higher proportion of COX-2 down-regulation in the entire group of papillary carcinomas could be related to the indolent behaviour of these tumours in comparison with other thyroid carcinomas. Siironen et al. [21] postulate that with the older age group having a much worse prognosis and a higher expression of COX-2, COX-2 confers an adverse prognosis via either invasion or metastasis. An association among age, worse prognosis, and higher grade in thyroid pathology is well recognized in the literature [6].

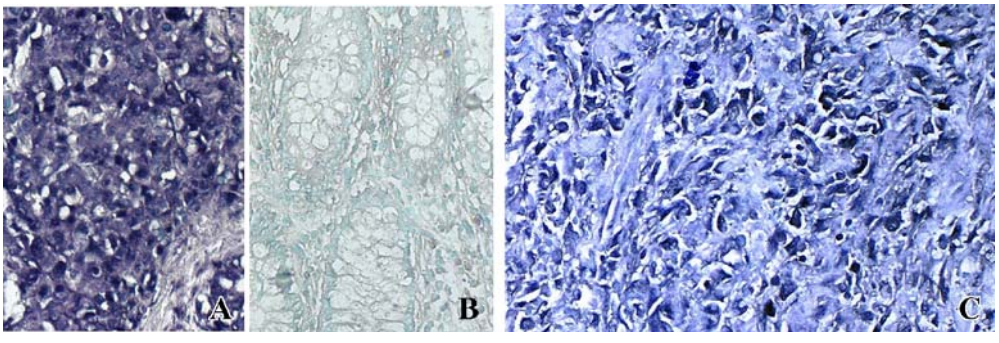


Fig. 2 In situ hybridisation for COX-2. **a** Positive control (carcinoma of the large bowel) (×200). **b** Negative control (normal mucosa of the colon) (×200). **c** Undifferentiated carcinoma of the thyroid showing strong positivity for COX-2 (×200)

In our series, however, we could not establish any relationship between COX-2 expression and patients' ages or lymph node metastases.

The cribriform-morular variant of papillary carcinoma is the sporadic counterpart of the thyroid carcinoma that occurs in patients with familial adenomatous polyposis [3, 4, 6]. *APC* mutations may represent a rare mechanism for COX-2 up-regulation in familial adenomatous polyposis-associated thyroid tumours [18]. However, among our cases of cribriform-morular variant of papillary carcinoma, including one case with germline mutation of the *APC* gene, we found weak but diffuse COX-2 expression in the only case with somatic, but not germline mutation of the *APC* gene [4]. A disturbance of the Wnt signal transduction pathway due to *β-catenin* gene mutations is more significant in the carcinogenesis of the cribriform-morular variant of papillary carcinoma [31].

Solid variant is a rare and poorly characterised variant of papillary thyroid carcinoma [16] whose a less favourable prognosis could correlate with expression of COX-2.

The immunoprofile of the rich lymphoid stroma in Whartin-tumour-like variant of papillary carcinoma is similar to that of chronic lymphocytic thyroiditis [6, 28]. The expression of COX-2 in lymphocytic thyroiditis, Hashimoto's thyroiditis and some thyroid tumours has been proposed as a basis for the relationship between carcinogenesis and autoimmunity [5, 17, 21].

A stepwise increase in immunoreactivity scores for COX-2 staining was found by Nose et al. [17] from follicular adenomas to papillary carcinomas, well-differentiated and poorly differentiated types and follicular carcinomas (with anaplastic carcinoma included in the poorly differentiated papillary carcinoma group). We found a strong COX-2 expression in more than 90% of both follicular carcinomas and poorly differentiated carcinomas. In our series, up-regulation of COX-2 was found in all cells of 93% of undifferentiated carcinomas, and the stain was stronger in undifferentiated areas in the two cases with residual poorly differentiated foci. These findings deserve special consideration due to the ominous prognosis of undifferentiated thyroid carcinoma [6], as well as to the fact that selective COX-2 inhibitors were found to enhance thoracic tumour response to radiation in preclinical studies [15].

Acknowledgements The authors are grateful to Dora C. Insua Santamaría for technical assistance. We also thank Deborah L. Randall for her linguistic supervision. This work was supported by research grant (PGIDE99PXI90201B) sponsored by Xunta de Galicia, Spain.

References

1. Agoff SN, Brentnall TA, Crispin DA, Taylor SL, Raaka S, Haggitt RC, Reed MW, Afonina IA, Rabinovitch PS, Stevens AC, Feng Z, Bronner MP (2000) The role of cyclooxygenase-2 in ulcerative colitis-associated neoplasia. Am J Pathol 157:737–745
2. Boolbol SK, Dannenberg AJ, Chadburn A, Martucci C, Guo XJ, Ramonetti JT, Abreu-Goris M, Newmark HL, Lipkin ML, DeCosse JJ, Bertagnolli MM (1996) Cyclooxygenase-2 overexpression and tumor formation are blocked by sulindac in a murine model of familial adenomatous polyposis. Cancer Res 56:2556–2560
3. Cameselle-Teijeiro J, Chan JKC (1999) Cribriform-morular variant of papillary carcinoma: a distinctive variant representing the sporadic counterpart of familial adenomatous polyposis-associated thyroid carcinoma? Mod Pathol 12:400–411
4. Cameselle-Teijeiro J, Ruiz-Ponte C, Loidi L, Suárez-Peñaranda JM, Baltar J, Sobrinho-Simoes M (2001) Somatic but not germline mutation of the *APC* gene in a case of cribriform-morular variant of papillary thyroid carcinoma. Am J Clin Pathol 115:486–493
5. Cornetta AJ, Russell JP, Cunnane M, Keane WM, Rothstein JL (2002) Cyclooxygenase-2 expression in human thyroid carcinoma and Hashimoto's thyroiditis. Laryngoscope 112:238–242
6. Chan JKC (2000) Tumors of the thyroid and parathyroid glands. In: Fletcher CDM (ed) Diagnostic histopathology of tumors, 2nd edn. Churchill Livingstone, Edinburgh, Scotland pp 959–1056
7. Cheuk W, Chan JK (2004) Subcellular localization of immunohistochemical signals: knowledge of the ultrastructural or biologic features of the antigens helps predict the signal localization and proper interpretation of immunostains. Int J Surg Pathol 12:185–206
8. DuBois RN (2000) Review article: cyclooxygenase—a target for colon cancer prevention. Aliment Pharmacol Ther 14(Suppl 1): 64–67
9. Farrow DC, Vaughan TL, Hansten PD, Stanford JL, Risch HA, Gammon MD, Chow WH, Dubrow R, Ahsan H, Mayne ST, Schoenberg JB, West AB, Rotterdam H, Fraumeni JF Jr, Blot WJ (1998) Use of aspirin and other nonsteroidal anti-inflammatory drug and risk of esophageal and gastric cancer. Cancer Epidemiol Biomarkers Prev 7:97–102
10. Fosslien E (2000) Molecular pathology of cyclooxygenase-2 in neoplasia. Ann Clin Lab Sci 30:3–21
11. Hashimoto Y, Kondo Y, Kimura G, Matsuzawa I, Sato S, Ishizaki M, Imura N, Akimoto M, Hara S (2004) Cyclooxygenase-2 expression and relationship to tumour progression in human renal cell carcinoma. Histopathology 44:353–359
12. Ito Y, Yoshida H, Nakano K, Takamura Y, Miya A, Kobayashi K, Yokozawa T, Matsuzuka F, Matsuura N, Kuma K, Miyauchi A (2003) Cyclooxygenase-2 expression in thyroid neoplasms. Histopathology 42:492–497
13. Kelley DJ, Mestre JR, Subbaramaiah K, Sacks PG, Schantz SP, Tanabe T, Inoue H, Ramonetti JT, Dannenberg AJ (1997) Benzo[*a*]pyrene up-regulates cyclooxygenase-2 gene expression in oral epithelial cell. Carcinogenesis 18:795–799
14. Koga H, Sakisaka S, Ohishi M, Kawaguchi T, Taniguchi E, Sasatomi K, Harada M, Kusaba T, Tanaka M, Kimura R, Nakashima Y, Nakashima O, Kojiro M, Kurohiji T, Sata M (1999) Expression of cyclooxygenase-2 in human hepatocellular carcinoma: relevance to tumor dedifferentiation. Hepatology 29:688–696
15. Liao Z, Milas L, Komaki R, Stevens C, Cox JD (2003) Combination of a COX-2 inhibitor with radiotherapy or radiochemotherapy in the treatment of thoracic cancer. Am J Clin Oncol 26:S85–S91
16. Nikiforov YE, Erickson LA, Nikiforova MN, Caudill CM, Lloyd RV (2001) Solid variant of papillary thyroid carcinoma: incidence, clinical-pathologic characteristics, molecular analysis, and biologic behavior. Am J Surg Pathol 25:1478–1484
17. Nose F, Ichikawa T, Fujiwara M, Okayasu I (2002) Up-regulation of cyclooxygenase-2 expression in lymphocytic thyroiditis and thyroid tumors: significant correlation with inducible nitric oxide synthase. Am J Clin Pathol 117:546–551

18. Oshima M, Dinchuk JE, Kargman SL, Oshima H, Hancock B, Kwong E, Trzaskos JM, Evans JF, Taketo MM (1996) Suppression of intestinal polyposis in Apc delta716 knockout mice by inhibition of cyclooxygenase-2 (COX-2). Cell 87:803–809
19. Preto A, Cameselle-Teijeiro J, Moldes-Boullosa J, Soares P, Cameselle-Teijeiro JF, Silva P, Reis-Filho JS, Reyes-Santias RM, Alfonsin-Barreiro N, Forteza J, Sobrinho-Simoes M (2004) Telomerase expression and proliferative activity suggest a stem cell role for thyroid solid cell nests. Mod Pathol 17:819–826
20. Sano H, Kawahito Y, Wilder RL, Hashiramoto A, Mukai S, Asai K, Kimura S, Kato H, Kondo M, Hla T (1995) Expression of cyclooxygenase-1 and -2 in human colorectal cancer. Cancer Res 55:3785–3789
21. Siironen P, Ristimaki A, Nordling S, Louhimo J, Haapiainen R, Haglund C (2004) Expression of COX-2 is increased with age in papillary thyroid cancer. Histopathology 44:490–497
22. Soslow RA, Dannenberg AJ, Rush D, Woerner BM, Khan KN, Masferrer J, Koki AT (2000) COX-2 is expressed in human pulmonary, colonic, and mammary tumors. Cancer 89:2637–2645
23. Specht MC, Tucker ON, Hocever M, Gonzalez D, Teng L, Fahey TJ III (2002) Cyclooxygenase-2 expression in thyroid nodules. J Clin Endocrinol Metab 87:358–363
24. Subbaramaiah K, Telang N, Ramonetti JT, Araki R, DeVito B, Weksler BB, Dannenberg AJ (1996) Transcription of cyclooxygenase-2 is enhanced in transformed mammary epithelial cells. Cancer Res 56:4424–4429
25. Sung JJ, Leung WK, Go MY, To KF, Cheng AS, Ng EK, Chan FK (2000) Cyclooxygenase-2 expression in *Helicobacter pylori*-associated premalignant and malignant gastric lesions. Am J Pathol 157:729–735
26. Tiano H, Chulada P, Spalding J, Lee C, Loftin C, Mahler J, Morham S, Langenbach R (1997) Effects of cyclooxygenase deficiency on inflammation and papilloma development in mouse skin. Proc Am Assoc Cancer Res 38:1727
27. Tucker ON, Dannenberg AJ, Yang EK, Fahey TJ III (2004) Bile acids induce cyclooxygenase-2 expression in human pancreatic cancer cell lines. Carcinogenesis 25:419–423
28. Urano M, Abe M, Kuroda M, Mizoguchi Y, Horibe Y, Kasahara M, Tanaka K, Sudo K, Hirasawa Y (2001) Warthin-like tumor variant of papillary thyroid carcinoma: case report and literature review. Pathol Int 51:707–712
29. Vane JR, Bakhle YS, Botting RM (1998) Cyclooxygenases 1 and 2 Annu Rev Pharmacol Toxicol 38:97–120
30. Vidal S, Kovacs K, Bell D, Horvath E, Scheithauer BW, Lloyd RV (2003) Cyclooxygenase-2 expression in human pituitary tumors. Cancer 97:2814–2821
31. Xu B, Yoshimoto K, Miyauchi A, Kuma S, Mizusawa N, Hirokawa M, Sano T (2003) Cribriform-morular variant of papillary thyroid carcinoma: a pathological and molecular genetic study with evidence of frequent somatic mutations in exon 3 of the beta-catenin gene. J Pathol 199:58–67
32. Xu XC (2002) COX-2 inhibitors in cancer treatment and prevention, a recent development. Anticancer Drugs 13:127–137
33. Yoshimura R, Sano H, Masuda C, Kawamura M, Tsubouchi Y, Chargui J, Yoshimura N, Hla T, Wada S (2000) Expression of cyclooxygenase-2 in prostate carcinoma. Cancer 89:589–596
34. Zimmermann KC, Sarbia M, Weber AA, Borchard F, Gabbert HE, Schror K (1999) Cyclooxygenase-2 expression in human esophageal carcinoma. Cancer Res 59:198–204

Virchows Arch (2005) 447: 18–23
DOI 10.1007/s00428-005-1268-5

ORIGINAL ARTICLE

Bogdan Galusca · Jean Marc Dumollard · Sandrine Lassandre · Alain Niveleau · Jean Michel Prades · Bruno Estour · Michel Peoc'h

Global DNA methylation evaluation: potential complementary marker in differential diagnosis of thyroid neoplasia

Received: 24 December 2004 / Accepted: 3 April 2005 / Published online: 13 May 2005
© Springer-Verlag 2005

Abstract The implications of global DNA hypomethylation were recently reported in several models of tumorigenesis. Little is known about this epigenetic event in thyroid neoplasia. The study aimed to evaluate the status of global DNA methylation in several types of thyroid tumors using a monoclonal antibody specific for 5-methylcytidine (5-mc) and to define the diagnosis potential of this marker. 5-mc immunostaining scores were calculated in 17 papillary thyroid carcinomas (PTC), 6 follicular thyroid carcinomas (FTC), 16 follicular adenomas (FA), 19 nodular goiters (NG) and ten Hürthle cells adenomas (HCA). The expression of galectin-3 was also evaluated. Computerized image analysis showed a significant lower level of 5-mc immunostaining in thyroid carcinoma when compared with benign tumors or adjacent normal thyroid parenchyma ($P<0.0001$). Overall, 5-mc accuracy to distinguish malign from benign thyroid tumors was similar to that of galectin-3 (89% versus 87%, $P>0.05$). The combination of 5-mc with galectin-3 led to an excellent accuracy level of 96%. Among follicular neoplasia 5-mc accuracy to differentiate malign tumors trends to be higher than galectin-3 one (90% versus 66%, $P=0.06$). These data stress the necessity of epigenetic events evaluation among thyroid nodules and propose global DNA methylation assessment as a potential diagnostic tool to combine with other valuable markers.

Keywords DNA methylation · Thyroid neoplasia · Galectin-3

B. Galusca (✉) · S. Lassandre · B. Estour
Endocrinology, CHU,
Saint Etienne, France
e-mail: bgalusca@yahoo.com
Tel.: +33-63-0974041
Fax: +33-47-7120493

B. Galusca
Endocrinology, UMF Gr.T.Popa,
Iasi, Romania

J. M. Dumollard · M. Peoc'h
Pathology, CHU,
Saint Etienne, France

J. M. Dumollard · M. Peoc'h
EA6063, Inserm,
Saint Etienne, France

A. Niveleau
UPRESA 5082 CNRS, Joseph Fourier University,
Grenoble, France

J. M. Prades
ORL, CHU,
Saint Etienne, France

Introduction

Thyroid nodules represent a very common endocrine pathology, although only a small number are diagnosed as cancers. Over the last few decades, fine-needle aspiration biopsy (FNA) has had the central role in the management of thyroid nodules [21, 22]. Despite good accuracy initially declared [22], classical cytodiagnosis include an important number of indeterminate or non-diagnostic results [2, 11]. Generally, these cases undergo surgery, and up to 70% of them will be shown to be benign [2]. Moreover, a significant number of operated tumors with a certain overall appearance will display opposite patterns over the time for whom inadequate protocols were applied [25, 26, 45]. In consequence, additional tools are mandatory in order to improve the decisional selectivity before and after the surgery.

Several tumoral markers are currently assessed [3, 10, 18]. Over the last few years, a certain homogenous group of studies of histo and cytochemistry promoted galectin-3 as an overall differentiating solution of thyroid nodules [3, 4, 19, 20, 37, 38, 44]. Less enthusiastic researchers, namely those employing semiquantitative or real time RT-PCR, constantly stressed the limits of galectin-3 regarding the follicular neoplasia differentiation [6, 9, 14, 30, 34, 40]. Some studies reported up to 74% false results among follicular thyroid neoplasia [27, 32, 41, 46].

Multiple associations, including galectin-3, HBME-1, MET, fibronectin-1 and cytokeratin-19, have also been in-

vestigated. However, none of these attempts reached very high levels of accuracy [10, 41, 43]. A recent study reported the ability to differentiate malign from benign nodules using microarray technology and molecular profiling [16, 17]. The analysis produced a large list of genes that were significantly differentially expressed between carcinoma and benign thyroid lesions. In all cases, an overlap of gene expression was found between benign and malign tumors in favor of a continuity in tumor progression. Given such variety of gene expression abnormalities, a question arises regarding a "conspirative" trigger event. Consequently, new hypotheses concerning epigenetic-genetic interaction were advanced [15].

Literature data demonstrated recently that global genomic hypomethylation represents an epigenetic difference in cancer susceptibility [35]. Recently, preliminary results were published on the status of global DNA methylation in a small number of thyroid neoplasia [13]. The aim of this study is to verify the possibility of quantifying this phenomenon among thyroid neoplasia and to evaluate its diagnostic potential in distinguishing malign thyroid tumors, isolated or in combination with other valuable markers.

Materials and methods

Tissue samples

We evaluated thyroid neoplasms, including 17 papillary thyroid carcinomas (PTC), six follicular thyroid carcinomas (FTC), 16 follicular adenomas (FA), 19 nodular goiters (NG) and ten Hürthle cells adenomas (HCA). The tumors were classified according to widely accepted histopathologic criteria [29]. Papillary carcinomas were diagnosed based on characteristic cytological features, and architectural (papillary or follicular) patterns. Follicular carcinomas were distinguished from adenomas on the basis of cytological patterns [28] and invasion of the edges of the tumor and/or invasion of blood vessels in or beyond the capsule. Tumors were classified as Hürthle cell neoplasm when the predominant cell subtype (almost 75% of cells) had oncocytic features [29].

Immunohistochemistry (IHC)

All thyroid specimens were fixed in 10% formalin for 24 h. In all cases, immunohistochemical analysis was performed on routinely paraffin-embedded sections. The tissues were sectioned onto positively charged slides (SuperFrost Plus, Menzer-Glaser, Freiburg, Germany) and dewaxed with xylene and alcohol.

Global DNA methylation (5-mc) Antigen retrieval was performed in two steps: 40 min with citrate buffer (pH 3.4) in a water bath at 97°C and 30 min in 3 N HCl for at 37°C. Thereafter, slides were incubated with a hybridoma supernatant containing anti-5-methylcytidine monoclonal antibody at a concentration of 5 μg/ml for 1 h at room temperature on a DAKO TechMate 500 Plus. Arguments in favor of the accessibility of these antibodies have already been published [23, 35, 36].

Galectin-3 (gal-3) Antigen retrieval was performed in 10 mM citrate buffer (pH 6.0). Thereafter, slides were incubated with the primary antibody (NCL-GAL3, IgG2a, 1:200, Novocastra Laboratories, UK) for 40 min at room temperature on a DAKO TechMate 500 Plus.

The EnVision detection system and DAB (diaminobenzidine) chromogen (K4006, DAKO Corporation, Carpinteria, Calif., USA) were used for both antibodies.

Cell immunostaining evaluation

Visual analysis Two independent observers, blinded to clinical data previously established, evaluated galectin-3 immunostaining. Galectin-3 cytoplasmic staining was semiquantitatively scored by a method previously described [1, 5]: (0) no reactivity, (1) faint or weak, (2) moderate positivity, (3) strong positivity.

Computerized image analysis The optical density of the nuclei of epithelial cells stained with anti-5-methylcytidine antibody was measured in 20 microscopic fields belonging to the pathologic portion of the sample and in 20 fields of the normal tissue when possible, in a computerized system (SAMBA Technologies, Lyon, France), connected to a Leica D.M.R. microscope (100× objective). Every tissue was analyzed using the same optical conditions (luminosity). An average staining score was automatically calculated by SAMBA Technologies software.

Statistical analysis

Data are presented as mean±SE. Differences were assessed by Mann-Withney Rank sum test (unpaired) or Wilcoxon test (paired). Significance level was assigned at $P<0.05$. For every marker, ROC curves were calculated (MedCalc Software) in order to evaluate the accuracy of differentiation between benign and malign tumors (area under ROC curve—AUC). AUC values were automatically compared. The output data of every marker ROC analysis included also a cut-off value corresponding to a optimal sensitivity/specificity ratio.

The same statistics were employed in the subgroup of follicular neoplasia (malign and benign).

Results

General group (n=68)

Global DNA methylation Variable nuclear staining was noted in all studied specimens. Visual inspection reported in papillary carcinoma a higher labeling in the periphery of nuclei (compacted heterochromatin) (Fig. 1).

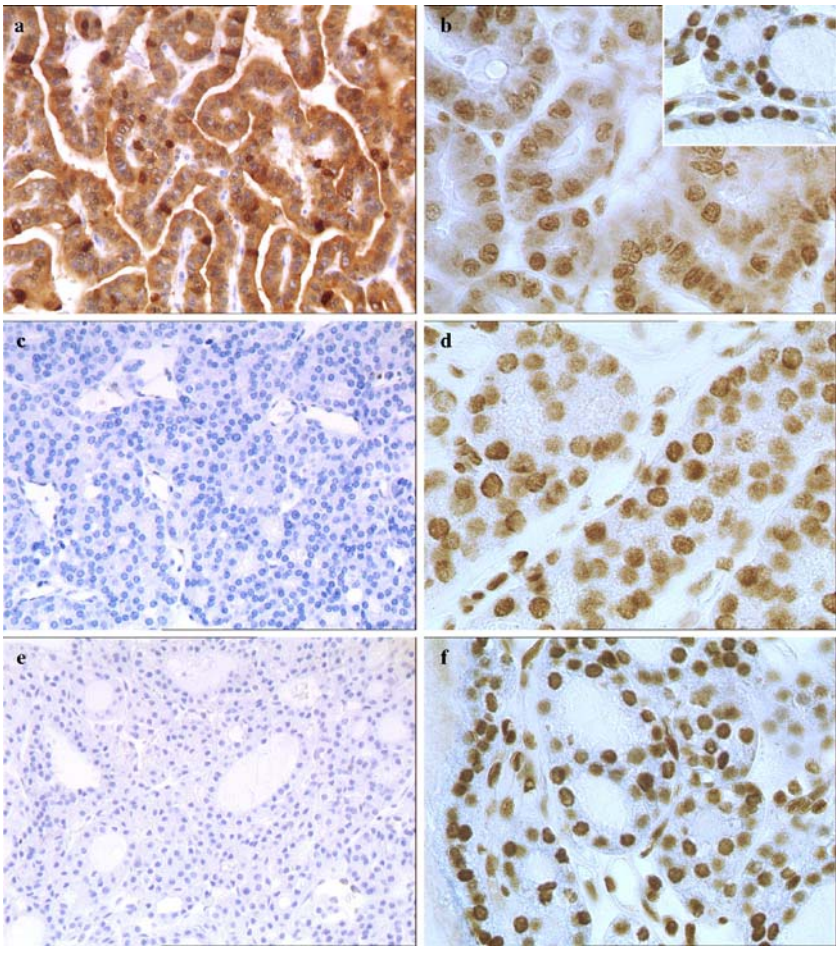


Fig. 1 DNA methylation (*right column*, ×100 magnification) and galectin-3 (*left column*, ×40 magnification) expresion in thyroid neoplasia. **a**, **b** papillary thyroid carcinoma; normal tissue is presented in Fig. 1**b** cartoon. **c**, **d** follicular thyroid carcinoma. **e**, **f** follicular adenoma

Computerized image analysis showed a significantly lower level of 5-mc immunostaining in thyroid carcinoma (PTC and FTC) compared with benign tumors (FA, HCA and NG) ($P<0.0001$, Mann-Witney test) (Fig. 2) or adjacent normal thyroid parenchyma ($P<0.0001$, Wilcoxon test). No difference was found between benign neoplasia and normal thyroid tissue ($P=0.3$). Receiver operator characteristics (ROC) performed to distinguish malign and benign tumors displayed a good accuracy of 89±3% and a optimal cut-off value of 35 with 96% sensitivity and 75% specificity (Table 1).

Galectin-3 Constant strong cytoplasmatic staining was found in PTC, while FTC revealed variable levels (Fig. 2).

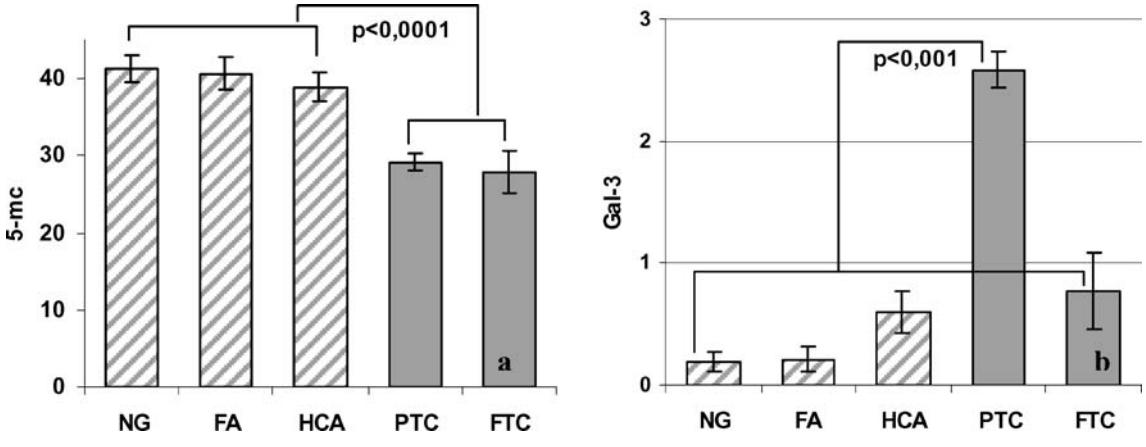


Fig. 2 **a** The mean levels of global DNA methylation assessed immunohistochemically, displayed a significant difference when comparing benign and malign thyroid neoplasia. **b** Gal-3 staining mean level was increased only in PTC. *NG* nodular goiter; *FA* follicular adenoma; *HCA* Hürthle cells adenoma; *PTC* papillary thyroid carcinoma; *FTC* follicular thyroid carcinoma

Table 1 Immunohistochemical results of 5-mc and galectin-3 in thyroid neoplasia

Diagnosis	5-mc* (%)	Gal-3** (%)
Normal thyroid tissue	0/17 (0)	0/17 (0)
Nodular goiter	3/19 (15,7)	2/19 (10,5)
Follicular adenoma	5/16 (31,2)	2/16 (12,5)
Hürthle cell adenoma	3/10 (30)	1/10 (10)
Papillary thyroid carcinoma	16/17 (94)	14/15 (93,3)
Follicular thyroid carcinoma	6/6 (100)	3/6 (50)

*Hypomethylated cases and **galectin-3 positive cases were differentiated according to cut-off values set automaticaly by employing MedCalc software: 5-mc≤35; galectin-3>0.5 (these values corresponding to an optimal specificity/sensibility ratio are orientative)

Gal-3 was found to be absent in almost all FA and NG. ROC curve performed to differentiate benign/malign tumors had an AUC of 87±4%, meaning a good accuracy level (Table 1). On a staining score scale from 0 to 4, an optimal cut-off value was set at 0.5 to differentiate benign and malign tumors with 80% sensitivity and 89% specificity.

A virtual marker was calculated for each specimen by combining gal-3 and 5-mc: GM=5-mc/10—galectin-3. ROC curve of this marker displayed an excellent accuracy level of 96±2%. This value was significantly greater than the accuracy of each marker assessed separately (P<0.001). No difference was found between the two parameters accuracies.

Global DNA methylation and galectin-3 accuracies in detecting papillary thyroid carcinoma presented no significant difference (88% versus 90%, P=0.72).

Follicular neoplasia (n=22)

ROC calculated accuracy of 5-mc IHC assessment trends to be significant grater than gal-3 one (90% versus 66%, P=0.06) in this type of tumors. Moreover, opposite to galectin-3, DNA methylation evaluation preserve its ability to differentiate FA from FTC (P=0.18 versus P=0.0018, Mann-Witney tests).

Discussion

The epigenetics of cancer was recently characterized as a complex dysregulation including global hypomethylation, individual gene hypomethylation and hypermethylation, chromatin modification and altered genomic imprinting [15]. Aberrant methylation and hypomethylation in particular were described in neoplasia as early events [12, 39]. The causes of this hypomethylation are not well known. Functionally, hypomethylation may contribute to chromosomal instability in cancer and, perhaps, to increased expression of selected affected genes [15].

To date, several cancer-associated regional DNA hyper- or hypomethylations have been identified in thyroid tumors [7, 8, 24, 31, 33, 42, 47, 48]. Recently, immunohistochemical techniques were developed in order to assess global methylation of DNA in individual cells [35, 36]. In the present study, we quantified this epigenetic feature in thyroid tumors by employing anti-5-methyl citidine antibodies.

Computerized image analysis allowed us to conclude that benign tumors (follicular or Hürthle cell adenoma, nodular goiter) had a significant higher global DNA methylation level than studied thyroid carcinoma (P<0.001). These results are in line with those previously published concerning 5–methylcytidine level in lung cancers cells [35, 36], breast carcinoma [39] or colorectal adenocarcinomas [23]. A recent study performed on eight cases of thyroid cancer and one multinodular goiter reported similar preliminary results [13].

In contrast to other tissues, benign tumors (stomach, breast) [12, 39], in thyroid follicular lesions the level of global methylation seems to be identical to that from normal thyroid parenchyma. Thus, we supposed that loss of methyl groups in thyroid neoplasia DNA is not such an early event as described in other tumorigenesis models [12, 39].

To better analyze the 5-mc diagnostic qualities, we evaluate this marker in parallel with galectin-3, a well-known, lately promoted marker in thyroid neoplasia differentiation [3]. In our study, the 5-mc diagnostic accuracy in differentiating thyroid tumors proved to be similar to that displayed by galectin-3 IHC assessment. A significant improvement was noticed when combining the evaluation of these two markers (accuracy—96%). In thyroid follicular neoplasia, a category for which galectin-3 differential abilities are controversial, 5-mc evaluation accuracy tends to be significant higher (90% versus 66%, P=0.06). These data propose an extension of global DNA methylation evaluation in thyroid cytologic smears.

In this paper, we stressed the diagnostic potential of global methylation evaluation among thyroid nodules. Our data corroborate a recent hypothesis in which epigenetic alteration contribute to tumor progression. It further suggest that recent microarray analysis revealing several overexpressed genes in thyroid carcinoma [16, 17] should be appended with an extensive approach of epigenetic dysregulation.

References

1. Aratake Y, Umeki K, Kiyoyama K, Hinoura Y, Sato S, Ohno A, Kuribayashi T, Hirai K, Nabeshima K, Kotani T (2002) Diagnostic utility of galectin-3 and CD26/DPPIV as preoperative diagnostic markers for thyroid nodules. Diagn Cytopathol 26:366–372
2. Baloch ZW, Fleisher S, LiVolsi VA, Gupta PK (2002) Diagnosis of "follicular neoplasm": a gray zone in thyroid fine-needle aspiration cytology. Diagn Cytopathol 26:41–44
3. Bartolazzi A, Gasbarri A, Papotti M, Bussolati G, Lucante T, Khan A, Inohara H, Marandino F, Orlandi F, Nardi F, Vecchione A, Tecce R, Larsson O (2001) Application of an immunodiagnostic method for improving preoperative diagnosis of nodular thyroid lesions. Lancet 357:1644–1650

4. Bartolazzi A, Papotti M, Orlandi F (2003) Methodological considerations regarding the use of galectin-3 expression analysis in preoperative evaluation of thyroid nodules. J Clin Endocrinol Metab 88:950; author reply 950–951
5. Beesley MF, McLaren KM (2002) Cytokeratin 19 and galectin-3 immunohistochemistry in the differential diagnosis of solitary thyroid nodules. Histopathology 41:236–243
6. Bernet VJ, Anderson J, Vaishnav Y, Solomon B, Adair CF, Saji M, Burman KD, Burch HB, Ringel MD (2002) Determination of galectin-3 messenger ribonucleic Acid overexpression in papillary thyroid cancer by quantitative reverse transcription-polymerase chain reaction. J Clin Endocrinol Metab 87:4792–4796
7. Boltze C, Schneider-Stock R, Quednow C, Hinze R, Mawrin C, Hribaschek A, Roessner A, Hoang-Vu C (2003) Silencing of the maspin gene by promoter hypermethylation in thyroid cancer. Int J Mol Med 12:479–484
8. Boltze C, Zack S, Quednow C, Bettge S, Roessner A, Schneider-Stock R (2003) Hypermethylation of the CDKN2/p16INK4A promotor in thyroid carcinogenesis. Pathol Res Pract 199:399–404
9. Buchs AE, Zehavi S, Sher O, Yeheskely E, Muggia-Sulam M, Sherman Y, Rapoport MJ (2003) Heparanase, galectin-3, and tissue factor mRNA are expressed in benign neoplasms of the thyroid. Endocrine 22:81–84
10. Casey MB, Lohse CM, Lloyd RV (2003) Distinction between papillary thyroid hyperplasia and papillary thyroid carcinoma by immunohistochemical staining for cytokeratin 19, galectin-3, and HBME-[1] Endocr Pathol 14:55–60
11. Chow LS, Gharib H, Goellner JR, van Heerden JA (2001) Nondiagnostic thyroid fine-needle aspiration cytology: management dilemmas. Thyroid 11:1147–1151
12. Cravo M, Pinto R, Fidalgo P, Chaves P, Gloria L, Nobre-Leitao C, Costa Mira F (1996) Global DNA hypomethylation occurs in the early stages of intestinal type gastric carcinoma. Gut 39:434–438
13. de Capoa A, Grappelli C, Volpino P, Bononi M, Musolino A, Ciardi A, Cavallaro A, Cangemi V (2004) Nuclear methylation levels in normal and cancerous thyroid cells. Anticancer Res 24:1495–1500
14. Feilchenfeldt J, Totsch M, Sheu SY, Robert J, Spiliopoulos A, Frilling A, Schmid KW, Meier CA (2003) Expression of galectin-3 in normal and malignant thyroid tissue by quantitative PCR and immunohistochemistry. Mod Pathol 16:1117–1123
15. Feinberg AP (2004) The epigenetics of cancer etiology. Semin Cancer Biol 14:427–432
16. Finley DJ, Arora N, Zhu B, Gallagher L, Fahey TJ III (2004) Molecular profiling distinguishes papillary carcinoma from benign thyroid nodules. J Clin Endocrinol Metab 89:3214–3223
17. Finley DJ, Zhu B, Barden CB, Fahey TJ III (2004) Discrimination of benign and malignant thyroid nodules by molecular profiling. Ann Surg 240:425–436; discussion 436–427
18. Galusca B, Dumollard JM, Chambonniere ML, Germain N, Prades JM, Peoc'h M, Estour B (2004) Peroxisome proliferator activated receptor gamma immunohistochemical expression in human papillary thyroid carcinoma tissues. Possible relationship to lymph node metastasis. Anticancer Res 24:1993–1997
19. Gasbarri A, Marchetti C, Iervasi G, Bottoni A, Nicolini A, Bartolazzi A, Carpi A (2004) From the bench to the bedside. Galectin-3 immunodetection for improving the preoperative diagnosis of the follicular thyroid nodules. Biomed Pharmacother 58:356–359
20. Gasbarri A, Martegani MP, Del Prete F, Lucante T, Natali PG, Bartolazzi A (1999) Galectin-3 and CD44v6 isoforms in the preoperative evaluation of thyroid nodules. J Clin Oncol 17:3494–3502
21. Gharib H (2004) Changing trends in thyroid practice: understanding nodular thyroid disease. Endocr Pract 10:31–39
22. Gharib H, Goellner JR (1993) Fine-needle aspiration biopsy of the thyroid: an appraisal. Ann Intern Med 118:282–289
23. Hernandez-Blazquez FJ, Habib M, Dumollard JM, Barthelemy C, Benchaib M, de Capoa A, Niveleau A (2000) Evaluation of global DNA hypomethylation in human colon cancer tissues by immunohistochemistry and image analysis. Gut 47:689–693
24. Huang Y, de la Chapelle A, Pellegata NS (2003) Hypermethylation, but not LOH, is associated with the low expression of MT1G and CRABP1 in papillary thyroid carcinoma. Int J Cancer 104:735–744
25. Ito Y, Tomoda C, Uruno T, Takamura Y, Miya A, Kobayashi K, Matsuzuka F, Kuma K, Miyauchi A (2004) Papillary microcarcinoma of the thyroid: how should it be treated? World J Surg 28:1115-1121
26. Ito Y, Uruno T, Nakano K, Takamura Y, Miya A, Kobayashi K, Yokozawa T, Matsuzuka F, Kuma S, Kuma K, Miyauchi A (2003) An observation trial without surgical treatment in patients with papillary microcarcinoma of the thyroid. Thyroid 13:381–387
27. Jakubiak-Wielganowicz M, Kubiak R, Sygut J, Pomorski L, Kordek R (2003) Usefulness of galectin-3 immunohistochemistry in differential diagnosis between thyroid follicular carcinoma and follicular adenoma. Pol J Pathol 54:111–115
28. Kini SR, Miller JM, Hamburger JI, Smith-Purslow MJ (1985) Cytopathology of follicular lesions of the thyroid gland. Diagn Cytopathol 1:123–132
29. LiVolsi VA (1990) Thyroid tumors. In: LiVolsi VA (ed) Surgical pathology of the thyroid. Saunders, Philadelphia, pp 131–212
30. Martins L, Matsuo SE, Ebina KN, Kulcsar MA, Friguglietti CU, Kimura ET (2002) Galectin-3 messenger ribonucleic acid and protein are expressed in benign thyroid tumors. J Clin Endocrinol Metab 87:4806–4810
31. Matsuo K, Tang SH, Zeki K, Gutman RA, Fagin JA (1993) Aberrant deoxyribonucleic acid methylation in human thyroid tumors. J Clin Endocrinol Metab 77:991–995
32. Mehrotra P, Okpokam A, Bouhaidar R, Johnson SJ, Wilson JA, Davies BR, Lennard TW (2004) Galectin-3 does not reliably distinguish benign from malignant thyroid neoplasms. Histopathology 45:493–500
33. Pichon B, Christophe-Hobertus C, Vassart G, Christophe D (1994) Unmethylated thyroglobulin promoter may be repressed by methylation of flanking DNA sequences. Biochem J 298 Pt 3:537–541
34. Pineda P, Rojas P, Liberman C, Moyano L, Goecke I (2003) [Detection of malignancy markers in thyroid nodules by reverse transcriptase polymerase chain reaction (RT-PCR)]. Rev Med Chil 131:965–972
35. Piyathilake CJ, Frost AR, Bell WC, Oelschlager D, Weiss H, Johanning GL, Niveleau A, Heimburger DC, Grizzle WE (2001) Altered global methylation of DNA: an epigenetic difference in susceptibility for lung cancer is associated with its progression. Hum Pathol 32:856–862
36. Piyathilake CJ, Johanning GL, Frost AR, Whiteside MA, Manne U, Grizzle WE, Heimburger DC, Niveleau A (2000) Immunohistochemical evaluation of global DNA methylation: comparison with in vitro radiolabeled methyl incorporation assay. Biotech Histochem 75:251–258
37. Saggiorato E, Aversa S, Deandreis D, Arecco F, Mussa A, Puligheddu B, Cappia S, Conticello S, Papotti M, Orlandi F (2004) Galectin-3: presurgical marker of thyroid follicular epithelial cell-derived carcinomas. J Endocrinol Invest 27:311–317
38. Saggiorato E, Cappia S, De Giuli P, Mussa A, Pancani G, Caraci P, Angeli A, Orlandi F (2001) Galectin-3 as a presurgical immunocytodiagnostic marker of minimally invasive follicular thyroid carcinoma. J Clin Endocrinol Metab 86:5152–5158
39. Soares J, Pinto AE, Cunha CV, Andre S, Barao I, Sousa JM, Cravo M (1999) Global DNA hypomethylation in breast carcinoma: correlation with prognostic factors and tumor progression. Cancer 85:112–118
40. Takano T, Miyauchi A, Matsuzuka F, Yoshida H, Kuma K, Amino N (2003) Ubiquitous expression of galectin-3 mRNA in benign and malignant thyroid tumors. Cancer Lett 199:69–73

41. Teng XD, Wang LJ, Yao HT, Li J, Ding W, Yan LP (2004) Expression of cytokeratin19, galectin-3 and HBME-1 in thyroid lesions and their differential diagnoses. Zhonghua Bing Li Xue Za Zhi 33:212–216
42. Venkataraman GM, Yatin M, Marcinek R, Ain KB (1999) Restoration of iodide uptake in dedifferentiated thyroid carcinoma: relationship to human Na+/I-symporter gene methylation status. J Clin Endocrinol Metab 84:2449–2457
43. Volante M, Bozzalla-Cassione F, DePompa R, Saggiorato E, Bartolazzi A, Orlandi F, Papotti M (2004) Galectin-3 and HBME-1 expression in oncocytic cell tumors of the thyroid. Virchows Arch 445:183–188
44. Volante M, Bozzalla-Cassione F, Orlandi F, Papotti M (2004) Diagnostic role of galectin-3 in follicular thyroid tumors. Virchows Arch 444:309–312
45. Wang TS, Dubner S, Sznyter LA, Heller KS (2004) Incidence of metastatic well-differentiated thyroid cancer in cervical lymph nodes. Arch Otolaryngol Head Neck Surg 130:110–113
46. Weber KB, Shroyer KR, Heinz DE, Nawaz S, Said MS, Haugen BR (2004) The use of a combination of galectin-3 and thyroid peroxidase for the diagnosis and prognosis of thyroid cancer. Am J Clin Pathol 122:524–531
47. Xing M, Tokumaru Y, Wu G, Westra WB, Ladenson PW, Sidransky D (2003) Hypermethylation of the Pendred syndrome gene SLC26A4 is an early event in thyroid tumorigenesis. Cancer Res 63:2312–2315
48. Xing M, Usadel H, Cohen Y, Tokumaru Y, Guo Z, Westra WB, Tong BC, Tallini G, Udelsman R, Califano JA, Ladenson PW, Sidransky D (2003) Methylation of the thyroid-stimulating hormone receptor gene in epithelial thyroid tumors: a marker of malignancy and a cause of gene silencing. Cancer Res 63: 2316–2321

Virchows Arch (2005) 447: 24–30
DOI 10.1007/s00428-005-1250-2

ORIGINAL ARTICLE

Asiye Safak Bulut · Esra Erden · Serpil Dizbay Sak · Hatice Doruk · Nazmiye Kursun · Dilek Dincol

Significance of inducible nitric oxide synthase expression in benign and malignant breast epithelium: an immunohistochemical study of 151 cases

Received: 10 December 2004 / Accepted: 4 March 2005 / Published online: 10 June 2005
© Springer-Verlag 2005

Abstract The role of calcium independent inducible nitric oxide synthase (iNOS) in breast carcinoma is controversial, and the implications of iNOS expression on prognosis are not known. In this study, we aimed to investigate the significance of immunohistochemical iNOS expression in 100 invasive ductal carcinomas. In addition, 11 normal breast tissues, 20 cases of usual ductal hyperplasias (UDHs) and 20 fibroadenomas were included. We found that 78% of malignant and 75% of benign cases showed iNOS immunoreactivity. However, the intensity and the quantity of iNOS expression were significantly higher in the cancer group when compared with benign breasts ($P<0.001$), suggesting a role of iNOS in breast carcinogenesis. We were unable to show a correlation between iNOS expression and tumor grade, axillary lymph node status, and estrogen receptor expression. In 50 axilla negative cases having 5–12 years follow-up, disease free survival (DFS) rate was significantly lower in cases showing strong iNOS expression ($P=0.05$). As strong iNOS expression was correlated with short DFS, we concluded that further studies would be necessary to elucidate if iNOS expression might be a useful prognostic marker in breast carcinoma, especially in the axilla negative group.

Keywords Nitric oxide synthase · Benign breast disease · Breast carcinoma · Immunohistochemistry

Part of this study was presented at XXIVth International Congress of the International Academy of Pathology, Amsterdam, The Netherlands on 5–10 October 2002 as a poster presentation.

A. S. Bulut · E. Erden · S. D. Sak
Department of Pathology,
Medical School of Ankara University,
Ankara, Turkey

H. Doruk · D. Dincol
Department of Medical Oncology,
Medical School of Ankara University,
Ankara, Turkey

N. Kursun
Department of Biostatistics,
Medical School of Ankara University,
Ankara, Turkey

A. S. Bulut (✉)
Ankara Universitesi Tip Fakultesi, Patoloji ADB,
Sihhiye/Ankara, Turkey
e-mail: asafakbulut@yahoo.com
Tel.: +90-312-3103010
Fax: +90-312-3106370

Introduction

Nitric oxide (NO), a free radical, is involved in several regulatory mechanisms as an intracellular second messenger, but the role of NO in tumor biology is poorly understood. NO seems to have a dose dependent and biphasic effect on tumor growth resulting from its influence on apoptosis and angiogenesis [3]. NO is generated from L-arginine by NO synthase (NOS), which is present in three isoforms, neuronal (nNOS), endothelial (eNOS) and calcium independent inducible (iNOS or NOSII) [3, 7]. iNOS generates a high amount of NO over a prolonged period, whereas the effect of the other two isoforms is smaller with regard to the amount of NO generated and the duration of their effects.

In recent studies, iNOS expression has been reported in human pharynx, esophagus, pancreas, colon, gallbladder, lung, bladder, cervix, ovary, prostate and thyroid carcinomas, cutaneous adnexal tumors, primary malignant mesotheliomas and metastatic malignant melanomas [1, 4, 6, 8, 12–15, 18, 21, 23, 25–27, 29–31, 34, 36–40]. There are also some studies on primary breast carcinomas and benign breast lesions with conflicting results [5, 10, 19, 20, 28, 33, 35]. In a few previous studies, iNOS expression was evaluated with regard to some prognostic clinicopathological parameters (axillary lymph node status, estrogen receptor status, grade) [5, 19, 20, 28, 33], but there is only one previous study on the implication of iNOS expression on survival rate [20].

The aim of this study was to examine iNOS expression immunohistochemically, in a large series of primary breast carcinomas, to determine the possible relationships be-

tween iNOS expression and clinicopathological parameters such as axillary lymph node status, tumor grade, estrogen receptor status and prognosis. In addition, it was aimed to investigate the iNOS expression with a special emphasis on the possible differences within the spectrum of normal to highly proliferative benign breast epithelium.

Materials and methods

Patients

Group 1 (malignant)

Archival sections from operation specimens of 100 patients with invasive ductal carcinoma, diagnosed between 1990 and 2002, and treated with modified radical mastectomy (n=78), lumpectomy/quadranectomy (n=22) and axillary dissection (n=99), were re-evaluated. Axillary lymph node status, tumor grade according to the modified Bloom and Richardson system and estrogen receptor status as determined by immunohistochemistry were recorded. Five to 12 years follow-up information was available for 50 patients. All of the 50 patients with follow-up information were axilla negative breast carcinoma patients evaluated for a previous study. Recurrences, metastases and/or death due to the disease in the follow-up period were considered as a poor prognosis, while no evidence of disease was considered as a good prognosis. DFS and OS rates were also evaluated.

Group 2 (benign)

Archival sections from tissue samples of 40 patients operated on for benign breast disease (20 fibroadenomas and 20 usual ductal hyperplasias (UDHs)) and normal breast tissue from 11 reduction mammoplasty specimens were re-evaluated. UDHs were graded as severe (formation of epithelial bridges across the lumen or filling and distention of the duct), moderate (tufting and the tendency to cross lumens) or mild (three to four cells layers above the basement membrane) [32]. All tissues were fixed in 10% neutrally buffered formalin and embedded in paraffin.

Immunohistochemistry

Sections 5 μm thick were cut from representative blocks and deparaffinized. Without using any pretreatment, sections were washed with PBS. Endogenous peroxidase activity was blocked by incubating with 3% H_2O_2. Histostain-Plus Kit (Zymed Laboratories, San Francisco, Calif., USA) was used as the secondary system. Protein blocking solution in the kit was used as a blocking agent. Sections were then incubated with a primary antibody (Onkogene, Calbiochem, San Diego, Calif., USA; anti-nitric oxide synthase (1131–1144), inducible, rabbit pAB–Cat. No. 482728; dilution:1:1750) against iNOS, without any cross-reactivity with nNOS or eNOS, at room temperature for 2.5 h. Sections were then washed with PBS and incubated with biotinylated secondary antibody for 15 min. After a further step of washing with PBS, sections were incubated with Streptavidin-HRP conjugate for 15 min. After washing in PBS, amino-ethyl carbazole was used as chromogen and finally Mayer's hematoxylin was used for counterstaining. Sections from a known iNOS positive colon carcinoma were used as positive control. Negative controls substituting PBS for the primary antibody were included for each slide run.

The scoring system suggested by Soini et al. was used for iNOS evaluation [30]. Cytoplasmic granular and/or diffuse staining pattern was taken as positive. According to this system, the quantity of iNOS-positive cells was evaluated in the mostly stained area of each tissue subjectively and scored as 0–4 as follows: 0: no positive immunostaining; 1: <25%; 2: 25–50%; 3: 50–75%; 4: >75% of cells showing cytoplasmic positivity. The intensity of staining was estimated visually by dividing the staining reaction in five groups: 0: no positive immunostaining; 1: weak; 2: moderate; 3: strong; 4: very strong staining intensity.

The scoring system suggested by Leake et al. was used for estrogen receptor (ER) evaluation [17]. Only nuclear staining was taken as positive. According to this system, the percentage (quantity) of ER-positive tumor cells was calculated by counting the number of positive cells on a total of 500 cells in the mostly stained area of each tissue and scored as follows:

0: no positive immunostaining; 1: <1%; 2: 1–10%; 3: 11–33%; 4: 34–66%; 5: 67–100% of tumor cells showing nuclear positivity. The intensity of staining was estimated visually by dividing the staining reaction in four groups: 0: no positive immunostaining; 1: weak, 2: moderate, 3: strong staining intensity.

The intensity and quantity scores for each antibody were added together and a total staining score (TSS) was obtained. TSS was then divided into three main groups: no immunostaining (score 0), weak immunostaining (score 1–4) and strong immunostaining (score 5–8).

In evaluation of the immunohistochemical stainings, scoring was performed by two different observers independently and when the scores were inconsistent, a third observer was also asked to score and the results were discussed.

Statistical analysis

SPSS for Windows was used for statistical analysis. Mann-Whitney U, Pearson correlation, Student t-test and Kaplan-Meier survival analysis were performed to detect the associations between clinicopathological parameters and iNOS expression. A P-value of equal to or less than 0.05 was considered as significant.

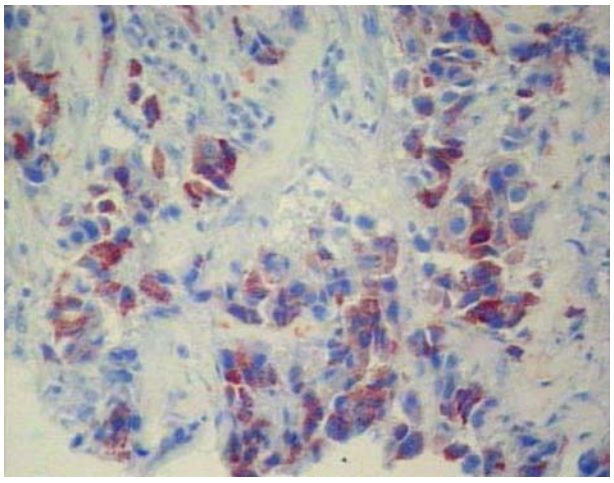


Fig. 1 Strong and widespread iNOS immune staining in a grade II invasive ductal carcinoma; original magnification is ×400

Results

The age of the patients in group 1 ranged from 28 to 76 years, with a mean of 49.4 years. In group 2, ages were 30–68 (mean 46.9), 14–47 (mean 39.3) and 16–63 (mean 35.7) years for UDHs, fibroadenomas and normal breasts, respectively. Thirty-two out of 99 patients had axillary lymph node metastasis at the time of operation; axillary lymph node dissection was not available in one patient. 22 tumors were grade I, 54 were grade II and 24 were grade III. In the second group, UDHs were graded as severe in seven, as moderate in seven and as mild in six patients.

Staining for iNOS was observed in the epithelial component of non-malignant tissues and in tumoral and/or nontumoral epithelial cells in carcinoma cases, either in granular or diffuse cytoplasmic pattern (Fig. 1). Generally, the staining pattern was not homogenous within a single case. Strongly stained cells were observed adjacent to non-stained cells (Figs. 2, 3). Stromal cells did not show immunoreactivity for iNOS.

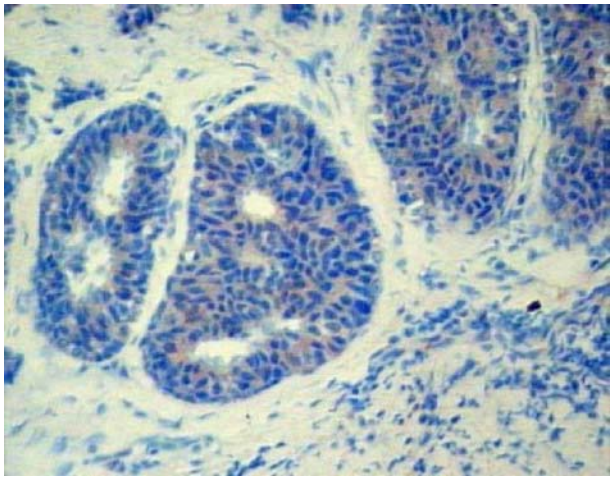


Fig. 2 Mild iNOS immune staining of epithelial cells in UDH; original magnification is ×200



Fig. 3 Focal and strong iNOS immune staining in a fibroadenoma; original magnification is ×100

Positive iNOS immunostaining was detected in 78% of carcinomas (Fig. 1). In the second (benign) group, 13/20 (65%) UDHs, 18/20 (90%) fibroadenomas and 7/11 (63.6%) normal breasts showed iNOS expression (Figs. 2, 3). TSS was significantly higher in the malignant group ($P<0.001$) (Table 1). In UDHs, 6/7 (85.7%) cases with severe, 4/7 (57.1%) cases with moderate and 3/6 (50%) cases with mild hyperplasia showed iNOS positivity. Although the percentage of strongly stained cases increased by the hyperplasia grade, the number of UDH cases was too small to make a statistical analysis between TSS of different hyperplasia grades. (Table 1).

iNOS expression did not show any significant correlation with tumor grade, axillary lymph node status and ER status (Table 2).

In 50 carcinoma patients having 5–12 years follow-up, disease free survival (DFS) and overall survival (OS) rate was 73% and 87%, respectively. Within the follow-up period, 11 cases showed a poor prognosis (four local recurrences, four distant metastasis, three recurrences and metastasis) and four of these patients died of the disease. Thirty-nine cases showed a good prognosis and remained free of the disease. Seventy-three percent of cases with poor prognosis and 41% of cases with good prognosis showed strong iNOS immunoreactivity. OS rates showed no significant difference between tumors showing strong and no/weak iNOS expression, but DFS rate was significantly lower in tumors showing strong iNOS expression ($P=0.05$), suggesting a negative impact of strong iNOS positivity on prognosis in axilla negative cases (Table 3) (Figs. 4, 5).

Discussion

Nitric oxide (NO), a free radical generated from L-arginine by NO synthases, is an important mediator of physiological functions such as vasodilatation, inhibition of platelet aggregation and neurotransmission in low concentrations. Although the role of NO in tumorigenesis and tumor progression is not clearly understood, experimental and

Table 1 iNOS expression in malignant and benign breast lesions and in normal breast

Groups	iNOS expression			Total *n*
	No (TSS:0) n (%)	Weak (TSS:1–4) n (%)	Strong (TSS:5–8) n (%)	
Group 1 (malignant)	22 (22.0)	32 (32.0)	46 (46.0)	100
Group 2 (benign)				
UDH				
Mild	3 (50.0)	2 (33.3)	1 (16.7)	6
Moderate	3 (42.8)	2 (28.6)	2 (28.6)	7
Severe	1 (14.4)	3 (42.8)	3 (42.8)	7
Fibroadenoma	2 (10.0)	16 (80.0)	2 (10.0)	20
Normal breast	4 (36.4)	6 (54.5)	1 (9.1)	11

clinicopathological data suggest that it has biphasic, dose and organ dependent effects. The role of NO in carcinogenesis is probably due to a combination of its dose-dependent and biphasic effects on apoptosis, tumor cell invasiveness and angiogenesis [3]. Although there are at least three different isoforms of NOS generating NO, iNOS gains special attention because it generates higher levels of NO and it has a prolonged activity [7].

In the literature, iNOS expression is observed in malignant cells of different tumors such as bladder, colon, prostate, esophagus, thyroid, pancreas, liver, lung and laryngeal carcinomas; brain tumors, malignant mesotheliomas, malignant melanomas and bone metastases of different tumors [2, 6, 9, 11–14, 18, 24, 30, 31, 36, 37, 39]. In some of these studies, stromal cells such as vascular smooth muscle, macrophages and endothelium have also been shown to be positive for iNOS [10, 13].

According to studies in the literature, 35–61% of breast carcinomas show iNOS expression [5, 19, 28, 33]. To our knowledge there are only three studies, with conflicting results, in which benign breast lesions have been studied and only in one study expression of iNOS in normal breast has been evaluated [19, 28, 33]. In the present study, we observed iNOS positivity in 78% of the cases, in a series of 100 invasive ductal carcinomas. Most of the UDHs, fibroadenomas and normal breasts also showed iNOS expression. Therefore, we suggest that iNOS expression cannot be used for distinguishing malignant epithelial cells from benign ones. However, TSS was remarkably higher in malignant group and this finding suggests a possible role of iNOS in breast carcinogenesis.

iNOS expression was evaluated in two studies on four and eight fibroadenomas in the literature and iNOS expression was not observed [19, 28]. However, in our series consisting of 20 fibroadenomas, iNOS positivity was present in 90% of fibroadenomas. In the literature, there is only one study on iNOS expression in proliferative benign breast lesions [19] in which iNOS expression was not observed in 15 cases. In our study, we found that 65% of 20 UDHs expressed iNOS. Although the percentage of stained cases increased with the hyperplasia grade, the number of UDH cases was too small to make a statistical analysis to show the correlation between iNOS expression and hyperplasia grade. There is only one study about iNOS expression in normal breasts. In this study, Tsugguel et al. showed iNOS expression in most of the epithelial cells in four normal breast tissues [33]. In our study, we also observed iNOS expression in normal breasts. In the previous studies, different polyclonal [19] and monoclonal [28, 33] primary antibodies were used. The discordance between the results concerning iNOS staining in benign breast epithelium may be related to the use of different primary antibody sources and technical procedures in these studies.

There are a few studies on the association of iNOS expression with prognostic parameters in breast carcinomas. The relationship between tumor grade and iNOS expression is controversial. Although NOS activity was more prominent in low-grade tumors in two studies [28, 33],

Table 2 iNOS expression in invasive ductal carcinomas with regard to clinicopathological parameters and prognosis

Parameters	iNOS			*P* value
	No n (%)	Weak n (%)	Strong n (%)	
Axillary lymph node[a]				
(−) n:68	17 (25.0)	17 (25.0)	34 (50.0)	0.2962
(+) n:31	5 (16.1)	14 (45.2)	12 (38.7)	
Grade				
I n:22	6 (27.3)	6 (27.3)	10 (45.4)	0.9850
II n:57	10 (17.6)	19 (33.3)	28 (49.1)	
III n:24	6 (25.0)	7 (29.2)	11 (45.8)	
Prognosis[b]				
Good n:39	13 (33.3)	10 (25.7)	16 (41.0)	0.0639
Poor n:11	1 (9.1)	2 (18.2)	8 (72.7)	
ER expression				
No/weak n:29	7 (24.2)	11(37.9)	11 (37.9)	0.3008
Strong n:71	15 (21.1)	21(29.6)	35 (49.3)	

[a]Axillary lymph node status was not available in one patient
[b]Prognostic information was available for 50 patients

Table 3 iNOS expression and OS, DFS rates in 50 axilla negative patients

	iNOS		*P* value
	No/weak (TSS:0–4)	Strong (TSS:5–8)	
OS rate	95%	77%	0.25
DFS rate	87%	56%	0.05

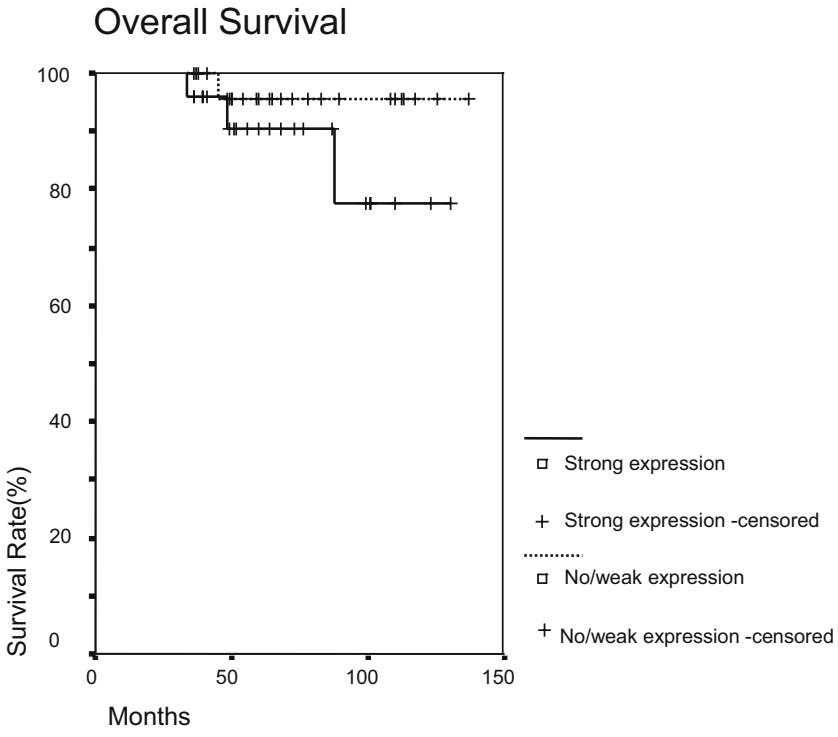


Fig. 4 Overall survival rates of strong and weak iNOS expressing malignant cases

detection of iNOS was positively correlated with decreasing tumor differentiation in another study [20]. There was no correlation in one other study, consistent with our findings [5]. We did not detect any significant correlation between axillary lymph node status and iNOS expression like Reveneau et al.'s study. However, Duenas-Gonzales et al. observed that most of the axilla positive cases were iNOS positive and a trend toward a lower median number of involved nodes was observed in iNOS positive tumors by Loibl et al. [5, 19]. There are only two previous studies investigating the correlation of iNOS expression with ER, and no relation was observed between ER and iNOS expressions either in the present or in previous studies [5, 20].

There are controversial reports about the relationship between iNOS expression in cancer cells from different carcinomas and prognosis. Kong et al., Pukkila et al. and Oka et al. reported that the expression of iNOS shows no prognostic value in pancreatic, pharyngeal and cervical

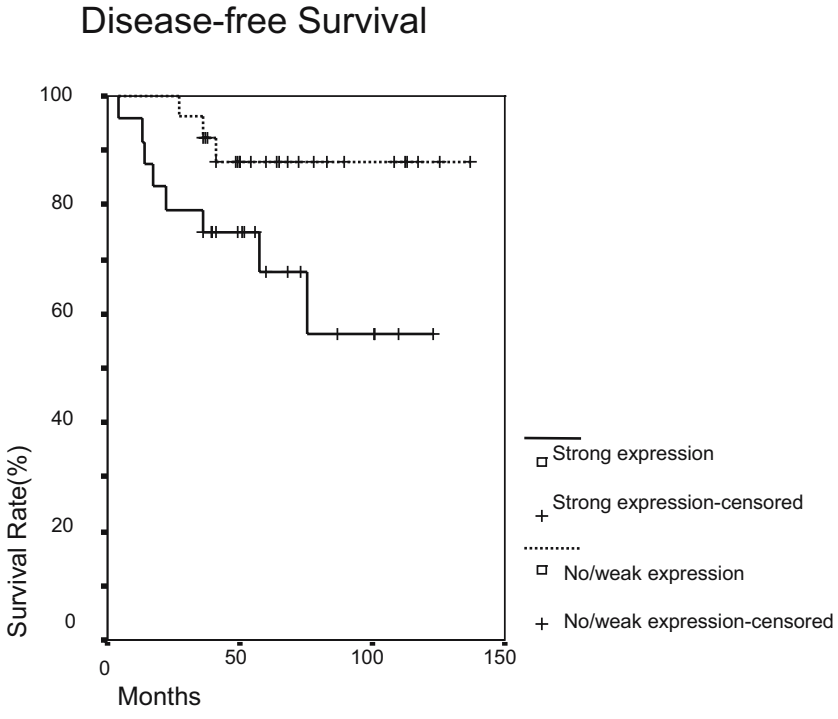


Fig. 5 Disease free survival rates of strong and weak iNOS expressing malignant cases

carcinomas, respectively [15, 23, 26]. On the other hand Ekmekcioglu et al., Raspollini et al., Niu et al., Huang et al., Nozoe et al. and Lagares-Garcia et al. reported that iNOS expression strongly correlated with poor survival and aggressive biological behavior in metastatic melanomas, ovarian serous carcinomas, primary gallbladder carcinomas, supraglottic squamous cell carcinomas and colorectal carcinomas, respectively [6, 9, 16, 21, 22, 27]. Conversely, Ropponen et al. and Puhakka et al. reported that patients with tumors showing high expressions of iNOS and other NOS izozymes had better survival rates in colorectal and non-small cell lung carcinomas [25, 29]. Loibl et al. have studied the impact of iNOS expression on prognosis recently and patients with iNOS positive breast carcinomas were found to have a significantly worse overall survival rate versus those with negative stains [20]. In the present study, in a series of 50 axilla negative invasive ductal breast carcinomas, we observed that patients showing strong iNOS expression had a lower DFS rate than those showing no/weak iNOS expression. This finding suggests that strong iNOS positivity may be a predictor of poor prognosis in axilla negative invasive ductal carcinomas and further studies are needed in this patient group.

In conclusion, iNOS expression can be observed in both benign and malignant mammary epithelium and it cannot be used as an indicator of malignancy. Expression of iNOS is an expected finding in benign epithelium, considering the various physiological functions of nitric oxide [10]. However its stronger expression in carcinomas suggests that it may have a role in pathogenesis of breast carcinoma. Nitric oxide produced by increased iNOS expression may help angiogenesis combined with an increase in tumor blood flow [10, 19]. We believe that strong iNOS expression in the majority of axilla negative breast carcinoma cases with poor prognosis deserves further studies. iNOS expression might prove useful in selection of the cases candidate for more aggressive therapy.

References

1. Aaltomaa SH, Lipponen PK, Viitanen J, Kankkunen JP, Ala-Opas MY, Kosma VM (2000) The prognostic value of inducible nitric oxide synthase in local prostate cancer. BJU Int 86:234–239
2. Brennan PA, Sharma S, Bowden JR, Umar T (2003) Expression of inducible nitric oxide synthase in bone metastasis. Eur J Surg Oncol 27:619–623
3. Chinje EJ, Stratford IJ (1997) Role of nitric oxide in growth of solid tumors: a balancing act. Essays Biochem 32:61–72
4. Choe W, Kim S, Hwang TS, Lee SS (2003) Expression of inducible nitric oxide synthase in thyroid neoplasms: immunohistochemical and molecular analysis. Pathol Int 53:434–439
5. Duenas-Gonzales A, Isales CM, Abad-Hernandez MD, Gonzalez-Sarmiento R, Sangueza O, Rodriguez-Commes J (1997) Expression of inducible nitric oxide synthase in breast cancer correlates with metastatic disease. Mod Path 10:645–649
6. Ekmekçioğlu S, Ellerhorst J, Smid CM, Prieto VG, Munsell M, Buzaid AC, Grimm EA (2000) Inducible nitric oxide synthase and nitrotyrosine in human metastatic melanoma tumors correlate with poor survival. Clin Cancer Res 6:4768–4775
7. Forstermann U, Closs EI, Pollock JS, Nakane M, Schwarz P, Gath I, Kleinert H (1994) Nitric oxide synthase isozymes. Characterization, purification, molecular cloning, and functions. Hypertension 23(part 2):1121–1131
8. Hong SK, Gul YA, Ithnin H, Talib A, Seow HF (2004) Expression of beta-catenin, COX-2 and iNOS in colorectal cancer: relevance of COX-2 and iNOS inhibitors for treatment in Malaysia. Asian J Surg 27:10–17
9. Huang Z, Zeng ZY, Peng HW, Xia LP, Hou JH (2003) Inducible nitric oxide synthase and basic fibroblast growth factor expression as prognostic factors in supraglottic squamous cell carcinoma. Aizheng 22:978–981
10. Jadeski LC, Hum KO, Chakraborty C, Lala PK (2000) Nitric oxide promotes murine mammary tumor growth and metastasis by stimulating tumor cell migration, invasiveness and angiogenesis. Int J Cancer 86:30–39
11. Kato S, Esumi H, Hirano A, Kato M, Asayama K, Ohama E (2003) Immunohistochemical expression of inducible nitric oxide synthase (iNOS) in human brain tumors: relationship of iNOS to superoxide dismutase (SOD) proteins (SOD1 and SOD2), Ki-67 antigen (MIB-1) and p53 protein. Acta Neuropathol 105: 333–340
12. Kitano H, Kitanishi T, Nakanishi Y, Suzuki M, Takeuchi E, Yazawa Y, Kitajima K, Kimura H, Tooyama I (1999) Expression of inducible nitric oxide synthase in human thyroid papillary carcinomas. Thyroid 9:113–117
13. Klotz T, Bloch W, Volberg C, Engelmann U, Addicks K (1998) Selective expression of inducible nitric oxide synthase in human prostate carcinoma. Cancer 82:1897–1903
14. Kojima M, Morisaki T, Tsukahara Y, Uchiyama A, Matsunari Y, Mibu R, Tanaka M (1999) Nitric oxide synthase expression and nitric oxide production in human colon carcinoma tissue. J Surg Oncol 70:222–229
15. Kong G, Kim EK, Kim WS, Lee KT, Lee YW, Lee JK, Paik SW, Rhee JC (2002) Role of cyclooxygenase-2 and inducible nitric oxide synthase in pancreatic cancer. J Gastroenterol Hepatol 17:914–921
16. Lagares-Garcia JA, Moore RA, Collier B, Heggere M, Diaz F, Qian F (2001) Nitric oxide synthase as a marker in colorectal carcinoma. Am Surgeon 67:709–713
17. Leake R, Barnes D, Pinder S, Ellis I, Anderson L, Anderson T, Adamson R, Rhodes T, Miller K, Walker R (2000) Immunohistochemical detection of steroid receptors in breast cancer: a working protocol. J Clin Pathol 53:634–635
18. Liu CY, Wang CH, Chen TC, Lin HC, Yu CT, Kuo HP (1998) Increased level of exhaled nitric oxide and up-regulation of inducible nitric oxide synthase in patients with primary lung cancer. Br J Cancer 78:534–541
19. Loibl S, Von Minckwitz G, Weber S, Sinn HP, Schini-Kerth VB, Lobysheva I, Nepveu F, Wolf G, Strebhardt K, Kaufmann M (2002) Expression of endothelial and inducible nitric oxide synthase in benign and malignant lesions of the breast and measurement of nitric oxide using electron paramagnetic resonance spectroscopy. Cancer 95:1191–1198
20. Loibl S, Buck A, Strank C, von Minckwitz G, Roller M, Sinn HP, Schini-Kerth V, Solbach C, Strebhardt K, Kaufmann M (2005) The role of early expression of inducible nitric oxide synthase in human breast cancer. Eur J Cancer 41:265–271
21. Niu X-J, Wang Z-R, Wu S-L, Geng Z-M, Zhang Y-F, Qing L (2004) Relationship between inducible nitric oxide synthase expression and angiogenesis in primary gallbladder carcinoma tissue. World J Gastroenterol 10:725–728
22. Nozoe T, Yasuda M, Honda M, Inutsuka S, Korenaga D (2002) Immunohistochemical expression of cytokine induced nitric oxide synthase in colorectal carcinoma. Oncol Rep 9:521–524
23. Oka K, Suzuki Y, Iida H, Nakano T (2003) PD-ECGF positivity correlates with better survival, while iNOS has no predictive value for cervical carcinomas treated with radiotherapy. Int J Radiat Oncol Biol Phys 57:217–221

24. Peng JP, Zheng S, Xiao ZX, Zhang SZ (2003) Inducible nitric oxide synthase expression is related to angiogenesis, bcl-2 and cell proliferation in hepatocellular carcinoma. J Zhejiang Univ Sci 4:221–227
25. Puhakka A, Kinnula V, Napankangas U, Saily M, Koistinen M, Paakko P, Soini Y (2003) High expression of nitric oxide synthases is a favorable prognostic sign in non-small cell lung carcinoma. Acta Pathol Microbiol Immunol Scand 111:1137–1146
26. Pukkila MJ, Kellokoski JK, Virtaniemi JA, Kumpulainen EJ, Johansson RT, Halonen PM, Kosunen AS, Nuutinen J, Kosma VM (2002) Inducible nitric oxide synthase expression in pharyngeal squamous cell carcinoma: relation to p53 expression, clinicopathological data, and survival. Laryngoscope 112:1084–1088
27. Raspollini MR, Amunni G, Villanucci A, Boddi V, Baroni G, Taddei A, Taddei GL (2003) Expression of inducible nitric oxide synthase and cyclooxygenase in ovarian cancer: correlation with clinical outcome. Gynecol Oncol 92:806–812
28. Reveneau S, Arnould R, Jolimoy G, Hilpert S, Lejeune P, Saint-Giorgio V, Belichard C, Jeannin JF (1999) Nitric oxide synthase in human breast cancer is associated with tumor grade, proliferation rate, and expression of progesterone receptors. Lab Invest 79:1215–1225
29. Ropponen KM, Kellokoski JK, Lipponen PK, Eskelinen MJ, Alanne L, Alhava EM, Kosma VM (2000) Expression of inducible nitric oxide synthase in colorectal cancer and its association with prognosis. Scand J Gastroenterol 35:1204–1211
30. Soini Y, Kahlos K, Puhakka A, Lakari E, Saily M, Paakko P, Kinnula V (2000) Expression of inducible nitric oxide synthase in healthy pleura and malignant mesothelioma. Br J Cancer 83:880–886
31. Tanaka H, Kijima H, Tokunaga T, Tajima T, Himeno S, Kenmochi T, Oshiba G, Kise Y, Nishi T, Chino O, Shimada H, Machimura T, Tanaka M, Makuuchi M (1999) Frequent expression of inducible nitric oxide synthase in esophageal squamous cell carcinoma. Int J Oncol 14:1069–1071
32. Tavassoli FA (1999) Ductal intraepithelial neoplasia. In: Tavassoli FA (ed) Pathology of the breast, 2nd edn. Appleton & Lange, Stamford, Connecticut, p 212
33. Tschugguel W, Schneeberger C, Unfried G, Czerwenka K, Weninger W, Mildner M, Gruber DM, Sator MO, Waldhör T, Huber JC (1999) Expression of inducible nitric oxide synthase in human breast cancer depends on tumor grade. Breast Cancer Res Treat 56:145–151
34. Umar T, Bowden J, Cameron S, Willy PJ, Anand R, Baker Ilankoran V, Brennan PA (2003) Expression of inducible nitric oxide synthase in cutaneous adnexal tumors of the head and neck. Int J Oral Maxillofac Surg 32:534–538
35. Vakkala M, Kahlos K, Lakari E, Paakko P, Kinnula V, Soini Y (2000) Inducible nitric oxide synthase expression, apoptosis, and angiogenesis in in-situ and invasive breast carcinomas. Clin Cancer Res 6:2408–2416
36. Vickers SM, MacMillan-Crow LA, Green M, Ellis C, Thomsen JA (1999) Association of increased immunostaining for inducible nitric oxide synthase and nitrotyrosine with fibroblast growth factor transformation in pancreatic cancer. Arch Surg 134:245–251
37. Wang J, Torbenson M, Wang Q, Ro JY, Becich M (2003) Expression of inducible nitric oxide synthase in paired neoplastic and non-neoplastic primary prostate cell cultures and prostatectomy specimen. Urol Oncol 21:117–122
38. Wolf H, Haeckel C, Roessner A (2000) Inducible nitric oxide synthase expression in human urinary bladder cancer. Virchows Arch 437:662–666
39. Yagihashi N, Kasajima H, Sugai S, Matsumoto K, Ebina Y, Morita T, Murakami T, Yagihashi S (2000) Increased in situ expression of nitric oxide synthase in human colorectal cancer. Virchows Arch 436:109–114
40. Zhang M, Pan JW, Ren TR, Zhu YF, Han YJ, Kuhnel W (2003) Correlated expression of inducible nitric oxide synthase and p53, Bax in benign and malignant diseased gallbladder. Ann Anat 185:549–554

Virchows Arch (2005) 447: 31–44
DOI 10.1007/s00428-005-1246-y

ORIGINAL ARTICLE

H. Hůlková · J. Ledvinová · B. Asfaw · K. Koubek · K. Kopřiva · M. Elleder

Lactosylceramide in lysosomal storage disorders. A comparative immunohistochemical and biochemical study

Received: 14 October 2004 / Accepted: 1 March 2005 / Published online: 26 May 2005
© Springer-Verlag 2005

Abstract Immunohistochemical studies of the presence of lactosylceramide (LacCer) in lysosomal storage disorders (LSDs) were done using anti-LacCer monoclonal antibody of the CDw17 type (clone MG-2). No sign of an association between LacCer and the lysosomal system in normal cells was observed, except for histiocytes active in phagocytosis. A comparative study of a group of LSDs showed a general tendency for LacCer to increase in storage cells in Niemann-Pick disease type C (NPC), and types A and B, GM1 gangliosidosis, acid lipase deficiency, glycogen storage disease type II and mucopolysaccharidoses. LacCer accumulated in storage cells despite normal activity of relevant lysosomal degrading enzymes. The accumulation of LacCer displayed variability within storage cell populations, and was mostly expressed in neurons in NPC. An absence of the increase in LacCer in storage cells above control levels was seen in neuronal ceroid lipofuscinoses (neurons and cardiocytes) and in Fabry disease. Gaucher and Krabbe cells showed significantly lower levels, or even the absence, of LacCer compared with control macrophages. Results of immunohistochemistry were corroborated by semiquantitative lipid thin-layer chromatography (TLC). It is suggested that different associations of LacCer with the lysosomal storage process may reflect differences in glycosphingolipid turnover induced by the storage-compromised lysosomal/endosomal system.

H. Hůlková · J. Ledvinová · B. Asfaw · K. Kopřiva · M. Elleder (✉)
Institute of Inherited Metabolic Disorders,
Charles University,
First Faculty of Medicine and University Hospital,
Bldg. D, Division B, Ke Karlovu 2 128 08,
128 08 Prague 2, Czech Republic
e-mail: melleder@beba.cesnet.cz
Tel.: +42-022-4918283
Fax: +42-022-4919392

K. Koubek
Institute of Haematology and Blood Transfusion,
Prague, Czech Republic

Keywords Lactosylceramide · Immunohistochemistry · Lysosomal storage disorders

Introduction

Lactosylceramide (LacCer) [βGal (1→4) βGlc (1→1′) Cer] belongs to the group of neutral glycosphingolipids (GSLs). Its synthesis starts from glucosylceramide on the cytosolic site of the Golgi apparatus. After translocation into the Golgi lumen, catalyzed presumably by transporters, LacCer synthase (UDP-galactose: glucosylceramide β-1,4-galactosyltransferase) transfers galactose from UDP-Gal to glucosylceramide, generating a β-1,4-glycosidic linkage [9]. In the lumen of the Golgi cisternae LacCer serves as a substrate either for GM3 ganglioside synthesis by sialyltransferase or gives rise to the specific glycolipid series: globo-, isoglobo-, ganglio-, lacto- (at the level of triglycosylceramides), and neolacto- (at the level of tetraglycosylceramides).

From the Golgi complex, LacCer is translocated via transport vesicles or via monomeric transport through the cytosol to various destinations inside the cells [50, 74]. One of the most important targets is the plasma membrane, where LacCer with other GSLs contributes to the creation of specialized microdomains called "rafts" [10, 57]. LacCer is present in both central and peripheral myelins [46, 69], which are derivatives of glial cell membrane. Its localization at the subcellular level has been studied in granulocytes of the neutrophil series, where it represents two-thirds of glycolipids. LacCer was found mainly in secondary granules and at lower levels in primary granules [70]. In rabbit skeletal muscle it has been localized to the sarcoplasmic reticulum [54]. There is evidence that LacCer plays a role as a signal molecule in various cellular processes [2–5, 36, 37, 43, 47, 48, 52, 79, 81]. Some of these functions have been studied in relation to atherogenesis [31].

In addition to granulocytes, LacCer is abundantly present in some blood cells, including platelets, monocytes, a subset of B lymphocytes [23], and in red blood cells [68].

LacCer has been found to be increased in atherosclerotic lesions [34, 53, 60], and in proximal tubular cells in homozygotes for familiar hypercholesterolemia [32, 33].

There are a number of reports describing the relationship between LacCer and the endosomal/lysosomal system. According to studies of the endocytotic pathway using a fluorescent LacCer analogue carried out in living cells, the lipid is transported under normal conditions directly to the Golgi by a specific pathway, whereas in a number of sphingolipid storage disorders the transport is directed to the late endosomal system [35, 61]. Targeting of the lipid is influenced by the amount of intracellular cholesterol [61]. This points to a temporary relationship of LacCer to the endosomal/lysosomal system, which might reflect raft cholesterol dynamics [66] regulated possibly by the NPC1 protein [49].

LacCer is a pivotal intermediate in lysosomal degradation of numerous complex GSLs. There are two lysosomal β-galactosidases, GM1-β-galactosidase and galactocerebroside-β-galactosidase, participating in its degradation and mutually substituting. However, this efficient LacCer degradation depends on the availability of functional sphingolipidhydrolase activator proteins (SAPs) A and B [64].

LacCer has been found to be increased in various tissues of several lysosomal storage disorders (LSDs) (see Discussion), especially in Niemann-Pick type C disease (NPC) [76] and in prosaposin deficiency [6, 27, 30].

We took advantage of having access to a highly specific monoclonal antibody against LacCer to study the association of LacCer with the lysosomal system in controls and in a representative set of LSDs. The results point to marked differences in the association of LacCer with subsets of LSDs. Moreover, data on LacCer in situ distribution provide important complementary information to biochemical lipid studies.

Materials and methods

Materials

Tissues

Samples of unfixed control post-mortem and biopsy tissues (brain, spinal medulla, liver, spleen, palatine tonsil, lymph node, heart, skeletal muscle and appendix) were frozen in liquid nitrogen and stored frozen until use. They were used for comparison with their counterparts from affected individuals with a set of lysosomal storage disorders (Table 1).

Post-mortem samples archived in formaldehyde from the heart and kidney of a Fabry hemizygote with a complex phenotype and of a Fabry heterozygote [29], and from the heart of a patient with Fabry disease cardiac variant [21] were examined for LacCer by TLC immunostaining. Fixed samples of heart and kidney served as controls. Cultured skin fibroblasts from recent patients with prosaposin deficiency (n=1, manuscript in preparation) and NPC (n=2) and from controls (n=4) were used as well.

Table 1 List of archived frozen tissues of LSDs available for studies

LSD	Number of samples	Tissues available
NPA	1	Brain, liver, spleen
NPB	1	Spleen
NPC (juvenile)[a]	2	Brain, liver, spleen, appendix
NPC1 (early onset)[b]	1	Brain, liver, spleen, appendix
GM1 (infantile)	1	Brain
KD (infantile)	1	Brain
MPS I	1	Adenoid tonsil
MPS II	1	Brain, liver
MPS IIIA	1	Brain
NCL6	2	Brain, liver, appendix (n=1); heart, skeletal muscle (n=1)
NCL1 (infantile)[c]	3	Brain
CESD (adult) [22]	1	Liver
GSD II (infantile)	1	Liver, heart, skeletal muscle
GD I (early onset)	1	Spleen[d]
GD I (adult)	2	Spleen[d] (n=1); bone marrow (n=1)
FD	4	Heart[e] (n=1); skin[f] (n=3)

NPA Niemann-Pick disease type A, *NPB* Niemann-Pick disease type B (acid sphingomyelinase deficiency), *NPC* Niemann-Pick disease type C, *NPC1* Niemann-Pick disease type C1, *GM1* gangliosidosis (acid β-galactosidase deficiency), *KD* Krabbe disease (galactocerebroside β-galactosidase deficiency), *MPS* II mucopolysaccharidosis type II (iduronosulphate sulphatase deficiency), *MPS IIIA* mucopolysaccharidosis type IIIA (heparan sulphamidase deficiency), *NCL6* neuronal ceroidlipofuscinosis type 6, *NCL1* neuronal ceroidlipofuscinosis type 1, *CESD* cholesteryl ester storage disease (acid lipase deficiency), *GSD II* glycogen storage disease type II (acid α-glucosidase deficiency), *GD I* Gaucher disease type I (acid β-glucosidase deficiency), *FD* Fabry disease (α-galactosidase A deficiency)

[a] Age at death 19 and 27 years

[b] Age at death 6 years, classified as NPC1 by complementation studies (M.T. Vanier, Lyon, France)

[c] Brain samples of NCL1 were kindly supplied by Dr. Jaana Tyynela-Vesterinen (University of Helsinki, Finland)

[d] Material from one patient with Mantle cell lymphoma with Gaucher-like Ig-loaded macrophages was studied for comparison

[e] Heart auricular muscle of Fabry hemizygote with complex phenotype

[f] Skin biopsies of Fabry hemizygotes with complex phenotype

Monoclonal antibodies

Three CDw17 clones were tested for LacCer specificity and sensitivity: MEM-74 (purified monoclonal mouse IgM; Exbio, Prague, Czech Republic); Huly-m13 (purified monoclonal mouse IgMκ; Ancell, Bayport, Minn.); MG-2 (monoclonal mouse IgM available as supernatant of hybridoma fluid, produced by conventional techniques [44]).

Lipids used for antibody testing in TLC

Individual glycolipids used as standards (glucosylceramide, galactosylceramide, lactosylceramide, globotriaosylceramide, globoside, sulphatide, GM1, GM2 and GM3

gangliosides) were prepared and characterized in this laboratory or purchased from Sigma (St. Louis, Mo.). Total lipid extracts from different human tissues (liver, spleen, kidney, brain, adrenal glands and erythrocytes) were prepared as described below.

Methods

The majority of samples were used for both immunostaining of cryostat sections and preparation of total lipid extracts used for TLC immunostaining (Table 2).

Preparation of tissue extracts

Selected tissues (Table 2) were weighed, homogenized and extracted successively with mixtures of chloroform/methanol/water (20:10:1, 10:20:1; v/v/v) [55] and finally with chloroform/methanol (1:1; v/v). Formaldehyde-fixed tissues were washed in water overnight before homogenization.

TLC immunostaining

Glycolipids were separated on Polygram Sil G sheets (Macherey-Nagel, Düren, Germany) in a solvent mixture consisting of chloroform/methanol/water (65:25:4; v/v/v). After blocking (1% ovalbumin and 1% polyvinylpyrrolidone in phosphate-buffered saline, PBS, for 1 h at 37°C), the TLC sheets were incubated overnight at 4°C with the tested antibody against LacCer: MG-2 (1:2 dilution with 1% bovine serum albumin, BSA, in PBS) and Huly-m13 (1:100 dilution with 1% BSA in PBS). MEM-74 was not tested in TLC. Repeated usage of MG-2 antibody for TLC

Table 2 LacCer detection in selected tissues in LSDs comparing the results of immunohistochemical in situ staining with those of TLC densitometry

Entity	Method	Liver		Spleen	Brain cortex (cerebral grey matter)
		Hepatocytes	Kupffer cells	Macrophages	Neurons
Control	IH	−	+++	+++	−
	TLC	100%		100%	100%
NPA	IH	−/±	+++	++/+++ (v)	++/+++ (v)
	TLC	243%		379%	279%
NPB	IH	NA		+++ (v)	NA
	TLC	NA		162%	NA
NPC case 1 (juvenile)	IH	+	+++	+++	++/+++ (v)
	TLC	187%		407%	255%
NPC case 2 (juvenile)	IH	+	+++	+++	++/+++ (v)
	TLC	145%		326%	205%
GM1 case 1	IH	NA		NA	++ (v)
	TLC	NA		NA	268%
GM1 case 2	IH	NA		NA	+/++ (v)
	TLC	NA		NA	143%
MPS II	IH	+	++	NA	++/+++ (v)
	TLC	146%		NA	175%
MPS IIIA	IH	NA		NA	++/+++ (v)
	TLC	NA		NA	209%
CESD	IH	++	++ (v)	NA	NA
	TLC	87%[a]		NA	NA
Gaucher disease case 1 (early onset)	IH	NA		–/±	NA
	TLC	NA		112%[b]	NA
Gaucher disease case 1 (adult)	IH	NA		–/±	NA
	TLC	NA		82%	NA
NCL1 case 1	IH	NA		NA	–
	TLC	NA		NA	72%[c]
NCL1 case 2	IH	NA		NA	–
	TLC	NA		NA	59%[c]
NCL1 case 3	IH	NA		NA	–
	TLC	NA		NA	17%[c]
NCL6 case 1	IH	+	++	NA	–
	TLC	83%		NA	48%[c]
GSD II[d]	IH	++	+++	NA	NA
	TLC	125%		NA	NA

Further details of the storage process are given in the text. The immunohistochemistry (*IH*) results represent a semiquantitative evaluation of staining intensity in situ: − negative, ± just detectable, + discrete, ++ intermediate, +++ strong. The TLC results are presented as densitometric percentage in relation to the mean control values (liver n=5, spleen n=6, brain cortex n=4). *NA* samples not available for analysis, *(v)* admixture of storage cell population of lesser staining intensity (−/±)

[a]Decrease explainable as admixture of cancerous foci, which were devoid of both storage and LacCer [22]

[b]Values of LacCer in splenic samples of Gaucher disease, which were still within the range of controls

[c]Decrease given by less admixture of myelin (hypo- or demyelinization), as confirmed by presence of sulphatides and galactosylceramide on TLC (data not shown)

[d]In the heart sample from the same GSD II patient the value of LacCer was 266% of the mean of control value; The LacCer in the skeletal muscle of the GSD II patient was increased 1.57-fold over the value in the myocardium

immunodetection was possible. The sheets were then washed six times with PBS, blocked for 30 min at 37°C with 1% BSA in PBS, exposed to secondary peroxidase-conjugated goat anti-mouse IgM (Pierce, Rockford, Ill.), diluted 1:200 for 90 min at 37°C, washed again six times with PBS and developed with 4-chloro-1-naphthol. Chromatograms were evaluated densitometrically using a Camag TLC scanner II (Cats3; Camag Scientific, Wilmington, N.C.) in reflection mode.

Immunohistochemistry

Cryostat sections, 5 or 10 μm thick, prepared from unfixed tissues, were allowed to dry and then treated with anhydrous acetone [19] for 20 min at room temperature (no differences from extraction at +4°C or at −20°C), dried for 30 min and fixed with 2–10% phosphate-buffered paraformaldehyde at 4°C for 5 min. After washing with distilled water, the sections were subjected to standard blocking of endogenous peroxidase (1% sodium azide, 0.3% H_2O_2 for 10 min) and a blocking procedure with 5% bovine fetal serum in PBS for 30 min at room temperature. The sections were then incubated for 1 h at 4°C or overnight at 4°C with primary antibody: MG-2 undiluted, Huly-m13 diluted 1:10 or 1:50, or MEM-74 diluted 1:10 or 1:100 (5% bovine fetal serum in PBS was used as the dilution buffer). After washing with PBS, secondary peroxidase-conjugated antibody (goat anti-mouse IgM; Pierce) diluted with 5% bovine fetal serum in PBS 1:100 was used for 1 h at 37°C, followed by PBS and diaminobenzidine (Sigma, St. Louis, Mo.). The sections were counterstained with Harris haematoxylin and mounted in Immu-Mount (Shandon, Pittsburgh, Pa.).

Parallel sections were stained after delipidation with the following total lipid extraction procedure: 50% ethanol (10 min at room temperature) and chloroform/methanol/water (4:8:3; v/v/v) followed by chloroform/methanol (2:1; v/v), both for 30 min at room temperature. Finally, sections were rinsed in 50% ethanol and fully hydrated.

Slides with intact cells (smears, cultured cells) were treated similarly, with or without addition of saponin to primary and secondary antibodies (final concentration 0.02%). For washing, distilled water was substituted by PBS. Cultured cells were prevented from drying.

Cell cultures

Fibroblasts were cultured in Dulbecco's modified Eagle's medium (Sevapharma, Czech Republic) supplemented with 10% bovine foetal serum (PAA Laboratories, Cölbe, Germany). Cells were grown on glass cover slips treated for good cell growth in HCl in 70% ethanol (1:99) and placed in plastic Petri dishes (Sarstedt, Germany or TPP, Switzerland).

Colocalization studies of LacCer in peripheral gut neurons

The colocalization of LacCer in peripheral gut neurons was investigated in cryostat sections of control appendix using a Nikon Eclipse E 800 microscope equipped with a C1 confocal module with EZC1 software supplied by Nikon. Neurites were stained with mouse IgG1 anti-heavy neurofilament protein antibody (NF-01) and mouse IgG1 anti-α-tubulin antibody (TU-01), both from Exbio. Late endosome/lysosome compartment (in both controls and the NPC autopsy sample) was detected using mouse IgG1 antibody against LAMP-2 (clone H4A3; Developmental Studies Hybridoma Bank, University of Iowa). Primary antibodies were visualized using Alexa Fluor 488 goat anti-mouse IgG1 and Alexa Fluor 568 goat anti-mouse IgM secondary antibodies (Molecular Probes, Eugene, Ore.). Primary antibodies were incubated successively for 1 h (anti-LacCer at 4°C and the others at 37°C) while the secondaries were incubated together.

Results

Testing of anti-LacCer antibodies and optimization of the experimental procedure

Immunohistochemistry

Optimal results for in situ detection of LacCer were obtained using cryostat sections of unfixed tissues and MG-2 antibody. This antibody bound the reference control structures (see below) and the binding was entirely removed by lipid pre-extraction. In some instances, e.g., in keratinocytes, there was a slight tendency of the lipid to form discrete in situ aggregates pointing to its relatively loose binding to membranes. Short post-fixation with 2% paraformaldehyde was an optimal treatment for cryostat sections of unfixed tissues. The addition of 0.02% saponin to primary and secondary antibody increased staining intensity and uniformity in *intact cells* (smears, cultured cells). Extensive methodological studies showed that the immunospecificity and sensitivity were completely lost when standard frozen sections were prepared from fixed samples by a routine immersion procedure. Unless otherwise stated, the sections were stained for LacCer and counterstained with Haematoxylin.

TLC immunostaining

LacCer was selectively and sensitively detected with MG-2 antibody (Fig. 1). Binding intensity with Huly-m13, which also cross-reacted with galactosylceramide, was much lower.

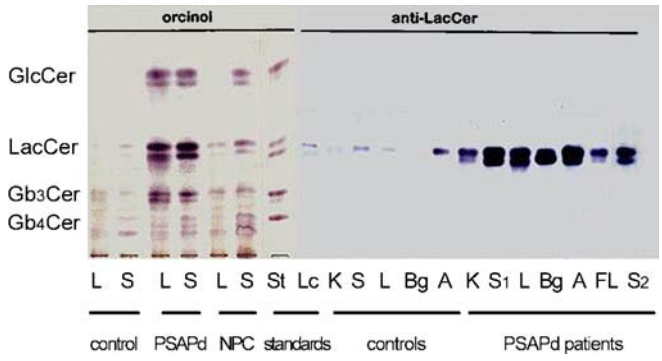


Fig. 1 Verification of anti-LacCer monoclonal antibody (clone MG-2) specificity: TLC immunodetection of LacCer in normal tissues and in tissues of prosaposin deficiency. Aliquots of 5 mg (orcinol) and 0.1 mg (immunodetection) tissue wet weight were applied on Polygram G TLC sheet (Macherey-Nagel, Germany). Solvent system: C:M:W (65:25:4; v/v/v). Abbreviations: L liver; S spleen (in prosaposin deficiency from two patients S_1 and S_2); K kidney; Bg brain grey matter; A adrenal cortex; FL foetal liver; Lc lactosylceramide; St mixture of glycosphingolipid standards; PSAPd prosaposin deficiency; GlcCer glucosylceramide; LacCer lactosylceramide; Gb_3Cer globotriaosylceramide; Gb_4Cer globoside

Inhibition of MG-2 antibody binding was tested with lactose, saccharose and N-acetyllactosamine (50 and 10 mg/ml for 2 h at 37°C for each). Lactose strongly inhibited the immunodetection of LacCer on TLC (Fig. 2), whereas N-acetyllactosamine blocked the LacCer immunostaining only partially (data not shown). Saccharose was without any effect (Fig. 2).

Because MG-2 antibody gave the best results for immunohistochemical analyses as well as for TLC immunodetection, only this antibody has been used in all further experimental work.

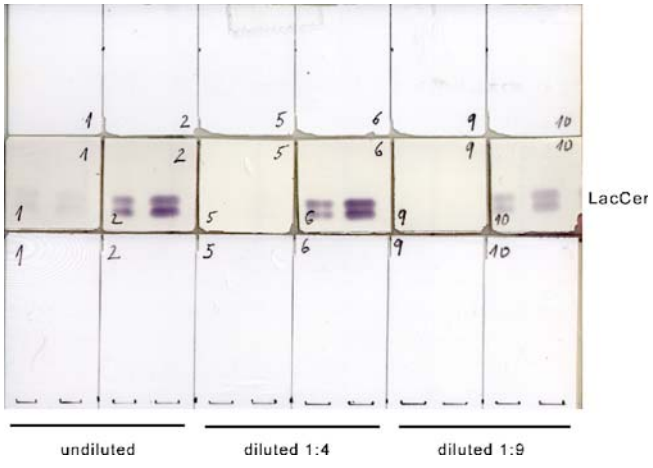


Fig. 2 Inhibition of anti-LacCer monoclonal antibody (clone MG-2) binding by disaccharides. Samples: 125 and 250 ng of LacCer were applied on TLC Polygram sheet. Solvent system: C:M:W (70:30:5; v/v/v). Immunodetection: MG-2 antibody was pre-incubated with 50 mg per ml disaccharide (1, 5, 9=lactose; 2, 6, 10=saccharose). Secondary antibody: goat anti-mouse IgM/Px, (Pierce, USA), dilution 1:500. Visualization: 4-chlor-1-naphtol

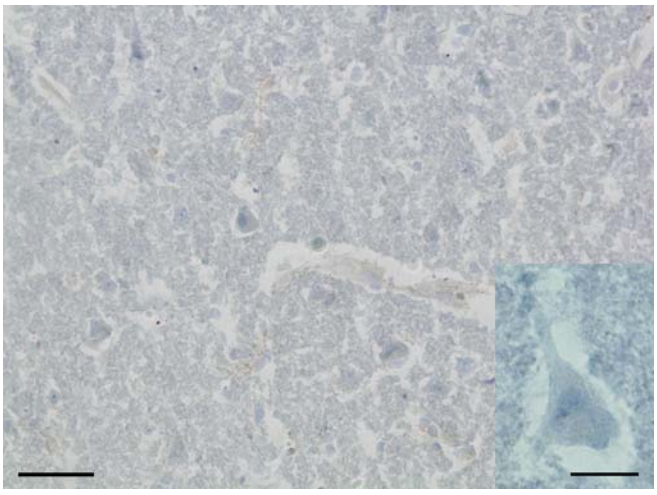


Fig. 3 Cortical neurons in control brain. Absence of detectable LacCer staining (*bar* 100 μm). *Insert* detail of a neuron (*bar* 30 μm)

LacCer in tissues

Nervous system

Controls Neurons of the brain cortex (Fig. 3), thalamus, basal ganglia, brain stem and spinal medulla were consistently LacCer-negative, as were the resting microglia and astrocytes. Occasional perivascular phagocytosing microglia (gitter cells) displayed LacCer positivity. Myelin (both central and peripheral) was stained strongly. Gut neurons in appendix displayed homogeneous LacCer staining of the perikaryon and fibrillar positivity of the neurites in both muscular and submucosal plexi (Fig. 4). Colocalization of LacCer with markers of microtubules and neurofilaments was not observed, although there was a close association with the neurofilaments. There was no sign of colocalization of LacCer with lysosomes (data not shown).

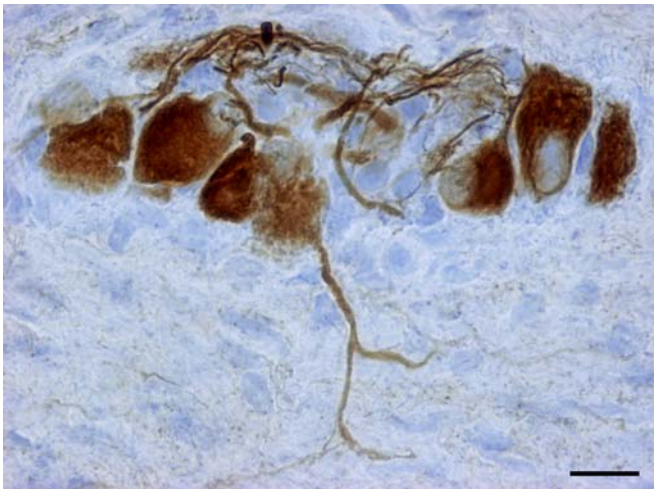


Fig. 4 Peripheral neurons in control appendix. LacCer staining pattern in myenteric plexus (*bar* 50 μm)

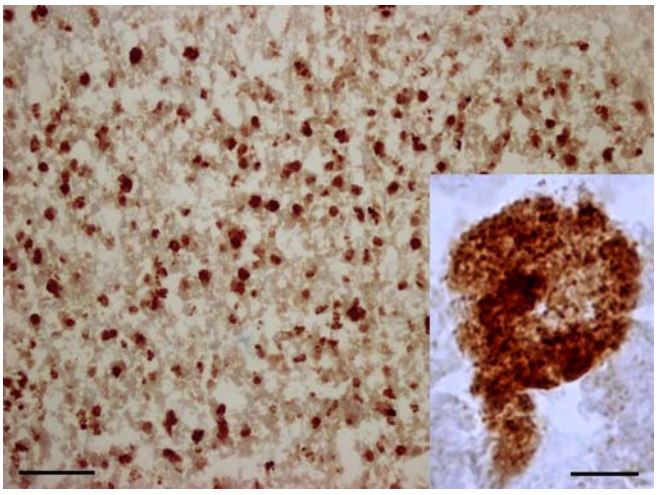


Fig. 5 NPA. Brain. Low magnification (*bar* 500 μm) showing dense population of LacCer-rich cortical neurons. *Insert* detail of a storage neuron (*bar* 30 μm)

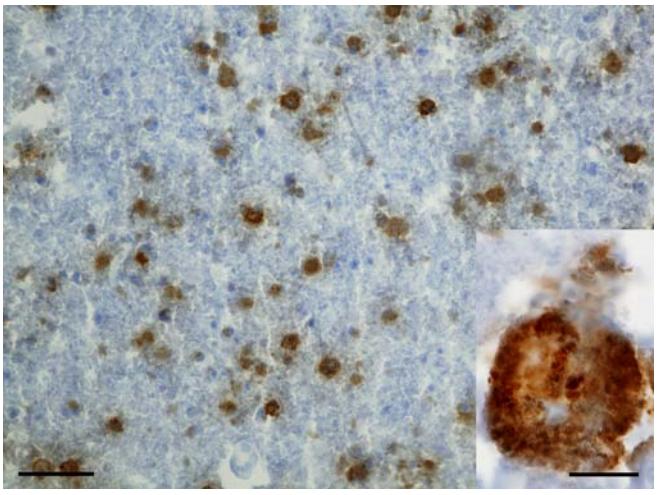


Fig. 7 NPC. Brain. Low magnification (*bar* 200 μm) showing LacCer in a population of cortical neurons displaying a higher degree of variability than in NPA (cf. Fig. 5). *Insert* detail of a storage neuron (*bar* 30 μm)

Neurons in LSDs Storage in cortical neurons was accompanied by strong LacCer staining in the majority of cells in NPC, NPA (Fig. 5), GM1 gangliosidosis, and MPS II and IIIA (Table 2). A small population of storage neurons were LacCer-negative (e.g., in NPA; Fig. 6). In some of the storage neurons LacCer staining was restricted to the cell periphery. In NPC and MPS the areas devoid of LacCer often displayed lipopigment accumulation (Fig. 7).

NPC brain Both the cortical and subcortical regions of NPC brains displayed notable regional heterogeneity of LacCer staining. The less storage distended cortical neurons were strongly positive (Fig. 8). However, the intensively storing ballooned neurons in subcortical areas (basal ganglia, thalamus and spinal medulla) were either devoid of any LacCer staining or displayed slight rim-like LacCer accumulation at the periphery of the neuronal body (Fig. 9). Spheroids of the extensive neuroaxonal dystrophy typically seen in early-onset NPC were LacCer negative.

Peripheral gut neurons in NPC Staining of storage peripheral gut neurons in NPC was either decreased or comparable to that of controls in the perikaryal-neurite complex (Fig. 10), and was not colocalized with lysosomal markers (data not shown). The voluminous submucosal axonal spheroids displayed variable LacCer staining.

Cortical storage neurons in NCL6 Cortical storage neurons in NCL6 were consistently LacCer-negative (Fig. 11

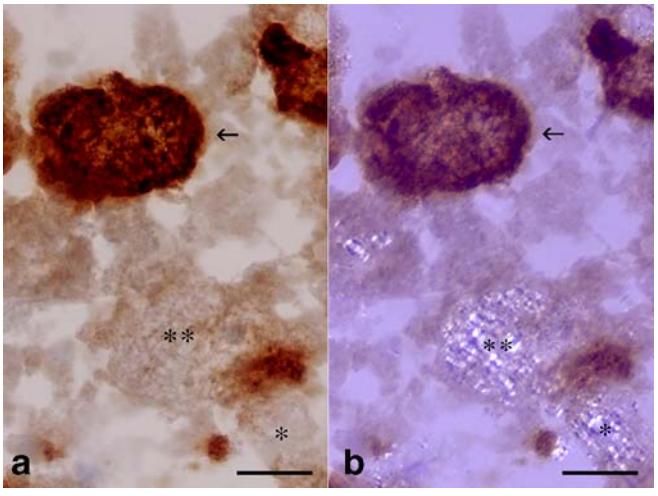


Fig. 6 NPA. Brain. Variability of neuronal LacCer accumulation. LacCer-stained section (**a**) also examined under polarized light (**b**). The LacCer-negative neuron (**a**) displays birefringence of sphingomyelin liquid crystals (**b**) (lipopigment was absent). The corresponding neurons are marked by *asterisks* and *arrows* (*bars* 50 μm)

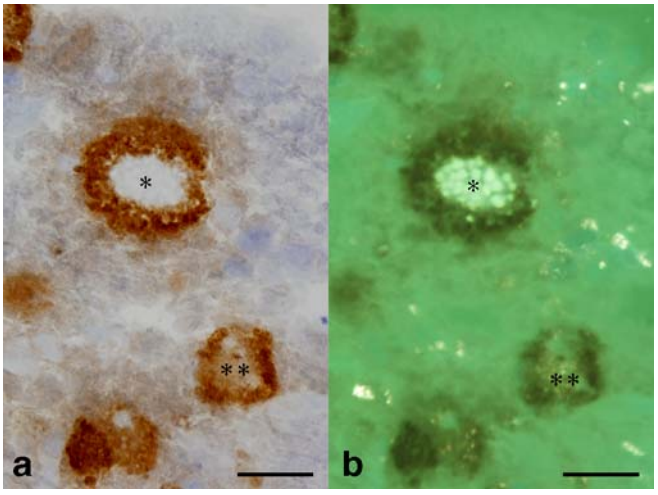


Fig. 8 NPC. Brain. Variability of neuronal LacCer storage. LacCer-stained section (**a**) also examined under UV light (**b**). LacCer least-stained areas (**a**) are rich in autofluorescent lipopigment (**b**). The corresponding areas are marked by *asterisks* (*bars* 50 μm)

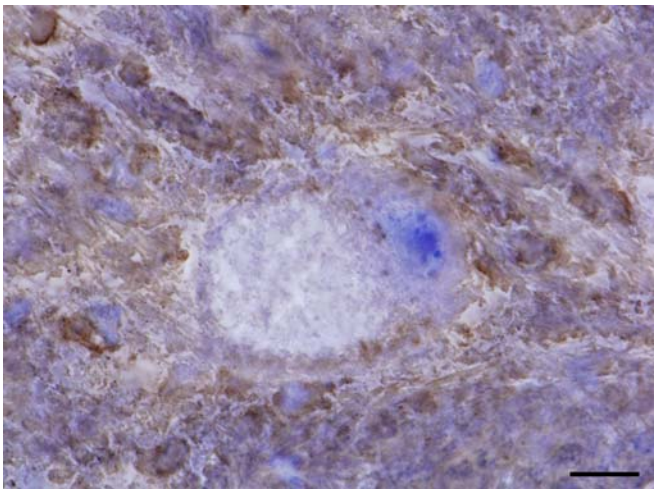


Fig. 9 NPC. Thalamus. Ballooned storage neuron free of detectable LacCer surrounded by positive myelin (*bar* 30 μm)

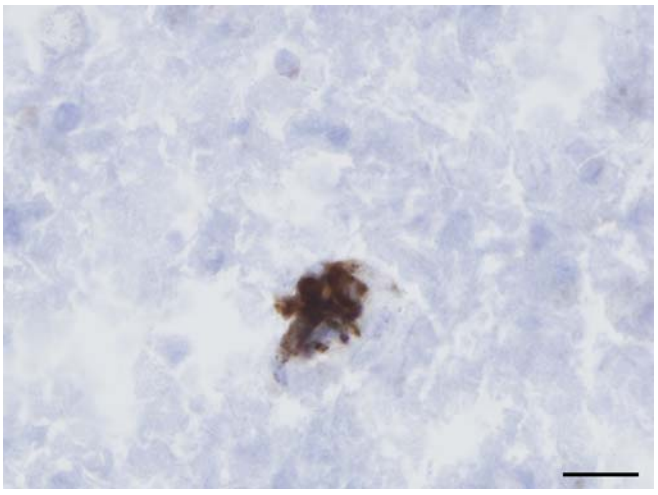


Fig. 11 NCL6. Brain cortex. Strong LacCer staining restricted to the coarse perikaryal lumps of aggregated storage material present in a single neuron. The surrounding storage cells are negative (*bar* 50 μm)

and Table 2), with the only exceptions being infrequent coarse globular or spheroidal perikaryal deposits which were strongly stained (Fig. 11). These deposits corresponded to the transformed storage material described elsewhere [17]. Storage gut neurons in NCL6 displayed decreased perikaryal staining whereas the amount of LacCer in their neurites was similar to that of controls. The cortical population in NCL1 was LacCer-negative with the exception of a small subset of microglia (Table 2). The persisting neurons were negative (Fig. 12).

Hepatocytes

LacCer staining was negative in control hepatocytes. In LSDs LacCer accumulation was seen in the narrow peribiliary zone of hepatocytes in NPC, NCL6 and CESD. It was distinctly expressed in foamy hepatocytes in MPS II and GSD II, whereas heavily storing hepatocytes in NPA were almost LacCer-negative (Table 2).

Macrophages and blood cells

Control macrophages in splenic red pulp, lymph nodes, palatine tonsil, liver and bone marrow displayed strong, coarsely granular cytoplasmic staining for LacCer (Fig. 13). Granulocytes and some lymphocytes and red blood cells in lymphoid organs and in bone marrow were positively stained for LacCer. In bone marrow smears thrombocytes and megakaryocytes belonged to strongly stained elements, the latter (megakaryocytes) being stained to various degrees according to the extent of maturation.

Storage histiocytes were generally strongly stained for LacCer (Fig. 14), irrespective of the type of lysosomal



Fig. 10 Appendiceal myenteric plexus in NPC. Decreased LacCer staining mainly in the storage-enlarged neuronal perikarya (*bar* 50 μm)

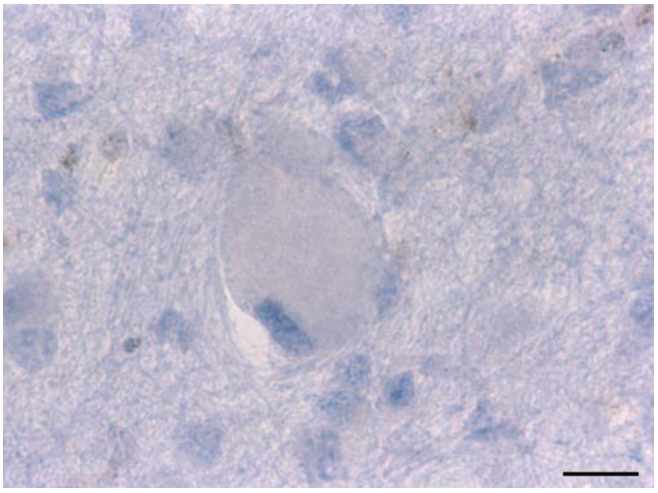


Fig. 12 NCL1. Brain cortex in an advanced stage of the storage process. The persisting ballooned neuron is LacCer-negative similar to the surrounding glial storage cells (*bar* 20 μm)

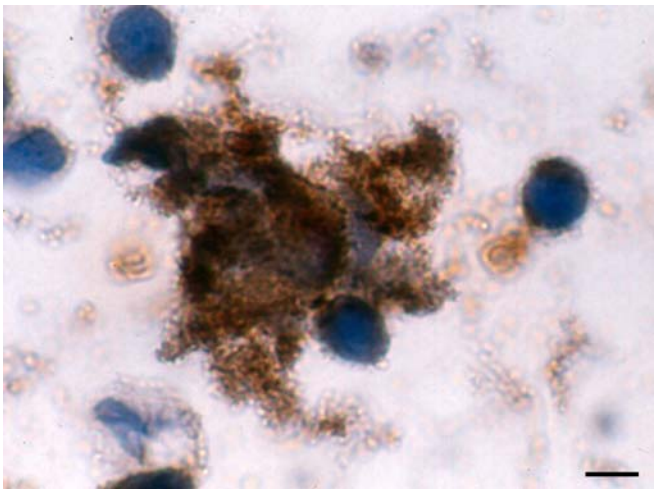


Fig. 13 Control bone marrow with strong staining of LacCer in a normal histiocyte. The histiocyte is active engaged in phagocytosis and has a characteristic stelate appearance (*bar* 20 μm)

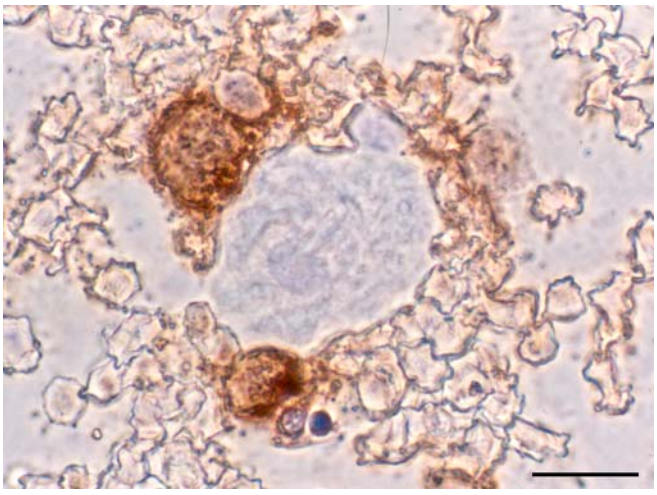


Fig. 15 Bone marrow smear with Gaucher cell showing no detectable LacCer. Note strong staining in the surrounding granulocytes. Phase contrast (*bar* 20 μm)

disorder, differing from the control counterparts by lower degree of uniformity, rounded appearance and larger size (Table 2). The decrease or negativity of LacCer in some of them was associated with deposition of lipopigment.

Krabbe cells and similarly Gaucher cells in the spleen and in bone marrow smears showed a strong decrease or even an absence of immunodetectable LacCer (Figs. 15 and 16a; Table 2). Negative LacCer staining in Gaucher cells sharply contrasted with strongly stained Gaucher-like cells in mantle cell lymphoma (Fig. 16b).

Skeletal muscle

In controls there was discrete mosaic punctuate LacCer staining, which did not correlate with the scarce subsarcolemmal lysosomal population (Fig. 17, insert). Its distribution fits well with localization of LacCer to sarcoplasmic reticulum described for rabbit muscle [54].

In LSDs marked LacCer staining was seen in GSD II obscuring all the sarcoplasmic structures due to massive lysosomal involvement (Fig. 17; Table 2). The relatively numerous discrete autofluorescent lysosomal deposits in NCL6 did not show detectable LacCer, but exhibited the staining pattern seen in control sections (see above).

Heart

Both conductive and contractile cardiocytes in controls were generally LacCer-negative (Fig. 18 insert), with the exception of dispersed LacCer-positive cardiocytes integrated into the fibres and fusiform cells closely associated with them (detailed studies of these cells are in progress).

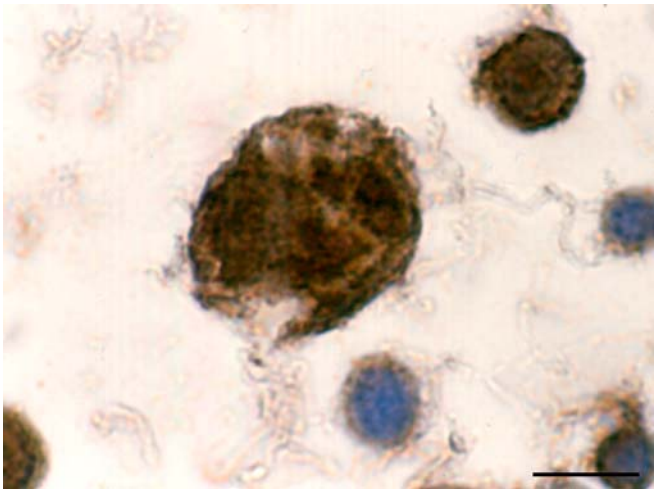


Fig. 14 Bone marrow storage histiocyte in NPC. The strongly stained cytoplasm is rounded and enlarged as compared with that of controls (cf. Fig. 13). The surrounding nonstorage cells display physiological LacCer staining (*bar* 20 μm)

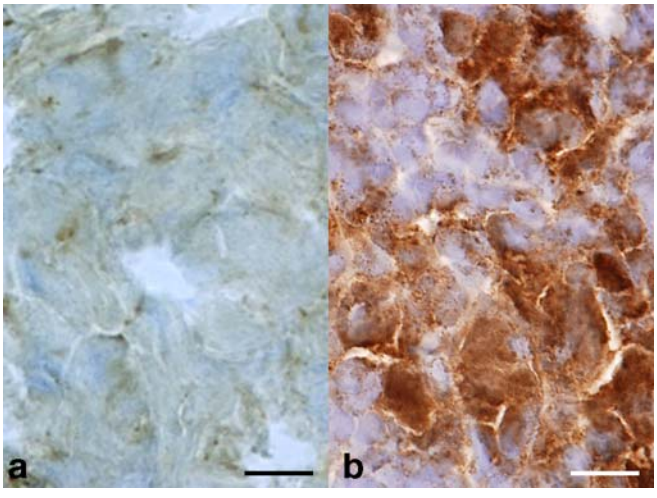


Fig. 16 Gaucher disease. Cryostat section of spleen with numerous Gaucher cells with just detectable cytoplasmic LacCer staining (**a**) contrasting with strong staining of Gaucher-like cells in mantle cell lymphoma (**b**). Slight positivity on membranes of surrounding lymphocytes is apparent (**b**) (*bars* 30 μm)

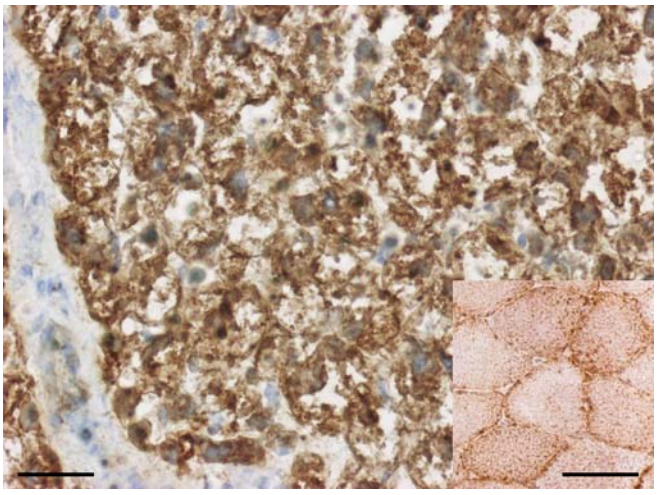


Fig. 17 GSD II. Storage in skeletal muscle with high degree of LacCer accumulation (*bar* 100 μm) contrasting with discrete punctate staining of skeletal muscle in control section (*insert bar* 50 μm)

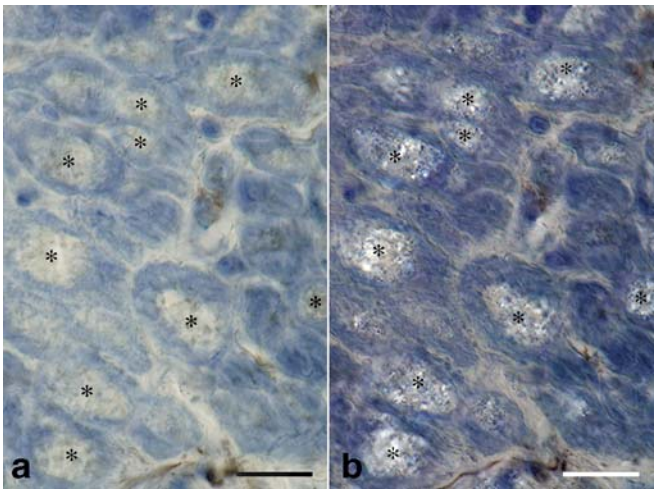


Fig. 19 Fabry disease. Heart auricle. Perinuclear storage lysosomes without detectable LacCer with only minimal lipopigment (**a**), but distended with liquid crystals of globotriaosylceramide with positive birefringence (**b**). Distended lysosomal regions are marked by *asterisks*. Positively stained small nerves are apparent in the interstitium (*bars* 50 μm)

Storage cardiocytes displayed strong LacCer staining in GSD II (Fig. 18; Table 2), which contrasted with the absence of detectable LacCer in lipopigment-loaded cardiocytes in NCL6. Fabry heart auricular cardiocytes displaying lipid and lipopigment storage were completely LacCer-negative (Fig. 19). The dispersed LacCer-positive cardiocytes seen in control sections (see above) did not express storage in either disorder. By TLC (Fig. 20), heart glycolipids in adult Fabry disease (formaldehyde-fixed samples used only for TLC analysis) showed a decrease in immunodetectable LacCer compared with control sections: Fabry hemizygote with complex phenotype 15%, Fabry hemizygote cardiac variant 10%, and Fabry heterozygote 60% of the mean control levels. A comparable decrease was seen in the kidneys of these patients: Fabry hemizygote with complex phenotype 20%, and Fabry heterozygote 17% of the mean of control levels.

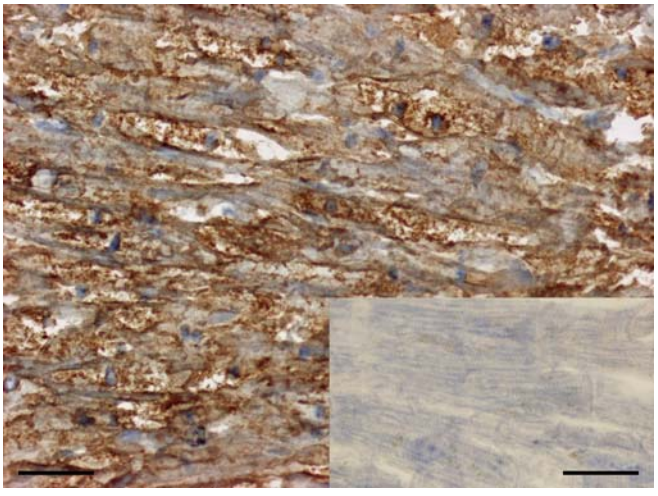


Fig. 18 GSD II. Storage cardiomyocytes strongly stained for LacCer in the expanded perinuclear storage regions (*bar* 100 μm), which contrasts with the absence of staining representing the bulk of control cardiocytes (*insert bar* 50 μm) which showed only the discrete brownish native colour of lipofuscin

Skin

In controls LacCer was found closely associated with the cell membrane of keratinocytes. A decreasing gradient of intensity was observed from the basal layer to several suprabasal layers. The granular and cornified layers were negative (Fig. 21, insert). A discrete, finely granular

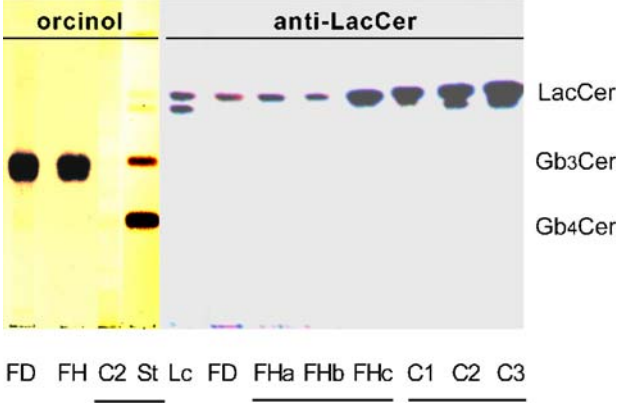


Fig. 20 TLC immunostaining of LacCer in formaldehyde-fixed myocardium from patients with Fabry disease and controls. Aliquots of 4 mg (orcinol) and 0.6 mg (immunodetection) tissue wet weight were applied to a Polygram G TLC sheet. Solvent system: chloroform/methanol/water (65:25:4; v/v/v). Immunodetection with anti-LacCer monoclonal antibody (clone MG-2). *FD* Fabry hemizygote with complex phenotype; *FH* Fabry heterozygote; *FHa*, *FHb*, *FHc* different samples from myocardium of Fabry heterozygote (heterogeneity reflecting either mosaicism in tissues of heterozygotes or different cellular composition of samples); *C1–3* controls; *St* mixture of glycosphingolipid standards; *Lc* lactosylceramide; LacCer lactosylceramide; *Gb3Cer* globotriaosylceramide; *Gb4Cer* globoside

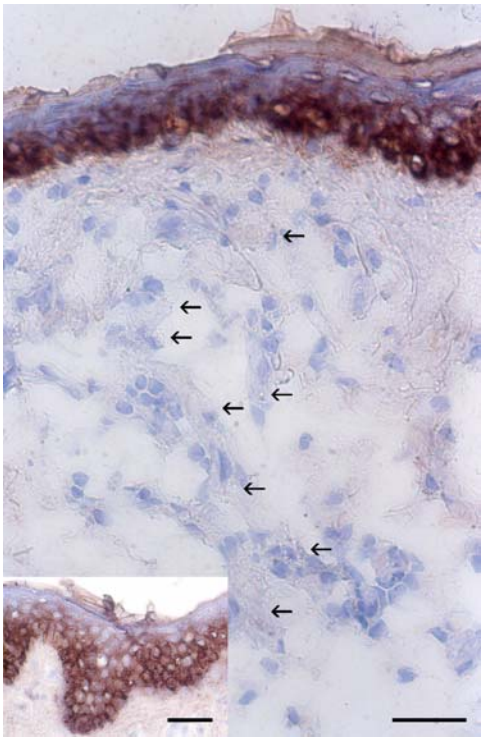


Fig. 21 Skin in Fabry disease (without angiokeratoma). Strong staining for LacCer in keratinocytes (*bar* 100 μm) equal to that of control sections (*insert bar* 50 μm). The storage capillary endothelium shows no staining in (*arrows*)

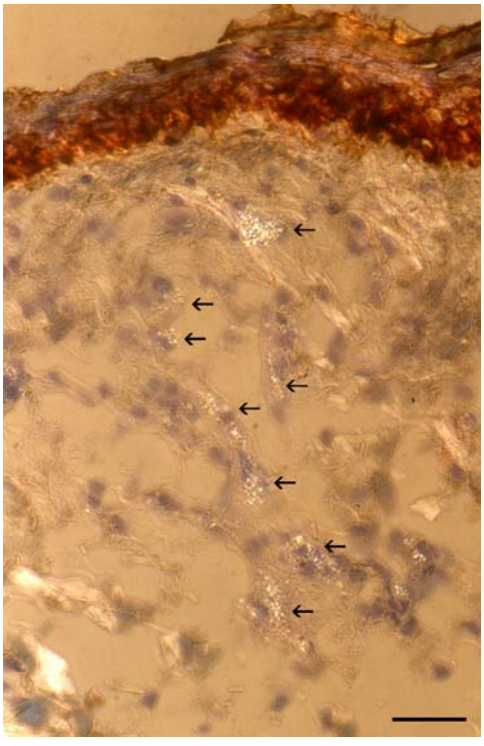


Fig. 22 The same section as in Fig. 21. The stored globotriaosylceramide in dermal capillaries can be visualized in a LacCer-stained section because of its birefringence (*bar* 100 μm). The corresponding structures are marked

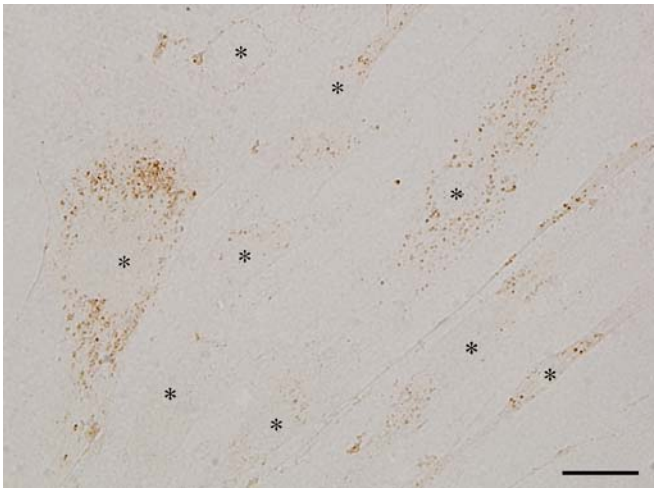


Fig. 23 Cultured fibroblasts (*asterisks*) from a patient with mitochondrial disorder serving as a control. Discrete variable punctate LacCer staining is apparent (*bar* 50 μm)

LacCer reaction in smooth muscle cells (musculus arrector pili) and in ducts of eccrine glands was seen.

The LacCer staining pattern of keratinocytes in Fabry disease was unchanged. Strongly storing eccrine glands in Fabry disease were negative.

Endothelium

In controls the endothelium was generally unstained or displayed just detectable positivity. Mild and variable LacCer staining in LSDs was noted in the spleen sinusoids (NPA, NPB and NPC) and in the capillary endothelium in NPA, GM1 gangliosidosis, NCL1 and NCL6, with the strongest being in the arterial endothelium in GSD II. Dermal capillaries in Fabry disease showed no detectable LacCer despite pronounced lysosomal storage (Figs. 21 and 22).

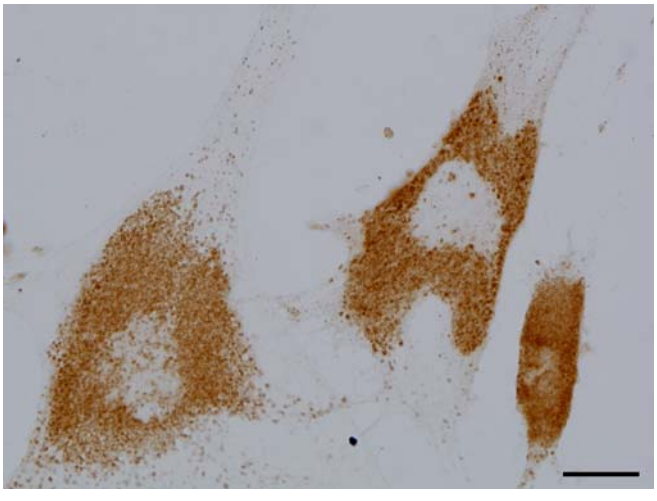


Fig. 24 Prosaposin deficiency. Cultured fibroblasts with strong granular cytoplasmic staining for LacCer (*bar* 50 μm; cf. Fig. 23)

TLC studies with densitometric evaluation of LacCer that were carried out in a majority of cases corroborated the immunohistochemistry results (Table 2).

Tissues in prosaposin deficiency

Tissues in this disorder displayed a large increase in LacCer on TLC. However, in fixed tissues a total loss of immunodetectability of the lipid in situ and an enormous increase in background staining were seen (see above). The cultured fibroblasts exhibited a strong uniform LacCer staining of the mass of storage vacuoles which exceeded by manyfold the staining in both control (cf. Figs. 23 and 24) and NPC fibroblasts.

Discussion

Our results provide evidence of heterogeneity of LacCer expression at both the tissue and cellular levels. The data show that in the lysosomal system of normal human tissues, LacCer is present in immunodetectable amounts in active phagocytes only. The lysosomal storage process, depending on the type of lysosomal disorder, leads to variable induction of LacCer expression.

LSDs associated with increased LacCer

The increase in LacCer in storage cells in GSD II (Figs. 17 and 18) represents the first description of abnormal lipid composition in this lipid-unrelated storage disorder. Our observations that an increase in LacCer occurs in a subset of LSDs (Table 2) corroborates the lipid biochemical studies in the respective entities (e.g., in NPA brain [24] and liver [11], in NPC [20, 40, 59, 76], in GM1 gangliosidosis, albeit inconstantly [1, 41, 72], in human MPS IIIB [25, 26], and in canine MPS I [13]). The association with the storage process leaves no doubt about the close relationship between LacCer and the storage-expanded lysosomes, although its exact position at the subcellular levels could not be specified. Our studies, based on in situ detection, enabled us to unravel the heterogeneity of the increases in LacCer, either within the storage-affected cell population or between different storage-affected cell types. The variability ranged from low in cortical neurons in NPA (Figs. 5 and 6) to high in neurons in NPC (Figs. 7, 8, 9). The remarkable heterogeneity in neurons in NPC suggests a loose association of LacCer with the disorder under the same loss of NPC1 sterol/glycolipid sensing protein function [12]. The variability in LacCer storage sharply contrasts with widespread deposition of GM2 and GM3 gangliosides in neurons in the NPC mouse model [80]. Studies of other glycolipids and cholesterol are therefore planned. The moderate increase in LacCer in the liver in NPC [75] was, in our patients, caused mainly by the sinusoidal macrophage storage pool (Table 2). The LacCer increase in the liver in NPA was also caused mainly by storage macrophages.

LSDs without detectable LacCer induction

By an absence of immunodetectable LacCer in three storage sites (skin, capillary endothelium as shown in Figs. 21 and 22, cardiocytes as shown in Fig. 19, and eccrine glands), Fabry disease differs from the above-mentioned storage disorders. Results of immunohistochemistry were corroborated by studies of lipid extracts of the Fabry heart and kidney, where the amount of LacCer (detected by immunostaining) was always lower than in the controls. The current stored lipid analyses in Fabry disease are mainly concerned with the digalactosylceramide, which has the same mobility on standard TLC analysis using general detection reagents for sugars (e.g., orcinol). Consequently, the absence of immunodetectable LacCer represents a biochemical feature of the storage process in α-galactosidase A deficiency. A satisfactory explanation is not available. Decreased synthesis or partial shunting to GM3–GD3 or other products is theoretically possible. It is doubtful whether the absence of LacCer is solely due to interrupted lysosomal degradation of globotriaosylceramide in that the influx of LacCer may come from other glycolipid series (e.g., lacto- and neolacto-) and from LacCer-rich cell membranes. Moreover, with functioning LacCer-degrading lysosomal enzymes, LacCer is promptly degraded and its immediate amount in lysosomes must be under the limit of in situ immunodetection.

In NCLs of both types examined detectable LacCer was absent. It is noteworthy that the process of transformation of deposits in NCL6 [17] was accompanied by significant LacCer accumulation (Fig. 11), suggesting their different lysosomal processing. Otherwise, secondary lipopigment deposition in NPC neurons and in macrophages was generally associated with either absence of LacCer (Fig. 8) or minimal staining, the only exception being MPS brain neurons, where the LacCer–lipopigment coincidence was frequent, however.

LSDs with progressive decrease in LacCer against control counterparts

The pronounced decrease or absence of LacCer in Gaucher cells (Figs. 15 and 16) is particularly notable as this suggests that Gaucher cells (and Krabbe cells) differ significantly from all other macrophages, with the exception of macrophages modified by high lipopigment load. Lack of LacCer expression in Gaucher disease was seen only in macrophages, i.e. in the storage-affected cell type. The low levels of LacCer in serum in Gaucher disease [15, 78] correlate well with the LacCer deficiency in Gaucher cells.

Results of immunohistochemistry were corroborated by TLC analysis of Gaucher spleen (Table 2). The findings fit well with published data on TLC analyses of Gaucher

spleen lipids showing glucosylceramide as the principal glycolipid [16, 45, 56, 58, 67]. All TLC analyses must consider admixture of LacCer from granulocytes and lymphocytes in spleen samples and the fact that the LacCer pool has been reported to be increased in granulocytes [42].

Our findings suggest significant depletion of the substrate for β-galactosidase, highly active in Gaucher cells [18], which normally provides the main substrate influx for the deficient glucocerebrosidase. The influx is suggested to be based on phagocytosis of glycolipid-rich senescent blood cells by macrophages [7]. The paucity of LacCer might therefore be due to decreased phagocytosis of mature Gaucher cells, provided there is no other significant source of LacCer. A similar situation might exist in Krabbe cells, which in their mature form may be deprived of phagocytosed myelin rich in LacCer precursors. Decreased synthesis with lower availability of LacCer in Gaucher cells does not seem to be a possibility, as GM3 ganglioside, the product of LacCer sialization, has been found to be increased two- to sixfold in Gaucher spleens [56]. This suggests possible recycling of the stored glucosylceramide to the synthetic compartment [63], which is also though to occur in the case of gangliosides [80]. Anyway, loss of LacCer increases the list of features by which Gaucher cells differ from the other storage macrophages [14, 19].

Significance of LacCer levels in LSDs

Decreased degradation because of β-galactosidase deficiency could contribute to LacCer increase. For instance, in MPS I–III (the group deficient in heparan sulphate-degrading enzymes) activity of β-galactosidase is inversely proportional to the degree of storage [73]. However, in GM1 gangliosidosis, which is inherently deficient in one of the critical LacCer-degrading enzymes, the increase in LacCer in the cerebral grey matter (see above) is associated with its normal or even increased degradation rate [8]. In contrast to our finding of a significant increase in LacCer in GSD II (Table 2), β-galactosidase activity has been found to be increased in this disorder [28].

Our conclusion is that the increase in LacCer observed in both lipid and nonlipid (e.g., GSD II) storage disorders, and regardless of the enzymopathic or nonenzymopathic nature of the defect (cf. cortical neurons in NPA with NPC1 protein deficiency, Figs. 5 and 7), can hardly be explained by a decrease in lysosomal degradation. The variable amount of LacCer in a given storage cell population is consistent with this view. The only exception is the deficiency of prosaposin with inactivation of both critical galactosidases [64], leading to massive lysosomal LacCer accumulation (Fig. 24) [30]. Yet, even in this condition one cannot exclude the possibility that a nonenzymopathic mechanism participates in the LacCer increase.

We further suggest that the variable levels of LacCer in LSDs reflect altered homeostatic control of the glycosphingolipid turnover (synthesis, degradation and recycling) that is a consequence of the primary defect. This notion fits well with results of immunohistochemical studies of gangliosides in LSDs [77], as well as with the recently presented hypothesis of deregulation of raft lipids in LSDs [49, 66].

Another lipid—bis(monoacylglyceryl) phosphate (BMP)—similarly reflects lysosomal storage indirectly. BMP has been shown to be increased differently in several storage disorders. In the visceral storage pool it has been found to be highly increased (e.g., in NPA [39, 62] and in NPC [65, 71, 75], but not in Gaucher disease [62] or other LSDs [38]). The lipid has recently been assigned a regulatory function in protein and lipid trafficking through late endosomes [51].

In any event, the varied association of LacCer with LSDs reflects a new aspect of molecular pathology of the lysosomal system worth further study.

Acknowledgements The excellent technical assistance of Miss Jana Sovová is gratefully acknowledged. The study was supported by research project of the Ministry of Education of the Czech Republic (VZ 111100003) and by the Grant Agency of Charles University (GAUK 16/2002/c).

References

1. Abe T, Okada R (1972) Lipid analysis of a case of GM1-generalized gangliosidosis. Jpn J Exp Med 42:543–551
2. Angstrom J, Teneberg S, Milh MA, Larsson T, Leonardsson I, Olsson BM, Halvarsson MO, Danielsson D, Naslund I, Ljungh A, Wadstrom T, Karlsson KA (1998) The lactosylceramide binding specificity of Helicobacter pylori. Glycobiology 8:297–309
3. Arai T, Bhunia AK, Chatterjee S, Bulkley GB (1998) Lactosylceramide stimulates human neutrophils to upregulate Mac-1, adhere to endothelium, and generate reactive oxygen metabolites in vitro. Circ Res 82:540–547
4. Bhunia AK, Han H, Snowden A, Chatterjee S (1996) Lactosylceramide stimulates Ras-GTP loading, kinases (MEK, Raf), p44 mitogen-activated protein kinase, and c-fos expression in human aortic smooth muscle cells. J Biol Chem 271:10660–10666
5. Bhunia AK, Arai T, Bulkley G, Chatterjee S (1998) Lactosylceramide mediates tumor necrosis factor-alpha-induced intercellular adhesion molecule-1 (ICAM-1) expression and the adhesion of neutrophil in human umbilical vein endothelial cells. J Biol Chem 273:34349–34357
6. Bradova V, Smid F, Ulrich-Bott B, Roggendorf W, Paton BC, Harzer K (1993) Prosaposin deficiency: further characterization of the sphingolipid activator protein-deficient sibs. Multiple glycolipid elevations (including lactosylceramidosis), partial enzyme deficiencies and ultrastructure of the skin in this generalized sphingolipid storage disease. Hum Genet 92:143–152
7. Brady RO, King FM (1973) Gaucher's disease. In: Hers HG, Van Hoof F (ed) Lysosomes and storage diseases. Academic Press, New York, pp 381–394
8. Brady RO, O'Brien JS, Bradley RM, Gal AE (1970) Sphingolipid hydrolases in brain tissue of patients with generalized gangliodosis. Biochim Biophys Acta 210:193–195
9. Brooks SA, Dwek MV, Shumacher U (eds) (2002) Functional and molecular glycobiology. BIOS Scientific Publishers, Oxford
10. Brown DA, Rose JK (1992) Sorting of GPI-anchored proteins to glycolipid-enriched membrane subdomains during transport to the apical cell surface. Cell 68:533–544
11. Brunngraber EG, Berra B, Zambotti V (1973) Altered levels of tissue glycoproteins, gangliosides, glycosaminoglycans and lipids in Niemann-Pick's disease. Clin Chim Acta 48:173–181

12. Carstea ED, Morris JA, Coleman KG, Loftus SK, Zhang D, Cummings C, Gu J, Rosenfeld MA, Pavan WJ, Krizman DB, Nagle J, Polymeropoulos MH, Sturley SL, Ioannou YA, Higgins ME, Comly M, Cooney A, Brown A, Kaneski CR, Blanchette-Mackie EJ, Dwyer NK, Neufeld EB, Chang TY, Liscum L, Tagle DA, et al (1997) Niemann-Pick C1 disease gene: homology to mediators of cholesterol homeostasis. Science 277:228–231
13. Constantopoulos G, Shull RM, Hastings N, Neufeld EF (1985) Neurochemical characterization of canine alpha-L-iduronidase deficiency disease (model of human mucopolysaccharidosis I). J Neurochem 45:1213–1217
14. Cox TM (2001) Gaucher disease: understanding the molecular pathogenesis of sphingolipidoses. J Inherit Metab Dis 24 [Suppl 2]:106–121 (discussion 87–88)
15. Dawson G, Oh JY (1977) Blood glucosylceramide levels in Gaucher's disease and its distribution amongst lipoprotein fractions. Clin Chim Acta 75:149–153
16. Ebato H, Abe T, Yamakawa T, Nagashima K (1980) Characterization of the cytoplasmic inclusion bodies of the spleens from patients with adult form Gaucher's disease. J Biochem (Tokyo) 88:1765–1772
17. Elleder M (1978) A histochemical and ultrastructural study of stored material in neuronal ceroid lipofuscinosis. Virchows Arch B Cell Pathol 28:167–178
18. Elleder M, Jirasek A (1981) Histochemical and ultrastructural study of Gaucher cells. Acta Neuropathol Suppl (Berl) 7:208–210
19. Elleder M, Lojda Z (1971) Studies in lipid histochemistry. VI. Problems of extraction with acetone in lipid histochemistry. Histochemie 28:68–87
20. Elleder M, Jirasek A, Smid F, Ledvinova J, Besley GT (1985) Niemann-Pick disease type C. Study on the nature of the cerebral storage process. Acta Neuropathol (Berl) 66:325–336
21. Elleder M, Dorazilova V, Bradova V, Belohlavek M, Kral V, Choura M, Budesinsky M, Harzer K (1990) Fabry's disease with isolated disease of the cardiac muscle, manifesting as hypertrophic cardiomyopathy. Cas Lek Cesk 129:369–372
22. Elleder M, Chlumska A, Hyanek J, Poupetova H, Ledvinova J, Maas S, Lohse P (2000) Subclinical course of cholesteryl ester storage disease in an adult with hypercholesterolemia, accelerated atherosclerosis, and liver cancer. J Hepatol 32:528–534
23. Goyert SM (1996) CDw17 workshop panel report. In: Kishimoto T (ed) Leucocyte typing VI, Kobe, Japan. Garland Publishing, New York, pp 971–972
24. Greenbaum M, Hoffman LM, Schneck L (1976) Ceramide hexosides in Niemann-Pick disease brain. J Neurol 213:251–255
25. Hadfield MG, Ghatak NR, Nakoneczna I, Lippman HR, Myer EC, Constantopoulos G, Bradley RM (1980) Pathologic findings in mucopolysaccharidosis type IIIB (Sanfilippo's syndrome B). Arch Neurol 37:645–650
26. Hara A, Kitazawa N, Taketomi T (1984) Abnormalities of glycosphingolipids in mucopolysaccharidosis type III B. J Lipid Res 25:175–184
27. Harzer K, Paton BC, Poulos A, Kustermann-Kuhn B, Roggendorf W, Grisar T, Popp M (1989) Sphingolipid activator protein deficiency in a 16-week-old atypical Gaucher disease patient and his fetal sibling: biochemical signs of combined sphingolipidoses. Eur J Pediatr 149:31–39
28. Hers HG, de Barsy T (1973) Type II glycogenosis (acid maltase deficiency). In: Hers HG, Van Hoof F (ed) Lysosomes and storage diseases. Academic Press, New York, pp 197–217
29. Hulkova H, Ledvinova J, Poupetova H, Bultas J, Zeman J, Elleder M (1999) Postmortem diagnosis of Fabry disease in a female heterozygote leading to the detection of undiagnosed manifest disease in the family. Cas Lek Cesk 138:660–664
30. Hulkova H, Cervenkova M, Ledvinova J, Tochackova M, Hrebicek M, Poupetova H, Befekadu A, Berna L, Paton BC, Harzer K, Boor A, Smid F, Elleder M (2001) A novel mutation in the coding region of the prosaposin gene leads to a complete deficiency of prosaposin and saposins, and is associated with a complex sphingolipidosis dominated by lactosylceramide accumulation. Hum Mol Genet 10:927–940
31. Chatterjee S (1998) Sphingolipids in atherosclerosis and vascular biology. Arterioscler Thromb Vasc Biol 18:1523–1533
32. Chatterjee S, Sekerke CS, Kwiterovich PO Jr (1982) Increased urinary excretion of glycosphingolipids in familial hypercholesterolemia. J Lipid Res 23:513–522
33. Chatterjee S, Kwiterovich PO Jr, Gupta P, Erozan YS, Alving CR, Richards RL (1983) Localization of urinary lactosylceramide in cytoplasmic vesicles of renal tubular cells in homozygous familial hypercholesterolemia. Proc Natl Acad Sci U S A 80:1313–1317
34. Chatterjee S, Dey S, Shi WY, Thomas K, Hutchins GM (1997) Accumulation of glycosphingolipids in human atherosclerotic plaque and unaffected aorta tissues. Glycobiology 7:57–65
35. Chen CS, Patterson MC, Wheatley CL, O'Brien JF, Pagano RE (1999) Broad screening test for sphingolipid-storage diseases. Lancet 354:901–905
36. Iwabuchi K, Nagaoka I (2002) Lactosylceramide-enriched glycosphingolipid signaling domain mediates superoxide generation from human neutrophils. Blood 100:1454–1464
37. Iwamoto T, Fukumoto S, Kanaoka K, Sakai E, Shibata M, Fukumoto E, Inokuchi Ji J, Takamiya K, Furukawa K, Kato Y, Mizuno A (2001) Lactosylceramide is essential for the osteoclastogenesis mediated by macrophage-colony-stimulating factor and receptor activator of nuclear factor-kappa B ligand. J Biol Chem 276:46031–46038
38. Kahma K, Brotherus J, Haltia M, Renkonen O (1976) Low and moderate concentrations of lysobisphosphatidic acid in brain and liver of patients affected by some storage diseases. Lipids 11:539–544
39. Kamoshita S, Aron AM, Suzuki K (1969) Infantile Niemann-Pick disease. A chemical study with isolation and characterization of membranous cytoplasmic bodies and myelin. Am J Dis Child 117:379–394
40. Kannan R, Tjiong HB, Debuch H, Wiedemann HR (1974) Unusual glycolipids in brain cortex of a visceral lipidosis (Niemann-Pick disease?). Hoppe Seylers Z Physiol Chem 355:551–556
41. Kasama T, Taketomi T (1986) Abnormalities of cerebral lipids in GM1-gangliosidoses, infantile, juvenile, and chronic type. Jpn J Exp Med 56:1–11
42. Klibansky C, Ossimi Z, Matoth Y, Pinkhas J, de Vries A (1976) Accumulation of lactosyl ceramide in leukocytes of patients with adult Gaucher's disease. Clin Chim Acta 72:141–146
43. Kojima N, Shiota M, Sadahira Y, Handa K, Hakomori S (1992) Cell adhesion in a dynamic flow system as compared to static system. Glycosphingolipid-glycosphingolipid interaction in the dynamic system predominates over lectin- or integrin-based mechanisms in adhesion of B16 melanoma cells to non-activated endothelial cells. J Biol Chem 267:17264–17270
44. Koubek K, Korinkova P, Hruba A, Hausner P (1988) Human leukocyte markers defined by monoclonal antibodies. I. Expression of X-hapten structure on cells of myeloid lineage. Folia Haematol Int Mag Klin Morphol Blutforsch 115:913–926
45. Kuske TT, Rosenberg A (1972) Quantity and fatty acyl composition of the glycosphingolipids of Gaucher spleen. J Lab Clin Med 80:523–529
46. Ledeen RW, Yu RK, Eng LF (1973) Gangliosides of human myelin: sialosylgalactosylceramide (G7) as a major component. J Neurochem 21:829–839
47. Lingwood CA (1998) Oligosaccharide receptors for bacteria: a view to a kill. Curr Opin Chem Biol 2:695–700

48. Lund-Johansen F, Olweus J, Horejsi V, Skubitz KM, Thompson JS, Vilella R, Symington FW (1992) Activation of human phagocytes through carbohydrate antigens (CD15, sialyl-CD15, CDw17, and CDw65). J Immunol 148:3221–3229
49. Lusa S, Blom TS, Eskelinen EL, Kuismanen E, Mansson JE, Simons K, Ikonen E (2001) Depletion of rafts in late endocytic membranes is controlled by NPC1-dependent recycling of cholesterol to the plasma membrane. J Cell Sci 114:1893–1900
50. Malinina L, Malakhova ML, Teplov A, Brown RE, Patel DJ (2004) Structural basis for glycosphingolipid transfer specificity. Nature 430:1048–1053
51. Matsuo H, Chevallier J, Mayran N, Le Blanc I, Ferguson C, Faure J, Blanc NS, Matile S, Dubochet J, Sadoul R, Parton RG, Vilbois F, Gruenberg J (2004) Role of LBPA and Alix in multivesicular liposome formation and endosome organization. Science 303:531–534
52. Moore RM, Lundgren DW, Silver RJ, Moore JJ (2002) Lactosylceramide-induced apoptosis in primary amnion cells and amnion-derived WISH cells. J Soc Gynecol Investig 9: 282–289
53. Mukhin DN, Chao FF, Kruth HS (1995) Glycosphingolipid accumulation in the aortic wall is another feature of human atherosclerosis. Arterioscler Thromb Vasc Biol 15:1607–1615
54. Muthing J, Maurer U, Neumann U, Kniep B, Weber-Schurholz S (1998) Glycosphingolipids of skeletal muscle: I. Subcellular distribution of neutral glycosphingolipids and gangliosides in rabbit skeletal muscle. Carbohydr Res 307:135–145
55. Natomi H, Sugano K, Iwamori M, Takaku F, Nagai Y (1988) Region-specific distribution of glycosphingolipids in the rabbit gastrointestinal tract: preferential enrichment of sulfoglycolipids in the mucosal regions exposed to acid. Biochim Biophys Acta 961:213–222
56. Nilsson O, Mansson JE, Hakansson G, Svennerholm L (1982) The occurrence of psychosine and other glycolipids in spleen and liver from the three major types of Gaucher's disease. Biochim Biophys Acta 712:453–463
57. Parkin ET, Turner AJ, Hooper NM (2001) Differential effects of glycosphingolipids on the detergent-insolubility of the glycosylphosphatidylinositol-anchored membrane dipeptidase. Biochem J 358:209–216
58. Philippart M, Rosenstein B, Menkes JH (1965) Isolation and characterization of the main splenic glycolipids in the normal organ and in Gaucher's disease: evidence for the site of metabolic block. J Neuropathol Exp Neurol 24:290–303
59. Philippart M, Martin L, Martin JJ, Menkes JH (1969) Niemann-Pick disease. Morphologic and biochemical studies in the visceral form with late central nervous system involvement (Crocker's group C). Arch Neurol 20:227–238
60. Prokazova NV, Mukhin DN, Orekhov AN, Gladkaya EM, Vasilevskaya VV, Mikhailenko IA, Sadovskaya VL, Bushuev VN, Bergelson LD (1989) Neutral glycolipids of atherosclerotic plaques and unaffected human aorta tissue. Eur J Biochem 180:167–171
61. Puri V, Watanabe R, Dominguez M, Sun X, Wheatley CL, Marks DL, Pagano RE (1999) Cholesterol modulates membrane traffic along the endocytic pathway in sphingolipid-storage diseases. Nat Cell Biol 1:386–388
62. Rouser G, Kritchevsky G, Yamamoto A, Knudson AG, Simon G (1968) Accumulation of a glycerophospholipid in classical Niemann-Pick disease. Lipids 3:287–290
63. Saito M, Rosenberg A (1985) The fate of glucosylceramide (glucocerebroside) in genetically impaired (lysosomal beta-glucosidase deficient) Gaucher disease diploid human fibroblasts. J Biol Chem 260:2295–2300
64. Sandhoff K, Kolter T, Harzer K (2001) Sphingolipid activator proteins. In: Scriver CR, Beaudet AL, Sly WS, Valle D (eds) The metabolic and molecular bases of inherited disease. McGraw-Hill, New York, pp 3371–3388
65. Seng PN, Debuch H, Witter B, Wiedemann HR (1971) Augmentation of bis(monoacylglycerin)phosphoric acid in sphingomyelinosis (M. Niemann-Pick?). Hoppe Seylers Z Physiol Chem 352:280–288
66. Simons K, Gruenberg J (2000) Jamming the endosomal system: lipid rafts and lysosomal storage diseases. Trends Cell Biol 10: 459–462
67. Suomi WD, Agranoff BW (1965) Lipids of the spleen in Gaucher's disease. J Lipid Res 58:211–219
68. Suzuki A, Kundu SK, Marcus DM (1980) An improved technique for separation of neutral glycosphingolipids by high-performance liquid chromatography. J Lipid Res 21:473–477
69. Svennerholm L, Vanier MT, Mansson JE (1980) Krabbe disease: a galactosylsphingosine (psychosine) lipidosis. J Lipid Res 21:53–64
70. Symington FW, Murray WA, Bearman SI, Hakomori S (1987) Intracellular localization of lactosylceramide, the major human neutrophil glycosphingolipid. J Biol Chem 262:11356–11363
71. Tjiong HB, Seng PN, Debuch H, Wiedemann HR (1973) Brain lipids of a case of juvenile Niemann-Pick disease. J Neurochem 21:1475–1485
72. Van Hoof F (1973) GM1-gangliosidosis. In: Hers HG, Van Hoof F (eds) Lysosomes and storage diseases. Academic Press, New York, pp 305–322
73. Van Hoof F (1973) Mucopolysaccharidoses. In: Hers HG, Van Hoof F (eds) Lysosomes and storage diseases. Academic Press, New York, pp 218–262
74. van Meer G, Lisman Q (2002) Sphingolipid transport: rafts and translocators. J Biol Chem 277:25855–25858
75. Vanier MT (1983) Biochemical studies in Niemann-Pick disease. I. Major sphingolipids of liver and spleen. Biochim Biophys Acta 750:178–184
76. Vanier MT (1999) Lipid changes in Niemann-Pick disease type C brain: personal experience and review of the literature. Neurochem Res 24:481–489
77. Walkley SU (2004) Secondary accumulation of gangliosides in lysosomal storage disorders. Semin Cell Dev Biol 15:433–444
78. Whitfield PD, Nelson P, Sharp PC, Bindloss CA, Dean C, Ravenscroft EM, Fong BA, Fietz MJ, Hopwood JJ, Meikle PJ (2002) Correlation among genotype, phenotype, and biochemical markers in Gaucher disease: implications for the prediction of disease severity. Mol Genet Metab 75:46–55
79. Yeh LH, Kinsey AM, Chatterjee S, Alevriadou BR (2001) Lactosylceramide mediates shear-induced endothelial superoxide production and intercellular adhesion molecule-1 expression. J Vasc Res 38:551–559
80. Zervas M, Dobrenis K, Walkley SU (2001) Neurons in Niemann-Pick disease type C accumulate gangliosides as well as unesterified cholesterol and undergo dendritic and axonal alterations. J Neuropathol Exp Neurol 60:49–64
81. Zimmerman JW, Lindermuth J, Fish PA, Palace GP, Stevenson TT, DeMong DE (1998) A novel carbohydrate-glycosphingolipid interaction between a beta-(1-3)-glucan immunomodulator, PGG-glucan, and lactosylceramide of human leukocytes. J Biol Chem 273:22014–22020

Virchows Arch (2005) 447: 45–52
DOI 10.1007/s00428-005-1248-9

ORIGINAL ARTICLE

Hyun Sook Jung · Bo Hyun Yoon · Jong Kwan Jun · Miha Kim · Young Ah Kim · Chong Jai Kim

Differential activation of mitogen activated protein kinases and nuclear factor-κB in lipopolysaccharide-treated term and preterm amnion cells

Received: 28 July 2004 / Accepted: 4 March 2005 / Published online: 1 June 2005
© Springer-Verlag 2005

Abstract Intrauterine exposure to amniotic sac infection elicits an inflammatory response from the fetus, which is associated with elevated levels of fetal plasma proinflammatory cytokines, i.e. interleukin-6 (IL-6). We have recently demonstrated that the severity of fetal inflammatory response in terms of gestation period is greater in preterm fetuses than in term fetuses. The activation of mitogen activated protein kinases (MAPKs) and nuclear factor kappa B (NF-κB) is known to be associated with up-regulation of proinflammatory cytokine gene expression in many cell types. In the present study, therefore, we studied patterns of MAPK and NF-κB activation following treatment with bacterial lipopolysaccharide (LPS) in amnion cells obtained from placentas of varying gestational ages to assess whether or not MAPKs and NF-κB are differentially regulated during gestation. MAPK phosphorylation was investigated by immunoblot analysis with phosphospecific antibodies. Transient phosphorylations of extracellular signal-regulated kinase (ERK) 1/2 and c-Jun N-terminal kinase (JNK) were observed in LPS-treated amnion cells, with the degree of phosphorylation being more pronounced in preterm cases. The results of NF-κB-dependent reporter gene expression and electrophoretic mobility shift assay (EMSA) of NF-κB were similar to those of ERK 1/2 and JNK activity. To assess whether the results of in vitro observations reflected in vivo results, we further analyzed amniotic fluid and cord blood IL-6 levels in preterm deliveries with placental inflammation. The analysis also revealed a significantly higher level of IL-6 in cases of ≤31 weeks gestation when compared with those of more than 31 weeks ($P<0.001$). All these findings strongly suggest that there is an inverse relationship between gestational age and fetal inflammatory response during human gestation, and that differences in the intensity of MAPK activation and NF-κB-dependent transcription pathways are elements of the major underlying mechanism.

Keywords Amnion · Interleukin-6 · Lipopolysaccharide · JNK · ERK 12 · NF-κB

H. S. Jung · Y. A. Kim · C. J. Kim (✉)
Department of Pathology,
Seoul National University College of Medicine,
28 Yongon-dong, Chongno-gu,
Seoul, 110-799, South Korea
e-mail: cjkim@plaza.snu.ac.kr
Tel.: +82-2-7603549
Fax: +82-2-7457966

H. S. Jung · B. H. Yoon · J. K. Jun · C. J. Kim
Laboratory of Fetal Medicine Research,
Clinical Research Institute,
Seoul National University Hospital,
Seoul, South Korea

B. H. Yoon · J. K. Jun · M. Kim
Department of Obstetrics and Gynecology,
Seoul National University College of Medicine,
Seoul, South Korea

Introduction

Intrauterine infection is emerging as a major cause of preterm deliveries, and exposure to bacterial lipopolysaccharide (LPS) in infected amniotic sac elicits fetal and placental inflammatory responses that are associated with elevation of proinflammatory cytokines in fetal plasma, amniotic fluid, and even in cervical fluids [15, 19, 35]. The severity of the fetal inflammatory response correlates with the levels of proinflammatory cytokines such as IL-1β, IL-6, and IL-8 in fetal plasma, with major perinatal morbidities and also with the severity of placental inflammation [14, 24, 26]. The cytokines subsequently activate matrix metalloproteinases (MMPs) and prostaglandin E_2 (PGE_2), which exert important effects on the degradation of extracellular matrix (ECM) and induce stimulation of preterm labor [4, 5, 1, 21, 32]. We have recently shown that the inflammatory response to intrauterine infection is more severe in preterm than in term fetuses. Preterm cases had a significantly higher incidence of acute funisitis at advanced stages and a higher level of fetal plasma IL-6 [20].

Mitogen activated protein kinases (MAPKs), which include extracellular signal-regulated kinases (ERKs), c-Jun

N-terminal kinases (JNKs), and p38, are members of a family of serine/threonine kinases that participate in signaling pathways initiated by a variety of infectious and inflammatory stimuli. MAPK signal transduction pathways have been well characterized. MAPK kinase kinase activates MAPK kinase (MAPKK), which in turn activates MAPK. The ERK pathway (ERK 1/2) is activated by the dual phosphorylation of MAPKK MEK1 and MEK2. Likewise, MAPKK MKK 4/7 potently activates JNK (SAPK) and MAPKK MKK 3/6 activates p38 [9, 33]. MAPK activation is a hallmark of LPS-induced cellular response [16], and Fig. 1 is a schematic representation of the MAPK signaling pathway.

The transcription factor NF-κB is also known to play a central role in the production of proinflammatory cytokines after exposure to LPS [6, 10]. NF-κB is a homo- or heterodimeric transcription factor, which usually consists of two proteins, a p50 subunit and a p65 subunit (also called RelA) [8]. In unstimulated cells, NF-κB is retained in the cytoplasm by an interaction with inhibitory proteins known as inhibitor of NF-κB (IκB). Many stimuli induce phosphorylation and subsequent proteolytic degradation of IκB via the ubiquitination-proteasome pathway [29, 38]. The release of NF-κB from IκB leads to translocation of NF-κB into the nucleus, where it binds to specific sequences in the promoter regions of many genes involved in immune and inflammatory responses.

Activation of MAPKs and NF-κB by infectious stimuli such as LPS were demonstrated in many cell types [17, 18, 25, 28], and these are also important regulators of various proinflammatory cytokine genes, including IL-1β, IL-6, IL-8, and tumor necrosis factor-alpha (TNF-α) [2, 3, 23]. However, the patterns of MAPKs and NF-κB during inflammation in the human gestational tissues have not been analyzed. We postulated that they would play a central role in the differential regulation of fetal inflammatory response according to gestational age, and therefore conducted the present study to assess patterns of MAPK and NF-κB activations in LPS-treated human placental tissues, especially of amnion. Activation of MAPK and NF-κB following LPS treatment were more pronounced in preterm amnion cells than in their term counterparts in vitro. An additional analysis of amniotic fluid and cord plasma IL-6 levels in preterm births was also conducted to determine whether this inverse relationship reflects fetal inflammatory response in vivo. The levels of amniotic fluid and cord plasma IL-6 were significantly higher during the earlier gestational period, which strongly supports the relevance of our observation in vitro.

Materials and methods

Tissue culture and LPS treatment

Placentas and amniotic membranes were obtained from Caesarean sections at different gestational periods (n=7; 23, 28^{+1}, 34^{+4}, 35, 37^{+3}, 38, and 39^{+1} weeks). Placental villous tissues were minced and meticulously washed with sterile PBS. The tissues were incubated in RPMI 1640 containing antibiotics without serum at 37°C for 30 min to remove residual red blood cells. After washing with RPMI 1640, amnions were cut into pieces of 3 cm^2. Amnion and villous explants were put into six-well plates containing medium supplemented with antibiotics and incubated overnight in CO_2 incubator. On the next day, the tissues were treated with LPS at the concentration of 1 μg/ml for the specified periods of time. The samples were then subjected to immunoblotting analysis and electrophoretic mobility shift assay.

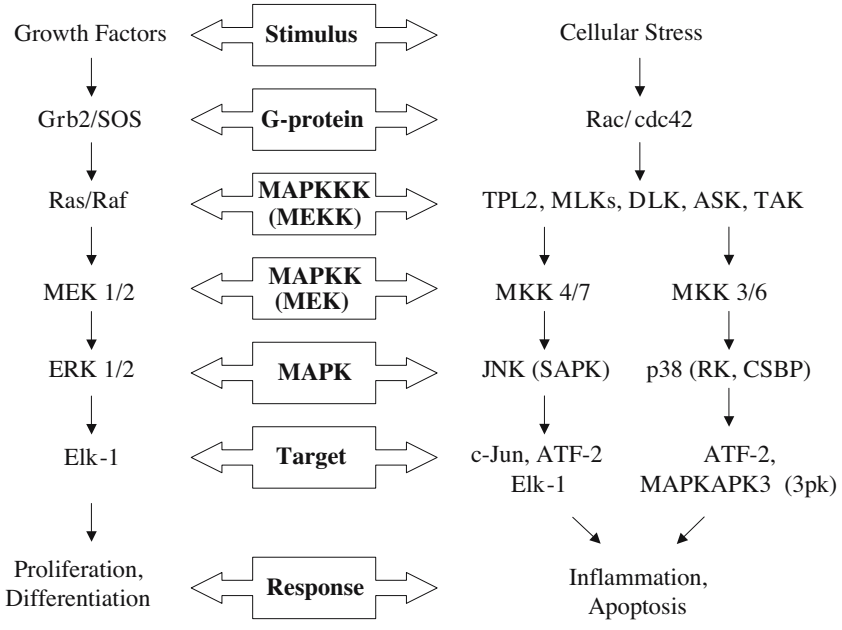


Fig. 1 Schematic drawing of MAPK signaling pathway

Immunoblotting

The cells were lysed in lysis buffer containing 10 mM Tris buffer (pH 7.4), 0.5 mM EDTA (ethylenediaminetetraacetic acid; Sigma Chemical Co., Steinheim, Germany), 0.25 M sucrose, and protease inhibitor with a Dounce homogenizer. The samples were then put on ice for 30 min. Pellets were removed by centrifugation at 6300 *g* for 30 min. The protein concentration was determined with a BCA kit (Pierce, Rockford, Ill., USA). For immunoblotting, a total of 30 or 50 μg protein was subjected to 10% SDS-polyacrylamide gel electrophoresis (SDS-PAGE) and transferred onto a nitrocellulose membrane. Non-specific binding was blocked by soaking the membrane with 3% non-fat milk in TBS (50 mM Tris, 150 mM NaCl) containing 0.1% Tween 20 (TBS-T) at room temperature for 1 h. p44/42, phospho-p44/42, JNK, phospho-JNK, p38, phospho-p38, p65 and actin were probed with rabbit polyclonal anti-p44/42, phospho-p44/42, JNK, phospho-JNK, p38 and phospho-p38 antibodies (Cell Signaling Technology, Beverly, Mass., USA.) and mouse monoclonal anti-p65 and anti-actin antibodies (Santa Cruz Biotechnology, Inc., Santa Cruz, Calif., USA), respectively. The membrane was incubated with 1:1000 diluted antibodies for 90 min at room temperature and washed 4 times for 15 min each with TBS-T. After washing, the blot was incubated with horseradish peroxidase-conjugated secondary antibodies. Signals were detected using enhanced chemiluminescence reagents (Amersham Life Science, Inc., Arlington Heights, Ill., USA).

Primary amnion cell cultures

Amnion cells were harvested from six additional fetal membranes of varying gestational ages (22^{+4}, 23^{+4}, 33, 37^{+4}, 38^{+3} and 38^{+6} weeks). Two cases (37^{+4} and 38^{+3} weeks) were also used for EMSA. Placentas were obtained from Caesarean section at different gestational periods. All of the cases were free of histologic chorioamnionitis. The institutional review board of Seoul National University Hospital approved the use and collection of the materials and information for research purposes. The amniotic membrane was washed with PBS (sterile phosphate-buffered saline) and initially treated with 0.5% collagenase in PBS for 20 min in a shaking water bath at 37°C, followed by vigorous shaking for 15 min at 15-min intervals over 90 min in 0.25% collagenase at 37°C. Amnion cells were collected using a sieve, centrifuged at 1000 *g* for 5 min, and washed again with PBS. The cells were then subjected to transfection and luciferase assay.

Transfection and luciferase assay

The cells were split in a six-well plate at a density of 4×10^5 cells/well, and cultured overnight in RPMI 1640 containing 10% fetal bovine serum and antibiotics. The cells were transfected with 1 μg of pNFκB-Luc (Stratagene, La Jolla, Calif., USA) using LipoFectamine (Invitrogen, Carlsbad, Calif., USA) and treated with Bacto® LPSs (Difco Laboratories, Inc., Detroit, Mich., USA) at a concentration of 1 μg/ml for 24 h after transfection in the presence or absence of 25 μM of tosyl-phe-chloro-methylketone (TPCK), an inhibitor of NF-κB. After incubation for another 24 h, luminometry was performed using a luminometry kit (Stratagene) according to the manufacturer's instructions. Luciferase activity was normalized to β-galactosidase activity.

Electrophoretic mobility shift assay

Placental villous tissue and amnion were liquid nitrogen-pulverized with a mortar and a pestle. Nuclear extracts were obtained from LPS-treated amnion cells from five placentas (24, 29, 37^{+4}, 38^{+3} and 39^{+1} weeks). After washing twice with hypotonic solution [10 mM 4-(2-hydroxylethyl)-1-piperazineethanesulfonic acid, 1.5 mM $MgCl_2$, 10 mM KCl, 0.1 mM EDTA], the samples were suspended in hypotonic solution containing 0.6% NP-40 and proteinase inhibitors (Completed; Boehringer-Mannheim, Basel, Switzerland) for 5 min on ice and centrifuged at 6300 *g* for 10 min. The supernatant was used as cytoplasmic fractions, and the pellets were dissolved in 20 mM HEPES, 0.4 M NaCl, 1 mM EDTA, 0.6% NP40, 1 mM DTT and proteinase inhibitors for 30 min on ice and centrifuged at 6300 *g* for 30 min. The supernatant was used as nuclear protein and subjected to EMSA. For EMSA, oligonucleotides comprising the consensus sequences for NF-κB (5′-AGTTGAGGGGACTTTCCCA GGC-3′) were end-labeled with [γ-^{32}P]-dATP (Amersham, Piscataway, N.J., USA) using T4 polynucleotide kinase (Promega Corporation, Madison, Wisc., USA). Nuclear extracts (20 μg) were incubated at binding conditions (4% glycerol, 1 mM $MgCl_2$, 0.5 mM EDTA, 0.5 mM DTT, 50 mM Tris-HCl, pH 7.5, 50 μg/ml poly (dI-dC)) for 10 min at room temperature. Radiolabeled probes were then added and the mixture was incubated at room temperature for 20 min. Protein-DNA complexes were analyzed on a 5% non-denaturing polyacrylamide gel. Gels were dried on 3 MM paper and exposed to Kodak X-ray film overnight at -80°C.

Immunoassay of amniotic fluid and cord blood IL-6

The amniotic fluid and cord blood IL-6 was assayed from 265 consecutive, singleton preterm births (≤36 weeks gestation) delivered at the Seoul National University Hospital (Seoul, Korea) between May 1993 and May 2000. All cases were diagnosed with placental inflammation. Many of the patients included in this study had undergone transabdominal amniocentesis either for evaluation of microbiologic status of the amniotic cavity or for assessment of fetal lung maturity. Umbilical cord blood was collected in an EDTA-containing blood collection tube by venipuncture of the umbilical vein at birth. The samples were centrifuged at 700 *g* for 5 min, and supernatants stored in polypropylene tubes at –70°C until assay. The IL-6 in the amniotic fluid and cord plasma was measured using a commercially

available, enzyme-linked immunosorbent assay kit (R & D Systems, Minneapolis, Minn., USA). The sensitivity of the test was less than 0.1 pg/ml and both inter-assay and intra-assay coefficients were less than 10%.

Analysis of major perinatal morbidity

Major perinatal morbidity was defined as the presence of any of the following conditions, as diagnosed according to the definitions previously reported in detail [35]: congenital neonatal sepsis, suspected sepsis, respiratory distress syndrome, congenital pneumonia, bronchopulmonary dysplasia, intraventricular hemorrhage, or necrotizing enterocolitis. Clinical chorioamnionitis was diagnosed when the temperature was elevated to 37.8°C or higher and two or more of the following four criteria were satisfied: uterine tenderness, malodorous vaginal discharge, maternal leukocytosis (>15,000/mm^3) and fetal tachycardia (>160 beats/min) [13].

Statistical analysis

Comparisons of continuous variables were preformed using the Mann-Whitney *U*-test and comparisons of proportions were performed with Fisher's exact test.

Results

Activation of MAPKs in amnion cells

It is well known that LPS treatment leads to activation of three families of MAPKs, ERK 1/2, JNK, and p38, in murine macrophages and human monocytes [17, 28]. To investigate the patterns of MAPK activation in human gestational tissues, placental villous tissues and amnion obtained from caesarean section at different gestational periods were treated with LPS. Four preterm and three term placentas (23, 28^{+1}, 34^{+4}, 35, 37^{+3}, 38, and 39^{+1} weeks) were used to analyze JNK and ERK 1/2 activation. Experiments were performed at least twice. Placental villous and amnion cell extracts were then examined for the active forms of MAPKs by immunoblotting. As shown in Figs. 2 and 3, both JNK and ERK 1/2 were phosphorylated in amnion cells. Although JNK and ERK 1/2 were also phosphorylated in placental tissues by LPS treatment, the response was much weaker than that of amnion (data not shown). Activation of p38 was not found in either placenta or amnion. In amnion obtained at 23 weeks of gestation, there was a 1.51-fold increase in JNK phosphorylation at 15 min after LPS treatment, which quickly declined. In amnion cells at 28^{+1} weeks of gestation, JNK phosphorylation was found at 15 min after stimulation and was sustained for over 1 h with a 3.86-fold increase at peak when compared with control. In amnion cells obtained at 35 weeks, maximal phosphorylation of JNK reached 1.29-fold

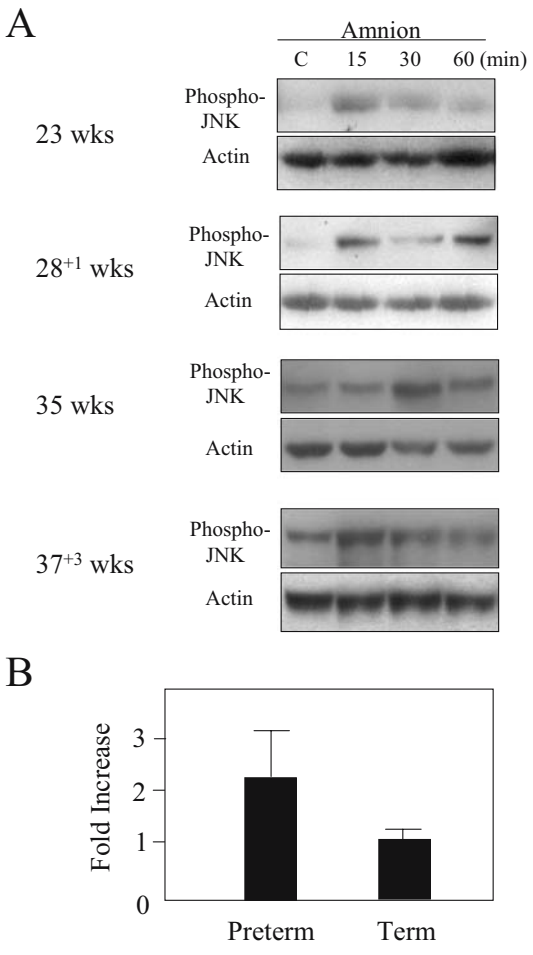


Fig. 2 Patterns of activation of JNK by LPS in amnion cells. (**a**) The amnion cells obtained at different gestational periods were treated with LPS at the concentration of 1 μg/ml for the specified periods of time. After homogenization of amniotic membranes, JNK phosphorylation was determined by immunoblotting with phosphospecific anti-JNK antibody. Aliquots of 50 μg total proteins were electrophoresed in 10% SDS-PAGE, electrotransferred onto a nitrocellulose membrane, and then the signals were detected by chemiluminescence. (**b**) Graph showing densitometric determined JNK activations at 15 min after LPS treatment in preterm (n=3) and term (n=3) amnion cells. The data were quoted as a percentage of control at 0 min

of the control, while LPS treatment had little effect on the levels of phosphorylated JNK in term cases (Fig. 2).

The phosphorylation of ERK 1/2 also increased at 15 min after LPS treatment, with a mean peak level of 1.38-fold in preterm amnion cells (23, 28^{+1}and 34^{+4} weeks; range), and then gradually decreased, showing that LPS causes a transient activation of ERK 1/2 in preterm amnion cells. However, there was only a mean 1.12-fold increase in phosphorylated ERK 1/2 in term amnion cells (Fig. 3).

Activation of NF-κB in term and preterm amnion cells

NF-κB is an obligatory transcription factor in inflammation and innate immunity. Accordingly, luciferase assay of

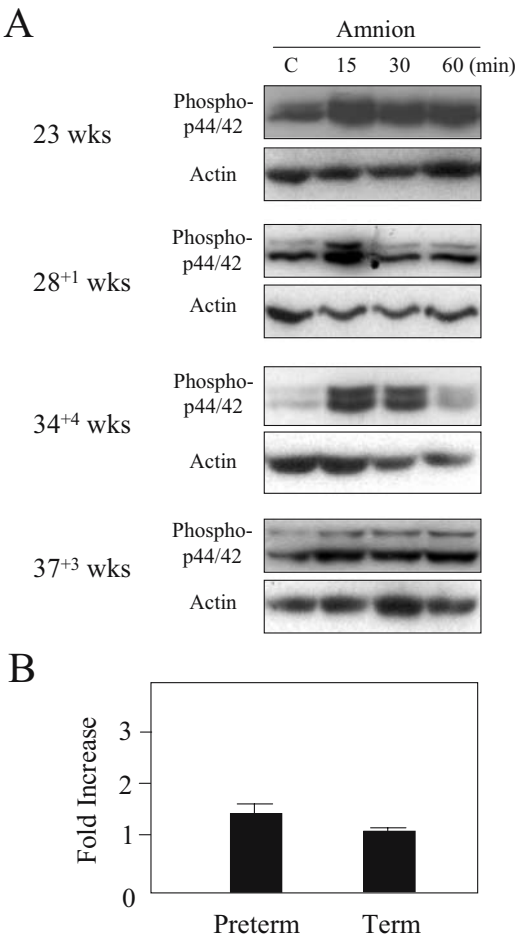


Fig. 3 Patterns of activation of ERK 1/2 by LPS in amnion cells. (**a**) The amnion cells obtained at different gestational periods were treated with LPS at a concentration of 1 μg/ml for the specified periods of time. After homogenization of amniotic membranes, phosphorylation of ERK 1/2 was determined by immunoblotting with phosphospecific anti-p44/p42 antibody. Aliquots of 30 μg total proteins were electrophoresed in 10% SDS-PAGE, electrotransferred onto a nitrocellulose membrane, and then the signals were detected by chemiluminescence. (**b**) Graph showing densitometrically determined ERK 1/2 activations at 15 min after LPS treatment in preterm (n=3) and term (n=3) amnion cells. The data were quoted as a percentage of control at 0 min

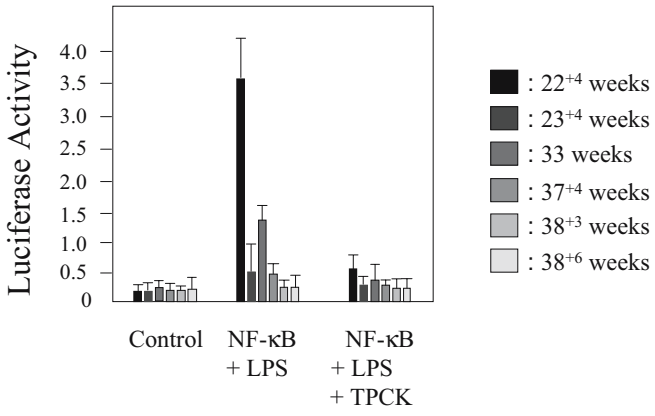


Fig. 4 Reporter gene analysis. Primary amnion cell cultures were transfected with 1 μg of pNFκB-Luc, and treated with LPS at the concentration of 50 ng/ml for 24 h after transfection in the presence or absence of 25 μM TPCK. The results clearly show an inverse relationship between gestational age and luciferase activity and also the inhibition of NF-κB activation by TPCK. The luciferase activity was normalized to β-galactosidase activity and is quoted as a percentage of control. LPS: lipopolysaccharide, TPCK: tosyl-phe-chloro-methylketone

NF-κB dependent gene expression by transient transfection of amnion cells obtained at varying weeks of gestation (n=6; 22^{+4}, 23^{+4}, 33, 37^{+4}, 38^{+3} and 38^{+6} weeks) demonstrated that the magnitude of NF-κB activation after LPS treatment was greater in preterm cases than in term counterparts. The relationship between magnitude of NF-κB activation following LPS treatment and gestational age is shown in Fig. 4. We also examined NF-κB activity by EMSA and western blot analysis using p65 specific antibody in nuclear extracts obtained from LPS-treated amnion cells (24, 29, 37^{+4}, 38^{+3} and 39^{+1} weeks). Competition experiments were carried out to determine the specificity of LPS-induced NF-κB DNA binding activity observed in the oligo NF-κB site. The binding activity was profoundly inhibited by the 50-fold molar excess of an unlabeled NF-κB oligonucleotide, whereas the 50-fold molar excess of an unlabeled oligo AP1 only slightly impaired the binding activity (Fig. 5a). In amnion cells at 24 weeks of gestation, a 2-fold increase in NF-κB activation was observed within 15 min, which gradually decreased at 30 min. The activity after 1 h of LPS exposure was similar to the control activity. At 29 weeks, densitometric analysis of NF-κB activation revealed an approximately 2.6-fold increase after 15 min, which was sustained until 1 h after LPS exposure (Fig. 5b). There was no significant change in NF-κB activation in term amnion cells. These data were consistent with the results of immunoblotting using p65 specific antibody.

Amniotic fluid and cord plasma IL-6 in preterm births

In a separate analysis, IL-6 levels in amniotic fluid and cord blood obtained from preterm deliveries were compared with placental inflammation to assess whether or not the fetal cytokine response during the preterm period is also gestational age-dependent. The level of significance was greatest when the preterm cases with placental inflammation were dichotomized for analysis at the gestational age of 31 weeks (Fig. 6). The amniotic fluid and cord blood IL-6 levels were significantly higher in cases born at or before the gestational age of 31 weeks than in preterm cases born after 31 weeks (amniotic fluid IL-6: median, 16.5 ng/ml; range, 0.1-92.5 ng/ml; versus median, 1.9 ng/ml; range, 0.1-115.2 ng/ml, respectively; cord blood IL-6: median, 68.1 pg/ml; range, 0.6-18107.5 pg/ml; versus median, 7.7 pg/ml; range, 0.0-4897.0 pg/ml, respectively; P<0.001 for all). When the IL-6 concentrations of amniotic fluid and cord plasma in cases with advanced stage of placental inflammation (chorion-decidua grade=3 and umbilical cord

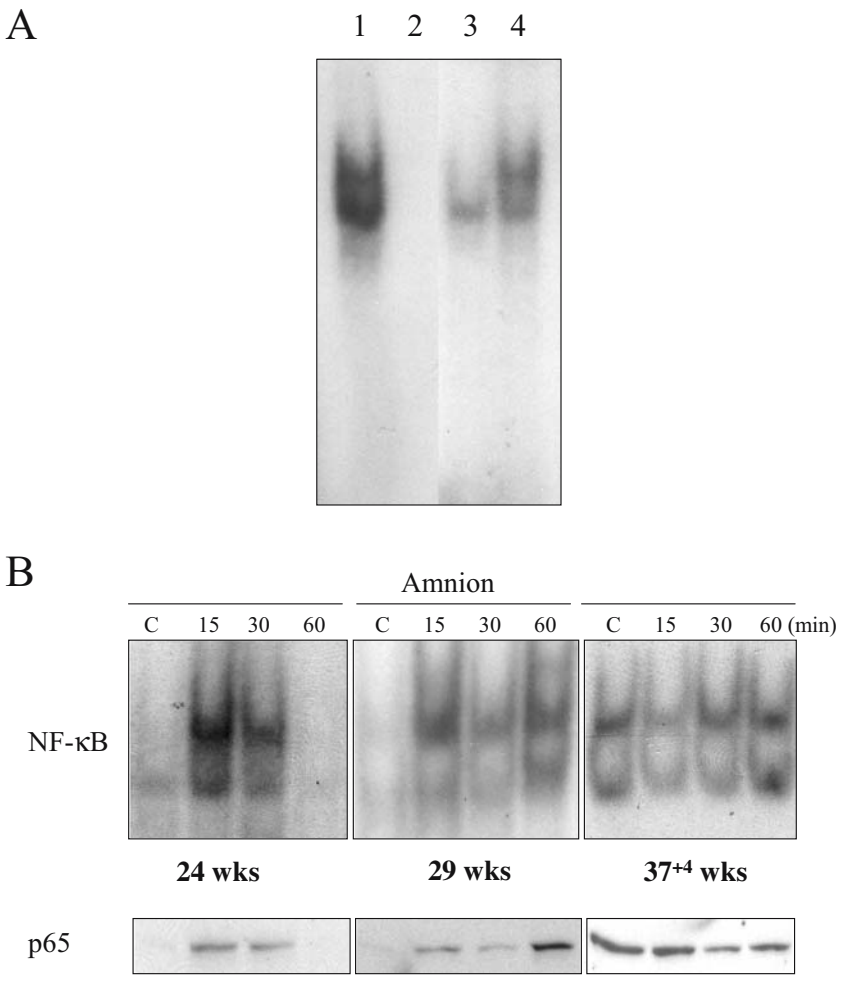


Fig. 5 NF-κB binding activity in response to LPS. Nuclear proteins were prepared and incubated with radiolabeled probes corresponding to the consensus binding site for NF-κB, and their DNA binding activity was determined by electrophoretic mobility shift assay (EMSA). (**a**) Competition experiments. Lane 1: positive control (^{32}P-labeled NF-κB oligonucleotide); lane 2: negative control; lane 3: specific competitor (^{32}P-labeled NF-κB oligonucleotide in the presence of a 50-fold molar excess of unlabeled NF-κB oligonucleotide); lane 4: non-specific competitor (^{32}P-labeled NF-κB oligonucleotide and unlabeled AP-1 oligonucleotide). (**b**) Amnion cells obtained from term and preterm placentas were treated with 1 μg/ml LPS for the specified periods of time

grade=2; [30]) were compared according to gestational age, the IL-6 concentrations of amniotic fluid and cord plasma were also found to be significantly increased in patients delivered at or before 31 weeks of gestation compared with those delivered after 31 weeks of gestation (amniotic fluid IL-6: median, 18.7 ng/ml; range, 0.2-

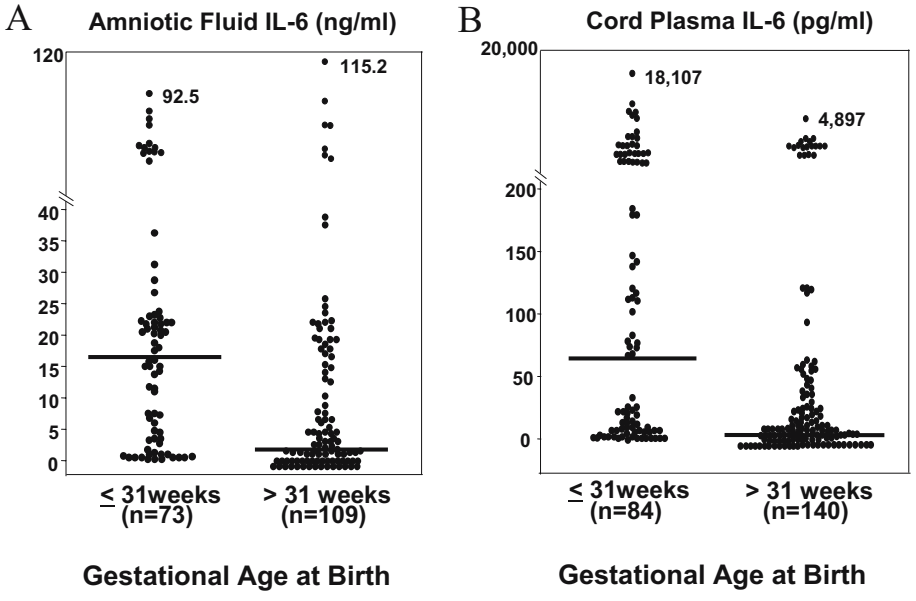


Fig. 6 IL-6 levels in amniotic fluid and cord blood in preterm cases. Amniotic fluid (**A**) and fetal plasma (**B**) IL-6 levels are significantly higher at or before the gestational age of 31 weeks than after the gestational age of 31 weeks (P<0.001). IL-6 levels were measured by specific immunoassay

92.5 ng/ml; versus median, 8.0 ng/ml; range, 0.1-115.2 ng/ml, respectively; P=0.016; cord plasma IL-6: median, 138.5 pg/ml; range, 4.4-7400 pg/ml; versus median, 51.9 pg/ml; range, 0.1-4897.0 pg/ml, respectively; P=0.023). The prevalence of major perinatal morbidity was also significantly higher in cases born at or before the gestational age of 31 weeks (P<0.0001).

Discussion

The intrauterine infection-associated complex of biological reactions occurring in the fetus has been designated as "fetal inflammatory response syndrome" (FIRS) [14]. Increased production of proinflammatory cytokines and fetal plasma cytokines, i.e. IL-6, is an essential component of FIRS, and we have recently shown that preterm fetuses respond more rigorously in terms of IL-6 response to intrauterine infection than their term counterparts [20, 37]. The relationship between the severity of fetal inflammatory response and gestational age led us to speculate that the cause may be the differential activation of signaling cascades activated by amniotic sac infection.

LPS, a surface component of Gram-negative bacteria, binds to cell surface CD14 and activates tyrosine kinases, protein kinase C, MAPKs and NF-κB. As demonstrated in various cell types, LPS can induce activation of ERK 1/2, JNK, and p38. These molecules in turn act as primary regulators of proinflammatory cytokine expression [17, 23, 24]. LPS treatment has been used as an in vitro mimic of bacterial infection in many experimental systems. Although LPS is a potent activator of many cell types including macrophages, microglial cells and embryo cardiomyocytes, these cells often play unique tissue-specific roles and exhibit different sensitivities to LPS. We observed the patterns of MAPK and NF-κB activation in human amnion cells. Although amnion cells do not belong to the fetus per se, they do comprise one of the major sources of proinflammatory cytokines in amniotic sac infection, as well as affording a relevant experimental system for cytokine research [12, 20, 27]. The patterns of JNK and ERK 1/2 activation by LPS in human amnion cells were similar to those reported in other type of cells [17, 18, 25, 28]. LPS increases binding between NF-κB and DNA and cytokine secretion by gestational tissues such as human placenta and amnion. NF-κB also plays a key role in the regulation of the expression and secretion of phospholipase enzymes in gestational tissues [22]. The present study did not address the exact mechanism of the differential activations of MAPK and NF-κB in amnion cells during human gestation. As LPS exerts its effects through CD14 and toll-like receptors [31], we presume that the expression levels of these molecules may be related. Further investigations on these molecules and other components related to innate immunity are necessary to elucidate the nature of the mechanisms underlying our observations.

The results of amniotic fluid IL-6 assay in preterm cases were also consistent with the results of ERK 1/2, JNK, and NF-κB analysis. The biological significance of this differential MAPK and NF-κB activation in amnion cells remains unclear, and further investigation is required to elucidate whether or not this is an organ- or cell type-specific phenomenon. Nevertheless, the results of the present study strongly suggest that critical biological responses potentially related to parturition differ according to gestational age. Elevation of proinflammatory cytokines in the fetus and placental compartments can induce delivery via activation of biological mechanisms that are related to parturition, such as MMPs and prostaglandin, as amnion cells are major sources of MMPs and PGE2 [7, 11, 32]. Such exaggerated cytokine response is also known to be able to induce significant tissue damage [34, 36] and thus may be related to the well-documented correlation between the incidence of major perinatal morbidities and the gestational age of the fetus.

In conclusion, we demonstrated that MAPK (ERK 1/2 and JNK) and NF-κB mediated signaling pathways, which are critical regulatory elements of cytokine gene expressions, are differentially activated by LPS in human amnion during gestation. These findings strongly imply that this differential regulation is the underlying mechanism of the inverse relationship between fetal inflammatory response and gestational period.

Acknowledgements Supported in part by a grant of the Korea Health 21 R&D Project, Ministry of Health and Welfare, Republic of Korea (01-PJ1-PG1-01CH07-0002), and in part by the 2003 BK21 Project for Medicine, Dentistry and Pharmacy.

References

1. Arechavaleta-Velasco F, Ogando D, Parry S, Vadillo-Ortega F (2002) Production of matrix metalloproteinase-9 in lipopolysaccharide-stimulated human amnion occurs through an autocrine and paracrine proinflammatory cytokine-dependent system. Biol Reprod 67:1952–1958
2. Awane M, Andres PG, Li DJ, Reinecker HC (1999) NF-κB-inducing kinase is a common mediator of IL-17-, TNF-alpha-, and IL-1 beta-induced chemokine promoter activation in intestinal epithelial cells. J Immunol 162:5337–5344
3. Borger P, Koeter GH, Timmerman JA, Vellenga E, Tomee JF, Kauffman HF (1999) Proteases from Aspergillus fumigatus induce interleukin (IL)-6 and IL-8 production in airway epithelial cell lines by transcriptional mechanisms. J Infect Dis 180: 1267–1274
4. Brown NL, Alvi SA, Elder MG, Bennett PR, Sullivan MH (1998) A spontaneous induction of fetal membrane prostaglandin production precedes clinical labour. J Endocrinol 157:R1–R6
5. Brown NL, Alvi SA, Elder MG, Bennett PR, Sullivan MH (1998) Regulation of prostaglandin production in intact fetal membranes by interleukin-1 and its receptor antagonist. J Endocrinol 159:519–526
6. Burgermeister E, Tibes U, Stockinger H, Scheuer WV (1999) Activation of nuclear factor-κB by lipopolysaccharide in mononuclear leukocytes is prevented by inhibitors of cytosolic phospholipase A2. Eur J Pharmacol 369:373–386
7. Casey ML, MacDonald PC, Mitchell MD (1984) Characterization of prostaglandin formation by human amnion cells in monolayer culture. Prostaglandins 27:421–427
8. Chen F, Castranova V, Shi X, Demers LM (1999) New insights into the role of nuclear factor-kappa B, a ubiquitous transcription factor in the initiation of diseases. Clin Chem 45:7–17

9. Cobb MH, Goldsmith EJ (1995) How MAP kinases are regulated. J Biol Chem 270:14843–14846
10. DiDonato JA, Hayakawa M, Rothwarf DM, Zandi E, Karin M (1997) A cytokine-responsive I-kappa B kinase that activates the transcription factor NF-kappa B. Nature 388:548–554
11. Fortunato SJ, Menon R, Lombardi SJ (1997) Collagenolytic enzymes (gelatinases) and their inhibitors in human amniochorionic membrane. Am J Obstet Gynecol 177:731–741
12. Furuta I, Yamada H, Sagawa T, Fujimoto S (2000) Effects of inflammatory cytokines on prostaglandin E(2) production from human amnion cells cultured in serum-free condition. Gynecol Obstet Invest 49:93–97
13. Gibbs RS, Blanco JD, St Clair PJ, Castaneda YS (1982) Quantitative bacteriology of amniotic fluid from women with clinical intraamniotic infection at term. J Infect Dis 145:1–8
14. Gomez R, Romero R, Ghezzi F, Yoon BH, Mazor M, Berry SM (1998) The fetal inflammatory response syndrome. Am J Obstet Gynecol 179:194–202
15. Greci LS, Gilson GJ, Nevils B, Izquierdo LA, Qualls CR, Curet LB (1998) Is amniotic fluid analysis the key to preterm labor? A model using interleukin-6 for predicting rapid delivery. Am J Obstet Gynecol 179:172–178
16. Guha M, Mackman N (2001) LPS induction of gene expression in human monocytes. Cell Signal 13:85–94
17. Hambleton J, Weinstein SL, Lem L, DeFranco AL (1996) Activation of c-Jun N-terminal kinase in bacterial lipopolysaccharide-stimulated macrophages. Proc Natl Acad Sci USA 93: 2774–2778
18. Jiang JX, Zhang Y, Ji SH, Zhu P, Wang ZG (2002) Kinetics of mitogen-activated protein kinase family in lipopolysaccharide-stimulated mouse Kupffer cells and their role in cytokine production. Shock 18:336–341
19. Jun JK, Yoon BH, Romero R, Kim M, Moon JB, Ki SH, Park JS (2000) Interleukin 6 determinations in cervical fluid have diagnostic and prognostic value in preterm premature rupture of membranes. Am J Obstet Gynecol 183:868–873
20. Kim CJ, Yoon BH, Park SS, Kim MH, Chi JG (2001) Acute funisitis of preterm but not term placentas is associated with severe fetal inflammatory response. Hum Pathol 32:623–629
21. Kossakowska AE, Edwards DR, Prusinkiewicz C, Zhang MC, Guo D, Urbanski SJ, Grogan T, Marquez LA, Janowska-Wieczorek A (1999) Interleukin-6 regulation of matrix metalloproteinase (MMP-2 and MMP-9) and tissue inhibitor of metalloproteinase (TIMP-1) expression in malignant non-Hodgkin's lymphomas. Blood 94:2080–2089
22. Lappas M, Permezel M, Georgiou HM, Rice GE (2004) Regulation of phospholipase isozymes by nuclear factor-kappaB in human gestational tissues in vitro. J Clin Endocrinol Metab 89:2365–2372
23. Mancuso G, Midiri A, Beninati C, Piraino G, Valenti A, Nicocia G, Teti D, Cook J, Teti G (2002) Mitogen-activated protein kinases and NF-kappa B are involved in TNF-alpha responses to group B streptococci. J Immunol 169:1401–1409
24. Naccasha N, Hinson R, Montag A, Ismail M, Bentz L, Mittendorf R (2001) Association between funisitis and elevated interleukin-6 in cord blood. Obstet Gynecol 97:220–224
25. Park J, Gores GJ, Patel T (1999) Lipopolysaccharide induces cholangiocyte proliferation via an interleukin-6-mediated activation of p44/p42 mitogen-activated protein kinase. Hepatology 29:1037–1043
26. Perenyi A, Johann-Liang R, Stavola JJ (1999) Assessment of cord blood IL-6 levels as an indicator of neonatal sepsis. Am J Perinatol 16:525–530
27. Potter S, Hansen WR, Keelan JA, Mitchell MD (1999) Characterization of the amnion-derived AV3 cell line for use as a model for investigation of prostaglandin-cytokine interactions in human amnion. Prostaglandins Leukot Essent Fat Acids 61: 373–379
28. Pyo H, Jou I, Jung S, Hong S, Joe EH (1998) Mitogen-activated protein kinases activated by lipopolysaccharide and beta-amyloid in cultured rat microglia. Neuroreport 9:871–874
29. Regnier CH, Song HY, Gao X, Goeddel DV, Cao Z, Rothe M (1997) Identification and characterization of an IkappaB kinase. Cell 90:373–383
30. Salafia CM, Weigl C, Silberman L (1989) The prevalence and distribution of acute placental inflammation in uncomplicated term pregnancies. Obstet Gynecol 73:383–389
31. Triantafilou M, Triantafilou K (2002) Lipopolysaccharide recognition: CD14, TLRs and the LPS-activation cluster. Trends Immunol 23:301–304
32. Vadillo-Ortega F, Gonzalez-Avila G, Furth EE, Lei H, Muschel RJ, Stetler-Stevenson WG, Strauss JF (1995) 92-kd type IV collagenase (matrix metalloproteinase-9) activity in human amniochorion increases with labor. Am J Pathol 146:148–156
33. Waskiewicz AJ, Cooper JA (1995) Mitogen and stress response pathways. MAP kinase cascades and phosphatase regulation in mammals and yeast. Curr Opin Cell Biol 7:798–805
34. Yoon BH, Romero R, Jun JK, Park KH, Park JD, Ghezzi F, Kim BI (1997) Amniotic fluid cytokines (interleukin-6, tumor necrosis factor-alpha, interleukin-1 beta, and interleukin-8) and the risk for the development of bronchopulmonary dysplasia. Am J Obstet Gynecol 177:825–830
35. Yoon BH, Romero R, Kim CJ, Jun JK, Gomez R, Choi JH, Syn HC (1995) Amniotic fluid interleukin-6: a sensitive test for antenatal diagnosis of acute inflammatory lesions of preterm placenta and prediction of perinatal morbidity. Am J Obstet Gynecol 172:960–970
36. Yoon BH, Romero R, Kim CJ, Koo JN, Choe G, Syn HC, Chi JG (1997) High expression of tumor necrosis factor-alpha and interleukin-6 in periventricular leukomalacia. Am J Obstet Gynecol 177:406–411
37. Yoon BH, Romero R, Moon J, Chaiworapongsa T, Espinoza J, Kim YM, Edwin S, Kim JC, Camacho N, Bujold E, Gomez R (2003) Differences in the fetal interleukin-6 response to microbial invasion of the amniotic cavity between term and preterm gestation. J Matern Fetal Neonatal Med 13:32–38
38. Zandi E, Rothwarf DM, Delhase M, Hayakawa M, Karin M (1997) The IkappaB kinase complex (IKK) contains two kinase subunits, IKKalpha and IKKbeta, necessary for IkappaB phosphorylation and NF-kappaB activation. Cell 91:243–252

Virchows Arch (2005) 447: 53–60
DOI 10.1007/s00428-005-1275-6

ORIGINAL ARTICLE

Naoya Nakamura · Hidenori Hase · Daisuke Sakurai · Sachiko Yoshida · Masafumi Abe · Nobuhiro Tsukada · Jun Takizawa · Sadao Aoki · Masaru Kojima · Shigeo Nakamura · Tetsuji Kobata

Expression of BAFF-R (BR3) in normal and neoplastic lymphoid tissues characterized with a newly developed monoclonal antibody

Received: 10 January 2005 / Accepted: 12 April 2005 / Published online: 14 June 2005
© Springer-Verlag 2005

Abstract BAFF-receptor (BAFF-R) is required for the successful maturation and survival of B-cells. We developed an anti-human BAFF-R monoclonal antibody (mAb), 8A7. The reactivity of 8A7 in normal and neoplastic tissue was examined by performing immunohistochemistry on paraffin-embedded sections. 8A7 reacted with lymphocytes in the mantle and marginal zones, but not with lymphocytes in the interfollicular area. Lymphocytes in the germinal centers were found to be negative or occasionally weakly positive for 8A7. BAFF-R expression was found only in B-cell lymphoma (44/80, positive cases/examined cases): B-lymphoblastic lymphoma 0/3, B-chronic lymphocytic leukemia/small lymphocytic lymphoma 4/4, mantle cell lymphoma 9/11, follicular lymphoma 10/14, diffuse large B-cell lymphoma (DLBCL) 11/25, marginal zone B-cell lymphoma 8/10, lymphoplasmacytic lymphoma 2/2, plasma cell myeloma 0/2, and Burkitt lymphoma 0/9, but not in T/NK cell lymphomas (0/19) or Hodgkin lymphoma (0/10). BAFF-R was expressed in most low-grade B-cell neoplasms and a small number of DLBCL, suggesting that BAFF-R may play an important role in the proliferation of neoplastic lymphoid cells. Thus, the mAb is very useful for further understanding of both healthy B-cell biology and its pathogenic neoplasms.

Keywords BAFF · BAFF-R · Monoclonal antibody · Immunohistochemistry · B-cell lymphoma · Diffuse large B-cell lymphoma

N. Nakamura (✉) · S. Yoshida · M. Abe
Department of Pathology,
Fukushima Medical University,
Hikarigaoka-1,
Fukushima-shi, 960-1295, Japan
e-mail: nao@fmu.ac.jp
Tel.: +81-24-5484488
Fax: +81-24-5484488

H. Hase · D. Sakurai · T. Kobata
Department of Immunology,
Dokkyo University School of Medicine,
Tochigi, Japan

N. Tsukada · J. Takizawa · S. Aoki
First Department of Internal Medicine,
Niigata University Medical Hospital,
Niigata University,
Niigata, Japan

M. Kojima
Department of Pathology,
Dokkyo University School of Medicine,
Tochigi, Japan

S. Nakamura
Department of Pathology and Molecular Diagnostics,
Aichi Cancer Center,
Nagoya, Japan

Introduction

B-cell-activating factor of the tumor necrosis factor (TNF) family (BAFF), also known as BLyS, THANK, TALL-1 and zTNF4, is a fundamental survival factor for B-cells, and BAFF functionality is indispensable for B-cell maturation [13, 18, 27, 28]. BAFF is a trimeric membrane-bound or soluble factor and is expressed by monocytes, macrophages, neutrophils and dendritic cells. Whereas BAFF-deficient mice lack mature B-cells, BAFF-transgenic mice, characterized by overexpression of BAFF, have increased the number of B-cells and develop autoimmunity [3, 4, 9, 12]. In particular, transitional type 2 (T2) B-cells and marginal zone B-cells are expanded in BAFF-transgenic mice. BAFF blockade does not inhibit germinal center (GC) formation or somatic hypermutation of immunoglobulin (Ig) genes, indicating that BAFF is required for the normal maintenance of B-cells, but not for the initiation of the GC reaction, although B-cell maturation and mature functions are severely impaired [35]. Recently, it was reported that BAFF is directly involved in B cell malignancy [2, 7, 22, 23].

Three receptors for BAFF have been established: B-cell maturation antigen (BCMA), transmembrane activator and

calcium-modulator, and cyclophilin ligand interactor (TACI) and the BAFF-receptor (BAFF-R, also called BR3) [3, 14, 32, 33]. All three receptors are expressed on B-cells, while TACI is also expressed on activated T-cells [13]. Whereas TACI and BCMA are found to bind to a proliferation-inducing ligand (APRIL), BAFF-R binds only to BAFF [13, 32]. TACI is known to negatively control B-cell homeostasis and T-cell independent immune responses from evidence obtained from TACI deficient mice [30, 34, 37]. Although BCMA was recently reported to be essential for the survival of plasma cells [1, 24], mice lacking BCMA possess normal-appearing B lymphocyte compartments [27]. Thus, only BAFF-R is clearly a key receptor involved in the successful survival and maturation of B-cells [13]. However, the distribution of BAFF-R in normal and malignant human lymphoid tissue has not been made fully clear.

Only a few reports on BAFF-R in malignant B-cells have appeared to date. Briones et al. examined the BAFF binding activity in 43 cases of non-Hodgkin's lymphoma (NHL) with flow cytometry [2]. Although all cases of NHL express receptors for BAFF, BAFF-R expression was not specifically classified. Chronic lymphocytic leukemia/small lymphocytic lymphoma (CLL/SLL), mantle cell lymphoma (MCL), follicular center lymphoma, Burkitt lymphoma (BL) and diffuse large cell lymphoma were reported to express BAFF-R mRNA [7, 22], and multiple myeloma (MM) was reported to express cell surface BAFF-R [23].

In this investigation, we established the mouse anti-human BAFF-R monoclonal antibody (mAb) and examined its reactivity in normal and neoplastic lymphoid tissues using immunohistochemistry. We found a high degree of significance in its distribution in normal lymphoid tissue and low-grade B-cell neoplasms as well as in a small part of diffuse large B-cell lymphoma (DLBCL).

Materials and methods

Cell preparation and cell cultures

Human peripheral blood mononuclear cells were isolated from pooled healthy donors by Ficoll-Hypaque density-gradient centrifugation. After the depletion of monocytes by adherence to the plastic surface of the culture dishes, E rosette-negative populations were collected with 5% sheep erythrocytes and Ficoll-Hypaque. Purified B-cells were isolated by depleting the non B-cells using a B-cell isolation kit and auto MACS (Miltenyi Biotec, Auburn, Calif., USA). The resultant B-cell population was <2% $CD14^+$, <1% $CD3^+$, <2% $CD57^+$, and >95% $CD20^+$. All cultures were conducted in RPMI 1640 medium supplemented with 25 mM HEPES (*N*-2-hydroxyethylpiperazine-*N*′-2-ethanesulfonic acid), 10% fetal calf serum, 2 mM L-glutamine, 1 mM sodium pyruvate, 5.5×10^{-2} mM 2-mercaptoethanol, 100 IU/ml penicillin, and 100 IU/ml streptomycin (all from Invitrogen, Carlsbad, Calif., USA).

Antibodies and reagents

Polyclonal anti-human BAFF-R antibody (C-20), control mouse IgG2a, and FITC-labeled goat antibody to mouse IgG were purchased from Santa Cruz Biotechnology (Santa Cruz, Calif., USA), Sigma-Aldrich (St Louis, Mo., USA), and CALTAG (Burlingame, Calif., USA), respectively.

Establishment of human BAFF-R transfectant

To construct a human BAFF-R expression vector, a cDNA encoding full-length human BAFF-R protein (GenBank No. AF373846) was custom-synthesized (Takara, Shiga, Japan), inserted into pBluescript SK (+) (Stratagene, La Jolla, Calif., USA) at the *Eco*RI and *Bam*HI sites, and finally into the pBCMGSneo expression vector [8] at the *Xho*I and *Not*I sites (pBCMGS-BAFF-R). Murine pre-B-cells (cell line 300-19) were electroporated with pBCMGS-BAFF-R and stable transfectants were selected with G418 treatment. Cells with high-density BAFF-R were cloned with a fluorescence-activated cell sorter (FACS). The vector alone-transfected cells (mock) have been described previously [6].

Generation of anti-human BAFF-R mAb

A BALB/c mouse was immunized with human BAFF-R-expressing transfectant cells 3 times at 10-day intervals. Three days after the final immunization, the splenocytes were fused with NS-1 cells (purchased from Human Science Research Resources Bank), and HAT (hypoxanthine-aminopterin-thymidine) selection and cloning of hybridomas were performed simultaneously using a hybridoma cloning kit (ClonaCell-HY; StemCell Technologies, British Columbia, Canada). Anti-human BAFF-R designated 8A7 (mouse IgG2a, κ) was established.

Immunoblot analysis

PBS-washed cell pellets were resuspended with 0.5% SDS solution and boiled for 5 min. Proteins (5–8 μg) were separated with SDS-PAGE, transferred to an Immobilon-P membrane (Millipore, Billerica, Mass., USA), blocked with 5% skim milk, and immunoblotted with arbitrary Ab and HRP-labeled secondary Ab. The immunoblots were developed by using the enhanced chemiluminescent substrate (SuperSignal West Pico; Pierce Chemical Co., Rockford, Ill., USA) and visualized with a LumiVision analyzer (Taitec Co., Tokyo), as previously described [5].

Flow cytometric analysis

Flow cytometric analysis was performed using FACScalibur and the associated Cell Quest software (both from Becton Dickinson, San Jose, Calif., USA). FITC-labeled

goat antibody to mouse IgG was used as a second Ab. An isotype-matched mouse IgG2a control was used throughout the studies and always reacted with <5% of the cells.

Tissues and immunohistochemistry

Formalin-fixed paraffin-embedded tissues were used in this study. Tonsils resected due to chronic tonsillitis, lymph nodes resected due to non-neoplastic lymphadenopathy, spleens resected because of non-lymphoma and bone marrow clots without malignancy were used for the non-neoplastic lymphoid tissues. Neoplastic lymphoid tissues from 109 cases were used in this study and comprised the following: three cases of B-lymphoblastic lymphoma (B-LBL), four cases of CLL/SLL, 11 cases of MCL, 14 cases of follicular lymphoma (FL), 25 cases of DLBCL, ten cases of marginal zone B-cell lymphoma (MZBCL), two cases of Lymphoplasmacytic lymphoma (LPL), two cases of plasma cell myeloma (PCM), nine cases of BL, three cases of T-lymphoblastic lymphoma, four cases of angioimmunoblastic T-cell lymphoma, five cases of peripheral T-cell lymphoma, unspecified, two cases of adult T-cell lymphoma, one case of systemic anaplastic large cell lymphoma, four cases of NK/T cell lymphoma and ten cases of Hodgkin lymphoma (HL). All cases of CLL/SLL and MCL expressed CD5. Cyclin D1 was immunohistochemically detected in all but one case of MCL. FL consisted of four cases of grade 1, four cases of grade 2 and six cases of grade 3. All cases of FL expressed CD10. DLBCL included three cases with CD5 (+) CD10 (−), three cases with CD5 (−) CD10 (+) and 19 cases with CD5 (−) CD10 (−). HL consisted of three cases of nodular lymphocyte predominance Hodgkin lymphoma (NLP-HL), four cases of mixed cellularity classical Hodgkin lymphoma (MC-CHL) and three cases of nodular sclerosis classical Hodgkin lymphoma (NS-CHL).

The de-paraffinized tissue section was pre-treated in citrate buffer with microwave oven heating. The section was incubated with the primary antibody at 4°C overnight and then the streptavidin-biotin complex method (Dakocytomation, Kyoto, Japan) was used. Neoplasms with >10% positive cells were judged as positive.

Results

Establishment of the anti-human BAFF-R mAb, 8A7

To evaluate the role of the interactions between BAFF and BAFF-R in human B cell responses, we developed an anti-human BAFF-R mAb. For this purpose, we first estab-

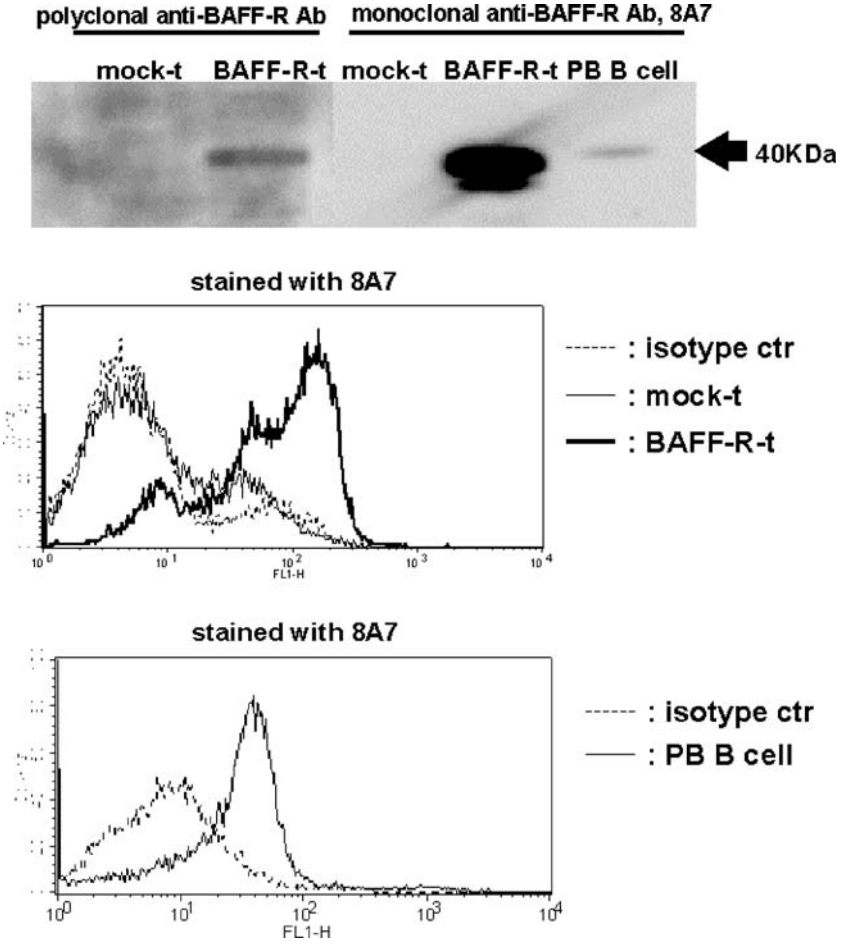


Fig. 1 8A7 mAb detects human BAFF-R. (**a**) Cell lysates prepared from BAFF-R- and mock-transfectants, and peripheral blood B cells, were subjected to immunoblot analysis using anti-human BAFF-R polyclonal Ab or 8A7 mAb. (**b**) Flow cytometric analysis of BAFF-R expression using 8A7 mAb. BAFF-R- and mock-transfectants and peripheral blood B cells were stained with 8A7 mAb or isotype-matched control Ab (IgG2a) followed by FITC-conjugated Ab to mouse IgG. Data shown are representative of three different experiments

lished a transfectant stably expressing human BAFF-R. Stable expression of human BAFF-R on the cDNA transfectant, but not on mock-transfected cells was verified using immunoblot analysis (Fig. 1a). Immunoblot analysis using commercially available polyclonal anti-human BAFF-R Ab revealed that BAFF-R cDNA-transfected cells expressed the BAFF-R molecule. We then immunized a BALB/c mouse with the BAFF-R-transfectant and fused the splenocytes with NS-1 myeloma cells. The hybridomas producing anti-human BAFF-R mAb were screened for specific reactivity to the BAFF-R-transfectant. As shown in Fig. 1a, one obtained mAb, designated 8A7, bound to BAFF-R-transfectant and peripheral blood B cells but not to mock-transfectant. Flow cytometric analysis revealed that the 8A7 mAb reacted with almost all peripheral blood B cells and BAFF-R-transfectant, but not with peripheral blood T-cells, monocytes, or mock-transfectant (Fig. 1b, data not shown).

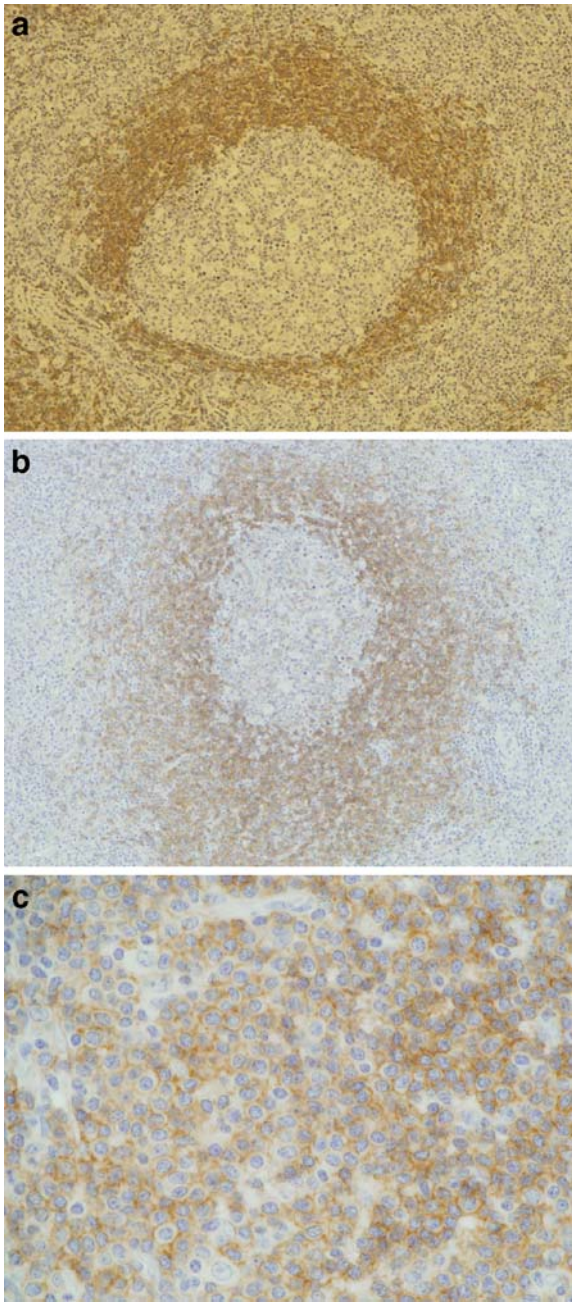


Fig. 2 BAFF-R expression in normal lymphoid tissues according to immunohistochemistry (IHC) on the paraffin-embedded section (strept/ABC method). 8A7 reacts with lymphocytes in the mantle zone of the secondary lymphoid follicles in the lymph node (**a**: IHC, original magnification ×50) and with lymphocytes in the mantle and marginal zones of the splenic white pulp (**b**: IHC, ×50). Marginal B-cells with a clear cytoplasm are positive for 8A7 (**c**: IHC, ×200)

Immunohistochemistry of non-neoplastic lymphoid tissue

8A7 reacted with lymphocytes in the mantle zone of the secondary lymphoid follicles in the tonsil (Fig. 2a) and the non-neoplastic lymph nodes. In the spleen, 8A7 reacted with lymphocytes in the mantle and marginal zones of the white pulp, but not with the interfollicular area (Fig. 2b,c). Lymphocytes in germinal centers (GCs) were found to be negative or occasionally weakly positive for hyperplastic GC. 8A7 failed to stain hematopoietic cells in the bone marrow. Plasma cells were negative for 8A7.

Immunohistochemistry of the neoplastic lymphoid tissue

Expression of BAFF-R in neoplastic lymphoid tissue detected by 8A7 is shown in Table 1 and Fig. 3. BAFF-R expression was only found in B-cell lymphoma (44/80, positive cases/examined cases), but not in T/NK cell lymphoma (0/19) or in Hodgkin lymphoma (0/10).

Discussion

An anti-human BAFF-R mAb, named 8A7, was developed using a transfectant stably expressing human BAFF-R to evaluate the role of interactions between BAFF and BAFF-R in human B-cell responses and malignancy. In this paper, reactivity and distribution in normal and malignant lymphoid tissues was addressed by means of immunohistochemistry with paraffin-embedded tissue.

The distribution of BAFF-R in human lymphoid tissue has not been heretofore reported, except in a recent report by Ng et al. [21]. They stated that the BAFF-R was expressed at a high level on all B-cells and at very low levels on T-cells in human peripheral blood. It is also expressed in tonsil B-cells, but B-cells with a GC phenotype ($CD38^+$, $CD27^+$, $CD39^-$, $CD24^-$ and IgM^-) exhibited lower levels of BAFF-R according to flow cytometry [21]. Intense staining of B-cell follicles and weaker staining of the GCs were observed in the immunohistochemistry using frozen sections [21]. We demonstrated that BAFF-R was strongly expressed on B-cells situated both in the mantle zone and the marginal zones of the secondary lymphoid follicles and weakly expressed on GC B-cells occasionally

Table 1 Reactivity of 8A7 in 109 neoplastic lymphoid tissues according to immunohistochemistry (Positive cases/examined cases). *NLP-HL* nodular lymphocyte predominance Hodgkin lymphoma; *MC-CHL* mixed cellularity classical Hodgkin lymphoma; *NS-CHL* nodular sclerosis classical Hodgkin lymphoma

B-lymphoblastic lymphoma	0/3
Chronic lymphocytic leukemia/Small lymphocytic lymphoma	4/4
Mantle cell lymphoma	9/11
Follicular lymphoma	10/14
Grade 1	4/4
Grade 2	4/4
Grade 3	2/6
Diffuse large B-cell lymphoma	11/25
Marginal zone B-cell lymphoma	8/10
Lymphoplasmacytic lymphoma	2/2
Plasma cell myeloma	0/2
Burkitt lymphoma	0/9
T-lymphoblastic lymphoma	0/3
Angioimmunoblastic T-cell lymphoma	0/4
Peripheral T-cell lymphoma, unspecified	0/5
Adult T-cell lymphoma	0/2
Anaplastic large cell lymphoma	0/1
NK/T cell lymphoma	0/4
Hodgkin lymphoma	0/10
NLP-HL	0/3
MC-CHL	0/4
NS-CHL	0/3

in the GCs. The intensity of BAFF-R in GC B-cells may vary between each GC. Marginal zone B-cells have somatically hypermutated immunoglobulin (Ig) genes and express CD27 at a level equivalent to memory B-cells [10]. It is widely considered that marginal zone B-cell development and survival are likely to directly or indirectly depend on BAFF [13]. Since the present data indicate that marginal B-cells express BAFF-R, it is likely that BAFF directly contributes to the maturation of marginal zone B-cells. BAFF-R was also expressed strongly on mantle zone B-cells, which are naive B-cells that exhibit unmutated Ig genes and mainly co-express IgM and IgD [11]. On the other hand, GC B-cells that undergo affinity maturation of their antigen receptors and express CD10 and CD38 [25] were observed to be negative or weakly positive for BAFF-R. Thus, BAFF-R is widely distributed on un-stimulated B-cells and antigen-stimulated B-cells during B cell differentiation, except for GC B-cells. This pattern of BAFF-R expression during different stages of B-cell differentiation seemed to be similar to that of Bcl-2 expression. GC B-cells express low levels of BAFF-R and the anti-apoptotic factor Bcl-2, and high levels of the apoptotic factor Fas [17, 39].

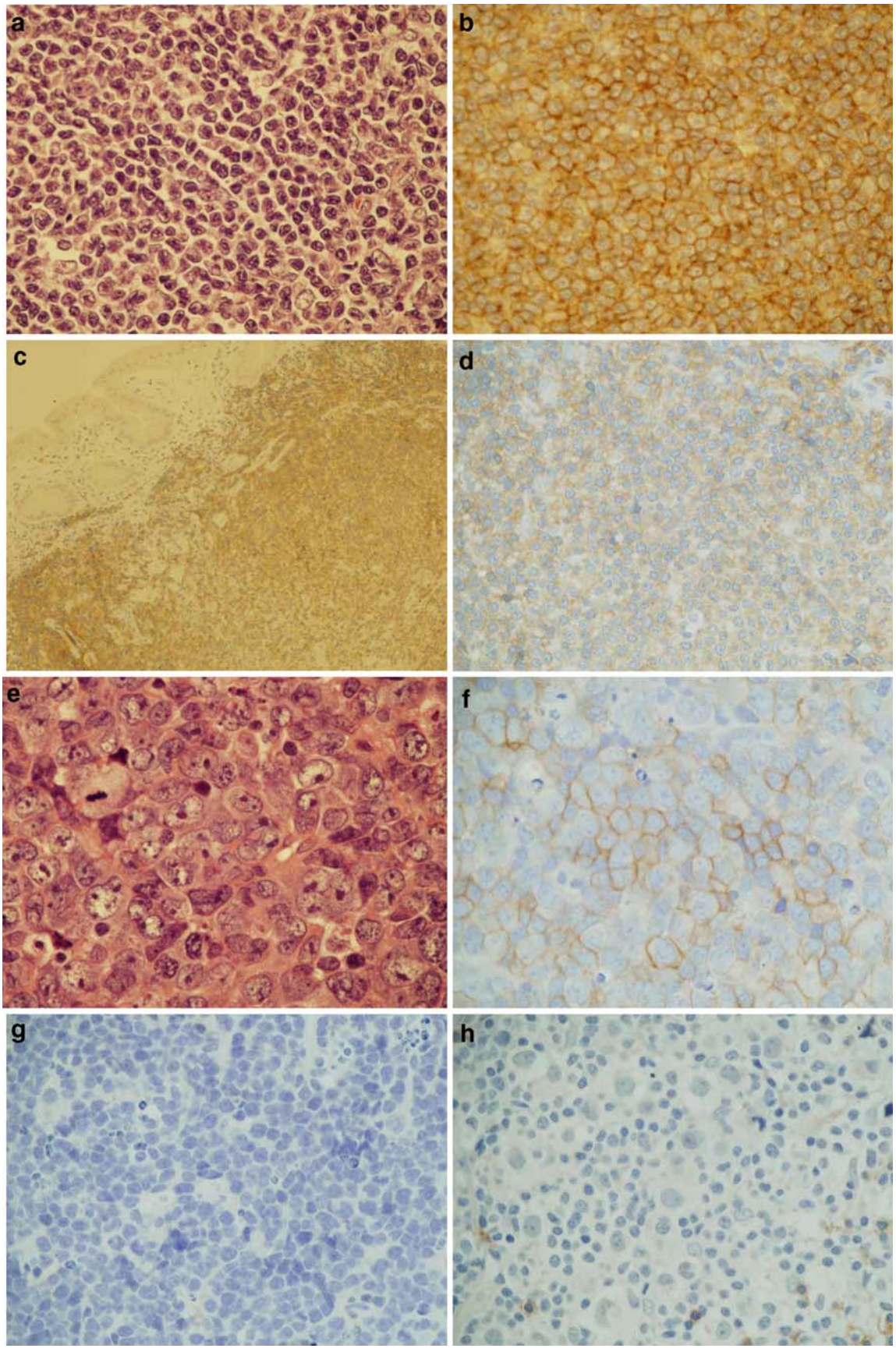
Novak et al. reported the cell surface expression of BAFF-R on both CD5 (+) peripheral blood B-cells as well as CD5 (−) peripheral blood B-cells [23]. Mice transgenic for TACI-Ig, and BAFF-deficient mice display a developmental block of B-cell maturation in the periphery, leading to a severe depletion of marginal zone and follicular B2 B-cells, but not of peritoneal CD5 (+) B1 B-cells [4, 13, 29]. Interactions between BAFF and BAFF-R may be needed for CD5 (+) B1 B-cell maturation as much as CD5 (−) B2 B-cell maturation in humans.

The reactivity of anti-BAFF-R mAb against neoplastic lymphoid tissue is of considerable interest. It is likely that BAFF-R expression was only found in B-cell lymphoma, but not in T/NK-cell lymphomas, for reasons related to the fact that BAFF-R expression is normally found only on healthy B-cells [21]. Only a small number of studies reporting BAFF-R expression in malignant B-cells have appeared to date. Seven of seven B-CLL samples, as well as normal B-cells, expressed BAFF-R mRNA [22]. None of the five MM cell-lines but two of the three mononuclear cells of patients with MM expressed cell surface BAFF-R [23]. Six of six NHLs, including CLL/SLL, MCL, FL, BL, and DLBCL, expressed BAFF-R mRNA [7]. In the present study, however, we demonstrated somewhat different results for BAFF-R expression.

Most of the low-grade B-cell neoplasms of B-CLL/SLL, MCL, LPL and MZBCL strongly exhibited BAFF-R. Among them, MCL and MZBCL are believed to be neoplasms derived from mantle zone B-cells and marginal zone B-cells, respectively. The normal counterpart cells of B-CLL/SLL are a neoplasm of CD5 (+) B-cells of the peripheral blood [15, 29]. These normal counterpart cells are all BAFF-R (+) and these B-cell neoplasms seemed to maintain BAFF-R expression. Low-grade B-cell lymphomas may require the interaction of BAFF and BAFF-R for survival and proliferation of the neoplastic B-cells.

Although normal GC B-cells exhibited a negative reaction or an occasionally weakly positive reaction for 8A7, both grade 1 and 2 FLs strongly expressed BAFF-R. FL consists of small-cleaved lymphoma cells with intermingled large sized centroblasts. Grade 1 and 2 FLs include less than 50 centroblasts and 50–150 centroblasts per ten high-power fields, respectively. Both grades 1 and 2 FLs retain a follicular growth pattern supported by a network of follicular dendritic cells (FDCs), and the lymphoma cells express CD20, CD10, Bcl-2 and Bcl-6 [20]. It has recently been shown that FDCs express BAFF [6]. On the other hand, in grade 3 FL, 2/3 in grade 3a and 0/3 in grade 3b were positive for 8A7. This may indicate that lymphoma cells of grade 1 and 2 FLs require the interaction of BAFF and BAFF-R for their survival and growth. Certain lymphoma cells of some grade 3 FL act autonomically in terms of proliferation.

BAFF-R was expressed in a lower number of cases of aggressive B-cell lymphomas. LBL and BL were negative for 8A7. Eleven out of 25 DLBCLs exhibited a positive reaction with anti-BAFF-R mAb, which supports the recent report by He et al. [7]. Among these, the expression of BAFF-R was found in CD5 (+) DLBCL as well as CD5 (+) CLL/SLL and MCL. BAFF-R (+) in many cases of CD5 (+) B-cell neoplasms was independent of their aggressiveness and clinical behavior. These findings may prove to be useful for the continual improvement of understanding of the biology of CD5 (+) B-cells and B-cell neoplasms, especially for CD5 (+) DLBCL, which is reported to have a poorer clinical outcome than CD5 (−) DLBCL [19, 36].


a
b
c
d
e
f
g
h

◀ **Fig. 3** BAFF-R expression in neoplastic lymphoid tissues according to immunohistochemistry (IHC) on the paraffin-embedded sections (strept/ABC method). 8A7 is strongly expressed in CD20 (+) CD5 (+) cyclin D1 (+) mantle cell lymphoma (**a**: HE, **b**: IHC, original magnification ×200). 8A7 reacts with the lymphoma cells of gastric MALT lymphoma, but not with the glandular epithelium (**c**: IHC, ×50; **d**: IHC, ×200). 8A7 expressed on some of the lymphoma cells of CD20 (+) CD5 (+) diffuse large B-cell lymphoma (**e**: HE, **f**: IHC, ×200) (**g**: IHC, ×200). Expression of 8A7 is not found in Hodgkin/Reed-Sternberg cells of Hodgkin lymphoma, but in a small number of small lymphocytes (**h**: IHC, ×200) Burkitt lymphoma is negative for 8A7

We analyzed the clinical profiling between BAFF-R (+) and BAFF-R (−) subgroups in all DLBCL examined. When analyzing these between the BAFF-R (+) and BA FF-R (−) subgroups in CD5 (−) CD10 (−) DLBCL, we found a significant difference in LDH. The number of patients with LDH >2-fold of the normal limit in the BAFF-R (+) subgroups was greater than that in the BAFF-R (−) subgroup (detailed data not shown). This may mean that the volume of lymphoma cells in patients with BAFF-R (+) DLBCL is high and may affect the treatment strategy for patients with BAFF-R (+) DLBCL. We found no significant differences in the overall survival curves between the two subgroups due to the small number of patients in this study, and more cases are needed for an accurate estimation. BAFF-R is a possible marker for sub-grouping of DLBCL. On the other hand, two out of three CD5 (+) DLBCL exhibited more than 2-fold the normal limit of LDH, but both cases of CD10 (+) DLBCL exhibited LDH within the normal limit.

The HRS cells of all cases of HL including NLP-HL, MC-CHL and NS-CHL were negative for BAFF-R. This is a marked difference from the finding that more than half of HL cases express the bcl-2 protein, an anti-apoptotic factor [26]. HL is a neoplasm derived from GC B-cells with a hypermutated Ig gene, as disclosed by single cell PCR analysis, and lacks Ig mRNA, which is different from the cases of DLBCL [16, 38]. Since the expression of BAFF-R is regulated by immunoglobulin, it is possible that HL is not able to express BAFF-R [31]. It is, however, odd that the NLP-HL that expresses Ig was also negative for 8A7.

In conclusion, we developed an anti-human BAFF-R mAb and addressed its reactivity and distribution in normal and malignant lymphoid tissues by performing immunohistochemistry with paraffin-embedded tissues. BAFF-R was found to be expressed on B-cells situated in the mantle and marginal zones, but not on B-cells in GC. We demonstrated that BAFF-R was expressed on most low-grade B-cell neoplasms and in some DLBCL.

Acknowledgements We thank Dr. Hajime Karasuyama for the pBCMGSneo expression vector, Dr. Hidefumi Kojima for helpful discussion, and Ms. Yumiko Kanno for participating in technical assistance. We also thank the Laboratory Animal Research Center and the Laboratory of Analytical Instruments, Institute for Medical Science, Dokkyo University School of Medicine, for the use of their facilities.

A grant-in-aid for Scientic Research (c) from the Ministry of Education, Culture, Sports, Science and Technology of Japan (KA KENHI 16590410 to T.K.) and The Science Research Promotion Fund from the Promotion and Mutual Aid Corporation for Private Schools of Japan (to T.K.)

References

1. Avery DT, Kalled SL, Ellyard JI et al (2003) BAFF selectively enhances the survival of plasmablasts generated from human memory B cells. J Clin invest 112:286–297
2. Briones J, Timmerman JM, Hilbert DM, Levy R (2002) BLyS and BlyS receptor expression in non-Hodgkin's lymphoma. Exp Hematol 30:135–141
3. Gross JA, Johnston J, Mudri S, Enselman R, Dillon SR, Madden K, Xu W, Parrish-Novak J, Foster D, Lofton-Day C, Moore M, Littau A, Grossman A, Haugen H, Foley K, Blumberg H, Harrison K, Kindsvogel W, Clegg CH (2000) TACI and BCMA are receptors for a TNF homologue implicated in B-cell autoimmune disease. Nature 404:995–999
4. Gross JA, Dillon SR, Mudri S, Johnston J, Littau A, Roque R, Rixon M, Schou O, Foley KP, Haugen H, McMillen S, Waggie K, Schreckhise RW, Shoemaker K, Vu T, Moore M, Grossman A, Clegg CH (2001) TACI-Ig neutralizes molecules critical for B cell development and autoimmune disease. Impaired B cell maturation in mice lacking BLyS. Immunity 15:289–302
5. Hase H, Kanno Y, Kojima H, Morimoto C, Okumura K, Kobata T (2002) CD27 and CD40 inhibit p53-independent mitochondrial pathways in apoptosis of B cells induced by B cell receptor ligation. J Biol Chem 277:46950–46958
6. Hase H, Kanno Y, Kojima M, Hasegawa K, Sakurai D, Kojima H, Tsuchiya N, Tokunaga K, Masawa N, Azuma M, Okumura K, Kobata T (2004) BAFF/BLyS can potentiate B-cell selection with the B-cell co-receptor complex. Blood 103:2257–2265
7. He B, Chadburn A, Jou E, Schattner EJ, Knowles DM, Cerutti A (2004) Lymphoma B cells evade apoptosis through the TNF family members BAFF/BLyS and APRIL. J Immunol 172:3268–3279
8. Karasuyama H, Kudo A, Melcher F (1990) The proteins encoded by the VpreB and lambda 5 pre-B cell-specific genes can associate with each other and with mu heavy chain. J Exp Med 172:969–972
9. Khare SD, Sarosi I, Xia XZ, McCabe S, Miner K, Solovyev I, Hawkins N, Kelley M, Chang D, Van G, Ross L, Delaney J, Wang L, Lacey D, Boyle WJ, Hsu H (2000) Severe B cell hyperplasia and autoimmune disease in TALL-1 transgenic mice. Proc Natl Acad Sci USA 97:3370–3375
10. Klein U, Rajewsky K, Kuppers R (1998) Human immunoglobulin (Ig)M+IgD+ peripheral blood B cells expressing the CD27 cell surface antigen carry somatically mutated variable region genes: CD27 as a general marker for somatically mutated (memory) B cells. J Exp Med 188:1679–1689
11. Klein U, Goossens T, Fischer M, Kanzler H, Braeuninger A, Rajewsky K, Kuppers R (1998) Somatic hypermutation in normal and transformed human B cells. Immunol Rev 162:261–280
12. Mackay F, Woodcock SA, Lawton P et al. (1999) Mice transgenic for BAFF develop lymphocytic disorders along with autoimmune manifestations. J Exp Med 190:1697–1710
13. Mackay F, Schneider P, Rennert P, Browning JL (2003) BAFF and APRIL: a tutorial on B cell survival. Annu Rev Immunol 21:231–264
14. Madry C, Laabi Y, Callebaut I et al. (1988) The characterization of murine BCMA gene defines it as a new member of the tumor necrosis factor superfamily. Int Immunol 10:1063–1702
15. Maes B, De Wolf-Peeters C (2002) Marginal zone cell lymphoma—an update on recent advances. Histopathology 40:117–126
16. Marafioti T, Hummel M, Foss HD, Laumen H, Korbjuhn P, Anagnostopoulos I, Lammert H, Demel G, Theil J, Wirth T, Stein H (2000) Hodgkin and Reed-Sternberg cells represent an expansion of a single clone originating from a germinal center B-cell with functional immunoglobulin gene rearrangements but defective immunoglobulin transcription. Blood 95:1443–1450

17. Martinez-Valdez H, Guret C, de Bouteiller O, Fugier I, Banchereau J, Liu YJ (1996) Human germinal center B cells express the apoptosis-inducing genes Fas, c-myc, P53, and Bax but not the survival gene bcl-2. J Exp Med 183:971–977
18. Moore PA, Belvedere O, Orr A, Pieri K, LaFleur DW, Feng P, Soppet D, Charters M, Gentz R, Parmelee D, Li Y, Galperina O, Giri J, Roschke V, Nardelli B, Carrell J, Sosnovtseva S, Greenfield W, Ruben SM, Olsen HS, Fikes J, Hilbert DM (1999) BLyS: member of the tumor necrosis factor family and B lymphocyte stimulator. Science 285:260–263
19. Nakamura N, Abe M (2003) Histogenesis of CD5-positive and CD5-negative B-cell neoplasms on the aspect of somatic mutation of immunoglobulin heavy chain gene variable region. Fukushima J Med Sci 49:55–67
20. Nathwani BN, Harris NL, Weisenburger D, Isaacson PG, Piris MA, Berger F, Muller-Hermalink HK, Swerdlow SH (2001) Follicular lymphoma. In: Jaffe ES, Harris NL, Stein H, Vardiman JW (eds) Tumours of haematopoietic and lymphoid tissues. IARC Press, Lyon, France pp 162–167
21. Ng LG, Sutherland AP, Newton R, Qian F, Cachero TG, Scott ML, Thompson JS, Wheway J, Chtanova T, Groom J, Sutton IJ, Xin C, Tangye SG, Kalled SL, Mackay F, Mackay CR (2004) B cell-activating factor belonging to the TNF family (BAFF)-R is the principal BAFF receptor facilitating BAFF costimulation of circulating T and B cells. J Immunol 173:807–817
22. Novak AJ, Bram RJ, Kay NE, Jelinek DF (2002) Aberrant expression of B-lymphocyte stimulator by B chronic lymphocytic leukemia cells: a mechanism for survival. Blood 100: 2973–2979
23. Novak AJ, Darce JR, Arendt BK, Harder B, Henderson K, Kindsvogel W, Gross JA, Greipp PR, Jelinek DF (2004) Expression of BCMA, TACI, and BAFF-R in multiple myeloma: a mechanism for growth and survival. Blood 103:689–694
24. O'Connor BP, Raman VS, Erickson LD, Cook WJ, Weaver LK, Ahonen C, Lin L-L, Mantchev GT, Bram RJ, Noelle RJ (2004) BCMA is essential for the survival of long-lived bone marrow plasma cells. J Exp Med 199:91–97
25. Pascual V, Liu YJ, Magalski A, de Bouteiller O, Banchereau J, Capra JD (1994) Analysis of somatic mutation in five B cell subsets of human tonsil. J Exp Med 180:329–339
26. Rassidakis GZ, Medeiros LJ, Vassilakopoulos TP, Viviani S, Bonfante V, Nadali G, Herling M, Angelopoulou MK, Giardini R, Chilosi M, Kittas C, McDonnell TJ, Bonadonna G, Gianni AM, Pizzolo G, Pangalis GA, Cabanillas F, Sarris AH (2002) BCL-2 expression in Hodgkin and Reed-Sternberg cells of classical Hodgkin disease predicts a poorer prognosis in patients treated with ABVD or equivalent regimens. Blood 100:3935–3941
27. Schiemann B, Gommerman JL, Vora K, Cachero TG, Shulga-Morskaya S, Dobles M, Frew E, Scott ML (2001) An essential role for BAFF in the normal development of B cells through a BCMA-independent pathway. Science 293:2111–2114
28. Schneider P, MacKay F, Steiner V, Hofmann K, Bodmer JL, Holler N, Ambrose C, Lawton P, Bixler S, Acha-Orbea H, Valmori D, Romero P, Werner-Favre C, Zubler RH, Browning JL, Tschopp J (1999) BAFF, a novel ligand of the tumor necrosis factor family, stimulates B cell growth. J Exp Med 189:1747–1756
29. Schneider P, Takatsuka H, Wilson A, Mackay F, Tardivel A, Lens S, Cachero TG, Finke D, Beermann F, Tschopp J (2001) Maturation of marginal zone and follicular B cells requires B cell activating factor of the tumor necrosis factor family and is independent of B cell maturation antigen. J Exp Med 194:1691–1697
30. Seshasayee D, Valdez P, Yan M, Dixit VM, Tumas D, Grewal IS (2003) Loss of TACI causes fatal lymphoproliferation and autoimmunity, establishing TACI as as inhibitory BLys receptor. Immunity 18:279–288
31. Smith SH, Cancro MP (2003) Cutting edge: B cell receptor signals regulate BLyS receptor levels in mature B cells and their immediate progenitors. J Immunol 170:5820–5823
32. Thompson JS, Bixler SA, Qian F et al. (2001) BAFF-R, a newly identified TNF receptor that specifically interacts with BAFF. Science 293:2108–2111
33. von Bulow GU, Bram RJ (1997) NF-AT activation induced by a CAML-interacting member of the tumor necrosis factor superfamily. Science 278:138–141
34. von Bulow GU, van Deursen JM, Bram RJ (2001) Regulation of the T-independent humoral response by TACI. Immunity 14: 573–582
35. Vora KA, Wang LC, Rao SP, Liu ZY, Majeau GR, Cutler AH, Hochman PS, Scott ML, Kalled SL (2003) Germinal centers formed in the absence of B cell-activating factor belonging to the TNF family exhibit impaired maturation and function. J Immunol 171:547–551
36. Yamaguchi M, Seto M, Okamoto M, Ichinohasama R, Nakamura N, Yoshino T, Suzumiya J, Murase T, Miura I, Akasaka T, Tamaru J, Suzuki R, Kagami Y, Hirano M, Morishima Y, Ueda R, Shiku H, Nakamura S (2002) De novo CD5+ diffuse large B-cell lymphoma: a clinicopathologic study of 109 patients. Blood 99:815–821
37. Yan M, Wang H, Chan B et al. (2001) Activation and accumulation of B-cells in TACI-deficient mice. Nat Immunol 2:638–645
38. Yatabe Y, Oka K, Asai J, Mori N (1996) Poor correlation between clonal immunoglobulin gene rearrangement and immunoglobulin gene transcription in Hodgkin's disease. Am J Pathol 149:1351–1361
39. Yoshino T, Kondo E, Cao L, Takahashi K, Hayashi K, Nomura S, Akagi T (1994) Inverse expression of bcl-2 protein and Fas antigen in lymphoblasts in peripheral lymph nodes and activated peripheral blood T and B lymphocytes. Blood 83:1856–1861

Virchows Arch (2005) 447: 61–65
DOI 10.1007/s00428-004-1191-1

ORIGINAL ARTICLE

Gian Kayser · Ulrike Gerlach · Axel Walch · Roland Nitschke · Sabine Haxelmans · Klaus Kayser · Ulrich Hopt · Martin Werner · Silke Lassmann

Numerical and structural centrosome aberrations are an early and stable event in the adenoma–carcinoma sequence of colorectal carcinomas

Received: 7 October 2004 / Accepted: 2 December 2004 / Published online: 1 June 2005
© Springer-Verlag 2005

Abstract *Aims:* Numerical and structural centrosome changes have been described for and linked with genetic instability in solid tumors. Here, we specifically address centrosome aberrations in the adenoma–carcinoma sequence of colorectal cancer by detailed evaluation of γ-tubulin staining patterns. *Methods:* Formalin-fixed and paraffin-embedded specimens (normal colonic epithelium n=21; low-grade intraepithelial neoplasia n=27, high-grade intraepithelial neoplasia n=16 and invasive adenocarcinomas n=33) were stained by an anti-γ-tubulin antibody using standard immunofluorescence. Three-dimensional image stacks of the stainings were recorded (Zeiss LSM510 confocal microscope), followed by numerical and structural data analysis (DIAS software package) and statistical evaluation (NCSS-software). *Results:* The mean centrosome signal per cell differed significantly (P<0.0001) between normal colonic epithelium (0.8775) and each low-grade intraepithelial neoplasia (1.787), high-grade intraepithelial neoplasia (2.259) and invasive carcinomas (2.267). Similarly, both the centrosomes' structural entropy (SE) and minimal spanning tree (MST) differed significantly (P< 0.001) between normal (SE=3.956, MST=38.78) and each low- (SE=6.39, MST=26) and high-grade intraepithelial neoplasia (SE=5.75, MST=26.97) and invasive carcinoma (SE=6.86, MST=28.08). *Conclusion:* Numerical and structural centrosome dysregulation is seen as early as in low-grade dysplastic lesions of the adenoma–carcinoma sequence of colorectal carcinomas and may, as such, play an initial role in the carcinogenic process.

Keywords Centrosomes · Adenoma–carcinoma sequence · Colon cancer · Genetic instability · Syntactic structure analysis

G. Kayser · U. Gerlach · M. Werner · S. Lassmann
Institute of Pathology, University Hospital Freiburg, Germany

R. Nitschke · S. Haxelmans
Institute of Biology I, Developmental Biology, Life Imaging Center, University Freiburg, Germany

K. Kayser
UICC-TPCC, Charite, Berlin, Germany

U. Hopt
Department of Surgery, University Hospital Freiburg, Germany

M. Werner (✉)
Institute of Pathology, University Hospital Freiburg, Albertstrasse 19, 79104 Freiburg, Germany
e-mail: direktion-pathologie@uniklinik-freiburg.de
Tel.: +49-761-2036737
Fax: +49-761-2036818

A. Walch
GSF-Forschungszentrum, Institute of Pathology, Neuherberg, Germany

Introduction

The formation and organization of centrosomes is essential for proper cell division and the generation of two diploid daughter cells [1, 25]. During interphase, centrosomes are involved in the organization of the cytoplasmatic microtubule network and thereby also influence cell movement and cell polarity. Parallel to the cell cycle, centrosomes duplicate, mature and separate by moving to the opposite poles of the cell, ensuring mitotic-spindle formation and attachment. At mitosis, centrosomes are directly involved in proper chromosome segregation. Changes in either the number and/or location of centrosomes may negatively influence chromosomal segregation and cell ploidy and thereby promote chromosomal instability in malignancy [1, 25].

Indeed, centrosome aberrations have been demonstrated in several types of cancer [2, 3, 4, 18, 22], both in cell lines [7, 23, 27, 32] as well as in solid [8, 17, 19, 26] and hematopathological [5, 21] tumors. In fact, both supernumerary and structurally altered centrosomes have been

described for especially aneuploid cell lines [7] and tumors [18, 19]. Moreover, direct manipulation of centrosome regulation in cell culture models was shown to induce aneuploidy and transformation [32], supporting the concept of a potentially causative role of centrosome aberrations in malignant progression. A recent in situ study of precursor lesions implicated centrosome defects in the carcinogenesis of tumors of the uterine cervix, prostate and breast [24].

In colorectal cancer, concomitant phenotypic and genotypic changes characterize the progression of normal epithelium to adenoma to invasive carcinoma [6, 11, 12, 16]. The genetic alterations accompanying the adenoma–carcinoma sequence are generally divided into two pathways, resulting in either chromosomal unstable, frequently aneuploid tumors (CIN) or microsatellite unstable (MIN), mostly diploid tumors. Specific small genetic alterations, such as point mutations, and/or gains and losses of entire genes have been associated with chromosomal and microsatellite instability [9]. However, whether or not centrosome aberrations and the associated chromosome missegregation are primarily involved in or contribute to the carcinogenesis of colorectal tumors, particularly the CIN-type aneuploid carcinomas, is still unclear.

In the present study, we have therefore investigated centrosome alterations in the adenoma–carcinoma sequence of colorectal cancer by examining numerical and structural changes of the centrosome-specific marker γ-tubulin in situ, using formalin-fixed and paraffin-embedded tissue sections of normal epithelial cells, low-grade intraepithelial neoplasia (LGIN), high-grade intraepithelial neoplasia (HGIN) and invasive adenocarcinoma.

Materials and methods

Tissue specimens

Colorectal specimens (n=76; surgically removed polypectomies and small biopsies), all formalin fixed and paraffin embedded, were selected from the archives of the Pathological Institute of Freiburg. Upon reclassification (GK, MW) according to the World Health Organization 2000 [10] guidelines, these specimens included 27 samples of LGIN, 16 samples of HGIN and 33 samples of adenocarcinomas of the colon. Normal epithelial samples (n=21) were analyzed in some of the above specimens from adjacent tissues.

Immunohistochemistry

Tissue sections (8 μm) were deparaffinized, hydrated using standard measures and subjected to antigen retrieval using Pronase E (0.05%). Subsequently, tissue sections were incubated with a primary mouse anti-γ-tubulin antibody (1:100; clone GTU-88, Sigma), followed by incubation with a fluorescein isothiocyanate (FITC)-labeled goat-anti mouse IgG (1:200; Dianova). Finally, nuclei were counterstained with 4′6′-diamidino-2-phenylindole-2-hydrochloride (DAPI).

Data collection and in-situ parameter analysis

For data collection, five microscopic areas were selected (63 objective, zoom 2), and three-dimensional image stacks, consisting of 16 planes with a distance of 0.5 μm in the z-axis, were acquired with a confocal laser-scanning microscope (Zeiss LSM 510Meta, PlanNeofluar 63×/1.2 water, zoom 2). Excitation of fluorescent dye was at 351 nm for DAPI and 488 nm for FITC-labeled γ-tubulin. Image stacks were converted into a projection image of all recorded slices and were analyzed semi-automatically with respect to the number of cells (DAPI) and γ-tubulin signals by programs based on the DIAS software package [13, 14]. Furthermore, structural image analysis was performed by measuring the structural entropy of γ-tubulin signals, which quantifies the degree of signal perturbation within a given environment (i.e. selected tissue area), as well as the minimum spanning tree (MST) of γ-tubulin signals, which quantifies the shortest connection of all γ-tubulin signals as mean distance within the selected tissue area [15, 31]. The total number of analyzed cells was between 250 and 300 cells per case.

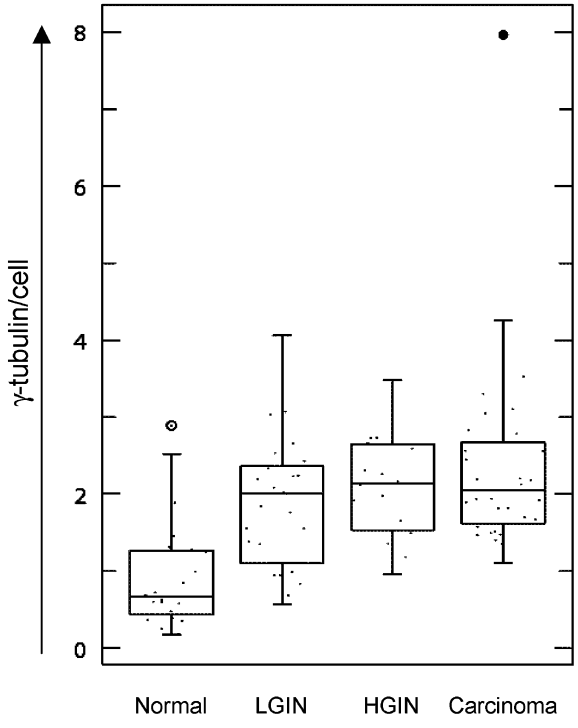


Fig. 1 Summary of the numerical changes of centrosomes along the adenoma–carcinoma sequence of colorectal adenocarcinoma. *Box plots* depict the measured γ-tubulin signals per cell for normal epithelial cells, low- and high-grade intraepithelial neoplasia (LGIN and HGIN) and invasive carcinoma. Each individual sample is indicated by a *dot*, minimum and maximum data points are indicated (*bar*, linked to the box by a line), and one statistical "outsider" (carcinoma) is shown by the *closed circle*

Table 1 Summary of the numerical changes of centrosomes within the adenoma–carcinoma sequence. *DAPI* 4′6′-diamidino-2-phenylindole-2-hydrochloride, *LGIN* low-grade intraepithelial neoplasia, *HGIN* high-grade intraepithelial neoplasia

Histology	γ-Tubulin/ DAPI (per cell)	Fold increase (relative to normal)	Significance (*P*) (relative to normal)
Normal	0.878		
LGIN	1.787	2.035	<0.0001
HGIN	2.259	2.573	<0.0001
Carcinoma	2.267	2.582	<0.0001

Statistical analysis

Statistical analysis was performed on the entire data set collected from all tissue samples using a commercially available software package (NCSS 2000, Number Cruncher Statistical Systems, Kaysville, Utah, USA) and included analysis of variance, the Mann-Whitney U test, the Wilcoxon-Rank test and the Kolmogorov-Smirnov test.

Results

Numerical changes of γ-tubulin staining in the adenoma–carcinoma sequence

In normal colonic epithelial cells (n=21), γ-tubulin staining showed a mean number of 0.88+/−0.6 signals per cell. In LGIN, an increase of γ-tubulin signals to 1.79+/−0.8 per cell was observed. These changes were even more obvious in HGIN, with 2.26+/−0.6 signals per cell, and invasive carcinomas, with 2.28+/−1.2 signals per cell (Fig. 1).

Statistical analysis (summarized in Table 1) of the numerical changes seen in γ-tubulin immunofluorescence stain revealed a significant alteration (P<0.0001) between: (1) normal cells and LGIN, (2) normal cells and HGIN and (3) normal and invasive carcinoma cells. However, the changes of γ-tubulin signals between LGIN and HGIN and invasive carcinoma showed no statistical significance.

Structural changes of γ-tubulin staining in the adenoma–carcinoma sequence

Whilst a regular, apical-orientated distribution of γ-tubulin was seen in normal epithelial cells, a progressively increasing sterical distortion of the γ-tubulin signals was observed in LGIN and HGIN and was most prominent in invasive carcinomas, with a complete loss of orientation (Fig. 2). To quantitatively measure these observations, we performed quantitative and syntactic analysis of: (1) the structural entropy of the γ-tubulin signals and (2) the MST between all γ-tubulin signals within the tissue images.

The structural entropy of the centrosomes within normal epithelium was 3.96+/−1.4 and was raised to 6.39+/−1.6 in LGIN, 5.75+/−1.6 in HGIN and to 6.86+/−2.1 in invasive carcinomas. As seen in the numerical γ-tubulin changes, the structural entropy measurements were also significantly different between normal and neoplastic epithelium (P<

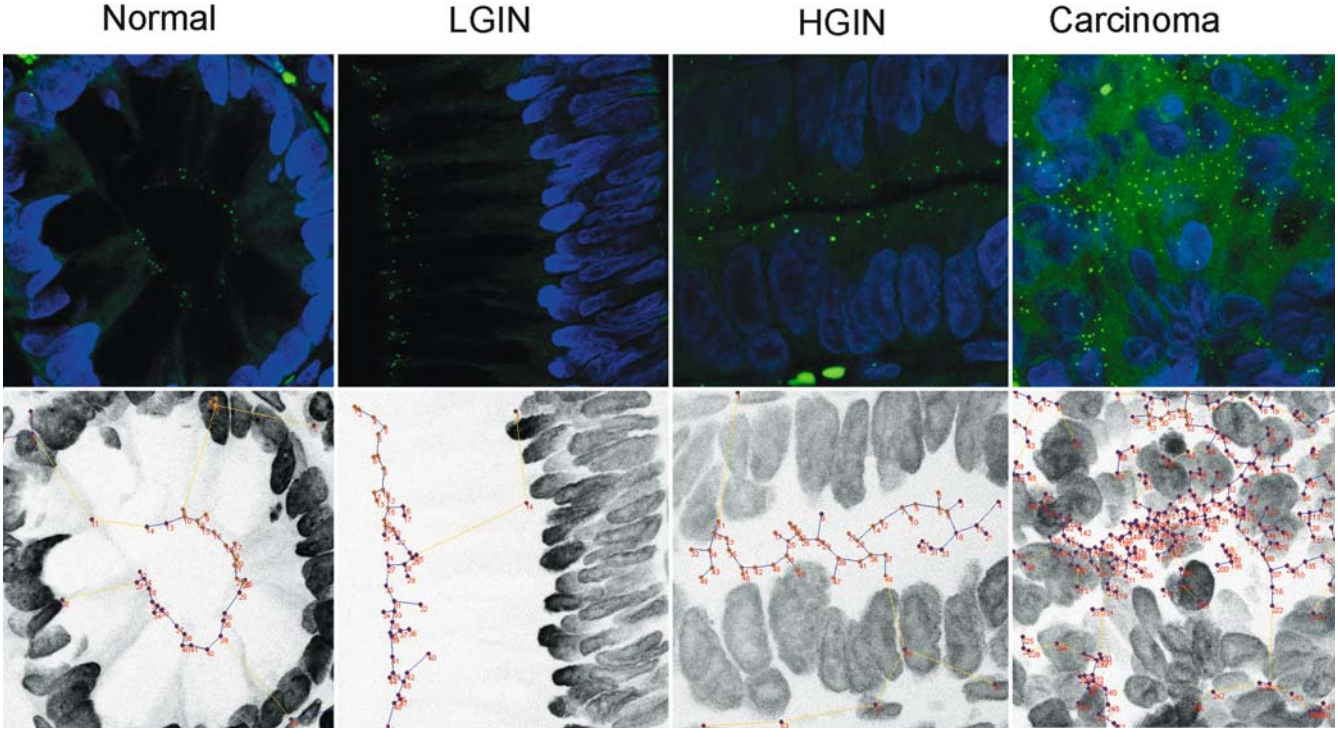


Fig. 2 Changes of centrosomes along the adenoma–carcinoma sequence of colorectal adenocarcinoma. Representative staining of centrosomes by γ-tubulin immunofluorescence (*top row*) and structural analysis of centrosome location by minimal spanning tree (*bottom row*). *Panels from left* normal epithelium, low- and high-grade intra-epithelial neoplasia and far right invasive adenocarcinoma. Magnification: 1260 (63 objective, zoom 2, camera ×10). γ-Tubulin signals are shown in *green*

Table 2 Summary of the structural changes of centrosomes within the adenoma–carcinoma sequence. *MST* minimal spanning tree, *LGIN* low-grade intraepithelial neoplasia, *HGIN* high-grade intraepithelial neoplasia

Histology	Entropy	Significance (relative to normal)	MST	Significance (relative to normal)
Normal	0.0396		38.78	
LGIN	0.0639	<0.001	26.00	<0.001
HGIN	0.0575	<0.001	26.968	<0.001
Carcinoma	0.0686	<0.001	28.08	<0.001

0.001) (Table 2). Together with an elevated number of γ-tubulin signals, this parallel increase of structural entropy may lead to a reduction of the mean distance between γ-tubulin signals, i.e., the MST. Indeed, the measurement of the MST of γ-tubulin signals also revealed significant differences between normal and neoplastic cells ($P<0.001$): the mean MST length in normal mucosa was 38.8+/−13.4 and shortened to 26.0+/−4.0 in LGIN, 27.0+/−3.3 in HGIN and 28.1+/−5.3 in invasive carcinoma.

Discussion

Centrosome dysfunction is closely associated with aneuploidy and chromosomal instability in cell-culture models [32], including colorectal cell lines [7], and has been implicated in a variety of human solid tumors [8, 17, 19, 26] as well as in lymphomas and leukemias [5, 21]. However, the association with and/or involvement of centrosome aberrations at early stages of malignant transformation, such as in dysplastic precursor lesions, have thus far only been addressed in a single study [24].

The present study is, therefore, the first in situ analysis of centrosomes within a large series of normal colonic epithelium, LGIN, HGIN and invasive carcinoma samples of colorectal cancer patients. By visualizing centrosomes with γ-tubulin, a highly conserved component of centrosomes [29, 30], we found not only numerical but also structural aberrations of centrosomes within the adenoma–carcinoma sequence. Moreover, these numerical and structural centrosome changes were already evident at the transition of normal epithelium to LGIN, suggesting that centrosome alterations may represent a very early event in the carcinogenesis of colorectal cancer. In fact, centrosome signals increased twofold from normal to LGIN and threefold from normal to HGIN and invasive carcinoma (Table 1). These observations are in accordance with earlier studies demonstrating that supernumerary centrosomes may occur in pre-invasive lesions of the uterine cervix, prostate and female breast [24], as well as in pre-invasive lesions of the cervix in association with human papilloma virus infections [28].

Centrosome dysfunction may occur not only at the level of numerical changes but also in the failure of structural organization [17, 20, 23]. We, therefore, evaluated whether structural and/or sterical alterations might additionally be involved in centrosomal dysfunction in colorectal carcinogenesis. Indeed, semi-automated image analysis of the structural entropy and MST [13, 14, 15, 31] of γ-tubulin-stained tissues revealed statistically significant changes in centrosome orientation and localization. Concomitantly with the numerical changes, these structural alterations were already present in LGIN.

Finally, the numerical and structural centrosome alterations observed from the transition of normal colonic epithelium to LGIN did not progress further along the adenoma–carcinoma sequence, remaining equally elevated in HGIN and invasive carcinomas.

Together, these results suggest early and stable numerical as well as structural alterations of centrosomes in the carcinogenesis of colorectal cancer. Whether these centrosome alterations are simply a consequence of the well-characterized genetic events of the adenoma–carcinoma sequence [6, 11, 12, 27] or whether they are a primary cause for the progression of a normal epithelium into an (aneuploid) invasive carcinoma remains an open question. However, the early occurrence of centrosome alterations, as seen in our samples of LGIN, may point toward a causative role of centrosome dysfunction in malignant transformation.

In fact, we have obtained further data supporting an early role of centrosome alteration in colorectal carcinogenesis by mRNA expression analysis of STK15, a serine-threonine kinase previously shown to be essential for centrosome function [32]. Similar to the pattern of γ-tubulin staining, STK15 mRNA increased significantly already in LGIN without any further increases in HGIN and carcinoma (Gerlach et al., unpublished observations). Moreover, our preliminary data also suggest that this increase of STK15 mRNA occurs preferentially in the carcinogenesis of chromosomal unstable colorectal tumors, and this appears to also be correlated with the number of γ-tubulin signals/cells. However, further studies have to prove the link of STK15 mRNA and γ-tubulin, i.e., centrosome aberrations, particularly in the development of chromosomal unstable colorectal cancers.

In summary, we have shown that centrosome aberrations are an early event in the adenoma–carcinoma sequence of colorectal adenocarcinomas. These changes are characterized by supernumerary centrosomes and an increasing perturbation in the arrangement of centrosomes within the cells. Both of these alterations may be associated with the induction of aneuploidy in colorectal carcinomas, particularly those that are chromosomally unstable.

Acknowledgements We thank Mrs. E. Bokla for expert technical assistance. This study was supported by a grant to S.L. from the Forschungskommission (#LA56203/03), Medizische Fakultät Freiburg, Germany.

References

1. Brinkley BR (2001) Managing the centrosome numbers game: from chaos to stability in cancer cell division. Trends Cell Biol 11:18–21

2. D'Assoro AB, Lingle WL, Salisbury JL, et al (2002) Centrosome amplification and the development of cancer. Oncogene 21:6146–6153
3. Doxsey S (1998) The centrosome—a tiny organelle with big potential. Nat Genet 20:104–106
4. Duensing S, Munger K (2001) Centrosome abnormalities, genomic instability and carcinogenic progression. Biochim Biophys Acta 2:M81–M88
5. Duensing S, Lee BH, Cin PD, et al (2003) Excessive centrosome abnormalities without ongoing numerical chromosome instability in a Burkitt's lymphoma. Mol Cancer 2:30
6. Fearon ER, Vogelstein B (1990) A genetic model for colorectal tumorigenesis. Cell 61:759–767
7. Ghadimi BM, Sackett DL, Difilippantonio MJ, et al (2000) Centrosome amplification and instability occurs exclusively in aneuploid, but not in diploid colorectal cancer cell lines, and correlates with numerical chromosomal aberrations. Genes Chromosomes Cancer 27:183–190
8. Gisselsson D, Jonson T, Yu C, et al (2002) Centrosomal abnormalities, multipolar mitoses, and chromosomal instability in head and neck tumours with dysfunctional telomeres. Br J Cancer 87:202–207
9. Grady WM (2004) Genomic instability and colon cancer. Cancer Metastasis Rev 23:11–27
10. Hamilton S, Aaltonen L (2000) Pathology and genetics of tumors of the digestive system. WHO Classification of Tumors, IARC Press, Lyon
11. Hermsen M, Postma C, Baak J, et al (2002) Colorectal adenoma to carcinoma progression follows multiple pathways of chromosomal instability. Gastroenterology 123:1109–1119
12. Jass JR, Whitehall VL, Young J, et al (2002) Emerging concepts in colorectal neoplasia. Gastroenterology 123:862–876
13. Kayser K, Gabius HJ (1997) Graph theory and the entropy concept in histochemistry. Progress in histochemistry and cytochemistry. Gustav Fischer, Stuttgart 32
14. Kayser K, Stute H, Bubenzer J, et al (1990) Combined morphometrical and syntactic structure analysis as tools for histomorphological insight into human lung carcinoma growth. Anal Cell Pathol 2:167–178
15. Kayser G, Baumhakel JD, Szoke T, et al (2003) Vascular diffusion density and survival of patients with primary lung carcinomas. Virchows Arch 442:462–467
16. Lengauer C, Kinzler KW, Vogelstein B, et al (1997) Genetic instability in colorectal cancers. Nature 386:623–627
17. Lingle WL, Salisbury JL (1999) Altered centrosome structure is associated with abnormal mitoses in human breast tumors. Am J Pathol 155:1941–1951
18. Lingle WL, Barrett SL, Negron VC, et al (2002) Centrosome amplification drives chromosomal instability in breast tumor development. Proc Natl Acad Sci U S A 99:1978–1983
19. Mayer F, Stoop H, Sen S, et al (2003) Aneuploidy of human testicular germ cell tumors is associated with amplification of centrosomes. Oncogene 22:3859–3866
20. Meraldi P, Nigg EA (2002) The centrosome cycle. FEBS Lett 521:9–13
21. Neben K, Tews B, Wrobel G, et al (2004) Gene expression patterns in acute myeloid leukemia correlate with centrosome aberrations and numerical chromosome changes. Oncogene 23: 2379–2384
22. Nigg EA (2002) Centrosome aberrations: cause or consequence of cancer progression? Nat Rev Cancer 2:815–825
23. Pihan GA, Purohit A, Wallace J, et al (2001) Centrosome defects can account for cellular and genetic changes that characterize prostate cancer progression. Cancer Res 61:2212–2219
24. Pihan GA, Wallace J, Zhou Y, et al (2003) Centrosome abnormalities and chromosome instability occur together in preinvasive carcinomas. Cancer Res 63:1398–1404
25. Rieder CL, Faruki S, Khdjakov A, et al (2001) The centrosome in vertebrates: more than a microtubule-organizing center. Trends Cell Biol 11:413–419
26. Sato N, Mizumoto K, Nakamura M, et al (1999) Centrosome abnormalities in pancreatic ductal carcinoma. Clin Cancer Res 5:963–970
27. Sato N, Mizumoto K, Nakamura M, et al (2001) Correlation between centrosome abnormalities and chromosomal instability in human pancreatic cancer cells. Cancer Genet Cytogenet 126: 13–19
28. Skyldberg B, Fujioka K, Hellstrom AC, et al (2001) Human papillomavirus infection, centrosome aberration, and genetic stability in cervical lesions. Mod Pathol 14:279–284
29. Stearns T, Kirschner M (1994) In vitro reconstitution of centrosome assembly and function: the central role of gamma-tubulin Cell 76:623–637
30. Stearns T, Evans L, Kirschner M (1991) Gamma-tubulin is a highly conserved component of the centrosome. Cell 65:825–836
31. van Diest PJ, Kayser K, Meijer GA, et al (1995) Syntactic structure analysis. Pathologica 87:255–262
32. Zhou H, Kuang J, Zhong L, et al (1998) Tumour amplified kinase STK15/BTAK induces centrosome amplification, aneuploidy and transformation. Nat Genet 20:189–193

Virchows Arch (2005) 447: 66–73
DOI 10.1007/s00428-005-1225-3

ORIGINAL ARTICLE

Kaori Morimoto · Isao Nishimori · Tamotsu Takeuchi · Takuhiro Kohsaki · Nobuto Okamoto · Takahiro Taguchi · Shigeru Yunoki · Ryohei Watanabe · Yuji Ohtsuki · Saburo Onishi

Overexpression of carbonic anhydrase-related protein XI promotes proliferation and invasion of gastrointestinal stromal tumors

Received: 5 November 2004 / Accepted: 6 February 2005 / Published online: 8 June 2005
© Springer-Verlag 2005

Abstract Three isoforms of carbonic anhydrase-related protein (CA-RP) are evolutionally well conserved among the CA gene family but lack classical CA activity. Although the biological function of CA-RPs is unknown, overexpression of CA-RP VIII has been reported in certain tumor types. Based on the finding that CA-RPs are commonly expressed in the neuronal cells, we investigated expression of all three CA-RPs in gastrointestinal stromal tumor (GIST). In contrast to no detectable signal of any of the three CA-RPs in intestinal cells of Cajal, immunohistochemical analysis showed distinct cytoplasmic expressions of CA-RPs VIII and XI in 13 (59%) and 20 (91%) of 22 GIST tissue specimens, respectively. The positive signals for both CA-RPs VIII and XI were more intense in the periphery than in the central part of GISTs, whereas no significant signal for CA-RP X expression was observed in any of the GISTs. These expression patterns of CA-RPs were consistently observed by reverse transcription–polymerase chain reaction–Southern blot and immunocytochemistry in the cultured GIST cell line GIST-T1. Ectopic expression of CA-RP XI in GIST-T1 cells induced cell proliferation and invasion in vitro. These findings indicate that CA-RP XI plays a role in the development of GIST.

Keywords Carbonic anhydrase · Carbonic anhydrase-related protein · KIT · Intestinal cell of Cajal · Gastrointestinal stromal tumor

K. Morimoto · I. Nishimori (✉) · T. Kohsaki · N. Okamoto · S. Onishi
Department of Gastroenterology and Hepatology,
Kochi Medical School,
Nankoku, Kochi, 783-8505, Japan
e-mail: nisao@med.kochi-u.ac.jp
Tel.: +81-888-802338
Fax: +81-888-802338

T. Takeuchi · Y. Ohtsuki
Department of Pathology, Kochi Medical School,
Kochi, 783-8505, Japan

T. Taguchi
Division of Human Health and Medical Science,
Graduate School of Kuroshio Science, Kochi University,
Kochi, 783-8505, Japan

S. Yunoki · R. Watanabe
Division of Surgery, Matsuyama Shimin Hospital,
Matsuyama, Ehime, 790-0067, Japan

Introduction

Carbonic anhydrases (CA) are zinc metal enzymes that catalyze the reversible hydration of CO_2 in the reaction $CO_2+H_2O \leftrightarrow HCO_3^-+H^+$ [13]. Among the members of the expanding CA gene family, three isoforms that are evolutionally well-conserved but lack classical CA activity have been reported and designated as CA-related protein (CA-RP): CA-RPs VIII, X, and XI [9]. These three CA-RPs lack one or more histidine residues required to bind the zinc ion, which is essential for CO_2 hydration activity. Recently, CA-RP VIII was reported to bind inositol 1,4,5-triphosphate (IP_3) receptor type I (IP_3R1) and to inhibit IP_3 binding to IP_3R1 by reducing the affinity of the receptor for IP_3 [5]. However, the exact biological function of CA-RPs is still unknown.

We have been working with cDNA cloning and studying expressions of human and murine CA-RPs VIII, X, and XI. Whereas mRNA expressions of CA-RP X and XI are relatively limited to the central nervous system [3, 11, 17], CA-RP VIII is expressed in almost all tissue types [1, 17]. Immunohistochemical analyses showed that all three CA-RPs were expressed in the cytoplasm of neural or glial cells in the central nervous system [16, 17]. Interestingly, CA-RP VIII expression is remarkably increased in colorectal and non-small lung cancer cells as compared with that in their normal counterparts [1, 8]. Furthermore, CA-RP VIII is significantly expressed in the pulmonary epithelial cells in developing lungs [1]. These findings suggest that CA-RPs play some role in the growing process of certain tumor and fetal cells.

Gastrointestinal stromal tumor (GIST) is the most common mesenchymal tumor of the gastrointestinal tract [2]. Most GISTs express a constitutively activated KIT oncoprotein (CD117), a transmembrane tyrosine kinase receptor in which the extracellular portion binds a ligand known as a stem cell factor [4]. A significant proportion of GISTs are also immunopositive for CD34 [2]. These phenotypic markers for GIST are also expressed in the intestinal cells of Cajal (ICCs), intestinal pacemaker cells, which play a neuromotor role in normal gut motility [2]. Accordingly, GIST has been thought to originate from ICC. Being independent of immunoreactivity of KIT and/or CD34, some GISTs express smooth muscle actin or S-100 protein, indicating potential neuromyogenic differentiation of GIST [2]. Our previous study showed the expression of CA-RP VIII and XI in the neural ganglionic cells constituting both myenteric (Auerbach's) and mucosal (Meissner's) plexuses [10]. These findings prompted us to study the expression of CA-RPs in GIST. Along with the results from immunohistochemical studies, we report herein findings obtained in vitro by using cultured GIST cells transformed with the CA-RP XI cDNA.

Materials and methods

Tissue specimens

Surgically resected specimens from 22 patients with GIST (16 primary lesions arisen from the stomach, 2 from the duodenum, and 4 from the small intestine) were used for the immunohistochemical study. Positive KIT expressions were immunohistochemically confirmed in all GIST specimens. No patient had received either preoperative chemotherapy or radiation therapy. To study the expression of CA-RPs in ICC, tissue specimens of the stomach containing hyperplastic ICCs, which were resected from a patient with von Recklinghausen disease, were used. Conforming to the principles of the Declaration of Helsinki, informed consent was obtained from each patient.

GIST cell line

A human GIST cell line, GIST-T1 [15], was used for the transformation study with CA-RP XI. GIST-T1 was originally established from a pleural metastatic lesion in a Japanese patient with gastric GIST, in which heterozygous deletion of 57 bp in the juxtamembrane domain (exon 11) of the c-*kit* gene was identified, resulting in constitutive KIT activation. GIST-T1 cells were strongly positive for KIT and CD34 but not for desmin, S-100 protein, or smooth muscle actin. The cells were cultured in Dulbecco's modified Eagle's medium (Sigma, St. Louis, MO, USA) with 10% fetal bovine serum, 100 U/mL of penicillin G, and 100 μg/mL of streptomycin (Invitrogen, Carlsbad, CA, USA).

Monoclonal antibodies

We previously produced mouse monoclonal antibodies to human CA-RPs VIII, X, and XI that belonged to the IgM subclass [16]. Antibody specificity was evaluated by preabsorption of the positive staining on immunohistochemical analysis using the synthetic peptide, which, as previously reported, had been employed for the immunization of mice to produce the monoclonal antibody [16]. Phenotypic markers for GIST were also immunohistochemically studied: KIT (CD117), by using polyclonal rabbit antihuman c-kit antibody (Dako, Glostrup, Denmark) and CD34 antigens, by using monoclonal mouse anti-HPCA-1 antibody (Becton Dickinson, San Jose, CA, USA).

Immunochemical analyses

Immunohistochemical and cytochemical analyses were performed by means of the streptavidin–biotin peroxidase method without any pretreatment procedures, as previously reported [7, 16]. Briefly, GIST tissues were formalin-fixed and embedded in paraffin. The tissue sections were deparaffinized and incubated with fetal bovine serum. GIST-T1 cells with or without transfection of CA-RP XI were cultured up to approximately 70% confluence on a chamber slide (Nunc, Naperville, IL, USA). The cells on the slide were gently washed with phosphate-buffered saline (PBS) and fixed with 100% acetone for 5 min. The tissue and cultured cell sections were incubated with the monoclonal antibodies to three CA-RPs, KIT, or CD34 at 4°C overnight. After washing with PBS, immunodetection was performed using biotinylated anti-mouse or anti-rabbit immunoglobulin antibody and peroxidase-labeled streptavidin (Dako LSAB kit). Finally, the immunohistochemical reactants were developed with 3, 3′diaminobenzidine. Counterstaining was performed using hematoxylin.

Transfection of CA-RP XI into GIST-T1

A full length of the coding region in the CA-RP XI cDNA was obtained by reverse transcription–polymerase chain reaction (RT-PCR) from a human brain λTriplEx library (Clonetech, Palo Alto, CA, USA) and subcloned into a pCI-neo vector (Promega, Madison, WI, USA) as previously reported [7]. Subsequently, the CA-RP XI cDNA was transfected into GIST-T1 cells by using lipofectamin (Roche, Mannheim, Germany) as previously reported [14]. Transfectants were selected for a 2-week culture in the presence of 800 μg/mL of G418 (Invitrogen) and isolated by a single-cell manipulation technique [14]. Overexpressed mRNA and protein of CA-RP XI were confirmed in the isolated transfectants (GIST-T1-CA11) by RT-PCR–Southern blot and immunocytochemical staining, respectively.

Analyses for mRNA expression of CA-RPs

mRNA expressions of CA-RPs VIII, X and XI in GIST-T1 cells were quantified by real-time PCR and the results were reconfirmed by RT-PCR–Southern blotting. Total RNA was extracted using trizol reagent according to the manufacturer's recommended procedures (Life Technologies, Grand Island, NY, USA). RNA extracts were reverse-transcribed using random hexamers and avian myeloblastosis virus reverse transcriptase by employing a commercial kit (Takara, Kyoto, Japan). For real-time PCR, Assays-on-Demand primers and probes sets were purchased: Hs0018 7850 m1 for CA-RP VIII, Hs00220143 m1 for CA-RP X, and Hs00154213 m1 for CA-RP XI (Applied Biosystems, Tokyo, Japan). Gene-specific PCR products were measured continuously by an ABI PRISM 7000 Sequence Detection System (Applied Biosystems) according to the manufacture's instructions. The relative mRNA expression of three CA-RPs was normalized to the amount of glyceraldehyde phosphate dehydrogenase (GAPDH) in the same cDNA by using the standard curve method described by the manufacturer. For RT-PCR–Southern blotting, the reverse-transcribed cDNAs were amplified by PCR using CA-RP-specific primer pairs. The sequences of the primer pairs were as follows: 5′-TCCTGATGCTAATGGGGAATACC AG-3′ and 5′ CTAAGAGGCTGAGTGGGCCGAAAG-3′ for CA-RP VIII, 5′-AATCAGAGGATGGAAATAGTC TG-3′ and 5′-CTACTTGAGGAGCCATTCATTTA-3′ for CA-RP X, and 5′-GGCAGCAGGTAACATCGGACCAGC-3′ and 5′-GGTTAGAGGTACTGGCCACGTTGAC-3′ for CA-RP XI. The PCR consisted of 30 cycles with denaturation at 94°C for 30 s, annealing at 55°C for 30 s, and elongation at 72°C for 30 s. The PCR-amplified products were electrophoretically separated on a 2.0% agarose gel and transblotted onto a Hybond N+ membrane (Amersham, Tokyo, Japan) according to the previously published method [12]. The membrane was treated with 0.5 N NaOH and processed. DNA probes of three CA-RPs were obtained from poly(A) RNA of the human brain (Clonetech) by RT-PCR with the primer sets described above. The proper cDNA sequence of the probe was reconfirmed by direct sequencing and then used for Southern blotting. The probe DNAs were randomly labeled with digoxigenin using DIG-High Prime (Boehringer, Mannheim, Germany). Hybridization was carried out in Easy Hyb buffer (Roche) at 50°C overnight. After hybridization, the membranes were incubated with an anti-digoxigenin antibody conjugated with alkaline phosphatase buffer (Roche). Alkaline phosphatase reactions were developed on the membranes with CDP-Star

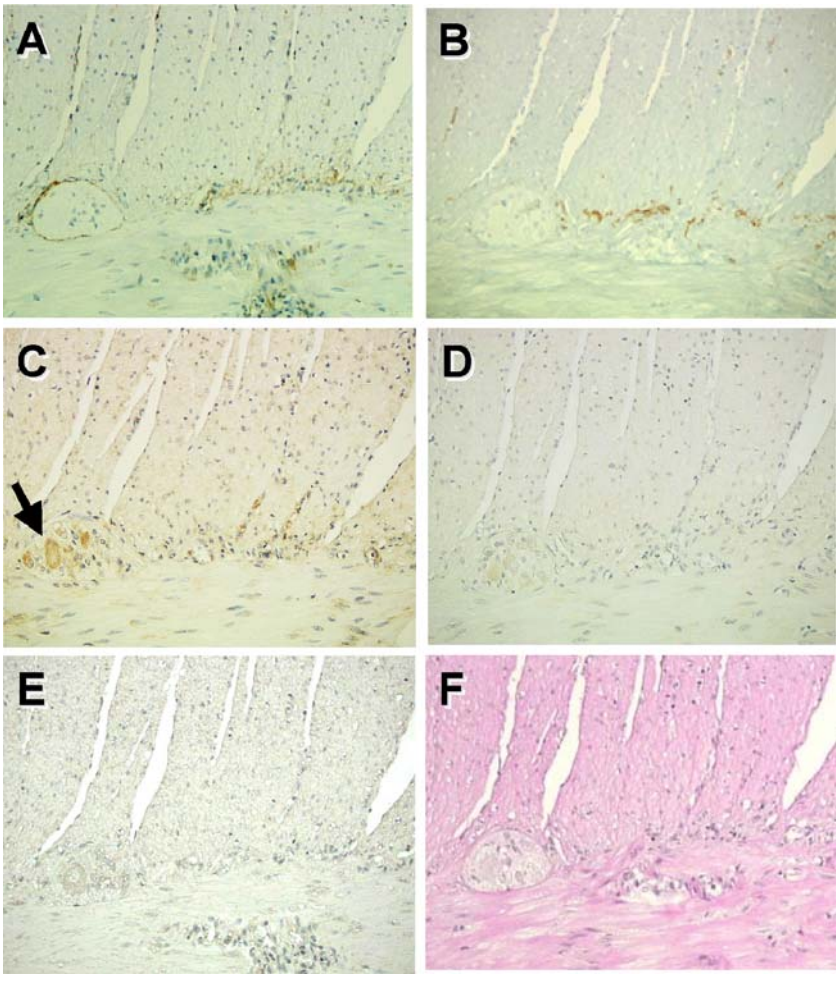


Fig. 1 Immunohistochemical analysis for expressions of CA-RPs, KIT, and CD34 in serial sections of the gastric tissue from a patient with von Recklinghausen disease. Significant signals for expressions of KIT (**a**) and CD34 (**b**) are observed in the myenteric plexus. Distributions of CA-RPs VIII (**c**), X (**d**), and XI (**e**) are completely different from those of KIT and CD34. CA-RPs are expressed in neural cell bodies. Among the expressions of the three CA-RPs, that of CA-RP VIII is most intense (*arrow*; **c**). Hematoxylin-eosin staining (**f**). (Original magnification×80)

Table 1 CA-RP expression in GIST

Location	No. of specimens	CA-RP VIII (%)	CA-RP X (%)	CA-RP XI (%)
Stomach	16	11 (69)	0 (0)	14 (88)
Duodenum	2	2 (100)	0 (0)	2 (100)
Small intestine	4	0 (0)	0 (0)	4 (100)
Total	22	13 (59)	0 (0)	20 (91)

buffer (Roche) and exposed to X-ray film (Fuji, Tokyo, Japan).

Cell proliferation and invasion assay

Cell proliferation and invasion properties of wild-type GIST-T1 and GIST-T1-CA11 were studied. Proliferation was determined by cell conversion of a tetrazolium salt into a formazan product with a commercial kit (CellTiter 96, Promega). The cells were resuspended at 1×10^5 cells per well in a 96-well plate (Nunc) and cultured for 24, 48, and 72 h. After the addition of 15 μL of a tetrazolium dye solution into the culture wells and incubation for 4 h, 100 μL of a solubilization-stop solution was added. The absorbance at 570 nm was recorded using a 96-well plate reader (Molecular Devices, Sunnyvale, CA, USA).

The property of cell invasiveness was studied by using a blind-well chemotaxis chamber containing an 8-μm pore-size filter with a thin layer of basement membrane Matrigel, which serves as a reconstituted basement membrane in vitro (BioCoat Matrigel invasion chamber, BD Biosciences, Bedford, MA, USA). The cells were resuspended at 1.25×10^5 cells per chamber and cultured for 48 h. The noninvading cells were removed from the upper surface of the filter by scrubbing with a cotton-tipped swab. The cells on the lower surface of the filter were stained with hematoxylin, and then the number of invading cells per high-power field was microscopically counted. Both assays were performed in triplicate.

Statistics

Where appropriate, values are expressed as means±standard deviation. Comparisons were made by Student *t* test, and differences with *P* values of <0.05 were considered significant.

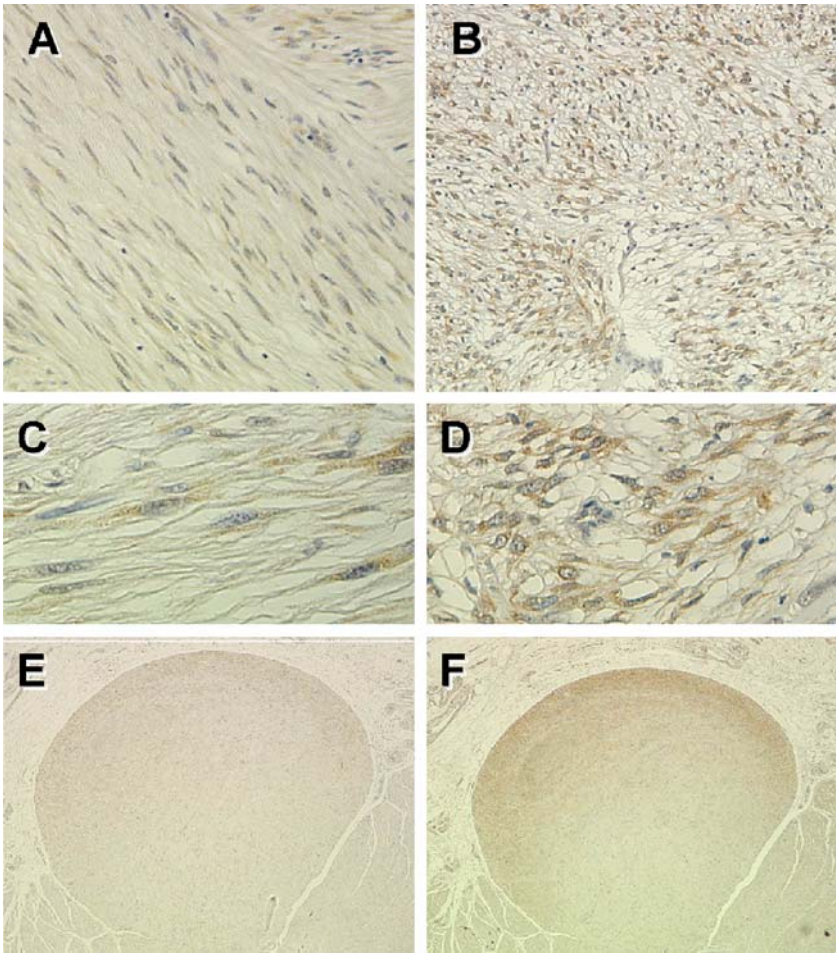


Fig. 2 Immunohistochemical analysis for expressions of CA-RPs VIII and XI in gastrointestinal stromal tumors (*GIST*). Significant signals for CA-RPs VIII (**a**, **c**, and **e**) and XI (**b**, **d**, and **f**) expression are observed in GISTs. Positive signals for both CA-RPs VIII and XI expression are observed in the cytoplasm of GIST cells (**c** and **d**). Expressions of CA-RP VIII and XI are more prominent in the invasive front of the tumor as compared with the central part of the tumor (**e** and **f**)

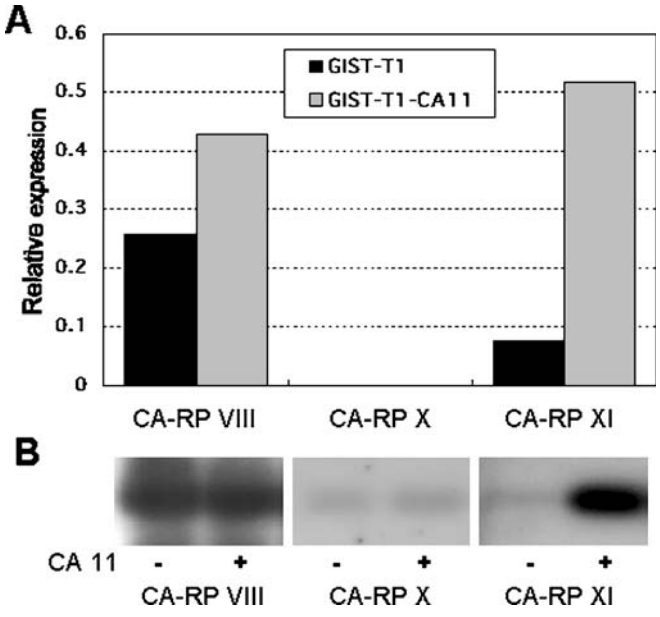


Fig. 3 Quantitative real-time PCR (**a**) and RT-PCR–Southern blot (**b**) for mRNA expression of three CA-RPs in wild-type and CA11-transfected GIST-T1 cells (*GIST-T1-CA11*). Real-time PCR shows 0.076 of relative expression of CA-RP XI mRNA normalized to GAPDH mRNA in GIST-T1 and 0.517 of that in GIST-T1-CA11, yielding 6.803 times increase in CA-RP XI mRNA expression by the CA11-transfection, which is consistent to the finding shown by RT-PCR–Southern blot. Intense signals for CA-RP VIII expression are seen in both GIST-T1 and GIST-T1-CA11 with 1.676 times increase by ectopic expression of CA-RP XI. In contrast, real-time PCR fails to show the standard curve to quantify CA-RP X mRNA expression, and RT-PCR–Southern blot shows very weak signals for CA-RP X in both GIST-T1 and GIST-T1-CA11

Results

CA-RP expression in ICC

Expression of three CA-RPs, KIT (CD117), and CD34 was studied in serial sections of the gastric tissue specimen in a patient with von Recklinghausen disease (Fig. 1). Immunohistochemical analysis revealed significant signals for expressions of KIT (CD117) and CD34 in the myeteric plexus (Fig. 1a, b, respectively). Distributions of all three CA-RPs (Fig. 1c–e) were completely different from those of KIT and CD34; CA-RPs were expressed in neural cell bodies. Among the expressions of the three CA-RPs in the neural cell bodies, that of CA-RP VIII was most intense (Fig. 1c, arrow).

CA-RP expression in GIST

Immunohistochemical analysis showed significant signals for CA-RP VIII and XI expression in 13 (59%) and 20 (91%) of 22 GIST tissue specimens, respectively (Table 1). In contrast, no significant signal for CA-RP X expression was observed in any of the GIST specimens studied herein. Positive signals for both CA-RPs VIII and XI expression were observed in the cytoplasm of GIST cells (Fig. 2a–d). Expressions of CA-RPs VIII and XI are more prominent in the periphery of the tumor as compared with the central part of the tumor (Fig. 2e, f).

CA-RP XI transfection into GIST-T1 cells

GIST-T1 cells were transfected with the CA-RP XI cDNA ligated into the expression vector (GIST-T1-CA11), and mRNA and protein expression of three CA-RPs were studied. Quantitative real-time PCR showed 0.076 of relative expression of CA-RP XI mRNA normalized to GAPDH in wild-type GIST-T1 and 0.517 of that in GIST-T1-CA11, yielding 6.803 times increase in CA-RP XI mRNA expression by the transfection (Fig. 3a). This was confirmed by RT-PCR–Southern blot analysis, showing remarkably increased expression of CA-RP XI mRNA in GIST T1-CA11 as compared to that in GIST-T1 (Fig. 3b). Immunocytochemical analysis also showed an increased expression of CA-RP XI protein in GIST-T1-CA11 as compared to GIST-T1 (Fig. 4). Intense signals for CA-RP XI expression were observed in the cytoplasm of GIST-T1 cell bodies.

Strong signals for mRNA and protein expression of CA-RP VIII were observed in both GIST-T1 and GIST-T1-CA11 (Figs. 3 and 4). Although there was no obvious difference in CA-RP VIII mRNA expression level between GIST-T1 and GIST-T1-CA11 (1.676 times increase by the transfection; Fig. 3a), interestingly, subcellular localization of CA-RP VIII protein was altered. CA-RP VIII was observed in the perinuclear area of GIST-T1, whereas in GIST-T1-CA11, it was seen in the whole cell body (Fig. 4). Real-time PCR failed to show the standard curve to quantify CA-RP X mRNA expression and RT-PCR–Southern blot showed a very weak signal for CA-RP X in both GIST-T1 and GIST-T1-CA11. Immunocytochemical analysis also showed no significant signal for CA-RP X expression in both GIST-T1 and GIST-T1-CA11. These findings indicate a trace level expression of CA-RP X in GIST-T1 and it is not influenced by ectopic expression of CA-RP XI.

Effects of CA-RP XI on proliferative and invasive properties of GIST-T1 cells

Cell proliferation assay showed no significant difference in cell growth between GIST-T1 and GIST-T1-CA11 after 24 h culture (Fig. 5a). After culture for 48 and 72 h, proliferative cell numbers of GIST-T1-CA11 had increased significantly more than that of GIST-T1 ($P<0.002$ and $P<0.005$, respectively). Meanwhile, cell invasion assay showed a significantly increased number of GIST-T1-CA11 (39.7±3.1/high-power field), which invaded through a thin layer of basement membrane Matrigel, as compared to that of GIST-T1 (6.7±4.6/high-power field; $P<0.005$) (Fig. 5b).

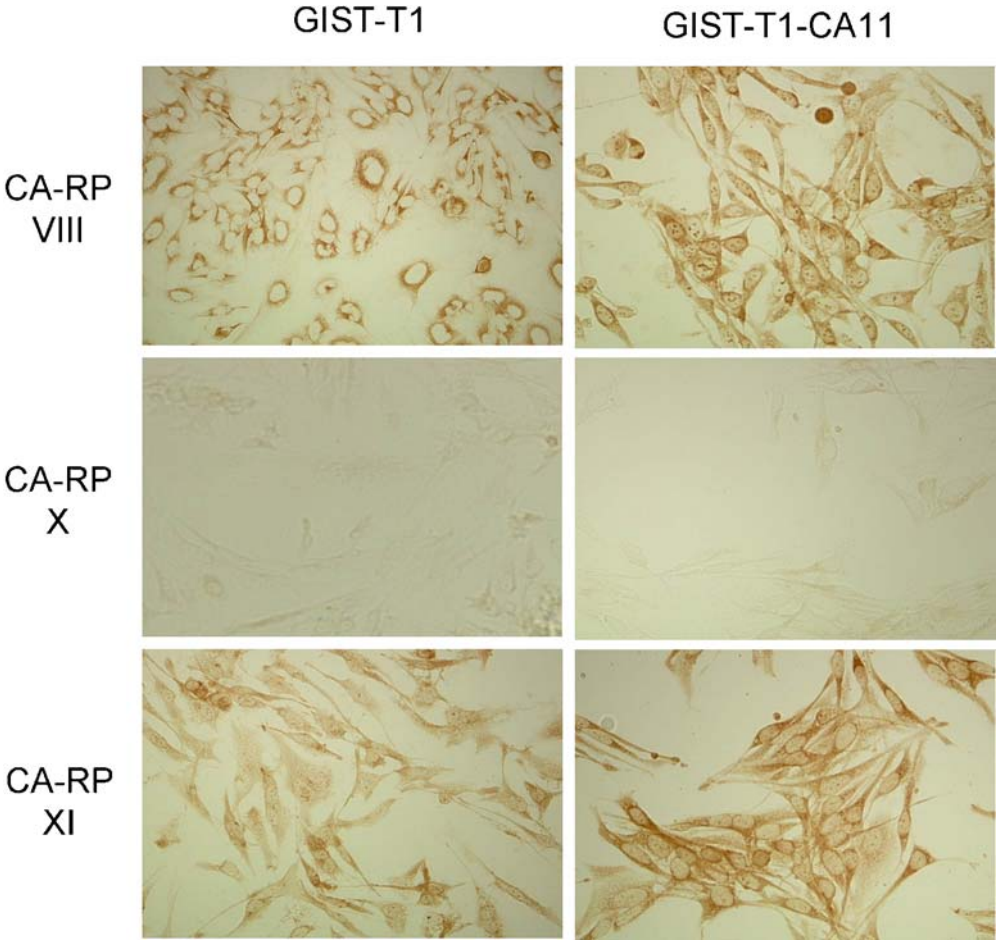


Fig. 4 Immunocytochemical analysis for expressions of three CA-RPs in wild-type and CA11-transfected GIST-T1 cells (*GIST-T1-CA11*). An increased expression of CA-RP XI protein is observed in the cytoplasm of GIST-T1-CA11 as compared to GIST-T1. In contrast, a trace level signal for CA-RP X is seen in both GIST-T1 and GIST-T1-CA11. CA-RP VIII is expressed in the perinuclear area of GIST-T1, whereas in GIST-T1-CA11, it is seen in the whole cell body

Discussion

To date, GIST has been believed to arise from ICC because both cell types express the characteristic phenotypic markers KIT and CD34 [2]. In this study, the distribution of CA-RPs was shown to be completely different from those of ICCs. Furthermore, ICCs exhibited no detectable signal for expression of any of the three CA-RPs, whereas GIST

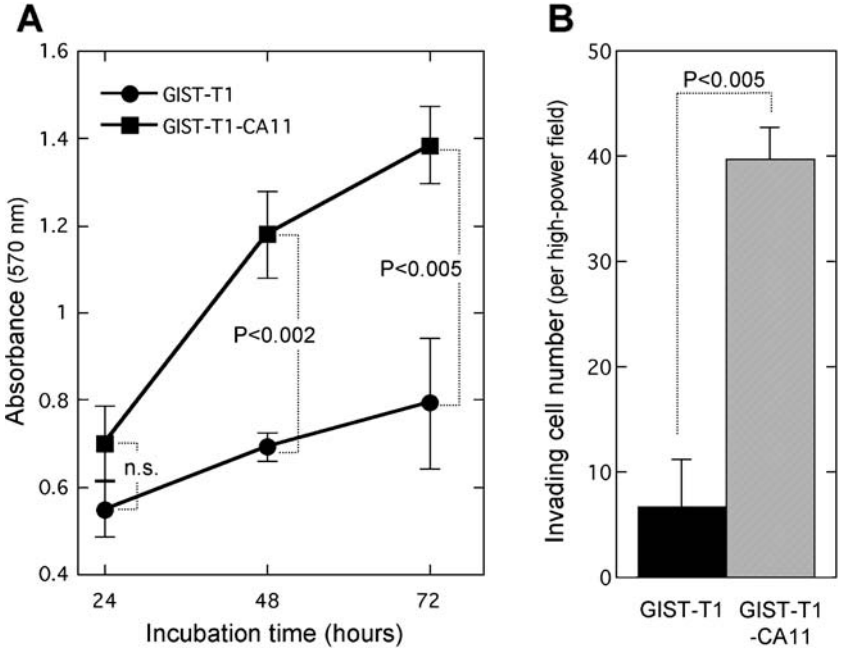


Fig. 5 Proliferation and invasion properties of wild-type and CA11-transfected GIST-T1 cells (GIST-T1-CA11). **a** Cell proliferation assay shows no significant difference in cell numbers between two cell types after 24-h culture. After culture for 48 and 72 h, proliferative cell numbers of GIST-T1-CA11 have increased significantly more than that of GIST-T1 ($P<0.002$ and $P<0.005$, respectively). **b** Cell invasion assay shows a significantly increased number of GIST-T1-CA11 (39.7±3.1/high-power field), which invades through a thin layer of basement membrane Matrigel, as compared to that of GIST-T1 (6.7±4.6/high-power field) ($P<0.005$)

cells significantly expressed CA-RPs VIII and XI in their cytoplasm. We previously reported that CA-RP VIII expression is remarkably up-regulated during carcinogenesis of lung and colorectal epithelial cells [1, 8] and also during fetal development of the pulmonary epithelium [1]. Although the exact biological function of CA-RPs has not yet been elucidated, these findings suggest that CA-RPs VIII and XI play a possible role for GIST development.

Most GISTs (91%, *n*=22) showed CA-RP XI overexpression. In contrast, CA-RP VIII expression was seen in 59% of GISTs, and there was no GIST showing a detectable signal for CA-RP X expression on immunohistochemical studies. These findings suggest that CA-RP XI has a more significant role in the progression of GIST than do the other two CA-RPs. Accordingly, we focused on the effect of CA-RP XI expression in vitro on biological properties of cultured GIST cells GIST-T1. We found that CA-RP XI-overexpressed GIST-T1 cells showed significantly increased capacities of cell proliferation and invasion as compared to wild-type GIST-T1 cells. We obtained similar findings in a previous study using the lung cancer cell line PC-9. CA-RP VIII-overexpressed PC-9 cells grew faster than wild-type PC-9 cells on laminin-coated dishes [7]. Furthermore, in the present study, expression of CA-RPs VIII and XI was much more intense in the marginal area of GISTs than in the central part of the tumor (Fig. 2). CA-RP VIII was also reported to be overexpressed at the invasion front of colorectal and lung cancer tissues [1, 8]. These findings indicate that not only CA-RP VIII but also CA-RP XI function to enhance the proliferation and invasion of certain tumor cells. CA-RP VIII and XI are evolutionally well-conserved isoforms [9]. The difference of CA-RP isotype expression between GIST and colorectal or lung cancer might be due to the different cell origins: that of the colorectal and lung cancers are derived from epithelial cells and that of the GIST arises from ICC, which belongs to the mesenchymal cell types [4].

The molecular mechanism by which CA-RP XI enhances proliferative and invasive properties of GIST cells is still uncertain. Although constitutive KIT activation was shown, GIST-T1 cells showed a low expression level of CA-RP XI. These findings indicate that enhancement of cell growth and invasion by CA-RP XI are not directly related to KIT. Interestingly, it was reported that malignant GIST cells had the gene amplification of chromosome 19q13 [6], on which the CA-RP XI gene has been reported to locate [4]. Although there was no direct evidence of an increased copy number of the CA-RP XI gene, gene amplification might be a possible explanation for the increased expression of CA-RP XI in GIST.

An additional finding obtained in the present study is the subcellular localization of CA-RPs in GIST-T1 cells. Consistent with immunohistochemical findings, CA-RPs VIII and XI were expressed in the cytoplasm of GIST-T1, but CA-RP X was undetectable in any part of the cell. Interestingly, whereas CA-RP VIII appears to be condensed in the perinuclear area in wild-type GIST-T1, CA-RP VIII was dramatically spread throughout the cytoplasm of GIST-T1-CA11 cells. Recently, CA-RP VIII was reported to bind inositol IP_3R1 and to inhibit IP_3 binding to IP_3R1 by reducing the affinity of the receptor for IP_3 [5]. IP_3R1 is known to be expressed on the membrane of the endoplasmic reticulum; thus, the perinuclear localization of CA-RP VIII suggests its colocalization with IP_3R1. This idea leads to further speculation; in GIST-T1-CA11 cells, ectopic CA-RP XI expression could substitute for CA-RP VIII to bind IP_3R1, resulting in the wide distribution of CA-RP VIII in the cytoplasm. To verify these hypotheses, an immunocoprecipitation study using a panel of antibodies reactive with three types of IP_3R and with three CA-RPs is currently underway.

In summary, although ICC showed no expression of any of the three CA-RPs, GIST cells demonstrated strong expression of CA-RPs VIII and XI. Overexpressed CA-RP XI possibly substitutes for CA-RP VIII in the cytoplasm and enhances the proliferation and invasion of GIST cells. Although the regulatory mechanism of CA-RP expression remains uncertain, these findings indicate that CA-RP VIII and XI play respective roles in the development of GIST.

Acknowledgements We thank Mr. Takuya Yamaguchi and Ms. Tomoko Minakuchi of the Kochi Medical School for their technical assistance. This work was supported in part by grants from the Japanese Ministry of Education, Science, Sports and Culture (1679 0382 and 15590656).

References

1. Akisawa Y, Nishimori I, Taniuchi K, Okamoto N, Takeuchi T, Sonobe H, Ohtsuki Y, Onishi S (2003) Expression of carbonic anhydrase-related protein CA-RP VIII in non-small cell lung cancer. Virchows Arch 442:66–70
2. Fletcher CD, Berman JJ, Corless C, Gorstein F, Lasota J, Longley BJ, Miettinen M, O'Leary TJ, Remotti H, Rubin BP, Shmookler B, Sobin LH, Weiss SW (2002) Diagnosis of gastrointestinal stromal tumors: a consensus approach. Hum Pathol 33:459–465
3. Fujikawa-Adachi K, Nishimori I, Taguchi T, Yuri K, Onishi S (1999) cDNA sequence, mRNA expression, and chromosomal localization of human carbonic anhydrase-related protein, CA RP XI. Biochim Biophys Acta 1431:518–524
4. Heinrich MC, Rubin BP, Longley BJ, Fletcher JA (2002) Biology and genetic aspects of gastrointestinal stromal tumors: KIT activation and cytogenetic alterations. Hum Pathol 33:484–495
5. Hirota J, Ando H, Hamada K, Mikoshiba K (2003) Carbonic anhydrase-related protein is a novel binding protein for inositol 1,4,5-trisphosphate receptor type 1. Biochem J 372:435–441
6. Knuutila S, Armengol G, Bjorkqvist AM, el-Rifai W, Larramendy ML, Monni O, Szymanska J (1998) Comparative genomic hybridization study on pooled DNAs from tumors of one clinical–pathological entity. Cancer Genet Cytogenet 100:25–30
7. Lu SH, Takeuchi T, Fujita J, Ishida T, Akisawa Y, Nishimori I, Kohsaki T, Onishi S, Sonobe H, Ohtsuki Y (2004) Effect of carbonic anhydrase-related protein VIII expression on lung adenocarcinoma cell growth. Lung Cancer 44:273–280
8. Miyaji E, Nishimori I, Taniuchi K, Takeuchi T, Ohtsuki Y, Onishi S (2003) Overexpression of carbonic anhydrase-related protein VIII in human colorectal cancer. J Pathol 201:37–45

9. Nishimori I (2004) Acatalytic CAs: carbonic anhydrase-related proteins. In: Supuran CT, Scozzafava A, Conway J (eds) Carbonic anhydrase: its inhibitors and activators. CRC, Boca Raton, pp 25–43
10. Nishimori I, Takeuchi T, Morimoto K, Taniuchi K, Okamoto N, Onishi S (2003) Expression of carbonic anhydrase-related protein VIII, X and XI in the enteric autonomic nervous system. Biomed Res 14:70–74
11. Okamoto N, Fujikawa-Adachi K, Nishimori I, Taniuchi K, Onishi S (2001) cDNA sequence of human carbonic anhydrase-related protein, CA-RP X: mRNA expressions of CA RP X and XI in human brain. Biochim Biophys Acta 1518:311–316
12. Sakurai S, Fukasawa T, Chong JM, Tanaka A, Fukayama M (1999) Embryonic form of smooth muscle myosin heavy chain (SMemb/MHC-B) in gastrointestinal stromal tumor and interstitial cells of Cajal. Am J Pathol 154:23–28
13. Sly WS, Hu PY (1995) Human carbonic anhydrases and carbonic anhydrase deficiencies. Annu Rev Biochem 64:375–401
14. Takeuchi T, Misaki A, Liang SB, Tachibana A, Hayashi N, Sonobe H, Ohtsuki Y (2000) Expression of T-cadherin (CDH13, H-Cadherin) in human brain and its characteristics as a negative growth regulator of epidermal growth factor in neuroblastoma cells. J Neurochem 74:1489–1497
15. Taguchi T, Sonobe H, Toyonaga S, Yamasaki I, Shuin T, Takano A, Araki K, Akimaru K, Yuri K (2002) Conventional and molecular cytogenetic characterization of a new human cell line, GIST-T1, established from gastrointestinal stromal tumor. Lab Invest 82:663–665
16. Taniuchi K, Nishimori I, Takeuchi T, Fujikawa-Adachi K, Ohtsuki Y, Onishi S (2002) Developmental expression of carbonic anhydrase-related proteins VIII, X, and XI in the human brain. Neuroscience 112:93–99
17. Taniuchi K, Nishimori I, Takeuchi T, Ohtsuki Y, Onishi S (2002) cDNA cloning and developmental expression of murine carbonic anhydrase-related proteins VIII, X, and XI. Brain Res Mol Brain Res 109:207–215

Virchows Arch (2005) 447: 74–80
DOI 10.1007/s00428-005-1224-4

ORIGINAL ARTICLE

Luigi Matturri · Giulia Ottaviani · Anna Maria Lavezzi

Early atherosclerotic lesions in infancy: role of parental cigarette smoking

Received: 18 October 2004 / Accepted: 6 February 2005 / Published online: 10 June 2005
© Springer-Verlag 2005

Abstract Cigarette smoking is associated with an increased incidence of atherosclerotic diseases. The aim of this study was to examine the progression of the preatherosclerotic lesions previously observed by us in coronary arteries of fetuses of smoker mothers and in infants with smoker parents. We examined the coronary arteries of 34 infants, aged 1–36 months, and the histological and biological [c-*fos*, proliferating cell nuclear antigen (PCNA), and apoptosis] features of the early atherosclerotic lesions. In 17 infants (50%), at least one parent smoked, generally more than five cigarettes a day. In 18 cases (53%), we observed variable thickening of the coronary walls from preatherosclerotic lesions to juvenile atherosclerotic plaques, related to parental smoking habit. This morphological progression of the lesions was accompanied by a sequence of biological changes in the smooth muscle cells of the tunica media. We suggest that the oxidants present in the gas phase of the parental cigarette smoke pass through the endothelium and induce at first the c-*fos* gene activation and subsequently the PCNA positivity, that is, a proliferative process.

Keywords Coronary arteries · Infancy · Early atherosclerotic lesions · Cigarette smoke

L. Matturri · G. Ottaviani · A. M. Lavezzi
Institute of Pathology, Lino Rossi Research Center for the Study and Prevention of Unexpected Perinatal Death (of term fetus—stillbirth- and neonatal) and Sudden Infant Death Syndrome (SIDS), University of Milan, Milan, Italy

L. Matturri (✉)
Institute of Pathology, University of Milan,
Via della Commenda, 19,
20122 Milan, Italy
e-mail: luigi.matturri@unimi.it
Tel.: +39-02-5419521
Fax: +39-02-54198538
URL: http://users.unimi.it/~pathol/pathol_e.html

Abbreviations SMCs: smooth muscle cells · PCNA: Proliferating Cell Nuclear Antigen · PBS: phosphate-buffered saline · TUNEL: TdT-mediated dUTP Nick End Labeling

Introduction

The atherogenic role of cigarette smoking is well-known. In particular, numerous epidemiological studies have shown that cigarette smoking is a major cause of cardiovascular diseases [3, 24, 32, 42, 44]. Tobacco smoking has been implicated both in the initiation and the progression of atherosclerotic vascular lesions [21, 41, 43, 44], but the precise mechanism by which cigarette smoke induces atherosclerosis is not yet fully established.

Recently, we demonstrated the presence of preatherosclerotic coronary artery lesions in human fetuses and infants of smoker mothers [28–30]. Our findings prompted us to continue the search to appraise whether there is progression of such lesions in infants with smoker parents. In this study, we examined on serial sections the coronary arteries of 34 subjects who died during the first years of life, including 21 cases of sudden infant death syndrome (SIDS). Our purpose was to correlate the possible presence of structural alterations of the vessel walls with one or both parents' smoking habit. In addition, following the protocol previously applied to fetal and infants' coronary arteries [28–30], we investigated the possible presence of some biological markers, namely, high expression of the proliferating cell nuclear antigen (PCNA), activation of the proto-oncogene c-*fos*, and apoptosis, which we previously described in the active atherosclerotic process [25, 26, 29, 30].

Materials and methods

We examined the coronary arteries of 34 infants, 20 males and 14 females, aged from 1 to 36 months. Twenty-one were victims of SIDS and 13 died of other causes (Table 1).

Table 1 Case profiles with morphological and biological results

Case no.	Age/sex (months)	Diagnosis of death	Parental smoking	Coronary lesions	Biological markers immunohistochemistry		
					c-*fos*	PCNA	Apoptosis
1	1/M	SIDS	m	A	+	−	−
2	1/M	SIDS	–	–	−	−	−
3	1/F	SIDS	p	–	−	−	−
4	1/M	Hypertrophic cardiomyopathy	m	B1	+	−	++
5	2/F	SIDS	m	A	++	−	−
6	2/F	SIDS	–	–	−	−	−
7	2/M	SIDS	m	B1	+	−	++
8	3/M	SIDS	–	–	−	−	−
9	3/M	SIDS	–	–	−	−	−
10	3/M	SIDS	m, p	B1	++	−	++
11	4/F	SIDS	m, p	B1	−	+	−
12	4/M	SIDS	p	B1	−	−	−
13	5/F	SIDS	–	–	−	−	−
14	6/M	SIDS	p	B2	−	+	−
15	6/F	Cardiac fibroma	–	–	−	−	−
16	7/M	SIDS	m, p	B2	−	+	−
17	8/F	SIDS	–	–	−	−	−
18	8/M	SIDS	–	–	−	−	−
19	9/M	Micronodular cirrhosis	m, p	B2	−	+	++
20	10/M	Congenital toxoplasmosis	–	B1	−	−	−
21	10/F	SIDS	–	B1	−	−	−
22	10/F	SIDS	–	–	−	−	−
23	10/M	SIDS	m, p	B2	−	+	−
24	11/M	SIDS	p	–	−	−	−
25	12/F	Acute glomerulonephritis	–	B2	−	−	−
26	12/M	Extrahepatic biliary atresia	m	B2	−	+++	−
27	12/M	SIDS	–	–	−	−	−
28	14/F	Conduction system alterations	–	–	−	−	−
29	15/M	Hypertrophic cardiomyopathy	–	–	−	−	−
30	18/F	Bronchopneumonia	m, p	B1	+	+++	−
31	21/M	Acute glomerulonephritis	–	–	−	−	−
32	25/F	Peritonitis	m	B2	−	+	−
33	34/M	Myeloid acute leukemia	–	–	−	−	−
34	36/F	Mucopolysaccharidosis	m, p	B2	−	+++	−

Immunohistochemistry evaluation: −=no positive cell, or presence of weakly immunostained cells, +=a number of positive cells 30% or less (low positivity), ++=a number of positive cells more than 30% and less than 60% (moderate positivity), +++=a number of positive neurons 60% or more (high positivity)

m Maternal smoking, *p* paternal smoking, *A* preatherosclerotic lesion, *B* juvenile plaque (*B1* initial plaque, *B2* advanced soft plaque), *SIDS* sudden infant death syndrome

Pregnancy in all cases had run a normal course. The mothers, aged between 24 and 34 years, were all healthy and under good socioeconomic conditions. All the subjects considered in this study were breast-fed.

Clinical data collected for each case included any parental cigarette smoking habit (mother's cigarette smoking before and/or during pregnancy, postnatal cigarette smoking of one or both parents, and in all cases, the number of cigarettes smoked daily). In 17 cases (50%), at least one parent smoked, generally more than five cigarettes a day, keeping or even increasing the smoke habit after the child's birth. In the smoker mothers, the smoking habit had started before pregnancy.

Coronary arteries examination According to the protocol followed by Roberts and Jones [37], the hearts were fixed in formalin for at least 1 day. The four major epicardial coronary arteries (left main, left anterior descending, left circumflex, right) were excised transversely to the longitudinal axis into segments approximately 2–4 mm long. Each segment was labeled sequentially either from its aortic ostium or from its origin from the left main coronary artery, dehydrated, embedded in paraffin block, and serially cut. The first serial sections of each block were stained with hematoxylin–eosin, trichromic Heidenhain (Azan) for histological examination, Alcian blue at pH 0.5 and 2.5 for acid mucopolysaccharides analysis, hyaluronidase–

Alcian blue for hyaluronic acids detection, and Weigert for elastic fibers identification. The following sections were submitted to specific immunohistochemical methods for lymphocyte, monocyte, and smooth muscle cell (SMC) typing and for PCNA, c-*fos*, and apoptosis detection.

Cellular typing

Immunophenotyping of the cells present in each lesion was performed using the immunoperoxidase technique with the following primary antibodies (Dako, Carpinteria, CA): anti-α-smooth muscle actin (1A4, Dako) to identify SMCs, anti-CD68 (EBM11, Dako) to identify monocytes, and anti-CD20 (L26, Dako) and anti-CD45RO (UCHL-1, Dako) to identify B- and T-lymphocytes, respectively.

Biological marker immunohistochemistry

Proliferating cell nuclear antigen Sections were air-dried overnight at room temperature and immunostained with the monoclonal antibody PC 10 at a dilution of 1:200, using an immunoperoxidase method (ABC complex) with light hematoxylin counterstaining. Only nuclei with intense immunostaining were considered to be PCNA positive.

c-fos Sections were deparaffinized in xylene and rehydrated. Endogenous peroxidase was blocked by incubating with 3% hydrogen peroxide for 5 min. After washing in phosphate-buffered saline (PBS), the sections were incubated with 10% normal goat serum and then with 1:100 diluted polyclonal anti-c-*fos* antibody (SC-52P, Santa Cruz Biotechnology, Santa Cruz, CA) at room temperature for 1 h. After washing in PBS for 5 min, the sections were incubated for 30 min with the biotinylated goat antirabbit IgG antibody supplied in the kit, then incubated with streptavidin–peroxidase for 30 min, stained with 3-3′-diaminobenzidine tetrahydrochloride (DAB, Sigma, St. Louis, MO) solution (30 mg of DAB and 0.5 ml of 0.3% hydrogen peroxide in 100 ml of 0.05 M Tris–HCl, pH 7.6), and counterstained with Mayer's hematoxylin. The cells with intense brown immunostaining were considered to be c-*fos* positive.

Apoptosis The sections were deparaffinized and incubated with 20 μg/ml proteinase K (Sigma St. Louis, MO 63178). After blocking the endogenous peroxidase with 3% H_2O_2, deoxynucleotidyl transferase (TdT 0.3 U/ml) was used to incorporate digoxigenin-conjugated deoxyuridine (dUTP 0.01 mM/ml) into the ends of DNA fragments. The TdT-mediated dUTP nick end labeling (TUNEL) signal was then detected by an antidigoxigenin antibody conjugated with peroxidase (Apoptag Peroxidase In Situ Apoptosis Detection kit, Oncor, Gaithersburg, MD). Apoptotic nuclei were identified by the presence of dark brown staining. Counterstaining was performed by immersing the slides in methyl green for 10 min.

All the sections obtained from the above immunohistochemical techniques were examined using a ×40 lens. For all the immunohistochemical methods, negative controls were prepared replacing the respective primary antibodies with PBS in the incubation. In these procedures, staining always failed to occur.

Immunohistochemistry evaluation

To evaluate the immunoreactivity for c-*fos*, PCNA, and apoptosis, we applied for each method a rating system based on the examination of all the immunostained sections. Only cells with very intense brown staining were considered to be positive. We have quantified the scoring for each case as − (no positive cell or presence of weakly immunostained cells), + (a number of positive cells 30% or less, low positivity), ++ (a number of positive cells more than 30% and less than 60% or less, moderate positivity), and +++ (a number of positive neurons 60% or more, high positivity).

The scores, referred to bilateral sides of every nucleus, were assigned by two independent and blinded observers, and comparison among the data was performed to evaluate the interobserver reproducibility. In case of discordance among the investigators, the case was reviewed and discussed until the same result was obtained.

Statistical analysis

The statistical value of the results was determined using the analysis of variance test (*F* test). The selected level of significance was $p<0.05$.

Definition of terms

Preatherosclerotic lesions

The earliest morphologically recognizable alterations are characterized by fragmentation of the tunica media with intense infiltration of SMCs, often arranged perpendicularly in columns or tangentially to the axis of the tunica itself. These SMCs infiltrate the intima, which tends to be thickened, also due to initial mucopolysaccharide deposits, mainly composed of type A and C chondroitin sulfates and of hyaluronic acid. Rare monocytes and B-lymphocytes are also present. The endothelium is morphologically intact. The internal elastic membrane appears to be focally fragmented [28, 29].

Juvenile soft atherosclerotic plaques

Such lesions are characterized by wide myointimal thickness with alteration of elastic fibers and of the tunica media. They are defined as "soft plaques" as they have abundant SMCs, associated with moderate infiltration of

monocytes and rare lymphocytes. Amorphous deposits of acid mucopolysaccharides, mainly composed of B chondroitin sulfates, are present, occasionally also in the internal portion of the tunica media. There is evident fragmentation of the elastic fiber system and of the tunica media. The endothelium is morphologically intact. Reduction of the lumen varies from approximately 10–15% to 30–40% [25, 29, 30].

Results

Table 1 shows the relationships between the results obtained from the morphological examination of the coronary arteries of the 34 victims, the parental smoking habit, and the biological markers.

At the histological study, a normal structure was found in 16 cases. In 18 cases (53%), there was a variable thickening of the walls: in 2 cases (cases 1 and 5), the lesions were preatherosclerotic (Fig. 1), mostly located in the anterior descending branch of the left coronary artery, whereas in 16 cases, juvenile soft atherosclerotic plaques of variable entity were observed in all the coronary branches, with a lumen decrease of up to 30–40% (Fig. 2).

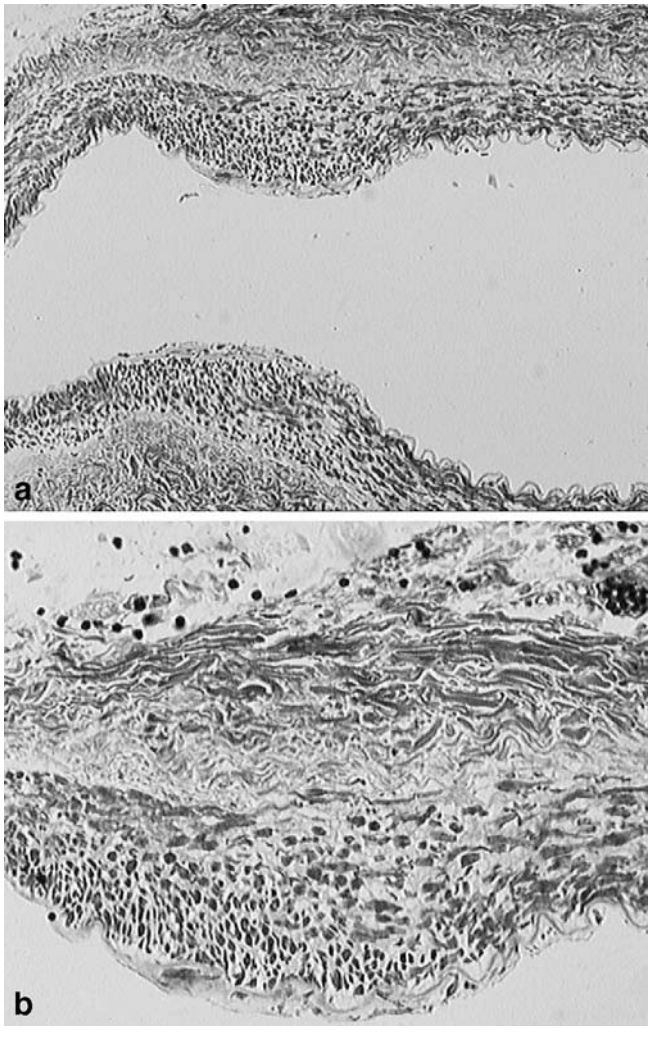


Fig. 1 Preatherosclerotic lesion in an epicardial coronary artery (left anterior descending branch) of an infant aged 2 months (case 5). The focal thickness consists of medial SMCs, perpendicularly oriented. Azan stain, **a** ×100; **b** ×200

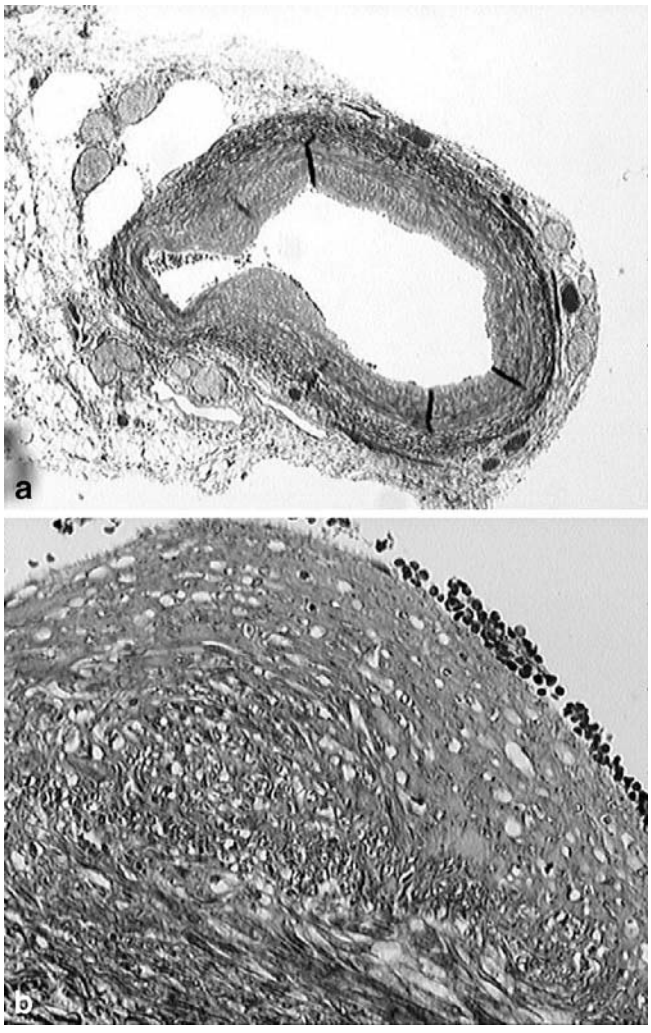


Fig. 2 Juvenile soft atherosclerotic plaque in an epicardial coronary artery (left anterior descending branch) of an infant aged 4 months (case 12). The myo-intimal thickness shows numerous SMCs and increased amounts of mucoid ground substance. Azan stain, **a** ×25; **b** ×200

We found a significant correlation ($p<0.05$) between such atherosclerotic lesions and the parental smoking habit, referred in 17 cases (50%). Only in three cases (20, 21, and 25) arterial lesions were observed in infants with nonsmoker parents, and only in two cases (3 and 24) with a smoker father did the coronary walls show a normal structure.

The preatherosclerotic lesions observed in two infants, aged 1 and 2 months, respectively, with a smoker mother, are characterized by initial alteration of the architecture of the tunica media, which appears focally fragmented and presents columns of SMCs perpendicularly located to the axis of the media itself (preatherosclerotic lesions). Together with rare monocytes and B-lymphocytes, these elements infiltrate the tunica intima, which tends to be

thickened, also due to the initial deposit of mucopolysaccharides. Focal alterations of the elastic fibers system, characterized by detachment and fragmentation of the fibers, were detected.

In infants older than 2 months with smoker parents, a progression of such coronary lesions is generally observed. The lesions are characterized by the formation of initial plaques that gradually increase mainly after the first 6 months, have abundant SMCs, and markedly reduce the coronary lumen, even up to 40% (juvenile soft atherosclerotic plaques).

Our findings demonstrate a correlation between the infants' age and the lesions' histological and biological aspects and progression. In fact, in the first 3 months of age, preatherosclerotic or juvenile plaques (B1) are found, mainly characterized by c-*fos* and apoptosis positivity. In infants 4 months or older, the SMCs are PCNA positive whereas are mostly c-*fos* and apoptosis negative. The percentage of PCNA-positive SMCs increases with age.

The most frequent result of the biological analysis was PCNA positivity observed in a relatively low number of SMCs in 9 of the 18 observed lesions (50%), having the prevalent appearance of juvenile soft plaques. The number of PCNA-positive SMCs was increased in cases 26, 30, and 34, corresponding to subjects aged 12, 18, and 36 months, respectively, whose plaques were advanced.

In six lesions (33%), a moderate number of c-*fos*-positive SMCs, and in four cases (22%), a moderate (++) apoptotic index were observed. Positivity for both the c-*fos* gene and apoptosis was a prevalent feature of infants aged a few months.

Discussion

In our previous works [28, 30], we have reported preatherosclerotic lesions in the coronary arteries of fetuses after the 35th gestational week, demonstrating a significant correlation with the mothers' smoking habit during pregnancy. We then described the early atherosclerotic lesions in infants, particularly if bottle-fed and with smoking parents [29, 30].

In the present study, we showed the progression of these lesions up to the development of juvenile soft atherosclerotic plaques in infants and pinpointed the fundamental atherogenic role of cigarette smoke. In fact, we detected a significant correlation between the atherosclerotic lesions in infant coronaries and the parental cigarette smoking habit. Other atherogenic factors were not identified. All the analyzed infants were the products of uncomplicated pregnancies of healthy mothers under good socioeconomic conditions, and all were breast-fed.

We noticed different morphological aspects of the coronary lesions in relationship to the infant's age and, therefore, to the duration of exposure to the noxious action of cigarette smoke.

The first early alterations of preatherosclerotic type were observed in the first 2 months of life. These lesions are characterized by alterations of the tunica media that become focally fragmented with intense infiltration of SMCs. Such fibrocells seem to lose their polarity and migrate toward the intima in columnar structures, progressively contributing, together with the initial deposition of acid mucopolysaccharides, to the formation of myointimal thickness.

As the lesions progress, myointimal thickening grows and successively soft atherosclerotic plaques appear.

This progression in the morphological appearance of the coronary lesions is accompanied by a sequence of biological changes. In fact, in the atherosclerotic lesions observed in the first months of life, the activation of the c-*fos* gene is evident. The proto-oncogene c-*fos* belongs to the family of "immediate early genes," so defined for their ability to become rapidly activated in the presence of noxious signals in a variety of vascular and nonvascular cells, because they do not require de novo protein synthesis [6, 14, 33].

In some of these primary lesions, immunopositivity of the SMCs for apoptosis was also observed. Many authors have provided morphological and biochemical evidence of apoptotic cell death in both experimental and human advanced atherosclerotic plaques [9, 10, 12, 16].

Cell death by apoptosis occurs during different stages of the evolution of the progression of the atherosclerotic process in a coordinate and highly regulated fashion that requires the expression of certain groups of genes critical for cellular signal transduction and metabolism. Besides, complex interactions between extracellular microenvironmental factors and intrinsic gene products occur before apoptosis begins [10]. In advanced atheroma, cell death may contribute to aneurysm formation and to weakening of the fibrous cap, enhances thrombogenicity of the lesion core, and increases the risk of plaque disruption.

Our observation of apoptotic cells in initial phases of atherosclerosis cannot have similar significance. This finding can be interpreted, as suggested by several authors [13, 19], as a beneficial physiological attempt to prevent the evolution of the atherogenic process and to preserve the wall structure under normal conditions.

Atherosclerotic progression is testified by the biological events in the coronary walls of infants aged more than 4 months. These consist prevalently of a moderate number of PCNA-positive SMCs that are increased in the more advanced lesions observed in older infants. This finding suggests that c-*fos* gene overexpression could promote a proliferative process. In fact, PCNA, principally expressed during the S phase of the cell cycle, is a specific marker of cellular replication [23, 26, 27].

Based on the biological data obtained in this study and on the observation in our previous works [26, 28] of intense overexpression of the proto-oncogene c-*fos* in preatherosclerotic lesions of coronary arteries of fetuses with smoker mothers, we can postulate that the first morphologically detectable signal of human atherosclerosis determined by cigarette smoke is c-*fos* gene alteration in the SMCs of the tunica media. Activation of the c-*fos* gene seems to promote a process of SMCs transformation with loss of

the differentiated state and acquisition of the ability of ameboid movement, then migration toward the intima.

Several authors [5, 7, 20, 40] have reported that in atherosclerosis, there are two types of SMCs, the contractile or quiescent type, characterized by the presence of typical SMCs contractile proteins, such as α-actin and SM myosin, and inability to undergo cytokinesis, and the synthetic or activated type, characterized by the loss of contractile function, a decrease of contractile proteins with a typical switch in actin expression from α- to β-form, an increase in rough endoplasmic reticulum, and increased synthetic and proliferative capacity. The dedifferentiated cells we observed to be involved in intimal thickening correspond to activated type SMCs and also to cells defined by Schürch et al. [39] as "myofibroblasts," having features in common with both SMCs and fibroblasts [8, 31].

Recently, experimental studies [11, 22, 36] have shown that in vascular SMCs, proto-oncogene expression, and in particular, c-*fos* levels, can be stimulated by exogenous and endogenous oxidants. Besides, Ikebuchi et al. [15] demonstrated that in cell cultures, exogenously added O_2 could also cause a rapid increase in intracellular pH and, subsequently, cytoplasmic alkalinization, considered to be an important early signal for the initiation of DNA synthesis.

More than 4,000 individual constituents that have been identified in cigarette smoke include polycyclic aromatic hydrocarbons such as benzopyrene, cadmium, nicotine, and also oxidants [1, 2, 4, 17]. Oxidative stress produced by cigarette smoke has been demonstrated by some authors in experimental studies to contribute to the pathogenesis of atherosclerosis, directly influencing the oxidation of plasmatic low-density lipoproteins (LDLs), which are taken up by macrophages to form foam cells [31, 35, 38, 45, 46].

We suggest, also based on interpretations by others' report on this issue [18, 22, 34, 36], that the oxidants present in the gas phase of cigarette smoke could determine the sequence of biological events in the arterial walls observed in this study. First, the oxidants pass through the endothelium, without causing morphologically identifiable alterations, and induce immediate and intense stimulation of the c-*fos* gene in the SMCs of the media. These cells, so activated, reacquire the primordial characteristic of ameboid movements and leave the media to move through the intima toward the lumen. Subsequently, again, due to the oxidative effect of the cigarette smoke, the c-*fos* gene exerts its mitogenic effect. This is confirmed by the presence of PCNA-positive SMCs in the coronary arteries of older infants.

Therefore, we can maintain that parental cigarette smoking is associated with an increased risk of coronary atherogenesis that begins very precociously in fetal life, as demonstrated in our previous work [28], and, persisting the parents' smoke habit, progresses through definite morphological and biological sequential stages toward true atherosclerotic plaques.

All the findings presented herein underline the severe atherogenic effect of cigarette smoke and the need to prevent cardiovascular diseases already during prenatal life.

Acknowledgements This study was supported by the Ministry of Foreign Affairs (joined project of particular relevance no. 269/P/0085087 "Anatomopathologic and genetic study of the unexplained perinatal death and SIDS").

The authors thank Mrs. Lorella Terni and Mrs. Graziella Alfonsi for their precious technical assistance.

References

1. Benowitz NL, Gourlay SG (1997) Cardiovascular toxicity of nicotine: implications for nicotine replacement therapy. J Am Coll Cardiol 29:1422–1431
2. Burns DM (1991) Cigarettes and cigarette smoking. Clin Chest Med 12:631–642
3. Burns DM (2003) Epidemiology of smoking-induced cardiovascular disease. Prog Cardiovasc Dis 46:11–29
4. Church DF, Pryor WA (1985) Free-radical chemistry of cigarette smoke and its toxicological implications. Environ Health Perspect 64:111–126
5. Cremona O, Muda M, Appel RD, Frutiger S, Hughes GJ, Hochstrasser DF, Geinoz A, Gabbiani G (1995) Differential protein expression in aortic smooth muscle cells cultured from newborn and aged rats. Exp Cell Res 217:280–287
6. Dony C, Gruss P (1987) Proto-oncogene c-*fos* expression in growth regions of fetal bone and mesodermal tissue. Nature 299:711–714
7. Gabbiani G, Kocher O, Bloom WS, Vandekerckhove J, Weber K (1984) Actin expression in smooth muscle cells of rat aortic intimal thickening, human atheromatous plaque and cultured rat aortic media. J Clin Invest 73:148–152
8. Gabbiani G (1998) Evolution and clinical implication of the myofibroblast concept. Cardiovasc Res 38:545–548
9. Geng YJ, Libby P (1995) Evidence for apoptosis in advanced human atheroma: colocalization with interleukin-1 beta-converting enzyme. Am J Pathol 147:251–265
10. Geng YJ, Libby P (2002) Progression of atheroma. A struggle between death and procreation. Arterioscler Thromb Vasc Biol 22:1370–1380
11. Greene EL, Velarde V, Jaffa AA (2000) Role of reactive oxygen species in bradykinin-induced mitogen-activated protein kinase and c-*fos* induction in vascular cells. Hypertension 35:942–947
12. Han DK, Haudenschild CC, Hong MK, Tinkle BT, Leon MB, Liau G (1995) Evidence for apoptosis in human atherogenesis and in a rat vascular injury model. Am J Pathol 147:267–277
13. Hasdai D, Sangiorgi G, Spagnoli LG, Simari RD, Holmes DR, Kwon HM, Carlson PJ, Schwartz RS, Lerman A (1999) Coronary artery apoptosis in experimental hypercholesterolemia. Atherosclerosis 142:317–323
14. Herrera DG, Robertson HA (1996) Activation of c-*fos* in the brain. Prog Neurobiol 50:83–107
15. Ikebuchi Y, Masumoto N, Tasaka K, Koike K, Kasahara K, Miyake A, Tanizawa O (1991) Superoxide anion increases intracellular pH, intracellular free calcium, and arachidonate release in human amnion cells. J Biol Chem 266:13233–13237
16. Isner JM, Kearney M, Bortman S, Passeri J (1995) Apoptosis in human atherosclerosis and restenosis. Circulation 91:2702–2711
17. Jaakkola MS, Jaakkola JJK (1997) Assessment of exposure to environmental tobacco smoke. Eur Respir J 10:2384–2397
18. Komai N, Morishita R, Yamada S, Oishi M, Iguchi S, Aoki M, Sasaki M, Sakurabayashi I, Higaki J, Ogihara T (2002) Mitogenic activity of oxidized lipoprotein (a) on human vascular smooth muscle cells. Hypertension 40:310–314
19. Kockx MM (1998) Apoptosis in the atherosclerotic plaque: quantitative and qualitative aspects. Arterioscler Thromb Vasc Biol 18:1519–1522
20. Kocher O, Gabbiani F, Gabbiani G, Reidy MA, Cokay MS, Peters H, Hottner I (1991) Phenotypic features of smooth muscle cells during the evolution of experimental carotid artery intimal thickening. Lab Invest 65:459–470

21. Krupski WC (1991) The peripheral vascular consequences of smoking. Ann Vasc Surg 5:291–304
22. Kunsch C, Medford RM (1999) Oxidative stress as a regulator of gene expression in the vasculature. Circ Res 85:753–766
23. Kurki P, Vanderlaan M, Dolbeare F, Gray J, Tan EM (1986) Expression of proliferating cell nuclear antigen (PCNA/cyclin) during the cell cycle. Exp Cell Res 166:209–219
24. Lakier JB (1992) Smoking and cardiovascular disease. Am J Med 93:88–128
25. Lavezzi AM, Milei J, Grana DR, Flenda F, Basellini A, Matturri L (2003) Expression of c-*fos*, p53 and PCNA in the unstable atherosclerotic plaque. Int J Cardiol 92:73–77
26. Lavezzi AM, Ottaviani G, Matturri L (2005) Biology of the smooth muscle cells in human atherosclerosis. APMIS 113: 112–121
27. Mathews MB, Bernstein RM, Franza BR, Garreis JL (1984) Identity of the proliferating cell nuclear antigen and cyclin. Nature 309:374–376
28. Matturri L, Lavezzi AM, Ottaviani G, Rossi L (2003) Intimal preatherosclerotic thickening of the coronary arteries in human fetuses of smoker mothers. J Thromb Haemost 1:2234–2238
29. Matturri L, Ottaviani G, Corti G, Lavezzi AM (2004) Pathogenesis of early atherosclerotic lesions in infants. Pathol Res Pract 200:403–410
30. Matturri L, Ottaviani G, Lavezzi AM, Rossi L (2004) Early atherosclerotic lesions of the cardiac conduction system arteries in infants. Cardiovasc Pathol 13:276–281
31. Mezzetti A, Lapenna D, Pierdomenico SD (1995) Vitamins E, C and lipid peroxidation in plasma and arterial tissue of smokers and non-smokers. Atherosclerosis 112:91–99
32. McGill HC (1988) The cardiovascular pathology of smoking. Am Heart J 115:250–257
33. Muchnok JP, Klishis ML, Roberts JR, Antonini JM, Whong WZ, Ong T (2001) Cadmium-induced cell transformation and tumorigenesis are associated with transcriptional activation of c-*fos*, c-*jun* and c-*myc* proto-oncogenes: role of cellular calcium and reactive oxygen species. Toxicol Sci 61:295–303
34. Nishio E, Watanabe Y (1998) Cigarette smoke extract is a modulator of mitogenic action in vascular smooth muscle cells. Life Sci 62:1339–1347
35. Pryor W, Stone K (1993) Oxidants in cigarette smoke. Radicals, hydrogen peroxide, peroxynitrate, and peroxynitrite. Ann NY Acad Sci 686:12–27
36. Rao GN, Berk BC (1992) Active oxygen species stimulate vascular smooth muscle cell growth and proto-oncogene expression. Circ Res 70:593–599
37. Roberts WC, Jones AA (1979) Quantitation of coronary arterial narrowing at necropsy in sudden coronary death: analysis of 31 patients and comparison with 25 control subjects. Am J Cardiol 44:39–45
38. Scheffler E, Wiest E, Woehrle J (1992) Smoking influences the atherogenic potential of low-density lipoprotein. Clin Invest 70:263–268
39. Schürch W, Seemayer TA, Path FR, Gabbiani G (1998) The myofibroblast: a quarter century after its discovery. Am J Surg Pathol 22:141–147
40. Schwartz SM, Campbell GR, Campbell JH (1986) Replication of smooth muscle cells in vascular disease. Circ Res 58:427–444
41. Strohschneider T, Oberhoff M, Hanke H, Hannekum A, Karsch KR (1994) Effect of chronic nicotine delivery on the proliferation rate of endothelial and smooth muscle cells in experimentally induced vascular wall plaques. Clin Invest 72:908–912
42. Thomas D (1993) Tobacco smoking and cardiovascular diseases. Rev Prat 143:1218–1222
43. Weintraub WS (1990) Cigarette smoking as a risk factor for coronary artery disease. Adv Exp Med Biol 273:27–37
44. Witteman JC, Grobbee DE, Valkenburg HA, van Hemert AM, Stijnen T, Hofman A (1993) Cigarette smoking and the development and progression of aortic atherosclerosis. A 9-year population-based follow-up study in women. Circulation 88:2156–2162
45. Yamaguchi Y, Matsuno S, Kagota S, Haginaka J, Kunitomo M (2001) Oxidants in cigarette smoke modify low-density lipoprotein in the plasma and facilitate atherogenesis in the aorta of Watanabe heritable hyperlipidemic rabbits. Atherosclerosis 156:109–117
46. Yokode M, Kita T, Arai H, Kawai C, Narumiya S, Fujiwara M (1988) Cholesteryl ester accumulation in macrophages incubated with low density lipoprotein pretreated with cigarette smoke extract. Proc Natl Acad Sci U S A 85:2344–2348

Virchows Arch (2005) 447: 81–86
DOI 10.1007/s00428-005-1220-8

ORIGINAL ARTICLE

Nestor M. Pakasa · Basile Pasquier · Marie-Laure Chambonnière · Alan L. Morrison · Abir Khaddage · Anne Gentil Perret · Jean Marc Dumollard · Fabrice G. Barral · Michel Péoc'h

Atypical presentations of solitary fibrous tumors of the central nervous system: an analysis of unusual clinicopathological and outcome patterns in three new cases with a review of the literature

Received: 20 October 2004 / Accepted: 28 January 2005 / Published online: 31 May 2005
© Springer-Verlag 2005

Abstract Central nervous system (CNS) solitary fibrous tumors (SFTs) are rare mesenchymal neoplasms recognized less than a decade ago. Approximately 60 cases of SFT have been reported in the central nervous system. We describe three atypical SFTs of the CNS, two intracranial and one within the spine. One intracranial SFT arose from the sella turcica and expanded into the suprasellar areas. It relapsed twice during the 3 years following partial resection, and the MiB1 labeling index steadily increased without obvious malignant transformation. The second SFT arose from the confluence of the sinuses, widely invaded the lateral sinus and adjacent bones, had a low MiB1 index and has not recurred after 5 years. The intraspinal tumor occurred at T5–T7 in a patient with multiple café-au-lait spots, was predominantly myxoid and developed a second similar lesion at S3–S5 14 years later. The MiB1 index was lower in the second tumor. Immunohistochemistry confirmed that all were SFTs. These atypical presentations gave us an opportunity to provide further information about the natural histological course of CNS SFTs.

Keywords Central nervous system tumors · Solitary fibrous tumor · Sella turcica · Spinal cord · Biological potential

N. M. Pakasa · M.-L. Chambonnière · A. Khaddage · A. G. Perret · J. M. Dumollard · M. Péoc'h
Department of Pathology,
Centre Hospitalier
Universitaire de Saint-Etienne,
Saint Etienne, France

B. Pasquier
Department of Pathology,
Centre Hospitalier Universitaire de Grenoble,
Grenoble, France

A. L. Morrison
Department of Pathology,
Naval Hospital Pensacola,
Pensacola, FL, USA

F. G. Barral
Department of Radiology,
Centre Hospitalier Universitaire de Saint-Etienne,
Saint Etienne, France

M. Péoc'h (✉)
Service d'Anatomie Pathologique,
Centre Hospitalier Universitaire,
Hopital Bellevue,
42055 Saint Etienne Cedex 02, France
e-mail: michel.peoch@chu-st-etienne.fr
Fax: +33-4-77120916

Introduction

The new World Health Organization classification of tumors of the nervous system [19] includes SFTs among the mesenchymal, non-meningothelial tumors [3, 10, 11, 31]. This category encompasses a wide variety of rare lesions with histological features resembling extracranial soft tissue tumors. SFTs of the meninges were first described by Carneiro and co-workers in 1996 [4]. The identification was based on distinctive immunohistochemical features common to soft tissue SFTs, including immunoreactivity for CD34, CD99, Bcl2 and vimentin but not for early membrane antigen (EMA) or S100 protein. This immunohistochemical profile differs from that encountered in fibrous meningiomas or hemangiopericytomas [4, 8, 32, 34]. Approximately 60 cases of SFT have been reported in the CNS. We present 3 additional cases of SFT, 2 intracranial and 1 within the spine, with emphasis on atypical features and outcomes, including a histological and MiB1 index analysis in sequential recurrences and in multicentric lesions.

Table 1 Immunohistochemical stains and results in sequential lesions. + positive, ++ very positive, − negative, *1A* patient 1 *1B* recurrence 1, *1C* recurrence 2, *2A* patient 2, *3A* patient 3, *3B* 2nd tumor

Antibody	1A	1B	1C	2A	3A	3B	Dilution	Source
CD34	+	++	++	++	++	++	1:100	Dako
CD99	+	++	++	++	++	++	1:100	Dako
Bcl-2	++	++	++	++	++	++	1:100	Dako
Vimentin	++	++	++	++	++	++	1:600	Dako
CD117	−	−	−	−	−	−	1:400	Dako
MiB-1[a]	20	63	110	3	56	21	1:50	Dako

[a]Corresponds to the number of immunostained cells over ten high-power fields

Materials and methods

All of the surgical specimens were fixed in 10% buffered formalin and embedded in paraffin. Histological sections were stained with hematoxylin–eosin with or without saffron counterstaining, periodic acid–Schiff and reticulin. Mitoses were counted by examining ten high-power fields (HPF), three times for each tumor, and determining an average number per ten HPF. Immunohistochemical studies were performed using the standard labeled streptavidin–biotin technique or Envision peroxidase method (Dako S.A., Trappes, France), as detailed in previous reports [13, 30]. Primary antibodies, dilutions and sources used in the current study are listed in Table 1.

Results

Clinical findings

Patient 1

A 66-year-old woman presented in 2000 with a history of several months of reduced visual acuity and visual field loss in the left eye. CT and magnetic resonance imaging (MRI) showed a lesion in the pituitary fossa radiologically consistent with a pituitary adenoma. Intraoperative observations revealed an intrasellar tumor with upward expansion. The mass was incompletely resected and recurred twice in the same location within 3 years (2002, 2003) with extension to the optic chiasm, carotid arteries and left cavernous sinus. The patient is alive with residual disease.

Patient 2

This 53-year-old male presented with a 6-month history of fronto-temporal headaches, visual disturbances and poor memory. CT revealed a homogenous right temporal supratentorial 6.5×3×6-cm growth radiologically consistent with a meningioma. MRI demonstrated that the mass arose from the cerebellar tentorium and extended into the supra- and infratentorial spaces. Intraoperatively, a well-circumscribed mass arose at the confluence of the sinuses and widely invaded the lateral sinus and adjacent bone. The lesion was completely resected. The patient is disease free 5 years post-surgery.

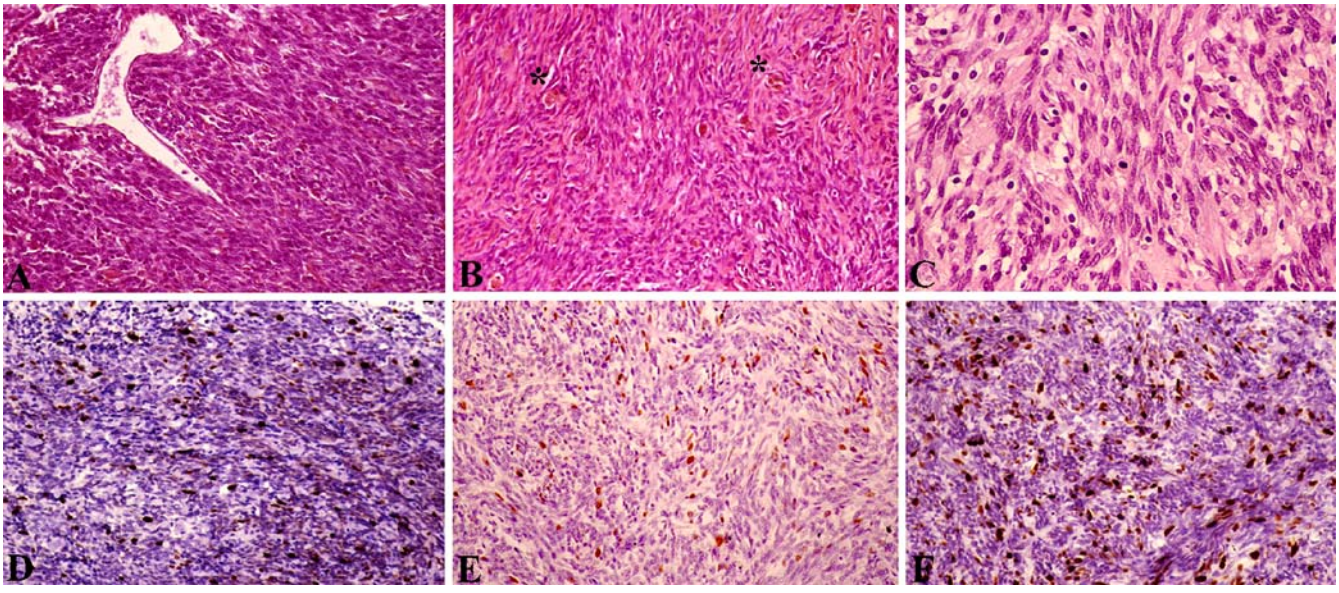


Fig. 1 Patient 1 primary solitary fibrous tumor of the sella turcica. **a** Bland spindle cells, a patternless growth pattern, collagen-rich network and a staghorn vascular pattern [hematoxylin and eosin (H&E) ×200]. **b** First recurrence. Bland spindle cells, patternless growth pattern, abundant collagen-rich matrix and hemosiderin-laden macrophages (*asterisk*) are conspicuous (H&E, ×200). **c** Second recurrence. Hyperchromatic spindle cells, patternless growth pattern and scattered mitoses (H&E, ×200). **d–f** Increasing MiB-1(*Ki-67*) labeling index in consecutive recurrences

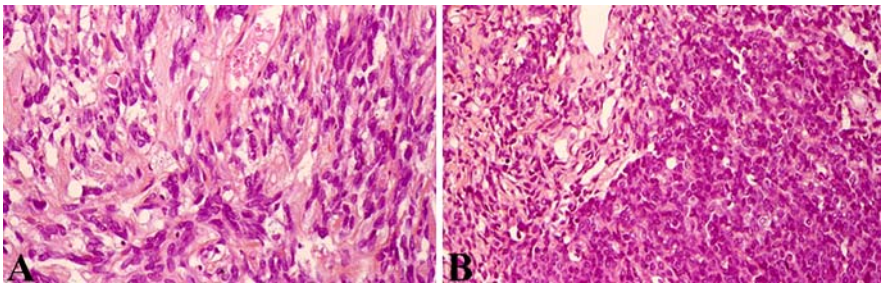


Fig. 2 Patient 2 primary solitary fibrous tumor of the posterior-fossa. **a** Spindle-shaped cells in a patternless growth pattern and collagen-rich matrix [hematoxylin and eosin (H&E), ×200]. **b** Cluster of spindle and oval cells, patternless pattern and collagen-rich matrix (H&E, ×200)

Patient 3

A 27-year-old male presented with recurrent back pain in 1987. He had multiple "café-au-lait" spots without a history of neurofibromatosis type 1 or other anomalies. MRI revealed an intradural extramedullary T5–T7 lesion measuring 2.5×2×2 cm consistent with a schwannoma. Intraoperatively, the tumor extended into the spinal cord and posterior nerve roots and was incompletely resected. The patient complained of nocturnal severe lower back pain 14 years later. MRI revealed an intradural extramedullary tumor of the distal dural sac. Intraoperatively, a tumor consistent with a schwannoma was located between S3 and S5 and the coccygeal nerve roots. The mass was surgically removed.

Histopathology

The primary sellar SFT (patient 1) was hypercellular with spindle-shaped cells arranged in a random pattern with thin bands of collagen between the cells (Fig. 1a) and rare myxoid areas. Increased collagen deposition between the spindle-shaped cells, hemosiderin-laden macrophages (Fig. 1b), resolving hemorrhage (Fig. 1b asterisk) and focal brain invasion were noted in first recurrence. The second recurrence (Fig. 1c) had spindled cells with increased mitotic activity, a collagen-rich background and a complete absence of myxoid changes. The increased proliferative activity in the sequential recurrences roughly correlated with the MiB-1 labeling index, ranging from less than 3% up to 6%, (Fig. 1d–f; Table 1).

The histological appearances of the tumor in the region of the confluence of the sinuses (patient 2) are illustrated in Fig. 2. The lesion was well circumscribed and encapsulated. There was a collagen-rich network between hypocellular and hypercellular areas of spindle- or oval-shaped cells that had bland nuclear features (Fig. 2a) and were typically arranged in a patternless growth pattern. Myxoid changes were noted in about 25% of the tumor. A prominent staghorn vascular pattern (Fig. 2a) and foci of round cells were also identified (Fig. 2b). The MiB1 index was below 0.5% (Table 1).

The spinal cord tumor (patient 3) was well circumscribed, encapsulated and multinodular (Fig. 3a). Loose myxoid areas (approximately 50–70%) (Fig. 3b) predominated over the solid hypo- and hypercellular zones (Fig. 3c). Spindled fibroblast-like cells showed bland features with occasional mitoses. They were arranged in a patternless growth pattern (Fig. 3a–c) with a prominent staghorn vascular pattern (Fig. 3a). The histological appearance of the recurrent tumor at S3–S5 was similar to the primary lesion at T5–T7 (not shown). The MiB1 labeling indices were 5% and 3%, respectively, in the primary and in the recurrent lesions.

None of these lesions exhibited cellular whorl arrangements or psammoma bodies suggestive of a meningioma. The tumors also did not have nuclear pleomorphism or tumor necrosis, which have been associated with aggressive behavior in SFTs.

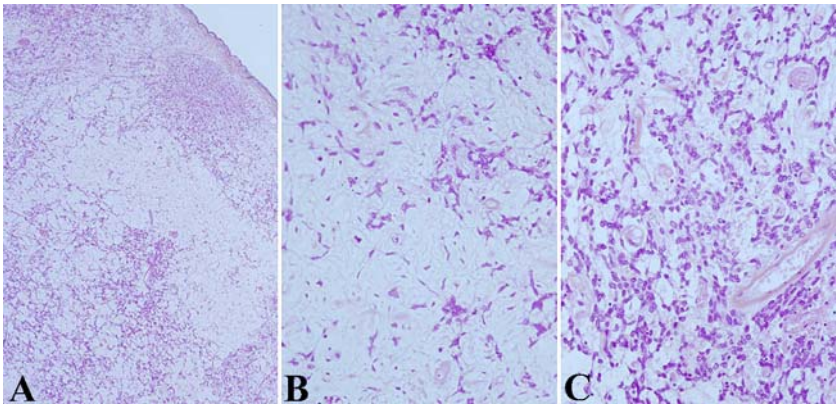


Fig. 3 Patient 3 primary solitary fibrous tumor (SFT) of the spinal cord. **a** Solid, myxoid and staghorn changes are seen as well as the fibrotic capsule at low magnification [hematoxylin and eosin (H&E), ×100]. **b** Detail of predominantly loose hypocellular myxoid changes (H&E, ×200). **c** Detail of hypercellular areas in predominantly myxoid SFT (H&E, ×200)

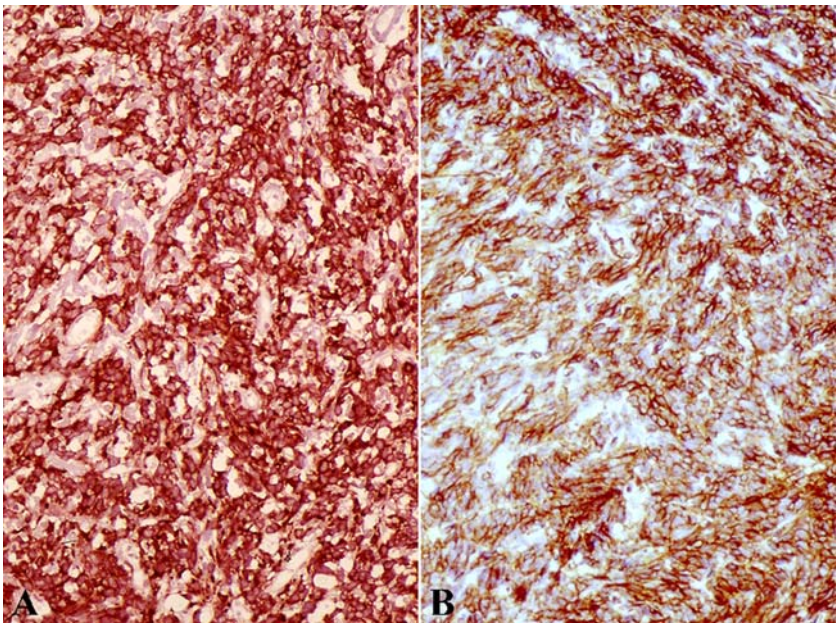


Fig. 4 Representative immunostaining for CD34 (×200) (**a**) and for Bcl-2 (×200) (b)

Immunohistochemistry

The immunophenotype of the spindle-shaped cells is shown in Table 1. The cells displayed strong diffuse cytoplasmic immunoreactivity for CD34 (Fig. 4a), CD99, Bcl-2 (Fig. 4b) and vimentin. Cytokeratins AE1/AE3, CD117 (c-kit), h-caldesmon, calretinin, estrogen receptors, cerb2, EMA, desmin, actin and the S-100 protein were negative. Progesterone receptors expressed diffuse weak staining.

Discussion

CNS SFTs are recently recognized distinctive dural-based neoplasms of the CNS [3, 10, 11, 31]. They are considered as counterparts of similar lesions initially identified in the pleura by Klemperer and Rabin in 1931 [20], which subsequently have been reported in numerous extrapleural sites and soft tissue [15, 26]. In the CNS, they are known to arise from the meningeal coverings [3, 4, 10, 11, 31] without meningothelial differentiation and are classified as mesenchymal nonmeningothelial tumors. Current studies suggest they are derived from vascular mesenchymal cells [8, 14]. Since their recognition in the CNS [4], approximately 60 cases have been recorded in the CNS literature. The actual incidence is unknown, in part because they were long overlooked in the differential diagnosis of solid CNS tumors and classified as fibrous meningiomas. Most SFTs occur in adulthood and show a slight male predominance [6]. A few cases have been described in children [18, 33]. While headaches predominate with intracranial lesions, visual disturbances, poor memory and occasional symptoms have also been reported [6, 23]. Back pain often occurs in intraspinal SFTs [1, 2, 17, 36].

Although MRI has proved the modality of choice for detecting, characterizing and staging most soft tissue tumors, a consensus MRI study regarding CNS SFTs is not yet available. In addition, this entity is still poorly recognized among the imaging community. As a consequence, most SFTs are still radiographically misdiagnosed and/or mistaken for meningiomas or schwannomas. With increased recognition of SFTs, radiological studies are reporting imaging features for solitary fibrous tumors [6, 18, 21, 22]. It appears that meningeal SFTs show a tendency to arise in the posterior fossa (26%) and spine (25%) [6].

SFTs are usually well-circumscribed encapsulated lesions resembling meningiomas, hemangiopericytomas or schwannomas. Histologically, SFTs exhibit spindled cells with scant eosinophilic cytoplasm growing in short fascicles, sheets, storiform patterns or irregular arrangements commonly referred to as a "patternless" pattern. Thin parallel bands of collagen are located between the spindled cells, and a hemangiopericytoma-like staghorn vascular pattern is often present [3, 10–12, 14]. Myxoid changes have been reported in SFTs, particularly in the spinal cord lesions, but pure myxoid variants are extremely rare [1, 2, 17, 36]. Hyperchromatism, nuclear pleomorphism, mitotic figures and tumor necrosis have been infrequently documented in the so-called malignant variants [4, 7, 14]. The unifying characteristic of all SFTs remains the strong reactivity of the spindle cells for CD34, CD99, Bcl-2 and vimentin plus their negative staining for S100 protein, EMA and muscle markers [4, 8, 34, 35]. In this study, staining for CD117 was negative. Ultrastructural studies have shown features consistent with fibroblasts or mesenchymal cells [4, 8].

The treatment of choice is surgical resection. Local recurrences have been reported with incomplete surgical excision [3, 4]. Some cases with malignant potential have also been reported, as well as metastases [7, 18, 28, 37]. Predictors of long-term outcome have not been well defined. The cytogenetics of SFTs is not well developed [9, 12, 14, 24]. A translocation involving chromosome 4q13 has been reported in two cases involving the pleura and peritoneum

[9]. A study on meningeal solitary fibrous tumors reported a loss of chromosome 3, deletions in the region of 3p21, losses in 4p15, 8q22, 10, 11q24, 17q11 and 21 and gains of 18p11, 1p11 and 20q11 [24].

This study includes a case of a spinal cord SFT and pigmented skin abnormalities (patient 3) not previously reported in the literature. Our patient had no history of neurofibromatosis. The primary SFT was resected, and 14 years later the patient developed a new lesion distant from the primary site with identical histological and immunohistochemical features. The decreased MiB1 labeling index in the second tumor is suggestive of a new lesion rather than metastasis from the original resection and may represent a genuine multifocal process. Multicentric CNS SFTs have not been previously reported in the literature. There is a single case report of a double primary localized fibrous tumor of the pleura and the peritoneum [16] and a case report of a multifocal primary intracerebral malignant fibrous-histiocytoma [25]. The importance and the nature of these findings, whether coincidental or part of a new syndrome, await further elucidation.

Only one other SFT has been reported involving the pituitary fossa [5]. In a parallel study of the radiological anatomy of the sella turcica and the histopathology of the pituitary gland in 205 autopsy specimens, Muir and co-workers found three cases of solitary tumors not otherwise specified in the anterior lobe, in the pre-immunohistochemistry era [27]. Our patient's lesion (patient 1) was incompletely excised and experienced several recurrences. Ogawa and co-workers [29] reported a case of a meningeal SFT, which locally relapsed four times and finally metastasized to the lung and invaded in the cerebellum over a period of 26 years. Similar to their experience, our patient expressed a steady increase of cellularity and of the MiB1 labeling index with each occurrence, suggesting a worse prognosis and a potential malignant transformation risk. Cerebral microinvasion was noted in the second occurrence, but this finding has not generally been regarded as a sign of malignant transformation but as an expression of increased local aggressiveness [7]. It is well known that repeated local reoccurrences may result in distant metastases over time [28, 29, 37], stressing the need for careful follow-up.

Our last patient (patient 2) had a well-circumscribed encapsulated intracranial SFT located in the posterior fossa. The lesion widely invaded adjacent structures and the lateral sinuses but had a very low MiB1 index. Since the posterior fossa has been identified as the most common site for intracranial SFTs [6], the imaging and pathological differential diagnosis of lesions in this area should include SFTs. This tumor showed focal round-shaped cells without noticeable features of malignity (Fig. 2b), which were strongly Bcl-2 and vimentin positive but negative for CD34 and CD99. Round-shaped tumor cells have been also recorded by others in cerebral SFTs [8], but this immunophenotype has not drawn much attention and will require further investigation. In summary, our study further shows the unpredictable nature and variability of the natural course of CNS SFTs.

Acknowledgements The authors would like to thank the technical staff of the Department of Pathology Bellevue Hospital for their invaluable assistance.

References

1. Alston SR, Francel PC, Jane JA Jr (1997) Solitary fibrous tumor of the spinal cord. Am J Surg Pathol 21:477–483
2. Bohinski RJ, Mendel E, Aldape KD, Rhines LD (2004) Intramedullary and extramedullary solitary fibrous tumor of the cervical spine. Case report and review of the literature. J Neurosurg 100:358–363
3. Burger PC, Scheithuaer BW, Vogel FS (2002) Solitary fibrous tumor. In: Surgical pathology of the nervous system and its coverings, 4th edn. pp 71–73
4. Carneiro SS, Scheithauer BW, Nascimento AG, Hirose T, Davis DH (1966) Solitary fibrous tumor of the meninges: a lesion distinct from fibrous meningioma. A clinicopathologic and immunohistochemical study. Am J Clin Pathol 106:217–224
5. Cassarino DS, Auerbach A, Rushing EJ (2003) Widely invasive solitary fibrous tumor of the sphenoid sinus, cavernous sinus and pituitary fossa. Ann Diagn Pathol 7:169–173
6. Caroli E, Salvati M, Orlando ER, Lenzi J, Santoro A, Giangaspero F (2004) Solitary fibrous tumors of the meninges. Report of four cases and literature review. Neurosurg Rev 27: 246–251, Epub May 08
7. Castilla EA, Prayson RA, Stevens GH, Barnett GH (2002) Brain-invasive solitary fibrous tumor of the meninges: report of a case. Int J Surg Pathol 10:217–221
8. Cummings TJ, Burchette JL, McLendon RE (2001) CD34 and dural fibroblasts: the relationship to solitary fibrous tumor and meningioma. Acta Neuropathologica 102:349–354
9. Debiec-Rychter M, de Wever I, Hagemeijer A, Sciot R (2001) Is 4q13 a recurring breakpoint in solitary fibrous tumors? Cancer Genet Cytogenet 131:69–73
10. Ellison D, Lowe S, Chimelli L (2004) Mesenchymal non-meningothelial neoplasms. In: Neuropathology, 2nd edn. Mosby pp 730–731
11. Fletcher CDM (2000) Mesenchymal, non-meningothelial tumors. In: Diagnostic histopathology of tumors, Vol 2, 2nd edn. Churchill Livingstone, Philadelphia, pp 1661–1663
12. Fletcher C.D.M, Dal Cin P, de Wever I, Mandahl N, Mertens F, Mitelman F, Rosai J, Rydholm A, Sciot R, Tallini G, van den Berg H, Vanni R, Willén H (1999) Correlation between clinicopathological features and karyotype in spindle cell sarcomas. A report of 130 cases from the CHAMP study group. Am J Pathol 154:1841–1847
13. Gentil Perret A, Mosnier JF, Duthel R, Brunon J, Barral F, Boucheron S (1999) Tumeur fibreuse solitaire des méninges. Ann Pathol 19:532–535
14. Graadt van Roggen JF, Hogendoorn PC (2004) Solitary fibrous tumour: the emerging clinicopathologic spectrum of an entity and its differential diagnosis. Curr Diagn Pathol 10:229–235
15. Hasegawa T, Matsuno Y, Shimoda T, Hasagewa F, Sano T, Hirohashi S (1999) Extrathoracic solitary fibrous tumors: their histological variability and potentially aggressive behavior. Hum Pathol 30:1464–1473
16. Ibrahim NBN, Briggs JC, Corrin B (1992) Double primary localized fibrous tumours of the pleura and retroperitoneum. Histopathology 22:282–284
17. Kim DS, Kim TS, Choi JU (1996) Intradural extramedullary xanthoma of the spine: a rare lesion arising from the dura mater of the spine: case report. Neurosurgery 39:182–185
18. Kim KA, Gonzalez I, McComb JG, et al (2004) Unusual presentations of cerebral solitary fibrous tumors: report of four cases. Neurosurgery 54:1004–1009
19. Kleihues P, Cavanee KW (2000) Pathology and genetics of the tumours of the nervous system (WHO). International Agency for Research in Cancer, Lyon

20. Klemperer P, Rabin CB (1931) Primary neoplasms of the pleura. Arch Pathol 11:385–412
21. Kocak A, Cayli SR, Sarac K, Aydin NE (2004) Intraventricular solitary fibrous tumor: an unusual tumor with radiological, ultrastructural, and immunohistochemical evaluation: case report. Neurosurgery 54:213–216
22. Lo CP, Chen CY, Lin CK, Chin SC, Juan CJ, Hsueh CJ (2004) Parasellar solitary fibrous tumor of meninges: magnetic resonance imaging features with pathologic correlation. J Neuroimaging 14:281–284
23. Martin AJ, Fisher C, Igbaseimokumo U, Jarosz JM, Dean AF (2001) Solitary fibrous tumours of the meninges: case series and literature review. J Neurooncol 54:57–69
24. Martin AJ, Summersgill BM, Fisher C, Shipley JM, Dean AF (2002) Chromosomal imbalances in meningeal solitary fibrous tumors. Cancer Genet Cytogenet 135:160–164
25. Mitsuhashi T, Watanabe M, Ohara Y, et al (2004) Multifocal primary intracerebral malignant fibrous histiocytoma—case report. Neurol Med Chir 44:249–254
26. Morimitsu Y, Nakajima M, Hisaoka M, Hashimoto H (2000) Extrapleural solitary fibrous tumor: clinicopathologic study of 17 cases and molecular analysis of the p53 pathway. APMIS 108:617–625
27. Muhr C, Bergstrom K, Grimelius L, Larsson SG (1981) A parallel study of roentgen anatomy of the sella turcica and the histopathology of the pituitary gland in 205 autopsy specimens. Neuroradiology 21: 55–65
28. Ng HK, Choi PC, Wong CW, To KF, Poon WS (2000) Metastatic solitary fibrous tumor of the meninges. J Neurosurg 93: 490–493
29. Ogawa K, Tada T, Takahashi S, Sugiyama N, Inaguma S, Takahashi SS, Shirai T (2004) Malignant solitary fibrous tumor of the meninges. Virchows Arch 444:459–464
30. Pasquier B, Péoc'h M, Morrison A.L, Gay E, Pasquier D, Sindou M, Kopp N (2002) Chordoid glioma of the third ventricle. A report of two new cases, with further evidence supporting an ependymal differentiation, and a review of the literature. Am J Surg Pathol 26:1330–1342
31. Paulus W, Scheithauer BW (2000) Mesenchymal, non-meningothelial tumours. In: Kleihues P, Cavanee KW (eds) Pathology and genetics of the tumours of the nervous system (WHO). International Agency for Research in Cancer. IARC, Lyon, pp 185–189
32. Perry A, Scheithauer BW, Nascimento AG (1997) The immunophenotypic spectrum of meningeal hemangiopericytoma: a comparison with fibrous meningioma and solitary fibrous tumor of meninges. Am J Surg Pathol 21:1354–1360
33. Ramdial PK, Madaree A (2001) Aggressive CD34-positive fibrous scalp lesion of childhood: extrapulmonary solitary fibrous tumor. Pediatr Dev Pathol 4:267–275
34. Suzuki SO, Fukui M, Nishio S, Iwaki T (2000) Clinicopathological features of solitary fibrous tumor of the meninges: an immunohistochemical reappraisal of cases previously diagnosed to be fibrous meningioma or hemangiopericytoma. Pathol Int 50:808–817
35. Tihan T, Viglione M, Rosenblum MK, Olivi A, Burger PC (2003) Solitary fibrous tumors in the central nervous system. A clinicopathologic review of 18 cases and comparison to meningeal hemangiopericytomas. Arch Pathol Lab Med 127:432–439
36. Vorster SJ, Prayson RA, Lee JH (2000) Solitary fibrous tumor of the thoracic spine. Case report and review of the literature. J Neurosurg 92:217–220
37. Winfree CJ, Mack WJ, Sisti MB (2004) Solitary cerebellar metastasis of malignant pleural mesothelioma: case report. Surg Neurol 61:174–220

Virchows Arch (2005) 447: 87–93
DOI 10.1007/s00428-005-1245-z

ORIGINAL ARTICLE

Anja Dankof · Maximilian Schmeding · Lars Morawietz · Raphaela Günther · Manfred G. Krukemeyer · Birgit Rudolph · Martin Koch · Veit Krenn · Ulf Neumann

Portal capillary C4d deposits and increased infiltration by macrophages indicate humorally mediated mechanisms in acute cellular liver allograft rejection

Received: 22 November 2004 / Accepted: 1 March 2005 / Published online: 10 June 2005
© Springer-Verlag 2005

Abstract Almost no data exist concerning the role of antibody-mediated mechanisms in human acute cellular liver allograft rejection (ACR). Therefore, the aim of this study was to determine whether ACR is associated with depositions of complement split products and increased infiltration by B-lymphocytes, plasma cells and macrophages. A total of 35 liver biopsy specimens (ACR n=22, controls n=13) were analyzed by immunohistochemical single and double staining. The average numbers of $CD20^+$, $CD38^+$ and $CD68^+$ cells per portal tract were established while the presence of C4d and C3d deposits was evaluated semiquantitatively. Significantly greater numbers of $CD20^+$ (P=0.029) and $CD38^+$ (P=0.014) cells were found in the ACR specimens than in the control specimens. Additionally, 50% of patients diagnosed with ACR showed C4d deposits along portal capillaries, which was associated with a significantly increased portal infiltration by macrophages (P=0.007). Taken together these results support the involvement of humorally mediated mechanisms in some cases of ACR.

Keywords Liver transplant rejection · Acute cellular rejection · C4d · Macrophages

A. Dankof · L. Morawietz · R. Günther · M. G. Krukemeyer · B. Rudolph · M. Koch · V. Krenn (✉)
Institute of Pathology,
University Hospital Charité,
Humboldt-University,
Schumannstrasse 20/21,
10117 Berlin, Germany
e-mail: veit.krenn@charite.de
Tel.: +49-30-450536134
Fax: +49-30-450536907

M. Schmeding · U. Neumann
Department of Surgery,
University Hospital Rudolf Virchow,
Humboldt-University,
Augustenburger Platz 1,
13353 Berlin, Germany

Introduction

Evidence for the existence of humorally mediated acute rejection (AHR) of human kidney and heart allografts has increased over the last few years, mainly due to improved immunohistochemical detection of C4d, an enzymatic cleavage product of the complement component C4 [4, 5, 12]. Proteolytic cleavage of C4 results from the classical pathway of activation of complement by immunocomplexes. Its final split product C4d exposes a thioester group which leads to the formation of a covalent bond to the closest protein or carbohydrate near the site of C4 activation and therefore allows immunohistochemical detection. Today AHR is accepted as a separate entity associated with kidney and heart allograft rejection. In line with this, humorally mediated mechanisms are suspected to be responsible for several pathological alterations in organ transplants other than heart and kidney.

So far only a few investigations have been carried out concerning the role of a humoral element of immunity in acute cellular liver allograft rejection (ACR) [19, 20]. In a recent study, we were able to show a significantly increased immigration of B-lymphocytes and plasma cells as well as depositions of C4d along portal capillaries in patients with ACR with a high rejection activity index, which indicates an association of acute liver allograft rejection with humoral immunity [8]. Additionally, IgVh analysis in a patient with ACR has demonstrated that B-cells in the transplanted liver tissue express a restricted V-gene repertoire and have a selected pattern of somatic mutations [15].

Although most investigators have focused on C4d as a marker for AHR of renal allografts, additional markers seem to provide supplementary information [2]. Deposits of C3d, a degradation product of C3, derived from both the classical and the alternative pathway of activation of the complement cascade, have been found to be associated with a worse clinical outcome in patients with renal AHR [9]. The occurrence of macrophages marks more severe renal allograft rejection and differentiates clinical from

subclinical rejection [3, 6]. A correlation between immigration of macrophages into the glomeruli and deposition of C4d on peritubular capillaries has been demonstrated [10].

Therefore our aim was to clarify whether these markers, as well as being useful in diagnosis of renal AHR, also provide additional information in acute rejection of liver allografts.

Materials and methods

Patients and tissues

A total of 35 liver biopsy specimens (n=35) taken between 1993 and 2003 from patients who had undergone liver transplantation due to various indications were selected for this study (Tables 1 and 2). Biopsies were taken 5 days to 3 years after transplantation. Of the 35 biopsies, 22 (9 from female patients, 13 from male patients; age 18–62 years) showed histologically proven ACR, and 13 (7 from female patients, 6 from male patients; age 20–65 years) were without clinical and histopathological signs of ACR and served as a comparison group.

Histopathological evaluation of acute rejection was done according to the Banff schema for grading liver allograft rejection [1]. Nine patients were diagnosed with mild, 12 with moderate and 1 with severe acute rejection. Patients with HCV reinfection were ruled out by selecting only those with a distinct histopathological diagnosis of acute rejection and without any histopathological signs of HCV reinfection.

Immunohistochemistry

Immunohistochemical single staining (CD20, CD38, C4d, C3d, CD68)

Paraffin-embedded sections were deparaffinized, demasked (pressure cooker, citrate buffer, pH 6) and stained with commercially available mouse monoclonal antibodies specific for CD20, CD38 and CD68. For C4d and C3d staining rabbit polyclonal antibody was used.

Primary antibodies were diluted as follows: CD20 (DAKO, Glostrup, Denmark) 1:100; CD38 (Novocastra, Newcastle upon Tyne, UK) 1:100; CD68 (DAKO) 1:50; C4d (Biomedica Austria, Vienna, Austria) 1:10; and C3d (DAKO) 1:800.

In chronically inflamed tissue and in blood, CD38 is expressed on B-lymphocytes (memory cells, germinal center cells) and on plasma cells. As CD138, another plasma cell marker, is also expressed by bile ducts, it was not used in this study. While anti-CD20 antibodies specifically stain B-lymphocytes, anti-CD68 antibodies identify monocytes and macrophages.

C4d and C3d, enzymatic cleavage products of the complement components C4 and C3, both expose a thioester group which enables them to bind covalently to the clos-

Table 1 Clinical and immunohistochemical data of 22 patients with ACR

ACR group	Sex	Age (years)	Etiology of liver disease[a]	Time between transplantation and biopsy (days)	Rejection severity grade	C4d
1	M	54	C2	5	Moderate	+
2	M	44	C2	6	Mild	−
3	F	44	HCV	11	Mild	+
4	F	62	HCC	6	Mild	+
5	F	41	PBC	24	Moderate	−
6	M	41	C2	7	Moderate	+
7	F	28	AIH	9	Moderate	+
8	F	51	HCV	11	Moderate	+
9	M	18	Acute liver failure/HAV	7	Moderate	+
10	M	48	HCV, C2	96	Moderate	+
11	F	59	Polycystic degeneration	24	Mild	+
12	F	50	PBC	126	Moderate	+
13	F	50	C2	120	Severe	−
14	M	27	HBV, retransplantation	7	Moderate	−
15	M	55	HCV	6	Moderate	−
16	M	57	C2	15	Mild	−
17	M	45	HCV	11	Mild	−
18	M	48	HCV	240	Mild	−
19	M	58	HCV	60	Mild	+
20	F	49	Cryptogenic cirrhosis	9	Mild	−
21	M	30	PSC	9	Moderate	−
22	M	49	HCV	5	Moderate	−

[a]*C2* alcohol-induced cirrhosis, *HAV* hepatitis A virus infection, *HBV* hepatitis B virus-induced cirrhosis, *HCV* hepatitis B virus-induced cirrhosis, *HCC* hepatocellular carcinoma, *PBC* primary biliary cirrhosis, *PSC* primary sclerosing cholangitis, *AIH* autoimmune hepatitis

Table 2 Clinical and immunohistochemical data of 13 patients without ACR

Comparison group	Sex	Age (years)	Etiology of liver disease[a]	Time between transplantation and biopsy (years)	Degree of inflammation	C4d
1	M	55	HBV	1	Mild	−
2	F	53	C2	1	Mild	−
3	M	60	Cryptogenic cirrhosis	3	No inflammation	−
4	F	65	Cryptogenic cirrhosis	3	Mild	−
5	F	37	Hereditary hemorrhagic telangiectasia	1	No inflammation	−
6	M	20	AIH	1	Mild	−
7	M	42	HBV, HDV, retransplantation	1	No inflammation	−
8	F	58	Hemangioendothelioma	1	Mild	−
9	M	58	Cryptogenic cirrhosis	1	Mild	−
10	F	56	CCC	1	Mild	−
11	F	60	C2, HCC	1	Mild	−
12	F	41	C2	3	Mild	−
13	M	62	C2	1	Mild	−

[a] *C2* alcohol-induced cirrhosis, *HBV* hepatitis B virus-induced cirrhosis, *HDV* hepatitis D virus-infection, *HCC* hepatocellular carcinoma, *CCC* cholangiocellular carcinoma, *AIH* autoimmune hepatitis

est protein or carbohydrate. Thus they are considered to be residues of a humorally mediated immunoresponse.

Staining was done using the labeled streptavidin-biotin method (LSAB Kit+, DAKO). Peroxidase-linked streptavidin binds to biotin, which again is linked to the secondary antibody. DAB (3,3-diaminobenzidine; DAKO) was used as a chromogen for the reaction with peroxidase. Endogenous peroxidase was blocked using H_2O_2. In a final step nuclear counterstaining with hematoxylin was performed according to the method of Mayer. Tonsil tissue treated as described above was used as a positive control; negative controls were obtained by omitting the primary antibody.

Immunohistochemical double staining (C4d/CD68)

For immunohistochemical double staining of C4d and CD68 the ENVISION Doublestain system (DAKO) was used according to the manufacturer's instructions. After epitope demasking (pressure cooker, citrate buffer, pH 6), anti-C4d antibody (polyclonal; Biomedica) and anti-CD68 antibody (DAKO) were successively added. DAB (CD68) and Fast Red (C4d) were used as chromogens. Tonsil tissue served as a positive control; negative controls were obtained by omitting the primary antibody. Double staining was performed on 11 biopsy specimens showing C4d positivity in immunohistochemical single staining.

Immunofluorescence (C4d/CD68)

As immunofluorescence serves as a gold standard in the diagnosis of renal allograft rejection, this technique was used to validate the results derived from immunohistochemical staining. Thus C4d/CD68 double stainings were performed on three biopsy specimens showing C4d positivity in immunohistochemical single staining. After deparaffinizing the sections (1–3 μm), demasking the epitopes (citrate buffer, pH 6) and blocking nonspecific binding sites, primary antibodies were diluted (CD68 1:50; C4d 1:10) and simultaneously added. Avoiding light exposure, slides were incubated simultaneously with secondary antibodies, Cy2-conjugated donkey anti-rabbit (1:100; Dianova, Hamburg, Germany) and Cy3-conjugated donkey anti-mouse antibody (1:200; Dianova). Finally, nuclear counterstaining was performed. While Cy2 fluoresces green (C4d), Cy3 emits a red signal (CD68).

Histopathological evaluation and statistical analysis

Immunostainings were evaluated by two pathologists (V.K., A.D.). The intensity of C4d and C3d staining was graded semiquantitatively, distinguishing diffuse, focal and weak positivity from completely negative specimens. Only diffusely and focally positive findings were considered a significant pathological result.

For the analysis of CD20, CD38 and CD68 staining, immunohistochemically positive cells in five portal tracts per specimen were counted, followed by calculation of the arithmetic mean and the standard deviation.

For further statistical analysis the nonparametric Mann-Whitney and Kolmogorov-Smirnov tests, and for metric parameters the *t*-test for unpaired samples were performed. *P* values less than 0.05 were regarded as statistically significant.

Results

Immunohistochemical single staining

CD20

All examined tissue sections contained $CD20^+$ cells, predominantly localized in the portal tracts. Additionally biopsies from patients with ACR showed small clusters of

$CD20^+$ cells without formation of follicular structures. Furthermore, the evaluated biopsies revealed a noticeable difference in B-cell content of individual portal tracts. While in some portal fields no $CD20^+$ cells were detected, other portal tracts in the same biopsy showed strong infiltration by B-lymphocytes.

Quantitative analysis of $CD20^+$ cells demonstrated a significant increase in B-lymphocytes in biopsies from patients with ACR (mean 32.4, median 33.6, range 1.0–113.0) compared to biopsies from patients without ACR (mean 14.1, median 6.6, range 1.6–38.6; P=0.029).

CD38

$CD38^+$ cells were detected in all biopsy specimens. The mean number of $CD38^+$ cells per portal tract differed significantly between biopsies from patients with ACR (mean 17.0, median 10.1, range 0.4–106.4; Fig. 1) and from those without ACR (mean 3.4, median 2.0, range 0.2–17.0; P=0.014). No significant difference was seen between biopsies from $C4d^+$ and $C4d^-$ ACR patients.

C4d

Out of 22 liver biopsies from patients with ACR, 3 showed diffuse and 8 showed focal C4d positivity according to the semiquantitative grading used for evaluation of the immunohistochemical staining for C4d (Fig. 2). These biopsies were considered as definitely $C4d^+$. While 1 biopsy expressed weak C4d positivity, 10 showed no positivity (11/22; 50%). C4d deposits were seen attached to endothelial cells of portal vessels. As they were not restricted to venous endothelium, but could in some cases also be demonstrated along endothelial cells of portal arteries and portal capillaries, no distinct distribution pattern of the C4d staining was apparent regarding vascular structures in the portal fields. Nevertheless, C4d deposits were not detected attached to hepatic veins or along sinusoidal endothelium.

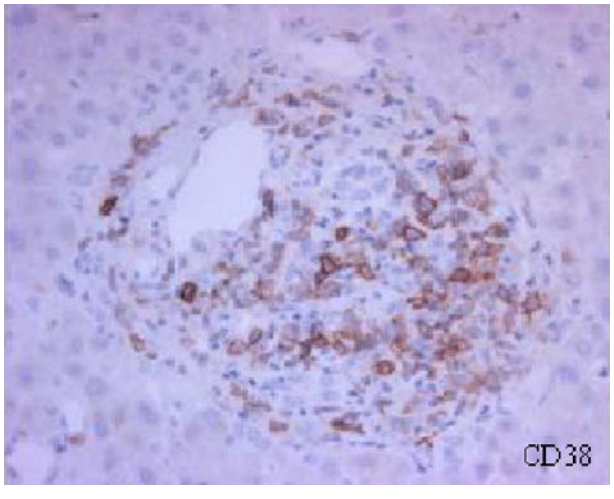


Fig. 1 $CD38^+$ cells in a portal field of a biopsy showing ACR (original magnification ×400)

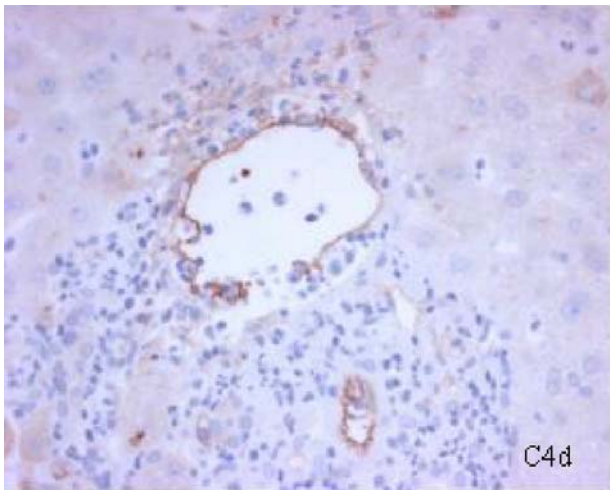


Fig. 2 Immunohistochemical staining of C4d deposits along portal vessels in ACR (original magnification ×400)

None of the control biopsies was considered $C4d^+$ (three biopsies showed only weak positivity and the remaining ten were negative). This represents a significant difference between ACR and control biopsies (P=0.013). No correlation was found between C4d positivity and rejection severity grade. There was also no statistically significant difference in the mean delay between transplantation and biopsy in patients with ACR between those with $C4d^+$ and $C4d^-$ biopsies (33 and 41 days, respectively).

CD68

$CD68^+$ macrophages were detected in all biopsies. The portal tracts of ACR biopsies contained a mean of 66.7 $CD68^+$ cells (median 53.5, range 15.5–164.8) compared to

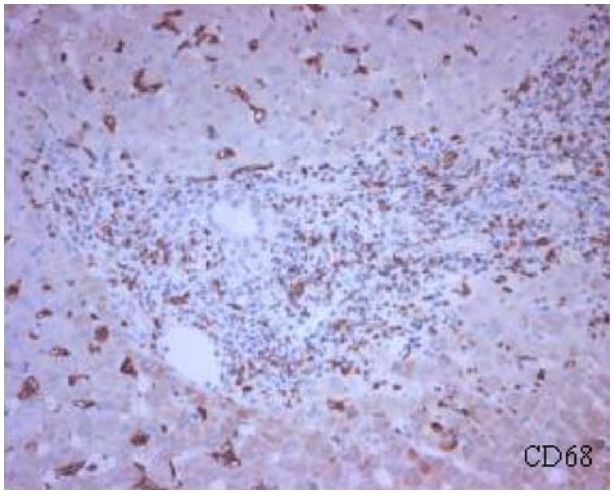


Fig. 3 $CD68^+$ macrophages in the portal tract as well as numerous $CD68^+$ Kupffer cells in the lobules of a rejected allograft (original magnification ×200)

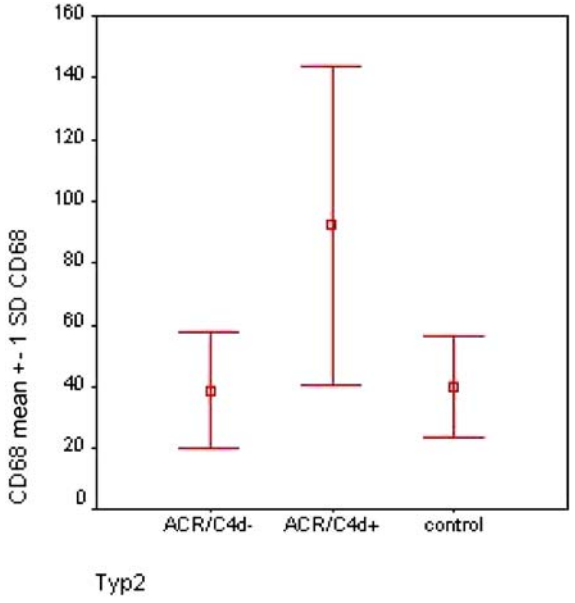


Fig. 4 C4d$^+$ biopsies from patients with ACR (*ACR/C4d*$^+$) showed a significant increase in CD68$^+$ cells per portal tract compared to C4d$^-$ biopsies from patients with ACR (*ACR/C4d*$^-$) and controls (*P*=0.007)

40.0 CD68$^+$ cells (median 41.8, range 13.7–63.4) in control biopsies. There was a highly significant difference in the mean of CD68$^+$ macrophages per portal tract between C4d$^+$ and C4d$^-$ ACR biopsies. In C4d$^+$ biopsies, there were 92.4 CD68$^+$ cells per portal field (median 80, range 27.3–164.8) compared to an average of 38.5 CD68$^+$ cells per portal field (median 39.5, range 15.5–71.3) in C4d$^-$ ACR biopsies (*P*=0.007; Figs. 3 and 4). CD68$^+$ cells were widely distributed across the portal fields.

C3d

C3d deposits were seen in 21 biopsies from patients with ACR (14 with focal positivity, 7 with diffuse positivity), whereas 1 biopsy remained unstained. In the comparison group positive staining was seen in 12 biopsies (9 diffusely positive, 3 focally positive), while 1 biopsy was negative. The number of positive biopsies was therefore not significantly different between patients with ACR and the control group.

Immunohistochemical double staining

C4d/CD68

Double staining was performed on 11 biopsies, which were demonstrated to be C4d$^+$ in immunohistochemical single staining. Results derived from immunohistochemical single staining were confirmed. In some biopsies an attachment of CD68$^+$ cells to C4d$^+$ endothelium could be demonstrated (Fig. 5).

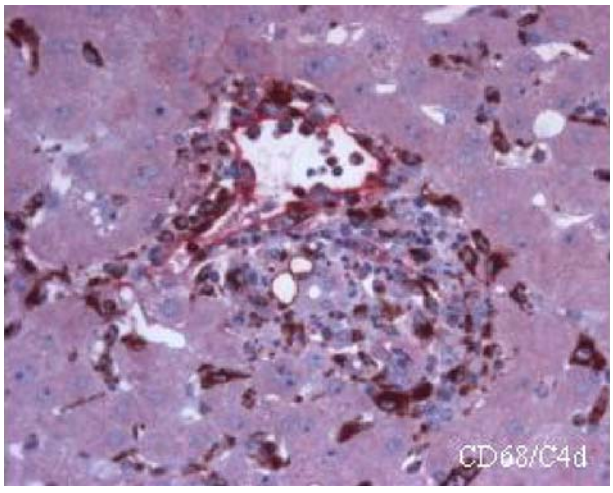


Fig. 5 Immunohistochemical double staining for C4d and CD68. CD68$^+$ cells are apparent in the vicinity of C4d deposits along the venous endothelium (original magnification ×400)

Immunofluorescence

C4d/CD68

Immunofluorescence single and double staining was conducted in three C4d$^+$ biopsy specimens to validate the results obtained by immunohistochemistry (Fig. 6). C4d$^+$/CD68$^+$ signals were detected in all biopsies. While bright focal and diffuse C4d deposits were seen along the portal capillary endothelium, CD68$^+$ cells were disseminated across the portal fields with slight accumulation at sites with strong C4d staining (Fig. 7).

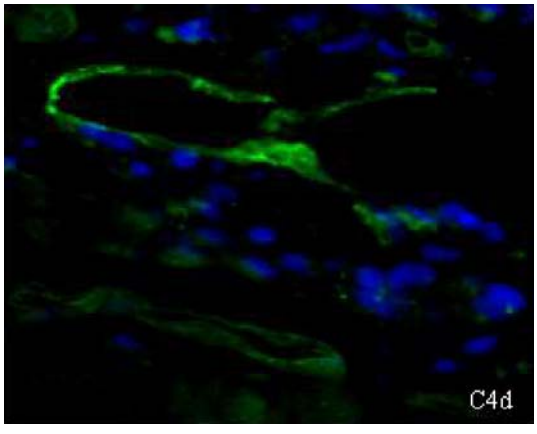


Fig. 6 Immunofluorescence staining of C4d deposits along portal endothelium in a rejected liver allograft (original magnification ×400)

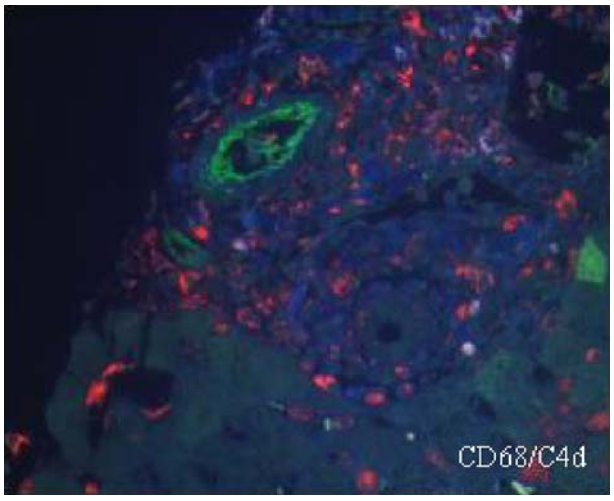


Fig. 7 Immunofluorescence double staining of C4d and CD68. Bright green C4d deposits are apparent along endothelial cells of a portal artery together with diffusely distributed red macrophages (original magnification ×400)

Discussion

Acute liver allograft rejection is considered to be primarily driven by T-lymphocytes. Histopathologically it is reflected by mononuclear infiltration of portal tracts by $CD3^+$ T-cells, and injuries to the bile ducts and venous endothelium [1]. Only few data exist concerning the role of antibody-mediated mechanisms in acute liver allograft rejection, but several studies have demonstrated an association between circulating anti-donor antibodies and rejection and graft loss [7, 11, 19]. Furthermore our group has recently identified C4d deposits along portal capillaries in liver biopsies from patients with ACR [8]. C4d has been shown to be a reliable marker of humoral immunoresponse to renal transplants so that today there is consent about AHR being an independent entity in renal allograft rejection [14].

IgVh analysis in a patient with ACR has demonstrated that B-cells in the transplanted liver tissue express a restricted V-gene repertoire and have a selected pattern of somatic mutations [15], indicating activation and clonal expansion of B-cells in liver tissue. Since no lymphatic follicles can be detected and immunohistochemical double staining of CD20 and Ki-67 does not demonstrate co-localization [8], an antigen-selected migration seems to be responsible for the colonization of portal fields by B-cells in ACR [15].

Although these studies have revealed new insight into the pathogenetic role of humorally mediated mechanisms in ACR, a systematic analysis of a larger population of ACR patients accompanied by validation of immunohistochemistry by immunofluorescence has yet to be carried out.

Immunohistochemical staining revealed a significant increase in $CD20^+$ and $CD38^+$ cells in biopsies from patients with ACR compared to control biopsies. These results are consistent with data recently published by Krukemeyer et al. who found a significantly increased accumulation of B-lymphocytes and plasma cells during acute rejection [8]. No significant difference was seen between $C4d^+$ and $C4d^-$ ACR patients.

However, concerning the histopathological evaluation of the comparison group, one major objection has to be considered. Protocol biopsies from patients who have undergone liver transplantation often reveal histopathological signs of a nonspecific inflammatory reaction despite fulfilling the criteria for ACR. The degree of this inflammation may be mild or moderate, and in some cases even severe. While three biopsies from the comparison group showed no signs of inflammation, ten protocol biopsies were diagnosed with mild inflammation. Statistical analysis of $CD20^+$ and $CD38^+$ cells in biopsies from ACR patients and the comparison group, disregarding biopsies without signs of inflammation, did not indicate significant differences. Therefore the possibility that increased infiltration of B-lymphocytes and plasma cells may be due to nonspecific inflammation rather than the hallmark of humoral immunoresponse in ACR cannot be ruled out completely. Nevertheless, the mere presence of B-lymphocytes and plasma cells challenges the concept of a pure cellular immunoresponse in ACR. Together with the finding that B-cells in acute liver allograft rejection express a restricted V-gene repertoire and have a selected pattern of somatic mutations [15], the results may suggest that antigen-induced selection, subsequent clonal expansion and final immigration of B-cells are part of the pathogenesis of ACR.

C4d deposits were seen along the endothelium of portal capillaries, portal veins and portal arteries in 50% of the biopsies from ACR patients, whereas no such deposits were seen in the protocol biopsies. C4d deposits were restricted to portal structures as they were not detected attached to hepatic veins or along sinusoidal endothelium. The specificity of the immunohistochemical staining was confirmed by immunofluorescence. As C4d is derived from the classical activation pathway of the complement cascade and specifically marks sites of humorally mediated reactions [2, 16, 17], this further supports involvement of a humoral immunoprocess in ACR. Although Krukemeyer et al. demonstrated C4d deposits in severely inflamed portal tracts [8], C4d positivity did not turn out to be correlated with rejection severity grade in this study. There was also no statistically significant difference concerning the mean delay between transplantation and biopsy between $C4d^+$ and $C4d^-$ biopsies from patients with ACR. Moreover no preponderance of late onset ACR was seen among $C4d^+$ biopsies.

Immunohistochemical detection of C3d, another proteolytic cleavage product of the complement cascade, was also performed. Almost all analyzed tissue specimens showed C3d deposits in the portal fields. This corresponds with the finding that normal renal tissue contains less C4d than C3d [2]. Furthermore, C3 shows the highest serum

concentration of all complement proteins and is capable of diffusing into interstitial spaces due to its molecular size [2]. But above all, it is the central link in the complement cascade, activated by the classical as well as the alternative pathway. Via an amplification loop, C3b is able to boost its own production, which reinforces complement-mediated reactions [2]. This may explain the occurrence of $C4d^{-}/C3d^{+}$ biopsies.

As C3d deposits were detected in almost all biopsies from the comparison group, one may question the significance of C3d immunostaining, but exclusive activation of the complement cascade via the alternative pathway triggered by a nonspecific inflammatory reaction could explain C3d deposits in these cases.

Despite the concern that, comparing biopsies from ACR and control patients, an increased infiltration of $CD68^{+}$ cells may again be a nonspecific sign of inflammation, this study showed that increased infiltration of macrophages is associated with C4d positivity in biopsies from patients with ACR. This association was first demonstrated in renal allograft rejection by Magil and Tinckam [10]. In another study investigating humoral rejection in cardiac transplantation macrophages served as a marker for AHR [13]. Accumulation of macrophages marks more severe renal allograft rejection and differentiates clinical from subclinical rejection [3, 6]. Macrophages are known to be activated by the formation of immunocomplexes by IgG and complement components (C5a) [18] and are capable of synthesizing complement factors (C4, C3).

Taken together the results of this study demonstrate an increased infiltration of portal tracts by B-lymphocytes and plasma cells in patients with ACR. Examining a larger population for the first time, C4d deposits were detected in 50% of biopsies from patients with ACR. Furthermore a significant association between the detection of C4d deposits and an increased infiltration of portal fields by macrophages in biopsies from patients with ACR was shown.

Thus we conclude that the frequent occurrence of macrophages, B-lymphocytes and plasma cells in portal tracts together with the presence of C4d deposits along portal capillaries indicate that there is actually more to acute liver allograft rejection than a mere cellular immunoresponse. The results suggest the involvement of humorally mediated mechanisms and innate immunity in some ACR patients. Whether the histopathological findings also mirror differences in the clinical course has yet to be determined.

Acknowledgements The authors thank G. Fernahl, J. Karle and K. H. Friedrich for providing excellent technical assistance. The study was supported by SFB 421 (Z3).

References

1. Anon (1997) Banff schema for grading of liver allograft rejection: an international consensus document. Hepatology 3:658–663
2. Baldwin WM, Kasper EK, Zachary AA (2004) Beyond C4d: other complement-related diagnostic approaches to antibody-mediated rejection. Am J Transplant 4:311–318
3. Croker BP, Clapp WL, Abu Shamat AR et al (1996) Macrophages and chronic renal allograft nephropathy. Kidney Int Suppl 57:S42–S49
4. Feucht HE, Felber E, Gokel MJ et al (1991) Vascular deposition of complement-split products in kidney allografts with cell-mediated rejection. Clin Exp Immunol 86:464–470
5. Feucht HE, Schneeberger H, Hillebrand G et al (1993) Capillary deposition of Cad complement fragment and early renal graft loss. Kidney Int 43:1333–1338
6. Grimm PC, McKenna R, Nickerson P et al (1999) Clinical rejection is distinguished from subclinical rejection by increased infiltration by a population of activated macrophages. J Am Soc Nephrol 10:1582–1589
7. Kasahara M, Kiuchi T, Takakura K et al (1999) Postoperative flow cytometry crossmatch in living donor liver transplantation: clinical significance of humoral immunity in acute rejection. Transplantation 67(4):568–575
8. Krukemeyer MG, Moeller J, Morawietz L et al (2004) Description of B-lymphocytes and plasma cells, complement, and chemokines/receptors in acute liver allograft rejection. Transplantation 78:65–70
9. Kuypers DRJ, Lerut E, Evenepoel P et al (2003) C3d deposition in peritubular capillaries indicates a variant of acute renal allograft rejection characterized by a worse clinical outcome. Transplantation 76:102–108
10. Magil AB, Tinckam K (2003) Monocytes and peritubular capillary C4d deposition in acute renal allograft rejection. Kidney Int 63:1888–1893
11. Manez R, Kelly RH, Kobayashi M et al (1995) Immunoglobulin G lymphocytotoxic antibodies in clinical liver transplantation: studies toward further defining their significance. Hepatology 21(5):1345–1352
12. Mauiyyedi S, Crespo M, Collins AB et al (2002) Acute humoral rejection in kidney transplantation: II Morphology, immunology, and pathologic classification. J Am Soc Nephrol 13:779–787
13. Michaelis PJ, Espejo ML, Kobashigawa J et al (2003) Humoral rejection in cardiac transplantation: risk factors, hemodynamic consequences and relationship to transplant coronary artery disease. J Heart Lung Transplant 22:58–69
14. Michaelis PJ, Fishbein MC, Clovin RB (2003) Humoral rejection of human organ transplants. Springer Semin Immunopathol 25:119–140
15. Moeller J, Krukemeyer MG, Morawietz L et al (2005) Molecular case report: IgVH analysis in acute humoral and cellular liver allograft rejection suggests a selected accumulation of effector B cells and plasma cells. Virchows Arch 446:325–332
16. Nickeleit V, Mihatsch MJ (2003) Kidney transplants, antibodies and rejection: is C4d a magic marker? Nephrol Dial Transplant 18:2232–2239
17. Sacks SH, Chowdhury P, Zhou W (2003) Role of the complement system in rejection. Curr Opin Immunol 15:487–492
18. Shushakova N, Skokowa J, Schulman J et al (2002) C5a anaphylatoxin is a major regulator of activating versus inhibitory FcgammaRs in immune complex-induced lung disease. J Clin Invest 110:1823–1830
19. Takakura K, Kiuchi T, Kasahara M et al (1999) Humoral immunity in acute cellular rejection after living-donor liver transplantation. Transplant Proc 31:526–527
20. Vella JP, Magee C, Vos L et al (1999) Cellular and humoral mechanisms of vascularized allograft rejection induced by indirect recognition of donor MHC allopeptides. Transplantation 67:1523–1532

Virchows Arch (2005) 447: 94–98
DOI 10.1007/s00428-005-1273-8

ORIGINAL ARTICLE

S. Sandhyamani · J. K. Sindhu · S. Sriramachari

Recolorization of museum specimens: a modification of Romhanyi's technique based on pyridine/nicotine hemochromogen reactions

Received: 28 February 2005 / Accepted: 12 April 2005 / Published online: 14 June 2005
© Springer-Verlag 2005

Abstract Romhanyi's technique for preservation and restoration of color in museum specimens is almost unknown outside Hungary. The technique was based on the use of pyridine, nicotine and sodium dithionite (sodium hydrosulphite) for restoring the natural red color of formalin-fixed gross specimens. We developed a modification of the original technique using a mounting medium containing citrate-phosphate-dextrose (CPD) buffer and glycerin to control pH and osmolality. Specimens recolorized with the modified and improved Romhanyi technique remained stable with a natural red color, and no histological deterioration, for more than 18 years. The technique demonstrates the formation of red colored complexes between nicotine and pyridine and ferro-hemochromes such as hemoglobin, myoglobin and other cytochromes in tissues, giving specimens a natural color. The modified technique enables further improvement for the old process of recolorization of museum specimens. In addition, it opens up new methods for demonstration of nicotine, pyridine and their analogues in biological tissues.

Keywords Pathology museum specimens · Recolorization technique · Color preservation · Pyridine hemochromogen · Nicotine hemochromogen

S. Sandhyamani
Department of Pathology, Sree Chitra Tirunal Institute for Medical Sciences and Technology,
Trivandrum, India

S. Sandhyamani (✉)
Laavanya,
D-11, Pillaveedu Nagar, Kesavadasapuram,
Trivandrum, 695 004, India
e-mail: sandhyamani@gmail.google.com
Tel.: +91-471-2524605
Fax: +91-471-2562116

J. K. Sindhu · S. Sriramachari
Institute of Pathology (Indian Council of Medical Research),
New Delhi, India

Introduction

Formaldehyde is used universally to fix biological tissues and prevent their decomposition. Although formalin-fixed specimens can be stored for long periods, they appear dull, grey-brown and featureless. During the last century, several methods were attempted to make anatomical and pathological museum specimens look natural, fresh and more appealing to the eye. Numerous museum techniques were developed, the most widely followed one being that of Kaiserling [5, 6]. These used formalin for fixation, with or without alcohol (ethyl and methyl) for restoring the red colour and mixtures of salts and glycerin for preservation of the specimen and its colour [3, 5, 8], but were generally found to be unsatisfactory or unstable over time.

An important technique by Pulvertaft [11], further modified by Wentworth [15, 16], used sodium dithionite (sodium hydrosulphite) to recolourize museum specimens. A less known but more important technique based on the hydrosulphite method was developed by the late Professor Romhanyi in Hungary, using pyridine and nicotine for recolorization of formalin-fixed tissues [12]. The technique (Table 1), obtained from Professor Romhanyi and brought to India by the third author (S.S.), produced specimens that had a near-natural colour and appearance. However, it did not become popular for various reasons. If care was not taken to follow the procedure strictly, the red colour disappeared with time or deteriorated irreversibly to a dirty-brown colour in some of the specimens.

We report modifications made in Romhanyi's technique to improve restoration and preservation of the natural red color of museum specimens. We successfully used combinations of glycerin with salts, with modification of the citrate-phosphate dextrose (CPD) buffer, commonly employed for storage of blood [4]. This paper highlights the stability of the tissues and preservation of their red color for more than 18 years, using the modified technique. The studies also indicate that nitrogenous substances such as pyridine and nicotine may have a long-lasting binding effect on hemoglobin, myoglobin and possibly other cytochromes present in blood and tissues.

Table 1 Romhanyi's technique[a]

Solution I (Fixative)	
Formaldehyde 40% solution	1 l
Common salt	300 g
Distilled water	5 l
Place in solution I for 1 week, rapidly wash in tap water, transfer to solution II	
Solution II (Colour Restorative)	
Formaldehyde 40% solution	1 l
Distilled water	5 l
Sodium dithionite	100 g
Potassium carbonate	30 g
Pyridine	10 ml
Nicotine (5% in distilled water)	10 ml
Change the solution every 2 or 3 days, at least 3 replacements	
Mount in fresh change of solution II	

[a]Personal communication, to Sriramachari

Materials and methods

The compositions of solutions used for the modified Romhanyi technique are given in Table 2. In order to avoid shrinkage or swelling of the tissues, initially a double concentration of CPD is employed, to ensure osmolality even after subsequent dilution with equal quantities of glycerin-distilled water mixture in the mounting medium. Thus, the final pH of approximately 6.3–6.4 in the final mounting medium is best suited for ensuring the optimum hue and saturation. In the recolorized specimen, hemoglobin attains a red colour (bright-red with pyridine and a darker shade of red with nicotine); muscle becomes brownish-red in colour. The quantities of pyridine and nicotine may be varied to get the desired shades in the specimens. It is important to use only laboratory grade reagents and chemicals. Only sodium dithionite ($Na_2S_2O_4$), also called sodium hydrosulphite should be used for this procedure and not sodium thiosulphate or "hypo" ($Na_2S_2O_3$), a fact correctly pointed out by Wentworth [15].

Procedure The specimen is dissected with minimum exposure to tap water, dabbed with cotton-wool to remove surface blood and fluids and placed in solution I for at least 1 week for proper fixation. The specimen is then taken out, trimmed and mounted on appropriate acrylate or Perspex sheet or suspended within a glass frame and placed in a fresh change of solution I for 3–4 days to remove loose fragments of tissue, blood etc. from the surface. Any further contact of the specimen with tap water is to be avoided. The specimen is placed in solution II for 7–10 days, until the entire specimen becomes uniformly recolorized. Solution II should be changed every 3 days, at least twice. Thereafter, the specimen is transferred to the mounting medium (solution III), taking care to deposit a layer of sodium dithionite (solid pieces or coarse powder) at the bottom of the jar, and the jar is "filled to the brim", before permanent sealing. Museum jars made of glass or Perspex may be used. A 1 ml aliquot of 40% formaldehyde or 1 g of camphor introduced into the mounting medium may prevent growth of microorganisms and repel insects. The mounting medium may need to be changed occasionally, if it develops a brownish discoloration due to any excess pyridine or nicotine seeping out of the specimen.

Table 2 Modified Romhanyi's technique for recolorization of museum specimens: composition of solutions

Solution I (Fixative)	
Formaldehyde 40% solution	1 l
Sodium chloride	300 g
Distilled water	5 l
Solution II (Color Restorative)	
CPD (×2 concentration)*	1 l
Distilled water	1 l
Sodium dithionite	100 g
Pyridine	10 ml
Nicotine (5% v/v in distilled water)	10 ml
Solution III (Mounting Medium)	
CPD (×2 concentration)*	1 l
Glycerin	250 ml
Distilled water	750 ml
Sodium dithionite	100 g
***CPD (×2 concentration) - composition adapted from Dacie and Lewis [4]**	
Trisodium citrate	52.60 g
Citric acid	6.60 g
Sodium dihydrogen phosphate	4.44 g
Dextrose anhydrous	51.00 g
Distilled water, make up to	1 l

Results

Color restoration begins immediately and takes 2–3 days for larger specimens. The brilliant red color of the specimens is best viewed with oblique and top illumination (Fig. 1a–c). Good preservation of the tissue, as evidenced by histology, was present even after the lapse of 18 years in a recolorized specimen of myxoma of the heart (Fig. 1d). Old specimens, primarily fixed in buffered formalin, can also be recolourized (Fig. 1c), but the red color may not be as stable and of optimum saturation as in fresh specimens, directly fixed in solution I. Imperfect initial or primary fixation may result in leaching out of hemoglobin from the erythrocytes forming "pools" within the lumen of the blood vessels as illustrated in a poorly fixed intestinal specimen (Fig. 1e). By contrast, the cytomorphological features were well preserved in a specimen of placenta fixed directly in solution I (Fig. 1f).

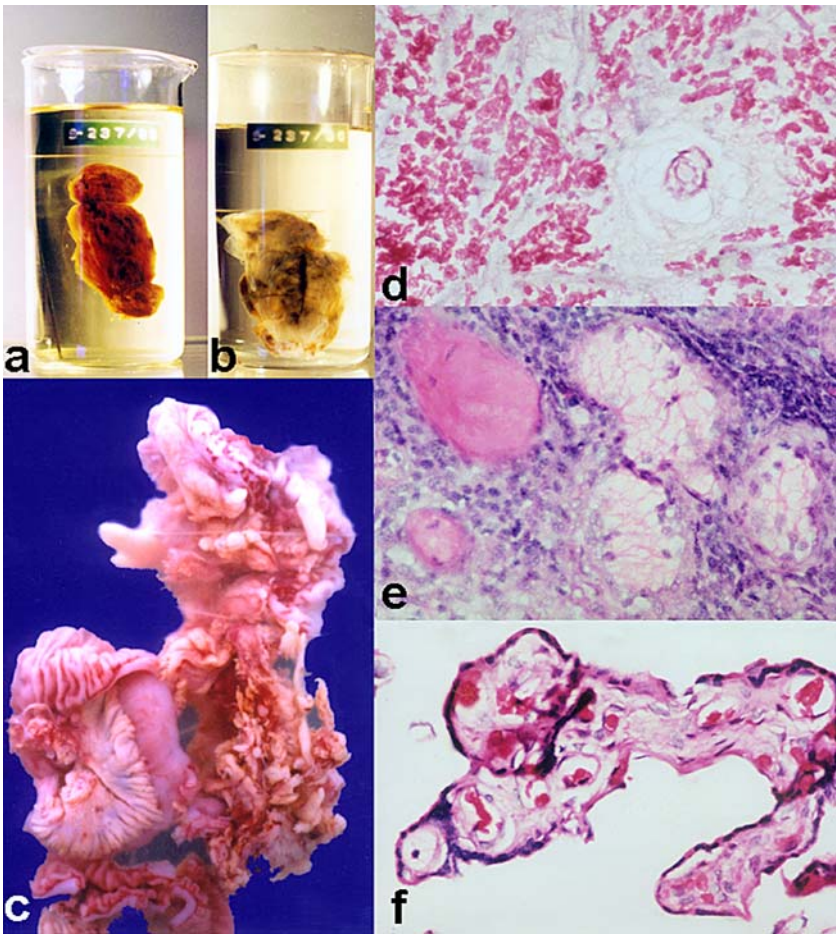


Fig. 1 Dark red color of right ventricular myxoma recolorized with the modified Romhanyi technique is in sharp contrast to the drab gray-brown appearance of its other half in 10% buffered formaldehyde (**a**,**b**). Bright red color is restored with the modified Romhanyi technique in a 2-year-old formalin-fixed specimen of small intestine and mesentery (**c**). Histology shows intact well-preserved erythrocytes and double-layered blood vessel in the recolorized myxoma specimen even after 18 years (**d**). Extracellular hemoglobin within capillaries (**e**) indicates improper primary formalin-fixation of the intestine specimen shown in (**c**). Intact erythrocytes and good staining characteristics are seen in a placental villus fixed directly in solution I prior to color restoration (**f**). [**d**,**e**,**f**: hematoxylin and eosin *385]

Discussion

After some preliminary trials, the authors succeeded in developing an improved method of recolorization that is quite stable over long periods of time. From a perusal of Romhanyi's original publication [12] and his personal communications to the third author (S.S.), the process involved pyridine, nicotine and sodium dithionite as the main constituents. However, in the details of the personal communication, the specimen is first fixed in solution I, containing formaldehyde and common salt, which probably acts as an osmotic factor; and later it is transferred to solution II containing formaldehyde, sodium dithionite, potassium carbonate, pyridine and nicotine (Table 1).

Although Romhanyi's modified technique gave excellent results initially, the rich red colour of the specimen slowly turned reddish brown and after a year or two in many instances there was a gradual seepage of colour into the mounting medium. In some cases, the colour turned a dull brown with development of a dirty brownish-white precipitate that formed a sediment over the surface of the specimen. Probably due to the presence of formalin in the mounting medium, the red colour developed was not rich and brilliant enough. It is well known that even though formaldehyde denatures and fixes tissues, there is with time, a slow disintegration of tissues and leaching out of colour and cell contents, especially evident from tissues rich in fat. To overcome these problems, we omitted formaldehyde and potassium carbonate from solution II (recolourization medium) and solution III (mounting medium). Formalin is necessary only for primary fixation of the specimen and not required after that in the recolorization and mounting solutions. Further, formalin fixation results in better preservation of tissues and many of their histochemical reactions (including the recolourization processes), only if buffered solutions are used for primary fixation and during long-term storage. Therefore, a combination of glycerin and salts (CPD) was introduced in solution III (mounting medium) to maintain pH and osmolality, as advocated for erythrocyte preservation by Dacie [4] and several museum technologies [5]. This was found to be a better combination to obtain a stable rich red color and its retention within the specimen over long periods. Histological examination of our specimens continued to show maintenance of cyto-architecture and intact erythrocytes within hemorrhagic areas (Fig. 1d) even after the lapse of 18 years.

In a series of experiments using pellets of fresh and formalinized erythrocytes and pieces of tissue samples, it was found that sodium chloride in fixative solution I had the effect of pickling the tissues. It prevented tissue lysis and release of cellular components, particularly hemoglo-

bin. However, we found that a cloudy precipitate forms if sodium chloride is mixed with pyridine or nicotine. In Romhanyi's method (see Table 1), after fixing the specimen in solution I with formalin and common salt, the specimen was rapidly and thoroughly washed in tap water, possibly to remove sodium chloride on the surface. Instead in the present modified technique, it was observed that dabbing the surface with cotton wool was better than washing with tap water, as it helped to exclude any microorganisms and deleterious effects of variations in salt composition and pH of tap water from different places.

The most important modification by us was introduction in solutions II and III of double-concentrated CPD initially and later adjusting it supplemented with glycerin and distilled water to finally attain "unit-concentration of CPD". It is well known that CPD is very effective in lengthening the storage and prolonged preservation of blood for transfusion purposes in blood banks. With added glycerin, blood could be stored for a longer term [2, 4]. Citric acid present in CPD may have helped to keep hemoglobin in a reduced (ferrous) state and so enhance the effect of sodium dithionite, as described below. The action of citric acid may be similar to that of ascorbic acid used in McCormick's technique [9]. It was found that CPD, along with glycerin gave better control of tissue shrinkage and swelling and retention of color within the specimen. Glycerin lends a translucency to dull-brown opaque formalin-fixed tissues, prevents bacterial growth, helps to control osmolality and being of high refractive index, it gives a crystal-like sparkle to the mounting medium. Hence although is costly, glycerin has been introduced in the mounting medium.

From Professor Romhanyi's personal communication (S. Sriramachari, personal communication), it would appear that pyridine and nicotine form respective "complex hemochromogens" with hemoglobin and myoglobin in the specimen resulting in red colored compounds. The term "hemochromogen" was later renamed "ferrohemochrome" and was considered to be a complex formed by the combination of heme with a nitrogenous substance such as pyridine, ammonia, glycine or denatured globin [1]. The red colored compound formed on addition of pyridine and nicotine resembles the colour of oxyhemoglobin. Pyridine gives a bright red colour and nicotine a darker shade of red. Similar reactions with myoglobin and possibly cytochromes also present may give rise to various shades of pink and brown in the specimen. The colour changes are more obvious in formalin fixed-tissues and blood samples than in fresh unfixed materials. Hence the direct binding effects of pyridine and nicotine on hemoglobin and other cytochromes may have gone unnoticed by scientists. We postulate that formalin-denatured globin may remain attached to heme in the tissue and form a complex compound called formaldehyde-globin-ferrohemochrome that is kept in a reduced state (ferrous iron form) by sodium dithionite.

Preliminary studies carried out by the first author (unpublished observations) suggest that pyridine and nicotine combine with the globin part of hemoglobin and affect its absorption spectrum in the region of the Soret band and also alter its affinity to oxygen. This is in contrast to the effect of carbon monoxide on hemoglobin to produce a cherry-red compound, carboxyhemoglobin, by displacing oxygen. Coal gas was bubbled into the fixative solution to produce carboxyhemoglobin for recolourizing museum specimens in Pick's technique and its modification by Schultz [3, 5]. Although the pyridine hemochromogen reaction was known as a test for identifying blood stains [1], it was not used in any technique other than Romhanyi's, to restore colour in museum specimens. Piperazine, a possible analogue of pyridine, was used for colour restoration, but the method published in Hungarian, was not known outside Europe [7]. The effect of nicotine on museum specimens and its reaction with hemoglobin and myoglobin were also not known in the literature.

If hemoglobin does become oxidized to a ferric state (ferrihemochrome), then the resultant complex with pyridine and nicotine will no longer be red in color and the tissue develops a dirty white or dull brown color. This reaction is irreversible. Such a change is usually the result of remnant detergents in the jar when a brownish-white powdery precipitate forms in the medium and sediments all over the specimen. Therefore, thorough washing and cleaning procedures are required for all glassware used for preparation of fixative and mounting solutions and even the specimen jars, supports or frames used for final storage of specimens. Good quality glass or Perspex museum jars may be used, but one must ensure that they are scrupulously cleaned. All traces of cleaning detergent should be removed by thorough washing of glassware and museum jars with distilled water. Failure to follow these procedures will result in suboptimal results and irreversible deterioration of colour.

The red colored compounds, pyridine- and nicotine-formaldehyde-ferrohemochromes do not decompose in the specimen as they are denatured and "fixed" by formaldehyde. Being "ferrohemochromes" they can become oxygenated and remain stable even on exposure to air. However their oxidation to a ferric state (ferrihemochromes) must be prevented by all means, using reducing substances, buffering salts, maintaining pH and excluding any oxidizing agents or detergents from the medium. Sealing the museum jar is not absolutely essential; it is done mainly to exclude contamination by microorganisms. Slow oxidation of the colored complex in the presence of air or bleaching on exposure to direct sunlight cannot be totally ruled out. Hence there may be a need to exclude air from the jar by boiling the mounting medium before use, as recommended by Wentworth [16], or degassing the medium under vacuum. Such procedures were, however, not done for our specimens, exposed to indirect sunlight and regular room illumination, but the colour remained stable for over 18 years.

Although Romhanyi's technique produced the most spectacular results, it did not become popular in India, even after distribution of the methodology to various medical

colleges and institutions as a personal communication by the third author (S.S.). Due to non-availability of some of the ingredients, particularly nicotine, and the above-mentioned technical difficulties, the procedure resulted in unstable colors. Therefore, the technique failed to arouse the curiosity of pathologists in general, who were keen on improving teaching methodologies [13], barring a few who could reproduce the technique with some success [10].

It was Kaiserling's lifetime desire and effort to produce near-natural fresh-looking museum specimens that did not deteriorate in color and appearance even after many decades [5]. Although alcohol treatment did not always give uniformly good results, his technique remained the most popular one for want of better methods and continues to be followed despite introduction of the "dry-mounting" technique of plastination [14] in some of the museums. Romhanyi's technique was far superior to all other methods of recolorization. The technique was almost lost in oblivion till the present authors revived it when they realized its importance not only as a unique museum technique but also as one that provided definite evidence regarding hitherto unknown tissue-binding effects of nicotine, pyridine and related compounds. It is hoped that in due course the technique may prove to be useful in the demonstration of deleterious tobacco products in biological tissues at the subcellular levels.

Acknowledgements The authors wish to thank the present and past Directors of Sree Chitra Tirunal Institute for Medical Sciences and Technology, Trivandrum, Dr. K. Mohandas and Dr. M.S. Valiathan, and Dr. Ashok Mukherjee, former Director, Institute of Pathology, New Delhi, for their interest in the work and encouragement shown, and staff of Medical Illustration Unit for technichal assistance.

References

1. Bell GH, Davidson JN, Scarborough H (eds) (1965) Textbook of physiology and biochemistry, 6th edn. The ELBS and E and S Livingstone Ltd, Edinburgh, pp 418–429 (Chapter 25)
2. Boorman KE, Dodd BE, Lincoln PJ (eds) (1977) Blood group serology, 5th edn. Churchill Livingstone, Edinburgh, London, New York, pp 465–467
3. Culling CFA (ed) (1974) Handbook of histopathological and histochemical techniques (including museum techniques), 3rd edn. Butterworth, London, pp 529–535
4. Dacie JV, Lewis SM (eds) (1991) Practical haematology, 7th edn. ELBS with Churchill Livingstone, Edinburgh, p 536
5. Edwards JJ, Edwards MJ (eds) (1959) Medical museum technology. Oxford University Press, London, New York, Toronto, pp 3–90
6. Kaiserling C (1922) Verhandlungen der Deutschen Pathologischen Gesellschaft. Virchows Arch 237:467–474
7. Krutsay M (1989) Re-coloration of pathological preparations exhibited in museums. Morphol Igazsu Orv Szle 29:204–206 (Hungarian)
8. Legault KM, Huang SN (1979) Colour preservation of gross specimens for teaching and medical illustration. Arch Pathol Lab Med 103:300–301
9. McCormick JB (1961) Color preservation of gross museum specimens. Arch Pathol 72:96–99
10. Patoria NK (1981) Restoration of natural colour to pathology specimens. Ind J Pathol Microbiol 24:195–197
11. Pulvertaft RJV (1950) Museum techniques: a review. J Clin Pathol 3:1–23
12. Romhanyi G (1956) Einfaches Verfahren zur Konservierung in naturlichen Farben. Virchows Arch 328:573–575
13. Singh MK, Chopra P (1987) Colour preservation and restoration in gross specimens. Ind J Pathol Microbiol 30:413–414
14. von Hagens G, Tiedman K, Kriz W (1987) The current potential of plastination. Anat Embryol (Berlin) 175:411–421
15. Wentworth JE (1942) The preservation of museum specimens in war-time. J Pathol Bacteriol 54:137–138
16. Wentworth JE (1947) The hydrosulfite method of preserving museum specimens. Bull Int Assoc Med Museums 27:201–204

Virchows Arch (2005) 447: 99–102
DOI 10.1007/s00428-005-1266-7

CASE REPORT

Makoto Endo · Tadashi Hasegawa · Takashi Tashiro · Umio Yamaguchi · Yuki Morimoto · Fumihiko Nakatani · Tadakazu Shimoda

Bizarre parosteal osteochondromatous proliferation with a t(1;17) translocation

Received: 19 January 2005 / Accepted: 30 March 2005 / Published online: 31 May 2005
© Springer-Verlag 2005

Abstract Bizarre parosteal osteochondromatous proliferation (BPOP) is a benign lesion that tends to recur repeatedly. Histologically, BPOP contains three components (cartilage, bone, and spindle cells) in differing amounts. The histological findings of BPOP are similar to those of florid reactive periostitis (FRP) and subungual (Dupuytren's) exostosis. Some authors have postulated that all of these conditions are reactive proliferative lesions representing different phases of reactive processes. Whether BPOP is a reactive proliferative lesion or a neoplastic lesion, however, remains controversial. Recently, a t(1;17)(q32;q21) translocation in BPOP was detected using chromosome banding and fluorescence in situ hybridization (FISH) analyses. Here, we describe a 39-year-old Japanese female with BPOP arising in the proximal phalanx of her third toe. A cytogenetic analysis revealed a t(1;17)(q42;q23) translocation. The breakpoints in this case are located close to those of previously reported cases. These results suggest that t(1;17) is a distinct translocation of BPOP and that BPOP is a neoplastic lesion, rather than a reactive proliferative process.

Keywords Bizarre parosteal osteochondromatous proliferation (BPOP) · Nora's lesion · Translocation · Fluorescence in situ hybridization

M. Endo · T. Tashiro · U. Yamaguchi · Y. Morimoto · F. Nakatani · T. Shimoda
Divisions of Orthopaedic Oncology and Clinical Laboratory,
National Cancer Centre Hospital and Research Institute,
Tokyo, Japan

T. Hasegawa (✉)
Department of Clinical Pathology,
School of Medicine,
Sapporo Medical University,
South 1, West 16, Chuo-ku,
Sapporo, 060-8543, Japan
e-mail: hasetada@sapmed.ac.jp
Tel.: +81-11-6112111
Fax: +81-11-6151418

Introduction

Bizarre parosteal osteochondromatous proliferation (BPOP), also known as Nora's lesion, is a rare tumorous lesion first described by Nora et al. in 1983 [7]. The lesion occurs in young adults and predominantly involves the small tubular bones of the hands and feet [5]. Radiologically, BPOP presents as a mass with distinct margins arising from the cortical surface of the affected bone. Cortical flaring of the adjacent bone or continuity of the central part of the tumor with the underlying osseous medulla, as seen in typical osteochondroma, is not present in BPOP. The histological features of BPOP resemble those of a reactive lesion, including the presence of cartilage, bone, and spindle cells. Although the cartilage is hypercellular and contains double-nucleated cells, neither hyperchromasia nor cytologic atypia are seen in the spindle cells. Mitotic figures are common, but none is atypical. Surgical excision is the treatment of choice. Although local recurrences frequently occur, BPOP is considered to be a benign lesion because it does not metastasize. Whether BPOP is a neoplasm or a reactive proliferative lesion remains uncertain. Recently, Nilsson et al. reported a t(1;17)(q32;q21) translocation in five cases of BPOP, as revealed by chromosome banding and fluorescence in situ hybridization (FISH) analyses [6]. Here, we present an additional case of BPOP with a t(1;17) translocation occurring in the foot of a 41-year-old Japanese woman.

Clinical history

A 39-year-old Japanese female complained of right foot pain after kicking a ball. She underwent a thorough medical examination at a local clinic, but no abnormal findings were found. At the age of 41 years, the pain recurred at the same site, without any traumatic episode, and began to worsen. She consulted a doctor and was referred to our hospital because of a suspected bone tumor. Clinical examination revealed a solid hard mass fixed to the proximal phalanx of the third toe. The mass was tender to palpation,

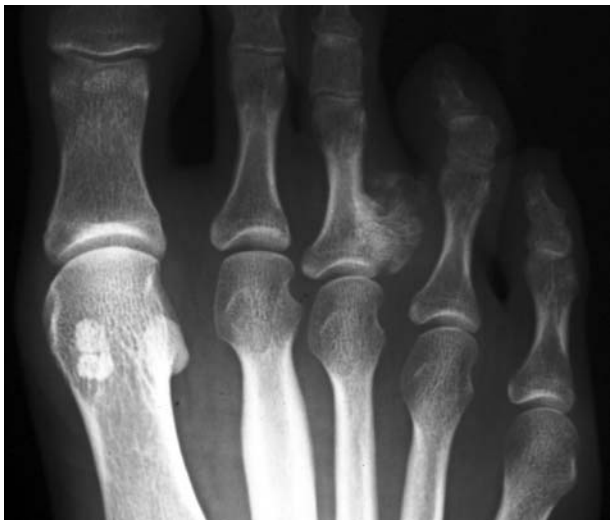


Fig. 1 Plain radiograph showing an oval mass with a distinct margin and heterogeneous patchy opacity adjacent to the lateral aspect of the base of the proximal phalanx of the third toe

but the overlying skin was intact. No neurovascular complications in the third digit were observed. Plain radiographs demonstrated a solid, 1.6×0.9 cm calcified mass with distinct margins arising from the cortical surface on the lateral aspect of the proximal phalanx (Fig. 1). Flaring of the cortex was not visible on an X-ray. Continuity with the osseous medulla was not seen using computed tomography. T1-weighted magnetic resonance imaging (MRI) showed a low-intensity mass adjacent to the proximal phalanx. Fat-suppressed T2-weighted images showed a heterogeneous, high-intensity mass with a well-defined convex border against the surrounding tissue. With regard to the proximal phalanx, neither cortical nor medullary abnormalities were seen. $^{99\ m}$Tc-and ^{201}Tl-scintigraphies demonstrated an abnormal uptake in the right foot lesion, while the uptake in other parts of her body was normal. All laboratory data were within the normal range. An open biopsy was performed, and a diagnosis of bizarre parosteal osteochondromatous proliferation was established. The mass was excised completely, and the patient has remained free of any evidence of local recurrence or metastasis for 3 months after the surgery.

Materials and methods

Histology and immunohistochemistry

The biopsy and excised specimens were fixed in formalin. Paraffin-embedded tissue was examined using standard histopathological techniques. Immunohistochemical staining was performed using antibodies against vimentin (V9; 1/200; DakoCytomation, Glostrup, Denmark), desmin (D33; 1/100; DakoCytomation), smooth-muscle actin (SMA) (1A4; 1/100; DakoCytomation), cytokeratin (AE1/3; 1/100; DakoCytomation), muscle-specific actin (MSA) (HHF35; 1/100; Enzo, New York, USA), epithelial membrane antigen (EMA) (E29; 1/100; DakoCytomation), S-100 protein (polyclonal antibody; 1/2000; DakoCytomation), CD34 (my10; 1/100; DakoCytomation), CD68 (KP1; 1/1000; DakoCytomation), p53 (DO7; 1/50; DakoCytomation), and Ki-67 (MIB-1; 1/100; DakoCytomation).

Cytogenetic and FISH analysis

A fresh fragment of the lesion obtained at the time of surgery was prepared for cytogenetic analysis using collagenase. The specimen was cultured in RPMI 1640 medium supplemented with 10% fetal bovine serum and antibiotics. Slides were stained using a previously described G-banding technique [3].

Multicolor FISH (M-FISH) [8] was performed using the SpectraVysion assay system (Vysis, Downers Grove, Ill., USA). The hybridization of the probe was visualized using fluorescence microscopy.

Results

Histopathological features

The histological evaluation showed a gross appearance consisting of a cancellous bone matrix partially covered by an irregular cartilaginous cap. Microscopically, three components (cartilage, bone, and spindle cells) were observed in differing amounts. The cartilage and bone interface showed irregular endochondral ossification, and the bone

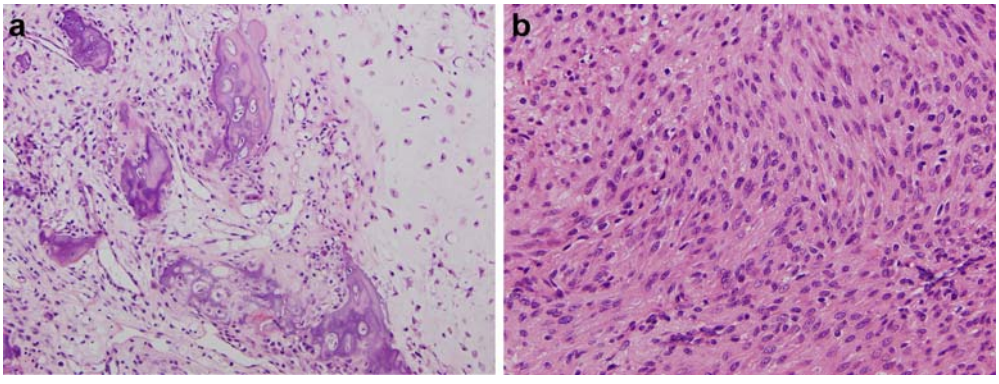


Fig. 2 Microphotographs of the lesion. **a** The cartilage and bone interface shows irregular ossification, and the formed bone trabeculae are characteristically stained blue [Hematoxylin and eosin (HE); original magnification, ×100]. **b** The spindle cells show monotonous proliferation without cytologic atypia (HE; original magnification, ×200)

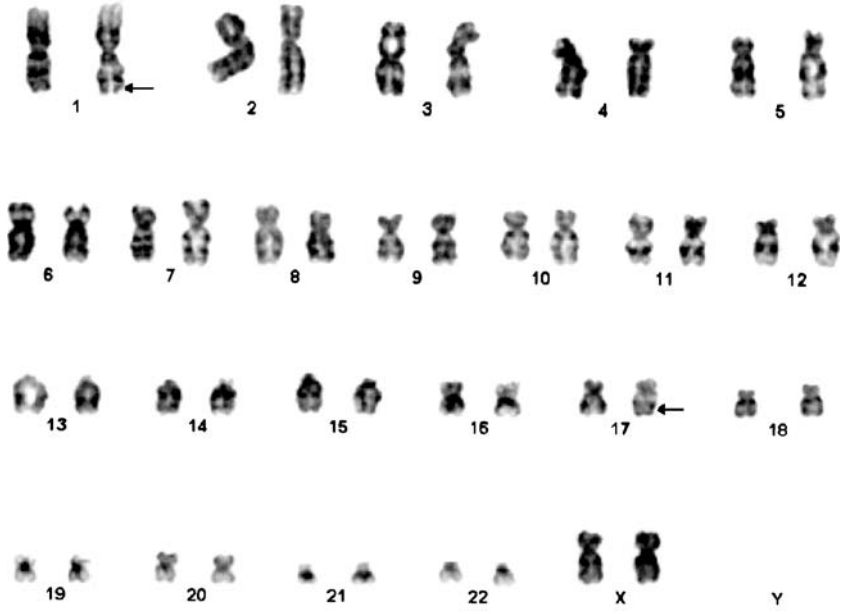


Fig. 3 G-banded karyotype showing a t(1;17)(q42;q23) translocation

trabeculae formed were characteristically stained blue with hematoxylin and eosin (Fig. 2a). The cartilage was partially hypercellular with moderately enlarged nuclei and contained large chondrocytes. The spindle cells were uniform without any cytologic atypia (Fig. 2b) and were loosely arranged between the bony trabeculae. Mitotic figures were occasionally seen, but none was atypical. Immunohistochemical examination showed that the spindle cells were positive for SMA. Desmin was expressed in the spindle cells and some chondrocytes, and vimentin was positive in almost all cell types within the lesion. MSA, cytokeratin, EMA, S-100 protein, CD34, CD68, and p53 tested negative. The MIB-1 labelling index was about 1% in the spindle cells.

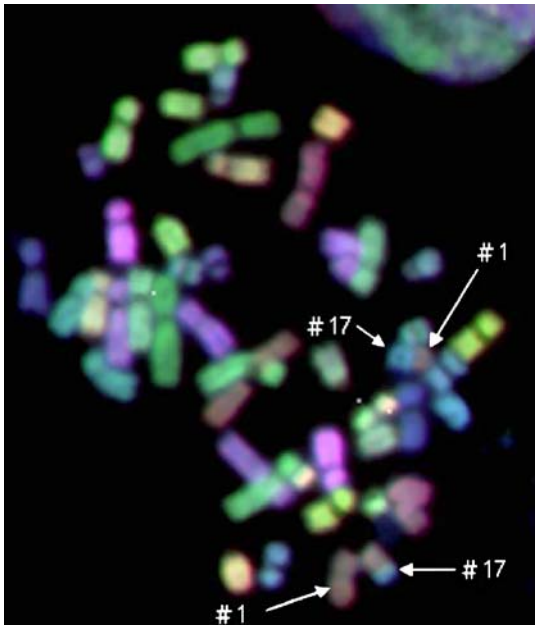


Fig. 4 Multicolor FISH analysis of a metaphase cell showing a t(1;17)(q42;q23) translocation. The colors representing chromosomes 1 and 17 are grey and light blue, respectively

Cytogenetic and FISH analysis

Cytogenetic analysis of the lesion revealed a karyotype with a t(1;17)(q42;q23) translocation (Fig. 3). The reciprocal translocation was further characterized by M-FISH analysis (Fig. 4).

Discussion

Recently, chromosomal aberrations in BPOP were reported by Nilsson et al. [6] and Zambrano et al. [12]. Nilsson et al. reported the cytogenetic findings of five cases of BPOP using G-banding and FISH analyses [6]. They reported the t(1;17)(q32;q21) translocation to be a recurrent and unique aberration in BPOP [6]. On the other hand, Zambrano et al. reported an abnormal clone characterized by additional ring chromosomes derived from chromosome 12 in one case [12]. In our experience, cytogenetic analysis of the lesion revealed a karyotype with a t(1;17)(q42;q23) translocation. Nilsson et al. used 1q32-and 17q21-specific bacterial artificial chromosome (BAC) probes to produce a detailed map of the breakpoints on chromosome 1 and 17 [6], but the BAC probes were unavailable for use in our analysis. The identification of the translocation breakpoints in our analysis might be rather approximate, and the present cytogenetic findings might actually express the same translocation as that reported by Nilsson et al. [6].

BPOP has a tendency to recur repeatedly, but it is regarded as a benign lesion because it does not metastasize [5]. Whether BPOP is a neoplastic lesion or a reactive proliferative lesion remains controversial. Although an antecedent traumatic history, which has been reported in

some cases [12], may support a reactive theory, a traumatic history cannot be documented in most cases. The histological features, primarily the maturation from cartilage to bone, support a reactive process akin to heterotopic ossification [5]. However, the monotonous proliferation of spindle cells, as seen in our case, suggests a neoplastic process, particularly one characterized by a genetic abnormality. If BPOP is a reactive lesion, the remarkable tendency to recur after excision would be difficult to explain. Although chromosomal aberrations have been reported in some soft-tissue lesions considered to be reactive, such as nodular fasciitis and proliferative myositis [1, 4, 9, 10], these were all single case reports that have not yet been corroborated. The t(1;17) translocation in BPOP is a distinctive cytologic abnormality that has been confirmed in at least six cases of BPOP, including the present one [6]. These histological and cytologic features support a neoplastic theory.

Some authors have proposed that several separately described entities, such as florid reactive periostitis (FRP), BPOP, and subungual exostosis, represent different phases of reactive processes initiated by trauma and subperiosteal hemorrhage, with subsequent organization and maturation [11]. The clinical and histological findings of BPOP resemble those of FRP and subungual exostosis. Zambrano et al. [12] and Dal Cin et al. [2] reported a t(X;6) translocation in four cases of subungual exostosis and suggested that subungual exostosis was a neoplastic lesion. Our chromosomal translocation findings in the present BPOP case were different from those found in subungual exostosis, so these two lesions might be distinct clinicopathologic entities with a different molecular pathogenesis. Concerning FRP, no cytogenetic abnormality has been reported.

In summary, we present an additional case of BPOP with a clearly demonstrated t(1;17) translocation. This finding suggests that BPOP is a neoplastic lesion, rather than a reactive proliferative lesion. Additional cases should be studied to determine the consistency of this finding, and further studies may help to elucidate the role of this translocation in the onset of BPOP.

References

1. Birdsall SH, Shipley JM, Summersgill BM, Black AJ, Jackson P, Kissin MW, Gusterson BA (1995) Cytogenetic findings in a case of nodular fasciitis of the breast. Cancer Genet Cytogenet 81:166–168
2. Dal Cin P, Pauwels P, Poldermans LJ, Sciot R, Van den Berghe H (1999) Clonal chromosome abnormalities in a so-called Dupuytren's subungual exostosis. Genes Chromosomes Cancer 24:162–164
3. Gustashaw KM (1991) Chromosome stains. In: Barch MJ (ed) The ACT cytogenetics laboratory manual. Raven, New York, pp 205–269
4. McComb EN, Neff JR, Johansson SL, Nelson M, Bridge JA (1997) Chromosomal anomalies in a case of proliferative myositis. Cancer Genet Cytogenet 98:142–144
5. Meneses MF, Unni KK, Swee RG (1993) Bizarre parosteal osteochondromatous proliferation of bone (Nora's lesion). Am J Surg Pathol 17:691–697
6. Nilsson M, Domanski HA, Mertens F, Mandahl N (2004) Molecular cytogenetic characterization of recurrent translocation breakpoints in bizarre parosteal osteochondromatous proliferation (Nora's lesion). Hum Pathol 35:1063–1069
7. Nora FE, Dahlin DC, Beabout JW (1983) Bizarre parosteal osteochondromatous proliferations of the hands and feet. Am J Surg Pathol 7:245–250
8. Speicher MR, Gwyn Ballard S, Ward DC (1996) Karyotyping human chromosomes by combinatorial multi-fluor FISH. Nat Genet 12:368–375
9. Velagaleti GV, Tapper JK, Panova NE, Miettinen M, Gatalica Z (2003) Cytogenetic findings in a case of nodular fasciitis of subclavicular region. Cancer Genet Cytogenet 141:160–163
10. Weibolt VM, Buresh CJ, Roberts CA, Suijkerbuijk RF, Pickering DL, Neff JR, Bridge JA (1998) Involvement of 3q21 in nodular fasciitis. Cancer Genet Cytogenet 106:177–179
11. Yuen M, Friedman L, Orr W, Cockshott WP (1992) Proliferative periosteal processes of phalanges: a unitary hypothesis. Skelet Radiol 21:301–303
12. Zambrano E, Nose V, Perez-Atayde AR, Gebhardt M, Hresko MT, Kleinman P, Richkind KE, Kozakewich HP (2004) Distinct chromosomal rearrangements in subungual (Dupuytren) exostosis and bizarre parosteal osteochondromatous proliferation (Nora lesion). Am J Surg Pathol 28:1033–1039

Virchows Arch (2005) 447: 103–106
DOI 10.1007/s00428-005-1223-5

CASE REPORT

Dmitry V. Kazakov · Radek Sima · Michal Michal

Hemosiderotic fibrohistiocytic lipomatous lesion: clinical correlation with venous stasis

Received: 23 December 2004 / Accepted: 3 February 2005 / Published online: 10 June 2005
© Springer-Verlag 2005

Abstract Hemosiderotic fibrohistiocytic lipomatous lesion (HFLL) is a recently proposed lipomatous entity. HFLL was originally suggested to be a benign reactive lesion arising due to an antecedent trauma. We report two patients with HFLL who also suffered from chronic vein insufficiency due to varicose involving deep veins of the low limbs. Both patients were middle-aged women with solitary, poorly circumscribed subcutaneous lesions on the lower extremities. Histopathological examination revealed typical features of HFLL. We think that the consistent clinical features such as advanced age, female sex predilection, and specific location along with distinctive histopathological features allow the suggestion that impaired blood circulation, to wit, venous stasis is involved in the pathogenesis of HFLL. We hypothesize that the proliferation of spindled fibroblastic and myofibroblastic cells and capillaries, erythrocyte extravasation, and hemosiderin deposition with lipomatous tissue of HFLL may simply represent an exaggerated tissue response to venous stasis in which elevated venous and capillary pressures, oxygen saturation, and edema stimulate the proliferation of the abovementioned elements and lead to erythrocyte extravasation. A similar histopathological pattern is seen in acroangiodermatitis of Mali and vascular transformation of lymph node sinuses, and these conditions are also associated with impaired blood circulation.

Keywords Adipose tissue · Acroangiodermatitis · Vascular sinus transformation of lymph nodes · Vein insufficiency · Stasis · Varicose · HUMARA

D. V. Kazakov · R. Sima · M. Michal (✉)
Sikl's Department of Pathology,
Medical Faculty Hospital, Charles University,
Alej Svobody 80,
304 60 Pilsen, Czech Republic
e-mail: michal@medima.cz
Tel.: +420-19-603886633
Fax: 420-19-377104650

Introduction

In 2000, a new entity within the group of adipose tumors was proposed [7]. It was called hemosiderotic fibrohistiocytic lipomatous lesion (HFLL) by the authors who identified 10 patients with this condition among all benign lipomatous lesions at the AFIP files over the preceding 24 years [7]. Its reproducible clinical and histopathological findings suggested that HFLL merits designation as a separate entity. HFLL was found to mainly occur in middle-aged women in the low extremities, especially in the foot/ankle region. Histopathological features included proliferation of bland or slightly pleomorphic spindled cells within well-delineated mature adipose tissue in a background of mixed inflammatory infiltrate and hemosiderin deposition. Immunohistochemically, the spindled cell component was demonstrated to represent a mixture of myofibroblasts, fibroblasts, and histiocytes. HFLL was originally suggested to be a benign reactive lesion arising due to an antecedent trauma [7]. Most recently, however, Folpe and Weiss [4] suggested that HFLL might represent a variant of pleomorphic telangiectatic tumor. We have seen two patients with HFLL who also had varicose involving deep veins of the low limbs. We suggest that impaired blood circulation due to varicose may also be implicated or even dominate in the pathogenesis of HFLL.

Case reports

Both patients were women (48 and 60 years old) suffering from varicose of deep veins of the low extremities with chronic venous insufficiency with known recurrent ulcerations of the skin of the calves. Both clinically presented with a solitary, poorly circumscribed subcutaneous mass located over the extensor surface of the right foot with extension onto the ankle. In the first patient, the lesion had previously been surgically removed twice, but recurred in the same site 3 years and 1 year after surgical interventions, respectively. The history of the second patient was irrelevant. The mode of treatment in both cases was surgical

removal of the lesion. Both patients were without signs of further recurrence or metastasis after the last excision 1 year and 6 months, respectively.

Material and methods

Tissues were fixed in 4% formaldehyde embedded in paraffin. The paraffin blocks were cut into 5-μm-thick sections and stained with hematoxylin and eosin, Giemsa, PAS with and without diastase pretreatment, Fontana, and Prussian blue stains.

Immunohistochemical studies were performed on formalin-fixed paraffin-embedded tissue. Primary antibodies against S-100 protein (polyclonal, 1:4,000, DakoCytomation, Glostrup, Denmark), CD34 (clone QBEnd/10, 1:100, DakoCytomation, Glostrup), CD68 (KP1, 1:200, DakoCytomation, Carpenteria), α-smooth muscle actin (ASMA) (1A4, 1:200, DakoCytomation, Glostrup), muscle-specific actin (MSA) (HHF-35, 1:5,000, DakoCytomation, Carpenteria), calponin (CALP, 1:1,000, DakoCytomation, Carpenteria), desmin (D33, 1:500, DakoCytomation, Glostrup), vimentin (V9, 1:200, DakoCytomation, Glostrup), melanosomes (HMB-45, 1:400, DakoCytomation, Glostrup), antigen Ki-67 (MIB-1, 1:150, Biotex, Westinghouse), epithelial membrane antigen (EMA) (E29, 1:700, DakoCytomation, Glostrup), and lysozyme (polyclonal, 1:200, DakoCytomation, Glostrup) were used. Immunostaining was performed according to standard protocols using an alkaline phosphatase–anti-alkaline phosphatase method or avidin–biotin complex labeled with peroxidase or alkaline phosphatase. Appropriate positive and negative controls were applied.

A polymerase chain reaction (PCR) with primers KSHV-1 (5′-AGCCGAAAGGATTCCACCAT-3′) and KSHV-2 (5′-TCCGTGTTGTCTACGTCCAG-3′) for human herpes virus 8 (HHV8) detection was performed as described elsewhere [12].

Clonality analysis was performed by a previously described method based on digestion of genomic DNA with methylation-sensitive restriction enzymes followed by PCR amplification of the CAG repeat at the human androgen receptor gene (HUMARA) locus at the X chromosome [1]. The primers used were as follows: 2A (5′-TCC AGA ATC TGT TCC AGA GCG TGC-3′) and 2B (5′-ATG GGC TTG GGG AGA ACC ATC CTC-3′) [10]. The amplification program consisted of denaturation for 14 min at 95°C, then five rounds of 2.5 min at 95°C, 1 min at 60°C, 1.5 min at 72°C, followed by 30 cycles of 1 min at 95°C, 1 min at 60°C, and 1.5 min at 72°C. Amplification program was finished by a final extension at 72°C for 10 min. All PCR products were examined by fragment analysis on 8% ReproGel High Resolution (AP Biotech, Uppsala, Sweden) using an ALFexpress automated sequencer and fragment analyzer (AP Biotech). All samples were analyzed in duplicate. Peak intensities of the two alleles were measured for each specimen. A corrected ratio (CR) was first assessed by dividing the ratio (allele 1/allele 2) of the *Hpa*II digested samples by the ratio (allele 1/allele 2) of the non-digested sample. A final clonality ratio was determined by dividing the CR of the lesional DNA by the CR of the nonlesional DNA. Samples were considered as monoclonal if the final ratio was 1.5 or greater [11].

Results

Gross findings

Only the lesion from the first patient, representing the second recurrence, was available for gross pathological examination. It had an overall appearance of adipose tissue, the size of 6×5×4 cm. The cut surface was homogeneously tan with tiny foci of hemorrhage.

Histopathological findings

Both lesions demonstrated mature adipose tissue with foci of proliferation of bland spindled cells around individual homogeneous adipocytes, small blood vessels, and along fibrous septa (Fig. 1a–c). There also were scattered infiltrates composed of small lymphocytes, mast cells, plasma cells with occasional Russell bodies, and rare granulocytes. Occasional normal mitotic figures were seen. The cellular proliferations were invariably associated with erythrocyte extravasations and hemosiderin deposits (as verified by Fontana and iron stains), and small areas of fibrosis. Small and medium-sized blood vessels appeared to be slightly increased in number and occasionally demonstrated a somewhat thickened wall and plump endothelial cells. All these changes were more prominent in the first case. In addition, the biopsy from this patient displayed rare multinucleated cells with prominent nucleoli and slight myxoid degeneration of small nerve twigs. There were no pleomorphic cells, nuclear crowding, lipoblasts, or abnormal mitotic figures.

Immunohistochemical findings

The spindled cells variably coexpressed CD34, calponin, lysozyme, vimentin, and CD68, and were negative for desmin, ASMA, MSA, and EMA. Proliferation index was low. S-100 protein stained adipocytes and nerves. HMB-45 reacted negatively.

Human herpes virus 8 PCR

The PCR failed to detect HHV8 DNA in the lesional tissues.

HUMARA analysis

One case was homozygous in locus HUMARA and was thus unsuitable for analysis of clonality. The analysis of the

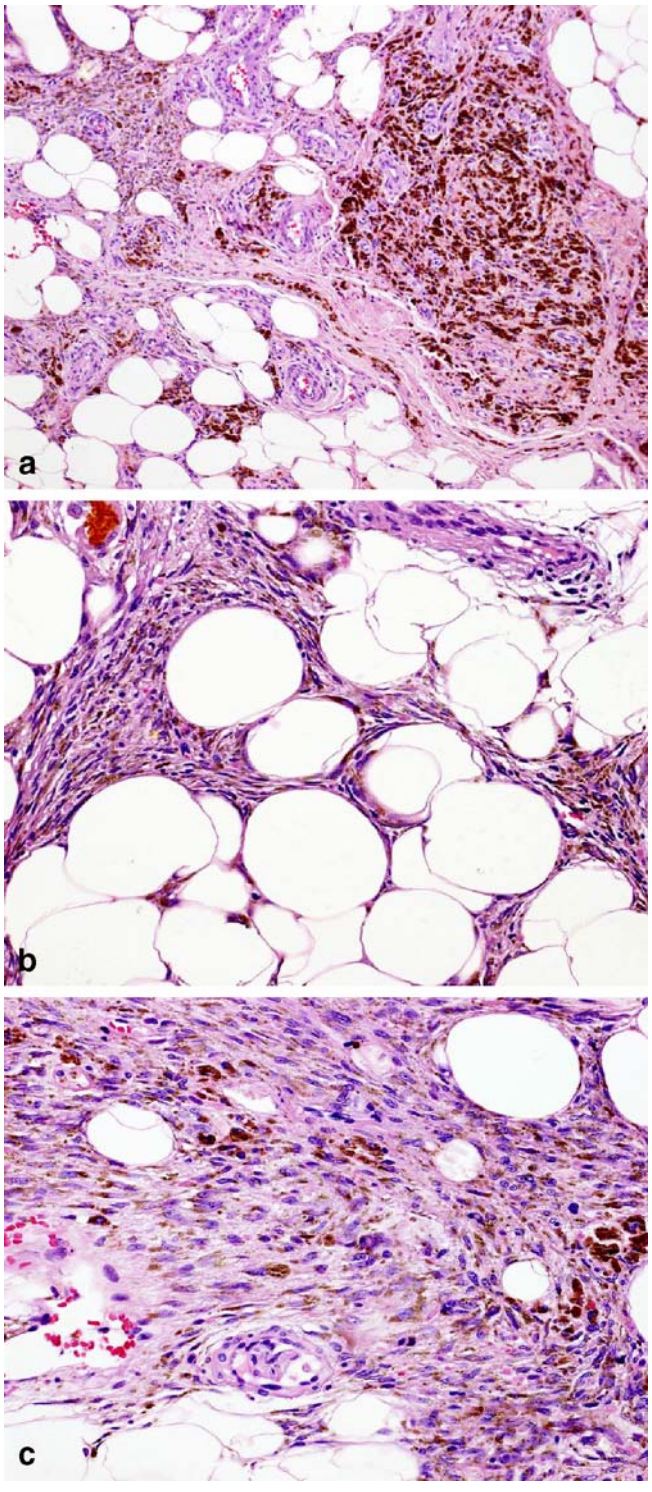


Fig. 1 **a** Mature adipose tissue with hemosiderin deposits, small areas of fibrosis, and proliferation of spindled cells along the fibrous septum and blood vessels. **b** Proliferation of spindled cells around individual lipocytes. **c** A close-up view: plump, relatively uniform spindled cells

HUMARA gene in the other patient showed partial loss of one allele in samples digested with restriction enzyme *Hha*I (*Hpa*II). Signal intensity ratio of nondigested and digested DNA was 1.55.

Discussion

Because a history of an injury (specific injury and/or multiple repeatable traumas) was given by the majority of the patients of the original series, it was suggested that HFLL occurs as a result of these [7]. Not denying this, we think that another factor may play a role in the pathogenesis of this condition. The predilection site of HFLL is the lower extremities, and the lesion usually occurs in middle-aged to old women. This very anatomic area of soft tissue in women is likely to suffer from impaired blood circulation as a result of venous insufficiency. Because this area is prone to traumas anyway, we think that it is not possible to deny the close association of HFLL with an injury. We therefore believe that the consistent clinical features such as advanced age, female sex predilection, and specific location along with distinctive histopathological features may lend credit to the suggestion that impaired blood circulation, to wit, venous stasis is involved in the pathogenesis of HFLL. This possibility was mentioned by Marshall-Taylor and Fanburg-Smith [7] while discussing the differential diagnosis of HFLL and acroangiodermatitis of Mali, but finally discarded by the authors, because none of their patients were known to have vascular insufficiency. In many women, the signs of congestions are, however, often mild and are only subclinically apparent, and still, these patients are prone to injuries, which often results in ulceration of the skin on the calves. Our patients had severe chronic venous insufficiency secondary to varicose of deep veins of the low extremities. Further, the histopathological pattern of HFLL and that of acroangiodermatitis of Mali is basically the same, namely, the proliferation of spindled fibroblastic and myofibroblatsic cells and capillaries, erythrocyte extravasation, and hemosiderin deposition. This pattern simply represents an exaggerated tissue response to venous stasis in which elevated venous and capillary pressures, oxygen saturation, and edema stimulate the proliferation of the abovementioned elements and lead to erythrocyte extravasation. The differences are only in the location: in acroangiodermatitis of Mali, the histopathological changes are confined to the upper dermis, and the main response is seen as the proliferation of capillaries that often assume a lobular pattern [6]. In HFLL, a deeper tissue, mainly fat, is involved. In respect to the skin, similar histopathological features are seen in patients with Stewart–Bluefarb syndrome (unilateral acroangiodermatitis secondary to congenital arteriovenous malformation) [2, 14] and in patients on hemodialysis as a consequence of an arteriovenous fistula [5]. The same pattern (proliferation of endothelial cells, spindle-shaped fibroblasts, erythrocyte extravasation, and hemosiderin deposition) is also seen in "vascular transformation of lymph node sinuses" [9, 13] especially in the nodular spindle cell variant of this lesion [3, 8]. This condition also occurs due to local impaired blood circulation after occlusion of efferent lymphatic vessels and veins by a tumor arising in the adjacent tissue or may be reproduced experimentally [13]. In fact, microscopically vascular sinus transformation of lymph node, acroangiodermatitis of Mali, and HFLL, and

other spindle cell mesenchymal lesions caused by congestion look identical; all these lesions have a similarity to Kaposi's sarcoma. Half of the patients with HFLL in the original series with follow-up had a local recurrence or residual disease within 3 years, requiring reexcision [7]. This was also seen in one of our patients and further supports our hypothesis, because the main underlying pathogenic mechanism, impaired blood circulation, persists and predisposes to recurrence.

In summary, we suggest that impaired blood circulation due to varicose may also be involved in the pathogenesis of HFLL. Further observations would be necessary to support or decline our hypothesis.

References

1. Allen RC, Zoghbi HY, Moseley AB, Rosenblatt HM, Belmont JW (1992) Methylation of *Hpa*II and *Hha*I sites near the polymorphic CAG repeat in the human androgen-receptor gene correlates with X chromosome inactivation. Am J Hum Genet 51:1229–1239
2. Bluefarb SM, Adams LA (1967) Arteriovenous malformation with angiodermatitis. Stasis dermatitis simulating Kaposi's disease. Arch Dermatol 96:176–181
3. Cook PD, Czerniak B, Chan JKC, Mackay B, Ordóñez NG, Ayala AG, Rosai J (1995) Nodular spindle cell vascular transformation of lymph nodes. A benign process occurring predominantly in retroperitoneal lymph nodes draining carcinomas that can simulate Kaposi's sarcoma or metastatic disease. Am J Surg Pathol 19:1010–1020
4. Folpe AL, Weiss SW (2004) Pleomorphic hyalinizing angiectatic tumor: analysis of 41 cases supporting evolution from a distinctive precursor lesion. Am J Surg Pathol 28:1417–1425
5. Kim TH, Kim KH, Kang JS, Kim JH, Hwang IY (1997) Pseudo-Kaposi's sarcoma associated with acquired arteriovenous fistula. J Dermatol 24:28–33
6. Mali JW, Kuiper JP, Hamers AA (1965) Acro-angiodermatitis of the foot. Arch Dermatol 92:515–518
7. Marshall-Taylor C, Fanburg-Smith JC (2000) Hemosiderotic fibrohistiocytic lipomatous lesion: ten cases of a previously undescribed fatty lesion of the foot/ankle. Mod Pathol 13:1192–1199
8. Michal M, Koza V, Fakan F (1992) Myoid differentiation in vascular transformation of lymph node sinuses due to venous obstruction. Immunohistochemical and ultrastructural study. Zentralbl Pathol 138:27–33
9. Michal M, Koza V (1989) Vascular transformation of lymph node sinuses—a diagnostic pitfall. Pathol Res Pract 185:441–445
10. Nakamura H, Hirota S, Adachi S, Ozaki K, Asada H, Kitamura Y (2001) Clonal nature of seborrheic keratosis demonstrated by using the polymorphism of the human androgen receptor locus as a marker. J Invest Dermatol 116:506–510
11. Paradis V, Laurent A, Flejou JF, Vidaud M, Bedossa P (1997) Evidence for the polyclonal nature of focal nodular hyperplasia of the liver by the study of X-chromosome inactivation. Hepatology 26:891–895
12. Serfling U, Lukowsky A, Audring H, Sterry W (1997) Search for Kaposi's sarcoma-associated virus DNA in hemangioproliferative disorders and cutaneous malignant lymphoma. J Cutan Pathol 24:298–304
13. Steinmann G, Foldi E, Foldi M, Racz P, Lennert K (1982) Morphologic findings in lymph nodes after occlusion of their efferent lymphatic vessels and veins. Lab Invest 47:43–50
14. Stewart WM (1967) Fausse angiosarcomatose de Kaposi par fistules arteriovenulaires multiples. Bull Soc Fr Dermatol Syphiligr 74:664–665

Virchows Arch (2005) 447: 107–110
DOI 10.1007/s00428-005-1218-2

CASE REPORT

Michal Michal · Ondrej Hes · Dmitry V. Kazakov

Primary signet-ring stromal tumor of the testis

Received: 10 November 2004 / Accepted: 19 January 2005 / Published online: 21 May 2005
© Springer-Verlag 2005

Abstract We present, in a 47-year-old man, the first case of the signet-ring stromal tumor of the testis. The tumor was located beneath the tunica albuginea surrounded by the testicular tubules and rete testis. It was sharply circumscribed by a thin and irregular fibrous capsule. Histologically, it was composed of cells with a widespread signet-ring cell change separated by fibrous stroma. In some places, the signet-ring cells formed vague Indian files, thus resembling metastatic carcinomas with signet-ring cell morphology. Under high magnification, most of the cytoplasm of the tumor cells was seen to be replaced by an empty clear vacuole which pushed the nuclei to the periphery of the cells. Some of the nuclei were indented by the cytoplasmic vacuoles, others were without indentation. Only in a small area did the tumor show cells without a signet-ring cell change. They looked like epithelioid fibroblasts forming abortive and vaguely tubular structures. Mitoses and necroses were absent. Mucicarmine and PAS stains were negative. Immunohistochemically, the tumor was vimentin positive and it was negative with antibodies to cytokeratins, inhibin, prostatic acid phosphatase, prostate-specific antigen, smooth muscle actin, S-100 protein, EMA and calretinin. The signet-ring stromal tumor of the testis is thus similar morphologically and immunohistochemically to the signet-ring stromal tumor of the ovary. The patient was free of recurrence and metastasis 3 years after the excision.

M. Michal · O. Hes · D. V. Kazakov
Department of Pathology, University Hospital Plzen,
Pilsen, Czech Republic

M. Michal (✉)
Sikl's Department of Pathology,
Laboratore Spec.
Diagnostiky Medical Faculty Hospital,
Alej Svobody 80,
304 60 Pilsen, Czech Republic
e-mail: michal@medima.cz
Tel.: +42-603-886633
Fax: +42-37-7104650

Keywords Testis · Signet-ring cell stromal tumor

Introduction

Signet-ring stromal tumor is a rare type of ovarian tumor and it has never before been described in the testis. Microscopically, this ovarian neoplasm is characterized by a proliferation of stromal spindle-shaped cells merged with rounded cells containing eccentric nuclei and single vacuoles, resembling signet-ring cells [1, 3, 7–10, 12]. The signet-ring cells may either be diffuse or represent only a focal change in an otherwise typical fibroma. We present a case of signet-ring stromal tumor of the testis identical to that of the ovary. To the best of our knowledge, this is the first case of signet-ring stromal tumor of the testis ever to be published.

Materials and methods

Tissue was fixed in 4% formaldehyde and paraffin embedded. Sections (5 μm thick) were stained using routine staining methods.

The case was examined by means of immunohistochemistry on the formaldehyde-fixed, paraffin-embedded material. As a detection system, we employed the avidin–biotin complex or streptavidin–biotin complex labeled with peroxidase or alkaline phosphatase (DakoCytomation). We used microwave antigen pretreatment prior to the application of the primary antibodies. Automated immunostaining employing Lab Vision autostainer was used. Antibodies against cytokeratins (CAM 5.2, Becton-Dickinson), AE1–AE3 (Boehringer), epithelial membrane antigen (EMA; E29, DakoCytomation), S-100 protein (polyclonal, DakoCytomation), neuron specific enolase (NSE; polyclonal, DakoCytomation), prostate specific antigen (polyclonal, DakoCytomation), prostate acid phosphatase (polyclonal, DakoCytomation), glial fibrillary acidic protein (polyclonal, DakoCytomation), CD 34 (QBEnd 10, DakoCytomation), calretinin (DC8, Zymed), vimentin (V9,

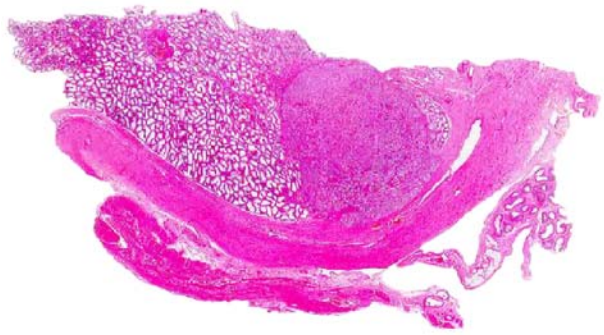


Fig. 1 A low-power view showing that the tumor lies beneath the tunica albuginea surrounded by the testicular tubules and rete testis

DakoCytomation), smooth muscle actin (1A6, DakoCytomation), desmin (D33, DakoCytomation), placental alkaline phosphatase (8B6, DakoCytomation), melanosome (HMB45, DakoCytomation), estrogen and progesterone receptors (Immunotech), androgen receptors (AR 441 DakoCytomation) and Ki67 (MIB1, Immunotech) were used.

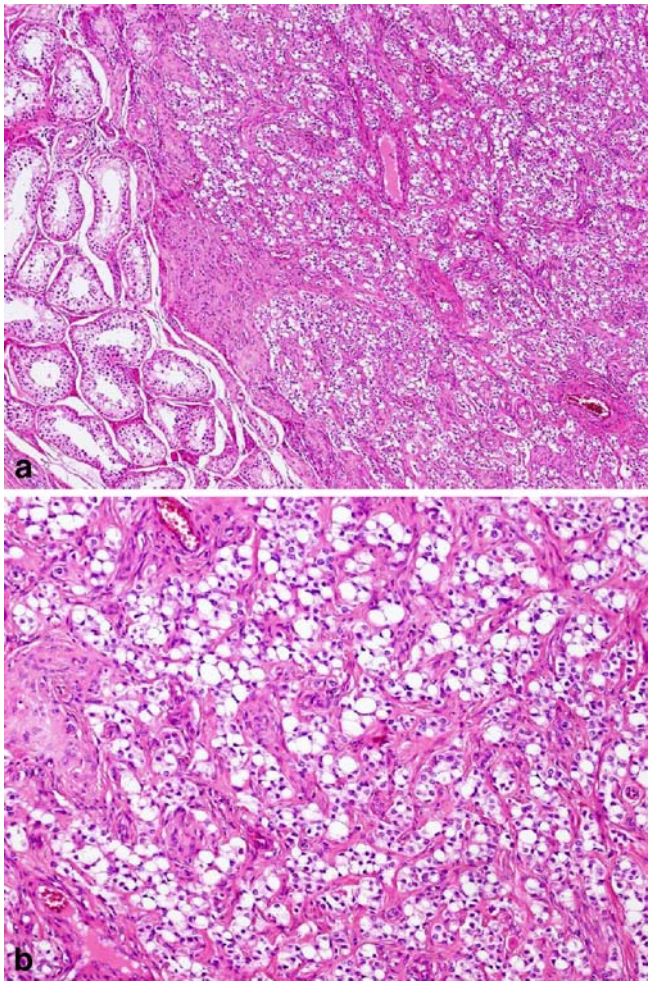


Fig. 2 The tumor is well circumscribed (**a**) and is formed by cells with widespread signet-ring cell change separated by fibrous stroma (**b**)

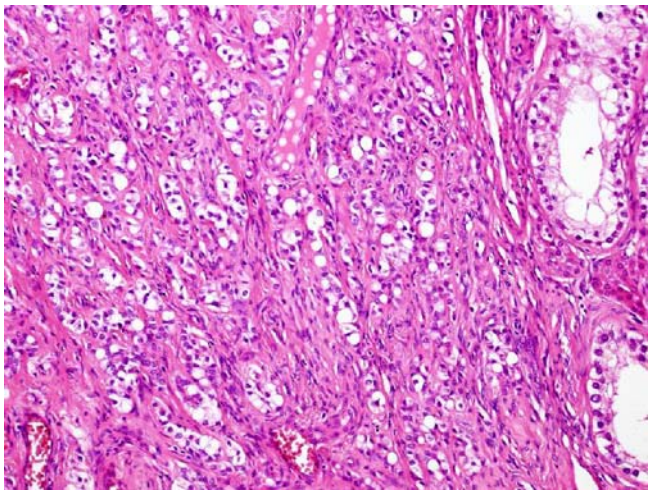


Fig. 3 In some places, the signet-ring cells form vague Indian files, thus having a resemblance to metastatic signet-ring cell carcinomas

Tissue material for ultrastructural examination was not available.

Results

Case report

A 47-year-old patient was found to have a round-shaped tumor 1 cm in largest diameter in the right testis. The tumor was surgically removed. Grossly it was white in color and hard in consistency. The patient is without signs of recurrence and metastasis 3 years after the excision.

The tumor was located beneath the tunica albuginea surrounded by the testicular tubules and rete testis. It was sharply circumscribed by a thin and irregular fibrous capsule (Fig. 1). Histologically, it was composed of irregular and variously shaped trabeculae of cells with a widespread

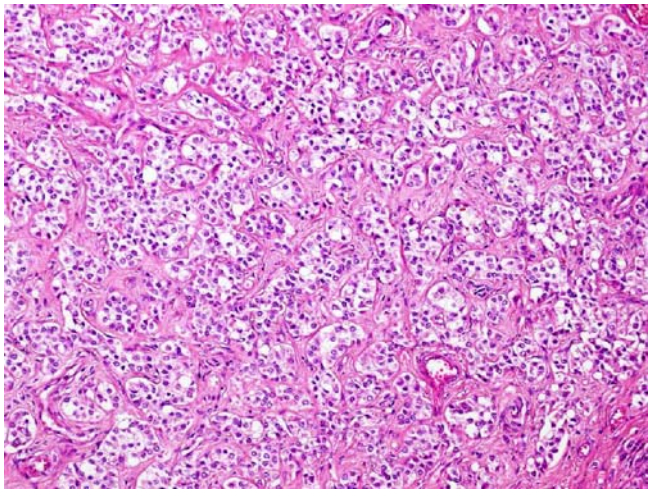


Fig. 4 The tumor cells in this area have the appearance of epithelioid fibroblasts

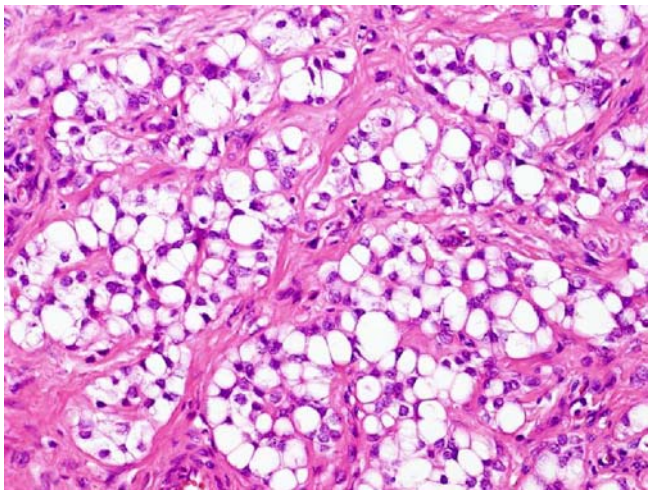


Fig. 5 Under high magnification, most of the cytoplasm is shown to be replaced by an empty clear vacuole that has pushed the nucleus to the periphery of the cell. Some of the nuclei are indented by the cytoplasmic vacuoles, while others are not

signet-ring cell change separated by fibrous stroma (Fig. 2). In some places the signet-ring cells formed vague Indian files, thus resembling metastatic signet-ring cell carcinomas (Fig. 3). Only in a small area were there cells without signet-ring cell change. The tumor cells in this area had the appearance of epithelioid fibroblasts arranged in abortive and vaguely microalveolar structures (Fig. 4). Under high magnification, most of the cytoplasm of the majority of the tumor cells was seen to be replaced by an empty clear vacuole which pushed the nucleus to the periphery of the cell. Some of the nuclei were indented by the cytoplasmic vacuoles, others were without sign of indentation (Fig. 5). Mucicarmine and PAS stains were negative. Mitoses and necroses were absent.

Immunohistochemically, the tumor cells reacted strongly with antibody to vimentin; and all other antibodies—including those against MIB1 and estrogen, progesterone and androgen receptors—reacted negatively.

Discussion

Benign fibrous tumors of the testis are quite unusual. Most of these tumors within this category are paratesticular and they have been considered variants of fibrous pseudotumor [11]. Jones et al. [4] coined the term "fibroma of gonadal stromal origin" for a group of rare testicular tumors in order to delineate these neoplasms from all other types of testicular lesions for which the term "fibroma" was used. However, in none of the cases of testicular fibromas of gonadal stromal origin was the observation of a signet-ring cell change ever published [2, 4].

Our case seems to have many similarities to the rare ovarian neoplasm called "signet-ring stromal tumors of the ovary" (SSTO). SSTO shown a spindle cell fibroblastic component which merges imperceptibly with rounded cells containing eccentric nuclei and large vacuoles resembling signet-ring cells. Ultrastructural examination showed that in some cases of SSTO the vacuoles result from generalized edema of the cytoplasmic matrix, from a swelling of mitochondria or from cytoplasmic pseudoinclusions of an edematous extracellular matrix [3]. Similar to this tumor, our case revealed a fibroblastic component without signet-ring vacuoles, which merged with PAS and mucicarmine negative signet-ring cells [3]. In addition, immunohistochemical vimentin positivity and immunohistochemical negativity with antibodies to cytokeratins, inhibin, smooth muscle actin, S-100 protein, EMA, and calretinin confirm that the immunoprofile of our case was identical to that of SSTO [3, 12]. Absence of mitoses, necroses, immunohistochemical negativity with MIB1 antibody and sharp circumscription of the lesion point to the benign nature of signet-ring stromal tumor of the testis.

There are very few lesions from which signet-ring stromal tumor of the testis should be differentiated. In contrast to the ovary, metastasis of gastric adenocarcinoma (Krukenberg tumor) with signet-ring cell morphology is an extremely rare event in the testis [5, 6]. Sharp circumscription, lack of mitoses, PAS, mucicarmine negativity and immunohistochemical negativity with antibodies to MIB1, EMA and cytokeratins clearly distinguish the visceral metastases with signet-ring cell morphology from the primary signet-ring stromal tumor of the testis. The authors are not aware of any other primary testicular tumor with so widespread a signet-ring cell morphology.

In summary, we describe the first example of the signet-ring stromal tumor of the testis, which had similar features to the SSTO. It is different from any other known primary testicular neoplasm and it can easily be differentiated by morphology and by immunohistochemical means from visceral metastatic carcinomas with signet-ring cell morphology.

References

1. Cashell AW, Jerome WG, Flores E (2000) Signet ring stromal tumor of ovary occurring in conjunction with Brenner tumor. Gynecol Oncol 77:323–326
2. de Pinieux G, Glaser C, Chatelain D, Perie G, Flam T, Vieillefond A (1999) Testicular fibroma of gonadal stromal origin with minor sex cord elements: clinicopathologic and immunohistochemical study of 2 cases. Arch Pathol Lab Med 123:391–394
3. Dickersin GR, Young RH, Scully RE (1995) Signet-ring stromal and related tumors of the ovary. Ultrastruct Pathol 9:401–419
4. Jones MA, Young RH, Scully RE (1997) Benign fibromatous tumors of the testis and paratesticular region: a report of 9 cases with a proposed classification of fibromatous tumors and tumor-like lesions. Am J Surg Pathol 21:2996–2305
5. Muir GH, Fisher C (1995) Gastric carcinoma presenting with testicular metastasis. Br J Urol 75:114–115
6. Ozdal OL, Yakupoglu YK, Cicek A, Erdem O, Memis L, Memis A (2002) Epididymal metastasis from gastric signet ring cell adenocarcinoma. Can J Urol 9:1498–1499
7. Ramzy I (1976) Signet-ring stromal tumor of ovary. Histochemical, light, and electron microscopic study. Cancer 38: 166–172

8. Shimokawa K, Ikeda T, Ojima A (1986) Sclerosing stromal tumor of the ovary. Gan No Rinsho 32:2021–2025
9. Su RM, Chang KC, Chou CY (2003) Signet-ring stromal tumor of the ovary: a case report. Int J Gynecol Cancer 13:90–93
10. Suarez A, Palacios J, Burgos E, Gamallo C (1993) Signet-ring stromal tumor of the ovary: a histochemical immunohistochemical and ultrastructural study. Virchows Arch A Pathol Anat Histopathol 422:333–336
11. Ulbright TM, Amin MB, Young RH (1999) Tumors of the testis, adnexa, spermatic cord, and scrotum. In: Atlas of tumor pathology. Armed Forces Institute of Pathology, Washington, DC, Series 3, Fascicle 25
12. Vang R, Bague S, Tavassoli FA, Prat J (2003) Signet-ring stromal tumor of the ovary: clinicopathologic analysis and comparison with Krukenberg tumor. Int J Gynecol Pathol 23:45–51

Virchows Arch (2005) 447: 111–112
DOI 10.1007/s00428-005-1234-2

LETTER TO THE EDITOR

N. Volkan Adsay · David S. Klimstra

Not all "mucinous carcinomas" are equal: time to redefine and reinvestigate the biologic significance of mucin types and patterns in the GI tract

Received: 6 January 2005 / Accepted: 15 February 2005 / Published online: 8 June 2005
© Springer-Verlag 2005

We read with great interest the study by Solcia et al. [14], published in the December 2004 issue of *Virchows Archives*. Their results reaffirm that the muconodular (or colloid) type of mucinous carcinoma is associated with a significantly better prognosis than other types of mucinous carcinomas (or the conventional carcinomas of the respective organs), not only in the breast [8] and pancreas [2], but in the stomach as well. As such, this study adds another major blow to a long-held dogma that mucinous carcinomas of any type are particularly aggressive in the gastrointestinal (GI) tract.

It has long been known that "pure mucinous" carcinomas of the breast, also referred to as colloid carcinomas [7, 9, 10, 13], are associated with an excellent prognosis, even better than that of some in-situ carcinomas of this organ [7]. It is also noted that, interestingly, even a small component of the usual ductal carcinoma negates this survival benefit [4, 8]. The same seems to apply to the pancreas; pancreatic carcinomas composed almost entirely of the colloid pattern have a very good prognosis [2], whereas mixed-mucinous carcinomas are highly aggressive tumors [12].

Why is pure colloid carcinoma indolent, but not mixed-mucinous carcinoma? We believe the answer lies in the pathogenesis of the colloid carcinoma pattern. It has been speculated that in colloid carcinoma, the mucin acts as a containing factor, exerting a function similar to that of the basement membrane in in-situ carcinomas [1, 7]. Indeed, the survival advantage and indolent behavior of colloid carcinomas appear to be most evident when most of the cells are floating within the mucin, without any non-mucinous glands infiltrating into the stroma. What causes the tumor cells to float within the mucin rather than invading the stroma? One characteristic feature of the colloid pattern is that the cells have reversed polarity (as evidenced by both immunohistochemical and ultrastructural studies) [1], in which the secretory pole of the cells is oriented toward the stroma-facing surface of the cells, leading to the accumulation of mucin in the stroma, which in turn acts as a barrier to the spread of the cells. Furthermore, the mucin secreted by these cells appears to be distinctive, with inhibitory properties [1]. MUC2, which is a tumor suppressor, is highly expressed in this type of mucinous carcinoma but not others. Why then is it that even a small component of ordinary carcinoma negates the survival advantage of the colloid pattern? One can speculate that once the cells of a colloid carcinoma acquire the properties that allow them to overcome the mucin and independently invade the stroma, these cells may represent a more aggressive phenotype than even ordinary invasive carcinomas.

Does the colloid (muconodular) pattern have the same implication in the GI tract as in the breast and pancreas? The studies by Solcia et al. [14] and others [3] show that it probably does. But in fact, there were already several questions regarding the significance of mucin production in the GI tract. First, appendiceal mucinous neoplasms that have a predominantly colloid pattern are associated with a protracted clinical course even if they give rise to pseudomyxoma peritonei. There are several observations that support this impression [5, 6]. The invasive (disseminated) component of the cases, referred to as "disseminated peritoneal adenomucinosis" by Ronnett et al. [6] or "low-grade mucinous neoplasm" by Misdraji et al. [5], typically shows a predominant colloid pattern and has a much better prognosis than those with less of a colloid pattern. There is yet

N. V. Adsay (✉)
Department of Pathology,
The Karmanos Cancer Institute and Harper University Hospital,
Wayne State University,
Detroit, MI, USA
e-mail: adsayv@med.wayne.edu
Tel.: +1-313-9932965
Fax: +1-313-7459299

D. S. Klimstra
Department of Pathology,
Memorial Sloan–Kettering Cancer Center,
NewYork, NY, USA

N. V. Adsay
Department of Pathology,
Harper University Hospital,
Detroit, MI, 48201, USA

another emerging set of data supporting the supposition that there may be distinct subsets of "mucinous" carcinoma in the GI tract: patients with hereditary nonpolyposis colorectal cancer (HNPCC) syndrome. Recent studies suggest that HNPCC-associated colorectal carcinomas have a better clinical outcome [15] (beyond that which can be explained by the younger age of the patients), and it has been also shown that HNPCC-associated colorectal carcinomas are commonly mucinous [11]. All of this evidence raises the question of whether different types and patterns of mucin production may have different clinical implications in the lower GI tract as well.

To determine the significance of mucin production in different sites, a more uniform approach to the definition of "mucinous carcinoma" is necessary. As discussed above, there is mounting evidence that the muconodular (colloid) pattern ought to be defined strictly as well-delineated lakes of mucin, in which most of the cells are floating unattached to the stroma. If a substantial number of the cells are clinging to the stroma or if the mucin lakes are ill defined, this should not be regarded as the muconodular (colloid) pattern. For a given case, the percentage of the colloid pattern in the tumor ought to be recorded. The goal for investigators, then, would be to determine what percentage of colloid pattern qualifies a case as a "colloid (or a muconodular or low-grade mucinous) carcinoma" so that the significance of this phenomenon can be verified.

References

1. Adsay NV, Merati K, Nassar H et al (2003) Pathogenesis of colloid (pure mucinous) carcinoma of exocrine organs: coupling of gel-forming mucin (MUC2) production with altered cell polarity and abnormal cell–stroma interaction may be the key factor in the morphogenesis and indolent behavior of colloid carcinoma in the breast and pancreas. Am J Surg Pathol 27:571–578
2. Adsay NV, Pierson C, Sarkar F et al (2001) Colloid (mucinous noncystic) carcinoma of the pancreas. Am J Surg Pathol 25:26–42
3. Gurbuz Y, Kahlke V, Kloppel G (2002) How do gastric carcinoma classification systems relate to mucin expression patterns? An immunohistochemical analysis in a series of advanced gastric carcinomas. Virchows Arch 440:505–511
4. Komaki K, Sakamoto G, Sugano H et al (1988) Mucinous carcinoma of the breast in Japan. A prognostic analysis based on morphologic features. Cancer 61:989–996
5. Misdraji J, Yantiss RK, Graeme-Cook FM et al (2003) Appendiceal mucinous neoplasms: a clinicopathologic analysis of 107 cases. Am J Surg Pathol 27:1089–1103
6. Ronnett BM, Zahn CM, Kurman RJ et al (1995) Disseminated peritoneal adenomucinosis and peritoneal mucinous carcinomatosis. A clinicopathologic analysis of 109 cases with emphasis on distinguishing pathologic features, site of origin, prognosis, and relationship to "pseudomyxoma peritonei". Am J Surg Pathol 19:1390–1408
7. Rosai J (1996) Ackerman's surgical pathology, vol 2. Mosby, St. Louis, pp 1607–1609
8. Rosen PP (2001) Rosen's breast pathology. Lippincott-Raven, Philadelphia
9. Rosen PP, Saigo PE, Braun DW Jr et al (1981) Predictors of recurrence in stage I (T1N0M0) breast carcinoma. Ann Surg 193:15–25
10. Roses DF, Bell DA, Flotte TJ et al (1982) Pathologic predictors of recurrence in stage 1 (TINOMO) breast cancer. Am J Clin Pathol 78:817–820
11. Shia J, Ellis NA, Paty PB et al (2003) Value of histopathology in predicting microsatellite instability in hereditary nonpolyposis colorectal cancer and sporadic colorectal cancer. Am J Surg Pathol 27:1407–1417
12. Siedel G, Iacobuzio-Donahue C, Adsay NV et al (2001) Almost all infiltrating colloid carcinomas of the pancreas and periampullary region arise from in-situ papillary neoplasms: a study of 33 cases (abstract). Mod Path 14:202A
13. Silverberg SG, Kay S, Chitale AR et al (1971) Colloid carcinoma of the breast. Am J Clin Pathol 55:355–363
14. Solcia E, Luinetti O, Tava F et al (2004) Identification of a lower grade muconodular subtype of gastric mucinous cancer. Virchows Arch 445:572–579
15. Watson P, Lin KM, Rodriguez-Bigas MA et al (1998) Colorectal carcinoma survival among hereditary nonpolyposis colorectal carcinoma family members. Cancer 83:259–266

Virchows Arch (2005) 447: 113–114
DOI 10.1007/s00428-005-1230-6

LETTER TO THE EDITOR

Ricardo Fonseca · Ana Raquel Tomás · Saudade André

Absence of Epstein-Barr virus EBER transcripts in male breast cancer

Received: 16 December 2004 / Accepted: 10 February 2005 / Published online: 31 May 2005
© Springer-Verlag 2005

Sir,

Epstein-Barr virus (EBV) is a ubiquitous human herpesvirus infecting more than 90% of the adult population worldwide. Since its discovery in 1964, EBV DNA has been demonstrated to be associated with several malignancies (e.g. Burkitt lymphoma, Hodgkin lymphoma, lymphomas occurring in immunodeficient individuals, and nasopharyngeal carcinoma) where it is almost always found in the latent state. Recently, it has been proposed that breast carcinomas should also be included in the list of EBV-related neoplasms [4]. Infection with EBV results in the establishment of a life-long carrier state, associated with the expression of a restricted set of viral antigens which encode two non-translated nuclear RNAs (EBER-1 and -2), six nuclear antigens (EBNAs), three integral membrane proteins (LMPs), and a polypeptide (RK-BARF0). Three forms of latent infection, referred to as latency types I–III, have been demonstrated in EBV-carrying B-cell lines and EBV-carrying tumour biopsy samples.

The viral EBER-1 and EBER-2 transcripts persist throughout the EBV infection cycle and accumulate to very high copy numbers in the nucleus, making them ideal candidates for identification of latent EBV infection. Male breast cancer is a rare entity (fewer than 1% of cases of breast cancer), and most of the knowledge about its biology has been extrapolated from its female counterpart. It occurs predominantly in old men (average 60 years of age, 10 years older than female breast cancer patients). The oestrogen receptor is expressed in most cases (80–93%), and it has been associated with an unfavourable outcome. In male breast cancer an eventual association with EBV would have implications for both prevention and therapy.

R. Fonseca (✉) · A. R. Tomás · S. André
Serviço Patologia Morfológica, Instituto Português de Oncologia de Francisco Gentil CROL S.A.,
Rua Professor Lima Basto,
1099-023 Lisbon, Portugal
e-mail: ricardo.fonseca@netcabo.pt
Tel.: +351-21-7229825
Fax: +351-21-7229825

We studied a sample of 23 invasive male breast carcinomas from southern Portugal for the presence of a latent EBV infection by detecting the EBER transcripts using chromogenic in situ hybridization (CISH). ISH was performed on paraffin-embedded sections using the INFORM EBER assay (Ventana Medical Systems, Frankfurt, Germany) according to the manufacturer's instructions (regarding positive and negative controls, and RNA preservation controls within samples). A nasopharyngeal carcinoma was used as a positive control. The patients' ages ranged from 39 to 87 years (mean 64.3 years). All samples were invasive ductal carcinomas of not otherwise specified (NOS) type. Tumour differentiation was assessed using the Elston and Ellis grading system: 3 (13.1%) samples were classified as grade 1, 13 (56.5%) as grade 2, and 7 (30.4%) as grade 3.

No EBER transcripts were found in our 23 male breast cancers. No EBV-positive lymphocytes were detected. The presence of EBV transcripts has been studied in female breast cancer using immunohistochemistry (IHC), PCR and ISH. In studies using IHC/PCR, EBV DNA was detected in 10–51% [4, 5] of female breast cancers, while in studies using ISH no EBV was detected in female breast cancers [2, 3] and or in male breast cancers [5]. The disparity in the results may have been due to differences in the sensitivity of the probes used for the detection of EBV infection. Herrman and Niedobitek [3] have suggested that EBV DNA detected by PCR in breast carcinoma tissues is likely to be related to the presence of EBV-infected lymphocytes in the tumour stroma, and thus does not indicate infection of the tumour cells by the virus. The study of DNA extracts by PCR is clearly unsatisfactory since it does not indicate the cellular source of any viral genome detected. In recent studies [1, 6] laser capture microdissection combined with real-time quantitative *Bam*HIC PCR has been used in an attempt to overcome this problem, but even with such techniques the results are controversial.

In conclusion, our findings corroborate those of Glaser et al. [2], and do not support an association between an EBV latent infection and the pathogenesis and/or progression of male breast cancer. Although we cannot totally

exclude an association of EBV within particular histological subtypes (e.g. medullary carcinoma/lymphoepithelioma-like carcinoma) that were not represented in our series of male breast cancer, the results of studies of these histological subtypes of breast cancer in females argue against this association [7].

References

1. Fina F, Romain S, Quafik LH, Palmari J, Ben Ayed F, Benharkat S, Bonnier P, Spyratos F, Foekens JA, Rose C, Buisson M, Gérard H, Reymond MO, Seigneurin JM, Martins PM (2001) Frequency and genome load of Epstein-Barr virus breast cancers from different geographical areas. Br J Cancer 84:783–790
2. Glaser SL, Ambinder RF, DiGiuseppe JA, Horn-Ross PL, Hsu JL (1998) Absence of Epstein-Barr virus EBER-1 transcripts in an epidemiologically diverse group of breast cancers. Int J Cancer 75(4):555–558
3. Herrmann K, Niedobitek G (2003) Lack of evidence for an association of Epstein-Barr virus infection with breast carcinoma. Breast Cancer Res 5:R13–R17
4. Labrecque LG, Barnes DM, Fentiman IS, Griffin BE (1995) Epstein-Barr virus in epithelial cell tumors: a breast cancer study. Cancer Res 55:39–45
5. Grinstein S, Preciado MV, Gattuso P, Chalay P, De Matteo E, Gould V (2002) Demonstration of Epstein-Barr virus in carcinomas of various sites. Cancer Res 62:4876–4878
6. Murray P, Lissauer D, Junying J, Davies G, Moore S, Bell A, Timms J, Rowlands D, McConkey C, Reynolds G, Ghataura S, England D, Caroll R, Young L (2003) Reactivity with a monoclonal antibody to Epstein-Barr virus (EBV) nuclear antigen 1 defines a subset of aggressive breast cancers in the absence of the EBV genome. Cancer Res 63:2338–2343
7. Dadmanesh F, Peterse J, Sapino A, Fonelli A, Eusebi V (2001) Lymphoepithelioma-like carcinoma of the breast: lack of evidence of Epstein-Barr infection. Histopathology 38:54–61

Virchows Arch (2005) 447: 115–116
DOI 10.1007/s00428-005-1260-0

LETTER TO THE EDITOR

Fabio De Giorgio · Antonio Abbate · Giuseppe Biondi Zoccai · Vincenzo L. Pascali · Arnaldo Capelli · Vincenzo Arena

Fatal choking due to amyloid infiltration of the laryngeal plexus

Received: 20 February 2005 / Accepted: 23 March 2005 / Published online: 20 May 2005
© Springer-Verlag 2005

Sir,

We hereby report the case of an elderly patient with undiagnosed amyloidosis, who died by choking after food inhalation—caused by unnoticed extensive amyloid infiltration of the laryngeal plexus.

Amyloidosis is a chronic, potentially fatal disease, caused by amyloid deposits in several areas, with heterogeneous clinical manifestations [3]. Peripheral neuropathy may be part of its syndromic context [5], but, very often, the disease is diagnosed late after onset and the pathogenesis of the underlying symptoms remains elusive [3, 5]. Careful post-mortem examination can unravel some puzzling clinical patterns.

In the case under our observation, we were faced with an 82-year-old woman, admitted to the UCSC Emergency Department after a car accident. At arrival the patient was awake, orientated and with transient postural instability. Past medical history was significant for hypertension and paroxysmal atrial fibrillation. A primary physical survey did not disclose significant abnormalities. A cranial CT scan ruled out fractures, intracranial haemorrhages, space-occupying lesions or oedema. Results of routine laboratory tests (including markers of myocardial necrosis) and electrocardiography were within normal limits, and chest X-ray showed mild ectasia of the aorta and pulmonary emphysema. After admission to the ward, the patient remained asymptomatic for over 48 hours. On the third day, however, shortly after lunch and in the absence of other symptoms, she suddenly experienced suffocation, which quickly evolved into respiratory arrest.

Post-mortem examination was requested because of the absence of any obvious medical diagnosis and because of the recent car accident. At gross dissection, in the absence of significant traumatic pathology, we found left ventricular and atrial hypertrophy and coronary atherosclerosis. CNS examination was also irrelevant, and pulmonary embolism could be ruled out. Eventually, a massive alimentary bolus was found, obstructing the bronchial tree bilaterally. In the context of a morphologically normal larynx, abnormal tissue deposits were noticed surrounding the perilaryngeal plexus, together with bilateral diffuse infiltration of cranial nerves IX–X. Histological examination of haematoxylin/eosin and Congo-red stained tissue led us to recognize the typical extracellular amyloid deposits (Fig. 1). Other deposits were also discovered in sections from ventricles, atria and pericardial nervous network. No further regions were apparently involved. Whether we were in the presence of primary or secondary amyloidosis remained unclear.

In the light of such evidence, *ab ingestis* suffocation by abnormal deglutition reflex was assumed as the ultimate cause of death, caused by perineural amyloid infiltration. By questioning the patient's relatives, we then learned about recurrent cough paroxysms that would shake the elderly patient while she was eating.

The present case illustrates sudden death by suffocation, caused by amyloid infiltration of IX–X cranial nerves.

The course of amyloidosis typically encompasses unpredictable morbidity and mortality, with long-lasting asymptomatic intervals and sudden life-threatening episodes. Unexpected symptoms and localizations are, therefore, part of its classical nosology.

F. De Giorgio (✉) · V. L. Pascali
School of Medicine, Institute of Legal Medicine,
Catholic University of the Sacred Heart,
L.go F. Vito 1,
00168 Rome, Italy
e-mail: fdegiorgio@tiscalinet.it
Tel.: +39-06-35507031
Fax: +39-06-35507033

A. Abbate
Department of Internal Medicine,
Virginia Commonwealth University,
Richmond, VI, USA

G. B. Zoccai
Institute of Cardiology,
Catholic University of the Sacred Heart,
Rome, Italy

A. Capelli · V. Arena
Institute of Pathological Anatomy,
Catholic University of the Sacred Heart,
Rome, Italy

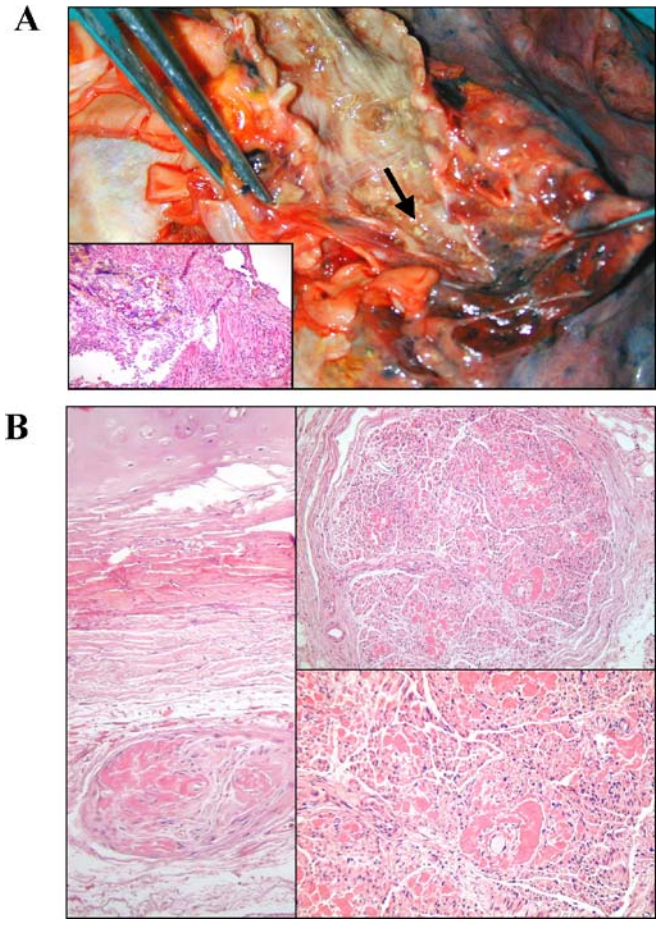


Fig. 1 **a** Macroscopic findings in the lung. Food material in a medium-sized bronchus is confirmed by histology. **b** Peribronchial branches of cranial nerves IX and X with amyloid deposits

Whereas clear-cut motor/sensitive symptoms—the expression of neural region involvement—have a firm place in the clinical descriptions of amyloidosis, the effects of autonomous nervous system involvement have been so far underrated. The same is true for laryngeal localization [1, 2, 4]. Indeed, to the best of our knowledge, sudden death by choking has never, as yet, been reported as a cause of death.

In view of the peculiarly elusive quality of abnormal swallowing symptoms and the uncertainty regarding the real incidence of significant laryngeal amyloid deposits in patients with amyloidosis, this clinical vignette emphasizes that the experienced clinician should regard *ab ingestis* suffocation as one of the most fearful amyloidosis complications. Thus, careful assessment of glottis function should be carried out in any patient with an established diagnosis of amyloidosis.

References

1. Chadwick MA, Buckland JR, Mason P, Randall CJ, Theaker J (2002) A rare case of dysphagia: hypopharyngeal amyloidosis masquerading as a post-cricoid tumour. J Laryngol Otol 116: 54–56
2. Finsterer J, Wogritsch C, Pokieser P, Vesely M, Ulrich W, Grisold W, Mamoli B (1997) Light chain myeloma with oropharyngeal amyloidosis presenting as bulbar paralysis. J Neurol Sci 147:205–208
3. Gillmore JD, Hawkins PN, Pepys MB (1997) Amyloidosis: a review of recent diagnostic and therapeutic developments. Br J Haematol 99:245–256
4. Nordborg C, Kristensson K, Olsson Y, Sourander P (1973) Involvement of the autonomous nervous system in primary and secondary amyloidosis. Acta Neurol Scand 49:31–38
5. Rajkumar SV, Gertz MA, Kyle RA (1998) Prognosis of patients with primary systemic amyloidosis who present with dominant neuropathy. Am J Med 104:232–237

Virchows Arch (2005) 446: 117
DOI 10.1007/s00428-005-1285-4
© Springer-Verlag 2005

ANNOUNCEMENTS

22–23 September 2005
Breast Diagnostic Histopathology Update
Hammersmith Hospital (Imperial College), London, UK

A 2-day course designed for pathologists at Consultant and Senior Trainee level. The course is a shorter version of the week long course and is also suitable for those who have previously attended that course and wish to participate in discussing new developments in the field. The course will be based on 30, mostly new, cases derived from the arcives of Hammersmith, Charing Cross, Nottingham City and Cambridge Addenbrook's Hospitals and is slanted to practical diagnostic pathology with special emphasis on areas that pose diagnostic difficulties. The participants will be given ample time to study histological preparations, followed by illustrated discussion of the cases. In addition there will be several talks on specific topics, given by breast pathology specialists followed by discussions. The topics will include issues in the interpretation of breast biopsies, examination of breast biopsies after neo-adjuvant chemotherapy, breast immunohistochemistry, dealing with the gross specimen, fibro-epithelial and spindle cell lesions; papillary, lobular, apocrine and metaplastic lesions, proliferative lesions/carcinoma in situ and sentinel lymph node biopsy. The faculty will include Ian Ellis, Mary Falzon, Andrew Lee, Sarah Pinder and Sami Shousha.

Further details from:
Wolfson Conference Centre,
Hammersmith Hospital,
Du Cane Road,
London W12 ONN, UK
Tel.: (44) 20 8383 3117/3227/3245
Fax: (44) 20 8383 2428
E-mail: wcc@imperial.ac.uk

1–2 December 2005
International Symposium on "Salivary Gland Tumours; Present Concepts of Diagnosis and Management"
Amsterdam, The Netherlands

For further information please contact congress secretariat
Mrs. D. Chavalking
Vrije Universiteit Medical Center (Vumc)
Department of Oral and Maxillofacial Surgery/Oral Pathology
PO Box 7057
1007 MB Amsterdam
The Netherlands
Tel.: +31-20-444-4039
Fax: +31-20-444-4046
E-mail: d.chevalking@vumc.nl
Internet: www.vumc.nl

391296.qxd 11.08.2005 13:44 Uhr Seite 119

Virchows Arch (2005) 447:119–123
DOI 10.1007/s00428-005-1296-1

EUROPATH NEWS 3/2005

European Society
of
Pathology

Editors
Dr. Grete Krag Jacobsen
University Department of Pathology,
Teilumbuilding Rigshospitalet
Blegdamsvej 9,
DK-2100 Copenhagen Ø, Denmark
Tel.: +45 3545 5450
Fax: +45 3545 5414
e-mail: grete.krag.jacobsen@rh.hosp.dk

Dr. Bjørn Risberg
Department of Pathology
The Norwegian Radium Hospital
0310 Oslo, Norway
Tel.: +47-22934174
Fax: +47-22508554
e-mail: brisberg@labmed.uio.no

Newsletter of the European Society of Pathology

Dear Members,

In this newsletter you have the Presidential Address before the Paris Congress – excellently reviewing the activities of the society since the last international congress in Ljubljana. Read it before you attend the ESP General Assembly on Wedensday, September 7.

Notice the members nominated as new ordinary members of the Executive Committee 2005–2007.

Some of the Working Groups report on their activities and announce Pre-congress Meetings, do not miss it. And finally the Application form for Membership of the Society is included in case you have colleagues who have still not applied.

We are all looking forward to the 20th European Congress of Pathology.

Sincerely yours,
Grete Krag Jacobsen

Presidential Address

Dear Members,

After the Ljubljana Congress, September 2003, when I assumed the Presidency, it was generally perceived by the membership that the scientific structures of the ESP had undergone a series of important and rapid modernising changes over recent years. They were considered satisfactory for the time being, but it was also felt that the legal and administrative regulations of the ESP had not evolved at a similar pace or so successfully. Therefore, it had become clear that a substantial change of these regulations was very much required. With these priorities so defined, I started working together with the new Executive Committee to achieve the needed changes. Now, almost two years later, the time has arrived to report on the facts and prospects resulting from my term as President.

In October 2003, following the mandate of the General Assembly in Ljubljana, a ballot was conducted to unlock the process of election of the President-elect. By over 70% this approved the decision of the previous Executive Committee to recommend Prof. Niki Agnantis as the next President-elect. An Extraordinary General Assembly took place on 7th February, 2004 in Paris. There, Prof. Agnantis was unanimously elected as President-elect. Roderick Simpson was also elected as Secretary until the Paris Congress 2005, replacing Prof. Jahn Nesland, who had resigned in Ljubljana. Revised Statutes of the ESP were approved in Paris and, after the pertinent adaptation to Belgian law, were officially accepted by the Belgian Ministry of Justice and published in the official Belgian Gazette on 26th November 2004.

Following a recommendation of the Extraordinary General Assembly held in Paris, new rules for election of officers were drawn up by a Constitutional Committee led by Prof. Michael Wells. These were approved by the Executive Committee in Barcelona on 19–20th November 2004.

On 16th April 2005, the Executive Committee met in Porto and, in accordance with the procedure approved in Barcelona, made the following nominations for the term 2005–2007: Fred Bosman as President-elect, Roderick Simpson as Secretary, as well as Mirian Marichal, Nina Gale, Thomas Kirchner and Fernando Schmitt as ordinary members of the Executive Committee. Also in Porto, the Executive Committee asked the Constitutional Committee to finish the new Bylaws, a task that was satisfactorily accomplished in Brussels on 27th May 2005. All these items will be presented for proper approval by the next General Assembly in Paris.

The fifth edition of the Members Handbook "blue book" 2005, will be issued at the Paris Congress by our Treasurer Han van Krieken, and it will contain as its most significant feature the new Statutes and Bylaws. Also, as in previous editions, updated directories of ESP Members, Committees, Bodies, Past Presidents, Honorary Members and Congresses are included. Even though all these data are available at

Important Information

EuroPath News appears in *Virchows Archiv* four times a year, i.e. February, May, August and November. ESP members who want to publish information in *EuroPath News* should send the manuscript by e-mail to the editor (GKJ) *2 months ahead* of publication. Information only for the website should be sent to the editor of the website (BR).

e-mail: grete.krag.jacobsen@rh.hosp.dk
e-mail: brisberg@labmed.vio.no

For further information look at the ESP home page: http://129.240.38.9/espl

391296.qxd 11.08.2005 13:44 Uhr Seite 120

our website (www.europathology.org), the "blue book" continues to be a very helpful tool to the ESP membership by providing on the spot precise and unambiguous guidelines. Consequently, we have not hesitated to continue this handy symbol of the ESP identity.

Biennial Congresses are the main and most conspicuous activity of the ESP, and they have become in recent years the second largest attended meeting of pathology in the world. The upcoming 20th Congress, organised by Prof. Pierre Bedossa in Paris, September 3–8, 2005, will have almost one hundred sessions, distributed over five days, more than one thousand posters and free papers, as well as a record figure of attendance of two thousand participants from more than 30 countries, and will certainly mark a new milestone in the history of our successful Congresses. The next scheduled biennial Congresses will take place in Istanbul, Turkey in 2007 and in Florence, Italy in 2009.

Through the imaginative foresight of Manuel Sobrihno-Simoes, the ESP successfully introduced the Intercontinental Congresses, which are currently held every four years. The first of them was hosted in May 2000 on the Island of Madeira, and the second was held in June 2004 in Iguaçu Falls, Brazil, jointly organised with the Latin American and Brazilian Societies of Pathology. The next Intercontinental Congress has been already scheduled for May 2008 in Barcelona. Whereas the main objective of the Biennial Congresses is the exchange of knowledge amongst pathologists in Europe, the Intercontinental Congresses aim to exchange knowledge between our pathologists and those of other continents.

Intercongress Meetings, which mainly focus on the scientific activities of the Working Groups, take place in the years between the main European Congresses of Pathology alternating with the Intercontinental Congresses. The first Intercongress was successfully hosted by Prof. Gianni Bussolati in 2002 in Baveno, Italy. The second Intercongress Meeting has been scheduled for May 2006 in Ioannina, Greece, where an attractive scientific and social programme has already been prepared. It is hoped that a large number of pathologists from throughout Europe will visit this beautiful and largely undiscovered area of Greece for what is expected to be a most valuable scientific meeting. The third Intercongress is planned in 2010.

The increasing complexity of the organisation of all these congresses, which are now every year, requires the appointment of a specific Congress Coordinator. This position was approved by the Executive Committee in Porto in April 2005. Written Guidelines for the Organisation of ESP Congresses are expected to be ready by the end of the current year and will assist the Congress Coordinator as well as the Congress Organisers. It is expected that in this way the trade mark ***ESP CONGRESS*** can be even better. This goal will also mean additional efforts by the Executive Committee, and in particular by the Treasurer and by the Financial Committee, in order to improve and secure the budgets of these congresses.

The Advisory Council acquired great relevance under the previous chairmanship of Prof. Antonio Llombart-Bosch. At present, it continues to be very successfully led by Prof. Günter Klöppel. Its role is to reinforce the links between the ESP and the National Societies thus ensuring a versatile flow of information in both directions. The Advisory Council and the national Societies have greatly contributed to the development of the scientific programme of the Paris Congress.

The newsletter "Europath News", periodically inserted in Virchows Archiv continues to provide a flow of information between the ESP and the membership, as also does the ESP Website. Grete Krag Jacobsen and Bjørn Risberg, their respective editors, continue to adapt the Newsletter and the Website to requests for a more rapid flow of information.

The European School of Pathology (EScoP), established in 1991, is an emblematic body of the ESP and is led by Prof.Gianni Bussolati, acting as a promoter of intensive and practically oriented courses. They are hosted annually in Turin, Italy and in recent years have been progressively extended to Kraków, Poland, Craiova, Romania and Ankara, Turkey. Similar courses are also held in Ioannina in Greece. All of them contribute quite decisively to the continuing improvement in the standards of diagnostic pathology throughout Europe, and have been attended by many hundreds of young pathologists.

Right from the outset, the ESP was eager to promote basic research in Pathology. This crucial aim has been very effectively accomplished, during the past 16 years, through one of the most emblematic bodies of our Society, Euro Cell Path, which is at present led by Prof. Fred Bosman. Founded in 1989, its courses were designed to provide information and standardise practical knowledge in modern cellular and molecular pathology. They are devoted to the most timely topics, efficiently and effectively contributing to the knowledge of numerous young pathologists. These courses are organized yearly, so far always in a different city of Europe. The 14th meeting of Euro Cell Path was held in May 2004 in Girona, Spain, organised by Josep Lloreta, and the 15th in June 2005 in Montebello, Norway was organised by Jahn Nesland.

Due to financial shortages, mainly because of increasing difficulties in attracting European Union funds, EScoP and Euro Cell Path courses need to be rethought. After a recent discussion between EScoP and Euro Cell Path leaders, any possible fusion of the two was felt at present not to be a valid option. The focus of their courses is totally different; the organisational structure and the programme concept of each could not be unified without significant loss for either one or both. However, the present situation of two entirely separate and autonomous bodies, was also viewed as no longer tenable. It was therefore considered as essential that EScoP and Euro Cell Path cross-fertilize, constructing coherent complementary postgraduate education policies within the ESP remit. I am confident that in the near future imaginative and at the same time practical alternatives will progressively develop. The approval of the European Institute for Continuing Medical Education in Pathology, encompassing EScoP and Euro Cell Path, points in the right direction.

The Working Groups have developed as true "European Task Forces of Specialisation in Pathology" and at the same time evolved as a crucial link between applied and basic research by areas of specialty. They are becoming very efficient in assembling by fields of interest previously disconnected pathologists. The number of Working Groups (eleven at present) is progressively increasing, as well as the number of their members and of institutions collaborating with each of them. In this way, the Working Groups are uncovering a large potential for collective stimulation of new ideas, for increasing opportunities of access to larger casuistic and to more sophisticated methodologies, in joint clinical and basic research projects. The Working Groups are therefore emerging as true backbones of the pathology by areas of specialisation. The Meeting of Chairpersons of Working Groups held in Ljubljana for the first time, helps to coordinate activities and administrative structures. Most Working Groups function well or in fact extremely well, but a few groups have encountered occasional difficulties, probably related to uncoordinated rapid growth. It is expected that any problems will solve themselves, as a result of implementing the specific regulations in the new Bylaws.

Very good news is coming from Virchows Archiv. This journal has been central to pathology in Europe for over 150 years, and it is now the Official Journal of the ESP. At its Editorial Board meeting on 18th February 2005 in Frankfurt, general satisfaction was expressed by all participants, (Springer, Editor-in-chief, managing Editors and ESP representatives) at the substantial rise in the impact factor of the Journal in 2004, reflecting the improved scientific vitality of the ESP and of the efforts of the past Editor-in-Chief, Prof. Günter Klöppel and of his successor, Prof. Heinz Höfler. The latter was quite optimistic about possibilities for further improvement. Moreover, it was widely felt that the continuing joint venture between Springer and ESP, offered opportunities for a much closer relationship that was bound to be beneficial for both partners. In this context, negotiations for renewal of the contract started in Frankfurt and were continued at the Executive Committee meeting of last April in Porto. There a net profit

391296.qxd 11.08.2005 13:44 Uhr Seite 121

share of 50% was agreed. This accounts for an initial annual revenue of about 50,000 Euros for the ESP and will considerably improve our financial situation. The new contract will be submitted for approval to the next General Assembly in Paris.

During the last two years, the Executive Committee became increasingly aware of the need to provide the Society with a well equipped and strategically located permanent office, as soon as reasonably possible. The rising organisational complexity of the ESP and its prospects for development in the near future very much require it. Both our Treasurer and Secretary very much endorse this move, as it would greatly facilitate and improve the fulfilment of their tasks. The office should offer facilities for a secretarial assistant and for an accountant, and also a place for meetings of the Executive Committee. Other possible functions are as editorial office of the ESP Journal and, if pertinent, as the centre for our Website. The cities of Brussels and Leyden are the two alternatives under serious consideration. Both offer logistic and financial advantages and disadvantages that need careful comparative evaluation. Renting or buying would be further decisions to make, keeping in mind that the latter seems more attractive in the long run. A proposal, currently under elaboration by the Treasurer and the Financial Committee, will be presented to the General Assembly on 7th September 2005.

At the end of the Paris Congress I will have completed my term as ESP President. Therefore, the time has arrived to express my very best wishes to Niki Agnantis, who will lead the Society towards the Congress of Istanbul, September 2007. I had a very close working relationship with her during the last two years, and I am fully confident in her energy and knowledge of the Society. My best wishes are also extended to Gianni Bussolati, who leaves the position of Past-President, as well as to Günter Klöppel, who continues to chair the Advisory Council, and also to the two continuing officers, Roderick Simpson, Secretary, and Han van Krieken Treasurer. Four members of the Executive Committee will leave after completion of their terms: Fatima Carneiro, Christiane De Wolf-Peters, Rastko Golouh and Grete Krag Jacobsen. Four experienced members will continue for the next two years: Frédérique Capron, Veli-Peka Lehto, Michael Wells and Dilek Yilmazbayhan. All of them have been very kind and extremely collaborative, carrying out time consuming tasks and helping to solve quite complicated issues in the best interest of our Society, and I thank them all both personally and on behalf of all the membership.

Last but not least, I want to express my thanks to you all for your generous support, as well as to my predecessors in office and to the previous and present officers, members of committees and organisers of congresses for their brilliant dedication, tremendous amount of work, and invaluable contributions to the success of the ESP. I am confident that in spite of the momentary political uncertainties in our continent, the vibrant European Society of Pathology that was born, grew and spread throughout Europe even during the difficult times of the Iron Curtain, will continue to thrive even more in the future.



Members nominated as ordinary members of the Executive Committee 2005-2007: Thomas Kirchner, Germany, Nina Gale, Slovenia, Miriam Marichal, Belgium and Fernando Schmitt, Portugal.

Antonio Cardesa
President
Barcelona, June 2005

ESP Working Group on Cytopathology

The Working Group has, in association with the organizers of the 20th European Congress of Pathology, to be held in Paris on 3–8 September 2005, prepared a special programme for participants devoted to cytopathology: A slide seminar, chair by Z.Pohar-Marinsek and Fernando Schmitt with presentation of challenge cases that will be discussed by young cytopathologists supervised for seniors ones, a symposium: How far can we go with cytology? chaired by W. Olszewiski and P. Viehl that will discussed the real possibilities of the cytology in the diagnosis of thyroid, breast, lung, soft tissue and lympho-proliferative diseases, and a short course: Role of bronchoalveolar lavage in pulmonary pathology, chaired by F. Thivolet and H. Popper. This course is a joined activity between the WG on Cytopathology and the WG on Pulmonary Pathology In our business meeting, before our regular administrative meeting we will have a interesting section exploring FNA in gastrointestinal, liver and pancreas pathology, with the participation of some invited guests from US (Andrea Abati and Ricardo Bardales) together with European cytopathologists (L. Skoog, F. Schmitt and V. Sviatoha).

For 2006, the WG will participate in the 2nd Inter-Congress of the ESP that will be held on Ioannina on 25–27 May. The main focus of this meeting is the activities of the ESP Working Groups and our purpose is to organize slide seminars, courses and plenary sections together with the others WGs.

For 2007, the WG was invited for the President of IAC (Matias Jymenez Ayala) to organize together with the Liaison Committee IAC-ESP a Satellite Symposium in the XVI International Congress of Cytology that will be held on Vancouver, Canada on 13–17 May, 2007.

Professor Fernando Schmitt
Chairman Cytopathology WG-ESP

391296.qxd 11.08.2005 13:44 Uhr Seite 122

ESP Working Group on Head and Neck Pathology

At the Annual Spring Meeting of the IAP-Finnish Division, which took place in Kökar Island, Finland from May 12.–15.2005 the following presentations were given by members of the Head and Neck Working Group:

- P Slootweg, Nijmegen: New aspects of odontogenic tumors and fibro-osseous lesions in the WHO classification.
- P Slootweg, Nijmegen: Head and neck squamous cell lesions: Clonal analysis, margins, micrometastasis and arrays as predictors of metastasis.
- R Simpson, Exeter: Salivary gland tumors in the new WHO classification.
- R Simpson, Exeter: Advances in salivary duct carcinoma and new entities of salivary gland neoplasia.
- I Leivo, Helsinki: Slide seminar: "Problems of head and neck".

In association with the 20th European Congress of Pathology in Paris, a one-day Pre-Meeting of the Working Group on Head and Neck Pathology of the ESP and the North American Society of Head and Neck Pathology of the United States and Canadian Academy of Pathology will be organized on **FRIDAY, SEPTEMBER 02, 2005 FROM 08:00 TO 17:30**, **LA PITIÉ-SALPÊTRIÈRE HOSPITAL, BABINSKI BUILDING AUDITORIUM**, **47-83 BOULEVARD DE L'HÔPITAL, PARIS 13ÈME, FRANCE.**

An expert panel will discuss approximately 20 cases which in daily practice resulted in diagnostic difficulty or the differential diagnostic considerations resulted in significantly different prognostic implications. Time for discussion from the audience and between panel members will be sufficient to engender lively exchange of ideas about how to make the diagnosis, special techniques, treatment implications, and future research endeavors.

See for additional information, and registration: http://www.pathology-congress.com/en/ecp.asp

Pieter Slotweg
Chairman of the WG of
Head and Neck Pathology

ESP Working Group on Nephropathology

The activities of the WG have been focused on collecting data about the current state of nephropathology in Europe by means of questionnaires. A database of pathologists and other scientists involved in renal pathology has been completed. The main task in 2005 has been the preparation of the scientific programme for the 20th European Congress of Pathology in Paris. There will be four sessions devoted to nephropathology and transplantation at the Congress: Short Course "Microangiopathies and Vasculitides in Kidney", Slide Seminar "Current Issues in Diagnostic Nephropathology", Short Course "Current Topics in Transplantation Pathology, and Business Meeting "Nephropathology in Europe".

In addition, all pathologists are kindly invited to attend the **Nephropathology Pre-congress Meeting "Updates in Nephropathology and Transplantation"** to be held in Paris, Palais des congres on September 3, 2005, 08.30–17.00, on the opening day of the Congress.the day. There will be four scientific sessions: "Genomics in Renal Pathology", "Berger's IgA Nephropathy and Henoch-Schönlein Purpura", "Current Issues in Kidney Diseases", and Special Workshop "Decoy Cells: Diagnosis and Clinical Significance" (Slide Seminar using virtual microscopy).

The speakers at both the Congress and the Pre-congress Meeting will be internationally recognized experts in the relevant fields. The Pre-congress Meeting will also provide an opportunity for informal contacts. There will be **no Registration Fee** for the scientific programme, Book of Proceedings, coffee breaks and modest lunch at the Pre-congress Meeting.

Dušan Ferluga
Chairman of the WG on Nephropathology

The European Society of Pathology

Dear Colleague,

It will surely not have escaped your attention that *Virchows Archiv* is now the Official Journal of the European Society of Pathology.

But did you realise what benefits membership in the society offer you?

- A subscription to the journal *Virchows Archiv* at no extra charge – this is automatically sent to every member every month.
- Access to the journal online (take a look at http://link.springer.de). If you are already a member of ESP but have not yet registered for your free electronic access, you will find the necessary form to complete online here too.
- A discount of 20% on most titles published by Springer. To take advantage of this, simply send your order directly to the publisher, with details of your membership.
- Attendance at the Society's conferences at a reduced fee.

If you have not yet joined the European Society of Pathology, why not do so now?
Simply complete and return the form enclosed.

We look forward to welcoming you as a member in 2005

Yours sincerely

A. Cardesa
President
European Society of Pathology

H. van Krieken
Treasurer
European Society of Pathology

H. Höfler
Managing Editor
Virchows Archiv

391296.qxd 11.08.2005 13:44 Uhr Seite 123

Application for Membership of the EUROPEAN SOCIETY OF PATHOLOGY



For formatting of old application, please follow old application (old Newsletter, p. 238)
This application can also be downloaded from our website:
http://www.Europathology.org

Please complete the following form (block capitals please) and return it to the Office of the Treasurer

FAMILY NAME: .....

First Name(s): .....

Male ❑ Female ❑

Place and date of birth: .....

Title/Present Position: Prof. ❑ Dr. ❑ Resident ❑

Other: .....

Please clearly indicate which one of the following addresses should be used for subsequent correspondence, mailings, and listing in the Members Handbook:

❑ PRIVATE ADDRESS:

Name: .....
Street: .....
Postcode .....
City: .....
Country: .....

❑ INSTITUTE / OFFICE ADDRESS:

Name Institute: .....
Department: .....
Street: .....
Postcode: .....
City: .....
Country: .....
Telephone: .....
Telefax: .....
E-mail: .....

FIELDS OF INTEREST: .....

Date: ..... Signature of Applicant: .....

Please mail or fax the completed application form to:

ESP – OFFICE OF THE TREASURER,
Prof. Dr. H. VAN KRIEKEN,
University Medical Center Nijmegen
Dept. of Pathology / 437 PA
P.O.Box 9101
6500 HB NIJMEGEN, The Netherlands

Tel.: +31-24-3614352
Fax: +31-24-3540520
e-mail: j.vankrieken@pathol.umcn.nl

Your acceptance as a member of E.S.P. will be confirmed in due course.

20th European Congress of Pathology

Paris, France, September 3-8, 2005

Abstracts



Virchows Archiv

Official Journal of the European Society of Pathology

20th European Congress of Pathology

Free papers (oral communications)

Sunday, Sept. 4	
Head & Neck	O 1 to O 14
Kidney Pathology	O 15 to O 23
Molecular Pathology	O 24 to O 29
Gastrointestinal Pathology	O 30 to O 38
Liver Pathology	O 39 to O 47
Foetopathology	O 48 to O 53
Hematopathology	O 54 to O 65
Pediatric Pathology	O 66 to O 72
Monday, Sept. 5	
Gastrointestinal, Liver and Pancreas Pathology	O 73 to O 80
Uropathology	O 81 to O 86
Pulmonary Pathology	O 87 to O 94
Transplantation Pathology	O 95 to O 100
Gynecopathology	O 101 to O 108
Gastrointestinal Pathology	O 109 to O 116
Tuesday, Sept. 6	
Pulmonary Pathology	O 117 to O 125
Endocrine Pathology	O 126 to O 131
Dermatopathology	O 132 to O 139
Soft Tissue Pathology	O 140 to O 144
Gastrointestinal Pathology	O 145 to O 153
Soft Tissue Pathology	O 153 to O 159
Endocrine Pathology	O 160 to O 167
Head & Neck	O 168 to O 173
Uropathology	O 174 to O 183
Gynecopathology	O 183 to O 192
Wednesday, Sept. 7	
Uropathology	O 193 to O 207
Breast Pathology	O 208 to O 216
Infectious Diseases, Miscellaneous	O 217 to O 222
Cardiovascular Pathology	O 223 to O 228
Breast Pathology	O 228 to O 237
Neuropathology	O 238 to O 243
Cardiovascular Pathology	O 244 to O 249
Neuropathology	O 250 to O 255
Breast Pathology	O 256 to O 264

Posters

Displayed on Sunday, Sept. 4	
Breast Pathology	P 1 to P 75
HematoPathology	P 76 to P 139
FoetoPathology	P 140 to P 151
Gastrointestinal Pathology	P 152 to P 202
Liver Pathology	P 203 to P 237
Pulmonary Pathology	P 238 to P 263
Displayed on Monday, Sept. 5	
CytoPathology	P 264 to P 279
Gastrointestinal Pathology	P 280 to P 329
Head & Neck Pathology	P 330 to P 359
UroPathology	P 360 to P 396
GynecoPathology	P 397 to P 425
Pediatric Pathology	P 426 to P 451
Kidney Pathology	P 452 to P 471
Pulmonary Pathology	P 472 to P 502
Displayed on Tuesday, Sept. 6	
Gastrointestinal Pathology	P 503 to P 529
Liver Pathology	P 530 to P 552
Head & Neck Pathology	P 553 to P 581
Endocrine Pathology	P 582 to P 629
Soft tissue, joint and bone Pathology	P 630 to P 664
UroPathology	P 665 to P 707
Cardiovascular Pathology	P 708 to P 734
Electron microscopy	P 735 to P 743
Displayed on Wednesday, Sept. 7	
GynecoPathology	P 744 to P 813
Soft Tissue, Joints and Bone	P 814 to P 837
UroPathology	P 838 to P 886
Miscelaneous	P 887 to P 913
DermatoPathology	P 914 to P 951
NeuroPathology	P 952 to P 998

Free papers (oral communications)

O-1
INFLUENCE OF TGF-B1 IN P-AKT EXPRESSION AND CELL PROLIFERATION-RELATED PROTEINS IN ORAL SQUAMOUS CELL CARCINOMA CULTURED CELLS

SALLES Felipe Torquato
PINTO JR Decio Santos
University of Sao Paulo School of Dentistry, Department of Oral Pathology

TGF-b is a molecule believed to play a crucial role in cellular growth, development and differentiation. Many studies point it out as an important tumor suppressor, and its absence has been related to tumor aggressiveness and invasiveness, especially in oral squamous cell carcinoma, the most frequent malignancy of the oral cavity. In order to evaluate p-Akt expression, as well as cell cycle and apoptosis related proteins, five cell lineages were used: HN6, HN19, HN30, HN31 and HaCat as normal keratinocytes. TGF-b1 (5ng/ml) was applied over cell monolayers during 18h periods and the expressions of p-Akt, cyclin D1, caspase-3 and Bad were evaluated through western-blot and immunofluorescence. The results revealed an increased p-Akt expression in all cell lines, especially HaCat, HN6 and HN30. Cyclin D1 exhibited similar results, except for HN31, where a decrease was noticed. Caspase-3 maintained similar levels in all cell lines, but decreased in HaCat and increased in HN30. Bad levels increased in all cell lines but HaCat. Immunofluorescence revealed cyclin D1 normal nuclear location after treatment, and cytosolic in HN31. These results suggest, according to recent findings, that TGF-b might not always function as a tumor suppressor. Depending on tumor progression stage and its molecular profile, this molecule may exert an adjuvant function in tumor growth. These data may provide evidence for an accurate revaluation of TGF-b role, as well as its use as a tumor marker.

O-2
STROMAL VERSICAN OVEREXPRESSION IS AN UNFAVORABLE PROGNOSTIC SIGN IN ORAL SQUAMOUS CELL CARCINOMA

BÖHM Jan *, PUKKILA Matti **, KOSUNEN Ari **, ROPPONEN Kirsi *, VIRTANIEMI Jukka **, KELLOKOSKI Jari **, KUMPULAINEN Eero ***, PIRINEN Risto *, NUUTINEN Juhani **, JOHANSSON Risto ***, KOSMA Veli-Matti.*
Departments of Pathology and Forensic Medicine*, Otorhinolaryngology**, Oncology***, University of Kuopio and Kuopio University Hospital, Kuopio, Finland.

Introduction and purpose: Versican is a large extracellular chondroitine sulphate proteoglycan expressed in several malignant tumors, suggesting involvement in the development and progression of cancer. Versican promotes tumor growth by disturbing cell adhesion. It also stimulates cell proliferation along with angiogenesis. Purpose of the study was to evaluate the prognostic role of versican in oral squamous cell carcinoma (OSCC).
Methods: Versican expression was analyzed immunohistochemically in paraffin embedded specimens of 139 OSCC patients treated in Kuopio University Hospital district between 1979 and 1998. Patients were followed-up until death or June 2002. All relevant clinical data were reviewed for tumor characteristics, primary treatment, follow-up and possible tumor recurrence. The stained stromal part in proportion to whole stromal area around invasive carcinoma nests was assessed on a continuous (0–100%) scale. The most prevailing versican staining intensity was graded into 3 groups: weak = 1, moderate = 2 or strong = 3. Stromal versican staining score (SVSS) was obtained by multiplying the percentage with intensity. The cell proliferation index was determined using immunohistochemical Ki-67 staining.
Results: The median age of the patients was 64 (range 10-88) years. The median SVSS was 100, which was used as a cut-off for statistical analyses. The median disease-free survival (DFS) time was 9.2 months and median disease-specific survival (DSS) was 17 months. Tumor recurrence and cell proliferation index were related to SVSS with borderline significance. Univariate survival analysis showed that lymph node involvement, Karnofsky performance status, SVSS and cell proliferation index were significant prognostic factors for DFS ($p<0.05$ for all). Significant prognostic factors for DSS were the size of the tumor, lymph node involvement, tumor stage and histological grade ($p<0.01$, $p<0.001$, $p<0.001$, $p<0.01$, respectively) along with Karnofsky performance status, SVSS and cell proliferation index ($p<0.05$, $p<0.01$, $p<0.05$, respectively).
In multivariate analysis histological differentiation, stage and SVSS were significant prognostic factors for DSS ($p<0.05$, $p<0.01$, $p<0.05$, respectively).
Conclusion: Our results suggest that the high stromal versican expression is associated with unfavorable outcome of OSCC patients, and may be a useful marker in deciding more aggressive treatment procedures.

O-3
SENTINEL NODE BIOPSY AND SUBCLINICAL LYMPH NODE METASTASES IN PATIENTS WITH ORAL SQUAMOUS CELL CARCINOMA ,T1-T2, N0, M0.

THERKILDSEN Marianne Hamilton(1), BILDE Anders(2),von BUCHWALD Christian(2).
Dept. Pathology (1) and Dept. Otolaryngol, Head & Neck Surgery (2), H:S Rigshospitalet, Copenhagen University Hospital, Copenhagen, Denmark

Introduction
In Denmark (5 million inhabitants) the incidence of malignant tumours of the oral cavity is 310 cases per year the majority being squamous cell carcinomas (SCC).
The presence of clinical lymph node metastasis in head and neck cancer is the single most important prognostic factor reducing survival by 50%. The impact of oral subclinical lymph node metastases including micrometastases is not known.
In oral cancer, clinical and radiological assessments seem unreliable in demonstrating spread to the lymph nodes of the neck.
The sentinel node (SN) concept states that the sentinel node is the first node to which a tumour will metastasize. Furthermore it is believed that the pathological status of SN reflects the histology of the remaining regional lymph nodes.
Purpose
The purpose of the study is to perform sentinel node biopsy in a consecutive material of oral SCC stage T1-T2N0M0 operated at our institution in order to: 1) To establish if the sentinel node biopsy (SNB) procedure is an adequate tool in the detection of metastases thereby reducing the incidence of elective neck dissection in the N0 neck. 2) To gain insight in the frequency of subclinical metastases including micrometastases.
Material and method
The study was initiated September 2004. The SN is identified by means of an isotope. Following resection of the primary tumour, SNB is performed with a subsequent selective neck dissection as part of a learning curve. All sentinel nodes are examined using step serial sectioning cut at 150-øm intervals. The sections are stained with hematoxylin and eosin (H&E) and broadspectrum anticytokeratin antibody AE1/AE3, respectively in order to detect metastases.

Results and conclusion
As of March 2005 18 patients have been included in the study. The number of SN varies between 1 and 4 nodes per patient. Two patients had metastases in the SN leading to upstaging of 11% (2/18) of the patients. The study will continue and further patients will be included with an adequate follow-up to establish the value of the technique.

O-4
PROGNOSTIC SIGNIFICANCE OF INTRATUMORAL HETEROGENEITY FOR CATHEPSIN D AND CYCLIN D1 EXPRESSION IN LARYNGEAL SQUAMOUS CELL CARCINOMA.

CORIC Marijana, BATELJA Lovorka, BUMBER Zeljko, DJANIC Davor, SEIWERTH Sven.
Institute of Pathology; ENT Clinic, Medical Faculty University of Zagreb, Croatia

Intratumoral heterogeneity is defined as the parallel existence of different (e.g. diploid and aneuploid) clones within a given tumor. This implies that different tumor parts could express different behavior (e.g. propensity to invade or metastasize, resistance against chemo- or radiotherapy). Current investigations mostly neglect intratumoral heterogeneity in general and completely ignore the possibility of regional intratumoral heterogeneity. The goals of this investigation were to define intratumoral heterogeneity of cyclin D1, cathepsin D and nm23 protein as well as nm23H1 gene in three different tumor regions (tumor center, invasive margin and transformation region), to establish potential prognostic significance of regional factors and to establish potential correlation between the investigated factors and classical prognostic factors (T, N, M, histological grade).
We performed the study on a group of 170 patients with laryngeal cancer undergoing partial or complete laryngectomy. After standard paraffin embedding immunohistochemistry was performed using manufacturers protocols (DAKO, Oncogene Sci.). Immunoreactivity was accessed using semiquantitative score. Follow up of patients was minimum 60 months for survivors. Statistics was performed using Statistica for Windows and RPART statistics.
Results of our study clearly show that the intratumoral heterogeneity is not a random event, but that there is a clear areal distribution of immunoreactivity to cathepsin D and cyclin D1, with the invasive margin expressing the strongest immunoreactivity followed by the tumor center. There is positive correlation for expression of cathepsin D in tumor cells with T (p=0,003), and negative correlation for stromal expression of cathepsin D with T (p=0,006), N (p=0, 01) and histological grade (p=0, 02). Areal expression of cathepsin D and cyclin D1 showed prognostic significance on Kaplan-Meier curves (cathepsin D (p=0,001) cyclin D1 (p=0,008)). Using RPART statistics the expression of cathepsin D in tumor stromal cells of tumor center was demonstrated as being a classificator equal to standard prognostic parameters.
These findings strengthen the concept that areal intratumoral heterogeneity should not be neglected neither in research nor in diagnostic work.

O-5
RASSF1A, VHL AND FHIT GENE IN SQUAMOUS CELL CARCINOMA OF LARYNX AND HYPOPHARYNX

M. Volavšek, D. Podpeènik, D. Glavaè, N. Gale
Institute of Pathology, Faculty of Medicine, Ljubljana, SLOVENIA

INTRODUCTION. Loss of heterozygosity (LOH) on short arm of chromosome 3p is frequently found in squamous cell carcinoma of larynx and hypopharynx (LHSCC). It is considered to represent an early step of LHSCC carcinogenesis. This chromosomal region contains three tumor supressor genes, Rassf1, VHL and FHIT.
AIMS. We wanted to determine whether Rassf1, VHL and FHIT changes contribute to LOH on 3p and influence survival of LHSCC patients.
MATERIALS AND METHODS. DNA was isolated from tumor and adjacent normal tissue from 77 LHSCC patients using standard procedure. Non-isotopic LOH analysis was performed with microsatellite markers D3S1007, D3S1038, D3S1233, D3S1285, D3S1300. Presence of mutations in exons 1-6 of Rassf1A gene and exons 1-3 of VHL gene was tested. PCR-non-isotopic conformation analysis was used for mutation analysis. Mutated regions were directly sequenced with ABI Prism Genetic analyser. Molecular analysis results were correlated with disease parameters. Survival analysis was performed.
RESULTS. Most of 77 patients were male (73), aged 36-77 years (58,3 ± 10,17) with laryngeal (56; 72,7%), moderately differentiated cancer (46; 59,7%). LOH at 3p was detected in 47 (61%) cases. There were 17 Rassf1A missense mutations discovered in 16 (20,8%) cases (1 homozygous), located in Rae 3 in 16 and in Rae 5 in one case. We found no pathogenic VHL mutations (3 polymorphisms). Presence of Rassf1A mutations didn't correlate with LOH in general, but there was significant correlation with LOH detected with each individual marker in informative cases(p=0,006 to p=0,020). Molecular analysis results didn't correlate with disease parameters or cancer specific survival.
CONCLUSIONS. Our results confirm LOH at 3p chromosome being a frequent event in LHSCC. Significant correlation between Rassf1A mutations and LOH on sites covered by each individual microsatellite marker is rather surprising, since the markers used cover all three gene sites. According to our results we can exclude possible impact of VHL changes. On the other hand, it is impossible to delineate shares of Rassf1A and FHIT alterations. Regions involved in LOH in individual cases could have spread over both genes. To determine the significance of each gene additional investigations including gene expression profile and methylation status are needed. Nevertheless, our results suggest that Rassf1A and FHIT gene changes contribute significantly to LOH at 3p and are involved in early steps of LHSCC

O-6
CELL CYCLE DISREGULATION IN LARYNGEAL DYSPLASIA.

Santiago Montes Moreno1, Socorro María Rodríguez Pinilla2, Lydia Sánchez Verde2, Monserrat Sánchez Céspedes2*, Francisco Martinez Tello1*.
1. Departamento de Anatomía Patológica. Hospital Universitario 12 de Octubre. Madrid. Spain.
2. Grupo de Cáncer de Pulmón. Programa de Patología Molecular. Centro Nacional de Investigaciones Oncológicas (CNIO). Madrid. Spain.
* Co-directors.

Introduction: In the larynx, dysplasia is strongly associated with smoking and affects more frequently the vocal cords. The progression from dysplasia to the development of invasive squamous cell carcinoma is well documented. Moreover, it has been noted a positive correlation between the degree of the dysplasia and the probability to develop an invasive carcinoma. Nevertheless, the molecular mechanisms that underlie the different steps of the progression to laryngeal carcinomas are poorly understood.
Aims: To further our understanding on the implications of cell cycle alterations in laryngeal cancer progression and to identify markers with value in predicting the development of invasive carcinoma or recurrence, we evaluated the levels of

proteins involved in cell cycle control in patients diagnosed with laryngeal keratosis or dysplasia.
Material and Methods: Two tissue microarrays were made containing 114 specimens (18 keratosis , 26 LIN I, 42 LIN II and 25 LIN III) obtained from biopsy material. Expression of the following proteins, RB, P63, Cyclin D1, P53, P27, P21, CDK2, CDK1, CDK4, CDK6, P16, Cyclin A, Cyclin E and Survivin were evaluated by immunohistochemistry. Results according to the percentage of positive cells and their distribution along the different epithelial layers were correlated with clinical and pathological characteristics.
Results: Our observations revealed that Cyclin A and P63 protein levels increased as the dysplasia progresses ($p=0.003$ and $p=0.036$ for Cyclin A and P63, respectively). Cases were considered positive when more than 2% and 60% of epithelial cells showed reactivity to cyclin A and P63, respectively. Conversely, CDK6 protein levels decreased and its expression was lost in basal and parabasal layer of the epithelium as the degree of dysplasia increased, distinguishing mainly between LIN II and LIN III ($p=0.017$ and $p=0.0001$, respectively). The correlation with the clinical parameters are being evaluated.
Conclusions: Our results provide information on the molecular profile of cell cycle components in laryngeal dysplasia and identify several cell cycle components as potential markers for dysplasia progression.

O-7
COMPUTERIZED IMAGE ANALYSIS ASSESSMENT OF CELL CYCLE RELATED PROTEINS (P16, P21, P27, P53, CYCLIN D1) AND E-CADHERIN IN 289 LARYNGEAL CARCINOMAS – A TISSUE MICROARRAY STUDY

KRAM Andrzej, TERESINSKI Leszek, OKAMOTO Natsumi*, DOMAGALA Wenancjusz.
Dept. of Pathology, Pomeranian Medical University, Szczecin, Poland
* Nara Medical University, Nara, Japan

Introduction: Laryngeal carcinoma is one the most common cancer of the head and neck. Surgery and radiotherapy are generally accepted as the treatment options. The laryngectomy is usually accompanied by lymph nodes surgical excision due to the risk of metastasis. However, there are cases in which the pathologic examination of resected lymph nodes reveals no metastasis. This study was done on laryngeal carcinoma tissue microarrays (TMA) in order to investigate the possible correlation between cell cycle related proteins (p16, p21, p27, p53, cyclin D1) and E-cadherin to the clinical and pathological parameters, with the special emphasis on lymph nodes status. Design: The immnohistochemical stains were done on three TMAs containing 289 laryngeal carcinomas. Tumor location, T- stage, grade and lymph nodes status were examined. Immunohistochemical staining and calculations of positive expression of p16, p21, p27, p53, cyclin D1 and E-cadherin protein with the use of computerised Quantimet 600S Image Analyser (Leica) were performed. Results were related to the clinical (location, T-stage) and pathological (grade and lymph nodes status) parameters of the tumors. Results: The mean age of patients was 54 years, 86.2% cases were male and 13.8% female. The positive expression of p16, p21, p27, p53, cyclin D1 and E-cadherin proteins was shown in 10%, 22%, 15.8%, 45.4%, 29% and 18% of cases respectively. None of the examined proteins was related to location, grade, or lymph node status. However, a significant adverse correlation (chi-square test, $p<0.05$) was found between the p27 protein expression and T-stage. Conclusion: In this study we showed the practical power of TMA technology in rapid immunohistochemical examination of large group of laryngeal carcinomas. Our results indicate that the risk of lymph node metastasis is not related to the expression of cell cycle proteins and E-cadherin. The adverse correlation between p27 protein expression and T-stage was not previously observed.

O-8
PROGNOSTIC VALUE OF TUMOR INFILTRATING CD4+T CELL SUBPOPULATIONS IN HEAD AND NECK CANCERS.

BADOUAL Cécile, HANS Stéphane , RODRIGUEZ José, PEYRARD Séverine, KLEIN Christophe, BRUNEVAL Patrick , FRIDMAN Wolf Herman, BRASNU Daniel , TARTOUR Eric

Background : CD4+T cells play a central role in initiating and maintening anticancer immune responses. However, the regulatory CD4+CD25+T cells which express Foxp3 have also been shown to inhibit anti-tumor effector T cells. In face of this heterogeneous CD4+T cell populations, the aim of this study was to determine the prognostic value of different populations of tumor-infiltrating CD4+T cell in head and neck squamous cell carcinoma (HNSCC).
Methods : 84 newly diagnosed untreated patients with primary histologically proven HNSCC were included in this study. Immunofluorescence staining was performed to assess and count the different subpopulations of tumor infiltrating CD4+T cells. CD4+CD69+T cells, regulatory CD4+Foxp3+T cells and the mixed CD4+CD25+T cells comprising both activated and regulatory T cells were analyzed in this study.
Results : In the univariate analysis, CD4+CD69+T cell infiltrating tumors were the only CD4+T cell subpopulations which positively correlated with both locoregional control ($p = 0.0027$) and survival ($p = 0.006$). Levels of regulatory Foxp3+CD4+T cell infiltration have no impact on clinical outcome. Multivariate analysis showed that the only significant prognostic factors independently related to locoregional control were T stage ($p = 0.008$) and CD4+CD69+T cell infiltration ($p = 0.018$) and the same two variables influenced overall survival probability : T stage ($p = 0.02$) and CD4+CD69+T cell infiltration ($p = 0.007$)
Conclusion : High levels of CD4+CD69+T cells tumor infiltration are significantly associated in both univariate and multivariate analysis with a better survival and locoregional control in head and neck cancer patients.

O-9
PULMONARY SQUAMOUS CELL CARCINOMA FOLLOWING HEAD AND NECK SQUAMOUS CELL CARCINOMA: METASTASIS OR SECOND PRIMARY?

Tom Geurts(1), Petra Nederlof(2), Michiel van den Brekel(1&3), Laura van ’t Veer(2), Daphne de Jong(2), August Hart(4), Nico van Zandwijk(5), Houke Klomp(6), Alfons Balm(1&3) and, Marie-Louise van Velthuysen(2)
Department of ORL, Academic Medical Center (1), and departments of Pathology (2), Head and Neck Oncology (3), Radiotherapy (4), Pulmonology (5), and Surgery (6) of the Netherlands Cancer Institute / Antoni van Leeuwenhoek Hospital, Amsterdam, The Netherlands.

Purpose: To distinguish a metastasis from a second primary tumor in patients with a history of head and neck squamous cell carcinoma (SCC) and subsequent pulmonary SCC, using clinical, histological and molecular characteristics.
Experimental Design: Of 46 patients with a primary SCC of the Head and Neck followed by a SCC of the lung, clinical data, histology and analysis of loss of heterozygosity (LOH) were used to differentiate metastases from second primary tumors.
Results: Clinical scoring suggested 40 patients with metastases and 6 with second primaries. LOH on different

chromosome arms was observed not to be an independent event. Therefore a novel interpretation strategy based on biological insight was developed and tested. Based on this strategy LOH analysis indicated metastatic disease in 21 cases and second primary SCC in 24 cases. In one case LOH analysis was inconclusive. For 27 patients LOH supported the clinical scoring and in 18 cases it did not. These 18 discordant cases were all considered to be second primary tumors by LOH analysis.
Conclusions: A considerable number of lung lesions (in this study 50%) clinically interpreted as metastases, are suggested to be second primaries by LOH analysis, justifying a surgical approach with curative intent in these cases.

O-10

SIMPLE IDENTIFICATION OF ATYPICAL CELLS IN BRUSH BIOPSIES OF ORAL MUCOSA VIA LAMININ-5 IMMUNOCYTOCHEMISTRY

KOSMEHL Hartwig (1), DAHSE Regine (1), BERNDT Alex (2), DRIEMEL Oliver (3), PISTNER Hans (4)
(1) HELIOS Klinikum Erfurt; Institute of Pathology, D-99089 Erfurt, Germany
(2) University of Jena, Institute of Pathology, D-07740 Jena, Germany
(3) University of Regensburg; Clinic of Craniofacial Surgery, D-93042 Regensburg
(4) HELIOS Klinikum Erfurt; Clinic of Craniofacial Surgery, D-99089 Erfurt, Germany

Brush Biopsy is a promising and critically discussed method to detect epithelial oral pre-cancerous and malignant lesions. The gamma2-chain of Laminin-5 (Ln-5) and its proteolytic fragments are an invasive factor in many carcinomas. We studied the impact of Ln-5 immunocytochemistry in cytological analysis of brush biopsies.
Material and Methods: 60 consecutive brush biopsy specimen: normal oral
mucosa (n=10), inflammatory (n=11) and benign (n=22) hyperproliferative lesions, oral carcinomas (n=17) with histopathological diagnosis. Standardised immunocytochemistry. Ln-5 monoclonal antibodies: D4B5 (Chemicon) or 4G1 (DakoCytomation), Detection: ChemMate; Autostainer (DakoCytomation).
Results: 100% specificity was achieved, e. e. no false positive results (atypical or immunostained cells in normal, inflammed or benign hyperproliferative mucosa). Bacteria colonies were stained false positive.
Oral squamous cell carcinoma brush biopsies demonstrated the following immunocytochemical pattern: a) cytoplasmic staining, b) ribbon-like staining between the epithelial cells, c) positive halo around epithelial cells. 4 out of 17 carcinomas could not be diagnosed by conventional cytology (sensitivity of conventional cytology 76%). 3 of the 4 carcinomas not identified by cytology were detected by
Ln-5 immunocytochemistry (sensitivity of conventional cytology + Ln-5 immunocytochemistry 94%).
The positive predictive value of cytology plus immunocytochemistry was 100%; the negative predictive value reached 91% for conventional cytology and 98% for the combination.
Conclusions: 1. The immunocytological Ln-5 staining simplifies the identification of atypical cells in brush biopsies fundamentally. 2. The Ln-5 pattern represents an independent information which confirms cytology. 3. The increased sensitivity of the immunocytologically enhanced brush biopsy recommends oral brush biopsy as an easily interpretable and reliable method.

O-11

LYMPHOMAS OF ORAL CAVITY. CLINICAL-PATHOLOGICAL STUDY OF 46 CASES AND REVIEW OF LITERATURE.

ASIOLI Sofia, FOSCHINI Maria P.,*ASIOLI Silvia, MAGRINI Elisabetta, COCCHI Roberto,°PILERI Stefano A.
Department of Anatomic Pathology, University of Bologna and Dept. of Maxillo-Facial Surgery at Bellaria Hospital, Bologna, Italy.
° Chair of Pathology, Institute of Haematology "L. and A. Seràgnoli" , University of Bologna, Bologna, Italy.
*Service of Anatomic Pathology, S. Maria Nuova Hospital, Reggio Emilia, Italy.

Introduction: Although several clinico-pathologic studies on extra-nodal oral cavity lymphomas have been reported, our understanding of these tumours is incomplete. This is mainly because oral lymphomas are quite rare and the opportunity to apply modern techniques to their classification is limited.
Propose: The aim of this study was to determinate both the histotype and phenotype of lymphomas presenting in the oral cavity.
Materials and methods: Cases were classified according to the World Health Organization Classification of Tumours of Haematopoietic and Lymphoid Tissues 2001. Immunohistochemical stains were performed on tissue microarrays (TMA).
Results: Forty-four cases of non-Hodgkin's lymphoma (NHL) and 2 cases of primitive Hodgkin's lymphoma (HL) were observed, with a slight female predominance (21M; 25F). Forty cases of NHL were primitive of the oral cavity, while six cases were secondary lesions. NHL were divided into five groups: 1) diffuse large B-cell lymphoma (DLBCL: 33 cases); 2) follicular lymphoma (FL: 5 cases); 3) extranodal marginal zone B-cell lymphoma (MZL: 3 cases); 4) mantle cell lymphoma (MCL: 1 case); 5) peripheral T-cell lymphomas, not otherwise specified (PTCL, NOS: 2 cases). HL occurred in two males, aged 25 and 65 years respectively. Both cases were diagnosed as nodular sclerosing HL.
The lesions were variably located in different sites of the oral cavity, commonly affected sites being the soft and hard palate and tongue. The most frequent clinical appearance was a sub-mucosal mass (34 cases). Dental waving was present in 5 cases and actinomycotic infection in one. Six cases appeared as slightly raised whitish lesions. Two cases (1 NHL and 1 HL) appeared in HIV infected patients.
Conclusion: The present series shows that malignant lymphomas of the oral cavity more often represent de novo primary growths. The most frequent event is DLBCL affecting elderly patients in the palate or tongue. Although rare, HL should be considered among primary oral cavity lymphomas.

O-12

CHONDROSARCOMA OF THE LARYNX

PAGLIARI Angelo Virgilio °, KLINGER Francesco *, KLINGER Marco *
° U.O. ORL - Azienda Ospedaliera di Crema
* Istituto di Chirurgia Plastica e Ricostruttiva
Università degli Studi di Milano - I.C. Humanitas

Introduction Chondrosarcoma is an uncommon malignant neoplasm accounting about 0,5% of all laryngeal primary tumours. The commonly affected laryngeal subsites are thyroid and cricoid cartilage and epiglottis
Methods We report a case of laryngeal chondrosarcoma of the larynx arising from cricoid cartilage with special regard to diagnostic aspects.
Results The patient referred to us for dysphonia, hoarseness and dyspnoea. A laryngoscopy showed a lesion in a area bordered inferiorly by the lower margin of the cricoid

cartilage and superiorly below the free margin of the true vocal cord and a CT scan of the larynx confirmed a heterogeneous calcified mass originated by the cricoid cartilage. Ultrasound-guided fine needle aspiration biopsy was performed and potentially malignant chondroid neoplasm was diagnosed. The snear was composed of metachromatic amorphons myxoid matrix with sparse chondrocyte often binucleated and plurinucleated characterized by plump and slighty irregular nuclei. The patient underwent a partial subglottic laryngectomy with temporary tracheotomy. The lesion was predominantly composed of lobules of well-differentiated hyaline cartilage with rare foci of calcification and chondrocytes showing moderatly hyperchromatic nuclei, plump with slight irregularities. Intermingled with these there were areas more hypercellulated with more marked nuclear irregularities and bi- and pluri-nucleation. Necrosis was not observed and mitoses were rare and limited to hypercellular areas.
Conclusion In the diagnosis of chondrosarcoma the histological distinction between the different degree of malignacy constitutes one challenge for the pathologist. The biological behaviour is characterized by locoregional recurrent in direct correlation with the degree od dedifferentiation. Metastasis in chondrosarcoma is a poor prognostic sign but is very rare.

O-13
EVALUATION OF EXPRESSION AND POTENTIAL PROGNOSTIC IMPORTANCE OF METALLOPROTEINASES 1 I 2 (MMP-1 I MMP-2) AND THE INHIBITOR OF METALLOPROTEINASE-3 (TIMP-3) IN CHOSEN ODONTOGENIC NEOPLASMS AND CYSTS.

Jozef Kobos*, Joanna Grodecka**
*Department of Pathology of the Age of Development and Department of Pathology Konopnicka Memorial Hospital Medical University of Lodz, Poland
**Department of Maxillofacial Surgery Medical University of Lodz, Poland

Currently used classification do not allow to predict precisely the biological behavior of odontogenic neoplasms and cysts. Real mechanisms of neoplastic transformation of epithelial and stromal components of odontogenic tumors remain unknown. Recently published data indicate the significance of metalloproteinases and their inhibitors in the phenomenon of local progression of neoplasms.
The aims of the study were evaluation of expression as well as potential prognostic importance of metalloproteinases 1 i 2 (MMP-1 i MMP-2) and the inhibitor of metalloproteinase-3 (TIMP-3) in a group of odontogenic neoplasms and cysts. For our research we used material from 74 patients (18 with ameloblastomas, 14 with other odontogenic tumors and 42 with odontogenic cysts) treated in the Maxillofacial Surgery Clinic of the Medical University of Lodz. For immunohistochemical evaluation Novocastra Company antibodies were applied. The intensity of immunohistochemical reaction was scored semiquantitatively.
Results
Intense expression of MMP-1 was observed in odontogenic cysts with strong inflammatory reaction.
There was no such dependency concerning the expression of MMP-2 and TIMP-3.
The expression of MMP-1 and TIMP-3 was noted in patients with odontogenic neoplasms presenting unfavourable clinical course and the intense expression of MMP-2 was observed in patients with no relapse.
Conclusions
Strong expression of MMP-1 was related to the intensity of inflammatory reaction in odontogenic cysts.
The expression of MMP-2 was related to favourable and the expression of MMP-1 and TIMP-3 to unfavourable clinical course in patients with odontogenic neoplasms.

O-14
EXPRESSION OF P16 IN SINONASAL MALIGNANT MELANOMA

FRANCHI Alessandro, ALOS Llucia, GALE Nina, MASSI Daniela, SANTUCCI Marco, ZIDAR Nina, CARDESA Antonio

Aim: p16 gene is one of the most frequently altered genes observed in various human neoplasms including malignant melanoma. It encodes a negative regulatory protein which prevents cell cycle progression from G1 to S phase by inhibiting the catalytic activity of CDK4 or CDK6/cyclin D complex and subsequently Rb protein phosphorylation. Little is known about the relationship between the clinical feature of the patients with sinonasal malignant melanoma and the expression of tumor suppressor gene products. The purpose of this study is to investigate the expression of p16 in relation with the histopathologic features and the clinical course in patients with malignant melanoma of the sinonasal tract.
Methods: Formalin-fixed, paraffin embedded sections from 34 cases of sinonasal malignant melanoma were immunostained with a monoclonal antibody against p16. The immunostaining was scored semiquantitatively as: negative, focal positivity (1-10% of neoplastic cells), moderate positivity (11-50%) and diffuse positivity (>50%).
Results: Nuclear and cytoplasmic immunoreactivity for p16 was observed in 14 melanomas (42.2%); immunostaining was also present in surface and glandular epithelia. Twenty melanomas (57.8%) showed loss of p16 expression. All cases with spindle or mixed cytology showed loss of p16, while this was present in 50% of tumours with epithelioid appearance (p=0.02). Loss of p16 expression was more frequently seen in melanomas with alveolar architecture (75%) than in tumours with diffuse architecture (61.6%), but this difference was not significant (p=0.68). Of 31 patients with available follow-up, 15 (48.3%) died of disease (follow-up ranging between 2 and 201 months; mean 30.3 months). There was no correlation between p16 expression and presence of lymph node or distant metastases (p=0.38 and 0.67, respectively). In addition, p16 status did not influence overall survival (p=0.2).
Conclusions: Loss of p16 expression is a frequent event in sinonasal malignant melanoma, which may be involved in the development of this tumour. Immunohistochemical analysis of p16 is not helpful in defining the prognosis of patients affected by sinonasal melanoma.

O-15
CHRONIC CALCINEURIN INHIBITOR TOXICITY IS ASSOCIATED WITH HYALINE SCLEROSIS OF THE RENAL VASA RECTA.

Hallgrimur Benediktsson, Min Yi Ngae, Serdar Yilmaz, Kevin McLaughlin and Rodger Loutzenhiser, University of Calgary, Calgary Laboratory Services and Calgary Health Region, Calgary, Alberta, Canada.

Introduction. Calcineurin inhibitor toxicity (CIT) is a common complication in renal allografts, and is associated with functional deterioration of the graft. While acute CIT is not associated with consistent morphologic changes, chronic CIT is characterized by nodular hyaline changes in the efferent arterioles, as well as interstitial fibrosis, tubular atrophy, and glomerulosclerosis, global and/or segmental. Changes have not been described in the post-glomerular vascular bed. We describe hyaline vascular sclerosis occurring in the renal vasa recta (VRHS) in patients with CIT.
Design. We selected 373 renal biopsies from our biopsy database for evaluation of the vasa recta. 143 cases were

excluded due to inadequate medulla sampling.The remaining 230 biopsies were scored semi-quantitatively for VRHS, as well as glomerulosclerosis, arterial fibrointimal thickening, arteriolar hyalinosis, tubular atrophy, cortical and medullary fibrosis. Transplant biopsies included 35 cases with original diagnoses of chronic allograft nephropathy (CAN), 29 with CIT, 23 transplant baseline biopsies, and 34 early post-transplant biopsies with or without acute rejection. Non-transplant cases included diabetic nephropathy (24), IgA nephropathy (33), focal segmental glomerulosclerosis (FSGS) (22), hypertensive nephrosclerosis (10) and various types of glomerulonephritis (20).
Results: Significant VRHS was frequently found in biopsies from patients with chronic CIT (24/29), and was often associated with nodular arteriolar hyalinosis. It was found less often in CAN (11/35), early post-transplant biopsies (6/34), FSGS (8/22), IgA nephropathy (8/33), and diabetic nephropathy (6/24). Mild changes were rarely seen in baseline transplant biopsies (2/23) and in biopsies from various types of glomerulonephritis (3/20). None of 10 biopsies with nephrosclerosis showed VRHS. Marked VRHS was most often seen in association with CIT.
Conclusion: VRHS occurs at significant frequencies in late transplant biopsies, particularly in association with evidence of CIT. It is seen infrequently in native FSGS, IgA nephropathy, and diabetic nephropathy and is not as severe as in transplant biopsies. The pathogenetic mechanism for this lesion is not clear. Increased transmitted blood pressure is a possible mechanism, however toxic drug effects and inflammation may also play a role. VRHS is an under-recognized lesion which may aid in the diagnosis of CIT, and may have significant functional correlates.

O-16
HUMAN IMMUNODEFICIENCY VIRUS ASSOCIATED NEPHROPATHY PATHOGENESIS: DOES VASCULAR ENDOTHELIAL GROWTH FACTOR (VEGF) PLAY A ROLE?

BROCHERIOU Isabelle*, IZZEDINE Hassane §, LAUNAY-VACHER Vincent §, DERAY Gilbert §, CAPRON Frederique*. Departments of *Pathology and §Nephrology, Pitié-Salpêtrière Hospital, Paris, France.

Background: Vascular endothelial growth factor (VEGF) is a major regulator of blood vessel biology and is highly expressed in presumptive and mature podocytes within the glomerulus. It has been suggested that overexpression of this factor may play a role in collapsing focal segmental glomerulosclerosis (cFSGS); however, definitive proof that it plays a pathogenic or developmental role in the Human immunodeficiency virus-associated nephropathy (HIVAN) has remained elusive. The aim of this study was thus to determine if the angiogenic peptide VEGF is required for glomerular ischemia-associated HIVAN.
Methods: Twenty renal biopsies from patients were selected from our tissue bank of frozen renal biopsy material. Five renal biopsies proven of HIVAN cases were studied immunohistochemically for expression of the VEGF. An equal number of, normal adult control kidneys, not HIV-associated cFSGS and other HIV-associated nephritis were tested for the same antibodies.
Results: VEGF protein was localized exclusively in glomeruli, predominantly in podocytes and the level of tubular expression was much lower or inexistant than that found in glomeruli in normal kidney tissue. In glomeruli with segmental or global sclerosis, cells expressing VEGF protein were not present in the sclerotic areas, as well as in epithelial tubular cells. In HIV-related nephritis without cFSGS cells expressing VEGF protein were markedly reduced in number in the glomeruli and tubules. However, in HIVAN, expression of VEGF protein was markedly increased in collapsing glomeruli and in epithelial cells of the microcystic dilated tubules.
Conclusion: Expression of VEGF by glomerular visceral epithelial cells and dilated tubule cells is increased in HIVAN, and this may have an important role in this disease.

O-17
ET-1/ETB-RECEPTOR IN COL4A3 KNOCKOUT MICE

Ch. Licht1, O. Gross2, M. Odenthal3, H.-P. Dienes3, D.V. Michalk1, M. Weber2,
J.W.U. Fries3
Department of Pediatrics1 and Pathology3 of the University of Cologne, and
Department of Internal Medicine I, Merheim Medical Center2, Cologne, Germany

Objectives:Tubulointerstitial injury (TI) is a common pathway of chronic renal disease and determines the loss of renal function. Chronic proteinuria causes
TI, but it is still controversial by what mechanism. Purpose of the present study was to find out whether ET-1/ETB-receptor is involved in the TI caused by
proteinuria. We made use of the COL4A3 -/- animal model mimicking Alport syndrome (AS), which is characterized by hematuria and proteinuria leading to progressive renal failure. Untreated COL4A3 -/- mice die from renal failure
after about 70 days. However, treatment with ramipril delays onset and reduces extent of proteinuria thereby increasing the lifespan by more than 100%. - The
model of the ramipril treated COL4A3 -/- mice was used to study the role of the endothelin (ET) - system in the development of the proteinuria caused tubulointerstitial fibrosis.
Methods:COL4A3 wild type and knockout mice were treated with 10 mg/kg/day ramipril in the drinking water starting at 4 wks of age and compared to controls (placebo). Animals were sacrificed following 7.5 and 9.5 wks. Kidneys
were rapidly harvested and either processed for immunohistochemistry or used for extraction of total RNA. TI was characterized by incubation with a-smooth
muscle actin (aSMA) antibody identifying myofibroblasts. Expression of ET-1 and ETB receptor was quantified by real time RT-PCR with b-actin as housekeeping-gene.
Results: Wildtype controls showed normal kidneys and no upregulation of ET-1 or ETB receptor expression. However, untreated COL4A3 -/- mice showed increasing amounts of aSMA positive cells and a with time increasing expression of ET-1 (7.5 wks: 2.05; 9.5 wks: 4.73) but not of ETB receptor (7.5 wks: 0.29; 9.5 wks: 0.13). Ramipril treatment did not affect renal histology in wildtype control animals, nor did it alter expression of ET-1 or ETB receptor. However, ramipril treated COL4A3 -/- mice developed less TI; ET-1 expression was increased (7.5
wks: 2.47; 9.5 wks: 2.98) but did not reach the level of placebo treated COL4A3-/- animals. ETB receptor expression was only slightly different from placebo treated animals (7.5 wks: 0.30; 9.5 wks: 0.59).
Conclusions:
(1) renal ET-1 expression is increased and ETB receptor expression is decreased in chronic proteinuria
(2) the protective effect of ramipril treatment against renal TI is linked to a reduced increase of ET-1 expression.
ET-1/ETB receptor may be important for mediating TI caused by proteinuria.

O-18
AN ADENOVIRUS-PROMOTER-CONSTRUCT TO STUDY RENAL MYOFIBROBLAST FORMATION IN VITRO AND IN VIVO

M Odenthal, J Wallraf, T Roth, C Licht*, HP Dienes and JWU Fries.
Department of Pathology and * Pediatrics, University of Koeln, Koeln, Germany

Objective: Myofibroblastic differentiation in the kidney is characterised by the presence of smooth muscle actin (SMA) in mesangial cells in glomerulosclerosis and in the interstitium following ureteral obstruction. To further study this process, we developed a convenient system in living cells allowing readily detection of early mesangial activation by using different mediators applicable to in vitro and in vivo investigation.
Methods: Human mesangial cells (HMCs, Cambrex Bioproducts)in subculture 6-9 were subjected to different commercially available transfection reagents (Lipofectin, Fugene, Lipofectamine, CaCl2, DEAE-dextran) or electroporation with the nucleofactor (Amaxa) using a CMV-ß Gal reporter plasmid for evaluation of transfection efficency. Also, adenoviral-mediated infection was performed with recombinant reporter expression driven by the CMV or the SMA promoter. Infection efficiency was monitored by GFP reporter fluorescence of CMV reporter infected mesangial cells. Recombinant reporter expression directed by the SMA promoter was quantitatively analysed by the Bioanalyszer (Agilent) during the myofibroblastic transition upon glucose (4 vs. 30mM) and mechanical strain (15, 30, 60 cycles/min)treatment of HMCs for up to 48 hrs. To test the inducibility of this construct in vivo, unilateral renal perfusion after 1.5 nephrectomy or ureteral ligation are used as models.
Results: Adenovirus-mediated transgene transmission and recombinant expression in HMCs was successful in 100% of the cells after 24 hrs. of infection with 10 MOI (multiplicity of infection) of an adenoviral CMV promoter driven reporter construct. From the commercially available transfection mediators only DEAE-dextran yielded positive cells (about 5%). Electroporation failed. In contrast to constitutive expression of CMV driven GFP, fluorescence of the SMA promoter GFP construct could be induced after 24 hrs by mechanical strain and by glucose. Maximal GFP intensity was achieved after glucose stimulation for 7d, lasting for at least 3 weeks after switching to normal feeding medium. In the in vivo models, the adenovirus-promoter construct was detected primarily in the epithelium of the proximal tubules, facilitating studies of epithelial-mesenchymal transition.
Conclusion: Adenovirus-mediated infection is an efficient way to achieve HMC manipulation. Using GFP, the inducibility of any promoter construct can be easily monitored and its in vitro and in vivo applicability tested.

O-19
IMMUNOHISTOCHEMICAL EXPRESSION OF ACTIVATED CASPASE-3 AS A MARKER OF APOPTOSIS IN HUMAN LUPUS NEPHRITIS

JERUC Jera, VIZJAK Alenka, FERLUGA Dušan
Institute of Pathology, Medical Faculty, University of Ljubljana, Ljubljana, Slovenia

Introduction. The significance of renal cell apoptosis in human lupus nephritis (LN) is not clear. One of the key events in the process of apoptosis is activation of caspase-3. Recently, antibodies that recognize activated caspase-3 have become commercially available. Studies on various experimental models of apoptosis suggest that activated caspase-3 is a reliable indicator of apoptotic rate, with a favourable comparison against the widely used TUNEL assay.
Aim of the study. We investigated the expression of activated caspase-3 in the glomeruli of LN patients and its relationship to histomorphologic changes, activity (AI) and chronicity (CI) indexes and renal function.
Material and methods. Kidney tissue samples of 36 patients with systemic lupus erythematosus were classified according to the current ISN/RPS 2003 classification of LN. In addition, AI and CI were calculated. Immunohistochemistry was performed by a sensitive peroxidase-streptavidin method on formalin fixed, paraffin-embedded tissue, using monoclonal antibodies against activated caspase-3 (Cell Signaling, MA, USA) and proliferative marker Ki-67.
Results. There were five cases of class II, 11 cases of class III and 20 cases of class IV LN. Among class IV, there were 9 cases of diffuse segmental and 11 cases of diffuse global LN. Active caspase-3 positive cells were identified in the glomeruli of all but three patients (two class II and one class III). The number of glomerular apoptotic cells was significantly higher in class III compared to class II LN ($p<0.005$) and in class IV compared to class III ($p<0.05$). There were more positive cells in global compared to segmental class IV LN, but the difference was not significant. The number of glomerular apoptotic cells correlated with AI, proliferation of glomerular cells and proteinuria ($r = 0.54$, 0.57 and 0.42, $p < 0.05$), but not with CI and renal function.
Discussion and conclusions. Our study shows that the apoptotic rate assessed by activated caspase-3 is higher in severe, active glomerular lesions in human LN. The results suggest that increased apoptosis of glomerular cells may be involved in the progression of human LN. Inhibitors of caspases are highly effective in preventing apoptotic cell death in both in vitro and in vivo models of apoptosis and should therefore be investigated among further therapeutic modalities of human LN.

O-20
PLASMA CELL DYSCRASIA AND DIAGNOSTIC INTRACELLULAR CRYSTALS IN THE URINE

LEH Sabine (1), IMMERVOLL Heike (1), LØVØ Mona Grete Skivenesvåg (2), BOSTAD Leif Henry (1)
(1) Department of Pathology and (2) Department of Medicine, Haukeland University Hospital, Bergen, Norway
sabine.leh@helse-bergen.no

Introduction: Crystalloid tubulopathy is a rare but well documented renal complication in plasma cell dyscrasia. The entity is usually diagnosed by histologic and ultrastructural investigation of a kidney biopsy. In our case tubular cells with crystalline inclusions were detected in the urine.
Case report: A 56-year-old man was admitted to the outpatient clinic with hypertension, slight increase of serum creatinine and slight proteinuria. Antihypertensive therapy resulted in nearly complete normalisation of blood pressure, but the serum creatinine value continued to increase over a period of 6 months. A renal ultrasound examination showed slightly reduced kidney size with reduced cortical parenchyma.
Subsequently monoclonal immunoglobulin IgG kappa was detected in serum, and urine analysis revealed monoclonal kappa light chains (16100 mg/l). The bone marrow smear contained 11% plasma cells. There were no osteolytic foci in an X-ray examination of the skeleton. A plasma cell dyscrasia was diagnosed.
The kidney biopsy showed massive intracellular deposition of crystals in proximal tubules. A few tubular lumina contained single needle shaped crystals. In addition benign nephrosclerosis with arterio/arteriolosclerosis and slight to moderate tubular atrophy was found. Ultrastructurally proximal tubular epithelial cells contained numerous partly membrane bound polygonal crystals without identifiable substructure.
Proximal tubular epithelial cells were seen in urine by cytological examination. Alcohol fixed Papanicolau stained cytospin preparations showed many tubular cells with clear polygonal inclusions. The staining pattern of these inclusions in a cell block preparation was identical to that seen in histological sections. The shape of the crystals in cytologic, histologic and ultrastructural preparations was similar.

Conclusion: This case of monoclonal gammopathy and crystalloid tubulopathy exemplifies that tubular cells with crystalline inclusions are easily recognised by urine microscopy. Urine analysis could therefore contribute considerably to establish the diagnosis in this rare entity.

O-21
NCAM POSITIVE INTERSTITIAL CELLS ARE INCREASED IN DIFFERENT FORMS OF GLOMERULONEPHRITIS

MARKOVIC-LIPKOVSKI Jasmina, MÜLLER Claudia, KLEIN Gerd, FLAD Thomas, KLATT Tatjana, BLASCHKE Sabine, WESSELS Johannes, MÜLLER Gerhard
Institute of Pathology, School of Medicine, University of Belgrade, Serbia & Montenegro;
Section for Transplantation Immunology and Immunohematology, ZMF, University Medical Clinic, Tübingen, Germany;
Department of Nephrology and Rheumatology, Center of Internal Medicine, Georg-August University, Göttingen, Germany

In adult human kidneys, NCAM expression is restricted to rare interstitial cells with dendritic morphology, which are neurofilament-negative and predominantly localised in the outer medulla. In this study NCAM expression was analyzed on interstitial cells in different forms of glomerulonephritis (5 IgA nephropathy, 7 focal segmental glomerulosclerosis, 5 membranous glomerulonephritis and 3 rapidly progressive glomerulonephritis) by immunohistochemistry and Western blot analysis. NCAM+ renal interstitial cells were characterized by double immunofluorescent staining using antibodies against alpha smooth muscle actin, vimentin, alpha-5-beta-1 integrin and the potential progenitor cell markers CD34, CD117, CD133, CD24 and cadherin-11.
The number of NCAM+ interstitial cells increased in the initial phases of interstitial fibrosis in different forms of glomerulonephritis such as IgA nephropathy, focal segmental glomerulosclerosis, membranous glomerulonephritis as well as in early phase of rapidly progressive glomerulonephritis. NCAM isoform of 140 kDa was detected in renal tissue of IgA nephropathy. In normal renal tissue NCAM positive cells are very conspicuous, single located and some subpopulation of them co-express the hematopoietic stem cell markers CD34 and CD133. However, in different forms of GN in the areas with slight interstitial interstitial fibrosis, the accumulated NCAM positive interstitial cells do not share CD34 and CD133 and they are also negative for alpha smooth muscle actin.
These data indicate that a rare subpopulation of NCAM+ interstitial cells in normal adult kidneys could represent renal progenitors. The number of NCAM+ interstitial cells is increased in the initial phase of interstitial fibrosis in different forms of glomerulonephritis and these cells are probably involved in this process.

O-22
HANTAVIRUS NEPHROPATHY IN MECKLENBURG-VORPOMMERN (NORTH GERMANY)

STROPAHL Gerhard1, FÜHRER Andreas2, STROPAHL Karsten2, JONAS Ludwig3, NIZZE Horst1
Institute of Pathology1, Clinic of Internal Medicine2, Electron Microscopic Centre3, University of Rostock, Germany

Hantaviruses are regarded as “emerging” viruses that have been detected in the Americas, Asia, and Europe. Their natural hosts are rodents (mice and rats). As zoonotic pathogens they cause human hemorrhagic fever with renal syndrome (HFRS) as well as the hantavirus pulmonary syndrome, each with varying degrees of severity. In Central Europe infections are normally caused by viruses type Dobrava and Puumala leading to a mild or moderate HFRS with prominent renal symptoms (Nephropathia epidemica). Due to differential-diagnostic problems a renal biopsy is carried out in some cases.
In the region of Mecklenburg-Vorpommern 23 cases with infectious diseases by hantaviruses were registered in the last 6 years (17 men, 6 women, age: 14-66 years). In 7 cases the virus type could be differentiated (6x Central European variant of Dobrava, 1x Puumala). 18 patients showed clinical and paraclinical signs of a nephropathy. The remaining 5 cases had only influenza-like symptoms. Mostly hantavirus nephropathy manifested suddenly with high fever, headache, back and/or abdominal pain. The majority of the cases showed proteinuria (> 3 g/d), microhematuria, increased serum creatinine level (> 310 µmol/L), thrombocytopenia (< 100,000/µL). Oliguria and subsequent polyuria were frequent. In 3 of the cases kidney biopsies were performed because of suspected acute or rapidly progressive glomerulonephritis. Histologically in one case only uncharacteristic changes of an acute renal failure with swelling, vacuolization, and single cell necrosis of tubular epithelium were detected. Specimen of the second patient showed fresh spot-shaped interstitial hemorrhages in the renal marrow in addition to the acute tubular kidney damage. Lesions of a moderate acute interstitial nephritis characterized the third case. Electron-microscopically virion particles with spherical or ovoid form (80-120 nm in diameter) were proved in tubular epithelium.
The diagnosis was established either by demonstration of antibody titer elevation or by culturing the virus from the urine. The renal failure was transient and patients recovered spontaneously.
In conclusion, an unclear acute renal failure with a sudden febrile onset, in particular with additional interstitial hemorrhages or an acute interstitial inflammation in the kidney tissue, can indicate a hantavirus nephropathy and should be clarified by serological tests. The suspected diagnosis can be supported by electron-microscopic examinations.

O-23
GLOBAL PROTEOMICS IN CONGENITAL OBSTRUCTIVE NEPHROPATHY

LIAPIS Helen and TOWNSEND Reed. Department of Pathology & Immunology and of Internal Medicine, Washington University, St Louis, MO, USA

Proteomics is a major spin off of the human genome project. We have previously studied congenital obstructive nephropathy in humans and in animal models and performed genomic analysis in human kidneys. In this study we aim to characterize the proteome.
We used three congenitally obstructed kidneys and equivalent controls. Fifty micron thick sections were used for total protein extraction. High throughput proteomics to profile protein changes was performed. Proteins were labeled with Cy dyes and separated by 2-D DIGE. Images were analyzed using DeCyder image analysis software to determine fold differences between obstructed and control kidneys. Selected spots were excised from the gels, trypsinized in situ and analysis was performed by matrix-assisted laser desorption ionization-time-of flight (MALDI-TOF/TOF) or by LC MS/MS mass spectrometry.
A total of 48 proteins were differentially expressed; 35 were positively identified, while 11 were not identified in the protein data bases that are currently available. In segmentally scarred kidneys, there was increased HSP, Albumin, Glyceraldehyde-3-phosphatedehydrogenase (GPH) and Tubulin. In contrast, Lumican, Vimentin, Collagen I and Osteoglycin were markedly increased in globally scarred obstructed kidneys and GPH was decreased. Other proteins

were variably expressed included tropomyosin. Of these, Lumican was previously found increased in experimental ureteral obstruction models by genomic analysis. Albumin is considered a urine marker for progressive kidney disease. Osteoglycin is expressed in the renal interstitium and thought to regulate collagen fibril spacing and to inhibit embryonic renal cell growth in vitro. Tubulin a both cytoplasmic and nuclear protein is currently a drug target in RCC.
Our findings are the first to report on the proteome of congenital obstructive nephropathy, a common cause of ESRD in children. Proteomics is a promising new tool for identification of biomarkers to shed more light in the natural history of this disease and to identify molecular endpoints for therapeutic intervention.

O-24
CELL CONTACT AND FAK INFLUENCE VEGF EXPRESSION THROUGH IRS-2

M. NEID(1), K. DATTA(2), D. MUKHOPADHYAY(2), A. TANNAPFEL(1) AND CH. WITTEKIND(1)
(1)Institut für Pathologie des Universitätsklinikums, Liebigstr. 26, 04103 Leipzig, Germany
(2)Biochemistry and Molecular Biology and Cancer Center, Mayo Clinic, Rochester, MN 55905, USA

Introduction: Under hypoxic conditions, tumour cells produce the Vascular Endothelial Growth Factor (VEGF) to induce tumourangiogenesis. We have shown recently that the Insulin Like Growth Factor-1 receptor (IGF-1R) and its downstream molecules Insulin Receptor Substrate-1 (IRS-1) and IRS-2 regulate VEGF expression in different ways. IRS-1 leads to a Hypoxia Inducible Factor-1 (HIF-1) dependent VEGF transcription whereas IRS-2 activates the transcription factor SP1.

Purpose of the study: In this study, we wanted to characterize factors that influence the expression of IGF-1R, IRS-1 and IRS-2, hence having an indirect impact on VEGF transciption. Data in the literature show a crosstalk between IRS-1 and integrin dependent signaling through Fokal Adhesion Kinase (FAK). This suggests an influence of the extra cellular matrix (ECM) on VEGF expression.
Methods: AsPC-1 pancreatic cancer cells were cultured either on plastic or on different extracellular matrices (fibronectin, ECL). VEGF transcription was measured by luciferase assays using either the full length VEGF promoter (2.6kb), containing HIF-1 binding sites, or a 0.35kb promoter construct with SP1 bingin sites only (hypoxia independent). Functional deactivation of FAK was achieved using a dominant negative mutant (dN FAK). Cell confluency experiments were carried out by putting the same amount of AsPC-1 cells, transfected with the VEGF promoter, onto a variably dense matrix of non-transfected AsPC-1. mRNA of IRS-1, IRS-2, IGF-1R were measured by RT real time PCR using a light cycler.
Results: ECM did not influence neither 2.6kb nor 0.35kb VEGF transcription. We observed colony forming of AsPC-1 and found that high cell confluency increased 0.35kb VEGF transcription and decreased 2.6kb VEGF transcription. In highly confluent cells, IRS-1 and IRS-2 were upregulated, but the total amount of IRS-2 exceeds the one of IRS-1. Although ECM did not change VEGF transcription, blocking FAK revealed the same changes in VEGF transcription pattern as in highly confluent cells. Moreover, dN FAK increased the IRS-2 and decreased the IRS-1 mRNA level. No change was observed in IGF−1R mRNA expression.
Conclusion: Extra cellular matrix does not influence VEGF transcription in the pancreatic cancer cell line AsPC-1. Abundant cell contacts increase hypoxia independent VEGF transcription (via SP1) through IRS-2. This is modulated by the integrin kinase FAK.

O-25
DEVELOPMENT OF A RAPID SCREENING APPROACH FOR CANDIDATE GENE SETS IN CANCER

R. Wittig1, R. Salowsky2, S. Blaich1, S. Lyer1, JS. Maa3, O. Müller2, J. Mollenhauer1, and A. Poustka1.
1Molecular Genome Analysis, Deutsches Krebsforschungszentrum (DKFZ), Heidelberg, Germany, 2Agilent Technologies, Waldbronn, Germany, and 3Maxim Biotech, San Francisco, CA, U.S.A.

Background: During the last decade, microarray-based gene expression analysis gave rise to a large number of candidate genes for the diagnostics and therapy of cancer. Bioinformatic approaches delivered gene sets, the expression patterns of which were predictive for certain cancer phenotypes. A synergy between these advances and the development of screening tools for a rapid and reliable screening of marker gene expression represents an important step towards an improved treatment of cancer.
Methods: For the semi-quantitative expression screening of eleven candidate genes for drug resistance in melanoma, we combined multiplex RT-PCR (mRT-PCR) with subsequent microfluidic fragment analysis.
Results: The functionality of this approach was demonstrated by low inter-experimental variations of amplicon quantities after endpoint analysis. Applied to RNA samples derived from drug-sensitive and -resistant melanoma cell lines, mRT-PCR delivered results qualitatively concordant with data obtained from Northern blot- and array-analyses. A preliminary screen of four additional melanoma cell lines points to IL1B, APOD, and CYR61 as interesting candidates for drug-resistance associated genes. First tests using an automated on-chip electrophoresis platform indicate the applicability of this approach for high throughput measurements.
Conclusion: mRT-PCR combined with on-chip electrophoresis reveals a rapid and easy-to-handle method for candidate gene set evaluation from limited amounts of mRNA. Using gene sets indicative for different tumor phenotypes, this procedure may represent an alternative for future cancer diagnostics.

O-26
DEFINING AGGRESSIVE PROSTATE CANCER USING A 12 GENE MODEL

BISMAR Tarek A.1,2, DEMICHELIS Francesca3,4, RIVA Alberto2,5, KIM Robert1, VARAMBALLY Sooryanarayana, HE Le1, KUTOK Jeff1,2, ASTER Jonathan C.1,2, TANG Jeffery1,2, KUEFER Rainer7, HOFER Matthias D.1,2, FEBBO Phillip G.2,8, CHINNAIYAN Arul M.6, and RUBIN Mark A.1,2,8
1 Department of Pathology, Brigham and Women's Hospital, Boston, MA
2 Harvard Medical School, Boston, MA
3 Bioinformatics, SRA Division, ITC-irst, Trento, Italy
4 Department of Information and Communication Technology, University of Trento, Trento, Italy
5Children's Hospital Informatics Program, Children's Hospital, Boston MA.
6 Department of Pathology and Urology, University of Michigan, Ann Arbor, MI.
7 University Hospital of Ulm, Ulm, Germany
8 Dana Farber Cancer Institute, Boston MA

Background: The critical clinical question in prostate cancer research is to develop means of distinguishing aggressive from indolent prostate cancer. Expression array technology has lead to the development of discrete molecular signatures but the development of a robust signature to characterize aggressive prostate cancer has yet to be achieved. We

describe a multi-stage approach to develop a model of prostate cancer progression.
Methods: A recent study from our group employed high-throughput immunoblotting using antibodies against 1383 distinct proteins or post-translational modifications in order to interrogate tissue extracts derived from benign prostate, clinically localized prostate cancer, and metastatic prostate cancer. An integrative analysis of this compendium of proteomic alterations and transcriptomic data derived from 8 prostate cancer profiling studies was used to select a smaller set of genes that demonstrated concordance between protein and transcript levels. 41 of these genes could be evaluated on archival tissue samples. Using a prostate cancer progression tissue microarray, the protein products of these genes were tested using quantitative analysis of immunohistochemistry. The best model was validated using prostate cancer expression array data with associated clinical outcomes data.
Results: Linear discriminant analysis determined that the optimal model consisted of 12 proteins. This 12 protein model accurately distinguishes stages of prostate cancer progression. Intriguingly, the transcriptional levels of the 12 genes encoding for these proteins predict PSA-failure in 80 men following surgery for clinically localized prostate cancer (p=0.0015).
Conclusion: This study demonstrates that cross platform models can lead to predictive models with the possible advantage of being more robust through this selection process.

O-27
BPC 157 ALTERS CELL GROWTH, DIFFERENTIATION AND SIGNAL TRANSDUCTION IN SHSY5Y HUMAN NEUROBLASTOMA CELL LINE

Sanja Radeljak, Sven Seiwerth, Ljiljana Hlupic and Predrag Sikiriæ, Lab. Of Molecular Pathology Dept. of Pathology and Dept. Of Pharmacology, School of Medicine, University of Zagreb, Salata 12, 10000 Zagreb, Croatia

Neuroblastoma is among the most aggressive cancers in humans predonimantly affecting children. Gastric pentadecapeptide BPC157 (GEPPGKPADDAGLV) is a novel small peptide molecule with various pharmacological effects on different organs in vivo in rat experimental models and it was never tested on human cancer cells. Various pharmacologic inhibitors are implicated in the mitogen-activated protein kinase (MAPK) path. This was supported by the finding that expression of a constitutively activated component of the MAPK path, MAPK kinase (MEK), decreased N-myc levels. Human neuroblastoma cells (NB) were grown in cell culture under standard conditions, treated with BPC157, VEGF and the combinations of these agents during 24-48 h. Changes in cell morphology were observed daily and photomicrographs were taken. After harvesting cells were prepared for flow cytometry and Western blot analysis of MAPK kinase signal transduction pathway.Western blot analysis of MAPK pathway was performed using ERK as primary antibody and phosphorylated (activated) ERK (pERK) as secondary antibody. Morphological changes in NB cells were most striking after 48 h treatment with BPC157 in concentrations of 2 and 10 ng/ml and after combined treatment of cells with BPC157 (10ng) and VEGF (10ng). Decrease in cell density, disapperance of cell clusters and mitosis were most prominent after treatment of cells with 10 ng of BPC 157 and after adding 10ng of BPC 157 to VEGF stimulated cells. Futhermore, cells were fully differentiated into neuronal-like phenotype, with long extensions of neurites, formed cellular network and visible synapses. Flow cytometry analysis showed 20% decrease percentage of cells entering S-phase of cell cycle, after treatment with 2 and 10ng of BPC157. Decrease of 15 % of S-phase cells were observed with combination of VEGF stimulation folowed by BPC157 treatment (10ng). Consistent with these findings, BPC157 acts as an antiproliferative and differentiating agent in neuroblastoma cell culture, affecting the G1-S transition state of cell cycle. Finally, BPC 157 exerts its antimitogenic properties by inhibition of ERK phosphorylation before and after VEGF stimulation, thus it blocks mitogenic signal along the MAPK kinase pathway. Our results indicate that BPC157 is selectively involved in downregulation of ERK phosphorylation. Here, we propose that BPC157, may act as a novel inhibitor of MAPK kinase signaling pathway and it could be of particular clinical interest.

O-28
SOCS-3 IS FREQUENTLY METHYLATED IN HEAD AND NECK SQUAMOUS CELL CARCINOMA AND ITS PRECURSOR LESIONS AND CAUSES GROWTH INHIBITION

Anette Weber; Dept. of Otorhinolaryngology, University of Leipzig
Iris Tischoff; Institute of Pathology, University of Leipzig
Christian Wittekind;Institute of Pathology, University of Leipzig
Andreas Dietz;Dept. of Otorhinolaryngology, University of Leipzig
Andrea Tannapfel;Institute of Pathology, University of Leipzig

The suppressors of cytokine signaling (SOCS) are inhibitors of cytokine signaling that function via the Janus kinase (JAK)/signal transducers and activators of transcription (STAT) pathway. Recently, methylation of SOCS-1 and SOCS-3 has been implicated in the tumorigenesis of liver and lung cancer. This study was performed to elucidate the role of SOCS-1 and SOCS-3 in squamous cell carcinoma of the head and neck (HNSCC) and its precursor lesions. HNSCC of 94 patients and corresponding normal mucosa, lymph node metastases as well as 16 high and 21 low grade squamous cell dysplasias were studied by using methylation-specific PCR (MSP) for the SOCS-1 and SOCS-3 promoter after microdissection. The presence of SOCS-3 mRNA transcripts was confirmed by semiquantitative real-time PCR, and the SOCS-3 protein was analyzed immunohistochemically. SOCS-3 hypermethylation was found in 85/94 HNSCC (90%) and in 10/16 high and 9/21 low grade dysplasias (63% and 43%, respectively). SOCS-1 promoter hypermethylation was detected in 10/94 HNSCC samples (11%) and in 2/16 high grade and 1/21 low grade dysplasias (13% and 5%, respectively). Lymph node metastases exhibited an identical methylation status as the primary tumors. Methylation of the SOCS-3 promoter correlated with downregulation of SOCS-3 transcripts and protein expression in these tumors and various cell lines. In the cell lines tested, SOCS-3 and SOCS-1 transcripts increased upon treatment with the demethylation compound 5-aza-2-deoxycytidine (5-AZA-DC). Overexpression of wild type SOCS-3 in carcinoma cells with methylated SOCS-3 resulted in the induction of apoptosis and growth suppression as well as downregulation of STAT3, bcl-2 as well as bcl-xL. Our data suggest that promoter methylation and subsequent transcript downregulation of SOCS-3 transcripts and, to a much lesser extent, SOCS-1 are involved in the multistep carcinogenesis of HNSCC. Due to its involvement in tumor growth, restoration of SOCS-3 may hold treatment potential for HNSCC.

O-29
SOMATIC AND GERMLINE MUTATION IN GRIM-19, A DUAL FUNCTION GENE INVOLVED IN MITOCHONDRIAL METABOLISM AND CELL DEATH, IS LINKED TO MITOCHONDRION-RICH (HÜRTHLE CELL) TUMOURS OF THE THYROID

Sobrinho-Simões M1,2,3, Maximo V1, Botelho T1, Capela J4, Soares P1,2, Lima J1, Magalhães J2,3, Taveira A1,4, Amaro T5, Barbosa A P6, Preto A1, Harach R7, Williams D8.
1.IPATIMUP (Institute of Molecular Pathology and Immunology of the University of Porto, Porto, Portugal; 2.Department of Pathology, Medical Faculty of University of Porto; 3.Department of Pathology, Hospital de São João, Porto, Portugal; 4.Department of Surgery, Hospital de São João, Porto, Portugal; 5.Department of Pathology, Portuguese Oncology Institute, Porto, Portugal; 6.Department of Endocrinology, Portuguese Oncology Institute, Porto, Portugal; 7.Pathology Service, "Dr. A. Oñativia Hospital, Salta, Argentina; 8.Strangeways Research Laboratory, University of Cambridge, Cambridge, United Kingdom.

Oxyphil or Hürthle cell tumours of the thyroid are characterized by their consistent excessive number of mitochondria. A recently discovered gene, GRIM-19, has been found to fulfil two roles within the cell: as a member of the interferon-beta and retinoic acid-induced pathway of cell death, and as part of the mitochondrial Complex I assembly. In addition, a gene predisposing to thyroid tumours with oxyphilia (TCO) has been mapped to chromosome 19p13.2 in one family. A cluster of genes involved in mitochondrial metabolism occurs in this region; one of these is GRIM-19. We have searched for GRIM-19 mutations in a series of 52 thyroid tumours. Somatic missense mutations in GRIM-19 were detected in 3 of 20 sporadic Hürthle cell carcinomas. A germline mutation was detected in a Hürthle cell papillary carcinoma arising in a thyroid with multiple Hürthle cell nodules. No mutations were detected in any of the 20 non-Hürthle cell carcinomas tested, nor in any of 96 blood donor samples. In one of the sporadic Hürthle cell papillary carcinomas positive for GRIM-19 mutation we have also detected a RET/PTC-1 rearrangement. No GRIM-19 mutations were detected in any of the six cases of known familial Hürthle cell tumours tested, so that our results do not support the identification of GRIM-19 as the TCO gene. The GRIM-19 mutations we have detected are the first nuclear gene mutations specific to Hürthle cell tumours to be reported to date; we propose that such mutations can be involved in the genesis of sporadic or familial Hürthle cell tumours through the dual function of GRIM-19 in mitochondrial metabolism and cell death.

O-30
COMPARISON OF 3 COMMERCIALLY AVAILABLE IMMUNOHISTOCHEMICAL TESTS FOR EGFR EXPRESSION IN COLORECTAL CANCERS. IS IMMUNOHISTOCHEMITRY (IHC) RELIABLE ?

F. M. Penault-Llorca, A. Cayre,L. Arnould, F. Bibeau, M. Bralet, P. Rochaix, J.C Sabourin

IHC appears to be the required test for the selection of patients for a monoclonal antibody based targeted treatment with C225 (Erbitux®). To validate the usefulness of IHC, confirmation of assays and scoring systems are mandatory. PURPOSE OF THE STUDY :In an attempt to standardize the immunohistochemical detection of EGFR, we have retrospectively evaluated three commercially available EGFR kits or antibodies and analyzed the discrepancies between the tests in terms of percentage of positive cells, intensity, cut off value and fixatives. METHODS: we extracted 230 paraffin embedded samples from a metastatic colorectal cancer trial. For all cases, EGFR expression have been assessed with the FDA approved Dako EGFR pharmaDx kit, the Zymed EGFR kit and the Ventana CONFIRMTM EGFR 3C6 antibody. Different cut off were tested, intensity was scored 0, 1+,2+, 3+ following the suppliers' recommendations.
RESULTS: number of positive cases
Dako Zymed Ventana
Cut off >0% 75 % 86% 93%
Cut off 5% 61% 78% 80%
Cut off 10% 48% 60% 72%
Performances of the tests i)percentage of positive cells: Ventana > Dako ($p<10-7$), Zymed > Dako ($p = 0{,}000002$), Ventana > Zymed ($p=0{,}75$, ns); ii) The intensity of staining was correlated to the percentage of positive cells for Ventana ($p < 10-6$) and Zymed ($p < 10-5$). iii) No interaction with staining was identified for any of the fixative, or with the nature of samples.Each technique has pros: full automation for Dako and Ventana tests, easier interpretation with Ventana's test (counterstaining), lower costs for Zymed kit.
CONCLUSION: our data showed a higher number of positive cases detected by Ventana and Zymed, whatever the cut off value for positivity was. No scoring system showed, to date, its accuracy, and more studies have to be conducted with an evaluation of response to C-225. Whether and how the EGFR status has to be tested for the selection of patients for C225 is still a non-answered question. The proper selection might be through a co-evaluation of other markers involved in EGFR regulation.

O-31
IMPACT OF PREOPERATIVE RADIOTHERAPY IN LYMPH NODES STATUS AFTER MESORECTAL EXCISION FOR RECTAL ADENOCARCINOMA

RULLIER Anne (1), LAURENT Christophe (2), CAPDEPONT Maylis (2), VENDRELY Veronique (3), BELLEANNEE Genevieve (1), RULLIER Eric (2)
Departments of (1)Pathology, (2)Surgery and (3)Radiotherapy-CHU Bordeaux-France

The number and status of lymph nodes analyzed is a crucial issue for optimal tumor staging and adjuvant treatment. The impact of preoperative radiotherapy in the number of lymph nodes retrieved in rectal specimen is still controversial. The aim of the study was to define influence of preoperative treatment in the number of both lymph nodes retrieved and positive lymph nodes after rectal excision for cancer.
From January 1994 to December 2004, 495 rectal adenocarcinomas underwent rectal excision. Preoperative radiotherapy (45 Gy in 5 weeks) was given in 332 patients (248 with concomitant chemotherapy) whereas 163 patients were treated by surgery alone. Influence of 11 clinical and pathological variables on nodal status (total number and positive lymph nodes) was assessed by univariate and multivariate analyses.
The mean number of lymph nodes retrieved per specimen was 14.6. The four variables influencing independently the number of lymph nodes were preoperative radiotherapy, tumor size, pathological tumor staging and surgical treatment. The mean number of lymph nodes retrieved after preoperative radiotherapy was smaller than after surgery alone (13 vs 17). Concomitant chemotherapy did not influence the number of lymph nodes retrieved whereas a boost of 10 Gy did influence ($p=0.008$). The mean number of positive lymph nodes was 1.6. The six variables influencing independently the number of positive lymph nodes were preoperative radiotherapy, tumor size, pathological tumor staging, tumor differentiation and vascular invasion. The mean number of positive lymph nodes retrieved after preoperative radiotherapy was smaller than after surgery alone (1.2 vs 2.3). The number of positive lymph nodes correlated with the number of lymph nodes retrieved ($p<0.001$).
Compared to surgery alone, preoperative radiotherapy decreases the number of both lymph nodes retrieved and positive lymph nodes after rectal excision for rectal cancer. However, further studies are needed to assess the optimal lymph nodes number to analyze after preoperative radiotherapy for rectal cancer.

O-32
REACTIVATION OF P16INK4A AND RASSF1A GENES AND INHIBITION OF C-MYC AND HTERT EXPRESSION BY AS2O3 IN COLORECTAL CANCER CELLS

Xing CUI1, Toshifumi WAKAI2, Katsuyoshi HATAKEYAMA2 and Seishiro HIRANO1
£¨1Environmental Health Sciences Division, National Institute for Environmental Studies, 2Division of Digestive and General Surgery, Niigata University Graduate School of Medical and Dental Sciences, Japan

Background & Aims
Inactivation of tumor suppressor genes and overexpression of DNA methyltransferase 1 (DNMT1), c-myc, and human telomerase reverse transcriptase£¨hTERT£©have been reported in human colorectal carcinoma (CRC). Arsenic trioxide (As2O3), an effective anticancer agent for the treatment of malignant hematopoetic diseases, has been shown to induce apoptosis and suppression of hTERT in leukemia cells. On the other hand, arsenic has been shown to induce DNA hypomethylation by depletion of methyl donor pool. In the present study, we investigated effects of As2O3 on restoration of some major tumor suppressor genes, p16INK4a, RASSF1A, and inhibition of DNMT1, c-myc, and hTERT in CRC cell lines.
Materials & Methods
HCT116 and SW480 cells were treated with 2-20 mM of As2O3 and/or 2 mM of demethylating agent, 5-aza-2'-deoxycytidine (5-aza-CdR) and/or trichostatin A (TSA), a histone deacetylase inhibitor, for 24, 48 and 72 h. DNA and RNA were extracted from these cells. The methylation status of the CpG island around the promoter regions of p16INK4a and RASSF1A was detected by a methylation-specific polymerase chain reaction (MSP). The mRNA and protein levels of above two genes in addition to c-myc, DNMT1 and hTERT were determined by quantitative real-time RT-PCR, immunohistochemical analysis. DNMT enzyme activity was also estimated in the cells treated with or without As2O3.
Results
CpG methylation of the p16INK4a and RASSF1A genes was correlated to the reduction of mRNA levels in CRC cell lines, and its mRNA expression was indeed restored by low concentrations (2-6 mM) of As2O3 through demethylation, as well as 2 mM of 5-Aza CdR and/or combined with 50 ng of TSA. Immunohistochemical analysis showed that expression of p16INK4a and RASSF1A was significantly enhanced after the treatment with a low concentration of As2O3. In contrast, high concentrations (10-20 mM) of As2O3 damaged cell membranes and markedly suppressed immunoreactivity. With nuclear extracts as the enzyme source and polydeoxyinosine-deoxycytosine as the substrate, As2O3 dose-dependently inhibited DNMT activity. Moreover, a low concentration of As2O3 suppressed expression of DNMT1, c-myc, and hTERT in CRC cells.
Conclusions
In conclusion, a low concentration of As2O3 can reactivate partially/fully silenced tumor suppressor genes through demethylation, and also inhibits expression of proto-oncogene such as c-myc and hTERT.

O-33
THE SIGNIFICANCE OF BETA-CATENIN, E-CADHERIN, AND P-CADHERIN EXPRESSIONS IN COLORECTAL ADENOMA-CARCINOMA SEQUENCE: AN IMMUNOHISTOCHEMICAL STUDY USING TISSUE ARRAYS

Berna Savas, Arzu Ensari, Sibel Percinel, Isinsu Kuzu, Ayhan Kuzu, Nazmiye Kursun.
Ankara University, Medical Faculty, Department of Pathology, Department of Surgery and Department of Biostatistics, Turkey

Introduction: Alterations in APC gene are known to be early events in colorectal adenoma-carcinoma sequence, causing activation of Beta-catenin/TCF pathway. Alterations of Beta-catenin together with its binding partner, E-cadherin are commonly observed in colorectal carcinogenesis. Increased nuclear Beta-catenin expression together with downregulation of E-cadherin was observed in the neoplastic progression of adenomas in previous studies.
Aim: To investigate the role of Beta-catenin, E-cadherin and P-cadherin in colorectal adenoma-carcinoma sequence.
Methods: Core tissue biopsies of 4 mm in diameter were prepared from paraffin-embedded tissue blocks of 167 cases, including 95 colorectal adenomas, 10 hyperplasic polyps, 8 serrated adenomas, 28 colorectal carcinomas and 26 normal colon mucosae. Of 95 adenomas, 17 were tubular; 41 were tubulovillous and 37 were villous adenomas. Fourteen adenomas contained microscopic foci of intramucosal carcinoma. Immunohistochemistry was performed using antibodies to Beta-catenin, E-cadherin, P-cadherin. Distribution of positivity was assessed using percentage expression while an arbitrary grading scale was used for staining intensity.
Results: Beta-catenin expression was either cytoplasmic-membranous or nuclear where as both E-cadherin and P-cadherin expressions were confined to cytoplasmic-membranous compartments. Cytoplasmic-membranous expression of Beta-catenin was significantly higher in adenomas including serrated adenomas compared with hyperplastic polyps and normal mucosae ($p<0.001$) while no such difference was observed between adenomas and carcinomas. Nuclear expression of Beta-catenin showed a mean of $8 \pm 14,4$ in TA, $2,97 \pm 7,5$ in TVA and $8,96 \pm 25,7$ in VA while adenomas with intramucosal carcinoma and carcinomas had significantly higher expression ($p<0.001$). Nuclear Beta-catenin expression showed a positive correlation with the grade of dysplasia in adenomas ($p<0.01$). No such difference was observed in E-cadherin, P-cadherin expressions.
Conclusions: The increase of nuclear expression of Beta-catenin correlating with the grade of dysplasia in adenomas and increased Beta-catenin nuclear staining intensity in carcinomas support the previous studies regarding the role of Beta-catenin in colorectal carcinogenesis. The presence of E-cadherin and P-cadherin expressions in adenomas suggests that these molecules are also involved in adenoma formation though not necessarily involved in neoplastic progression.

O-34
CYTOPLASMIC PHOSPHOLIPASE A2 EXPRESSION IN HUMAN COLON CARCINOMAS : A STUDY OF 65 TUMORS AND 8 CELL LINES

Dominique Wendum (1,2), Valentine Panel (2), Pierre-Yves Boëlle (3), Jesus Ayala-Sanmartin (2), Anne-Marie Jouniaux (2), Richard Hamelin (4), Joëlle Masliah (2), Germain Trugnan (2), Jean-François Fléjou (1,4)
(1) Department of Pathology, Hôpital Saint-Antoine, AP-HP, 184 rue du Faubourg Saint-Antoine, 75571 Paris Cedex 12
(2) Unité INSERM U538 and (3) U444, Faculté de Médecine Saint-Antoine, Université Pierre et Marie Curie, 27 rue Chaligny, 75571 Paris Cedex 12
(4) INSERM U434, Fondation Jean Dausset-CEPH, 27 rue Juliette Dodu 75010 Paris

Cyclooxygenase (COX) is a key enzyme for prostaglandin production and is directly involved in colorectal tumor development mainly via generation of prostaglandin E2 (PGE2). However, prostaglandin production is also directly

dependent on arachidonic acid availability. Cytoplasmic PLA2 (cPLA2) preferentially hydrolyses arachidonic acid that is the limiting substrate for COX mediated prostaglandin production. Because of this key role in prostaglandin production, the role of cPLA2 in intestinal tumorigenesis has been suggested. However, contradictory data are found in the literature.
In this study we evaluated cPLA2 expression in colon carcinomas and determined if cPLA2 expression could contribute to PGE2 production.
cPLA2 and COX-2 protein expression were evaluated in 65 colon carcinomas by immunohistochemistry and in 8 colorectal cancer cell lines by Western Blot. Furthermore, basal PGE2 production and PGE2 production after cPLA2 stimulation by calcium ionophore were evaluated in the cell lines by enzyme immunoassay and correlated to cPLA2 and COX-2 expression. As the presence of microsatellite instability influences COX-2 expression, we also investigated the relationship between cPLA2 expression and microsatellite instability assessed by PCR.
Twenty -five carcinomas had microsatellite instability. A moderate or strong cPLA2 expression in carcinomas was observed in 49 % of all the cases. Within a same tumor cPLA2 expression positively correlated with COX-2 expression (p=0,0003). Although a low COX-2 expression correlated with the presence of microsatellite instability (p=0,0002) there was no association between cPLA2 expression and microsatellite instability (p=0,69). Both cPLA2 and COX-2 protein expression were detected in 4 cell lines and COX-2 protein expression was detected in one additional cell line. In the cell lines, levels of cPLA2 and COX-2 protein expression correlated (p=0.008). Basal PGE2 production was correlated with COX-2 levels (p=0.03) but not with cPLA2 levels (p=0,2). The increase in PGE2 production after a 30 minutes stimulation by calcium ionophore was correlated with cPLA2 levels (p=0.002) but not with COX-2 levels (p=0.06).
Conclusion: A moderate or strong cPLA2 protein expression exists in about half of colon carcinomas, and is often associated with a moderate or strong COX-2 expression. cPLA expression in colon carcinomas seems to be involved in prostaglandin E2 production and could contribute to colon tumor development.

O-35
EVALUATION OF REVISED BETHESDA GUIDELINES FOR HEREDITARY NON-POLYPOSIS CANCER IN A CONSECUTIVE SERIES OF 225 COLORECTAL CARCINOMAS

JULIÉ Catherine, MUTI Christine, COULET Florence, TRESALLET Christophe, BROUQUET Antoine, SOUBRIER Florent, BOILEAU Catherine, NORDLINGER Bernard, ROUGIER Philippe, PENNA Christophe, FRANC Brigitte, RADVANYI Hélène. CHU Ambroise Paré, Boulogne; CHU Tenon, Paris, France (AP-HP)

Introduction: Hereditary non-polyposis cancer (HNPCC) is an autosomal dominant cancer predisposition syndrome caused by germline mutations in DNA mismatch repair (MMR) genes. Defective MMR results in microsatellite instability (MSI) phenotype, which has been almost always found in HNPCC tumors, and in only 10-15% of sporadic colorectal tumors. The Bethesda guidelines developed in 1996 to guide who should undergo MSI analysis were recently revised to further aid in the identification of HNPCC kindred for genetic testing. Among the 5 revised criteria, 1 focuses on the histopathological features. Our aim was to evaluate the validity of the revised Bethesda criteria.
Methods: A consecutive series of 225 resected colorectal invasive adenocarcinomas from 214 patients was collected in our institution. All patients were seen by a clinical geneticist and personal and familial cancer history were collected. For all patients, age at diagnosis, location, stage and pathological characteristics of the tumor were collected. All tumors were reviewed by a senior pathologist. Tumors were analysed for MSI status using the five markers of the original NCI microsatellite panel. Germline mutations in the MMR genes pointed by immunohistochemistry were searched for MSI-high (MSI-H) tumor patients.
Results: Eighty-six patients (40%) fulfilled at least one of the 5 Bethesda criteria, but 75 of these Bethesda-positive patients (87%) fulfilled only 1 criteria. Among our 214 patients, 21 (8 Bethesda-positive and 13 Bethesda-negative) had a MSI-H tumor. Five out the 8 Bethesda-positive patients with MSI-H tumor presented a germline mutation of one of the MMR genes (4 hMSH2 mutations, 1 hMLH1 mutation). For the 3 remaining patients, search for mutation is ongoing, but there is some evidence for HNPCC (familial history (2/3), loss of expression for hMSH2 (2/3), rectal location (1/3)). Among the 13 Bethesda-negative patients with MSI-H tumor, 2 presented a germline mutation (1 hMLH1 mutation and 1 hMSH6 mutation).
Conclusion: In our study, the revised Bethesda criteria were not very selective: 40% of our unselected patients were retained using these criteria, only 9% of them had a MSI-H tumor. All the Bethesda-positive patients with MSI-H tumor presented a proven or likely HNPCC. On the other hand, we found 2 HNPCC cases in Bethesda-negative patients, showing that in our series, the revised Bethesda criteria were not sufficient to identify all HNPCC patients.

O-36
MICROSATELLITE INSTABLE (MSI+) COLORECTAL CANCERS COMPLICATING INFLAMMATORY BOWEL DISEASE MAY HAVE A DIFFERENT GENETIC PATHWAY FROM MSI+ SPORADIC COLORECTAL CANCERS

SVRCEK Magali (1, 2), DUVAL Alex (2), HAMELIN Richard (2), COSNES Jacques (3), BEAUGERIE Laurent (3), TIRET Emmanuel (4), PARC Rolland (4), FLEJOU Jean-François (1, 2)
Departments of Pathology (1), Gastroenterology (3), Digestive Surgery (4), Saint-Antoine Hospital, AP-HP, University Pierre et Marie Curie ; INSERM U434 (2), CEPH, Paris, France

Twelve to 15% of sporadic colorectal cancers (CRC) display defective DNA mismatch repair (MMR), manifested as microsatellite instability (MSI). In this group of cancers, the MMR deficiency is due to silencing of hMLH1 by methylation of its promoter, resulting in loss of hMLH1 protein expression.
Patients with inflammatory bowel disease (IBD) face an increased risk of CRC in ulcerative colitis (UC) and Crohn's disease (CD), and of small intestinal adenocarcinoma (SIA) in CD. MSI has been found to be a feature of some IBD-associated intestinal cancers, with a frequency still debated.
The aim of this study was to assess the prevalence of MSI in IBD-associated CRC and SIA in a referral hospital. We also compared the expression of MMR proteins and the clinicopathological variables of MSI+ cancers complicating IBD to those of a series of 21 MSI+ sporadic CRC observed in the same centre.
Paraffin embedded tissues from 53 CRC in 37 patients with UC and 17 CRC and 6 SIA in 21 patients with CD were studied. We evaluated MSI by PCR on 5 mononucleotide markers and immunohistochemistry (IHC) of hMLH1, hMSH2 and hMSH6.
15 cancers complicating IBD were suitable only for IHC. 61 were investigated using both techniques.
10/70 CCR (14%) and 0/6 SIA exhibited MSI. These 10 cancers were observed in 6 patients (2 with CD and 4 with

UC) (1 patient with UC had 5 cancers). IHC revealed a loss of expression of one MMR protein in 9/10 MSI+ cases (5 of 6 patients). One case showed loss of hMLH1, 3 cases hMSH2 and 5 cases (1 patient) hMSH6. All MSI+ sporadic CRC showed a loss of expression of hMLH1. MSI+ CRC complicating IBD were seen more frequently in left colon and rectum than sporadic CRC (50% vs 5%, p<0.01). The mean age at diagnosis of cancer was younger in the group of IBD-associated cancers (57 yrs, range 50-65 vs 74 yrs, range 49-91, p<0.01). Tumours in the two groups of patients shared many pathological features, in particular mucinous or partially mucinous differentiation (50% in IBD and 71% in sporadic, respectively), expanding margins (30% and 38%) and Crohn's-like lymphoid infiltrate (30% and 29%).
In conclusion, the prevalence of MSI in IBD related CRC is similar to that observed in sporadic CRC. The immunohistochemical pattern of MMR protein expression suggests that different genetic events may be involved in tumorigenesis of these two groups of cancers. MSI seems to be a rare event in IBD related SIA.

O-37
THYMIDILATE SYNTHASE QUANTITATION, VASCULAR ENDOTHELIAL GROWTH FACTOR AND P53 PROTEIN OVEREXPRESSION, AND POINT K-RAS MUTATION IN COLORECTAL CARCINOMA: RELATIONSHIPS WITH TUMOR RECURRENCE AND SURVIVAL

USAJ Slavica, KRTOLICA Koviljka*, BOGDANOVIC Andrija**, CEROVIC Snezana, BRAJUSKOVIC Goran, TARABAR Dino***
Institute of Pathology, Military Medical Academy; *Institute of nuclear science, Vinca, **Clinic of Hematology, School of Medicine, Belgrade University, *** Clinic of Gastroenterology, Military Medical Academy, Serbia and Montenegro

Introduction. Tumor angiogenesis, K-ras mutation and p53 protein overexpression are commonly involved in colorectal tumorigenesis, but their interrelationship and clinicopathological effects remains inconclusive. The expression of thymidilate synthase (TS) determines the response of patients with colorectal carcinoma (CRC) to fluorinated-pyrimidine based chemotherapy, but there are a few reports regarding prognostic value of TS expression on recurrence and overall survival of patients treated with curative surgery alone. The aim of this study was to examine the immunohistochemical expression of vascular endothelial growth factor (VEGF), p53 protein, and TS as wall as the presence of K-ras mutation in CRC tissue, their relationships and their significance in predicting tumor behavior and clinical outcome in CRC patients. Material and methods. Paraffin embedded tumor tissue specimens of 81 curatively resected colorectal carcinomas (Dukes stage A-21, stage B-24, and stage C-36 patients) were studied by immunohistochemical methods for detection of VEGF, TS and p53 protein and by polymerase chain reaction (PCR) for identification of mutations in the 12th and 13th codon of the K-ras gene. Median follow up was 31.4 month (range, 2-66 months). Results. TS, VEGF expression, nuclear p53 protein overexpression and K-ras mutation were found in 44.4%, 66.7%, 58.0% and 40.7% of CRC tissue, respectively. In high TS expressing group there were significantly more frequent VEGF and p53 protein overexpression as wall as the presence of K-ras mutation than in low TS group (86.1%, 77.8% and 63.9% versus 51.1%, 42.2% and 22.2% respectively, p value < 0.01)). Survival analysis showed that high value of TS, VEGF and p53 protein expression as wall as the presence of K-ras mutation in tumor tissue significantly correlated with early recurrence and poor overall survival (p ¡Ü 0.01) of CRC patients. Conclusions. The investigated molecular markers may be useful for prediction of outcome and recurrence rate in curatively treated CRC patients. In conjunction with clinical and pathological staging, they may provide a stronger indication of clinical outcome than staging alone and help better selection of therapeutic options in CRC patients.

O-38
CHARACTERIZATION OF MOLECULAR CHANGES FROM FROZEN, PARAFFINED, AND DEPARAFFINED SECTIONS OF NORMAL AND ADENOCARCINOMATOUS HUMAN COLONIC TISSUES BY NEAR-INFRARED RAMAN MICROSPECTROSCOPY

GUILLOU Pierre-José, BELJEBBAR Abdelilah, BOUCHE Olivier, THIEFIN Gérard, MANFAIT Michel, PALOT Jean-Pierre, DIEBOLD Marie Danièle
Laboratoire Central d'Anatomie et de Cytologie Pathologiques, Service de Chirurgie générale, Service d'Hepato-gastro-enterologie, CHU de Reims, Avenue du Général Koenig, 51092 REIMS CEDEX, France
Unite MeDIAN, CNRS UMR 6142, UFR de Pharmacie, 51 rue Cognacq-Jay, 51096 REIMS CEDEX, France

Raman spectroscopy is a vibrational spectroscopic technique that can be used to probe molecular changes associated with tissue malignancy and prognosis. A previous study conducted on 52 tissues (26 normal mucosa and 26 tumors) human fresh colonic samples has shown the potential of Raman spectroscopy to discriminate between normal and tumor tissues on frozen sections. The aim of this work was to investigate the effect of formalin-fixation and deparaffination on human colonic tissues by near-infrared Raman microspectroscopy. Raman spectral images were recorded from paraffin-embedded, deparaffined, and frozen normal (n=3) and tumor (n=3) tissue sections. A mathematical routine involving vector algebra was developed to substract the paraffin contribution in each spectrum (virtual deparaffination). Multivariate statistical analysis was performed to identify the molecular composition (lipids, proteins, and collagen) in normal and malignant tissues. The comparison between the information obtained from frozen, paraffined, and deparaffined sections showed i) some significant spectral changes in protein content due to formalin-fixation, ii) the absence of lipid as expected after paraffin inclusion process iii) less information from protein and collagen spectra after deparaffination. Unsupervised hierarchical cluster analysis was used to classify the data obtained from frozen, paraffined, and deparaffined sections. This analysis permitted to classify tissues into two groups, normal and adenocarcinomas whatever the tissue preparation. In conclusion this study demonstrates that Raman spectroscopy can be applied on fixed tissues as well as on fresh tissues.

O-39
ACCUMULATION OF LEPTIN AND ADIPONECTIN WITH INCREASED EXPRESSION OF ADIPONECTIN RECEPTORS IN THE LIVER OF PATIENTS WITH NON-ALCOHOLIC FATTY LIVER DISEASE

CERVERA Pascale, LEMOINE Maud, WENDUM Dominique, CHARLOTTE Frédéric, KIM Minji, BASTARD Jean-Philippe, POUPON Raoul, HOUSSET Chantal, FLEJOU Jean-François, CAPEAU Jacqueline, SERFATY Lawrence.

Fat-secreted adipokines leptin and adiponectin are possibly involved in the pathogenesis of non-alcoholic fatty liver

disease . While a profibrogenic action of leptin and an antiinflammatory action of adiponectin are suggested by animal experimental studies, it is not known whether hepatic levels of leptin, adiponectin or adiponectin receptors are modified in patients with non-alcoholic steatohepatitis (NASH).
To address this question, we investigated 49 patients with biopsy-proven NASH (age 50±13, sex ratio 1, BMI 29.2±4.4), 14 with steatosis only (age 49±13, sex ratio 1.2, BMI 26.9±4.3) and 6 controls without steatosis who underwent liver surgery (age 63±8, sex ratio 2, BMI 24.4±1.5). In all subjects, insulino-resistance index, serum leptin and adiponectin levels were measured, intrahepatic leptin and adiponectin immunoreactivity was analyzed by immunohistochemistry, and hepatic expression of adiponectin receptors RI and RII was quantified by real-time RT-PCR.
Results : Patients with NASH, steatosis and controls were significantly different for insulino-resistance index (6.3±5.4 vs 3.1±2.4 vs 0.5±0.4, p=0.01) and serum adiponectin/leptin ratio (0.97±1 vs 1.6±1.4 vs 3.8±4.7, P=0.001). Liver adiponectin immunoreactivity was higher in patients with NASH than in patients with steatosis or controls (mean score 1.55±1.06 vs 0.93±0.3 vs 1±0 respectively, p<0.05), whereas leptin immunoreactivity was similar in the 3 groups. There was no relationship between serum concentrations and hepatic contents of leptin or adiponectin. Among patients, the amount of adiponectine immunoreactivity was positively related to the degree of steatosis and necrosis (p<0.0001 and p=0.02). The amount of leptin immunoreactivity was related only to the degree of steatosis (p=0.02). Leptin or adiponectin mRNAs were undetectable by RT-PCR in the liver both of patients and controls. Adiponectin RII mRNA levels were significantly higher in patients with NASH than in patients with steatosis and controls (4.9±2.6 vs 3.5±1.9 vs 2.2±1 respectively, p=0.01).
Conclusion : In patients with non-alcoholic fatty liver disease, 1) adiponectin and leptin accumulate within the liver, in the absence of significant local synthesis, 2) NASH is associated with higher amounts of hepatic adiponectin and its receptor RII as compared to patients with steatosis or to controls, 3) the amount of hepatic adiponectin, is related to the degree of steatosis and of necrosis.

O-40
A COMPARISON OF STELLATE CELL ACTIVATION AND TGF-Â EXPRESSION IN PATIENTS WITH HEPATITIS C AND WITH COMBINED HEPATITIS C/ DIABETES MELLITUS

M Rivera- NYPH-Weill Cornell Medical Center, New York, NY
F Ahmed- NYPH-Weill Cornell Medical Center, New York, NY
E Hyjek- NYPH-Weill Cornell Medical Center, New York, NY
LM Petrovic- NYPH-Weill Cornell Medical Center, New York, NY

Backround: Hepatits C virus (HCV) infection is a major cause of chronic liver disease.Hepatic stellate cell activation, manifested by the expression of smooth muscle actin (SMA) and TGF-â arekey factors in liver fibrogenesis.
Aim: The aim of this study was to assess and compare the degree of stellate cell activation in liver biopsies of patients with HCV alone and in patients with HCV/DM.The pattern of TGF-â expression was examined in selected cases.
Design: 69 liver biopsies were evaluated: HCV (n=39), and HCV/DM (n=30).All biopsies were immunostained for SMA, and 26 (13 from each group) randomly selected cases for TGF- â.A grading scale was applied (range: 0-3) reflecting the percentage of stellate cell activation which occurred in each zone of the hepatic acinus. A similar scale was applied in evaluating TGF-â expression.T-test and Wilcoxon rank-sum tests were implemented comparing stellate cell activation with the grade, stage, and degree of steatosis between the two groups.TGF-â expression was compared between the two groups.
Results: The mean stage of fibrosis for the HCV/DM and HCV group were 2.8 and 1.6 respectively (p<.0001).The mean grade of inflammation for the HCV/DM group and HCV group were 1.9 and 1.5 respectively (p=0.03).The mean grade of steatosis for the HCV/DM and HCV group were 1.1 and 0.5 respectively (p=0.01). The average grade of stellate cell activation for all zones for the HCV/DM group and HCV group was 1.3 and 1.2 respectively (p=.39). In both diagnostic groups combined, a significant stellate cell activation was observed in the zone 1 of the acinus and portal tracts for higher stages of fibrosis (>2) vs lower stage disease (p<.0001). A statistically significant increase in stellate cell activation was also observed in zone one for the HCV/DM group as compared to the HCV group (p=.02).The average grade of TGF-â expression in the HCV/DM and HCV group were 0.69 and 0.83 respectively (p=0.32).In advanced stages, prominent staining of septal myofibroblasts by TGF-â was seen.
Conclusion: Activated stellate cells are predominantly present in zone 1 of the acinus, correlating with advanced stages of fibrosis.Zone 1 stellate cell activation is significantly increased in the HCV/DM group as compared to the HCV group.TGF-â expression is increased in lower stage disease with prominent staining of septal myofibroblasts in high stage disease.This may reflect the role of stellate cell activation and TGF-â in early fibrogenesis.

O-41
EXPRESSION OF PROTEASE-ACTIVATED RECEPTORS AND TISSUE FACTOR IN HUMAN LIVER

Anne Rullier1,2, Nathalie Senant1, Walter Kisiel3, Paulette Bioulac-Sage1,2, Charles Balabaud1, Brigitte Le Bail1,2 and Jean Rosenbaum1.
1 INSERM, E362, 33076 Bordeaux France ; Université Victor Segalen Bordeaux 2, 33076 Bordeaux France ; IFR 66, 33076 Bordeaux France, 2 CHU de Bordeaux, Hôpital Pellegrin, Department of Pathology, Bordeaux France, and 3 University of New Mexico School of Medicine, Department of Pathology, Albuquerque, New Mexico, USA.

Thrombin, acting via its receptors called Protease-Activated Receptors (PARs) and tissue factor (TF) are major actors of haemostasis and are also known to be involved in inflammation and tissue repair processes and in tumorigenesis. Hepatocellular carcinomas (HCC) usually complicate chronic liver diseases characterized by inflammation and fibrosis. Thus, the aim of this study was to describe the expression of PARs and of TF in normal liver, cirrhosis and HCC.
We performed an immunohistochemical detection of the thrombin receptors PAR-1, PAR-3, PAR-4 and of human TF in formalin-fixed paraffin-embedded human tissue samples from 19 subnormal livers, 33 cirrhosis and 30 HCCs. PAR-1 was found on endothelial cells of sinusoids and larger vessels in all samples. In cirrhosis, spindle-shaped cells within septa and T lymphocytes were also PAR-1-positive. A few PAR-1-positive tumor cells were found in only 10% of HCCs. Whatever the nature of the tissue sample, PAR-4 expression was restricted to macrophages, B lymphocytes and nerves. The expression of PAR-3 was rarely seen. Unexpectedly, TF was found expressed in 95% of normal livers, 94% of cirrhotic livers, but only as in 50% of HCCs (p<0.001). Staining was mostly found in hepatocytes, and sometimes in neovessels and spindle-shaped cells within cirrhotic septa. No association was found between TF labelling and clinicopathological characteristics of HCC.

In conclusion, the pattern of expression of PARs confirms their role in the course of chronic liver disease by promoting inflammation via immune cells and neurogenic stimulation. However, PARs and TF expressions do not support their implication in HCC progression .

O-42
EXPRESSION OF CELLULAR RETINOL-BINDING PROTEIN-1 (CRBP-1) AND FIBRILLIN-1 IN HUMAN FŒTAL LIVER: AN IMMUNOHISTOCHEMICAL STUDY OF 28 CASES.

LEPREUX Sébastien (1,2), DESMOULIÈRE Alexis (2), PELLUARD-NEHME Fanny (1), CARLES Dominique (1), CHAPONNIER Christine (3), BALABAUD Charles (2), BIOULAC-SAGE Paulette (1,2)
(1) Service d'Anatomie Pathologique, Hôpital Pellegrin, CHU Bordeaux, France (2) GREF/INSERM E0362, Université Victor Segalen Bordeaux 2, France, (3) Département de Pathologie CMU Genève, Suisse.

In adult human liver, the CRBP-1 (which is involved in vitamin A metabolism) is a relevant marker of the quiescent hepatic stellate cells (HSC). CRBP-1 is also expressed in biliary cells and with a lower intensity in hepatocytes. Fibrillin-1, a component of microfibrils found in elastic fibers, is expressed without elastin as a regular network in the Disse space and is reinforced along the biliary ducts. Little is known on the expression of CRBP-1 and fibrillin-1 in the Disse space and biliary tree during the development of human fœtal liver.
Materials and methods: Twenty-eight fœtal livers at different stages of development (between 7 and 31 weeks of development (WD)) were studied. Immunohistochemistry was performed using antibodies against CRBP-1 on formalin fixed tissue (n=28) and against fibrillin-1 on frozen tissue (n=20).
Results: 1- Disse space. Until the 13th WD (n=13), CRBP-1 was expressed in 0/rare (n=9) or many cells (n=4). After the 13th WD (n=15), all cases showed CRBP-1 expressing cells in the Disse space with a similar density than adult liver in 13/15 cases. CRBP-1 expressing cells were fusiform in the majority of cases before the 16th WD and stellate after the 18th WD. Cellular bodies were stained as well as cytoplasmic processes, but no cytoplasmic lipid droplets were outlined by the staining, in contrast with HSC in adult liver. The expression of fibrillin-1 in the Disse space was discontinuous and irregular, but increased progressively with the age of development.
2- Biliary tree. From the 11th WD, all levels of ductal plate remodeling were observed. Whatever the stage of maturation, biliary cells showed a granular cytoplasmic CRBP-1 staining, lower than in HSC, but higher than in hepatoblasts. No fibrillin-1 staining surrounded the ductal plate. During the remodeling, an irregular deposition of fibrillin-1 surrounded progressively some isolated tubular biliary structures. At the late stage of the ductal plate remodeling, strong and regular deposition of fibrillin-1 around the biliary ducts was observed, as found in adult liver.
Conclusions: These data illustrate i/ the progressive organization of the Disse space with maturation of the HSC and gradual fibrillin-1 deposition, both participating in the sinusoidal architecture and control of the microvasculature tone; ii/ the CRBP-1 expression during the differentiation of biliary cells suggesting that biliary compartment could be early involved in vitamin A metabolism.

O-43
FIBROSING CHOLESTATIC HEPATITIS AFTER LIVER TRANSPLANTATION FOR HEPATITIS C VIRUS

GARRIDO Marta, MIQUEL Rosa., GARCIA Montserrat, FORNS Xavier, RIMOLA Antoni and BRUGUERA Miquel .
Pathology Department and Liver Unit.
Hospital Clinic. IDIBAPS. University of Barcelona.

Introduction. Fibrosing cholestatic hepatitis (FCH) is an infrequent severe histologic form of viral hepatitis that leads to a rapid and usually fatal early liver failure. Initially described in hepatitis B infected renal transplant recipients, it has also been reported exceptionally in other organ transplant recipients with hepatitis C or B infection, and in subjects with HIV-HCV/HBV co-infection and in HBV infected patients receiving chemotherapy.
Objective. The aim of this study was to investigate the incidence, clinical and histological data and outcome of the FCH in liver transplant (LT) recipients, in our institution.
Patients and Methods. A cohort of 116 consecutive HCV-infected patients undergoing 117 LT in our center between March 2000 and August 2003 were followed-up, including HVC-RNA quantification and systematic liver biopsies. The median follow-up was of 22 months.
Results. The liver biopsies of 7 of the patients (6 %) showed histologic characteristics of FCH, with marked irregular and expansive periportal fibrosis associated with mild inflammatory activity, presence of periportal ductular proliferation and periportal hepatocyte ballooning and cholestasis. Bile duct disorders were excluded clinically in each of these patients. FHC was diagnosed at a median of 12 months postransplant (5-18 months). The mortality of the group of patients with FHC was statistically significative higher (p=0.029) than the rest of the series. The development of FHC was associated with a young recipient age (p=0.032), and a trend to have higher pretransplantation (p=0.089) and higher HCV viral load at 1 and 3 months after transplantation (p=NS) was observed. The type of donor (cadaveric or living), old donor age, and administration of steroid boluses did not correlate with the presence of FCH.
Conclusions. Fibrosing cholestatic hepatitis is an aggresive form of viral C hepatitis that has been identified in 6% of the patients with HCV recurrence after LT in our series, emphasizing the importance of the histologic recognition of this condition because it represents a major cause of graft loss and dead. Further studies are needed in order to investigate the potential benefit of antiviral treatment in these patients.

O-44
LIVER HISTOLOGICAL LESIONS IN MULTIDRUG-RESISTANCE-3P-GLYCOPROTEIN HETEROZYGOUS GENE MUTATIONS CARRIERS : A CASE CONTROL STUDY IN ADULTS

ZIOL Marianne (1), FRASSATI-BIAGGI Annonciade (1), HANDRA-LUCA Adriana (1), BEAUGRAND Michel (2), GANNE-CARRIE Nathalie (2).
1:Pathology Department and 2: Liver Unit, CHU Jean Verdier and Paris 13 University, Bondy, France

Multidrug-resistance-3 P-glycoprotein (MDR3) is a canalicular phospholipid translocator involved in the biliary secretion of phospholipids. MDR3 gene mutations result in a spectrum of cholestatic liver diseases including adult cholelithiasis, intrahepatic cholestasis of pregnancy and progressive familial intrahepatic cholestasis type 3 (PFIC). Apart from PFIC, histological liver lesions have been very rarely described in other MDR3 mutation related phenotypes. We aimed to report clinical and biological characteristics and to describe histological liver lesions in 10 adults with MDR3 gene mutations.
Methods: 19 patients (16-57 years) referred for unexplained anicteric cholestasis and/or increased aminotranferases had both liver biopsy and MDR3 gene sequencing. Previously, the main causes of chronic liver disease and obstructive extrahepatic biliary disease were ruled out. Liver biopsies were retrospectively analyzed by 2 pathologists (MZ and

AFB). Clinical, biological and histological characteristics of patients with and without MDR3 gene mutations were compared.
Results: 10 patients had heterozygous gene point mutations (group A) and 9 had no mutation (group B). No significant differences were found between the groups for age (mean 34,6 vs 37 for group A and B respectively), sex ratio (H/F:8/10 vs 7/9), biliary lithiasis related symptoms (n=3 vs n=2), and alkaline phosphatases (2x upper limit of normal vs 1,8). Liver biopsies from the 10 patients with MDR3 mutation showed in all cases characteristic biliary fibrosis ranging from portal fibrous enlargement without septa (n=5) to septal fibrosis (n=5) with varying degrees of ductular proliferation. Slight alterations of interlobular bile duct epithelium with discrete lymphocytic exocytosis were observed in all cases except 2 showing severe ductopenia. No florid nor sclerosing cholangitis or lobular lesions was observed. In group B, biliary fibrosis and ductular proliferation were observed in 2 of 9 cases (one patient with severe ductopenia, one with advanced sclerosing cholangitis). Two biopsies did not show any significant lesions, 2 were suggestive of nodular regenerative hyperplasia, one of non alcoholic steatohepatitis and one of chronic hepatitis.
Conclusion: The results of this case-control study 1) underscore that anicteric cholestasis without biliary symptoms could be added to MDR3 mutation phenotype and 2) show that heterozygous MDR3 can result in significant liver biliary fibrosis.

O-45
EXPRESSION AND ROLE OF GAS6 AND OF ITS RECEPTOR AXL IN HEPATIC REGENERATION FROM OVAL CELLS.

COUCHIE Dominique*, LAFDIL Fouad*, MARTIN Nadine#, LAPERCHE Yannick*, ZAFRANI Elie Serge *#, MAVIER Philippe *. INSERM U581* and Département de Pathologie#, Hôpital Henri Mondor, Université Paris XII-Val de Marne, 94010 Créteil cedex, France.

Introduction. After submassive necrosis or when hepatocyte replication is severely impaired, hepatocyte regeneration takes place from precursor cells called oval cells. These cells proliferate in periportal areas and differentiate into hepatocytes. Gas6 is a vitamin K-dependent protein that binds to the Axl subfamily of tyrosine kinase receptors. Gas6 has anti-apoptotic and proliferative properties and plays a role in development and tissue remodeling.
Aim of the study. To evaluate the expression and role of Gas 6 and of its receptor Axl in hepatic regeneration from oval cells.
Methods and results. Hepatic regeneration from oval cells was induced by treating rats with acetylaminofluorene followed by partial hepatectomy. Rats were sacrificed the day of surgery and at days 1, 5, 9, 14 and 21 after partial hepatectomy. Oval cell accumulation was moderate at day 5, marked at day 9 and 14 and declined thereafter. Oval cells expressed Gas6, as demonstrated at the mRNA level by in situ hybridization and at the protein level by immunohistochemistry. Oval cells also expressed Axl by immunohistochemistry, and Axl mRNA level, measured by quantitative RT-PCR, paralleled the degree of precursor cell accumulation. Gas6 and Axl expression was also demonstrated in vitro by RT-PCR and immunoblotting in WB-F344 cells, a hepatocytic precursor cell line. We studied the effect of recombinant Gas6 on WB-F344 survival. After a 7 day-incubation in serum-free medium, the percentage of viable cells assessed by MTS test was 76% in the absence of Gas6 and 93% in its presence ($p<0.01$). In addition, inhibition of 15-d-prostaglandin J2-induced WB-F344 cell apoptosis by Gas6 was demonstrated morphologically and by a 45% decrease of caspase 3 activity in cells incubated with Gas6. Gas6 did not stimulate WB-F344 proliferation measured by thymidine incorporation.
Conclusion. Oval cells express in vivo Gas6 and its receptor Axl during hepatic regeneration from precursor cells. In vitro, the Gas6/Axl couple protects from apoptosis a hepatocytic precursor cell line. These results strongly suggest that the Gas6/Axl couple favours oval cell accumulation in regenerating liver by an autocrine/paracrine mechanism.

O-46
DETECTION OF HEPATITIS B VIRUS CCCDNA IN LIVER BIOPSY SPECIMENS

KOTOULA Vassiliki, SOULTOYANNIS Ioannis, AKRIVIADIS Evangelos, KOUSTIANI Georgia, NIKOLAKAKI Eleni, PAPADIMITRIOU Constantine, HYTIROGLOU Prodromos.
From the Departments of Pathology and Internal Medicine, Aristotle University Medical School, Thessaloniki, Greece.

Introduction: The major transcriptional template of hepatitis B virus (HBV) is the covalently closed circular DNA (cccDNA). Chronicity of infection and resistance to treatment are believed to be due to inability of the immune system and antiviral agents to clear hepatocytes of cccDNA. Molecular methods for detection of cccDNA have recently been described.
Purpose of study: To assess the presence of cccDNA in liver biopsy specimens of patients with chronic HBV infection, and to correlate the findings with pathologic features.
Methods: A real-time polymerase chain reaction (PCR) methodology for quantitative assessment of cccDNA and HBS gene sequences was developed. Total DNA was extracted from 37 needle liver biopsy specimens, obtained from 33 patients with chronic HBV infection and 4 patients with other diseases. Thirty of the 33 patients were HBeAg-negative in serum. A small fragment of each biopsy specimen was used for DNA extraction, while most of the material was processed for histologic and immunohistochemical examination. Real-time PCR reactions were run in an Opticon DNA Engine. The detection standard limits for cccDNA and HBS DNA were 1.5fg and 7.5fg, respectively.
Results: On histologic evaluation, the biopsies from the 33 patients with HBV infection showed the following grades of necroinflammatory activity: minimal: n=6 ("inactive carriers"); mild: n=11; moderate: n=9; severe: n=7. Fibrosis was staged as: absent: n=3; mild: n=6; moderate: n=11; severe: n=10; cirrhosis: n=3. Positive immunohistochemical staining for HBsAg and HBcAg was observed in 30 and 14 biopsies, respectively. HBS gene sequences were detected by real-time PCR in 30 out of the 33 specimens. The values ranged from 0.3pg to 94.7pg. Detectable cccDNA was found in 12 out of the 33 specimens. cccDNA values were low and ranged from <0.1fg to 0.2pg. In 2 of these 12 cases, necroinflammatory activity was mild, in 4 moderate, and in 6 severe ($p<0.01$). There was a clear-cut association between detectable cccDNA and positive immunostaining for HBcAg ($p<0.001$). No cccDNA or HBS gene sequences were detected in specimens from patients without HBV infection.
Conclusions: 1) Detectable cccDNA in liver biopsy specimens from patients with chronic HBV infection correlates with the grade of necroinflammatory activity, as well as with positive immunohistochemical staining for HBcAg. 2) In this predominantly HBeAg-negative patient population, the level of cccDNA in liver tissue is generally low.

O-47
HEPATIC TUMORS WITH SPINDLE CELL COMPONENT : A RARE AND HETEROGENEOUS GROUP WITH A HIGH RATE OF MALIGNANCY

ANDRIAMAMPIONONA Francine (1), BIOULAC-SAGE Paulette (1), BLANC Jean-Frédéric (2), SARIC Jean (3), LE BAIL Brigitte (1)

(1) Service d'Anatomie Pathologique, Hôpital Pellegrin; (2) Services d'Hépato-Gastroentérologie et (3) de Chirurgie Digestive, Hôpital Saint-André, CHU Bordeaux, France.

Spindle cell tumors, either primitive or secondary seem to be rare in the liver and the diagnosis is difficult.
Our aims were to evaluate the prevalence of hepatic tumors with spindle cell component (HTSC), their histological type, the proportion of primitive and secondary neoplasms and to determine the appropriate panel of antibodies to use for diagnosis.
We perform a retrospective review of HTSC seen in our institution from January 1994 to March 2005, either in liver biopsies or operative specimens.
During this period, only 42 HTSC were found. The prevalence among all hepatic tumors during the 6 last years was 2.9%. In 26 (61.9%)HTSC, spindle cells constituted the only/main component of the tumor and in the remaining ones (16 = 38.1%), spindle cells were in minority and associated with other cell types. The tumors were classified as malignant in 31 cases (73.8%), either primitive (n=18) or metastatic (n=13). The most common diagnosis were vascular tumors in 23.8%, with a high rate of angiosarcoma (80%); metastatic spindle cell melanoma (14.3%); leiomyosarcoma (11.9%); metastatic GIST (9.5%); solitary fibrous tumor, angiomyolipoma, and undifferentiated hepatic sarcoma (7.1% each). The origin of metastasis was mainly melanoma whereas primitive malignant tumors were mostly angio- and leiomyosarcomas. Primitive hepatic carcinomas were unfrequent : spindle cell hepatocellular carcinoma , spindle cell cholangiocarcinoma and hepatoblastoma with spindle cell component, 1 case each. Among benign tumors, solitary fibrous tumors were the most frequent (n = 3), followed by angiomyolipomas and epithelioid hemangioendotheliomas (2 each).The most usefull markers were: endothelial (CD 34 and CD 31) and muscular (AML and caldesmone) ones for sarcoma and solitary fibrous tumor, HMB45 and PS100 for melanoma and angiomyolipoma, CD 117 for metastatic GIST, CK 7 and Pancytokeratin for spindle cell carcinoma, anti-Hepar and anti-AFP for undifferentiated hepatocellular carcinoma; vimentine was totally aspecific.
Conclusion: in our series, HTSC represent 2.9% of hepatic tumors. 74% are malignant, mostly of mesenchymal origin with vascular or muscular differentiation. A restricted panel of markers (less than 12) is usefull, depending on the histology and on the patient's clinical history. The search of a primitive tumor may be necessary, especially for a GIST or a cutaneous or ocular melanoma. Benign tumors are rarer, mostly represented by solitary fibrous tumors.

O-48
CHORION NODOSUM: A PLACENTAL HALLMARK OF THE LIMB BODY WALL COMPLEX/SHORT UMBILICAL CORD SYNDROME

STANEK Jerzy, ADENIRAN Adebowale. Department of Pathology and Laboratory Medicine, University of Cincinnati College of Medicine, Cincinnati, OH, U.S.A.

Recently we reported the statistically significant association between amnion nodosum (AN) and clinical oligohydramnios, macerated stillbirths, malformations, and chronic twin-twin transfusion syndrome. On microscopic examination of some chorionic discs devoid of amnion (extraamniotic pregnancies), we noticed vernix-containing nodules identical to those of AN, but attached directly to the chorionic mesenchyme, which we named chorion nodosum (ChN). This study was undertaken to characterize the clinical setting of ChN.

Our surgical pathology (placentae and previable fetuses) and perinatal autopsy database, and relevant histology slides were reviewed to identify all AN and ChN cases examined from 1994 to 2004.

Among all consecutive 4356 placentae, there were four placentae with ChN (0.1%). Among 450 perinatal autopsies and 521 surgical pathology examinations of previable fetuses, six limb-body wall complex/short umbilical cord syndrome (LBWC) cases were identified (0.6%). The diagnosis of LBWC was based on coexistence of at least two of three features: exencephaly/encephalocoele/facial clefts, thoraco/abdominoschisis, and limb defects. All four ChN cases were associated with LBWC. In those cases, mean gestational age was 22 weeks, fetal weight 499 gm, fetal length 24 cm, and placental weight 165 gm. In two cases of LBWC without placental ChN, the corresponding means were: 18.5 weeks, 255 gm, 25 cm, and 130 gm.

ChN is a relatively infrequent finding (17 times less frequent than AN in our material). Severe oligohydramnios seems to be operational in the pathogenesis of AN and ChN. We believe that absence of the underlying amnion in ChN justifies a formal separate designation, distinct from AN. The term AN in such situation would be a misnomer because the nodules are attached directly to the chorionic mesenchyme and not to the amnion. ChN is a lesion characteristic of the spectrum of the LBWC. The pathomechanism of ChN is most probably related to prolonged direct contact of the fetal body with the chorionic mesenchyme denuded of amnion because we did not observe ChN in any case of the oligohydramnios sequence, early amnion rupture sequence, or extraamniotic pregnancies without LBWC. The absence of ChN in two cases of LBWC may be due to sampling, but it is likely that the duration of direct fetal-placental contact may be important, since the mean gestational age at delivery in these two cases was 3.5 weeks shorter than in the LBWC cases with ChN.

O-49
FOCALLY INCREASED AMOUNT OF INVASIVE INTERMEDIATE TROPHOBLASTS IN MATERNAL FLOOR IN OCCULT PLACENTA ACCRETA

DRUMMOND Zarius, STANEK Jerzy. Department of Pathology and Laboratory Medicine, University of Cincinnati College of Medicine, Cincinnati, Ohio, USA

We reported about the absence of significant differences in intensity of immunostaining for galectin 3 and E-cadherin in implantation site intermediate trophoblasts (isit) in placentae with basal plate myometrial fibers (bpmf). Increased number of isit was found in hysterectomy specimens with placenta creta but we are not aware of quantitative isit studies in spontaneously delivered placentae with bpmf. Consequently, the aim of this study is to verify whether the cell number, thickness and density of isit are different in the basal plates of such placentae in patients without clinical signs and symptoms of abnormal placental separation.

Among consecutive 4040 placentae, there were 25 cases (0.6%) in which routine histopathologic examination revealed the presence of bpmf apposed to chorionic villi or isit, but without intervening decidua ("occult" placenta creta, study group, sg). The control group (cg) comprised 25 placentae matched for gestational age (23-41 weeks) but without bpmf. There were no hysterectomies, cesarean sections, obstetric hemorrhage or manual extraction of placenta in either group. Archival formalin-fixed, paraffin embedded placental sections were immunostained for CD146 (Vector Laboratories), a cell adhesion molecule that highlights the intermediate trophoblasts. Number of isit cells was counted and thickness of the isit layer between chorionic villi and bpmf (sg) or chorionic villi and decidua (cg and sg away from bpmf) was measured by micrometry at two non-contiguous areas at bpmf spots and away from bpmf. From these measurements, density of isit was calculated. The results were compared statistically by ANOVA.

The micrometry thickness and cell number of isit were statistically significantly ($p<0.005$) larger in sg at sites with bpmf than away from bpmf and in cg (0.6 ±0.3, 0.3± 0.1, 0.4±0.1 mm, and 11.4±6.5, 6.7± 3.5, 7.0±3.5 cells, respectively), while the isit density was statistically not different ($p>0.05$) between sg at or away from bpmf, and in cg (20.4±10.4, 19.8± 7.6, 17.2± 22.6 cells/mm respectively).

In conclusion, the occult placenta accreta features an increased amount of proliferating isit in its basal plate only at sites of bpmf, but not in the remaining maternal floor. This may be related to the pathogenesis of placental ingrowth in placentae cretae. Pathogenetically, the occult placenta creta fills the gap between normal placental implantation and the symptomatic placenta creta.

O-50
STUDY OF BIRTH DEFECTS DETECTED IN A SERIES OF 2019 CONSECUTIVE PEDIATRIC AUTOPSIES

Piram, Adriana, MD – Department of Genetics, Faculty of Medicine of Ribeirão Preto, University of São Paulo, Ribeirão Preto, São Paulo, Brazil
Peres, Luiz Cesar, MD – Department of Pathology, Faculty of Medicine of Ribeirão Preto, University of São Paulo, Ribeirão Preto, São Paulo, Brazil
Pina-Neto, Joao Monteiro, MD – Department of Genetics, Faculty of Medicine of Ribeirão Preto, University of São Paulo, Ribeirão Preto, São Paulo, Brazil

Birth defects are an important cause of infant and child morbidity and mortality. A series of 2019 consecutive autopsies performed on patients aged 0 to 14 years of age from a referral university hospital was studied to determine the frequency and the pattern of birth defects or genetic diseases. We reviewed the records of autopsies performed over a 10 years period (1994-2003) at the Department of Pathology of the University Hospital at the School of Medicine of Ribeirão Preto, São Paulo University. The data of all pediatric autopsies were reviewed, summarized and catalogued according to the age, sex, and categories of the main cause of death. Cases presenting birth defects and genetic diseases were selected, and data from medical charts, photographic documentation, radiological studies, and records from the Departments of Pathology and Medical Genetics were reviewed and analyzed. Perinatal disorders were the leading cause of death (51.8%), followed by birth defects (29.3%) and infections (15.6%). Birth defects or genetic disorders related or not to the cause of death were found in 712 (35.3%) cases of which 183 (25.7%) had a confirmed isolated defect and other 70 (9.8%) had a probable isolated defect; 159 (22.3%) had a confirmed sequence and 7 (1.0%) had a probable sequence. Multiple defects were observed in 260 (36.5%) cases, of which 183 (25.7%) presented a defined diagnosis. Other genetic conditions such as metabolic or inherited neurological disorders were confirmed in 30 (4.2%) cases, and 3 (0.4%) were suspected. Birth defects and genetic diseases are an important cause of pediatric mortality pointing to the need for a collaborative study between Pathology and Medical Genetics using the available diagnostic resources in order to define the clinical and etiological diagnosis after which the recurrence risk, the ultimate and fundamental information for genetic counseling to the families, can be known.

O-51
PATHOLOGY OF SELECTED DEVELOPMENTAL VESTIGES

SOTELO-AVILA Cirilo , deMELLO Daphne, SOTELO-RAMPY Andrea K. Department of Pathology, SSM Cardinal Glennon Children's Hospital, St. Louis, MO, USA

Developmental Vestiges (DV), a topic of confusion and misunderstanding among pathologists, are defined as surviving traces, residues, marks or signs of something that existed during normal human embryonic or fetal development. "Something" applies not only to an anatomic structure but also to a condition or quality serving as indication of its former existence, e.g., ventricular septal defect (VSD), patent ductus arteriosus (PDA) and patent foramen ovale (PFO).

DV are important to pathologists because of their

· tendency to manifest clinically through hyperplastic or neoplastic growth causing compression of surrounding anatomic structures; tendency to undergo cystic dilation, infection, inflammation or torsion thus presenting as acute medical emergencies; occasional functional continuity from intrauterine to extrauterine life beyond newborn period with devastating consequences if not corrected, e.g., VSD, PDA, PFO; relative frequency in routine surgical pathology and in postmortem examinations. A complete understanding of normal embryologic and fetal development of these lesions along with the natural history and significance are as essential as their correct diagnosis. DV may

remain dormant for years and eventually undergo spontaneous involution and disappearance; undergo hyperplastic growth or neoplastic induction to form benign or malignant tumors in children and adults, but most commonly, they mature into dysplastic structures.

DV are classified as normal or common when they are present in most individuals, e.g., appendix testis and paraovarian ducts, and; abnormal or uncommon when they are absent in most individuals, e.g., branchial cysts, notochord remnants, etc.

A 23-year review of the surgical pathology files of SSM Cardinal Glennon Children's Hospital (72,735 specimens) disclosed numerous examples of common and some uncommon DV including caudal vestiges, pilonidal sinuses with subcutaneous neuroglia and ependymal rests, glomus coccygeum, tails and tailgut cysts, sequestered meningoceles of the scalp and some rare associations such as a sacrococcygeal dedifferentiated chordoma with malignant fibrous histiocytoma. Common and uncommon examples will be illustrated.

O-52
EXPRESSION OF P53/HGF/C-MET/STAT3 SIGNAL IN FETUSES WITH MALFORMATION OF NERVOUS SYSTEM.

TROVATO Maria1, D'ARMIENTO Maria2, LAVRA Luca3, ULIVIERI Alessandra3, DE STEFANO Nicoletta3, DOMINICI Roberto4, ZEPPETELLA DEL SESTO Filomena Stella2, GROSSO Maddalena1, VECCHIONE Raffaela2, BARRESI Gaetano1, SCIACCHITANO Salvatore3-5.
1Dipartimento di Patologia Umana, Università di Messina, Italy;
2Dipartimento di Scienze Biomorfologica e Funzionale, Sezione di Anatomia Patologia, Università Federico II di Napoli, Italy;
3Centro di Ricerca Osp.S.Pietro Fatebenefratelli, AFaR, Roma, Italy;
4Istituto di Neurobiologia Medicina Molecolare, CNR, Roma, Italy;
5II Facoltà di Medicina e Chirurgia, Osp. S. Andrea, Università La Sapienza di Roma, Italy.

HGF/c-met/STAT3 signaling pathway plays a role in cellular morphogenesis and organogenesis. Placentas of malformed fetuses showed low expression levels of proteins involved in this pathway, when compared with fetuses without any malformation. This observation suggests a possible role of this pathway in the pathogenesis of malformations. However, no data are currently available on the expression levels of any

member of this pathway, directly evaluated in the malformed organ. TP53, exerting a stimulatory effect on transcription of both murine HGF and c-met genes, may regulates cell growth as well as differentiation, even if its role in organogenesis is not well established yet.
Aim of our study is to evaluate the mRNA expressions of HGF, c-met and STAT3 in placentas and organs of fetuses with nervous system malformations (NSM)s and to correlate this results with p53 expression levels. Four fetuses, dead between 16th and 28th week of gestation, showing NSMs but non-malformed lungs and kidneys, have been selected for the study. Total RNA was extracted from malformed nervous system, lung, kidney and placenta of each fetus and analyzed by Reverse Transcriptase-PCR, using specific primers for HGF, c-met STAT3 and p53. Reduced expression or absence of HGF, c-met and STAT3 transcripts has been observed in all malformed nervous systems, as well as in the placentas. The reduced expression of all the members of HGF/c-met/STAT3 pathway, observed in both malformed nervous systems and in placentas, correlates with the absence of p53 in all these samples. On the contrary, detectable expression levels of p53, as well as HGF, c-met and STAT3 have been observed in non-malformed lungs and kidneys from the same fetuses.
In conclusion, the correlation between expression levels of p53 and of HGF/c-met/STAT3 pathway members suggests a role of this transcription factor in the pathogenesis of NSMs. The demonstration of occurrence of the same alterations in both malformed nervous systems and in the placentas, raises the possibility to perform the analysis of expression levels of these genes in placental tissue to diagnose NSMs during gestation.

O-53
ETHANOL AND NEURAL TUBE DEFECT IN MICE.

Cristiane Minot Gutierrez and Luiz Cesar Peres
Associate Professor, Department of Pathology, Faculty of Medicine of Ribeirao Preto, University of Sao Paulo

The clinical and experimental teratogenic effects of ethanol are well recognized. Nevertheless it is still the most important exogenous teratogen widely used by women in childbearing age. Ethanol has been implicated in congenital heart disease, limb anomalies and Neural Tube Defect (NTD). The aim of the present study was to determine the effects on the fetuses of low and high doses of ethanol given to pregnant mice. Female Swiss mice were randomized into Control (C), low ethanol (E1) and high ethanol (E10) groups with six animals each, kept in individual plastic cages in a controlled environment with commercial mouse chow and water ad libitum throughout the experiment. On the 8th, 9th, and 10th day of gestation all animals received intraperitoneal injections. Group C received saline, the experimental groups received ethanol diluted in saline 25% (v/v) of a dose of 0.4 g/Kg body weight for Group E1 and 4.0 g/Kg for Group E10. The animals were killed on the 19th gestational day in a CO2 chamber. The number of implants, resorptions, late fetal death, presence of NTD, weight and length of fetuses and placentas were recorded. NTD was found only in Group E10 (2.86%). Statistically significant difference was observed for late fetal death, body weight and length of male, female or both fetuses of Group E10 when compared to Groups C and E1($p<0.05$). No difference was observed for implants, resorptions, and the number of live fetuses in all groups as well as for all parameters between groups C and E1. Body weight and length was statistically different between male and female fetuses in each respective group. The finding of NTD only in group E10 indicates that the teratogenic effects of ethanol are dose dependent. Group E1 received ethanol equivalent to 28 g/Kg of body weight in man, a dose corresponding roughly to 2 cans of beer. Group E10 received a dose high enough for the mice to become comatose. Low ethanol dose in mice do not interfere with fetal survival and development, the opposite of high dose. In conclusion, high ethanol dose induces developmental restriction, late fetal death and NTD in Swiss mice when administered for a short period in early pregnancy. Since Swiss mice suffer less deleterious effects when exposed to ethanol during pregnancy than C57B, which present more resorptions and NTD, caution in the interpretation of results must be taken in respect to the teratogenic effects of ethanol.

O-54
COMPARISON OF MORPHOLOGY, GRADE, AND CYTOGENETIC ABNORMALITIES IN T(14;18) AND NON-T(14;18) FOLLICULAR LYMPHOMAS: DOES ANYTHING CORRELATE?

KELLER Christian, College of Physicians and Surgeons, Columbia University, VAKIANI Efsevia, College of Physicians and Surgeons, Columbia University, MURTY Vundavalli, College of Physicians and Surgeons, Columbia University, FRIZZERA Glauco, Joan and Sanford I. Weill Medical College, Cornell University, ALOBEID Bachir, College of Physicians and Surgeons, Columbia University, BHAGAT Govind, College of Physicians and Surgeons, Columbia University

Background: Two subtypes of follicular lymphoma (FL), with and without t(14;18) have been described. Distinct cytogenetic abnormalities have also been reported in the different subgroups of FL3. We investigated whether we could 1) stratify FL diagnosed at our institute, according to specific cytogenetic abnormalities and 2) discern morphologic and cytogenetic abnormalities between the t(14;18) and non-t(14;18) groups. Methods: We obtained 33 successive cases of FL from our departmental files with an informative karyotype, diagnosed between 1997-2004. Morphologic features and grade were reviewed by 2 pathologists, blinded to the cytogenetic findings. All cases were graded according to the current WHO criteria and divided into 2 groups; FL with t(14;18) or without t(14;18). Cases were further subdivided according to the presence or absence of 3q27 abnormalities. Statistical analysis was performed using Fisher's exact and Student's t-tests. Results: 24 of 33 (73%) cases had t(14;18) group I, while 9 cases lacked t(14;18) group II. In group I, 20 cases lacked group 1a and 4 cases had 3q27 abnormalities group Ib. Group II consisted of 6 cases without group IIa and 3 cases with 3q27 aberrations group IIb; 3q27 abnormalities consisted of translocations (n=4), inversions (n=2) and deletions (n=1). Signet ring cell differentiation (n=2) was only seen in group I while large, expansile follicles (n=3) and plasma cell differentiation (n=1) was seen in group II. No significant differences in grade of FL or number of cytogenetic abnormalities were seen within and between groups I and II (mean 8.1 vs. 6.6). Groups Ib and IIb had a higher number of chromosomal abnormalities (means 10.8 and 10.3) compared to groups Ia and IIa (means 7.6 and 4.7) (p=0.04), but no significant differences were seen on comparing similar grades. FL3a was more common in group 2 (n=3) compared to group 1 (n=1) (p=0.05); FL3b (n=1) was only seen in group 1. Two of three FL3a in group II but none of the FL3a (or 3b) in group I had a 3q27 abnormality. All cases in group Ib were FL2 while group IIb comprised of FL2 (n=1) and FL3a (n=2). Conclusions: Morphologic variants unique to t(14;18) and non-t(14;18) groups were observed. Overlapping and non-significant differences in the number of cytogenetic abnormalities were seen across all 3 grades of FL in both groups. We did not observe any correlation between presence of 3q27 abnormalities and specific grades of FL, contrary to prior reports.

O-55
IDENTIFICATION OF GENE EXPRESSION SIGNATURES THAT PREDICT THE OUTCOME OF FOLLICULAR LYMPHOMA PATIENTS.

Olivier RAMUZ (1,3,4), Reda BOUABDALLAH (2,4), Agnes GROULET-MARTINEC (5), Elisabeth DEVILARD (1,3,4), Françoise BIRG (3,4), Daniel BIRNBAUM (3,4, Luc XERRI (1,3,4)
From the
1 Departments of Biopathology, and 2 Haematology, Institut Paoli-Calmettes, 232 boulevard de Sainte-Marguerite, BP 156, 13273 Marseille Cedex 9, France
3 UMR 599, Marseille, France
4 Cancéropôle PACA, France
5 Ipsogen Inc., Luminy Biotech Entreprise, Case 923, 163 Av. de Luminy, 13288 Cedex 9 Marseille, France

We used DNA-microarrays analyses to identify gene expression signatures (GES) that could predict the outcome of Follicular Lymphoma (FL) patients. Gene expression profiling was performed using DNA-microarrays on 21 FL samples. These FL samples were all collected at the time of initial diagnosis prior to any systemic therapy for all patients. These tumour samples were either grade 1 or grade 2 FL according to the 2001 WHO classification of tumours of lymphoid tissues.
We identified 2 distinct gene GES that allowed a clear segregation between relapsing and non relapsing FL patients ("relapse" GES), and alive and dead FL patients ("survival" GES), respectively. No FL patient was misclassified. Among the 13 genes included in the "relapse" GES, the T-cell marker CD2 was overexpressed in non relapsing FL patients. Further more, the pro-apoptotic factor BID was overexpressed, whereas cytochrome b-5 (CYB5) was underexpressed in relapsing patients. Among the 17 genes included in the "survival" GES, the transcription factor HOXA2 was underexpressed, whereas the interferon-inducible protein viperin (CIG5) was overexpressed in alive FL patients. No prognostic relevance of the T-cell marker CD3 was evidenced by immunohistochemistry (IHC) on tissue-microarrays.
Our results provide insights into FL biology and suggest that, in agreement with previous reports, T-cell immune response may have an effect on FL patients outcome. The lack of prognostic relevance of CD3 IHC expression may imply that the T-cell effect on FL outcome is probably more qualitative than quantitative. The prognostic GES we evidenced herein need further validation on prospective studies before clinical application may be considered.

O-56
ASSESSMENT OF PROGNOSTIC FACTORS IN PLASMA CELL MYELOMAS ON TISSUE MICROARRAYS USING IMMUNOHISTOCHEMISTRY AND FISH ANALYSIS

Jenni Bettina1,2, Reineke Tanja1, Korol Dimitri2, Kofler Andreas2, Moch Holger1, Probst-Hensch Nicole-M2,Tinguely Marianne1

Aim
Plasma cell myeloma (PM) exhibits a clinical and molecular heterogeneity. Traditional morphological and immunohistochemical prognostic factors in PM are of limited value. In PM, translocations involving the IgH are observed in up to 80% of patients. Some of those have a prognostic impact on the disease outcome and/or a predictive value for the success of particular treatments. In situations, where no fresh samples are available, inter-phase FISH analysis is a method to specifically search for distinct translocations on formalin fixed, paraffin embedded tissues.
We investigated PMs from bone-containing surgical biopsies on a tissue microarray (TMA) for prognostic factors, including IHC and FISH analysis. We looked for translocations with a favourable (t(11;14)) and unfavourable (t(4;14)) behaviour. The correlation of the IHC with FISH and the molecular data with the survival of the patients were analysed.
Materials and Methods
49 formalin fixed, paraffin embedded specimens (44 osseous, 5 extra-osseous) from 41 patients with PM were arranged on a TMA. From each biopsy, two tissue scores were punched out. The investigations included morphology, IHC (CD20, CD79a, CD38, CD138, CD56, CyclinD1 and MIB1) and inter-phase FISH analysis specific for the t(4;14) and t(11;14).
Results
Biopsies were regarded as eligible, if at least one of the scores contained 30% of tumour cells.
All of the 49 samples fulfilled these criteria for morphology and IHC. Overall, in 26/41 (61%) patients and in 21/36 (58%) of the osseous biopsies, the FISH analysis was interpretable. 4/26 (15%) of PM showed a t(11;14) and 2/26 a t(4;14) (8%). Cyclin D1 was positive in 8/41 PMs and was concordant with FISH and either associated with a t(11;14) or an amplification of the bcl1 gene. A tendency of higher Mib1 expression in CyclinD1 positive PMs, was not significant (p=0.06). The mean survival time from diagnosis was 65 and 34 mo in patients with t(11;14) and t(4;14) respectively.
Conclusions
TMAs are applicable on bone-containing tissues. The percentage of t(11;14) and the mean survival time for both translocations is in agreement with the one reported in the literature, suggesting, that TMAs are suitable for testing new prognostic markers including molecular analysis in PM. The results need to be validated and statistically underlined by extending the series. Prospectively, optimized decalcification procedures should lead to a higher yield of interpretable FISH.

O-57
RELATION BETWEEN PHENOTYPE AND CHROMATIN TEXTURE IN ACUTE LEUKEMIAS

Metze K, Silva RC, Adam RL, Pereira FF, Leite NJ, Lorand-Metze I
Department of Pathology Department of Internal Medicine, Faculty of Medicine, Institute of Computing, State University of Campinas, Brazil

Chromatin structure is a fundamental hallmark for morphological diagnosis in routine cytology. Changes of chromatin arrangement as well as the expression of cytoplasmic or membrane proteins reflect the degree of cellular differentiation. The aim of our study was to correlate chromatin texture features with the expression of membrane and cytoplasmatic proteins in blasts of patients with acute leukemia. We examined the diagnostic bone marrow aspirates from 32 patients with acute lymphatic leukaemia (ALL) and 31 patients with acute myeloid leukemia (AML). Diagnosis was based on cytologic features, phenotype (determined by flow cytometry) and cytogenetic analysis. Texture analysis was done on gray-scale transformed digitalized images of 100 cells of routinely stained May-Grünewald-Giemsa smears. We measured granulometric features (using the gray level height of the basins as filter parameter) as well as Shannon´s entropy and the fractal dimension in images after application of thick and thin contour detection. Antigen expression was quantified by mean flourescence intensity (analysis: Paint-a-gate software; 10 000 cells / case).
In ALL, there was a negative correlation between the expression of immunoglobulins (light chains) and the number of granulometric residues at lower gray levels (r = - 0.54; p =

0.005). Furthermore, we found a positive correlation between the CD20 expression and the fractal dimension after morphologic gradient filtering (r = 0.39; p = 0.036).
In AML patients, the number of granulometric residues at lower gray levels had a negative correlation with CD7 (= - 0.50; p = 0.004) and myeloperoxidase expression (r= - 0,42; p=0,036). A positive correlation was found between CD45 and the number of granulometric residues at higher gray levels (r = 0,45; p = 0,038).
We conclude that, in acute leukemias, changes of chromatin structure may express differences in maturation measured by quantitative expression of antigens routinely used in diagnosis.
Supported by FAPESP, FAEP, CNPq

O-58
EXPRESSION OF TP73L IS A HELPFUL DIAGNOSTIC MARKER OF PRIMARY MEDIASTINAL LARGE B-CELL LYMPHOMAS

ZAMÒ Alberto (1), MALPELI Giorgio (1), SCARPA Aldo (1), DOGLIONI Claudio (2), CHILOSI Marco (1) and MENESTRINA Fabio (1).
(1) Department of Pathology, University of Verona, Verona, Italy
(2) Department of Histopathology, San Raffaele Hospital, Milan, Italy

Introduction. Primary mediastinal large B-cell lymphoma (PMLBCL) is a well-defined lymphoma entity whose molecular pathogenesis is incompletely understood, and also lacking well-established diagnostic markers. Recently, the presence of overlapping features between Classical Hodgkin's Lymphoma (CHL) and PMLBCL was highlighted by gene expression profiling as well as morphological studies. Purpose of the study. We investigated the expression of TP73L (commonly known as p63) isoforms in PMLBCL at both protein and mRNA level by immunohistochemistry and Real-Time PCR. Results. We demonstrated the exclusive presence of transactivating (TA) isoforms in all cases, and that TP73L is expressed in a subset of germinal center B-cells (GCBC), as well as in some Diffuse Large B-cell Lymphomas (DLBCL), but it is never present in CHL. Nodular Lymphocyte Predominance Hodgkin's Lymphoma (NLPHL) also showed TP73L positivity by immunohistochemistry. Isoform analysis by Real-Time PCR showed that TA-TP73L alpha is the most represented in PMLBCL, but TA-TP73L gamma is the most differentially expressed in comparison to both GCBC and DLBCL. Conclusions. TP73L expression proved a useful diagnostic marker of PMLBCL, and gave new insights in the molecular pathways playing a role in this lymphoma.

O-59
CORRELATION BETWEEN MOLECULAR AND HISTOPATHOLOGICAL DIAGNOSES OF BONE MARROW SPECIMENS IN B-CELL NEOPLASMS

KAYASUT Kanita, LE TOURNEAU Agnès, AUDOUIN Josée, DIEBOLD Jacques, DEVEZ Francis, DUCRUIT Véronique, BOUCHET Pierre-Etienne, MOLINA Thierry Jo.
Department of Pathology, Hôtel-Dieu, AP-HP, Université Paris 5, Paris, France

Introduction. Histopathological study of bone marrow (BM) biopsy is routinely performed for evaluation of lymphoma involvement during diagnosis, staging and follow-up. Polymerase chain reaction (PCR) for antigen receptor gene and oncogene rearrangement has been shown to detect a clonal population below the morphological threshold.
Purpose of the study. To correlate the morphological and immunohistochemical evaluation of B-cell lymphoid neoplasms in BM biopsies with immunoglobulin heavy chain (IgH) gene and Bcl-2 rearrangement by PCR in concurrently obtained aspirates.
Methods. We retrospectively evaluated 99 BM specimens from 78 patients with B-cell neoplasms (81 small B-cell and 18 large B-cell lymphomas) which were selected according to the presence of a clonal marker of the disease (IgH or Bcl-2). PCR analysis was performed, using Bcl-2 MBR and the consensus IgH primers (FR1, FR2, FR3).
Results. Considering IgH-PCR alone, a monoclonal B-cell population was detected in 87% (55/63) and 30% (11/36) in the histopathologically (H) positive and negative groups, respectively. The concordant rate was 80% (55 H+, PCR+ and 25 H-, PCR-). The discordant group (H+, PCR-) contained 8 cases, including 6 follicular lymphoma (FL) and 2 mantle-cell lymphoma (MCL). Four FL showed at least 20% BM involvement while all two MCL showed minimal (= 10%) and focal involvement. All these 6 FL although IgH PCR-, were Bcl2 MBR+. We identified a clonality in H- group, including 4 diffuse large B-cell lymphomas (DLBCL), 1 FL and 6 other small B-cell lymphomas. When considering Bcl-2 MBR, we additionally detected a clonality of 5 DLBCL (3 associated with FL) and 8 FL.
Conclusion. The sensitivity (87%) for the IgH-PCR assay in BM aspirates in our study is higher than the published studies due to our selection criteria. However, IgH-PCR alone missed few cases of strongly histopathological positive in FL, probably due to ongoing somatic mutation whereas they had a Bcl-2 MBR marker. When lymphoma involvement was focal and minimal, IgH-PCR might be negative probably due to sampling problem. Complementary use of Bcl-2 MBR can increase detection rate of monoclonality in both H+ and H- groups of FL. Therefore, we suggest that especially in FL, IgH-PCR alone is not good enough for BM assessment. On the other hand when Bcl-2 MBR is a marker of disease, this molecular test on BM aspirates may replace BM biopsy for evaluation of disease.

O-60
NPM-ALK REGULATED ACTIVATION OF THE AP-1 TRANSCRIPTION FACTOR IN ANAPLASTIC LARGE CELL LYMPHOMAS (ALCL)

VESELY Paul(1), STABER Philipp B.(2), MOSER Gerit(1), SCHAUER Silvia(1), DIRKS Wilhelm(3), KADIN Marshall E.(4), STERNBERG David W.(5), HOEFLER Gerald(1).
1 Institute of Pathology, Medical University Graz, Austria
2 Department of Internal Medicine, Division of Hematology, Medical University Graz, Austria
3 DSMZ, Braunschweig, Germany
4 Department of Pathology, Beth Israel Deaconess Medical Center and Harvard Medical School, Boston, USA
5 Division of Hematology/Oncology, Mount Sinai School of Medicine, New York, New York

Introduction: Translocation (2;5)(p23;35) causing a nucleophosmin-anaplastic lymphoma kinase (NPM-ALK) fusion gene leading to high expression of the ALK tyrosine kinase is the defining feature of the majority of anaplastic large cell lymphomas (ALCL).
Purpose of the study: To identify molecular events regulated by NPMALK, we studied consequences of the kinase activation on gene expression and on the proteomic level.
Methods: SSH libraries were created using mRNA from pools of NPM-ALK positive and negative ALCL cell lines as well as human embryonic kidney (293) cells transfected with active and kinase-dead NPM-ALK constructs. mRNA expression patterns were analyzed in individual cell lines using cDNA arrays utilizing cDNA clones resulting from the SSH libraries as well as genes relevant for cancer development. Quantitative RT-PCR of 20 selected genes

validated the mRNA expression data. The activation status of key proteins was determined using EMSA and Western-blot analysis.
Results: In 293 cells, the active NPM-ALK construct confers significant changes in the expression of 38 genes. Expression of 102 genes distinguishes NPM-ALK-negative (FE-PD, MAC-2A) from NPM-ALK-positive ALCL cell lines (SU-DHL-1, JB-6, SUP-M2, SR-786, DEL and Karpas 299). The majority of these genes are involved in regulation of cell cycle and apoptosis. A specific subset of genes regulated by NPM-ALK indicates increased activation of AP-1 transcription factors. We verified NPM-ALK dependent AP-1 DNA binding activity by electrophoretic mobility shift assays using lysates from 293 cells transfected with active or kinase-dead NPM-ALK constructs, Ba/F3 murine hematopoietic cells expressing stably or doxocyclin induceable NPM-ALK, as well as NPM-ALK positive and negative ALCL cell lines. Super Shift experiments revealed JunB to be the major AP-1 transcription factor involved.
Conclusion: In this study we present a set of genes regulated by NPM-ALK and demonstrate that this fusion gene enhances AP-1 activation by selectively up-regulating JunB. Our data might indicate a new mechanism for regulation of AP-1 activity.

O-61
PTEN AND P27 EXPRESSION IN MATURE T-CELL AND NK-CELL NEOPLASMS

Ayþegül H. Üner1, Arzu Saðlam1, Ünsal Han2, Mutlu Hayran3, Arzu Sungur1, Þevket Ruacan1,4
1 Department of Pathology, Hacettepe University Medical Faculty,
Sihhiye, Ankara,Turkey
2 Department of Pathology, Social Security Training Hospital, Ankara,
Turkey
3 Department of Preventive Oncology, Hacettepe University Oncology
Institute, Sýhhiye, Ankara, Turkey
4 Current Address: Mesa Hospital, Ankara, Turkey

Background: PTEN is a tumor suppressor gene located on chromosome 10q23 and is amongst the most commonly mutated genes in human cancers. The lipid phosphatase activity of Pten enables it to dephosphorylate PIP3, hereby antagonizing growth factor stimulated PI3-kinase signaling mediated by AKT/PKB. The growth inhibition effect of PTEN has been shown to be mediated by p27 which is one of the important effector molecules downstream of the AKT pathway. Recently the importance of Pten and PKB/AKT pathway in the regulation of the immune system and development of hematological malignancies have been shown.
Materials and methods: Loss of Pten and p27 expressions were examined immunohistochemically in 45 patients with peripheral T and NK cell lymphoma.
Results: Partial or complete loss of Pten was detected in 66.7% of the cases of anaplastic large cell lymphoma (ALCL) compared to only 12.5% of all other mature T/NK cell lymphomas combined. Loss of p27 was identified in 64.9% of cases, which showed a positive correlation with Pten loss.
Conclusion: In this study, we showed that loss of Pten is more frequent in ALCL as compared to other mature T/NK cell lymphomas, which strongly correlates with the loss of p27 expression. Our findings provide further evidence for the importance of the deregulation of the PI3K-AKT pathway in ALCL.

O-62
PRIMARY NASAL NK/T CELL LYMPHOMA: CYTOLOGY AND LEVEL OF THE ANTIAPOPTOTIC PI9 PROTEIN HAVE PROGNOSTIC RELEVANCE.

Céline Bossard 1*, Karim Belhadj 2*, Felix Reyes 2, Nadine Martin-Garcia 1*, Alain Kümmer 3*, Françoise Berger 4*, Josette Brière 5*, Anne-Catherine Baglin 6*, Odile Casiraghi 7*, Eric Lepage 8* and Philippe Gaulard, for the GELA 1*. 1 Département de Pathologie et Inserm U617, Hôpital Henri Mondor, Créteil, France; 2 Service d'Hématologie Clinique, Hôpital Henri Mondor, Créteil, France; 3 Department of Pathology, Free University Hospital, Amsterdam, Netherlands; 4 Service d'Anatomie et de Cytologie Pathologiques, Centre Hospitalier Lyon Sud, Pierre Benite, France; 5 Département de Pathologie, Hôpital Saint Louis, Paris, France; 6 Département de Pathologie, Hôpital Foch, Suresnes, France; 7 Département de Pathologie, Institut Gustave Roussy, Villejuif, France and 8 Département d'Information Médicale, Hôpital Henri Mondor, Créteil, France.

Nasal NK/T cell lymphoma is a rare disease entity characterized by a nasopharyngeal presentation, a common origin from NK cells, an association with EBV and a predilection for Asians and South Americans contrasting with its rarity in Western countries. Several studies (Chim CS, 2004; Li CC, 2004) indicate that the disease has a poor outcome following conventional combined chemoradiotherapy treatments, which might be related to resistance to therapy-induced apoptosis. It has been shown (Hermine O, 1996; Ten Berge R, 2002) that high level of expression of antiapoptotic proteins by lymphoma cells is associated with poor outcome in a variety of lymphomas.
In a retrospective analysis of 37 patients treated with first-line chemotherapy (n=34) or chemoradiotherapy (n=3) according to the LNH87, LNH93 and LNH98 trials of the GELA, we have analyzed by immunohistochemistry the expression of the granzyme B-protease inhibitor 9 (PI9) regarded as an inhibitor of apoptosis, and of the active form of caspase-3 (aC-3), an effector of apoptosis. The diagnosis was based on biopsies of the upper respiratory tract showing a proliferation of neoplastic cells with a CD3+/CD5- (100%), CD56+ (90%), TIA1/GrB+ (100%) phenotype and EBV association (100%). Among the 37 patients, 73% were < 60y, 68% were male. 76% had stage I, 5% Stage II, 19% stage IV and 68% had an IPI score of 0-1. With a median follow-up of 6.3 y, 5y-event-free and overall survivals were 38% and 47%. According to cytology, tumors were subclassified into predominantly small cell (52%) and large cell (48%) categories. PI9 was scored as positive (>10% of tumor cells) in 68% of the cases, whereas 35% were assigned a high number (>10 per field at high magnification) of aC-3 positive tumor cells. Univariate analysis showed that small cell cytology and absence of PI9 expression were associated with poor outcome. By multivariate analysis, cytology and PI9 downregulation were shown to independently affect event-free (P=0.01 and 0.05) and overall survival (P=0.009 and 0.006).
We conclude that nasal NK/T cell lymphomas disclose cytological heterogeneity which has prognostic relevance. We also found that downregulation of PI9 is associated with poor outcome, an unexpected finding in view of the known antiapoptotic function of this protein. Since PI9 is constitutively expressed by normal NK cells, it might be postulated that its impaired expression in tumor cells reflects a yet unknown mechanism associated with progression

O-63
BLASTOID AND COMMON VARIANTS OF MANTLE CELL LYMPHOMA EXHIBIT DISTINCT IMMUNOPHENOTYPIC AND INTERPHASE FISH FEATURES

Marie PARRENS (1), Marc-Antoine BELAUD-ROTUREAU (1), Olivier FITOUSSI (2), Nathalie CARERRE (1), Krimo

BOUABDALLAH (2), Gérald MARIT (2), Pierre DUBUS (1), Antoine de MASCAREL (1), Jean-Philippe MERLIO (1)
1: Department of Pathology and Tumor Biology, CHU and Equipe 2406 University of
Bordeaux 2, France
2: Department of Hematology, Hopital of Haut-Lévêque, 33604 Pessac, France

To further characterize blastoid variant (BV) of mantle cell lymphoma (MCL), 18 MCL cases were analyzed for their clinicopathological features, proliferation MIB-1 index, CDK4 and cyclin D1 expression and CCND1 genetic profile. Thereafter, 14 cases were recognized as common MCL and 4 cases as BV-MCL including one secondary BV-MCL.
Despite common clinical features at presentation. BV-MCL vs common MCL was characterized by a shorter overall duration of response after first line therapy (11 months vs 28 months) and shorter overall survival (20 months vs 42 months). Interphase FISH showed a characteristic t(11;14) fusion pattern in the 14 tested cases. Furthermore, the 4 blastoid cases were characterized by extracopies of CCND1 signals. Using additionnal probes of chromosomes 11, 18, 21, these signals were shown to be the result of hypotetraploidy and not of a specific amplification of the normal or the translocated CCND1 allele. There was no significant difference in the overexpression level of cyclin D1 isoforms transcripts between BV and common MCL cases as determined by real-time RT-PCR. However the BV-MCL cases were characterized by a combined percentage of cyclinD1 and/or CDK4 immuno-positive cells with a proliferation MIB1 (Ki67) index above 50%. Such features allowed the recognition of areas of large cell transformation in the secondary BV-MCL case. Since distinction between BV and common MCL is of clinical relevance, our data underline the need to add phenotypic and cytogenetic criteria for a better recognition of BV-MCL

O-64
MOST PRIMARY CENTRAL NERVOUS SYSTEM LYMPHOMAS DISPLAY AN ACTIVATED IMMUNOPROFILE

CAMILLERI-BROET Sophie 1,2,3, CRINIERE Emmanuelle 4, BROET Philippe 5, DELWAIL Vincent 2,6, MOKHTARI Karima 4,7, MOREAU Anne 2,8, KUJAS Michele 4,7, RAPHAEL Martine 2,9, IRAQI Wafae 11, SAUTES-FRIDMAN Catherine 3, COLOMBAT Philippe 2,10, HOANG-XUAN Khe 4,11, MARTIN Antoine 2,12.
1Anatomie Pathologique, Hôtel Dieu, AP-HP, Faculté de médecine Paris 5, Paris
2GOELAMS (Groupe Ouest Est des Leucémies et Autres Maladies du Sang), France
3INSERM U255, Université Paris 6, Centre de recherche biomédical des Cordeliers, Paris
4INSERM U 711, Groupe hospitalier Pitié Salpetrière, Université P. et M. Curie Paris VI
5Sante Publique, Hôpital Paul Brousse, AP-HP, Faculté de médecine Paris-Sud, Villejuif
6Oncologie hématologique et thérapie cellulaire, Hôpital Bernard, Poitiers
7Laboratoire de Neuropathologie R. Escourolle, Groupe hospitalier Pitié Salpetrière, Paris
8Anatomie Pathologique, Hôtel Dieu, Nantes
9Service d'hématologie et Immunologie Biologiques, Cytogénétique, INSERM E109, CHU Bicêtre, Université Paris-Sud 11, Le Kremlin Bicêtre
10Hématologie, hôpital Bretonneau, Tours
11Service de Neurologie Mazarin, Groupe hospitalier Pitié Salpetrière, AP-HP, Paris
12Anatomie Pathologique, hôpital Avicenne, AP-HP, Faculté de médecine Paris XIII, Bobigny

Primary central nervous system lymphomas (PCNSL) of immunocompetent patients are usually diffuse large B-cell lymphomas (DLBCL), which are characterized by a poorer prognosis as compared to systemic cases. Systemic DLBCL is a heterogeneous entity, with at least two identified subgroups: germinal centre (GCB) and activated B-cell like (ABC). GCB subgroup is characterized by a better prognosis than ABC. In the literature, a GCB origin of PCNSL has been hypothesized based on BCL-6 expression and presence of ongoing mutational activity. The goal of the present study was to determine by immunohistochemistry the proportion of GCB and ABC cases in a large series of 83 PCNSL and to determine its prognostic significance. CD10, BCL-6 and MUM1 were expressed by tumour cells in 2.4%, 56% and 92.6% of the cases, respectively. None of the tested cases expressed CD138. All but three cases were classified in the ABC subgroup. Half of these ABC cases displayed BCL-6+/MUM1+ co-expression, favouring an 'activated GCB' origin whereas the others showed an 'activated non GCB' pattern, as demonstrated by MUM1 expression alone. These findings lead to new insights in interpreting the poor prognostic of PCNSL, which may be due in part to biological aggressiveness related with the activated B-cell like pattern of tumour cells.

O-65
THE RELATIVE LEVELS OF CYCLIN D1 [A] [B] ALTERNATE TRANSCRIPTS IN MANTLE CELL LYMPHOMA MAY DEPEND MORE ON THE SAMPLE ORIGIN THAN ON CCND1 GENE POLYMORPHISM.

Nathalie Carrère, Marc-Antoine Belaud-Rotureau, Pierre Dubus, Marie Parrens, Jean-Christophe Garoste, Antoine de Mascarel, Jean-Philippe Merlio
Pathology Laboratory, Hôpital Haut-Lévêque, Pessac, France and Histology and Molecular Pathology Laboratory, Victor Segalen University, Bordeaux, France

Background and Objective: The t(11;14)(q13;q32) leads to cyclin D1 overexpression in mantle cell lymphoma (MCL). Two [a] and [b] transcripts of CCND1/cyclinD1gene may be alternatively expressed. Real-time RT-PCR was used to determine the relative amount of [a] and [b] transcripts in a series of typical MCL. We also investigated whether genetic polymorphism at position 870 may influence the overexpression of each isoform.
Design and methods: 39 MCL samples and 2 CLL samples were analyzed by real-time RT-PCR. The relative amount of each isoform was normalized and expressed as a cyclin D1 to GAPDH ratio. Overexpression of cyclin D1 was also determined by ratio calculation over the basal expression rate in the same tissue category.
Results: Both a and b isoforms were detected in tumoral and control tissues. At least a five-fold overexpression was observed for both isoforms in 28/39 MCL cases and for only one isoform in 10/39 MCL (7 a and 3 b). No correlation was observed between genotype and overexpression of either a or b CCND1 isoforms. Their relative level varied according to the tissular origin and may also depend on the relative amount of tumoral cells.
Interpretation and Conclusions. Cyclin D1 overexpression was found above a five-fold threshold in all MCL samples except in one case with RNA degradation. The interest of monitoring of each cyclin D1 isoforms should be evaluated in homogeneous samples such as peripheral blood because the basal expression of both isoforms is very low at this level in healthy donors.

O-66
LOCALIZED NEUROBLASTOMA: PROGNOSTIC SIGNIFICANCE OF CD44 AND TRKA EXPRESSION.

K. Ernestus 1,2, B. Hero 2, R. Spitz 2, F. Berthold 2
1 Department of Pathology, University of Cologne
2 Childrens Hospital, Department of Pediatric Oncology and Hematology, University of Cologne

Introduction: Neuroblastoma is the most common solid pediatric tumor except from brain tumors. Clinical behaviour is variable, ranging from spontaneous regression to progression and death. MYCN amplification, stage, age, and deletion 1p, are known and utilized as prognostic factors.
Purpose: This retrospective study was performed to analyse the prognostic significance of trkA and CD44 expression in a large series of unselected neuroblastoma focussed on localized neuroblastoma.
Methods: Frozen tumor sections from 248 neuroblastic tumors without treatment prior to biopsy were investigated by semiquantitative immunohistochemistry for CD44 and trkA expression. MYCN amplification and deletion 1p were analysed by FISH.
Results: In localized neuroblastoma 92% of the tumors expressed CD44, while trkA was expressed in 82%, respectively. In these cases expression of trkA or CD44 correlated with a significant better outcome (CD44: 3-year event free survival (EFS) positive 87±3% versus negative 36±16%, $p<0.0001$). The subgroup of localized neuroblastoma without MYCN amplification demonstrated inferior EFS for trkA negative tumors, while CD44 expression did not discriminate. In a multivariate analysis, including the variables MYCN amplification, trkA and CD44 expression both MYCN amplification and trkA expression were determined as independent prognostic factors.
Conclusions: In localized neuroblastic tumors absence of trkA expression is a strong independent prognostic factor. In particular, in the subgroup of MYCN non amplified tumors absence of trkA expression defines patients with unfavourable outcome.

O-67
ALTERATIONS OF THE PULMONARY SURFACTANT SYSTEM IN PEDIATRIC PATIENTS WITH ABCA3 MUTATIONS.

F. Brasch1,2*, S. Schimanski3*, G. Johnen4, M. Griese5, M. Ochs2, H. Schroten6, E. Mildenberger7, E. Prüter8, V. Rigourd9, L. Chevret10, M. Bahlmann11, A. Haverich12, K.-M. Müller1, and G. Schmitz3.
* Both authors contributed equally to this work.
1Institute of Pathology, University Hospital Bergmannsheil, Bochum, Germany; 2Division of Electron Microscopy, University of Göttingen, Germany; 3Institute for Clinical Chemistry and Laboratory Medicine, University of Regensburg, Germany; 4Institute of Occupational Medicine (BGFA), Ruhr University, Bochum, Germany; 5Dr. von Haunersches Children's Hospital, Ludwig-Maximilians-University, Munich, Germany; 6Pediatric Infectious Diseases, Department of General Pediatrics, Heinrich-Heine-University, Düsseldorf, Germany; 7Department of Pediatrics, Free University Berlin, Germany; 8Department of Pediatrics, Bethesda Hospital, Wuppertal, Germany; 9Service de réanimation néonatale, institut de puériculture et de périnatalogie, Paris, France; 10Service de réanimation pédiatrique, CHU de Bicêtre, Le Kremlin-Bicêtre, France; 11Department of Pediatrics and 12Department of Thoracic and Cardiovascular Surgery, Hannover Medical School, Germany

The integrity of pulmonary surfactant is of paramount importance for lung function. Previously, ABCA3 mutations were described in newborns with fatal surfactant deficiency. By means of immunohistochemistry, transmission, and immuno electron microscopy (EM), as well as Western blotting, we studied the pulmonary surfactant system in consanguineous and non-consanguineous full-term babies with unexplained respiratory distress syndrome (URDS). In eight patients with a variable combination of histological patterns of non-specific interstitial pneumonia, desquamative interstitial pneumonia, and pulmonary alveolar proteinosis, we found an abnormal staining pattern or lack of ABCA3 by means of immunohistochemistry. At the ultrastructural level, we found membrane bound electron dense bodies instead of lamellar bodies in type II pneumocytes. Sequencing of the ABCA3 gene revealed homozygote splice site, frameshift, and missense mutations in consanguineous as well as compound heterozygote frameshift and missense mutations in non-consanguineous patients. Since all but one patient showed clinical symptoms of severe neonatal surfactant deficiency and died shortly after birth due to respiratory insufficiency, immunohistochemical, immuno-EM, and Western blot analyses of lung tissue and BAL fluids for SP-B were performed. In line with low levels of mature SP-B in the alveolar surfactant, type II pneumocytes showed only a weak dot-like staining pattern. By means of immuno-EM, SP-B was localized over the dense core and the lysosomal aspartic protease cathepsin D over the matrix of electron dense bodies. Since lung function improved in one patient after high dose steroid treatment, successful heart-lung transplantation could be performed at the age of 18 months. Surprisingly, in the explanted lung we found not only electron dense bodies but also a few typical lamellar bodies in type II pneumocytes. In conclusion, our data indicate that ABCA3 mutations are associated not only with an abnormal distribution or lack of ABCA3 but also the formation of aggregates of mature SP-B in lysosomal organelles in type II pneumocytes leading to severe alterations of the pulmonary surfactant system. High dose steroid treatment might be helpful to improve respiratory function in a subset of patients. Our findings highlight the importance of immunohistochemistry and electron microscopy in the examination of lung tissue from babies with URDS.

O-68
SKELETAL MUSCLE BIOPSY AND POST MORTEM RETROSPECTIVE STUDIES IN CHILDREN WITH LEIGH SYNDROME CAUSED BY SURF1 GENE MUTATIONS.

Maciej Pronicki1, Ewa Matyja2, Dorota Piekutowska-Abramczuk3, Ewa Popowska3, El¿bieta Karczmarewicz4, Ewa Pronicka5.
1 Department of Pathology, Children’s Memorial Health Institute, Warsaw
2 Department of Neuropathology, Polish Academy of Sciences, Warsaw
3 Department of Medical Genetics Children’s Memorial Health Institute, Warsaw
4 Department of Biochemistry and Experimental Medicine, Children’s Memorial Health Institute, Warsaw
5 Department of Metabolic Diseases, Clinic of Pediatrics, Children’s Memorial Health Institute, Warsaw

Leigh syndrome (LS) is one of the most frequent presentations of respiratory chain dysfunction in children. The discovery of SURF1 gene and its mutations leading to autosomal recessive cytochrome oxidase deficient Leigh syndrome was the breakthrough in mitochondrial medicine.
Retrospective pathological studies were performed in 22 children from 21 families with LS clinical phenotype and SURF1 gene mutations. In all patients in whom the biopsy was performed spectrophotometric study confirmed the presence of complex IV deficit. Nineteen skeletal muscle samples and 4 autopsies were reassessed.

Skeletal muscle consistently showed diffuse total or pronounced histochemical cytochrome oxidase deficiency, variable degree of lipid increase, and mild to moderate variability in muscle fibre size. Electron microscopy revealed focal intermyofibrillar or subsarcolemmal accumulations of structurally normal mitochondria with accompanying increase of small lipid droplets. Neither ragged red fibers nor other ultrastructural alterations of mitochondria were seen. Three patients showed mixed or microvesicular liver steatosis of severity ranging from mild to severe. One girl showed lipid accumulation in cells lining proximal convoluted tubules. Central nervous system revealed typical LS lesions, some of them detectable only microscopically. In two children the lesions were obscured by post mortem changes.
Conclusions: In children with SURF1 dependent COX deficient LS - skeletal muscle shows reproducible abnormalities with COX deficit as a salient feature; omitting of COX histochemical assessment may lead to misinterpretation of biopsy; post mortem detection of CNS lesions requires careful microscopical assessment; variable degree of liver steatosis may be present.

O-69
EFFECT OF ETHANOL AND ALLOXAN INDUCED DIABETES IN THE OUTCOME OF THE PREGNANCY IN THE MOUSE.

Camila Nunes Ribeiro, postgraduate student, Department of Pathology, Faculty of Medicine of Ribeirao Preto, University of Sao Paulo, Brazil.
Luiz Cesar Peres, MD, Department of Pathology, Faculty of Medicine of Ribeirao Preto, University of Sao Paulo, Brazil.

Congenital anomalies in fetuses born to diabetic mothers are 2 to 3 times more frequent than normal ones. Ethanol is the most widely exogenous teratogen used by women in childbearing age, being implicated in NTD, congenital heart disease and limb abnormalities as diabetes. The aim of this study was to investigate the effects of diabetes, ethanol and the association of both on the outcome of pregnancy. Swiss mice were randomly allocated into 4 groups with 6 animals each: Control (C), Diabetes (D), Ethanol (E), and Diabetes and Ethanol (DE). Animals of groups D and DE received an i.v. dose Alloxan (40mg/Kg) prior to mating. Animals of groups E and DE received an i.p. injection of ethanol 4g/Kg of a saline solution 25% (v/v) on the 7th gestational day, while animals of groups C and D received saline. Killing was in a CO2 chamber on the 18th gestational day and the number of implantations, resorptions, late fetal death, and live fetuses with and without NTD, and placental weight and diameter were recorded. Blood glucose level was normal on the 18th gestational day in groups C and E and elevated in groups D and DE, being highest in D. There was no difference for implantation for all groups and for all parameters between groups C and E. Resorption was highest in group D and late fetal death in group E. Group D fetuses and placentas were smaller and lighter than those of group C. Group DE placentas and female fetuses, but not male, were smaller and lighter than group C and E ones. Fetal length, but not weight, was different between groups D and DE. Tail length was smaller in group D. High single dose of ethanol given to pregnant swiss mice on the 7th gestational day did not induce IUGR and placental growth and as did diabetes, associated or not to ethanol. When given to diabetic mice, ethanol improves male fetal weight and length indicating that female fetuses are more prone to the detrimental effects of diabetes. Ethanol reduces resorptions but increases late fetal death and also enhances the effects of diabetes inducing NTD. Diabetes has a negative effect on the placenta that is not affected by ethanol. These results may indicate that ethanol may have a favorable action in early gestation probably by contributing to energy metabolism but it is known to increase cell damage that will eventually result in NTD, late fetal death and reduction of the placental mass.

O-70
EVALUATION OF HEPATIC FIBROSIS IN THE PEDIATRIC POPULATION : WHICH HISTOLOGICAL STAGING SYSTEM AND WHAT ALTERNATIVE ?

Brigitte Le Bail (1, 2), Paulette Bioulac-Sage (1,2), Victor de Lédinghen (3), Laurent Rebouissoux (3), Laurent Castéra (3), Juliette Foucher (3), Monique Darriet (4), and Victor de Lédinghen (1,3), Thierry Lamireau (1,5).
(1) INSERM E362 IFR66 Université Victor Segalen, 33076 Bordeaux; (2) Service d'Anatomo-Pathologie, Hôpital Pellegrin, C.H.U. Bordeaux, 33076 Bordeaux; (3) Service d'Hépato-Gastroentérologie, Hôpital Haut Lévêque, C.H.U. Bordeaux, 33604 Pessac; (4) Laboratoire de Biochimie, Hôpital Pellegrin, C.H.U. Bordeaux, 33076 Bordeaux, France;(5) Département de Pédiatrie, Hôpital Pellegrin, CHU Bordeaux, 33076 Bordeaux.

The prevalence of chronic liver disease in children is low , but the etiologies are multiple and a severe fibrosis at presentation is frequent. Although very invasive, liver biopsy remains the gold standard to evaluate and to follow up fibrosis in this population. Unfortunately, there is no consensus about the best histological system of staging of fibrosis in this heterogeneous group of patients. Recently, novel non-invasive methods to assess liver fibrosis have been validated in adult patients, such as Fibrotest®, based on biochemical seric markers, and transient elastography (FibroScan®), a rapid (< 5 mn) bedside ultrasound based method measuring liver stiffness. Preliminary results suggest that this last method would be very accurate in children.
The aims of this prospective study was to evaluate two histological scores for liver fibrosis in children with chronic liver disease as compared with 2 non invasive tests : FibroScan® and Fibrotest®.
33 consecutive children (20 boys, mean age 11 years (4 months – 20 years)) with chronic liver disease underwent liver biopsy, fibrotest and Fibroscan and were included. The most frequent pathologies were Wilson's disease, biliary atresia, polycystic fibrosis, and autoimmune hepatitis. Fibrosis was evaluated using METAVIR score, from F0 to F4, basing on portal fibrosis, and a more complex semi-quantitative score adapted from Chevallier and coll. (SQS), which takes into account fibrosis in portal tracts, central veins, sinusoids and also consider the number, thickness and lenght of septa. Correlation of histological values with non invasive datas were analyzed using the Spearman coefficient of correlation.
According to METAVIR, fibrosis was F1 in 4 cases, F2 in 6 cases, F3 in 7 cases, and F4 in 16 cases. SSQ ranged from 1 to 23, with 15 cases > 15. FibroScan® and Fibrotest® values ranged from 2.9 to 75 kPa, and 0.004 to 0.97, respectively. Correlation coefficients and associated probability (p), determined on the 19 first cases were : METAVIR score : 0.676 ($p = 0.001$) with Fibroscan and 0.478 (NS)with Fibrotest; SQS : 0.712 ($p < 0.0001$) with Fibroscan and 0.544 ($p = 0.004$) with fibrotest.
Conclusions: In this pediatric series, severe hepatic fibrosis was very frequent and Chevallier's semi-quantitative score correlated better than METAVIR score with FibroScan® and Fibrotest non invasive tests. FibroScan® could avoid liver biopsy in many cases and its usefulness in the follow-up of children should be evaluate

O-71
ACTIVATION OF THE WNT/ß-CATENIN PATHWAY IN HEPATOBLASTOMA

Carolina ARMENGOL (1), Stefano CAIRO (1), Monique FABRE (2), Claire-Angélique RENARD (1), Laurence BRUGIÈRES (3), Véronique LAITHIER (4), and Marie Annick BUENDIA (1)
(1) Unité d'Oncogenèse et Virologie Moléculaire, Inserm U579, Institut Pasteur, Paris; (2) Anatomie et Cytologie Pathologiques, CHU de Bicêtre, Le Kremlin-Bicêtre; (3) Département de Pédiatrie, Institut Gustave Roussy, Villejuif; (4) Service de Pédiatrie, CHU de Besançon, Besançon, France.

Hepatoblastoma (HB) is the predominant type of malignant liver tumors in childhood. The etiology of HB is unknown, but an association with congenital abnormalities is well established. HBs are characterized by the proliferation of immature hepatocytes, showing 4 patterns: fetal, embryonal, macrotrabecular, and small anaplastic (undifferentiated) type. Mixed epithelial-mesenchymal tumors also contain myofibroblastic, chondroid and osteoid tissues, and occasional teratoid features, suggesting that they derived from uncommitted stem cells. Genetic analysis has uncovered a high frequency of mutations in the ß-catenin or Axin genes, leading to constitutive activation of the Wnt pathway in a majority of HB cases.
In this study, we aimed to identify downstream genes of Wnt/ß-catenin signaling implicated in the molecular pathogenesis of HB. To this end, we have collected frozen and fixed HB samples from French hospitals. Most patients were enrolled in the international clinical trials of the SIOPEL group. Extensive pathological and clinical annotations were obtained. The ß-catenin mutational status was determined by RT-PCR over exons 3 and 4, and ß-catenin localization was examined by immunohistochemistry. Finally, gene expression profiles were analyzed in 35 tumors and 4 liver samples by using Affymetrix arrays.
Hierarchical cluster analysis clearly separated tumors from normal liver and identified two tumor groups: (i) cluster A: localized tumors with fetal histology, and (ii) cluster B: invasive tumors with less differentiated patterns and bad prognosis.
Supervised analysis according to ß-catenin status (mutated or wild type) revealed significant differences between deregulated genes within each cluster. Overexpression of known ß-catenin target genes related to fatty acid or amino acid metabolism, such as glutamine synthetase (GS), was predominant in cluster A, but not in less differentiated tumors. Conversely, ß-catenin targets related to proliferation and cell cycle, such as c-myc, were strongly activated in cluster B and downregulated in cluster A. Microarray data are currently validated by immunohistochemistry.
In conclusion, the molecular signature of Wnt/ß-catenin signaling in hepatoblastoma seems to be mainly imposed by liver environment, but differs according to developmental stage. This work was supported by grants from the Ligue Nationale contre le Cancer (programme Carte d'Identité des Tumeurs) and from the GIS Institut des Maladies Rares.

O-72
AN IMMUNOHISTOCHEMICAL (IH) AND ELECTRON-MICROSCOPIC (EM) STUDY OF IMMATURE GLOMERULI IN CHILDREN WITH NEPHROTIC SYNDROME (NS) GLOMERULOPATHIES (WITH REFERENCE TO CLINICAL FINDINGS).

Aldona Wozniak1, Wieslawa Salwa-Zurawska1, Jakub Zurawski1, Danuta Ostalska-Nowicka2
Departments of Clinical Pathomorphology1 and Pediatric Nephrology2, Karol Marcinkowski University of Medical Sciences, Poznan, Poland

INTRODUCTION
We were not able to find any reports in the available literature on the presence of immature glomeruli in other childhood glomerulopathies than Alport's syndrome, thin membranes syndrome or Finnish type congenital NS. LM evaluation of immature glomeruli is difficult, because hypercellularity masks pathological changes. The aims were: 1/ to determine the relationship between the presence of immature glomeruli and the clinical findings initially and in response to treatment in children with NS glomerulopathies 2/ to carry out an EM and IH study of immature glomeruli.
MATERIAL AND METHODS
The study group consisted of 53 children with minimal change disease (MCD), mesangioproliferative gn (MES GN) and focal segmental glomerulosclerosis (FSGS) (44, 7 and 2 cases, respectively. Control group (no signs of immaturity) consisted of 92 children (43 with MES GN, 49 with MCD), also hospitalized due to the first episode of NS. The paraffin sections were incubated with monoclonal antibodies to vimentin (VIM), CD34, CD31, SMA, synaptopodin (SYN), VEGF and WT1.
RESULTS
EM study confirmed the diagnosis of MCD in 37 cases. MES GN was diagnosed in 14 cases (mesangial cell proliferation and electron dense deposits were evident). Clinical analysis has demonstrated that significantly lower number of children from study group responded to steroids ($p=0.0105$ for MES GN and $p=0.002$ for MCD). Patient age exceeding 1 year ($p=0.0163$ for MES GN and $p=0.017$ for MCD) and serum albumin concentration above 1 g/dl ($p=0.0163$ for MES GN and $p=0.017$ for MCD) have proven to represent favourable prognostic factors. The mesangial cells exhibited very weakly and focally SMA (as immature glomeruli in the late M stage), whereas podocytes strongly expressed VIM. The CD31 IH staining pattern of capillary endothelial cells was similar to normal adult and immature glomeruli. The loss of CD 34 immunostaining, typical for adult glomerular endothelial cells, was not evident. Podocytes of immature glomeruli expressed SYN in MCD less intensively. VEGF expression was not different in immature glomeruli.
CONCLUSIONS
The results obtained indicate the usefulness of EM verification to reveal lesions undetectable by LM. The analysis exhibits significantly more frequent steroid resistance in children with immature glomeruli. The IH staining pattern of glomerular cells did not differ from the results obtained in normal – i.e. healthy immature glomeruli.

O-73
CLAUDINS IN ESOPHAGEAL NEOPLASMS AND BARRETT'S ESOPHAGUS

GYORFFY Hajnalka1, HOLCZBAUER Agnes1, KISS Andras1, NAGY Pal2, KUPCSULIK Peter3, PASKA Csilla1, SZABO Zsuzsa4, SCHAFF Zsuzsa1
12nd Department of Pathology, 3 1st Department of Surgery, Semmelweis University,
2Department of Pathology, National Medical Center, 4 St. Laszlo Hospital, Budapest, Hungary

Introduction
Claudins (CLDN), the main transmembrane proteins of tight junctions (TJ), are key molecules participating in cell adhesion, polarity and paracellular transport. Several studies suggested that changes in CLDN expression pattern might play role in carcinogenesis. The aim of the present study was to investigate the changes in the pattern of CLDN 1,2,3,4 and 7 expression in specialized intestinal metaplasia (SIM) of the Barrett's esophagus (BE) and adenocarcinoma (ACC) in comparison to foveolar glandular epithelium, esophageal

normal squamous epithelium and squamous carcinoma (SCC).
Materials and methods
Formalin fixed, paraffin embedded samples of 25 human BEs, 25 ACCs, 25 glandular epithelia from the lower esophageal tract, 25 esophageal normal squamous epithelia and 25 squamous carcinomas were studied by immunohistochemistry. Mouse monoclonal antibodies for CLDN 2 and 4, rabbit polyclonal antibodies for CLDN 1, 3, and 7 were analyzed and scored for areas of positive cells. Significant alterations were analyzed for mRNA expression by Real-Time RT-PCR, using relative quantification with GAPDH as internal control.
Results
CLDN1 and 7 were highly expressed in all groups without significant differences. CLDN3 and 4 were increased in BE and ACC compared to foveolar epithelium (p=0,0022, p=0,0064, p=0,0107). CLDN2 was higher in ACC than in BE and foveolar epithelium (p=0,0001, p=0,0022, resp).
Conclusion
CLDN 3 and 4 show increased expression in BE and ACC, which differentiates these lesions from foveolar glandular epithelium. In addition elevated CLDN 2 expression is characteristic to the carcinoma stage. CLDN expression pattern can be used for differentiation of benign, premalignant and malignant glandular epithelium. Similarities and differences of CLDN pattern in BE and ACC might indicate a sequence of molecular alterations in carcinogenesis, and support the view that BE is a precancerous stage of ACC.
This project was supported by grants NKFP-1A/0023/2002; NKFP-1A/002/2004 and OTKA-T037838.

O-74
GUANYLYL CYCLASE C EXPRESSION IN BARRETT'S ESOPHAGUS

BOMBONATI Alessandro MD (1-2), MITROO Pradnya MD (3), BIRBE Ruth MD (4), RHONDA Walters (2), PALAZZO Juan Pablo MD (2), SCHULZ Stephanie PhD (1), WALDMAN Scott A. MD, PhD (1)
(1)Division of Clinical Pharmacology, Departments of Medicine and Biochemistry and Molecular Pharmacology, Thomas Jefferson University, Philadelphia, PA 19107, USA
(2)Department of Pathology, Anatomy and Cell Biology, Thomas Jefferson University, Philadelphia, PA 19107, USA
(3)Division of Gastroenterology, Department of Medicine, Thomas Jefferson University, Philadelphia, PA 19107, USA
(4)Department of Pathology, Fox Chase Cancer Center, Philadelphia, PA 19111, USA

Introduction:
Barrett's esophagus (BE) is a metaplastic process in which the squamous epithelium of the esophagus is replaced by a specialized columnar epithelium. The presence of goblet cells is regarded as pathognomonic of this condition. However in endoscopic biopsies with small foci of BE, the identification of unequivocal goblet cells can be difficult. Guanylyl cyclase C(GC-C) is a receptor selectively expressed in apical membranes of epithelial cells from the duodenum to the rectum, but not by normal esophageal or gastric mucosae in humans. Recent studies demonstrated that GC-C is a useful immunohistochemical marker to identify intestinal metaplasia (IM), dysplasia and adenocarcinomas in the gastrointestinal tract.
Purpose of the study:
To evaluate the expression of GC-C in BE and its utility as a sensitive and specific marker for detecting cells undergoing IM in esophagus.
Methods:
26 biopsies from the lower esophagus exhibiting IM with unequivocal goblet cells in hematoxylin-eosin stains; 6 samples of normal gastroesophageal junction(GEJ) and 6 samples of cardiac-type mucosa (CTM) without IM were evaluated. Formalin fixed paraffin-embedded biopsies were stained for GC-C employing purified IgG from rabbit serum immunized with a peptide derived from human GC-C. Epithelial cells exhibiting apical membrane staining were considered positive for GC-C expression. All specimens were obtained under an IRB-approved protocol.
Results:
GC-C was expressed in all 26 (100%) cases of BE. All goblet cells, either in the surface of the mucosa or in glands, exhibited distinct membrane staining at their apex. No cytoplasmic or nuclear staining was present. Of significance, GC-C reactivity also was present in columnar cells adjacent to goblet cells. In contrast, 6 normal GEJ and 6 CTM did not stain. Moreover, normal squamous epithelia were negative in all cases.
Conclusions:
GC-C is 100% sensitive for BE, since it was consistently expressed in all areas of IM containing "classic" goblet cells. Similarly, GC-C is 100% specific for BE, demonstrated by the absence of staining of normal GEJ, CTM, and normal squamous epithelia. Of importance, GC-C was expressed by columnar cells adjacent to goblet cells in regions of BE. These data underscore the utility of GC-C as a highly sensitive and specific immunohistochemical marker for BE, particularly in histopathologically equivocal biopsies lacking the presence of pathognomonic goblet cells required for the diagnosis

O-75
NUCLEAR BETA-CATENIN EXPRESSION PREDICTS RESPONSE AND SURVIVAL AFTER NEOADJUVANT RADIOCHEMOTHERAPY OF OESOPHAGEAL CARCINOMAS

BALDUS Stephan E., ROTHE Birgit, MÖNIG Stefan P., METZGER Ralf, BOLLSCHWEILER Elfriede, MÜLLER Rolf-Peter, THIELE Jürgen, HÖLSCHER Arnulf H., DIENES Hans P., SCHNEIDER Paul M.
Institute of Pathology, Department of Visceral and Vascular Surgery, Department of Radiation Oncology, University of Cologne, Kerpener Str. 62, D-50931 Cologne

Introduction: Patients with locally advanced oesophageal cancer have a poor prognosis. Therefore, neoadjuvant therapeutic approaches have been developed. However, such therapies are expensive and associated with increased complication rates. Consequently, predictive molecular markers indicating response or non-response to neoadjuvant treatment may be of special clinical interest.
Purpose: In the present study, we investigated the expression of beta-catenin in a larger series of patients with oesophageal carcinomas in order to evaluate possible correlations with the response to neoadjuvant radiochemotherapy as well as survival.
Material and methods: Our study included 62 patients with locally advanced oesophageal carcinomas (cT2-T4, cNx, cM0 according to the TNM classification) comprising adenocarcinomas as well as squamous cell carcinomas. After bioptic confirmation of the diagnosis, standardised neoadjuvant radiochemotherapy was performed. Biopsies from 49 patients and the resected specimens of all patients were available and could be included. The grade of regression was assessed histomorphologically. A presence of less than 10 % vital residual tumour cells (VRTC) after therapy was defined as major response, the presence of more than 10 % VRTC was considered as minor response. Beta-catenin was visualised immunohistochemically and its membranous as well as nuclear expression were evaluated semiquantitatively followed by a thorough statistical analysis of the data.
Results: In general, nuclear beta-catenin expression was significantly up-regulated in resected carcinoma specimens as compared with the biopsies. Whereas only 12 % of the biospies contained more than 20 % of tumour cells exhibiting nuclear beta-catenin, about 35 % of the resected specimens

showed the same pattern. Additionally, up-regulation of nuclear beta-catenin expression was associated with a significantly worse response to neoadjuvant radiochemotherapy. Furthermore, a strong nuclear beta-catenin expression in the resected specimens correlated with a reduced survival probability.
Conclusions: An up-regulated beta-catenin expression in oesophageal carcinomas is predictive for a worse response to neoadjuvant radiochemotherapy as well as an unfavourable prognosis of the patients. Therefore, the immunohistochemical beta-catenin determination in such patients may present clinically valuable information.

O-76
IMMUNOHISTOCHEMICAL DETECTION OF MYCOPHENOLIC ACID IN GASTROINTESTINAL BIOPSIES OF MYCOPHENOLATE MOFETIL TREATED RENAL TRANSPLANT PATIENTS WITH CHRONIC DIARRHOEA

DERAEDT Karen°, MAES Bart°°, SHIPKOVA Maria°°°, ECTORS Nadine°, GEBOES Karel°
°Department of Pathology, University Hospital Gasthuisberg, Leuven, Belgium
°°Department of Medicine, Division of Nephrology, University Hospital Gasthuisberg, Leuven, Belgium
°°°Department of Clinical Chemistry, Georg-August-Universität, Göttingen, Germany

Introduction. Mycophenolate mofetil (MMF) is used for prevention of rejection. Chronic diarrhoea is a common adverse effect. Studies have shown that diarrhoea in patients treated with MMF is frequently infectious. In a subset of patients Graft-versus-host-like or Crohn's disease-like changes are observed in biopsies. Since reduction of MMF was the effective therapy for the diarrhoea, metabolites of MMF may be a possible cause.
Aim. After oral intake, the inactive MMF is absorbed and completely conversed into the active metabolite mycophenolic acid (MPA). The aim of the study was to investigate the presence of MPA and its distribution in the gastro-intestinal mucosa.
Materials and methods. Biopsies from renal transplant patients receiving MMF and presenting with chronic diarrhoea were snap frozen at -80°C. Samples were available from 7 patients, 4 males, 3 females (age between 30 and 60 years, mean 49.1 years). In one patient the drug was stopped for one year. Samples consisted of gastric and duodenal biopsies in 6 patients and ileal and colonic biopsies in 3 patients. Cryostat sections were stained with haematoxylin and eosin, and with the monoclonal antibody against MPA (DADE international; immunoperoxidase) and analysed without prior knowledge of clinical data.
Results. Gastric biopsies revealed no alterations (n=2), mild reactive gastropathy (n=1), inactive mildly chronic gastritis (n=2), and mildly active, chronic Hp-positive gastritis (n=1). Duodenal biopsies showed no alterations (n=1), architectural alterations and epithelial damage (n=3) and epithelial damage only (n=2). In ileum and colon, mildly active (ileo)colitis (n=2) or minor architectural alterations (n=1) were observed. In 3/6 gastric biopsies, cytoplasmic staining for MPA was observed in parietal cells. In 4/6 duodenal biopsies, focal positivity for MPA was noticed in cytoplasm and brush border of enterocytes. One negative biopsy was from the patient in which the drug was stopped. All samples of ileum and colon were negative for MPA.
Conclusion. Gastric lesions were not mainly Hp-related. Small intestinal and colonic lesions showed IBD-like features. Immunohistochemistry with the monoclonal antibody against MPA revealed focal positivity in the brush border of duodenal enterocytes in patients treated with MMF and suffering from chronic diarrhoea. MPA can thus be detected in the tissue. This technique may help to identify those patients in which diarrhoea and lesions are drug-induced.

O-77
SMALL INTESTINAL FOLLICLE ASSOCIATED EPITHELIUM AND VILLUS EPITHELIUM COMPARED BY GENE EXPRESSION PROFILE

P. Verbrugghe, P. Demetter, J. Vandesompele(1), W. Waelput, C. Cuvelier, Academic Department of Pathology, Ghent University, Belgium; (1)Center for Medical Genetics, University Hospital, Ghent, Belgium

INTRODUCTION: The follicle associated epithelium (FAE) overlying the lymphoid follicles of Peyer's patches mediates transcytosis of antigens to the underlying lymphoid tissue, mainly by the presence of M-cells. By its antigen handling function it plays an important role in the pathogenesis of inflammatory bowel diseases (IBD), especially Crohn's disease. A detailed knowledge of the FAE and in particular the M-cell phenotype is lacking. So far, the molecular and biochemical characterization of the FAE and M-cells is at an early stage and few specialized M-cell or FAE specific characteristics are known.
AIMS: In order to identify possible new molecules important for the role and function of FAE and M-cells in normal and IBD small intestinal mucosa, the gene expression profile of FAE was compared with that of villus epithelium (VE).
METHODS: Epithelium was isolated from adult Balb/c murine Peyer's patches and non-Peyer's patch small intestine. Total RNA was extracted from the FAE and VE with the Qiagen RNeasy mini kit. Agilent Mouse Development Oligo microarrays were used to obtain a broad picture of differences in gene expression between FAE and VE. To confirm FAE specific expression of candidate genes, Q-PCR was performed with the iCycler real-time PCR detection system (Biorad).
RESULTS: After microarray analysis and Q-PCR, significant differences (in a range of 2-fold to 10-fold) between FAE and VE were detected for the expression profile of 20 genes. These included previously undescribed genes encoding adhesion molecules, cytokines, cytoskeleton molecules and cathepsin.
CONCLUSION: The finding of gene expression differences in the FAE compared with the VE contributes to a better characterization of the FAE phenotype. The main differences are related to molecules involved in cellular transport and antigen handling. In a next phase, immunohistochemistry and electron microscopy will be performed to detect more M-cell specific molecules.

O-78
MICROSCOPIC COLITIS AND UNEXPLAINED DIARRHEA: IS IT WORTHWHILE TAKING MULTIPLE BIOPSIES IF A COLONOSCOPY IS NORMAL? IS IMMUNOHISTOCHEMICAL STAINING OF TENASCIN HELPFUL IN "MINIMAL" COLLAGENOUS COLITIS DIAGNOSIS?

ORLOWSKA Janina[1]*, JAROSZ Dorota[1]*, CWIKLA Maria*, OSTROWSKA Joanna[2], BUTRUK Eugeniusz*, KUPRYJANCZYK Jolanta**
Histopathology Laboratory[1]*, Department of Gastroenterology*, Medical Centre for Postgraduate Education, Oncology Centre; Department of Molecular Pathology**, Oncology Centre; Department of Pathology, Prof. W. Orlowski Clinical Hospital[2], WARSAW, POLAND

Introduction: Collagenous colitis (CC) and Lymphocytic Colitis (LC) belong to the group of Microscopic Colitis (MC), which is a cause of chronic watery diarrhea. Both entities are

possible to establish only when serial biopsies are taken from macroscopically normal colons. CC relies on the histological presence of subepithelial bands of collagen deposits of =10µm in well-oriented sections. Sometimes they may be presented only focally or are too subtle to allow a definitive diagnosis upon routine stainings. Tenascin can better visualize these deposits. The basic histological criterion for LC is increased number of intraepithelial lymphocytes (IEL) = 20/100 surface epithelial cells.
The purpose of this study was:
1. To investigate the diagnostic yield of biopsies taken from patients referred for unexplained chronic diarrhea with macroscopically normal colonoscopy,
2. To estimate the value of Tenascin for the identification histologically "minimal" form of CC.
Material and Methods: The cases had been collected prospectively between July 1999 and March 2005. Slides were stained with H&E, AZAN and Van Gieson or Trichrome in order to visualize the collagenous bands. The monoclonal anti-human Tenascin antibody (1:400, cat. no MAB19101, Chemicon Int.) was used for immunohistochemistry (IHC) in the specimens taken from 11 pts with CC, 9 pts with CCS and 6 control pts. Its expression was scored semiquantitatively as negative (0-0,1) or positive (1, 2, 3).
Results: There were 28 pts with CC, 13 pts suspected for CC (CCS) and 7 pts with LC during the study period: 4M: 24F with CC of average age 61,2; 7M: 6F with CCS of average age 56,5 and 7F with LC of average age 64,8. We have shown that the IHC detection of increased amounts of Tenascin (1, 2 or 3) in subepithelial zone was a specific marker for CC (9/11patients = 81,8%), but it was mostly negative in CCS (8/9 patients = 88,8%). Only in one woman Tenascin staining helped to change a doubtful diagnosis of CCS to CC. Histologically normal specimens taken from 6 pts with normal colon mucosa were negative for Tenascin.
Conclusions:
1. Serial biopsies taken from endoscopically normal colon from patients with unexplained diarrhea are necessary to establish diagnosis.
2. Though Tenascin IHC is useful to better identify the intensity of CC, its most important value concerns the possibility of excluding the doubtfully positive cases of CCS avoiding an unnecessary treatment of patients.

O-79
ASSESSMENT OF "MOLECULAR DIGESTIVE BIOPSIES": COMPARISON OF DNA ARRAYS AND TISSUE MICROARRAYS RESULTS FROM SPECIMENS OF PATIENTS WITH INFLAMMATORY BOWEL DISEASES

LASSALLE Sandra (1, 2), HOFMAN Veronique (1, 2), ABAKAR-MAHAMAT Abakar (3), SELVA Eric (2), HEBUTERNE Xavier (3), HOFMAN Paul (1, 2).
(1) Laboratory of Clinical and Experimental Pathology, (2) Tissue Biobank Unit, (3) Department of Gastroenterology, University of Nice, Nice, France

New molecular techniques such as cDNA, protein or antibody arrays allow for highthroughput identification of thousands of potentially disease-related markers on the genome, transcriptome and proteome level. However, these molecular techniques have been mainly developped from surgical specimens. Some human diseases such as inflammatory bowel diseases or IBD [Crohns'disease (CD) and ulcerative colitis (UC)] are most of the time diagnosed from small biopsies taken during endoscopy. The aim of this work was, 1) to assess if some molecular techniques (cDNA arrays and tissue microarrays) can be developped from biopsies obtained in IBD, 2) to correlate from biopsy specimens taken in patients with IBD, data obtained from DNA microarray and from tissue microarray techniques. The quantity and the quality of extracted RNA from digestive biopsies were assessed from the results obtained by bioanalyze (Agilent 2100) and were largely compatible with DNA array experiments (by using a 2500 genes home made array). The results obtained by DNA arrays were always controled by RT-PCR. Among, the different molecules which were upregulated in CD (for example, DAF/CD55 and ubiquitin D) and in UC (for example lipocalin 2 and C4PBP), a strong correlation was most often seen between the transcriptomic results and the levels of corresponding proteins quantified on tissue microarrays. These preliminary data were obtained from heterogeneous populations, without any selection of cohorts of patients. Current works using these molecular approaches are making on different groups of patients with similar epidemiological, and clinical profiles.

O-80
THREE-DIMENSIONAL VIRTUAL MICROSCOPY OF COLORECTAL BIOPSIES

Authors:
WU Mark Li-cheng(1), VARGA Viktor Sebestyen(2), KAMARAS Viktor(2), FICSOR Levenete(2), TAGSCHERER Attila(2), TULASSAY Zsolt(2) and MOLNAR Bela(2)
Affiliations:
(1)University of California, Irvine College of Medicine, Irvine, California, USA and
(2)Digital Microscopy Laboratory, 2nd Department of Internal Medicine, Semmelweis University, Budapest, Hungary

Introduction: Conventional microscopy produces diagnostic errors due to incomplete sampling because only a small fraction of the specimens is visualized, and diagnostic errors due to poor orientation because many institutions randomly embed specimens. Furthermore, attempts to avoid these errors by obtaining additional sections or by re-embedding can prolong turnaround time. Purpose: We describe new technology that may eliminate these problems by enabling pathologists to rapidly examine entire specimens and convert poorly oriented mucosa to well oriented mucosa. Methods: Material from biopsies of a putative cecal polyp, for which initial sections appeared normal, was exhaustively sectioned. These sections were digitized using the HI-Scope system then analyzed using the 3D-Scope program. The HI-Scope system is a fully automated digitizer capable of rapidly digitizing hundreds of slides at a time at high resolution. The 3D-Scope program evaluates the 2D digitized images of serial sections with virtual 2D and 3D microscopy. The complete array of 2D digitized images of serial sections may be displayed simultaneously as a gallery of essentially the entire specimen. The 2D images may be automatically stacked and aligned to form a 3D image. This image may be rotated about any axis or sectioned along any plane. Results: From the gallery of 2D images, a tubular adenoma in well oriented mucosa, and a poorly oriented focus were immediately evident in the image of each additional serial section. We selectively cropped the poorly oriented focus from the image of 1 serial section, and the corresponding focus from the images of all other serial sections was then automatically cropped, stacked and aligned to reconstruct a 3D image of the poorly oriented focus. We interacted with the program to rotate the 3D image about various axes and to section the 3D image along various planes until several crypts were sectioned longitudinally, effectively converting the poorly oriented mucosa to neo-well oriented mucosa. This required only a few seconds. Scanning, 3D reconstruction, and diagnosis by virtual microscopy together required only 2.5 hours. Conclusions: We describe new technology, which incorporates exhaustive sectioning, three-dimensional reconstruction and virtual microscopy, that may eliminate problems innate to conventional microscopy by enabling pathologists to rapidly examine entire specimens and convert poorly oriented mucosa to well oriented mucosa.

O-81
IMPACT OF LONG TERM FINASTERIDE TREATMENT ON PROSTATE CANCER MORPHOLOGY

Yves Allory (1,2), Mark A. Rubin (3,4), Vincent Molinié (5), Wei Huang (3,4), Xavier Leroy (6), Adam Kuten (3,4), Laurent Salomon (1,2), Claude Abbou (1,2), Dominique Chopin (1,2), Alexandre de la Taille(1,2)
1 CHU Mondor, AP-HP, Créteil, France
2 EMI 0337, INSERM, Créteil, France
3 Brigham and Women's Hospital
4 Harvard Medical School
5 Hôpital Saint-Joseph, Paris, France
6 CHU Lille, Lille, France

Introduction: The Prostate Cancer Prevention Trial (PCPT) reported a decreased incidence of prostate cancer for patients treated by finasteride. However, when cancer was present, the finasteride treated men had significantly higher Gleason grade cancer. One possible explanation was an overgrading due to changes in the tumor architecture following long term finasteride treatment similar to that seen with LHRH agonists. Aim of this work: to study the morphologic impact of finasteride on prostate cancer. Methods: Between 1996 and 2004, 53 prostate cancer patients who received finasteride for at least 6 weeks (6-624) were reviewed. A control group of 42 matched patients (age, PSA, digital rectal exam and Gleason score) and a group of 21 patients who had 3-month LHRH agonist before radical prostatectomy were included. Two genitourinary pathologists reviewed the cases in a blinded manner using standard criteria for evaluating hormonal treatment effect such as apoptosis, vacuolated cytoplasm, pyknotic nuclei and small irregular glands. Hormonal effect was scored as either not present (score=0), suspicious for (score=1) or highly suggestive of hormonal treatment (score=2). Results: The mean reviewed Gleason scores were 7.0, 7.4 and 7.3 for the control, finasteride and LHRH groups, respectively. Initial Gleason scores were 6.8, 6.7 and 6.9 respectively. Only the difference between initial Gleason score of finasteride group and reviewed Gleason score was statistically significant. Overall mean treatment scores were 0.33, 0.41 and 1.38 for control, finasteride and LHRH groups, respectively. Surprisingly, there was no significant morphologic treatment effect seen in 73% of the finasteride treated cases. The 27% with treatment effect did not differ from the 25% of control patients who were scored with either suspicious for or highly suggestive of treatment effect. Ki-67 index was assessed in half of control and finasteride patients. It revealed no difference between control and finasteride group. Patients treated with more than 2 years of finasteride (versus less than 2) had higher Gleason (8.4 vs 6.9, $p<0.001$) and treatment scores (1.18 vs 0.22, $p<0.001$). Conclusion: We did not observe any consistent hormonal therapy effects with finasteride as compared to LHRH agonists. Therefore while other aspects of the PCPT design might account for the higher Gleason grades in the study arm, morphologic changes due to long term finasteride treatment are not a likely cause.

O-82
RISK OF NON SIGNIFICANT PROSTATE CANCER AFTER AN EXTENSIVE SATURATION 21-NEEDLE BIOPSY PROTOCOL : A STUDY OF 1050 PROCEDURES.

Yves Allory (1,2), Alexandre de la Taille (1,2), Laurent Salomon (1,2), Zahira Mérabet (1), Eric Bonte (1), Dimitri Vordos (1,2), Andras Hoznek (1,2), René Yiou (1,2), Dominique Chopin (1,2), Claude Abbou (1,2).
1 CHU Henri Mondor, Assistance Publique-Hôpitaux de Paris, Créteil, France
2 EMI 0337, INSERM, Créteil, France

Introduction: extensive saturation biopsy is performed to increase prostate cancer detection rate but the potent risk of detecting non significant cancer could limit the clinical interest of this protocol. Aim of this work: to evaluate prospectively the risk of detecting non significant prostate cancer using an extended 21-needle biopsy protocol. Methods: 860 patients underwent prospectively a 21-needle biopsy protocol (peripheral zone, 6; far lateral, 6; transition zone, 6; middle peripheral zone, 3) resulting in 1050 procedures (including 651 "1st biopsy sets", 252 "2nd biopsy sets" and 147 "3rd or more biopsy sets"). Median serum PSA was 12 ng/mL (2-590) and digital rectal examination was T1c (n=654) or T2/T3 (n=206). The results obtained with 21 biopsy protocol (BP) were compared to those obtained in the same patients if a restricted 6 BP (sextant), 12 BP (sextant + far lateral) or 18 BP (sextant + far lateral + transition zone) had been performed respectively. Results: prostate cancer incidence was 25.6 % (6 BP), 31.6 % (12 BP), 34.5% (18 BP) and 35.1 % (21 BP) respectively, with a significant detection rate increase between 6 BP, 12 BP and 18 BP ($p<0.01$). In patients with a preoperative risk of non significant cancer (T1c, PSA <10 ng/mL, only 1 positive biopsy with a total tumor length <3 mm and a Gleason score <7), radical prostatectomy examination showed a significant cancer (stage pT3 or 4, and/or tumor volume >0.5cc and/or Gleason score >=7) in 12/23 (52%) (6 BP), 14/24 (58%) (12 BP), 16/24 (66%) (18 BP) and 7/16 (44%) (21 BP). Of note, among these patients with a preoperative risk of non significant cancer, 29 and 9 patients would not have been diagnosed by 6 BP and 12 BP, 18 (62%) and 5 (55%) of them with a significant cancer in radical prostatectomy, respectively. Conclusion : 1) the prostate 21-needle biopsy protocol is useful in increasing the cancer detection rate without increasing immoderately the rate of non significant cancer detection, 2) the preoperative criteria are not sufficient to predict the risk of non significant cancer and should be improved.

O-83
DOES SAMPLES SURFACE VARIABILITY HAVE ANY IMPACT ON CENTRALLY-REVIEWED PROSTATE CANCER DIAGNOSIS OF PSA-BASED SCREENING BIOPSIES ?

MAZEROLLES Catherine, ZAIRI Anas, SERRES Isabelle, GROSCLAUDE Pascale, RISCHMANN Pascal, DELISLE Marie-Bernadette, VILLERS Arnaud, MALAVAUD Bernard.

Within the ERSPC program, 50-70 years old male participants are offered PSA testing and addressed for 6 TRUS-guided biopsies when PSA >3ng/ml. The initial 94 sets of biopsies (n=878 biopsies) have been centrally reviewed for consistency in diagnosis in relation to the surface of the biopsies.
Materials and Methods: All biopsies were blinded and reviewed by 2 reference pathologists for prostate cancer diagnosis and also assessed in terms of PIN, extensive chronic inflammation, lesion suspect but not diagnostic for malignancy. The surface of all analyzed materials, was measured by image analysis (Image J°). Results are expressed as mean+/-SD.
Results: The mean number of biopsies was 11.3+/-2.5 with a mean surface of 240 +/- 88 mm2 analyzed per patient. The surface ranged from 70 to 510 mm2. Prostate cancer was evidenced in 25 cases by the local pathologists, 3 additional cases being found on central review. The inter-judge kappa coefficient was 0.92 ($p<0.0001$), showing excellent concordance. The three discrepancies befitted the definition of focal cancer (<3mm, one positive biopsy) and were observed in significantly smaller samples than the concordant diagnosis (142+/-32 vs. 243+/-88 mm2, $p=0.05$).

There were no relationships between the surface analyzed and the diagnosis of cancer (220+/-86 vs. 245+/-90 mm2, p=0.250), of isolated PIN (253+/-98 vs. 246+/-88, p=0.82), of acute inflammation or extensive atrophy, while extensive chronic inflammation was associated with significantly larger samples (280+/-87 vs. 230+/-87, p=0.049).
Conclusion: Despite the ERSPC recommendations, we observed some variability in the urologists' practices, with a mean number of biopsies exceeding largely the number recommended in the protocol (11.3 vs.6 per patient). Such variability was even more evident when considering the surface of biopsies available for analysis, albeit it had no overall impact on the diagnosis of prostate cancer and isolated PIN. While inter-judge concordance was good (kappa 0.92), three additional cases of cancer were found at central review, all in significantly smaller samples than in the cases of concordant diagnosis.

O-84
CONCORDANCE BETWEEN HISTOPATHOLOGY AND MRI IN PROSTATE CANCER

Compérat E (1), Renard-Penna R (2), Just PA (1), Mozer P (3), Delcourt A (1), Bitker MO (3), Akakpo J-P (2), Richard F (3), Grenier P (2), Capron F(1).
(1) Service d'Anatomie et Cytologie Pathologique
(2) Service de Radiologie
(3) Service d'Urologie
CHU La Pitié-Salpêtrière
75013, Paris

Introduction: Histopathology is the gold standard to evaluate prostate cancer on radical prostatectomy. Accurate localization of prostate cancer within the gland is of increasing clinical importance for the treatment of these patients. It is of tremendous therapeutical importance to examine, whether these patients display uni-, bilateral or extracapsular extension of their prostate cancer. To precise evaluation of these parameters, preoperative MRI imaging is employed routinely. Our retrospective study compared preoperative MRI and postoperative histological findings.
Materials and Methods: Fourty-seven patients with biopsy proved prostate cancer underwent endorectal MRimaging before radical prostatectomy. Images were interpreted by two independent radiologists. After prostatectomy, prostates were treated according to the recommendations of the Stanford protocol. Prostate specimens were examined by two independent and experimented pathologists. Invasion of the capsule, extracapsular extension and invasion of the periprostatic tissue were assessed, and results compared to MRI findings.
Results: In 43 (91%) of 47 cases, invasion or integrity of the capsule was predicted by IRM and confirmed by histopathology. 39 cases (82%) with irregular capsule in IRM displayed capsular invasion in histology. Four cases (9%) did not have any sign of capsular invasion in MRI, results were confirmed by histology. Discordance was found in 4 cases (9%).
Concerning extracapsular spread concordance was found in 23 cases (49 %).
In 9 cases (19%) MRI predicted extracapsular spread, histology found extracapsular adenocarcinoma in 12 cases (26%). In 21 cases (44%) MRI suspected extracapsular tumor spread, histology could not confirm these findings. In 14 (30%) cases neither MRI nor histology found extracapsular tumor growth.
Conclusion: Preoperative MRI imaging seems to be a good tool to predict prostate capsule invasion. Concerning extracapsular growth MRI displays weaker specificity, either because tumor spread is confined to one gland, which might be difficult to detect even in light microscopy. On the other side prostate gland does not display a real capsule, fibrosis and inflammation especially surrounding adenocarcinoma may mimic extracapsular growth in radiology. Histology still remains the gold standard although MRI has become a very sensitive tool.

O-85
DETECTION OF PTEN DELETION IN PROSTATE CANCER BUT NOT PROSTATIC INTRA-EPITHELIAL NEOPLASIA BY FLUORESECENCE IN SITU HYBRIDIZATION ON TISSUE MICROARRAYS

CUTZ J-C (1,2), YOSHIMOTO M (1), NUIN PAS (4), BAYANI J (1), ZIELENSKA M (5,6), EVANS AJ (1,3,5), SQUIRE JA (1,5)
1 Molecular and Cellular Biology, Ontario Cancer Institute - Princess Margaret Hospital, Toronto, Ontario, Canada; 2 CIHR Molecular Oncologic Pathology Program, Toronto, Ontario, Canada; 3 Dept. of Pathology, Princess Margaret Hospital, Toronto, Ontario, Canada; 4 Dept of Biology, McMaster University, Hamilton, Ontario, Canada; 5 Laboratory Medicine and Pathobiology, University of Toronto; and 6 Dept. of Pathology and Laboratory Medicine, The Hospital for Sick Children, Toronto, Ontario, Canada

Introduction: Although somatic PTEN alterations have been reported in prostate cancer, including loss of heterozygosity or homozygous deletions, point mutations, and promoter hypermethylation, the relationship between genomic alterations of PTEN and prostatic neoplasia (PIN)remains unclear.
Purpose: The purpose of this study was to determine whether PTEN deletion, as assessed by FISH, is associated with the progression of PIN to invasive cancer.
Methods: Archival formalin-fixed, paraffin embedded tissues from 25 radical prostatectomy specimens were used for tissue microarray (TMA) assembly. Arrayed tissues were examined by haematoxilyn and eosin staining and scored according to Gleason grading criteria. Standard dual-color FISH was performed using commercially-available DNA probes for band 10q23 (PTEN locus) and band region 10p11.1-q11.1 (centromere of chromosome 10). At least 100 nonoverlapped intact interphase nuclei were scored in areas of cancer, PIN, benign glandular epithelium and stroma. The signal counts for areas of neoplasia were compared against those obtained from benign and stromal cell nuclei. Standard immunohistochemistry (IHC)was performed on a contiguous TMA section to evaluate immunoreactivity for total PTEN protein. IHC scoring was performed in areas of PIN, benign and malignant epithelium and stroma taking into account intensity and extent of diaminobenzidine (DAB) staining. Comparisons between PIN and cancer cell PTEN immunoreactivity were made once normalized against stromal cell immunoreactivity in the same tissue core.
Results: Six of 6 (100%) cases of benign hyperplasia and 16/16 cases (100%) of PIN were found to be PTEN deletion-negative while 17/25 (68%) of cancer samples were PTEN deletion-positive ($P < 0.01$). Homozygous PTEN losses appeared to be uncommon in the PTEN deletion-positive group (8%). A negative correlation was observed between PTEN deletion status and intensity of IHC staining for PTEN protein. In silico analysis of the PTEN locus revealed a high frequency of duplicons flanking the PTEN gene.
Conclusions: The results of this study suggest that PTEN deletion plays a role in the progression of PIN to cancer and that local microhomology at 10q23 may provide a mechanism of gene deletion. Further, PTEN deletion appears to be reflected as a relative decrease in immunoreactivity in the affected cells.

O-86
PROTOCADHERIN-PC: A POTENTIAL BIOMARKER FOR HORMONE REFRACTORY PROSTATE CANCER AND ITS ASSOCIATION WITH TUMOR PROGRESSION

TERRY Stephane 1, GIL-DIEZ-de-MEDINA Sixtina 1, QUEIRES Luis 1, FAUCON Hugo 1, De la TAILLE Alexandre 1,2, ALLORY Yves 1,2, CHEN Min-Wei 3, ABBOU Clément-Claude 1,2, BUTTYAN Ralph 3, CHOPIN Dominique 1,2 and VACHEROT Francis 1
1 INSERM E 03-37, Université Paris XII,2 Department of Urology of CHU Henri Mondor, Assistance Publique des Hôpitaux de Paris, Créteil, France
3 The Departments of Urology and Pathology of The College of Physicians and Surgeons of Columbia University, New York, NY

Introduction : Previously, we reported the characterization of a novel gene product, protocadherin-PC (PCDH-PC), specifically expressed by apoptosis-resistant variants of the human prostate cancer cell line, LNCaP. In this study, we tested by using LNCaP xenografts models if PCDH-PC could induce a state of hormone-resistance and we examined PCDH-PC mRNA expression level and its localization in human normal prostate and prostate cancer tissues.
Methods : parental and PCDH-PC transfected LNCaP cells were tested for their ability to form tumor xenografts (in intact or castrated male immunodeficient mice). PCDH-PC mRNA expression and its localization were studied by semi-quantitative RT-PCR and by in situ hybridization (ISH) performed on tumor xenografts and human prostate tissues.
Results : By an in situ hybridization procedure, we showed evidence that PCDH-PC mRNA was dramatically upregulated in LNCaP xenografts during the acquisition of hormone resistance following castration of the host. In order to investigate whether protocadherin-PC expression might directly convert parental LNCaP cells to a hormone-resistant state, we implanted into castrated nude male mice either control LNCaP cells or PCDH-PC–transformed LNCaP cells. In contrast to control-transfected cells, PCDH-PC transfected LNCaP cells were able to form tumors in castrated male nude mice. Semi-quantitative RT-PCR procedure demonstrated that normal human prostate cells and tissues expressed little or no PCDH-PC-related mRNA and that this low level of expression was maintained in untreated CaP cells. ISH showed that expression of PCDH-PC-homologous transcripts was restricted to some epithelial cells in normal tissue and to CaP cells in tumors. In contrast, hormone-resistant CaP cells were found to express significantly higher levels of PCDH-PC-related mRNA, by both RT-PCR and ISH analysis. Comparison of PCDH-PC mRNA and androgen receptor mRNA levels in hormone refractory CaP did not show correlation between the overexpression of these two molecules.
Conclusions : Our findings suggest that PCDH-PC may be involved in the generation of hormone-resistance of human prostate cancer.

O-87
PATHOLOGY OF HONEYCOMB LUNG –A REAPPRAISAL: SOME HETEROGENEITY AMONG USUAL INTERSTITIAL PNEUMONIA (UIP) OF DIFFERENT ETIOLOGIES

HONMA Koichi, ARAKAWA Hiroaki
Departments of Pathology and #Radiology, Dokkyo University School of Medicine Mibu, Tochigi 3210293, JAPAN

Introduction and Purpose of Study

Honeycomb lung (HL) constitutes a cardinal feature of usual interstitial pneumonia (UIP) regardless of its etiology. There is some morphologic spectrum involving HL. The heterogeneity includes type of honeycomb cysts, some of which still retain at least part of the mural structure of a conducting airway. To find out any relation between morphology of HL and UIP of different etiology, the composition of honeycomb cysts is compared between idiopathic pulmonary fibrosis (IPF)-UIP and exposure-associated (EA)-UIP.
Materials and Methods
Cases showing high-resolution CT features consistent with UIP and confirmed at autopsy as having UIP were used for the study. They consisted of 8 cases with IPF (69.9+/-9.8 yrs) and 17 cases associated with occupational exposure to dust (74.5+/-5.4 yrs). The total number of honeycomb cysts (Nc) which appeared on the representative histologic slides was counted, if they measured greater than 3 mm in diameter and among them, the proportion of airway-type cysts (Nb) was identified. Remodelling index (RI) which presumably indicates stage of evolution in UIP, was defined as: RI = (Nc – Nb)/Nc x 100 (%). The number of fibroblast foci (FF) also was counted in each case on the same microscopic slides used for counting cysts.
Results
A total of 321 cysts were evaluated in IPF-UIP lungs, in which 110 Nb-type cysts were found (RI = 65.8%). EA-UIP had 620 Nb cysts among 1180 cysts (RI = 47.5%). An average of 2.3 FF was found in IPF-UIP per microscopic slide (ca. 4 cm2) in contrast to 0.93 FF per slide in EA cases. These differences were not statistically significant.
Discussions and Conclusions
EA-UIP has more airway-type cysts involving HL than does IPF-UIP. IPF-UIP may represent a more advanced stage of disease and its remodeling process appears to remain ongoing as suggested by a higher FF count.

O-88
MORPHOGENESIS AND MECHANISMS OF PROGRESSION OF DIFFERENT VARIANTS OF IDIOPATHIC DIFFUSE INTERSTITIAL PULMONARY DISEASES

Kogan E.A.

Idiopathic diffuse interstitial pulmonary diseases (IPD) are classified as idiopathic pulmonary fibrosis (IPF) and variants of idiopathic interstitial pneumonias.Particular morphological features, clinical symptoms, prognosis and answer to steroid therapy characterize different variant of IPD. Morphogenesis and mechanisms of progression of different variants of IPD are contradictory in many aspects.The aim of our study was to analyze morphogenesis and mechanisms of progression of different variants IPD in accordance with immunohistochemical, clinical, functional, high resolution CT dates at early and late stages of the disease.102 IPF patients were studied. Open lung biopsy by formal thoracotomy (77 cases), video-assisted thoracoscopy (6 cases) and transbronchial biopsy (19) were performed. Histological classification based on criteria for IPD (European Respiratory Society and American Thoracic society, 2004) was used. CD34 (Novocastra), bTGF (Biosourse International), FRF (DAKO), TNFa (DAKO), p53 (DAKO), Ki-67 (DAKO), PCNA (DAKO), bcl-2 (DAKO), c-myc (Novocastra), CD68 (DAKO), EMA (DAKO) were detected in paraffin sections.Results. Usual interstitial pneumonia (UIP) was found in all cases of IPF. It is characterized by active production of cytokines by interstitial macrophages at early stages that induced proliferation of myofibroblasts, endothelial and epithelial cells. Late stage of UIP results in honeycomb lung and adenomatous hyperplasia without/with cell atypia. Wide spectrum of epithelial changes was found, including new entities, such as atrophy of bronchial and

alveolar epithelium and neuroendocrine hyperplasia in oval structures with background sclerosis. Desquamative interstitial pneumonia differs from UIP by more active alveolar macrophages that induce second type pneumocyte proliferation with “septal” sclerosis and squamous metaplasia. Nonspecific interstitial pneumonia, respiratory bronchiolitis and cryptogenic organizing pneumonia contained cells with cytokine’s production in alveolar lumen and tissue infiltrates, that results in light and moderate rate of pneumosclerosis and epithelial proliferation.Conclusion. The dramatic progression of UIP comparing with other IPD is based on progressive interstitial fibrosis and prominent reconstruction of pulmonary tissue that are induced by cytokine deregulation.

O-89
CHILDHOOD PULMONARY INTERSTITIAL GLYCOGENOSIS ASSOCIATED WITH SELECTIVE POLYSACCHARIDE ANTIBODY DEFICIENCY

deMELLO Daphne, BECKER Brad, SOTELO Cirilo, NOYES Blake. Departments of Pathology and Pediatrics, Saint Louis University School of Medicine and Cardinal Glennon Children's Hospital, St. Louis, MO , U.S.A.

Pulmonary interstitial glycogenosis (PIG), is a new description for the entity of infantile cellular interstitial pneumonitis which causes lung dysfunction. Immaturity of lung interstitial cells is the presumed basis for the glycogenosis. We report two children with PIG who also have selective antibody deficiency with normal immunoglobulins (SAD), suggesting an associated immune disorder.
A girl born at term, had unexplained respiratory distress and hypoxia, and at 12 days of age, a lung biopsy showed PIG. PIG is characterized by the presence of plump interstitial cells with clear cytoplasm, causing widening of interalveolar septa. The cells contain cytoplasmic glycogen, demonstrable by the periodic acid-Schiff (PAS) reaction, and by electron microscopy as monoparticulate pools of cytoplasmic glycogen. At 16 months, because of recurrent respiratory symptoms, fever, and pneumonia, immunologic studies showed normal immunoglobulins, but poor antibody responses to conjugate pneumococcal and tetanus vaccines. Lymphocyte studies were normal except for poor proliferation to antigens, which improved with IL-2. She was weaned off oxygen and placed on intravenous immunoglobulin (IVIG, approximately 500mg/Kg/dose); at 40 months of age she still has occasional wheezing spells.
Patient 2 is a term boy whose lung biopsy was done at 5 weeks of age for respiratory distress. It showed PIG and subsequently he had recurrent respiratory symptoms, fever, and pneumonia that prompted immune studies at 42 months of age. He had normal immunoglobulins, but no antibody response to the polysaccharide pneumococcal vaccine, normal antibody responses to protein antigens and normal lymphocyte studies.
These cases suggest an association of pulmonary interstitial glycogenosis and selective antibody deficiency to polysaccharide antigens. There may be a therapeutic role in these patients for IVIG. The cases also illustrate the importance of considering PIG in infants with cellular interstitial pneumonitis and of the diagnostic role of histochemistry and electron microscopy in the pathologic evaluation of infantile interstitial pneumonia.

O-90
ROLE OF BRONCHOALVEOLAR LAVAGE IN CHILDREN WITH CHRONIC PULMONARY ASPIRATION

RIZZO Stefania, GIACOMETTI Cinzia, BARBATO Angelo, PANIZZOLO Cristina, SAETTA Marina, VALENTE Marialuisa, CALABRESE Fiorella
University of Padova Medical School, Padova, Italy

INTRODUCTION: Chronic pulmonary aspiration (CPA) is a common cause of persistent respiratory diseases, particularly in children with gastroesophageal reflux (GER). PURPOSE OF THE STUDY The aims of the study were to establish: a) the accuracy of Lipid-laden Macrophage Index (LLMI) as test for GER-related CPA; b) the role of GER in CPA. Clinico-pathological correlations between ¡°aspirators¡± and ¡°non-aspirators¡± patients (pts) were also performed. METHODS: We prospectively evaluated 37 pts (12 F, 25 M, mean age 4,8 yrs) with chronic respiratory symptoms. All pts underwent esophageal ph-metry and bronchoscopy with bronchoalveolar lavage (BAL) for LLMI analysis. Functional and clinical data, including asthma and atopy were recorded in all pts. GER-related CPA was diagnosed in presence of suggestive clinical history, pathological pH-metry and LLMI¡Ý75% (aspirators). Aspirators (8 pts) were compared with non-aspirators (8 pts) in terms of clinical parameters and molecular viral infections detected on BAL. RESULTS: LLMI sensitivity and specificity were 60% and 67% respectively; the positive and negative predictive value 40% and 82% respectively. GER frequency was detected in 22% of pts. Aspirators were older (mean age 6.4 vs 3.5), less atopic (25% vs 87%) and with lower frequency of laryngitis (12 vs 50%) than non-aspirators (p¡Ü0,05). CONCLUSIONS: LLMI may role out the presence of GER due to its high negative predictive value. GER plays an important role in the development of CPA. Atopy can not be considered a predisposing factor for GER-related CPA.

O-91
REDUCED BRONCHIAL EPITHELIAL SMAD7 PROTEIN EXPRESSION IN COPD

ZANDVOORT, Andre 1,2, POSTMA, Dirkje S 2, JONKER, Marnix R 1, NOORDHOEK, Jacobien A 2, VOS Johannes TWM 1 and TIMENS, Wim 1. 1
Dept. Pathology, and 2 Pulmonology, University Medical Center Groningen, Groningen, THE NETHERLANDS.

Introduction: Degradation and repair of the extracellular matrix (ECM) are essential processes in the pathogenesis of COPD. Previously, we have demonstrated an altered decorin expression in the peribronchial area of COPD patients reflecting an alteration in ECM modulation. Decorin transcription is known to be regulated by Smad7, an inhibitory component of the TGF-beta -Smad pathway. This pathway is the key intracellular signal route for ECM gene transcription.
Objective: To determine whether Smad proteins are differentially expressed in lung tissue of COPD patients compared to controls.
Method: Using immunohistochemistry, Smad protein expression was compared in lung tissue of GOLD stage II (n=11) and stage IV (n=8) COPD patients and controls (n=8). Expression was semi-quantitatively analysed.
Results:
In GOLD stage II as well as GOLD stage IV patients, we found a significantly lower epithelial expression of the inhibitory Smad, 7. In addition, we found a significantly lower epithelial expression of TGF-beta in stage II patients.
Discussion: The TGF -Smad pathway appears to be aberrantly regulated in COPD patients, most likely resulting in an atypical ECM modulation. Reduced expression of Smad7 in bronchial epithelial cells could play a role the reduced presence of decorin in the peribronchial area of COPD patients.
Funded by the Dutch Asthma Foundation.

O-92
MALIGNANCY ARISING IN KAOLIN PNEUMOCONIOSIS OF GEORGIA

Beverly Y. Wang, Cameron C. Avant, Elizabeth D. Loomis, Richard Hessler, Lawrence J. Freant.
Department of Pathology, Medical College of Georgia, Augusta, GA, USA

Background: Kaolinite (Al2O3*SiO2*2H2O) is widely used in rubber, paint, adhesives, fillers in plastics, paper, and as an absorbant. Kaolin clay in Georgia constitutes one of the major open mining operations in the United States. The product is relatively free of silica. Exposure to kaolin has been linked to the development of pneumoconiosis. Rare cases of lung cancers arising in kaolin-related pneumoconioses have been reported. We have examined 4 cases of carcinoma associated with kaolin exposure.
Designs: Four archival specimens from the file of the Medical College of Georgia including wedge excisions and lobectomies obtained between years 2002-2004. The specimens were routinely processed, formalin-fixed and paraffin embedded. Sections were stained with Hematoxylin and Eosin. Review of patient charts and clinical follow-up were performed (Table).
Results: All 4 cases had a histologic background of interstitial lung disease (Fig 1). 3 patients were smokers with emphysema (#1,2,3). One lived in the mining area and was exposed to airborne dust for many years. 2 cases developed adenocarcinoma (#1,4, Fig 2, 3), one had large cell carcinoma (#2, Fig 4), and one squamous cell carcinoma (#3, Fig 5). 3 patients are alive after surgery, 1 is lost to follow up.
Conclusions: 4 kaolin-exposed patients from Georgia USA had kaolin-related interstitial lung disease, and developed a superimposed lung carcinoma. Kaolinosis may be a risk factor for carcinomas of the lung with or without smoking.

O-93
EVALUATION OF MEDIASTINAL NODES AND MASSES BY ENDOSCOPIC ULTRASOUND (EUS)-GUIDED FINE-NEEDLE ASPIRATION BIOPSY (FNAB): A SERIES OF 156 CASES.

DRAK ALSIBAI Kinan (1), FABRE Monique (1), HOMSI Toufik (2), LAZURE Thierry (1), DE PINIEUX Isabelle (2), BALATON André (2), MOLINIE Vincent (2). Anatomie et Cytologie Pathologiques, AP-HP Hôpital de Bicêtre (1), Le Kremlin-Bicêtre; Hôpital saint-Joseph (2), Paris, France

Introduction: FNAB has become an important tool in the evaluation of pancreatic masses, mostly done using EUS allowing both the initial staging and the diagnosis of cancer. Currently, the role of EUS-FNA in identifying mediastinal lesions is under evaluation and early results have been quite promising in the diagnosis and staging of lung cancers.
Aim of the study: To determinate the EUS-FNAB diagnostic performance in mediastinal nodes and masses by retrospective study from two institutions.
Patients and methods: 156 consecutive patients (110 male), median 58 yrs (23-85) who underwent EUS-FNAB for suspicious mediastinal lesions, were studied from January 2003 to January 2005. Mediastinal nodes (n=129) and/or mediastinal masses (n=43) were sampled, using a linear array echoendoscope equipped with Wilson-Cook or Olympus 19 or 22-G needles. An average of 1.8 (1-3) needle passes were performed. The aspirated specimens were analyzed further by using conventional and liquid-based smears (Cytyc Corp.) (n=142) and/or microbiopsy using cytoblock® preparations (n=156).
Results: No serious complications were noted (abdominal pain). In 3/156 specimens (1.9%) no sufficient cell/tissue material could be aspirated. In the remaining 153 specimens, a benign lesion was found in 63/153 cases (41.1%): reactive lymphadenopathy (n=34), tuberculosis (n=14), sarcoidosis (n=11), silicosis (n=2), bronchogenic cyst (n=2). A malignant lesion was found in 90/153 (58.8%). The primary site of metastases was the lung in 65 cases (72.2%) including SCLC (n=27), adenocarcinoma (n=22), SCC (n= 16) and others various organs in 17 cases: kidney (n=6), cardia (n=3), prostate (n=2), breast (n=2) and one case in thyroid, larynx, bladder and testis. Five lymphoma and three sarcoma were also diagnosed. Immunostaining was performed in 66 cases with a mean of 10 antibodies (1-16).The global accuracy of EUS-FNA was 96.8%
Conclusion: This study demonstrates that EUS-FNAB 1) is a safe and minimally invasive diagnostic technique, 2) plays an important role in the diagnostic of benign mediastinal lesions such as granulomatous adenitis when previous pleural, lung and bronchial biopsies are negative, 3) allows an accurate cyto/histologic diagnosis of mediastinal nodal status in patients with lung cancers avoiding invasive mediastinoscopy or thoracotomy. EUS-FNAB is a key step to identify a subgroup of downstaged patients who are not candidates for surgery but are firstly for radio/chemotherapy.

O-94
GRANULOMETRIC ASSESSMENT OF NUCLEAR TEXTURE IN BRONCHIAL BRUSH CYTOLOGY

Adam RL(1,2), Silva PVVT(1), De Carvalho RB(1), Leite NJ(2), Metze K(1)
(1) Department of Pathology, Faculty of Medicine, UNICAMP, Campinas, Brazil
(2) Institut of Computing, UNICAMP, Campinas, Brazil

The assessment of the chromatin texture plays an important role for the diagnosis of cellular differentiation. Wheras classic morphometry does not describe precisely nuclear heterochromatin, granulometry characterizes quantitatively the coarseness of an image in a hierarchical way. It obtains an ordered and complete description of an image from morphologic residues, which are defined as the difference between two consecutive granulometric levels. The aim of this study was to study the chromatin texture in rotine bronchial brush cytology by granulometry in order to characterize cell differentiation. We compared nuclear images of HE-stained bronchial brush cytology of 54 patients (17 without neoplasia, 22 squamous cell carcinomas, 6 small cell carcinomas and 9 adenocarcinomas). In every case final diagnosis was confirmed by subsequent histologic examination. Texture analysis was based on grayscale transformed images. From each granulometric level of gray scale images the residues were extracted by progressive filtering (openings and geodesic reconstruction)with the following filter parameters : 1.height of the basins (in gray levels), 2.area, and 3.volume. Number of seeds and residues were extracted. Comparison was done by analysis of variance. Least density of residues of lower level basins was found in non-neoplastic cells, followed by small cell carcinoma, squamous cell carcinoma, and highest density was seen in adenocarcinomas. At medium and higher basin levels lowest density of residues was calculated for adenocarcinomas, followed by squamous cell carcinoma and small carcinomas, whereas highest values appeared in non-neoplastic epithelium. The area of basins was largest in adenocarcinomas, followed by squamous cell carcinoma, small cell carcinoma, and finally non-neoplastic epithelial cells. The density of seeds was minimum in non-neoplastic epithelium, followed by small cell carcinomas, epidermoid carcinomas and highest in adenocarcinomas. In other words, the three neoplasias and the non-neoplastic cells reveal different ramification pattern of basins, which characterizes the chromatin organization. Neoplastic cells reveal larger heterochromatin clumps, with the maximum values in adenocarcinomas, follwed by squamous cell carcinomas and

small carcinomas. Thus we conclude , that quantification of granulometric residues in digitalized images of bronchial brush cytology may be useful for differential diagnosis.
Supported by FAPESP, FAEP, CNPq.

O-95
DO VASCULAR CHANGES IN DONOR KIDNEYS HAVE AN IMPACT ON LATE GRAFT-DYSFUNCTION?

KEMÉNY Éva, NAGY-FRICSKA Adrienn, KISS Andrea, SZEDERKÉNYI Edit, ELLER József, MORVAY Zita, IVÁNYI Béla, SZENOHRADSZKY Pál
Departments of Pathology, Surgery, Radiology and Informatics, University of Szeged, Hungary

Introduction: Morphological studies of "zero-hour" kidney donor biopsies have produced controversial findings over what type of vascular changes -if any- are associated with late graft-dysfunction. Hence we carried an original clinicopathological study involving morphometry to assess this question.
Materials & Methods: 94 consecutive pretransplant "zero-hour" biopsies from cadaver kidney grafts were studied. We examined the frequency and severity of arteriolar hyalinisation (AH), intimal fibroelastosis (IFE), tubular atrophy (TA), interstitial fibrosis (ISF) and glomerulosclerosis (GS) semi-quantitatively. The wall thickness/lumen (W/L) ratio of each vessel present in the biopsy was determined by morphometry. Groups were then differentiated according to their blood vessel size: G1: d<79µm, G2: d=80-149µm, G3: d=150-300µm. Statistical analyses were done to examine the clinicopathological correlations. Follow up examinations were made 48 months after each transplantation.
Results: There was a significant correlation between the mean elevated serum creatinine (SCR) level at 48 months after transplantation and (a) the age of the donors ($p<0.05$), along with (b) the frequency of intracranial hemorrhage as the cause of donor-death ($p<0.05$). In the "zero-hour" biopsies non-specific morphological changes were frequently observed: AH: 84.0%, IFE: 76.6% (moderate: 26.6%), ISF: 25.5%, TA: 71.3% and the mean proportion of sclerotic glomeruli was 5.01%. Among the vascular changes studied only the moderate IFE ($p<0.01$) revealed a significant correlation with SCR at 48 months. In IFE there was also a significant correlation (a) with the non-specific morphological lesions studied ($p<0.001$), and (b) with the frequency of intracranial hemorrhage as the cause of donor death ($p<0.01$). By morphometry a significant association was found between the mean W/L ratios of arteries in the G3 group and the degree of IFE ($p<0.01$).
Conclusion: Our results suggest that donor kidneys with a moderate degree of intimal fibroelastosis -occuring significantly more frequently in kidneys from older donors, and whose cause of death is intracranial haemorrhage- do indeed have a higher risk of late graft-dysfunction. This should be taken into consideration in optimal donor selection.

O-96
POLYOMAVIRUS-ASSOCIATED NEPHROPATHY (PVAN): ROLE OF JC VIRUS

HIRSCH Hans 1, DRACHENBERG Cinthia 2, MUNIVENKATAPPA Raghava 2, MCKINNEY Jamie 3, WALI Ravinder 3, NOGUEIRA Joseph 3, CANGRO Charles 3, RAMOS Emilio 3, PAPADIMITRIOU John C 2
1 Transplantation Virology, and Infectious Diseases, University Hospital Basel, Basel, Switzerland, 2 Departments of Pathology and 3 Medicine, University of Maryland School of Medicine, Baltimore, MD, USA

Background:
PVAN in renal transplants is mainly caused by BK virus, but rare cases have implicated JC virus.
Design and Results:
Over a period of 19 months, 1280 ambulatory renal transplant patients (pt) were screened for decoy cells in urine cytology (n=2845). We identified 139 (10%) with 1 to 11 urine samples positive for decoy cells. In 122 patients with decoy cell-positive urines and at least 12 months of follow up, BK and JC viral load was quantified in urines and in plasma. Patients were classified according to the type of virus present in urine as: BK only (42%), BK+JC (28.6%) and JC only (29.4%). The type of viruria was correlated with the biopsy findings and creatinine (Cr). Patients biopsied were BK:39, BK+JC:27, only JC 26. Serum Cr at biopsy was 2.58 (1.2-7.5), 1.74 (1-3.3) and 1.58 (.9-2.6) respectively. Last Serum Cr was 3.49 (1-10.1), 1.81 (1-4.3) and 1.66 (.9-3.8) respectively. PV nephritis was found in 33/39, 13/27 and 5/26 patients respectively.
Graft loss occurred in 6 patients with BK viruria, 1 patient with BK and JC viruria and in no patient with JC only viruria. A larger proportion of patients with BK viruria had clinical dysfunction, PVAN and graft loss. JC viruria persisted in some patients independently of BK viruria, BK viremia, PVAN or response to intervention including clinical improvement and disappearance of BK viremia.
Conclusions:
Urine cytology identifies high-level replication of both, BK and JC virus. The pathogenic implications and clinical consequences appear to be significantly different in patients shedding one virus or the other. JCV shedding may be associated with histological PVAN in 20%, but graft dysfunction is absent in most patients.

O-97
GLOMERULAR AND TUBULAR CHIMERISM IN RENAL ALLOGRAFTS

FERLICOT Sophie (1), PLES Raluca (1), CREPUT Caroline (2), GUETTIER Catherine (1), DURRBACH Antoine (2)
Services (1) d'Anatomie Pathologique, (2) de Néphrologie, CHU de Bicêtre, le Kremlin-Bicêtre.

Background. After transplantation, many pathologic conditions can damage the kidney and lead to acute renal failure. Regeneration of necrotic cells was initially thought to be based on self-renewal tissues. Recent studies have underlined that cells of donor origin can be found in recipient tissues after transplantation of any solid organ. We investigated whether cells of recipient origin were present in kidney allograft secondary to episodes of kidney injuries.
Methods. To test the hypothesis in humans that extrarenal cells can participate in tissue remodeling, we examined the origin of glomerular and tubular cells in 10 male patients who received a kidney transplant from a female donor. Among these patients, three had no histopathological signs of rejection, one had acute rejection and six had signs of chronic allograft nephropathy. Four patients had developed acute tubular necrosis following transplantation. Fluorescent in situ hybridization was used to detect Y chromosome on frozen biopsies.
Results. All patients showed an intragraft chimerism in interstitial, tubular and glomerular cells. A mean of 8% of tubules and 23% of glomeruli contained Y chromosome cells. No correlation to morphology was found.
Conclusion. Regeneration after injury is not exclusively based on self-renewal of allograft-tissues. This is consistent with the concept that circulating pluripotent progenitor cells exist, capable of differentiating into tubular and glomerular cells. The presence of chimeric cells in a higher level in glomerular cells than in tubules remains unclear.

O-98

LIVER INDUCES IMMUNE TOLERANCE IN PEDIATRIC INTESTINAL TRANSPLANTATION

Damotte Diane, Jugie Myriam , Canioni Danielle , Le Bihan Christine, Sarnacki Sabine, Révillon Yann, Jan Dominique, Lacaille Florence , Cerf-Bensussan Nadine,Goulet Olivier, Brousse Nicole.
Intestinal Transplantation Unit, Necker-Enfants Malades and HEGP Hospital, Paris, INSERM EMI 0212, U255, U580, Faculté Necker, Université René Descartes, Paris V, France

Background and Aims: Small bowel transplantation remains a challenge due to the intestine septic and immune conditions, therefore graft and patient outcome are difficult to predict. In order to assess the putative tolerogenic role of the liver in combined transplantation, and to find new predictive markers of the transplantation outcome, we compared two groups of pediatric intestinal transplantation, seven small bowel graft (SbTx) and eight combined liver-small bowel graft (LSbTx) receiving the same immunosuppressive therapy.
Methods: Fifteen single-center children who underwent small bowel transplantation between 1994 and 1998, were retrospectively reviewed and compared to fifteen controls (normal and inflammatory small bowel mucosa). Transplant and patient overall survival, acute rejection episodes of each group were analysed and compared to epithelial apoptotic body count and to the immunostaining of NF-kB (p65) transcription factor, caspase-3 (CPP-32) and Bax pro-apoptotic factors from day 0 to 20 after transplantation.
Results: LSbTx had a higher graft and patient survival at five years (75% and 75%) as compared to the SbTx (43% and 57% respectively). Small bowel histological analysis recorded a constant higher apoptotic body count in LSbTx ($p=0.05$ at day 5 and $p<0.01$ thereafter). Endothelial, epithelial and lymphoid cells from both groups displayed differential NF-kB and Bax immunostaining at day 0 ($p<0.05$).
Conclusions: Concomitant liver transplantation improved intestinal graft and patient survivals and was associated with different apoptotic body count and NF-kB, Bax staining within the small bowel. Although not clearly demonstrative, these results in pediatric transplantation strenghten the hypothesis of immune tolerance induced by liver.

O-99

PANCREATIC ISLETS PROGENITOR/STEM CELLS IN MICE. THEIR ROLE IN PANCREATIC ISLETS TRANSPLANTATION

Koryna Socha* 1, Marcin Socha 2, Igor Jakoniuk 1, Piotr Fiedor 2. 1 Military Medical Institute, Warsaw; 2 Warsaw School of Medicine, Warsaw. Poland

According to the data which indicates the presence of pancreatic islet progenitor cells in pancreatic ducts, in case of transplantation of nonpure islets suspension, these particular duct cells could also differentiate into hormone producing cells and participate in the process of remodelling and growth of islet grafts.
In this study the syngeneic transplantation of C57BL/6 mice pancreatic islets into the kidney subcapsular space of diabetic recipient (streptozotocine 100mg/kg bw i.p.) was performed. To distinguish cells' origin the graft we used transgenic B.6. mice expressing EGFP under the b actin promoter or sex mismatched model. After the graftectomy (day 14, 30, 100) an immunohistochemical analysis and FISH were performed.
We found that 0.6% of b cells were in the cell cycle (Ki67 expression), the number of Ki 67 positive endocrine cells within pancreas was not significantly lower. In the syngeneic grafts the presence of 1 per 30HPF proliferating bcell of recipient phenotype was showed. We confirmed the coexpression of early pancreatic islets markers and CD 45 in cells of recipient phenotype. Recipient origin cells were found within graft vessels and nerves. An increase of ßcells cross section area, revealed between the 14 day and 100 day grafts, indicated the ßcells growth and this process was significantly increased in case of nonpure islets transplantation.
The results of this study underline the complexity of pancreatic graft cells indicating the presence of cells which can differentiate/transdifferentiate into hormone producing cells and other graft elements. Data points that pancreatic hormone producing cells can enter the cell cycle but also underlines the possible role of the exocrine tissue remnatns in this process. Maiority of insulin producing cells were of the donor origin but the presence of single recipient derived b cells indicates that certain adult cells population can differentiate into islet cells. The important finding is the possible beneficial role of duct cells present within the graft which, if contain progenitor cells, can influence pancreatic islets engraftment. This study remains an indication that adult stem/progenitor cells can be considered as an alternative cell source supplying cell transplantation and also the results underline the regenerative capacity of pancretic islets.

O-100

MINOR SALIVARY GLAND DAMAGE AFTER BONE MARROW TRANSPLANTATION IN PATIENTS WITH AND WITHOUT C-GVHD

Cintra ML 1, Alborghetti MR 1, Corrêa MEP 2, Adam RL 1, Coracin FL 2, de Souza CA 2, Metze K 1.
Department of Pathology, Faculty of Medicine 1, Bone Marrow Transplantation Center Hematology /Hemotherapy Center 2 - State University of Campinas, Brazil.

Histological alterations of minor salivary glands (MSG) in patients after bone marrow transplantation (BMT) may be due both to chronic graft-versus-host disease (cGVHD) as well as to pre-transplant treatment. The aim of our study was to evaluate the influence of these factors on the histological changes in MSG. Sequential biopsies performed during cGVHD therapy were evaluated in 14 patients after BMT. As control group, biopsies of 9 BMT patients without cGVHD were used. Histological grading of cGVHD was done by two blinded observers according to Horn's classification. An objective assessment of the volume of secretory units was obtained with the help of digitalized images of standardized PAS-stained sections using a software for texture analysis. The density of inflammatory infiltrate per area was obtained in leukocyte common antigen stained sections. In each patient a detailed clinical history was available. The histological variables as well as Horn's grades in the MSG were closely associated with the diagnosis of cGVHD. Both, the use of antihypertensive drugs and chronic basic disease reduced significantly the volume of PAS+ (acinar) material in a linear multiple regression. The degree of the inflammatory infiltration was related to later biopsy after transplantation and longer duration of pre-transplant disease. In a multivariate regression only cGVHD was predicitive of fibrosis in MSG. Even after treatment glands of cGVHD patients showed still significantly less acinar PAS+ volume when compared to the glands of BMT patients without cGVHD at day 100+. We could not find significant differences of PAS+ acinar volume, leukocyte index, fibrosis and Horn's grades when comparing the glands of all patients before and after treatment of cGVHD. Changes in the Horn score between the two biopsies were only dependent of the patient´s age. Only patients with less than 40 years showed a decrease in the severity of cGVHD. We conclude that MSG functional and structural damage is the result of both: prexisting systemic disease treatment and cGVHD. Even after cGVHD treatment there is no significant recovery of the MSG secretory unit, which explains the persistence of clinical symptoms, such as xerostomia.
supported by CNPq, FAPESP, FAEP.

O-101
EXPRESSION PROFILING OF ENDOMETRIAL STROMAL CELLS TREATED WITH ESTRADIOL AND PHYTOESTROGENS

O'TOOLE Sharon, LAIOS Alex, SHEPPARD Brian, SMYTH Paul, O'REGAN Esther, SHEILS Orla, O'LEARY John.
Departments of Obstetrics and Gynaecology and Pathology, Trinity College Dublin.

Introduction:Phytoestrogens are chemicals that originate from plants and have estrogenic activity. Considerable interest has been shown in these compounds as an alternative for hormone therapy.
Aim: Little is known about the molecular pathways initiated or mediated by these compounds so the aim of this study was to examine the transcriptome profile of normal endometrial stromal cells treated with estradiol and the phytoestrogens tectorigenin, irigenin and apigenin.
Methods:A normal endometrial stromal cell line was cultured and treated with 0.1µM of estradiol and 0.1µM of the phytoestrogen extracts. RNA was extracted from the treated and untreated control cells and processed into Digoxigenin labelled cRNA by reverse transcription-in vitro transcription (RT-IVT). Gene expression analysis was performed using the chemiluminesence based Applied Biosystems array 1700 system which has 31,077 probes and targets a complete annotated and fully curated set of 27,868 human genes from the public and Celera databases. Technical replicates were performed for each sample.Data was normalised using 5% trimmed mean. Genes were filtered based on a signal/noise ratio of greater than 3 in more that 75% of the arrays. Students t-test and bon ferroni analysis were carried out and additional multitest analysis using the R package.
Results: Good reproducibility was seen in technical replicates. Various signaling pathways and transcription factors were initiated by estradiol and the phytoestrogens. Expression was compared to untreated controls and also each extract was compared to estradiol. Of interest was the upregulation of hypoxia inducible factor-1 (HIF-1) by estradiol and tectorigenin. Among the 70 target genes of HIF-1 known so far several are involved in angiogenesis, cell proliferation and cell viability and some of these target genes such as cyclin G2 and PIK3CA were upregulated in this study by estradiol and tectorigenin.
Conclusion: Gene targets are currently been validated using Taqman PCR. The HIF-1 pathway will be further investigated as a possible mechanism for endometrial hyperplasia. The molecular pathways initiated by phytoestrogens need to be fully elucidated before these extracts can be used as an alternative for hormone therapy.

O-102
FOCAL ADHESION KINASE EXPRESSION IN ENDOMETRIAL CANCER: CORRELATION WITH CLINICOPATHOLOGICAL VARIABLES

THEOCHARIS Stamatios1, VOULGARIS Zannis2, PAPASPIROU Irini1, SOUMAKIS Konstantinos1, RODOLAKIS Alexandros1, VLACHOS Georgios1, DIAKOMANOLIS Emmanuel1, KYROUDI Aspasia3
Departments of Forensic Medicine-Toxicology1, 1st Obstetrics and Gynecology2 and Histology-Embryology3, Medical School, University of Athens, Athens, Greece

Background-Aims: Focal adhesion kinase (FAK) is an enzyme of the tyrosine kinase group linked to signalling pathways between cells and their extracellular matrix. In tumor cells in vitro, FAK expression was correlated with their ability for invasion and metastasis. The aim of this study was to assess FAK protein expression in tumor samples from 40 patients with endometrial adenocarcinoma and to correlate it with clinicopathological variables.
Patients and Methods: FAK protein expression was examined immunohistochemically on paraffin embedded tissue sections of 40 endometrial adenocarcinoma cases. FAK positivity, overexpression (positivity in more than 75% of tumoral cells), and intensity of staining (mild, moderate, intense) were correlated with clinicopathological variables as patients' age, TNM status, tumor histological type, grade, and proliferative capacity (Ki-67 labeling index).
Results: Thirty-five out of 40 endometrial adenocarcinoma cases (40%) were FAK positive, and 4 out of 40 (10%) presented FAK protein overexpression. In endometrial adenocarcinoma cases examined, FAK positivity was correlated with TNM stage (p=0,031), but not with the other clinicopathological variables. FAK protein overexpression was correlated with tumor proliferative capacity, as tumors that present FAK protein overexpression also present increased Ki-67 labeling index (p=0.045). FAK protein overexpression was not correlated with the other clinicopathological variables. Additionally, FAK intensity of staining did not correlate with any of the examined clinicopathological variables.
Conclusions: In endometrial adenocarcinoma, FAK protein expression was correlated with important clinicopathological variables for patients management, being correlated with TNM stage and tumor cells' proliferative capacity. Further molecular and clinical studies are required in order to delineate the significance of FAK protein expression in endometrial neoplasia.

O-103
ANGIOGENESIS IN UTERINE MALIGNANT MULLERIAN TUMORS OF THE UTERUS.

NÄYHÄ Veera, STENBÄCK Frej. DEPARTMENT OF PATHOLOGY, UNIVERSITY OF OULU, OULU, FINLAND

Malignant mixed mullerian tumors are a heterogeneous group of aggressive malignant neoplasms that contain both carcinomatous and sarcomatous elements. They have a dismal prognosis, current treatment strategies have therapeutic limitations and prognostic indicators are lacking. Angiogenesis is associated with prognosis in epithelial cancers of many organs; studies on angiogenesis of carcinosarcomas are few and inconclusive.
The present study comprises 25 patients with uterine conditions diagnosed as carcinosarcomas of the ovary or uterus. Clinical data, history and follow up were obtained from each patient. To assess vessel involvement, the number, size, shape, structure and locations of vessels in the stroma were determined using quantitative densitometry and morphometry of histological specimens stained with an antibody to vascular endothelium, CD34. All neoplasms diagnosed as carcinosarcomas were classified based on vessel arrangement in immunohistochemistry and automated image analysis.
Angiogenesis was distinct in all neoplasms, related to the number of different sized vessels, resulting in a significant increase in total vessel area and associated with decreased survival. Those with the shortest survival had the largest, most irregular vessels and the highest antibody staining intensity. In solid tumour areas vessel number increased compared to non-neoplastic tissue. Vascular arrangements surrounded these cellular areas in a garland type pattern, vessel arrangement in bursts was uncommon, directional angiogenesis was rare. Fibrillary type neoplasms commonly contained few, regular and diffusely arranged vessels. Vessel dilatation was prominent in all specimens, vessel sprouting, and extensions of vessels, occurred as increased vessel shape factor/vessel area.
This study showed angiogenesis to be a fundamental part of the biological behaviour of neoplasms of this type. A distinct separation of different components is needed to establish

angiogenesis as an independent predictor of clinical behaviour.

O-104
HISTONE DEACETYLASE 2 EXPRESSION IS HIGHLY INCREASED IN ENDOMETRIAL STROMAL SARCOMAS: HDACS INHIBITORS AS CANDIDATES FOR TREATMENT OF ENDOMETRIAL STROMAL TUMORS

HRZENJAK Andelko, MOINFAR Farid, KREMSER Marie-Luise, STROHMEIER Bettina, ZATLOUKAL Kurt, DENK Helmut
Institute of Patohology, Medical University Graz, Auenbruggerplatz 25, A-8036 Graz, Austria

Covalent modifications of histones, in particular de/acetylation of lysine residues, play an important role in the regulation of gene transcription. These processes, which regulate the accessibility of transcriptional regulatory proteins to chromatin templates, are controlled by histone acetyltransferases (HATs) and histone deacetylases (HDACs). A controlled equilibrium between HATs and HDACs is essential for normal cell growth. Nowadays it is obvious that de/acetylation of histones plays an important role in different types of tumors. However, there have been no investigations about these processes in mesenchymal tumors. Endometrial stromal sarcomas are rare uterine malignancies and molecular mechanisms involved in their pathogenesis are poorly understood. Beside surgical excision, quite often followed by recurrences, other therapeutic methods, like chemotherapy, seem to be somewhat neglected.
The present study shows differences in the HDAC2 expression in endometrial stromal tumors and cognate ESS-1 cell line in comparison to healthy endometria. We also examined wheter sodium-valproate, an HDAC inhibitor that preferentially inhibits class I enzymes, is able to mediate cell differentiation, cell cycle arrest and expression of other genes related to malignant phenotype of endometrial stromal tumors. Here we show for the first time that HDAC2 expression is highly increased in endometrial stromal tumors in comparison to healthy endometrial stroma. Furthermore, HDAC2 expression appears to positively correlate with the tumor stage, being further increased in high-grade undifferentiated endometrial sarcomas. In vitro experiments with the endometrial stromal sarcoma cell line (ESS-1) showed that specific HDAC2 inhibitor, Na-valproate, led not only to expected HDAC2 decrement but also to cell differentiation. HDAC2 inhibition in ESS-1 cell caused also significant changes in the cell cycle by inhibiting the G1/S transition. Using QRT-PCR we showed that mRNA amount of secreted frizzled-related protein 4, an important reppressor of the wnt-signalling pathway, was 9-fold increased after HDAC2 inhibition. Regarding immunohistochemical data the HDAC2 expression in endometrial stromal sarcoma seems to correlate with the expression of ß-catenin, another important member of the wnt-signalling pathway.
Taken together this study suggests that HDACs in general and HDAC2 in special might be considered as potential drug-targets in the therapy of endometrial stromal tumors.

O-105
PDGFR ALPHA AND BETA, BUT NOT C-KIT ARE EXPRESSED IN ENDOMETRIAL STROMAL SARCOMAS - A THERAPEUTIC OPTION FOR TYROSINE KINASE INHIBITORS

Bernadette LIEGL, Olaf REICH* and Sigrid REGAUER
Institute of Pathology and * Department of Gynecology and Obstetrics, Medical University of Graz, Austria

Aims: Endometrial stromal sarcomas (ESS) are among the rarest primary uterine malignant tumors. The etiology and the genetic mechanisms in the oncogenesis of ESS are still unknown. ESS are hormone sensitive tumors which respond to anti-hormone treatments. Treatment modalities based on oncogene expression, however, are not available for ESS. Stromal tumors in other organs such the gastro-intestinal tract (GIST) expressing the proto-oncogene c-KIT have somatic mutations of the transmembrane tyrosine kinase receptor, which makes them suitable for treatment with tyrosine kinase inhibitors, such as Gleevec. Gleevec has convincing treatment success in GIST through an inhibitory effect on multiple class-3-receptor tyrosine kinase members such as platelet-derived growth factor receptor alpha and beta (PDGFRa, PDGFRß) and c-KIT. C-KIT expression and genetic mutations in mesenchymal unterine tumors are rare and it has been suggested that patients with ESS are unlikely to benefit from treatment with the presently available tyrosine kinase inhibitors. Recent studies on a small group of GIST lacking KIT mutations, however, suggest that patients with c-kit negative GIST can also benefit from Gleevec therapy, based on the identification of PDGFRa mutations as an alternative oncogenic mechanism in GIST. The aim of this study was to investigate the immunohistochemical expression of c-KIT, PDGFRa and PDGFRß in ESS.
Methods: Formalin-fixed,paraffin-embedded tissues of 14 archival ESS were analysed using antibodies against PDGFR-a, PDGFR-ß (Santa Cruz Biotech, CA) and c-KIT (Dako Cytomation Denmark) according to standard procedures. Cases were scored positive when >10% tumor cells showed a positive reaction.
Results: All ESS were negative for c-KIT, only 2/14 cases showed individual single cell staining (<10% of tumor cells). 7/14 ESS showed a strong staining in 80% of tumor cells for PDGFRß, while 2/14 cases were focally and weakly positive in <50% of tumor cells. 5/14 ESS showed no staining for PDGFRß. For PDGFRa, 3/14 ESS showed a strong positivity in >50% of tumor cells. 4/14 cases were focally and weakly positive and 7/14 cases were negative for PDGFRa.
Conclusion: c-KIT negative ESS express PDGFRß in >50% and PDGFRa in 25%. Our observations suggest that some patients with ESS may benefit from treatment with tyrosine kinase inhibitors. Further studies are necessary to prove that immunohistochemical PDGFRa/ß staining correlates with genetic mutations of PDGFRa/ß.

O-106
INCREASED EXPRESSION OF METALLOPROTEINASE-2 IN ENDOMETRIAL CARCINOMA

RASPOLLINI Maria Rosaria1, CASTIGLIONE Francesca1, ROSSI DEGL'INNOCENTI Duccio1, GARBINI Francesca1, SUSINI Tommaso2, and TADDEI Gian Luigi1
1Department of Human Pathology and Oncology, 2Department of Gynecology, Perinatology and Reproductive Medicine, University of Florence, School of Medicine – Florence, Italy

The growth of a tumoral mass requires remodeling of the extracellular matrix. The matrix metalloproteinase (MMP) are a family of endopeptidases that can degrade almost all the extracellular matrix components. Recent immunohistochemical studies have suggested that expression of MMP-2 and MMP-9 in endometrial carcinoma might play a critical role in neoplastic tissue invasion or metastasis, while cyclooxigenase-2 (COX-2) expression was related to immunomodulation and neoangiogenesis. Aim of this study was to investigate the role of MMP in endometrial carcinoma and the possible correlation with COX-2 expression.
mRNA expression of MMP-2 ,MMP-9 and COX-2 genes in 30 paraffin-embedded endometrial carcinomas and in 20 non neoplastic endometrial samples obtained from matched controls were investigated. Amplification of mRNA was

detected by reverse transcription-polymerase chain reaction (RT-PCR) assay and was measured quantitatively.
Amplification of MMP-2, MMP-9 and COX-2 was detected respectively in 62.5%, 25% and 25% of the endometrial carcinoma cases, while it was not detected in any non neoplastic endometrial samples. We observed a relation between the quantitative expression of MMP-2 in 1B and 1C FIGO stages compared to 2 and 3 stages. There was no significant relationship between the expression of MMP-9 and COX-2 and FIGO stages nor grade of differentiation nor clinical outcome possibly because of the low amplification. Interestingly, we observed a relationship between the expression of MMP-9 and of COX-2 possibly indicating a common role on tumor related angiogenesis. To our knowledge this is the first report describing MMPs and COX-2 quantitative expressions in endometrial cancers by molecular biology techniques.

O-107
THE ROLE OF LEIOMYOCITE'S PROLIFERATION, HYPERTROPHY AND APOPTOSIS IN UTERUS LEIOMYOMAS.

PhD VE Ignatova
Prof. EA Kogan

Introduction. The mechanisms of growth of benign and malignant tumors are different. Uterus leiomyomas are benign tumor but sometimes they may grow very rapidly . So the purpose was to investigate the role of leiomyocite's proliferation, hypertrophy and apoptosis in uterus leiomyoma's histological variants.
Methods. The research was conducted basing on operating materials, which were taken from 75 patients of age from 18 up to 76 years old with diagnosis of Lm of uterus. Histological researches were conducted with paraffin slides with hematoxylin and eosin staining. Immunohistochemical staining was carried out on serial paraffin slides according to the standard methods with antigen retrieval in microoven and with the usage of primary antibody to EGF (Santa Cruz Biotechnology, 1:100), EGF-R (Santa Cruz Biotechnology, 1:100), PDGF (Calbiochem, 1:100), IGF-1 (Pepro Tech EC LTD, 1:100), Ki-67 (DAKO, 1:50), PCNA (DAKO, 1:100), Fas receptor (DIANOVA, 1:50). LSAB KIT (DAKO) was used for secondary antibodies and visualizing system.
Results. The leiomyoma (Lm) and her variants cellular and mitotically activite Lm distinguish themselves in morphological structure and the mechanisms of growth. The main pathological processes in the growth of Lm are: proliferation, hypertrophy and apoptosis of leiomyocites, stroma formation and secondary changes in the growth. In the different types of Lm, the correlation of these processes may vary. The maximum level of proliferation markers is observed in mitotically activite Lm and defines the development of the tumor. The highest level of apoptosis of leiomyocites is detected in Lm. The lowest level of apoptosis – in the cellular and mitotically activite Lm, what may contribute to the prolongation of the life cycle of leiomyocites in combination with relatively high proliferation of cells accumulation and the development of the tumor growth. The correlation of proliferation processes and apoptosis in the Lm and her variants cellular and mitotically activite Lm varies, and according to this fact, we draw the conclusion about the different mechanisms of their growth. The increase of size of Lm is the result not only of proliferation of tumor cells, but also of hypertrophy under the influence of EGF, EGF-R, IGF-1, PDGF and also the proliferation of stroma elements and its secondary modifications.

O-108
OVARIAN CARCINOMA CELLS AND IL-1BETA ACTIVATED HUMAN PERITONEAL MESOTHELIAL CELLS ARE POSSIBLE SOURCES OF VASCULAR ENDOTHELIAL GROWTH FACTOR IN INFLAMMATORY AND MALIGNANT PERITONEAL EFFUSIONS

STADLMANN Sylvia,1 AMBERGER Albert,2 POLLHEIMER Juergen,3 GASTL Guenther,4 OFFNER Felix Albert ,5 MARGREITER Raimund,2,6 ZEIMET Alain Gustave 7

Objective: Inflammatory or malignant peritoneal diseases are associated with high levels of ascitic vascular endothelial growth factor (VEGF). We compared the VEGF secretion by human peritoneal mesothelial cells (HPMC) and ovarian carcinoma (OVCA) cells and its regulation by pro-inflammatory cytokines.
Material and methods: VEGF secretion in cultured HPMC, established human OVCA cell lines, and inflammatory or OVCA-associated ascites was determined by enzyme linked immunosorbent assay.
Results: HPMC constitutively produced VEGF at median levels of 43 ± 7 pg/105 cells. Treatment of HPMC with 1 ng/ml IL-1? (567 ± 213 pg/105 cells;) or TNF-? (89 ± 1 pg/105 cells) resulted in a 13-fold ($p < 0.01$) or 2-fold ($p < 0.05$) elevation of the VEGF secretion. In OVCA, the constitutive VEGF expression was 8-fold higher than VEGF levels in HPMC (364 ± 185 pg/105 cells; $p < 0.001$). VEGF secretion in OVCA cells was also increased by IL-1? (514 ± 105 pg/105 cells; $p < 0.01$) or TNF-? (458 ± 168 pg/105 cells; $p < 0.01$) reaching similar levels as in IL-1? activated HPMC. Median VEGF levels in malignant ascites (2,761 ± 1549 pg/ml) were 11-fold higher compared with levels in inflammatory fluids (244 ± 170 pg/ml; $p < 0.01$). VEGF levels in both, inflammatory- and OVCA-associated fluids, correlated with ascitic IL-1? levels ($p < 0.05$).
Conclusion: We identified ovarian cancer cells and/or IL-1? activated peritoneal mesothelial cells as important sources of ascitic VEGF. The present data indicate that IL-1? triggered VEGF production by neoplastic and normal cells is a common pathomechanism for ascites formation in both inflammatory and malignant conditions.

O-109
USE OF MESOTHELIN IN DIAGNOSING PANCREATIC CARCINOMA ON FNA SPECIMENS.

Molinié Vincent (1), Marty Olivier (2), De Pinieux Isabelle (1), Homsi Toufik (1), Balaton André (1). Pathology (1) and gastro enterology (2) department Hôpital saint Joseph Paris France.

Background: diagnosis of fine needle aspiration (FNA) of pancreatic carcinoma can be difficult due to morphologic overlap with reactive processes. Mesothelin is a 40kDa glycoprotein attached to the cell surface by phosphatidylinositol. Overexpression of mesothelin has been reported in the majority of the pancreatic ductal carcinoma but not non-neoplastic ductal epithelium. This objective of the study is to evaluate the use of mesothelin as a marker for pancreatic ductal adenocarcinoma on FNA specimens.
Design: 30 cell blocks of pancreatic EUS-FNA from 30 patients (18 females and 12 males with a median age of 62 years) were retrieved. All cases were AFA fixed an paraffin embedded. Sections were cut at 4 microns and immunostained with anti-mesothelin antibody (clone: 5B2; dilution 1:60; Novocastra Lab Ltd., New Castle upon Tyne, UK). Immunostaining was performed on an automated stainer (Dako stainer). Seven FNAs were from patients with reactive/inflammatory conditions. The remaining 23 FNAs included 16 pancreatic ductal carcinoma, 1 intracystic papillary mucinous carcinoma (IPMT), 5 neuroendocrine cell neoplasm, 1 lymphoma. The presence of immunoreactivity in

more than 10% of the tumor cells, irrespective of level of intensity, was considered positive for mesothelin expression.
Results: 80% of the pancreatic ductal carcinomas and the IPMT demonstrated positive staining with mesothelin, ranging to focal to diffuse. Positive staining epithelial cells showed intense cytoplasmic staining especially at the apical (luminal) aspects with variable membranous staining. None of the benign aspirates was positive for mesothelin. None of the non-ductal neoplasms demonstrated mesothelin expression. The difference in mesothelin expression between pancreatic ductal carcinoma and other lesions was statistically significant ($p<0.0001$, Fisher exact test). The sensitivity and specificity of mesothelin as a marker for pancreatic ductal carcinoma were 97% and 90%, respectively.
Conclusions: Mesothelin is overexpressed in pancreatic ductal carcinoma with an intense apical cytoplasmic and variable membranous staining pattern. Our results suggest that the phenotypic expression of mesothelin can be used as a diagnostic marker of pancreatic ductal adenocarcinoma in EUS-FNA specimens.

O-110
DIFFERENT PATTERN OF P16 AND P53 PROTEIN EXPRESSION IN INTRADUCTAL PAPILLARY-MUCINOUS NEOPLASMS AND PANCREATIC INTRAEPITHELIAL NEOPLASIA

KUME Keiko, SUDA Koich, YAMASAKI Sigetaka, SONOUE Hiroshi, MITANI Keiko, NOBUKAWA Bunsei
Department of Pathology I, Juntendo University School of Medicine, Tokyo Japan

Introduction Intraductal papillary-mucinous neoplasms (IPMNs) are precursors of invasive ductal adenocarcinoma of the pancreas as the same way pancreatic intraepithelial neoplasias (PanINs) are. Their morphological similarity causes some confusions of their nomenclature and criteria. An illustrated consensus classification of the intraepithelial lesions in the pancreatic ducts, PanINs and IPMNs, are achieved in 2004. Though IPMN is recognized as a distinct group of lesions apart from PanINs, their genetic progression models for pancreatic cancer are thought to be considerably common.
Purpose The purpose of this study is to examine aberrations and differences of cell cycle regulatory proteins between IPMNs and PanINs.
Materials and Methods The protein expression of p16, p53 and 14-3-3ƒÐ were examined by immunohistochemistry both in 47 IPMN lesions (22 hyperplastic lesions, 12 adenomas and 13 adenocarcinomas) from 26 patients with IPMN and in 40 PanIN lesions (12 PanIN1, 20 PanIN2 and 8 PanIN3) from 11 patients with invasive pancreatic ductal cancer. We compare the percentage of immunohistochemical positivity between groups as follows: PanIN1 and hyperplastic lesion of IPMNs, PanIN2 and adenoma of IPMNs, PanIN3 and carcinoma in situ of IPMNs. Ki-67 labeling index (LI) was also counted in each lesion. Statistical analysis was conducted with Fisher• fs exact test and Kruskal-Wallis test, respectively.
Results Loss of p16 protein expression was much more frequently observed in PanIN3 than in intraductal papillary-mucinous carcinoma (IPMC) ($p=0.046$). Overexpression of p53 protein was much more prominent in PanIN1 and PanIN2 than in hyperplastic lesions and adenoma of IPMNs ($p=0.011$ and 0.004, respectively). Ki-67 LI was correlated with histological grades of both PanINs and IPMNs ($p=0.0001$, $p=0.0001$). The percentage of 14-3-3ƒÐ protein expression was not significantly different between IPMNs and PanINs.
Conclusion Loss of p16 protein expression might be a supportive factor for distinction between PanIN3 and IPMC. It may be possible to distinguish PanIN1 and PanIN2 from IPMNs showing the same as degree of dysplasia by using p53 immunohistochemical stain.

O-111
FROZEN-SECTIONS OF THE PANCREATIC CUT SURFACE DURING PANCREATECTOMY FOR INTRADUCTAL PAPILLARY AND MUCINOUS TUMOURS (IPMT) ARE USEFUL AND RELIABLE: A PROSPECTIVE EVALUATION.

COUVELARD Anne (1), KIANMANESH Reza (2), HAMMEL Pascal (3), COLNOT Nathalie (1), LEVY Philippe(3), RUSZNIEWSKI Philippe (3), BEDOSSA Pierre (1), BELGHITI Jacques (2), SAUVANET Alain (2). Departments of Pathology (1), Digestive Surgery (2) and Gastroenterology (3), Beaujon hospital, AP-HP, University Paris VII, Clichy, France.

Introduction: IPMT are associated with a significant risk of malignant transformation which is higher for main-duct (MD) types than branch-ducts (BD). Preoperative imaging is not reliable for precise evaluation of tumour topography. Frozen-sections (FS) of the pancreatic cut surface have been proposed into guide pancreatic resection.
Aims: Evaluate the accuracy of FS of the pancreatic cut surface during pancreatectomy for IMPT and its influence on the surgical procedure.
Patients and Methods: From 1996 to 2004, 154 pancreatectomies were performed for IPMT at our institution. IPMT type included: 56 BD and 98 MD or mixed variants, with no dysplasia (IMPT-adenoma [A]; n=55), moderate dysplasia (IPMT-borderline [B]; n=27), carcinoma in situ (CIS; n=35) or infiltrating carcinoma (n=37). FS was performed in 127 procedures, including 90 pancreaticoduodenectomies (with 1-4 successive FS, giving a total number of 132 FS), 23 distal pancreatectomies (1-2 FS; total=26) and 14 medial pancreatectomies (2-4 FS; total=30). Pancreatectomy was extended if FS revealed at least IPMT-adenoma on the main duct or IPMT-borderline on branch ducts (so-called “significant” lesions).
Results: (a) Results of FS (n=188): MD epithelium was normal (n=120), eroded (n=15) or revealed A (n=33), B (n=11) or CIS (n=5) lesions. BD epithelium was normal (n=106) or revealed A (n=65), B (n=8) or CIS (n=5) lesions. FS revealed infiltrating carcinoma in 4 cases. Overall, 54/188 (29%) of FS revealed « significant » lesions. (b) Comparison FS-definitive pathology: definitive pathology and FS were identical in 176/188 cases (94%). 12 conflicting results included 9 cases of «underestimation» and 3 cases of «overestimation» by FS. (c) Influence of FS on surgery: 54 FS with significant lesions lead to 46 additional resections (n=38 patients, 30%). Additional resection was not performed in 8 cases due to either high operative risk or simultaneous diagnosis of infiltrating carcinoma of poor prognosis. The 134 FS without «significant» lesions were associated with additional resection in 7 patients, due to either macroscopic suspicion of tumour in another localization or erosion of epithelium. Inadequate results of FS resulted in inadequate resection in 4 patients (3%).
Conclusions: During pancreatectomy for IPMT, frozen sections of the pancreatic cut surface is useful since it changes the extent of resection in 30% of patients. It is reliable, resulting in adequate resection in 97% of patients.

O-112
ENDOCRINE PRECURSOR LESIONS ARE ASSOCIATED WITH DUODENAL GASTRINOMAS IN PATIENTS SUFFERING FROM MULTIPLE ENDOCRINE NEOPLASIA TYPE 1

ANLAUF Martin*, PERREN Aurel**, MEYER Cora L.*, SCHMID Sonja**, SAREMASLANI Parvin**, KRUSE

Marie L.***, WEIHE Eberhard****, KOMMINOTH Paul**, HEITZ Philipp U.**, KLÖPPEL Günter*
*Department of Pathology, University of Kiel, Germany
**Department of Pathology, University Hospital Zürich, Switzerland
***1st Department of Medicine, Laboratory for Molecular Gastroenterology and Hepatology, University of Kiel, Germany
****Department of Molecular Neuroscience, Institute of Anatomy and Cell Biology, Philipps-University of Marburg, Germany

Introduction: The identification of precursor lesions has a great impact on the understanding of tumorigenesis. Precursor lesions of endocrine tumors are known to occur in the setting of the MEN1 syndrome. Purpose of the study: The aim of this study was to test the hypothesis of the development of MEN1-associated duodenal gastrinomas from preneoplastic gastrin cell proliferations. This hypothesis is based on the fact that MEN1-associated duodenal gastrinomas are usually multiple, in contrast to sporadic gastrinomas. Methods: The distribution of endocrine cells in the nontumorous duodenal tissue was analyzed qualitatively and quantitatively in 25 patients, who underwent surgery for duodenal gastrinoma. The MEN1 status was assessed clinically and by PCR based mutational analysis. Results: Fourteen of 25 gastrinoma patients had proliferative, hyperplastic lesions consisting of gastrin cells in the nontumorous duodenal mucosa similar to the gastric ECL cell lesions observed in chronic atrophic gastritis. All ZES patients with proven MEN1 had such proliferative gastrin cell lesions, and all ZES patients without precursor lesions were MEN1 negative. Conclusions: Duodenal gastrinomas in MEN1, but not sporadic duodenal gastrinomas, are associated with gastrin cell proliferation within the nontumorous mucosa. It is likely that these lesions precede the development of MEN1-associated duodenal gastrinomas.

O-113
MARKEDLY ALTERED EXPRESSION OF TIGHT JUNCTION PROTEINS DIFFERENTIATE PRIMARY HUMAN HEPATOCELLULAR CARCINOMAS AND METASTATIC LIVER TUMORS.

KISS Andras1, PASKA Csilla1, ORBAN Erika1, SZIJARTO Attila2, KUPCSULIK Peter2 and SCHAFF Zsuzsa1
1 2nd Inst. of Pathology, Semmelweis Medical University, Budapest, Hungary
2 1st Dept. of Surgery, Semmelweis Medical University, Budapest, Hungary

Background: Tight junction proteins as claudins, occludin and JAM or peripheral zonula occludens (ZO) proteins are widely implicated in carcinogenesis. Claudins (1-24) have been recently identified as integral proteins of the tight junction strands. Claudin-4 has not been found in normal hepatocytes or bile duct epithelium. Claudin 3 and 4 can function as the receptor of the Clostridium perfringens enterotoxin. Further, downregulated claudin 1 is associated with poor prognosis of colon carcinoma and claudin 10 expression is associated with the recurrence of hepatocellular carcinoma (HCC). Aim: The objective was to characterize the expression of claudin 1-4, 7, occludin, JAM 1-2 and ZO 1-3 in human HCCs and liver metastases. Material and methods: 19 human HCC, 15 colon metastasis samples, surrounding nontumorous livers and 7 normal livers were examined by real-time RT-PCR, immunohistochemistry and Western blotting. Results: Claudin 4 in HCCs was found downregulated 3.4 folds and 43 folds compared to normal livers and metastases, respectively. Western blot data confirmed minimal expression of claudin 4 in HCC, however, immnohistochemistry detected the presence of claudin-4 on bile ducts. Claudin 3 mRNA epression was 12 fold higher in metastases compared to HCC. Metastatic tumors showed strong claudin-3 and 4 immunolabeling while HCC cells gave only partial and weak positivity. Claudin 1, nevertheless, showed 3 fold higher expression in HCCs. Claudin 2 in HCCs revealed 3 fold downregulation in comparison to normal liver, however, there was no significant difference between HCCs and metastases. Claudin 7 mRNA expressions were eleveted in metastases and HCCs in comparison to normal liver but there was no significant difference between primary and metastatic liver tumors. Western blot analysis supported the results found by immunohistochemistry. ZO-2 and JAM-2 mRNA expression was found significantly decreased in HCCs compared to the surrounding tissue: 4 and 3 fold, respectively. Conclusion: Taken together, pronounced downregulation of claudin 3 and 4 and higher expression of claudin 1 might differenciate primary hepatocellular carcinomas from metastatic colorectal tumors. The high level of claudin 3 and 4 in liver metastases might serve as target of adjuvant therapy. Biological role and significance of altered claudin expression should be elucidated. The project was supported by grants: NKFP-1/0023/2002, NKFP-1A//002/2004, OTKA T-049559

O-114
GENOTYPE-PHENOTYPE CORRELATIONS IN HEPATOCELLULAR ADENOMAS SUGGEST A NEW CLASSIFICATION

ZUCMAN-ROSSI Jessica1, JEANNOT Emmanuelle1, TRAN VAN NHIEU Jeanne2, SCOAZEC Jean-Yves3, GUETTIER Catherine4, REBOUISSOU Sandra1, BACQ Yannick5, LETEURTRE Emmanuelle6, PARADIS Valérie7, MICHALAK-PROVOST Sophie8, WENDUM Dominique9, CHICHE Laurence10, FABRE Monique11, MELLOTTEE Lucille1, LAURENT Christophe12, PARTENSKY Christian3, CASTAING Denis4, ZAFRANI Elie Serge2, LAURENT-PUIG Pierre13, BALABAUD Charles12,14, BIOULAC-SAGE Paulette 14,15.
1Inserm U674-CEPH-Paris, 2AP-HP-hôpital Henri-Mondor-Créteil, 3hôpital Edouard Herriot-Lyon, 4AP-HP-hôpital Paul Brousse-Villejuif, 5hôpital Trousseau-Tours, 6CHRU- Lille, 7AP-HP-hôpital Beaujon-Clichy, 8CHU-Angers, 9AP-HP-hôpital Saint-Antoine-Paris,10CHU Caen,
11AP-HP, hôpital Bicêtre-Paris,12CHU-hôpital Saint-André-Bordeaux, 13Inserm-U490-UFR Saints-Pères-Paris, 14Inserm-E362-Université Bordeaux 2-Bordeaux,15CHU-hôpital Pellegrin- Bordeaux, France

Background: Hepatocellular adenomas are benign tumors that can be difficult to diagnose. To refine their classification, we performed a comprehensive analysis of their genetic, pathological and clinical features.
Methods: A retrospective multicentric series of 96 liver tumors with a firm or possible diagnosis of hepatocellular adenoma was reviewed by a panel of liver pathologists. In all cases, the genes coding for hepatocyte nuclear factor 1alpha (HNF1alpha) and ß-catenin were sequenced.
Results: No tumors was mutated in both HNF1alpha and ß-catenin enabling tumors to be classified into 3 groups, according to genotype. Tumors with HNF1alpha mutations formed the most important group of adenomas (44 cases). They were phenotypically characterized by marked steatosis ($p<10^{-4}$), lack of cytological abnormalities ($p<10^{-6}$) and inflammatory infiltrates ($p<10^{-4}$). In contrast, the group of tumors defined by ß-catenin activation included 13 lesions with frequent cytological abnormalities and acini foci ($p<10^{-5}$). In the third group of tumors, without HNF1alpha or ß-catenin mutation, we identified a subgroup of 17 inflammatory lesions, resembling telangiectatic focal nodular hyperplasias, with frequent cytological abnormalities ($p=10^{-3}$), ductular reaction ($p<10^{-2}$) and dystrophic vessels ($p=0.02$). In this classification, hepatocellular carcinoma associated with adenoma or borderline lesions between carcinoma and adenoma is found in 46% of the ß-catenin

mutated tumors whereas they are never observed in inflammatory lesions and are rarely found in HNF1alpha; mutated tumors (p=0.004).
Conclusions: The molecular and pathological classification of hepatocellular adenomas permits the identification of strong genotype-phenotype correlations and suggests that non-inflammatory adenomas and particularly those with ß-catenin activation have a higher risk of malignant transformation.

O-115
COMBINED HEPATOCELLULAR-CHOLANGIOCARCINOMA IN A SINGLE EUROPEAN CENTER: CLINICO-PATHOLOGIC FEATURES AND OUTCOME.

D Cazals-Hatem, F Dondero, V Paradis, O Farges, F Durand, C Francoz, J Belghiti, P Bedossa.
Departments of Pathology, Hepatology and Surgery, Hôpital Beaujon, 92118 Clichy, France

Backgrounds: Combined hepatocellular-cholangiocarcinomas (HCC-CC) are rare and described in Asia as an aggressive hepatocellular carcinoma (HCC) variant. In United States, none of the HCC-CC recently reported arose in cirrhosis. Clinical, pathological and prognostic features of HCC-CC observed in Europe are not established.
Patients & Methods: between 1988 and 2004, 712 patients underwent liver resection or transplantation for primary liver cancer in a single center; HCC-CC was diagnosed in 29 patients on histological analysis. Clinical, pathological, immunohistochemical and follow-up data were retrospectively analyzed (using antibodies of cytokeratin (CK)7, CK19, CK20, of Hep Par 1 and p53).
Results: All patients (mean age at diagnosis: 58 yo) were Caucasian and 90% were men (26 out of 29 patients). The prevalence of positive hepatitis B or C serology and of genetic hemochomatosis cirrhosis were 38% and 10% respectively. Twelve patients (41%) displayed cirrhosis and 12 (41%) a normal background liver. Mean tumor size was 6.2 cm; 19 patients (66%) needed a major hepatectomy and 7 patients (24%) were transplanted. Most HCC-CC presented with a single mass with admixed hepatoid and cholangiolar components both positive for CK7 and/or CK19; p53, Hep Par1 and CK20 expression were present in 50%, 41% and 23% of them respectively. Vascular invasion, satellite nodules and metastasis were observed in respectively 90%, 62% and 21% of all HCC-CC. The median overall survival after resection was 34 months. One, 3, 5 years survivals were respectively 69%, 45% and 36%. Five of the 7 transplanted patients were alive at 3 years without recurrence (48±28 months).
Conclusion: HCC-CC in Europe presented with intermediate clinico-pathologic features between Eastern and Western series and similar adverse outcome. LT should offer curative treatment for HCC-CC if Milano criteria are respected, similarly to HCC.

O-116
EXPRESSION OF CLASS I MHC MOLECULES AND TAPASIN IN PRIMARY HUMAN HEPATOCELLULAR CARCINOMA

FRANCESCHINI Barbara (1, 3), GRIZZI Fabio (1, 3), BOSSI Paola (2), CEVA-GRIMALDI Giorgia (1, 3), DIOGUARDI Nicola (1, 3), CHIRIVA-INTERNATI Maurizio (4)
1) Scientific Direction and 2) Pathology Department, Istituto Clinico Humanitas, Rozzano, Milan, Italy; 3) “M. Rodriguez” Foundation, Milan, Italy; 4) Department of Microbiology and Immunology, Texas Tech university, Lubbock, TX, USA.

Introduction. Major histocompatibility complex (MHC) class I molecules present short peptides, produced in cytosol through proteolytic breakdown of antigens, to cytotoxic T lymphocytes. The stable assembly of MHC class I molecules with peptides in the endoplasmic reticulum involves several resident chaperones. One of these accessory proteins is called Tapasin. It is a trasmembrane protein that mediates the binding of MHC class I molecules to the peptide transporter associated with antigen processing. Tapasin also plays a quantitative role in antigen presentation, and deficient tapasin expression appears to be a frequent event in human neoplastic cells of unrelated histological origin. Purpose. To investigate the expression of MHC class I molecules and tapasin in primary hepatocellular carcinomas (HCC). Methods. MHC class I molecules [heavy chain (HC-10) and ß2-microglobulin] and tapasin expression were recognized by immunohistochemistry in paraffin-embedded and formalin-fixed specimens taken from patients free of neoplastic liver disease (n=5), and affected by primary HCC (n=20). Results. All the investigated proteins were found in scattered normal hepatocytes and infiltrated T lymphocytes. Biliary cells were also found immunopositive, while sinusoids express only MHC class I molecules, but not tapasin. Although trabecular HCCs were immunonegative, the pseudoglandular histotype was found lowly immunopositive for all the investigated antigens. Conclusions. The obtained results demonstrate that liver parenchymal cells moderately express MHC class I molecules and tapasin. This seems linked to the liver complex organismal functions. Interestingly, pseudoglandular tumour express MHC class I molecules and tapasin. However the un-expression of these molecules in some HCCs (i.e. trabecular histotype) stimulate us to further investigate their association with the prognosis of the neoplastic disease, and to explore this peculiar behavior as tumor escape mechanism.

O-117
MDM2 EXPRESSION IN BRONCHIAL PRENEOPLASTIC LESIONS AND ITS CORRELATION WITH P53

HALLER Annick (1), MASCAUX Céline (2+3), MARTIN Benoît (3), FEOLI Francesco (1), NINANE Vincent (4), SCULIER Jean-Paul (3), VERHEST Alain (1)
(1) Department of pathology, Institut Jules Bordet, Brussels, BELGIUM
(2) Research Fellow FNRS(National Fund of Scientific Research), BELGIUM
(3) Department of Intensive Care and Thoracic Oncology, Institut Jules Bordet, Brussels, BELGIUM
(4) Department of Pneumology, Saint-Pierre University Hospital, Brussels, BELGIUM

Background:P53 is one of the most important genes in oncogenesis and in the development of lung cancer. MDM2 is one of the proteins playing an essential role in p53 regulation.
The objective of the present study is to assess MDM2 expression in different grades of bronchial squamous precursor lesions and in invasive squamous cell carcinoma (SQCC). We also tried to correlate MDM2 and p53 expression in the same biopsies.
Patients and methods: An immunohistochemical assessment of MDM2 and p53 expression was performed in 91 biopsies obtained by fluorescence bronchoscopy in patients at high risk for lung cancer.
Results: 38 biopsies (46%) overexpressed MDM2. Overexpression of MDM2 was found in 23 % of normal tissues, 25% of hyperplasias, 40% of epidermoid metaplasias, 86% of mild dysplasias, 83 % of moderate dysplasias, 83 % of severe dysplasias, 100% of carcinomas in situ and in 75 % of invasive carcinomas. MDM2 expression was found to be significantly different in low versus high grade lesions. When MDM2 expression was increased, the positive predictive

value (PPV) to be a high grade bronchial premalignant lesion was 26%. With reference to high grade dysplasia, lack of MDM2 overexpression had a negative predictive value (NPV) of 95.5%.
Seventy-two percent of the biopsies were positive for p53. We found a high statistically significant association between positivity for MDM2 and p53 (p=0.0015). When the biopsy was overexpressing neither MDM2 nor p53, the NPV for a high grade lesion was 92.7%.
Conclusion: MDM2 which is an important negative regulator of p53, is overexpressed early in bronchial preneoplastic lesions from the stage of mild dysplasia, playing thus an early role in lung SQCC carcinogenesis. Lack of MDM2 expression predicted the absence of high grade lesion better than the negativity of the p53 protein.

O-118
KLF-4 AND C-FOS ARE DOWNREGULATED IN NON-SMALL CELL LUNG CARCINOMAS. A GENE EXPRESSION AND TISSUE MICROARRAY ANALYSIS

GOMEZ-ROMAN Jose Javier, RODRIGUEZ Ana1, LOPEZ-BREA Marta2, MONS Roberto3, CUEVAS GONZALEZ Jorge, VAL-BERNAL J. Fernando
Dpto Anatomía Patológica, 1Genómica SAU. Madrid, 2S. Oncología Médica, 3S. Cirugía Torácica. Hospital Universitario Marqués de Valdecilla. Santander (Spain)

Background: Lung cancer can be classified in two groups Small and Non small cell carcinomas, because the different clinical setting, biological behaviour, molecular properties, and treatment. On the other hand, genetic changes contributing to tumor development determine tumor phenotype. Thus, markers based on those genetic changes should provide predictive power and robust diagnostic tools. In this sense, DNA array technology is a powerful tool to monitor the expression of thousands of genes. The term gene expression profiling means the process of establishing the pattern of expression of thousands of individual genes simultaneously in a given cell or tissue sample by extracting its RNA, converting it to cDNA and hybridizing the labeled cDNA or cRNA to a DNA microarray. We show here the results of a collaborative project between the Pathology Department of the Hospital Universitario Marqués de Valdecilla in Santander (Spain) and Genomica SAU (Madrid). Our aims were to describe the gene expression pattern in pulmonary non-small cell carcinomas.
Methods: 29 non-small cell lung carcinomas and 18 pulmonary non-neoplastic tissue samples from the frozen sample tissue bank of the Pathology department (Spanish tumor network), were evaluated by cDNA microarrays. A 9128-cDNA clonal elements microarray from a commercial library (Human UniGene 1, Incyte Genomics) was constructed (MICROGRID II, Biorobotics). In each microarray the expression profiling of tumoral and non-neoplastic samples was compared to the results of a control cell line. In all cases, we perform a sample morphological control (frozen section H&E stained). Moreover, as an internal control, a set of Housekeeping Genes was included in each assay. KLF-4 and c-Fos were validated by quantitative RT-PCR. Tissue microarray immunohistochemistry was performed in 146 carcinomas.
Results: We have found several groups of genes differentially expressed in adenocarcinomas, squamous cell carcinomas and large cell carcinomas, as well as differences between clinicopathological stages. In supervised bioinformatic analysis, 78 genes were capable to discriminate between neoplastic and non neoplastic samples with a positive predictive value higher than 83%. KLF-4 and c-Fos were both downregulated in mRNA and protein validation studies.
Conclusions: It is possible to establish a molecular signature in non-small cell lung carcinomas. KLF-4 and c-Fos could act as tumor suppressor genes in these kind of neoplasms.

O-119
TUMOUR EXPRESSION AND ACTIVITY OF MMP-2 AND MMP-9 METALLOPROTEINASES IN NON SMALL CELL LUNG CANCER ACCORDING TO TFPI-2 GENE EXPRESSION.

BLECHET Claire, ROLLIN Jerome, IOCHMANN Sophie, LEMARIE Etienne, REVERDIAU Pascale, GUYETANT Serge, GRUEL Yves.
INSERM U618 "Protéases et vectorisation pulmonaire" and IFR 135 Faculté de médecine 10 Bd Tonnelé 37032 TOURS Cedex

Background
MMP-2 and MMP-9 are two metalloproteinases that degrade components of extracellular matrices (ECM) and thus are playing a key role in tumour invasion. Their activation in ECM could be regulated by Tissue factor pathway inhibitor 2 (TFPI-2), a serine protease inhibitor that reduces tumour invasion. We recently demonstrated that TFPI-2 gene expression was decreased in part of non small cell lung cancer (NSCLC). The aim of this study was therefore to determine MMP-2 and MMP-9 expression and activity in NSCLC and to investigate if a relationship could be found in NSCLC between tumour TFPI-2 expression and levels of activated MMP-2 and -9.
Methods
MMP-2 and MMP-9 mRNA expression was first evaluated by specific real-time PCR in tumours and non-affected lung tissues of 57 patients who had underwent surgical excision for NSCLC. We then established, by immunohistochemistry, immunostaining scores of stromal cells and tumour cells for both proteins, and we studied the MMP-2 and MMP-9 activity by gelatine zymography in 27 patients selected according to TFPI-2 tumoral expression that was previously quantified by real-time PCR. In 14 NSCLC tumours (“TFPI-2 low”), less than 300 TFPI-2 mRNA copies were measured while in the 13 other cases (“TFPI-2 high”) TFPI-2 gene expression was higher (> 2000 copies).
Results
The expression of MMP-9 was significantly higher in lung tumours than in corresponding normal tissues (95 vs 30 mRNA copies, p=0,0005) whereas MMP-2 mRNA levels were not significantly different (4382 vs 4241 mRNA copies, p=0,51). The levels of MMP-2 and MMP-9 mRNA in tumours were negatively related to lymph nodes status (p=0.05 and p=0.025 respectively).
All tumours expressed MMP-2 and MMP-9 proteins. However, MMP-2 immunostaining scores were higher in stromal cells that in cancerous cells (80 vs. 20 respectively, p=0.004) whereas MMP-9 scores were higher in cancerous cells than in stromal cells (110 vs. 40 respectively, p=0.0016). The relative amounts of activated forms of MMP-2 and MMP-9 were significantly higher in tumours compared with non-affected tissues, but without significant difference between “TFPI-2 high” and “TFPI-2 low” groups.
Conclusions
MMP-2 and MMP-9 are mainly expressed by different cells in NSCLC, i.e. cancerous cells for MMP-9 and stromal cells for MMP-2. A low TFPI-2 gene expression does not appear to be associated with increased amounts of activated MMP in NSCLC tumours as evaluated by zymography.

O-120
IDENTIFICATION OF EPIDERMAL GROWTH FACTOR RECEPTOR (EGFR) MUTATIONS IN ADENOCARCINOMA OF THE LUNG WITH

BRONCHIOLOALVEOLAR CARCINOMA (BAC) COMPOUND.

DANEL Claire(1), BLONS Hélène(2,3), CÔTE Jean-François(1,3), LE CORRE Delphine(3), RIQUET Marc(4), LAURENT-PUIG Pierre(2,3).
1)Service d'Anatomie Pathologique,
2)Service de Biochimie,
4)Service de Chirurgie Thoracique,
Hôpital Européen Georges Pompidou, Paris, France
3) INSERM U 490, Université Paris 5, France

Lung cancer is a leading cause of mortality worldwide and despite progress in management the 5 years survival rate remains under 15%. In this group of cancers, it is known that non small cell lung cancer (NSCLC) is genetically and morphologically heterogeneous. Classifying cancer upon genetic abnormalities has become a challenge since the evidence that the success of targeted therapy is closely related to the existence of specific molecular alterations One evidence in NSCLC is the recent identification of a subgroup of patients with obvious response to gefitinib (Iressa), an inhibitor of EGFR. It was shown that sensibility to gefitinib was linked to the presence of EGFR mutations in tumors. EGFR activates intracellular proliferative and anti-apoptotic signaling pathways. The inhibition of mutated EGFR by getifinib leads to dramatic tumor response.
The goal of this work was to individualize tumors based upon EGFR pathway abnormalities. Ninety-four patients (48 men and 46 women) with surgery as first line treatment for NSCLC were enrolled in this study. Clinicopathological parameters were collected (age at surgery, smoking status, histology and tumor stage). For each subjects a frozen tumor sample was speared for DNA extraction and pathological control. Moreover Immunochemistry (IHC) with anti EGFR antibody was performed on paraffin sections. Tumors were screened for mutations in EGFR, HER2, HER3, K-ras and TP53 and in major down stream effectors by direct sequencing.
Fourteen patients harbored EGFR mutated tumors (14/96) and showed a particular phenotype. EGFR alterations were statistically linked to female gender, absence of smoking, adenocarcinoma with a BAC compound and absence of K-ras mutation. No correlation was found with TP53 mutations or anti EGFR IHC analysis.
The finding that EGFR mutations segregated essentially in BAC or in adenocarcinoma with BAC compound, raised the question of which adenocarcinoma subtypes harbor the mutated allele. To answer this question, EGFR mutation screening in microdissected tumors harboring adenocarcinoma with BAC compound will be undertaken separately on each subtype. The restriction of the mutation to a cluster of tumor cells could have important consequences on gefitinib response rates and the quantification of the BAC compound in adenocarcinoma could have major clinical impacts.

O-121
SARCOMATOID CARCINOMAS OF THE LUNG – ARE THESE HISTOGENETICALLY HETEROGENEOUS TUMOURS?

Markus Blaukovitsch, Iris Halbwedl, Hannelore Kothmaier, Helmut H. Popper
Laboratories for Molecular Cytogenetics, Environmental and Respiratory Tract Pathology, Institute of Pathology, Medical University of Graz, Austria

Introduction: Sarcomatoid carcinomas (SC) of the lung are a heterogeneous group of poorly differentiated, rare non-small cell lung carcinomas (NSCLC) containing a sarcoma or sarcoma-like component. SC may represent malignant epithelial neoplasm undergoing divergent tissue differentiation originating from a single clone. Furthermore, epithelial mesenchymal transition (EMT) best describes the origin of the sarcoma-like appearing components of the SC.
Purpose: The aim of this study was to find any concordant chromosomal aberrations within the subgroups of SC and how they correlate with the EMT hypothesis.
Methods: 23 cases of SC were investigated by means of chromosomal comparative genomic hybridisation (c-CGH). Immunohistochemical staining was performed with antibodies reactive with E-Cadherin (epithelial marker) and Snail, TGFß1, c-Fos (EMT related proteins).
Results: In contrast to the predominant NSCLC-types, where gains and losses are equally distributed, in our study gains occurred more frequently than losses (70, 5 % versus 29, 5 %). The shortest regions of overlap were gains on 8q and 7 followed by 1q, 3q and 19. We were also able to detect gains on chromosomes 11, 12p, 17q, 20q and 22q; losses were found on chromosomes 4q, 5q, 6q, 10q, 11q, 13, 15 and 16q.
The IHC revealed in 13 of 23 (56, 5 %) cases a negative and in 5 of 23 (22 %) cases a weak reaction for E-Cadherin. 20 of 23 (87 %) and 21 of 23 (91 %) cases were positively stained for TGFß1 and Snail, respectively. In addition 18 (78 %) of 23 cases had a positive reaction for c-Fos.
Conclusion: To our knowledge this is the first c-CGH study in SC. Our data show a homogenous pattern of chromosomal aberrations, which would support the single clone hypothesis. The corresponding IHC results suggest that the sarcomatoid appearing components of SC have undergone EMT and are of epithelial origin. To further elucidate EMT other members of this pathway will be investigated by IHC.

O-122
MALIGNANT LYMPHOMA INITIALLY DIAGNOSED IN THE LUNG – WHAT IS NECESSARY?

Ulrike Gruber-Mösenbacher1, Christine Beham-Schmid[2], Felix Offner1, Johannes Rothmund[2], Helmut H.Popper[3], Institutes of Pathology1, Department of Pulmology2, Academic Teaching Hospital Feldkirch1, and Medical University Graz3, Austria

Introduction: Malignant lymphomas affecting the lung are rare, especially primary non-Hodgkin-lymphomas (NHL). Secondary involvement of the lung in extrapulmonary NHL is reported in 25-40% of cases, but initial manifestation in the lung has rarely been reported. Especially clinically "indolent" courses of lymphomas tend to be overlooked and not included into the clinical differentials.
Material and Methods: 19 cases of NHL, initially diagnosed in the lung, were reviewed and classified according to the WHO. Demographic data, clinical and radiological diagnoses, extension of the infiltrates and types of diagnostic procedures were compared. All cases were immunotyped using a panel of CD-antibodies.
Results and Discussion: The histological diagnoses were: 6 diffuse large B-cell lymphomas (DLBCL), 6 marginal zone B-cell lymphomas of the mucosa-associated lymphoid tissue (MALT) type, 3 lymphomatoid granulomatoses (LYG), 2 peripheral T-cell-lymphomas, 1 post-transplant lymphoproliferative disease (PTLD). All DLBCL formed masses, and were easily diagnosed in the first biopsy (endobronchial or transbronchial) by routine stains and immunohistochemistry. The 6 marginal zone B-cell lymphomas were clinically uncharacteristic, presented radiologically as longstanding and often therapy-resistant "pneumonias" or atelectases. Three of them could be diagnosed in endo-or transbronchial biopsies, one of them in the third repeated biopsy. Three cases were only diagnosed in biopsies obtained by video-assisted thoracoscopic surgery (VATS). In the 2 peripheral T-cell-lymphomas the diagnosis could be established in small endoscopic biopsies, however, in these cases diagnosis was challenging. One of the lymphomatoid granulomatoses cases was diagnosed in CT-

guided needle biopsies, the two other cases of LYG were seen in wegde-resections.
Establishing the diagnosis in marginal zone B-cell lymphomas, lymphomatoid granulomatosis, and also in peripheral T-cell-lymphomas requires experience and may in some cases be exceedingly difficult. Especially when dealing with small endobronchial or transbronchial biopsies, the diagnostic features may be easily missed. Frequently there are also reactive changes, such as interstitial pneumonia, which may obscure the tumor cell infiltration. Molecular analyses of B-cell clonality or T-cell rearrangement may be necessary to firmly establish the diagnosis in some cases. Good clinical information is important for a timely diagnosis.

O-123
E-CADHERIN, N-CADHERIN, TTF-1 AND CD56 - ANTIBODIES THAT MAY HELP DISTINGUISH MESOTHELIOMATOUS FROM CARCINOMATOUS SPINDLE CELLS IN THE LUNG AND PLEURA.

FABRE Aurelie, PELLING Nathalie, RYAN Deirdre, NICHOLSON Andrew
Department of Histopathology, Royal Brompton and Harefield NHS Trust, London

Whilst well established for epithelioid neoplasms, the role of immunohistochemistry in differentiating malignant spindle cell lesions within lung and pleura is less certain.
Purpose of the study: We have therefore compared the immunophenotype of malignant spindle cells in 28 mesotheliomas to those in 23 primary pulmonary carcinomas.
Methods: Single tumour blocks (archival formalin-fixed paraffin-embedded tissue) from 28 mesotheliomas (sarcomatoid (n=21), biphasic (n=7)) and 23 primary pulmonary carcinomas (pleomorphic (n=21), spindle cell (n=1) carcinosarcoma (n=1)) were stained using the antibodies: anti-pan cytokeratins (CK) (MNF116), anti-TTF-1, a “mesothelioma” panel (anti-CK5/6, anti-calretinin anti-thrombomodulin) anti-CD56, anti-E-cadherin and anti-N-cadherin, Staining was assessed semi-quantitatively for intensity (strong = +++, moderate = ++, weak = +) and distribution (3 = > 50%, 2 = 10-50%, 1= <10% of cells).
Results: In terms of at least moderate intensity and distribution, 100% of mesotheliomatous and 96% carcinomatous spindle cells were positive for MNF116 (negative in carcinosarcoma only). All cases showed nuclear positivity for E-cadherin, but only carcinomatous spindle cells showed membrane staining with E-cadherin (0% vs 35%). This was mainly seen when spindle cells were part of cohesive sheets of tumour. N-cadherin (61% vs 4%) and CD56 (36% vs 0%) showed good specificity for mesotheliomatous spindle cells although weaker staining (1+) was more frequently seen (82% vs 26% and 60% vs 8% respectively). TTF-1 only stained carcinomatous spindle cells (30% vs 0%). Calretinin (65% vs 39%) and thrombomodulin (35% vs 17%) showed greater sensitivity for mesotheliomas but specificity was low. CK5/6 stained more carcinomas (8% vs 9%).
Conclusion: TTF-1, anti-E-cadherin (membranous staining), anti-N-cadherin, and CD56 antibodies may help in differentiating malignant spindle cell lesions of pleural mesotheliomas and pulmonary carcinomas, although interpretation must be in the context of histological appearance and clinical presentation.

O-124
AMPLIFICATION OF TOPOISOMERASE 2A GENE (TOP2A) IN MALIGNANT MESOTHELIOMA CELL LINES INVESTIGATED BY FLUORESCENCE IN SITU HYBRIDIZATION.

ORECCHIA Sara, SCHILLACI Francesca, SALVIO Michela, LIBENER Roberta, BETTA Pier-Giacomo. Pathology Unit. Dept of Oncology. Azienda Sanitaria Ospedaliera. Alessandria. Italy.

Introduction. Malignant mesothelioma (MM) is a tumour type that is particularly refractory to a number of different chemotherapy agents, yet the mechanisms by which resistance occurs are poorly understood. The pattern of resistance is consistent with disruption of topoisomerase (topo) function or expression. Topo enzymes help to relieve helical winding and DNA tangling problems produced by transcription or replication complexes tracking along DNA. The human genome contains five family members: topo I, IIA, IIB, IIIA and IIIB. Topo IIA is encoded by TOP2A gene adjacent to the HER2 oncogene at the chromosome location 17q12-q21. TOP2A amplification is often accompanied by HER2 gene amplification, e.g. in breast and bladder cancers. Amplification or deletion of TOP2A may account for sensitivity or resistance to topo II targeting drugs.
Purpose of the study. As part of an effort to evaluate the contribution of topo II alterations to drug sensitivity and resistance in MM, we have sought to identify the frequency of amplification of the TOP2A gene in a panel of human MM cell lines in which immunohistochemistry and fluorescence in situ hybridization (FISH) had previously demonstrated neither HER2 gene amplification nor overexpression.
Methods. 15 human MM cell lines established from pleural effusion samples from histologically confirmed MM patients, were analyzed by FISH using TOP2A FISH pharmDx™ Kit (DakoCytomation), designed to determine the copy number of the TOP2A gene related to the centromere of chromosome 17 (the TOP2A/CEN-17 ratio; ratio >2: TOP2A gene amplified).
Results. We found that 7/15 MM cell lines had disomy of TOP2A gene copy; in a MM cell line TOP2A gene and centromere 17 signals were located in two different chromosomes. Polysomy was present in 6/15 MM cell lines and the increase of TOP2A gene copies was related to chromosome 17 aneuploidy (4-5 copies/cell). TOP2A gene amplification was detected in 2/15 MM cell lines: two 17 isochromosomes were found in a MM cell line and in the other MM cell line the TOP2A/CEN-17 ratio was > 2.
Conclusions. While further study is required, we present preliminary evidence that the TOP2A gene amplification may occur without HER-2 coamplification, at least in one MM subset. This finding also highlights the importance of screening for TOP2A gene copy number aberrations when topo II inhibitors are considered either alone or combined with other chemotherapeutic drugs for the targeted treatment of MM patients.

O-125
TTF-1 EXPRESSION IN PLEOMORPHIC CARCINOMAS FROM THE LUNG AND PLEOMORPHIC MESOTHELIOMAS; THE EXPERIENCE OF THE MESOPATH GROUP

PACIENCIA Maria(1), ROULEAU Vincent(1), FLEURY Céline(1), DE QUILLACQ Anne(1,2,3), LAUNOY Guy(2), GALATEAU-SALLE Françoise(1,2,3) on the Behalf of the Mesopath Group(1) and under the auspices of the PNSM(3).
(1)Departement of Pathology-CHU de Caen, France
(2)INSERM ERI3-CHU Caen, France
(3)InVs, Hopital St Maurice, France

Background: Mesothelioma is a great mimicker of adenocarcinomas, other carcinomas and sarcomas and may be source of diagnostic difficulties.
The new 2004 WHO classification of lung tumors had proposed a new concept and unified a heterogenous group of non small cell carcinoma that contain sarcoma and sarcoma-like component under the designation: carcinoma with pleomorphic,sarcomatoid or sarcomatous elements (PC).

Mesothelioma was classified in four categories: epithelioid, sarcomatoid, desmoplastic and biphasic. Both sarcomatoid and epithelioid poorly differentiated mesothelioma may present pleomorphic features (PM) that are very misleading with PC.
The aim of this study is to analyse the relevancy of immunohistochemistry in the diagnosis of neoplasms with pleomorphic features and to evaluate the value of TTF1 alone or in combination with other markers to differentiate PM and PC.
Methods: 1779 mesotheliomas were selected from the Mesopath group diagnosed between April 1996-2003 and were validated according to the procedure of certification instituted by the Mesopath group. 2080 primary lung carcinomas were retrieved during the same period of time from the files of the departement of pathology CHU Caen.
Immunohistocheminal staining was performed using Ventana automated stainer with avidin-biotin-peroxydase methods. Negative control were included in each test by omission of the primary antibody and alveolar type 2 positive were used as a positive control for TTF1 and pan CK's, squamous cell carcinoma for CK5/6 and brain for calretinin. A tumor was considered postive if>10% of the neoplasic cells reacted with a clear cut signal on the relevant localization.
Results: 30 PM out of 1779 mesotheliomas were retrieved (<1,6%) and 31 PC out of 2080 primary lung carcinoma according to the WHO classification 2004 (<1,4%). AE1/AE3, KL1 and CK5/6 expression was observed respectively in 81%, 58% and 10% of PC and in 77%, 43% and 37% of PM. Calretinin expression was observed in 73% PM and in none PC while TTF1 expression was observed in 32% PC and in none PM.
Conclusion: We found that the combination of both calretinin and TTF1 was extremely useful in differentiating PM from PC. Additionally, we found that KL1 expression (80%) was more sensitive than AE1/AE3 expression (40%) for the diagnosis for PM while CK5/6 was poorly sensitive in both tumors (PC 10% and PM 32%).

O-126
WHAT ABOUT A SCALED SCORE FOR PAPILLARY CARCINOMA OF THE THYROID?

VERHULST Priscilla(1), DEVOS Patrick(2), AUBERT Sebastien(1), BUOB David(1), CRANSHAW Isaac(3), CARNAILLE Bruno(3), WEMEAU Jean-Louis(4), LETEURTRE Emmanuelle(1).
from departements of Pathology(1), Biostatistics(2), General and Endocrine Surgery(3) and Endocrinology(4), Lille, France.

The gold standard for the diagnosis of papillary thyroid carcinoma (PTC) remains morphologic criteria. This diagnosis, especially for the follicular variant of PTC, is subjective and variable even among experienced thyroid pathologists. The purpose of the study was to analyse the frequency of PTC morphologic features classically described in a series of 132 thyroid tumours. Then, we created a scaled score based on these morphologic features. We hoped this would illustrate the variety of morphologic presentations of follicular adenoma (FA) and PTC. Methods: 66 PTC and 66 FA were selected and matched for age, sex and presence of thyroiditis. Two independent observers delineated the following PTC morphologic features: papillary architecture; psammoma bodies; nuclear pseudoinclusion and grooves; enlarged, ground glass, ovoid, irregularly shaped and overlapping nuclei; lack of polarization in the cells; dark staining colloid; irregular contours of follicles; multinucleated macrophages. Statistical analyses were performed. Results: Under univariate analysis, all the PTC morphologic features were significantly more frequent in PTC than in FA (p<0,05). Under multivariate analysis, the most important criteria were: dark staining colloid (>25% of the tumour), nuclear grooves, enlarged nuclei, ovoid nuclei (>5% of tumour cells) and lack of polarization in the cells. Using factorial discriminant analysis, these 5 criteria allowed us to define a scaled score (range 0-79). If the threshold score for malignancy was set at >30, the score had a sensitivity of 98,5% and a specificity of 100% for the original diagnosis of PTC. On a validation population (29 PTC/29 FA), a score >30 was in agreement with the original diagnosis of PTC with a sensitivity of 72% and a specificity of 100%. 21/29 PTC scored >30 and 8/29 PTC scored <30 but >7. The majority of FA (21/29) scored < or =7, but a minority (8/29) had a score between 7 and 30. Therefore, there was a "grey zone" for cases which scored between 7 and 30. The original diagnosis for these cases included both FA and PTC. Conclusion: This score illustrates the variety of morphologic presentation of FA and PTC. However, we were unable to demonstrate a clear cut-off between the diagnoses of FA and PTC. The "grey zone" we have defined could argue for a category of "well differentiated tumour of uncertain malignant potential". The score could help in evaluation of new molecular markers for the diagnosis of PTC.

O-127
POST MENOPAUSE IS A PREDICTOR OF RECURRENCE IN PAPILLARY THYROID CARCINOMA AND IS ASSOCIATED WITH EPIDERMAL GROWTH FACTOR RECEPTOR – EGFR- EXPRESSION AND HIGHER FOLLICULAR CELL PROLIFERATION

GAMBOA-DOMINGUEZ Armando, SAQUI-SALCES Milena, ROCHA Brenda, CANDANEDO-GONZALEZ Fernando.
Patología. Instituto Nacional de Ciencias Médicas y Nutrición Salvador Zubirán. Mexico

Background: Papillary thyroid carcinoma (PTC) has worse prognosis after 45 years age. Aim: Identify if hormonal changes in women with PTC correlate with TNM, recurrence, EGFR and Ki-67 expression.
Design: Case control study nested in a retrospective cohort. Clinical data, hormonal status, follow-up, size, multicentricity and extra thyroid invasion were obtained from charts. Staging and classification were performed using AJCC/WHO systems. Post menopause was defined as absence of uterine bleeds >1 year and all were submitted to similar surgical procedures. Tissue arrays including one of remnant thyroid were constructed. EGFR (EGFRpharmDx) and Ki-67 (Dako) immunohistochemistry detection were performed; EGF-R was graded as 0, 1, 2, 3, and Ki-67 as an index of +ve cells. Post menopause, age and stage correlate with each other, and were analyzed separately. Uni and multivariate analysis were performed.
Results: 215 women were included, 154 pre and 61 postmenopausal with a mean follow-up of 71 months. At the time of diagnosis no differences were observed in pT, pM and higher pN was identified in pre menopause. Recurrences were observed in 30 patients (14%); mainly post menopause (p=0.008). Cox regression model controlled by size, node or distant metastases and, extra thyroidal invasion showed that post menopause had adverse effect on recurrence-free survival (p=0.041). EGFR was mainly expressed in postmenopausal (p<0.02) with higher Ki-67 indexes.
Conclusions: Postmenopausal status is an adverse factor in women with differentiated PTC and is associated with EGFR/Ki-67 +ve tumors. This is a biological explanation for currently used UICC/AJCC 45 y-o prognostic cutoff.

O-128
LYMPHATIC VESSEL DISTRIBUTION AND VEGF-C/VEGF-D PRODUCTION IN PAPILLARY CARCINOMA OF THE THYROID

Arianna Di Napoli*, Flavia Melotti*, Stefania Scarpino* and Luigi Ruco*
*Dipartimento di Diagnostica di Laboratorio, Ospedale Sant¡¦Andrea, Università ¡§La Sapienza¡¨, Roma, Italia

Introduction Lymphatic metastatization is the initial step of generalized spreading of papillary carcinoma of the thyroid. Because of the absence of specific markers for lymphatic endothelium, very few information is available about the lymphatic vascularization of papillary carcinoma, In the present study we have investigated the lymphatic vessel distribution in 22 cases of papillary carcinoma, and we have attempted a correlation with the levels of VEGF-C and VEGF-D present in tumour tissue and in primary cultures of papillary carcinoma.
MethodsThe lymphatic vessel distribution and the presence of VEGF-D were demonstrated in paraffin sections of 22 cases of papillary carcinoma using a mouse monoclonal antibody(IgG1) raised against podoplanin,1:50 dilution and a mouse monoclonal antibody(IgG1) anti human VEGF-D1:200dilution.
Total RNA was extracted from the tumour and from the peri-tumoral normal thyroid tissue microdissected from 6-8 ƒÝm frozen sections in 14 cases of PTC.RNAtranscripts for VEGF-C and VEGF-D, were evaluated by real time quantitative RT-PCR using the ICycler System.VEGF-C and VEGF-D expression was also investigated in RNA extracts obtained from 6 cases of primary cultures of PTC.
Results In all the investigated cases, podoplanin-positive lymph vessels could not be demonstrated inside the tumour. Large lymphatic lacunae, lined by podoplanin-positive flat endothelial cells, were frequently observed in the peritumoral normal thyroid; these latter showed occasional images of invasion by tumour cells. Quantitative analysis of RNA transcripts for VEGF-C and VEGF-D has indicated that these growth factors were more abundantly produced in the normal thyroid tissue as compared with the corresponding tumour tissue. VEGF-D mRNA transcripts were completely absent or poorly present in 6/6 cases of primary cultures of papillary carcinoma cells. Immunostaining for VEGF-D could be demonstrated in some normal thyroid follicles lined by tall cells.
Conclusion Our findings clearly indicate that most cases of papillary carcinoma do not contain intratumoral lymph vessels. This implies that metastatization to the lymph nodes requires tumour cell invasion of lymphatic vessels of the surrounding normal thyroid. Our study indicate that a defective production by tumour cells of growth factors involved in lymphangiogenesis such as VEGF-D and VEGF-C may be one of the molecular mechanism leading to a poorly developed intratumoral lymphatic vascularization.

O-129
USEFULNESS OF CYTOKERATIN 19 AND GALECTIN-3 IN THE DIAGNOSIS OF FOLLICULAR VARIANT OF PAPILLARY THYROID CARCINOMA.

BELLA Maria Rosa, ORELLANA Ruth, COMBALIA Neus, GIMENEZ-PEREZ Gabriel*, CASALOTS Alex, MARQUÈS Gabriel**, FERNANDEZ Sara, DINARÉS Maria Carme, PARRA Tamara, ESCODA Maria Rosa, REY Mercè. Pathology Dept., Endocrinology Unit*, Surgery Dept**. Corporació Sanitària Parc Taulí – UDIAT-CD. Sabadell (Barcelona). Spain.

INTRODUCTION: Follicular variant of papillary thyroid carcinoma (FVPC) is not an unusual neoplasm that can raise diagnostic problems in fine needle aspiration biopsy (FNAB) and in surgical specimens. On the other hand, immunohistochemical markers as Cytokeratin 19 (CK19) and Galectin-3 (Gal3) are usually positive in papillary carcinoma (PC).
PURPOSE OF THE STUDY: To determine the expression of CK19 and Gal3 in FVPC compared to other entities included in its differential diagnosis.
METHODS USED: 26 FVPC, 5 nodular hyperplasia, 5 follicular adenomas (FA) and 5 follicular carcinomas (FC) were examined by immunohistochemistry (IHC) for CK19 and Gal3. Semiquantitative evaluation of each marker alone (0 to 3+) and combined (0 to 6+), and analysis of the results were performed.
RESULTS: Considering positive 2+ and 3+, Gal3 and CK19 have a sensitivity of 100 and 92 %, and a specificity of 92 and 75% respectively for FVPC in histologic specimens. Adding the two immunostaining results, values of 5+ or more give a sensitivity of 88%, but specificity reaches 100%. Cases of FVPC that don't reach 5+ correspond to macrofollicular variant or had focal oncocytic change.
In 7 cases of FVPC, a conclusive diagnosis of PC was not established in the previous FNAB (neoplasm, suspicious of PC, undetermined, benign). IHC on the cell blocks would favour PC diagnosis in 3/7, in which Gal3 was positive and combined values of 5+ or more were reached. The four remaining cases correspond to macrofollicular variants or cases with focal oncocytic change.
Gal3 is more specific, supported by the evidence that only two cases of other entities (1 FA and 1 FC) reached values of 2+ on histologic material, and never exceeded 1+ on FNAB cell block.
CONCLUSION: Cytokeratin 19 and Galectin-3, preferably together, can be useful in the diagnosis of FVPC, both in surgical specimens and in FNAB, with some limitations in macrofollicular and oncocytic variants.

O-130
VIRTUAL MICROSCOPY AND THYROID PATHOLOGY QUALITY ASSURANCE ON A NATIONWIDE SCALE IN FRANCE

FRANC Brigitte 1, BERGER Nicole 2*, CAILLOU Bernard 3*, CAVERIVIÈRE Paul 4*, COURTIN Philippe 5*, DE MICCO Catherine 6*, ETTORE Francette 7*, FOULET Armelle 8*, FROMENT Nicolas 9*, GUYÉTANT Serge 10*, KETTANI Sami 11*, KADI-HANIFI Anne-Marie 12*, BELLOCQ Jean Pierre 13**, PATEY Martine 14*
*Members of Committee n°6 "thyroid", working on behalf of **AFAQAP (French Association for Quality Assurance in Pathology).1 Department of Pathology, A. Paré Hospital (APHP), 92100, Boulogne-Billancourt, France, 2, 3, 4 , 5, 6 , 7 , 8, 9 , 10, 11, 12 , 13. (Lyon, Villejuif, Toulouse, Lille, Marseille, Nice, Le Mans, Metz, Tours, Angers, La Roche Sur Yon, Strasbourg, Reims

Several studies testing observer variation in borderline thyroid lesions had underlined their low diagnostic reproducibility. Little is known about typical thyroid lesion general practice assessment in France.
Virtual slides (VS) offered the opportunity to regularly test diagnostic performances on a wide scale. After the test, participants had access to the comments associated with the slides.
The test, performed with the NAVIQAP® (VS) system (Samba Technologies), was composed of a set of 10 thyroid lesions (3 benign: oncocytic adenoma [OA], Graves' disease [GD], hyalinizing trabecular adenoma [HTA], and 7 malignant: insular carcinoma [ITC], medullary thyroid carcinoma [MTC], widely invasive follicular thyroid carcinoma oncocytic variant [WIFTCOV), diffuse papillary sclerosing variant [DPSV], papillary carcinoma follicular variant [PTCFV], minimally invasive follicular carcinoma [MIFTC], and widely invasive follicular carcinoma with anaplastic carcinoma [WIFTC-ATC]). A total of 133 general pathologists, either private or public practitioners, (43% and

57% respectively) belonging to 118 different French laboratories filed the associated questionnaire.
The median global score was 15/20: 7% of the pathologists were quoted between 4 and 10, 40% between 11 and 15; 4% of the pathologists perfectly diagnosed all ten diagnoses.
Malignancy was recognised by 94% to 100% of the participants except the MTC and the WIFTCOV identified as malignant by 82% and 87% of the participants. Benignity was identified by 83% to 87% of the participants according to cases. When considering the malignant diagnosis, an almost perfect diagnosis was reached by 41%, 80%, 12%, 51%, 89%, 63% and 34% of the participants, for ITC, MTC, WIFTCOV, PDSV, PTCFV, MIFTC, WIFTC-ATC respectively. Difficulties with a malignancy diagnosis concerned ITC, MTC, and WIFTCOV, which were not diagnosed as malignant by 6%, 18% and 13% of the participants respectively. In addition, ITC and WIFTC-ATC were misdiagnosed as MTC by 3% and 8% of the participants respectively. The WIFTCOV was considered as MTC by 4,5% of the participants or as partly or completely anaplastic by 4,5% of them.
Those results permitted to focus teaching efforts on obvious mistakes such as under-diagnosis of WIFTCOV and under- or over-diagnosis of MTC.
Virtual microscopy appeared to be a splendid tool in identifying diagnostic difficulties on a nationwide scale and to provide the participants with a learning aid.

O-131
SETTING UP OF A NON TUMORAL AND TUMORAL THYROID TISSUE BANK FOR CLINICAL RESEARCH: MAIN DIFFERENT ISSUES TO GET A HIGH LABEL OF QUALITY

HOFMAN Véronique (1, 2), LASSALLE Sandra (1, 2), BUTORI Catherine (1), GUEVARA Nicolas (3), GAVRIC-TANGA Virginie (2), TRIPAULT Frédérique (2), SELVA Eric (2), AMBROSETTI Damien (1), HAVET Katia (1), SANTINI José (3), HOFMAN Paul (1, 2).
(1) Laboratory of Clinical and Experimental Pathology, (2) Tissue Biobank Unit, (3) Department of Oto-Rhino-Laryngology, Pasteur Hospital, University of Nice, Nice, France

With the current explosion of new technologies fitting to human tissue (such as DNA microarray, protein array, high-density tissue array, and laser capture microdissection methods), it is actually crucial to control the different steps between the resection of the human tissue specimens and these different analysis. One of the goal of a biobank tissue should be to ensure these controls before using tissue for research studies. In this regard, we began to set up a thyroid tissue bank following several procedures allowing us to get tissue and tissue products (RNA and DNA) with a high label of quality. All specimens stored in the bank are accompagnied by a signed agreement of the patient; selection of representative specimens is made by a well trained pathologist; time between the surgical excision and the frozen procedure is less than 15 min; several specimens are taken both in lesions and in adjaccent normal areas; all specimens are weight before freezing; visual control of a section from a “mirror sample” is obtain in regard of the frozen tissue; RNA quality is assess by the Agilent bioanalyser; complete histological, epidemiological and clinical data are recording; moreover, paraffin tissue blocks of the corresponding tissue are available to set up tissue microarrays (TMAs). Thus, from September 2004 to March 2005, we have collected, according to this procedure, more than 120 thyroid specimens (from both lobectomies and thyroidectomies). Among these specimens, there are 38 carcinomas (13 papillary carcinomas and 6 microcarcinomas, 10 medullary carcinomas, 5 follicular carcinomas, 4 anaplastic carcinomas); 62 adenomas or nodular hyperplasias; 17 lymphocytic thyroiditis and 13 Graves’ disease. A mean of 18 frozen tissue specimens (both from lesional and normal areas; 15 mg to 80 mg) was obtained by each thyroid. Mean RNA 28s/18s ratio was 1.39; mean DNA 260 nm/280 nm ratio was 1.79. In parallel, TMAs were set up for each subgroup of lesion (with both adjacent non lesional and lesional tissues)

O-132
INTERNET EXPERT SYSTEMS FOR SKIN DISEASES (WWW.MUNI.CZ/ATLASES)

FEIT Josef
Institute of Pathology, University Hospital Brno, Czech Republic
JEDLICKOVA Hana,Department of Dermatology, St. Anna University Hospital, Brno, Czech Republic
MATYSKA Ludek, FRIML Tomas, Faculty of Informatics, Masaryk University, Brno, Czech Republic
KEMPF Werner, BURG Gunter,Department of Dermatology, University Hospital, Zurich, Switzerland

Introduction
The Internet atlas of skin pathology with clinical and histological images will be described. The atlas is equipped with expert systems to help the diagnostic process. Purpose of the study. To prepare the digital atlas of pathology with high resolution histological images and tools to make the diagnostic process easier.
Methods
The atlas is available through the Internet. The HTML document
is created from XML data sources. Users need an internet browser to access all features of the atlas. Special interfaces for the access to the high resolution images and to the expert systems are available.
Summary
The atlas of skin pathology has been available on the Internet since 1998. At present the atlas consists of about 3600 images, clinical and histological. Histological images are available in very high resolution (up to 7000×7000 px).The images are annotated and arrows pointing to important signs can be activated. In addition to the table of contents and extensive index a Diagnostic Key to the Epithelial Tumors and Cysts is available. This diagnostic tool is organized in a similar way to botanic keys: a sequence of questions leads to a diagnosis. About 200 diagnostic targets are available. The key is linked to the atlas, so that the target diagnosis can be easily verified. Thanks to the hypertext structure it is easy to backtrack when the diagnostic process reaches the dead end.. Another diagnostic tool will be demonstrated: the Expert System for Non-tumorous Skin
Diseases. The universal structure describing the main pathological changes of skin lesions was created and a database of descriptions of diagnostic units was prepared. The user during the consultation receives a three level menu, through which the lesion in question can be described. The data are sent to the server, where the description is compared with the database using fuzzy scoring function. According to the achieved score the diagnostic units are sorted and (together with the previous description) are sent back, so that the user can refine the descriptions and repeat the process if necessary. The system is designed to run on the Internet and does not require permanent relation to the server. The expert system and the atlas are continuously maintained. The number of diagnostic units is over 150 and new units are being added.
Conclusion
The atlas is available at www.muni.cz/atlases and serves as a source of image material and information.

O-133
MORPHOLOGICAL AND IMMUNOHISTOCHEMICAL STUDY OF 83 CASES OF DERMATOFIBROSARCOMA PROTUBERANS (DFSP): ELABORATION OF A GRADING.

MAMERI Saâdia (1) ZIANI Farid (2), OUAHIOUNE Wahiba (1), BOUZID-BENDISARI Kheira (3)
(1)Laboratory of Pathology,Hospital of Douera,Douera, Algiers Algeria
(2)Orthopaedics surgery unit, Hospital of Douera,Douera, Algiers Algeria
(3) Laboratory of Pathology,Hospital of Beni-messous,Algiers Algeria

Introduction: The DFSP is a malignant mesenchymal tumor of the skin, characterized by frequent recurrences, rarely metastasizant , which presents under several morphological aspects named variants: sclerosant, schwanian, myxoïd, withgiantcells, pigmented, atrophic, myofibroblastic ,fibrosarcomatous. Until now, there is no grading of DFSP.
Purpose of the study: This study aims, through the analysis of 83 cases of DFSP observed during 7 years, to repertory the histological criteria which can predict the behavior of the tumor.
Methods used: 83 cases of DFSP and their 128 recurrences are viewed prospectively and retrospectively. Sections on paraffin blocks are realized for all the cases, with hematoxylin-éosin-safran(H.E.S) stainings.Special histochemical stainings are achieved: P.A.S (Periodic acid of Schiff)-Blue Alcian-Fontana-Trichrome of Masson. An immunohistochemical study using a broad panel of antibodies is performed: .CD34 - CD117 or C.Kit-Protein S100- FactorXIIIA -FactorVIII - CD68-
Summary of the results: The global analysis reveals that the type of the variant, the cellular atypia, the mitotic index and necrosis are microscopic predictive factors for the evolution of the DFSP. They serve to set up a grading. This grading is obtained on the basis of a score which results from the quantification of all these criteria.
Conclusion: An histopronostical grading of DFSP is obtained from these microscopic factors, giving three grades; the first one of good prognosis , the second one of intermediate or median prognosis , and the last, of bad prognosis.

O-134
RECURRENT GENOMIC IMBALANCES OF TRANSFORMED MYCOSIS FUNGOIDES

Prochazkova Martina, Chevret Edith, Beylot-Barry Marie, Mainhaguiet Guillaume, Vergier Béatrice, Belaud-Rotureau Marc-Antoine and Merlio Jean-Philippe
Histology and Molecular Pathology Laboratory EA 2406, Victor Segalen University, Bordeaux, France

Mycosis fungoides (MF) is the most common form of cutaneous T-cell lymphoma, representing roughly half of all cutaneous lymphomas originating in the skin. MF is characterised by an epidermotropic infiltrate of malignant CD4+ helper T-cells that present in most cases a clonal T-cell receptor gene rearrangement. The clinical course is usually indolent, except when MF transforms to large T-cell lymphoma (T-MF), which occurs in 8% to 23% of patients. This transformation is associated with clinical progression and a short survival. Whereas histopathological features of T-MF are now well defined, little is known about the genetic mechanisms underlying the transformation. To address this issue, we analysed 19 tumours with T-MF obtained from 12 patients. We used comparative genomic hybridization (CGH) and in some cases chromosome banding, fluorescence in situ hybridisation (FISH) and DNA content analysis.
In 13 T-MF, DNA measurements of tumour skin nuclei isolated from formalin embedding tissues revealed a DNA content elevated above the diploid value (DNA indices range from 2.4n to 3.2n, mean 2.72n +/- 0.34, P = 0.001). Karyotypes and FISH analysis of 5 T-MF tumours revealed recurrent near-tetraploidy karyotypes whereas such abnormality was not detected by the analysis of peripheral blood lymphocytes. Hence, we suggest that polyploidisation observed at the skin level is a recurrent T-MF abnormality comparably to blood findings for large cells transformation of Sézary syndrome, a leukemic variant of MF.
In 19 T-MF tumours, CGH analysis identified imbalances in 89% of the cases (17/19). Imbalances were recurrently observed for chromosomes 1 (82%), 7 (47%), 9 (76%), 10 (35%), 17 (59%) and 19 (47%). The minimally involved regions were gain of 1p36, 7, 9q34, 17q24-qter, 19 and loss of 9p21, 10p11-p13, 10q22, 17p. Previous cytogenetics studies in MF have already identified the presence of an isochromosome 17q, loss of chromosome 10 and a 9p21 deletion at both early and advanced stages of MF. However such studies have not discriminate tumour stage of MF without large cells from T-MT. Thus, these abnormalities cannot be considered as hallmark for T-MF although they may have biological impact on transformation. Therefore, we are screening whether the imbalances revealed by our CGH study may involve genetic pathways leading to polyploidisation.

O-135
GENETIC ALTERATIONS OF PRIMARY CUTANEOUS LYMPHOMAS ARE RELATED TO CLINICOPATHOLOGICAL SUBTYPES

Marc-Antoine Belaud-Rotureau (1, 2), Virginie Marietta (1), Beatrice Vergier (1, 2), Guillaume Mainhaguiet (1), Michelle Turmo (1), Marie Beylot-Barry (1, 3), Jean-Philippe Merlio (1, 2)
1: EA 2406 Histology and Molecular Pathology of tumours, University Victor Segalen, Bordeaux
2: Pathology Laboratory, Haut-Lévêque Hospital, CHU Bordeaux
3: Dermatology Department, Haut-Léveque Hospital, CHU Bordeaux

Few studies have investigated genetic alterations in primary cutaneous B-cell lymphomas (PCBCL). Therefore, we performed comparative genomic hybridization (CGH-array) and fluorescent in situ hybridization (FISH) assays on a series of 21 PCBCL.
Frozen cutaneous biopsies of 21 patients were selected : large cells lymphomas of the leg (LCLL, N=5), large cells lymphomas with another localisation than the leg (LCLA, N=5), small cells centrofollicular lymphomas with unique lesion of the head or trunk (CFU, N=4), small cells centrofollicular lymphomas with multiple lesions (CFM, N=3) and small cells mucosa associated lymphoid tissues lymphomas (MALT, N=4). All samples were assayed by CGH-array with the Array-300 (Abbott-Vysis). FISH analyses were also performed 1) to assess translocations or genes rearrangements (IGH, MALT1, IGH-CCND1, IGH-MYC, IGH-BCL-2) and 2) to confirm the data of the CGH-array assays (p16, AML1, TOP2A, 7ptel, 19qtel).
The FISH analysis demonstrated a t(8;14)(q24;q32) (IGH-MYC) in 2/5 LCLL. By contrast with lymphomas of the lymph nodes, no other abnormality was found. The CGH-array assays showed a more important number of total and/or recurrent genetic alterations in LLCL (mean 59, $p<0.05$) than in LCLA (mean 29, $p<0.05$). Inversely, MALT and CFM exhibited rare alterations (mean 6 and 10, $p<0.01$). Compilation of these data and FISH analyses led to the determination of genetic profiles associated with the LCLL

and LCLA. Particularly, recurrent deletions in 9p21 (p16) were a constant finding in LCLL (5/5). Inversely, LCLA demonstrated recurrent 1p36 deletions (4/5) without deletion in 9p21. Finally, these results suggest that the different prognosis of LCLL and LCLA is supported by specific genetic aberrations.

O-136
CD158K/KIR3DL2 FOR THE DIAGNOSIS OF ERYTHRODERMA IN SKIN SPECIMENS

ORTONNE Nicolas (1,2), WECHSLER Janine (1), BAGOT Martine (3), MARTIN-GARCIA Nadine (1), BENSUSSAN Armand (2).
1 : Département de Pathologie, hôpital Henri Mondor, Créteil
2 : Unité INSERM U659, faculté de Médecine de Créteil
3 : Service de Dermatologie, hôpital Henri Mondor

INTRODUCTION. Erythroderma may result from different causes, including cutaneous T-cell lymphoma (CTCL) and inflammatory diseases, and diagnosis on skin specimens is often problematic. It has been shown recently that CD158k/KIR3DL2 is a marker of Sezary cells, expressed in the blood and skin of Sezary syndrome (SS) patients. The aim of this study was to determine whether CD158k may help for the diagnosis of erythroderma in tissue samples.
METHODS. 35 skin specimens from erythrodermic patients were analyzed. 12 had CTCL (10 SS and 2 erythrodermic mycosis fongoides (EMF)) and 23 had erythrodermic inflammatory diseases (EID) (drug reactions, psoriasis, eczema). In 3 SS patients, the malignant T cell clone, identified in the blood, was shown to be present in the skin by the immunoscope technique. Immunohistochemistry for CD158k, CD3, CD4, CD8 was performed on frozen sections. The CD8/CD3 and CD158k/CD3 ratios were evaluated in the epidermis and in the dermis. In addition, RT-PCR for CD158k was performed in 12 cases.
RESULTS. All cases displayed subepidermal band-like lymphocytic infiltrates with epidermotropism. As expected, CD158k was positive in all CTCL, including EMF. However, CD158k+ cells were also observed in 17 EID. Erythrodermic CTCL displayed lower CD8/CD3 ratios in both the epidermis (mean CD8/CD3 ratio : 12% in CTCL versus 38 % in EID) and dermis (83% of CTCL vs 38% of EID had CD8/CD3<25%). Mean CD158k/CD3 ratios were similar in both groups in the epidermis. However, EID had a lower CD158k expression in the dermis (33% CTCL vs 74% EID with CD8/CD3<25%). RT-PCR, performed in 12 cases displaying similar CD158k+ infiltrates, showed a stronger expression of CD158k mRNA in CTCL.
DISCUSSION. A significant proportion of CD158k+ lymphocytes are present in the skin of erythrodermic patients. Whether these lymphocytes are recruited from the blood and expand in the skin, or correrspond to skin resident lymphocytes is an interesting issue. Although CD158k+ lymphocytes are present both in CTCL and EID, there is a stronger expression of CD158k mRNA in CTCL, what may suggest functional recruitment of CD158k by its ligands in this context.
CONCLUSION. CD158k may be expressed in EID but CTCL have a higher proportion of positive cells in the dermis. Whether the use of CD158k RT-PCR and immunohistochemistry in combination might be more accurate for the diagnosis of erythroderma in cutaneous specimens remains to be confirmed.

O-137
GRANULOMA FACIALE : A CLINICOPATHOLOGICAL STUDY OF 66 PATIENTS

ORTONNE Nicolas (1), WECHSLER Janine (1), BAGOT Martine (2), GROSSHANS Edouard (3), CRIBIER Bernard (3)
1:Département de Pathologie, Hôpital Henri Mondor, Créteil, France
2:Service de Dermatologie, Hôpital Henri Mondor, Créteil, France
3:Clinique Dermatologique de Strasbourg, Hôpital civil de Strasbourg, France

INTRODUCTION : Granuloma faciale (GF) is a rare cutaneous disease usually occuring on the face, that follows a chronic course and has a tendency for recurrence. Only case reports or small series of patients have focused on GF so that the frequency of morphologic changes has never been established. The aim of the study was to describe the clinicopathological characteristics of GF in a large series of 66 patients.
METHODS: 66 patients diagnosed with GF were rincluded in the study and 73 skin specimens were retrospectively analyzed. Among histopathological parameters, GF were categorized as having acute, chronic or mixed inflammatory infiltrates. Statistical analysis evaluated the correlation between histopathological criteria and duration of the lesions.
RESULTS: Mostly, GF presented a one or several, reddish or violaceous, plaques or nodules on the face of middle-aged adults, with a slight male predominance. Five patients had extrafacial lesions and multiple localisations were present in one third of cases. Diagnosis of GF was clinically proposed in only 10 cases whereas sarcoidosis, lymphoma, lupus, and basal cell carcinoma were the most frequent differential diagnoses. Most frequent histopathological features were presence of a grenz zone, neutrophils and telangiectases. Vasculitis was considered to be present in a half of cases, but vessels wall necrosis was very rare. Acute and chronic inflammatory changes were often associated and lesions of longer duration were more likely to have a larger size, what suggest a progressive course with reccurrent acute phases.
CONCLUSION: GF is often clinically misdiagnosed. Criteria usually considered to be of diagnostic value, such as eosinophil infiltration, may lack. Extrafacial localisations, evidences of vascular injuries, lack of eosinophils and presence of a patterned fibrosis in a significant number of cases suggest that GF, erythema elevatum diutinum and localized chronic fibrosing vasculitis may be related.

O-138
DRESS SYNDROME: IS THERE A SPECIFIC HISTOPATHOLOGICAL ASPECT ?

de FERAUDY Sébastien, GROSBER Martine, ORTONNE Nicolas, ALLORY Yves, ROUJEAU Jean-Claude, WECHSLER Janine
HOPITAL HENRI MONDOR (AP-HP)
51 AV. DU MARECHAL DE LATTRE DE TASSIGNY
94010 CRETEIL
FRANCE

INTRODUCTION: DRESS syndrome (DS) is a life-threatening drug hypersensitivity reaction, characterized by a febrile eruption, hypereosinophilia, and visceral involvement. Although skin biopsy belongs to diagnosis criteria, the morphologic changes in DS have never been investigated on large series. The aim of the study was to characterize whether DS has a distinctive histopathological aspect. METHODS: We retrospectively reviewed 43 cutaneous specimens from patients with a diagnosis of drug reaction with eosinophilia and systemic symptoms. Patients were clinically categorized in 4 drug reactions groups: DS definite (n=9); DS probable (n=14); DS not excluded (n=15) and DS excluded (n= 5). RESULTS: Mean age in definite and DS probable was significantly higher than in DS excluded (35 vs 60 years). In definite and probable DS, density of inflammatory infiltrate,

intensity of interface dermatitis and lymphocytic exocytosis were significantly more important than in DS excluded. Although eosinophils and atypical lymphocytes in the blood are diagnosis criteria for DS, eosinophils were absent in most of specimens and atypical lymphocytes were never seen. CONCLUSION: Although not specific, skin biopsy analysis provides help in differenciating DS from other cutaneous drug reactions. Absence of eosinophils and atypical lymphocytes on skin biopsy does not rule out the diagnosis of DS.

O-139

QUANTITATIVE ANALYSIS OF CXCL12 AND CXCR4 EXPRESSION IN HUMAN PRIMARY AND METASTATIC CUTANEOUS MALIGNANT MELANOMA.

MONTEAGUDO Carlos*, LOPEZ-GUERRERO José Antonio**, RAMOS David*, ALONSO Vicent***, JORDÁ Esperanza***, PELLIN Antonio*, LLOMBART-BOSCH Antonio*.
*Department of Pathology, University of Valencia, **Fundación Instituto Valenciano de Oncología, and ***Department of Dermatology, Hospital Clínico Universitario, Valencia, Spain.

Introduction: A role for the CXCR4 chemokine receptor in tumor cell migration during melanoma progression has been proposed. The fact that expression of CXCL12, the only CXCR4 ligand, is higher in lymph nodes, liver, bone marrow, and lung, than in normal skin supports the hypothesis that a gradient concentration of this chemokine might facilitate metastatic colonization. In this regard, CXCR4 antagonists are currently being tested in experimental models in order to prevent metastatic dissemination. Purpose: Our goal was to quantify CXCL12 and CXCR4 mRNA expression in primary and metastatic human cutaneous malignant melanomas in order to determine if there is a gradient expression of both molecules between primary and metastatic lesions which could support the value of a therapeutic blockade in order to inhibit the metastatic dissemination of human melanoma. Methods: CXCL12 and CXCR4 mRNA expression was evaluated by real-time quantitative PCR in 45 frozen tissue samples from primary and metastatic melanoma (<=1 mm, >1mm, in transit, lymph node, and distant metastasis). An immunohistochemical study was also performed in adjacent frozen sections with monoclonal antibodies to CXCL12 and CXCR4 (MAB350 and MAB172, R&D Systems) in order to evaluate the cell types responsible for chemokine ligand and receptor expression. Results: CXCL12 mRNA levels were much higher in thin primary melanomas than in thick primary tumors, lymph node metastases and distant visceral metastases (9, 10 and 83 fold respectively). CXCR4 mRNA levels were higher in lymph node metastases than in thin and thick primary tumors or distant metastases (1.2, 5.5 and 7.3 fold respectively). CXCL12 immunostaining was present in most tumor cells in primary and metastatic tumors as well as endothelial, and other stromal and dendritic cells. CXCR4 immunostaining was found in a subpopulation of tumor cells in primary and metastatic tumors as well as endothelial cells and lymphocytes. Conclusions: The fact that the highest CXCL12 mRNA levels are present in thin melanomas suggests that CXCL12 might retain CXCR4+ tumor cells in the primary site in these patients. In contrast, the lower levels of both CXCL12 and CXCR4 in thick melanomas support the potential dissemination of CXCR4+ tumor cells to lymph nodes or distant sites where mean receptor and ligand levels are similar or higher.

O-140

CLINICALLY DETECTED BENIGN NOTOCHORDAL CELL TUMORS: LESIONS THAT ARE IMPORTANT TO DISTINGUISH FROM INTRAOSSEOUS CHORDOMA

YAMAGUCHI Takehiko 1), IWATA Jun 2), SUGIHARA Shinsuke 3), McCARTHY Edward 4), KARITA Michiaki 5), MURAKAMI Hideki 5), KAWAHARA Norio 5), TSUCHIYA Hiroyuki 5), TOMITA Katsuro 5)
1) Department of Clinical Pathology, Sapporo Medical University School of Medicine, Sapporo, Japan
2) Department of Laboratory Medicine, Kochi Health Science Center, Kochi, Japan
3) Department of Orthopaedic Surgery, Kochi Health Science Center, Kochi, Japan
4) Department of Pathology, John Hopkins Hospital, Baltimore, USA
5) Department of Orthopaedic Surgery, Kanazawa University, Kanazawa, Japan

Introduction: Benign notochordal cell tumor is a recently discovered intraosseous benign lesion of notochordal cell origin that can be precursors of chordoma. The anatomical distribution is identical to that of chordoma. They are usually small and found at autopsy. The concepts or clinicopathological features have not been widely accepted although clinically found cases have been sporadically documented.
Purpose: To know clinicopathological features of clinically detected benign notochordal cell tumors.
Materials and Methods: We collected seven cases of clinically detected benign notochordal cell tumor and examined their histology and clinical records including follow-up information, conventional radiograph, computed tomography scan, and magnetic resonance imaging.
Results: The patient group consisted of 3 men and 4 women with an average age of 44 years old. Two patients had two lesions at different sites. The lesions involved the cervical spine in 4, lumbar spine in 2, sacrum in 2, and coccyx in 1. The most common symptom was mild pain. Two patients were found to have lesions incidentally on imaging study for unrelated conditions. Five patients underwent surgical procedure. All patients but one who died of surgical complications were well without recurrent or progressive disease for 13 to 84 months. X-rays did not reveal significant abnormality in 5 lesions. In one patient who was found to have two lesions, the tumors exhibited diffuse sclerotic changes. Computed tomography scan demonstrated increased density within the vertebral bodies. The lesions showed homogeneous low signal intensity on T1-weighted magnetic resonance imaging and high on T2-weighted imaging. Microscopically, the lesions consisted of sheets of adipocyte-like vacuolated cells without myxoid matrix. The nuclei were usually bland but occasionally polymorphic. The affected bone trabeculae were sclerotic. The tumor cells stained immunohistochemically positive for vimentin, S-100 protein, and epithelial markers.
Conclusions: Benign notochordal cell tumor is a benign bone lesion and may be clinically found in the cervical or lumbar vertebral body. The differential diagnosis includes fatty marrow, chordoma, and metastatic clear cell carcinoma. They do not require any surgical management until they undergo malignant transformation. Benign notochordal cell tumors should be recognized in pathologists, radiologists, and orthopedic surgeons to prevent unnecessary surgical management.

O-141

BENIGN NOTOCHORDAL CELL TUMORS: A COMPARATIVE HISTOLOGICAL STUDY OF BENIGN NOTOCHORDAL CELL TUMORS, CLASSIC CHORDOMAS AND NOTOCHORDAL VESTIGES OF FETAL INTERVERTEBRAL DISKS

YAMAGUCHI Takehiko, HASEGAWA Tadashi

Department of Clinical Pathology, Sapporo Medical University School of Medicine, Sapporo, Japan

Introduction: Chordoma has been believed to arise in residual notochordal tissue; however, we established a new concept intraosseous "benign notochordal cell tumor" that may undergo malignant transformation to classic chordoma.
Purpose: To know morphological and immunohistochemical features of benign notochordal cell tumors.
Materials and methods: The material consisted of 34 benign notochordal cell tumors found in 25 autopsy cases. The patient group consisted of 19 males and 6 females with a mean age of 63 years. This study attempted to define the morphological and immunohistochemical features of benign notochordal cell tumors by contrasting them with classic chordomas (n=3) and notochordal vestiges in fetal intervertebral disks (n=27).
Results: The average tumor size was 4 x 2 mm. The location of 34 tumors was as follows: 8 tumors were in the clivus, 6 in the coccyx, 5 in the second cervical vertebra (C2), 4 in the fourth segment of the sacrum (S4), 3 in S3, 2 each in the third lumbar vertebra (L3) and L4, and one each in C5, S1, S2, and S5. No lesions were found in the intervertebral disks. Benign notochordal cell tumors were morphologically characterized by well demarcated but unencapsulated sheets of adipocyte-like vacuolated and less vacuolated eosinophilic cells within axial bones. The round nuclei were mildly polymorphic but bland. The tumor cells often contained cytoplasmic eosinophilic hyaline globules and lacked any intercellular myxoid matrix or necrosis. The host bone trabeculae were often sclerotic without bone destruction. Vimentin, S-100 protein, epithelial membrane antigen, AE1/AE3, and CAM5.2 were positive in benign notochordal cell tumors, classic chordomas, and notochordal vestiges; however, only notochordal vestiges failed to demonstrate any positive reaction for cytokeratin 18.
Conclusions: The histological features were different from those of both notochordal vestiges in fetal intervertebral disks and classic chordomas. There was overlap in immunohistochemical reactivity of benign notochordal cell tumors and chordomas but notochordal vestiges failed to demonstrate cytokeratin 18 positivity. A more appropriate term for the lesions is "benign notochordal cell tumor" rather than "notochordal rest" or "notochordal hamartoma" as they are not rests and do not fulfill the definition of hamartoma. Benign notochordal cell tumors do not need any surgical procedure and must be adequately recognized in order to prevent unnecessary operations.

O-142
THE JNK AND ERK MAPK SIGNALING PATHWAYS ARE IMPLICATED IN PATHOGENESIS AND PROGRESSION OF HUMAN CHONDROSARCOMAS VIA COOPERATIVE UP-REGULATION OF THE ANGIOGENIC FACTOR VEGF

Dionysios J. Papachristou (1,2), Georgios I. Papachristou (2), Odysseas A. Papaefthimiou (1), Niki J. Agnantis (1), Effie K. Basdra (3), Athanasios G. Papavassiliou (2)
(1) Department of Pathology, School of Medicine, University of Ioannina, Ioannina, Greece
(2) Department of Biochemistry, School of Medicine, University of Patras, Patras, Greece
(3) Department of Orthodontics, School of Dentistry, Aristïtle University of Thessaloniki, Thessaloniki, Greece

Introduction: Chondrosarcoma is the second most common primary skeletal malignancy. Nonetheless, its pathogenesis has not been adequately explored. In vitro data have documented that the JNK and ERK MAP kinases, and their downstream effectors c-Jun and c-Fos (AP-1 transcription complex), are involved in chondroblastic differentiation/proliferation. These oncoproteins functionally interact with the transcription factor Runx2, which is also engaged in cartilage biology. Previous studies have shown that VEGF, a major angiogenic factor, is up-regulated in human chondrosarcomas through yet unidentified mechanisms.
Purpose: 1) To investigate the role of JNK–AP-1 and ERK signaling cascades, Runx2 and VEGF in cartilaginous tumors pathogenesis; 2) To assess these proteins as possible molecular markers for the prediction of chondrosarcomas' clinical behavior.
Materials and Method: We employed immunohistochemistry to examine normal cartilage and neoplastic cells in paraffin-embedded chondrosarcomas (n=45) and enchondromas (n=21). We evaluated the cellular levels of JNK2, p-JNK (phosphorylated/active form of JNK2), c-Jun (JNK's major substrate), pc-Jun (phosphorylated/active form of c-Jun), c-Fos, p-ERK (ERK's phosphorylated/active species), Runx2 and VEGF.
Results: Positive immunostaining for all proteins was observed in the majority of the chondrosarcomas but in a small percentage of enchondromas. Normal chondrocytes were devoid of these immunoreactivities. The cellular levels of all proteins were positively and significantly correlated to each other (Kendal's Tau = 0.44-0.809, $p<0.01$). Their expression levels were substantially augmented in high grade (G2, 3) compared to low grade (G1) chondrosarcomas, and in low grade tumors compared to benign enchondromas (Mann-Whitney test, $p<0.005$ for all). VEGF predicted accurately the grade in 88% of the chondrosarcomas (OR 43.7, $p<0.005$).
Conclusions: 1) The (JNK / ERK)–AP-1 / –Runx2 signal transduction pathways are up-regulated in chondrogenic tumors in a well-orchestrated fashion; 2) the JNK and ERK cascades are associated with chondroblastic malignant transformation and chondrosarcoma development, either independently or through up-regulation of VEGF; 3) VEGF can qualify as molecular marker to predict high grade chondrosarcomas; 4) the use of highly selective agents targeting the JNK/ERK pathways and VEGF might constitute a novel complementary therapy for chondrosarcoma patients.

O-143
EXTRACELLULAR AND INTRACELLULAR EXPRESSION OF CD52 IN SKELETAL TUMORS

GUENTHER Raphaela1, MORAWIETZ Lars1, GRUETZKAU Andreas3, MELCHER Ingo2, SCHASER Klaus-Dieter2, SERS Christine1, KRENN Veit1
1 Institute for Pathology, Charité University Hospital, Berlin, Germany
2 Center for Musculoskeletal Surgery, Charité University Hospital, Berlin, Germany
3 German Arthritis Research, Charité University Hospital, Berlin, Germany

CD52 is a GPI-anchored glycoprotein which is expressed abundantly on all lymphocytes, monocytes, macrophages and eosinophils as well as in the male genital tract. The sperm CD52 antigen differs from CD52 on lymphocytes by its carbohydrate structure, but the protein core is identical. To date, the physiological role of CD52 on lymphocytes is not clear. However, an antibody directed to CD52 called CAMPATH-1H is capable of complement activation as well as antibody-mediated cellular cytotoxicity leading to a depletion of lymphocytes. Presently, CD52-specific antibodies are used to treat lymphoproliferative disorders. Recently, we detected CD52 on giant cell tumours of the bone (GCT) by microarray analysis, suggesting a role of the CD52-antigen in bone tumorigenesis, especially in GCTs, osteosarcomas (OS) and chondrosarcomas (CS).
In this study we analyzed GCT, OS and CS tissues as well as cell lines by immunohistochemical staining and RT-PCR analysis to investigate the expression of CD52 mRNA and protein. We used flow cytometry to analyze the intensity of intracellular and extracellular expression of CD52.

Furthermore, western blot was used to determine differences in the size of CD52 on GCTs, OSs and CSs cells as compared to the lymphocyte-form of CD52.
With RT-PCR we could confirm the expression of the CD52 mRNA in GCTs, OSs and CSs both in vivo (tissue) and in vitro (cell lines). Immunohistochemical staining as well as the FACS scan revealed, that CD52 was not only expressed on the surface of the tumour cells, but also cytoplasmic with a golgi-association. By western blot analysis we confirmed the GPI-anchoring of the CD52 peptide. Multiple bands representing the glycosylation of the antigen were different from bands detected in lymphocytes. This suggested a cell type specific modification of CD52.
The current study demonstrated CD52-expression in GCT, OS and CS tissues as well as cell lines and suggested a role for CD52 in the development of bone tumours. Interestingly, the immunohistochemical as well as the FACS analysis revealed not only the extracellular GPI-anchored CD52, but also a cytoplasmic expression of CD52. In the future, we want to evaluate the expression of CD52 in normal bone and cartilage and the potential of the CAMPATH-1H antibody to recognize CD52 on GCTs and to activate the complement cascade for specific lysis.

O-144
HISTOPATHOLOGICAL GRADUATION OF RHEUMATIC AND NON-RHEUMATIC SYNOVECTOMY SPECIMENS

Morawietz L (1), Kriegsmann J (2), Koepenik A (3), Burmester GR (4), Krenn V (1)
(1) Institute for Pathology, University Hospital Charite, Berlin
(2) Group practice for Pathology, Trier
(3) Oligene GmbH, Berlin
(4) Department for Rheumatology, University Hospital Charite, Berlin

Aims: To establish a standardized and feasible graduation system ("synovialitis-score") for the degree of inflammation in synovectomy specimens, applicable to all forms of synovialitis irrespective of etiology.
Materials and Methods: Three features of chronic synovialitis are separately graded in a semiyuantitative manner (from 0=absent to 3=strong): enlargement of lining cell layer, activation of stroma (i.e. resident) cells, leukocytic infiltrate. The sum of the three criteria resembles the synovialitis-score, which is interpreted as follows: 0-1: no synovialitis, 2-3: slight synovialitis, 4-6: moderate synovialitis, 7-9: strong synovialitis. 559 synovectomy specimens were graded by two independent observers. Clinical diagnoses were osteoarthrosis (OA; n=212), posttraumatic arthritis (PtA; n=21), rheumatoid arthritis (RA; n=246), psoriatic arthritis (PsA; n=22), reactive arthritis (ReA; n=9), and controls (Co, n=49) from necropsies of patients without joint damage.
Results: Median synovialitis scores when correlated to clinical diagnoses were: Co 1.0, OA 2.0, PtA 2.0, PsA 3.5 ReA 5.0, RA 5.0. The differences in scores between Co and all other groups were highly significant ($p<0.001$). A synovialitis-score of 4 points and more was strongly associated with rheumatic joint diseases (sensitivity 84.1%, specificity 77.6%). The correlation between the two observers was high ($p<0.001$).
Conclusion: The proposed synovialitis-score is based on well definable histopathological criteria. It enables a standardized evaluation of synovectomy specimens in routine histopathology and may contribute to the diagnosis of rheumatic and non-rheumatic joint diseases. Furthermore, it represents a rational basis for usage of synovectomy specimens in experimental rheumatology. Tissue microarrays (TMAs) for experimental studies have been made (Oligene GmbH, Berlin, Germany) using synovectomy samples graded according to this graduation system.

O-145
STAT3 IS DIFFERENTIALLY EXPRESSED IN DIFFUSE AND INSTESTINAL TYPE OF GASTRIC ADENOCARCINOMA

Sergiu SUSMAN1, Dawi VERNEREY1, Raphaëlle BARNOUD2, Frédérique BIBEAU3, Francesco BORRINI4, Marc POCARD1, Jean-Christophe SABOURIN1,
1 DEPARTMENTS of PATHOLOGY and SURGERY, GUSTAVE ROUSSY INSTITUTE, VILLEJUIF, France,
2 DEP of PATHOLOGY, HOPITAL DE LA CROIX ROUSSE, LYON, France,
3 DEP of PATHOLOGY, CENTRE VAL D'AURELLE, MONTPELLIER, France
4 DEP of PATHOLOGY, UNIVERSITE LA SAPIENZA, ROME, Italie.

Purpose: It is well know that tumor cells resemble embryonic cells. As a result of the progress made lately in molecular biology it is possible to elucidate the molecular mechanisms that determine (induce) and control tumor phenotypes.
Signal transducers and activators of transcription (STATs) mediate biological actions such as differentiation, cell proliferation and survival in response to cytokines and growth factors. STATs are also important in epithelial–mesenchymal transition during gastrulation, organogenesis and cancer progression. Recently, a relationship between STAT3 and E-caderin bas been reported in digestive tumor: STAT3 seems to decrease E-cadherin expression in tumor cell which could lead to cell mobility. In this study we investigate the role of STAT3 and molecular adhesion proteins (E-cadherin, a and b cathenin) in gastric cancer in order to distinguish the eventual difference of expression in intestinal and diffuse type.
Patients and methods: 120 patients with intestinal type adenocarcinoma and 75 patients with diffuse type adenocarcinoma were analyzed by Immunohistochemistry – Tissue array technique for STAT3, E-cadherin, a and b catenin. Mean expression levels were compared by "t" test.
Results: The expression of a, b catenin and E-cadherin were significantly higher in intestinal than in diffuse type: a-catenine (98% versus 38%, $p < 0.0001$), b-catenin (96% versus 48%, $p < 0.0001$) and E-cadherin (99% versus 62%, $p < 0.0001$). For Stat3 the expression is higher in diffuse type than in intestinal type (31% versus 14%, $p = 0.0029$).
Conclusion: The molecular mechanisms of adhesion molecules are different in intestinal and diffuse type adenocarcinomas. Stat3 molecule, which is involved in epithelial–mesenchymal transition during embryogenesis, seems to play an important role in determining tumor phenotype of diffuse type adenocarcinoma. Theoretically its aggressive nature might be decreased by partial or total inhibition of Stat3. Further investigation is needed to clarify these findings.

O-146
PROGNOSTIC IMPLICATIONS OF HIGH MICROSATELLITE INSTABILITY IN SPORADIC GASTRIC CANCER

NESI Gabriella1, OTTINI Laura2, SAIEVA Calogero3, GIRARDI Lucia Roberta1, FALCHETTI Mario2, LUPI Ramona2, SERA Francesco3, PALLI Domenico3
1Department of Human Pathology and Oncology, University of Florence, Italy; 2Department of Experimental Medicine and Pathology, University "La Sapienza", Rome, Italy; 3Molecular and Nutritional Epidemiology Unit, CSPO, Scientific Institute of Tuscany, Florence, Italy.

Aims: Microsatellite instability (MSI) is a frequent event in gastric carcinogenesis and shows a trend towards distinct clinical and pathological characteristics of gastric cancer (GC). We investigated the role of MSI in GC in order to

elucidate the possible clinical implications of MSI in GC prognosis.
Methods: A series of 159 GC cases were originally identified in the GC high-risk area surrounding Florence (Central Italy) and were actively followed up until recently. Formalin-fixed and paraffin-embedded histological specimens and information on clinico-pathological characteristics, vital status at 5 years, age and family history were available for all patients. A panel of six dinucleotide (D1S104, D2S123, D3S1611, D5S107, D17S261, D18S34) and two mononucleotide (BAT25, BAT26) markers were used to determine the MSI status. Tumours were classified as MSI-high when showing contraction(s) in BAT26 and/or BAT25, as MSI-low when instability was limited to dinucleotide loci, and as MSI negative when no instability was observed at the loci tested. GC cases with low-frequency MSI were included in the MSI negative group for statistical analysis.
Results: Overall, 132 (83.0%) tumours were classified as MSI negative and 27 (17.0%) as MSI-high. The MSI high-phenotype was positively associated with the female sex, but not with other individual characteristics (including age at diagnosis, GC family history, pT or pN status). A strong association was found with vital status at 5 years: 15/27 MSI high-positive cases (55.6%) were still alive at 5 years vs 44/132 MSI negative (33.3%) (p=0.04). A multivariate regression model, including terms for sex, age at diagnosis, pT and pN status, confirmed the positive association between MSI high-phenotype status and survival at 5 years (p=0.03).
Conclusions: MSI high-phenotype may have strong implications in the prognosis of GC, with MSI high-positive patients showing increased survival at 5 years.

O-147
ANGIOGENESIS AND LYMPHANGIOGENESIS IN GASTRIC CANCER.

Assia Bassarova 1,3, Dimitur Bulanov 2, Jahn M. Nesland 3
Department of Pathology, Medical University – Sofia, Bulgaria1
Department of Surgery, Medical University – Sofia, Bulgaria2
Department of Pathology, The Norwegian Radium Hospital, University of Oslo, Oslo, Norway3

Introduction: Vascular endothelial growth factor family is composed of four members: VEGF-A, VEGF-B, VEGF-C, VEGF-D. VEGF-A is a key regulator of blood vessel growth, whereas VEGF-C and VEGF-D regulate lymphatic angiogenesis. The effects of VEGF-A are mediated by binding to VEGF-R1 and VEGF-R2, receptor tyrosine kinases expressed on the surface of vascular endothelial cells, while VEGF-R3 is a receptor for VEGF-C and VEGF-D.
Purpose: The aim of the study was to examine the expression of VEGF-A, VEGF-C, VEGF-D and their receptors VEGF-R1, VEGF-R2, and VEGF-R3 in advanced gastric cancer.
Materials and methods: The study was performed on 106 surgical specimens. All cases were classified according Lauren classification; pTNM staging was performed using the last AJCC criteria from 2002. The expression of the three growth factors and corresponding receptors was evaluated immunohistochemically on both primary tumor and metastatic lesions. In addition microvessel density was assessed by using the pan-endothelial marker CD31 (DAKO) and D2-40 (DAKO), specific for lymphatic endothelium.
Results and discussion: We could not demonstrate expression of VEGF-A. All specimens (both primary and metastatic lesions) were completely negative. VEGF-A was detected only in small proliferating vessels. At the same time the assessment of angiogenesis by CD31 showed quite high microvessel density in the main tumor mass, as well as in many of metastatic lymph nodes and in haematogenous metastases. VEGF-C was expressed in 78 % of all primary tumors and 71 % of all positive carcinomas showed high, strong staining intensity in more than 50 % of the tumor cells. Diffuse type tumors or mixed carcinomas with diffuse component demonstrated stronger VEGF-C expression than intestinal carcinomas. That high expression of one of the regulators of lymphatic angiogenesis was in contradiction with relatively low lymphatic microvessel density. The new monoclonal antibody D2-40 (IgG1) detects an oncofetal antigen associated with germ cell neoplasia and is also a selective marker of lymphatic endothelium. We found a peculiar expression of that antigen by stromal fibroblasts and a condensation of stromal positive “hot spots” in the infiltrative board of the primary tumor.
It seems that in primary gastric cancer VEGF-A plays lesser role in the regulation of angiogenesis than VEGF-C. On the other hand M2A antigen, detected by D2-40 probably plays important role in tumor-stroma interactions.

O-148
GENE EXPRESSION PROFILING IN HUMAN GASTRIC ANTRAL AND CORPUS BIOPSIES INFECTED WITH HELICOBACTER PYLORI

HOFMAN Véronique 1, 2*, MOREILHON Chimène 3*, BREST Patrick 1, SICARD Dominique 4, RAYMOND Josette 5, LAMARQUE Dominique 6, BARBRY Pascal 3, HEBUTERNE Xavier 7 and HOFMAN Paul 1, 2
(1) INSERM 721, Faculty of Medicine, 06107 Nice cedex 01, (2) Laboratory of Clinical and Experimental Pathology, Pasteur’Hospital, 06002 Nice, (3) CNRS UMR 6097, Insitute of Molecular and Cellular Pharmacology, Valbonne, France,(4) Department of Bacteriology, Archet’Hospital, 06200 Nice,(5) Department of Bacteriology, Saint-Vincent de Paul’ Hospital, Paris, (6) Department of Gastroenterology, Hotel Dieu’Hospital, Paris (7) Department of Gastroenterology, Archet’Hospital, 06200 Nice

Introduction: There are sufficient data to suggest that Helicobacter pylori, through direct pathogenic mechanisms, contributes significantly to the gastric mucosal injury associated with this infection, and may enhance the suceptibility of gastric epithelial cells to carcinogenic conversion. Clinical outcome of H. pylori infection may be associated with specific virulence-associated bacterial genotypes. Moreover, polymorphism genotype in host gastric mucosa may be linked with different outcome of the disease. Thus, host genetic factors have been shown to be important in determining the immune response to H. pylori infection and the propensity to develop gastric atrophy, hypochlorhydria and gastric cancer. Aim : The aim of this study was to evaluate differential expression of genes in human gastric epithelial cells infected or not by H. pylori. Methods : We used microarray analysis to identify gene expression profiles among 29 patients infected by different strains of H. pylori and among 25 patients non infected by H. pylori. The obtained profiles were correlated with the H. pylori BabA2, vacAs1/s2, vacAm1/m2, and cagA status determinated by polymerase chain reaction. Antrus and corpus histopathology was examined according to the updated Sydney classification. Results: Of the 29 infected patients, 17 (58.6 %) harboured cagA+ strains, 13 (44.8%) BabA2 strains, 9 (31%) vacAs1m1 strains, 14 (48.2%) s1m2 strains and 5 (17.2%) s2m2 strains. CagA+ H. pylori strains were found to change the expression of gene encoding apoptosis proteins, metalloprotease-disintegrin proteins, tissue inhibitors of metalloproteinases, growth factors and cytokine/chemokines. Marked differences in gene expression profiles were observed following cagA+ and cagA- infection with 96 known genes being differentially expressed. This study demonstrated the usefulness of cDNA array analysis of human biopsies for investigating H. pylori-induced changes in host gene expression.

O-149
MDR PROTEINS IN GASTROINTESTINAL STROMAL TUMORS (GISTS) : SITE DEPENDANT EXPRESSION AND INITIAL RESPONSE TO IMATINIB

Théou N (1, 2), Gil S (3), Devocelle A (3), Julié C (4), Lavergne-Slove A (5), Alain Beauchet (6), Farinotti R (3), Le Cesne A (7), Lemoine A (2, 8), Faivre-Bonhomme L (1, 3), Emile JF (2, 4)
(1)Pharmacy Department, Paul Brousse hospital, Villejuif, (2)INSERM U602, Villejuif, (3)UPRES 2706, Faculty of Pharmacy, Chatenay Malabry, Université Paris XI, (4)Pathology department, Ambroise Paré hospital, Boulogne, and Faculty of Medicine Paris-Ile de France Ouest, Garches, (5)Pathology department, Lariboisière Hospital, Paris, (6)Public Health and Medical Information department, Ambroise Paré hospital, Boulogne, (7)Oncology department, Institut Gustave Roussy, Villejuif, (8)Biochemistry department, Paul Brousse hospital, Villejuif, France

Gastrointestinal stromal tumors (GIST) are the most frequent mesenchymal tumors of the digestive tract and are poorly responsive to chemotherapy. Recently, a treatment with a tyrosine kinase inhibitor, Imatinib Mesylate, was shown to have anti-tumor effects in metastatic patients. However, this drug is a substrate for multidrug resistance (MDR) proteins. We thus investigated the expression of Pgp and MRP1 by Western blot in 21 GIST and 3 leiomyosarcomas, and correlated these results with clinico-pathological characteristics. All the GISTs were positive for either Pgp or MRP1 expression, in 86% and 62% of the case respectively. Pgp was expressed in all gastric GIST, while in only 67% in other localization. By contrast, MRP1 was more expressed in non-gastric tumors (78% versus 42%). Furthermore, the levels of these MDR proteins in gastric GISTs were higher for Pgp (P=0.007) and lower for MRP1 (P=0.004), when compared to other localizations. No correlation was found between MDR expression and the risk assessment. None of the 6 patients treated with Imatinib was resistant, although all were positive for at least one MDR protein. These results confirm that gastric and non-gastric GISTs have different biological characteristics, and suggest that MDR proteins do not impair initial response to Imatinib.

O-150
GASTROINTESTINAL STROMAL TUMORS: A MULTICENTER STUDY OF 645 TURKISH CASES

GIST Working Group, Turkish Society of Pathology, Turkey

INTRODUCTION : Gastrointestinal stromal tumors (GISTs) are the most common mesenchymal tumors arising from the gastrointestinal tract, omentum, and retroperitoneum. The aim of this multicenter study was to determine the histopathological features and immunohistochemical profiles of GISTs diagnosed in Turkish patients.
METHODS: Twenty participating centers registered GIST cases on a nationwide database. The diagnosis of GIST relied upon H&E features and the results of immune antibody panel including CD117, CD34, Desmin, SM Actin, S-100 protein, and Ki67. The database consisted of parameters including patient age and gender, tumour location, size, number of mitoses/50 HPF and other histopathological and immuno-histochemical findings. Statistical analysis was performed using Kruskal Wallis and Multiple Comparison Tests.
RESULTS: From a total of 701 GISTs registered into the database, 645 cases with a male to female ratio of 1.34 and a mean age of 56.19 years were included in the study after eliminating the cases with incomplete data. Most common location was stomach (40.8%) followed by small intestine, omentum and peritoneum, large intestine, and esophagus (32.9%, 13.5%, 10.4%, 0.5%, respectively). The risk groups consisted of 5.7% very low, 20.3% low, 20.0% intermediate and 54.0% high risk cases. There were significant differences ($p<0.001$) between the risk groups and mean size and number of mitoses in relation to tumour location. Spindle pattern was inversely, however, mixed pattern was positively correlated with increasing risk ($p<0.001$). CD117 was positive in 94.3% of GISTs whereas 73.5% were CD34, 51.9% SMA, 10.7% Desmin, 21.2% S-100 positive. Though no significant relation was found between CD117 expression and tumour location, CD34, SMA, S-100 and Ki67 expressions significantly varied in different locations ($p<0.001$). A similar difference was observed in CD117, CD34, Desmin, Ki67 expressions in relation to risk groups: CD117and Ki67 expressions increased in parallel with the risk while CD34 and Desmin decreased.
CONCLUSIONS: The results of this multicenter study demonstrated that features other than tumour size and mitosis, and other immune markers besides CD117 and Ki67 included in the antibody panel also seem to be useful predicting risk factors. Studies with long follow-up and response to therapy of GIST cases will form the basis of our future projects in order to determine the biological behavior of these tumors in our country.

O-151
MORPHOLOGICAL, IMMUNOHISTOCHEMICAL AND GENE EXPRESSION OF GASTROINTESTINAL STROMAL TUMORS (GIST).(HIGH-THROUGHPUT ANALYSIS)

SIMONETTI Sara*,TORNILLO Luigi**,MASCOLO Massimo*, MIGNOGNA Chiara*,SCHNEIDER-STOCH Regine***,TERRACCIANO Luigi**,PETTINATO Guido*,INSABATO Luigi*
* Department of Biomorphological Sciences,Section of Pathology, University “Federico II” of Naples, Italy
** Institute of Pathology, University Basel, Switzerland
*** Department of Biometrics of the Otto-von-Guericke University Magdeburg,Germany

INTRODUCTION: Gastrointestinal stromal tumors (GISTs) represent the most common mesenchymal neoplasm of the GI tract. In the last few decades this entity has became of incredible interest given the new insights derived from the discovery of its derivation from the interstitial cells of Cajal, of the invariable C-kit immunoreaction and of its sensitivity to a RTKs inhibitor drug.
OBJECTIVE: To ascertain the clinicopathologic features and biologic behaviour of these tumors, we reviewed a large series of GISTs with an immunohistochemical and molecular analysis, along with a correlation with clinical outcome.
METHODS: 94 primary GIST were retrieved from the files of the Departments of Anatomic Pathology of Naples-Italy and Basel-Switzerland that we reviewed, both at morphological and molecular level. 9 known oncogenes (CMYC, MDM2, GLI1, CDK4, HER2, EGFR1, CCND1, FGF3, EMS) were analyzed by fluorescent in situ hybridization (FISH) on a tissue microarray (TMA). Moreover the above 94 tumors were included in a larger group of 284 GISTs , retrieved from the Department of Pathology of the University of Magdeburg, Germany. P16 protein expression was analyzed by immunohistochemical staining on TMA, as well as on large sections.
RESULTS: A significant correlation between necrosis, cellularity, mitoses and risk categories of tumors, and the overall survival was found. Amplification was found for CMYC in 3 of 90 (3.3%), for MDM2 in 5 of 94 (5.3%), for EGFR1 in 5 of 94 (5.3%), and for CCND1 in 7 of 79 (8.9%) evaluable cases. No amplifications were seen for HER2, GLI1, CDK4, FGF3, EMS. Amplifications of MDM2 and

CCND1 were associated with clinical and histological malignancy. P16 loss was found in 50% of GISTs. Patients having p16-negative tumors had a worse prognosis than those with p16-positive tumors (p=0.012) with a 2.3-fold relative increased risk of dying of disease.
CONCLUSIONS: Interestingly, we found in a quite large number of cases of GIST, an association of morphologic parameters to aggressiveness of tumors. Moreover, MDM2/CCND1 amplification, and p16 loss may represent respectively molecular and immunohistochemical features to determine subsets of GISTs with poor prognosis. In conclusion our data show clinicopathologic implications in the prognosis of patients with GIST.

O-152
EXPRESSION OF HEDGEHOG SIGNALING COMPONENTS IN STOMACH AND GASTRIC LESIONS

ALINGER Beate, DATZ Christian, KOLLMANN Karoline, BLAAS Leander, ESTERBAUER Harald, ABERGER Fritz, DIETZE Otto, HAUSER-KRONBERGER Cornelia
Department of Pathology, General Hospital Salzburg; Department of Internal Medicine, Oberndorf Hospital; Department of Molecular Biology, University of Salzburg.

The Hedgehog signaling cascade has been shown to play an essential role in embryogenesis, especially in patterning and specification of several tissues. The pathway is involved in the development of the gut and the differentiation of gastric glandular cells. Hedgehog signaling components like the ligand Sonic Hedgehog (Shh) and its receptor Patched (Ptch) have been demonstrated to be expressed within the embryonic stomach. Main components of the Hedgehog pathway are expressed within the adult stomach, proposing an active role of the signaling also in mature stomach. Mutation of just one of the Hedgehog signaling components can lead to disregulation of the pathway resulting in gastric dysfunction and gastric malformations like intestinal metaplasia, gastric atrophy or even cancer.
In the present study normal gastric tissues from human, mouse and rat were analyzed using immunohistochemical methods. The antibodies used are directed against the main components involved in the Hedgehog signaling cascade, including the ligands Sonic, Indian and Desert Hedgehog, the transcription factors Gli1, Gli2 and Gli3 as well as the receptor Patched. Additionally 34 cases of benign and malignant human gastric lesions had been examined. Benign lesions comprise antrum gastritis, hyperplastic polyps, tubular adenomas and intestinal metaplasia, and malignant lesions intestinal adenocarcinoma, diffuse adenocarcinoma, neuroendocrine carcinoma and epithelial dysplasia with early adenocarcinoma. Several components of the Hedgehog signaling cascade are localized in human, and also in mouse and rat normal stomach, indicating an active Hedgehog pathway in the mature stomach. The expression is mainly restricted to the chief and the parietal cells. This may indicate a communication between these main cell types of the gastric glands resulting in a well coordinated and balanced regulation of the number of cells and of digestive processes. Additionally the ligands, the receptor and the transcription factors have been demonstrated in neuroendocrine cells and the myenteric plexus. Case dependent expression pattern of components of the Hedgehog signaling cascade in benign and malignant lesions may correlate with an individual up- or down-regulation of the pathway.
Our findings leads to the presumption that defective proceeding of one or even more of the hedgehog signaling steps may induce gastritis, dysplasia or even gastric cancer.

O-153
CHRONIC URTICARIA INVOLVES THE GASTRODUODENAL MUCOSA AS WELL AS THE SKIN

F Minnei1, C Wetzels2, G De Hertogh2, P Van Eyken2, R Ambu1, G Faa1, A-M Kochuyt3, K Geboes2
Dpt of Cytomorphology, Division of Pathology, University of Cagliari, Italy (1)
Dpts of Morphology & Molecular Pathology (2) and Allergy – Immunology (3), University Hospitals KUL, Leuven, Belgium

BACKGROUND & AIM
Chronic urticaria (CU) is characterized by recurrent episodes of itching, raised smooth and pink skin eruptions twice a week for more than six weeks. It can be initiated by food intake and may be associated with digestive symptoms. Quantitative cell counts have revealed an increased number of mast cells in biopsies from skin lesions of CU. The aim of the present study is to detect a possible relationship between a clinical history of CU and the number of mast cells in the gastroduodenal mucosa.
MATERIALS & METHODS
Two groups were defined as follows: (1) CU patients: 52 Belgians (20 males; mean age 44 y); (2) controls: 16 Belgians (8 males, mean age 43y) and 34 Italians (9 males, mean age 39 y) with upper abdominal complaints and normal endoscopy and histology. Formalin-fixed, paraffin-embedded biopsy specimens were stained with haematoxylin and eosin for routine analysis. We then detected mast cells in the gastroduodenal mucosa using immunohistochemistry for tryptase and c-kit (CD117). The number of mast cells was counted in 5 high power fields (HPF).
RESULTS
All the biopsies from the controls showed a normal histology of the gastroduodenal mucosa. The mean number of c-kit + cells was 21.0/HPF in the stomach and 34.8/HPF in the duodenum. The mean number of tryptase + cells in the stomach was 19.9/HPF for the Belgian controls and 18.4/HPF for the Italian controls. The values for the antrum and the corpus were 19.9 and 20.7/HPF. In the duodenum the mean numbers of tryptase + cells were 32.0/HPF for the Belgian controls and 32.6/HPF for the Italian controls.
In the CU patients the number of tryptase + cells was 31.7 ± 10.9/HPF (mean ± standard deviation, SD) in the stomach and 44.4 ± 16.3/HPF in the duodenum.
CONCLUSIONS
The number of c-kit + cells in the gastroduodenal mucosa of controls was slightly higher than the number of the tryptase+ cells (c-kit also stains degranulated cells). The number of tryptase+ cells was the same in the normal gastroduodenal mucosa from Belgian and Italian controls. Therefore we presume that dietary habits have no influence upon the number of mast cells in the gastroduodenal mucosa. The number of tryptase + mast cells was significantly increased in the gastroduodenal mucosa from patients with CU when compared with controls ($P < 0.0001$). It thus appears that CU is a syndrome which may involve the gastroduodenal mucosa, with presence of associated digestive symptoms.

O-154
PLEOMORPHIC HYALINIZING ANGIECTATIC TUMOR OF SOFT PARTS: A RECENTLY DESCRIBED ENTITY. ULTRASTRUCTURAL ANALYSIS OF ONE CASE.

CAPOVILLA M (1, 2), BIREMBAUT P (1), DE SAINT-MAUR PP (2), CUCHEROUSSET J (1), FLEJOU JF (2), PLOTON D (1).
(1) Laboratoire Pol-Bouin, Hôpital Maison-Blanche, Reims, France.

(2) Service d'Anatomie Pathologique, Hôpital Saint-Antoine, Paris, France.

The Pleomorphic Hyalinizing Angiectatic Tumor (PHAT) is a rare lesion of uncertain lineage that occurs in the superficial soft tissues of the distal extremities and trunk. It was first described by Smith et al. in 1996 with a series of 14 cases and, to date, fewer than 100 cases have been reported. Morphologically, it shares common features with ancient schwannomas and malignant fibrous histiocytomas. In fact, it is characterized by the presence of prominent ectatic vessels with hyalinized walls, pleomorphic spindle stromal cells with intranuclear inclusions and a variable inflammatory component. Despite the presence of numerous atypical cells, mitotic rates are extremely low and this lesion seems to behave as a low-grade neoplasm with possible local recurrences but, not to date, metastases. Only 3 cases of PHAT have been previously studied by electron microscopy. They appeared constituted of primitive mesenchymal cells with bizarre nuclei and numerous intermediate-sized cytoplasmic filaments. The histogenesis and lineage of PHAT are currently unknown; some features are consistent with a reactive process secondary to vascular damages but a unique cytogenetic analysis is more in favour of a neoplastic lesion because of presence of additional ring chromosomes in the neoplastic nuclei. Some authors have recently reported a putative precursor lesion, so-called "early-PHAT". Thus, PHAT should be considered as a low-grade mesenchymal neoplasm and complete surgical excision may be the treatment of choice.

We report a case of PHAT arising from the right buttock of a 66 year-old man. Histologically, it presented areas of typical PHAT and two original features with the presence of a large central area of ischemic necrosis and ganglion-like cells. The tumor cells expressed vimentin and VEGF but not CD34. Ultrastructural analysis revealed primitive mesenchymal cells with pleomorphic nuclei, abundant granular endoplasmic reticulum and numerous intracytoplasmic intermediate filaments. A collagen-rich extracellular matrix with incomplete basal membranes surrounded each cell. The vascular walls were very thickened by abundant hyaline material.

This observation supports the hypothesis of a proliferation of primitive mesenchymal cells. However, further pathologic, cytogenetic and molecular analysis are needed to establish that PHAT is really a neoplastic lesion and to study its natural history.

O-155
NON-INVOLUTING CONGENITAL HEMANGIOMA PRESENTING AS ATYPICAL LARGE LESIONS IN THE NECK

WASSEF Michel (1), SALHI Aïcha (2), KOZAKEWICH Harry (3), BREVIERE George-Marie (4), MULLIKEN John (3), ENJOLRAS Odile (1)

(1) Department of pathology and Consultation des angiomes, hôpital Lariboisière, Paris, France. (2) Consultation des angiomes University Hospital Algiers, Algeria. (3) Center for vascular anomalies, Childrens hospital, Boston, USA. (4) Department of cardiology, hôpital Nord, Lille, France.

Aim: Non-involuting congenital hemangioma (NICH) is a recently described vascular tumor that generally manifests as a round or oval plaque-like or bossed lesion of limited extension, with an average size of 6 cm diameter, mainly affecting the face and the limbs. These lesions are clinically and histologically distinct from common hemangioma of infancy.

We describe a series of a peculiar vascular tumour, presenting as a large plaque-like lesion in the neck and shoulder, and histologically resembling NICH.

Patients: There were 11 patients in this series (8 females and 3 males).

Results: All lesions were congenital; none evidenced postnatal disproportionate growth; and subsequently either were stable or altered slightly. They involved the entire posterior and lateral aspect of the neck, from hairline to upper trunk, unilaterally in 7 patients, bilaterally in 4. Three also extended to the mandibular area. All resembled proliferating phase or involuting phase infantile hemangioma, rather than NICH. In addition, all had a distinctive peripheral bluish or white halo and scar-like atrophic areas. US/Doppler or arteriogram indicated fast-flow, without arteriovenous fistulas, causing diagnostic confusion with arterio-venous malformation.

Histological specimens were available for 8 patients and showed an admixture of veins and arteries, many of which appeared abnormal and lobular aggregates of small vessels. These vessels were lined by endothelial cells with barely visible cytoplasm and contained small, dark, hyperchromatic nuclei protruding in the lumen, creating a hobnailed appearance. Some anisokaryosis was present but mitoses were rare. In some specimens, small clusters of endothelial cells contained round, eosinophilic globules in their cytoplasm. These features were reminiscent of NICH.

Conclusion: Besides the limited plaque-like or bossed lesion initially described, non-involuting congenital hemangioma may present as large extensive lesion in the neck and shoulder area.

O-156
MDM2 AND CDK4 IMMUNOSTAININGS ARE USEFUL ADJUNCTS IN DIAGNOSING WELL-DIFFERENTIATED AND DEDIFFERENTIATED LIPOSARCOMA SUBTYPES. A COMPARATIVE ANALYSIS OF 561 SOFT TISSUE NEOPLASMS WITH GENETIC DATA.

BUI NGUYEN BINH Matthieu, SASTRE-GARAU Xavier, GUILLOU Louis, DE PINIEUX Gonzague, TERRIER Philippe, LAGACE Réal, AURIAS Alain, HOSTEIN Isabelle, COINDRE Jean Michel.

From the departments of pathology at the Curie Institute Paris (MBNB, XSG), the University Institute of Pathology, Lausanne, Switzerland (LG), Cochin University Hospital, Paris (GP), the department of pathology at the Gustave Roussy Institute (PT), Hotel-Dieu University Hospital, Montreal, Canada (RL), Bergonié Institute , Bordeaux (IS, JMC), University Victor Ségalen, Bordeaux (JMC) and INSERM Unit 509, the Curie Institute, Paris (AA).

Introduction: atypical lipomatous tumor - well differentiated liposarcoma (ALT-WDLPS) and dedifferentiated liposarcoma (DDLPS) may be difficult to distinguish from benign adipose tumors and from poorly differentiated sarcomas, respectively. Genetically, they are characterized by amplification of MDM2 and CDK4 genes on chromosome 12q13-15.

Purpose of the study: we studied MDM2 and CDK4 immunoexpression in a large series of soft tissue sarcomas to evaluate the correlation between staining, pathological diagnosis and genetic data.

Materials and methods: we examined a series of 559 soft tissue tumors (44 ALT-WDLPS, 61 DDLPS, 49 benign adipose tumors, and 405 non-ALT-WDLPS/DDLPS sarcomas) for MDM2 and CDK4 expression using immunohistochemistry either on whole tissue sections and/or tissue microarrays. MDM2 and CDK4 immunoexpressions were compared to gene amplification status (as assessed by quantitative PCR and/or comparative genomic hybridization) in 239 neoplasms.

Results: most ALT-WDLPS/DDLPS expressed MDM2 (97%) and CDK4 (92%) as opposed to few benign adipose tumors (MDM2: 5%; CDK4: 2%) and a limited number of

non-ALT-WDLSP/DDLPS sarcomas (MDM2: 18%; CDK4: 6%). The sensitivity and specificity of MDM2 and CDK4 immunostainings in identifying ALT-WDLPS/DDLPS among other soft tissue tumors were 97% and 92%, and 83% and 95%, respectively. MDM2 and CDK4 immunostainings were particularly useful to separate ALT-WDLPS from the large group of differentiated adipose tumors, and to distinguish DDLPS from poorly differentiated sarcomas. A strong correlation was observed between MDM2 and CDK4 stainings and gene amplification status. MDM2 and CDK4 stainings were comparable whether they were performed on tissue microarrays or on whole tissue sections.
Conclusion: MDM2 and CDK4 immunostainings, which correlate with gene amplification, are helpful adjuncts to differentiate ALT-WDLPS from benign adipose tumors and to separate DDLPS from poorly differentiated sarcomas.

O-157
EVALUATION OF MDM2 GENE AMPLIFICATION AND EXPRESSION AS POTENTIAL TOOLS FOR THE DIAGNOSIS OF ATYPICAL LIPOMATOUS TUMORS/WELL-DIFFERENTIATED LIPOSARCOMAS IN PARAFFIN-EMBEDDED MATERIAL

Speel EJM, Meulemans EV, Rüland AM, Pauwels P
Department of Pathology, University Hospital Maastricht, The Netherlands

The distinction between lipomas and atypical lipomatous tumours/well differentiated lipo-sarcomas (WDLs) may be difficult to make on basis of histology and is one of the most frequent problems encountered when consultative second opinions are sought. Lipomas are cytogenetically characterized by a variety of balanced rearrangements often including the chromosome 12q13-15 region, whereas in WDLs supernumerary ring and giant marker chromosomes have been reported containing amplified 12q sequences. The MDM2 gene, located within the 12q13-15 region, is an important candidate for amplification, which may result in protein overexpression. This may permit override of the block operated by the G1-S cell cycle checkpoint on cell proliferation. The goal of this study was to determine if overexpression of MDM2 and/or MDM2 gene amplification can be used as (a) diagnostic marker(s) for the differential diagnosis of lipoma and WDL. For this purpose, we analyzed paraffin-embedded material of a series of 18 lipomas (including 4 arguable cases) and 9 liposarcomas (7 WDL, 2 dedifferentiated tumors) for MDM2 protein accumulation by routine immunohistochemistry and for MDM2 gene amplification by multicolor fluorescence in situ hybridisation (FISH) using MDM2 and centromere 12-specific probes. Three of the 18 lipomas showed MDM2 overexpression, particularly in areas with inflammation, whereas no gene amplification was detected in these tumors. In the liposarcomas, 8 tumors showed MDM2 protein accumulation except for 1 WDL. FISH analysis, however, revealed MDM2 gene amplification in this WDL as well as in 6 additional tumors, but showed two copy numbers per nucleus for both probes in 1 WDL and 1 dedifferentiated liposarcoma positive for MDM2 protein expression. Thus, although MDM2 immunostaining and MDM2 gene amplification detection by FISH show a high amount of concordance, the latter approach might be preferred in the differential diagnosis of lipoma and liposarcoma, because MDM2 immunostaining is unreliable in case of inflammatory infiltrates present in the tumor.

O-158
LOCAL RECURRENCE OF MYXOFIBROSARCOMA IS ASSOCIATED WITH INCREASE IN TUMOUR GRADE AND CYTOGENETIC ABERRATIONS, SUGGESTING A MULTISTEP TUMOUR PROGRESSION MODEL.

WILLEMS Stefan M (1), DEBIEC-RYCHTER Maria (3), SZUHAI Karoly (2), SCIOT Raf (4) and HOGENDOORN Pancras CW (1)
Departments of (1) Pathology and (2) Molecular Cell Biology, Leiden University Medical Center,Leiden, The Netherlands;
Departments of (3) Human Genetics and (4) Pathology, Catholic University of Leuven, Leuven, Belgium

Myxofibrosarcoma is one of the most frequent soft tissue tumours in elderly patients, mostly arising in the extremities. Low-grade lesions are only locally aggressive whereas intermediate and high-grade lesions have metastatic potential. The differential diagnosis contains several other benign myxoid soft tissue tumours. A number of sarcomas are characterized by specific cytogenetic aberrations, giving not only insight in their biological pathways; they also serve as helpful molecular markers in difficult diagnosis. However, cytogenetic data on myxofibrosarcomas are scarce with only a few isolated cases described in the literature. No specific chromosomal aberrations have been detected so far. Moreover, molecular pathways in tumorigenesis and progression of myxofibrosarcomas are barely understood.
Here we describe the clinicopathologic data and karyotypes of 32 myxofibrosarcomas. These include 8 low-grade, 8 intermediate-grade and 16 high-grade lesions. Twenty-two were primary tumours, nine were local recurrences and 1 a lymph node metastasis. Complex cytogenetic anomalies were found in all grades, including the presence of ring chromosomes. However, no tumour-specific chromosomal abnormalities could be withdrawn. Local recurrences showed increase in grade compared to their primary lesions. Interestingly, these local recurrences showed more complex cytogenetic aberrations. Thus increase in grade parallels increase in cytogenetic aberrations and malignant potential. Since the chromosomal aberrations found were not tumour type specific, we think that they are rather the result of secondary events in tumour progression. Based on these findings, we suggest that tumorigenesis of MFS is mainly a multistep genetic process.

O-159
DETECTION OF LOW-GRADE FIBROMYXOID SARCOMA (LGFMS) T(7;16) (FUS-CREB3L1/2) TRANSLOCATION IN PARAFFIN-EMBEDDED TISSUES, USING RT-PCR. A USEFUL DIAGNOSTIC ADJUNCT.

Louis Guillou (1), Carole Gengler (1), Jean-Michel Coindre (2), Gabrielle Gallagher (1), Dominique Ranchère-V. (3), Jean Benhattar (1), and the Members of the French Sarcoma Group. University Institute of Pathology, Lausanne, Switzerland (1), Bergonié Institute, Bordeaux (2), and Léon-Bérard Cancer Center, Lyon (3), France.

Introduction. Separating LGFMS from benign mimics (e.g. desmoid tumors, perineuriomas,..) is often problematic for pathologists. Over 90% of LGFMS bear the t(7,16) (q32-34;p11) translocation, involving either FUS and CREB3L2 (BBF2H7) genes (95% of cases) or FUS and CREB3L1 genes (5%). FUS-CREB3L1/2 fusion transcripts are detectable in frozen tissues, using RT-PCR. Experience regarding their detection in paraffin-embedded tissues is limited.
Purpose of the study. To develop a sensitive and reliable method to detect FUS-CREB3L1/2 fusion transcripts in paraffin-embedded tissues.
Materials and methods. 35 fixed, paraffin-embedded soft tissue neoplasms (30 primaries, 3 local recurrences, 2 lung metastases) with morphologic features suggestive of LGFMS,

and 31 non-LGFMS tumors were examined for the presence of FUS-CREB3L1/2 transcripts.
Results. PCR products were detected in 59 of 66 (89.4%) neoplams, including 34 (97%) potential LGFMS and 25 (80%) non-LGFMS. 26 of 34 (sensitivity: 76.5%) neoplams showing morphologic features most consistent with LGFMS contained detectable FUS-CREB3L2 (25/26; 96%) and FUS-CREB3L1 (1/26) fusion transcripts. In addition, 2 non-LGFMS, initially diagnosed as sclerosing epithelioid fibrosarcomas contained FUS-CREB3L2 transcripts; all other (n=23) non-LGMFS neoplasms were negative for FUS-CREB3L1/2 transcripts (specificity: 92%), including 9 desmoid tumors, 4 cellular myxomas, 3 sclerosing epithelioid fibrosarcomas, 3 ossifying fibromas, 1 desmoplastic fibroblastoma, 1 low-grade myxofibrosarcoma, and 2 unclassified non-LGFMS fibromyxoid sarcomas. Patients with t(7;16)-positive tumors (n=28) included 15 females and 13 males, aged from 13 to 75 years (median: 39.5 years). Tumor size on 19 cases varied between 3 and 19 cm (median: 8 cm). Tumor sites included lower extremity (11/28, 9 in the thigh), trunk wall (9), buttock (1), internal trunk (4), head and neck (2), and upper extremity (1). All but one neoplasms were deep-seated. Immunohistochemically, t(7;16)-positive LGFMS expressed epithelial membrane antigen (15/20), at least focally, but were consistently negative for S100 protein (0/23), CD34 (0/22), smooth muscle actin (0/22), desmin (0/19), and keratins (0/16).
Conclusion. The t(7;16) FUS-CREB3L1/2 translocation seems to be specific for LGFMS but fusion transcripts are detected in only 76.5% of those neoplasms initially diagnosed as potential LGFMS. 75% of t(7;16)-positive LGFMS express EMA.

O-160
CHROMOSOMAL INSTABILITY PREDICTS THE MALIGNANT PHENOTYPE IN SPORADIC INSULINOMAS

Ernst-Jan M. Speel1, Yvonne M.H. Jonkers1, Sandra M.H. Claessen1, Aurel Perren2, Sonja Schmid2, Paul Komminoth3, Albert A. Verhofstad4, Leo J. Hofland5, Ronald R. de Krijger6, Piet J. Slootweg7, Frans C.S. Ramaekers1
1Department of Molecular Cell Biology, University of Maastricht, The Netherlands, 2Department of Pathology, University Hospital Zurich, Switzerland, 3Department of Pathology, Hospital Baden, Switzerland, 4Department of Pathology, University Medical Center Nijmegen, 5Department of Internal Medicine and 6Department of Pathology, University Medical Center Rotterdam, 7Department of Pathology, University Medical Center Nijmegen, The Netherlands

Insulinomas are the most frequently encountered functioning endocrine pancreatic tumors to occur in humans. The metastatic potential of insulinomas can frequently not be predicted using histopathological criteria, and also molecular markers indicating malignant progression are unreliable because of the small number of cases per subtype studied so far. For the identification of reliable indicators of metastatic disease, we studied 62 sporadic insulinomas (44 benign and 18 tumors with metastases) by means of comparative genomic hybridization (CGH). In addition, the role of MEN1 gene mutations was determined to assess specific chromosomal alterations associated with dysfunction of this endocrine tumor-related tumor suppressor gene. Only one case with a somatic MEN1 mutation was identified (1527del7bp), indicating that the MEN1 gene plays a minor pathogenic role in sporadic insulinomas. CGH analysis revealed that 1) the total number of aberrations per tumor differs strongly between the benign and the malignant group (4.2 vs 14.1; $p<0.0001$), and 2) chromosome 9q gain is the most frequent aberration in both benign and malignant insulinomas, whereas chromosome 6q losses and 12q, 14q and 17pq gains are strongly associated with metastatic disease. Our study shows that chromosomal instability, as defined by 5 or more gains together with 5 or more losses, or a total number of gains and losses of 8 or more, rather than parameters such as tumor size, is the most powerful indicator for the development of metastatic disease in patients with sporadic insulinoma. Furthermore, the identified genetic changes may indicate novel genes important in the tumorigenesis of insulinomas.
This study was supported by grants from the Association for International Cancer Research and the Netherlands Foundations Vanderes and Sacha Swarttouw-Hijmans.

O-161
THE PROGNOSTIC SIGNIFICANCE OF CYTOKERATIN 19 EXPRESSION IN PANCREATIC ENDOCRINE TUMORS (PETS)

LA ROSA Stefano, BIANCHI Veronica, RIGOLI Elena, UCCELLA Silvia, CAPELLA Carlo
Dept. of Pathology, Ospedale di Circolo and University of Insubria, Varese, Italy

Introduction: pancreatic endocrine tumors are a heterogeneous group of neoplams showing different clinical, morphological and molecular features. They are currently classified according to the criteria of the recent WHO classification into well and poorly differentiated tumors. The latter represent a very aggressive category with poor outcome and well defined histology. Well differentiated tumors include benign, malignant or borderline subtypes and their prognosis is difficult to establish on a pure morphological background. In recent years, several attempts have been made to identify prognostic markers and, among them, the expression of cytokeratin 19 (CK19) has been recently proposed as an indicator of unfavorable outcome. However, this finding remains to be verified and to be compared with more used prognosticators such as Ki67 and mitotic index, vascular and/or perineural invasion.
Aim: was to evaluate the expression and the role of cytokeratin 19 as prognostic marker in PETs.
Methods: 145 well characterized PETs have been immunohistochemically studied using two different anti-CK19 monoclonal antibodies (BA17 and RCK108). Results were statistically compared with clinicopathological features, Ki67 and mitotic index and vascular and perineural invasion.
Results: By univariate analysis, only the CK19-immunoreactivity obtained with the RCK108 antibody correlated with prognosis. In particular, RCK108 staining correlated with prognosis when the whole group of PETs was considered and in the group of insulinomas. On the contrary, it did not show a prognostic meaning among nonfunctioning neoplasms. Ki67 index, mitotic count, vascular and perineural invasion were all statistically correlated with prognosis at the univariate analysis. However, at the multivariate Cox test analysis, only the Ki67 index (>2%) proved to be an independent prognostic marker.
Conclusion: CK19 expression when tested with the RCK108 antibody correlates with the prognosis of patients with PETs, and especially for those harboring insulinomas. However, Ki67 index appears to be a more significant prognostic predictor.

O-162
DOES EXPRESSION OF CYTOKERATIN 19 IN PANCREATIC ENDOCRINE TUMORS CORRELATE WITH THE WHO CLASSIFICATION?

KAPRAN Yersu*, OZTURK A. Sanem*, GULLUOGLU Mine G.*, ERBIL Yesim**, GILES Yasemin**, BILGE Orhan**, DIZDAROGLU Ferhunde*
*Istanbul University Istanbul Faculty of Medicine, Department of Pathology

**Istanbul University Istanbul Faculty of Medicine, Department of General Surgery

Expression of cytokeratin 19 in islets is restricted to fetal pancreas, whereas strong expression remained in the ductal cells of the adult pancreas. In compatible with this feature ductal carcinomas positively stain with CK19, while CK19 expression has not been systematically investigated in pancreatic endocrine tumors (PETs). A recent study suggests that CK19 positivity is a highly specific marker of adverse outcome in PETs. Our aim was to evaluate the expression of CK19 in PETs classified according to the WHO classification. Our study included 22 tumors of which 8 were well-differentiated benign PETs, 10 well-differentiated PETs with uncertain behavior and 4 well-differentiated malignant PETs. In the benign group only one tumor showed focal weak CK19 positivity (1/8), while all tumors in the uncertain behavior (10/10) and malignant group (4/4) had diffuse and moderate to strong positivity ($p<0.001$). Our results indicate a close association between CK 19 immunoexpression and WHO classification. CK19 can be used to discriminate the benign tumors from other groups, though it does not show any difference between tumors with uncertain behavior and malignant ones.

O-163
ACTIVATION OF THE WNT SIGNALING PATHWAY IS A FREQUENT EVENT IN BOTH BENIGN AND MALIGNANT ADRENOCORTICAL TUMORS

TISSIER Frédérique (1,2), CAVARD Catherine (3), GROUSSIN Lionel (2,4), PERLEMOINE Karine (2), FUMEY Gwladys (2), HAGNERE Anne-Marie (1), RENE-CORAIL Fernande (2), JULLIAN Eric (2,5), GICQUEL Christine (6), BERTAGNA Xavier (2,4,7), VACHER-LAVENU Marie-Cécile (1), PERRET Christine (2), BERTHERAT Jérôme (2,4,7)
(1) Department of Pathology, Cochin Hospital, APHP, René Descartes-Paris V University, Paris, France
(2) Department of Endocrinology, Institut Cochin, INSERM U567, Paris, France
(3) GDPM, Institut Cochin, INSERM U567, CNRS UMR 8104, IFR116, René Descartes-Paris V University
(4) Department of Endocrinology, Cochin Hospital, APHP, Paris, France
(5) Oncogenetics Unit, Cochin Hospital, APHP, René Descartes-Paris V University, Paris, France
(6) Department of Physiology, Trousseau Hospital, APHP, Paris, France
(7) COMETE NETWORK, Paris, France

Introduction: Adrenocortical carcinoma is a rare cancer with a very poor prognosis. The genetic alterations identified to date in adrenocortical tumors (ACT) are limited. Activating mutations of the Wnt signaling pathway have been observed in more frequent cancers, particularly digestive tract tumors. We investigated whether Wnt pathway activation is involved in ACT tumorigenesis.
Material and methods: Sporadic adrenocortical tumor (other than Conn's adenoma) was diagnosed in 39 adult patients. Immunohistochemical study with an anti ß-catenin antibody was performed from formalin-fixed tissue embedded in paraffin. For mutation analysis exon 3 and the flanking intronic sequences of the beta-catenin gene were amplified by PCR from tumoral as well as leucocyte DNA.
Results: Immunohistochemistry (IHC) revealed abnormal cytoplasmic and/or nuclear accumulation of ß-catenin in 10 of 26 adrenal adenomas (AA) and 11 of 13 adrenal carcinomas (AC). An activating somatic mutation of the ß-catenin gene was demonstrated in 7 AA (7/10 with abnormal IHC) and 4 AC (4/11); most of these mutations were point mutations altering the serine 45 of exon 3 (in the consensus GSK3ß/CK1 phosphorylation site), although deletions were also observed in two ACT. This is the first molecular defect to be reported with the same prevalence in both benign (7/26) and malignant (4/13) ACT. ß-catenin mutations are also the most frequent genetic defect currently known in AA. In AA, ß-catenin alterations seem to be more frequent in non functional tumors, suggesting that ß-catenin pathway activation might be involved in the development of non secreting AA and AC. The very frequent and substantial accumulation of ß-catenin in AC suggests that other alterations might also be involved as APC or axin mutations.
Conclusion: The finding of activating mutations of the Wnt signaling pathway in adrenocortical tumors may contribute to new therapeutical approaches targeting the Wnt pathway in malignant ACT, for which only very limited medical therapy is available.

O-164
CONVENTIONAL AND 1P-SPECIFIC MICROARRAY-BASED CGH ANALYSIS OF SPORADIC AND SYNDROME-RELATED PHEOCHROMOCYTOMAS

Speel EJM1, Aarts M2, Dannenberg H2, Claessen SMH1, DeLeeuw RJ3, Van Nederveen F2, Verhofstad AA4, Dinjens WNM2, Lam WL3, De Krijger RR2
1Department of Molecular Cell Biology, University of Maastricht, Departments of Pathology, 2Josephine Nefkens Institute, Erasmus University Medical Center Rotterdam and 4University Medical Center Nijmegen, The Netherlands and 3Department of Cancer Genetics and Developmental Biology, British Columbia Cancer Research Center, Vancouver, Canada

Pheochromocytomas (PCCs) are relatively rare neuroendocrine tumors, mainly of the adrenal medulla. They occur sporadically or as part of inherited cancer syndromes, such as MEN2, NF1 or VHL. Because to date no reliable histological or molecular markers are available to distinguish benign from malignant PCCs, and VHL-related PCCs exhibit genetic alterations different from sporadic PCCs, we used conventional CGH analysis to identify chromosomal alterations involved in tumor development and metastatic progression in 55 sporadic, 10 MEN2- and 3 NF1-related PCCs. In addition, 24 of these tumors were analyzed by CGH on a microarray of 642 overlapping BAC clones mapped to 1p11.2-1p36.33 to identify the critical regions on this most frequently lost chromosome arm in PCCs. ArrayCGH showed that the consensus regions of deletion involved 1cen-1p32.3 and 1p34.3-1p36.33. Conventional CGH analysis revealed that 1) 1p and 3q losses are frequent, 2) amplifications in each of 3 sporadic tumors are detected at 7p13-q22, 10q11.2 and 19p13.2-13.3, 3) the average number of alterations, gains and losses per tumor differed significantly between benign sporadic and MEN2-related PCCs, i.e. 5.4 versus 9.6 ($P<0.0001$), 1.2 versus 3.5 ($P=0.003$) and 4.1 versus 6.1 ($p=0.007$), respectively, 4) losses of 3q, 8q, 9p and 13q and gains of 1q, 17q and 20q were more often observed in MEN2-related PCCs, whereas losses of 6q and 11p were exclusively found in the sporadic PCCs, 5) benign tumors are significantly smaller than malignant ones (d= 6.2 versus 10.5 cm; $P=0.001$), 6) the total number of aberrations per tumor differs strongly between benign and malignant PCCs (5.4 versus 9.4; $P=0.004$), as does the number of gains (1.2 versus 2.9; $P=0.04$) and losses (4.1 versus 6.6; $P=0.008$), and 7) losses of 8p and 18p and gains of 5p, 7p and 12q are detected significantly more frequent in malignant PCCs (P¡Ü0.047). Our study indicates that losses of 1p and 3q are early genetic events in the pathogenesis of sporadic and syndrome-related PCCs, but that sporadic and MEN2-associated tumors further evolve along different genetic pathways. Malignant PCCs appear to be associated with chromosome 8p and 18p losses and 5p, 7p and 12q gains. The identified chromosomal

regions may lead to the discovery of novel genes that play a role in PCC tumorigenesis and may help to predict their biological behavior.
This study was supported by the Netherlands Van Walree Fund and the Dutch Cancer Society.

O-165
CORRELATION OF ACCUMULATION OF MICROSATELLITE ABNORMALITIES AND SOMATIC DOWN-REGULATION OF MISMATCH REPAIR PROTEINS IN MALIGNANT PHEOCHROMOCYTOMAS

Salvador J. Diaz-Cano(1,2) and Alfredo Blanes(2)
(1) King's College Hospital-GKT School of Medicine, London, UK
(2) University of Malaga School of Medicine

Background: Adrenal pheochromocytomas (PCC) have been extensively studied at the molecular level, but no information is available on the microsatellite profile by topographic compartments of malignant and locally-invasive PCC. The contribution of DNA mismatch repair abnormalities to this profile remains unknown.
Design: Microdissected samples from the peripheral and internal zones of 143 PCC (95 sporadic, 48 associated to MEN 2A) were selected for loss of heterozygosity (LOH) and single nucleotide polymorphism (SNP) analyses. Five polymorphic DNA regions from TP53, RB1, WT1, and NF1 were systematically studied by polymerase chain reaction-denaturing gradient gel electrophoresis. PCC were classified malignant (16 sporadic tumors with distant metastases), locally invasive (30 sporadic tumors showing showing retroperitoneal infiltration only), and benign (all remaining tumors). Statistical differences were evaluated using Fisher's exact test. Mismatch repair was assessed by mlh1 and msh2 sequencing and immunostaining in PCC with >2 abnormal microsatellite loci.
Results: LOH/SNP involved TP53 in 40/134 informative cases (29.9%), RB1 in 22/106 informative cases (20.8%), WT1 in 32/120 informative cases (26.7%), and NF1 in 32/80 informative cases (40.0%). More genetic abnormalities involving the peripheral compartment were revealed in 34 PCC (23.8%): 12/16 malignant, 10/30 locally invasive, and 12/97 benign. Multiple and coexistent genetic abnormalities characterized malignant PCC ($p<0.001$), whereas locally invasive PCC showed significantly higher incidence of NF1 alterations ($p<0.001$).
A significant decrease of MLH1/MSH2 protein expression was observed in the peripheral compartment, but with no gene mutations identified in PCC with high microsatellite instability.
Conclusions: 1. Somatic topographic down-regulation of mismatch repair proteins contributes to both the accumulation of microsatellite lesions in the peripheral compartment and intratumor heterogeneity, the trwo key features characterizing malignant PCC and supporting multistep tumorigenesis for these neoplasms. 2. In contrast, locally invasive PCC frequently reveals single locus alterations, especially involving NF1.

O-166
CORTISTATIN AND MRGX2 RECEPTOR EXPRESSION IN HUMAN NEUROENDOCRINE TISSUES AND RELATED TUMORS.

VOLANTE Marco1, ALLIA Elena1, TARABRA Elena2, ROSAS Rosj3, CAPPIA Susanna3, MUCCIOLI Giampiero2, PAPOTTI Mauro3.
1Department of Biomedical Sciences & Oncology
2Division of Pharmacology, Department of Anatomy, Pharmacology and Forensic Medicine
3Departments of Clinical & Biological Sciences at San Luigi Hospital Orbassano
University of Turin, Torino, Italy

Introduction. Cortistatin (CST) is a novel hormone firstly described in the rat, mouse and human cerebral cortex, with structural and functional similarities to somatostatin (SRIF). CST binds to all five somatostatin receptors, and, differently from SRIF, also to other receptors, such as the growth hormone secretagogue receptor (GHS-R) type 1a and MrgX2, recently identified as its specific receptor. Little is known on CST and MrgX2 distribution in peripheral non-tumoral and neoplastic tissues, although the presence of CST has been reported in the human endocrine pancreas and immune system.
Purpose of the study. Our aim was to determine CST and MrgX2 distribution, at both protein and mRNA level, in human non-tumoral and neoplastic tissues, with special reference to neuroendocrine ones.
Methods. CST and MrgX2 immunohistochemistry and mRNA analysis (RT-PCR) were performed in 56 non-tumoral and 108 tumoral human tissues. Co-localization experiments with double-label immunofluorescence and immunohistochemistry were also performed.
Results. Despite the high amount of CST mRNA expression in non-tumoral and tumoral (both neuroendocrine and non-neuroendocrine) tissues, the presence of immunoreactive CST was confirmed in a subset of gastroenteropancreatic (GEP), parathyroid, and pituitary non-tumoral cells only, and, focally, in 24/43 neuroendocrine tumors. No immunoreactivity was observed in non-neuroendocrine tumors. Colocalization experiments in the GEP system demonstrated that the normal CST producing cells are ä cells, while in the adenohypophysis no preferential co-localization of CST with any of the pituitary hormones was observed. MrgX2 mRNA was variably detected in the hypothalamus, pituitary, thyroid, lung, GEP tract, testis and ovary, and was negative in the cerebral cortex, parathyroid and adrenal, as well as in a variety of tumor types. Conversely, immunolocalization of MrgX2 protein was restricted to neurohypophysis and testis, being all tumors analyzed negative. Moreover, MrgX2 protein was widely detected in blood vessels, scattered lymphocytes and gastrointestinal ganglia, of both normal and neoplastic samples.
Conclusion. Our findings demonstrate a selective distribution of CST in normal and neoplastic neuroendocrine tissues suggesting that CST might have a broader functional role than previously assumed. In tumors, autocrine/paracrine CST actions are probably mediated by receptors (ie somatostatin receptors) other than MrgX2.

O-167
GALECTIN-3 IMMUNOHISTOCHEMICAL DETECTION IN THE DIFFERENTIAL DIAGNOSIS OF PARATHYROID LESIONS.

VOLANTE Marco*, BERGERO Nicoletta, RAPA Ida, ROSAS Rosj, SACERDOTE Carlotta*, GASPARRI Guido, BUSSOLATI Gianni*, PAPOTTI Mauro
Departments of Clinical & Biological Sciences at San Luigi Hospital Orbassano, and of *Biomedical Sciences & Oncology, University of Turin, Torino, Italy

Introduction. The differential diagnosis and classification of parathyroid lesions needs complementary evaluation of clinical data and morphologic features. No strict microscopic criteria have been unequivocally defined, especially in the identification of malignant lesions without clear-cut invasive growth or metastases. Proliferation markers (Ki-67 and others) have been proposed to distinguish adenomas from carcinomas, but a some overlap exists between benign and malignant lesions, thus limiting their diagnostic applicability.

Purpose of the study. We aimed to analyze the expression of galectin-3 (gal-3), a well-established marker of malignancy in thyroid follicular nodules, as a possible diagnostic adjunct in the classification of parathyroid hyperplastic/neoplastic lesions.
Methods. A retrospective series of 112 parathyroid lesions, including 26 carcinomas (PC) (diagnosed on the basis of capsular/vascular invasion in 26 cases, extra-parathyroid infiltration in 16 cases, local recurrence in 9 cases and distant metastases in 6 cases), 35 adenomas (PA), 4 primary hyperplasias (PHP), 50 secondary hyperplasias (SPH) and 7 tertiary adenomas (TPA), was collected and screened by immunohistochemistry for Ki-67 and gal-3. Results were statistically validated in terms of sensitivity, specificity and p values determined by Fisher and Mann-Whitney tests.
Results. As expected, Ki-67 proliferative index was higher in PC (mean 6.7%) than PA (2.2%), PHP (0.3%), SHP (1,8%), and TPA (0.1%) ($p<0.001$). Gal-3 was expressed by 92.3% of PC (24/26) and 3.3% of PA (1/35) ($p<0.001$). All metastatic PC cases were gal-3 positive. The association of gal-3 with Ki-67 (using a cut-off of 6%) increased sensitivity to 96.2% and specificity to 90%. PHP and TPA were gal-3 negative in all but one case each, while SPH showed gal-3 immunoreactivity in 62% of cases, with a slightly higher expression (percentage of case and also intensity) in recurrent cases.
Conclusion. In highly proliferating (Ki-67 >6%) primary parathyroid lesions, gal-3 expression is a valuable additional tool to support a diagnosis of PC. By contrast, gal-3 over-expression in most SHP is unrelated to malignancy, and, although limiting its diagnostic utility in secondary hyperparathyroidism, may suggest a possible role of specific gal-3 modulators linked to renal failure and active in its up-regulation.

O-168
HIGH INCIDENCE OF HPV16 IN TONSIL CARCINOMA

1De Crémoux P., 2Jouffroy T., 1Fréneaux P., 1Thioux M., 1Rosty C., 1Nicolas A., 2Rodriguez J., 1Sastre-Garau X.
Departments of 1Tumor Biology and 2Surgery,
Institut Curie, 26, rue d'Ulm, 75248 Paris.

Background: HPV DNA sequences are associated with the large majority of genital cancer but the oncogenic role of these viruses in head and neck tumors is less documented. We have analyzed a series of cases to determine whether tumors of the oral cavity were more likely to be linked to HPV.
Material and Methods. A series of 80 cases of oral invasive squamous cell carcinoma has been analyzed. These cases corresponded to tumors developed in the tonsil (51 cases) or in other localizations of the oro-pharyngeal region (tongue, gingiva …) (29 cases). For each case, a DNA extraction and HPV typing have been performed by PCR using primers specific for HPV16, HPV18, HPV6/11, HPV33, HPV45 or using consensus primers.
Results: HPV DNA sequences were found in 38 of the 80 cases analyzed (48%). A striking difference was observed between the HPV positive rate in tonsil carcinoma (61%) and that in other localizations (24%). Most of the HPV positive carcinoma of the tonsil were found associated with HPV16 (25/31;81%). In contrast, only 3 of the 7 tumors at other localizations were associated with this type of virus.
Conclusion: A high incidence of HPV 16 is observed in tonsil carcinoma, in contrast with that found in other tumors of the oral cavity. Further studies are in progress to determine whether clinical, pathological and epidemiological features distinguish HPV positive from negative carcinoma of the tonsil. These data may be important for a better knowledge of the pathogenesis of head and neck tumors and for the development of specific therapy.

O-169
HPV 16 IN RELATION TO SMOKING AS PROGNOSTIC INDICATORS FOR PATIENTS WITH TONSILLAR CARCINOMAS

Speel EJM1,3, Hafkamp HC2, Schepers M2, Bot FJ3, Haesevoets A1, Claessen SMH1, Voogd AC4, Hopman AHN1, Ramaekers FCS1, Manni JJ2.
1Departments of Molecular Cell Biology and 4Epidemiology, University of Maastricht, and Departments of 2Otorhinolaryngology, Head and Neck Surgery and 3Pathology, University Hospital Maastricht, The Netherlands

Apart from alcohol and tobacco, oncogenic human papillomavirus (HPV) is a causative agent for a subgroup of head and neck squamous-cell carcinomas (HNSCC), particularly tonsillar carcinomas. The literature, however, is controversial with respect to the physical status of HPV DNA (episomal and/or integrated) in the tumor cells, the use of p16INK4A overexpression as a surrogate marker for HPV detection, and the clinical course and prognosis of HPV-related HNSCC. Formalin-fixed, paraffin-embedded tissue sections of 81 tonsillar carcinomas were subjected to HPV 16-specific fluorescence in situ hybridization (FISH) and p16INK4A-specific immunohistochemistry to assess the frequency of tumors exhibiting HPV integration and p16INK4A overexpression. Medical records were screened for (clinical) patient data, and results were statistically evaluated. FISH detected HPV 16 integration in 33/81 (41%) carcinomas, 32 of which also showed p16INK4A accumulation. Only 5/48 HPV-negative carcinomas did stain for p16INK4A. The presence of HPV in the tumor thus correlates very strongly with p16INK4A overexpression ($P<0.0001$), as well as with low amounts of tobacco and alcohol intake, poor differentiation grade, small tumor size, presence of local metastases and a decreased recurrence rate (P,,T0.039). Kaplan Meier analysis revealed that particularly non-smoking patients with HPV-containing tumors show a remarkable improved disease-specific survival as compared to smoking patients with or without detectable HPV. In conclusion, our data show that approximately half of the tonsillar carcinomas harbor integrated HPV 16 DNA. Virus integration is strongly correlated with p16INK4A accumulation, suggesting that p16INK4A may be considered as an alternative biomarker for HPV detection in tonsillar carcinomas. HPV 16-associated tonsillar tumors predict an improved prognosis in non-smokers.
Supported by the Medical Research Foundation of the University Hospital Maastricht.

O-170
A FRENCH STUDY OF 58 TONSILLAR CARCINOMAS: HPV TESTING AND EXPRESSION OF P16 PROTEIN

GUILLOU Pierre-José, COISSARD Cyrille, VITRY Fabien, LORENZATO Marianne, CHAYS André, PLUOT Michel, BIREMBAUT Philippe, DIEBOLD Marie Danièle, CLAVEL Christine, MEROL Jean-Claude
Laboratoire Central d'Anatomie et de Cytologie Pathologiques, Laboratoire Pol Bouin, Unité d'Aide Méthodologique et Service d'Oto-Rhino-Laryngologie
CHU de Reims, 45 rue Cognacq-Jay, 51092 REIMS CEDEX, France

Oncogenic Human Papillomavirus (HR-HPV -High Risk HPV-), the causal agent of cervical cancer, appears to be involved in the etiology of the cancers of oropharynx, especially in tonsillar carcinomas (TC). Interactions between HR-HPV oncoproteins (E6/E7) and cell cycle proteins as p16 encoded by the CDKN2A tumor suppressor gene are involved in carcinogenesis and p16 overexpression is postulated to be a

specific biomarker of cervical neoplasia. The prevalence of HPV detection may vary depending on the population and the detection procedure. Our aim was to evaluate the frequency and type of HPV DNA in a retrospective series of TC and its association with 3 immunohistochemical markers: p16, p53 and MIB1. 58 case patients with TC were recruited in this retrospective study in the C. H. U. of Reims from 1987 to 2004: 54 men (mean age: 55.7) and 4 women (mean age: 54.1). Patients were mainly heavy smokers and drinkers. All the tumors were squamous carcinomas: 53 well or moderately differentiated and 5 poorly differentiated. Total DNA was extracted from paraffin-embedded tissues. HPV detection and genotyping were performed using the Line Blot Assay (Roche). This assay allowed the genotyping of 21 HR-HPV and 16 LR-HPV (low risk HPV). Immunohistochemistry was processed using p53, p16 and MIB1 antibodies. P16 immunostaining was scored according to Klaes. The threshold of p53 positivity was 10%. We detected HPV DNA in 20.7% of cases, represented by HPV-16 in 66%. 21 % of all tumors were positive for p16 protein. P53 was detected in 47% of cases. For MIB1, the mean value of positivity was 44% +/- 25. 58% of HPV positive tumors were p16 positive versus 11% of HPV negative tumors (p=0.001). There was no significant difference between the two groups with p53 and MIB1. HPV status was correlated neither with histological differentiation nor TNM staging. Analysis showed less smokers (10/12 vs 45/46) and drinkers (9/12 vs 44/46) among patients with a HPV + tumor. Age and gender were not different between the two groups. The rate of HPV positivity in our study is inferior to previously published results for tumors at the same site and similar to HPV prevalence reported in the head and neck carcinomas in general. In spite of a tendency of less smokers and drinkers in HPV + patients, the 2 groups were characterized by heavy tobacco and alcohol exposure which may explain these results. P16 expression was correlated with HPV status with less specificity than previously reported.

O-171
EVALUATION OF FROZEN SECTION VERSUS DEFINITIVE PATHOLOGIC DIAGNOSIS IN 721 PAROTID GLAND LESIONS

BADOUAL Cécile (1), ROUSSEAU Audrey (1), HEUDES Didier (1), CARNOT Françoise (1), BRUNEVAL Patrick (1), BRASNU Daniel (2), LACCOURREYE Ollivier (2).
(1) Department of Pathology,
(2) Department of Otorhinolaryngology - Head & Neck Surgery,
Hôpital Européen Georges Pompidou, Assistance Publique des Hôpitaux de Paris, Université Paris V, Paris, France.

We report a large series of 721 patients operated on for a parotid mass. In each case, a frozen section was performed during surgery. Results of frozen section examination were evaluated in comparison with the corresponding definitive pathologic diagnosis.
On frozen section, 97 (13.5%) and 624 (86.5%) specimens were considered as malignant and non malignant, respectively. On definitive examination, 124 patients (17.2%) presented a malignant tumor and 597 patients (82.8%) had a benign lesion. For malignant versus benign lesion assessement, frozen section examination had a sensitivity of 74% and a specificity of 99%, with 6 false positive (0.83%) and 24 (3.5%) false negative cases. Carcinoma was correctly diagnosed in 74.1% malignant cases, as was adenoma in 95.9% benign lesions. But the exact tumor type could be established in only half cases, with the exception of Warthin tumor and pleomorphic adenoma which were accurately diagnosed in more than 90% cases. Cysts were interpreted as benign lesions in all instances. Lymphoma was correctly identified in 65% cases and was mostly misdiagnosed as adenopathy in the remaining cases. Metastases and non epithelial tumors were accurately interpreted in more than 90% cases. Frozen section examination during surgery is a useful diagnostic tool in correlation with clinico-radiological and preoperative cytological data if both the surgeon and the pathologist are aware of its performance and difficulties.

O-172
ANGIOGENIC AND LYMPHANGIOGENIC MICROVESSEL DENSITY IN CARCINOMA EX PLEOMORPHIC ADENOMA AT AN EARLY PHASE OF THE CARCINOMATOUS TRANSFORMATION

SOARES Andresa*,JULIANO Priscila*, METZE Konradin*, ARAUJO Vera **, ALTEMANI Albina*
* Department of Pathology, Medical Science Faculty, University of Campinas - UNICAMP, Brazil
** CPO São Lepoldo-Mandic, Campinas, Brazil

Carcinoma ex pleomorphic adenoma (CXPA) is an epithelial malignancy that arises in or from a pleomorphic adenoma (PA). Based on the extent of invasion beyond the PA capsule, the carcinoma may be classified as intracapsular, minimally invasive, and frankly invasive. Intracapsular and minimally invasive carcinomas have been considered low-grade tumors that behave benignly. However, metastases have recently been reported in intracapsular CXPA and minimally invasive CXPA. As angiogenesis and lymphangiogenesis are critical processes for tumor growth and invasion, the aims of this study were to evaluate the microvessel density and the presence, if any, of lymphatic vessels in intracapsular and in minimally invasive CXPA comparing the benign and malignant areas of the tumor. We measured blood and lymphatic vascular microvessel density in 7 CXPAs (3 intracapsular and 4 minimally invasive) using immunohistochemical vascular marker CD34 and lymphatic marker D2-40 (both from Dakocytomation). No patient presented metastasis. Vessels were counted in representative high magnification fields in benign and malignant areas and then the mean microvessel density for CD34 and D2-40 was calculated for each one. In six cases (85.7%), the carcinoma was high-grade with nuclear pleomorphism ranging from moderate to severe. Lymph vessels were found neither in the benign nor in the malignant areas of the tumor. The peritumoral lymphatics were morphologically similar to normal tissue vessels. Microvessel density within individual tumors was heterogeneous and correlated directly with the cellular density. The carcinomatous areas, which were highly cellular in all cases, presented microvessel density (mean 4.29, std ±0.81) similar to the benign portions of the cellular type (mean 4.94, std ±1.02), in which the epithelial element predominates. Benign areas composed largely of myxochondromatous element showed significantly lower microvessel density (mean 3.38,std ±0.72) than cellular portions of the lesion, regardless if the latter were benign or malignant. The peritumoral tissue around the microinvasive areas of the carcinoma beyond the PA capsule showed slight increase of the microvessel density. In conclusion, the malignant transformation in PA does not promote significant increase of the vascular proliferation. Similar to other solid glandular tumors there is absence of intratumoral lymph vessels in CXPA.

O-173
ACINAR CELL CARCINOMA VERSUS ADENOID CYSTIC CARCINOMA: THE PIVOTAL ROLE OF ELECTRON MICROSCOPY IN ASSESSING THE CORRECT DIAGNOSIS

RESTA Leonrado, FIORE Maria Grazia, SANGUEDOLCE Francesca, PISCITELLI Domenico
DAP-Department of Anatomic Pathology, University of Bari, ITALY

The importance of electron microscopy as an ancillary technique in pathology has decreased with the development of immunohistochemistry and molecular biology; nowadays, it still plays an important role in research, but seems to have little practical diagnostic use. We report here the case of a 62-year-old man who presented with a 1-year history of a mass located at left parotid region. CT scan revealed a well-defined solid tumor involving the middle third of the left parotid gland. Macroscopic examination of the surgical specimen showed an oval soft greyish tumor of 2,8 cm in its largest dimension. The light microscopy diagnosis, made on the basis of its architectural and cytological features, was of acinar cell carcinoma with microfollicular pattern. The case was submitted to ultrastructural examination within a review of parotid neoplasms, showing the presence of true glandular lumina and pseudocysts, and a reduplication of basal membrane surrounding myoepithelial cells; such findings allowed us to finally make the correct diagnosis of tubular type adenoid cystic carcinoma. A further confirmation came from immunohistochemistry, that revealed vimentin and CD117/c-kit positivity of neoplastic cells.
In our case, electron microscopy played a major role in assessing the diagnosis, thus confirming its importance in pathological practice especially in a field as tricky as salivary gland tumors.

O-174
INVOLVEMENT OF UBIQUITINATION AND SUMOYLATION IN URINARY BLADDER CARCINOGENESIS INDUCED BY PERSISTENT LONG-TERM LOW DOSE IONIZING RADIATION IN HUMANS

Prof. Alina Romanenko, Prof. Alexander Vozianov, Prof. Shoji Fukushima
Dept. of Pathology and Urology, Institute of Urology, Kiev(Ukraine), Dept. of Pathology, Osaka University Medical School (Japan)

Introduction.
The incidence of urinary bladder cancer in the Ukraine increased from 26.2 to 50.3 per 100, 000 population between 1986 and 2003 after the Chernobyl accident. Cesium 137 accounts for 90% of the internal radioactivity in the Ukrainian population and it is known to be eliminated via the urine. The present study was conducted to determine whether ubiquitination and sumoylation processes in cell proteolysis are altered in urinary bladder urothelium by chronic long-term persistent low doses of ionizing radiation (IR) in male patients with benign prostate hyperplasia and females with chronic cystitis living more than 19 years in Cesium 137 contaminated areas after the Chernobyl accident in Ukraine.
Material & Methods.
Bladder urothelial biopsies from 45 patients were subjected to histopathological and immunohistochemical studies of ubiquitin (Ub), the small Ub-related modifier 1 (SUMO1), SUMO E2 conjugating enzyme Ubc9, and the cell cycle inhibitors p53 and p27Kip1.
Results.
Chronic proliferative atypical cystitis ("Chernobyl cystitis"), featuring multiple foci of dysplasia, and carcinoma in situ (CIS) were observed in 23 (92%) and 19 (76%), respectively, of 25 group 1 patients from radio-contaminated areas, in addition to one small pTa grade 1 urothelial carcinoma. Chronic cystitis with areas of mild dysplasia and urothelial hyperplasia were detected in 2 (10%) and 3 (15%) of 20 patients in the control group 2 from so-called clean (without radio-contamination) areas of Ukraine. Strongly elevated levels of Ub, SUMO1, Ubc9 and p53 as well as decreased levels of p27Kip1, were evident for patients in group 1, as compared to group 2 (all $p < 0.001$).
Conclusion.
Activation of ubiquitination and sumoylation processes in Chernobyl cystitis might be a compensatory reaction in response to the insufficient proteolysis of aberrant p53 and, on the other hand, lead to unscheduled degradation of p27Kip1 cell cycle negative regulator occurred due to the long-term low dose rate IR exposure that may contribute to urothelial carcinogenesis caused by IR.

O-175
MOLECULAR ANALYSIS OF INVERTED TUMORS OF THE URINARY BLADDER: FGFR3 MUTATION STATUS AND KI-67 INDEX CAN RESOLVE DIFFICULT CASES.

Arndt Hartmann, Matthias Eiber, Joke Van Oers, Ellen Zwarthoff, Peter Wild, Robert Stoehr, Stephan Störkel, Theo Van der Kwast, Guido Sauter, John C. Cheville, Mahul Amin, Ferdinand Hofstaedter, Regine Schneider-Stock, Hagen J. Blaszyk. Institute of Pathology, University Regensburg, Germany, Institute of Pathology, Erasmus MC Rotterdam, The Netherlands, Clinic of Urology, University Regensburg, Germany, Institute of Pathology, Helios Clinic Wuppertal, Institute of Pathology, University Basel, Switzerland, Mayo Clinic, Rochester, MN, Institute of Pathology, Emory University Atlanta, GA, Institute of Pathology, University Magdeburg, Germany, Institute of Pathology, University of Vermont, VT

Purpose: Inverted papilloma of the urinary tract (IP) is thought to be benign, but some urothelial carcinomas show a prominent inverted growth pattern (invUC) which may pose a diagnostic dilemma. Ancillary markers may help to resolve diagnostically challenging cases. Design: 89 inverted urothelial lesions of the urinary tract were reviewed by five uropathologists. Four European pathologists diagnosed these lesions as inverted papilloma, low grade UC and high grade UC, whereas one American pathologist used the new WHO classification criteria (IP, PUNLMP, low grade UC, high grade UC).
Genetic alterations frequently found in non-invasive papillary UCC were investigated after microdissection. Deletion of chromosome 9p/q, 17p (LOH) and microsatellite instability (MSI) were determined by microsatellite analysis. Mutations in FGFR3 were analyzed by SNaPshot. Promotor methylation of p16, DAPK, E-cad, RASSF1 and hMLH1 was investigated by methylation sensitive PCR (MSP). Expression of p53, Ki67, CK20, hMLH1, hMSH2 and hMSH6 was studied immunhistochemically. Ploidy and deletion status of 9p21 (p16) was investigated by FISH (Urovysion®).
Results: MSI and loss of mismatch-repair-protein within the European consensus was very infrequent in contrast to inverted tumors of the upper urinary tract. LOH of chromosome 9q was detected in 7/53 IP with a higher percentage in invUC (8/22). Methylation was found in 18 of 53 IP (mostly in DAPK, hMLH1 and p16). Clinical data revealed a significant difference ($p=0.002$) concerning recurrence in IP (3/51) vs. invUC (6/14). No patient with IP showed a history of UCC, whereas 3/12 invUC did ($p=0.001$). Ki67 proliferation index and FGFR3-mutation correlated strongly with the histological diagnosis ($p<0.0001$). In contrast, with regard to the American diagnosis there was a lower significant difference between IP and invUC with Ki67 labeling index and FGFR3 status ($p=0.012$ and $p=0.041$, respectively) and no association to clinical data.
Conclusions: MSI, deletions in chromosome 9 and 17 and FGFR3 mutations are rarely seen in IPs. IPs does not show molecular changes associated with a malignant urothelial genotype. Our data strongly suggest that IP are benign urothelial lesions. In our view inverted tumors without clear features of malignancy should not be classified as a malignant lesion or PUNLMP. The presence of FGFR3 wildtype and a Ki67 proliferation index <5% favors a diagnosis of IP over invUC. This could help resolve ambiguous cases.

O-176
ALPHA-METHYLACYL-COA RACEMASE EXPRESSION IN TRANSITIONAL CELL CARCINOMA OF THE UPPER URINARY IS ASSOCIATED WITH DISEASE PROGRESSION

Cord Langner1, Gerhild Rupar1, Peter Rehak2, Gerald Hofler1, Richard Zigeuner3
1Institute of Pathology, 2Department of Surgery, Division of Biomedical Engineering & Computing and 3Department of Urology, Medical University of Graz, Austria

Introduction
Alpha-Methylacyl-CoA Racemase (AMACR) is a cytosolic enzyme that plays an important role in peroxisomal beta-oxidation of branched fatty acids. Recently, this protein has been identified as a marker of prostate cancer, whereas most benign prostates lack AMACR expression. AMACR is known to be present in a subset of transitional cell carcinomas (TCCs). However, data correlating AMACR expression with tumour stage, grade and morphologic features of aggressive tumour growth, such as angioinvasion, as well as patient outcome are currently lacking.
Methods
51 upper urinary tract TCCs were immunostained for AMACR using a tissue microarray technique. Immunoreactivity was analyzed semiquantitatively with respect to associations with pT-stage, tumour grade as well as lymphatic and/or venous invasion applying the Fisher¡¯s exact test. Specimens of normal pelvic urothelium, low and high grade intraurothelial neoplasia and urothelial carcinoma in situ were analyzed for comparison. The prognostic impact (regarding metastasis-free survival) was analyzed using the Kaplan-Meier method and the log-rank test. For multivariate analysis a Cox¡¯s proportional hazard regression model was used.
Results
Distinct finely granular cytoplasmic AMACR immunostaining was noted in 30/51 (59%) tumours. High AMACR expression (¡Ý50% of tumour cells) was correlated with high tumour stage (3/31 (21%) pT1/pT2 vs. 10/20 (50%) pT3; p=0.002) and high tumour grade (2/28 (7%) low grade vs. 11/23 (48%) high grade; p=0.001). However, AMACR expression was found to be independent from angioinvasion, since 5/12 (42%) tumours showing lymphatic and/or venous invasion showed AMACR immunoreactivity compared to 8/39 (21%) tumours lacking angioinvasion (p=0.3). Non-neoplastic urothelium lacked AMACR immunostaining, whereas intrauothelial neoplasia (high grade > low grade) and urothelial carcinoma in situ showed specific labelling. With respect to patient outcome, AMACR immunoreactivity proved to be a new independent prognostic marker in multivariate analysis with a risk ratio of 9.0 (95% confidence interval 1.8-45.6; p=0.008).
Conclusion
Our preliminary study suggests that AMACR is associated with tumour progression in upper urinary tract TCCs. Moreover, AMACR proved to be a independent prognostic marker with respect to metastasis-free survival. However, further studies including more patients are needed to substantiate our results.

O-177
ASSESSMENT OF ERBB2 MRNA EXPRESSION LEVELS IN A LARGE SERIES OF BLADDER TUMORS BY QUANTITATIVE REAL-TIME REVERSE TRANSCRIPTION POLYMERASE CHAIN REACTION (RT-PCR), CORRELATION WITH IMMUNOHISTOCHEMESTRY (IHC).

Delphine Amsellem-Ouazana*, Department of Urology, Paris, France; Vincent Molinié, Department of Pathology, Suresnes, France; Ivan Bièche, Sengül Tozlu, Genetic Oncology, Saint-Cloud, France; Annick Vieillefond, Department of Pathology, Paris, France; Henry Botto, Department of Urology, Suresnes, France; Bernard Debré, Department of Urology, Paris, France; Rosette Lidereau, Genetic Oncology, Saint-Cloud, France.

Introduction.ERBB2 (also known as HER2) is known to be implicated in bladder cancer. The ErbB2 protein encoded is the aim of new targeted therapies. The aim of this study was to assess ERBB2 expression levels in a large series of bladder tumors using both quantitative real-time RT-PCR (at the mRNA level) and IHC (at the protein level) and to compare the results of these two methods.
Methods: 73 tumors and 5 normal bladder samples were obtained by trans urethral bladder resection or cystectomy. Samples were staged and graded as follows: 22 pTaG1, 10 pTaG3, 21 pT1G3, and 20 T2-T4. Real time quantitative RT-PCR allowed to obtain quantitative values of ERBB2 mRNAs. IHC was performed with a polyclonal antibody. Beside the percentage of tumoral stained cells, the intensity of the staining was graded: 0/+/++/+++. Relationships between median ERBB2 mRNA levels and clinical, histological parameters were based on the Chi2 or Mann Whitney test.
Results: RT-PCR. ERBB2 mRNA levels ranged from 0.21 to 54.39 with a median value of 2.26 (median value for normal bladder samples was 1). Over-expression was noted in 23 tumors (31.5%); 7 pTaG1 (31.8%), 4 pTaG3 (40%), 6 pT1G3 (28.6%) and 6 T2-T4 (30%). ERBB2 expression levels were significantly higher in tumors versus normal bladder (p=0.0093), in pTaG1 versus normal samples (p=0.0033) and in T2-T4 tumors versus pTa+pT1 tumors (p=0.037).
IMMUNO-HISTOCHEMESTRY. Positivity of ErbB2 immunostaining was not different in tumors (78.7%) versus normal bladder (60%) (p=0.34). Moreover, positivity was not related to tumor stage (p=0.09). Intensity of immunostaining showed no difference as well.
COMPARAISON RT-PCR / IHC. ERBB2 mRNA quantification by RT-PCR was correlated to positivity (p=0.01) and intensity (p=0.00549) of immunostaining. The level of mRNA over-expression was correlated to the percentage of tumoral immunostaining (p=0.019).
Conclusions: Over-expression of ERBB2 mRNA occurs in one third of bladder tumors. Before an eventual anti ErbB2 protein targeted therapy, ErbB2 status could be assessed both by real-time RT-PCR assay and IHC.

O-178
QUANTITATIVE RT-PCR IN BLADDER CANCER REVEALS CHANGES OF GENE EXPRESSION DURING CARCINOGENESIS

Compérat E (1, 5), Bièche I (2), Dargère D (1), Ferlicot S (1), Laurendeau I (2), Benoît G (3), Vieillefond A (4), Capron F (5), Vidaud M (2), Bedossa P (1), Paradis V (1)
(1) CNRS UMR 8149, Faculte des Sciences Pharmaceutiques et Biologiques, Paris V
(2) Laboratoire de Genetique Moleculaire-UPRES EA 3618, Faculte des Sciences Pharmaceutiques et Biologiques, Universite Paris V
(3) Service d'urologie Le Kremlin-Bicêtre, Paris
(4) Service d'Anatomie et Cytologique Pathologique Hôpital-Cochin, Paris
(5) Service d'Anatomie et Cytologique Pathologique Hôpital La Pitié-Salpêtrière, Paris

Urothelial carcinoma (UC) has an incidence of 3000 annual new cases in France, mainly with transitional differentiation. UC are defined into 3 groups: superficial non invasive neoplasms (pTa), chorion invasive neoplasms (pT1) and muscle invasive cancers (pT2 to pT4). Their clinical outcome depends on the tumor stage, approximately 25 % of non invasive tumors may progress to invasive tumors with poor clinical outcome. The aim of our study was to detect changes of gene expression associated with bladder carcinogenesis

using a molecular approach able to identify some key-genes involved in the progression of the disease.
49 bladder tumors, including 18 pTa/pT1(12 pTa, 6 pT1) and 31 pT2-pT4 tumors(3 pT2, 20 pT3 and 8 pT4N+), from trans ureteral resections or cystectomy specimens, were studied. 12 control samples of histologically normal bladder were taken from the same specimens at tumor distance. mRNA levels of a set of 11 genes were quantified by real-time RT-PCR from dissected epithelial component for each case. Expression level of deregulated molecules was evaluated by immunohistochemistry in the same samples.
mRNA expression in normal bladder versus invasive tumors showed 5 genes significantly downregulated and 1 gene (STK-6, Aurora-A) upregulated in cancer samples. GJA1(connexine 43), was among the most discriminating between both groups ($p < 0.001$). Comparing pT2/pT3 group versus normal tissue, similar differential gene expression was seen, with significant increase of STK6 ($p<0.0001$) and GJB2 (Connexin 26) ($p=0.005$) and significant decrease of LYVE-1 ($p=0.02$), VEGF-D (vascular endothelial growth factor D)($p=0.004$) and PROK-1 (Prokinase-1)($p=0.005$) in tumoral samples. By comparing normal versus pTa/pT1 tumors we found significant deregulation for 6 genes, STK-6 was upregulated in tumoral tissues versus normal bladder ($p=0.0004$) and 5 downregulated (GJA2, VEGF-D, PROK-1, LYVE-1 (Lymphatic vessel hyaluronan receptor 1), TATP63 (transmembrane proteine 63)). Immunohistochemistry (IHC) for STK-6, connexin 26, p63 and VEGF confirmed gene expression data.
This study identified key-genes associated with different stages of bladder carcinogenesis. 6 of 11 selected genes studied were deregulated as soon as the earliest stage of bladder carcinoma such as pTa tumors. Our results suggest that these genes play a crucial role in cancer development, and a potential role in tumor progression. IHC may be a valuable tool to discriminate UC having poor evolution.

O-179
OVEREXPRESSION OF TELOMERASE COMPONENTS IN UROTHELIAL TUMOURS OF THE BLADDER: AN IN SITU HYBRIDIZATION AND IMMUNOHISTOCHEMISTRY STUDY OF 70 CASES.

LEPREUX Sébastien (1,2), AUBERT Incarnation (1), DEMINIERE Colette (2), FOURNIER Marie-Christine (1), CARTEYRON Monique (2), MEHAYE Catherine (2), PARIENTE Jean-Louis (3), FERRIERE Jean-Marie (3), BIOULAC-SAGE Paulette (2), BLOCH Bertrand (1,2), MARTIN-NEGRIER Marie-Laure (1,2).
(1) Laboratoire d'Histologie-Embryologie, UFR II, Université Victor Segalen Bordeaux 2, France; (2) Service d'Anatomie Pathologique, (3) Service d'Urologie, Hôpital Pellegrin, 33076 Bordeaux Cedex, France.

Backgrounds and aims: The prognostic markers of human urothelial tumours of the bladder are the histological determination of stage of invasion and tumour grades and recently the classification was revisited (WHO/OMS histological classification published in 2004). The aim of our study was to explore new diagnostic and pronostic perspectives offered by the detection of telomerase components including an RNA subunit (hTR) and a reverse transcriptase subunit (hTERT).
Materials and Methods: We investigated the expression of hTR and hTERT respectively by in situ hybridization and immunohistochemistry in bladder non-invasive tumours and infiltrating carcinomas at various grades and stage of invasion and non-tumoral urothelium (70 cases).
Results: The cells exhibited a hTR labeling in non-tumoral urothelium and in urothelial carcinoma, but the level of expression of hTR was significantly higher in urothelial tumours than in non-neoplastic urothelium ($p<0.05$). In non-invasive tumours, the number of cells which expressed hTERT protein at cytoplasmic level or/and at nuclear level was significantly higher than in non-neoplastic urothelium ($p<0.05$). In infiltrating carcinomas, the number of cells which expressed hTERT protein at cytoplasmic level was significantly higher than in non-neoplastic urothelium ($p<0.05$). There was no significant difference of expression of telomerase between the superficial part and the deep part of the infiltrating urothelial carcinomas (>pT1). There was no relation between the telomerase expression levels and the progression of tumour grades and/or stage.
Conclusions: This study demonstrates at the morphological level that the overexpression of telomerase is associated with bladder urothelial tumours and that the expression of telomerase in the superficial part of the deep infiltrating carcinomas that potentially produces exfoliating cells faithfully reflects expression of all tumoral cells.

O-180
PATHOLOGICAL FEATURES OF SURGICALLY TREATED PROSTATE CANCER IN THE "PSA ERA"

BOLLITO Enrico, BERGERO Nicoletta, TERRONE Carlo*, GRANDE Susanna*, GUERCIO Stefano#, BELLINA Maurizio#, SCARPA Roberto Mario*
Divisions of Pathology and of *Urology, University of Turin and San Luigi Hospital, Orbassano, and #Division of Urology, Rivoli Hospital, Turin, Italy

INTRODUCTION: In the last decade, the clinical routine use of serum prostate-specific antigen (PSA) dosage has highly modified the epidemiology of prostate carcinoma (PC). Furthermore, a remarkable tumour volume and pathological stage reductions have been reported in countries where PC screening became a common health policy. The aim of this study was to analyze the histomorphological features of PC treated with radical prostatectomy in two Italian institutions.
MATERIALS AND METHODS: In the period 1991-2005, 493 cases of PC were treated by radical prostatectomy in our Hospitals. PSA evaluation was done in all patients before the diagnosis of PC. Ninety-two patients who underwent neo-adjuvant therapy were excluded and in the remaining 401 (median age 65, range 46-76), the volume of the tumour and that of the whole prostate gland were calculated as proposed by the Italian Group of Uropathology in 2001. In addition, Gleason score and pathological TNM stage (6th ed., 2002) were evaluated. Statistical analysis was performed by Mann-Whitney U and Kruskal-Wallis tests.
RESULTS: The median serum PSA level was 8.5 ng/ml (0.8-60). A significant difference in median PSA values has been observed between the periods 1991-1999 and 2000-2005 (11.0 vs 8.0 ng/ml; $p< 0.001$). The PCs were staged pT2 in 222 patients, pT3a in 123, pT3b in 44, and pT4a in 12. In cases operated in years 2000-2005, a significant increase ($p<0.0001$) of the number of pT2 cases has been detected, compared to the cases operated in 1991-1999. No significant differences between the time periods considered above were observed in the median Gleason score (6, range 5-9), or in the median tumour volumes (3.5 ml, range 0.3-21). In these cases, the median prostate volume was 36.0 ml (15.9-152.5), and the median tumour/prostate volume ratio was 9.9% (0.6-45.4). A tumour volume <0.5 ml was encountered in only the 2.4% of the cases operated in both time periods.
CONCLUSION: These data, derived from a suburban area of Turin in which the routine use of PSA regular evaluations is established since 1991, indicate that the significant reduction of both median tumour volumes and high Gleason score tumours observed in areas covered by a PSA-based PC screening program was not observed. However, a significant reduction of median PSA values and of high (pT3-pT4) stage carcinomas was recorded in the last five years (compared to years 1991-1999), in association with regular PSA evaluation

by the adult male population.

O-181
HISTOPROGNOSTIC FACTORS OF PROSTATE CARCINOMA. A RETROSPECTIVE CORRELATIVE STUDY OF 80 CASES.

Armelle bardier(1), Pierre Levy(2), Jean-dominique Doublet(3), Marine Lefevre(1), Patrice Callard(1), Mathilde Sibony(1)
(1) Department of surgical pathology, Hopital tenon, 14 rue de la Chine, 75020 Paris, France.
(2) Department of statistics, Hopital tenon, 14 rue de la Chine, 75020 Paris, France.
(3) Department of urology, Hopital tenon, 14 rue de la Chine, 75020 Paris, France.

Prostatic cancer is considered as a latent cancer with a falling mortality rate due to large screening of prostate confined cancer on biopsies. This screening is a new challenge for uropathologists because it implies to diagnose prostate cancer on more and more small focuses. There is actually no consensus on criteria and treatment of small foci of cancer.
The aim of this analyse was to determine predictive factors of extraprostatic extension and tumoral volume. We correlated prostate needle biopsies findings with prostatectomy outcomes of 80 patients treated during 1998 and 2003. We were more particularly interested in focus carcinoma (one positive biopsy and three mm length).
Method : Preoperative factors and radical prostatectomy outcomes were analysed in this retrospective report of 80 consecutive prostate carcinoma cases collected in a single institution, from 1999 to 2003. Preoperative factors (PSA concentration, number of positive biopsies, length of cancer in mm, proportion of cancer on biopsies, Gleason score) were correlated with histopathological data on prostatectomy (tumoral volume in cm3, extraprostatic extension).
Results : In multivariate analysis, two histoprognostic factors of tumoral extension were pointed out (p=0,004) : number of positive biopsies (> 1 ; = 1) and length of cancer (>three mm ; ¡Ü three mm).
The 23 patients with one positive biopsy and length of cancer ¡Ü three mm had an intraprostatic cancer (pT2). On these 23 patients, 16 patients had a bilateral cancer (pT2c), 2 had more than half of a lobe involved (pT2b), 5 had half of a lobe or less involved (pT2a).
Among the 43 patients with more than one positive biopsy and length of cancer > three mm, 17 had an extraprostatic extension (pT3). Risk of extraprostatic cancer was 10-fold higher in this group (p=0,003). Among the 14 patients with either one positive biopsy or length of cancer ¡Ü three mm, 12 had an intraprostatic cancer and 2 patients had an extraprostatic extension. On the 31 patients with one positive biopsy, the length of cancer was not predictive of tumoral volume : 8 patients with focus carcinoma had non significant tumoral volume (<0,2 cm3), 2 patients with focus carcinoma had a tumoral volume between 0,2 and 0,5 cm3 and 21 patients had tumoral volume > 0,5 cm3 of which 13 had focus carcinoma.
Conclusion : One positive biopsy and length of cancer three mm on biopsies were predictive of intraprostatic cancer but were not predictive of tumoral volume.

O-182
CD 34 IN PROSTATIC BIOPSIES WITH ADENOCARCINOMA. A DOUBTFULL MARKER FOR MICROVESSEL DENSITY (MVD) ASSESSMENT.

ASIMAKI Niki, TANOGLIDI Anna, SAMARAS Vasilis, KALANTZAKIS Spyros, BARBATIS Calypso.
Department of Pathology, Hellenic Red Cross Hospital
Athens, Greece.

INTRODUCTION: Angiogenesis is essential for tumor growth. Studies on the importance of MVD in prostatic adenocarcinoma (pCa) as an independent predictor of biological behaviour after radical prostatectomy are controversial because of the problematic methodology of MVD measurements. CD34 a myeloid progenitor cell antigen expressed by endothelial and other mesenchymal cells has been reported as a better marker for intratumoral vessel counting, compared to other endothelial cell specific molecules.
AIM OF THE STUDY: To evaluate the expression of CD34 in normal and neoplastic prostatic tissue and its use for the assessment of MVD in pCa.
MATERIALS AND METHODS: 58 cases of prostatic biopsies with adenocarcinoma were included in the study: Gleason's score: 5(7), 6(9), 7(18), 8(13) and 9(4). The immunohistochemical method of Envision-HRP was used using an anti CD34 mAb. The specific endothelial cell marker CD31 was also studied in parallel sections.
RESULTS: CD34 was widely expressed in prostatic tissue.The endothelium of all blood vessels (capillaries, arterioles, veins, arteries) was CD34+. There was strong albeit focal CD34 positivity of stromal cells in benign areas with a characteristic linear distribution around normal prostatic glands and CD34 expression in nerve sheaths. A distinct concentric perivascular CD34+ spindle cell arrangement was also observed. In our study it was impossible to use CD34 as a marker for MVD assessment as there was marked stromal and periglandular CD34 expression concealing the capillaries in 45/58 tumors with the exception of solid, cellular areas of type 5 growth pattern, where intratumoral CD34+ capillaries with negative stroma could be identified. A distinct linear CD34 positivity around malignant glands was observed reminiscent of the normal tissue pattern.
There was an obvious marked increase in stromal CD34 expression in pCa, either diffuse or focal compared to the normal prostatic tissue.
CD31 stained the endothelium of large blood vessels and occasional capillaries but despite its specificity it lacks sensitivity for pCa angiogenesis.
SUMMARY: CD34 is widely expressed in normal epithelial prostatic cells with distinct distribution. The marked CD34 increase in the stroma of most pCas does not allow accurate MVD measurements, except in cases of high grade with solid hypercellular growth pattern and minimal stromal production.

O-183
CYTOKERATIN 5/6 AND ALPHA-METHYLACYL-COA RACEMASE (AMACR) ARE USEFUL IN EVALUATING PROSTATE SPECIMENS AFTER THERAPY

Kiril Trpkov and Asli Yilmaz. Anatomical Pathology, Calgary Laboratory Services and University of Calgary, Calgary, Alberta, Canada.

Introduction and purpose: Reliable evaluation of prostate specimens after radiotherapy (RT), cryotherapy (CT) and hormonal therapy (HT) remains a diagnostic challenge. Diagnostic utility of immunopanel that includes high molecular weight cytokeratin 5/6 (CK 5/6) and AMACR has not been examined in post-treatment prostate specimens.
Method: We evaluated prospectively 58 prostate biopsies (37 post-RT, 21 post-CT) and 4 prostate specimens post-HT (3 radical prostatectomies and 1 transurethral resection) using CK 5/6 and AMACR. Immunostains were performed to aid in establishing the final diagnosis and were correlated with the morphology. The results for both stains were scored as: negative (0), weak (1+), moderate (2+), or strong (3+).
Results: Final diagnosis of prostate cancer (pCa) was established in 37 cases (16 post-RT, 17 post-CT, 4 post-HT) and benign diagnosis (post-RT atypia and post-CT atypia) was rendered in 25 cases (21 post-RT and 4 post-CT). CK 5/6

did not stain any case of pCa after treatment (100% specificity). Moderate (2+) to strong (3+) basal cell staining for CK 5/6 was seen in all benign glands showing post-treatment atypia (both in cases with and without pCa). AMACR demonstrated combined sensitivity for post treatment pCa of 86.5% (87.5 % post-RT, 94% post-CT and 50% post-HT). Staining intensity for AMACR was moderate (2+) to strong (3+) in 88.9% of cases. All five pCa negative for AMACR (2 post-RT, 1 post-PC, 2 post-HT) were also uniformly negative for CK 5/6, which allowed to establish the final diagnosis of pCa. Of 6 AMACR positive cases with non-pCa diagnosis (3 each with 1+ and 2+), all 6 cases showed focal positivity for CK 5/6 (one with PIN, 4 with post-treatment atypia, and one with atypia of uncertain significance).
Conclusions: 1.) Majority of problematic foci in treated prostate specimens can be reliably diagnosed as pCa or benign post-treatment atypia using a panel of CK 5/6 and AMACR in correlation with the morphology. 2. The immunopanel allowed for confirmation of suspected pCa foci, establishing the extent of pCa on biopsy, as well as appreciating better the areas of post-treatment atypia 3.) In suspicious cases negative for AMACR, uniform lack of CK 5/6 staining supported a definitive diagnosis of pCa. 4.) Although we evaluated only few pCa specimens after hormonal therapy, AMACR expression appears to be variable in this setting.

O-184
INCREASED APOPTOSIS IN CERVICAL INTRAEPITHELIAL NEOPLASIA FROM HUMAN IMMUNODEFICIENCY VIRUS (HIV)-INFECTED WOMEN: ASSOCIATION WITH ONCOGENIC HUMAN PAPILLOMAVIRUS, CASPASES AND LANGERHANS' CELLS.

WALKER Francine (*§), ADLE-BIASSETTE Homa (*), MADELENAT Patrick (#), HENIN Dominique (*), LEHY Thérèse (§).* Department of Pathology, § INSERM U683, # Department of Gynaecology, Hôpital Bichat-Claude Bernard, Paris, France.,

Purpose : Increasing risk of squamous cervical intraepithelial neoplasia (CIN) exits in human immunodeficiency virus (HIV)-infected women. However, the relatively low incidence of invasive carcinoma in the untreated HIV-infected population suggests an imbalance between cell proliferation and apoptosis. We investigated apoptosis and caspases in cervical samples from this population comparatively to non HIV-infected and control subjects.
Experimental design : Apoptotic TUNEL method, immunohistochemistry for caspases -2, -3, -8, -9 and other apoptosis markers were performed on 12 normal cervical samples and 103 low- and high-grade cervical lesions, containing human papillomavirus(es), from 35 HIV-negative and 33 HIV-positive women before tritherapy advent.
Results : 1) The apoptotic index (AI) in epithelial cells did not vary between normal mucosa and condyloma acuminata infected or not with HIV; 2) AI augmented with the CIN severity in HIV-positive and HIV-negative women; 3) AI dramatically increased in oncogenic HPV-infected CIN of HIV-positive population compared to the CIN of similar grade in HIV-negative one. This was associated with a greater expression of caspase-8, active caspase-9 and active caspase-3 in those samples. Moreover, densities of Langerhans' cells - involved in apoptotic bodies engulfment- were greatly reduced in CIN of HIV-positive women. In samples, these densities were highly inversely correlated with AI ($r = - 0.88$, $P< 0.002$).
Conclusions : This study provides the first evidence for the strongly enhanced apoptosis levels and caspase expression in CIN of untreated HIV-infected women. We suggest that the reduction in Langerhans' cell number could contribute at least partly to apoptotic cell accumulation.

O-185
HUMAN PAPILLOMAVIRUS FINDINGS IN CERVICAL INTRAEPITHELIAL NEOPLASIA: A STUDY ON 416 SPANISH WOMEN, USING PCR FOR DETECTION AND TYPING OF HPV.

MEIZOSO Telma, GARRIDO María, ENGUITA Ana Belén, RODRIGO Maximiliano, NAVAS Rafael, SEGOVIA Beatriz, RODRIGUEZ José Luis.
SERVICIO DE ANATOMIA PATOLÓGICA. 12 DE OCTUBRE UNIVERSITY HOSPITAL, MADRID, SPAIN

INTRODUCTION:
Cervical cancer represents the second most common cancer in women worldwide.
This cancer is a consequence of an infection by some types of Human Papillomavirus (HPV) sexually transmitted.Twenty nine different types of HPV have been characterized, and classified into three diferent oncogenic risk categories: low, medium and high potential
There are esentially three different types of nucleic acid hybridization method formats for detecting HPV, including Southern blot, hybrid capture and polymerase chain reaction.
The aim of this study is to evaluate the HPV distribution in cervical diseases, specially in CIN lesions.
MATERIAL AND METHODS:
416 cervical lesions were collected from the pathology department files of "12 de Octubre" University Hospital, Madrid, Spain between 1998 and 2003 years.
The tissue was fixed in formalin, embedded in paraffin, stain with hematoxylin and eosin and diagnosed under light microscopy. On the other hand, DNA extraction and HPV detection were performed by PCR method.
RESULTS:
HPV DNA was detected in 174 specimens (41.9%) of all biopsies.
HPV 16 was present in 27.5% of this positive samples, HPV 18 in 4.6%, HPV 6/11 in 5.8%, HPV 31/33 in 2.9% and 54% of the cases HPV type were no classified.
HPV was detected in 73 of 94 (77,6%) high grade cervical lesions: in 38.3% of them were HPV 16, 6.5% HPV 18, 2.2% HPV 6/11 and 1.1% HPV 31-33. HPV was detected in 68 of 129 low grade cervical lesions: in 6.2% of them were HPV 16, 6.2% HPV 18, 2.3% HPV 31/33, and 3.1% HPV 6/11.
DISCUSSION:
HPV prevalence rate in high grade cervical intraepithelial neoplasia has been reported between 77 and 84.2%. In our study was 80.2%.
The distribution of HPV types varies with the histological diagnosis and its oncogenic risks. Therefore high risk viruses including HPV 16 or 18 were associated in our cases with CIN II-III (45.7%) and low risk types such as 6 were associated with condylomas (75%). These results agree with others Spanish and European studies but differs with assian´s ones.
In populations where cytology based programmes are established it would be beneficial to add HPV testing to the screening protocol. Prevention of exposure to high risk HPV types by vaccination would be the most efficent preventive intervention for cervical cancer. Nowadays this is not possible and the prevention and treatment of HPV infections are necessary.

O-186
MORPHOLOGICAL CHANGES IN UTERUS CERVIX AFTER RADIOCONIZATION UNDER THE CERVICAL INTRAEPITHELIAL NEOPLASIA (CIN)

DERIZHANOVA Irina, NECHITAILO Tatyana

The aim of the research is to study morphological changes in tissues and peculiarities in postoperative uterus cervix wound repair after radioconization under CIN. The Surgitron portable instrument was used. 224 uterus cervix pieces ablated from 56 patients, 30 cervical channel biopsies and 120 smears-prints of cervical surface (neutral zone, cervix channel, front and back lip) were studied at 1, 7 and 21 day. Histological and cytological pieces were colored in standard way. CIN II was found in 51 patients, CIN III in 3 cases, Ca in situ in 2 ones. Using PCR for all patients various HPV cultures were found, in 60% - types 16 and 18. Morphological changes in ecto- and endocervix after radioconization depend on radio-wave power and exposition. The fixed current with 45-50 W power seems to be optimal, the coagulant necrosis zone under it does not exceed 0.05-0.4 mm, epithelial dystrophic a! nd necrobiotic changes are not clearly shown and do not prevent histological CIN diagnostics in operation matter. Under radio wave exposure the vascular smooth muscles spasm accompanied by abrupt luminas narrowing down to obturation took place; there were endothelium desquamation, agglutination with nuclei pyknosis. During the first 7 days the necrotic tissues rejection from the wound surface occurred as very tiny fragments among fibrin and few neutrophilicus leukocytes. Bacillus and coccus flora, neutrophilicus leukocytes in phagocytosis and lysis stages predominated. In periphery zone the integument epithelium regeneration prevailed in form of layer clusters of parabasal cells.

At 21-day reconstruction of the cervix channel mucous membrane and epithelization of significant wound part occurred. Leukocytes infiltration is manifested poorly. Relative pathogenic flora was substituted by lactobacilli. Uterus cervix complete epithelization came in 30-45 days. In 6 month in biopsies the cervix and cervix channel complete reconstruction was observed. CIN signs were lacking. Only one patient got HPV infection relapse with condyloma forming.

Conclusion: radio-wave CIN treatment method in form of Uterus cervix conization leads to minimal tissue lesions and causes vessel changes, preventing bleeding; by changing microcenosis it accelerates wound healing.

O-187
P-53 IMMUNOSTAINING IN LICHEN SCLEROSUS IS RELATED TO ISCHEMIC STRESS AND NOT A MARKER OF DYSPLASIA AND D-VIN

Bernadette Liegl and Sigrid Regauer
Institut für Pathologie, Medizinische Universität Graz Austria

Introduction:"Differentiated VIN" (d-VIN), a postulated rapidly progressing precursor lesion for LS-associated vulvar squamous cell carcinoma (SCC), shows an atypical basal keratinocyte proliferation with p53-positive basal/suprabasal keratinocyte nuclei. p53-staining is considered a marker for progression to invasion.

Purpose of the study was (1) to investigate the frequency of d-VIN in LS and LS-associated SCC in our collective of over 200 patients with LS and (2) to identify the p-53 staining profile of different subtypes of LS and precursor lesions of vulvar SCC.

Material and Methodes: We analyzed archival formalin-fixed and paraffin-embedded tissue of 207 biopsies, excisions, vulvectomies and circumcisions for LS 148 patients,33 patients with vulvar SCC arising in LS, 26 pediatric patients with penile (23) and vulvar (3) LS. The control group included vulvar biopsies (15)and (15)circumcisions LS. H&E stained sections were evaluated for morphological citeria of HPV-infection, types of inflammatory infiltrates, vascular changes and Candida infections with a PAS reaction. Depending on the histological features, LS was divided into early (40), classical (78) and hypertrophic stages. Immunohistochemistry was performed with monoclonal antibody to p53 (DAKO Corp. Carpinteria, CA).p-53 staining was scored as negative, when LI was less than 10% of basal keratinocyte nuclei. p-53 staining was divided into discontinuous linear, continuous linear and basal and suprabasal staining of keratinocyte nuclei according to LI under 50% and at least 70% (continuous and basal and suprabasal) respectively.

Results and Summary: Nuclear p53 staining was observed in 175/ 207 LS of biopsies. 80% of early and 69% of pediatric LS showed p53-staining in basal keratinocytes. Classic LS showed no p-53 staining in 17%, discontinuous basal keratinocyte staining in 20%, continuous basal keratinocyte staining in 58%, basal/suprabasal staining in 5%. Hypertrophic LS revealed basal keratinocyte staining in 32% and basal/suprabasal staining in 61%. p53-staining showed a strong association with sclerosis of blood vessels and dermis, lymphoid infiltrates, vasculitis and hypertrophic LS. d-VIN was seen in 2% of lone LS and 24% of SCC-associated LS. p53-staining in LS was frequent and best explained as ischemic stress response due to poor oxygenation, vasculitis and inflammation. Evaluation of p-53 expression is a poor screening tool for identifying precancerous lesions in LS.

O-188
VULVAR SQUAMOUS CELL CARCINOMAS HARBOUR LOW AND HIGH RISK HPV GENOTYPES

REGAUER S, AIGELSREITER A, REICH O* and BEHAM-SCHMID Ch.
Institute of Pathology and *Gynecology and Obstestrics, Medical University of Graz, Austria

Aims: Vulvar squamous cell carcinomas (SCC) are divided traditionally into keratinizing lichen sclerosus (LS) associated SCC and basaloid Human Papilloma Virus (HPV)-induced SCC, mostly due to high risk HPV16 genotype. Classification of HPV is almost entirely based on molecular characteristics. PCR is the most widely used target amplification method. The aim of this study was to analyse the distribution of 25 different individual HPV genotypes in vulvar SCC with and without LS.

Methods: Formalin-fixed, paraffin-embedded material of 47 vulvar SCC (17 LS-associated SCC and 30 non-LS associated SCC) were analyzed with the INNO-LIPA HPV-Genotyping for individual HPV genotypes 6,11,16,18,31,33,34,35,39,40,42,43,44,45,51,52,53,54,56,58, 59,66,68,70,73,74. INNO-LIPA HPV-Genotyping is based on broad spectrum amplification of HPV genotypes using SPF10 primers, which amplify only 65 base pairs at the L1 region (Innogenetics, NL) . Selected SCC were also analysed with primers against E6 and E7 of HPV16 genotype with conventional PCR analysis. Five SCC had to be excluded due to poor DNA quality.

Results: No HPV-DNA was detected in 7/14 LS-associated SCC and 6/28 non-LS-associated SCC. One LS-associated SCC each revealed HPV-DNA genotypes 6, 18, 31, 33 and 6&16. Two SCC contained HPV 6&33. In the non-LS associated SCC group, HPV-DNA 6, 33 and 6&52 were detected in one SCC each, HPV-DNA 6&16,6&18 and 6&51 in two SCC each and HPV 6&31 in 3 SCC. HPV16 genotype alone was identified in 10/28 SCC. Detection of HPV16 genotypes using the INNO-LIPA HPV-Genotyping corresponded to results obtained by PCR analysis using primers against E6 and E7 of the HPV16 genotype.

Conclusion: 30% of LS-associated SCC were negative for the major HPV genotypes. 30% each were characterized by detection of only one HPV genotype and by co-infection of a low risk and a high risk HPV genotype. HPV16 genotype was identified in only 1/14 LS-associated SCC. In the basaloid SCC group, only 20% of SCC contained no HPV genotypes. A single HPV genotype, mainly HPV16, was identified in

45% of basaloid SCC and two HPV genotypes, a low and a high risk genotype, were identified in 35%. Multiple HPV genotypes (>2) were not detected in our analysis. Demonstration of HPV genotypes in LS-associated SCC is more common than previously assumed. Although HPV16 genotype is the most common individual infectious agent in non-LS-associated basaloid vulvar SCC, co-infections with two HPV genotypes are common.

O-189
PATTERN OF MIB-1 IMMUNOSTAINING ASSISTS IN THE DIAGNOSIS OF SQAMOUS INTRAEPITHELIAL LESIONS OF THE UTERINE CERVIX

DJORDJEVIC Biljana, MIHAILOVIC Dragan, VELICKOVIC Ljubinka, ZIVKOVIC Vesna, MILENTIJEVIC Maja, STANOJEVIC Zorica*
Institute of Pathology, Medical Faculty University of Nis, Serbia and Montenegro
* Clinic of Oncology, Medical Faculty University of Nis, Serbia and Montenegro

The aim of this study was to compare pattern of MIB-1 immunostaining in normal squamous epithelium (NSE), metaplastic squamous epithelium (MSE), low grade squamous intraepithelial lesions (LSIL), and high grade squamous intraepithelial lesions (HSIL) of the uterine cervix.
Material and methods. Formalin fixed and paraffin embedded tissue from 20 NSE, 20 MSE, 20 LSIL, and 40 HSIL was immunostained for MIB-1 (DAKO). For the analysis of the staining a four-tired scale was used both for the intensity of nuclear staining (negative, weak, moderate, strong) and the percentage of positive nuclei (<10%, 10-50%, 50-80%, >80%). A total score was obtained by multiplying both parameters. Score 1-3 was classified as weakly, 4-8 as moderately, and 9-12 as strongly positive.
Results. MIB-1 expression was exclusively confined to the basal and parabasal layers of NSE and MSE. There were no significant differences of MIB-1 immunostaining between NSE and MSE. In SIL specimens, the staining was markedly increased in the basal and parabasal layers and MIB-1 positive cells were also distributed in the intermediate (LSIL) or all layers (HSIL) of squamous epithelium. Significant differences for MIB-1 staining were found in comparations between NSE or MSE and SILs and between LSILs and HSILs.
Conclusions. These results indicate that MIB-1 immunostaining is useful in evaluating of squamous intraepithelial lesions of the uterine cervix.
Key words. Uterine cervix, Squamous intraepithelial lesions, MIB-1

O-190
CERVICAL NEOPLASIA OR A BENIGN MIMIC?

Ring M, Heffron CCBB, Murphy N, Astbury K, Martin C, Hughes C, O'Leary JJ.
Department of Pathology, Coombe Women's Hospital, Dublin 8 and Trinity College Dublin, Ireland.

Background: Differential diagnosis of cervical neoplastic lesions from their 'mimics' is fraught with difficulty. An ongoing search for a specific and sensitive marker for cervical dysplasia is occurring. The tumour suppressor protein, p16 INK4A, has been widely reported to be of significant diagnostic utility in identification of cervical squamous and glandular dysplasia. However, it is occasionally expressed in benign glandular lesions giving rise to a false impression of malignancy. Our group has evaluated a panel of biomarkers for use in these diagnostic dilemmas. A number of proteins play an important role in the control of DNA replication, these include the mini chromosome maintenance proteins (MCM) of which, MCM 2, MCM3 and MCM5 were assessed along with cell division cycle protein 6 (CDC6)) and topoisomerase II alpha. In addition, a marker of cell proliferation MIB 1(Ki-67), and bcl2 were assessed.
Design: 100 cases in total were assessed. Benign lesions included normal and reactive squamous lesions, benign glandular lesions (microglandular hyperplasia, reactive atypia, tuboendometrioid metaplasia). Cervical lesions included cervical intraepithelial neoplasia (CIN) grades 1,2,3, cervical glandular intraepithelial neoplasia (cGIN), invasive squamous carcinoma, and invasive adenocarcinoma (including villoglandular adenocarcinoma). All cases were retrieved from the pathology files of the Coombe Women's Hospital. Immunohistochemical staining with antibodies for p16 INK4A, MIB1, bcl2, MCM2, MCM3, MCM5, CDC6 and topoisomerase II alpha was performed on all cases. A score of 0 – 3 was given for each antibody in each case.
Results: Immunopositivity was noted in the majority of pre-malignant and malignant cervical lesions for p16 INK4A, MIB1, MCM 2,3,5, CDC6 and topoisomerase II alpha while bcl2 was negative or focally positive.
In the benign cervical lesions analysed, bcl2 was strongly positive with focal positivity for p16 INK4A, MIB1 was negative in normal cervical glands although positive in the basal cells of the squamous epithelium, and MCM 2/3/5 and CDC6 showed variable staining.
Conclusion: The accurate diagnosis of cervical dysplasia from its 'mimics' can be time consuming and difficult. We propose that a panel of biomarkers should be available for the diagnosis of such cases. Biomarkers that may prove most useful when used in addition to p16 INK4A include MIB1, bcl2, and MCM3.

O-191
INCIDENCE OF HIGH-GRADE DYSPLASIAS IN PATIENTS WITH ASCUS-H PAP SMEARS

S. Latif 1, J. Matthews-Greer1,2, R. Reyes1, D. Rivette 1, E. A. Turbat-Herrera 1, Department of Pathology1 and Pediatrics2, Louisiana State University HSC, Shreveport, LA

Introduction: The diagnostic category for atypical squamous cells, cannot exclude high-grade dysplasia (ASCUS-H) is a recent addition and was first introduced in Bethesda 2001 to differentiate between immature squamous metaplasia and high-grade squamous intra-epithelial lesions (HSIL). At present, in the USA many institutions are performing HPV reflex testing for ASCUS; the most common test done is for HR HPV. It is known that young women, particularly adolescents, are more likely to get dysplasia and rapid progression of their dysplasia as a result of HPV infection. In our adolescent patient population the prevalence of cervical abnormalities, namely (ASC-US and above) is high 24%. HPV testing is performed in our institution using the Hybrid Capture II (HCII) assay.
Purpose of the study: This study was undertaken to establish the prevalence of HSIL in our ASCUS-H patients and determine their high risk HPV status.

Methods: Twenty patients with ages ranging 19-79 years underwent cervical biopsy for ACUS-H at our institution. Liquid-based pap smears were prepared in the standard fashion. The remaining sample was submitted for HCII assay for detection of HR-HPV using a cut-off of 1.2 to prevent true positives from being missed.
Results: Out of twenty cervical biopsy specimens, 7 were positive for HSIL, 9 for LSIL and four biopsies were normal. All HSIL were positive for HR-HPV. In the low-grade (LSIL) group, all five cases tested were negative for HR- HPV.
Conclusion: Thirty-five percent of ASCUS-H pap smears were diagnosed as high-grade dysplasia on cervical biopsy and forty-five percent as low-grade. We believe as more cases of ASCUS-H are studied we will understand the implications of this entity better.

O-192
MITOGEN-ACTIVATED PROTEIN KINASE (MAPK) ACTIVATION HAS DIFFERENT CLINICAL SIGNIFICANCE IN CANCER CELLS OF OVARIAN, BREAST AND MESOTHELIAL ORIGIN IN EFFUSIONS

VINTMAN Lina, M.Sc.1, KONSTANTINOVSKY Sophya, M.Sc.1, RISBERG Björn, MD PhD2, BERNER Aasmund, MD PhD2, NESLAND Jahn M., MD PhD2, REICH Reuven, PhD1, DAVIDSON Ben, MD PhD2
1 Department of Pharmacology and Experimental Therapeutics, School of Pharmacy, Faculty of Medicine, The Hebrew University of Jerusalem, Jerusalem 91120, Israel
2 Department of Pathology, The Norwegian Radium Hospital, Montebello N-0310 Oslo, University of Oslo, Norway

Introduction: The mitogen-activated protein kinase (MAPK) pathway mediates major intracellular signaling events, including proliferation and apoptosis. Molecular events related to intracellular signaling in cancer cells in effusions are poorly defined.
Purpose: To compare the expression (level) and phosphorylation status (activity) of the three MAPK, extracellular-regulated kinase (ERK), c-Jun amino-terminal kinase (JNK) and high osmolarity glycerol response kinase (p38), in ovarian and breast carcinoma, malignant mesothelioma (MM) and reactive mesothelium (RM) in effusions.
Methods: 135 pleural and peritoneal effusions from patients diagnosed with ovarian carcinoma (=64), breast carcinoma (=25), MM (=32) and RM (=14) were studied using immunoblotting with antibodies detecting the total (pan-) and activated fraction (phospho-,
p-) of ERK, JNK and p38. Values for pan-MAPK and p-MAPK expression and the
p-MAPK/pan-MAPK ratio were compared. Results were corroborated using immunocytochemistry in selected cases. The predictive value of MAPK expression and activation was analyzed in breast carcinoma and compared to previous data for ovarian carcinoma.
Results: Pan-ERK, -JNK and -p38 expression and activation was found in the majority of specimens. Ovarian and breast carcinomas showed significantly higher activation of ERK and p38 compared to MM ($p=0.001$ for both). MM and RM showed similar MAPK expression, activation and activation ratio (Mann-Whitney test, $p>0.05$). Higher p38 activation ratio predicted worse disease-free (DFS, $p=0.018$) and overall (OS, $p=0.004$) survival in breast carcinoma. Conversely, pan-ERK ($p=0.008$), pan-JNK ($p=0.038$) and p-ERK ($p=0.034$) predicted better OS in ovarian carcinoma.
Conclusions: This study presents the first evidence of in vivo activation of MAPK in malignant effusions. The similar MAPK profile in benign and malignant mesothelium, and their correlation with better survival in ovarian carcinoma question the validity of MAPK as molecular therapeutic targets in these cancers. MAPK activation may be a molecular marker of disease aggressiveness in breast cancer.

O-193
MULTICENTRIC DETERMINATION OF THE BEST INTEROBSERVER CONCORDANCE USING THE FUHRMAN GRADING SYSTEM IN RENAL CELL CARCINOMA.

LINDNER Véronique(1), De FROMONT Marc (2), MOLINIE Vincent (3), LETOURNEUX Hervé (4), MEYER Nicolas (5), LANG Hervé (4), JACQMIN Didier (4).
(1) University Hospital, Pathology, Strasbourg, France (2) University Hospital, Pathology, Marseille, France (3) St Joseph Hospital, Pathology, Paris, France (4) University Hospital, Urology, Strasbourg, France (5)University Hospital, Statistics, Strasbourg, France.

Introduction :
The Fuhrman grading system is the nuclear grade most often used in the world for renal cell carcinoma (RCC). This grading is recognized as an significant prognostic factor. However according to the few previous studies, its reproductibility appears to be low.
Material and method :
Between 1980 and 1990, 255 RCC (pT1, pT2, pT3a and b, N0 M0)were treated by radical nephrectomy. In a retrospective multicentric study, three pathologists independently classified 241 cases according to the Fuhrman grading system. We analysed the concordance between the three pathologists. We then searched the best interobservers concordance by collapsing into a three, then a two level grading system. At the same time, the overall survival curves were evaluated for each pathologist according to the classical 4-scheme and for the scheme giving the best concordance. The statistical analysis used the kappa index to measure concordance between each pair of observers and the Cox model for multivariate survival analysis.
Results :
The mean interobserver kappa value was 0.22 (0.09 to 0.36). The best concordance was obtained by collapsing to a low grade (grades 1 and 2) versus a high grade (grades 3 and 4): kappa = 0.44 (0.22 to 0.55). The Fuhrman grading system was an independent prognostic factor for each pathologist ($p=0.01$, $p<0.0001$, and $p=0.004$). With the 2-grade scheme, the nuclear grade remained an independent factor for each pathologist ($p=0.004$, $p=0.0003$ and $p=0.005$).
Conclusions :
Reducing the Fuhrman system to a 2-grade scheme improves the interobserver agreeement and remains an independant prognostic factor.

O-194
PLATELET-ACTIVATING FACTOR RECEPTOR EXPRESSION IN HUMAN RENAL CELL CARCINOMA

MITROPOULOS Dionissios1,2, SERAFETINIDES Efraim1, KYROUDI Aspasia2, KITTAS Christos2, THEOCHARIS Stamatios3
Departments of Urology1, Histology-Embryology2 and Forensic Medicine- Toxicology3, Medical School, University of Athens, Athens, Greece

Background-Aims: Platelet-Activating factor (PAF) is a potent lipid mediator, participating via its specific receptor (PAF-R) in inflammatory and physiological responses. It has been reported that PAF and other PAF-like lipids could inhibit cell proliferation and invasive capacity of tumoral cells. The aim of this study was to examine the expression of PAF-R in human renal cell carcinoma (RCC) cases and to correlate it with clinicopathological variables and patients' survival.
Materials and Methods: PAF-R expression was examined immunohistochemically
on paraffin embedded tissue sections of 37 RCC cases. PAF-R positivity, overexpression (positivity in more than 40% of tumoral cells), distribution (cytoplasmic, nuclear, cytoplasmic and nuclear pattern) and intensity of immunostaining were correlated with patients' sex, age, clinical stage, tumor histological type and grade and patients' survival.
Results: Thirty six out of 37 (97%) RCC cases were PAF-R positive, while PAF-R overexpression was noted in 30 out of 37 (81%). PAF-R cellular distribution was mainly cytoplasmic and nuclear. In the majority of cases, moderate or intense immunostaining was noted. PAF-R positivity, distribution and intensity of staining were not correlated with

any of clinicopathological variables examined and patients' survival. PAF-R overexpression was statistically significantly correlated with patients' survival (p=0.034) but not with the other clinicopathological variables examined.
Conclusions: Our data suggest a possible involvement of the lipid mediating PAF-R in RCC. Further experimental data at clinical and molecular levels are needed to delineate the implication of PAF/PAF-R system in renal neoplasia.

O-195
VASCULAR ENDOTHELIAL GROWTH FACTOR IS AN INDEPENDENT PROGNOSTIC FACTOR IN PT3 RENAL CELL CARCINOMAS.

Nathalie Rioux-Leclercq, Karim Bensalah, Emmanuelle Leray, Florence Jouan, Pascale Bellaud, Sebastien Vincendeau, Alejandro Rodriguez, Andrea Manunta, Francois Guille, Bernard Lobel, Jean-Jacques Patard.
Departement d'Anatomie et Cytologie Pathologique, Service de Santé Publique, Service d'Urologie, CHU, Faculté de Médecine, Rennes.

Objective: To evaluate the prognostic value of angiogenesis measured by VEGF immunostaining in a series of pT3 renal tumors.
Material and methods: 112 patients were included in this retrospective study. Tumors were classified according to the 2002 revised TNM and Fuhrman grade systems. All slides were reviewed by a single pathologist. VEGF was determined by immuno-histochemistry. The following variables were evaluated, using univariate and multivariate analysis, for their impact on the risk for death from renal cancer: age, gender, tumor size, fat, adrenal or vein invasion, inferior vena cava involvement, Fuhrman grade, ECOG performance status and VEGF expression.
Results. There were 71 men and 41 women and mean age at surgery was 65 years. A total of 62 patients were dead at last follow-up, including 49 (43,8%) from RCC. A 30% VEGF cut-off was determined according to Roc curves. Tumor size, nodal invasion, distant metastasis, fat invasion, VEGF expression ($p<0.01$), and Fuhrman grade (p:0.02) were significantly associated to survival in univariate analysis. Only the following variables remained significant in multivariate analysis: Fuhrman grade, fat invasion, renal vein invasion, distant metastasis ($p<0.01$) and VEGF expression (p:0.01) (Odd ratio: 3,187 [1,248 – 8,140]).
Conclusion: In this study, VEGF expression was confirmed as being an independent prognostic factor for predicting survival in pT3 renal tumors. Utilizing it, in addition to the known TNM and Fuhrman variables, may provide a rationale for including high-risk pT3 renal cancer patients in trials with adjuvant angiogenesis inhibitors.

O-196
THE USE OF E-CADHERIN, P53, CK19 AND 34BE12 IN SUBTYPING RENAL CELL CARCINOMA (RCC). AN IMMUNOHISTOCHEMICAL STUDY.

SAMARAS Vasilis*, TANOGLIDI Anna*, NOMIKOS Alexandros*, TSAMOURI Magdalini*, KEFALA Maria*, POULIAS Hercules**, BARBATIS Calypso*.
Hellenic Red Cross Hospital, Departments of Pathology* and Urology**. Athens. Greece.

INTRODUCTION: RCC represents almost 2% of all human carcinomas with definite prognostic factors the histological grade, type and stage. Correct classification of RCCs and the assessment of probable prognostic factors are constantly investigated with emphasis on molecules related to tissue organization, survival and cell differentiation.

AIM: An immunohistochemical study of E-cadherin, p53, CK19 and 34BE12 in subtyping RCCs and their relationship with pT stage and histological grade.
MATERIALS-METHODS: 40 RCCs were studied; 31 Conventional (cRCCs), 4 Papillary (pRCCs), 4 Chromophobe (chrRCCs) and one collecting duct (cd). Histological grade: G1 (9), G2 (20), G3 (7), G4 (4), pT-stage: T1 (20), T2 (11), T3a (1), T3b (2) according to Fuhrman's and UICC/AJCC/TNM classification systems, respectively. With the immunohistochemical method of Envision-HRP and the use of monoclonal antibodies, the topography of the cell adhesion molecule E-cadherin, the nuclear phosphoprotein p53 and two types of cytokeratins that are expressed along the distal nephron were studied.
RESULTS: E-cadherin: we confirmed the E-cadherin expression in Bowman's capsule, distal tubules collecting ducts as it has been reported in a few studies but focal, minimal expression was seen only in 3/31 cRCCs, in contrast to all 4 chrRCCs where a diffuse cytoplasmic membrane positivity was observed. pRCCs and collecting duct cases were negative.
P53: p53 nuclear expression >5% was observed in 2/4 pRCCs, 1/31 cRCC and one cd. Only grade 3 and 4 tumors were expressing p53.
CK19: strong cytoplasmic, diffuse positivity was observed in 3/4 pRCCs and the collecting duct. All conventional types were negative but scatter CK19 (+) cells were observed in one chrRCC.
34BE12: Strong diffuse positivity characterised the collecting duct and 1/4 pRCCs. All other cases were negative.
CONCLUSIONS: E-cadherin expression was undetectable in all, exept the chromophobe subtype of RCCs. P53 was uncommon in all types of RCCs hence it couldn't be used as a prognostic factor. CK 19 is commonly expressed in pRCC and 34BE12 is also a marker of distal nephron differentiation.

O-197
PREVALENCE OF VON HIPPEL-LINDAU GENE MUTATIONS IN SPORADIC RENAL CELL CARCINOMA: RESULTS FROM THE NETHERLANDS COHORT STUDY

VAN HOUWELINGEN Kjeld P (1),VAN DIJK Boukje AC (2), HULSBERGEN-VAN DE KAA Christina A (3), SCHOUTEN Leo J (2), GORISSEN Hanneke JM (1),SCHALKEN Jack A (1), VAN DEN BRANDT Piet A (2), OOSTERWIJK Egbert (1).
(1)Department of Urology, University Medical Center Nijmegen, P.O. Box 9101, 6500 HB Nijmegen, the Netherlands.
(2)Department of Epidemiology, NUTRIM, Maastricht University, P.O. Box 616, 6200MD Maastricht, the Netherlands.
(3)Department of Pathology, University Medical Center Nijmegen, P.O. Box 9101, 6500 HB Nijmegen, the Netherlands

INTRODUCTION
Biallelic Von Hippel-Lindau (VHL) gene defects, a rate-limiting event in the carcinogenesis, occur in approximately 75% of sporadic clear-cell Renal Cell Carcinoma (RCC). In 19% of sporadic clear-cell RCC, methylation of the VHL gene promoter appeared to be involved, and in 10%-20% no alteration in the VHL alleles was detected, indicating that other genes are involved.
Several risk factors for developing RCC have been identified e.g. tobacco smoking, hypertension and/or its medication, and occupational exposures. Multiple and specific types of VHL mutations in RCC have been associated with exposure to trichloroethylene. Consumption of vegetables and citrus fruit decreased the frequency of VHL mutations among smokers.

Therefore, mutational patterns in the VHL gene may serve as an etiological imprint to factors causing renal cancer.
PURPOSE
We studied the VHL mutation status of RCC cases identified within a population-based cohort of 120,852 men and women which was recruited in the Netherlands to study associations between dietary habits, lifestyle and cancer occurrence.
METHODS.
Within this Netherlands cohort study, after 11.3 years of follow-up, 337 incident cases with histologically confirmed epithelial cancers were identified. DNA was isolated from paraffin material collected from 51 pathology laboratories and revised by one pathologist, leaving material from 235 cases with RCC. VHL mutational status was assessed by SSCP followed by direct sequencing, after testing SSCP as a screening tool in a subsample.
RESULTS
The number of mutations was significantly higher for clear-cell RCC compared to other histological types. We observed 131 mutations in 114 out of 187 patients (61%) with clear-cell RCC. The majority of mutations were truncating mutations (47%). The mean tumor size was 72.7 mm for mutated tumors compared to 65.3 mm for wildtype tumors (p=0.06). No statistically significant differences were observed for nuclear grade and TNM stage. In other histological types, we observed 8 mutations in 7 out of 48 patients (15%), 1 mutation in 1 of 6 oncocytoma, 3 mutations in 2 of 7 chromophobe RCC, 2 mutations in 2 of 30 papillary RCC, no mutations in 1 collecting duct carcinoma and 2 mutations in 2 of 4 unclassified RCC.
CONCLUSIONS
VHL mutations were detected in 61% of sporadic clear-cell RCC and in 15% of non-clearcell RCC. VHL mutated and wildtype clear-cell RCC did not differ with respect to most investigated parameters.

O-198
TFE3 IMMUNOSTAINING IS A USEFUL TOOL TO IDENTIFY RENAL CELL CARCINOMAS ASSOCIATED WITH THE XP11.2 TRANSLOCATION - A STUDY OF 21 TFE3 IMMUNOPOSITIVE RENAL CELL CARCINOMAS.

VASILIU Viorel, CAMPARO Philippe, COUTURIER Jérôme, SIBONY Mathilde, FERLICOT Sophie, FROMONT Gaëlle, LEROY Xavier, BOCCON-GIBOD Liliane, LAE Marick, VIEILLEFOND Annick
1.Service d'Anatomie Pathologique - Hôpital Necker, Paris, 2.Service d'Anatomie Pathologique, - Hôpital Val de Grace, Paris, 3.Service de Génétique Oncologique - Institut Curie, Paris, 4.Service d'Anatomie Pathologique - Hôpital Tenon, Paris, 5.Service d'Anatomie Pathologique – CHU de Bicêtre, 6.Service d'Anatomie Pathologique – CHU de Poitiers, 7.Service d'Anatomie Pathologique – CHRU de Lille, 8.Service d'Anatomie Pathologique - Hôpital Armand-Trousseau, Paris, 9.Service d'Anatomie Pathologique - Institut Curie, Paris, 10.Service d'Anatomie Pathologique - Hôpital Cochin, Paris.

Background: Recently, a new entity was individualized in the 2004 WHO classification of tumors of the kidney: renal cell carcinomas (RCCs) associated with Xp11.2 translocations/ TFE3 gene fusions. These neoplasms, that mainly affect children and young adults, were formerly recognized as « juvenile renal carcinoma » (JRC). The diagnosis is supported by cytogenetic and /or molecular analysis demonstrating several different translocations, always involving Xp11.2, all resulting in gene fusions involving the TFE3 transcription factor gene. Interestingly, the TFE3 antibody, directed against the C-terminal part of the TFE3 protein, is a sensitive and specific marker of RCCs associated with Xp11.2 translocations as experimented by Argani et al., 2003 (1).
Design: We sought to evaluate TFE3 immunohistochemical expression on paraffin-embedded tissue sections. We studied a panel of 28 RCCs with JRC features and 50 adult-type RCCs, including 23 clear cell, 10 papillary and 17 unclassified RCCs. The 28 tumors with JRC features presented intermigled papillary and clear cell pattern and/or occured in children or young adults. A cytogenetic study was performed for 8 tumors with JRC features : 7 tumors presented a t(X;1)(p11.2;q21) and 1 tumor a t(X;17)(p11.2;q25).
Results: A strong nuclear expression of TFE3 was observed in 20 (including the 8 cytogenetically studied tumors) of the 28 tumors displaying JRC features. The 20 patients (6 males and 14 females) were young adults (age ranging from 8 to 42 years old with a mean of 21 years). In contrast, only one of the adult-type RCCs expressed TFE3 (unclassified tumor occurring in a 78 years old man).
Conclusion: We recommend to evaluate the TFE3 immunohistochemical expression in RCCs with mixed papillary and clear cell pattern, especially in young patients but also in older patients with unclassified RCCs. Diagnosis of RCCs associated with Xp11.2 translocations is therefore possible, even retrospectively, on paraffin-embedded tissue sections when fresh or frozen materiel was not available for cytogenetic and/or molecular biology analysis. This new tool will allow a better evaluation of the frequency and prognosis of these neoplasms.

O-199
INTERPHASE CYTOGENETIC IN METASTATIC CHROMOPHOBE RENAL CELL CARCINOMA (RCC).

BRUNELLI Matteo (1,3), COSSU ROCCA Paolo (2), PEA Maurizio (1), MENESTRINA Fabio (1), BONETTI Franco (1), SCARPA Aldo (1), CHILOSI Marco (1), COLOMBARI Romano (3), MINA Maria Mihaela (1), GOBBO Stefano (1), BADOUAL Cecile (4), MARTIGNONI Guido (1,2).
Department of Pathology, Università di Verona (1) and Sassari (2), Arzignano Hospital, Vicenza (3), Italy, Hopital Europeen George Pompidou, Paris (4), France.

Introduction. Chromophobe RCC is a low grade malignancy which can metastatize many years after the nephrectomy. Primary chromophobe RCC shows frequent genetic anomalies as the losses of multiple chromosomes from among chromosomes 1, 2, 6, 10, and 17 but little is known about the genetics of their rare metastases.
Purpose. To characterize the genetic anomalies associated with metastatic disease, we assessed the status of three chromophobe RCCs in matched primary and metastatic samples.
Material and Methods. Three classic variant primary chromophobe RCCs and their metastatic lesions that occurred in the lung, pancreas and retroperitoneal lymph-nodes respectively 10, 12 and 5 yrs after the nephrectomy were studied. The samples were investigated by interphase fluorescence in situ hybridization on 5 micron paraffin-embedded tissue sections with centromeric probes for chromosomes 1, 2, 6, 10, and 17 (Vysis, Abbott). Signals were counted in 100-200 neoplastic nuclei from each tumor.
Results. In two cases (67%) both the primary and the metastatic tumors showed loss of chromosomes 1, 2, 6, 10 and 17 (single signal ranged from 79-88% of neoplastic nuclei) whereas no chromosomal losses were detected in the third primary chromophobe RCC and its lymph-nodal metastases.
Conclusions. We conclude that 1) primary and metastatic chromophobe RCCs show the same genetic patterns; 2) metastases of chromophobe RCC show presence (67%) or absence (33%) of losses of chromosomes 1, 2, 6, 10, and 17;

3) the presence or absence of losses of chromosomes 1, 2, 6, 10, and 17 could be related to the haematogenous (67%) and the lymphatic (33%) neoplastic spreading respectively.

O-200
EXPRESSION OF ALPHA-METHYLACYL-COA RACEMASE (AMACR/P504S) IN RENAL NEOPLASMS.

Molinié Vincent (1), De Pinieux Isabelle (1), Guillou Louis (2), Homsi Toufik (1),Balaton André (1). Pathology department, Hôpital Saint Joseph (1), Paris France, CHU Lausanne (3) Suisse.

Background: Alpha-methylacyl-CoA racemase (AMACR), also known as P504S, has recently been utilized as a biomarker for prostate carcinoma. Expression of AMACR is also recognized in normal renal tubules. The aim of the present study was to evaluate the expression of AMACR/P504S in different subtypes of renal tumors.
Design: 110 cases of renal neoplasms were selected from the surgical pathology files of 2 department of pathology, including conventional clear cell type (n=25), papillary renal cell carcinoma (n=55) (type 1 n = 33, type 2 n = 22), mucinous tubular and spindle cell carcinoma (n=5), chromophobe carcinoma (n=6), oncocytoma (n=9), urothelial carcinoma (n=2), angiomyolipoma (7), and bellini carcinoma (n=1). One paraffin block of representative renal tumor and normal kidney in each case were studied. Sections were cut at 4 microns and stained with AMACR/P504S monoclonal antibody (Prédiluted, Menarini Diagnostics) on an automated immunostainer (Dakostainer). AMACR/P504S staining was evaluated as negative, focally positive, or diffusely positive. The percentage of positive cells were evaluated in each case.
Results: No expression of AMACR/P504S was observed in Bellini and urothelial carcinoma. A weak and focally expression of AMACR/P504S was observed in conventional clear cell carcinoma (16%), chromophobe carcinoma (16%), and oncocytoma (7%). In papillary renal cell carcinoma 3.6% (2/55), and 96.4 % (53/55) of papillary carcinoma showed focally and diffusely positive for AMACR, respectively, without no difference expression in different subtype (Type 1 or 2). All 5 mucinous tubular and spindle cell carcinoma were strongly positive for AMACR/P504S.
Conclusions: High expression of AMACR/P504S is found in papillary renal cell carcinoma (even type 1 or 2), and in mucinous tubular and spindle cell carcinoma. This should be exercised in using P504S immunohistochemical staining for the diagnosis of papillary renal cell carcinoma, and particularly in case of biopsy to differentiate different eosinophilic renal tumor. A weak and focal AMACR staining could be present in case of clear cell and chromophobe carcinomas, and even in oncocytoma.

O-201
PAX2: A RELIABLE IMMUNOHISTOCHEMICAL MAKER FOR NEPHROGENIC ADENOMAS

TONG Guo-Xia1, MELAMED Jonathan2, MANSUKHANI Mahesh1, MEMEO Lorenzo1, WAISMAN Jerry2
1Department of Pathology, Columbia University Medical Center, 2 Department of Pathology, New York University Medical Center, New York NY.

INTRODUCTION: The diagnosis of nephrogenic adenoma (NA), characterized by a proliferation of small tubules and cystic structures in the lamina propria, sometimes with polypoid papillary projections on the surface of the urinary tract is usually straightforward. However, misdiagnosis may occasionally occur. Immunohistochemical markers to differentiate NA from adenocarcinomas have had only partial success. The demonstration of the origin of NA from renal tubular epithelium in renal transplant patients, suggests that its histogenesis may help differentiate it from tumors of the urinary tract.
PURPOSE: We investigated the value of the expression of PAX2 - a renal transcription factor - CD10, and uroplakins, to differentiate NA from adenocarcinoma of prostate gland (AOP), and urothelial carcinoma (UC) of the urinary tract.
METHODS: 39 cases of non-renal transplant related NA - 25 vesical, 1 ureteral, 11 prostatic urethral and 2 distal urethral - retrieved from Tisch Hospital of NYU Medical Center and Columbia University Medical Center, and tissue microarrays (TMA) of 100 AOP, 47 invasive UCs of the urinary bladder, and 100 samples of normal prostate tissue were used in the study. Normal urothelium and normal prostate acini in the NA specimens were used as internal controls. Immunohistochemical staining for Pax2 (Zymed), CD10 (Dako) and uroplakins (kindly provided by Dr. T.T. Sun in NYU) were performed with biotin-avidin method following antigen retrieval.
RESULTS: Strong nuclear staining of PAX2 was found in all 39 cases of NA (100%) regardless of histologic pattern. PAX2 was not detected in AOP, invasive UC, normal prostate, and normal urothelium. Focal CD10 was detected in 6 of 13 NA, mainly in the superficial papillary component. In addition, CD10 was detected in normal prostate tissue, normal urothelium, AOP, and UC. No uroplakins were detected in any NA.
CONCLUSION: In this study, we found that NA in non-renal transplant patients consistently expressed PAX2, consistent with a renal tubular origin. Distinct nuclear staining in all NA, but not AOP or UC indicates that PAX2 is useful in distinguishing NA from common lower urinary tract malignancies.

O-202
MCM3 AND KI67 AS PROGNOSTIC MARKERS FOLLOWING SURGERY FOR RENAL CELL CARCINOMA.

MEMEO Lorenzo 1, MITCHELL Robert 2, PARSONS Ramon 1, HIBSHOOSH Hanina 1, ASSAAD Adel 1, MCKIERNAN James 2, MANSUKHANI Mahesh 1.
1 Department of Pathology and 2 Department of Urology, Columbia University Medical Center, New York NY.

INTRODUCTION: Minichromosome maintenance proteins (MCM2-7) accumulate in cycling cells, enabling DNA replication in a process called “licensing”. Ki-67, another marker of cycling cells, starts to accumulate later in G1.
PURPOSE: We undertook this study to evaluate the role of Ki-67 and MCM3 expression in predicting lymph node or distant metastases and survival following radical or partial nephrectomy for renal cell carcinoma (RCC).
METHODS: Immunohistochemical analysis for Ki-67 and MCM3 was performed on tissue microarrays containing tumor tissue from 99 patients who underwent nephrectomy for renal cortical carcinomas at our institution between 1999 and 2004. Pathologic variables (tumor diameter, grade, histology, lymph node status) and follow-up data pertaining to these patients were obtained from the Columbia University Comprehensive Urologic Oncology Database. The proportion of tumor cell nuclei expressing these proteins was estimated and scored as “0” through “4”. Expression of Ki-67 was correlated with that of MCM3. Using logistic regression and Cox proportional hazards models, the impact of the expression of these proteins in estimating hazard of lymph node and distant metastases, and overall survival, disease free survival, and disease specific survival was evaluated.
RESULTS: The expression of Ki-67 linearly correlated with that of MCM3 (Pearson correlation coefficient, 0.571, $p<0.001$). Tumors expressing high levels of Ki-67 (“3” and “4”) were 9.25 times more likely to be associated with lymph

node or distant metastases at the time of surgery (p=0.001). On univariate analysis of recurrence free survival, Ki-67 and MCM expression showed a statistically significant negative impact on disease free survival (p<0.001 and p= 0.032). Using a multivariate model (including diameter, grade, histology, and Ki-67), Ki-67, grade, and diameter were statistically significantly associated with an increased hazard of disease recurrence (p=0.030, 0.013, and 0.026, respectively).
CONCLUSIONS: This study demonstrates a correlation between MCM3 and Ki-67 expression, and confirms the prognostic importance of Ki-67 as an independent marker for disease progression

O-203

EXPRESSION OF PDGFR-ALFA IN 140 RENAL CELL CARCINOMAS USING TISSUE MICROARRAYS

GASPA Albert*, PETIT Anna*, TRUAN David^, MELLADO Begonya', PALACIN Antonio*, FERNANDEZ Pedro, MALLOFRE Carme*.
Department of Pathology*, Oncology' and Urology^. Hospital Clinic de Barcelona. IDIBAPS. University of Barcelona.

SHORT INTRODUCTION:Platelet derived growth factor receptor alfa (PDGFRa) is a transmembrane tyrosin kinase receptor that is considered a therapeutic target because it can be specifically inactivated by small-molecule tyrosine kinase inhibitors such as Imatinib (STI-571). The expression of PDGFRa in Renal Cell Carcinoma (RCC) has not been extensively studied in vivo and has interest because there is currently no effective treatment for patients with metastatic or recidivant RCC.
PURPOSE OF THE STUDY:The aim of the study is to evaluate the immunohistochemical expression of PDGFRa in different subtypes of RCC using tissue microarrays in order to assess whether Imatinib could be a potentially useful therapeutic target in these neoplasms.
METHODS USED:We constructed five tissue microarrays with representative areas from 140 RCC: 60 Clear Cell RCC (CCRCC), 36 Chromophobe RCC (ChRCC), 29 Papillary RCC (PRCC) and 15 RCC with Sarcomatoid differentiation (SRCC). Immunohistochemical study was performed using polyclonal antibody PDGFRa (c-20, Santa Cruz, dilution 1:100). The percentage of positive staining cells was categorized as focal (1-25% of tumor cells), moderate (25-50%) and diffuse (>50%).The intensity of expression was evaluated on a three-grade scale and the staining pattern (cytoplasmic, membranous, or nuclear) was also considered. In the cases of SRCC only the sarcomatoid part of the tumour was analysed.
RESULTS: 98% of CCRCC, 88% of ChRCC, 86% of PRCC and 100% of SRCC expressed PDGFRa. Of the positive CCRCC, 64% showed membranous, 50% cytoplasmic and 40% nuclear staining. In all these cases the expression was weak (intensity 1/3) and 55% presented focal positivity. ChRCC and PRCC exhibited a weak cytoplasmic staining pattern in >80% of cases. All SRCC showed cytoplasmic positivity for PDGFRa that was diffuse in 77% of cases and with moderate intensity (2/3) in 66% of cases.
CONCLUSIONS:Most of RCC show expression of PDGFRa being the cytoplasmic staining pattern and the weak intensity (1/3) the most frequent ones. However 65% of CCRCC also showed a membranous staining pattern and only SRCC reveal a more intense and diffuse cytoplasmic positivity for PDGFRa compared with the rest of the subtypes. The meaning of the expression of this protein and its role in the pathogenesis of RCC is not clear and deserve further studies in order to consider its possible use as a therapeutic target.

O-204

IMMUNOHISTOCHEMICAL STUDY OF 310 ADULT RENAL CELL TUMOURS USING TISSUE MICROARRAYS TECHNOLOGY

Céline Bazille (1), Philippe Camparo (2), Yves Allory(3), Vincent Molinié (4), Marine Lefèvre (5), Patrice Callard (5), Annick Vieillefond (6), Mathilde Sibony (5).
(1) Hôpital Lariboisière, Paris. (2) Hôpital du Val de Grâce, Paris. (3) Hôpital Henri Mondor, Créteil. (4) Hôpital St Joseph, Paris. (5) Hôpital Tenon, Paris. (6)Hôpital Cochin, Paris.

Background: While most adult renal epithelial tumours can be classified according histologic criteria and cytogenetic data, some morphologic aspects may be confusing. As renal tumours have different prognoses, it would therefore be of interest to establish distinctive immunophenotype patterns.
Materials and methods: Using Tissue Micro-Array technique, we analysed the immunoprofile of the four main renal epithelial tumours occurring in adults, with emphasis on uncommon lesions such as chromophobe renal cell carcinomas and oncocytomas. 310 tumours were analysed : 75 clear cell renal cell carcinomas (ClCRCC), 89 papillary renal cell carcinomas (PRCC), 50 chromophobe renal cell carcinomas (CRCC) and 96 oncocytomas (ONC). Immunostaining was performed in all cases using a large panel of antibodies.
Results: Main antibodies and percentage of positivity in each subtype tumour (ClCRCC, PRCC, CRCC and ONC) are for CK7 (0;79;81 and 9%), Vim (54;85;0 and 2%), CD10 (86;65;39 and 14%), RCC (38;55;0 and 2%), CD117 (0;0;57, and 57%), E-Cadherin (12;16;100 and 48%) Racemase (3;87;0 and 0%) and Aqp1 (8;53;0 and 2%).
AE1-AE3, EMA, CK19, cyclin D1 and Muc-1 were variably expressed in all kinds of tumours. 34betaE12 and C-erbB2 were positive in rare cases. CK5/6, CK10/13, CD15, Aquaporine 2, Aquaporine 3 and CD99 were negative in all tumours. These antibodies were not useful for diagnosis.
When combining antibodies, we obtained some immunohistochemical profiles. Antibodies patterns suitable as routine tools with sensibility (Se) and specificity (Sp) are :
ClCRCC CK7- Racemase- Vim+/- CD10+ (Se 74,5%, Sp 92%)
PRCC CK7+ Racemase+ Vim+/- CD10+/- (Se 68,5%,Sp 100%)
CRCC CK7+ Racemase- Vim- CD10+/- (Se 80%, Sp 97%)
ONC CK7- Racemase- Vim- CD10- (Se 68%, Sp 97,5%)
Conclusion : In case of unclear morphological features, antibody panel (CK7, Racemase, Vim and CD10) permits to determine with more precision histological subtypes of epithelial renal cell tumors. CD117, and E-Cadherin may be helpful as second line panel.

O-205

PRIMARY EWING'S SARCOMA/PNET OF KIDNEY. CLINICOPATHOLOGIC AND MOLECULAR ANALYSIS OF 7 CASES.

Carole Gengler (1), Annick Vieillefond (2), Dominique Ranchère (3), Philippe Beuzeboc (4), Gabrielle Gallagher (1), Jean Benhattar (1), Louis Guillou (1). University Institute of Pathology, Lausanne, Switzerland (1), Departments of Pathology (2) and Medical Oncology (4) , Cochin Hospital, Paris, and Léon-Bérard Cancer Center, Lyon (3), France.

Introduction. Ewing's sarcoma (ES) is mostly observed in bone and soft tissue. Its occurrence in viscera, including kidney, is a rare event.
Purpose of the study. To report the clinicopathologic features of seven translocation-positive ES primary of kidney.
Materials and methods. 7 ES primary of the kidney were retrieved from the consultation files of the authors. Histology and immunohistochemical features were reviewed. Molecular

analysis was performed on formalin-fixed, paraffin-embedded tissue, using RT-PCR.
Results. There were 5 males and 2 females, aged from 17 to 52 years (median, 35 yrs). 4/6 tumors were located in the right kidney (missing data, 1). Tumor size varied from 6 to 26 cm (median, 11 cm). Tentative pathologic diagnoses included, in addition to ES, nephroblastoma (2), poorly-differentiated synovial sarcoma (1), and small cell carcinoma (1). All tumors, which were fixed in formalin, presented histologically as primitive small round cell proliferations. Immunohistochemical findings were as follows: CD99+ 6/6, Fli-1+ 3/4, keratins+ 1/6, EMA+ 1/6, S100 protein+ 0/5, chromogranin-A+ 0/5, synaptophysin+ 1/5, desmin+ 0/5. EWS-FLI1 fusion transcripts were detected in all paraffin-embedded tumors, using RT-PCR. Breakpoints included EWS exon 7-FLI1 exon 6 (EWS-FLI1 - type 1) (2/7), EWS ex 7-FLI1 ex 5 (EWS-FLI1 - type 2) (3/7), EWS ex 10-FLI1 ex 6 (1/7), data not available (1/7). For 2 cases, breakpoints which have previously been identified in another laboratory (Curie Institute, Paris, F; Drs E. Guilbert & O. Delattre) using frozen tissue samples and multiplex RT-PCR, were identical in both frozen and corresponding paraffin-embedded tissue samples. Unusual transcripts were confirmed by sequencing. Clinical data were available for 6 cases. Five patients had localized disease at diagnosis. Two patients recurred locally 10 and 27 months after diagnosis, and two additional patients developed distant metastases to lung and femur 7 and 17 months after diagnosis. Two patients were alive without disease at 6 and 56 months, 2 were alive with disease at 22 and 29 months, and 2 died of disease 12 and 18 months after diagnosis. Median overall survival was 20 months (range: 6-56 months).
Conclusion. Similarly to ES of bone and soft tissue, ES primary of kidney are rare, highly aggressive neoplasms, of which most seem to bear the t(11;22) EWS-FLI1 translocation.

O-206
PRIMARY EWING'S SARCOMA (ES) / PNET OF URINARY BLADDER AND PROSTATE. CLINICOPATHOLOGIC AND MOLECULAR ANALYSIS OF 6 CASES.

Carole Gengler (1), Gérard Bertrand (2), Gabrielle Gallagher (1), Jean Benhattar (1), Louis Guillou (1). University Institute of Pathology, Lausanne, Switzerland (1), and Anatomic Pathology Center, Angers, France (2).

Introduction. ES most commonly develops in bone and soft tissues of adolescents and young adults. Its occurence in prostate and urinary bladder is exceptional. 85-90% of ES bear the t(11,22) (q24;q12) translocation involving EWS and FLI1 genes. EWS-FLI1 fusion gene transcripts which are specific for ES can be detected in frozen and paraffin-embedded tissues, using RT-PCR.
Purpose of the study. To report the clinicopathologic and molecular features of 6 ES primary of the urinary bladder and prostate.
Materials and methods. 6 ES primary of the urinary bladder (n=4), of prostate (n=1), and of both organs (n=1) were retrieved from the consultation files of the authors. Histology and immunohistochemical features were reviewed. Molecular analysis was performed on formalin-fixed, paraffin-embedded tissue (6/6), using RT-PCR.
Results. There were 4 males and 2 females, aged from 20 to 53 years (median, 28 yrs). Four patients (2 females and 2 males, median age, 25 yrs) presented with large locally infiltrative masses of the urinary bladder (median size, 6 cm), one patient had a 6 cm tumour confined to the left prostatic lobe, and one patient had a 9 cm pelvic mass centered on the prostate and urinary bladder. All but one patients had localized disease at diagnosis. Histologically, all neoplasms presented as primitive small round cell proliferations that expressed CD99 (6/6) and EMA (1/6, focal reactivity) but were negative for keratins, desmin, S100 protein, chromogranin-A, synaptophysin, and CD45 (0/6, each). EWS-FLI1 fusion transcripts were detected in all cases. Breakpoints included EWS exon 7-FLI1 exon 6 (type 1) (4/6) and EWS ex 7-FLI1 ex 5 (type 2) (2/6). Treatments consisted of varying combinations of surgery, chemotherapy and radiation therapy. Three patients were alive and well 6, 8, and 13 months after treatment completion. The patient who presented with a large pelvic mass died of disease at 27 months. One patient who was metastatic at presentation died at 7 months, and one patient died of treatment complications (radiation colitis) at 12 months.
Conclusion. This study shows that ES/PNET can (rarely) develop in the urinary bladder and prostate as a primary neoplasm. Clue to diagnosis include CD99 positivity, negativity for epithelial, muscular, and lymphoid markers, and the detection of ES translocations and/or fusion transcripts.

O-207
THE TESTICULAR BIOPSY IN THE ASSESSMENT FOR FERTILITY TREATMENT

YOUNG Rebecca, HAMILTON Judith, CHANDRA Ashish

Introduction: The current standard method for assessment of infertility on testicular biopsy is the Johnsen Maturity Index (JMI), in which 10 randomly chosen seminiferous tubules are each assigned a score of 1-10 according to the stage of spermatogenesis, their mean score providing the JMI. Fertility treatment is offered to patients on the assumption that mature spermatozoa are unlikely to be harvested with JMI <4.5. However, spermatozoa may be demonstrated on biopsies with JMI <4.5 and the converse is also true.
Method: This study was designed to investigate the reproducibility of JMI and offer an improvement on the current reporting of testicular biopsies. The details of 50 patients with testicular biopsies for infertility during the period 2000-03 were obtained from the archives. The original histological sections were reviewed for the following information - 1. Total number of seminiferous tubules in the biopsy, 2. JMI and 3. Percentage of tubules containing spermatozoa. The original histology report was then reviewed for comparison.
Results: Of the 40 patients studied, 6 had biopsies with originally reported JMI <4.5; review revealed small numbers of mature spermatozoa in these cases. In retrospect, we believe that these additional 6 (15%) cases could have been offered IVF. In 3 cases, mature spermatozoa in small numbers were seen in >10% tubules on the biopsy.
Two cases with JMI >4.5 showed no spermatozoa on the biopsy.
On review, JMI varied from the original by >1.0 in 7 patients including 3 cases where it was revised to >4.5.
Conclusions: These findings highlight drawbacks of using JMI alone, the most important being that it does not identify all men to whom sperm harvesting for IVF could be offered. Also, significant variation between observers is more likely with as many as 10 numeric scores for each tubule.
We propose a system of reporting testicular biopsies that combines a score of highest maturity with the extent of spermiogenesis for selection of men for sperm harvesting.

O-208
DEVELOPING EXTERNAL QUALITY ASSURANCE IN BREAST SCREENING PATHOLOGY IN THE GERMAN POPULATION BASED PROGRAMME: FIRST RESULTS

DECKER Thomas, HUNGERMANN, Daniela, BÜRGER Horst, KERSTING Christian, BÖCKER Werner
Gerhard-Domagk-Institute of Pathology
University of Muenster

Introduction: In 2005, a population based mammography screening program for Germany based on the European guidelines will start. Without improving the pathology service, the benefit of screening may be reduced or even lost. Especially specimens from minimal invasive diagnosis (MIB) of screened women provide pathologists with problems. To prepare pathologists who intend to participate in the program the authors provide courses on breast screening pathology for continuous education as the most important tool within an external quality assurance scheme.
Purpose of the study: 1. to evaluate the effect of the training courses on diagnostic performance, 2. to assess the performance of German pathologists interested in breast cancer screening, and 3. to identify the diagnostic problems.
Methods: Till November 2005 about 280 pathologists will participate in 16 diagnostic courses, each for 20 participants. Each course includes 4 microscopic tutorials and 8 presentations. It starts and ends with a diagnostic test using the same set of 11 slides of MIB specimens selected within broad diagnostic categories (only cases with complete agreement among the coordinators). Participants reading the slides use a form planned as standard reporting form for the German Screening Project including the B category according to the EU Guidelines. Kappa statistics are calculated separately for the entry and the closing test. The advantage of these statistics is that kappa values are independent of the diagnosis; they simply reflect the consistency of ratings by the participants. The following limits were used for interpretation: <0.0: poor, 0.0-0.2: slight, 0.21-0.4: fair, 0.41-0.6: moderate, 0.61-0.8: substantial, and 0.81-1.0: very good. (180 participants by September 2005).
Results: (preliminary 100 participants) 1. After the course the rate of cases with substantial and very good consistency rises from 7 to 9/11 cases. 2. The overall consistency of the participants' B-categories is 0.68. 3. There are 4 cases with poor to fair agreement: columnar cell change, columnar cell hyperplasia, DCIS low grade, and phyllodes tumor.
Conclusions: 1. The training course improves the consistency of the diagnosis in MIB. 2. The consistence of attending German pathologists in MIB diagnosis is in general at least substantial (kappa >0.6) 3. To improve the performance further education should include columnar cell lesions and non-high nuclear grade DCIS / ductal hyperplasia, respectively.

O-209
ATYPICAL DUCTAL HYPERPLASIA, FLAT EPITHELIAL ATYPIA AND BREAST CANCER RISK

DAUPLAT Marie-Mélanie, MISHELLANY Florence, FOUILHOUX Genevieve, DELATOUR Monique, FEILLEL Viviane, LEBOUEDEC Guillaume, LEMERY Sylvie, PENAULT-LLORCA Frédérique;

Background: With the development of breast screening mammography atypical ductal hyperplasia (ADH) and the recently described flat epithelial atypia (FEA) or columnar cell atypia are frequently reported. Those lesions are considered as potential markers of risk of breast cancer. Their finding on core biopsies for micro calcifications implies a surgical procedure. But their involvement in breast carcinogenesis remains still badly defined. Material and methods: We conducted a retrospective study on 394 patients operated on for benign lesions between 1986 and 1998, in order to revalue the presence of atypical breast lesions and to study their relationship to the risk of cancer. The slides were reviewed, blindly by two pathologists. Follow up was 13.1 years. Results: Middle age was 55.6 yearss. 116 patients (29.5%) had family history including 23% at first degree. 196 patients took a hormonal treatment (oral contraception (6.3%), progestative treatment (10.4%) and hormonal replacement therapy (HRT)(33%)). Atypical breast lesions: ADH (14%), FEA (20%) and both (5%). Among these 394 patients, 9.5% developed a breast cancer (in situ or invasive) during their follow up. The middle age at the occurence of the cancer was 56.5 years. 28% of the patients had family history at first degree and 36% received a hormonal treatment. 55.5% had atypical lesions (28% ADH, 19.5% FEA and 8% both lesions). A significant increase in the relative risk (RR) was observed in case of ADH (RR=2), FEA in a context of family history (RR=2.5%) and, ADH associated either family history (RR=3.5) or HRT (RR=4.5%) or progestative treatment (RR=8.4).
Conclusion: Our data support the breast cancer risk associated with atypical breast mesions, especially in case of an association with a hormonal treatment. Only prospective studies with molecular tests will make possible the understanding of their behaviour.

O-210
DOES DIAGNOSTIC MANIPULATION OF THE PRIMARY BREAST CANCER INCREASE INCIDENCE OF SENTINEL LYMPH NODE METASTASIS?

M Amini L Costarelli, FR Piro, L Fortunato (*), M Farina (*), CE Vitelli (*), A dell'Osso (°)
"San Giovanni Addolorata" Hospital, Department of Pathology and Surgical (°) – Roma, Italy "MG Vannini" Hospital, Department of Surgery (*) – Roma, Italy

Introduction: Sentinel lymph node biopsy has been stated by numerous studies. It can be helpful to identify positive cases, as it may avoid patients' morbidity of surgical excision of axillary lymph nodes. Recent publications reported that a previous fine needle aspiration (FNAC) or core biopsy (CB) or incisional biopsy (IB) of the primary tumor are associated with passive dislodgement of tumor cells in the sentinel lymph node.
Purpose: We present 503 cases of primary breast cancer that were retrospectively evaluated to assess if a previous manipulation of primary tumors increases incidence of metastases in sentinel lymph node, actually.
Methods: 503 consecutive patients (meadian age 61 yrs) with primary breast cancer (median diameter 1,5 cm) were retrospectively evaluated. They came from two different institutions (SGA and MGV). A group of patients, coming from SGA, were studied preoperatively with FNAC, core biopsy or incisional biopsy of the primary breast tumor; the other group, coming from MGV, were studied intraoperatively and breast tumor and SLN were excised simultaneously. All sentinel lymph nodes were evaluated by conventional staining and immunoistochemistry according to our step analysis protocol. First section obtained from each SLN was called Level 0 and routinely processed; if negative, at least six additional couples of section were obtained at 100 micron of distance and were analysed with conventional staining and immunoistochemistry. SLN metastases were called micrometastases (MICRO) when less than 2mm in diameter and isolated tumor cells (ITC) when less than 0,2 mm in diameter.
Results: FNAC (n=88), CB (n=16), or IB (n=100) was performed in 204 cases from 4 to 60 days (median time 11 days) before SLN biopsy procedure. FNAC and CB cases represented GROUP 1, IB cases represented GROUP 2. After intraoperative examination, a simultaneous excision of primary breast tumor and SLN was performed in 299 patients (GROUP 3).We observed SLN+ in 37,5% GROUP 1, 33% GROUP 2 and in 42,1% GROUP 3 (p=0,2). Macrometastases were 18 in GROUP 1, 18 in GROUP 2 and 77 in GROUP 3 (p=0,1). Micrometastases were 11 in GROUP 1, 5 in GROUP 2 and 31 in GROUP 3 (p=0,2). ITC were 10 in GROUP 1, 10 in GROUP 2 and 18 in GROUP 3 (p=0,2).
Conclusions: We could not identify any increased incidence of sentinel lymph node MICRO or ITC after diagnostic

manipulation of the primary tumor. These results are not in accord with other studies.

O-211
INTRAOPERATIVE EXAMINATION OF SENTINEL LYMPH NODES FREQUENTLY CHANGES SURGICAL MANAGEMENT IN WOMEN WITH BREAST CANCER

M Amini, L Costarelli, FR Piro, L Fortunato (*), Massimo Farina (*), A Dell'Osso (°), CE Vitelli (*)
"S.Giovanni Addolorata" Hospital, Department of Pathology and
Surgical (°) – Roma, Italy
"MG Vannini" Hospital, Department of Surgical – Roma, Italy

Introduction: Sentinel lymph node (SLN) biopsy has rapidly changed the surgical management of patients with breast cancer. Intraoperative identification of positive cases can be helpful, as it may avoid patients' return to the operating room.
Methods: We studied 418 consecutive patients (median age 64 years) with primary breast cancer (median diameter 1.5 cm) who underwent SLN biopsy from January 1999 to August 2003. At the discretion of the operating surgeon, an intraoperative examiation (IE) of the SLN was obtained, and the material stained with toluidine blue. After surgery, SLN's were step sectioned, and at least six additional couples of sections obtained from each SLN at 75 micron distance were analysed with conventional staining and immunohistochemistry (IHC – MNF 116).
Results: IE was obtained in 236 patients (56%) with either frozen section (FS; n=68) or with touch prep cytology (TP; n=168), according to different periods of the study. Intraoperative examination resulted in an accuracy of 89% (209/236), but identified only 52/77 positive cases (sensitivity 68%). There were 25 false negative cases (9%), of which 7 cases were represented by macrometastases and 18 cases by micrometastases ($p < 0.001$). Six of the macrometastases were missed by TP, and one by FS ($p= 0.9$). A change in surgical management with IE, resulting in synchronous axillary dissection, occurred in 10% of patients with tumors less than 1 cm in diameter (6/63), in 20% of those between 1-2 cm (24/119), and in 34% of those more than 2 cm in diameter (18/53) ($p=0.05$). In additional 14 cases isolated tumor cells (ITC) were diagnosed at final SLN analysis with IHC, and IE failed to identify them in 12 cases. Lobular histology, but not tumor diameter or age, was the only factor associated with the presence of ITC ($p=0.008$).
Conclusions: IE is highly accurate, but has mediocre sensitivity, particularly for micrometastases. FS and TP are roughly equivalent. The advantage of the latter is mainly represented by the preservation of tissue for subsequent step analysis and IHC. IE is particularly helpful in larger tumors. An accurate and feasible method of intraoperative examination needs to be standardized.

O-212
PRONOSTIC VALUE OF PROLIFERATION MARKERS IN SMALL SIZE NODE NEGATIVE BREAST CANCER. A RETROSPECTIVE STUDY OF 104 CASES

S. Bellefqih1, A. Al Ghuzlan1, M. Caly1, L. Gambotti2, A. Vincent-Salomon1,
L Chneker1, M. Lae1, V. Dieras3, B Sigal-Zafrani1, X Sastre-Garau1
Department of Pathology1, Biostatistics2, and Oncology3,
Institut Curie, 26 rue d'Ulm 75248 Paris, France

Background :
Biological prognostic parameters in node negative breast cancer are needed to select patients (pts) likely to take benefit from adjuvant chemotherapy. We have retrospectively analysed the prognostic value of Ki67 (MIB1) and mitotic index (MI) in T1/T2 breast cancer with long follow-up.
Material and methods :
A series of 104 cases of node negative breast cancer (mean pathological size 15.6 mm) treated by surgery without adjuvant chemotherapy between 1995 and 1996 has been retrospectively analysed. Ki67 and MI were assessed for all pts. Overall survival (OS), metastasis free survival (MFS) and disease-free survival (DFS) were calculated using the Kaplan-Meier estimates and comparisons for survival curves are based on the log-rank test.
Results :
The mean age of pts was 55.6. Median follow up was 92 months (9-109 m). The MI was <10 mitosis in 60 cases, 10 - 19 mitosis in 24 cases and >20 mitosis in 20 cases (mean 10,88; median 7). The MIB1 score was <33% in 70 cases, 34-66% in 18 cases and 67-100 in 16 cases (median = 15%). MIB1 score was a parameter significantly associated with MFS ($p=0.04$) and OS ($p=0.03$) but not with DFS ($p=0.5$). Also, MI was more significantly associated with MFS ($p=0.002$) and OS (0.01), underlying a trend for DFS ($p=0.05$).
Conclusion :
In this study, both MI and KI67 scores were significant predictors of the outcome of small size node negative breast carcinoma but the discriminative value of MI was higher than that of MIB1. A larger series of cases will be analysed to confirm this result. Proliferation index should be considered as a biological marker of value to take into account for the indication of adjuvant chemotherapy

O-213
ASSESSMENT OF EPIDERMAL GROWTH FACTOR RECEPTOR (EGFR) BY IMMUNOHISTOCHEMISTRY AND CHROMOGENIC IN SITU HYBRIDIZATION (CISH) IN METAPLASTIC CARCINOMAS OF THE BREAST

Milanezi F 1,2, Reis-Filho JS 3, Carvalho S 1, Simpson PT 4, Lakhani SR 4, Schmitt FC 1,5.
1 IPATIMUP- Institute of Molecular Pathology and Immunology of Porto University, Porto – Portugal; 2 School of Health Sciences, University of Minho, Braga – Portugal; 3 The Breakthrough Toby Robins Breast Cancer Research Centre, Institute of Cancer Research, London – UK; 4 Molecular & Cellular Pathology, Mayne Medical School, University of Queensland, Queensland Institute of Medical Research and Royal Brisbane and Women's Hospital, Brisbane, Australia; 5 Medical Faculty of Porto University, Porto – Portugal

INTRODUCTION: Metaplastic breast carcinomas (MBCs) account for less than 1% of all invasive mammary carcinomas. They are a heterogeneous group of neoplasms generally characterized by an intimate admixture of adenocarcinoma with dominant areas of spindle cell, squamous, and/or mesenchymal differentiation. These tumours are reported to show an aggressive biological behaviour. In previous studies, we have demonstrated that up to 80% of MBCs overexpress the epidermal growth factor receptor (EGFR). HER2 and EGFR have received great attention in the medical literature over the last few years owing to the fact that humanised monoclonal antibodies against HER2 and therapies against the extracellular ligand binding domain or the intracellular tyrosine kinase domain of EGFR have proven to be successful for the treatment of certain types of human cancer.

AIM: To investigate the presence of overexpression and amplification of EGFR and HER2 in MBCs.
METHODS: EGFR and HER2 protein levels were assessed by IHC in 24 formalin-fixed, paraffin-embedded MBCs using a monoclonal antibody (31G7) for EGFR and a polyclonal antibody for HER2 and scored according to the Herceptest scoring system. Gene amplification was evaluated by chromogenic in situ hybridisation (CISH) using digoxigenin-labeled EGFR probe. The results were evaluated by bright-field microscopy under a 63x objective lens.
RESULTS: Nineteen tumours had strong expression of EGFR protein (79.2%), two had weak staining (8.3%) and three were negative (12.5%). Five cases (20.8%), 2 carcinomas with squamous differentiation and 3 spindle cell carcinomas, showed EGFR amplification as defined either by large gene clusters or >10 signals/nucleus. The 19 remaining cases (79.2%) showed a normal gene status (up to 2 dots/nucleus). All the tumours with EGFR amplification had overexpression at the protein level. All tumours lacked HER2 overexpression (3+).
CONCLUSION: MBCs frequently show EGFR overexpression which is associated with EGFR gene amplification in approximately 20% of the cases. On the other hand, MBCs proven not to harbour HER2 overexpression. Take together; our findings suggest that some patients with MBCs might benefit from the new developed therapies that target the EGFR. As some MBCs show EGFR overexpression without gene amplification, further studies evaluating EGFR activating mutations are warranted.

O-214
HER-2/NEU AMPLIFICATION AND EXPRESSION ASSESSMENT : COMPARISON OF IMMUNOHISTOCHEMISTRY, QUANTITATIVE PCR AND RT-PCR.

LABERGE-LE COUTEULX Sophie1, CORNIC Marie1, BLOT Emmanuel2, GUILLEMET Cécile2 et PICQUENOT Jean-Michel1. Service d'Anatomie et Cytologie Pathologique, Service d'Oncologie Médicale, CLCC Henri-Becquerel, Rouen, FRANCE.

INTRODUCTION: HER-2/neu overexpression/amplification is described in 30% of breast carcinomas and has prognostic and therapeutic implications. Conventional methods to detect it includes immunohistochemistry (IHC) and fluorescent in situ hybridization(FISH). Molecular biology offers new methods which can be automated and less expensive, though reliabililty of such methods is not well established.
MATERIAL AND METHODS: We studied 200 consecutives samples of breast carcinomas from january 2001 to december 2002 using quantitative PCR (Q-PCR) of exons 3 and 23 regions on paraffin embedded tissue and snap frozen tissue, quantitative RT-PCR(Q-RT-PCR) of exons 3 and 23 regions on snap-frozen tissue and IHC on paraffin embedded tissue. Discordant results between methods and positive IHC samples were assessed by FISH.
RESULTS: DNA extraction from paraffin embedded tissue was suitable in 166 samples (79%), from 199 (99,5%) snap frozen tissue and RNA extraction from 147 (73%)samples. A total of 119 samples from 113 patients was analyzed with all methods. Average tumor size was 26mm, with 48 (42%) patients with metastatic lymph nodes. Mean age was 61 years with 64% of post-menopause patients. Eighty-five percent of cases were invasive ductular carcinoma non special type, 9% of lobular carcinomas and 6% of others, 80% of cases expressing hormonal receptors. IHC revealed 11(10%) cases 3+, 2 cases 2+ and the remaining cases negative. Results for molecular biology showed 14(13%) cases positive in paraffin embedded tissue by Q-PCR, 24 (22%) positive samples in snap frozen tissue and 12(10%) samples were positive by Q-RT-PCR. All IHC positive samples (except one 2+ case) were positive in molecular biology. Q-PCR on frozen tissue was found to be the more sensitive and more specific method, though false positive cases were often aneuploid for chromosome 17. Interestingly, some cases showed augmented HER-2/neu RNA with negative IHC and without amplification. In rare cases, there was an imbalance between copy of exon 23 and exon 3. With a follow-up of 3,5 years there was no correlation between either IHC, Q-PCR or Q-RT-PCR and disease free survival (15 patients are metastatic).
CONCLUSION: Q-PCR on snap frozen tissue is a reliable and relatively cheap method to assess HER-2 amplification on large series of patients and can easily be done in routine. Confirmation by either IHC or FISH allows a great specificity. Cost effectiveness evaluation needs larger series to be don.

O-215
NEOADJUVANT CHEMOTHERAPY FOR INVASIVE LOBULAR CARCINOMAS OF THE BREAST: A POOR PATHOLOGICAL RESPONSE BUT SAME PROGNOSIS THAN INVASIVE DUCTAL CARCINOMA

Anne Vincent-Salomon, Chantal Gautier, Brigitte Sigal-Zafrani, Paul Fréneaux, Marick Laé, Christophe Rosty, Bernard Asselain, Rémy Salmon, Jean-Yves Pierga, Xavier Sastre-Garau.
Institut Curie, 26 rue d'Ulm 75005 PARIS, France

Background: Invasive Lobular Carcinomas (ILC) at initial presentation are larger tumors, with a low proliferative rate and higher hormonal receptors positivity compared to invasive ductal carcinomas (IDC), characteristics known to be negative predictive factors for response to neoadjuvant chemotherapy. Our aim was to retrospectively analyse the overall response rate of the ILC to neoadjuvant chemotherapy and compared it to those of ductal carcinomas (IDC).
Material and methods: We selected from our database, patients presenting a T2T3 (< 7cm) N0-N1a N1b ductal or lobular unilateral breast carcinoma, treated with neoadjuvant chemotherapy (4 cycles of anthracyclines-based chemotherapy) from 1990 to 1999. All slides of lobular carcinomas were retrospectively reviewed. The E-cadherin expression was assessed by immunohistochemistry. We retrospectively analysed, the clinical and pathological response rates to chemotherapy of the lobular compared to the ductal carcinomas. We also determined the conservative treatment and the survival rates (overall OS, disease-free DFS and metastasis-free survival MFS) for patients in each group.
Results: 802 patients were studied (median follow-up: 109 months), 86 with an ILC and 716 with an IDC. All ILCs except 3 were E-cadherin negative. The pathological characteristics showed that ILC, when compared to IDC, were more frequently grade I (39% for ILC, 12% for IDC, $p< 0.0001$) and ER positive (77% for ILC and 64% for IDC, $p= 0.02$) and PR positive (75% for ILC and 61% for IDC, $p=0.02$). A conservative surgery was possible for 53% of the ILC and for 64% of the IDC ($p=0.04$). Pathological response was available for 584 patients (532 IDC, 52 ILC) and showed that only one patient with ILC presented a complete pathological response contrasting with to 32 complete pathological response in the IDC group. The DFS, MFS and OS were identical within the two groups of patients.
Conclusion: We showed that after neoadjuvant chemotherapy, a conservative treatment was less frequently possible for ILC than for IDC and that no complete pathological response to neoadjuvant chemotherapy was observed in ILC. But patients with ILC presented the same outcome than patients with IDC. This poor response to neoadjuvant chemotherapy can be related to the biological characteristics of ILC. As one of the major goal of neoadjuvant chemotherapy is to increase breast conservative surgery, the ILC patients are not good candidates for this treatment.

O-216
PLEOMORPHIC LOBULAR CARCINOMA OF THE BREAST: ROLE OF COMPREHENSIVE MOLECULAR PATHOLOGY IN CHARACTERIZATION OF AN ENTITY

Jorge S. Reis-Filho, MD1,2, Pete T Simpson, PhD 1,3*, Chris Jones, PhD 4, Dawn Steele, BSc 1, Alan Mackay, BSc1, Marjan Iravani, BSc 1, Kerry Fenwick, BSc 1, Haukur Valgeirsson, BSc, 1, Maryou Lambros, BSc 1, Alan Ashworth, PhD 1, Jose Palacios, MD 5, Fernando Schmitt, MD, PhD 2, Sunil R Lakhani, MBBS, MD, FRCPath 3
1 ¡V The Breakthrough Toby Robins Breast Cancer Research Centre, Institute of Cancer Research, London, SW3, 6JB, UK
2 ¡V IPATIMUP ¡V Institute of Molecular Pathology and Immunology, University of Porto, Porto, Portugal
3 ¡V Molecular & Cellular Pathology, Mayne Medical School, University of Queensland, Queensland Institute of Medical Research and Royal Brisbane and Women¡¦s Hospital, Brisbane, Australia.
4 ¡V Section of Paediatric Oncology, Institute of Cancer Research, Sutton, UK
5 ¡V Centro Nacional de Investigaciones Oncologicas, Madrid, Spain.

Introduction: Immunohistochemical analysis of E-cadherin has changed the way lobular neoplasia is perceived. It has helped to classify difficult cases of carcinoma in situ with indeterminate features and led to the identification of new variants of lobular carcinoma. Pleomorphic lobular carcinoma (PLC) and pleomorphic lobular carcinoma in situ (PLCIS), recently described variants of invasive and in situ classic lobular carcinoma, are reported to be associated with more aggressive clinical behaviour. Although PLC/PLCIS show morphological features of classic lobular neoplasia and lack E-cadherin expression, it is still unclear whether these lesions evolve through the same genetic pathway as lobular carcinomas or are high grade ductal neoplasms that have lost E-cadherin.
Material and Methods: A 44-year-old female patient presented with a breast lump in the left upper outer quadrant. Histological and immunohistochemical analysis revealed extensive PLCIS and invasive PLC associated with foci of E-cadherin negative carcinoma in situ with indeterminate features. Multiple foci of preinvasive and invasive carcinoma were analysed with i) immunohistochemistry with antibodies for E-cadherin, beta-catenin, estrogen receptor (ER), progesterone receptor (PgR), androgen receptor (AR), HER2, epidermal growth factor receptor, p53 and p63; ii) chromogenic in situ hybridisation with probes for HER2, EGFR and c-myc and centromeric probes for chromosomes 7 and 8; iii) high resolution comparative genomic hybridisation (CGH) and iv) array-based CGH with the 4.6K Breakthrough Breast Cancer Research Centre Array CGH platform, which has a resolution of <1Mb.
Results: All lesions lacked E-cadherin and *f*Ò-catenin, were positive for hormone receptors and showed gain of 1q, 7p, 8p, 9p and 20p and loss of 1p and 16q. In addition, HER2 overexpression (3+) and amplification of c-myc and HER2 were detected in the PLCIS and invasive PLC.
Conclusion: The combination of gain of 1q and loss of 16q associated with lack of E-cadherin and beta-catenin expression are typically observed in lobular carcinomas and not seen in high grade ductal lesions. Amplification of c-myc and HER2 may account for the high grade features in this case and the reported aggressive clinical behaviour of PLC. Taken together, these data suggest that at least some PLCs may evolve from the same precursor or through the same genetic pathway as classic lobular carcinomas.

O-217
TUBERCULOSIS IN RHEUMATOID ARTHRITIS

Miklós Bély MD, PhD, DSc1 and Ágnes Apáthy MD2
1Department of Pathology,
Policlinic of the Hospitaller Brothers of St.John of God, Budapest, Hungary
2Department of Rheumatology,
National Institute of Rheumatology and Physiotherapy, Budapest, Hungary

Objective
Tuberculosis is one of the most important diseases accompanying rheumatoid arthritis (RA). The risk of miliary dissemination of post-primary tuberculosis is high, because of the poor immune status of elderly patients with an autoimmune disease which is treated with steroids, and/or immunosuppressive drugs.
The aim of this study was to determine
1. the prevalence of post-primary fibrous, or fibrocaseous tuberculosis (Tb) in RA
2. the incidence of miliary disseminated tuberculosis (mTb) in RA
3. the incidence of organ involvement by Tb and mTb
4. the relationship between Tb and mTb in RA.
Patients and Methods
A randomized (non-selected) autopsy population of 234 in-patients with RA was studied. RA was confirmed clinically according to the criteria of the ACR.
Post-primary fibrous, or fibrocaseous tuberculosis, and miliary dissemination of tuberculosis was confirmed histologically. The link between tuberculosis and disseminated miliary tuberculosis was determined by c;²-tests.
Results
1. Post-primary fibrous, or fibrocaseous tuberculosis accompanied RA in 27 (11.54 %) of 234 cases. Post-primary tuberculosis was localized to the lung. Twelve of 27 post-primary Tb cases were histologically fibrocaseous, and 15 of 27 revealed only fibrous scars due to documented tuberculosis.
2. Eight (3.4%, 29.6 rel%) of 27 post-primary fibrous, or fibrocaseous tuberculosis cases were complicated by disseminated miliary tuberculosis.
3. Proliferative, or exudative epithelioid granulomatous tuberculosis involved different organs, such as lungs, liver, spleen, adrenal glands, synovial membrane, vertebrae, pituitary gland, and/or lymph nodes.
4. There was a statistically significant association between Tb and mTb ($Chi^2 = 54.84$, $p<0.0001$, $q=1$), or fibrocaseous character of Tb and mTb ($Chi^2 = 68.9$, $p < 0.0001$).
Conclusion
A focus of post-primary fibrocaseous tuberculosis (mostly in the lung) represents a high risk of miliary dissemination in RA.
In our autopsy material the miliary dissemination of tuberculosis was the result of exacerbation of endogenous Tb, based on the high value of Youle's association coefficient.
The miliary dissemination of tuberculosis may be considered as a terminal phenomenon, because the limited number of granulomas involved only a few organs.
The exudative character - beside proliferative epithelioid granulomas - must be regarded as histological evidence of impaired immunologic reactivity.

O-218
CHARACTERIZATION OF RABBIT MODEL FOR EPSTEIN-BARR VIRUS-ASSOCIATED LYMPHOPROLIFERATIVE DISEASE WITH HEMOPHAGOCYTIC SYNDROME AND ITS THERAPEUTIC TRIALS.

K. Hayashi, K. Takashima, Y. Kitamura, W. Oda, I. Ogahara, M. Ohashi,* T. Sairenji.*
Divisions of Molecular Pathology and Biomedical Science,* Tottori University Faculty of Medicine, Yonago-city, Japan

Introduction: Epstein-Barr virus associated hemophagocytic syndrome (EBV-AHS) is often associated with T-cell lymphoproliferative diseases (LPD). The therapy of this disease is one of the most challenging goals in medicine. Purpose: To elucidate the exact nature of fatal LPD observed in Herpesvirus papio (HVP)-induced rabbit LPD with hemophagocytic syndrome (HPS), we analyzed sequential development of HVP-induced rabbit LPD and their cell lines. To develop some therapeutic interventions for EBV-AHS, we examined the effectiveness of antiviral agent or chemotherapy, using this rabbit model. Methods & Results: All of the seven Japanese White rabbits inoculated intravenously with HVP died of fatal LPD or HPS 18 to 27 days after inoculation. Sequential autopsy revealed splenomegaly and swollen lymph nodes, often accompanied by bleeding. Atypical lymphoid cells with HVP-RNA-1 expression infiltrated many organs with a 'starry sky' pattern, frequently involving the spleen, lymph nodes and liver. HVP-ISH of immunomagnetic purified lymphoid cells from spleen or lymph nodes revealed HVP-EBER1+ cells in each CD4+, CD8+ or CD79a+ fraction. Hemophagocytic histiocytosis was observed in the lymph nodes, spleen and bone marrow. HVP-DNA was detected in the infected rabbits by PCR or Southern blot analysis. Six IL-2 dependent rabbit T-cell lines were established from transplanted scid mice tumors of LPD. Three of them showed tumorigenicity in nude mice. Furthermore, three HVP-infected rabbits treated with vidarabine died of HPS between days 23 and 28, which were not different from the untreated rabbits. Three of the infected rabbits that were treated with CHOP treatment died of HVP-induced LPD and HPS with a bleeding tendency and/or with opportunistic infections. They died on the 26th, 62nd and 105th day, respectively. The most interesting finding of this experiment was observed in the rabbit with the longest survival time: HVP-negative lymphomas surrounded by HVP-induced LPD developed in the larynx and ileum of this rabbit. Conclusion: HVP-induced fatal LPD with HPS in rabbits are almost reactive oligoclonally in nature, but contain some pre-neoplastic T-cell clones. Our data from therapeutic trials using EBV-AHS rabbit model indicate that vidarabine is not effective to treat HVP-infected rabbits, and even the cytotoxic chemotherapy of CHOP is not sufficient to cure the HVP-infected rabbits. Further studies will be required to develop better therapies to treat EBV-AHS.

O-219
SIALIC ACID EXPRESSION IN PAEDITRIC AND ADULT RESPIRATORY TRACTS

NICHOLLS John, BOURNE Anthony, PEIRIS Malik

INTRODUCTION:
Influenza virus infection of humans involves binding of the virus to cells of the respiratory tract and sialyoligosaccharides are responsible for the viral-cell interactions. Human strains preferentially agglutinate red blood cells with N-acetylneuraminic acid (sialic,SA) alpha 2-6 Gal linkages and avian strains preferentially bind alpha 2-3 sequences. Previous research indicated that ciliated cells primarily display SA alpha 2-6Gal sequences whilst goblet cells contain the SA alpha 2-3Gal sequence. Recent studies on cultured human tracheo-bronchial epithelium however appeared to show a contrary view. These differing findings are of importance for the understanding of the development of avian influenza infection in humans, which appeared first in Hong Kong in 1997 and has recently resulted in outbreaks in Thailand, Vietnam and Cambodia.

PURPOSE OF STUDY
It was felt that it was necessary to readdress the distribution of the SA alpha 2-6Gal and SA alpha 2-3Gal in human tissues to determine whether the culture model could be applied to human cases and to determine if there was real variation in the distribution of these two receptors.
METHODS USED:
Archival fetal and neonatal autopsies, biopsy specimens of children with congenital cystic adenomatoid malformation (CCAM) and biopsy specimens of bronchial mucosa.
RESULTS:
There is greater expression of SA alpha 2-3Gal in perinatal and paediatric respiratory epithelium than in adults with ciliated epithelium as well as goblet cells showing membranous and cytoplasmic staining. In adult tissues metaplastic mucosa shows increased staining of SA alpha 2-3Gal.
CONCLUSION:
The increased expression of SA alpha 2-3Gal is one explanation for the high incidence of avian influenza in a paediatric population and may also serve to highlight susceptible populations for this type of influenza

O-220
INTER-LABORATORY VALIDATION OR PCR-BASED DETECTION OF MYCOBACTERIUM TUBERCULOSIS IN PARAFFIN-EMBEDDED TISSUE

C. SCHEWE, T. GOLDMANN*, M. GROSSER°, A. ZINK", S. PAHL, A. NERLICH", G.B. BARETTON°, M. DIETEL, E. VOLLMER*, I. PETERSEN
Institute of pathology, Charité Campus Mitte, Berlin, FRG
*Laboratory of clinical and experimental pathology, Research Center Borstel, FRG
°Institute of pathology, Technical University Dresden, FRG
"Institute of pathology, Hospital München-Bogenhausen, FRG

The present study is based on an initiative for quality assurance of the German Society of Pathology and the Professional Association of German Pathologists. Four panel laboratories with experience and expertise in PCR detection of M. tuberculosis were selected to establish the prerequisites for continuous external laboratory trials, in particular by providing pre-tested specimens and evaluation criteria for participating institutes.
In a first step, the four panel laboratories performed an internal trial to test their own reliability and reproducibility.
Paraffin sections and DNA preparation from 32 clinical specimens and 2 experimentally generated tissues totalling to 66 samples were evaluated by each panel institute according to their own protocols using different methodologies. Despite these differences, a high degree of inter-laboratory reliability was achieved. The correlation with the histological findings revealed that the extent of necrosis was the only significant parameter being associated with PCR positivity. The detailed results will be published (Virchows Archiv, 2005, in press) providing recommendations for applying PCR-based methodology for the detection of mycobacterial DNA in surgical specimens of pathology.
Pre-tested specimens are now available for the external trail and can be ordered from the steering institute via Oligene (www.oligene.com). All molecular pathology laboratories are invited to participate in this quality assurance initiative.

O-221
CONCENTRATION OF SERUM IS ONE OF THE DETERMINING FACTORS AFFECTING THE PURITY AND THE QUANTITY OF OBTAINED SCHWANN CELLS

Vahid Bayati, Farideh Etesam, Abbas Abdolvahhabi, Mohammad Ali Shokrgozar, Aligholi Sobhani*, Mohammad Barbarestani

Abstract:

Aims of Investigation: Finding a way to gain Schwann cells (SCs) with maximal purity and numbers in order to use them for autologous cellular transplant was the aim which made us to study the role of various concentrations of Fetal Bovine Serum (FBS) on SCs culture in RPMI-1640 medium.

Methods and Materials: We used adult rat sciatic nerve model (one to three nerve per primary culture) after a 10 days period of in vivo predegeneration of nerve induced by surgery, followed by isolating SCs and subcultivating two times during a week. Then the obtained cells were cultured in 8 groups with various concentrations of FBS (5%, 2.5%, 1.25%, 0.625%) and different times of application (4 dishes containing these concentrations to day 4 and from day 5 to 10, without any serum supplementation and the other 4 dishes containing the same concentrations to day 10) to the RPMI-1640 medium for 10 days. Finally the SCs were immunocytochemically (using rabbit anti- S100 antibody) and morphologically characterized and counted using fluorescence Microscope equipped with phase-contrast, fluorescein optics.

Results: This investigation demonstrated that the RPMI-1640 supplemented with 0.625% FBS results in 360×10^3 cells with the approximate purity of 99% in a 35mm dish.

Conclusion: According to results we conclude that the manipulation of serum concentrations may be a new approach for purifying SCs culture during isolation.

Key Words: Adult Schwann cell, Purity, Fetal bovine serum, Subcultivation

O-222
DIAGNOSIS OF METASTATIC CARCINOMA IN CHOROID BY FNA: REPORT OF THREE CASES.

DREHER IRION Luciane Cristina 1, CORRÊA Zelia Maria 2, MARCON Italo 2, GAIGER Ana Maria 3.

1.Consultant Histopathologist The Royal Oldham Hospital, UK and Laboratório Patologistas Reunidos, Porto Alegre, Brasil.

2.Ophthalmologist Complexo Hospitalar Santa Casa/FFFCMPA, Porto Alegre, Brasil.

3.Head Pathologist Laboratório Patologistas Reunidos, Porto Alegre, Brasil.

Introduction: Although uncommon, metastatic lesions in the eye ball should be kept in mind, and the differential diagnosis with a primary tumour, especially melanoma, is fundamental. Clinical data: Two male patients (case 1: 35 years old and case 2: 56 years old) and one female patient (case 3: 39 years of age) had subito loss of sight, ocular pain and conjunctival hyperaemia. Ultra-sonound scans showed partial retinal detachment and a choroidal mass. Patient 1 was undergoing an investigation of a pulmonary lesion. Patient 2: history of surgery for renal carcinoma 6 years before and case 3: the ocular lesion was the 1st clinical sign. Diagnostic methods: After US scans with suspicious choroidal lesions, a FNA has been performed in each case in order to differentiate between primary and metastatic lesion. The transvitreal FNA has been done with indirect binocular ophthalmoscopy under peribulbar anaesthetics and sedation. Microscopic findings: The aspirate from all cases was satisfactory and a Papanicolaou stain was used. Case 2 has shown malignant looking large epithelial cells and haemorrhage, in keeping with metastatic lesion from renal tumour due to past history. Cases 1 and 3: malignant epithelial cells demonstrated and immunocytochemistry has been performed for differential diagnosis. In both cases AE1/AE3, CK7 and TTF1 were positive and CK20, S100 and HMB45 were negative, suggesting metastatic carcinoma from lung as primary source. Comment: The possibility of intraocular metastases should be kept in mind. In experienced hands, a FNA along with immunocytochemistry can be helpful for a definite diagnosis.

O-223
CORONARY THROMBOSIS IS FREQUENTLY INITIATED DAYS OR WEEKS BEFORE THE CLINICAL ONSET OF MYOCARDIAL INFARCTION

VAN DER WAL Allard, RITTERSMA Saskia, KOCH Karel, PIEK Jan, DE WINTER Rob Academic Medical Center, Amsterdam, The Netherlands

Introduction.

Acute Myocardial Infarction (AMI) is caused by fibrous cap disruption of a coronary atherosclerotic plaque, leading to occlusive thrombosis. Both the onset of plaque complications (rupture) and the onset of symptoms (chest pain) can be seen as acute events, but at present there is limited insight in the time lag between both processes. In order to relate the onset of thrombus formation with the clinical onset of AMI ,we systematically studied the age of intracoronary thrombi of AMI patients using histopathological and immunohistochemical parameters.

Methods.

Percutaneous intracoronary thrombectomy (thrombosuction) was performed in 211 AMI patients prior to angioplasty (balloon dilation with or without stent implantation). The aspirated material was collected in a bottle, fixed in formalin, filtered and embedded in paraffin. Sections were cut at 6 levels and stained with Haematoxlin and Eosin and Elastic van Gieson stains. Additional immunohistochemistry was performed with monoclonal antibodies anti-CD68, anti-CD31, anti-CD61 and anti-smooth muscle actin. Thrombus age was classified as 1:fresh thrombus (layers of intact platelets, fibrin, erythrocytes and granulocytes) 2:lytic thrombus(colliquation and karyorrhexis, 1 to 5 days old) and 3:organized thrombus, (more than 5 days up to weeks old).

Results.

In 199 of 211 patients (95%) materials were retrieved;in 114 of 199 patients (54%) only thrombus was found, in 12 patients (5%) only plaque components were identified and in 85 patients (41%), both thrombus and plaque fragments were aspirated. Plaque materials consisted in all instances of soft plaque constituents: CD68+ foamcell macrophages and extracellular lipid debris with cholesterol clefts. In 101 of 199 patients who showed thrombus (51%) the age of thrombus was classified as at least partially lytic (35%, 1 to 5 days old) or at least partially organized (16%, older than 5 days). In organized thrombus the ingrowth of actin + immunostained smooth muscle cells could be demonstrated, with or without deposition of young collagen and in some instances in combination with ingrowth of CD31+ microvessels.

Conclusion.

Intracoronary materials retrieved from AMI patients is frequently heterogenous of composition in terms of thrombus age. In 51% of cases older thrombus is present, indicating an important discrepancy (in terms of days up to weeks)between the time of onset of thrombosis and the occurence of acute clinical symptoms.

O-224
INCREASED MMP-2/-9 ACTIVITIES IN THE MYOCARDIUM CORRELATE WITH IMPAIRED CARDIAC FUNCTION AND APOPTOSIS DURING EARLY MULTIPLE ORGAN FAILURE IN SHEEP

Jeremias Wohlschlaeger1, Henning D. Stubbe2, Klaus J. Schmitz1, Naomasa Kawaguchi1, Atsushi Takeda3, Nobuakira Takeda3, Frank Hinder2 , Hideo A. Baba1

1Institut für Pathologie, Universität Essen, Germany, 2Klinik und Poliklinik für Anästhesiologie und operative Intensivmedizin, Universität Münster, Germany and 3Department of Internal Medicine, Jikei University, Tokyo, Japan

Objective: Matrixmetalloproteinases (MMP) degrade extracellular matrix (ECM) and are involved in systemic inflammation and heart failure. We investigated the roles of MMP-2, MMP-9, MT1-MMP, focal adhesion kinase (FAK) and Paxillin in ovine hearts during early multiple organ failure induced by norfenefrine-masked hypovolemia and endotoxinemia.
Design: Fifteen adult instrumented sheep were randomly assigned to one of three groups: 1. norfenefrine-masked hypovolemia plus endotoxemia (NMH+ENDO), 2. norfenefrine-masked hypovolemia without endotoxemia (NMH), 3. recurrent endotoxemia during normovolemia (ENDO). Three healthy sheep served as untreated controls (CONTROLS).
Measurements and results: Cardiac tissue was analysed by gel zymography and Western blots. Apoptosis was determined by TUNEL-staining. Gel zymography revealed significantly increased MMP-2 activity in NMH+ENDO compared to ENDO and controls. MMP-9 activity was significantly elevated in all experimental groups.
MMP-2 was significantly increased on the protein level, while MMP-9 was unaltered. MT1-MMP was not significantly altered in any group.
MMP-2 and -9 activities correlated positively with heart rate and negatively with parameters of cardiac function. MMP-2/-9 activity and p-Paxillin expression correlated positively with cardiomyocyte apoptosis.
Conclusions: MMP-2 and -9 activities are significantly increased in combined vasoconstrictor-masked hypovolemic and endotoxinemia shock in sheep. Increased MMP-2 activity appears to be mainly due to enhanced synthesis, whereas increased MMP-9 activity obviously follows posttranslational activation of pro-MMP-9. Increased cardiac apoptosis during MOF is probably partly due to MMP-associated ECM degradation. This study provides evidence to the pivotal roles of MMPs in acute cardiac dysfunction during early multiple organ failure.

O-225
INCREASED EXPRESSION AND ACTIVITY OF MATRIX METALLOPROTEINASES CHARACTERIZE EMBOLIC CARDIAC MYXOMAS

Augusto Orlandi1, Alessandro Ciucci1, Amedeo Ferlosio1, Antonio Pellegrino2, Luigi Chiariello2, Luigi Giusto Spagnoli1
1Anatomic Pathology, Tor Vergata University, Rome, Italy
2Cardiovascular Surgery, Tor Vergata University, Rome, Italy

Myxomas are the most frequent primary cardiac neoplasms, accounting for 50% of all tumors. Myxomas are considered tumors with an endocardial origin whose name derives from their prevalent myxoid extracellular matrix, rich in mucopolysaccharides. Cardiac myxomas are benign tumors which are unable to infiltrate the myocardium or give rise to metastases. Nevertheless, they are considered “clinically malignant” tumors because of their susceptibility to embolize to distant organs, that occurs in 30 to 50% of all cases, cardiac myxoma, but the causes are still uncertain. Matrix metalloproteinases (MMPs) are a large family of zinc-dependent proteolytic enzymes that degrade the extracellular matrix in both normal and pathological processes. Many MMPs are released into the extracellular milieu in a pro-enzyme state with affinity to specific extracellular matrix proteins. Purpose of the study was to evaluate MMP activity in cardiac myxomas with the hypothesis of its possible role in the pathogenesis of tumor embolism. Methods used: we examined 27 left atrium-sided myxomas; 10 of them showed clinical signs of peripheral embolism. Immunohistochemistry in all cases and Western blotting, in situ and in-gel zymography in 4 embolic and 6 non-embolic consecutive tumors. MMP expression was also evaluated in myxoma cells in vitro. Summary of the results: we observed in embolic myxomas a higher expression and activity of MT1-MMP, pro-MMP-2 and pro-MMP-9, whereas pro-MMP-1, MMP-3 and TIMP-1 levels were similar to those of non-embolic tumors. RT-PCR demonstrated that increased MMP activity was due, at least in part, to increased transcription and also documented increased TIMP-2 transcripts in embolic myxomas. In vitro, embolic tumor cells retained higher MT1-MMP and pro-MMP-2 levels in basal condition and after stimulation with IL-1b and IL-6. Conclusions: our results show in embolic cardiac myxomas an increased MMP expression and activity. The latter may induce an excessive degradation of tumor extracellular matrix, with consequent increase of the tumor friability, and/or an increased risk of detachment of superficial thrombi.

O-226
HISTOMORPHOMETRIC SEMIQUANTITATIVE ASSESSMENT OF EFFECTS OF PARTIAL LEFT VENTRICULECTOMY: ONE-YEAR FOLLOW-UP:

VASILJEVIC D. Jovan, OTAŠEVIC Petar, POPOVIC V. Zoran , GRADINAC Siniša, GLUMAC Sofija , NEŠKOVIC Aleksandar
Institute of Pathology, Belgrade University School of Medicine, Serbia and Montenegro; Dedinje Cardiovascular Institute, Belgrade, Serbia and Montenegro

INTRODUCTION: left ventricular contractility may be improved by partial left ventriculectomy (PLV) in patients with severe heart failure.
PURPOSE: histological assessment by using semiquantitative morphometric parameters of the left ventricle after surgery, and endomyocardial biopsies (EMB) one-year postoperatively.
MATERIAL AND METHOD: The study group consisted of 15 consecutive PLV survivors, predominantly male (13/15), aged 45+12 years. Surgical specimens were taken from the inferior- and/or lateral wall of the LV, processed routinely, and stained with Masson-trichrome. Postoperative EMB, 3 to 5 per patient, were taken 12 months later and processed in the same manner. The following morphometric parameters were assessed: (1) degree of hypertrophy and attenuation (fibre diameter); (2) nuclear evidence of hypertrophy (diameter); (3) myofibrilar volume fraction; (4) degree of degenerative, vacuolar changes, and (5) fibrosis volume fraction. These parameters were graded in the usual fashion (0-none, 1-mild, 2-moderate, 3-severe).
RESULTS: Both NYHA functional class and EF improved 12 months following operation as compared to preoperative values (2.40+0.69 vs. 3.33+0.49, $p<0.001$, and 33.21+12.05% vs. 20.21+9.07%, $p<0.001$, respectively). Semiquantitative morphometric analysis demonstrated postoperative decrease in the degree of attenuation as compared to preoperative values (1.40+0.51 vs. 2.47+0.64, $p<0.01$), as well as decrease in fibrosis volume fraction (2.07+0.80 vs. 2.67+0.49, $p<0.001$) and nuclear hypertrophy (1.27+0.46 vs. 1.67+0.62, $p<0.05$). There was postoperative increase in myofibrilar volume fraction (1.87+0.61 vs. 1.40+0.61, $p<0.01$). There was no difference in post- and preoperative degree of myofibrilar hypertrophy and degenerative changes.
CONCLUSION: One-year postoperatively, PLV had favourable effects on myocardial morphology that parallels

improvement in patient's functional status and LV systolic function.

O-227
LYMPHATIC VASCULATURE IN HUMAN HEARTS IN CHILDREN AND ADULTS

1KHOLOVÁ Ivana, 2HÁJKOVÁ Petra, 1HAZES Thierry, 1KASKENPÄÄ Nina, 2ŠTEINER Ivo, 1YLÄ-HERTTUALA Seppo
1Department of Molecular Medicine and Biotechnology, A.I.Virtanen Institute for Molecular Sciences, University of Kuopio, Kuopio, Finland
2Fingerland Department of Pathology, Charles University Hospital, Hradec Králové, Czech Republic

Introduction: Gene therapy of myocardial ischaemia using vascular growth factors has raised the question of the arrangement of lymphatics in normal/diseased human heart. Recent establishment of lymphatic specific antibodies enables to study the presence and relationship of lymphatic vasculature in the human heart.
Purpose of the study: To analyze the presence and arrangement of cardiac lymphatics in different compartments of the heart under normal and pathological conditions both in children and adults.
Materials and methods: Using commercially available LYVE-1 antibody we studied lymphatics in autopsied hearts in children (n = 25, age range 1 months - 18 years) and adults (n = 10).
Results: In ventricles, lymphatic capillaries form an arcade net in epicardium and a ramified net is also present in endocardium. In myocardium lymphatics are only scarcely present. In atria, the lymphatic net is less developed. Under normal conditions, lymphatics are collapsed, but dilatation accompanies cardiac fibrosis.
Conclusions: Lymphatic specific antibodies were found as a useful tool to study cardiac lymphatic system. Other lymphatic markers will also be discussed. The profound knowledge of cardiac lymphatic system has an impact on further studies on therapeutic vascular growth and improvement of new therapeutic approaches.

O-228
LEFT ATRIAL MYOCARDIAL EXTENSION INTO PULMONARY VEINS AND ITS POTENTIAL ROLE IN ATRIAL FIBRILLATION: AN AUTOPSY STUDY OF 100 HEARTS

STEINER Ivo
Department of Pathology
Charles University Faculty of Medicine and University Hospital, Hradec Kralove
Czech Republic

Atrial fibrillation (AF) is the commonest cardiac arrhythmia and particularly prevalent in the older population. Electrophysiological studies have established the critical role of pulmonary veins (PVs) in the initiation of AF, but there is a paucity of data about PV morphology as an arrhythmogenic substrate.
The venous wall comprises a thin endothelium, an irregular media of smooth muscle and fibrous tissue, and a thick fibrous adventitia. Extensions of left atrial myocardium into PVs, known as 'myocardial sleeves', are positioned externally on the adventitial side. These myocardial sleeves are considered responsible for the generation of ectopic beats.
In-depth morphological analysis was undertaken of atrial myocardium in the PVs of 100 human hearts obtained at autopsy from 50 patients with and 50 without AF. This is the largest series on this aspect of cardiac pathology so far studied and the first to examine the presence of senile isolated atrial amyloid (IAA) in the myocardial sleeves.
Cross sections of the complete PV circumference were obtained in 3-4 mm increments from the pulmonary hilum to the veno-atrial junction. A total of 1151 sections was stained with H and E and by the elastica-Van Gieson method and IAA was sought with the Sirius red stain and by immunohistochemical localization of atrial natriuretic peptide.
Of the total 393 PVs examined, myocardial extensions (sleeves) were revealed in 349 veins (88.8 %). In all hearts, at least one PV had a sleeve. The sleeves were longer in the upper veins than in the lower ones, and in the left than in the right. Histologically, in the myocardium of the sleeves, there was focal fibrosis (scarring) in 89 hearts and deposition of IAA in 58. The extent of both of these changes was graded semiquantitatively by visual assessment of the microscopic images. The lesions were more pronounced in patients with AF as compared with patients without this arrhythmia.

O-229
HETEROGENOUS IMMUNOHISTOCHEMICAL EXPRESSION OF HER2/NEU IN AXILLARY LYMPH NODE NEGATIVE BREAST CARCINOMAS

ERGUN Dilhan*, PERCÝNEL Sibel*, DÝZBAY SAK Serpil*, KUZU Isinsu*, ELHAN Atilla Halil**, ERDEN Esra*
Departments of Pathology* and Biostatistics**, Ankara University School of Medicine, Ankara, Turkey

Introduction: HER2/neu (c-erbB2) is an important prognostic parameter in node positive breast carcinoma patients and it is also helpful in the selection of therapeutic regimen. Although flourescence in situ hybridization (FISH) has disadvantages, it is safer and more objective in the evaluation of HER2/neu status especially in small biopsy specimens when compared with immunohistochemistry (IHC).
Aims: 1. To determine HER2/neu status by IHC and FISH in axillary lymph node negative breast carcinoma patients, using low density manual tissue microarray and to correlate the results with prognosis.
2. To determine heterogeneity by IHC and FISH within a single tumor using multiple tissue cylinders.
Materials and Methods: Tissue cylinders of 4 mm diameter from paraffin blocks of 85 invasive breast carcinomas were arrayed in 25 recipient paraffin blocks. We analyzed HER2/neu status of 85 carcinoma cases (2-5 cylinders/case) by IHC (DAKO), using streptavidin biotin immunodetection system and 75 carcinoma cases (2 cylinders/case) by FISH (Q-biogene).
Results: Immunohistochemically, 35.2%, 25.9%, 20% and 18.9% cases were scored as 0, +1, +2 and +3 respectively. Seventy-five cases were evaluated by at least two tissue cylinders and immunohistochemical scores of different cylinders (2-5 cylinders/case) of the same tumor were compared. In 52% of the cases, same immunohistochemical score was observed in all tissue cylinders from the same case. In 4 cases, there was important discordance between the scores of cylinders that could affect the treatment regimen of the patients.
Two tissue cylinders/case were used in 44 cases by FISH. Amplification was obtained in 16% of the cases. There was no evidence of HER2/neu gene amplification in the cases scored as 0 and +1 by ICH. Only 1/15 of immunohistochemically +2 tumors was FISH positive. 83.3% of +3 cases was positive by FISH. However, 2 cases that were scored as +3 by IHC, were found to be negative by FISH. There was no discordance between the two cylinders with respect to amplification.
No correlation was detected between the clinicopathological and prognostic parameters and immunohistochemical and amplification findings.

Conclusion: 1. Evaluation of HER2/neu by IHC may be risky that could affect the treatment regimen of the patients in small biopsy specimens because of tumor heterogeneity
2. FISH is safer and more objective in the evaluation of HER2/neu in small biopsies when compared to IHC.

O-230
NATIONAL PROGRAM OF HER2 BREAST CARCINOMA TESTING: EXPERIENCES FROM SLOVAKIA FROM THE PERIOD 2003-2004

PLANK Lukáš, KAJO Karol, JANÁKOVA ¼uba, KVIATKOVSKÁ Zuzana
Department of Pathology, Comenius University, Jessenius Medical Faculty and Faculty Hospital, Martin, Slovak Republic

Introduction: For the selection of an appropriate therapy of the patients with invasive breast carcinoma, the HER2 protein and gene testing of biopsy material seem to be a condition sine qua non. Purpose of the study: To develop a national system of a standardized HER2 testing of all diagnosed breast carcinomas and its quality control. Methods used: Due to a cooperation of the Slovak pathologists and on the basis of accepted regional centralization, a national network system of a breast carcinoma biopsy diagnosis was introduced in Jan. 2003. The network consists of 8 regional and university departments using a standardized diagnostic approach, incl. immunohistochemical HER2 protein testing (HercepTest, DAKOCytomation). In the cases showing 2+ or 3+ protein positivity, the HER2 gene amplification may be confirmed by FISH and/or CISH techniques in the centrum of the project. All the results are reported in standardized biopsy protocols. The quality of HER2 protein testing was controlled by 'a panel of experts' using blind testing cases being examined in the involved centres. The control was followed by an educational joint conference of the departments. Summary of the results: Biopsy examinations of 2260 cases diagnosed in 2003-2004 in 8 centres proved HER2 protein positivity in 523 cases (23.1%): 3+ positivity in 283 (12.5%)and 2+ in 240 (10.6%). After first 9 months, some technical problems and problems of HER2 protein positivity grade interpretation were identified by the quality control and discussed by the educational conference. Finally, all immmunohistochemically 2+ and 3+ positive cases tested by CISH, FISH or by both the techniques showed HER2 gene amplification, in few cases minor differences in the amplification degree were recognized. In addition, the correlations of HER2 status and other parameters (incl. histological grade, ER, PR and lymph node status) seem to be statistically significant. Conclusions reached: The described program brought standardized results representing a good basis for the therapeutical considerations and for further optimization of HER2 testing and studies of all the parameters of the disease. The program continues also in 2005.

O-231
INTRAOPERATORY CYTOLOGICAL IMPRINT AND METASTASIS DETECTION OF MAMMARY CARCINOMA IN SENTINEL LYMPH NODES

VILELA Rafael Sarlo, MOURÃO Mario, OSÓRIO Cynthia A B Toledo. Research and Medical Center Hospital do Cancer, São Paulo, Brazil.

INTRODUCTION: The study of sentinel lymph node (SLN), in the attempt to increase detection of metastasis, was intensified since 2002, when it was included in the TNM staging of breast cancer.
AIM: Relate the effectiveness of detection of mammary carcinoma metastasis (MCM) by cytological imprint (CI).
MATERIALS AND METHODS: We studied 148 SLN from 83 patients. The SLN were identified by vital blue coloring or colloidal albumen injection with radioactive markers. The CI was obtained of the transversal cutting faces of SLN during surgery. Subsequent histological interpretation of slides from paraffin embedded tissue were performed. Negative cases for MCM in paraffined tissues had been submitted to immunohistochemical reaction with cytokeratin AE1/AE3 for diagnostic confirmation or detection of micrometastasis. This reaction was not carried in negative specimens of patients with 1 or more metastatic SLN, previously detected by CI or paraffined tissues.
RESULTS: Malignant epithelial cell plugs measuring 2 mm or less were considered micrometastasis. Of 148 SLN analised in this study, 11 showed positivity in the CI (one micrometastatic lesion measuring 0,76 mm and 10 macrometastasis measuring 3 to 20 mm). Of the 83 patients involved in this work, 18 presented positive SLN. 9 patients presented positive SLN in the CI and had been submitted to axillary lymphadenectomy in the same surgical act. The 9 remaining patients showed positivity in paraffined tissues. 3 of them were submitted to axillary lymphadenectomy in the first surgical act, defined by clinical criteria, 4 of them in a second surgical intervention and the last 2 ones were not submitted to new surgeries until the moment. Of the 137 negative SLN in the CI, 11 became positive in paraffined material (6 micrometastasis measuring 0,32 to 1,75 mm and 5 macrometastasis measuring 2,95 to 8 mm). The immunohistochemical reaction of the negative SLN in CI and paraffined tissue previous analyses showed no positivity in all specimens.
DISCUSSION: CI showed high effectiveness detecting metastasis. This fact helps to prevent second surgeries in patients with metastatic axillary lymph nodes. Moreover, surgical specimens are preserved for accomplishment of immunohistochemical reactions, if necessary.
CONCLUSION: Our results showed the importance of CI in the study of the SLN. Surgical interventions can be avoided, propitiating reduction of costs and morbidity.

O-232
IGF II EXPRESSION IN BREAST CANCER (BC) TISSUES. RELATIONSHIP WITH THE MOST IMPORTANT PREDICTIVE PARAMETERS IN BREAST MALIGNANCY.

E.Giustarini, A.Pinchera, D.Campani*, P.Fierabracci, M. E. Lippman°, C.Giani
Dipartimento di Endocrinologia e Metabolismo, University of Pisa. *Dipartimento di Oncologia, University of Pisa (Pisa, Italy). °V.T. Lombardi Cancer Research Center Georgetown University (Washington DC, USA).

Recent in situ hybridization data showed high content of IGF-II mRNA in the stroma of breast cancer. The aim of this study was to examine the relationship between IGF-II protein expression and several prognostic parameters in 75 ductal infiltratimg carcinoma (DIC) of the breast.
The tissue sections were evaluated for proliferating activity, IGF II protein, ER, PR, p53, P21 expression using immunohistochemical procedures. The amoumt of the stromal proliferation was assessed. The menopausal status. the axillary nodes and the nuclear degree were known . Thirty-five patients (44.3%) were pre-menopausal and 47 (62.6%) had node metastases. Marked stromal proliferation was found in 34 (45.3%) specimens and high nuclear grade in 20 (26.5%). Eighteen tumors (24%) showed no IGF-II immunostaining. In the positive cases, IGF-II was detected in the stroma as well as in the cytoplasm of epithelial cancer cells: marked IGF-II content was found in 12 specimens (16.0%) , slight in 14 (18.7%) and moderate in 31(41.3%). Twenty-four tumors (32.0%) showed high proliferating activity. Both ER and PR were expressed in the nucleus of cancer cells: 49 tumors (65.3%) were ER positive (ER+) and 34 (45.3%) PR positive (PR+). p21 protein was detected in 37

tumors (49.6%) and p53 in 12 (16%). IGF-II protein was not related with menopausal status. lymph-node metastases, nuclear grade, proliferating activity, ER and p53 oncogene. In contrast, IGF-II was strongly correlated with stromal proliferatiom ($p<0.001$), with PR ($p:0.04$) and with p21 oncogene ($p:0.01$). The results of this study demonstrate that in DCI of the breast IGF-II protein is expressed in the epithelium as well as in stroma of the majority of tumors and that it is correlated with stromal amount, with PR and p21 oncogene expression. These findings indicate that in breast cancer, IGF-II expression is connected with the stromal proliferation and with two important regulators of breast cancer growth and differentiation.

O-233
DIFFERENTIAL GENE EXPRESSION IN OVARIAN TUMORS REVEALS DUSP 4 AND SERPINA 5 AS KEY REGULATORS FOR BENIGN BEHAVIOR OF SEROUS BORDERLINE TUMORS

SIEBEN Nathalie(1,2), OOSTING Jan (2), FLANAGAN Adrienne (3), PRAT Jaime (4), ROEMEN Guido (1), KOLKMAN-ULJEE Sandra (2), VAN EIJK Ronald (2), CORNELISSE Cees (2), FLEUREN Gert Jan (2), VAN ENGELAND Manon (1)
Depts. of Pathology, University of Maastricht (1) and Leiden University Medical Centre (2), The Netherlands and University College London (3), United Kingdom and Autonomous University of Barcelona (4), Spain

Introduction
Ovarian serous borderline tumors (SBTs) are characterized by arborizing edematous papillae lined by stratified epithelial cells resembling those of the fallopian tube, varying degree of nuclear atypia and absence of frank stromal invasion. Originally, these tumors have been classified as 'borderline' because they behaved in a remarkably indolent manner despite pathological features suggesting malignancy. Even with widespread tumor deposits called implants at laparotomy and the presence of lymph node involvement the prognosis of such lesions generally remains excellent.
Tumor biology studies of SBTs are in progress. High-prevalence of B-RAF/K-RAS mutations in SBTs in contrast to serous carcinomas (SCAs) indicates that the mitogenic RAS-RAF-MEK-ERK-MAP-kinase pathway is crucial for the pathogenesis of SBTs.
The purpose of this study was to further unravel the genetic pathways through which SBTs develop with a special focus on explaining the in general benign SBT behavior despite its frequent widespread disease and activated mitogenic pathway.
Materials and Methods
We generated RNA expression profiles of 38 ovarian serous neoplasms including 11 SBTs, 10 low-grade SCAs, and 15 high-grade SCAs. Global Test pathway analysis and Significance Analysis of Micro arrays (SAM) of the expression profiles was performed.
Results
Global Test analysis of the expression profiles showed that in SBTs the mitogenic RAS-RAF-MEK-ERK-MAP kinase pathway and genes involved in downstream protease activation are uncoupled. This was substantiated by the finding that in SBTs the matrix metalloproteinase 9 (MMP-9) mRNA expression value was 2.1-fold decreased compared to SCAs, which was confirmed on a biological level by MMP-9 zymography. SAM analysis enabled us to identify two candidate key-regulator genes involved in uncoupling the mitogenic pathway and downstream genes involved in ECM: (ERK-inhibitor) Dusp 4 and (uPA-inhibitor) Serpina 5. Both genes were consistently down regulated in the SCAs when compared to the SBTs. The mean mRNA Dusp 4 expression for SCAs was 3.1 fold decreased compared to SBTs. The mean Serpina 5 mRNA expression for SCAs was 5.3 fold decreased compared to SBTs. The microarray data on Dusp 4 and Serpina 5 were substantiated for all 38 cases by q-RT-PCR assays.
In conclusion, we propose that the putative tumor suppressor genes Dusp 4 and Serpina 5 provide a major clue to the indolent behavior of the large majority of SBTs.

O-234
DIFFERENT ROLES FOR THE NERVE GROWTH FACTOR RECEPTORS TRKA AND P75 ALONG TUMOR PROGRESSION IN OVARIAN CARCINOMA

ØDEGAARD Elin 1, ABELER Vera M. 2, KOPOLOVIC Juri 3, ONSRUD Mathias 1, LAZAROVICI Philip 4, REICH Reuven 4, STAFF Anne Cathrine 1, DAVIDSON Ben 2
1 Department of Gynecology, Ulleval University Hospital N-0407 Oslo, Norway
2 Department of Pathology, The Norwegian Radium Hospital, University of Oslo, Montebello
N-0310 Oslo, Norway
3 Department of Pathology, Sheba Medical Center, Tel Aviv University, Tel-Hashomer
52620, Israel
4 Department of Pharmacology and Experimental Therapeutics, School of Pharmacy, Faculty of Medicine, The Hebrew University of Jerusalem, Jerusalem 91120, Israel

Introduction: The biological effect of nerve growth factor (NGF) is mediated through the effects of two receptors, p75 (low affinity) and the tyrosine kinase receptor TrkA (high affinity). We previously showed that the activated p-TrkA is a predictor of poor survival in advanced-stage ovarian carcinoma.
Purpose: To analyze p-TrkA and p75 expression in ovarian borderline tumors and FIGO stage I carcinomas and compare it to the expression in advanced-stage (FIGO stage III-IV) tumors.
Methods: Sections from 50 borderline tumors, 50 FIGO stage I invasive ovarian carcinomas and 56 advanced-stage carcinomas were evaluated for expression of the TrkA and p75 using immunohistochemistry.
Results: p-TrkA membrane expression was significantly higher in advanced-stage carcinomas compared to both borderline and stage I tumors ($p<0.001$, Chi-square test), with opposite results for cytoplasmic expression. p75 membrane expression was comparable in the three groups ($p>0.05$).
Conclusions: Expression of biologically active p-TrkA receptor at the cell membrane is upregulated along tumor progression in ovarian carcinoma, while p75 expression remains unaltered. These data provide further proof to the clinical role of p-TrkA in ovarian carcinoma.

O-235
HISTOPATHOLOGICAL AND CLINICAL STUDY OF 70 SEROUS BORDERLINE TUMORS OF OVARY

NOHRA Olivier, KAMBLE Meenal, MISHELLANY Florence, CANIS Michel, DAUPLAT Jacques, PENAULT-LLORCA Frederique
Centre JEAN PERRIN-CLERMONT-FERRAND-FRANCE

Introduction: International community of pathologists is still divided about serous borderline tumor of the ovary (SBOT). In one hand, a minority of pathologists wishes to split SBOT in 2 separates entities. In the other hand, other pathologists wish to retain this category.
Purpose of the study: try to draw prognostic factors of recurrence of SBOT. Assess the effect of histopathological subtype (including micropapillary (MP) and slight MP category), implants, benign associated lesions and treatment on SBOT behavior.

Method used: a retrospective and descriptive clinicopathological study of SBOT was performed on 70 patients (PTS) between 1986 and 2004. Both in academy hospital and in anti cancer center of Clermont-Ferrand, France, PTS were retrieved by using ADICAP computing database. All PTS clinical files were reviewed and added to the database. All histopathological slides were reviewed by two pathologists following 2003 WHO classification of SBOT.
Summary of the results: there were only six consultation cases. The mean follow-up was seven years. FIGO stage : 63 stage I, 4 stage II and 3 stage III. Recurrence rate was 17% and was only relevant to stage I. For 1 PT, the recurrence was an invasive adenocarcinoma. All recurrences occurred after conservative surgery. Seven patients were treated by adjuvant chemotherapy. Mean time from diagnosis to recurrence was 7.1 years. Mean time from recurrence to last news was 3.8 years. No patient died of the disease. The predictive factor suggestive of recurrence was conservative surgery (p=0.025). A trend to recurrence was present when endosalpingiosis was diagnosed (p=0.068), and when SBOT was exophytic (p=0.24). A correlation was found between exophytic tumors and peritoneal implants (p=0.013). There was no correlation between aneuploid tumors and recurrences (p=0.90). We could not draw any conclusion about the MP subtype of SBOT because our series contained only 2 cases. Furthermore, no correlation was found between 21 SBOT with slight MP structure and recurrences.
Conclusion reached: a minimal five years or 10 years follow-up is recommended for patients treated by conservative surgery. Besides, among FIGO stage I, laparoscopic follow up is needed to avoid recurrences.

O-236
PARP, CAF-1 AND DNA PLOIDY AS FACTORS INFLUENCING PROGNOSIS IN OVARIAN GRANULOSA CELL TUMORS.

STAIBANO Stefania°, MIGNOGNA Chiara°, MASCOLO Massimo°, MEZZA Ernesto°, SALVATORE Gaetano^, DI BENEDETTO Maria^, NUGNES Loredana°, NAPPI Carmine*, DE ROSA Gaetano°.
°Department of Biomorphological and Functional Sciences, Pathology Section, ^Department of Medicine and *Department of Obstetrical-Gynaecological and Urological Sciences and Reproductive Science, “Federico II” University, Naples, Italy.

Ovarian granulosa cell tumors (OGCT) are sex-cord stromal tumors that represent 1.5-3% of primary ovarian tumors. OGCT have a low/moderate potential of malignancy. However, metastases have been reported from 7% to 53% of cases in a ten-years interval. Classical clinical-pathological parameters are unable to predict the biological behaviour of these tumors.
Chromatin assembly factor I (CAF-1) is a heterotrimeric protein complex formed of three subunits, p150, p60, and p48, involved in cell replication and DNA repair. P150 interacts directly with proliferating cell nuclear antigen (PCNA) and seems responsible of the DNA-repair process; the p60 subunit has been directly correlated with cell proliferation, and has been proposed as a novel sensible proliferation marker in tumors. Overall, it has been hypothesized for CAF-1 a role as a new prognostic indicator in human cancer.
Poly(ADP-ribose) polymerase 1 (PARP-1) is a zinc finger DNA-binding protein involved in the control of genomic stability, DNA repair and regulation of apoptosis. Its potential role in carcinogenesis has not been evaluated. During apoptosis, PARP is cleaved by caspases. Recent studies reported the over-expression of full-length PARP-1 in a variety of tumors with aggressive phenotype and poor clinical outcome. The aim of this study was to establish if a correlation exists between the immunohistochemical expression of PARP-1 and CAF-1 p60 and p150, DNA-ploidy pattern and clinical behavior of OGCT.
We found that a high expression of the uncleaved form of PARP-1 and CAF-1 p60, aneuploidy and low expression of CAF-1 p150 were statistically correlated with a worse prognosis. On the contrary, a prevalent expression of cleaved PARP-1, low levels of CAF-1 p60, euploidy or aneuploidy associated with an euploid cell population and appreciable levels of CAF-1 p150 were found in tumors with a clinical “indolent” behaviour.
These preliminar results suggest that CAF-1 p60 may have a role as new proliferation marker in OGCT. Moreover, variation of its expression are correlated with altered expression of PARP-1, CAF-1 p150 and DNA ploidy pattern in a subset of tumors, suggesting the potential role of these factors as prognostic markers in OGCT.

O-237
ANALYSIS OF BRAF/ERK AND P16 IN OVARIAN ENDOMETRIOID LESIONS

SCHLOSSHAUER Peter, IDREES Muhammad, NEZHAT Farr, DELIGDISCH Liane, DONG Jianli

Introduction: Either activation of the BRAF/ERK pathway or inactivation of the tumor suppressor p16 have been reported in a variety of neoplasms including ovarian carcinomas.
Purpose of study: To explore the correlation between BRAF/ERK activation and loss of p16 in ovarian endometrioid lesions.
Methods: 22 cases of pelvic (including 19 ovarian) endometriosis, 13 ovarian endometrioid adenofibromas (AF), and six cases of ovarian endometrioid adenocarcinoma (OEC) arising in an AF were analyzed. Formalin fixed, paraffin embedded tissue sections were immunostained for p16, total (t-) and phosphorylated (p-) ERK and evaluated by three pathologists. PCR-RFLP and direct sequencing were used for mutational analysis of BRAF codon 600 on genomic DNA extracted from laser capture microdissected epithelial cells.
Results: Nuclear p16 expression was seen in 11/21 (52%) of endometriosis cases and 8/13 (62%) of adenofibromas, ranging from sporadic to 20% of epithelial cells. Cytoplasmic staining for p16 was present in 17/21 (81%) endometriosis cases and 11/13 (85%) adenofibromas, including all cases with nuclear positivity. One of six (17%) carcinomas showed strong nuclear but no cytoplasmic expression in 10% of the cells from both the AF and OEC components. 4 of 6 (66%) carcinomas had weak cytoplasmic p16 expression in 10-50% of cells of both AF and OEC elements. ERK expression was generally strong in endometriosis, intermediate in AF and variable in OEC. P-ERK tended to be less diffusely present and more concentrated within nuclei than t-ERK. No oncogenic BRAF mutations were identified.
Conclusions: While cytoplasmic p16 expression is present in the majority of all types of ovarian endometrioid lesions, nuclear p16 expression appears to decrease during tumor progression from adenofibromas to carcinomas. One carcinoma case showed nuclear staining only, which may be associated with inactivating p16 mutations. Our results suggest that (1) The co-expression of p-ERK and p16 in benign lesions inhibits ERK-driven cell proliferation; (2) In carcinomas, even weak p-ERK activity may have a proliferative effect in the absence of functioning p16; (3) Oncogenic BRAF mutations appear not to be a pathogenetic factor in ovarian endometrioid tumorigenesis; (4) The BRAF/ERK/p16 profile in ovarian endometrioid neoplasms differs from that in serous tumors, confirming that morphologically distinct ovarian lesions are associated with different molecular pathogenetic mechanisms.

O-238
EXPRESSION ANALYSIS OF BMI1 IN MEDULLOBLASTOMAS AND CORRELATION

TO HISTOLOGICAL AND MOLECULAR CHARACTERISTICS.

RODUNER Sarah, LEUNG Carly, SUTTER Catherine, STORZ Martina, MOCH Holger and MARINO Silvia
Institute of Clinical Pathology, University Hospital, Zürich, Switzerland

Medulloblastomas, highly aggressive embryonic tumors of childhood, originate from deregulated proliferation of cerebellar granule cell progenitors. The Sonic Hedgehog (Shh), Notch and Wnt pathways are well known regulators of the proliferation and differentiation of these progenitor cells during embryonic and postnatal cerebellar development and have been implicated in medulloblastoma pathogenesis. We recently identified BMI1, a member of the Polycomb group of transcription repressors, as a crucial player in controlling proliferation and possibly differentiation of granule progenitor cells in the mouse.
The aim of this study was to determine BMI1 expression in human medulloblastomas and to correlate it to the expression of other key players of the Sonic Hedgehog, Notch and Wnt pathways.
A tissue microarray with 63 human and 24 experimental murine medulloblastomas was constructed to allow high throughput analysis of gene expression by means of immunhistochemistry and mRNA insituhybridization. BMI1 expression was correlated with histologic characteristics of medulloblastomas and with expression of PTCH1, Gli1, Gli2, Hes1, Hes5, bcatenin and CyclinD1.
Overexpression of BMI1 did not correlate with the histological subtype of the tumors or with the degree of neuronal and glial differentiation. The data showed that activation of the Wnt pathway is rare in medulloblastoma and is not associated with BMI1 overexpression. However, overexpression of PTCH1 in all tumors overexpressing BMI1 suggested that activation of the Sonic Hedgehog pathway is involved in the development of the majority of human medulloblastoma.

O-239

PROGNOSTIC SIGNIFICANCE OF SURVIVIN EXPRESSION AND APOPTOTIC RATE IN MEDULLOBLASTOMA

Joze Pizem1, Andrej Coer2, Lorna Zadravec-Zaletel3, Mara Popovic1
1 Institute of Pathology, Medical Faculty, Ljubljana, Slovenia
2 Institute for Histology and Embryology, Medical Faculty, Ljubljana, Slovenia
3 Institute of Oncology, Ljubljana, Slovenia

Introduction. To improve the treatment of medulloblastoma, new prognostic markers are needed. Survivin is a member of the inhibitor of apoptosis protein family, which is over-expressed in many human cancers. Apoptosis is a major contributor to cell loss in medulloblastoma, either spontaneous or induced by therapy.
Purpose. Our aim was to analyse survivin expression in medulloblastoma, its association with aberrant activation of the WNT (wingless) pathway and apoptotic rate. We tested prognostic significance of survivin expression and apoptotic rate.
Methods. We immunohistochemically analysed survivin expression and localisation of â-catenin, a downstream mediator of the WNT pathway, in 56 cases of medulloblastoma. We also determined the apoptotic rate using an antibody against cleaved caspase 3, a specific marker of apoptotic cell death.
Results. Survivin was detected in the nuclei of tumour cells in all cases, but the proportion of positive nuclei varied from 0.5 to 31.3%. Survivin expression tended to be higher in medulloblastomas with an aberrant activation of the WNT pathway (nuclear localisation of â-catenin), but did not correlate with histological type, age group or dissemination via cerebrospinal fluid pathways. The apoptotic rate varied considerably among medulloblastomas (0.1-25.9%, median 1.1%). Apoptotic cells were relatively evenly distributed in 38 cases, while in 18 cases, an uneven distribution with foci of an increased number of apoptotic cells and their clustering was observed. Clusters of apoptotic cells were found around necrotic areas, in contrast, necrotic cells were caspase 3 negative. The apoptotic rate was higher in medulloblastomas with CSF dissemination, tended to be higher in desmoplastic medulloblastomas, but there was no association with age group, sex or survivin expression. In the analysis of disease-specific overall survival, the apoptotic rate had no prognostic value, while survivin expression and dissemination status were two independent negative prognostic variables.
Conclusions. Survivin is up-regulated in medulloblastomas. It is a negative prognostic marker and a potential therapeutic target. The variation in apoptotic rate among medulloblastomas is very likely predominantly associated with variations in tumour microenvironment, as supported by apoptotic cell clustering and rimming around necrotic areas. The apoptotic rate in medulloblastoma resection specimens does not seem to be of prognostic value.

O-240

FISHING FOR CYCLIN-D1 IN GLIOMAS. IS THERE ANY CORRELATION BETWEEN HISTOLOGY AND GENETICS?

Kathryn McFadden#, Diana Ionescu#, Kathy Cieply#, Dafna Fernandez Burguera, Alicia Gude+, Ester Anton Valenti*, Clayton Wiley#, Marta E. Couce Matovelle*. # University of Pittsburg Medical Center, Pittsburg, USA.,+ Facultad de Matemáticas, Universidad de Santiago de Compostela, Spain. *Hospital Universitario Son Dureta and Hospital Son Llatzer, Palma de Mallorca, Spain.

Introduction and Purpose of the study: Gliomas frequently show aberrations in genes coding for cell cycle regulatory proteins involved in the control of G1/S phase transition. The D-type cyclins promote cell cycle progression from G1 to S phase by binding to and activating cyclin dependent kinases. Overexpression of cyclin D1 has been shown in many tumors, but there are still some controversies regarding the significance of overexpression of cyclin D1 in gliomas. The purpose of this study was to identify cyclin D1 amplification in gliomas, and to analyze the potential correlation of this amplification with histologic diagnosis, other genetic aberrations, and prognosis.
Methods: The study was approved by the Institutional Review Board of the University of Pittsburgh Medical Center. Thirty five patients with glial tumors were identified in the archives of the University of Pittsburgh Medical Center. Cytogenetic aberrations of the gene locus at chromosome 11q13 (Cyclin D1) were evaluated using fluorescence in situ hybridization (FISH). Mutational genotyping was performed using polymorphic microsatellites situated within or adjacent to known tumor suppressor genes or genomic sites potentially involved in human brain carcinogenesis, at 1p, 9p, 10q, 17p and 19q. PCR amplification products were analyzed for loss of heterozygosity (LOH) by capillary gel electrophoresis using a multi-color fluorescence-based DNA analysis system (ABI Prism 3100 Genetic Analyzer, Applied Biosystems, Foster City, CA).
Results and Conclusions: The analysis showed a statistically significant association between the histologic diagnosis of oligodendrogliomas or oligoastrocitomas and the presence of cyclin-D1 amplification (Fisher exact test, alpha >= 0,001). We also demonstrated that amplification of Cyclin-D1 was more common in low grade gliomas. Although there was no significant correlation between cyclin-D1 amplification and survival in these patients; its presence was more common in those cases with better outcome. The occurrence of other

variables, such as young age at presentation and low grade tumors were strongly linked to survival. Additionally, there is no statistically significant association between Cyclin-D1 amplification and the presence of LOH for any of the genes examined.
In summary, the detection of Cyclin-D1 amplification by FISH in gliomas could represent an important adjuvant technique for diagnosis.

O-241
AUTOMATIC ASSESSMENT OF 1P36-19Q13 STATUS IN GLIOMAS BY INTERPHASE FISH ASSAY

Marc-Antoine Belaud-Rotureau (1, 2), Nelly Meunier (1), Sandrine Eimer (3), Michelle Turmo (1), Pierre Dubus (1, 2), Anne Vital (3), Hugues Loiseau (4), Jean-Philippe Merlio (1, 2)
1: EA 2406 Histology and Molecular Pathology of tumours, University Victor Segalen, Bordeaux
2: Pathology Laboratory, Haut-Lévêque Hospital, CHU Bordeaux
3: Pathology Laboratory, Pellegrin Hospital, CHU Bordeaux
4: Neurosurgery Department, Pellegrin hospital, CHU Bordeaux

The histological classification of glial tumours is not sufficient for the prediction of patient prognosis and therapeutic response to chemotherapy. Genetic analyses have shown that combined 1p36 and 19q13 losses are associated with chemosensitivity and a longer survival in oligodendrogliomas (O). The prognostic significance of such deletions in astrocytomas (A) and mixed oligoastrocytomas (OA) is still a matter of debate. The 1p/19q status can be determined either by fluorescent in situ hybridization (FISH) assay or by molecular testing for loss of heterozygosis (LOH). Frozen samples of 25 patients with a grade II or III glioma (5 O, 14 A, 6 OA) were selected and checked on cryostat sections. Thereafter, touch imprints of this representative frozen material were collected and stored at room temperature until use. The interphase FISH assay was performed using the LSI 1p36/LSI 1q25 - LSI 19q13/19p13 Dual-Colour Probe Sets (Abbott-Vysis) in comparison with previously assayed probes. The automatic assessment of hybridization patterns was performed using the Metafer 4 software (Metasystems) in comparison with visual analysis by two independent observers. Results were interpreted according to the guidelines of the International Society of Pediatric Oncology for studies of peripheral neuroblastic tumours.
The use of both LSI-probes and frozen imprints of control tissues allowed to establish a cut-off threshold at 6% (mean + 3 SD). Frozen tumour imprints provided few truncated nuclei and strong and compact fluorescent signals were observed. The automatic assessment of the hybridization patterns provided similar results to the visual count and was 3 times more rapid. It allowed an objective capture of all the nuclei and a better standardization of the assay.
FISH analysis demonstrated a combined 1p-19q losses for 5 patients (1A, 2O, 2OA). No isolated 1p36 or 19q13 deletion was detected. A complex profile with 1p-19q imbalance was observed in one patient. Despite the low size of our cohort, the clinical follow-up of our patients suggested that 1p-19q losses may be associated with a significant higher time to progression and overall survival in gliomas with an astrocytic component (A and OA). Finally, automated FISH analysis of fresh or frozen tumour imprints allow a powerful assessment of the 1p/19q status in gliomas. The prognostic relevance of such deletions in gliomas with an astrocytic component needs to be confirmed on larger series

O-242
METALLOTHIONEIN EXPRESSION IN NEUROBLASTOMA

THEOCHARIS Stamatios1,2, KLIJANIENKO Jerzy1, FRENEAUX Paul 1, MICHON Jean 1, COUTURIER Jerome1, BRISSE Hervé1, VIELH Philippe1, SASTRE-GARAU Xavier1
1Departments of Tumor Biology, Pediatrics and Radiology, Institut Curie, Paris, France
2Department of Forensic Medicine and Toxicology, Medical School, University of Athens, Athens, Greece

Background-Aims: Neuroblastoma is an heterogenous tumor of neural crest origin cells that form the adrenal medulla and sympathetic ganglia. Metallothionein (MT) is a multifunctional protein implicated in cell cycle-apoptosis, drug and radiotherapy resistance and several aspects of carcinogenic evolution. The aim of this study was to examine immunocytochemically the expression of MT in neuroblastoma cells obtained at initial diagnosis by Fine-Needle Aspiration (FNA) from neuroblastoma patients in order to estimate any possible clinical significance.
Materials and Methods: Ultrasound-guided FNA aspirates from 30 patients were obtained and maintained as ThinPrep preparations. Tumor cells were immunostained using the streptavidin-biotin immunoperoxidase technique in order to evaluate MT expression. MT positivity and overexpression (positivity in more than 50% of tumor cells), pattern (cytoplasmic, nuclear, cytoplasmic and nuclear) and intensity of immunostaining (mild, moderate, intense) were correlated with clinicopathological variables as patients' clinical stage, tumor cells' DNA ploidy and proliferative capacity (estimated as S-phase fraction) and MYCN oncogene amplification that is associated with a more aggressive clinical outcome.
Results: All of our cases proved MT positive, while in 24 out of 30 (80%) MT overexpression was also noted. Neither MT positivity nor MT overexpression were correlated with patients' clinical stage, tumor cells' DNA ploidy and proliferative capacity or MYCN oncogene amplification. MT distribution and intensity of staining in neuroblastoma tumor cells were not correlated with any of the clinicopathological variables examined.
Conclusions: MT expression and overexpression are prominent in human neuroblastoma cases examined, nevertheless no correlation was found with clinicopathological parameters important for their outcome. Our data suggest that involvement of MT in diagnosis or management of neuroblastoma patients is uncertain.

O-243
THE SIGNIFICANCE OF IMMUNOHISTOCHEMICAL EXPRESSION OF KI-67, P53, P21, AND P16 IN MENINGIOMA TISSUE ARRAYS

TERZI Aysen, BARAK Anil, SOYLEMEZOGLU Figen
Hacettepe University, Faculty of Medicine, Department of Pathology and Biostatistics, Ankara, Turkey

Although histologic grading of meningiomas has prognostic and clinical implications, in some cases it is difficult to predict the outcome of patients. There has been several efforts to evaluate the use of different immunohistochemical markers for predicting meningioma prognosis.

In this study we aimed to determine the prognostic utility of Ki-67, p53, p21, and p16 proteins in meningiomas. We analyzed the immunohistochemical expression of Ki-67, p53, p21, and p16 proteins in 130 meningiomas (64 benign, 39 atypical, and 27 malignant, including 5 papillary and 15 rhabdoid variants). The tumours were graded according to WHO 2000 classification. The study was carried out on tissue arrays.

There was a statistically significant corelation between the expression of Ki-67, p53, p21, p16 and the grade of

meningiomas (p<= 0,001). By ordinal logistic regression; p53 and Ki-67 were significantly associated with grade, and an increase of 1% in labeling index, resulted in an increase in the risk of raising the grade by 2,17 and 1,49, respectively.

Histologic grade, p53 and Ki-67 labeling indeces were strongly associated with decreased recurrence free survival in univariate analysis. In contrast multivariate analysis revealed that only tumour grade is an independent factor for predicting meningioma recurrence.

We conclude that the Ki-67 and p53 labeling indeces are useful additional tools in discriminating atypical from benign or anaplastic meningiomas, especially in histologically borderline cases.

O-244
FAMILIAL AORTIC ANEURYSM AND DISSECTION WITH CYSTIC MEDIAL NECROSIS CAUSED BY SMOOTH MUSCLE MYOSIN HEAVY CHAIN (SM-MHC) GENE MUTATION: THE NEW CONCEPT OF CONTRACTILE PROTEIN SMOOTH MUSCLE CELL DISEASE OR VASCULOMYOPATHY

BRUNEVAL Patrick(1), ZHU Limin(1), KHAU VAN KIEN Philippe(2), JEUNEMAITRE Xavier(1). (1) Hopital Europeen Georges Pompidou, Paris and (2) CHU de Dijon. France.

Cystic medial necrosis and vascular smooth muscle cell (VSMC) loss are frequently, but inconstantly, observed in the media from cases of aortic aneurysms and/or dissections. These histologic changes are not specific: although they are sometimes related to a clearly characterized Marfan's syndrome, most frequently they are not associated with any clear-cut disease. For that latter condition, an extracellular matrix (ECM) involvement, not yet characterized, is usually considered as a potential culprit.

Thoracic aorta aneurysm tissues from two male patients of 37 and 56 year-old respectively were obtained during surgical repair and were studied to assess aorta wall structure (H&E and elastic stains) and VSMC phenotype (immunohistochemistry for alpha-smooth muscle actin, h-caldesmon, vimentin, and SM-MHC). These patients belong to a large kindred characterized by an unusual incidence of sudden death, aortic aneurysms or dissections, and patent ductus arteriosus. Genetic analysis performed in this kindred showed a mutation in the MYH11 gene encoding for SM-MHC.

Both thoracic aortas showed similar figures of media thinning, cystic medial necrosis with severe involvement of elastic fibers, and dramatic loss of VSMC. VSMC normally expressed alpha-smooth muscle actin, h-caldesmon, and vimentin. For the expression of SM-MHC, four different commercially available antibodies raised against different epitopes of SM-MHC were tested. VSMC in the patient aortas were negative with an antibody, the one directed against the mutated epitope of SM-MHC, and positive with the three others, whereas VSMC from normal and Marfan's syndrome control aortas were constantly positive for all antibodies.

It can be concluded that: 1) Alterations of a major VSMC contractile protein can lead to an arterial phenotype characterized by aneurysms or dissections with cystic medial necrosis, elastic fiber and VSMV loss, as do Marfan's syndrome, the best characterized ECM genetic disease. Thus, besides ECM protein diseases, VSMC diseases or vasculomyopathies, i.e. contractile protein diseases, should be now considered as a possible mechanism leading to cystic medial necrosis; 2) The variability of reaction of different antibodies against mutated proteins precludes the use of immunohistochemistry for the reliable detection of some genetic defects as those affecting SM-MHC.

O-245
DISTINCT PHENOTYPE OF HUMAN ARTERIAL SMOOTH MUSCLE CELLS EXPRESSED PLATELET-ACTIVATING FACTOR RECEPTOR. FUNCTIONAL IMPLICATIONS.

BROCHERIOU Isabelle*°, STENGEL Dominique*, KARABINA Sonia-Athina*, DURAND Hervé*, PICKERING Geoffrey#, CAPRON Frederique*° and NINIO Ewa*.

*INSERM U525, Paris, France; Institut Fédératif 14, Paris, France; Université Pierre et Marie Curie and Faculté de Médecine Pitié-Salpêtrière, Paris, France; °Service d'Anatomie-pathologie, Hôpital Pitié-Salpêtrière, Paris, France; # Robarts Research Institute (Vascular Biology Group), London Health Sciences Centre, Departments of Medicine, Biochemistry, Medical Biophysics, University of Western Ontario, London, Canada.

Objective- Platelet-activating factor (PAF) and its structural analogues formed upon low density protein oxidation are involved in all stages of atherosclerotic plaque formation and may signal through a specific G-protein coupled receptor, PAF-receptor (PAF-R) found in human macrophages and in certain smooth muscle cells (SMCs) in the media, but rarely in the intima of human plaques. The diversity of SMC phenotypes in normal arteries has been described and led to the suggestion that distinct subsets of SMC might participate in the lesion development.

Methods and results- Circulating SMC progenitors and two phenotypically distinct clones of proliferative, epithelioid phenotype vs contractile, spindle-shaped SMCs from the media of a single fragment of adult internal thoracic artery were studied for the presence of PAF-receptor (PAF-R). Only the subset of SMCs of spindle-shaped of synthetic phenotype expressed both mRNA and PAF-R protein and in the functional test only these cells migrated in the presence of PAF. Two unrelated, specific PAF-R antagonists inhibited PAF-induced migration, but did not modify the migration initiated by PDGF.

Conclusions- The observation that the arterial spindle-shaped SMCs of synthetic phenotype express PAF-R opens new avenues concerning the migration of these cells from the media into the intima and atherosclerotic plaques formation.

O-246
ANALYSIS OF INTERCALATED DISC REMODELING IN EXPLANTED HEARTS FROM CHILDREN WITH CONGENITAL HEART DISEASES OR DILATED CARDIOMYOPATHY

P. Francalanci, A. Tessa°, F.M. Santorelli°, F. Diomedi Camassei, F. Parisi^, R. Devito, R. Boldrini, F. Callea. Dep. of Pathology, ° Molecular Medicine and ^Dep. of Cardiology and Cardiac Surgery, Bambino Gesù Children's Hospital, Rome, Italy

The cadherin family of trans-membrane proteins mediates mechanical junctions at the level of intercalated discs (ID) where the ends of thin and intermediate filaments are anchored to polar sarcolemma via adherents junctions (AJ) and desmosomes, respectively. In the AJ, the barb ends of actin of terminal sarcomeres are believed to link N-cadherin through binding to alfa-actinin or vinculin, which joins a-catenin, which links beta- or gamma-catenin.

Previous study in hamster and human hypertrophic cardiomyopathy demonstrated a remarkable accumulation of N-cadherin and beta-catenin in disarrayed ID and that the alteration of this pathway could play a key role in modulation of genes directly related to the onset of the hypertrophic phenotype.

Purpose: Aim of this study is to evaluate whether in end-stage cardiac hypertrophy due to dilated cardiomyopathy (DCM) or congenital heart disease (CHD) the ID remodeling is associated with abnormal expression of cadherin/catenin complex in AJ as well as of connexin 43 (Cx43) in gap junction (GJ).
Methods: Ventricular samples of explanted hearts obtained from 11 children (aged 1-15 years) with DCM and from 7 children (aged 9-24 years) with CHD were studied by light microscopy, immunohistochemistry and Western blot analysis.
Results: Both DCM and CHD displayed hypertrophic and disarrayed myocells with disorganized morphology of the IDs. N-cadherin expression was nearly normal in both DCM and CHD. In disarrayed ID, beta-catenin immunostaining was increased and fragmented in all samples, while gamma-catenin stain was almost regular in DCM and faint in CHD. Cx43 expression was abnormal in all, showing a distribution over the entire surface of the myocytes, consistent with neonatal distribution. By Western blotting analysis, beta-catenin was significantly increased in 12 samples, 7 DCM (+53%) and 5 CHD (+31%). Contrariwise, gamma-catenin expression was unaffected in DCM, whereas it was reduced (-25%) in 4/7 patient with CHD. N-cadherin and Cx43 were normal.
Conclusions: This study suggests that beta-catenin deposits occur at the AJ in end-stage hypertrophic ventricular myocytes, regardless of the primitive heart pathology, either DCM or CHD. This seems not associated with simultaneous down-regulation of gamma-catenin, at least in DMC, or with modification of N-cadherin. Remodeling of adhesions junctions does not lead to a quantitative changes of Cx43, although the expression of this protein can be abnormal.

O-247
EXPRESSION OF PROINFLAMMATORY CYTOKINE AND CHEMOKINE IN LYSOPHOSPHATIDIC ACID-TREATED VASCULAR SMOOTH MUSCLE CELLS: A ROLE OF MITOGEN-STIMULATED SMOOTH MUSCLE CELLS IN THE VASCULAR INFLAMMATORY SYSTEM.

KANEYUKI Utako1,2, KATO Seiya2, UEDA Seiji1, YAMAGISHI sho-ichi3, INAGAKI Yosuke3, YOSHIMURA Junko1,2, IMAIZUMI Tsutomu3, OKUDA Seiya1. Departments of 1Nephrology, 2Pathology, and 3Internal Medicine III and the Cardiovascular Institute, Kurume University School of Medicine, Kurume, Japan.

Atherosclerosis is recognized as a chronic inflammatory disease, however functional involvement of each vascular constituent has not been clearly understood. Vascular smooth muscle cells (SMC) are major constituent of the vascular structure. At the site of vascular insult, mitogens promote proliferative (myofibroblastic) phenotype of SMC, resulting in the neointimal hyperplasia. Here we tested the hypothesis that mitogen-stimulated SMC may contribute to the vascular inflammatory system other than proliferative response. Lysophosphatidic acid (LPA), a platelet-activating component of mildly oxidized low-density lipoprotein, has been known to act as a SMC mitogen via the activation of intracellular protein kinases. Cultured human aortic SMC are stimulated with 10-100uM of LPA in the serum-free condition. NADPH-driven reactive oxygen species (ROS) generation and proinflammatory gene expressions were examined. HMG-CoA reductase inhibitor, Pitavastain, was also tested for the inhibition of LPA-induced inflammatory response. LPA-treated SMC showed up-regulation of mRNA levels of p22phox and gp91phox, membrane components of NADPH oxidase, and intracellular ROS generation, which were completely inhibited by diphenylene iodonium (DPI), an inhibitor of NADPH oxidase, as well as by Pitavastatin. LPA also stimulated the expression of interleukin-18 and monocyte chemoattractant protein-1 genes in SMC, which were significantly prevented by DPI, N-acethylcystein, an antioxidant, and Pitavastatin. Our data suggested that mitogen-stimulated SMC potentially produce proinflammatory cytokine and chemokine via the up-regulation of intracellular ROS. Proliferating SMC may involve in the vascular inflammatory system at least two ways: One is as myofibroblastic proliferating cells for the vascular remodeling, and the other is as inflammatory cells directly producing inflammatory mediators. The lipid-lowering agent, Pitavastatin, would exert the atheroprotective property in mitogen-stimulated SMC with the anti-oxidative and anti-inflammatory effects.

O-248
STRUCTURAL-FUNCTIONAL STATUS, NUCLEAR PLOIDY IN INTERVENTRICULAR SEPTUM CARDIOMYOCYTES FROM CHILDREN AND ADULTS WITH OBSTRUCTIVE HYPERTROPHIC CARDIOMYOPATHY.

Rybakova M1, Gudkova A2, Borisov K3, Selivanova G4, Vlasova T4, Parfenov V3,
Bokeria L3 and Schlyakhto E2.
1)Pathology Department, State Pavlov Medical University, St.Petersburg, Russia
2- Faculty Therapy department, State Pavlov Medical University, St.Petersburg, Russia
3)Bakulev Reseach Center of Cardiovascular Surgery, Moscow, Russia
4)Cytology Research Institute, St.Petersburg, Russia

Aim: to study structural-functional status and nuclei ploidy of adult and children cardiomyocytes from patients with obstructive hypertrophic cardiomyopathy (OHCMP).
Material and methods: material from 61 patients with OHCMP was included into the study. Among those, 19 were below 21 y.o. and named as "children". The rest 41 patients were over 21 y.o. and named as "adults". The material was obtained upon the surgical interventions as well as upon express autopsies from the right side of the interventricular septum. The samples were stained with hematoxylin-eosin technique and by the method of nucleolar organizer regions silver staining. Histological index was estimated according to Noorden (1971). Nuclear area was calculated by morphometry. DNA content was estimated by Felgen method on dissociated cardiomyocyte nuclei and assessed by cytophotometry. One hundred tissue lymphocytes were used as a control for diploidal DNA content.
Clinical and echocardiographic data were obtained from case histories.
Results: There was no statistical difference between children and adults in LVMI and IVS thickness in the outflow tract. Histological index in children varied from 80 to 100 % with a mean 94,2¦ 2,3 and was significantly higher, then in adults (71,1%¦ 1,4 p<0,05). There was no significant difference in nuclear area between children and adult group (94,8¦ 2,6 and 93¦ 2, p>0,05), however, severe nuclear polymorphism was noticed in children group. In this group the percentage of "huge" cardiomyocyte nuclei with area >200,0 was significantly higher, then in adult group (21,2% 1,5 and 11,5%¦ 1,6, p<0.000). The percentage of micronuclei (area <30%od mean cardiomyocyte area) was significantly higher in children group as well (10,2%¦ 1,7 and 5,4%¦ 1 p<0,017). There was significant increase in pared nuclei content (11,6%¦ 0,1 and 7,5%¦ 0,6 p<0,017) and a tendency to the multiple nuclei cardiomyocytes (8,4%¦ 1,6 and 4%¦ 0,4) in children group. The average DNA content ! was higher in

children group a (15,2¦ 2,2 and 9,9 ¦ 0,7 correspondingly, p<0,017).
Conclusion: the children group with OHCMP is characterized by highest degree of myocardial hypertrophy, accompanied by increase nuclear polymorphism and nuclear area. The significant increase of pared nuclei, cardiomyocytes with multiple nuclei (caryokinesis without cytokinesis), the percentage of hyperploidy and average DNA content in cardiomyocytes characterizes the grow potential of hypertrophic and hyperplasia processes in children.

O-249
THE ROLE OF ELECTRON MICROSCOPY IN THE DIAGNOSIS OF SYSTEMIC VASCULITIS IN RHEUMATOID ARTHRITIS

Miklós Bély1, Pál Kapp1, Tamás Szentjóbi Szabó1, and Ágnes Apáthy2
1Department of Pathology,
Policlinic of the Hospitaller Brothers of St.John of God, Budapest, Hungary
2Department of Rheumatology,
National Institute of Rheumatology and Physiotherapy, Budapest, Hungary

Introduction
Systemic vasculitis is the most likely lethal complication; moreover it is missed clinically with a high probability in rheumatoid arthritis.
The high prevalence of vasculitis in the peripheral nerves and skeletal muscles makes biopsy of the sural nerve (with surrounding muscles) a good target for the confirmation of suspected systemic vasculitis (with, or without visible involvement of the skin).
The aim of this study was to demonstrate the ultrastructural changes in sural nerves, and to demonstrate the value of electron microscopic examination in the diagnosis of systemic vasculitis.
Patients and Methods
Biopsy samples of 25 sural nerves, and 31 samples of skeletal muscle (surrounding the nerve) were studied from 36 autopsy patients who had rheumatoid arthritis with histologically confirmed systemic vasculitis.
The tissue samples were examined by light and electron microscopic methods.
Results
Vasculitis of nutrient vessels was confirmed by light microscopy in 13 (18.7%, 52 rel %) of 25 sural nerves, and in 17 (19.7%, 54.8 rel %) of 31 samples of skeletal muscle.
Ultrastructural changes of neurons were present in all 25 tissue samples, with or without visible vasculitis by light microscopy.
The changes included loss of myelinated fibers, thinning of myelin sheeths, demyelization, degeneration of Schwann cells and intracytoplasmic onion bulbs (indicating active demyelization), furthermore axonal degeneration. The myelinated nerve fibre density decreased, and axonal clusters developed.
The ultrastructural changes were accompanied by endo- and perineural increase of collagen fibrils.
The ultrastructural alterations were present with different degrees of severity and in different stages of its development.
Discussion
Vasculitis involves a segment, or a sector of the vessel walls. Sporadic vasculitis (because of the lower density of inflammatory segments in the vessel walls) may be missed by traditional light microscopic examination of sural nerve biopsies.
Vasculitis of the nutrient vessels around the neurons is accompanied by secondary (longitudinal) changes [degeneration, demyelization, or endo- and perineural fibrosis].
Early stages or mild forms of neural degenerative processes (ultra- structural changes) may be detected only by electron microscopy.
The ultrastructural changes of neurons may indirectly indicate the presence of vasculitis in case the inflamed segments are not in the plane of sectioning

O-250
HIPPOCAMPAL ANGIOGENESIS AND PATHOLOGICAL REMODELING IN HUMAN TEMPORAL LOBE EPILEPSY

RIGAU Valérie (1,2), CRESPEL Arielle (2,3), RAYNAUD Pierre (1), COUBES Philippe (3), DE BOCK Frédéric (2), ROUSSET Marie-Claude (2), BALDY-MOULINIER Michel (3), BOCKAERT Joël (2), BALDET Pierre (1), LERNER-NATOLI Mireille (2)
(1) Pathology Unit, CHU Gui de Chauliac
(2) IGF, CNRS UMR5203, INSERM U661
(3) Epileptology Unit, CHU Gui de Chauliac
Montpellier FRANCE

We recently described an increased number of microvessels in chronic epileptic foci, particularly in case of severe lesions and neuro-glial reorganization.
Here we attempted to evidence an angiogenesis in chronic foci of adult patients with intractable temporal lobe epilepsy (TLE). To approach the mechanisms of this neo-vascularization, we looked for the kinetic of angiogenic processes in murine models of TLE.
Human subjects: hippocampi were obtained in 30 patients who underwent surgery for intractable TLE (with various etiologies and different degrees of neuronal loss) and in 4 non epileptic, autopsied patients (NE).
Animal model: 20 rats underwent status epilepticus after lithium-pilocarpine injection and developed a chronic limbic epilepsy.
Hippocampi were used for immunohistochemistry and western blotting to check the expression of angiogenic factors or their receptors and markers of immature endothelial cells.
:
In human, microvessels were more numerous in the hippocampus of TLE patients than in NE hippocampi. Particularly in case of hippocampal sclerosis, neo-microvessels were positive for various markers of immature endothelial cells in injured areas and in the dispersed dentate granular layer. In most patients, VEGF was strongly expressed by pyramidal and granular neurons and also by astrocytes. In animals, angiogenic factors were rapidly detected in hippocampal neurons and astrocytes after experimental seizures.
Angiogenic processes appear to be concomitant to the neuro-glial reorganization which occurs in lesional epilepsy of adult patients. Even if VEGF expression reflects a protective mechanism triggered by the seizure itself, the neo-vascularization could participate in the pathological remodeling of the chronic focus (gliosis, inflammation, blood brain barrier leakage and drug resistance).

O-251
NEUROPATHOLOGIC CORRELATES OF NEW IMAGING TECHNIQUES: SUSCEPTIBILITY WEIGHTED IMAGING AS A PROMISING NEW TECHNIQUE FOR EARLY DETECTION OF CRITICAL NEUROLOGIC ABNORMALITIES

Neuropathologic correlates of new imaging techniques: susceptibility weighted imaging as a promising new technique for early detection of critical neurologic abnormalities

1RAGHAVAN Ravi, 1WYCLIFFE Nathaniel, 1OBERNAUS Andy, 1TIAN h R, 1ASHWAL Stephen, 2HACKE e M, 1KIDO Daniel
1Departments of Pathology and Neuroradiology, Loma Linda University Medical Center, CA, USA; 2MRI Institute of

Biomedical Research and Wayne State University, Detroit, MI, USA

Introduction: A relatively new method of data acquisition and image processing called susceptibility weighted imaging (SWI), that exploits susceptibility differences between signals from various tissue types, can provide more accurate information in the early diagnosis of vascular lesions, brain trauma, stroke, and tumors. Unlike conventional neuroimaging, it also has the unique capability of detecting microscopic hemorrhages, mineralization, and alterations in iron metabolism in vivo, and is a potentially useful research tool in cerebrovascular and neurodegenerative disease. Purpose of study: Till recently, very little validation of SWI has occurred from a neuropathologic perspective. An earlier retrospective study from the group had indicated that SWI is highly sensitive in detecting microscopic hemorrhages in human acute cerebral infarcts, and our group is actively involved in evaluating this technique in animal models. Methods:In a pilot experiment (approved by the Institutional Animal Care and Use Committee), four spontaneous hypertensive adult rats underwent monofilament middle cerebral artery (MCA) occlusion for 90 minutes using standard methods for inducing focal cerebral ischemia in rodents.. The monofilament was withdrawn and human recombinant tPA was administered intravenously for 30 minutes. The rats underwent neuroimaging in a Micro CT scanner, and MR imaging including spin-echo T1, T2, diffusion-weighted imaging, and SWI scans at 24, 48 and 72 hours. At 72 hours, the rats were sacrificed, and brain was examined with H&E and Prussian Blue stained sections. Results and Discussion: All rats showed infarcts in the MCA territory, of which two showed associated hemorrhage. The extent of hemorrhage seen on SWI was larger and more accurate than conventional imaging, and was confirmed by histopathology. More animals are under study to further explore the sensitivity of this technique, and additional findings will be presented. Other ongoing projects, including a rodent model for validation of SWI as a means of studying brain iron metabolism will also be discussed.

O-252
SPORADIC CREUTZFELDT-JAKOB DISEASE. CLINICAL, PATHOLOGICAL AND MOLECULAR STUDY OF 8 CASES FROM THE GALICIAN COMMUNITY.

RIVAS Eloy*, TEIJEIRA Susana*, BARROS Francisco**, SAN MILLAN Beatriz*, NAVARRO Carmen*
* Department of Pathology and Neuropathology, Hospital Meixoeiro, Vigo (Spain)
** Molecular Medicine Unit, Hospital Clinico Universitario, Santiago de Compostela (Spain)

INTRODUCTION: Sporadic Creutzfeldt-Jakob disease (sCJD) is the more common form of human transmissible spongiform encephalopathies (TSE) that may present as sporadic, genetic or infectious diseases. TSE are fatal neurodegenerative disorders caused by prions, pathological isoforms (PrPsc) of the normal cellular prion protein (PrPc). Accumulation of these protease-resistent isoforms of PrP in neural cells leads to vacuolization and cellular death. Sporadic CJD typically presents as a rapidly progressive dementia often associated with cerebellar ataxia, myoclonus, periodic sharp-wave encephalographic (EEG) activity and death within the first 6 months. Different clinical profiles can be correlated with the type of PrPsc glycoform, based on Western blot migration patterns, and the genotype at codon 129 of the prion protein gene(PRNP). We present clinical, pathological and molecular data from 8 cases of sCJD.
MATERIAL AND METHODS: From 2002 to 2004, brains from 8 patients fulfilling clinical criteria of probable CJD were studied in our Centre. Neuropathological evaluation was carried out using standard histological stains and immunohistochemistry with GFAP, b-amyloid and PrP antibodies. Western blot analysis was performed, allowing PrP differentiation of type 1 (21 kDa) and type 2 (19 kDa) based on electrophoretic mobility. Genomic DNA was extracted from brain tissue and used to determine the genotype at codon 129.
RESULTS: All cases were sporadic. Ataxia was the most frequent clinical presentation (5/8). Myoclonus was present in all cases, characteristic EEG in 5/8, positive 14-3-3 protein in CSF in 7/7, and typical MRI findings in 3/8. All but one died before 6 months after the onset. Cortical spongiosis was severe in 5/8 cases. All cases had moderate-severe lesions in basal ganglia and cerebellum. In 5 out of 7 cases, type 1 PrP isoform was detected and the other two corresponded to type 2.
CONCLUSIONS:This study confirms the phenotypic variability in sCJD and predominance of the PrP type 1 isoform. Moreover, some correlations could be established: the two cases with PrP type 2 showed atypical EEG, predominant subcortical and cerebellar involvement, plaque-like pattern of PrP deposit and a longer disease-duration in one of the two cases. The use of Western blot analysis in Neuropathology laboratory is a useful diagnostic tool in cases of TSE, allowing a rapid confirmation of the diagnosis, the differentiation of PrP isoforms and the type of prion disease.

O-253
INCREASED EXPRESSION OF PRECURSOR NERVE GROWTH FACTOR AND NEUROTROPHIN RECEPTOR P75 IS ASSOCIATED WITH NEURONAL DEGENERATION

Hun-Taek Kim1, Gina Lungu1, Paul K. Y. Wong2, George Stoica1,
1Department of Pathobiology , Texas A&M University, College Station, Texas 77843
USA;
2Department of Carcinogenesis, The University of Texas M.D. Anderson Cancer Center Science Park-Research Division, Smithville, Texas, USA

Neuronal degeneration in mice infected with the retrovirus MoMuLV-ts1 is a model for human immunodeficiency virus (HIV)-induced neurodegeneration in humans. The precursor of the neurotrophin nerve growth factor (NGF), proNGF, has been suggested to be a death-inducing ligand for the neurotrophin receptor p75 (p75NGFR) which is also induced by various injuries to the nervous system. We investigated whether expression of p75NGFR and proNGF are increased in the brainstem tissues of ts1-infected mice. Levels of proNGF and p75NGFR mRNAs and proteins were increased in the brainstem tissues of ts1-infected mice compared with controls. We demonstrate that proNGF is the predominant form of NGF in the brainstem tissues of ts1-infected mice, whereas little or no mature NGF is detected. In brainstem sections, we found that astrocytes surrounding spongiform lesions contain increased amounts of immunoreactive NGF, but little in microglial cells, and that immunoreactive p75NGFR was located in the neurons undergoing degenerative changes. Together, these data suggest that ts1 infection-mediated neuronal degeneration in mice may result from the proNGF/p75NGFR signaling pathway.

O-254
CEREBRAL AMYLOID ANGIOPATHY IS INFLUENCED BY ALZHEIMER DISEASE PATHOLOGY

Johannes Attems (1), Monika Huber (1), Kurt A.Jellinger (2), and Felix Lintner (1)

(1) Pathologic Institute, Otto Wagner Hospital, Baumgartner Höhe 1, 1140 Vienna, Austria
(2) Institut for Clinical Neurobiology, Kenyong. 18, 1070 Vienna, Austria

Background: Cerebral amyloid angiopathy CAA is defined by beta-amyloid peptide (Ab) depositions in cerebral vessels and is associated with Alzheimer disease (AD). In addition CAA has been shown recently to be an independent risk factor for cognitive decline. The relationship between sporadic CAA and AD is poorly understood and the origin of Ab in CAA remains unclear. The aim of our study was to further investigate the relationship between CAA and AD.
Material and methods: 113 autopsy brains (61.1% female, 55.8% clinically demented, age range 54-102, mean 83.5 ±9.9 years) underwent standardized neuropathological assessment of AD using CERAD, Braak stages, and NIA-RI Criteria. CAA was evaluated in frontal, frontobasal, hippocampal and occipital regions. For detection of Ab in cerebral vessels sections were immunostained with commercially available Ab antibody (4G8, Signet). The severity of Ab depositions in vessels was assessed semiquantitatively for each region separately. In 53 cases APOE genotype was evaluated using real time PCR.
Results: CAA was present in 77 cases (68.1%), with the occipital region being affected significantly more often and more severe than other regions (P<0.01). The overall prevalence of CAA was significantly higher in cases with high grade AD pathology compared to cases with no to medium grade AD pathology (P<0.01). 23.5% of brains without any AD pathology revealed CAA, while 24% with AD pathology did show no CAA. The severity of CAA significantly increased with increasing AD pathology, in the occipital region significantly stronger than in all other regions, respectively (P<0.01). Univariate ANOVA to test the combined influence of CAA, CERAD, Braak stages, NIA-RI-Crit., age, and APOE e4 on clinical dementia, revealed that only each CAA (P<0.05), CERAD, Braak stages, and NIA-RI-Crit. (P<0.01) remained significant. When controlling the positive correlation between CAA and clinical dementia seperately for each CERAD, Braak stages, and NIA-RI-Criteria, however no significance was observed.
Discussion: Our results do not unequivocally support the concept of CAA being an independent risk factor for cognitive decline but suggest a strong association of AD with CAA. There are, however, cases with severe CAA lacking AD pathology and vice versa. We conclude that CAA might be an entity of its own, which is aggravated by AD pathology and that evaluation of the occipital region is mandatory in the diagnosis of CAA.

O-255
DEVELOPMENTAL EXPRESSION OF CELLULAR PRION PROTEIN (PRPC) IN HUMAN CEREBRAL CORTEX

ADLE-BIASSETTE Homa (1,2), VERNEY Catherine (2), PEOCH Katell (3), DAUGE Marie-Christine (1), RAZAVI Féreshté (4), CHOUDAT Laurence (5), GRESSENS Pierre (2), BUDKA Herbert (6), HENIN Dominique (1,2)
1- Service d'Anatomie Pathologie, Hôpital Bichat-Claude Bernard, 75877 Paris France, 2- INSERM E9935, Hôpital Robert-Debré, 75019 Paris, France, 3- Service de Biochimie, Hôpital Lariboisière, Paris 75018, France, 4- Service d'Histologie Embryologie, Hôpital Necker-Enfants Malades, 75015 Paris, France, 5- Service d'Anatomie Pathologie, Hôpital Robert Ballanger, 93602 Aulnay sous bois Cedex, France, 6- Institute of Neurology, Medical University Vienna, AKH 4J, POB 48, A-1097, Austria

The cellular prion protein (PrPc) is an ubiquitous copper-binding membrane sialoglycoprotein. Its posttranslational modifications in prion diseases leads to the accumulation of the protease resistant conformer (PrPsc). The functions of PrPc are unknown. In adult central nervous system, PrPc is mainly a synaptic protein. We investigated the developmental expression of PrPc in the cerebral cortex of fetuses in whom was searched the polymorphism of codon 129 of PrPc gene. Five anti PrPc monoclonal antibodies (12F10, KG9, 6H4, 3F4 and BG4) were used for immunohistochemistry. Double immunofluorescence and confocal microscopy were performed using GFAP, Iba-1, MAP2, doublecortin, calretinin, synaptophysin, synapsin and GAP-43. PrPc-immunoreactivity (IR) followed the rostrocaudal gradient of development. At 11-15 gestational week (GW) PrPc IR was observed in elongating fiber tracts and in the molecular layer. Between 17 and 22 GW, in addition to growing fibers tracts, some positive neurons were detected in the subplate and in the cortical anlage. Microglial cells were also immunoreactive. From 24 WG until the perinatal period PrPc immunoreactivity was still strongly expressed in fiber tracts in the subplate. In parallel, PrPc labelling of synaptic profile increased until the perinatal period. In contrast in adults, PrPc IR was very weakly detected in the white matter and extensively present in the neuropil of the gray matter. At all ages, choroid plexus was strongly immunoreactive but ependymal staining was absent in adults. In some pathological cases, over expression of PrPc was observed in vessels, perivascular (micro)glial cells, in some neurons and axonal bundles. Our results show that during development PrPc is predominantly expressed in axonal growth cones and in synapses along synaptogenesis. It is also expressed in various nonneuronal cells. Several presumed functions of PrPc are plausible.

O-256
THE PATHOLOGICAL RESPONSE TO NEOADJUVANT TAMOXIFEN THERAPY IS ASSOCIATED WITH ERB EXPRESSION IN INVASIVE BREAST CARCINOMA

Christophe Rosty, Jerome Verine, Fabien Reyal, Patricia de Cremoux, Brigitte Sigal-Zafrani, Marick Lae, Paul Freneaux, Veronique Girre, Remy Salmon, Xavier Sastre-Garau, Anne Vincent-Salomon
Institut Curie, 26 rue d¡¯Ulm, 75005 Paris

Introduction and purpose of the study: Neoadjuvant endocrine therapy is a therapeutic option for post-menopausal women with advanced stage hormone receptor-positive invasive breast carcinoma. Estrogen receptor b (ERb) is an isoform of ER which was shown to be associated with the response to adjuvant tamoxifen therapy. To determine if ERb expression may predict response to neoadjuvant endocrine therapy, we conducted a retrospective study on 55 women treated with tamoxifen before breast surgery.
Methods: Selected patients were diagnosed with invasive breast carcinoma on needle core biopsy with significant expression of ERa, and treatment by tamoxifen during at least 3 months, followed by surgical excision of the residual tumor. Pathological response was evaluated in the surgical tumor specimen by decrease in the mitotic index (MI), using the deltaMI ratio defined as (MI before therapy ¨C MI after therapy) divided by MI before therapy. A tumor with a deltaMI value of 50% or greater was considered as responsive to therapy. Immunohistochemistry for ERb was performed using the PPG5/10 antibody (Serotec). Cases with ¡Ý10% nuclear immunostaining were considered positive.
Results: All 55 selected patients were post-menopausal women with a mean age of 70.6 ¡À 6.5 years (range: 52-83). Initial diagnosis was invasive ductal carcinoma in all cases (grade I: 36%; grade II: 53%; grade III: 11%). A clinical partial response was present in 37 patients (67%) while the remaining 25 patients had no response (4 patients, 7%) or stable disease (14 patients, 26%). deltaMI was ¡Ý50% for 21 tumors (41%), which were considered as pathological

responsive to tamoxifen. We did not observe any correlation between PR expression and the pathological response. ERb was expressed in all invasive breast carcinomas with 1% to 80% stained nuclei. The percentage of stained tumor cells was positively associated with the deltaMI ratio (r= 0.36, P = 0.01). With a 50% cut-off to define tamoxifen-responsive tumors, we found that 17/32 (53%) of ERb-positive breast carcinomas had a pathological response to therapy whereas only 4/19 (21%) ERb-negative breast carcinomas responded (P = 0.04).
Conclusion: High expression of ERb in invasive breast carcinoma is associated with a better pathological response to neoadjuvant tamoxifen therapy in post-menopausal women. This result suggests that the determination of ERb expression may be used to select patients who may benefit from neoadjuvant tamoxifen therapy.

O-257
ALLELIC IMBALANCES IN LOCALLY ADVANCED BREAST CANCERS BEFORE AND AFTER HIGH DOSE ANTHRACYCLIN / CYCLOPHOSPHAMIDE CHEMOTHERAPY

VARNA Mariana (1), SOLIMAN Hany (2), FEUGEAS Jean-Paul (2), TURPIN Elisabeth (2), ESPIE Marc (3), CHAPELIN Dominique (2), MISSET Jean-Louis (3), JANIN Anne (1), de THE Hugues (2), BERTHEAU Philippe (1)
(1) INSERM U728 and Department of Pathology, (2) Department of Biochemistry, (3) Department of Oncology, Hosp St-Louis, Paris, France

Locally advanced breast cancers (LABC) are best treated by first line chemotherapy. We previously showed in non inflammatory LABC that complete pathologic responses to high dose epirubicin / cyclophosphamide chemotherapy were observed in 60% tumours with TP53 mutations, while no complete response was observed among tumours without TP53 mutations. We hypothesized that the absence of response in tumours without TP53 mutations could be linked to epirubicin induced p53 dependant cell cycle arrest and subsequent resistance to cyclophosphamide while tumours with TP53 mutations would accumulate genetic alterations leading either to tumour progression or to complete tumour response through mitotic catastrophes.
In order to explore genetic alterations in these tumours, we analyzed allelic profiles in 32 LABC with or without TP53 mutations (10 and 22 cases, respectively), biopsied before and mastectomized after 6 courses of high dose epirubicin / cyclophosphamide, and having not responded to that treatment. After laser tissue microdissection, PCR were performed for 10 microsatellites located on chromosomes 3, 5, 7, 8, 11, 13, 16 and 17. Allelic profiles before and after chemotherapy were compared, looking for improvement or worsening of imbalances as well as new alleles. For each tumour, we analyzed the global changes of the ten allelic profiles after chemotherapy defining four categories : better, worse (including new alleles), unchanged and combined better/worse.
Our results showed 7 tumours with a “better” profile and 10 with a “worse” profile, distributed in similar proportions in both TP53 mutated and not mutated tumours. 15 tumours had “unchanged” or “combined better/worse” profiles. Clinical data and follow-up did not show significant differences between groups.
In conclusion, important changes in allelic profiles can be observed after high dose chemotherapy in LABC, with both improved and worsened profiles. Tumours showing complete disappearance of allelic imbalances after chemotherapy raise questions about the mechanisms involved in tumour cells targeting by treatments. Unexpectedly, p53 did not prove to be an important regulator of genetic changes in these settings.

O-258
PROGNOSTIC SIGNIFICANCE OF OCCULT AXILLARY LYMPH NODE METASTASIS IN EARLY BREAST CARCINOMA

FRKOVIC GRAZIO Snjezana, SUSNIK Barbara*, BRACKO Matej
Institute of Oncology Ljubljana, Slovenia
*Medical College of Wisconsin, Milwaukee, USA

Background and aims: The most relevant factor for the assessment of risk in operable breast cancer in general remains the axillary nodal status and the number of lymph nodes involved. Our study was undertaken to assess the prognostic value of occult metastases in axillary lymph nodes in patients in whom metastases were not seen on initial assessment of H&E sections and to evaluate their relative importance with regard to traditional prognostic factors and some immunohistochemical markers.
Methods: Lymph nodes from 222 patients with breast carcinoma that were originally categorized as T1N0M0 were reassessed with 3 additional H&E levels and IHC for cytokeratin. Histologic features of the primary tumour (size, type and grade, lymphovascular invasion and mitotic index) and staining for ER, PR, CEA, HER-2, p53, bcl-2 and MIB-1 were also evaluated. The results were correlated with cancer specific (CSS) and metastasis-free (MFS) survival in univariate and multivariate analysis.
Results: During the follow up (median, 15.7 years), there were 68 occurrences of distant metastasis and 53 cancer related deaths. Lymph node tumour deposits were found in 40 (18%) out of 222 cases and were classified as macrometastasis (>2 mm) in 5 cases, as micrometastasis (>0.2 mm and up to 2 mm) in 17 cases, and as individual cells or clusters (ITC, up to 0.2 mm) in 18 cases; 22 cases (10%) were thus upstaged to T1N1M0 category. Whereas the presence of ITC was of no prognostic significance, CSS and MFS were significantly worse in the group of patients with upstaged disease (P=0.02 for CSS and P=0.002 for MFS).
Apart from upstaged nodal status, mitotic index, vascular invasion, HER-2 and CEA expression were also significant predictors of MFS and CSS in univariate analysis. In multivariate analysis of the whole group, upstaged nodal status, HER-2, lymphovascular invasion and mitotic index were significant independent prognostic factors for both MFS and CSS, whereas histologic type influenced only CSS and expression of CEA only MFS. The presence of ITC was of no prognostic significance in the 'new' T1N0M0 group of patients.
Conclusions: In our study the presence of occult macro- and micrometastases but not ITC in axillary lymph nodes proved to be a significant independent prognostic factor for CSS and MFS in the group of patients with breast carcinomas that were initially regarded as T1N0M0.

O-259
C-MYC EXPRESSION IN BREAST LESIONS ASSOCIATED TO MICROCALCIFICATIONS DETECTED BY ROUTINE MAMMOGRAPHY.

LOGULLO ângela, MAZZINI renato, TAKANO daniela, OSHIMA celina, KEMP Claudio. Departamentos de Patologia e Mastologia da UNIFESP

Introduction: c-myc is a proto-oncogene associated to cell cicle control. Amplification and super-expression of c-myc is involved in early stage of many human neoplasias. Recently a possible role of c-myc in breast carcinogenesis has been hypothesized in literature.
Objective: To evaluate c-myc expression in biopsies from early detected breast lesions by mamography. To compare c-myc expression to histopatological and clinical variables.
Methods: in a retrospective analysis 51 female patients

diagnosed and treated at Universidade Federal de São Paulo from 1998 to 2003 were elected. All cases were submitted to percutaneous biopsy of breast lesions containing microcalcifications classified as BI-RADS 4 and 5 in routine mamomagraphy. Morphology and immunohistochemistry were analysed by two independent observers. Final diagnosis sub-divided the cases in two groups, non-malignant lesions and malignant lesions. C-myc expression was evaluated with standard ABC immunohistochemical essay considering nuclear staining as positive.
Results: median age was 53,7 years. From 51 cases, 20 were malignant (39,2%), including infiltrative and in situ ductal or lobular carcinoma, and 31 cases (60,8%) non-malignant (fibrocistic changes and ductal hiperplasias). C-myc was positive in 19 (37,3%) cases and negative in 32 (62,7%). Among the malignant cases, 9 (45%) were c-myc negative and 11 (55%) positive, whereas between the 31 non-malignant lesions, 8 (25,8%) exhibited c-myc expression and 23 (74,2%) were negative; with a significant association (p=0,035). However, clinical variables (age, Gynecological history, hormone therapy, evolution) did not correlate to c-myc expression in both groups.
Conclusion: c-myc protein identification was more frequent in malignant than non-malignant early detected breast lesions suggesting that alterations in c-myc expression is not a early event in breast carcinogenesis. The role of c-myc expression on detecting potential malignant lesions must be further addressed.

O-260
PROGNOSTIC SIGNIFICANCE OF A COMBINED CLINICOPATHOLOGIC SCORE FOR RESPONSE TO PRIMARY SYSTEMIC THERAPY IN LOCALLY ADVANCED BREAST CANCER

BERTHEAU Philippe, LEREBOURS Florence, MOUNIER Nicolas, DE ROQUANCOURT Anne, ESPIE Marc, CLOT Philippe, SERVANT Jean-Marie, MISSET Jean-Louis, MARTY Michel, JANIN Anne

The response to chemotherapy is one of the best indicators of prognosis in locally advanced breast cancer (LABC). The pathologic response (pR) of 108 LABC patients was analysed and compared with their clinical response (cR). Our aim was to define a new combined clinicopathologic response score (cpR) and to explore its correlation with survival data.
The 108 stage IIB to IIIB breast carcinomas were first treated with high-dose anthracycline-based chemotherapy. Standard criteria were used to assess cR. Pathologic analysis of surgical specimens allowed the definition of 5 types of pR. Three groups of combined clinicopathologic response were defined.
Twenty-two patients (20%) had complete or almost complete pR. Most patients (88, 81%) had partial cR. This large group of partial cR was very heterogeneous, ranging from pR1 to pR5 and from cpR1 to cpR3. In univariate analysis, pR and cpR both strongly correlated with EFS. cR, pR and cpR all correlated with OS. Subgroups of incomplete pathologic responses were not prognostically different. In multivariate analysis, only cpR correlated strongly with both EFS and OS ($p<0.002$), identifying good (20%), intermediate (61%) and poor (19%) prognosis patients.
In conclusion, in 108 stage IIB to IIIB breast cancer patients initially treated by high-dose chemotherapy, combined grading of clinical and pathologic responses in a single score allowed accurate prediction of outcome.

O-261
DENSITY OF VEGFR-3 POSITIVE VESSELS IN SMALL BREAST CARCINOMAS IS RELATED WITH TUMOR CELLS POSITIVITY BUT NOT WITH METASTATIC SPREAD IN AXILLARY DISTRICT

G. Canavese (§), A. Bernardi (§), G. Candelaresi (§), E Margaria (§), R. Bussone (*), R. Giani (*), E. Berardengo (§).
(§) Department of Pathology, Ospedale S. Giovanni Antica Sede, Turin, Italy
(*) Department of Surgery, Ospedale S. Giovanni Antica Sede, Turin, Italy

INTRODUCTION Neoplastic embolization and metastatic dissemination are widely recognised as main factors affecting breast tumors behaviour. Immunohistochemical expression of Flt-4/VEGFR-3, a protein involved in tumoral lymphatic angiogenesis that could have a significant role in these processes, is still scarcely indagated in these tumors. AIM OF THE STUDY To evaluate the expression of the protein Flt-4 in a group of patients with limited breast tumors and to investigate its predictive value in tumor embolization and tumor metastatic aptitude towards axillary district. METHODS 47 cases of pT1 staged (< 2 cm size) tumors treated with conservative surgery and SN resection were selected from July 2004 to january 2005 Sections from breast lesions were stained with PoAb Ftl-4 (Santa Cruz Biotech.). RESULTS Normal duct epithelium had intense membrane staining (pos+++) for Flt-4, and sporadic vessels were faintly stained in normal parenchyma. 20 tumors (46%) had good (pos++) cytoplasm positivity, associated with an intense membrane staining in 8 cases. Most intensely stained areas were mainly in peripheral portion of the tumors. In 17 cases tumor cells cytoplasm were faintly stained (pos+) with the PoAb and 3 of them presented membrane staining. 10 cases were negative. In 20 carcinomas out of 46 cases evaluated (42%) we could detect a good positivity of several small vessels (>10xHPF) in peritumoral stroma; 3 ITC and 2 metastases were detected in SN in this subgroup, and 4 of this cases had evidence of embolization in peritumoral vascular structures. In 8 cases only a small number of vessel were present (2 metastasis in SN, 3 cases with embolization), and 18 case no vascular structure were stained (1 ITC and 1 metastasis in SN, 6 cases with embolization). Only 2 of the 10 negative tumors belonged to the first group, while 8 out of the 20 tumors with intense staining fit in the same group. CONCLUSION In our study Flt-4 stained peritumoral vascular structures in 42% of the selected carcinomas: we could not find statistical relations between the occurrence of peritumoral Flt-4 positive vessels and the presence of tumoral cells (ITC and metastasis) in SN, tumoral neoangiogenesis, and evidence of peritumoral vascular embolization. Moreover, immunohistochemical expression of the protein Ftl-4 was detected in cancer cells in 46 % of cases This feature was statistically related with the occurrence of Ftl-4 positive vessels in peritumoral stroma (p= .03).

O-262
ABNORMAL EZRIN EXPRESSION IN INVASIVE BREAST CARCINOMAS

Socorro María Rodríguez-Pinilla, 1 David Sarrió,1 Ana Dotor, 2 David Hardisson, 3 and José Palacios.1
1 Breast and Gynaecological Cancer Group, Molecular Pathology Programme, Centro Nacional de Investigaciones Oncológicas (CNIO), Madrid, Spain;
2 Spanish National Tumour Bank Network, Molecular Pathology Programme, Centro Nacional de Investigaciones Oncológicas (CNIO), Madrid, Spain;
3 Department of Pathology, La Paz Hospital, Madrid, Spain;

Introduction: The membrane-cytoskeleton crosslinker ezrin is associated with malignant progression and metastasis in human neoplasias.
Material and Methods: We assessed ezrin expression in 577 breast carcinomas using tissue microarrays. Immunohistochemical staining for ezrin, p53, ki-67, phospho-

Akt, HER2, and estrogen (ER) and progesterone (PR) receptors was performed. Ezrin expression was also studied in breast cancer cell lines by confocal microscopy and western blot.
Results: Ezrin staining in normal breast epithelium localized at the apical cell surface, whereas, in most breast tumor cases (298, 64%), it localized in the cytoplasm. Complete membranous staining occurred in 114 (24%) samples, and apical staining was seen in 57 (12%) cases. Only 48 (9.3%) breast tumors did not express ezrin. There were significant positive associations between cytoplasmic ezrin localization and adverse tumor characteristics, such as higher grade, high Ki-67, p53 positivity, ER and PR negativity, and lymph-node metastases. Apical ezrin staining was associated with favorable clinicopathological features, and membranous ezrin staining with stronger p-Akt expression. Weak ezrin staining or its complete absence was associated with the presence of lymph-node metastasis, ER negativity and reduced p-Akt expression. Western blot revealed no clear differences in total ezrin levels among the breast cancer cell lines studied. However, immunofluorescence staining revealed that ER-positive, noninvasive and nontumorigenic cell lines concentrated ezrin at the apical surface, whereas invasive cell lines had more diffuse, cytoplasmic staining.
Conclusion: The abnormal ezrin expression, either negative or diffusely positive in the cytoplasm, is correlated with adverse features in invasive breast tumors and cancer cell lines.

O-263
KIT IS HIGHLY EXPRESSED IN ADENOID CYSTIC CARCINOMA OF THE BREAST, A "BASAL-LIKE" CARCINOMA ASSOCIATED WITH A FAVORABLE OUTCOME.

AZOULAY Sandy 1, LAE Marick 1, FRENEAUX Paul 1, MERLE Solange 1, ROSTY Christophe 1, AL GHUZLAN Abir 1, SIGAL-ZAFRANI Brigitte 1*, SALMON Rémy 2, FOURQUET Alain 3, SASTRE-GARAU Xavier 1, VINCENT-SALOMON Anne 1.
Departments of 1Pathology, 2 Surgery, 3 Radiotherapy, * on behalf of the Breast Cancer Study Group. Institut Curie, 26 rue d'Ulm, 75248 Paris Cedex05, France.

The objective of this study was to assess the clinical, morphological and immunophenotypic characteristics of adenoid cystic carcinoma (ACC) of the breast. Eighteen cases were identified from our files. Clinical information was available for 16 patients with a follow-up ranging from 1 to 15 years. Fifteen patients were treated by surgery followed by radiotherapy for 9 of them and one by exclusive radiotherapy. Fourteen patients were alive. Two of them presented a local recurrence. Two patients died, one of the disease (the patient was treated by radiotherapy exclusive) and one of another cause. Morphologically, all tumors were graded according to the system used for ACC of the salivary glands. Seven out of the 18 cases studied were grade I (39%), 7 grade II (39%) and 4 grade III (22%). Immunophenotype was assessed with anti ER, PR, HER-2, KIT, ''basal'' and luminal cytokeratins (CK5/6, CK8/18), Smooth Muscle Actin (SMA) and p63 antibodies. All cases were ER, PR and HER-2 negative and in contrast, all cases (100%) were KIT positive. The 18 cases were labeled with basal CK5/6, luminal CK8/18, myoepithelial p63 and SMA markers. Epithelial cells were strongly positive around glandular lumens. P63 and SMA labeled cells in solid areas and cells surrounding pseudocystic spaces. In addition, different populations of cells were identified: stem cells (CK5/6+), glandular precursor cells (CK5/6+/CK8/18+), glandular cells (CK8/18+) and myoepithelial cells (p63+/ SMA+.
Our study has showed that ACC of the breast is a special type of "basal like" breast carcinoma, harboring an excellent prognostic with a specific immunophenotype ER, PR, HER-2 negative and KIT highly positive.

O-264
IMMUNOREACTIVITY OF A SIALYLATED MUC1 EPITOPE AS DETECTED BY MONOCLONAL ANTIBODY MY1.E12 PREDICTS A BETTER PROGNOSIS OF MAMMARY CARCINOMA PATIENTS

BALDUS Stephan E., WIENAND Jens R, WERNER Jan P., LANDSBERG Stephanie, HANISCH Franz-Georg, DIENES Hans P.
Institute of Pathology and Center of Biochemistry, University of Cologne, Kerpener Str. 62, 50931 Cologne, Germany

Introduction: MUC1 represents a promising marker in breast cancer. However, due to the structural complexity of the MUC1 glycoprotein, multiple epitopes can be detected by monoclonal antibodies. This fact may be responsible for the contradictory results of previous investigations regarding the clinical and prognostic relevance of MUC1 expression in breast cancer.
Purpose: Therefore, we tried to evaluate the role of different glycosylated and non-glycoslyated MUC1 epitopes as well as other mucin-associated peptides (MUC2) and carbohydrates (Thomsen-Friedenreich antigen, sialyl-Lewis a, sialyl-Lewis x) as predictors of the clinical course and prognosis in mammary carcinomas.
Material and methods: An immunohistochemical study applying numerous monoclonal antibodies (mabs) was performed to characterize the expression of a selected panel of MUC1 epitopes, and of MUC2, Thomsen-Friedenreich antigen, sialyl-Lewis a, and sialyl-Lewis x in a series of 140 patients with breast cancer. The results were correlated with clinicopathological variables as well as overall survival.
Results: Generally, more than 90 % of the mammary cancers, were strongly stained with the MUC1-specific mabs. Especially ductal and lobular carcinomas were strongly MUC1 and sialyl Lewisa positive, whereas MUC2 binding was significantly elevated in mucinous neoplasms. Associations between the immunoreactivity of any mab under study and tumor progression as reflected by pTNM staging could not be observed. However, expression of the sialylated MUC1 epitope detected by mab MY1.E12 revealed as a favourable independent prognostic factor.
Conclusions: These results confirm that MUC1 is generally strongly expressed in mammary carcinomas. As an exception, mucinous carcinomas are significantly less MUC1 reactive, but express strongly MUC2. Our data suggest that only the presence of a sialylated short-chain MUC1 glycoform is associated with a better prognosis, whereas the other molecules under study are not correlated with the course of disease and survival probability.

Posters

P 1

CLINICAL, HISTOPATHOLOGIC AND IMMUNOHISTOCHEMICAL CHARACTERISTICS OF BREAST CANCERS PRESENTING DURING PREGNANCY OR LACTATION

Mazyar Shadman , MD.
Mohammad Sadegh Fazeli , MD.
Isa Jahanzad , MD
Shahram Nikbakhtian
Imam Khomeini General Hospital, Cancer Institute

Introduction:
As a rare condition, pregnancy associated breast cancers are of the most challenging medical issues. The poor prognosis and disappointing nature of these kinds of cancers have made them an area of research interest in the past years. There been controversy regarding the independent role of pregnancy alone in making such poor outcomes. We conducted this descriptive cases series study to determine the different aspects of this kind of breast cancer.
Method and Materials:
All the charts and medical records of breast cancer patients presenting in Cancer Institute of Imam Khomeini General Hospital were reviewed to find the patient who were pregnant or had a childbirth 6 months before the diagnosis of breast cancer. The patients were evaluated regarding the presenting complaint, diagnosis method, tumor histopathologic pattern and immunohistochemical studies like Estrogen and Progesterone receptors positivity and determining HER-2/neu (c-erb-B2) and P53. Immunohistochemical studies performed using pathologic blocks if IHC data was insufficient for the study purposes.
Results:
We found 10 patients, 7 of which were pregnant, 2 were lactating and one was in the postpartum period but not lactating. Mean age was 32 (27-38) and the mean weight was 70.9(63-81). The mean gestational age was 17.4 weeks (6-35) and the mean number of previous pregnancies was 1.8 (1-3). Seventy percent of patients had a positive history of breast-feeding with a mean of 20 months. Eight patients (80%) presented with a breast mass and two with nipple bloody discharge. One patient was in the Stage 1 (10%), 6 patients in Stage 2 and 3 in the stage 3. The most common histopathologic pattern has been Invasive ductal Carcinoma (7 Patients, 70%) followed by Invasive lobular (1 Patients, 10%) and Mocinous (1 Patients, 10%) and pure DIC (1 Patients ,10%).
50% of patients were ER positive , 62.5 % PR positive and 57.1 % were positive for both. P53 and HER-2/neu has been positive in 50% and 33% of patients, respectively.
Conclusion:
Most of the obtained results were comparable with previous studies. Because of the controversial nature of the disease, further studies for comparison between such patients and non-pregnancy associated breast cancer patients are needed considering the different confounding factors. Because of determination of most important confounding factors, Data of current study can be used as a base for further cohort studies.

P 2

TNM STAGING AND CLASSIFICATION OF BREAST CANCER (FAMILIAL AND NON-FAMILIAL) IN JORDANIAN FEMALES

Dr. Manr Atoum and Dr. Salem Akel

Introduction: Cancer becomes one of the most common diseases in our lives today, and breast cancer is the women's worst enemy.
Purpose: Staging or morphology of breast tumor has important implications for treatment and prognosis and it would be of interest to determine the relation between various morphological types and age of patient as well as the frequency of each stage among familial and non-familial breast cancer.
Results: Out of ninety-nine breast cancer females enrolled in this study, forty three were familial females and fifty six were non-familial females. Breast cancer cases were staged depending on the combination of TNM category into in situ, early invasive, advanced invasive and metastatic.
One female breast cancer Jordanian females was diagnosed with in situ cancer, fifty cases were in early stages of invasive cancer. The remaining was diagnosed with advanced invasive (29 cases) and metastatic (19 cases) breast cancer.
Stage 2b was the most common stage of early invasive cases and represented 48% of the staged cases. On the other hand, among cases diagnosed with advanced invasive breast cancer, stage 3a was the most common stage and represented 89.6% of cases. Interestingly, all cases of stage 3a belonged to TNM stages of T2N2M0 and T3N1M0. The tumor size in all cases of Jordanian females diagnosed with advanced invasive breast cancer exceeded the 2 cm size.
The incidence of non familial breast cancer was slightly higher (56.4%) than that of familial type (43.4%) among studied Jordanian females. Sixty two percent of cases diagnosed as early invasive belonged to familial breast cancer type. In contrast, most (72% and 84%) of advanced invasive and metastatic breast cancer cases, respectively were of non familial type.
Young females below 40 years were diagnosed with in situ (5.2%), early invasive (26.3%), advanced invasive (31.6%) and metastatic (36.8%) breast cancer. Among females older than 40 years, frequency of early invasive stage was higher (56.3%) than that of advanced invasive (28.7%) and metastatic (15.0%). Among age of 51-60 years, cases of early invasive represented 63.9% of cases.
Conclusion: Non-familial breast cancer is more common than familial breast cancer, most breast cancer females were diagnosed at early invasive stage. Non familial breast cancer were more frequent at lower stage, while familial breast cancer were more frequent at higher stage.

P 3

PAGET DISEASE (PD) OF THE NIPPLE MAY BE DERIVED FROM LOBULAR CARCINOMA IN SITU (LCIS).

Sabine Fransis, MD; Isabelle Vandenbempt; Maria Drijkoningen, MD, PhD.
Pathology Department, University Hospital Leuven, Leuven, Belgium.

PD occurs in about 1-4% of patients with breast cancer and is characterized by the presence of neoplastic "glandular" cells within the epidermis of the nipple-areola complex. PD is usually associated with poorly differentiated ductal carcinoma in situ (DCIS) located in the lactiferous ducts, with or without invasive ductal adenocarcinoma (IDC). DCIS and PD show similar morphological features and an identical immunocytochemical (ICC) profile: both are positive for low molecular weight cytokeratins (CK), HER-2/neu and carcino-embryonic antigen (CEA).Therefore, PD is regarded as a high grade DCIS that is present in the epidermis. The intra-epidermal location of PD cells may be explained by epidermotropic migration of cells of the underlying DCIS, facilitated by the HER-2/neu receptor.
In our lab, 11 of the 570 mastectomies received between 1/8/2001 and 31/12/2004, showed PD. 8/11 cases were associated with poorly differentiated DCIS and IDC. However, in 3/11 cases LCIS and invasive lobular carcinoma (ILC) were present. In all 3 cases, LCIS extended into the

lactiferous ducts and PD consisted of single cells only. Cells of ILC, LCIS as well as PD expressed CK 8/18, epithelial membrane antigen (EMA) and CEA, but were consistently negative for epithelial cadherin (E-cadherin) and HER-2/neu. Expression of CK8/18, EMA and CEA is suggests glandular differentiation, while absence of E-cadherin typically points towards a lobular phenotype. However, in PD cells the absence of staining for E-cadherin was difficult to corroborate, since they are sprinkled as single cells in between E-cadherin positive keratinocytes. The strongest evidence against an origin from DCIS in these 3 cases lies in the absence of HER-2/neu overexpression by PD cells.
In conclusion, morphologic as well as ICC findings indicate that in these 3 cases PD is not derived from DCIS, but from LCIS. To our knowledge, only one such case has been previously reported by Rosen et al, 2002. As a consequence, the mechanism by which PD cells end up in the epidermis has to be re-evaluated , since it is obvious that in PD derived from LCIS, there is no role for HER-2/neu as an facilitator of intra-epidermal migration of adenocarcinoma in situ cells.

P 4
PROGNOSTIC FACTORS OF NODE METASTASES IN PT1 BREAST CANCER
L Costarelli, FR Piro, L Fortunato(*), CE Vitelli(*), M Farina(*) M Giordano, M Taffuri, I Nofroni(°) and M Amini
"S.Giovanni Addolorata" Hospital, Department of Pathology - Roma, Italy
"MG Vannini" Hospital, Department of Surgery (*) – Roma, Italy
"La Sapienza" University of Rome, Department of Experimental Pathology and Medicine-Medical Statistics (°) – Roma, Italy

Introduction: The axillary lymph node status of patients with newly diagnosed breast cancer remains the most important prognostic information available at the moment. The incidence of metastases in axillary lymph node (MAL) is related with the neoplasia's diameter. In breast cancer < cm1 in diameter, it has been observed a low incidence of MAL, because only a minority of patients presents with such node metastases at diagnosis. It may be possible to forecast the MAL by prognostic factors variation other than axillary lymph node dissection.
Purpose: We reviewed our database to find which factors are associated with MAL.
Methods: We studied 500 consecutive cases of breast cancer < or equal 2 cm in diameter (pT1) from 1999 to 2004 and we evaluated immunoistochemistry expression of the estrogenic and progestinic receptors and prognostic factors pS2, Ki67, bcl2, p53 e c-erbB2 (neu). We considered positive the nuclear (ER, PgR, p53), cytoplasmatic (pS2 e bcl2) and complete of membrane (neu) expression in over than 10% cells. Proliferative Index was calculated with immunoistochemitry expression of Ki67. These dates are related with MAL, grade and istotype of the tumor, diameter of the neoplasia, patient's age, multifocale tumoral nodes. The statistical analysis was performed with c2 test and a multiple regression logistic model.
Results: Significative statistical resultes were observed as like as MAL and age (p<0,01), MAL and tumoral grade (p<0,001), MAL and tumoral size (p<0,001), MAL and P.I. (p<0,001) and MAL and p53 expression (p<0,01). We did not observed statistical correlance between MAL and tumoral type, multifocal tumor, ormonal receptrors expression , PS2, bcl-2 and c-erbB2. Cut off was 6.5 with sensivity of 77,2% and specifity of 50%. ROC-curve result was 0,69.
Conclusion: We found that age inferior to 50 years, high grade, diameter superior to cm 1, elevated ki-67 and expression of oncogene p-53 are all factors associated with lymph node metastases

P 5
SENTINEL LYMPH NODE IN BREAST CANCER: IS IT POSSIBLE A STANDARD EXAMINATION?
M Amini, L Costarelli, FR Piro, L Fortunato (*), M Farina (*), A Dell'Osso(**), CE Vitelli (*)
"San Giovanni Addolorata Hospital", Department of Pathology and
Surgical (**) Rome - Italy
"MG Vannini Hospital", Department of Surgical (*) Rome - Italy

Introduction: Sentinel lymph node (SLN) biopsy allows enhanced pathology through serial sections and immunoistochemical analysis of the retrieved node, with detection of micrometastases (MICRO) and isolated tumor cells (ITC) not otherwise recognized and this tecnique is usually applied in most of surgical oncology centers.
Purpose: We present our experience with an effective protocol for analysis of SLN in breast cancer.
Methods: We studied 416 consecutive patients (median age 63 years) with primary breast cancer (median diameter 1.5 cm) who underwent SLN biopsy from March 2001 to December 2004 in two different hospital. After surgery, SLN's were step sectioned. First section obtained was called "Level 0" and routinely processed. If first section was negative, at least six additional couples of sections were obtained from each SLN at 100 micron distance (Level I, II and III) and were analysed with conventional staining and immunohistochemistry (IHC–MNF 116). SLN metastases were classified according to TNM 2002 and called MICRO when less than 2mm in diameter and ITC when less than 0,2 mm in diameter.
Results: With conventional analysis, SLN was positive al Level 0 in 25% of cases (106/416). Further metastases or ITC was discovered in 14,5 cases (61/416): 8,9% at Level I, 4% at Level II and 1,6% at level III, of which ITC were 62% (38/61), MICRO were 36% (22/61) and 2% were macrometastases (1/61). Our protocol discovered MICRO or ITC in 13% of patients with tumors less than 2 cm in diameter (T1) and in 15% of those more than 2 cm in diameter (T2) (p=0.7). Evidence of MICRO and ITC at level III was 1,3% in T1 patients and 3,8% in T2.
Conclusions: SLN step analysis is most useful to discover MICRO and ITC in a good percentage of cases. This tecnique allows to study more accurately women with breast cancer. Our protocol seems best possible because in our experience the incidence of MICRO and ITC at Level III is very low, expecially in T2 tumors. Currently, it doesn't known which is prognostic relevance of MICRO and ITC

P 6
FINE NEEDLE ASPIRATION CYTOLOGY OF MAMMARY CARCINOMA WITH OSTEOCLAST-LIKE GIANT CELLS. A REPORT OF NINE CASES
GONZALEZ-PERAMATO Pilar, JIMENEZ-HEFFERNAN Jose A, VICANDI Blanca, LOPEZ-FERRER Pilar, PEREZ-CAMPOS Ana, HARDISSON David, VIGUER Jose M.
Departments of Pathology, University Hospitals Guadalajara and La Paz, Madrid, Spain

Inroduction: Carcinoma with osteoclast-like giant cells (OCGC)is an uncommon neoplasm characterized by giant cells, prominent vascularization, haemorrhage and areas of cribriform epithelial growth with moderate atypia. Multinucleated giant cells have been described in several other breast lesions raising an interesting differential diagnosis, mainly with benign disorders. Due to its rarity few cases have been described cytologically.
Purpose of the study: To determine if mammary carcinoma with OCGC shows cytologic features characteristic enough to

permit a specific preoperative diagnosis using fine needle aspiration.
Methods: We retrospectively reviewed 13 fine needle aspiration samples from 9 patients with this variant of carcinoma. Nine corresponded to breast tumours and four to axillary, liver, subcutaneous and mediastinal metastatic lesions. The expression of CD68 by giant cells was evaluated immunocytochemically in six cases. All patients had a complete pathologic study of the breast neoplasm.
Results: Smears showed a double component of epithelial and giant cells. Epithelial clusters were predominantly of intermediate size with irregular contours. Most were cohesive but others showed cellular dissociation with scarce to moderate cellular pleomorphism. Giant cells had a well defined, deeply stained cytoplasm and round to elongated morphology. Two metastatic cases were devoid of them. Hemosiderin-laden macrophages were common in smears from breast tumors. In the six cases tested CD68 was expressed in multinucleated giant cells. Except for one case that was diagnosed as suspicious of malignancy all the cytologic diagnoses were of carcinoma. There were no false negative diagnosis.
Cconclusion: Cytologic features of mammary carcinoma with osteoclast-like giant cells correlate closely with the histologic ones. Most cases are clearly recognizable as malignant but in others cytologic atypia may be minimal mimicking a benign lesion. In difficult cases the presence of hemosiderin-laden macrophages and the histiocytic nature of the MGC are helpful diagnostic features.

P 7

PATHOLOGY EVENTS (MALIGNANT OR NOT) IN PATIENTS WITH BREAST CANCER TREATED WITH TAMOXIFEN WITH OR WITHOUT CHEMOTHERAPY

Arapantoni-Dadioti P., Britsou M., Terzi M., Trihia H., Tzaida O., Lekka J.
Pathology Dpt. METAXA Cancer Hospital , PIRAEUS - GREECE

The benefit from prolonged use of tamoxifen in reducing the incidence of breast carcinoma is considered sufficiently great to justify its use as a chemopreventive agent despite the risk of undesirable side effects.
AIMS: To determine the spectrum of pathological findings in breast cancer patients treated with tamoxifen.
METHODS: The study population comprised 109 breast cancer patients, out of 1009 diagnosed with the disease in our laboratory over a period of five years (1997-2001). The above patients were treated with tamoxifen and presented with secondary pathological findings, other than metastatic disease. The data were collected retrospectively and included 73 patients with D&C and hysterectomy/oophorectomy specimens for tamoxifen-associated gynaecological symptoms and 36 patients with other than gynaecological pathology.
RESULTS: Of the 73 patients who underwent D&C or surgery for gynaecological symptoms, 28 had normal endometrium (16 atrophic), 15 simple hyperplasias, 30 hyperplastic endometrial polyps, 5 endometrial carcinomas, 5 endometrial sarcomas, 18 leiomyomas, 8 adenomyomatosis, 6 ovarian cysts, 2 ovarian endometriosis, 1 ovarian adenocarcinoma, 6 ovarian stromal tumors, 1 ovarian teratoma, 2 Brenner tumors, 3 CINIII and 1 squamous carcinoma of the cervix.
In 12 patients, a second malignancy, other than gynaecological, was diagnosed: 3 in the contralateral breast, 2 renal cell carcinomas, 3 thyroid carcinomas, 1 urothelial carcinoma, 1 adenocarcinoma of the colon, 1 Hodgkin's disease and 1 multiple myeloma.
In 9 patients there were diagnosed 3 adenomas of the colon, 2 neurofibromas and 1 GIST.
In the remaining 15 patients, the specimens concerned gallbladders with lithiasis or chronic cholecystitis.
CONCLUSIONS: In our study 67% of the women treated with tamoxifen presented with gynaecological-related pathology concerning the endometrium and the ovaries, 16,4% of which were malignant in nature. In 11% malignant disease in other organs was diagnosed. Interestingly 13,7% of the patients showed biliary tract- related problems, propably due to tamoxifen-producing cholestasis.

P 8

PLEOMORPHIC LOBULAR NEOPLASIA (PLN) OF THE BREAST NEEDS TO BE EXCISED AND BEHAVES LIKE A PRE-INVASIVE ENTITY: AN HISTOLOGIC AND PHENOTYPIC STUDY FROM A SERIE OF 15 NEEDLE CORE BIOPSIES (NCB) AND THEIR SUBSEQUENT SURGICAL SPECIMENS

BIBEAU frédéric 1, CHATEAU marie-christine 1, MICHENET patrick 2, BORRELLY cécile 1, ESSLIMANI-SAHLA majida 1, DELFOUR christophe 1 , LAVAILL rosy 1, BOISSIERE florence 1, MASSON Bruno 1. 1 Pathology and Radiology Departments, Val d'Aurelle Cancer Center, Montpellier, France, 2 Pathology Department, Hôpital La Source, Orléans, France.

Introduction: Lobular neoplasia is considered to be a marker of cancer risk, but its appropriate management is still controversial. The increasing use of percutaneous NCB for non palpable breast lesions, has highlighted evolving entities such as PLN.
Purpose: Our goal is to emphasize this pleomorphic variant, whose presentation differs from the classical form of lobular neoplasia and whose recognition has clinical relevance.
Methods: Fifteen PLN were primarly diagnosed from fourteen 8 or 11 Gauge (G) Mammotome® procedures, using stereotactic mammography and one 14 G biopsy, using ultrasound guidance. All PLN, but one, were mammographically detectable, because of microcalcifications. Subsequent surgical specimens were obtained in 13 cases, during which 7 sentinel lymph node procedures or 3 axillary dissection were performed. An immunohistochemical study for estrogen and progesteron receptors (ER, PR), c-erbB2, E-Cadherin and high molecular weight cytokeratin 34 beta E-12 (HMW-CK), was realized on NCB and excision specimens.
Results: Among the 15 PLN cases, 5 were associated with an invasive lobular carcinoma (ILC) and 3 with a microinvasive lobular carcinoma. Seven invasive or microinvasive cases were already identified on NCB. One ILC was identified on the surgical resection alone. ILC and microinvasive carcinoma were always closely located to the PLN areas, both on biopsies and surgical specimens. Morphologically, PLN cases were composed of pleomorphic, dyshesive cells with comedo-like, apocrine and signet ring features. Comedo-like patterns with central necrosis were associated with microcalcifications. PLN presented the following phenotype: ER 13+/15, RP 5+/15, CerbB2 3+/15, E-cadherin 0+/15, HMW-CK 15+/15. PLN and their invasive/microinvasive counterparts shared a similar phenotype. Two metastatic axillary involvement were noted.
Conclusions: These clinical, histological and phenotypic data support the evidence that PLN looks more like a preinvasive lesion than a marker of increased risk. Thus, percutaneous biopsies with PLN should be evaluated diligently for the presence of an invasive or microinvasive lobular component and require a subsequent surgical excision. Pathologists, as well as physicians involved in the management of breast disease, should be aware of this mammographically detectable entity, which has distinct histologic patterns and behaviour.

P 9

PROGNOSTIC FACTORS IN PRIMARY MUCINOUS BREAST CARCINOMAS

Ulrika Klopèiè, Snježana Frkoviæ-Grazio*, Marija Us-Krašovec
Department of Cytopathology and Department of Pathology*, Institute of Oncology, Zaloška cesta 2, 1000 Ljubljana, Slovenia

Background
Pure and mixed mucinous breast carcinomas (MCs) are separate morphological entities, with different biological potential and prognosis. The recent WHO classification of breast carcinomas suggests that 100%, and not the generally used 90% cut-off value, of mucinous component must be present for a diagnosis of pure MC.
Aims of the study
To analyse clinical, cytological and histological features of MCs of the breast and to determine their prognostic significance.
Material and methods
Altogether 98 patients with primary breast MCs were included in the study. A mucinous component of 90% has been routinely required for pure MCs at our institution. Clinical (age of patient, tumour size, regional lymph nodes status, distant metastases, treatment), cytological (amount of mucin, sample cellularity, nuclear pleomorphism, cytoplasmic features, presence of capillaries), histological (grade, amount of mucin) parameters, and DNA ploidy were assessed and their influence on survival was analysed.
Results
Among 98 breast MCs, 64 were classified as pure and 34 as mixed. Regional lymph node metastases were found in 5 of 60 pure MCs and in 21 of 30 mixed MCs. Distant metastases were present in 5 of 64 pure MCs and in 17 of 34 mixed MCs. Overall 5 and 10 year survival for pure MCs was 89.0% and 83.0%, and 78.9% and 46.5% for mixed MC. The difference in survival was statistically significant ($p=0.004$).
Univariate analysis revealed that histological type, axillary lymph node status, tumour size and cytologically assessed nuclear pleomorphism had a statistically significant impact on survival ($p<0.05$). The histological type and size of tumour influenced survival of patients without axillary lymph node metastases. Axillary lymph node status and tumour size were found by multivariate analysis to be independent prognostic factors.
The 5 and 10 year survival was 93.7% for MCs with 100% of mucinous component, but dropped to 85.3% and 65.1% for MCs containing about 90% of mucinous component ($p>0.05$).
Conclusions
Regional lymph node status is the most important independent prognostic factor for breast MCs, followed by tumour size.
The present study supports the recent recommendations by WHO classification of breast carcinomas that 100% and not 90% of mucinous component is required for pure MCs. Since the component other than mucinous has a great influence on the survival of patients with MCs of the breast, a meticulous sampling of the tumour is necessary.

P 10

METASTATIC INVOLVEMENT IN INTERPECTORAL (ROTTER'S) LYMPH NODES RELATED TO LOCATION, SIZE AND GRADE OF BREAST CANCER

VELIMIR VRDOLJAK Danko, KNEŽEVIÆ Fabijan
University Hospital for Tumors, Zagreb, Croatia

Aims and background: The study was aimed at analyzing metastatic involvement in interpectoral (Rotter's) lymph nodes related to site, size and grade in primary breast cancer.
Methods: The study includes 210 female patients undergoing surgery for breast cancer at the University Hospital for Tumors, Zagreb, Croatia from November 2001 to March 2004. In addition to the standard surgical procedure, interpectoral (Rotter's) lymph nodes were removed in all of the patients. Metastatic involvement of interpectoral lymph nodes was confirmed by histological and immunohistocemical examinations.
Results: Rotter's lymph nodes were identified in 66,2% of the patients, with metastatic involvement revealed in 18,5% of the Rotter's nodes. Metastatic involvement of Rotter's nodes in patients with negative and positive axillary lymph nodes was 2,8% and 34,6%, respectively. Considering location of the tumor in patients with metastatic involvement of Rotter's nodes, it was shown that tumors located in the upper breast quadrants were more prone to metastasis to Rotter's nodes, demonstrating a significant positive correlation between tumor location within the breast and positive Rotter's lymph nodes ($r=0.93$, $p=0.02$). As regards tumor size, Rotter's nodes were identified in 15%, 20% and 60% of stage T1 (<2 cm), T2 (2-5 cm) and T3 tumors (>5 cm), respectively with a significant positive correlation ($r=0.759$, $p=0.09$). Also considering tumor grade it was shown that metastatic involvement of Rotter's lymph nodes was 3,8%, 17,6% and 31,6% of histological grade I,II and III, respectivly with a significant positive correlation ($r=0.993$, $p=0.08$).
Conclusions: The results show that almost one-fifth of breast cancer patients, or even one-third of them with positive axillary lymph nodes, are discharged with positive interpectoral lymph nodes that remain undiagnozed and non-extirpated. As the interpectoral nodes can be surgically removed without additional mutilation, the exploration of Rotter's lymph nodes should be introduced into routine clinical practice. In upper breast quadrants tumors were more prone to metastase in to Rotter's nodes, as well as higher tumor size and grade.
Key words: breast cancer, interpectoral (Rotter's) lymph nodes

P 11

OUTCOME OF PURE AND ATYPICAL MEDULLARY CARCINOMAS OF THE BREAST

KARAYIGIT Ebru (*), YAVUZ Ekrem (*), TUZLALI Sýtký (*), ILHAN Rýdvan (*), DERIN Duygu (†), GUNEY Neþe (†), ASOGLU Oktar (**), AKHAN Süleyman (***), IPLIKCI Altan (*)
Istanbul University, Istanbul Faculty of Medicine, Departments of Pathology (*), General Surgery (**) and Gynecology & Obstetrics (***)
Istanbul University, Institute of Oncology, Department of Medical Oncology (†), Turkey

Pure medullary carcinoma (PMC) of the breast is a rare neoplasm. Using strict morphologic diagnostic criteria, it usually displays a favourable outcome. Atypical medullary carcinoma (AMC) of the breast has some medullary features and its prognostic significance is controversial. In this study, we aimed to compare our PMC and AMC cases, using clinicopathological findings and to reach a conclusion, concerning the diagnostic criteria of breast carcinomas with medullary features. For this reason, we retrieved 19 cases of PMC and 106 cases of AMC from almost 4000 breast carcinomas that were diagnosed at our department between years of 1988 and 2004. Of these, 7 PMC and 48 AMC cases with available follow-up were compared. The following data, including patient age, menopausal status, tumor size, grade, stage, lymph node status, estrogen and progesterone receptor status, existence of distant metastasis, disease free survival (DFS) and overall survival (OS) were recorded as well. The median follow-up time was 55 (range 8-156) months for all the cases (n=55), 96 (range 13-145) months for PMC cases (n=7) and 48 (range 8-156) months for AMC cases (n=48). All of the PMC cases were lymph node-negative, while 20 AMC cases showed lymph node metastasis. None of the PMC patients has died, while 8 patients with AMC had died during the follow-up. No recurrence was noted, except for a patient

who developed a new primary PMC at the contralateral breast 7 years after the diagnosis, among the PMC cases. Cumulative survival rates of the AMC cases was 69.7 % at sixty-five months with Kaplan Meier analysis (SE: 0.091). There was no significant difference between the survival curves of two groups by log-rank test with Kaplan Meier analysis (log-rank:1.86, df:1, p:0.172). We concluded that a favourable outcome can be expected for PMCs and some AMCs. Also, a redefinition of morphologic diagnostic criteria should be made for breast carcinomas with medullary features.

P 12
PANNICULITIS-LIKE INVASIVE CARCINOMA OF THE BREAST

ICHIHARA Shu, MORITANI Suzuko
Department of Pathology, Nagoya Medical Center

Introduction: In the boundary between the invasive mammary carcinoma and the adipose tissue, isolated or groups of infiltrating tumor cells are often blended with fat cells. This pattern is responsible for an echogenic rim surrounding the hypoechoic mass of invasive breast carcinoma observed by ultrasound. We termed this pattern panniculitis-like infiltration (PLI) because this pattern resembles inflammation of the adipose tissue. Invasive lobular carcinomas are occasionally composed predominantly of PLI without a significant desmoplastic reaction, resulting in a spider• fs web-like structure. However, the clinicopathological significance of such pattern in non-lobular invasive carcinomas are not known. Methods: We reviewed all the histological slides of 155 consecutive invasive carcinomas of the breast and classified the degree of PLI into three degrees; PLI-1 (<10%), PLI-2 (10-50%) and PLI-3 (>50%) according to the extent of this pattern in invasive area. The relationships between PLI and histological types, grade, steroid receptors, lymph node status were examined. Results: We found that the number of cases in invasive mammary carcinoma with PLI-1, PLI-2 and PLI-3 were 113 (73%), 30 (19%) and 12 (8%), respectively. Invasive mammary carcinoma with PLI-3 was composed of 9 panniculitis-like invasive ductal carcinomas (PLIDC) and 3 panniculitis-like invasive lobular carcinomas (PLILC). Remarkably, two PLIDC were composed purely (>90%) of this pattern and presented echogenic masses without hypoechoic cores in fatty breast of the elderly women. Pure PLIDC and PLILC may be overlooked unless the examiners keep this unusual ultrasound pattern of invasive carcinoma in mind. Mammographically, most PLIDC presented distortion or spiculated masses less dense than common invasive ductal carcinoma. Most (11/12) PLIDC and PLILC showed estrogen-receptor positive and HER2 negative immuno-phenotypes (P<0.05). In spite of relatively small size by palpation, the half cases had positive axillary lymph nodes. Definite diagnosis by aspiration cytology was unsuccessful in five cases. This is due to hypocellularity and frequent co-existence of benign ductal elements in the cytological specimens. Core needle biopsy may be a more reliable tool for pre-operative diagnosis of PLIDC and PLILC.
Conclusions: Panniculitis-like invasive carcinoma is a new clinicopathological entity with unique histopathological and ultrasound features.

P 13
ACCURACY OF TYPING AND GRADING MAMMARY LESIONS ON CORE BIOPSIES AND COMPARISON WITH THE EXCISIONAL SPECIMENS.

CATTANI Maria Grazia
U.O. Anatomia Patologica, Ospedale Maggiore, Azienda USL Bologna, Bologna (Italy)

INTRODUCTION. Needle core biopsy of palpable lesion (NCB;14 gauge) and stereotactic vacuum assisted biopsy (SVAB;11 gauge) of non-palpable mass are the majors preoperative methods of breast diagnosis. The UKNHS Breast Screening Project recommends the use of a core biopsy reporting form that recognize five diagnostic categories (B1-B5). Purpose of this study was to evaluate the incidence and the predictive value of the two categories: B4 (suspicious of malignancy) and B3 (lesion of uncertain malignant potential) in lesions diagnosed by NCB and SVAB and to assess the accuracy of the two methods in typing and grading infiltrating and in situ breast carcinomas.
MATERIALS AND METHODS. 2170 core biopsies (893 NCB and 1277 SVAB) were performed between January 2000 and February 2005. In 879 cases, the correlation between biopsy results and subsequent surgical excision was available.
RESULTS. The frequency of B3 diagnosis was 8 % (72 cases) in NCB and 9 % (115 cases) in SVAB. The B4 category was reported in 7 % (62 cases) of NCB and in 3 % (38 cases) of SVAB. At definitive histology, 24 % of B3 (NCB:32 cases, SVAB:12 cases) and 87 % of B4 (NCB: 54 cases, SVAB: 33 cases) showed invasive carcinomas or ductal carcinoma in situ. Type and grade of the invasive and in situ carcinoma, were determined in both biopsy and definitive excision and the results compared. For histological type, 12 % of NCB and 3 % of SVAB were changed to a different category. The agreement with overall grade was of 85 % with SVAB and of 62 % with NCB. On 94 cases that differed, 98 % differed by one grade and 63 % were upgraded.
CONCLUSIONS. SVAB has been shown to have a greater accuracy in diagnosis, mainly because of the increased quality and quantity of tissue obtained. However, the incidence of B3 category is comparable with SVAB and NCB methods. This behaviour could be explained considering that the B3 category often refers to atypical intraductal epithelial proliferation, most frequently associated to clustered microcalcifications sampled by SVAB. Grading based on NCB is not as accurate as SVAB, and its evaluation should be delayed until the surgical specimen examination.

P 14
AUTOMATIC CLASSIFICATION OF CLUSTERED MICROCALCIFICATIONS IN BREAST CANCER

Marek Ustymowicz1 and Katarzyna Guziñska-Ustymowicz2
1 Technical University of Bialystok, Mechanical Department, Bialystok, Poland,
2 Medical University of Bialystok,

Introduction: Breast cancer is a significant public health problem worldwide. Plenty of mammographic screening programs resulted in the detection of breast carcinomas at early stage. The presence of microcalcifications in mammogram not only correlates with breast cancer in many cases, but also sometimes is the only early sign of this disease. Nowadays, Computer Aided Diagnosis (CAD) systems may help radiologists detecting and classifying clustered microcalcifications, which is vital for proper treatment.
Objectives: The objective of this work was to evaluate the performance of the computerized classification method for automatically detected clusters of microcalcifications.
Materials and Methods: In our research we used 106 images from Digital Database for Screening Mammography (DDSM), among which 67 presented malignant and 39 benign cases. Our experiments were carried out in two steps: automatic detection and automatic classification. For the detection, previously developed morphological method has been used. Before the classification task was conducted, the whole set of mammograms was divided into two groups: training and testing sets, including the same number of images. Only images from training set were used to train the

Support Vector Machine (SVM) classifier. The performance of the classifier has been tested on images from testing set.
Results: Automatic classification of clustered microcalcifications in mammograms is a final stage of CAD system which helps the radiologist in diagnosis. According to ROC analysis the presented algorithms yielded Az=95,23%.
Conclusions: The SVM classifier used in experiments gave very good results and will be used in further research on complex CAD system.

P 15
BILATERAL BREAST CARCINOMA – THE HISTOLOGICAL PATTERN
P. Wisniewski MD, K. Socha MD PhD*, J. Patera MD, W. Kozlowski MD PhD
Department of Clinical Pathology, Military Medical Institute, Warsaw, Poland

Histological grade and tumor biology remain important predictors of clinical behaviour of breast carcinomas. The aim of this study was to compare the histopathological and genetical / BRCA-1 mutation/ patterns of breast carcinomas in women who underwent a surgery due to invasive carcinomas and in which the bilateral invasive carcinoma presence was ascertained.
From 1995 to 2004 year 542 women underwent mastectomy in our Military Medical Institute. In 13 patients /2.4%/ a bilateral invasive carcinoma was diagnosed. There were 9 synchronous and 3 metachronous breast carcinoma patients. In order to estimate the estrogen /ER/ and progesteron /PR/ receptors status and an overexpression of HER2 in primary tumors immunohistochemical examinations were performed. Furthermore, these receptors rates/expression was evaluated in metastases to regional lymph nodes and in remote metastases. In 10 patients the presence of the invasive ductal carcinoma was ascertained in one breast at least; in 6 cases the ductal carcinoma was bilateral. The tubular carcinoma was diagnosed in 4 patients / in 1 woman it was bilateral/. The lobular carcinoma was diagnosed in 3 cases /in 2 cases it was bilaterally/.
There was no difference found in the status of ER, PR in patients with bilateral tumors of the identical histopathological pattern. No correlation of receptor's status was stated in all other cases. In metastases the ER and PR status corresponded with the receptor's status of one of primary tumors. BRCA-1 mutation analysis confirmed its presence in 1.4% of 427 examined breast carcinoma cases but none woman with bilateral cancer carried such mutation. Compare to unilateral cancers the bilateral one was mostly present in women under the 40 year of age. Thus, also the other genetical risk factors should be searched in order to predict the development of bilateral breast cancer. Our findings indicate that synchronous bilateral breast carcinoma showed a higher frequency of invasive ductal carcinoma. Also they indicate problems in estimating the TNM status of bilateral cancers, especially concerning metastases into regional lymphnodes. The examination of receptors rates and HER2 overexpression of both tumors in bilateral breast carcinomas and their metastases is required and their analysis remains an important predictor of the clinical behaviour of breast carcinomas.

P 16
PANNICULITIS-LIKE BREAST CANCER
ICHIHARA Shu, MORITANI Suzuko
Departmant of Pathology, Nagoya Medical Center

Background: In the boundary between the invasive mammary carcinoma and the adipose tissue, isolated or groups of infiltrating tumor cells are often blended with fat cells. This pattern is responsible for an echogenic rim surrounding the hypoechoic mass of invasive breast carcinoma observed by ultrasound. We termed this pattern panniculitis-like infiltration (PLI) because this pattern resembles inflammation of the adipose tissue. Invasive lobular carcinomas (ILC) are occasionally composed predominantly of PLI without a significant desmoplastic reaction, resulting in a peculiar spider'
s web-like structure. However, the frequency and clinicopathological significance of such lace-like pattern in invasive ductal carcinomas (IDC) is unknown. Material and Methods: We reviewed all the histological slides of
155 consecutive invasive carcinomas of the breast and classified the degree of ! PLI into three degrees; PLI-1 (<10%), PLI-2 (10-50%) and PLI-3 (>50%) according to the extent of this pattern in invasive area. The relation of PLI to histological types, grade, hormone receptor and lymph node status were examined. Results: We found that the number of cases in invasive mammary carcinoma with PLI-1, PLI-2 and PLI-3 were 113 (73%), 30 (19%) and
12 (8%), respectively. Invasive mammary carcinoma with PLI-3 was composed of
9 IDC and 3 ILC. Remarkably, two IDC with PLI-3 were composed solely (>90%) of this pattern and presented pure echogenic masses without hypoechoic cores in fatty breast of the elderly women. Pure panniculitis-like IDC and ILC may be overlooked unless the examiners keep this unusual ultrasound pattern of invasive carcinoma in mind. Mammographically, most panniculitis-like IDC presented distortion or spiculated masses less dense than common IDC. Most
(11/12) invasive carcinomas with PLI-3 showed estrogen-receptor positive and! HER2 negative immuno-phenotypes ($P<0.05$). In spite of relatively s mall size by palpation, the half cases showed positive axillary lymph nodes metastasis. Definite diagnosis by aspiration cytology was unsuccessful in five cases. This was due to hypocellularity and frequent co-existence of benign ductal elements in the cytological specimens. Core needle biopsy may be a more reliable tool for pre-operative diagnosis of invasive carcinomas of PLI-3.
Conclusions: Predominant panniculitis-like infiltration is associated with unique histopathological and ultrasound features and occurs in a subset of IDC as well as ILC.

P 17
PROGNOSTIC VALUE OF PLASMOCYTOID DENDRITIC CELLS INFILTRATE IN POOR PROGNOSTIC BREAST CARCINOMAS.
M C. Mathieu , F. André, A. Dunant, L. Zelek, M. Spielmann, P.Chomarat, and L. Zitvogel. Departments of Pathology, of Statistics, of Medical Oncology Institut Gustave Roussy, Villejuif, France

Lymph node status is the most important prognostic factor to select high-risk patients for chemotherapy. However, the classical progostic factors did not explain the 30% 10-year survival of patients with a large axillary involvement (> 8N+) without chemotherapy. Our purpose was to determine the prognostic impact of dendritic cells (DC) for this group of patients.
In a retrospective series of 248 patients with > 8 N+ treated at the IGR between 1972 to 1983 without chemotherapy, a group of 37 patients without relapse within 15 years was matched to 37 patients who relapsed and dead within 15 years. The matching was done on number of N+, grade, estrogen receptor status, year of diagnosis, age
Immunohistochemistry staining was used to determine the infiltration of immature DC (CD1a, Immunotech), mature DC (DC-lamp and p55, Schering Plough), plasmocytoid DC (CD 123, Schering Plough). The staining was assessed using a semi-quantitative grading system and consider negative for absent or low infiltrate and positive for intermediate and high infiltrate.
In long terms survivors, 16%, 21%, 37% of tumors contained CD1a, p55, DC-lamp cells. These infiltrates did not

significantly differ from those of matched control tumors. A significant higher infiltrate of plasmocytoid DC (pDC) (CD 123+) was observed in long survivors patients (38%) compared to control group (13%) (p = 0.006). Plasmocytoid DC were localized in the stroma of the tumor. The presence of pDC was not correlated to number of N+, grade and estrogen receptor status.
These results allow us to hypothesize a protective role of plasmocytoid DC infiltrate in this group of high-risk tumors. pDC may produce interferon type I who promote their differentiation into antigen presenting tumor cells and may also hamper tumor cell growth.
Further studies are thus needed to determine the role of pDC and their potentiel therapeutic use.

P 18
SENTINEL LYMPH NODE IN BREAST CARCINOMA: THE EXPERIENCE OF DEPARTMENT OF PATHOLOGICAL ANATOMY - BARI

GIARDINA Carmela, TRAVERSI Carmela, D'EREDITA' Giovanni***, PASCAZIO Francesco**, NAPOLI Anna, CIAMPI Luigia, INGRAVALLO Giuseppe, SERIO Gabriella, FIORE Grazia, RUBINI Giuseppe* and MAIORANO Eugenio.
Dipartimento di Anatomia Patologica; *Dipartimento di Radiologia; **Dipartimento di Scienze Chirurgiche e Specialistiche; **U.O. di Chirurgia Generale II - BARI (Italy)

Introduction:Assessment of axillary lymph node status in breast cancer is a collaborative and multidisciplinary work between surgeons and pathologists. Sentinel lymph node (SLN) biopsy can truthfully predict the axillary nodal status in clinically node-negative breast cancer patients. The pathological examinations of SLN typically involves the evaluation of multiple tissue levels and/or keratin in immunohistology.
Purpose: of our study was to estimate the usefulness of SLN examination by evaluation of multiple-level sectioning in SLN and to assess the value of SLN as the only method in nodal staging in breast cancer patients.
Matherial and Methods: From January 1999 to December 2004, 253 patients underwent SLN procedure for breast cancer. The mean age was 56 (range 30-82). The tumors were: 27 Tis (10%), 64 T1b (25%), 105 T1c (41%) and 57 T2 no larger than 3 cm.
A mean number of 1.4 nodes were examined per case for a total of 354 lymph nodes.
SLN was completely and serially examined after wax embedding and E-E staining. Cytokeratin were performed only in case of dubious metastasis. The mean number of histologic section for each SLN was 19,2.
One hundred seventy six of patients also underwent axillary dissection.
Results: SLN revealed in 55 (21.7%) cases metastatic deposits: 38 (69%) macrometastases (> 2 mm) and 17 (31%) micrometastases (<= 2 mm). In 27 (49%) cases SLN was the only metastatic node
In 198 cases SLN was metastasis free; of these patients 121 underwent also axillary dissection; metastases in non sentinel node (NSLN) were detected in 9 of them. The false-negative rate (FNR) was 8%. In five of these cases only one other node was involved, in one case 2 nodes and in three cases 3 nodes. In two cases there were micrometastases.
The comparison between these cases and the other ones, did not show any relevant differences.
Micrometastases in SLN were associated with axillary involvement in 4 (23.5%) cases: in 3 cases one only other node was involved, in one case four nodes.
Macrometastases were associated with axillary involvement in 23 cases (60.5%).
No cases of in situ carcinoma showed metastatic involvement of SLN.
Conclusions Our results confirm the importance of this method to avoid unnecessary axillary dissection in node negative patients and of the extension of metastases in the SLN in relation to the different rate of axillary involvement.

P 19
CORRELATIONS BETWEEN NUCLEAR PLEOMORPHISM AND INTRATUMORAL STROMAL COMPONENTS IN INVASIVE DUCTAL CARCINOMA OF THE BREAST

ENACHE Stelian Danut***, PLESEA Iancu Emil*, ZAHARIA Bogdan*, POPESCU Carmen***, GILUSI Mirela***, MUNTEANU Marian****, GHEONEA Dan Ion*, ALEXANDRU Dragos**
*Department of Pathology, **Department of Informatics, University of Medicine and Pharmacy Craiova, Romania
***Department of Pathology, ****Department of Surgery, Universitary Hospital, Craiova, Romania

Introduction, Aims: The authors made a preliminary assessement of possible correlations between the degree of nuclear pleomorphism and the amount of fibrillary components and capillaries of intratumoral stroma in 20 cases with invasive ductal carcinoma of the breast.
Methods: The samples were fixed in buffered formalin and included in paraffin wax. Stromal components were marked silver staining (Gömöri) and antibodies for CD34 Classs I. Five fields with no necrosis were selected randomly using x10 objective, for each case, from the most representative slide for the tumoral pattern. The selected tumoral areas were aquired using a Nikon DN100 digital camera and a LuciaNet 1.16.2 soft. The quantitative determinations were performed, after image calibration, with analySIS Pro 3.2 soft. The 100 selected fields were subdivided in three groups following the degree of nuclear pleomorphism: group I (mild atypia), group II (moderate atypia), group III (severe atypia). The studied parameters for each group were: area occupied by stromal fibrillary elements, area occupied by malignant cells and capillary densities related to tumoral area, to malignant cells area and to stromal fibrillary components.
Results. The group with moderate nuclear atypia on the field area was the most numerous. Stromal fibrillary component ranged between 25,85% in group II, with a good Confidence Level (95%) of 2,93, and 34,9% in group III but with a Confidence Level (95%) of 9,07 (group III). Vascular density related to whole tumoral area was higher in groups with intermediate and severe pleomorphism but with a better Confidence Level (95%) of 5 for group II only. Vascular density related to epithelial malignant cells had an increasing trend from group I to group III, but the latter had a small number of analysed fields and a large range of values, reflected in a Confidence Level (95%) value of 13,23. Vascular density related to stromal fibrillary components had high mean values in the second group (193/mm2) but with large intervals of range in all three groups and especially in the third.
Conclusions. Our preliminary data showed that severe nuclear atypia seems to be present in tumoral areas with an increased amount of stromal fibrillary components No significant correlation was found between the vascular density and the degree of nuclear atypia, despite the relative increasing trend of vascular density related to tumoral parenchyma from areas with mild to those with severe atypia.

P 20
CORRELATIONS BETWEEN TUBULE FORMATION AND INTRATUMORAL STROMAL COMPONENTS IN DUCTAL INVASIVE CARCINOMA OF THE BREAST

PLESEA Iancu Emil*, ENACHE Stelian Danut***, GEORGESCU Claudia*, COMANESCU Violeta***, POP Oltin Tiberiu*, STANCULESCU Diana***, PASALEGA Marin****, BADEA Petrica**

*Department of Pathology, **Department of Informatics, University of Medicine and Pharmacy, Craiova, Romania
***Department of Pathology, ****Department of Surgery, Universitary Hospital, Craiova, Romania

Introduction, Aims. The authors made a preliminary assessement of possible correlations between the amount of fibrillary components and capillary network of intratumoral stroma and the degree of glandular formation in 20 cases of invasive ductal carcinoma of the breast.
Material and Methods. The samples were fixed in buffered formalin and included in paraffin wax. Stromal components were marked silver staining (Gömöri) and antibodies for CD34 Classs I. Five fields with no necrosis were selected randomly using x10 objective, for each case, from the most representative slide for the tumoral pattern. The selected tumoral areas were aquired using a Nikon DN100 digital camera and a LuciaNet 1.16.2 soft. The quantitative determinations were performed, after image calibration, with analySIS Pro 3.2 soft. The 100 selected fields were subdivided in three groups following tubule formation: group I (score 1), group II (score 2), group III (score 3).
The studied parameters for each group were: area occupied by stromal fibrillary elements, area occupied by malignant cells and capillary densities related to tumoral area, to malignant cells area and to stromal fibrillary components.
Results. The group with less than 10% tubule formation (score 3)on the field area was the most numerous, followed by the group with score 2. Fibrilary component represented between 27,6% (group II) and 30% (group III), with a Confidence Level (95%) between 4,52 (group I) and 3,66 (group III). Vascular density related to whole tumoral area ranged between 39/mm2 (group I) and 43/mm2 (group II) with a Confidence Level (95%) between 8,72 (group I) and 4,68 (group III). Vascular density related to epithelial malignant cells was higher (around 66/mm2) in groups II and III, with a Confidence Level (95%) between 8,18 (group II) and 7,1 (group III). Vascular density related to stromal fibrillary components had its highest value in third group (191/mm2) but with large intervals of range in all three groups.
Conclusions. These preliminary data showed no significant variations of the intratumoral stroma and capillaries amounts in different areas of ductal invasive breast carcinomas and also no significant correlation between stromal components variations and the degree of tubule formation.

P 21
FINE NEEDLE ASPIRATION CYTOLOGY AND CORE NEEDLE BIOPSY BY MAMMOTOME IN THE EVALUATION OF NON PALPABLE BREAST LESIONS.

GIARDINA Carmela, INGRAVALLO Giuseppe, GUERRIERI Angela*, CASSANDRO Giovanna*, ZACCARIA Monica, CIMMINO Antonella, NAPOLI Anna and RICCO Rosalia.
Dipartimento di Anatomia Patologica - Università di Bari;*Servizio Autonomo di Radiologia a Indirizzo Senologico - Policlinico di Bari (Italy)

Introduction: Radiologically dubious breast lesions, often requires a second diagnostic step, generally consisting in a FNAC (Fine Needle Aspiration Citology) or in a core biopsy.
Purpose: -to evaluate the distribution of lesions in C1-C5 and B1-B5 categories and the meaning of them in respect to the final diagnosis -to compare the quality assurance of the two methods.
Matherial and Methods: During the last 5 years 1519 patients underwent FNAC under stereotactic or ultrasound guidance (needle 23-24 gauge) and 504 patients had a core needle biopsy by Mammotome (11 gauge). All patients had non palpable breast lesions.
Cytological smears were classified as: C1: 433(28.5%), C2: 590(38.8%), C3: 100 (6.5%), C4: 131(8.6%), C5: 265(17.4%); Mammotome biopsies as: B1: 3(0.6%), B2: 279(55.2%), B3: 36(7.3%), B4: 6(1.2%), B5: 180(36%).
Results: histology was available in 365 cases of cytologies: 46 C1 (10.6%), 36 C2 (6%), 25 C3 (25%), 61 C4 (46%), 147 C5 (55%).
C1 were malignant in 29 (60%), benign in 16 (33%); one case (2%) was diagnosed as atypia.
C2 resulted malignant (false negative) in 19 (52.7%) and benign in 17 (47.2%).
Of C3 lesions 12 (48%) resulted benign and 13 (52%) malignant.
C4 were malignant in 43 cases (70%), benign in 17 (28%); one case was atypia.
C5 were malignant in 144 cases (98%), atypical in 2 cases (1.37%) and benign (false positive) in one case (0.6%).
183 cases of core biopsy had definitive histology: B1: No case had surgery. Of B2: two were benign one was a cancer (liponecrosis on the Mammotome). Of B3: 15 were benign and 2 malignant.
Among B4 cases (4) having surgery: three were atypical, one was a DCIS. A definitive histology was available in 159 of B5 cases. Diagnosis was confirmed in 151 cases (95 in situ and 56 invasive), 7 cases did not show tumor any more and one case (0.6%) was atipical duct hyperplasia.
Sensibility was 71% for FNAC and 97.8% for core biopsy. Specificity was 96.7% for FNAC and 99.6% for core biopsy. PPV of cytology was 99.2 (C5), NPV was 96.8%. PPV of microbiopsy was 99.4% (B5), NPV was 99.6%.
Conclusions: “C” and “B” categories showed a different distribution of lesions with a different meaning in relation to the final diagnosis.
Core biopsy presented a higher specificity, sensibility, PPV and NPV than FNAC; it, in spite of its high rate of inadeguate samples, probably due to the small dimension of the lesions, can be still considered a valid approach for breast lesions.

P 22
STEROID AND HER2 RECEPTORS’ STATUS IN BREAST CARCINOMA – 4493 CASES FROM POPULATION-BASED STUDY IN POLAND

OLSZEWSKI Wlodzimierz, OLSZEWSKI Wojciech, MROZKOWIAK Anna. Department of Pathology, Institute of Oncology, Warsaw, on behalf of HER2 Polish Working Group

The study is a part of national HER2 screening project in Poland, which started in 2002 and continues. Until April 2004, 11 557 cases of invasive breast carcinoma cases were included.
Breast cancer diagnostics, aside from well-established prognostic and predictive factors (e.g. histological type, histological grade, pTNM, lymph node status) employs the assessment of other parameters in order to make pathological report sufficient for oncological management. These parameters are estrogen (ER), progesterone (PGR) and HER2 status.
The aim of the study was the description of dependency between HER2 and estrogen/progesterone status.
Materials and methods: The study was performed on 4493 non-selected cases of breast cancer. The data originated from 14 oncological centers in Poland and were collected between April 2003 and March 2004. The estrogen, progesterone and HER2 receptor status were evaluated immunohistochemically (IHC).
HER2 IHC results were classed into 4 groups (DAKO criteria system: 0,1+, 2+, 3+). The cases classed as 0, 1+ and 2+ were considered to have negative HER2 status. The remaining cases (3+) were clinically HER2-positive.

Steroid receptors positive cases were grouped by presence of 10% or more positively stained cancer nuclei, regardless of strength of the stain. ER/PGR status was stated positive, when the presence of ER/PGR receptors was detected. A mixed group consisted of cases, in which one steroid hormone was present.
Results: The group of cases described by IHC as "0", "1+" and "2+" showed the presence of at least on steroid receptor expression in more than two thirds of all cases (71%, 80,1% and 79,1%, respectively). Among the tumors exhibiting very strong HER2 receptor expression (3+), 48,2% were steroid receptors negative.

Discussion: The results indicate the difference between the expression of estrogen and progesterone receptors and HER2 status. Results suggest necessity of independent evaluation of both steroid receptors and HER2 status. The probability of existence of positive steroid receptor status in clinically HER2-positive group is much lower, than in clinically HER2-negative groups (0, 1+, 2+).

P 23
THE USE OF FISH METHOD IN HER2 EVALUATION ALGORITHM IN BREAST CANCER
MROZKOWIAK Anna, OLSZEWSKI Wojciech, PIASCIK Agata, SZEWSKI Wlodzimierz, Department of Pathology, Institute of Oncology, Warsaw

There are two main techniques of evaluation of HER2 status: immunohistochemistry (IHC) for the protein expression and fluorescence in situ hybridisation (FISH) for amplification of HER2 gene.
During the year 2004, in our Department of Pathology, 1409 consecutive cases of invasive breast carcinoma were diagnosed and included in the study. Among them 365 were described by IHC as 2+. According to the algorithm of the diagnostic procedure, those cases were additionally examined with FISH method.
The aim of the study was to compare the results obtained by IHC and FISH methods in determination of HER2 status in breast cancer.
Materials and Methods: The material originated from 414 patients operated in Institute of Oncology in Warsaw. FISH method was preformed in every 2+ (365) case and, in randomly selected cancers exhibiting 0/1+ (14 cases) and 3+ (35 cases) IHC stain. IHC was performed with DAKO HercepTest. The results were classed into 4 groups, accordingly to the four-tier DAKO criteria system (0,1+, 2+, 3+). FISH evaluation was performed with PathVysion (Abbott) reagents. The results were divided into three groups: NA - no amplification, LA - low amplification and HA - high amplification. The number of copies of chromosome 17 was also assessed.
Over 90% of cases described by IHC as 3+ exhibited amplification of HER2/neu gene. The majority of cases classed by IHC as 2+ were negative by FISH (74,5%) or showed no amplification of HER2/neu gene combined with aneuploidy of chromosome 17 (6,6%). Almost one fifth of IHC 2+ tumours presented gene amplification (18,9%). All cases described by IHC as 0/1+ were HER2-negative by FISH.
IHC is well-established method of assessing HER2 status in breast cancer. Nonetheless, group of cases described as 2+ should be additionally examined using FISH. The results obtained by the latter method are more reliable. With FISH method twenty percent of clinically negative 2+ group are potential beneficiates from Herceptin therapy.

P 24
EVALUATION OF C-ERB-B2/HER-2/NEU EXPRESSION IN INFILTRATING BREAST CARCINOMA IN A GREEK POPULATION COHORT OF 1100 CASES BY IMMUNOHISTOCHEMISTRY AND CHROMOGENIC IN SITU HYBRIDIZATION. EARLY DATA OF THE GREEK MULTICENTER STUDY.
C.Valavanis1a,b ,K.Koutsoubi2, S.Kouneli3, N.Kapranos4, M.Sotiropoulou5, F.Patakiouta6, H.Trihia1a, G.Morphopoulos7, E.Papaspyrou5, E.Georgiadou7, H.Arvaniti3,H.Kokka7, Th.Toliou6, S.Markaki5, E.Bairaktari3, N.Apostolikas2, P.Arapantoni-Dadioti1a
1.a. Dept. of Pathology – b. Molecular Pathology Unit, METAXA Cancer Hospital, Piraeus, Greece, 2. Dept. of Pathology, St.Savvas Cancer Hospital, Athens,Greece, 3. Dept. of Pathology, H.Venizelou General Hospital, Athens,Greece, 4. Dept. of Pathology/Molecular Pathology, Mitera General Hospital, Athens,Greece, 5. Dept. of Pathology, Alexandra General Hospital, Athens,Greece, 6. Dept. of Pathology, Theageneio Cancer Hospital,Thessaloniki,Greece, 7. Dept. of Pathology, A.Fleming General Hospital, Athens,Greece

OBJECTIVE: To evaluate the expression of c-erb-B2/HER2/neu in infiltrating breast carcinomas in Greek patients by immunohistochemistry, to compare the reactivity against HER2 of three different antibodies and to correlate HER2 expression levels to its gene amplification by CISH.
MATERIALS AND METHODS: In this study, 1100 specimens of infiltrating breast carcinoma (ductal and lobular) were analysed immunohistochemically, using three different antibodies against HER2 , AO485 (DAKO), TAB-250 (Zymed) and CB11 (Biogenex). Immunostaining was evaluated as membranous, and the intensity was graded 0 (negative), 1+ (weak), 2+ (moderate) and 3+ (strong). Cases been evaluated as 1+ and 2+ in IHC were analysed by CISH (Zymed kit) to determine the presence or not of HER2 gene amplification. Gene amplification was graded as negative (2-5 gene copies/nucleus), low amplification (6-10 gene copies/nucleus) and high amplification (>10 gene copies/nucleus).
RESULTS AND CONCLUSIONS:
1. By using the commonly used AO485 antibody, 22.81% of the tumors were 3+, 16.50% showed 2+ and 27.66% exhibited 1+ HER2 reactivity.
2. There was discordance in evaluating HER2 expression among the three different antibodies, especially in the cases that have been graded as 1+ and 2+.
3. Concerning CISH, among 1+ IHC cases, 92.59% had no gene amplification,4.93% displayed low gene amplification and 2.47% high gene amplification. On the other hand, 2+ cases showed low gene amplification in 11.69%, high gene amplification in 11.69% and no amplification in 76.62% of the cases. We conclude that CISH is a highly accurate method in evaluating HER2 gene status, more sensitive than IHC and should be used not only in 2+ IHC cases but also in 1+ IHC ones.

P 25
ASSESSMENT OF HER2 STATUS IN BREAST CANCER BY FLUORESCENCE IN SITU HYBRIDISATION
PLASTIRA1Konstantina, ANGELOPOULOU1 Roxani, POTHOS2Alexios, GOUTAS3 Nikolaos, VLACHODIMITROPOULOS3 Dimitrios., KOUNELI4 S.
1 Department of Histology and Embryology, Faculty of Medicine, University of Athens.
2Department of Obstetrics and Gynecology, Helena Venizelou Maternity Hospital, Athens Greece.
3Department of Forensic Medicine and Toxicology, Faculty of Medicine, University of Athens.
4Department of Pathology, Helena Venizelou Maternity Hospital, Athens Greece.

Introduction

The aim of this study was to analyse the presence of gene amplification and/or overexpression of the HER-2/neu (c-erbB-2) proto-oncogene in invasive breast carcinomas. Furthermore, to ascertain the ability of our laboratory to create specific for HER-2/neu probe and test it versus the commercially available assay (Abbott ¨C Vysis, Downers Grove, IL).
Materials and Methods
Forty cases of invasive breast carcinomas were evaluated by immunohistochemistry (IHC). Interpreted 2+ borderline reactions were considered inconclusive and referred to FISH analysis (Guidelines of HER-2/neu, 2003). The amplification of the HER-2/neu gene was determined by dual-colour FISH using the c-erbB-2 specific probe (SpectrumOrange) and the chromosome 17 centromere specific probe (SpectrumGreen) from the commercially available kit (Abbott ¨C Vysis). FISH probe, generated by our team, from BAC clone, specific for HER-2/neu gene, was also tested and both, the Vysis assay versus ours were compared in order to evaluate their efficacy.
Results
According to the scoring criteria, HER-2/neu to chromosome 17 ratio < 2 signifies non amplification of the HER-2/neu gene, whereas HER-2/CEP17 ¡Ý 2 is considered amplified.
From the studied cases 31 of 40 (77.5%), showed no amplification of the c-erbB-2 gene and 4 (10%) demonstrated amplified signals after FISH examination. The test failed in the remaining five cases (12.5%) because the intensity of the hybridization signals was too faint to be counted. Both the generated probe of HER-2/neu gene and the commercially available probe (Abbott ¨C Vysis) showed the same results with the same intensity and hybridization efficacy in FISH analysis.
Discussion
Despite the tendency of IHC interpreted 2+ cases to present HER-2/neu amplification, a high percentage of non-amplified cases (77.5%) was observed. Although, a possible failure in IHC cannot be excluded due to non-specific staining and the subjective nature of interpretation that led to misclassification, further number of new cases will allow statistical analysis to be performed for final conclusions.

P 26
THE ASSOCIATION OF HER-2/NEU OVEREXPRESSION IN RELATION WITH P53 NUCLEAR ACCUMULATION, HORMONAL RECCEPTOR STATUS AND COMMON CLINICOPATHOLOGICAL PROGNOSTIC PARAMETERS IN A SERIES OF EGYPTIAN WOMEN WITH INASIVE DUCTAL CARCINOMA
u, Mona M. Rashed; MD
v Noha M. Ragab; MD
wManal K. Galal; MD
uw General Organization for Teaching Hospitals & Institutes; Cairo – Egypt
v Medical Research Institute, Alexandria University; Alexandria – Egypt

Introduction: HER2/neu protein has garnered a great deal of interest in the popular media. However, it has long been known amongst pathologists and oncologists for its potential role as a tumor and prognostic marker. This protein exists on the surface of epithelial cells and functions in the normal cell as a receptor for a cellular growth factor. Aim of the study: is to determine the association of HER-2/neu and p53 as well as hormonal receptor status with conventional common pathologic parameters in a series of Egyptian women with invasive ductal carcinoma of breast. Methods: expression of HER-2/neu and p53 was examined by immunohistochemistry in samples of breast tissue from 50 patients with invasive ductal carcinoma and their significance for prognosis was analyzed. Results: Of the 50 carcinoma tissue samples, 26% were positive for HER2 over-expression. In the present study there was a high significant association between HER-2 over expression and the accumulation of nuclear p53 (p=0.0017) also there was an inverse significant association with ER (p=0.0001) and PR status (p=0.0003). There was a significant association between HER-2 over expression and the increased size of tumor (p=0.0115) as well as the high grade tumors (p=0.0001). Meanwhile no significant association was there as regard number of the invaded lymph nodes, grade of tumor necrosis and menopausal status. Conclusion: The study had indicated that Her-2/neu may be a powerful predictor of poor prognosis as it's over expression was strongly directly correlated with p53 nuclear accumulation, tumor size, tumor grade and inversely correlated with hormonal receptors status, of breast carcinoma. Meanwhile; no significant associated for number of invaded lymph nodes and the menopausal status.
Key words: Immunohistochemistry, Her-2/neu, p53, hormone receptors, clinicopathological prognostic parameters & breast cancer

P 27
COMMON EXPRESSION OF EGFR (HER-1) IN METAPLASTIC BREAST CARCINOMAS: POTENTIAL RELEVANCE TO ADJUVANT THERAPY WITH EGFR-INHIBITORS?
LEIBL Sebastian, MD, MOINFAR Farid, MD
Department of Pathology, Medical University of Graz, Austria

Metaplastic carcinomas (MCs) of the breast rarely express steroid receptors and Her-2, which minimizes the options for adjuvant therapy in patients with advanced disease.
We immunohistochemically assessed the expression of steroid receptors and 4 members of the EGFR/Her-family (EGFR/Her-1, Her-2, Her-3 and Her-4) in a collective of 20 MCs (8 MCs with heterologous elements, 7 spindle cell MCs, 4 carcinosarcomas and 1 matrix producing carcinoma). 14 out of 20 MCs (70%) showed positive reactions for EGFR (Her-1). Among these cases, 1+, 2+ and 3+ reactivity was observed in 2, 4 and 8 cases, respectively. Her-2 was only present in one MC with 1+ reactivity. Her-3 (1+ reactivity), Her-4 (2+ reactivity) and Androgen receptors (2+ reactivity) were also expressed by one tumor. Estrogen and Progesterone receptors (3+ reactivity each) were only detected in the epithelial component of 2 carcinosarcoma-type MCs.
Compared to collectives of not otherwise specified (NOS) breast carcinomas investigated in previous studies, the MCs in our study expressed EGFR considerably more frequently. Therefore, we conclude that they represent a promising subject for future studies (especially molecular analyses to detect specific mutations in EGFR-exons) on EGFR expression in breast carcinomas. Androgen receptor targeted therapy or anti-Her 2 therapy do not seem to be an option for adjuvant treatment of MCs according to our results, but patients suffering from this aggressive variant of breast carcinoma might benefit from treatment with protein kinase inhibitors such as gefitinib or cetuximab.

P 28
PROX-1, A LYMPHATIC-ENDOTHELIUM ASSOCIATED TRANSCRIPTION FACTOR, IS OVEREXPRESSED BY BREAST CANCER CELLS
Authors: LONGATTO FILHO Adhemar1, 2, MARTINS Albino1, TOMAREV Stanislav3, REIS Rui M1, COSTA Sandra1, MILANEZI Fernanda1, 5, SCHMITT Fernando C4, 5.
1- Life and Health Sciences Research Institute, Health Sciences School, University of Minho, Braga, Portugal, 2- Pathology Division, Adolfo Lutz Institute, São Paulo, Brazil, 3- Section of Molecular Genetics, Laboratory of Molecular and Developmental Biology, National Eye Institute, Bethesda, MD, USA, 4- Medical Faculty, Department of Pathology, University of Porto, Porto, Portugal, 5-

IPATIMUP – Institute of Molecular Pathology and Immunology of University of Porto, Porto, Portugal.

Introduction: The study of lymphatic vessels and lymphatic-derived tumours is frequently complex, due to common characteristics of morphological features between blood and lymphatic endothelial cells, as well as to the lack of specific lymphatic endothelial markers. Prox-1, a homebox gene cloned by homology with the Drosophila gene prospero, that codifies a nuclear transcription factor that plays a major role during embryonic lymphangiogenesis and is supposed to be a useful marker to differentiate lymphatic from blood endothelial cells. Purpose: We studied a series of breast carcinomas in order to observe the specificity of this marker in lymphatic vessels. Methods: Tissue–array from formalin-fixed and paraffin-embedded samples of 116 invasive ductal carcinomas recovered from the Pathology files of IPATIMUP, Porto, Portugal were immunostained with a primary antibody raised against Prox-1 (diluted 1:133; Research Diagnostics, Inc., Flanders, NJ, USA). Results: Prox-1 immunostaining highlighted the lymphatic vessels, and was also detected in the cytoplasm and nuclei of neoplastic cells in 94.8% (110/116) of the cases. Conclusion: Our results suggest that invasive breast carcinoma cells can express Prox-1. Further studies are needed to understand the real meaning of this finding.

P 29

UNUSUAL CYTOPLASMIC IMMUNOPOSITIVITY FOR MIB1 IN BREAST CARCINOMA

CHARFI Lamia (1), PALLUD Claude (1), CHAMPY Odile (1), BELICHARD Catherine (2), GUINEBRETIERE Jean Marc (1)
(1) Department of pathology (2) Department of surgery. Rene Huguenin centre. 35 Dailly street. 92210 Saint Cloud. France

INTRODUCTION:
Tumour cell proliferation can be assessed by a large number of antibodies: Ki-67, PCNA, KiS1… MIB1, the most commonly used, is a monoclonal antibody raised against the recombinant part of the Ki67 antigen. It reacts with cells in the late G1, S, G2 and M phases of the cell cycle and only stains nuclei with various intensity.
We report herein 2 cases of breast carcinoma with cytoplasmic immunoreactivity for MIB1.
POPULATION:
One occurred in a 62 year-old women, a 12 cm invasive ductal carcinoma, histoprognostic SBR grade 3. The second occurred in a 54 year-old women, a 23mm invasive ductal carcinoma, histoprognostic SBR grade 1. None of these patients received preoperative treatment.
Immunohistochemistry was done with MIB1 (Dako) after antigen retrieval (water bath) with LSAB kit and DAB revelation. The test was repeated at different times and with different blocks of the fixed tumour (Formaline, AFA) with the same results. The others immunohistochemistry (RE, RP, HER) didn't shown abnormal staining (nuclear staining for RE and RP, cytoplasmic staining for HER).
DISCUSSION:
In 1995, Hirokawa and al, first reported the cytoplasmic immunoreactivity for MIB1 in hyalinizing trabecular adenoma of the thyroid. Recently, two reports showed this unusual staining in atypical pleomorphic adenoma of the salivary gland and sclerosing haemangioma of the lung. To the best of our knowledge, this immunoreactivity hasn't been reported in breast tumours. Significance of this unusual staining is still unknown. There was no correlation between the properties of the cells stained and the mitotic count which suggests a cross-reaction of this immunostaining.
CONCLUSION:
Pathologists should be aware of this unusual MIB1 cytoplasmic staining. This pattern of reactivity of MIB1 in breast carcinoma may be a result of cross-reaction of the antibody.

P 30

IGF-II MRNA EXPRESSION IN BREAST CANCER (BC) TISSUES AND CLINICAL OUTCOME.

C.Giani, P.Fierabracci, E.Giustarini, D.Campani*, K.Cullen. Dipartimento di Endocrinologia e Metabolismo, Università di Pisa. *Dipartimento di Oncologia, Università di Pisa. V.T. Lombardi Cancer Research Center Georgetown University, Washington Dc, USA.

Insuline like growth factor II (IGF II) is an important regulator of neoplastic growth and it is generally expressed in stroma of BC tissues. Estrogen and Progesterone receptor (ER, PR) are considered a good prognostic predictors in BC. The aim of the study was to evaluate the impact of IGF II mRNA expression in clinical outcome in a large series of BC. The study group included 75 women (mean age +/- SD= 53.3+/-15.6 yr) submitted to radical mastectomy for ductal infiltrating breast carcinoma. The BC specimens was assessed for IGF II mRNA using in situ hybridization method and ER and PR by immunohistochemistry. Five years clinical follow-up was available in 65/79 BC (82.3%) and 46/65 (70.8%) were still alive and relapse free. ER+ was found in 39/65 (60%), PR + in 30/65 (46.2%) and stromal IGF II mRNA expression (IGF II +) in 33/65 (50.8%). 22/65 (33.8%) BC were IGF II+ ER+ and 19/65 (29.2%) IGF II+ PR+. No relationship was found between ER, PR, IGF II separately examined and clinical outcome. The better 5 yr survival was found in ER+ IGF II+ (16/22: 72.7%) and IGF II+ PR+ BC (14/19: 73.7%) and in contrast, the worse survival was found in IGF II+ ER- (6/11: 54.5%) and IGF II+ PR- (57.1%) groups. (p=0.006, p=0.02, respectively). These data indicate that stromal IGF II may be considered a new important predictive factor in BC and suggest that this growth factor may have a role in both differentiation or proliferation of BC cells

P 31

CORRELATION BETWEEN CYCLOOXYGENASE-2 EXPRESSION AND CELL PROLIFERATION IN INVASIVE DUCTAL BREAST CANCER

ŠARÈEVIÆ Božena,MILAS Ivan,KUJUNDŽIÆ-TILJAK Mirjana,MARUNICA Jelena
University Hospital for Tumours, Depart.of Pathology Medical School

INTRODUCTION:Cyclooxigenase-2(COX-2)is overexpressed in breast cancer and may have a role in tumor development and progression.There has been inconsistency in the literature regarding the precise significance of this.Some studies have found no clinicopathological relevance at all, while others have concluded Cox-2 expression is an important biomarker in invasive disease, correlating with poor prognosis features.The aim of this study was to determine the relationships between Cox-2 expression and cell proliferation in breast cancer, and to correlate the expression of this enzyme with classic clinicopathological parameters.
MATERIAL AND METHODS:We retrospectively analyzed 150 breast tumors in paraffin embeded tissue and from medical records, obtained clinicopathological data.Regarding to tumor grade we had three groups of patients and each group consisted of 50 patients.Cox-2 expression was investigated by immunohistochemistry using monoclonal antibody. Immunohistochemistry was done following protocol on DAKO TechMate Horizon automated immunostainer.S-phase fraction (SPF)determined by flow cytometry used as a marker of cell proliferation.
RESULTS:Cox-2 expression was detected in 86%of all tumors studied.The preliminary results have shown that Cox-2 protein expression significantly correlates only with tumor

grade but not with SPF.We have found statistically significant difference in expression of Cox-2 in different grade of tumors (p=0.02).Comparing different grade with SPF we found statistically significant higher SPF in poorly differentiated tumors (p<0.001).
CONCLUSIONS:We have confirmed that Cox-2 expression does occur in invasive breast ductal cancer and is associated with tumor grade.It remains to be investigated whether treatment with selective inhibitors of Cox-2 may be an additional therapeutic option for patients with breast cancer.

P 32
IMMUNOHISTOCHEMICAL ANALYSIS OF RET AND ITS LIGAND GDNF IN 139 CASES OF BREAST CANCER

Gordillo, J.; Moreno, J.; San José, C.; Limón, M. and Pichel, J.G.*
Department of Pathology and Laboratory of Investigation, Hospital de Mérida, Mérida, Spain. *IBMCC/CSIC. Centro de Investigación del Cáncer, Salamanca. Spain.

Introduction: The RET proto-oncogene tyrosine kinase receptor is activated by a ligand complex comprising glial cell line-derived neurotrophic factor (GDNF) and GDNF family receptor alpha1 (GFRalpha1). They are expressed in multiple organs during development and in some types of human tumors in adults. In this study we evaluated the expression of RET, and GDNF in different types of breast cancer.
Material and Methods: RET, expression was analyzed in samples of formalin-fixed tissues from tumoral zone, from 139 patients with different types of breast cancer: 109 IDC; 5 IC; 7 ILC; 6 mucinous carcimomas; 4 medullary carcinomas; 3 papillary carcinomas 2 tubular carcinomas and others (3) using immunohistochemical methods.
Results: A total of 98/137 (71,6%) of breast tumors showed citoplasmic immunoreactivity for RET, and 130/138 (71,6%) for GDNF. By statistical analysis based on 111 months follow up showed that RET expression was associated with less tendency to the regional lymph nodes metastases (p<0,0001); less tendency to relapse (p<0,004); increase of overall survival (p<0,0004); There was no statistically significant correlation of RET or GDNF expression with the histological grade, microscopic type, size or stage. Those findings were not supported by multivariant analysis.
Conclusions: We found that RET and its GDNF/GFRalpha1 ligand complex were expressed in normal breast tissues and in a high percentage of different types of breast tumors using immunohistochemical methods. The presence of RET did not show clear association with any particular light microscopic growth pattern or special tumor subtype, but interestingly, this expression was associated with less tendency to the lymph nodes metastases and increase of overall survival. In summary RET determination by immunohistochemical analysis could be used as a prognostic factor in breast cancer.

P 33
PROGNOSTIC VALUE OF MIB1 PROLIFERATION INDEX AND C-ERBB2 IN PATIENTS WITH STAGE II BREAST CANCER AND LYMPH NODE INVOLVEMENT

Soriano P1, Vicente F2, Guerrero D3, Miranda C2, Mart¨ªnez-Peñuela JM4, C¨®rdoba A4, B¨¦rtolo C3, Caballero MC4, Amat I4, Lera JM2
1Servicio Cirug¨ªa General. Fundaci¨®n Hospital de Calahorra. 2Servicio de Cirug¨ªa General y Digestiva, Hospital de Navarra. Servicio Navarro de Salud. 3Centro de Investigaci¨®n Biom¨¦dica, Servicio Navarro de Salud 4Servicio de Anatom¨ªa Patol¨®gica, Hospital de Navarra. Servicio Navarro de Salud.

INTRODUCTION: Breast cancer is the first leading cause of cancer in women from Spain, and its incidente rates have increased in the recent last years. Study of prognostic value of different factors in breast cancer patients with lymph node involvement can identify subgroups of patients with high risk for more effective clinical management. C-erbB2 that encodes HER2/ Neu protein (p185HER2), and MIB1 proliferation index are useful parameters to assess this issue.
PURPOSE: The goal of this study was to evaluate if the prognostic role of c-erbB2 and MIB-1 proliferation index, p53, S-phase, were dependent or independently useful to characterise more aggressive breast tumors.
PATIENTS AND METHODS: 87 positive-node infiltrating breast cancer patients classified as stage II (T2N1). C-erbB2, p53, MIB-1 proliferation index, estrogen (ER) and progesteron receptors (PR) were determined immunohistochemically by assigning a score with an analysis image software. C-erbB2 membrane expression was graded negative, indeterminate, 1+, 2+, 3+ when ¡Ý5%, 20%-30%, 30%-50%, and more than 50% of cells were stained, respectively. Comparisons in distributions were analyzed by ANOVA and Pearson tests, using SPSS. Differences in disease-free and overall survival were evaluated by using the log-rank test.
RESULTS: 48.3% of the patients resulted to be negative for c-erbB2, whereas 12.6%, 18.4%, 15% and 5.7% of the patients were indeterminate, 1+, 2+ and 3+, respectively. C-erbB2 immunostaining was correlated to node involvement and number of positive nodes (P= 0.022, P=0.023, respectively), tumor size (P= 0.037) and PR (P=0.03). There are no correlations between c-erbB2 immunostaining, age, ploidy, MIB-1 and ER. The median follow-up time was 90 months. Disease-free survival is inversely correlated to c-erbB2 immunostaining (P= 0.027), number of positive nodes (P=0.037) and tumor size (P=0.042), being nearly significant for MIB1 (p=0.09). Predictive value for c-erbB2 was confirmed with a relative risk of 2.5 times in multivariate analysis.
CONCLUSIONS: 1. Higher proliferation index is a bad prognosis factor in patients with infiltrating breast cancer patients, stage II tumors and lymph node involvement. 2. C-erbB2 oncogene is an indicator of bad prognosis in these patients. 3. Patients that were negative for proliferation index and C-erb-B2 presented longer overall survival.

P 34
PLATELET-DERIVED GROWTH FACTOR RECEPTOR-ALPHA (PDGFR-ALPHA) EXPRESSION IN INVASIVE BREAST CARCINOMAS

Ines Carvalho, BSc1,2; Fernanda Milanezi, MD1,2; Albino Martins, BSc2; Rui Reis, MD PhD2; Fernando Schmitt, MD PhD1,3
1IPATIMUP, Institute of Molecular Pathology and Immunology of Porto University, Porto, Portugal
2 School of Health Sciences, University of Minho, Braga, Portugal
3 Medical Faculty of Porto University, Porto, Portugal

Introduction: Receptor tyrosine kinases have been extensively studied due to their frequently abnormal activation in the development and progression of many human cancers. Platelet-derived growth factor receptors (PDGFRs) are receptors with intrinsic tyrosine kinase activity that regulate several functions in normal cells and are widely expressed in a variety of malignancies. After the demonstration that GISTs without c-kit mutations harbour PDGFR-alpha activating mutations, and that it is also a therapeutic target for imatinib mesylate, the interest for this receptor increased considerably. Since breast cancer is one of the most frequent neoplasia in women worldwide, and there are only one study reporting PDGFR-alpha expression in breast carcinomas, the aim of this work was to investigate the potential meaning of PDGFR-alpha expression in invasive mammary carcinomas.

Methods: We used immunohistochemistry to detect PDGFR-alpha overexpression on a series of 181 formalin-fixed paraffin-embedded invasive ductal breast carcinomas and associated its expression with known prognostic factors. We also performed PCR-SSCP and direct sequencing in order to screen for PDGFR-alpha gene mutations.
Results: PDGFR-alpha expression was demonstrated in 39.2% of the breast carcinomas and showed an association with lymph node metastasis (p=0.0079), HER-2 expression (p=0.0265) and Bcl2 expression (p=0.0121). It was also found a correlation with PDGF-A ligand expression (p=0.0194). Screening for mutations revealed the presence of the 2500 A>G and 2529 T>A alterations in exon 18, the 2472 C>T (exon 18) and 1701 G>A (exon 12) missense mutations, and also the presence of the intronic insertion IVS17-50insA at exon 18 in all sequenced cases. These mutations did not correlate with PDGFR-alpha expression.
Conclusions: PDGFR-alpha is expressed in invasive breast carcinomas and is associated with biological aggressiveness factors. The mutations found did not show any correlation with PDGFR-alpha expression.

P 35
CA-125 IS A USEFUL TUMOURMARKER IN BRCA2 ASSOCIATED BREASTCANCER AND IN POORLY DIFFERENTIATED SPORADIC TUMOURS.
L. Luts 3, H. Olsson 1,2, A. Borg 1, N. Loman 1.
From Departments of 1) Oncology, 2) Cancer Epidemiology, and 3) Pathology, University Hospital, Lund, Sweden.

CA-125 is a useful tumour marker for ovarian cancer. As such the marker is not specific for ovarian cancer. A number of other tumours diseases and conditions have been found to be related to elevated plasma levels of CA-125. In breast cancer overall 5-80% (median 30%) have been found to be positive for CA-125.
In twenty one consecutive patients with BRCA2 germ line mutations the breast tumours were stained for Ca-125 immunoreactivity. 8/21 BRCA2 tumours showed moderate to strong immunostaining and in the sporadic tumours 8/17 showed similar immunostaining. 5/8 BRCA2 tumours where classified as histological grade 3 tumours while all of the the tumours that showed positive immunoreactivity for CA-125 where classified as histological grade 3 tumours. Two of the BRCA2 patients had a recurrence and the tumour recurrence correlated with an elevation of plasma Ca-125. The elevation occurred before metastatic symtoms. Further one of the patients progressed twice while first responding favourably to endocrine therapy and later to chemotherapy with the tumour status strongly correlated with Ca-125 levels.
Immunohistochemistry and serum assay were used to detect CA-125.
Tumour cells diplaying Ca-125 were demonstrated in eight of twenty one BRCA2 tumours. Six of these tumors were ductal carcinomas and two were lobular carcinomas. Five of these eight tumors expressed both estrogen –and progesterone receptor immunoreactivity. Three men with breast cancer were included and none of them expressed CA-125 immunoreactivity in their breast tumours.
In the sporadic tumours Ca-125 immunoreactivity were demonstrated in eight of seventeen tumours. All of these tumors were ductal carcinomas and the tumours were poorly differentiated and classified as histological grade 3 tumours. Six of these eight tumors were negative for both estrogen – and progesterone receptor immunoreactivity.
The data demonstrate that Ca-125 is a useful early tumour marker in a subset of breast cancer patients associated with BRCA2 mutations and possibly also in other high grade tumours in the breast.
This knowledge is of importance as Ca-125 is used to screen for ovarian tumours in BRCA1/2 patients. The finding that Ca-125 is an early marker of breast tumours in a subset of BRCA2 cases lends hope that this marker also could be used in therapeutic settings.

P 36
ESTROGEN RECEPTOR (ER) NEGATIVE INVASIVE BREAST CARCINOMAS FREQUENTLY EXPRESS MYOEPITHELIAL MARKERS
Emanuele Dainese, Selenia Casnedi, Donata Micello, Cristina Riva, Carlo Capella, Fausto Sessa
Department of Pathology, University of Insubria, Varese, Italy

Introduction: Luminal, basal and myoepithelial cell differentiation have been reported in ductal breast cancer (BC), using several markers, including cytokeratins (CKs) 5, 14, 8, 18, actin, S100, and vimentin. Luminal type BCs are associated with ER and PgR positivity and a good prognosis. Few studies documented basal and myoepithelial markers expression in relationship to p53 positivity and tumor grade. The aim of our study was to investigate the expression of basal (CK5 and CK14) and luminal (CK8 and CK18) cytokeratins in high-grade p53+, ER- and PR- BCs, and to correlate them with the expression of myoepithelial markers (a-smooth muscle actin, vimentin and S100).
Design: Formalin-fixed, paraffin-embedded sections from 60 selected p53+, ER-, PgR-, c-erb-B2-negative BCs, including 56 NOS invasive ductal and 4 medullary carcinomas, were immunostained for CK14 (Novocastra), CK5 (Novocastra), CK8 (Dako), CK18 (Novocastra), a-smooth muscle actin (Sigma), S100 (Dako) and vimentin (Dako).
Results: All cases were G3, ER-, PR-, c-erb-B2-negative, p53-positive BCs. The mean age was 59 years ranging from 29 to 87. Twenty of sixty cases (33%) had lymph node metastases (15 N1 and 5 N2). The most common morphological features were the presence of large sheets of cells sometimes with spindle appearance, festoon-like pattern, pushing margins and occasional large central acellular zones, represented by foci of tissue infarction and deposits of collagenous or hyaline-like material. The proliferative index (Ki-67) and p53 expression were high in all cases (mean percentage of 63% and 81% respectively). Forty-four of 60 (73%) BCs were positive for S100, 31/60 (52%) for vimentin, 5/60 (8%) for a-smooth muscle actin, 43/60 (72%) for CK5, 20/60 (33%) for CK14, 55/60 (92%) for CK8 and 31/60 (52%) for CK18. Coexpression of basal and luminal CKs was seen in 43 cases (72%); 39 of these cases were positive for at least a myoepithelial marker.
Conclusions: Our study suggests that a subset of high grade ER/PR/c-erb-B2- and p53+ BCs frequently displays an intermediate luminal/basal phenotype (immunoreactive both for basal and luminal CKs), often coexpressing myoepithelial markers. This particular phenotype could be the result of a peculiar pathway of breast carcinogenesis of great clinical relevance because of the high rate of lymph node metastasis. The results suggest that p53+, ER-, BCs should be investigated for the expression of basal and myoepithelial markers.

P 37
PROGNOSTIC SIGNIFICANCE OF TOPOISOMERASE II ALPHA IN BREAST CANCER PATIENTS
OZTURK Figen, OZKAN Metin, SOYUER Isin, SOYUER Serdar
Department of Pathology, Medical Oncology and Radiation Oncology,
Medical Faculty of Erciyes University

Introduction: There are many studies that show tumors overexpressing TOPO II have better response to anthracyclines. In our study we aimed to show the expression

of this enzyme at high and low risk breast cancer patients and the effect of this activity on prognosis of this disease.
Material and Methods: Thirty-seven operable breast cancer patients including 21 high risk and 16 low risk who were followed at Erciyes University Medical Oncology clinic between March 1999 and June 2003 were enrolled into this study. High risk patients received adjuvant chemotherapy consisting taxane and anthracycline and radiotherapy, 3 of the low risk patients received no adjuvant therapy, 4 adjuvant hormonal therapy, 9 adjuvant CT. Only one patient received RT in this group. TOPO II alpha expression was categorized in 4 groups according to cell numbers showing nuclear staining, 35% and higher expression (3+ and 4+ nuclear staining) was accepted as positive and others negative.
Results: Median age of all patients was 42 years (range 23-78). Histopathologically 32 patients(86.5%) were diagnosed as IDC. Two patients were stage I, 15 stage II, 20 stage III. Median follow-up time was 32.5 months (range 18-64). TOPO II alpha expression was positive in 45.9% of the patients. Ten patients (58.8%) among 17 patients showing TOPO II expression had also HER-2 expression. There was statistically significant relationship between TOPO II alpha expression and tumor grade (p=0.015), diameter (p=0.019), lymph node positivity (p=0.001), increased number of lymph nodes (p=0.033) and age (p=0.039). There was statistically significant relationship between disease free survival (DFS) and lymph node positivity and increased number of lymph nodes (p=0.04 and 0.03, respectively), however no significant relation was detected between TOPO II alpha expression and DFS (P=0.14). Discussion: TOPO II alpha expression seemed to be related to the aggressive behavior of the tumor in this study, however there is a need to confirm these findings in larger studies. High expression of TOPO II alpha and HER-2 in this group may be due to many factors, and this may also show that tumor behavior and anthracycline response may be different in our patients compared to other group of patients.

P 38
EXPRESSION OF CD10 IN STROMAL FIBROBLASTS IN INVASIVE BREAST CANCER
1 - Nurija Bilalovic, MD PhD;
2 - Semir Vranic MD;
1 - Department of Pathology, Sarajevo University School of Medicine, Sarajevo, Bosnia and Herzegovina
2 - Sarajevo University School of Medicine, Sarajevo, Bosnia and Herzegovina

Aim: To explore presence and prognostic value of CD10 in stromal fibroblasts in invasive breast cancer and its correlation with other basic histopathological parameters, hormonal status (Estrogen receptor, ER and Progesterone receptor, PR), bcl-2 and cyclin D1.
Material and methods: Medical records of 46 patients, diagnosed in 1998, from Central Database of Institute of Oncology, Clinical Center University of Sarajevo were analysed. The median follow-up was 67 months (range: 4-103 months). Routine histopathological evaluation was performed for 46 formalin fixed and paraffin embedded tissue samples. For immunohistochemical staining we used monoclonal antibodies for ER, PR, bcl-2, cyclin D1 and CD10.
Results: Twenty three (50%) out of 46 samples were negative for CD10; 9 (19.6%) showed expression 1, 8 (17.4%) expression 2 and 6 (13%) expression 3. Expression of CD10 inversely correlated only with ER (p=0.05)) and no significant correlation was found with other parameters analysed in our study. Patients with higher CD10 expression had shorter overall survival but not relapse-free survival (p=0.006). Cox regression analysis for overall survival (OS) showed that lymph node status, tumor size, age, bcl-2 and CD10 expressions were independent prognostic factors (p=0.009, 0.029, 0.019, 0.034 and 0.049, respectively).
Conclusion. Expression of CD10 is associated with worse disease outcome in invasive breast cancer.
Key words: Breast cancer, CD10, stromal fibroblasts, prognostic factors.

P 39
HIF-1 ALPHA AND CA IX : TWO PROGNOSTIC FACTORS IN INVASIVE BREAST CARCINOMA
Cynthia Trastour1, Francette Ettore2, Emmanuel Benizri1, Alain Ramaioli3, André Bongain4, Jacques Pouysségur1, and Edurne Berra1
1Institute of Signaling, Developmental Biology and Cancer Research, CNRS UMR-6543, Centre Antoine Lacassagne, 33 Avenue Valombrose, 06189, Nice, France.
2Department of Pathology, Centre Antoine Lacassagne.
3Department of Biostatistics, Centre Antoine Lacassagne.
4Department of Gynecology-Obstetrics, University Archet II Hospital, 151 route St-Antoine de Ginestière, BP 3079 06202 cedex 3 Nice, France.

Introduction : Hypoxia inducible factor 1 (HIF-1) is a key regulator of oxygen homeostasis and controls the expression of several genes involved in various aspects of cancer progression (metabolic adaptation, angiogenesis and cell survival). Among those genes, ca9 (carbonic anhydrase 9) plays a role in extra-cellular pH regulation. HIF-1a, one of the 2 subunits of HIF-1 is stabilized by hypoxia.
We retrospectively studied the impact of HIF-1a and CA IX expressions on the outcome of patients with breast cancer.
Methods : Immunohistochemical stainings of HIF-1a and CA IX were evaluated in an unselected cohort of 132 patients with invasive breast carcinoma. The follow-up was more than 10 years. We examined overall survival, distant metastasis-free and disease-free survivals by univariate and multivariate analyses. Correlations to clinicopathological parameters (tumour size, nodal status, histological grade, hormonal receptors and carcinoma in situ associated with the invasive tumour) were performed using Chi-square test. The level of significance was 5% (P<0.05).
Results: No significant correlation exists between tumour size or nodal status and the expression of HIF-1a or CA IX. HIF-1a or CA IX staining is however statistically associated with the histological grade (P<0.0001 et P=0.0004, respectively). Both markers are in general negative in low grade tumours and HIF-1? is positive in high grade tumours. HIF-1a and CA IX are significantly positive when hormonal receptors are lost, mainly estrogen receptors (P<0.0001). HIF-1a is also expressed in tumours associated with carcinoma in situ (P=0.0022).
Expression of HIF-1a or CA IX is correlated to worse overall survival (P=0.0005 and 0.048, respectively), distant metastasis-free survival (P=0.0001 and 0.0066) and disease-free survival (P<0.0001 and P=0.0129). Stromal CA IX expression is correlated with worse overall survival (P=0.0014). Multivariate analysis, regarding overall survival and including all parameters correlated with HIF-1a, shows that the grade is the most significant factor. HIF-1a positive immunoreactivity is more significant than CA IX's.
Conclusion : This preliminary study confirms that HIF-1a and CA IX are poor prognostic factors in breast cancer, but mainly related with the grade in our hands. One larger study is ongoing to confirm these results and evaluate the impact of these markers in therapeutic response to establish a putative predictive role.

P 40
MICROSATELLITE INSTABILITY AND LOSS OF HETEROZYGOSITY IN BREAST CARCINOMA
*SEO Seung-Won, *JAEGAL Young-Jong, KIM Hyun-Joong, NAM Jong-Hee, PARK Chang-Soo
Department of *Surgery and Pathology, Chonnam National University Medical School, Gwangju, Korea

Previous studies have shown that younger women exhibit more aggressive pathologic features of breast cancer in comparison with older women. Young age could be an independent predictor of adverse prognosis. In order to evaluate any existing differences in the molecular progression of breast cancer between younger and older women, Microsatellite instability (MSI) and loss of heterozygosity (LOH) was investigated in paired tumour and normal tissue DNA from 32 younger (less than 40 years old) and 32 older (more than 50 years old) breast cancer patients for 12 simple repeated primer sets.

MSI was observed at a single locus in 5 (15.6%) of younger patients and 8 (25.0%) of older patients. LOH was noted at a single locus in 7 (21.8%) and at multiple loci in 22 (68.7%) of 32 younger patients. In older patients, LOH was revealed at a single locus in 9 (28.1%) and at multiple loci in 15 (46.9%). Greatest frequency of LOH was at loci UT5320 (37.5%), D8S321 (34.4%), D9S242 (31.3%), and D19S394 (31.3%) in younger patients and L17686 (34.4%) and D19S394 (28.1%) in older patients. LOHs at D19S394 and L17686 were highly identified in both age groups. LOHs at D9S242 and D8S321 were significantly higher in the carcinoma of younger women. LOH status was unrelated to clinical stage, nodal status, tumour size, histologic grade or estrogen receptor (ER) status. LOH at D8S321 was associated with tumor size and LOH at UT5320 was associated with histologic grade and ER status. Amplification of CyclinD1 was relatively higher and was associated with histologic grade, nodal status and clinical stage in the younger women, indicating its prognostic significance.

These results indicate that the pattern of chromosomal alterations are not exactly same, especially at D9S242 and D8S321, in the carcinomas in the two age groups and suggest that the molecular pathogenesis of the carcinomas is not similar.

P 41

EVALUATION OF CYCLIND1 EXPRESSION IN DUCTAL CARCINOMA OF BREAST AND ITS CORRELATION WITH CLINICOPATHOLOGIC ASPECTS

Introduction:

Breast carcinoma is the most common malignant tumor and the leading cause of carcinoma death in women.CyclinD1 is a key cell cycle regulatory protein with demonstrated oncogenic activity in a variety of malignancy including breast cancer. We analyzed expression of cyclinD1 in ductal carcinoma of breast and its correlation with clinicopathologic parameters such as age, lymph node status, tumor size and grade.

Materials& Method

Formalin fixed tissue samples from 54 patients diagnosed as ductal carcinoma of breast were analyzed by Immunohistochemistry .We designed a Scoring system based on intensity and percentage of staining cells. Then we performed a statistical analysis to investigate the relationship between clinicopathologic parameters and cyclinD1 expression.

Result:

CyclinD1 expression was observed in all of cases with cytoplasmic pattern. We found positive significant correlation between intensity of staining and number of involved lymph nodes (P=0.013) .Also we observed positive significant correlation between percentage of positive cells and tumor size (P=0.016). No relationship was seen between tumor grade and cyclinD1 expression (P>0.05). Also no relationship was seen between patient's age and cyclinD1 expression (P>0.05). In additional studies we found positive correlation between tumor grade and number of involved lymph nodes (P=0.01).

Conclusion:

According to our finding we conclude evaluation of cyclinD1 expression could be useful for evaluation of lymph node status, tumor size and thus prognosis.

Keyword:
Cyclin D1 , Ductal carcinoma , Grade , Immunohistochemistry.

P 42

EXPRESSION OF THE INSULIN RECEPTOR SUBSTRATE 1 IN PRIMARY TUMORS AND LYMPH NODE METASTASES IN BREAST CANCER: CORRELATIONS WITH ERÁ, KI-67, BCL-XL AND BAX PROTEINS.

KODA Mariusz, SULKOWSKA Mariola, KANCZUGA-KODA Luiza, GOLASZEWSKA Jolanta, BALTAZIAK Marek, KISIELEWSKI Wojciech, RESZEC Joanna, WINCEWICZ Andrzej, SULKOWSKI Stanislaw
Department of Pathology, Medical University of Bialystok, Waszyngtona 13, 15-269 Bialystok, Poland

Insulin receptor substrate 1 (IRS-1) transmits signals from insulin-like growth factor I receptor (IGF-IR) and insulin receptor (IR) and it has been associated with pathogenesis of cancer disease. IRS-1 down-regulation was suggested with breast cancer progression, but simultaneous assessment of IRS-1 expression in primary and metastatic breast cancer have never been reported before. Consequently, we examined by immunohistochemistry IRS-1 expression in 109 samples of primary breast cancer and in 42 matched pairs of primary and metastatic tumors. Additionally, we correlated IRS-1 expression with selected clinicopathological features, including the ERá status and proliferation marker Ki-67 as well as with antiapoptotic Bcl-xL and proapoptotic Bax proteins. We found positive, cytoplasmic IRS-1 immunostaining in 69.7% and 76.2% of studied primary and metastatic tumors, respectively. Both IRS-1-positive and IRS-1-negative primary tumors were found to produce IRS-1-positive as well as IRS-1-negative metastases. IRS-1 expression in primary tumors correlated with poorly differentiated (G3) breast cancer ($p<0.005$) and with lymph node involvement ($p<0.05$). In primary tumors as well as in lymph node metastases, IRS-1 expression did not significantly correlate with ERá and Ki-67 expression. However, in the subgroup of ERá-positive primary tumors IRS-1 expression positively correlated with Ki-67 ($p<0.02$, $r=0.351$). In primary tumors, we found a significant positive correlation between IRS-1 and Bcl-xL ($p=0.001$, $r=0.315$) as well as between IRS-1 and Bax expression ($p<0.0001$, $r=0.346$). Additionally, in lymph node metastases we also observed positive correlation between IRS-1 and Bcl-xL ($p=0.004$, $r=0.447$) as well as between IRS-1 and Bax expression ($p=0.037$, $r=0.356$). Thus, our results could suggest that IRS-1 might affect turnover of cancer cells and breast cancer progression through activation of mitogenesis and participation in the regulation of the balance between anti- and proapoptotic pathways. Moreover, we suppose that knowledge about heterogeneity between primary and metastatic tumor might help to understand mechanisms of breast cancer progression as well as lead to the development of more effective anti-cancer drugs.

P 43

PROLACTIN RECEPTOR EXPRESSION IN BENIGN AND MALIGNANT BREAST LESIONS OF MALE AND FEMALE PATIENTS

FERREIRA Marco, MESQUITA Marta, QUARESMA Manuela, ANDRÉ Saudade
Serviço de Anatomia Patológica, Instituto Português de Oncologia Francisco Gentil CROL SA, Lisboa, Portugal

Background: Despite the well established function of prolactin (PRL) in normal breast development, the role of this

pituitary hormone in breast cancer pathogenesis is still controversial. PRL activity is dependent on the activation of a transmembrane protein, the PRL receptor (PRLR). The expression of PRLR is common in female breast carcinoma (FBC), but, to our knowledge, no studies were reported in male breast carcinoma (MBC).
Objective: Evaluate and compare PRLR expression in male and female breast carcinoma, as well as in gynaecomastia and benign female breast lesions.
Methods: PRLR expression was detected immunohistochemically, using a monoclonal antibody (clone B6.2), in formalin-fixed paraffin-embedded tissue of 30 cases of gynaecomastia, 30 cases of benign female breast lesions (including ductal hyperplasia, fibroadenoma, sclerosing adenosis, papilloma and radial scar), 30 cases of MBC and 30 cases of FBC (all invasive ductal carcinomas NOS). The whole series was also assessed for estrogen receptors (ER), progesterone receptors (PR) and androgen receptors (AR). A cut-off of 10% was used as positivity criteria. Histological type was evaluated according to the WHO classification. Tumour differentiation and pathological stage were assessed using the Elston & Ellis grading system and TNM-UICC system, respectively. Statistical analysis was performed with Fisher's Exact Test.
Results: PRLR positivity was seen in 20% of gynaecomastia cases, in 20% of benign female breast lesions, in 60% of MBC and in 50% of FBC. PRLR expression was significantly higher in MBC than in gynaecomastia (p=0,003). Likewise, it was significantly higher in FBC than in benign female breast pathology (p=0,029). No statistically significant differences between gynaecomastia and benign breast lesions or between MBC and FBC were found (p=1,000 and p=0,604, respectively). There was no statistically significant correlation between PRLR expression and ER, PR, AR, pTNM, histological grade or patients' age.
Conclusions: The results indicate that: 1) there is no difference in PRLR expression between male and female benign breast lesions; 2) there is no difference in PRLR expression between MBC and FBC; 3) PRLR is significantly more expressed in invasive carcinoma than in benign male and female breast lesions, suggesting a role of PRL in breast carcinogenesis.

P 44
THE BRMS1 (BREAST METASTASIS SUPPRESSOR GENE 1) GENE IS RELATED TO TUMOR PROGRESSION IN HUMAN BREAST CANCER
LOMBARDI Grazia, DI CRISTOFANO Claudio, CAPODANNO Alessandra, ARETINI Paolo, ISOLA Patrizia*, TANCREDI Mariella, COLLECCHI Paola, NACCARATO Giuseppe, BEVILACQUA Generoso, CALIGO Maria Adelaide.
Division of Surgical, Molecular and Ultrastructural Pathology, Department of Oncology, University of Pisa and Pisa University Hospital, Pisa, Italy;
*Department of Pathology B.M.I.E, University of Pisa, Pisa, Italy.

The BRMS1 (Breast Cancer Metastasis Suppressor Gene 1) gene has been identified by differential display, using mRNA extracted from the metastatic cell line of human mammary carcinoma (MDA-MB-435) and from the parental cell line stably transfected with chromosome 11. Experimental evidences show that BRMS1 reduces the metastatic ability, without affecting tumorigenicity, of both human and murine breast cancer cells in vivo metastasis assays. Preliminary studies into the mechanism of the observed metastasis suppression suggest that BRMS1 is a protein involved in a complex that represses gene expression, and that it is associated with regulation of cell-cell communication.
So far, BRMS1 gene involvement in human cancer has not been demonstrated. Aim of this study is to determine if BRMS1 might play a role in tumor progression by using an in vivo system (paired samples from human primary breast tumors and local metastasis) and to verify the correlation between BRMS1 expression and cell proliferation in vitro (human breast carcinoma cell line Hs578T).
BRMS1 mRNA expression was quantified by TaqMan assay in peritumoral, carcinoma tissues and in lymph-nodal metastasis of breast cancer patients with at least 10 years follow-up and in Hs578T cell line. Total cellular RNA has been extracted from laser-microdissected cells isolated from fresh frozen tissues.
The BRMS1 mRNA is expressed in all tissues analyzed. BRMS1 expression in carcinoma cells is generally higher than in matching normal cell populations (10/14 cases; p=0,0005), it decreases then in lymph-nodal carcinoma cells (9/15 cases; p=0,001). The BRMS1 mRNA was then quantified in 47 breast cancers from selected patients with a good (free from disease and/or alive) or a poor (recurrence and/or breast cancer mortality) outcome. Univariate (Log-Rank test: p=0,007) and multivariate analysis (Cox regression: HR=4,0; p=0,054) have shown that BRMS1 higher expression is associated with a shorter disease free survival and overall survival of breast cancer patients. BRMS1 higher expression was not related to cell proliferation rate of tumor cells as shown by an in vivo (breast carcinoma tissues) and in vitro system (Hs578T).
This study is the first and a preliminary evidence of BRMS1 involvement in human breast carcinoma. The BRMS1 expression decreases during tumor progression. However our data suggest that BRMS1 higher expression in primary breast carcinoma is correlated to a poor prognosis.

P 45
EXPRESSION OF MISMATCH REPAIR PROTEINS IN SPORADIC AND FAMILIAL INVASIVE AND IN SITU BREAST CARCINOMA
1Arkoumani E, 1Stefanou D, 1Batistatou A, 1Balasi E, 2Briasoulis E, 3Kontostolis E and 1Agnantis NJ.
1Department of Pathology, 2Department of Medical Oncology, 3Department of Obstetrics and Gynaecology, University of Ioannina, Medical School, Ioannina, 45110, Greece

Introduction:Microsatellite instability appears to be one of the various genetic alterations found in breast tumors, however the results differ considerably in various studies concerning sporadic as well as familial breast cancer. It is not clear yet whether defects in the mismatch repair system accompany this instability.
Aim:The purpose of this study is to explore the expression of two of the proteins encoded by the DNA mismatch repair genes, namely MLH1 and MSH2, in sporadic and familial in situ and invasive breast carcinoma.
Materials and Methods:MLH1 and MSH2 expression was monitored immunohistochemically using the monoclonal antibodies MLH1 and MSH2 (BIOCARE MED-Menarini Diagnostics) in 60 sporadic breast carcinomas (20 in situ and 40 invasive of various types and grades) and in 30 familial breast carcinomas (ductal and lobular type) defined based on published criteria. In the familial cases we examined concomitantly the invasive and the in situ component.
Results:Nuclear staining for MLH1 and MSH2 was observed in all cases of sporadic in situ carcinoma examined.In only one case of DCIS, papillary type the staining for MLH1 was stronger than that of the adjacent normal breast tissue while the staining for MSH2 was similar.Immunostaining for MLH1and MSH2 revealed preservation of expression in all cases of sporadic invasive carcinoma.Regarding MLH1 only one papillary carcinoma exhibited decrease in percentage and intensity of staining.Interestingly, 6 out of 8 papillary carcinomas displayed increase in MSH2 staining intensity compared to normal tissue.In contrast, in familial breast

carcinomas we found loss of expression of MLH1 in 8/30 (26%) and of MSH2 in 4/30 (13%) of the cases examined. Three carcinomas (10%) were negative for both MLH1 and MSH2. Staining for both antibodies was observed in all cases in the adjacent in situ carcinoma, however a clear degradation in the expression was noted in the in situ foci of MLH1 and MSH2 negative cases.Although not statistically significant, there was an association between loss of expression of MLH1 and MSH2, negative estrogen receptor status and higher grade of the tumor.
Conclusions:Our data suggest that the DNA MMR pathway may be involved in the development of familial breast cancer. Regarding sporadic neoplasms, the increased expression of MSH2 in papillary carcinomas can be another clue of their unique differentiation profile. Further molecular studies are necessary for definite conclusions.

P 46
HORMONE RECEPTORS AND ONCOGENE EXPRESSION IN APOCRINE CARCINOMAS
Kaya H1, Erbarut I1, Bozkurt SU1, Gulluoglu B2, Elder J3
Marmara University Hospital, Department of Pathology, Istanbul, Turkey
Marmara University Hospital, Department of Surgery, Istanbul, Turkey
Countess of Chester Hospital, Department of Histopathology, Chester, UK

Introduction:Apocrine carcinomas are 1%-2% of breast carcinomas. 98% of apocrine lesions have been reported as ostrogen and progestron receptors negative. Androgen receptor expression was found to be high rates in this rare type of tumors comparing to more common types of the breast as ductal carcinoma or lobular carcinoma.
Purpose of the study: The main aim of the study was to search the GCDFP-15, ostrogen receptor (ER), progesteron receptor (PR), androgen receptor (AR), p53 and c-erbB-2 immunoexpressions in apocrine carcinomas of the breast.
Methods: In Marmara University Hospital, Department of Pathology we have diagnosed 13 (2.47%) cases from 526 breast biopsies as apocrine carcinoma of the breast. In thirteen cases, we determined ER, PR, AR, GCDFP-15, c-erbB-2 and p53 immunoexpression with Sr.ABC/HRP.
Result: All of the cases were GCDFP-15 positive. ER was positive in five cases (38.5%), PR was positive in four cases (30.8%), AR was positive in eight cases (61.5 %), c-erbB-2 was positive in eleven cases (84.6%), and p53 was positive in five cases (38.5%).
Conclusion: High rates of AR and c-erbB-2 expression brings the discussion of spesific treatment protocols in apocrine carcinomas rather than the classical treatment protocol of the breast carcinomas.

P 47
LYMPHATIC INVASION AND METASTASIS IN BREAST CANCER IN THE ABSENCE OF INTRATUMORAL LYMPHATICS
Dimitrios Stefanou(1), Panayiotis A. Kyzas (1), Silvana Geleff (2), Evdokia Arkoumani (1), Ann Gousia (1), Niki J. Agnantis (1)
(1): Department of Pathology, Medical School, Universtiy of Ioannina, Greece
(2): Department of Pathology, Medical School, Universtiy of Vienna, Austria

Introduction: Lymph node metastasis is a frequent complication in breast cancer. However, the extent to which this depends on lymphangiogenesis or on invasion of pre-existing lymphatic vessels remains controversial.
Purpose: To address this issue, we investigated lymphatic vasculature in 60 primary breast cancer patients.
Experimental Design: We used immunostaining for the specific lymphatic endothelium marker podoplanin. We examined whether intratumoral lymphatics were present in our tissue samples, and quantified peritumoral lymphatic density. Furthermore, we recorded the presence of peritumoral lymphatic invasion, and addressed the association of all the above parameters with various clinicopathological features.
Results: We did not observe any intratumoral lymphatic vessels. Podoplanin positive lymphatic vessels were confined to tumor periphery, and their density was generally low. Higher peritumoral lymphatic density was associated with lower differentiation (x2 p=0.019) and higher incidence of peritumoral lymphatic invasion (x2 p=0.002). We observed a trend towards a correlation of higher peritumoral lymphatic density with the presence of lymph node metastasis at diagnosis, but the observed association was not formally significant (Mann Whitney p=0.07).
Conclusion: The above results are in accordance with previous studies, and suggest that breast carcinomas preferentially invade and metastasize via pre-existing peritumoral lymphatics rather than promoting lymphangiogenesis.

P 48
PURE MUCINOUS CARCINOMAS OF THE BREAST: PROGNOSTIC INTEREST OF DNA-FLOW CYTOMETRY.
Morand C.1, Verrièle V.2, Valo I.2, Paillocher N.3, Chassevent A.4.
1 Département de radiothérapie, Centre Paul Papin, 2 rue Moll 49933-Angers Cedex 9, France ; 2 Service d'anatomo-pathologie, Centre Paul Papin ; 3 Service de gynécologie-obstétrique, CHU Angers ; 4 Laboratoire de cytométrie, Centre Paul Papin.

Pure mucinous carcinomas (PMCs) of the breast are considered as a quite specific entity which represents less than 2% of all breast cancers and are said to have a favorable prognosis. There is a lack of investigation concerning DNA-ploidy and S-Phase fraction (SPF) as prognostic factors for this histologic subtype. This study included 69 patients with pure mucinous carcinomas where DNA flow cytometry was performed on fresh or frozen samples in this purpose.

A tumor size higher than 2 cm was observed in 56.5% of cases. A lymph node involvement concerned only 12% of all patients and just 3% when tumor size was lower than 2 cm. Hormone receptors were negative in only 16% of cases. Aneuploidy concerned 26% of tumors which is a lower rate comparing with invasive ductal carcinomas. A high SPF was observed in only 7.5% of cases.

A higher tumor size (> 2cm) was predictive (p=0.03) of shorter disease-free survival (DFS) and overall survival (OS). No correlation was found between nodal involvement, hormone receptor status, S phase fraction and DFS or OS. DFS was shorter for patients with aneuploid tumors compared to diploid ones (p=0.048). A prognostic classification based on tumor size and DNA-ploidy was obtained (p<10-3 for OS and DFS): a bad prognosis concerned six patients with large (>2cm) aneuploid tumours whose 5-year DFS rate was 16.7%.

Conclusion: the good prognosis of PMCs has to be questioned and this study discriminates a bad prognosis group of patients taking into account tumour size and DNA-ploidy.

P 49
ALTERNATIVE SPLICING OF CYCLIN D1 TRANSCRIPTS HAVE DIFFERENT EFFECTS ON CELL CYCLE REGULATION IN BREAST CANCERS
Cheng-Ping YU, Department of Pathology, Tri-Service General Hospital, Taipei, Taiwan, R.O.C.

Jyh-Cherng YU, Division of General Surgery, Tri-Service General Hospital, Taipei, Taiwan, R.O.C.
Yia-Tang YIANG, Department of Pathology, Armed Forces Taichung General Hospital, Taiping,
Taichung, Taiwan, R.O.C.
Sheng-Chuan HSI, Division of General Surgery, Armed Forces Tao-Yuan General Hospital, Tao-Yuan, Taiwan, R.O.C.

Introduction
The cyclin D1 (CCND1) plays a key role in early G1 phase progression of cell cycle. The amplification and/or overexpression of CCND1 gene have been detected in different types of cancer, such as esophagus, stomach, liver, lung, urinary bladder, head and neck, and breast. It has been reported that a A/G single nucleotide polymorphism (SNP) at the intron 1-exon 1 junction (G870A)of CCND1 gene, and the A-allele has higher risk for cancer generally. This SNP can produce two transcripts (a and b) by alternative splicing, and they may have different functions in cell cycle regulation.
Purpose of Study
In this study, we analyze this G870A SNP of CCND1 gene, the expression levels of CCND1 transcripts a and b, and correlate with cell proliferative index in breast cancers, to evaluate their functions in cell cycle proliferation.
Materials and Methods
The study population consisted of 97 sporadic infiltrating ductal carcinoma of breast who were treated at Tri-Service General Hospital between September 1997 and March 2002. All patients were diagnosed histologically with specimens both fresh and paraffin-embedded. Clinical and histologic information were obtained from patient charts and pathologic reports. Tumor stage was assigned according to the tumor-node-metastasis (TNM) staging system. Pathologic grade of tumors was determined according to the Modified Bloom-Richardson histologic grading criteria. The SNP of G870A was analyzed by PCR-RFLP methog from fresh tissue extracted genomic DNA. The expression levels of transcripts a and b were determined by RT-PCR method. The proliferative index of cancer cells was evaluated by immunohistochemistry of Ki-67 (A0047, Dako, Denmark). One-Way ANOVA and Independent-Samples T tests were applied for statistic analysis.
Summary of Results
The A-allele of CCND1 G870A is more prevalent in breast cancer than the G-allele. Compared with GG or AG+GG, the AA genotype has higher proliferative index. Compared with GG, the AA genotype has higher levels of transcript b. The levels of proliferative index have no significant correlation with the expression levels of transcripts a and b. Higher levels of transcript a have higher tumor grade.
Conclusions
The A-allele of CCND1 G870A is a risk factor for breast cancers. The genotypes of G870A have effects on differential expression of CCND1 transcripts in breast cancer, and this differential expression is grade-related but not proliferation-related.

P 50
EXPRESSION OF TOPOISOMERASE IIÁ IN BREAST CANCER. CORRELATION WITH CERBB2 AND OTHER PREDICTIVE FACTORS

ANDREI Florin 1, CEAUSU Mihai 1, NEAGU Maria 1, BUTUR Georgeta 1, ARDELEANU Carmen 1
1. Victor Babes National Institute of Pathology, Bucharest, Romania

Top2a is a fairly new molecular marker, involved in prediction of response to anthracycline therapy in breast cancer. Prior studies described a possible correlation between Top2a and Her2 neu. Aim of this study was to assess the expression of Top2a related to commonly used markers in breast cancer.
Indirect tristadial ABC method was performed on formalin fixed paraffin embedded tissue from serial file biopsies of 142 patients using the following antibodies: TOP2A, CerbB2, ER, PGR, and PCNA. The cases with strong expression for CerbB2 were confirmed by FISH.
From 110 cases that presented low or negative expression of CerbB2, 20 were positive for Top2A (18.2%); from 20 cases with moderate expression of CerbB2, 9 were positive for Top2A (45%); from 11 cases with strong expression of CerbB2, 2 were positive for Top2A (18.2 %). After removal of 92 cases with no expression of both markers, using multiple regressive analysis, a negative correlation between Top2A and CerbB2 was found (r=-0.43) with a high statistical significance (p=0.001). A very low correlation with no statistical significance was found between Top2a and PCNA (r=0.2, p=0.09) and a direct positive correlation between PGR and CerbB2 was found (r=0.97) with statistical significance (p=0.02). A low negative correlation with statistical significance was found between ER, PGR and TOP2A (r=-0.2 and -0.3, p=0.006).
In conclusion overexpression of CerbB2 associates high levels of Top2A but they show a significant reverse proportional correlation, and TOP2A expression proved to be independent to hormonal receptors and proliferating index.

P 51
FASCIN AND CAVEOLIN EXPRESSION ARE ASSOCIATED WITH THE BASAL –LIKE SUBTYPE OF INVASIVE BREAST CARCINOMA.

Socorro Mª Rodríguez-Pinilla1, David Sarrió1, Ginés Hernández2, Yolanda Rodríguez Gil3, Lucía Hernández3, Francisco Calero2, David Hardisson4, José Palacios1.
1. Programa de Patología Molecular. Breast and Ginecological Laboratory. CNIO. Spain.
2. Department of Ginecology. La Paz Hospital. Madrid. Spain.
3. Department of Pathology. 12 de Octubre Hospital. Madrid. Spain.
4. Department of Pathology. La Paz Hospital. Madrid. Spain.

INTRODUCTION: Using cDNA expression profiling, previous studies classified breast carcinomas into different groups: the “luminal” (estrogen receptor positive), the “normal breast-like”, the “HER2 positive”, and the “basal-like” subtypes. The latter two groups have also been associated with poor outcomes. Basal-like tumours are typically negative for estrogen receptor (ER), progesterone receptors (PR) and HER2, but positive for basal cell (myoepithelial) markers, such as cytokeratins 5/6 (CK5/6) and Epidermal Growth Factor Receptor (EGFR). However, basal-like tumours remain poorly characterized. Caveolin and fascin proteins are expressed by breast myoepithelial cells. Furthermore, caveolin was identified as a tumor suppressor gene, whereas fascin has been involved in cell-to-matrix interactions, and tumour invasion.
AIMS: To study caveolin and fascin expression in breast tumors, and to assess whether these makers are associated with the basal-like phenotype.
MATERIALS AND METHODS: We studied caveolin and fascin expression in a tissue microarray (TMA) including 226 node-negative invasive breast carcinomas. In addition, we evaluated ER, PR, HER2, CK5/6, EGFR, p53, and ki-67 expression.
RESULTS: Overall, 21 (9.3%) and 56 (24,8%) breast carcinomas expressed caveolin and fascin, respectively. The basal-like phenotype (RE-/HER2-/CK5+ and/or EGFR+) was found in 28 (12,4%) carcinomas. Interestingly, 25% (7/28) of tumours with the basal-like phenotype, but only 7.1% (14/197) of non-basal tumours expressed caveolin. Likewise,

fascin was more frequently expressed in basal-like tumours (14/27, 52%) than in non-basal carcinomas (42/196, 21,4%). Therefore, a direct statistically significant correlation was found between caveolin and fascin expression and the basal-phenotype (p=0,007 and p=0,001 for caveolin and fascin, respectively).
CONCLUSION: These data indicate that caveolin and fascin expression is associated to breast cancers with basal phenotype and thus, they could serve to identify more accurately this subgroup of tumours.

P 52
THE EFFECT OF PHYSICAL CONDITIONS AND SLIDE AGING ON STINING QUALITY OF BREAST CARCINOMAS FOR C-ERB-B2, ESTROGEN (ER) AND PROGESTERON (PR) RECEPTORS
OLTULU Turkuler, SAK Serpil D, PERCINEL Sibel , KUZU Isinsu.
Department of Pathology , School of Medicine, Ankara University, Turkey

Fixation and tissue processing conditions effect the staining quality and may create difficulties on interpretation of immunostaining for receptors (ER, PR) and c-erb-B2 in breast carcinomas. There are also evidences about the negative effects of tissue section's age (slide age) and storage temperature on the staining intensity of these prognostic markers. Today slide aging is becoming more important, because of the need for storage of hundreds of tissue microarray sections for future planned studies concerning immunohistochemistry (IHC) or in-situ hybridisation methods. Our aim in this study was to examine the effects of age and the storage conditions on immunostaining quality of ER, PR, and c-erb-B2 on breast carcinoma cases.
MATERIALS AND METHODS:
Tissue cores optained form 14 donor paraffin blocks of different breast carcinomas previously scored for receptors and c-erb-B2, were re-bloked in an order to prepare the tissue array block. Four micron sections of the tissue array block were stored for 36, 24, 12 weeks in 4 different conditions: 1- Room temperature dry, 2- Room temperature humid, 3- Room temperature sealed by paraffin, 4- at 4oC. The slides were stained with primary antibodies against ER (NCL-ER-6F11, 1/50), PR (NCL-PGR, 1/600) and cer-b-B2 (Neomarkers e2-4001+3B5,1/700) by using Ventana Benchmark autostainer on the same session. The results of the staining intensity of all groups were compared with newly cut paraffin section. Freidman test was used for statistical analysis.
CONCLUSIONS
We examined that the staining intensity of immunostaining for breast cancer prognostic markers were decreased when the paraffin slides are stored in humid conditions.
Sealing the slides by paraffin does not have any conservative effect on staining quality.
The staininig quality of the slides decrease by the length of the storage period.
Keeping the slides at 4oC can decrease the negative effect of slide aging on immunostaining.

P 53
HORMONE RECEPTORS AND ONCOGENE EXPRESSION IN APOCRINE CARCINOMAS
Kaya H1, Erbarut I1, Bozkurt SU1, Gulluoglu B2, Elder J3
Marmara University Hospital, Department of Pathology, Istanbul, Turkey
Marmara University Hospital, Department of Surgery, Istanbul, Turkey
Countess of Chester Hospital, Department of Histopathology, Chester, UK

Introduction:Apocrine carcinomas are 1%-2% of breast carcinomas. 98% of apocrine lesions have been reported as ostrogen and progestron receptors negative. Androgen receptor expression was found to be high rates in this rare type of tumors comparing to more common types of the breast as ductal carcinoma or lobular carcinoma.
Purpose of the study: The main aim of the study was to search the GCDFP-15, ostrogen receptor (ER), progesteron receptor (PR), androgen receptor (AR), p53 and c-erbB-2 immunoexpressions in apocrine carcinomas of the breast.
Methods: In Marmara University Hospital, Department of Pathology we have diagnosed 13 (2.47%) cases from 526 breast biopsies as apocrine carcinoma of the breast. In thirteen cases, we determined ER, PR, AR, GCDFP-15, c-erbB-2 and p53 immunoexpression with Sr.ABC/HRP.
Result: All of the cases were GCDFP-15 positive. ER was positive in five cases (38.5%), PR was positive in four cases (30.8%), AR was positive in eight cases (61.5 %), c-erbB-2 was positive in eleven cases (84.6%), and p53 was positive in five cases (38.5%).
Conclusion: High rates of AR and c-erbB-2 expression brings the discussion of spesific treatment protocols in apocrine carcinomas rather than the classical treatment protocol of the breast carcinomas.

P 54
P53, C-ERBB-2, OSTROGEN AND PROGESTERON RECEPTOR EXPRESSION: CORRELATION WITH THE HISTOPATHOLOGICAL PROGNOSTIC PARAMETERS IN DUCTAL CARCINOMAS OF THE BREAST
Kaya H1, Erbarut I1, Bozkurt SUB1, Gulluoglu B2, Aribal E3
1Marmara University Hospital, Department of Pathology, Istanbul, Turkey
2Marmara University Hospital, Department of Surgery, Istanbul, Turkey
3Marmara University Hospital, Department of Radiology, Istanbul, Turkey

Until today many prognostic factors have been studied on ductal carcinomas of the breast in order to find out the clinical and therapeutic implications.
The aim of this study was to search the p53, c-erbB-2, ostrogen receptor (ER) and progesteron receptor (PR) expression in ductal carcinomas of the breast and correlation with the well known histopathological prognostic parameters.
Material-Method:
55 cases of invasive ductal carcinomas were retrieved from the archives of Marmara University Hospital, Department of Pathology. Immunohistochemical detection was performed by the StreptAvidin-Biotin complex method on 5 ? m sections from archival representative paraffin embedded blocks.
Results: The cut of values for p53, ER and PR were 10%. The cut of value for c-erbB-2 was considered as positive when we have revealed ++ and/ or +++ spessific membranous staining.
31% of the cases had immunoexpression with c-erbB-2. 41% of them were positive with p53. 53% of the cases were also positive with ER/PR, 65% of the same cases were advanced stages as T2, T3 or T4, 88% were either grade 2 or 3 and 47% of them had lymph node metastasis .
35% of the invasive ductal carcinoma cases were positive with p53. p53 positive cases demonstrated 68% ER/PR positivity, 79% were advanced stages, 89% were either grade 2 or 3, and 42% had lymph node metastasis.
Discussion:
In the literature, c-erbB-2 protein overexpression is shown to be independently associated with poor prognosis in women with node-positive breast cancer. In this recent study immunoexpression results of c-erbB-2 have concordance with the literature as
c-erbB-2 has a statistically significant correlation with the tumor grade, stage and lymph node metastasis. Although

ER/PR positivity are known to be as good prognostic parameters we have revealed ER/PR positivity of 53% of the c-erbB-2 positive cases. ER/PR positivity have also been observed in p53 positive cases. p53 positivity have also been revealed in advance stages and high grades.
Conclusion: Results of our study is concordance with the literature except the high immunoexpression ratios of the ER/PR. This result could be attributable to the geographic, social differences with Western Europe.

P 55
CELL CYCLE CONTROL RELATED PROTEINS (P53, P21, AND RB) AND TRANSFORMING GROWTH FACTOR-BETA (TGF-BETA) IN 'IN SITU' AND INFILTRATING HUMAN BREAST CANCER: AN IMMUNOHISTOCHEMICAL STUDY.
GARCÍA-TUÑON Ignacio, RICOTE Mónica, FRAILE Benito, PANIAGUA Ricardo and ROYUELA Mar
Department of Cell Biology and Genetics, University of Alcalá. 28871 Alcalá de Henares. Madrid. Spain. E-mail: ignacio.tunon@uah.es

INTRODUCTION: It has been reported that several regulators of the cell cycle –including mtp53, p21, pRB, and TGF-beta are altered in many malignant tumors.
PURPOSE: The aim of this study was to investigate the expression patterns of p53 (mutated form), p21, Rb, pRb and TGF-beta in order to elucidate the possible roles of this cell cycle regulatory system in breast cancer.
METHODS AND METHODS: A comparative study of the products of the cell cycle control genes p53 (mutated form), p21, Rb (non-phosphorylated and phosphorylated form) and TGF-beta was performed by immunohistochemistry and Western blot, in 17 benign breast disorders and 62 breast cancer (17 'in situ' and 45 infiltrating tumors) samples.
RESULTS: For these proteins studied, the relative numbers of positively stained cells were higher in 'in situ' carcinoma than in benign breast diseases. In infiltrating breast tumors the relative numbers of positively stained cells were even higher than in 'in situ' tumor, except for the percentage of pRb immunostained cells, which decreased slightly in infiltrative tumors. For the other proteins, the percentages of positively stained cases were similar to those found in 'in situ' tumors. In the three groups of patients, TGF-beta immunoreaction appeared in the cytoplasm while immunoreactions to p53, p21, Rb and pRb were always found in the nucleus, except for p21 in 'in situ' tumors, which showed cytoplasmic immunoreaction to this protein.
CONCLUSIONS: Present results suggest that accumulation of mutated p53, cytoplasmic p21, and pRb in breast gland epithelium might be a crucial point in the development of 'in situ' adenocarcinoma. In the infiltrating tumors, the expression of p21 in the nuclei and the decrease in pRb expression suggest an insufficient attempt to hinder cell proliferation.
ACKNOWLEDGEMENTS: This work was supported by grants from Fondo de Investigaciones Sanitarias (PI020383) and the University of Alcalá.

P 56
INTERFERON-GAMMA AND ITS FUNCTIONAL RECEPTORS IN IN SITU AND INFILTRATING HUMAN BREAST CANCER: AN IMMUNOHISTOCHEMICAL STUDY.
GARCÍA-TUÑON Ignacio, RICOTE Mónica, FRAILE Benito, PANIAGUA Ricardo and ROYUELA Mar
Department of Cell Biology and Genetics, University of Alcalá. 28871 Alcalá de Henares. Madrid. Spain. E-mail: ignacio.tunon@uah.es

INTRODUCTION: Interferons are a group of proteins that trigger multiple responses including prevention of viral replication, inhibition of cell growth, and modulation of cell differentiation. In different mammary carcinoma cell lines IFNgamma induces growth arrest at mid-G1. At the present there are no in vivo studies in human breast.
PURPOSE: The aim of this study was to investigate the expression patterns of IFNgamma and its two receptors (IFNgamma-Ralpha and IFNgamma-Rbeta) in order to elucidate its role in the different types of human breast cancer (in situ and infiltrative).
METHODS AND METHODS: A comparative study of IFNgamma and its two receptors (IFNgamma-Ralpha and IFNgamma-Rbeta) was performed by immunohistochemistry and Western blot, in 17 benign breast disorders and 62 breast cancer (17 in situ and 45 infiltrating tumors) samples.
RESULTS: For IFNgamma, IFNgamma-Ralpha and IFNgamma-Rbeta, the relative numbers of positively stained cells were higher in benign breast than in carcinoma. In in situ tumors the relative numbers of positively stained cells were even higher than in infiltrating breast. In the three groups of patients, IFNgamma and IFNgamma-Ralpha immunoreactions appeared in the cytoplasm while IFNgamma-Rbeta also was found in the nucleus.
CONCLUSIONS: The decreased expression of IFNgamma and its receptors in cancer could be regarded as an attempt, although insufficient, to inhibit the uncrontrolled cell proliferation. The mechanism causing the antiproliferative effect could be related to the other factors variation as wild p53 or Rb.
ACKNOWLEDGEMENTS: This work was supported by grants from Fondo de Investigaciones Sanitarias (PI020383) and the University of Alcalá.

P 57
THE STATUS OF EPIDERMAL GROWTH FACTOR RECEPTOR (EGFR), GRADE AND AXILLARY LYMPH NODES INVOLVEMENT IN PRIMARY BREAST CANCER
Jalali Nadoushan Mohammad Reza,Neisani Elham,Valaei Naser
Shahed University

Introduction: The breast cancer is the most common worldwide malignancy of women. The number of prognostic factors in breast cancer has grown recently. A conceptual framework is now emerging that outlines how certain principles of EGFR may be employed in the future management of patients with Breast cancer.
In this study, we want to show the status of EGFR and its correlation with grade and axillary lymph nodes involvement in primary breast cancer.
Material and Methods: In a cross-sectional double-blind study, 57 paraffin blocks from patients with breast cancer from pathology department of shaheed Mostafa Khomeini hospital, since 2000-2003 were obtained and from each one, 3 micron sections were provided. One of the tumoral section and one of the lymph node section were stained by H & E. We determined size and type of tumor, number of lymph nodes and grade according to Natingham modification of Bloom-Richardson criteria. We studied EGFR on the other section by IHC. We had 10-parraffin blocks without breast cancer.
Result: Our study showed that 89.5% were positive and 10.5% were negative for EGFR. The most patients were Grade III (43.9%) and the lowest patients were Grade I (22.8%). 66.7% had axillary lymph nodes involvement. In this study, we didn’t find significant correlation between EGFR and axillary lymph nodes involvement.
Conclusion: The high expression of EGFR in patients with breast cancer is important to note as a prognostic factor in the world and Iran, but further investigions with more specimens and follow-up are required to clarify the exact role of EGFR in prognosis of breast cancer.

P 58

ANDROGEN RECEPTORS ARE FREQUENTLY EXPRESSED IN MAMMARY AND EXTRAMAMMARY PAGET`S DISEASE.

LIEGL B. (1), L.C. HORN (2), F. MOINFAR (1)
(1)Institut für Pathologie, Medizinische Universität Graz Austria
(2)Institut für Pathologie, Universität Leipzig Deutschland

Aims: Mammary paget`s disease (MPD) and Extramammary paget`s disease (EMPD) are rare intraepithelial neoplasms. MPD is almost exclusively associated with underlying invasive breast carcinoma (IDC) or high grade Carcinoma in situ, DCIS (ductal intraepithelial neoplasia, DIN). EMPD arises in areas rich in apocrine glands and is thought to have apocrine gland origin. The aim of the study was to investigate the presence of estrogen receptor (ER), progesterone receptor (PR), androgen receptor (AR) and Her2/neu in a large number of cases.
Methods: We investigated 81 cases of MPD (58 cases) and EMPD (23 cases). Formalin fixed and paraffin-embedded tissues were analyzed using antibodies against AR, PR, ER and Her2/neu according to standardized guidelines.
Result: In MPD, positive immunoreactions for Her2/neu, AR, and ER were observed in 56 of 58 (97%), 51 of 58 (88%), and 6 of 58 (10%) cases, respectively. All cases of MPD were negative for PR. MPD showed a co-expression of Her2/neu and AR in 51 out of 58 cases (88%). In EMPD, positive immunoreactions for AR, Her2/neu, and ER were observed in 18 of 23 (78%), 12 of 23 (52%),and 1 of 23 (4%)cases, respectively. All cases of EMPD were negative for PR. EMPD showed a co-expression of AR and Her2/neu in 12 out of 23 cases (52%).
Conclusion: In contrast to ER and PR, AR and Her2/neu are commonly expressed in MPD and EMPD. The immunohistochemical determination of AR in paget`s disease could lead to the development of a new adjuvant therapy, particularly in patients with recurrent disease.

P 59

CLINICOPATHOLOGIC AND IMMUNOHISTOCHEMISTRY FEATURES ASSOCIATED TO THE BASAL PHENOTYPE OF INVASIVE BREAST CARCINOMAS

Alfredo Ribeiro-Silva, MD, PhD
Leandra Náira Zambelli Ramalho, MD, PhD
Sérgio Zucoloto, MD, PhD
Department of Pathology, Faculty of Medicine of Ribeirão Preto, University of São Paulo, Brazil

In the normal breast, the majority of luminal cells express the cytokeratins 7, 8, 18 and 19, while the basal myoepithelial cells express the cytokeratins 5, 14, 15 and 17. However, there is a subset of normal mammary luminal cells that are positive for CK5/6 and negative for CKs 8/18/19. These cells have the capacity to differentiate toward a glandular phenotype (CKs 8/18/19 positive) with intermediate populations that are positive both for CK5 and CKs 8/18/19. Considering that all of these cells can undergo malignant change, the breast carcinomas can be classified as expressing a basal (CK5+ CKS 8/18/19- or CK5+ CKs 8/18/19+) or a luminal phenotype (CK5- CKS 8/18/19+). This work aims to study the immunoprofile of CK-5 positive breast carcinomas and its relationship with pathologic features of clinical significance. Immunohistochemistry with the antibodies CK5, CK8/18, p63, BRCA1, estrogen receptor, progesterone receptor, p53, c-erbB-2, and Ki67 were performed in 102 formalin-fixed paraffin-embedded samples of invasive ductal carcinomas. The clinical data were collected from the medical files. Conventional clinical features were evaluated, including age, menstrual status, pathological grading, tumor size and lymph node metastasis. Focal expression of CK5 was seen in 18.6% of carcinomas. CK5 expression was significantly correlated with younger age, high tumor grade, positive nodal status, negativity for hormonal receptors, and high proliferative rate. There was a strong relationship between CK5 and p63 expression in breast carcinomas indicating that p63, like CK5, may be considered a marker for the basal phenotype of breast cancer. There was also a strong relationship between reduced expression of BRCA1 with both p63 and CK5 expression as well as there was an inverse correlation between p63 and CK8/18 expression suggesting that lost of p63 expression is required for the transition between the basal to luminal phenotype of breast carcinomas. Since p63 is thought to be a marker of stem cells and may act as an oncogene our data reinforce that BRCA1 acts as stem cell regulator.

P 60

PROGNOSTIC SIGNIFICANCE OF P63-POSITIVE NEOPLASTIC CELLS IN INVASIVE BREAST CARCINOMAS

Alfredo Ribeiro-Silva, MD, PhD
Heveline Becker de Moura, MD
Sérgio Zucoloto, MD, PhD
Department of Pathology, Faculty of Medicine of Ribeirão Preto, University of São Paulo, Brazil

P63 is a p53 homologue gene located on chromosome 3q27-29. P63 protein is highly expressed in embryonic ectoderm and in the nuclei of basal cells of many epithelial tissues in the adult including skin, oral epithelium, prostate and urothelium In the normal mammary gland p63 is considered to be a myoepithelial cell marker but p63-positive neoplastic cells may be found in up to 11% of invasive breast carcinomas. The prognostic significance of this finding, however, is still unknown. This work aims to study the overall survival and the disease-free survival associated with p63-positive breast carcinomas. Immunohistochemistry with the antibody p63 (clone 4A4) was performed in 100 formalin-fixed paraffin-embedded samples of invasive ductal carcinomas diagnosed between 1992 and 1995. Clinical data concerning the outcome of the patients were retrieved from the medical files. Sixteen of 100 carcinomas showed rare and scattered neoplastic cells stained for p63 and were interpreted to be p63-positive. The median age of patients (n=100) included in this study was 54.2 years (range 25-85 years). Median follow-up was 6.5 years (range 1-10 years). The average overall survival of patients whose tumors were positive and negative for p63 was 6.5 and 6.9 years, respectively (p=.8134). The average disease-free survival of patients whose tumors were positive and negative for p63 was 4 and 5.8 years, respectively, with the difference being statistically significant (p=.0474). These data indicate that p63 might be used in routine practice to identify patients at high risk of precocious recurrence or metastasis.

P 61

IMMUNOPROFILE OF P63-POSITIVE INVASIVE BREAST CARCINOMAS

Alfredo Ribeiro-Silva, MD, PhD
Heveline Becker de Moura, MD
Sérgio Zucoloto, MD, PhD
Department of Pathology, Faculty of Medicine of Ribeirão Preto, University of São Paulo, Brazil

P63 is a p53 homologue gene that is essential for the maintenance of a stem cell population in several epithelial tissues. P63 expression is associated with several malignancies including squamous cell carcinomas of the head and neck, primary cutaneous adnexal neoplasms, lung carcinomas, endometrial carcinomas, esophageal squamous cell carcinomas, transitional cell carcinomas of the urinary tract, and papillary thyroid carcinomas. These data indicate

that p63 may act as an oncogene in the genesis of these tumors. In breast carcinomas, p63 expression correlates with several indicators of aggressiveness, including advanced pathologic stage, tumor size, lymph node metastasis, high histological grade, and negativity for estrogen receptors. Very little is known about the molecular profile of p63-positive carcinomas. Thus, this study was carried out to study the expression of several key regulators of the cell cycle including oncogenes and apoptosis-related proteins in p63-positive carcinomas. Immunohistochemistry with the antibodies BAG-1, Bcl-2, c-erbB-2, c-erbB-3, Checkpoint Kinase 2 (CHK2), Cyclin D1, Epidermal Growth Factor Receptor (EGFR), Telomerase (hTERT), Osteopontin (OPN), p16, p21, and p27 was performed in 100 formalin-fixed paraffin-embedded samples of invasive ductal carcinomas. Association between p63 expression and other markers was determined by the Fisher exact test. Sixteen of 100 carcinomas expressed p63-positive neoplastic cells. P63 correlated only with the expression of hTERT. The transcriptional activation of telomerase is considered to be a crucial step in the development of malignancy and is responsible for the continued growth and immortalization of cancer cells. In breast carcinomas hTERT is associated with aggressiveness and a poor clinical outcome. It is frequently activated in early breast carcinogenesis and this activity is associated with nodal metastases and cellular proliferation. These data suggest that differential regulation of h-TERT in p63-positive breast carcinomas may contribute to the clinically more aggressive behavior of these neoplasms.

P 62
BRCA1 EXPRESSION IN SPORADIC BREAST CARCINOMAS: A CLINICOPATHOLOGIC AND IMMUNOHISTOCHEMICAL STUDY

Alfredo Ribeiro-Silva, MD, PhD
Sergio Zucoloto, MD, PhD
Department of Pathology, Faculty of Medicine of Ribeiro Preto, University of São Paulo, Brazil

Although mutations in BRCA1 are rare in non familiar breast carcinomas, it is common the lost of expression of the protein codified by this gene probably due to epigenetic changes. The prognostic importance of this finding is not well established. This work aims to analyze the immunohistochemistry expression of BRCA1 in sporadic breast carcinomas and to compare the results with clinical and histopathologic data of prognostic significance.
Immunohistochemistry with the antibodies BRCA1, estrogen receptor, progesterone receptor, p53, c-erbB-2, and Ki67 was performed in 102 formalin-fixed paraffin-embedded samples of not otherwise specified invasive ductal carcinomas. BRCA1 expression was graded as follow: 0/+ (negative or positivity in less than 25% of neoplastic cells), ++ (positivity between 25 to 50% of neoplastic cells), and +++ (positivity in more than 50% of neoplastic cells). Conventional clinical features were evaluated, including age, menstrual status, pathological grading, tumor size and lymph node metastasis. The clinical data were retrieved from medical files. Association between BRCA1 expression and other pathologic variables was determined by the Fisher exact test (2 groups) or ÷2 test (3 or more groups). In normal epithelium, BRCA1 showed only nuclear staining, while the carcinomas showed either nuclear or cytoplasmatic staining. The histological analysis of BRCA1 showed that 25.5% of carcinomas were graded as 0/+, 25.5% were graded as ++, and 49% were graded as +++. Carcinomas with reduced expression of BRCA1 (0/+) were poorly differentiated, with high proliferative rate, negative for hormonal receptors, and positive for c-erbB-2. There was not correlation between BRCA1 expression with age, menstrual status, tumoral size, lymph nodes status, pathologic stage, and p53 expression. The mean survival and disease-free survival of patients which tumors expressed less and more of 25% of neoplastic cells stained for BRCA1 were 4.2 and 3.9 ($p<0,001$); and 7.8 and 6.3 ($p=0,0095$) years respectively. In conclusion, BRCA1 may be considered a useful marker in identification of sporadic carcinomas of poor prognosis that is in high risk for precocious recurrence.

P 63
THE RELATIONSHIP BETWEEN CYTOKERATIN 5, CYTOKERATINS 8/18, P63 AND MATRIX METALLOPROTEINASE-19 IN MAMMARY CARCINOMAS INDUCED BY 7,12 DIMETHYLBENZ[A]ANTHRACECENE IN MICE FED WITH FAT DIET

Alfredo Ribeiro-Silva, MD, PhD1
Leandra Náira Zambelli Ramalho, MD, PhD1
Fernando Silva Ramalho, MD, PhD2
Sérgio Zucoloto, MD, PhD1
Departments of Pathology1 and Surgery & Anatomy2, Faculty of Medicine of Ribeirão Preto, University of São Paulo, Brazil

Human Breast carcinomas usually express cytokeratins 8/18 (CK8/18) but a reduced expression of CK8/18 may be found in up to 40% of poorly differentiated tumors. CK5 is a 58 kD protein found in many non-keratinizing stratified squamous epithelia. There is a subset of human breast carcinomas that express CK5. P63, unlike its homologue p53, is not a classical tumor suppressor gene, being essential for the maintenance of a stem cell population in several epithelial tissues. The expression of CK5 and p63 in experimentally induced mammary tumors is still unknown. Unlike most matrix metalloproteinases, MMP-19 is downregulated during malignant transformation and histologic dedifferentiation. This study was carried out to verify the expression of p63 and cytokeratin 5 (CK5), as well as their relationship with cytokeratins 8/18 (CK8/18) and metalloproteinase 19 (MMP19), in DMBA-induced mammary tumors in mice fed a diet enriched with linoleic acid. Sixty 8-week-old virgin female balb-c mice were given by gavage 1 mg of 7,12 dimethylbenz[a]anthracecene (DMBA) dissolved in 1 ml of corn oil once a week for 6 weeks. Linoleic acid was supplied as 15 g of corn oil for each 100 g of standard diet. When tumors reached 1 cm in size, euthanasia was performed and mammary tissue was pooled for analysis. Formalin-fixed paraffin-embedded tumors were submitted to immunohistochemical study with CK5, p63, CK8/18 and MMMP19. Sixteen animals developed poorly differentiated adenosquamous carcinomas which were diffusely positive for CK5 and p63 and focally positive for CK8/18 and MMP19. Like p63, CK5 stained the poorly differentiated areas as well as the foci of squamous differentiation, suggesting that they may be used together in immunohistochemical panels to characterize squamous differentiation in poorly differentiated carcinomas. The focal positivity for CK8/18 may be attributed to suppressed gene expression or accelerated protein degradation. MMP19 expression indicates that progression towards an invasive phenotype and neoplastic dedifferentiation led to the disappearance of MMP-19 from tumor cells. In conclusion, the addition of linoleic acid to the diet of mice given DMBA induces mammary carcinomas with immunoprofile similar to the poorly differentiated human carcinomas suggesting that a fat diet may be involved in the pathogenesis of these neoplasms.

P 64
BREAST TUMOR RESEMBLING THE TALL CELL VARIANT OF PAPILLARY THYROID CARCINOMA

CAMESELLE-TEIJEIRO José1, ABDULKADER Ihab1, RUIZ-PONTE Clara2, REYES-SANTÍAS Rosa1, BARREIRO Francisco3, SOBRINHO-SIMÕES Manuel4

1Department of Pathology, 2Molecular Unit, and 3Department of Surgery, Hospital Clínico Universitario, University of Santiago de Compostela, Santiago de Compostela, Spain; 4Institute of Molecular Pathology and Immunology, University of Porto, Porto Portugal

The breast tumor resembling the tall cell variant of papillary thyroid carcinoma (BTRPTC) is a very unusual mammary carcinoma whose histologic and predominant nuclear features mimic a papillary thyroid carcinoma. We report a case of BTRPTC with cytologic, pathologic and molecular analysis. A 64-year-old woman presented with a palpable nodule in the right breast. Fine needle aspiration of breast mass disclosed abundant cellularity with isolated cells, sheets and papillary formations of epithelial cells with nuclear grooves. The tumor measured 5.2 cm. Histologically, the neoplastic cells were arranged in a solid to papillary architecture, with areas showing a follicular or cribriform pattern of growth. The neoplastic nests and papillae were made up of columnar to cuboidal cells with eosinophilic cytoplasm. In addition, the neoplastic cells showed numerous nuclear grooves and occasional eosinophilic pseudo-inclusions. Tumor cells were positive for cytokeratins (CAM5.2 and AE1/AE3), estrogen receptor-alpha and –beta, progesterone receptor, androgen receptor, CEA, and bcl-2. Thyroglobulin, thyroperoxidase, calcitonin, TTF-1, chromogranin, synaptophysin, vimentin, and galectin-3 were consistently negative. Because of the peculiar nuclear appearance of the cells of the BTRPTC, a previous study for RET/PTC rearrangements had been reported in the literature with negative results. Due to the fact that RET/PTC rearrangements and BRAF mutations are mutually exclusive etiopathogenetic events in papillary thyroid carcinomas we also searched for BRAF mutations, but no mutations were found. The awareness of the existence of mammary tumors that histologically mimic the tall cell variant of papillary thyroid carcinoma will avoid unnecessary clinical investigations. This work was supported by research grant (PGIDE 99PXI 90201B) sponsored by Xunta de Galicia, Spain.

P 65

PRIMARY ANGIOSARCOMA OF THE BREAST: CLINICOPATHOLOGICAL AND IMMUNOHISTOCHEMICAL ANALYSIS ON 4 CASES

OZLUK Yasemin(*), TUZLALI Sitki(*), YAVUZ Ekrem(*), DERIN Duygu(**), ASOGLU Oktar(***), ILHAN Ridvan(*), Iplikçi A(*)
(*)Istanbul University, Istanbul Faculty of Medicine, Department of Pathology
(**)Istanbul University, Institute of Oncology, Department of Medical Oncology
(***)Istanbul University, Istanbul Faculty of Medicine, Department of Surgery

Primary angiosarcoma of the breast (PAB) is an unusual neoplasm with an adverse outcome. The incidence of its association with pregnancy is reported as 6% of PAB.

The aim of this study is to detect the incidence, the hormonal status and the prognostic indicators of PAB.

The archieve material of our department was reviewed to identify clinicopathological features of PAB. Immunohistochemical analyzes were performed for antibodies CD31, CD34, ER, PR and Ki-67. During a 17-year period 4 cases of PAB were established out of almost 5000 breast biopsies. All patients clinically presented with a palpable mass. Two patients were at the end of their first trimester in pregnancy. The mean patient age at diagnosis was 40.8 years (29-56). All patients underwent simple mastectomy after an initial diagnosis on either excisional or incisional biopsy. None of the patients had received prior radiotherapy. Grossly, all tumors had hemorrhagic cystic spaces with solid, white coloured areas and ill-defined borders. The mean tumor size was 8.37 cm (2.5-12). One case revealed two masses of PAB, 9 cm and 1.3 cm in diameter. Two of the tumors were Grade I, one of the tumors was Grade II and one was Grade III, histologically. Immunohistochemistry revealed positivity for CD31 in all tumors and CD34 in 3. The mean score of Ki-67 index was 28.6% (2-54.6%). The tumor without CD34 immunoreactivity was Grade III and exhibited the highest Ki-67 index (54.6%). Two patients with Grade I tumor and with the lowest Ki-67 index were alive with no evidence of disease 7-8 years after surgery. One of the pregnant patients, having two foci of Grade II tumor, is still alive after 1 year follow-up with distant metastasis 5 months after surgery and has been receiving radiotherapy and chemotherapy. The patient with Grade III tumor died with disseminated disease one year after initial diagnosis.

Since, it was previously stated that grading is the most important prognostic indicator, we suggest that Ki-67 proliferation index may also be used for the same purpose. We also propose that at least two endothelial markers must be used in differential diagnosis, especially in poorly differentiated tumors in which expression of endothelial markers may be lost. No evidence of an association with hormonal status could be drawn, therefore, the occurrence with pregnancy should be related to the age of incidence. These statements need further investigations on large series of PAB.

P 66

LYMPHOEPITELIOMA-LIKE CARCINOMA OF THE BREAST: IS IT A DISTINCT ENTITY?

Reguero ME, Camarasa N, Gª Martos M, Santon A, Gª-Cosio M, Capote LF, Gonzalez-Palacios JF.

INTRODUCTION:
Lymphoepitelioma (LE), a tumor originally described within the nasopharynx, is an undifferentiated carcinoma with prominent lymphoid infiltration and with variable expression of the Epstein-Barr virus (EBV) genome within the tumor cells. There are only 13 cases of lymphoepitelioma involving the breast described in the literature, none of them associated with EBV. It is considered to be a less aggressive type of breast carcinoma.
MATERIALS AND METHODS:
A set of 30 breast cancer with prominent lymphoid intersticial infiltration were examined and selected from a total of 1226 reviewed biopsies. There were excluded from the study cases following the criteria for medullary carcinoma, cases with syncitial growing patterns higher than 75%, papillary areas, glands or carcinoma in situ, and cases with morphological features not consistent with LE.
The presence of EBV was subsequently analysed in 14 histologically confirmed cases of LE by immunohistochemistry (LMP-1), in situ hybridisation (EBERs) and PCR (LMP-1 terminal region and EBNAs). Morphological and complementary data (hormonal receptors, proliferation index, p53, and Her-2) were also evaluated.
RESULTS:
None of the cases were associated with EBV, 11 of them were N+, and all of them showed histological findings suggestive of high grade tumors (GIII), high proliferative activity (>25%), negative hormonal receptors (13) and high p53 expression (10). Two cases were HER 2 (+++).
CONCLUSIONS:
There is no evidence to considerer LE as a distinct entity of infiltrating breast carcinoma.

P 67

NON-HODGKIN'S LYMPHOMAS OF THE BREAST

P. Xirou1, V. Christoforidou1, D. Anestakis1, A. Bousoulegas2, F. Patakiouta1
Departments of Pathology1 and Breast Surgery2, "Theagenion" Anticancer Hospital, Thessaloniki, Greece

Introduction: Primary non-Hodgkin's lymphoma of the breast is a rare disease, constituting less than 1% of malignant mammary neoplasms. Lymphomas secondarily involving the breast are also uncommon. A lymphoma is considered primary if the breast is the first or major site of presentation, without concurrent nodal disease except for the involvement of ipsilaterar axillary nodes and with no previous history of extramammary lymphoma.
Materials and Methods: We report 5 cases of breast lymphoma, 3 primary and 2 secondary. All patients were female, ranging in age from 42 to 85 years. Of the 3 primary cases, one was classified as extranodal marginal zone B-cell lymphoma of MALT type, one as diffuse large B-cell lymphoma arising in a pre-existing maltoma and one as Burkitt lymphoma. In the other 2 cases, breast was secondarily involved by a MALT lymphoma of salivary gland and a nodal diffuse large B-cell lymphoma.
Discussion: Primary non-Hodgkin's lymphomas of the breast are uncommon. Two distinct clinicopathologic types have been described. One type occurs in pregnant or lactating young women as massive bilateral breast swelling and corresponds to a Burkitt lymphoma. The second and larger type usually affects postmenopausal women and presents with clinical features identical to those of carcinoma of the breast. This latter type, histologically, is usually a diffuse large B-cell lymphoma.
Differentiation must be made from benign lymphocytic infiltrations and non lymphoid neoplasms of the breast.
Primary lymphomas of the breast behave in a way similar to lymphomas of corresponding type and stage in other sites. Therapeutic management is controversial and consists of various combinations of surgery, radiation therapy and chemotherapy.

P 68
DIABETIC MASTOPATHY: REPORT OF FIVES CASES
S Hannachi Sassi, I Kadri, K Mrad, R Dhouib, I Abbes, M Driss, K Ben Romdhane.
Department of Pathology, Salah Azaiez Institute, Tunis, Tunisia.

Introduction: The diabetic mastopathy (D.M) is a benign disease of the breast parenchyma but may clinically simulate a breast carcinoma. This mastopathy usually occurs in women who suffered from insulin-dependent diabetes mellitus for some years.
Aims: To describe the clinical, radiological, histological features of this benign disease. M.D is little known by clinician, radiologist and pathologist.
Materials and methods: Five cases of M.D were examined during 7-year period from 1997-2003. We analysed the clinocopathological and immunohistochemical findings of the lobular lymphocytic infiltrate. Immunohistochemical profile (CD20 and UCHL-1) was analysed using avidin-biotin-immunoperoxidase technique.
Results: All cases were female. Three cases had type 1 insulin-dependant diabetes and one case had type 2 insulin-independant diabetes. In one case the type of diabetes was unknown. The mean age at presentation was 40.8 years (33-57). The mean duration of diabetes was 18.25 years (12-24). In one case the patient was treated 6 years ago for a medullary carcinoma of the homolateral breast (T1N0M0). All the palpable lesions were dense at mammography. Macroscopically, the mean size was 5.7 cm (2.5-8). The parenchyma was found to be a white and fibrotic plaque indistinctly separate from surrounding normal breast tissue. Histologically, the lesion was characterized by the association of three elements: a lobular lymphocytic infiltrate, perivascular lymphocytic infiltrate of variable intensity, often organized in lymphoid nodules and stroma fibrosis with myofibroblast hyperplasia. The lymphocytic infiltrate was predominantly of B phenotype in 2 cases, predominantly of T phenotype in 2 cases and equally B and T phenotype in 1 case.
Conclusion: Our epidemiological, clinical and radiological findings are in agreement with published data. The diagnosis of M.D is based on the confrontation of the clinical context, radiological and characteristic histological features.

P 69
GYNAECOMASTIA IN HIV-INFECTED MEN ON HIGHLY ACTIVE ANTIRETROVIRAL THERAPY: A CASE REPORT AND REVIEW OF THE LITERATURE
CARVALHO Leda, BOMBONATTI Fernanda, DALTRO Barbara, BRANDÃO Luis Felipe, ALVES Gustavo, TARRICONE Vicente
Faculty of Medicine – Fundação Lusíada/ Hospital Guilherme Álvaro-Santos, SP, Brazil.

An estimated 610.000 individuals were infected with HIV/AIDS in Brazil in 2001. The rate of reported AIDS cases increased from 10.6 per 100.000 in 1992 to a high of 18.7 per 100.000 in 1998. Brazil has experienced a stabilizing trend with rates of 16.5, 16.4, and 14.8 per 100.000 in 1999, 2000, and 2001, respectively. Since 1998, the death rate from AIDS has stabilized at 6.3 per 100.000. This tendency is attributed to Brazil´s guarantee of access to free antiretroviral drugs since 1996. HIV-infected patients who are treated with highly active antiretroviral therapy (HAART) can developed breast enlargement due to benign and malignant diseases. Benign disorders comprise gynaecomastia (GM), pseudoangiomatous stromal hyperplasia and lipomastia. We describe a case of HAART-induced left-sided gynaecomastia in a 42-year-old HIV-infected man treated with lamivudine and efavirenz for 2 years and discuss the pathogenesis of these lesions according to the literature. Physical examination showed a nontender, freely mobile nodular mass in the periareolar area of left breast measuring 6.5x5.0 cm. The patient underwent a complete excision of the lesion. The pathological examination revealed gynaecomastia with extensive pseudoangiomatous stromal hyperplasia. The patient developed GM of the contralateral breast after 7-month follow-up period. Gynaecomatia is not uncommun in HIV-infected men under HAART, especially in those taking efavirenz and didanosine.The role of antiretroviral therapy on GM development is still discussed.

P 70
SOLITARY FIBROUS TUMOR OF THE MALE BREAST: A CASE REPORT
CARVALHO Leda* , PERUSSO Vanessa* , TROCOLI Felipe* , SANTOS Erika* , GAVINO Joyce*, TARRICONE Vicente*, PEREIRA Emilio**
*Faculty of Medicine- Fundacao Lusiada/ Hospital Guilherme Alvaro- Santos, SP, Brazil
**Salomao e Zoppi Laboratories- Sao Paulo, SP, Brazil

Solitary fibrous tumor is currently recognized as a benign soft tissue neoplasm that may occur in almost every site in the body. The breast is rarely involved. We describe a case of this rare lesion with the clinicopathological and immunohistochemical findings. A 64-year-old- white man presented a left breast mass that grew in a 18-month period. He denied any steroid abuse and did not disclose any sign or symptom of endocrinopathy. Physical examination showed a large, firm, round, well circumscribed tumor measuring 14x12 cm, replacing the entire left breast. Contralateral breast was normal. The patient underwent a simple mastectomy. The gross appearance was that of a well circumscribed but unencapsulated solid nodule. On cut section, the tumor was pale white to grayish. Histological examination showed a spindle cell tumor with pushing borders, which was

composed of bland spindle cells, haphazardly arranged and admixed with collagen fibers. There were hypercellular areas alternated with hypocellular fibrotic areas. Mitosis, necrosis and haemorrhages were not seen. Immunohistochemistry revealed that the tumor cells were diffusely positive for vimentine, CD34 while myogenic markers (Desmine [D33], á-smooth muscle actin [1A4]), cytokeratin AE1/AE3 and S-100 protein were negative. The pathological diagnosis was Solitary Fibrous Tumor of the breast on the basis of the gross, histological and immunohistochemical findings. No recurrence or any other clinical problems have been noted in the 6-month follow-up period. The structural and immunohistochemical characteristics of these tumors are similar to those of a myofibroblastoma. Some investigators attempted to distinguish between the two entities and the diagnosis of solitary fibrous tumor is reserved for lesions actin-negative and CD34-positive.

P 71
CLINICOPATHOLOGIC FEATURES OF PHYLLODES TUMORS
AMALINEI Cornelia*, BALAN Raluca*, RADULESCU Doinita*, PRICOP Florentina**, COTUTIU Coriolan*
*Department of Pathology
**Department of Obstetrics and Gynecology
University of Medicine and Pharmacy Iasi, Romania

Phyllodes tumor represents a type of fibroepithelial breast tumor, previously named cystosarcoma phyllodes or periductal stromal tumor. The purpose of our study was the evaluation of the variability of clinicopathological features and its correlation with prognosis in this type of breast tumor. We present 6 cases of phyllodes tumors, diagnosed in patients of 34-59 years old. Fine needle aspiration cytology (FNAC) or needle core biopsies were applied in 3 cases, followed by intraoperatory examinations, in 2 cases. Fragments from the excisional biopsies were stained with usual stainings. Immunohistochemistry for vimentin, actin and desmin was applied. The clinical aspect was that of a firm, palpable, solitary, unilateral breast tumor, larger than 4 cm diameter (maximum 8.5 cm) and in only one case the tumors were multifocal, with diameter of 1 and 2 cm respectivelly, and history of rapid growth. Mammography revealed a rounded, lobulated, opaque mass, sharply defined in 4 cases and with indistinct borders in 2 cases. Cytology aspect was that typical of a fibroepithelial tumor, with excess bipolar stromal cells and fragments in the background. Gross pathology revealed nonencapsulated, well circumscribed external surface of nodules in 4 cases and a less circumscribed surface in 2 cases. Sections presented firm, bulging gray tissues, with papillary aspects. In 2 cases, small foci of necrosis and hemorrhage were observed. The main histologic hallmark was represented by an exaggerated structure of intracanalicular fibroadenoma (rising also issues of differential diagnosis) with increased cellularity, with epithelial-lined clefts and variable degree of epithelial hyperplasia. Three cases were diagnosed as benign, exhibiting well defined border, only few mitoses, modest cellular overgrowth and slight cytologic pleomorphism, with a correlation between the degree of epithelial proliferation and appearance of the stroma. 1 case presented invasive aspect, in the form of secondary fibroepithelial stromal overgrowth. One case presented the aspect of low-grade malignant phyllodes tumor, exhibiting microscopically invasive border, less than 5 mitoses/ 10 hpf, and moderate stromal cellularity. Immunohistochemistry expressed vimentin postivity, actin and desmin variable positivity. In one case a local recurrence was registered, corresponding to the high grade of the initial tumor.

P 72
EFFECTS OF ESTROGEN THERAPY IN POST-MENOPAUSAL WOMEN BREAST TISSUE MORPHOLOGICAL AND IMMUNOHISTOCHEMICAL EVALUATION.
LOGULLO angela, ELIAS Simone, HEINKE thais, KEMP Claudio BARACAT Edmund.

Introduction: Estrogen replacement therapy, isolated or combined with progestin has been prescribed widely in the past decade. However, many studies associate hormone replacement therapy (HRT) over 5 years with increased risk of breast cancer. Despite this important evidence, not much is known about the mechanisms by which hormones act on normal breast epithelium.

Objective: To analyze breast tissue of postmenopausal women before and after 6 months of continuous HRT with combined estrogen-progestin (0.625 mg of conjugated equine estrogens associated with 2.5 mg of medroxyprogesterone acetate).

Methods: All patients were evaluated before and considered clinically eligible to the HRT. Samples were obtained from the upper outer left quadrant, through a percutaneous large-core breast biopsy. All microscopic variables were evaluated by two independent observers. Morphology assessment included epithelial density and nuclear volume on hematoxylin-eosin stained slides. Morphometry was graphically analyzed with the use of IMAGELAB 2000 software, after image capture by the VIDCAP 32 system. Immunohistochemical reactions used a standard ABC method and included epithelial proliferative activity (Ki-67 index), expression of the estrogen and progestin receptors, and angiogenesis (CD-34).

Results: After 6 months of estrogen-progestin HRT, there was a significant increase in nuclear volume in late postmenopausal women. There was no difference in epithelial density, neither in Ki-67 labeling index and angiogenesis. Estrogen and progestin receptors expression did not change with the HRT.

Conclusions: Estrogen-progestin HRT during 6 months induced an enhanced nuclear volume of breast epithelial cells, suggesting an increase in their metabolic activity. However, it is this finding was observed only in late postmenopausal women. Other factors such as the exposure length, the type of hormone utilized, the timing of therapy initiation, the treatment regimen used and individual characteristics must be further evaluated.

P 73
MYOEPITHELIAL CARCINOMA ARISING IN AN ADENOMYOEPITHELIOMA OF THE BREAST: A CASE REPORT WITH IMMUNOHISTOCHEMICAL AND MUTATIONAL ANALYSIS
Ichiro Mori, Bo Han, Misa Nakamura, Yasushi Nakamura, Kennichi Kakudo
Department of Pathology, Wakayama Medical University

Adenomyoepithelioma of the breast is an uncommon tumor characterized by biphasic proliferation of both epithelial and myoepithelial cells. It was first recognized by Hamperl in 1970, and approximately 140 cases of adenomyoepithelioma in breast have been reported in English literature. Although most of adenomyoepithelioma has been considered to be benign, they can progress a malignant change and give rise to metastases in rare instances. Malignant transformation may involve epithelial, myoepithelial or both cellular elements of an adenomyoepithelioma. We report a 69-year-old female with a 2.5 cm mass in her right breast. Histological examination revealed a highly cellular neoplasm, consisting of a predominantly spindle cell proliferation admixed with scattered glandular epithelial lined spaces. The spindle cell component, which was surrounding the latter, proliferated in broad sheets, strands or multinodular fashion, and was separated by hyalinized collagenous stroma of varying thickness. Immunohistochemically, the spindle cells of the

tumor were diffusely positive for S-100, ƒ¿-SMA, GFAP (Glial fibrillary acidic protein), p63, and cytokeratin (CK) 14, whereas the glandular epithelial cells were strongly positive for EMA, CK19. Both glandular and myoepithelial cells were consistently negative for estrogen receptor (ER), progesterone receptor (PgR) and HER2/neu. These results confirmed biphasic epithelial and myoepithelial character of the tumor. On the basis of overall architecture, the tumor was classified as the spindle cell type of adenomyoepithelioma, and diagnosed as • gmyoepithelial carcinoma arising in an adenomyoepithelioma• h because of cytological atypia, high mitotic rate, and local invasion of the myoepithelial component. MIB1 index was high (>70%) in myoepithelial cells. Immunohistochemical study also revealed strong expression of P53 and phosphorylated extracellular signal-regulated kinase (ERK) 1/2 in myoepithelial carcinoma cells, but not glandular epithelial component. We hypothesized that myoepithelial cells in this tumor might possess p53 gene mutation. Laser capture microdissection (LCM) technique and mutational analysis revealed point mutation of p53 gene (T->C transversion at codon 176) in myoepithelial cells but not in glandular epithelial component and adjacent normal ductal epithelium. To our knowledge, this is the first report using mutational analysis on a malignant adenomyoepithelioma of the breast.

P 74
MYOEPITHELIAL LESIONS OF THE BREAST- THE DIAGNOSTIC PROBLEMS

CHMIELIK Ewa, SMOK-RAGANKIEWICZ Anna, WOLOSZYNSKA-PREIDL Krystyna, PONIKIEWSKA Dorota, STOBIECKA Ewa, JAWORSKA Magdalena, , SZCZENIAK-KLUSEK Bogna, GORAJ-ZAJAC Aleksandra , LANGE Dariusz
Department of Tumor Pathology, Centre of Oncology, M. Sk³odowska-Curie Institute, Gliwice, Poland

Introduction The myoepithelial cells are an integral part of the normal histology of the mammary glands. Lesions with striking overgrowth of myoepithelial cells are rare. Histologically and cytologically they may disclose different patterns, and some additional features may result in diagnostic errors.
Aim We report two cases of adenomyoepithelioma (tubular variant and spindle cell variant) and one case of adenomyoepithelial adenosis.
Material and methods We analysed their histologic, cytologic, immunohistochemical features and their differential diagnosis. The tumors were characterized by a bicellular pattern of gland-forming epithelial cells and proliferative myoepithelial cells. They showed foci of monotonous growth of myoepithelial cells devoid of glands with low mitotic rate (1-2 figures/10HPF) or middle mitotic rate (3-6 figures/10 HPF). Immunohistochemically myoepithelial cells were reactive with SMA, Actin, Calponin, but negative for Desmin. The cytologic features of adenomyoepitheliomas characterized by hypercellularity and clusters of regular polygonal cells with abundant pale cytoplasm (tubular variant) or sheets of spindle cells (spindle cell variant). The nuclei were round to oval with dispersed chromatin and small nucleoli.
Conclusion Failure to recognize adenomyoepithelioma or adenomyoepithelial adenosis may lead to an inappropriate diagnosis such as fibroadenoma, sclerosing adenosis, tubular adenoma, and even invasive carcinoma. Immunohistochemical examination is needed to distinguish epithelial cell proliferation from myoepithelial cell proliferation.

P 75
ADENOMYOEPITHELIOMA OF THE BREAST

N. Vladika, F. Patakiouta, P. Xirou, Ch. Tsompanidou, A. Bousoulegas*
Departments of Pathology and Breast Surgery*, Theagenion Anticancer Hospital, Thessaloniki, GREECE

Introduction: Adenomyoepithelioma (AME) of the breast is a very rare low-grade malignant biphasic tumor, morphologically and immunohistochemically identical to epithelial-myoepithelial cell carcinoma of salivary gland.
Materials and methods: We report 10 cases of adenomyoepithelioma of the breast. All patients were female, ranging in age from 27 to 87 years (average 58 years). One patient had a history of chronic lymphocytic leukemia, two patients had coexistent ductal carcinoma and another one had fibroadenomas in both breasts.
All tumors presented as palpable nodules, ranging from 1-7 cm in maximum diameter and were located in the peripheral portion of the breast (8 cases) or near the areola (2 cases). Patients were treated by local excision.The excised tumors had the typical macroscopical, histological and immunohistochemical features of adenomyoepithelioma.
Discussion: Breast and salivary gland tumors can share morphological features, but often differ in incidence and clinical behavior. Breast tumors showing pure myoepithelial or epimyoepithelial differentiation are rare.
AME of the breast is a biphasic tumor, with a distinctive architectural growth pattern (tubular, papillary or solid), that is composed of two cell types, epithelial and myoepithelial. It usually affects adult female patients and presents as a palpable nodule. Tumors are treated by local excision.
AMEs of the breast are currently classified as low grade malignant tumors that may recur and rarely metastasize, but their histoprognostic factors are not yet defined.
The prognosis of adenomyoepithelioma is usually good. Local recurrences can occur when the primary tumor has a tubular growth pattern and has been incompletely excised. Tumors consisting mainly of myoepithelial cells and/or with increased mitotic activity (> 2/10 H.P.F) can behave in a malignant fashion. Lung is the most frequent site of distant metastases.
As regards our patients, all are well, without recurrences and distant metastases.

P 76
EVALUATION OF FREQUENCY OF EPSTEIN-BAR VIRUS (EBV) IN VARIOUS HISTOLOGICAL SUBTYPES OF HODGKIN'S DISEASE

SHARIFI Noorieh MD , KATEBI Mehrdad MD

Introduction: The incidence of Hodgkin's disease (HD) shows marked heterogeneity according to age, gender, race, geographical state, socioeconomic position and histological subtypes. Recently, multiple studies in different countries applied by newer technologies such as Immunohistochemistry (IHC) and polymerase chain reaction (PCR), to being more familiar with the pathogenesis of this neoplasm. The Epstein-Barr virus (EBV) is detected with high incidence in HD cases, approximately 40-50% in developed countries and much more (up to 95% of cases) in developing countries. There is evidences that mixed cellularity (MC) Hodgkin's disease is more likely to be EBV-associated which is against association of nodular sclerosis (NS) subtype.
Purpose of the study: With regard to the geographical location of Iran and absence of similar documented research in our knowledge, it is need to perform studies like this.
Methods & Materials: This study was done by IHC method with antibody against latent membrane protein-1 (LMP1) antigen of EBV for assessment of relationship between EBV infection and parameters such as age, gender and histological subtype. We collected 30 paraffin section samples of HD and positive cytoplasmic reactivity of Reed-Steinberg (RS) cells was evaluated.

Results: From 30 cases that surveyed in this study only 2 cases were not immunoreactive for EBV marker which both was NS subtype in two adult male .We confirm frequency of 93% EBV associated HD in our cases and also confirm the above histological subtype distribution and that childhood cases are more likely to be EBV-associated than adult cases. There is possible female predominant of EBV associated HD. This survey as a pilot study needs further studies with more cases for distinct confirmation.
Conclusion:
It seems EBV is a strong etiologic factor especially in developing countries like Iran and in childhood cases.

P 77
EXPRESSION OF T-CELL MARKERS IN CLASSICAL HODGKIN LYMPHOMA IS RARE: A TISSUE MICROARRAY STUDY
ZIMPFER Annette 1, BOURGAU Caroline 1, KAISER Alexandra 2, PILERI Stefano A. 3, WENT Philip 1, TZANKOV Alexandar 2 and DIRNHOFER Stephan 1
1 Institute of Pathology, University Hospital Basel, Switzerland
2 Institute of Pathology, Medical University of Innsbruck, Austria
3 Chair of Pathologic Anatomy & Lymphoma Unit, Institute of Hematology and Clinical Oncology "L. & A. Seràgnoli", University of Bologna, Italy

Abstract (265 words)
Introduction and purpose of the study: In most instances, Hodgkin and Reed-Sternberg cells (HRSC) of classical Hodgkin lymphoma (cHL) are of B-cell origin. Nevertheless, expression of T-cell related antigens on HRSC has been observed in some cases, pointing to a possible T-cell origin. We comprehensively analyzed the expression of a panel of T-cell antigens in a large serie of classical Hodgkin lymphoma (cHL) cases under standardized conditions using the tissue microarray (TMA) technique.
Methods: A TMA containing 330 cHL cases was used. Expression of the T-cell antigens CD2, CD3, CD4, CD5, CD7 and CD8 was analyzed immunohistochemically. A case was considered positive if >20% of HRSC demonstrated specific staining. The HRSC of T-cell marker positive cases were microdissected (75 to 120 HRSC per case) and analyzed by a multiplex PCR for clonal immunoglobulin heavy chain- and T-cell receptor gamma (TCRg) gene rearrangements.
Results : Twelve cases (5%) expressed at least one T-cell marker in the following order: CD2 in 10 cases, CD4 in 5 cases, CD3 in 2 cases and C5 and CD8 in 1 case each. There was no CD7-positive case. The expression of more than one T-cell antigen was seen in 5 cases (2%). In the positive cases, a mean fraction of 40% of the HRSC (range 20-100%) expressed the T-cell markers analyzed. In two cases (<1%) a clonal TCRg gene rearrangement was demonstrated.
Conclusions: The expression of T-cell antigens in HRSC of cHL is rare (5%) and in most cases due to aberrant expression of these markers on HRSC of B-cell origin. Only isolated cHL cases may be true clonal T-cell proliferations.

P 78
SENSORY NEUROPATHY REVEALING A HODGKIN'S LYMPHOMA.
O.LAOUAR*, C.KAIDI*, N.OUKID*, N.LANKAR**, M.TAZIR**, A.LANKAR*
* Laboratoire d'Anatomie et de Cytologie Pathologiques CHU Annaba-Algérie.
** Service de Neurologie CHU Mustapha Alger-Algérie

Association of a sensory neuropathy with a Hodgkin's lymphoma is rare.
Causes of a such neuropathy might vary. They are either due to the Hodgkin's lymphoma itself, infiltrating the peripheral nervous tissue, to opportunistic infections, viral in particular such as the HIV, to neurotoxic effects of chemotherapy or to a systemic reason leading to a paraneoplastic syndrome.
Hereby, we report a case in which a young woman aged 30 years presented progressive worsening gait troubles for 8 months with pain and lower limbs heaviness, a fall of 15 kg weight and a pruritus on trunk and hands.
Bilateral upper and lower limbs reflexes were abolished, with tactile and vibratory hypoaesthesia. EMG confirmed the sensory neurogenic fit.
Chest and abdominal scanner showed large mediastinal and intra and retroperitoneal adenopathies. It also revealed the presence of numerous micro-nodules in lung, liver and spleen.
Biopsy of a right upon-clavicle node which appeared during hospitalization concluded to a scleronodular form of Hodgkin's lymphoma.
Medullary and sural nerve biopsy did not show any tumoral cells infiltration.
As far as etiopathogeny is concerned, the retained hypothesis is the one of a systemic origin

P 79
OSSEOUS PRESENTATION OF HODGKIN'S DISEASE: A CASE REPORT AND REVIEW OF THE LITERATURE
R. Dogan Koseoglu* Atilla Senaylý ** Unal Býcakcý** Nurper Onuk Filiz* Taner Sezer *** Tiraje Celkan****
*Department of Pathology, Gaziosmanpasa University Medical School, Tokat, Turkiye
**Department of Pediatric Surgery, Gaziosmanpasa University Medical School, Tokat, Turkiye
***Department of Pediatrics, Gaziosmanpasa University Medical School, Tokat, Turkiye
****Department of Pediatric Oncology, University of Istanbul, Cerrahpasa Medical School, Istanbul, Turkiye.

Although bone involvement in the later stages of Hodgkin's disease is an expected phenomenon, bone involvement in early stages of the disease are very rare. About forty-nine cases of Hodgkin's disease presented with bone involvement were reported in the literature. We reported a 14 years old boy initially evaluated with the pain at the left ilium localization. Although all the radiological examinations were targeting an osseous anomaly, pathologic evaluations of the pelvic lymphadenopathies determined the disease. We discussed the possible differential diseases and reviewed the literature for the osseous presentation of Hodgkin's disease.

P 80
EPSTEIN-BARR VIRUS INDUCED B-CELL PROLIFERATION OF HODGKIN AND REED-STERNBERG CELL GENO- AND PHENOTYPE MAY DEVELOP IN PERIPHERAL T-CELL LYMPHOMAS
PAJOR László, KAJTÁR Béla, JÁKSÓ Pál, LACZA Ágnes, LÁSZLÓ Renáta
Department of Pathology, Faculty of Medicine, University of Pécs, Pécs, Hungary

Introduction. Peripheral T-cell lymphoma (PTCL) can display not only a morphological, but also an immunophenotypical overlap with classical Hodgkin lymphoma (cHL) as PTCL may contain CD30 and CD15 as well as T-marker positive Hodgkin-Reed-Sternberg (HRS) cells of cHL type in a mixed inflammatory background of eosinophils, lymphocytes, histiocytes and plasma cells . The distinction between PTCL and cHL is further complicated by the rare variant of PTCL resembling cHL because of the presence of HRS type of cells which are constantly Epstein-Barr virus (EBV) and CD30 positive. Single cell molecular analysis of these cells indicated B-cell genotype, but lack of monoclonality.

Purpose of the study. To clarify the nature of the scattered HRS-like cells, without the aspecific inflammatory background of cHL, in PTCLs.
Methods. Three cases of PTCLs with scattered giant cells of HRS type, resembling classical cHL because of the inconspicuous to moderate atypia of the PTCL cells, are described. Immunohistochemistry, in situ hybridization for EBV encoded RNA (EBER) and immunoglobulin (Ig) light chains, antigen receptor gene rearrangement studies on whole tissue as well as sequencing and mutational analysis of the FRI-J region on DNA obtained from EBER+, flow sorted nuclei were performed.
Results. Monoclonal rearrangement of the T-cell receptor gamma gene in whole tissue DNA extract as well as constant EBV association (EBER+, LMP-1+) of the HRS cells could be proved in all three cases. In one tumor, the HRS cells exhibited the CD15-, CD20+, CD30+, CD45+ phenotype and polyclonal Ig heavy chain (IgH) gene rearrangement in flow sorted, EBER+ nuclear preparation. In the other two lesions, however, the HRS type cells exhibited the CD15---/+, CD20--/+, CD30+, CD45- phenotype, lacked any light chain mRNA expression and showed clonal IgH gene rearrangement. In one of these two cases the IgH-V gene mutation and Ig gene associated transcription factor (Oct2, BOB.1/OBF.1) expression patterns corresponded to those of HRS cells in cHL.
Conclusion. EBV induced B-cell proliferation in a PTCL related immunosuppression may range from a polyclonal activation state even to HRS cells being indistinguishable in pheno- and genotype from those in cHL of B-cell origin and these latter cells might be the neoplastic precursor cells for a pathomorphologically overt cHL.

P 81

TITLE: IMMUNOHISTOCHEMICAL MARKERS CAN BE OF PREDICTIVE VALUE IN HODGKIN'S LYMPHOMA RESPONSE TO TREATMENT. A PRELIMINARY STUDY OF 23 CASES.

CANIONI Danielle, DEAU Bénédicte, TAUPIN Pierre, DELARUE Richard, VASILIU Viorel, BROUSSE Nicole, HERMINE Olivier.
Pathology, Hematology and Biostatistics Departments, Hôpital Necker, Paris, France and Université René Descartes, Paris V, France.

Hodgkin's lymphoma (HL) belong to the most curable tumor diseases in adults and about 80% of patients can be cured with modern treatment strategies. However, some HL are primary refractory to usual treatments and only clinical factors are considered as relevant for prognosis. In the current study we evaluate immunohistochemical markers of apoptosis, proliferation and of the environmental non neoplastic cells in HL in order to predict their prognostic value in treatment response. A retrospective study was performed on pre-treatment biopsy specimen of 23 patients presenting with HL, 8 with primary refractory HL and 15 responding well to chemotherapy and free of disease for 2 or 3 years. These patients ranged in age from 23 to 52 years old (median= 36.5 years) for refractory HL and from 21 to 75 years old (median = 37.9 years) for responding patients. All refractory HL, except one for whom histological type could not be precised(too small biopsy), had a nodular sclerosis (NS) histological type. The histological type was NS in 13 responding patients and mixed cellularity for the 2 others. The semi-quantitative immunohistochemical study used CD30, bcl2, p53, Ki67, TiA1 and c-kit antibodies. The results were statistically evaluated using a Wilcoxon sum rank test. CD30 and Ki67 were strongly expressed on Hodgkin (Hg) and Reed-Sternberg (RS) cells whatever patients were refractory or responded well to chemotherapy. By contrast, p53 and bcl2 had a significantly higher expression on Hg or RS cells in refractory patients (median = 90% & 60%) compared to responding HL (median = 42.5% & 8%) (p=0.0001 & p=0.026 respectively). The cytotoxic marker TiA1 stained a significantly higher number of small lymphocytes in refractory HL (median=53 per high power field (hpf)) compared to responding patients (median=24 per hpf) (p= 0.0003). C-kit antibody was negative in Hg or RS cells but stained significantly more mastocytes in refractory HL (median=13 per hpf) comparing to responding HL (median=3.8 per hpf) (p= 0.001). These results indicate that some immunohistochemical markers may be useful for predicting the response to therapy of HL. A high expression of bcl2 and p53 in refractory HL supports the notion that an intact apoptosis cascade is essential for cell killing effect of chemotherapy. The increasing of TiA1 and c-kit positive cells raises the importance of the environmental non-neoplastic cells in HL. A larger study is mandatory to confirm these preliminary results.

P 82

EPSTEIN-BARR VIRUS (EBV) AND HODGKIN'S DISEASE IN A MOROCCAN CENTRE

L. Jabri*, F. Marnissi*, M. Karkouri*, A. Madani**, A. Iraqi*
* Pathology Department, ** Hematology and pediatric oncology; University Hospital Ibn Rochd, Casablanca, Maroc

The Epstein-Barr virus (EBV) has been implicated as a contributing factor in the development of Hodgkin's disease (HD). Western cases of Hodgkin's disease have shown the presence of EBV in tumoral cells in approximately 50%. The presence of EBV varied according to the histological subtype. Mixed cellularity HD is more like to be EBV-positive compared with nodular sclerosis. The purpose of our study is to analyse the prevalence of EBV in this disease in a Moroccan population using immunohistochemical detection of latent membrane protein LMP-1.
We studied a total of 62 cases of classical Hodgkin's disease, diagnosed between January 2004 and December 2004. Of 10 patients (16 %) less than 15 years of age (childhood), 5 had a nodular sclerosis subtype, 4 mixed cellularity, and one unclassified. Of the 52 from patients aged 15 years and above, 30 (58%)
had nodular sclerosis, 20 (38,50 %) mixed cellularity, and 2 unclassifiable. 11 patients were 50 years and above (5 sclerosis nodular, 5 mixed cellularity and 1 unclassified). All the cases were tested for CD30 and CD15. 95% were CD30 positive and 83% were CD15 positive.
Positive immunostaining for LMP1 was demonstrated in 39 / 62 cases (63 %) respectively 50% in sclerosis nodular and 47 % in mixed cellularity . In the younger age group, 7 of the 10 cases (4 mixed cellularity, 2 nodular sclerosis) showed the presence of EBV (70 %). In the older age group, EBV was detected (61,50%) in the following proportion: 33% nodular sclerosis, 29 % mixed cellularity.
The results of the current study showed that nodular sclerosis HD is more frequent (53 %) than mixed cellularity (42%), without bimodal distribution. The peak of incidence was between 15 and 50 years. The findings suggest also, a strong association of EBV with Hodgkin's disease in Moroccans (39/62, 63%), especially in children when it reach 70%. In this study there was no evidence of predominance association of EBV in mixed cellularity HD. Our results must be confirmed by in situ hibridization.

P 83

B-CELL DIFFERENTIATION IMMUNOPHENOTYPES IN CLASSICAL HODGKIN LYMPHOMAS

V. Panoulas (1), A. Papoudou-Bai (2), S. Kamina (1), N. Horianopoulos (1), P. Kitsoulis (2), K. Stefanaki (3), D. Rontogianni (4), N.J. Agnantis (1), P. Kanavaros (2), M Bai (1)

Department of Pathology (1) and Department of Anatomy-Histology-Embryology (2), Medical Faculty, University of Ioannina, Department of Pathology, Agia Sophia Hospital, Athens (3), Department of Pathology, Evangelismos Hospital, Athens (4), Greece

The bcl6/CD10/MUM1/CD138 B-cell differentiation immunophenotypes were analyzed in 101 cases of classical Hodgkin lymphomas (cHL) in order to gain further insight in their histogenesis.
Three major bcl6/CD10/MUM1/CD138 immunophenotypes were distinguished on the basis of the immunohistochemical positivity of Hodgkin and Reed-Sternberg (H/RS) cells: a) the late germinal center (GC)/early post GC B-cell-like immunophenotype (bcl6-/CD10-/MUM1+/CD138-); 59/101 cases (59 %), b) the post GC B-cell-like immunophenotype (bcl6-/CD10-/MUM1+/CD138+); 24/101 cases (24 %) and c) the indeterminate immunophenotype 18/101 cases (18 %) (bcl6+/CD10-/MUM1+/CD138-: 14 cases and bcl6+/CD10-/MUM1+/CD138+: 4 cases).
The above findings indicate that H/RS cells in most cHL display bcl6/CD10/MUM1/CD138 immunophenotypes consistent with late GC/early post GC or post GC B-cell differentiation. In addition, H/RS cells in a small fraction of cHL display indeterminate bcl6/CD10/MUM1/CD138 immunophenotypes which are characterized by simultaneous expression of GC, late GC/early post GC and post GC B-cell differentiation proteins. These immunophenotypes do not correspond to the differentiation immunophenotypes of normal B-cells and their identification in a part of cHL suggests that the differentiation process of H/RS cells is not complete in a fraction of these cells and/or is still ongoing at the time of observation.

P 84
PROLIFERATION PROFILE OF CLASSICAL HODGKIN'S LYMPHOMAS. INCREASED EXPRESSION OF THE PROTEIN CYCLIN D2 IN HODGKIN AND REED-STERNBERG CELLS.

E. Tsanou (1), A. Goussia (1), S. Kamina, (1), C. Grepi , (1), K. Stefanaki (2), D. Rontogianni (3), V. Galani (4), N. J. Agnantis (1), P. Kanavaros (4), M. Bai (1)
Department of Pathology, Medical Faculty, University of Ioannina (1), Department of Pathology, Agia Sophia Hospital, Athens (2), Department of Pathology, Evangelismos Hospital, Athens (3), Department of Anatomy-Histology-Embryology, Medical Faculty, University of Ioannina (4), Greece

There is accumulating evidence that Hodgkin and Reed-Sternberg cells of classical Hodgkin's lymphomas display multiple and concurrent alterations in different pathways and checkpoints of the cell cycle. However, the expression of cyclin D2 and its relation to other major cell cycle proteins has not been analyzed in classical Hodgkin's lymphomas.
The aim of the present study was to assess expression of cyclin D2, Ki67, cyclin A, cyclin B1, cyclin D1, cyclin D3, cyclin E, p53, Rb, p16 and p27 proteins in order to gain further insight in the proliferation profile of classical Hodgkin's lymphomas.
Overexpression of cyclin D2 in Hodgkin and Reed-Sternberg cells was detected in 64/89 (72%) cases of classical Hodgkin's lymphomas. This finding, in view of recent in vitro data showing that constitutive activation of nuclear factor (NF)-kB could upregulate cyclin D2 expression in part via signal transducer and activator of transcription (STAT)-5a, suggests that induction of cyclin D2 expression may support the proliferation of Hodgkin and Reed-Sternberg cells. In addition, the present study showed that 1) increased p27 expression status was significantly correlated with higher levels of cyclin A expression ($p=0.048$) and 2) increased p53 expression status was significantly correlated with higher levels of cyclin A ($p<0.001$) and cyclin B1 ($p=0.040$) expression. The association between increased p27 and p53 expression status and higher expression levels of G2/M cyclins suggests that the impairment of the growth inhibitory activity of the p27 and p53 tumor suppressor pathways may promote the proliferation of Hodgkin and Reed-Sternberg cells.

P 85
RECTAL EPSTEIN BARR VIRUS POSITIVE HODGKIN LYMPHOMA IN A PATIENT WITH CROHN'S DISEASE

S. Kamina (1), M. Economou (2), K. Katsanos (2), Ch. Bali (3), E. Arkoumani (1), E, Balasi (1), E. Sintou-Mantela (1), A. Kappas (3), E. Tsianos (2), M. Bai (1)
Department of Pathology (1), Departnent of Hepato-Gastroenterology (2) and Department of Surgery (3), Medical Faculty, University of Ioannina, Greece

Primary gastrointestinal Hodgkin lymphomas arising in the setting of Crohn's disease (CD) are rare. Only ten cases have so far been reported. A strong association with Epstein Barr virus (EBV) infection, similar to that found in post-transplantation immunosuppression-related lymphoproliferative disorders, has been suggested.
We present a 35-year-old man with ileocolonic Crohn's disease diagnosed at the age of 27, several months after an operation for a colorectal adenocarcinoma. Patient was on maintenance treatment with immunosuppressants and additionally he received two doses of infliximab. Seven years after adenocarcinoma diagnosis, the patient presented with anal pain and diarrhea. At that time digital examination revealed a small rectal area, which was thick in digital contact leaving blood traces at palpation. Rectosigmoidoscopy and subsequent biopsies from this area located 5 cm above the anal ring were compatible with rectal Hodgkin lymphoma. Histopathological examination revealed extensive ulcerations of the mucosa and diffuse infiltration composed by a mixed inflammatory cell population and numerous Hodgkin and Reed-Sternberg cells. The tumor cells showed the immunophenotype of classical Hodgkin lymphoma (CD15+, CD30+, CD45-, CD20-, CD3-, EMA-). In situ hybridization study with EBV RNA 1/2 (EBER 1/2) probes and immunohistochemistry for the latent membrane protein-1 (LMP-1) showed that almost all tumor cells carried EBV infection. No peripheral lymph nodes were noticed and CT examination showed no evidence of visceral lymph node enlargement or hepatosplenic lesions. Anal ultrasonography showed a hypo-echogenous lesion (1.5X2 cm2) extending to the one third of the whole rectal wall perimeter. Perirectal fat was invaded. Bone marrow biopsy was normal. Infliximab administration was discontinued and patient underwent chemotherapy. After a eighteen-month follow up, the patient does well with no evidence of secondary lesions or further local progression.
We present herein a primary rectal EBV positive Hodgkin lymphoma metachronous to a colorectal adenocarcinoma in a Crohn's disease patient who was on maintenance treatment with immunosuppressants. It is suggested that immunosuppressive drugs may facilitate the emergence of a EBV-positive neoplastic clone, but this scenario still remain only theoretical.

P 86
THE COMPARISON OF IMMUNOHISTOCHEMICAL EXPRESSION OF CD34, VEGF AND CD44 IN LYMPH NODE AND BONE MARROW INFILTRATES BY HODGKIN'S LYMPHOMA

CEMERIKIC-MARTINOVIC Vesna,*TERZIC Tatjana, PERUNICIC Maja, BOGDANOVIC Andrija, PETROVIC Milan, MIHALJEVIC Biljana, JANKOVIC Snezana, NEDELJKOV-JANCIC Ruzica, TOMIN Dragica, BOSKOVIC Darinka.

Institute of Hematology, Clinical Center of Serbia, Belgrade, Serbia and Montenegro,
*Institute of Pathology, School of Medicine, University of Belgrade, Belgrade, Serbia and Montenegro

Introduction: Bone marrow (BM) infiltration is present in 5-15% of patients with Hodgkin's lymphoma. It is usually associated with prominent fibrosis and proliferation of blood vessels. Limited information exists about the significance of neoangiogenesis and expression of "homing receptor" CD44 in Hodgkin's lymphoma.
Aims: In this study we analyzed immunohistochemical expression of CD34, VEGF and CD44 in lymph node (LN) and BM infiltrate by Hodgkin's lymphoma.
Methods: We identified 40 patients (29 male and 11 female, median age 45 years) with BM infiltration by Hodgkin's lymphoma. The most frequent histological type was nodular sclerosis (28/40). Slides from paraffin embedded LN and BM biopsy of the same patient were stained with haematoxylin&eosin and reticulin fibers (Gordon-Sweet). Microvessels were visualized by immunohistochemical staining for CD34. We counted the number of vessels per 400x high power field (hpf) in the area of most dense vascularization. All samples were further analyzed for the expression of VEGF and CD44 in neoplastic Hodgkin-Reed-Sternberg (HRS) cells. The intensity of staining was graded as weak, moderate and strong.
Results: In majority of patients (31/40) we found marked increase of microvessels density, which correlated with the number of VEGF-positive HRS cells. Expression of CD34 was almost twice lower in BM than in LN in majority of patients. We observed that mean vessels count per hpf in LN was 12.0, but in BM this count was 7.5/hpf. The intensity of VEGF expression in HRS cells was usually strong in LN and moderate in BM infiltrate of the same patient. Immunohistohemical expression of CD44 both in LN and BM was high in HRS cells in majority of patients (35/40), but in this group of 35 cases, in 4 cases HRS cells lost CD44 expression in BM infiltrate.
Conclusion: Our findings suggest that neoangiogenesis in BM infiltrates by Hodgkin's lymphoma was extensively increased. Therefore, the density of microvessels and expression of VEGF may provide useful prognostic information. The results of CD44 expression might suggest causal involvement of this marker in the progression of Hodgkin's lymphoma, especially nodular sclerosis type.

P 87

EXPRESSION OF NITRIC OXIDE SYNTHASES IN CLASSICAL HODGKIN LYMPHOMA: ROLE ON APOPTOSIS DEREGULATION AND INFLUENCE ON CLINICAL OUTCOME

Campos AHJFM(1), Aldred VL(2), Ribeiro KCB(3), Nonogaki S(4), Neves JI(1), Santos OP(1), Ferreira SS(1), Braga CEN(1), Vassalo J(5), Soares FA(1).
Department of Pathology, Centro de Tratamento e Pesquisa Hospital do Câncer A C Camargo, São Paulo(1), Department of Pathology, Faculty of Medicine, University of São Paulo, São Paulo(2), Cancer Registry, Centro de Tratamento e Pesquisa Hospital do Câncer A C Camargo, São Paulo(3), Ludwig Institute for Cancer Research, São Paulo(4), Department of Pathology, Faculty of Medical Sciences, State University of Campinas, Sao Paulo(5). BRAZIL

Introduction: Hodgkin Lymphoma (HL) is a monoclonal neoplasm in which the neoplastic cells, named Hodgkin-Reed&Sternberg (H-RS) cells, bear somatic mutations in immunoglobulin genes, inactivating immunoglobulin production. Unlike normal B lymphocytes, which suffer apoptosis when failing to produce immunoglobulins, H-RS cells, by mechanisms not fully understood, are capable of escaping apoptotis. Nitric oxide (NO), a molecule involved in multiple steps of carcinogenesis, is produced by a family of enzimes known as the nitric oxide synthases (NOS), which have been shown to be overexpressed in many human tumors. NOS expression and NO production in HL have not been described yet. Objective: This study analyzed the role of NOS and apoptosis-related proteins expression in HL, to test the hypothesis that NOS expression and NO production are involved in the defective apoptotic program of HL. The role of EBV on NOS expression and NO production was also studied. Finally we investigated the influence of NOS expression on the clinical outcome of HL's patients. Material and methods: 171 cases of HL were retrieved from the archives of the Departamento de Patologia do Hospital do Câncer A C Camargo. Relapse biopsies and HIV-associated HL were excluded. Immunostains with antibodies against NOS1, NOS2, nitrotyrosine, bcl-2, bax, p53, fas, fasL and LMP1 were performed. Cases were also tested for EBV status using in situ hybridization for EBER-1. Results: NOS1 and NOS 2 expression were detected in 42.1% and 55% of the cases, respectively. Nitrotyrosine expression was observed in 18.7% of the cases. Bcl-2, bax, p53, fas, fasL and LMP1 expression were positive in 35.1%, 44.4%, 44.4%, 93,6%, 5.8% e 49.7% of the cases, respectively. EBER-1 was detected in 46.8% of the cases. Significant associations were established between bax and p53 (p=0.036), bax and fasL (p=0.046), NOS1 and p53 (p=0.006), bax and NOS2 (p=0.022); and between bcl-2 e NOS2 (p=0.034). An inverse correlation was observed between EBV (LMP-1) and NOS2 (p=0.018), and between EBV and bcl-2 (LMP-1, p=0.002; EBER, p=0.006). NOS2 expression was associated with a shorter overall survival (p=0.0098). It also predicted a poor prognosis in cases treated with MOPP/ABVD (p=0.0003). Conclusions: H-RS cells express NOS and produce NO, which appear to play a role in the defective apoptotic program of HL. NOS2 may be involved in bcl-2 overexpression in EBV-negative HL. NOS2 expression is associated with a poor outcome in HL.

P 88

FREQUENT ASSOCIATION OF BOB-1 AND MUM-1 IN EBV INFECTED EGYPTIAN CLASSIC HODGKIN LYMPHOMA

H. Abd El All, P. Gaulard

Background: Previous studies concerning the expression of Bob-1, MUM-1 and Bmi-1 in classic Hodgkin lymphoma (CHL), confirmed the expression of Bmi-1 and MUM-1 in Hodgkin/Reed-Sternberg (H/RS) cells, while almost all the researchers agree on the lack of Bob-1 expression pointing out to a defect in transcription machinery associated with lack of immunoglobulin gene expression. Objectives: To study the expression of Bob-1, MUM1 and Bmi-1 proteins in Egyptian CHL and to correlate this expression with EBV viral load. Methods: Paraffin sections of randomly selected 24 CHL cases were included: 3 lymphocyte rich (LR), 6 mixed cellularity (MC), 13 nodular sclerosis (NS) and 2 lymphocyte depletion (LD). Results: All the cases except five (two MC and three NS) were positive for EBV by in-situ hybridization and immunostaining for LMP-1. Unexpectedly, strong to moderate nuclear Bob-1 expression was observed in 94% of cases ranging from 25-100% of the neoplastic cells. Moderate MUM-1staining, observed in 94% of cases, was nuclear, nucleolar and cytoplasmic. The percentage of MUM-1+ cells ranged from 25-75%. Mild to moderate nuclear bmi-1 positivity was observed in 56% of cases; few to 25% of bmi-1+ cells were identified. There was a frequent co-expression of Bob-1/MUM-1 in all the cases ($p<0.005$). This expression parallels the EBV positive H/RS cells. Conclusion: These findings concerning the expression of Bob-1, MUM-1 and Bmi-1 in the Egyptian population are different from the Western ones denoting different genetic and environmental factors. Does this difference should be taken into

consideration in the treatment strategy? A point under consideration.

P 89

CLINICOPATHOLOGIC PROFILE OF HODGKIN DISEASE IN A MOROCCAN CENTRE. ABOUT 269 CASES

L Jabri*, F. Marnissi*, A. Madani**, S Zamiati*, A Iraqi*
*Central Department of Pathology,
**Hematology and pediatric oncology department Ibn Roshd University Hospital, Casablanca, Morocco

Epidemiological distribution of Hodgkin disease (HD) show in developping countries two peaks occurence, one in childhodfor boys and another in older adults. The subtype of HD that occurs most often in this countries is cellularity mixed. In developping countries ther is a bimodal age specific incidence rate with early peak in adulthood and another in advanced age.
In order to define epidemiologic and histoprognosis aspects of the Hodgkin disease, we conduct a retrospective study on 269 cases recorded at the departement of Pathology, Ibn Rochd University Hospital, Casablanca, between 1997 and 2001. The mean age of our patients is 40 [04-84 years]. The sex-ratio is 1,5. Incidence according to age finds a peak between 17 and 35 years, without bimodal repartition. Actually, 74,3% of our patients are less than 40, 17% only are under 14. The predominant histologic type is the sclerosisnodular (SN) (70,5%) versus 26,8% for the cellularity mixed subtype (CM) . The SN subtype is predominant without regard of age (< 14 years, 14-40 years and >40 years). The bone morrow biopsy showed invasion in 30% . The immunohistochemistry study was realised in 80 cases (29,7%). CD15 was positive in 84,4 % and CD 30 in 93,7% . Stage III et IV constitute 64,43%. The rate of complete remission is 69,5%. This rate is 89% for the under 40 years old and only 64,4% for the more 40 years old.
Factors that influe on the complete remission rate are : the advanced age (the rate of complete remission of the patients <40 ans is 89>% versus 64,4 % for patients under 40 years old; the histologic subtype, but we find that complete remission in mixed cellularity subtype is higher than sclerosis nodular subtype.
The absence of bimodal distribution according to age, predominance of the SN subtype and the diffuse stages are the main characteristics of our study.

P 90

NODULAR LIVER INVOLVEMENT IN A PATIENT WITH MULTIPLE MYELOMA

I.D.Venizelos1, E.Mandala2, Z.A.Tatsiou1, I.Paradias2, L.Kampas1 , D.Sioutopoulou1

1 Department of Pathology, Hippokration Hospital, Thessaloniki
2D' Department of Internal Medicine, Aristotelian University of Thessaloniki, Hippokration Hospital, Thessaloniki, Greece

Multiple myeloma (MM) is a malignant plasma cell disorder characterized by the production of a monoclonal immunoglobulin. Recurrent infections, anemia, osteolytic lesions and renal insufficiency are the typical clinical manifestations. Liver involvement in the form of solitary or multiple nodules is extremely rare.

We report the case of a 42-year –old male, who presented in our hospital due to pathologic fracture of his right femur. From the hematological examination, bone marrow aspiration and biopsy, the diagnosis of IgG-k MM was made. The patient was treated with oral melphalan and prednisone. Three years later, at the time of reevaluation, it was found pancytopenia, multiple lytic bone lesions, diffuse osteopenia, renal function impairement, but normal liver function. Bone marrow biopsy showed an hypocellular marrow and infiltration by plasma cells (30%). He was treated with VAD regimen for only one cycle, because of severe cardiac complications, and pulse dexamethasone. Whole blood cell counts and renal function improved, but he developed progressive impairment of liver biochemical parameters. A CT scan revealed multiple hypodense liver lesions. A fine needle CT-guided biopsy of a liver nodule was performed to rule out metastasis of another origin. Histological examination showed infiltration of the liver by plasma cells which were positive for CD138 and k-light chain. A bone marrow biopsy at the same time showed plasma cell infiltration (60%). The patient underwent treatment with proteasome inhibitor bortezomib, showing improvement of renal function but progressive hepatic failure with portal hypertension and ascites.

We present this case because liver involvement by MM in the form of multiple nodules is extremely rare in living patients. Conclusively, liver infiltration should be suspected in a case of nodular liver lesions in patients with known MM.

P 91

MYELODYSPLASTIC LESIONS IN THE BONE MARROW OF PATIENTS WITH MULTIPLE MYELOMA AT FIRST DIAGNOSIS.

Hadjileontis C1, Zervas K2, Papaioannou M2, Papadimitriou C1, Kaloutsi V1.
Technicians1: Tsatsaroni A, Avgoloupi A.
1. Pathology Dept, Medical School, Aristotle University of Thessaloniki, Greece.
2. Haematology Clinic, Theagenion Cancer Hospital of Thessaloniki, Greece.

INTRODUCTION: The myelodysplastic lesions (MDL) in the bone marrow (BM) of patients with multiple myeloma (MM) that are more widely known are the ones related to the therapeutic treatment. Studies on MDL as a result of the toxicity that myeloma cells may have on the haemopoietic BM and are present at first diagnosis have not until now been reported.
PATIENTS AND METHODS: We investigated the presence of MDL in BM biopsies (H+E stains) as well as in BM and peripheral blood imprints (May Gruenwald Giemsa stains) of 80 patients with newly diagnosed MM. Each case was evaluated by two observators. The presence of MDL was statistically correlated with the percentage of infiltration for each case (paired t-test) and the survival of the patients (Spearman's and Kruskal-Walis's tests).
RESULTS: MDL were present in 35% of the patients and they were similar to those observed in myelodysplastic syndromes, but of less severity. They concerned mainly the red cell line (33,75%), secondarily the granulocytic line (10%) and less often the megakaryocytic line (6,25%), while MDL from two of the three lines were found in 10% of the cases and from all the three lines in 3,75% of the cases. Statistical analysis brought up a significant correlation between the presence of MDL and the percentage of MM infiltration ($p<0,01$), as well as between MDL and patients' survival ($p<0,01$).
CONCLUSIONS: We demonstrate the prognostic value and therefore the diagnostic significance of the presence of MDL in the BM of patients with MM. Due to the absence of other relevant data in the current literature more research should be performed.

P 92

BONE MARROW FIBROSIS IN PATIENTS WITH MULTIPLE MYELOMA

Janusz Dzieciol, Dorota Lemancewicz, Janusz Kloczko, Katarzyna Zietara

Bone marrow fibrosis is a reactive process that results from an increased stimulation of fibroblast proliferation and collagen synthesis. Multiple myeloma (MM) is a malignant neoplasm characterised by the increase of clonal plasma cells in bone marrow. The levels of cytokines, which are responsible for fibrosis, are raised in patients with MM as compared to healthy patients. Histopathological examination of bone marrow by bone marrow trephine biopsy (BMT) makes possibility for evaluation of the degree of reticulin fibrosis (an increasing number of argentophylic fibres) and collagen fibrosis (an increasing number of collagen fibres). BMT is also used for the assessment of bone marrow involvement by plasma cells. The aim of the study was to determine the degree of bone marrow fibrosis in patient with multiple myeloma. The specimens were obtained by BMT from 82 patients with multiple myeloma, as initial examinations prior to any treatment, from the postero-superior iliac spine using the Jamshidi needle. Bone marrow tissue was carried out in Oxford solution and paraffin embedding. Hematoxylin and eosin, Gomori's, AZAN staining was applied. The degree of bone marrow fibrosis using Kundel criteria with Bauermeister modification was determined. The morphometric tests were done using the image analysis (DP 12) for evaluation the percentage of plasma cells infiltration. Nodular and diffuse patterns of infiltration in bone marrow by plasma cells were observed in 67 patients. In the most of patients the marrow was infiltrated in diffuse pattern. The infiltration was accompanied by an increase in the number of reticulin fibres. The frequency of reticulin fibrosis was positively correlated with advanced clinical stage according to the classification of Durie and Salmon. Collagen fibrosis was found in 13 patients. BMT is a useful method for assessing the degree of myelofibrosis in MM. It has prognostic value, because when the collagen fibrosis is present, only partial regression after treatment is possible.

P 93

PLASMABLASTIC MICROLYMPHOMA ASOCIATED WITH A MULTICENTRIC CASTLEMAN DISEASE IN A HIV+ PATIENT

DE PINIEUX Isabelle,MOLINIE Vincent, BALATON André, HOMSI Toufik, departement of pathology
AUPERIN Isabelle, departement of internal medicine
hospital Saint Joseph, 182 rue R. Losserand, 75014 Paris

Multicentric Castleman's disease (MCM)in HIV+ is associated with human herpes virus 8 (HHV8)infection. Most of the patients present a mixed histological pattern : hyaline-vascular variant and plasma cell variant. HHV8 infected cells are plasmablasts localized within the mantle zone or organized in small sheets of large plasmablastic cells or in a microlymphoma toward aggressive NHL.
Aim of the study: evaluation of HHV8 antibody in a plasma cell variant of MCM in a HIV+ 34 year's old man who presented cervical polyadenopathy with night sweats, fever and inflammmatory biological abnormalities.
Materiel and methods: immunostaining were performed on formol fixed, paraffin embedded 3microns sections on a Dakostainer with CD3(1/75),CD20(1/150), CD68(1/500),CD138 (1/50), CD15(1/200), CD30(1/200), EMA(1/50), HHV1 et 2 (2/2500), kappa (1/15000), lambda (1/15000) Dako;CMV(1/300)Biosoft and HHV8(1/25)Novocastra.
Results : histological evaluation of one of these adenopathy revealed atrophic lymphoid follicles with small germinal centers and peripheal onion lymphoid arrangement, hyaline vascular proliferation, mixed with regular plasma cells sheets in the interfollicular zone. In small foci, the peripheral sinus exhibites small sheets of large lymphoid cells with atypical nuclei and prominent nucleoli. These atypical cells were HHV8+ whereas plasma cells were negatives. These large cells were also CD138+. They didn't exhibit any immunostaining with CD20, CD3, CD30, CD15 and EMA antibodies. The diagnosis of a plasmablastic micro lymphoma associated with a MCM was retained in presence of a restricted monotypic phenotype IgMlambda.
Conclusion : In case of lymphadenopathy in a HIV+, the HHV8 staining is helpful to detect plasmablastic microlymphoma and even aggressive NHL.

P 94

IN VIVO WNT-SIGNALING ANTAGONIST SFRP3 EXPRESSION IN MULTIPLE MYELOMA: ANOTHER POTENTIAL PATHWAY IN MYELOMA BONE DISEASE.

Raynaud Pierre(1), Poizat Flora (1), Rigau Valérie (1), Baldet Pierre (1), Klein Bernard (2), Costes Valérie (1).
(1) Laboratoire d'Anatomie Pathologique, CHU de Montpellier, France.
(2) Institut de Recherche en Biothérapies, CHU de Montpellier, France.

Multiple myeloma (MM) is commonly associated with lytic bone lesions. Although the mechanisms of increased osteoclast activity are partially understood, comparatively little is known about the mechanisms that lead to the observed decrease in osteoblast number and activity.
Wnt glycoproteins comprise a family of extracellular signaling ligands that play essential roles in cell proliferation and differentiation during normal developmental processes. Recently, secreted frizzled-related proteins (sFRPs) have been identified as possible modulators of the Wnt signal transduction pathway, based on their ability to bind and sequester the Wnt ligands. The sFRP3 glycoprotein suppress osteoblast cell number, acting as a decoy receptor for Wnt proteins that promote osteoblast proliferation.
Methods: Using a double-immunostaining (CD138/sFRP3) on tissue microarrays (TMA), we analysed plasma cells (PCs) sFRP3 expression in 59 fixed paraffin-embedded bone marrow samples (BMS) from patients with newly diagnosed MM (according to International Myeloma Working Group criteria (2002)) versus 43 control normal BMS.
All BMS were Bouin's (alcohol-based) fixed, decalcified in EDTA and paraffin embedded. The TMA consisted of 2 cores (2mm in diameter) from each BMS.
The percentage of CD138/sFRP3-positive PCs was determined by counting all PCs in normal samples to 400 PCs in MM samples in areas with the impression of highest expression ("hot spot") at low magnification.
Results: Depending on sample, the percentage of positive PCs varied from 0% to 100%.
We found consistent, uniform cytoplasmic sFRP3 expression for an average of 80% of the PCs (mean: 90%) in MM samples, versus 19% (mean: 16.4%) of the PCs in normal BMS (p-value < 0.0001).
If we considered as positive for sFRP3 expression, BMS with more than 50% of PCs sFRP3/CD138+, 88.1% of MM samples were positive as opposed to 11.6 % of normal samples ($p<0.001$).
Conclusion: Using bone marrow TMA for the first time, we observed, by double-immunostaining, significant differences in the relative expression of sFRP3 between PCs of newly diagnosed MM and normal BMS. The production and secretion by myeloma cells of sFRP3, which is an inhibitor of osteoblast proliferation, is a new potential pathway in myeloma bone disease. We propose that sFRP3 inhibits the proliferation of osteoblasts and shift the balance between osteoblasts and osteoclasts, thereby diminishing bone formation and enhancing the development of lytic lesions.

P 95

PLASMA CELL MORPHOLOGY AND PROLIFERATION FRACTION IN MULTIPLE

MYELOMA ASSESSED IN TREPHINE BIOPSIES: RELATION TO CLINICAL STAGE

BAYKOV Vadim
Dept pathology, St Petersburg medical university

Multiple myeloma (MM) is a haematologic malignancy, built of terminally differentiated B-cells with morphological features of plasma cells and their predecessors. Morphological presentation of the tumour is well known, but little data exist on cellular architecture assessed in paraffin sections and related to clinical stage and proliferation rate.
The OBJECTIVE of the study was to evaluate cellular composition and proliferation fraction of the tumour in different clinical stages.
The study was based on 62 trephine biopsies (TB), containing myeloma clone. TB were taken from patients (aged 47-78) for diagnostic and follow-up purposes with informed consent. 9 patients were in Durie stage I, 24 – in stage II and 29 in stage III. Routinely HE and Romanovsky-Giemsa stains were performed, as well as immunostaining for CD138 and Ki-67 (Dako Cytomation, Denmark). CD138 immunoreactivity contributed greatly to recognition of abnormal or immature plasma cells and in some cases increased the total myeloma cell count up to 30% as compared to HE stain alone. The cell sub-classification protocol, proposed by J.E.Goasguen et al. (1999) for cytological purposes, was applied to histological sections. It appeared possible to put over 85% of myeloma cells into four groups - plasmablastic, proplasmacytic I and II and plasma cell using "positive selection" methodology. Statistically significant increase in plasmablastic cells was documented in patients in stage III of the disease in comparison with those in stage I (14% against 2%), accompanied by concomitant decrease in mature plasma cells (30% against 68%). Proliferation index was 0,9 in stage I and 9,5 in stage III. Values in stage III showed substantial variation, entirely because of 3 cases included in the group with predominantly blastic morphology. These cases taken separately showed plasmablastic cell count 39% and proliferation index of 40%. Interestingly, plasmablastic cell count performed in aspirate smears showed mean of 22%.
WE CONCLUDE that blastic cell count and proliferation rate assessed in bone marrow TBs correlate with clinical stage of MM. In bone marrow sections plasmablastic cell count is higher than reported in smears - possibly due to differential ability of mature and immature bone marrow cells to get aspirated.

P 96

CD20 ABERRANT EXPRESSION OF MULTIPLE MYELOMA

M. Melachrinou, V. Zolota, P. Matsouka*, T. Kourelis*, I. Xagoraris, P. Aroukatos, D. S. Bonikos.
Departments of Pathology and *Internal Medicine, Division of Hematology, University of Patras Medical School, Patras, Greece.

Introduction It is well known that reactive and neoplastic plasma cells may express various hematopoietic and non-hematopoietic antigens. However, there are few reports that correlate the aberrant immunophenotype of multiple myeloma (MM) with the survival of patients. The aim of this study was to investigate whether the expression of particular B-cell antigens by myeloma cells is suggestive of a more aggressive phenotype.
Material and method A total of 102 routinely processed bone marrow biopsy specimens from untreated MM patients were immunostained with anti-LCA (CD45), L26 (CD20), anti-CD79a and anti-syndecan-1 (CD138) monoclonal antibodies using Envision detection kit.
Results All the specimens showed a strong positive immunostaining for CD138 in almost 100% of neoplastic cells. CD20- and CD79a-expression (>5% of myeloma cells) was detected in 24.5% and 43.1% of cases, respectively. The great majority to 100% of the myeloma cells were reacted with anti-CD20 and anti-CD79a antibodies in 14 (13.7%) and 15 (14.7%) cases, respectively. Overall survival of patients was not associated with CD20 and/or CD79a expression by myeloma cells ($p = 0.30$). A significant percentage of CD45 positive neoplastic plasma cells was observed in only two specimens.
Conclusions Syndecan-1 appears to be a reliable marker for plasma cells. A positive CD20-immunostaining does not exclude the possibility of a plasma cell tumor, especially in the case of an extramedullary neoplasm (e.g. plasmacytoma). CD20 and/or CD79a expression by myeloma cells does not seem to be of significant value in predicting survival. Myeloma cases with a strong CD20 expression may respond to treatment with anti-CD20 monoclonal antibody, in combination with the standard therapy.

P 97

EXPRESSION OF PI3K/PTEN/AKT-HIF-1 SIGNALING PATHWAY PROTEINS, THEIR RELATION WITH CELL PROLIFERATION AND CLINICAL OUTCOME IN PATIENTS WITH MULTIPLE MYELOMA (MM)

KAYGUSUZ Gulsah [1], KUZU Isinsu [1], CEKIN Nilgun 3, BEKSAC Meral [2], TOPRAK Selami K [2], SOYDAN Ender [2], KIZIL Merih [2], SAHIN Fikret 4, ELHAN Atilla H 5
Departments of Pathology[1], Haematology2, Microbiology4, Biostatistics5, School of Medicine and Biotechnology Institude3, University of Ankara, TURKEY

The factors related with the expansion of the malignant clone in MM, are enhanced proliferation and resistance to apoptosis. Recent studies have focused on different related pathways stimulating proliferation or suppressing apoptosis. The phosphotidylinositol-3-OH kinase (PI3K) signal pathway integrates receptor tyrosine kinase signaling which could be the major candidate regulating the apoptotic cascade related to the survival and proliferation of myeloma cells. One mediator of PI(3)K signaling is the Akt/protein kinase B, which phosphorylates multiple downstream effectors that ultimately regulate a variety of cell functions including glucose metabolism, cell proliferation and survival. mTOR and HIF-1 are among these mediators. And tumor suppressor protein PTEN is one of major inhibitors of Akt phosphorylation.
In this study we aim to examine the expressions of the phosphorylated proteins PI3K/PTEN/Akt, related downstream proteins mTOR, HIF-1 on bone marrow biopsy specimens of MM patients and to analyze their relation between the proliferative activity and survival.
PATIENTS AND METHODS:
Fourty seven myeloma patients diagnosed in our department between 2002-2004, aged 54(33-77), whose bone marrow biopsy specimens could be retrieved were included in this study. All patients were treated with VAD or MP as first line treatment.
Immunohistochemical staining was performed using monoclonal antibodies against phospho- PTEN (Cell Signaling Tech), phospho-Akt (Cell Signaling Tech), phospho-mTOR (Cell Signaling Tech), HIF1 alpha (abcam) and Ki67 (Labvision) with Zymed ABC Px Kit manually or Ventana Benchmark automated immunostainer for secondary visuilisation. Negative control was present in each experiment.

CONCLUSIONS:
Loss of PTEN expression (10 of 35 patients) was correlated with high proliferative activity examined by Ki67 staining ($p=0.014$, Mann-Whitney U test).
Akt activation was seen in 20% of the cases which was not correlated with the survival.

There were no correlations between survival, proliferation status of the myeloma cells and expressions of the proteins involved in PI3K/PTEN/Akt, HIF-1 pathway.
The cases having loss of PTEN expression by immunohistochemistry did not show increased Akt expression. It seems that Akt activation on the way of proliferation may be related to the other stimulating factors rather than the negative control of PTEN.

P 98
EXPRESSION PROFILES OF CYCLIN A, D1, D2, D3 AND CYCLIN DEPENDENT KINASE INHIBITORS (CDKI) P16 AND P21 IN PATIENTS WITH MYELOMA ON BONE MARROW SPECIMENS
KUZU Isinsu [1], KAYGUSUZ Gulsah [1], BEKSAC Meral [2], TOPRAK Selami K [2], SOYDAN Ender [2], KIZIL Merih [2], ELHAN Atilla H 3
Departments of Pathology[1], Haematology2 and Biostatistics3, School of Medicine, University of Ankara, TURKEY

INTRODUCTION
Cyclins are expressed during specific phases of the cell cycle and are controlled by cell cycle dependent kinase inhibitors (CDKI). p16 and p21 control Cyclin D and Cyclin A, respectively. The sequential role of Cyclin A and p21 has not been determined yet. We aimed to analyze the cyclin and CDKI's in marrow plasma cells by immunohistochemistry.
PATIENTS and METHODS
Fourty five myeloma patients diagnosed in our department between 2002-2004, aged 54(33-77), M/F:21/13 whose bone marrow biopsy specimens could be retrieved were included in the study. All patients were treated with VAD or MP as first line treatment.
Immunohistochemical staining was performed using monoclonal antibodies: Cyclins A, D1, p16, p21(LabVision), Cyclin D3(DAKO), Cyclin D2 (Santa Cruz) and Ki67 (Labvision) with Zymed ABC Px Kit manually or Ventana Benchmark automated immunostainer for secondary visuilisation. Negative control was present in each experiment.
CONCLUSION
We could not find any correlation between the expression profiles of Cyclins A, D1, D2, D3, p16, p21, Ki67 and survival. But there was an inverse correlation between p16 and cyclin A expressions as expected.

Cyclins and their inhibitors can be expressed in different combinations by plasma cells. A decreased expression of cyclin A or D and a relevant CDKI's increased expression was evaluated as a low proliferative situation (P min).
P min was observed 5/45 of the patients, resulted with 80% overall response and 100%survival at 5 years.
On the contrary P max patients (high Cyclin and low CDKI expressing patients) were observed more frequently(19/45). 10/19 of these patients responded and performed 57% Survival. Pmax and P interm patients responded (7/17) and survived similarly.
Prognostic factors such as age, B2MG and CRP were similar between Pmin, P max or P interm groups thus did not influence the response and survival effect.
Cyclin-CDKI patterns are associated with bone disease: P max patients had bone lesions more frequently (11/14) whereas P min patients had none(p=0.008). The role of bone disease as a prognostic factor has been shown before by other investigators. This association supports the prognostic role of cell cycle regulators and inhibitors.

P 99
MUC1 EXPRESSING PLASMA CELLS IN BONE MARROW EXHIBITING INVOLVEMENT BY PLASMA CELL MYELOMA
BALDUS Stephan E., PALMEN Christine, THIELE Jürgen
Institute of Pathology, University of Cologne, Kerpener Str. 62, D-50931 Cologne

Introduction: MUC1 represents a mucin molecule expressed in various epithelial tissues and neoplasms as well as normal haematopoietic cell lines. Additionally, its presence could be demonstrated in diffuse large B cell lymphomas as well as plasma cell myelomas. However, a thorough analysis of the clinical as well as pathological importance of MUC1 positive plasma cells in bone marrow involved by plasma cell myeloma was not performed up to now.
Purpose: In the present study, we tried to evaluate the expression of MUC1 in a larger series of bone marrow specimens with plasma cell myeloma involvement in order to evaluate possible correlations with histopathological parameters as well as survival data.
Material and methods: Trephine biopsy specimens with involvement by plasma cell myelomas derived from 105 patients were investigated immunohistochemically visualizing syndecan-1 (CD138) and MUC1 positive myeloma cells. Initially, the percentage of CD138 positive plasma cells was determined. Additionally, MUC1-specific monoclonal antibodies (mabs), anti-epithelial membrane antigen (EMA) as well as HMFG-2 were applied. The rate of MUC1 positive plasma cells was evaluated semiquantitatively. Possible correlations with pathological variables (grade, fibre content, pattern of infiltration) as well as survival were analysed statistically applying chi square tests as well as survival analyses.
Results: About 55 % of the cases showed EMA expression and 47 % HMFG-2 immunoreactivity in more than 5 % of the plasma cells in the bone marrow. In cases exhibiting a so-called packed marrow, EMA immunoreactivity was reduced. However, MUC1 positivity as assessed semiquantitatively did not show a statistically significant correlation with the cytologic grade of differentiation or the fibre content, respectively. Correlations with survival probability could also not be observed.
Conclusions: About 50 % of the cases with plasma cell myeloma involvement of the bone marrow exhibited an expression of MUC1 in plasma cells. This observation may be of special interest with regard to recently published data. For example, enrichment of MUC1-specific T cells or MUC1 vaccination may represent new aspects in the therapy of plasma cell myeloma and MUC1 expression in plasma cell myeloma may be regulated by interleukin 7. However, MUC1 expression by bone marrow-infiltrating plasma cells did not correlate with most histomorphological parameters or patients' prognosis according to our results

P 100
EXTRANODAL LYMPHOMA : A CLINICOPATHOLOGIC STUDY OF 87 CASES
AYADI Lobna, BAHRI Ibticem, GHARIANI Mekki, GOUIAA Naourez, MNIF Hela, SELLAMI Ahmed, BOUDAWARA SELLAMI Tahya

Introduction:
Primitive extranodal lymphomas (PENL) constitute 25 % of whole non Hodgkin lymphomas. They are defined as localised lymphomas which appear in extranodal tissue with or without invasion of regional nodes.
Objectives:
The purpose of this study is to specify the clinicopathologic and immunohistochemical characteristics of the principal locations of extranodal lymphomas and to discuss their prognosis.
Patients and methods:
Our study is retrospective relating to 87 cases of PENL diagnosed in the period between January 1995 and December 2000 at the Pathologic Department of Habib Bourguiba Hospital (Sfax –Tunisia). This study is based on the

clinicopathologic and immunohistochemical findings. All cases were analysed and reclassified using the latest WHO (2000) classification.
Results:
The mean age of patients was 45 years (extreme: 3 and 84 years). There was a male prevalence with a ratio of 1,7. Primitive lymphomas of the digestive tract (PLDT) were the most common (44 cases : 50,6%) followed by Waldeyer's ring lymphoma (17 cases : 19,5%), cutaneous lymphomas (9 cases : 10,5 %), lymphomas of the central nervous system (6 cases: 6,9 %), centrofacial lymphomas (5 cases : 5.8 %), osseous lymphomas (2 cases : 2,3 %), splenic lymphoma, thymic, orbital, and salivary glands lymphoma (one case for each location : 1,1 %). The association of a digestive lymphoma to a lymphoma of the ring of Waldeyer were observed among 4 patients (9 % of PLDT). The most common histologic type was diffuse large B-cell lymphoma (56 cases : 64,4 %) followed by MALT- lymphoma (10 cases : 11,6%). Treatment policies adopted as well as the outcome were documented for each location
Conclusion:
The PENL represent a very hetregenous group of neoplasms . They are not always easily identified on routinely stained sections and their diagnosis need immunohistochemical analysis and even molecular biology. Their outcome is variable depending on the site and the histological type.

P 101
ABSENCE OF MICROSATELLITE INSTABILITY IN GASTRIC LYMPHOMA : AN IMMUNOHISTOCHEMICAL STUDY OF HMLH1 AND HMSH2 PROTEIN EXPRESSION
CUILLIERE-DARTIGUES Peggy, FABIANI Bettina, DUMONT Sylvie, COPIE-BERGMAN Christiane, COUVELARD Anne, MOLINA Thierry, FLEJOU Jean-françois

Defective DNA mismatch repair results from genetic or epigenetic alterations that most frequently inactivate the genes hMLH1 and hMSH2. This pathway is known to be involved in the pathogenesis of a subset of solid neoplasm, most prominently encountered in hereditary non polyposis colorectal cancer (HNPCC) syndrome, characterized by microsatellite instability (MSI). However its role in lymphomagenesis is not well established. In gastric lymphoma of mucosa-associated lymphoid tissue (MALT) type, contradictory results concerning the prevalence of MSI have been reported in few studies using molecular testing.
The aim of this study was to identify tumours with a mutator phenotype by detection of abnormal MMR gene protein expressionin a large series of gastric lymphoma.
Immunohistochemestry was performed in 111 low grade MALT lymphomas and in 44 diffuse large B cell lymphomas using two monoclonal mouse antibodies that react against hMLH1 and hMSH2 protein. In all cases with contributive immunohistochemestry (80), tumours showed nuclear expresion of both proteins.
These results suggest that defects in DNA mismatch repair, due to inactivation of hMLH1 and hMSH2, do not seem to contribute significantly to the molecular pathogenesis of gastric MALT lymphoma.

P 102
CASTLEMAN'S DISEASE OF THE HEAD OF THE PANCREAS: UNUSUAL ASSOCIATION WITH ADENOMATOUS HYPERPLASIA OF THE PAPILLA VATERI
COSIC MICEV Milena 1, MICEV Marjan 1,2, TODOROVIC Vera 2, MILICEVIC Miroslav 1, DOJCINOV Stefan 3
1 Institute of Digestive Diseases, Clinical Centre of Serbia, Belgrade, Serbia and Montenegro
2 Institute for Medical Research, Belgrade, Serbia and Montenegro
3 Department of Pathology, University Hospital of Wales, Heath Park Cardiff, UK

INTRODUCTION: Castleman's disease has been described in a variety of anatomical sites including the peripancreatic retroperitoneum. We present a case of its unusual intrapancreatic presentation associated with simoultaneous hyperplasia of the papilla Vateri.
A CASE PRESENTATION: A 54 years old female patient suffered back pain, abdominal discomfort and short interval intermittent jaundice. The ultrasound finding suggested cystic lesion and after CT scan examination pancreatic mass was diagnosed in the head of the pancreas. There were no other significant or conclusive laboratory findings. Intraoperative surgical examination found well circumscribed tumor occupying the posterior part of the head of the pancreas and peripancreatic fat in the proximity of obstructive enlargement of the papilla Vateri. Frozen section biopsy was misinterpreted as non-representative peripancreatic lymph node and Whipple's cephalic pancreatico-duodenectomy was performed.
METHODS AND RESULTS: Gross examination revealed well circumscribed mass measuring 64 mm in greatest diameter in the head of the pancreas with small part extruding to peripancreatic fat. Histologically, nodular architecture of lymphoid infiltrate was composed of follicle-like structures with hyalinised and vascularised centres and onion skin-like distribution of surrounding small lymphoid cells. Immunostaining showed B-cell phenotype (CD20+, CD5-, CD10-, CD43-) with CD21+ rich dendritic cell networks, focally mantle zone-like areas (focal expression of CD10+ and bcl-6+) and a lack of bcl-2 immunoexpression in germinal centres, but CD3+/CD5+ positive small T lymphocytes among polymorphous interfollicular lymphoid infiltrate. PCR analysis with Biomed 2 primers (FR1, FR2, FR3) showed a polyclonal pattern. In addition, slight fibrotic ampullary stenosis and adenomatous hyperplasia of the papilla Vateri were found, not accompanied with epithelial atypia or simoultaneous myomatous hypertrophy. In 14 months follow-up there was no relapse or any signs of the disease.
CONCLUSION: Very unusual anatomical presentation of Castleman's disease with profound ingrowth of the lymphoid proliferation within the head of the pancreas associated with obstructive adenomatous hyperplasia of the papilla Vateri was initially misunderstood as pancreatic cancer. This broadens differential diagnosis of obstructive periampullary and pancreatic lesions.

P 103
CHEMOKINE RECEPTOR EXPRESSION IN NONGASTRIC MUCOSA-ASSOCIATED LYMPHOID TISSUE (MALT)-TYPE LYMPHOMAS
AIGELSREITER Ariane (1), DEUTSCH Alexander (2), STEFAN Martina (3), BEHAM-SCHMID Christine (1), BEHAM Alfred (1), LANZER Gerhard (4), STELZL Evelyn (5), LINKESCH Werner (2), SCHAIDER Helmut (3) and NEUMEISTER Peter (2)
1 Department of Pathology, 2 Division of Hematology, 3 Department of Dermatology
4 Department of Blood Group Serology and Transfusion Medicine, 5 Institute of Hygiene, Medical University Graz, Austria

Introduction: Chemokine receptors mediate the migration and activation of lymphocytes through binding of their ligands. Several recent studies have revealed important contributions of chemokine receptors and their ligands to the development and progression/dissemination of hematopoietic neoplasms. By promoting tumor dissemination CXCR3 has recently been

identified as a major contributor in the pathogenesis of mucosa-associated lymphoid tissue (=MALT) lymphomas. Little is known about the chemokine receptor expression profile of nongastric MALT lymphomas.
Purpose: The aim of our study was to identify the expression pattern of all 17 currently known and characterized chemokine receptors in nongastric MALT-lymphomas in comparison to normal, surrounding tissue.
Material and Methods: 10 extragrastric MALT lymphomas of the parotid gland were selected from the archives of the Department of Pathology, Medical University Graz. As control specimens 5 pooled non-malignant parotid glands were included.
Makrodissected tissue containing >80% lymphoma cells from paraffin embedded MALT lymphomas of the salivary gland were processed for RNA isolation. Semiquantitative Real Time PCR was performed on a GeneAmp® 5700 Sequence Detector. Peripheral blood from healthy donors served as calibrator, due to the broad expression of all chemokine receptors investigated. Expression of 17 chemokine receptors was determined in triplicate and the number of cycles was compared to the reference gene HPRT and peripheral blood, based on calculations of 2-deltadeltaCT.
Results: Compared to normal tissue we demonstrated de novo expression of CCR4 and CCR8.
As opposed to non-malignant control tissues, receptor upregulation occurred in CCR5, CCR6, CCR7, CCR9, CXCR3, CXCR4, CXCR5 and XCR1. Equal expression could be observed in CCR1, CCR2, CCR3, CXCR1, CXCR2 and CX3CR1, whereas the chemokine receptor CCR10 was down-regulated. In the CC receptor family the most pronounced upregulation could be attributed to the family members CCR6 (57,6 times) and CCR7 (31,8 times), whereas CXCR4 (20 times) was highest expressed in the CXC receptor family group.
Conclusion: Hence, our data support a model of the etiopathogenesis of extragastric MALT lymphomas involving a complex interplay of multiple interacting signals mediated by chemokine receptors, where differentially regulated members of the CXC as well as CC receptor family might play a crucial role in the dissemination/homing of malignant B-cells.

P 104

INDUCIBLE NITRIC OXIDE SYNTHASE AND APOPTOSIS IN HUMAN B CELL LYMPHOMAS

* ATÝK Esin, **ERGÝN Melek, **ERDOĐAN Þeyda, **TUNCER Ýlhan
(*)Department of Pathology, Mustafa Kemal University, Faculty of Medicine, Antakya-Hatay / Turkey
(**) Department of Pathology, Çukurova University, Faculty of Medicine, Adana/ Turkey

Purpose: Nitric oxide synthases (NOS) are isoenzymes that catalyse the synthesis of nitric okside (NO). NO plays both pathological and physiological roles depending on its rate of synthesis and concentration in cellular source and microenvironment.
Apoptosis is an important biological factor in lymphomas.
This study evaluates expression of inducible nitric oxide synthase (iNOS) in human lymphomas and its relation with apoptosis.
Material and Methods: This study comprised 46 cases of B-cell lymphoma. The lymphomas were classified as 3 mantle cell, 5 marginal zone, 4 follicular, 2 Burkitt, 25 diffuse large cell, 2 anaplastic large cell, 3 lymphoblastic, 2 lymphoplasmacytic according to WHO classification of lymphoid neoplasms. .
Hematoxylin eosin slides of the cases were reviewed and immunoperoxidase technique was performed iNOS and Caspase monochlonal antibodies to selected sections of each case. Antigen staining was carried out with iNOS and Caspase proteins and Ultravision Polyvalent, Rabbit, HRP-AEC kit (Neomarkers- Biogen USA).
For the evaluation of iNOS and Caspase, tumor areas with a high density of expression were chosen. Positive stained cells were counted in 5 different areas at a magnification X40 by an Olympus BX51 microscope in each case.
The iNOS and Caspase expressions were independently recorded by two pathologists and the results were averaged.
Results: Our study revealed that there is a positive relation between iNOS expression and apoptosis (p= 0.032 spearman correlation). This relation might be promising new agents in therapeutic protocols.

P 105

SYNCHRONOUS PRESENTATION OF NON-HODGKIN'S LYMPHOMA AND MALIGNANT MELANOMA

I.D.Venizelos1, Z.A.Tatsiou1, L.Kampas1, D.Sioutopoulou1, V.Perifanis2, V.Garipidou2

1 Department of Pathology, Hippokration Hospital, Thessaloniki
2B Department of Internal Medicine, Aristotelian University of Thessaloniki, Hippokration Hospital, Thessaloniki, Greece

The association of malignant melanoma (MM) with different neoplasias is uncommon but not exceptional. Over the past 2 decades, both MM and non-Hodgkin's lymphoma (NHL) incidence rates, have increased substantially. Several epidemiological studies have suggested an association between MM and NHL and an interaction between genetic and environmental factors in the pathogenesis of these tumors.

We report the case of a 72-year-old man who presented in our hospital due to enlarged, not painful cervical, axillary and inguinal lymph nodes, persisted for 6 months. On physical examination it was found peripheral lymphadenopathy with no hepatosplenomegaly. Hematological examination was normal. CT scan of the chest and abdomen revealed generalized lymphadenopathy, with no hepatosplenomegaly. An inguinal lymph node was excised and histological examination showed morphological and immunohistochemical features of B-cell small lymphocytic lymphoma (SLL). At the same time, a melanocytic lesion on the frontal region of the head was excised due to recent enlargement and change of the colour. Histological examination of the lesion showed features of superficial spreading MM, Clark's level IV and Breslow's depth of invasion 2,5 cm, for which he received no further treatment. The patient received 10 courses of systemic chemotherapy with mabthera, 1 course with fludarabine, decadron and mitoxantron for SLL, and remained in partial remission. One year later he presented with neurological signs due to brain metastasis, and multiple skin nodules on the tract. Histological examination of an excised skin nodule showed the features of MM. One month later he died due to complications of CNS involvement.

In the present study we report a rare case of synchronous presentation of NHL and MM. Although it is rare, we should suspect this association and make the correct diagnosis using the appropriate immunohistochemical stains.

P 106

MORPHOIMMUNOHISTOCHEMICAL DIFFERENTIAL DIAGNOSTICS OF "GREY ZONE" LARGE LYMPHOMAS.

Kovrigina A, Probatova N.

INTRODUCTION: Overlape between Hodgkin's lymphoma and large-cell lymphomas creates the difficult task for morphological diagnostics. At the last time "grey zone" is

complicated for the account of T-cell/histiocyte-rich B-cell lymphoma (TCRBCL), anaplastic variant of diffuse B-cell large lymphoma (DBCL), primary mediastinal B-cell lymphoma (PMBL), anaplastic large-cell lymphoma.
Purpose of study was to investigate group of "grey zone" lymphomas.
MATERIALS AND METHODS. We have studied 143 lymph nodes biopsies of "grey zone" lymphomas using immunohistochemical method with wide panel of monoclonal antibodies: CD3, CD4, CD8, CD10, CD15, CD20, CD21, CD23, CD30, CD43, CD45, CD57, Granzyme B, ALK, EMA, bcl-2, bcl-6.
RESULTS: We have diagnosed 21 cases of TCRBCL (m:f 0,7:1,0; mediana 47 years, range 16-67). Diffuse growth was marked in 20 cases and nodular growth in 1 case, that demands differential diagnostics with nodular lymphoid-predominant of Hodgkin's lymphoma. PMBL was diagnosed in 35 pts (m:f 1,0:3,5, mediana 31,5 years, range 16-62) with immunophenotype of neoplastic cells: CD45-positive and CD20-positive (all cases), CD30 (75%), CD23 (48%), bcl-6 (33%) and all cases were IgM-negative. 2 cases of anaplastic variant DBCL were revealed. ALCL was diagnosed in 39 pts (mediana 22 years, m:f 1,0:1,0; range 4-79).
ALK-positive cases were observed in 58% (till 40 years) but any case in 40 years and more senior. The others cases were referred toHodgkin's lymphoma (mixed cellularity, NS II subtypes).
CONCLUSION: "Grey zone" lymphomas may be diagnosed only by using wide panel of antibodies. ALK-negative with 0-immunophenotype cases of ALCL are generated

P 107
CYTOTOXICITY OF THE SMALL MOLECULE BCL-2 ANTAGONIST, HA14-1, AND SELECTED ANTICANCER DRUGS IN FOLLICULAR LYMPHOMA B-CELLS.
Joanna Skommer (1), Donald Wlodkowic (1), Mikko Mattö (1), Mine Eray (2), Jukka Pelkonen (1,3)

The Bcl-2 overexpression is a hallmark of follicular lymphoma (FL). Since patients with FL often suffer from progressively resistant to chemotherapy refractory disease, the development of new regiments is required. In this study we analyzed for the first time the effects of a Bcl-2 antagonist, HA14-1, alone and in combination with antineoplastic agents commonly used against follicular lymphoma, in human FL cell lines with t(14;18). The cell lines were established from patient samples send for PAD analysis and earlier analysed in detail. All cells were sensitive to HA14-1 induced cytotoxicity (the LC50s of 4.5 to 12.6μM) and apoptosis. Moreover, HA14-1 enhanced dexamethasone and doxorubicin mediated (in schedule independent and dependent manner, respectively) cytotoxicity and apoptosis, but antagonized with vincristine, in all FL cells. Together these findings warrant further in vivo studies and provide conceptual basis for therapeutic intervention in follicular lymphoma.

P 108
TUMORS OF HEMATOPOIETIC AND LYMPHOID TISSUES IN CHERNOBYL CLEAN-UP WORKERS (1996-2004)
GLUZMAN Daniel, SKLYARENKO Lilia, NADGORNAYA Valentina, ZAVELEVICH Michael, SIMONET Marie-Laurence
R.E. Kavetsky Institute of Experimental Pathology, Oncology and Radiobiology, National Academy of Sciences of Ukraine, Kyiv, Ukraine
French-Ukrainian Center "Children of Chernobyl"

The role of ionizing radiation as a causative factor of various biological types of leukemias and lymphomas after Chernobyl is still controversial. Different predictive models on the incidence of hematopoietic malignancies in Ukrainian Chernobyl clean-up workers have been suggested up to present. Nevertheless, the actual data are still lacking mainly because of the inconsistency in the primary findings preventing the precise diagnosis of hematopoietic malignancies.
The aim of the study was to characterize in details the major forms and cytological variants of oncohematological diseases in Chernobyl clean-up workers exposed in 1986-1987 to radiation at a dose within the range of 7.5-25 cGy.
The data on 200 consecutive cases of malignant diseases of hematopoietic and lymphoid tissues in Chernobyl clean-up workers diagnosed in Reference Laboratory of R.E. Kavetsky Institute of Experimental Pathology, Oncology and Radiobiology in 1996-2004 on the basis of up-to-date techniques of cytomorphology and immunophenotyping in accordance with novel WHO classification have been summarized. The specimens were analyzed using immunocytochemical techniques (PAP, APAAP, ABC) and panel of monoclonal antibodies to differentiation antigens of leukocytes employed for immunophenotyping of leukemic cells. The patterns of the main forms of hematopoietic malignancies in Chernobyl clean-up workers have been compared with that in general population.
Practically all the main forms of malignant diseases of hematopoietic and lymphoid tissues were revealed in the group of Chernobyl clean-up workers under study. The comparison of relative distribution of the particular forms of hematopoietic malignancies in the patients diagnosed among Chernobyl clean-up workers demonstrates increasing multiple myeloma rate and the tendency to increasing non-Hodgkin's lymphoma and CML rates as compared to general population.
The peculiar feature of AML in clean-up workers under study consists in the development of leukemia on the background of preceding myelodysplastic syndromes in 50% of all AML cases studied. 4 cases of large granular lymphocyte leukemia were recorded among clean-up workers. Strongly alkaline phosphatase-positive villous cells identified in bone marrow stroma in clean-up workers suffering from malignant as well as non-malignant diseases of hematopoietic and lymphoid tissues seem to represent a response to incorporation of the osteotropic heavy metals including radionuclides.

P 109
EBV ASSOCIATED EXTRA-NODAL NK CELL LYMPHOMA NASAL TYPE OF THE BREAST IN BEHCET DISEASE: A CASE REPORT
L. Jabri, S. Zamiati, M. Karkouri, A. Iraqi
Central Department of Pathology, Ibn Roshd University Hospital, Casablanca, Morocco

Primary non Hodgkin lymphoma of the breast is uncommon. Most are of B-cell phenotype, with only rare cases showing a T-cell phenotype, NK-cell lymphomas are extremely rare, only 2 cases are reported so far in the literature. The association of Behcet's disease with malignancies has rarely been reported. Only 6 cases of lymphoma have been reported, of whom one is a nasal NK-cell lymphoma.
We report a case of NK-cell lymphoma extranodal nasal type of the breast
It is a 20 year-old woman followed up for Behcet disease under immusuppressive treatment for 4 years. She presented with a mammary nodule of 3 cm.The biopsy of the lesion revealed the infiltration of medium to large sized lymphoma cells with necrosis and angiocentric pattern. The cells were positive for cytoplasmic CD3, CD56, CD8, TiA1 and Granzyme B, negative for surface CD3. Analysis of T-cell receptor fails to show clonal rearrangement. EBV studies show clonal episomal integration of EBV (EBER-1 positive). She underwent chemotherapy and radiotherapy and achived complete remission.

To our Knowledge this case report is the first to describe NK-cell lymphoma of breast arising in Behcet disease.

P 110
REAL-TIME QUANTITATIVE PCR DETECTION OF FUSION GENE ALK/NPM IN PATIENTS WITH ALCL: RESIDUAL DISEASE MONITORING AND A CORRELATION WITH THE DISEASE STATUS

KALINOVA Marketa, KRSKOVA Lenka, HILSKA Irena, KOPECKA Pavla, KODET Roman
Department of Pathology and Molecular Medicine, 2nd Faculty of Medicine, Charles University in Prague, Czech Republic

Introduction: Anaplastic large cell lymphoma (ALCL) represents a heterogeneous group of malignant lymphoproliferative diseases. Most of the cases are of T cell origin. ALCL is frequently associated with t(2;5)(p23;q35)coding for NPM/ALK fusion gene - anaplastic lymphoma kinase (ALK) gene is fused with nucleophosmin (NPM) gene. The NPM/ALK chimeric gene encodes a constitutively activated tyrosin kinase that has been shown to have potent oncogenic properties. The NPM/ALK fusion protein is found in up to 75% of pediatric ALCL.
Purpose: To monitor residual disease using real-time quantitative reverse-transcription PCR (RQ-RT-PCR) of NPM/ALK fusion gene.
Methods: RQ-RT-PCR is a recently developed technique for nuclear acid quantification. We developed an assay using RQ-RT-PCR for the quantitative assessment of minimal residual disease (MRD) in childhood ALCL by using a hydrolysis probe for quantification of NPM/ALK and hybridization probes for quantification of housekeeping gene (Beta-2 microglobulin gene), which was used as internal cDNA quality and quantity control. We constructed plasmid standards with NPM/ALK fusion gene and Beta-2 microglobulin gene. Normalized expression of NPM/ALK (NPM/ALKn) was determined as a ratio between NPM/ALK and Beta-2 microglobulin levels assessed by RQ-RT-PCR.
Results: We analysed NPM/ALK expression levels at diagnosis and/or relapses (cryopreserved and/or paraffin-embedded tissues) from affected lymph nodes and residual samples during the treatment in a group of 6 patients (4 – 19 years). All of them presented hyperexpression of NPM/ALKn (median 17321 copies) suitable for the MRD detection. Combined analysis of NPM/ALKn levels, qualitative RT-PCR NPM/ALK (1st vs 2nd round positivity) and the course of disease in 49 residual samples (bone marrow, peripheral blood) showed a clear correlation.
Conclusion: RQ-RT-PCR-based analysis of NPM/ALK expression is a promising and rapid approach for monitoring MRD in patients with ALCL. The impact of NPM/ALK various levels found during monitoring the residual disease on the treatment and prognosis needs further clarification.
Supported by grants from the Czech Ministry of Health #00064203, Czech Ministry of Education #0021620813 and Charles University GAUK #66/2004

P 111
MOLECULAR CHARACTERIZATION OF COMPOSITE MANTLE CELL AND FOLLICULAR LYMPHOMA

ZAMÒ Alberto (1), ZANOTTI Roberta (2), LESTANI Maurizio (1), OTT German (3), KATZENBERGER Tiemo (3), SCARPA Aldo (1), PIZZOLO Giovanni (2), MENESTRINA Fabio (1) and CHILOSI Marco (1)
(1) Department of Pathology, University of Verona, Verona, Italy
(2) Department of Haematology, University of Verona, Verona, Italy
(3) Department of Pathology, University of Würzburg, Würzburg, Germany

Introduction. Composite lymphomas are rare associations of two distinct lymphoma types at the same anatomical sites. Reporting of such cases is important since they pose major biologic, diagnostic and therapeutic dilemmas. Purpose of the study. We describe the third reported case of Mantle Cell and Follicular lymphoma. Methods. We performed accurate immunohistochemical, FISH and molecular studies in order to verify molecular hallmarks of the two components and to define the mono- versus bi-clonal nature of this neoplasm. We used both manual and LASER-capture microdissection combined to multiple molecular approaches for clonality determination, including detection of heavy and light chain recombination, as well as presence of kappa /Kde recombination. Results. By immunohistochemistry and FISH we confirmed the presence of two distinct lymphoma types characterised by specific translocations (namely, t(11;14) and t(14;18)), while by molecular techniques we demonstrated two distinct and not clonally related cell populations. Conclusions. Composite lymphomas are a diagnostic and pathogenetic dilemma, that should be investigated using multiple combined approaches. Care should be taken in the definition of mono- vs bi-clonality. The light chain approach, and particularly the kappa /Kde recombination detection, proved very useful for solving the clonality issue.

P 112
CUTANEOUS T-CELL LYMPHOMA, FLOW CYTOMETRIC IMMUNOPHENOTYPING AND ASSESSMENT OF CYTOKINE PRODUCTION

MANDAKOVA Petra, CAMPR Vit, KORTANKOVA Hana, MACHOVCOVA Alena*
Department of Pathology and Molecular Medicine, *Department of Dermatology, Charles University, 2nd Medical Faculty, Prague, Czech Republic

Background: The diagnosis of cutaneous T-cell lymphoma (CTCL), a tumor predominantly of T-helper cell origin (Th, CD4+), may be facilitated by flow cytometry (FC). If the precise immunophenotype of tumor cells is known, it is possible to study the cytokine production, which may help in explanation of interrelationships between neoplastic and tumor infiltrating cells (TIL). It is known, that Th1 and Th2 cytokines have distinct roles in proliferation and elimination of tumor cells. Th1 cells producing e.g. INF gamma or IL2 may activate cytotoxic T lymphocytes (CTL), but Th2 cells producing e.g. IL4 may inhibit antitumor CTL.
Purpose: The purpose of this study was to assess a contribution of FC to the diagnosis of CTCL and elucidate the relationships between TIL/CTL and tumor cells in CTCL. We presumed that tumor cells might produce the Th2 cytokines and thus inhibit TIL/CTL.
Patients and methods: 20 skin biopsies from 17 patients with the clinical suspicion of primary CTCL were examined. The suspension of lymphocytes for FC was prepared by enzymatic digestion of skin biopsy. After an immunophenotyping with a standard panel of antibodies the spontaneous and induced (by ionomycin and PMA i.e. phorbol 12-myristate 13-acetate) production of IL2, INF gamma and IL4 by tumor lymphocytes was examined.
Results: The suspension of lymphocytes was obtained in 70% of the cases. In this group the aberrant immunophenotype of T-cells was found in 70% and the findings were conclusive for T-cell lymphoma. Tumor cells produced IL2 only. No production of IL4 or INF gamma even after activation by ionomycin and PMA was showed.
Conclusion: If the lymphocytic infiltrate of the skin is not dense (as assessed from a frozen section) and only sporadic tumor cells are present, obtaining a representative sample is problematic. In such cases FC does not seem to be a diagnostic method of choice. Inconclusive results of FC may be caused by an absence of aberrant immunophenotype on

tumor cells and/or because of "masking" of the tumor cells by prevailing populations of TIL.
Furthermore, our results did not confirm our hypothesis, that tumor cells produce Th2 cytokine. Tumor cells produced mainly IL2. It is possible, that they may locally activate themselves by autocrine loop and may contribute to the tumor cell proliferation.
Supported by Research Project FNM MZO 00064203 and Internal grant of FNM 9729.

P 113
IMMUNOHISTOCHEMICAL DETECTION OF STAT1 AND TRAF1 IN MEDIASTINAL LARGE B-CELL LYMPHOMA
CAMPR Vit, MRHALOVA Marcela, NERADOVA Marie, PYTLIK Robert*
Department of Pathology and Molecular Medicine,
Charles University, 2nd Faculty of Medicine and Teaching Hospital Motol;
*Department of Internal Medicine, Charles University, 1st Faculty of Medicine;
Prague, Czech Republic

Background: Mediastinal large B-cell lymphoma (MLBCL) is a subtype of diffuse large B-cell lymphoma (DLBCL) defined by its clinicopathological features. Recent studies on the gene expression profile identified a molecular link between MLBCL and classical Hodgkin's lymphoma (cHL). These two tumors share similar pathogenetic mechanisms different from those of most non-mediastinal DLBCLs, with a decreased expression of B-cell receptor signalling cascade components, with an increased expression of cytokine pathways components, and an activation of NF-kappaB pathway. The tumor cells were shown to express among other proteins STAT1 (signal transducer and activator of transcription-1) and TRAF1 (tumor necrosis factor receptor-associated factor-1).
Purpose of the study: The aim of our study was to analyze the immunophenotype of MLBCL focusing on STAT1 and TRAF1 expression and to compare it with cHL and non-mediastinal DLBCL.
Patients and methods: Formalin fixed and paraffin-embedded tissue from 27 cases of MLBCL with a classical immunophenotype (18 females and 9 males, age 21 - 64, average 33 y, median 29 y) and a set of mediastinal nodular sclerotic subtype of cHL and non-mediastinal DLBCL was investigated. The expression of STAT1 (BD Biosciences) and TRAF1 (Santa Cruz) was evaluated by a standard immunohistochemical technique.
Results: The expression of STAT1 and TRAF1 was detected in most MLBCL tumor cells in all cases, the positivity was strong, cytoplasmic. Tumor cells of cHL were also strongly positive. The cells of DLBCL also expressed both proteins, but the positivity was in most cases moderate. Small T cells revealed a weak cytoplasmic positivity and stromal cells were negative.
Conclusion: Our study confirms that MLBCL and mediastinal cHL are characterized by a strong expression of STAT1 and TRAF1. However, the expression of these proteins does not discriminate reliably between MLBCL and non-mediastinal DLBCL which are positive as well, though the positivity of the latter group is weaker.
Supported by Research Project FNM MZO 00064203 and IGA NR 8231/3.

P 114
BONE MARROW BIOPSY FINDINGS IN T-CELL LARGE GRANULAR LYMPHOCYTIC LEUKEMIA (LGL): REPORT OF 4 CASES
BOVERI Emanuela (1), RIBONI Roberta (1), ARCAINI Luca (2), PASSAMONTI Francesco (2), INVERNIZZI Rosangela (3), IPPOLITI Giovanbattista (4), CASTELLO Alessandro (1), MAGRINI Umberto (1)
(1) Institute of Surgical Pathology, (2) Institute of Haematology, (3) Institute of Internal Medicine, IRCCS Policlinico San Matteo and University of Pavia, Pavia (Italy); (4) Division of Internal Medicine, Ospedale Civile, Voghera

Introduction: T cell large granular lymphocytic leukemia (T-LGL) is a rare disease, with indolent clinical course, often associated with autoimmune conditions (rheumatoid arthritis), hematological disorders (myelodisplastic syndromes, aplastic anemia) or neoplasias (hairy cell leukemia, myeloma). Diagnosis can be made on marrow aspirate and peripheral blood by cytological, immunophenotypical and molecular findings (assessment of T cell receptor/TCR rearrangement). However, presenting features can overlap with other low grade lymphomas and a bone marrow biopsy (BMB) is performed.
Purpose of the study: to describe the clinico-pathologic findings in 4 cases of T-cell LGL.
Patients and methods: 4 patients (M : F= 3:1; mean age: 56 years, range 48-70) presented cytopenia (particularly, neutropenia), lymphocytosis (4/4) and hepatosplenomegaly (2/4); in all cases, the clinical picture had been present relatively unchanged for more than 1 year before BMB (range: 1-24 years); one patient showed associated pulmonary hypertension. Paraffin embedded BMBs were used for morphological and immunophenotypical studies; flow cytometry and molecular assessment of the TCR rearrangement were performed on peripheral and/or marrow blood.
Results: in all cases, the hemopoietic matrix was partially (20-40%) replaced by an interstitial lymphoid population of medium-sized cells, with clear cytoplasm. By immunostains, underscoring a constant sinusal involvement, these cells had a T (CD2+, CD3+, CD5+, CD7+, CD20-) activated cytotoxic phenotype (CD8+, CD4-, CD57+, CD56-, TIA1+, granzyme B+, perforin+); they were TCR alpha-beta+, gamma-delta- by flow cytometry and carried a monoclonal TCR rearrangement by molecular analysis. A decreased leuco-erythroblastic ratio and a mild diffuse fibrosis were seen. In 1 patient, sequential BMBs, after therapy, at 1 and 2 years from diagnosis, showed overlapping morphofunctional features, with a mild decrease of lymphoid infiltration.
Conclusion: T-cell LGL is a rare diagnosis in hematopathologist's practice; its distinction from other lymphoproliferative diseases both of B (hairy cell leukemia, splenic marginal zone lymphoma) and T cell origin (hepatosplenic T cell lymphoma) is of paramount importance, as these entities carry a worse prognosis and require specific or more aggressive therapy. In our cases, the final diagnosis could be reached only by combining different techniques, thus underlining the need of a multidisciplinary approach.

P 115
RETROPERITONEAL FOLLICULAR DENDRITIC CELL SARCOMA
ALEXANDROU Paraskevi, LIAPIS George, TZIRAKIS Mixalis, GIASLAKIOTIS Konstantinos, ANDROULAKI Athina. Affiliations: Department of Pathology, Laiko Hospital, University of Athens

Follicular dendritic cell sarcoma (FDCS) is an extremely rare neoplasm with only a few reported cases in the literature reviewed, arising from antigen-presenting immune accessory cells in nodal and extranodal sites. It is considered to be an intermediate grade malignancy with a significant recurrent and metastatic potential. We report a case of excisional biopsy of a retroperitoneal mass performed in a 33 years old woman. The tumor tissue was gray to tan, 5cm in the greatest dimension. On microscopic examination, the prominent histological feature was the presence of sheets, fascicles and trabeculae formed by spindle to ovoid cell with indistinct cell borders, oval nuclei, dispersed chromatin and inconspicuous

nucleoli. There were also scattered multinucleated cell forms and marked necrosis. Striking lymphocyte and plasma cell infiltrations with increased focal vascularity were also present. The neoplastic cells showed positive reaction to vimentin, CD21, CD23 and negative to CD1a, HMB-45 and cytokeratins, an immunoprofile consistent with FDCS. There is an overlap of the immunoprofile among various dendritic cell lesions, which makes the differential diagnosis complicated. The combination of CD21 and CD23 markers is found primarily in FDCS, thus it is of great importance in the diagnostic distinction.

P 116

COMPARISON OF FASCIN TO DF3/MUC-1 EXPRESSION IN RELATIONSHIP TO TCR-¦Ã CLONALITY, NPM/ALK CHIMERIC PROTEIN EXPRESSION AND 2P23 REARRANGEMENT FINDINGS IN ANAPLASTIC LARGE CELL LYMPHOMAS

BOBOS Mattheos, KOSTOPOULOS Ioannis, KOTOULA Vassiliki, KARAYANNOPOULOU Georgia, PAPADIMITRIOU S. Constantine
Department of Pathology, Aristotle University Medical School, Thessaloniki, 54006, Greece

Introduction.Fascin is expressed in almost all cases of Hodgkin disease (except lymphocyte predominance type) and in a high percentage in anaplastic large cell lymphomas (ALCLs) and peripheral T cell lymphomas. DF3/Muc-1 mucin-like glycoprotein is aberrantly overexpressed in most adenocarcinomas and in a variety of hematopoietic cell malignancies as T and B-cell lymphomas and myelomas. It is also frequently expressed in ALCL. The aim of this study is to investigate the expression of fascin and DF3/Muc-1 in ALCL in comparison with other markers used in these neoplasms.
Material and Methods. A total of 52 cases of ALCL (46 of T-cell and 6 null-cell type) from various sites (39 systemic ALCL, 10 primary cutaneous [C-ALCL] and 3 HIV-related ALCL) were analyzed for fascin and DF3/Muc-1 expression by immunohistochemistry (IHC). Molecular assessments PCR and RT-PCR) and cytogenetic investigation (FISH) were performed in 42 and 43 cases respectively. Tissue sections from 11 ALCL and tissue microarray blocks containing 41 cases of ALCL were used for IHC and FISH. Chi-Square (¦Ö2) tests of significance were performed using the statistical software SPPS 12.0.
Results. Fascin was expressed in the cytoplasm of tumor cells in 41/52 (78,8%) cases; 34 systemic and 7 C-ALCL, (p¡Ü0,001); 37 of T-cell and 4 of null-cell phenotype. Fourteen out of 15 (93,3%) ALK+ and 27/37 (72,9%) ALK- tumors, as well as all ALCL bearing ALK rearrangements were positive for fascin. The majority of ALCL positive for TCR-¦Ã stained for fascin (20/21) (95,2%).
Cytoplasmic and membraneous expression of DF3/Muc-1 was detected in 18/52 (34,6%) of ALCL cases; 15 systemic ALCL and 3 C-ALCL; 15 of T-cell and 3 of null-cell type. Muc-1 was positive in 60% ALK+ and in 24,3% ALK- tumors ($p<0,05$). Ten out of 21 (55,6%) cases with clonal rearrangement and 5/12(41,7%) cases with 2p23 region rearrangement showed Muc-1 expression. Seventeen out of 18 cases with Muc-1 expression were also positive for fascin ($p<0,05$).
Fascin and/or DF3/Muc-1 were detected 42 (80,8%) cases. The two antibodies were also expressed in the majority of systemic (34/39) or C-ALCL (8/10), (p¡Ü0,001) cases. None of the HIV-related ALCL cases was positive for fascin or DF3/Muc-1.
Conclusion. Fascin is widely expressed in ALCL, in contrast to DF3/Muc-1. Up-regulation of fascin protein and its clinical usefulness in these tumors have not yet been determinated. It seems that this aberrant expression is more common finding in ALK+ ALCL

P 117

PROGNOSTIC SIGNIFICANCE OF THE APOPTOSIS-RELATED PROTEINS BAX, BAK, BCL-2, MCL-1, CASPASE 3, ACTIVATED CASPASE 3 AND CASPASE 9 IN ACUTE MYELOID LEUKEMIA

ZOLOTA Vassiliki, SIRINIAN Chaido, TSAMANDAS Athanassios, A. KOURAKLIS-SYMEONIDIS Alexandra*, SYMEONIDIS Argyrios*, MELACHRINOY Maria.
Department of Pathology and *Hematology Division, Department of Internal Medicine, University of Patras, Medical School, Rion, Patras, Greece.

Background: Acute myeloid leukemia (AML) is an aggressive disease with generally poor prognosis. Common mechanisms of resistant disease are defects in apoptotic pathways. Apoptosis is regulated by i) mitochondrial-mediated and ii) receptor-mediated pathways. This study investigates the expression of mitochondrial related apoptotic genes bcl-2, bax, bak and mcl-1, and the apoptosis enzymes caspase-3 and caspase-9 in AML and their potential correlation with patients' outcome.
Material and methods: Paraffin-embedded sections of 40 bone marrow biopsies, from equal number of patients with newly diagnosed AML (34 de novo not otherwise categorised AML cases classified as follows: M0(n=1), M1(n=9), M2(n=8), M3(n=2), M4(n=10), M5(n=4), AML following MDS(n=6)) were analyzed immunohistochemically using antibodies against bcl-2 (Dako), bax (Dako), bak (Dako), mcl-1 (Neomarker), caspase 3 (Neomarker, epitope not determined), activated caspase 3 (Chemicon, cleaved p17 fragment) and caspase 9 (Neomarker, middle fragment of caspase molecule). Patients were followed up for 0-78 (mean14.45) months.
Results: The mean indices for bax, bak, bcl-2, caspase 3 and caspase 9 were: 52.45 (15-100), 47.1 (11-90), 39.26 (5-88), 27.5 (0-95) and 39 (0-90) respectively. In all cases, activated caspase 3 was detected in a very small percentage of tumor cells (mean 2.9%-range 0-5). Mcl-1 was detected only in 4 cases. Bax/bcl-2 ratio mean index was 2.36 (0.26-9.00). A direct correlation was recorded between i) caspase 3 and caspase 9 expression ($p<0.01$) ii) bax, bak and caspase 3 expression ($p<0.05$ respectively) and iii) bax/bcl-2 ratio and caspase 3 expression ($p<0.05$). No significant relationship was observed between the expression of the above markers and disease free or total survival. Cases expressing bax/bcl-2 ratio >1.5 showed longer total survival compared with those expressing bax/bcl-2 <1.5 but this was not statistically significant. Histologic subtyping showed no correlation with any of the markers studied.
Conclusions: Overexpression of bax and bak as well as increased bax/bcl-2 ratio suggest that the apoptotic pathway mediated by mitochondria seems to be activated in AML. However, failure of caspase 3 activation seems to exist and results in accumulation of uncleaved caspase-3 in leukemic cells. Whether this deficit is sufficient to block bax-induced cell death or apoptosis signal may be mediated by other pathways, remains to be evaluated.

P 118

INTERDIGITATING DENDRITIC CELL SARCOMA OF THE TONSIL

ALEXANDROU Paraskevi, LIAPIS George, TZIRAKIS Mixalis, GIASLAKIOTIS Konstantinos, ANDROULAKI Athina. Affiliations: Department of Pathology, Laiko Hospital, University of Athens

Interdigitating dendritic cell sarcomas (IDCSs) derive from antigen-presenting cells of the lymph node paracortex and deep cortex, the splenic periarteriolar lymphoid sheaths and the interfollicular space of mucosa-associated lymphoid tissue. They are extremely rare, generally occur in adults with male predominance and usually show an aggressive course.

We report a case of a 55 years old male presented with a painless enlargement of the right tonsil, having no past medical history. A bilateral tosilectomy was performed. The affected tonsil exhibited a polypoid mass measuring 15 X 15 X 6 mm. On light microscopy, the normal architecture of the tonsil had been replaced by a diffuse infiltration of large irregularly shaped histiocytoid cells with clumped chromatin and indistinct cell borders. Spindle shaped, polylobated and multinucleated forms were also present. The tumor cells were moderately to strongly immunoreactive for vimentin, S-100, CD1a and lysozyme. Other immunostains including cytokeratin, actin, desmin, HMB-45, B-cell markers and T-cell markers, CD30 and follicular dendritic cell markers including CD21 and CD35 were negative. Based on morphological and immunohistochemical profile a diagnosis of IDC was suggested. Ultrastuctural study eliminated the minor possibilities of misdiagnosis. The IDCSs exhibit significant overlap with other malignancies such as undifferentiated metastatic carcinoma, primary and metastatic sarcoma, malignant melanoma, anaplastic large cell lymphoma and histiocytic-dendritic cell proliferations. The phenotypic heterogenity of the IDSCs renders the combination of a thorough pathological and clinical investigation necessary for an accurate diagnosis.

P 119

EXPRESSION OF SURVIVIN IN LEUKEMIC CELLS IN RESPONSE TO INITIAL PREDNISONE THERAPY IN CHILDREN WITH ACUTE LYMPHOBLASTIC LEUKEMIA: RELATION TO OTHER PROGNOSTIC FACTORS.

Elzbieta Kamienska1, Tomasz Ociepa1, Lucyna Pawluch1, Michal Matysiak3, Andrzej Kurylak4, Mariusz Wysocki4, Tomasz Urasinski1, Elzbieta Urasinska2
1I Clinic of Pediatrics, Pomeranian Medical University, Szczecin, Poland, 2Dept. of Pathology, Pomeranian Medical University, Szczecin, Poland, 3Clinic of Pediatrics, Hematology and Oncology, Medical University, Warszawa, Poland, 4Clinic of Pediatrics, Hematology and Oncology, Collegium Medicum UMK, Bydgoszcz, Poland

BACKGROUND: Decreased apoptosis associated with overexpression of endogenous inhibitors of apoptosis, e.g. survivin (SUR) may be responsible for treatment failure in children with acute lymphoblastic leukemia (ALL). This study aimed to assess time resolved changes of SUR expression and its intracellular distribution (nucleus versus cytoplasm) in peripheral blood mononuclear cells, collected prior to and after 6 and 12 hours of prednisone administration as well as the relation between expression of SUR and other prognostic factors (age, risk factor group, peripheral blood leukemic cell count at the diagnosis and immunophenotype).
METHODS: The study comprised 26 children with de novo ALL. Cytospin preparations of mononuclear cells isolated on density gradient were stained with mouse anti-SUR antibody followed by goat anti-mouse antibody conjugated with APC. Cellular DNA was counterstained with PI/RNase A. SUR–associated long red fluorescence excited by HeNe (633nm) was measured simultaneously over the nucleus and the rim of cytoplasm (2 pixels width) by laser scanning cytometer (CompuCyte).
RESULTS: Expression of SUR measured: (1) over the nucleus and over cytoplasm before and after 6 and 12 h from prednisone administration was significantly higher in children in medium/high risk groups then in standard risk group ($p<0.005$), (2) over the nucleus before and 12 h after treatment was significantly higher in children with peripheral blood leukemic cell count more then 20 000/uL ($p<0.05$), (3) over the nucleus before treatment was higher in ALL-T then ALL-B ($P<0.05$).
CONCLUSION: The association of high expression of SUR and poor prognostic factors in ALL suggest that SUR may be responsible for higher rates of treatment failures in children with ALL. Further studies are needed to confirm this preliminary observation.

P 120

MANTLE CELL LYMPHOMA IN TAIWAN: A CLINICOPATHOLOGIC AND MOLECULAR STUDY OF 21 CASES EXCLUSIVELY IN MALE PATIENTS

CHUANG Shih-Sung1, 2, CAMPO Elias3, COLOMER Dolors3, HUANG Wan-Ting4, HEISH Pin-Pen5, CHANG Hui-Mei6, CHO Chi-Yi7, HUANG Shih-Hung8, LU Yin-Che 9, WU Jiann-Der10
Department of Pathology, 1Chi-Mei Foundation Medical Center, 2Taipei Medical University, 4Chang Gung Memorial Hospital, Kaohsiung Medical Center; 5Veterans General Hospital-Kaohsiung, 6Changhua Christian Hospital, 7St. Martin de Porres Hospital, 8Cathay General Hospital, Departments of 9Oncology and 10Pathology, Chia-Yi Christian Hospital, Taiwan; 3Laboratory of Pathology, Hospital Clinic, University of Barcelona, Barcelona, Spain

INTRODUCTION: Mantle cell lymphoma (MCL) is a rare and aggressive B-cell lymphoma and has never been fully characterized in Taiwan.
PURPOSE OF THE STUDY: We conducted this multi-institutional study in an attempt to have a better understanding of MCL in Taiwan.
METHODS: Retrospective study with morphology, immunohistochemistry, and real time RCR for cyclin D1 mRNA using paraffin sections.
SUMMARY OF RESULTS: A total of 21 cases, all male patients, were identified with a median age at 61.0 (mean, 60.7; range, 41-75). The most common organs of involvement at diagnosis were lymph node (19 patients, 90.5%), bone marrow (15, 71.4%), spleen (8, 38.1%), and gastrointestinal tract (5, 23.8%). Four patients (19.0%) developed multiple lymphomatous polyposes including 3 at diagnosis and 1 at disease progression. Eighteen (85.7%) were at high-stage disease. The 1- and 5-yr survival rates were 77.8% and 16.7%, respectively. The most common growth pattern in non-marrow tissue was mixed nodular (mantle zone) and diffuse patterns (9/20, 45%); while in the marrow, interstitial pattern (12/13, 92.3%). Cytologically, 18 (85.7%) cases were of classic variant; and 3, blastoid. The tumor cells expressed CD20, Bcl2, and IgM (in 100% cases), cyclin D1 (95.2%), CD5 (85.7%), CD43 and IgD (61.9%), CD52 (60.0%), and Bcl6 (5%). No tumor expressed CD23. There was no statically significant impact of p21, p27, and p53 expression and Ki67 labeling index on survival. Real time PCR for cyclin D1 mRNA was performed on 11 cases. One case was not amplifiable; the single cyclin D1-negative case showed a low level of mRNA while the remaining 9 cyclin D1-positive cases showed extremely high levels.
CONCLUSION: We confirm that the usual morphologic variants and aberrant immunophenotype of MCL in the West occur in Taiwan and this disease carry a poor prognosis. Real time PCR for cyclin D1 mRNA is a useful adjunct for surporting the diagnosis of cyclin D1-negative MCLs.

P 121

ANGIOGENESIS IN CHRONIC MYELOPROLIFERATIVE DISEASES DETECTED BY CD34 EXPRESSION.

K. Panteli (1) , N. Zagorianakou (2), A. Goussia (2), A. Zioga (2), A. Katsaraki (2), K. Bourantas (1), N. J. Agnantis (2), M. Bai (2)
Department of Hematology (1) and Department of Pathology (2), Medical Faculty, University of Ioannina, Greece.

Increased bone marrow angiogenesis estimated as bone marrow microvessel density (MVD) or as serum angiogenic factor levels and/or immunohistochemical expression of these

factors in bone marrow biopsy has been demonstrated in a variety of hematological disorders including chronic myeloproliferative diseases (MPDs).
The aim of this study was to investigate the MVD in 25 cases of myelofibrosis with myeloid metaplasia (MMM). MVD was estimated by CD34 immunohistochemical expression in bone marrow biopsies. A control group of 27 patients without bone marrow disease, eight cases of polycythemia vera (PV), 41 cases of essential thrombocythemia (ET) and nine cases of chronic myeloid leukemia (CML) were also studied. Moreover, in cases with MMM and cases with ET, MVD was correlated with clinical, laboratory, histological parameters and the outcome of the patients.
Our study confirmed a significantly higher degree of angiogenesis in MMM, PV, ET and CML compared with controls ($P < 0.001$, $P = 0.0007$, $P < 0.001$ and $P = 0.0008$, respectively). Angiogenesis was higher in MMM than PV, ET and CML cases ($P < 0.001$, $P < 0.001$ and $P = 0.008$). Increased angiogenesis was correlated with hypercatabolic symptoms in MMM patients ($P = 0.009$). No correlation with other clinicopathological parameters or clinical outcome was found. In ET cases, increased angiogenesis was not correlated with clinical, laboratory, bone marrow histopathological parameters or clinical outcome.
Definitive conclusions regarding the prognostic value of increased angiogenesis may require additional follow-up and a larger group of patients.

P 122
ASSOCIATION BETWEEN MEDIASTINAL GERM CELL TUMOR AND ACUTE MYELOÏD LEUKEMIA
CAMPARO P (1), DESANGLES F (2), MOSSAFA H (3), SOULEAU B (4), BRANQUET D (5)
Laboratoire d'histologie pathologique (1) Laboratoire de cytogénétique (2); HIA du Val de Grâce, 74 boulevard Port Royal Paris. (3) Laboratoire CERBA, (4) Service d'Hématologie Clinique, (5) Laboratoire d'Anatomie Pathologique, HIA Percy

Introduction : Acute myeloïd leukemia (AML) in the follow up of other malignant tumors are usually chemotherapy-induced and may present treament specific chromosomic alterations. We report a case of AML occuring in the short follow up of a mediastinal germ cell tumor (MGCT) that was not therapy-induced, but cytogenetically proved to originate from the germ cell tumor.
Observations : A mediastinal tumor was discovered in an asymptomatic 24 years old man. Histologically, this tumor consisted of a mixed germ cell tumor associating seminoma and teratoma with some foci of myeloïd differenciation. It was first treated by chemotherapy. Ten months later the remaining mediastinal tumor was partially removed by surgery while a myelemia occured (35000 WBC). No Phi chromosome was observed on blood cell cultures (myelodysplasic syndrom MDS/MPS). Because of bad general condition, second chemotherapy was delayed and four months later the MDS/MPS transformed into AML (110 000 WBC with 28 % of blast cells). The patient died two month later.
Discussion : 60 cases of such an association between mediastinal germ cell tumor (MGCT) and AML have been discribed. The leukemia is usually of M7 type accordind FAB classification (our case). It occurs during the 5 years following the diagnosis of the germ cell tumor, a too short period for a chemotherapy-induced leukemia. The germ cell tumor is usually mixed with seminoma and yolk sac components.
The proof of a commun ancestor between germ cell tumor and leukemia is made by cytognetic analysis that shows the specific germ cell tumors i(p12) in both tumors, while others genetic alterations commonly observed in induced leukemia are absent (7q32-35 or 11q23). Only ten of such cases have been fully documented.
Conclusion : Association between GCT and AML is rare. The link between the two tumors is proved by cytogenetic analysis. These patients show poor clinical outcome with death occuring in the year following the acutisation.

P 123
B-CELL PROLYMPHOCYTIC "LEUKEMIA" (B-PLL): A HETEROGENEOUS DISORDER WITH EMPHASIS IN ITS CLINICAL, HISTOLOGICAL AND GENETIC CHARACTERISTICS
LOME-MALDONADO Carmen 1, MARTÍNEZ-BENÍTEZ Braulio 1, LARA César 1, VELA-CHAVEZ Teresa 1, QUINTANILLA-MARTÍNEZ Leticia 2, FEND Falko 2, ÁNGELES-ÁNGELES Arturo 1.
1 Pathology, Instituto Nacional de Ciencias Médicas y Nutricion "Salvador Zubirán", Mexico City, Mexico and 2 Institute of Pathology, Technical University, Munich, Germany.

Background: B-PLL is an infrequent disease, defined by the WHO as an aggressive lymphoid neoplasia, characterized by splenomegaly without lymphadenopathy and peripheral lymphocytosis with > 55% prolymphocytes.
We report 3 cases with morphologic and immunohistochemical features of B-PLL with unusual clinical and genotypic features shared by mantle cell lymphomas. Based on these findings we consider the wider term B-cell prolymphocytic leukemia/lymphoma more appropriate and discuss its use.
Design: Retrospective, descriptive.
Results: Patient 1: 51year-old male with splenomegaly and cervical lymphadenopathy, lymphocytosis (>55%),infiltrated bone marrow.
Patient 2: 54 year-old female with fever and generalized lymphadenopathy. CBC without lymphocytosis, infiltrated bone marrow.
Patient 3: 59 year-old male with fever and generalized lymphadenopathy. CBC without lymphocytosis, bone marrow without infiltration.
Lymph nodes in all cases had prolymphocytic differentiation.
All three patients had the next immunophenotype in lymph nodes: CD20+, IgM+, CD5-, CD23-, CD43-, cyclin D1-, with variable expression of Ki-67(5-50%), and p53(5-70%).
Genotyping studies using FISH probes showed t(2;8)(p12;q24) in patient 1. Patients 2 and 3 showed t(11;14) in 20% and 40% of the analyzed cells respectively.
Discusion: B-cell prolymphocytic lymphoproliferations constitute a heterogeneous group of disorders in which c-myc rearrengement can be present in very few cases. However, direct involvement of c-myc specifically affecting 8q24 has been proposed as an important factor in B-PLL pathogenesis, as detected in patient 1.
Patients 2 and 3 correspond to a B-cell prolymphocytic lymphoproliferation with isolated lymph node involvement without leukemic component. To our knowledge, this presentation is very uncommon, and is not part of the WHO classification scheme. Although it has been considered that some cases of B-PLL could represent a variant of mantle cell lymphoma, our cases were CD5 and cyclin D1 negative, partially ruling out this possibility. However, using FISH we documented t(11;14) in both patients. Our clinical and genetic data support the idea that these B-prolymphocytic disorders can be considered as B-cell prolymphocytic lymphoma/leukemia they shares a broad and still undefined genetic spectrum.

P 124
CD56 EXPRESSION WITH OR WITHOUT CYTOTOXIC PHENOTYPE IN T-CELL NON-HODGKIN INTESTINAL LYMPHOMAS
LARA César, MARTÍNEZ-BENÍTEZ Braulio, VALERIO Juan Carlos, VELA-CHAVEZ Teresa, ONTIVEROS

Patricia, LANGUREN Marisol ÁNGELES-ÁNGELES Arturo, LOME-MALDONADO Carmen.
Instituto Nacional de Ciencias Médicas y Nutrición "Salvador Zubirán", México.

In the WHO classification two major neoplasms derived from mature NK/T cells are recognized; the nasal/nasal-type T/NK-cell lymphoma and the aggressive NK cell leukemia lymphoma. Recent papers have documented the expression of CD56 in non-Hodgkin T-cell lymphomas in a variety of anatomic locations, like cutaneous lymphomas, where CD56 expression has been associated with a poor prognosis. The aim of our study is to identify the cases of NH-T cell intestinal lymphoma in our institution, describe in detail their morphologic features and to classify them according to their CD56 expression.
Material and methods: Paraffin blocks from 9 cases of T-cell intestinal NHL were evaluated, by clínical, morphological, immunophenotypical (CD3, CD20, CD4, CD8, CD7, CD5, CD 56, granzyme, LMP-1, and EBER-ISH), and molecular biology analysis (TCRg and IgH by PCR) in most of them.
Results: We identified 67 intestinal lymphomas from 1980-2004; 46 of them were B-cell lineage and 21 of T-cell lineage. Nine cases had available material for immunohistochemical studies. Of these, 6 cases were NK-(CD56-); one with expression of citotoxic granules (granzime +) and two without it. Three cases were NK + (CD56+); one with expression of citotoxic granules and 2 negative. A variable expression of CD4 and CD8 markers was found, showing no correlation with either CD56 or cytotoxic phenotype. Epstein-Barr virus presence was detected in all NK – (CD56-) cases and in none of NK + (CD56+) cases.
Discussion: We describe herein three unusual cases of intestinal large NK/like T-cell lymphomas with or without cytotoxic phenotype and without evidence of enteropathic damage. These cases had morphologic characteristics similar to those described in nasal and nasal-type NK-T cell lymphomas as angiocentric lesions and necrosis. Interestingly, EBV infection was not documented in our CD56+ cases. The particularly aggressive behavior of our cases was confirmed by clinical follow-up.
Conclusions: Our results demonstrated that T-cell intestinal NHL represent a heterogeneous group of neoplasms in which expression of CD56 can be present, with an apparent poor clinical prognosis. Theses cases could be considered as part of the group of NK-T cell nasal type lymphomas or as a particular group of CD56 + (cytotoxic or not) intestinal NHL.These items are open to future investigations with larger series of cases.

P 125
CEREBRAL INVOLVEMENT IN CHRONIC LYMPHOCYTIC LEUKEMIA
TERZIC Tatjana, SKENDER-GAZIBARA Milica, SUVAJDZIC Nada*, MITROVIC Dragan, RADOJEVIC Sanja,CVETKOVIC-DOZIC Dubravka
Institute of Pathology, School of Medicine, University of Belgrade; *Institute of Hematology, Clinical Center of Serbia, Belgrade, Serbia & Montenegro

Introduction: Central nervous system (CNS) involvement is an extremely rare complication of chronic lymphocytic leukemia (CLL). We reviewed 26 autopsy cases of CLL with special attention on pathological findings in CNS.
Patients: The study group consisted of 18 males and 8 females aged 45-75 years (average 62 years). The diagnosis of CLL was obtained on review of the hematoxylin and eosin-stained slides and immunophenotype data.
Results: Leukemic infiltration of CNS was evident clinically and grossly in two cases. The first patient was 53-years-old man with CLL of 3 years' duration, who developed a sensomotoric aphasia with right-sided hemiplegia six weeks prior to death. At autopsy, a large (6x6x4cm) ill-defined tumor mass was found in the temporo-occipital region of the left cerebral hemisphere with temporal herniation. Histologically, tumor tissue was very cellular, composed of large cells with vesicular nuclei, prominent nucleoli and occasionally giant and Reed Sternberg-like cells admixed with a small number of mature lymphocytes. Immunohistochemically, both types of malignant proliferation (small and large cells) stained positively for CD20 (pan-B marker). The diagnosis of cerebral diffuse large cell lymphoma in CLL (Richter syndroma) was obtained. The second patient was 70-years-old man with CLL of one year's duration, who developed a polyradiculoneuropathia one month prior to death. At autopsy, infiltration of spinal roots and cranial nerves as well as diffuse leptomeningeal dissemination ("leukemic meningitis") were found. Histologically, peri- and endoneural leukemic infiltration, leukostasis and perivascular leukemic infiltration (prevalent in the brainstem and spinal cord) and meningiosis were presented. Histopathological findings (without evidence of a mass lesion) in 2/26 CLL cases without neurological signs were in the form of petechial hemorrhages with leukostasis and perivascular leukemic infiltration, localized in the white matter of the cerebral hemispheres. In all other cases of CLL (22/26, 84,6%) cerebral leukemic infiltration was not present.
Conclusions: The clinicopathological features of these cases indicate that, despite of rarity of CNS involvement in CLL, any neurological manifestation in CLL patients should be aware of the possibility of this complication.

P 126
EXPRESSION LEVEL OF CASPASE-3 IN DIFFUSE LARGE B-CELL LYMPHOMA: CORRELATION WITH GERMINAL CENTRE EXPRESSION PROFILE.
PANDELEON Barbara, KATIKOS Evangelos, VAMVOUKA Chrysanthi, STEFANAKI Kalliopi, PAPPA Vasiliki, ECONOMOPOULOS Theofanis, HARHALAKIS Nikolaos, RONTOGIANNI Demetra.
Departments of Pathology and Hematology, Evangelismos Hospital, and Second Department of Internal Medicine-Propaedeutic Clinic, Athens University.

Background: Abnormalities in programmed cell death frequently induce drug and/or radiation resistance in non-Hodgkin's lymphoma (NHL). Caspase-3 is an enzyme crucial to the apoptotic process and is activated in both major apoptotic pathways, including stress-induced pathway and a cell surface death receptor signalling pathway, leading to final execution of apoptosis. Recent study showed that the expression of caspase-3 in NHLs can reflect proper functioning of apoptotic pathways. Diffuse Large B-Cell Lymphomas -DLBCLs- are a group of tumours with heterogeneous clinical, morphological, immunophenotypic, cytogenetic and molecular features.
Purpose of the study: In order to elucidate whether good prognosis of germinal centre cell DLBCLs is related to well functioned caspase apoptotic pathway, we studied the expression of active form of caspase-3 (activated CCP32) in 46 cases of DLBCLs which were classified in four groups according to bcl-6 protein, CD10 and MUM-1 antigen expression: I) bcl-6 positive 16/46, II) bcl-6 positive, CD10 positive, germinal centre cell immunophenotype 14/46, III) bcl-6 positive, MUM-1 positive 10/46 and IV) bcl-6 negative 6/46. Chi-square was used as the statistical test.
Results: 1) Group I -bcl-6 positive- showed significantly higher expression of caspase-3 than the group IV -bcl-6 negative-. 2) Group II -bcl-6 positive, CD10 positive- showed significantly higher expression of caspase-3 than the groups I -bcl-6 positive-, and III -bcl-6 positive, MUM-1 positive-.
Conclusions: Our results indicate that DLBCLs with germinal cell immunophenotype maintain well functioning apoptotic

pathway which can explain good response to current chemotherapeutic agents.

P 127
EXTRANODAL DETERMINATION OF ANAPLASTIC LARGE-CELL LYMPHOMA

DOBREA Camelia 1,2, SIMION Alina 3, VASILESCU Florina 1,4, IOSIF Cristina 1,5, MIHAI Mihaela 1,6, ANDREI Florin 1, COLITA Adriana 2, COLITA Dan 2, ARDELEANU Carmen 1
1-"V Babes" National Institute, Bucharest, Romania
2-Dept of Haematology, "Fundeni" Clinical Institute, Bucharest, Romania
3-student, "Carol Davila" University, Bucharest, Romania
4- Central Military Hospital, Bucharest, Romania
5-"Sfanta Maria" Clinical Hospital, Bucharest, Romania
6-Dept of Pathology, "Fundeni" Clinical Institute, Bucharest, Romania

T/null Anaplastic Large-Cell Lymphoma (ALCL) is a very rare Malignant Lymphoma (~5% incidence), frequently with extranodal determination. 45 cases of systemic ALCL diagnosed in ours laboratories were studied, and a pathological and clinical study was performed. The 45 patients(M/F = 2.75, 66% T-cell ALCL and 33% null ALCL, 56.5% expressing ALK)presented extranodal disease in 42% of cases. Only in 3 cases the first presentation was extranodal (bone-1 case and digestive-2 cases). The most frequently sites were: bone (8 cases), cutaneous (6), bone marrow (4), digestive (4), pulmonary(4), hepatic (4), central nervous system (3). Four patients presented more than 3 extranodal determinations. The pediatric population presented particularly cutaneous and bone marrow infiltration. The phenotype of the malignant cells was more frequently T-cell (28% of the T-ALCL and 18% of the null-ALCL). More than 50% of the ALCL ALK negative presented extranodal disease (half of the cases with more than 2 localizations), and only 38% of the ALCL expressing ALK. The presence of extranodal disease in ALCL is an important characteristic of these malignancy and, sometime, pose problems of diagnosis and treatment.

P 128
IMMUNOHISTOCHEMICAL ANALYSIS OF T-CELL RECEPTOR SIGNALING ACROSS THE SPECTRUM OF CELIAC DISEASE ASSOCIATED LYMPHOCYTIC PROLIFERATIONS

KELLER, Christian, College of Physicians and Surgeons, Columbia University, New York, USA, CATTORETTI, Georgio, College of Physicians and Surgeons, Columbia University, New York, USA, VAKIANI, Efsevia, College of Physicians and Surgeons, Columbia University, New York, USA, GREEN, Peter, College of Physicians and Surgeons, Columbia University, New York, USA, BHAGAT, Govind, College of Physicians and Surgeons, Columbia University, New York, USA

Background: Small bowel biopsies with increased intraepithelial lymphocytes (IELs) are commonly seen in patients with celiac disease (CD). In individuals with refractory CD (RCD) the IELs display an abnormal phenotype, persist despite gluten withdrawal and are often clonal, possibly representing cryptic enteropathy associated T-cell lymphomas (EATLs) in a subset. We evaluated for possible dysregulation of the T-cell receptor (TCR) associated signaling proteins as well as mediators of the NF-kappa B pathway across the spectrum of CD associated IEL proliferations to determine whether any differences exist between IEL expansions in active CD, RCD, and EATL.
Material and methods: Immunohistochemical (and in a subset immunofluorescent) staining of duodenal biopsies from patients with active CD (n=2), RCD with polyclonal IELs (n=2), RCD with clonal IELs (n=1), EATLs (n=4), normal individuals (n=2), and suitable controls was performed with antibodies against Zap-70, Bcl-10, CD25, c-REL, p65, and junB by immunohistochemistry. IELs were also phenotyped by staining for the pan-T-cell antigens, CD30, and TIA-1.
Results: IELs in all cases were ZAP-70+, CD25-, c-REL-, p65-, and junB-; Bcl-10 staining was equivocal in a few cases. One EATL was CD4+ TIA-1-, while the remaining 3 were CD4- CD8- TIA-1+, 2 of these were also CD30+, CD25+, and Bcl-10+. All EATLs were ZAP-70+. None of the EATLs stained with c-REL and p65. Both the CD30+ EATLs showed intense nuclear junB staining while CD30- EATL showed only scattered junB+ cells.
Conclusions: We did not observe any differential expression of TCR associated proteins in CD associated IEL expansions. A lack of CD25 expression by the IELs suggests the role of cytokines besides IL-2 in cell survival and proliferation. No detectable elevation in proteins of the classical NF- kappa B pathway in EATLs suggests the possible role of other signaling pathways. Lastly, nuclear accumulation of junB in a subset of EATLs appears to be the consequence of CD30 activation, as has been demonstrated for other subsets of T-cell lymphomas.

P 129
STUDY OF TRANSLOCATION T(11;18)(Q21;Q21)(API2/MLT1) AND EXPRESSION OF BCL10 IN PRIMARY CUTANEOUS MARGINAL ZONE B-CELL LYMPHOMAS

V.Baena1, C.Barranco1, F.Gallardo1, B.Belosillo1, S.Boluda1, M.Jimeno1, M.Iglesias1, N. Juanpere1, M. Garcia1, R. Esgueva1, A. Ariza2, F.Solé1, R. Pujol1, J. Lloreta1, S.Serrano1. Pathology and Dermatology Departments. Hospital del Mar-IMAS1. Pathology Department. Hospital Universitari Germans Trias i Pujol2.

Background
Primary cutaneous marginal B-cell lymphoma (C-MZL), an usually benign low-growth fraction neoplasm, is probably the most frequent form of primary B-cell lymphoma of the skin. API2/MLT1 fusion transcripts due to (11;18)(q21;q21) and aberrant bcl10 nuclear expression have been described in some noncutaneous marginal zone lymphoma subtypes, but little is known about cutaneous-MZL genetic alterations. Our aim was to evaluate a possible implication of API2/MLT1 fusion transcripts and bcl10 expression in primary cutaneous-MZL.
Design
A total of 42 patients diagnosed with cutaneous-MZL on the basis of WHO/EORTC criteria were studied. Skin biopsies from every patient were routinely tested with a wide panel of monoclonal antibodies. Additionally, MLT1 fusion transcripts were performed in 21 instances.
Results
Aberrant nuclear bcl10 expression, demonstrated in 15 cases, was related to a more aggressive clinical behaviour. Translocation t(11;18)(q21;q21) was absent in all evaluated samples.
Conclusion
The API2/MLT1 fusion, strongly associated with extracutaneous MALT lymphomas, does not seem to play a role in cutaneous marginal zone lymphoma pathogenesis. However, bcl10 aberrant nuclear expression could be a significant prognostic factor in cutaneous marginal zone lymphoma, signalling a more aggressive clinical course and a higher risk of extracutaneous involvement.

P 130
BCL 2 AND BAX INTERACTION IN PERIPHERAL BLOOD B – LYMPHOCYTES IN PATIENTS WITH CHRONIC LYMPHOCYTIC LEUKEMIA

BRAJUSKOVIC Goran, OROLICKI VUKOSAVIC Slobodanka*, CEROVIC Snezana, USAJ KNEZEVIC Slavica, MARJANOVIC Slobodan**, ROMAC Stanka***
Institute of Pathology and ** Clinic of Hematology, Military Medical Academy, Belgrade, Serbia and Montenegro; * Novartis Research Foundation WRO, Friedrich Miescher Institute, Basel, Switzerland, *** Faculty of Biology, University of Belgrade, Belgrade, Serbia and Montenegro

Chronic lymphocytic leukemia (CLL) is neoplastic disease characterized by the accumulation of morphologically mature monoclonal CD 5+ B cells in the early phase (G0/G1) of the cell cycle. The accumulation of neoplastically transformed B lymphocytes (CLL cells) is primarily the consequence of the blockade of apoptosis in these cells. The Bcl 2 proteins are well-known modulators of this process. Some of these proteins are anti-apoptotic while other are pro-apoptotic. All contain at least one of the four conserved regions called Bcl 2 homology domains (BH1-BH4). Evidence indicates that Bcl 2 and Bax form homo- and heterodimers. The antiapoptotic effect of Bcl 2 protein is based on its possibility to bind Bax protein in the heterodimer form, and in that way blocks forming Bax/Bax proapoptotic homodimers. The ratio of Bcl 2 / Bax represents a cell autonomous rheostat which determinates the type of cell reaction to an apoptotic stimulus. We used the co – immunoprecipition method to determine the level of interaction between these two proteins in CLL cells. Our study included the analysis of 20 peripheral blood speciments from 20 patients with CLL, and 20 peripheral blood specimens of healthy persons who represented the control group. Simultaneously we analysed the level of binding Bcl 2 protein to Bax (IP: Bcl 2 / WB: Bax) and reversed (IP:Bax / WB: Bcl 2). The intensity of Bcl 2 and Bax protein binding compared to the control samples of the peripheral blood of healthy persons, was increased in CLL cells. Results IP: Bax / WB: Bcl 2 showed a high level of »free« Bcl 2 protein which is not bound in the heterodimer form to Bax protein. Simultaneously IP: Bcl 2 / WB: Bax has showen that a higher quantity of Bax protein was bound in the heterodimer form to Bcl 2 protein, than the rest of the potential homodimer bound to bax protein. Further studies involving larger groups of patients are necessary to explore potentional significance of Bcl 2 / Bax protein ratio determination as a prognostic parameter in CLL treatment.

P 131

AGGRESSIVE SYSTEMIC MASTOCYTOSIS WITH PRIMARY PRESENTATION IN GASTROINTESTINAL TRACT. CASE REPORT

Ugnius Mickys, Auðrinë Barakauskienë
National Centre of Pathology, Vilnius, Lithuania
Chris De Wolf-Peeters, Karel Geboes
Department of pathology, K.U. Leuven, Belgium

Introduction
The WHO classifies mastocytic proliferations into: 1. Cutaneous mastocytosis. 2. Indolent systemic mastocytosis. 3. Systemic mastocytosis with associated other clonal hematological disease. 4. Aggressive systemic mastocytosis. 5. Mast cell leukemia. 6. Mast cell sarcoma. 7. Extracutaneous mastocytoma.
Aggressive systemic mastocytosis is characterized by clonal mast cell proliferation in skin, bones, lymph nodes and the gastrointestinal tract.
Our aim is to report a rare case of primary presentation of aggressive systemic mastocytosis in small and large bowel.
Materials and methods
A 46 years old woman suffered from watery diarrhea, vomiting, abdominal pain, weakness and weight loss for 6 months. No skin lesions were documented. Clinical and other investigations revealed ascites, massive edema of the legs, leucocytosis, anemia, hypoproteinemia and patchy erosive lesions in the large and small bowel (endoscopically). Small and large bowel biopsies, cytological smear of ascitic fluid and a bone marrow biopsy were evaluated with routine staining (haematoxylin and eosin), histochemical stainings (PAS, Giemsa, Ziehl-Neelsen, Toluidin, Leder). Hmmunohistochemical stainings using antibodies directed against: S-100, CD1a, CD68, mast cell tryptase, CD117 (c-kit) and myeloperoxidase (MPO).
Results
Routine staining revealed an accumulation of large cells with pale cytoplasm in the lamina propria of duodenum and large bowel. PAS, Giemsa, Ziehl-Neelsen and Toluidin blue stainings performed for the identification of these cells were negative. The immunophenotype of the cells was S-100 (-), CD1a (-), MPO (-), CD 68 (+), c-KIT (CD117) (+) and mast cell tryptase (+) which is consistent with mast cells. Infiltrates of mast cells occupied 50% of bone marrow space with collagen fibrosis. Giemsa (+) violet granules and Leder (+) red granules were found in mastocytes. Cytological evaluation of ascitic fluid was negative.
Conclusions
A diagnosis of primary mastocytosis in a visceral localization is very difficult, because this presentation is unusual and it is really a diagnosis of exclusion.
The main clue for the diagnosis of mastocytosis is the detection of mast cell tryptase immunohistochemically. Immunoreactivity of mast cells for CD68, CD117, MPO and positivity for Giemsa and Leder stains histochemically may suggest the diagnosis but the results of these stainings may vary according to the localization and in malignant mast cell proliferations.

P 132

CDK9/CYCLIN T1 EXPRESSION DURING NORMAL LYMPHOID DIFFERENTIATION AND MALIGNANT TRANSFORMATION

DE FALCO Giulia, LEUCCI Eleonora, ONNIS Anna, TILLI Chiara, COCCO Mario, BELLAN Cristiana, GIORDANO Antonio and LEONCINI Lorenzo
Department of Human Pathology and Oncology, University of Siena, Italy

Cdk9 is a member of the CDC2-like family of kinases. Its cyclin partners are members of the Cyclin T family (T1, T2a and T2b) and Cyclin K. Cdk9/Cyclin T1 complex is very important in controlling specific differentiative pathways of several cell types. Limited data are available regarding the expression of Cdk9/Cyclin T1 in haematopoietic and lymphoid tissues. We analyzed the expression of this complex in lymphoid tissue, in order to assess its role in B and T cell differentiation and lymphomagenesis. Cdk9/Cyclin T1 expression was found by immunohistochemistry in precursor B and T cells. In peripheral lymphoid tissues, Cdk9/Cyclin T1 were expressed in germinal center cells and scattered B and T cell blasts in interfollicular areas, while mantle cells, plasma cells and small resting T lymphocytes displayed no expression of either molecule. Therefore Cdk9/Cyclin T1 expression appears to be related to particular stages of lymphoid differentiation/activation.
To monitor the expression level of Cdk9/Cyclin T1 during normal lymphoid differentiation, we isolated different B and T cell populations by magnetic separation, based on their surface antigens, to check the expression levels of the complex at different stages of activation of B and T cells. After isolation, the expression levels of the Cdk9/Cyclin T1 complex was monitored by RT-PCR in Real Time. We observed that the expression level of Cdk9/Cyclin T1 seems to increase in activated cells, compared to un-stimulated ones. Differentiation is achieved through the direct involvement of proteins of the basic helix-loop-helix family, which are specifically activated during differentiation. Different members of this family are involved in different

differentiation systems. In lymphoid cells the E2A gene products, E12 and E47, are specifically activated during differentiation. We investigated whether Cdk9 was able to promote lymphoid differentiation by interacting with E12 and E47. Our results showed that Cdk9 interacts, with the E2A gene products, both in vitro and in vivo, thus suggesting an active role for the Cdk9/Cyclin T1 complex during lymphoid differentiation, through physical binding with E12 and E47.
These preliminary results suggest that the Cdk9/Cyclin T1 complex may affect the activation and differentiation program of lymphoid cells. However, through which molecular mechanism Cdk9/Cyclin T1 complex is altered in malignant transformation still needs to be elucidated.

P 133
THE VASCULAR CHANGES IN LYMPHADENOPATHIES

MIHAILOVICI Maria-Sultana, TELEMAN Sergiu, FERARIU Dan, DANCIU Mihai, BUTCOVAN Doina, TERINTE Cristina, CIOBANU Delia
Pathology Department, University of Medicine and Pharmacy "Gr. T. Popa", IASI, ROMANIA

Disorders primarily affecting the lymph node vessels are certainly uncommon in comparison with those that primarily involve lymphoid tissue. The vascular changes are commonly manifest, either in ischaemic lesions in the nodal parenchyma, or in vascular proliferation and modify the histopathological appearances in both reactive and neoplastic lymphadenopathies.
Aims: We conducted a study to establish vascular lesions from lymph nodes with valuable signification in the positive or differential diagnosis of reactive, inflammatory and neoplastic lymphadenopathies.
Material and methods: Our study included lymph node biopsies from 1701 patients, using histological and immunohistochemical techniques.
Results: Histopathological aspects of 1701 specimens of lymph nodes evidenced: 568 (33.4%) reactive lymph nodes, 969 (57.2%) neoplastic lymphadenopathies; 164 (9.4%) were biopsies that didn't contain lymphoid tissue. The neoplastic lymphadenopathies were primary NHL (432 cases – 25.4%), HL (207 cases - 12.2%) and metastatic neoplasm (330 cases – 14.4%). In the reactive lymphadenopathy cases, we observed a variety of vascular lesions as: diffuse vasodilatation, vascular granulation tissue formation, vascularization of lymph node sinuses, capillary vascular proliferation, post-capillary venule proliferation, vasculitis and total or subtotal, segmental or focal infarction, vasoproliferation in reactive states (angio-immunoblastic lymphadenopathy) or marked proliferation of small blood vessels in Castleman's disease and angiomatosis/haemangiomatoids in axillary lymph nodes draining breast carcinomas. Vasoproliferation in malignant neoplasms was evident whether the lymph nodes were occupied by malignant lymphomas of metastatic tumor.
Conclusions: Vascular transformation of sinuses is a pattern of fibrosis formation in chronic lymphadenitis with atrophy of lymphoid tissue. Reactive proliferation of blood vessels is one of the central features of hyperimmune angiofollicular and plasmacytic polyadenopathy, and angio-immunoblastic lymphadenopathy. Primary vascular lesion of lymph node was infarction with various intensity degrees, mainly in NHL. Capillary proliferation in primary malignant lymphadenopathies was present in Hodgkin's lymphoma, in lymphoplasmacytic neoplasms while in T cell NHL we saw a marked proliferation of post-capillary venules. In latter condition, differetial diagnosis with hyperplasia and stimulation of the paracortical areas is needed.

P 134
EXPRESSION OF TELOMERASE COMPONENTS IN NEUTROPHILS.

LEPREUX Sébastien (1,2), DOUDNIKOFF Evelyne (1), BIOULAC-SAGE Paulette (1), BLOCH Bertrand (1,2), MARTIN-NEGRIER Marie-Laure (1,2).
(1) Laboratoire d'Histologie-Embryologie, UFR II, Université Victor Segalen Bordeaux 2, France (2) Service d'Anatomie Pathologique Hôpital Pellegrin, 33076 Bordeaux Cedex, France.

Backgrounds and aims: Human telomerase comprises an RNA subunit (hTR) and a catalytic protein subunit with reverse transcriptase activity (hTERT). Telomerase extends chromosome ends in compensation for the attrition of the telomeres during replication. Telomerase is normally expressed in germinal or stem cells during the adult life and during cellular immortalisation and tumorigenesis in pathology. Even though hTERT protein is a key component controlled the telomerase activity, some data indicate that hTERT protein expression level did not always correlate with telomerase activity. In this work, we explore the expression of hTR and hTERT protein in neutrophils, which are highly differentiated cells without hTERT mRNA expression and telomerase activity.
Materials and methods: We investigated the expression of hTR and hTERT protein, respectively by in situ hybridization with a S35-labeled specific probe and immunohistochemistry with two different antibodies, in neutrophils of the stroma in 10 cases of bladder carcinomas. hTERT protein expression was also studied by immunoelectronmicroscopy in neutrophils of non-neoplastic liver tissues with "surgical hepatitis" in 3 cases of partial hepatectomy.
Results: Like others non-tumoral cells, neutrophils expressed hTR. hTERT protein was strongly expressed in the cytoplasm of neutrophils with the 2 antibodies. The ultrastructural study showed that the gold particles were not associated with specific organelles but scattered in the cytosol. No significant nuclear labeling was observed in neutrophils.
Conclusions: This study demonstrates that hTERT protein is expressed in the cytoplasm of neutrophils. We hypothesize that complex qualitative changes, i.e. post-traduction modification, compartimental protein sequestration could be of importance in the enzyme activity level control. The functional significance of cytoplasmic hTERT protein without telomerase activity remains to be elucidated.

P 135
ULTRASONIC DECALCIFICATION IS RAPID AND SUITABLE FOR FISH ANALYSIS

T. Reineke, B. Jenni, P. Zubler, S. Frigerio, H. Moch, M. Tinguely
Institute of Clinical Pathology, University Hospital Zurich, Switzerland

Aim
In haematopathology, the requisite analyses on bone marrow biopsies are increasing; in addition to morphology and immunohistochemistry (IHC), molecular analysis (MA) like FISH is now demanded in order to improve diagnostic accuracy. Certain chromosomal alterations in particular, are known to be of prognostic or predictive value. In some circumstances, e.g. surgical biopsy, "packed marrow", only formalin fixed, bone-containing tissue is available for MA. Since the various decalcification procedures can impair DNA quality, there is an urgent need for standardized decalcification protocols allowing FISH analysis on these materials. Our aim was to set up a routinely applicable protocol to optimise the MA method whilst preserving morphology and IHC results.
Materials and Methods
Bone marrow specimens were fixed in 4% buffered formalin. The decalcification procedures were carried out in an EDTA solution (Usedecalc, Medite, Burgdorf, Germany) with or without the use of an ultrasonic decalcifier (USE33, Medite,

Burgdorf, Germany). Decalcification solutions containing either formic or acidic acid were compared. The decalcification times varied from one and a half hours up to 24 hours. Thereafter, the ultrasonic decalcified tissue was dehydrated, paraffin embedded and, depending on the sample size, again incubated in the EDTA solution. Samples were stained with H+E and Giemsa, and IHC for nuclear (Mib1, Glycophorin A) and cytoplasmic markers (CD20, CD3, CD61, MPO) was performed. Interphase FISH analysis with a double colour, double fusion probe (Abbott Molecular Diagnostics, Illinois, USA) specific for the translocation t(11;14) was applied according to the manufacturers instructions.

Results

Ultrasonic decalcification allows reduction of the decalcification time. Overall, the best results for morphology, IHC and FISH analysis were obtained by 3-5 hours of ultrasonic decalcification using an EDTA solution. Of interest, FISH analysis was successfully applied only on samples positive for Mib1 IHC, thus being predictive for DNA quality of the sample.

Conclusion

The combination of ultrasound and EDTA for decalcifying bone-containing tissue samples is a rapid and easy method resulting in an excellent morphology comparable to plastic embedded bone marrow trephines. Most importantly, the same protocol permits successful interphase FISH analysis. Current investigations will reveal whether this decalcification approach is also suitable for PCR studies.

P 136

HEDGEHOG SIGNALLING IN B-CELL DIFFERENTIATION

BLAAS Leander, KOLLMANN Karoline, ALINGER Beate, REGL Gerhard, ABERGER Fritz, DIETZE Otto, HAUSER-KRONBERGER Cornelia

Department of Pathology, Gerneral Hospital Salzburg and Department of Molecular Biology, University of Salzburg, Austria

The Hedgehog signalling pathway plays a crucial role in embryonic tissue development and differentiation and has also been shown to function in adult self-renewing tissues.

Apparently, the pathway is also involved in the development of the hematologic system. It has been published that the ligand Sonic hedgehog (Shh) is involved in development of primitive human hematopoietic cells and T-cells. Together with the receptors Patched (Ptch) and Smoothened (Smo) Shh also ensures survival of germinal center B-cells.

Recently published findings showed expression of Shh by follicular dendritic cells and expression of the pathway receptors Ptch and Smo by germinal center B-cells.

Lately, we could show that the Hedgehog signalling pathway is involved in differentiation of human B-cells. Especially the transcription factor Gli2 is expressed in B-cells of the bone marrow.

In the present study we examined the expression of members of the Hedgehog pathway in normal and malignant B-cell development. Formalin-fixed and paraffin-embedded tissues of normal bone marrow and secondary lymphatic tissues were immunohistochemically analyzed using antibodies against ligands, receptors and transcription factors involved in the Hedgehog pathway. Non-Hodgkin's lymphomas and B-cell leukemias were investigated as each disease entity shows an increased proliferation of specific stages of B-cell development.

Lymphatic tissues displaying Precursor B-lymphoblastic lymphoma/leukemia (n=5), Precursor B-cell acute lymphoblastic lymphoma/leukemia (n=5), B-cell chronic lymphatic leukemia/small lymphocytic lymphoma (n=5), B-cell prolymphocytic leukemia (n=5), Lymphoplasmacytic lymphoma (n=5), Plasma cell myeloma/Plasmacytoma (N=5), Extra-nodal marginal zone B-cell lymphoma of MALT type (n=5), Follicular lymphoma (n=5), Diffuse large B-cell lymhoma (n=5), Burkitt's lymphoma (n=10), and Hodgkin's lymphomas (n=10) were examined. By using CD markers in double fluorescence stainings cells with an active pathway were assigned to their hematopoietic lineages.

The results showed pathway activity in several stages of B-cell development. CD79a positive B-cells showed strong expression of Ptch and Gli2. Additionally, only a small minority of plasma cells showed pathway activity. In conclusion, active Hedgehog signal transduction plays a role in the differentiation of B-lymphocytes.

P 137

STUDY OF EC CELLS IN PATIENTS WITH PERNICIOUS ANEMIA

MAÈUKANOVIÆ-GOLUBOVIÆ Lana, KATIÆ Vuka, RANÈIÆ Gorana,MILENOVIÆ Mladen,MARJANOVIÆ Goran,VUKIÈEVIÆ Tomislav,ÈOJBAŠIÆ Irena,GOLUBOVIÆ Ivan,DJORDJEVIÆ Goran

Enterochromathophine (EC) cells are the members of diffuse neuroendocrine system and are classified according to ultrastructure characteristics as ECl-intestinal type; EC2-duodenal type and ECn-gastric type. Gastric type EC cells are argirophylic and argentaphylic in 10-20%.They are localized in antral and corporal gastric mucosa. In pathologic conditions EC cells can change their number, morphology and cytochemical characteristics, so as a functional properties.

The aim of this study is to investigate presence, type and granularity EC cells in patients with pernicious anemia(PA).

During the period from l977 to 2005(Clinic of Hematology-Niš), 78 patients with PA were examined as well as 30 patients with dyspeptic syndrome(control group).Classical (HE) histological method was used for pathological evaluation of gastric mucosa.Grimelius(argyrophilic) and Massons(argentaphilic) methods were used for the identification of EC cells.

Hyperplasia, metaplasia and hypergranularity of EC cells were found in corporal mucosa of PA patients. The number of EC cells was increased proportionally to the changing of gastric mucosa and the grade of intestinal metaplasia(22 to 43 cells per field). Sometimes, EC cells hyperplasia is of so high grade that resemble intramucous carcinoidosis. EC cells were transformed from close type to the open type: they become triangle shape and high amount of serotonin in them.

These results can confirm that new formed, intestinal type of EC cells secrete high quantity of serotonin increasing permeability and inducing the retrograde diffusion of H ions in gastric mucosa. In the way, H ions induce acidosis and inhibit cellular metabolism, leading to citolysis of all attached cells. Serotonin stimulates synthesis of acid mucins and has an inhibition effect on HCL secretion.

Hyperplasia and metaplasia of EC cells could be important for the cancer genesis through serotonine effects.

P 138

D2-40 - SELECTIVE MARKER OF LYMPHATIC ENDOTHELIUM AND A PUTATIVE FOLLICULAR DENDRITIC CELL MARKER.

Assia Bassarova, Jahn M. Nesland, Jan Delabie

Department of Pathology, The Norwegian Radium Hospital, University of Oslo, Oslo, Norway

Introduction: M2A antigen is an oncofetal antigen associated with germ cell neoplasia, present in testis on fetal gonocytes and re-expressed on carcinoma in situ (CIS) and germ cell tumours. It was shown that the antigen is an O-linked sialoglycoprotein containing a simple mucin-type carbohydrate epitope. A specific monoclonal antibody named D2-40 (IgG1) against the antigen was developed. It was then

observed that D2-40 is a selective marker of lymphatic endothelium.
Purpose: The aim of the study was to examine the expression of D2-40 in various haematopoietic and lymphatic tissues.
Materials and methods: The study was performed on 60 cases, distributed as followed: 34 lymph node samples, 14 spleens and 8 bone marrow specimens. Half of the lymph nodes were involved by metastatic carcinoma and half were involved by various lymphoma types – 1 small lymphocytic lymphoma, 2 mantle cell lymphomas, 2 marginal zone lymphomas, 4 follicular lymphomas, 4 diffuse large B cell lymphomas, 2 with peripheral T cell lymphoma and 3 lymph nodes with angioimunoblastic T cell lymphoma. Most of the spleen specimens (8) were with reactive changes, 3 were affected by lymphoma. Bone marrow was predominantly with reactive changes and 2 with lymphoma infiltration. The expression of D2-40 was evaluated immunohistochemically. Except for that on several specimens double immunofluorescence with D2-40 and CD21 was performed.
Results and discussion: All metastatic lymph nodes showed specific D2-40 expression in the preserved lymphoid follicles. In all specimens positive reaction was observed in both lymphatic vessels and follicular dendritic cells. In lymphomas the staining intensity in the follicular dendritic cells was generally weaker. In the spleen no immunoreactivity was detected. The same pattern was observed in the bone marrow. Except for a specific marker for lymphatic endothelium M2A antigen, detected by D2-40 monoclonal antibody detects also a subset of follicular dendritic cells. Further investigations should to be performed to clarify the function and significance of this marker in reactive conditions and lymphoproliferative diseases.

P 139
FATAL NECROTIZING HERPES SIMPLEX VIRUS LYMPHADENITIS IN A PATIENT WITH CHRONIC LYMPHOCYTIC LEUKEMIA AND SEVERE HYPOGAMMA GLOBULINEMIA

B.Chibaudel (1), T.Hanslik (1), F. Rosenberg (2), F. Le Deist (3), J.Prinseau (1), A.Baglin (1), J.F.Emile (4).
(1)Service de médecine interne, Hôpital Ambroise Paré, Faculté de médecine PIFO, Boulogne, (2)Service de virologie, Hôpital Saint Vincent de Paul, Paris, (3)Service d'immunologie et hématologie pédiatrique, Hôpital Necker, Paris, (4)Service d'anatomie pathologique, Hôpital Ambroise Paré, Faculté de médecine PIFO, Boulogne, France

Necrotizing lymphadenitis is a rare manifestation of herpes simplex virus (HSV) infection. We report a 80-year-old patient with fever, retroperitoneal necrotic lymphadenopathy and thrombosis of the lower vena cava, revealing a lymphocytic leukemia and a necrotizing HSV lymphadenitis mimicking Richter's transformation. Lymph node biopsy revealed a diffuse necrosis, with an infarct like pattern. Necrosis contained karyorrhectic bodies and numerous cells with Cowdry A inclusions. HSV was detected within a lymph node biopsy by immunohistochemistry. HSV type II DNA was detected within blood and bone marrow samples by PCR. The patient had a severe hypogammaglobulinemia and normal T cell repertoire. No skin nor mucosal lesion were present. Clinical and biological symptoms improved rapidly with acyclovir and immunoglobulins, however the patient died with pulmonary embolism. HSV lymphadenitis may be misdiagnosed with Richter's transformation. Humoral immunity seems to be the main defense in human against severe HSV infections.

P 140
APOPTOSIS AND PROLIFERATIVE ACTIVITY OF HUMAN TROPHOBLAST CELLS IN SPONTANEOUS ABORTIONS WITH NORMAL AND PATHOLOGIC KARYOTYPES

I.N. Voloschuk, J.V. Gorbacheva, M.A. Paltsev

Introduction. Apoptosis and proliferation are interrelated processes, that supply normal implantation of an ovum and development of pregnancy. Disturbances of these processes in cases of spontaneous abortions (SA) may reflect the pathogenesis of pregnancy loss. From this point of view it is interest to compare the apoptotic and proliferation rates in SA caused by chromosomal aberrations and in SA with normal karyotype.
Materials and methods. Proliferation and apoptosis in villous and extravillous trophoblast was estimated in SA with pathologic karyotype (15 cases), SA with normal karyotype (15 cases) and in normal early pregnancy (20 cases of elective abortions). Proliferative activity (PA) was determined as the rate of Ki-67-positive cells. Estimation of apoptotic index (AI) was performed using the ApoTag Peroxidase Kit ("Biotech", USA).
Results. In normal early pregnancy specimens Ki-67 was strongly expressed in villous cytotrophoblast (VCT) and extravillous trophoblast (EVT). Syncytiotrophoblast (ST) was negative for proliferation marker. Signs of apoptosis were mainly observed in ST, syncytial knots, VCT, some villous stromal cells and in EVT. PA of VCT was low in both groups of SA as compared to control group. The significant differences in rate of apoptosis between SA with normal and pathologic karyotypes was revealed. The rate of villi with apoptotic VCT was significantly higher in SA with pathologic karyotype (26.20 %) than that in SA with normal karyotype (7.6%) and normal first trimester pregnancies (16.65 %). AI of EVT was also higher in group of SA with pathologic karyotype (7.67±3.31) as compared to SA with normal karyotype (2.78±2.56). Furthermore, SA with pathologic karyotype showed uncorrelation between AI and PA in EVT: the level of AI was the highest whereas PA was minimal. The highest frequency of apoptosis in combination with minimal proliferative activity of EVT in SA caused by chromosomal pathology indicates active invasion restriction of chorion with pathological karyotype.

P 141
HUMAN PLACENTA AND FETAL IUGR AT 20-22 WEEKS OF GESTATION

RESHETNIKOVA Olga, KONONENKO Olga, MOROZOV Sergiy
Dept. of Pathologic Anatomy, Medical University, Lugansk, Ukraine.

It is reported that some adult diseases has intrauterine 'programming' mechanism. Disproportions and restrictions of placental and fetal growth could be the marker for the high risk group of newborns.
The aim of the present study was to identify which organs are principally affected in cases of fetal growth restriction (FGR) at 20-
22 weeks of gestation.
Methods: 8 cases with fetal growth restriction (FGR) and high (0.41±0.04) placenta/fetal weight index (PFI) were compared with 10 controls (PFI= 0.26±;0.01) in cases of induced abortions for psychotherapeutic reasons at 20-22 weeks of gestation. Weights of placenta (PW) and fetus (FW), fetus length (FL), head (Ch), chest (Cch), abdominal (Ca) circumferences, fetal kidneys (KW), pancreas (Pn W), liver (LW) and heart (HW) as well as some indices were recorded.
Results: FGR group had smaller parameters of FW (390+2.0 vs 610+2.6 g, $p<0.001$), FL (26+0,9 vs 30+0,6 cm, $p<0.001$), Cch (15+0.6 vs 18+0.4 cm, $p<0.001$), Ch (18+0.04 vs 22+0.4 cm, $p<0.001$), Ca (13+0.4 vs 15+0.3 cm, $p<0.001$). All FGR cases had decreased LW (16+0.2 vs 29+0.2 g, $p<0.001$); PnW (0.2+0.01 vs 0.4+0.07 g, $p<0.001$); KW (4+0.3 vs 6+0.2 g, $p<0.001$); HW (2.1+0.2 vs 3.4+0.2 g, $p<0.001$). PW was unchanged (160+12 vs 160+8 g, $p>0.05$).

Conclusions: these results suggest that the discrepancy between fetal and placental growth at 20-22 weeks of gestation is associated with fetal kidneys, pancreas, heart and liver growth retardation. Pathological alterations of organs could be a structural basis of adult pathologies.

P 142

HISTOLOGIC AND PLACENTAL ABNORMALITIES CORRELATE WITH SEVERITY OF PREECLAMPSIA AND ITS COMPLICATIONS

STANEK Jerzy, WENG Eric, LEVIN Linda. Department of Pathology and Laboratory Medicine and Environmental Health, University of Cincinnati College of Medicine, Cincinnati OH, U.S.A.

We have previously reported that the frequency and severity of placental lesions in preeclampsia (PE) are gestational age-dependent. This analysis was undertaken to identify the clinical and placental factors that are associated with severity of PE and its complications

In years 1994-2004, 332 consecutive placentae from patients with PE with gestational age at delivery of 20 weeks or more were examined (7.9% of all placentae examined). 112 women had mild PE (Group 1), 172 severe PE (Group 2), 36 HELLP syndrome (Group 3), and 12 eclampsia (Group 4). Univariate contingency table analyses were carried out to assess associations between possible risk factors and PE groups. When cell frequencies were sufficiently large, ordinal and nominal factors were analyzed using Mantel-Haenszel and likelihood ratio Chi-square statistics, respectively. For small sample sizes, 2-by-2 tables were analyzed using Fisher's exact test.

Statistically significant differences were found in the following 8 of 14 maternal/fetal clinical risk factors and outcomes, and 7 of 27 gross and microscopic placental features in Groups 1-4, respectively: average gestational age at delivery (36,33,30,30 weeks), maternal diabetes mellitus (14,7,5,0%), abnormal fetal heart rate (26,24,6,8%), meconium-stained amniotic fluid (12,3,3,0%), fetal weight (2594,1822, 1456,1250 gm), one (7,6,5,4) and five minute (8,7,7,5) apgar scores, cesarean sections (45,64,83,67%), placental weight (439,311,274,265 gm), hyperplastic decidual arteriolopathy (20,36,36,33%), decidual atherosis (10,27,44,41%), villous infarctions (29,55,56,58%), maternal floor trophoblastic giant cells (18,40,44,25%), diffuse villous hypoxia (23,32,36,33%), and meconium staining on histology (29,15,16,8%).

The significant overlap of frequencies of various clinical and placental factors in mild and severe PE and its complications indicates that they represent a spectrum of essentially the same process. While the frequency of abnormal maternofetal factors in general decreased from Group 1-4, possibly in relation to increasing frequency of cesarean sections, the frequency of decidual vascular lesions and placental hypoxic changes, except for the histologic evidence of meconium staining, increased from Group 1-4. Therefore, placental examination is a useful tool for retrospective evaluation of PE confirming the important role of uteroplacental hypoxia in fetal distress in PE.

P 143

LETHAL OSTEOCHONDRODYSPLASIA: A FETOPATHOLOGICAL STUDY OF 31 CASES

A.Lahmer*, M.T.Yacoubi*, S.Hmissa*, A.Ben Abdelkader*, L.Belaid*, S.Hidar**, M.Mokni*, S.Korbi*
*Department of pathology
*Department of gynecology
F.Hached Hospital
Sousse Tunisia

Introduction:

Skeletal dysplasia is a large heterogeneous group of diseases characterized by malformation, disproportionate growth and deformation of the skeleton or of individual bones or groups of bones. They are common birth defects. Their prevalence differs between populations and in various studies. Lethal osteochondrodysplasia is generally tracked down during the third or the fourth month of pregnancy, or during the antenatal ultrasonography.

Materials and methods:

Our study is retrospective and descriptive of 31 cases of lethal osteochondrodysplasia: 22 foetuses, 6 new-born and 3 dead-born.

Cases were brought from 6 hospitals of the center of Tunisia during a period of 13 years from 1991 to 2004. Foetopathological examination was done for all cases including autopsies, radiography of skeleton and histological examination of bone.

Results:

Mothers were aged between 20 and 39 years. Consanguinity was found in 6 cases. The disorder was revealed on antenatal ultrasonography in 24 cases and showed micromelia in all cases, narrow trunk in 5 cases and spina-bifida in 3 cases. Correlation between radiographics and fetopathological examination, identified 8 cases of achondrogenesis type I, 3 cases of achondrogenesis type II, 9 osteogenesis imperfecta, 4 thanatophoric dwarfism, 4 schneckenbecken dysplasia, 2 short-rib dysplasia with polydactyly (Majewski-type) and one case of asphyxiating thoracic dysplasia (Jeune).

Conclusions:

Severe ostéochondrodysplasia seems more frequent in the center of Tunisia. Correlation between radiographic and histological data must be undertaking for the management of these bone anomalies in order to make adequate genetic counselling.

P 144

ISOLATED OLIGOMEGANEPHRONIC HYPOPLASIA OF THE FETAL KIDNEY: A RARE CAUSE OF FETAL ANAMNIOS

M.T.Yacoubi*, M.Mokhtar*, W.Stita*, A. Ben Abdelkader*, S.HMissa*, A. Achach* L.Belaid*, S.Hidar**, A.Trabelsi*, M.Mokni*, S.Korbi*
* Department of pathology
* Departement o gynecology and Obstetrics
F.Hached Hospital, Sousse, Tunisia

Oligomeganephronic hypolasia of the kidney is a rare condition leading to anamnios.

We report the first case diagnosed in our department.

It was a 28 week - old- aged female fetus.

The pregnancy was interrupted for anamnios and fetal hypotrophy objectivated by ultrasonography.

External fetal examination showed a diffuse oedema with deformartive sequence caused by the anamnios.

At the visceral examination, the kidneys were hypoplastic weighting 2g together.

The histological study confirms the hypoplastic feature of the kidneys with a reduced number of the nephrons, which are hyerptophic.

These signs support the diagnosis of the ologomeganephronic hypoplasia of the kidney.

Than, we discuss the morphological feature of this anomaly, the embryological and the genetic hypothesis.

P 145

BNOS EXPRESSION IN EARLY ENDOUTERINE FETAL DATH: AN IMMUNOHISTOCHEMICAL STUDY ON PARAFFIN-EMBEDDED PLACENTAS

RESTA Leonardo, SANGUEDOLCE Francesca, PISCITELLI Domenico, SBLANO Sara*, MARZULLO Andrea, GESUALDO Loreto°

DAP-Department of Anatomic Pathology, and * Institute of Forensic Medicine, University of Bari° Institute of Nephrology, University of Foggia, ITALY

Nitric oxide (NO) is a free radical that modulates vasodilatation, smooth muscle relaxation, inhibition of platelet aggregation and functions as an immune system mediator; during pregnancy there are increased levels of NO, partly due to autocrine secretion by feto-placental structures. It is the substrate of the nitric oxide synthase (NOS) enzyme, which is also present in endothelial cells from umbilical cord and placental resistance vessels, but not in term villi.
The aim of the present study was to evaluate the presence of the constitutive isoform of NOS (brain NOS or bNOS), mainly expressed in human nervous tissue, also in early pregnancy (first trimester) endometrium and placenta.
We examined 39 cases of early endouterine death and 5 control specimens of induced abortion. Formalin-fixed paraffin-emebedded tissues were submitted to heat-mediated antigen retrieval and immunohistochemistry with anti bNOS monoclonal antibody.
bNOS was detectable in endometrial decidua (both glands and stromal cells) and villous syncytiotrophoblast. In particular, its expression was reduced in syncytiotrophoblast and increased in deciduas from pathological cases in comparison to controls.
In conclusion, we demonstrated that immunohistochemistry with bNOS antibody can be performed also on paraffin-embedded material, by a proper antigen retrieval system. The difference between the two groups would suggest that early miscarriages may have a vascular pathogenesis.

P 146
CAUSES OF PERINATAL DEATH AT OSIJEK CLINICAL HOSPITAL, 1995-2004

MARJANOVIC Ksenija*, DMITROVIC Branko*, BLAZICEVIC Valerija*, BARTOLIC Kristina**, IVANOVIC Marko**, MARJANOVIC Mirjana***.
*Department of Pathology, Osijek Clinical Hospital, Osijek, Croatia.
**Faculty of Medicine, J. J. Strossmayer University, Osijek, Croatia.
***Health Center Beli Manastir, Beli Manastir, Croatia.

AIM. Perinatal mortality and the causes of perinatal death as determined by autopsy and by placental biopsy at the Osijek Clinical Hospital in the period 1995 – 2004 are presented.
METHODS. The data were collected at the Department of Pathology: the autopsy reports and the placental biopsy reports were reviewed. The causes of death were classified into 10 categories: intrauterine hypoxia and birth asphyxia, congenital malformations, infection, abnormal pulmonary function, intracranial hemorrhage, immaturity, other diseases, macerated fetus with no signs of asphyxia, tumors, and violent death. The asphyxia was later subdivided into 3 categories: failure of blood to become oxygenated in the placenta, obstruction to circulation through the cord, and of unknown cause. Descriptive statistics are presented.
RESULTS. There were 23.860 deliveries at the Osijek Clinical Hospital in the period 1995 – 2004. In this period, there were 540 children deaths, and the autopsy was performed in 534 cases (98.89%). Perinatal mortality values were: 21.31‰ (1995), 17.47‰ (1996), 12.73‰ (1997), 17.75‰ (1998), 13.23‰ (1999), 11.90‰ (2000), 7.97‰ (2001), 13.81‰ (2002), 13.35‰ (2003), and 10,38‰ (2004). The majority of deaths were in fetuses and infants who showed evidence of asphyxia (58.33%): 71.43% of those cases was attributed to the failure of blood to become oxygenated in the placenta, 9.21% to the obstruction to circulation through the cord, and the rest 19.36% were of unknown cause. Congenital malformations (11.49%) ranked second, abnormal pulmonary function (9.26%) third, both immaturity and macerated fetus (6.29% each) fourth, and other conditions were far behind. In the group of 66 congenital malformation, the most common were multiple organs malformations (50%), followed by central nervous system malformations (16.67%), and heart and large blood vessel malformations (12.12%). In the early perinatal period, the most common causes of death were intrauterine hypoxia (53.62%), immaturity (14.01%), and macerated fetus with no signs of asphyxia (13.52%).
CONCLUSIONS. Whether death should be attributed to one cause or another is often subject to variable opinion because of the much overlap among groups. Most of the deaths attributed to asphyxia were explained by placental biopsy report. The placental biopsy report must be an integral part of a autopsy report in the cases of the perinatal death.

P 147
COMPLETE TRISOMY 9: PRESENTATION OF TWO AUTOPSY STUDIES

FERRERES Joan C, TORAN Nuria, VENDRELL Teresa*, PEG Vicente, SALCEDO M Teresa, ESPINOZA Paul.
Departament of Pathology and Genetics Unit*.
Hospital Vall d'Hebron. Universitat Autònoma de Barcelona. Barcelona, Spain

Objective: To present the autopsy study of two cases of complete trisomy 9 (CT9). This is a very infrequent chromosomal abnormality, which in most cases results in spontaneous abortion during the first 3 months of the pregnancy. To our knowledge only about 30 cases have been reported previously.
Case 1: A 35-year-old gravida III woman was referred for amniocentesis at 20 weeks' gestation (wg) because ultrasonography showed a lumbosacral neural tube defect, malposition of hands and micrognathia. A genetic study revealed a karyotype of 47,XY,+9 in all the amniocytes. The pregnancy was terminated at 22 wg. The foetus body weight was 290 g.
Case 2: A 25-year-old primigravida woman was referred to our hospital for evaluation at 32 wg because of an ultrasonographic Dandy-Walker malformation suspicion. The patient underwent amniocentesis with the result of 47,XX,+9 in all the cells. A 1934 g stillborn infant was delivered at 37 wg after spontaneous labour.
Autopsy findings: Both foetuses presented multiple congenital anomalies. In both cases we observed similar craniofacial anomalies: bulbous nose, enophtalmus, small mouth, retromicrognathia, microglosia, a short and thick neck and low-set malformed ears; clenched hands with two oblique palm folds, dysplastic nails (small with triangular form and profound implantation), absence of intergluteous fold, bilobed right lung, agenesis of dorsal pancreas, hypoplastic thymus and hypoplastic adrenal glands. Additional findings: Case 1: Intrauterine growth restriction, microstomia, anterior rotation of shoulders, dorsal cyphosis, small penis, myelomeningocele lumbosacral with Arnold Chiari malformation, diaphragmatic elevation with lung hypoplasia, liver calcification, agenesis of gallbladder, polylobed spleen, horseshoe kidney, atrial left isomerism and atrial septal defect. Case 2: anteroflexed right ankle, club feet, sacral pit, palatal pit, type II truncus arteriosus, aortic right arch, calcification in myocardial vessels, portal venous anomaly (esplenic and inferior mesenteric veins with drainage directly at cava inferior vein), pyeloureteral bilateral stenosis, three supernumerary spleens and Dandy Walker malformation.
Conclusion: Foetuses with CT9 have multiple anomalies and can be identified prenatally with sonographic studies. Some of these abnormalities have not previously been described. The CT9 diagnosis is always done through a genetic study, but some autopsy findings can suggest this diagnosis.

P 148

THE SIGNIFICANCE OF COLLAGEN IV STEREODYNAMICS IN METANEFROGENESIS. IMPLICATIONS IN PATHOLOGY

Dragoi G. S., Trasca T.E., Monica Banita, Catalina Pisoschi, Maria Magdalena Nuta
Academic Hospital Filantropia Craiova Romania
University of Medicine and Pharmacy from Craiova

Introduction. The collagen type IV, an important extra cellular matrix element greatly contributes to the building of reticular nets from lamina basalis of the metanefros structures.
Purpose of the study. The purpose of the study is to establish the stereo and topographic dynamics of the type IV collagen evolution in definitive kidney genesis.
Materials and methods. Renal fragments from 3 human embryos, 2 fetuses and 3 new born have been prepared using microanatomical techniques. The visualisation of the extracellular matrix elements was achieved by means of PAS, Gomori and Van Giesons stains.
Results. The knowledge of the type IV collagen stereo and topographic dynamics is possible by its identification inside tubular and vascular nefron micro anatomic structures. Corroborating the data observed on the differentiating kidney sections we noticed a variable distribution of glicosaminoglicans and type IV collagen inside lamina basalis. The determinant factor of type IV stereo and topographic dynamics is the existence of the reciprocal induction phenomena between urethral bud derivates and metanefrogen mesenchyma derived structures. In pediatric pathology the type IV collagen intervenes in the initiation of the glomerulosclerosis processes.
Conclusions. The type IV collagen is cause and effect in metanefrogenesis processes. It determines the mesenchyma cells migration for the establishment of the nefron structures. Its stereodistribution has as effect the differentiation of the lamina basalis inside tubular and vascular nefron structures.

P 149

VASCULOGENESIS – A DETERMINANT FACTOR IN THE TIME AND SPACE EVOLUTION OF THE METANEFROS STRUCTURES. IMPLICATIONS IN PATHOLOGY

Dragoi G.S., Rodica Silca, E.T. Trasca, P.R. Melinte, Nuta Maria Magdalena
Academic Hospital Filantropia Craiova Romania
University of Medicine and Pharmacy from Craiova

Introduction. The genesis and the evolution of the metanefros structures are multi factorial dependent. A determining factor of the renal glomerulus morphogenesis is represented by the phenotype transformation of the metanefrogen mesenchymal cells in order to achieve the sanguine capillaries.
Purpose of the study. Our purpose was to visualize the time and space apparition of glomerulus vascular structures from the metanefrogen mesenchyma and its integration in the forming stages of the glomerulus basal membrane.
Materials and methods. We used fragments from 3 human embryos (7 weeks old) and tissue fragments from 3 human fetuses (28 weeks old). The serried sections were stained using Hematoxilin Eosine, Van Gieson, Gomori and Giemsa methods.
Results. By analyzing the 300 serried sections through human embryos and the 200 serried sections through human fetus kidney we noted that the glomerulus structures genesis is based on the metanefros vasculogenetic mesenchyma. These elements appear between the proximal sinusoid vessels of the primordial contort tube. The process of the capillary genesis is determined by the presence of the primordial podocytes derived from the nefrogen mesenchyma and of the mezangiocytes from the vasculogen mesenchyma. The three newly formed structures establish contiguity relations for the formation of the plasma filtration structures.
Conclusions. The phenotype transformation of the metanefrogen mesenchymal cells and their integration inside the glomerulus structures represent the basis of the complex mechanisms of the renal glomerulus capillaries vasculogenesis.

P 150

FETAL THROMBOTIC VASCULOPATHY (FTV)

BALAN Raluca*, AMALINEI Cornelia*, SOCOLOV Razvan**, GHEORGHITA Vlad**,COTUTIU Coriolan*
*Department of Morphology, University of Medicine and Pharmacy "Gr.T.Popa" Iasi, Romania
**Department of Obstetrics and Gynecology, University of Medicine and Pharmacy "Gr.T.Popa" Iasi, Romania

Occlusion of a large fetal artery on the chorionic plate or of a fetal stem artery create a pattern of clustered avascular villi which is called fetal thrombotic vasculopathy (FTV). We report 3 cases of FTV. The chorionic plate vessels were grossly enlarged, distended, and hard. One case was associated with the rupture into the amniotic cavity. Microscopically, the downstream villi were avascular with densely collagenized, hyalinized stroma, and the nuclei of the syncytiotrophoblast cells were clustered into syncytial knots. The larger fetal stem vessels distal to the thrombus underwent septation and fibromuscular sclerosis, characterized by medial hyperplasia and intimal proliferation with eventual luminal obliteration. FTV diagnosis by histopathologic examination is important as it may be correlated with thrombotic lesions in the newborn.

P 151

OSTEOGENESIS IMPERFECTA TYPE 2: A FETAL CASE REPORT

A. Altavilla, A. Martinelli*, L. Resta, G. Caruso
Department of Pathological Anatomy. University of Bari. Italy
* Department of Radiology. Policlinico. Bari. Italy

Introduction
Osteogenesis Imperfecta, also known as brittle-bone disease, is a heritable disorder characterized by low bone mass, propensity to fracture, blue sclerae, hearing loss, loose joints, and growth deficiency, caused by a quantitative or qualitative defect in collagen synthesis. The underlying defect is a dominant negative mutation affecting COL1A1 or COL1A2 alleles, which encode the proA1 and proA2 chains of type I collagen, a protein of paramount importance for normal skin and bone development. On the basis of clinical presentation and bone architecture the disease is currently classified into seven types. We present a case of post-mortem diagnosis of osteogenesis imperfecta of a 22 weeks-old fetus with skeletal anomalies. The purposes of this paper are to describe this typical example of osteogenesis imperfecta and to value the importance of prenatal and post-mortem diagnosis in managing pregnancy and delivery.
Methods
On a female fetus with skeletal anomalies, the decision of pregnancy termination was based on ultrasound examination. A post-mortem radiographic study and autopsy were carried out. Placenta examination was also performed.
Results
The fetus presented short trunk, blue sclerae, small nose, micrognathia, hypertelorism, low set ears, scoliosis, arthrogryposis, and smallness for gestational age. Post-mortem radiographs showed mild angulation and shortening of long bones due to multiple intrauterine fractures, irregular callus formation, a barrel-shaped rib cage, and a poor ossification of the calvaria with a poor mineralization of the skull. Bone histology revealed a marked decreased in both cortical thickness and trabecular bone, and growth plate showed disorganization. In the fractured areas, the bony

spicules were disorderly arranged and associated with fibrosis and callus formation. Placenta histology showed the presence of hydropic villi and altered Hofbauer cells suggesting a genetic defect.
Conclusions
The wide spectra of clinical, imaging, grossly and hystologic features of the case studied led us to make the diagnosis of osteogenesis imperfecta type II. The differential diagnosis was made with hypophosphatasia, achondrogenesis, thorax dystrophy, osteosarcoma and battered child syndrome. Osteogenesis imperfecta is one of the commonest skeletal disorders with an incidence about one in 10,000 and it is often silent cause of adult osteoporosis for that reason is very important prenatal diagnosis.

P 152
FIBROBLASTIC POLYP OF THE COLON: CLINICOPATHOLOGIC ANALYSIS OF 10 CASES OF A NOVEL TYPE OF BENIGN COLORECTAL POLYP.
Gabriel M. Groisman, Sylvie Polak-Charcon, Henry D. Appelman
Departments of Pathology: Hillel Yaffe Medical Center, Hadera, Israel, Sheba Medical Center, Tel-Hashomer, Israel and University of Michigan, Ann Arbor, Michigan, USA.

Background: Benign fibroblastic polyp (FP) is a recently described, histologically distinctive type of colonic mucosal polyp. Herein we present the clinical, histological, immunohistochemical and ultrastructural features of a series of FP with the goal of further characterizing this entity.
Methods: Ten cases of FP were identified. Clinical and histologic features were reviewed. Immunohistochemistry was performed on formalin fixed paraffin embedded tissue using antibodies against vimentin, actin, desmin, CD-68, cytokeratin AE1/3, S-100 protein, COX-2, c-Kit and CD34. Ultrastructural examination was performed in two cases.
Results: All patients were asymptomatic adults (seven women, three men) with ages ranging from 44 to 63 years (median 59). Polyps ranged in size from 0.2 to 0.4 cm. Eight were located in the sigmoid colon, one in the descending colon and one in the ascending colon. Five cases were associated with hyperplastic polyps and two with tubular adenomas. Histologically, FP were characterized by a proliferation of uniform, bland spindle cells with focal periglandular or perivascular concentric arrangement. Five cases also showed superficial bundles of spindle cells arranged parallel to the surface. Eight lesions contained serrated (hyperplastic) crypts admixed with the fibroblastic cells and represented mixed fibroblastic/hyperplastic polyps (or FP with serreated crypts). Immunohistochemically, the spindle cells reacted to vimentin only. Ultrastructural examination revealed features supportive of fibroblastic differentiation.
Conclusions: 1) FP is a distinctive type of benign colorectal mucosal polyp characterized by its distal colorectal location, small size, frequent association with hyperplastic polyps, distinct morphologic appearance and typical immunonegativity for markers of specific differentiation. 2) FP with serrated crypts (mixed fibroblastic/hyperplastic polyp) represents a frequent variant of this polyp. 3) Pathologists should recognize FP and discriminate it from other types of colorectal polyps.

P 153
CLINICOPATHOLOGICAL STUDY ON CARCINOID TUMOR OF THE RECTUM - MAINLY ON COMPARISON OF CASES WITH METASTASIS AND THOSE WITHOUT METASTASIS
Seiji Haraoka, Akinori Iwashita*, Ikuko Iwashita**
*Department of Pathology, Chikushi Hospital, Fukuoka University, **Nishifukuoka Hospital, Fukuoka, Japan

Epidemiologic studies in Japan have found that gastrointestinal carcinoid tumors most commonly occur in the rectum. An increase in the size of rectal carcinoid tumors is associated with metastasis to regional lymph nodes and distant organs. Invasion to the muscularis propria or deeper also is a risk factor for metastasis. However, malignancy criteria of rectal carcinoid tumors remain to be established. The aim of our study is to clarify the clinicopathological factor relevant to the malignant potential of this disease.
Cases of rectal carcinoid tumor were divided into group A (12 lesions in 12 cases with metastasis) and group B (15 lesions in 14 cases without metastasis), and a comparative study was carried out from the clinicopathological standpoint. Nine of twelve cases of group A had metastasized to the regional lymph nodes at the time of surgery, and four of these cases metastasized to the liver. In seven cases of group A, the tumor had involved the liver.
There were significantly more cases in group A who manifested large tumor size, central depression and/or ulcer formation, deep infiltration, positive vascular invasion, a moderately elevated mitotic index, a moderately elevated Ki-67 labeling index, and appearance of P53 positive cells. Histologically, approximately 80 percent of cases of both group A and B showed Soga• fs classification type B and mixed type (type A+B), and there was no distinct difference between the two groups. From these results it could be pointed out that the findings of tumor size (more than 1.0cm), depth of invasion (muscularis propria or beyond), central depression and/or ulceration, mitotic index (>2/10HPF), vascular invasion and Ki-67 labeling index (>2%) are useful predictive criteria in the assessment of the malignant nature of these neoplasms. In addition, as a result of multivariate analysis of the above factors it was found that only tumor size was an independent and significant factor. Thus, it was concluded that the most important malignancy criterion of this neoplasm is tumor size.

P 154
CLINICOPATHOLOGIC CHANGES IN TATTOO OF COLONIC NEOPLASM WITH STERILE CARBON COMPOUND
DINARÈS Maria Carme, ORELLANA Ruth, BRULLET Enric*, CASALOTS Àlex, FERNANDEZ Sara, BELLA Maria Rosa, PARRA Tamara, ESCODA Maria Rosa, REY Mercè.
Corporació Parc Taulí, Pathology Dep, UDIAT-CD. Sabadell, Barcelona. Spain. *Corporació Parc Taulí, Endoscopy Unit. Sabadell, Barcelona. Spain.

BACKGROUND: Endoscopic marking of intestinal lesions, 'colonic tattooing', is used as a guide for the intraoperative identification of polypectomy sites and follow-up examinations. Many dyes, such as India ink and methylene blue, have been employed but may cause serious tissue injury and clinical complications, which must be recognised in pathological examination. Recently, a new sterile carbon compound (SPOT) has been used.
AIMS: To determine the histologic changes, safety and effectiveness of SPOT
METHODS: During the last year colonic tattooing with SPOT was performed in 20 cases of colonic polyps. Six of them turned out to have an infiltrating carcinoma in endoscopic polipectomy and underwent surgical resection. Clinical data and pathological findings were collected.
RESULTS: Six surgically resected specimens (5 sigmoid colon/ 1 rectum) were reviewed. The average age ranged from 52 to 86 years (mean, 70). The interval from endoscopic injection to pathologic examination varied from 1 to 48 days. No clinical complications ocurred. The SPOT was clearly

observed on gross examination in all cases during surgery. Tattoo was observed in submucosa (3 cases), submucosa and muscularis propia (1 case) and transmural (2 cases). No mucosal lesion was detected. Carbon particles were localized mainly in macrophages of the submucosa (5 cases) or as free particles involving the wall (1 case). Inflammatory infiltrate was predominantly neutrophilic and eosinophilic in 4 cases, and lymphocytic and histiocytic in 2 cases. Giant cell reaction was not observed. Areas of submucosal edema (2 cases), necrosis (2 cases) and fibrosis (2 cases) were noted (4 of them with haemorrhagic focus). The vascular injury observed was: endothelial hyperplasia (1 case), neovascularization (4 cases) and fibrinoid necrosis (1 case).
CONCLUSIONS: SPOT is a safe and effective marker for use in colonoscopy when surgical resection is required. It is also useful for endoscopic follow-up of patients who have not undergone surgery. There was no evidence of short-term clinical or histological complications although histologic changes were observed. Fibrosis was detected in cases with greater interval between injection and surgery. To determine long-term safety of colonic tatooing with SPOT, a longer follow-up studies should be performed.

P 155
MALIGNANCY AND OVERDIAGNOSIS OF MALIGNANCY IN PEUTZ JEGHERS POLYPOSIS
MICU Gianina*, ZURAC Sabina*, VRABIE Alexandra*, GRAMADA Eliza*, ZAHARIA Anca*, LAVRIC Luciana*, ANDREI Razvan*, STANICEANU Florica*, VOIOSU Radu**, SIMION Sorin***,
*Department of Pathology, Colentina Universitary Hospital
**Department of Gastroenterology, Colentina Universitary Hospital
***Department of Surgery, Colentina Universitary Hospital
Bucharest, Romania

Peutz Jeghers (PJ) polyps are rare hamartomatous tumors of the gastrointestinal tract frequently associated with skin and mucosal pigmentation. Despite their benign nature there is a certain increased risk of progression to malignancy in some cases, justifying a sustained follow-up of the patients.
We present 6 cases of Peutz Jeghers polyposis (PJP) diagnosed in our hospital during the last year on gastrointestinal specimens obtained by endoscopy and by opened surgery. We analyzed different degrees of dysplastic changes, epithelial intussusception, association with other types of polypoid lesions and others various aspects that might be related with disease progression. Clinico-pathological correlations were made.
Two of these cases consisted in two women, mother and daughter; both of them were operated in another hospital for small bowel tumors with a subsequent diagnosis of adenocarcinoma. The daughter (28 years old) was referred to our hospital for endoscopic follow-up; a small polyp of the transverse large bowel was excised by colonoscopy with a histopathologic diagnosis of PJ polyp; a careful histopathologic reevaluation of the both specimens of enterectomy (slides and paraffin blocks) revealed overdiagnosis of cancer due to the epithelial cystic dilatation and pseudoinvasion in both patients.
The other 4 cases showed diagnostic changes of PJP and also various aspects of hyperplastic (1 case) and adenomatous polyps (3 cases), one of them with mild and moderate dysplastic changes.
When a PJ polyp is diagnosed, the possibility of pseudoinvasion should be kept in mind, in order to avoid malignancy overdiagnosis; also, due to the fact that the malignant transformation of a PJ polyp is still on debate (hamartoma – dysplasia – carcinoma progression versus malignant transformation of an adenomatous aria of a hamartoma versus coincidental association of a digestive cancer due to genetic aberrations of PJP), all the other associated microscopic aspects of the lesion should be carefully analyzed.

P 156
ALTERATIONS IN THE EXPRESSION OF MUCIN ANTIGENS IN COLONIC ADENOMAS HARBORING INVASIVE CARCINOMAS
AHISKALI Rengin, EREN Funda, OZKAN Naziye
Marmara University School Of Medicine Department of Pathology, Istanbul, Turkey

Alterations in the synthesis of mucin glycoproteins have been shown to be related to both neoplastic transformation and malignant progression. We studied the expression patterns of four gastrointestinal mucins in colonic adenomas harboring invasive carcinomas with the aim of establishing the alterations that correlate with malignant progression.
MATERIAL METHODS
Immunohistochemical staining for muc1, muc2, muc5AC, muc6 were performed on 44 cases of colorectal carcinomas arising in adenomas. For each mucin antibody, nonneoplastic mucosa, adenoma and carcinoma areas were evaluated for the percentage of epithelial cells with mucin expression and for the staining intensity semi quantitatively. Qualitative changes of mucin expression in different areas of the same tumor were also evaluated.
RESULTS
Adenomas and carcinomas had aberrant expression of mucin antigens which are not normally synthesized in colonic mucosa. When compared to normal mucosa both adenomas and carcinomas had highly significant alterations of all four mucin types($p<0.01$). Although there is no correlation between the expression patterns of non-neoplastic mucosa and neoplasms, adenomas and carcinomas had a significant correlation($r=.6-.7$). Intratumoral heterogeneity of mucin expression were detected in all the neoplastic components. Although there were differences of mucin distribution patterns in adenomas and coexisting carcinomas it did not reach statistical significance.
COMMENTS
The high correlation of alterations in mucin expression patterns of adenomas and invasive carcinomas may be useful for the detection of adenomas which are more likely to develop invasive carcinomas.

P 157
ADENOCARCINOMA OF SIGMOID COLON WITH CHORIOCARCINOMATOUS DIFFERENTIATION.
NADIA KOURDA, ILHEM BETTAIB, ZERMANI RACHIDA, SOUMAYA RAMMEH , BALTAGI BEN JILANI SARRAH Service d'anatomie et cytologie pathologiques,
Hôpital Charles Nicolle BOULEVARD 9 AVRIL 1006 TUNIS

Colorectal carcinomas presenting with choriocarcinomatous differentiation are exceedingly rare; only six prior cases have been reported. We report a new case of carcinoma with germ cell differentiation developed in de novo ulcerative colitis after renal transplantation in a 42-year-old woman. Clinically, the patient presented ulcerative colitis 8 years after renal transplantation, developed colon cancer with liver metastasis 2 years after diagnosis and died one month after operation. Histologically, the removed tumor was composed of two distinctive elements consisting of an adenocarci,noma and a choriocarcinoma. The metastatic foci in the liver were exclusively composed of choriocarcinoma. Identification as choriocarcinoma was made on the basis of typical histologic appearance, immunohistochemical demonstration of human chorionic gonadotropin (hCG) in the tumor cells and the high hCG level in patient's serum, unrelated to trophoblastic disease.

In this report, pathogenesis is briefly discussed and clinical conditions are reviewed.

P 158
ATHOLOGICAL REPORTS OF COLORECTAL CANCER SPECIMENS ON A NATIONWIDE SCALE IN FRANCE: IMPACT OF A CONSENSUS CONFERENCE.
Jean-François Fléjou, Jean-Yves Scoazec, and the members of Committee n°5 “Digestive tract”, working on behalf of AFAQAP (French Association for Quality Assurance in Pathology).

The pathological assessment of surgical specimens is a crucial issue in the management of patients with colorectal cancer (CRC). Tumour stage and lymph node (LN) status are major prognostic factors, circumferential margin is a predictor of local recurrence in rectal cancer, and the presence of LN metastasis is the only criterion to indicate adjuvant chemotherapy. Several studies have demonstrated regional differences in practices in various countries including France. A consensus conference on colon cancer was held in France in 1998, with recommendations on the features that have to be included in pathological reports.
The aim of this study was to evaluate practices in France regarding the reporting of CRC, before and after the consensus conference. All the reports made by pathologists from 82 laboratories throughout the country from June to December 1997 and 2000 were collected, and the items recommended were systematically recorded. The mean number of reports per structure was 30 in 1997 (range 2-158) and 34 in 2000 (6-130). The stage of tumour invasion was present in 99.9% (1997) and 100% (2000) of reports. The longitudinal margins were specified in 94.1% (1997) and 97.1% (2000) of reports. In rectal cancer, the circumferential margin was present in 12.8% (1997) and 51.7% (2000) of reports ($p<0.001$). The number of sampled and metastatic LN was specified in 99.8% (1997) and 99.5% (2000) of reports ($p<0.05$). The pTNM stage was indicated in 19.2% and 80.9% (2000) of reports ($p<0.001$). The mean number of LN per report increased from 9.67 in 1997 to 12.1 in 2000 ($p<0.05$). The percentage of reports with less than 8 sampled LN decreased from 45.65% in 1997 to 26.04% in 2000 ($p<0.05$).
In conclusion, this study suggests that practices have improved in France regarding the reporting of CRC after a consensus conference held in 1998. However, there are still reports with insufficient data, especially regarding the number of LN sampled and the circumferential margin in rectal cancer. These features may be improved by the use of standardized report forms.

P 159
FEATURES OF COLORECTAL CANCERS ARISING ADJACENT TO SESSILE SERRATED ADENOMA
Markus J. Mäkinen, Karoliina Tuppurainen, Susannah M. Harrison, Tuomo J. Karttunen
University of Oulu, Department of Pathology, Oulu, Finland.

Background: Sessile serrated adenoma (SSA) is a novel subtype of colorectal polyps. It has been shown to be temporally associated with microsatellite instable colorectal cancer, but direct evidence on its neoplastic nature and malignant conversion is not well established.
Aims: To find out the prevalence and features of colorectal cancers associated with SSAs.
Materials and methods: Altogether 466 colorectal cancer cases were included in the study. SSA component was sought immediately adjacent to cancer tissue as previously described.
Results: Six colorectal cancers associated with SSA were discovered, with 1.3% prevalence in this study. In addition, 29 other serrated adenocarcinomas were detected (prevalence 6.2%) Four of SSA-associated carcinomas were found from female patients, four of them were located in the proximal colon, and DNA microsatellite instability was present in three cases. SSA component was characterized by a large slightly elevated tumor composed of hyperplastic-like epithelium. Cellular atypia was evident in all cases. Carcinomatous component consisted of serrated clear or slightly eosinophilic serrated epithelial proliferation with a great resemblance to the adenomatous component. Colorectal cancers associated with SSA were more often mucinous than conventional colorectal cancers (67% vs. 8%; P=0.001), but did not differ from other serrated adenocarcinomas (67% vs. 38%, P=0.36). However, they were less often well differentiated than other serrated adenocarcinomas (0% vs. 50%; P=0.017).
Conclusions: SSA is a rare precursor of colorectal cancer. It shares both clinical and morphological features with serrated adenoma and commonly represents MSI. As SSA has been proposed to be more frequent than serrated adenoma, lower frequency of SSA-associated cancers in this study could indicate less frequent malignant conversion rate for SSAs compared to serrated adenomas.

P 160
IS THERE A ROLE OF INFLAMMATION IN SPORADIC COLORECTAL CANCER? A STUDY OF COMMON POLYMORPHISMS IN INFLAMMATORY RESPONSE-RELATED GENES
NONNI Aphrodite1, THEODOROPOULOS George2, GAZOULI Maria2, GAKIOPOULOU Hariklia1, LAZARIS Andreas1, THOMOPOULOU Georgia1, BRAMIS John2, PATSOURIS Efstratios1
Depts of Pathology1 and Biology2, Medical School, University of Athens, GREECE

Epidemiological observations suggest that environmental and host immunological factors could significantly contribute to the initiation and the progression of colorectal cancer (CRC). Genetic polymorphisms can play a role in determining how individuals respond to various environmental factors. Although rather limited, evidence exists linking common polymorphisms in immune system related genes and CRC tumorigenesis.
The aim of the study was to investigate the association between common single nucleotide polymorphisms (SNPs) in the inflammatory response related genes interleukine (IL)-6, IL-8, tumor necrosis factor á (TNFá), peroxisome proliferators-activated receptor ã (PPARã), and intercellular adhesion molecule-1 (ICAM-1) and the risk of colorectal cancer in a group of Greek patients.
The study group consisted of 222 CRC patients and 200 healthy controls. Genotyping was performed using allele-specific PCR of PRC-RFLP and the results were confirmed by sequencing. We have studied the association of SNPs in the IL-6 (-174G>C), IL-8 (-251T>A), TNFá (-308G>A), ICAM-1 (R241G and K469E), and PPARã (Pro12Ala) genes and the risk of CRC.
The IL-6 -174G, R241 and K469 alleles are associated with increased risk of CRC (OR = 1.927 [CI95%: 1.508 to 3.336], OR = 1.833 [CI95%: 1.235 to 2.719] and OR = 1.546 [CI95%: 1.174 to 2.034], respectively). The IL-8 and the TNFá polymorphisms had no effect. Whereas the PPARã Ala12 genotype was associated with reduced risk of disease (OR = 0.588 [CI95%: 0.416 to 0.832]).
The association between common SNPs in immunologic response related genes with CRC is reported in the present study. Apart from shedding light on the mechanisms of malignancy initiation and progression, SNPs may improve appropriate screening for risk sub-population.

P 161
MORPHOLOGICAL FEATURES OF HEREDITARY NON-POLYPOSIS COLORECTAL CARCINOMAS COMPARED TO OTHER EARLY ONSET AND

SPORADIC COLORECTAL CARCINOMAS IN THE WESTERN CAPE, SOUTH AFRICA.

H Holm, P de la M Hall, N Allie, R Ramesar.* Divisions of Anatomical Pathology and Human Genetics* University of Cape Town and Groote Schuur Hospital NHLS

Background:
Families with hereditary non-polyposis colorectal carcinoma (HNPCC) are not uncommon along the West-Coast of South Africa. These patients present with early onset carcinomas, mostly colorectal, predominantly in the right colon. They may develop tumours of other organs, including uterus, breast, stomach and skin.
Objectives:
1. To evaluate and compare the microscopic characteristics of three groups of colorectal carcinomas (HNPCC, early onset colorectal carcinomas and sporadic colorectal carcinomas).
2. To determine the features most characteristic of the HNPCC group in the South African population.
Methods:
Coded sections of formalin-fixed paraffin-embedded tissue from patients with
(1) sporadic colorectal carcinomas (58 cases)
(2) early onset (<45 years) colorectal carcinomas (93 cases) and
(3) HNPCC (30 cases) are evaluated and graded on the following features:
intratumoral lymphocytes (TL),
stromal lymphocytes (SL),
lymphoid aggregates in the vicinity of the tumour (LA),
presence and type of necrosis (Ne),
percentage of mucin (Mo = 0%, M1 = <25%, M2 = 25-50%, M3 = 50-75%, M4 = >75%) and
histological grade based on the standard criteria of gland formation (G1 to G4).
Results and conclusions:
Intratumoral lymphocytes and lymphoid aggregates are fairly sensitive markers for HNPCC, the former being more specific than the latter. Stromal lymphocytes are a third, even more sensitive marker for HNPCC, but less specific than the other two. The other parameters tested are of no help in the differential diagnosis except for presence of necrosis which is more typical of sporadic and early onset colorectal carcinoma than of HNPCC.

P 162
ONCOCYTIC MODIFICATIONS IN RECTAL ADENOCARCINOMA

Ambrosini Spaltro Andrea*, Betts Christine M**, Salvi Fabrizio§, Frezza Giovanni P§, Baccarini Paola§, Baldoni Cristina†, Foschini Maria P§ and Viale Giuseppe*.
§ Dept. Of Oncologic Sciences, Sections of Anatomic Pathology and Radiotherapy at Bellaria Hospital, University of Bologna, Bologna, Italy.
† Dept. of Anatomic Pathology, Maggiore Hospital, Bologna, Italy.
** Dept. Of Experimental Pathology, University of Bologna, Bologna, Italy.
* Post-graduate Medical School in Anatomic Pathology, University of Milan, Milan, Italy.

Introduction. Oncocytes are granular, eosinophilic cells, with mitochondria occupying more than 40% of the cytoplasm. Tumors composed mainly of oncocytes are distributed in many organs, although thyroid and kidney are the most frequent. Oncocytic modifications have been reported after radiotherapy in salivary glands. To date few data are available on oncocytic modifications in adenocarcinomas of the colon-rectum.
The purpose of the study was to evaluate whether oncocytic modifications are present before radiochemotherapy (RCT) and if oncocyte-rich rectal carcinomas are resistant to RCT.
Materials and methods. 17 cases of advanced rectal carcinoma, treated preoperatively and simultaneously by 5-fluorouracil (200-225 mg/m2) and 46 Gy in 23 fractions were studied. All patients were biopsied before RCT and underwent surgery within six weeks after RCT. Specimens were routinely processed, stained with hematoxylin and eosin (H&E) and immunohistochemistry was performed using anti-mitochondria antibody (clone 113-1; dilution 1:500; Biogenex). In two cases, both pre and post RCT tissues were examined at ultrastructural level.
Results. All tumors were adenocarcinomas. Pre-RCT features: oncocytic changes were difficult to find on H&E, while at immunohistochemistry, anti-mitochondria antibody stained 5 to 100% of neoplastic cells (mean 59%). Post RCT features: Oncocytic cells were detected in all 17 cases on H&E and constituted 10 to 100% of the residual neoplastic population (mean 61%). With immunohistochemistry, the anti-mitochondria antibody confirmed the oncocytic changes, highlighting a larger number of neoplastic cells (range from 5 to 100%, mean 73%). Ultrastructural examination revealed large and bizarre mitochondria in tumor cells in both pre and post RCT tissues.
Conclusion. The present data suggest that rectal carcinomas can be “mitochondria rich” tumors. After pre-operative RCT, residual neoplastic cells may acquire a definite oncocytic phenotype. It is likely that the mitochondria enhance neoplastic cell survival.

P 163
PATTERNS OF MORPHOLOGICAL FEATURES IN RECTAL CARCINOMA AFTER PREOPERATIVE RADIATION OR CHEMORADIATION AND CLINICAL OUTCOME.

CHMIELIK Ewa (1), STOBIECKA Ewa (1), WOLOSZYNSKA-PREIDL Krystyna (1), JAWORSKA Magdalena (1), LANGE Dariusz (1), KRYJ Mariusz (2), ZEMAN Marcin (2), ZEMBALA-NOZYNSKA Ewa(3), NOZYNSKI Jerzy (4)
(1)Department of Tumor Pathology, Center of Oncology, M.Sklodowska-Curie institute, Gliwice, Poland
(2)Department of Surgery, Center of Oncology, M.Sklodowska-Curie institute, Gliwice, Poland
(3)Chair and Department of Pathomorphology, Silesian Medical School, Zabrze, Poland
(4)Department of Histopathology, Silesian Center for Heart Diseases, Zabrze, Poland

Introduction Pre-operative radiation(RT) and chemotherapy (CRT) improve outcome in patients with rectal adenocarcinoma (ACA).
Aim Analysis of histological features in residual rectal carcinoma following preoperative RT or CRT and their prognostic significance.
Materials and methods Resection specimens from 54 patients with T1-T4 advanced rectal ACAs treated with RT and CRT before surgery were analyzed for the following features:
tumor treatment response (pPR1, pPR2, pPR3), histological architecture structures
(cribriforme, tubular, papillary, cystic), degree of cytological alteration, extent of damaged tubular structures(0-30%, 30-60%, >60%), inflammatory or histiocytic reaction in the tubular structures, microfoci of carcinoma, tumor necrosis, mucus degeneration of stroma, inflammatory or fibroinflammatory reaction of stroma, cytoplasmic eosinophilia , cytoplasmic basophilia, neoplastic or post-irradiation ulceration. The data obtained were statistically analyzed using ANOVA, Kruskal-Wallis method, median test, ch^2 test and Mann Whitney test.
Results There were no significant correlations between the histological architecture structures and other features.

There was correlation between 30% extent of damaged tubular structures and RT type (42-60Gy) p=0.022; type of ulceration and microfoci of carcinoma (p=0.036), sex (ch^2 test p=0.045) and treatment response (ch^2 test p=0.0001); cytoplasmic basophilia with the time of recurrence (p=0.024); sex and time of recurrence onset of relapse?) (p=0.024).
Conclusion In our study we characterized histomorphology of post-irradiated rectal ADAs and report morphological features associated with the time of recurrence.

P 164
PROGNOSTIC VALUE OF THE CLASSIFICATION OF FIBROTIC STROMA IN COLORECTAL CANCER
Sanei Mohammad Hossein MD, Nooshin Afsharmoghadam MD
, Department of pathology, Isfahan university school of Medicin, Isfahan

Abstract:
Introduction:
Various factors influence prognosis of colorectal cancer including local extension, lymph node involvement, tumoral growth pattern and lymphocytic infiltration at the tumor margin. There is controversy about the role of amount of fibrotic stroma but there are a few studies on the type of stroma. The aim of this study is evaluating the prognostic value of classification of stroma by means of Astlre and coller staging system.
Materials & Methods :
Ninety two cases of colorectal cancer were examinated.we classified fibrotic stroma in front of tumor extension based on Uneo and colleague criteria to three category:typA,multiple fine and mature fiber were stratified ;typeB,broad hyalinized collagen(keloid-tyoe) were intermingled;type C,myxoid stroma.we exited cancers were superimposed on IBD and familial polyposis.Then the data were analyzed by chi-square test..
Results:
45% of cases had typeA stroma, 18% type B stroma. And 37% type C.
The prevalence of type A stroma in the various stages of tumor was such:A=100%,B1=68%,B2=26%,C1=60%,C2=33% and the prevalence of type C stroma in the various stages of tumor was such: A=0, B1=16%, B2=49%, C1=40%, C2=48%.
In order to identify amount of correlation we employed pearson index (R=0.43).
Discussion:
The results showed a decreasing in type A stroma when the stage of disease increase (stage A=100%, stage B1-68%, stage B2= 27%, stage C1=60%, stage C2=33%) and increasing in type C(stage A=0, stage B1=16%, stage B2=49%, stage C1=40%, stage C2=48%).
The result was statically significant and classification of stromal pattern had independent prognostic value same as lymph node involvement, lymphocytic infiltration and growth pattern.
Keywords:
Colon cancer, fibrotic stroma, Collagen, myxoid stroma

P 165
RESPONSE TO PREOPERATIVE CHEMORADIOTHERAPY ON RECTAL ADENOCARCINOMA: HISTOPATHOLOGICAL EFFECTS AND RELATIONSHIP WITH LEVEL OF P53 AND PCNA EXPRESSION.
RAMOS Paloma*, DIEZ Manuel**, OLMEDILLA Gabriel*, RUIZ Antonio* and ALVAREZ Isabel***.
*Dpt. of Pathology, Principe de Asturias University Hospital, Alcala de Henares, Madrid, Spain.
**Dpt. of General Surgery, Principe de Asturias University Hospital, Alcala de Henares, Madrid, Spain.
***Dpt. of Pathology, Ramon y Cajal University Hospital, Madrid, Spain.

INTRODUCTION: Adjuvant chemoradiotherapy delivered before surgery has been used to improve control and to reduce the likehood of local recurrence in selected patients with rectal cancer. Although the status of p53 gene and the expression of Proliferating Cell Nuclear Antigen (PCNA) has been widely studied in these tumors, little is known about their value to predict responsiveness of rectal cancer to chemoradiation.
AIMS: To assess effects of preoperative chemoradiation in advanced rectal adenocarcinoma.
METHODS: We examined the histopathologic effects of chemoradiotherapy on 73 rectal tumors and correlated the efficacy of treatment with the level of p53 and PCNA proteins expression in pretreatment biopsies.
RESULTS: Three patients showed no primary tumor in the resection specimen. Another eight carcinomas showed a good response to chemoradiation with only small nests of viable tumor cells. Grouping these two categories, we considered that the tumor response had been total or subtotal in 11 cases (15%). Nuclear accumulation of p53 protein was detected in 53 (72%) specimens. Thirty five tumors showed a high PCNA index (48%). No obvious relationship seemed to exist between pretreatment p53 immunostaining and response to chemoradiotherapy. Tumors with high PCNA index were more likely to respond to chemoradiation: 8/35 (72%) versus 3/38 (43%)(p=0.07).
CONCLUSIONS: Knowledge of proliferative activity of rectal cancer, as determined by PCNA immunostaining, should be useful in predicting the likehood of response to preoperative chemoradiation.

P 166
THE CHANGES OF THE TYPES OF COLONIC MUCINS IN THE BENIGN ,PREMALIGNANT AND MALIGNANT LESIONS
Dr.Ibrahim Ghada(M.B.CH.B,F.I.C.Pathology), supervised by professor dr .Alkaptan Ikbal (F.R.C.Path.,M.r.c.Path)

the aim of study
To clarify the changing pattern of colonic mucins in colonic tumours, and to evaluate the benefit of the staining methods in diagnosis and prognosis of colorectal lesions ,for early detection of premalignant changes and compare this mucin pattern with western researches.
materials and methods
95 biopsies were selected and stained with haematoxylin and eosin,PAS stain ,Alcian blue ph(2.5) and Shikata`s modified orcein/alcian blue
Results
sulphated mucin is the predominant mucin in normal colon.Mucin pattern in adenoma is variable. Adenoma with mild dysplasia mucin pattern is similar to normal.,these with moderate to severe dysplasia and carcinoma in situ,mucin production is decreased or absent and if it is present it is amixture of sialo and sulphated mucin (sialomucin is more predominant)
in ulcerative colitis with dysplastic changes mucin also is vairiable according to the degree of dysplasia
ie in mild and moderate dysplasia mucin pattern is close to normal (both types is present however sulphated mucin is predominant) while in Ulcerative colitis with severe dysplasia the mucin pattern is differ as the amount of mucin is decrease and pattern is change predominantly to sialomucin
In all carcinomas,reduction of mucin is evident,less marked in well differentiated adenocarcinoma in which three types of mucin is present(sialo ,sulphated and neutral mucin)

In Moderately differentiated carcinoma mucin is mainly (intraluminal)sialomucin.In poorly differentiated carcinomas, mucin is scanty or absent.
Conclusion
The study of mucin pattern of colon is rewarding in detection of early malignancy ,classification of polyps.assesment of their malignant potential ,(increased sialylation is important in transition from adenoma to carcinoma and for determining prognosis in patients with colorectal cancer

P 167
COLONIC PSEUDOCARCINOMA-CASE REPORT
Simona Mocan1, Simona Stolnicu2, Doina Milutin1, Doinita Radulescu3
1Department of Pathology, County Clinical Hospital Targu Mures, Romania
2Department of Pathology, University of Medicine Targu Mures, Romania
3Department of Pathology, University of Medicine Iasi, Romania

Aims. Misplaced epithelium within an adenoma (pseudocarcinoma) is a rather common findings but currently there are no clinical or endoscopic methods available in differentiate adenomas with epithelial misplacement from those with adenocarcinoma.
Material and methods. We present the case of a 64-year-old female presented with bright red blood per rectum. Previous medical history was not significant. Upon colonoscopy, two pedunculated polyps were identified in the lower sigmoid, which were excised endoscopically and submitted to pathology for evaluation. The tumors were excised, fixed in formaline, embedded in paraffin and the sections were stained with H-E, PAS-ALCIAN blue. We performed also immunohistochemical staining: with Cytokeratin, Vimentin, Collagen IV and p53.
Results. The gross appearance was similar for both polyps. The histological features were different. An adenomatous polyp, with tubulo-villous architecture and misplaced epithelium in the submucosa stalk, mucinous pools lined, represented one of the polyps by dysplastic epithelium similar to that seen at the surface of the polyp. The second polyp was represented by an adenomatous polyp with villous architecture and high-grade dysplasia, focally with irregular, variably sized crypts, without lamina propria, with irregular mucous pools containing floating malignant cells within the stalk of the polyp. The immunohischemical results were different in the two cases.
Conclusions. The most common differential diagnosis of adenomas with epithelial misplacement are adenomas that contain invasive adenocarcinoma, but several other entities may on occasion, be confused with the former lesions, such as solitary rectal ulcer syndrome-associated polyps, Peutz Jeghers polyps, hyperplastic polyps. Unfortunately, the diagnosis it cannot be made just based on the histologic appearance.

P 168
ANALYSIS OF CYCLOOXYGENASE-2 EXPRESSION IN COLON CANCER AND NORMAL COLON USING TISSUE MICROARRAY
Díez A1, García R2, Acuña MJ1, Pajares R1, Ibarrola C2, Lopez-Alonso G2, Sánchez-Verde L1, and Ballestín C2.
Histology & Immunohistochemistry Unit, Biotechnology Program, Spanish National Cancer Center (CNIO), Madrid, Spain1, Department of Pathology, Hospital 12 de Octubre, Madrid, Spain.2

Introduction:
Recent studies have shown that cyclooxygenase (Cox-2) may be involved in colorectal carcinogenesis.
Cyclooxigenase-2 is an inducible enzyme involved in the response of cells to growth factors, tumour promoters, and cytokines that induce its expression. Given its role in synthesizing prostaglandins, Cox-2 is therefore of interest in studying immune response regulation. Is also induced by a wide variety of other stimuli and was initially identified as an immediate-early growth response gene.
Aims: To analyse expression of COX-2 in colorectal carcinomas, and to compare this expression between normal and tumoral colon cells in a series of 35 patients.
Material and Methods:
Tissue samples of primary sporadic colorectal carcinoma and adjacent normal mucosa samples from 35 patients were included in a Tissue Microarray.
Cox-2 expression was first evaluated in a Tissue Microarray with normal tissue samples (thyroid, placenta, tonsil, mammary gland, colon mucosa, appendix, spleen, liver, kidney and lung) in order to establish the best protocol, using Immunohistochemical staining in 3um Tissue Microarray sections, with Cox-2 antibody from Neomarkers. This protocol was then applied to the tumoral and normal colon Tissue Microrrays.

The specimens were graded based on the intensity and extent of staining as follows:
1+: 30% positive cells
2+: 30%-60% positive cells
3+: 60%-100% positive cells
Also the homogeneity and heterogeneity of the staining were validated.
Results:
From a total of 35 patients included in the study, the expression of COX-2 was:
· Normal samples were (3+) homogeneous positively with a very strong level of positivity
· From 35 tumour samples, one sample was not evaluated
17 cases (50%) 3+ homogeneous and with strong intensity
3/34 cases (8.8%) 3+ homogenous and weak expression
5/34 cases (14,7%) 2+ homogenous and weak expression
2/34 cases (5,8%) 1+ homogenous and weak expression
5/34 cases 14.7% heterogeneous expression
2 cases were completely negative
Conclusions:
1.- The data presented in our study show that Tissue Microarrays are a useful tool for identifying expression profiles and expression changes of proteins, allowing comparisons between normal and tumoral regions.
2.-Cox-2 is expressed intensively and homogeneously in normal mucosa colon
3.- Colorectal cancer shows lower intensity in number of cells compared with their normal mucosa colon counterpart
4.- Some tumours show

P 169
CYCLOOXYGENASE-2 (COX-2) EXPRESSION IN POLYPS AND CARCINOMAS OF HEREDITORY NON-POLYPOSIS COLORECTAL CARCINOMA (HNPCC) AND SPORADIC COLORECTAL CARCINOMAS IN THE WESTERN CAPE, SOUTH AFRICA.
H Holm, P de la M Hall, N Allie, R Ramesar*
Division of Anatomical Pathology and Human Genetics,*
Groote Schuur Hospital/University of Cape Town, South Africa

Background:
COX-2 inhibitors are being used as chemoprevention in familial adenomatous polyposis. If COX-2 is also expressed in HNPCC there might be a role of COX-2 inhibitor treatment for patients with a known mismatch repair gene defect - either

to inhibit progression of tumours or to prevent the onset of carcinogenesis.
Objectives:
1. To evaluate COX-2 expression in colonic adenomas and carcinomas in patients with genetically proven HNPCC.
2. To compare COX-2 expression in HNPCC cases with that in sporadic tumours.
Methods:
Coded sections of formalin fixed paraffin embedded tissue from patients with known hMLH1 or hMSH2 mutations (6 polyps and 12 carcinomas) and sporadic tumours (5 polyps and 39 carcinomas) where immunohistochemically stained with an antibody to the COX-2 (Santa Cruz). Expression of COX-2 in the tumours was scored on both intensity and distribution and compared to the adjacent normal epithelium.
Results:
Normal colonic epithelium does not express COX-2. HNPCC: 1/6(17%) polyps and 5/12(42%) carcinomas express COX-2. Sporadic tumours: 3/5(60%) polyps and 26/39(67%) carcinomas express COX-2.
Conclusions:
COX-2 is generally more expressed in sporadic compared to HNPCC tumours. Furthermore COX-2 expression is more often expressed in infiltrating lesions compared to the expression in polyps. Chemoprevention is probably indicated in a selected number of HNPCC individuals.

P 170
EPIDERMAL GROWTH FACTOR RECEPTOR STATUS IN PRIMARY VERSUS METASTATIC SITES OF COLORECTAL ADENOCARCINOMAS

DURZYNSKA Monika, OLSZEWSKI Wlodzimierz T, KRZAKOWSKI Maciej.
Departament of Pathology, Departament of Thoracic and Lung Tumor
The Maria Sk³odowska – Curie Memorial Cancer Center and Institute of Oncology, Warsaw

The epidermal growth factor receptor (EGFR) is expressed in 40% to 80% of colorectal cancers. It is well known that EGFR expression in tumor cells is not early event and it changes in time in opposition to HER2 status. Data from literature have shown different EGFR status comparing primary and metastatic lesions. Relation between EGFR status and respons to specific treatment is still under investigation.

The aim of our study was to compare EGFR status on primary colorecatal tumors with corresponding metastases to determine whether assesment EGFR status in primary tumor is reliable for planing EGFR - targeted therapy.

Patients and Methods: EGFR expression was evaluated by immunohistochemistry in primary tumors and related metastases in 50 pacients with colorectar adenocarcinomas. In 35 (70%) cases metastatic sites were lungs and in 15 (30%) – liver. EGFR status was evaluated as positive if the percentage of membrane stained tumor cells was > or = 1% of all tumor cells.

Results: 33 (66%) of 50 specimens from primary tumor were EGFR positive. In 9 (27%) specimens from related metastses EGFR status was negative. 3 (17%) specimens from metastatic sites were EGFR positive whereas corresponding primary tumor specimens were negative.

Conclusion: Our data suggest that due to differences in EGFR expression on primary and metastatic sites of colorectal adenocarcinomas, for planning EGFR - targeted therapy EGFR status should be evaluated on specimens taken from at the moment exisiting tumor focus - metastates or recurrent lesions.

P 171
EXPRESSION OF EGFR IN COLON CARCINOMAS AND THEIR CORRELATION WITH

POPOVSKA Savelina, MARKOVA Elena, BETOVA Tatyana.
Department of General and Clinical Pathology
Medical University, Pleven

Background: Epidermal growth factor receptor (EGFR) is commonly overexpressed in a number of epithelial malignancies and is often associated with an aggressive phenotype advanced stages of cancer and a poor prognosis for the patient.
Aims: The expression of EGFR was analyzed in 50 cases of colon carcinoma, using immuhistochemical technique of paraffin sections. A correlation was made between the EGFR expression in primary tumour and the following clinicopathological parameters: histological type, histological grade and stage of the disease.
Methods: The patients had undergone curative surgical resection at the Oncology Centre in University Hospital - Pleven. EGFR expression was examined by immunohistochemistry using the Dakocytomation's EGFR PharmDx (Dako Cytomation) in paraffin-embedded colon tumors and graded as percentage of cells stained. The correlation statistical analisys was used.
Results:EGFR immunoreactivity was detected in 34 (68%) cases of colorectal carcinomas.
High levels of EGFR protein were observed in 10/50 (20 %) samples. Thirteen (26%) show moderate of EGFR expression in tumor cells and 11/50 (22 %) show slight level of EGFR expression. Sixteen of tumors were totally negative (32%).
Most of the cases showed complex and heterogenous patterns of EGFR-expression.
No association was found between the expression of studied EGFR protein and histological grade and type of primary tumor. Similarly, no correlation was detected between EGFR immunostaining and stage of colorectal adenocarcinoma.
Conclusions: Prospective multicentric studies should be conducted to confirm overexpression of EGFR as a prognostic factor.
Key words: EGFR, colorectal adenocarcinoma

P 172
HER 2/NEU EXPRESSION IN COLON CANCER AND ITS CORRELATION WITH CLINICOPATHOLOGIC VARIABLES

K.Ghaffarzadegan,M.D.*,N.Sharifi,M.D.*,H.Vosooghynia,M.D.**,T.Shakeri,Ph.D***,
Sh.Ghanad Kafi,M.D.****M.Ghavam Nadir,M.D.*****
*Pathology Department,Ghaem hospital,Mashad University of Medical Sciences(MUMS)
**Gasteroenterology Department, Ghaem hospital,Mashad University of Medical Sciences(MUMS)
*** Community medicine Department ,faculty of medicine, , Mashhad University of Medical Sciences (MUMS)
****Resident of pathology, Ghaem hospital,Mashad University of Medical Sciences(MUMS)
*****Oncology Department,Omid hospital, ,Mashad University of Medical Sciences(MUMS)

Abstract
Aims:Colon cancer is a prevalent human malignancy.HER2/neu is an important oncogene in breast cancer,but its prevalence and significance in colon cancer have been poorly documented.
Aim of our study is to determine the rate and pattern of HER2/neu expression in colon carcinoma by immunohistochemistry(IHC).
Material and Methods:Sixty-nine archival ,paraffin wax embedded colon carcinoma specimens were chosen.IHC for HER2/neu was performed.Clinicopathologic data and IHC results were analyzed.
Results : Most of the carcinoma cases were well differentiated and located in the left side .There is positive

HER2/neu staining in a high percent of cases (41 Cases ,59.4 %) with both cytoplasmic (27cases.65.9%) and membranous-cytoplasmic (14cases,34.1%) staining .
In higher stages , the rate of positive staining were decreased but there was higher rate of strong membranous staining .Also, in higher grades , the rate of HER2/neu staining was decreased (P=0.04) and there was more membranous staining .
There were no correlation between HER2/neu expression and age , sex, site and type of tumor .
Conclusion : The rate of HER2/neu expression in colon carcinoma is high. Because of more prominent membranous staining in higher stages and grades,the Herceptin therapy could be helpful in patients with lymph node or distant metastases.
Keywords: coloncarcinoma, HER2/neu, immunohistochemistry

P 173
IMMUNOHISTOCHEMICAL ASSESSMENT OF EPIDERMAL GROWTH FACTOR RECEPTOR (EGFR) EXPRESSION IN PRIMARY COLORECTAL CARCINOMA AND THEIR RELATED METASTASES. A COMPARATIVE STUDY ON TISSUE SECTIONS AND TISSUE MICROARRAY
BIBEAU frédéric1, BOISSIERE florence 1, SABOURIN jean-christophe 2, GOURGOU sophie 1, PENAULT-LLORCA frédérique 3, ROCHAIX philippe 4, ARNOULD laurent 5, BRALET marie-pierrre 6, AZRIA david 1, YCHOU marc 1 and the GETCO group. 1 Val d'Aurelle Cancer Center Pathology, Biostatistics and Oncology Departments, Montpellier, 2 Pathology, Institut Gustave Roussy, 3 Pathology, Centre Jean Perrin, 4 Pathology, Institut Claudius Regaud, 5 Pathology, Centre Georges-François Leclerc, 6 Pathology, Institut Paul Brousse and Le Groupe d'Etude des Thérapeutiques Ciblés en Oncologie, France.

Introduction: Recently approved new EGFR-targeted treatment (Cetuximab®) in metastatic colorectal carcinoma (CCR), requires an immunohistochemical assessment for patient eligibility. Controversial and limited data are available on the EGFR status in distant metastases.
Purpose: Because of clinical implications, we studied EGFR expression of primary CCR and their related metastases, to assess whether EGFR status was equivalent on both sites.
Methods: EGFR immunohistochemistry (IHC) on tissue sections was retrospectively assessed from primary tumors and related synchronous metastatic sites in 32 CCR patients (colon: 21; rectum: 11). Metastatic sites analyzed were liver (31) and ovary (1). IHC standardized assay was used (EGF-R pharm Dx, DakoCytomation) and EGFR positive status (EGFR +) was defined by a percentage of stained cells >1%, displaying a membranous pattern. In addition to tissue sections, EGFR was assessed on two triple core tissue microarrays (TMA), in order to find out if this high throughput technique was valuable for EGFR screening (diameter of the core: 0,6 mm, punched in the deepest region of the tumor invasion known to contain the strongest immunoreactivity).
Results: EGFR + tissue sections were observed in 84% of the primary cases (27/32) and 94% of the metastases (30/32). All patients displayed an EGFR + status either in the primary site (2/32), in the metastasis (5/32) or both (25/32). Discordant cases (i.e primary positive/ metastasis negative and inversely) were not statistically significant (p=0.453). Additionally, the number of EGFR + cells in the primary site was significantly correlated with that observed in their metastasis (r^2= 0.616, p= 0.0002). EGFR status on TMA was significantly under-evaluated on both sites, when comparing with tissue sections (p=0.0001 and p=0.0015 for primitive and metastatic sites, respectively). Moreover, using the TMA technology, we failed to find any correlation of EGFR expression between both sites.
Conclusion: Our results suggest that EGFR expression is frequent and equivalent on both primary and metastatic sites. Moreover, all patients exhibit an EGFR + status when combining EGFR status from the primary and from the metastatic site. Consequently, patient exclusion for Cetuximab® therapy should not be based on EGFR negativity from one single site. Our results also demonstrated that TMA is not a suitable tool for EGFR assessment in CCR, since it significantly underestimates its status.

P 174
Â-CATENIN, E-CADHERIN AND CYCLIN D1 EXPRESSION AT THE INITIAL STAGES OF THE ADENOMA-CARCINOMA SEQUENCE
AKMAN Hatice, DEMIRKAN Nese, DUZCAN Ender

Introduction and aims:
Most of the colorectal carcinomas originate from adenomatous polyps and this process is known as adenoma-carcinoma sequence. â-Catenin play an important role at Wnt signaling pathway and E-cadherin-catenin complex is essential at the maintenance of normal tissue architecture. An alteration of any of the components of E-cadherin-catenin complex are believed to result in the loss of cell-cell adhesion and to contribute to carcinogenesis. This study aimed to determine expression and cellular distribution of E-cadherin, â-catenin, and its target gene cyclin D1 and c-myc during tumor progression and malignant transformation in colon and to reveal its diagnostic or prognostic usefulness.
Methods:
Following histopathological examination, immunohistochemical staining of E-cadherin, â-catenin, cyclin-D1 and c-myc were performed at each section of 60 tumor samples and 31 polyp samples taken from 61 patients diagnosed as colorectal carcinoma and/or adenomas.
Results:
At polyps, the frequent loss of membraneous expression of E-cadherin was found at high dysplastic lesions however it was not significant (p: 0,07). Cytoplasmic and/or nuclear expression of â-catenin and nuclear expression of cyclin D1 was correlated with the degree of dysplasia (p: 0,01, p: 0,003, respectively).
At the tumors; the membraneous expression of E- cadherin was negatively correlated with lymph node metastasis (p:0,04). Nuclear cyclin D1 was expressed more at well differentiated tumors and at early stage (p:0,02, p:0,04, respectively). The increase of nuclear cyclin D1 positivity was correlated with cytoplasmic â-catenin positivity (p:0,034). Tumors of less than 5 cm diameter have more cytoplasmic and/or nuclear â-catenin positivity than tumors of more than 5 cm diameter (p: 0,039). No specific expression pattern were detected at c-myc expression related to adenoma-carcinoma sequence.
Conclusion:
This study demonstrated a significant loss of membraneous expression of E-cadherin during tumor progression at colon carcinomas. We hypothesized that loss of membrane staining of E-cadherin might be an indicator of worse prognosis at colon carcinomas. We propose to use nuclear expression of â-catenin as a marker of invasiveness in adenomas. As the overexpression of cyclin D1 is an early event in adenoma-carcinoma sequence, cyclin D1 may account for good prognostic parameter in colon carcinomas.

P 175
E-CADHERIN EXPRESSION PATTERN IN PRIMARY COLORECTAL CARCINOMAS AND THEIR METASTASIS REFLECT DISEASE OUTCOME
Adam Elzagheid 1,2,Riyad Bendardaf 1, Hanan Lamlum 1,Yrjo Collan 2, Kari Syrjanen1, Seppo Pyrhonen 1.

1Department of Oncology and Radiotherapy, Turku University Hospital, Savitehtaankatu 1 PB 52, FIN-20521, Turku, Finland,
2Department of Pathology, University of Turku, Kiinamyllynkatu 10, FIN-20520, Turku, Finland,

Aim: We using immunohistochemistry to examine the levels of E-cadherin expression in primary tumours and their metastasis from a series of 42 colorectal cancer (CRC) patients. Material and Methods: E-cadherin expression was separately analysed in membrane and cytoplasmic location by calculating two indices (MI and CI) in a series of 42 CRC and their metastases. Univariate and multivariate survival analyses were used to assess the value of these two E-cadherin indices as predictors of both disease-free (DFS) and disease-specific (DSS) survival.
Results: E-Cadherin MI was significantly higher in primary tumours as compared to their metastasis (p=0.0001), whereas CI did not show such a difference. Both MI and CI in the primary tumour were higher among patients who developed subsequent metastasis (p=0.022 and p=0.007, respectively). Interestingly, both indices were higher in metastasis of the liver than in those at other anatomic sites (p=0.034 and p=0.022), respectively. In univariate analysis, CI in the primary tumour was a significant predictor of DFS (p=0.042), and retained its predictive power also in multivariate Cox model, with a strong inverse correlation between CI and DFS (p=0.006). In the multivariate model, MI in the primary tumour proved to be a significant independent predictor of DSS, higher indices being associated with more favourable outcome (p=0.016).
Conclusions: The examining E-cadherin expression and distribution in colorectal tumours can be extremely valuable in predicting disease recurrence. The observation that aberrant cytoplasmic expression of E-cadherin can predict disease recurrence is obviously of great importance for both the patient and the clinician and affects significantly decisions concerning patient therapy and management.

P 176
EXPRESSION OF E-CADHERIN IN BUDS AT THE INVASIVE FRONT OF COLORECTAL CANCER (CRC) IN ASSOCIATION WITH LYMPH NODE INVOLVEMENT.

Katarzyna Guzinska-Ustymowicz, Mariusz Gryko, Andrzej Kemona, Jolanta Czyzewska
Department of General Pathomorfology, Medical University of Bialystok,Poland

Introduction:
Tumor budding refers to microscopic clusters of undifferentiated cancer cells just ahead of the invasive front of the carcinoma. It has been suggested that dysfunction E-cadherin-mediated cell adhesion is associated with tumour invasion and metastasis.
That why the aim of this study was to evaluate the relationship of tumour budding to chosen anatomoclinical features of colorectal cancer, and to E-cadherin expression in the main tumour mass, lymph node metastases and in the buds.
Methods: Tumors from 55 patients with colorectal cancer (CRC) were assessed by immunohistochemistry. Tissue sections were fixed in 10% buffered formaldehyde solution, embedded in paraffin and stained immunohistochemically with anti-human E-cadherin and â-catenin antibody.
Results:
It has been found that loss of membrane E-cadherin expression at the invasion front of primary tumour and tumour budding correlate with lymph node involvement. A different location of E-cadherin expression was also observed in buds. A statistically significant correlation between localization of E-cadherin expression in buds and presence of lymph node metastases ($p<0.01$) was found. We also noted a statistically significant correlation between changes at the site of E-cadherin expression in primary tumor, buds and localization of E-cadherin expression in lymph node metastasis.
Conclusion: These date suggest that different aggressiveness of tumors may depends of changes at the location of E-cadherin expression in buds at the invasion front of colorectal cancer.

P 177
EXPRESSION OF E-CADHERIN, BETA-CATENIN AND CD44V6 IN COLON CANCER: CORRELATION WITH CANCER METASTASIS.

Delektorskaya V.V., Perevoschikov A.G., Kushlinsky N.E.
N.N.Blokhin Russian Cancer Research Centre RAMS,Moscow,Russia.

Adhesion molecules are closely involved in the development and growth of metastatic tumours. The aim of the present study was to invastigate the level of expression and cellular distribution of E-cadherin, beta-catenin and CD44v6 and to assess the role of proteins in progression of colon carcinoma. Immunohistochemical analysis for E-cadherin, beta-catenin and CD44v6 was carried out on formlin-fixed paraffin-embedded sections of colon cancer tissues by streptavidin-biotin immunoperoxidase method. We examined the expression patterns of these molecules in 84 primary colon, 92 liver and 35 lymph node metastatic tumours, obtained from 84 patients and 45 non-metastatic colon carcinomas as control. The presence of membranous, cytoplasmic and mixed staining for E-cadherin were found in tumour tissues. Loss of normal membranous staining and reduced E-cadherin expression were detected more freqwently in the primary tumour with liver metastasis (64/84,76%), than in those without secondaries(14/45,31%)(p=0,014). In addition, the expression of E-cadherin had an inverse relationship with level of differentiation of the tumour.The expression level of E-cadherin was markedly decreased in the cancer cells of metastasis in lymph nodes and liver. Beta-catenin immunoreactivity was increased with cytoplasmic accumulation and nuclear translocation in more than 80% of the neoplasms with distant metastasis and in metastasis in lymph nodes and liver. Nuclear localization of beta-catenin was significantly higher in the invasive magin of some tumours in metastatic group (70/84,83%) when compared with the localized one (15/45,33%) (p=0,01). No significant difference in beta-catenin' expression was found between primary tumours and their lymph node and hepatic metastasis. There was no correlation between the expression of CD44v6 and lymph node involvement or liver metastasis of colon carcinoma. Expression of CD44v6 in metastasis showed no consistent relationship to that in the primary tumours.These results indicate that decreased expression of E-cadherin and nuclear accumulation of beta-catenin in colon cancer tissues are closely related to liver metastasis. There may be no association between CD44v6 expression and metastatic ability of colon carcinoma. In conclusion, our study suggest that both E-cadherin and beta-catenin play an important role in invasion and metastasis of colon cancer and may become a significant prognostic markers for tumour behaviour.

P 178
ASSOCIATION BETWEEN PRESENCE OF TUMOUR BUDDING AND EXPRESSION OF CATHEPSIN B AT THE INVASION FRONT OF COLORECTAL CANCER (CRC).

Katarzyna Guzinska-Ustymowicz, Andrzej Kemona, Mariusz Gryko, Jolanta Czyzewska
Department of General Pathomorphology, Medical University of Bialystok, Poland

AIM: Recent studies concerning the prognostic factors in colorectal cancer (CrC) have paid attention to tumor budding

as a prognostic factor. Cathepsin B play an important role in cancer invasion and metastases by degrading extracellular matrix components and basement membrane. However, the correlation between cathepsin B and presence of tumor budding at the invasion front of colorectal cancer has not yet been presented. The aim of this study was to clarify the association between the expression of cathepsin B in main mass of tumor, budds, and lymph node metastases, and presence of tumor budding at the invasion front of CRC, and lymph node involvement.
METHODS: A standard avidin-biotin immuno-peroxidase method (ABCu-NCL) staining technique was performed on 4im paraffin-embedded tissue section with a mouse anti-human cathepsin B monoclonal antibody (Novocastra/NCL-CATH-B).
RESULTS: A tumor budding was observed in 78.2% cases out of 55 colorectal adenocarcinomas. It has been observed that tumor budding at the invasion front was strongly associated with lymph node metastases. Positive immunohistochemical staining for cathepsin B was observed in 52.7% cases. Statistically significant correlation was found between expression of cathepsin B in main mass of tumor and lymph node involvement ($p<0.01$). The expression of cathesin B in primary tumor was also associated with tumor budding and vascular invasion ($p<0.01$)

P 179
CERBB2 AND P53 OVEREXPRESSIONS ARE POOR PROGNOSTIC PREDICTORS IN PATIENTS WITH COLORECTAL CARCINOMA
ERDAMAR Sibel, DOGUSOY Gulen, GOKSEL Suha, DIRICAN Ahmet,Aydin Ovgu
Cerrahpasa Medical College Pathology Deparment, Istanbul

Aim and background:To assess biological markers of primary colorectal carcinima (CRC) that may improve clinical staging and provide useful information for the application of novel therapeutic strategies, we investigated the protein product of the c-erb B2/HER-2 oncogene and p53 expression.
Method: Formalin-fixed paraffin embedded histopathological samples from 41 patients with CRC treated radical surgery in different stage were analysed to determine HER-2 and p53 protein expression by immunohistochemistry using Avidin-Biotin complex. Spearman Rank correlation test and Kaplan Meier survival tests were used in statistical analyses.
Results: Follow-up period was 12-84 months (mean; 27,6 ms) in study group. It's found that there was Lymph node metastases (LN met) in 21 cases (51,2%), perineural invasion (PI) in 13 cases (31%). There was not any expression of HER-2 in 10 cases (24%). There was Her-2 expression (+):n=5, 12%; (++): n=13, 31,7%; (+++): n=13, 31,7%. Expression of Her-2 was correlated with poor prognosis ($p<0.05$). P53 expression was less than 15% in 21 cases, whereas it was 15% or higher in 20 cases. Overexpresion of p53 was found poor prognostic indicator. Both markers were correlated with LD met.
Conclusion: Our study suggest that analysis of cerb B2/HER2 and p53 expression may provide relevant prognostic information about CRC patients that should be added in our pathology reports.

P 180
CLINICAL SIGNIFICANCE OF P53, K-RAS, DCC GENE ALTERATIONS AND EXPRESSION OF P53, RAS P21 ONCOPROTEIN IN THE EARLY STAGE COLORECTAL CANCERS
Mustafa Akkiprik*, Cigdem Ataizi Celikel**, Fikret Dusunceli***, Ozgur Sonmez*, Bahadir Gulluoglu***, Aydin Sav**, Ayse Ozer*
Marmara University School of Medicine, Departments of Medical Biology1, Pathology2 and Surgery3

Genetic alterations of p53, K-ras and DCC genes have a pivotal role in the colorectal colorectal tumorigenesis. Clinical significance of these genetic changes includes contradictory results. The aim of this study was to clarify the association between point mutation of K-ras oncogene codon 12/13, p53 aberrations, DCC loss of heterozygosity (LOH) and p53, ras p21 immunoexpression with the patient outcome and tumor characteristics in the early stage colorectal cancer patients.
Fifty-three stage I-II colorectal cancer patients who underwent surgical treatment with no postoperative adjuvant therapy were included in the study. Follow-up data were available for 43 patients with a median follow up 76 months (range, 6-168). Mutations in exons 5-8 of the p53 gene and codon 12 and/or 13 of the K-ras gene were assayed by PCR-SSCP and then confirmed by DNA sequencing. DCC LOH was studied by PCR-RFLP. p53, using the monoclonal antibody DO7 and ras p21 expression were evaluated by using immunohistochemistry on paraffin-embedded tissue sections.
Mutations of the p53 and K-ras genes were found in 15 and 5 tumors, respectively. DCC LOH was found in 5 cases. The most common combination of these alterations was DCC and p53, whereas p53 and K-ras was extremely rare. Cases with mutation of guanine to thymine (Gà T) which occurred in K-ras codon 12 and DCC LOH were found to be more aggressive than other cases with codon 12 mutations and DCC wild-type phenotype. Fourteen patients developed recurrence, 7 of whom had tumors with p53 or K-ras mutations or DCC LOH. K-ras gene mutations were found mostly in presence of a mucinous component within the tumor ($p=0.06$).
Nuclear staining of p53 was found in 54 % of the cases. Overexpression of the ras p21 were detected in 76% of the tumors. Ras p21 overexpression did not correlate with any of the clinicopathological parameters examined. Many tumors with p53 overexpression were localized at the left site ($p=0,005$). The 5-year disease free and overall survival rates indicated that no significance exists between the patients with or without these genetic alterations.
In conclusion, although none of these genetic alterations showed a significant prognostic value, specific mutation of K-ras gene and DCC LOH phenotype might have a predictive prognostic implication in colorectal cancer. Furthermore, distinct genetic patterns might be involved in the tumoregenesis of the left and right colon and mucinous colorectal adenocarcinomas.

P 181
DNA FLOWCYTOMETRIC ANALYSIS AND CYTOGENETIC ABERRATIONS DETECTED BY FLUORESCENCE IN SITU HYBRIDIZATION (FISH) OF COLORECTAL CARCINOMA
RAAFAT Amira,Professor of Pathology ,National Cancer Institute- Cairo University , Egypt; SHOMAN Soheir,Professor of Patholgy ,National Cancer Institute, Cairo Univ.,Egypt;
MOSTAFA Naglaa , Assistant Lecturer of Pathology, National Cancer Institute, Cairo Univ. Egypt and ABOULELA Mounir, Professor of surgery , National Cancer institute,Cairo Univ. Egypt

Colorectal cancer is one of the leading cancer sites in developed countries. It is also one with high mortality rates. Inspite of the utilization of numerous histopathologic and tumour markers, the clinical behaviour of colorectal cancer is highly variable with unpredictable prognosis.New prognostic markers and increased biologic understanding of the growth of the tumour are therefore needed which would help to identify patients at risk of recurrence and therefore aid in improving treatment strategies. This study was conducted on

45 cases of Egyptian colorectal carcinoma. Detection of DNA content and calculation of S-phase fraction (SPF)was performed by flowcytometry(FCM). Also, detection of numerical chromosomal aberrations of chromosomes 7, 17and 18 using FISH technique was done.It was found that 56.7%of cases were aneuploid, 52.9% in the hypotetraploid range , 23.5% in the near diploid and 11.8% for each of triploid and tetraploid ranges.SPF had a mean of 15.59%, ranging from 3.3% to 37.8%. Aneuploidy correlated with tumour size, grade, lymph node (LN) state and there was a tendency for aneuploid cases to be of metastatic Dukes C/D and to be distally located.Cases with high SPF tended to be more in distal tumours,metastatic Dukes C/D and in cases with more than 3 LNs and correlated significantly with tumour size.Aneusomy for at least 1 of the investigated chromosomes were present in 63.3%, being 53.3%, 26.7% and 43.3% for chromosomes 7, 17 and 18 respectively. Statistically significant correlation existed between chromosomes 7, 17,18 and LN deposits, chromosomes 7,17 aneusomies and tumour size and grade with high tendency of metastatic Dukes C/D to harbour high number of aneusomies.Statistically significant correlation existed between ploidy as detected by FCM and chromosomal aneusomies as detected by FISH and between chromosomes 7,17 and SPF.In conclusion, FCM is a rapid, sensitive and accurate method in evaluating thousands of nuclei for their DNA content and proliferative activity. Ploidy state correlated with tumour size, grade and number of LNs. Also, FISH is a more sensitive technique than classic cytogenetic ones, allowing rapid and straightforward result interpretation. The use of these techniques ,thus can help in improving treatment strategies for patients with colorectal carcinoma.

P 182
DNA PLOIDY, S PHASE FRACTION, P53 EXPRESSION AND CHROMOSOME # 17 COPY NUMBER ANEUSOMY IN COLORECTAL CARCINOMA IN EGYPT.

SHOMAN sohair,ABOU EL-ELA mounir, RAAFAT amira.
Departments of Pathology and Surgery, NCI, Egypt.

INTRODUCTION:
In Egypt high proportion of colorectal carcinoma(CRC) occurs below the age of 35 years and are associated with advanced disease at presentation .
AIM OF THE STUDY:
DNA ploidy, S-phase fraction (SPF), p53 Immunohistochemistry (IH) and chromosome # 17 aneusomy studied in a series of 30 patients below 35 years undergoining resective surgery for primary operable CRC to investigate whether these alternations have any clinical value in predicting CRC patient's prognosis.
METHODS:
DNA ploidy & SPF performed on tumour frozen tissues by flow cytometer (FMC) FAC scan B-D, chromosome copy number changes using non-radioactive fluorescent Insitu hybridization (FISH) using centromer specific DNA probe (D17Z1) for chromosome # 17 and p53 over expression by IH (M3566 –Dako cytomation) on paraffin embedded tissues. The median follow up time was 36 months.
RESULTS:
The majority of cases were males (79%) , distal colon in 46.6% with tumors > 5 cm in 70% of patients. DNA ploidy was associated with high Histologic grade (G3) ($p<0.05$), high SPF (>15.6) in 43 %, lymph node metastases ($P<0.01$), advanced Duke's stage (C&D) ($P<0.01$), lymph node metastases ($P<0.01$) and distal tumours ($P<0.001$). FISH showed chromosome #17 aneusomy in 26.6 %, (20 % deletion and 6% gain) while p53 over expression by IH in 59.4 %. No association detected between chromosome #17 aneusomy by FISH and p53 expression by IH.
CONCLUSIONS:
DNA aneuploidy, high SPF, p53 over expression are the hallmark of CRC in young Egyptian patients and are predictors of poor outcome.

P 183
EXPRESSION OF FASCIN PROTEIN IN COLORECTAL CARCINOGENESIS; RELATIONSHIP TO DECREASED EXPRESSION OF E-CADHERIN PROTEIN

Jin Hee Sohn, Seoung Wan Chae, Min Kyung Kim, Eo-Jin Kim
Department of Pathology, Kangbuk Samsung Hospital, Sungkyunkwan University School of Medicine, Seoul, Korea

Background: Fascin is an actin-bundling protein that induces cell membrane protrusions and increased motility, and is highly expressed in various transformed cells, and in specialized normal cells including neuronal, endothelial and dendritic cells. Methods: We evaluated the expression of fascin by immunohistochemistry in normal colonic mucosa, tubular adenomas and colorectal carcinoma, and investigated its relationship with E-cadherin expression and the various clinicopathologic factors. Results: Overall, variable fascin immunoreactivity was detected in 0% of 13 normal colonic glandular epithelium, and weakly in 52.6% of 16 adenomas, and weak to strongly in 40.9% of 115 colonic adenocarcinomas under study. Fascin immunoreactivity was high in poorly differentiated group compared with well to moderately differentiated group ($p<0.01$). And right side colon cancer showed slightly increase of fascin expression than left side one. Interestingly, fascin expression was inversely correlated with E-cadherin expression ($p<0.01$). And there was no significant correlation with the tumor size, metastasis or pathologic staging. Conclusions: In the multistep pathogenesis of colonic adenocarcinoma, fascin overexpression seemed to be a late event, and was associated with down-regulation of E-cadherin protein.

P 184
EXPRESSION OF TGF-Â2 AND SMAD4 IN COLON CARCINOMAS

Kouvidou Ch.(1), Karatapanis S.(2), Latoufis C.(3), Lianou E.(1), Kouvatseas G.(1), Anagnostakis D.(1), Vrettou-Aravani V.(1)
Departments of Pathology(1), Gastroenterology(2) and Oncology(3), "ELPIS" Hospital, Athens, Greece.

INTRODUCTION: TGF-â2, a potent natural antiproliferative agent, is believed to play an important role in suppressing tumorigenicity. This effect is mediated through Smad4, a tumour-suppressor gene, at chromosome 18q21.1, that affects gene transcription and controls cell growth.
PURPOSE: To study the expression of TGF-â2 and Smad 4 in colon carcinomas and to correlate them with pathological parameters and patient's survival.
MATERIALS AND METHODS: Formalin-fixed paraffin embedded tissue from 50 cases of colon carcinoma was stained by immunohistochemistry for TGF-â2 and Smad4 protein. Statistical analysis was performed using the Fisher's exact test, Kaplan-Meier method and log-rank test.
RESULTS: Smad4 nuclear and cytoplasmic staining was absent or reduced in 29/50 (58%) colorectal carcinomas, while in the remaining 21 (42%) Smad4 expression comparable with colonic mucosa was observed. A subset of poorly differentiated and mucinous carcinomas revealed normal Smad4 expression. TGF-â2 cytoplasmic staining expressed in all colon carcinomas and was overexpressed in 25/50 cases. We observed a tendency for a relationship between Smad4 and TGF-â2 in a subset of poorly differentiated and in advanced stage carcinomas. No statistical relationship between the above markers and survival was detected.

CONCLUSIONS: In poorly differentiated carcinomas the normal Smad4 protein expression may be linked to TGF-â2 overexpression, findings that may represent activation or dysregulation of the TGF-â2 signalling pathway. Inactivation of TGF-â2 gene occurs at an early stage of colorectal carcinogenesis, while inactivation of Smad4 is likely to be a late event.

P 185

HISTOLOGICAL AND IMMUNOHISTOCHEMICAL STUDY OF SPORADIC POORLY DIFFERENTIATED COLORECTAL ADENOCARCINOMAS

DANCIU Mihai*, IVAN Luminita**, FLOREA Niculina***, FERARIU Dan***, PLAMADEALA Petru*, MIHAILOVICI Maria-Sultana*
* Pathology Department, University of Medicine and Pharmacy "Gr. T. Popa", Iasi, ROMANIA
** Pathology Department, Armed Forces Hospital, Iasi, ROMANIA
*** Pathology Derpartment, Universitary Hospital "Sf. Spiridon", Iasi, ROMANIA

Sporadic poorly differentiated adenocarcinoma of colon and rectum are unusual findings. Although, TNM or Dukes systems of stages are the most important in establishing the five-year survival rate, the prognostic depends also on the histological type of the tumor. Hence, the necessity of distinction between these carcinomas and other variants (neuroendocrine carcinoma, large cell carcinoma).
Aims: Our purpose was to analyze the histological and immunohistochemical pattern of sporadic poorly differential colon carcinomas, in order to find reliable additional criteria in differentiating them from other types.
Material and methods: We studied eight cases of sporadic poorly differentiated enteric type colon adenocarcinomas. Selection of these cases was made considering histological aspects. All tumors were routinely processed (paraffin embedded, HE, van Gieson and Alcian blue staining). Immunohistochemical labeling included antibodies to Cytokeratin (cocktail), Chromogranin A and Neuron Specific Enolase and was considered to be positive if present in at least 10% of the tumor cells.
Results: Macroscopically, seven tumors were exophytic, large (mean size of 5.4 cm), ulcerated, infiltrating the subserosa of the colon. Only one tumor, localized in cecum, was 7 cm large, circumpherential, infiltrating the colon wall and penetrating an ileal loop situated at about 30 cm from ileo-cecal valve. Microcopically, all tumors were poorly differentiated, enteric type adenocarcinomas: large atypical tumor cells disposed in irregular cords or nests, with reduced glandular formation (under 10% of tumor mass). Immunostaining for Cytokeratin cocktail was largely positive in all tumors. The intensity of immunoreaction was similar in areas with reduced differentiation, glandular formation and in adjacent mucosa (with or without dysplasia). On the contrary, immunoreactivity for Chromogranin A and Neuron Specific Enolase was negative in these areas for all studied cases. Localization of the tumor, age and sex of the patient had no influence on immunoreactivity intensity.
Conclusions: Chromongranin A and Neuron Specific Enolase are important immunohistochemical markers helpful in distinguishing between poorly differentiated colorectal adenocarcinomas (with no neuroendocrine differentiation) and neuroendocrine carcinomas, when histological aspects are similar.

P 186

HYPOXIA INDUCIBLE FACTOR - 1Á INFLUENCES ANGIOGENESIS AND PROGNOSIS IN LOCALLY ADVANCED RECTAL CANCER

GAKIOPOULOU Hariklia1, THEODOROPOULOS George2, THOMOPOULOU Georgia1, LAZARIS Andreas1, NONNI Aphrodite1, PANOUSSOPOULOS Dimitrios2, BRAMIS John2, PATSOURIS Efstratios1
Depts of Pathology1 and Surgery2, Medical School, University of Athens, GREECE

Hypoxia-inducible factor 1á (ÇIF-1á) is a critical regulatory protein of cellular response to hypoxia and is closely related to the triggering of the angiogenic process through activation of the vascular endothelial factor (VEGF) gene. The disruption of apoptosis, which is mainly regulated by the bcl-2 anti-apoptotic gene and the death promoting p53, causes loss of programmed cell death and tumour progression. We investigated the relationship between hypoxia, angiogenesis and apoptosis and their prognostic impact in patients with advanced rectal cancer.
HIF-1á tissue immunostaining, assessment of angiogenesis profile, quantitation of apoptosis (apoptotic index) and expression of p53 and bcl-2 were carried out in formalin-fixed paraffin-embedded tumour tissue samples retrieved from 92 patients with locally advanced rectal cancer (T3,4/N+).
HIF-1á high reactivity was noted in 47.8% of the examined cases and its expression correlated significantly with lymph node metastasis ($p< 0.001$), low rectal location ($p = 0.016$), infiltrative growth pattern ($p = 0.039$), absence of peritumoural lymphocytic infiltration ($p = 0.037$), depth of invasion (pT4) ($p = 0.04$) and vascular invasion ($p = 0.001$). VEGF positive expression was detected in 44.6% of tumour samples. VEGF expression and microvessel density were associated with lymph node involvement ($p<0.001$). VEGF was found more frequently in larger in size and low-lying rectal carcinomas ($p = 0.003$ and $p = 0.029$). HIF-1á expression was directly correlated with VEGF up-regulation ($r = 0.64$, $p < 0.001$) and MVD ($r = 0.41$, $p<0.001$). VEGF expression was also closely interrelated with MVD ($r = 0.75$, $p<0.001$). In univariate analysis advanced grade, low rectal location, infiltrative pattern of tumour growth, vascular invasion, positive lymph node status, HIF-1á expression, VEGF upregulation and p53 accumulation were related to decreased disease-free survival. Regarding overall survival, all aforementioned variables, except for tumour location and p53 status, were proved to be statistically significant negative prognosticators. In multivariate analysis only high HIF-1á reactivity and positive lymph node status were emerged as independent variables of adverse prognostic significance.
HIF-1á and VEGF may play an important predictive and prognostic role in patients with locally advanced rectal cancer. HIF-1á may serve as a prognostic marker of

P 187

MOLECULAR MARKERS PREDICTORS OF SURVIVAL AND METASTASIS IN COLORECTAL CANCER

Ana María Dotor de Lama 1, Marina Pollán 2, Jose A. Aramburu 3, Mercedes Butrón 4, Rufo Rodríguez 5, José Palacios 1, Manuel Morente 1.
1 Molecular Pathology Program. Spanish National Cancer Centre (CNIO).
2 Cancer Epidemiology Unit. National Centre for Epidemiology. Carlos III Institute of Health.
3 Pathology Department of Hospital Universitario, Getafe.
4 Pathology Department of Hospital Xeral, Vigo.
5 Pathology Department of Hospital Virgen de la Salud, Toledo.
1 Breast and Gynaecological Cancer Group Leader . Molecular Pathology Program. Spanish National Cancer Centre (CNIO).
1 CNIO ´Spanish National Tumour Bank Network Leader.. Molecular Pathology Program

Introduction: Colorectal cancer is the second most common neoplasia in men and women and the second most deathful cancer in the west world.
Up to date, the most important variable in the outcome from colorectal cancer is the stage of disease at diagnosis (Dukes or TNM stage). Nevertheless, those classifications are not helpful enough to predict the prognosis of patients, mainly when intermediate levels of disease appear (Dukes B and C stage). In order to solve this issue, it is very important to identify molecular markers clearly associated to the outcome of patients.
Material and methods: With this objective, we analysed 198 (52% Dukes B and 48% Dukes C stage) colorectal carcinomas selected from the archives of 3 different Spanish hospitals. All cases were removed between 1997 and 1998. After the surgery 47% were treated with adjuvant chemotherapy (5-FU) while 53% of patients did not receive any additional treatment. Sixty two out of the total amount of the patients have developed metastasis after surgery. After a 5-year follow-up period, 47% of patients had died and 53% were still alive.
Four tissue microarrays (TMA) were constructed with paraffin embedded tissue samples. Thirty molecular markers were examined by inmunohistochemistry, including markers of apoptosis, cell cycle, proliferation, signalling, adhesion, repair genes and immunologic response. Conventional histopathological features of colorectal cancer were also evaluated.
Results: In the univariate analysis, most of molecular markers did not show any significant association with survival or metastasis. However, the over-expression of p21 and cyclin B1 were related with recurrent disease (p= 0,028 and p=0,039), and the loss of expression of p16 was also linked to distance metastasis (p= 0,007).
In addition, the over expression of cyclin D1 was associated with shorter survival (p= 0,037).
However, in current study the presence of lymphovascular invasion was considered the most relevant risk factor for disease recurrence, distal metastasis and survival in general (p<0,0001).
Conclusion: As a conclusion, this inmunohistochemical study of B and C Dukes stage of colorectal carcinoma on TMA reveals that the expression of p21, p16, cyclin B1 and Cyclin D1 could be used as prognostic markers of metastasis or survival.

P 188
PROGNOSTIC EVALUATION OF CD44 EXPRESSION IN CORRELATION WITH BCL-2 AND P53 IN COLORECTAL CANCER
ZIZI-SERBETZOGLOU Adamantia, ZAVRlDIS Harris, KATSAMAGOU Eleftheria,PAPATHEOFANIS Ioannis,ELEMENOGLOU Ioannis
Department of pathology, Tzaneio General Hospital, Piraeus, Greece

Colorectal cancer results from a series of genetic events which disorder the normal mechanisms controlling cell growth. The aim of this study was to investigate the expression of CD44 in colorectal carcinoma and examine its association with clinicopathological features,bcl-2,p53 and long term outcome.
MATERIALS and METHODS:A series of 100 patients underwent surgical resection of primary colorectal carcinoma at the III Department of Surgery , Tzanneio Hospital of Piraeus between 1995 and 1999.Colorectal cancer cases in non-inherited polyposis in adenomatous polyposis and in ulcerative colitis were not included in this study.Colorectal cancer cases which death occured in the immediate postoperative period were also excluded.
Paraffin embedded specimens from 61 patients with Dukes stage B and 39 patients with Dukes stage C colorectal adenocarcinoma were assessed. We determined the expression of CD44,bcl-2,P53 with 5year follow up.
RESULTS:ln our study low CD44 expression‹10%)was present in 30%,moderate CD44 expression (10%-50%) in 30% and extensive CD44 expression(>50%)in 40% of cases.Expression of CD44 was unrelated to patient sex and age but was related to tumor differentiation(p=0.0295),tumors stage (p=0.009)and tumor site. No significant association was demonstrated between CD44 and bcl-2 status. However there was significant evidence of an association between CD44 and P53 status in the 66 cases in which P53 had previously been assessed.When entered into a multivariate analysis model, which also included bcl-2 and P53,CD44 staining emerged as prognostic indicator variable.
CONCLUSSIONS: CD44 expression may be an indicator of poor prognosis in colorectal cancer patients.

P 189
PROGNOSTIC SIGNIFICANCE OF NUCLEOLAR ORGANIZER REGIONS (AGNORS) IN ADENOCARCINOMAS OF THE RECTUM
RADULESCU Doinita*, AMALINEI Cornelia*, STOLNICU Simona**, MOCAN Simona***
*Department of Pathology, University of Medicine and Pharmacy Iasi, Romania
** Department of Pathology, University of Medicine Targu-Mures, Romania
***Laboratory of Pathology, Municipality Hospital Targu-Mures, Romania

The prognostic significance of silver-binding nucleolar organizer regions (AgNORs) was evaluated in tissue sections of biopsies from 45 primary adenocarcinomas of the rectum prior to their curative resection. AgNOR index was correlated with five-year survival rate and various morphological parameters of the primary tumors such as malignancy grade, tumor and lymph node stage. A significant correlation between five-year survival rate as well as pT categories and the mean AgNORs number per tumor cell was found. There was no significant relationship between AgNORs content and grade of malignancy or pN categories. The most valuable variable to predict a poor prognosis were pN, pT, and mean AgNORs index. The analysisi of AgNORs may represent a useful pretherapeutic evaluation of the aggressiveness of the rectum adenocarcinoma.

P 190
RACK1 OVEREXPRESSION ASSOCIATES WITH HIGH GRADE AND LYMPH NODE METASTASES IN COLORECTAL CARCINOMAS
CUATRECASAS Miriam, ESPINOZA Paul, IGLESIAS Carmela, ROJO Federico, ALLENDE Helena, DE TORRES Ines, JIMENEZ Jose, TABERNERO Jose*, RAMON Y CAJAL Santiago
Pathology and Oncology* Departments, Vall d'Hebron University Hospital, Barcelona. Spain.

Introduction: The receptor for activated C kinase 1 (RACK1) is a protein kinase C-mediated (PKC) signaling enzyme. RACK1 is an adaptor protein that contains many domains that mediate protein-protein interactions, anchors activated PKC isozymes and other signaling enzymes and regulates cell growth. The function and levels of expression of RACK1 may help elucidate signaling pathways leading to carcinogenesis and could result in the identification of novel therapeutic targets.
Purpose of the Study and Methods: RACK1 expression was evaluated in 116 colorectal carcinomas between 2001 and 2003 in a prospective study, to asses the clinical utility of the levels of expression of RACK1 protein. Tissue microarrays (TMAs) representative of normal mucosa and colorectal carcinoma of all cases were performed, including areas from

the centre and infiltrative margin of the tumor. When present, additional TMAs from metastatic lymph nodes or adenomas where done. In order to assure the representativity of the areas we included 3 cores of 1,2 mm of each selected zone. Positivity was scored using the Hscore (range from 0 to 300) resulting from multiplying the intensity (0 to 3) by the percentage of positive staining. RACK1 levels were determined by immunohistochemical staining, using a monoclonal antibody (BD610177). Results were correlated with clinical, histopathological parameters, and survival. In a subset of cases Western-blot was also performed.
Results: RACK1 overexpression was observed in 61'2% (71) cases. Overexpression of RACK1 correlated with poor differentiation (grade) p=0.036 and presence of lymph node metastases (p=0.049). No differences were observed between RACK1 expression and tumor localisation, stage or depth of tumor infiltration. Interestingly RACK1 expression in adenomas showed only 16'6% overexpression (2/12), compared to 70% in concomitant carcinomas (p=0.010). No differences in RACK1 immunostaining were observed between the centre of the tumor and the infiltrative margin, neither between the primary tumor and metastatic lymph nodes (p=0.927). Western-blot analysis confirmed the high levels of the protein. Disease-free survival was not related to RACK1 expression (p=0.356).
Conclusions: We have found significant differences in expression of RACK1 in high grade and lymph node metastatic colorectal carcinomas. We propose that RACK1 expression can be a potential marker of worse prognosis in colon carcinoma and be used as a novel therapeutical marker.

P 191
SCREENING FOR ASSOCIATION OF HEREDITARY NON-POLYPOSIS COLORECTAL CANCER (HNPCC) WITH GENOMIC REARRANGEMENT IN HMSH2 OR HMLH1 GENES USING LEUKOCYTE-DERIVED GENOMIC DNA FROM PATIENTS
R. Salehi, M. Salehi, M. Mousazadeh, A. Karimi
Department of Genetics and Molecular Biology, School of Medicine, Isfahan University of Medical Sciences, Isfahan Iran

Background & Objectives:
Hereditary non-polyposis colorectal cancer (HNPCC) is an autosomal dominant disease due to germline mutations of human mismatch repair genes (MMR), mainly hMLH1 and hMSH2. Colorectal cancers associated with the HNPCC syndrome usually present in younger patients, show loss of mismatch repair (MMR) gene expression, and exhibit microsatellite instability (MSI). About 12% of sporadic colorectal cancers also show MMR loss and MSI.
Methods & Materials:
To evaluate the status of genetic lesions in hMLH1 and hMSH2 MMR genes in the peripheral lymphocytes of the patients and find out a prognostic criteria for detection of those who are at high risk to develop the disease in future, 25 individuals diagnosed with HNPCC included in this study.
A DNA sample isolated from peripheral blood leukocytes obtained from each of these probands was examined for genomic rearrangement using the multiplex ligation-dependent probe amplification (MLPA) method. The probe mixture included probes for each of the 19 exons of the hMLH1 gene as well as for each of the 16 exons of the hMSH2 gene.
Results:
Seventy percent of the individuals (18/25) were shown to have a genomic rearrangement resulting in the deletion of one or more exons of one of these two genes. Family cancer histories predictive of a high risk of HNPCC significantly associate with a genomic rearrangement in hMSH2 or hMLH1.
Conclusions:
Based on our results it is concluded that using MLPA to identify genomic rearrangements in the above mentioned genes could be considered an economic first step in screening for HNPCC as an initial assessment of gross genomic integrity in leukocyte-derived genomic DNA. This would be especially valuable when individuals undergoing testing are identified by clinical history to be at high risk, as this approach would bypass the logistical difficulties of tumor analysis (assessment of microsatellite instability and immunohistochemistry.

P 192
THE ROLE OF P53,C-ERB-B2 AND BCL2 IN COLORECTAL TUMORS
Suhail N Abdullah Al-Salam
Pathology department, Faculty of medicine and health sciences, United Arab Emirates University, Alain, UAE.
P.O.17666

Introduction
Colorectal carcinoma is the most common gastrointestinal malignancy and one of the three most common causes of cancer death in western industrialized societies. An important role for P53 gene mutation and c-erb-B2 and bcl2 genes overexpression in the development of colorectal carcinoma had been described .Difficulties in the diagnosis of superficial endoscopic biopsies from papillary rectal neoplasms do exist and this study admits a suggested tool to help the pathologists in making their decision on these lesions.
Objective
The aim of the study is to evaluate the use of immunohistochemical stains of p53, c-erb-B2 , and bcl2 in the diagnosis of papillary colorectal tumours in endoscopic biopsies and
to determine their roles in the pathogenesis of colorectal carcinoma.
Materials and methods
Seventy endoscopic biopsies of colorectal tumours were selected . Fifty biopsies were colorectal adenocarcinomas, 10 were villotubular adenomas, and 10 were villous adenomas .Another 10 biopsies of normal and chronic inflammatory bowel disease were also selected . 4 – micrometer sections were prepared and stained with streptavidin –biotin immunohistochemical method using monoclonal antibodies against P53,c-erb-B2,and bcl2 (DAKO).One section of each biopsy was stained with H&E stain. Suitable positive and negative controls were used. Diaminobenzidine (DAB) was used as a chromogen.
The results were compared with surgical specimens of total colectomy and proctocolectomy .
Results
Forty two(84%)biopsies of colorectal carcinomas , one tubulovillous adenoma (10%) and two villous adenomas (20%)showed positive staining for P53 while no case of chronic inflammatory bowel disease or normal mucosa showed any staining for P53.
Forty eight (96%) biopsies of colorectal carcinoma ,6(60%) tubulovillous adenomas,7(70%) villous adenomas,3 (60%)of the chronic inflammatory bowel disease biopsies and 2 (40%)biopsies of normal colonic mucosa showed positive staining for c-erb-B2. Twenty eight (56%) biopsies of colorectal carcinomas , 4 (40%)tubulovillous adenomas,6(60%)villous adenomas ,2 (40%)chronic inflammatory bowel disease biopsies showed positive staining for bcl2.While no stain for bcl2 was noticed in normal intestinal mucosa biopsies.
Conclusions
P53 immunostaining is an important tool in the differentiation between benign and malignant papillary colorectal neoplasms in endoscopic biopsies especially when combined with c-erb-B2 and bcl2 .

P 193
THYROID TRANSCRIPTION FACTOR-1 IMMUNOREACTIVITY IN COLORECTAL CARCINOMA
MICHALAK Sophie, KOFFI Emmanuel, JOSSELIN Nicolas, TRIAU Stéphane, SAINT-ANDRE Jean-Paul
Department of Pathology, University Hospital, 4 rue Larrey, 49933 ANGERS cedex 09, France

Introduction : Metastatic adenocarcinoma of unknown primary origin is a common but perplexing problem. Among the useful immunohistochemical markers, thyroid transcription factor-1 (TTF1) has revealed to be a sensitive and specific marker for adenocarcinomas of lung and thyroid origin. Two patients with a multinodular liver without known malignancy underwent liver biopsies at Angers Hospital ; the liver specimens showed an adenocarcinoma CK7- CK20+ TTF1+. A colorectal cancer (CRC) was discovered in each patient but no lung tumor. The aim of this study was to investigate TTF1 immunohistochemical expression in CRC.
Methods : We studied TTF1 immunoreactivity of 53 consecutive cases of CRC diagnosed between may to December 2004 on coloscopic biopsies (8 cases), surgical resections (34 cases) or both (11 cases).
Results : A nuclear TTF1-reactivity was observed in 5 cases (9%) : 2 cases with strong reactivity in more than 50% of cells, 3 cases with weak and focal reactivity in less than 5% of cells. When biopsies and tumor were evaluated for the same patient, the immunophenotype was the same.
Conclusion : TTF1 is a useful but not specific marker for lung and thyroid cancer. It must be used with other immunohistochemical markers to guide the clinician toward the primary tumor.

P 194
TUMOR HYPOXIA AND ACIDITY DRIVE STROMATOGENESIS AT THE INVADING TUMOR EDGE OF COLORECTAL CARCINOMAS
A Giatromanolaki(1), Ch. Charalampidis(1), MI Koukourakis(2), E Sivridis(1)
1Department of Pathology, Democritus University of Thrace Medical School, Alexandroupolis, Greece.
2Department of Radiotherapy/Oncology, Democritus University of Thrace Medical School, Alexandroupolis, Greece.

Stromatogenesis, i.e. the formation of new stroma at sites of tumour invasion for tumour invasion itself, occurs in complicity with host's peritumorous fibroblasts (Sivridis et al, 2004 Int J Surg Pathol 12: 1-9); it is a phenomenon of utmost importance for tumour growth and progression. In this study, we investigated the activation status of host's fibroblasts at the invading tumour edge, assessed as MIB1 proliferation index and thymidine phosphorylase (TP) expression. Our results were related to vascular density (VD), and certain qualities expected to occur in invading cancer cells, such as MIB1 proliferation activity, expression of TP, expression of endogenous markers of hypoxia (hypoxia inducible factor-1á or HIF-1á) and acidity (lactate dehydrogenase 5 or LDH5). Standard immunohistochemical techniques were applied in a series of 150 colorectal adenocarcinomas. Normal fibroblasts confronting the tumour edge showed a median MIB1 index of 2%, significantly more than the 0.3% growth fraction found in normal submucosal fibroblasts and significantly less than the median MIB1 index of 40% estimated in cancer cells. Normal peritumorous fibroblasts with a proliferation rate above median were virtually loaded with TP and supported by an increased vascular network. Cancer cells confronting these fibroblasts were characterized by a high MIB1 proliferative index, high HIF1á and LDH5 reactivity, and a clear trend to extramural extension. All these associations were statistically significant. It is suggested that an activated fibroblastic status at the invading tumor front, sets the stage for stromatogenesis and new blood vessel formation, facilitating deep transmural invasion in colorectal adenocarcinomas. This complicity of peritumorous fibroblasts in the overall aggressiveness of the colorectal tumours, occurring within the framework of cancer-stromal cell interactions, is apparently favoured from the altered micro-environmental conditions of hypoxia and acidity.

P 195
HEDGEHOG PATHWAY IN COLONIC LESIONS
ALINGER Beate, KRENNBAUER Stefan, DATZ Christian, ESTERBAUER Harald, ABERGER Fritz, BLAAS Leander, KOLLMANN Karoline, DIETZE Otto, HAUSER-KRONBERGER Cornelia

Colorectal cancer is one of the major forms of cancer in industrialized countries. About 10% of the colorectal cancer cases have a hereditary basis, including defined syndromes like familial adenomatous polyposis (FAP) and hereditary nonpolyposis colorectal cancer (HNPCC). The remaining 90% of colorectal cancers occur sporadic by spontaneous mutation of single genes.
Hedgehog signaling is a main regulation cascade in embryonic differentiation of the whole gastrointestinal tract and mutations of some components have been associated with birth defects like gut malrotation, imporforate anus or intestinal transformation of the stomach. In addition to their function in the embryo, the Hedgehog pathway members are present in postnatal and adult tissues including stomach, pancreas, small intestine and colon. Therefore unusual expression of Hedgehog components has been associated with benign and malignant lesions of stomach and pancreas, leading to our current investigations.
In the present study we examined the presence of the Hedgehog pathway in normal human colon using immunohistochemical methods. The antibodies used are directed against the majority of the components involved in the Hedgehog signaling cascade, including the ligands Sonic, Indian and Desert Hedgehog, the transcription factors Gli1, Gli2 and Gli3 as well as the receptor Patched. Additionally, 14 cases of benign and 14 cases of malignant lesions of the human colon have been investigated to prove alteration of the expression pattern. Malignant lesions of the colon mostly comprise adenocarcinoma and benign lesions comprise tubular, villous and tubulo-villous adenoma and hyperplastic polyps. Up- or down-regulation of the Hedgehog pathway has been examined.
In the normal colon tissue we detected expression of the ligands Sonic (Shh) and Desert Hedgehog (Dhh) within the lining epithelium, as well as the receptor Patched and the transcription factors Gli1 and Gli2 along the whole colonic crypts. Within all benign lesions a positive staining of Shh, Dhh, Gli1, Gli2 and Ptch was detected, but expression was not consistently distributed within the lesions than rather restricted to single cell aggregates. Some malignant lesions also displayed the same unique staining pattern, though Hedgehog activity was not detected in all malignancies examined. We conclude that the Hedgehog signaling cascade may be involved in the normal physiological renewing process of the colonic lining.

P 196
APPLICATION OF SPECIFIC ANTI-SENSE OLIGONUCLEOTIDS AGAINST HUMAN TELOMERASE RNA (HTR) ON CCL-247 COLON CANCER CELL LINE
Mansoor Salehi and Rasoul Salehi
Dept. Of Genetics and Molecular Biology
Medical School
Isfahan University of medical Sciences

Isfahan
Iran

Background & Objectives: Inhibition of telomerase activity is one of the most promising targets for cancer therapy, because telomerase activity is present in most malignant cells but undetectable in most normal somatic cells. Unlike an ordinary enzyme, telomerase has RNA and a protein component that are both necessary for telomerase activity. We targeted the RNA component, the telomerase RNA (HTR), which contains the template for the telomere sequence. It is shown that the majority of gastric cancers express high levels of HTR that is essential for cellular survival. In this study, we evaluated the ability of anti sense oligonucleotides against HTR (anti-HTR) to inhibit telomerase activity in human colon cancer cells.
Methods & Materials: Thio-phosphoramidated anti-sense oligonucleotides against HTR were transfected into the CCL-247 colorectal cancer cell line using FUGENE6-mediated DNA transfection technology. Different concentration of anti-HTR was applied and cell growth and cell cycle parameters were analyzed. Telomerase activity was measured by TRAP assay and the apoptotic features were studied by PI and Hoechst 33258 staining. Control oligonucleotides and normal fibroblast were used as control.
Results: Anti-sense oligonucleotides against HTER were successfully transfected to the cells and reduced the cell viability to 28%. This treatment also inhibited the telomerase activity of the cells by 70%, in a dose-dependent manner. The apoptotic cells rate was also increased to 33%.
Conclusions: Our results demonstrated that application of anti-HTR is a powerful approach that can inhibit telomerase activity in colon cell line and therefore probably have the potential to be considered for anti-cancer therapy.

P 197

LABEL-FREE ANALYSIS OF MICROSATELLITE INSTABILITY IN COLORECTAL CARCINOMA BY ON-CHIP ELECTROPHORESIS.

BARTA Nora, BALDUS Stephan E., DIENES Hans Peter, SALOWSKY Rüdiger*, and ODENTHAL Margarete.
Institute for Pathology, University Clinic Cologne, and
*Agilent Technologies Waldbronn Germany

Microsatellite instability (MSI) is caused by a failure of the DNA mismatch repair system and occurs frequently in various types of cancer. Since sporadic MSI are associated with approximately 10 to 15% of colorectal, gastric or endometrial carcinoma and impact clinical prognosis, MSI analysis is an important tool in clinical research and molecular diagnostics.
Aim: Given that conventional techniques used for MSI detection – e.g. polyacrylamide gel electrophoresis (PAGE) or capillary electrophoresis - turned out to be laborious or expensive, this study aimed to develop a simple and efficient procedure of MSI detection.
Methods: Forty cases with no (26 cases) or with MSI (14 cases) were selected out of a panel of 150 patients with colon carcinoma. Amplicons derived from areas of non-tumor (N) and tumor (T) tissues were analyzed by microfluidic based on-chip electrophoresis on the Agilent 2100 bioanalyzer.
Results: The results presenting a pattern of five microsatellite loci were compared with the findings obtained by fluorochrome-associated PAGE technology. In all cases, label-free microfluidic separation of the PCR amplicons resulted in highly resolved, distinct patterns of each of the five microsatellite loci. Detection of MSI could be demonstrated by microsatellite loci-associated, well defined deviations in the electropherogram profiles of tumor and non-tumor material and confirmed the classification of the MSI cases performed by conventional technology (95% concordance rate).
Conclusion: The presented data demonstrate that microfluidic chip technology is a simple, reliable and robust technology for MSI detection, which allows label-free analyses of microsatellite amplicons within 30 minutes.

P 198

ANTIBIOTIC-ASSOCIATED HEMORRHAGIC COLITIS CAN BE INDUCED BY KLEBSIELLA OXYTOCA IN AN IN VIVO RAT MODEL

Cord Langner1, Christoph Hoegenauer2, Eckhard Beubler3, Thomas A. Hinterleitner2
1Institute of Pathology, 2Department of Internal Medicine and 3Institute of Experimental and Clinical Pharmacology, Medical University of Graz, Austria

Introduction
Antibiotic-associated hemorrhagic colitis (AAHC) is a serious side effect of antibiotic treatment occurring mainly with broad-spectrum penicillins. Its cause is unknown, however, Klebsiella oxytoca can be found in the stool of affected patients, whereas Clostridium difficile is absent. Concomitant intake of non-steroidal anti-inflammatrory drugs (NSAIDs) by patients is common.
Methods
A strain of K. oxytoca resistant to amoxicillin-clavulanate (AC) was isolated from the stool of a patient with AAHC. Sprague Dawley rats received either K. oxytoca, AC and indomethacin [A], AC and indomethacin [B], K. oxytoca and AC [C], K. oxytoca [D], indomethacin [E] or AC [F]. Four days after exposure to K. oxytoca the animals were sacrificed and the colon was analyzed for presence of inflammation, epithelial damage, mucosal hemorrhage, submucosal edema and erosions applying an arbitrary histological score (0-3 points).
Results
Histological changes were most prominent in the right-sided colon while changes in the distal colon were less severe. Inflammation was seen only in group [A] and [C] animals with median scores of 1.4 and 1.0, respectively. Marked epithelial damage was seen in group [A] and [C] animals with median scores of 1.7 and 1.3, respectively, whereas the animals in the other four groups showed only focal epithelial alteration (median scores 0.2-0.3). Mucosal hemorrhage was again noted in group [A] and [C] animals only with median scores of 1.0 and 0.6, respectively. Submucosal edema was prominent in group [A] and group [E] animals with median scores of 2.2 and 2.3, respectively. However, mild changes were also seen in groups [B], [C] and [E] with median scores of 0.5-1. Finally, severe erosive changes were detected in group [E] animals (median score 2.5), and group [A] animals (median score 1.4), while in groups [B] and [C] mild changes (median scores 0.1-0.2) were found.
Conclusions
K. oxytoca isolated from a patient with AAHC induces a predominantly right-sided hemorrhagic colitis in an in vivo rat model. The administration of NSAIDs enhances the severity of disease.

P 199

INVESTIGATION OF CMV INFECTION AND ANGIOGENESIS IN PATIENTS WITH REFRACTORY CHRONIC ACTIVE ULCERATIVE COLITIS

Hadjileontis C, Fericean A, Kardasi M*, Alexopoulou E., Gerovassilis F*
Technicians: Assimori B, Apostolou G
Pathology and Gastroenterology* Departments
"Achillopouleion" General Hospital, Volos, Greece

OBJECTIVE: A number of cases with chronic ulcerative colitis (UC) are resistant to therapy. Cytomegalovirus (CMV) infection has been reported to be a cause of it. Besides, angiogenesis has also been reported to have a potent role in the course of the disease. This pilot study investigates the

impact of both CMV infection and angiogenesis in patients with refractory UC.
PATIENTS AND METHODS: Twenty patients with UC were studied (ten with chronic active and ten with chronic quiescent form). Six of the cases were resistant to steroid, 5ASA and/or azathioprine therapy. All cases were investigated for the presence of CMV both morphologically and immunohistochemically. Angiogenesis was evaluated quantitatively by measuring the number of newly formed vessels expressing CD34 and VEGF in sections of the bioptic material. Measurements were performed through an ocular millimetric grid at 400X magnification, by two different observers and were expressed as microvessels per square millimeter. Ten intestinal biopsies with normal findings were used as a control group for the above investigation.
RESULTS: There were no viral inclusions in H&E stained sections nor was the presence of CMV detected immunohistochemically in any of our cases. Microvessel density (MVD) was increased in all the cases with chronic active disease compared to both the quiescent form and the control groups ($p<0.05$). Furthermore all patients with refractory UC showed higher MVD within the lamina propria of the inflamed mucosa compared to the responding to therapy cases.
CONCLUSIONS: The above results do not indicate that CMV infection is responsible for resistance to therapy in our cases of refractory UC. We however suggest that a deficient response to therapy in chronic active UC may be due to increased angiogenesis which, together with other factors, seems to play an important role in the mechanism of tissue inflammation, ulceration and regeneration in UC

P 200
DIFFUSE ENDOCRINE SYSTEM AND LYMPHOCYTE SUBSETS IN COLONIC MUCOSA IN ULCERATIVE COLITIS
Botina AV, Solovyeva OI*, Rybakova MG (Dept pathology, St Petersburg state medical university; *Dept therapy, St Petersburg medical academy postgraduate study)

The diagnostics of ulcerative colitis (UC) is based on a complex of methods with obligatory colonoscopy and colon biopsy. The diagnostics is difficult, UC remains largely the diagnosis of exclusion. So, thorough evaluation of all the components of the mucosa could make the diagnostics more reliable. Cellular lining of the mucosa carries out multiple functions including antigen transfer to MALT of the gut and certain endocrine activity. Little attention has been paid to possible role of APUD elements of the mucosa in progression of the disease and their interaction with lymphocytes of the lamina propria.
THE OBJECTIVE of the present investigation was to study the lymphocyte subsets and endocrine cells in the colonic mucosa with special reference to EC-cells.
MATERIAL, METHODS AND RESULTS. 141 colon biopsies (3 from each of 47 patients with UC - from macroscopically inflamed and non-inflamed bowel) were studied by means of conventional morphology, morphometry and immunohistochemistry. Patients were placed in 3 groups, varying from remission to exacerbation, according to the degree of activity of the inflammation, judged by lymphocyte and leukocyte count. Endocrine cells were revealed by argyrophilic reaction as well as with antibodies against chromogranin A, serotonin (Dako Cytomation, Denmark). Differential lymphocyte subset count was performed in slices immunostained for CD20, CD8 (Dako Cytomation, Denmark), CD3, CD4 (Novocastra Lab, UK).
The total population of endocrine cells was increased in inflamed bowel, especially in exacerbation, with EC-cells comprising the majority of the population (up to 70%). T/B ratio showed considerable decrease, CD4/CD8 appeared to be slightly decreased. Statistical analysis showed negative strong correlation between total lymphocyte count and total population of endocrine cells in remission, in exacerbation the correlation was strong and positive. CD8+ lymphocyte count was high in both inflamed and non-inflamed bowel in exacerbation of UC.
IN CONCLUSION we speculate that endocrine cells of the bowel may be involved in the pathogenesis of UC.

P 201
RADIATION COLITIS: A DETAILED HISTOPATHOLOGIC STUDY AND CORRELATION WITH ENDOSCOPIC FINDINGS
Panelos I1, Batistatou A1, Katsanos KH2, Briasoulis E3, Tsekeris P4, Economou M2, Christodoulou DK2, Bai M1, Capizzello A2, Karavasilis V3, Tsianos EV2, Agnantis NJ1
1Department of Pathology, 2Hepato-Gastroenterology Unit (1st Department of Internal Medicine), 3Department of Oncology, 4Department of Radiotherapy, University Hospital of Ioannina, Ioannina , Greece

Introduction: Ionizing radiation is known to cause radiation colitis (RC). The histopathological features of irradiation-induced early and late changes in bowel mucosa have not been analyzed in detail
Aim: The aim of the study was to characterize the histopathologic features of radiation-induced colitis and to correlate them with the endoscopic findings.
Patients-Methods: Twenty-three patients (12 females, 11 males; median age 63 years), suffering from rectal, cervical or prostate cancer were enrolled in the study and were followed up for a median of 13.5 months (range 6-32 months). All patients were treated by a linear accelerator (6 MV, box technique), with a median daily radiation dose of 1.9 Gy and a mean number of fractions, 28. They also underwent three endoscopies (sigmoidoscopies): before initiation of radiotherapy, immediately after the end of radiotherapy and at least six months after the end of radiotherapy. During sigmoidoscopy at least three colonic mucosa biopsies were taken. A new endoscopic grading system based on the RTOG/EORTC late radiation morbidity scale for large intestine and on endoscopic grading systems for inflammatory bowel disease was used for endoscopic grading of bowel mucosa. Clinical diagnosis of RC was based on patient symptoms, on sigmoidoscopy findings and on laboratory tests.
Results: Based on the histological features noted, the cases were allocated to one of four groups: no changes, acute injury, early regenerative changes and late regenerative changes. In total 12/23 patients (52.2%) were diagnosed with radiation colitis (RC). Acute radiation colitis was diagnosed in 4/23 patients (17.4%). None of these cases exhibited "eosinophil crypt abscesses." The correlation of histologically defined phases of RC and clinical/endoscopic findings was poor.
Conclusion: Radiation colitis is very frequent in patients irradiated in the pelvic area. The discordance between clinical/endoscopic and histopathologic findings could reflect the absence of relation between the presence and extend of histologically-defined radiation colitis and radiation-induced morbidity and mortality. Furthermore, it strengthens the need for a more global concept of radiation-induced bowel injury, incorporating bowel symptoms, performance status, radiation characteristics (dose-duration-timing), a new endoscopy grading system, a detailed histological analysis, laboratory tests and hospitalization.

P 202
FULMINANT CYSTIC FORM OF PNEUMATOSIS COLI ASSOCIATED WITH KAPOSI'S DISEASE IN A MAN WITH A KIDNEY GRAFT.
BARDIER-DUPAS A (1), HOANG C (1), MOUQUET C (2), TURRIN N (3), MENEGEAUX F(3), CAPRON F (1)

(1) Department of surgical pathology, (2) Anesthesia-intensive care unit, (3) Department of digestive surgery, Hôpital de la Pitié – Salpêtrière, 91 bd. de l'hôpital 75634 Paris cedex 13.

We report a first case of fulminant cystic form of pneumatosis coli associated with Kaposi's disease. A 57 year-old-man with Kaposi's disease (skin and lymph nodes), who had a kidney transplantation five years before because of nephroangiosclerosis, suffered from a pyelonephretic syndrome. TDM revealed a wide parietal pneumatosis coli. A right ileocolectomy was performed. Grossly, pneumatosis coli appeared as round, polypoid lesions covered by normal mucosa. It was associated with several black spotty maculas. Microscopic analysis demonstrated multiple empty spaces in the submucosa lined by histiocytes. The maculas were Kaposi's lesions anti-HHV8 +.

Pneumatosis is primary in only 15% of cases. The other cases are secondary to various predisposing conditions. The fulminant form of pneumatosis coli rarely occurs in adults, in whom it is associated with drugs, chemotherapy or with ischemic and pseudomembranous enterocolitis. Pneumatosis coli is also described in acquired immunodeficiency syndrome (AIDS). Such cases have been reported to follow a benign course, even when associated with infectious colitis. Benign form of pneumatosis coli resolves spontaneously in up to 50 % . Rare cases of pneumatosis coli require immediate surgery.

P 203

THE EFFECT OF LAMIVUDINE TREATMENT ON THE PROGRESS OF HBE NEG-ANTI HBE POS CHRONIC HEPATITIS B (CHB). A THREE YEARS STUDY.

BARBATIS Calypso*, DELLADETSIMA Ioanna**, NOMIKOS Alexandros*, VASILIADIS Themis***, KITIS George****, EVGENIDIS Nikolaos***, PAPAIOANOU Maria*****, VOGIATZIS George*****
Deps of Pathology Hellenic Red Cross*, Laikon** Hospitals,Athens, Deps of Medicine Ippokration***, Papageorgiou**** Hospitals, Thessaloniki, Glaxo Smith Kline***** Athens, Greece

Introduction: Lamivudine is an effective drug for the treatment of CHB. Its long term effect on the activity and stage of CHB is still under investigation as it may induce viral mutations responsible for drug resistance and recurrence of inflammation.
Purpose of the study: A multicenter clinicopathological study of three years duration was undertaken in order to assess the long term effect of Lamivudine in patients with Hbe neg- anti Hbe pos CHB.
Materials: 137 patients entered the study (115• ‰, 22• Š) age 46.7+/- 11.7 years . A liver biopsy was performed at zero time (124/137), 12 months (109/124) and 36 months (39/124). HBV DNA serum levels were annually investigated.
Methods: Histological grade and stage were diagnosed using Ishak• fs classification system. Hbs and Hbc antigens were immunohistochemically detected, their topography was assessed and a semiquantitative method was used for evaluating the extent of their expression in hepatocytes. Statistical analysis was performed with the Wilcoxon Signed Rank Test and Mc Nema• fs chi Square statistic for alterations of grade, stage, Hbc, Hbs and serum HBV-DNA at zero time, 12 and 36 months (ms).
Results: Low HBV-DNA levels were sustained in 77% of patients at 36 ms (p=0.003) and they were unrelated to grade, stage or Hbs expression but with the extent of Hbc expression. There was statistically significant reduction of grade at 12 ms (p=0.0001) which was not altered at 36 ms. The stage of the disease remained steady throughout the study period with the exception of 3 cases with cirrhosis at 12 ms which returned to stage 3-4. There was marginal statistical significance of Hbc and grade (p=0.067) at zero time, which became significant at 12 and 36 ms (p=0.035, p=0.006 respectively). The quantity of Hbs expression was not altered throughout the study but an increase in submembranous localization was observed at 12 ms (p=0.035) with subsequent stabilization.
Conclusion: Lamivudine is a very effective drug for the treatment of CHB patients. It reduces the necroinflammatory response (grade), stabilizes the fibrotic process (stage) and results in sustained low HBV-DNA serum levels.

P 204

SIGNIFICANCE OF CORRELATION BETWEEN SEROLOGICAL MARKERS OF HEPATITIS B AND PATHOHISTOLOGY AND ULTRASTUCTURAL FINDINGS

DIMITRIJEVIC Jovan, DJOKIC Milomir*, BRAJUSKOVIC Goran**, KNEZEVIC USAJ Slavica**, ALEKSIC Anastazija***, NOZIC Darko*, SKARO MILIC Andjelija**
Department of Pathology, Institute of Urology and Nephrology, Clinic Centre of Serbia; *Clinic of Infective and Tropic Diseases and **Institute of Pathology, Military Medical Academy; ***Institute for Medical Research, Belgrade, Serbia and Montenegro

Needle biopsy of liver as reliable method in evaluation of disease activity with serological markers of Hepatitis B infection enable more detailed realization of histopatologic diagnosis. This study includes light microscopy (LM) and electron microscopy (EM) analyses of needle biopsy of 101 patients with Hepatitis B. Results of this analysis were compared with the level of serologic markers and antigens of HBV infection, which were collected contemporary with the biopsy. Analyzing of biopsy specimens demonstrated further types of lesions in liver tissue: minimal lesion (ML) in 10 biopsies and acute hepatitis (AH) in 17; chronic persistent hepatitis (CHP) in 51 biopsies; chronic active hepatitis (CAH) in 20 biopsies and cirrhosis (CH) in 3 biopsies. By recognition of pathohistological finding and correlation with serological markers of HBV infection we found that histology findings with advanced (high grade) necrosis in AH and CAH most frequently demonstrated the presence of HBeAg in distinction to the other antigens and antibodies of HBV infection, which were present with significantly lower quantity. In addition, the EM analysis in these morphologic categories most distinct demonstrated the ultrastructural lesions, particularly affection of the nucleoli of hepatocytes in the presence of HBeAg. This serological marker represents the viral infectivity factor and manifests the viral replication and hepatocyte destruction. This study confirms a direct proportion between hepatocyte necrosis, presence of HBeAg and changes in hepatocyte nucleoli, and therefore it contributes the recognition of pathogenesis of virus B hepatitis.

P 205

CORRELATION BETWEEN TGF-BETA1, VEGF, HGF, EGF, TGF-ALPHA AND FGF SERUM LEVELS AND NECROIMFLAMMATORY ACTIVITY AND FIBROSIS IN CHRONIC HEPATITIS C.

E. Janczewska-Kazek1, B. Marek2, D. Kajdaniuk 2
1. Department of Infectious Diseases, Medical University of Silesia, Chorzów
2. Department of Pathophysiology, Medical University of Silesia, Zabrze

Introduction: Liver fibrosis can be a result of chronic inflammatory processes of different etiology. The meaning of fibrosis is the accumulation of extracellular matrix components in liver parenchyma. This process is the result of disturbed balance between extracellular matrix protein

synthesis and degradation. It is supposed that growth factors taking part in classic 'wound healing' reaction may play the meaningful role in the similar process in the liver and their serum levels may reflect the intensity of liver lesions.
Aims: The aim of the study was evaluation of the mutual correlation between TGF-beta1, VEGF, HGF, EGF, bFGF, TGF-alpha levels and inflammatory activity grade and fibrosis stage, as an attempt to assess the role of growth factors in chronic hepatitis and fibrosis formation.
Methods: Study group included 100 chronic hepatitis C (CHC) patients (52 men and 48 women, mean age 42) with fibrosis (Scheuer score: inflammatory activity 1-4 points, fibrosis 1-4 points). Control group consisted of 30 HCVAb positive subjects (16 men and 14 women, mean age 41) with normal ALT level, none or minimal necroinflammation (Scheuer: 0 points) and without fibrosis (Scheuer: 0 points). Serum levels of TGF-beta1, VEGF, HGF, EGF, bFGF, TGF-alpha were measured by immunoenzymatic method. Correlation between studied growth factors levels and inflammatory activity grade and fibrosis stage was evaluated.
Results: Levels of TGF-beta1, HGF and TGF-alpha were significantly higher in study group than in control group (TGF-beta1 35,89 vs 32,37 ng/ml, p=0,023; HGF 1506,34 vs 1017,11 pg/ml, p=0,034; TGF-alpha 1,85 vs 0,26 pg/ml, p=0,0001). The significant negative correlation between VEGF, bFGF and TGF-alpha serum levels and the grade of inflammatory activity was observed (VEGF R=-0,40, p<0,01; bFGF R=-0,40, p<0,05; TGF-alpha R=-0,34; p<0,05). Only VEGF level correlated negatively with the stage of fibrosis (R=-0,30, p<0,05).
Conclusions:
1) HGF and TGF-alpha may play the role in chronic inflammation and liver fibrosis formation as well as TGF-beta1, which is well known fibrogenetic factor.
2) Increasing inflammatory activity is connected with decrease of VEGF, bFGF and TGF-alpha levels. All these factors have angiogenetic potential. It may suggest that liver tissue inflammation is connected with impaired angiogenesis. Levels of VEGF were also lower in patients with advanced fibrosis and cirrhosis.

P 206
IMPACT OF HEPATITIS C VIRUS PROTEINS ON HEPATIC PROLIFERATION
G Granier (1), U Hibner (2), E Antoine (2), Ch Marty-Double (1).
Y Service d'anatomie pathologique, Groupe Hospitalo-Universitaire Carémeau, CHU Nîmes.
f Institut de Génétique moléculaire, Centre National de Recherche Scientifique, Unité mixte de Recherche 5535, IFR 122, Montpellier. France

The development of the liver carcinoma during chronic Hepatitis C is barely known. Mice transgenic for the full Hepatitis C Virus (HCV), which we have bred, develop hepatocarcinoma without immune disease. That suggest that HCV proteins are sufficient to induce the liver carcinogenesis. The aim of this work was to study the role of hepatocytic proliferation in carcinogenesis during infection with HCV. The liver is the only organ that can regenerate by multiplication of hepatocytes after hepatectomy at least 70%. Materials: 16 C57Bl6 male mice transgenic for the full HCV open reading frame (FL-N/35 lineage): HCV+, and 15 control mice: HCV-, were used. 27 animals underwent hepatectomy of 75% (12 HCV+, 15 HCV-) and were compare to 4 mice which underwent a white laparotomy. The anaesthesia used was an association of Ketamine-Rompin (1mg/kg). Animals were sacrified at 4 points of kinetic (1, 4, 18 and 48 hours after hepatectomy). The evaluation of hepatocytic proliferation was analysed by 3 methods: a-quantification of the weight of liver after death of mouse compared without weight considered left in place after hepatectomy. b-Immunochemistry detection of BrdU after nuclear incorporation. c-transcriptional analysis by Dot blot technical of 9 genes whose expression during hepatic regeneration is known (early expression: cfos, cmyc, MKP1; delayed expression: p53, p21, mdm2, gadd45; late expression: cyclin A and E). Results: liver regeneration were incomplete 48 hours after partial hepatectomy in the mice HCV+ and HCV-. The liver weight quantification and nuclear marking with BrdU reveals a delay of regeneration of HCV+ hepatocytes. Cyclin A, 48 hours after hepatectomy, is the only gene to have been activated in HCV+ hepatocyte compared to control mice and HCV- mice. The difference transcriptional expression of cyclin A between HCV+ and HCV- animals is compatible with an entry of HCV+ hepatocyte delayed in phase S. Discussion: The delay of liver regeneration in mice HCV- observed in our study is different from the data in the literature. That can be explained by the hepatotoxicity of anaesthesia. Indeed we observed an early transitory toxic microvacuolar steatosis in all mice. No excessive proliferation of hepatocyte were observed in HCV+ mice. Besides our results suggest delay of liver regeneration in HCV+ animals. These results could be the direct consequence of HCV proteins expression in liver.

P 207
THE POTENTIAL ROLE OF STELLATE CELL ACTIVATION IN LIVER BIOPSIES WITH HEPATITIS C COMPARED WITH HEPATITIS C/DIABETES MELLITUS
AC Tsamandas, D Dimitropoulou*, A. Liava, C Gogos*, CD Scopa.
Departments of Pathology and *Internal Medicine University of Patras Greece

Background: Hepatits C virus (HCV) infection is a major cause of chronic liver disease. Steatosis is a common finding both in HCV and in diabetes mellitus (DM). Hepatic stellate cell activation, manifested by the expression of smooth muscle actin (áSMA), is a major factor responsible for fibrosis and its progression in chronic liver disease. In this study we assessed and compared the degree of stellate cell activation in liver biopsies of patients with HCV alone and in patients with HCV/DM.
Patients and Methods: A total of 50 liver biopsies were evaluated: HCV (n=35), and HCV/DM (n=15). All biopsies were immunostained with the antibody for smooth muscle actin (áSMA). A grading system on a scale of 0-3 was applied reflecting the percentage of stellate cell activation which occurred in each zone of the hepatic lobule. Statistical analysis (t-test and Wilcoxon rank-sum test) was implemented to determine if stellate cell activation differed at a given stage of fibrosis, grade of inflammation and steatosis in comparing the aforementioned groups.
Results: The mean stage of fibrosis for the HCV/DM and HCV group were 2.8 and 1.6 respectively (p<.0001). The mean grade of inflammation for the HCV/DM group and HCV group were 1.9 and 1.5 respectively (p=0.03). The mean grade of steatosis for the HCV/DM and HCV group were 1.1 and 0.5 respectively (p=0.01). The average grade of stellate cell activation for all zones for the HCV/DM group and HCV group was 1.3 and 1.2 respectively (p=.39). However, in both diagnostic groups combined, a significant stellate cell activation was observed in periportal areas (zone 1) and portal tracts for higher stages (>2) vs lower stages (<2) of fibrosis (p<0.0001). In addition, a statistically significant increase in stellate cell activation was observed in zone 1 for the HCV/DM group (mean=1.5) as compared to the HCV group (mean=1.2) regardless of stage of fibrosis (p=0.02).
Conclusions: The results of this study imply that the activated stellate cells are predominantly present in periportal areas (zone 1), which correlates with advanced stages (>2) of fibrosis. Periportal stellate cell activation is significantly

increased in the HCV/DM group as compared to the HCV group.

P 208

THE ROLE OF SIGNALING PROTEINS STAT, JAK, SOCS AND PIAS IN RESPONSE TO COMBINED INTERFERON THERAPY FOR CHRONIC HEPATITIS C.

Jiøí Ehrmann jr. 1, Kvìtoslava Aiglová 2, Jiøí Ehrmann 2
1 Laboratory of Molecular Pathology & Department of Pathology, Faculty of Medicine, Palacký University, Olomouc, Czech Republic
2 IInd Department of Internal Medicine, Faculty of Medicine, Palacký University, Olomouc, Czech Republic

The currently used standard treatment for chronic hepatitis C using a dual combination of IFN alpha/RBV is only successful in 50% cases. With the exception of some clinical and biochemical factors, degree of inflammation (grading) and degree of fibrosis (staging), there are no other known markers which may serve as valid predictors of response to therapy. Interference of HCV with signaling pathways modulated by JAK-STAT, ERK1/2, NF-kappa B and MAP proteins is one mechanism which may influence the interaction between HCV and interferon. These proteins regulate different cell processes such as activation of cytokines, activation of apoptosis, regulation of cell proliferation etc. Therefore, it is possible that impaired signaling or inhibition/dysregulation of some of these proteins by HCV infection may cause resistance to IFN alpha treatment.
The aim of study was immunohistochemical assessment and analysis of expression of STAT 2, 3 proteins, their inhibitors SOCS 2, 3 and PIAS 3 and proteins JAK 1 and ERK1/2 in liver biopsies of 23 patients with chronic hepatitis C treated by dual combination IFN alpha/RBV and subsequent correlation of the results of immunohistochemical analysis (histoscore) with histological picture and clinical response to treatment.
The results show increased expression of STAT 3, STAT 2 and ERK 1 proteins and decreased expression of SOCS 3 and SOCS 2 in hepatocytes of patients with more marked inflammation and fibrosis. In patients with sustained virological response there was increased expression of SOCS 3 and JAK 1 and decreased expression of SOCS 2. Relapse was associated with increased expression of SOCS 3 and PIAS 3. However, owing to the small sample size, the results only approximated statistical significance, but we suggest that proteins of STAT family and their inhibitors SOCS and PIAS probably play an important regulatory role during response to treatment for chronic hepatitis C
Supported by IGA MZ CR NR 7814/03 and MSM 6198959216

P 209

SPECTRUM AND INCIDENCE OF SYSTEMIC MANIFESTATIONS IN CHRONIC HEPATITIS C OF LOW ACTIVITY.

T.P.Nekrasova,S.Yu.Karpov,P.E.Krel,T.N.Lopatkina,T.N.Krasnova,S.Yu.Milovanova

The aim of the present study is to evaluate extrahepatic manifestations of chronic HCV-infection with low grade and stage. In 58 patients with chronic hepatitis C (CHC) liver biopsy tissue specimens were histologically investigated. The spectrum of changes from mild piecemeal necrosis in few portal areas, mild or moderate lobular necrosis to mild or moderate portal inflammation and fibrous portal expansion was defined. Grading was done according to Knodell scoring system, and staging - according to Scheuer system. The histology activity index fell between 3 and 8. The stage was 1 in all cases. Systemic manifestations were observed in 23 patients. In 12 of them they were associated with cryoglobulinemia. Systemic manifestations included cryoglobulinemic vasculitis with skin and joint involvement, cryoglobulinemic glomerulonephritis, arthralgia without cryoglobulinemia. Independent risk factors for development of systemic disorders in CHC of low activity comprised gender, age over 45, the disease duration and presence of cryoglobulinemia. CHC with low activity is characterized by high occurrence of systemic manifestations primarily associated with cryoglobulinemia.

P 210

ULTRASTRUCTURAL EVIDENCES OF THE LYMPHOCYTE APOPTOSIS IN CASE OF HEPATITIS C VIRUS INFECTION

Valerie Groma (1), Valda Zalcmane (1), Natalja Makarova (1), Faina Nigmatjanova (2), Baiba Rozentale (2)
1 - Laboratory of Electron microscopy, Institute of Anatomy and anthropology, Riga Stradins university, Riga, Latvia
2 - Latvian Center of Infectology, Riga, Latvia

Recent studies do not provide a definite answer on whether the effect of hepatitis C virus infection (HCV), with respect to other etiologic factors of liver damage, is more an up- or a down-regulation of apoptotic process. An electron microscopy still remains a significant contributor to the study of events in apoptosis. Cell membrane blebbing and nuclear chromatin changes are hallmarks of the apoptotic cell death. This study aimed an ultrastructural characterization of the intralobular lymphocyte involvement in apoptotic process along the course of an acute HCV.
The liver tissue biopsies obtained from patients (11) with an acute HCV were processed for conventional transmission electron microscopy and further analysis of apoptotic events taking place within the liver lobule. The intrahepatic lymphocytes distributed within the sinusoids lumen, sinusoidal wall, perisinusoidal space, and along the intercellular space between the hepatocytes were selectively estimated in this study.
A prominent condensation of lymphocyte nuclear chromatin, compaction of cytoplasmic organelles, blebbing, and fragmentation into a great number of rather small apoptotic bodies were constantly present within the lumen of sinusoids. Macrophages detected ultrastructurally and using an appropriate (CD 68) immunohistochemical marker were detected in the close vicinity to the apoptotic bodies. Paired lymphocytes were rather often in the perisinusoidal space. Lymphocytes apoptotic changes were much more less common in this area comparing with the sinusoids lumen. Lymphocytes invading the intercellular spaces between the hepatocytes were single and paired, in some cases invading lymphocytes extended deep enough toward the bile canaliculi. Many of them caused a prominent depression on the hepatocyte surface, and expansion of the intercellular space. Some of these lymphocytes showed a prominent nuclear chromatin condensation, compaction of cytoplasm, and blebbing. Detection of the hepatocyte apoptosis was rare, and was restricted to the cell cytoplasmic shrinkage.
We can conclude that electron microscopy used in this study provides the evidences on the cellular behavior during apoptosis, and reveals the peculiarities in the lymphocyte distribution, type of invasion and cell death events along the acute HCV.

P 211

IMPACT OF APOPTOSIS ON THE SEVERITY OF CHRONIC HEPATITIS C

Akl M*., Zakaria S**., El Hindawi A.***, Hammam O*., Yehia H.**, El Raziky M.**,
Ibrahim R#, Fakhry S.#, El Behairy N#
Pathology* , Tropical Medicine# , Electron Microscope** Departments ,Theodor Bilharz Research Institute. Tropical Medicine** and Pathology ***Departments, Faculty of Medicine, Cairo University.

Realizing that chronic hepatitis c (CHC) is one of the important health problems in Egypt, this work is designed to study the impact of apoptosis on the parameters concerned with the severity of the disease. The study involved 57 patients diagnosed as pure CHC, according to full clinical history , examination and laboratory investigations to exclude any other associated pathology. All patients were subjected to pelvi-abdominal sonography, upper endoscopy, rectal snips, liver needle biopsies, serological tests for viral markers and liver functions . Immunohistochemical (IHC) studies using both the monoclonals; anti-fas and anti p53 mutant gene were performed on liver sections. Five control cases were included. Electron microscopic (EM) study for a sample of 8 cases was performed.

Apoptosis was focally demonstrated in liver sections by Hx and E stain and via IHC technique by detecting the localization and distribution of Fas antigen (for apoptosis) within the liver tissue. Pathologically patients were classified according to the grades of inflammatory activity into 3 classes; patients with mild inflammatory activity (Gr 1); 38.6%, patients with moderate inflammatory activity (Gr 2); 29.8% and those with severe inflammatory activity (Gr 3); 31.6%, Clinicopathologically; significant elevation of ALT and AST levels were detected with Grs 2 and 3 inflammatory activity compared to both control and Gr 1, inflammatory groups. Fas positivity within hepatic tissue sections was found significantly correlated with the increasing grades of inflammatory activity, stages of fibrosis, serum ALT, AST, ALP, Albumin and HCV-RNA viremia levels in all the studied patients. EM study identified early and advanced ultrastrctural hepatocytic apoptotic changes . P-53 was over expressed in 29.8% of the studied liver cases and showed significant direct correlation with the increase in inflammatory activity.

It was concluded that apoptosis through Fas antigen is a main mechanism of liver cell injury in Egyptian pattern CHC and is in parallel correlation with its biological markers and grades of inflammatory activity. Hepatocytes in variable stages of apoptosis could be localized in periportal areas by fas antigen, light microscope and EM. Mutant p53 is over expressed in the precocious stages of CHC-related liver damage before carcinogenesis. We suggest the term: “apoptotic activity” instead of 'necro-inflammatory' activity, in describing CHC interface areas.

P 212

HEPATIC EXPRESSION OF ENDOTHELIAL NITRIC OXIDE SYNTHASE (ENOS) AND VASCULAR ENDOTHELIAL GROWTH FACTOR (VEGF) IN CHRONIC HEPATITIS C AND SCHISTOSOMAL LIVER DISEASE

BADAWY Afkar, and HAMMAM Olfat.
Department of Pathology, Theodor Bilharz Research Institute. Cairo, Egypt

Immunohistochemical hepatic tissue expression of endothelial nitric oxide synthase (eNOS) that has important function in inflammation and vasoregulation, and vascular endothelial growth factor (VEGF) which plays a role in new vascularization in liver tissue of patients with chronic hepatitis C (n=25),schistosomal liver disease (n=6) ,and mixed schistosomal and chronic hepatitis C infection (n=7) were semiquantitated and correlated to hepatic histological features of inflammation and fibrosis. Control liver tissue (n=5) were collected during cholecystectomy. In control liver eNOS and VEGF were expressed in endothelial cells lining sinusoids and portal vessels and in hepatocytes. Hepatic tissue with chronic hepatitis C or Schistosomal liver disease over expressed both eNOS and VEGF, this over-expression was insignificant versus control group and between each other. Hepatic tissue with concomitant chronic hepatitis C and Schistosomiasis had significant endothelial over-expression of eNOS versus livers with chronic hepatitis C ($p > 0.05$) and control liver ($p > 0.01$) ,and of VEGF versus livers with chronic hepatitis C ($p > 0.05$). Endothelial expression of eNOS and hepatocytic expression of VEGF significantly raised in higher degree of inflammatory activity and in higher fibrotic stage ($p > 0.05$) in hepatic tissue of chronic hepatitis C (with or without Schistosomal co-infection) .

In conclusion: endothelial NOS and VEGF over expressed in chronic hepatitis C and in Schistosomal liver disease without definite correlation between their expression suggesting different regulatory mechanisms. Endothelial NOS is expressed mainly by endothelial cells and to a lesser extent by hepatocytes which are the main cells expressing VEGF. Co-incidence of Schistosomiasis with chronic hepatitis C accentuates over expression of both eNOS and VEGF proteins indicating that Schistosomiasis is a risk factor for haemodynamic disturbance in chronic viral hepatitis.

P 213

POSITIVE CORRELATION BETWEEN IGF-IR EXPRESSION AND EXTENSION OF PARENCHYMAL LESIONS IN CHRONIC HEPATITIS C

Stefano JT 1, Correa-Giannella ML 1 , Ribeiro CMF 2, Alves VAF 1, Massarollo PCB 1 Machado MCC 1, Giannella-Neto D 1
University of Sao Paulo School of Medicine 1
Santa Casa de Misericordia de Sao Paulo 2

The Insulin-Like Growth Factor (IGF) system is an attractive target of study, since it may be modified by liver diseases and, reciprocally, it might play a relevant role in the evolution of some hepatic diseases. This system is comprised of two ligands, IGF-I and IGF-II, their specific receptors, IGF-IR and IGF-IIR, and the IGF-binding proteins. IGFs are peptides involved in proliferation, differentiation and inhibition of apoptosis of several cell types. IGF-IR was shown capable to mediate both IGF-I and IGF-II signalling, whereas IGF-IIR is only able to decrease the bioavailability of IGF-II. Although increased IGF-IR gene expression has been reported in hepatocellular carcinoma and in human hepatoma cell lines, studies assessing IGF-IR in chronic hepatitis C (CHC) and cirrhosis are scarce.

The objective of this study was to evaluate the hepatic expression of IGF-IR in patients with CHC. Thirty five patients with CHC were selected according to clinical, serological, and biochemical criteria. IGF-IR expression was determined by semi-quantitative RT-PCR and by immunohistochemical analysis of liver fragments obtained before treatment. In ten patients, liver biopsy was performed within one month after the end of combined treatment with *f*Ñ-2a or *f*Ñ-2b interferon and ribavirin for 48 weeks.

An increase of IGF-IR mRNA content was observed in hepatic tissue from all patients in comparison to normal liver. The immunohistochemical findings suggested these raises in mRNA content are related to increased IGF-IR expression in hepatocytes. There was a positive correlation between IGF-IR mRNA expression and the extension of parenchymal lesions. A statistically significant decrease in IGF-IR mRNA content was observed in patients who achieved sustained virological response after therapy with interferon-*f*Ñ and ribavirin, suggesting an improvement in hepatic damage. Previous studies demonstrated that normal hepatocytes in vitro do not proliferate in response to IGF-I probably due to downregulation of IGF-IR promoted by locally produced IGF-I. The finding of increased IGF-IR expression in hepatocytes in CHC raises the question whether IGF-I, together with other growth factors such as HGF and TGF*f*Ñ, directly participate in liver regeneration in this condition. It remains to be elucidated if IGF-IR upregulation results from direct activation of IGF-IR gene by HCV or if it is a consequence of chronic aggression to hepatic parenchyma.

P 214
POST-TRANSPLANT RECURRENT HEPATITIS C - IMMUNOHISTOCHEMICAL DETECTION OF HCV CORE ANTIGEN AND POSSIBLE PATHOGENIC IMPLICATIONS

Mario G Pessoa, Venancio A F Alves, A Wakamatsu; G Maertens, B van der Borght, Joaquim Guanaes; Linda Ferrell, Teresa Wright
Sao Paulo University, Sao Paulo, Brazil; InnoGenetics, Ghent, Belgium; University of California, San Francisco, CA

Background: The mechanisms by which severe cholestatic hepatitis develops after liver transplantation are not fully understood. Reports on immunohistochemical distribution of HCV antigens are still scarce, but recently, HCV immunostaining was suggested for early diagnosis of cholestatic forms of recurrent hepatitis C in liver grafts. Design: After purification, Rb246 pab anti-core (aa1-68) yielded specific, granular cytoplasmic staining in hepatocytes. Signal amplification through Peroxidase-anti-Peroxidase avoided endogenous biotin. Rb246 was applied to liver samples of explants of 14 transplant recipients, 7 with the most severe form of posttransplantation recurrence (group 1) and 7 with mild recurrence (group 2). We also detected immuno-reactivity at 2 time-points posttransplantation (6 mos and 2 years) in both groups. HCV-core Ag was semi-quantified from 0 to 3+ in each time-point. HCV-RNA was also measured on the different time-points by branched DNA. Results and Conclusions: In the early post-transplant time-point, 1 patient had a mild staining (1+) and 2 patients had a moderate staining (2+) in group 1, compared to 6 patients with no staining (0) and 1 patient with mild staining (1+) in group 2. Late post-transplant liver samples were not available in all patients, but only 2 had a mild staining in group 1, compared with no patients in group 2. Strikingly, on the pre-transplant samples, HCV immunostaining was strongly positive in group 1 and mildly positive in group 2. HCV-RNA was significantly higher in group 1, on both time-points post-transplantation. HCV-core Ag was not direct associated to HCV-RNA on the different time-points. These preliminary results suggest that strong HCV immunostaining in the explant is predictive of more severe disease recurrence.

P 215
GRANULOMAS IN LIVER BIOPSIES OF CHRONIC HEPATITIS C VIRUS.

MULARCZYK Marius (1), THEBAULT Sophie (1), DANJOUX Marie (2), CUZIN Lise (3), BARANGE Karl (4), KAMAR Nassim (5), VALMARY Sèverine (2), SELVES Janick (2).
1: Service de Médecine Interne, 2: Service d'Anatomie Pathologique, 3: Service des Maladies Infectieuses, 4: Service d'Hépatologie, CHU Purpan, place du Dr Baylac, 31059 Toulouse. 5: Service de Néphrologie, CHU Rangueil, Avenue J Poulhès, 31403 Toulouse.

Introduction : Granulomas are well known findings in the liver biopsies of hepatitis C Virus (HCV)-infected patients. Frequency of those lesions is variously appreciated, from less than 1 to more 10%. The prevalence of granulomas and their relation to the severity of the liver disease will be discussed.
Methods : Between 01/01/2000 and 31/12/2003, 1654 liver biopsies were done in HCV-infected patients and read in a single pathology university laboratory. All results were retrospectively analysed in search for granulomas.
Results : Sixty four biopsies (4%) showed granulomas. Among those, 34 were steatosis-associated lipogranulomas, and 30 corresponded to true epithelioid granulomas. Only the 30 epithelioid granulomas were included in further analysis. They were classified in 3 groups. Group 1 consisted of 13 biopsies, showing granulomas surrounding exogenous inclusions (9 from patients undergoing dialysis and 4 drug-induced granulomas). Group 2 consisted of 7 biopsies with known aetiology: 2 sarcoidosis, 2 tuberculosis, 2 primary biliary cirrhosis (PBC), and 1 atypical mycobacterial infection in an HIV-positive patient. Group 3 consisted of 10 biopsies (0.6% of 1654) with no evident aetiology apart from HCV-infection. Two out of these were portal tracts' epithelioid granulomas surrounding biliary ducts, with associated cirrhosis. These patients had negative anti-mitochondrial antibodies (AMA). The last 8 presented with small and lobular epithelioid granulomas, with moderate fibrosis (less or equal to F2 for METAVIR score) excepted in one patient who had cirrhosis.
Conclusion: In our study, HCV-related granulomas without any other known aetiology were rare (0.6%) and of mild severity. Nevertheless, we found 2 isolated cases with particular pathological features consisting of cirrhosis with portal epithelioid granulomas surrounding biliary ducts in patients with negative AMA. These histological lesions evoke "PBC-like" disease.

P 216
STEATOSIS IN CHRONIC HEPATITIS C. CORRELATION WITH SPECIFIC HCV GENOTYPE AND METABOLIC CO-FACTORS

TZIOUFA Valentini1, RAPTOPOULOU Maria2, SINAKOS Emmanouel2, BOBOS Mattheos1, ORPHANOU Eleni2, LALA Thaleia2, GIGI Eleni2, VRETTOU Eleni1
1 Department of Pathology
2 2nd Department of Internal Medicine, Hippokration Hospital
Both of Aristotle University of Thessaloniki, Medical School

Introduction: Liver steatosis plays a central role in the pathogenesis and disease progression of chronic hepatitis C. Evidence has shown that HCV genotype 3 infection is associated with higher rates of steatosis and this is due to a cytopathic viral effect. The aim of the present study was to correlate the occurrence and severity of liver steatosis with the presence or absence of co-factors in chronic HCV genotype 1 and 3 infection.
Material and Methods: We have retrospectively assessed steatosis in biopsy specimens from 239 patients with chronic hepatitis C. Biopsies were divided in a) Group A: 125 biopsies from patients with no metabolic co-factors and Group B: 114 biopsies from patients with metabolic co-factors (alcohol intake, type II diabetes, obesity, lipidemia). Our results were further analyzed according to HCV genotype.
Results: Group A: Steatosis was found to be present in a significantly higher rate in patients with HCV-3 infection (70.7%) compared to 56.2% of patients with HCV-1. In both HCV-1 and 3 infection steatosis was mainly of low grade (HCV-3: grade 1, 44.8%, grade 2, 12.2%, grade 3, 8.6% HCV-1: 37.5%, 12.5%, 6.3% respectively). Group B: The results were similar to those of Group A (57.1% for HCV-1, 70% for HCV-3). However, higher grades of steatosis were noticed, mainly in HCV-3 infection (HCV 3: grade 1, 25%, grade 2, 21.7%, grade 3, 23.3%. HCV-1: 31.4%, 29% and 5.7% respectively).
Conclusions: Our results show that a) HCV-3 infection is more frequently associated with the occurrence of hepatocyte steatosis b) Steatosis is mainly related to a viral effect and c) Metabolic factors aggravate steatotis produced by the virus itself.

P 217
LIVER CELL APOPTOSIS AND PROLIFERATION IN HCV INFECTED RENAL TRANSPLANT PATIENTS

Ioanna Delladetsima1, Paraskevi Alexandrou1, Mina Psichogiou2, George Nikolopoulos2, Alkiviadis Kostakis3, Angelos Hatzakis2, John Boletis3

1Dept of Pathology, Laiko General Hospital, 2Dept of Hygiene and Epidemiology, National Retroviral Center, Athens University Medical School, 3Transplantation Center, Laiko General Hospital, Athens, Greece.

Background-Aims: The role and prognostic significance of hepatocellular apoptosis and regeneration in liver disease of HCV infected renal transplant patients (RTx) remain unclear. In the present study hepatocellular apoptosis and proliferation activity (PA) were assessed in liver biopsies (LBs) of RT patients with HCV infection and were correlated with hepatitis-necroinflammatory activity (grade and stage), disease outcome, viremia and genotype.
Methods: Ninety liver biopsies including 31 follow up biopsies were examined histologically. DNA fragmentation was detected by TUNEL assay and PA by immunohistochemical ki67 expression. Apoptotic index (AI) and PA were defined by the number of positive hepatocytes per 10 High Power Fields (1000 cells)and were classified in three categories ranging from 0-5 cells and from 0-1,35 cells respectively. HCV RNA levels and genotype were also determined.
Results: Histological evaluation revealed no significant changes in 8 (13,6%), acute hepatitis in 2 (3,4%) and chronic hepatitis in 49 (83%) cases. A low apoptotic index (AI) (0-2,5) was observed in 31 (52, 5%) and a high (>5) in 12 (20,3%) cases. There was no PA in 22 (37,9%) cases whereas it was >1,35 in 17 (29,3%). By univariate analysis the AI showed a significant correlation with viral load, resulting in 1 log10 higher HCV RNA levels in those patients with high number of apoptotic cells (p=0,003). This finding was verified by multivariate analysis (OR=6,67, 95% CI 1,4-30,9, p=0,015). Both variables did not show any significant correlation with hepatitis grade and stage, disease progression and genotype, whereas a significant positive correlation was observed between AI and PA (p=0,03).
Conclusions: Apoptotic cell death seems to be pathogenetically associated with high viral load probably through a direct cytopathic pathway. The low PA points towards a suppressed liver cell proliferation, which may be linked to viral effects and/ or the immunosuppressive therapy.

P 218
A STANDARDIZED AND COMPUTERIZED PATHOLOGICAL REPORT FOR CHRONIC HEPATITIS C : A SIX YEARS EXPERIENCE.
LE BAIL Brigitte, BIOULAC-SAGE Paulette

Since 1999, we have been using a standardized and computerized pathological report (SCPR) for liver biopsies with chronic hepatitis C in our department of Pathology, with annual revision of its content. Here we present the initial SCPR, its evolution, and the evaluation made by clinicians and pathologists.
The SCRP was developed by one of us in May 1999 on Diamic ® laboratory sofware (Infologic, France), based on a Word interface. It consists in a basic text with missing items to be filled using a panel of predetermined and preregistered answers, with either simple or multiple choice; after that, modifications/addition of data can be made. At first, the basic text and the answers were stricly based on the grid and the algorithm for histological evaluation published by the METAVIR group.
For 6 years, 1718 reports were made by 3 pathologists. They used the SCPR immediately and systematically. This adhesion was favored by the previous use of a paper form for METAVIR grid. Further changes included the introduction of new answers, the development of multiple choice items and of an arborescence of answers, all resulting in more accuracy and flexibility in the description of histological parameters, and in the conclusion, possibility to notify the degree of diagnostic fiability, and to add a secondary diagnosis with clinical consequences, such as steatohepatitis, auto-immune hepatitis, iron overload, or liver cell dysplasia. As a mean, the SCPR is now one full page, 400 words, and 31 lines. During the last revision based on 200 consecutive SCPR, we found 149 (74.5%) reports to be strictly conform to the bible text; for the remaining 25.5%, the small variations observed had to do with the evaluation of fibrosis: difficulties in establishing the stage of fibrosis (n=22) or quantification of peri-centrolobular/-cellular fibrosis, which lead us to the last modifications.Clinicians find this SCPR very well adapted for the diagnosis, prognosis and follow up of patients with hepatitis C, either isolated or associated with other hepatopathies. Pathologists appreciate the quickness of the making the report (120 seconds as a mean), and its didactic and pedagogic values. Furthermore, all necessary data are present and ready for statistical evaluation without reexamination of the slides.
In conclusion, the SCPR for hepatitis C reporting appears as a simple, quick, systematic, reproductible and flexible tool adapted to the clinicians and pathologists needs.

P 219
CORRELATION BETWEEN INTRAHEPATIC EXPRESSION OF HLA-DP / DR, INTERCELLULAR ADHESION MOLECULES AND T HELPER LYMPHOCYTES IN CHRONIC VIRAL B AND C HEPATITIS
BUTUR Georgeta 1, CEAUSU Mihai 1, VASILESCU Florina 1, IOSIF Cristina 1, FLOREA-GRAMADA Zenaida 1, ANDREI Florin 1, ARDELEANU Carmen 1
1 – "Victor Babes" National Institute of Pathology, Bucharest, Romania

The specific cellular immune response in the liver against HBV and HCV chronic infections requires the cooperation between professional and occasional antigen presenting cells (APC) e.g.: Kupffer cells, macrophages, hepatocytes, endothelial cells and lymphocytic subpopulations.
The aim of the study was the assessment of HLA-DP / DR expression and intercellular adhesion molecules on hepatocytes, correlated with activated level of CD4 helper T cells in chronic viral hepatitis.
Indirect tristadial immunohistochemical ABC method was performed on liver biopsies taken from 20 patients with single and double infections, using HLA-DP, HLA-DR, CD54, CD44, CD4 antibodies.
Using regressive biostatistic analysis, a positive direct correlation between HLA-DP/DR and CD44 was observed ($r = 0.46$) with statistical significance ($p = 0.04$). In double infections ($n = 5$ cases), HLA-DP/DR expression had a positive correlation with CD4 ($r = 0.56$), but without statistical signification ($p = 0.3$). In HCV infections, a positive correlation statistically highly significant, between CD44 and CD54 was found ($r = 0.78$, $p = 0.002$). Between CD44 expression and CD4+ infiltrating cells, a negative correlation statistically significant was established ($r = - 0.6$, $p = 0.008$). Activated level of CD4+ lymphocytes assessed by CD44 had a negative relationship ($r = -0.44$), statistically significant ($p = 0.04$).
During hepatic chronic viral infections, decreasing of T helper cells number in inflammatory infiltrate is associated with a significant activation degree of the same lymphocytes and with an increased expression of accessory molecules on hepatocytes, suggesting a by-pass of professional APC which can maintain a necro-inflamatory microclimate.

P 220
HEPATOCYTE APOPTOSIS IN CHRONIC HEPATITIS C: A PROMINENT FEATURE OF DISEASE SEVERITY IN EGYPTIAN PATIENTS

Akl M*., Zakaria S**., Hammam O*., El Raziky M.**
Yehia H.**, Fakhry S.#, Seyam M# ,Ibrahim R#, , El Hindawi A.***, El Behairy N#
Departments of* Pathology , #Tropical Medicine , and **Electron Microscopy ,Theodor Bilharz Research Institute, Departments of **Tropical Medicine ,and ***Pathology, Faculty of Medicine . Cairo University.

Background and Aims: Chronic hepatitis C virus (HCV) is a major health problem in Egypt, where genotype 4 is the most prevalent. There is increasing evidence, from recent studies, suggesting that liver damage in chronic HCV genotype 1 and 3 is mediated by the induction of apoptosis. The aim of this study were to assess hepatocytic apoptosis in chronic HCV patients, correlate it with disease severity, and to identify possible mechanisms of apoptosis induction.
Methods: The study included 57 selected patients diagnosed on clinico-pathological and virological basis as chronic HCV , in addition to five control cases. Liver specimens were studied according to the grade of inflammation, stage of fibrosis and extent of steatosis. Immunohistochemical (IHC) studies using both the monoclonals; anti-Fas and anti-p53 mutant gene were performed. Electron microscopic (EM) study for 8 cases were done.
Results: Apoptosis was focally demonstrated in routinely stained liver sections and intensely by detecting Fas antigen expression in 84.2% of patients compared to no expression in controls. A positive correlation was observed between Fas expression and grades of inflammation , stages of fibrosis, serum alanine amino-transferase (ALT), aspartate amino-transferase (AST), alkaline phosphatase (ALP) , and viral load. p53 was over expressed in 29.8% of patients, showing significant direct correlation relative to the grades of activity, stages of fibrosis, serum albumin and bilirubin levels, ALP and viral load. Significant direct correlation were detected between hepatic steatosis and both Fas and p53 positivity. EM study identified the ultrastructural features of apoptotic changes within hepatocytes.
Conclusions: Hepatocyte apoptosis through Fas antigen expression is significantly increased in Egyptian patients with chronic HCV and correlates with disease severity. We suggest the term "apoptotic activity" instead of "necroinflammatory activity" in describing chronic HCV interface areas. Mutant p53 is over expressed in the precocious stages of HCV related liver damage before carcinogenesis indicating close follow-up.

P 221
HISTOPATHOLOGICAL STUDY OF CHRONIC HEPATITIS C: EVALUATION OF PERISINUSOIDAL FIBROSIS AND COMPARISON OF SCORING SYSTEMS

CELIKEL Cigdem Ataizi*, AKPULAT Sertac*, TIFTIKCI Arzu**, AVSAR Erol**
Marmara University School of Medicine, Departments of Pathology* and Gastroenterology**

Background/Aims: Needle liver biopsy has been shown to be the "gold standard" in assessing the histopathological degree of liver damage which is essential for the routine care of patients with chronic hepatitis C virus (HCV) infection. Several scoring systems have been proposed to standardize the morphological features seen in HCV. Although it is a characteristic feature for steatohepatitis, it is well known that perisinusoidal fibrosis may also be seen in viral hepatitis. In this study, our aims were to determine 1) the interobserver reliability of the different scoring systems, 2) the correlation between the scoring systems, 4) the correlation of necroinflammatory activity in different scoring systems with the serum transaminase levels, 3) the incidence of pericellular fibrosis in HCV and its relation with different histopathological features. Methods: Liver biopsies stained with H&E and trichrome from 96 chronic HCV cases were re-examined and scored by two independent pathologists using Knodell, METAVIR, Scheuer, and Ishak systems. Pericellular fibrosis was scored semiquantitatively according to Brunt et al. (0= no fibrosis, 1= <33%, 2= 33-66%, 3= >66%). The results were analysed using Kappa statistics and chi-square test. Results: While all the systems used produced moderate agreement when necroinflammatory score (NIS) was assessed, the ISHAK system produced slightly higher (k=0.64) values. NIS showed poor correlation with serum transaminases in all systems (k< 0.30) except Ishak score which was moderate (k=0.47). Concordance between the different scoring systems is good for NIS, and excellent for fibrosis score. Perisinusoidal fibrosis was present in 54.2 % of the cases and no correlation could be identified with any of the histopathological features including degree of steatosis and pericentral necrosis. Conclusions: While all systems produced reasonable agreement, this was greater in the Ishak system, especially concerning NIS. Perisinusoidal fibrosis was not a rare morphological change which had no relation with any of the histopathological features examined and its role in the prognosis of HCV patients needs to be determined with prospective studies.

P 222
CORRELATION BETWEEN IFN-MEDIATED SIGNAL PROTEINS EXPRESSION LEVELS IN LIVER TISSUE AND THE PREVALENCE OF HCV INFECTION.

Dolores Bautista*, Alicia Millan* and Elena Baixeras§.
*Department of Pathology and §.Fundación IMABIS. Hospital Regional Universitario Carlos Haya. Málaga. Spain.

Hepatitis C virus (HCV) affects to 2% of occidental population. Interferon (IFN) is the main antiviral agent. At present, patients with chronic hepatitis C are treated with recombinant IFNa in combination with ribavirin. However, only 30% of patients are responders to this therapy. The molecular mechanisms of HCV and IFNa interactions are not fully solved. IFNa subtypes constitute a family of 13 polypeptides coded by different genes that interact with the same receptor while eliciting distinct antiviral and antiproliferative actions. Recently, in vitro data demonstrated that HCV is able to counteract the IFN signal at very early stages affecting Jak/STAT pathways. Thus, it suggests that HCV bypasses endogenous IFN-mediated signal probably making useless the current therapies with IFN in the majority of patients. In the present study we focus our interest on the expression of proteins involved in IFNa mediated signalling pathways in tissue liver samples from HCV patients and control donors. We sought to determine the correlation between the presence of HCV and the physiological expression levels of STAT proteins and their protein activation modulators (SOCS) that could explain the failure of IFN treatment in the majority of HCV patients. To this aim, we have developed tissue arrays technology and analysis by microscopy. We found robust and higher expression levels of STAT1 and STAT2 in HCV patients when compared with healthy donors. Moreover, expression of these proteins are restricted to nuclear localization in hepatocytes, thus indicating that at least the early-IFN response is functional in these patients. SOCS protein expression were also investigated and results are discussed.

P 223
HEPATIC STEATOSIS IN EGYPT . A CLINICAL AND PATHOLOGICAL PROFILE

Zakaria S, Akl M*, Nosseir M*, El Raziky M,Zakaria S, Akl M*, Nosseir M*, El Raziky M, Amer A, Anwar H, Abu-Madian A.
Department of Tropical Medicine, Faculty of Medicine, Cairo University,
Pathology Department*, Theodor Bilharz Research Institute.

Cairo - Egypt
C,Anwar H, Abu-Madian A.
Department of Tropical Medicine, Faculty of Medicine, Cairo University,
Pathology Department*, Theodor Bilharz Research Institute.
Cairo - Egypt

Bright liver is not an uncommon abdominal ultrasonographic finding in the daily medical practice. Objectives: This study aims at evaluation of the clinical, laboratory and pathological aspects of cases presenting with Simple Steatosis (SS) and Non Alcoholic Steato-Hepatitis (NASH) in Egypt.
Methods: Seventy five subjects with bright liver by abdominal ultrasonographic examination were enrolled for this study. According to their virological markers they were selected so as: 60 subjects were sero- negative for chronic hepatitis B(HBV)and chronic hepatitis C (HCV), whereas 15 subjects were anti- HCV sero- positive. All patients were subjected to full clinical and laboratory investigations with special emphasis on risk factors of hepatic steatosis, and to needle liver biopsy.
Results: Hepatic Steatosis is a disease of both sexes, female: male ratio is 1.9:1. It occurs mostly in the fourth and fifth decades of life. Risk factors are: obesity, diabetes mellitus, hypertriglyceridemia. Main complaints are easy fatigue, right hypochondrial pain. On histopathological assessment: NASH was present in 60% of the studied patients among whom mixed micro and macro vesicular hepatocytic steatosis was noted with moderate and severe affection. Eighty-seven percent of patients with SS had a micro steatotic pattern with minimal to mild degree of affection. Chronic hepatitis C patients exhibited micro vesicular pattern in 46.7% and mixed pattern in 53.3% of biopsies. ALT and triglycerides were significantly higher in NASH than SS with positive correlation between their levels and histopathological scoring of hepatic steatosis. AST/ALT ratio was <1 in 90% of cases.
Conclusion: NASH is an emerging disease entity in Egypt which might be a cause of progressive chronic liver disease.

P 224

MORPHOMETRICAL STUDY OF HEPATIC FIBROSIS AND NECROINFLAMMATORY GRADE BY REPEAT LIVER BIOPSY IN PATIENTS WITH CHRONIC HEPATITIS C (HCV), THE ROLE OF VIRUS GENOTYPE AND TREATMENT.

KIRICHENKO Yury, MATSIONIS Alexandre,
*ROMANOVA Elena, *AMBALOV Yury, POVILAITITE Patritsia
Rostov Regional Bureau of Pathology,
*Rostov City Centre of Hepatology, Rostov-on-Don, Russian Federation

Introduction. Prognosis of chronic HCV infection depends on fibrosis progression in the liver. Previous data concerning rate of fibrosis progression and results of HCV therapy show possible significance of virus genotype and necroinflammatory grade. Semi quantitative assessments of fibrosis and necroinflammation are currently regarded as a routine procedure, but it is obvious that these methods are subjective. Alternative method is comparative morphometrical analysis of repeat liver biopsies.
Aim. The aims of this study were to assess rate of fibrosis progression by investigation of primary and repeat liver biopsy HCV-infected patients and to identify factors, connected with prognosis.
Methods. Paired liver biopsies from 60 patients (age 26-45 years) with chronic HCV were studied. RT-PCR was used for detection of HCV-RNA and its genotype. Patients were non-treated before primary biopsy, 20 patients were treated by _ interferon/riboverin in standard dose between biopsies. The same pathologist scored paired biopsies from the same patient, applied V.J.Desmet (1994) and R.G.Knodell (1981) semi quantitative assessments. Software SigmaScan Pro 5.0 was used for morphometrical analysis. Sections were stained by Masson Trichrome method. Fibrosis index (FI) was calculated as collagen area divided all section area.
Results. Our results showed that 66,6% of patients had 1b genotype of HCV. Genotypes 2a and 3a were found rarely (12,5% and 37,5%). 12,5% of patients were with mixed genotype 1b-3a. Investigation of primary liver biopsy showed predominantly mild and moderate necroinflammation and fibrosis of liver in case of 1a or 1b HCV genotype, without significant difference (Knodell 5, Desmet 1-2, IF 0,01-0,03). Significantly marked necroinflammation (Knodell 9 and more) were in the biopsies from patients, that were infected 3a or mixed 1a-3b HCV genotype. Liver fibrosis stage (IF, Desmet) did not correlate to inflammation degree. Morphometrical investigation of paired biopsies showed that the majority of treated patients showed no progression of fibrosis (invariable IF, or moderate reducing from 0,03 to 0,01). Our data indicated fibrosis progression in repeat biopsy if patients were older than 40 years or had marked fibrosis (Desmet 3, IF 0,1) in primary liver biopsy.
Conclusion. Our results suggest good correlation between histological activity and HCV genotype. Success of therapy depends on fibrosis range and age of patients at the time of primary biopsy.

P 225

LIVER HISTOLOGY IN PATIENTS WITH SPORADIC ACUTE HEPATITIS E : A STUDY OF 11 PATIENTS FROM SOUTH-WEST FRANCE.

MISSOURY Réda (1), POIRSON Hélène (2),PERON Jean-Marie (2), VINEL Jean-Pierre (2),MANSUY Jean-Michel(3), BUREAU Christophe (2), IZOPET Jacques(3), BROUSSET Pierre (1), SELVES Janick(1).
1: Service d'Anatomie Pathologique, 2: Service d'Hépato-gastro-entérologie, 3: Laboratoire de virologie, CHU Purpan, Place du Dr Baylac, 31059 TOULOUSE

Hepatitis E virus (HEV) is responsible for acute hepatitis predominantly in developing countries. Sporadic cases have been described in industrialized countries but information on hepatic histology in these cases is scarce. We describe a series of 11 patients with sporadic acute hepatitis E and a liver biopsy. Methods: Liver biopsy was performed because of clinical suspicion of underlying chronic liver disease or uncertain etiology of the acute episode of hepatitis despite though diagnostic evaluation. HEV IgG antibodies were detected using an immuno-enzyme assay. HEV RNA was detected in the serum and feces with a real time PCR. All serums were negative for hepatitis B virus antibodies and DNA, hepatitis C virus RNA and antibodies, immunoglobulin-M class to hepatitis A virus, CMV and EBV. Anti-nuclear, anti smooth-muscle and anti LKM antibodies were also negative. Toxic and drug induced hepatitis were ruled out on anamnesis. Results: Eleven patients, 3 females and 8 males diagnosed with acute hepatitis E from march 1997 to march 2004 had a liver biopsy. Mean +/- SD age was 61 +/- 13. Overall 45% of the patients had an exaggerated alcohol consumption. Liver biopsy was transjugular in 5 cases. Five patients had confirmed histological micronodular cirrhosis. Four had exaggerated alcohol consumption on anamnesis (> 40 g/d). Two of these had lesions of acute alcoholic hepatitis including Mallory bodies, neutrophil infiltrates and steatohepatitis. The other 2 had mild steatohepatitis without Mallory bodies. All the other patients (1 with cirrhosis, 1 with mild fibrosis and 5 without fibrosis) had important spotty necrosis of hepatocytes with polymorph inflammation in the lobule. Anisocaryosis was present in most patients. Ballonisation was observed in only one case. No viral inclusions or epithlioïd granuloma were observed. In portal tracts, inflammation was marked with numerous neutrophils in almost all cases and moderate piecemeal

necrosis in only 2 cases. Bile duct damage was mild and ductular proliferation various. Cholestasis was observed in 4 cases. There was no phlebitis. Conclusion. Cirrhosis and alcohol consumption was frequent in this population of patients hospitalized for acute hepatitis E raising the question of their interaction. Characteristic pathology signs of acute hepatitis E were hepatocyte intralobular necrosis, polymorph inflammation and neutrophils in portal tract.

P 226

THE SIGNIFICANCE OF SMAD4 EXPRESSION IN THE PROGNOSTIC EVALUATION OF THE CHRONIC HEPATITIS

Esra Erden, Aysegul Yalcinkaya, Berna Savas, Hulya Cetinkaya, Hakan Bozkaya, Cihan Yurtaydýn
Ankara University, Medical Faculty, Department of Pathology and Department of Gastroenterology,Turkey

Introduction and Objective: We aimed to compare SMAD4 expression and fibrosis in the pre and post-treatment hepatic biopsies
in cases with chronic hepatitis B, chronic hepatitis C and chronic hepatitis D.
Materials and Methods: We examined the hepatic biopsies of thirty one chronic hepatitis C and 40 chronic hepatitis B cases, 4 chronic D hepatitis which were diagnosed at our department. The cases were reexamined, staged and graded according to modified Ishak and Metavir scoring systems. Immunohistochemistry was performed using antibody against SMAD4 and nuclear SMAD4 staining in perisinusoidal cells having oval nuclei and sprouting vacuolar cytoplasm was accepted as positive.
Results: When SMAD4 cut-off value 0,263 was chosen, 89 percent of the patients having SMAD4 expression below this level showed regression in fibrosis. Patients having SMAD4 expression more than 0.263 cut-off value showed fibrosis progression. This progression was calculated as 77,7 percent when the cases evaluated according to Metavir system and 81 percent when they were evaluated according to the modified Ishak. In cases with SMAD4 cut-off value below 0,184 the stage decreased in 96 percent of the patients. Median SMAD4 expression was found significantly higher in cases with chronic hepatitis C.
Conclusions: Our results showed a significant correlation between SMAD4 expression and fibrosis. Therefore, we conclude that it is necessary to observe the SMAD4 expression in pretreatment hepatic biopsies while defining the prognosis of the cases with chronic viral hepatitis.

P 227

HISTOPATHOLOGIC PARTICULARITIES OF HEPATITIS D VIRUS CHRONIC HEPATITIS

ZURAC Sabina*, LAVRIC Luciana*, VRABIE Alexandra*, MICU Gianina*, GRAMADA Eliza*, ZAHARIA Anca*, ANDREI Razvan*, STANICEANU Florica*, STREINU-CERCEL Adrian**, VOIOSU Radu***
*Department of Pathology, Colentina Universitary Hospital
**Department of Infectious Disease, Matei Bals Institute
***Department of Gastroenterology, Colentina Universitary Hospital
Bucharest, Romania

Hepatitis D virus (HDV) chronic hepatitis (which is frequent in Romania) shows no specific histopathologic lesions comparing with other viral etiologies.
MATERIAL AND METHODS: We studied 58 cases of HBV-HDV chronic hepatitis and 355 cases of HBV chronic hepatitis diagnosed in our department in 14 months; we analyzed various histopathologic parameters (portal and lobular inflammation, interface hepatitis, spotty necrosis, confluent necrosis, apoptosis, fibrosis, ground glass cells, large cell dysplasia, ductal lesions) using Ishak semicantitative score to assess necro-inflammatory activity and fibrosis; the results were compared with a group of 355 cases of HBV chronic hepatitis; a statistical analysis was performed – CHITEST, FISCHER and STUDENT tests were used with a level of statistical significance (P) of 0.05.
RESULTS: In HBV-HDV chronic hepatitis there were significant more abundant lobular inflammation (P=0.004), interface hepatitis (P=0,002), spotty necrosis (P=0,005), steatosis (P=0.025), Kupffer cells hyperplasia (P=0.007), necro-inflammatory activity (P=2,25428x10-07) and fibrosis (P=9,83716x10-07); the portal inflammatory infiltrate and ballooning degeneration were more prominent in HBV-HDV chronic hepatitis but P values were outside of the confidence range (P=0.052 and P=0.057); there was more hepatocytic hemosiderin deposition, less polymorphic inflammatory infiltrate, more prominent ductal lesions and large cell dysplasia. No significant differences were recorded in matter of sex, age, number of ground glass cells, distribution of portal inflammatory infiltrate or confluent necrosis.
CONCLUSIONS: Based on our data (higher necro-inflammatory activity with an elevation of all histopathologic parameters of necrosis and inflammation except confluent necrosis, higher hepatocytic degeneration (ballooning degeneration and steatosis), higher fibrosis) a more aggressive histopathologic appearance is recorded in HBV-HDV chronic hepatitis.

P 228

IMMUNOHISTOCHEMICAL CHARACTERIZATION OF HEPATIC DUCTULAR REACTION IN WILSON'S DISEASE

NAGY Peter
Semmelweis University, Ist Dept. of Pathology and Experimental Cancer Research, Budapest, Hungary

The so called ductular reaction is a misterious histological response of the human liver. It occurs in a wide variety of hepatic diseases, but its origin and importance is still debated. In the present study the immunophenotype of the ductular cells was investigated in three livers from patients of Wilson's disease.
The immunohistochemistry was performed on paraffin embedded liver tissue by ABC technique using diaminobenzidine as chromogen.
The ductular cells were cytokeratin(CK)7+/19+/14- and were surrounded by smooth muscle actin positive stellate cells. Occasionally, large polygonal, hepatocyte like cells were present in the ductules, which lost CK7 staining but gained nuclear hepatocyte nuclear factor 4 (HNF 4) positivity. Ki 67 staining was confined exclusively to the ductular structures, but copper/orcein positive granules were present only in hepatocytes. Alfa-fetoprotein, deleted in malignant brain tumor-1 (DMBT-1) reactions were negative, CD 34 antibody decorated only the endothelial cells.
These results suggest that the ductular reaction in Wilson's disease represents a stem cell derived regenerative response and shows certain similarity to the oval cell proliferation in the rat liver.

P 229

HISTOPATHOLOGICAL SCORING OF THE NECRO-INFLAMMATORY ACTIVITY AND FIBROSIS IN AUTOIMMUNE HEPATITIS: A COMPARISON OF TWO SCORING SYSTEMS

K.Ghaffarzadegan M.D.*, M.Sotoudeh M.D. **, MH. Derakhshan M.D. **, M. Mohammadzadeh M.D. *, S. Haghazali M.D. **, H. Saadatnia M.D. *, H. Vossoghinia M.D. *, S. Amoian M.D. *, L. Kafami M.D. *, A. Mehrnami M.D. **, N. Rakhshani M.D. **, B. Abedi-Ardakani M.D. **, R. Malekzadeh M.D.**
*Mashhad University of Medical Sciences, Mashhad, Iran

**Digestive Diseases Research Center (DDRC), Tehran University of Medical Sciences, Tehran, Iran

Background and Aims:
Histopathological scoring of grade of necro-inflammatory process and stage of fibrosis is widely used for chronic viral hepatitis and the same scoring systems are also applied to the biopsy samples of patients with autoimmune hepatitis. We aimed to compare the results of scorings by Modified Histological Activity Index (HAI) and the METAVIR systems and their validity for determination of severity of disease in Iranian patients with autoimmune hepatitis.
Materials and Methods:
Blind histological examination of 20 liver biopsy slide sets from patients with autoimmune hepatitis was performed by two independent pathologists. Grades and stages of the liver lesions were determined according to the HAI and METAVIR systems. The correlations of the scores of the two systems were determined by weighted kappa analysis. Correlation of necroinflammatory activity and fibrosis with serum levels of aminotrasferases was analyzed by the Spearman's rho test.
Results:
There was moderately well to good correlation between grades and stages obtained by the two systems (weighted kappa 0.58 and 0.56 respectively). However, the scores of none of the two systems showed a significant correlation with serum levels of aminotransferases.
Conclusion:
Concordance between HAI and METAVIR scoring systems is good for the histological grading and staging of autoimmune hepatitis. However, neither of the two systems proved to be valid for determination of the activity of the disease when compared to the levels of serum aminotranferases. We conclude that HAI and METAVIR systems give comparable results in autoimmune hepatitis but a more valid system has to be devised for histological scoring of this group of liver diseases.
Key words:Autoimmune hepatitis,Scoring,Metavir,Modified HAI

P 230
EFFECT OF SPLENECTOMY ON LIVER FIBROGENICITY IN PORTAL HYPERTENSION PATIENTS
Zeinab S. Omran, M.D.***, El Batanouny M.M.D.**, Mohamed M. Essawy, M.D.*, Abdel-Rahman Elbee, M.D.**, Hussein Ezzat, M.D.*, Mohamed Abbas, M.D*, Mona M. Nosseir, M.D.***, and Iman A. Khaled, MD.****
*General Surgery, ***Pathology and ****Hematology Departments, Theodor Bilharz Research Institute and **General Surgery Department of Kasr El-Aini, Cairo University, Egypt.

This study was designed to assess the role of the spleen on the presence and localization of liver fibronectin, to measure the amount of hepatic collagen and serum level of fibronectin and procollagen III in cases of portal hypertension.
The study was performed on 40 patients divided into two groups: Portal hypertension group (20 patients) included one pure schistosomal hepatic fibrosis, three mixed schistsomal and virus C cirrhosis, ten virus C hepatic cirrhosis, two virus B hepatic cirrhosis and four mixed B&C infections. Control group (20 patients) presented with different splenic insults without hepatic affection. In the first group, through clinical examinations and sonographic findings revealed hepatosplenomegaly and grade III & IV varices with history of injection sclerotherapy in 65% of cases.
Preoperatively, marked hepatic fibronectin deposition in portal tracts and around blood vessels raised the stage of fibrosis. This was accompanied by decrease in plasma level of fibronectin and increase of serum level of procollagen III in relation to the control group.
Six months post-operatively, tissue fibronectin, collagen content and serum procollagen III were insignificantly decreased. However, plasma level of fibronectin was increased significantly.
These results denoted that fibronectin is one of the predominant early fibrogenic components in chronic liver diseases, stimulating further collagen deposition. It is concluded that the role of the spleen in the development of hepatic fibrosis seems ancillary. Multifactorial influences, including etiology, timing of splenectomy, hepatic vascular adjustment, and factors associated with the biology of extracellular matrix of the liver, probably play a more significant role. Further studies were recommended to assess the role of splenectomy on liver fibrogensis at different stages of fibrosis. Intervention with splenectomy could improve or reverse fibrogenic activity at early stages.
Key words: Splenectomy, fibrogenicity, fibronectin, procollagen III, liver fibrosis, portal hypertension.

P 231
PRIMARY SCLEROSING CHOLANGITIS SIMULTANEOUSLY WITH ANCA-ASSOCIATED VASCULITIS
Honsova E, Kostolna E, Trunecka P, Jaresova M.

Primary sclerosing cholangitis (PSC) is a chronic cholestatic liver disease characterized by inflammation and fibrosis of the intra- and/or extrahepatic bile ducts. Anti-neutrophil cytoplasmatic antibodies (ANCA) are a heterogeneous group of autoantibodies directed against cellular components of the polymorphonuclear leucocyte. ANCA directed to proteinase 3 (PR3-ANCA) or myeloperoxidase (MPO-ANCA) are closely associated with systemic necrotizing vasculitis. Atypical anti-neutrophil specific antibodies (atypical p-ANCA) are detected in the majority of patients with PSC.
Methods: Retrospective analysis of patients with diagnosis of PSC between the years 2002-2004.
Results: A total of 38 patients in whom ERCP features of PSC and liver biopsies were evaluated - 25 (65,8%) men, 13 (34,2%) women. Of the 38 patients, 26 (68,4%) suffered from inflammatory bowel disease. 3 patients (2 men, 1 woman) had skin palpable purpuric rash, and underwent skin biopsy with morphological diagnosis of vasculitis. Simultaneously positive ANCA antibodies directed to proteinase 3 were detected in the sera of all of them. All of these patients had been suffering from migrating polyartralgia. None of them had any renal abnormalities.
Conclusion: The underlying pathophysiology of PSC is unknown but genetic and immunological mechanisms may play a role. Patients with PSC can have positive tests not only to atypical pANCA but also to PR3-ANCA. Some of the extrahepatic complications of PSC can be associated with systemic vasculitis, and these patients need more extensive monitoring of the disease and especially adequate therapy to prevent a more serious course of the disease.

P 232
CELL REACTION OF PERISINUSOIDAL FIBROSIS DURING NONALCOHOLIC STEATOHEPADTIS.
Petrov S.B., Kiyasov A.P., Odintsova A.

Nonalcoholic steatohepatitis (NASH) is characterized by perisinusoidai fibrosis, which develops on early stages of the disease. The cellular sources of fibrillar collagens and other matrix proteins are endothelial cells (EC), hepatic cells and mainly hepatic stellate cells (HSC) which proliferate after liver injury and undergo activation to a myofibroblast - like phenotype. Capillarization is a process in which the liver sinusoid became consecutive capillaries with evident basement around and it is followed by expression of CD34 by EC.

Aims: To determine the connection between the development of perisinusoidal fibrosis, activation of HSC and capillarization of sinusoids during NASH. Methods: 36 liver biopsies from the patients with NASH were studied. We analyzed correlation between grade of disease activity and stage of the disease and expression of a- SMA (activation of HSC) and CD34 (capillarization). Results: Perisinusoidal fibrosis is revealed in all stages of NASH and followed by activation of HSC. Expression of CD34 arises on the basis of perisinusoidal fibrosis, activation of HSC and correlates with the grade of activity. Conclusion: Perisinusoidal fibrosis is the result of HSC activation, leads to capillarization and to change of EC phenotype and expression of CD34.

P 233

BETA-AMINOISOBUTYRIC ACID ALLEVIATES STEATOHEPATITIS IN A MURINE MODEL OF DIABETES AND OBESITY.

ABBEY-TOBY A.(1,2), BEGRICHE K.(2), IGOUDJIL A.(2), LETTÉRON P.(2), DUBOIS S.(1), FROMENTY B(2).
1-Service d'Anatomie Pathologique, Hôpital Beaujon, 100 Bd du Général Leclerc, CLICHY, France
2-Inserm U-481, Faculté de Médecine X.Bichat, PARIS, France.

Non-alcoholic fatty liver diseases (NAFLD) are characterized either by isolated steatosis or by steatosis associated with necroinflammation, thus constituting non-alcoholic steatohepatitis (NASH). NASH can evolved toward more severe liver diseases such as fibrosis, cirrhosis and hepatic carcinoma. NASH is mainly observed in metabolic diseases such as type 2 diabetes and obesity.
Background: we previously reported that administration in lean (Swiss) mice of 100 mg/kg/d of beta-aminoisobutyric acid (BAIBA, a natural catabolite of thymine) for 6 weeks was associated with increased hepatic fatty acid oxidation (FAO) and decreased body fat mass (BFM). In genetically obese and diabetic ob/ob mice this dose of BAIBA stimulated FAO at a lesser extent and did not decrease BFM.
Aims: the first goal of the study was to determine whether higher doses of BAIBA and/or a longer exposure could decrease BFM in ob/ob mice. In addition, we asked whether BAIBA could improve liver function and lesions and oxidative stress in this model of obesity. Lastly, we wished to know more regarding the mechanisms whereby BAIBA is able to increase hepatic FAO.
Materials and Methods: 100 or 500 mg/kg/d of BAIBA were administered to ob/ob mice for 4 months. BFM was assessed by DEXA before and at the end of the experiment. ALT and LDH were determined in plasma and liver histology was performed with standard stains (hematoxylin-eosin, Masson trichrom, picrosirius). In addition, apoptosis was assessed with a TUNEL assay. mRNA expression of 2 mitochondrial FAO enzymes (L-CPT-1, MCAD) was assessed with a RiboProtection Assay. Finally, hepatic glutathion and lipid peroxidation were measured.
Results: we showed that administration in ob/ob mice of high dose of BAIBA for 4 months did not decrease BFM. Although hepatic steatosis was not decreased in ob/ob mice, periportal and perisinusoidal fibrosis and necroinflammation and apoptosis were alleviated by BAIBA. This histologic improvement was associated with a trend toward lower ALT and LDH. Hepatic expression of L-CPT-1 and MCAD was increased and oxidative stress was lessened.
Conclusion: although the natural compound BAIBA does not decrease fatness in ob/ob mice, it improve liver function in this model. However, despite increased expression of FAO enzymes, steatosis in ob/ob mice was not decreased suggesting that a compensatory de novo lipogenesis may occur in liver. BAIBA is being tested in other models of dysmetabolic diseases.

P 234

HEPATIC DYSFUNCTION IN ANOREXIA NERVOSA: CLINICAL, HISTOLOGICAL, ULTRASTRUCTURAL AND PROGNOSTIC ANALYSES

D Cazals-Hatem, PE Rautou, G Feldmann, C Francoz, G Arcangelli, A Grodet, F Durand, D Valla, P Bedossa.
Departments of Pathology and Hepatology, Hôpital Beaujon, 92118 Clichy, France

Liver tests abnormalities have been described in anorexia nervosa. However, the mechanisms of liver dysfunction in this context are not well established and histological reports are rare.
Aims: To analyze the clinical, pathological and prognostic features of hepatic dysfunction observed in patients with severe anorexia nervosa.
Patients & methods: 9 patients with anorexia nervosa (7 females, 2 males, mean age: 27.3) were investigated in Hôpital Beaujon because of acute liver failure. The clinical and biological parameters were recorded. Liver biopsy was performed in every patient with electron microscopy study in two cases.
Results: At admission, the mean BMI was 11.3 ± 1 kg/m2, (range 9.6 – 13.2). Transaminase ranged from 18.1-105.5N; prothrombin time was below 50% in all patients. Five patients were hospitalized because of hypoglycaemic coma and cardiac explorations revealed cardiac dysfunction in 4 out of the 5 patients (left ventricular ejection fraction below 50%). Hepatic gradient was normal in all patients who underwent a transjugular biopsy (8/9).
Liver biopsies performed days 2 to 9 after admission showed swelling and clear hepatocytes in all cases, corresponding to spongiocytic steatosis as proven by Soudan red staining in only 1 case. Periodic acid-Schiff staining showed decrease glycogen amount in all cases and abundant ceroid pigments in hepatocytes of the centrilobular zone, associated with hepatocytic atrophy and inconspicuous sinusoidal fibrosis in 4 of the 9 cases. Centrilobular necrosis without inflammation or congestion was observed in one case. Ultrastructurally, hepatocytes displayed a low density of glycogen particles and few organelles. Endoplasmic reticulum was slightly altered. Phagolysosomes with dense osmiophilic bodies were prominent. Clinico-pathological confrontations showed a higher proportion of centrilobular lesions in patients with cardiac dysfunction and/or severe hypoglycemia. The patient with microvesicular steatosis presented with recurrent vomiting before admission. After glucose therapy, complete normalization of prothrombin time was achieved in all patients. Only one patient with cardiac dysfunction needed dobutamine therapy.
Conclusion: Severe hepatic abnormalities may occur in anorexia nervosa with favorable evolution after glucose infusion. Microscopically, fatty deposit was infrequent but hepatocytic lesions were common but mild, possibly related to hypoglycaemic coma and/or cardiac dysfunction.

P 235

HISTOLOGICAL STUDY OF POLYCYSTIC LIVER DISEASE REVEALS SIGNIFICANT VASCULAR CHANGES IN NON-CYSTIC LIVER PARENCHYMA.

L Catherine (1), M Ronot (2), C. Francoz (3), O. Farges (4), F. Durand (3), J. Belghiti (4), P. Bedossa (1), V Vilgrain (2), V Paradis (1).
(1) Pathology Dpt, (2) Radiology Dpt, (3) Hepatology Dpt (4) Liver surgery Dpt, Beaujon hospital, Clichy France.

Background : Polycystic liver diseases are made of heterogeneous entities associated with specific genetic mutations. Histological analysis focused on liver cysts' characteristics and failed to describe morphological aspects of non-cystic parenchyma. The aim of this study was to assess

histological changes of the non-cystic parenchyma, which could explain the pejorative clinical evolution of some cases.
Patients and Methods: Forty-six liver resections obtained from patients with polycystic liver disease were retrospectively examined. The sex ratio was 41 women / 5 men, with a mean age of 50 years + 9 (range: 33-66). The liver resection consisted in a left hepatectomy (n=19), a right hepatectomy (n=12), or a total hepatectomy performed in the context of liver transplantation (n=15). Twenty-two patients had also kidney polycystic disease involvement. Histological analysis evaluated the following features in a semi-quantitative assessment: portal fibrosis (0: absent, 1: mild enlargement of portal tracts, 2: few fibrotic septa, 3: numerous fibrotic septa, 4: cirrhosis), centro-lobular fibrosis (0: absent, 1: discrete perisinusoidal fibrosis around the centrolobular vein, 1: perisinusoidal fibrosis involving < 1/3 of the lobule, 2: perisinusoidal fibrosis involving > 1/3 of the lobule), sinusoidal dilatation and congestion (0: absent, 1: few foci, 2: extensive areas), regenerative nodular hyperplasia (incomplete or complete). The presence of venous thrombosis, venular portal dilatation or other parenchyma anomalies were also noted.
Results: In addition to the presence of numerous cysts disseminated throughout the liver, 40 cases (87%) displayed significant morphological changes in the non-cystic parenchyma. All patients had bilobar disease and 32 of them have complicated cysts (28 hemorrhagic cysts, 9 infected cysts). Significant portal fibrosis (> score 2) and centrolobular fibrosis (score 2) were noted in 16 (34.7%) and 25 (54.3%) cases, respectively. In 18 cases (39%), both sinusoidal dilatation and congestion were extensive. Venous thrombosis was present in 12 cases and venular portal dilatation in 41 cases. Architectural disorders, including regenerative nodular hyperplasia-like and regenerative nodular hyperplasia, were observed in 16 cases (34.7%). Peliosis and steatosis were reported in 12 and 7 case, respectively.
Conclusion: This study shows that non-cystic parenchyma of polycystic liver disease display significant morphological disorders, especially vascular changes, including regenerative nodular hyperplasia, and also fibrosis in at least 1/3 of cases. Such modifications, potentially induced by the secretion of cytokines and growth factors by the liver cyst epithelial cells, may be involved in the progression of the disease.

P 236
EVALUATION OF THE ANTI-SCHISTOSOMAL ACTIVITY OF THYMOQUINONE IN MURINE SCHISTOSOMIASIS MANSONI: INFLUENCE ON NITRIC OXIDE, ICAM-1 AND COLLAGEN
.SAMIRA SALEH, MADIHA MAHMOUD1, HANAN E1-ABHAR, ZEINAB OMRAN2
Department of Pharmacology and Toxicology. Faculty of Pharmacy. Cairo University: Kasr El-Aini st. 11562 Cairo. Egypt. Department of 1Pharmacology and 2Pathology, Theodor Bilharz Research Institute. Imhaba, Giza 12411 Egypt

We have proved previously that Nigella Sativa oil reduced Schistosoma mansoni (S. mansoni) induced hepatic fibrosis, the total worm burden, egg load and granuloma formation. Therefore, we aimed here to study the possible antischistosomal effect of one of its active constituent's thymoquinone (TQ). The drug was given to S. mansoni infected mice in two dose levels (5 and 10 mg/kg, p.o.) for two weeks, and its effect was compared to that of the standard antischistosomal drug, praziquantel (PZQ). Two weeks later, the following parameters were estimated, viz., worm load and distribution, oogram changes, egg load in liver and intestine, granuloma diameter, collagen deposition and intercellular adhesion molecule-1 (ICAM-1) expression. Moreover, serum levels of L-alanine aminotransferase (ALT) and nitric oxide (NO), as well as NO hepatic level were estimated. Mice treated with TQ showed a significant reduction in total number of worm burden, both in liver and portomesentric blood vessels. The oogram pattern recorded a decrease in immature and mature ova, and an elevation in dead ova. Tissue egg load was reduced in both liver and intestine. In infected mice treated with TQ, the elevated serum ALT activity leveled off. However, neither serum NO level was altered, nor in the infected group nor in those treated with TQ or PZQ. In liver homogenate, infection decreased NO level, which was not corrected with PZQ, but in-groups treated with TQ, a further reduction was reported. TQ caused shrinkage in granuloma diameter, and a diminution in collagen deposition. On the other hand, PZQ failed to reduce collagen deposition. Both TQ and PZQ decreased ICAM-1 expression in Kupffer and inflammatory cells. However, neither TQ nor PZQ affected it in endothelial cells. These results point to a possible antischistosomal role of TQ, which may be correlated with modulation in the immune system.
Key words: schistosomiasis mansoni; nitric oxide; granuloma; intercellular adhesion molecule-l (ICAM-l), collagen; thymoquinone; praziquantel.

P 237
HEPATIC STELLATE CELLS IN HUMAN SCHISTOSOMIASIS: A COMPARATIVE IMMUNOHISTOCHEMICAL STUDY WITH LIVER CIRRHOSIS.
Leandra N.Z. Ramalho 1,Daniel Chang 1, Fernando S. Ramalho 2,
Ana L.C. Martinelli 3, Maria I. Fernandes 4, Sergio Zucoloto 1.
Departments of 1Pathology, 2Surgery and Anatomy, 3Medicine and 4Pediatrics
Faculty of Medicine of Ribeirão Preto, University of São Paulo, Ribeirão Preto, SP, Brazil

Hepatic schistosomiasis (SCH) frequently results in liver fibrosis, but in the most of cases without functional loss of the liver. Chronic hepatitis C virus hepatitis (HCV) often curses with cirrhosis and liver failure. The hepatic stellate cells (HSC) are involved in both disease, but it is not clear if the proportion of quiescent or activated HSC and their rates of proliferating can be associated with the clinical outcomes. The present study intends to verify if exist difference in quiescent and activated hepatic stellate cells and their proliferating capacity, between SCH and HCV. The liver biopsies were reviewed and the diagnoses were confirmed. It was performed a immunohistochemistry study, with double staining for proliferating cell nuclear antigen and glial fibrillary acid protein (for detection and quantification of proliferating quiescent HSC), and double staining for proliferating cell nuclear antigen and smooth muscle á-actin (for detection and quantification of proliferating activated HSC). In SCH patients, there was observed a lower number of activated HSC than in HCV patients ($p<0.05$), without any difference considering the quiescent HSC ($p>0.05$). The rates of proliferating, both to quiescent and activated HSC were similar in SCH and HCV patients ($p>0.05$). Thus, the activation state of HSC is more important than proliferating rates. The HSC are important to SCH fibrosis, but, the activated HSC profile, the more proliferating, is predominant in cirrhosis. Probably, the evident inflammatory stimuli present in HCV can activate a higher number of HSC than in SCH, that present a mechanical mechanism of fibrogenesis and curses with lower fibrosis and less important clinical repercussion.

P 238
PULMONARY EPITHELOID HAEMANGIOENDOTHELIOMA (IVBAT)
Fillinger J.,Soltész I.,Kerényi A.,
Marosi M.,Molnár É.,Agócs L.

In our Institute four cases were diagnosed by the authors,they also review the clinicopathologycal features, differential diagnostic problems and the literature.The epitheloid haemangioendothelioma (EHE)can occur everywhere in the human body, most often in liver, soft tissue, bone and lung.In the literature mentiones occurences in central nervous system, mamma, head- neck region and lymph nodes. The opinions are divided but the mostly accepted is that EHE is a low grade sarcoma. The tumors that are normally progressing from soft tissue and bone are more agressive than the ones of other origin.
Pulmonary origin is relatively rare.Patientes are usually without complaint and the condition is dicovered accidentally. Occurence in women is four times more frequent.The average age is under forthy.
In pulmonary EHE on X-ray and CT scan shows most often subpleural soliter or multiplex nodules. Nodules can reach 2 cm in diameter but most are under 1 cm.Radiomorphology shows metastatic tumor progression.Nevertheless repetedly scans can not show any progression.The differential diagnostic approach needs to considers multiplex benign tumors,vasculitis, bronchiolitis and granulomatous diseases.
Survival of patientes are variable from a few month to 15 years and depends on the site of tumor.Pulmonary origin with pleural and lymph node spreading indicates poorer outcome.Therapy is variable, can only be observation or chemotherapy too.

P 239

LUNG OSTEOMA – A NEW BENIGN LUNG LESION

Eva Markert, Ulrike Gruber-Mösenbacher, Christian Porubsky, Helmut H. Popper
Institutes of Pathology, Medical University of Graz and Teaching Hospital Feldkirch, Department of Thoracic and Hyperbaric Surgery, Medical University of Graz, Austria

Introduction: The most common benign neoplasm's' of the lung are hamartomas. A primary osteoma in the lung has never been reported. Within its differentials hamartoma with osseous foci, osseous metaplasia, secondary ossification, and nodular amyloidosis have to be discussed.
Material and Methods: A 38 year-old man presented with a solitary well limited tumor in the right middle lobe. He was treated with chemotherapy and interferon because of multiple myelomas and got a bone marrow transplantation 2 years and a few months before this lesion appeared. The patient underwent surgical resection. Usual routine pathologic work-up followed.
Results: The tumor presented with a well defined fibrous capsule and consisted of mature bone. Within the tumor a fatty tissue was seen much as it would be seen in mature bone. Focally most often at the edges small bone spicules could be discerned, most probably the area of new bone formation and appositional growth. There was no amyloid deposition, no immature epithelial tubules as in hamartomas, and no normal lung structure within the tumor, such as in osseous metaplasia.
Discussion: We have named this lesion osteoma, because it looks like any other extrasceletal osteoma. For comparison with similar lesions to be excluded, nodular amyloidosis, hamartomas, and various forms of osseous metaplasias will be exemplarily shown. To the best of our knowledge, this is the first case of osteoma arising in the lung.

P 240

LYMPHOEPITHELIOMA-LIKE CARCINOMA OF THE LUNG: REPORT OF TWO CASES

KASAI Kiyoshi
Divison of Basic and Clinical Medicine, Department of Nursing,
School of Health Sciences, Sapporo Medical University, Sapporo, Japan

Introduction The term lymphoepithelioma-like carcinoma (LELC) has been proposed for histologically unique neoplasms characterized by an undifferentiated malignant epithelial neoplasm with a markedly prominent lymphoid infiltrate. LELC of the lung is a rare lung tumour and is classified as a variant of large cell carcinoma. The aim of the present study is to describe the histopathological features of 2 LELCs and to analyze the association with EBV of LELC.
Materials and methods I report two patients (females) with LELC, who underwent surgery. Tumor specimens were routinely fixed and processed. Deparaffinized sections were stained by HE and examined immunohistochemically with cytokeratin, EMA, CEA, LMP-1 and ZEBRA protein expression. For the detection of EBV, non-radioactive DNA-RNA in situ hybridization for EBV-encoded small RNAs (EBER-1) was carried out.
Results Tumor cells of the 2 lobectomy specimens showed a syncytial growth pattern of undifferentiated cells. Cancer cells consisted of oval nuclei with a clear to vesicular chromatin pattern and a few prominent nucleoli. The neoplastic epithelial cells were accompanied by an intense lymphoid infiltrate and admixed intimately with small lymphocytes. Some areas of squamous differentiation in the form of well-defined cell borders and focal keratinization were observed within the tumors. The tumor cells of both cases stained positive for cytokeratin and EMA but not for CEA. EBER1 expression was intense and was present in most tumor cells of both cases. No expression of EBV-related proteins (LMP-1 and ZEBRA) was detected in tumor cells.
Conclusion I believe that careful histopathological examination of the large cell carcinomas of the lung may help to establish the exact diagnosis of LELC. Although the typical LELC of the lung consists of undifferentiated carcinoma, EBV-infected LELC in Asians is not restricted to undifferentiated carcinoma and includes more differentiated carcinomas

P 241

UNDIFFERENTIATED ' LYMPHOEPITHELIOMA - LIKE 'CARCINOMA OF THE LUNG A DISTINCT ENTITY WITH BETTER PROGNOSIS

HAMEL Nadia*, ASSELAH Fatima*, CAPRON Frédérique**
* Departement of pathology CHU Mustapha Algiers- Algeria
**Departement of pathology Hopital de la Pitié Paris- France

BACKGROUND
lymphoepithelioma – like carcinoma (LELC) is a large cell carcinoma histologically similar to nasopharyngeal lymphoepithelial carcinoma with nests of large malignant cells in a lymphoid rich stroma. LELC of the lung is very rare in western countries, but not in southeast Asia where it is frequently associated with Epstein-Barr virus. Algeria is endemic for Epstein-Barr virus infection and nasopharyngeal carcinoma and Burkitt lymphoma are relatively frequent in our population.
OBJECTIVE
to attempt to identify cases of LELC from a large series of lung cancer and to asses their association with Epstein-Barr virus and their particularities.
METHODS
A total of 70 cases of poorly differentiated lung carcinoma reviewed. EBV research was performed by in situ hybridation technique (IHS) using EBER arrays associated with immunohistochemical (IHC) technique for expression of LMP-1 protein.
RESULTS
10 cases of LELC identified (08 squamous carcinomas and 02 undifferentiated carcinomas with lymphoid stroma).The patients were aged 45 to 79 years (median, 52 years), ratio M/F= 5. All the mens were smokers.

We found a high expression of LMP-1 by IHC and EBER-1 by HIS in the two cases of undifferentiated carcinomas with lymphoid stroma. The two patients are females, 60 years old and non smokers. LELC of the lung occurring in Asians is an EBV-associated neoplasm ; it also associated with young age, a history of not smoking, high bcl-2 immunoreactivity, and better survival rate (Fen Fen Chen,1998)
IN SUMMARY
These are the first cases of LELC associated to EBV reported in Algerians. The role of EBV in the oncogenesis is poorly understood. LELC is histologically and biologically distinct entity with a better prognosis.

P 242
MEDISTINAL LOW-GRADE FIBROMYXOID SARCOMA (A CASE REPORT)
Sanei Mohammad Hossein MD *, Tabatabaie Seid Abbas MD †, Mahzooni Parvin MD * , Sanei Behnam MD †
*Department of pathology, Isfahan university school of Medicin, Isfahan †Department of Thorasic Surgery ,Isfahan university school of Medicin ,Isfahan

Sanei Mohammad Hossein MD *, Tabatabaie Seid Abbas MD †, Mahzooni Parvin MD * , Sanei Behnam MD †
*Department of pathology, Isfahan university school of Medicin, Isfahan †Department of Thorasic Surgery ,Isfahan university school of Medicin ,Isfahan
Abstract:
We report the second case of Low-grade fibromyxoid sarcoma of the mediastinum, a very rare tumor, in a 55-year-old woman presented with dyspenea. Chest X-ray and computed tomography (CT) on admission showed a 30cm mass in the anterior mediastinal space, compressing the lungs and adhered to chest wall. A diagnosis of benign peripheral nerve sheate tumor was established by a CT-guided percutaneous needle biopsy. Systemic examination revealed no metastasis to the contralateral pleural cavity or other distant organs, and the mediastinal mass was resected. Tumor cells were positive for vimentin and negative for actins, EMA, CD34, keratins, and S-100 protein .Pathological and immunohistochemical analyses confirmed a diagnosis Low-grade fibromyxoid sarcoma. The patient is alive without recurrence 10 months after his operation
Key word ; Low-grade fibromyxoid sarcoma- mediastinum

P 243
LEIOMYOMA OF THE BRONCHUS: A CASE REPORT AND REVIEW OF LITERATURE
MAEDA Mitsuhide, HARADA Hiroshi, KANEYUKI Utako, YOSHIMURA Junko, KOJIRO Masamichi
Department of Pathology, Kurume University School of Medicine, Kurume, Japan

Leiomyoma of the lower respiratory tract is a rare benign neoplasm and only limited numbers of cases have been described in the English literature. We recently encountered a case arising in the intrapulmonary bronchus of a Japanese young adult and present clinical and histological summary with breif literature review. A 33-year-old woman complained of old pneumonia and persistent cough for three years and was referred to our hospital in late 2004. Chest computed tomography showed a well circumscribed and enhanced mass lesion as well as a dilation of the distal bronchus and pneumonia. The mass was measured 15 mm in the largest dimension and was located in the eighth segment of the left bronchus. Bronchoscopy demonstrated a smooth whitish mass, which obstructed left basal bronchus. The left lower lobulectomy was performed and gross specimen included a polypoid lesion 21• ~11• ~10 mm in dimension, which was covered by the intact bronchial mucosa. Histological examination revealed a spindle cell tumor with bland cellular morphology and readily recognized fascicular arrangement. Nuclei showed typical bland-end shape and rare mitosis. Neither destructive growth nor infiltration into surrounding tissue was observed. Immunohistochemically, the tumor cells were positive for myogenic markers such as desmin, alpha-smooth muscle actin, HHF35, calponin and h-caldesmon. Post-operative course is not eventful for six months after operation. Leiomyomas of the lower respiratory tract are uncommon and account for less than 2% of all benign tumors of the lung. They were subdivided into three anatomical varieties: parenchymal, bronchial, and tracheal leiomyomas. As far as we know, less than 75 cases have been reported with female predominance of 1.5:1, and are found rarely in the aged or in children. Bronchial obstruction with atelectasis, pneumonia and hyperlutency are common symptoms as seen in the present case. Outcome is generally excellent.

P 244
INFLAMMATORY MYOFIBROBLASTIC TUMORS – LUNG NEOPLASMS WITH UNPREDICTABLE BEHAVIOUR
STOJSIC Jelena, RADOJICIC Jelena, MILENKOVIC Branislava, ADZIC Tatjana,
TODOROVIC Vera, DRNDAREVIC Neda
Institute for Lung Diseases and Tuberculosis, Belgrade, Serbia, Institute for Medical Research, Belgrade, Serbia

Background: Inflammatory myofibroblastic tumor (IMT) is a mesenchymal lung neoplasm accoding to a recent WHO classification of lung tumors. Methods: We analysed biological behavior of 20 IMTs diagnosed in last ten years on operated tissue obtained as segmental resection, lobectomy or pneumonectomy. Results: 17 IMTs were solitar nodules without necrosis and 3 IMTs were multinodular with one central, large nodule surrounded by a few smaller ones. Some of “satellite” nodules involved mediastinal pleura, penetrating in mediastinal fat tissue. Morphologicaly, tumor contained spindle cells arrayed in fascicles with or without mild nuclear pleomorphism and seldom mitoses. Spindle cells showed myofibroblastic differentiation, histochemicaly by van Gieson, Masson – trichrome and Periodic –Acid – Shiff (PAS) caracteristic stains and immunohistochemically by desmin and vimentin positivity. After surgery 17 solitar IMTs didn’t recidive. Three multinodular, agressive IMTs were treated as malignant mesenchimal tumors with adequate oncologic therapy. Conclusion: IMTs are mesenchimal neoplasms with benign or locally invasive, malignant growth pattern. The criteria for IMTs malignancy, despite cellular pleomorphism and mitoses, are their multinonodular, agressive growth pattern accompanied with presence of necrosis. Postsurgery oncologic treatment was required in such cases. It means that IMTs are truly neoplasms not pseudotumors.

P 245
GRANULAR CELL TUMORS OF THE LUNGS-THREE CASES
Tatjana ADZIC, Jelena STOJSIC
Institute for lung diseases and tuberculosis, Clinical Center of Serbia, Belgrade, Serbia and Montenegro

Background: Granular cell tumors (GCT) are rare tumors most often located in oral cavity, skin or subcutaneous tissue. The occurrence of this tumor in the tracheobronchial tree is extremely rare.
Methods: We describe three cases of GCT found in our institution during fiftheen years
period (1990-2004). At all three cases biopsies of tumors were obtained, microscopically examined and pathohistologicaly diagnosed.
Results: In the first patient, male, 45-years old, the diagnosis was confirmed, after recurrent bronchopneumonias by

bronchological examination, with endoscopic pendular tumor in the left upper lobe.
In the second patient, female, 63-years old, after hemoptysis, the diagnosis was established by bronchological examination, with tumor in the proximal wall of main left bronchus.
In the third patient, male, 84-years old, the diagnosis was confirmed, after fine needle aspiration biopsy.
The histopathologic study of the specimens, supported by histochemical and immunohistochemical techniques, determined the lesions to be a GCT. In all three cases on pathohistological examination large cells with acidophilic cytoplasm were found. In the first case a mild nuclear pleomorphism was present. Tumor cells showed histochemicaly extremely PAS sensitivity and immunohistochemicaly S-100 positivity.
All patients were treated locally, with complete remission in two patients.
One year after resection, the first patient developed malignant GCT, with metastatic diseases in the left parietal bone and in the left suprarenal gland and was treated with chemotherapy.
Conclusion: Pathohistological examination of each lung tumor is requested because of adequate oncologic treatment, especcialy in cases of rarity as GCT. Endobronchial granular cell tumors are in the majority of cases a benign tumors with a good prognosis. Local treatment gives the best results.

P 246
CONGENITAL CYSTIC LUNG DISEASE AND LUNG CANCER
Titl:
L.Shestakova,PhD; A.Charny,PhD, E.Kogan,MD and M.Paltsev, MD. Central Hospital N1 RGD,
Moscow Medical Setchenov's Academy, Moscow, RUSSIA.

BODY: A retrospective study was carried out on 642 cases. 81 cases / 13%/ were malignant lung tumors arising within congenital malformation areas. There were 72 males / 89%/ and 9 females /11%/ with ages ranging from 23 to 65 years. In 18 cases /22%/ congenital lung malformations were revealed 1-15 years earlier lung cancer development. Morphologic analysis revealed two groups:58 cases were different grade squamous cell carcinoma inside hypoplasia,
congenital cystic adenomatoid malformations of the lungs;23 cases were malignant carcinoid or adenocarcinoma or bronchioloalveolar multifocal cancer inside hypoplasia with congenital cystic disease of the lung, introlobar sequestration or congenital bronchioloectatic emphysema.
Signatura of Presenting Autor:
Dear colleagues!
A promt reply would be appreciated.
God bless you!

P 247
PULMONARY CYSTIC DISORDER RELATED TO LIGHT CHAIN DEPOSITION DISEASE
COLOMBAT Magali (1), GROUSSARD Odile(2), FOURNIER Michel (3), STERN Marc (4),VALEYRE Dominique (5), HERSON Serge (6), MONNET Isabelle (7), DANEL Claire (8).
(1)Service d'anatomie pathologique, Hôpital Tenon, Paris, France
(2)Service d'anatomie pathologique et (3) de pneumologie, Hôpital Beaujon, Clichy, France
(4)Service de pneumologie, Hôpital Foch, Suresne, France
(5)Service de pneumologie, Hôpital Avicenne, Bobigny, France
(6)service de medecine interne, Groupe Hospitalier Pitie-Salpetriêre, Paris, France
(7)Service de pneumologie, Centre Hospitalier Intercommunal, Creteil, France
(8)Service d'anatomie pathologique, Hôpital Europeen Georges Pompidou, Paris, France

Light chain deposition disease (LCDD) is a rare entity that very uncommonly affects the lung. We report 3 cases of LCDD presenting as a bilateral cystic lung disorder with severe outcome leading to lung transplantation. In all cases, a presumptive diagnosis of lymphangioleiomyomatosis or Langerhans'cell histiocytosis was proposed based on clinical and radiological data. The diagnosis of LCDD was finally established in 2 cases, on an open lung biopsy specimen, and in 1 case, on the explanted lungs.
In these cases, the disease was characterized by progressive dyspnea associated with numerous joining cysts, diffusely distributed in both lungs. Nodules were also observed in 1 case. Lung function tests showed an obstructive pattern. The histological examination demonstrated an amorphous eosinophilic Congo red negative material located in the alveolar walls, small airways and vessels. It was most often surrounded by multinucleated giant cells. Emphysematous changes were present at the edge or at distance from these deposits. Many small airways were also dilated. Immunofluorescence disclosed staining for ê but not for ë light chains within abnormal deposits and basement membranes. Electron microscopy revealed coarsely granular electron-dense deposits in the same localizations. No other extrapulmonary deposition was ever found except for 1 case in minor salivary glands. No immunoproliferative disorder could be evidenced.
In summary, this report demonstrated that LCDD may 1) primarily affect the lungs, 2) present as a cystic disease resembling lymphangioleiomyomatosis and Langerhans'cell histiocytosis on radiological grounds, and 3) lead to severe respiratory failure.

P 248
THYROID TRANSCRIPTION FACTOR-1 EXPRESSION IN LUNG CANCER
R. Tringidou, K. Papadopoulou, P. Kalkandi, J. Vamvakaris,M. Apostolidou, M. Fotinou
Pathology Dpt., Athen's General Hospital for Thoracic Diseases - Greece

Introduction: It is known that tissue-specific transcription factors control cell determination and differentiation. TTF-1 is a tissue specific transcription factor expressed in the epithelial cells of thyroid gland and the lung.
Aim: In this study we detected the expression of TTF-1 in normal human lung and in lung adenocarcinomas primary or metastatic, by immunohistochemistry, in order to find its diagnostic value, if TTF-1 can be used to distinguish between lung and nonlung origin of a tumor.
Methods: Using AvidinBiotin-Complex / Alkaline Phosphatase immunohistochemical technique method and TTF-1 MAb clone 8G7G3 (DAKO) for the detection of TTF-1 in a retrospective study from our laboratory material (177 adenocarcinomas, 64 diagnosed in biopsies tissue, and 113 in surgical specimens, 20 NE neoplasms and 40 small cell lung carcinomas / SCLCs).
Results: (1) TTF-1 was detected in normal human lung with nuclear immunoexpression in bronchial and alveolar epithelial cells (2) Nuclear immunoreaction of TTF-1 was detected in the majority of lung adenocarcinomas (157/177) (3) TTF-1 was not expressed in neoplasms having a NE cell origin (4) Expression of TTF-1 was identified in 35 cases of SCLCs.
Conclusions: TTF-1 immunoreaction was absent in 20 cases of metastatic lung tumor with clinical or histological suspicion (from colon, breast, renal cell adenocarcinoma) and this finding supports the potential diagnostic value of this marker in lung and nonlung origin of a tumor.

P 249

CONGENITAL CYSTIC ADENOMATOID MALFORMATION OF THE LUNG AND BRONCHIOLOALVEOLAR CARCINOMA IN A YOUNG WOMAN

MUKENSNABL Petr, PESEK Milos, SPIDLEN Vladimir, MINARIK Marek, HADRAVSKA Sarka, CHUDACEK Zdenek
Medical Faculty Hospital, Plzen, Czech Republic
Genomac International, Prague, Czech Republic

Introduction: Congenital cystic adenomatoid malformation (CCAM) is a hamartomatous mass of lung tissue that has varying degree of cystic changes. CCAM is a relatively uncommon pulmonary lesion that presents mainly in neonates, rarely this lesion manifests in older children and adults. There are on records only a few patients with CCAM or history of CCAM who has developed bronchioloalveolar carcinoma.
Case report: A 29-year-old nonsmoking woman was admitted to Department of pulmonary diseases because of persisting fever, cough and the left chest pain suspicious of chronic pneumonia in the last several months. On the chest X-ray paracardial consolidation of the left lung was found. Physical examination was unremarkable. Chest CT-scan revealed a picture suspicious of intralobar pulmonary sequestration. However, the chest and abdominal aortography did not confirm the diagnosis. Lung functions were within normal limits and bronchoscopy did not reveal any abnormality of bronchial tree, or other pathology.
Results: Resection of the left lower lobe was performed. Grossly and histologically there was found a congenital cystic adenomatoid malformation in the excised tissue containing areas with numerous mucinous cells, which in some foci had transitions to mucinous bronchioalveolar carcinoma. Molecular genetic investigation revealed a deletion mutation located on the exon 19 of EGFR gene. Patient recovered without major complaints after surgery. In the follow-up period, the chest X-ray and CT-scan did not show progression of tumor.
Conclusion: CCAM with transition to bronchioalveolar carcinoma is an extraordinary rare disorder. The presence of mucinous epithelium in CCAM may led to the suspicion, that this epithelium is premalignant. Mutation of EGFR gene is currently recognized as a marker of early phase of cancerogenesis in this lesion. Because this type of tumor becomes growth factor-dependent, it typically shows a good response to biological therapy and the prognosis of such patients, who undergo radical surgery, is usually favourable.

P 250

COMBINED AND SYNCHRONOUS PULMONARY TUMOURS-CASES REPORT

VASILESCU Florina 1,2 DUMITRESCU Marius 1, FLOREA – GRAMADA Zenaida 2, LUCA Lacramioara 1, TOMA Liana 1, BULATA Rodica 1, CUREA Marius 1.
1- Military Hospital of Bucharest
2- Victor Babes Institute of Pathology

We report two cases of rare lung tumours. The first case is a 51-years-old-male which on CT of the chest had a single centro-hilar tumour. The bronchoscopy revealed a polypoid intrabronchial mass infiltrating the lung parenchima. On bronchoscopic biopsy the histologically diagnosis was typical carcinoid. Also, on frozen sections, the right tracheobronchial lymph node has shown micrometastases of typical carcinoid. The surgery specimen, represented by the middle lobe of the right lung, had a tumour of 5 cm in the main diameter. On routine stain (H&E), we diagnosed two different histo-pathological patterns: typical carcinoid (IHC positive diffuse for chromogranin and synaptophysin) and squamous cell carcinoma (IHC negative for neuroendocrine markers). The second case is a 59-years-old-male which presented in the superior lobe of the left lung two tumours: the first one was a polypoid intrabronchial mass of 2.5 cm which at light microscope had a basaloid scuamous cell carcinoma apearance. The second one was a peripheral mass measuring 3 cm in diameter which microscopically proved to be an adenocarcinoma. The two cases of combined and synchronous lung tumours are rare occurrence. The clinical significance of these types of tumours are uncertain.

P 251

PRIMARY LYMPHOID NEOPLASMS OF THE LUNG

KAVANTZAS Nikolaos 1, KORKOLOPOULOU Penelope 1, AGROGIANNIS George 1, THYMARA Irini 1, ZACHILAS Dimitrios 2, ADAMOPOULOU Marina 2, ANASTASIOU Nikolaos 2, PATSOURIS Efstratios 1
1.Department of Pathology, School of Medicine, National and Kapodistrian University of Athens, Athens, Greece
2.Department of Thoracic Surgery, 1st IKA Hospital, Athens, Greece

Introduction: Primary lymphoma of the lung is a rare clinical entity (0.5-1% of the primary malignancies of the lung). Less than 100 cases of primary Hodgkin disease of the lung have been reported in the literature, worldwide. We present five cases of primary lymphoid neoplasms of the lung.
Patients and Methods: Over a 6 years period, 5 patients (3 men, 2 women, mean age: 70.6 years) were admitted with symptoms of bronchial occlusion and/or signs of parenchymal disease. Minimal invasive diagnostic techniques were performed to all patients. Radiologically, 4 patients demonstrated signs of diffuse nodular lesions, while 2 of them had concomitant pleural effusion. Lower lobe atelectasis was demonstrated in one patient. Bronchoscopy was performed in one patient, Medical Thoracoscopy (MT) in one patient and Video-assisted Thoracic Surgery (VATS) in 3 patients. In all cases histological examination of the excised specimens was followed.
Results: Primary non-Hodgkin lung lymphoma was diagnosed in 3 patients (one patient with solitary endobronchial lesion). Primary Hodgkin disease of the lung was diagnosed in 2 patients. All patients received appropriate treatment. One patient with non-Hodgkin lung lymphoma died 4 months after the diagnosis, due to treatment complications, while the other 2 patients with non-Hodgkin lung lymphoma died 12 and 13 months respectively, from non disease-related causes. Two patients with primary Hodgkin disease of the lung are disease-free 9 and 10 months respectively from the time of diagnosis.
Conclusions:
The tremendous progress in the fields of histopathology and immunochemistry along with the advent of minimally invasive diagnostic techniques (MT, VATS) have facilitated the diagnostic approach to the primary lymphoid lung neoplasms. With the use of these minimally invasive techniques by which large sized biopsy specimens can be obtained, unnecessary diagnostic thoracotomies can be avoided.

P 252

SCLEROSING HEMANGIOMA OF THE LUNG: REPORT OF 5 CASES WITH IMMUNOHISTOCHEMICAL AND CLINICOPATHOLOGICAL FINDINGS

OZLUK Yasemin(*), GULLUOGLU Mine G.(*), TOKER Alper(**), KALAYCI G(**), YILMAZBAYHAN Dilek(*)
(*) Istanbul University, Istanbul Faculty of Medicine, Department of Pathology
(**) Istanbul University, Istanbul Faculty of Medicine, Department of Thoracic Surgery

Sclerosing hemangioma of the lung (SHL) is a rare tumor which is thought to be benign. Although the differentiation of tumor cells has been controversial, it is believed to be

originated from fetal pulmonary epithelial cell. Also, with various histological patterns, it leads to diagnostic difficulties having no specific immunohistochemical marker.

The aim of this study is to demonstrate the immunohistochemical profile of SHL in addition to the analysis of clinicopathological features.

The clinicopathological features of 5 SHLs were reviewed and analyzed. Immunohistochemical analysis could be performed in 3 cases for antibodies TTF-1, Surfactan protein-B, NSE, Chromogranin A, Synaptophysin, CD31, CD34, estrogen and progesteron receptors, Cytokeratin 7, EMA, p53 and Ki67.

All patients were female with an average age of 54.4 years (36-65). The tumor size ranged from 2 to 5 cm with a mean of 3.7 cm. The combination of observed histological patterns was different in each case. Four cases revealed papillary pattern, 1 case revealed sclerotic pattern, 4 cases revealed solid pattern and 3 cases revealed hemorrhagic pattern. No mitotic activity was detected in all cases. Ki-67 proliferation index ranged from 1.4 to 2.2% with an average of 1.8%. Both the surface and round stromal cells were diffusely positive for EMA and TTF-1 in two cases, whereas NSE was demonstrated focally in all. Only in one tumor TTF-1 and Surfactan protein-B were detected to be weakly focal positive, but EMA was diffusely strong positive. None of the tumors exhibited positivity for endothelial markers. Cytokeratin7 and Surfactan protein-B were both positive in only surface cells. Progesteron receptor was detected both in surface and round stromal cells but estrogen receptor was negative.

SHL is most probably a benign tumor of primitive pulmonary epithelium with various histological patterns. There is no specific immunohistochemical marker for SHL but EMA, TTF-1 and Surfactan proteins are helpful in differential diagnosis. This entity must always be kept in mind in the diagnosis of solitary pulmonary nodules because of its similarity to the histology and immunophenotype of the primary and metastatic pulmonary tumors. Positivity for progesterone receptor antibody may be associated with the female predominancy of SHL. However, this suggestion is needed to be studied on large series of SHL.

P 253

TTF-1 IMMUNOHISTOCHEMISTRY AS AN INTRA-OPERATIVE DIAGNOSTIC TOOL AT FROZEN SECTION FOR DISTINCTION BETWEEN PRIMARY AND SECONDARY LUNG TUMOURS

BUTCHER David, GOLDSTRAW Peter, LADAS George, DUSMET Michael, SHEPPARD Mary, NICHOLSON Andrew.
Departments of Histopathology and Thoracic Surgery, Royal Brompton Hospital, Sydney Street, London SW3 6NP, UK.

Although undertaking frozen sections is a well established, diagnostically accurate procedure in intra-operative lung cancer diagnosis, differentiation of primary from metastatic carcinomas remains problematic. This study assesses the value and practicality of undertaking immunohistochemistry (IHC) for thyroid-transcription factor-1 (TTF-1) at the time of frozen section when faced with this clinical situation.

Thirteen patients presented with a mass in the lung and a history of previous carcinoma (colon n= 8, renal n= 1, breast n=3, thyroid n=1). Specimens were taken during operation for confirmation of malignancy and at this time additional sections were taken for intra-operative localisation of TTF-1. The antigen was visualised using the Envision® System with abridged methodology. Slides were assessed as positive, equivocal or negative. Conventional IHC was then repeated both on the paraffin block from the frozen section and a separate tumour block from the resection specimen for comparison.

Of 13 cases, seven cases were positive for TTF-1 at frozen section, one of which was metastatic thyroid carcinoma. The remaining six were either positive (n=5) or equivocal (n=1) on the subsequent paraffin section and positive on resection specimen (n=6) and felt morphologically to be primary pulmonary adenocarcinomas. Six cases were negative on frozen section. However, one case of colonic carcinoma showed focal staining for TTF-1 on sections from subsequent paraffin block and resection. IHC confirmed metastatic disease in the resection specimens (colonic carcinoma (n=5), cytokeratins (CK)20 +ve, CK7 –ve TTF-1 –ve; renal cell carcinoma (n=1), TTF-1 -ve with clear cell morphology). The average time above that of the basic frozen section was 24 minutes per frozen section. The extra cost per test was £32 per slide.

Frozen section IHC using TTF-1 shows specificity and sensitivity similar to those seen for fixed tissues, and appears feasible within the time frame of a thoracotomy. However, its practice should be properly planned within an operative procedure as liberal usage will likely have significant staff and cost implications.

P 254

COX-2 EXPRESSION IN NEUROENDOCRINE TUMOURS OF THE LUNG

Tötsch M, Krzysik M, Schmid KW.
Department of Pathology, University of Essen, Westgerman Tumour Centre, Germany

Background:
Recent studies have highlighted the role of COX-2 in human cancers and the protective effect of COX inhibitors. Cox-2 can be found in a large proportion of lung adenocarcinoma and squamous cell carcinoma. However, little is known about the frequency of COX-2 expression in neuroendocrine tumours of the lung.
Materials and Methods:
Paraffin-embedded material from 64 neuroendocrine tumours were retrieved from the archives. Immunohistochemistry showed COX-2 staining in all twelve carcinoids (100%), in two of four atypical carcinoids (50%) and in 13 of 48 small cell carcinomas (27%). While a dense and intensive cytoplasmic COX-2 staining (++ - +++) could be seen in carcinoids, the findings in the two positive cases of atypical carcinoids were weak respectively moderate. In SCLC, seven cases showed a weak (+) expression of COX-2, four cases presented a moderate staining (++). Normal bronchial epithelium showed an apical staining, pneumocytes II were positive in regions with chronic inflammation.
Conclusion:
This study is one of the first to investigate systematically the expression of COX-2 in neuroendocrine tumours of the lung. It demonstrates that the different entities of these tumours show a very distinct immunohistochemical pattern. The clinical impact of these findings has to be further investigated.

P 255

EXPRESSION AND PROGNOSTIC IMPLICATIONS OF APOPTOSIS-RELATED PROTEINS IN LOCALLY ADVANCED NON-SMALL CELL LUNG CANCERS.

FOKKEMA, Eelco 1, TIMENS Wim 2, DE VRIES, Elisabeth G.E. 3, DE JONG, Steven 3, FIDLER, Vaclav4, MEIJER, Coby 3, GROEN, Harry J.M. 1.
Departments of Pulmonary Diseases1, Pathology2, Medical Oncology3, and Biostatistics and Epidemiology4, University Medical Center Groningen, The Netherlands.

Introduction: In advanced lung cancer at present little prameters are available to predict outcome.
Purpose: To evaluate prognostic significance of apoptosis related proteins in locally advanced non-small cell lung cancer (NSCLC).
Patients and Methods: Bronchoscopically procured tumor biopsies of NSCLC patients were stained

immunohistochemically and rated for expression of eight different cellular proteins. Staining ¡Ü 10% of the tumor cells was classified as negative, > 10% was considered as positive. Patients were treated with 60 Gy radiotherapy with or without carboplatin as radiosensitizer.
Results: Apoptotic proteins in tumors that showed positive staining were the highest for Bax (99%), Fas (92%), FasL (87%), Rb (87%), p21(WAF1) (73%), and p53 (70%), and the lowest for c-myc (58%) and Bcl-2 (58%). In the Cox regression analysis stage (stage 3B versus stage 3A, relative risk (RR) = 0.63, 95% CI, 0.43-0.92, p<0.02), the presence of mediastinal lymph nodes (N2 versus N3, RR=1.69, 95% CI, 1.02-2.8, p=0.04) and Bcl-2 positivity (RR=0.61, 95% CI, 0.37-0.98, p=0.04) were predictive for overall survival. Only Bcl-2 staining percentage (RR10 (RR associated with an increase in stained cells of 10%) = 0.93, 95% CI, 0.89-0.99), p53 (RR10=0.94, 95% CI, 0.89-0.99, p=0.027) and FasL (RR10=0.92, 95% CI, 0.86-0.99) were predictive for a longer time to progression. No specific constellation of apoptotic proteins was associated with tumor response except that the loss of Rb expression was associated with the absence of any tumor response.
Conclusion: Bcl-2 expression in tumor tissue of patients with locally advanced NSCLC predicts a better overall survival, while Bcl-2, p53, and FasL expression predict for a longer time to progression.

P 256
EXPRESSION OF SOMATOSTATIN RECEPTORS 2-5 IN NEUROENDOCRINE TUMOURS OF THE LUNG
Tötsch M, Krzysik M, Schmid KW.
Department of Pathology, University of Essen, Westgerman Tumour Centre, Germany

Background:
Somatostatin receptors 1-5 can be found in a large proportion of human tumours. Due to the fact, that receptor-positive tissue can be detected by scintigraphy , several investigations have taken place to demonstrate somatostatin-receptors also at the immunohistochemical level. Recent studies have concentrated mainly on the detection of the Somatostatin receptor type 2 (SSTR2) in small cell carcinoma. We were interested to investigate systematically the presence of SSTR 2-5 by immunohistochemistry in various entities of neuroendocrine tumours of the lung.
Materials and Methods:
Paraffin-embedded material from 45 neuroendocrine tumours were retrieved from the archives. Of twelve carcinoids, 8 expressed SSTR2, three SSTR3. None were positive for SSTR 4 or 5. All four atypical carcinods were negative for SSTR2, in 3 cases a cytoplasmic staining for SSTR3 was found. One case was weakly positive for SSTR4 and two cases for SSTR5. In 10 of 28 small cell carcinoma SSTR2 was found, 13 cases were positive for SSTR3, 3 cases for SSTR4 and one case for SSTR5. The case of large cell neuroendocrine carcinoma was positive for SSTR3 and SSTR4, SSTR2 and SSTR5, however, were negative.
Conclusion:
This preliminary study may help to correlate the findings by receptor autoradiography with immunohistochemical results in various types of lung neuroendocriene tumours. This may provide further information concerning diagnosis as well as therapeutic approach in these tumours.

P 257
PULMONARY METASTASIS SECONDARY TO "BURNED OUT" TESTICULAR TUMOR. A CASE REPORT.

SAINT-BLANCARD Patrick (1), GUIGAY Joel (2)
Department of Pathology (1),
Department of Respiratory Diseases (2)
Hôpital, d'instruction des armées, Percy, 92141 Clamart France.

Metastatic germ-cell tumor of the primary testicular lesion has rarely reported. The majority of cases described described in the literature have occured in patients with retroperitoneal metastasis. The autors present a case of pulmonary metastasis with complete regression of the primary testicular tumor.
A 34-year-old Caucasian man presented with a 3-month history of chronic cough. The chestX-ray and the thoracic computed tomography scan showed a 10x14 cm mass in the lower lobe of the left lung without lymph node involvement. The flexible bronchoscopic examination revealed an obstructive mass in the upper segment of the left lower lobe. Histological examination proved the mass to be a malignant germ-cell tumor containing embryonal carcinoma elements. Serum ƒÒ-human chorionic gonadotropin and ƒÑ-fetoprotein were elevated. Ultrasonography visualized a heterogeneous testicular mass. Histological examination of the testicular tumor showed stromal fibrohyalinosis with no evidence of a tumor. The patient was successfully treated with orchiectomy, chemotherapy and lung surgery. Four years later, he remains disease free.
Confronted with a young man presented an isolated pulmonary tumor and apparently normal testes, the physician should suspect a metastatic malignancy, especially metastatic germinal germ-cell tumor with regression of the primary testicular tumor. Tumor marker assays and ultrasonography should be performed and in-deph histological examination of the testis in essential when lesions are identified.

P 258
THYROID TRANSCRIPTION FACTOR-1 (TTF-1) IN THE DIFFERENTIAL DIAGNOSIS OF THE PRIMARY AND METASTATIC LUNG CANCER. OUR 4-YEAR FOLLOW-UP STUDY.
Jäckel,M1., Moldvay,J2., Bogos,K3., Soltész,I3., Agócs,L3., Kovács,G3. and Schaff,Zs4.:
1Central Hospital of Hungarian Defence Forces, Department of Pathology , Budapest , 2County Hospital of Pulmonology, Torokbalint, 3National Institute of Pulmonology, Budapest, 4Semmelweis University Budapest, 2nd. Department of Pathology, Hungary

Introduction: Lung adenocarcinoma is very frequent in adult population. The tumor may be primary, but metastasis from malignancies of other organs often appears as a solitary nodule. From the treatment's point of view it is very important to know if the tumor is of primary or metastatic origin. TTF-1 is a sensitive marker for pulmonary and thyroid adenocarcinomas.
Material and methods: In order to determine the usefulness of TTF-1 in distinction between primary and metastatic lung adenocarcinoma we have examined the expression of TTF-1 in 100 solitary pulmonary nodules. They included 50 stage I. peripheral primary bronchial adenocarcinomas and 50 metastatic pulmonary adenocarcinomas of different origin such as breast, colon, rectum, kidney, stomach and thyroid gland. TTF-1 was performed on formalin-fixed and paraffin-embedded tissues. All primary adenocarcinomas were diagnosed in 2000. In November, 2004 follow-up study was performed. We investigated the correlation between the strong and the weak nuclear immunostaining and the survival of patients.
Results: We found immunopositivity in 46/50 cases, among them 30 cases showed strong nuclear immunostaining. In the remaining four cases the immunopositivity was localized to the cytoplasm. All metastatic adenocarcinomas were negative, apart from the 2 thyroid carcinoma metastases that showed strong immunopositivity. Follow-up data were available in 49/50 patient. There was no tumor recurrence in 27 cases (12 strong immunopositivity), in 6 cases the disease progressed (5

strong immunopositivity), and 14 patients died (9 weak immunopositivity). Kaplan-Meier survival analysis and chi square test showed strong correlation between strong immunopositivity and free survival time (p=0.03)
Conclusion: Our results confirm, that the TTF-1 immunohistochemistry is a very sensitive and highly specific method in the differential diagnosis of primary and metastatic lung adenocarcinomas and should be used in the everyday routine practice. Moreover, TTF-1 immunopositivity proved to be a good prognostic factor in stage I lung adenocarcinomas.

P 259
TISSUE MICROARRAY IMMUNOPHENOTYPING OF PRIMARY NSCLC AND BRAIN METASTASES
PÁPAY Judit,1 MOLDVAY Judit,2 KRENÁCS Tibor,3 TAMÁSI Anna,1 STELKOVICS Éva,3 FURÁK József,4 KOPPER László1
1Department of Pathology and Experimental Cancer Research, Semmelweis University, Budapest, 2County Hospital of Pulmonology, Törökbálint, 3Laboratory of Tumor Pathology and Molecular Diagnostics, Bay Zoltan Foundation for Applied Research, Szeged, 4Department of Surgery, University of Szeged, Szeged, Hungary

Introduction. A proportion of non small-cell lung cancers (NSCLC) form metastases almost exclusively into the brain irrespectively of their primary sizes. Purpose. To identify markers which can predict metastatization of NSCLC into the brain. Methods. Twenty one squamous cell carcinomas and 5 adenocarcinomas of the lung with brain metastases using immunohistochemistry with a selected panel of antibodies were tested. Twenty squamous cell carcinomas and 15 adenocarcinomas with no brain involvement were used as a control. Tissue cores of 2 mm in diameter were incorporated into 24-sample microarray blocks resulting in 117 samples in 5 paraffin blocks using duplicate samples in most cases. Tested antibodies were specific for molecules of cell adhesion (e.g. BP180/Collagen XVII, CD44, E-Cadherin, b-Catenin), cell growth (e.g. Akt1, EGFR, nm23) cell cycle regulation (e.g. Cyclin D1, -D3; Ki67, p16, p21waf1/Cip1, p27kip1, DNA repair (Topoisomerase IIa) and apoptosis (e.g. Bax, Bcl-2, CAS, Caspase-3, -8,-9, FAS, p53). The results were assessed by 2 independent observers a 4-scale scoring system (0 negative, 1 weak, 2 moderate, 3 strong), where cut-off levels were based on literature data considering the patho/biological role of the given marker. The concensus based final scores were converted using the TMA-Deconvoluter software. Non-supervised hierarchical clustering was applied for all data and for selected data groups, which then were visualized using the TreeView program. Results. Phenotypic marker expression of primary NSCLC and their brain metastases showed very similar profile without major loss or gain of any marker. None of the exclusive groupings of markers, i.e. analyzing cell cycle, apoptosis or cell adhesion associated markers grouped separately, resulted in obvious clustering of our cases. However, when the expression profile was set up combining immunoreactions for Cyclin D1, Cyclin D3, Ki67, p16, Collagen XVII/BP180 molecules, the majority of brain tumors clustered with a high positive correlation (0.86) with these markers. Conclusion. Based on tissue microarray analyses, the metastatic capacity of NSCLC cases into the brain seems to be associated with cell cycle activation and the upregulation and delocalization of the hemidesmosomal Collagen XVII/BP180 antigen. Analyses of further restricted combinations involving the expression of a few more marker molecules are still under way.

P 260
STROMAL TUMOR OF THE ILEUM WITH PULMONARY METASTASIS.
SAINT-BLANCARD Patrick (1), JANCOVICI Rene (2), Department of Pathology (1) and Department of Thoracic Surgery (2), Hôpital d'instruction des armées, Percy, 92141 Clamart, France.

Gastrointestinal stromal tumors (GISTs) constitue the largest category of primary non-epithelial neoplasms of gastrointestinal tract. Extra-abdominal metastases of GISTs occur in less 10 percent of patients.
A 34-year-old Caucasian man was admitted for abdominal pain, anorexia, nausea vomiting occur, weight loss of 10 kg. No abdominal mass was found. The endoscopic findings were not specific. Abdominal computed tomography scan showed multiple intramural masses of jejunum and ileum. Thoracic CT scan showed a right hilar mass with small mediastinal lymph nodes. The intestinal masses were resected by laparotomy and hilar mass by mediastinoscopy. Histological and immunohistochemical studies on the surgical resection specimens revealed a GIST with pulmonary metastases. The patient died after 2 years.
GISTs are rare and represent the 0.2% of all malignancy of this site. They occur predominantly in older individuals over 40 years of age with equal sex incidence. They are most common in stomac (60-70%), followed by small intestine (20-30%), colon and rectum (5 %), oesophagus (*f*¬ 5 %), and occasionnally in omentum and mesentery. Recent work has indicated that the interstitial cells of Cajal, which exhibit both myoid and neural features, could be candidates for tumor histogenesis.
20-30 % of GISTs show malignant behavior, including peritoneal dissemination and hematogenous metastases. Metastases are often present at the time the primary tumor is discovered. The most common metastatic sites are the peritoneal surfaces and liver, following by retroperitoneal soft tissues. Lymph nodes, bone and lung metastases are rare. The survival rates at 5 years of malignant tumors vary of 19 to 54 %.

P 261
UNUSUAL METASTATIC PATTERN OF A RADIATION INDUCED ANGIOSARCOMA OF THE SKIN – A CASE REPORT
KNOLLE Jürgen, HEGE Stefanie, SCHREIBER Christel, SCHREIBER Jens
Municipal Hospital Dessau, Academic Teaching Hospital, Institute of Pathology and Dept. of Pulmonology, 06847 Dessau, Germany

We report on a 67 year old female patient in whom hysterectomy and oophorectomy as well as adjuvant telecobalt radiation were performed 27 years ago. 25 years later multiple tumours occurred in the abdominal wall. Histological examination of these tumours showed an epitheloid neoplasm with vascular proliferation and a fine framework of reticular fibres. Immunohistochemistry (pancytokeratin, cytokeratin 8/18, CA125 and CD45 negative, vimentin and CD31 positive, CD34 focally positive) revealed angiogenic differentiation and an angiosarcoma was diagnosed. It was treated surgically.
Another two years later the patient was admitted to hospital with severe dyspnoea. Chest x-ray and CT-scans showed abundant bilateral predominantly interstitial infiltrates in both lungs. Bronchoscopy revealed a diffuse thickening of the bronchial mucosa. Bronchoalveolar lavage, biopsies of the bronchial mucosa and transbronchial lung biopsies were performed. A malignant small round blue cell tumour was identified in all specimens. Immunohistochemistry (cytokeratin and CD45 negative, CD31 intensely positive) confirmed metastases of the angiosarcoma.
Post-mortem examination revealed relapse of the angiosarcoma in the abdominal wall as well as metastases in the lungs, which showed a predominantly interstitial and

peribronchial growth pattern. Further metastases were found in the lymph nodes, in the myocardium, in the abdominal fatty tissue and additionally in a synchronous renal cell carcinoma. Radiation induced angiosarcoma is very uncommon. Furthermore the metastatic pattern with the clinical presentation as an interstitial lung disease on the one hand and with a metastasis in another malignant tumour, which occurred independently, on the other hand are extreme rarities.

P 262
ASSOCIATION BETWEEN MALIGNANT MESOTHELIOMA OF THE PLEURA AND OTHER MALIGNANCIES

Claudio Bianchi, Tommaso Bianchi, Lucia Ramani
Center for the Study of Environmental Cancer, Italian League against Cancer, Hospital of Monfalcone, 34074 Monfalcone, Italy

The association between malignant mesothelioma and other primary tumors has repeatedly been described. In such reports, however, a denominator is frequently not available. In the present study, a series of 169 malignant pleural mesotheliomas, examined at necropsy at the Hospital of Monfalcone, Italy, in the period 1980-2002, were reviewed.The group included 139 men and 30 women. All mesotheliomas were classified as asbestos-related. The co-existence of mesothelioma with other malignancies had been detected in 33 cases (19.5%). Four different tumors were seen in two cases. A 77-year-old men showed, besides mesothelioma, a lung carcinoma, a small carcinoma of the kidney, and a small carcinoma of the prostate. A 85-year-old woman showed three carcinomas of the large bowel.Triple malignancies were observed in 6 cases; in particular, non-Hodgkin lymphoma or leukaemia were associated with mesothelioma in three cases, and prostate adenocarcinoma in two. Double tumors were observed in 25 cases, with prostate adenocarcinoma (5 cases), bladder carcinoma (4 cases), and hepatocellular carcinoma (3 cases), being the most frequent additional malignancies. Of the four non-Hodgkin lymphomas observed in the whole series, two were extra-nodal. In some of the present cases the co-existence of different tumors was a cause of major difficulties in the clinical diagnosis. Only small percentages of people exposed to asbestos develop mesothelioma. The analysis of the cancer varieties associated with mesothelioma may furnish information about the background, in which mesothelioma develops, and/or about the co-factors playing a role in the genesis of asbestos-related mesothelioma. The co-existence of mesothelioma with non-Hodgkin lymphoma or with hepatocellular carcinoma may suggest a role of immune impairment in the genesis of mesothelioma.

P 263
CELL PROLIFERATION RATE AND TELOMERASE ACTIVITY IN THE DIFFERENTIAL DIAGNOSIS BETWEEN BENIGN AND MALIGNANT MESOTHELIAL PROLIFERATIONS

CAKIR Caglar, GULLUOGLU Mine G., YILMAZBAYHAN Dilek.
Istanbul University, Istanbul Faculty of Medicine, Department of Pathology

The differential diagnosis of malignant mesothelioma (MM) from benign mesothelial proliferations (BMP) based on histopathologic criteria is sometimes not satisfying and causes diagnostic problems for the histopathologists. We investigated whether the immunohistochemically determined cell proliferation rate and telomerase activity, using Ki-67 and hTERT immunohistochemistry, respectively, are useful in the differential diagnosis of MM from BML. Sixty six cases of MM (33 epithelioid, 30 biphasic and 3 sarcomatoid) and 22 cases of BML (15 reactive mesothelial proliferations and 7 fibrous pleuritis/pericarditis) were included in this study. The mean value of Ki-67 proliferation index (pi) in MMs was significantly higher than that of BMLs. Biphasic MMs have higher Ki-67pi than epithelioid and sarcomatoid types. Ki-67 immunohistochemistry has the sensitivity of 86%, specificity of 74% and positive predictive value of 94% in detecting MM. hTERT immunohistochemistry detected MM with sensitivity and specificity of 68%. Furthermore, the sensitivity and specificity of hTERT for detecting MM among the cases with low Ki-67pi were 58% and 78%, respectively. As a result, being cheap and simple methods, Ki-67 and hTERT immunohistochemistries can be used in differentiating malignant and benign mesothelial lesions in routine formalin-fixed, paraffin-embedded material.

P 264
DIAGNOSTIC VALUE OF PSEUDOINCLUSION IN THYROID PAPILLARY CARCINOMA AND HASHIMOTO'S LYMPHOCYTIC THYROIDITIS

Dr Ezatollah Rafie Alavi,Dr Amir Khashayar Varkoohi,Samira Roshani

Objectives and background:Papillary carcinoma is the most common malignant tumor of the thyroid.
Intranuclear inclusions(pseudoinclusions)that represent an invagination of the cytoplasm into the nucleus are frequently seen in papillary carcinoma ,and in fact this is one of characteristic features.
Chronic lymphocytic thyroiditis(Hashimoto's);is one of the thyroid diseases that could be present with thyroid cold nodule and FNA is recommended for evaluation.
Materials & Methods:This is an experimental study .In this study 33 cases of patients with cold nodules or diffuse enlargment of one or both lobes of thyroid were candidated for FNA.In clinical studies, these 33 cases were diagnose as suggested for malignancy or Hashimoto's thyroiditis. All prepared smears were staine with papanicolao and geimsa,and studied.
.Findings: In all cases showed nuclear pseudoinclusion in papanicolao and geimsa stain.
Cytologic findings in 16 smears included variable degrees of lymphocytic infiltration with some hurthle cells in scanty colloid background and diagnosed chronic lymphocytic thyroiditis(Hashimoto's thyroiditis).17 of them were diagnose as suggested for papillary carcinoma,due to seen pseudoinclusion,but in histologic study of them showed hashimoto's thyroiditis and the result of TPO test in these 17 cases was positive
As a result , pseudoinclusion showed clearly in smears stained with papanicolao.
Conclusion: Most of cytomorphologic findings in FNA of papillary carcinoma are not specific ,for example ;papillae could be seen in papillary hyperplasia,nuclear features ,so ground-glass chromatin,longitudinal folds or nuclear groove,although are important for papillary carcinoma ,but are neither constant nor specific.Psammoma bodies are observed in a small number of cases which are not specific to papillary carcinoma of the thyroid, because they also have been described in other lesions such as toxic diffuse goiter and Hashimoto's thyroiditis. In contrast to previous reports,nuclear pseudoinclusion are not characteristic for papillary carcinoma of thyroid and it could be seen in Hashimoto's thyroiditis

P 265
ACCURACY OF FINE NEEDLE ASPIRATION CYTOLOGY IN THYROID NODULES.

Authors:
Dr.Enssieh Shafigh,MD.AP*,
Dr.Sepideh Siadati,MD.ACP,
Dr.Zoleikha Moazezi,MD,Internist,Endocrinologist.

Place: Department of Pathology, Shahid Beheshti Hospital, Babol, Iran.
* Correspondence author.

Introduction: FNAC has become accepted as a cost-effective procedure in the assessment of thyroid nodules and is an important first-line diagnostic test for the evaluation of goiter and the single most effective test for the preoperative diagnosis of a solitary thyroid nodule. To evaluate the accuracy of FNAC in the diagnosis of thyroid nodules did this study.
Material & Methods: This study was carried out at Shahid Beheshti Hospital in Babol Medical University during the period of 1998 and 2003. There were 745 FNACs of which 98 had definite histology after thyroidectomy. FNAC was correlated with histology and sensitivity, specificity, accuracy with NPV and PPV were calculated.
Results: The overall sensitivity of FNAC detecting thyroid neoplasia was 86.84%, specificity 73.3% and accuracy 78.57%. NPV and PPV were 89.79%, 69.38%, respectively. There was no false positive malignant FNAC. 32 malignant cases were detected, that of 22 males, 13 (59%) had malignancy compared with 19 of 76 females (25%).
Conclusion: FNAC is a useful test in assessment of solitary thyroid nodules especially in males who have high index of suspicion of thyroid cancer. Malignant or suspicious for malignancy cytology are absolute indicators for thyroidectomy.
Keywords: Solitary thyroid nodule, FNAC, Thyroid neoplasia, Accuracy.
Address for correspondence:
Dr. Enssieh Shafigh, Department of Pathology, Shahid Beheshti Hospital, Babol, Iran.
Tel: 0098-111-2252071-5. Fax: 0098-111-2251664.
Email: eshafigh@yahoo.com.

P 266
HISTIOCYTOID-LIKE CELLS IN FINE-NEEDLE ASPIRATION BIOPSY (FNAB)OF THE THYROID
ORELLANA Ruth1, BELLA Maria Rosa1, COMBALIA Neus1, FERNÁNDEZ Sara1, GIMÉNEZ Gabriel2, CASALOTS Alex1, ESCODA Maria Rosa1, DINARÈS Maria Carme1, REY Mercé1.
1Corporació Parc Taulí, Pathology Dep. Sabadell, Barcelona. Spain
2 Corporació Parc Taulí, Endocrinology Dep. Sabadell, Barcelona. Spain

INTRODUCTION: Histiocyte-like cells, characterised by vacuolated cytoplasm without classic nuclear changes of papillary carcinoma (PC), isolated or in clusters, have been described recently as highly specific for PC in thyroid FNAB specimens.
AIMS: Immunohistochemical study and cytohistologic correlation in cases with histiocyte-like cells at FNAB without classic features of PC.
MATERIAL AND METHOD: 327 FNA of thyroid were performed in our Hospital last year. Cases with histiocyte-like cells observed isolated in both smears and cell blocks were selected; Cytokeratin 19 (CK-19) (Novocastra, b170), Galectin 3 (Gal-3) (Novocastra, 9C4) and CD-68 (DAKO, PG-M1) were performed on the cell block; histologic correlation with surgical specimen was made.
RESULTS: Of 327 FNAB, only in 3 cases histiocyte-like cells were identified in both smears and cell block. These cells were immunoreactive for CK-19 and Gal-3, and were negatives for CD-68. All resection specimens correspond to nodular hyperplasia (NH), showing at microscopic level cystic follicles lined by follicular cells with histiocytic appearence like those identified in cytologic samples.
CONCLUSIONS: Histiocyte-like cells are a rare finding. Although these cells present the same immunohistochemical profile as PC cells, they are not pathognomonic, raising a potential pitfall for the interpretation of thyroid FNAB. These cells could be altered follicular cells from the cyst lining, in NH, with repair-like features or scamous metaplasia based on their immunoreactivity.

P 267
OUR EXPERIENCE IN THE EFFECT OF FINE-NEEDLE ASPIRATION ON THE PAPILLARY THYROID CARCINOMA SCAN
SOPTA Jelena., TATIC Svetislav , HAVELKA Marija., ATANACKOVIC Mirjana., MARKOVIC Ljiljana

Papillary carcinoma represents approximately 75-85% of all thyroid malignancies. We report comparative analyses: fine-needle aspiration (FNA) cytology before operation and definitive histopathology undergo surgical excision in evaluation of it.
During the last 2 years in 600 exanimate thyroid aspirates 19 cytological diagnosis of papillary carcinoma was made. These diagnostic guidelines were used: so-called “tumor cellularity” of smears, papillary arrangement of cells, tumor cells are larger then normal follicular cells with slight anisocytosis, ground-glass nuclei, presence of intranuclear inclusions and scanty or absent colloid. Tumor was more frequent in females in 74%. The middle ages (51,2) was older then expected. Classic cytological characteristics had 89% aspirates. One papillary carcinoma contained psammoma body. In 26,3% degenerative changes (hemorrhage and necrosis) were presented. In 2 smears papillary carcinoma were associated with Hashimoto`s thyroiditis and oxyphilic lesion.
Definitive histopathology undergo surgical excision was confirmed papillary carcinoma (15, or 79%), Hashimoto`s thyroiditis with degenerative changes (2), nodular goiter with degenerative changes (1) and oxfphilic lesion (1).
We conclude that FNA cytology has a high sensitivity and specificity for the diagnosis of papillary carcinomas. Significant number of thyroid papillary cancers could be detected by fine-needle aspiration before operation.

P 268
FINE NEEDLE ASPIRATION CYTOLOGY IN THE BREAST SCREENING PROGRAM IN VERONA. FIVE YEARS OF EXPERIENCE.
Manfrin E 1 , Mariotto R 2, Reghellin D1, Remo A1, Dalfior D1, Eccher A1, Bonetti F1.
1 Department of Pathology, University of Verona (Italy), 2 Breast Screening Unit ULSS 20 Verona (Italy)

Introduction: Fine needle aspiration cytology (FNAC) is a quick, low expensive diagnostic technique widely used in the management of breast lesions both in screening programs and clinical senology. Efficacy of cytology is variable in different experiences. A European standard system of reporting the classification of cell samples (C1-C5) is now used to perform quality assurance statistics in cytology units. This system allows to compare results between units with different experience. Purpose of the study: To evaluate the cytology quality standard in Breast Screening Program (BSP) in first five years of activity according to the European guidelines.
Material and methods: Compared with the “classic” screening, the Verona program has a different organization, similar to that of a Breast Clinic, and operates in a building exclusively devoted to the BSP. First level mammograms and all second level exams (US, FNAC, core biopsy, mammotome) are performed in the same structure by a staff composed of two radiologists, two cytopathologists, four technicians and two nurses. All women are submitted to a double projection mammography with real time analysis of mammograms by Radiologists. Results are immediately communicated. Negative patients are dismissed after

reassurances; suspicious patients are immediately submitted to second level examination. FNAC is evaluated in real time for adequacy and a diagnostic report is immediately given to the Radiologist. Results: 1374 FNAC have been performed; the cytology diagnosis was C1: 10.8% (149 cases); C2:51.7% (710cases); C3:6%(83 cases); C4: 9.2% (124cases); C5:22.3% (308cases). Absolute sensitivity was 73%, Complete sensitivity:95.4%, Specificity (full):75.2%, PPV:99%, False positive rate:0.4%, False negative rate:2.1%, Inadequate rate:10.8%, Inadequate rate from cancers:2.4%, Suspicious rate:15%. Conclusions: In the Verona BSP all thresholds for FNAC quality performance are within the preferable value suggested by European quality guidelines for screening programs. From our results it seems that FNAC can be highly effective particularly within a screening program with real time microscopic analysis coupled with multidisciplinary consult between radiologist and pathologist.(Supported by Fondazione Cassa Risparmio VR-VI-BL-AN.Bando 2004.Progetto Cr.Mammella)

P 269
CLINICAL AND CYTOLOGIC FEATURES OF PAPILLARY NEOPLASMS OF BREAST

CHOI Yoo-Duk, *GONG Gyung-Yub, *KIM Mi-Jung JUNG, KIM Hyun-Joong, LEE Ji-Shin, NAM Jong-Hee, JUHNG Sang-Woo, CHOI Chan
Department of Pathology, Chonnam National University Medical School, Gwangju, South Korea
*Department of Pathology, Asan Medical Center, University of Ulsan, Seoul, South Korea

INTRODUCTION: The cytologic pattern of papillary neoplasm of the breast is described as a cellular aspirate with complex papillary fronds and a variable number of single, high, columnar epithelial cells. Differentiating a benign papillary lesion from an atypical or malignant one is difficult using fine needle aspiration cytology owing to their overlapping cytologic features.
OBJECTIVE: To compare the cytologic features of benign and malignant papillary breast lesions.
STUDY DESIGN: We reviewed the clinical and cytologic features in 29 cases of intraductal papilloma and 26 cases of atypical papilloma or papillary carcinoma that had been diagnosed by histologic examination. The diameter of the mass was examined as a clinical feature. The cytologic features evaluated were as follows: bloody background, row of tall columnar cells, naked bipolar nuclei, hemosiderin-laden macrophages, myoepithelial cells, single scattered atypical cells, cellularity, nuclear atypia, nuclear grade, apocrine metaplasia, eosinophilic cytoplasmic granules, papillary clusters, small papillae, cell balls, and large sheets.
RESULTS: Of the features evaluated, the diameter of the mass, naked bipolar nuclei, and cell ball differed significantly between benign and atypical or malignant papillary neoplasm. The average diameter of a benign papillary neoplasm was 1.8 cm, and that of an atypical or malignant papillary neoplasm was 2.2 cm (p=0.042). Naked bipolar nuclei were found in 27 cases of benign papillary neoplasm (93.1%) versus 19 cases of atypical or malignant papillary neoplasm (73.1%) (p=0.050). Cell balls were found in 14 (48.3%) and 21 (80.8%) cases, respectively (p=0.012). All six cases in which cell balls were present and naked bipolar nuclei were absent proved to be atypical or malignant papillary neoplasm. Of 17 cases where cell balls were absent and naked bipolar nuclei present, 13 (76.5%) were benign papillary neoplasm.
CONCLUSION: Most of the cytologic features overlap in benign and atypical or malignant papillary neoplasm. Although they were not pathognomic, naked bipolar nuclei and cell balls were cytologic features that differed significantly between benign and atypical or malignant papillary neoplasm. When papillary neoplasm of the breast is suspected in a cytologic smear, the combination of clinical examination, mammography, and cytologic features should be considered to make the correct diagnosis.

P 270
THE ROLE OF FINE NEEDLE ASPIRATION CYTOLOGY (FNAC) IN CLINICAL DECISION MAKING FOR PATIENTS WITH ADVANCED BREAST CANCER

Chiara Casadio*, Mara Lusiardi*, Anna Cardillo°, Giuseppe Renne*

Background: Fine needle aspiration cytology (FNAC) is a well established procedure for the diagnosis of primary tumor, recurrence, and metastasis. Biomarkers of breast cancer cells (hormone receptor status and Her-2 oncogene expression) play a key role in the prognosis and treatment response. These biomarkers can become modified during progression of disease (PD).
Purpose: To demonstrate the utility of FNAC to confirm the clinical diagnosis and to re-evaluate the biomarker status in recurrent disease.
Materials and Methods: From January 2003 to April 2005, fine needle aspiration was performed on 98 cutaneous nodules or lymph nodes from 86 women. Smears were alcohol fixed (95%) and/or air-dried and stained with hematoxylin and eosin (H&E), Papanicolaou stain, or May-Gruenwald Giemsa. In 42 cases, the remaining specimen was rinsed in a 50% alcohol solution prior to preparation in a paraffin-embedded cell block. Slides from the cell block were submitted for H&E, and when necessary, immunohistochemistry (IHC) and fluorescent-in situ hybridization-dual colour (FISH) were performed. Cytomorphology, IHC, and FISH results were compared with those of the primary tumour, when possible.
Results: The majority of FNAC were positive (76 cases) for recurrent disease. 14 cases were negative and 8 were unsatisfactory for evaluation. 56 of the 76 positive cases were re-assessed for biomarker status. There was an 83.9% concordance in biomarker status (hormone receptor status and Her-2 expression) in the recurrent tumour when compared to the primary tumour. The discordant rate was 16.1% giving rise to the hypothesis that in a few cases one tumour cell clone has dominated and metastasized.
Conclusions: FNAC is a well-tolerated procedure that is easy to perform and less invasive. A well managed cytologic specimen is sufficient for establishing a diagnosis and biological characterization. IHC and FISH can be easily performed on FNAC and facilitate the management of breast cancer patients with PD.

P 271
CYTOLOGICAL FEATURES OF PROSTATIC INTRAEPITHELIAL NEOPLASIA

Alexander Valdman. Department of Urology, Karolinska Hospital, Stockholm, Sweden.
Sara Jonmarker. Department of Pathology and Cytology, Karolinska Hospital, Stockholm, Sweden.
Peter Ekman. Department of Urology, Karolinska Hospital, Stockholm, Sweden.
Lars Egevad. Department of Pathology and Cytology, Karolinska Hospital, Stockholm, Sweden.

INTRODUCTION. Fine needle aspiration cytology (FNAC) is an acknowledged method for diagnosing prostate cancer. Although core biopsies have become more common, FNAC is still useful in elderly men and in patients with advanced disease. False positive results are uncommon but concerns have been raised that prostatic intraepithelial neoplasia (PIN) could be misinterpreted as carcinoma. PURPOSE. The aim of this study was to describe cytological features of PIN.
METHODS. Macroscopically normal areas of peripheral zone in 177 radical prostatectomy specimens were sampled by scraping cells from cut surfaces. The obtained material was

smeared, air-dried and Giemsa-stained. Histological slides from these areas were reviewed and 17 samples with high-grade PIN and no invasive cancer were selected. An equal number of smears from invasive cancer were randomly chosen for comparison. The cytological specimens were reviewed without knowledge of the histological diagnosis.
RESULTS. Cancer smears showed high cellularity and dissociation, while PIN smears only contained a few clusters of atypical cells. Pronounced nuclear atypia, prominent or multiple nucleoli and mucin were more often seen in cancer than in PIN. Crystalloids, cytoplasmic granules and size of atypical clusters did not distinguish between PIN and cancer.
CONCLUSION. PIN should not be diagnosed by FNAC alone. However, a highly cellular smear with pronounced nuclear atypia seems to preclude PIN.

P 272
URINE CYTOLOGY IN THE PREVENTION OF NEPHROPATHY BY POLYOMAVIRUS IN PATIENTS WITH RENAL TRANSPLANTATION.
ALVAREZ M. (1), GONZALEZ-OBESO E. (1), RUIZ E. (1), LOPEZ-FERRER P. (2), VICANDI B. (2), VIGUER J.M. (2).
(1) Trainee resident; (2) M.D.

INTRODUCTION: The polyomavirus (PV) is a member of the papovavirus family; two strains are associated with disease in humans: BK virus and JC virus. It has a small size (45 nm. diameter), it is not enveloped, and it contains a double-stranded DNA genome. Primary infection occurs in childhood, having an asymptomatic course, and residing in a latent state that can be activated without clinical consequences. 0.3% of the inmunocompetent individuals have asymptomatic virurias, 3% of the pregnant women, and 30-40% of the recipients of a renal allograft. In this last group the reactivation can lead to nephropathy and allograft rejection.
PURPOSE OF THE STUDY: We aim to demonstrate the usefulness of urine cytology in the detection of reactivation of PV infection in patients with renal allograft.
MATERIALS AND METHODS: The 26 transplanted patients in the study were randomly asigned into two groups: group A with 17 patients with monthly control cytologies and group B with 9 patients without urine cytological studies. A cytology was considered to be positive when PV-infected intranuclear inclusion cells (decoy cells) were found. When positive, an additional cytology was made 15 days later, and, if positive too, the inmunosuppression treatment of the patient was reduced. Besides, if renal dysfunction was found a biopsy was performed.
RESULTS: 11% of the patients of group B developed PV nephropathy, while none of the patients of group A developed it, in spite of having 29% of positive urine cytologies.
CONCLUSIONS: The repeated detection of decoy cells in urine cytologies of patients with renal transplantation allows the modulation of the inmunosuppression treatment in order to control the viremia and to prevent the nephropathy that could lead to the loss of the renal allograft. As a consequence, in our hospital the patients with a renal allograft follow periodic urine cytology controls.

P 273
FNAB OF LYMPH NODES – IS IT WORTH USING THIS DIAGNOSTIC METHOD?
Székely Eszter dr., Istók Roland dr., Szabó Ildikó, Hegedûs Ágnes, Járay Balázs dr.
Semmelweis University, II. Department of Pathology

Introduction: Although lymph node examination by fine needle aspiration biopsy (FNAB) is a quick and cost-effective method, which is well tolerated by the patient, it is not widely used by hematologists. In our opinion, it is partly due to misapprehension and bad local experience.
Our purpose was to give a non-aligned statistical proof of the efficacy of this diagnostic method, based on our data.
Method: Between 1st of January 1995 and 31st of December 2004, 2796 ultrasound (US) guided lymph node FNABs were performed in the neighbouring US laboratories, that were examined by our cytological team. (734 aspirations were performed by radiologists, the rest by cytopathologist). The smears were wet fixed with ethanol, stained with H&E.
The results are the following: lymphadenopathy – 1334, metastatic disease-880, unsatisfactory for diagnosis - 307 , (264 of them were performed by the clinician, the rest by the cytopatologist), hematological malignancy: 152 cases, „other" 119 (the latter are cases, in which the smears are staisfactory, but the result cannot be pushed into either of the above-mentioned categories. 76 of the hematological malignancies were non Hodgkin lymphomas (NHL), and found 18 HL. 17 of the 18 HL diagnosed by FNAB, were histologically confirmed. In further 58 cases, the cytological examination raised the possibility of a hematological malignancy, which was confirmed in 41 patients. (No more data in 9 patients). In 8 cases, the histological examination proved no malignancy (fals postitive by cytology). In this series of 2796 lymph node FNAB, one single false negative case was found.
Conclusion: our data prove, that FNAB of enlarged lymph nodes is a very efficient method in the diagnosis of different hematological and non- hematological diseases in experienced hands . The examination can be repeated in case of the suspicion of false negativity. We suggest the use of this easy, cost effective and quick method, by which unneaded operations might be avoided, and based on the quick diagnosis many patients can benefit. We would like to share some of our „favourite cases" with the audience.

P 274
EFFECT OF VITRIFICATION ON FERTILIZING CAPACITY OF SPERMATOZOA IN FERTILE AND INFERTILE MEN
FASLI Hassan, GHAFFARI NOVIN Marefat, PEIROVI Tahmineh, SOLEIMANIRAD Jafar
Department of Reproductive Endocrinology and Embryology, Reproductive Biology and Biotechnology, Infertility Center, Tehran, Iran
Department of Histology, Urimia University of Medical Sciences, Urimia, Iran
Infertility Center, Tabriz University of Medical Sciences, Tabriz, Iran

Cryopreservation is widely used in Assisted Reproductive Techniques to maintain male fertility. Evaluation of the acrosome and its disruption and motility are important tasks within the diagnostic tests of male infertility to predict the fertilizing capacity of sperm. The aim of the present study was to evaluate the effect of vitrification on acrosome reaction and motility of sperm in fertile and infertile men. Semen samples were collected from ten fertile and twenty infertile men after a minimum of 3 days of sexual abstinence. After seminal liquefaction, a routine semen analysis was performed using Semen Analyzer Quality to determine sperm concentration and motility according to World Health Organization specifications. This was immediately followed by the evaluation of acrosome quality by triple staining technique. The remainder of each sample was immediately cryopreserved by vitrification method and thawed after two weeks. Analyses of concentration, motility and acrosome quality were performed after thawing and the results were statistically analysed by paired t-test.
After vitrification, the percentage of live spermatozoa with intact acrosome was significantly decreased from 33.37 ± 4.07 to 9.87 ± 2.97 ($p<0.002$) in fertile and from 26 ± 3.64 to 11.16 ±1.82 ($p<0.001$) in infertile groups. The percentage of sperm progressive motility (a + b) were significantly

decreased from 60 and 35 to 40 and 20 in fertile and infertile groups after vitrification, respectively. It is concluded that vitrification impairs fertilizing capacity of sperm in fertile and infertile men.

P 275
SECONDARY TUMORS TO THE PANCREAS. STUDY OF 17 CASES WITH FINE NEEDLE ASPIRATION CYTOLOGY

Manfrin E°, Capelli P°, Zamboni G*, Eccher A°, Remo A°, Reghellin D°, Dalfior D°, Bonetti F°, Menestrina F°.
° Department of Pathology, University of Verona.
* Anatomina Patologica, Ospedale Sacro Cuore Don Calabria, Negrar Verona

Introduction: Secondary tumors to the pancreas are inusual and in most cases part of an advanced metastatic disease. They account for 3-16% of all pancreatic malignancies. They present as solitary or multiple lesions, sometimes with clinical and radiological features that can be confused with a primary pancreatic adenocarcinoma. Fine needle aspiration cytology (FNAC) is a quick, low-expensive technique that allows a rapid identification of metastatic carcinoma and the patient's management in pre-surgical diagnostic phase.
Purpose: To report the clinical and cytological findings of secondary tumors to the pancreas observed in the Department of Pathology of Verona University.
Methods: Between January 1990 and December 2004, we studied 17 secondary tumors to the pancreas diagnosed by FNAC.
Summary: The mean age of patients was 62 years. 10 patients were males (59%) and 7 females (41%). In 16 cases (94%) FNAC was performed with ultra-sonography guide on outpatients and in 1 case FNAC was performed during abdominal laparothomy for suspected pancreatic adenocarcinoma.. The metastatic lesion involved the head of the pancreas in 41% of cases (7/17) and the body-tail in 35% (6/17). In 24% of cases (4/17) the anatomic site of pancreatic metastasis was not available. Radiological imaging showed in 94% of cases (16/17) a suspicious solitary mass and in a single case multiple lesions; the diameter of suspicious nodules ranged from 2 to 8 cm. The histotype of metastasis was renal cell carcinoma, classic type: 35%(6/17), large bowel carcinoma: 18%(3/17), gastric carcinoma 6%(1/17), breast carcinoma: 4%(1/17), prostate carcinoma: 6%(1/17), carcinoma of the lung:6%(1/17). In 24% of cases the primitive site of neoplasia could not be assessed. The clinical history was available in all cases of renal cell carcinoma with a mean interval of 13 years between the primitive renal carcinoma and the pancreatic metastasis.
Conclusion: Most secondary tumors to the pancreas occur as a solitary lesion, both on the head and tail of pancreas, simulating a primary pancreatic carcinoma. The most frequent metastatic tumor to the pancreas is renal cell carcinoma, often many years after the primary renal tumor. FNAC allows a distinction between primary pancreatic cancer and secondary tumors and represents an important diagnostic tool in the follow up of oncologic patients.

P 276
VIRAL MARKERS IN CYTOLOGIC AND HISTOPATHOLOGIC PREPARATIONS OF CERVICAL LESIONS

AMALINEI Cornelia*, BALAN Raluca*, RADULESCU Doinita*, PRICOP Florentina**, DOBRESCU Gioconda*, COTUTIU Coriolan*
*Department of Pathology
**Department of Obstetrics and Gynecology
University of Medicine and Pharmacy Iasi, Romania

Consistent epidemiologic evidence had demonstrated that human papillomavirus (HPV) infection plays a central role in the development of cervical cancer precursors and invasive cervical cancers. Over 20 types of HPV are associated with cervical intraepithelial lesions and cervical carcinomas. The purpose of our study was to analyze viral markers expression in cervical lesions. 105 Pap smears and 84 biopsies were selected as they exhibited viral cytopatic effects. We performed immunohistochemical staining for HPV on both types of preparations, in cases with SIL diagnosis. Cytologic aspects were: koilocytosis associated with diskeratocytes, and parabasal cells (± atypia), low grade squamous intraepithelial lesion (L-SIL) and high grade squamous intraepithelial lesion (HG-SIL). Histology revealed chronic cervicitis, condyloma acuminatum, L-SIL and H-SIL. HPV was detected in 61.1 % of smears, exhibiting a double localisation: nuclear and cytoplasmic and in 65.71 % of biopsies, with a nuclear localisation and an enhanced expression within superficial layers of condylomas. Concluding, HPV may be evidentiated in cytologic and histologic preparations from cervical lesions, the negative preparations being atributed to (co)existence of other infectious agents or to the limited sensitivity of the immunohistochemical method.

P 277
COMPARATIVE STUDY OF CONVENTIONAL AND LIQUID-BASED CYTOLOGY IN A POPULATION WITH OPPORTUNISTIC CYTOLOGICAL SCREENING

HADZI-NICHEVA Biljana,1 GRNCHAROVSKA Zlata,1 PRODANOVA Irina,2 YASHAR Genghis,2 KUBELKA-SABIT Katerina,2 POPOVSKA Zora,1 BASHESKA Neli2
1Department of Gynecological Cytology, Clinic of Obstetrics and Gynecology, 2Department of Histopathology and Clinical Cytology, Institute of Radiotherapy and Oncology, Medical Faculty Skopje, Republic of Macedonia

Background: In the last decade the conventional Pap smear (CPS) has frequently been replaced by the liquid-based cervical cytology (LBC) in the routine clinical practice due to improved technical quality and increased efficacy in detecting squamous intraepithelial lesions (SIL) and cervical cancer by LBC.
Aims: The purpose of this study is to report the preliminary results of the performances of LBC versus those of CPS, in a country with an opportunistic cytological screening and a high incidence of cervical carcinoma.
Methods: This comparative retrospective study is an initial part of a wider project, anticipated to assess the validity of the new method and its impact on clinical practice. It includes two groups of women referred to a tertiary centre for gynaecologic care, in different six-month periods. In each group, the Pap smear was taken by one of the methods. Data from unselected, consecutive series of 3,261 LBC tests and of 4,102 CPSs were analysed. Cytological diagnoses were classified using the Bethesda system. The differences in specimen adequacy and the rates of atypical squamous cells (ASC) category between the two groups were compared using *fÓf¢* test. The histological correlation with histopathological findings could be established in 901 patients with the LBC and in 1,408 with the CPSs. Sensitivity, specificity, positive predictive value (PPV), negative predictive value (NPV) and diagnostic accuracy of the findings were evaluated as well.
Results: The improvement in the specimen adequacy for LBC was documented by the more than fivefold reduction of the proportion of unsatisfactory specimens (0.4% for LBC vs. 2.1% for CPS, P<0.001). The rate of ¡§satisfactory but limited by¡¨ was also reduced by 40% for LBC (P<0.001). However, the rate of ASC category was similar in both methods (0.9% for LBC vs. 1.2% for CPS). The performances of LBC for detection of cervical SIL or cancer lesions versus those of CPS, such as sensitivity (94% vs. 79%), PPV (85% vs. 69%) and NPV (90% vs. 66%) were significantly different (P<0.001). There was no statistically significant difference in

specificity between the methods (65% vs. 62%, P<0.15). Ultimately, the diagnostic accuracy was higher in LBC than in CPS (84% vs. 73%, P<0.001).
Conclusions: Our preliminary results suggest that the implementation of LBC significantly improved the technical quality of the smears and resulted in statistically significant improvement of the diagnostic value of the Pap test.

P 278
IMMUNOPHENOTYPING OF CSF SPECIMENS BY SLIDE BASED LASER SCANNING CYTOMETRY
JASTANIA Raid, BOERNER Scott, GEDDIE William

Background:
In cerebrospinal fluid (CSF) cytology analysis of cell surface markers is frequently required for diagnosis or subtyping of lymphoproliferative disorders, but insufficient cells may be present for flow cytometry. Laser scanning cytometry provides a simplified and inexpensive means of immunophenotyping paucicellular samples. We have assessed our experience with this method in CSF samples requiring immunophenotyping over an 18-month period.
Materials and Methods: Cytocentrifugation and rapid Giemsa stain were used for immediate assessment of 521 consecutive CSF samples. Slide based immunophenotyping by Clatch's method was attempted in 60 samples that showed some increase in lymphoid cells. Twenty-five cases had a history of previous hematolymphoid malignancy, and in 12 HIV positive patients neurologic decompensation led to suspicion of CNS lymphoma. 37 samples contained 10,000 cells or less, with the remainder ranging up to 150,000 cells total. In 12 samples with over 60,000 cells a full immunophenotyping panel of 20 antibodies was performed. In the samples with fewer cells at least kappa and lambda light chains and CD19 were initially assessed. By repetitive re-staining of the unfixed cells on the slide more surface antigens could be documented. After fixation and permeabilization intracellular markers could be assessed. All analyses were performed in the cytology laboratory using an LSC (Laser Scanning Cytometer - Compucyte®)
Results: 43 cases showed a reactive immunophenotype and a diagnosis of negative or chronic inflammation was rendered. The 17 remaining cases were diagnosed as suspicious for lymphoma (7) or malignant lymphoma (10). In 3/7 suspicious cases the LSC result was supportive of, but not conclusive for, lymphoma. In the remainder it was not contributory. In the 10 definite lymphoma cases the LSC immunophenotype confirmed B-cell clonality or an abnormal T-cell phenotype consistent with the clinical and morphologic diagnosis.
Conclusions: Slide based cytometry using Clatch's method is useful in the evaluation of CSF samples containing a hematolymphoid population suspicious for lymphoma, allowing specific reactive or malignant diagnoses in a number of cases containing inadequate cells for flow cytometry.

P 279
UTILITY OF CYTOLOGIC IMPRINTS IN INTRAOPERATIVE DIAGNOSIS
Garza-Guajardo Raquel MD FIAC, Mendez-Olvera Nora MD, Ancer-Rodriguez Jesús MD, Barboza-Quintana Oralia MD FIAC
Anatomic Pathology and Cytopathology Service, Universitary Hospital “Dr. José E. González”, UANL, Monterrey, México

Intraoperative diagnosis has been traditionally based on frozen histologic sections because provide architectural information, cytologic smears allow us to evaluate morphology on well preserved cells, without the well-known artifacts associated with freezing. Both methods thus complement each other. However, utilizing only the cytologic technique is possible if performed by experienced hands in special situations.
Material and Methods
We study 416 consecutive specimens submitted for intraoperative biopsies over a two-year period, Imprint cytologies were done on all specimens, and frozen sections were performed on 384 of them. The diagnoses obtained from both methods were recorded and compared with the final diagnosis yielded by the definitive histological sections.

Results
9 of 416 cases (2.2%) were misdiagnosed by IC, and there were diagnostic errors in 8 / 384 (2.1%) cases by frozen sections. Diagnostic accuracy was 97.8% for imprint cytology and 97.9% for frozen sections. Six cases of 416 (1.4%) were misdiagnosed by both imprint cytology and the frozen section. The accuracy rate of both methods used jointly was 98.5%.
Conclusions
Intraoperative imprint cytology is a quick, easy-to-perform, and low-cost technique that provides morphological details on intact cells without the artifacts resulting from freezing. It is therefore a highly valuable adjunct to the frozen section.
The benefits obtained from the use of imprint cytology are unquestionable, particularly under the following situations and considerations: 1) assessment of small specimens; 2) necrotic lesions; 3) to prevent cryostat contamination in infectious processes; 4) to facilitate identification of micro-organisms; 5) no special equipment is required; 6) to preserve material for special studies (ultrastructure, immunohistochemistry, etc.); 7) for the assessment of some specimens for which it is not possible to perform frozen sections, such as bone specimens; 8) it shows cytogenetic characteristics (e.g. parathyroid tissue, cytological type of lymphoma); and 9) experience is gained in cytology.

P 280
THE IMPORTANCE OF P-16’S EXPRESSION CORRELATED WITH KI-67 IN ESOPHAGEAL INTRAEPITHELIAL HPV-INDUCED SQUAMOUSE LESION
Authors : Maria Sajin , Alina Chefani, Anca Lazaroiu, Anca Simona Constantin,Ana-Maria Sajin,
Bucharest Universitary Hospital, Carol Davila Medicine Faculty, Bucharest

BACKGROUND The esophageal malpighian epithelium may be the siege of HPV infections, thus determining intraepitheial squamouse lesions, similar to thoes found at the level of the uterine cervix. P-16 is an cyclin-dependent kinases inhibitor and a key regulator of the G1-S, and check point in the cell cycle. The over-expression of P-16 marker has been observed in CIN and invasive carcinomas, associated with high-risk hPV types.. Ki-67 is a nuclear antigen expressed in g1-S-G2-M phases, also being an agrssivity indicator.
DESIGN A number of 31 esophageal byopsies and 8 esophagectomy specimen material was fomalin-fixed, paraffin embedded , HE stained and analised immunohistochemicaly using speciffic antibodies against Ki-67 and P-16 by ABC immunoperoxidase procedure. Out of thoes 31 byopsies, 7 were showing HPV-induced low grade intraepithelial squamouse lesion ,and 18 were showing high grade intraepithelial squamouse lesions (CIN II-6, CIN III-9, CIS-3) and 6 cases of inavsive carcinoma.
RESULTS :Our study demonstrates that HSIL-s have uniform and diffuse nuclear staining (Ki-67+) 100% (24 cases) and (P-16+) 80% (19 cases) thruout all cell layers of the lesion. None of our 7 LSIL cases showed (+) Ki-67 in the supperficial layer. In the lower third of the epithelium our LSIL cases showed positive staining for both P-16 and Ki-67 but the upper third of the epithelium showed no such staining for either of them.
CONCLUSION Although the classical morphological features are the main diagnostic mean in the case of HPV

infection, the P16 and Ki-67 immunohistochemical markers and their staining patterns are useful in distinguishing between two biologically different groups of esophageal neoplastic lesions.

P 281
INTESTINAL METAPLASIA AT THE GASTRO-ESOPHAGEAL JUNCTION: PREVALENCE AND ASSOCIATED CONDITIONS

Fiocca R, Mastracci L, Musizzano Y, Spaggiari P, Savarino V, Zentilin P, Dulbecco P, Mansi C, Conio M.
DICMI, Department of Pathology;
DIMI,Department of Gastroenerology;
University of Genova

AIM: Junctional intestinal metaplasia (JIM) is defined as intestinal metaplastic change found at the esophago-gastric junction and its pathogenesis is controversial. The aim of our study was to determine the prevalence of JIM and the frequency of coexisting esophageal and gastric lesions. METHODS: we studied a continuous series of 485 unselected patients with various digestive symptoms who underwent upper GI endoscopy including multiple esophageal, junctional, and gastric biopsies (body and antrum). All samples were stained with Haematoxylin-eosin, PAS-Alcian blue and Giemsa for H. pylori detection. All the slides were simultaneously revised by two expert GI pathologists who assessed the presence of microscopic esophagitis, Barrett's metaplasia, intestinal metaplasia at the junction and in the stomach and gastritis in accordance with the up-dated Sydney system.
RESULTS: JIM was found in 91/485 cases (18.8%); 11 had complete-type metaplasia, 77 incomplete-type and 3 both types. The male/female ratio was 1,5/1 for cases with JIM and 1/1 in 394 controls without JIM and the median age was 59.5 in the former and 53.3 in the latter group (p=0.0003). The prevalence of associated lesions in cases with and without JIM respectively was as follows: microscopic esophagitis 50.5% vs 58.6%, Barrett's esophagus 31.9% vs 0%, H. pylori gastritis 22.0% vs 23,9%, gastric intestinal metaplasia 27.5% vs 17.3% (p=0.037), no gastro-esophageal lesions 4.4% vs 24.1%. Since numerous patients showed more than one associated lesion the sum of % exceeds 100%.
CONCLUSIONS: both esophageal and gastric lesions may be found in association with JIM with a trend of esophageal lesions to be more frequent in cases with JIM than in controls. The very low prevalence of normal esophageal and gastric findings in cases with JIM as compared with controls suggests that JIM is not an isolated change but esophageal, gastric or combined factors contribute to its pathogenesis.

P 282
ESSENTIAL MARKERS FOR THE EVALUATION OF METAPLASIA, DYSPLASIA AND CANCER IN BARRETT'S ESOPHAGUS

Semyon Petrov, Timur Akhmetov, Michael Burmistrov, Eugeni Sigal
Kazan Cancer Center, Kazan State Medical University, Dept. Pathology,
Kazan, Russian Federation

Introduction:The last 20 years are characterized by increased incidence of distal esophageal adenocarcinoma, being considered as a complication of gastroesophageal reflux disease and Barrett's esophagus. The major risk factors for adenocarcinoma are intestinal metaplasia and high grade dysplasia.
The purpose of this study was to select essential markers of dysplasia and metaplasia that could be included in standard panel for diagnostics of precancerous conditions of distal esophagus.
Methods: In 2003 – 2004 we performed an immunohistochemical (IHC) analysis of distal esophagus biopsy specimens (histologically showing features of metaplasia and/or dysplasia) in 42 patients (38 male and 4 female). Our common panel included antibodies to the following proteins: markers of intestinal or cardial differentiation (CK ¹7 and CK ¹20, villin), markers that could be used for evaluation of dysplasia grade (CEA, p53) and marker of proliferation (Ki67). In difficult cases (where cancer is being supposed) we defined additional markers: basement membrane marker - collagen IV, marker of histiocytes - CD 68, vimentin and a wider set of cytokeratins.
Results: The high grade dysplasia and adenocarcinomas were revealed due to the strong uniform cytoplasm reaction for CEA with nuclear reaction for p53 and a higher proliferation index. Using the above mentioned panel of markers we have diagnosed the following cases: 16 (38,2%) - Barrett's esophagus with cardial metaplasia, 8 (19,2%) - Barrett's esophagus with intestinal metaplasia, 7 (16,6%) adenocarcinoma, 7 (16,6%) squamous-cell carcinoma, 2 (4,7%)–poorly differentiated carcinoma and 2 (4,7%) - chronic esophagitis.
We have concluded that the usage of the wider panel of biomarkers could significantly help to diagnose the distal esophagus precancerous conditions and to determine effective treatment.

P 283
EVALUATION OF BARRETT'S MUCOSA IN TERMS OF CK7, CK20, KI67, P53, AND COX2 EXPRESSIONS USING CHROMOENDOSCOPIC OESOPHAGEAL BIOPSIES

Berna Savaþ, Arzu Ensari, Necati Örmeci*, Iþýnsu Kuzu, Murat Palabýyýkoðlu*, Þahin Çoban*, Nazmiye Kurþun+
Ankara University Medical School, Departments of Pathology, Gastroenterology*, and Biostatistics+, Ankara, Turkey

P 284
GLYCOPROTEIN EXPRESSION PATTERNS IN THE BIOPSIES OF GASTROESOPHAGEAL JUNCTION : A PRELIMINARY STUDY

CELIKEL Cigdem Ataizi*, SAVCI Dilara*, ERBARUT Ipek*,OZKAN Naziye*,AVSAR Erol **
Marmara University School of Medicine, Departments of Pathology* and Gastroenterology**

To determine incomplete intestinal metaplasia (IM) in endoscopic biopsies obtained from the gastroesophageal junction or proximal, may represent IM of the cardia (CIM) due to H. pylori (HP) and gastroesophageal reflux disease (GERD) or Barrett's esophagus (BE), which have different clinical implications. In this study, we aimed to determine the glycoprotein expression patterns in BE, CIM (HP and GERD related), multilayered epithelium(ME) and columnar blues (CB) in order to relate their expression to BE development. Archival biopsies and endoscopy reports of 138 patients biopsied from gastroesophageal junction (or proximal) were re-evaluated. CIM was demonstrated in 51% of 64 patients diagnosed as carditis due to GERD. Fifty-eight patients had HP carditis with complete and incomplete intestinal metaplasia in 16% and 27% of the cases, respectively. BE was determined in 16 patients, 3 biopsies revealing dysplasia. ME was detected in 3 BE and 12 GERD associated carditis. CB was identified in 4 HP related carditis, 16 GERD related carditis and 12 BE. Sequencial sections of representative formalin-fixed paraffin-embedded tissue sections in 16 BE, 12 GERD and 8 HP associated CIM were stained by immunohistochemistry for Human Gastric Mucin (HGM), MUC1, MUC2, MUC5AC. Submucosal glands of esophageal mucosa expressed MUC5B, whereas squamous epithelium

MUC1. MUC1 was rarely expressed in BE and CIM compared to ME and CB ($p < 0.05$). All BE cases showed gastric mucin (MUC5AC, HGM), but only 53.4% MUC2 expression. Gastric mucins (MUC5AC, HGM) were detected in all CIM cases, but expression intensity was low in columnar cells and usually HGM staining was limited to goblet cells in HP associated CIM cases. MUC2 expression differed between GERD and HP associated CIM being 45% and 22%, respectively. Gastric mucins (MUC5AC, HGM) with low intensity of staining was limited to basal cytoplasm in CB, but to the superficial columnar cells in ME. Our preliminary results suggests that ME may be a precursor in the development of BE. In regard to mucin expression the specificity of any pattern is insufficient for distinction in individual cases with BE and CIM in GERD are virtually indistinguishable, limiting their use in this differential and raising the question of whether they are biologically related.

P 285

IMMUNOHISTOCHEMICAL MARKERS IN THE DIAGNOSIS OF BARRET'S ESOPHAGUS AND ESOPHAGEAL ADENOCARCINOMA

IMMUNOHISTOCHEMICAL MARKERS IN THE DIAGNOSIS OF BARRET'S ESOFHAGUS AND ESOPHAGEAL ADENOCARCINOMA

IMMUNOHISTOCHEMICAL MARKERS IN THE DIAGNOSIS OF BARRET'S ESOFHAGUS AND ESOPHAGEAL ADENOCARCINOMA

A.Kotsev, M.Kamenova, N.Sarbianova, K.Tschernev, Al.Tcherveniakov

Bulgaria, Medical University, Sofia, :Medical Institute of Emergency,Sofia

Introduction: Barrett's esophagus /BO/ is associated with increasing incidence of the adenocarcinoma of the esophagus. Histopathological staging of BO is associated with high inter- and intraobserver variation .There have been many attempts to find adjunctive methods for improving the diagnose.

Purpose: As the progression of Barrett's metaplasia to adenocarcinoma is related to impaired control of cell cycle the question arised whether the application of tumor markers involved in increased proliferation and inhibition of apoptosis could be useful for an exact diagnosis. ..

Material and methods: Tissue samples from 25 patients were examined: eight with BO and seventeen with adenocarcinoma, associated with BO. The tissue pieces for the immunohistochemistry analysis were obtained by endoscopic biopsy or after surgical resections and included in paraffine blocks. Several tumor markers involved in cell proliferation and apoptothic pathways were studied: Ki-67, PCNA, RB, p16, p53, Bcl-2 and Bax .Routine immunohistochemical procedures were applied with antibodies produced from Dako, Denmark.

Results:Expression of the markers for proliferation Ki-67 and PCNA was increased in adenocarcinoma, especially in undifferentiated forms.Mutated tumor marker-p53 was strongly expressed in adenocarcinoma and Barrett's epithelium with high grade of dysplasia.Expression of the proapoptotic marker Bax was increased in adenocarcinoma.The antiapoptotic marker Bcl-2 showed no expression in most of the samples; in some samples the staining was weak in tumor cells and strong positive in immune cells of the lamina propria. Expression of the markers associated with cell cycle-p16 and Rb was increased in adenocarcinoma and high grade Barrett's epithelium .

Conclusion: The results suggest that the investigation of tissue tumor markers may contribute to improve the diagnosis , assessment of the prognosis and risk of progression .

P 286

PROGNOSTIC AND POTENTIALLY PREDICTIVE FACTORS IN EARLY GASTRIC CANCER

Ma³gorzata Malinowska, Anna Nasierowska-Guttmejer

Department of pathology,Oncology Center,Warsaw

BACKGROUND: The incidence of gastric cancer is decreasing worldwide, but the prognosis is still generally poor. It is the second cause of death in men and fourth one in women. Detection of the early gastric carcinoma is the crucial factor to improve the results
of treatment. 5 -year survival rate in T1 stage is 80-95%. Lymph node metastasis are observed in 10.4% of early gastric cancer. The depth of invasion and lymph node metastasis are the most significant prognostic factors in the early gastric cancer. AIM: The E-cadherin-catenin complex is important for cell-cell adhesion of epithelial cells. We analyze the E-cadherin expression with clinicopathological features of the early gastric cancer. METHODS: 39 patients were diagnosed and total gastrectomy with lymphadenectomy was done. Histological report included: location and size of the tumor, surgical margins, histologic type and grade, pTNM stage. Immunohistochemical staining of E-cadherin was performed. Normal membrane E-cadherin staining was observed in control gastric mucosa. RESULTS: Abnormal expression of E –cadherin was demonstrated in 37 cases (94.9%). High (3+) membranous expression of E-cadherin was seen in 2 well differentiated adenocarcinomas (5.1%). Less or absent immunoreactions of E-cadherin was observed in 14 well differentiated adenocarcinomas and all (23) poorly differentiated adenocarcinomas or diffuse type of Lauren classification. Moreover, abnormal expression of E-cadherin occurred more frequently in macroscopic ulcerated type (0-IIc, 0-I II) and was associated with lymph node metastasis. CONCLUSION: We suggest that E-cadherin play an important role in the macroscopic growth as well as microscopic differentiation of the early gastric carcinoma.

P 287

HISTOLOGIC CHANGES OF THE GASTRIC MUCOSA ASSOCIATED WITH GASTRIC CARCINOMAS AND PRIMARY LYMPHOMAS

RAMADAN Saime Sezgin, CELIKEL Cigdem

Marmara University School of Medicine, Department of Pathology, Istanbul, Turkey

In order to formulate proper surveillance and therapy protocols in epithelial changes of the gastric mucosa, it is important to determine the frequency and type of preneoplastic lesions in gastric carcinogenesis. For comparative purposes, we evaluated gastric mucosa surrounding 93 gastric adenocarcinomas (GCa), 19 primary gastric lymphomas (PGL) and gastric mucosa of 30 autopsy cases who died of reasons other than gastric malignancies, according to the updated Sydney System and Padova International Classification. In addition, in order to determine the role of G-cell and enterochromaffin-like cell hyperplasia in gastric carcinogenesis, we studied gastrin and chromogranin A (ChrA) immunohistochemistry in the surrounding mucosa of each case. In our study; atrophy, intestinal metaplasia (IM) type I and III, foveolar hyperproliferation (FHP) were all observed in high frequencies in gastric carcinoma cases ($p<0.001$). Hyperproliferative intestinal metaplasia (HIM), low (LGD) and high grade dysplasia (HGD) were only detected in carcinoma cases. When diffuse (n=43) and intestinal (n=50) type of GCa cases were compared, atrophy, IM type III, HPIM, LGD, and HGD were statistically more common in intestinal GCa's ($p<0.05$). High H.pylori density and FHP were recorded mainly in diffuse GCa's. In our study, gastrin and ChrA overexpression were observed in GCa and PGL cases but not in autopsy cases. Gastrin expression was related to intestinal metaplasia ($p<0.05$) but not to the H. pylori

density and atrophy. ChrA expression was related to intestinal metaplasia ($p<0.01$) and atrophy ($p<0.05$) but not to the H. pylori density. G cell hyperplasia corelated well with the lineer and diffuse neuroendocrine cell hyperplasia ($p<0.05$). Our study revealed that FHP and HPIM which comprises inconspicious for dysplasia group in Padova International Classification were associated with carcinoma cases in high frequencies. We think that these lesions could be preneoplastic lesions rather than being a part of a regenerative process. Our results show that although intestinal GCa's develop as a consequence of a sequence of events, some mechanisms acting in the active phase of gastritis could be an important factor in the carcinogenesis of the diffuse type. Our data related to gastrin and ChrA immunohistochemistry gives the idea that both G cell and enterochromaffin cell hyperplasia may be involved in gastric carcinogenesis.

P 288

INTESTINAL AND DIFFUSE TYPES OF GASTRIC ADENOCARCINOMA: CLINICOPATHOLOGIC FEATURES

RAMADAN Saime Sezgin, CELIKEL Cigdem, KULLU Sevgi
Marmara University School of Medicine, Istanbul, Turkey

Gastric carcinoma is classified into intestinal type (IC) and diffuse type
adenocarcinoma (DC) by Lauren histological classification. There are reports that these two types have different prognostic implications according to different clinicopathological factors. We examined 40 DC and 49 IC in radical gastrectomy specimens to determine the importance of factors affecting prognosis within these two groups of carcinomas. Patients' age, sex and tumor localisation were determined from clinicopathologic files. We retrospectively evaluated all the H&E stained
slides of the cases and recorded histological grade,WHO histological types, invasion patern(submucosal, pushing or infiltrative), depth of invasion, venous, lymphatic and perineural invasion, intratumoral and peritumoral lymphocytic infiltration, desmoplasia,metastatic foci in lymph nodes and other organs. In our study, we observed that both types were more common in males and IC was more frequent in elderly. In the literature; lymph node metastases, perinodal, perineural, serosal invasion,surgical margin positivity are features accepted as determinants of poor prognosis and these are all observed in high frequencies in our DC cases. No statistical difference was found between the two groups in respect to WHO histological types but DC mostly had signet ring cell component. In our study, we also found that the two types had different invasion paterns: DC,infiltrative or submucosal; IC, infiltrative or expansile. There were no difference in intratumoral lymphocytic infiltration (including lymphoid agregate and follicle formation) between two histological types. Although no statistical difference could be found in regard to desmoplasia formation between the two groups, the extend of desmoplasia was higher in IC. In summary, factors defined as poor prognostic factors in the literature were more common in DC and we conclude that these altogether bring out the poor outcome in DC.

P 289

HISTOLOGICAL CHANGES IN HYPERPLASTIC POLYPS AND SURROUNDING GASTRIC MUCOSA

ALTINOK Gulcin*, GUREL Bora*, CAKAR Mustafa**, HIMMETOGLU Cigdem*, SOKMENSUER Cenk*, BAYRAKTAR Yusuf**, GEDIKOGLU Gokhan*,
Departments of Pathology* and Gastroenterology**, Hacettepe University School of Medicine, Ankara, Turkey

Introduction: Hyperplastic polyps were considered to represent the regenerative changes in a background mucosa with chronic atrophic gastritis and rarely harbor true precancerous lesions themselves.
Aim: The aim of this study was to determine on which morphological background gastric hyperplastic polyps develop and to assess the frequency of precancerous changes in the hyperplastic polyps and background mucosa.
Material and Method: We studied 73 patients with gastric hyperplastic polyps and characterized endoscopic and histologic features of the polyps (topographic location, multiplicity and the presence of dysplasia and adenocarcinoma) and the background gastric mucosa (intestinal metaplasia, dysplasia, carcinoma, and classification of gastritis). The histopathologic features seen within the hyperplastic polyp and the background mucosa were assessed according to the revised (2004) Vienna classification.
Results: Hyperplastic polyps were most common in the antrum (42.5%) followed by the corpus (27.4%), both antrum and corpus (15.1%) and the site of anastomosis (15.1%). There were multiple polyps in 37% of the patients which were mostly situated in antrum (40.7%), followed by both antrum and corpus (33.3%). Intestinal metaplasia of the polyp was present in 19% and low-grade dysplasia in 9.5% of patients. Only one patient (1.3%) had intramucosal adenocarcinoma within the polyp which also showed adenocarcinoma in the surrounding mucosa. Evaluation of the surrounding gastric mucosa showed intestinal metaplasia in 36% of patients, at least low-grade dysplasia in 12%, and synchronous carcinoma in 9%. Of the seven cases with hyperplastic polyps harboring low grade dysplasia, four also demonstrated low grade dysplasia in the surrounding gastric mucosa. All hyperplastic polyps with dysplasia were located in the antrum and all but one were multiple. Ninety percent of the hyperplastic polyps were associated with various forms of gastritis, most commonly superficial gastritis (44.2%), followed by chronic active H. pylori gastritis (23.1%), chronic atrophic gastritis (21.2%) and chemical gastritis (11.5%).
Conclusion: These results show a strong association between mucosal inflammation and development of hyperplastic polyps. As the frequency of dysplasia and adenocarcinoma in the background mucosa was higher than that of hyperplastic polyps, a meticulous endoscopic examination and multiple biopsies of the surrounding mucosa would reveal early precancerous changes.

P 290

EFFECT OF TRANSFORMING GROWTH FACTOR-BETA (TGF-B) ON PROLIFERATION OF GASTRIC EPITHELIAL CELLS IN CULTURE

GHAINI M.Hosswin, Pathologist

BACKGROUND: Helicobacter pylori has a well-established role in the development of gastric cancer. In vitro studies reveal increased proliferation of the gastric mucosa in the presence of H. pylori infection. It has been also shown that production of some cytokines, such as interleukin-1 beta (IL-1b) is increased in H. pylori infection. In addition, IL-1b increases proliferation of gastric epithelial cell in culture study. In this study, The effect of transforming growth factor beta (TGF-b) on gastric epithelial cell proliferation has been examined.
METHODS: AGS cells were cultured with TGF-b. DNA synthesis was assed by bromo-deoxyuridine (BrdU) test and total viable cell numbers by MTT assay.
RESULTS: TGF-b decreased DNA synthesis and cell numbers. This effect was both time- and dose-dependent ($p<0.05$). Both tests, BrdU test & MTT assay revealed this suppressive effect, but it was more evident in BrdU test. Simultaneous exposure to TGF-b & IL-1b, obliterated the results of each one, alone.
CONCLUSIONS: TGF-b suppresses proliferation of malignant gastric epithelial cells. It appears that modulatin of tyrosine kinase activity is essential to anti-proliferative effect

of TGF-b. This effect is reversed by IL-1b, and it may be due to opposed effects of these cytokines.

P 291

PROGNOSTIC VALUE OF BAX, BCL-2 PROTEINS AND FAS/FASL SYSTEM IN PATIENT WITH GASTRIC AND COLON CANCER.

N.Belushkina, V.Obukhova, A.Samokhvalov, S.Kharnas
Sechenov Moscow Medical Academy, Russian Federation

Background. The inhibition of apoptosis is one of possible mechanism of tumor formation. The family Bcl-2 proteins and Fas/FasL system play the important role in apoptosis regulation. The family Bcl-2 protein includes the proteins-inhibition of apoptosis (such as Bcl-2), and activators of apoptosis (such as Bax). Fas protein is known to induce cell death by apoptosis in susceptible cells. Change of a level gene expression these protein lead to disturbed of apoptosis regulation. The prognostic importance of Bax, Bcl-2 proteins and Fas/FasL system in this tumor is yet to be evaluated.
Aims. To examine the prognostic significance of Bax, Bcl-2 and Fas protein expression in patient with gastric and colon adenocarcinoma.
Methods. The content of proteins Bcl-2, Bax and Fas was definite in fragments of the frozen tissues by immunohistochemical research serial paraffin section both tumor and not transformed tissues along patients (n=15) with the streptavidin-biotin method.
Results. It was establish the modification in level Bcl-2 and Bax protein in gastric and colon cancer. The level of Bcl-2 protein in tumor tissue increase in 1,5 time in comparison with not transformed tissue. The Bax level is increased or remains like not transformed tissue. Is shown, there is the high level of Bcl-2 and Bax in majority of cells in gastric and colon cancer. Fas expression were noted in all cancer specimens and all their noncancerous counterparts. The level of Fas-positive cells was significantly lower in patient without metastasis (by 89%, p=0,04) and then in non cancerous tissue (by 54%, p=0,04)
Conclusion. The increase of synthesis Bcl-2, apparently, is one of mechanisms of apoptosis inhibitors in tumor cells. The increase of Bax level testifies to activation apoptosis-inducing mechanisms in tumor cells. However the determining importance has not a level of protein in a cell, and its ability to carry out the function. By us is earlier shown, that the gene Bax frequently changes at gastric and colon cancer. Expression of Fas in gastric and colon epithelium is progressively reduced during the malignant transformation and is frequently associated with metastasis in gastric and colon adenocarcinoma.

P 292

CLAUDIN 1, 3, 4 AND 5 IN GASTRIC CARCINOMA, LOSS OF CLAUDIN EXPRESSION ASSOCIATES WITH THE DIFFUSE SUBTYPE

Y Soini M.D.(1), S Tommola M.D. (2), H Helin M.D.(3), P. Martikainen (2)
Department of Pathology, University Hospital of Oulu and Oulu University, PO Box 5000 (Aapistie 5) 90014 Oulu, Finland (1)
Department of Pathology, Tampere University Hospital, PO Box 2000, FIN-33521, Tampere, Finland (2)
HUSLAB, Division of Pathology, Helsinki University Central Hospital, PO Box 400, FI-00029, HUS, Helsinki, Finland (3)

Introduction: Claudins are tight junctional proteins present in epithelial and endothelial cells.
Purpose of the study: Purpose was to study the expression of claudins 1, 3, 4 and 5 in gastric carcinomas and their significance for tumor behaviour
Methods: 118 cases of gastric carcinoma including additional samples from 50 metastatic lesions were collected. Immunohistochemistry was performed for claudins 1, 3, 4 and 5 Ki67 and E-cadherin. Additionally, cases were studied for apoptosis by the TUNEL method.
Results: Expression of all these claudins could be seen in gastric carcinoma, most prominently for claudin 4 and least expression was found for claudin 5. All claudins showed significantly more expression in gastric carcinomas of intestinal type. Their expression was significantly associated with each other. Expression of claudin 4 and 5 was associated with E-cadherin. Strong expression of claudin 5 was associated with higher cell proliferation and apoptosis. Claudin 3 expression had an association with a better prognosis of the patients, especially in the intestinal type.
Conclusions: The results show that expression of claudins 1, 3, 4 and 5 is lower in diffuse type gastric carcinomas. Possibly they play a role in determining the diffuse phenotype and lowered cohesion of cells in diffuse type of gastric carcinoma in a similar manner as E-cadherin. The loss of their expression does not clearly associate with poorer prognosis of the patients, except for claudin 3 where strong expression was associated with a better outcome of the patients, a feature especially related to intestinal type tumors.

P 293

CYTOKERATIN EXPRESSION PATTERNS OF GASTRIC CARCINOMAS ACCORDING TO LAUREN AND GOSEKI CLASSIFICATION

*Ye°im Gürbüz, *Nur Köse,
*Kocaeli University Medical Faculty Pathology Department

INTRODUCTION: Goseki system is a new gastric carcinoma classification proposal that classifying gastric carcinomas as according to their gland formation and mucin production patterns. In Goseki system, grade I tumors are in intestinal type; grade II tumors correspond to mucinous tumors; grade III tumors include mucin poor, diffuse infiltrating morphology and grade IV tumors contain signet ring cell carcinomas. The signet ring cell carcinoma of the stomach is believed to be originated from superficial foveoler epithelium of the gastric mucosa while mucinous carcinoma is a specific entity originating from goblet cell metaplasia. It seems likely that the main advantage of Goseki classification is to separate signet ring cell carcinomas, mucin poor diffuse infiltrating carcinomas and mucionus carcinomas of the gastric mucosa in to different groups. Cytokeratin 7 (CK7) is observed only in chronically inflamed gastric mucousa and co-exists with incomplete intestinal metaplasia. CK20 can be observed in the superficial foveoler epithelium and mature goblet cells.
PURPOSE: The aim of this study was to examine the cytokeratin expression profiles in gastric carcinomas that are classified according to both Goseki and Lauren systems.
MATERIAL METHOD: CK7, CK8, CK19 and CK20 were applied to the paraffin sections of 66 gastric carcinoma cases. The cytokeratin expression patterns of cases were grouped as CK20(+)/CK7(+), CK20(+)/CK7(-),CK20(-)/CK7(+), CK20(-)/CK7(-).The results were compared statistically with chi-square test.
RESULTS: CK20 immunoreactivity was observed in 18% of the grade I carcinomas, 24% and 31% of grade III and IV case respectively. CK20(+)/CK7(-) pattern was observed in 20% of the grade IV and 66.7% of the grade II carcinomas and was not observed in the grade I or grade III tumors ($p<0,0001$).
CONCLUSION:In conclusion, bouth Goseki grade III and IV carcinomas originate from superficial gastric mucousa but grade III carcinomas are poorly differentiated. Goseki grade II carcinomas have a specific immunophenotype than inthestinal type gastric tumors. Goseki classification seems to be superior in identifying poorly and well differentiated forms of diffuse infiltrating carcinomas and mucinous carcinomas.

P 294
UNEXPECTED TTF-1 EXPRESSION IN GASTRIC CARCINOMA
ONEA Alina, WALTER Paul, MARIN Cristi, LAURENT Camille, CHENARD Marie Pierre.
Hôpital de Hautepierre, CHU de Strasbourg

Background: Thyroid transcription factor 1 (TTF-1) is a nuclear transcription factor selectively expressed in thyroid, lung and diencephalon. Immunoreactivity against TTF-1 in an adenocarcinoma is thought to be highly specific for pulmonary or thyroid origin.
Design: The morphologic characteristics of a case of gastric adenocarcinoma exhibiting strong staining for TTF-1 are reported and relevant literature data is reviewed.
Results: A biopsy specimen from a polypoid lesion of the cardia in a 68-year-old caucasian patient showed neoplastic glands with immunoreactivity against TTF-1 (MAb 8G7G3/1). Exploration of lung and thyroid was unremarkable. After surgical resection, the gastrectomy specimen revealed a mixed diffuse-type and intestinal type adenocarcinoma of the oesocardial junction, with strong nuclear TTF-1 positivity limited to the intestinal-type component. Moreover, TTF-1 staining was also focally present in the surrounding gastric mucosa, within intramucosal glandular cysts partly lined by metaplastic ciliated epithelium. Distant mucosal changes in stomachs resected for carcinoma and especially ciliated metaplasia are common findings in Japanese patients, but are rarely observed in European subjects. Expression of TTF-1 in ciliated metaplasia has never been reported before. Among the numerous studies concerning TTF-1 expression in carcinomas other than those derived from lung and thyroid, positivity in gastric carcinoma has only be shown in two cases, without details of histological data.
Conclusions: We describe a case of gastric carcinoma showing strong nuclear TTF-1 positivity within the tumor cells themselves and in intramucosal glandular cysts partly lined by ciliated epithelium. This finding suggests that the rare gastric cancers with TTF-1 expression may possibly derive from ciliated metaplastic cells. Moreover, detection of TTF-1 in a gastric carcinoma calls into question the absolute specificity of this marker for thyroid or pulmonary cancer.

P 295
RCAS1 EXPRESSION IN GASTRIC CANCER: CORRELATION WITH CLINICOPATHOLOGICAL VARIABLES AND PATIENTS' OUTCOME
THEOCHARIS Stamatios1, EFKARPIDIS Themistocles2, GIANGINIS Konstantinos1, SFINIADAKIS Ioannis1, SPILIOPOULOU Chara1, KOURAKLIS Gregorios2
Departments of Forensic Medicine-Toxicology1 and Propaedeutic Surgery2, Medical School, University of Athens, Athens, Greece

Background-Aims: The tumor associated antigen "receptor-binding cancer antigen expressed on SiSo cells" (RCAS1) inhibits the growth of receptor expressing cells and induces apoptosis. In this study, RCAS1 expression was examined in tumor samples obtained from gastric cancer patients and was correlated with histopathological parameters and patients'survival.
Materials and Methods: RCAS1 protein expression was examined immunohistochemically in paraffin embedded tissue sections from 38 gastric cancer cases. RCAS1 protein positivity, overexpression (positivity in more than 75% of tumor cells) and intensity (mild, moderate, intense) of staining were correlated with patients'age, gender and TNM stage, tumor histological type, grade, proliferative capacity (Ki-67 labeling index), and the patients' final outcome.
Results: RCAS1 protein positivity was noted in all of the examined cases, while in 15 out of 38 (39%) RCAS1 protein was overexpressed. RCAS1 overexpression and intensity of staining were statistically significantly correlated with tumor histological type, being mainly expressed in tumors of intestinal type ($p=0.027$ and $p=0.002$, respectively). The other clinicopathological parameters examined and patients' survival were not correlated with RCAS1 protein overexpression and intensity of staining.
Conclusions: RCAS1 protein is widely expressed in gastric cancer cases and its overexpression is correlated with intestinal type gastric tumors, suggesting the participation of RCAS1 in gastric carcinogenesis.

P 296
RELATION OF NEUROENDOCRINE DIFFERENTIATION TO TGF-ALPHA AND EGFR EXPRESSION IN GASTRIC ADEOCARCINOMAS: THEIR PROGNOSTIC IMPLICATIONS
CELIKEL Cigdem*, EREN Funda*, GULLUOGLU Bahadir**, TURHAL Serdar***
Marmara University School of Medicine
Departments of Pathology*, General Surgery**, and Oncology***

Coexpression of transforming growth factor-alpha (TGF-a) and epidermal growth factor receptor (EGFR) in carcinomas is believed to confer growth advantage to tumor cells. It is well known that TGF-a is one of the products of neuroendocrine cells, but there is no evidence concerning the possible effect of neuroendocrine differentiation (NED) in gastric adenocarcinomas (GCa) on the expression of TGF-a and EGFR. In order to assess this and their role on the survival of carcinoma patients, we analyzed Chromogranin A (ChrA), TGF-a and EGFR immunohistochemistry (IHC) in partial/total gastrectomy specimens of 101 GCa (diffuse type = 41, intestinal type = 60) cases. ChrA IHC was performed on the tissue sections prepared from formalin fixed paraffin embedded tissue blocks containing GCa areas. ChrA IHC was evaluated semiquantitatively (0-4). For each case IHC was performed for TGF-a and EGFR in sequential sections of a representative block selected based on NED. Evaluation of the IHC staining for TGF-a and EGFR was done according both to the intensity (0-2) and quatification of the positively stained areas (0-3). When a total score (sum of the intensity and quantification measurements) was 4 or greater, the tumor was considered positive for either TGF-a and EGFR. According to the results of TGF-a and EGFR staining the carcinomas were scored as 0 if neither TGF-a and EGFR was stained, as 1 if either TGF-a or EGFR was stained, and as 2 if both TGF-a and EGFR were stained. Follow-up data was available in 54 patients. Twenty seven patients was alive, while 27 died of disease with a follow-up of 7-101 and 1-131 months, respectively. NED in GCa's was related to TGF-a expression ($p<0.01$) but not to EGFR expression and TGF-a / EGFR coexpression. The percentage of cases expressing ChrA was higher in diffuse type GCa's, not with statistical significance ($p>0.05$). When the cases were grouped according to Lauren's classification, NED correlated with TGF-a but not with EGFR in both intestinal and diffuse type GCa's. Correlation of NED with TGF-a / EGFR coexpression reached statistical significance only in diffuse type GCa's. Although histologic type, NED, and TGF-a had no effect on survival, EGFR ($p<0.05$) and TGF-a / EGFR coexpression (<0.001) were related to survival. The results of our study suggest that the autocrine mechanism between TGF

P 297
EXPRESSION OF HUMAN GASTRIC MUCUS AND PCNA IN INTESTINAL METAPLASIA ASSOCIATED WITH GASTRIC CARCINOMA: AN IMMUNOHISTOCHEMICAL STUDY AND A PRELIMINARY REPORT

AKBULUT Metin, BIR Ferda, DOGANAVSARGIL Baþak, DEMIRKAN Neþe

Background: Gastric adenocarcinoma is in important cause of cancer related death and historically is known to be frequently associated with intestinal metaplasia (IM). Because IM is an important intermediary in the gastric carcinogenic sequence, understanding how an IM progress to cancer is important. HGM is a well known gastric phenotypic mucus marker that expressed in normal gastric epithelial cells and various carcinomas.To clarify the heterogeneous nature and significance of IM, we have examined the relationship between proliferating cell nuclear antigen (PCNA) and human gastric mucus protein (HGM) expression in areas of IM adjacent to gastric cancer and chronic gastritis.
Methods: In this study, we reevaluated biopsy samples obtained from 110 cases of chronic gastritis associated with IM (CG+IM) and 30 cases of gastric carcinoma associated with IM (GC+IM). We examined PCNA and HGM expression in the proliferating zone, in the areas of IM and tumor separately via immunohistochemically and correlated with each groups of CG+IM and GC+IM. Immunohistochemical study could not evaluated in all of the cases due to technical problems.
Results: The immunohistochemical staining of HGM were positive in normal gastric mucosa adjacent to CG+IM and GC+IM groups. In CG+IM group, HGM expression of the areas of IM was shown lower than GC+IM groups, this was statistically significant according to Mann Whitney-U test (p: 0,005). Although statistically insignificant, PCNA labeling index of the IM areas in GC+IM was higher than in CG+IM (p: 0,07).
Conclusion: The findings suggest that cases of IM with overexpression of HGM and high PCNA labeling index are more commonly observed in GC+IM group. We concluded that, overexpression of HGM and evaluating the PCNA labeling index may be useful for early detection of IM with high risk of gastric carcinoma. But it is necessary to study these parameters within large series to establish the precise decision.

P 298
EXPRESSION OF MUCINS IN GASTRIC CARCINOMA AND THEIR CLINICOPATHOLOGICAL SIGNIFICANCE.

Gursan N1, Gursan MS2,
1Department of Pathology, Ataturk University, Medical Facult, Erzurum,Turkey
2Department of Surgery, Ataturk University, Medical Faculty, Erzurum,Turkey

AIM: To investigate the expression of three types of mucin (MUC1, MUC2, MUC5AC) and in human gastric carcinomas and their clinical significance
METHODS: Tumours were classified according to WHO criteria. The mucin phenotype was determined immunohistochemically using markers for MUC1, MUC2, MUC5AC in 95 cases of human gastric cancer.
RESULT: There were significant correlations between MUC1 and MUC2 expression and types of cancer. MUC1 and MUC2 expression was showed the tendency to lower expression in well and moderately differentiated tubular adenocarcinoma and higher expression in advanced stage cancers (poorly differentiated adenocarcinoma, signet-ring cell carcinoma and mucinous carcinoma) (P>0.05); MUC5AC expression was showed the tendency to higher expression in well and moderately differentiated tubular adenocarcinoma and lower expression in advanced stage cancers (P>0.05);
CONCLUSIONS: MUC1 ve MUC2 is significantly influenced by histological grade,. These findings suggest that MUC1 ve MUC2 expression may be an indicator for prognosis of gastric cancer patients and correlated with early tumorigenesis and initiation of invasive growth in gastric cancer.

P 299
HELICOBACTER PYLORI GASTRITIS-UPDATED SYDNEY CLASSIFICATION APPLIED IN OUR MATERIAL

Manxhuka-Kerliu S, Kerliu A, Telaku S, Baruti-Kelmendi A, Pruthi D, Juniku-Shkololli, Maloku I.

Institute of Pathology, Faculty od Medicine, University of Prishtina.

Hp inhabits the stomach more than 50% of humans and is the most frequent cause of chronic gastritis worldwide.
The purpose of this research was to present the importance of combining topographical, morphological and etiological information of diagnostic evaluation on grading gastritis in our material according to Updated Sydney Classification.
There have been investigated 154 cases of gastric mucosa (endoscopic biopsies) which were fixed in buffered neutral formalin and embedded in paraffin. Tissue sections (5mm thick) were cut and stained with H&E, May Grunwald Giemsa and Silver stain.
The biopsy cases were analyzed in attempt to assess the major histopathological features of gastritis. The histopathological variables (Hp density, neutrophil infiltration, mononuclear infiltration, atrophy, intestinal metaplasia and dysplasia were graded on a scale of 3 (mild, moderate and severe). Minor histopathological features were not graded, but simply assessed in case of their presence or absence.
36 (23.37%) cases were positive for Hp (22.2%, 72.2%, 5.5%) . The atrophy was positive in 23 (14.93%) cases with the scale (47.8%; 47.8%; 4.34%). Dysplasia was positive in 13 (8.44%) cases with the scale (84.6%; 7.6%; 7.6%). Intestinal metaplasia was positive 25 (16.2%) with the scale (76%; 20%, 4%).
After eradication of Hp, neutrophils disappeared for 6-8 weeks, but chronic inflammation persisted longer as well as other major Hp features.
There were 6 (3.8%) cases of MZL, which were treated properly.
The presence of H. pylori increases the chances of developing adenocarcinoma and MALT lymphoma; therefore, it is important to look for possible early eradication of H.pylori to prevent the eventual development of gastric cancer. These findings should influence the treatment of gastric cancers.

P 300
COMPARING 200 GASTRIC TOUCH CYTOLOGY STAINED BY GIEMSA AND GRAM METHODS WITH HISTOLOGY STAINED BY H&E FOR HELICOBACTER PYLORI INFECTION

Seyed Mohammad Owji M.D., Mehrbod Karimi M.D.
Pathology Department,Shiraz Univ. Med Sciences,Shiraz-Iran.

Introudction and purpose:
Many observations suggesting that Helicobacter pylori (H.Pylori) to be closely associated with acute gastritis (Type B) and gastric ulcer,and some malignancy of stomach. Multiple tests are available for determining H.pylori infection. Culture is the standard method, but as the histologic examination the result is delayed .Serologic method and phase contrast microscopy is also used for detection of H.pylori.
Among the methods based on endoscopic biopsies only the rapid urease test and cytology may give result available before the patient leaving endoscopy room. The purpose of this study is to compare histologic examination with t ouch cytology stained by Giemsa and gram methods in 200 cases.

Materials and Methods:
For each patients 2-5 biopsies were obtained put into 10% formalin for histologic examination.. Additional single gastric biopsy was transferred from the biopsy forceps to a glass slide then delicately rolled onto the surface of the slide. This technique is called touch cytology. Then the slides were air dried. For each patient one slide stained by Giemsa and another slide stained by Gram method.
Results:
In histologic examination 93 out of 200 cases were positive for H.pylori. In Giemssa method 135 out of 200 cases, and in Gram method 92 cases out of 200 were positive for H.pylori. Additional result consist of 4 cases of Candida albicans with yeast –like organism and pseudohyphea in touch cytology stained by Giemsa or Gram method but not detected in histologic examination.
Conclusion:
We believed that touch cytology method is useful ,simple and rapid in diagnosis of mucosal infection of stomach with H.pylori organism, specially when the level of infection is mild. Touch cytology stained by Giemsa method yield more positive result and easier and faster to screen the smear , but in touch cytology stained by Geram method no advantage obtained over histologic examination. The combination of the histologic examination with touch cytology examination(Giemsa) are the test of choice for detection of H,.pylori and evaluation of inflammation and degree of injury/

P 301
EFFECT OF TRIPLE THERAPY IN HELICOBACTER PYLORI ASSOCIATED GASTRITIS.
C.W. Hsueh, Y.Y. Tsai, S.C. Wen, N.H. Feng, T.M. Lee*.
Depts. of Internal Medicine and Pathology*, Kaohsiung Armed Forces General Hospital, Kaohsiung, Taiwan.

Helicobacter pylori (HP) infection is a cause of gastritis in most of the patients with duodenal ulcer. Clearance of the organism leads to improvement or even total resolution of gastritis.
Aim: To evaluate the histological outcome of gastritis in the patients with duodenal ulcer after HP eradication.
Methods: A total 87 patients with duodenal ulcer with positive HP, were given triple therapy for one week. The gastric antral biopsies were made before and 6 months after the end of treatment. Histological investigation was performed according to the Sydney system on a four-point scale.
Results: The scores of gastritis histological feature before and after HP eradication are as following: 1) 2.1 and 0.9 for inflammatory cells infiltration, 2) 0.7 and 0.4 for atrophic changes, 3) 0.2 and 0.2 for intestinal metaplasia, 4) 0.4 and 0.3 for lymphoid follicles. Gastric mucosa was normalized in 58.6 % (51 / 87) out of the patients.
Conclusions: In this study, HP eradication improved gastritis in the patients with duodenal ulcer. Gastric mucosa normalizes in 58.6 % of the patients, 6 months after triple therapy.

P 302
REGRESSION OF GASTRIC MALT LYMPHOMA AFTER HELICOBACTER PYLORI ERADICATION.
AMIR Zine-Charaf, ASSELAH Fatima
Department of Histopathology, CHU Mustapha Algiers - ALGERIA

Background : Helicobacter pylori (H p) is considered the leading cause of gastric mucosa associated tissue lymphoid (MALT) lymphoma (GL) and the majority (60 – 90%) of low grade gastric MALT lymphoma are reported to regress after eradication of H p (Fischbach, 2004).
Objective: to evaluate the histologic response of low grade gastric MALT lymphoma after eradication of H p.
Methods and results: 186 cases of gastric MALT lymphoma were analyzed at the pathological department during eight years (1996 – 2003). They represent 30, 8% of all gastric cancer diagnosed during the same period. Sex ratio was 0, 97 and median age was 42 years (17 – 80 y). Abdominal pain was the most common presenting symptom (81%); a suspect antral ulceration was the endoscopic finding in 80%.
124 patients (66%) had low grade gastric MALT lymphoma. Hp infection was found in all cases. 61 of them (53%) were treated with triple therapy (amoxicillin, proton pump inhibitor and metronidazol) for seven days. Subsequently, they were followed up by sequential endoscopy and biopsy. Eradication of Hp infection was achieved in all patients; 35 of them were free of lymphoma (complete remission, 28 months median follow up); 03 patients were in partial remission (median follow up, 10 months). 02 patients relapse after 21 and 27 months; they had surgical cure and adjuvant chemotherapy.
Eradication therapy permitted the regression of more than 50% of early low grade gastric MALT lymphoma. Our results are similar to those reported in the literature
Conclusion: Actually, GL therapy isn't well codified. However eradication of Helicobacter pylori in low grade gastric MALT lymphoma is widely accepted as a first line therapy. Although complete Hp eradication is necessary and a long time follow up needed to confirm the regression.

P 303
MOLECULAR DETECTION AND GENOTYPING OF HELICOBACTER PYLORI STRAINS FROM GASTRIC BIOPSY SPECIMENS USING PCR-RFLP
R. Salehi, F. Navabakbar, M. Salehi, AR. Sabahi
Department of Genetics and Molecular Biology, School of Medicine, Isfahan University of Medical Sciences, Isfahan 81744-176, Iran

Helicobacter pylori is a gram-negative microaerophilic organism that colonizes human gastric mucosa. It has been proved that H. pylori is an etiologic agent of chronic gastritis and peptic ulcer diseases and is also a risk factor for gastric cancer. The World Health Organization has classified H. pylori as a class I carcinogen. Epidemiological studies have shown that H. pylori infection occurs world wide at a high prevalence rate.

Recurrence of infection after apparent eradication has also been reported and is associated with recurrence of ulcers. However, it is unclear whether the recurrence of ulcers following H. pylori eradication therapy is due to recrudescence of the previous infection or to exogenous re-infection by another strain. An accurate method for the detection and differentiation of H. pylori strains in patients both before and after therapy is therefore of great importance for diagnosis, monitoring of treatment, and reduction of the long-term consequences of continued but undetected disease.

Attempts to differentiate H. pylori strains have been made using a variety of conventional typing schemes, like haemagglutination, biotyping, cytotoxin activity, plasmid profiles and immunobloting. However, each of these methods due to some inherent difficulties did not gain widespread use for precise differentiation of H. pylori strains.
Gastric biopsy specimens were obtained from 79 patients, 36 women and 43 men. Extracted DNA amplified using primers specific for UreC gene. The amplified products were purified using PCR products purification kit and then digested with 10 U of CfoI, MboI and AluI restriction enzymes separately for at least 3h at 37°C.
Five patterns for MboI, five patterns for AluI and 4 restriction patterns for CfoI were observed. The patterns were classified based on the number of bands detectable by gel electrophoresis.
From our study it is concluded that, the PCR-based RFLP technique is a useful approach for genotyping of specific H. pylori strains. Using this method we can determine

reinfection, infection with new strains, recrudescence or drug resistance in H. pylori infected patients.

P 304

THE POSSIBILITIES OF IMMUNOHISTOCHEMICAL STAINING METHOD FOR DETECTION OF HELICOBACTER PYLORI (HP) INFECTION IN CASES WITH CHRONIC GASTRITIS, ULCERS AND GASTRIC CANCER AND GASTRIC LYMPHOMA

BRACHKOVA Yordanka, MARKOVA Elena

Background: The HP infection affects more than 50% of the human population and plays an important role in the pathogenesis of chronic gastritis, chronic peptic ulcer of stomach and duodenum, gastric cancer and gastric lymphoma. Thus the eradication of HP has definite therapeutic and preventive effect.

Aims: 1. To improve the diagnosis of HP infection putting into practice the immunohistochemical / IHCh/ staining of bacteria on endoscopic biopsies.2. Determine the rate of HP infection in patients with chronic gastritis, chronic peptic ulcers, gastric cancer and gastric lymphoma.

Methods: Two hundred forty endoscopic biopsies prepared with routine histological and histochemical methods (HE, V.G., PAS) are studied retrospectively and analyzed. Two hundred twenty three (92%) are stained with Giemsa for HP and 99 (42%) are tested immunohistochemically with Polyclonal rabbit anti HP antibody (DACO}

Results: Analyzing the material we found that the identification of HP with Giemsa staining was respectively 55% and 58% in cases with chronic gastritis and ulcers and 66% and 69% in the surrounding mucosa in patients with gastric cancer and gastric lymphoma. Immunohistochemically HP was detected in 83% and 93% in chronic gastritis and ulcers and 70% and 77% in gastric cancer and lymphoma. The efficiency of the proposed method in number detection is mostly evident in the group of patients with chronic gastritis, where all the negative and suspicious for HP cases were examinated immunohistochemically. The percentage of cases with identified HP bacteria in this group increased from 55% to 93%. For the group of ulcers the rise is from 58% to 83%, while for gastric cancer and lymphoma cases it was inconsiderable. The reason for this is the lack of appropriate material from the surrounding mucosa in the tissue samples for IHCh staining. Conclusions:The examination with IHCh staining is a reliable method for identification of HP infection in gastric mucosa. By the means of this method we reduce the number of suspicious cases. The increased exposure of HP is due to the detection of the attached to the cell membranes bacteria and the coccoid forms too.

Key Words: HPylory, immunohistochemical detection, gastroscopic biopsies.

P 305

HELICOBACTER PYLORI INFECTION IN CHILDREN: CORRELATION BETWEEN CAGA, ICEA AND VACA GENOTYPES AND HISTOPATHOLOGICAL CHANGES IN GASTRIC MUCOSA

Boštjan Luzar, Mario Poljak*, Matjaž Homan**, Boštjan J. Kocjan*, Gabriela Panter*, Maja Shrestha*, Maja Kveder*, Tina Moèilnik*

Institute of Pathology, Microbiology and Immunology*, Medical Faculty University of Ljubljana, and Department of Paediatrics**, Clinical Centre, Ljubljana, Slovenia

Background

Despite strong association of distinct Helicobacter pylori (HP) genotypes with degree of histological changes in gastric mucosa of adults, such an association is still controversial in paediatric population.

Aims of the study

To analyse correlations between cagA, iceA and vacA HP genotypes and the degree of histological changes in the gastric mucosa in paediatric population.

Material and methods

The entry criteria for the study was a positive rapid urease test, and subsequent detection of ureA and/or ureC genes by polymerase chain reaction (PCR) in the same tissue specimen. Histological changes in gastric mucosa were graded according to the updated Sydney system. The cagA gene, signal (s) and middle (m) regions of vacA gene and iceA gene were determined by PCR in the total DNA, isolated from tissue samples used for the rapid urease test.

Results

Altogether 186 samples of gastric mucosa (158 from antrum and 28 from corpus) from 140 children, aged from 4 to 18 years (mean age 13 years) were analysed histologically. The degree of activity and chronicity in antrum and corpus correlated with the density of HP colonisation ($p<0.05$). A statistically significant decrease in the degree of activity and chronicity after HP eradication was observed only in antral mucosa ($p<0.05$). The HP eradication rate was 69% for antrum and 75% for corpus. cagA was detected in 63% (75 of 119) of samples and correlated with the degree of activity and chronicity in antrum ($p<0.05$). No correlation was found between iceA and histological changes. Regardless of the subtype, a borderline statistical association was present between vacA s and antral intestinal metaplasia ($p=0.05$), and between vacA m and corpus atrophy ($p=0.03$). Co-infection with various HP strains, found in 8% of antral mucosa samples, did not correlate with histological changes.

Conclusions

Our results confirm the need for treatment of symptomatic children with HP infection in order to diminish and/or abolish the damaging effect of acute and chronic inflammation on the gastric mucosa, a hallmark of HP infection. Both have been previously shown in adults to correlate with the subsequent development of atrophy and intestinal metaplasia, possible precursor lesions in gastric carcinogenesis. Finally, it appears that at least the cagA gene influences the degree of activity and chronicity in antral mucosa of children, and that the mechanism of mucosal damage by HP is different in corpus and antrum.

P 306

GASTROINTESTINAL LYMPHOMAS AND HELICOBACTER PYLORI INFECTION – CLINICOPATHOLOGIC STUDY

BRACHKOVA Yordanka, MARKOVA Elena

Medical University of Pleven, Bulgaria

Background: Chronic Helicobacter Pylori /HP/ infection is strongly associated with the development of primary gastric B-cell lymphoma of MALT type. The choice for gastric surgery or stomach concerning treatments, should be based on an accurate histopathological diagnosis, grading and clinical staging. The effect of curing HP infection on the course of a high-grade gastric MALT lymphoma is uncertain.

Aims: 1. To study the primary gastrointestinal lymphomas /GIL/ for the last 5 years, obtained gastroscopically, after surgical treatment or diagnosed on autopsy.

2. To follow up and analyze the effect of HP eradication therapy /HPET/ and chemotherapy on gastroscopic biopsies.

Patients and methods: For the period 2001-2005, 36 patients between 38 and 84 years with primary GIL were studied /32 of the stomach, 3 on small bowel and 1 on large bowel/. Twenty six cases were diagnosed on gastric biopsies, 5 after surgical biopsy and 5 after autopsy. All lymphomas were immunophenotype identificated, graded and clinical staged by Ann Arbor and Musshoff system.

Results: From 36 GIL 35 were classified as B-cell NHL and 1 as high grade T-cell NHL, 28 were high-grade B cell

lymphoma /HGBCL/ or diffuse large B cell lymphoma /DLBCL/ and 7 low-grade B cell lymphoma /LGBCL/. A follow up examination, about 30-36 months, was performed on 7 cases/3 with HGBCL and 4 with LGBCL/. Complete histological remission was found in 2 patients with successful HPET and chemotherapy /CHOP, MABTHERA/ and unsuccessful HPET with incomplete histological remission in 5 cases. Twelve patients /aged 50-57/ with DLBCL were operated in stage IIE -10 gastric and 2 intestinal. Half of them were with large ulcerated lesions. All GIL diagnosed after autopsy were in advanced stage /1 high-grade T-cell and 4 DLBCL/.
Conclusions: Our results revealed that primary GIL were mostly high grade B-cell/DLBCL and in 80% were associated with HP infection. The effect of HPET was not successful in most cases. We found that they were rarely suspected by clinicians and were diagnosed mostly in IIE clinical stage. This settled down the question about revision of HPET and the responsiveness of lymphomas to the therapy.
Key words: Gastrointestinal lymphoma, Low grade MALT, DLBCL, HP eradication, Chemotherapy, Surgical treatment.

P 307
GASTROINTESTINAL STROMAL TUMOUR: ROUND CELL ANAPLASTIC TYPE LACKING C-KIT/CD117 IMMUNOEXPRESSION
MICEV Marjan 1,2, TODOROVIC Vera 2, MITROVIC Olivera 2, COSIC MICEV Milena1, PESKO Predrag 1, BORICIC Ivan 3
1 Institute of Digestive Diseases, Clinical Centre of Serbia, Belgrade, Serbia and Montenegro
2 Institute for Medical Research, Belgrade, Serbia and Montenegro
3 Institute of Pathology, Medical Faculty, University of Belgrade, Serbia and Montenegro

INTRODUCTION AND AIMS: Gastrointestinal stromal tumors (GISTs) are the most common mesenchymal tumors of the gastrointestinal tract with the stomach as the most common site. CD117/KIT immunoexpression has been accepted as a specific marker for GISTs preferentially used for confirmation of the diagnosis. However, GISTs constitute a group of phenotypically heterogenous mesenchymal neoplasms with uncertain biological behaviour that often coexpress CD34 and/or myoid, neural and other markers.
MATERIAL AND METHODS: We reexamined clinically, histologically and immunohistochemically 121 cases of paraffin-embedded GISTs noted in the Tumor Registry of Clinical Centre of Serbia from the total of 412 patients operated for abdominal mesenchymal mostly visceral tumours between 1992 and 2004. In addition, evaluation of malignancy of GISTs was based on clinico-pathological criteria proposed both by Fletcher in 2002 and Bucher in 2004.
RESULTS: Most of gastric GISTs were composed of spindle cells (73%), epithelioid cells (20%) or both and/or rare cell types (7%), and nearly 30% showed obvious clinical malignant behavior. We present three cases of primary GISTs with similar small round cell morphology, two gastric (in 47 year old male and 56 year old female patients) and one esophageal (63 year-old male patient). In one case, hepatic metastases were resected during primary surgery, in two other cases they developed after 8 and 11 months. None of them were treated with imatinib (Glivec) and only one patient had conservative chemotherapy. Follow-up showed short survival interval (9 to 16 months). All cases expressed only strong vimentin immunoexpression and were preexcluded for other small round cell differentiation. Immunohistochemical examination showed weak cytoplasmic CD117 expression in one case, evident CD34 expression in two of cases (one of them exlusively CD34 positive) and confirmed non-myogenic and non-neurogenic differentiation. In addition, all cases showed Ki-67 index higher than 10% and PCNA higher than 30%.
CONCLUSION: Round cell anaplastic type of GIST might represent small distinct clinically aggressive subgroup of these tumours with incomplete immunophenotypic expression or dedifferentiated type of GISTs different from immunohistochemically similar group of so-called fibroblastic, mostly spindle cell type of GISTs (GIFT).

P 308
GASTROINTESTINAL STROMAL TUMORS OF THE DUODENUM.
MARIÑO Ana, BACCHI Carlos,PANUNCIO Ana,DI MATTEO Carina,DE ARMAS Rafael.
Department of Pathology,Clinicas Hospital University of Uruguay.

Abstract
Introduction:The mayority of gastrointestinal tumors (GIST) express c-kit, a growth factor receptor with tyrosine kinase activity .Mutations in the c-kit proto-oncogene may lead to constitutive ligand-independent activation of c-kit and subsequent neoplastic transformation, but alterations in chromosomes 14 and 22 may also play a role in the molecular pathogenesis.The purpose of the study is to distinguish GISTs from the other mesenchymal tumors of the GI tract and specially duodenal tumors,because of differences in natural history, as well as the efficacy of treatments targeting the GIST tyrosine kinase.
On immunohistochemical staining, tumor duodenal cells were positive for vimentin, CD34, CD117(c-Kit), Ki-67 and negative for muscle-specific actin, desmin, S100, neurofilament and keratin.GISTs tumors have a spectrum of clinical behavior at all sites of their ocurrence. Tumors that show low mitotic frecuency (5 or fewer mitoses per 50 HPF) usually have a benign behaviour. However, there is a definite percentage of mitotically inactive tumors that subsecuently metastasize, emphasizing the fact that low mitotic count does not rule out a malignant behaviour. GISTs with mitotic counts over five per 50 HPF are customarily designated as malignant, and tumors over 50 mitoses per 50 HPF are designated as high-grade malignant
The small intestinal tumors and duodenal tumors were more agresive than other localizations, in our cases the tumors shows high risk and malignant potential in comparison with gastric tumors. Tumor size, location,mitotic and proliferation indices, and mutations in the juxtamembrane domain of c-kit (exon 11) appear to correlate with risk of malignant behaviour.
The molecular targeting of the critical pathogenetic mechanism underlying GIST has given patients new hope, and has provided physicians with a highly effective and well tolerated therapeutic option for a disease for which no systemic therapy existed previously.
Moreover GISTs serve as the model solid tumor for a molecular biology-based diagnosis and treatment of cancer.

P 309
CLINICOPATHOLOGIC FEATURES AND IMMUNOHISTOCHEMICAL STAINING FOR C-KIT PROTEIN (CD117) IN METASTATIC AND PRIMARY MALIGNANT MELANOMA OF THE GASTROINTESTINAL TRACT
ALTINOK Gulcin*, HIMMETOGLU Cigdem*, GUREL Bora*, SAVAS Berna**, ENSARI Arzu**, DURSUN Ayse***, SOKMENSUER Cenk*, GUNGEN Yucel*, GUNHAN Omer****, GEDIKOGLU Gokhan*
Departments of Pathology, Hacettepe University School of Medicine*, Ankara University School of Medicine**, Gazi University School of Medicine***, Gulhane Military Medical Academy ****, Ankara, Turkey

Introduction: Malignant melanoma (MM) is the most common metastatic tumor of the gastrointestinal tract and can present with fairly common constitutional symptoms. The small and large intestines are the most common sites for metastases from cutaneous MM. However, primary MMs in these sites are exceedingly rare. Genuine primary MM of the gastrointestinal tract is a rare, highly malignant anorectal neoplasm of poor prognosis.
Aim: This investigation was performed to determine the clinicopathologic features and immunohistochemical staining for c-kit protein in metastatic and primary gastrointestinal malignant melanomas.
Material and Method: 26 gastrointestinal MM cases were retrieved from the archives of pathology departments of four different medical schools and were evaluated for histologic features. Formalin-fixed, paraffin-embedded tissue sections were immunostained with c-kit protein by the avidin-biotin-peroxidase procedure.
Results: These cases included 17 anorectal, 6 small intestinal, 2 duodenal, and 1 gastric MM. Most of the anorectal MMs (56.2%) were presented with gastrointestinal hemorrhage, whereas small intestinal (SI) MMs with intussusception (44.4%) and acute abdomen. Comparison of gender and tumor size (median, 5.5cm in anorectal MM, and 5cm in SI) showed no significant difference. Patient age at presentation (median, 62 years in anorectal, and 49 years in SI) was not statistically different (p=0.08). Resection materials revealed that anorectal cases were solitary (12/12), whereas small intestinal cases were multiple (4/4), p=0.0005. Histologically, tumor cell (epitheloid and spindle) type (p=0.667), and diffuse and intense cytoplasmic expression of c-kit did not differ significantly in between the anorectal, small intestinal and duodenal MM (p=0.627).
Conclusion: Metastatic MM in the gastrointestinal tract should be suspected in patients with history of melanoma of the skin and acute gastrointestinal symptoms. Other than clinical presentation, location and multiplicity, the clinicopathologic parameters did not differ between primary and metastatic MM. This study also emphasizes on diffuse positive immuno-expression of c-kit protein in gastrointestinal MMs which diminishes the discriminatory value of c-kit protein for differential diagnosis between the cases of gastrointestinal stromal tumor and poorly pigmented malignant melanoma.

P 310
FIRST RESULTS OF THE NATIONAL PROGRAM OF STANDARDIZED GISTS DIAGNOSIS IN SLOVAKIA: RETROSPECTIVE VERSUS PROSPECTIVE ANALYSIS

SZÉPE Peter, KAJO Karol, MACHÁLEKOVÁ Katarína, KVIATKOVSKÁ Zuzana, Poliaková Katarína*, STRAKA ¼ubomír*, PLANK Lukáš
Dept. of Pathology, Komenius University Jessenius Medical Faculty and Faculty Hospital in Martin
Dept. of Pathology, Faculty Hospital in Prešov*

Introduction: The definition of gastrointestinal stromal tumors (GIST) has evolved over time and its true incidence is still unknown, probably underestimated. GIST showing an increasing incidence after molecular discovery (KIT gene) and clinical-pathological diagnostic tools (CD117) represent targets for new treatment by anti-CD117 therapy.
Purpose of the study: Comparation of incidence, morphology and clinical data of GIST of two series: The 1st series representing a retrospective study of 10 years material reported at ESP Congress in Ljubljana (2003) versus (vs) 2nd series of GIST diagnosed during the last 2 years under cooperation with other Slovak departments involved in national program.
Methods used: For both the series, identical methodology and interpretation of the findings based on the criterias of Fletcher et al. (2002) were used. In addition to histological stainings, the immunohistochemical analysis included primary antibodies against vimentin, desmin, actins, S-100 protein and CD117 (all DakoCytomation) and CD 34 (Immunotech). Because of lacking molecular biology examinations, only CD117-positive cases were included to the study.
Summary of results: The 1st series includes 32 and the 2nd 33 cases. The tumors of both the series showed predominant localisation in the stomach (18 vs 13 cases) and small intestine (11 vs 15 cases), while other localisations were rare (colon 1 vs 2 cases, extramural GIST 2 vs 2 cases). One of the 2nd series cases represented a liver metastasis of the case diagnosed previously as „gastric leiomyoma“ 19 years ago, without a possibility for the review. However, both the series showed different distribution of the risk categories: predominance of the lower risk categories in the 1st series (2 cases of very low, 16 of low, 8 of intermediate and 6 of high risk category) vs predominance of high risk categories in the 2nd series (4 cases of very low, 8 of low, 7 of intermediate and 14 of high risk category).
Conclusion reached: In contrast to literary data and results of our 1st series, the intestinal localisation was predominating in the 2nd series. Although both files are relativelly small, the localisation might be related to the increased number of the higher risk categories cases. The study shows first benefits of the program, resulting in a higher „sensitivity“ of the pathologist to recognize the GIST. Therefore the program will continue and should involve molecular diagnostic techniques of GIST diagnosis.

P 311
GASTROINTESTINAL STROMAL TUMOR AND OTHER SPINDLE CELL TUMORS; PATHOLOGICAL AND CLINICAL ANALYSIS OF 30 CASES.

HERLEA Vlad, STOICA-MUSTAFA Elena, HORTOPAN Monica, MIHAI Mihaela, PECHIANU Catalin, VASILESCU Catalin, TOMULESCU Victor, IONESCU Mihnea and POPESCU Irinel
Department of Pathology, Fundeni Clinical Institute, Bucharest, Romania
Department of General Surgery, Fundeni Clinical Institute, Bucharest, Romania

BACKGROUND: Gastrointestinal stromal tumors (GISTs) are mesenchymal neoplasms of the gastrointestinal tract. These lesions have been a source of controversy in regards to classification, histogenesis, differentiation and biologic potential. Recently with the advent of new therapeutic interventions, proper characterization and conceptualization of these tumors has acquired a new meaning, and emphasis is being placed on the role that various diagnostic techniques play in the evaluation of these neoplasms.
PURPOSE OF THE STUDY: We conducted a study to identify true GISTs with known pathological and immunohistochemical criteria from other tumors of the gastrointestinal tract.
METHODS: We selected from clinical records of patients with diagnosis of schwannoma, leiomyoma, leiomyosarcoma and tumor of uncertain biological behavior of the gastrointestinal tract, 79 cases. All the cases studied were surgically treated. To confirm the usefulness of an immunohistochemical panel of antibodies and histological analysis we have been selected 30 cases of GISTs . The antibodies used were : c-kit/CD117, CD34, desmin, smooth muscle actin (SMA), S-100 protein.
RESULTS: Thirty cases of GISTs were identified, based on histological and immunohistochemical analysis. All the confirmed GISTs were positive at immunohistochemistry for c-kit expression and most of them for CD34, desmin and S-100. SMA have only limited value. The two predominantly location of the tumors were the stomach (75%)and small intestine (6%). Various pathological and clinical parameters have been evaluated (size, mitotic rate, invasion into mucosa,

presence or absence of coagulative necrosis, status of surgical margins, location, chronic or acute bleeding).
CONCLUSIONS: Tru GISTs can be recognized from other tumors by histological analysis. Immunohistochemistry to identify c-kit protein expression is useful to certified the diagnosis. For predicting behavior in GISTs, the authors proposed some criteria .

P 312
IDENTIFICATION OF GASTROINTESTINAL STROMAL TUMORS IN PRIMARY BENIGN AND MALIGNANT MESENCHYMAL NEOPLASMS OF THE GASTROINTESTINAL TRACT AND INCIDENCE IN DOUBS COUNTY. CLINICOPATHOLOGICAL RETROSPECTIVE STUDY OF 230 CASES FROM 1990 TO 2000.
RINGENBACH F. (1), VIENNET G. (1), MONNIEN F. (2), MERCIER M. (2), DANZON A. (3), MANTION G. (4), BOSSET J.F. (2), KANTELIP B. (1).
(1) Pathology, (2) Radiotherapy, (3) Tumors Registry, (4) Digestive Surgery department, CHU Jean Minjoz. 25030 BESANCON CEDEX. France.

Gastrointestinal stromal tumors (GISTs) are KIT-positive spindle cell or epithelioid mesenchymal tumors (MTs) occurring anywhere in the gastrointestinal (GI) tract or abdomen. The majority of GI-MTs are therefore now considered as GISTs. However, the frequency of GISTs in GI-MTs is not well known and their incidence too. The purpose of this study is to identify GISTs in the Franche-Comté region (eastern France) in a ten year-period (1990-2000) in all primary benign or malignant MTs of the GI-tract and abdomen.
This study includes MTs diagnosed in all Franche-Comté region pathology laboratories as leiomyomas, leiomyosarcomas, leiomyoblastomas, schwannomas, schwannosarcomas, neurofibromas, fibromas, fibromatosis, spindle cells sarcomas, and GISTs. The Franche-Comté (population : 1,200,000) is a region composed of 4 counties in particular the Doubs county (population : 499,062). Over the 10 year-period, 230 cases were retrieved. For each case, a standard morphologic study and an immunohistochemical study using anti-CKIT, CD34 antibodies was carried out. The proliferative index was performed with the Ki67 (MIB-1) antibody. The diagnosis was drawn up according to GIST Symposium 2002 criteria.
Out of the 230 cases, 29 were initially identified as GISTs (13 %). After this second study, 102 / 230 are GISTs (44 %), and 28 / 29 are true GISTs. In stomach 67 / 81 are GISTs (83 %), in small bowel 24 / 40 (60 %), in omentum 4 / 5 (80 %), in mesentery 3 / 9 (33 %), in colon 3 / 53 (6 %), in retroperitoneum 1 / 12 (8 %). In esophagus (21 tumors), in liver (5), in anus (2), in appendix (1) and in gallbladder (1), no GIST was identified. GISTs were developed in stomach in 66 % of cases, in small bowel in 24 %, in omentum and mesentery in 7 %, in colon in 3 % and in retroperitoneum in 1 %. Over 102 GISTs, 47 patients live in Doubs county at time of diagnosis. The mean “floor” limit of the raw incidence rate was estimated at 1 case / year / 100,000 in Doubs county. The proliferative index over 10 % of neoplastic cells stained was correlated with poor prognostic.
The occurrence of GISTs in our study is close to that reported in literature. Stomach and small bowel locations are the most frequent. Furthermore, our study show that 74 benign or malignant GI-MTs were reclassified as GISTs and that GISTs are the most common mesenchymal neoplasm in the gastrointestinal tract.
Supported by grants from the French Research Ministry (PHRC 2003), NOVARTIS, and Ligue Contre le Cancer

P 313
NATIONAL PROGRAM OF A STANDARDIZED BIOPSY DIAGNOSIS OF GASTROINTESTINAL STROMAL AND NEUROENDOCRINE TUMORS OF THE GI-TRACT IN SLOVAKIA
PLANK Lukáš, SZÉPE Peter, KAJO Karol, MACHÁLEKOVÁ Katarína, KVIATKOVSKÁ Zuzana

Introduction: The gastrointestinal stromal and neuroendocrine tumors (GISTs, resp. NETs) of the gastrointestinal tract show unique biological behavior. Their appropriate managment requires a standardized approach and methods used for the biopsy diagnosis.
Purpose of the study: Because of their relativelly low incidence, the experiences of the pathologists with the biopsy diagnosis and differential diagnosis of GIST and NET are limited. Therefore the aim was to develop a national system offering a standardized biopsy examination and interpretation of all the clinical and laboratory results for the patients with GIST and NET.
Methods used: The authors introduced in 2004 a retrospective analysis of previously diagnosed GISTs and NETs and attended the Italian course INTUIT („Identification and New Treatment of Uncommon Intestinal Tumors“). Due to a cooperation of Slovak pathologists and involved clinical specialists, a national network system of a GISTs and NETs biopsy diagnosis based on the accepted regional centralisation and using standardized protocol for all the obtained data was introduced in Jan. 2005. The system includes a second look biopsy examination of the cases at accepted specialized centres in relation to clinical data evaluation. In addition to the unified panel of morphologic and immunohistochemical methods of the GISTs and NETs biopsy diagnosis, all hormonal and necessary prognostic markers may be examined in situ at the coordination centrum of the project.
Summary of the results: The early preliminary results summarizing first months of the project document its first benefits, e.g. increasing number of the bioptically identified GIST cases. An integral part of the project is represented by the educational activities. In association with the traditional IAP meetings of the Slovak pathologist, first two minisymposias discussing the topics of GIST and NET biopsy diagnosis were organized and the project was introduced at the national conference of the gastroenterologists. Next educational activities will involve also other specialists, incl. the participations of the molecular biologists.
Conclusions reached: The described program starts to offer: a./ for clinical practice standardized results representing a good basis for the managment and therapeutical considerations in the cases of GISTs and NETs, incl. their targeted therapy, b./ good outcomes for further optimization of their diagnosis including also molecular biological techniques.

P 314
VARIABILITY ASSESSMENT OF IMMUNOPHENOTYPICAL PATTERN OF DIFFERENTIATION IN GASTROINTESTINAL STROMAL TUMORS
CEAUSU Mihai 1,2, ARDELEANU Carmen 1,2, BUTUR Georgeta 2, ANDREI Florin 2, FLOREA-GRAMADA Zenaida 2, CONSTANTIN Laura 1
1 - « Carol Davila » University of Medicine and Pharmacy, Bucharest, Romania
2 - “Victor Babes” National Institute of Pathology, Bucharest, Romania

Gastrointestinal stromal tumors (GIST) are mesenchimal neoplasms of gut with origin in interstitial cells of Cajal which express the tyrozin-kinazic receptor of c-kit (CD117). According to phenotypical features, GIST’s can be classified in tumors with smooth muscle differentiation, neural, mixt or non neuro-muscular diferentiation.

The aim of the study was to investigate and to test the efficiency of a panel of antibodies in immunophenotypical pattern variability analysis of diferentiation in GIST.
The indirect tristadial ABC method was performed on formalin fixed paraffin embedded tissues taken from 13 patients with GIST, using 5 antibodies : CD117, CD 34, vimentin, actin, S-100.
GIST's were immunoreactive to CD117 in 80% cases, to CD34 in 91% cases. Using regresive biostatistics analysis, it was observed a direct positive correlation between CD117 and CD34 ($r = 0.7$) and highly significant ($p = 0.002$). Between CD117 and actin, a positive polynomial relation was found ($r = 0.4$), without statistical signification ($p = 0.6$). Between CD34 and actin, a slightly positive liniar correlation ($r = 0.3$) was observed, as it was between CD34 and S-100 ($r = 0.23$), but none with statistical signification ($p = 0.2$). Tumors with a diffuse stain to CD117 and CD34 shown a focal expression to S-100, actin and vimentin.
The study confirmed the coexpression between the main diagnostic markers of GIST's - CD117 and CD34 ; CD34 high percentage in correlation with actin and S-100 expression, may provide to this heterogen antigenic association, a significant diagnostic value with future therapeutical involvements.

P 315
INFLAMMATORY CELL-RICH GASTROINTESTINAL STROMAL TUMOR IN THE STOMACH: A CASE REPORT
DILEK Fatma Husniye,MD, AKTEPE Fatma,MD, SAHÝN Dursun Ali,MD, DÝLEK Osman Nuri,MD,FACS.

We report the case of a 62-year-old woman with two primary neoplasms: adenocarcinoma of the colon with hepatic metastase and stromal tumor of the stomach, that had unusual histologic findings. Abdominal-pelvic ultrasonography and computed tomography revealed that there was wall widening in the descending colon and posterior wall of the antrum. Preoperative endoscopic examination revealed a hemispheric submucosal tumor in the anterior wall of the antrum. Histologic diagnosis of colon mass was adenocarcinoma and tumor metastased to liver. The tumor of the stomach, which was 3 cm in diameter, was resected by antrectomy. Histologic examination revealed that it was composed of spindle shaped cells with elongated nuclei and no mitoses. Inflammatory cells were intense and patchy throughout the tumor and a peripherial cuff of lymphoid aggregates was observed in the tumor. Tumor cells expressed vimentin, S-100 protein and CD117 strongly and diffusely and neuron-specific enolase weakly and focally. Tumor was uniformly negative for smooth muscle actin, desmin, cytokeratin, CD34, synaptophysin, and chromogranin. A positive reaction for MIB-1 was only a few. This appears to be the first report of the stromal tumor which has a cuff of lymphoid cells in peripheral and dense plasma cells in GISTs.

P 316
C-KIT MUTATIONS ANALYSIS OF A SERIES OF GISTS FROM PORTUGUESE PATIENTS
GOMES Ana 1, BRITO Maria 2, MILANEZI Fernanda 1,3, SCHMITT Fernando 3,4, REIS Rui 1
1- Life and Helath Sciences Research Institute (ICVS), School of Helath Sciences, University of Minho, Braga, Portugal, 2 - Hospital Garcia de Orta, Almada, Portugal, 3 - IPATIMUP, Porto Portugal and 4 - Medical Faculty, Porto University, Porto, Portugal

Gastrointestinal Stromal Tumors (GISTs) are rare primary mesenchymal tumors of the gastrointestinal system. GISTs diagnosis is partially dependent on the immunohistochemistry c-Kit over expression, a type III tyrosine kinase receptor. The majority of GISTs have a constitutively active form of oncogene c-kit, which is the reflex of activation mutations in the extracellular domain (exon 9), juxtamembrane domain (exon 11), and intracellular kinase domains (exons 13 and 17). Approximately 80% of c-kit mutations occur in exon 11, and are clinically important due to their association with high sensitivity and response to Imatinib, a specific kinase receptor inhibitor, when compared to mutations in the other c-kit exons. The reported frequency of c-kit mutations ranges from 20 to 70% of GISTs cases. In Portugal, the incidence of c-kit mutations in GISTs tumors is, to the best of our knowledge, unknown.
The aim of this work was to assess the frequency of oncogene c-kit mutations, in a Portuguese series of GISTs and other mesenchymal tumors, to determine the frequency of patients that would benefit from Imatinib therapy.
DNA was extracted from formalin-fixed and paraffin-embedded tissues of 22 GISTs and 7 mesenchymal non-GISTs tumors (3 Leiomyosarcomas, 1 Malignant Triton, 2 Leiomyomas, 1 Sarcoma). Mutation analysis of c-kit exons 9, 11, 13 and 17 was done by PCR-SSCP. Samples with a SSCP pattern different from the normal blood pattern were further sequenced to confirm the genetic alteration.
Of the twenty-two GISTs cases, eight (36.4 %) contained a mutation in exon 11, one (4.5 %) in exon 9, and no mutation was identified in exons 13 and 17. Mutations in exon 11 included four deletions, two duplications and two base substitutions. The mutation in exon 9 was duplication. All deletions and duplications were in-frame. In total, c-kit mutations were present in 9/22 (41%) of GISTs. No mutation was found in any of the mesenchymal non-GIST cases studied.
We characterized for the first time the occurrence of c-Kit mutations in Portuguese GISTs series. The incidence of c-kit mutation is 41%, in agreement with described range. As previously reported, the great majority (8/9, 89%) of mutations are located in exon 11, and lead to constitutive activation of c-kit kinase activity. No mutations were identified in non-GISTs stromal tumors.

P 317
A NATIONAL STUDY OF GISTS IN GREECE
M. DEMONAKOU, C. PATSIOURA, D. APESSOU, P. ARAPANTONI,
S. ASIMAKH, C BARBATI, I GIGONTI, CH. KALEKOU, C. KAFIRI,
A. KRIAKA, E. MACHERA, K. MEDITZKOU, E NENOPOULOU,
K. PARASI, F. PATAKIOUTA, C. PETRAKI, S. SAVVA,
M. SOTIROPOULOU, E VRETOU, J. VENIZELOS, S. PAPADOPOULOS
Gastrointestinal study group of HELLENIC SOCIETY OF PATHOLOGY

GISTs are rare neoplasms of the GI tract with unpredictable prognosis, differentiating towards Cajal cells; most GIST express CD117 and carry genetic changes in chromosome 11 which encodes for the c-kit receptor, a tyrosine-kinase transmebrane molecule get involved in cell signaling. An inhibitor of this molecule has been discovered recently, giving rise to new therapies.
The aim of this study is to investigate the incidence of GIST in Greece and analyze the morphological and immunohistochemical characteristics, so as to create a GIST database in Greece.
The mesenchymal neoplasms of GI tract and mesentery diagnosed in 23 laboratories in Greece during a 5-year period (1998-2002) were collected. They were studied by ten couples of Pathologists for morphological subtypes, mitotic activity (50hpf), necrosis, cystic degeneration and atypia in H&E and by immunostaining with CD117 for the staining pattern and the percentage of positive cells (DAKO 1/100,

polyclonal, without pretreatment, using the Ventana automated NeXes system). Follow up the patients for 24 –96 months for overall survivor, partial or complete remission and relapsing in comparison to the morphological and immunohistochemical characteristics of GISTs.
209 out of 311 cases of mesenchmyal neoplasms were positive for CD117 (67.2%). 60.3% of the patients were 61-80 years old, 51% were men and 41% \women (M/F: 1.44). 57.8% of GISTs affected stomach, 28.6% small bowel, 6.6% large bowel and 3% mesentery. 48.2% of neoplasms were measured < 2cm, 36% >2<5cm, 37.6% >5<10 and 21.60% >10cm. Less than <2 mitoses per 50hpf were counted in 48.2% of the cases, 2-5 in 20.3%, >5<10 in 13.7% and >10 in 17.8%. The most common neoplasm was the spindle cell type (52.50%) with moderate atypia (54%). In 51.2% of GISTs 81%-100% of neoplastic cells express KIT protein. A diffuse staining pattern was found in 80.2% of the cases. Since now we follow up 80 patients.
Epidemiology and Histology of GISTs in Greece share the same characters with GISTs worldwide apart from a lower expression of KIT protein, a finding needing further investigation. Follow up of patients is in process and the results should be discussed.

P 318
MULTIPLE GASTROINTESTINAL STROMAL TUMORS IN SMALL BOWEL
SOYUER Isýn,KALA Mehtap,GÜRSOY Sebnem, OK Engin,TURAN Cuneyt,ÖZDEMÝR Mehmet Akif,ÖZKAN Metin, SOYUER Serdar,
Department of Pathology, Department of Gastroenterology,Department of Surgery,Department of Pediatric Surgery, Department of Pediatric Hematology and Oncology,
Department of Oncology,Department of Radiation Oncology, University of Erciyes, Medical Faculty, Kayseri, Turkey

Objectives: In most cases, gastrointestinal stromal tumors (GIST) are sporadic in nature, however, they may occur as multiple lesions in familial forms associated with KIT or PDGFRA germline mutations, but may also develop in the setting of type 1 neurofibromatosis. In these situations, GISTs arise in a background of interstitial cell of Cajal hyperplasia and may be associated with systemic manifestations including skin hyperpigmentation and mast cell disorders. We report four patients with multiple GIST in small bowel and one of them was a child who was diagnosed as a very rare multiple GISTs and gastrointestinal autonomic nerve tumor (GANT).
Methods and Results: We identified four patients with multiple GISTs in small bowel. One of the adult patients has also type 1 neurofibromatosis. Rests of the patients have no type 1 neurofibromatosis and familial disorders. Immunostains for CD117, CD34, desmin, actins, S-100 protein, and keratins were performed on all of the tumors. Patient's ages/genders were 66/M, 65/F, 48/F, 10/M. All of the patients had multiple GISTs in small bowel, large bowel mezothelial surface (operation findings); at least 10 nodules and average 3.0 cm (0.2mm-12cm). First patient also had pancreatic adenocarcinoma, third patient with type 1 neurofibromatosis also had periampullary somatostatinoma. Our child patient had suffered from diarrhea and had familial tuberculosis history. He had multiple (the largest was 12cm diameter) serozal nodules. Tumor cells appear like ganglion cells and immunostains for CD117 was focal positive, NSE, Synapthophysin were diffuse positive,CD34, desmin, actin, myoglobulin were negative.
Our cases had no hepatic metastases. However they had multiple residual tumor nodules, only child patient has been treated with Imatinib Mesylate for two months.
Conclusions : Multiple GISTs are unusual tumors that have been rarely described in children. GISTs require resection and close observation for hepatic metastases.

P 319
REDUCED PROLIFERATIVE ACTIVITY DOES NOT EXPLAIN LOSS OF AVIDITY ON PET SCAN, IN A CASE OF METASTATIC GIST
HEMMINGS Chris*, YIP Desmond#
*Department of Anatomic Pathology and #Department of Medical Oncology, The Canberra Hospital, ACT, Australia

INTRODUCTION
Positron Emission Tomography (PET) is commonly used to monitor disease progression in patients with metastatic Gastrointestinal Stromal Tumour (GIST). We report a case of Imatinib-refractory disease with very low avidity on PET scan.
A malignant GIST was resected from the stomach of a 60 year old woman in 2000. She represented with metastases in the liver and lesser sac in 2001, and was treated with Imatinib. In 2003 further metastases were identified, although tracer uptake on PET was so low that the scan was initially reported as negative. One possible explanation for this could be that the chemotherapy had resulted in a metabolically inactive tumour, which would not take up tracer. A likely result of this would be lower proliferative activity; therefore the pathology was reviewed in an attempt to ascertain whether this could provide an adequate explanation.
METHODS
All slides were reviewed from both the original resection specimen and the subsequently resected metastatic tumour. Mitotic counts were performed on two separate tissue blocks from each specimen, along with immunoperoxidase staining for Ki-67 (MIB-1, Dako). For the mitotic counts, 50 high power fields (hpf)per block were examined, and only definite mitotic figures were counted. Ki-67 staining was assessed by counting the number of positively stained cells per 100 tumour cells, conducting several counts over each slide.
RESULTS
In the original specimen, there weer 55 and 66 mitotic figures (mf) in 50hpf; up to 4mf/hpf and 40mf/10hpf. In the metastatic tumour the counts were 58 and 51mf/50hpf; up to 4mf/hpf and 29mf/10hpf.
Ki-67 staining showed zonal variation in both instances, with staining per centages ranging from 2-58% in the primary tumour and 2-54% in the metastasis. In both cases, the overall average staining rate was estimated at around 40%.
CONCLUSION
There does not appear to be any significant difference in proliferative activity between these tumours, whether assessed by traditional mitotic counts or by staining for Ki-67. Thus differences in proliferative activity do not explain the lack of tracer uptake in this case. It is postulated that Imatinib therapy may have been sufficient to inhibit tracer uptake and/or phosphorylation, but insufficient to inhibit tumour cell proliferation. Regardless of the cause, this loss of avidity has important implications for therapeutic monitoring of patients with recurrent GIST.

P 320
THE HISTOPATHOLOGIC PATTERN OF GASTRO - INTESTINAL STROMAL TUMORS (GIST) AFTER TREATMENT BY IMATINIB.
MICHEJ Wanda, NASIEROWSKA – GUTTMEJER Anna

INTRODUCTION – Mesenchymal neoplasms derived from stroma of gastrointestinal tract (GIST) are restive for classic chemotherapy. These tumors become from Cajal cells and show immunopositivity for tyrosine kinase receptor – CD 117. This reaction is a base to recognize them and allows to treat by Imatinib (Glivec). It is no a predictive factor.
MATERIALS AND METHODS – Thitry patients with GISTs were treated by Imatinib in Cancer Center in Warsaw

between 2001 and 2004 year because of dissemination of neoplasms. Eight cases become from stomach, twelve from small intestine, ten tumors were of unknown origin. The response of treatment was monitorring by computer tomography. The cases with radiologically regression were resected. The resected specimen were fixed in 10% formalin and futher tissue sections were stained with routin hematoxylin and eosin. Immunohistochemical anaysis for CD 117 were also done.
AIM – To show histopathologic curative effects in GISTs treated by Glivec RESULTS – Comlete response appeared in 3 cases, partial response in 20 ones, in others (8) there were no any changes. Grossly: Tumors of diameter from 2 to 6 cm with gelatinous consistensy were present with many haemorrhages and necrotic slough. Microscopically – the cells of neoplasm show a little degree of damage (about 30% of neoplasm volume). The remainder or tumors cells were confirmed by positive reaction CD 117. The results of therapy were: necrosis, haemorrhage, foci of connective tissue, hyaline deposits.
CONCLUSION – Partial or complete regression of GISTs was observed in patients cured by Imatinib. This medicine makes possible to resect non – operative tumors within healthy limits.

P 321

IMMUNOHISTOCHEMICAL EVALUATION OF P16, MCM-2, AND KI-67 EXPRESSION AS MARKERS OF TUMOR PROGRESSION IN GISTS BY TISSUE MICROARRAY AND CORRELATION WITH THE RISK CLASSIFICATION OF THE NIH CONFERENCE CONSENSUS

Chien-Feng LI^, Ching-Nan LIN^, Wen-Wei HUANG$, Hsuan-Ying HUANG*
Department of pathology, Chi-Mei foundation Medical Center, Tainan, Taiwan^
Department of Family Medicine, National Cheng Kung University, Tainan, Taiwan$
Departemnt of Pathology, Chang Gung Memorial Hospital, Kaohsiung Medical Center, Kaohsiung, Taiwan*

Introduction: Risk stratification for gastrointestinal stromal tumors (GISTs) is crucial but sometimes remains challenging if based on histology alone. Inactivation of p16 gene is common in human cancers, which results in aberrant loss of its encoding protein and consequently promotes G1/S progression of cell cycle. Minichromosome maintenance protein-2 (MCM-2) is associated with cell proliferation and represents one member of the MCM hexamers that unwind DNA during replication. Few series have addressed the role of dysregulated p16 in disease progression of GISTs with a sufficiently large sample size. Moreover, the prognostic value of MCM-2 has never been examined in GISTs. Purpose: We attempted to elucidate the association between expression of p16, MCM-2, and Ki-67 and disease progression in GISTs by tissue microarrays (TMAs). Methods: Six TMAs were prepared from 343 GISTs conformed by CD117 and/or PKC-£cwith each case punched in quadruplicate. All cases were stratified by NIH consensus criteria and immunostained with p16 (Novacastra), Ki-67 (DAKO), and MCM-2 (Novacastra). Only cases with ¡Ù2 preserved cores were scored for statistic analysis. Results: Of cases with scoring data, aberrant loss of p16 (<15%) was observed in 63% of GISTs: 47/88 (53%) of very low/low-risk (VL/L-R) cases and 134/201(67%) of intermediate/high-risk (I/H-R) GISTs (p=0.032). Overexpression of Ki-67 (¡Ù5%) and MCM-2 (¡Ù10%) was found in 34% and 48% of GISTs, respectively: 15/81 (18%) of VL/L-R cases and 79/192 (41%) of I/H-R GISTs for Ki-67 (p<0.001); 29/82 (35%) of VL/L-R cases and 106/197 (54%) of I/H-R GISTs for MCM-2 (p=0.005). Both Ki-67 and MCM-2 were highly related to mitoses (p<0.0001 for each) and tumor size (p<0.0001 for Ki-67, p=0.017 for MCM-2), but aberrant loss of p16 was not so. Besides, MCM-2 labeling was not only highly correlated with (p<0.0001) but also significantly higher (p<0.0001) than that of Ki-67. However, expression of p16 was inversely associated with MCM-2 labeling alone (p=0.011). Conclusions: I/H-R risk GISTs preferentially express higher MCM-2, higher Ki-67, and loss of p16, indicating their roles in tumor progression. However, aberrant loss of p16 protein still occurs in a considerable proportion of early GISTs, which may contribute to tumorigenesis by promoting G1/S transition with a consequent increase in cell proliferation. MCM-2 may help identify non-high risk GISTs that will behave aggressively because of the higher sensitivity than Ki-67.

P 322

GIST AS UNEXPECTED CAUSE OF DYSPHAGIA IN MULTIPLE SCLEROSIS PATIENT

BULIMBASIC Stela1, NIKOLIC Igor2, KRIZANAC Simun3
1Department of Pathology, General Hospital “Sveti Duh”, Zagreb, Croatia
2Department of Thoracic Surgery, University Hospital “Jordanovac”, Zagreb, Croatia
3Institute of Pathology, Zagreb Medical School, Zagreb, Croatia

Introduction: Gastrointestinal stromal tumors (GISTs) are the most common mesenchymal tumors of the gastrointestinal tract. Majority of cases arise in stomach and small intestines, while occurrence in other sites is rare. We report a case of GIST causing dysphagia in patient with multiple sclerosis.
Patient and methods: A 50 year old female patient with multiple sclerosis suffered from dysphagia of unknown cause. Preoperative endoscopic and CT procedures discovered large tumor mass in the lower posterior mediastinum. Left posterolateral thoracotomy revealed tumor basis emerging from the esophageal wall. Excided tumor was pathohistologically analyzed using standard HE and immunohistochemical stains against vimentin, S-100, SMA, CD34 and CD117.
Results: Tumor mass measured 9.5 cm in diameter. Cut surface was fleshy with areas of cystic degeneration and necrosis. Histologically tumor consisted of short fascicles of spindled cells mixed with areas of epitheloid cells, both positive for CD34, CD117 and vimentin, while S-100 and SMA were negative. There were 8 mitosis per 50 high power fields.
Discussion: Less than 2% of GISTs occur in the esophagus, mostly in the lower parts, causing dysphagia. High majority of patients are middle-aged males without other symptoms which makes GIST difficult to diagnose. Rareness of such cases explains why there is only one study found in literature that reports 17 patients with GIST of esophageal localization. That survey enabled Miettinen and associates to undoubtedly confirm that size of tumor and high mitotic index are major prognostic factors. According to these prognostic elements, GIST revealed in our patient was characterized with high risk of aggressive behavior. The specific targeted medication therapy was recommended. Postoperative period was uneventful and patient was discharged on the ninth postoperative day.
The occurrence of GIST in patient with multiple sclerosis is considered to be coincidental; tumor symptoms were masked by known neurological disease and proper diagnostic evaluation was delayed. Overall survival will depend not only on response to given therapy but also to concomitant neurological disease.
Conclusion: Although rare, GIST ought to be considered in differential diagnosis of tumor masses in posterior mediastinum. Pathologist should be aware of this possibility because adequate gross and microscopic examination followed by immunohistochemical analysis is essential.

P 323

SMALL INTESTINAL STROMAL TUMORS: A CLINICOPATHOLOGIC STUDY OF 7 CASES

KOURDA Nadia*, FERCHICHI Leila *, ZERMANI Rachida*, RAMMEH Soumaya*, CHELBI Emna*, FAREH-KLIBI Faten*, NAJAH Nabil***, ZAOUCHE Abdjelil**, BALTAGI BEN JILANI Sarrah*
* Service d'Anatomie et de Cytologie Pathologiques, Hôpital Charles Nicolle, Tunis
** Service de chirurgie B, ***Service de chirurgie A, Hôpital Charles Nicolle, Tunis

Introduction: Stromal tumors of the digestive tract, or gastrointestinal stromal tumors (GIST), originate from Cajal cell. Small intestinal stromal tumors (SIST) are infrequent tumors. Their worse prognosis compared to other GIST is clearly established. The aim of this study was to report the clinicopathologic features and immunohistochemical characteristics of SIST through a series of 7 cases.
Material and methods: We identified seven cases of c-kit positive SIST from 40 cases of GIST reviewed in our center over a 13-year period (from January 1990 to December 2002).
Results: Three patients were men, four were women and the average patient age was 56 years. Five tumors were located in the ileum, two in the duodenum and one in the jejunum. The presenting clinical symptoms were gastrointestinal bleeding, either acute or occult, in 4 cases and abdominal pain in 2 cases. In the remaining patient, SIST was an incidental finding during abdominal ultrasonography for unrelated condition. Tumour size was ranged from 2 to 10 cm (median: 5.5 cm). Histologically, the majority of tumours in this group (6 cases) were composed of spindle cells with relatively scant amounts of cytoplasm. In all 6 of these tumours, the cells were arranged in a predominant fascicular growth pattern. In one tumour (case 3), the majority of cells had an epithelioid morphology and a focal organoid growth pattern was seen. Nuclear pleomorphism was absent in two cases, moderate in 3 and severe in 2 tumors. Mitotic counts ranged from 0 to 10 mitotic figures per 50 HPF. Treatment options were segmental intestine resection in all cases. None of the patient had lymph node involvement or distant metastasis at time of surgery. Four of five patients on whom there was follow-up information were free of disease. One patient died at 8 days from postoperative complications.
Conclusion: The authors discuss the clinicopathologic features including immunohistochemical staining profile of the SIST and define morphologic criteria which can help the pathologist to distinguish between low and high malignant potential SIST. The SIST express CD117, and mutations of the c-kit gene are central to their pathogenesis and likely the key to effective therapeutic intervention(Gliveec®).

P 324

IMMMUNOHISTOCHEMICAL EXPRESSION OF CYCLOOXYGENASE-2 AND CYTOKERATIN 8/18 IN GASTROINTESTINAL STROMAL TUMORS

F. Patakiouta, P. Xirou, D.Tzilves*, N. Vladika, Z. Antonopoulos*, I. Katsos*
Departments of Pathology and Gastroenterology-Oncology*, "Theagenio" Anticancer Hospital, Thessaloniki, Greece

Introduction: Cyclooxygenase (COX) is the key enzyme in the prostaglandins synthesis, catalyzing the conversion of arachidonic acid to PGH2 and exists in two isoforms (COX-1 and COX-2). The inducible form COX-2 plays an important role in tumorigenesis and has been shown that it is expressed in colorectal cancer, as well as in lung, breast and prostate cancer. Little is known about the expression of COX-2 in nonepithelial tumors, such as the gastrointestinal stromal tumors (GISTs). As regards expression of cytokeratin in GISTs, it seems to be very rare.
Purpose: To examine the expression of COX-2 and cytokeratin 8/18 in GISTs.
Materials and Methods: Twenty-six patients (15 females and 11 males, median age: 63.8 years, range: 36-79), with GISTs were evaluated. Paraffin-embedded tumor tissue sections were stained with hematoxylin-eosin. COX-2 and cytokeratin 8/18 expression were determined immunohistochemically.
Results: COX-2 expression was noted in the cytoplasm of tumor cells in 19 of 26 tumors (73,1%), with variable intensity of staining. The expression was stronger in epithelial than in spindle cell tumors and in epithelial areas of mixed tumors. There was no statistically significant difference of the COX-2 expression between benign and malignant tumors, but there was a greater extent of expression in tumors located within the stomach. Cytokeratin 8/18 expression was focally found in tumor cells in 2 gastric tumors (7,7%), one benign and one malignant.
Discussion: COX-2 is upregulated in many epithelial tumors, particularly in those of the gastrointestinal tract. The enzyme is implicated in the process of carcinogenesis and its overexpression has correlated with tumor size, infiltrative growth, local recurrence, haematogenous metastasis and reduced survival. However, up to now little is known about the expression of COX-2 in non epithelial tumors. COX-2 expression has been described in the sarcomatoid component of some uterine tumors, in pleural tumors and in sarcomas of infancy. It is also known that expression of simple epithelial keratin in GISTs is much rarer than that observed in typical leiomyosarcoma and occurs especially in malignant epithelioid tumors.
Conclusions: COX-2 overexpression was noted in the majority of cases of GISTs, suggesting the possible role of the enzyme in the tumor growth and the use of COX-2 inhibitors in treatment. On the contrary, expression of cytokeratin 8/18 in GISTs was very rare.

P 325

GASTRITIS IN CHILDREN AND ADULTS : A COMPARATIVE HISTOPATHOLOGIC STUDY.

Bettaieb I, Mrad K, Sassi S, Driss M, Abbes I, Dhouib R, B. Zouari*, Ben Romdhane K.
Pathology department, Institut Salah Azaiez, *epidemiology and medical statistics, Faculty of medicine, 1006, Bab saadoun, Tunis, Tunisia.

Introduction : Helicobacter pylori (HP) is highly associated with gastritis, peptic ulcer, gastric carcinoma and lymphoma. Since HP infection usually occurs in childhood and remains for life unless treated, we compared gastric biopsies in children and adults.
Material and methods : The study was performed on random biopsies from gastric mucosa of 100 patients (50 adults and 50 children). Sex and age were recorded for each patient. Following parameters were evaluated on H&E biopsies according to Sydney system: HP infection (0/1/2/3+), lymphocyte infiltrate (0/1/2/3+), activity (0/1/2/3+), atrophy (0/1/2/3+), and intestinal metaplasia (present/absent). Comparison of histologic variables between two groups (children and adults) was performed using the Fisher exact test or khi-2 analysis, as appropriate.
Results : The male to female ratio was 1.17 in both groups. HP was present in 90% of children biopsies and 82% of adult biopsies (p=0.249). A significant trend toward increased lymphocyte infiltrate in children was detected (p=0.019), but there was no difference in the prevalence of follicular pattern (p=0,838). There was no statistical difference in activity (p=0.58).The mucosa in children (18%) showed significantly less atrophy than in adults (36%) (p=0.043). Intestinal metaplasia was positively correlated with age (22% in adults/2% in children, p=002).
Conclusion : In children, gastritis shows increased lymphocyte infiltrate and less damaged epithelium. In adults,

the immune response seems to be decreased and the capability of epithelium regeneration is altered since atrophy and metaplasia are increased.

P 326

IMMUNE RESPONSES INDUCED AFTER MUCOSAL ADMINISTRATION OF THE NON TOXIC CHOLERA B SUBUNIT IN HUMAN VOLUNTEERS: USEFULNESS OF ELISPOT METHOD

CUBURU Nicolas (1), BERTO Frederick (2), TRIPAULT Frederique (2), GAVRIC- TANGA V (2), CZERKINSKY Cécil (1), HOFMAN Paul (1, 2).
(1) INSERM 721 and (2) Laboratory of Clinical and Experimental Pathology, Pasteur Hospital, University of Nice, Nice, France

Oral administration of antigens, including allergens and autoantigens, maybe an efficient way to prevent diseases associated with untoward immune responses to self- and non-self antigens. However, this approach has met with limitations because it usually requires repeated administrations of large doses of antigen. Tolerance induction, based on oral administration of small amounts of antigens conjugated to the B subunit of cholera toxin (CTB), may find broad applications for preventing untoward immune responses. The aim of this study was, by using a commercial CTB (SBL vaccine), 1) to evaluate the CTB-specific systemic and mucosal immune responses after oral, nasal, or sublingual human immunization; 2) to evaluate the predictive markers of immunogenicity. We showed that homing receptor expression profile depends on the site of immunization: 100% of CTB-specific IgA SCs express alpha4 beta7 after oral, nasal and sublingual immunization; 100% of CTB-specific IgA SCs express CD62L after nasal and sublingual immunization, whereas 40% of CTB-specific IgASCs express CD62L after oral immunization. The detection of CTB-specific antibody-secreting cells in blood was performed in cell suspensions par ELISPOT method. According to the route of immunization and systemic or mucosal CTB-specific response, ELISA (IgA2) or search for antibody secreting-cells in blood (IgA and IgG ELISPOT) were performed. Moreover, a selection of cells expressing chemokine receptor or integrin such as CCR9, CCR6, CCR10 and integrin alpha4 beta7 was performed by magnetic cell sorting and detection of antibody secreting-cells in positive and negative fraction was done by ELISPOT.

P 327

GASTRIC MUCOSAL ENDOCRINE CELLS IN THE EXPERIMENTAL BREAST CARCINOGENESIS.AN IMMUNOCYTOCHEMICAL STUDY

Maric Lj.Ivana, Jancic A Slavisa, Rosic L. Gvozden, Jancic A.Snezana
Oncology Clinic,University Medical School,Nis,Serbia and Montenegro
Institute of Pathology and Phisiology,University Medical School,Kragujevac,Serbia and Montenegro

It is well known the role of many regulatory peptides in clinical course of human cancers.However,these are no reported data about endocrine cells of the stomach in the experimental breast carcinogenesis.Because of that,the aim of this report is to study G-,EC-,ECL- and D-gastric mucosal cells,during chemically induced breast carcinogenesis.
We used the female albino Wistar rats,42 days old and 120±10gr. of weight.One miligram of 9,10 dimethyl-1,2 benzanthracene(DMBA) was implanted in the 5-th mammary gland.The experimental group includud 15 rats,as well as control group.The animals were killed after 60 days after the implantation.
Specimens from stomach were taken only from the rats with developed mammary gland cancer.Five micrometer thin sections were routhynly stained with HE and immunocytochemical SAB-method with antibodies against gastrin,serotonin,histamin and somatostatin.Obtained results were statisticaly analysed by Students T test.
We have found a characteristic hyperplasia of endocrine cells,with hyperplastic G,EC and ECL-cells,compared to these cells of control animals.Simultaneously in this study revealed revealed the development of multifocal dysplastic lesions in the antral mucosa.
The authors suggests direct stimulatory effects of DMBA on endocrine cells of the gastric mucosa.It can be concluded that DMBA cause preneoplastical effects on the gastric mucosa in rats.

P 328

AUTOMATED PROLIFERATION/APOPTOSIS DETERMINATION IN GASTROINTESTINAL FRESH FROZEN SECTIONS USING TRIPLE FLUORESCENT LABELLING AND SCANNING FLUORESCENT MICROSCOPY CORRELATES TO IMMUNHISTOCHEMICAL STAINING AND VISUAL COUNTING

BOCSI József *, SIPOS Ferenc, FICSÓR Levente, VARGA Viktor, MOLNÁR Béla, TÁRNOK Attila *
* Children's Heart Center, Uni. Leipzig, Germany
Cell Analysis Lab, II.Dept. of Medicine, Semmelweis Uni, Budapest Hungary

Background: Proliferation/ apoptosis balance is an important information in gastrointestinal ulcerative and malignant diseases. Until now immunhistochemical staining and visual counting was the routine procedure. Recently we reported a new scanning fluorescent technique for automated motorised microscopes (SFM).
Aims: development of triple fluorescent labelling method for proliferating/apoptotic/ resting cells and application of SFM for the automated analysis and counting on gastric biopsy specimen.
Materials and methods: Routine gastroscopy antral biopsy specimen (30) were fresh frozen and 5 um sections were prepared. Proliferation was detected using a PCNA antibody and an antimouse-rhodamine labelling system. Apoptosis was labelled using the TUNEL reaction with FITC bound nucleotids. DAPI nuclear counter staining was applied.
The labelled sections were scanned and digitised in the three fluorescent channel. SFM was modified to detect epithelial surface, glands in the biopsy specimen. Automated nuclei detection, PCNA and Tunnel detection was performed, ratio was calculated. In paralell standard biopsy specimen were labelled with PCNA and AEC labelling . TUNEL reaction was performed also performed.Visual counting was performed upto 1000 epithelial cells.
Results: The mean PCNA labelling in healthy samples were 45,3+12,4%, TUNEL positivity was found in 23,2+ 7,8%. Significant correlation in apoptosis/proliferation ratio between the two methods could be observed ($p<0,05$). The SFM procedure proved to be more time efficient both in the labelling, both in the detection procedures.
Conclusions: Triple fluorescent labelling and automated fluorescent microscopy is an applicable tool for the proliferation, apoptosis determination in fresh frozen samples.

P 329

EXPERIENCES IN AUTOMATIC CLASSIFICATION OF COLON AND GASTRIC DIGITAL SLIDES

FICSÓR Levente, MOLNÁR Béla, TULASSAY Zsolt
Cell Analysis Laboratory, 2nd Department of Internal Medicine, Semmelweis University

INTRODUCTION
Thanks to the fast evolution of digital microscopy new ways have been opened for image analysis on whole histological

tissue slides. Moreover recently new pattern recognition techniques were introduced for cell detection on the complicated histological images working on single field of views.

AIMS

The aims of present study were to adopt new development of image processing algorithm for whole biopsy slides to detect higher structures as gland, epithelium surface and finally to automatically classify gastric and colon samples using digital slide format.

METHODS

Altogether 69 colon (24 normal, 11 aspecific colitis, 25 colitis ulcerosa and 9 crohn disease) and 79 gastric (14 normal, 17 atrophy, 6 gastritis with intestinal metaplasia, 12 gastritis and 30 adenocarcinoma)well oriented mucosal biopsy specimens were selected. To digitalize the selected H/E stained slides Zeiss Mirax slide scanner system was used. Automatic histological evaluation modules were developed in C++. Altogether 45 parameters described the area, cell density and cellular characteristics of the basic tissue components as the surface epithelium, glands, connective tissue and the inflammatory cell compartment. Area and contained cell number ratios of different tissue compartments were calculated which we named to tissue cytometric features.

RESULTS

We could find that that newly developed tissue cytometric features efficiently can be used to classify both gastric and colon digital slides by their disease state. The most important parameter was the ratio of total cell number and cell number in interstitial region (Colon: healthy 1.57±0.17; aspecific colitis 1.34±0.16; colitis ulcerosa 1.18±0.09; Crohn disease 1.28±0.11, $p<0.01$ - Gastritis healthy 1.43±0.12; gastritis 1.23±0.13; carcinoma 1.1±0.05 $p<0.01$).

CONCLUSION

This preliminary study proved again that the development and evaluation of quantitative tissuemetric features can be used in the automated classification of histological colon biopsy specimen.

P 330

WEGENER'S GRANULOMATOSIS MASQUERADING AS MASTOIDITIS: REPORT OF AN UNUSUAL CASE

NAGY Pál*, SALAMON Ferenc*, Z. SZABÓ László**, DOMJÁN Gyula***, BALOGH Károly****

*Dept. of Pathology, National Medical Center, Budapest, Hungary

**Dept. of Otorhinolaryngology, National Medical Center, Budapest, Hungary

***Dept. of Medicine, Szent Rókus Hospital, Budapest, Hungary

****Dept. of Pathology, Harvard Medical School, Boston, USA

Introduction: Wegener's granulomatosis is a rare, immunologically mediated inflammatory disease (WHO, 1991). The diagnosis is based on the clinical picture, the presence of cANCA by immunofluorescent microscopy and by biopsy of the affected tissue. Our purpose is to present a case in which the unusual clinical picture and the atypical histologic findings posed a diagnostic problem.

Material and methods: A 27 year old woman was referred to our hospital (NMC) with symptoms of severe mastoiditis. During a period of 7 months she had 7 operations in 4 different hospitals for progressive chronic inflammation of the right mastoid process. Microsopically, all surgical specimens showed nonspecific granulation tissue with chronic inflammation, fibrosis, and once, suppurative granulomatous inflammation. This process also involved adjacent bone, causing focal osteonecrosis. Laboratory tests, including bacteriologic cultures failed to reveal a definite etiology of the progressive, destructive process which later necessitated also resection of a part of the first cervical vertebra. The patient's condition deteriorated and she became critically ill. Consultation was requested and the entire histologic material was reviewed (K.B). Special stains (Gram, PAS) for microorganisms, fungi and parasites, as well as immunohistochemical reactions to exclude differential diagnostic considerations were all negative.

Results: The main features of the reviewed histologic material were

- •Ulcerative granulomatous inflammation with focal fibrosis and destruction of underlying tissues
- •Capillaritis and venulitis without arteritis
- •Confluent, partly well circumscribed histiocytic granulomas with central microabscesses
- •Irregular („geographic") necrosis (in one small area only)

These histologic characteristics and the exclusion of differential diagnostic considerations (infectious granuloma, sarcoidosis, histiocytosis, eosinophilic granuloma) strongly suggested a localized variant (" forme fruste") of Wegener's granulomatosis and was confirmed by the cANCA test, which initially was negative. The patient was treated with steroids and cyclophosphamide and has been in remission for almost two years. Follow-up studies failed to disclose any upper respiratory, pulmonary or renal involvement.

Conclusion: In young or middle age patients "mastoiditis " resistant to conventional medical or surgical therapy may be due to Wegener's granulomatosis.

P 331

A CLINICOPATHOLOGICAL STUDY OF KIMURA'S DISEASE IN THE HEAD AND NECK REGION. A REPORT OF THREE CASES.

Bellefqih S*, Le Pelletier F*, Charlotte F*, Meningaud J-P**, Pitak-Arnnop P**, Barete S***, Bertrand J-C**, Capron F*, Fouret P*.

Dpts of Pathology*, Maxillofacial Surgery**, and Internal Medecine***, Groupe Hospitalier Pitie-Salpetriere, Paris, France.

Background: Kimura's disease (KD) is an uncommon inflammatory disorder of unknown aetiology, primarily seen in young Asian males. Its characteristics are painless subcutaneous masses in the head and neck region, blood and tissue eosinophilia, and markedly elevated serum IgE.

Material and methods: Over a ten-year period, 3 cases of KD of the head and neck region were diagnosed in our department and retrospectively reviewed.

Results: The three male patients (25, 26, and 29 years old at diagnosis) were natives from Madagascar, Cambodia and Mauritius. All had hypereosinophilia and elevated serum IgE with normal renal function. The first patient presented with a parotid localization, while the second had a temporal dermohypodermic nodule with ipsilateral involvement of parotid gland. The third patient showed a preauricular mass. Histologically, the soft tissue and the parotid gland were infiltrated by lymphoid follicles with folliculolysis and eosinophils forming eosinophilic abcesses. There were numerous thin walled vessels with neither epithelioid nor vacuolated endothelial cells. Adjacent lymph nodes also showed hyperplastic follicles with paracortical eosinophilia and folliculolysis. The immunohistochemical studies revealed CD20+ follicles with prominent staining of dendritic reticular cell CD23+, surrounded by numerous interfollicular CD3+ and CD4+ or CD8+ T-cells. CD1a, HHV-8, and LMP1 were negative. In situ hybridization confirmed the lack of EBV infection. FVIII-related antigen and CD34 decorated the thin-walled blood vessels.

Recurrence was observed in the first patient both at original and contralateral sites.

Conclusion: KD is a rare chronic inflammatory disease with genetic predisposition that typically presents as a deep pre-auricular nodule and/or parotid gland involvement. The

immunohistological study confirms its reactive nature. Excision is considered as the treatment of choice, but recurrences can occur even in a prolonged period.

P 332
MORPHOFUNCTIONAL PECULIARITIES OF THE GUM TISSUES AT PATIENTS WITH CHRONIC PERIODONTITIS AND PRE-IMPLANTATION TREATMENT
MUDRAYA Valentina, RESHETNIKOVA Olga
Department of Operative Dentistry and Department of Pathologic Anatomy, Medical University, Lugansk, Ukraine.

Periodontal diseases have high incidence rate worldwide.Quite often treatment plans involving tooth replacement, are used for sites diagnosed with chronic periodontitis (CP). Thus, there is a problem of finding pathogenically based methods of structural changes correction in a gum. Present study was undertaken to help further evaluate gum tissues remodelling with and without pre-implantation treatment of CP.
Methods. 30 volunteers were enrolled while receiving dental care. 10 gums biopsies were taken from patients without CP symptoms (group of comparison), 10- from patients with CP undergoing surgical operation without preoperational therapy (group 1) and 10- from CP patients with pre-implantation treatment by glutarginum and vector-therapy (group 2). Histological slides were stained with H&E, Van Gison, and then stereological evaluation by point count method was performed. The volume fractions of inflammatory infiltrates, vascularity, areas of dystrophy and necrosis of connecting tissue and others were determined. Collagen I and ? type's expression were studied immunohistochemically with the use of specific antibodies.
The results have shown that the increase of volume fractions of inflammatory infiltrates, vessels, foci of periodontal connective tissue dystrophy and necrosis are determined in group I. Immunohistochemical analyses showed that both expression and distribution of the I type collagen was diminished here too. Unlike this, the ? type collagen was registered here more often with increased intensity of expression.
The data in group 2 demonstrate a reduction of hyperemia, vessels number, inflammatory infiltrates and areas of connecting tissue dystrophy. The collagen type's distribution has changed to the mode seen in group of comparison: type I collagen predomination over the ? type collagen.
Conclusion. These findings suggest that chronic periodontitis stimulates the forming of immature connective tissue and persistent inflammation in a gum. On this background there is braking of repair processes, which can unfavorably affect implant osteointegration. The use of glutarginum, possessing antioxidant and membranes protective properties, in conjunction with the mechanical debridement by vector-therapy, allows normalizing gum tissue's metabolism, to recover the normal parameters of collagen stromal components. These seem to be effective in maintaining structure and function of the gums and periodontal tissues at pre-implantation period.

P 333
PRESENCE AND DISTRIBUTION OF MERKEL CELLS IN ORAL MUCOSA.
RIGHI Alberto, MARUCCI Gianluca, **MARCHETTI Claudio,**MONTEBUGNOLI Lucio, FOSCHINI Maria P.
Department of Oncological Sciences, Section of Anatomic Pathology, University of Bologna.
** Department of Oral Sciences, University of Bologna.

Introduction: Merkel cells (MC) are endocrine elements located in the basal layer of epidermis and oral mucosa. MC are difficult to be found by routine light microscopy; but can be visualized by electron microscopy and immunohistochemistry. Cytokeratin 20 (ck20) is a sensitive marker for MC. A few data are available on the distribution of MC in human oral mucosa. The aim of the present paper is to better define the presence and distribution of MC in normal and pathological oral mucosa.
Materials and Methods: 89 surgical consecutive biopsies of oral mucosa were evaluated. Patients age ranged between 3 and 84 years (mean 48). Sections were stained with haematoxylin\eosin and immunohistochemistry applying a monoclonal antibody anti ck20 (Dako, clone KS 20.8, diluted 1:40). Semiquantitative evaluation of ck20-positive cells, consistent with MC, was performed on 300 basal keratinocytes, in the area with higher number of MC. Location (basal or supra-basal) of MC and shape (oval or dendritic) were recorded.
Results: MC Distribution according to the site: the highest number of MC was observed in the gingiva (range 1 to 80 MC, mean 14 MC), palate (range 1 to 40 MC, mean 11 MC) and buccal mucosa (range 2 to 19 MC, mean 11), while MC were rare in the tongue (1 to 8 MC, mean 4 MC), and cheek (no more than 1 MC for biopsy), and were not observed in tonsil mucosa. Distribution according to the histological diagnosis. MC were present in 7\14 biopsies from normal oral mucosa (range 1 to 27 mean 8); 7\14 in acute inflammation with ulceration (range 3 to 18, mean 8); 9\11 chronic inflammation with hyperkeratosis (range 1 to 80, mean 18); 4\6 lichen (range 1 to 14, mean 5); 7\12 epithelium overlying chorion fibrosis (range 1 to 33, mean 13); 12\15 epithelium overlying salivary gland tumours and ameloblastoma (range 1 to 40, mean 13); 3\17 dysplasia and in situ carcinoma (range 1 to 8, mean 5). MC were not localized in the ulcerated or dysplastic epithelium, but when present they were observed in the epithelium adjacent to the lesion. In all cases MC were oval or dendritic in the same proportion., they were mainly located in the basal layer, in two cases only reaching the superficial layers of the epithelium.
In conclusion the present data confirm that MC are mainly localized in gingival, palate and buccal mucosa. In addition their number increases in chronically damaged mucosa, thus suggesting a possible function in reparative processes.

P 334
HPV GENOTYPING BY DNA CHIP STUDY IN AMELOBLASTOMA
Hye-Kyoung Yoon, Mi-Seon Kang, Woo-Hyung Kim
Dept. of Pathology, Pusan Paik Hospital, Inje University, Pusan, Korea

Background: Ameloblastoma is a relatively common tumor, however, the etiologic factor or biologic activity are not clearly defined. This study is designed to determine the relation of ameloblastoma with a possible etiologic factor, human papilloma virus (HPV), and to evaluate the clinicopathologic characteristics of HPV-positive ameloblastoma.
Methods: The materials were 31 formalin-fixed, paraffin-embedded tissue samples from 22 ameloblastoma patients. HPV DNA chip study was done, and clinicopathologic parameters were compared according to the recurrence and HPV status.
Results:
1. In sixteen cases without recurrence, HPV DNA was not detected. However, three of 15 tissue samples from six recurred cases were HPV 16-positive. One of them showed positive for HPV 16 and HPV 40.
2. Nine of 16 cases without recurrence were under 20 years old, in contrast, there was no case under 20 years old in 6 recurred cases.
3. There were no significant differences of sex ratios and tumor locations according to the recurrence.

4. Radiologically three of 16 cases without recurrence was multicystic mass, but four of 6 recurred cases were multicystic. Three HPV DNA-positive cases were also multicystic.
5. Ten of 16 cases without recurrence and five of 6 recurred cases were follicular type histologically, and one recurred cases showed conspicuous cytologic atypia.
6. Two of 3 HPV-positive cases showed relatively rich stromal component, and remaining one case exhibited conspicuous inflammatory reaction.
Conclusion: In the half of recurred ameloblastoma cases, HPV 16 was detected, in contrast, no HPV-positivity in 16 cases without recurrence. The results suggest that HPV could be regarded as a possible etiologic factor of ameloblastoma with a tendency of recurrence. In addition, the risk of recurrence might be increased in cases showing multicystic mass, follicular type with cytologic atypia or rich stromal components and HPV-positivity.

P 335
AMELOBLASTOMA WITH MALIGNANT TRANSFORMATION: A CASE REPORT - 20 YEARS EVOLUTION
PAIVA Geise Rezende, ANDRADE Rodrigo Guimarães, VILELA Rafael Sarlo, PINTO Clóvis Antonio Lopes.
Research and Medical Center Hospital do Cancer, São Paulo, Brazil

INTRODUCTION: Ameloblastomas comprise nearly 1% of the oral tumors. They have slow growth, but they are locally aggressive. Malignant transformation and metastasis occurrence are described in the literature. In 1971 Malignant ameloblastoma was included in WHO's classification of odontogenic tumors.
OBJECTIVE: Report a case of ameloblastic carcinoma in jaw.
CASE REPORT: We present a case of a 30 year-old female patient, with primary ameloblastoma in left jaw, without evidence of metastatic disease to the diagnosis. This patient was submitted to partial resection of the left jaw. The evolution demonstrated local progression, with eight recurrences in jaw, buccinator muscle, infratemporal fossa and cervical area, in 20 years of observation, showing evident maligant transformation in the last three recurrences.
DISCUSSION: The term malignant ameloblastoma and ameloblastic carcinoma have been raising discussions in the literature. Peter et al revising WHO's odontogenic tumors classification (1992) suggests a subdivision of malignant potential ameloblastic tumors, proposing the terms malignant ameloblastoma and ameloblastic carcinoma. The literature demonstrates that the expression of P53 and a high proliferation index is related to a higher tendency of tumor's recurrence and aggressiveness. Morphologically we observed a neoplasia composed of strings or islands of basaloid epithelial cells, with fence appearing outlying cells, intermixed with a reticular colagenized stroma. Pleomorfic cells with atypical and hipercromatic appearing nucleus, beyond numerous mitosis, were observed in the last three recurrences, as well as the high p53 and Ki67 expression. Indeed, it is a highly aggressive tumor with evident malignant transformation, testified by cytological alterations, initial negative expression for p53 protein, which is over expressed in the last three recurrences, and the cellular proliferation index progression (Ki67).
CONCLUSION: The term ameloblastic carcinoma can be applied to our case. It demonstrated malignant cytological alterations, besides the classical ameloblatoma morphology. The morphological and immunohistochemical features of this case can represent a tumoral progression model of the ameloblastic tumors.

P 336
EWING'S SARCOMA OF THE JAW BONES. A REPORT OF THREE CASES.
Bellefqih S*, Gruffaz F*, Handra-luca A*, Couturier J***, Meningaud J-P**, Pitak-Arnnop P**, Bertrand J-C**, Capron F*, Fouret P*.
Dpt of Pathology* and Dpt of Maxillofacial Surgery**, Groupe Hospitalier Pitié-Salpêtrière;
Dpt of Genetics***, Institut Curie, Section Médicale. Paris, France.

Background: Ewing's sarcoma is an uncommon neoplasm usually arising in long bones or pelvis. The involvement of jaw bones is very rare.
Patients and methods: Three patients with Ewing's sarcoma of jaw bones treated between 1996 and 2005 were clinicopathologically reviewed. The diagnosis was based on the histological, immunohistochemical and genetic molecular data.
Results: Two women and one man were 22, 24, and 25 years-old at diagnosis. Two tumours localized in the mandible, while the other was in the maxilla. The dominant symptoms were pain, as well as a rapidly destructive and expansile mass. Histologically, the tumour consisted of sheets of small, round and undifferentiated cells that were PAS-positive. Abundant blood vessels, haemorrhagic foci, and necrotic areas were seen. Immunohistochemical study revealed that the tumour cells were reactive for CD99 (MIC2) and vimentine, but EMA, pancytokeratin, S-100 protein, chromogranine A, and CD45 negative. The Ki-67 proliferation rate was 10, and 80% in two cases. In one case CD117 (c-Kit) was slightly expressed as well as p53 in 30% of cells. MDM2 was negative in each case. EWS rearrangement was evidenced by FISH in one case and RT-PCR in another case. Patients were treated by surgery followed by chemotherapy. One patient had three local recurrences without metastasis during a 5 years follow up.
Conclusion: Ewing's sarcoma is a rare and aggressive tumour of jaw bones that occurs in young adults. Immunohistochemical and genetic molecular analyses are essential for diagnosis. The recurrence is quite common and the prognosis is poor.

P 337
ATYPICAL LIPOMATOUS TUMORS OF THE TONGUE
1Aleš Ryška, 2Thomas Mentzel, 1Helena Hornychová, 1Aleš Kohout
1Department of Pathology, Charles University Medical Faculty and University Hospital, Hradec Králové, Czech Republic
2Dermatopathologische Gemeinschaftspraxis, Friedrichshafen, Germany

Aims: To report 5 cases of rare low grade lesion, atypical lipomatous tumor (ALT) of the tongue.
Patients: The patients were 3 males and 2 females, aged 11-78 years (average 51.2 years, median 65 years). The tumors were in all cases present at the lateral side of the tongue. In one case, there were multiple tumor nodules, localized at both sides of the tongue. Follow up was available in four cases (8-96 months). After surgical excision, none tumor recurred or metastasized.
Results: The size of the tumors ranged from 7 mm to 20 mm (average 11.2 mm, median 10 mm). All cases shared similar microscopic features. They showed infiltrative growth into surrounding structures (skeletal muscle, fibrous tissue). They were of lobular arrangement, composed of adipocytes with slight variation of size and shape. Isolated sparse lipoblasts (both univacuolar and multivacuolar) were present. In two cases, there was prominent interstitial sclerosis and the features thus coped more with the diagnosis of sclerosing ALT, whereas three cases had the features of lipoma-like

o cases, isolated spindle-shaped primitive looking found, presumably of precursor nature. Mitotic s very low, only several typical mitoses were found s examined. Immunohistochemically, the tumor ed positivity of vimentin (4/4), S100 protein (4/4),) and CDK4 (3/4). Proliferative antigen Ki-67 was isolated cells only (less than 0.5 %). Two cases xamined by FISH. Amplification of mdm-2 gene in both cases, whereas amplification of CDK-4 resent in one case only.
s: Atypical lipomatous tumors of the tongue are ver, they have characteristic morphologic features her with typical immunophenotype, enable their agnosis. The herein presented results are in with conclusions of the previously reported series. ve in an indolent fashion; they can recur if y excised, however they virtually never .
vas in part supported by the Ministry of Health blic, Grant No. MZO 00179906

GIOPERICYTOMA OF THE OCCIPITAL CASE REPORT

C Ksenija ,DOZIC Branko ,JEZDIC Zoran
t of Oral pathology Faculty of Stomatology
linic for Maxillofacial Surgery Faculty of
y Belgrade,Serbia and Montenegro.

n: Haemangiopericytoma (HPC) a rare neoplasm in somatic soft tissue, or in a central nervous C of central nervous sustem is highly cellular and larised tumour almost always attached to the dura. ty of meningeal haemangiopericytomas can be ut local reccurences are almost inevitable in the while postoperative irradiation appears to delay .
fication 1979 still contained " haemangiopericytic of meningioma, however this concept has now olete.
scull, HPC occurs more often in occipital region, confluens sinuum.
: 69 years old female patient reffers to the Clinic facial Surgery, Faculty of Stomatology Belgrade, f swelling in occipital region. From personal t could be concluded that pathological formation m duration (" since childhood").
c feature tumor was slightly lobulated, firm, cut fleshy and yellow white to red brown, with zones rhage and necrosis.
ogy : Highly cellular lesions with numerous anels (" stag-horn type") surrounded by and thin nests of spindle-shaped cells. The nuclei was imes elongated with moderate chromatin density. r atypia was found as well as prominent mitotic nse reticulin network surrounded individual tumor

efinitive diagnosis was made : pericytoma WHO grade II.

USCULAR MYXOMA OF THE TEMPORAL CASE REPORT

nko, BODLOVIC Ksenija, JEZDIC Zoran,
rko
t of Oral pathology Faculty of Stomatology
Clinic for Maxillofacial Surgery Faculty of
y Belgrade,Institute of Oncology et Radiology
erbia and Montenegro

n : Myxomas are commonly found in the heart, jaw oft tissues of the body; however these lesions are unusual in the soft tissue of the head and neck. The lesion is composed of undifferentiated stellate cells set in a myxoid stroma.
Case report : In june 2000, a 63-year-old male was evaluated for a slowly growing, asymptomatic mass in his left temple region, which had been present for more than 4 years.
Clinical examination showed a ,5x4x2 cm,firm ,smooth,painless,oval mass in the left temporal region.The cup surfaces was yellowich and gelatinos.
Microscopic examination showed a rellativelly well circumscribed lesion. The spindle and stellate cells embedded in an abundant myxoid stroma with a reticulin fiber network. No cellular pleomorphism or mitotic activity was evident. A diagnosis of intramuscular myxoma was made. 3 years after surgery, there was no evidence of reccurence.
Discussion: In the head and neck, intramuscular myxoma is extremely rare, because it commonly arises from large sceletal muscles.
It is difficult to diagnose this lesion before biopsy, because of the lack of typical clinical manifestations or features in radiographic studies. It usually appears as a painless and slow-growing mass.
The basic histology of intramuscular myxoma is indistinguishable from myxoma that occurs elsewhere in the body; however, on close inspection, the delicate fibrous capsule is incomplete, and most of all lesions infiltrate adjacent muscle.
Differential diagnosis of intramuscular myxoma must include malignant tumors such as myxoid liposarcoma, malignant hystiocytoma and myxoid chondrosarcoma.
Treatment for intramuscular myxoma is surgical excision. There is no report of metastasis or malignant changes, but occasionally recurrences resulting from incomplete exccision.

P 340

APOPTOSIS DISORDERS IN SJOGREN'S SYNDROM

K. BELLIL*, I. BEN GHORBAL**, A. MEKNI*, S. BELLIL*, N. KCHIR*, MH. HOUMAN**, MM. ZITOUNA*, S. HAOUET*
* Service d'anatomie pathologique – hôpital la Rabta– Bab saadoun 1007 – tunis – tunisie
** Service de médecine interne – hôpital la Rabta– Bab saadoun 1007 – Tunis – Tunisie

It has been suggested that defects in the modulation of programmed cell death (apoptose) might lead to autoimmune disease, such as sjögren's syndrome (SS).
OBJECTIVES: The aim of our study is to determine the role of apoptosis in Sjögren'syndrome. MATERIAL AND METHOD: Salivary glands biopsies from 21 patients suffering of primary and secondary SS (Chisholm 3 and 4) were analysed by apoptosis regulators: Bcl-2, Bax, P53 and Fas (CD95) using immunohistochemisty method. Control group had 15 normal subjects. RESULTS: Bcl-2 was strongly expressed in lymphocytic lesions of all cases. Its associated with a bax and a p53 reactivity respectively in 76% (16/21 cases) and 85% (18 cases/21)of acinar and ductal epithelial structures. A fas antibody was detected in 5 cases only in epithelial component and none in lymphocytic area.
CONCLUSION: Present data suggest a lymphoid defective apoptosis, by Bcl2 activation, inducing lymphoid infiltrate. SS salivary epithelial cell death requires the cooperation of both Fas and Bax. However, P53 duct expression may be a defensive mechanism that provides ductal cells with time to repair DNA damage.

P 341

STUDY OF B-CELL MONOCLONALITY, HELICOBACTER PYLORI AND BCL-10 EXPRESSION IN SJOGREN'S SYNDROME.

Kouvidou Ch.(1), Piperi E.(2), Chrysomali E.(2), Tsakistou G.(1), Anagnostakis D.(1) and Vrettou-Aravani V(1).

(1) Department of Pathology, "ELPIS" hospital, Athens, Greece
(2) Department of Oral Pathology and Medicine, Dental School, National and Kapodistrian University of Athens, Greece

INTRODUCTION: Sj'gren's Syndrome (SS) is an autoimmune disorder characterized by lymphocytic infiltration and MALT acquisition at the exocrine glands, as well as an increased risk of developing malignant lymphoma, especially extranodal marginal zone lymphoma of MALT type.
Helicobacter pylori (Hp)-gastritis predisposes to the development of acquired MALT and eventually MALT lymphoma, associated in 5% of cases with the mutant form of Bcl-10, while the bacterium is a common habitant of oral microbial plaque and saliva, only rarely investigated in salivary lymphoid tissues in SS.
PURPOSE: To evaluate the presence of acquired MALT and B-cell monoclonality at the labial salivary glands of patients with SS and their possible association with Helicobacter pylori and Bcl-10 expression.
MATERIALS AND METHODS: Formalin-fixed paraffin embedded tissue from 40 cases with SS and 20 control cases with non-specific sialadenitis was stained by immunohistochemistry for CD3, CD20, kappa, lambda, Helicobacter pylori and Bcl-10 protein.
RESULTS: Acquired MALT was observed in 26/40 (65%) cases with SS, while 9/26 (34,6%) showed areas of light chain restriction. 7/26 cases (27%) were positive for Hp, 3 of which were also monoclonal (43%). Cytoplasmic expression of Bcl-10 was observed in lymphoid follicles in all 26 cases, while no nuclear expression was detected. None of the controls showed either MALT and B-cell monoclonality or Hp. and Bcl-10 expression. Acquired MALT, Helicobacter pylori, and Bcl-10 expression statistically significant correlated with the emergence of B-cell monoclonality (p value < 0,05).
CONCLUSIONS: Helicobacter pylori may be linked to MALT acquisition and B-cell clonality in SS, at least in some cases. Adherence to saliva may facilitate lipopolysaccharide (LPS) activation of Toll-like receptors on ductal cells and Bcl-10-mediated NFêÂ antigenic signalling of B-cell receptor (BCR) may result in persistent B-cell proliferation in genetically susceptible individuals, thus predisposing to the emergence of pathologic clones. Alternatively, Hp. presence in the salivary glands may induce MALT accumulation as a result of acquired gastric MALT dissemination, as observed in MALT lymphomas, through á4â7-associated recruitment of gastric memory B-cells. Bcl-10 may be of importance in the interruption of the neoplastic cascade, while further studies are needed to clarify Hp's precise role in SS's pathobiology.

P 342

ROLE OF EPSTEIN BARR VIRUS IN PATHOGENESIS OF SJOGREN'S SYNDROME

K. BELLIL*, I. BEN GHORBAL**, A. MEKNI*, S. BELLIL*, N. KCHIR*, MH. HOUMAN**, MM. ZITOUNA*, S. HAOUET*
* Service d'anatomie pathologique – hôpital la Rabta– Bab saadoun 1007 – tunis – tunisie
** Service de médecine interne – hôpital la Rabta– Bab saadoun 1007 – Tunis – Tunisie

Sjogren's syndrome (SS) is a chronic autoimmune disease characterized by lymphocytic infiltration of salivary and lachrymal glands which results in xerostomia and keratoconjonctivitis sicca. The pathogenesis of this syndrome remains unclear but viral infections have been suggested as a possible aetiologic factor.
OBJECTIVES: The aim of our study is to determine the potential role of Epstein Barr Virus (EBV) in pathogenesis of SS. MATERIAL AND METHOD: Salivary glands biopsies from 35 patients suffering of primary and secondary SS were analyzed to determine the presence of EBV by immunohistochemistry method (LMP, ZEBRA, EBNA-2) and in situ hybridization study with EBV-encoded small RNAs termed EBER1 and early lytic PNA probe. Control group had 15 normal subjects. RESULT: 14 cases were positive for ZEBRA, 17 were positive for LMP and EBNA-2. All cases were EBV positif after in situ hybridization. None case of control group was EBV (+). CONCLUSION: EBV has a strong salivary tropism. Our results suggest that EBV could be implicated in the pathogenesis of SS. Its T-cell responses might contribute to labial salivary gland destruction and could have a role in lymphoid proliferation.

P 343

INVASIVE SPHENOID ASPERGILLOSIS: A CASE REPORT WITH AN UNUSUAL PRESENTATION

Mneimneh W, Cazals-Hatem D, Mosnier I, Bellier C, Sterkers O, Bedossa P
Departments of Pathology, ENT and Internal Medicine, Hôpital Beaujon, 92118 Clichy, France

Backgrounds: Fungal sphenoid sinusitis is rare, and aspergillus fumigatus is the most common pathogen. The invasive form of the disease is usually encountered in immunocompromised hosts with a potentially unfavorable outcome. We report a case of invasive sphenoid aspergillosis with pseudo-tumoral features on imaging, developed in an immunocompetent patient.
Observation: A 51-year-old male patient presented in January 2005 with a right otorrhea. He underwent in November 2004 a total thyroidectomy which revealed a multifocal papillary micro-carcinoma of the thyroid. He presented with an eight-year history of a chronic intermittent headache with a negative complete work up. Physical examination was unremarkable except for a right tympanic perforation, and no neurological defect was noted. A computed tomography revealed a 4x2.7cm mass of the left sphenoid sinus associated with bone erosion and suspicious for metastasis. Biopsies of the mass were performed. Histologic examination showed an extensive granulomatous inflammatory process invading the mucosa and bone, with fungal hyphae, identified as Aspergillus flavus by culture. Serologies for soluble aspergillus antigen and HIV were negative. The diagnosis of chronic invasive aspergillosis of the sphenoid sinus was established, and one-year of voriconazole treatment was started.
Discussion: In addition to immunosuppression states, predisposing factors for sinus invasive mycosis include maxillofacial trauma, drug sniffing and radiotherapy, none of which was present in our patient. The disease is usually symptomatic, most frequently with headache, followed by visual changes, cranial nerve palsies, seizures and pain in the trigeminal distribution. Diagnosis relies on endoscopy, imaging and biopsy for histologic examination and culture.
Conclusion: Sinus invasive aspergillosis is a rare condition, encountered most frequently in immunodeficient patients. We present an unusual case of a pauci-symptomatic sphenoid invasive aspergillosis in an immunocompetent patient with a pseudotumoral aspect. This entity should be kept in mind in the differential diagnosis of pseudo-tumoral lesions of this area.

P 344

THE SIGNIFICANCE OF HISTOLOGICAL ESTIMATION IN FUNGAL INFECTIONS OF THE ORAL AND MAXILLOFACIAL REGION

MAKOS Christos1, NIKOLAIDOU Anastasia2, DIMITRAKOPOULOS John3
1 Registrar, Oral and Maxillofacial Department, General Hospital of Kilkis, Kilkis, 61100 Greece

2 Registrar, Pathology Department, General Hospital of Kilkis, Kilkis, 61100 Greece
3 Associate Professor, Aristotelian University of Thessaloniki, Oral and Maxillofacial Clinic, "G. Papanikolaou" General Hospital, Exohi, Thessaloniki, Greece

Introduction: Mucormycosis (zygomycosis, phycomycosis) is an opportunistic and often fatal fungal infection caused by aerobic saprophytic fungi of the class Zygomyces (Phycomycetes), order Mucorales, family Mucoraceae and most common genera Absidia, Mucor, Rhizopus and Rhizomucor. Different clinical forms are described and most common the rhinocerebral form. Aspergillosis of the maxillary and paranasal sinuses is an endemic disease in countries with hot and dry climate. The causative factor is Aspergillus fungus of Actinomyces race. Recent studies have shown an increasing incidence of the disease in mild and cool climates. The non invasive (localised and allergic) and invasive (benign and fulminant) forms are accepted. Most cases of the non invasive form are prescribed in otherwise healthy individuals imitated an acute, chronic or allergic sinusitis with a remarkable resistance in a classical therapy of sinusitis.

The purpose of this work is to discuss about the significance of histological estimation in relation to diagnosis, treatment and prognosis in cases with these fungal infections.

Methods: The clinical, radiographical and histological pictures in cases with mucormycosis and aspergillosis in oral and maxillofacial area are presented and the particularities in histological sections and stains are referred.

Conclusion: Definite diagnosis in the above mentioned fungal infections is emphasized by histological evidences. The systematic laboratory examination of the excretions, material and tissues of the affected oral and maxillofacial areas is the exclusive method for the earliest diagnosis and a successful treatment of the disease, even if negative clinical and radiographical evidences exist.

P 345

ROLE OF NERVE GROWTH FACTOR RECEPTOR IN ATROPHIC SALIVARY GLAND IN CASE OF SIALOLITHIASIS

Valerie Groma (1), Janis Dumpis (2), Girts Salms (3), Andrejs Skagers (3)
1 - Institute of Anatomy and Anthropology, Riga Stradins University, Riga, Latvia
2 - Private Dental practice, Riga, Latvia
3 - Department of oral and maxillofacial surgery, Riga Stradins University, Riga, Latvia

Involvement of nerve growth factor cell surface receptor p75 (p75) has been shown to be essential in maintaining the integrity of the salivary glands. Furthermore, in human salivary glands no immunoreactivity for the p75 was observed in the serous or mucous acinar cells. This study was undertaken to analyze a possible role of p75 in human submandibular gland atrophy in case of sialolithiasis using immunohistochemistry.

The study was carried out on 14 human salivary glands obtained along sialadenectomy performed because of the presence of intraglandular sialoliths. The salivary glands were morphologically subdivided into two groups on the basis of the presence (9 cases) and absence (5 cases) of parenchymal atrophy. Formalin fixed, paraffin embedded tissue sections were processed for a traditional streptavidin-biotin-peroxidase technique.

p75 immunoreactivity was restricted to the ductal myoepithelial cells and nerve fibers supplying salivary glands. There was a co-localization of p75 and an alpha-smooth muscle actin reactivity within the myoepithelial cells. A ductal p75 expression was much more stronger displayed in cases with a prominent gland atrophy and severe fibrosis. This ductal p75 expression correlated with a degree of ductal wall cell proliferation assessed by routine morphological visualization and proliferating cell nuclear antigen immunohistochemistry.

The present study revealed a strong co-incidence between p75 expression and proliferation within a ductal wall in case of prominent salivary gland parenchymal atrophy. These findings suggest that p75 present on the surface of the myoepithelial cells may be intimately involved in the pathophysiology of salivary gland disturbances in case of sialolithiasis contributing to the interplay of multiple factors that balance homeostasis at the appropriate level.

P 346

P63 EXPRESSION IN SALIVARY GLAND TUMOURS: ROLE OF DELTANP73L IN NEOPLASTIC TRANSFORMATION.

FOSCHINI Maria P., GAIBA Alessia, COCCHI Roberto°, PENNESI Maria G.°, PESSION Annalisa.
Department of Oncological Sciences, Section of Anatomic Pathology , University of Bologna, at Bellaria Hospital, Bologna.
°Department of Maxillo-Facial Surgery, Bellaria Hospital, Bologna.

Introduction: p63 gene has two different functions: TAp63 favours cell differentiation, whereas DeltaN p63 favours cell proliferation. Two new isoforms have been described, Delta4TAp63 and DeltaNp73L, lacking exon 4. DeltaNp73L is present in squamous cell carcinoma, but absent in normal epithelium.

Purpose of the present study was to illustrate the role of p63 and its truncated variants in salivary gland tumours.

Materials and methods: Twenty three consecutive tumours and six normal salivary glands were studied immunohistochemically with anti-p63 monoclonal antibody (NeoMarkers, Freemont, USA, clone 4A4, diluted 1:200) and by RT and Nested PCR to detect p63 isoform expression.

Results: Normal salivary glands: p63 antibody stained basal and myoepithelial cells; by RT and nested PCR, the two main isoforms, TAp63 and DeltaNp63 were present, whereas DeltaNp73L was absent.

Tumours: p63 antibody was positive in 20 out of 23 cases, specifically in Warthin tumour (WT) (3/3), oncocytoma (OC) (1/1), pleomorphic adenoma (PA) (7/7), polymorphous-low-grade adenocarcinoma (PLGA) (3/3), adenoid-cystic carcinoma (ADCC)(3/4), epithelial-myoepithelial-cell carcinoma (EMC)(1/1), myoepithelial-cell carcinoma (MCC)(1/1). By RT and nested PCR all tumours expressed p63 irrespective of their morphological differentiation. Furthermore the DeltaNp73L isoforms were present in neoplastic tissue but absent in normal salivary gland.

In conclusion, p63 antibody stained basal and myoepithelial cells in normal and neoplastic salivary gland tissues. By RT and nested PCR all salivary gland tumours appeared to express at least one isoform of p63. The DeltaNp63 variant lacking exon 4, named DeltaNp73L, was present only in neoplastic lesions, whereas it was lacking in normal salivary gland tissue, a feature that indicates the crucial role of this molecule in neoplastic transformation.

P 347

A CASE OF MUCIN-RICH VARIANT OF SALIVARY DUCT CARCINOMA EX PLEOMORPHIC ADENOMA

Tohru Kaku, Tomoyuki Ohuchi, Masaaki Satoh, Tatsuru Ikeda, Hiroko Asanuma, Kyogo Azuma, Hideki Kobayashi
Department of Oral Pathology, School of Dentistry• @, Health Sciences University of Hokkaido
Department of Clinical Pathology, Sapporo Medical University

Salivary duct carcinoma (SDC) is an established aggressive salivary gland neoplasm resembling intraductal and infiltrative ductal carcinoma of the breast. Diagnostic criteria and concept of SDC have been expanded along with subtype and new entity case reports such as sarcomatoid SDC, minor salivary gland origin SDC, invasive micropapillary SDC, and mucin-rich variant SDC. SDC often occurs as the malignant component of carcinoma ex pleomorphic adenoma.• @ Lewis et al. reported that SDC was many as the malignant component of carcinoma ex pleomorphic adenoma next to adenocarcinoma, not other specified from retrospective study (Hum Pathol 32: 594, 2001). Mucin-rich variant SDC was first reported by Simpson et al. (Am J Surg Pathol 27: 1070, 2003). They reported four mucin Ðrich variant SDC cases. However, there is no report of other mucin-rich variant SDC case after SimpsonÕs description. Here we report a case of mucin-rich variant of SDC ex pleomorphic adenoma arising from submandibular gland.

A 73-year-old Japanese male had noticed a painless swelling at the right submandibular area for about 35 years. This lesion had rapidly increased in size for a period of about 10 months. Macroscopically, the resected tumor was a solid mass with multiple mucinous cysts and necrotic areas in the submandibular gland. Microscopically, large areas of tumor nests infiltrated to normal salivary gland with aboundant fibrous and/or hyalininzing connective tissue. Malignant tumor has many forms, such as, arranged solid, ductal, cribriform, and mucinous (colloid) carcinoma-like patterns. Some nests exhibit Roman bridge-like appearance, central necrosis, and intraductal patterns. In the mucinous carcinoma-like area, irregularly shaped small nests with fibrous connective tissue floated in pools of mucin. In this tumor it was composed of large atypical round to polygonal eosinophilic cells with round shaped nuclei. Most of these tumor cells were positive for diastase-PAS and mucicarmine, and androgen receptor, gross cystic disease fluid protein-15 and Her2/neu, histochemical and immunohistochemical stainings respectively. Immunohistochemistry of this tumor was the same as general SDC. In a small part of tumor, we recognized small bilayered duct and mixed appearance-like regionm,such as resembling pleomorphic adenoma in strongly hyalinized stroma. Furthermore• @this case has a long term history. Finally,we diagnosed this tumor as a mucin-rich variant of of SDC ex pleomorphic adenoma.

P 348

LYMPHOEPITHELIAL CA OF PAROTID GLAND. REPORT OF TWO CASES

Tzaida O., Iakovidou J., Valavanis C., Simoulis A., Petridis N.,Arapantoni-Dadioti P.
Pathology Department , METAXA Cancer Hospital Piraeus , GREECE

Two cases of lymphoepithelial Ca, a rare salivary gland malignant epithelial neoplasm, are presented. This neoplasm is also referred to as “malignant lymphoepithelial lesion” and “undifferentiated Ca with lymphoid stroma”.
The patients were males 50 and 61 years old and presented a slowly growing, painless mass located at the left parotid gland, measuring 3 and 2.5 cm, respectively.
In the case of the elder patient a biopsy of a left cervical LN preceded the tumor’s surgical excision. The diagnosis on this material was a metastatic high-grade undifferentiated Ca resembling the nasopharyngeal lymphoepithelioma. A simultaneously performed nasopharynx biopsy was negative.
The microscopical examination of the two subtotal parotidectomies revealed malignant epithelial tumors. The neoplasms consisted of irregular shaped islands of large, anaplastic, eosinophilic, epitheliod cells within a mature type lymphocytic–rich stroma. Presence of epimyoepithelial islands, characteristic finding of benign lymphoepithelial lesion, was also evident. The immunohistochemical study confirmed the epithelial nature of the neoplasms and the concomittant benign lymphoepithelial lesion . EBV infection was revealed by a positive expression to LMP1 .
Particularities of this tumor, problems of differential diagnosis and terminology, are discussed.

P 349

EPSTEIN-BARR VIRUS AND WARTHIN TUMOR IN TUNISIA: MOLECULAR AND IMMUNOHISTOCHEMICAL STUDY

TRIMECHE Mounir, ZIADI Sonia, AMARA Khaled, HMISSA Sihem, MESTIRI Sarra, MOKNI Moncef, KORBI Sadok
Laboratoire d’Anatomie et de Cytologie Pathologiques, CHU Farhat Hached de Sousse, Tunisia

Purpose: Tunisia belongs to a zone at high risk for several neoplasms associated to Epstein-Barr virus (EBV), particularly for the nasopharyngeal carcinoma. The salivary glands are considered as one of the major reservoirs of replication and latency of this virus. Warthin tumor of the salivary gland is composed of oncocytic epithelium with a prominent follicular lymphoïd infiltrate. The histogenesis of this tumor is still debated and its association with EBV is controversial. The purpose of this study was to determine the prevalence of EBV in Warthin tumor in Tunisia.
Methods: Nineteen formalin-fixed, paraffin-embedded blocks of Warthin tumors from the parotid gland were examined for the presence of EBV, using polymerase chain reaction (PCR), EBERs in situ hybridization and immunohistochemistry for the detection of LMP1, EBNA2 and ZEBRA.
Results: Thirteen cases were PCR b-globin positive. The EBV was detected by PCR in 2 of 13 cases (15,4%). In the two EBV positive cases, EBERs in situ hybridization showed a positivity in few lymphocytes; these cells does not express LMP1, EBNA2 or ZEBRA.
Conclusions: The low frequency of EBV in Warthin tumor indicate that the virus is not the cause of this tumor, however the possibility that the virus acts as a cofacteur cannot be ruled out.

P 350

MUCINOUS ADENOCARCINOMA OF THE SUBMANDIBULAR SALIVARY GLAND

FARAH-KLIBI Faten*, ZEDDINI Abdelfatteh*, ZERMANI Rachida*, FERCHICHI Leila*, RAMMEH Soumaya*, CHELBI Emna*, FERJAOUI Mohamed**, BEN JILANI Sarrah*.
*: Laboratory of pathology.
**: Oto-rhino-laryngology service.

Mucinous adenocarcinoma is a rare malignant neoplasm characterized by large amounts of extracellular epithelial mucin that contains cords, nests and solitary epithelial cells. It is a tumor analogous to mucinous eccrine carcinoma and mucinous carcinoma of the breast and colon. Few cases of primary salivary gland mucinous adenocarcinoma have been reported and all these cases arose in the major salivary gland.
We report a new case in 41-year-old man presented with an enlarging, painless left submandibular mass. On physical examination, a 6-cm firm mass was noted and no adenopathy was detected. Ultrasonography revealed a 4-cm heterogeneous mass. The patient underwent excision of the submandibular gland and lymph node dissection. Histological study concluded at mucinous adenocarcinoma without lymph node metastasis. After two years, the follow-up has been good.
The aim of this study is to review diagnosis difficulty of this rare entity and differential diagnosis.

P 351

IMMUNOPROFILE OF REACTIVE SALIVARY MYOEPITHELIAL CELLS IN AREAS OF IN SITU CARCINOMA EX-PLEOMORPHIC ADENOMA.

Vera Cavalcanti de Araújo-Research Center SL Mandic,Campinas, Brazil,
Albina Altemani- Department of Pathology UNICAMP, SP, Brazil
Cristiane Furuse-Research Center SL Mandic,Campinas, Brazil
Marília Trierveiler Martins-Deparment of Pathology USP,SP, Brazil,
Ney Soares de Araújo- Department of Pathology USP, SP, Brazil

Myoepithelial cell (MEC) is the component of various secretory glands including salivary and breast glands and it is located between the basement membrane and the luminal cells. The MEC has pinocytic vesicles, microfilaments and dense bodies resembling smooth muscle cells and they are recognized immunohistochemically by the positivity of myofilaments. Since the beginning, its function as a contractile cell which facilitates the excretion of the products of both salivary and breast glands is well known. With the scientific advances in molecular and biologic studies, new functions were added. The studies in this area are controversial since some have indicated a tumour suppressor function and others a tumour facilitating function for the MEC. In order to increase some knowledge to this subject, we have investigated the immunoprofile of benign MEC in areas of in situ carcinoma ex-pleomorphic adenoma (ISCXAP) comparing with the MEC in areas of pleomorphic adenoma (PA) source of the malignant tumour. Tissue samples from 4 cases of ISCXAP have been selected for immunohystochemistry study using MEC markers (SMA, calponin, CK14, p-63), extracellular matrix protein (laminin) and protease inhibitor (maspin). The results revealed that all MEC markers plus laminin and maspin are stronger expressed in benign MEC of ISCXAP areas than in benign MEC of pleomorphic adenoma . These results have led us to conclude that MEC which surrounds the malignant epithelial component of ISCXAP is phenotypically altered and more differentiated than the benign MEC of pleomorphic adenoma and probably, exerts, at this moment of the oncogenesis process, a tumour suppressive function. Further studies are necessary in order to clarify if the MEC is also implicated in the transition of in situ to invasive carcinoma.

P 352

CD10 EXPRESSION USEFULNESS IN DIFFERENTIAL DIAGNOSIS OF PRIMARY AND METASTATIC CLEAR CELL TUMOURS OF SALIVARY GLANDS

Alos L, Morente V, Garrido M, Mozos A, Ordi J, Cardesa A.
Department of Pathology, Hospital Clinic, IDIBAPS, University of Barcelona, Spain.

INTRODUCTION: The expression of CD10, or common acute lymphoblastic leukemia antigen, has been widely studied in normal tissues and neoplasms. CD10 is characteristically expressed in renal clear cell carcinomas, a neoplasm with tendency to metastatize in the head and neck region. Its positivity has been shown to be helpful in the differential diagnosis with other tumours with clear cells in other organs such as the ovary. However, the expression of CD10 in clear cell neoplasms of salivary gland origin has not been previously studied in detail.
PURPOSE OF THE STUDY: To study the expression of CD10 in primary clear cell tumours of salivary glands and metastatic renal cell carcinoma, in order to determine the uselfulness of this marker for the differential diagnosis.
MATERIAL AND METHODS: Thirty-five tumours of salivary glands with a major clear cell component were selected. Thirty-two were primary tumours and three were metastatic renal clear cell carcinomas. The immunohistochemical study for CD10 (Novocastra Laboratories. Newcastle, UK. Dilution 1:25) was performed in all cases from from formalin-fixed and paraffin embedded material.
RESULTS: All primary tumours composed of myoepithelial cells showed a strong and diffuse cytoplasmic CD10 positivity: myoepitheliomas (4/4), myoepithelial carcinomas (3/3), and epithelial-myoepithelial carcinomas (3/3). CD10 was also positive in other primary tumours with clear cells: mucoepidermoid carcinomas (3/6) showed a predominant apical and luminal positivity in glandular differentiated areas; some acinic cell carcinomas (2/8) and oncocytomas (1/3) had a cytoplasmic pattern.Three salivary gland clear cell carcinomas and two sebaceous differentiated tumours were negative for CD10. Metastatic renal clear cell carcinomas showed a strong membrane positivity (3/3).
CONCLUSION: CD10 is expressed in a variety of primary tumours of salivary glands, with a cytoplasmic or luminal pattern; whereas this marker shows a strong membrane positivity in metastatic renal cell carcinoma. The different immunoreactivity pattern may be useful for differentiating renal cell carcinoma metastasis from other primary salivary gland tumours.

P 353

EXTRA PAROTID PARAPHARYNGEAL SPACE TUMOR WITH BIPHASIC PATTERN.

DINU* Carmen, TOUBLANC* Marianne, WASSEF** Michel, GEHANNO*** Pierre, HÉNIN* Dominique
*Pathology department, ***ENT department, Bichat hospital; **Pathology department, Lariboisière hospital, Paris, France.

A 54 year old woman presented with a nodular lesion of the parapharyngeal space. This lesion was well-circumscribed hypoechogene on echography, separated from the parotid gland by a narrow band of fat tissue on CT scan. On MRI a possible connection with the parotid gland and a T2 moderate hypersignal were noticed. At surgery the tumor appeared as a firm encapsulated greyish nodule, 3,5 x 5,5 cm, without connection with the parotid gland.
Microscopically, tumor was predominantly composed of spindle cells intermixed with mature adipose tissue and epithelial cells, forming small solid nests with squamoid features, rarely tubes or microcysts. No necrosis was observed. Both epithelial and spindle cells were strongly positive for AE1/AE3. Spindle component was PS100 + and faintly smooth muscle actin +. Proliferation index was less than 3% . Cells were not stained by CD34, desmine, GFAP and CD99 antibodies. Diagnosis of ectopic hamartomatous thymoma was first proposed on account of location at the skull base without connection with parotid gland, predominant spindle shaped pattern and squamoid features, but PS100 positivity was unusual. On serial sections cartilage tissue was found, leading to the diagnosis of pleomorphic adenoma.
Tumors in the parapharyngeal space (PPS) are rare and constitute less than 0.5% of head and neck neoplasm. Of these, pleomorphic adenoma (PA) is the most common (40%) followed by schwannoma and paraganglioma. PA can arise either de novo from accessory salivary glands or from the deep lobe of the parotid gland and extend through the stylomandibular tunnel into the PPS. Typical PA has a biphasic appearance resulting from the intimate admixture of epithelium and myoepithelial cells, and generally contain myxochondroid areas and sometimes adipous tissue. Some pleomorphic adenomas are extremely cellular, the tumor cells being either round or spindle shaped. The myoepithelial component is immunoreactive for keratins, myosin, fibronectin, PS-100 and often for actin. The main differential diagnosis include ectopic hamartomatous thymoma, biphasic

synovial sarcoma, schwannoma, malignant peripheral nerve sheath tumor and myoepithelioma of soft tissue.
Conclusion: Immunohistochemical study is important for the diagnosis of parapharyngeal space tumor with biphasic pattern.

P 354
PRIMARY AMYLOIDOSIS OF THE LARYNX
PAGLIARI Angelo Virgilio °, KLINGER Francesco *, KLINGER Marco *
° U.O. ORL - Azienda Ospedaliera di Crema
* Istituto di Chirurgia Plastica e Ricostruttiva
Università degli Studi di Milano-I.C. Humanitas

Introduction In 1851 Virchow coined the word amyloid to describe the strachlike reaction of a waxy material when treated with iodine and sulphuric acid. Amyloidosis is defined as a pathologic proteinaceous substance deposited between the cells of tissues and organs leads to various clinico-pathologic conditions. Localized and idiopathic amyloidosis in the head and neck is a rare and benign process.
Methods We present a clinical case of a 63 years female with hoarseness due to a laryngeal mass and also a review of literature regarding localized amyloidosis. A laryngoscopic examination revealed a smooth, non ulcerated submucosal mass involving the ventricle, false cord extended to vocal process. Physical and laboratory evaluation showed no evidence of systemic amyloidosis or multiple myeloma. The lesion was treated by endoscopic laser excision.
Results At light microscope amyloid is a homogeneous acellular eosinophilic and extracellular material with haematoxylin and eosin stains. It stains metachromatically purple red with crystal violet and characteristically manifests a Congo red staining of its fibrils with apple-green birefrigence. Amyloid stains dark brown with iodine. Exposure of the Congo red to potassium permanganate and diluite sulphuric acid may be used to partly subclassify amyloid. Immunohistochemical examination revealed a polyclonal staining pattern of light chain of immunoglobulins.
Conclusion Localized amyloidosis of head and neck region is rare. Borow in 1873 first reported amyloidosis of the larynx and at the present about 350 cases were reported in literature. It should be recognized, understood, evaluated and properly treated.

P 355
ANGIOLEIOMYOMA OF THE NECK MIMICKING THYROGLOSSAL DUCT CYST
SALERNO Angela*, MARLIA Enrico°, FONTI Giulio°.
*Servizio di Anatomia e Istologia Patologica e Citodiagnostica. Ospedale Maggiore. Bologna.
°Unità Operativa di Chirurgia Generale. Ospedale G. Dossetti. Bazzano (Bologna). ITALY

INTRODUCTION. Angioleiomyoma (AL) is an uncommon benign tumour composed of smooth muscle cell and vascular endothelium. After Shout reported the first 11 cases in 1937, about another thousand have been reported and most authors have accepted that angioleiomyoma originates from the smooth muscle in the wall of vascular channels. In 1973 Morimoto proposed to subdivide AL into capillary (solid), cavernous and venous type. Clinically AL is more frequent in female; they are usually located in lower extremities and present as a solitary, painful cutaneous or subcutaneous mass of solid type. Only about 10% of AL arises in the head and neck area and they usually present as a painless mass of venous or cavernous type. Frequently imaging study or cytological examination is not helpful for preoperative diagnosis. Recurrence is rare.
PURPOSE OF THE STUDY. In this paper we report the case of an angioleiomyoma of the neck mimicking a thyroglossal duct cyst and to our knowledge this is the first case described in this location.
METHODS. A 67-year-old male presented with a painless mass of the neck. Physical examination revealed a 2 cm subcutaneous solid mass in the upper neck. There was neither associated lymphadenopathy nor abnormality of the skin. Ultrasound examination showed a 20 x 15 x 21 mm solid hyperechogenic mass, with hypoechogenic peripheral rim. The preoperative diagnosis was of a thyroglossal duct cyst. The patient underwent surgery and a 2 cm solid mass was found attached to the geniohyoid muscle but without relation with the hyoid bone.
RESULTS. Histologic examination showed a well demarcated nodule composed of smooth muscle with thick-walled venous vessels with inner layers of smooth muscle and without lamina elastica. The tumour contained also mature fat cells. Immunohistochemistry for smooth muscle actin was positive and confirmed the diagnosis of angioleiomyoma of venous type.
CONCLUSION. AL is a rare benign tumour in head and neck area. This lesion is difficult to diagnose before surgery, especially when it occurs as a painless mass and is in a site where other lesions are more frequent. Surgical excision is necessary to make a correct diagnosis and gives good results with rare recurrence.

P 356
EWING /PNET FAMÝLY SARCOMA ARISING FROM BRANCHIAL CYST WALL
DERVISOGLU Sergulen, OZ Buge, SAR Mehmet

INTRODUCTION:The Ewing sarcoma family tumors (ESFT) include Ewing sarcoma, peripheral primitive neuroectodermal tumor, neuroepithelioma, atypical Ewing sarcoma, and Askin tumor. ESFT research is ongoing to further characterize the biology of the EWS/FL1 fusion protein and it's role in transformation, cell growth and chemosensitivity. Unusual location of such tumors may cause diagnostic problems and cytogenetic analysis on tumor tissue samples may solve the problem in diagnostic approach. We present an ESFT arising from a branchial cleft cyst and discussed the diagnostic difficulties.
CASE: A 21 year old female complained dysphagia for 2 years duration. During the last 2 months a mass was palpated on the right side of the neck. Physical examination revealed cystic cervical, nontender mass with 4x3x3cm diameters, located along the lower one third of the anterior border of the sternocleidomastoid muscle between the muscle and overlying skin. Histopathological examination of the excised mass showed cystic wall lined with partially stratified squamous and respiratory epithelium. Lymphoid tissue was seen in the cyst wall in accordance with branchial cleft cyst. Next to this lymphoid area a malignant neoplasm consisting primitive cells arranged in cords and with a vague nesting pattern was observed. Immunohistochemical studies showed CD99 positivity, while cytokeratin, CD45, NSE, S-100, chromagranin, synaptophysin, smooth muscle actin, and desmin were all negative.Cytogenetic analysis performed by using RT-PCR technique on paraffin embedded tumor tissue demonstrated the chimeric fusion transcripts EWS/FLI-1 and confirmed the diagnosis of ESFT.
CONCLUSION:This location was unique when we rewieved the English written literature as far as we could reach .
Because the ESFT is a rare tumor in extraskeletal site it is often not considered in clinical differential diagnosis until a biopsy reveals a small blue round cell tumor.Especially unusal presentation like the presented case, a panel of immunohistochemistry may not be helpful in all instances. Cytogenetic analysis may solve the problem if the material belongs to a tumor with a known characteristic transformation. In our case EWS/FL-1 fusion which is present in 85% of ES/PNET cases was helpful in dignostic approach.

Because of the cystic nature and branchial cyst association malignancy was not in the differential diagnosis clinically, consultation with an oncologist is critical.

P 357
SPINDLE CELL PROLIFERATION IN FOLLICULAR ADENOMA OF THE THYROID. CASE REPORT IN PATIENT TREATED FOR HIGH GRADE LYMPHOMA

Manfrin E°, Martignoni G*, Remo A°, Reghellin D°, Dalfior D°, Eccher A°, Bonetti F°.
°Department of Pathology, University of Verona
*Department of Pathology, University of Sassari

Introduction: Spindle cell proliferations of the thyroid are rare and they include anaplastic carcinoma and mesenchimal tumors. There are few reports of spindle cell change in epithelial tumors of the thyroid as such as have been described in follicular adenoma and papillary carcinoma.
Purpose: to report the clinical and pathological features of a thyroid adenoma with diffuse spindle cell change in a patient treated for high grade lymphoma.
Methods: In 2003, a 31-year-old woman was admitted to "G.B.Rossi" hospital of Verona University and underwent chemotherapy because of high grade lymphoma. In 2004, she received bone marrow transplantation (BMT). During follow-up, a Positron Emission Tomography (PET) was performed and a suspicious single nodule in the thyroid was detected. Following fine needle aspiration cytology (FNAC) was not conclusive and the nodule was surgically removed.
Summary: Cytologically, the lesion was composed by cohesive, plump spindle cells with amphophylic cytoplasm, irregular nuclei with granular cromatin. No bizarre nuclei nor necrosis or mitoses were detected. On gross examination, the nodule was 2.5 cm in diameter, with whitish cut surface and a well-defined capsule. Histologically, it was composed, almost completely (90%), of spindle cells growing in diffuse, haphazard pattern, surrounding residual thyroid follicles. There was no vascular neither capsular invasion. Immunohistochemically, spindle cells were strongly positive with TTF-1, CK8-18 and vimentin, positive with keratin, but negative with CD34, S-100, desmin, HMB-45 and calcitonin. Spindle cells showed weak and focal immunoreactivity for thyroglobulin. Immunoistochemical results demonstrated the follicular origin of the lesion and suggested a diagnosis of spindle metaplastic transformation in follicular adenoma.
Conclusion: Spindle cell adenoma of thyroid is an extremely rare lesion. In our case FNAC was not conclusive and histological examination was necessary for a correct diagnosis. An association between spindle cell adenoma and the treatment for lymphoma cannot be ruled out.

P 358
EVALUATION OF FIBRONECTIN EXPRESSION IN LARYNGEAL CANCER: AN IMMUNOHISTOCHEMICAL STUDY*

PIETRUSZEWSKA Wioletta (1), KOBOS Jozef (2), GRYCZYNSKI Maciej (1)
(1) Department of Otolaryngology, Barlicki University Hospital, Medical University of Lodz
(2) Department of Pathology, Medical university of Lodz

Fibronectin is one of the extracellular matrix glycoprotein, that plays an important role in cancer invasion and progression. Our purpose was to evaluate fibronectin expression and its possible prognostic value in laryngeal cancer. Forty-one patients (six female and thirty-five male) surgically treated for laryngeal cancer were included in the study. The expression and distribution of fibronectin was immunohistochemically determined by using monoclonal antibody against fibronectin. Low expression of fibronectin was detected around the individual carcinoma cells, but large amounts were present in the invasive tumour front and the cancer surrounding stroma was strongest positive for fibronectin. By univariate analysis the level of fibronectin expression on the border of the invasive tumour front was proved to be correlated with tumor stage ($p=0,03$). There was a significant association between the defect of ECM and overall survival ($p>0,05$). These observation indicates that testing the distribution and the expression of ECM seems to be useful to evaluate the histological grading of malignancy of laryngeal cancer and to be helpful to prognosticate the overall survival while measured on the border of tumour proliferative front in laryngeal patients. The results demonstrate that fibronectin amount may be useful in evaluating the invasion potential of the tumour.

P 359
MALT LYMPHOMA IN SJOGREN'S SYNDROME

KATIÆ Vuka, KRASIÆ Dragan, BURIÆ Nikola, TRENKIÆ Marija, KATIÆ Katarina.
Institute of Pathology, Medical Faculty of Niš University, Niš, Serbia and Montenegro

Introduction and aim: Sjogren's syndrome is a chronic autoimmune and rheumatic disorder with prominent sicca complaints from the mucous membranes because of lack of proper exocrine secretions. A large number of autoantibodies have been reported in Sjogren's syndrome where the antibodies are correlated with the extent and severity of disease. It is world-wide disease and may occur in all ages.However, the peak incidence is in the fourth and fifth decades of life with a female/male ratio of 9:1. Mucosa Associated Lymphoid Tissue (MALT) accounts for about 7,2% of all of non-Hodgkin's lymphomas.Most arise at sites without lymphoid tissue and appear following a period of chronic inflammation. This is the result of autoimmune disease as occurs in the thyroid or salivary glands, or in the stomach following local bacterial infection. In contrast to many reports on MALT lymphoma induced H.pylori chronic infection, on MALT lymphoma in salivary glands induced autoimmune disease there are a few data, that is the reason for our study.
Material and methods: Five patients with tumours of the parotid glands and surrounding lymph nodes, were surgically treated and sent to pathologist for histological analysis.Formaldehyde-fixed and paraffin- emmbedded tumorous tissue were cut and stained with H&E,AB-PAS, Van Gieson's and immunohistochemical LSAB2 methods. For immunohistochemical analysis, antibodies to cytokeratin and to CD20 and CD45RO antigens were used.
Results: MALT lymphoma in the salivary glands has a mean age incidence 56 years with a female to male ratio of 3:1. Macroscopical characteristics are not specific. Histological characteristic of MALT lymphoma was the presence of lymphoid follicles and diffuse infiltrate of lymphocytes occupying the marginal zone and both infiltrating and replacing glandular epithelium (pathognomonic lymphoepithelial lesion). The marginal zone, more developed, contained a mixed population of cells, with plasma cells and many mature B-cells,including centrocytoid and monocytoid B-cells.The pathognomonic lymphoepithelial lesions were more numerous than in
gastric MALT lymphoma. Immunohistochemically, lymphoepithelial lesions and B-cell origin of MALT lymphoma were confirmed.
Conclusion: MALT lymphoma in Sjogren's syndrome is autoimmune genesis.Characteristics of
MALT lymphomas induced by chronic H.pylori infections are symilar to characteristics of MALT lymphoma in Sjogren's syndrome.

P 360

MICROPAPILLARY CARCINOMA OF THE BLADDER: REPORT OF TWO CASES

CHELBI Emna (1), RAMMEH Soumaya (1), ZERMANI Rachida (1), BEN MOUALLI Sami(2), FARAH Faten (1), KOURDA Nadia (1), FERCHICHI Leila (1), AYED Mohsen (2), BEN JILANI Sarrah (1)
(1) Departement of Pathology, Charles Nicolle Hospital, Tunis.
(2) Departement of Urology, Charles Nicolle Hospital, Tunis.

INTRODUCTION
Micropapillary carcinoma (MC) of the bladder, first described in 1994, is a rare and highly aggressive variant of urothelial cell carcinoma (UCC) that accounts for 0.6% to 1% of all urothelial carcinoma. Histologically, the micropapillary component (MPC) is characterized by superficial pattern of slender, filiform processes or small papillary clusters of tumor cells and a deep pattern of tight infiltrating clusters contained within tissue retraction spaces. Herein, we report two additional cases of MC of the bladder including one with a long follow-up.
CASE 1:
A 68-year-old man presented with macroscopic hematuria. Ultrasonography and cystoscopy showed a sessile papillary tumor of 4 cm involving the anterior wall. The transurethral excision was complete. Microscopic findings demonstrated a grade G3 TCC with focal superficial and deep MPC (20%). Evidence of vascular invasion without muscular extension was found. A complementary BCG therapy was delivered. Four months later, the tumor relapsed and complete transurethral resection showed a recurrent pTa G1 UCC without MPC. He benefited from a second BCG therapy cure. He is now free of disease since more than six years.
CASE 2:
A 70-year-old man, treated for terminal chronic renal failure of unknown cause, exhibited a gross hematuria. Ultrasonography coupled with cystoscopy were consistent with a multifocal papillary tumor. The pathological examination after complete transurethral resection revealed a G3 papillary UCC with extensive MPC (60%) which infiltrate the lamina propria. The resection did not include muscle tissue. No cystectomy nor BCG therapy were scheduled due to his poor general condition. Currently, the follow-up is only one month.
DISCUSSION
While MC of the bladder is considered as a highly aggressive tumor with a high grade and stage at presentation, its prognosis is not very well documented due to the low number of cases in the literature. We report two additional cases including one with a favourable clinical course, the follow-up is too short for the second one. The prognosis depends on the extent of the invasion and on the proportion of the MPC. Deep muscle biopsies are recommended to rule out invasion when MPC is encountered. BCG therapy benefit should be better evaluated. A review of a large number of cases is needed to conclude whether or not the prognosis of patient with MC is poorer than that of patients with UCC G3 bladder cancer.

P 361

PROGNOSTIC IMPACT OF INVASIVE PATTERN, SQUAMOUS DIFFERENTIATION AND SARCOMATOID TRANSFORMATION IN TRANSITIONAL CELL CARCINOMA OF THE UPPER URINARY TRACT

Cord Langner1, Peter Rehak2, Richard Zigeuner3
1Institute of Pathology, 2Department of Surgery, Division of Biomedical Engineering & Computing and 3Department of Urology, Medical University of Graz, Austria

Introduction
Initial tumour stage and grade and extent of surgery have been documented as major prognostic factors in patients with upper tract transitional cell carcinoma (TCC). Our study aimed to evaluate the prognostic impact of other histopathological factors, such as invasive pattern, squamous differentiation and sarcomatoid transformation, in a large series of consecutive patients.
Methods
239 consecutive patients underwent surgery for upper urinary tract TCC between 1984 and 2004 at our institution. Patients with non-invasive TCCs (pTa) and multifocal (both pelvic and ureteral) TCCs were excluded. H&E slides of the remaining 188 cases (133 pelvic and 55 ureteral TCCs) were systematically re-evaluated regarding invasive pattern (nodular, trabecular and infiltrative), squamous differentiation and sarcomatoid transformation. The prognostic impact (regarding metastasis-free survival) was analyzed using the Kaplan-Meier method and the log-rank test. For multivariate analysis a Cox proportional hazard regression model including tumour stage and grade was used.
Results
The pattern of invasion was nodular in 47%, infiltrative in 31% and trabecular in 22% of cases, respectively. Squamous differentiation was identified in 22%, sarcomatoid transformation and marked tumour cell anaplasia were noted in 8% of cases, respectively. Follow-up data were available from 182/188 (97%) patients. After a mean follow-up of 4.1 years, metastatic disease was noted in 80/182 (44%) patients. Mean time to progression was 22 months. Significant prognostic factors in univariate analysis were pattern of invasion ($p<0.001$), squamous differentiation ($p=0.009$) and sarcomatoid transformation ($p=0.002$). In multivariate analysis, infiltrative pattern of invasion ($p<0.001$, risk ratio [RR]=7.1, 95% confidence interval [CI]=2.4-19.8) and pT category > 1 ($p<0.001$, RR=4.0, 95%CI=1.9-8.3) proved to be independent predictors with respect to metastasis-free survival, whereas for sarcomatoid transformation only a trend was noted ($p=0.06$).
Conclusions
The infiltrative pattern of invasion proved to be a new independent predictor of metastasis-free survival in upper tract TCCs, whereas squamous differentiation and sarcomatoid transformation lacked independent influence on patient outcome.

P 362

PROGNOSTIC IMPACT OF TUMOUR STAGE, GRADE AND ANGIOINVASION IN TRANSITIONAL CELL CARCINOMA OF THE UPPER URINARY TRACT

Cord Langner1, Peter Rehak2, Richard Zigeuner3
1Institute of Pathology, 2Department of Surgery, Division of Biomedical Engineering & Computing and 3Department of Urology, Medical University of Graz, Austria

Introduction
Initial tumour stage and grade and extent of surgery have been documented as major prognostic factors in patients with upper tract transitional cell carcinoma (TCC). However, data are limited due to small sample size and the new two-tired grading system of the WHO has not yet been systematically tested with respect to prognostic significance. Therefore, our study aimed to evaluate possible conventional prognostic factors, such as tumour stage and grade as well as angioinvasion, in a large series of consecutive patients.
Methods
239 consecutive patients underwent surgery for upper urinary tract TCC between 1984 and 2004 at our institution. Patients with non-invasive TCCs (pTa) and multifocal (both pelvic and ureteral) TCCs were excluded. The slides of the remaining 188 cases (133 pelvic and 55 ureteral TCCs) were systematically re-evaluated regarding pT-category, tumour grade according to the recent revision of the WHO classification and angioinvasion (L1, V1). The prognostic

impact (regarding metastasis-free survival) was analyzed using the Kaplan-Meier method and the log-rank test. For multivariate analysis a Cox proportional hazard regression model was used.
Results
Follow-up data were available from 182/188 (97%) patients. After a mean follow-up of 4.1 years, metastatic disease was noted in 80/182 (44%) patients. Mean time to progression was 22 months. Significant prognostic factors in univariate analysis were pT-stage > 1 (p<0.001), high tumor grade (p<0.001) and angioinvasion (p<0.0001). No significant prognostic influence was observed for tumour location. In multivariate analysis, pT-stage > 1 (p<0.001, risk ratio [RR]=4.7, 95% confidence interval [CI]=2.3-9.5) and angioinvasion (p<0.001, RR=4.9, 95%CI=2.7-8.9) proved to be independent predictors with respect to metastasis-free survival, whereas for high tumour grade only a trend was noted (p=0.09).
Conclusions
Advanced tumour stage and presence of angioinvasion were independent predictors of metastasis-free survival in upper tract TCCs. No impact was seen for tumour localization (pelvic vs. ureteral), thus supporting the current concept of the TNM system to summarize pelvic and ureteral TCCs in one tumour category.

P 363
CORRELATION BETWEEN APOPTOSIS AND HISTOLOGICAL GRADE OF TRANSITIONAL CELL CARCINOMA OF URINARY BLADDER
Bahram Mofid,Mohammad Reza Jalali Nadoushan, Hamideh Peivareh

Purpose: TO evaluate the relationship between histological Grade and Apoptotic Index (AI) in TCC of urinary bladder .

Methods & Materials: Formalin-fixed and paraffin-embedded tissue blocks from 75 patients with TCC who underwent Transurethral resection (TUR) were studied. One 3 micron sections were provided from each TUR samples. In one section after Hematoxylin and Eosin (H&E) staining, grade was determined according to WHO/ISUP criteria. The apoptotic cells were determined using a terminal deoxynucleotidyl transferase (TdT) mediated dUTP biotin nick end labeling (TUNEL) technique. Apoptotic index was then obtained as the percent of TUNEL positive cells from observations of at least 1000 cells in each section.

Results: Forty-nine patients were men and 26 were women. The mean age was 56.34,,b9 years. The mean AI was 2.30,,b0.50. The relationship between grade and AI was significant (P=0.000, rs=0.551). A higher grade was associated with a higher AI.

Conclusion : The AI has a direct correlation with bladder TCC grade. For determination of definite role of it in prognosis, other analytical studies are needed.

Key Words: Transitional cell carcinoma, Grade, Apoptotic Index, Tunnel

P 364
THE RELATIONSHIP BETWEEN C-ERB B2 ONCOPROTEIN OVER EXPRESSION AND HISTOLOGIC GRADE ON TRANSITIONAL CELL CARCINOMA OF URINARY BLADDER
Jalali Nadoushan Mohammad Reza,Jouian Neda,Zaeri Farid
Shahed University

Background and Objective: Transitional cell carcinoma of urinary bladder is the fourth most common cancer in men and eighth in women. Similar to other cancers, this cancer needs to determination of prognosis and type of treatment, after diagnosis. Several parameters such as clinical and pathological parameters, chromosomal and genetically abnormalities and molecular factors in cells surface have rules in determination of prognosis. In this research, for the first time in Iran, abundance of c-erb B-2 oncoprotein and it's relation with tumor grade were evaluated.
Material and Method: A prospective cross-sectional study was performed in paraffin embedded tissue from 75 patients with TCC of urinary bladder. Two 3m sections were provided. In one section, according to WHO/ISUP grading system, grade of tumor was determined, by H&E staining. In the other section, the presence of c-erb B-2 oncoprotein was determined by IHC Method.
Results: Increasing in number of patient with c-erb B-2 protein over expression, was associated to increase in grade of tumor, and a meaningful relation between over expression of c-erb B-2 and grade of tumor was found.
Conclusion: c-erb B-2 oncoprotein over expression had a direct relation with tumor grade. Results of this study are the same as often previous; therefore c-erb- B-2 oncoprotein over expression could be a prognostic factor in TCC of urinary bladder. Other studies for confirmation of this hypothesis are recommended.

P 365
IMMUNOHISTOCHEMICAL EXPRESSION OF CK 7, CK20, P53, AND MIB1 IN UROTHELIAL LESIONS
Molinié Vincent (1), Lebret Thierry (2), Hervé Jean Marie (2), Botto Henry (2). Pathology department (1), Hôpital saint Joseph, Paris, and Urology department (2) Hôpital Foch, Suresnes, France.

Morphological aspect in vesical lesion is sometimes difficult to distinguish from a reactional dystrophy, and it could be difficult to distinguish low and high grade carcinoma, specilally in G2 tumour. In these cases immunohistochemistry with p53 and Mib1 may be useful.
Aim of the study : to evaluate the expression CK 20 in the diagnosis of urothelial carcinoma, and to compare to the expression of p53 and Mib1 and CK 7.
Materials and methods : 69 cases of urothelial carcinoma (54 TUR and 15 biopsies), interesting 3 reactional dystrophic lesions, 32 low grade urothelial carcinoma, 34 high grade urothelial carcinoma ; corresponding in 59 superficial tumours (38 pTa, 16 pT1a, 5pT1b) and 8 infiltrative tumours (pT2). For each cases one paraffin block of representative with normal urothelium were tested with CK 7 (Immunotech, 1/50); CK 20 (Immunotech, 1/50); p53 (Dako, 1/80) and Mib1 (Ki67, Dako, 1/100), after antigenic restoration, on an automate stainer Nexes Ventana ®.
Results : Normal superficial cells expressed CK7 in 98,5% of the cases. With CK 20, in normal urothelium, and low grade tumors, only superficial cells were stained. In high grade tumours all the height of the urothelium was stained. CK 20 expression was correlated with grade p = 0,01 (WHO 73: G1 vs G2 vs G3 or WHO 2004: High grade vs Low grade), but not with stage p = 0,15. Expression of p53 and Mib1 varied from 5 to 90%. Mib1expression was strongly correlated with grade : p = 0,013 (WHO 2004: High grade vs Low grade or WHO 73: G1 vs G2 vs G3) and with stage p = 0,05. p53 expression was correlated neither with the grade p = 0,58 nor stage p = 0,18.
Conclusion : High expression of CK 20 and Mib1 is found in high grade urothelial carcinoma and in CIS. This should be exercised in using CK 20 and Mib1 immunohistochemical staining for the diagnosis of papillary urothelial tumour of intermediate grade (G2, OMS 73), or in case of atypical plane lesion

P 366
SIGNIFICANCE OF P21 AND C-MYC EXPRESSION IN BLADDER UROTHELIAL LESIONS

Badawy Afkar, El-hindawy Aly, Khattab Hany*, Abo-Shousha Tarek, El-Shahat Noha, and Omran Zeinab.
Pathology department, Theodor Bilharz Research Institute and * Faculty of Medicine, Cairo University, Egypt.

Immuno-histochemical tissue expression of the anti-proliferative marker P21 and the oncogenic marker C-myc were estimated in 40 cases with non-neoplastic and neoplastic urinary bladder lesions with or without schistosomal infection to assess the significance of their urothelial expression as a diagnostic tool in patients with higher risk of developing cancer bladder and as a prognostic indicator in malignant lesions. P21 expression was detected randomly in normal urothelial nuclei, while 50% of simple cystitis cases and all cases with premalignant changes were positive for P21 immuno-reactivity expressed into about 16% of urothelial cells. Eighty five percent of malignant cases expressed P21 in 48-55% of urothelial cells without significant variance between different histologic tumor types. Extent of P21 expression inversely correlated with bilharzial association, upgrading of malignancy and tumor invasiveness.

C-myc was detected in 50% of normal urothelium (as cytoplasmic staining), in 80% of simple chronic cystitis cases (75% cytoplasmic, 25% cytoplasmic and nuclear expression), and in all cystitis cases with premalignant changes (as cytoplasmic and nuclear expression). Eighty nine percent of cancer cases were C-myc positive with predominance of nuclear expression to be seen in 16.7% and mixed with cytoplasmic expression in another 58.3% of positive cases. Malignancy upgrading and invasiveness raised C-myc positivity. In conclusion: P21 expression increases in an attempt to check cellular proliferation, but when the matter is out of hand, P21 is down- regulated, while the increase in the oncogen C-myc goes ahead. Loss of P21 and increased C-myc expression in a malignant lesion is a predictor of malignancy progress to higher grade or stage.

P 367

IMMUNOHISTOCHEMICAL PROGNOSTIC FACTORS OF UROTHELIAL CARCINOMA.

Frank G.A., Zavalishina L.E., Andreeva Yu.
Hertsen Research Oncological Institute, Moscow, Russian Federation

AIMS : Immunohistochemical study structural component of extracellular matrix and cellular adheson mollecules in bladder urothelial carcinoma of different grade.
METHODS : Using formalin – fixed and paraffin – embedded tissue, we examined by immunohistochemical method tenascine, collagen IV, laminin, E-cadherin, beta-catenin, CD44 in 39 cases of urothelial carcinoma: G1 – 15, G2 – 12 and G3. Staining intensity of E-cadherin, beta-catenin and CD44 were evaluated using a 0 to 3+ scale.
RESULTS: The strong positive staining (3+) with antibody to E-cadherin was observed in most of cases G1 carcinoma. Low intensive (0/1+) reaction was found in all cases G3 urothelial carcinoma. Immunohistochemical staining with antibody to beta-catenin was the same in localisation and inteisity of expression with E-cadherin: G1 carcinoma – 3+ and 2+ in 80%, G2 – 2+ in 40% and 1+ in 60%, G3 – 0/1+ in 100% cases. It is impotant, that it was low expression E-cadherin and beta-catenin (0/1+) in a few cases high-grade urothelial carcinoma.
CD44 level was high in tumor cells in G1 and low – in extracellular matrix. But in G3 cases we observed strong reaction in extracellular matrix and low reaction – in tumor cells membrane.
Expression collagen IV and laminin was high intensivety around tumor complexes in G1 carcinoma, but low – in cases G3. The overexpression of tenacsine was found only in bladder carcinoma G1.
CONCLUSAON: Our data suggest, that expression E-cadherin, beta-catenin, CD44, tenascine, collagen IV and laminin may play a role of prognostic factores in urothelial carcinoma and they correlate with different level of malignancy. .

P 368

PROGNOSTIC VALUE OF THE IMMUNOHISTOCHEMICAL EXPRESSION OF : KI67, P53, PCNA AND BCL2 IN THE SUPERFICIAL TUMORS OF THE BLADDER.

RAMMEH-ROMMANI Soumaya *, ZERMANI Rachida *, SFAXI Mohamed **, ZOUARI B¨|chir ***, FARAH Faten *, KOURDA Nadia *, AYED Mohsen **, BEN JILANI-BALTAGI Sarrah *.
* Departement of Pathology, Charles Nicolle Hospital, Tunis.
** Departement of Urology, Charles Nicolle Hospital, Tunis.
*** Departement of Preventive and community Medicine, Faculty of Medicine, Tunis.

Introduction: Superficial tumors of the bladder present 2 prognostic problems: a risk of recurrence and a risk of progress in grade and in stage. Predictive factors of recurrence and of tumoral progress were identified.These factors are essentially endoscopical and pathological ones. Recent works underlined the prognostic value of the immunohistochemical study of the markers of cellular proliferation and of apoptosis in these tumors.
Aims: To study a series of superficial tumors of the bladder and to assess the prognostic significance of p53, Ki67, PCNA and bcl2 in these tumors.
Materials and methods: We studied 59 bladder tumors: 43 pTa and 16 pT1. All Patients had cystoscopy 3 months after the resection and tumors that did not recur had a minimum follow up of 5 years.
Results: Age more than 65 years (p = 0,001), multifocality (p = 0,022) and tumoral size ¡Ý 3 cm (p = 0,022) were correlated with the recurrence. The expression of p53 was correlated with the recurrence in the year following the tumoral resection (p = 0,035). That of of Ki67 was correlated with the histological grade (p = 0,03) and stage (p = 0,002).
Conclusion : Our results suggest to practise regular endoscopic controls during the first year following the resection of the primitive tumor if it expresses p53. The immunohistochemical expression of Ki67 being correlated with the grade, this marker could help to better classify the tumors of intermediate grade.

P 369

KI67 EXPRESSION IN RECURRENCE PAPILLARY TRANSITIONAL CELL BLANDER CARCINOMA

NIKOLAIDOU Anastasia1, TSOBANIDOU Chrysoula 2, HASAKIOILIS Pantelis 3, KLAMBATSAS Athanasios 3, TOLIOU Theano 2
TOLI A 2 Tehnician
1Department of Pathology, General Hospital of Kilkis, Kilkis, Greece
2Department of Pathology, “Theagenio” Anticancer Institute, Thessaloniki, Greece
3Department of Urology, General Hospital of Kilkis, Kilkis, Greece

This work has been sent
but the category miscellaneous is fault
The category of this work is uropathology
We beg your pardon.

P 370

EXPRESSION OF TETRANECTIN IN INVASIVE AND NON-INVASIVE PAPILLARY BLADDER CANCER

BRUNNER Andrea, ENSINGER Christian, CHRISTIANSEN Michael*, HEISS Simone, MIKUZ Gregor, TZANKOV Alexandar
Institute of Pathology, Medical University of Innsbruck
Department of Clinical Biochemistry, Statens Serum Institute, Copenhagen*

Introduction: Tetranectin is a plasma protein, which can be detected immunohistochemically in many normal cells. It is able to bind to the kringle-4 region of plasminogen and to participate in proteolytic processes that are considered to play an important role during tumor invasion and metastasis. Tetranectin expression was reported in breast, gastric and colon cancer being associated with a reduced survival in breast cancer.
The aim of the study was to investigate the expression of tetranectin in the normal bladder and bladder cancer.
Material and methods: Expression of tetranectin was studied in 20 invasive and non-invasive bladder tumors, including 9 low grade (5 grade 1, 4 grade 2 tumors) and 11 high grade tumors (3 grade 2, 8 grade 3 tumors) and in normal urothelium by means of immunohistochemistry using a monoclonal antibody against human tetranectin.
Results: Tetranectin was detected in normal urothelial cells, in the extracellular matrix, in inflammatory cells, in the smooth muscle of the bladder wall and in endothelial cells.
Non-invasive bladder tumors showed a weak tetranectin expression in superficial and intermediate cells.
In invasive tumors high expression of tetranectin was found in the invasive tumor component.
The extracellular matrix stained positive for tetranectin in non-invasive and invasive tumors, exhibiting a more intense staining around invasive tumor.
Conclusion: Stromal tetranectin expression is observed in the normal bladder and bladder cancer. The significance of this finding remains to be clarified.
The observed high cytoplasmic expression in invasive tumor cells suggests a potential role for tetranectin during invasion of bladder cancer.

P 371
MINICHROMOSOME MAINTENANCE PROTEIN (MCM) 2 AND 5 EXPRESSION IN MUSCLE INVASIVE UROTHELIAL CANCER : A MULTIVARIATE SURVIVAL STUDY INCLUDING PROLIFERATION MARKERS AND CELL CYCLE REGULATORS

KORKOLOPOULOU Penelope 1, GIVALOS Nikolaos 1, SAETTA Angelica 1,
GOUDOPOULOU Athina 1, GAKIOPOULOU Hariklia 1, THYMARA Irene 1,
DIAMANTOPOULOU Kalliopi 2, THOMAS-TSAGLI Euphemia 2, PATSOURIS Efstratios 1.
1 Department of Pathology, Athens University, Medical School, Athens GR 115 27 Greece
2 Department of Pathology, Asklepeion Voula Hospital, Athens GR 166 73 Greece

Minichromosome maintenance (MCM) proteins are components of the prereplicative complex and thus essential for eukaryotic DNA replication. Their presence only in proliferating cells suggests a role as a novel proliferation marker. There is no previous study investigating MCMs in muscle-invasive bladder carcinomas. We analyzed immunohistochemically the expression of MCM-2 and MCM-5 proteins in 65 patients with muscle-invasive urothelial bladder carcinomas, in relation with clinicopathological parameters, patients' overall and disease-free survival and the expression of the conventional proliferation index Ki-67 and other cell-cycle modulators (p53, pRb, p21WAF1 and p27Kip1).
MCM-2 and MCM-5 levels were significantly higher in high grade ($p<0.0001$), advanced stage ($p=0.001$) and non-papillary tumors ($p<0.0001$). MCM-2 and MCM-5 protein ex-pression significantly associated with the conventional proliferation index Ki-67 ($p=0.0001$ for each protein). MCM-2 or MCM-5 expression positively correlated with p53 labeling index ($p=0.014$ and $p=0.009$ respectively). Also median p21WAF1 labeling index was higher in MCM-5 high expressors ($p=0.028$). Finally, both MCM-2 and MCM-5 associated significantly with adverse patients` outcome in both univariate ($p=0.0072$ and $p=0.0074$ respectively) and multivariate ($p=0.0001$) analysis.
In conclusion, MCM-2 and MCM-5 proteins appear to be reliable proliferative indices and useful prognostic markers in patients with muscle-invasive urothelial bladder carcinomas.

P 372
QUALITATIVE AND QUANTITATIVE ANALYSIS OF ANGIOGENIC FACTORS IN TRANSITIONAL CELL BLADDER CARCINOMA: RELATIONSHIP WITH CLINICAL COURSE AT 10 YEARS FOLLOW-UP

NESI Gabriella1, BARTOLETTI Riccardo2, CAI Tommaso2, GIRARDI Lucia Roberta1, SARDI Iacopo3, RIZZO Michelangelo2, TADDEI Gian Luigi1
1Department of Human Pathology and Oncology, University of Florence, Italy; 2Department of Urology, University of Florence, Italy; 3Department of Paediatrics (Onco-Haematology Unit), University of Florence, Italy

Aims: Many authors have shown that tumour hypoxia exerts its own influence on malignant progression by inducing angiogenetic factors and new blood vessels toward and within the tumour. This event usually suggests poor prognosis and/or aggressive tumour behaviour. The objective of this study is to compare molecular analysis of angiogenetic factors with microvessel density (MVD) in bladder cancer.
Materials and methods: Twenty-nine consecutive patients underwent transurethral or open surgery for bladder tumours. Neoplastic tissue samples, normal-appearing bladder mucosa and blood samples were taken from each patient. All the tissues underwent mRNA extraction and Northern Blot analysis, marked with specific probes for inducible Nitric Oxide Synthase (iNOS), Cycloxygenase-2 (COX-2) and Vascular Endothelial Growth Factor (VEGF), and evaluated by gel-electrophoresis. MVD, a quantitative analysis for neoangiogenesis, was also evaluated by using CD31 immunohistochemical assay and compared with molecular analysis and patient follow-up. Two follow-ups for recurrence or progression were performed at 74 months and 10 years from surgery, respectively.
Results: Pathological evaluation demonstrated the presence of superficial transitional cell carcinoma (sTCC) in 15 patients, while 14 had an invasive bladder tumour (iBT). At both 74 months and 10 years follow-up, all patients with lower MVD had a shorter survival time. No significant results were obtained by comparing disease progression or survival rate with VEGF, iNOS and COX-2 levels. A proportional increase of VEGF expression and MVD associated with poor prognosis was the expected outcome of our study. These results were disregarded at both the first and the second follow-up. A strong correlation between MVD >20 and survival rate was noted both in sTCC ($p=0.024$) and iBT ($p<0.001$) patients.
Conclusions: These results confirm that MVD could be considered a good prognostic factor. The angiogenetic cytokine overexpression found in control tissue samples of sTCC could have clinical significance in either a macroscopically unidentified diffuse carcinogenetic process or a systemic immune response against tumour cells.

P 373
MICROSATELLITE INSTABILITY AND SOMATIC DOWN-REGULATION OF MISMATCH REPAIR CHARACTERIZE SOLID MUSCLE-INVASIVE

TRANSITIONAL CELL CARCINOMA OF THE BLADDER

Alfredo Blanes(1) and Salvador J. Diaz-Cano(1,2)
(1) University of Malaga School of Medicine, Spain
(2) King's College Hospital-GKT School of Medicine, London, UK

Background: Histologic patterns have been demonstrated prognostically useful in transitional cell carcinomas (TCC) of the bladder, but no information is available on the prognoistic significance and genetic profile of muscle-invasive TCC by infiltration pattern. The contribution of DNA mismatch repair abnormalities to this profile remains unknown.
Design: The predominant infiltration patterns of 72 muscle-invasive TCC was assessed in the deep compartment and classified as "solid" (diffuse infiltration effacing the muscle fibers, 45 cases) or "single-file" (tumor infiltration dissecting the muscle and inducing an intense stromal reaction, 27 cases). Tumors were studied by compartments (superficial and deep to muscularis mucosa), DNA being extracted from both compartments to analyze the microsatellite pattern of TP53, RB1, WT1, and NF1 by polymerase chain reaction-denaturing gradient gel electrophoresis. Mitotic indexs, Ki67 index, in-situ end labelling (ISEL) and DNA ploidy analyses were evaluated in the same areas. Statistical differences were tested using ANOVA and Fisher's exact test. Mismatch repair was assessed by mlh1 and msh2 sequencing and immunostaining in TCC with >2 abnormal microsatellite loci.
Results: Single file TCC showed lower cell turnover (Ki67 index 14.94±4.28, ISEL 14.1±10.0), lower incidence of aneuploid DNA content, and shorter mean survival (20 months) than solid TCC (Ki67 index 20.65±4.94, ISEL index 20.2±22.7, and 37-month survival, respectively).
The genetic profile was demonstrated significantly different for RB1 (p=0.0003) and NF1 (p=0.0023) only. Single-file TCC showed a low incidence of genetic deletions/single nucleotide polymorphism(s), not involving RB1 locus, and very occasionally NF locus (2 cases, 13%). A significant decrease of mlh1/msh2 protein expression (absence of any of these proteins) with no gene mutations were identified in TCC with high microsatellite instability and solid growth pattern.
Conclusions: 1. Somatic down-regulation of mismatch repair proteins (mlh1/msh2) in solid muscle-invasive TCC results in microsatellite instability characterized by deletion/single nucleotide polymorphism(s) in RB1 and NF1. 2. This microsatellite instability profile correlates with the higher cellular turnover (both proliferation and apoptosis) and longer survival observed in patients with solid TCC (as compared with those of single-file TCC).

P 374

CYTOKERATIN 20 EXPRESSION IN UROTHELIAL CARCINOMA OF THE BLADDER: A HIGH-THROUGHPUT TISSUE MICROARRAY ANALYSIS CONFRONTING THE PRIMARY TUMOR AND ITS METASTASIS.

C. Mallofré, M. Castillo*, A. Gaspa, A. Petit , E. Campo .
Dpt. of Pathology, Hospital Clínic de Barcelona i Hospital Universitari de Bellvitge*

Introduction
Cytokeratin 20 (CK20) expression has been reported in a high percentage of urothelial carcinomas (UC) of the bladder, with no clear correlation with stage or grade, and it has poorly been studied in metastatic carcinoma.
The aim of our study was to determine whether CK20 was consistently expressed in metastatic UC.
Material and Methods
We studied all the cistectomy cases performed in our department from 1995 until 2004 with a diagnosis of UC, and found 45 cases which had developed metastatic disease. A Tissue Microarray (TMA) was built with duplicates of 0,6 mm cores of the 45 primary UC and their metastasis (31 nodal, 4 pulmonary, 4 osseous, 4 peritoneal and 2 to the urogenital area). CK20 immunohistochemistry was performed on 5mm sections (clon Ks20.8, Dako, dilution: 1/400).
Results
CK20 was positive in 45,4% of the primary UC and in 42,9% of the metastasis. In 54% of the cases, primary and metastatic disease showed the same pattern of expression (23% both positive, 31% both negative), while in 19% of cases there was a loss of CK20 expression in the metastasis compared to primary tumor. Unexpectedly, 27% of the primary UC were negative for CK20 and their metastasis were positive.
Conclusions
CK20 is generally considered a good marker of UC of the bladder, specially in combination with CK7. In our series, less than half of the primary UC express CK20, probably owing to high-grade histology. Furthermore, there is a decrease of CK20 expression in metastatic disease compared to primary UC. We think that CK20 is a good marker of UC of the bladder, specially in combination with CK7, and specially in low-grade and low-stage UC.

P 375

EXPRESSION OF CELL CYCLE PROTEINS IN BLADDER CARCINOMA

A. Goussia (1), V. Kordela (2), E. Sintou-Mantela (1), A. Zioga (1), I. Panelos (1), A. Charchanti (3), S. Dimou (1), N.J. Agnantis (1), M. Bai (1)
Department of Pathology (1) and Department of Anatomy-Histology-Embryology (3), Medical faculty, University of Ioannina, Department of Pathology, General Hospital of Preveza (2), Greece

The cell cycle is known to be deregulated in cancer. We therefore analyzed the immunohistochemical expression of cell cycle related proteins p53, Rb, p21, p16, p27 and cyclin D1 in 128 cases of transitional cell bladder carcinomas. The proliferation status was determined by Ki67, cyclin A and cyclin B1 protein expression. The expression of the proteins was correlated with clinicopathological parameters.
High expression of p53, p21 and cyclin D1 proteins (>10% of neoplastic cells)was detected in 64.7%, 16.5% and 32.5% of the cases, respectively. Low expression (<10% of neoplastic cells) of pRb, p16 and p27 proteins was found in 55.65%, 22.10% and 9% of the cases, respectively. Expression of Ki67, cyclin A and cyclin B1 proteins was found in all cases. Significant positive correlations were found between a) p53 and p21, Ki67, cyclin A, cyclin B1, b) pRb and Ki67, cyclin A, c) p21 and cyclin D1, cyclin A, when their expression was compared as continuous variables.
The following combined p53/p21 expression patterns (p53 pathway) were observed: p53+p21+ (13.91%), p53+/p21- (53.04%), p53-/p21+ (3.48%), p53-/p21- (29.56%). The combined Rb/p16/cyclin D1 expression patterns (Rb pathway) were: Rb+/p16+/cyclin D1+ (9.63%), Rb+/p16+/cyclin D1- (25.3%), Rb+/p16-/cyclin D1- (3.6%), Rb+/p16-/cyclin D1+ (7.23%), Rb-/p16+/cyclin D1+ (15.67%), Rb-/p16+/cyclin D1- (26.5%), Rb-/p16-/cyclin D1- (10.84%), Rb-/p16-/cyclin D1+ (1.20%). A significant correlation was found between combined p53/p21 expression patterns and cyclin A (p=0.002) and cyclin D1 (p<0.0001) expression. Moreover, cyclin A expression was correlated with combined Rb/p16/cyclin D1 expression patterns(p=0.040).
High expression of p53, Ki67, cyclin A and cyclin B1 (>10% of neoplastic cells) was negatively correlated with the papillary morphology of the tumor (p=0.026, p<0.0001, p<0.0001 and p=0.001, respectively) and positively with tumor grade (p=0.014, p<0.0001, p=0.002 and p=0.027, respectively) and T-stage (p=0.014, p<0.0001, p=0.004 and p=0.025, respectively).

These results suggest that alterations of cell cycle regulatory proteins are common in bladder carcinomas and may act in cooperative or synergistic ways to promote tumor progression.

P 376
HER-2/NEU OVEREXPRESSION AND AMPLIFICATION IN METASTATIC UROTHELIAL CARCINOMA OF THE BLADDER.
M. Castillo, A. Gaspa*, A. Petit *, C. Mallofré*. Dpt. of Pathology, Hospital Universitari de Bellvitge i Hospital Clínic de Barcelona*

Introduction
Studies reporting Her2Neu expression, both immunohistochemical and by fluorescence in situ hibridization (FISH) have shown varying results: some authors have suggested that Her2Neu gene amplification rates are low, in comparison with protein overexpression. The pattern of expression of Her2Neu in metastatic disease has not been almost studied.
The aim of our study was to determine Her2Neu status by immunohistochemistry (IHC) and FISH in metastatic bladder cancer.
Material and Methods
We studied all the cistectomy cases performed in our department from 1995 until 2004 with a diagnosis of UC, and found 45 cases which had developed metastatic disease. A Tissue Microarray (TMA) was built with duplicates of 0,6 mm cores of the 45 primary UC and their metastasis (31 nodal, 4 pulmonary, 4 osseous, 4 peritoneal and 2 to the urogenital area). FISH was performed using the Pathvysion kit (Vysis, Abbott), and IHC was performed on 5mm sections (CB11, Ventana) and evaluated as 0, 1+, 2+, and 3+.
Results
Only 6% of the primary UC and 8,6% of the metastasis show amplification by FISH, and correspond to the 3+ results by IHC. 91,1% and 3% of the primary neoplasms and 80% and 11,4% of the metastatic tumors are IHC negative and show 2+ positivity for Her2Neu, but none of them are amplified by FISH.
Conclusions
Her2Neu is not frequently amplified in bladder carcinoma, not even in metastatic disease. All the cases with a 2+ IHC result are not amplified in our series, and perhaps the performance of FISH is not necessary in those cases.

P 377
IMMUNOHISTOCHEMICAL EXPRESSION OF UROPLAKIN-III IN PRIMARY BLADDER ADENOCARCINOMAS AND LESIONS WITH GLANDULAR PHENOTYPE.
HATZIANASTASSIOU Dimitris (1),(2), GIASLAKIOTIS Constantinos (1), ANDROYLAKI Athina (1), KARAMERIS Andreas (3), and DELLADETSIMA Johanna (1).
Department of Pathology, Laiko University Hospital of Athens, Greece (1)
Laboratory of Histology - Embryology, Medical School, National & Kapodistrian University of Athens, Greece (2)
Department of Pathology, Veterans Administration Hospital of Athens, Greece (3)

Introduction: Primary bladder adenocarcinomas (PBAs) represent a small fraction of bladder tumors (1-2%). Their differential diagnosis from other metastatic adenocarcinomas can be difficult on histological basis alone, and the combined use of Cytokeratin (CK) 7 & 20 does not always seem to resolve the problem. Relatively new, urothelial specific diagnostic markers, such as Uroplakin-III (UPIII), are commercially available for immunohistochemistry.
Purpose: To investigate the possible diagnostic value of UP-III immunohistochemical detection in PBAs, as well as, in a small number of lesions with true glandular differentiation, arising in the bladder.
Methods: Seven cases of PBA, one villous adenoma with mucin producing cells and two cases of enteric type urothelial metaplasia were retrieved from our files. The material was re-evaluated and stained with monoclonal antibodies against CK7, CK20 and UPIII using appropriate positive and negative controls, according to standard procedures. A streptavidin-biotin based detection system was employed, using diaminobenzidine as chromogen. The staining reaction was assigned semiquantitatively; the cut-off point was set at 5%.
Results: Regarding the panel of CK7/20 four PBAs were (+/+); one (+/-); two (-/+). The adenoma and the metaplastic lesions were (+/+). UPIII was positive in almost all cases (9/10), including (6/7) PBAs regardless of their histologic subtype. The staining pattern was cytoplasmic with focal membrane accentuation. The staining intensity and the percentage of positive cells were variable.
Conclusions: UPIII seemingly represents a valid, constant diagnostic immunohistochemical marker for PBA and can contribute to their differential diagnosis, providing evidence for their urothelial origin, even in cases with frankly enteric phenotype.

P 378
LOH AND FISH ANALYSIS FOR THE DETECTION OF BLADDER CANCER FROM VOIDED URINE SPECIMENS: A PRELIMINARY STUDY REPORT
FRIGERIO Simona (1), PADBERG Barbara (1), STREBEL Räto (2), LENGGENHAGER Daniela (1), MESSTHALER Angelika (1), ABDOU Marie-Therèse (1), MOCH Holger (1), JOHN Hubert (2) and ZIMMERMANN Dieter (1)
Department of Pathology (1), and Department of Urology (2), University Hospital Zürich, Switzerland

Introduction: Successful treatment of bladder cancer depends largely on early detection of primary and recurrent disease. As cytology alone is too unreliable to serve as a basis for therapy decision, improved laboratory tests are needed. Today, loss of heterozygosity (LOH) and fluorescence in situ hybridization (FISH) are the most promising assays to detect early tumor-specific genetic alterations in cytological specimens. We chose to set up and validate a LOH method, which involves analysis at 10 microsatellite loci on chromosomes 8p, 9q, 9p, 13q, 16q and 17p. Ambiguous cases were additionally analysed by FISH.
Methods: Matched biopsies and urines from patients scheduled for tumor resection were collected prospectively and examined by routine histology and cytology. LOH analysis was performed using fluorescence-labeled primers and capillary electrophoresis. FISH analysis was done according to the manufacturer's recommendations (UroVysion, Vysis).
Results: Preliminary analysis were performed on 62 urine samples from patients with histological confirmed diagnosis of bladder cancer (carcinoma in situ pTis: 8; non-invasive papillary pTa: 10 G1, 22 G2, 3 G3; invasive papillary pT1: 2 G2, 9 G3 and pT2: 8 G3). Chromosomal aberrations were detected in 47 urine samples (76%), while 15 were LOH negative (mostly pTa G1-2 tumors). Remarkably, the sensitivity of LOH for low grade tumors (G1-2) was superior to cytology (69% vs. 26%). Most genetic aberrations were associated with losses at 9p and 9q, confirming a pivotal role of these regions for bladder tumorigenesis, while LOH on chromosome 8p, 13q, 16q and 17p rather correlated with advanced tumor grade and stage. To date, FISH analysis was performed on 13 urines. There were 10 histologically positive carcinoma cases (2 pTa G1-2, 2 pTa G3, 3 pT1-2 G3 and 3 pTis), of which 7 exhibited chromosomal instabilities, while 3 were scored as normal. Out of 3 histologically tumor-free cases, 2 were FISH-negative and 1 FISH-positive. Comparing

the two methods, identical LOH and FISH positive as well as negative results were documented in 7 histologically corresponding cases. Clinical follow-up is currently ongoing for the other 6 ambiguous cases.
Conclusions: Preliminary data show that both LOH and FISH analysis improve the sensitivity of voided urine specimens for the detection of bladder cancer.

P 379
DETECTION OF PRIMARY UROTHELIAL CARCINOMA IN VOIDED URINE SPECIMEN USING FOUR PROBE FISH ASSAY COMBINED WITH AUTOMATED MICROSCOPIC SYSTEM, A PROSPECTIVE STUDY

PAJOR Gábor(1), KNEIF Maria(1), CSALA Judit(1), FARKAS László M.D.(2), SOMOGYI László M.D.(2), PAJOR László M.D.(1), SÜLE Norbert M.D.(1)
(1) Department of Pathology, University of Pécs Medical School
(2) Department of Urology, University of Pécs Medical School

INTRODUCTION: The gold standard to diagnose urinary cancer is urinary cytology combined with cystoscopy. The low-grade urothelial cancer and early detection of recurrences are the greatest diagnostic challenges and many attempts are made to make the urinary cytology screening more sensitive and specific especially in these two critical cases. The literature is flooded with different methods including different immunologic and genetic testings like microsatellite instability assays and FISH. It seems that FISH assays will play an important role in the future in the cytology laboratory.
PURPOSE: Determination of the effectiveness of an automated microscopic system in the detection of chromosomal changes in uroepithelial cancer.
METHODS: We have analyzed 19 patients with primary uroepithelial cancer. Conventional urinary cytology coupled with cystoscopy and biopsy in each case was performed. From the collected voided urine we have analyzed three preparations processed with three methods. After optimizing the cell count in cyto-chamber we used the alcohol fixed specimen for FISH analysis. The preparations were evaluated by Zeis Axioplan2 automated microscope combined with Metasystem/Metacyte-Metafer4 software and/or manually counted (150-300 cells).
RESULTS: Histologically evident uroepithelial carcinoma was present in 16 cases (grade I/II/III: 3/8/5 respectively). The cytology evaluation of the voided urine specimen could prove the presence of neopastic cells in 10 cases (62.5%) and was suspicious in 4 cases (25%). One result was negative and one was unsatisfactory. Automated detection system could identify surprising number of chromosomal abnormality even in histologically negative cases (average 31 cell; 7.81%). The number of cells carrying chromosomal abnormality was significantly lower in low grade vs. high grade tumors (G1:45 cells; 5,18% vs.G2:248,5; 16,77% and G3:146,8; 17,39%). Similar correlation could be observed in in situ vs. invasive (pTa:78 cells, 7,41%;vs. pT1:272,67, 19,67%; pT2:102,5, 16,3%). The control manual counts gave similar results.
CONCLUSION: Using Zeis Axioplan2 automated microscope combined with Metasystem/Metacyte-Metafer4 software is a powerful method to detect chromosomal changes in voided urine cytology specimen. The criteria defining positive diagnosis need to be adjusted, because the original Urovysion criteria was established on manual evaluation which required only the presence of 25 morphologically abnormal cells.

P 380
LIMPHOEPITHELIOMA-LIKE CARCINOMA OF THE BLADDER. CASE REPORT AND REVIEW OF THERAPEUTIC MANAGEMENT

TERRASA fernando, GARCÍA magdalena, ARRIVI antonio, REBASSA miguel.

Introduction
Lymphoepithelioma-like carcinoma (LELC) of bladder is an extremely rare tumor. In the bladder, Zuckerberg and col. first describe this tumor as a part of a series of carcinoma simulating lymphoma. The origin of this tumor is unknown although it is suspected that it originates from modified urothelial cells. Initially it was classified as a neoplasm with a poor prognosis, but actually it is recognized its sensitivity to chemotherapy and a more long-term prognosis when compared with other types of carcinomas of bladder of equivalent stage and grade.
Case report
We present, a case of LELC diagnosed and treated at our Institution. The case is that of a 70 years old male with two years history of hematuria. A transurethral resection (TUR) of the bladder tumor was carried out after multiple inconclusive imaging studies, cystoscopy and urine cytologies. The histologic diagnosis of LELC with tumor infiltration of the muscle layer, led to 4 cycles of chemotherapy treatment with cysplatin and ethoposide based regimens, and no additional surgical interventions. 18 months later, the patient was well and free of disease.
Results and conclusion:
Microscopically, the tumor showed a neoplastic cell proliferation composed of sheets and nests of atypical cells with scarce eosinophilic cytoplasm and large vesicular nuclei with prominent nucleoli and numerous mitosis. The tumor invaded into the muscle layer of the bladder, and was accompanied by a prominent inflammatory reaction. The bladder mucosa was focally ulcerated, and we did not identify areas of carcinoma in situ or conventional bladder carcinoma elsewhere. Immunohistochemically, tumor cells showed strongly positive cytoplasmic staining for Keratin (CK) AE1/AE3 and epithelial membrane antigen; and were focally positive for CK 7 and 8. Neoplastic cells were negative for CK 20. Immunostaining for Epstein-Barr virus was negative. All these findings are concordant with those of reported LELC cases in this location. Invasive LELC of bladder, according to the criteria of Amin et al., are classified as pure (all lymphoepithelial elements), predominant (more than half) or focal (less than half). It is well established that the two first types, are tumors that respond well to chemotherapy. It is important to recognize these tumors, and distinguish them for conventional transitional tumors with focal LELC differentiation, in order to administrate appropriate treatment and avoid cystectomy in these patients.

P 381
PRIMARY SMALL CELL NEUROENDOCRINE CARCINOMA OF THE URINARY BLADDER : AN IMMUNOHISTOCHEMICAL STUDY OF 15 CASES.

TRIAU Stéphane(1), KOFFI Emmanuel(1), LAVOINE Eric(2), JOSSELIN Nicolas(1), SAINT-ANDRE Jean-Paul(1), ROUSSELET Marie-Christine(1).
(1) Department of Pathology, University Hospital, 4 rue Larrey, 49933 Angers Cedex 09 France. (2) Pathology Center, 2 rue de l'Appentis, 49022 Angers, France.

Introduction : Primary small cell neuroendocrine carcinoma (SCC) of the urinary bladder is a very rare entity (0.5% of urinary bladder tumors). Its morphology may overlap with poorly differentiated urothelial carcinoma but SCC must be clearly distinguished because of differences in treatment and prognosis. We investigated the immunohistochemical expression of epithelial growth factor receptor (EGFR) and some other markers in a series of 15 SCC.
Methods : We studied synaptophysin, CD56, chromogranin A and B, cytokeratin (34betaE12) p16, p53 and EGFR reactivity in 15 consecutive cases diagnosed between 1990 to 2005 on

transurethral resection (9 cases), radical cystectomy (1 case) or both (5 cases). Ten cases were fixed in formalin, 5 in Bouin's fluid.
Results : In 13 cases (87%), the SCC was associated with an urothelial carcinoma which was a minor component in all but one case and was invasive in 8 cases, in situ in 2 cases or both in 3 cases. A reactivity with 2 or more neuroendocrine markers was observed in all cases. Synaptophysin was positive in all cases, CD56 in 13 cases (87%), chromogranin A in 12 cases (80%) and B in 9 cases (60%). 34betaE12 was always negative on SCC but was expressed by the urothelial carcinoma component while p16 was positive on both components in all cases. All tumors fixed in formalin presented a high expression of p53. Nine SCC (60%) expressed EGFR in at least 5% to more than 50% of cells.
Conclusion : In poorly differentiated tumors of urinary bladder, neuroendocrine markers must be used with 34betaE12 to differentiate SCC from poorly differentiated urothelial carcinoma. As in small cell carcinoma of the lung, we found an over-expression of p53 and p16 that might be related to a disruption of the Rb pathway. EGFR is expressed in a majority of SCC of the urinary bladder thus suggesting a possible therapeutic role for EGFR inhibitors.

P 382
NEUROENDOCRINE DIFFERENTIATION IN PRIMARY ADENOCARCINOMAS OF THE URINARY BLADDER
BOLLITO Enrico °, PACCHIONI Donatella*, VOLANTE Marco*, DE POMPA Roberta°, CAPPIA Susanna°, LOPEZ-BELTRAN Antonio§, PAPOTTI Mauro°
Divisions of Pathology of °San Luigi Hospital, University of Turin, Orbassano, *San Giovanni Hospital, Torino, Italy, and §Reina Sofia Hospital, University of Cordoba, Spain.

Indroduction: Adenocarcinoma (AC) of the bladder is a rare entity and has several architectural variants: the “enteric-type” is the most common one and shares morphological and immunophenotypic features with conventional colorectal carcinoma. Although the occurrence of neuroendocrine (NE) differentiation in ACs from various sites, lung, colon and prostate, among the most relevant has been widely reported, in the bladder only rare case reports have been documented. cells, as known in colorectal, prostatic (but not in urothelial) carcinomas, among others.
The purpose of this study was to investigate the occurrence of NE differentiation in bladder AC and non–neoplastic glandular lesions.
Methods: Sixteen primary bladder ACs (6 urachal) and 4 urothelial carcinomas with glandular differentiation (UGCC) were collected. The UGCC had high grade urothelial carcinoma areas admixed with enteric-type glands (5-80% of the tumor). ACs were subclassified into enteric-type (7), mucinous (6) and NOS (3 cases) variants. To classify a case as “urachal adenocarcinoma” we applied the criteria proposed by Johnson and coworkers [1985]. In addition 20 glandular cystitis, 3 urachal cysts, 15 urothelial carcinomas and 3 small cell carcinomas were also collected as control groups. NSE, synaptophysin and chromogranin A immunostainings were performed. Clinico-pathological and outcome data were available for all but one case.
Results: Panendocrine markers gave heterogeneous results: NSE was negative, synaptophysin was focally positive in two cases, and chromogranin-A revealed NE differentiated cells in 12/20 cases (60%) (all enteric-type and mucinous carcinoma variants). All urachal cysts and 70% of glandular cystitis also had chromogranin-A reactive cells. Control urothelium and urothelial carcinomas (but not 3/3 small cell carcinoma) were chromogranin-A negative. No correlation was found between NE differentiation and clinical (including outcome) or pathological parameters. At follow up, 50% of patients had fatal outcome. In patients died of disease, the mean survival was 40 months (ra

P 383
PARAGANGLIOMA OF THE URINARY BLADDER: REPORT OF THREE CASES
KILICASLAN Isin*, OZTURK A. Sanem*, MIROGLU Cengiz**, BOZBORA Alp***, UYSAL Veli*
*Istanbul University, Istanbul Faculty of Medicine, Department of Pathology
**Sisli Etfal Training and Research Hospital, Department of Urology
***Istanbul University, Istanbul Faculty of Medicine, Department of General Surgery

We present three cases of urinary bladder paraganglioma. One of them is a tumor resection of a patient with typical micturition attacks. The other two are transurethral resection materials consultated to our department. One of these two patients was diagnosed as urothelial carcinoma and the other one was diagnosed as adenocarcinoma and urothelial carcinoma in two different pathology departments. As we learned later, one of these patients had an hipertension attack during the biopsy procedure.
Microscopical examination of all three cases revealed the typical cellular and vascular arrangement of paragangliomas. Focal pleomorphism was remarkable in one of the cases. Submucosal invasion was detected in the transurethral resection materials. In the partial cystectomy material the tumor was located in the muscular layer. The negative immunohistochemical reaction of the tumor cells with pancytokeratin, cytokeratin 7 and cytokeratin 20 helped to rule out urothelial carcinoma. The tumor cells showed diffuse immunoreactivity with chromogranin A, synaptophysin and neuron specific enolase and the sustentacular cells stained positive for S100 protein. Based on these immunohistochemical findings we diagnosed the tumors as paraganglioma. The Ki67 proliferation index of the tumors were 1-2%.
The invasion of lamina propria and the muscular layer of paragangliomas is the misleading point of the transurothelial resection materials. The pathologist must take paraganglioma into consideration in the differential diagnosis of these materials not to miss out the cases.

P 384
PARAGANGLIOMA OF URINARY BLADDER
GHAINI M.Hossein, FROOTAN Kazem, SAKI Soheil

Urinary bladder is a rare site of paraganglioma. We describe a paraganglioma of the urinary bladder in a 51-year-old female who presented with painless gross hematuria. Abdominal ultrasonography revealed a protruding well-defined mass, about 3Cm. in diameter over the left lateral wall of the urinary bladder. The tumor was not completely resected by transurethral resection of bladder tumor (TURBT) due to involvement of the bladder wall. Histologic examination of the tumor indicated clustersof polygonal chromaffin cells, arranged in nests (zellballen). Although there was marked pleomorphism and atypia in nuclei, no evidence of recuurence or metastasis has seen since about 1 year. There is no reliable method for predicting their clinical behavior, so long-term follow-up is required. We also provide a brief review of the literature for comparison.

P 385
SARCOMATOID TRANSITIONAL CELL CARCINOMA OF URACHUS:A CASE REPORT
SETARESHENAS Roya,AZIZI Rasoul,
Assistant Professors of Iran Medical Science University.

Tumors of urachus duct which is remnant of embryonic

allantoic duct are rare.We report a case of transitional cell carcinoma of urachus in a 54 Y/O man with chief complaint of abdominal wall mass.The mass had adhesion to anterior abdominal wall and also extension to dome of bladder.By operation the mass and small part of wall of bladder were excised.

Cut section of mass showed a cyst inside,with tumoral lesion around.Histilogically the tumor was transitinal cell carcinoma of variable degrees and also sarcomatoid pattern in some areas.Smooth muscles of urachus wall and also bladder wall were invaded by tumor,but surgical margins and two detected lymph nodes were free.

It seems that this patient is the first reported case of sarcomatoid carcinoma of urachus.

P 386

SARCOMATOID TRANSITIONAL CARCINOMA OF URACHUS(A CASE REPORT)

SETARESHENAS Roya,AZIZI Rasoul

Urachus duct which is remnant of embryonic allantois duct,may show neoplastic lesions rarely.The most common tumor of urachus is adenocarcinoma,but squamous cell carcinoma and transitional cell carcinoma(TCC) has also been reported.

We report a case of sarcomatoid TCC of urachus in a 54 year old male who presented with abdominal wall mass.

Abdominal CT-Scan and sonography detected a mass in lower abdomen between umbilicus and symphisis of pubis with minor attachment to bladder.Cystoscopy was normal.

Operation consisted of exicion of mass and small part of bladder wall.Cut section of mass showed a cyst inside with tumoral lesion including necrosis around,surrounded by muscular and fatty tissues.

Microscopically the tumor was TCC with variable degrees and also sarcomatoid patterin some areas. Smooth muscle of urachus and bladder wall were invaded by tumor but striated muscles,surgical margins and 2 detcted lymph nodes were free.

It seems this is the first reported case of sarcomatoid carcinoma of urachus.

P 387

HISTOPATHOLOGIC ASSESSMENT OF ANGIOGENIC RESPONSE IN DIFFERENT URINARY BLADDER LESIONS.

NOSSEIR Mona, AKL Maha.
Pathology Department. Theodor Bilharz Research Institute

This study was designed to evaluate the angiogenic activity in chronic bladder lesions (chronic cystitis and schistosomal cystitis) in comparison to bladder tumors, as well as its relation to the stage of invasiveness of bladder carcinoma. The pattern and state of vascularization of bladder lesions could provide novel therapies using anti-angiogenic agents.
Methods: The current study included 75 cases of urinary bladder lesions representing 12 cases of chronic non-specific cystitis, 12 cases of schistosomal cystitis, 31 cases of transitional cell carcinoma (TCC), 13 cases of squamous cell carcinoma (Sqcc), 7 cases of urothelial dysplasia; in addition to 5 control cases of apparently normal bladders. All cases were first diagnosed and studied by hematoxylin and eosin. Then all were assessed for the expression of both basic fibroblast growth factor (bFGF); within epithelial cells, endothelial cells, fibroblasts and macrophages, and Factor VIII-related antigen (von Willebrand Factor ,vWF); delineating endothelial cells at the wall of blood vessels, using a standard immunohistochemical technique. Positive expression for bFGF was scored as 3+,2+&1+, while microvascular density (MVD) was calculated through counting the microvessels positively stained for Factor VIII-related antigen in five successive hot spots. Results: Expression of bFGF and MVD were significantly higher in malignant bladder cases, especially in advanced stages, compared to chronic cystitis cases. Schistosomal cystitis cases showed marked angiogenic activity. Conclusion: High angiogenic response in non-invasive early stage of bladder cancer could predict recurrence and metastatic potentiality. Tumor invasive capability is directly correlated to the increase in its angiogenic activity. Marked angiogenesis in schistosomal cystitis could provide a favorable environment for tumorigenesis, thus they are commonly recorded in association.

P 388

ADENOCARCINOMA OF THE URINARY BLADDER ASSOCIATED WITH SCHISTOSOMIASIS IMMUNOHISTOCHEMICAL PROFILE

NADJI mehredad**, SHOMAN sohair*, EISSA saad*, NASSIRI mahdy**.
Departments of Pathology, NCI, Egypt* and University of Miami, Florida, USA**.

INTRODUCTION
Primary nonurachal intestinal adenocarcinomas of the urinary bladder are frequently associated with chronic irritation of bladder mucosa and a background of intestinal metaplasia and/or intestinal type cystitis glandularis.
PURPOSE OF THE STUDY
The morphology and immunophenotype of 102 cases of bladder adenocarcinoma associated with schistosomiasis were reviewed, and special attention was paid to the presence of associated metaplastic or preneoplastic changes.
MATERIAL & METHODS
One hundred two partial or radical cystectomy specimens performed at the National Cancer Institute, Cairo, Egypt with the diagnosis of primary adenocarcinoma were studied. Biographic data and clinical information including clinical stage, type of therapy and follow-up were reviewed. The histopathology of tumor, pathologic stage and variation in cell type was recorded in all samples. Special attention was paid to the status of non-involved bladder mucosa for the presence of intestinal metaplasia and/or cystitis glandularis. Five representative paraffin blocks from each case were selected for immunohistochemical studies.
Four micron paraffin sections were stained by a standard labeled streptavidin-biotin method using antibodies against cytokeratin 7 and cytokeratin 20 (M7018 and M7019), p53 (M3566), HER-2/ neu (A0485) and Cathepsin D (A0561) [DakoCytomation, Carpinteria, CA], heat-induced antigen retrieval using citrate buffer in a vegetable steamer. DAB was used as chromogen in the presence of hydrogen peroxide. The presence, pattern and intensity of immunohistochemical reactions were evaluated in both tumor cells and in non-neoplastic epithelium.
RESULTS
The tumors occurred predominantly in trigone, lateral, or posterolateral walls. None of the tumors involved bladder dome or the anterior wall. The study cohort consisted of 64 male and 38 female patients (male-female ratio, 1.7:1.0) ages 25 to 78 (mean, 50.3 years). Most frequent presenting symptoms were hematuria and irritation. In all patients, partial or radical cystectomy was performed followed by radiation therapy. The clinical stage of disease and the follow up data are as follows; 73 patients (72%) presented with advanced disease (T3 and T4), 56 of whom (78%) were either dead from the disease or alive with cancer during the 36month follow up period. Five patients with the predominant signet ring cell type adenocarcinoma were all dead of the disease in less than 15 months after the diagnosis.

P 389

PREVALENCE OF P53 AND KI-67 IMMUNOREACTIVITY IN CHRONIC URINARY BLADDER LESIONS

BADAWY Afkar, NOSSEIR Mona,and MOUSSA Mona.
Pathology Department, Theodor Bilharz Research Institute.Cairo,Egypt.

Early detection of alterations affecting p53 and/ or ki-67 control pathways will affect the clinical course of the disease and tumor progression.
The aim of this study was to investigate the expression of mutant p53 oncoprotein and the proliferative marker ki-67 in a series of non-neoplastic and neoplastic urinary bladder lesions with or without schistosomal infection using immunohistochemical staining on formalin-fixed, paraffin embedded sections. Its relation to traditional prognostic indicators (grades and stages) of malignant lesions was assessed.
Cystoscopic biopsies from (66) cases, received in the Pathology Department of TBRI were examined including; 22 cases of chronic cystitis (16 were schistosomal in etiology and 10 were associated with premalignant changes) and 44 cases of malignancy (34 cases of transitional cell carcinoma (TCC) and 10 cases of squamous cell carcinoma (SqCC)). Four normal controls were also added. Grades and stages of malignant cases according to World Health Organization Scheme were studied in sections stained with Hx.&E.. Scoring of the immunohistochemical nuclear expression of p53 and ki-67 for all cases was performed . Results were compared with those of control bladder specimens. Nuclear staining for p53 could not be detected in normal urothelium or in cases with cystitis (whether bilharzial or not) , but it was expressed in presence of premalignanant changes with significant over-expression in bilharzial versus non bilharzial cases. p53 over-expression accentuated in malignant lesions and correlated with upgrading of malignancy. Ki-67 was variably expressed in hyperplastic urothelium of cystitis cases, over-expressed in premalignant and malignant lesions with significant correlation to schistosomal association in malignant cases, to grade of tumor differentiation, and to p53 overexpression.
Assessment of both markers can yield prognostic information that is more powerful than what behavior alone can provide.

P 390

E-CADHERIN AND EPITHELIAL MEMBRANE ANTIGEN EXPRESSION IN SCHISTOSOMAL URINARY BLADDER LESIONS .

BADAWY Afkar and HAMMAM Olfat.
Department of Pathology, Theodor Bilharz Research Institute. Cairo, Egypt.

Urothelial immunohistochemical tissue expression of the epithelial cell-to-cell adhesive molecules: E-cadherin and Epithelial Membrane Antigen (EMA) were assessed in 66 cases with chronic urinary bladder lesions (benign, premalignant, and malignant) with or without schistosomal infestation to estimate a possible role of schistosomiasis in disruption of these adhesive antigens with its consequent relationship to pathological prognostic features of bilharzial related bladder carcinoma versus non bilharzial one. Normal urothelium expressed E-cadherin and EMA as uniformly membranous immunostaining of high intensity, localized to epithelial cell membranes. The staining intensity of both E-cadherin and EMA declined in chronic non specific cystitis, with significant limitation in extent of positively stained urothelial cells in chronic schistosomal cystitis. In advance, both antigens were expressed in a heterogenous pattern with loss of staining in basal urothelial layers and its preservation in superficial cells in cystitis cases with dysplastic changes. In malignant cases, the extent and intensity of staining of both antigens significantly diminished with alteration of their membranous immunoreactivity into heterogenous staining pattern and even cytoplasmic or nuclear accumulation which was more evident in T.C.C than in Sq.C.C cases. Upgrading and invasiveness of malignancy correlated with changing pattern of expression of E.M.A and E-cadherin, and with loss of urothelial positivity extent and intensity of E-cadherin rather than EMA. Schistosomal association in malignant cases correlated with more diminution in staining intensity of both antigens, and with advanced alteration in their pattern of expression which may facilitate tumor invasiveness and explain presentation of schistosomal associated cancer bladder at advanced stages.

In conclusion, it is the altered expression of E-cadherin and EMA that reflect neoplastic urothelial process rather than percentage of stained cells or their staining intensity. Schistosomal cystitis progressively minimize EMA and E-cadherin secretion than do non specific cystitis with advanced alteration in their expression pattern when complicated by malignancy process versus non schistosomal related bladder malignancy. Assessment of E-cadherin and EMA immunoreactivity may be a useful histologic prognostic marker in schistosomal cystitis and schistosomal related cancer bladder.

P 391

COMPARATIVE PATHOLOGIC ANALYSIS OF RENAL NEOPLASMS DEVELOPED IN PATIENTS WITH ERDS AND BACKGROUND RENAL CHANGES

SULE Norbert, YAKUPOGLU Ulkem, SHEN S. Steven, KRISHNAN Bhuvaneswari, TROUNG D. Luan

INTRODUCTION:
Patients with end-stage renal disease (ESRD) show increased incidence of acquired cystic kidney disease (ACK) and development of renal tumors. In a recent study demonstrated prominent calcium oxalate (CO) deposition in these carcinomas.
PURPOSE:
Complete phenotypic and immunologic profiling of benign and malignant neoplasm and determination the extent of CO deposition in the tumors and parenchyma.
METHODS:
We performed a retrospective analysis in a 13-year period to identify ACK-associated renal neoplasms. We compared the main pathologic features, immunologic profile and proliferative rate of the malignant and benign tumors. The severity of CO deposition was semiquantitated (0-4+) under polarizing microscope. RCC Marker, CD10, EMA and kidney specific cadherin (KSC) stains were performed and the intensity was graded (0-4+). The number of proliferating cell was determined by Ki-67 in 10 high power fields.
RESULT:
We identified 30 renal cell carcinomas with background changes of ESRD. Two histologic appearances were dominant: clear cell carcinoma (13, 43.33%) and oxalate type (8, 26.67%). We also identified 4 papillary (13.3%), 1 chromophobe (3.33%) and 1 sarcomatoid carcinoma (3.33%). Three tumors were necrotic and were not classified in either group. CO deposition was present in 8 neoplasms. Immunologic profile of the clear cell and the 3 necrotic tumors, which probably represented also clear cell carcinoma judged by the residual morphological features, showed EMA positivity (>3+; 76.92% and 100%, respectively); oxalate and sarcomatoid type had dual expression of RCC marker (>3+; 62.5% and 100%, respectively) and CD10 (>3+; 100% both). Papillary carcinoma expressed strongly EMA (4+; 100%) and had and intermediate CD10 intensity (2+; 100%). Chromophobe type displayed a combined expression of EMA and KSC (4+ each). No increased mitotic activity was detected. In the kidneys we identified 21 adenomas: one necrotic and 20 with either oxalate (8, 38.09%) or papillary phenotype (12, 57%). CO was identified in 4 cases, all associated with oxalate phenotype. Cystic changes were

present in all kidneys and combined with CO crystals in 11 cases.
CONCLUSION:
CO deposition in ACK-associated renal lesions is common. Distinct, recently described tumor morphology is evident, which defies the current classification. Proximal tubular cell differentiation in conjunction with ESRD-mediated high serum level of CO may be important in the pathogenesis

P 392
MORPHOLOGIC, ULTRASTRUCTURAL AND HISTOCHEMICAL STAINING CHARACTERISTICS OF CHROMOPHOBE RENAL CELL CARCINOMAS

Bahram Shahgoli(1), Natasha Djurdjevic(2),Slobodan Bojovic(2)
Department of pathology, University Clinical-hospital center "Zvezdara" Belgrade,Serbia&Montenegro

Morphologic, ultrastructural and histochemical staining characteristics of
Chromophobe Renal Cell Carcinoma
Introduction: Approximately 5% of renal cell carcinoma in surgical series are chromophobe renal cell carcinoma.It is rare in the first two decades of life.Althought obesity,smoking,hypertension and exposure to industrial chemicals have been implicated as risk factors in the genesis.An association with von Hippel-Lindau disease is seen in occasional cases.Associations also exist with tuberous sclerosis and autosomal dominant polycystic kidney disease.The genetic hallmark of chromophobe renal cell carcinoma is the loss of multiple chromosomes.
Case: 70 years old male presented with complaint of hematuria and pain in the flank.Ultrasonography and computerized tomographic scan show a solid mass in the left kidney.The diagnosis was obtained of the hematoxylin and eosin (H&E), histochemical stained slides and ultrastructural findings..
Results: On gross examination a well –circumscribed,solid tan mass is identified.Microscopically ,characterized by mosaic pattern composed of large and small cells with reticular cytoplasm,well-defined thick cytoplasmic membranes.The Hale's colloidal iron stain colors the cytoplasm blue.Ultrastructurally,the cytoplasm of chromophobe cells is crowded with many small vesicles.
Conclusion: The eosinophilic variant of chromophobe cell renal cell carcinoma was recognized.This variant shares the ultrastructural and colloidal iron staining features of the typical variant but in H&E stained slides often closely resembles renal oncocytoma.For this reason,it is worthwhile routinely to collect specimens for electron microscopy from renal tumors,especially those which do not have the yellow color characteristic of clear cell renal cell carcinoma.

P 393
YOLK SAC TUMORS : A REPORT OF 9 CASES
MNIF Hela, KHABIR Abdelmajid, AYADI Lobna, GHARIANI Mekki, BAHLOUL ALI, BOUDAWARA SELLAMI Tahya

Introduction
A single institution review of epidemiological, clinico-pathological and immunocytochemical features, and prognosis of yolk sac tumor
Materiels and Methods
We report a retrospective study performed of 9 cases of yolk sac tumor accessioned at the pathologic anatomy and cytology laboratory of the University Teaching Hospital of Sfax between 1983 and 2003.
Results:
Presentation occurred at a median age of 18 months (range 8 months to 24 months).The interval between children¡¯s first symptoms and diagnosis was 2,2 months (rang 1 to months). Clinical presentation occurred most often (88, 88%) with testicular lump. Seven patients had stage I and two patients had stage II according to the Baden classification.
The anatomopathological study confirmed the diagnostic. The germinal testicular tumor presented a structors that showing the yolk sac of the human embryon. Two pathognomical histological signs were most often presents (66, 66): the Schiller Duval body and hyaline globules. The immunohistochemical study showed that this tumor over expressed the ¦Á-foetoprotein (AFP) in 100% of the cases. The radical orchidectomy was indicated in all cases. It was associated with chemotherapy in advanced tumors.
Prognostic factors included age, clinical stage, rate of AFP, vascular or lymph node involvements, local extension, tumor¡¯s size, proliferated molecular factors = AND¡¯s index, proliferated cellular nuclear Antigen PCNA, ki 6l and molecular genetically factor= oncogen hst-1
Conclusion:
The testicular tumors in pr¨¦pubertal children and especially the yolk sac tumors have an excellent prognosis the overall 5 years survival range 95 to 100%.
Prospective study will be effective to establish a therapeutical consensus between differents equips.

P 394
TWO UNUSUAL SITES OF SOLITARY FIBROUS TUMOR (SFT)
TANOGLIDI Anna*, SAMARAS Vasilis*, ABOU-ASABEH Lydia*, AGELIDIS Panagiotis**, POULIAS Hercules**, KATSIFOTIS Charilaos***, BARBATIS Calypso*.
Hellenic Red Cross Hospital,Department of Pathology* and Urology**.
Polycliniki, Department of Urology***.
Athens,Greece.

INTRODUCTION
Solitary fibrous tumor is a rare spindle-cell neoplasm of uncertain histogenesis and with potentially aggressive behaviour.It usually arises on serosal surfaces with infrequent involvement of other sites.Renal and paratesticular SFTs are extremely rare and only 9 intrarenal,intrapelvic and parapelvic and 3 paratesticular cases have been reported in the international literature respectively.
AIM
Two cases of SFTs,one large renal and one paratesticular are reported with review of the literature and emphasis on the differential diagnosis from other mesenchymal or epithelial spindle cell neoplasms.
MATERIALS - METHODS
Case 1.A 79 years old man was operated for an asymptomatic solid tumor of the left kidney at CT-scan.The tumor was 12 cms in greatest diameter,well circumscribed,round,with smooth surface,firm consistency,whorled appearance and grey-white in colour with hemorrhagic areas without involvement of the pyelocalycic system.
Case 2.A 27 years old male had a palpable,nodular,painless left intrascrotal mass.At operation,a well circumscribed 3 cms binodular tumor between the tunica vaginalis and the dartos was removed.Sections were examined with H+E,PAS,PAS-D and the immunophenotype was determined with the Envision-HRP method for the detection of MCK,Vimentin,Desmin,a-SMA,CD31,CD34,CD99,CD68,Bcl-2,HMB-45,GFAP,NSE,NF,Ki-67 and C-kit.
RESULTS
Both tumors were encapsulated,non-invasive,composed of spindle cells with storiform,diffuse or fascicular growth pattern of varying cellular density and scattered wide collagen bundles.The renal tumor at the centre was vascular with loosely arranged cells and an atypical mitosis.Additional features:myxoid areas with scattered multinucleated cells,a marked chronic perivascular inflammation and focal

hyalinization of the vascular walls.The neoplastic cells of both tumors were Vimentin,CD34 and CD99 positive.Bcl-2 expression was either diffuse in the paratesticular SFT or reduced/absent in the central vascular area of the renal SFT.NSE and CD68 focal positivity was observed in the paratesticular SFT.Ki67<2% and <2 mitoses per 10 HPF.
CONCLUSIONS
SFT has a characteristic growth pattern and immunophenotype(Vimentin,CD34,CD99,Bcl-2 +)which enables differential diagnosis from other tumors of fibroblastic,myofibroblastic or epithelial origin.Follow-up,even after complete excision is recommended as it may recur or even metastise regardless of cellular atypia.

P 395
MYCOPLASMOSIS OF MALE UROGENITAL TRACT IN IRAN
AMIRMOZAFARI Nour , HARIRI Ali
Azad University, Lahijan Branch, Microbiology Department, Lahijan, Iran

Mycoplasma are the smallest bacteria capable of growth in artificial media. Their contribution to male urogenital infections and infertility are lesser known. The most common complaints of male patients who refer to urologists include urogenital tract irritations and infertility problems. Although the cause of these complications are very diverse and multifactorial, urogenital infections with Mycoplasma and Ureaplasma are among the known etiological factors. Very little attention has been paid to these infections in the male patients in Iran. A total of 302 clinical samples including semen, urethral secretions, and first urine drops were enriched and cultured for Mycoplasma. We also sought to compare the isolation rate for the bacteria by the filteration (0.45 um pore size) versus non-filteration (multi-antibiotic use) method of enrichment. The bacteria were cultured from 27 of these samples. Of these, 11 were contaminated with Mycoplasma hominis, 9 with Ureaplasma urealyticum, and the remaining 7 individuals were co-infected with both of these bacteria. Six percent of the sperm secretions, 10% of the first urine drop samples, and 11% of the urethral discharges were culture positive. Co-infections were seen only in the first urine drops. Overall, Mycoplasma and Ureaplasma were cultured in 8.9% of the male samples collected. This points to the relatively high prevalence of mycoplasmosis among sexually active male population in Iran. It also emphasizes a probable detrimental role mycoplasmosis plays in the overall quality of sperm cells.

P 396
MOLECULAR AND IMMUNOHISTOCHEMICAL STUDY OF CELL CYCLE REGULATORS IN URINARY BLADDER TUMORS
RAMOS David1, YURAKH Andriy1, LÓPEZ-GUERRERO José Antonio2, CALABUIG-FARIÑAS Silvia, PELLÍN Antonio, RUBIO José2, SOLSONA Eduardo2, LLOMBART-BOSCH Antonio1
Department of Pathology, University of Valencia1. Fundación Instituto Valenciano de Oncología2. Valencia, Spain.

INTRODUCTION: The optimal management of patients with bladder neoplasms requires the assessment of multiple predictive markers in addition to classical clinical and pathologic (grade and stage) factors. PURPOSE: Our main goal was to quantify diverse molecular and immunohistochemical (IHC) markers in order to accurately predict the clinical evolution of these patients in terms of tumor recurrence, progression and survival. METHODS: Clinical and pathologic data from 84 patients were collected including all tumor grades and stages. DNA from all these cases was analyzed for the presence of loss of heterozygosity (LOH) of the 9p21 locus; homozygous deletions (HD) and promoter methylation of the p14ARF, p16INK4A and p15INK4B genes; gene amplification of the MDM-2, CCND1 and CDK4; and P53 mutations; by means of diverse PCR-based techniques. Paraffin-embedded material from the cases was also studied at the IHC level by means of p53, Ki-67 (MIB1), p14, p16, p21, p27, pRb, MDM-2, and cyclin D1 antibodies using the avidin-biotin peroxidase procedure. Statistical analyses were performed with a specific software program package (STATISTICA version 6.0, Statsoft Inc, USA). RESULTS: In univariate studies, HD of the p14ARF, p15INK4A, and p16INK4B genes showed a statistical correlation with recurrence prediction; whereas CDK4 and CCND1 amplifications together with Ki-67 labeling index (LI), p27, p53, p16 and pRb immunoexpression were statistically associated with tumor progression. Likewise, LOH of the 9p21 locus along with p14, p53 and cyclin D1 protein expression showed strong statistical correlation with relapse-free survival (RFS). In multivariate studies, tumor stage and Ki-67 LI appeared to be independent prognostic factors in relation to overall survival, whereas HD of the 9p21 locus was related to RFS. CONCLUSION: Three factors demonstrated in the present study independent prognostic significance: clinical tumor stage, overexpression of Ki-67 antigen and HD of the 9p21 locus.
Supported with grant: Beca de la Fundación para la Investigación en Urología (FIU), 2001. “PREMIO PEDRO CIFUENTES DÍAZ”

P 397
HEAVY EOSINOPHILIC INFILTRATE OF THE BREAST
JM Radhi, C Otero, S Reid
Department of Pathology, Diagnostic Imaging and Surgery, McMaster University, Hamilton Ontario, Canada

Introduction: Significant eosinophilic infiltrate of the breast is encountered in eosinophilic mastitis granulomatous mastitis, Churg-Strauss syndrome, Crohn's disease, parasitic infection and rarely in carcinoma.
Aim: Our aim is to identify cases of breast reported with heavy or significant eosinophilic infiltrates.
Materials & Methods: Seven cases were identified after reviewing all breast cases reported during the period of 1999-2005. Three cases diagnosed as granulomatous mastitis, one eosinophilic mastitis, two ductal carcinoma and one gynecomastia. The ductal carcinoma cases exhibited florid eosinophilic infiltrates with periductal fibrosis and destruction. One case associated with prior history of herbal medication.
Conclusion: Significant eosinophilic infiltrate is identified in cases of mastitis and rarely in ductal carcinoma. Although eosinophils can degranulate and release toxic inhibiting factors into tumours, they are uncommonly encountered in breast carcinoma.

P 398
FEMALE MALIGNANT BREAST TUMORS IN CAMBODIA
MONCHY Didier, HOU SEREY Vannak, SOK KIM Eng
Pathology Department, Institut Pasteur du Cambodge
Phnom Penh Cambodia

Background: Little is known about breast cancer in Cambodian women living in Cambodia.
Objectives: To describe the various histological types of invasive breast cancers, their frequency, grade and stage.
Methods: We selected all breast biopsies and surgical specimens that were processed during 2003 and 2004 in our newly set up laboratory in Phnom Penh. Tissue samples were embedded after 10% formalin fixation and sections were stained by H&E. Pathology reports were written according to international recommendations. Carcinomas were graded

using the Nottingham modification of the Bloom-Richardson system and staging was established according to the 2003 TNM classification. Detection of hormone receptors by immunohistochemistry was not available in Cambodia at this time.
Results: A total of 107 ladies from Phnom Penh and different provinces in Cambodia, aged 16 to 76, presented with malignant tumors of whom 12 (11.2%) had biopsy then surgery, 81 (75.7%) directly had surgery and 14 (13.1%) solely had biopsy. Lesions included 96 (89.7 %) carcinomas, nine (8.4 %) Phylloides tumors and two (1.9%) lymphomas. The mean age of patients with carcinoma was 48.2 (23-76). Among these patients, invasive ductal type was the most frequent, identified in 79 ladies (82.3%) and high histological grade was found in 74.7% of cases. Radical surgery was performed in 63 of the 79 affected patients and proportions of T1, T2, T3 and T4 were respectively 9.6%, 41.2%, 15.9% and 33.3%. Lymphadenectomy was performed in 31 of 63 patients (49.2%) and lymph node metastases were observed in 26 of 31 (83.9%). Medullary carcinomas accounted for 11.4% (11/96) of the ladies, whose mean age was 46.4 (40-59). Metaplastic, papillary, mucinous and mixed histological types of carcinoma were rare and no case of invasive lobular carcinoma was diagnosed.
Conclusion: Our findings demonstrated a high frequency of medullary carcinomas and malignant phylloides tumors in Cambodian ladies. In contrast, no case of lobular carcinoma was found. The fact that most of our cases were at late stage of the disease, may suggest that early detection of the disease should be strengthened in Cambodia. In addition, standardized surgical procedures should be established so that lymphadenectomy, for instance, is systematically performed at the time of tumor excision.

P 399
TUMOUR GRADE AND TUMOUR MARKER EXPRESSION IN INVASIVE BREAST CARCINOMA WITH INTRA-DUCTAL COMPONENT.
Lacerda M.*; Figueiredo P.*; Schmitt F.**
*C.R.O.C.I.P.O.F.G. –Coimbra –Portugal
** I.P.A.T.I.M.U.P.-Porto - Portugal

Introduction: Ductal carcinoma in-situ is regarded as a precursor to invasive breast cancer. Trying to find steps in this progression. we compared the grade and expression of some tumour markers (ER, PR, c-erb-B2, MIB-1, P53 and Bcl-2) of both components in 74 cases of invasive carcinoma with an intra-ductal component. Materials and methods: Both components (intra-ductal and invasive) were classified independently according the guidelines of the European Commission Working Group on Breast Screening Pathology. The results of the staining were analyzed in the intra-ductal and in the invasive components separately. We worked with the cut-off limits generally accepted.
Statistical analysis: For comparison between the two components the chi-square test was used. Statistically significant differences were assumed when $P<0.05$.
Results: 1)Tumour grade – a): high grade of the intra-ductal and grade of the invasive component: in 28% cases the invasive component was grade 3; in 57% cases the invasive component was grade 2 and in 14,3% the invasive component was grade 1;b)intermediate grade plus low grade of the intra-ductal component: in 34% cases the invasive component was grade 2; in 56,6% the invasive component was grade 1. Only in 5 cases (9,4%) the invasive component was grade 3. 2) ER expression: in 62,2% cases both components were ER+ and in 27% cases both components were ER-. 3) PR expression: in21, 6% cases both components were RP+ and in 66,2% both components were RP- 4) c-erb-B2: in 17,6% cases c-erb-B2 was over-expressed in both components; in 77% cases c-erb-B2 was negative in both components. In no one case we observed c-erb-B2negative in the intra-ductal component and over-expression in the invasive component. 5) MIB-1: in 12,2% cases MIB-1 was high in both components but in 18,9% cases its expression move on to low in the invasive component; in 64,9% cases MIB-1 was low in both components. 6) P53 expression: in 66,2%cases both components were P53+ and in 10,8%cases P53- in both components. 6) Bcl-2 expression: in 27% cases Bcl-2 both components were Bcl-2+ and in 63,5% cases both components were Bcl-2-.
Conclusion These results allow us to conclude that the step between in-situ and invasive carcinoma, seems to occur independently of tumour grade. The tumour markers that we studied were not clearly associated with the progression from in-situ to invasive; the expression of these tumour markers are almost identical in the two components.

P 400
ROUND/OVAL SHAPE IN BREAST LESIONS. A MARKER OF BENIGN LESION? CYTO-HISTOLOGICAL STUDY OF 544 CASES FROM THE VERONA BREAST SCREENING PROGRAM.
Manfrin E1, Mariotto R2, Dalfior D1, Remo A1, Reghellin D1, Eccher A1, Bonetti F.1
1 Department of Pathology, University of Verona (Italy), 2 Breast Screening Unit ULSS 20 Verona (Italy)

Introduction: The round/oval shape is a radiological feature suggesting a diagnosis of benign breast lesion.
Purpose: To evaluate the pathologic and mammographic correlation of round/oval-shaped breast lesions.
Methods: Between 1999 and 2004, we studied the cytological and histological features of breast lesions with ultrasonographic and/or mammographic circular shape within the Verona Breast Screening Program (BSP).
Results: Out of 544 round breast lesions, 125 (22,9%) were malignant and 419 (77,1%) benign. Malignant lesions were all invasive; histotype was ductal: 105 cases (84%), lobular: 13 cases (10,4%), mucinous: 4 cases (3,2%), medullary: 2 cases (1,6%), tubular: 1 case (0,8%). The TNM of malignancy was pT1: 102 cases (81,6%); pT2: 18 cases (14,4%); pT3: 2 cases (1,6%) and pT4: 3 cases (2,4%).
Nodal status, available in 98% of cases, was N+: 24.4% and N-:75.6%. All benign lesions were investigated with cytology and so stratified: fibroadenoma: 188 (44,9%); cyst: 53 (12,6%); benign lesion, NAS: 54 (12,9%); fibrocystic change: 32 (7,6%); steatonecrosis: 17 (4%); adenosis: 15 (3,6%); adipose nodule: 12 (2,9%); papilloma: 7 (1,7%); intramammary lymph node: 5 (1,2%) and other(focal fibrosis, granulomas, abscess): 36 (8,6%). Surgery was performed in 14 cytological benign lesions; histology was benign in 9 cases, atypical in 5.
Conclusion: In our series, round/oval-shaped breast lesions were malignant in 23% of cases. The most frequent histotype was infiltrating ductal cell carcinoma. The most common benign lesion was fibroadenoma. From our data we conclude that follow-up is not adequate in breast lesions with round-oval imaging, but further investigations are necessary. (Supported by Fondazione Cassa di Risparmio VR-VI-BL-AN. Bando 2004. Progetto Carcinoma Mammella)

P 401
BREAST SCREENING PROGRAM IN VERONA. CYTO-HISTOLOGICAL FINDINGS OF FIVE YEARS OF ACTIVITY AND COMPARISON WITH OTHER SCREENING PROGRAMS IN EUROPE.
Manfrin E1, Mariotto R2, Remo A1, Reghellin D1, Dalfior D1, Eccher A1, Bonetti F1.
1Department of Pathology, University of Verona (Italy), 2 Breast Screening Unit ULSS 20 Verona (Italy)

Breast Screening Program (BSP) for women with age comprised between 50 and 69 years started in Verona in

1999. Compared with the "classic" screening, the Verona program has a different organization, similar to that of a Breast Clinic, and operates in a building exclusively devoted to the BSP. First level mammograms and all second level exams (US, FNAC, core biopsy, mammotome) are performed in the same structure by a staff composed of two radiologists, two cytopathologists, four technicians and two nurses. All women are submitted to a double projection mammography; the Radiologists perform real time interpretation of mammograms. Results are immediately communicated. Negative patients are dismissed after reassurances; suspicious patients are immediately submitted to second level examination. FNAC is evaluated for adequacy and a diagnostic report is immediately given to the Radiologist. Core-biopsy and mammotome specimens are centrally collected in Pathology Department of University of Verona. Result of histological exams are communicated within two days. Results: In the first five years of activity (1999-2004) 55.000 women have been evaluated by screening. The participation rate was 61% in initial screening, 89% in subsequent screening. Among 513 cases sent to surgery, 424(83%) were malignant, 24(5%) atypical hyperplasia, 65(12%) benign. The ratio benign vs. malignant was 0.18. The detection rate for cancer was 9.6‰ in the first round and 4.9‰ in the following rounds. The pre-operative diagnosis of malignancy was done in 85% of cases with FNAC and in 15% of cases with core biopsy/mammotome. The TNM of malignancy was pTis: 23.4%, pT1:63.9%, pT2:10.3%, pT3:0.9%, pT4:1.4%. Nodal status was N+:21% and N- :79%. Surgery was conservative in 80% with 20% mastectomy. TNM(M0) staging was St0:23.4%; StI:54.5%, StII:15.3%, StIII:6.8%, StIV:0. Interval cancers rate was 8.6%.Conclusions: Compared with other screening program, the results of the Verona screening program are all within the preferred results of the European guidelines. The peculiar organization of the program, with its centralized integrated radio-pathological activity seems a major factor for a successful screening program.(Supported by Fondazione Cassa Risparmio VR-VI-BL-AN.Bando 2004. Progetto Cr. Mammella)

P 402

MALE BREAST CARCINOMA : A CLINICO-PATHOLOGICAL STUDY OF 21 CASES

MNIF Hela, MAKNI Saloua, FAKHFAKH Ines, SELLAMI Ahmed, BOUDAWARA SELLAMI Tahya

Introduction:
Breast carcinoma rarely occurs in males and information regarding this pathology are limited. The aims of this study were to document epidemiological, clinico-pathological and immunocytochemical features of this cancer and to establish which factors would predict prognosis.
Materiels and Methods:
A retrospective study was performed of 21 cases of male breast carcinoma accessioned at the pathological anatomy and cytology laboratory of the University Teaching Hospital of Sfax between 1992 and 2003.
Results:
The patients' mean age was 65,4 years. The average duration of signs and symptoms before the diagnosis was 10,4 months. Presentation occurred most often (85,7%) with self-detected lump. Clinically the majority of the cases presented advanced cancers. Three patients had stage 0, 5 had stage II, 4 had stage III, 9 had stage IV disease. Histology found: 13 canalar infiltrating carcinoma, 3 neuroendocrin carcinoma, 1 papillary carcinoma and 4 ductal carcinoma in situ. Four Paget's disease were diagnosted. The histological grad of SBR was precised: 2 patients had grad I, 8 had grad II, 7 had grad III. Lymph node involvement was found in 52,3% of the cases. Immunohistochemicaly data were reviewed: 65% of tumors were oestrogen receptor positive, 80% were progesterone receptor positive, 23,5% over expressed CerbB2, 40% over expressed Bcl2 and P53 and 15% exprimed vimentin. The overall 5 years corriged survival was 61,9%. The disease stage, high histological grad, lyph node involvement and the over expression of the biological biomarkers (receptor of oestrogen, P53, , CerbB2, vimentine) were correlated with poor prognosis.
Conclusion:
The poor prognosis of male breast cancer is related to older age at diagnosis in advanced stage of disease at presentation.We find that to get better prognosis, it is important to improve medical and technical means, to increase information and to promote early detection.

P 403

PRELIMINARY ANALYSIS OF THE HISTO-PROGNOSTIC POWER OF A HETEROGENEITY INDEX FOR BREAST CANCER

Venus Sharifi-Salamatian, Lab. d'Analyse d'Image en Pathologie Cellulaire (AIPC) Hôpital Saint-Louis, Paris, France
Joelle Simony-Lafontaine,Majida Esslimani, Nadine Lequeux, Laboratoire d'Anatomie Pathologique, Centre Regional de Lutte Contre le Cancer (CRLCC), Montpellier, France

In 1998, the Kananaskis Tumour Heterogeneity working group conjectured that there should be a correlation between the level of intratumoral heterogeneity and the seriousness of a carcinoma. This group emphasized the need for a reproducible and quantifiable measure of heterogeneity to test this hypothesis.
In this paper, we use a recently developed Intratumoral Spatial Heterogeneity Index (ISHI) complying with the Kananaskis group requirements. This index has been shown to be very useful in characterisation of breast cancer tumours. In particular it was shown that the ISHI for various blocks of a single tumour was invariable, regardless of the fact that various blocks differ in size and in number of marked cells. We present in this paper our preliminary results about the histo-prognostic ability of the ISHI.
The ISHI has been derived on a set of 78 blocks coming from 56 breast carcinoma patients and labelled by monoclonal anti-MIB-1 marker. A complete analysis of the ISHI and its correlation with SBR grade assigned by a pathologist has been conducted and some interesting results are obtained. The analysis shows clearly that blocks coming from patient with a SBR grade I, have also low level of heterogeneity (ISHI close to 1). ISHI separates well (as validated by a statistical test) SBR grade I from grade II and III, but grade II and III are not well separated.
We conducted a survival analysis of a sub-sample of 37 breast carcinoma patients with 10 to 12 years of follow-up, to evaluate the histo-pronostic value of the ISHI. For this purpose we divided the set of 37 patients into three equal size sets containing patients with decreasing value of ISHI; group 1 with low heterogeneity (ISHI between 1 and 0.9), group 2 with medium heterogeneity (ISHI between 0.9 and 0.82), group 3 with large heterogeneity (ISHI from 0.82 to 0.67). We therefore compared the survival curve of the 3 group. It appears that no mortality has been reported in group 1 (with low heterogeneity) and that the survival curve of the group 3 is clearly below the group 2 and 1 (as validated by a logrank statistical test). This could be seen as a preliminary validation of the histo-pronostic value of the ISHI.
Even if the number of samples used in this study is not enough to reach to a definitive answer, however this gives some indications that motivate us to conduct a larger scale survival study.

P 404

SPORADIC INVASIVE CARCINOMAS OF THE BREAST WITH MEDULLARY FEATURES SHOW BASAL-LIKE CHARACTERISTICS.

Yolanda Rodríguez-Gil1, Socorro María Rodríguez-Pinilla2, Mª del Carmen Martín Guijarro3, David Sarrió2, David Hardisson4, Lucía Hernandez1, Juan C. Cigudosa3, José Palacios2.

1. Department of Pathology. 12 de Octubre Hospital. Madrid. Spain.
2. Programa de Patología Molecular. Breast and Ginecological Laboratory. CNIO. Spain.
3. Programa de Patología Molecular. Citogenetic Laboratory. CNIO. Spain.
4. Department of Pathology. La Paz Hospital. Madrid. Spain.

INTRODUCTION: Tumours from women with germline BRCA1 mutations have a basal-like phenotype: estrogen receptor (ER) negative, HER2 negative, cytokeratin 5 (CK5) and/or epidermal growth factor receptor (EGFR) positive. Moreover, they show high cyclin E expression and frequently show medullary features.

AIMS: To investigate whether or not atypical medullary sporadic breast carcinomas have a basal-like phenotype.

MATERIAL and METHODS: We studied a group of 39 sporadic invasive breast cancers that displayed features of atypical medullary carcinoma according to the 2003 WHO criteria, and a series of 76 consecutive sporadic breast tumors (as a control group). They were analysed inmunohistochemically for ER, PR, p53, Her2neu, ki-67, cyclin E, CK5 and EGFR expression. Cyclin E alterations were also analysed by fluorescence in situ hybridization (FISH). Both studies were performed on paraffin-embedded tumours included in tissue-microarrays (TMA).

RESULTS: In the medullary carcinoma group, 100% and 92,3 % of the cases were negative for Her2neu and ER whereas 28,2%, 61,5% and 66,7% were positive for EGFR, CK5/6 and cyclin E, respectively. The three ER positive cases were negative for both CK5/6 and EGFR. Interestingly, we observed that cyclin E gene was amplified in 15,4% of the cases. On the other hand, in the control group 76,3% and 22,3% of the cases were negative for Her2neu and ER, respectively. We found positivity for CK 5/6 and EGFR in 8 (10,5%) and 11 (14,5%) cases, respectively but only 5 (6,6%) cases fulfilled all the criteria to be included in the basal-phenotype group. Cyclin E was overexpressed in 36,8% of the cases but no gene amplification was found.

CONCLUSION: These data indicate that as well as in BRCA1-mutated tumours, sporadic invasive breast cancers with medullary features show the characteristics of the basal phenotype. Interestingly, medullary breast tumours show a high percentage of cyclin E gene amplification , a fact not previously been reported in breast tumours.

P 405

WIDESPREAD BREAST CANCER METASTASES TO THE UTERUS AND LEIOMYOMA - REPORT OF TWO CASES

AKBULUT Metin, Pamukkale University School of Medicine, Department of Pathology,Denizli, Turkey
BIR Ferda, Pamukkale University School of Medicine, Department of Pathology,Denizli, Turkey
AKMAN Hatice, Pamukkale University School of Medicine, Department of Pathology,Denizli, Turkey
DEMIRKAN Neþe, Pamukkale University School of Medicine, Department of Pathology,Denizli, Turkey
SOYSAL Mehmet Emin, Pamukkale University School of Medicine, Department of Obstetrics & Gynecology,Denizli, Turkey
DUZCAN Süleyman Ender, Pamukkale University School of Medicine, Department of Pathology,Denizli, Turkey

WIDESPREAD BREAST CANCER METASTASES TO THE UTERUS AND LEIOMYOMA - REPORT OF TWO CASES

Background: Breast carcinoma is the most common malignancy in the female population. Frequent sites of metastases include lymph nodes, liver, lung and bone. Widespread gynecologic and leiomyoma metastases from breast carcinoma is a well-known but extremely rare phenomenon and had only been reported sporadically in the literature.

We present two cases of gynecologic and leiomyoma metastases from invasive ductal and lobular carcinoma of the breast respectively. Immunohistochemical studies including CEA, estrogen, progesteron, C-erb–2 and human milk fat globulin was performed for differential diagnosis.

Case I: An 62-year old multigravid woman with a history of breast cancer and tamoxifen therapy presented with abnormal uterine bleeding. After the diagnosis of malignancy was made on cervical smear, biopsies were taken from cervix and endometrium, which revealed an infiltrating moderately differentiated ductal adenocarcinoma consistent with breast metastasis. A total abdominal hysterectomy, bilateral salpingo-oophorectomy, and pelvic lymph node sampling were performed. The uterus measured 10x6x4 and it was markedly distorted with multiple gray-white cervical, intramural and endometrial tumor nodules with the maximum diameter of 3 cm. Final pathology examination revealed metastatic ductal carcinoma of the breast including vagina, cervix, endometrium, myometrium and fallopian tubae.

Case II: A 49-year-old multigravid woman was admitted to the hospital with the complaint of uterine bleeding and abdomino-pelvic pain. Her gynecologic history was unremarkable, however, 4 months previously, she was underwent a right sided modified radical mastectomy for invasive lobular carcinoma. At the time of admission, her physical and genital examinations showed no abnormalities except multiple leiomyomas. After the vaginal hysterectomy and bilateral salpingo-oophorectomy; microscopic examination revealed metastatic foci of invasive lobular carcinoma in the leiomyoma and ovary

Conclusion: Metastases to the female genital tract from extragenital cancers are uncommon. It should be kept in mind that abnormal uterine bleeding may be the first sign of metastatic disease in a woman with a history of malignant disease as in our cases.

P 406

IMMUNOHISTOCHEMICAL EXPRESSION OF P21 WAF1/CIP1, BAG-1, BAX, MCL-1 PROTEINS IN BREAST CARCINOMAS. CORRELATION WITH PROGNOSTIC FACTORS

1L Zakhartseva, 2I Shchepotin, 2O Lobanova
1Kiev City Oncology Hospital
2National Medical University

Introduction Identification of apoptosis factors and cell proliferation carries valuable information about specific features of tumor clinics, treatment sensitivity and survival of patients. Cell cycle progression is governed by cell cycle regulators and inhibitors such as cyclin dependent kinases, p21 WAF1/Cip1, BAG-1, BAX, and Mcl-1.

Material and methods Immunohistochemical analysis for estrogen/progesterone receptors (ER/PR), c-erb B2, p21 WAF1/Cip1, BAG-1, BAX, Mcl-1 was performed on formalin-fixed infiltrating ductal (81%) and lobular (19%) breast carcinomas of 64 patients with

Ò1-2 N0 M0 G2-3. They were undergone mastectomy and chemotherapy therapy taking into account c-erb B2 expression. Two groups of patients were studied in terms of survival. The first group with more than 3 years survival (53), the second – less than 3 years (11).

Results The tumors of the first group of patients had positive reaction ER/PR in 83% cases, c-erb B2 in 18%, p21 WAF1/Cip1 – 75% (tumor having more then 20% staining cells were considered to be positive), BAG-1and BAX in 100% in c-erb B2 positive tumors and 25% in c-erb B2 negative tumors , Mcl-1 in 20% in c-erb B2 positive tumors and 36% in c-erb B2 negative tumors. The tumors of the second group patients had positive reaction ER/PR in 38%cases, c-erb B2 in 25%, p21 WAF1/Cip1 – 83%, BAG-1 and BAX in 30%, Mcl-1 in 20%.
Conclusion Higher expression of BAG-1, BAX, Mcl-1, as well as ER/PR, is indicates good prognostic factors of survival.

P 407
INCREASED LEVEL OF FATTY ACID SYNTHASE AND PROGESTERONE RECEPTOR PROTEINS IN PREMALIGNANT MAMMARY LESIONS AND IN SITU CARCINOMA

ESSLIMANI-SAHLA Majida1,2, KRAMAR Andrew3, SIMONY-LAFONTAINE Joelle2, THEZENAS Simon3, LAVAILL Roselyne2, BIBEAU Frederic 2, BALDET Pierre4, MAUDELONDE Thierry1,4, CHALBOS Dany1 and ROCHEFORT Henri1,4
1INSERM U540, Endocrinologie Moléculaire et Cellulaire des Cancers; Departments of 2Pathology and 3Biostatistics, Cancer Center Val d'Aurelle; 4CHU; Montpellier, France

While progestins increase the risk of breast cancer after menopause (the WHI trials 2002 and 2004), the mechanism of this effect is unclear. One approach is to estimate the level of proteins related to progestin action in different mammary preinvasive lesions compared to adjacent normal mammary glands, in an attempt to define at which stage of carcinogenesis progestin action could be increased. We previously found that Fatty acid synthase (FAS) was overexpressed in invasive breast cancer and induced by progestins and growth factors. FAS was then described by others as corresponding to a mammary and prostate nutritional oncogene.
We now estimate by immunohistochemistry, FAS and progesterone receptor (PgR) expression in "benign" breast disease (BBD) of increasing histological risk according to Dupont and Page (non proliferative, proliferative without atypia, proliferative with atypia) and in situ breast carcinomas (of lobular and ductal subtypes). This study was performed in archive paraffin embedded tissues from 116 patients with 164 BBD and in situ carcinomas, compared to their adjacent normal ducts and lobules, using a rabbit polyclonal FAS antibody (raised by D. Chalbos in our laboratory) and a PgR monoclonal antibody (clone PgR636-Dako). The expression level of these markers was quantified by computer image analyser. A statistical analysis was performed to compare staining level in normal glands to that in the different lesions and to correlate FAS and PgR levels with MIB-1 proliferation index and clinical parameters (age, menopausal status and hormone therapies).
Results will be given showing at which premalignant lesion the expression level of these two markers was found to be significantly increased.

P 408
THE STATUS OF C-ERBB-2/HER-2/NEU AND EXPRESSION OF E-CADHERIN IN INVASIVE LOBULAR AND DUCTAL CARCINOMAS OF THE BREAST

TURASHVILI Gulisa 1, BOUCHAL Jan 1, BURKADZE George 2, KOLAR Zdenek 1
1 - Institute of Pathology and Laboratory of Molecular Pathology, Palacky University, Olomouc, Czech Republic
2 - Department of Pathology, Tbilisi State Medical University, Tbilisi, Georgia

Introdution. E-cadherin (E-CD) is considered to be the most important cell adhesion molecule in mammary gland. Some studies suggest that downregulation of E-CD and subsequent loss of cellular adhesiveness correlate with poor prognosis and metastasis but this is not confirmed by other studies. Many investigations suggest that E-CD protein is not expressed in invasive lobular (ILC) in comparison with invasive ductal carcinoma (IDC) of the breast. A few papers report that E-CD mediated cell adhesion system can be disrupted by oncoprotein c-erbB-2/HER-2/neu in c-erbB-2-positive breast carcinomas despite ductal or lobular type. Purpose of study. To evaluate the relationship between expression of HER-2/neu and E-CD in ILC and IDC and analyze an association with lymph node positivity. Methods. We reviewed 106 cases of breast cancer: 91 IDC and 15 ILC including 3 pleomorphic lobular carcinomas (PLC). All cases were examined in our laboratory for suspicioion for c-erbB-2 overexpression. Nottingham histologic grade, immunohistochemical staining for estrogen and progesterone receptors (ER and PR), proliferating cell nuclear antigen (PCNA), E-CD; fluorescense in situ hybridization for HER-2/neu gene amplification; and lymph node positivity were evaluated. Results. HER-2/neu gene amplification was observed in 60.5% of IDC and 26.7% of ILC including one case of PCL and positively correlated with higher histological grade and lymph node positivity. Strong positivity for PCNA was observed in 84.2% of IDC and positively correlated with histological grade and HER-2/neu positivity. IDCs were negative for ER in 50%, and PR in 57.8% of cases. ILCs were negative for ER in 40%, PR in 46.7% of including one case of PLC. ER/PR-negativity was associated with histological grade, HER-2/neu gene amplification and lymph node positivity. Majority (80%) of ILC including two cases of PLC showed negative staining for E-CD. E-CD expression was lost in 10 cases (26.3%) of 38 IDCs and positively correlated with histological grade, HER-2/neu gene amplification and lymph node positivity. Conclusion. The loss of E-CD expression can be a feature of some typical invasive ductal carcinomas of the breast. E-CD negativity seems to be associated with higher histological grade, HER-2/neu gene amplification and lymph node positivity suggesting that c-erbB-2 may act as a regulator of E-CD expression in most human breast carcinomas in vivo.
This work was supported by grants NR7844-3 and MSM6198959216.

P 409
PATHOLOGICAL AND IMMUNOPHENOTYPICAL RESPONSE TO TRASTUZUMAB THERAPY IN HER2 POSITIVE BREAST CANCER. ARGUMENTS IN FAVOR OF ANTIBODY-DEPENDENT CELLULAR CYTOTOXICITY (ADCC).

GELLY-MARTY Marion, ASSOUS Dorothee, PENAULT-LLORCA Frederique, BONNETAIN Franck, MIGEON Colette, CABARET Veronique, Philippe BERTEAU, COUDERT Bruno and ARNOULD Laurent.
Centre G-F LECLERC, Dijon, France ; Centre J PERRIN, Clermont, France ; Centre A VAUTRIN, Nancy, France ; Centre O LAMBRET, Lille, France ; CHU, Limoge, France, CHU-Saint Louis, Paris, France

Background: Treatment with trastuzumab (T) has shown excellent clinical response in patients with HER2-overexpressing breast cancer (BC). However, the exact mechanisms of action of T has not been fully characterized and appears to be complex. The objective of this study was to dertermine, in vivo, whether the immune response is a mechanism of action of T in human BC.
Material and Methods : 23 patients with BC characterized as 3+ HER2 by immunochemistry (IHC) were enrolled to receive T + docetaxel (D) primary systemic therapy (PST) as

part of the 'TAXHER01' trial. Following surgery, they were 9 (40%) pathological complete response (pCR). The remaining 14 BC displayed partial (N =13) or no (N=1) pathological response. Additionally, 23 BC treated with D-containing PST, and 23 BC treated with anthracycline-containing PST were analyzed as non-T groups. Each cases of the 2 control subgroups was chosen to be matched (same pathological response) with those of the case group. Of these 69 surgical specimens, residual tumors areas or pCR areas were blindly analyzed by morphology and IHC. B-lymphocytes were stained with anti-CD20. T-lymphocytes were stained with CD3, CD4 and with CD8. Macrophages were stained with CD68. Dendritic cells were stained with PS100 and CD1a. Natural Killer (NK) cells were stained with CD56 and with NK1. Potential cytolytic cells were stained with Granzyme B and with TIA-1. HER2 status was also analyzed by IHC on residual tumor cells. These analyses were performed by 2 independent pathologists.
Results : All residual tumor cells from the cases group were HER2 postive on IHC and there were no differences in HER2 status before and after T PST in the case group. The number, topography, and activation status of various type of immunocompetent cells were generally different between the case group and the two control groups. Significantly more NK cells were in contact with tumor cells in the case group than in controls. In addition, there was significantly greater expression of Granzyme B and Tia1 by lymphoid cells in the case group than in controls.

Conclusion : This study provides evidence in favor of the immune response as one of the mechanisms of action of T in BC. NK cells in particular, that are able to mediating antibody-dependent cell toxicity against antibody-coated cells via their expression of FcãRIII, seemed to play an important role. This finding may have further implications for the management of T treatment in BC.

P 410
IMMUNOHISTOCHEMICAL DETECTION OF ERBB RECEPTORS OVEREXPRESSION IN HUMAN BREAST CARCINOMAS

Ravazoula P,Lykaki-Karatza E, Koumoundourou D, Androutsopoulos G, Michail G, Kourounis G.
Departments of Pathology, Radiology and Obstretrics-Gyneacology, School of Medicine, University Hospital of Patras, Greece

Abstract
ErbB receptors are expressed in various tissues, in which they are involved in the control of diverse biological processes such as proliferation, differentiation, migration and apoptosis. Cerbb-2 overexpression has been implicated in many types of human cancers and is associated with poor prognosis.
The aim of our study is to identify the expression of cerbB-3, cerbB-4 and cerbB-2 in human breast carcinomas.
Materials and Methods: The study comprised 47 breast cancer specimens of 47 women with follow up period 3-10 years. Histological examination showed 3 in situ ductal carcinomas and 44 ductal invasive carcinomas common type (11 grade I, 23 grade II and 10 grade III). Eight out of 44 women with invasive carcinoma had a recurrent disease. Immunohistochemistry was carried out by using polyclonal antibodies against cerbB-3 and cerbB-4 (Santa Cruz Biotechnology) and a monoclonal antibody against cerbB-2 (Biogenex). Tumors were scored by the proportion of tumor cells stained.
Results: Expression of cerbB-3 was evident in all in situ and in 10 (22,72%) invasive carcinomas. One out of the 10 women with invasive carcinoma had a local recurrence (9%). CerbB-4 expression was evident in 1 in situ carcinoma and in 28 (63,6%) invasive carcinomas. Seven out of the 28 women with invasive carcinoma had a recurrent disease (24,13%). CerbB-2 expression was evident in all in situ and in 7 invasive carcinomas (~15%). Two out of the seven women with invasive carcinoma had a recurrent disease (28,57%).
Conclusions: Our results demonstrate that erbB receptors are expressed early in human breast carcinoma. ErbB-2 and erbB-4 overexpression is correlated with recurrent disease.

P 411
CERB B2 OVEREXPRESSING BREAST CANCER CEELS REVEAL DISTINCTIVE NUCLEAR FEATURES BY IMAGE CYTOMETRY

DR.BALOGLU H,DR.YILDIRIM S,HAHOLU A,DR.YILMAZ I,DR.BERBER U,DR.,DR.CERMIK H,DR.ERGUR R*.
DEPTARTMENT OF PARTHOLOGY & OBGYN* GATA-HEH,ISTANBUL,TURKEY.

Background: To understand if CerbB2 over-expressing breast cancer cells have distinctive phenotypic features.
Design: N0 Grade II twelve invasive breast cancer cells showing heterogenous CerbB2 protein over-expression were included in the study. For measurements, 100 CerbB2 immunoreactive tumor cells, and 100 non-reactive tumor cells were selected for each case from their paraffin embedded tumor tissue sections stained immunohistochemically with mouse antihuman CerbB2 antibody (BioGenex, CA, USA). Nuclear area, nuclear perimeter, and nuclear form factor of these selected cells were determined on SAMBA 4000 image analysis workstation. Discriminative analysis was performed whether measured parameters are accurate to identify CerbB2 positive and negative cellular phenotype.
Results: Nuclear area was found to be the most distinctive feature for CerbB2 over-expression second to the nuclear perimeter ($p<0,05$). CerbB2 expressing cells have bigger nuclear area and bigger nuclear perimeter significantly ($p<0,05$).
Conclusion: CerbB2 protein expression was found consistent with distinct nuclear features in invasive breast carcinoma cells that may be identified by image cytometry.

P 412
EXPRESSION OF HEDGEHOG SIGNALING COMPONENTS IN BREAST CANCER

KOLLMANN Karoline,BLAAS Leander, ALINGER Beate, ESTERBAUER Harald, ABERGER Fritz, DIETZE Otto, HAUSER-KRONBERGER Cornelia
Department of Pathology, General Hospital Salzburg and Department of Molecular Biology, University of Salzburg, Austria.

The hedgehog signal transduction pathway plays an important instructional role during the development of vertebrates. This pathway includes hedgehog ligands (Sonic hedgehog, Shh; Desert hedgehog, Dhh; Indian hedgehog, Ihh) binding to the membrane receptor patched (ptch) and the trans-membrane protein smoothened with its intracellular effectors (Gli1, Gli2, Gli3). Mutations of the receptor ptch are known to induce human tumours, i.e. the basal cell carcinoma (BCC).
Lately, hedgehog has been described to play a crucial role in the carcinogenesis, differentiation and proliferation of breast cancer.
The aim of the present study has been to reveal the expression of single components of the hedgehog pathway in normal tissues, precancerous lesions, non-invasive and invasive cancer of the breast.
Formalin fixed and paraffin embedded human normal (n=3) tissue, precancerous lesions (atypical hyperplasia, DCIS; LCIS n=15) and invasive ductal and lobular carcinoma tissues (n=25) have been investigated. Additionally breast cancer tissue arrays and breast cancer cell lines were analyzed for the expression of components of the hedgehog pathway using immunohistochemistry. The ligands (Shh, Dhh, Ihh), the

receptor Patched and the transcriptionfactors (Gli1, Gli2, Gli3) as main partners of an activated pathway were analyzed. Twelve breast cancer cell lines (MDA-231, SK-BR-3, BT-20, MDA-361, HS-578, T-47 D, ZR 751, MCF-7, HBL-100, 734B, MTSV 1-7, ALAB) have been examined by real-time polymerase chain reaction for the quantification of mRNA.
The results suggest a constitutively activated hedgehog pathway in all breast carcinoma tissues. Furthermore, there are differences in the expression of the hedgehog components. Invasive ductal carcinomas apparently show an increased expression of Shh, Gli1, Gli2, Gli3 and Ptch. In addition to the over-expressed components in invasive ductal carcinoma, ductal carcinomas in situ indicate an intensive staining of Ihh. Shh, Ihh, Gli1, Gli2, Gli3, and Ptch are expressed in invasive lobular carcinomas and in LCIS.
Elucidation of the role of hedgehog signalling pathway in breast cancer could contribute to a new therapeutic approach by obstructing the hedgehog pathway cascade with cyclopamine or antibody therapy.

P 413
A MODIFIED APPROACH FOR EVALUATION OF ERBB2 (HER2) GENE COPY NUMBER IN MODERATELY AMPLIFIED INVASIVE DUCT CARCINOMAS (IDC) OF THE BREAST
MRHALOVA Marcela, NERADOVA Marie, KODET Roman
Department of Pathology and Molecular Medicine, 2nd Faculty of Medicine, Charles University in Prague, V Uvalu 84, Prague 5 – Motol, 150 06, Czech Republic

INTRODUCTION: In IDC of the breast ERBB2 gene FISH status is reported as a ratio of a total number of ERBB2 signals and a total count of chromosome 17 centromere signals (ERB/CEP17). Using this system, interpretation of borderline findings may be difficult. PURPOSE: To introduce a more accurate approach to describe ERBB2 gene status in cases with a borderline ERBB2 gene amplification. METHODS: We investigated ERBB2 gene status in tissue imprints (92 IDC) and histological sections (127 IDC) using FISH PathVysion (Abbott/Vysis). We evaluated 100 tumor cells in each case and classified the nuclei according to the number of ERBB2 signals in three categories: without the gene amplification, with a moderate (<10 signals) and with a strong (>10 signals) amplification. The evaluation of ERBB2 signals was performed relatively to the number of CEP17 signals in each counted cell. The IDCs were classified as strongly amplified if more than 10% of tumor cells had the strong amplification. A case with a moderate amplification was defined as having more than 10% of tumor cells with the gene moderately amplified. SUMMARY OF THE RESULTS: A group of tumors which were by our system of evaluation strongly amplified had the ERB/CEP17 ratio >2 (101 IDC; 2,11-16,14; median 6,81), and a group of tumors without amplification had the ratio <2 (90 IDCs; 0,84-1,90; median 1,07). However, in 28 cases classified as moderately amplified by our system the ERB/CEP17 ratio varied from 1,18 to 4,77 (median 1,96) – 10 cases with imprints 1,18-2,96 (median 1,84), 18 patients with tissue sections 1,30-4,77 (median 2,12 – reflecting the cutting of the nuclei). We found that neither approach to FISH evaluation of borderline cases has a correlate to the protein status. CONCLUSION: In a majority of IDCs the ERB/CEP17 ratio describes ERBB2 gene status in a comparable way with our system. In cases with a borderline ERBB2 gene amplification ERB/CEP17 ratio may lead to misinterpretation of the result. Evaluation of histological sections should be done with a caution because centromeres may be cut off dysproportionally to the ERBB2 signals resulting in an increase of ERB/CEP17 ratio. On the other hand, ERB/CEP17 ratio may hide a minor tumor cell clone with a strong amplification. From this reason it is more useful to report the percentage of tumor cells with a strong and with moderate amplification. The result must be carefully confronted with the ERBB-2 protein status. FNM MZO 00064203

P 414
ESTROGEN RECEPTOR BETA EXPRESSION IN HIGH GRADE BREAST CANCER PATIENTS MAY PREDICT METASTASIS AND MORTALITY
VELA Teresa, PÉREZ Victor, MORA Arcelia, DUBON Elsa, HERNÁNDEZ-RODRÍGUEZ Norma; Instituto Nacional de Cancerología, México, México

Background: The two isoforms of estrogen receptor (ER)alpha and beta are involved in breast tumorigenesis and progression. ER alpha is a well established prognostic and predictive factor for anti-estrogen therapies in breast cancer, and predicts a favorable disease outcome, ER beta potential as a clinical prognostic marker remains to be defined. The aim of this study was to identify the potential of ER beta as a predictor of metastases and mortality in high grade breast cancer patients.
Methods: In a group of 50 patients with confirmed diagnostic of ductal carcinoma and a SBR of 8-9, we assesed by immunoblotting and IHQ (using specific monoclonal antibodies directed against ER alpha and ER beta) the distinct expression pattern of this ER isoforms in primary tumor samples. Chi-square and log rank tests were used to determine differences between proportions of each ER isoform and mortality and survival distributions respectively. A P value <0.05 were considered significant.
Results: The median follow up of this case series was 80 months (2-107) months.Twenty-three (46%)of 50 patients developed metastases, and 25 of 50 (50%) were positive for expression of ER alpha and ER beta respectively. We found a high frequency of metastasis (13 of 25; 52%) among those cases that express ER beta. Similar to 17 of 25 (68%)observed in ER alpha negative samples. This relationship was very significant (P=0.0000) when compared to the rest of the group. We also found a statistically significant correlation between patients with positive ER beta and negative ER alpha and higher mortality (P=0.03 and P=0.0038 respectively).
Conclusions: These findings suggest that ER beta expression in high grade samples from ductal carcinoma histologic subtype may be used as a poor prognostic marker in breast cancer patients.

P 415
NY-BR-1 REPRESENTS A NEW DIFFERENTIATION ANTIGEN IN INVASIVE BREAST CANCER, WHICH REMAINS STABLE DURING METASTATIC PROCESS.
THEURILLAT Jean-Philippe, JAEGER Dirk, SASSE Bernd, FREI Claudia, MOCH Holger, VARGA Zsuzsanna

NY-BR-1 is believed to represent a new differentiation antigen in breast cancer that represents a potential target antigen for antibody based therapies. We investigated immunohistochemical expression of NY-BR-1 invasive breast cancer cases by using a monoclonal antibody. The retrospective study involved 124 invasive breast cancer cases comprising well (G1), moderately (G2), and poorly (G3) differentiated carcinomas. Lymph node metastases were examined in 38 cases. NY-BR-1 was detected in all normal breast samples and all ductal carcinoma in situ components (100%). Among invasive carcinomas, NY-BR-1 was detected in 76% of G1 , 63% of G2 and 51% of G3 carcinomas. Expression profile of NY-BR-1 remained remarkably stable in the lymph node metastases. Our data could provide further evidence that NY-BR-1 is a differentiation antigen by being ubiquitously expressed in normal breast tissue and ductal carcinoma in situ, and its expression was decreasingly detected by dedifferentiation. NY-BR-1 might possibly play

an invasion suppression function at least in a subset of breast cancer cases. As NY-BR-1 exhibits organ specificity, it might be of practical use at routine practice by unknown primaries. Whether NY-BR-1 could be seen as a potential target for immunotherapy, needs to be investigated by further studies.

P 416
THE MULTIFUNCTIONAL ROLE OF SMAD2 PROTEIN IMMUNOHIS-TOCHEMICAL EXPRESSION IN INVASIVE BREAST CARCINOMAS

Mylona E, Liapis G, Alexandrou P, Athanassiadou S, Nikolaou I, Markaki S, Keramopoulos A, Nakopoulou L
2nd Department of Pathology, "Attikon" Hospital, National and Kapodis-trian University of Athens, Athens, Greece

Introduction: Smad2 participates in the Transforming Growth Factor- beta (TGFbeta) signaling pathway, where, in a complex with other Smad proteins, cooperates with transcription factors to regulate expression of defined genes. The purpose of the present study was to investigate the expression of phosphorylated smad2 (pSmad2) in association with clinicopathological parameters and various biological markers of prolif-eration and invasion.
Methods: A two step immunohistochemical method (Envision) was applied on paraffin embedded sections from 164 patients with invasive breast carcinomas to detect the expression of the proteins pSmad2, Ki-67, topoisomerase II alpha (topoII alpha), Extracellular Signal Regulated Kinase-2 (ERK2), catenin p120, Matrix Metalloporteinases (MMP)-14, -2 and Tissue Inhibitor of Metalloproteinase-2 (TIMP-2). The results were subjected to statistic analysis.
Results: pSmad2 protein was detected in the nuclei in the 68.1% of ma-lignant cells and in the fibroblasts of the tumor (55.2%). Nuclear pSmad2 was inversely correlated with histological grade (p=0.047) and the normal immunoexpression of catenin p120 (p=0.028). Both nuclear and stromal pSmad2 were inversely correlated with lymph nodal status (p=0.054 and p=0.053 respectively), Ki67 (p=0.003 and p=0.043 re-spectively) and topoIIa (p=0.021 and p=0.035 respectively), whereas their relation with MMP-14 of tumor cells (p=0.012 and p=0.008 respec-tively) and ERK2 of tumor fibroblasts (p=0.008 and p<0.0001 respectively) was found to be parallel. Stromal pSmad2 was further positively related with MMP-14 of stromal cells (p=0.006) and TIMP-2 of cancer cells (p=0.022) and nuclear pSmad2 with MMP-2 of stromal cells (p=0.038).
Conclusion: In the present study, pSmad2 was found to play both tumor suppressive and invasive role, probably via its collaboration with MAP kinase pathway.

P 417
PROGNOSTIC SIGNIFICANCE OF THE IMMUNOHISTOCHEMICAL EXPRESSION OF VASCULAR ENDOTHELIAL GROWTH FACTOR (VEGF)-C AND ITS RECEPTOR, FLT-4, IN INVASIVE BREAST CARCINOMA

Mylona E, Alexandrou P, Giannopoulou I, Nikolaou I, Athanassiadou S, Markaki S, Keramopoulos A, Nakopoulou L
2nd Department of Pathology, "Attikon" Hospital, National and Kapodistrian University of Athens, Athens, Greece

Introduction: The vascular endothelial growth factor (VEGF) family currently includes five members. Among them, VEGF-C is a ligand for VEGF receptor-3 (VEGFR-3 or flt-4). Both show some selectivity toward lymphatic endothelial cells but their role in cancer is largely unknown. The aim of the present study was to investigate the role of VEGF-C and its receptor, flt-4, in invasive breast carcinomas through their correlation with classic clinicopathological parameters, biological markers indicative of aggressive tumor phenotype, such as proliferation markers (Ki67, topoII alpha), invasion markers [Metalloproteinase(MMP)-11 and abnormal e-cadherin], c-erbB-2 and patients' survival.
Methods: Immunohistochemistry was applied on paraffin embedded sections from 169 patients with invasive breast carcinomas to detect the expression of the proteins VEGF-C, flt-4, c-erbB-2, Ki67, topoisomerase II alpha (topoII alpha), (MMP-11) and e-cadherin. Results were subjected to statistic analysis.
Results: VEGF-C was detected in the cytoplasm and the membrane of malignant cells in 86% and 32% of the cases respectively, whereas flt-4 was found to be expressed in the nuclei of cancer cells (41.4 %) and tu-mor fibroblasts (65%). Membranous VEGF-C showed a parallel correlation with proliferation markers Ki67 and topoII alpha (p-0.006 and p=0.026 respectively), stromal MMP-11 (p=0.012) and abnormal e-cadherin (p=0.035) and it was further found to be an independent prognosticator of patients' shortened disease-free survival (p=0.03), while cytoplasmic VEGF-C had an independent unfavorable effect on patients' overall survival (p=0.016). Flt-4, on the other hand, when detected in the nuclei of malignant cells showed a parallel correlation with topoII alpha (p=0.039), whereas stromal flt-4 was positively associated with c-erbB-2 (p=0.017) and a shortened overall survival of postmenopausal patients (p=0.058). Patients who expressed simultaneously membranous VEGF-C and stromal flt-4 were found to have the worst prognosis as far as both disease-free and overall survival is concerned (p=0.012 and p=0.039 respectively).
Conclusion: VEGF-C and its receptor, flt-4, were associated with biological markers indicative of aggressive tumor phenotype. Furthermore, VEGF-C seems to exert an unfavorable effect on patients' survival, suggesting that it may be an independent prognosticator for invasive breast carcinomas.

P 418
HER2 OVEREXPRESSION PREDICTS SURVIVAL IN STAGE II AND III OF BREAST CANCER PATIENTS TREATED WITH NEOADJUVANT DOCETAXEL PLUS EPIRUBICIN

Daniel Guimarães Tiezzi, Jurandyr Moreira de Andrade, Alfredo Ribeiro-Silva, Marcelo Guimarães Tiezzi, Heitor Ricardo Cosinski Marana, Fábio Eduardo Zola, Joaquim Moraes Sarmento-Filho.
Departments of Obstetrics & Gynecology and Pathology, Faculty of Medicine of Ribeirão Preto, University of São Paulo, Brazil

Objective: The study was designed to evaluate the importance of biological markers to predict response to neoadjuvant chemotherapy and the overall survival in stage II and III of breast cancer patients. Patients and methods: Fifty-two patients received preoperative docetaxel (75 mg/m²) in combination with epirubicin (50 mg/m²) in i.v. infusion in D1 every 3 weeks after incisional biopsy. They received adjuvant chemotherapy with CMF or FEC according the axillary status following definitive breast surgery. Clinical and pathologic response rates were determined after preoperative therapy. We evaluated the response rate to neoadjuvant chemotherapy and the prognostic significance of clinicopathologic and immunohistochemical parameters (p53, HER2, p21, RE and RP). Median patient age was 50 years with a median follow up of 46 moths from time of diagnosis. Results: Preoperative treatment achieved clinical response in 73% and complete pathologic response in 5.7%. The p53 overexpression was associated with an increased rate of objective response (P= 0.04). Among all clinicopathologic and immunohistochemical parameters, only HER2 overexpression, the axillary status (>2 positive LN) and age (under 41 years old) were associated with decrease in disease free survival (P= 0.004, P= 0.001 and P< 0.0001, respectively). The overall survival was reduced in HER2 overexpression patients (P= 0.02) and in patients with

more than seven axillary lymph node metastasis (P= 0.03).
Conclusions: p53 overexpression is associated with a higher objective response rate and HER2 overexpression is associated with poor prognostic in stage II and III of breast cancer patients treated with neoadjuvant taxanes/anthracyclin based chemotherapy.

P 419
IMMUNOHISTOCHEMICAL ANALYSIS OF CHROMOGRANINE A, SYNAPTOPHYSINE AND KI67 IN PURE MUCINOUS BREAST CARCINOMA.
Mrad K, Kacem D, Driss M, Sassi S, Abbes I, Dhouib R, A. Bouziani*,
Ben Romdhane K.
Institut Salah Azaiez, 1006, Bab Saadoun, (*) HMPIT, Tunis, Tunisia

Introduction : Breast mucinous carcinoma (BMC) are characterized by their favourable prognosis but they are not completely homogenous at microscopic level.
Aim of the study : to analyse endocrine differentiation and ki67 in BMC.
Material and method : Only pure BMC are eligible for the study. They were classified as follows according to the proportion of tumor cells/the whole tumor surface : A:<20%, B: 20-50%, C>50% and the presence (1) or absence (2) of cytoplasmic mucus. The following parameters were analyzed: age, follow-up, tumor size, lymph node status, Elston and Ellis grade. Immunohistochemical study of the following antibodies (Dako, dilution : 1/50) was performed : chromogranine A, synaptophysine and Ki67 (clone KiS5).
Results : Endocrine markers are positive in 7 cases. Chromogranine A is positive in 4 cases and synaptophysine in 5 cases with co-expression of the two markers in 2 cases. Two phenotype groups are distinguished :
- group I : immunolabeling of more than 50% of the cells (1+ to 3+)
- group II : immunolabeling of a low number of cells (20% : 1 case, few cells : 2 cases) with high intensity (2+ and 3+).

Expression of neuroendocrine markers is more frequent when the stroma is less abundant (type B and C) and when the cells contain cytoplasmic mucous (type 1). There's no difference for other parameters (size, lymph node, Elston and Ellis grade, survival).
Rates of Ki67 expression was distributed as follows : <1% : 11 cases, <10% : 7 cases, >20% : 4 cases. The rate is not correlated to the cellular type, neither to the the proportion of tumor cells/tumor surface
Conclusion : Endocrine differentiation doesn't influence the outcome of the tumor. The low rate of Ki67 expression could explain the favourable course of the tumor.

P 420
AN IMMUNOHISTOCHEMICAL STUDY OF EXTRAMAMMARY PAGET'S DISEASE
SCHELFOUT Katrien, TJALMA Wiebren, VAN DEN EYNDEN Gert, NAIK Raj, LOPES Tito, VAN MARCK Erik, MONAGHAN John, COLPAERT Cecile

Introduction: Extramammary Paget's disease (EPD) has diverse histogenetic pathways, some lesions originating primarily from cutaneous adnexal structures (primary EPD), while others resulting from secondary involvement of the skin by a subjacent carcinoma (secondary EPD). In primary EPD, most Paget cells seem to be cytokeratin (CK) 7+/CK 20-/gross cystic disease fluid protein (GCDFP-15)+, while CK20+/GCFDP-15- Paget cells suggests the presence of a subjacent cancer with a corresponding immunophenotype, most often a rectal carcinoma or a transitional cell carcinoma (TCC). Mammary and extramammary Paget cells share histopathological similarities. The receptor complex of heregulin-alpha consisting of HER2/neu, HER3 and HER4, is present in almost all cases of mammary Paget's disease. Published studies report a variable (0-88%) overexpression of HER2/neu in EPD. Expression of HER3 and HER4 in EPD has not been studied before.
Aim: To immunophenotype 15 cases of EPD and evaluate the expression of HER2, HER3 and HER4.
Methods: Immunohistochemical stains were performed on formalin-fixed, paraffin–embedded tumour tissue from 15 patients with EPD, using antibodies to CK7, CK20, GCDFP-15, TAB250, CB11, HER3 and HER4. HER2 oncogene amplification was assessed by fluorescence in situ hybridization (FISH).
Results: Mean age at diagnosis was 68.3 years (range 38-84). The EPD involved the vulva and/or perineum or urethra in all females (n=9). In the males (n=6), the EPD was located in perianal, scrotal and/or inguinal regions and symphysis. Eleven tumours were intraepithelial and 4 were invasive. Four patients had a subjacent cancer: 2 rectal carcinomas, 1 in situ TCC and 1 mucinous/endometrioid carcinoma of the vagina. The CK7+/CK20-/GCDFP-15+ immunophenotype was found in 6 cases, all without an associated carcinoma, and CK20+/GCDFP-15- in another 6 cases, including 1 associated TCC and 2 associated rectal carcinomas. The CK7+/CK20-/GCDFP-15- immunophenotype was found in 3 cases, including 1 associated mucinous/endometrioid carcinoma. Three cases of EPD showed HER2/neu oncogene amplification. HER3 and HER4 was expressed in 7 and 9 cases respectively, pointing at a role for heregulin-alpha in the chemotaxis of extramammary Paget cells.
Conclusion: We confirm that immunophenotyping of EPD with CK7, CK20 and GCDFP-15 is valuable in predicting the risk of an associated cancer. New therapies targetting the frequently expressed HER3 and HER4 might be promising.

P 421
VASCULAR ENDOTHELIAL GROWTH FACTOR (VEGF)-A IMMUNOHISTOCHEMICAL EXPRESSION IS ASSOCIATED WITH AN AGGRESSIVE PHENOTYPE IN INVASIVE BREAST CARCINOMA
Mylona E., Giannopoulou I., Alexandrou P., Athanassiadou S., Nikolaou I., Zoumpouli C., Nakopoulou L.
2nd Department of Pathology, "Attikon" Hospital, National and Kapodistrian University of Athens, Athens, Greece.

Introduction: Angiogenesis is a complex process which includes the protelolysis of the basal vascular membrane and intercellular matrix, migration and proliferation of endothelial cells and the formation of tubular structures. Tumor growth is dependent on angiogenesis that is regulated by peptide growth factors of which vascular endothelial growth factor (VEGF)-A is one of the most selective and potent. In the present study we investigated the role of VEGF-A in invasive breast carcinoma through its correlation with classic clinicopathological parameters (menopausal status, tumor size, histologic type, grade, lymph nodal status, stage of the disease, ER, PR), biological markers indicative of aggressive tumor phenotype (p53, c-erbB-2) and invasiveness [Membrane type1- Matrix Metalloproteinase (MT1-MMP)] and patients' survival.
Methods: A three step immunohistochemical method (ABC/HRP) was applied on paraffin embedded sections from 162 patients with invasine breast carcinoma to detect the expression of the proteins VEGF-A, p53, c-erbB-2 and MT1-MMP. Results were subjected to statistic analysis.
Results: VEGF-A was detected in the cytoplasm of malignant cells and the tumor stroma in 49.6% and 48.4% of the cases respectively. Cytoplasmic VEGF-A showed a parallel correlation with accumulative, non functional p53 and c-erbB-2 (p=0.007 and p=0.028 respectively). Additionally, parallel was found to be the correlation between cytoplasmic VEGF-A and MT1-MMP in cancer and stromal cells

(p=0.018 and p=0.020 respectively) as well as MT1-MMP of vascular endothelial cells (p=0.018). VEGF-A was found to have no significant relation to the clinicopathological parameters and patients' disease free or overall survival.
Conclusion: VEGF-A expression seems to be associated with the emergence of an aggressive tumor phenotype through its correlation with p53 and c-erbB-2. Moreover, VEGF-A correlation with MT1-MMP indicates its participation in angiogenesis, which further supports its contribution to the aggressive behavior of breast carcinoma.

P 422
NATURE OF C-KIT ALTERATIONS IN BREAST CANCER. A PUTATIVE NEW PROGNOSTIC AND THERAPEUTIC FACTOR
Isabel Arranz, Sebastian Luna and Dolores Bautista.
Department of Pathology. Hospital Regional Carlos Haya. Málaga. Spain.

Mutations of protooncogen c-kit (CD117)are believed to have a pathogenetic role in several neoplasms. Detected in most gastrointestinal stromal tumors (GIST), are highly relevant for treatment, determining a target for tyrosine kinase receptors inhibitors as Imatinib. C-kit mediated signal pathway is important for the development of breast cancer cell lines and c-kit gene expression seems to be lost in most breast neoplasms. However, an increase of c-kit expression has been associated with aggressiveness and poor outcome. The mechanism of these changes of expression and its importance in breast cancer biology and treatment have not been determined.
In order to study the nature and relevance of c-kit alterations in breast cancer, we have analyzed 85 invasive ductal carcinoma for c-kit expression at protein level, by immunohistochemistry (IHC) using a polyclonal antibody from DAKO, and at mRNA level by Quantitative RT-PCR. We also analyzed DNA for point mutations in exons 9, 11, 13 and 17 of the gene.
Normal ductal epithelia was always positive for c-kit protein but most neoplastic samples lost this expression when analyzed by IHC. However, 11 (12'9%)tumors showed overexpression of the protein, most of them (7 out of 11) of high histologic grade (WHO grade III). None of these cases contained point mutations when DNA was analysed, and the single detected mutation was present in a case negative by IHC. mRNA expression of c-kit in tumor tissues did not correlate with protein expression patterns nor presence of point mutation, suggesting a different origin. The nature, mechanism and significance of c-kit overexpression in breast cancer will be discussed.

P 423
PHYLLODES TUMOURS OF BREAST: A RETROSPECTIVE STUDY OF 18 CASES
GHARIANI Mekki, BAHRI Ibticem, AYADI Lobna, KHABIR A, SELLAMI Ahmed, BOUAZIZ Younes, BOUDAWARA SELLAMI Tahya

Introduction:
Phyllodes tumours (PT) are rare accounting for 0,3 to 1% of all primitive tumours of the breast. They constitute a spectrum of tumours ranging from benign to malignant form.
Objective:
The purpose of this study is to discuss the clinic and pathologic characteristics, the course and the prognosis of PT of breast.
Material and methods:
We report a retrospective study of 18 cases of PT diagnosed in the pathology department of Habib Bourguiba Hospital (Sfax-Tunisia) over a five years period (1999 - 2003)
Results:
The mean age of patients was 40 years (extremes: 17 and 60 years). Most patients (72,3%) gave a history of a slowly enlarging mass. The mammographic aspect was in favour of a benign tumour in ??? cases (71,4%). Macroscopically, the tumour size ranged from 1,5 to 22 cm (mean size : 7,9 cm). 11 PT were benign (61,2%), 4 borderline (22,2%) and 3 malignant (16,6%). A tumorectomy was carried out in 17 cases followed by a mastectomy in 4 cases. One benign PT and one borderline PT recurred after a follow up of 12 and 24 months. Two borderline PT and one phyllode sarcoma metastasised after a mean follow up of 12 months. A complete remission was observed in 15 case (83,3%) with a mean follow up of 32 months (extremes : 2 and 60 months).
Conclusion:
PT are usually benign but relapses and metastases are not uncommon. The clinical course can not be predicted reliably from histologic grading.

P 424
INDUCTION OF APOPTOSIS PREDICTS THE RESPONSE TO THE NEOADJUVANT CHEMOTHERAPY IN LOCALLY ADVANCED BREAST CANCER
Daniel Guimarães Tiezzi, Jurandyr Moreira de Andrade, Alfredo Ribeiro-Silva, Francisco José Cândido dos Reis, Heitor Ricardo Cosiski Marana, Sérgio Bighetti, Antônio Plácido Pereira.
Departments of Obstetrics & Gynecology and Pathology, Faculty of Medicine of Ribeirão Preto, University of São Paulo, Brazil

Objective: This study was designed to evaluate the relationship between the apoptosis induced by chemotherapy and the clinical response in breast cancer. Patients and methods: We studied the Apoptotic Index (AI) and the overexpression of the protein p53 in 44 breast tumors from patients submitted to neoadjuvant chemotherapy. Objective response (OR) to primary chemotherapy was observed in thirty-seven (84%) and no response (NR) in seven. The AI was measured by the rate of apoptotic cells identified by morphological criteria in hematoxylin and eosin stain. The p53 protein expression was evaluated by the immunoperoxidase technique. The cases were interpreted as positive if more than 2/3 of tumors cells exhibited a dark brown nuclear staining. Results: The median AI change (AI initial – AI post-chemotherapy) observed in the patients with objective response was 0.84 while in patients with no response the median AI change was -0.01 (r= 0.40; P= 0.006). P53 protein overexpression was observed in 16.6% of OR patients and 42.8% of NR patients (r= -0.32; P= 0.034). The median AI change in p53-positive cases was 0.75, and in p53-negative cases, it was 1.72 (r= 0.44; P= 0.0029). Conclusion: We find a positive correlation between the increase in the AI and the clinical response and a negative correlation between the p53 expression and the clinical response, in patients with breast cancer submitted to neoadjuvant chemotherapy.

P 425
ADHESIVENESS IN SHORT-TERM PRIMARY CULTURES DERIVED FROM INFILTRATING DUCTAL BREAST CANCER AND THEIR ASSOCIATION WITH CLINICOPATHOLOGICAL VARIABLES
Bértolo C1, Guerrero D1, Vicente F2, Martínez-Peñuela JM3, Córdoba A3, Miranda C2, Ojer A1, Balen E2, Lera JM2
1Centro de Investigación Biomédica, Servicio Navarro de Salud. 2Servicio de Cirugía General y Digestiva, Hospital de Navarra. Servicio Navarro de Salud. 3Servicio de Anatomía Patológica, Hospital de Navarra. Servicio Navarro de Salud.

INTRODUCTION: Breast cancer is the most commonly diagnosed non-skin malignancy in women, being its incidence

and death rates increasing world-wide. E-cadherin adhesion molecule is involved in morphogenesis, maintenance of tissue cytoarchitecture and cellular migration. Short-term primary cultures isolated from ductal breast tumors are more reliable as a tool to study the specific cellular behaviour than commercial cell lines.
PURPOSE OF THE STUDY: We have studied the possible correlation between E-cadherin expression and pathological variables (histologic grade, c-erbB2 amplification…), metastasis, disease-free and survival time periods. The role of E-cadherin and histologic grade in growth pattern and metastatic properties of short-term primary cultures were also evaluated.
PATIENTS AND METHODS: We studied 30 patients that were preoperatively diagnosed with infiltrating ductal breast cancer and were informed about the study and gave their consent. The infiltrating ductal breast cancer tumors (IDC) were classified according to TNM stage, Nottingham prognostic index combined histological grade (NPI) and histologic grade (G1, G2, G3). Cells fractions were isolated and maintained for a short-period of time in 19 viable epithelial cultures derived from breast tumors. Tumor cell invasion was evaluated using a modified Boyden chamber invasion assay. E-cadherin expression was evaluated by immunohistochemistry and Western Blotting.
RESULTS: The median follow-up value was 33.2 months. 63.3% of the tumors were cultured, and their growth rate is associated with G3 (P= 0. 009). Lack of expression of E-cadherin by Western Blot is directly correlated to invasion properties (P= 0.027) and inversely correlated to c-erbB2 overexpression (P=0.008). There is no association between cell invasion and metastasis in vivo (P=0.51). E-cadherin expression did not associate with estrogen and progesterone receptor expression (P= 0.35, P=0.16, respectively) or growth rate (P=0.65). Histological grade is closely associated with ER and PR status (P=0.003, P=0.041, respectively), proliferative index (P=0.005) and overall survival (P=0.009).
CONCLUSIONS: 1. Viability of cultures is closely associated to unfavourable histological grade 2. E-cadherin expression is correlated with invasive properties in cell cultures.

P 426

CARDIOMEGALY AND MYOCARDIAL INFARCTION IN AN INFANT OF A DIABETIC MOTHER

HERVA Riitta, HIRVIKOSKI Pasi, VÄÄRÄSMÄKI Marja and AIKIO Outi
Oulu University Hospital, Oulu, Finland

Introduction
Pregnancy in diabetic women is a risk state that involves increased somatic size or macrosomia, an increased incidence of perinatal death and prematurity, hypertrophy of the islets of Langerhans with B-cell hyperplasia and hyperinsulinemia, and an increased frequency of congenital malformations.Today, diabetes is the most common chronic disease complicating pregnancy and its occurrence is especially high in Finland. The onset of diabetes occurs at an increasingly young age and vascular complications are thus becoming more common. The strain on maternal care services is also increasing. We describe an unhappy case with many complications of diabetic pregnancy.
Case report
The case consists of the second pregnancy and delivery of a 27-year-old female. The mother has had insulin-treated DM1 for 17 years. The first pregnancy in 2003 ended in birth at 38 + 2 weeks. The weight of the baby was 4435g. During the present pregnancy the patient's diabetes was in satisfactory control after the first trimester. In the third trimester, however, she developed pre-eclampsia. Emergency Caesarean section was done at 38 + 3 weeks because of CTG changes. The weight of the male baby was 5370g (+4SD) and length 59cm. Apgar score was 3/5/7 at 1/5/15 minutes. The infant's appearance was typical of diabetic macrosomia. Thorax X-ray and ultrasonography showed a hypertrophic heart. The baby died at 13 hours of age. Autopsy revealed ventricular and septal myocardial hypertrophy and mild obstruction of the outflow canal. There was a recent infarction in the septal myocardium and disorganized structure. The islets of Langerhans in the pancreas were hyperplastic and increased.
Conclusions
In Finland insulin-treated diabetes complicates about 4-5/1000 births. Many pregnant women have had diabetes long enough to develop diabetic vascular complications because the onset of diabetes occurs at a young age. Although hypertrophic cardiomyopathy is uncommon, the findings and the outcome of the present case indicate the importance of third trimester echocardiographic monitoring of fetal heart function when the mother has diabetes.

P 427

RESPIRATORY CHAIN DYSFUNCTION IN "NON-MITOCHONDRIAL" GENETIC DISORDERS – THE ROLE OF PATHOLOGICAL EXAMINATION OF SKELETAL MUSCLE

Maciej Pronicki1, Ewa Matyja4, El¿bieta Czarnowska1, Hanna Mierzewska2, El¿bieta Karczmarewicz3, Ewa Pronicka2
Department of Pathology1, Division of Metabolic Diseases Department of Paediatrics2, Department of Biochemistry and Experimental Medicine, 3 Children's Memorial Health Institute, Warsaw, Poland
Department of Neuropathology Polish Academy of Sciences, Warsaw, Poland4

Detection of respiratory chain (RC) complex deficits in spectrophotometric assay of muscle and fibroblasts consists an important contribution to diagnosis of mitochondrial disorders (MD). However RC complexes may show defective activity in several disorders not primarily related to genes/proteins involved in structure and function of the RC.
Out of 300 skeletal muscle and fibroblast samples obtained from children suspected for MD 130 showed RC dysfunction in spectrophotometric assay. In 51 patients eventually molecular genetic studies of mtDNA and nDNA confirmed the diagnosis of MD. In 27 patients with RC complex deficits other diagnosis was finally confirmed. The diagnoses include: Duchenne and Becker muscular dystrophy, spinal muscular atrophy, myotubular myopathy, glycogen storage disease type II, vanishing white matter leukodystrophy, Lowe syndrome, LCHAD deficiency, Fanconi Bickel syndrome, hereditary fructose intolerance and others. Histological and histochemical assessment of skeletal muscle in children with RC complex deficits revealed: diagnostic pattern of mitochondrial or other non-mitochondrial disease; non-specific lesions; or normal morphology. The mechanisms of RC deficits in patients with diagnoses other than MD are probably diverse and subject to further investigation.
Conclusions: Repiratory chain defects may be associated with various „non mitochondrial'' disordes. Morphological examination remains useful in differential diagnosis of secondary respiratory chain defects. Disregard of morphological examination may lead to misdiagnosis.

P 428

DISEASE OF LETTERER-SIWE: A CASE REPORT

CHEDDADI F.

The Langerhans'cell histiocytosis has an incidence of 5 per million and often occurs in childhood with a male predominance.
Its clinical translation and its forecast are very variable and depend on the age of occurred (lower than two years) and of the organs reached. Pathologies of benign evolution and pathologies of bad forecast are thus defined.

The Langerhans'cell histiocytosis is characterized by a more or less polymorphic inflammatory infiltrate but always containing cells of lang¨¦rhans with notched nucleus which express the CD1a antigen intensely.
The diagnosis of LCH per defect is not posed any more with the advent of the antibody 010.It is necessary to avoid the diagnosis by excess met more and more in inflammatory pathologies or an increase in the histiocytes is observed.
It acts, in the observation which we report of a 4 month old nourrisson which presents:
- a cutaneous eruption generalized prevailing on the level of the folds of inflection,
- three masses of three cm large axis each one, occupying the right and left skull area,
- a hypertrophic gingivitis with early dental eruption,
- a chronic diarrhea,
and a multiple gaps of the dome of the skull with osseous lysis of the internal table.
The diagnosis of LCH was posed on fragments biopsic coming from the left skull mass, gum and the bone.
The cutaneous, oral and osseous attack concomitant realize the board of LCH in its traditional form multi focal and multi systemic and which returns within the framework of the clinical entities of bad forecast.
The marking of the molecule of adherence (¦ÁE¦Â7) could not be done for a digestive attack search.
Conclusion: the disease of LETTERER - SIWE is rare. The majority of the LCH cases corresponds to a focal disease (eosinophilic granulom solitary).the role of the histopathology in the diagnosis of the LCH largely profited from the Ag CD1a.
Unfortunately there are not criteria histopathologic of bad forecast from where major importance of confrontation anatomo-clinic.

P 429
OVERCOMING THE BLOOD BRAIN BARRIER WITH HIGH DOSE ENZYME REPLACEMENT THERAPY IN THE MURINE MUCOPOLYSACCHARIDOSIS VII MODEL OF LYSOSOMAL STORAGE DISEASE
VOGLER Carole, GRUBB Jeffrey, LEVY Beth, GALVIN Nancy, TAN Yun, KAKKIS Emil, PAVLOV Nadine, SLY William S.
Department of Pathology and Edward A. Doisy Department of Biochemistry and Molecular Biology, Saint Louis University School of Medicine, 1402 South Grand Blvd., St. Louis, MO 63104, USA and Division of Medical Genetics, Department of Pediatrics, Harbor-UCLA Research and Education Institute, Torrance CA USA and BioMarin Pharmaceutical Inc., Novato, CA USA

Enzyme replacement therapy (ERT) with recombinant enzyme is effective in reducing lysosomal storage in patients with several of the lysosomal storage diseases although improvement in CNS disease has been limited because the blood brain barrier restricts access of enzyme to the CNS. ERT with recombinant beta-glucuronidase (GUS) is not yet available for human MPS VII. However, there is a good murine model for this disorder in which glycosaminoglycan storage in the CNS produces severe cognitive disability. Studying this model, we found that the CNS is accessible to and improved by infused recombinant human GUS (rhGUS) in the newborn period but not improved by treatment begun after age 2 weeks. We recently reported that this enzyme delivery to brain in the newborn period is dependent on transcytosis of phosphorylated enzyme across the blood brain barrier by the mannose 6-phosphate/IGF-2 receptor. Down-regulation of this receptor mediated delivery system by age 2 weeks appears to explain the lack of response in the adult MPS VII mouse. In the current study we asked whether the obstacle to enzyme delivery to the CNS in the adult could be overcome by administering much higher doses of enzyme than used in conventional trials. We measured reduction in lysosomal storage for doses of 0.3-40 mg/kg body weight of rhGUS administered i.v. for 1 – 13 weeks to MPS VII mice tolerant to GUS. Mice treated for only 3 weeks with 0.3-5 mg/kg enzyme weekly had a slight reduction in meningeal storage but no change in storage in neurons. When mice received doses of 1-4 mg/kg/week for 13 weeks, there was a dose-based therapeutic effect on meninges, parietal neocortical and hippocampal neurons and glia. Only mice treated with 4 mg/kg showed a response in both neocortex and hippocampus. However, doses of 20-40 mg/kg GUS given 3 times over 1 week failed to reduce storage in any area of the CNS except the meninges. On the other hand, mice given 20 mg/kg weekly for 4 weeks, showed a decrease in neuronal, glial and meningeal storage and, on average, 2.5% of wild type GUS activity in brain. Our results indicate therapeutic enzyme can be delivered across the blood brain barrier in the adult MPS VII mouse if 1) one administers higher doses of enzyme than used in conventional ERT trials and 2) if these high doses of enzyme are administered over a sufficient period of time. These results have important implications for ERT for human lysosomal storage diseases.

P 430
SOLID PSEUDOPAPILLARY TUMOR OF THE PANCREAS IN CHILDREN
NICULESCU Liviu 1,CITU Rafira 2,ARDELEANU Carmen 3,PETRESCU Amelia 4
1.University of Medicine and Pharmacy "Carol Davila",2."Grigore Alexandrescu" Children Hospital,3."Victor Babes" Institute of Pathology, 4."Prof Dr.Th.Burghele" Clinical Hospital,Bucharest,Romania

Introduction:Solid pseudopapillary tumors of the pancreas are rare and their origin is unknown.The aim of this work is to report a new case diagnosed at a child.Thus ,we present the case of 14 years old girl hospitalised for complaining of severe epigastric pain. The radiological examination demonstated a well- demarcated pancreatic mass.The sugeons decided to remove the tumor.
Macroscopically examination carried out the removed tumor showed a 5 cm.diameter,well circumscribed and capsulated tumor with a gray-whitish colour on cut surface,soft consistency and haemorrhage zones.
Material and methods: Fragments of the tumor were fixed in formaldehyde 10% included in paraffin and the sections were stained with HE,VG and immunohistochemical markers like Vimentine (VIM), progesteron receptors(PR),neuron-specific enolase(NSE) and glucagone.
Results:The histological examination revealed proliferation of uniform cells with basophilic cytoplasm without atypia arranged in nests;between nests we observed giant multinucleated cells ,cholesterol crystals within a haemorrhagic stroma and pseudopapillary features.Immunohistochemical analysis : VIM positives, PR diffuse positives,NSE diffuse positives,glucagone positives
Conclusions: All these findings plead for the diagnosis of solid pseudopaillary epithelial tumor of the pancreas.

P 431
SOME IMMUNOPATHOLOGICAL CHARACTERISTICS OF EPITHELIAL CHANGES IN JUVENILE POLYPS OF COLON AND RECTUM IN CHILDREN
A. S. Tertychnyy, D. M. Konovalov, N. S. Marenich, A. G. Talalaev, Russian State Medical University, Moscow, Russia

The aim of this study was to outline variants of morphological epithelial changes in solitary juvenile colorectal polyps.
Material and methods: Formalin fixed paraffin embedded tissues were obtained from 30 patients with solitary juvenile polyps (JP) of colon and rectum. Patients were 6 months - 9

years old (median age 4.3 years). Localization of polyps was the rectum (n=22) and sigmoid colon (n=8). Size of JP varied from 0.5 to 5.0 cm (median 3.4 cm). H&E, histochemical (van Gieson, periodic acid Shiff (PAS) and Gomori's aldehyde fushcin - Alcian-blue (GAF-AB) stains and immunohistochemical (expression of Ki-67, p53 and carcinoembryonic antigen (CEA)) analyses were performed.

Results: The following morphological variants of epithelial changes were observed: in 25/30 JP comprised reactive regenerative changes within focal complex glandular structures, with high mitotic counts and expression of Ki-67. 22/30 cases showed hypertrophic epithelial changes, consisting of enlarged and pseudostratified goblet cells, suggestive of so called transitional mucosa. In 19/30 cases we observed focal cytoplasmic expression of CEA. 12/30 cases showed eosinophilic epithelial changes consisting of glands with abundant eosinophilic cytoplasm and centrally located small round nuclei. Expression of Ki-67 and CEA was negative in this group. In 7/30 cases we observed Paneth cell metaplasia, and in 5/30 cases, mild dysplasia with expression of p53 in less than 10% of nuclei in polyp glands.

Conclusion: JP showed a board spectrum of epithelial changes that might represents degenerative, regenerative and metaplastic processes. The main diagnostic pitfall is early dysplasia. Level of expression of p53 in JP may aid in differential diagnosis between reactive, regenerative changes and dysplasia.

P 432

HETEROTOPIC ORAL GASTROINTESTINAL CYST : REPORT OF A CASE

Nona Zabolinejad,MD*,Mehran Hiradfar**
*Department of Pathology,**Department of Pediatric Surgery
Dr. Sheikh Children Hospital,Mashhad-IRAN

Heterotopic gastrointestinal cyst of the oral cavity is an extremely rare lesion which fewer than 40 cases have been reported in the English language literature. They usually involve the soft tissue of the floor of the mouth and the tongue. The lining of these lesions resembles gastric or intestinal mucosa. In this report we describe an oral heterotopic gastrointestinal cyst of tongue in a 1-month-old boy and discuss its pathogenesis.

P 433

A CASE OF A COMPLETE PYLORIC PANCREATIC HETEROTOPIA AT CHILD CAUSING GASTROESOPHAGEAL REFLUX

NICULESCU Liviu 1, CATU Rafira 2 , ARDELEANU Carmen 3, PETRESCU Amelia 4
1."Carol Davila" University of Medicine and Pharmacy ,Bucharest,Romania 2.“Grigore Alexandrescu” Children Hospital, Bucharest, Romania 3.“Victor Babes” Institute, Bucharest, Romania 4.“Prof.Dr. Th. Burghele”Hospital, Bucharest, Romania

Introduction and aim: Heterotipic pancreas is usually found incidentally. Despite many cases having been reported heterotopic pancreas causes diagnostic difficulties for clinicians.Authors report a case of 1 year 1 month baby boy hospitalized for a history of vomiting, bleeding, gastroesophageal reflux and weight loss.
Plain abdominal radiograph showed a “trumpeting elephant” image.Endosonographical examination revealed a pyloric mass and a surgery was conducted to explore the area for tumor ablation.
Macroscopic examination showed a small tumor with a diameter of 6mm, firm, yellow, sharply circumscribed from the surrounding tissues, located beneath a mucosa;central umbilication was present.
Material and methods: Fragments of the tumor were fixed in formalin 10%, embedded in paraffin and sections were stained with HE. Immunohistochemical tests have been done:CD 56, Chromogranine, Glucagone, Insuline, Somatostatine, Sinaptophizine and VIP.
Results: Microscopic examination revealed a tumor proliferation consisting of acini‘s group, pancreatic ducts, Langerhans island on the pyloric sub- mucous and hypertrophyc muscular layer. The tumor was positive for insuline, glucagone, VIP,CD 56
Conclusions:The morphological appearance and immunohistochemical results enabled us to the diagnosis of complet form of heteritopic pancreas.It is important to differentiate between a cancer, an ectopic pancreas , a metastasis of a tumour and a pancreatic metaplasia of gastric mucoasa. Thus,an ectopic pancreas must be considered in the differential diagnosis of gastroesophageal reflux.

P 434

IDENTIFICATION OF THE MOTILIN CELLS IN DUODENAL EPITHELIUM OF PREMATURE INFANTS

NISHIKUBO T1), YAMAKAWA A2), NISHINO M3), NAKAJIMA M4), TAKAHASHI Y5), NAKAYAMA M6), KITAJIMA H7) AND FUJIMURA M7)
1)Neonatal Intensive Care Unit, 2)Clinical Laboratory Division, and 3)Department of Pediatrics, Nara Prefectural Hospital, 4)Department of Pediatrics and 5)Neonatal Intensive Care Unit, Nara Medical University Hospital, Nara, 6)Department of Pathology and 7)Neonatal Intensive Care Unit, Osaka Medical Center and Research Institute for Maternal and Child Health, Osaka, Japan

Introduction: Motilin is one of the gastrointestinal hormones, and originates in the endothelial cells of the upper small intestine. Motilin regulates the gastrointestinal motility via migrating motor complex (MMC) activity. Most preterm infants of <32 weeks gestation are considered to lack MMC activity.
Purpose: The aim of the present study was to examine the presence of motilin in the duodenal epithelial cells of premature infants of <32 weeks gestation.
Methods: Specimens from 10 deceased infants (gestational age: 26.4 • } 2.7 weeks and birthweight: 808 • } 303 g) were examined as subjects. All infants died of severe cardiopulmonary disorder or intraventricular hemorrhage (grade IV). The average survival period was 3.1 • } 1.9 days. Autopsies were performed and formalin-fixed duodenums were immunostained with rabbit antiserum to motilin by the labeled streptavidin-biotin (LSAB) method. An adult duodenum obtained by pancreatoduodenectomy was also examined for the presence of motilin as a positive control specimen. An absorption test using motilin peptide was performed to prove the specificity of the binding with rabbit antiserum to motilin.
Results: Motilin-containing cells were detected in the adult specimen, and the binding by rabbit antiserum to motilin was completely inhibited by excess amounts of motilin peptide, indicating that this binding was specific to motilin. All 10 infants had presence of motilin antigen in the epithelial cells of their duodenums.
Conclusion: This preliminary study indicates that the immunohistological analysis is specific to detect motilin-containing cells, and certifies the presence of motilin in duodenal epithelial cells of premature infants of <32 weeks gestation, including one at only 22 weeks gestation.

P 435

KARYOMETRIC ANALYSIS OF THYMOCYTES IN DOWN SYNDROME

MIHAILOVIC Dragan, KUTLESIC Cedo, DJORDJEVIC Biljana, MIJOVIC Zaklina, GOVEDAREVIC Nenad
Institute of Pathology, University of Nis, Serbia

Introduction. Down syndrome (trisomy 21) is the most common numeric aberration of autosomal chromosomes in man; the incidence in newborn is about 1 in 700. Intrauterine growth retardation is a consistent finding in infants with Down¡¦s syndrome. The common anomalies, in order of frequency, are cardiac defects, duodenal obstruction, talipes equinovarus, cataracts, imperforate anus, cleft lip or palate, congenital megacolon, and meningomyelocele. Endocrine disorders in patients with Down¡¦s syndrome include hypothyroidism, occasionally associated with precocious puberty or diabetes mellitus. T-cell immunodeficiency in Down syndrome has been well documented.
Purpose of the study. To estimate nuclear size and integrated optical density of thymic lymphocytes in patients with Down¡¦s syndrome and control group.
Material and Methods. During the years 1988 to 2000, fourteen cases of Down¡¦s syndrome were found (eight male and six female). Ten babies without congenital anomalies, died with respiratory distress syndrome, were analyzed as a control group. Karyotyping was performed in all cases during life. After standard pediatric autopsy, 5 ƒÝm thick sections were stained with hematoxilin and eosin. Karyometric analysis was done using ImageJ software, NU-1 microscope (Carl Zeiss, Jena, Germany), at objective x63 (NA=0.65), after manual editing of a binary image.
Five nuclear variables were estimated: mean number of lymphocyte nuclei per visual field, area, perimeter, circularity, and integrated optical density (IOD), in both cortex and medulla.
Results.In the thymic cortex, the mean number of lymphocyte nuclei was significantly lower in patients with Down syndrome. Integrated optical density of thymocyte nuclei was significantly higher in Down syndrome patient, compared to control group. Thymocytes nuclei were smaller in Down syndrome patients, but this difference was not statistically significant.
Conclusions. In Down syndrome patients the thymus is usually small and may be dysplastic with lymphocyte depletion; a small, contracted cortex and loss of corticomedullary demarcation resemble thymic involution. Large Hassall¡¦scorpuscles with calcification and cystic change in the thymus has been suggested as a marker for Down syndrome. The present results suggest altered gene expression in excessive genetic material, disordered maturation of cortical lympohocytes, with decreased number and increased chromatin density.

P 436
MORPHOLOGIC AND ULTRASTRUCTURAL FEATURES OF SOFT PALATE AND PHARYNGEAL MUSCLES IN CHILDREN WITH CLEFT PALATE
CECCHETTI Denise, *LUCCHESI Paolo, POLLINA Luca Emanuele, **SANSEVERO Stefano, **MASSEI Alessandro, FUNEL Niccola, BEVILACQUA Generoso, VIACAVA Paolo
Division of Surgical, Molecular and Ultrastructural Pathology, Department
of Oncology, University of Pisa, Pisa, Italy
* Department of Human Morphology and Applied Biology, University of Pisa, Pisa, Italy
** Department of Plastic Surgery, Hospital of Pisa, Pisa, Italy

Introduction. Palate and lip muscle alterations in patients with cleft are poorly known. Few studies have focused attention on lip muscle, while very rare data are reported on the pathologic features of palate muscles. The morphological alterations of palate and pharyngeal muscles in infants with cleft palate could be responsible for a persistent postsurgical velopharyngeal insufficiency with consequent inadequate functional recovery especially for speech and swallowing.
Purpose. Based on this, we decided to analyze the histologic features of the superior pharyngeal constrictor muscle and right and left palatopharyngeal muscles in a series of 11 patients affected by isolated cleft palate and 9 patients affected by unilateral or bilateral cleft lip and palate. In 4 cases ultrastructural analysis was also performed. Methods. A muscle biopsy was done during palatoplasty. Muscle sections were stained with hematoxylin-easin, modified Gomori trichrome, PAS and NADH-TR. The analyzed parameters were: organization and type of muscle fibers, presence of ragged red fibers, characteristics of nuclei, degree of fibrosis, presence of adipose tissue and inflammatory infiltrate.
Results. Our results showed the presence in both type of muscle of dystrophic-like alterations such as variability of fiber size, increase of connective tissue and presence of adipose tissue. No ragged red fiber, inflammatory infiltrate or neurogenic atrophy was observed. Electron microscopy evidenced focal areas of disruption of myofibrils containing amorphous materials. Conclusions. The marked alterations of palate muscles in children with cleft suggest that muscle damage could represent a significant pathogenetic factor in this type of malformation. The degree of muscle alterations may be responsible for a persistent postsurgical velopharyngeal insufficiency despite successful surgical repair. Muscular biopsy during palatoplasty could offer useful functional prognostic information in patients with cleft lip and palate.

P 437
HYPOPHYSEAL DUPLICATION WITH FRONTONASAL AND CNS MALDEVELOPMENT
González-Obeso E.(1), Morales C (2), Mariño A (1), García-Fernández E (1), Rodríguez JI(2).
Department of Pathology. La Paz University Hospital. Madrid. Spain.
(1) Tranee resident; (2) Medical Doctor.

INTRODUCTION: Hypophyseal duplication is an uncommon malformation that appears isolated or associated with craniofacial malformations. About 24 cases have been reported since 1880.
PURPOSE OF THE STUDY: To present a new case and review the central nervous system (CNS) and craniofacial anomalies associated with hypophyseal duplication in the autopsy cases reported in literature.
METHODS: Clinical reports, scanner images, and autopsy study of a girl (46, XX) 2 months and 20 days old.
RESULTS: The propositus had frontonasal malformation (hypertelorism, broad nasal bridge, bifid nasal tip and bifid anterior cranium), macrostomia, retrognathia, and bifid tongue. She also presented maxilomandibular bony fussion, as well as fussion of the tongue to the palate and to the inferior lip by a hairy polyp, both corrected surgically.
In the cranium, the sella turcica was broadened, with little prominence of the clinoid apophyses, and with two cavities that contained two complete hypophyses with two infundibules. The three cranial fosae where narrowed antero-posteriorly.
The CNS had both olfactory bulbs and corpus callosum agenesis, anomalous morphology of the brain stem and spinal cord, and neuronal heterotopia in occipital white matter and leptomeningeal heterotopia.
CONCLUSIONS: There are seven previous autopsy cases of hypophyseal duplication that associate, in order of frequency, the following frontonasal malformations: hypertelorism (6 cases), an intraoral mass –epignatus- (4), bifid tongue (3), duplication of the anterior groove of the spinal cord (1), and "V" shaped hairline (1). The associated anomalies of the CNS reported were broadened sella turcica and hypothalamic anomalies (7); corpus callosum agenesis (5) and olfactory bulbs agenesis (2), and glial and/or neuronal heterotopias (1).
The present case has several common features with the one described by Hori et al. in 1983, that, in addition, had cleft palate, abnormal circle of Willis, duplication of the spinal

cord groove extended to the thoracic level, but it had no olfactory bulbs agenesis.
There are several hypothesis about the origin of the hypophyseal duplication and the associated malformations, yet none of them is definitive.

P 438
MELANOTIC NEUROECTODERMAL TUMOR OF INFANCY IN THE RETROAURICULAR REGION: A CASE REPORT.
EFSTRATIOU Ioannis (1), ZAVITSANAKIS Athanassios(2), NEOFYTOU Andreas (2), PETROPOULOS Anastassios(2).
1. Institute of Pathology
2. Department of Children Surgery, Papageorgiou Hospital Thessaloniki Greece

EFSTRATIOU Ioannis, ZAVITSANAKIS Athanassios, NEOFYTOU Andreas, PETROPOULOS Anastassios.
Melanotic neuroectodermal tumor of infancy in the retroauricular region: a case report.
Melanotic neuroectodermal tumor of infancy (MNTI) is a very rare neoplasm arising in the first year of life and localized mainly in the craniofacial region. It grows rapidly and has a high rate of recurrence.
We report a case of MNTI because of its unusual extraosseous localization. The tumor has been investigated by means of histology and immunhistochemistry,
A 10 month-old male infant presented with a swelling of the left retroauricular region. Ultrasonography showed a soft tissue lesion 1 cm in diameter with poor vascularisation without destruction of the scull. A dermoid cyst was suspected.
The surgical specimen measured 1,5x1x0,5 cm and had a whitish focally black color with elastic consistency.
Histologically the tumor consisted of alveolar nests and tubules within fibroblastic tissue. These formations were composed of two cell populations, large melanin-containing cells around smaller neuroblast-like cells with smashed nuclei. Immunhistochemically the melanocyte-like cells expressed cytokeratin and HMB-45. The smaller ‘blue cells’ didn’t stain for any marker due to the smudging artefact. Histological and immunhistochemical characteristics of the tumor confirm the diagnosis of MNTI. Six months later the patient has no evidence of recurrence.
MNTI is a dysembryogenetic tumor of neural crest occurring commonly in the maxilla and in the mandible. In our case the tumor had a very infrequent site. The vast majority of these tumors behave in a benign fashion after local excision. However follow-up for at least 2 years is necessary because of the high recurrence rate.

P 439
DIFFERENTIATED MELANOTIC NEUROECTODERMAL TUMOR OF INFANCY
PARK So Yeon, HYUN Chang-Lim, LEE Youn Kyung, LEE Hye Seung, CHUNG Jin Haeng, CHI Je Geun, CHOE Gheeyoung
Department of Pathology, Seoul National University Bundang Hospital, Seoul National University College of Medicine

A three-month-old male infant was admitted due to left temporal mass. He was born at full term by vaginal delivery. His birth weight was 2.8 kg and his head circumference was within normal limits. A mass was noted on left temporal area at the age of one month, and the mass progressively increased in size. Brain CT revealed an extra- and intra-dural tumor with calcification and destruction of overlying calvaria. Temporoparietal craniotomy with near-total removal of the tumor was done. On operation, the tumor involved left temporal bone, periosteum, dura and cerebral cortex. Microscopically, the tumor consisted of lobules and solid clusters of monomorphous small cells admixed with gland-like or tubular arrangements of pigmented epithelium. Both pigmented melanin-containing epithelial cells and a small-cell component resembling neuroblasts were present, and the diagnosis of melanotic neuroectodermal tumor of infancy (MNTI) was made. The patient received 18 cycles of ¡°8 drugs in 1 day¡± chemotherapy for 15 months. Follow-up CT disclosed a residual mass attached to the petrous bone with a peritumoral cyst. The mass showed strong contrast enhancement. Second operation was done 11 years after the first operation, and the residual mass was excised. The surgical specimen of second operation was a 3 cm-sized, pigmented mass with focal calcification. Microscopically, the tumor consisted of two different components. In the center of the tumor, pigmented epithelial cells formed clusters, glands or tubules. In the peripheral region of the tumor, lobules of mature ganglion cells, immature ganglion cells and abundant neuropil were surrounded by pigmented epithelial cells and fibrovascular septa. Compared to the original tumor, the residual tumor revealed extensive maturation of neuroblast-like small cells. We diagnosed this case as a differentiated MNTI.
MNTI is a rare but well-documented lesion of neuroectodermal derivation. Maturation of the neural elements has been reported only occasionally. To the authors' knowledge, this case is the first one of MNTI in which neuronal differentiation of the neuroblastic cells is convincingly demonstrated in a residual tumor over 10 years, and in which chemotherapy might have induced differentiation of the neuroblastic cells.

P 440
1H MRS STUDY OF THE BRAIN IN NORMAL CHILDREN AND IN CHILDREN WITH SEIZURE DISORDERS
ROGOZHYN Vladimir, ROZHKOVA Zina, KIRILLOVA Lyudmila
Radiological Center of the Academy of Medical Sciences of Ukraine, Kiev, Ukraine

Purpose: We propose the quantitative indicators for the characteristics of regional and age-related peculiarities of brain metabolism in normally developing children and in children with seizure disorders.
Materials and Methods: Two groups of children are examined by 1H MRS using 1.5T Magnetom Vision (SIEMENS). The 1st group (NG) consists of 10 healthy children (in the age from 1 months to 16 years). The 2nd group (PG) includes 24 developmentally delayed children with seizure disorders (in the age from 2 weeks to 10 years). In all children 12x12 spectral matrixes in supraventricular region parallel to the canthomeatal line are obtained. 2DCSI 1H spectra are recorded with: TR/TE=1500/135 ms, NS = 1.
Results: In each voxel of the spectral matrix we introduce two indicators: the metabolite content AM as the peak area and the metabolite concentration CM as the ratio of the peak area to the sum of all the peak areas S: CM=AM/S. We describe the metabolic state in each voxel by the triad T* ={ACho, ACr, ANAA}, where ACho, ACr, and ANAA are the peak areas of the signals from Cho, Cr and NAA. For each of the areas we assign three values: 1, 2 and 3, to obtain six symbolic spectral configurations:1* ={1,2,3}, 2* = {2,1,3}, 3* ={1,3,2}, 4* ={3,2,1}, 5* ={3,1,2} and 6* ={2,3,1}. We analyzed the temporal alterations of the triad distributions during neurodevelopment. In the NG during infancy (from 1month to 1 year) the most frequent configurations in gray and white matter are 3*, 4* and 5*. During childhood (from 1year to 11 years) in the NG triads 1* and 2* dominate in all voxels of VOI. In the PG in the electrically defined seizure focus the triads 5* and 6* are observed. Signal of lactate is elevated only in children of PG, who had seizures immediately before MRS-examination.

Conclusion: The triad distributions in developing brain give us a quantitative way for the estimation neurodevelopmentally abnormalities.

P 441

THE CHILD'S CEREBRAL TUMORS

Hanane Rais, Fatiha Benadra, Badiaa Belaabidia
Department Of Pathology, CHU Mohammed VI - Marrakec-Morroco

The child's cerebral tumors (CCT) are rare. They represent 20% of the child's malignant tumors. They constitute the second malignant tumors in pediatrics after the leukemias 34,5% and the first cancer strong tumor, just before the lymphoma 7-10%. The object is to value through a set of 52 cases of CCT the epidemiological and pathologic features of this pathology. It is a retrospective review (survey carrying) on 210 cases of cerebral tumors collected to the service of anatomy pathology between June 2001 and August 2004.
The CCT represent 24,76% of the cerebral tumors. The median age at diagnosis was 8.9 years (range 2-16 years). The sex-ratio was 2 with a masculine predominance. The cerebral tumors of the posterior fossa cerebral occupied the first rank with 68.18%. The médulloblastoma represents 51,9% followed of the astrocytoma 19,23%. The CCT are highly heterogenous, so in every case the histological diagnosis should be obtained. They distinguish themselves to the one of the adult by a particular topographic and histological distribution: Big frequency of the tumors of the posterior fossa cerebral, clean predominance of the astrocytoma, médulloblastoma. Their diagnosis require an anatomo-clinical and radiological confrontation. Prognostic factors are the degree of histologic malignancy and the extent of surgical resection.

P 442

ENCEPHALOCELE ASSOCIATED TO AN AGENESIS AND A LIPOMA OF CORPUS CALLOSUM : A CASE REPORT.

ELBAKKOURI Jalila (1), RAIS Hanane(1), ALATAWNA Hind (1), ELATTAR Hicham(1), LOQA C. (2), BELAABIDIA Badia (1), AIT BENALI (2).
(1) Department of anatomopathology – (2) department of neurosurgery.
CHU Mohammed VI - Marrakech

Lipomatous hamartomas are rare disorders affecting the central nervous system. Forty percent of all lipomas develop in the anterior third of the corpus callosum. In 48% of the cases, there is partial agenesia of the corpus callosum. In 50% of the cases, there is no clinical expression.

We report the case of a 30 months old boy with frontal tumefaction since his birth. The neurological examination was normal. There were no associated malformations. The brain computed tomography scanning showed a lipoma and an agenesis of the corpus callosum. An hydrocephaly of the temporal and occipital corns has been found. Surgery was indicated. The mass was composed of typical adipose tissue in which a large number of blood vessels were present. The evolution was marked by post-surgery meningitis.

Our purpose was to describe a very rare association of an encephalocele, agenesis and lipoma of the corpus callosum.

P 443

IMMUNOHISTOCHEMICAL EXPRESSION OF CELL CYCLE REGULATORS IN PEDIATRIC EMBRYONAL BRAIN TUMOURS

STEFANAKI Kalliopi,ARGYRAKOS Theodore,VAN VLIET-CONSTANTINIDOU Catherine,MOSCHOVI Maria,PATERELI Amalia,SAKELLIADIS Emmanuel ,HADJIGEORGI Christiana,SFAKIANOS George,PRODROMOU Fivos,KARENTZOU Ourania.
Dept.of Pathology,Computerized Tomography,Neurosurgery of "Aghia Sophia Children's Hospital,Dept.of Oncology-Haematology First Pediatrics Clinics of Athens University,Athens Greece

Background:Embryonal brain tumours in children are aggressive neoplasms with overlapping clinical and histological features.The distinction between Medulloblastomas(MB)and Atypical Teratoid Rhabdoid tumours(ART)has prognostic and therapeutic value.
The purpose of this study was to investigate the immunophenotypic features and the expression of cell cycle regulators,p27,Cyclin D3,Cyclin E,in 35 pediatric embryonal brain tumours in correlation with Ki-67 and p53,bcl-2 proteins.
Our material comprised 29 MB and 6 ART.The Streptavidin-Biotin HRP method was performed on paraffin sestions for the detection of Synaptophysin(SY),GFAP,Neurofilaments(NF),EMA,Cytokeratin AE1/AE3,Cytokeratin 8,Vimentin(VIM),Smooth muscle actin(SMA),Desmin,Ki-67/MIB-1,P53(DO7),bcl-2,p27(1B4),Cyclin D3,Cyclin E with monoclonal antibodies.
The immunophenotype of MB was:29+/29 SY,9+/29NF,5+/29 GFAP,0/29 EMA and AE1/AE3,while the ART were:6+/6 VIM,5+/6 EMA,6+/6 AE1/AE3 and Cytokeratin 8,4+/6 NF,5+/6 GFAP,4+/6 SMA.
High expression of Ki-67(>25%)and p27(>50%)was observed in 89,6%(26/2)]and 79%(23/29) of MB respectively with increasing p27 expression in areas of neuroblastic differentiation.Cyclin D3 and Cyclin E were detected in 25%(6/24)and 62,5%(15/24)of MB.
High Ki-67/high p27 was observed in 68,9%(20/29) of MB with detection of Cyclin E in 65%(13/20) and a parallel Cyclin D3 expression in 3 MB.P-53 and bcl-2 proteins were detected in 75%(22/29)and 27,5%(8/29) of MB respectively.
High Ki-67(>25%) and p53(>10%)expression was revealed in all ART,while high bcl-2 and p27 expression was observed in 5. Cyclin E and Cyclin D3 were detected in 6 and 1 ART respectively.
In conclusion,the complex immunophenotype including the detection of epithelial markers contributes significantly in the differential diagnosis of ART from MB.
The parallel high Ki-67/p27 expression in correlation with Cyclin E detection in a considerable number of MB and ART suggests that dysregulation of G1/S transition may play an important role in their pathogenesis.

P 444

CHILDREN'S KAPOSI'S SARCOMA IN CAMEROON(CENTRAL AFRICA) WITHIN THE ONGOING AIDS EPIDEMIC AN ENDEMIC AREA

NKEGOUM Blaise(1),GESSAIN Antoine(2),DOUMBE Pierre(3)
1- Service of Pathology, University Teatching Hospital-Yaondé-Cameroon email: nkegoum@yahoo.fr
2-Unit of Viral Oncology,Pasteur Institute-Paris-France
3-Department of Pediatric,Unit of Children oncology-Yaoundé-Cameroon

Background: Cameroon (Central Africa) was known to be an endemic area af Kaposi's sarcoma even before the unset of AIDS epidemic. Jensen and al reported 16 cases of Kaposi's sarcoma in cameroonian children between 1968 and 1974. An increase in the incidence of Kaposi's sarcoma have being noted in AIDS patients
allover the world nowadays. The aim of this study was to show the anatomoclinical aspects of Kaposi's sarcoma within the ongoing AIDS epidemic in Cameroon.

Materials and methods: we carried out this retrospective study over a period of 18 years (from 1987 to 2004).All cases of children Kaposi's sarcoma were retrieved. We noted:
- the total number of Kaposi's sarcoma within the period of study,
- the ages and gender of the patients,
- the clinical signs,
- the HIV status,
- the pathological aspects,
- the treatment received and the evolution under treatment.
Results: among the 575 cases of Kaposi's sarcoma noted, 4% were aged 0 to 15 years. The youngest patient was aged 3 months and was HIV positive. The male to female ratio was 3/1. The most common site of involvement was cervical lymph nodes. All the chidren presented with fever and weight loss. Skin and lymph nodes were simultaneously involved in 2 cases. Only 4 cases of HIV positive serology were observed in this serie of children and their mothers. The pathological aspect most frequently observed was advanced stage Kaposi's sarcoma. Less than 10 children received fulldose of chemotherapy made up of cyclophosphamide, vincristine and prednisone. Only one child survived 9 years after chemotherapy.
CONCLUSION: Children Kaposi's sarcoma is still a rare disease in Central Africa for the moment.

P 445
INTRAMEDULLARY OSTEOID OSTEOMA: A CASE REPORT.
ELBAKKOURI Jalila (1), BELAABIDIA B. (1), KASSIMI Nabil (2), OULED SAID (2).
(1) department of anatomopathology -
(2) department of Paediatric Surgery.
CHU Mohammed VI - Marrakech

Osteoid osteoma is a benign bone tumour. It accounts for 2 to 3% of the whole of bones tumours. The intramedullary localization is rare and poses diagnosis problems at the radiological stage.
We report the case of an 8 years old boy without particular pathological antecedents. He has consulted for pains of the left leg appeared 6 months before. Plane radiographes objectified a medullary tibial hyperdensity and a cortical thickening. The computed tomography showed intramedullary calcifications.
A biopsy exerèse of the tumour was carried out. The anatomo-pathological examination confirmed the diagnosis of the osteoid osteoma.

Intramedullary osteoid osteoma is rare. It poses a real radiological diagnosis problem. Its final diagnosis is anatomo-pathological. The characteristics of our case are the unusual localization of the osteoid osteoma associated with intense reactive bone sclerosis.

P 446
CONGENITAL BILATERAL ADRENAL NEUROBLASTOMA WITH MULTIPLE METASTASES: A CASE REPORT
SPASEVSKA Liljana, JANEVSKA Vesna, PETRUSEVSKA Gordana, JOVANOVIC Rubens, RISTOVSKI Milco, BANEV Saso
Institute of Pathology, Faculty of Medicine, Skopje, R. Macedonia

We report a case of bilateral congenital neuroblastoma (NB) with multiple metastases found at autopsy.
The neonatus was born by normal vaginal delivery in a local hospital at 40 weeks of gestation and weighted 3000g. Maternal history was unremarkable. His abdomen was markedly distended, suspected to congenital malformation. Prenatal ultrasound was not peformed. He was urgently transported to the Central Hospital but died on the way two hours after birth.

Postmortem examination, revealed a relatively well demarcated huge tumors in the both adrenal glands with necrosis and hemorrhage. The kidneys were not involvded by tumors. The left tumor measured 4x4x2cm and weighed 120g and the right tumor measured 6x4x2cm , weighed 140g. The left tumor was ruptured with massive intraabdominal bliding (300ml). Multiple metastatic nodules in the liver (500g), lung and in the brain were noted. The other organs were grossly unremarkable. Microscopically the tumors were composed of small poorly differentiated neuroblasts with minimal stroma and without fibrillary background. The diffuse pattern of growth was accompanied with necrosis, hemorrhage, angiomatoid and pseudovascular formations. The tumor cells were immunoreactive for neuron specific enolase, chromogranin and synaptophysin, while desmin, MIC2, and leucocyte comman antigen were negative. The microscopical findings of the liver, lung and brain were similar. A diagnosis of NB with multiple metastases was made. The NB was classified on the basis of INPC (Shimada) classification as one of the stroma-poor tumors, poorly differentiated, with mitosis karyorrhexis index of less than 200 - faborable histology.

P 447
RENAL DYSPLASIA. ANALYSIS AND CLASSIFICATION OF 16 POST-NATAL CASES.
SALERNO Angela.
Servizio di Anatomia e Istologia Patologica e Citodiagnostica. Ospedale Maggiore. Bologna. ITALY

INTRODUCTION.
Renal dysplasia (RD) is the major cause of renal failure in children. It consists of a heterogeneous group of disorders with different etiologies and it is classified according to well-recognised histopathologic criteria. RD may affect the whole kidney or may be focal or segmental and may have a broad spectrum of severity. RD shows usually unilateral involvement of a kidney. Most forms of dysplasia have associated cysts suggesting common etiopathogenetic mechanisms. One of them is the disruption of renal branching morphogenesis. The more frequent forms of RD include the isolated multicystic dysplastic kidney, the dysplastic kidney from early fetal ureteric obstruction and the dysplastic kidney associated with a genetic syndrome.
PURPOSE OF THE STUDY.
To evaluate the clinical data and the microscopic feature of the post-natal dysplastic kidneys submitted to the Pathology Department in the last ten years according to the most used classification (Osathanondh and Potter 1964) and using a semiquantitative evaluation, devised by Tarantal et al. in 2001 in their experimental model, to grade dysplasia.
METHODS.
Clinical data and pathological material of 16 patients with RD registered between 1995 and 2005 were retrieved and reviewed.
RESULTS.
The 16 patients included 11 males and 5 females. Their ages ranged from 1 to 29 months with a mean age of 10 months (ten patients were less than 12- months old). Only one patient had bilateral RD (postmortem case) and 7 out of 16 had segmental disease. The malformations most frequently associated were ureter duplication (9 cases) and ureteral stenosis or atresia (4 cases). The microscopic features of the renal parenchyma including renal architecture, cyst, alterations in collecting tubules, primitive ductal structures, fibromuscular rings, changes in the metanephric mesenchyme, growth of primitive glomeruli and tubules and evidence of islands of cartilage has been scored. Cysts were very scanty in 2 cases and cartilage was absent in 9 cases (5 females). The dysplasia was less severe in female patients. Chronic inflammation was usually present.
CONCLUSION.

The prevailing classification of RD takes into account the clinical manifestations and the pathological changes but a completely satisfying classification system, encompassing new data from molecular studies on morphogenesis and traditional histology, is still missing.

P 448
EVALUATION OF PROGNOSTIC IMPORTANCE OF THE 2001 SIOP PROTOCOL IN CHILDREN WITH NEPHROBLASTOMAS. A PRELIMINARY STUDY.
Jozef Kobos*, Katarzyna Taran**
*Department of Pathology of the Age of Development and Department of Pathology Konopnicka Memorial Hospital Medical University of Lodz, Poland
** Department of General Pathology and Department of Pathology Konopnicka Memorial Hospital Medical University of Lodz, Poland

The application of modern complex therapeutic protocols in children with Wilms' tumor caused a spectacular increase in the curing rate up to 85-90% cases. Histopathological classification is a vital part of these protocols and morphological diagnosis determines the schedule of subsequent treatment.
The new Revised SIOP Working Classsification of renal Tumor of Childhood (2001) was introduced in our center.
For our research we used formalin-fixed and paraffin-embedded archival material from 48 patients with nephroblastomas cured in our Hospital.
For histopathological evaluation of tumors we applied the previously used system and also the new Revised SIOP Working Classsification of renal Tumor of Childhood (2001). Statistical analysis was based on Kaplan-Meier survival method and Kruskal-Wallis as well as Chi2 tests.
The aim of our study was to correlate the prognostic importance of both classifications.
Results:
The presence of regular and irregular blastemal component in evaluated nephorblastomas was related to poor prognosis. Children with Wilms' tumor with low differentiated epithelial component did similiarly as patients with nephroblastomas which contained regular and irregular blastemal component. The application of the former classification showed the correlation between the histological grade of the tumor and the presence of metastases and relapses as well as with the presence of deaths from the disease.
The use of new SIOP (2001) classification also showed a strong correlation between the histological grade of the tumor and the presence of deaths from the disease.
Conclusion:
The new SIOP classification is an excellent tool in both the diagnosis and treatment of children with Wilms' tumor. The subdivision of cases fulfilling criteria for intermediate-risk tumors depending on either high or low epithelial differentiation might be useful for further prognostic analysis.

P 449
IMMUNOHISTOCHEMICAL ANALYSIS OF PROTEIN P16 IN WILMS TUMOR
S. Radojevic-Skodric1, G. Basta-Jovanovic1, S. Djuricic2, D. Brasanac1, S. Glumac1,
T. Terzic1, J. Sopta1, I. Baralic3
1-Institute of pathology, Medical school, University of Belgrade
2-Mother and Child Health Institute of Serbia "dr Vukan Cupic", Belgrade

SUMMARY: Cyclin-dependent kinase (CDK) inhibitors represented by the INK4 family (including p16(INK4a), p15(INK4b), p18(INK4c), and p19(INK4d) are regulators of the cell cycle shown to be aberrant in many types of human cancer. AIM: The aim of our study was to investigate p16 protein expression in Wilms tumor, to compare it with the expression in normal renal tissue as well as to see if there is a correlation between p 16 expression in Wilms tumor with tumor stage, histological type and prognostic group. METHODS: 28 cases of Wilms tumor (2 cases with metastasis) and 2 samples of normal kidney tissue were studied using streptavidin-biotin-complex technique. P16 expression levels were semiquantitatively scored. RESULTS: The expression of p16 was observed in the majority of cases (96%). There was statistically significant relationship between p16 expression and tumor stage (p=0.015) that is, tumors of higher stage (III/IV/V) more often expressed p16 then tumors of lower stage (I/II). Expression of p16 was detected in various histological types of Wilms tumor, but there was no statistically significant association (p=0.82). p16 was found more frequently in high risk tumors then in tumors with good prognosis (p=0.02). P16 immunostaining was observed in two cases of metastasis. CONCLUSION: Although, p16 is inhibitor of CDK, the results of our investigation show that nephroblastoma cells may proliferate in the presence of elevated levels of p16.

P 450
ROLE OF THE ? TYPE COLLAGEN IN FORMING OF CONNECTIVE TISSUE ELEMENTS OF HUMAN FETAL KIDNEYS AT IUGR CASES IN 20-22 WEEKS OF GESTATION
SYSOENKO Olexander, RESHETNIKOVA Olga, MOROZOV Sergiy
Department of Pathologic Anatomy, Medical University, Lugansk, Ukraine.

It is suggested that fetal intrauterine growth retardation (IUGR) may lead to hypertension in adults. Alteration of kidneys tissue maturation may play an important role in the pathogenesis of a hypertension too. The aim of present study was to determine the distribution of the III type collagen in forming of connecting tissue of the fetal kidneys in cases of IUGR. Methods: 20 pairs of fetal kidneys (including 10 pairs of kidneys in cases of IUGR) from the late medical abortions because of psychotherapeutic reasons at 20-22 weeks of gestation were weighted, studied macroscopically and microscopically, and then the distribution of the III type collagen with the help of antibodies was investigated. Results have shown that kidneys in IUGR group have macroscopic and histological signs of both organ and tissue growth restriction. The intensity of the III type collagen expression and the area of its distribution increased, mainly in the perivascular connective tissue, kidneys cortex and medulla's stroma. Conclusion: Fetal IUGR is accompanied with the lesion of renal tissue formation. The intensified synthesis of collagen ? may be a marker of tissue remodeling when connective tissue formation and sclerosis outrun the parenchyma elements growth and maturation.

P 451
PENTALOGY OF CANTRELL : AN EARLY CASE REVEALED AT 12 W.G.
Loget Philippe (1, 2), Mouchel François (1,3), Mouchel Jack (1,3), Krizeck Marie-Christine (1,4), Martin Dominique (1) Chevé Marie.Thérèse (1), Foulet-Rogé Armelle (2)
1: Prenatal Diagnosis Center of Le Mans, 2: Service d'anatomie pathologique, Hôpital Le Mans. 3 Clinique du Tertre Rouge, Le Mans, 4 : Laboratoires de biologie associés, unité de cytogénétique, Nantes.

We present the case of a 39 years old female foetus with termination of pregnancy at 14 W.G. for a polymalformation syndrome with: a midline supra umbilical wall defect, ectopia cordis, anterior diaphragmatic defect, defect of the lower sternum and omphalocele.

The G4P1A1 woman (2 miscarriages), with no history of systemic illness or familial disease, showed at the first obstetric ultra sonogram (12 W.G.) an increased nuchal translucency (6 mm), omphalocele, wall defect with ectopia cordis evocative of the Pentalogy of Cantrell. The autopsy showed a normal growth male foetus (Karyotype: 46, XY), with the full spectrum of the Pentalogy and also club feet, nuchal oedema without cystic hygroma, persistent left vena cava and probably a septal ventricular defect. The X ray films were normal.
The Pentalogy was first described by Cantrell in 1958 with five cases. The full Pentalogy occurs rarely and such early cases are very rare. The pathogenesis has not been elucidated. Cases are generally sporadic even if some families, monozygotic twins and rare chromosomal abnormalities (triploidy and trisomy 18) have been described.
We present this case because of its rarity and to stress on the importance of the examination of the foetus even in very early termination of pregnancy for an appropriate genetic counseling.

P 452
HISTOPATHOLOGICAL AND HISTOCHEMICAL STUDY OF THE EFFECTS OF TEUCRIUM POLIUM ON THE KIDNEY IN RAT
TALAEI KHOZANI Tahereh , DEHGHANI Farzaneh, PANJEHSHAHIN Mohammad Reza, KARBALAY-DOOST Saeed, Anatomy Department, Shiraz Medical School, Shiraz University of Medical Sciences

Teucrium Polium is commonly used in Iran traditional medicine for decreasing of blood sugar level. The aim of this project was to study of the effects of Teucrium Polium water extract on histologic structure of kidney in male rats. To examine such effects, 50 Spragu-Dawly rats were divided randomly to four experimental and one control groups. Experimental groups were fed with Teucrium Polium water extract (4gr/kg, 3gr/kg, 2 gr/kg, 1gr/kg) for 14 days. The rats were scarified, their kidneys were removed, and fixed, histological sections were prepared and stained with PAS/alcian blue and toluidin methods.
The results indicated that histological structure did not change but the extract affected on extracellular matrix. There was a mild precipitate of metachromatic material around the renal tubules of the cortex. Increasing amount of acidic glycoconugates and metachromatic components were observed in extracellular matrix of medulla and it was dose dependent.
It seems that this extract causes some kinds of changes in renal extracellular matrix, therefore it is recommended that this extract should be used cautiously and it needs more research to find its complications.
Keywords: Teucrium Polium, kidney

P 453
ESTIMATION OF GLOMERULAR VOLUME ON GLYCEROL-INDUCED ACUTE RENAL FAILURE IN RAT
DEHGHANI Farzaneh, DEZFULIAN Rahman, PANJEHSHAHIN Mohammad Reza, ZAHIRI Shahla Anatomy Department, Shiraz Medical School, Shiraz University of Medical Sciences

Backgroud:The use of stereological methods in evaluation of volume changes in vital organs such as kidney is very important. In this study, the volume of glomeruli in glycerol-induced acute renal failure in rat was determined.
Methods: 48 Sprague-Dawley male rats were divided into 2 groups (1control, 1experiment). Experimental group 10ml/kg of 50% glycerol was injected intramuscularly. And control group the same volume of saline was injected. After 48h, animals were dissected under deep anesthesia, and right kidneys were fixed by vascular perfusion. Microscopic slides were stained with H-E. Glomerular volumes were calculated using projecting microscope, point counting and cavalieri principal.
Finding: The results indicated that renal failure induced-glycerol didn't effect on glomerular volume
Conclusions:It seems that estimation glomerular volume can not be useful variable in identifying of acute renal failure induced glycerol, but further investigation is needed to clarify the issue.
Key Word:Kidney, Stereology, Mean Volume

P 454
POLYOMA (BK) VIRUS INFECTION IN TRANSPLANTED PATIENTS.
Cinzia Giacometti, Fiorella Calabrese, Francesco Marchini*, Paolo Rigotti** and Marialuisa Valente.
Institute of Pathological Anatomy, * Division of Nephrology, **Clinica Chirurgica 3, Department of Medical and Surgical Sciences, University of Padua, Medical School, Padova, Italy

INTRODUCTION: Polyoma (BK) virus nephropathy was first described in 1971. In immunocompetent patients it has a high prevalence but a low morbidity. Urinary tract is usually affected. Ureteric stenosis, hemorrhagic cystitis and interstitial nephritis had been described in renal graft before introducing cyclosporine A and Induction therapy. Afterwards BK infection was rarely reported for decades.
MATERIAL AND METHODS. From July 2001 to May 2003 132 adult patients underwent kidney transplantation at the University of Padua. Among these 7 patients developed BK infection with histological proven interstitial nephritis. The patients were 5 males and 2 females, mean age 42 years. Time interval between transplant and infection ranged from 6 to 79 months (mean 25,5). Triple therapy was performed in all cases : FK-506, Mycophenolate Mofetil and Steroids was performed in 5, Cyclosporine, Mycophenolate Mofetil and Steroids in 1 case and Cyclosporine, Rapamycin and Steroids in 1 case. Biopsy was performed in all cases due to increase in serum creatinine level. Diagnosis was suspected at histology on haematoxylin and eosin stain and confirmed by PCR method. Three patients experienced graft loss.
CONCLUSIONS. Polyoma (BK) infection is becoming more frequent in renal grafts. This may be related either to new immunosuppressive agents or to total level of immunosuppression. Reaching biopsy diagnosis following creatinine elevation, is usually too late in order to allow graft survival, because nephrotoxicity of antiviral therapy. Role of surveillance biopsies and PCR on bioptic material for earlier viral detection should be considered in heavily immunosuppressed transplanted patients.

P 455
TWO CASES OF CRYPTOCOCCOSIS DIAGNOSED ON KIDNEY GRAFT BIOPSY
MEHRENBERGER Marion (1),RIBES David (1), PILLET Adèle (1), ROSTAING Lionel (1), DURAND Dominique (1), BROUSSET Pierre (2), MODESTO Anne (2).
(1)Service de Néphrologie Dialyse et Transplantation, Hôpital Rangueil, 1, Avenue J. Poulhes, TSA 50032 Toulouse Cedex 9, France
(2) Service d'Anatomie et Cytologie Pathologiques, Hôpital Purpan, 1, Place Dr Baylac, TSA 50032, 31 059 Toulouse cedex, France

Cryptococcus neoformans accounts for 4% of the fungal infections after renal transplantation, and mortality remains high despite therapy (30 to 60%). Diagnosis relies on isolation of the yeast or its capsular antigen in biological samples. We report on two cases of neuromeningeal cryptococcosis that have been diagnosed on histologic study of renal graft biopsy.

Mrs D, 62-year-old, had received a kidney graft for polykystic disease . Immunosuppression associated thymoglobulins, mycophenolate mofetil, tacrolimus and steroïds. Two years after transplantation, a graft biopsy performed for nephrotic syndrom and progressive renal failure revealed an allograft glomerulopathy, with arterial fibrosis and membranoproliferative pattern. Immunofluorescence was positive for IgM deposits. Hepatitis serologies were negative. Suspecting chronic rejection, she received anti CD20 antibody therapy. Two months later, she died from a terrifying (foudroyant?) meningoencephalitis of unknown origin. Diagnosis was made on post-mortem graft analysis,which revealed cryptococcal yeasts in small renal vessels. It was secondary confirmed by blood cultures.
Mr S, 46-year-old, had chronical replicative hepatitis C, and type III cryoglobulinemia. Twenty years prior before, he had been transplanted for childhood malformative uropathy, and was treated by azathioprine, ciclosporine and steroïds. In 2003, azathiopine was replaced by mycophenolate mofetil because of chronic allograft nephropathy. One year later, he presented a neuromeningeal cryptococcosis, diagnosed on lumbar puncture. The same month, immunosuppression discontinuation and end-stage graft failure led to transplantectomy. Endovascular cryptococcal yeasts were noted on transplant biopsy. Antifungal therapy led to complete recovery.
Histologic diagnosis of C. Neoformans infection must be evocated in front of capsulated yeast that are strongly Periodic Schiff Acid positive . They are typically stained by Grocott coloration and Alcian Blue staining.
Cryptococcal infection occurs in cell immunity deficient patients, such as AIDS, prolonged steroid therapy, malignancies, sarcoïdosis and transplantation,especially under heavy immunosuppressive therapy. Because of its systemic spreading, the pathologist must be able to recognize such yeasts in peripheral organs, such as kidney graft in transplanted patients.

P 456

UNUSUAL DIFFERENTIAL DIAGNOSIS FOR VASCULAR ACUTE REJECTION : EARLY RENAL GRAFT PYELONEPHRITIS

MEHRENBERGER Marion (1), LAVAYSSIERE Laurence (1), ROSTAING Lionel (1), MODESTO Anne (2), BROUSSET Pierre (2), DURAND Dominique (1)
(1)Service de Néphrologie Dialyse et Transplantation, Hôpital Rangueil, 1, Avenue J. Poulhes, TSA 50032 Toulouse Cedex 9, France
(2) Service d'Anatomie et Cytologie Pathologiques, Hôpital Purpan, 1, Place Dr Baylac, TSA 50032, 31 059 Toulouse cedex, France

Accelerated acute rejection occurs within a few days after renal transplantation, due to preformed cytotoxic antibodies. It is often responsible for early graft loss. Histologic studies show evidence of vascular lesions with thrombosis, and polymorphonuclear leukocytes infiltrating glomeruli. We report on a case of acute graft pyelonephritis that mimicked an accelerated acute rejection.
Mrs B., a 34-year-old woman, developed 32 % panel-reactive antibodies to HLA class I after a prior kidney transplantation for lupic nephropathy. Fourteen years later, she underwent a second renal allograft, with a pre-transplantation negative crossmatch , but a low positive crossmatch against B lymphocytes, on a one-year-old serum . The patient received anti-thymocyte globulins, mycophenolate mofetil, tacrolimus and steroïds. After initial normalization of renal function, she became anuric on the 5th day. Clinical examination and Doppler ultrasound of the graft were normal . There was no fever, nor biological markers of inflammation or haemolysis. Bacteriological screening returned negative. The patient received two steroïd pulses and two plasma exchanges for suspected accelerated acute rejection.
Graft biopsy, performed on the 8th day, showed major polymorphonuclear (PN) cell infiltration of glomeruli, invading urinary space,as well as numerous PN casts stating the diagnosis of pyelonephritis. Interstitium examination revealed diffuse oedema, but only moderate PN leukocytes infiltrate. Rare glomerular thrombi were noted. The following day, urine and blood cultures returned positive for Escherichia Coli, and inflammatory markers elevated. Infection and renal function improved under antibiotherapy.
Urinary tract infections are the most frequent infections in renal transplant recipients, favored by immunosuppression and urologic surgery. Although most of them are benign, they can sometimes threaten graft function, especially in early post-transplant period . In such cases, the differential diagnosis with acute rejection can be difficult, because of attenuation of physical and biological signs by steroid therapy , and
then relies on kidney graft biopsy.

P 457

RELATIONSHIP BETWEEN POLY (ADP-RIBOSE) POLYMERASE WITH COLD ISCHEMIA AND DELAYED RENAL FUNCTION IN TRANSPLANT. DEMONSTRATION IN A PARP-1 KNOCKOUT MOUSE MODEL.

O'VALLE Francisco, GOMEZ-MORALES Mercedes, Del MORAL Raimundo MG, BENITEZ Maria del Carmen, AGUILAR Mariano, MARTIN-OLIVA David, OLIVER F Javier, Del MORAL Raimundo G.
Department of Pathology, San Cecilio University Hospital, Granada. Institute of Parasitology and Biomedicine, CSIC, Granada, Spain.

Kidney allografts undergo pre-transplant cold ischemia and consequent ischemia-reperfusion injury (IR). Poly (ADP-Ribose) Polymerase (PARP-1) overactivation leads to massive NAD+ consumption and ATP depletion with induction of cellular necrosis under ischemic conditions, which may lead to an increase in acute tubular necrosis (ATN) and a delay in total recovery of renal function (RFR) of the transplanted organ. Objetive: Our aim was to demonstrate that the expression of PARP-1 are relationship with ischemia, develop of acute tubular necrosis and delayed of renal function.
Material and Methods: We studied the semiquantitative nuclear expression of PARP-1 in tubular cells by immunohistochemistry with the monoclonal antibody PAR01 in kidney transplant biopsies from expanded-criteria donors (ECD) (N=166), and allografts with ATN (N=94), and by immunohistochemical and western blot expression of parp-1 in knockout mice ischemia /[45 min.]/reperfusion [6 and 48 hours] model.
Results: In 50% of ATN biopsies, more than 50% of tubular nuclei were immunostained for PARP-1. PARP-1 expression was higher in ATN biopsies than in those from ECD (2.40 ± 0.74 vs 0.92 ± 1.13, p=0.0001 Mann-Whitney). PARP-1 showed a statistically significant relationship with the time required to achieve effective diuresis (Rho:0.608, P=0.0001 Spearman test), with serum creatinine, and with duration of cold ischemia (Rho:0.650, P<0.0001 Spearman test); these relationships were stronger in the biopsies with ATN (Rho: 0.774; Rho:0.806, P=0.0001 Spearman test, respectively). In IR experimental model we induced tubular lesion in PARP-1wild-type mice and we reduced the severity of renal injury in PARP-1 knockout mice and in PARP-1 wild-type mice chemical blocks with PARP inhibitor.
In conclusion, multivariate analysis demonstrated that PARP-1 expression and cold ischemia duration in kidney biopsies with ATN predicted the short-term RFR (delay in total recovery of renal function, and serum creatinine in the first

month) It is proposed that PARP-1 plays a pivotal role in the pathophysiology of I/R injury of the human kidney.

P 458

BK –VIRUS NEPHROPATHY FREQUENCY IN RENAL TRANSPLANT BIOPSIES.

ÇAKALAĐAOĐLU Fulya, ERBARUT Ýpek, TUĐLULAR Serhan*, KAYA Handan.
Department of Pathology, Division of Nephrology-Department of Internal Medicine*, Marmara University School of Medicine. Ýstanbul-Turkey.

BK virus nephropathy is the most common type of viral disease following renal transplantations. Although the frequency is differs according to the transplantation centres, the rate is between 1.5% and 20%. The diagnosis can be established histologically by renal allograft biopsy.
The aim of this study is to search the frequency rate of the BK-virus nephropathy which causes the graft rejection in our cases.
The material of this study consists of the graft rejection cases that we received in last two years. The biopsies are diagnosed routinely according to the Banff criterias. We have found 5 cases (15.6%) of BK virus in 32 cases. All of the cases have been treated by immunosuppresive drugs following the transplantation surgery. Biopsies have been performed because of the disturbance of the renal functions. Only one case have had urinary examination.
Morphological diagnosis of BK virus nephropathy has been followed by serological examination.
The most frequent morphological changes with our BK virus infection are basophilia, nuclear inclusions, nuclear enlargement, on the tubul epithelium. Decoy cell has not been found in the only case who had urinary examination.
The treatment of immunosuppresion of the cases with BK virus nephropathy has been reduced and antiviral treatment has been started.
BK virus nephropathy should be kept in mind in the differential diagnosis of transplant rejection and drug toxicity.

P 459

IGNORED ALPORT SYNDROME REVEALING BY QUICKLY PROGRESSIVE GLOMERULONEPHRITIS ON RENAL BIOPSY OF TRANSPLANT

ALHAMANY Zaitounia(1) ,RAHOU Hakima(2),ROUAS Lamiaa(1),BENTATA Yasmine(2) ,CHERRADI Nadia(1) MALIHY Abderrahman(1) LAMALMI Najat (1) OUZEDDOUNE Naima(2),BALAFREJ Leila(2)
(1) :Laboratoire d'Anatomie Pathologique C HU Ibn Sina Rabat Maroc (2) :Laboratoire d'Anatomie Pathologique C HU Ibn Sina Rabat Maroc

Miss KA, born in 1983, eldest child of six with consanguineous parents of first degree followed on hemodialysis since 2000 for chronic renal insufficiency developed after ignored initial nephropathy: (focal segmental glomerulosclerosis ?). Family history: * a sister dead at 4years ago in a swollen syndrome, * another 20 years ago sister has renal insufficiency and * a brother of 16years ago has proteinuriea higher than 3g/24h. TRANSPLANTATION of KA in June 2003 with the kidney of her mother of 43years ago. Good evolution under immunosuppressor therapy.
EVOLUTION of the transplant :* At 6 months (01/01/04) after surgery, occurrence of a arterial stenosis of the renal graft successfully cured. *At 18 months (01/01/05) after transplantation,occurrence of hématuria with progressive increased creatinin and serum urea suggesting acute rejection or toxicity in Cyclosporine?Two biopsy were performed
Renal biopsy 1: extra-capillary diffuse glomerulonephritis with linear IgG and C3deposits , leading to diagnosis of a quickly progressive glomerulonephritis by anti-glomerular basement membrane(GBM) antibody developed in ignored Autosomal Recessive Alport 's Syndrome . No recovery even after plasmatic exchanges and bolus of solumedrol and endoxan .Renal Biopsy 2 performed one month and half after the first one showed important lesions of chronicity.
Patient given in hemodialysis. Discussion: For this rare complication the diagnosis is against all new transplantation and must lead to the meeting of a genetic council

P 460

TYPE III COLLAGENOFIBROTIC GLOMERULOPATHY ASSOCIATED WITH IGA MESANGIAL DEPOSITS

Mihaela Gherghiceanu,
"Victor Babes" National Institute of Pathology
E. Mandache
"Dr. Carol Davila" Hospital of Nephrology. Bucharest. Romania

The collagenofibrotic glomerulopathy is a recently described entity that is characterized by massive accumulation of banded collagen fibers in glomerular mesangial and subendothelial zones. Abnormal accumulations of banded collagen are an ultrastructural pathologic hallmark of nail-patella glomerulopathy. In this disease the banded collagen occur predominantly within the glomerular basement membranes, whereas in the collagenofibrotic glomerulopathy the abnormal collagen fibers occur predominantly in the subendothelial zone and mesangium.
Collagenofibrotic glomerulopathy is a rare disease that usually presents with nephrotic syndrome and renal insufficiency. It has been first reported in 1979 by Masaaki Arakawa. In 1993 M-C. Gubler et al. reported 10 children with collagenofibrotic glomerulopathy who had evidence for familial renal disease with an autosomal recessive transmission.
The pathogenesis of this disease is unknown. Some patients have elevated serum levels of type III procollagen suggesting up regulation of collagen synthesis.
A case of collagenofibrotic glomerulopathy has been diagnosed in a series of over 500 renal biopsies. This is the first internationally reported association of type III collagenofibrotic glomerulopathy and IgA mesangial deposits. A 22-year-old male was admitted with recurrent macroscopic hematuria. Physical examination revealed normal blood pressure and no edema. Laboratory values - normal blood tests. Hematuria: 30-60/mm3. Proteinuria: 250 mg/24h
The diagnostic was established after performing immunohistochemistry on frozen sections, light microscopy and a thorough electron-microscopic investigation. The light microscopy showed slight mesangial proliferation. The immunofluorescence emphasized IgA mesangial deposits. These IgA deposits have been clearly identified as dense paramesangial spots in electron microscopy too. In electron microscopy, type III collagen fibers, having a diameter of about 100 nm and a standard periodicity, were found arranged as clusters in the mesangial matrix and less in the sub endothelial area. Only a few fibers were found in the glomerular capillary basement membrane and in the capsular basement membrane. Not all the glomeruli showed type III collagen fibers. In the renal interstitial area, especially around the glomeruli, the strips of collagen fibers were more conspicuous then usual.

P 461

THE MORPHOMETRIC STUDY OF IMMUNOFLUORESCENT C3D INTERSTITIAL DEPOSITS IN IGA GLOMERULONEPHRITIS

E. Mandache (a, b), Mihaela Gherghiceanu (a), M. Penescu (b),
(a)"Victor Babes" National Institute of Pathology, Bucharest, Romania

(b)"Carol Davila" Clinical Hospital of Nephrology, Bucharest, Romania

The IgA glomerulonephritis (IgAGN) is one of the most common primary glomerulonephritis and has a variable and difficult to predict evolution toward the end-stage nephrosclerosis. The deposition of C3d complement component in peritubular capillaries (PTCs) indicates a variant type of acute rejection while C3d deposition in primary glomerulonephritis (GN) is poorly documented.
The aim of this study is to examine C3d expression in peritubular capillaries (PTCs) and its correlation with the severity of renal injury in IgA glomerulonephritis. Since these interstitial, immunofluorescent deposits have tiny and poorly structured shapes our investigation applied some computerized morphometry programs. Thus we could demonstrate the occurrence of the C3c IF deposits in strict connection with the peritubular capillaries in either cross or longitudinal section. Polyclonal FITC conjugated rabbit anti-human C3c and C3d antibodies were used for direct immunofluorescent evaluation of the C3c and C3d deposits in 24 kidney biopsies with IgA glomerulonephritis.
The study revealed that the C3d deposits in peritubular capillaries were associated with known predictor aspects for rapid progression of IgAGN such as: glomerular sclerosis (63,6%), atrophic tubules (90,9%) and interstitial sclerosis (81,8%). The intensity of the C3c glomerular immunofluorescent deposits was related with active lesions. Thus, the predictive value of C3d deposition on PTCs in IgAGN is worth to be taken into consideration as an unfavorable outcome of the disease and request further long run investigations.

P 462
MEMBRANOPROLIFERATIVE GLOMERULONEPHRITIS COMPLICATING DIABETIC NEPHROPATHY

L.Grcevska (1), G.Petrusevska (2), S.Kostadinova (2), S.Dzikova (1)
1. Department of Nephrology, Clinical Center, Skopje, Macedonia
2. Institute of Pathology, Faculty of Medicine, Skopje, Macedonia

Renal diseases other than diabetic nephropathy (DN) can be found in diabetic patients. Various forms of primary and secondary glomerular diseases were reported, but membranoproliferative glomerulonephritis (MPGN) is rare. We noted 4 patients with MPGN associated with DN at our Department for the past 3 years.
Two of the patients had enlarged lobular glomeruli due to mesangial and endocapillar hypercellularity. Intraglomerular cells consisted of monocytes, rare neutrophils, mesangial and endothelial cells. Mesangial matrix was enlarged with focal hyaline-sclerotic areas. The silver methenamine staining showed duplication of glomerular basement membrane (GBM). Visceral epithelium was hypertrophic and adherent to parietal epithelium. Interstitial edema with slight fibrosis was visible. Intrarenal blood vessels presented hyaline insudative changes. This was followed with deposition on immunofluorescence of granular deposits of IgA, IgM, IgG, C3, C4 and Fibrinogen. The whole histopathology in these two patients suggested nodular form of DN with diffuse MPGN.
The other two patients presented diffuse diabetic glomerulosclerosis. Inflammatory cellular mesangial proliferation with intracapillary influx of neutrophils was also present, with duplication and partial destruction of GBM. Part of the glomeruli presented diffuse changes, and the rest presented segmental changes. Tubular epithelium showed degenerative changes and the interstitium was edematous with diffuse mononuclear cell infiltration. Changes of intrarenal blood vessels affected only the vascular poles. The immunofluorescent analyses showed granular deposits for the above mentioned antibodies.
The renal structure and function in both diseases are similar. Pathological changes in DN include thickening of all renal extracellular basement membranes and the mesangial matrix. Mesangial expansion is related to proteinuria, hypertension and declining GFR. Interstitial volume may be increased in insulin-dependent diabetes mellitus particularly in areas containing sclerotic glomeruli or marked tubular atrophy. Parallel findings were documented for type I MPGN in which the increased mesangial volume was related to decreased GFR, increased glomerular permeability to protein and hypertension. The cortical interstitial volume is correlated with functional abnormalities both in DN and MPGN. Besides these similaritites, hyperperfusion injury characteristic for DN, can also be found in MPGN.

P 463
THE ROLE OF VIRAL INFECTION IN ORIGIN AND PROGRESSION OF PRIMARY GLOMERULONEPHRITIS AND SOME NEPHROPATHIES

V.A. Varshavsky (1), E.P. Golitsyna (1), P.N. Rybin (2), D.N. Fedorov (1)
(1) I.M. Sechenov Moscow Medical Academy, 119992, Moscow
(2) N.N. Burdenko Main Military Clinical Hospital, 105229, Moscow

It is known that viral infection has a high profile in origin and progression of glomerulonephritis and noninflammatory nephropathies in children and adults.
The aim of our study was to determine the role of different viruses in development of glomerulonephritis and some nephropathies.
Methods and materials. 136 biopsies from patients (aged from 1,5 to 58 years) with unspecified viral presence (group I) and 68 biopsies from patients with proven viral infection (group II) were studied. Biopsies were examined by means of light microscopy, immunohystochemistry and electron microscopy. Viral typing was performed by means of PCR and IFA.
Results and discussion. Electron microscopy has revealed viral inclusions in 70 of 136 cases from group I. 12 types of viruses were determined in 68 cases of group II. It was revealed that single viruses as well as viral associations (from two to three viral types) play a role in progression of glomerulonephritis and noninflammatory nephropathies. The most commonly encountered were Herpes simplex virus (HSV), adenoviruses, hantaviruses and their associations. The correlation analysis between type of virus and morphology of nephropathy was performed. The most common morphological form of glomerulonephritis was mesangioproliferative glomerulonephritis (31 cases): in 30 cases single-type virus was revealed (adenovirus type 8 or 11, HSV type 1 or 2, Coxsackie-virus, RS-virus, hantaviruses (Hantaan and Puumala viruses), and cytomegalovirus). Membranoproliferative glomerulonephritis was revealed in 15 cases: membranoproliferative glomerulonephritis type I with 2 virus type combination was diagnosed in 7 most serious cases. Parvovirus B19 was revealed exceptionally in segmental-focal sclerosing glomerulonephritis and arteriolohyalinosis (6 cases). Herpes simplex virus type II was found in 1 case of segmental-focal sclerosing glomerulonephritis. Antiviral therapy resulted in strongly beneficial effect.
Conclusion. As a result of our study we confirmed viral infection participation in development and/or progression of glomerulonephritis and some nephropathies. However further investigations are needed in order to determine the role of viruses as an etiological factor, or as disease progression factor originated from corticosteroid therapy of.

P 464

DYNAMIC GD-ENHANCED MRI, IN VIVO ¹H MRS AND T₂ RELAXOMETRY STUDY OF HUMAN KIDNEYS

ROGOZYN Vladimir, ROZHKOVA Zina, Vozianov Sergei
Radiological Center of the Academy of Medical Sciences of Ukraine, Kiev, Ukraine

Purpose:We propose quantitative analysis of Gd-enhanced MRI (time-intensity curves), in vivo ¹H MRS, and T₂-relaxation time for differential diagnosis of renal tumors.
Materials and Methods: 44 patients are examined by 1.5 T Magnetom Vision System (SIEMENS). MRI are obtained after i.v. bolus of 0.1 mM/kg body weight of Gadovist 1.0 (Schering) with breath-hold sequence: FLASH-2D sequence:FA=70^o,TR/TE=160/6ms,TA=22s which was repeated every minute for 10 minutes. ¹H MR-spectra are recorded with SVS-STEAM sequence:TR/TE = 1500/60 ms. In T₂-relaxation time measurement the ¹H MR-spectra are recorded in and outside of the tumors with SVS-STEAM sequence:TR/TE = 1500/60,80,100,140ms.
Results:The following enhancement patterns were established for the normal renal medulla (NRM, maximal signal intensity (mSI) in the 2-4 min after Gadovist 1.0 injection), renal cell carcinoma (RCC, mSI in the 1min), and the transitional cell carcinoma (TCC, flat curve, enhancement weaker than in the NRM). In the case of angiomyolipoma the enhancement was not different from the RCC. From ¹H MR spectra the peak areas of main metabolite signals: water (4.7ppm), lipids(1.5,2.3-2.5,5.4ppm), creatine+creatinine(Cr,3.0ppm), choline-containing compounds(Cho), and betaine (3.25-3.9ppm) are obtained. For NRM the following mean values of T₂ are calculated: T₂^{NRM}(Wat)=(114.3+-9.6)ms before and (92.4+-3.5)ms after Gadovist 1.0 injection. The following mean values of T₂ are obtained: for RCC the mean values of T₂^{RCC}(Wat)=(83.2+-4.7)ms before and (61.7+-5.2)ms after Gadovist 1.0 injection, and for TCC T₂^{TCC}(Wat)=(72.6+-4.3)ms before and (53.7+-4.2)ms after Gadovist 1.0 injection.
Conclusion: This work is very helpful for study of kidney metabolism and for differential diagnosis of renal tumors.

P 465

TWO FAMILIAL CASES OF ANCA-ASSOCIATED VASCULITIS

Honsova E, Rihova Z, Jancova E, Lodererova A.

Antineutrophil cytoplasmatic autoantibodies (ANCA) directed to proteinase 3 (PR3-ANCA) or myeloperoxidase (MPO-ANCA) are closely associated with systemic necrotizing vasculitides (AAV). However, ANCA alone are not sufficient, as based on clinical and experimental data, and other, probably exogenous factors, seem necessary for disease induction. Besides, various genetic factors are most likely involved in disease susceptibility.
Case Reports
We report on two familial cases of AAV. In the first family, the father had presented with an acute renal failure due to PR3-ANCA-associated disease three years before his daughter had exactly the same manifestation. However, at the time of his admission to the hospital she had already had E.N.T. involvement, which was later attributed to Wegener´s granulomatosis. There were also very similar morphological features in their kidney biopsies. The second family involved two sisters, who were diagnosed with microscopic polyangiitis (MPO-ANCA associated) with a more gradual decline of renal function within four months of each other. The younger sister actually suggested the diagnosis of her sibling based on her symptoms and probably saved her a significant amount of renal function.
Conclusion
As in other autoimmune diseases, the etiology of AAV is heterogenous and basically unknown. Different predisposing factors probably play differential etiopathogenic roles in various groups of AAV. The two familial cases support the hypothesis that genetic predisposition plays an important, although not yet fully understood role.

P 466

FREQUENCY OF DETECTION OF EPSTEIN-BARR VIRUSES (EBV) IN THE RENAL BIOPSIES: VALUE OF ULTRASTRUCTURAL FINDINGS AND POLIMERASE CHAIN REACTION.

REZNIKOVA Galina, MATSIONIS Alexandre,
KIRICHENKO Yury, POVILAITITE Patrisia.
Rostov Regional Bureau of Pathology

Introduction. Concomitant viral infection exerts negative influence on the basic process and treatment of chronic renal pathologies. Intranuclear virion-like inclusions are often seen during diagnostic electron microscopy of renal biopsies, but it is difficult to identify these unusual inclusions for lack of specificity of its ultrastructure. We used within one year not only electron microscopy, but also polimerase chain reaction (PCR) and immunohistochemistry for analysis of all renal biopsies.
Aim. The purpose of the present study was the revelation and exact identification of viruses in the renal biopsies and also characteristic of accompanying alterations.
Methods. Renal biopsies with preliminary diagnosis chronic glomerulonephritis (n=145) were the subjects of the study. The material was prepared by the standard methods for light microscopy, immunohistochemistry and electron microscopy (EM-208/Philips). Identification of EBV was confirmed by PCR, we isolated DNA from non-fixed or formalin-fixed, paraffin-embedded tissue.
Results. In the biopsy samples DNA of EBV was detected by PCR most frequently (16 positive reactions, 10% of cases). For the same period DNA of a Herpes-virus (1-2 types) was found out in one case, and in one case DNA of cytomegalovirus. Ultrastructural analysis of these samples showed the specific alterations of nucleus - small or large electron dense chromatin formations with a light halo, numerous nuclear bodies, inner nuclear membranes thickening. The same abnormal nucleus ultrastructure was in the mesangial and visceral epithelial cells and in the interstitial monocytes. Light microscopic examination has detected presence of numerous limphocytes in the inflammatory infiltrate of the interstitium. Immunohistochemical examination of EBV antigen (Dako anti-EBV primary antibody, clone LMP) has demonstrated distribution of LMP in the cytoplasm of the glomerular podocytes, rarely in the infiltrating cells and in the tubular epithelial cells. The most frequent forms of basic pathology - amyloidosis, minimal change glomerulopathy and membranous glomerulonephropathy, are accompanied by tubulointerstitial alterations.
Conclusion. Our results show the high level of concomitant EBV infection in the renal biopsy samples from patients with chronic renal pathologies. Ultrastructural identification of intranuclear inclusions is helpful for early determination of EBV and other Herpesviruses in the renal tissue.

P 467

COMPUTERIZED ANALYSIS OF RENAL CORPUSCLE MORPHOLOGY IN RAPIDLY PROGRESSIVE GLOMERULONEPHRITIS

CARUNTU Irina-Draga(1), HARTAN Alexandra(1), SAJIN Maria(2), DOBRESCU Gioconda(1)

(1) University of Medicine and Pharmacy "Gr.T.Popa" Iasi, Romania
(2) University of Medicine and Pharmacy "Carol Davila" Bucuresti, Romania

Purpose: The evaluation by computerized morphometry of the morphologic elements characterizing the renal corpuscles in rapidly progressive glomerulonephritis (RPGN), pointing out several gravity stages that induce a quantitative-type classification and justify distinct attitudes in the clinical approach.
Material and methods: We analyzed 10 cases diagnosed by renal biopsy as RPGN. The measurements were automatically performed on 100 renal corpuscles (10 per biopsy), relying on the procedure COREN, developed by us for running under KS400 (Zeiss) software. COREN exploits the RGB segmentation to accurately individualize the corpuscle (cor) and its entities presenting interest for the quantitative analysis: capillaries (cap), nuclei (nuc), connective tissue of the mesangium and crescent (cot), Bowmann space (bos). For each considered corpuscle (i=1 to 100), COREN measures the areas (square microns) of the corpuscle (denoted by A(i)cor) and of the aforementioned entities (denoted by A(i)x, where x=cap, nuc, cot, bos), computes the corresponding percentages relative to A(i)cor (denoted by P(i)x=A(i)x/A(i)cor) and stores the results in a data base. Next, for each case (c=1 to 10), COREN extracts the adequate information from the data base and calculates the mean values per case denoted by A(c)cor, A(c)x and P(c)x=A(c)x/A(c)cor. Finally, COREN provides the mean values characterizing the entire lot of biopsies, denoted by Acor, Ax and Px=Ax/Acor.
Results: For the analyzed biopsies we have obtained the following mean areas: Acor=3485, Acap=460, Anuc=355, Acot=2140, Abos=260, which, in percentage terms, yield Pcap=13,2%, Pnuc=10,2%, Pcot=61,4%, Pbos=7,4% and 7,7% for other elements (i.e. erythrocytes). Based on appropriate comparisons between the above values and the values corresponding to the 10 reported cases (not reproduced here for brevity reasons), we have studied the role of P(c)x in the classification of the cases, reflecting different gravity degrees, which cannot be rigorously evaluated by the usual microscopic exam. Further evolutions of our cases have shown that the proposed separation in classes is fully motivated from the point of view of the medical practice.
Conclusions: The morphometric approach opens new perspectives for the analysis of the renal biopsy in the sense of refining the diagnosis and, consequently, the therapy. Future researches should focus on the general validity of the classification criteria, by enlarging the number of studied cases.

P 468
EXERCISED-INDUCED APOPTOSIS IS MEDIATED BY BOTH ANGIOTENSIN II AT1 AND AT2 RECEPTORS IN RATS KIDNEY

PODHORSKA-OKOLOW Marzena*, DZIEGIEL Piotr*, GOMULKIEWICZ Agnieszka*, KISIELA Dagmara**, CEGIELSKI Marek*,DOLINSKA-KRAJEWSKA Barbara*, CARRARO Ugo***, ZABEL Maciej*#
*Department of Histology and Embryology, Medical University, Wroclaw, Poland
**Department of Biochemistry, Pharmacology and Toxicology, The Faculty of Veterinary Medicine, Agricultural University of Wroclaw, Poland
***Department of Biomedical Science, University of Padua, Italy
Department of Histology and Embryology, University of Medical Sciences, Poznan, Poland

Excessive physical exercise may lead to disturbance of the entire homeostasis in the body, including the damage not only in skeletal muscles but also in many distant organs. Among the mechanisms responsible for the exercised-induced changes could be an oxidative stress or angiotensin II. We previously showed that acute exercise led to apoptosis in kidney but not as a result of oxidative stress. In this study, we examined the role of angiotensin II and its receptors AT1 and AT2 in mediating exercised-induced apoptosis in kidney. We clearly demonstrated that an acute physical exercise induced apoptosis in renal distal tubular cells. Moreover, those cells displayed an increased expression of both AT1 and AT2 angiotensin II receptors and p53 protein. These results suggest that angiotensin II could upregulate p53 expression via both AT1 and AT2 receptors in renal distal tubular cells what might be a crucial mediating mechanism of apoptosis occurrence in kidney after excessive exercise.

P 469
ROLE OF INDUCED NITRIC OXIDE SYNTHASE (I-NOS) IN UNILATERAL OBSTRUCTIVE NEPHROPATY

BAHAR AKKAYA1, H.ELIF PESTERELI1, SHERIEF LABIB2, ASSEM EL SHERIEF2

Background: Obstructive nephropathy leads to tubulointerstitial fibrosis and loss of function. Nitric oxide has been shown to have antifibrotic properties. We explored induced nitric oxide synthase (i-NOS) expression in kidneys from rats underwent obstruction- release of unilateral ureteral obstruction.
Methods: Experiments were performed using a total 63 male Sprague-Dawley rats. The rats were either subjected to left proximal unilateral ureteric obstruction (UUO) or sham operation. The duration of UUO differed according to the group (1 day, 7 days, or 14 days obstruction). At each time point (1, 7 and 14 days) groups of rats (n =5) were sacrificed without relieving the obstruction to evaluate the severity of the obstructive injury. Other rats had their obstruction relieved and were left for another 15 days before sacrifice to evaluate the extent of structural recovery. Controls animals (n = 5) were sacrificed in parallel at each time point. Paraffin sections were stained CD68 and iNOS expression and assessed by immunohistochemistry.
Results: A significant increase in cortical interstitium macrophage number on CD68 immunolabelling was shown between obstruction- release and control group. By contrast no differences were observed on renal cortical and medullar interstitium in control groups. A significant difference in macrophage infiltration in cortex and medulla interstitium was found between obtruction-release group and control group. (p¡Ü0.05)
Significant increase on iNOS expression in cortex and medulla tissue of obstruction release group compared to control group was observed. (p¡Ü0.05) On the contrary, difference on i-NOS expression in cortex of control group compared to medulla of control group was found. But a significant increase on iNOS expression in medulla tissue of obstruction release group compared to cortex at the same group was detected.
Conclusion: In kidneys with UUO an expression of iNOS in medulla and cortex was increased. These results provide evidence for the iNOS expression in the renal cortex induced by inflammatory cytokines at medulla tissue of UUO kidneys. It is suggested a possible link in the pathogenesis of post ¨Cobstruction renal fibrosis.

P 470
A RENAL INTRAVASCULAR LARGE B- CELL LYMPHOMA REVEALED BY PROTEINURIA.

ZIDANE Merzouka (1), BABINET François (2), ROUSSELET Marie-Christine (1), SAINT-ANDRÉ Jean-Paul (1).
(1)Department of Pathology, University Hospital, 49933 Angers Cedex 09. France

(2)Nephrology, Center Hospital, 72037 Le Mans cedex 01. France

Intravascular lymphoma is a rare subtype of large B-cell lymphoma. The lumina of small vessels are plugged with large lymphoid cells, especially in the brain, skin or lungs, without tumor mass or leukemia. Symptoms are non specific, related to vascular occlusion, and clinical diagnosis is difficult unless a microscopic examination of an affected organ is performed. This lymphoma has a propensity to rapid systemic dissemination and many cases have been diagnosed only at autopsy.
Case report : a 73-year-old male with a medical history of hypertension, repeated pulmonary embolism, heart deficiency and mellitus diabetes was hospitalized for a 38°C fever and weight loss without adenopathy, neither hepatosplenomegaly or neurological symptoms. Laboratory investigation disclosed proteinuria near the nephrotic range (2.2 to 3.3 g/24 hours), a severe inflammatory syndrome (C-reactive protein 115 mg/l, fibrinogen 7.3 g/l) and a mild elevation of serum lactate dehydrogenase (LDH) (473 UI/l). Immunoserology was negative (ANCA, antinuclear antibody). A kidney biopsy showed large atypical lymphoid cells only localized in glomerular capillaries, without other glomerular changes and a mild chronic interstitial nephritis. Tumor cells were immunostained by the CD45, CD20 and CD79a antibodies but negative for CD5 and CD10. There was no other tumor localization on brain, spine, skeletal, thorax and abdominal imaging as well as on bone marrow aspiration and biopsy. Laboratory tests quite suddenly worsened with a high LDH titer (> 1000 UI/l), hemoglobin concentration at 7 g/dL, and signs of microangiopathic haemolysis. Combination chemotherapy was initiated and after six cycles, the patient was alive and well, with normal laboratory tests. Nine months after the diagnosis, a second renal biopsy showed focal hyaline scars in glomeruli with no residual lymphoma cells.
Comments: this case of intravascular large B-cell lymphoma appeared limited to the kidney, and, as in a few other reported cases, revealed by proteinuria. An early diagnosis by renal biopsy was followed by combination chemotherapy usually effective in high-grade non-Hodgkin's lymphoma and leading to complete remission.

P 471
CONTRIBUTIONS TO THE KNOWLEDGE OF THE EVOLUTIVE POTENTIAL OF THE METANEFROGEN MESENCHYMA

Dragoi S.G., Trasca E.T., Rodica Silca, Melinte P.R., Popescu M., Riza L
Academic Hospital Filantropia Craiova
University of Medicine and Pharmacy from Craiova, Romania

Introduction. Oscar Hertwig (1881) proposed the term of mesenchyma as a morphogenetic entity instead of mezoblast. Today, it must be defined as an ancestral system endowed with variable differentiation potentialities in fundamental structures (cardiac, angiogenetic, nefrogenetic).
Purpose of the study. The purpose of this paper is to submit anatomic arguments for the knowledge of the differentiation ability of the metanefrogen mesenchyma.
Materials and methods. Our research has been achieved on human material (6 embryos, 4 fetus, 5 new born). We used classical micro anatomical staining techniques (Hematoxilin Eosine, Van Gieson, Gomori, PAS, Giemsa).
Results. The knowledge of the evolutive potentialities of the metanefrogen mesenchyma has been achieved due to our efforts in understanding the genesis and the evolution of the tubular and vascular nefron structures. By analyzing the serried section through tissue fragments in different stages of metanefrogenesis, we observed the existence of the dual differentiation potentiality of the metanefrogen mesenchyma – a part generated the walls of the Muller-Bowman capsule and of the contort and Henle renal tubes; another part formed the glomerular capillaries.
Conclusions. We consider that the differentiation of the metanefrogen mesenchyma is determined by the inductive action of the urethral bud for the genesis of the nefron and tubular structures and by the neural crest migrated cells for the formation of the nefron vascular structures.
Key words: metanefrogen mesenchyma, Bowman capsule, nefron

P 472
PROSPECTIVE STUDY OF EPIDERMAL GROWTH FACTOR RECEPTOR (EGFR) AND C-KIT EXPRESSION IN NON SMALL CELL LUNG CANCER (NSCLC) AND NEURO-ENDOCRINE CARCINOMAS (NEC)

Patrick Saint-Blancard (1), Hélène Laize (2), Jacques Margery (2), Joël Guigay (2)
Service d'Anatomie Pathologique, (2) Service des Maladies Respiratoires.
Hôpital d'Instruction des Armées Percy, 101, avenue Henri Barbusse, 92141 Clamart, France.

The new target therapies are designed molecular missiles, aimed at specific cancer cellular command centers. Kit (CD117), the product of the proto-oncogene c-kit, is a tyrosine-kinase transmembrane receptor. Kit positivity is in fact a definitive feature of GIST. EGFR is another important cellular receptor, with EGFR-targeted agents such as gefinitib, OSI-774, and cetuximab in current development.
We decided to analyse the CD117 and EGFR immunohistochemical profiles of majors types of lung tumors on surgical specimens or lung biopsies. This prospective study of expression of EGFR and c-kit was assessed on 49 adenocarcinomas, 8 squamous tumors and 8 small cell lung carcinomas (SCLC) or neuro-endocrine carcinomas (NEC). Material was formalin-fixed, paraffin-embedded tissue , obtained by thoracoscopic wedge biopsies, bronchial biopsies or resection specimens.
44/49 adenocarcinomas, 6/8 squamous epitheliomas, and 1/8 SCLC or NEC, revealed increased expression of EGFR. 5/49 adenocarcinomas, 1/8 squamous epitheliomas, and 5/8 SCLC or NEC, revealed increased expression of c-kit CD117 immunoreactivity was also more frequent for the patients with SCLC or NEC lung carcinomas (p=0.001). For 46 adenocarcinomas, 6 squamous carcinomas and 6 SCLC or NEC, we evaluated if the expression of EGFR or CD117 immunoreactivity was correlated with differents variables as clinicopathological characteristics (gender, tobacco's status), therapy (surgery or chemotherapy) or response to chemotherapy. Statistical analysis used a Fisher's exact test. None of the tested parameters was significative for the squamous carcinomas or adenocarcinomas. There was no statistical link between tobacco's status and EGFR overexpression.CD117 immunoreactivity was correlated with a good response to chemotherapy and a lack of progression for the patients with SCLC or NEC (p=0.07).
The success of imatinib in the treatment of metastatic GIST has stimulated interest in understanding the functional sence of kit immunoexpression in others tumors. This therapeutic's way could be attractive for the SCLC or the NEC, as they often overexpress c-kit. Although a recent study with a little number of patients with SCLC was negative, it should be interesting to assess this molecule's efficacy in the other NEC.

P 473
PROGNOSTIC VALUE HER-2/NEU ONCOGENE AND ESTROGENE RECEPTOR EXPRESSION IN NSCLC PATIENTS

Jasminka Jakic-Razumovic, M.D., Ph.D, Ivan Aleric, M.D. Ph.D. 1

Department of Pathology, Clinical Hospital Center Zagreb, Croatia, Clinical Hospital for pulmonary diseases Jordanovac, Zagreb, Croatia 1

Introduction: Lung cancer is the leading cause of cancer mortality worldwide. Patients prognosis partially depends on some traditional patohistological parameters and clinical stage, but in recent time many studies try to find some additional risk factors which would be able to divide patients with better disease-free and overall survival from those who will have early tumor recurrence and metastatic disease. Patients and methods: Clinical information and pathological slides and paraffin blocks from 132 consecutive patients with non-small cell lung carcinoma (NSCLC) were collected to evaluate HER-2/neu oncogene and oestrogen receptor (ER) expression, as well as their correlation with patients survival. All tumors were reviewed to verify histological parameters as histological type, tumor and nuclear grade, quantity of lymphocytic infiltrates, mitotic rate, and degree of tumor necrosis. Additionally, clinical data as sex, smoking habits, preoperative clinical stage, and overall survival were collected. HER-2/neu and ER status were determined immunohistochemicaly and correlated with clinical and pathohistological data. Results: The results showed statistically significant correlation between HER-2/neu and nuclear grade (p=0,010). Additionally correlation between ER expression and histological type of tumor (p=0,043), and mitotic rate (p=0,008) was found. Kaplan-Meier analysis showed statistically significant correlation of patients overall survival with TNM status (p<0,0001) and degree of tumor necrosis (p=0,0153). Cox proportional hazards regression analysis showed that male gender (p=0.01214), histological type (p=0.0303), high degree of necrosis (p=0.0064), and higher histological grade (p=0.0370) had significant influence on patient's survival. Relative risk of death was 2.7 times higher for male gender, 2.2 times for adenocarcinomas in comparison with squamous carcinoma, and 3.4 times higher for tumors with prominent necrosis in comparison with tumors without necrosis. Conclusion: Our findings indicate that some traditional histological parameters are important for determination of NSCLC patient's prognosis, but that ER and HER-2/neu expression might be of potential usage in clinical practice for assessment of certain group of patients who might benefit of specific treatment.

P 474

EVALUATION OF EPIDERMAL GROWTH FACTOR RECEPTOR AND C-ERBB2 IN DIFFERENT TYPE OF NON SMALL CELL CARCINOMA OF LUNG

FAHKRJOU ASHRAF M.D.,MONTAZERI VAHID M.D.

INTRODUCTOIN:The aim of this study was to evaluate the effects of EGFR(epidermal growth factor receptor) and c-erbB2 in the different type of non small cell lung cancer ,and to compare the results with normal lung tissue and different stages of tumor.
METHOD: For this study ,79 paraffin blocks were obtained for 64 patients having a confirmed pathological report of non small cell lung cancer and 15 normal lung tissue as a control group.All of specimens were stained with monoclonal antibodies against EGFR and c-erbB2.
Results:In this study 30 patients with SCC(sqamous cell carcinoma) , 30 patients with AC(adenocarcinoma),2 cases of large cell cacinoma and 2 patients with carcinoid tumorwere selected.In 27(90%) patients with SCC ,EGFR was positive and in 20(66%) patients with adenocarcinoma,c-erbB2 was positive.None of large cell carcinoma and carcinoid tumor were positive for these factors.
CONCLUSION:According to the results of this research there is sinificant difference between SCC and AC of lung that can help for adjuvant treatment after surgery of tumor.
key words:Lung cancer,non small cell cancer,c-erbB2,EGFR.

P 475

PROGNOSTIC SIGNIFICANCE OF KI67, CD44,AND CD 105 TUMOUR MARKERS IN SURGICALLY TREATED NON-SMALL CELL LUNG CANCER (NSCLC)

Maria CHORTIS, Evangelia VLETSI, Nikolaos TRAKAS, Nikolaos MAOUNIS, Phillipos PALAMIDAS, Stella LEGAKIS, Stella ZOUGRIS, Heleni ANAGNOSTOPOULOU,Laura MANOLIA, Nikolaos TAMVAKIS
Department of Pathology , Sismanoglio General Hospital, Athens, Greece.

Introduction:Given the fact of an ominous prognosis in surgically treated non-small cell lung cancer (NSCLC), even in early stage cases, more specific prognostic factors could be of help in the preoperative categorisation of these neoplasms.
Aim of the study:We examined the expression of Ki67 (nuclear proliferation index), CD44 (adhesive molecule) and CD105 (vascular index)in surgically treated NSCLC and correlated these markers with histological type, stage and size of the tumour.
Material and methods:41 specimens of surgically treated NSCLC were included in this study, 23 adenocarcinomas (56.1%),13 squamus (31.7%)and undifferentiated (12.2%).22 patients were staged as Ia-Ib (61.1%)and 14 as IIa-IIb (38.95%)
Immunohistochemical staining was perfofmed on paraffin sections.Our results were correlated to the clinical and pathological parametres(size,histology,stage).The evaluation of CD105 vessels positivity was based on microvessel density technique (MVD).
Results:All results were statistically assessed using Pearson chi2 score.Statistical significance was observed in Ki67 expression in adenocarcinomas (p<0.014)which could be explained by an increased agressiveness of this type of cancer.CD105 was also overexpressed and correlated to a more advanced stage of disease which apparently seems to be related to a worse disease prognosis.CD44 did not present with significant statistical advantage and awaits further investigation considering the fact that a larger number of cases may be apparently required to provide us with more conclusive results.

P 476

PROGNOSTIC SIGNIFICANCE OF NK CELLS AND TNFA IN SURGICALLY TREATED NON-SMALL CELL LUNG CARCINOMAS

RIGAS Angelos1, STYLIANOU Paraskevi1, CHORTI Maria2, TRAKAS Nikos2, LEGAKI Stella2, PALAMIDAS Filippos1, MAOUNI Niki3, ANAGNOSTOPOULOU Helen2, ZIOTOPOULOS Panayiotis1, TAMVAKIS Nikolaos2. 1 1st Department of Respiratory Medicine, Sismanoglion General Hospital, Athens, GREECE; 2 Pathology Department, Sismanoglion General Hospital, Athens, GREECE; 3 Cytology Department, Sismanoglion General Hospital, Athens, GREECE.

Aim: To assess the prognostic significance of NK cells (CD56) and TNFa in biopsy specimens with non-small cell lung cancer (NSCLC).
Materials and methods:104 patients who underwent surgery because of NSCLC were investigated as follows: tumors were classified as squamous cell carcinoma (n=53) or adenocarcinoma (n=51), and age, tumor stage, and tumor size were assessed. Expression of TNFa in lung cancer cells and the NK cells were estimated with the use of monoclonal antibodies. Samples showing >10% of TNFa positive tumor cells were considered positive. Samples with 20-30% infiltration with CD56 were considered positive and >30% strongly positive for the NK cells.Results were assessed

statistically using Pearson chi square. Life tables were estimated by Kaplan-Meier statistics and survival curves were compared using the long-rank test (SPSS 10.0).
Results: 28 samples (26.9%) were TNFá positive and 76 samples (73.1%) were TNFá negative. The survival for negative samples was 56,97 months and 37,52 for positive (p=0.01). There was also a positive correlation between the TNFá expression and more advanced stages IIIA and IIIB (p=0.01). 43 (43%) specimens were CD56 negative, 44 (44%) CD56 positive and 13 (13%) were strongly positive. There was no correlation of CD56 positive expression with the stage and survival (p=0,1000/p=0,2392 respectively). No relation was found with the size of the tumour, the histological type and the age.
Conclusion: The current study could support a role for TNFa as a prognostic factor for patients with non-small cell lung cancer.

P 477
EXPRESSION OF MATRIX METALLOPROTEINASES 7 AND 9 IN NON-SMALL CELL LUNG CANCER; RELATION TO CLINICOPATHOLOGICAL FACTORS, PROGNOSIS AND BETA-CATENIN

PIRINEN Risto (1), LEINONEN Tero (1), BOHM Jan (1), JOHANSSON Risto (2), ROPPONEN Kirsi (1), KOSMA Veli-Matti (1)
1) Department of Pathology and Forensic Medicine,
2) Department of Oncology
University of Kuopio and Kuopio University Hospital, Kuopio, Finland

INTRODUCTION: Lung tumour aggressiveness is based on its invasive and metastatic properties probably regulated by different cell–cell and cell-matrix interactions. Matrix metalloproteinases have an important role in many physiological processes and cancer cell behaviour.
PURPOSE OF THE STUDY: The present study was undertaken to analyze the expression and prognostic value of MMP-7 and MMP-9 in non-small cell lung cancer (NSCLC). The relationship of MMP-7 with beta-catenin was also evaluated.
MATERIAL AND METHODS: The study consists of 212 patients with resected NSCLC. The representative tumour samples were collected and stained immunohistochemically. The expression of MMP-7 and MMP-9 was evaluated in both tumour cells and peritumoural stromal tissue. Results were compared to beta-catenin expression and clinicopathological factors of the patients.
RESULTS: The normal bronchial epithelium was either MMP-7 negative or showed weak positivity mainly in apical cells. In MMP-9 stainings the positive staining signal was noted through the whole bronchial epithelium. The dysplastic epithelium was seen in 11 cases. Three out of 11 cases were weakly positive for MMP-7, whereas high MMP-9 staining was seen in all cases throughout the dysplastic epithelium. A high staining of MMP-7 and MMP-9 in tumour cells was noted in 62 (30%) and 113 (57%) cases, respectively. Expression of MMP-7 in cancer cells was associated with histological type of tumour (p=0.022). High cancer cell associated MMP-7 was related to less advanced tumour (p=0.037) and better tumour differentiation (p=0.005). High MMP-7 was also correlated with normal beta-catenin expression in tumour cells (p=0.001). High MMP-9 expression in tumour cells was related to poor tumour differentiation (p=0.016). The stromal signal for MMP-9 was observed in 58 (32%) cases and was linked with higher tumour grade (p=0.031). In survival analyses the significant predictors of survival were histological type of tumour and tumour stage (p=0.0009 and 0.0012, respectively). MMP-7 or MMP-9 expressions were not related to patient`s outcome.
CONCLUSION: The results indicate that in NSCLC high MMP-9 expression both in cancer cells and tumour stroma is a sign of more aggressive tumour, while high MMP-7 expression correlates with less advanced disease.

P 478
MORPHOMETRIC INTRATUMORAL MICROVESSEL AREA EVALUATION: USEFUL INDICATOR FOR COADJUVANT THERAPY IN RESECTED NSCLC

DREHER IRION Luciane Cristina 1, PROLLA Joao Carlos 2, HARTMANN Antonio 3, SILVA Vinicius 4, MARCHIORI Edson 5.
1.Master in Pathology (FFFCMPA, Porto Alegre, Brasil) and Consultant Histopathologist at The Royal Oldham Hospital.
2.Professor Head of Adult Medicine Dept of UFRGS and Professor of Post-graduation Programme in Pathology of FFFCMPA, Porto Alegre, Brasil.
3.Professor Assistant of Pathology Dept of FFFCMPA and Professor of Post-Graduation Programme in Pathology, Porto Alegre, Brasil.
4.Professor Assistant of Pathology Dept of PUCRS, Porto Alegre, Brasil.
5.Professor of Post-Graduation Programme of UFRJ, Rio de Janeiro, Brasi.

Introduction: Despite improvements on diagnosis and treatment, the prognosis of non small cell lung cancer (NSCLC) still is reserved. There has been much research on new biological parameters and prognostic markers for innumerable malignancies. Studies have demonstrated that angiogenesis can be considered as an independent prognostic factor in several neoplasias including those from lung. Computed assisted analysis of angiogenesis has been performed in some types of tumours by assessment of the number of tumour vessels. This study, however, includes also the area of tumour vessels with image analysis in NSCLC as well as survival rates in Brazilian patients. Purpose: To accomplish the tumour vascular area measurement and the microvessel count with computed assistance through microscopic images from NSCLC, and verify the correlation between these measurements and patient survival in a 5-year period. Material and methods: Paraffin blocks from 107 surgical specimens for NSCLC from Pavilhao Pereira Filho - Santa Casa (Porto Alegre, Brazil). Immunohistochemistry with anti-CD34 monoclonal antibody (QB-End10; Dako Corporation) was performed on paraffin-embedded tissue sections in order to highlight the vessels. The tumour vascular area and the microvessel count were obtained through Image Pro Plus - 3.0 program. 6 images (200x) from 3 hot spots have been taken from each case, totalling 18 images per case. With this software, the vascular area and the number of tumour vessels images have been obtained. The vascular area of each case was assumed as the mean value of its all 18 images. The cases were then separated into high or low vascular area groups, the cut-off being the mean from all 107 cases. Similar process has been made to the microvessel count method. Results: the 5-year survival rate of high vascular area group was 21.7 months „b 2.5, significantly lower (P<0.0001) than the low vascular area cases, 38.9 months „b 3.0. The correlation coefficient between the microvessel area and the microvessel count was 0.5 (P=0.001). The tumour vascular area showed higher correlation to survival (correlation coefficient: 0.48 / P= 0.001) than the tumour microvessel count (correlation coefficient:0.2 / P=0.03). Conclusion The tumour vascular area measurement with computed assistance can be used as a prognostic marker in NSCLC.

P 479
THE IMPACT OF IMMUNOHISTOCHEMICAL DETECTION OF POSITIVE LYMPH NODES ON STAGING AND PROGNOSIS IN EARLY LUNG CANCER

ERSEV Ayse, TEZEL Cagatay, KIRAL Hakan, UREK Senol, DUDU Canan, ARMAN Bulent

Detection of micrometastatic disease is an interesting topic about lung cancer. In early stage, some researchers showed its prognostic impact on survival. Therefore we conducted a study to determine whether the detection of mediastinal lymph node spread by immunohistochemical analysis affects the risk of recurrence and metastasis.
Between 1997 and 2003 21 patients underwent complete resection with mediastinoscopy and systemic nodal dissection for early stage (Stage I and II) lung cancer in our clinic. 426 lymph nodes from 21 patients were analysed. Epithelial spesific antigen Ab-9 and Keratin Pan Ab-1 were used as immunohistochemical markers. Based on nodal spread four of the 21 patients (19.04%) were upstaged after the immunohustochemical analysis. One patient with stage IB (T2N0) were upstaged to IIIA (T2N2); two patients staged as IIB (T2N1) were upstaged to IIIA (T2N2). only one of the 11 patients who had pN0(i)developed local recurrence. On the other hand three of four patients who had both pN1(i) and pN2(i) disease, developed either local recurrence or metastatic disease. Statistical analysis showed that the lymphatic dissemination detected with immunohistochemical analysis was associated with reduced disease-free-survival.
Our study provides some verification that patients with lymphatic micrometastasis have a reduced disease free survival. These results suggest that adjuvant therapies may have a role in early stage lung cancer. Before the new TNM staging system will be commonly used more information is needed to understand the prognostic impact of micrometastatic dissemination.

P 480
DIFFERENTIAL DIAGNOSTIC OF SMALL-CELLED LUNG CANCER USING PLOIDOMETRY
Fedorina TA, Yugina OV
Samara State Medical University, Samara, Russia

Background. The problem of early differential diagnostics of small-celled and non-small-celled lung cancer is particularly important in the light of different approaches to clinical management depending on a tumor type.
Aim: to use ploidometry research for studying the epithelial cell clones in the lung tumors to determine objective criteria of diagnostics of small-celled and non-small-celled lung cancers.
Methods. Computer ploidometry test was carried out for nuclei of epithelial cells in bronchial biopsy specimens, taken from 50 patients with small-celled and squamous cells carcinomas in different stages of cancerogenesis. Bronchial epithelium nuclei taken from 10 healthy individuals were used as control. Histological preparations of 8 micron thickness, stained by Feulgen's technique, were subject of the research. Nuclei's ploidy was defined by means of the computer image analyzer "Imager-CH" ("Avtan-San" software version). The "tissue ploidy standart" (2c) was used for obtaining the data of 1856 bronchial epithelium nuclei. Inter-phase cell nuclei of clones of normal bronchi epithelium, small-celled and squamous cells carcinomas in different stages of differentiation were the subjects of investigation.
Results: In comparison with the average ploidy value of the normal bronchial epithelial cells nuclei, the average ploidy index increases 1,7 times in small-celled cancers. 2 times in well differentiated squamous cells carcinomas and 2,5 times in poorly differentiated squamous cells carcinomas. The study results showed that tumor cells proliferative activity and nuclei ploidy increase in parallel with the increased disdifferentiation of squamous cells carcinomas. In routine diagnostics of bronchial biopsy specimens morphological identification between small-celled and poorly differentiated squamous cells carcinomas is particularly complicated and equally important for further clinical management. The average ploidy of nuclei significantly differs between clones of small-celled and squamous cells cancers (4.2 c versus > 6.3 c) which makes the ploidy index a useful differential diagnostic criteria.
Conclusions: Computer ploidometry may be used in differential diagnostics of small-celled and squamous cells lung cancers. Use of ploidometry data in morphological diagnostics of lung tumors can be an objective tool for taking justified clinical decisions.

P 481
THYMUS TUMORS ON OPEARTIVE TISSUE MATERIAL
STOJSIC Jelena1, RADOJICIC Jelena1, ADZIC Tatjana1, JOVANOVIC Dragana1, TODOROVIC Vera2, DRNDAREVIC Neda2 Institute for Lung Diseases and Tuberculosis, Belgrade, Serbia1
Institute for Medical Research, Belgrade, Serbia2

Background: Thymus tumors are the most frequent tumors of anterior mediastinum. It is a great challenge for surgical pathologist to estimate a precise type of thymus tumor.
Methods: We analysed 75 operated tumors of anterior mediastinum of thymus origin in last fourteen years. Thymus tumors were classified and reclassified according to the most recent classification. Thymus cysts were included in a group of anterior medisatinum operated tumors of thymus origin.
Results: Only on 14 (18.6%) preoperative percutaneuos needle biopsies pathohistological diagnosis of thymoma was established. They measured approximatively 79mm in the greatest diameter. Operated tumors were mostly encapsulated by smooth capsule, lobulated by wide septas, mostly solid or partly cystic. Eleven of them penetrated capsula and involved surrounding tissues. The most frequent was thymoma of A type - 18 (24%), then of AB type – 12 (16%), of B1 – 8 (10.66%), of B2 - 4 (5.33%) and B3 – 4 (5.33%), of C type 6 (8%). Also 3 Hodgkin lymphoma and 3 germ cell were diagnosed, each of 4%. One thymolipoma and one carcinoid tumor of thymus were also estimated – each of 1.33%. Very frequent were diagnosed thymus cysts – 15 (20%).
Conclusion: Preoperative percutaneuos needle biopsies is helpful to distinguish thymus tumors from to other tumors of anterior mediastinum, especially mesenchimal tumors and Hodgkin and B and T non Hodgkin lymphoma. According to their morphology and immunophenotype the precise pathohistological diagnosis could be established and adequate therapy, operated or else oncologic, applied. On small tissue samples the tumor biological behaviour, penetration of thymus capsula and involving of surrounding tissues, can not be estimated. It is only possible on operated thymus tumors.

P 482
MUCINOUS CYSTIC TUMOR OF THE THYMUS: A DOCUMENT OF AN EXTREMELY UNCOMMON CASE
HARADA Hiroshi, YANO Hirohisa, TAKAMORI Shinzo*, MATSUO Toshihiro*
Department of Pathology, Kurume University School of Medicine
Department of Surgery, Kurume University School of Medicine*

Pure epithelial benign neoplasms without lymphoid element are extremely rare in the thymus, although several examples of thymic adenocarcinoma have been described in the literature. We recently encountered a cystic tumor almost purely composed of goblet cell-like mucus-producing cells of the thymus arising in a middle aged Japanese male and describe herein its histological features with brief discussion regarding to the histogenesis. The patient was a 54-year-old male, who was pointed out of enlargement of the

mediastinum in 2004. But he had no complaint such as pain and remained untreated approximately for a year. At the initial presentation to our hospital in early 2005, computed tomography revealed a tumor of the medistinum and surgical removal of the thymus was performed. Gross specimen presented a unilocular cystic lesion containing abundant mucin, which was surrounded by thymic tissue and measured 8x5.5x4.5cm. Dense fibrous tissue occasionally associated with calcification intervened between the lesion and the thymic tissue. Microscopic examination revealed a cystic tumor consisting of bland mucus-producing cells resembling goblet cells and forming tiny daughter cysts within the dense fibrous capsule. In some areas, pseudostratified columnar cells were recognized as well as flattened cells showing slight atypia and nuclear enlargement in the basal layer. No destructive growth or infiltration into surrounding thymic tissue was observed. Thus, the tumor should be regarded as a mucinous cystic tumor of the thymus, probably • gmucinous cyst adenoma• h. Immunohistochemically, tumor cells showed positive reaction for AE1/AE3, CAM 5.2, but negative for 34betaE12 and involucrin. Only a few cells were reactive for p63. Two hypotheses are to be discussed on histogenesis; this tumor is likely considered to have developed from a thymic cyst on basis of pseudostratified columnar cells occasionally identified among mucinous cells. Otherwise, it might have a close relationship to mucoepidermoid carcinoma rarely found also in the thymus, although definite evidence of squamous differentiation was not confirmed. Anyway, the present case is an extremely common neoplasm which has not been described.

P 483

EXPRESSION OF OCT4 AND CELL CYCLE-REGULATORY PROTEINS IN SEMINOMA AND EMBRYONAL CARCINOMA ORIGIN IN THE MEDIASTIUM

Pao-Hsien Chu, Shih-Ming Jung, The First Cardiovascular Department; Department of Pathology, Chang Gung Children Hospital and University, Taipei, Taiwan

Background. Primary germ cell tumor is a relatively rare tumor usually located in the anterior mediastinum. A previous study has postulated that OCT4 is a nuclear transcription factor that is expressed in pluripotent embryonic germ cells. The cell cycles in the germ cell tumors have not been well documented. This study attempted to identify and characterizations of OCT4 expression and cell cycles in the specific germ cell tumors, seminoma and embryonal carcinoma.

Methods. A retrospective study conducted between 1983 and 2005 included 10 consecutive patients with seminoma and embryonal carcinoma in the mediastinum whose tumors had been surgically excised. Overexpressions of OCT4, Ki-67, p16, p53 and p63 genes were studied by immunohistochemistry.

Results. Of the 10 seminoma and embryonal carcinoma in the mediastiun patients, all were men (age 26.8 ¡Ó 15.5 y). Clinical presentations included asymptomatic (38%), chest pain (49%), and dyspnea (13%). The study group contained 10 (100%) men, with a mean age of 26.8 ¡Ó 15.5 years and follow-up 37.2 +/- 18 months. Over-expression of the OCT4 (66.7¡Ó38.3%), p53 (68.6¡Ó31.3%), and p16 (55.5¡Ó34.7%) were considerably higher than Ki-67 (31.4¡Ó27.6%).

Conclusions. This work first examined the immunohistochemical over-expression of OCT4 and cell cycle (Ki-67, p16 and p53) in seminoma and embryonal carcinoma in the mediastinum. This approach demonstrates OCT4 is highly sensitive and specific for the diagnosis; and distinguishes the potential roles of cell cycle in the development of seminoma and embryonal carcinoma.

Dr Chu is supported by NHRI, Taiwan (NHRI-EX91-9108SC, NHRI-EX92-9108SC, NHRI-EX-93-9108SC and NHRI-EX94-9108SC), and CMRPG32057 from Chang Gung Memorial Hospital at Taiwan. Dr. Jung is supported by CMRPG33044 from Chang Gung Memorial Hospital at Taiwan.

P 484

CLINICOPATHOLOGIC STUDY OF THYMOMAS (ABOUT 40 CASES)

BRAHAM Emna, ISMAIL Olfa, AYADI Aida, KILANI Tarek* and EL MEZNI Faouzi
Service d'Anatomie Pathologique,
Service de Chirurgie, Hôpital A Mami, Ariana, Tunisia.

INTRODUCTION

Thymomas are primary tumors that arise from epithelial cells of the thymus. They account for more than 50% of anterior médiastinal masses and approximatively 20% of all médiastinal tumours. These neoplasms are most commonly associated with parathymic syndromes, especially myasthenia gravis.

PURPOSE:

We present the clinical and histologic features of thymomas and review the literature.

METHODS

From January 1994 until December 2004, microscopic slides of 40 cases of thymomas were reviewed retrospectively and reclassified according to the new World Health Organization histologic classification. The stage was determined according to Masaoka's classification. Clinical records were collected from medical folders.

RESULTS

There were 23 females and 17 males. Mean age was 51,05 years (range14-76). At presentation 4 patients were asymptomatic and 7 presented with myasthenia gravis. Diagnosis was achieved on surgical specimen in 29 cases and on biopsy in 11 cases .The distribution of histologic subtype was type A (n=1), type AB (n=7), type B1 (n=6), type B2 (n=17), type B3 (n=6), micronodular thymoma (n=2), metaplastic thymoma (n=1). 10 patients were in stage I, 10 in stage II, 8 in stage IIIa, 5 in stage IIIb, 5 in stage IVa and 1 in stage IVb.

CONCLUSION

The predominant histological type in our study was B2 and half of patients were stage I and II of Masaoka. Surgery was the mainstay of treatment, and complete resection with clinical stage seem the most important prognostic factors in this disease.

P 485

MEDIASTINAL GANGLIONEUROMAS: A REPORT OF 7 CASES

ISMAIL Olfa, LIMAIEM Faten, BRAHAM Emna, HALTITI Raja,AYADI Aida, LAGHA Mohamed,DJILANI Habiba, and EL MEZNI Faouzi.
Department of Pathology,
Department of Thoracic surgery,
Department of Pneumology, Tunisia.

INTRODUCTION

Peripheral neuroblastic tumors include neuroblastoma, ganglioneuroblastoma and ganglioneuroma. These tumors were classified on depending of neuroblastic differentiation and the degree of schwannian stroma. Ganglioneuroma was a mature and benign form of them. It was rare slow-growing tumor, localized commonly in the posterior mediastinum and retroperitoneum

PURPOSE

The aim of the study is to describe the clinical and pathological characteristics of mediastinal ganglioneuroma in our institution.

METHODS

We retrospectively analyzed seven cases of mediastinal ganglioneuroma diagnosed between January 1993 and December 2004. Medical records and microscopic slides were reviewed.
RESULTS
Patients were 2 males and 7 females. Mean age was 22.14 years (4-84 years) and there were 4 pediatric cases. The most common symptoms were cough and chest pain. One patient presented with Claude-Bernard-Horner's syndrome. Two presented supraclavicular lump and one patient was fortuitously diagnosed. CT scan showed posterior mediastinal mass with dumbbell type in one case. Six patients underwent total tumorectomy. In macroscopy, 5 tumors were firm in consistency, one was soft and other was cystic with calcifications. The mean size was 5.9 cm (3.5 – 9 cm). In histological examination, tumors were composed of nerve fibers and mature ganglion cells. Lymphocytes were observed in 4 cases, fibrous capsule in three cases and calcifications in one case.
CONCLUSION
Ganglioneuromas tend to develop in children and young adults. They are asymptomatic in 50% of cases and symptoms are related to the mass effect. The mean tumor size reported in literature is 8 cm. In our study, tumors were litter and paradoxically the most of them were symptomatic (6 cases).
The definitive diagnosis is histological and the presence of neuroblasts excludes ganglioneuroma. So, complete surgical resection is necessary for ultimate diagnosis and it' is the best chance of cure.

P 486
NEUROGENIC TUMORS OF THE MEDIASTINUM IN ADULTS: A REPORT OF 44 CASES.
ISMAIL Olfa, KLAI Khedija, SMATI Belhassen*, AYADI Aida, DJILANI Habiba*,
KILANI Tarek* and EL MEZNI Faouzi.
Department of pathology
Department of thoracic surgery, Hôpital A Mami, Ariana, Tunisia.

INTRODUCTION
Neurogenic tumors originate in the embryonic neural crest cells, which constitute the ganglia, paraganglionic and parasympatic systems. In mediastinum, they are relatively uncommon, though they represent 20% of all primary mediastinal tumors in adults and occur almost exclusively in the middle and posterior compartments.
PURPOSE
We retrospectively reviewed our institutional experience of mediastinal neurogenic tumors in adults with emphasis on the clinical and pathologic characteristics.
METHODS
Between January 1993 and January 2005, 44 mediastinal neurogenic tumors were diagnosed in patients older than 14 years. Clinical records (demographic data, clinical presentation, diagnostic investigations, operative procedures and follow up) were analysed and all microscopic slides were re-examined. Comparison for parameters to distinguish malignant forms to benign, was made by X2 test.
RESULTS
Patients were 16 males and 28 females and ranged from 14 to 84 years of age. 9 patients were asymptomatic, otherwise, chest pain was the main symptom. 4 patients presented a thoracic lump and three a Recklinghausen disease. The tumors had the following characteristics: 38 of them were located in the post medistinum and 3 tumors showed an intraspinal extention, the so called dumbbell-type. They were 36 benign and 8 malignant tumors with 21 schwannomas, 10 neurofibromas, 7 malignant peripheral nerve tumors, 3 ganglioneuromas, one ganglioneuroblastoma and 2 paragangliomas. Resected was performed for all benign tumors and 4 cases of malignant tumors.
With a X2 test, we founded that tumor size¡Ý 8 cm, extension in TDM, dyspnea, thoracic lump and general status alteration were the predictive factors for malignancy.
CONCLUSION
Most studies of mediastinal neurogenic tumors compared pediatric and adult forms and age seem the most important clinical parameter for distinguishing between histological type and rate of malignancy for these tumors. In adult population, it appears that tumor size and some symptoms were the predictive factors of malignancy, especially
general status alteration that seem the only independant factor.

P 487
EFFECTS OF MELATONIN ON HISTOPATHOLOGICAL CHANGES AND OXIDANT-ANTIOXIDANT STATUS IN RABBITS EXPOSED TO SMOKE
Mehmet Unlu 1, Fatma Fidan 1, Levent Tetik 1, Onder Sahin 2, Hidir Esme 3, Tulay Koken 4, Murat Sezer 1
1Department of Pulmonary Medicine, Afyon Kocatepe University Faculty of Medicine
2Department of Pathology, Afyon Kocatepe University Faculty of Medicine
3Department of Thoracic Surgery, Afyon Kocatepe University Faculty of Medicine
4Department of Biochemistry, Afyon Kocatepe University Faculty of Medicine

ABSTRACT:
Objectives: To show the effects of smoke exposure in rabbits to the histopathological changes in lungs, oxidant-antioxidant status, and the effects of melatonin on these changes.
Methods: Four groups each with five rabbits are formed. A glass box (80x80x80 cm) is used. Group 1 (control) is exposed to cigarette smoke, group 2 (melatonin) is given melatonin only, group 3 (smoke+melatonin) is both exposed to smoke and given melatonin in a duration of 1 month for 1 hour daily and group 4 (control) is the control group. Then lung tissues are examined histopathologically . Protein sulfhydryls (SH), carbonyl, prostaglandin F2á (PG F2á), melandialdehyde (MDA), glutathion peroxidase (GPX), superoxide dismutase (SOM) levels in blood are measured.
Results: Histopathologically intraparenchimal vascular congestion and thrombosis, intraparenchimal hemorrhage, respiratory epithelial proliferation, macrophages in alveolar and bronchial lumens, and bronchoalveolar hemorrhage scores were significantly higher in group 1(smoke) than group 4(control). The scores of bronchoalveolar hemorrhage is significantly decreased in group 3(smoke+melatonin) than group 1 (smoke). Levels of SH and PG F2á were significantly higher and levels of SOD were significantly lower in group 1(smoke) than group 4(control). Carbonyl levels were significantly lower in group 3(smoke+melatonin) than group 1(smoke).
Conclusion: Exposure to cigarette smoke causes severe histopathological changes and negatively effects the oxidant-antioxidant status on rabbits. Melatonin treatment has no healing effect on histopathological changes and oxidant-antioxidant status.

P 488
TRANSTHORACIC FINE NEEDLE BIOPSY OF THE LUNG
REPŠE-FOKTER Alenka, KERN Izidor

BACKGROUND AND AIMS: Transthoracic fine needle biopsy of the lung is one of the basic invasive diagnostic procedures in patients with lung diseases. It is safe, cost effective and successful, especially in detecting of malignant diseases. Our objective was to assess the correlation between cytologic and histologic diagnoses.

MATERIAL AND METHODS: We analysed cytologic and histologic diagnoses of 39 patients in whom transthoracic fine needle biopsy of the lung was performed between January 2002 and December 2004.
RESULTS: The patients were 31 – 84 years old (mean 59). The cell samples were insufficient for cytologic diagnosis in 8 cases (20,5%), 5 of them were insufficient also for histologic diagnosis. In 13 out of 31 representative cases cytologic diagnoses were correctly interpreted as benign changes (41,9%). There were two cases of hamartoma and two cases of abscedent inflammation among benign lesions, remaining 9 were reported as non-specific benign changes. In 5 patients cytologic diagnoses were suspicious for carcinoma. In three of them histologic diagnosis confirmed epidermoid carcinoma, in one mesotelioma. One of cytologically suspicious cases was suspicious also after histologic examination. 13 out of 31 representative cases were correctly diagnosed as malignant. Among malignant lesions 4 were adenocarcinomas, 3 epidermiod carcinomas, 2 non-small cell carcinomas and 2 small cell carcinomas. Histologic examination of the two malignant tumors with very unusual cytomorphologic picture revealed synovial sarcoma in one case and PNET in the other.

CONCLUSION: Transthoracic fine needle biopsy of the lung and cytologic examination is a reliable method in distinguishing benign or malignant nature of lung lesions. It is successful also in differentiation of malignant tumors. However, histologic examination is more reliable in further classification of benign changes.

P 489
DIFFUSE PULMONARY OSSIFICATION: A FORGOTTEN ENTITY IN CHRONIC LUNG DISEASE
Ruiz E.(1), Gonzalez-Obeso E.(1), Nistal M.(2).
(1) Trainee resident; (2) MD, pHD.
Department of Pathology. Universitary Hospital La Paz. Madrid. Spain

INTRODUCTION: Diffuse pulmonary ossification (DPO) is an uncommon chronic process characterized by progressive metaplastic lung parenchima ossification. Clinical course is usually asymptomatic, although mild symptoms and restrictive pulmonary physiology have been described in some cases.
OBJECTIVE: To present two cases of DPO and correlate the clinical, radiographical, and pathological features of this entity.
METHODS: Lung biopsies and adult autopsies performed at the University Hospital of La Paz from 1966 to 2004 were reviewed to identify the cases of DPO. One case of DPO was identified out of 9,964 lung biopsies and the other out of 4,051 adult autopsies.
RESULTS: The biopsy was obtained from a 72 year-old man clinically diagnosed of pulmonary restrictive disease. The other case was a 81 year-old man with biventricular hipertrophy and a peacemaker who died of bilateral bronchoneumonia. Radiographically, both patients presented signs that could sugest DPO. Histologically, lungs from both patients presented a nodular pattern of DPO (lamellar deposits of calcified osteoid material located within the alveolar spaces). Even though, the underlying pathology of the first patient has been associated to the dendriform or branching pattern of DPO.
CONCLUSIONS: DPO is an unusual entity seen incidentally at autopsy. Since it is hardly ever considered by clinical physicians, it is rarely diagnosed. A better understanding of the process of DPO formation, its associated diseases, and radiographical appearance is important in order to avoid misdiagnosis with other types of calcium accumulation in the lungs.

P 490
CENTRAL AND PERIPHERAL AIRWAYS EXPRESSION OF NF-KBP65 AND HDAC2 IN NONSMOKERS, ASYMPTOMATIC SMOKERS AND COPD
ISAJEVS Sergejs, TAIVANS Immanuels, KOPEIKA Uldis, STRAZDA Gunta
Department of Pathology, Faculty of Medicine, University of Latvia

Introduction. Airways inflammation and oxidant/antioxidant imbalance is a major cause of lung damage in COPD. An oxidative stress lead to redox-sensitive transcription factor nuclear factor-kB (NF-kB) activation, which regulates the transcription of inflammatory mediators. The molecular mechanism by which inflammatory genes are switched off is mediated by chromatin deacetylation by histone deacetylase (HDAC2).
Purpose of the study. The aim of our research was to compare inflammatory changes in central and peripheral airways in nonsmokers, asymptomatic smokers and in smokers with COPD.
Patients and methods. The study population was composed of 17 subjects undergoing lung resection for a solitary peripheral carcinoma. They have been subdivided into three groups: 5 subjects was nonsmokers and had normal lung function, 5 subjects were smokers with normal lung function and 7 subjects had COPD (FEV1/VC<70%). Immunohistochemical methods were used to identify NF-kB p65 and HDAC2 positive cells. The alveolar destruction index was calculated by formula DI (destruction index)={D/(D+N)}*100%, where D-is destroyed, but N-normal alveolar walls.
Results and discussion. Asymptomatic smokers had more NF-kBp65 positive cells in central compared to peripheral airways and alveolar walls. Subjects with COPD had more NF-kBp65 positive cells in alveolar walls and peripheral airways compared to central airways. The NF-kBp65 was activated both in macrophages and bronchial epithelial cells. In nonsmokers NF-kBp65 expression was found mostly in cytoplasm, but in smokers in cell nucleus. In central airways of asymptomatic smokers there was a positive correlation between the number of NF-kBp65 positive cells (p=-0,04; r=0,65) and smoked pack-years. In patients of all groups there was a positive correlation between macrophages in alveolar walls and destruction index (p=-0.04; r-=0,68). HDAC2 was expressed in all inflammatory cells. HDAC2 expression was suppressed in smokers.
Conclusion. It has been suggested that NF-kB was activated both in asymptomatic smokers and in smokers with COPD. In COPD NF-kBp65 positive cells mostly infiltrate alveolar walls and peripheral airways. The HDAC2 activity was suppressed in smokers.

P 491
PARTICULARITY OF CHRONIC DIFFUSE LUNG DISEASE IN PATIENTS LIVED AT RADIOACTIV-POLLUTED TERRITORIES OF SEMIPALATINSK REGION
Sagindikova G., Kogan E.

Aim. To study diseases, mortality and morphological peculiarities of chronic diffusion diseases of lung in persons lived at radioactive-polluted territories of Semipalatinsk region over a long period of time.
Materials and methods. The analysis of 631 postmortem examination reports with the diagnosis chronic diffusion disease of lungs and archival paraffin autopsy, surgical and biopsy material from 300 patients with CDLD who lived near to polygon and were exposed to the radiation over a long period of time since childhood up to 2003 (annual dose of the irradiation exceeded 0,1 bar). Light microscopy with painting by haemotoxilin and eosin; Van-Gison were performed;

chromogranin À (DAKO) were studied by immunohistochemically.
Results. In the presence of CDLD except known morphology particularities we can point to: sclerosis of walls of bronchus and interstitial; vessel pathology with development of hemosiderosis; accumulation of dust as an indirect index of deposit of radionuclide; hyperplasia of neuroendocrine cells; displease of bronchus epithelium.
Conclusion. The analysis of diseases, mortality, and decrease of these indexes after closing of the polygon and morphology data and information from the literature showed that radiation has a very high mean in pathogenesis of CDLD.

P 492
THE FIRST YEAR OF TRANSBRONCHIAL BIOPSY (TBB) AFTER LUNG TRANSPLANTATION (LT). THIRTEEN YEARS EXPERIENCE.
E.Caballero-Mendoza*,R Vilallonga,I de Torres, M Ferran, R Broto, J Ancer*,S Ramon y Cajal,J Majo. Hospital Vall Hebron, Barcelona, Spain. * Pathology Department, Faculty of Medicine, UANL, Monterrey, Mexico.

Objective.
To analyze the evolution of the mean, indications and diagnostics of 700 TBB performed in the first year from 241 lung transplants performed between 1990 and 2003
Design.
We divided our TBB database for LT into two groups, the historical group (HG) (80 LT& 345 TBB, between 1990 to 1997), and the recent group (RG) (161 LT & 355 TBB, between 1998 to 2003). Each of them were divided into early postransplant period (EPT) (<45 days), and late postransplant period (LPT) (45 to 365 days). We also considered wether the biopsy was clinically indicated (Bcli) or it was a survillance biopsy (Bsurv)
Results.
There is a current decrease in the mean TBBs, principaly in the LPT, in both Bsurv and Bclin compared the HG and RG. The frecuency of TBB in EPT were similar in Bsurv and Bclin in the HG and RG
Historic Group: TBB* 345 (I:4.3); EPT 114 (I:1.42); LTP* 231 (I:2.88); B surv* 163 (I:2.06); B surv EPT 45 (I:0.56); B surv LTP* 118(I:1.47); B clin 182 (I:2.27);B clin EPT 69 (I:0.86); B clin LPT* 113 (I:1.41).
Recent Group: TBB* 355 (I:2.2); EPT 214 (I:1.32); LTP* 141 (I:0.85); B surv* 150 (I:0.93); B surv EPT 88 (I:0.54); B surv LTP* 62(I:0.38); B clin 205 (I:1.27);B clin EPT 126 (I:0.78); B clin LPT* 79 (I:0.49).
* $p<0.05$
In Bcli, in TBB from the recent group we can see an increase of diagnostic biopsies of acute rejection (AR) from 32 to 61 cases (17.6% in HG vs 29.8% in RG, $p<0.05$) and bronchitis/bronchiolitis from 3 to 17 cases (1.6 in HG vs 8.3% in RG, $p<0.05$) and decrease of non-diagnostic biopsies (ND) from 38 to 26 cases (20.9% in HG vs 12.7% in RG, $p<0.05$).
In Bsurv observed an increase of AR diagnostics from 32 to 48 cases (19.6% in HG vs 32% in RG, $p<0.05$) and bronchitis/bronchiolitis from 4 to 20 cases (2.5% in HG vs 13.3% in RG, $p<0.05$)
Conclusions.
1) We are currently managing LT with less TBB before.
2) Present better definitions of clinical settings (i.e. chronic airway rejection) see to improve the percentage of diagnostics in B cli
3) Better recent biopsy protocolization provides Bsurv with some wortwhile indications, not only in the early PT period, but also in late non far PT period

P 493
DISCREPANCIES OF CLINICAL AND POSTMORTEM DIAGNOSIS IN PULMONARY CASES.
Kleina Regina, Aboltins Arnis

The aim of our study is to analyze frequency and reasons of undiagnosed lung diseases in hospitals of Riga (Latvia) during 1999-2004.
Material and methods.We have evaluated autopsy protocols, histological specimens, cases reports of 51 patients with nonspecific inflammation processes and tuberculosis. All dates were evaluated with SPSS 10 program.
Results. In State Center of Pathology (Riga) in six years were made 3600 necropsies. The level of uncoincidence between clinical and pathological diagnosis was 10, 6 %. The comparison of clinical cause of death and autopsy diagnosis showed misdiagnosis of lung diseases in 16, 1 % of cases. Between undiagnosed lungs diseases were: 64 % with lobar pneumonia (LP), 19 % -bronchopneumonia (BP), 5 %-chronic bronchitis (CHB), 12 % -tuberculosis (T). Hospitalization time of patients with LB. was 5days. These were cases with such complications as empyema and purulent meningitis. BP. cases were mainly with abscesses. Persons dead due to CHB were very old people. In misdiagnosis of T. clinical doctors ignored bone tuberculosis in anamnesis and T. was not proved by X- ray examinations.
Instead of lung diseases clinical doctors had diagnosed pathologies of CNS (33, 3 %), coronary heart disease (12%), gastrointestinal system 18, 5% and other pulmonary problems (28%). Duration of patient's hospitalization was average 2, 6 days; ratio male to female was 1, 9:1, average age of men -49, female 60 years. Diagnostic difficulties were also due to severe concomitant diseases of liver and cardiovascular system.
Conclusions. Misdiagnoses of lung diseases were mainly due to short hospitalization time of patient. Doctors ignored patients complains and overlooked X-ray findings, leukocytosis, high ESR, coughing, dyspnoe.

P 494
EXPRESSION OF EXTRACELLULAR MATRIX METALLOPROTEINASE INDUCER (EMMPRIN) IN INTERSTITIAL LUNG DISEASES.
CAULET-MAUGENDRE Sylvie*, GUILLOT Stéphanie**, MARTIN-CHOULY Corinne**, JOUNEAU Stéphane***, DELAVAL Philippe***,LAGENTE Vincent**.
* Laboratoire d'Anatomie Pathologie, ** INSERM U620, Université de Rennes 1, *** Service de Pneumologie, CHU RENNES. France.

Background : Extracellular matrix metalloproteinase inducer (EMMPRIN) is a transmembrane glycoprotein, member of the immunoglobulin superfamily, which stimulates the production of various matrix metalloproteinases (MMPs) from mesenchymal cells. Several MMPs (MMP-1, MMP-2, MMP-9, MMP-14) are involved in lung tissue remodeling and fibrotic processes in experimental and human interstitial lung diseases, as Usual Interstitial Pneumonia (UIP), Non Specific Interstitial pneumonia (NSIP), Chronic Organizing Pneumonia (COP or BOOP), diffuse alvolar damage (DAD), or sarcoidosis.
Purpose of the study : This study aimed to analyse the EMMPRIN expression in various human interstitial lung inflammatory diseases, with or without fibrosis, to precise the cellular source and relationships between EMMPRIN, inflammation and fibrosis.
Methods : The expression was evaluated by immunohistochemistry on surgical lung biopsies in 14 UIP (7 idiopathic or IPF and 7 with associated disease), 4 other interstitial pneumonia (1 NSIP, 1 COP, 2 without specific histologic pattern), 5 DAD, 5 sarcoidosis, 5 pneumoconiosis at early stages, 5 localized fibro-bullous disease and 4 histological normal tissues.
Results : In normal lung, EMMPRIN was slightly expressed in alveolar macrophages and in bronchiolar epithelial cells. In all cases, EMMPRIN was mainly localized in alveolar and

tissue macrophages and bronchiolar cells, with an increased cytoplasmic staining in interstitial pneumonia. In UIP and DAD, pneumocytes of type II present in areas of fibrosis (honeycomb pattern or fibroblastic foci) expressed EMMPRIN according a membranous pattern, along the basement membrane and the cellular interfaces. Pneumocytes of type I, observed in preserved areas of UIP or in all other diseases, were never stained.
Conclusion : EMMPRIN, as an inducer of MMPs, is implicated in the migration/proliferation and phenotype change of the fibroblasts to myofibroblasts with subsequent accumulation and remodeling of extracellular matrix. In UIP and DAD, the increase and peculiar expression of EMMPRIN demonstrated that both the inflammatory (macrophages with activation) and epithelial (alveolar epithelial cells with injury/activation) pathways play a major role in the development of fibrosis. This could be underlined in these two interstitial pneumonia for therapeutical research, because their dramatic evolution towards fatal fibrosis with no or limited response to classical anti-inflammatory drugs.

P 495
METAPLASTIC CHANGES IN BRONCHIAL GLANDS ON THE PLACE OF THE PREVIOUS BIOPSY
GAJANIN Radoslav, BABIC Bozana, KLEM Istvan, ERI Zivka, GAJANIN Vesna, ZRNIC Bogdan

INTRODUCTION: In the bronchi on the place where the previous biopsy had been done, we noticed presence of regenerative changes, while in the bronchial glands we discovered changes with necrotizing sialometaplasia characteristic, which can be wrong diagnostic like mucoepidermoid or squamous cell carcinoma.
MATERIAL AND METHODS: Research includes 141 biopsy samples, which was get by repeated biopsy (rebiopsy). From 141 biopsy samples, changes in bronchial glands are noticed in 44 biopsy samples. The main goal of this research is discovered morphological changes in bronchial glands at the place of previous biopsy.
RESULT: Morphological changes which are discovered on the place of previous biopsy in bronchial glands are: lobular look of changes (59,09% all cases), lesion on the surface (or mucous membrane)(86,36%), fibrin (90,91%), granulations tissue (100%), squamous cells in fibrin (75%), reparative defect in the cartilage (66,67%), granulocytes in the epithelium (93,18%), cylindrical epithelial hyperplasia (93,02%), mucus in the interstitial tissue (77,27%), cystic formation (70,45%), dyskeratotic changes (70,45%), nuclear polymorphism (56,81%) and hyperchromatism (36,36%), multinuclear cells (15,91%), emphasized nucleolus (90,91%), mitosis (47,73%), necrosis (13,64%), 'capture' squamous cells in the granulation tissue (90,91%).
CONCLUSIONS: The characteristic changes in the bronchial glands on the place of previous biopsy are: lobular look of lesion with defect on the surface field up with fibrin or granulation tissue inside who accumulated islands squamous cells with cellular polymorphism, emphasized nuclei who are mitotic active, intraepithelial and stromal granulocytes, reparative defect in cartilage, goblet and cylindrical cells, mucus in the interstitium and cystic formation. The above facts could be wrong diagnostic like mucoepidermoid or squamous cell carcinoma.
KEY WORDS: bronchi, rebiopsy, bronchial glands, regeneration

P 496
INTERACTIVE TELEPATHOLOGY WITH THE COOLSCOPE, IN CONSULTATIVE DIAGNOSTICS OF THE DISPERSED LUNG LESIONS.
SLODKOWSKA Janina, *SIEMIATKOWSKA Krystyna, **WOJCIECHOWSKI Michal
National Tuberculosis and Lung Diseases Research Institute [NTB&LDRI], Warsaw. *Kujawsko-Pomorskie Center of Pulmonology [KPCP], Bydgoszcz; **Nikon, Warsaw. POLAND

The term „dispersed lung lesions" [DLL] is a common preliminary clinical diagnosis accompanying the lung biopsy specimen for the histological examination. Actually, DLL is a radiological term used for an undefined lung lesions, does not correlate with their extension nor anatomic distribution. The clinical interpretation of DLL includes: diffuse interstitial lung diseases [DILD], infections, neoplasms (primary or secondary), thrombembolic and cardiovascular diseases, ARDS. Many diseases (especially DILD) have various manners of manifestations and histologic patterns; need complex analysis of the patient data and create the diagnostic problems for the pathologist who will need the second opinion. As our previous studies showed the static telepathology has limited value in the teleconsultations of DILD.
The study was performed to assess the usability of a new generation of telemicroscopy - the coolscope system (NIKON, Japan) for the interactive teleconsultations of DLL.
40 cases of lung biopsy with the preliminary diagnosis "DLL" entered the interactive teleconsultations between KPCP and NTB&LDRI. The coolscope was installed at the workstation with 10 MB network transfer capacity; the viewing workstation used 2 MB transfer capacity (17 inches flat panel monitor with 1,3 mln pixles). For the voice Internet communication the Windows Messenger software was used. The telediagnoses were verified with the light microscope.
The viewing time of a complete microscopic slide ranged from 10 to 60 minutes/case and was depended on the case difficulty and time of image downloading (30' - 7'). The main diagnostic problems encompassed: classification of idiopathic interstitial pneumonias (usual v. non-specific interstitial pneumonia; mixed multilobular patterns; honeycomb stage) - 20 cases; granulomatous inflammatory pattern (extrinsic allergic alveolitis, sarcoidosis, aspergillosis) - 9; occupational diseases - 4; lymphoproliferative diseases - 2; infections - 2; thrombembolic disease - 2; bronchiolitis - 1. An overall diagnostic accuracy was 95% (38/40), 2 cases needed additional immunostaining.
The benefit from this technical development is a very high diagnostic accuracy in DLL teleconsultations combined with the high efficiency of the system (the standard Internet connection, free time access to the system, independent platforms, cheep and good quality of the service).

P 497
ISOLATED AMYLOIDOSIS OF THE TRACHEA
KORKOLOPOULOU Penelope 1, KAVANTZAS Nikolaos 1, THALASSINOS Nikolaos 2, ZACHILAS Dimitrios 2, PREZAS Loukas 2, LOUTRARIS Christos 1, ANASTASIOU Nikolaos 2, PATSOURIS Efstratios 1
1. Department of Pathology, School of Medicine, National and Kapodistrian University of Athens, Athens, Greece.
2. Department of Thoracic Surgery, 1st IKA Hospital of Athens, Athens, Greece.

Introduction: Respiratory amyloidosis is a rare disease that occurs in three forms: tracheobronchial, nodular parenchymal and diffuse parenchymal involment. Tracheobronchial amyloidosis is characterized by focal or diffuse deposition of amyloid in the submucosa of the trachea and proximal bronchi.
Clinical and laboratory features: A female 55–year-old patient presented in the Department of Thoracic Surgery with symptoms of dyspnea on exertion the last 2 years. She reported previous hospitalization for sangeinous sputum and bronchiectasis. On physical examination she had rales and

prolongation of the expiratory phase. Her chest radiography was negative and the CT scan showed thickness of the posterior wall of trachea. On bronchoscopy, soft, whitish, sponteneously bleeding patches were discovered and biopsed. One of the lesions was obstructing the opening of the left main bronchus. Histological examination showed isolated amyloidosis of the trachea, without any involvement of the larynx or the bronchi. The diagnosis was confirmed by the Congo Red histochemical stain. The patient was initially treated with endoscopic laser surgery. Given that obstruction of the left main bronchus persists, the patient is a candidate for stent placement.
Conclusion: Primary isolated amyloidosis of trachea is a rare and probably recurrent disease. Airway compromise can be a persistent problem. Repetitive laser or cryotherapy interventions and use of stent is a palliative therapy for this disease with poor prognosis.

P 498
NON AMYLOÏDOTIC BRONCHOPULMONARY DEPOSITS OF IMMUNOGLOBULIN IN WALDENSTRÖM'S MACROGLOBULINEMIA
Alexandre VASILJEVIC (1), David MEYRONET (1), Lara CHALABREYSSE (1), GINDRE Dominique (1), Frédérique DIJOUD (2), Jean-François CORDIER (3), Françoise THIVOLET-BEJUI (1)
(1)Service d'anatomie et cytologie pathologiques , hôpital Louis Pradel , Lyon
(2)Service d'anatomie pathologique , hôpîtal Debrousse, Lyon
(3)Centre des maladies orphelines pulmonaires , hôpital Louis Pradel, Lyon

We report the case of a 49 years old woman, followed up since 2001 for Immunoglobulin M (IgM) kappa monoclonal gammopathy of undetermined significance and presenting for 4 years evolutive dyspnea with bronchorrhea.
Paraclinical evaluation has shown non-infectious proximal diffuse bronchiectasis associated with parenchymatous destruction by chest tomodensitometry ; a decrease of CO diffusion ; « candle stains » lesions of bronchi by endoscopy. A high rate of monoclonal IgM, previously undervalued because of a cryoglobulinic pattern, was found. There wasn't Bence Jones proteinuria. A bone marrow biopsy led to the diagnosis of Waldenström's macroglobulinemia.(WM)
MATERIAL AND METHODS :
The bronchic and pulmonary biopsies sampled by endoscopy and thoracotomy were fixed or frozen for optical microscopy , electronic microscopy and immunofluorescence.
RESULTS :
Under optical microscopy , bronchic submucosa exhibited deposits of a perivascular and intersitial amorphous eosinophilic material. Pulmonary tissue showed proximal acinar emphysema and bronchiolar dilatation. Congo red and T thioflavin stains showed these deposits to be non amyloïdotic. Immunofluorescence of the deposits were positive for anti kappa and anti mu immunoglobulin chains antibodies. They were granular under electronic microscopy. Similar but smaller deposits were found in alveolar wall.
DISCUSSION :
There are two classical types of lung involvement in WM : AL amylosis and primary lymphomatous invasion. The reported case is original because :
the bronchopulmonary presentation (proximal bronchiectasis) is exceptional
the nature of the deposits made of complete or fragmentary light chain and heavy chain of IgM is non amyloidotic
CONCLUSION :
This case represents an original anatomo-clinical syndrom. The pathological mechanism which explains that the monoclonal IgM kappa cryoglobulin forms deposits at bronchopulmonary level and leads to these clinical manifestations is still undetermined.

P 499
MUCORMYCOSIS MIMICING LUNG CANCER (CASE REPORT)
Fillinger J.,Soltesz I.,Udud K.,Csekeõ A.,Kludák I.

The authors introduce two cases, whose history includes diabetes mellitus.Either of them after ketoacidic coma were found to have unilateral pulmonary infiltration. Bronchoscopy showed cone shape stricture of the right main bronchus. the surface of the mucus membrain was rough and looked like a tumor. Histology did not find anything other than fungal infection.
In one case the regulary done investigation found a tumor, suspected,infiltration of the left lower lobe.The resected lobe has undergone histopathological investigation and showed infection of mucormycosis.
In the literature mucormycosis stands in forth place among opportunistic pulmonary fungal infection.Backround of the recent years recognised growing incidence of well known immundefficiency and increasing number of diabetes mellitus.

P 500
IMPROVED PCR-BASED DETECTION AND DIFFERENTIATION OF MYCOBACTERIUM TUBERCULOSIS COMPLEX IN PARAFFIN-EMBEDDED TISSUES BY APPLICATION OF THE HOPE*-TECHNIQUE
E. Vollmer1, D. Hillemann2§, T. Kubica1, G. Zissel3, J. Müller-Quernheim3, J. Galle1,
T. Goldmann1
1Clinical and Experimental Pathology, Research Center Borstel, Borstel, Germany.
2National Reference Center of Mycobacteria, Research Center Borstel, Borstel, Germany
3University Freiburg, Dept. for Pneumology, Freiburg, Germany

Introduction: Detection of mycobacterial DNA by PCR in formalin fixed, paraffin-embedded specimens may lack sensitivity due to degradation of nucleic acids.
Purpose of the study: To improve the results we set up an approach by application of the novel HOPE-fixative in PCR-detection of mycobacteria in paraffin-embedded tissues.
Methods used: PCR, Real time PCR, Spoligotyping.
Summary of the results: Comparison of PCR-results using DNA extracted either from HOPE- or formalin-fixed specimens in BCG-infected SCID-mice revealed a more than 100fold enhanced sensitivity for the HOPE-fixed material. Due to the preservation of DNA from degradation in HOPE-fixed tissues even differentiation within the M. tuberculosis complex was possible by spoligotyping.
Conclusions reached: We demonstrate that the HOPE-technique is a useful tool for molecular pathology, which enhances the sensitivity of PCR-based methods for detection of pathogens in paraffin embedded tissues compared to formalin-fixation. Due to the better preserved DNA improved differentiation of mycobacteria from archived materials is possible. These results promise new and substantially enlarged possibilities in the field of molecular pathology.
*(Hepes-Glutamic acid buffer mediated Organic solvent Protection Effect

P 501
HISTOLOGICAL DIAGNOSIS OF LUNG BACTERIAL NECROTIZING INFECTION: A STUDY OF 4 FULMINANT CLINICAL CASES
LASSALLE Sandra (1, 2), HOFMAN Véronique (1, 2), BUTORI Catherine (1), HOFMAN Paul (1).
Laboratory of Clinical and Experimental Pathology, Pasteur' Hospital, University of Nice, Nice, France

We report the clinical and histological findings of four cases of pulmonary infection due to bacteria which were associated with a lung extensive necrosis. These infections were fulminant with a fatal course within a few hours. Histological findings were very similar in these 4 cases and were characteristics of these infections by associating an extensive hemorrhagic tissue necrosis, large layers of bacteria observed inside the alveola and/or in the connective tissue, and most often, a very weak or no inflammatory infiltrates. These infections were due to group A Streptococcus in two cases, Staphylococcus aureus in one case, and Haemophilus influenzae in one case. The histological features observed in these infections are due to the production of large amounts of different necrotizing toxins. These dramatic infections are extremely rare and can occur, both in immunodeficient and in immunocompetent patients without any apparent underlying disease. The differential diagnosis includes a viral infection which can be very difficult to be eliminate histologically. The precise diagnosis is always based on a correlation between the histological and the microbiological results. These data confirm the reappearance of some highly invasive strains, such as strain of group A streptococci, capable of producing a variety of fulminant diseases, including shock and diffuse pulmonary necrosis. The nonspecific presentation and fulminant progression require that the treating physician, the microbiologist, and the pathologist be both knowledgeable and vigilant.

P 502

LOH AT 9P21 (P16 LOCUS) AND 17Q13 (P53 LOCUS) CAN BE DETERMINED IN ORAL EXFOLIATIVE CYTOLOGY FROM NON-SMALL-CELL-LUNG-CANCER PATIENTS.

J Sanz-Ortega 1, J Sanz-Esponera 1, S Hernandez 2, M Saez 1, F Roig 3, L Callol 3 and A Munoz

Background: LOH at different loci is a frequent genetic alteration detected in non-small-cell lung cancer. Identical allelic deletions were found in most cases in normal bronchial cells adjacent to tumor Smoking exposure has been involved with these genetic changes in oral, larynx and lung tumorigenesis. Therefore, demonstration of LOH in any of these locations may detect patients with a higher risk of cancer. Design: Oral exfoliative cytology was obtained from 64 patients divided in 3 groups: 23 current smokers in which NSCLC was detected, 24 current smokers with no evidences of malignancies (3-5 years follow-up) , and 17 non-smokers control population.Results: We found LOH at 17q13 in 3/15 (20%) and LOH at 9p21 in 2/12 (16.6%) of the informative tumor cases. In total, 5 out of 18 (27,5%) patients that were informative for either alleles showed deletions. LOH was not found at any locus in oral mucosae from any non-tumoral case, smoker or non-smoker.
Conclusion: LOH at 9p21 (p16) and 17q13 (p53) can be determined not only in normal bronchial cells adjacent to NSCLC but also in oral exfoliative cytology. In our series these somatic genetic changes were unusual in patients with similar age and sex distribution with no evidences of malignancies. LOH assessment in oral exfoliative cytology may be useful in screening to detect smoker patients at a higher risk of malignant transformation.

P 503

THE POTENTIAL ROLE OF INCREASED CD68 POSITIVE MACROPHAGES AND MACROPHAGE MICROACCUMULATIONS PRESENCE, IN CASES OF CROHN'S COLITIS AND THEIR CONTRIBUTION IN ITS DISTINCTION FROM ULCERATIVE COLITIS

TSAMANDAS Athanassios, LIAVA Anna, ZOLOTA Vassiliki, SCOPA Chrisoula
Department of Pathology, University of Patras Greece.

Background: Previous studies have demonstrated that macrophage microaccumulations (MA) are present in gastric and small bowel mucosal biopsies from patients with Crohn's disease (CD). However, their presence in inflammatory diseases of the colon has not been fully elucidated. In this study we investigated whether CD68 immunostaining and MA can be used to distinguish CD from ulcerative colitis (UC).
Design: The study included 123 routinely processed colonic mucosal biopsies, including 72 specimens obtained from 30 patients with CD (mean age: 47 yrs, M/F: 10/20), 33 specimens from 20 patients with UC (mean age: 33 yrs, M/F: 5/15) and 18 specimens from 18 normal controls (mean age: 63 yrs, M/F: 8/10). On paraffin sections a standard streptavidin-biotin peroxidase method was applied using the anti-CD68 antibody. The total number of CD68(+)cells in 10 consecutive intercrypt regions (ICR) of the lamina propria was recorded in each biopsy specimen. The number of MA, defined as loose collections of at least 5 macrophages identifiable only by CD68 immunopositivity, and not by H&E staining, present in 10 consecutive ICRs was also recorded. Finally we employed statistical analysis in order to compare the results from the different patient groups.
Results: There were no significant differences in the number of subepithelial or basal lamina propria CD68(+)cells between the three patient groups. However, the mean number of CD68(+) macrophages in the mid lamina propria was higher in CD (29±4) than UC (19±8, $p<0.05$) and normal controls (23±3, $p>0.05$). MA were present in 24 biopsies from 19 (63%) CD patients, compared to 6 biopsies from 5 (25%) UC patients ($p<0.01$) and none (0%) of the normal controls ($p<0.0001$). Furthermore, only CD cases contained >1 MA (9 biopsies from 6 patients, $p<0.01$). None of the UC or control patients had >1 MA.
Conclusions: The study demonstrates that small aggregates of CD68(+)macrophages are more frequently present in CD than in UC and multiple MA are found exclusively in CD. Thus, the presence of multiple MA may contribute to the distinction of CD from UC in colonic biopsies.

P 504

AN ANALYSIS OF THE RELIABILITY OF DETECTION AND DIAGNOSTIC VALUE OF VARIOUS PATHOLOGICAL FEATURES IN CROHN'S DISEASE

Engin Cigerciogullarý*, Suha Goksel*, Gulen Bulbul Dogusoy*, Sibel Erdamar Cetin*, Aykut Ferhat Çelik**, Yusuf Erzin**, Ismail Hamzaoglu***
University of Istanbul, Cerrahpasa Medical Faculty, *Department of Pathology, ** Department of Gastroenterology, *** Department of General Surgery

Introduction. Due to the relatively high frequency of intestinal tuberculosis (IT) and intestinal involvement of Behçet's disease (BD) in Turkey, the differential diagnosis of Crohn's disease (CD) is difficult. This difficulty is valid for the pathologic investigation of both endoscopic and surgical GIT material. The aim of this study is to specify the pathological features of CD that will differentiate from the other conditions, and to analyze the reliability and diagnostic value of these features.
Material and Methods. In this study, 26 standardized patients, that have been diagnosed as CD through standard clinical, laboratory, radiological, endoscopic, microbiological procedures and further operated, have been investigated. The preoperative endoscopic biopsies, the surgical specimens and the immediate mucosal punch biopsies of the resected intestine have also been revised.
Results. In the resection specimens of 23 patients, fissure formation, transmural lymphoid follicle infiltration, submucosal fibrosis, neuronal hyperplasia, subserosal

fibrosis, which are the classical findings of CD were observed. The striking point in this regard was the infrequent presence of granuloma formation in these patients (30%). In the remaining 3 patients, even though some of the above findings exist, the classical Crohn's picture was not established. In the endoscopic biopsies the most presenting finding was antral metaplasia, and the most interesting finding was increase in eosinophils. In 2 of the patients the coexistence of BD and CD was observed.
Conclusion. Granuloma formation which a finding of CD is not observed too frequently among the patients in Turkey. The presence of antral metaplasia and increased eosinophils in the endoscopic biopsies of the chronic patients may be useful for diagnostic approach when combined with other histological findings. Due to the incidence of coexistence of BD and CD, the investigation of standardized BD and IT groups, are subjects of our ongoing studies.

P 505
A NEW SIMPLIFYED HISTOLOGICAL CLASSIFICATION OF COELIAC DISEASE
VILLANACCI Vincenzo * CORAZZA Gino Roberto
*2nd Department of Pathology - Spedali Civili di Brescia, Italy
First Department of Medicine IRCCS Policlinico S. Matteo University of Pavia, Italy

The diagnosis of Coeliac disease (CD) is still based on the biopsy-proven presence of duodenal-jejunal mucosal lesions which improve after gluten-free diet.
It is believed that the currently used criteria are often the source of disagreement between pathologists and clinicians.Marsh proposed a four stage grading: type1 infiltrative lesion, normal mucosal architecture with an increased number of intraepithelial lymphocytes (IELs), type 2 hyperplastic lesion, an increase in crypt depth without villous flattening, type 3 destructive lesion, villous atrophy .Oberhuber et al subsequently proposed a new standardized report scheme, based on the Marsh classification, in which stage 3 was split further into 3a, 3b and 3c, characterised respectively by mild villous flattening, marked villous flattening and completely flat mucosa. How can the Marsh-Oberhuber classification be simplified to improve its reproducibility without reducing its diagnostic accuracy with respect to CD? Obviously, type 1 infiltrative lesion – cannot be put aside. This lesion can in fact be the only evidence of a gluten-sensitive enteropathy in dermatitis herpetiformis and a sensitive, marker of latent CD. More recently, the upper limit of the normal range has been established as being 25 IELs/100 epithelial cells and we therefore feel that IELs counts above this figure allow the diagnosis of a type 1 infiltrative lesion. As regards type 2 hyperplastic lesion, we doubt its usefulness in the diagnosis of new patients – who would, in any case, already be identified by the increased IELs . As regards the substages 3a and 3b characterised by mild and marked villous flattening but not yet by flat mucosa, we suggest that these should be grouped in a single stage. Finally, as regards type 3c there is no doubt that this stage should be maintained. A simplification of the current histological classifications of CD is necessary in order to make the work of pathologists more uniform and to facilitate the relationship between pathologists and clinicians. We therefore propose that the lesions characterising celiac disease be divided into non-atrophic (grade A) and atrophic (grade B) and that the latter be further split into grade B1, in which the villus/crypt ratio is less than 3/1 with still detectable villi, and grade B2 in which the villi are no longer detectable.

P 506
ROLE OF OXYGEN FREE RADICALS ON THE MOTILITY OF RAT ILEUM:
NASTARAN EIZADI-MOOD(1) AND KAILASH PRASAD (2)
1 Assistant Professor of Isfahan University of Medical Sciences, Isfahan, Iran
2 Professor of department of Physiology, College of Medicine, University of Saskatchewan, Saskatoon, Saskatchewan S7N
OWO, Canada

ABSTRACT
The major objective of the present study was to characterize the effects of oxidants which generated by xanthine (X) plus xanthine oxidase (XO) on isolated rat ileum motility. The effects of three concentrations of X/XO on the basal tone of the rat ileum preparation were studied for 20 minutes. Developed tensions were measured in mg/mg tissues and then expressed as percentage of baseline tension. Also the effects of 2X concentration of X/XO in the presence and absence of Superoxide dismutase, catalase ,mannitol, histidine, and deferoxamine were evaluated.The result were expressed as mean +- SE. Xanthine plus xanthine oxidase produced relaxation of ileum. Superoxide dismutase (a superoxide anion metabolizer) and catalase (a hydrogen peroxide scavenger) did not protect ileum from effects of X/XO, suggesting that neither superoxide anion nor hydrogen peroxide involve in X/XO-induced relaxation of ileum. The results of this study suggest that hydrogen peroxide formed extracellularly by X/XO may enter the cells and interact with intracellular iron to form a highly reactive oxidant, hydroxyl radical. The finding that two powerful hydroxyl radical scavengers, dimethylthiourea (DMTU) and mannitol offered protection against X/XO-induced relaxation of ileum suggest formation of hydroxyl radical within the cells. Pretreatment with deferoxamine, a potent iron chelator, reduced the relaxation of ileum, indicating that hydroxyl radical plays an important role in mediating the X/XO-induced relaxation of ileum. In addition, the ability of exogenously administered histidine to reduce relaxation suggests that singlet oxygen is another oxygen derivatives which is responsible for relaxation of ileum-induced by X/XO.
Key Words: Ileum Strips; Xanthine; Xanthine oxidase; Hydroxyl radical; Singlet oxygen; Superoxide dismutase; Catalase; Dimethylthiourea; Manntiol; Histidine; Deferoxamine

P 507
THE EFFECT OF GINGER ON SMALL INTESTINE CHANGES INDUCED BY DIABETES IN RATS
ESKANDARI Mehdi *, SHIRPOOR Alireza **, GOL Ali **, ILKHANIZADE Behrooz ***
* Department of physiology & Pharmacology, Zanjan university of medical sciences
** Department of physiology & Pharmacology, Urmia university of medical sciences
*** Department of pathology, Urmia university of medical sciences

In the present study, we investigated the effect of ginger consumption on the morphological and histological changes in the small intestine of diabetized rats. Eighteen male wistar rats with average body weight 250 gr and 8 months old were chosen to do the study. They were divided into three equal groups (n= 6): the first group rats were nondiabetic; the second group rats were diabetized by streptozocine (60 mg/kg body weight) which received normal diet, and the third group rats were also diabetized which received normal diet and ginger (6 percent of daily diet weight). After 6 weeks abdominal cavity was opened and mesentery was separated carefully by using scissors. Then the small intestine was taken from pyloric sphincter and ileocecal sphincter. After weighing and measuring the length of small intestine, from three parts of small intestine including duodenum, jejunum and ileum 5

cm long samples were taken. After filling the lumen with 10% formalin buffer and ligature of it, they were put into formalin. After sectioning and staining, villi length, crypt depth and muscle thickness of samples was measured. The weight and length of small intestine, length of villi, depth of crypt and muscle thickness increased in non-treated rats comparing to those of nondiabetic rats. The mentioned parameters did not show any significant difference comparing to two groups of ginger-treated and healthy rats. The study showed that ginger as an antioxidant probably prevented changes caused by diabetes in small intestine.

P 508

MUCOSAL LYMPHATIC VESSELS IN IDIOPATHIC BOWEL DISEASE

STÖMMER Peter E.(1), BAYER Ingrid
(1) Gemeinschaftspraxis für Pathologie,Augsburg

Introduction
The lamina propria of normal colorectal mucosa contains only some small lymphatic vessels near the muscularis mucosae. New monoclonal antibodies (MoAbs) fascilitate their differentiation from blood capillaries.
Purpose of study
Chronic inflammations induce lymphatic angiogenesis in different organs. We investigated number and localisation of intramucosal lymphatic vessels in chronic idiopathic bowel disease (IBD), in respect of their contribution to the pathogenesis of colitis ulcerosa (C.u.) and Crohn's disease (CD)
Materials and Methods
MoAb D2-40 (reacting with lymphatic endothelium specific O-linked sialoglycoprotein MW 40K;DCS Hamburg; RTU) and LYVE (reacting with a lymphatic hyaluronanreceptor; DCS Hamburg; RTU) were used as markers for lymphatic vessels. Proliferation was quantified by nuclear Ki-67 (DCS Hamburg; Clone SP6).
Results
Colitis ulcerosa
In the interface of mucosa and muscularis mucosae, there are dense networks of thinwalled lymphatic vessels; they are oriented parallel to the circumference of the colon; their endothelial cells have activated nuclei, though they are negative for proliferation marker Ki-67.Numerous lymphatic vessels are found in the lower third of the mucosa; the middle third of the lamina propria contains less lymphatic channels; the upper third is free of lymphatics. Only rarely, there are perpendicularly oriented lymphatic vessels (mostly near lymphatic follicles).
The density of lymphatic vessels correlates well with the duration of C.u and the proliferative activity of crypt epithelia; the extension of inflammation and proliferative activity of lymphoid cells in the mucosa does not influence the density of lymphatic vessels.
Carcinoma in C.u. shows high density of lymphatic vessels in between of the neoplastic glands, correlating perhaps to its aggressive course.
Crohn's Disease
In contrast to C.u., the density of lymphatic vessels is augmented not only in the lower third of the lamina propria, but also in the middle and upper parts of the mucosa. High density is seen in fibrotic areas and in parts with enteral metaplasia. Their number correlates to the intensity of inflammation.
Conclusions and hypothesis
Proliferation of mucosal lymphatic vessels, consequence of elevated levels of VEGF in IBD, contributes to the differences in pathogenesis of late phases of C.u. and MC.

P 509

BCL-2 PROTO-ONCOGEN EXPRESSION IN ISCHEMIC MAMMALIAN SMALL BOWEL MUCOSA IN RELATION TO THE DURATION OF ISCHEMIA. (PRELIMINARY REPORT).

Grigoriou M*, Gerasimidou D**, Karayannopoulou G**, Atmatzides C*, Papadimitriou C.S**.
*2nd Surgical Department, Aristotle University Medical School, Thessaloniki, "G.Gennimatas" Hospital Greece.
**Department of Pathology, Aristotle University Medical School, Thessaloniki. Greece.

Introduction. Bcl-2 proto-oncogen is a key factor in the prevention of apoptosis in lymphoid and epithelial tissues. The aim of this study is to evaluate the role of Bcl-2 expression in ischemia-induced apoptosis of small intestinal mucosal cells.
We investigated the appearance of apoptosis at various time points of ischemia in comparison to the expression of the Bcl-2 protein.
Materials and methods. We examined samples obtained from mammalian small intestine (New Zealand White Rabbits) following ischemia induced by strangulation-obstruction of 5cm of jejunum. Samples were taken preoperatively and progressively at 30, 180 and 360 min from the onset of strangulation. Tissue sections were stained for H&E for the estimation of mucosal ischemic damage. Tissue sections taken from the same samples were stained immunohistochemically for Bcl-2 protein.
Observations from both H&E and Bcl-2 staining were compared to estimate the correlation of Bcl-2 expression with the severity of the ischemic injury.
Results. Histological changes were observed in the jejunum concerning the upper third, the upper two thirds and the whole length of the villi respectively at 30, 180 and 360 min from the onset of ischemia. Cytoplasmic expression (++++) of Bcl-2 protein was observed at villous epithelial cells, while it was barely obvious at the crypts at the onset of ischemia. Minimal reduction (++) of Bcl-2 expression at the apical third of the villi at 30 min and increased reduction concerning the two thirds of the villi at 180 min after the induction of ischemia was observed. Only scattered apoptotic epithelial cells were observed expressing the protein after 360 min of ischemia.
Discussion. Progressive suppression of the Bcl-2 proto-oncogen expression on ischemic injured small intestinal mucosal tissue suggests a key role of the Bcl-2 protein in the apoptotic pathway induced by ischemia. The correlation of this phenomenon to the severity of ischemic injury at consequent time intervals leads to the assumption that this is not a triggered effect but a dynamic process aggravated by the progression of ischemia.

P 510

INTESTINAL VASCULITIS MIMICKING A COLONIC NEOPLASM. REPORTING OF A CASE.

CASALOTS Alex, PARRA Tamara, ORELLANA Ruth, FERNANDEZ Sara, DINARES Carme, ESCODA Maria-Rosa, ANDREU Javier, REY Mercè.
Corporació Parc Taulí, Pathology Dept., UDIAT-CD, Sabadell, Barcelona. Spain.

INTRODUCCION
Vasculitis of the gastrointestinal (GI) tract is known to occur as a part of a systemic process such as Panarteriitis Nodosa, Churg-Strauss angiitis, Behcet's disease, giant-cell arteritis, Buerger's disease, systemic Eritematous Lupus, Henoch-Schölein purpura and rheumatoid arthritis. Systemic and isolated vasculitis classification is based on the predominant type and size of the vessel involvement. Polyangiitis overlap syndrome proposed by Leavitt and Fauci is defined as systemic vasculitis that does not fit precisly into a single category of classical vasculitis or overlaps several of the categories.
CASE REPORT

A 77-year-old woman presented with 2-days history of abdominal pain, bowel obstruction and abdominal distention. An abdominal computed tomography scan was performed and showed swelling and bowel wall thickening of the sigmoid colon. With the clinical diagnosis of a malignant tumor, the sigmoid colon was resected. Pathological examination of the resected colon segment revealed an stenotic pseudotumoral lesion (3-4 cm.), mucosal ulceration and severe obstruction that compromise 70% of the circumference. Microscope examination showed severe mucosal ischemic necrosis associated with necrotizing vasculitis involving medium and small-sized arteries and heavy infiltration of eosinophils. No granuloma formation was observed.

DISCUSSION

The main differential diagnosis has to be made within the group of vasculitis involving medium and small sized arteries. Wegener's granulomatosis is distinguished by its predilection to affect the upper and lower respiratory tract and kidneys, positive C-ANCA titer and GI involvement is uncommon.

Churg-Strauss syndrome is a disorder characterized by clinical features such as asthma, allergic rhinitis, hypereosinophilia and histological features of necrotizing vasculitis, eosinophilic infiltration and granulomas. GI involvement is about 50%.

PAN is a systemic disease that showed acute arteritis with fibrinoid necrosis of the vessel wall. GI involvement is relatively frequent (40-70%).

In our case, according to the clinical and pathological findings, we suggest the diagnosis of a polyangiitis overlap syndrome with some features of allergic granulomatous angiitis and Polyarteritis nodosa.

P 511

PRIMARY RHABDOID CARCINOMA OF THE ILEUM: REPORT OF THE SECOND CASE IN THE LITERATURE WITH EXTENSIVE IMMUNOHISTOCHEMICAL (IHC) WORK-UP AND OVERVIEW OF DIFFERENTIAL DIAGNOSIS.

TOTH Laszlo(1), NEMES Zoltan(1), GOMBA Szabolcs(1), ASZTALOS Laszlo(2), SZENTIRMAY Zoltan(3), MOLNAR Peter Pal(1).

University of Debrecen, Medical & Health Sciences Center (DE-OEC), Department of Pathology, (2)DE-OEC, 1st Department of Surgery, Debrecen, Hungary; (3)National Institute of Oncology, Institute of Pathology, Division of Molecular Pathology, Budapest, Hungary.

Introduction: Primary rhabdoid tumors of the small intestine are very rare but do occur as we demonstrate herewith.

Purpose: To describe the second case of primary rhabdoid carcinoma of the ileum with multiple recurrences.

Material and methods: The 81-y-old male patient had been treated for ischemic heart disease, arteriosclerosis and a benign papilloma of the urinary bladder. In November 2004 he was admitted and urgently operated on because of melena and progressive ileus. Abdominal examination revealed a firm, left parumbilical mass, easily palpable that was cca. 8 cm in diameter. A 20 cm long ileum-segment was removed. Its wall was widely infiltrated by a cauliflower-like, extensively hemorrhagic, ulcerated tumor. The invaded segment firmly adhered to the parietal peritoneum hence the resection included that part as well. Since the 1st operation the tumor has recurred twice (in 01/05 and in 03/05), each time breaking through the wall of the small intestine from the peritoneal surface and causing mucosal ulceration. These tumors were removed and re-excision of the surgical wound was also necessitated by local neoplastic re-growth. Presently tumorous infiltration along the surgical incision is evident again, but the patient refuses further surgery. The formol-fixed, paraffin embedded tumors comprised large necrotic-hemorrhagic areas and solid, highly cellular, solid sheets with focal loss of cellular cohesion. The round or polygonal cells were intermingled with bizarre, pleomorphic, often multinucleated forms. The nuclei were large, often polymorphic and eccentric with prominent nucleoli and numerous abnormal mitoses. The Mib-1 labeling index was 50-75%. Characteristic, pathognomonic, homogeneous eosinophilic cytoplasmic inclusions ("hyalin-globules") were seen. IHC revealed diffuse, strong vimentin, panCK and focal EMA positivity. CD30, Bcl-6, S100, HMB45, c-kit, CK7, CK20, p27-kip1, E-cadherin, SM actin, desmin, caldesmon and CD34 were negative. CD3, CD20 and LCA decorated the reactive lymphoid elements. Monoclonal p53 was diffuse positive. Some areas reacted with neu oncoprotein (++). All lymphnodes were reactive-hyperplastic but tumor-free. So far no distant metastases occurred.

Discussion: IHC and light microscopic morphology prove rhabdoid cancer excluding lymphoma, adenocarcinoma or leiomyosarcoma. EM and molecular tumor-analysis are in progress, the results will be presented. Literature-search disclosed only 1 earlier jejunal case by 04/05.

P 512

APPENDICEAL MUCINOUS NEOPLASMS: A ROLE IN PSEUDOMYXOMA PERITONEI

Kwang-Sun Suh, Moon-Il Park, Kyu-Sang Song, Wan-Hee Yoon*

Departments of Pathology and Surgery*, Chungnam National University School of Medicine

Mucinous neoplasms of the appendix are rare and associated with colonic or ovarian neoplasms, and pseudomyxoma peritonei (PMP). PMP is a rare form of dissecting gelatinous ascites associated with multifocal peritoneal and omental implants that secrete copious globules of extracellular mucin. Recent immunohistochemical and molecular genetic evidence suggests the appendix to be the primary site. We analyzed 30 cases of appendiceal mucinous tumors (22, mucinous cystadenoma; 4, borderline mucinous tumor; 4, malignant mucinous tumor), seven of which were accompanied by PMP. An immunohistochemical study for MUC2, MUC5AC, CK7, and CK20 was also performed to confirm the origin of PMP. Among 30 appendiceal mucinous tumor cases, four cases had right colon cancer, one case exhibited Peutz-Jeghers syndrome, one case endometriosis, and one diverculosis of the right colon. Seven PMP cases showed both appendicial and ovarian mucinous tumors. The appendiceal, peritoneal, and ovarian mucinous tumors showed the same immunoprofile (MUC2+/MUC5AC+/CK7-/CK20+). One case of appendiceal mucinous cystadenoma was associated with ovarian mucinous cystadenoma of borderline malignancy with no evidence of PMP. The appendiceal lesion was MUC2+/MUC5AC-/CK7-/CK20+. In contrast, the ovarian lesion was MUC2-/MUC5AC+/CK7+/CK20-. Therefore, these lesions are considered to be synchronous. In conclusion, the MUC2+/CK7-/CK20+ expression profile supports an appendiceal rather than ovarian origin for PMP.

P 513

ARE GOBLET CELL CARCINOIDS OF THE VERMIFORM APPENDIX CRYPT CELL CARCINOMAS?

Susanne van Eeden(1), G. Johan A. Offerhaus(1), Augustinus A.M. Hart(2), Lucy Boerrigter(3), Petra M. Nederlof(3), Marie-Louise F. van Velthuysen(3)

(1)Department of Pathology, Academic Medical Center, Amsterdam, The Netherlands

(2) Department of Radiotherapy, Het Nederlands Kanker Instituut/ Antoni van Leeuwenhoek Ziekenhuis, Amsterdam, The Netherlands

(3)Department of Pathology, Het Nederlands Kanker Instituut/ Antoni van Leeuwenhoek Ziekenhuis, Amsterdam, The Netherlands

Introduction and aim of the study:

Goblet cell carcinoids (GCC) of the vermiform appendix are rare neoplasms of uncertain histogenesis, with features reminiscent of both classical carcinoids (CC) and conventional colonic adenocarcinomas (CAC). This study was performed to investigate whether GCCs should be regarded as a separate entity or as a variant of CCs, of CACs or of other primary appendiceal tumors, i.e. mucinous cystadeno(carcino)mas (MCA).
Material and Methods:
The immunohistochemical expression pattern of 19 different markers in 16 GCCs was compared with the expression pattern in 14 CCs, 19 CACs and 10 MCAs. The mutation status of KRas codon 12 was determined in all tumors by a mutant-enriched PCR method. The results were subjected to a stepwise linear discriminant analysis.
Results:
GCCs could be distinguished from the control groups and were characterized by diffuse positivity for CAM5.2, CDX2 and CEA, frequent coexpression of Ck7 and Ck20, scattered positivity for endocrine markers in up to 50% of the cells and a proliferative activity (Ki67 positivity) intermediate between that of CCs and CACs. Alterations in KRas codon 12, TP53, DPC4 and in the Wnt-signaling pathway were rare or absent in GCCs. Histologically, GCCs showed a typical growth pattern and contained different cell types reminiscent of the neoplastic counterparts of normal crypt cells.
Conclusion:
The results suggest, that GCCs should be regarded as a separate entity, probably arising from a crypt progenitor cell as previously suggested. Therefore, the formerly used term 'crypt cell carcinoma' may be more appropriate than GCC and this diagnosis also better reflects the more aggressive clinical behaviour of these tumors.

P 514
TOXIC EFFECTS OF WATER EXTRACT OF TEUCRIUM POLIUM ON THE RAT INTESTINE
PANJEHSHAHIN Mohammad R., DEHGHANI Farzaneh, KARBALAEEDOOST Saeed
Department of Pharmacology, Faculty of Medicine, Shiraz University of Medical Sciences, Shiraz, Fars,Iran.

Teucrium Polium is traditionally used to lower blood sugar in diabetic patients in Iran and some other parts of the world. However, some gastro-intestinal side effects have been reported by the patients who have used this remedy. The aim of this investigation was to study of the effects of Teucrium Polium water extract on the structure of the small intestine in male rats . Fifty wistar rats were randomly divided to four experimental and one control groups. The experimental groups were fed different doses (4 g/kg, 3 g/kg, 2 g/kg,1 g/kg) of the Teucrium Polium extract by oral rout for 14 days. The rats were then scarified and histological sections were prepared. The result indicated that the extract could cause vascular delitation as well as lymphoid cell, macrophage and neutrophile infiltration in the intestinal tissues. Apoptosis was also observed in liver tissue. It seems that this extract may cause damage and changes to the small intestine, therefore, it is recommended that the extract of Teucrium Polium should be used cautiously. More investigation is needed to find its complications and mechanisms of damages induced by this extract.

P 515
LACK OF CLAUDIN 4 EXPRESSION AND HIGH EXPRESSION OF CLAUDIN 3 AND CLAUDIN 7 DIFFERENTIATE PANCREATIC ENDOCRINE TUMORS FORM PANCREATIC DUCTAL CARCINOMA
BORKA Katalin, KISS András, KALISZKY Péter*, KUPCSULIK Péter*, SCHAFF Zsuzsa
2nd Department of Pathology and *1st Department of Surgery, Semmelweis University, Budapest, Hungary

Introduction: A new family of tight junction (TJ) proteins called claudins was discovered in 1998. These transmembrane proteins are responsible for cell adhesion, polarity and paracellular permeability. Although changes in permeability of TJs were noted in several cancers, the role of claudins in carcinogenesis is controversial. Claudin 4 overexpression was reported in primary and metastatic pancreatic adenocarcinomas. These findings support use of claudin 4 as target for novel therapeutics of pancreatic cancers.
Purpose: To analyse different claudin expressions in human pancreatic endocrine tumors and ductal carcinomas using a panel of polyclonal (claudins 1, 3, 7) and monoclonal (claudins 2, 4) antibodies.
Methods: Twenty formalin fixed, paraffin embedded pancreatic endocrine tumors and ten pancreatic ductal carcinomas were studied, and immunohistochemical evaluation performed to analyse claudin 1, 2, 3, 4 and 7 expressions. Semiquantitative evaluation was used for the area of extension (0-5) and intensity (0-3) of reaction.
Results: Claudins 1, 2 proved negative in all endocrine tumors. The majority (7/10) of ductal carcinomas was positive for claudin 4, while endocrine tumors were negative. In contrast, claudin 7 showed high expression in all endocrine tumors, however, ductal carcinomas did not express the protein. Claudin 3 was detected in 80% (16/20) of endocrine tumors, while ductal carcinomas were negative. Claudin 7 expression was significantly higher in endocrine tumor cells, compared with claudin 3 ($p<0,0032$).
Conclusion: Our findings support that claudins 3 and 7 are specific marker for endocrine pancreatic tumors in contrast to ductal carcinomas. Further studies are necessary to assess the biological role of these proteins in pancreatic carcinogenesis.

Supported by grants NKFP-1A/0023/2002, NKFP-1A/002/2004, OTKA-T037838

P 516
GASTROENTEROPANCREATIC ENDOCRINE TUMORS: HISTOPATHOLOGIC FEATURES AND CATEGORIZATION ACCORDING TO WHO CLASSIFICATION
Deniz Peker, Gulen Bulbul Dogusoy, Sibel Erdamar Cetin, Suha Goksel
University of Istanbul, Cerrahpasa Medical Faculty, Department of Pathology

INTRODUCTION: Although gastrointestinal and pancreatic endocrine tumors (GEPs) are relatively rare they represent a complex tumor entity. The aim of this study was to determine the histopathological features and immunohistochemical profiles of GEPs diagnosed in our department.
METHODS: Of the 125 cases of GEP diagnosed between the years of 1995 and 2004, we reviewed cases based both on histologic patterns common to GEP and immunohistochemical results. Immune antibody panel included Chromogranin A, Synaptophysin, NSE, PGP 9.5 to all, Serotonin, Gastrin, Somatostatin, Glucagon, Insulin, VIP and some other peptides like ACTH, GRH to some sporadic cases. Ki67 expression was investigated to determine the proliferation index. Due to results of examination all cases were categorized according to new WHO classification.
RESULTS: 125 cases were collected from the archives of our department with a male to female ratio of 1.21 and a mean age of 61 years. The most common location was large intestine (43.2 %) followed by stomach, small intestine, pancreas and appendix (39%, 7.2%, 6.4%, 4.0% respectively). 64.8% of the cases were pure GEP whereas others were mixed endocrine- exocrine tumors. Among the pure GEP group, 11.1% were benign, 6.2% uncertain behavior tumors,

13.6% well differentiated and 69.1% poorly differentiated carcinomas. Synaptophysin was the most common immune marker observed and Ki67 indexes were correlated significantly with the biologic behavior categories ($p<0.05$)
CONCLUSIONS: The results of this study demonstrated that the distribution of our GEP cases in gut and the biologic behavior categories varied however malignancy –predictive factors including Ki67 index and immune profile were in accordance with previous reports.

P 517
IMMUNOHISTOCHEMICAL STUDY OF 29 SOLID PSEUDOPAPILLARY NEOPLASMS OF THE PANCREAS ON TISSUE MICROARRAYS

Virginie AUDARD (1), Hubert RICHA (2), Muriel INFANTE (1), Anne COUVELARD (3), Benoît TERRIS (4), François PAYE (2), Jean-François FLEJOU (1)Department of Pathology (1) and Digestive Surgery (2), Hôpital Saint Antoine, Paris; Department of Pathology, Hôpital Beaujon (3), Clichy; Department of Pathology, Hôpital Cochin (4), Paris, AP-HP France

Background : Solid pseudopapillary neoplasm of the pancreas is a rare tumour of uncertain histogenesis, that may raise difficult diagnostic issues.
Aim: To examine in a series of solid pseudopapillary neoplasm the expression of proteins of potential diagnostic and histogenetic interest by immunohistochemistry on tissue microarrays.
Methods : 29 solid pseudopapillary neoplasms of the pancreas were analysed. The expression of the following proteins was studied: CD10, oestrogen receptor, progesterone receptor, vimentin, cytokeratin (KL1), chromogranin A, synaptophysin, Mismatch Repair proteins (hMLH1, hMSH2, hMSH6), p53, b-catenin, E-cadherin.
Results : Tumours expressed the various antibodies with the following frequency: CD10 100%, progesterone receptor 100%, vimentin 93%, cytokeratin 72%, synaptophysin 46%, chromogranin A 0%, oestrogen receptor 0%. None of the cases presented a loss of expression of hMLH1, hMSH2 or hMSH6. There was no overexpression of p53 protein. In all cases a strong nuclear immunostaining of b-catenin was present in most tumour cells, with a “dot-like” cytoplasmic expression of E-cadherin that showed no membranous expression.
Conclusion: CD10, progesterone receptor, vimentin and b-catenin are expressed in solid pseudopapillary neoplasms of the pancreas, and are useful diagnostic markers for this rare tumour type. The pattern of b-catenin and E-cadherin expression that we observed suggests a major role for these proteins in the development of this tumour. The particular localisation of E-cadherin could be due to an abnormal trafficking of the protein to the membrane and/or to an endocytosis of this protein. Although solid pseudopapillary neoplasm develops in young patients and has a good prognosis, there is no immunohistochemical argument for the presence of microsatellite instability in these tumours.

P 518
SOLID AND CYSTIC PAPILLARY NEOPLASM OF THE PANCREAS

YILMAZ Banu, SAKIZ Damlanur,KABUKÇUOÐLU Fevziye, POLAT Nedim, KÖKSAL Hakan*
Þiþli Etfal Education and Research Hospital, Department of Pathology and Department of General Surgery*, Ýstanbul, Turkey

OBJECTIVE: Solid and papillary cystic neoplasm of the pancreas (SCPN) is a rare primary pancreatic neoplasm of unknown etiology, occurring most commonly in young women. Four patients with solid and cystic papillary tumor of the pancreas are evaluated to discuss the histopathological and immunohistochemical findings with the clinical course and surgical treatment.
PATIENTS AND METHODS: Three cases of SCPN located in the tail of the pancreas and one located in the head of the pancreas are presented. In two patients distal pancreatectomy with splenectomy were performed. Spleen was preserved in one of the patients. Whipple’s operation was performed for the patient with the tumor at the head of pancreas. The cases located in the tail of the pancreas were a 14 year old female, a 73-year-old female and 69-year-old male with the diameter of the masses as 6 cm, 2,5 cm and 6,5 cm respectively. The fourth case was a 17-year-old woman with a 5 cm mass in the head of the pancreas. In all patients the pancreatic lesions were shown by ultrasonography and a computed tomography scan. Histological diagnosis was made by performing haemotoxylene-eosin and PAS staining, immunohistochemical staining for progesteron receptors, vimentin, chromogranin A, EMA, NSE, cytokeratin, synaptophysin, CEA, Ki-67, CD10 and CD56.
RESULTS: The histological findings showed large encapsulated tumors with the section of the tumors surrounded by hemorrhagic and necrotic areas. The solid areas were composed of small and medium size tumor cells, which had no obvious atypia. Pseudopapillary structures were found in the cystic degeneration areas. Immunohistochemically,all of the tumors were positive for CD56,vimentin and progesterone receptor, negative for EMA, CEA.Two tumors stained for chromogranin or synapthophysin and one tumor stained for cytokeratin and synapthophysin. One tumor stained for CD10. Three tumors (Case 1,2,3) were, 1% nuclear positive and one of the tumors (Case 4) was, 5% nuclear positive for Ki-67.Case 4 showed an infiltrative growth into the surrounding pancreatic parenchyma.In the follow-up period (1-5 years) all patients are alive with no evidence of recurrence.
CONCLUSIONS: Solid and cystic papillary neoplasm of the pancreas (SCPN) is a neoplasm with a low malignancy and show favorable prognosis after surgical removal.In spite of the characteristic macroscopic and microscopic aspects, the immunohistochemical profile is nonspecific.

P 519
PANCREATIC SOLID AND CYSTIC HAMARTOMA IN ADULTS: CHARACTERIZATION OF A NEW TUMOROUS LESION

Ursula Pauser, M.D.1, Markus Kosmahl, M.D.1, Božo Krušlin, M.D. 2, Maria Teresa Simões da Silva, M.D. 3, Jörg Placke, M.D.4, David S. Klimstra, M.D.5, Günter Klöppel, M.D.1
Department of Pathology, 1University of Kiel, Germany, 2Sestre Milosrdnice University Hospital, Zagreb, Croatia, 3University of Coimbra, Portugal, 4Dinslaken, Germany, 5Memorial Sloan-Kettering Cancer Center, New York, NY, USA

Introduction: Nonneoplastic tumor-forming lesions in the pancreas are uncommon. They include cystic and noncystic varieties that have to be clearly distinguished from malignancies.
Patients, Materials and Methods: We report on a solid and cystic tumor-like lesion of the pancreas that occurred in 4 adult patients. Because of the unclear nature of these lesions, resection was performed. Formalin-fixed, paraffin-embedded tissues from the specimens were investigated by means of immunohistochemistry.
Results: The four resection specimens each contained a firm, gray, well demarcated nodule with focal cystic changes. The size ranged from 2 to 7 cm in diameter. The surrounding pancreatic tissue was unaffected. Histologically, the tumors showed a disorderly arrangement of well differentiated endocrine and exocrine pancreatic tissue that was embedded in a fibrous stroma. The cystic structures were lined by duct-

like cells. Immunohistochemically CD34 and c-kit coexpression was seen in the spindle cell component in two cases. Scattered insulin-producing cells were detected between acinar and ductal cells. Islets were lacking.
Discussion: The four pancreatic tumors showed a histologic pattern compatible with that of a hamartoma of the pancreas.

P 520
ECHO ENDOSCOPIC ULTRASONOGRAPHY FINE NEEDLE ASPIRATION (EUS-FNA) IN PANCREATIC LESIONS. EXPERIENCE AT HOPITAL SAINT-JOSPEH.
DE PINIEUX Isabelle 1, HOMSI Toufik 1, , BALATON André 1, MARTY Olivier 2, MALLET Laurent 2,MOLINIE Vincent 1. Department of Pathology (1) and Gastroenterology (2), Hôpital Saint-Joseph, Paris, France.

Background: Endoscopic ultrasonograpghy (EUS) fine needle aspiration (FNA) is a new safe procedure used to explore non accessible pancreatic lesions.
Objectives: Evaluation of our early experience of EUS-FNA in pancreatic lesions.
Methods: The study was performed until 2003, by an experimented operator (OM), using a ultrasound transducer echoendoscope, with microbiopsy (FNA 22 G), without antibiotics prophylaxy (expected in cystic lesions). For each case 1 to 4 FNA was performed and pull in 1 or 2 AFA containers. For eache case the reporting data consisted in : clinical setting with echographic results, endocopic procedure (exact position of the trasducer, and transfixed organ) and site of biopsy. The pathological procedure consited in parrafin inclusion, after centrifugation. For histologic analysis a set of 5 slides were obtained with a single 3 HES staining sections, and 5 slides for histochemistry (PAS or Alcian Blue) or immunohistochemistry study.
Results: 50 EUS-FNA were performed in 30 patients (12 M/ 18 F) 62 years old mean (40 - 80). Echoendoscopic results were : 5 cystic lesions, 5 singl masses, 16 unresectable tumors. The maximal diameter was 26 mm (7-42), and 2 patients had a pancreatitis history.The site of biopsy was : body 3, head-isthmus 18, tail 9. The transfixed organ was stomach 52%, duodenum 48%. The number of biopsy studied was 1.8 (1-4).A non concluent diagnosis was performed in only 1 case (cystic lesion). The diagnosese were : malignant in 22 cases (Pancreatic carcinoma 16, Pancreatic endocrine tumor 5, lymphoproliferation 1) and benign in 7 cases (Abces 1, Tuberculosis 1, Normal pancreas 2, Pancreatitis 2, Mucinous cystadenoma 1).
Conclusion: The fiability of EUS-FNA in pancreatic lesion in our experience is 94%, similar to the fiability reported in the literature. In our experience, EUS-FNA is a vailable method even in small tumors, and specially in pancreatic adenocarcinoma. Cooperation between pathologist and gastro-enterologist is necessary to obtain the best organization for the best diagnosis.

P 521
ADENOCARCINOMAS OF THE AMPULLA OF VATER AND OF THE HEAD OF PANCREAS HAVE DIFFERENT EXPRESSION OF MUC1, MUC2, MUC5AC, AND MUC6 APOMUCINES
Fausto Sessa, Francesca Franzi, Clementina Zampatti, Carlo Capella
Department of Pathology, University of Insubria, Varese, and Ospedale di Circolo di Busto Arsizio, Varese, Italy

Background: Adenocarcinomas (AC) arising from the ampulla of Vater (AV) and the head of pancreas (HP) have similar morphologic features, clinical presentation and a common surgical treatment (Whipple procedure) but a different outcome. AV-AC are histologically classified as intestinal type (IT) and biliopancreatic type (BPT) ACs. The classification is based on the histological pattern, Cdx-2 expression and/or cytokeratin 20 positivity for IT ACs and cytokeratin 7 positivity for BPT ACs. Apomucines have different expression according to the site of the tumor or to the phenotypic differentiation. The de novo expression of MUC1 is indicated as a negative prognostic marker, while MUC2 seems to be involved in the tumor suppression of colorectal cancer.
The aim of this study was: a) to investigate the expression of MUC1, MUC2, MUC5AC and MUC6 and b) to explore the utility of apomucines in differentiating the HP ACs from the AV ACs.
Design: Forty four surgically resected invasive AV-ACs, previously classified as IT (28) and as BPT (16) by using Cdx2 immunoreactivity, were immunostained for MUC1, MUC2, MUC5AC and MUC6 using avidin-biotin-complex method, including positive and negative controls.
Results: Twenty-seven out 44 AC of AV (61%) were positive for MUC1. MUC5AC was present in 15/44 (34%), MUC6 in 13/44 (29%) and MUC2 in 11/44 (25%) cases. MUC1 was present in 14/28 (50%) IT AC and in 13/16 (81%) BPT AC. MUC2 was present in 8 AV AC classified as IT and in 3 cases classified as BPT. MUC5AC and MUC6 had no difference in their distribution in relationship to IT or BPT phenotype. In HP ACs we found 30/35 (86%) cases expressing MUC1, 25/35 (71%) MUC5AC, 7/35 (20%) MUC6 and 2/35 (6%) cases expressing MUC2. Follow up was available for 32 patients, 13 of which alive with a mean survival of 58 months and 19 dead of the disease after a mean survival of 20 months. Twelve of 13 alive patients express one or both intestinal markers.
Conclusions: The adenocarcinomas of AV and HP have different pattern of MUC expression. MUC1 and MUC5AC are much more expressed in HP ACs, in association with the poor prognosis of pancreatic cancer. AV-BPT adenocarcinomas show a pattern very similar to HP ACs. Only MUC2 is preferentially observed in AV-AC and it can be useful as marker of intestinal type differentiation of AV AC, related to a better prognosis of this type of cancers.

P 522
DIFFERENTIATION PATHWAYS IN AMPULLARY CARCINOMAS: COMPARATIVE STUDY ON MUCIN PEPTIDE CORE ANTIGENS (MUC1, MUC2, MUC5AC) AND CDX2 EXPRESSION, INCLUDING GASTRIC AND COLON CARCINOMAS.
Gursan N1, Gursan MS2,

A broad histomorphologic spectrum of ampullary carcinomas of Vater make a reproducible histologic classification difficult. The aims of this study were to determine histologic subtype of ampullary carcinomas kullanarak mucin peptide core antigens and CDX2 in comparison with gastric and colorectal carcinomas. We examined immunohistochemically for expression of MUC1, MUC2, MUC5AC, and CDX2 in ampullary carcinoma(30), gastric carcinomas (30) and colon carcinomas (30). sixty-four percent of the gastric carcinomas and sevety-five of the ampullary carcinoma expressed MUC1, whereas none of the colorectal carcinomas did. MUC2 mucin was highly expressed in colorectal carcinomas In ampullary carcinoma, gastric carcinomas expressed MUC2 89%, 83%, respectively. Immunohistochemically, MUC5AC were frequently expressed in gastric carcinoma. fifty-five of the ampullary carcinoma expressed MUC5A. The nuclear expression of CDX2 was closely associated with the expression of MUC2 in colon carcinomas . In ampullary carcinoma, gastric carcinomas expressed CDX2 75%, 62%, respectively. Moreover, the expression of MUC1. MUC2 MUC5A and CDX2 was a useful to determine histologic subtype of tumors derived from the ampulla of Vater.

P 523

HEP PAR 1 IMMUNOEXPRESSION IN THE TUMOURS OF PERIAMPULLARY REGION AND HEAD OF THE PANCREAS

GULLUOGLU Mine G.(*), KARAYÝGÝT Ebru(*), OZDEN Ilgin(**), KAPRAN Yersu(*), CEVÝKBAS Ugur(*), DÝZDAROGLU Ferhunde(*).
*Istanbul University, Istanbul Faculty of Medicine, Department of Pathology
**Istanbul University, Istanbul Faculty of Medicine, Department of General Surgery, Hepatopancreatobiliary Surgery Unit

Ampullary carcinomas may arise from two different types of mucosa and comprised of two different histologic types; intestinal and pancreatobiliary. It is important to distinguish them from each other since they have different therapeutic and prognostic implications. Monoclonal antibody Hep Par 1 which shows hepatocytic differentiation is generally used in the differential diagnosis of hepatocellular carcinomas. Some authors advocate that this antibody indirectly shows small intestinal differentiation. The aim of this study is to evaluate the Hep Par 1 immunoexpression in pancreatic, duodenal and extrahepatic biliary tract carcinomas including periampullary tumours and to explore the utility of this antibody in differentiating pancreatic ductal adenocarcinoma and ampullary adenocarcinoma of pancreatobiliary type from the intestinal type ampullary carcinoma.
We studied Hep Par 1 immunoexpression in 61 cases of periampullary (n=40), pancreatic (n=16), duodenal (n=4) and mid-choleductal (n=1) carcinomas. Twentytwo (55%) periampullary carcinomas, 14 (87.5%) of the tumours originating from head of the pancreas and two (50%) of the duodenal tumours were negative for Hep Par 1 ($p<0.05$). Fourteen of the 18 intestinal type periampullary tumours (77.7%) were positive for Hep Par 1 whereas only three of the 21 pancreatobiliary type tumours (14%) showed focal immunoreactivity ($p<0.0001$). There was no significant difference between the Hep Par 1 expressions of the pancreatic carcinomas and the ampullary carcinomas of pancreatobiliary origin.
In conclusion, we suggest that the ampullary tumours of intestinal origin can be seperated from the tumours of pancreatobiliary origin either ampullary or pancreatic by Hep Par 1 immunohistochemistry.

P 524

PROGNOSTIC SIGNIFICANCE OF EGFR AND HER2/NEU(C-ERB2) IN PANCREATIC CANCER

ZIZI-SERBETZOGLOU Adamantia,KATSAMAGOU Eleftheria,SPANOS Ilias,VASSILAKAKI Thivi,ELEMENOGLOU Ioannis
Department of pathology, Tzaneio General Hospital, Piraeus, Greece

Pancreatic duct carcinoma is a malignant tumor with an extremely poor prognosis. The mechanisms of the aggressive growth and metastasis are not completely understood.
Recent studies have shown that some growth factor receptors with tyrosine-kinase activity,e.g.,the epidermal growth factor receptor (EGFr) and the Her2/neu(c-erb2)oncoprotein,are associated with aggressive biologic behaviour in a variety of tumors.
The aim of this study was to detect the relation of EGFr and c-erb2 to the progression and metastasis of pancreatic duct carcinoma and analyze the correlation between EGFr and c-erb2 expression pattern
and clinicopathological factors.
MATERIAL and METHODS:We examined the immunohistochemical expression of c-erb2 and EGFr in formalin-fixed paraffin embedded tissue samples from 42 patients with pancreatic ductal adenocarcinoma,4 patients with carcinoma of Vater's ampulla and 10 patients with chronic pancreatitis.
RESULTS: 19 of 42(43.6%)samples of pancreatic cancer stained positive for EGFr and 23 of 42(53%) for c-erb2. 3 of 4 samples of carcinoma of Vater's ampulla expressed EGFr and 2 of 4 expressed c- erb2.1 of 10 samples with chronic pancreatitis expressed EGFr and 1 of 10 c-erb2. The coexpression rate of the two proteins was 28%(16/42).This coexpression in the pancreatic duct adenocarcinoma groups was correlated with histopathological grades and metastatic status of TNM classification ($p<0.01$).
CONCLUSSIONS: The immunohistochemical expression of EGFr and c-erb2 can be used as a marker of aggressive biological behaviour including recurrence and metastasis of pancreatic duct adenocarcinoma.

P 525

IS THE PERITUMORAL REGION IN EXOCRINE PANCREAS CARCINOMA DIFFERENT FROM NORMAL PARENCHYMA?

HERLEA V1,PASLARU L1,LAZAR V2,HOREANGA I3,TAIEB J 4,BOISSIN H5,POPESCU I1.
1 - Fundeni Clinical Institute, Bucharest, Romania, 2- Gustave Roussy Institute, France,3- Rntech, Romania, 4- Pitié Salptriérè Hospital, Paris, France
5- Rntech, France

Background: Ductal adenocarcinoma and its variants make up over 90% of all pancreatic tumours. Adenocarcinoma of the pancreas is characterized by local tumor growth that infiltrates vascular structures, nerves and lymphatics, and causes early hematogenous spread to the liver. Studies of pathologic characteristics of the primary or metastatic tumor have failed to define high-low risk subgroups of clinical significance, mainly because most patients experience rapid disease progression. Purpose: We conducted a study to identify histological quantitative and qualitative modifications in the region surounding exocrine pancreas carcinomas (peritumoral region) compared with normal parenchyma.Methods: We have studied 28 cases of ductal adenocarcinoma localized in the head, body, and tail of pancreas who underwent surgical resection. We defined the peritumoral region, as the portion of apparently not affected parenchyma in 1 centimeter surrounding the tumor. In this region we have been analyzed the inflammatory infiltrate (using an immunohistochemicaly technique with the antibody for CD 68)and angiogenesis (with antibody for CD 34)comparative within the tumor and to the parenchyma from distance . Results: In the studied cases, the inflammatory infiltrate was slight increased in the peritumoral region than the tumoral and normal, and there was a significant positive staining for CD68 (expressed on macrophages and monocytes). The expression of CD34 was not significant modified. Various pathological parameters have been evaluated (size, mitotic rate, vascular -perineural invasion, lymph node metastasis, necrosis, surgical margins, location).
Conclusion: Although the cell kinetics of the pancreas are not understood, it seems likely that there is a continuous slow turnover of cells, fed from a stem cells population in the ducts, and that the controls on the production rate of each cell type are local rather than systemic.The surounding inflammatory infiltrate(especialy macrophages)in the exocrine pancreas tumors is important in prognosis.This parameter can be important for tumoral behavior and therapeutic strategies.

P 526

MIXED DUCTAL ENDOCRINE CARCINOMA OF THE COMMON BILE DUCT

Authors and Affiliations:LIAPIS George, ALEXANDROU Paraskevi, TZIRAKIS Mixalis, ANDROULAKI Athina, KIRIAKOU Vasiliki.

DEPARTMENT OF PATHOLOGY LAIKO HOSPITAL, ATHENS

The mixed bile duct endocrine/ductal carcinoma is a rare neoplasm and only a few cases have been reported in the literature reviewed. We present a case of a carcinoma of the common bile duct with mixed histological features in a 71 years old man who presented with jaundice and a cholestatic biochemical profile. The carcinoma measuring 2,2 x 1 cm, arose in the wall of the common bile duct and invaded the gallbladder neck and the pancreas forming an intrapancreatic tumor mass of 3 cm in diameter. Histologically the tumor tissue consisted of a poorly differentiated endocrine carcinoma (small cell carcinoma) and a carcinomatous component with features of ductal adenocarcinoma. The two neoplastic elements showed a separate or merging growth pattern while biphasic structures exhibiting both cell types were also encountered. Interestingly, the pancreas was infiltrated exclusively by the small cell carcinoma. The endocrine immunophenotype was confirmed by the expression of chromogranin, NSE, synaptophysin and CD56 while the ductal adenocarcinoma showed a positive reaction to EMA, CEA, CD15 and cytokeratin 19. Regarding histogenesis the intimate topographical coexistence of the heterogeneous cell populations is very likely to represent their histogenetic association with a multipotential precursor cell.

P 527

IMMUNOHISTOCHEMICAL STUDY OF GENETIC ALTERATIONS, MUC1 AND MUC2 EXPRESSION IN INTRADUCTAL AND INVASIVE DUCTAL TUMORS OF THE PANCREAS

AYDIN Ovgu, GOKSEL Suha, ERDAMAR Sibel, GOCENER Selda, BULBUL Dogusoy Gulen

Pancreatic carcinoma is a highly malignant neoplasm that still carries a very poor prognosis. Majority of pancreatic carcinomas are malignant. So the classification has a clinical and prognostic significance. The ductal adenocarcinomas(DA) arising from Intraductal Papillary Mucinous Neoplasia (IPMN) are said to have a much beter prognosis than the classical adenocarcinoma.Also the pancreatic intraductal lesions, named as Pancreatic Intraepithelial Neoplasia (PanIN) have been classified by WHO. Multiple genetic alterations are involved in development of pancreatic neoplasm. In this study, pancreatic tissue obtained from 135 operations were examined for PanIN lesions. The frequency of PanIN in tumoral and nontumoral pancreata were compared and DA cases were evaluated for presence of IPMN.Then we investigated expression of p21, p53 and DPC4, the major apomucins (MUC1, MUC2)in PanIN lesions and tumors of the IPMN related carcinomas and the classical DA by immunohistochemical method. p21 and p53 expression increased progressively with the severity of the lesion. p21 expression was (-) in normal pancreatic tissue, PanIN1a, PanIN1b, PanIN2 lesions and was (+) in 2 PanIN3 lesions both of which were sampled from IPMN(-) DA (2/20) and 10 invasive carcinoma area most of which belonged to IPMN (-) DA. p53 expression was (-) in normal pancreata, PanIN1a, PanIN1b, PanIN2 lesions and was (+) in most of PanIN3 and invasive carcinoma samples. DPC4 was highly expressed in normal pancreata, PanIN1a, PanIN1b lesions and DPC4 expression decreased with the severity of lesions (PanIN2:%61, PanIN3:%57, TM: %43). IPMN(-) tumors highly express MUC1 and only 1 case was (+) for MUC2. On the other hand most of IPMN (+) cases were (+) for both MUC1 and MUC2. The most frequent PanIN lesion was PanIN3 in tumor cases. A positive correlation between PanIN1a, PanIN1b, PanIN2 and chronic pancreatitis was found. There was no correlation between chronic pancreatitis in DA and high grade PanIN lesions. Vascular invasion and lymph node metastasis were significantly less in IPMN(+) DA compared to IPMN (-) DA. This finding supports the hypothesis that IPMN(+) adenocarcinomas have a beter prognosis than a classical DA. DPC4 expression is especially present in low grade carcinomas in IPMN(-) tumors and loss of DPC4 expression increases with the grade of IPMN(+) tumors. p21 and p53 expression were both found to be late events in development of pancreatic neoplasia according to our results.

P 528

NON-INVASIVE INTRADUCTAL PAPILLARY MUCINOUS TUMORS OF THE PANCREAS. EXPERIENCE OF THE HOSPITAL CLINIC OF BARCELONA.

MIQUEL Rosa, GARRIDO Marta, PETIT Ana, BOMBÍ Josep-Antoni, COLOMO Lluís, SOLÉ Manel, SANCHEZ Marcelo, SORIANO Antonio, FERNANDEZ-ESPARRACH Gloria, NAVARRO Salvador and FERNANDEZ-CRUZ Laureano.
Departments of Pathology, Radiology, Gastroenterology and Surgery.
Hospital Clinic, IDIBAPS, University of Barcelona

Introduction. Intraductal Papillary Mucinous Neoplasms (IPMN) of the pancreas are intraductal tumors characterized by variable amount of mucin production, cystic dilatation and papillary growth, that have increased its frequency in the last past years. They display a wide spectrum of cytologic and architectural atypia, from benign adenomatous lesions to invasive carcinomas.
Objective. The purpose of these study was to report the clinicopathological features of non-invasive IPMN in our hospital.
Material and Methods. We reviewed the histologic material from surgical pancreatic resections performed between 1995 and April 2005 at the Hospital Clinic of Barcelona in wich the words mucinous, cystic or papillary formation were identified in the pathology reports, in order to identify and classify IPMN according the current WHO definition of these neoplasms. The clinical history and image studies of each patient were also reviewed.
Results. A total of 27 IPMN were identified of wich 14 (52%) were non-invasive. Ten of the 14 patients were man and 4 female, with a mean age of 72 years. In two patients the lesion was discovered because of abdominal pain and 1 for a constitutional sindrome. In 5 patients (36%) IPMN were discovered incidentally whereas a history of recurrent acute pancreatitis was found in 6 patients (43%). Most of the lesions were localized at the pancreatic head (10 71%) and 3 at the body/tail. The mean size was of 3 cm (1.3 to 5.8). In 9/14 cases USE-FNA was performed previous to surgery, obtaining mucin and ductal cells with or without atypia. Histologically, 10 cases displayed features of IPM adenoma, 2 moderate dysplasia and 2 high grade dysplasia/in situ carcinoma. Branch-type was the most frequent IPMN type found (11/14 79%) and in the other 3 cases the main pancreatic duct and its branches were affected. None of the patients had recurrence or died of the disease after a median follow-up of 22 months (from 1 to 88).
Conclusion. IPMN represents a group of pancreatic neoplasms that have increased its frequenty in the recent last past years, mostly due to their recognition in early phases as incidental lesions by the improvement and the most extended use of image techniques, specially in asymptomatic patients, as has been observed in 36% of the patients of our series of non-invasive IPMN.

P 529

MORPHOLOGY OF THE GALLBLADDER MUCOSA IN VARIOUS TYPES OF CHRONIC CHOLECYSTITIS

Dariusz Lange1, Ewa Zembala-No¿yñska2 , Miros³aw Œnietura1, Micha³ Zembala3, Jerzy No¿yñski3

1 Dept. of Tumor Pathology, Centre of Oncology, M.Curie-Sk³odowska Institute, Gliwice, Poland
2 Chair and Dept of Pathomorphology, Silesian Medical University, Zabrze
3 Dept. of Histopathology, Silesian Centre For Heart Diseases, Zabrze, Poland

Background: Chronic inflammation of gallbladder comprises simple form with mucosa with slight atrophy and rarely chronic hyperplastic form with arboriform hyperplasia of mucosa, suggesting neoplasia.
Aim: The aim of this study was the comparison of the morphology, proliferative activity and karyometry of mucosa cells in both types of cholecystitides.
Material and methods: 25 cases of simple chronic cholecystitis and 30 of chronic hyperplastic cholecystitis were collected. The morphological analysis of mucosa architecture was done using confocal laser scanning microscopy, proliferative activity was assessed with Ki-67 reaction, karyometric measurements included: nuclear area, length, breadth, perimeter, roundness, aspect and mean grey level.
Results: Simple chronic cholecystitis was characterized by monolayered glandular epithelium, in cases of hyperplastic chronic inflammation the multilayered epithelium was observed moreover, Ki-67 was positive in almost all epithelial cells, whereas in simple chronic inflammation only single cells were Ki-67-positive.
Conclusion: Chronic hyperplastic cholecystitis shows the different architecture of epithelium, increased proliferative activity and different karyometric characteristics, including rounding and widened nuclei with predominance of euchromatin.

P 530
LIVER CELL DYSPLASIA IN PERCUTANEOUS LIVER BIOPSY IN CHRONIC HBV OR HCV HEPATITIS

ZURAC Sabina*, STANICEANU Florica*, VRABIE Alexandra*, MICU Gianina*, GRAMADA Eliza*, ZAHARIA Anca*, ANDREI Razvan*, LAVRIC Luciana*, STREINU-CERCEL Adrian**
*Department of Pathology, Colentina Universitary Hospital
**Department of Infectious Diseases, Matei Bals Institute
Bucharest, Romania

The role of hepatitis B virus (HBV) and hepatitis C virus (HCV) infections in the etiopathogeny of the hepatocellular carcinoma (HCC) is well established.
Material and methods
We studied the presence of large cell changes (LCC) and small cell dysplasia (SCD) according to the etiology, age, necroinflammatory activity and fibrosis in a group of 1173 percutaneous liver biopsies from patients with chronic viral hepatitis B, C and D. The necroinflammatory activity and fibrosis were assessed based on Ishak semiquantitative score. A statistical analysis was performed using CHITEST (X 2) with a level of statistic significance (P) of 0.05.
Results
LCD was exclusively revealed in HBV+/-HDV infection (P=1x10-54); SCD was more frequent in HCV infection (P=9x10-6).
There were significant association between high necroinflammatory activity and LCC in HBV infection (P=2x10-27) and HBV+HDV infection (P=1x10-5); also, SCD and low necroinflammatory activity were associated with HCV infection (P=2x10-6) and HCV+HBV infection (P=6x10-6).
Advanced stages of fibrosis were associated with LCC and HBV infection (P=4x10-31), LCC and HBV+HDV infection (P=2x10-17), SCD and HBV infection (P=1x10-18), SCD and VHC infection (P=0.01) and SCD and VHC+VHB infection (P=1x10-212).
Conclusions
LCC appear in chronic hepatitis with high grades of necroinflammatory activity and advanced stages of fibrosis (they need a long time to develop – important fibrosis – but it seems they are elicited by the hepatocytic lesions – important activity). SCD also need advanced stages of fibrosis (long time to evolve) but low grades of necroinflammatory activity (SCD are caused by accumulations of genetic alterations in the hepatocytes)

P 531
USEFULNESS OF FINE NEEDLE ASPIRATION BIOPSY (FNA) AND THIN NEEDLE CORE BIOPSY (NB) FOR THE DIAGNOSIS OF HEPATIC NODULES LESS THAN 2 CM IN CIRRHOTIC PATIENTS

MOZOS Ana, SALA Margarita, VILANA Ramon, BIANCHI Lluis, BRUIX Jordi, SOLÉ, Manel
Departments of Pathology and Radiology, and Liver Unit. Hospital Clínic. IDIBAPS. University of Barcelona.

Introduction: Systematic screening of cirrhotic patients for the early diagnosis of hepatocellular carcinoma (HCC) results in the detection of nodules less than 2 cm that cannot be fully characterized by imaging techniques. The role of biopsy in this setting remains controversial, due to the risk of sampling error and to the assumed very well differentiated nature of the tumors.
Purpose: To evaluate the efficacy of a prospective diagnostic approach based on the combination of FNA and NB for the diagnosis of small (<2cm) nodules in cirrhotic patients.
Material and methods: 45 cirrhotic patients undergoing systematic ultrasonographic (US) screening in which a nodule less than 2 cm (17 out of them 1cm or less) was detected. FNA (45 cases) with cell block when enough sample was obtained (43 cases) and NB with a 20G cutting needle when allowed by the location of the lesion (16 cases) were performed. Both cytologic and histologic diagnoses were based on previously published criteria. Cases were classified in five categories: 1. Negative 2. Benign nodule (regenerative vs. low grade dysplastic) 3. Suspicious (high grade dysplastic vs well differentiated HCC) 4. Malignant 5. Insufficient. Cases in the 3 and 4 categories were treated accordingly. Nondiagnostic and benign cases were followed-up for a period ranging from 3 to 12 months and rebiopsied according to the same protocol when indicated by the imaging features (US-Sonovue, computed tomography and magnetic resonance) or nodule growth (21 rebiopsies in 17 patients).
Results: 22 patients were classified in the categories 3 or 4 after the first biopsy, and other 7 after a second (6 cases) or a third biopsy (sensitivity for the first biopsy 75,7%). 3 out of the 7 false negative cases were classified in category 5 in the first biopsy, and the other 4 in category 1. 7 cases diagnosed as category 3 or 4 measured 1cm or less; 6 were diagnosed at the first biopsy and the other in the second biopsy. FNA (cytology + cell block) failed to diagnose 4 out of 29 lesions classified as 3 or 4, whereas NB missed 4 out of 12 lesions in which this procedure was performed.
Conclusions: FNA combined with NB is an efficient method for the diagnosis of small nodules in cirrhotic patients. Failures in diagnoses seem to be related to sampling rather than to diagnostic difficulties by the pathologist. FNA comprising cytology and microhistology of cell blocks is more sensitive than NB, probably due to better sampling.

P 532
FINE NEEDLE ASPIRATION BIOPSY OF FOCAL LIVER LESIONS – THE EXPERIENCE OF 2111 CASES

Székely Eszter dr., Istók Roland dr., Székely Tamás,Járay Balázs dr
Semmelweis University, II. Department of Pathology, Budapest, Hungary

Introduction: Ultrasound (US)-guided fine needle aspiration biopsy (FNAB) of focal liver lesions is a cost effective diagnostic method, by which the nature of the lesion (benign / malignant, primary / metastatic) is easily diagnosed in most cases. Clinicians and pathologists of those centers, that lack an experienced team needed for these examinations usually deny the efficacy of cytological examinations, and prefer thick needle – core- biopsies.
Our purpose was to show our data, demonstrate the most relevant, most frequently occurring technical and diagnostic difficulties, and to show the role of FNAB in the diagnostic armory.
Method: In the past 20 years, 2111 US guided liver FNABs were performed in the neighbouring US laboratories, that were examined by our cytological team. The smears were wet fixed with ethanol, and stained with H&E.
The results are the following: Benign lesion (cyst, adenoma, FNH, etc) 405 cases. Malignant lesion:1046 - in this group 206 hepatocellular carcinomas (HCC) 719 metastatic diseases were found. In further 121 cases in this group malignant disease was diagnosed without comment, whether the lesion was primary or secondary. In the next category, „suspicious for malignancy"(122 cases). Malignancy could not be proven in 290 cases. In 145 cases, the smears were unsatisfactory for any diagnosis or opinion. In 60 % of these cases clinical follow up and/or histology or autopsy confirmed the nature of the hepatic lesion. No false positive case was found. In four cases metastatic disease was suspected, that turned out to be HCC, or mixed HCC-cholangiocarcinoma.
Conclusion: Our data may persuade those colleagues, who deny or haven't yet experienced the usefulness of liver FNAB-s, to use this easy method as a diagnostic modality, of which we do believe the patients benefit the most. We would like to share some of our „favourite cases" with the audience.

P 533
REGRESSION OF LIVER ADENOMATOSIS AFTER WITHDRAWAL OF ORAL HORMONAL CONTRACEPTIVE : A CASE REPORT

SVRCEK Magali (1), JEANNOT Emmanuelle (2), POUPON Raoul (3), ARRIVE Lionel (4), FLEJOU Jean-François (1), ZUCMAN-ROSSI Jessica (2), WENDUM Dominique (1).
(1) Department of Pathology, Saint-Antoine Hospital, AP-HP, Paris, (2) INSERM U434, CEPH-Fondation Jean Dausset, Paris (3) Department of Hepatology, Saint-Antoine Hospital, AP-HP, Paris, (4) Department of Radiology, Saint-Antoine hospital, AP-HP, Paris.

Liver adenomatosis (LA) is a rare disease characterized by the presence of multiple hepatocellular adenomas. Initially, LA was considered as a separate clinical entity from isolated hepatic adenoma by no relation with oral contraceptive use. However, recently, frequent biallelic inactivation of TCF1 gene encoding Hepatocyte Nuclear Factor -1*f*Ñ (HNF-1*f*Ñ) was identified in both hepatocellular adenomas and LA, suggesting a possible overlap of these two entities. Pathogenesis of LA is unclear. One case of LA regression is described in the literature after hormonal therapy withdrawal, but without any information concerning the TCF1 gene status. We report the second case of regressive LA after withdrawal of hormonal therapy. In this case, TCF1 was not inactivated.
A 48-year-old woman was admitted to our hospital in April 1990 because of a polynodular liver. Ultrasonography (US), computed tomography (CT) and magnetic resonance imaging showed at least eight masses in the liver: the largest one (6 cm) was located within segments VIII-VI. One of these masses, in the left lobe, was typical of angioma. Histological diagnosis of hepatocellular adenoma was made on laparoscopic liver biopsy performed on 2 nodules.
The patient had no diabetes and had been taking oral contraceptives for 10 years at the time of diagnosis. After withdrawal of hormonal therapy, she was examined regularly once a year by US and CT over a period of 10 years, and partial regression of the adenomas was documented. She died in June 2000 because of a pancreatic cancer. Necropsy showed a pancreatic cancer corresponding to an anaplastic carcinoma. Macroscopic and microscopic examination of the liver showed an hemangioma in the left lobe and revealed only one hepatocellular adenoma in the right lobe measuring 3 cm with large areas of ischemic necrosis, haemorrhage and fibrosis. A few microadenomas with steatotic hepatocytes were also present.
The immunohistochemical analysis for estrogen receptors and progesteron receptors performed on the partially regressive adenoma was negative. Neither somatic nor germline inactivation or mutation of TCF1 was found in the hepatocellular adenoma and the normal liver tissue.
With this case report, we demonstrate that LA, without inactivation of TCF1 gene, may almost completely regress after hormonal therapy withdrawal. Exogenous hormonal therapy probably has an important role in some cases of this disease and it seems indicated to avoid it in these patients.

P 534
ASSESSMENT OF IMMUNOHISTOCHEMICAL PROFILE IN HUMAN HEPATOCARCINOMAS

CEAUSU Mihai 1,2, BUTUR Georgeta 1, ARDELEANU Carmen 1,2, CEAUSU Maria 3, GRAMADA Zenaida Florea 1
1 – "Victor Babes" National Institute, Bucharest, Romania
2 – "Carol Davila" University of Medicine and Pharmacy, Bucharest, Romania
3 – "St. Andrew" County Hospital, Galati, Romania

The immunoprofile of human hepatocarcinoma (HCC) has a more or less diagnostic value, doing difficult the differential diagnosis with cholangiocarcinoma or metastasis of adenocarcinoma.
Our aim was to investigate and to test the efficiency of a selected panel of antibodies for assessing the immunohistochemical profile (IHC) of HCC for positive diagnosis.
We performed the indirect tristadial ABC method of IHC for 7 antibodies: CK 7, CK 8, CK 18, CK 19, AFP, CD 34, OCH1E5 on formalin fixed paraffin embedded tissues taken by biopsies from 33 cases with HCC.
Hepatocarcinomas were immunoreactive to CK 8 and 18 in 65% cases, the tumors being positive especially to CK 18; the immunoreaction intensity was higher to CK 18 than CK 8 in tumor and peritumoral hepatic tissue. Alpha fetoprotein was positive in 85% of cases, showing a great sensibility in all tumoral types. Well differentiated tumors stained strongly to CD34, with a perisinusoidal pattern of vessels; low differentiated tumors with compact pattern stained weekly to CD34 (with random distribution of vessels) or negative. OCH1E5 is a liver specific antibody (positive in over 75% of tumors, and in 100% of peritumoral hepatic tissue), but it is pretentious, requiring special technical pretreatments.
Despite of tumoral immunoreaction variability , this 7 antibodies panel proved to be a usefull tool with significant diagnostic value of human hepatocarcinomas.

P 535
HEPATOCYTE GROWTH FACTOR AND ITS RECEPTORS C-MET AND C-MYC IN HEPATOCELLULAR CARCINOMA

Khalil A El Halfawy(1), Shaden Muawia (1), Mohamed A Osman (1) , Mohamed El-Hasafy(2), Shwikar M Abdel Salam(3), Nahla AF Kamel(4)
(1)Molecular biology Department,Molecular Engineering Institute,Minufya University, (2)Internal Medicine,

(3)Microbiology, (4) Patholgy departments,Faculty of Medicine, Alexandria University./egypt

Despite a variety of therapeutic strategies, HCC remains a significant cause of cancer death. Therefore ,to study the HCC pathogenesis is of the utmost importance for the prevention and treatment of this disease. In the present study markers known of regeneration(HGF/c -met system) and cell proliferation(c-myc oncogene) were studied in a series of 20 HCC cases. HGF concentration was estimated in serum by ELISA &in tumor tissues by immunohistochemistry, c-myc & c-met mRNA were detected by RT-PCR. HGF concentration in sera of HCC cases was higher than normal controls(mean value 52.2 versus 20.7 pg/ml). However it was not detected by immunohistochemistry in any of tumor tissues. The elevated levels of HGF had significant correlation with less differentiated and bigger size tumor tissue. c-met was detected in 45% of cases and c-myc in 30% of cases.There was a significant correlation between HGF&c-met &tumor size while no significant correlation between HGF/c-met system and c-myc.

P 536

THE POTENTIAL ROLE OF ACTIVATED CASPASE-3 EXPRESSION IN HEPATOCELLULAR CARCINOMA

TSAMANDAS Athanassios, PAGONI Niki*, PAPATHANASSIOU Zefi**, PETSAS Theodore**, KARATZA Chrisoula*, SCOPA Chrisoula. Departments of Pathology, *Internal Medicine and **Radiology, University of Patras, Greece

Background: Caspase 3 is a downstream effector cysteine protease in the apoptotic pathway. Previous studies have shown that caspase-3 is expressed in 52% of hepatocellular carcinoma (HCC) by immunohistochemistry. Nuclear survivin, present in 42% HCC, correlated with poor prognostic survival parameters. In this study we investigated caspase 3 expression in HCC and related it to survivin overexpression, prognostic parameters, and outcome.
Patients and Methods: Formalin-fixed, paraffin-embedded 4ìm sections obtained from 76 HCC hepatectomy specimens, were subjected to immunohistochemistry (streptavidin-biotin peroxidase) using polyclonal antibodies for activated caspase-3 and survivin (SantaCruz, USA). Human tonsils were used as positive controls. Immunostaining was evaluated in the cytoplasm and nucleus of hepatocytes and Kupffer cells. Results followed moprhometric analysis and were expressed as % of positive cells. Mean follow up time was 27.19 months (range 1.5-83 months).
Results: In HCC, activated caspase 3 was expressed within hepatocytes in 69/76 (90.7%) and within Kupffer cells in 52/76 (68,4%) cases. The stain was cytoplasmic and nuclear. Survivin was present in 34/76 (44.7%) and the stain was cytoplasmic and nuclear. Caspase expression was correlated with lower grade ($p<0.05$), higher disease free ($p<0.01$) and higher total survival ($p<0.01$). Caspase 3 expression was reversely correlated with cytoplasmic survivin expression ($p=0.024$).
Conclusions: Activated caspase 3 expression is correlated with higher disease free survival and higher total survival; in addition it displays a reversed correlation with survivin expression which is considered as a poor prognostic parameters given the fact that suppresses apoptosis. The higher caspase-3 expression probably reflects the fact that apoptosis is associated with good prognosis in cases of HCC.

P 537

GLUTATHIONE S- TRANSFERASE M1 (GSTM1) NULL GENOTYPE AND RISK OF HEPATOCELLULAR CARCINOMA IN HCV CIRRHOTIC PATIENTS.

Gabriela Perdomo Coral MD, PhD; Venâncio Avancini Ferreira Alves MD, PhD; Evandro Sobrosa de Mello MD, PhD; Gilka Jorge Figaro Gattás, PhD; Luiz Carlos da Costa Gayotto MD, PhD.
Department of Pathology/ LIM 14 & Oscar Freire Institute/ LIM 40, University of São Paulo School of Medicine, São Paulo, Brazil.

Glutathione S- transferase M1 (GSTM1) gene has a polymorphism and there are large differences in the prevalence of its null genotype among ethnic groups. Patients with GSTM1 null genotype are more susceptible to some cancers and other diseases. Although a few publications have assessed the link between GSTM1 null genotype and hepatocellular carcinoma (HCC), to our knowledge no one has assessed the impact of this polymorphism on cirrhosis due to HCV, the main etiological factor for HCC. The aim of this study was to investigate the modifying effect of GSTM1 null genotype on hepatocarcinogenesis in patients with cirrhosis secondary to HCV infection. Forty-three patients with cirrhosis secondary to hepatitis C virus infection were evaluated. Of these patients, 16 had HCCs (37.2%) and three had high-grade dysplastic nodules (HGDN). Age, gender, prior alcohol intake, grade of necroinflammatory activity and genetic polymorphism of GSTM1 were studied. DNA was extracted from paraffin blocks of explanted cirrhotic livers and their respective gallbladders. GSTM1 polymorphism was determined by PCR technique. The prevalence of GSTM1 null genotype was 13/43 (30.23%). Only GSTM1 null genotype was associated with HCC/HGDN in explanted HCV-related cirrhotic livers (RR: 4.49; 95% CI, 1.108-18.266; $P = 0.046$). In conclusion, this association of GSTM1 null genotype with HCC/HGDN in patients with cirrhosis secondary to HCV might represent the identification of a subgroup with a high risk of HCC development.

P 538

THE GLUTAMINE SYNTHETASE GENE IS A RELIABLE MARKERS OF MUTATED-ß-CATENIN HUMAN HEPATOCELLULAR CARCINOMAS

Jessica Zucman-Rossi1, Cécile Godard2, Sandrine Boyault1, Frédérique Tissier3, Gisèle Grimber2, Charles Balabaud4,6, Antonio Sa Cunha7, Paulette Bioulac-Sage5,6, Christine Perret2.
1Inserm U674, IFR105 Paris Saint-Louis, CEPH, 27 rue Juliette Dodu, 75010 Paris, France
2Institut Cochin, INSERM U567, UMR CNRS 8104, Département de Génétique, Développement et Pathologie Moléculaire, Université Paris V, 24 rue du Faubourg St Jacques, 75014 PARIS, France
3 Service d'Anatomie Pathologique, Hôpital Cochin, Paris, France
Département d'Hepatologie4 et de Pathologie5, Centre Hospitalier Universitaire de Bordeaux, France
6GREF Inserm E0362, Université Bordeaux 2, France
7Service de Chirurgie Digestive Hôpital Saint-André CHU Bordeaux

Activation of Wnt/ ß-catenin signalling is a frequent event in human hepatocellular carcinomas (HCC). We evaluated various ß-catenin target genes as molecular markers of aberrant activation of the ß-catenin pathway in ß-catenin and Axin1 mutated HCC. A collection of 45 HCC was characterized for activating ß-catenin and inactivating Axin1 mutations and analyzed for expression of the glutamine synthetase (GS), glutamate transporter (GLT-1), ornitho-aminotransferase (OAT), Gpr49, LECT2, c-myc and cyclinD1 genes by real-time RT-PCR. A subset of HCC was analyzed for ß-catenin and GS by immunohistochemistry. We found a significant correlation between ß-catenin mutations and over-abundance of mRNA for GS, GPR49 and GLT-1 ($p=0.0001$), but not for OAT, LECT2, c-myc or cyclin D1.

GS appears to have the best predictive value for ß-catenin activation and is a faithfull immunohistochemical marker of ß-catenin activation in human HCC. Interestingly, in Axin1-mutated tumors, none of the liver ß-catenin target genes validated in human HCC was overexpressed and accordingly, no aberrant accumulation of ß -catenin was observed. In conclusion, our results show that overexpression of each GS and GPR49 are reliable markers of HCC carrying an activated ß-catenin mutation. Surprisingly, HCC presenting inactivated Axin1 mutation do not show anomalous expression of the same genes.

P 539

THE VALUE OF IMMUNOHISTOCHEMICAL MARKERS (IMS) FOR THE DIAGNOSIS OF LIVER TUMORS IN CT-GUIDED LIVER BIOPSY

NOMIKOS Alexandros*, SAMARAS Vasilis*, TANOGLIDI Anna*, TSIKOU-PAPAFRAGOU Aikaterini*, KOKKINAKI Anna**, MYLONA Sofia**, THANOS Loukas**, BARBATIS Calypso*.
Departments of Pathology* and Radiology** Hellenic Red Cross Hospital. Athens, Greece.

Introduction: Guided and not blind liver biopsy is essential for diagnosing primary or metastatic liver tumors. Combination of IMs are useful for detection of specific antigens indicative of cell differentiation/maturation/function and their selective use is mandatory for a correct diagnosis.
Purpose of the study: To evaluate the usefulness of IM panels designed according to histological patterns and clinical history for the diagnosis of liver tumors.
Materials-Methods: 50 cases of CT-guided liver biopsies (Bs) were studied (43 males, 7 females). 10 patients had suffered from another primary malignancy, hepatocellular carcinoma was suspected in 9 cases of chronic hepatitis B and 40 were investigated for unknown primary tumor. Formalin fixed Bs were diagnosed with H+E, PAS, PAS-D, Masson Trichrome and Gordon's and Sweet's reticulin stain. The immunohistochemical method Envision-HRP was used for detection of mixed cytokeratins, CK7, 8,18,19, 20, CEA, Ca19-9, Ca125, c-erb-B2, TTF1, chromogranin A, oestrogen/progesterone receptors and the HepPar1 antibody which is normally expressed in hepatocytes.
Results: In 10/50 cases with another primary malignancy the selective use of IMs confirmed liver metastasis from the primary tumor. 9 hepatocellular carcinomas were diagnosed but attention sould be paid to the focal or absent expression of HepPar1 in high grade tumors. Primary site was suggested in 40 cases and confirmation of a correct liver biopsy diagnosis was available in 16/40 surgical specimens. 24 patients with proposed diagnosis were not traced as they were treated in other hospitals. Discordance was observed in two adenocarcinomas with immunophenotype (Ca19-9 +, CK7 +, CK20 -). The upper GI tract was proposed as primary site but colonic adenocarcinoma was diagnosed in another hospital. Comparison of liver and colonic tumors was unavailable.
Conclusion: CT-guided liver biopsy is a useful method for distinguishing primary from metastatic liver tumours and for the recognition of primary site. As the pool of IMs increases, a logical approach is needed for achieving high specificity and sensitivity

P 540

EVALUATION OF APOPTOTIC CELL TURNOVER AND P62 EXPRESSION IN THE PROCESS OF NEOPLASTIC TRANSFORMATION BEGINNING FROM CHRONIC HEPATITIS TO HEPATOCELLULAR CARCINOMA

Gülen Akyol, Özlem Erdem, Güldal Ýylmaz
Gazi University School of Medicine Department of Pathology

Background and Aim: It is well known that reduced apoptosis plays a significant role in hepatic carcinogenesis. Actin fragment, which is produced by caspase 3 during apoptosis, can be recognized by fractin and it has been demonstrated that fractin expression in tissues has a place in the evaluation of apoptosis. p62 is a tumor-related insulin-like growth factor which is shown that approximately one-third of hepatocellular carcinomas exhibited high expression of p62 protein immunohistochemically, whereas adjacent non-malignant parenchymal liver cells had no detectable staining. The aim of this study is to evaluate fractin and p62 expressions in cases of chronic viral hepatitis, cirrhosis and hepatocellular carcinoma to reveal out the possible impact of these proteins in hepatocellular carcinogenesis.
Material and Methods: Fractin expression has been evaluated in paraffin embedded sections by immunohistochemistry in cases of 13 mild, 11 moderates and 3 severe chronic hepatitis, 8 cirrhosis and 7hepatocellular carcinoma. Nuclear and cytoplasmic staining percentage was used for statistical comparisons
Results: Although fractin expression did not differ between groups of different degree of hepatitis, the difference was significant between cases of chronic hepatitis, cirrhosis and hepatocellular carcinomas. While the apoptotic rate was highest in chronic hepatitis, it was lower in hepatocellular carcinomas. In contrast to the literature, we could not detect p62 in hepatocellular carcinoma cases. However, it was found weakly positive in 1 hepatitis B and 1 cirrhosis case.
Conclusion: It has been suggested that apoptosis that evaluated by fractin antibody could be more helpful for defining preneoplastic lesions during hepatic carcinogenesis than p62 expression.

P 541

TGF-BETA PATHWAY CORRELATES WITH APOPTOTIC INDEX IN NEOPLASTIC HUMAN LIVERS

GIACOMETTI Cinzia, PONTISSO Patrizia, VALENTE Marialuisa, CALABRESE Fiorella
University of Padova Medical School, Padova, Italy

INTRODUCTION TGF-beta1 plays a central role in regulation of cell growth and differentiation. The signalling pathway is complex and its effect is dependent by the activation of specific transduction factors. PURPOSE OF THE STUDY The aim of the present study was to investigate the expression of TGF-beta pathway (TGF-beta1, SMAD 1-2 and TGF-beta type II receptor) in neoplastic human livers. METHODS 43 HCC tissue samples obtained form 12 liver biopsies and 31 surgical resections, 20 normal liver tissues, 6 cirrhotic and 20 viral hepatitis were investigated for the TGF-beta1 and its signalling pathway (TGF-beta1 type II receptor and SMAD) expression. Semi-quantitative RT-PCR for the detection of TGF-beta1 was performed on all frozen liver tissues. Apoptotic index was evaluated by TUNEL technique and proliferation index was analysed with MIB1 (Ki-67 antigen). Results TGF-beta expression (mRNA and protein) was higher in HCC compared with normal liver but it was significantly lower than cirrhosis and hepatitis. RESULTS A concordant expression of TGF-beta1 with RII and SMAD 1-2 was observed in the majority of cases ($p<0.05$). A positive correlation was observed between apoptotic index and TGF-beta pathway. No correlation was observed between TGF-beta pathway and other clinical and pathological parameters. CONCLUSIONS TGF-beta is markedly low expressed in HCC compared to inflammatory and degenerative processes. TGF-beta pathway plays an important role in the arrest of cell growth in HCC.

P 542

SCREENING OF SERUM BIOMARKERS IN HEPATOCELLULAR CARCINOMA BY SELDI TECHNIQUE

Jianzhong Zhang, Yanhua Zheng, Kai Feng
Department of Pathology and Laboratory Medicine
Beijing 306 Hospital
9 North Anxiang Road, Beijing 100101, China

Objective: Liver cancer is one of the diseases with higher incidence and mortality. New technologies for the earlier detection of liver cancer are urgently needed. The aim of this study was to screen serum biomarkers in patients with hepatocellular carcinoma by using surface-enhanced laser desorption and ionization time-of-flight mass spectrometry (SELDI-TOF-MS) Methods: Proteomic spectra were generated by mass spectroscopy in 88 cases, including 34 cases of hepatocellular carcinoma that had been pathologically confirmed with aged 45 to 94 years, and 34 cases of healthy control aged 20 to 78 years. 68 spectra obtained were used to train and develop a decision tree classification algorithm.
Results: A total of 17 distinguished proteomic peaks were detected, two of which were used to build a proteomic pattern. The results yielded a sensitivity of 91.18£¥ (33/34), specificity of 97.06£¥(32/34), and positive predictive value of 96.88£¥.
Conclusion: SELDI-TOF-MS offers a unique platform for the earlier detection of tumor. It also offers a noninvasive method to study the local microenvironment associated with the development and progression of liver cancer.

P 543

THE MESENCHYMAL HAMARTOMA OF THE LIVER IN ADULTHOOD: REPORT OF TWO CASES WITH IMMUNOHISTOCHEMICAL PROPHYLE, CLINICAL AND HISTOPATHOLOGICAL FEATURES

Gürbüz Y*, Turan G*, Utkan Z**, Alponat A**
*Kocaeli University Medical Faculty Pathology Department
**Kocaeli University Medical Faculty General Surgery Department

INTRODUCTION: Mesenchymal hamartoma is an uncommon cystic mass of the liver occur primarily in children. However there are a few reports of adulthood mesenchymal hamartoma of the liver (MHL).
CASE REPORTS: In this paper we present two cases of MHL in two female patiens 54 and 51 years old. In radiological examination of bouth of the cases the patiens had multiple cystic lesions in the liver accompanied a kidney cyst In microscopic examination a multilocular cyst lined by flattened epithelium surrounded by a mesencymmal component composed of mature connective tissue, arterial and venous vascular structures, peripheric nerve bundles, and ductal structures was observed. An immunohistochemical panel composed of desmin, smooth muscle actin, S-100, vimentin, CD34, CEA, Pan cytokeratin, cytokeratin 7 (CK7), CK8, CK17, and CK20 was applied to the paraffin sections. CK7 and CK19 immunoreactivity was observed in cystic epithelium and in ductal structures. Focal and patchy desmin immunoreactivity was observed in connecting tissue. S-100 was positive only in pheripheric nerve bundles.
CONLUSION: In conclusion MHL of aduthood is a localised tumoral abnormality that precedes birth which had delayed clinical presentation. These lesions seems to be in a maturation process just like the hosts carrying them. The stomal component consist of immature ebematous spindle cells stroma rich in mucopolicassatides convert to mature paucicellular hyalinised coonecting tissue. This maturation process may be also related with lost of precancerous potential of these tumors observed in juvenyl forms.

P 544

HIGH EXPRESSION OF CLAUDIN-4 IN BILIARY CARCINOMAS

LODI Csaba (1), SZABO Erzsebet (1), BATMUNKH Enkhjargal (1), HOLCZBAUER Agnes (1), PAKU Sandor (2), KISS Andras (1), KUPCSULIK Peter (3), ILLYES Gyorgy (1), SCHAFF Zsuzsa (1).
(1) 2nd Department of Pathology, Semmelweis University, Budapest, Hungary,
(2) First Department of Pathology and Experimental Cancer Research, Semmelweis University, Budapest, Hungary,
(3) First Department of Surgery, Semmelweis University, Budapest, Hungary.

BACKGROUND/AIMS: Cell adhesion molecules play an important role in carcinogenesis, especially claudins, being part of tight junctions. It has been shown the importance of certain claudins in development of several tumors, and some of them even suggested as a future therapeutic target. For this reason, the aim of our study was to analyse the expression of claudins in biliary carcinomas (BCs).
METHODS: A tissue microarrays comprising 24 biliary carcinomas, arising from different localisations (gallbladder, common bile duct, hepatic ducts, intrahepatic bile ducts) were constructed to investigate claudin-1,2,3,4,7 expression by immunohistochemistry on formalin fixed, paraffin embedded slides. Claudin-4 was further investigated by Western blot analysis on 5 human surgically resected, snap frozen BC specimens. Subcellular localisation of claudin-4 was detected by confocal laser scanning microscopy.
RESULTS: Intensive membranous immunolabeling was found for claudin-4 in BCs of different origin. A single band of the expected size was detected on Western immunoblots and revealed a strong expression of claudin-4. Confocal microscopy confirmed the increased expression of claudin-4 on the membrane of BC cells.
CONCLUSIONS: Our data report the first time a significantly increased claudin-4 expression in BCs. The results represent a novel feature of BCs and claudin-4 protein could well become a potential diagnostic marker and therapeutic target for biliary carcinomas, as it has been suggested for pancreatic and ovarian cancers.
The project was supported by grants: NKFP-1/0023/2002, ETT- 077/2003, OTKA-T037838.

P 545

DETECTION OF RESPONSE-PREDICTING MUTATIONS IN THE KINASE DOMAIN OF THE EPIDERMAL GROWTH FACTOR RECEPTOR GENE IN CHOLANGIOCARCINOMAS

KIM Young-A1, PARK Jong-Moo2,GWAK Geum-youn3, AHN Young-Joon4, YOON Jung-Hwan3
1Department of Pathology, Seoul National University Boramae Hospital, 2Department of Neurology, Eulji University School of Medicine , 3Department of Internal Medicine, Seoul National University College of Medicine, 4Department of Surgery, Seoul National University Boramae Hospital

Purpose: Epidermal growth factor receptor (EGFR) signalings have recently been implicated in the genesis and progression of cholangiocarcinomas. Thus, the EGFR kinase inhibitor appears to be promising in the treatment of this cancer. The response-predicting mutations in the tyrosine kinase domain of EGFR gene have recently been detected in non-small cell lung cancers. This study was, therefore, to investigate if these mutations are also found in cholangiocarcinomas. Methods: Twenty-two consecutive cholangiocarcinoma patients who underwent surgical resection were enrolled. Their resected paraffin-embedded cholangiocarcinoma specimens were used for mutation analysis, which was performed by DNA sequencing of exons 18, 19 and 21 in the EGFR gene. Clinical characteristics were compared between each group

according to the presence or absence of mutations. Results: Three patients (13.6 %) harbored EGFR mutations. All the mutations found were deletions in exon 19. Mutations were more common in intra-hepatic or poorly differentiated tumors. Differences in age, sex, stage at diagnosis and survival were not observed between mutation-positive and -negative patients. Conclusions: This study, for the first time, demonstrates that a subset of cholangiocarcinoma patients has response-predicting EGFR mutations. Therefore, a highly selected application of the EGFR kinase inhibitor would be therapeutically effective in these patients.

P 546

HEREDITARY HEMOCROMATOSIS ASSOCIATED WITH A FULL SPECTRUM OF BILE DUCT LESIONS: CHOLANGIOCARCINOMAS, BILE DUCT ADENOMAS AND BILIARY MICROHAMARTOMAS.

GARCIA Adriana, MOYANO Susana, LANDOLFI Stefania, SANCHEZ Marcelo, GARCIA-VALDECASAS Juan-Carlos, BRUGUERA Miquel and MIQUEL Rosa.
Departments of Pathology, Radiology, Surgery and Liver Unit.
Hospital Clinic, IDIBAPS, University of Barcelona.

Genetic hemochromatosis (GH) is a relatively common inherited disorder associated with chronic liver damage and cirrhosis. Iron overload has been also associated with an increased risk for the development of primary liver tumours. Although hepatocellular carcinoma is the malignant tumor most frequently found in these patients, a wide spectrum of biliary lesions and cholangiocarcinoma have also been described. Von Meyenburg complexes and bile duct adenomas are two well known lesions associated with cholangiocarcinomas and considered putative precursor lesions.

We present a case report of a 64–years-old man with liver cirrhosis associated with GH, homozygotic for the C282Y mutation, and treated for the last 4 years with venesections. The patient was admitted to our hospital for the study of two hepatic focal lesions suspicious of metastasis. After the diagnosis of a well differentiated adenocarcinoma by a fine-needle aspiration of one of the nodules, and exclusion of a primary tumor in other localization, the patient was submitted for hepatic resection. A segmentectomy II-III, V and a percutaneous liver biosy of the left lobe were performed. Macroscopically five white nodules were observed, from 2.5 to 0.2 cm, in a micronodular background. The non-tumoral liver parenchyma showed cirrhosis with a moderate iron deposition. Microscopically the two largests nodules were cholangiocarcinomas. A total of 7 bile duct adenomas and numerous von Meyenburg complexes were also identified in the adjacent liver tissue of all the specimens. No morphological transition between benign and malignant lesions was observed. Immunohistochemical studies using citokeratin 7 and 20, EMA, CEA, p53, Mucins and Ki-67 antibodies were performed.

In GH individuals, primary liver tumors may present with a wide morphological spectrum, from hepatocyte-derived malignancies to cholangiocyte-derived lesions. A carcinogenic effect has been proposed for iron overload by both direct or indirect pathways. The unusual case we present shows a full spectrum of biliary lesions with biliary microhamartomas, bile duct adenomas and cholangiocarcinomas.

P 547

SOLITARY FIBROUS TUMOR OF THE LIVER: REPORT OF THREE CASES ONE OF THEM SHOWING MALIGNANT FEATURES

Peña C*, Rullier A*, Laurent C°, Le Bail B*, Bioulac-Sage P*.
*Department of Pathology and °Surgery CHU Pellegrin, Bordeaux, France.

Solitary fibrous tumors (SFT) are rare neoplasm arising from mesenchymal cells, which are difficult to diagnose. They have been reported in a wide range of anatomical sites usually benign, but malignant transformation has been described. SFT of the liver are exceptionally described and always benign.
We report three cases of SFT of the liver diagnosed during last ten years in our department. All were located in the right liver and surgically resected. Case 1 and case 2 were benign SFT diagnosed in 69 and 57 year-old women. The main clinical manifestation was abdominal pain with weight loss for case 1. Tumor size varied from 9 to 10.5 cm in diameter. The external surface was typically smooth, of firm consistency and well defined. The cut surface was light tan to gray-white with whorled texture with foci of cystic degeneration. Histologically, tumors showed alternating cellular and paucicellular areas. The former included spindle-shaped cells with finely disperse chromatin and uniform nuclei. The latter were made of abundant hyalinization and collagen deposits. The tumor vascular supply was well developed. Mitotic activity did not go beyond 4 mitoses/10 HPF. All tumor cells expressed CD34 and vimentin whereas cytokeratins, alpha smooth muscle actin, S100 protein and c-kit were negative. Proliferative index was low. The patients were alive without recurrence since 9 years and five months for cases 1 and 2 respectively .
Case 3 concerned a 70 year-old woman presenting with persistent abdominal pain. Tumor size was 16 cm with similar macroscopical characteristics as previous cases. Histologically the aspects were identical to previous tumor at one exception. An expansive and basophilic nodule was found in the cellular area with dense cellularity, fascicular pattern and, high mitotic activity (8 mitoses/10 HPF) and proliferative index. No necrosis nor lymph node metastasis were observed. The immunophenotype of tumor cells was identical as previous cases even in the atypical nodule. The patient is still alive without recurrence since three months.
Solitary fibrous tumor of the liver are exceptional. They are usually benign, but tumor with malignant features can occur with unknown prognosis.

P 548

SYNCHRONOUS PERIVASCULAR EPITHELIOID CELL TUMORS (PECOMA) INTRAHEPATIC, AND OF THE ROUND LIGAMENT OF THE LIVER.

ALFARO Luis, RAYÓN Miguel, FROUFE Agustín, SANJUÁN Fernando, MIR José.
Hospital La Fe. Valencia. Spain.

Perivascular Epithelioid tumors (PEComas) is a recently introduced concept to describe a family of lesions sharing peculiar features: co-expresion for muscular and melanocytic markers, spindle or epithelioid cell shapes, pale or clear cytoplasm, arrangement around blood vessels, melanosomes or premelanosomes in its ultrastructure, and absence of a normal precursor cell.
We present a case of double PEComa developed in left hepatic lobe, and round ligament, in a 24-year-old woman. She sufferered acne, in treatment with oral contraceptives, and came to the hospital with slight dyspepsia. On the echographic exploration two hepatic lesion were seen. Magnetic resonance confirmed a 8 cm lesion dependent of umbilical vein, and a second intrahepatic 3’5 cm lesion, located in segment IVb. No signs of tuberous sclerosis were found. Both lesions were resected, and showed on microscopical examination identical appearance. The tumors were composed of uniform spindle to round cells, with clear cytoplasm, and slightly pleomorphic nuclei. A prominent vascular component subdivided the cells in fascicles and nests. Mitotic activity was lower than 1/10 high power fields. Some areas had cells with prominent cytoplasmic melanic pigmentation.

Immunohistochemically the cells in both tumors strongly expressed HMB-45, smooth muscle actin and Melan-A. S-100 protein, keratin and desmin were all negative. C-kit, and CD99 were positive in more than 80% of tumor cells; and Ki-67 showed a proliferation index lesser than 1%. Electron microscopy study revealed oval cytoplasmic inclusions with dark staining granules, and some with cross striated structures, characteristic of melanosomes.
These kind of lesions had been suffering a controversy regarding its histogenesis and even its real existence a clinicopathological entity. Generally considered as benign lesions, some cases have been described with malignant evolution or sarcomatous transformation. Our case raised also the possibility of a metastatic intrahepatic lesion from and initial ligamentous tumor. However and, in spite of the exceptionality of these lesion and especially for multiples ones, they are usually considered as multicentric processes and not true metastatic lesions.

P 549
TWO CASES OF BILIARY ADENOFIBROMA OCCURING IN PATIENTS WITH HOMOZYGOUS HEMOCHROMATOSIS, ASSOCIATED WITH PRIMARY LIVER CARCINOMA AND OTHER BILIARY LESIONS.

DE LAJARTE-THIROUARD Anne-Sophie (1), BOUDJEMA Karim (2), ZAFRANI ELie-Serge (3), TURLIN Bruno (1)
(1) Department of Pathology, CHU Pontchaillou, Rennes, France
(2) Department of Surgery, CHU Pontchaillou, Rennes, France
(3) Department of Pathology, CHU Henri Mondor, Créteil, France

Hepatocellular carcinoma (HCC) and cholangiocarcinoma (CC) are reported as complications of genetic hemochromatosis (GH). We report two cases of GH with several benign and malignant lesions, including biliary adenofibroma (BAF).
For the first patient, of 68 years old, followed and treated by phlebotomy for 30 years, two hepatic nodules were found. Left hepatectomy was performed. Four nodules were macroscopically identified, mesuaring 0.5, 1.5, 1.5 and 5 cm. They corresponded, respectively, to bile duct adenoma, focal nodular hyperplasia, BAF and HCC. For the second patient, of 72 years old, GH and hepatic nodules were diagnosed at the same time. Abdominal imaging revealed four nodules in the right hepatic lobe. Histologically, 3 of them were HCCs and the fourth was BAF. In both patients, non neoplastic liver showed extensive fibrosis but no cirrhosis and multiple von Meyenburg complex (VMC). In the second case, the parenchyma showed severe siderosis with numeral iron free foci.
BAF is a rare benign neoplasm with only three previously reported cases in the litterature. It is characterized by a microcystic and tubuloglandular architecture composed of a biliary epithelium supported by a fibroblastic stroma scaffolding. Here we report the 2 first cases of BAF in GH patients. Existence of several biliary lesions, developped in a non cirrhotic liver in two patients with GH, suggest a relationship between iron overload and these lesions. BAF, as suggested Varnholt et al, could be an intermediate step in biliary carcinogenesis from VMC to CC. In this setting, occurrence of CC in GH have been already reported in association with VMC. Morcos et al, studying liver cancer in GH, have shown a wide histologic spectrum including VMC and CC.

P 550
HISTOLOGICAL CHANGES OF NON TUMORAL LIVER IN RIGHT HEPATECTOMY FOR METASTATIC COLORECTAL CANCERS. CORRELATIONS WITH PREOPERATIVE IMAGING.

A. Abbey-Toby (1), M. Ronot (2), D. Goere (3), P. Bedossa (1), J. Belgithi (3), V. Vilgrain (2), V. Paradis (1).
(1) Pathology Dpt, (2) Radiology Dpt, (3) Liver surgery Dpt, Beaujon hospital, Clichy France

BACKGROUND : Neo-adjuvant systemic chemotherapy is largely used in patients with liver metastastatic colorectal cancers. The impact of such treatment on non-tumoral liver tissue is still poorly investigated. The aim of this study was to (1) describe the morphological changes of non-tumoral liver tissue on surgical specimens, (2) correlate the microscopic findings with the preoperative radiological constatations in a prospective cohort of patients with right hepatectomy.
PATIENTS AND METHODS: From March 2002 to February 2004, 58 consecutive patients with liver metastases had a right hepatectomy. Among them, 43 had chemotherapy, associated with a right portal vein embolization in 8 patients. Liver specimens were reviewed by 2 pathologists and the following features were semi-quantified: steatosis (0: absent; 1 <30%, 2 > 30%), sinusoidal dilatation (0: absent; 1: few foci, 2: numerous foci involving 2/3 of the lobular surface, and 3: extensive areas associated with regenerative nodular hyperplasia), portal fibrosis (0: absent or mild: portal tracts normal or minimally enlarged, 1: extensive fibrosis). Preoperative imaging included CT and MRI in all patients. The following signs were analysed in consensus by 2 radiologists: morphologic changes of the liver, steatosis, abnormal enhancement patterns and signs of portal hypertension.
RESULTS: At pathology, 52 out of 58 (90%) post-chemotherapic liver specimens displayed significant liver changes. Steatosis was observed in 35 cases (60 %), mild and moderate in 29 and 6 cases, respectively. Vascular changes were present in 28 cases (48 %), mild and moderate in 18 and 4 cases, respectively. In 6 patients (10%), regenerative nodular hyperplasia was diagnosed. CT and MRI had a sensitivity to diagnose steatosis of > 30 % and between < 30% of 67% and 7%, respectively with a specificity of 100%. Among patients with microscopic vascular abnormalities, only 3 had abnormal enhancement at imaging (30 %).
CONCLUSION: This study shows that significant morphological changes are observed in the context of neo-adjuvant systemic chemotherapy given in most patients for liver metastastatic colorectal cancers, with steatosis and vascular changes the most prevalent lesions. Among them, regenerative nodular hyperplasia was frequent in this series and may have an important clinical impact on postoperative outcome. The accuracy of combined CT and MRI to detect steatosis was high whereas it was low for the detection of vascular lesions.

P 551
EPIDERMAL GROWTH FACTOR RECEPTOR (EGFR) EXPRESSION IN COLORRECTAL CANCER LIVER METASTASES

Alfredo Matilla1, Luis Vicioso1, Isabel Sevilla2, Elena Gallego3, Martina Álvarez3, Eduardo Marquez4, Isabel Hierro5.
Servicio de Anatomía Patológica1, Oncología2 and Cirugía4 del Hospital Clínico Universitario Virgen de la Victoria de Málaga, Unidad de Apoyo a la Investigación Oncopatológica de la Universidad de Málaga3 and Servicio de Anatomía Patológica del Hospital de Antequera/Málaga5.

EGFR represents a molecular binding for several antineoplastic agents. Results of treatment are not always related to the level of EGFR expression. This could be related to a different expression of EGFR in the primary tumor (PT) and in liver metastatic disease (LM).

Of the 48 cases 36 were EGFR positive in the PT and 12 were negative.Of the 36 positive patients in the PT 24 were also positive in the LM but in 12 LM EGFR were negative. From the 12 primary tumors EGFR negative 7 had EGFR negative LM and in 5 EGFR were positive in the LM. Besides the 48 cases 3 developed a second PT and in 2 of them EGFR expression of the second primary was the contrary of the first tumor. Seven of the 48 cases presented a second LM after a time (14.28 months), of these 4 presented a level of expression contrary to the first metastases.
In conclusion, EGFR expression in the colon PT and LM can be a prognostic factor for recurrence and response to anti-EGFR therapy.

P 552
EXPRESSION OF CLAUDINS IN HUMAN HEPATOBLASTOMA
HALÁSZ Judit(1), KISS András (1), HOLCZBAUER Ágnes (1), PÁSKA Csilla (1), KOVÁCS Margit (1), BENYÓ Gábor (2), GALÁNTAI Ilona (3), SCHAFF Zsuzsa (1)
2nd Department of Pathology, Semmelweis University, Budapest, Hungary (1)
1st Department of Pediatrics, Semmelweis University, Budapest, Hungary (2)
Madarasz Pediatrics Hospital, Budapest, Hungary (3)

P 553
METASTATIC RENAL CELL CARCINOMA IN THE SINONASAL TRACT-REPORT OF A CASE
Simona Mocan1, Simona Stolnicu2, Doinita Radulescu3
1Department of Pathology, County Clinical Hospital Targu Mures, Romania
2Department of Pathology, University of Medicine Targu Mures, Romania
3Department of Pathology, University of Medicine Iasi, Romania

Aim. Few sinonasal tumours can manifest, histologically, as clear cell neoplasia, the most frequent encountered being metastatic renal cell carcinoma.
Material and methods.We present a case of a 63 years old men presented with a six-month history of right-sided epistaxis associated with nasal obstruction. Previous medical history was significant for renal cell carcinoma. The clinical examination revealed a tumor mass localized in the anterior right nasal cavity. A craniofacial resection was performed for tumor extirpation. The tumor was fixed in formaline, embedded in paraffin and the sections were stained with H-E, PAS-ALCIAN blue. Immunohistochemical examinations were performed for Cytokeratin, Vimentin, S-100, EMA, CEA and HMB 45.
Results. Histologically, the tumor was represented nests and tubular structures of tumor cells and little stroma with prominent vascularity. The cells were large, with abundant clear cytoplasm and distinct cytoplasm membranes, the nuclei were rounded, centrally located with reduced nuclear pleomorfism. The tumor was ulcerated on the surface. Histochemistry confirmed the presence of tumor glycogen but no mucin. Immunohistochemistry confirmed strong expression for Cytokeratin, Vimentin and EMA.
Conclusions. Sinonasal tumors that can appear as clear cell malignancies include primary squamous cell carcinoma, salivary tumors (such as mucoepidermoid carcinoma, acinic cell carcinoma, clear cell carcinoma, epithelial myoepithelial carcinoma), metastatic tumors (from renal cell carcinoma and follicular thyroid carcinoma) and recently described entity as “sinonasal renal cell like carcinoma”. The differential diagnosis is made on histochemical, immunohistochemical and ultrastructural features.

P 554
THYROID METASTASIS FROM UNDIFFERENTIATED NASOPHARYNGEAL CARCINOMA: A CASE REPORT
ELLOUZE Sameh, GOUIAA Naourez, KHABIR Abdelmajid, CHTOUROU Imen, MAKNI Saloua, AYADI Lobna, GHORBEL Monem, BOUDAWARA SELLAMI Tahya

Introduction:
Metastatic lesions in the thyroid gland are rarely reported; they account less than 4% of malignant thyroid tumors ; but the number of cases seems to be increased in recent years, with routine use of fine-needle aspiration biopsy. The metastatic involvement of the thyroid gland does not appear to be dependent on age but is more common in females. The most common site of origin was the kidney closely followed by breast and lung. Thyroid metastasis from undifferentiated nasopharyngeal carcinoma (UCNT) has not been reported in the literature;
Objective:
The purpose of this work is to report the clinical and morphological characteristics of this unusual metastatic lesion in the thyroid gland.
Case report:
we report an original case of metastasis to the thyroid from UCNT occurring in a 47-year-old man, 8 years after the diagnosis of the original primary nasopharyngeal tumor treated by chemoradiotherapy. Clinical examination revealed a multinodular goiter. Thyroid gland was voluminous with intact capsule and showed many nodules of different size, witch were diagnosed as metastasis from UCNT. On immunohistochemistry study, the neoplastic cell showed a focally positive immunoreactivity for LMP1 and were negatives for thyroglobulin.
Conclusion:
The thyroid metastasis from UCNT are not always easily identified on routing stained sections and their diagnosis need clinical findings and even immunohistochemical analysis.

P 555
EXPRESSION OF MLH1, MSH2 AND EGFR IN 35 INTESTINAL-TYPE SINONASAL ADENOCARCINOMAS
Flora Poizat (1), Pierre Raynaud (1), Renaud Garrel (2), Valérie Rigau (1), Pierre Baldet (1), Valérie Costes (1).
(1) Department of pathology, (2) Department of head and neck surgery, CHU Gui de Chauliac, Avenue Augustin Fliche 34295 Montpellier Cedex 5

Introduction : Intestinal-type sinonasal adenocarcinomas (ITAC) are malignant epithelial tumors that show histological, and immunochemical features reminiscent of colorectal adenocarcinomas. Unlike ITAC, colorectal adenocarcinoma is one of the most widely studied human malignancies. We have worked on the hypothesis that similarities between ITAC and colorectal adenocarcinoma might reflect equivalent genetic alterations and carcinogenesis.
Purpose of the study : The phenomenon of microsatellite instability (MSI) caused by mutation or methylation in the MLH1 and MSH2 mismatch repair (MMR) genes is a way of pathogenesis involved in 10-15% of sporadic colorectal adenocarcinoma. The aim of our study was to assess MSI status in ITAC by standardised immunochemistry in order to determine if the similarities between ITAC and colorectal adenocarcinoma extend beyond the light microscopic level to an eventual identical way of carcinogenesis.
Futhermore, overexpression of Epithelial Growth Factor Receptor (EGFR) is a common event in colorectal adenocarcinoma. We attempted to determine if such consistent expression of EGFR was also observed in ITAC.
Methods : MLH1, MSH2 and EGFR expression were

investigated in paraffine sections of resection specimens of 35 ITAC using standardised immunochemistry with antigen retrieval.
The expression of MLH1 and MSH2 was considered positive if there was definitive nuclear staining in any of the tumoral cells.
Membrane staining of EGFR was evaluated in the neoplastic cells and graded using a semiquantitative score (0-3+).
Results : All of the 35 carcinomas examined showed preserved nuclear expression of MLH1 and MSH2 with most cases showing strong nuclear staining.
There was no staining of neoplastic cells for EGFR in 8 cases (23%, score 0). Staining was weak in 9 cases (25%, score 1+), moderate in 10 (29%, score 2+), and strong in 8 (23%, score 3+).
Conclusions : First, these results suggest that defective DNA mismatch repair does not play an important role in the pathogenesis of ITAC and confirms the previous investigation of Perez and coll. in 10 patients.
Secondly, we show for the first time that most of the ITAC (77%) stained positively for EGFR with a frequency quite similar to colorectal adenocarcinoma (74 to 97%). On the basis of the already proven antitumoral effect of agents acting as EGFR inhibitors, it is suggested that patients with ITAC might benefit from these agents.

P 556
A MORPHOLOGIC AND IMMUNOHISTOCHEMICAL STUDY OF NASAL MUCOSA IN LEATHERWORKERS OF THE PROVINCE OF FLORENCE AND PISA, ITALY

PALOMBA Annarita*, BIANCALANI Mauro*, IAIA Tonina Enza†, CONTI Stefano?, BATTISTA Giuseppe‡, FRANCHI Alessandro**.
*Division of Anatomic Pathology, Department of Laboratory Medicine, “S. Giuseppe” Hospital, Empoli, †Department of Prevention, USL11, Empoli, ? Division of Otolaryngology Head and Neck Surgery, “S. Verdiana” Hospital, Castelfiorentino, ‡ Department of Prevention, University of Siena, **Department of Human Pathology and Oncology, University of Florence, Italy

Aims: An increased risk for developing sinonasal intestinal type adenocarcinoma has been ascertained in individuals occupationally exposed to leather manufacturing, but no conclusive data have been reported concerning the morphological precursors of these tumors. The purpose of this study is to investigate early histologic changes and modification in the phenotype of epithelial cells in nasal mucosa of leatherworkers, with specific reference to the presence of intestinal metaplasia.
Subjects and methods: 75 male subjects (age 38-75 years) who had a long-time exposure to leather manufacturing (range 7-48 years) underwent biopsy of the nasal mucosa of the lower turbinate. Samples were fixed in formalin and routine processed for histology. Serial sections were stained with haematoxylin and eosin, PAS diastase and immunostained for cytokeratin 20, CDX-2 and MUC-2.
Results: In the majority of the biopsies (66.6%) the normal ciliated epithelium showed areas of squamous metaplasia, which was associated with mild to moderate dysplasia in 24 cases (32%). Another frequent histopathologic finding was the presence of a chronic inflammatory infiltrate (90.6%). In 13 biopsies (17.3%) we observed an increased number of goblet cells, which showed an intense cytoplasmic positivity for MUC-2, while no immunostaining was observed for cytokeratin 20 and CDX-2 in any epithelial cell of surface or glandular epithelium.
Conclusions: As for woodworkers, the most common epithelial changes in the nasal mucosa of leatherworkers are squamous metaplasia (with or without dysplasia) and goblet cell hyperplasia. Intestinal metaplasia, with acquisition of CDX-2 and cytokeratin 20 expression, is not observed in nasal mucosa of leatherworkers, and may be a late event in the pathway leading to development of sinonasal intestinal type adenocarcinoma.

P 557
NASOPHARYNGEAL PAPILLARY ADENOCARCINOMAS. INCLUDING TWO CASE OF THYROID LIKE CARCINOMAS EXPRESSING TTF-1

LUNA Mario, PINEDA Keyla, NETO Antonio
Department of Pathology. M.D. Anderson Cancer Center

Introduction: Nasopharyngeal papillary adenocarcinomas (NPPAs) are uncommon neoplasms with different histogenesis and histomorphology.
Purpose: To characterize the behavior, and IHC of NPPAs.
Design: 19 neoplasms coded as NPPAs were identified in our files. Demographic data and histomorphology were reviewed. IHC for CKs 5/6 , 7 and 19 , S-100 protein, thyroglobulin (THYG) and TTF-1 were performed.
Results: 11 females and eight males ranged in age from 9 to 79 years(mean 47.5 yrs). NPPAs were reclassified as: 8 primay low grade nasopharyngeal adenocarcinomas (LGNPA),7 polymorhous low grade adenocarcinomas (PLGA), and two each thyroid-like papillary carcinomas and metastatic papillary thryoid carcinomas (MPTC).The only children in the study had TLPC. S-100 protein was expressed only in PLGA, CK 5/6 was postive only in LGNPA. TLPC and MPTC immnoreacted to CK 7, CK 19 and TTF-1, wheras only MPTC expressed THYG. All patinets were treated surgically, the pts with MPTC in addiiton received postoperative radiotherapy. All pts are alive without tumor. Pts with MPTC are alive with residual or recurrent tumor.
Conclusions:Differentiating these adenocacinomas has therapeutic and prognostic implications. Our findings document a strong correlation between histomorphology and IHC expression., allowing this distinction. Since THYG may not be express in metastatic papillary thyroid carcinomas,the diagnosis of TLPC is based in the absence of carcinoma in the thyroid gland

P 558
SEBASEOUS CARCINOMA OF THE NASAL VESTIBULE: A CASE REPORT

BIR Ferda, Pamukkale University, School of Medicine, Department of Pathology
AKBULUT MMetin, Pamukkale University, School of Medicine, Department of Pathology
SEN Nilay, Pamukkale University, School of Medicine, Department of Pathology
KELTEN Esra Canan, Pamukkale University, School of Medicine, Department of Pathology
TOPUZ Bulent, Pamukkale University, School of Medicine, Department of Otorhinolaryngology
DEMIRKAN Nese, Pamukkale University, School of Medicine, Department of Pathology

Abstract
Background: Sebaceous carcinomas are cutaneous appendageal tumors that may be extremely rare in the nasal vestibule. These lesions are relatively rare, but some have a predilection for the head and neck region and can easily be misdiagnosed as more common lesions. To our knowledge, only 19 examples of nasal sebaceous carcinomas have been reported in the literature.
Case report: Here the authors described a case of a 90-year-old man who presented with an ulcerated mass in the right nasal vestibule with a history of basal cell carcinoma of the same area. The patient stated that the lesion had been present for 18 months. The examination revealed a destructive, irregularly shaped mass measuring 1.5 cm in maximum diameter. At follow-up, 12 months later, a new lesion of 0.5

cm in diameter had appeared in the same area. Histologic examination of the mass was composed of small basaloid cells and large foamy cells. Sebaseous differentiation was evident in some tumor islands. The sebaseous cells were well defined and variably sized and contained minimally pleomorphic, centrally located, vesicular-shaped nuclei with prominent nucleoli, and had poorly defined cellular outlines. A lot of smaller, darkly staining, basaloid cells with oval shaped nuclei and prominent nucleoli are also frequently identified. The basaloid cells exhibited strong reactivity with 34beta12 and sebaseous cells in tumoral islands stained positive with CEA and EMA. No staining was observed with vimentin, actin and S-100. Mucicarmine stain and periodic acid Schiff stains with and without diastase were negative, confirming that the vacuolated clear cells were neither mucus cells nor glycogen-rich squamous cells. As a result histology revealed a sebaceous carcinoma.
Conclusion: Sebaseous carcinoma can be highly malignant, due to its histological differentiation. It is usually a slowly growing tumor, which is locally aggressive and capable of metastatic spread to regional lymph nodes and distant sides. Historical data indicate a nearly 30% local recurrence rate with standard surgical excision. Careful pathological examination with clinical correlation is essential in the diagnosis and the differential diagnosis of common tumors of the face should include this rare malignancy.

P 559
SPERM PROTEIN 17 EXPRESSION DEFINES TWO SUBSETS OF PRIMARY ESTHESIONEUROBLASTOMA

GRIZZI Fabio (1, 2), BUMM Klaus (3), FRANCESCHINI Giorgia (1, 2), CEVA-GRIMALDI Giorgia (1, 2), SINHA K. Uttam (4), DIOGUARDI Nicola (1, 2), IRO Heinrich (3), KAST Martin W. (5), CHIRIVA-INTERNATI Maurizio (6)
1. Scientific Direction, Istituto Clinico Humanitas, IRCCS, Rozzano and 2. Foundation "M. Rodriguez", Milan, Italy; 3. Department of Otorhinolaryngology, Head & Neck Surgery, Friedrich-Alexander-University Erlangen-Nuremberg, Erlangen, Germany; 4. Department of Otolaryngology, Head & Neck Surgery, Keck School of Medicine of the University of Southern California, Los Angeles, California, USA; 5. Norris Comprehensive Cancer Center, University of Southern California, Los Angeles, California, USA; 6. Department of Microbiology and Immunology, Texas Tech University Health Science Center and Southwest Cancer Treatment and Research Center, Lubbock, Texas, USA.

Introduction. Esthesioneuroblastomas (ENBs) are rare malignant tumors of the nasal vault whose origin, diagnosis and management are still subjects of discussion. The fact that there is no related prognostic factor or generally recognized therapeutic regimen highlights the need for further analyses of its underlying biological features and investigations of new marker proteins that allow more reliable clinical testing. Purpose. To investigate whether Sperm protein 17 (Sp17) is expressed in ENBs and to compare whether Sp17 expression is correlated with other well characterized ENBs markers. Methods: The analyzed tissues came from 42 patients (23 males and 19 females with a median age of 54.5 years; range: 10-84) treated at the University of Erlangen-Nuremberg and the University of Southern California. Two-micrometer thick sections were cut and processed for immunohistochemistry. The immunohistochemical expression of the antibodies (Sp17, Ki-67, chromogranin, S100, synaptophisin, neurofilament) was evaluated by means of light microscopy of all of the available tissues for each patient at 20 x and 40x objective magnifications. Results. We here show that Sp17 is expressed in the ciliated cells of the normal olfactory epithelium and in a proportion of primary ENB lesions. We found an association between Sp17 expression and metastases at relapse ($p = 0.035$), cromogranin expression ($p = 0,014$), and female gender prevalence. A statistically non-significative relation was also found between Sp17 and S-100, synaptophisin, and neurofilament expression. No relation was also found between Sp17 expression and the proliferative capacity of the lesion that was evaluated with the Ki-67 immunohistochemistry. Conclusion. Our results extend previous findings showing that the ciliated cells of the respiratory system and male and female reproductive systems are immunopositive for Sp17, and suggest that Sp17 may be a useful new protein marker for distinguishing two subsets of ENB lesions. Furthermore, they may represent a first step towards the characterization of this histologically heterogeneous family of tumors going under the same name.

P 560
EXPRESSION AND DISTRIBUTION OF MASPIN PROTEIN IN POLYMORPHOUS LOW-GRADE ADENOCARCINOMA

MARTINS Marília, MACARENCO Cíntia, FONTES Alexandra, ARAÚJO Vera, SOUSA Suzana.
Oral Pathology Department, University of São Paulo, BRAZIL

Introduction. Polymorphous low-grade adenocarcinoma (PLGA) is a malignant neoplasm that affects almost exclusively minor salivary gland, representing, in these sites, the second or third most frequent malignant tumour, according to the published series. Despite the recognised clinical importance of the PLGA little is known about its biology. Maspin is a member of the serpin family of serine protease inhibitors with a peculiar role as tumour suppressor. It inhibits cell motility, invasion and metastasis and loss or reduction in maspin expression has been associated with tumoral progression. Maspin is mainly associated with myoepithelial cell and it was already demonstrated, by our group, to be present in a series of salivary gland tumours with myoepithelial cell participation. The aim of this study was to investigate the presence and distribution of the maspin protein among the different histological patterns of PLGA.
Material and methods: Immunohistochemistry for maspin was performed on archival formalin-fixed, paraffin-embedded samples of 19 cases of PLGA, using the labelled-polymer method.
Results: All cases studied were positive for maspin but the pattern and extent of staining varied among the histological patterns. Maspin was abundant in the lobular, more densely cellularized areas, while cribriform, tubular and trabecular showed part of the cells positive and papillary and single file pattern showed only occasional cells positive for maspin. It was also possible to notice, among the usually described medium-sized cell, with nuclei revealing fine chromatin and inconspicuous nucleoli, the scattered presence of a smaller cell, which showed hyperchromatic nucleus. This cell was always negative for maspin. When visible, the periphery of the lesions showed no positivity.
Conclusions: Maspin expression was more abundant in highly cellular areas suggesting that maspin needs cellular contact to be expressed. Although the well-recognized cytological uniformity it seems that there is possibly less differentiated cell in PLGA which does not express maspin. In salivary gland, maspin is not exclusive of cells with myoepithelial differentiation.

P 561
IN SITU HYBRIDIZATION SIGNALING OF HOXA7 AND TGIF TRANSCRIPTS IN ORAL SQUAMOUS CELL CARCINOMA.

MATIZONKAS-ANTONIO Luciana Fasanella*, ACQUAFREDA Thaís*, SILVA-VALENZUELA Maria das Graças*, LIBÓRIO Tatiana Nayara*, SPENER Roberta*, MICHALUARTE Pedro**, NUNES Fabio Daumas*.
* School of Dentistry, University of São Paulo, Brazil.

** Hospital das Clínicas of São Paulo, Brazil.

Oral cancer is one of the most frequent cancers worldwide. Although different types of cancers can affect the oral cavity, approximately 90% are squamous cell carcinoma (OSCC). The literature shows an extensive search for biomarkers which could predict OSCC behavior. Homeobox genes comprise a family of developmental regulators that are vital for several aspects of growth and differentiation. Recent studies demonstrated genetic alterations in homeobox genes or its expression in many cancers including homeobox HOXA7 and TGIF. HOXA7 may act as a repressor of transcription and down-regulates multiple differentiation specific genes during keratinocyte proliferation. HOXA7 was correlated with leukemia, epithelial ovarian tumors and mouse skin carcinoma. TGIF encodes a protein that is a transcription regulator. TGIF amplification and over-expression was observed in esophageal SCC. The involvement of HOXA7 and TGIF in OSCC has not been demonstrated yet. The purpose of this study was to verify the presence of HOXA7 and TGIF transcripts in OSCC and adjacent non-tumoral tissues (NT), and to see if there is a relation with the cells morphology. Biopsy specimens of OSCC were obtained from Hospital das Clínicas of São Paulo, Brazil. Samples of NT and OSCC tissues were collected and divided in two parts. One half was used for RNA extraction and transcripts amplification by RT-PCR. The other half was submitted to in situ hybridization (ISH) with sense and antisense digoxigenin labelled riboprobes on frozen tissues sections placed in silanized slides. Amplification of HOXA7 was seen in 72.73% of cases, 13.64% only in NT tissues, 40.91% only in OSCC samples and 18.18% in both tissues. TGIF was amplified in 81.81% of cases, 4.54% only in NT tissues, 18.18% only in OSCC samples and 59.09% in both tissues. ISH signal was similar for both transcripts, but more intense for TGIF. In NT tissues there was an intense expression in the epithelium, either in basal and suprabasal layers or disperse and more intense in the spinous layer. In OSCC transcripts were localized in all tumoral cells, but in poorly differentiated areas the signal was less intense and in a few cases it was negative. These results show that OSCC express HOXA7 and TGIF transcripts, mostly in well differentiated regions, suggesting a participation of these genes in OSCC development or progression.

P 562

ORAL SQUAMOUS CELL CARCINOMA: AN IMMUNOHISTOCHEMISTRY COMPARATIVE STUDY BETWEEN THE TUMOR AND THE PERILESIONAL MUCOSA

Lucinei Roberto de Oliveira
Alfredo Ribeiro-Silva
Leandra Náira Zambelli Ramalho
Sérgio Zucoloto
Department of Pathology, Faculty of Medicine of Ribeirão Preto, University of São Paulo, Brazil

Oral squamous cell carcinoma (OSCC) is the most frequent malignant neoplasm of the head and neck region. Conversion of normal cells to cancer cells is achieved through a multi-step process that is closely associated with the accumulation of multiple gene changes including both oncogenes and tumour suppressor genes. This work aims to study the relationship between the immunoprofile of the OSCC and the corresponding perilesional normal tissue.
Immunohistochemistry with the antibodies p53, p63, p16, p21, p27, Ki-67, cyclin D1, BAG-1, matrix metalloproteinase 1 (MMP-1), MMP-2, CD34, vascular endothelial growth factor (VEGF), Checkpoint kinase 2 (CHK2), telomerase, epithelial growth factor receptor (EGFR), c-erbB-2, c-erbB-3, and Bcl-2 was performed in a formalin-fixed paraffin-embedded sample of human OSCC and the adjacent non tumoral mucosa. The immunostaining was evaluated as negative (-), weak to moderate/focal (+), or strong/diffuse (++). In the perilesional mucosa there was no reaction for CD34, EGFR, c-erbB-2, c-erbB-3, VEGF, Bcl-2, p21, p16, MMP-1 e MMP-2. The positivity for cyclin D1, BAG-1, p53 e CHK2 was graded as + while the positivity for Ki-67, p27, telomerase, and p63 was graded as ++. The carcinoma was negative for BAG-1, CD34, c-erbB-2, c-erbB-3, Bcl-2, p16, MMP-1, and MMP-2. None markers in carcinoma were classified as +. The positivity for Ki-67, cyclin D1, p21, p27, p53, p63, telomerase, EGFR, VEGF e CHK2 was graded as ++. These data indicate that the expression of p53, p21, EGF, VEGF, CHK2, BAG-1 e cyclin D1 changed from perilesional mucosa to the carcinoma. P21, p53 and CHK2 modulate multiple cellular functions, such as gene transcription, DNA synthesis and repair, cell cycle arrest, senescence and apoptosis. Mutations in these genes can abrogate their functions, leading to genetic instability and progression to cancer. Cyclin D1 overexpression plays a role in the carcinogenesis. BAG-1 has an anti-apoptotic effect, so its downexpression is a stimulus for the cellular proliferation. EGFR is a transmembrane protein, which is implicated in the progression of many epithelial cancer types. VEGF play a critical role in cancer progression by promoting new blood vessel formation. A better understanding of the molecular biology involved in the progression of OSSC is essential for new therapeutic approaches.

P 563

SQUAMOUS CELL CARCINOMA OF THE SUPRAGLOTTIC LARYNX.SURVIVAL RATE-FIVE YEAR STUDY

Slavisa A.Jancic,Milan Mijailovic,Ivana Lj.Maric,Snezana Jancic
Oncology Clinic,University Medical School-Nis,Serbia and Montenegro
Pathology Clinic,University Medical School-Kragujevac,Serbia and Montenegro
Radiology diagnostic Center-KC Kragujevac,Serbia and Montenegro

Having in mind dissimilarity of scientific reports regarding the survival rate the patients with squamous cell carcinoma of the supraglottic region,the aim of our research was to present our 5 year experiance in radiotherapy of this neoplasm.
Our study includes 171 patients with squamous cell carcinoma of the supraglottic larynx with various degree of the pathohistological differenciation and stage of illness(T1-T4).
Patients iradiated after surgical treatment from 1994-1998 have been analised at the Oncology Clinic University Medical School-Nis.Megavoltage therapy with x-rays of 10 MEV and electrontherapy of 6-14 MEV were utilized for the radiotherapy treatments.
In the group of patients iradiated after surgical treatment 3 years survival rate vary from 100%-12,5%,depending on the illness stage.In the same group of patients 5 years survival rate was recorded within 80%-12,5% cases.
Patients who were radicaly iradiated(iradiation alone)have had 3 years survival rate,recorded among 64%-8% and 5 years survival rate among 57%-4%.
The study discuss the influence of degree of tumor differentiation on the choise of the radiotherapy plan and the effects of side factors on radiotherapy (in)efficiency.

P 564

LYMPHANGIOGENESIS IN HEAD AND NECK SQUAMOUS CELL CARCINOMA: EVIDENCE AND PROGNOSTIC IMPLICATIONS.

Panayiotis A. Kyzas1, Silvana Geleff 2,3, Anna Batistatou1,4, Niki J Agnantis1,5 Dimitrios Stefanou1,3.

1: Department of Pathology, University of Ioannina, Medical School, Ioannina, Greece.
2: Department of Pathology, Vienna Medical University, Vienna, Austria
3: Associate Professor
4: Assistant Professor
5: Professor

ABSTRACT
Purpose: Exploring the mechanisms of tumor lymphangiogenesis is necessary for understanding the metastatic behavior of epithelial neoplasms. The aim of this study was to investigate this phenomenon in head and neck squamous cell carcinoma (HNSCC) and address its possible clinical implications.
Methods: We examined 81 tissue specimens of patients with HNSCC using immunostaining for the specific lymphatic endothelium marker podoplanin. We assessed intratumoral lymphatic density (ILD) and peritumoral lymphatic density (PLD). We also quantified lymphatic invasion and examined the possible associations of all the above parameters with clinicopathological features and outcome. Finally, we used double staining with podoplanin and the cell proliferation marker ki-67 in order to evaluate intratumoral lymphangiogenesis.
Results: Both high ILD and high PLD were significantly associated with the presence of lymph node metastasis at the time of diagnosis ($p<0.001$ and $p=0.007$ respectively). We also noticed a significant correlation between ILD and lymphatic invasion. Patients with higher ILD exhibited shorter overall survival (OS, log rank $p<0.001$), whilst PLD had no influence on outcome. The correlation remained significant after multivariate analysis (Cox $p=0.04$) indicating that ILD is an independent prognostic factor for OS. Double staining revealed the existence of proliferating intratumoral lymphatics, in which tumor emboli were occasionally observed.
Conclusions: The above results indicate that lymphangiogenesis indeed occurs in HNSCC; that newly formed vessels are targets of invasion by cancer cells; and that ILD might be used as a criterion to separate patients at higher risk.

P 565
PROGNOSTIC FACTORS FOR SQUAMOUS CELL CARCINOMA IN ORAL CAVITY WITH EMPHASIS ON P53 PROTEIN EVALUATION

TADIC LATINOVIC LJiljana 1, ERI Zivka 2, KLEM Istvan 2, JANICIC Dusan 3
1 Department of Pathology, Clinical Center Banja Luka, Bosnia and Herzegovina
2 Institute of Pulmonary Diseases, Sremska Kamenica, Serbia and Montenegro
3Department of Thoracic Surgery, Clinical Center Banja Luka Serbia and Montenegro

INTRODUCTION An alteration in the p53 tumor suppressor gene is the most frequent genetic abnormality in human cancers. The aim of the present study was to evaluate the overexpression of p53 protein, histological grade, stage of the disease and tobacco habit in oral squamous carcinomas in order to relate them with progression and prognosis of these tumors.
MATERIAL AND METHODS Primary tumors were studied on a series of 30 patients. Immunohistochemystry has been applied on paraffin sections of oral squamous carcinomas using DO7 antibody.
RESULTS Overexpression of the p53 protein has been found in 40% of patients. Overexpression of the p53 protein has been correlated with histological grade of the tumor (p¡Ü0,1) and lymph node metastases (p¡Ü0,05). Overexpression of p53 protein in well differentiated carcinomas (33,3%) was significantly higher than in poorly differentiated tumors (0%). Relaps of the disease and stage of the TNM has been correlated with prognosis in patients with this tumor. The higher TNM stage correlates with shorter survival of patients (p¡Ü0,05). No significant correlations were found between overexpression of p53 protein with stage of disease, tobacco habit and survival of patients.
CONCLUSIONS Study showed that immunohistochemical examination of p53 has no prognostic significance in oral squamous carcinomas. Overexpression of p53 protein correlates with histological grade and lymph node metastases.

P 566
HEAD AND NECK SQUAMOUS CELL CARCINOMAS (HNSCC): EPIDERMAL GROWTH FACTOR RECEPTOR (EGFR) PROTEIN EXPRESSION AND EGFR GENE COPY NUMBERS

MRHALOVA Marcela*, PLZAK Jan**, BETKA Jan**, KODET Roman*
* Department of Pathology and Molecular Medicine, 2nd Faculty of Medicine, Charles University in Prague, V Uvalu 84, Prague 5 – Motol, 150 06, Czech Republic
** Department of Otorhinolaryngology and Head and Neck Surgery, 1st Faculty of Medicine, Charles University in Prague, V Uvalu 84, Prague 5 – Motol, 150 06, Czech Republic

INTRODUCTION: EGFR protein is expressed on membranes of squamous cells and it is overexpressed in HNSCC. The protein is coded by EGFR gene at 7p12. An antibody against the EGFR protein (cetuximab) may be used therapeutically in patients overexpressing the protein. PURPOSE OF THE STUDY: To introduce the treatment with cetuximab it may be important to establish the extent and type of the EGFR protein expression, and to find out whether the overexpression of the EGFR protein is caused by the EGFR gene amplification and/or by increased copy numbers of chromosome 7 or not. METHODS: We used tissue sections from 33 patients with HNSCC. The EGFR protein expression was tested immunohistochemically (IHC) using EGFR pharmDx (DakoCytomation). FISH to determine EGFR gene and chromosome 7 copy numbers (Abbott/Vysis) was applied. SUMMARY OF THE RESULTS: We found the EGFR protein expression in 31 of 33 patients. The EGFR protein expression had a variable pattern. In one case there were only scattered positive individual tumor cells. In 12 cases we found a variable intensity of the expression in the tumor cells (from 1+ to 3+). In 5 cases the tumor cells were 3+ positive at the periphery of the tumor nests. In 13 cases all tumor cells overexpressed the EGFR protein strongly (3+). The investigation of the EGFR gene revealed its amplification in 7 of 33 patients. The amplification was present in up to 50% of the tumor cells in an individual patient (median 33%). Increased numbers of chromosome 7 centromere signals were found in 23 of 33 patients. We did not find any correlation between the subtypes of the EGFR protein expression and amplification of the EGFR gene and/or increased copy numbers of chromosome 7. CONCLUSION: In patients with HNSCC the overexpression of the EGFR protein was found in a significant number of cases. This phenomenon is not caused by the EGFR gene amplification or by increased numbers of chromosome 7. Hence, the evaluation of the EGFR gene copy number and the number of chromosome 7 signals does not contribute to the decision whether to put these patients on cetuximab treatment or not. The evaluation of the EGFR protein expression by IHC testing appears satisfactory for this purpose. The type of the EGFR protein expression should be taken into consideration when evaluating the responsiveness of patients treated with cetuximab in future studies. Research Project FNM MZO 00064203

P 567
EXPRESSION OF C-ERBB-2 IN LARYNGEAL CARCINOMAS OF MALAYSIAN PATIENTS
HAFIZA A, SITI-AISHAH M.A, HARISFAZAL M.B, CLARENCE-KO C.H, JULIA M.I, EZANEE-AZLINA M.H,SHARIFAH N.A, ABDULLAH-SANI M.

Introduction: The c-erbB-2 (HER-2/neu)oncogene encodes for a 185-KD cell-membrane glycoprotein receptor sharing homologies with growth factor receptor. Overexpression of c-erbB-2 protein is a frequent and prognostically relevant event in a variety of human cancers. The aim of this study was to evaluate c-erbB-2 expression in laryngeal lesions and correlate the carcinomas with other available clinicopathological parameters.
Materials & Methods: We examined a total of 89 cases consisting of 47 cases of carcinomas (median 64.0; range 47-79 years), 10 papillomas, and 21 nodules or polyps diagnosed between 1995 and 2003 in Hospital Universiti Kebangsaan Malaysia. The specimens were obtained by laryngectomy or biopsies. Cases of the laryngeal carcinomas (44,[93.6%]males) included 45 squamous cell carcinomas (SCC), 1 sarcomatoid carcinoma and 1 spindle cell carcinoma. Immunohistochemistry was performed in 89 formalin-fixed, paraffin-embedded specimens using c-erbB-2 protein (DAKO A0485,1:300) by the streptavidin-biotin method. Membrane c-erbB-2 immunostaining was used and scoring was according to standard criteria, 0,1+,2+or3+. In addition, the 2+ case was evaluated using fluorescent in-situ hybridization (FISH) for HER-2 gene amplification. Clinical information was obtained from the medical records.
Results:Of the 89 patients, only 1(1.1%)case of SCC was c-erbB-2 protein-positive (2+) while the rest of the specimens were negative. This positive case showed gene amplification for HER-2. Clinical follow-up information was available for 35 patients, ranging from 2 months to 77 months (mean 31.2 months). Five (15.6%) of these patients died of the disease. There was no correlation between c-erbB-2 expression with histopathological grade of differentiation of laryngeal carcinoma, age, sex, lymph node metastases and stage of the patients.
Conclusion:c-erbB-2 protein is rarely expressed in laryngeal lesions and may not play a prominent role in laryngeal carcinomas.

P 568
LOCALIZATION OF PMX1 TRANSCRIPTS IN ORAL SQUAMOUS CELL CARCINOMA BY IN SITU HYBRIDIZATION.
ACQUAFREDA Thaís, MATIZONKAS-ANTONIO Luciana Fasanella, SILVA-VALENZUELA Maria das Graças, LIBÓRIO Tatiana Nayara, FERRAZ Alberto, NUNES Fabio Daumas

Oral squamous cell carcinoma (OSCC) is the most frequent cancer of the oral cavity being responsible for 95% of all oral malignancies and is the eighth most common cancer worldwide. Several studies have demonstrated that cancer and development share common features since both exhibit shifts between cell proliferation and differentiation. The homeobox gene family is responsible for encoding transcriptional factors during development bringing our attention for its potential role during carcinogenesis. Paired Mesoderm Homeobox 1 (PMX1, PRX1 or PHOX1) is a non-clustered homeobox gene and as all other members of this family has a homeodomain motif which is responsible for DNA binding. This gene has been related with mesenchyma throughout development such cardiovascular system and skeletal elements. The relation between PMX1 and tumor is not well established yet. The purpose of this study was to verify the presence of PMX1 transcripts in OSCC and adjacent non-tumoral tissues. For such study, tissues were obtained from Hospital das Clínicas (HCFMUSP), with patients' agreement, and divided in two halves. One was used for RNA extraction and transcripts amplification by RT-PCR. Sense and antisense probes were generated by in vitro transcription and labeled with non-radioactive digoxigenin. The other part was fixed in 4% paraformaldehyde, treated with 1X PBS and 30% sucrose before freezing. For in situ hybridization (ISH), serial sections were placed in silanized slides. In the adjacent non-tumoral tissues ISH signaling were detected at the basal and parabasal layers. In the OSCC the signaling was spread all over the tissue becoming more intense in areas with isolated carcinoma cells. Our findings suggest a participation of PMX1 in oral carcinogenesis and its expression in poorly differentiated carcinomas is being analyzed in detail. It is known that PMX1 is mainly expressed in mesenchyme and it is responsible for the maintenance of appropriate level of gene expression in the epithelium. For the first time PMX1 transcripts are detected in oral epithelium and in oral squamous cell carcinoma.

P 569
CORRELATION OF TSG101 AND E-CADHERIN EXPRESSIONS WITH TUMOR BEHAVIOR AMONG SUQAMOUS CELL CARCINOMA OF HEAD AND NECK
Chao-Cheng Huang, Chih-Yen Chien, Ching-Mei Chen, Chih-Ying Su, Chung-Feng Hwang, Jiin-Tsuey Cheng
Departments of Pathology and Otolaryngology, Chang Gung Memorial Hospital at Kaohsiung, Taiwan; Chang Gung University School of Medicine, Taiwan; Department of Biological Sciences, National Sun Yat-Sen University, Taiwan.

Tumor susceptibility gene TSG101 plays an important role to maintain genomic stability and cell cycle regulation. Aberrant expression of TSG101 has been associated with tumorigenesis in some carcinomas. Down regulation of E-cadherin has been known to be related to tumor invasion and metastasis. To study the clinical significance of TSG101 and E-cadherin expression among squamous cell carcinoma of head and neck, we retrospectively performed the immunohistochemical study on the surgical specimens of suqamous cell carcinoma among head and neck region from 65 patients who had received primary surgical treatment from 1986 to 1997. In the mean time, we used TSG101 antisense probe to study mRNA expression of these tumors by in situ hybridization. We found that TSG101 together with E-cadherin homogenously expressed over the suprabasal, granular and cornified layers but not the basal layer among the normal squamous epithelium and the well differentiated squamous cell carcinomas. The expression of TSG101 significantly correlated with that of E-cadherin ($p<0.001$). Besides, down regulation of either TSG101 or E-cadherin expression among tumor cells was significantly associated with poor differentiation of the tumor ($p<0.001$). Moreover, both TSG101 and E-cadherin expression significantly correlated with nodal status ($p<0.001$) but not tumor stage. The mRNA expression detected by in situ hybridization well correlated with protein expression by the immunohistochemical study. In conclusion, studies on TSG101 and E-cadherin expressions among squamous cell carcinoma of head and neck may be useful for the evaluation of the tumor differentiation and the risk of nodal metastasis. Further study on the close relationship between TSG101 and E-cadherin expressions in squamous cell carcinoma would be of interest and would potentially disclose their role to control cell differentiation and behavior.

P 570
B-CATENIN/CYCLIN D1 PATHWAY IS CRUCIAL FOR ORAL SQUAMOUS CELL CARCINOMA

GROWTH AND SUSCEPTIBLE TO WORTMANNIN ACTION

SALES Katiuchia Uzzun, ALVES Jr. Sergio Melo, SALLES Felipe Torquato, PINTO Jr. Decio Santos

B-catenin and cyclin D1 are crucial proteins related to tumor proliferation and progression. The complex composed by free cytoplasmic b-catenin and transcription factor LEF/TCF migrates to nucleus, activating several target genes such as cyclin D1. In order to evaluate possible correlations between b-catenin and cyclin D1 in oral squamous cell carcinoma (OSCC), the expression of these proteins was analyzed by immunohistochemistry on tissue sections and in OSCC cells lines treated with 2nM wortmannin for 10min. Protein expression was assessed in five cell lineages, HN6, HN19, HN30, HN31 and HaCat as control keratinocytes, analyzed by immunofluorescence and western-blot. Immunohistochemical results showed a strong correlation between cyclin D1 overexpression and b-catenin cytosolic and/or nuclear presence. No significant alterations in b-catenin expression in treated and control cells were observed by immunofluorescence. Wortmannin promoted cyclin D1 fast relocation to the cytosol. Western blot analysis confirmed the decrease of cyclin D1 levels after wortmannin treatment. This last molecule is able to simulate the PTEN pathway, blocking PI3K and consequent activation of proliferation pathways. Taken together, these results point out the crucial role that b-catenin/cyclin D1 and PTEN pathways might play together in OSCC, and may provide the development of more effective therapeutical approaches regarding this frequent neoplasm.

P 571

PSEUDOVASCULAR ADENOID SQUAMOUS CELL CARCINOMA OF THE ORAL CAVITY

ZIDAR Nina, GALE Nina
Institute of Pathology, Medical Faculty, University of Ljubljana, Ljubljana, Slovenia

Pseudovascular adenoid squamous cell carcinoma (PASCC) is an uncommon histopathologic variant of squamous cell carcinoma characterised by acantholysis of the tumour cells, creating anastomosing spaces and channels, thus mimicking an angiosarcoma. PASCC has been reported in the skin of the head and neck as well as in other organs, such as the breast, lungs, vulva, uterine cervix and urinary bladder. It has been suggested that PASCC has a more aggressive behaviour and a worse prognosis than conventional squamous cell carcinoma, but the number of patients reported so far is too small to draw firm conclusions.

We report two cases of PASCC in the oral cavity. One occurred on the buccal mucosa in a 59-year-old man who was a heavy smoker but denied alcohol abuse. The other occurred on the floor of the mouth in a 79-year-old woman who denied smoking and alcohol abuse. In both patients, radical tumour excision and neck dissection were performed. The bulk of both tumours was histologically consistent with PASCC, and contained foci of squamous cell carcinoma suggesting the correct diagnosis. In one patient, they consisted of conventional squamous cell carcinoma, and in the other, they consisted of a spindle cell carcinoma. Immunohistochemically, the tumour cells expressed keratin and vimentin; they did not express CD31 and the vast majority of the tumour cells did not express E-cadherin. Both patients had no metastases at the time of diagnosis, and are alive and well 2 years later.

Pathogenesis of PASCC is not completely understood. It has been suggested that acantholysis is the underlying pathogenetic mechanism. Consistent with this suggestion, we observed in our cases loss of immunohistochemical expression of E-cadherin, one of the major adhesion molecules of epithelial cells. E-cadherin was expressed only in areas of both tumours which exhibited the morphology of conventional squamous cell carcinoma or spindle cell carcinoma. We speculate that loss of E-cadherin expression might lead to the loss of the tumour cell-cell adhesion and acantholysis characteristic for this particular type of squamous cell carcinoma.

In conclusion, eventhough the prognostic significance of PASCC in the head and neck is at present unknown, its recognition is important because it may mimic angiosarcoma which may result in erroneous treatment. The study of our two cases suggest that PASCC might be pathogenetically related to the loss of E-cadherin expression.

P 572

LARYNGEAL SQUAMOUS CELL CARCINOMAS AND THEIR LYMPH NODES METASTASES COMPARED BY MULTIVARIATE STATISTICAL ANALYSIS OF DIFFERENT HISTOLOGICAL AND IMMUNOHISTOCHEMICAL PARAMETERS – RAISING THE QUESTION OF THEIR PRACTICAL VALUE.

GEORGIU Carmen*, GEORGIU A.**, OLINICI C.D.*
* Department of Pathology – University of Medicine and Pharmacy "Iuliu Hatieganu" Cluj Napoca, Romania
** Individual Medical Center 81, Cluj Napoca, Romania

Aims. Some of the histological and immunohistochemical parameters of laryngeal squamous cell carcinomas are frequently quantified for each patient but some of them raise more and more the question of their practical value in the prognostic and treatment of the patients.

Methods. A number of 40 primary tumors of squamous laryngeal carcinomas with and without lymph nodes metastases (20 cases of each one) were investigated by different histological and immunohistochemical parameters: grade of differentiation - G OMS, morphometric grade - MG (the percentage of suprabasal keratinocytic cells versus spinous and fully differentiated keratinocytes), type of tumor cells cohesion at the invasion front - IF, mitotic index corrected per volume - M/V (volume of tumor occupied by tumor cells and not connective tissue), MIB-1 proliferation index (percentage of MIB-1 positive tumor cells), p53 index, microvascular density index - MVD (the number of CD-31 positive microvascular endothelial cells) and the grade of peritumoral inflammatory infiltrate - ii. Results. The multivariate statistical analysis of these parameters suggests that the more elevated metastasizing potential have the tumors with the combination of high MIB-1, IF, M/V, MG, ii and G OMS. The most important indicators were the number of cells in cell cycle and the lack of cohesion between the tumors cells at the invasion front (both were three times higher than in the tumors without metastases). The MG was more important than G OMS suggesting that the differentiation pattern of tumor cells (number of spinous cells and the keratin production) may overshadow the real proliferating suprabasal keratinocytes. The p53 index did not affect the process of metastasis but the cells selected in this process were those with high p53 index (in the lymph nodes the p53 index was much higher than in the primary tumors). The high MVD influenced the metastasis, but MVD had much lower values in the lymph nodes than in the primary tumors. The metastasizing potential depends on the neoangiogenesis by the propensity of the tumor cells to create their minimal new ecosystem in the lymph nodes and not for other reasons.

P 573

MOLECULAR TARGETS FOR THERAPY IN PRENEOPLASTIC AND NEOPLASTIC LESIONS OF OROPHARYNX AND LARYNX

IOSIF Cristina Ileana 1, VASILESCU Florina 1, DOBREA Camelia 1, ANDREI Florin 1, BUTUR Georgeta 1, CEAUSU Mihai 1, MIHAI Mihaela 1, ARDELEANU Carmen 1, SARAFOLEANU Codrut 2.

1 Victor Babes National Institute of Pathology, Bucharest, Romania
2 "St Mary" Hospital, Bucharest, Romania

Introduction: EGFR, COX-2 and cerbB2 are known as molecular targets for antitumoral and antiangiogenic therapy. The aim of our study was to evaluate by immunohistochemical(IHC) method the expression of EGFR, COX2, and cerbB2 in preneoplastic and neoplastic lesions of larynx and oropharynx.
Materials and methods: We performed an IHC study on 30 biopsies from patients with preneoplastic and neoplastic lesions of the larynx and 20 squamous cell carcinomas of the oropharynx (ABC tristadial IHC method; EGFR from SIGMA-USA, COX-2 from Novocastra, cerbB2 from DAKO)
Results: In larynx neoplastic lesions we found EGFR expression in small vessels at the invasion front of the tumor, and lack of positivity in neoplastic cells; in premalignant lesions of the larynx EGFR expression decrease with the degree of dysplasia; the same expression we found for COX-2; for cerbB2 the positivity was inconstant; in neoplastic lesions of oropharynx we founded positive correlation between the expression of EGFR and COX-2; for cerbB2 the expression was focal and inconstant
We concluded that EGFR and COX-2 could be considered as valuable targets for antitumoral therapies in preneoplastic and neoplastic lesions of larynx and oropharynx; cerbB2 is expressed but require further investigation.

P 574
RETINOBLASTOMA GENE AND PROTEIN EXPRESSION IN EVALUATION OF LARYNGEAL SQUAMOUS CELL CARCINOMA*

PIETRUSZEWSKA Wioletta (1), KOBOS Jozef (2), GRYCZYNSKI Maciej (1)
(1) Department of Otolaryngology, Barlicki University Hospital, Medical University of Lodz
(2) Department of Pathology, Medical university of Lodz

The identification of possible genetic alternations in cancer involves inactivation of tumor suppressor genes or activation of proto-oncogenes. In cell cycle, most of the regulatory actions occur at the so-called restriction point (R) in the late G1 phase. Tumor suppressor genes; Rb, p53 and p21 are among the most important of the agents suppressing transition through R point. Changes in the expression of Rb (retinoblastoma) gene which is localizated in 13q14, correlate with the presence of Rb protein and they are believed to be an early event in carcinogenesis. This issue seems to be not plainly defined in laryngeal cancer. Our purpose was to investigate 13q14 LOH and expression of Rb protein and their possible prognostic value in laryngeal cancer. Surgical specimens were obtained from 41 patients with 5-year time observation who underwent surgical treatment at the Department of Otolaryngology Medical University of Lodz. Paraffin-embedded tissue sections were immunohistochemically stained with a monoclonal antibody raised against Rb protein. PCR-based techniques were used for investigating 13q14 LOH. The products of PCR reaction were fractionated on acrylamide gel. There were assessed correlation between the expression of Rb gene and Rb protein presence and clinical and histological implications (patients age, localisation of tumour origin, tumour size and nodal status based on TNM system, local and nodal recurrences, overall and disease free survival rate after surgical treatment and histological grading). Based on this findings it can be deduced that investigation of Rb gene expression and its protein product makes it easier to understand the process of cancerogenesis in laryngeal cancer and to establish its prognostic value further research and observations need to be attempted.

*This study was supported by grant No 502-11-132 from Medical University of Lodz

P 575
THE EXPRESSION OF P53 PROTEIN AND HUMAN PAPILLOMAVIRUS INFECTION IN CONJUNCTIVAL AND EYELID BENIGN AND MALIGNANT LESIONS

RESZEC Joanna, KODA Mariusz, SULKOWSKA Mariola, KANCZUGA-KODA Luiza,SULKOWSKI Stanislaw
Department of Pathology, Medical University of Bialystok, Waszyngtona 13, 15-269 Bialystok, Poland

Purpose: Squamous cell papillomas of eyelid and conjunctiva are common benign neoplasm of ophthalmological interest. Squamous cell and basal cell carcinomas are respectively the most common malignancy of conjunctiva and eyelid skin. Human Papillomavirus (HPV) infection as well as P53 protein function lost has been identified as frequent events in varies of human tumors.
The aim of our study was the evaluation of P53 protein expression and HPV infection in 45 benign (papillomas) and 38 malignant conjunctival and eyelid lesions (27 cases of basal cell carcinomas and 11 cases of squamous cell carcinomas).
Methods: Using monoclonal antibody for P53 protein (DAKO) performed the immunohistochemical reaction; LSAB technique and DAB detect the complex antigen-antibody. To detect HPV infection PCR-RFLP technique was performed, using specific set of primers (TaKaRa) and for identification of HPV types 16,18, 33 the PCR products were enzymatic digested at 37¢ªC.
Results: P53 protein expression was observed in 30 out of 45 (66,6%) squamous cell papillomas. In SCC and BCC groups P53 positivity was noticed in 31 out of 38 carcinomas and there was a statistically significant correlation between histological type of tumor and P53 protein expression. Malignant type HPV 16 and HPV 18 were detected in 3 squamous cell papillomas, 2 cases of BCC and 1 of SCC. However we observed P53 protein expression only in 2 HPV positive papillomas and 1 infiltrative type of BCC.
Conclusions: The results suggested P53 protein role in development of conjunctival and eyelid tumors, however the role of P53 protein in malignant transformation should be carefully investigated in the future. HPV seems to occur rarely, although in some cases it¡¯s role in pathogenesis of conjunctival and eyelid tumorigenesis should be considered.

P 576
STUDY OF KIT (CD 117) EXPRESSION IN PRIMARY UVEAL MELANOMAS AND METASTASES OF UVEAL MELANOMAS.

Lichvansceva V.G, Anurova O.A, Vereschagina M.V.

Nevertheless, uveal melanoma (UM) rate is about 1% of all human cancers, UM mortality rate is about 18% from dissemination. Comparison of these indexes let us think that UM is most malignant tumor. In the recent years with the help of immunohistochemistry it was achieved a great progress in investigation of tumor progression mechanisms. The KIT-gene encodes proto-oncogene c-kit, that has tyrosine kinase activity. Mutation in any exones of c-kit gene in tumor cells activates oncogene and stimulates production of mutant protein KIT in the lack of ligand. The result of all these mutatins is activation of mitotic activity of cells and tumor progression. Hyper expression of CD 117 detected in UM is the way of application of inhibitors of tyrosine kinases in the treatment of these tumors.

Purpose: To study CD 117expression in primary uveal melanomas and metastases of UM.

Materials and methods: Expression of c-kit was analysed in 39 paraffin-embedded sections of primary UM and 4 paraffin-embedded sections of UM metastases. Immunohistochemistry

was performed using the polyclonal anti-CD117 antibody from Dako.

Results: Immunohistochemistry for CD 117 was negative in 6 cases (15%), weakly positive in 11 cases (28%), moderately positive in 10 cases (26%) and strongly positive in 12 cases (31%) of primary UM. In 4 metastases (100%) of UM the reaction for CD 117 was strongly positive.

Conclusion: It appears justified to investigate the utility of imatinib mesylate in the treatment of these patients in clinical researches.

P 577

CENTRAL FACIAL DESTRUCTIVE GRANULOMA FOLLOWING COCAINE ABUSE

PAGLIARI Angelo Virgilio°,Klinger Francesco *, Klinger Marco *
° U.O.ORL Azienda Ospedaliera di Crema
* Istituto di Chirurgia Plastica e Ricostruttiva Università degli Studi di Milano-I.C.Humanintas

Introduction The use and consuption of cocaina by snorting and sniffing exploded into a full blown epidemic. The adverse effects of cocaine nasal passages have long been recognized. Only recently a cocaine complex mimicking the rare condition of massive facial midline necrosis is described.
Methods Four patients referred to us with extensive necrotizing lesions of naso-sinusal tract and midface are described. Diagnostic and treatment are discussed with a literature review.
Results On physiacal examination all patients had a severe crusting, granulation tissue, purulent discharge and necrosis of nasal septum, lateral cartilages and hard palate. None other medical conditions were associated. Biopsies of nasal tissue revealed chronic inflammation without evidence of vasculitis or granulomatosis. There were onion skin deposits of perivascular fibrosis with numerous eosinophils. Plasma cells and lymphocytes primary T cells were present.
Conclusion Massive facial midline necrosis continues to be a diagnostic challenge. The aetiology comprises autoimmune disorders and certain tropical diseases. We underlines as a possible cause the cocaine abuse. Ischemic necrosis due to vasoconstriction and prolonged anaesthesia may be factors causing tissue destruction.

P 578

A CASE OF : NASAL GLIAL HETEROTOPIA

JOSSELIN Nicolas(1), LACCOUREYE Laurent (2), DUBIN Jacques (2), TRIAU Stéphane (1), ROUSSELET Marie-Christine (1)
(1)Department of pathology
(2)Department of otorhinolaryngology
Hospital of Angers, 4 rue larrey- 49933 Angers

We observed a baby born at terms with an apgar of 10, presenting an inspiration dyspnea on its second day of life . Endoscopy discovered a tissular mass filling the right sinus. The imagery made favoured a teratoma.Under microscopy, areas of mature glial tissue of variable cellularity were embedded in the nasal mucous membrane. The cells of this cellularity, sometimes multi nucleic or of dystrophic aspect showed immunochemistry which varied depending on the areas of glial and neuron markers.There were not noticed numerous mitosis nor atypical cyto nuclears. The diagnosis of glial nose heterotopia was proposed.
Median congenital face malformations occur every 20000 to 40000 births. Among the most frequent, we note hemangioma, dermoid cysts, and encephaloceles. Nasal glial heterotopia is less frequent with only 250 cases observed. This pathology only concerns babies, mostly during the first month of life. After an asymptomatic period of time, the children had a weight loss which was due to alimentation problems because of nose obstruction. The location of 60 per cent of the lesions is extra nasal, 30 per cent of them is intra nasal and the remaining 10 per cent are mixed. They are probably due to confinement of an encephalocele during fœtal life which sometimes leaves a fibrous cord. Microscopically, these lesions are composed of glial tissue areas of variable cellularity made of non atypical and little proliferative astrocytes. A are association is that of a neuron component.
In presence of congenital median facial lesions, establishing diagnosis through biopsies is not indicated. Indeed in the case of encephaloceles this might open a (meningo) gap which could be responsible for a iatrogenic meningitis.
An MRA examining possible communication between intra cranial structures and lesions is compulsory before Therapeutic treatment. This consists presently of an endoscopy which avoids the complications of surgery needed by craniotomy.

P 579

CYTOGENETIC ANALYSIS OF ORAL LICHEN PLANUS

FARNEDI Anna, MAGRINI Elisabetta, PESSION Annalisa, **MONTEBUGNOLI Lucio, **MARCHETTI Claudio, FOSCHINI Maria P.
Department of Oncological Sciences, Section of Anatomic Pathology, University of Bologna.
** Department of Oral Sciences, University of Bologna.

Introduction: oral lichen planus (OL) is an inflammmatory lesion having controversial malignant potential, sometimes evolving to squamous cell carcinoma (SCC). SCC develops along a multistep pathway and thus accumulate genetic hits in functional targets relevant to tumour evolution. Recent studies suggest that chromosome instability increases with the degree of histologic changes from normal tissues to carcinomatous lesions. To date, there are no classic cytogenetic data on OL.
Purpose of the present study is to describe chromosomal alterations of a series of OL studied with classic cytogenetic technique.
Matherial and methods: fresh biopsies were divided in two specimens: one was formalin-fixed and paraffin embedded for histological and immunohistochemical analysis for p53 (DAKO, clone p53, diluted 1: 50) and Ki 67 (Dako, clone MIB-1, diluted 1:100) . The other was used for classic G-banding cytogenetic analysis on short term cultures.
20 cases having typical clinical and histological featuresof OL were obtained. No dysplasia was present in the lesions. Results were compared with 9 cases of normal gingival mucosa from tooth extraction.
On histology, all the cases showed OL typical inflammatory infiltration with basal membrane disruption, vacuolization and apoptosis of the basal cheratinocytes. Immunohistochemistry: p53 and Ki67 were expressed in 15 to 40% of basal and suprabasal cheratinocytes in OL, while they stained no more than 15% of basal cheratinocytes in normal gingival mucosa. Cytogenetic results: clonal alterations were found in 3/20 cases (gain of a chromosome 18 copy was present in two cases), while Non Clonal Alterations (NCA) were detected in14/20 cases. The most frequent NCA were: losses of chromosomes 21, 14, 9 and gains of chromosome 18. Alterations (i.e. gains and losses) involved also chromosomes 6 and 3. No clonal nor NCA alterations were found in cultures from normal gingival mucosa.
Discussion: present histological and immunohistochemical results show that, in cases of OL, oral mucosa shows a high proliferation activity. Cytogenetic analysis shows aneuploidy as the more frequent alteration, suggesting presence of chromosomal instability in these lesions. Althought we cannot identify, to date, the meaning of single gains or losses, we suggest that the chromosome instability in OL might indicate a risk of malignant transformation.

P 580

IMMUNOHISTOCHEMICAL ASSESMENT OF HEAT SHOCK PROTEIN 70 IN ADENOID TISSUE

AKTEPE Fatma*, SAHIN Onder*, DILEK Hüsniye.*, YILMAZ Deniz**, KAHVECI Orhan**, DEREKOY Sefa**
*Department of Pathology, **Department of Otolaryngology, University of Afyon Kocatepe, Faculty of Medicine, Afyon, Turkey.

Objectives: To evaluate the expression of heat shock protein 70 (HSP70) and its relation to histopathologic parameters in adenoid hyperthrophy. In addition, HSP70 expression in adenoid tissue was compared with in adult and childhood.
Materials and Methods: Parafin-embedded adenoid tissue sections were obtained from 17 childhood and 17 adult patients. Expression of HSP70 was evaluated by immunohistochemical staining using anti-HSP70 monoclonal antibody and correlated with histopathologic parameters.
Results: Positive HSP70 expression was observed mainly in the mucosal epithelium, lymphocytes in germinal centers, interfollicular lymphocytes, subepithelial plasma cells and vascular endothelium. HSP70 immunoreactivity in the metaplastic mucosal epithelium with severe intraepithelial lymphocytic infiltration was higher than in the respiratory epithelium. The decrease in plasma cells showing HSP70 positivity was corraleted with age.
Conclusions: These results suggest that intraepithelial lymphocytic infiltration is induce HSP70 expression in mucosal epithelium of adenoid.

P 581

SEVERITY OF EPITHELIAL DYSPLASIA IS ASSOCIATED WITH LOSS OF MASPIN EXPRESSION IN ACTINIC CHEILITIS

FONTES Alexandra, SOUSA Suzana, MARTINS Marília.

Introduction: Maspin is a member of the serpin superfamily of protease inhibitors and it is known to have tumour suppressor functions. It was demonstrated that maspin is expressed in normal cells, down-regulated in neoplastic cells and absent in metastatic cells. It was also inversely associated with increased dysplasia degree in mammary gland and gastric epithelium. Maspin is expressed in oral squamous cell carcinoma associated with a favourable prognosis. Actinic cheilitis is a potentially malignant lesion that is caused by long exposure to sunlight. Many authors consider that lip squamous cell carcinoma is always preceded by actinic cheilitis. Histologically this lesion is characterized by different degrees of epithelial dysplasia.
This study had the aim of evaluating the maspin expression in actinic cheilitis and comparing the findings to the degree of epithelial dysplasia.
Material and methods. Twenty nine cases histologically diagnosed as actinic cheilitis were retrieved from our files. The cases were represented by 13 cases with mild epithelial dysplasia, 9 moderate, and 7 intense dysplasia. The sections were submitted to the anti-maspin antibody (BD Pharmingen, 1:100) using the streptavidin-biotin method of immunohistochemistry. Immunostaining was semi-quantitatively evaluated and graduated: 0 (no staining), 1 (<5% of cells positive), 2 (5 to 50% of cells positive), 3 (<50% of cells positive).
Results: All the cases with mild dysplasia were graduated 3. In moderate dysplasia 2: 66.6% were graduated 2 and 33.3% received 3. All the cases with intense dysplasia were graduated 1. When the extent of staining was evaluated in the different epithelial layers, it was possible to notice that basal layer was abundantly stained only in 5 cases of mild epithelial dysplasia. In the other cases this layer showed scattered or no cells positive for maspin. In general, positivity in the layers decreased with the increase of atypias, from the basal to the surface.
Conclusions: Maspin expression was very abundant in actinic cheilitis with mild dysplasia and this expression decreased with the increase of the dysplasia degree. The first layer to lose maspin positivity was basal layer and successively upper layers lost positivity with the increased degree of dysplasia. In conclusion, this data suggests that in actinic cheilitis maspin expression is inversely related with progression of the lesion towards malignancy.

P 582

EFFECT OF IRON REPLETION AND CORRECTION OF IRON DEFICIENCY ON THYROID FUNCTION TESTS IN IRON-DEFICIENT IRANIAN ADOLESCENT GIRLS

Mohammad Hassan Eftekhari, Ph.D1, Mohammad Reza Eshraghian, Ph.D2,Mahmood Jalali, Ph.D3, Seyed Ali Keshavarz, Ph.D3, Navid Saadat, MD4, Fereidoun Seyasi, Ph.D3, Najmeh Moeenvaziri,GP5
1-Department of Nutrition, School of Public Health, Shiraz University of Medical Sciences
2-Department of Biostatistics, School of Public Health and Institute of Public Health Research, Tehran University of Medical Sciences
3-Department of Nutrition and Biochemistry, School of Public Health and Institute of Public Health Research, Tehran University of Medical Sciences
4-Endocrine Research Center, Shaheed Beheshti University of Medical Sciences
5-School of Medicine, Shiraz University of Medical Sciences

Study objective: To investigate whether iron supplementation can improve thyroid hormone function in iron-deficient adolescent girls.
Design: A double-blind intervention study.
Setting: The study was performed in 2002 through 2003 in a region in southern I.R.Iran.
Subjects: A total of 103 iron deficient subjects that fulfilled all of the inclusion criteria were chosen. In all 94 subjects successfully completed this study.
Interventions: Patients were randomly assigned to one of two groups and treated with a 300 mg ferrous sulfate 5 times/week (n=47) and placebo 5 times/week (n=47) for 12 weeks.
Main outcome measures: At the beginning and at the end of study blood samples were collected and assayed for hemoglobin, hematocrit, serum ferritin, iron, total iron binding capacity (TIBC), Thyroid stimulating hormone (TSH), total thyroxine (TT4), total triiodothyronine (TT3), free thyroid hormones (FT4 and FT3), triiodothyronine resin uptake (T3RU), reverse triiodothyronine (RT3), selenium and albumin concentrations.
Results: There was a significant increase in iron indices in iron treated group after intervention. Indices of thyroid at the end of study revealed a significant increase in TT4, TT3, T3RU, and a significant decrease in rT3 concentration in comparison to initial values in iron treated group, and a significant difference when compared to placebo group. Alterations in FT3 and TSH concentration were not significant, but concentration of FT4 revealed a significant difference between beginning and end of the study in iron treated group.
Conclusions: Our results indicate that improvement of iron status was accompanied with improve in some indices of thyroid hormones.

P 583

ANALYSIS OF PARAFOLLICULAR-C CELLS IN POLYNODOSE COLOID GOITRE OF THYROID GLAND

Ljiljana Vuckovic, Marija Havelka, Svetislav Tatic, Zivka Eri, Istvan Klem, Dragutin Savjak, Slavica Usaj Knezevic, Mileta Golubovic, Filip Vukmirovic, Tatjana Nenezic

INTRODUCTION: C cells of thyroid gland belong to a diffuse neuroendocrine system of the organism. There are different data in literature about usual normal number of C cells in thyorid gland. Colloid goitre is an after effect of an insufficient synthesis of thyorid hormones, and it results with assembling of great quantities of inactive colloid in follicules. Diameter of follicules becomes larger and due to the pressure, the height of follicular cells decreased. As the illnes progresses, the thyorid gland are enlarged at first diffusing and then due to the increase of connective tissue, a nodes is created.
PURPOSE: A connection between a number of C cells and height of follicular cells, size of follicules and quantity of colloid in polynodose colloid goitre of thyroid gland were analysed.
MATERIALS AND METHODS: There were analysed 96 polynodose colloid goitres, which were operated from year 2001 to 2004. The slides were fixed in formaldehyde and formed in paraffin blocks, and then they were colored with hematoxilin-eosin and immunohistochemical coloring on calcitonin.
RESULTES: The sample wes devided into groups, according to C cells and height of follicular cells, size of follicules and quantity of colloid, and all the resultes are semiquantitative. The results were statistically elaborated and they show high statistic significanse of C cells connection with height of follicular cells, although there is no significant connection between C cells and follicules size and quantity of colloid in observed sample.
DISCUSSION AND CONCLUSIONS: It is possible to conclude, according to the final data, there is a connection between C cells and height of follicular cells in polynodose colloid goitre of thyroid gland, but there is no connection with size of follicules and quantity of colloid.

P 584
CONCOMITANT USE OF FINE-NEEDLE BIOPSY AND LARGE-NEEDLE BIOPSY IN THE DIAGNOSIS OF THYROID NODULES
MIZUKAMI Yuji, *MICHIGISHI Takatoshi, TAKEMURA Akihiro, ONOGUCHI Masahisa, TAKAYAMA Teruhiko
Department of Radiological Technology, School of Health Sciences, *Department of Nuclear Medicine, Faculty of Medicine, Kanazawa University

Fine-needle asplration biopsy (FNA) and large-needle (cutting) biopsy (LNB) were performed on 109 patients with thyroid nodule or goiter who later underwent thyroidectomy. FNA alone provided a correct diagnosis in 84 (77%) of the 109 cases and LNB alone in 84 (77%) of the 109 cases, with the two methods yielding the same accuracy rate. Ninety-nine (91%) of the 109 cases were diagnosed correctly when both results were considered together. As to the causes for the discrepancies between the FNA or LNB results and the corresponding surglcal diagnoses, the most common one was cytologic interpretive errors and, in descending order, insufficient material and sampling errors in FNA. On the other hand, in LNB, histologic interpretive errors were less but sampling errors were more frequently found compared with FNA. The present study indicated a need to concomitantly perform FNA and LNB in the diagnosis of thyroid nodules. Careful attention is required to distinguish between the follicular variant of papillary carcinoma and follicular adenoma, between encapsulated follicular carcinoma and follicular adenoma, and between malignant lymphoma and chronic thyroiditis at FNA as well as LNB diagnosis.

P 585
COINCIDENCE OF HYPERPARATHYROIDISM AND THYROID CANCER FOUND AT THE TIME OF PARATHYROIDECTOMY
CEROVIC Snezana, IGNJATOVIC Mile*, BRAJUSKOVIC Goran, KNEZEVIC USAJ Slavica, HRVACEVIC Rajko**
Institute of Pathology, * Clinic of Surgery and ** Clinic of Nephrology, Military Medical Academy, Belgrade, Serbia and Montenegro

INTRODUCTION: A few reports have suggested an association between hyperparathyroidism (HPT) with thyroid cancer (TC) previous to surgery. Synchronous thyroid disease was found in 7% to 18% of primary HPT patients undergoing surgery, while 12% of thyroid lesions were found to be malignant. Association between non-medullary TC and primary HPT has been frequently reported. There is also some evidence for an association between secondary and tertiary HPT and thyroid cancer.
METHODS: This is a retrospective study of all cases of thyroid cancer in association with parathyroid disease treated surgically in our hospital from January 2000 to January 2004.
RESULTS: There were 280 surgical procedures for HPT in 274 patients. All patients had an elevated preoperative serum level of parathyroid hormone and serum calcium levels. Intraoperatively, 4 parathyroid adenomas and 270 parathyroid hyperplasia were diagnosed. In 50 patients (18.2%) thyroid resection was performed simultaneously. Three patients (1.1%) were found to have papillary thyroid cancer at the time of parathyroidectomy (PTX): one patients had primary HPT, one patients had secondary HPT, and one patient had tertiary HPT. Two cases were associated with metastatic spread to local lymph nodes. In those cases, total thyreodidectomy was performed, and frozen section revealed a small papillary microcarcinoma (diameter< 1cm in size). None of the patients with thyroid cancer had a prior history of head and neck irradiation .
CONCLUSION: These data suggest that the association between thyroid cancer and HPT is rare and coincidental. The association of simultaneous pathology in the two glands justifies preoperative thyroid imaging and fine-needle aspiration (FNA) biopsy to determine the best surgical approach for patients with HPT.

P 586
AN UNUSUAL NODULE OF THE THYROID: ECTOPIC MICROINVASIF THYROID THYMOMA OF AB TYPE(MIXTE)
Compérat Eva (1), Dinu Carmen (1), Menegaux Fabrice (2), Rouxel Agnes (3), Capron Frederique (1), Hoang Catherine(1).
(1) Service d'Anatomie et Cytologique Pathologique,
(2) Service de Chirurgie Générale Digestive et Endocrinienne
(3) Service de Médecine Nucléaire
CHU-Est La Pitié Salpetrière, Paris.

We report a rare case of ectopic thyroid thymoma of AB type. A 56 years old patient presented a left sided thyroid nodule discovered by palpation. Scintigraphic examination displayed a cold nodule, which measured 38 mm. Strong adhesion with the left loge was observed; the nodule predominated in the inferior pole of thyroid gland. Histologically the proliferation corresponded to a thymoma of AB type with neoplasic embols and extension to the adjacent adipous tissue. The jugulo-carotidic pick-up did not find any metastatic lymph nodes.
Ectopic cervical thymoma is a part of epithelial tumors with thymic differentiation of the neck. Incomplete descending or persistence of the cervical part of thymus is considered as the origin of ectopic thymus. These tumors are revealed by more or less compressive cervical masses without paraneoplasic syndromes. They present the same histological sub-types as their mediastinal homologue, but do not show any genetic anomaly. Differential diagnostic problems might be seen by extension of a mediastinal thymoma to cervical region, with an undifferentiated carcinoma, squamous cell carcinoma or

with lymphoma. Evolution remains local; relapses are never seen if surgery is complete. No prognostic factor is known nowadays.

P 587
CONNECTION OF THE LYMPHOCYTES PHENOTYPE AND PROTEIN OF APOPTOSIS IN LYMPHOCYTIC THYROIDITIS
Ljiljana Markovich MD PhD, Jelena SoptaMD PhD,Mirjana Atanackovich MD PhD,

In persons diseased on thyroiditis the number and function of CD8+ lymphocytes have been normal.It has been shown that iodide induces apoptosis of thyroid cells in culture and demonstrated that KI can do the same to rats with induced goiter. Impairment Bcl-2 and Bax genes on thyrocytes, have been detected as a direct consequence of administration of of iodine in potassium iodide-KI. Wistar rats having been receiving KI, KCl, NaI or NaCl. The Determinations of Peripheral Blood and Thymocyte Subpopulations of Rats have been done by FACScan.The double staining used FITC (CD8).and SA-PE(CD4). Immunohistochemical staining have been done with DAB on avidin-biotin and peroxidase using ARK, stained them with antibodies to:Bcl2 oncoprotein and Bax.We evaluated the intensity and distribution of positive DAB staining on a scale of 0 to 4.We perform statistic analisis by ANOVA and Student T-test.The histological analyses of thymus, spleen and thyroid have shown the changes in the thyroid as a diffuse mononuclear cell infiltration in the follicles and in the spaces between destruction of the acini, proliferation of connective tissue have been seen began between 5th and 10thday.So KI induced the symptomless LT in rats.Significant differences between individual groups ($p > 0.05$) nor in comparison to the non-treated controls ($p > 0.05$)has not been presented .Bcl-2 and Bax gene expression was significantly higher in rats with LT iodine induced and correlated with the extent of lymphocytic infiltratio. Bcl-2-expression was constantly seen in regular thyrocytes and in the mantle-zone of lymphofollicular infiltrates.Bcl-2 and Bax gene expression were not in conection with lymphocyte subgroups in peripheral blood. This work was partiali supported by MNS of Serbia, grant 1997

P 588
ABSENCE OF BRAF MUTATIONS IN HYALINIZING TRABECULAR TUMORS OF THE THYROID
CAMESELLE-TEIJEIRO José1, RUIZ-PONTE Clara2, ABDULKADER Ihab1, DURANA-TONDER Cristina1, ALFONSÍN-BARREIRO Natividad4, BARREIRO Francisco3, SOBRINHO-SIMÕES Manuel5
1Department of Pathology, 2Molecular Unit, and 3Department of Surgery, Hospital Clínico Universitario, Santiago de Compostela, Spain; 4Deparment of Pathology, Hospital do Meixoeiro, Vigo, Spain; 5Institute of Molecular Pathology and Immunology, University of Porto, Porto Portugal

Hyalinizing trabecular tumor (HTT) of the thyroid is a rare tumor of follicular cell origin with a trabecular pattern of growth and marked intratrabecular hyalinization. The etiology of HTT is unknown but nuclear features, association with conventional papillary carcinoma, and RET/PTC rearrangements in some of these tumors suggest a relationship with papillary thyroid carcinoma. The majority of studies find that RET/PTC rearrangements and BRAF mutations are mutually exclusive in papillary carcinomas; however, one study considered that BRAF mutations may cooperate with RET/PTC rearrangements in the development of papillary carcinoma. RET/PTC rearrangements were detected previously in 28.6-75% of HTT. We examined six hyalinizing trabecular adenomas and two hyalinizing trabecular carcinomas for BRAF mutations All tumors showed positivity for thyroglobulin and TTF-1 and lacked immunoreactivity for calcitonin, chromogranin A, and synaptophysin. DNA was isolated from paraffin-embedded tumor tissues and the exon 15 of the BRAF gene was sequenced directly. No mutations were found in any tumor samples analyzed. Our results show that BRAF mutation do not seem to play, at variance with RET/PTC, a role in the etiopathogenesis of HTT (neither the typical V600E mutation nor the mutation associated to the follicular variant of PTC-K600E, was detected in any HTT). This work was supported by research grant (PGIDE 99PXI 90201B) sponsored by Xunta de Galicia, Spain.

P 589
THYROID FNA – QUALITY CONTROL
VILCHEZ JOse*, MANITA Isabel**, SARAIVA Catarina**, SANTOS Sofia*, PORTUGAL Jorge** and BRITO Maria-Jose*
Departments of Histopathology* and Endocrinology**
Hospital Garcia de Orta, Almada, Portugal

Introduction: Thyroid FNA is a widely available diagnostic method with different results according to different series.
Aim: To evaluate thyroid FNA diagnostic accuracy (DA), sensitivity (S), specificity (Sp), false negative (FN) and false positive (FP)values and predictive values, positive (PPV) and negative (NPV), in the present series.
Material and methods: All thyroid FNA performed between April 2000 and December 2004 (n=1044)were rewied and compared with histological diagnosis in 148 cases. Patients age varied between 11 and 85 years old, 87.74% were females.
Results: FNA were classified as diagnostic in 70.2%: 707 benign (goitre and thyroiditis) and 26 malignant (papillary carcinoma, medullar carcinoma and lymphoma); 29.79% were non diagnostic: 36 undetermined (follicular tumour and suspicious) and 12 insufficient. In 148 cases histological diagnosis was available: 83 corresponding to negative FNA, 17 to malignant FNA, 36 to undetermined FNA and 12 to insufficient FNA. FN (n=5) and FP (n=1) were 23.8% e 1.3%, respectively. The PPV was 94.1%, NPV was 93.9%, S was 76.2%, Sp was 98.7% and DA was 94.0%.
Conclusions: Our findings are in the range reported in literature. FNA is a good diagnostic tool in our hospital.

P 590
THYREOIDECTOMY INDUCED MORPHOLOGICAL ALTERATIONS IN MAMMARY GLAND OF THE RATS
Jancic A.Snezana,Rosic L. Gvozden,Jancic A.Slavisa and Maric Lj.Ivana
Institute of Pathology and Phisyology,Medical School,Kragujevac,Serbia and Montenegro
Clinic of Oncology,Medical Center Nis,Serbia and Montenegro

The mechanizm of the influence of lower level of thyreoid hormons on breast tissue is not enough explored.There is a suggestion in literature that the deficit of thyreiodea can predispose the development of the breast tumor.
The aim of our work is the influence of partial thyreidectomy on mammary glands of the rat.
We used for experiment virgo female albino Wistar rats,weight 120±10gr.,45 days old.The animals were treated with ethar narcosis during the partial thyreoidectomy.There were 18 rats as well as in the control group.The animals were sacrified after 70 days and there was used a tissue of the breast for PH analisys.
All specimens were fixed in Bouins solution.The tissue was embedded in paraffin wax,and sections were cut at 4-5 micrometar and stained with HE and immunocytochemical ABC-method with antibodies against beta TSH,EGF and PNA-lectin.

The significate hyperplasion of the acinus and ductulus was observed with PH analysis.until they looked kike microadenoma.In cytoplasma of the cell there are present a large number of vesiculas wich are often confluence,forming an macrodroped aspect.Mastocits,hypergranulated and polymorph,are present in the lipomatosa stroma around ductulus and acinus.
In comparision to normal mammary gland,in epithel of hyperplastical acinuses and ductuluses was found beta TSH,PNA-lectin and EGF.
Exept in epithel of the hyperplastical acinuses and ductuluses,EGF is found also in fibroblasts and fibrocites and in the epithel of the acinuses and ductuluses in mammary glands of control group of rats.
In this work we discuss about the mechanizm of the influence of the deficite of thyreoidal hormones on the mammary gland of the rats,as well as the influence of breast carcinogenesis.

P 591

OVEREXPRESSION OF EPIDERMAL GROWTH FACTOR RECEPTOR IN THE SOLID CELL NESTS OF THE THYROID AND THE CYSTIC TUMOR OF THE ATRIOVENTRICULAR NODE OF THE HEART

CAMESELLE-TEIJEIRO José1, ALFONSÍN-BARREIRO Natividad2, ABDULKADER Ihab1, PRETO Ana3, SOARES Paula3, REYES-SANTÍAS Rosa1, SOBRINHO-SIMÕES Manuel3
1Department of Pathology, Hospital Clínico Universitario, University of Santiago de Compostela, Santiago de Compostela, 2Department of Pathology, Hospital do Meixoeiro, Vigo, Spain; 3Institute of Molecular Pathology and Immunology, University of Porto, Porto, Portugal

Solid cell nests (SCNs) are a normal component of the human thyroid gland that play a putative stem cell role. The cystic tumor of the atrioventricular node (CTAVN) of the heart is a benign cystic mass located at the base of the atrial septum of the heart, in the region of the atrioventricular node. Recently, we proposed that CTAVN of the heart is the cardiac equivalent of the SCNs (ultimobranchial rests) of the thyroid. Both entities are identical and basically composed of solid and/or cystic nests of squamoid cells (main cells) with a minor population of neuroendocrine cells (C cells). Epidermal growth factor (EGF) has widespread growth effects, and overexpression of EGF and epidermal growth factor receptor (EGFR) were found in dyshormonogenetic goiters, follicular adenomas, and well differentiated and undifferentiated (anaplastic) carcinomas of the thyroid. For this reason we investigated a series of seven cases of SCNs and one of CTAVN immunohistochemically with a mouse monoclonal antibody directed against EGFR (EGFR pharmDX kit, DAKO). In all cases, the main cells of SCNs and CTAVN revealed a distinct membranous staining pattern with weak cytoplasmic reactivity. Normal follicular cells were totally negative for this staining. The overexpression of EGFR fits with our previous findings of a higher proliferative index in main cells and supports the idea of these structures having an active biological role. This work was supported by a research grant (PGIDE 99PXI 90201B) sponsored by Xunta de Galicia, Spain.

P 592

COX2 AND MULTIDRUG RESISTANCE PROTEIN 2 (MRP2) IN MEDULLARY THYROID CARCINOMAS (MTC).

RUGGERI Rosaria Maddalena1, SCIACCHITANO Salvatore2-3, VITARELLI Enrica4, TRIMARCHI Francesco1, BENVENGA Salvatore1, BARRESI Gaetano4, TROVATO Maria1-4.
1Sezione di Endocrinologia - Dipartimento Clinico Sperimentale di Medicina e Farmacologia, University of Messina, Messina, Italy;
2II Facoltà di Medicina e Chirurgia, Osp. S.Andrea, Università La Sapienza di Roma, Rome, Italy;
3Centro di Ricerca Osp.S.Pietro Fatebenefratelli, AfaR, Rome, Italy;
4 Dipartimento di Patologia Umana, University of Messina, Messina, Italy.

The characterization of the mechanisms regulating the expression of multidrug-resistance proteins (MRPs) is crucial to plan an adequate treatment of cancers that display different degrees of resistance to chemotherapic drugs. COX2, a key enzyme in the conversion of arachidonic acid to prostaglandins, is an up-regulator of a MRPs member, namely, MPRP-1. To determine whether COX2 is a potential regulator of MRP2 in MTC we evaluated the expression of MRP2 and COX2 in MTC.
We investigated the expression of MRP2 and COX2 in 12 MTC nodules, 10 colloid nodules and 6 normal thyroids by immunochemistry. The 22 nodules were studied paired with the adjacent non-nodular (normal) tissue.
Only MTC nodules showed immunoreaction: 9/12 (75%) were positive for MRP2 and 12/12 (100%) for COX2. The proportion of MRP2 positive cells (10% to 40%, mean 25%) was inversely related with the proportion of COX2 positive cells (10 to 100%, mean 54%); $r = 0.96$, $P < 0.05$. Both immunoreactions exhibited levels of intenstity from moderate to strong and were localized on the apical side pertaining to plasma membrane (MRP2) and to cytoplasm (COX2).
The results indicate that COX2 is a possible regulator of MRP2 expression in MTC and suggest its role in the limited response to chemotherapic agents.

P 593

THE SURVEY OF PATHOLOGICAL LESIONS IN THE AUTOPSY OF THYROID GLAND, ISFAHAN ,IRAN.

REISIFAR Malek, NAJAFI Farideh,NAJAFI Mohammad Reza

Background;thyroid gland autopsy is the suitable and exact way to consider the morphology of thyroid gland.
methods;this study is descriptive-analytic type.The thyroid gland were dissected carefully,weighthed and measured and fixed in %5 formalin for 72h and sliced for microscopic examination and histopathologic study by two pathologists.
Results;251 whole of thyroid glands were collected at autopsy who had no known cilnical history of thyroid disease(208 m;43 f,ratio4:84) and intend in anatomic study and 202 whole thyroid glands (159 m and43 f,ratio 3.7)were collected in pathologic study.normal histopathology in125case (4.85%) goiter 41cases (20.3%;nodular,diffuse) thyroididtis 22 ;neoplasia 15cases (12 papillary carcinoma and 3 follicular adenoma).
conclosion;normal thyroid gland can be lead cilnicaly to the great pathological finding in microscopic study in consideration of high malignant incidence and occult carcinoma.We should pay more attention to the smallest findings during clinical examinations in Isfahan city toward the other parts of the world such as Brazil.

P 594

PATTERN OF THYROID CARCINOMA AMONG UNITED ARAB EMIRATES NATIONALS A CLINICOPATHOLOGIC STUDY

* AL-SALAM Suhail , EL-TERAIFI Hassan **
* Pathology department, Faculty of medicine and health sciences, United Arab Emirates University, AlAin, UAE
** Pathology department, Twam Hospital, AlAin, UAE

Introduction

The United Arab Emirates (UAE) is a union of seven sovereign sheikhdoms of the Arabian Gulf, which was formed

in 1971. These sheikhdoms or emirates include Abu Dhabi (the largest), Ajman, Dubai, Fujairah, Ras AlKhaima, Sharjah and Um Al Quwain. Although the total population is estimated to be 4 millions, only about 600,000 people are 'nationals' or natives of the country, the rest representing an extensive expatriate population. The national or indigenous population is composed of Emirate Arabs who, historically, were registered into tribes that included pastoral nomads and small agricultural settlements .Thyroid cancer is the most common endocrine malignancy. In the UAE thyroid cancer is the sixth most common cancer among nationals and the second among females .

Objective:

The aim of this study is to analyze the distribution of various pathologic types of thyroid carcinomas in a native Arab population of the United Arab Emirates (UAE) at Twam hospital in AlAin.

Materials and methods:

Forty-nine patients with thyroid carcinoma diagnosed over a 14-year period (1991-2004) at Tawam Hospital ;the main oncology center in UAE were retrospectively studied clinically and morphologically and classified according to the World Health Organization (WHO) histologic classification .

Results

Forty-four patients (90%) were diagnosed before the age of 45 years with a mean age of 35.5 years. The overall peak incidence was in the 3rd decade. There was a high female to male ratio comprising 11:1.Of the 49 patients in the study, 86 % had papillary thyroid carcinoma (PTC), 12% had follicular thyroid carcinoma (FTC) and 2% had anaplastic thyroid carcinoma.

Conclusions

Thyroid carcinomas in the UAE are more common among females than males with a very high female to male ratio suggesting that female gender is a possible risk factor in their development. Since most of our cases were diagnosed before the age of 45 years; with expected good prognosis, the age before 45 years can be considered as an important prognostic factor as well as a possible risk factor. PTC predominates the histologic pattern of thyroid carcinoma in UAE, which is usually associated with iodide sufficient area.

P 595

ANAPLASTIC THYROID CARCINOMA IN A 14-YEAR-OLD CHILD. CASE REPORT.

Lange D, Wloch J, Szalecki M, Jarzab M, Nikiel B, Jarzab B.
Centre of Oncology, M.Curie-Sklodowska Institute, Gliwice, Poland

Anaplastic thyroid carcinoma is a highly malignant tumor with peak incidence during the sixth and seventh decade of life. The youngest patient described so far was 22 years old. A 14-year-old boy was admitted to the hospital in Kielce. Physical examination revealed in the right thyroid lobe a painless resilient tumor of 1.5 cm in diameter. A FNA biopsy was performed revealing the presence of atypical pleomorphic cells, arousing suspicion of medullary or papillary carcinoma. Chest X-ray showed numerous oval metastatic foci as well as enhanced stroma architecture. The patient had been referred to the Institute of Oncology in Gliwice. The patient underwent ADM+CDDP chemotherapy. Because of epilepsy onset, magnetic resonance was performed revealing numerous metastatic foci in the brain. Despite further chemotherapy the metastases in the central nervous system continuously progressed. The patient died on November 24, 2001, 17 months after initial diagnosis. Pathologic evaluation. In cross-sections of the right lobe a weakly separated tumor was found (2.0 cm in diameter). In microscopic assessment the majority of tumor texture was formed by anaplastic spindle-shaped cells with pleomorphic hyperchromatic nuclei. Numerous mitotic figures were seen. Foci of extensive necrosis and extravasated blood were noticeable in regions with anaplastic texture. Neoplastic texture fully occupied by anaplastic cancer with extensive necrosis was present in 4 lymph nodes measuring from 0.5 to 1.0 cm in diameter. Immunohistochemical study.In a few tumor cells showing features of papillary cancer thyroglobulin immunoassay was positive. The same tumor areas showed also expression of cytokeratin AE1/AE3 and cytokeratin 19. A weak reaction with cytokeratin was observed in some anaplastic cells both in the primary tumor and in node metastases. The majority of cancer cells present in metastases did not show, howeverthe presence of thyroglobulin. The fields of anaplastic, spindle-shaped cancer cells showed expression of p53 protein in ca. 50% of cell nuclei. Anaplastic histological features of the discussed neoplasm have been confirmed by the lack of reaction with TTF-1, a minimal reaction with thyroglobulin antibody and a very high, above 70% MIB-1 index in anaplastic fields of tumor. It appears symbolic that the birth date of a first child who died from anaplastic thyroid cancer is the same as the date of the Chernobyl disaster.

P 596

INSULAR CARCINOMA OF THE THYROID GLAND IN CHILDREN.

Rotin D.L., Pavlovskaya A.I., Savelov N.A., Smirnova E.A.
N.N. Blokhin Cancer Research Center RAMS, Moscow, Russia

INTRODUCTION: Insular carcinoma of the thyroid gland represents poorly differentiated tumors that are relatively infrequent. It is even rarer tumor in pediatric patients. It is written that this neoplasm occurs predominantly in patients elder than 50-60 years old. Currently, insular carcinoma is considered to be a tumor with very poor and unfavorable prognosis.

MATERIALS AND METHODS: We collected and investigated surgical thyroid specimens from 5 patients (age 9 to 15) with insular carcinoma. These specimens were routinely processed, stained with HE, PAS, van Gieson. Ultra structural and immunohistochemical investigations with monoclonal antibodies to vimentin, citokeratins, chromogranin A, thyroglobulin, calcitonin and Ki-67 were also performed. All case reports and follow-up were carefully evaluated.

RESULTS: The careful histological examination revealed the presence of insular pattern mixed with more differentiated (either papillary or follicular) thyroid carcinoma. We found no significant areas of necrosis in all cases, so peculiar and usual for this tumor. Ultrastructurely, all the features of follicular-cell differentiation were found. Immuhistochemically, all cases were positive for thyroglobulin, vimentin and citokeratins. In majority of tumors the activity of proliferation, evaluated by means of Ki-67 expression, was moderate to high. All these tumors were negative for calcitonin, chromogranin A. Clinically, no evidence either of distant metastasis or of local recurrence was seen in all 5 cases. Whole this group of patients is still alive, showing post-operative survivence from 2 to 5 years.

CONCLUSION: Insular carcinoma of the thyroid gland is very rare neoplasm in children and adolescence. In this age group it tends to have more favorable prognosis than it does in adults, where it often shows the evidence of distant metastasis and recurrence.In other words, the biological behavior of insular carcinoma in pediatric patients tends to have better than it seems by means of its histological appearance.

P 597

CYCLOOXYGENASE-2 IN NORMAL, HYPERPLASTIC, AND NEOPLASTIC FOLLICULAR CELLS OF THE HUMAN THYROID GLAND

GARCÍA-GONZÁLEZ Miguel, ABDULKADER Ihab, VÁZQUEZ BOQUETE Angel, LENS NEO Xosé Manuel, FORTEZA Jerónimo, and CAMESELLE-TEIJEIRO José
Departments of Nephrology and Pathology, Hospital Clínico Universitario de Santiago de Compostela

This study was undertaken to investigate cyclooxygenase-2 (COX-2) expression in follicular cells of the human thyroid. COX-2 expression was studied immunohistochemically in a total of 174 samples. COX-2 immunoreactivity was confined to the cell cytoplasm with the nuclei remaining unlabelled. COX-2 expression was observed in 5 cases (17.2%) of normal follicular cells and in one case (16.6%) of solid cell nests. Follicular carcinoma expressed COX-2 more frequently than follicular adenoma (93.4% vs. 21.1%) ($p<=0.001$). A higher percentage of cases of papillary microcarcinomas up-regulated COX-2 in comparison with all papillary carcinomas ($p<=0.05$). However, we could not establish any relationships between COX-2, patients' ages or lymph node metastases in papillary carcinomas. COX-2 expression was found in 12 (92.3%) poorly differentiated carcinomas and in 13 (92.8) undifferentiated carcinomas. We found that COX-2 is not always useful as a marker of malignancy. Our results suggests that COX-2 plays a role in progression of all thyroid carcinomas but, in papillary carcinomas, seems more important only in the early stages. COX-2 expression in the undifferentiated carcinoma deserves special consideration due to its prognosis and to the fact that selective COX-2 inhibitors were found to enhance tumour response to radiation in some studies. This work was supported by research grant (PGIDE 99PXI 90201B) sponsored by Xunta de Galicia, Spain.

P 598

CONCOMITANT GLOBAL DNA METHYLATION EVALUATION AND GALECTIN-3: POTENTIAL TOOL IN DIFFERENTIAL DIAGNOSIS OF THYROID NEOPLASIA

GALUSCA Bogdan 1,5, DUMOLLARD Jean Marc 2,4, VAUNOIS Brigitte 2, PRADES Jean Michel 3, ESTOUR Bruno 1, PEOC'H Michel 2,4
1 Endocrinology Department ; 2 Pathology Department ;3 ORL Department , CHU, Saint Etienne, France ; 4 EA6063, Inserm, Saint Etienne, France ; 5 Endocrinology, UMF Gr.T.Popa, Iasi, Romania

Introduction. The implications of global DNA hypomethylation were lately reported in several models of tumorigenesis. Little is known about this epigenetic event in thyroid neoplasia.
Over the last few years galectin-3 was promoted as an overall differentiating solution of thyroid nodules but it was also described limits of this marker regarding the follicular neoplasia differentiation.
This study aimed to evaluate concomitantely the status of global DNA methylation and galectin-3 in several types of thyroid tumors in order to define the diagnosis potential of this combination.
Materials and methods. 5-mc and galectin-3 immunostaining scores were evaluated by computerized image analysis in 17 papillary thyroid carcinomas (PTC), 6 follicular thyroid carcinomas (FTC), 16 follicular adenomas (FA), 19 nodular goiters (NG) and 10 Hürthle cells adenomas (HCA).
Results. We found a significant lower level of 5-mc immunostaining in thyroid carcinoma when compared with benign tumors or adjacent normal thyroid parenchyma ($p<0.0001$). Overall, 5-mc accuracy to distinguish malign from benign thyroid tumors was similar to that of galectin-3 (89% vs. 87%, $p>0.05$). The combination of 5-mc with galectin-3 lead to an excellent accuracy level of 96%. Among follicular neoplasia 5-mc accuracy to differentiate malign tumors trends to be higher than galectin-3 one (90% vs 66%, $p=0.06$).
Conclusions. These data stress out the necessity of epigenetic events evaluation among thyroid nodules and propose global DNA methylation assessment as a complementary diagnostic tool.

P 599

HBME - 1 MONOCLONAL ANTIBODY IN DIFFERENTIATION OF BENIGN AND MALIGNANT THYROID LESIONS

Mojgan Mokhtari , assistant professor of pathology Isfahan universisy.
Ardeshir Talebi, assistant professor of pathology Isfahan universisy.
Magid Sadeghi , Pathologist.

Abstract:
Introduction:
Monoclonal antibody HBME-1 was prepared using cells from an epithelial malignant mesothelioma as immunogen. It is an antimesothelial monoclonal antibody that recognized an unknown antigen on microvilli of mesothelial cells. The antibody is only relative specific for mesothelium and is helpful in the differential diagnosis between mesothelioma and adenocarcinoma, within the context of an appropriate immunohistochemical panel.Thyroid lesions have high incidence in human and distinction between benign and malignant lesions is very important for surgical approach.
In the past the only reliable method for diagnosis was H&E staining.
Purpose of the study:
The purpose of this study was to evaluate HBME1 monoclonal antibody staining for diagnosis of benign and malignat thyroid lesions.
Methods used:
This is an analytical descriptive study.90 formalin fixed and paraffin embedded thyriod lesions (45 benign and 45 malignant) were examined by immunostaining and light microscopy.Data were analysed with chi-square test and P value lower than 0.05 was determined significant.
Summary:
We found strong positive staining in the majority of papillary carcinoma (28/31), in some of follicular carcinoma (4/6), in a few follicular adenoma (2/17) and negative staining in oxiphilic cell adenoma (0/4), nodular goiter (0/13) and undifferentiated carcinoma(0/8)and thyroiditis(0/11).
Conclusion:
The results suggest that monoclonal antibody HBME-1 is useful in differentiating papillary and follicular carcinoma of the thyroid from benign lesions especially in more differentiated lesions. Strong and generalized immunoreactivity for HBME-1 in a follicular lesion should raise the suspicion of malignancy, but negative staining specially in poorly differentiated lesion does not rule out malignancy.

P 600

DIAGNOSTIC VALUE OF GALECTIN-3, HBME-1, P27, CYCLIN D1, CYTOKERATIN19, AND HIGH MOLECULAR WEIGHT CYTOKERATIN IN THE DIFFERENTIAL DIAGNOSIS OF THYROID TUMORS

Kyoung-Bun Lee, Hye Seung Lee, Jin Haeng Chung, Gheeyoung Choe, Seong Hoe Park, So Yeon Park.
Department of Pathology, Seoul National University Bundang Hospital, Seoul National University College of Medicine, Seongnam, Gyeonggi, Korea

The distinction of benign and malignant thyroid tumor is critical for the management of patients with thyroid nodules. Immunohistochemical markers, such as galectin-3, HBME-1, p27, cyclin D1, cytokeratin19 (CK19) and high molecular weight cytokeratin (HMWCK) have been suggested to be helpful in the distinction of thyroid malignancy and papillary

thyroid carcinoma. We applied immunohistochemical staining in 262 surgically resected thyroid nodules including 181 papillary carcinomas (PC; 147 conventional papillary carcinomas [CPC] and 34 follicular variant of papillary carcinomas [FVPC]), 22 follicular carcinomas (FC), 25 follicular adenomas, and 34 nodular hyperplasias, to determine the diagnostic accuracy of these markers. The expression of all markers was significantly associated with thyroid malignancy. The sensitivity for the diagnosis of thyroid carcinoma was 97.0% for galectin-3, 90.6% for HBME-1, 82.8% for p27, 63.5% for cyclin D1, 90.6% for CK19. The specificity of these markers was 93.2%, 71.2%, 76.3%, 86.4% and 79.7%, respectively. Among the four benign nodules which showed focal galectin-3 positivity, none showed staining to HBME-1, cyclin D1 and CK19. In comparison of PC and FC, the expression of galectin-3, cyclin D1, CK19 and HMWCK was significantly higher in PC than in FC. When comparing FVPC with FC, the expression of CK19 and HMWCK was significantly higher in FVPC. However, CK19 showed focal positivity in 32% and diffuse positivity in 9% of FC. Although the expression of HMWCK was confined to PC, the sensitivity for the diagnosis of PC was only 58.6%. In comparison of CPC and FVPC, the expression of galectin-3, HMWCK, cyclin D1 was significantly higher in CPC than in FVPC. We concluded that although galectin-3 has limitation due to focal staining in benign lesion, it is a useful marker in the distinction of benign and malignant thyroid tumors, especially when used in combination with HBME-1, CK19 and cyclin D1. CK19 and HMWCK can be aided in the diagnosis of PC. However, the low sensitivity of HMWCK and low specificity of CK19 may limit its utility.

P 601

IMPACT OF ACTIVATING BRAF MUTATION ON AGGRESSIVENESS IN PAPILLARY THYROID CANCER

Jin-Man Kim1 ,Young-Suk Jo, Jun-Chul Lee, Ki-Hyun Kwon, So-young Rha, Hyo-Jin Lee, Bon Jeong Ku, Young-Kun Kim, Heung-kyu Ro,Minho Shong
Departments of Pathology1 and Internal Medicine, Chungnam National University College of Medicine, Daejeon, Korea

Activating mutations in the BRAF kinase gene have recently been reported in human papillary thyroid cancers. The aim of the present study was to determine the frequency of BRAF mutations in thyroid cancer and their correlation with clinicopathological parameters and various immunohistochemical markers including VEGF. We analyzed exon 15 of BRAF gene in 190 frozen or paraffin-embedded thyroid tumor tissues. A missense BRAF mutation was found in exon 15 in 105 of 166 papillary carcinomas(63.3%), 0 of 18 benign disease, 0 of 5 follicular carcinoma and 0 of 1 medullary carcinoma.

Mutation of BRAF and concomitant ERK activation may also influence the progression of papillary carcinomas. Examination of 166 patients with papillary thyroid cancer showed that BRAF mutation did not have correlation with clinical stage and distant metastasis, but BRAF mutation was more common in palpable thyroid cancer (p-value<0.05).

Angiogenesis is very important process during the development and progression of solid tumors. Vascular endothelial growth factor (VEGF) is a major regulator of angiogenesis and could be produced by papillary thyroid cancer. To investigate the relationship between BRAF mutation and VEGF expression in the tumorigenesis of human thyroid, immunohistochemical study was performed. VEGF expression did not correlate with various clinicopathological parameters but, clearly correlated with tumor size. Papillary thyroid cancer with BRAF mutation exhibited more intensive VEGF expression (p-value<0.05).

Our results suggest that activating mutation of BRAF gene closely related to VEGF expression and more common in palpable thyroid cancer.

P 602

ROLE OF CYTOKINES AND DENDRITIC CELLS ON FIBROSIS IN THYROID PAPILLARY CARCINOMA AND HASHIMOTO• FS DISEASE

KAWAKUBO Yasuaki 1), SATO Yuichi 2), JIANG Shi-Xu 3), OKAYASU Isao 3)
1) Department of Pathology, School of Nursing, Kitasato University, 2) Department of Molecular Diagnostics, School of Allied Health Sciences, Kitasato University,
3) Department of Pathology, School of Medicine, Kitasato University

Introduction: Significant fibrosis is observed in both Hashimoto• fs disease (HD) and thyroid papillary carcinoma (TPC). TPC is a particularly suitable model to study the role of tumor-associated macrophages (MfÓ) and/or dendritic cells (DC), because it is frequently associated with signs of immune reaction, including lymphocytic infiltration. On the other hand, interstitial cells such as fibroblast, DC and MfÓ are known to secrete various cytokines which have effects on connective tissue cells and endothelial cells in fibrotic lesions. Purpose: We tried to clarify whether the released cytokines from interstitial cells were related to development of fibrosis in the diseased thyroid. Materials and Methods: The role of cytokines such as TGFfÀ1, CTGF, GM-CSF and TNFf¿ in the development of fibrosis was examined with immunohistochemical staining (IHC) and in situ hybridization (ISH) using paraffin sections of the TPC and HD. The phenotype of the interstitial cells was examined by IHC. In addition, in vitro assays were performed using cultured fibroblasts (WI-38), thyroid carcinoma cells (HTC/C3) and differentiated U-937 cells including immature DC, and MfÓ, to determine how the released cytokines act on fibroblasts. The levels of cytokines, both in the cytoplasm and the culture medium, were examined using IHC, ELISA and RT-PCR. Results: In TPC, there was significant expression of TGFfÀ1, CTGF, GM-CSF and TNFf¿, not only in fibroblasts and/or MfÓin the stroma of the tumors, but also in the tumor cells and infiltrating DCs around the tumor cells. In the HD, mature DCs were seen mainly in lymph follicles, and immature DCs were focally observed around the degenerative or destructive thyroid follicles. Using in vitro assay, differentiated U-937 cells (mainly MfÓ and DC) were shown to significantly release GM-CSF and TNFf¿. When co-cultured with differentiated U-937 and/or HTC/C3 cells, respectively, WI-38 cells showed elongation of the cytoplasm and expressed cytokines. Conclusion: The results from both the in vivo and in vitro assays suggest that cytokines such as GM-CSF and TNFf¿ released by fibroblasts and MfÓ as well as CD1a+ cells, involve in the proliferation and differentiation of fibroblasts. This may contribute to the fibrosis development in TPC. However, in HD, the relationships between fibroblasts, DC, MfÓ and their released cytokines and fibrosis remain unclear.

P 603

GALECTIN 3, ONCOFETAL FIBRONECTIN, EMMPRIN, CYTOKERATIN 19, CITED1, AND TPO EXPRESSION IN THYROID TUMORS

WILT Marc, MILLON Régine, THEOBALD Serge, EBER Michel, RODIER Jean-François, JEANDIDIER Nathalie, SCHNEEGANS Olivier, GHNASSIA Jean-Pierre
Centre de Lutte contre le Cancer Paul Strauss, Strasbourg, France
Service d'Endocrinologie, Hôpitaux Universitaires, Strasbourg, France

Background: Fine needle aspiration (FNA) has become the keystone diagnostic tool in the management of thyroid nodules. However this method has some limitations, such as its lack of sensitivity for follicular neoplasm and may not be informative in 5 to 20% of FNA samples. The use of molecular markers of malignancies could improve the diagnostic performance of these inconclusive or non-informative FNA. The choice for the most relevant markers needs to be performed on tissue samples.
The aim of this study was to determine the expression of 6 genes that may be effective in diagnosing cancer: galectin 3, oncofetal fibronectin, emmprin, cytokeratin 19, CITED 1, and TPO by analysing surgical thyroid tissue samples.
Design: Eighty six tissue samples were analysed and divided into 5 types: 11 normal thyroid tissue, 21 adenoma, 40 papillary carcinoma, 8 follicular carcinoma and 6 anaplastic carcinoma. For each sample, the gene expression was assessed compared to an ubiquitary gene RPLP0 using quantitative real time RT-PCR. The ratio concentration of studied genes over RPLP0 represented the level of expression of the studied gene in each sample. For the 6 studied genes, means and medians of these ratios were calculated for each type of tissue sample. These ratios were compared using an ANOVA and Scheffe tests (proc GLM Sas Institute).
Results: The emmprin and cytokeratin 19 levels of expression were comparable in all 5 types of tissue studied (p=0.6 and p=0.4). Galectin 3, fibronectin and CITED 1 levels of expression were significantly increased only in papillary carcinoma compared to normal tissue. The mean value of galectin was 1.19 (IC 95%:0.94-1.44) vs 0.13(IC 95% : 0.08-0.18), mean value of fibronectin was 4.48 (IC 95%:2.5-6.06) vs 0.04 (IC 95% : 0.02-0.07) and mean value of CITED 1 was 6.94 (IC 95%:4.80-9.07) vs 0.20 (IC 95%:0.15-0.26). TPO was significantly underexpressed only in papillary carcinoma compared to normal tissue. The mean value of TPO was 0.6 (IC 95%:0.12-0.69) vs. 1.68 (IC 95%:1.15-2.22).
Conclusion: The emmprin and cytokeratin 19 gene did not seem effective in distinguishing different tissue types. The significantly increased levels of fibronectin, galectin 3 and CITED 1 and decreased levels of TPO found in papillary carcinoma compared to normal tissue may confirm the interest in these 4 genes as molecular markers of papillary cancer. An evaluation of these genes in cytology samples is now being conducted.

P 604
DIFFERENTIATED THYROID CARCINOMAS : IMMUNOHISTOCHEMISTRY IS USEFUL TO PREDICT THE OCCURRENCE AND THE CHRONOLOGY OF LYMPH NODES METASTASES

HOANG Catherine(1), JUST Pierre-Alexandre(1), MENEGAUX Fabrice(2), LEENHARDT Laurence(3), TRESSALET Christophe(2), AUBRIOT-LORTON Marie-Helene(1), CAPRON Frederique(1)
(1)Anatomie et cytologie pathologiques, (2)Chirurgie generale, digestive et endocrinienne, (3)Medecine nucleaire. Groupe hospitalier Pitie-Salpetriere, 47-83 boulevard de l¡¯Hopital, 75651 Paris Cedex 13, France.

Background : The poor outcome of differentiated thyroid carcinomas is difficult to predict, specially in pT1 (¡Ü2cm) carcinomas. The diagnostic interest of various immunohistochemical markers has often been demonstrated but their prognostic value still remains unclear.
Objective : Are immunohistochemical findings in differentiated thyroid carcinomas correlated to the occurrence and the chronology of their lymph nodes metastases?
Material and methods : HBME-1, Galectin-3, Thyroperoxydase(TPO), Cytokeratin-19(CK19) and c-erbB-2 expression was studied in 41 thyroid carcinomas : 10 (N0) limited to the thyroid gland during a 7 to 9 years follow-up and 31 (N+) with lymph nodes metastases (12 with synchronous, 10 with metachronous and 9 with synchronous and metachronous lymph nodes metastases).
Results : The tumors were 35 papillary carcinomas (PTC) and 6 follicular carcinomas (FTC), including one oncocytic variant. 31PTC/35 coexpressed HBME-1, Galectin-3 and CK19, 2/35 expressed c-erbB-2 and 32/35 had a loss of TPO-expression (TPO staining in less than 60% of tumor cells). 6/6 FTC were stained with CK19, 5/6 with Galectin-3, 4/6 with HBME-1, 0/6 with c-erbB-2 and 6/6 had a loss of TPO-expression. 10/10 carcinomas with exclusive metachronous lymph nodes metastases were totally negative for TPO versus 8/21 others N+-carcinomas (p=0.001).
7/8 N0-PTC had an intense (in more than 70% of the tumor cells) HBME-1 staining versus 5/27 N+-PTC (p<0.001). None N+-carcinomas was negative for Galectin-3 contrary to 4/10 N0-carcinomas (p=0.002). 9/9 N+-pT1-PTC associated an HBME-1/Galectin-3 coexpression and a loss of TPO-expression versus 1/5 N0-pT1-PTC (p=0.005).
Staining in tumors and their lymph nodes metastases was globally the same for each antibody except for galectin-3.
Conclusion : HBME-1, Galectin-3 and CK19 (alone or associated to each others) and the loss of TPO-expression are highly sensitive for the diagnosis of PTC. A strong HBME-1 staining is often found in N0-PTC whereas galectin-3 had a 100% sensitivity for N+-carcinomas. A galectin-3/HBME-1 coexpression with a loss of TPO-expression is correlated to the occurrence of lymph nodes metastasis in pT1-PTC. A completely negative TPO-staining seems to be related to the occurrence of metachronous lymph nodes metastases. These results should prompt to modulate the actual consensual surveillance of patients with thyroid carcinomas, according to immunohistochemistrical pattern.

P 605
BRAF T1799A MUTATION IN HUMAN THYROID PAPILLARY MICROCARCINOMA

LUSHNIKOV Eugeny, LANTSOV Dmitry, ABROSIMOV Aleksandr, SEDLIAROU Ilya, SAENKO Vladimir, ROGOUNOVITCH Tatiana, NAMBA Hiroyuki, NAKASHIMA Masahiro, MEIRMANOV Serik, YAMASHITA Shunichi
Clinical-Morphological Department, Medical Radiological Research Center RAMS, Obninsk, Russia
Departments of Molecular Medicine, International Health and Radiation Research, and Tissue and Histopathology Section, Atomic Bomb Disease Institute, Nagasaki University Graduate School of Biomedical Sciences, Nagasaki, Japan

Background. A hotspot mutation in exon 15 of BRAF gene, the T1799A transversion, has been shown to be a prevalent (28.8% - 68.6% in various series from different countries) and highly specific genetic alteration in human papillary thyroid cancer (PTC) in adult patients. BRAF mutation associates with certain histological variants of the tumor being found in a large proportion of PTC with classic papillary morphology and, vise versa, underrepresented in the tumors with follicular architecture. At the same time, little is known about the involvement of BRAF mutation in early stages of thyroid carcinogenesis such as papillary thyroid microcarcinoma (PMC) and its role in tumor progression.
Purpose of the study. Our investigation was set out i) to determine the prevalence of BRAF mutation in PMCs in patients from two geographically distinct groups, Japan and Russia; and ii) to evaluate a correlation between the presence of mutated BRAF and PMC morphology and biological behavior of the tumor.
Materials and methods. Tumor tissue was microdissected from serial sections of 15 PMCs from Japanese patients and 31 PMCs from Russian patients. DNA was extracted using Proteinase K/phenol-chloroform protocol. Fragment of BRAF exon 15 was PCR amplified and analyzed by direct sequencing.

Results. Mutated BRAF was detected in 13/46 (28.2%) of the tumors: 9/31 (29.0%) and 4/15 (26.6%) in Russian and Japanese individuals, respectively, displaying no signs of discrepancy in the mutational rates in patients with differing genetic background seen in PTCs. Occurrence of the BRAF mutation did not significantly correlate with patients' gender, age at presentation, metastatic indices as well as with papillary, mixed papillary and follicular, and solid/trabecular PMC histotype. On the contrary, tumors with follicular morphology significantly associated with the mutation-free genotype (P=0.018). In the mixed-type tumors characterized by co-occurrence of well-differentiated and less differentiated components, the BRAF mutational frequency was significantly elevated (P=0.020).
Conclusion. Results indicate that PMCs may have a spectrum of genetic events partly overlapping with that of PTCs. The BRAF T1796A mutation occurs in about one-third of PMCs irrespectively of the genetic background of patients and positively or negatively associates with particular tumor architecture whereas no correlation could be found with patients' demography and biological behavior of the tumor.

P 606
BRAF T1799A MUTATION IN VARIOUS THYROID DISEASES

ABAKUSHIN Dmitri N., ABROSIMOV Aleksandr Yu., KONOVA Marina V., PETUKHOVA Natalia S, LUSHNIKOV Eugeny F.
Clinical-Morphological Department, Medical Radiological Research Center RAMS, Obninsk, 4 Korolev str., 249036, Russia
E-mail: abakushin@mrrc.obninsk.ru

BACKGROUND: High prevalence of activating T1799A transversion in B Raf kinase-encoding gene (BRAF V600E) has been reported specifically in papillary thyroid cancer (PTC) varying 29-69% in series from different countries, but not in follicular thyroid cancer (FTC) and benign follicular thyroid adenomas (FA). With regard to other types of thyroid diseases information remains rather limited.
PURPOSE OF THE STUDY: In this investigation we determined BRAF mutational rate in medullary thyroid cancer (MTC), FTC, FA, nodular goiter (NG) and lymphocytic thyroiditis (LT) tissues along with that in PTCs in an attempt to elucidate the difference in BRAF alteration frequency among these entities.
MATERIALS AND METHODS: For the study we collected 2 MTCs, 5 FAs, 5 NGs, 2 LTs, 4 FTCs (1 case with lymph node metastasis) and 11 PTCs including 5 cases of follicular variant of PTC, 2 multi-focal PTCs with 2 lymph node metastases from adult patients (2 males and 27 females) aged 30-69 years at operation, residents of central region of Russia. We collected normal thyroid tissues for analyzing in all that cases also. The pathological diagnoses of all the tumors were made in accordance with WHO classification criteria (1988). Genomic DNA was isolated from fresh frozen surgical tissue samples using TRIzol reagent (Invitrogen, Carlsbad, CA) and analyzed for the BRAF mutation by mutant allele specific polymerase chain reaction. DNA extracted from PTC tissue previously determined to harbor mutant BRAF was used as a positive control.
RESULTS: In this series, we found no BRAF T1799A mutation in all eleven PTC cases as well as in any other type of tissue analyzed.
CONCLUSIONS: Our data demonstrate the absence of BRAF mutation in thyroid diseases such as medullary and follicular cancer, follicular adenoma, nodular goiter and lymphocytic thyroiditis. On the other hand, the fact that we were unable to detect BRAF T1799A transversion in 11 cases of PTC indicates that BRAF mutational rate is not too high in adult Russian patients suggestive that frequency of BRAF gene alteration in PTC may be substantially different in the individuals with distinct genetic background (i.e. it is markedly lower in Russian patients in comparison with e.g. Asian individuals). Greater comprehension is necessary to correctly evaluate BRAF mutation prevalence in Russian patients with PTC.

P 607
A NEW BRAF GENE MUTATION DETECTED IN A CASE OF SOLID VARIANT OF PAPILLARY THYROID CARCINOMA

Magalhães J1,2, Trovisco V3, Soares P3, Soares R3, Sá Couto P4, Sobrinho-Simões M1,2,3
1.Department of Pathology. Medical Faculty of University of Porto; 2.Department of Pathology, Hospital de São João, Porto, Portugal; 3.IPATIMUP (Institute of Molecular Pathology and Immunology of the University of Porto); 4.Department of Surgery, Hospital de São João, Porto, Portugal.

BRAF gene mutations have frequently been detected in papillary thyroid carcinoma (PTC).
Moreover, there is a close association between the type of mutation and the PTC histotype: BRAFV600E is associated with conventional PTC and with histological variants of PTC displaying a prominent papillary growth pattern, whereas BRAFK601E is associated to the follicular variant of PTC.
We report the detection of a novel BRAF triplet deletion in a case of solid variant of PTC. The deletion leads to the replacement of a valine and a lysine by a glutamate in the BRAF activation segment (BRAFVK600-1E) thus mimicking partially the two BRAF mutations previously described. Our study reinforces the existence of a close relationship between the occurrence of some types of BRAF mutation and some PTC histotypes. The genetic study of more cases of the solid variant of PTC is necessary to find whether or not there exists a significant association between the occurrence of BRAFVK600-1E and such PTC histotype.

P 608
PAX8-PPAR*f*× TRANSLOCATION: ANOTHER COMMON FEATURE TO FOLLICULAR THYROID CARCINOMA AND FOLLICULAR VARIANT OF PAPILLARY CARCINOMA

Magalhães J 1,2, Castro P3, Rebocho A3, Soares R3, Roque L4, Soares P1,3, Sobrinho-Simoes M1,2,3
1.Department of Pathology, Medical Faculty of University of Porto; 2.Department of Pathology, Hospital de São João – Alameda, Porto 3.IPATIMUP (Institute of Molecular Pathology and Immunology of the University of Porto); 4.IPO (Portuguese Institute of Oncology), CIPM, Lisbon, Portugal.

Thyroid tumours are among the few epithelial tumours harbouring chromosomal translocations. Papillary thyroid carcinomas (PTC) may display RET/PTC and TRK rearrangements and follicular tumours often have the PAX8-PPAR*f*× translocation.
The follicular variant of papillary thyroid carcinoma (FVPTC) is characterized by the cytologic nuclear features of PTC with a follicular pattern of growth. At variance with conventional PTC these tumours display a low frequency of RET/PTC rearrangements, low frequency of B-raf mutations (and of a distinct type from those found in conventional PTC) and a higher frequency of ras mutations.
In an attempt to further characterize the FVPTC we investigated the presence of PAX8-PPAR*f*× translocation in FVPTC using interphase FISH, RT-PCR and immunohistochemistry.
By FISH analysis we found that 41% (9/22) of FVPTC cases display the PAX8-PPAR*f*× translocation. All the cases which harboured the PAX8-PPAR*f*× translocation showed a strong immunoreactivity for PPAR*f*×, and the translocation was confirmed by RT-PCR in two of the cases.

The presence of PAX8-PPAR*f*× translocation was associated with the presence of invasion and/or metastasization (p=0.0034) and with the presence of multifocality (p=0.04).
We conclude that follicular carcinomas and FVPTC share the presence of PAX8-PPAR*f*× translocation at a very similar frequency. We also found three cases of FVPTC displaying both PAX8-PPAR*f*× translocation and Ras mutations. Finally, our data, together with the data already published, shows that FVPTC may be more closely related with FTC than with classical PTC.

P 609
THE EXPRESSION PROFILE OF DIFFERENTIATED THYROID CANCER: MULTI-GENE CLASSIFICATION APPROACH
D. Lange, E. Chmielik, B. Nikiel, J. W³och, A. Czarniecka, A. Kukulska, Z. Wygoda, K. Fujarewicz, K. Simek, M. Oczko, M. Jarz¹b, M. Kowalska, A. Swierniak, B. Jarz¹b
Centre of Oncology, M.Curie-Sk³odowska Institute, Gliwice, Poland

The diagnosis of thyroid cancer is still a field of many controversies, even among experienced pathologists. There is a paucity of efficient markers, both to differentiate benign and malignant cases and to recognize cancer subtypes. Thus, we apply the oligonucleotide microarray technology to study the expression profile of differentiated thyroid cancer and to select transcripts which differentiate between subclasses. We use state-of-the-art bioinformatic techiques, based on Support Vector Machines algorithms, to select not only the single "solitary" markers but rather the sets of genes which are taken into account cooperatively to enhance the diagnosis accuracy.
We start our analysis from the simplest model, the comparison between papillary thyroid cancer and normal thyroid tissue, mainly specimens from thyroid lobe contralateral to tumor.
In total, 82 thyroid samples were investigated by high density oligonucleotide microarrays (HG-U133A, Affymetrix): 48 PTC samples, 25 samples of macroscopically unchanged thyroid tissue and 9 benign thyroid lesions. We recently proposed (Jarzab et al., Cancer Res. 2005) a 20-gene classifier, trained on the initial group of 16 PTC and 16 normal samples, which took into account the interactions between genes and in our group outperformed any single-gene approach. It included DPP4, GJB3, ST14, SERPINA1, LRP4, MET, EVA1, SPUVE, LGALS3, HBB, MKRN2, MRC2, IGSF1, KIAA0830, RXRG, P4HA2, CDH3, IL13RA1, MTMR4. In the study we validate this classifier on the separate group of 50 samples and obtain 93% accuracy. The few misclassified tissues usually exhibit a low percentage of tumor cells in collected sample.
We further extend the analysis to the set of follicular neoplasms (10 follicular cancers and 10 follicular adenomas), where the specification of differentiating genes is much more difficult and it results in significantly lower accuracy.
Conclusion: The high diagnostic accuracy of the recently proposed own multigene PTC classifier has been confirmed.

P 610
IMMUNOHISTOCHEMISTRY IN THYROID TUMOUR PATHOLOGY
Louis THIENPONT(1),Paul VAN CROMBRUGGE(2) Beatrix COCHAND-PRIOLLET(3), Jan S. WILLEMS(1) and Jean-Pierre GILLARDIN(4)
Histo- and Cytopath. Lab(1) Dept. Internal Medicine-Endocrinology(2) Dept. General Surgery(4) Onze-Lieve-Vrouw Ziekenhuis B9300 AALST, Belgium; Department of Pathology (3) Lariboisière Hospital, F75475 Paris, France

Background and Aims:
Traditionally invasive growth is the only criterion of malignancy in follicular tumours of the thyroid, while nuclear characteristics are the major criterion for papillary tumours, both papillary and follicular variant.
Our aim was to investigate the immunohistochemical phenotype of follicular epithelium and to characterize in more refined way follicular lesions of various origin.
Material and Methods:
Thyroid lesions and nodules encountered in daily practice over the last eighteen months were stained for various antibodies. Antibodies were used to demonstrate follicular cells (thyroglobulin, TTF1), oxyphilic cells (thyroglobulin, TTF1 and CK14) and C-cells (calcitonin, CEA and chromogranin A).
Thyroid malignancy associated antibodies used were: CK19, HMW keratin, HBME1, Galectin 3, RET-PTC and PAX8-PPARgamma.
Preliminary Results :
HBME1 showed to be a most interesting valuable marker for follicular tumours, helping to distinguish follicular carcinoma from adenoma. Other useful stains in case of follicular carcinoma are Galectin3 (Gal3)and PAX-PPARgamma.
In our experience Cytokeratin 19 is a very good marker for papillary carcinoma; papillary as well as follicular variants. Most papillary cancers stain for HBME1 and Gal3 as well.
Conclusions:
1. Immunohistochemical staining of thyroid nodules in general is mostly a valuable adjunct to confirm equivocal histopathological diagnoses.
2. In encapsulated, non-invasive tumours with follicular growth pattern but with focal papillary carcinoma nuclear features, in our hands a definite correlation was noted with CK19 positivity.
3. Oxyphilic cells stain for CK14.
Gal3 and HBME1 markers, helpful in distinguishing benign from malignant follicular tumours, may be positive in both benign as well as in malignant oxyphilic tumours.
4. In cellular areas in thyroid nodules and goitres, the positivity of some malignancy-associated markers is at present not well understood, but might be due to clonal heterogeneity.
Short Bibliography:
Fusco A., Chiapetta G., Hui P., Garcia-Rostan G., et al. AM.J.Path. 160, 2002 , p.1941-4
Hunt J.L., Baloch Z.W., Barnes E.L., LiVolsi Endocr. Path. 13,2002 p 321-9
Nikoforov Y.E. in Endocrine Pathology: Different. Diagn.& Mol.Adv. R.V. Lloyd Edt. Humana Press Totowa NJ 2004, p 191-209
Thienpont L., Schelfhout A-M. Willems J. Drijkoningen M. Cytopathology supp 2002 p. 73-4
Williams E.D. (Chernobyl Path. Gr.) Int.J.Path 2000, 8, p 181-3

P 611
HER2/NEU STATUS IN THYROID TUMORS: A STUDY OF 92 THYROID CASES BY IMMUNOHISTOCHEMISTRY AND FLUORESCENCE IN SITU HYBRIDIZATION
DÝZBAY SAK Serpil*, ERGUN Dilhan*, PERCÝNEL Sibel*, ERDEN Esra*, KUZU Isinsu*, KURSUN Nazmiye**
Departments of Pathology* and Biostatistics**, Ankara University School of Medicine, Ankara, Turkey

Introduction: HER2/neu overexpression and amplification have been shown in a variety of carcinomas particularly breast carcinomas. However, a limited information is available concerning thyroid neoplasms in this regard.
Aims: The aim of this study was to determine HER2/neu status by immunohistochemistry (IHC) and fluorescence in situ hybridization (FISH) in benign and malignant thyroid neoplasms using low density manual tissue microarray.
Materials and Methods: For immunohistochemical study and FISH analysis, tissue cylinders of 4 mm diameter taken from

paraffin blocks of 92 thyroid tumors were arrayed in 8 recipient paraffin blocks. We analyzed HER2/neu status of 9 follicular adenomas, 50 papillary carcinomas, 19 medullary carcinomas, 10 anaplastic carcinomas and 4 follicular carcinomas by IHC (DAKO), using streptavidin biotin immunodetection system and by FISH (Q-biogene).
Results: A cytoplasmic staining with an intensity score changing between +1 and +3 was detected in various ratios in all groups except anaplastic carcinoma group immunohistochemically However, none of the tumors showed diffuse strong membraneous staining. Cytoplasmic and/or membraneous staining was observed in 88%, 68.4%, 66.6% and 100% of papillary carcinomas, medullary carcinomas, follicular adenomas and follicular carcinomas, respectively. There was no statistically significant difference between papillary carcinoma group and other tumor groups with respect to staining. No statistically significant difference regarding staining was detected between papillary microcarcinoma and papillary carcinoma group, either.
Although HER2/neu amplification was detected in single tumor cells in some cases, HER2/CEP17 ratio was found to be lower than 2 in all tumors.
Conclusion: Cytoplasmic and/or membranous HER2/neu expression by IHC can be seen in thyroid tumors but the staining is not as strong or widespread as observed in breast carcinomas. Immunohistochemical expression does not correspond to a high level of amplification by FISH. The mechanisms and clinical impact of immunohistochemical HER2/neu expression remains unknown.

P 612
DIFFERENTIAL EXPRESSION OF DYSADHERIN IN PAPILLARY THYROID CARCINOMA AND MICROCARCINOMA: CORRELATION WITH E-CADHERIN EXPRESSION

Scopa CD, Batistatou A*, Nakanishi Y**, Charalabopoulos K***, Hirohashi S**, Agnantis NJ*
Department of Pathology, University of Patras Medical School, Patras, Greece, *Department of Pathology, University of Ioannina, Medical School, Ioannina, Greece, **Pathology Division, National Cancer Center Research Institute, Tokyo, Japan and ***Department of Physiology, Clinical Unit, University of Ioannina, Medical School, Ioannina, Greece

Introduction: Papillary carcinoma is the most common type of thyroid cancers. Microcarcinomas are small tumors (<1cm) of the same histologic type, usually clinically silent and frequently detecting as incidental findings. E-cadherin is a cell adhesion molecule involved in the progression of several malignant neoplasms. Dysadherin is a recently described cell membrane glycoprotein, which has an anti-cell-cell adhesion function and downregulates E-cadherin.
Purpose: The purpose of the study was to examine the expression of dysadherin and E-cadherin in papillary thyroid carcinomas and microcarcinomas and investigate whether there are differences in their expression.
Methods: The expression of E-cadherin and dysadherin was detected immunohistochemically in 20 papillary carcinomas and 20 microcarcinomas of the thyroid gland. The method was applied on formalin-fixed, paraffin-embedded tissue sections using the EnVision System (DAKO) and the monoclonal antibodies: NCC-M53 against dysadherin and E-cadherin (CM170B, Biocare Medical). The intensity, the expression pattern and the percentage of neoplastic cell staining was recorded and correlated with the histologic type.
Results: Dysadherin was not expressed in normal thyroid follicular cells. In papillary carcinomas low membranous expression was detected in 40%(8/20) of the cases, intermediate expression in 20%(4/20) and high expression in 15%(3/20). In microcarcinomas low expression was detected in 40%(8/20) of the cases, intermediate expression in 10%(2/20) and high expression in 0%(0/20). Immunoreactivity for E-cadherin was detected in non-neoplastic follicular cells. In papillary carcinomas low expression was detected in 30%(6/20) of the cases, intermediate expression in 45%(9/20) and high expression in 20%(4/20). In microcarcinomas low expression was detected in 10%(2/20) of the cases, intermediate expression in 50%(10/20) and high expression in 40%(8/20). Increased dysadherin expression was correlated with aberrant (cytoplasmic) E-cadherin expression in most tumors.
Conclusion: Since dysadherin is not normally expressed in non-neoplastic thyroid follicular cells, it is conceivable that it plays a pivotal role in the neoplastic transformation of thyroid gland. Moreover its expression correlates with tumor size. In papillary thyroid tumors, dysadherin appears to downregulate E-cadherin expression, at least in part.

P 613
FIBRILLIN 1 EXPRESSION IN THYROID CARCINOMAS .

TSELENI-BALAFOUTASofia 1,FANOURAKIS Galinos 1, VOUTSINASGerasimos 2, LITSIOUHelen 1, MITSIADESConstantine 3, MITSIADESNikolas 3,PATSOURIS Efstratios 1
1 Department of Pathology, Medical School,National University of Athens, Greece
2Institute of Biology,NCSR Demokritos,Athens
3.Dana Farber Cancer Institute,Harvard Medical School, Boston

Introduction:
Fibrillin is an extracellular matrix glycoprotein ,a main component of microfibrills , with sites recognizable by integrin receptors, suggested to support cell attachment and to impact cell differentiation and migration. The aim of this study was to investigate and to compare the fibrillin expression in thyroid carcinomas at mRNA and protein level in cell lines, commercial available tissue microarrays and archival specimens,
since ECM proteins are suggested to be of great importance for the metastatic potential of carcinomas.
Material and Methods:
RNA was extracted from 13 thyroid cell lines (9 papillary Ca , 2 anaplastic Ca , 1 follicular Ca,and 1 medullary Ca) .RT-PCR analysis for Fibrillin- 1 mRNA was followed, using gene-specific primers.
Furthermore we investigated the fibrillin expression by immunohistochemistry in a commercial available tissue microarray (IMGENEX IMH 319) including 42 papillary Ca, 7 follicular Ca, 1 PDC and 9 benign thyroid tissues, as well as in archival tissue from the files of the Pathology Department of the Athens University, including 33 thyroid carcinomas(15 papillary, 4 follicular, 5 Huerthle cell-, 1 anaplastic and 8 medullary Ca).For immunohistochemistry an antibody against fibrillin 1 (Santa Cruz H-109) was used at dilution 1:100 (overnight) .The stain was evaluated semiquantatively (0 - +++)
Results:
RT-PCR analysis revealed Fbn-1 mRNA expression in all thyroid carcinoma cell lines, with highest expression in the follicular Ca cell line WRO, the papillary SW579 and the medullary TT, whereas lowest expression was found in the two anaplastic cell lines (ARO, FRO) and 1 papillary (BHP 18)
Fibrillin has been demonstrated immunohistochemically in cytoplasmic location in the tissue microarray as well as in the archival sections in almost all papillary (39-14), medullary(5), Huerthle cell-4) ,anaplastic(1) and poorly differentiated Ca (1), whereas it was absent in all follicular carcinomas.The most intense stain has been observed in papillary carcinomas, with a slight increased intensity in advanced stages.
Conclusions:

Our data indicate that,fibrillin 1 is strongly expressed by the neoplastic cells of thyroid carcinomas in different degree in the various histologic types and might be implicated in cell-stroma interaction in terms of signaling ,attachment and migration.

P 614

DIAGNOSIS OF METASTATIC CARCINOMA OF THE THYROID GLAND BY FINE NEEDLE ASPIRATION CYTOLOGY. A REPORT OF CLINICAL AND MORPHOLOGICAL FEATURES OF A CASE WITH THYROID METASTASES FROM COLON ADENOCARCINOMA.

IVANOVA Radina, KARANOVA Penka, KANEV Nikolai, KOVACHEVA Russana
Clinical Center of Endocrinology, Medical University, Sofia, Bulgaria

Clinically evident, diagnosed and surgically resected thyroid metastases are uncommon. In a series of 42 cases with nonthyroid carcinoma and thyroid nodules, thyroid metastases were found in 4 cases (2 – lung cancer, 1 – breast cancer, 1 – colon cancer) by ultrasound-guided fine needle aspiration cytology of the thyroid gland. We report the clinical and morphological features of a case of colon adenocarcinoma metastatic to the thyroid gland. The patient was a 56- year- old woman with progressively enlarging goiter and compression symptoms. A history of left hemicolectomy for colon adenocarcinoma with extracellular mucinous production - T3N0M0 (6 years ago), right lower lobectomy for lung metastasis (4 years ago) and chemotherapy was present. Thyroid ultrasound found a big tumor mass in the right lobe and a small one in the left lobe, and numerous enlarged neck lymph nodes. Fine-needle aspiration cytology of the thyroid showed atypical tall cells with an acinar pattern. Total thyroidectomy and lymph nodes' extirpation was done. Histological examination confirmed the presence of metastatic colon adenocarcinoma with moderate differentiation. Immunohistochemical staining of the thyroid tumor was negative for thyroglobulin but positive for CEA and cytokeratin 19. In conclusion ultrasound scan and FNA biopsy of the thyroid gland with cytology appear to be useful methods for the differential diagnosis of thyroid nodules in cancer patients, including colorectal carcinoma. The recognition of thyroid metastases is essential for the appropriate staging and therapy of primary carcinoma.

P 615

UTILITY OF HBME-1, CYTOKERATIN 19 AND GALECTIN-3 IMMUNOSTAINING IN THE DIAGNOSIS OF THYROID MALIGNANCY.

Matos PS , Ferreira AP, Facuri FO, Assumpção LVM, Ward LS, Metze K.
Department of Pathology and Division of Endocrinology, Department of Internal Medicine, Faculty of Medicine (FCM) - State University of Campinas (UNICAMP), São Paulo, Brazil

The aim of our study was to investigate the usefulness of immunohistochemical expression and immunolocalization of a panel of markers including HBME-1, CK-19 and galectin-3 in thyroid neoplasias and non-neoplastic lesions.
We evaluated 170 thyroid lesions including 148 neoplasias (84 papillary carcinomas, 38 follicular carcinomas, 18 follicular adenomas, 1 hyalinizing trabecular tumor, 5 medullary carcinomas, 2 anaplastic carcinomas) and 22 non-neoplastic lesions (12 adenomatous nodules and 10 Hashimoto´s thyroiditis). The percentage of positive cells as well the pattern of staining were analysed. The three markers were usually negative in normal thyroid tissue. This was helpful to differentiate lesions with follicular pattern, when there was doubt regarding the nuclear features of papillary carcinoma. HBME-1, galectin-3 and CK-19 were expressed in 94%, 72.6%, 72.6% of the papillary carcinomas and in 63%, 21% and 21% of the follicular carcinomas. Furthermore, the staining pattern of the three markers (diffuse, focal segmental of focal cellular) was useful to differentiate neoplastic from non-neoplastic nodules. Lesions could be differentiated by their staining pattern. Diffuse reactivity predominated among papillary carcinomas, specially in the follicular variant of papillary carcinoma, in contrast to the focal segmental and focal cellular pattern found in follicular adenomas or carcinomas and adenomatous nodules. Counting the percentage of galectin-3 and CK-19 positive cells was useful for the differentiation between cases of follicular variant of papillary carcinoma and follicular carcinoma or adenoma.
Therefore we conclude that immunohistochemical staining features may be useful for the differential diagnosis of thyroid lesions. Diffuse positivity is indicative of malignancy. We also suggest that HBME-1 is a very sensitive marker for thyroid malignancy, but the three markers together may be helpful in special cases. This panel of markers discriminates the lesions with a follicular pattern, with special reference to the follicular variant of papillary carcinoma .
supported by FAEP, CNPq, FAPESP.

P 616

IMMUNOHISTOCHEMICAL EXPRESSION OF GALECTIN-3 IN BENIGN, MALIGNANT AND THYROID TUMORS OF UNCERTAIN MALIGNANT POTENTIAL

ABROSIMOV Aleksandr, LUSHNIKOV Eugeny

Background. Well differentiated encapsulated thyroid tumors with a follicular architecture are sometimes quite difficult for pathologists to make differential diagnosis between a definite malignant or definite benign category. Pathologists are compelled to classify the tumors having questionable nuclear changes and questionable or absent capsular invasion as well differentiated tumors of uncertain malignant potential (WDT-UMP). In a series of recent reports it has been found that galectin-3 immunostaining may be useful to distinguish benign and malignant thyroid tumors. Immunohistochemical expression of galectin-3, a human lectin, has been shown to be highly associated with a malignant behaviour of thyroid tumors.
Purpose of the study. We studied galectin-3 expression in a spectrum of obvious benign, tumors of border-line or uncertain malignancy and obvious malignant thyroid tumors.
Materials and methods. Sixteen papillary carcinomas, two follicular carcinomas, five well differentiated thyroid carcinomas not otherwise specified (NOS), seventeen follicular adenomas and twelve thyroid tumors of uncertain malignant potential were examined. Monoclonal antibodies specific to galectin-3 (Novocastra Laboratories) and indirect streptavidin-biotin complex immuno-reaction were used for immunohistochemistry.
Results. Positive cytoplasmic immunostaining of tumor cells was seen in 14 papillary, 2 follicular carcinomas, 4 well differentiated carcinomas NOS, 2 follicular adenomas and 5 well differentiated thyroid tumors of uncertain malignant potential.
Conclusion. Galectin-3 is a reliable marker of well differentiated thyroid carcinoma. It can sometimes be expressed in benign tumors. Group of well differentiated thyroid tumors of uncertain malignant potential is seems to be a heterogeneous. The significance of positive immunostaining of tumor cells in obvious benign tumors and in some of the border-line group of tumors as well as negative immunostaining in some of the obvious malignant tumors needs to be further investigated.

P 617

IMMUNOHISTOCHEMICAL EXPRESSION OF FASCIN IN GASTROENTEROPANCREATIC ENDOCRINE TUMORS

BOBOS Mattheos, KARAYANNOPOULOU Georgia, GERASIMIDOU Domniki, TELEVANTOU Despoina, KOLETSA Triantafyllia, PAPADIMITRIOU S. Constantine
Department of Pathology, Aristotle University Medical School, Thessaloniki, 54006, Greece

Introduction. Fascin is a globular protein that organizes F-actin into well-ordered, tightly packed parallel bundles in vitro and in cells. Fascin is normally expressed by basal layer cells of the epidermis, neurons, glial cells, dedritic cells, endothelial cells and macrophages. Abnormal expression of fascin was reported in almost all cases of Hodgkin disease (in Reed-Sternberg cells), in T-cell lymphomas and in various types of carcinomas. In studies of non-small cell lung carcinoma and gastric adenocarcinoma high fascin expression is correlated with poor survival. Its immunoreactivity is variable in endocrine tumors (ETs). According to our knowledge, studies concerning the expression of fascin-1 in gastroenteropancreatic (GEP) ETs have not been reported.
The aim of the present study is to investigate the expression of fascin in GEP-ETs.
Material and Methods. A total 30 cases of GEP-ETs were included in this study. A panel of immunohistochemical markers was used for diagnosis. GEP-ETs were classified according to the latest WHO criteria in 13 cases of well differentiated ETs "carcinoids" and 17 cases of endocrine carcinomas (well or low differentiated). The primary tumors were located in the foregut (13-43,3%), midgut (14-46,7%), or hindgut (3-10%) respectively. All the cases were immunohistochemically tested using the monoclonal antibody that recognizes the C-terminal region of the fascin molecule. Twenty pancreatic and gastrointestinal tissue speciments with non-specific reactive changes were also tested for fascin expression.
Results. Diffuse cytoplasmic staining of fascin was found in neoplastic cells of 4/17 GEP endocrine carcinomas. These tumors had a high MIB-1 labeling index (over >50% of neoplastic cells). All the well differentiated ETs were non-reactive for fascin. The endocrine cells of Langerhans islands of pancreas and those of the GI tract were also negative.
Conclusion. High expression of fascin is reported in large-cell neuroendocrine carcinomas of the lung and in all cases of small-cell lung carcinoma. In typical or atypical carcinoids of the lung fascin is detected in a small number of cases. In our study only 4/17 cases of GEP endocrine carcinomas were positive for fascin. On the contrary all the well differentiated GEP-ETs were non-reactive. These results show that overexpression of fascin-1 in GEP-ET is not a common finding. Further extensive studies are essential to define the role of fascin expression in these neoplasms.

P 618

RELATIONSHIP BETWEEN IMMUNOHISTOCHEMICAL EXPRESSION AND PLASMA CONCENTRATION OF TOTAL GHRELIN IN PATIENTS WITH GASTRIC NEUROENDOCRINE TUMOURS.

TSOLAKIS Apostolos V. *, STRIDSBERG Mats **, PORTELA-GOMES Guida M. §, GRIMELIUS Lars #, TIENSUU-JANSON Eva *.
Dept. of Medical Sciences, Section of Endocrine Oncology *, Section of Clinical Chemistry **, Dept. of Genetics and Pathology #, Uppsala University Hospital, Uppsala, Sweden. Centre of Nutrition, Lisbon University, Lisbon, Portugal §.

Background: Ghrelin is a 28-amino acid growth hormone secretagogue occuring predominantly in the gastric mucosa. Ghrelin-immunoreactive (IR) cells in normal stomach also express vesicular monoamine transporter-2 (VMAT-2). Ghrelin has been reported in ECLomas type I and III and in regions with ECL cell hyperplasia.
Aim: To characterise neuroendocrine (NE) tumours of the human gastric corpus with respect to the occurrence of ghrelin-IR cells and relate the findings to plasma (P) total ghrelin concentration.
Material and Methods: The study included ECLomas type I (n=4), type III (n=5), one gastric NE carcinoma and one malignant gastric ghrelinoma. Antibodies against chromogranin A, synaptophysin, synaptic vesicle protein 2, VMAT-1, VMAT-2 and ghrelin were used for immunohistochemistry. P total ghrelin was measured using a commercial RIA kit (Linco Research, Mi, USA).
Results: Ghrelin immunoreactivity was found in varying frequency in neoplastic cells of ECLomas type I (VMAT-2-IR) and in virtually all cells of the ghrelinoma (VMAT-2 negative), but were not observed in type III ECLomas nor in the NE carcinoma. Immunoreactivity for ghrelin was detected among the ECL hyperplastic cells in the mucosa of ECLomas type I. In ECLomas type III and in the NE carcinoma slight diffuse hyperplasia of ghrelin-IR cells was also seen in the peritumoural mucosa. P total ghrelin levels were within the reference range (<5 ìg/L) in all ECLomas and in the NE carcinoma, despite the presence of neoplastic and/or hyperplastic ghrelin-IR cells. Increased P concentration of total ghrelin was only observed in the patient with the malignant gastric ghrelinoma, who had more than 400-fold increase (2100 ìg/L).
Conclusion: In spite of neoplastic and hyperplastic ghrelin-IR cells in ECLomas type I and ghrelin cell hyperplasia in the surrounding mucosa of the neoplastic tissue in type III and in the NE carcinoma no elevation of P total ghrelin concentration was detected. However, in the patient with the ghrelinoma the P total ghrelin was markedly elevated. Thus, expression of ghrelin in neoplastic (excluding the ghrelinoma case) and hyperplastic cells in the gastric mucosa does not seem to give rise to elevated circulating levels of ghrelin.

P 619

PANCREATIC MICROADENOMATOSIS IN PATIENTS WITH AND WITHOUT THE MULTIPLE ENDOCRINE NEOPLASIA TYPE 1 SYNDROME

SCHLENGER Regina*, ANLAUF Martin*, PERREN Aurel**, SCHMID Sonja**, BAUERSFELD Juliane*, WIEBEN Daniel*, KOCH Christian A.***, KOMMINOTH Paul**, DRALLE Henning****, WEIHE Eberhard*****, HEITZ Philipp U.**, KLÖPPEL Günter*
*Department of Pathology, University of Kiel, Germany
**Department of Pathology, University Hospital Zürich, Switzerland
***Division of Endocrinology and Nephrology, University of Leipzig, Germany
****Department of General and Visceral Surgery, University of Halle, Germany
*****Department of Molecular Neuroscience, Institute of Anatomy and Cell Biology, University of Marburg, Germany

Introduction: Microadenomatosis of the endocrine pancreas has been suggested to represent a hallmark of multiple endocrine neoplasia type 1 (MEN 1). Purpose of the study: On the basis of several observations we hypothesize that microadenomatosis may also occur independently of MEN 1 and that it may show features distinct from those in MEN 1.
Methods: Pancreatic tissue specimens from 40 patients were analyzed, using immunohistochemisty, confocal laser scanning microscopy and morphometric methods. The MEN 1 and Von-Hippel-Lindau (VHL) status were assessed clinically and by PCR based mutational analysis. Results: Twenty seven of the 31 MEN 1 patients were found to have microadenomatosis in addition to single macrotumors. Most microadenomas and macrotumors expressed glucagon, with pancreatic polypeptide and insulin following in frequency. In

nine of the 40 patients with pancreatic microadenomatosis neither MEN 1 nor VHL germline mutations could be found. Five of these nine patients suffered from hyperinsulinism caused by multiple microinsulinomas, while the four others had multiple clinically silent microglucagonomas. The nontumorous pancreatic tissue from both MEN 1 and nonMEN 1 patients contained proliferative endocrine cell lesions in the ducts and the islets. Conclusions: Microadenomatosis in MEN 1 is the basis for the development of single macrotumors, which may cause a hormonal syndrome. Microadenomatosis is not specific for MEN 1 or VHL, but may occur independently and cause a functional syndrome. In both conditions microadenomatosis is preceded by various preneoplastic proliferative changes of endocrine cells.

P 620

ARE PANCREATIC ENDOCRINE TUMORS A MANIFESTATION OF THE NF1 PHENOTYPE? MOLECULAR ANALYSIS OF A PATIENT WITH VON RECKLINGHAUSENS SYNDROME

PERREN Aurel, WIESLI Peter, SCHMID Sonja, MONTANI Matteo, SCHMITT Anja, MOCH Holger, KONNINOTH Paul
Institute for Clinical Pathology, Department of Pathology, University Hospital Zürich
Division of Endocrinology and Diabetes, University Hospital Zurich (W.P.)
Institut for Clinical Pathology, Kantonsspital Baden, AG, Switzerland (K.P.)

Introduction: Patients with a von Recklinghausen syndrome (NF1) carrying NF1 germline mutations are predisposed to endocrine tumors including pheochromocytomas and duodenal somatostatinomas. It is unclear whether the rarely reported occurrence of pancreatic insulinomas in NF-1 patients represents a coincident finding or whether insulinomas are a rare manifestation of the NF1 syndrome.
Aims: To determine the relationship between NF1 and insulinomas, we analyzed blood and tumor tissue of an insulinoma for NF1 mutation, allelic loss of the NF1 gene and its expression in a patient with von Recklinghausen syndrome.
Patient: The NF-1 patient presented with recurrent episodes with weakness, sweating, and occasional loss of consciousness. A MRI showed a 2.5 cm tumor in the body of the pancreas. A tumor enucleation was performed and histology revealed a well differentiated pancreatic endocrine carcinoma (WHO 2004) with a micrometastasis in a peripancreatic lymph node. Immunohistochemistry showed expression of insulin and proinsulin.
Methods: Mutation analysis was performed by direct sequencing of the peripheral blood and tumor tissue. Allelic loss (LOH) analysis of the NF1 gene was done using the intragenic microsatellite markers D17S1166, NF1.PCR3 and D17S1849 on 17q11.2. For expression analysis, a RT-PCR was designed spanning intron 3 of the NF1 gene including the mutated site in exon 4.
Results: Mutation analysis of peripheral blood leukocytes confirmed a 4 base pair deletion in exon 4 starting at codon 167 (499 del TGTT). LOH analysis of tumor tissue revealed retention of both NF1 alleles. While RT-PCR of peripheral blood showed biallelic expression of both the wild-type NF1 and the mutated form, RT-PCR of tumor extracts showed a sole expression of the mutated NF1 allele.
Conclusion: These results suggests that the transcription of the wild type NF1 allele is suppressed, probably by epigenetic mechanisms. This is a strong indication for a causal relationship between the insulinoma and the von Recklinghausen disease. It can be hypothesized that insulinomas are a rare manifestation of the NF1 pheonotype. Furthermore, the NF1 gene must be considered as a candidate tumor suppressor gene for insulinomas and other PET, since the second allele can be inactivated by other mechanisms than 17q LOH.

P 621

NESIDIOBLASTOSIS: A RARE CAUSE OF HYPERINSULINEMIC HYPOGLYSEMIA IN ADULTS.

Gürbüz Y*, Filinte D*, Erçin C*, Cantürk NZ**, Cantürk Z***, Türemen E***, Tarkýn I***, Çetinarslan B***
*KOCAELI UNIVERSITIY MEDICAL FACULTY PATHOLOGY DEPARTMENT
**KOCAELI UNIVERSITIY MEDICAL FACULTY GENERAL SURGERY DEPARTMENT
***KOCAELI UNIVERSITIY MEDICAL ENDOCRINOLOGY DEPARTMENT

INTRODUCTION: Nesidioblastosis is an uncommon cause of hyperinsulinemic hypoglisemia in adults. In this case report we will present an adulthood nesidioblastosis.
CASE REPORT: 73 years old man was admitted to the emergency service of Kocaeli University Medical Faculty with the complaint of senkop. During first examinations, the blood glucose levels were between 10-29 mg/dl. Although there was not any preoperative radiological findings of pancreatic mass, decision of surgical examination for the diagnosis and treatment of insulinoma was made. During surgery, 85% distal pancreatectomy was performed because of the lack of pancreatic mass during operative exproration.
The resection material was in 12X4X1,5 cm dimentions. All the pancreas was embedded in 24 blocks. Serial sections were applied to each block for three times and tumoral mass was not observed. In histopathological examination abnormal shaped Langerhans islands, ductulo-insular complexes, endocrin buddings from ductal structures, small clustures and single endocrine cells were observed in the pancreas parachyma. The insulin immunostaining was observed more than 80% in Langerhans islands, small clustures and single cells in the parancyhima. The typical peripheric alpha cell ring was not observed in some islands in glucagon immunostaining. The mean Langerhans island diameter was 270µ.
After the operation the patient's general condition deteriorated because of his respratory problems and sent to intensive care unit. The blood glucose levels were fluctuated between 90-110 mg/dl. The patient died because of the respratory problems in postoperative 48. day.
CONCLUSION: The diagnosis of adulthood nesidioblastosis was made according to clinical and histopathological features. Although insulinoma is the most common reason of deep hyperinsulinemic hypoglycemia the entity of nesidioblatozis must be in mind for differential diagnosis of this situation.

P 622

SUBTOTAL PANCREATECTOMY FOR PERSISTENT HYPERINSULINAEMIC HYPOGLYCAEMIA – CASE REPORT

BOGOEVA Biljana, KOCOVA Mirjana, PETROVSKI Pero, CVETKOVSKI Petar
Institute of Pathology, Pediatric Clinic, Pediatric Surgery clinic

The syndrome of persistent neonatal and infantile hyperinsulinaemic hypoglicaemia(PHHI) has long recognized, its pathogenesis remain to be eluciated.Two different forms, focal and diffuse, have been reported. The diffuse form corresponds to the lesion previosly described as " nesidioblstosis". Persistent hyperinsulinemic hypoglycemia (PHHI) rarely appears after infancy. We present a normally developed 4.5 year old boy with severe hypoglycemia resistant to medications.Treatment with glucose infusions did not keep his glycemia normal. He was hypoglycemic (initial glycemia 1.9 mmol/l) and no ketosis was detected. He

required 140 mg/min iv glucose for maintenance of glycemia within normal range. The insulinemia was 44 mu ;IU/ml at glycemia of 2.2 mmol/l (ratio 20:1). Hyperinsulinemia was persistent. Imaging of the pancreas by ultrasound and CT was normal. Diasoxide in a dose of up to 6 mg/kg showed a transitional effect. After two months the child became severely hypoglycemic again requiring permanent high doses of iv glucose. Glucagon and somatostatin did not correct the hypoglycemia as confirmed by continuous glucose monitoring. Subtotal pancreatectomy was performed. Metods and results: Intra-operative frosen section were performed on small pancreatic specimens taken from the different parts of the gland allows one to determine the type of lesion (focal or diffuse). The paraffin block obtained from subtotal pancreatectomies were sliced and stained with routine staining HE, reticulin, PAS and immunohistochemical stains: insulin, proinsulin, somatostatin, glukagon, pancreatic polipeptid, P57 and SUR-1. Hystology of the pancreas showed numerous normally configured islets that are quite numerous with variably sized.They are irregulary distributed in the acinar tissue and interlobular stroma.The structure was normal with insulin cells in the center and glucagon, somatostatin and pancreatic polypeptide cells at the periphery. The islets were not at rest. Labeling for P57 and SUR-1 was normal.There was no excessive release of insulin. The child is in good health 14 months after surgery and does not require any treatment. Continuous glucose monitoring showed normal values of glycemia. Last check up showed normal HbA1c (5.0%) and insulin level (10.4 uIU/ml). Histology and the clinical course are not typical for a diffuse form or a PHHI.

P 623

ANEUPLOIDY AND LOW P21/WAF1 EXPRESSION IN MALIGNANT PARAGANGLIOMAS

Fernando A. Candanedo-Gonzalez, Brenda Barraza-Ibarra, Arturo Cerbulo-Vazquez, Milena Saqui-Salces, Armando Gamboa-Domínguez.
Departments of Pathology from Oncology Hospital at Nacional Medical Center and National Institute of Medical Science and Nutrition, and Department of Citometry, INPer. Mexico City.

Background: Clinical and histopathological features do not reliably distinguish between benign and malignant paragangliomas. Additional markers that might be useful prognostic indicators in the pathological assessment of these tumors are sought. Aim: to determine if p21/WAF1, p27Kip1, p53 and Ki-67 expression, and DNA content correlates with clinical behaviour of the paragangliomas. Design: Patients submited to surgery for sporadic paraganglioma from sites anywhere with follow-up, were included in this retrospective case-control study. Gender, age, tumor size and metastases were obtained from medical records. Malignancy was defined as the presence of metastasis and/or extensive local invasion. IHQ detection of p21/WAF1, p27 Kip1, p53 and MIB-1 against Ki-67 antigen, was blindly performed. The reactivity was evaluated as percentage of positive nuclear immunoreactivity. For measurement of DNA content one block of each case was selected. Student t test was used. Results: The study group included 31 patients, 23 women and 8 men. Mean follow-up was 41 months (range, 0-123). Twenty-seven were benign and 4 malignant tumors. Three of the malignant tumors were present in men. Mean age of patients with benign and malignant tumors was 48 ± 11.3 years and 33 ± 12.3 years, respectively (p=0.031). The mean size for benign and malignant tumors was 4.5 cm ± 1.9 and 7.5 cm ± 8.3, respectively (p=0.093). Recurrences were observed in 2 patients (7%). p21/WAF1 expression was positive in 50% malignant versus 89% benign tumors. Only one benign case was positive for p53. p27Kip1 and Ki-67 expression no showed significant differences between groups. All malignant tumors were aneuploid versus only 23% of benign tumors. Conclusions: The present study showed that malignant paragangliomas were related to less age, higher tumor size, aneuploidy and less p21/WAF1 expression. This results suggest that p21/WAF1 can be inactivated in malignant paragangliomas inducing proliferation of neoplastic cells.

P 624

ADRENAL LIPOMAS: REPORT OF TWO CASES AS INCIDENTAL AUTOSY FINDING.

JM Suárez-Peñaranda, Alvarez-Iglesias MT, JI Muñoz, MS Rodríguez-Calvo, JA Ortiz-Rey*, L Concheiro.
Department of Pathology and Forensic Sciences. University of Santiago de Compostela.
* Department of Pathology . POVISA Medical Center. Vigo Spain.

INTRODUCTION

Adrenal lipomas are extremely rare, benign, non-functioning neoplasms, with very few cases recorded in the medical literature. Most cases have been incidental findings, usually during autopsy investigation of deaths from an unrelated cause. The size can be variable, ranging from one up to twelve centimetres. The follow up is limited to exceptional cases diagnosed during life and the outcome of these patients have been excellent.

CASE REPORTS

Case 1: A 70-year-old man is found dead in a beach. Medico-legal investigation and autopsy confirm that the death was due to drowning. A small tumour is noted in the right adrenal gland. It is a soft, rounded, yellow mass, with 1 cm in its largest dimension. Histopathological examination reveals a typical lipoma.

Case 2: A previously healthy 45-year-old man collapsed and dies while taken to the hospital. Autopsy examination shows that both adrenal glands are enlarged. The left weights 92 gr and a yellow-tan mass occupies most of the cut surface. Histopathologically corresponds to a pheocromocytoma, which was considered responsible for the death.

The right adrenal gland weights 18 gr. and has a 2 cm, soft, yellow mass. Histopathological examination reveals a lipoma.

COMMENTS

We report two cases of adrenal lipomas, one of them associated to pheocromocytoma in the contraleteral adrenal gland. To the best of our knowledge, this association has not been previously reported. Since lipomas are very unusual in this location, in both cases the whole mass was submitted for histopathological examination to rule out other possibilities such as myelolipoma or liposarcoma.

Histopathologically, adrenal lipomas are similar to conventional lipomas arising elsewhere in the body, a feature non contributive to asses its pathogenesis, which remains unknown. The relation between myelolipoma and lipoma has been discussed and a continuum spectrum between both neoplasms has been proposed, but never proved.

Our cases are typical, since they were asymptomatic and only discovered at autopsy. Although they present little difficulty in the histopathological diagnosis, their kwnowledge is merit because the incidental discovery of these neoplasms has increased during the last years.

P 625

HISTOPATHOLOGICAL STUDY OF PRENATAL STRESS ON ADRENAL GLAND TOTAL VOLUME AND ABSOLUTE VOLUME OF GLOMEROLUSA, FASCICULATE, RETICULARIS LAYERS AND MEDULLA IN 21 DAYS NEONATE RATS: A STEREOLOGICAL STUDY

Bahmanpour S, Noorafshan A, Karimpour M, Dehghani F
Shiraz University of Medical Sciences, Shiraz, Iran

Pregnant mothers may expose to various stresses and it may impact on their embryos. It affects the structural development of brain, gland and body weight. The detail of this histopathlogical changes have been little researched. The base of this study was the prenatal stress effects on adrenal gland stereological.
Sprague-Dawely rats were kept in standard condition for two weeks. The two female with one male were caged overnight. Vaginal pluge and sperm detection in vaginal smear confirmed the pregnancy. Then 30 pregnant rats were divided into two groups as control and experimental. The experimental group was exposed to stress from the first to the end of the pregnancy. The stress was induced three times a day, each time lasting 45 minutes. 21 days after birth one animal from each dam was selected and its adrenal gland was removed for tissue processing, and sterological study. 12 sections were selected by random systemic sampling and the Cavalier's method was used to calculate the gland volume. The statistical analysis revealed significant differences between the total and absolute volume of glomerolusa, fasciculate, reticularis layers ($P<0.001$) and medulla ($P<0.05$) in control and experimental animals.
It can be concluded that prenatal stress causes total adrenal gland and cortical layers hypertrophy and reduces the volume of adrenal medulla.

P 626
DGGE MUTATION ANALYSIS OF RET, VHL, SDHB AND SDHD IN A SERIES OF EXTRA-ADRENAL PHEOCHROMOCYTOMAS

1 E. Korpershoek, 1 B. Petri, 1 F. van Nederveen, 1 W.N.M. Dinjens, 2 A.A. Verhofstad, 2 J.W. Lenders, 3 S. Schmid, 3 A. Perren, 3 P. Komminoth, 1 R.R. de Krijger
1 Department of Pathology, Josephine Nefkens Institute, Erasmus MC, Rotterdam, the Netherlands, 2 Department of Pathology and Internal Medicine, Radboud University Nijmegen, the Netherlands, 3 Department of Pathology, University of Zürich, Switzerland.

Pheochromocytomas (PCC) are rare tumours that generally arise from the chromaffin tissue of the adrenal medulla, but approximately 10% may also develop from extra-adrenal tissues. Twenty-five to 30% of patients with adrenal PCC show germline mutations in either rearranged during transfection protoocogene (RET, associated with multiple endocrine neoplasia type 2), VHL (associated with von Hippel-Lindau disease), succinate dehydrogenase subunit B (SDHB) or succinate dehydrogenase subunit D (SDHD). So far, little is known about the occurrence of mutations in these susceptibility genes in extra-adrenal PCC, as only few studies have investigated these tumours in limited numbers of patients. Therefore we have investigated a large group of extra-adrenal PCC for the presence of mutations in RET, VHL, SDHB and SDHD. We have performed denaturating gradient gel electrophoresis (DGGE) mutation analysis on a series of 32 extra-adrenal PCC. Mutation analysis of SDHD showed two patients with previously described mutations D92Y and L95P in exon 3, whereas there were three patients with previously undiscribed SDHB mutations: S100F and S123P in exon 4, and C243S in exon 7. No mutations were found in RET and VHL. We conclude that SDHB and SDHD might be involved in the development of a small proportion (15%) of the extra-adrenal PCC, whereas it seems that VHL and RET play no role.

P 627
EVALUATION OF HISTIDINE DECARBOXYLASE EXPRESSION IN NEUROENDOCRINE TUMORS OF DIFFERENT SITES BY IMMUNOHISTOCHEMISTRY AND REAL-TIME RT-PCR.

UCCELLA Silvia, CERUTTI Roberta,FURLAN Daniela, OLDRINI Rita, CARNEVALI Ileana, LA ROSA Stefano, CAPELLA Carlo.
Dept. of Human Morphology, University of Insubria, Varese

Immunohistochemical (IHC) expression of HDC has been proposed as a marker for normal ECL-cell of the stomach and related neuroendocrine tumors (NETs). HDC immunoreactivity (IR) has been recently detected in NETs other than gastric ECL-cell tumors, such as intestinal, bronchial and pancreatic well differentated NETs (WDNETs) and in poorly differentiated neuroendocrine carcinomas (PDNECs) of the lung. To date, the only available anti-HDC antibody is a polyclonal directed against the whole recombinant protein. This raises the possibility of a cross reaction with DDC, which shares a large piridoxal-5'-phosphate-dependent domain with HDC.
Aim of this work was to study the HDC-IR in a series of 107 NETs and to validate the IHC results in a subset of cases by the analysis of HDC and DDC mRNA expression using quantitative real-time PCR technique.
We studied 51 WDNETs (8 gastric and 43 extragastric) and 56 PDNECs (11 of the lung and 45 extrapulmonary). Anti HDC antibody (Eurodiagnostica, Malmo, SW) was employed with standard immunoperoxydase technique on sections from formalin fixed and paraffin embedded tumor samples. Fluorescence-based real-time RT-PCR assay was performed on 37 cases (26 WDNETs- 7 gastric, 5 ileal, 7 pancreatic, 7 bronchial- and 11 PDNECs of the lung), using specific probes and primers for HDC and DDC.
HDC-IR was observed in 43/51 WDNETs (84%) with no significant differences among various sites. 32/56 PDNETs (57%) were HDC-positive, including all lung carcinomas and a fraction ranging from 33% to 55% from other sites. Quantitative real-time PCR showed an increased expression of HDC in HDC-IR gastric, ileal and pancreatic WDNETs, while DDC expression was absent or lower than in normal controls. By contrast, HDC mRNA levels were very low in HDC-IR bronchial carcinoids, while DDC was highly expressed in all cases. In addition, all lung PDNECs showed HDC mRNA levels below the normal control, whereas high levels of DDC mRNA were found in all cases.
This study shows that anti-HDC antibody against the whole recombinant protein cross-reacts with DDC. Therefore, HDC-IR in NETs should be critically evaluated and validated with a specific molecular approach. Our data demonstrate that HDC is expressed in ileal and pancreatic WDNETs, in addition to gastric ECL-cell tumors. On the other hand, HDC-IR in bronchial WDNETs and in lung PDNECs should be considered as a cross reaction with DDC.

P 628
ANGIOGENESIS IN PITUITARY ADENOMAS BY VASCULAR ENDOTHELIAL MARKERS

Tanase Cristiana*, Codorean E.*, Popescu D.I.*, Raducan E.*, Cruceru L.**, Arsene D.*, Georgescu M.*, Ciubotaru V.***,Ogrezean I.***, Hinescu M.**, and Ardeleanu C.*
* National Institute of Pathology "Victor Babes", Bucharest, Romania
** "Carol Davila University of Medicine", Bucharest, Romania
*** "D. Bagdasar" Hospital, Neurosurgery Dept., Bucharest, Romania

Introduction
Angiogenesis is a dynamic process, essential for embryogenesis, morphogenesis, tumorigenesis and other biological processes, being the most important factor for growth and proliferation of tumors.
Aim

We proposed to evaluate angiogenic phenotype by quantified the vascular density for estimation the biological behavior and invasiveness to pituitary adenomas.
Materials and methods
For quantified the vascular density, we used histochemistry (Gomori stain) and immunohistochemistry analysis (for vascular endothelial markers CD31/CD34, FVIII and the most potent angiogenic molecule - VEGF).
Results
We have investigated 30 paraffin-embeded pituitary adenomas: 21 functioning and 9 non-functioning; 22 with local invasiveness, 16 invasive in cavernous sinus; 4 were recidives.
Immunohistochemical analyses of CD31/CD34, FVIII, demonstrate variable degrees of vascular density in different types of pituitary tumors. There were differences in the fields of the same tumor, and also in the different types of tumor, angiogenesis being more pronounced in the front of invasive than in the middle of tumor.
CD34 was expressed in 100% of cases, follow by FVIII in 83,3% of cases.
There is a good correlation between CD34 and FVIII expression.
We observed a positive correlation between vascular density and invasiveness, angiogenesis is more pronounced in invasive pituitary tumors.
VEGF expression is more prominent in certain adenoma subtypes; stronger in invasive pituitary adenomas.
Conclusions.
Analyses of vascular density may provide useful information regarding angiogenesis and their role in determining overall angiogenic phenotype and their tumor behavior.

P 629
ROLE OF NITRIC OXIDE IN THE MODULATORY EFFECTS OF OVARIAN HORMONES UPON BEHAVIORAL INDICES OF ANXIETY IN FEMALE RATS
SADEGHIPOUR RODSARI,Hamid Reza
Depte. of Physiology, Faculty of Medicine,Tehran University of Medical Sciences,Teharn, Iran

Nitric oxide, as neurotransmitter and neuromodulator is considered to be involved in several physiologic processes within the central nervous system. The objective of the present study is to determine the influence of this molecule on the indices of anxiety regulated by ovarian hormones.
The study was conducted on 150 sterilized female rats. Estradiol Benzoate (10 ìg/kg/SC), progesterone (25 mg/kg/SC), alone or both, were administered to the animals in different groups. Some groups received an additional dose of either L-name (60 mg/kg/IP) or L-arginine (100 mg/kg/IP) before the behavioral test. Then the anxiety indices based on open and closed arms exploration, were estimated in an elevated-plus maze test.
Finally, blood samples were obtained to measure serum nitrite-nitrate concentration (the metabolite of nitric oxide) using Griess reaction.
Our study showed an anxiolytic effect of progesterone and progesterone+L-name, along with a decrease in the nitrite-nitrate concentration. While the administration of estradiol alone or together with L-arginine showed an anxiogenic effect and a reduction in nitrite-nitrate concentration.
The findings suggest the possible involvement of nitric oxide in the process of anxiety induced by ovarian steroid hormones.

P 630
CHONDROMYXOÏD FIBROMA OF THE TIBIA. A CASE REPORT
AL ATAWNA Hind, EL BAKOURI Jalila, BENADRA Fatiha, RAIS Hanane, EL ATTAR Hicham, BELAABIDIA Badia
Pathology Department , Mohammed VI hospital , university of Marrakesh , Morocco

The chondromyxoïd fibroma (CMF) is a rare benign osseous tumour. It represents less than 1% of the primitive osseous tumours and 2% of the benign osseous tumours. Its radiological aspect is strongly evocative. Its histological aspect is misleading sometimes of a chondrosarcoma or a chondroblastoma. The diagnosis confirmation rests on anatomo-radiological confrontation.
A 28 years old man has consulted for metaphyso-epiphyseal tibial osseous pains . X-Rays demonstrated a metaphyso-epiphyseal lytic excentric limited tibial image without periosteal reaction nor invasion of the soft tissue.The anatomopathological exam for surgical curettage confirmed the diagnosis of CMF.
The CMF is a rare benign osseous tumour. It poses problems of differential diagnosis with a chondrosarcoma. The anatomo-clinical and radiological confrontation is needed for diagnosis confirmation. The prognosis of this entity is good.

P 631
ACTIVATION OF THE JAK1 – STAT3 SIGNAL TRANSDUCTION PATHWAY IS ASSOCIATED WITH PATHOGENESIS AND PROGRESSION OF HUMAN CHONDROSARCOMAS
D.J. Papachristou , O.A. Papaefthymiou , D. Strefanou, A. Batistatou and N.J. Agnantis
Department of Pathology, School of Medicine, University of Ioannina, Greece

Introduction: Chondrosarcomas represent the second most frequent primary bone malignancies. However, comprehension of the molecular mechanisms underlying their pathogenesis is far from thorough. The Signal Transducer and Activator of Transcription (STAT) family proteins are transcription factors pivotal in mediating cytokine signaling. Among them, STAT3 is frequently activated in human malignancies and transformed cell lines and is involved in tumorigenesis. Activation of STAT3 is regulated by JAK1, a member of the Janus Kinases family proteins. Recent studies have demonstrated that STAT3 interacts with the promoter of c-fos proto-oncogene, enhancing its transcription. In vitro and in vivo data suggest that the onco-protein c-Fos is overexpressed in human chondrosarcomas.
Purpose: To test the hypothesis that functional upregulation of the JAK1 – STAT3 pathway and induction of c-Fos, are implicated in the pathogenesis and progression of human chondrosarcomas.
Materials and method: We employed immunohistochemistry to assess the protein levels of JAK1, its substrate STAT3, the phosphorylated/activated form of STAT3, p-STAT3 and c-Fos, in 21 benign chondroblastic lesions (14 osteochondromas, 7 enchondromas), 36 chondrosarcomas (13 Grade 1, 15 Grade 2, 8 Grade 3) and in normal cartilage.
Results: Positive immunostaining for JAK1, STAT3, p-STAT3 and c-Fos was observed in 94.4%, 100%, 97.2% and 94.4% of the chondrosarcomas, and in 42.9%, 61.9%, 23.8% and 42.9% of the benign tumors, respectively. Normal cartilage was devoid of these immunoreactivities. The cellular levels of all proteins were significantly correlated to each other (Spearman's Rho 0.699-0.892, $p<0.001$ for each correlation). Significantly higher expression levels of all proteins were detected in grade 3 compared to grade 2/1 chondrosarcomas, and to benign chondroblastic lesions (Mann-Whitney U test, $p<0.001$ for each tumor grade pair, Kruscal Wallis $p<0.001$).
Conclusions: Our findings provide novel evidence that the JAK1/STAT3 signal transduction pathway and the onco-protein c-Fos are functionally operative in the neoplastic change of chondroblastic cells and the development and progression of human chondrosarcomas. Evaluation of the

expression levels of c-Fos and JAK1 - STAT3 signalling cascade components, may facilitate an improved prediction of the tumor's clinical behaviour and potentially be exploited in designing patient-tailored treatment regimens.

P 632
IMPLICATION OF JNK/ERK–AP-1/ –RUNX2 "CROSS-TALK" IN CARTILAGE LOAD-TRIGGERED CHONDROGENESIS

D.J. Papachristou (1,2), P. Pirttiniemi (3), T. Kantomaa (3), N.J. Agnantis (1), A.G. Papavassiliou (2), E.K. Basdra (4)
(1) Department of Pathology, School of Medicine, University of Ioannina, Ioannina, Greece
(2) Department of Biochemistry, School of Medicine, University of Patras, Patras, Greece
(3) Institutes of Dentistry, University of Oulu & University of Helsinki, Finland
(4) Department of Orthodontics, School of Dentistry, Aristïtle University of Thessaloniki, Thessaloniki, Greece

Introduction: Mechanical loads influence chondro-osteogenesis and thus skeletal morphology. However, the exact mechanisms by which mechanical stimuli are transduced in chondrocytes remain obscure. Recent data have documented the involvement of the JNK and ERK MAPK signaling pathways and the transcription complex AP-1 in chondroblastic differentiation, proliferation and maturation. Furthermore, in vitro studies have demonstrated the paramount importance of the transcriptional regulator Runx2 in chondroblast biology.
Purpose: To explore and characterize the mechanotransduction events occurring in chondroblasts under altered functional loading. To this end, the roles of JNK/ERK–AP-1 signaling cascades and Runx2 were investigated.
Materials and Method: Fourteen-day-old female Wistar rats were divided into 2 groups: the first group was fed whole pellets (simulating physiologic mastication), while the second group was fed soft diet (lowered temporomandibular joint (TMJ) loading). Animals were sacrificed at 6, 12, and 48 h post-experiment initiation and biopsy material was obtained from their TMJ condyles at each time point. Immunohistochemistry was performed to evaluate the expression levels of pc-Jun (c-Jun' s phosphorylated/active form), c-Fos (principal AP-1 partner of c-Jun), JNK2 (major c-Jun kinase), p-JNK (phosphorylated/active species of JNK2), p-ERK (ERK's phosphorylated/active counterpart) and Runx2, on each TMJ specimen.
Results: The protein levels of all the examined signaling mediators/effectors were markedly increased in animals fed with hard diet, throughout the experimental process (ANOVA, $p<0,001$ for all). Tukey post-hoc analysis revealed that protein expression levels were significantly higher in cartilage from the hard, compared to cartilage from the soft food group, at 48 and 12 h. The cellular levels of the proteins were positively and significantly correlated to each other (Kendall's tau = 0.601-0,812, $p<0.001$).
Conclusions: 1) Functional cartilage loading induces the MAPK cascades; 2) Coordinate targeting of AP-1 and Runx2 transcription factors by mechano-triggered JNK and ERK appears to "fine tune" chondroblastic differentiation/maturation; 3) Deciphering the molecular events underlying the mechanotransduction phenomena is important, in order to effectively combine mechanical therapy with pharmacological intervention to control cartilage growth, augment cartilage repair and prevent cartilage degeneration.

P 633
MESENCHYMAL CHONDROSARCOMA – MULTICENTRIC OR METASTATIC LESION

ATANCKOVIC Mirjana, SOPTA Jelena, NAGULIC Mirjana, TULIC Goran

We present a case of mesenchymal chondrosarcoma in a 25 year old man who had painless tumour of m.vastus lateris sinistri invented after trauma. Radiographic examination showed soft tissue mass with iregular calcification of femoral region.
Diagnostic evaluation disclosed a hematoma in obs., but MRI will show an aggressive soft tissue mass in the reg.femoris with areas of calcification.
One month later patient noticed a weal of eyelid inferior and sweling with protrusio bulbi oculi dextri. CT scans showed retrobulbar infiltrative mass soft tissue density. Tumor mass present at the right frontal sinus was 18-20 H.U.density.
Surgical resection was done at the same time of retrobulbar and reg.femoris tumors mass. Microscopically, tumours exhibited biphasic pattern, cellular and cartilage. The majority of the tumours were composed of sheets or aggregates of small round and spindl cells with hyperchromatic nuclei that resamble those of Ewing sarcoma. Somewhere cells were arranged in a manner suggestive of hemangioperycitoma. Poorly circumscribed cartilaginous areas are blend with the undifferentiated tumour cells. Rarely, the cartilaginous foci were well defined. The histological and imunohisthemical diagnosis was – mesenchimal chondrosarcoma.
Two months after operation it was marked on the skin small lesions of abdominal wall and reg. buccae. Pathohystological verification was done and diagnosis was – mesenchymal chondrosarcoma. At the same time on verthebral body of Th 2-4. Radiographic examination showed small osteolytic lesions, but those lesions didn't examinate pathohystologicali.
Chemotherapy (ADM) was apply 3,5 months after resection, but because of recurrens of retrobulbar tumour and its invasion at the cranium with simptoms of intracranial high pressure – patient died 8 months after diagnosis was made.
A critical step of presented case is to ascertain whether it is a multicentric soft tissue and bone mesenchymal chondrosarcoma or the first discovered localisation is primary tumour and the others - metastasis.

P 634
CONDROBLASTOMA, A RETROSPECTIVE STUDY OF 13 CASES OVER A PERIOD OF 6 YEARS.

POP Doina, POP Florinel

Condroblastoma is a rare benign tumor of the epiphysis encountered commonly in the 2nd decade benefiting exclusively from surgery.
Many histopathological pitfalls associated with this tumor make it a great mime of osseous tumors, especially of osteosarcoma, which is by far more frequent in this age interval and of giant cell tumor, sharing with it the same location. The extreme heterogeneity of this tumor coupled with its local aggressiveness, in long standing cases, awakes suspicion about malignancy. Because of extra compartmental involvement in 8 out of 13 cases, fine needle aspiration was the fist diagnostic procedure, which is a simple maneuver, sometimes in the range of the pathologist's competence and very often rewarding, if not with extreme precision of diagnosis at least as malignant/benign supposition.
Frequently our guess was giant cell tumor (5 out of 8 cases), and only in 1 case the condroblastoma diagnosis was carried out in this stage of diagnostic procedures. In two cases the aspirate was very cellular, mitoses were noticed as well as chondro and osteoid matrices, facts that arose suspicion of malignancy and urged for biopsy. As for the biopsy the pathologist task was not easy. histochemistry (Acid periodic-Schiff, Gordon-Sweet and Alcian Blau and immunohistochemistry(S-100 protein, neuron specific enolase, osteopontin, Ki-67 and PCNA) were performed and sometime contributory to the final right decision.

Those cases staged G1(Enneking), were submitted to surgical excision with thorough curetting after benign intraoperatory frozen sections .
The definitive paraffin diagnosis was carried out after scrupulous sampling and integration of all histopathological aspects some of which could be very intriguing if taken apart. Our presentation intends to show most of them which are related to the presence of condro-osteoid matrix, metaplastic areas and mitotic activity.

Immunohistochemisty was of little help in differential diagnosis so that one's experience and radiological correlation are essential.

Our study tries to catch the many faces of this tumor and establish an algorithm of diagnosis emphasizing on radiological-histopathological correlation.

P 635

PROTECTIVE EFFECTS OF VITAMIN D3 ON METHYLPREDNISOLONE ACETATE INDUCED LOSS OF BONE METABOLISM MARKERS AND BONE MINERAL DENSITY IN THE LUMBAR SPINE OF RAT.

Aligholi Sobhani Ph.D., Fatemeh Moradi, MSc., Parichehr Pasbakhsh Ph.D., Iraj Ragerdi Kashani, MSc.

Introduction: Although some vitamins have been shown to prevent glococorticoids induce osteoporosis in short time, the magnitude of this effect remains to be clarified. The aim of this prospective study is the evaluation of protective effect of vitamin D3 on methylprednisolone acetate induced osteoporosis in rats.

Methods and Materials: Total duration of the experiment was four weeks. Twenty-four male spargue Dawly rats (8 week old and 180 g weight) were randomly divided into four groups: Group A (n=6), was a base line control or normal animals. Group B (n=6), was treated only normal saline (0.9%), group C (n=6), was treated methylprednisolone acetate (0.2 mg/kg) subcutaneously for 4 weeks (3 times per a week) and finally group D (n=6) were administered methylprednisolone acetate resemble to group C and treated by Vitamin D3 (0.1 µg/kg dissolved in ethanol daily). For evaluation of biochemical agents changes in the serum, level of calcium, osteocalcine and acid phosphatase were measured before and after treatment. Also, bone mineral density (BMD) of lumber vertebrae was measured by dual energy x-ray absorptiometry (DEXA).

Results: The results showed that, the serum calcium level unaffected ($P>0.05$) by methylprednisolone acetate in all groups before and after treatment, but, the serum osteocalcine level and bone mineral density of lumbar vertebrae were significantly ($p=0.05$) decreased in group C compared with groups A and B. In group D serum osteocalcine level increased again significantly ($p<0.05$) but increasing of bone mineral density and bone mineral content were not significant ($P>0.05$). Also, the serum acid phosphatase level increasing in group C was treated by vitamin D3 (in Group D), but was not significantly ($p>0.05$).

Conclusions: The findings of present investigation indicate that by using of vitamin D3 in methylprednisolone acetate treated rats could increase bone formation and decrease bone resorption.

Key words: Methylprednisolone acetate, Vitamin D3, Osteoporosis, Bone Markers Metabolism, BMD and Rat.

P 636

FIBRONECTIN IN HUMAN BONE TISSUE REMODELLING

DAHSE Regine (1), ROSENHAHN Julia (2), KILIAN Olaf (3), KOSMEHL Hartwig (1)
(1) HELIOS Klinikum Erfurt; Institute of Pathology, Nordhäuser Str. 74, D-99089 Erfurt, Germany
(2) University of Jena, Institute of Human Genetics and Anthropology, Kollegiengasse 10, D-07740 Jena, Germany
(3) University of Giessen, Dept. of Trauma Surgery, Buchheimstr. 7, D-35392 Giessen, Germany

The extracellular matrix component fibronectin (fn) has fundamental functions in cell attachment, differentiation, proliferation and in cell migration. Embryonic forms of cellular fn, named EDA-fn and EDB-fn, are generated by alternative splicing. They are detected in proliferating tissue, wound healing and tumor invasion.
This study aimed to quantify fn and its splice variants in the most frequent highly malignant human bone tumor (osteosarcoma) in comparison to bone fracture healing tissue as a model for a physiological bone repair process.
Material and Methods: A real-time quantitative RT-PCR assay (LightCycler System, Roche) was developed to quantify levels of fn, EDA-fn and EDB-fn mRNA. Relative expression was correlated to cell proliferation and differentiation (detected immunohistochemically by Ki67 and CD31 marker) and to the level of osteoid formation.
Results: Both, osteosarcoma and bone fracture healing tissue, did express higher levels of the embryonic fn variants (EDA-fn, EDB-fn) compared to unspliced fn. No significant differences were found in the EDA-fn and EDB-fn mRNA expression comparing tissue remodelling in malignant or physiological repair processes. EDA-fn and EDB-fn expression in osteosarcoma did correlate to the osteoid formation.
Conclusions: Embryonic fn splice variants are a strong marker for active granulation and tissue remodelling processes in human bones comparable with wound healing processes. The stimulating effect of fn splice variants on reparative and proliferative processes can be found in physiological bone remodelling as well as in malignant transformation. EDA-fn and EDB-fn mRNA expression levels are a marker for the malignant differentiation in osteosarcoma.

P 637

TGF BETA 1 INFLUENCE ON OSTEOBLASTS IN PATIENTS WITH NONSYNDROMIC CRANIOSYNOSTOSIS

Severgina E, Leonova L, Severgina L, Lopatin A, Ovchinnikov S, Yassonov S.

Nonsyndromatic craniosynostosis (NC) is characterized by premature closure of cranial sutures in children. The aim of our investigation was to evaluate osteoblastic cell events that lead to NC. 10 children (from 8 months to 5 years old) incision biopsies were studied. All children had an isolated NC. Stenosed cranial sutures were removed during the cranioplastic operation, fixed, decalcified with the trilon B, paraffinized. Light microscopy, immunohistochemistry was performed with labeled, specific anti-TGF beta 1 and R1, Ki 67 antibodies.
We found mature osteons, fragments of the osteons, intermediate lamellas, osteon-like structures in the cranial biopsies. Osteoblastic cells lining the bone fronts were located on the inner side of sutures. We did not find in the biopsies the serrated margins of sutures in opposite to the control. We discovered the focuses of ossification as well as the areas of bone atrophy. Within affected sutures we revealed premature ossification, increased extent of subperiosteal bone formation and complete suture obliteration instead of connective tissue zone and osteogenic cells as seen in normal cranial sutures. The same criteria of the increased osteogenesis were seen about 3 cm from a closed suture. In conjunction with increased osteogenesis the morphological changes of the osteolysis were observed: the close situated serration resorption line, the dedifferentiation of the osteones,

the osteoclastic resorption, ”oncosis.” There were opened haversion canals and spaces in the inner plate of the bone.
The immunohistochemystry showed the expression of TGF beta 1 and R1 on the osteoblasts and overexpression of the same factor on the osteoblasts within the inner plate of the cranial bone. We found increased osteoblastic proliferation with deposition of Ki 67 in these areas. The TGF beta 1 is one of the factors regulating cell-to-cell and cell-to-matrix interactions, proliferation, differentiation and maturation of the osteoblasts. Also this factor stimulates osteogenic activity of osteoblasts and accelerates osteogenesis. The activated osteoblastic cells grew at a significantly increased rate and produced significantly more serum osteocalcin than the control (119,3 ng/ml vs. 31,5 ng/ml, $p<0,05$).
In general the morphological changes of the cranial bones were typical for cynostosis in all children, but the quantitative and qualitative features were different. Maximal TGF beta 1 expression in the cranial biopsies proposes a key role of this factor for NC due to stimulation of the osteoblast proliferation, differentiation and maturation. Our results indicate that an increased maturation of osteoblastic cells in the suture margins leads to the premature ossification in NC.

P 638
CLINICAL AND PATHOLOGICAL ASPECTS IN DISTAL FEMORAL PATHOLOGICAL FRACTURES DUE TO METASTASIS
P.Sirbu1, Doinita Radulescu2, Simona Stolnicu3, Simona Mocan3
1. Emergency Hospital, University of Medicine, Iasi, Romania
2. Department of Pathology, University of Medicine, Iasi, Romania
3. Department of Pathology, University of Medicine, Targu Mures, Romania

The present paper analyzed the clinical, pathological and therapeutic aspects in a group of 15 patients with surgically removed metastasis at the distal femur level. The mean age was of 52,5 years. 9 patients showed a history of malignancy (lung carcinoma- 5 cases, larynx carcinoma- 1 case, breast cancer- 2 cases and prostate cancer- 3 cases). All patients were operated fir the pathological fractures by tumor exeresis, cavity sealing with acrylic cement and internal fixation, with immediate mobilization. Histopathological examination showed similar differentiation degrees in metastasis and the primary tumor in 7 cases. 3 primary tumors were found while 3 metastasis remained with an unknown primary tumor. Even if the osteosynthesis was performed on pathological bone it insured the patient the required mobility that was balanced with the survival period.

P 639
THE FRA-1, FRA2 AND JUNB, JUND TRANSCRIPTION FACTORS ARE INVOLVED IN THE SIGNALING CASCADE TRANSDUCING MECHANICAL LOAD IN CONDYLAR CHONDROCYTES
Papachristou D.J. (1,3), Pirttiniemi P (2), Kantomaa T. (2), Agnantis N.J. (1), Papavassiliou A.G. (3), Basdra E.K. (4)
(1) Department of Pathology, School of Medicine, University of Ioannina, Ioannina, Greece
(2) Institutes of Dentistry, University of Oulu & University of Helsinki, Finland
(3) Department of Biochemistry, School of Medicine, University of Patras, Patras, Greece
(4) Department of Orthodontics, School of Dentistry, Aristïtle University of Thessaloniki, Thessaloniki, Greece

Introduction: The chondrocytes of articular condylar cartilage proliferate, hypertrophy and finally undergo apoptosis, being replaced by osteoblasts. Mechanical loading influences the growth of the condylar cartilage, and the mechanical environment of the temporomandibular joint (TMJ) regulates the biological and histological features of the cartilage tissue via differentiation of proliferative cells into mature chondroblasts. Animal studies have shown that changes in the amount of chewing force and reduced masticatory function result in alteration of the overall growth of the mandible, hence decreased condylar cartilage growth activity. The Jun (c-Jun, JunB, JunD) and Fos (c-Fos, Fra-1, Fra-2) family of proteins are components of the dimeric transcription factor AP-1. They are activated by extracellular stress and play critical roles in bone remodeling and programmed cell death/apoptosis.
Purpose: The aim of this study was to examine the implication of the AP-1 constituents Fra-1, Fra-2, JunB and JunD in the signaling pathway of mechanical loading in the condylar cartilage. Furthermore, the association of mechanical load to cell differentiation and apoptosis through the involvement of the above factors was investigated.
Materials and Method: Fourteen-day-old female Wistar rats were divided into 2 groups: the first group was fed hard food (simulating physiologic mastication), while the second group was fed soft diet (resulting in lowered TMJ loading). Animals from both groups were sacrificed at 6, 12 and 48 h after the experiment initiation and histologic sections were obtained from their TMJ condyles at each time point. The condylar cartilage of both groups was immunostained against Fra-1, Fra-2, JunB and JunD.
Results: Our data revealed up-regulation of all the examined members of the AP-1 transcription factor family in all stages of differentiation of chondrocytes derived from mandibular condylar cartilage.
Conclusions: Mechanical loading of condylar chondrocytes results in early apoptotic phenomena of these cells and subsequent replacement by osteoblasts, most likely affecting the overall growth of the condylar head. Elucidating the signaling pathways of mechanical load in condylar cartilage cells may unravel new routes for innovative treatment approaches of patients suffering from dentofacial deformities.

P 640
CALCANEUS AS A LOCALIZATION OF SOLITARY UNICAMERAL BONE CYST
SOPTA Jelena, ATANACKOVIC Mirjana

The calcaneus is a skeletal site no so frequently affected by solitary unicameral bone cysts (SBC). In the period of 30 years at the Bone Biopsy Register of the Institute of Pathology, School of Medicine, Belgrade in calcaneus have been registered:3 chondroblastomas, 5 osteochondromas, 2 morbus exostosans, 4 chondrosarcomas, 1 osteoid osteoma, 1 osteosarcoma, 1 Ewing sarcoma, 1 giant cell tumor, 3 aneurysmal bone cysts and 17 solitary bone cysts. Calcaneal SBC accounts 3,25% of SBC of all localizations and 44,7% of all diagnosed tumors in calcaneus.
The diagnosis of calcaneal SBC based on radiographic features was possible in almost all cases. On CT scans and MRI scans the cysts were filled with fluid. A CT scan showed a central hypodense area of -120 Hounsfield units representing fat in the fluid-fluid cyst (differential diagnosis intraoseous lipoma).
After curettage cystic membrane was pathological observed. Histological features of SBC in calcaneus, are slight different from SBC of long tubular bones. The cyst membrane is usually thinner (in 2 cases absent), the zone of bleeding are more marked (9 cases), with cholesterol crystals (7 cases). Histologic proof of cementum-like substance (8 cases) showed that calcaneal cysts are true SBC and excluded intraoseous lipoma. Cementum-like substance was diagnosed more frequent in cancaneal (43%) than in long bone (10%) SBC. In 2 cases were presented histological characteristic of superposed aneurismal bone cyst.

In 80% of cases cysts were diagnosed on a characteristic and typical location- the trochlear processus, Ravelli's calcaneal triangle. The nature and clinical importance of calcaneal cysts is controversial and not clear. The risk of pathologic fracture is unpredictable and surgical treatment is not always necessary. SBC in caslcaneus is "self-limited" disease, and in significant percent of cases were described spontaneous filling of the defect.

P 641
HISTOPATHOLOGICAL CLASSIFICATION OF PERIPROSTHETIC LOOSENING MEMBRANES

Morawietz L (1), Schroeder J (2), Dynybil C (2), Kriegsmann J (3), Krenn V (1)
(1) Institute for Pathology, University Hospital Charite, Berlin
(2) Department for Orthopedic Surgery, University Hospital Charite, Berlin
(3) Group practice for pathology, Trier

Aims: To find a consensus on defined histopathological criteria for a standardized evaluation of the periprosthetic membrane from loose hip and knee endoprostheses.
Methods: Based on histomorphological criteria, four types of the periprosthetic membrane are defined: Wear particle type (detection of foreign body particles; macrophages and multinucleated giant cells occupy at least 20% of the area; type I); infectious type (granulation tissue with neutrophilic granulocytes, plasma cells and few if any wear particles; type II); combined type (aspects of type I and type II occur simultaneously; type III); indifferent type (neither criteria for type I nor type II are fulfilled; type IV).
Periprosthetic membranes from 370 patients (f=217, m=153, mean age 67.6 years, mean time to revision surgery 7.4 years) were analyzed according to the abovementioned criteria.
Results: Incidences of the histopathological membrane types: type I 54.3%, type II 19.7%, type III 5.4%, type IV 15.4%, not assessable 5.1%. The mean time between primary arthroplasty and revision surgery was: type I 10.1 years, type II 3.2 years, type III 4.5 years and type IV 5.4 years. The inter-observer reproducibility (three pathologists) was sufficient (87.1%, Cohen's kappa=0.805). The correlation between histopathological and microbiological diagnosis was high (89.7%).
Conclusion: Together with numerous co-workers, we propose a feasible classification system, enabling a standardized diagnostic evaluation of periprosthetic membrane samples. Furthermore, the importance of non-infectious, non-particle-induced prosthesis loosening (membrane type IV), which was observed in 15.4%, is highlighted.

P 642
ONCOGENIC OSTEOMALACIA (OO): REPORT OF TWO CASES

JOSSELIN Nicolas(1), CROUE Anne(1), KOFFI Emmanuel(1), AUDRAN Maurice(2), ROUSSELET Marie-Christine(1), SAINT-ANDRE Jean-Paul (1)
(1) Department of Pathology, University Hospital, 49933 ANGERS cedex 09, France
(2) Department of Rheumatology, University hospital, 49933 ANGERS cedex 09, FRANCE

Oncogenic osteomalacia (OO) is rare and characterized by vitamin D inefficiency, hypophosphatasia and loss of phosphate in urine. OO is mostly linked to benign mesenchymatous tumours. We report two cases.
The first concerned a woman of 67 who benefited from treatment for postmenopausal osteoporosis. The second one concerned a 52-year-old man who had an initial diagnosis of male osteoporosis. Both were treated by alendronate and vitamin D. Despite this treatment, these patients showed bone fractures and progressively increasing asthenia. New biological exams assessed dramatic hypophosphatemia and an abnormal phosphate tubular absorption. Calcic metabolism was normal. A bone biopsy was performed on the woman showing osteoporosis and rickets. For each case, biological results allowed to exclude a carential etiology. Tumours were located using CT-scan. For the woman, the tumour measured 15 mm beneath abdominal subcutaneous fat. For the man the tumour was located under the sole of the foot and measured at 30 mm. Both tumours showed the same histological aspect. They were composed of fusocellular cells. These cells were not atypical. They were surrounded by an often mineralized myxoid stroma. Vascularization showed a hemangiopericitic pattern. Bone pain, clinical signs and hypophosphatemia normalized a few months after removing of the tumour.
Oncogenic osteomalacia are most often linked to benign mesenchymatous tumours mostly located in bone or soft tissue. They have several histological aspects. They secrete ' Fibroblast Growth Factor' FGF23 which leads to loss of phosphate in urine by inhibiting phosphate tubular reabsorption.

P 643
QUANTITATIVE ANALYSIS OF PERIOSTEAL CIRCULATION IN LONG BONES

ANTABAK Anko, BRCIC Luka, BATELJA Lovorka, DAVILA Slavko, SEIWERTH Sven.
Dept. Of Surgery Clinical Center Zagreb; Institute of Pathology, Medical Faculty, Zagreb, Croatia.

The important role that periosteum plays in healing bone injury and its use as a potential source of osteoprogenitor cells is of high clinical interest. Periosteum is important for bone vascularization and osteogenesis. Periosteal tissue is divided into an outer fibrosis and an inner - active and proliferative layer with intrinsic periosteal blood system. So far few data are available about the quality of periosteal circulation especially regarding different bones and different bone segments. Aim of this study was to quantify microcirculation of inner layer of intact periosteum. We examined periosteum of radius and tibia, taken from 4 sheep 1 to 2 years old. Material for microscopic examination was fixed in 10% neutral buffered formalin, decalcinated in a mixture of formic and sulfuric acid, embedded in paraffin and stained immunohistochemically for CD34 and von Willenbrands factor according standard protocol (DAKO, Denmark). Two samples from each periosteum, 1 cm length respectively, were processed. From each sample 5 fields were analyzed microscopically using a x25 objective and computer-based image analysis system (ISSA, VAMSTECH, Zagreb, Croatia). Periosteal thickness and capillary count were accessed. Capillaries were counted in inner periosteal layer in a determined field of 10 000im2. Analysis of intact periosteal microcirculation yielded a mean capillary number of 5, and a mean periosteal thickness of 100um. Our quantification of the periosteal capillaries indicates no significant differences between periosteum taken from radius and those taken from tibia. From our data we concluded that they represent a basis for studying periosteal capillary circulation during the process of healing or its damage caused by osteosynthesis.

P 644
REPAIR OF BONE DEFECTS BY ANIONIC COLLAGEN MATRICES

(1) Department of Pathology, Faculty of Medicine of Ribeirão Preto, University of São Paulo, Brazil, (2) Department of Pathology, Faculty of Medicine, (3) Institute of Computing, State University of Campinas, Brazil

The aim of this study was to evaluate the repair of critical-size bone defects by three anionic collagen matrices in rats. Samples of the collagen matrices with varying electric charge density were implanted in 4-mm cranial bone defects with empty defects as controls. Cranial bone was retrieved after 3,

7, 15, 30, 60 days and 1 year and submitted to radiological, histological, immunohistochemical and ultrastructural analysis. Texture analysis was done on digitalized microscopic images. Two of the matrices allowed a quick recovery of the bone structure. After two months, full recovery of the bone defects was seen. The collagen matrix with the highest electric charge density still had remnants at the periphery of the newly formed bone at the same period. The anionic collagen matrices were actively incorporated into the mineralized bone matrix, without signs of resorption prior to the mineralization process. At the beginning of the regeneration process insulin-like growth factor-I and bone morphogenetic proteins 2 and 4 were found in direct contact with anionic collagen matrices, revealing a possible mechanism of osteogenesis stimulation by the anionic collagen matrices. One year after implantation, all defects were fully recovered. Texture analysis showed decreasing values of entropy and the fractal dimension during the experiment. The changes of the fractal dimensions followed a power law for each matrix. Morphologically, the bone formed by the matrix with the highest charge density had a more mature aspect compared with the less electronegative matrices, which could also be demonstrated by comparison of the fractal dimensions. These results show that the anionic collagen matrices are effective osteoconductive biomaterials, showing a great potential for clinical application.
Supported by FAPESP, CNPq

P 645
THE ROLE OF THE EXTRACELLULAR MATRIX IN THE BONE LAMELLA ARCHITECTURE
A. F. Vreju (1), G. S. Drãgoi (1,2), Trasca E.T. (1)
1. University of Medicine and Pharmacy- Craiova
2. Academic Hospital Filantropia -Craiova

Objective: The bone lamella participates to the formation of two components of the bone, compacta and the spongy part of the bone. The bone lamella, a constitutive part of the bone extracellular matrix was studied using a microanatomic study of the endochondral ortomorphogenesis; a study of the bone lamellar elements in trabecular bones, and a study of the bone lamellar system in bones with mixed osteogenesis.
Materials and methods: 53 bones from the axial skeleton (vertebra, sternum), 54 bones from the lower limb skeleton (femur, tibia, calcaneus). Stains: HE, Van Gieson, Gömöri.
Results: The research on the extracellular matrix from the cortex of the tibia diaphisis showed us a continuity of the interosteonal collagen lamella fascicles with those from the osteon's periphery. This doesn't concord with the classic images. The collagen lamella fascicles' stereotopography can be studied using mathematical methods – the parametric equation of a Moebius band. The collagen fibers from the bone lamella in the osteons from compacta of tibia diaphisis are birefringent and parallel with each other. Some fascicles are tangent to the oval spaces.
Conclusions: The stereodistribution of the collagen lamella fascicles is variable with the osteogenesis and the mechanic forces hereupon the bones are or will be submitted. The application of the mathematic methods of algebra topology and the finite element opens new ways in the modeling and the creation of abstractisation of the bone lamella system, on one way and in the evaluation of the hemato-pathological lesions on the bone biopsy on the other way.

P 646
EPIDERMAL GROWTH FACTOR RECEPTOR (EGFR) EXPRESSION IN CHORDOMA
PTASZYNSKI Konrad, PEKUL Monika, PIASCIK Agata, FALKOWSKI Slawomir.
MCS CANCER CENTER, INSTITUTE, WARSAW, POLAND

Epidermal Growth Factor Receptor (EGFR) overexpression has been found in various tumors with poor outcome. Chordoma is a neoplasm arising from the embryonal rest of the notochord. The most common locations are both ends of the spine, sacral bone and head and neck locations. Surgery and radiation therapy are the most commonly used treatment modalities. Purpose of the study was to evaluate an EGFR expression status in 21 cases of chordoma diagnosed at the MCS Cancer Center Institute between 2002 and 2004. Immunohistochemistry with anti EGFR antibody as well as Fluorescence In Situ Hybridisation (FISH) were utilised on the slides obtained from the paraffin blocks. Ten cases showed strong expression of EGFR receptor, eleven cases were negative. At the time of the evaluation, six cases with EGFR expression presented with metastatic disease. Four cases negative for EGFR expression showed metastatic disease. In many cases of chordoma surgical and radiotherapy treatment is not effective. New treatment modalities are needed. Anti EGFR (cetuximab) treatment approach might be a supplementary method.

P 647
GIANT CELL TUMORS OF THE BONE: A RETROSPECTIVE STUDY OF 33 CASES.
S Hannachi Sassi1, S karray2, F Laddeb2, M Douik2, K Ben Romdhane1.
1 Department of Pathology, Salah Azaiez Institute, Tunis, Tunisia.
2 Department of Orthopaedical Surgery, Mohamed Taïb Kassab Institute, Tunis, Tunisia.

Introduction: Giant cell tumors (G.C.T) of the bone are rare. They represent 5 to 10% of all primary bone tumors and 20% of benign lesions. They are often locally aggressive neoplasm characterized by large numbers of uniformly distributed, osteoclast-like giant cells and a more diagnostically pertinent background population of plump, epithelioid to spindle mononuclear cells.
Aims: To describe the epidemiological, clinical, radiological features and test the relationship between histological grading of Jaffe et al., established in 1940, and the prognosis.
Materials and methods: Thirty three cases of G.C.T of the bone were examined during 28-year period from 1970 to 1997. After studying the epidemiological, clinical and radiological features, the histological criteria of Jaffe et al. (1940) were performed for each case.
Results: Thirty three cases of G.C.T were retrieved with a range of age between 16 and 66 years with an average of 32.8 years. Female outnumbered male (23 vs. 10). Ninety-four (94%) were located in the long bones, the most frequent sites being the lower end of the femur (10 cases), the upper end of the tibia (6 cases) and the lower end of the radius (6 cases). Twenty cases (64%) occurred around the knee. Radiologically, 24 cases (77.4%) occupied the epiphysial and metaphysial regions. The tumor was centrally placed in 23 cases (69.7%) and eccentrically placed in 10 cases (30.3%). The tumor showed an expanded lytic lesion with fine to moderately coarse trabeculations in 26 cases (78.8%) and a pure lytic appearance in 7 cases (21.2%). Histological grading of Jaffe et al. resulted in 12 cases of grade I, 20 cases of grade II with 3 cases of grade II+ and 1 case of grade III. Statistical analysis revealed no significant correlation between all morphological parameters and prognosis.
Conclusion: Our epidemiological, clinical and radiological findings are in agreement with published data. Furthermore, there is no relationship between the histological grading and the prognosis.

P 648
A RETROSPECTIVE MULTIVARIATE ANALYSIS OF MYXOFIBROSARCOMAS: WITH A SPECIAL

EMPHASIS ON MARGIN STATUS AS A CRITICAL PROGNOSTICATOR

Chien-Feng LI^, Ching-Nan LIN^, Hsuan-Ying HUANG*
Department of Pathology, Chi-Mei foundation Medical Center^, Tainan, Taiwan
Department of Pathology, Chang Gung Memorial Hospital, Kaohsiung Medical Center*, Kaohsiung, Taiwan

Introduction: Myxofibrosarcomas (MFS) are characterized by tumor progression with increased metastases after relentless local recurrences (LR). It remains challenging to predict outcomes without a prudent survival analysis to assess parameters of primary lesions. Previous series suggested that LR could not be predicted by any factor, whereas few have uniformly examined prognostic factors by appropriate multivariate analyses. Purpose: The aim of this study was to identify critical clinicopathological variables related to outcome by Cox regression model. Methods: 70 primary MFS were retrospectively identified after review and graded by the FNCLCC scheme. Survival was compared by log-rank test with regard to recurrence-free survival (RFS), metastasis-free survival (MeFS), disease-specific survival (DSS), and overall survival (OS). Results: Follow-up (FU) was obtained in 61 cases with a median duration of 32 months (range: 2-201). Among them, there were 32 men and 29 women with a median age of 61 years. The size of primary tumors ranged from 1.5 to 24 cm (median, 5.5). The surgical margins were considered positive in 21 cases (34%). At last FU, 27 patients developed at least 1 LR, 14 patients experienced distant metastasis, 13 patients died of MFS, and 4 patients died of other causes. The cumulative 3-year rates of RFS, MeFS, DSS, and OS were 51%, 72%, 80%, and 74%, respectively. By univariate analysis, positive margins (p=0.0003) were the only significant factor for worse RFS. Mitoses¡Ù20/10HPF, high grade (grade 2,3), positive margins, tumor necrosis(¡Ù10%), prominent nuclear pleomorphism, and AJCC stage 3 were significantly correlated with MeFS, while factors associated with reduced DSS and OS included the former 3, together with tumor necrosis and nuclear pleomorphism found respectively significant for DSS and OS. By multivariate analysis, only high mitoses (p=0.0009 for DSS; p=0.0034 for OS) and positive margins (p=0.0203 for DSS; p=0.0034 for OS) remained independent for poorer patient survival. However, tumor necrosis (p=0.0053) was independently associated with MeFS, apart from high mitoses (p=0.0086) and positive margins (p=0.0142). Conclusions: Margin status is a critical prognostic determinant in MFS, not only proved as the single significant factor for reduced RFS but also independently predictive of metastatic propensity and patient survival as is high mitotic activity. However, tumor necrosis¡Ù10% independently predicts worse MeFS alone.

P 649

CALCIFYING APONEUROTIC FIBROMA. THE FIRST CASE REPORT COMPRISING COMPLETE HISTOLOGICAL, IMMUNOHISTOCHEMICAL, ULTRASTRUCTURAL AND CYTOGENETIC CHARACTERISTICS OF TUMOUR AND A REVIEW OF THE LITERATURE

RYS Janusz*, WASILEWSKA Anna*, KRUCZAK Anna*, ILISZKO Mariola**, MARKIEWICZ Dorota*, SZPOR Joanna*, WYSOCKA Joanna*, MOSKAL Julia*, DRABIK Grazyna***, MIERZYNSKI Wojciech***
*Cracow Center of Oncology, **Dept of Biology and Genetics Medical University of Gdansk ***Polish-American Children's Hospital, Jagiellonian University, Cracow, Poland

Introduction: Calcifying aponeurotic fibroma (CAF) is a rare soft tissue tumour that primarily occurs in children and adolescents and has a strong predilection for hands and feet. It has been described as locally invasive, recurring tumour without the ability to metastasize. Since initial report by Keasby, more than 100 cases have been documented in the literature. However, only a few reports presented histological, immunohistochemical and ultrastructural characteristics of the tumour.
Aims: The aim of the study is a presentation of CAF with morphological, and cytogenetic analysis of tumour. This is the first description of ultrastructural features of CAF in childhood, as well as the first note concerning cytogenetic study of the tumour.
Material and methods: A 2 year-old girl was operated on because of a nodule, 2.5 cm in diameter, localized in soft tissue of hypothenar of the left hand. Surgical exploration of the lesion revealed a rather dull-separated tumour attached to ulnar nerve and vessels. The mass was excised non-radically. Small fragments of tumour tissue were taken for cytogenetic and ultrastructural studies. Finally the material was fixed in 10% buffered formalin's solution, and embedded in paraffin blocks. Paraffin-embedded material was examined histologically and with immunohistochemistry, using the LSAB2+ kit.
Results: The lesion was characterized by a fibromatosis-like proliferation of fibroblastic cells, admixed with cartilage-like islands with areas of calcification. Spindled fibroblasts infiltrated striated muscles as well as nerves and vessels, and they were usually organized in well-orientated fascicle. Chondroid-like foci were built of swollen cells lodged in lacunae. Despite the focal cellularity of the lesion, mitotic figures were scarce, and did not exceed 2 per 50 high-power fields. MiB-1 index reached 9.6. Both spindle and chondroid tumour cells were stained with antibodies against vimentin, H-caldesmon, CD99, and S100 protein (diffuse reaction), as well as smooth- and muscle- specific actin (focal reaction). On the contrary, they lacked keratins, EMA, desmin, BCL-2, CD34, CD57, ER, PR and P53 expression. On ultrastructural examination a biphasic texture consisting of fibroblasts and cartilage cells could also be distinguished. The karyotype of tumour cells was normal.
Conclusion: Our findings favor the origin of CAF from fibroblastic cells which differentiate into fibrocartilage and/or hyaline cartilage.

P 650

SOLITARY FIBROUS TUMOUR OF THIGH AND INGUINAL REGION. THE HISTOLOGICAL, IMMUNOHISTOCHEMICAL, ULTRASTRUCTURAL AND CYTOGENETIC CHARACTERISTICS OF TWO CASES AND A REVIEW OF THE LITERATURE

RYS Janusz, WASILEWSKA Anna, LACKOWSKA Bozena, SZPOR Joanna, KRUCZAK Anna, ILISZKO Mariola*, MARKIEWICZ Dorota, WYSOCKA Joanna, MOSKAL Julia, KOLODZIEJSKI Leszek
Cracow Center of Oncology, *Dept of Biology and Genetics Medical University of Gdansk

Introduction: Extrapleural solitary fibrous tumours (SFTs) are uncommon mesenchymal neoplasm. Slightly more than 100 cases were reported. Most of them were localized in the upper respiratory system and the soft tissues of head and neck region. SFTs of the extremities are exceptionally rare. We found only eight such cases in the available literature. They pose problems in the differential diagnosis, especially from synovial sarcoma.
Aims: The object of the study is the clinico-morphological characteristics of 11 (including our two cases) described SFTs of the thigh and inguinal region and the estimation of prognostic significance of selected morphological and cytometric parameters of the tumour.
Material and methods: A 61-year-old woman and a 39-year-old man were admitted to the Centre of Oncology with the circumscribed, palpable masses localized in soft tissue of the thigh and inguinal region. The tumours were totally excised and both patients live with no evidence of tumour recurrence

49 and 12 months, respectively. Tumour tissues for light microscopy were fixed in 10% buffered formalin and embedded in paraffin. Representative paraffin blocks were chosen for immunohistochemical studies. Small fragments of fresh tumour tissue were taken for ultrastructural, cytometric and cytogenetic studies.
Results: Histological texture of tumours was characterized by a combination of hypocellular and hypercellular areas separated from each other by thick bands of hyalinized collagen and hemangiopericytoma-like vessels. The tumour cells of both cases were positively stained with antibodies against CD34, BCL2, CD99, and progesterone receptor. The first tumour showed additionally the small foci of necrosis. The proliferative activity of tumours was variable. The cellular areas of the first tumour presented up to 13 mitoses per 10HPF and 11.0% MIB-1 index. FCM study of these cells revealed 7.2% S-phase fraction (SPF) and aneuploidy (DI= 2.08). Conversely, the second tumour was diploid and characterized by low mitotic rate (6/10 HPF), MiB-1 index (7.2%) and SPF (0.3%). Cytogenetic analysis of this tumour showed 46,XX normal karyotype.
Conclusion: 1)High proliferative activity, aneuploidy, and focal necrosis do not have to indicate the malignant behaviour of SFT. 2)Lack of the (X,18) translocation facilitates the differentiation between SFT and synovial sarcoma.

P 651
ACRAL MYXOINFLAMMATORY FIBROBLASTIC SARCOMA
DERVISOGLU Sergulen, DEMIRKESEN Cuyan, OZTURK Kilicaslan Tulin, MIDI Ahmet
ISTANBUL UNIVERSITY CERRAHPASA MEDICAL FACULTY PATHOLOGY DEPARTMENT

INTRODUCTION:Acral myxoinflammatory fibroblastic sarcoma (AMIFS) was described as different entity in the larger group of myxomatous soft tissue tumors in 1997 and 1998 by three different authors. These tumors have quite characteristic clinical presentation and morphology. The lesion has morphologically myxoid or myxohyalen presentation and multinodular growth pattern. In this present study we report on three cases of AMIFS seen in our department to discuss their clinicopathological features and emphasize the rare occurrence of it's invasion to neighboring bone tissue.
MATERIALS and METHOD:We found 3 cases of AMIFS in our register in 1999 to 2004. We applied routine H&E sections and also immunohistochemical stains as vimentin, CD68, CD34, S100 protein, SMA and cytokeratin. Clinical features were obtained from archive records.
RESULTS and CONCLUSION: All of the cases were adult men of ages 29, 36, and 56. Lesions occurred in the 4.th and 5.th metacarpophalangeal joints of the right hand (first case), in the right elbow wrist (second case) and in the right toe thumb distal interphalangeal joint (third case). Tumors were composed of epithelioid to spindle cells containing myxoid zones and various inflammatory cells. In some foci, Reed-Stenberg like giant cells were seen. Immunohistochemically, tumors were diffusely positive for vimentin. Various numbers of cells were also positive for CD 68. Only one case was poorly positive for CD34 and SMA. All of the cases were negative for S-100. In contrast to the previous literature, we observed neighboring bone invasion in two cases. In follow up period, one case had regional lymph node metastasis. This newly described, both morphologically and clinically distinct tumor must be kept in mind when dealing with a tumor locating in distal extremities and must be in differential diagnosis with epithelioid sarcoma and myxoid or inflammatory type malignant fibrous histiocytoma.

P 652
A SINGLE-TEAM EXPERIENCE OF LIMB SPARING APPROACH TO ADULTS WITH HIGH-GRADE MALIGNANT FIBROUS HISTIOCYTOMA
ISSAKOV Josephine, KOLLENDER Yehuda, NIRKIN Alex, BICKELS Jacob , FLUSSER Gideon, MELLER Isaac ,LIFSCHITZ-MERCER Beatris ,MERIMSKY Ofer

Introduction: Malignant fibrous histiocytoma (MFH) is the most common subtype of soft-tissue sarcoma (STS). When located in a limb, MFH, as well as other STS, are currently treated with limb sparing surgery (LSS) followed by radiation therapy (RT).
Patients: From October 1994 through October 2002, 42 adult patients with high-grade limb MFH were approached by LSS followed by RT.
Results: Our results reflect a single-team experience with multi-disciplinary limb sparing approach towards adult patients with limb high-grade MFH, and point to several important conclusions. High grade MFH can be treated by surgery and postoperative radiation therapy, and controlled to yield a 10-year relapse free survival of 62% and a 10-year overall survival rate of more than 80%. Recurrences of MFH tend to occur during the first 2 years of follow-up, and become less frequent thereafter. Relapse free survival was affected mainly by location in the lower limb versus the upper limb, irrespective of the tumor size. Patients who had their diagnostic biopsies in another medical center had a greater tendency to local and systemic relapse probably due to compartmental and systemic contamination with tumor cells. This observation supports the need for early referral of patients with limb masses suspicious of sarcomas, to a specialized center for careful diagnosis and multidisciplinary therapy.
Conclusions: Our results are satisfactory and are within the accepted ranges. It seems that the most important key words for disease-free survival is the team experience, starting with biopsy, surgery, and post-operative radiation therapy. All other factors are tumor-biology dependent, and thus far are beyond our control.

P 653
PRIMARY HEMANGIOPERICYTOMA OF THE TIBIA A CASE REPORT.
*F.Yassi, * F.Gheghessi, *A.Djenouni, **Z.Tebbi, ** R.Maza, * A.Lankar
*Laboratoire Central d'Anatomie et de Cytologie Pathologiques CHU Annaba-Algérie
**Service d'Orthopédie-traumatologie CHU Constantine-Algérie.

Primary hemangiopericytoma of the bone is a very rare vascular tumor. It can occur any where but the most common sites are pelvis, proximal femur, humerus, rachis, sacrum and mandible.
We report a case occurred in a patient aged 53 years who consulted in June 2004 for pain of the left knee evolving since 3 years and swelling.
Standard X-ray showed a lytic metaphyso- epiphysary tumor of the upper of the left tibia with cortical permeation and extension into surrounding soft tissues and fibula.
Giant cells tumor and chondrosarcoma were evoked. Biopsy concluded to a grade 2 hemangiopericytoma.
Immunohistochemical staining showed no expression of FVIII, actin and CK by tumoral cells.
The tumor was treated by en bloc resection followed by a chemotherapy.
The result was good. The patient presented neither recurrence nor metastasis 6 monthes after the treatment.

P 654
PECOMA OF ABDOMEN: A UNIQUE CASE

DEMONAKOU Maria, MACHERA Helen , MANOLIA Lora , RAPTIS Ioannis, TAMVAKIS Nikolaos, FINOKALIOTIS Nikolaos.
Department of Pathology and 2nd Department of Surgery Sismanoglion CH Marousi Athens Greece.
District General Hospital Attikis "KAT"

BACKGROUND: The World Health Organization recently recognized a family of neoplasms showing at least partial morphological or immunohistochemical evidence of a putative perivascular epithelioid cell (PEC) differentiation. These tumors include angiomyolipoma (AML), clear cell 'sugar' tumors of the lung (CCST), lymphangioleiomyomatosis (LAM), clear cell myomelanocytic tumors of the falciform ligament and distinctive clear cell tumors at various other sites. Pecomas are rare neoplams of pericytes, mainly affect young women. PCMs have been identified in uterus, lung,, vulva, breast, prostate, rectum, jejunum, liver, cardiac septum, falciform ligament soft tissue and in the abdomen with tuberous sclerosis.

CASE PRESENTATION: A 29 years old woman without previous history was admitted with a painless palpable mass in her abdomen. Laboratory tests were normal apart of ECHO revealing a mass up to 8c in her abdomen. The mass were easily identified and removed by laparoscopy. There were no sign of Tuberous Sclerosis.

The tumor was well circumscribed , encapsulated, measured 8x5x3cm.Cut surface was red, nodular, with visible blood vessels. Microscopy revealed a well developed vascular network in the vicinity of which a pleomorphic cellular component was recognised. Neoplastic cells at the immediate vascular location are epithelioid and spindled shaped whereas in areas away from vessels, resemble smooth muscle cells.

Epitheliod cells show variable morphology , some having clear cytoplasm and others eosinophilic with “ground glass “ configuration . Most display small, normochromatic round nuclei and other have large oval nuclei with prominent nucleoli. Immunostaining shows diffuse positivity in HMB-45 and SMA focal for S-100 , and negativity for cytokeratins and desmin.

Although most of these tumors have behaved in a benign fashion, they should be considered tumors of uncertain malignant potential given previous reports of recurrence and metastases. Our patient remains free of disease 36 months later.

P 655

LIPOMATOUS HEMANGIOPERICYTOMA (ADIPOCYTIC VARIANT OF SOLITARY FIBROUS TUMOR) OF THE ORBIT

FARAH-KLIBI Faten*, FERCHICHI Leila*, ZAIRI Issam**, ZERMANI Rachida*, RAMMEH Soumaya*, CHELBI Emna*,ADOUANI Ali**, BEN JILANI Sarrah*.
*: Departement of Pathology of Charles Nicolle Hospital.Tunis.Tunisia.
**: Departement of Maxillo-Facial Surgery of Charles Nicolle Hospital.Tunis.Tunisia.

Hemangiopericytoma (HPC) of the orbit is a rare tumor presenting with slowly progressive proptosis, ocular motility impairment and visual loss. In 1995, a newly variant of HPC termed lipomatous hemangiopericytoma (LHPC), was described. Only two cases arising in the orbit have been previously reported.

The authors describe a new case of orbital LHPC arising in a 64-year old woman who presented a 1-year history of pain in the right orbital region and a progressive right proptosis. Computed tomography scans revealed a well-delineated extraconal mass of 3x3x1,5cm affecting the superomedial area of the orbit. No signs of bony erosion or globe indentation were visible. Histological examination revealed an entirely encapsulated lesion composed of a haphazard proliferation of spindle, fibroblast-like cells alternating with hypocellular foci. The stroma was collagenous, with vascular spaces displaying a prominent hemangiopericytoma pattern (stag horn configuration) and lipomatous areas made of mature adipocytes was found. Mitotic figures were absent, and no cellular atypia, necrosis, or vascular invasion was observed. Immunohistochemical staining revealed an intense and diffuse positive reactivity to CD99, CD34 and bcl-2. The patient was free of recurrence when examined 9 months after surgery.

The aim of this study is to discuss the clinicopathologic features, including the immunohistochemical staining profile and ultrastructural appearance of this distinctive tumor, and briefly discuss the relationship between HPC and solitary fibrous tumor (SFT) of soft tissue, a neoplasm with many clinical and pathologic similarities.

P 656

ANGIOSARCOMA OF BONE

NIKOLAIDOU Anastasia1, PAPANIKOLAOU Athanasios2, KONSTANTINIDES Panagiotis3, MAKOS Christos4, TOPTSIS Konstantinos5
1 Registrar, Pathology Department, General Hospital of Kilkis, Kilkis, 61100 Greece
2 Registrar, Pathology Department, “Hippokratio” General Hospital of Thessaloniki, Thessaloniki, Greece
3 Orthopaedic Surgeon, Thessaloniki, Greece
4 Registrar, Oral and Maxillofacial Department, General Hospital of Kilkis, Kilkis, 61100 Greece
5Associate Director, Orthopaedic Department, “Hippokratio” General Hospital of Thessaloniki, Thessaloniki, Greece

The purpose of this work is to describe a rare case of an angiosarcoma of bone and to discuss about the low frequency and the variant behavior and histological appearance of the malignant vascular bone tumors.

Method and results: A male 47 years-old with a 4-year history of lower back pain was operated for a lumbar disk herniation, but during his transportation from the operation theater a pathological intertrochanteric fracture of the right hip was reordered.

The magnetic resonance imaging (MRI) showed a large soft tissue mass extending anteriorly with infiltration of the bone marrow to the cartilaginous level of the femur head. The histological examination revealed variable shapes of vascular anastomotic channels lined with large atypical endothelial cells with solid sheaths formations, pseudopapillary infolding arrangements and foci of necrosis. On immunohistochemical investigation many neoplastic cells were positive in factor-VIII and UEA-I endothelial markers. The treatment included a radiotherapy (300 rad/per day for 13 days) followed by an amputation and total hip replacement.

Conclusion: The malignant vascular bone tumors are very rare accounting less than 1% of the bone malignancies characterized by unknown etiology and variable biologic behavior and histological appearance.

P 657

MORPHOLOGICAL FEATURES OF 23 MALIGNANT VASCULAR TUMORS

KÖSEMEHMETOĐLU Kemal,MD and GEDÝKOĐLU Gökhan,MD,Professor

Introduction: Due to its rarety, information and experience about malignant vascular tumors are limited. Although many immunohistochemical techniques are available, determination of grade still requires a detailed morphological investigation.
Methods: We present histological features of 23 malignant vascular tumors, 8 of which had a prior diagnosis of angiosarcoma. Tumor size, mitotic index, pleomorphism, cellularity, presence of necrosis and grade are determined for

each case. Chi square test and linear regression analysis are used and $p<0.05$ is accepted as significant.
Results: Age at diagnosis was 6-77 years with a median of 35 years and male to female ratio was 1.5. Extremities(8) were most common primary site following head and neck(5); sacrum(3); parenchymal organs including colon (2), liver (1) and spleen(1); abdominal wall (1); inguinal (1) and breast (1). Tumor size, varied 1 cm up to 20 cm in diameter (median 5.5 cm), was >3 cm in 14 of cases, 9 of which were high grade lesions. Infiltrative pattern (15/23) and epitheloid cellular characteristic (15/23) were dominant. Majority of lesions were hemorrhagic (83%) and necrotic (70%). Mainly, pleomorphism and cellularity have contributed to grade of tumor. Decision giving for high grade tumor was directly associated with high pleomorphism ($p<0.00$) and tumor diameter (>3 cm, $p<0.02$). In cases of intermediate pleomorphism, cellularity has assisted on grading. After a total reexamination of all 23 vascular tumors 11 of them were categorised as high grade lesions. Follow up information were available for 7 of 23 patients: Five of them were alive for 5 years and 2 of them, both having high grade tumor, were dead of disease in 2 years.
Conclusion: Following an algorithm as consideration of pleomorphism, size and cellularity of malignant vascular tumors has a key role in determination of grade, thus the diagnosis of angiosarcoma. Still the need for more objective findings such as molecular studies is obvious on the way to specific diagnosis of malignant vascular tumors.

P 658
METASTATIC ANGIOSARCOMA ARISING IN AN EPITHELOID HEMANGIOENDOTHELIOMA OF AN LIGATED ARTERIOVENOUS FISTULA IN A IMMUNOSUPPRESSED PATIENT AFTER KIDNEY TRANSPLANTATION
Bodó K. 1, Liegl B. 1, S. Regauer 1, W. Weybora 1, E. Spuller 1
1: Institut of Pathology, Medical University, Graz, Austria

Introduction:
About one third of angiosarcomas develop in association with certain pre-existing conditions such as benign hemangiomas, synthetic vascular grafts or other foreign material. Immunosuppression in the setting of organ-transplantation is associated with the development of malignant tumors, most commonly carcinomas or lymphomas. Sarcomas are relatively infrequent. We report a male patient with chronic renal failure, who underwent kidney transplantation. The patient presented with an epitheloid hemangioendothelioma at the site of a ligated arteriovenous fistula constructed for haemodialysis at the left cubital region. Within 2 years a transformation into an angiosarcoma occurred. The patient died of multiple metastases.
Purpose of the study:
This is rare case of an epithelial hemangioendothelioma in an immunosuppressed patient at the site of an AV-fistula with malignant transformation into an angiosarcoma. It is important to keep in mind, that immunosuppressed patients can develop sarcomas in such circumstances.
Material and methods:
Formalin-fixed and paraffin-embedded archival material of biopsy and surgical specimen, as well as autopsy material of primary tumor and metastases were examined on HE-stained section and immunochemistry was evaluated using antibodies to CD31, CD34 and factor VII.
Results:
The initial biopsy and the surgical specimen showed a solid proliferation of a vascular tumor composed of short strands, cords and solid nests of rounded to slightly spindled eosinophilic endothelial cells, some of them with intracytoplasmic lumina containing erythrocytes. The autopsy specimens of the recurrent tumor at the primary site as well as the metastases (lungs, bone, axillary lymph nodes) showed classical features of an angiosarcoma with positive staining with antibodies against CD31, CD24 and factor VII.
Conclusion:
It is important to keep in mind, that immunosuppressed patients in addition to carcinomas or lymphomas may also develop sarcomas. Immunosuppressed patients with ligated AV-fistula do have an higher risk to develop a malignant tumor in the shunt. Especially we would like to draw attention, that angiosarcoma may arise in benign or intermediate vascular tumors under such circumstances.

P 659
EPITHELIOID HEMANGIOENDOTHELIOMA OF THE SOFT TISSUES IN A WOMAN'S ARM: A CASE REPORT AND REVIEW OF THE LITERATURE
I.Abbes, S.Sassi, R.Sallemi, K.Mrad, M.Driss, K.Ben Romdhane.
Department of Pathology, Salah Azaiez Institute, Tunis, Tunisia.

Introduction: Epithelioid hemangioendothelioma (EHE) is a rare vascular neoplasm arising in soft tissue, bone, lung and liver. This tumor is often considered to have an intermediately aggressive nature and a long clinical course depending on the sites involved.
Aims: To present the clinicopathologic and immunohistochemical features of a rare vascular tumor and to review differential diagnosis.
Material and methods: A 44-year-old woman presented with an expansive soft tissue mass of her left arm. Tumor resection was performed with light microscopic and immunohistochemical analysis.
Results: Macroscopic examination revealed a fusiform perivascular mass measuring 22 / 13 mm and infiltrating the surrounding adipocytic and skeletal muscle tissues. Histological examination revealed short strands, cords or solid nests of rounded to slightly spindled or epithelioïd eosinophilic cells. The stroma was hyalinized and focally calcified. Some tumor cells displayed endothelial differentiation as evidenced by intra-cytoplasmic lumina (vacuoles) containing erythrocytes. Mitotic activity was estimated as 1mitosis / 10 HPF. Immunohistochemical study revealed tumor cells immunoreactivity for CD 31, Ulex europeus and vimentin.
To date, neither recurrence nor metastases have been observed 10 months after initial diagnosis.
Conclusion: EHE of soft tissue is a rare borderline vascular tumor with unpredictable prognosis. This uncommon tumor should be considered in the differential diagnosis of other tumors such as carcinomas and malignant epithelioïd schwannoma. The role of immunohistochemistry is crucial.

P 660
VASCULAR MALFORMATIONS: CLINICOPATHOLOGIC CLASSIFICATION
WASSEF Michel (1-2), ENJOLRAS Odile (1-3), BISDORFF Annouk (1-3), MERLAND Jean-Jacques(3)
Consultation des Angiomes, (1) and Departments of Pathology (2)and Neuroradiology (3), Hôpital Lariboisière, 2 rue Ambroise Paré, 75475 Paris Cedex 10, France

Objectives:
The classification of vascular anomalies (vascular malformations and vascular tumours) has been a matter of debate. A first consensus was obtained at the International Society for the Study of Vascular Anomalies (ISSVA, Hamburg 1988) on separating infantile hemangiomas and other vascular tumours from vascular malformations. A common scheme of classification, based on the main vascular constituent was then adopted (Rome 1996). A more detailed classification of vascular malformations is still to be

achieved. We present the classification we have used for several years in our interdisciplinary group, based on clinical and pathological data.
Classification:
A - Troncular vascular malformations
Affecting arteries ,veins, or lymphatics
Anomalies of length, diameter, course, or number
Direct arteriovenous fistulas
B - Tissular (non troncular) vascular malformations
Capillary Malformations (Port Wine Stains and other telangectasias)
Venous Malformations (common, nodular, with glomus cells)
Lymphatic Malformations (capillary type, venous type, cystic type)
Arteriovenous Malformations
Soft Tissue Angiomatosis
C - Combined vascular malformations (associate 2 or more defined entities from A and/or B)
Hemo-lymphatic malformation
Arteriovenous-lymphatic malformation
…
D – Complex malformations
One or more from (A), (B) or (C) may be associated with non vascular anomalies of bone, soft tissues or viscera in eponymous syndromes.
Sturge-Weber syndrome, Klippel-Trenaunay syndrome, Parkes Weber syndrome, Bean syndrome, Proteus syndrome, etc.
Conclusion: This classification has proved to be convenient for our clinical, imaging, and pathological practice. The clinical and pathological features of the main types of vascular malformations will be illustrated.

P 661
CRANIAL FASCIITIS OF CHILDHOOD WITH UNDERLYING
Aneeta Jassar, VK Kumar, Ashok Kumar
Command Hospital (NC)
Udhampur J&K India

A ten-year old girl presented with a spontaneous, rapidly growing but painless subcutaneous mass over the left temporal region of the scalp. An initial biopsy of the
mass showed features of cranial fasciitis, a variant of nodular fasciitis first described by Lauer and Enzinger in 1980. Cranial fasciitis is considered a benign fibroblastic lesion of likely myofibroblastic origin but uncertain etiopathogenesis, though some authors have found an association with previous local trauma. Radiographically, there was a lytic skull lesion with destruction of both the inner and outer tables of left temporal bone. Computed tomography (CT) scan done to visualize extent of tumour showed intracranial extension and partial destruction of the greater wing of sphenoid but no midline shift. The tumour had destroyed the calvarial bone as well as part of the zygoma. Dura was pushed but not infiltrated. Peroperatively, there was a large, firm tumour of high vascularity. Cut section had a gritty feel and a 'honey-coombed' appearance. Histopathological examination showed cellular septae separating angiectoid cavernous spaces without endothelial lining. Multinucleated osteoclast-like giant cells and reactive bone formation were present. A
diagnosis of solid variant of aneurismal bone cyst was offered. Features of cranial fasciitis were restricted to the superficial part of the lesion which also showed
intercellular haemorrhages. The authors hypothesize that the cranial fasciitis in this child was a reactive response to intralesional haemorrhages from the aneurysmal bone cyst.
Thus cases of cranial fasciitis must be thoroughly worked up to rule out other underlying pathology. The child is well eight months post follow-up. This is the first such report in world literature.

P 662
ALTERATIONS OF THE ß-CATENIN PATHWAY IN SARCOMAS OF THE PULMONARY ARTERY(SPA)
Gaumann A1, Bode-Lesniewska B2, Zimmermann D2, Hofstädter F1, Dietmaier W1
1Institute of Pathology, University Regensburg, 2Institute of Pathology University of Zürich

Aims: The Wnt signaling pathway plays an important role in cell fate determination mediated by stabilization of the ß-catenin complex through APC. Thus, ß-catenin activation is an important step in the tumorigenesis through induction of transcription and proliferation via c-myc, cyclin A and cyclin D1. Since activation mutation of ß-catenin/APC has been shown to occur in a variety of tumors we investigated the expression and mutation of the involved molecules.
Methods: Expression of ß-catenin, cyclin A, cyclin D1 and mismatch repair proteins hMLH, hMSH2, hMSH6 were examined by immunohistochemistry in 18 SPA and microsatellite instability (MSI) using the recommended reference panel for colorectal cancer. In addition, sequencing of exon 3 of the ß-catenin gene was performed. Subsequently, survival analysis was performed for ß -catenin, cyclin A and cyclin D1.
Results: In 8 cases a membrane staining and in 3 cases additional cytoplasmic staining of ß-catenin was observed. 1 case showed some cells with nuclear staining and 3 cases were negative. Mutation analysis of ß-catenin revealed wildtype sequence of Exon 3 in all examined cases. Cyclin D1 was expressed in most cases while cyclin A was present in few tumors. MSI could only be detected in 2 cases of the SPA. Interestingly, this case also showed nuclear staining for ß-catenin. In addition, 4 cases revealed a LOH at the APC gene locus. Nuclear expression of hMLH1, hMSH2 and hMSH6 was detected in17cases. Survival analysis revealed a significant better survival for cyclin D1 positive tumors.
Discussion: LOH of APC was the prominent observation in our series supporting the view that misfunction of this tumor supressor gene may play a role in the tumorigenesis of some SPA. However, ß-catenin showed only nuclear translocation in 1 case, which was the only patient who had also MSI. Thus, alteration of the ß-catenin pathway and MSI seem to play a minor role in the proliferative activity of SPA in our series.

P 663
PREVALENCE AND SEVERITY OF AA AMYLOIDOSIS IN RHEUMATOID ARTHRITIS - A RETROSPECTIVE CLINICOPATHOLOGIC STUDY OF 161 AUTOPSY PATIENTS
Miklós Bély MD, PhD, DSc1 and Ágnes Apáthy MD2
1Department of Pathology,
Policlinic of the Hospitaller Brothers of St.John of God, Budapest, Hungary
2Department of Rheumatology,
National Institute of Rheumatology and Physiotherapy, Budapest, Hungary

Statement
AA amyloidosis (AAa) may exist in different stages of its development at the time of death.
AAa is a progressive cumulative process in each individual patient. The different stages of AAa found at death in a population of RA patients represent the progression of the pathological process of amyloid A protein deposition, i.e. the chronological development of AAa can be followed by studying its characteristics in individuals who died in various stages of the disease.
The aim of this study was to determine

(1) the prevalence of systemic AAa in RA, (2) the mortality due to AAa, (3) the clinically missed diagnosis of AAa, (4) the severity (extent) of amyloid A deposits in RA patients.
Patients and Methods
A randomized autopsy population of 161 in-patients with rheumatoid arthritis (RA) was studied.
AAa was diagnosed histologically.
The mortality and the clinically missed diagnosis of AAa were analyzed retrospectively by reviewing the clinical records and histological slides.
The degree of AAa was evaluated semi-quantitatively: the numerical values of amyloid A deposits were summarized in different tissue structures of the heart, kidneys, liver, and lungs of RA patients with AAa.
Results
(1) Systemic AA amyloidosis was observed in 34 (21.1%) of 161 cases. (2) Seventeen (50 rel%) of 34 patients died of uremia. (3) In 9 (26 rel%) of 17 amyloidosis was recognized clinically. (4) The severity of AAa distributed according to the curve of Gauss. Arranged according to increasing values the cases of 'severity' showed an exponential growth curve.
Discussion
Only about one quarter of existing amyloidosis was clinically recognized.
AAa was recognized clinically in end stage of the disease, characterized by severe amyloid deposits, and with clinical evidence of renal insufficiency and uremia.
Clinical signs of renal involvement (nephrotic syndrome) refer to an advanced stage of amyloidosis, with a worse prognosis.
Early clinical stages characterized by minimal, or small amounts of amyloid deposits remained clinically undetected.
In the autopsy population of this study minimal amyloid A deposits indicate the early stage of the pathological process; these patients died of other diseases before they developed massive deposits of AAa. In other words, by determining the extent and location of amyloid A protein deposition in different structures of various organs, one may estimate the stage of AAa in a given case. Staging has a prognostic value.

P 664
A VERY CURIOUS LESION OF THE SCALP
BOUILLOT-EIMER Sandrine (1), DAUTHERIBES Michel (2), LEPREUX Sébastien (1), COINDRE Jean-Michel (3)
Departments of Pathology (1,3), and Neurosurgery (2) – Pellegrin Hospital (1,2) and Bergonié Institute (3), Bordeaux – FRANCE

The presence of ectopic meningothelial tissue on the scalp can occur under different forms: typical or rudimentary meningocele, meningothelial hamartoma, primitive meningioma of the scalp, or extension of an internal or external skull meningioma on the scalp. Skin or subcutaneous hamartomas are extremely rare. A sixteen-month-old child presented with an hamartoma on the scalp with ectopic meningothelial elements. Since birth, this child had an occipital middle cyst, evoking a meningoencephalocele with associated lipoma. Clinically, this was a non evolutive unique lesion, measuring 1,4 cm, well-demarcated, rounded and soft, with no modification of the skin. The RMI scan showed a middle nodular tumor with liquid aspect looking like either a meningocele or an epidermal cyst. The lesion was removed, and the post-surgical course was uneventfull. Histologically, well-circumscribed mixture of vascular structures, conjonctive bundles and adipose cells was observed in the deep dermis, the entirety without specific architecture. The characteristic element was the presence of numerous epithelioïd cells, set up in irregular bundles or clusters, closely mixed with dermis. Some seemed to merge with the vessels, and sometimes seemed to form anastomotic structures which can mime a malignant vascular tumor. Immunostains witnessed the meningothelial origin of the epithelioid cells by the strong positivity of EMA and vimentin. Moreover, the negativity of CD34, CD31 and cytokeratin dismissed a vascular origin. The purpose of this case is to remind of the histological criteria of this rare entity. It also helps us to distinguish it from an atypical vascular proliferation and even from an angiosarcoma. Mix of meningothelial cells with conjonctive tissue and vessels, also allows to differenciate it from a cutaneous meningioma. On the histogenetic view, the presence of meningothelial component could be explained by ectopic meningothelial remnants on the scalp, and therefore must be considered as the part of an hamartomatous process.

P 665
RARE ASSOCIATION : OSTEOSARCOMA AND ANEURYSMAL BONE CYST
RAIS Hanane(1), BELAABIDIA Badia(1) MOUTCHOU Ahmed(2)
(1) Department Of Pathology, CHU Mohammed VI - Marrakech
(2) Department Of Pathology, Hospital HassanII -Agadir Morroco

The diagnosis of the lesions bony depends of the clinic, the radiology and the histology. However, the association of a malignant bony tumor and a pseudo tumor made this difficult diagnosis. The aneurysmal bone cyst is the result of a specific pathophysiologic change, which is probably the result of trauma or a tumor-induced anomalous vascular process. Osteosarcoma is rare preexisting lesion of aneurysmal bone cyst. A 38-year-old male presented with a painful progressive swelling in his right knee, without further complaints, which had been present for 5 weeks. Radiological examination was found to have a well-defined 5cm lytic lesion in the right tibial head and neck. The cortex was thinned. Surgical excision and histological exam showed a double tumorous proliferation:vascular and cellular. The diagnosis of aneurysmal bone cyst is the likeliest. However, an fibroblastic osteosarcoma cannot be eliminated. This rare association makes difficult to take therapeutic decision: curettage or amputation and chemotherapy. Bone tumors represent a group of tumors of various dignity. In spite of this, single tumor entities may display strong morphological resemblance to each other which can in turn result in deep difficulties in different diagnosis.

P 666
IMMUNOEXPRESION OF TNF-ALPHA AND P38 TRANSDUCTION PATHWAY MEMBERS IN NORMAL AND PATHOLOGICAL (BENIGN HYPERPLASTIC AND CANCER) HUMAN PROSTATE.
RICOTE Mónica, GARCÍA-TUÑON Ignacio, FRAILE Benito, PANIAGUA Ricardo and ROYUELA Mar
Department of Cell Biology and Genetics, University of Alcalá. 28871 Alcalá de Henares. Madrid. Spain. E-mail: monica.ricote@uah.es

P 667
AKT INHIBITION ENHANCES APOPTOSIS AFTER TNF-ALPHA ADMINISTRATION IN PROSTATE CELL LINE LNCAP BUT NOT IN PC3.
RICOTE Mónica*, GARCÍA-TUÑON Ignacio*, FRAILE Benito*, FERNÁNDEZ Carlos#, ALLER Patricio#, PANIAGUA Ricardo* and ROYUELA Mar*
*Department of Cell Biology and Genetics, University of Alcalá. 28871 Alcalá de Henares. #Centro de Investigaciones Biológicas, Consejo Superior de Investigaciones Científicas. Madrid. Spain. E-mail: monica.ricote@uah.es

INTRODUCTION: Akt/PI3K play an important role in TNF-alpha resistance because has been reported like a survival factor in addition to NF-kappaB. Akt interferes with the apoptotic machinery by phosphorylating thus sequestering the

pro-apoptotic Bcl-2 family protein, caspase-9 and promoting NF-kappaB-dependent cytoprotection via transcriptional activation of a plethora of downstream target genes. In neutrophils, PI3-K/Akt inhibition prevents p38 and ERK1/2 activation.
PURPOSE: The aim of this study was investigate Akt/PI3K role (pro- or anti-apoptotic) after TNF-alpha administration in prostate cancer cell lines (LNCaP and PC3).
MATERIAL AND METHODS: Two establish human prostate cancer cell lines LnCap (CRL-1740) and PC3 (CRL-1435) were used. TNF-alpha treatments were carried out with TNF-alpha at several concentrations and selectively with specific pharmacological Akt/PI3K (LY294002). Apoptosis determination was evaluated by DAPI and flow cytometry. MAPKs activation was measured by Western blot.
RESULTS: TNF-alpha induces apoptosis in LNCaP when we increased TNF-alpha concentration (10, 20, 50, 75, 100 ng/ml) while this treatment has no significant effect on PC3 cells viability. Akt inhibition by LY294002 showed a significative apoptosis increment in LNCaP but not in PC3.
CONCLUSION: Constitutively activate PI3-K/Akt promotes cellular survival and resistance to chemotherapy and radiation in prostate cancer cells. Furthermore, showed that Akt is involved in the activation of NF-kappaB by tumour necrosis factor alpha (TNF-alpha). In our study PI3-K/Akt seems to be involved in TNF-alpha apoptosis regulation in LNCaP and may be through different survival factors as NF-kappaB.
ACKNOWLEDGEMENTS: This work was supported by grants from Fondo de Investigaciones Sanitarias (PI020383) and the University of Alcalá.

P 668
CYCLOOXYGENASE-2 EXPRESSION CORRELATES WITH LOCAL CHRONIC INFLAMMATION AND MICROVESSEL DENSITY IN BENIGN PROSTATE HYPERPLASIA AND PROSTATE CANCER
Wanzhong Wang, Anders Bergh, and Jan-Erik Damber

BACKGROUND. Chronic inflammation has been suggested to be linked to the development and progression of prostate cancer. Up-regulated cyclooxygenase-2 (COX-2), which can be induced by elevated levels of proinflammatory cytokines, may play a role in influencing cell proliferation, differentiation, apoptosis, or angiogenesis. This study aimed to derive data from human BPH and prostate cancer tissues to investigate whether chronic inflammation and angiogenesis were correlated with the expression of COX-2. METHODS. Detection of COX-2 expression was performed on a total of 88 patients, including 45 BPH and 43 prostate cancers. Double-IHC technique were used with the combination of: COX-2/CD3, /CD68, /CD20, to investigate the COX-2 expression and the relationship with chronic inflammation; COX-2/Ki-67 and /Bcl-2, to determine the proliferation or apoptosis; COX-2/ CK34¦ÂE12 and /CK8, to detect the lay of epithelial cells; and COX-2/CD31, to show the microvessle density (MVD). RESULTS. A. In BPH, COX-2 expression was detected in prostate luminal epithelial cells in all 45 samples. The overall percentage of COX-2 positive glands was 7.5%, distributed as: 0.2% in normal prostate tissue, 25.7% in PAH, and 11.9% in simple atrophy. It was evidently that COX-2 expression was mainly found in atrophic glands, which commonly infiltrated with inflammatory cells. T-lymphocytes and macrophages were the predominant inflammatory cells related to the COX-2 expression. COX-2 expression was also associated with Bcl-2 immunostaining and the COX-2 positive epithelial cells had higher proliferation index. B, COX-2 positive staining was detected in 40/43 cancer samples with the very heterogeneous expression. Elevated COX-2 expression was associated with high Gleason score. COX-2-positive areas were noted with high T-lymphocyte and macrophage densities than COX-2 negative tumor areas. MVD were also found higher in COX-2-positive areas than in COX-2-negative tumor areas. CONCLUSIONS. This study demonstrates a novel relationship between COX-2 expression and the local chronic inflammation in situ. The data demonstrate that T lymphocytes and macrophages, by releasing pro-inflammatory cytokines, appeared to play an important role in the induction of COX-2 expression in prostate epithelium, both benign and malignant cells. It is likely that COX-2 may be an effective therapeutic target in prostate cancer treatment.

P 669
THE KI-67 EXPRESSION COULD BE USEFUL IN THE DIFFERENTIAL DIAGNOSIS OF PROSTATIC INTRAEPITHELMIAL NEOPLASIA AND DUCTAL ADENOCARCINOMA
N.Rioux-Leclercq, JJ. Patard, Emmanuelle Leray, Bernard Lobel, François Guillé, Florence Jouan, Pascale Bellaud, JI Epstein. Département d'Anatomie et de Cytologie Pathologiques, de Santé Publique et d'Urologie Faculté de Médecine,Rennes, France, and Departments of Pathology, Urology and Oncology, The Johns Hopkins Medical Institutions, Baltimore, Maryland, USA.

Background : Cribriform and /or papillary prostatic lesions observed on limited tissue, such as needle biopsy, can pose diagnostic dilemmas.One such area of difficulty is the distinction between papillary and/or cribriform prostatic high-grade intraepithelial neoplasia (HG-PIN) and ductal adenocarcinoma.
Design : Over 48 months, we identified 17 cases of ductal adenocarcinoma and 17 cases of HG-PIN from radical retropubic prostatectomy specimens. The HG-PIN lesions were in all cases associated with an acinar prostatic adenocarcinoma component. For each case, we evaluated the proliferative activity, assessed by Ki-67 immunohistochemistry. Results : The majority of ductal adenocarcinomas (82%) were composed of mixed papillary and cribriform patterns, with the remaining demonstrating pure papillary or cribriform patterns. The HG-PIN lesions showed a papillary, cribriform, or mixed papillary/cribriform architecture. The proliferative activity, defined as Ki-67 labeling index, was statistically higher in ductal adenocarcinoma (mean: 33%; range: 21%-66%) as compared to HG-PIN (mean 6%; range: 2%-15%), with no overlap in the Ki-67 indices (p,0.0001).
Conclusion : A combination of histologic features and measurements of cellular proliferation may be helpful to distinguish HG-PIN from ductal adenocarcinoma in limited prostatic tissue samples.

P 670
DOES AMACR/P63 ANTIBODY COCKTAIL DETECT NON SIGNIFICANT PROSTATIC CARCINOMA? A CORRELATIVE STUDY BETWEEN BIOPSIES AND RADICAL PROSTATECTOMIES.
Zahira Merabet (1), Alexandre de la Taille (1,2), Laurent Salomon (1,2), Eric Bonte (1), Sandy Azoulay(2), Hugo Faucon (2), Dimitri Vordos (1,2), René Yiou (1,2), András Hoznek (1,2), Dominique Chopin (1,2), Claude Abbou (1,2), Yves Allory (1,2).
1 CHU Henri Mondor, AP-HP, Créteil, France
2 EMI 0337, INSERM, Créteil, France

Introduction : AMACR/p63 antibody cocktail used in the context of atypical small acinar proliferations suspicious for malignancy provides an increased sensitivity in cancer diagnosis on prostate biopsies. However the risk to detect by this way non significant cancer is not estimated.
Aim of the study : to evaluate in radical prostatectomy the significance of prostate cancers that were diagnosed preoperatively using AMACR/p63 cocktail.

Methods : among the 525 prostate biopsies performed in year 2004, 37 cases were selected with cancer diagnosis made only after AMACR/p63 immunohistochemistry, 17 among these 37 cases were treated by radical prostatectomy and reviewed. Non significant cancer in radical prostatectomy was defined as an intraprostatic tumour with a Gleason score < 7 and a volume <0.5 cc.
Results : median number of biopsies was 21 (15-21) with tumour detected only in 1 biopsy (n=14), or 2 to 4 biopsies (n=3); Gleason score was 5 (n=1), 6 (n=15) or 7 (n=1), median total tumour length was 0.85 mm (0.4-4.6) with a median percentage involved of 0.3% (0.2-2.1). In radical prostatectomy, cancer was significant in 10 cases (Gleason score was 7 (n=9) or 8 (n=1), with a tumour volume above 0.5 cc in 5 cases (1.23-2.28), stage pT2 (n=8), pT3a (n=1) or pT4 (n=1) and positive margins in 3 cases). Cancer was not significant in other 7 cases but no stage pT0 was observed. Median PSA at diagnosis was 7.1 ng/mL in significant cancers (3.9-40) and 6.8 ng/mL in non significant cancers (5.2-14) without statistical difference.
Conclusion : the high rate of significant prostate cancer among those diagnosed preoperatively using AMACR/p63 immunohistochemistry confirms the strong interest of this ancillary technique in clinical practice.

P 671
ROLE OF TOUCH IMPRINT CYTOLOGY IN THE DIAGNOSIS OF PROSTATE CORE NEEDLE BIOPSIES
MANNWEILER Sebastian 1, PUMMER Karl 2, AUPRICH Marco 2, RATSCHEK Manfred 1, TSYBROVSKYY Olsksiy 1, MOINFAR Farid 1
1: Institute of Pathology, Medical University, Graz, Austria
2: Department of Urology, Medical University, Graz, Austria

Introduction: Patients at increased risk for prostate cancer with previously negative biopsies pose a diagnostic challenge.
Purpose: The aim of this study was to investigate the diagnostic accuracy of touch imprint cytology of core needle biopsies of the prostate.
Material and Methods: All patients were suspect for having prostate carcinoma. A total of 452 transrectal prostate needle biopsies were performed from 56 patients. The age ranged from 45 to 87 years, the median age was 68 years.
From each fresh biopsy cylinder two touch imprints were prepared which were stained with Diff-Quik and Papanicolaou methods. After formalin-fixation of the core biopsies a first histological diagnosis was made. The results of the touch imprints and the diagnosis of the first histological examinations were compared. Later on, up to 60 fine step serial sections from all biopsy cylinders, which were inconclusive or negative for carcinoma were prepared. The cytological and histological findings were evaluated by two pathologists.
Results: Needle biopsies: The routinely histologically examined slides of 352 biopsies and 259 touch imprints revealed no carcinoma. A carcinoma was diagnosed in 100 first histologically examined slides and in 193 touch imprints. In 93 touch imprints, a carcinoma was detected, which could not be identify in the first histological examination. While in the following serial sectioning in 336 slides no carcinoma was detected, 116 slides showed a carcinoma at deeper level. In 16 biopsy cylinders a carcinoma was diagnosed which was not identified in the first histological examination. In 77 imprints which were positive for carcinoma no carcinoma was detected even after serial sectioning.
Patients: While the routine histological examination of 27 patients revealed carcinoma, the touch imprint cytology showed carcinoma in 38 patients. In the following fine step serial sectioning of 29 histologically cancer-free patients, 26 patients remained to be negative. The fine step serial sectioning, however, displayed additional carcinomas in 3 patients who were initially negative in the first histological examination.
Conclusion: The additional use of touch imprint cytology of prostate core needle biopsies can improve the diagnostic accuracy. Touch imprint cytology of the prostate can particulary be useful as an adjunct in patients with repeated negative histology or in cases with previous inconclusive histological results.

P 672
EXPRESSION OF E-CADHERIN AND PROTEINS FROM THE CYCLINE-DEPENDENT KINASE INHIBITORS (CDKI) FAMILY IN PROSTATE ADENOCARCINOMA (PAC)
Ma³gorzata Janicka-Jedyñska, Aldona WoŸniak, Jakub ¯urawski, El¿bieta Kaczmarek, Joanna Bulak
Department of Clinical Pathology, Karol Marcinkowski University of Medical Sciences, Poznañ, Poland

INTRODUCTION: In the androgen-independent, metastatic PAC there is currently no successfull therapy. Therefore we need to improve our understanding of markers which can be helpfull in determining the metastasizing potential. It has been proposed that progression may be related to the presence of neuroendocrine differentiation, proteins from the CDKI family (p21, p27) and adhesion molecule E-cadherin. Decreased expression of this proteins may be associated with PAC invasion potential. The aim of our study was to evaluate if E-cadherin, p21 and p27 are valuable to identify individuals at risk for biologically active PAC.
MATERIAL AND METHODS: Archival tissues from 75 patients with PAC after total prostatectomy and 75 controls with BPH (and a 10-year PAC-free follow-up) were labeled for E-cadherin, p21 and p27. Analyzed neoplasms were subdivided into two groups: GL(5-6) (Gleason score 5-6) 48 cases (64%) and GL(7-9) 27 cases (36%). Immunoreactivity for E-cadherin was quantified using morphometric computer analysis. LM patterns were saved (mean 30 for case) and the percentage of cells with positive membranous reaction per 1000 cells was calculated. For p21 and p27 the percentage of positively stained nuclei was counted (per 1000). The results obtained were compared with the histological grade, Gleason score, staging system.
RESULTS: In BPH strong membranous reaction for E-cadherin was evident in all cases (in more than 80% of cells). Regions of PAC were less intensively stained. In the GL(5-6) the percentage of positive cells was above 80% in 34 cases (70.89%) when in the GL(7-9) group it was lower than 80% in 13 cases (48.74%) ($p<0.036$). Correlations between E-cadherin immunostaining pattern and histological malignancy were found. Decreased expression (less than 10% positively stained nuclei) for p27 was observed in 18 cases (66.71%) and 39 cases (81.25%) respectively in above mentioned groups ($p<0.032$). The percentage of positively stained nuclei was above 50% in all control cases. Loss of immunoreactivity was correlated with histological grading and staging. There were found no significant differences for p21.
CONCLUSIONS: The results obtained confirm the importance of E-cadherin and p27 as strong biomarkers for PAC. Decreased expression of this proteins is associated with aggressive phenotype in PAC and may provide additional information to decide which patients need more intensive monitoring or treatment (chemoprevention).

P 673
EXPRESSION OF MOLECULES OF INTERCELLULAR INTERACTION IN PROSTATE CANCER
MATSIONIS Alexander, MEDVEDEVA Larisa, MEDVEDEV Vladimir, RESNIKOVA Galina
Rostov Regional Bureau of Pathology, Rostov-on-Don, Russia

INTRODUCTION: It is known, that losses of an intercellular adhesion resulting in to disconnection of tumour cells, and also the changes of extracellular matrix can promote development of metastatic disease. It is doubtless, that the tumour cells at interaction, and also at construction of a stroma the same molecules use, as normal tissues, though the character expression of those or other factors in various phases of a cancerogenesis can be various. We investigated features expression of some adhesive molecules in prostate cancer.
MATERIALS & METHODS: Tissue samples were taken from 211 patients with prostate cancer, their age ranging between 51 and 82 years. Tissues sections were subjected to immunohistochemical study with a monoclonal antibody in to human ICAM-1 (clone My13), VCAM-1 (clone 1.4C3), CD31 (clone JC/70A), N-Cadherin (clone 3B9), P-Cadherin (clone NCC-CAD-299), E-Cadherin (clone HECD1), collagen 1Ó (clone C1Y 94), Laminin (clone 4C7), Tenascin (clone TN2) (Dako, Zymed). An EnVisionTM; +System (AES) complex staining kit (Dako) was used.
RESULTS: The obtained data allow revealing some differences of normal and tumour cells, and also nor-mal stroma and stroma shaped tumour. In particular, in samples of a normal tissue predominates expression of laminin, Ð- and Å-Cadherins in comparison with other molecules. We reveal ICAM-1 and tenascin rarely and absolutely misses VÑAM-1. At highly differentiated tumours reaction with laminin and collagen 1Ó increase reliable. At moderate differentiated tumours reliable decreases expression of Ð- and Å-Cadherins in comparison with a normal tissue and the expressiveness of reaction with CD31 and collagen 1Ó of increases. In poorly differentiated tumours cells demonstrate tenascin expression and absence or weak degree of reaction of remaining investigated molecules. It was founded that tumours demonstrating decreasing expression of cadherin (p=0,3) and laminin (p=0,3), and increasing expression of tenascin (p=0,05) are accompanied by the more frequent development of the biochemical relapse during three years after radical prostatectomy.
CONCLUSION. Thus, for the prostate cancer characterisation the most important are CD31, cadherin, laminin and tenascin. The changing of their expression is accompanied by the increasing of the frequency of the development of the biochemical relapse.

P 674
DIAGNOSIS OF LIMITED PROSTATE CANCER IN BIOPSY TISSUE: A BAYESIAN ANALYSIS.
DALTON Leslie
South Austin Hospital
Austin, TX USA

Background: Currently the threshold in the histologic diagnosis (dx) of prostate cancer (ca) from atypia/suspicious (A/S) is not fixed. Emphasis is now given to use as many methods as possible to increase sensitivity in the dx of ca. The question becomes whether or not continuing this approach has merit with respect to improving patient outcome (PO). A Bayesian approach was used to analyze the question.
Design: The existing relevant literature was searched for the numbers needed for input into the problem. Unlike prior considerations of this question, the initial point to begin calculating probabilities was where a single pathologist identifies a focus of A/S vs. ca. or even misses an A/S focus. From this point the logical progression of types of studies to review include: pathologist reproducibility (repro.) in the dx of prostate ca, use of immunohistochemistry (ihc) in dx, prostatectomy findings (pf) given a dx of limited ca, findings on repeat bx after dx of A/S or benign dx with persistent increase in PSA, disease progression (dp) based on pf, dp after biochemical failure, mortality/morbidity statistics, and watchful waiting (ww) as a tx.
Results: Studies of pathologist repro. in the dx of limited prostate ca are sparse. Repro. of the ihc methods currently being advocated to help in the decision of limited ca vs. A/S are virtually nonexistent. Possible coin flips therefore abound at the earliest phases of the problem. Then patients with a dx of A/S often show obvious ca after repeat bx., and conversely the dx of limited ca at bx often leads to insignificant ca found after prostatectomy. Ww in many clinical settings has not been proven to unfavorably compare with aggressive treatment. Pathologists rarely consider morbidity in their evaluation of patient outcome, and leave the input of this number as a blank.
Conclusions: At this juncture a defined threshold or set of specific criteria should be set before a dx of prostate ca should be given. Based on this study it appears that any questionable focus less than 0.5mm in a single bx core without Gleason grade 4 features could be regarded as A/S with ww recommended as tx. Diagnosis of ca in foci smaller than 0.5mm (GS <=6), despite many talented individuals feeling comfortable in doing so, should await better validation of technique.

P 675
THE ROLE OF LAMININ-5, VLA-6 AND TENASCIN IN PROSTATE ADENOCARCINOMA SPREADING
POPOVA-GLADSKIKH Olga, KUZNETSOVA Alla, DANILOVA Tamara, IVANOV Alexei, ANDREEVA Yulia*, SHEGAI Peter*, ALEXEEV Boris*, FRANK George*, PALTSEV Michael
Moscow Medical Academy, Moscow Research Institute of Oncology*, Moscow, Russia

Introduction. The process of tumor invasion is accompanied with the significant alterations in expression of different matrix components responsive for cell adhesion and cell migration and contribute to the carcinoma spreading. In prostate adenocarcinoma we investigated the expression of some matrix proteins and integrins have been reported to be highly expressed in many other cancers. The results were compared with respect to histological and clinical peculiarities.
Materials and methods. Cryostat sections and the primary cultures of prostate tissue from 20 patients were immunohistochemically examined using mAb against human tenascin, two forms of Fn, TSP-1, lam, lam-2, lam-5, VLA-2, VLA-6.
Results. Excepting laminin-5, VLA-6 and tenascin we didn't find any correlation with tumor characteristics and reveled variable patterns of expression of the other investigated antigens. All samples showed a complete loss of laminin-5 in focuses of invasion and in sharp contrast a strong positive staining of this antigen in adjacent hyperplastic benign areas. The loss or production of laminin-5 was exceptionally stable feature as it was confirmed in all primary cultures from histologically distinct zones. The immunostaining for VLA-6 was obviously positive in basal layer of all hyperplastic glands and generally negative or decreased in association with malignancy but it was newly observed and even further enhanced in only some cases at the invasive edge of tumor. Tenascin as well as VLA-6 showed positive staining in stroma of hyperlastic areas and it was highly prominent in a few samples, where it arose in epithelial carcinoma cells and partially increased in periglandular stroma of carcinoma foci. Analysis of the relationship of the VLA-6 and tenascin patterns with various clinicopathological characteristics and the patient state revealed that the tenascin presence in carcinoma cell cytoplasm and increased emergence of VLA-6 associated with lymph node metastasis and advanced clinical stage.

Conclusion. The complete loss of laminin-5 in prostate adenocarcinoma is a principal property of invasion and would suggest a less stable epithelial-stromal junction. Partial loss and later new reinforcing of VLA-6 and tenascin at the invasive margins of tumor could reflect a different stages of tumor growth or invasion and also indicate a contributive role of these antigens in migration of malignant cells and disruption of normal integrin signaling.

P 676

EZRIN EXPRESSION IN PROSTATE CANCER AND BENIGN PROSTATIC TISSUE

Alexander Valdman. Department of Urology, Karolinska Hospital, Stockholm, Sweden.
Xiaolei Fang. Department of Urology, Karolinska Hospital, Stockholm, Sweden.
See-Tong Pang. Division of Urology, Chang Gung Hospital, Tao-Yuan, Taiwan.
Bo Nilsson. Department of Biomedical Statistics, Karolinska Hospital, Stockholm, Sweden.
Peter Ekman. Department of Urology, Karolinska Hospital, Stockholm, Sweden.
Lars Egevad. Department of Pathology and Cytology, Karolinska Hospital, Stockholm, Sweden.

INTRODUCTION. The membrane-linking protein ezrin is highly expressed in several types of human cancers and correlations between its immunoreactivity and histopathological data as well as patient outcome have previously been shown. However, such studies have not yet been done on human prostate cancer.
PURPOSE. This study assesses ezrin protein expression in a series of clinical specimens.
METHODS. Immunohistochemical analysis was used to characterize patterns of ezrin expression in prostatic carcinoma and benign epithelium in 103 radical prostatectomy specimens. Ezrin immunoreactivity (IR) was scored 0 to 3 (absent, weak, moderate or strong staining). Agreement between three independent observers was calculated.
RESULTS. Ezrin IR in prostate cancers was moderate or strong in 70% of specimens while negative or only weakly positive in benign epithelium. Interobserver agreement of IR score was substantial (mean weighted kappa 0.70, range 0.67 - 0.73). Ezrin expression correlated with Gleason score ($p = 0.016$) and seminal vesicle invasion ($p = 0.006$) but not with extraprostatic extension or margin status. No correlation with biochemical recurrence after prostatectomy was found ($p = 0.19$). Urothelial and squamous metaplasia invariably showed moderate or strong ezrin expression. Epithelium of seminal vesicles and ejaculatory ducts was always intensely positive.
CONCLUSION. Ezrin was expressed in the majority of prostate cancers and correlated with adverse prognostic factors. Interestingly, high levels of ezrin IR were observed in benign metaplastic epithelium and in seminal vesicles.

P 677

CO-OPERATION BETWEEN THE ANDROGEN RECEPTOR AND THE ERBB FAMILY PROTEINS IN ANDROGEN-INDEPENDENT PROSTATE CANCER

Z. Kolar, V. Student, M. Hajduch, J. Bouchal, M. Svachova
Institute of Patology & Laboratory of Molecular Patology, Faculty of Medicine, Palacky University, CZ-77515 Olomouc, Czech Republic
Laboratory of Experimental Medicine, Faculty of Medicine, Palacky University, Olomouc
Department of Urology, Faculty of Medicine & Faculty Hospital, Palacky University, Olomouc

Introduction: The androgen receptor (AR) plays a crucial role in the development of androgen-independent prostate cancer (AIPC). There is also considerable evidence for significant activation of AR by growth factor receptors like the erbB family. Preliminary results have shown that the modulation of the AR function is mediated by the erbB-2/erbB-3 pathway and not by erbB-1 (EGFR).
Aim: To analyse the relationship between AR and erbB-1-4 expression in relation to AIPC development.
Material and methods: We used indirect immunohistochemistry for determination of the above mentioned expressions in prostate cancer samples obtained from 147 symptomatic AIPC patiens where prostatic biopsies were available both before the start of androgen deprivation and after AIPC development. Mild, moderate or strong membrane-specific staining was recorded semiquantitatively using H-score (intensity of staining 1-3 x % of positive cells). Relevant statistical methods were used to analyse the results.
Results: We found a statistically higher expression of erbB-1 and erbB-2 in cases with AIPC and a significantly shorter survival of patients with high expression of erbB-2 after AIPC development. The levels erbB-3 and erbB-4 proteins were unchanged. Expression of AR positively correlated with expression of erbB-2 in advanced cases with metastases.
Conclusions: These data suggest that the erbB family proteins pathway is a critical target in hormone-refractory prostate cancer and that pharmacological inhibition of these receptors may provide a powerful approach to treatment of advanced prostate cancers.
This work was supported by NC/7497-3.

P 678

IMMUNOHISTOCHEMICAL EXPRESION OF P21WAF1, P27KIP1, CYCLIN D1, P53 AND KI-67(MIB-1) IN PROSTATE INTRAEPITHELIAL NEOPLASIA AND ADENOCARCINOMA, WITH EMPHASIS ON PIN WITH MICROINVASION (PINMIC)

LUQUE Rafael J.(1), REGUEIRO Juan C.(2), LOPEZ-BELTRAN Antonio(2)
(1)Jaén and (2)"Reina Sofia" University Hospitals, Jaén and Cordoba, Spain.

INTRODUCTION: Prostate intraepithelial neoplasia (PIN) is the most likely precursor of adenocarcinoma (PCA) in the prostate, but the morphologic process in which PIN become PCA is poorly understood. Therefore, PIN with microinvasion (PINmic) could be the intermediate step in this morphologic continuum.
PURPOSE: The aim of this study is to present the differential expression of some G1-S modulators of the cell cycle in PINmic as compared with normal prostate (N), PIN, and PCA.
Thirty-seven formalin-fixed, paraffin-embedded samples from radical prostatectomies which contained foci of N (n=37), PIN (n=32), PINmic (n=22) and PCA (n=18) were used. Immunohistochemical expression of p21, p27, cyclin D1, p53 and MIB-1 was quantitated by the grid counting method and the corresponding labelling indices (LI) were determined. Statistical analysis included one-way ANOVA and Scheffe's test for post-hoc multiple comparisons.
RESULTS: We found an increase in the mean LI for all markers from N to PIN, PINmic and PCA. Significant differences between N and PIN, PINmic and PCA were characterized by down-regulation of p27 and up-regulation of the other markers investigated (ANOVA). Multiple group comparisons showed differences between all groups for cyclin D1 LI (N: 1.45±0.76, PIN: 2.49±0.99, PINmic: 3.68±1.02, PCA: 4.76±0.82) ($p<0.001$) and p53 LI (N: 1.55±1.09, PIN: 4.90±2.03, PINmic: 5.36±2.06, PCA: 9.02±4.02) ($p<0.001$), with PINmic showing values between PIN and PCA.
CONCLUSION: G1-S phase modulators of the cell cycle are frequently altered in a continuum from N to PIN, PINmic and PCA. PINmic should be considered an intermediate lesion from PIN to PCA and therefore it could be included as a morphologic variant of PIN.

P 679

FUSION OF MRI AND HISTOLOGY IMAGES IN PROSTATE CANCER: A HELPFUL TOOL FOR PROSTATE CANCER TREATMENT

Le Naour G (1), Bart S (2), Mozer P (2), Penna-Renard R (3), Grenier P (3), Hemar P (4), Troccaz J (4), Chartier-Kasteler E (2), Richard F (2), Delcourt A (1), Capron F (1), Compérat E (1).
(1) Service d'Anatomie et Cytologie Pathologique
(2) Servce d'Urologie
(3) Service de Radiologie, CHU La Pitié-Salpêtrière, 75013 Paris
(4) Laboratoire TIMC, Faculté de Médecine Domaine de la Merci-38706 La Troche

Prostate cancer (PC) is the first cancer in terms of incidence and the second leading cause of death among men in France with 40309 new cases and 10004 deaths in 2000. Needle core biopsy is used for the diagnosis of prostate cancer by urologists worldwide. MRI has shown to be sensitive and specific for prostate imaging and is a useful diagnostic tool. It is critical to acquire that the best possible protocols for biopsy to improve PC treatment. The aim of this study was (i) : to compare retrospectively preoperative MRI images with histological data in order to improve pre-therapeutic disease staging, (ii): to evaluate feasibility and precision of a system of fusion of IRM and histopathological data and (iii) to collect data in order to constitute a 3D computerized prostate surface model with the major sites of prostate cancer, thus to improve biopsy, but also in order to perform medical interventions through the use of passive, semi-active, or active guiding systems.
This study has included 4 cadaver prostates and 8 specimen of radical prostatectomy. MRI imaging was available for all specimens. Cadaver prostates were examined by MRI after resection, patients who underwent prostatectomy had MRI examination before surgery.
Before examination of the prostates after the recommendations of the Stanford protocol, size, weight and volume were evaluated. To be able to reconstruct histology, parallel needles were inserted into the prostate from the apex to the base. These biopsy tunnels were labelled by ink. After staining of the histological sections, all slices were reconstructed and scanned. Contours of organ and tumor were defined. Using deformable modeling techniques, 3D computerized prostate surface models were reconstructed from prostatectomy specimens with localized prostate cancer. A 3D computer simulation system was developed to accurately depict the anatomy of the prostate and all individual tumor foci.
Registration accuracy determined on composite images was visually estimated to about 2-3mm. The composite image quality may be rather limited for MRI retrospective analysis
Composite images of histology/MRI have been defined, to improve the cancer detection. Histological/MRI fusion is still very promising to improve the pre-therapeutic staging of PC, to optimize the biopsy strategy by application of a computer aided system of reference, to increase positive biopsy rate
This may

P 680

NEW DATA ABOUT ETHNIC PECULIARITIES OF LATENT CANCER OF PROSTATE OF THE INHABITANTS AROUND FORMER NUCLEAR TEST SITE (SEMIPALATINSK, EAST KAZAKHSTAN)

WHEELER Thomas, BARAKAT Marina, AYALA Gustavo, PRUGLO Yuriy
Baylor College of Medicine, Houston, TX, USA; State Medical Academy, Semipalatinsk, Kazakhstan

Introduction: The study of prevalence pathogenesis and morphogenesis of prostate cancer (PC) is relatively restricted in countries of Asia. Ethnic variations in cancer incidence in the region are unknown.
Purpose of the study: Study of ethnic peculiarities of latent cancer of prostate of the inhabitants of Semipalatinsk.
Materials and Methods: Morphological analysis of prostates was performed on sequential gross autopsy material of histotopographic sections among 778 inhabitants of Semipalatinsk region in eastern Kazakhstan. The population in this area consists mainly of Europeans (68.1%, mean age at death: 55.3 yrs) and Asians (31.9%, mean age at death: 45.4 yrs).
Results: Cancer of prostate was discovered in 223 cases, PC occurred 2.5 times more often among the persons of Europeans origin, than among the Asians (35.5% vs. 14.1%, $P<0.05$). Of interest also is that in Europeans PC incidence increased with age, while among the Asians it decreased up to the 7th decades, and later ($P<0.05$). HGPIN was also more frequent in the Europeans population than Asians (35.5% vs. 16.1%, $P<0.01$). However Asians had more HGPIN in the 4th and 5th decades and Europeans in the older population. Low Gleason scores (GS) were more frequent in younger Asians. Also Europeans tend to have more foci of cancer than Asians.
Conclusions: Ethnic peculiarities were discovered among the inhabitants of Semipalatinsk region, Kazakhstan with latent cancer of prostate. Asian patients have a lower incidence of PC that happens earlier in life and is less aggressive biologically. This is further evidence of ethnic predisposition to the cancer of this origin.

P 681

NEUROENDOCRINE DIFFERENTIATION AND ANDROGEN EXPRESSION IN BENIGN AND NEOPLASTIC PROSTATE EPITHELIUM

GHIKONTI Ioanna (2), TSIGKA Alexia (2), MIHALOPOULOU Anna (2), BAIRAKTARI Georgia (2), TAMVAKOS George (1), GORANTONAKIS George (1), CHAMILOS Efthymios (1), THEODOSOPOULOS Nikolaos (2), SKOULIDAKIS George (2), THEODOROPOULOS Vasilios (1)
(1) Departments of Urology and (2) Pathology, Agia Olga General Hospital, Athens, Greece.

Introduction. A substantial proportion of primary prostatic adenocarcinomas contain a subpopulation of malignant cells expressing a neuroendocrine phenotype. Neuroendocrine cells (NEC) are considered important for regulating prostatic cell growth and differentiation. Androgen, acting via the androgen receptor (AR), is associated with the development and progression of prostate cancer. We determined the incidence and pattern of distribution of NEC and AR in prostate hyperplastic and cancer tissue and correlated their expression with tumor differentiation and invasiveness.
Material and Method. Antibodies to chromogranin A (CgA) and neuron specific enolase (NSE) were used for the immunohistochemical detection of NEC in formalin fixed, paraffin embedded prostate tissue. We immunohistochemically evaluated 70 prostate cancer (PCa)- 30 well, 20 moderately and 20 poorly differentiated-, 55 prostate intraepithelial neoplasia (PIN)- 30 PIN1, 10 PIN2, 15 PIN3- and 60 prostate adenosis (PA) specimens for CgA, NSE and AR expressing tumor cells. Neuropeptide immunoreactivity was scored as (-) no staining, (+) <2%, (++) 2-25% and (+++) >25% of isolated cells staining positive. AR expression was categorized according to the scoring of the estrogen receptor expression in breast cancer.
Results. Neuroendocrine differentiation (NED) (1% of tumor cells) was noted in 16% of well, 25% of moderately and 50% of poorly differentiated PCa specimens; in 16% of PIN1 and 66% of PIN3; and in 17% of PA cases. AR expression was

positive (weak-moderate) in 50% of well and 100% of moderately differentiated PCa, and moderate-strong in 75% of poorly differentiated PCa specimens.
Conclusions. NED is upregulated in prostatic carcinogenesis, with higher levels of expression in PIN and carcinoma compared with normal cells and hyperplastic tissue. In prostate cancer, NED was increased with PCa dedifferentiation; the same percentage was demonstrated in PIN, which in turn increased in high PIN grades. AR immunoreactivity was more pronounced in benign than malignant prostatic epithelium and became stronger as the tissue became increasingly neoplastic. No negative association between NED status and AR expression was noted in prostate carcinoma. The NEC may play a key role in the regulation of prostatic growth and differentiation.

P 682
BASAL CELL CARCINOMA OF THE PROSTATE: REPORT OF ONE CASE.
LÓPEZ José Carlos, PUÑAL Lidia, CARAMÉS Nuria and ABDULKADER Ihab.
Department of Pathology
Hospital Clínico Universitario
C- Choupana /SN 15706-Santiago de Compostela SPAIN.

INTRODUCTION
Basal cell carcinoma (BCC) is a very rare neoplasm, with only a few cases published in the literature.
CASE REPORT
A 51-year-old male presented with urinary obstruction and hematuria. Serum PSA was normal. The cystoscopic examination showed a nodule located in prostatic urethra that was biopsied and diagnosed as basal cell carcinoma of the prostate.
A radical prostatectomy was performed.
MATERIALS AND METHODS
Formalin-fixed and paraffin-embedded tissue was available from the biopsy and the radical prostatectomy specimen.
Immunohistochemical analysis was performed using a universal second antibody kit that used a peroxidase-conjugated labeled-dextran polymer (EnVision, Peroxidase/DAB; Dako-Cytomation Glostrup, Denmark).
RESULTS
Histologically, there was a proliferation of solid nests of uniform basophilic cells with scant cytoplasm and large nuclei with prominent nucleoli. Mitotic figures were inconspicuous.
The immunohistochemical study showed strong and diffuse positivity for BCL-2 and a high proliferation index (MIB-1).
Cytokeratin -34betaE12 was focally positive. Cytokeratin -7 and p53 were also positive.
Prostate-Specific Antigen (PSA), Prostatic Acid Phosphatase (PAP), Leukocyte Common Antigen (LCA), chromogranin, synaptophysin, Neuron-Specific Enolase (NSE), S-100 and p63 were all negative.
Microscopic examination of the radical prostatectomy specimen showed a predominance of a basal cell type solid pattern, but focally there were some cribriform areas. The neoplasm involved more than one-half of the right prostatic lobe (pT2b) and contacted with the inked surface, but periprostatic adipose tissue and striated muscle were free of tumor. Perineural invasion was present. No vascular invasion was identified.
DISCUSSION
Basal cell proliferative lesions of the prostate include lesions ranging from the common basal cell hyperplasia to the uncommon basal cell carcinoma.
Histological features that help to distinguish benign from malignant lesions are the presence of atypical cells with large nuclei and prominent nucleoli showing an infiltrative pattern , perineural invasion, extraprostatic extension or invasion of the bladder neck, necrosis and stromal desmoplasia.
In the case described herein necrosis was only focally seen and the stroma showed areas of myxoid change.
However, the strong and diffuse positivity for BCL-2 and the presence of a high proliferation index are extremely helpful in the diagnosis.

P 683
KI 67 AND P53 IMMUNOHISTOCHEMICAL EXPRESSION IN PROSTATE CANCER
Silvia Lacramioara Roznovan*, Doinita Radulescu **, Laurette Graziella Cozma ***, Simona Stolnicu****, Simona Mocanu******
*Clinical Hospital"C. I Parhon", Iasi, ** University of Medicine and Pharmacy , Iasi, *** Institute of Public Health, Iasi , **** University of Medicine and Pharmacy , Tg Mures, ***** Clinical Hospital, Tg Mures.

Prostate carcinoma is the most common male cancer and represents a serious health problem.
The aim of this study is to correlate P53 tumor suppresor protein , with tumor grade and proliferative activity. Clinical data were obtained from case notes.
Materials and methods:
Paraffin-embedded samples from 23 patients with prostate carcinoma the were assessed for pattern, Ki 67 and P53 expression. Biotinylated secondary antibodies and the streptavidin-biotin peroxidase complex were applied according to the manufacturer`s instructions (LSAB2 kit, DAKO, Denmark).
Immunohistochemical analise was performed for the expression of Ki 67and p53.Target retrieval solution was used .
Results and Conclusions:. All the carcinomas expressed Ki67, 12 having > 25% nuclear marking. Four patients who was strongly positive for p53 and had a high Ki67 score survived only one year after diagnosis. Survival ranged from 1 to 13 years after diagnosis.
This study confirms that the the expression of P53 correlates with Ki67.

P 684
PROLIFERATING CELL NUCLEAR ANTIGEN ANALYSIS IN PROSTATIC NEEDLE BIOPSY – CORRELATION WITH PSA
Silvia Lacramioara Roznovan*, Doinita Radulescu **, Laurette Graziella Cozma ***, Simona Stolnicu****, Simona Mocanu******
*Clinical Hospital"C. I Parhon", Iasi, ** University of Medicine and Pharmacy , Iasi, *** Institute of Public Health, Iasi , **** University of Medicine and Pharmacy , Tg Mures, ***** Clinical Hospital, Tg Mures.

Effective management of prostate cancer is dependent on adequate pathological reporting of the surgical specimen. Immunohistochemistry has become an important tool in surgical pathology and the evaluation of PCNA and PSA, specific immunohistochemical marker for tumors of prostatic origin, became now routine practice.
Aims: To evaluate the expression of PCNA and PSA in prostate needle byopsy specimens and transurethral resection of the prostate and corelation with tisular PSA and other prognostic indicators including age, Gleasson score and surviving period for some patients.
Materials and methods:
Biological markers (PSA, PCNA) were performed on 61 patients with prostate cancer. Biotinylated secondary antibodies and the streptavidin-biotin peroxidase complex were applied according to the manufacturer`s instructions (LSAB2 kit, DAKO, Denmark).
Diaminobenzidine was used as a chromogen for visualization. The slides were counterstained with light hematoxylin.
Results and Conclusions:

PSA immunoreactivity decreased in adenocarcinomas with higher Gleason score.
PCNA increases progresively from well differentiated through poorly differentiated cancer; correlation with canser stage is strong. In the less differentiated cases , the percent of positive nuclei is higher than the average. PCNA correlates with clinical stadialization and degree of tumor metastasis .

P 685
VIRTUAL SLIDES QUALITY ASSESSMENT TEST FOR EARLY PROSTATE CANCER ON A NATIONWIDE SCALE IN FRANCE
Nicole BERGER, Laurent BIENVENU, Eric BOUCHER, Marc de FROMONT, Alain FONDIMARE, Vincent MOLINIE, Eric PELTIER, Dominique PIRON, Mathilde SIBONY, Frédéric STAROZ, Marie TRILLER, Annick VIEILLEFOND. For Committee n°6 « Urinary tract », working on behalf of AFAQAP (French Association for Quality Assurance in Pathology).

Background: PSA screening increases the number of cancer cells detected at a low stage (pT1c), with only small foci found on biopsy specimens. In order to reduce the number of potential over- and under-diagnoses, a study was carried out through a quality assessment test on a nationwide scale in France on virtual microscopic slides.
Materials and methods: Twelve cases of prostatic specimens (biopsies, TRUP) displaying carcinoma and their mimics were selected: prostatic carcinoma (n=6), mimickers of cancer (n=5), high grade PIN (n=1). Among carcinoma there were Gleason score £ 6 (n=2), Gleason score > 6 (n=4), with small focus (n=5). Mimickers were atrophy (n=2), cribriform clear cell hyperplasia (n=1), basal cell hyperplasia (n=1), and sclerosing adenosis (n=1).
For each case an H&E slide was digitalized on a CD-ROM with the NAVIQAP® virtual slide system from Samba Technologies.
The CD-ROM was sent to 191 junior or senior pathologists scattered all over the country. The answer form included main items like benign lesion, prostatic carcinoma, need for new biopsy, and secondary items for the sub-classification of the lesions and the Gleason score in case of malignancy. After the deadline for the responses, each participant was given access to the results and comments on the CD-ROM.
Results: 130 answers were analyzed. Some mimic lesions were misinterpreted as carcinoma: sclerosing adenosis (37%), atrophy (2 -10%), basal cell hyperplasia and cribriform clear cell hyperplasia (2% of the participants). HGPIN was misinterpreted as a benign lesion by 13%, and over-diagnosed as carcinoma by 5% of the pathologists. Small foci of carcinoma were misinterpreted as benign lesions in respectively 6, 7 and 18% in Gleason score > 6, and in 40 and 48% in Gleason score £ 6. Ductal carcinoma was misinterpreted as a benign lesion by 5% of the participants.
Conclusion: This study demonstrated the ability to test on a large scale the pathologist accuracy on usual prostate lesions. Its results can be used to focus teaching efforts on obvious potential mistakes in a “the real life” setting.

P 686
HER-2/NEU ONCOGENE EXPRESSION IN PROSTATE CARCINOMA: EVALUATION OF GENE AMPLIFICATION BY FISH
SERTÇELÝK Ayþe, KANKAYA Duygu, PERÇÝNEL Sibel, KUZU Iþýnsu, BALTACI Sümer

Introduction: The variability in the clinical and biological behaviour of prostate cancer and the inadequacy of markers used for assessing prognosis leads to investigate for new prognostic parameters. There has been an increasing interest on Her-2/neu oncogene and studies which investigate its role in prostate carcinomas have given variable results.
Aim: The aim of the present study is to investigate whether Her-2/neu oncogene has a role in the initiation and progression of prostate carcinoma.
Methods: Radical prostatectomy specimens from 74 patients who have prostate carcinoma were included in the study. Tissue array blocks were constructed by taking 2-6 cores 4mm in diameter for each tumour specimen using punch biopsy needle. Overexpression of Her-2/neu protein was assessed in areas of carcinoma, low grade intraepithelial neoplasia (LGPIN), high grade intraepithelial neoplasia (HGPIN), and benign prostate hyperplasia (BPH) by immunohistochemistry (IHC). Flourescence in-situ hybridization (FISH) method was used to investigate Her-2/neu gene amplification in areas of carcinoma in 56 cases. The results of both methods were compared in correlation with gleason grade, stage of tumour and preoperative serum prostate spesific antigen levels.
Results: Her-2/neu protein was expressed in a cytoplasmic/membranous manner in the study cases. The expression of Her-2/neu oncoprotein significantly increased from areas of BPH to PIN and reached the highest degree in areas of carcinoma (p=0). Her-2/neu overexpression by IHC was observed in 66,21 % of prostate carcinomas while Her-2/neu gene amplification by FISH was present in 4,05 % of prostate carcinomas. There was no relationship between the ratio of Her-2/neu protein expression or gene amplification and gleason grade, stage of tumour and preoperative serum prostate spesific antigen levels.
Conclusion: The degree of expression of Her-2/neu oncoprotein increased from areas of BPH to PIN and reached the highest degree in areas of carcinoma by IHC though no correlation with gleason grade, stage of tumour and preoperative serum prostate spesific antigen was found. Her-2/neu gene amplification was observed in very few of the carcinoma cases, thereby making it difficult to comment on the significance of Her-2/neu protein expression in prostate carcinoma. Therefore, studies on larger series of prostate carcinoma representing different stages are necessary to clarify its significance.

P 687
THE SIGNIFICANCE OF THE IMMUNOEXPRESSION OF KI 67 AND P21 IN PROSTATE BIOPSY TISSUE
VLAHOVA Aleksandrina,CHRISTOVA Svetla, SLAVOV Chavdar
Chair of General and Clinical Pathology
*Department of General Urology
Alexandrovska University Hospital
Medical University, Sofia, Bulgaria

The diverse clinical outcome of patients with prostate cancer necessitates additional examination of biopsy tissue to achieve individual approach of treatment. Some clue can be provided by immunohistochemical establish abnormal expression of p21 or Ki 67. The aim of this study was to investigate the expression of Ki67 and p21 and to analyze their relationship in BPH and prostate cancer. METHODS: The expression of the Ki67 and p21 was examined by immunohistochemistry on paraffin embedded tissues sections from patients with BPH, PIN and prostatic carcinoma. RESULTS: A total of 52 patients, from 52 to 81 years old, were diagnosed: 9 benign prostatic hyperplasia, 11 prostatic intraepithelial neoplasia and 32 adenocarcinomas. The specimens were examined by immunohistochemistry for Ki67 and p21 . We found that BPH and PIN showed no or weak immunostaining for p21 and Ki 67, ranging from 0 to 3%, with one exception. Ki 67 was found positive mainly in prostates with PIN, revealing the premalignant nature of the lesion. In Gleason score 2-6 group Ki 67 showed equal percentage of cells in proliferation, and no p21 expression. The adenocarcinomas with high Gleason score revealed high proliferative index. The incidence of expression and the

percentage of Ki 67 positive cells increased with Gleason score. In the examined biopsies, different zones revealed different expression of Ki67, with tendency to increase in less differentiated areas. Overexpression of p21 was found only in four cases mainly in the areas with high Ki67 index.
CONCLUSION: Although the immunoexpression of Ki67 and p21 cannot help to differentiate between BPH, PIN and cancer, it provides additional information to find patients needing close clinical follow up. Their expression serves as independent prognostic factor after PSA, Gleason score and stage, and shows the effect of treatment and AIPC turn down. If the data are known from biopsy before the operation they can help to choose the most efficient treatment. The high proliferative index in biopsies of patients without cancer screens those needing close clinical and biochemical control.

P 688

COMPARISON OF NUCLEAR VOLUME IN PROSTATIC INTRAEPITHELIAL NEOPLASIA AND PROSTATE CARCINOMA

1S. Roznovanu, 2D. L. Frincu, 3D. Radulescu, 2D.L. Calin
1Division of Pathology, Parhon Hospital, Departments of 2Anatomy and 3Pathology, University of Medicine and Pharmacy „Gr. T. Popa", Iasi, Romania

Introduction. Prostatic intraepithelial neoplasia (PIN) is the most precancerous lesion of prostatic carcinoma, one of the most common malignant diagnosed tumor and there are no accurate technique for predicting their evolution. Gleason system has been shown to accurately predict prognosis for low and high grades PINs, but for prostate carcinoma is of limited prognostic use. We have been interested in using a computer-based quantitative measurement to determine a more accurate assessment of nuclear dimension.
Materials and methods. There were analyzed histologic sections from 82 biopsies and 40 transrectal rezections of prostate carcinoma. The biopsy tissue block and tumor fragments were paraffin included and quantitative analysis was performed on hematoxylin and eosin-stained histological sections with a computer-based program. All distinguishable nuclei in a microscopic measurement field were systematically selected for the standard measurement and for stereologic estimation of volume-weighted mean nuclear volume by the „point-sampled intercept" method. The lesion measured in each samples of primitive tumor was always the most severe and 40 nuclei were measured in each case.
Results. The stereologic results indicate a significant increase in nuclear volume from low grade PIN (301.0532 ± 68.1322) to high grade PIN (387.11563 ± 74.5381) and prostatic carcinoma (400.2371 ± 88.5272). It is a significant difference between the two grades of PINs, but the differences between high grade PIN and prostatic carcinoma was not significant.
Conclusion. Our study provides a more-objective differentiation of the two grades of PINs and demonstrates that stereologic nuclear volumetry adds significantly to the correct and objective clasification and prediction of these lesions and is of capital importance in patient management.
KEY WORDS: NUCLEAR VOLUME MEASUREMENT, PROSTATE CARCINOMA, PROSTATIC INTRAEPITHELIAL NEOPLASIA.

P 689

EXPRESSION OF CLEAVED CASPASES 3 AND 8 IN HUMAN PROSTATE CARCINOMAS

DECAUSSIN-PETRUCCI Myriam 1,2, RUFFION Alain 2,3, DEVONEC Marian 2,3, MAUDUIT Claire 1,2,and BENAHMED Mohamed 2.
1Service d'Anatomie Pathologique, Centre Hospitalier Lyon Sud, 2 U407 Inserm, Facult¨¦ de M¨¦decine Lyon Sud, 3 Service D'Urologie, Centre Hospitalier Lyon Sud, Lyon, FRANCE

Prostate carcinoma (Pca), one of the most common cancer in men, is a major health problem, due to its morbidity and mortality in the growing elderly man population. New diagnostic and prognostic markers are needed, and the carcinogenesis of Pca remains to be clarified.
The disruption of the balance between cell proliferation and apoptosis in favor of apoptosis is responsible for the abnormal growth of the prostatic gland during neoplastic development. The chief effectors of the apoptotic pathway are the caspase family that induce cell death through activation ¡°in cascade¡± of different caspase members. Upstream, caspase 8, an initiator caspase, cleaves all other known caspases. Downstream, caspase 3, as executioner, is at the center of apoptotic process by cleaving cellular substrats and inducing DNA fragmentation.
The aim of this study was to evaluate the cleaved caspase 3 (Ccsp3) and 8 (Ccsp8) proteins expression in prostate cancers to better understand the role of the apoptotic pathway in these tumors.
Immunohistochemical study was performed on prostatic tumors (with tumoral and normal tissues in each case) from 30 patients. The cases were separated in low grade tumors (Gleason score ¡Ü6, n=12) and high grade tumors (Gleason score >6, n=18). For each case, paraffin sections was incubated with rabbit polyclonal antibodies raised against Ccsp3 or Ccsp8.
Ccsp 3 expression was significantly decreased (p= 0.0006) in cancers compared with normal tissues. Moreover, this expression was also decreased in tumoral tissues from low grade (p= 0.0025) and from high grade (p=0.0005) tumors, compared with normal tissues. By contrast, no significant changes (p>0.05) in Ccsp8 expression was detected in tumoral tissues from all the 30 cases or inside the subgroups (low or high grade) compared with normal tissues.
The loss of Ccsp3, -the key protein in the execution of apoptosis-, in prostate cancers compared with normal tissues suggests an inhibition of the apoptotic process in these tumors. Furthermore, the decrease in Ccsp 3 expression was observed even in low grade tumors, making of this activated protein a potential early marker of tumoral transformation. Nevertheless, how caspase 3 is inactivated in Pca remains unclear. It couldn¡¯t be accounted on the loss of activation of caspase 8 since its expression was not modified in Pca. A potential posttranscriptionnal deregulation of caspase 3 activation in Pca could be hypothesized.

P 690

INMUNOHISTOCHEMICAL CHARACTERIZATION OF LOCALIZED PROSTATE CANCER.

G.Olmedilla *, J.C. Tamayo**, P.Ramos *, A. Ruiz Villaespesa *, M. Sánchez Chapado **.
Departments of Pathology * and Urology **. Hospital Principe de Asturias. University of Alcalá de Henares. Alcalá de Henares, Madrid

Introduction: classical predictive factors for prostate cancer seem to be sometimes insufficient . Advances in molecular biology and inmunohistochemistry allow us to study molecules related with the cell cicle in prostatectomies with prostate cancer.
Aims: To define predictive value for prognosis of different molecules implicated in the biology of prostate cancer; using inmunohistochemistry for p-21, bcl-2 and ki-67 in radical protatectomies of localized prostate cancer in order to determine association with biochemical relapse.
Material and methods: We used inmunohistochemistry to analyze the expression of ki-67, p21 (waf1/cip1) and bcl2 protein in 96 radical prostatectomies with localized prostate cancer. The results were related with biochemical relapse (seric PSA more than 5ng/ml) using statistical analysis with Kaplan-Meyer curves and test log-rank. Gleason score and tumour stage were related.

RESULTS: Biochemical relapse was found in 22 cases (22%). Patients with overexpression of p21 and Bcl-2 were more prone to have biochemical relapse (36 months follow-up), but without statistical association. Patients with overexpression of Ki-67 had 3,15 more possibilities to have biochemical relapse, with statistical signification (p< 0,001).

CONCLUSIONS: Ki-67 overexpression seems to be a good prognostic predictive factor.

P 691

SINGLE-MINDED 2 HOMOLOG GENE (SIM2) IS OVEREXPRESSED IN PROSTATE CANCER

HALVORSEN Ole J., ROSTAD Kari, ØYAN Anne M., BØ Trond H., STORDRANGE Laila, OLSEN Sue, HAUKAAS Svein A., HOOD Leroy, JONASSEN Inge, KALLAND Karl-Henning, AKSLEN Lars A.
Section for Pathology and Sections for Microbiology and Immunology, The Gade Institute, Haukeland University Hospital, Department of Informatics, University of Bergen, Bergen, Norway, Institute for Systems Biology, Seattle.

The single-minded homolog 2 gene (SIM2) is present within the Down's syndrome critical region on chromosome 21 and encodes a transcription factor involved in development. A short (SIM2-s) and long (SIM2-l) isoform of the SIM2 transcript have been identified. In a recent study, we identified SIM2 among highly upregulated genes in 29 malignant prostate tumours (T), compared with 33 benign (B) prostate samples, using a 40k human cDNA microarray. SIM2 was identified as the second most consistently upregulated named gene in T versus B samples, only surpassed by AMACR. The purpose of our study was to validate the expression of the SIM2 gene and SIM2 isoforms, and examine the expression and prognostic impact of SIM2-s protein expression in prostate cancer. The upregulation of SIM2 was confirmed in a subset of samples using oligonucleotide microarrays. SIM2-s and SIM2-l specific and SIM2 total TaqMan Assays-by-design were employed for quantitative real time PCR (qRT-PCR) on an expanded material of 47 prostate T and 38 B total RNAs, including 31 T/B pairs. SIM2-s, -l and -total were significantly elevated in malignant vs. benign prostate tissues by 3.3, 6.3 and 3.8 fold (median), respectively. However, SIM2-s upregulation was paralleled by SIM2-l upregulation in tumours, contrasting previous studies. Low level expression of both SIM2 isoforms was also detected in benign prostate tissue. In order to examine a larger patient series, a tissue microarray consisting of paraffin embedded prostate cancers from 104 patients, treated by radical prostatectomy, was subjected to immunohistochemistry using an anti-SIM2-s specific antibody. A moderate/strong staining was noted in 44 of 103 carcinomas as opposed to a weak to negative staining in the remaining cases. Moderate/strong expression of SIM2-s was associated with adverse prognostic variables like high histological grade, extra-prostatic extension and elevated serum-PSA. The 13 year survival was 98.1 % vs. 72.8 % in patients with weak/negative vs. moderate/strong SIM2-s expression, respectively (P=0.008, log rank test). In conclusion, the SIM2 gene was upregulated in prostate cancer as validated by oligonucleotide microarrays and qRT-PCR, and SIM2-s protein expression was found to be associated with adverse prognostic variables and reduced patient survival. These findings may prove relevant as SIM2 has been proposed as a possible drug therapy target.

P 692

COMPARISON OF 34BE12 AND P63 IN VARIOUS LESIONS OF THE PROSTATE; ATYPICAL SMALL ACINAR PROLIFERATION (ASAP), LOW AND HIGH GRADE ADENOCARCINOMA AND HIGH GRADE PROSTATIC INTRAEPITHELIAL NEOPLASIA (PIN)

SAYGIN Tuzel, AKYILDIZ IGDEM Aysenur, SAHAN Elife, ERDOGAN Nusret
Department of Pathology, Taksim Training and Research Hospital, Istanbul, Turkey

Objective: The basal cell-specific cytokeratin antibody (34¥âE12) is widely used to aid diagnosis of prostate cancer. Recently p63, a nuclear protein, was identified as useful basal cell-specific marker.

In this study, specimens from prostate needle biopsies, transurethral resections of prostate (TURP), open enucleations and radical prostatectomies were examined. We compared staining patterns of 34¥âE12 and p63 on the lesions of atypical small acinar proliferation (ASAP), low and high grade adenocarcinoma and high grade prostatic intraepithelial neoplasia (PIN).

Results: It was a statistical significance in basal cell staining with 34¥âE12 and p63 in the foci of ASAP. In some cases, 34¥âE12 was stained basal cell layer as complet and strong, whereas p63 was stained fragmented and strong. In three cases, both stains did not stain basal cell layer.

In other lesions, ©¥t was not a statistical significance for staining of basal cell layer with 34¥âE12 and p63. However, some different features of both stains were observed.

Conclusion: ASAP is not a new tumor or precursor entity. Whereas the high predictive value of ©¥ts for subsequent adenocarcinoma warrants close follow-up and repeat biopsy.

The most commonly used ©¥mmunohistochemical marker in the diagnosis of prostate cancer is 34¥âE12. However, p63 is almost as sensitive and specific as 34¥âE12 in diagnosing prostate cancer in needle core biopsies. Both stains are usually equally effective in demostrating basal cells in benign glands. p63 is a basal cell- specific marker that could be used as a complemantary test for the traditionally used 34¥âE12 in diffucult cases. An important difference from 34¥âE12 is its consistent strong nuclear signal, which is easier to interpret.

P 693

CORRELATIONS OF SMALL (3MM OR LESS) FOCUS OF PROSTATE CARCINOMA ON NEEDLE BIOPSY WITH RADICAL PROSTATECTOMY SPECIMEN.

CAMPARO Philippe, DENOUX Yves, MOLINIE Vincent, HAUS Rachel, BARDIER Armelle, COMPERAT Eva, VIEILLEFOND Annick, SIBONY Mathilde.

Purpose of the study : In order to analyse the radical prostatectomy follow up of small foci of prostate cancer diagnosed on biopsies, we perfomed a multicentric retrospective study from1999 to2004.
Methods : We studied 107 consecutive patients, with a small focus of cancer (less or equal to (</=) 3 mm length) on only one biopsy core, a Gleason score </=7, and evaluated the pT stage and the tumour volume on subsequent radical prostatectomy specimen.
Results : Mean age of patients was 64,6 years (46-83 years). Mean PSA concentration was 9,12 (0,6-33) (no data available for 5 patients).
The average number of prostate cores per biopsy was 7,94 (5 – 21). Average total length biopsies was 83,69 mm (13-170). 45 patients had a focus </= 1mm, 30 between 1 and 2 mm and 32 between 2 and 3 mm. 15 patients had Gleason score </= 5, 73 of 6, and 19 of 7.
The whole prostate was embedded in paraffin ; cancer staging was reevaluated according to TNM 2002 classification. Volume of cancer was measured according to an elliptic model : length x width x heigth x 0.4. Average tumour volume at radical prostatectomy was 1,1cc (0,001 – 11,8).
pT Stages pT2a, pT2b, pT2c, pT3 (</= 1mm : 13, 3, 26, 3; 1-2 mm : 3,6, 13, 8; 2-3mm : 5, 4, 16, 7)

volumes </= 0,2 cc; 0,2-0,5cc;> 0,5cc (</= 1mm : 16, 6, 23; 1-2 mm : 7, 6, 17; 2-3 mm : 11, 6, 15)
A small focus </= 1 mm was statistically associated with an organ confined cancer (p=0,02), and associated with pT2a stage (p=0,04). Paradoxically, it was not associated with a small cancer volume (</= 0.5cc p=0.47 and </= 0.2cc p=0.77). PSA average value was correlated with cancer volume (p=0.02) and a volume </= 0.5cc was highly correlated with PSA<10ng/ml (p=0.001).
There was not a significant association between Gleason score and cancer volume (p= 0.47)
On multivariate analysis no association was found between cancer volume and length of cancer on biopsy, adjusted on PSA and gleason score (p>0.5).
Conclusion : This study demonstrates a strong association between small foci of tumour (</= 1 mm) on one prostate biopsie core and pT2a stage (but not with tumour volume) on prostatectomy. Those paradoxical results justify a prospective study on a series of patients with larger number of biopsies (i.e. 12 to 18) to determine wether length of tumour on biopsy can or not identify a subset of patients with good prognosis.

P 694
PATHOLOGICAL SECRETIONS IN PROSTATIC ADENOCARCINOMA
Lj Velickovic, B Djordjevic, V Katic, D Dimov, V Zivkovic

Introduction The presence of pathological intraluminal secretions in prostatic adenocarcinoma, ie. pink amorphous secretions, crystalloids, blue – tanged mucinous secretions, is always suspicious, but not diagnostic for prostate cancer. Between 10% and 23% of acinar – forming prostatic adenocarcinoma contain intraluminal crystal – like structures referred to as crystalloids, and are often associated with amorphous, intraglandular eosinophilic secretions. The aim of our study was to analysis the expression of these morphological signs in prostatic adenocarcinoma.
Methods Research was performed in 80 patients with prostatic adenocarcinoma, at the Institute of Pathology Clinical Centre Nis. The specimens were fixed in 10% formaldehyde and embedded in paraffin. The sections were stained with HE, PAS and HID-AB pH 2,5 methods.
Results The most common changes present in mucous secreting carcinomas were neoplastic glands lumen distension (43/80 – 53,75%), basophilic secretion (21/80 – 26,25%), presence of extracelular mucins (7/80 – 8,75%) and presence of crystalloids (22/80 – 27,5%). Presence of all morphological signs was recorded in carcinomas of Gleason grade 1-4A. Crystalloids were more often present in well differentiated and moderately differentiated neoplastic glands. Lumen distension was typical for Gleason grade 3 and 4A. The association of those morphological features with mucin secretion was confirmed with special methods for mucin detection (PAS and HID-AB).
Conclusions This study clearly showed that pathological intraluminal or extraluminal secretions are very often in prostatic adenocarcinoma and it can use as supportive features of prostatic cancer.

P 695
TUMOR MARKER DETECTION BY MEANS OF RT-PCR: ANALYSIS OF PARAFFIN-EMBEDDED SENTINEL LYMPH NODES OF PROSTATE CANCER PATIENTS
HAAS Christian J.*, CUBUKLUÖZ Figen*, WAGNER Benjamin*, WECKERMANN Dorothea**, ARNHOLDT Hans*, WAGNER Theo*
*Dept. of Pathology and **Dept. of Urology, Augsburg Central Hospital, Augsburg, Germany

Introduction: For the improvement of pathological diagnosis RT-PCR based expression analysis of tumor markers seems to be a highly promising method. However, the value of this technique for routine diagnosis has to be proven by application on paraffin-embedded tissue and direct correlation with immunohistochemical data.
Material and Methods: From 242 routinely paraffin-embedded SLNs obtained from 85 prostate cancer patients two immediately adjacent 8 µm sections were cut, one of which used for IHC and the other for RNA-extraction.
The obtained RNA was reverse transcribed and PCR for the detection of various tumor markers was performed. The specificity and sensitivity of these RT-PCRs was compared with the immunohistochemical results, as well as with the other pathological and clinical data of the respective patients.Moreover, for the RT-PCR positive specimen the tumor marker expression was quantified by real-time PCR and a correlation with the micromorphometric data was performed.
Results: For the tumor marker panel tested, the sensitivity of the RT-PCR as well as the negative predictive value was 99 % for detection of immunohistochemically identified tumor cells in the SLNs. All non-prostate cancer SLNs used as negative controls were RT-PCR negative. Of the 175 immunohistochemically negative prostate cancer SLNs 25 were RT-PCR positive. Of these 8 were from pN1(i+)(sn) patients and 14 from pN0(i-)(sn) patients with biochemical relapse. The real-time RT-PCR data corresponded well with the histopathological distinction between isolated tumor cells, micro- and macrometastases.
Conclusions: RT-PCR based techniques are feasible on single sections of paraffin material and thus can be used as a supportive methods in pathological diagnosis of prostate SLNs. This opens the possibility for extremely sensitive qualitative and even quantitative analysis of tumor marker expression. For prostate cancer patients RT-PCR analysis of appropriate tumor markers may be useful as an additional prognostic factor for the identification of patients with increased risk of biochemical relapse.

P 696
ANATOMO-PATHOLOGICAL FEATURES IN MUCINOUS PROSTATE CARCINOMA
ROZNOVANU Lacramioara Silvia*, RADULESCU Doinita**, AMALINEI Cornelia**, STOLNICU Simona***
*Laboratory of Pathology "Parhon" Hospital Iasi, Romania
**Department of Pathology, University of Medicine and Pharmacy Iasi, Romania
***Department of Pathology, University of Medicine Targu-Mures, Romania

Signet-ring adenocarcinoma of the prostate is an unusual variant of prostatic carcinoma, with a high grade of malignancy. But with increasing use of needle biopsies as the primary mode of diagnosis, pathologists should be familiar with the full range of aspects of this tumor and its mimics. We report the cases of two male patients, with ages of 65 and 72 years, presented with urinary retention. Seric Prostatic specific antigen (PSA) level was increased in both cases. Fine needle biopsies were performed and fragments were fixed in formalin and embedded in paraffin. Histochemical reactions (mucicarmin, Alcian blue) and immunohistochemical methods (PSA) were applied. Over 90% of prostate samples were infiltrated by a poorly differentiated carcinoma with mucinous and signet ring patterns. The signet-ring cells presented abundant clear or vacuolated cytoplasms and ovalar, vesicular, eccentrically placed nuclei, with small nucleoli. The overall grade was assesed as Gleason grade 5 and immunohistochemical staining for PSA was positive in both cases. This aggressive tumor is an uncommon but distinct variant of primary prostatic carcinoma which should be distinguished from metastatic disease. The expression of prostate associated antigens such as PSA represents the diagnostic of prostatic origin.

P 697

DUCTAL CARCINOMAS OF THE PROSTATE: A CLINICOPATHOLOGICAL AND IMMUNOHISTOCHEMICAL STUDY

ROZNOVANU Lacramioara Silvia*, RADULESCU Doinita**, AMALINEI Cornelia**, STOLNICU Simona***
*Laboratory of Pathology "Parhon" Hospital Iasi, Romania
**Department of Pathology, University of Medicine and Pharmacy Iasi, Romania
***Department of Pathology, University of Medicine Targu-Mures, Romania

The aim of our study was to confirm the expression of prostate specific antigen (PSA) in ductal carcinoma of the prostate, and to analyse p53, and Ki-67 expression in these tumors. Paraffin-embedded samples from 12 patients with ductal carcinoma of the prostate were assessed for pattern, mitotic count and the presence of a microacinar carcinoma component. There were 6 pure ductal and 6 mixed microacinar and ductal carcinomas. Sections were stained immunohistochemically for the expression of PSA, p53 and Ki-67. Six of the ductal tumors had a papillary pattern whilst the others had a cribriform appearance. The mitotic rates in the ductal areas were high in the tumors from 8 of the 12 patients. PSA immunohistochemistry was positive in all cases. Two of the tumors were strongly positive for p53 protein. All the ductal carcinomas expressed Ki-67. This study confirms the expression of PSA in ductal carcinomas of the prostate. The percentage of tumors expressing p53 was similar to that published for high-grade microacinar carcinomas. The results for Ki-67 suggest that ductal tumors have higher scores than microacinar tumors, but further studies are necessary to ascertain this aspect. As half of the patients with ductal tumors had co-existent microacinar tumors, we advise transrectal prostatic biopsies in patients diagnosed with pure ductal carcinomas on transurethral resection specimens, to exclude high-grade microacinar carcinomas.

P 698

EXPRESSION OF CYCLIN A, CYCLIN B1, AND HIGH MOLECULAR WEIGHT CYTOKERATIN (34-BETA-E12) IN PROSTATIC CANCER

GOVEDAROVIC Vitomir*, RADOSAVLJEVIC Radosav**, MITROVIC Dragan*, BRASANAC Dimitrije*, ACIMOVIC Miodrag**, HADZI-DJOKIC Jovan**, MARKOVIC-LIPKOVSKI Jasmina*
*Institute of Pathology, Medical Faculty, University of Belgrade
**Clinical Centre of Serbia, Belgrade

Cytokeratin 34-beta-E12 staining is a useful tool in confirming and establishing of prostatic cancer diagnosis. Our aim was to investigate, whether cyclin A and B1, as a proliferative markers, have additional importance.
Forty three cases of patients with primary prostatic adenocarcinoma obtained from needle biopsy in Department of Urology, Clinical Centre of Serbia, Belgrade.
Cyclin A, cyclin B1 and cytokeratin 34-beta-E12 proteins expression were immunohistochemically assessed by semiquantitative evaluation using anti-human cyclin B1 monoclonal antibody (M 3530, DAKO) and anti-human cytokeratin 34-beta-E12 monoclonal antibody (N1553, DAKO). We examined relationship of this immunohistochemical markers with values of Gleason score, PSA and F/T PSA in serum.
Cytokeratin expression and Gleason score were in inversion correlation ($p<0.05$). Decreased cytokeratin expression was followed by increased expression of cyclin A ($p<0.05$), but without statistically significant increase of cyclin B1 expression ($p>0.05$). However, strong correlation between cyclin A and cyclin B1 expression were observed ($p<0.01$). PSA value and Gleason score were in very strong direct correlation ($p<0.001$). We could not found any significant relationship between F/T PSA and other analysed parameters. Increase of Gleason score which has prognostical significance, clinically has been followed by higher serum PSA levels and immunohistochemically by decreased expression of cytokeratin. Direct significant connection between Gleason score and cyclin A and B1 has not found.
We conclude that only 34-beta-E12 staining is still reliable immunohistochemical marker which improves prostatic carcinoma diagnosis on needle biopsies.
Key words: prostatic cancer, Gleason score, cyclin A, cyclin B1, cytokeratin 34-beta-E12, PSA, F/T PSA, needle biopsy

P 699

INTRAOPERATIVE FROZEN SECTIONS ANALYSIS OF THE POSTEROLATERAL MARGINS DURING NERVE SPARING LAPAROSCOPIC RADICAL PROSTATECTOMY: TECHNICAL ASPECTS

L. Doucet (1), N. Dreux (1), G. Fournier(2), A. Valeri (2), N. Lagarde(1), A. Volant (1).
(1) Department of Pathology, University Hospital of BREST, FRANCE
(2) Department of Urology, University Hospital of BREST, FRANCE

Introduction : nerve sparing procedure during laparoscopic radical prostatectomy need to perform a dissection closer to the posterolateral margins than without preservation of the neurovascular structures. Using intraoperative frozen sections (IFS) analysis on the posterolateral margins was unfrequently reported before during open or laparoscopic radical prostatectomy and could be an improvement of the technique allowing more patients to benefit from nerve sparing for preservation of potency in case of negative margins.
Purpose of the study: describe the technical aspects of the technique that we currently use in patients candidates to a nerve sparing procedure.
Methods: A total of 242 (uni or bilateral) IFS analysis were realised during nerve sparing laparoscopic prostatectomy between April 2002 and March 2005 for potent patients with clinically localized prostate cancer (T1&T2). After completion of the nerve sparing procedure and interfascial dissection the prostate is immediately remove. A specimen (2.5/4cm x 1cm) is cut by the surgeon from base to apex on one or both side of the prostate posterolaterally on the area of contact of the neurovascular bundles. The specimen including the capsule and 4 mm of the underlying prostatic parenchyma is immediately sent to the pathologist. After inking of capsular side 12ìm frozen sections are performed followed by toluidine blue staining and analyzed. Positive surgical margins are defined as tumor at the inked surface. In case of positive margins the ipsilateral neurovascular bundle is removed at the end of the procedure.
Conclusions: The usefulness of IFS during laparoscopic radical prostatectomy remains to be proven but seems to allow the surgeon to offer a nerve sparing procedure more frequently without compromising cancer control.

P 700

A MORPHOLOGICAL STUDY OF STARTING SITES OF INVASION FROM PROSTATIC INTRAEPITHELIAL NEOPLASIA (PIN) TO PROSTATIC ADENOCARCINOMA

Mareyuki Endoh, Tai-Yi Jin, Mika Watanabe, Takuya Moriya, and Hironobu Sasano

Introduction: High-grade prostatic inraepithelial neoplasia (PIN) has been considered as the most likely preinvesive stage of prostatic adenocarcinoma. However starting mechanisms of invasion from PIN has not been completely investigated not only from the view of genetics but also

morphology admittedly. Thus we examined a large number of complete serial sections so as to find out starting sites of invasion, and also we reconstructed 3D- images from the sections in order to visualize the sites and to examine them morphologically.
Materials and methods: Used were two prostatectomy specimens having extensive PIN with multiple invasive foci. After formalin fixed and paraffin embedded, five blocks were selected and sectioned serially in 3um thickeness completely. After HE stained and immunohistostained for high molecular weight cytokeratin (34bE12) in aid of searching for micro-invasion, invasive lesions connected with PINs were searched microscopically. Then, the lesions were reconstructed into 3D-images with computer-assisted 3D-reconstruction system.
Results: Total amount of the serial sections reached 824 sheets containing many invasive lesions, while only six sites were considered to be invasive lesions apparently connected with PIN. Furthermore, serial sections and 3-D images revealed the early invasive sites were distinctly diminutive compared from the surrounding invasive lesions.
Conclusion: The study confirmed morphologically that PIN was preinvasive lesion of prostatic adenocarcinoma. While starting sites of invasion were hardly discovered and the area were obviously smaller than the surrounded invasive lesions.

P 701
EPIDERMAL GROWTH FACTOR RECEPTOR (EGFR) EXPRESSION IN BASAL CELLS OF NORMAL, ATROPHIC, HYPERPLASTIC PROSTATIC GLANDS, AND PIN. A TISSUE MICROARRAY STUDY
R. Esgueva 1, M. Iglesias 1, M. Jimeno, V. Baena, N. Juanpere, M. Garcia, J. A. Lorente 2, S. Hernandez 5, L. A. Rioja 4, A. Gelabert 2,6, S. Serrano 1,6 and J. Lloreta 1,5.

Background: Epidermal growth factor receptor (EGFR) is involved in the autocrine regulation of basal and luminal cell growth in the prostate. Basal cells (BC) of the prostate act as reserve-regenerative compartment, and are important in the maintenance of normal glands and in the development of prostatic diseases. Expression of EGFR in BC has been documented, but modification of this expression under pathologic conditions has received relatively little attention. The present tissue microarray (TMA) study has focused on EGFR expression in BC of normal (N), atrophic (A), hyperplastic (H), and dysplastic (PIN) glands from patients with prostatic adenocarcinoma (PCa).
Design: 227 radical prostatectomies were reviewed and 4 TMAs were
constructed, with a total of 849 cores (3.7 cores/case). In addition to representative foci of PCa, the cores included 451 areas with benign or dysplastic lesions (N:57; A,168; H,146; PIN, 80). The slides were immunostained with a monoclonal EGFR antibody (H11, DakoCytomation), using the Envision system (DakoCytomation, Glostrup, Denmark). The results were scored in a four-tiered scale (0, 1+, 2+, 3+). The percentages of cores with EGFR-positive BC in N, A, H or PIN glands in each intensity category were compared using a Chi-square test.
Results: The distribution and relative percentages of positive cores for each category are summarized in the table. None of the observed differences was statistically significant.
Conclusion: 1.EGFR expression in BC is predominantly of low (1+) intensity. 2.The EGFR expression profile of BC in hyperplasia is similar to that of atrophic, and only slightly different from that of normal glands. 3. Strong positivity (3+) is observed more often in BC of glandular hyperplasia, but moderate and strong positivity are overall more extensively observed in BC of PIN. 4. EGFR expression in BC may be relevant in the pathogenesis both of hyperplasia and PIN.

P 702
BASAL CELL HYPERPLASIA OF THE PROSTATE
Sosa G, Álvarez M, Álves J, Picazo M. Department of Pathology. Universitary Hospital La Paz, Madrid, Spain.

Introduction: Prostatic basal cell proliferations is a benign condition in a background of nodular hyperplasia typically found in the transition zone and usually identified in transurethral resection or prostatectomy specimens. Some studies report an incidence of BCH in prostate between 8.9% and 10.2%. BCH show a wide spectrum of morphologic features, ranging from focal basal cell hyperplasia to florid adenoid basal cell hyperplasia. Unusual hystological patterns are rare and the distinction between benign and malignant lesions is difficult to establish. Morphologic evidence of malignancy include infiltrative growth, extraprostatic extension, perineural invasion, local recurrence or metastases, necrosis and stromal desmoplasia. When the lesion is well delineated, the term adenoma has been used (BCA). Hyperplastic lesions and adenoid cystic carcinomas have cytoplasmatic immunoreactivity to high molecular weight keratins, but the basaloid carcinoma does not have it. Purpose of study: The aim of this study is to remark this entidity because basal cell proliferations are uncommon lesions and sometimes can mimic prostatic intraepitelial neoplasia and carcinoma. Materials and methods: A 65-year-old white male underwent a retropubic simple prostatectomy. The serum prostate-specific antigen (PSA) was 2,8 ng/ml. We collected 18 cases with the diagnosis of BCH and BCA that were reported in this Department over a 35 year period (1970-2005). Results: Gross abnormalities were multinodular masses of variable size. Sectioning showed multiples nodules tan-white and uniformly firm. The largest one measuring 2.5 cm. Microscopic findings: in a background of benign nodular hyperplasia the largest nodule was well circumscribed and containing small nests of basal cells of two or more cell layers thick surrounded by a few concentric layers of compressed stroma. The basal cells were plump, with large and uniform nuclei, scant cytoplasm and inconspicuous nucleoli. Our diagnostic was basal cell hyperplasia with nodular pattern. Conclusion: BCH are uncommon lesions in the prostatic gland and can exhibit a morphologic ranging. Accounted for 18 cases reported in our files emphasizing the unusual of these diagnosis and the architectural and citology features of ordinary and unusual patterns of BCH that even more closely mimic prostatic intraepithelial neoplasia and carcinoma.

P 703
RETRACTION CLEFTING AND PROSTATIC INTRAEPITHELIAL NEOPLASIA IN NEEDLE CORE BIOPSIES
Krušlin B, Tomas D, Odak Lj, Cupic H, Kos M, Belicza M Ljudevit Jurak Department of Pathology, Sestre Milosrdnice University Hospital, Zagreb, Croatia

Introduction: In comparison to normal glands retraction clefting is more common and prominent around neoplastic acini and therefore represents an additional criterion for the diagnosis of prostatic adenocarcinoma. Prostatic intraepithelial neoplasia (PIN) composed of abnormal proliferation within the prostate ducts, ductules, and large acini, premalignant foci of cellular dysplasia and carcinoma in situ without stromal invasion is the most likely precursor of prostatic adenocarcinoma. However, in the literature, we were not able to find data on the relationship between clefts and prostatic intraepithelial neoplasia.
Purpose of the study: To determine the presence and extent of retraction clefting in glands with prostatic intraepithelial neoplasia (PIN) in needle core biopsies.
Methods: We analyzed needle core biopsies from 35 consecutive biopsies of patients with PIN diagnosed at the Department of Pathology, Sestre milosrdnice Universty Hospital. Specimens were fixed in 10% buffered formaldehyde, embedded in paraffin, cut at 4 μm and

routinely stained with hematoxylin and eosin. Glands with PIN were analyzed on high power field (400x) and classified in three groups: group I (no clefting), group II (clefting in up to 50% of gland circumference) and group III (clefts in more than 50% of gland circumference). Normal glands within the same biopsy served as a control.
Results: The age of the patients ranged from 53 to 84 years (median 67.8 years), with the PSA value from 4.2 to 121 ng/ml. In glands with PIN, clefts in more than 50% of gland circumference were not found. There were 8 PIN (22.8%) cases with clefting in less than 50% of circumference (group II) and 27 (78.2%) cases with no clefting.
Conclusion: Our results showing the lack of retraction clefting in PIN cases suggest the influence of stromal reaction in the development of clefts around neoplastic acini of prostatic adenocarcinoma and therefore clefting should not be considered as an aid in the differential diagnosis of PIN.

P 704

METABOLIC AND T2-RELAXATION TIME MAPPING OF PROSTATE USING 1H MRS

ROGOZHYN Vladimir, ROZHKOVA Zina, VOZIANOV Sergei
Radiological Center of the Academy of Medical Sciences of Ukraine, Kiev, Ukraine

PURPOSE: We propose quantitative description of metabolic and T2-relaxation time alteration of prostate tissue for differential diagnosis between prostatic carcinoma (PC) and benign changes such as hyperplasia (BPH) and inflammation.
MATERIALS AND METHODS: Two groups of patients are examined by 1.5 T Magnetom Vision System (SIEMENS). The 1-st group (PG) includes 10 patients (age range 34-76), the 2-nd group (VG) consists of 4 healthy asymptomatic volunteers (age range 32-48). For building of the metabolic map the 1H MR-spectra are recorded with 2D CSI sequence:TR/TE = 1500/60 ms. In T2-relaxation time measurement the 1H MR-spectra are recorded in two regions of the prostate (in the central zone (CZ) and in the peripheral zone (PZ)) with SVS STEAM sequence: TR/TE = 1500/60,80,100, 140,180 ms. All spectra are recorded with and without of water suppression. The water signal of prostate tissue as an internal standard for calculating of content of main metabolites is used.
RESULTS: Lesions identified on T2-weighted images were analyzed using the following criteria: low-signal nodule (well circumscribed, rounded low-signal area), low-signal zone (irregular, less circumscribed low-signal area), heterogeneous zone (mixed, high- and low-signal area), central gland asymmetry. From 1H MR spectra the peak areas of main metabolite signals: citrate (Cit, 2.6 ppm), creatine (Cr, 3.0 ppm) and choline (Cho, 3.2 ppm) and the mean peak height ratios of R = Cit/(Cr+Cho) are obtained. The values R>1.12 are indicative for PC, R>2.30 – for BHP, R>4.14 – for normal regions of prostate tissue. In the VG the mean values of T2 for water (Wat), and for Cit, Cr, and Cho are the following: T2 CZ (Wat)=(71.3+-0.56) ms, T 2 CZ (Cit)=(170.2+-0.23) ms, T 2 CZ (Cr)= (134.5+-0.3) ms, and T 2 CZ (Cho)=(254.13+-0.81) ms; T 2 PZ (Wat)=(123.5+-0.74) ms, T 2 PZ (Cit) =(216.8+-0.79) ms, T 2 PZ (Cr)=(241.2+-0.15) ms, T 2 PZ (Cho)=(323.7+-0.2) ms. In the PG the values of T 2 (from 56. 4 to 93.2 ms) are indicative for water signal in PC, and (from 98.7 to 117.4 ms) - for BHP.
CONCLUSION: Metabolic and T2-relaxation time mapping can be helpful for diagnosis and characterization of clinically localized PC and also for the estimation of efficiency of therapy.

P 705

IS P63 A RELIABLE MARKER FOR PROSTATE BASAL CELL EPITHELIUM? IMPLICATIONS FOR PROSTATE CANCER DIAGNOSIS

GHIKONTI Ioanna (2), TSIGKA Alexia (2), MIHALOPOULOU Anna (2), BAIRAKTARI Georgia (2), ALEKSANDRAKIS Konstantinos (1), GORANTONAKIS George (1), GERZELIS Ioannis (1), THEODOSOPOULOS Nikolaos (2), SKOULIDAKIS George (2), THEODOROPOULOS Vasilios (1)

Introduction. The diagnosis of prostate malignancy is often based on the absence of basal cells. Diagnostically reliable identification of prostatic basal cells has depended on staining for high molecular weight cytokeratin. The p63 gene, a member of the p53 gene family, has also been shown to be expressed in the basal epithelial cells of normal human prostatic epithelium. Additionally, irregularities in p63 expression in multiple organs have been associated with epithelial carcinogenesis; p63 may protect prostatic epithelial cells against neoplastic transformation, perhaps through a tumor suppressor function. We examined the differential expression of p63 protein and cytokeratin 903 in prostatic adenocarcinoma (PCa), intraepithelial neoplasia (PIN), atypical adenomatous hyperplasia (AAH) and benign prostatic hyperplasia (BPH).
Material and Method. We performed immunohistochemistry with monoclonal antibodies for p63 and cytokeratin 903 on specimens of PCa (70 cases: 30 well, 20 moderately and 20 poorly differentiated), PIN (55 cases: 30 PIN1, 10 PIN2, 15 PIN3) and AAH (60 cases).
Results. 100% of the PCa specimens were negative for p63 and cytokeratin 903 immunoreactivity. In PIN1-3, p63 expression was weak-moderate and focal in 100%, and cytokeratin 903 staining was weak and focal in 89% of the cases. Weak-moderate and focal expression of p63, as well as weak and focal expression of cytokeratin 903 were also observed in 85% and 70% of AAH cases, respectively. In BPH, p63 glandular expression was more extensive than cytokeratin 903.
Conclusions. In contrast to normal and preneoplastic prostatic tissue, prostate adenocarcinomas do not express p63. The latter seems to be a reliable marker for prostate basal epithelium, such as cytokeratin 903, and can potentially increase the specificity for discerning cancer from high grade PIN or atypical prostate lesions, thereby reducing diagnostic uncertainty. In prostate cancer (PCa), p63 can be considered a potential reliable method for facilitating its pathologic diagnosis.

P 706

ATYPICAL PROSTATIC BASAL CELL PROLIFERATIONS: MORPHOLOGIC AND IMMUNOHISTOCHEMICAL STUDY OF 4 CASES

VASILIU Viorel, CAMPARO Philippe, LIARD-MEILLON Marie-Elisabeth,
VIRE Olivier, TISSEAU Laurent, VIEILLEFOND Annick
1.Service d'Anatomie Pathologique - Hôpital Necker, Paris, 2.Service d'Anatomie Pathologique, Hôpital Val de Grace, Paris, 3.Cabinet d'Anatomie Pathologique, Brive, 4.Cabinet d'Anatomie Pathologique, St Raphael, 5.Cabinet d'Anatomie Pathologique, Saint Brieuc, 6.Service d'Anatomie Pathologique - Hôpital Cochin, Paris

Background: Besides usual basal cell hyperplasia commonly observed in prostatic adenoma, atypical basal cell proliferations are observed in less than 0,1% of samples provided from transurethral resection (TUR) or adenomectomy. Florid and/ or adenoid hyperplasia can be observed on repeated resections during years without aggravation, but a small subset of lesions displays a malignant evolution with extra prostatic invasion and /or distant metastases.

Design: Because of the rare occurrence of these lesions and the limited follow-up information available in elderly population, the histologic criteria of malignancy are not clearly established. We report 4 cases of florid basal cell hyperplasia and/ or carcinoma in attempt to precise these criteria.
Results: Patients were respectively 58, 73, 90 and 92 years old without previous prostatic surgery. An unusual basal cell proliferation was observed in almost the whole prostatic tissue obtained by TUR (1 patient) or adenomectomy (3 others). The lesions varied from small to large lobular sheets of basaloid cells with frequent cystic patterns to basaloid and/or comedo-like patterns with central necrosis. In 2 cases, adenoid cystic (AC) like pattern surrounded by dense hyaline stroma was predominant. In the 2 other cases there were large sheets of basal cells associated with infiltrative patterns suspect of malignancy. P63 was expressed by 50 to 100% of basal cells at the periphery of the lobules in AC like patterns and was negative in basaloid ones. Mib-1 expression was respectively 40% and 60% in the 2 cases suspect of malignancy and 10 and 30% in the 2 others. Bcl-2 was intensely expressed in 100% of cells of basaloid and/or comedo-like patterns, weakly and heterogeneously elsewhere. Without additional treatment the 4 patients are free of disease 2 years after surgery.
Conclusion: Morphological differences exist among these lesions in correlation with immunohistochemical profile. Basaloid proliferations displaying large cohesive pseudoinfiltrative and comedo-like patterns suspicious of malignancy are associated with a Mib 1 index > 30%, a strong bcl-2 expression and a lack of p63 expression. Considering the difficulty to assess extra prostatic or perineural extension in limited samples and the accurate infiltration except on total prostatectomy specimen, these morphologic and immunohistochemical features could be used to induce a more agressive therapeutic approach in patients with long life expectancy.

P 707
PROSTATIC MIXED EPITHELIAL-STROMAL (PHYLLODE) TUMORS: A REPORT OF 4 NEW CASES

PLES Raluca (1), DIMET Stéphanie (1), COPPOLA Sylvie (2), LE MARC'HADOUR François (3), DARREYE Ghislaine (4), VIEILLEFOND Annick (5), FERLICOT Sophie (1)
(1)Service d'Anatomie Pathologique, CHU de Bicêtre, Le Kremlin-Bicêtre,
(2)Centre de Pathologie, avenue Jean Jaurès,30900 Nîmes,
(3)Centre de Pathologie, rue Général Ferrié, 38100 Grenoble
(4)Cabinet de Pathologie, rue Deverrine, 87000 Limoges
(5)Service d'Anatomie Pathologique, Hôpital Cochin, Paris

We report 4 additional cases of mixed epithelial-stromal tumor (phyllode tumor of the prostate) arising in men aged 27 to 64 years. The presenting clinical symptoms included urinary retention (2 cases), hematuria (1 case), and hematospermia (2 cases). The tumors formed prostatic masses measuring from 6 to 12 cm in diameter.
The diagnosis was suggested in 2 cases based on needle biopsy. In all cases the whole tumor was resected and patients were well from 4 months to 5 years after surgery.
Histologically, tumors showed a non-neoplastic epithelial component with cystic glands, an elongated cleft-like space and stromal proliferation with occasional high cellularity and cellular atypia. There was no increased mitotic activity. The epithelial component was positive for cytokeratin and PSA. The stromal cells were positive for vimentin in all cases, smooth muscle actin in 2 cases, desmin in 2 cases, and occasionally CD34.
These tumors are of uncertain malignant potential and need to be distinguished from benign lesions (leiomyomas and stromal hyperplasia with bizarre nuclei), and from stromal sarcomas and leiomyosarcomas.
These four cases as well as most cases reported in the literature behave in an indolent fashion but recurrences and progression to sarcoma can occur. Thus, when the diagnosis is suggested based on needle biopsy, total resection of the lesion is required.

P 708
RECIPIENT DERIVED COLLAGEN TYPE III IN HUMAN TRANSPLANTED HEARTS

PICHLER Martin1, TESSARO Brigitte1, KNIEPEISS Daniela2, KLEINERT Reinhold1, HOEFLER Gerald1.
1 Institute of Pathology, Medical University Graz, Austria
2 Department of Surgery, Medical University Graz, Austria

Introduction: Transplantation of donor hearts is often associated with progressive development of interstitial myocardial fibrosis and alterations in composition and organisation of the extracellular matrix. Changes in cardiac interstitial collagen network are thought to contribute to abnormal stiffness and loss of function of the myocardium. Fibroblasts are the main producers of type I and type III collagens, the major interstitial collagens found in the heart. In transplanted hearts, intragraft fibroblasts consist of two cell populations. Donor-derived fibroblasts pre-exist in donor organs, whereas host-derived fibroblasts are progressively immigrating as mesenchymal progenitors from the circulation to the allograft.
Purpose of the study: To determine the contribution of these two distinct fibroblast populations to progression of myocardial fibrosis, we studied endomyocardial biopsies from eight male patients who had received hearts from female donors.
Methods: In these sex-mismatched patients two frequent genetic polymorphisms at the collagen III locus were determined by polymerase chain reaction-based restriction enzyme digestion, both in donor allografts and in the corresponding explanted recipient heart. Based on differences the of collagen-genotype in donor and recipient tissue, we selected 40 endomyocardial biopsies by hematoxylin eosin staining and determined population-specific collagen expression using single nucleotide polymorphisms.
Results: Total number of donor derived cells in biopsies determined by short tandem repeat analysis was up to 70%. Chromogene in situ hybridization with probes specific for Y-chromosomes and immunohistochemistry staining for CD68 demonstrates the majority of macrophages to be of donor origin. The amounts of interstitial collagen type I and type III increased in a time-dependent manner within cardiac allografts. Years after transplantation a substantial number of Y-chromosome-positive recipient-derived cells was non-inflammatory, non-endothelial spindle-shaped fibroblast-like cell types. A considerable quantity of collagen III mRNA can be attributed to recipient-derived fibroblasts in transplanted hearts.
Conclusion: Our data confirm the existence of a substantial number of fibrosis-mediating immigrated recipient-derived fibroblasts in cardiac allografts. Furthermore, this suggests an active, essential role for recipient-derived fibroblasts in the process of fibrosis in transplanted human hearts.

P 709
PULMONARY LEUKOCYTOCLASTIC VASCULITIS AFTER HEART-LUNG TRANSPLANTATION: A NEW CASE SUGGESTING ACUTE HUMORAL REJECTION.

THOMAS DE MONTPRÉVILLE Vincent, CERRINA Jacques, DULMET Elisabeth, DARTEVELLE Philippe
Department of pathology and department of thoracic and vascular surgery and heart and lung transplantation
Centre Chirurgical Marie Lannelongue 133, avenue de la Résistance 92350 LE PLESSIS ROBINSON FRANCE

Acute pulmonary rejection is primarily cell-mediated and is characterized by perivascular mononuclear infiltrates. Acute vascular rejection with humoral component has only been suspected in few previously reported cases. Diagnostic criteria are not well established. We present a case of pulmonary vasculitis possibly related to such a rejection.
A 33-year-old female patient had an initially uneventful double lung transplantation for primary pulmonary hypertension. There were no panel-reactive anti-HLA antibodies. From day 19, she developed fever, progressive bilateral lung opacities with hilar lymphadenopathy and irregularities of the bronchial mucosa. Pulmonary function did not deteriorate. No was no sign of angiitis in other organs. No infection could be identified, beside the donor being HHV8+. Antineutrophil cytoplasmic antibodies were absent. Treatment with high doses of corticoids was started at day 58 and lead to rapid abatement of fever and progressive disappearance of lung opacities. The patient is well 6 months after her transplantation.
Bronchioloalveolar lavage at day 20 showed 90% of macrophages often containing nuclear debris and with important hemosiderosis. Transbronchial lung biopsy at day 20 was normal but bronchial and transbronchial biopsies at day 45 showed leukocytoclastic capillaritis. An open lung biopsy, performed at day 58 confirmed a widespread leukocytoclastic vasculitis involving capillaries, veins and arteries with foci of necrosis. A peribronchial lymph node was necrotic. Their was no usual criterion for acute resection. Special stains showed no micro-organism and there was no viral inclusion. Immunofluorescence on cryostat sections for C4d deposition was not conclusive. A second open lung biopsy, performed at day 109 during the treatment of a persisting pneumothorax, showed normal pulmonary parenchyma.
Acute humoral rejection is difficult to ascertain. However in rare cases similar to this one, clinical and pathologic data may suggest this diagnosis.

P 710
HUMAN HEART EXPLANT CONTAIN CELL POPULATION DIFFERENTIATING IN VITRO INTO MYOFIBROBLASTS
B.Wozniewicz, B.Cukrowska, E.Czarnowska, M.Pronicki, W.Grajkowska, T.Debinska-Szymanska, A Zajaczkowska .
Department of Pathology . CMHI Warsaw, Poland

Introduction. In human and experimental animal there is now incontrovertible evidence that new myocytes may be generated throughout life in responce to physiological and pathological stimuli.Adult heart stromal system has been proposed to consists of mesodermal stem cell that are capable of self -reneval into de novo cardiomyocytes. The rate of cell reneval is slow and low. Purpose. Sections from heart explants of patient endervent heart transplanation were cultured in vitro. This procedure was perform to obtain a population for future supporting failured heart with cultured 'stem cell' transplantation. Material.Multiple fragment from human heart explants were cultured in vitro.Method.Number of stainig procedures were performed to confirm phenotypes of growing cells (FGF, Titin, actin,myosin, vimentin, desmin, HLA class I and II, CD31, CD34, CD68 including electron microscopy. Results. The prolonged culture of heart fragments was the source of de novo growing cell population. Conclusion. It has been demonstraded that failured heart in contrast to normal has had precursor cells exchibits growth potentials to generate population of cells with immunocytochemical and ultrastructurel characters of myofibroblasts.

P 711
EXPRESSION OF PCNA GENE, NUCLEOLAR ORGANIZER REGION ACTIVITY AND NUCLEAR PLOIDY IN INTERVENTRICULAR SEPTUM CARDIOMYOCYTES FROM CHILDREN AND ADULTS WITH OHCMP
Rybakova M1, Gudkova A2, Borisov K3, Semernin E2., Selivanova G4, Vlasova T4, Parfenov V3, Bokeria L3 and Shlyakhto E2.
1 – Pathology Department, State Pavlov Medical University, St.Petersburg, Russia
2- Faculty Therapy department, State Pavlov Medical University, St.Petersburg, Russia
3 – Bakulev Reseach Center of Cardiovascular Surgery, Moscow, Russia
4 – Cytology Research Institute, St.Petersburg, Russia

Aim: to estimate PCNA expression, nucleolar organizer region activity and nuclear ploidy in interventricular septum cardiomyocytes from patients with obstructive hypertrophic cardiomyopathy (OHCMP).
Materials and methods: material from 61 patients with OHCMP was included into the study. Among those, 19 were below 21 y.o. and named as 'children'. The rest 41 patients were over 21 y.o. and named as 'adults'. The material was obtained upon the surgical interventions as well as upon express autopsies from the right side of the interventricular septum. The samples were stained with hematoxylin-eosin technique and by the method of nucleolar organizer regions silver staining. Expression of PCNA in cardiomyocyte nuclear was studied by immunohistochemistry. DNA content was estimated by Felgen method on dissociated cardiomyocyte nuclei and assessed by cytophotometry. One hundred tissue lymphocytes were used as a control for diploidal DNA content.
Clinical and echocardiographic data were obtained from case histories.
Results: the mean age in the children group was 14±1,1, ranging from 5 to 21 y.o. The mean age in the adult group was 46,4±1,9, ranging from 27 to 82 and being statistically different from the children group ($p<0,000$). The mean age of OHCMP diagnosis was 4,5±1,1 in children group, ranging from several days to 14 years. In the adult group this parameter was 38±2 and ranged from 2 to 69, being statistically different from children ($p<0,000$). There was no statistical difference between children and adults in LVMI (276,1±28,6±and 252,1±16g/m2) and IVS thickness in the outflow tract (2,89±0,14 and 2,54±0,08cm). In the children group compared to adult group there was a significant increase in AgNORs parameter (25,9±0,58 and 20,9±0,6, $p<0,000$), PCNA-positive cardiomyocytes (6,9% ±0,9 and 3,8%±0,4 $p<0,001$) and DNA content (15,2±2,2 and9,9 ±1,4 $p<0,017$). The mean number of maximal cardiomyocyte DNA content was higher in children group, then in adult group as well (53,5±7 and 30,7±2,2 $p<0,002$).
Conclusion: the children group with OHCMP is characterized by highest degree of myocardial hypertrophy, accompanied by increase in PCNA expression, increase in cardiomyocyte ploidy and increase in ribosomal biogenesis, estimated by AgNOR content in cardiomyocytes form right side of asymmetrically hypertrophied interventricular septum.

P 712
MORPHOLOGICAL CHANGES IN HIBERNATING MYOCARDIUM
Laky D., Parascan Liliana, Candea V.
Institute for Cardiovascular Diseases
Prof.Dr.C.C.Iliescu, Bucharest Romania.

Introduction:
Hibernating myocardium represent a prolonged but potentially reversible myocardium contractile dysfunction caused by chronic myocardial ischemia. The purpose of this study was to describe the morphological changes in diskinetical areas and their correlation with the functional investigations.

Material and methods:
In 48 patients with chronic ischemic heart diseases, areas of left ventricular hibernating myocardium were identified by angiography , thalium scintigraphy and dobutamine echography.On biopsies removed during by inter-ventions, ultrastructural and various histological and immunohistochemical investigation were effectuated.
Results:
The morphological changes are suggestive for embryofetals dedifferentiations and summarized as following: loss of the contractile structures, fragment glycogen granules, small mitochondria, absence of sarcoplasmic reticulum and T tubules, redistribution of chromatin, the presence of rough endoplasmic reticulum and a-smooth muscle actin , the decrease of cardiotonin, the expression of titin in puncted pattern. In the extracellular matrix were increased early matrix such for fibronectin, tenascin, collagen type I and III and fibroblasts. Also were observed stunned changes, cellular degeneration, apoptosis and reparative fibrosis.
Conclusions:
Hibernating myocardium is a transient incomplete adaptation to reduced coronary blood flow, an embryofetal dedifferentiation, that impose early revascularization.

P 713
EXPRESSION OF THE NUCLEOLAR ORGANIZER REGION'S ARGENTOPHYLLIC PROTEINS, TUMOR SUPPRESSOR GENE P53 AND CASPASE-3 IN CARDIAC SAMPLES FORM PATIENTS WITH IDIOPATHIC RESTRICTIVE CARDIOMYOPATHY.
Gudkova A1, Rybakova M2.
1 - Department of Faculty Therapy, St,Petersburg State Pavlov Medical University
2 – Department of Pathology, St.Petersburg Sate Pavlov Medical University

Aim
Our aim was to study the expression of argentophyllic proteins in the nucleolar organizer regions, tumor suppressor protein p53 and caspase-3 in cardiac samples from patients with idiopathic restrictive cardiomyopathy (IRCMP).
Material and methods
The express-autopsy cardiac samples from five patients with IRCMP were studied by hematoxylin-eosin, Van Gieson and Congo Red staining and well as by AgNOR staining. Immunostaining of p53 and caspase 3 were performed with DAKO monoclonal antibody. Cardiac samples from eight healthy people, died due an incidental cranial trauma were used as controls.
Results
In all study samples we found oxyphyllic amorphic protein depositions, which were positive for Congo Red staining only in two cases. Along with morphologically normal nucleoli in atrial and ventricular cardiomyocytes we identified micronucleolar, or atypical extranucleolar localization of argentophyllic proteins. The latter were more often seen in atria then in ventricles. The stromal cellularity was markedly increased, in some stromal cells 1-8 small, dot-like inactive nucleoli were observed. Positive staining for caspase-3 was present in cardiomyocyte cytoplasm and cardiomyocyte nuclei were positive for p53 staining. In the control samples, atipical extranucleolar localization of argentophyllic proteins were not present, as well as positive caspase-3 and p53 staining. Most of the stromal cells in the control cardiac tissue contain one dot-like nucleolus.
Conclusion
Cardiomyocyte nuclei from patients with IRCMP, complicated by terminal congestive heart failure, are characterized by increased p53 expression along with increased cytoplasmatic caspase-3 expression, which might illustrate p53-dependent apoptosis process. Atypical localization of argentophyllic proteins in cardiomyocyte and stromal cell nuclei as well as presence of micronucleoli might reflect the impairment of the protein synthesis. It is also important to note, that besides signs of structural and functional abnormality of the nucleoli in all study cases oxyphyllic amorphic protein depositions were found.

P 714
DISEASE GENETICAL SYNDROMS AND CONGENITAL HEART
LASTIC-MALETIC Sofija, KANJUH Vladimir, GLUMAC Sofija, POPOVIC Zoran, STOJSIC Zorica, RADOJEVIC-SKODRIC Sanja, VASILJEVIC D. Jovan
Institute of Pathology, Medical School, Belgrade, Serbia and Montenegro

INTRODUCTION: Congenital heart diseases (CHD) mainly develop as a consequence of multifactor influence, i.e. some develops as partially genetically induced anomalies. Therefore some CHD are often associated with different genetic syndromes.
PURPOSE: The aim of the study was to evaluate the incidence of CHD associated with genetic syndromes, as well as to analyze the types of CHD found in particular entity.
MATERIAL AND METHOD: At the Institute of Pathology, Medical School University of Belgrade, during the period from 1926-2004, a total number of 1399 cases of CHD were diagnosed. This investigation was made by analysis of data from standard autopsy protocols, and especially the designed forms for CHD cases. All autopsies were performed using standard or modified Rokitansky technique.
RESULTS: Our results showed that the most common association of CHD was with Down syndrome, found in 42 cases (3% of all CHD). Out of them, in 26 cases the atrio-ventricular septal defects (AVSD) was found; in 7 cases ventricular septal defect (VSD), in 6 cases atrial septal defect (ASD), and in 1 case there were trilogy of Fallot, aortic atresia and persistent ductus arteriosus. Besides Down syndrome, we found association of CHD with four cases of Edwards's syndrome, and one case of Turner syndrome. In three cases of Edwards's syndrome, isolated VSD was found, and in one case bivelar pulmonary valve with fibroelastosis of both ventricles was present. In only case of Turner syndrome, coarctacion of aorta and patent ductus arteriosus was found.
CONCLUSION: Our findings, made on very large autopsy series, indicate a relatively low percentage of CHD associated with different genetic syndromes. However these findings are in agreement with data from the literature, indicating that predominant influence in the development of CHD should be looked outside of genetic disorders.

P 715
ENDOMYOCARDIAL BIOPSY FINDINGS IN PATIENTS WITH MYOTONIC DYSTROPHY
VASILJEVIC D. Jovan, RAKOÈEVIC-STOJANOVIC Vidosava, GLUMAC Sofija, APOSTOLSKI Slobodan
Insitute of Pathology, Medical School, Belgrade, Serbia and Montenegro, ad Institute of Neurology, Clinical Center of Serbia, Belgrade

Introduction: Endomyocardial biopsies (EMB) are powerfull diagnostc tool in specific cardiomyopathies, including patients with different neuromuscular diseases and heart problems. Although among indications for EMB, usual non-pathognomonic findings in these entities are the reson for limmited series in the literature. In patients with myotonic dystrophy (MD) it has been shown changes such as myofibrillar degeneration, mitochondrial abnormalities, focal myocarditis, fibrosis and fatty infiltration of the myocardium, and especially changes in the conduction system.
Methods: This study presents the results of EMB findings in 10 patients with MD. The biopsies were carried out using King's bioptome, followed by routine histological procedure.

Results: In two patients with severe MD, biopsy specimens showed changes compatible with border-line myocarditis. In five patients with moderate to severe forms of MD, we found fibrosis and fatty infiltration of the myocardium, in addition to degenerative changes and hypertrophy of muscle fibers. Three patients with mild MD had non-specific degenerative and hypertrophic myocardial changes.
The histological changes described above were present in patients without cardiological symptoms and in those with normal ECG and echocardiographic findings. Only two of the 10 patients in whom EMB was performed complained of fatigue and occasional palpitations, while the rest of the patients were asymptomatic. One patient with focal myocarditis had ECG signs of left bundle branch block and echocardiographic evidence of reduced left ventricular contractility. Five patients with signs of endomyocardial fibrosis only had an abnormal Q-wave on ECG recordings. The remaining five patients with border-line myocarditis and/or with degenerative and hypertrophic myocardial changes had normal ECG and echocardiographic findings.
Conslusions: These results stress the significance of endomyocardial biopsy in detecting myocardial pathologic changes in patients with MD.

P 716
MYOCARDIAL FLUORESCENCE MEASUREMENTS AS MORPHOPATHOLOGICAL CRITERIA FOR DETERMINING THE DURATION OF MYOCARDIAL INFARCTION
ANESTIADI Vasile, TSIPLE Ilie
Centre for Pathobiology and Pathology, Academy of Sciences, Chisinau, Moldova

The study aimed towards finding new criteria for the determination of the duration in time of myocardial infarction (MI). 52 hearts from persons deceased from MI, in which MI beginning was documented clinically and by ECG, were selected. 30 hearts of persons deceased almost instantaneously from traumas served as controls. In each case we did 1000 measurements of myocardial primary fluorescence (MPF) at the wavelength of 360 nm, both in the necrotic (ischaemic) zone (NZ) and in extrainfarctic zones (EZ). During 8-12 hrs from MI beginning, the MPF decreased concordantly in both zones, being 89.6±2.3% of controls. At 24 hrs after MI onset MPF in NZ was 78.8±4.3%, in EZ 84.4±3.1% of controls. Minimal NZ MPF was at 4-5th and 9-10th days (66.3±2.5% and 62.6±2.1% of controls, $p<0.001$). EZ MPF at 4-5th days was 77.4±3.5%, at 9-10th days 82.3±2.2% and at 14-15th days 85.7±2.8%, remaining even up to 30-35th days of MI 7.3±0.8% below controls. MPF variations in time were approximated by splines. By solving a system of equations, which included formulae for EZ and NZ MPFs, it was possible to determine the time elapsed from the MI onset, with an accuracy of 9.6 hours.

P 717
APOPTOSIS IN ISCHEMIC CARDIOMYOCYTE INJURY
Rybakova MG, Kuznetsova IA (Dept. pathology, St Petersburg state medical university, St Petersburg, Russia)

It is believed that necrosis, apoptosis and reversible injury differentially contribute to cardiac functional loss in ischemia. Although apoptosis has been studied extensively as a pathogenic factor in cardiovascular pathology, its role in myocardial infarction remains not fully understood. THE AIM of the study was to evaluate apoptosis in ischemic myocardium and assess its pattern of distribution.
36 specimens of the myocardium were obtained during necropsy (performed within 6 h from death) from patients who died of acute cardiac failure within 24 h from the onset of the ischemic attack. M/F ratio was 1:1, median age – 62. Coronary arteries were 50-80% stenotic, with no signs of thrombosis. Myocardium from patients who died from brain hemorrhage was included for control purposes. Basing on clinical (ECG, enzyme assays) and morphologic data (basic fuchsin stain and polarized light microscopy). 5 groups were built with duration of ischemia from 0-1h, to over 24 h. Standard protocol was created for taking samples from the myocardium considering position towards ischemic region and heart anatomy. Bcl-2, caspase 3 and p53 were studied immunohistochemically (reagents from Dako Cytomation, Denmark).
Bcl-2 and caspase 3 were localized in peri-infarction zone, with increasing intensity from 6 to over 24 h of ischemia. Intranuclear positivity for p53 was demonstrated in isolated cardiomyocytes (CMs) and only in sudden cardiac death. TUNEL method was used to prove apoptotic DNA fragmentation. The distribution of TUNEL-positive CMs showed mosaic pattern in sudden cardiac death and was multifocal in peri-necrotic region in developed infarction. Marked chromatin clumping was seen in apoptotic cells. Strong statistical correlation between the apoptotic rate and contracture damaged cells in the myocardium was shown. By polarized light microscopy apoptotic CMs were localized in areas with marked contracture changes.
WE CONCLUDE that apoptosis contributes to the development of CM injury in ischemia. Apoptotic death of CMs may lead to electric instability of the myocardium in early ischemia and cause sudden cardiac death. Apoptosis of the peri-infarction CMs may precede extension of the necrotic area. Further studies of apoptotic death of CMs in ischemic heart disease may help to elaborate novel therapeutic strategies, aimed at regulation of apoptosis.

P 718
MORPHOLOGY OF CHOLINERGIC INNERVATION IN ISCHEMIC HEART DISEASE
Sorokina I.V., Yakovtsova A.F., Gargin V.V.

The sequence of changes in the vessels, cardiomyocytes and neurocytes in ischemic heart disease remains unsolved, but they are strategically important question for choice of pharmacological measures direction at the same time. The purpose of the present work was to study the morphological state of the parasympathetic innervation of the heart in ischemic heart disease.
The hearts of patients died with acute and chronic form of ischemic heart disease and hearts of persons who died due to cranial trauma were subjected to morphological study. The histological, histochemical, morphometric methods were used.
The results of the study have demonstrated that the parasympathetic plexuses had consistent topography with highest density near the heart hilum. The density of the ganglia was reduced in cardiosclerosis. Degenerative and sclerotic changes of all cholinergic elements were established. The number of the ganglia and density of the filaments did not correlate with level of coronary stenosis. The change of the form of perivascular neurocytes has been revealed with signs of perinuclear chromatolysis, edema, and augmentation of cell dimensions. Thus the vacuolization begins from periphery of the cells with the subsequent growth of vacuoles and movement of the nuclei to periphery. Study of cholinergic innervation revealed pronounced depression of acetyl cholinesterase activity.
The nervous fibers settle mainly along of vessels of microcirculatory bed. Both myelenic, and amyelenic nervous fibers are turgent, with signs of pronounced argyrophilia. Thus the fibers are impregnated irregularly with alternating of light and dark fields. The varicose thickenings, leakage of neuroplasm, microlocuses of destruction and fragmentation are marked; cytoplasm with signs of vacuolization.

So, deparasympathetization of myocardium could be one of the factors in pathogenesis of myocardial ischemia.

P 719
CARDIOMYOCYTE REMODELING, A NEW ASPECT OF ARRHYTHMOGENIC RIGHT VENTRICULAR CARDIOMYOPATHY
Czarnowska E.1, Pronicki M.1, Grajkowska W.1, Turska-Kmiec A. 2, Kawalec W. 2, WoŸniewicz B.1
1 Department of Pathology, and 2 Department of Cardiology, The Children's Memorial Health Institute, Warsaw, Poland

Background. Progressive deterioration of mainly right ventricular function due to fibro-fatty tissue infiltration and ongoing loss of myocytes is a characteristic feature of the arrhythmogenic right ventricular cardiomyopathy/dysplasia (ARVC/D). Histopathological investigations of endomyocardial biopsy samples have diagnostic value but till now were not dedicated to elucidate the cellular mechanisms underlying myocyte loss except apoptosis, and disease progression.
The study was aimed to show if structural cardiomyocytes remodeling might underlie the ARVC/D development and progression.
Methods. Endomyocardial biopsy specimens of the right ventricle wall were obtained from 7 paediatric pts. (4F, 3M, aged from 6 to 17 years) with ARVC/D established according to McKenna et al. (1994) criteria. Samples obtained from every heart were fixed in 4% buffered formaline and embedded in paraffin blocks, and in 2.5% glutaraldehyde in cacodylate buffer and embedded in Epon blocks. Serial paraffin sections stained hemotoxylin-eosin, AZAN, PAS and PAS with diastase, and immunohistochemically with antibodies anti-desmin, smooth muscle alpha-actin, vimentin were analysed. Ultrathin sections prepared from trimmed area bordering fibro-fatty tissue were routinely stained for EM examination.
Results. Some myocytes adjacent to fatty tissue showed vacuolisation, myolysis and accumulation of glycogen. Immunohistochemistry revealed that some of these cells exhibited abnormal pattern of desmin labelling at the level of Z-lines and positive staining for smooth muscle alpha-actin simultaneously. Electron microscopical studies showed in some cardiomyocytes lysis of contractile apparatus, accumulation of glycogen, loss of sarcoplasmic reticulum and T-tubules, polymorphic mitochondria and dispersion of nuclear chromatin. Both immunohistochemistry and electron microscopy presented related cell alterations probably.
Conclusions. Changes in ARVC/D in distribution and expression of proteins involved in contraction and excitation are probably phenotypic resemblance to fetal cardiomyocytes, what points the dedifferentiation of these cells. Dedifferentiation of cardiomyocytes might actually be considered survival states aimed to endure the altered conditions. Whether this state could be reversible needs further studies.
Acknowledgement. This work was supported by project QLG1-CT-2000-0191 financed by the UE.

P 720
QUANTITATIVE BASES OF COMPROMISED CARDIAC CONTRACTILITY DURING THE LATE STAGE OF SEPSIS
1L. L. Francu, 2A. Ciobanu, 1D. L. Calin,1 C. C. Ghibirsina
Departments of 1Anatomy and 2Infectious Disease, University of Medicine "Gr. T. Popa", Iasi, Romania

Introduction. Previously it is reported an association between sepsis and myocardial edema and histologic changes, but the anatomic base of sepsis-induced myocardial depression is incompletely understood. The objective of the present study was to determine whether are prerequisite morphometric myocardial parenchymal or microcirculatory changes for the development of contractile dysfunction in sepsis.
Material and methods. We have studied fourth-eight patients, who died of sepsis caused by abdominal infections and were been postmortem examination. The fragments from all cavities of the heart have been processed by paraffin technique and have been examined for qualitative diagnosis. The quantitative studies have been done with a video digital interactive program that utilized standard measurement of cardiac muscle fibers and stereology of percentual volumes of myocardial components.
Results. Our studies provide that histological changes are also a feature of myocardial injury in human sepsis. We noted alterations in the myocardium that consisted of interstitial miocarditis, interstitial edema, and muscle-fibers necrosis. We remarked differences between heart cavities, ventricles being more affected by myocytolisis and destruction of capillary wall. Morphometry relieved the increased of percentual volumes of interstitial space (22.1% vs. 13.5% in witness hearts) and myocardial capillaries occupied by leukocytes (16.8% vs. 4.1% in witness hearts).
Conclusion. We conclude that that objective myocardial structural changes and microcirculatory injuries may contribute to decreased ventricular contractility during sepsis.
KEY WORDS: CARDIAC CONTRACTILITY, MYOCARDIUM, QUANTITATIVE ANALYSIS, SEPSIS

P 721
HEMORRHAGIC MYOCARDIAL INFARCTION
Dariusz Lange1, Miros³aw Œnietura1, Ewa Zembala-No¿yñska2, Micha³ Hawranek3, Mariusz G¹sior3, Marek Gierlotka3, Jerzy No¿yñski3
1 Dept. of Tumor Pathology, Centre of Oncology, M.Curie-Sklodowska Institute, Gliwice, Poland
2 Chair and Dept of Pathomorphology, Silesian Medical University, Zabrze
3 Silesian Centre for Heart Diseases, Zabrze, Poland

Objective: Hemorrhagic myocardial infarction is one of the rarest kinds of myocardial necrosis. It is result from thrombolysis, hemorrhagic disturbances or mechanic trauma.
Aim: The aim of the work was the characterization of morphology of myocardial hemorrhagic infarction and its differences with ischemic myocardial necrosis (myocardial infarction).
Material and methods: The material consisted of 30 cases of macroscopically hemorrhagic myocardial infarction. Comparative group consisted of 20 cases of ischemic, pale myocardial infarction. The clinical history of disease was 48 hours. The studies were based upon histology and confocal laser scanning microscopy.
Results: Hemorrhagic myocardial infarction was characterized by the bulk of interstitial erythrorrhages, paucity of inflammatory infiltration, preserved continuity of cardiocytes hyperemia of coronary veins, compression of coronary arterioles and nerve trunks. In confocal laser microscopy the myocardial fibers shows no increased autofluorescence and fractures, but dominant feature was its thinning by interstitial hemorrhages.
Conclusion: Hemorrhagic myocardial infarction is a diverse morphological entity, closely resembled with hemorrhagic complications.

P 722
MYOFIBROBLASTS IN THE EVOLUTION OF HUMAN MYOCARDIAL INFARCTION
KOJC Nika, ZIDAR Nina

Recent studies have shown that cardiac fibroblasts and myofibroblasts play an important role in healing and remodeling processes after myocardial infarction (MI). Despite extensive research, the exact mechanisms are not

completely understood yet. The aim of our study was to analyze the distribution and immunophenotype of fibroblasts and myofibroblasts in the normal human heart and MI.
Methods. Autopsy samples of infarcted heart tissue from 15 patients with MI of different duration, and samples of heart tissue from 5 healthy persons who died in accidents, were included. Immunohistochemistry was performed by a sensitive peroxidase-streptavidin method on formalin fixed, paraffin-embedded tissue, using monoclonal antibodies against ¥á-smooth muscle actin (SMA), CD34, CD31, vimentin, desmin, activated caspase-3, Ki67, TGF©¬1 and TGF©¬1 receptors,.
Results. In normal hearts, there were scattered vimentin and CD34-positive fibroblasts in the subendocardial space and around intramyocardial blood vesssels. TGF©¬1 was focally expressed on capillary endothelial cells.
Myofibroblasts were found in MI which were at least 5 days old; they were vimentin and SMA positive and desmin negative ('VA' phenotype). Some were labeled with Ki67, and some with anti caspase-3. Myofibroblasts as well as most of inflammatory cells and endothelial cells also expressed TGF©¬1 and TGF©¬1 receptors.
In old scar, some myofibroblasts retained SMA and TGF©¬1 receptor expression.
Conclusions. 1. We found CD34-positive fibroblasts in the interstitium of the normal myocardium. These cells might be one of the origins of myofibroblasts, similarly to other tissues. 2. Myofibroblasts in MI were of the 'VA' phenotype. 3. Myofibroblasts, inflammatory cells and endothelial cells in MI also expressed TGF©¬1 and TGF©¬1 receptors suggesting that TGF©¬1 might be important in the healing process after MI as suggested by experimental studies 4. Some myofibroblasts were activated caspase-3 positive showing that apoptosis is an important mechanism in transformation of granulation tissue into a scar. 5. Some myofibroblasts in old scars after MI retained SMA expression, in contrast to dermal wound healing, where expression of SMA is transient. It has been suggested that this is due to the continuous mechanical stress caused by contraction and relaxation of the surrounding viable myocardium.

P 723
CLINICAL SPECTRUM OF CARDIAC LYMPHOMAS
Mary N Sheppard

Cardiac lymphmas are rare and there is often a delay in diagnosis. We present six cases where the clinical presentation varied from sudden death to infarction to pericardial effusion.
Two cases presented with large pericardial effusions in children. Both were T cell lymphomas. One child died suddenly after draining the effusion shortly after admission to hospital.
One T cell lymphoma presented as multiple areas of infarction due to vascular involvement with diagnosis only being made 6 months after presentation when a 29 year old male developed cutaneous lesions.
One large B cell lymphoma presented as a suspected bacterial endocarditis on an aortic homograft in a 57 year old male.
One case in an 81 year old presented with sudden death due to widespread infiltration by chronic lymphocytic leukaemia.
The final case presented as a sudden death in a 57 year old man ollowing cardiac transplantation six years previously. He had wiidespread microscopic involvement by a B cell lymphoma.
All these reflect the wide variation in cardiac involvement by lymphoma.

P 724
A NOVAL METHOD OF QUANTITATIVE FUNCTIONAL MORPHOLOGY ASSESSING CONTRACTILE RESERVES OF MYOCARDIUM USING HISTOLOGICAL SECTIONS
GHEVONDYAN Tigran.
Laboratory of Quantitative Functional Morphology,
Department of Pathological Anatomy of National Institute of Health, Yerevan, Republic of Armenia.

Introduction
The important information for cardiology and cardiosurgery obtained from morphological examination of heart muscle biopsies is the volume of the myocardial contractile potential. Currently this information can only be obtained by methods of quantitative functional morphology generally requiring electron microscopic examination (EME).
Aim
The aim of the study was to develop a method to determine the contractile reserve of the cardiac muscle using histological sections examined by light microscope (LM).
Materials and Methods
Cardiac muscle samples were collected and investigated as following: a) postmortem heart muscle from patients died of acute myocardial infarction and healthy people died in accidents, b) myocardium specimens from normal and physically exercised rats as well as animals with acute pancreatitis, c) the cardiac biopsy tissue from patients with valvular heart disease. We applied conventional histology, electron microscopy, stereology, micromechanography, statistics, mathematical modeling and quantitative functional morphology.
Results
A novel mathematical model was developed, which makes it possible to determine the contractile ability of cardiac muscle (fmyo) using quantitative morphological parameters obtained by LM. The parameters (Vv = volume density; Sv = surface density) take into account the most essential quantitative and qualitative changes of muscle fibres (mf), capillaries (cap) and interstitium (int). The following equation with a modular construction and an open architecture was derived:
fmyo=K•Vvmf•{ {
(1/Vvcap)+[1/(0,0064•Svcap)]+(Vvint/0,0073)+
[1/(0,0016•Svmf)]+
+(Vvmf/0,053) }•(1/v1)}-1,
The index (K) shows the relative level of myocytolysis. The ratio (1/v1) is considered the standard value for this model. The (-1) is the power for equation.
The statistically strongly correlated concordance of myocardial contractility data from the same hearts determined by using micromechanography from one side and by using EME, LM examination from the other side, supports the validity of the new mathematical model.
Conclusion
Our results demonstrated that the quantitative functional morphology using histological sections is a quick, reliable and easily applied method in assessing myocardial contractility. We suggest this noval method for routine evaluation of vital capacities of myocardium.

P 725
CARDIAC ANGIOSARCOMA
DOLENC - STRAZAR Zvezdana 1, GERSAK Borut 2, KOZELJ Mirta 3
1 Institute of Pathology, Medical Faculty, University of Ljubljana
2 Department of Cardiovascular Surgery, University Medical Center, Ljubljana, Slovenia
3 Department of Cardiology, University Medical Center, Ljubljana, Slovenia

Introduction:
Primary tumours of the heart are rare. 80-90% are benign. The most common malignant tumour is angiosarcoma, representing 40% of cardiac primary sarcomas. Patients are usually adult, more frequently men. We present a man with angiosarcoma of the right atrium.

Clinical history:
Otherwise healthy 22-year-old man was admitted to the hospital due to severe chest pain a day after a mild blunt chest trauma. ECG and chest x-ray were normal. Transthoracic echocardiogram demonstrated a moderate pericardial effusion and a mass measuring 3x3 cm, protruding into the right atrium above the tricuspid annulus, without obstruction of the orifice. The angiography showed abnormal vascularization originating from the right coronary artery. The tumour was excised but excision was not radical due to extension of the tumour. The patient refused urgent cardiac transplantation, which was performed six months later.
Macroscopically, the excised tumour was multilobular, dark, growing around right coronary artery. In explanted heart residual tumour measuring 6x4,5x3,5 cm infiltrating pericardium and a satellite tumour were found.
Microscopically, there were irregular vascular channels, papillary fronds lined by atypical endothelial cells, compressed capillary channels without recognizable lumina, sheets of anaplastic and spindle cells with extravascular erythrocytes. There were mitoses, some necrosis, invasion of blood vessels and nerves. Tumour extended to the resection margin in both samples.
Discussion:
Histologically, angiosarcoma of the heart has three major differential diagnostic possibilities, haemangioma with papilary endothelial hyperplasia, spindle cell and Kaposi sarcoma, which usually forms small nodules on pericardial surface with minimal infiltration of the heart. Most cases of cardiac angiosarcoma are diagnosed at the time of autopsy. Metastases, most often in lungs, are present at the time of presentation in 66-89% of patients. Prognosis is extremely poor, mean survival only 3 months, but survival up to 53 months has been reported. Complete resection is usually not possible, because of extensive local spread. Heart transplantation is the best option. Radiation therapy and chemotherapy may offer some temporary relief. Our patient is currently on radiation therapy, without any signs of disease, 11 months after presentation of the tumour.

P 726
METASTATIC SQUAMOUS CELL CARCINOMA MIMICKING CARDIAC MYXOMA
ELHAFEY Ahmed, PAPADIMITRIOU John C., BURKE Allen
Department of Pathology, University of maryland Medical School, USA

Introduction:
We report a case of squamous cell carcinoma of the uterine cervix, presenting with cardiac metastasis in a 42-year-old woman who had a radical hysterectomy for carcinoma of the cervix. The tumor was a poorly differentiated squamous cell carcinoma with extensive vascular invasion, involving the cervix, lower uterine segment, myometrium and parametrial soft tissue. The patient received radiotherapy and chemotherapy. Two years later the patient was admitted for symptomatic right atrial mass (clinical impression: Atrial myxoma).
Methods:
The original tumor and cardiac metastasis was analyzed for expression of low and high molecular weight cytokeratins, Ki-67, and p53.
Results:
The first intraoperative frozen sections exhibited prominent myxomatous stroma leading to an initial impression of myxoma. Subsequent intraoperative sections showed obvious squamous cell carcinoma.
Immunohistochemical study of the tumor showed expression of low and high molecular weight cytokeratins and high Ki-67 positivity. The original tumor and cardiac metastatic squamous cell carcinoma did not demonstrate any degree of p53 expression. Interestingly, the myxomatous stroma exhibited marked Ki-67 positivity.
Conclusion:
Patients with squamous cell carcinoma of the uterine cervix with extensive vascular invasion are at the risk of vascular invasion and hematogenous dissemination.
Metastatic squamous cell carcinoma to the right atrium can mimic atrial myxoma by CT and echocardiogram. Furthermore, a myxoid stromal reaction with high proliferative index can lead to an initial misdiagnosis of atrial myxoma.

P 727
PATHOLOGICAL FINDINGS IN SUDDEN CARDIAC DEATH
Burnley Hayley, Chase Deborah, Gallagher Patrick J, Roderick Paul. Southampton University Hospitals, Southampton SO16 6YD, UK

Sudden cardiac death results from an acute ischaemic evvent or a ventricular arrhythmia arising in an inflammed, scarred, hypertrophic or genetically abnormal heart. To determine the relative contributions of these causes we made a prospective study of all cases of sudden cardiac death in adults of any age over a one year period.
Three hundred and twenty one cases of out-of-hospital sudden cardiac death occuring within one hour of the onset of symptoms were studied. Each case was graded according to the certainity of the cause of death.Grade 1 cases were the certain result of ischaemia and had clear evidence of coronary artery thrombosis or myocardial infarction. Grade 2 cases had evidence of healed myocardial infarction and at least one coronary artery < 1mm in diameter. Grade 3 cases had coronary artery narrowing alone while Grade 4 had cardiac hypertrophy only. Grade 5 was unexplained cardiac death (SADS).In 107 cases (33%) there was coronary thrombosis or acute infarction. In 163 further cases there was coronary artery narrowing. 107(33%) had an associated myocardial scar (Grade 2) whilst 56 (17%) did not (Grade 3).In 45 cases (14%)non ischaemic heart dusease was present (Grade 4) and in 5 there was no obvious cardiac pathology (SADS).
The 33% incidence of acute ischaemia in sudden death is lower than in two studies from the 1990s (47% and 52%). Whether this is the result in changes in autopsy practice or a real change in the pattern of disease is uncertain. Our incidence of SADS is lower than in a recent UK study, but one that set an upper age of 65 years. Sudden death due to unexplained cardiac hypertrophy is important and has been underinvestigated.

P 728
SPONTANEOUS AORTIC DISSECTION. AN AUTOPSY STUDY OF 28 CASES.
ELD Mikkel(1), BANNER Jytte(2), KRISTENSEN Ingrid Bayer(2)
1) Institute of Pathology, Aarhus University Hospital, Aalborg Hospital, Denmark
2) Institute of Forensic Medicine, Aarhus University, Denmark

Background: Spontaneous aortic dissection is caused either by a tear in the intima or by an intramural haematoma preceded by rupture of the vasa vasorum. The dissection is caused by degeneration of the media, which is seen in different conditions like hypertension, heart valve diseases, pregnancy, cocaine abuse and certain syndromes.
Material and methods: In a 12-year period (1992 - 2003), 28 cases of sudden unexpected death were autopsied at the Institute of Forensic Medicine, University of Aarhus, and diagnosed as aortic dissection. The cases represent different clinical manifestations, diagnostic difficulties and different localizations of the dissection.

Results: Of the 28 cases 11 were females aged between 20-82 years (mean 47,2) and 17 were men aged between 31-80 years (mean 49,5).
In terms of De Bakey classification, 60 % were classified as Type I, 40 % as De Bakey Type II and none were classified as De Bakey Type III. Varying symptoms including, chest pain, nausea, dyspnoea, headache and sweating were reported in 68%, whereas 32% had been asymptomatic.60% had had medical contact and of these 21% had been hospitalized of which 50% had been misdiagnosed as coronary thrombosis, and two as gallstone and gastric ulcer. Aortic dissection was only diagnosed in one case by CAT-scan. The examinations done at admission were, electrocardiography (100 %), blood test (83 %), echocardiography (33 %), chest X-ray (16 %) and CAT-scan in the only pre-mortem correctly diagnosed case.
Conclusion: The diagnosis is difficult because the symptoms often mimic other conditions like gallstone, peptic ulcer and coronary thrombosis. With the symptoms in mind one should consider aortic dissection as a possibility, if the electrocardiography and blood tests are inconclusive for coronary thrombosis. The common used diagnostic procedures are CAT-scan, MR-scan, transoesophageal echocardiography and angiography, which have different accessibility, advantages and disadvantages.
The only chance of saving lives is to diagnose aortic dissection as early as possible, even though the prognosis is poor.
The only known treatment is surgery.

P 729
AUTOPSY FINDINGS IN CORRECTED TRANSPOSITION OF THE GREAT ARTERIES
LASTIC-MALETIC Sofija, GLUMAC Sofija, STOJSIC Zorica, POPOVIC Zoran, KANJUH Vladimir, VASILJEVIC D. Jovan
Institute of Pathology, Medical School, Belgrade, Serbia and Montenegro

Introduction: congenitally corrected transposition of the great arteries (C-TGA) represents the combination of atrio-ventricular and ventriculo-arterial discordance, with completely normal circulation, but with many associated cardiac anomalies.
Purpose: The aim of this study was to analyze the cases of C-TGA (sex, age and causes of death, atrial situs), and presence of associated cardiac and/or extra-cardiac anomalies.
Material and Methods: during the period from 1926-2004, a total number of 1.399 cases of congenital heart diseases (CHD) were diagnosed. All autopsies were performed using standard or modified Rokitansky technique. C-TGA was found in 24 cases (1.7 %).
Results: There were 15 males (62.5%) and 9 females (37.5%); in 20 cases the heart was in situs solitus (83.3%) and in 4 in situs inversus (16.7%). The viscera was always in situs solitus. Majority of the patients had 2 or more associated cardiac anomalies (20 ASD, 9 VSD, 3 AVSD, 2 PDA), and only 1 case had no communications between heart chambers; in 7 cases we found 1 communication, in 15 cases 2, and in 1 case 3. In addition, pulmonary atresia was present in 7 cases (29.2 %), and pulmonary stenosis in 4 (16.7%). Anomalous connection of pulmonary veins was found in 5 cases (20.8%), and anomalies of the coronary arteries too (hypoplasia in 3 and single coronary artery in 2). Majority of the patients died within the first month of life (13 or 54.2%), 6 within the first year (25%), 2 in the second year (8.3%), 1 in the third year (4.2%), and 2 lived over 20 years (8.3%). Extra-cardiac causes of death were predominant within the first year of life: bronchopneumonia (12 or 50%), athelectasis (4 or 16.7%), cerebral hemorrhage (3 or 12.5%), acute heart failure (2 or 8.3%), and myocarditis/endocarditis (1 or 4.2%).
Conclusion: Our results showed male predominance, situs solitus predominance, and the most often cause of death were extra-cardiac complications. Majority of patients died within the first year of life, and the most often associated cardiac anomalies were: ASD, VSD, pulmonary atresia or stenosis, and AVSD.

P 730
PECULIARITIES OF VULNERABLE PLAQUE FORMATION
PALTSEVA E.M., LYSENKO A.I., BELOV Iu.V., IVANOV A.A., PALTSEV M.A.

Vulnerable plaque formation exposed to rupture is the main cause of the acute coronary syndrome. The factors that promote the progression of atherosclerotic lesions instability are not clearly understood. In this study we showed the difference in extracellular matrix components and cellular distribution in vulnerable and stable plaques.
Methods and Results. Human carotid and coronary endarterectomy specimens (n=27) were obtained from patients with stenosis of >65%, as demonstrated by duplex ultrasonography and angiography. Plaques were histologically classified as either fibrous (stable), vulnerable (unstable) or plaques with features of instability – large lipid core, numerous inflammatory infiltrates and neovascularization but having thick fibrous cap. Immunohistochemical staining was used to analyze the expression of CD68, aSMA, collagen type III, fibronectin, laminin and thrombospondin-1. Macrophage (CD68 positive cells) infiltrates were greater in vulnerable plaques and plaques with features of instability. Laminin and thrombospondin-1 immunostaining was not detected in normal arteriers (n=5) and was larger in vulnerable plaques and plaques with features of instability than in stable plaques. The matrix components collagen type III and fibronectin showed variable distributions in all groups. There were no significant differences in aSMA immunostaining between different lesions also.
Conclusions. Our results suggest that laminin and thrombospondin-1 as well as CD-68 positive macrophages may be involved in the formation of vulnerable plaques and plaques with features of instability.

P 731
AORTIC DISSECTION, A LIFE THREATING DISEASE, TREATED BY USING „BIO-GLUE" SURGICAL ADHESIVE IN THE SURGICAL WALL REPAIR
Doina Butcovan, Cleopatra Borza - Department of Pathology Grigore Tinicã-Cardiology Center Iasi

Using Bio-Glue the cardiovascular surgery becomes a minimal invasive technique. Biologic glued anastomoses are obtained by applying a conventional technique of anastomosis indicated for severely altered aortic walls. We present a 55 years old man, without significant known history, having at presentation an anterior thoracic sudden violent pain, with duration of 1 hour and half. The patient was admitted at Cardiology Center Iasi with the suspicion of aortic dissection, which was confirmed after a complete cardiovascular evaluation. The histological examination of the surgical biopsic aortic specimens showed the morphological substrate of the disease represented by medial degenerative lesions that were evidentiated by using routine morphological techniques. The study revealed the importance of a complete cardiovascular evaluation and a rapid diagnostic for indicating an effective treatment and, in this way, for preventing an unpredictable complication. Concluding, we can appreciate that this biologic glue allows a good anastomosis, and a truly minimally invasive cardiovascular surgery may be possible.

P 732

CD44 IS LOCATED IN PLEXIFORM LESIONS OF IDIOPATHIC PULMONARY ARTERIAL HYPERTENSION

Keiko Ohta-Ogo, Hiroyuki Hao, Hatsue Ishibashi-Ueda

Introduction: The plexiform lesion in idiopathic pulmonary arterial hypertension (IPAH) is characterized by thin-walled microvessels with abnormal endothelial cells (ECs) proliferation. The pathogenesis of plexiform lesions has not been fully clarified. Recently, CD44 has been reported to regulate collateral artery formation via leukocyte trafficking and several growth factors. We hypothesized that CD44 is involved in formation of plexiform lesions of IPAH.
Methods: Expression of CD44 was examined on lung specimens including 46 plexiform lesions from 7 IPAH patients and normal lung tissues from 3 autopsy cases as control. To define localization of CD44, the following antibodies were used: CD31 for ECs, CD68 for macrophages, CD45Ro for T lymphocytes and alpha -smooth muscle actin for smooth muscle cells.
Results: ECs in 44 out of 46 plexiform lesions (96%) expressed CD44, while in patent muscular arteries from IPAH and muscular arteries from control lung tissue were negative for CD44. Intense expression of infiltrating leukocytes in plexiform lesions or perivascular accumulating leukocytes (mainly T lymphocytes) in lung tissue from IPAH was also observed.
Conclusion: CD44 expression was increased in ECs and leukocytes of plexiform lesions. The result indicates that CD44 might play an important role in the formation of plexiform lesions in IPAH.

P 733

CHAGAS´ DISEASE AND SUBSETS T CELL

Carmen E. Fuenmayor1 , Maria L. Higuchi2 , Hugo Carrasco1, Maryori García1 , Marcia M Reis2 , Julia Silvestre2 and Vera Aiello2 . Instituto de Investigaciones Cardiovasculares de la Universidad de los Andes, Mérida1, Venezuela. Instituto do CoraVão (InCor), São Paulo, Brasil2.

The present work reviewed endomyocardial biopsy specimens taken in the Instituto de Investigaciones Cardiovasculares de la Universidad de los Andes Mérida, Venezuela and Instituto do CoraVão, São Paulo, Brasil, from 1986 to 1998 and, looking for different CD4+/CD8+ T cell ratios in patients with chronic heart failure. For immunohistochemistry, T.cruzi antigens and CD4+ and CD8+ T cells in paraffin histological sections were quantified. The sections came from 4 groups of chagasic patients: A.- Acute phase (12 pts); B.- Indeterminate form (21 pts); C.- Cardiac form with arrhythmia (10 pts); and D.- Chronic heart failure (11 pts).
Groups A, B, C and D presented respectively: 100%, 10%, 40% and 45% of myocarditis; 58%, 0%, 10% and 0% with T.cruzi (+) antigens; with a mean CD4+/CD8+ T cell ratio of 0,75; 0,90; 1,17 y 0,79. The Pearson Correlation Test between mean numbers of CD4+ T and CD8+ T cells was high in groups A and B but not in groups C and D. Acute phase is characterized by myocardial inflammatory infiltrate with a balanced CD4+/CD8+ T cell immune response, associated with presence of parasite antigens. Indeterminate phase shows a lesser degree of myocarditis and balanced T cell immune response. Chronic cardiac forms are associated with myocarditis, but the quantity of T.cruzi antigens is much smaller and not detected by biopsy; an unbalanced immune response, with low CD4+/CD8+ T cell ratio, may be contributing to the persistence of active chronic myocarditis and injury of non-infected myocardial fibers.

P 734

PATHOLHISTOLOGICAL CHANGES IN AORTOCORONARY VENOUS GRAFTS

DUGANOVSKA Snezana, PETRUSEVSKA Gordana, BANEV Saso, FILIPOVSKI Vanja, TOLOVSKA Miljana, NIKOLOVSKI Momcilo
Institute of Pathology, Medical faculty, University "St Cyril and Methodius" Skopje, R. Macedonia

The aim of this paper is to present authopsy, histomorphological and immunohistochemical findings in aortocoronary saphenous vein bypass. Aortocoronary vein grafts removed at autopsy from 15 patients who died within one month up to 2 years after the bypass operation were examined. Histomorphological analysis was performed on paraffin sections stained with hemalaun eosin, Van Gieson elastica and Trichrome Masson. Immunohistochemical analysis for smooth cell actin, desmin, vimentin, CD 68, MAC 387, LCA, CD 20, and CD 43 (DACO products) was performed. A technique of LSAB+ immunoperoxidase (DAKO) was used with prior microwave antigen retrieval in citric acid buffer (pH 6,0). The main immunohistological finding were presence of intraluminal thrombotic masses, and endothelial damage with slight hyperplasia of tunica intima. Immunohistochemically we found a few smooth cell actin and vimentin positive cells in the intima. There were not found inflamatory cells, except at the anastomotic sites (CD68+, MAC 387+ and a few LCA+ cells). Positivity for the muscle cell actin in the intima suggests presence of adhesive molecules and cytokines that influence migration and hyperplasia of these cells, as well as in formation of atherosclerotic changes that occured in the wall of the vain grafts.

P 735

ULTRASTRUCTURAL ALTERATIONS OF THE PLACENTAL BARRIER UNDER HYPOXIA CONDITIONS

RESHETNIKOVA Olga, MILOVIDOVA Anna, MOROZOV Sergiy
Lugansk State Medical University,Ukraine

The electron microscopic investigation of placenta under hypoxia condition caused by maternal iron-deficiency anaemia and EPH-gestosis was carried.
Electronograms from 30 placentas, including 10 cases of EPH-gestosis, 10-maternal anaemia and 10-uncomplicated pregnancy (controls) were studied stereometrically by point count method at magnification X 5600.
Pathological ultrastructure's alterations of a placental barrier, including a damage of microvilli, thickening of basal membranes both of epithelium and endothelium, a stromal fibrosis were found. Compensatory proliferations of cytotrophoblast in cases of EPH-gestosis and in anaemia group; as well as hyperaemia of foetal vessels in EPH-gestosis group were seen too. The increase of the syncytiotrophoblast volume fraction (VF) in anaemia group (35,71±0,66 vs. 32,19± 0,26 % in controls), as well as cytotrophoblast, epithelium and endothelium basal membranes VF's both in anaemia (A) and gestosis(G) groups had registered
(correspondingly: A- 2,76± 0,04; 3,52±0,02; 0,57±0,06; G-1,05±0,03; 4,76±0,03; 0,74±0,04 vs. 0,76±0,04; 3,04±0,01; 0,38±0,12% in controls, $P<0,05$). The capillary lumen increased to 14,70±0,26% in gestosis group (13,5±0,21% VF in controls, $P<0,05$).
Pathological changes of a placental barrier could be a structural basis of a placental insufficiency. It was suggested that the process of ultrastructural remodelling of the placental membrane may compensate for different pathologies at the terminal parts of the villous chorion, which is essential base of the morphological correction of a placental insufficiency.

P 736

ULTRASTRUCTURAL STUDY OF THE EFFECT OF EXPERIMENTAL STAINING OF THE ANTERIOR LENS CAPSULE IN ALBINO RABBITS ON THE CORNEA AND ANGLE

Elham M. El-Shazli, M.D.
Ehsan El-Mehelmy, M.D.

Purpose: To study the value and safety of staining the anterior lens capsule in albino rabbits.
Methods: The experiment was divided into 3 stages. First, the capacity of different concentrations of crystal violet solution to stain the anterior lens capsule of postmortem albino rabbit eyes was tested. The toxicity of different concentrations of the dye (2% to 0.25%) was then tested to determine the highest concentration that was nontoxic to the cornea and trabecular meshwork. The third step was to detect possible toxicity of lower concentrations (0.1% to 0.05%). Different concentrations were injected into the anterior chamber of the rabbit eyes. The eyes were examined after 1 and 3 days, 1 week, and 1 month using light microscopy and scanning and transmission electron mcroscopy.
Results: Different concentrations of crystal violet stained the anterior lens capsule, allowing for easy capsulorhexis. The use of the 2% and 1% concentrations was accompanied with irreversible damage to all corneal layers. The use of the 0.5% concentration caused damage to stromal keratocytes and endothelium. The use of the 0.25% concentration did not damage any corneal layer of the trabecular meshwork. Lower concentrations of 0.1% and 0.05% also stained the capsule, providing good visibility for successful capsulorhexis, and were less toxic to the corneal endothelium.
Conclusion: Staining the anterior lens capsule with 0.25% ti 0.05% concentrations of crystal violet solution caused no injury to the cornea or trabecular meshwork in albino rabbit eyes.

P 737
LIVER INJURY IN HEAT STROKE: ELECTRON MICROSCOPY STUDY.

C.W. Hsueh, Y.Y. Tsai, N.H. Feng, T.M. Lee*
Depts. of Internal Medicine and Pathology*, Kaohsiung Armed Forces General Hospital, Kaohsiung, Taiwan.

It is common that thermal injury results in widespread injury of liver. The purpose of the study is to investigate the ultrastructural changes of liver in the patients with heat stroke.
Methods: A total 12 young soldiers with heat stroke, liver biopsy specimens were obtained within one week after the onset of heat stroke. Specimens were examined in electron microscope.
Results: Ultrastructural abnormalities of hepatic tissues were found in 11 cases. The changes of liver are as following: fat droplets in hepatocytes, increased autophagic vacuoles in cytoplasm, increased collagen fibers in space of Disse, dilated endoplasmic reticulum, cell debris and glycogen in sinusoid, and outer membrane disruption of hepatocytes. In one of the cases, the liver showed no remarkable change.
Conclusions: In this study, various degrees of liver injury were found in most of the patients with heat stroke. The histological changes of liver evidence that direct thermal injury and tissue hypoperfusion.

P 738
LET'S DO THE TWIST - A MODEL FOR THE ASSEMBLY OF CYTOPLASMIC AND NUCLEAR INTERMEDIATE FILAMENT PROTEINS

Bernd Sasse, Institute of Surgical Pathology, University Hospital Zurich, Switzerland
Ueli Aebi, Maurice E. Müller-Institute for Structural Biology, Biozentrum, University of Basel, Switzerland

Recently, intermediate filament (IF) proteins and especially the nuclear lamins have attracted wide attention as mutations in the lamin A-gene have been linked to various diseases such as lipodystrophy, dilative cardiomyopathy, muscular dystrophy, neurodegenerative disorders and progeria. Still the function of IF proteins is poorly understood. The ability of IF proteins to self-assemble into higher-order structures is conserved among species and thus seems to be key for protein function. Nuclear lamins and cytoplasmic intermediate filament proteins share the primary steps of assembly but ultimately form different structures in vivo.
Here we propose a model for the self assembly of nuclear lamins and cytoplasmic IF proteins which, on the basis of known interactions, explains the differences in assembly properties: IF proteins share a common tripartite architecture consisting of an alpha-helical central rod domain flanked by non-helical domains. The alpha-helices wind around each other resulting in dimeric coiled-coils. The dimers in a second step can interact basically in four different ways, one parallel and three anti-parallel, resulting in higher order structures such as unit-length filaments and ultimately filaments in case of the cytoplasic IF proteins and head-to-tail polymers and paracrystals in case of the nuclear lamins.
Nuclear lamins and cytoplasmic IF proteins are distinct in that nuclear lamins have a 42 amino acid insert in their rod domain. Our model explains, why this insert leads to a different behavior of assembly. We propose that IF filaments filaments are twisted structures emerging from surface lattices formed by dimetric IF proteins assembled via the known four basic dimer-dimer interactions and we extend this model onto the nuclear lamins, the geometry of which finally leads to other higher order structures.

P 739
THE ENDOMETRIAL PINOPODES INVESTIGATION IN WOMEN WITH UNEXPLAINED INFERTILITY.

ILYINA Olga, ZADOROZHNAYA Tamara, ILYIN Igor
Ukrainian Institute of Pediatrics,Obstetrics and Gynecology; Reproductive Genetics Institute; Kiev,Ukraine

Introduction The aim of the study was to evaluate the peculiarity of pinopodes formation in luminal uterine epithelial cells in women with unexplained infertility.
Materials and methods We have investigated the luminal epithelial cells morphology of endometrium in 16 patients with unexplained infertility and 10 healthy women from couples with male infertility. Double endometrium biopsy was taken on day LH+6/7 and LH+8/9. Specimens were examined with scanning electron microscopy for detection of pinopodes.
Results The SEM pictures of pinopodes were obtained in all the patients. Scanty pinopodes were present in 6 (37,5%) cases;the same stage of development in both biopsies or arrested pinopodes in 2 (12,5%) cases;high variability of the pinopodes shape and size in 8 (50%) cases;ciliated cells were absent in 4 (25%) cases.
In all the women from couples with male infertility were abundant or moderate pinopodes.
Conclusion We can consider,that the disturbances in pinopodes formation,maturation and ciliated cells quantity is one of the causes of implantation failure.

P 740
REVERSIBLE AND IRREVERSIBLE LUNG CHANGES AFTER EXOGENOUS SURFACTANT TREATMENT WITH IMMUNO-ELECTRON MICROSCOPY STUDIES

MARSZALEK Andrze, BICZYSKO Wieslawa

Exogenous surfactants are widely used in prevention and treatment of respiratory distress syndrome in newborns. There are also several attempts to use the same mode of therapy in

treatment of acute respiratory distress syndrome in adults but the results are still unsatisfactory.
The aim of the present study was evaluation of influence of exogenous surfactant on cells of air-blood barrier and the outcomes on its morphology in prolonged observations. The studies were conducted on animal model. The single dose of commercially available surfactant (Curosurf plus synthetic analogue of SP-B-HA) was introduced under anesthesia and intubation. Lung tissue samples were taken for morphologic evaluation after 1, 6, 24 hours and 5, 10, 21 and 42 days. Light and electron microscopic techniques as well as morphometric studies were used.
In the first periods of observation after administration of exogenous surfactant atelectasis, congestion, alveolar edema and erythrorrhagies were observed. After 5 days those changes started to decline and since the 10th day of observations first signs of alveolar fibrosis were recognized. Using the immuno-electron microscopic studies evidence of incorporation of exogenous surfactant into membrane systems of air-blood barrier cells was found.
In conclusion it should be stressed that exogenous surfactant internalize with cell membranes and cause lung injury. The injury of the lung parenchyma leads to alveolar fibrosis.

P 741
ULTRASTRUCTURE IN FAMILIAR HYPERTROPHIC CARDIOMYOPATHY WITH ARG723GLY MUTATION
BOMBÍ Josep Antoni, PETIT Ana, RAMÍREZ Josep, FRANCINO Antonio*, NAVARRO Francisco*.
Depts. of Pathology and Cardiology*. Hospital Clinic. University of Barcelona Medical School. Barcelona. Spain.

The Familiar Hypertrophic Cardiomyopathy is considered as the most prevalent (1/500) hereditary cardiomyopathy. At least ten genes are related to its appearance. In our hospital we have assessed a new mutation in three families over 30 carriers, that has demonstrated a worse prognosis. This is a Arg723Gly mutation in the gene that codifies for the heavy chain of beta-myosine. The carriers of this mutation show a non-obstructive form of the disease with evolution to clinical symptoms of cardiac failure that starts at the age of forty. The evolution of the patients is progressive heart failure leading to death at a mean age of 50 years, so they have to be treated with an implantable cardioverter-defibrilator or finally with heart transplant. Two of these patients needed a cardiac transplant, so we had the opportunity of studying these hearts histopathologically. Grossly they were within normal measurements, but a marked fibrosis was seen in the microscopical study. We performed electronic microscopy of both, that showed peculiar cytoplasmic granules, measuring 8-10 microns. These granules were dilated endoplasmic reticulum with granular material in dense areas.
As a conclusion this is the first time that a genetic based cardiomyopathy has been related to an abnormal morphological change. This contribution can be of help in order to make the diagnosis of these patients.

P 742
SOME EFFECTS OF ARTIFICIAL EXTRACELLULAR MATRIX ON FUNCTION AND MORPHOLOGY OF HUMAN ENDOMETRIAL EPITHELIAL CELLS IN VITRO.
NOURI Mohammad, GHAFFARI NOVIN Marefat
Infertility Center, Tabriz University of Medical Sciences, Tabriz, Iran
Department of Reproductive Endocrinology and Embryology, Reproductive Biology and Biotechnology, Avesina Research Center, Tehran, Iran

The importance of extracellular matrix (ECM) in development and function of different cells has been reported but little is known about its role in human endometrial epithelial cells. We have examined effects of artificial ECM (Matrigel) on the function and morphology of human endometrial epithelial cells using molecular techniques and electron microscopy. Endometrial samples were removed, with informed patient consent and Ethics Committee approval, from 17 previously fertile women undergoing total abdominal hysterectomy. The tissue was dissociated and centrifuged to provide an epithelial-rich suspension which was cultured either on plastic or seeded into Matrigel to produce polarized cells. Cells on plastic were undifferentiated, flattened and squamous but cells in polarized cultured were well-developed, tall, columnar and similar to secretory phase cells in vivo. The amount of total RNA in cells grown on Matrigel (23+1.5 pg/cell) was more than double that in cells grown on plastic (9.1+1.4 pg/cell). These results suggest that ECM plays an important role in function and morphology of human endometrial epithelial cells in vitro.

P 743
MULTIHORMONAL ADENOMAS OF PITUITARY. APPLICATION OF ELECTRON- AND IMMUNOELECTRON MICROSCOPY IN THE DIFFERENTIAL DIAGNOSIS
MAKSYMOWICZ Maria1, ZIELIÑSKI Grzegorz2, OLSZEWSKI W³odzimierz T.1, PODGÓRSKI Jan2
1- Institute of Oncology, 2 - Military Medical Institute, Warsaw, Poland

Pituitary adenomas are classified on the basis of hormones produced by the neoplastic cells detected by immunohistochemical stains. The pivotal part in pituitary tumors diagnosis is based on the electron microscopy investigation. Immunoelectron microscopy using single and double staining enables to identify cell types not detectable by routine methods. It is important to recognize some rare subtypes of pituitary tumors with specific biology and prognosis.
Aim. Evaluation of practical implementation of electron microscopic techniques in diagnosis of pituitary adenomas.
Material consists of 470 consecutive cases of surgically resected pituitary tumors. In pituitary adenomas were diagnosed (424 cases), clinically there were 147 patients with symptoms of acromegaly, 71 patients with hyperprolactinemia, 59 cases of Cushing's syndrome, 6 cases of Nelson syndrome, 3 cases of TSH hypersecretion and 138 clinically nonfunctioning adenomas. We selected 48 cases for current study.
Methods. All cases were diagnosed by routine histological examination and immunohistochemical identification of pituitary hormones (growth hormone, prolactin, ACTH, TSH, FSH, LH and alpha-subunit) and then examined with transmission electron microscope. Immunoelectron microscopy was done using a postembedding immunogold technique.
Results. Immunohistochemical analysis demonstrated the presence more than one pituitary hormone in the about 40% of pituitary adenomas. Immunopositivity was encountered in 27,5% of nonfunctioning tumors. Ultrastructural analysis provided proper diagnosis of selected cases (e.g. subtypes of silent corticotroph adenomas or mixed GH/TSH adenomas). Double immunogold labeling greatly facilitated the distinction among mixed growth hormone/prolactin, mammosomatotroph and acidophil stem cell adenomas.
Conclusions. Electron microscopy analysis was valuable to provide a useful informations regarding the diagnosis of rare multihormonal pituitary adenomas. At present, in the routine pathological diagnosis of pituitary tumors, immunoelectron microscopy (as well as molecular biologic methods) still are regarded as research tools. These methods has to be limited for cases in which they are necessary.

P 744

CYTOLOGICAL HISTORY OF 104 WOMEN WITH INVASIVE CERVICAL CANCER.

ALEJO María 1,DE SANJOSE Silvia 2,COMBALIA Neus 3,CULUBRET Montserrat 4,TARROCH Xavier 5,BADAL Josep 6,MENDEZ Imma 7,AUTONELL Josefina 1,BOSCH Xavier 2
1 Department of Pathology, Hospital of Vic, 2 Department of Epidemiology & Cancer Registry, Institut Catala d'Oncologia, Hospitalet of Llobregat, 3 Department of Pathology, Corporació Parc Tauli, Sabadell, 4 Department of Pathology, Hospital of Terrassa, 5 Department of Pathology, Hospital Mutua of Terrassa, 6 Deparment of Pathology, Hospital of Manresa, 7 Deparment of Pathology, Hospital of Granollers, Catalonia, Spain.

Objective: The aim of this study was to analyse the cervical cytological history of women with invasive cervical cancer.
Methods:Cases of invasive cervical cancer diagnosed between 2000-2003 were identified from six Pathology departments covering a Health Region in Catalonia (Spain). For each case we retrieve from the laboratories data base: age, histology, cervical smear histories in minimum 5 years preceding the diagnosis , time from last negative and time from last abnormal screen.
Results: During this period, we identified 104 patients with invasive cervical cancer. Seventy-five per cent of cases were squamous carcinoma and 26% adenocarcinomas. 81.8% (85/104) had not a cervical smear reported as negative one year before of the diagnosis of the cervical cancer. The average age of these patients was 57 years. Eleven patients (11%) had had an occasional normal cervical smear an average of four years before of the diagnosis. After review, we estimaded that 15% were reported as false negative
Conclusion: A majority of cases of invasive cervical cancer occur in women without evidence of cervical screening history. In a country with very low incidence rates of cervical cancer and opportunistic screening, specific actions to reinforce coverage among menopausic women may be justified.

P 745

NEW INSIGHT INTO THE EFFECT OF HIV ON HPV INFECTED CELLS

NYAGOL Joshua, LEUCCI Eleonora , CASTAGNINI Marta, COCCO Mario, ONNIS Anna, TILLI Chiara, DE FALCO Giulia, SANTOPIETRO Rosa, GIORDANO Antonio and LEONCINI Lorenzo
Department of Human Pathology and Oncology, University of Siena, Italy

The role of HPV in the carcinogenesis of intraepithelial and invasive anogenital lesions is currently well established. E6 and E7 oncoproteins of HPV 18/16 high risk genotype are known to inactivate p53 and pRb pathways. The role of HIV in cervical carcinomas associated with HIV infection is, however, less well known. Several studies have described an increased prevalence of both cervical HPV infection and invasive cervical cancer among HIV-positive women compared to HIV-negative ones. A high recurrence rate of invasive cervical cancer after standard treatment has been noted in HIV-positive women and the severity of these lesions seems to be inversely correlated to immune function. This combination of events typically results in a more aggressive phenotype. A primary means by which HIV infection may influence the pathogenesis of HPV-associated cervical pathology is by molecular interaction between HPV and HIV genes. Although not yet well defined, an upregulation of HPV E6 and E7 gene expression by HIV proteins such as Tat has been postulated by some authors. With this in mind, we investigated the role of HIV in cervical carcinomas both by transfecting HeLa cells, a cervical carcinoma cell line, with Tat and by analyzing HIV positive or negative cases.
Testing HIV negative cases by immunohistochemistry, we found a recurring pattern of pRb2/p130 expression. In precancerous lesions we found two distinct layers: a proliferating one, composed of Ki-67+/pRb2- cells, and a superficial one composed of Ki-67-/pRb2+ cells. In cancerous lesions all the cells showed staining for both markers, suggesting that the growth control exerted by pRb2/p130 may be lost due to the binding with HPV E6 and E7. We then tested the effect of the expression of the HIV-1 Tat protein in HeLa cells. After Tat over-expression in HeLa cells we observed a significant reduction of cell cycle inhibitor transcription and an increase in the levels of proliferating markers, such as Cyclin A, at the mRNA level.
These preliminary results seem to suggest that HIV may contribute to carcinogenesis by promoting cancer progression, because in HIV-positive women the disease may be aggressive and less responsive to treatment.

P 746

EXPRESSION OF CYCLIN-DEPENDENT KINASE INHIBITORS P16 INK4A IN PREMALIGNANT UTERINE CERVICAL LESIONS; ITS ASSOCIATION WITH DEGREE OF DYPLASIA, HUMAN PAPILLOMAVIRUS (HPV) STATUS AND COMPARISON WITH PROLIFERATION MARKERS LIKE KI67 AND AGNORS.

L. Baron, M. Postiglione, P. Beltotti , N. De Stefano, F. Quarto
U.O. di Anatomia ed Istologia Patologica e Citopatologia P.O. S.Leonardo, Castellammare di Stabia (NA), Italy

BACKGROUND:HPV is recognized as a casual agent for cervical carcinomas. Assimilation of HPV oncogenes E6 and E7 into the host DNA promotes upregolation of cyclin dipendent kinase inhibitor (CDKI) p16 detectable by monoclonal antibody in the developing cervical cancer cells.
STUDY DESIGN:The aim of this study is to examine the potential of p16 (INK4A) as a biomarker and to determine its utility as an HPV marker on a spectrum of cervical reactive and neoplastic lesions.
METHODS:A series of 172 cervical tissue samples (20 reactive, 88 CIN1, 54 CIN2, 10 CIN3) were analyzed by immunohistochemistry for expression of p16 (E6H4,CINtec™,DAKO) and Ki67 (Mib-1,DAKO) as well as by in situ hybridization for high risk HPV testing (INFORM® VENTANA) and by histochemical staining (Ploton) for AgNORs assessement. The distribuition of p16 staining was graded as patchy, diffuse basal and diffuse full thickness. Pearson's ÷2 test analyzed the relationship between p16, CIN, HPV, Ki67 and AgNORs expression.
RESULTS:In CIN1 p16 was positive in 48% ($p<0.001$) with 74% showing patchy, 21% diffuse basal and 5% diffuse full thickness; in CIN2 p16 was positive in 70% ($p<0.001$) with 3% showing patchy, 34% diffuse basal and 63% diffuse full thickness; in CIN3 p16 was positive in 100% ($p<0.001$) with 30% showing diffuse basal and 70% diffuse full thickness. The difference in the proportions of biopsies showing patchy p16 staining in CIN1 (LSIL) and diffuse full thickness staining in CIN2/3 (HSIL) was significant ($p<0.001$). High risk HPV increased from 52% in CIN1 to 94% in CIN2 and to 100% in CIN3 ($p<0.001$); in CIN1 39% of high-risk HPV positive biopsies were p16 positive ($p<0.001$) showing 61% patchy, 28% diffuse basal and 11% diffuse full thickness distribuition; in CIN2 69% were p16 positive (3% patchy, 29% diffuse basal and 68% diffuse full thickness) while all high-risk HPV positive CIN3 biopsies were p16 positive (30% basal and 70% diffuse full thickness).
Ki67 and AgNORs pattern of distribuition were similar: limited to basal layer in LSIL extending to middle and superficial layers in HSIL, correlated with degree of neoplasia, also if they were expressed in more reactive conditions than p16.

CONCLUSIONS:Diffuse full thickness p16 expression in lesion with high and intermediate-risk HPVs appears a good marker of persistent high risk HPV infection and might be useful to discriminate in equivocal cases HSIL from LSIL and to select LSIL with higher risk of neoplastic progression.

P 747

KI-67 EXPRESSION IN THE INVASION FRONT AS AN ADDITIONAL INDEPENDENT SIGNIFICANT PROGNOSTIC FACTOR INFLUENCING RECCURENCE IN EARLY STAGE CERVICAL CARCINOMAS

BASHESKA Neli, PRODANOVA Irina, KUBELKA-SABIT Katerina, YASHAR Genghis
Department of Histopathology and Clinical Cytology, Institute of Radiotherapy and Oncology, Medical Faculty, Skopje. Republic of Macedonia

INTRODUCTION: The attempts to determine the prognostic significance of biological markers and their relation to human papillomavirus (HPV) infection in cervical cancer have yielded controversial results.
AIMS: The aims of this retrospective study were to correlate alterations of cell proliferation, growth, differentiation and apoptosis regulatory proteins in early stage cervical carcinomas with HPV infection, histopathological and clinical parameters, and to estimate their prognostic significance.
METHODS: Expression of Ki-67, p53, mdm-2, bcl-2, c-erbB-2, EGFR protein, as well as estrogen and progesterone receptors was evaluated by immunohistochemistry in operative specimens of 83 patients with early stage cervical carcinoma. The results were assessed semiquantitatively in the surface area, center and invasion front of each tumor as a percentage of the immunostained cells and/or intensity of immunostaining for each protein. The presence of HPV was assessed by conventional in situ hybridization (ISH) technique and catalyzed reporter deposition signal amplification ISH using mixed biotinylated probes to identify types 6/11, 16/18 and 31/33 or 31/33/51.
RESULTS: In our case series 73 patients had a tumor limited to the uterine cervix less than 4 cm in diameter (pT1b1), while 10 patients had larger neoplasms belonging to pT1b2 category. Pelvic lymph node involvement was found in 20 patients. During the follow-up period (range, 65 -181, mean, 121 months) recurrences were observed in 9 patients. The 5, 10 and 15-year disease-free survival rate was 92.7%, 90.8% and 86.6%, respectively. Among the 18 variables pelvic lymph node involvement (P=0.0008), tumor diameter (P=0.035), depth of stromal invasion (P=0.029), histotype (P=0.0009), grade (P=0.056), HPV DNA presence (P=0.056), HPV type (P=0.043), as well as bcl-2 (P=0.035), mdm-2 (P=0.051), EGFR (P<0.0001), and Ki-67 (P=0.031) expression in the tumor's invasion front were identified as important predictive indicators of recurrence in the univariate analysis. Independent significant prognostic factors for disease-free survival in multivariate analysis were the histotype, HPV DNA presence and Ki-67 expression.
CONCLUSIONS: The invasive front of carcinomas proved to be the most important area for tumor prognosis. In addition to the detection of HPV presence and morphological parameters, Ki-67 evaluation could be used in selecting appropriate therapeutical approaches in patients with early stage cervical cancer.

P 748

HUMAN PAPILLOMA VIRUSES DO NOT PLAY AN AETIOLOGICAL ROLE IN ADENOSARCOMAS OF THE UTERINE CERVIX

GRAYSON Wayne, ALI Hasiena, TURTON Diane, MUMBA Everisto
Division of Anatomical Pathology, School of Pathology, University of the Witwatersrand and the National Health Laboratory Service, Johannesburg, South Africa

Primary adenosarcomas of the uterine cervix are exceedingly uncommon neoplasms. Although high-risk human papilloma virus (HPV) types have been linked to cervical carcinosarcomas, with demonstration of integrated virus in the nuclei of the malignant epithelial and sarcomatoid components, their role in the histogenesis of adenosarcomas is unclear. The aim of this study was to determine if HPVs play an aetiological role in cervical adenosarcomas. The HPV status of 7 adenosarcomas of the cervix was investigated by non-isotopic in situ hybridisation (NISH) and polymerase chain reaction (PCR). NISH was carried out using digoxigenin labelled probes to HPV types 6, 11, 16, 18, 31 and 33. PCR employed GP5+/GP6+ primers to the HPV L1 gene. Neither the benign epithelial components nor the malignant stromal components of the 7 neoplasms harboured nuclear NISH signals for the HPV types investigated. Amplimers of the HPV L1 gene could also not be detected by PCR in any of the tumours studied. HPVs do not appear to play an aetiological role in the pathogenesis of uterine cervical adenosarcomas. This suggests that a different histogenetic pathway for this rare tumour type must exist.

P 749

THE USEFULNESS OF HYBRID CAPTURE II (HC2) AS SCREENING OPTION IN LOW-RESOURCE SETTINGS OF LATIN AMERICA.

Adhemar Longatto-Filho1,2, M.Sc, Ph. D, PMIAC, Mojca Eržen3, M.D., PhD, MIAC, Margherita Branca4, M.D., PhD., MIAC, Cecília Roteli-Martins5, M.D., PhD, Paulo Naud,6 M.D., PhD, Sophie Marie F. Derchain7 M.D., PhD, Luciano Hammes6 M.D,Jean Matos6 M.D,Renata Gontijo7, M.D, Luis Otávio Sarian7, M.D, Temístocles P. Lima5 M.D, Marina Yoshiê Sakamoto Maeda1, M.Sc., Sílvio Tatti8, M.D., PhD,Stina Syrjänen9 D.D.S., PhD,Kari Syrjänen10. M.D., PhD, FIAC
1Instituto Adolfo Lutz, São Paulo, Brazil
2University of Minho, School of Sciences of Health, Braga, Portugal
3SIZE Diagnostic Center, Ljubljana, Slovenia
4Istituto Superiore di Sanità, Rome, Italy
5Hospital Leonor M de Barros, São Paulo , Brazil
6Hospital de Clinicas de Porto Alegre, Brazil
7Universidade Estadual de Campinas, Brazil
8First Chair Gynecology Hosp. de Clinicas, BA, Argentina
9Department of Oral Pathology, University of Turku, Finland
10Department of Oncology & Radiotherapy, University of Turku, Finland

Objective: Hybrid Capture II (HC2) to detect high-risk HPV (hr-HPV) in our ongoing multi-centre trial was performed and compared to other optional testing screening tools [cytology (conventional and liquid-based {LBC}, screening colposcopy, Visual Inspection with acetic acid (VIA), Visual Inspection with Lugol's Iodine (VILI): conventional and self-sampling], for cervical cancer in Brazil and Argentina, in order to test the potential use of HC2 as a primary option for cervical screening. Purpose: A cohort of 12.107 women attending four clinics (Campinas, Sao Paulo, Porto Alegre, and Buenos Aires) are randomised into the 8 diagnostic arms. Women testing positive with any of the tests are referred for colposcopy, and cervical biopsies are used as the gold standard to assess performance characteristics (SE, SP, PPV, NPV, ROC) of the HC2 test. Methods: All cases with cytological abnormalities were referred to colposcopy and biopsies were taken according clinical evaluation. The HC2 protocol was performed according to the instructions of the manufacturer (Digene Co., Gaithersburg, MD, USA). In estimation of the viral load, samples with relative light units

(RLU) > 20 were considered to harbour a high viral load and, those with 5-19.9 were intermediate, and those with 1-4.99 were low. Only high risk HPV was tested. Chi-square test was used to analyze correlations between categorical data, with Pearson's correlation and Fisher's exact test, and calculating OR and their 95%CI where appropriate. In all statistical analysis, the p<0,05 were regarded as significant. Results: The sensitivity and specificity for CIN3 were 96.5 (95.1-97.9) and 66.1 (62.6-69.6), respectively. For CIN 2 the results were quite similar: 90.4 (88.2-92.6) and 69.0 (65.6-72.4). When we adjusted the results for Roc Curve (Receiver Operating Characteristics) the Sensitivity and Specificity were very robust: 82.5% and 82.3¨for CIN3, and 83% and 76.3% for CIN2. Conclusion: In our settings, positive hr-HPV-DNA showed an important agreement with high-grade lesions of the cervix. The Public Health authorities should seriously evaluate the potential use of HC2 as primary option in order to optimize the sensitivity of cervical cancer screening. Moreover, HC2 performance might be improved by the association of cytology (preferentially, LBC) performed either after HC2 or concomitantly.

P 750
CERVICAL INTRAEPITHELIAL NEOPLASIAS POSSESS ANGIOGENIC ACTIVITY. IMMUNOHISTOCHEMICAL AND MORFOMETRIC STUDY
MRÈELA Milanka, ILIÆ-FORKO Jadranka, BABIÆ Damir

Introduction. Angiogenesis is the fundamental process through which new blood vessels are made. Angiogenesis is necesary for growth of solid tumors. On the other hand, cervical intraepithelial neoplasias (CIN) represents the proliferational state of the epithelium with biological caracteristics of carcinoma.
Purpose. This research was performed to answer whether cervical intraepithelial neoplasias are able to provoke neovascularisation - angiogenesis.
Methodes. The blood vessel count along the basement membrane of the epithelium and the total number of blood vessels of given microscopic view field were compared between 30 specimens of CIN 1, 30 specimens of CIN 2, 30 specimens of CIN 3 and two control groups each of them containing 30 specimens of cervical tissue without pathohistological abnormality and differing from each other in the fact that specimens of control group K 1 were taken from patients who underwent hysterectomy for reasons unrelated to CIN and group K 2 of specimens taken from patients with CIN 3 lesions but from parts with no pathohistological abnormality. Samples were treated with immunohistochemical methods using anti-F-VIII and anti-CD 31 markers. Quantitative parameters were processed using quantitative morphometric analysis in program 'ISSA for windows', produced by VAMS, Zagreb. The results were statistically analysed by method testing analyisis of variance (ANOVA) based on Fischer's (F-test) as the criterion of significance.
Results. Statistically significant difference was found in the blood vessel count directly below or along the basement membrane between CIN 1, CIN 2, CIN 3 and the control group K1 using both immunohistochemical methods (P<0,05) and betwen CIN 3 and the control group K 2 (P<0,05). Statistically significant diference was found in the total number of blood vessels between control groups K 1, K 2 and CIN 3 only using method F-VIII (P<0,05). The blood vessel count close to the basement membrane of epithelium between CIN 1 and CIN 3, and CIN 2 and CIN 3 in both immunohistochemical methods was significantly different (P<0,05)
Conclusion. Since there is a significant difference in the blood vessel count along the basement membrane between normal and dysplastic epithelium, and that number increases with the rise of CIN grade, it was concluded that CIN lesions are angiogenic.

P 751
P16 PROTEIN EXPRESSION IN HISTOLOLOGICAL MATERIAL OF CERVIX AND ITS CORRELATION WITH HPV INFECTION
TRAUNER Antonija, ALINGER Beate, MUSTAFA Georg, MUSTAFA Lisa, GRAF Anton-Helmut, DIETZE Otto, HAUSER-KRONBERGER Cornelia
Department of Pathology, General Hospital Salzburg, Mustafa´s Laboratory Salzburg, Austria

Cervical carcinoma is a multistage process. It arises from defined precursor as low-grade intraepithelial lesions (LSIL), referred to as high-grade intraepithelial lesions (HSIL). An important factor in the pathogenesis is the high-risk HPV types (HR-HPV) infection. The HSIL may be initiated by deregulated expression of HR-HPV oncogenes E6, E7 in replicating epithelial stem cells. An indicator of active expression of viral oncogenes is the overexpression of the cyclin-dependent kinase inhibitor p16.
A total of 339 routinely processed cytological specimen were analyzed. The material was taken consecutively for Pap test and for HPV-DNA hybrid capture assay (HC™, Digene). The cytological reports were negative for intraepithelial lesion or malignancy, LSIL to HSIL and cells of undetermined significance (ASC-US). HR-HPV positive cases were used for further investigation. Amplification of ß-Globin was followed by subtyping of HPV 16-DNA with conventional PCR. A total of 73 cases of cervical carcinoma and its precursor lesion were diagnosed out of these 339 cases of routinely cytological cervical specimen. The histological report showed condylomatous atypia, cervicitis, mild dysplasia (CIN I), moderate dysplasia (CIN II), severe dysplasia (CIN III), carcinoma in situ (CIS) and invasive cancer (Ca). Formalin-fixed, paraffin-embedded tissue blocks were used for the immunocytochemical expression of p16 protein with CINtec™ p16INK4a histology kit (DakoCytomation, DN).
23 specimens with histological reports of condylomata acuminata, cervicitis and CIN I showed positivity for HR-HPV (HC™) in 79%, HPV 16-DNA (PCR) in 37% and p16INK4a in 26%.
63% of the Pap-test cases were diagnosed as LSIL or negative for intraepithelial lesion and malignancy.
50 specimens with histological results of CIN II to CIN III, CIS and Ca showed HR-HPV (HC™) positivity in 97% and for HPV 16-DNA (PCR) in 76% and in 87% for p16INK4a. 49% of the Pap-test cases were diagnosed as HSIL, CIS, Ca and 16% of the Pap-cases were reported as ASC-US.
Our results indicate that the cyclin-dependent kinase inhibitor p16 is strongly overexpressed in correlation with the transforming activity of the viral oncogenes of all HR-HPV types, but particular the HPV 16. The p16INK4a expression increases with the progression of dysplasia.

P 752
EXPRESSION OF MMP-1, -2 AND TIMP-1, -2 IN CERVICAL INTRAEPITHELIAL NEOPLASIA AND INVASIVE CERVICAL CANCER
MI SEON KANG, HYE KYOUNG YOON.

Destruction of extracellular matrix is one of the most important step for the metastasis and invasion of cancer cells. Matrix metalloproteinase-2(MMP-2) specifically cleaves collagen type IV and MMP-1 digests interstitial collagen type I and III. These proteolytic activities are regulated by stoichiometric binding of specific, locally produced tissue inhibitor of metalloproteinases(TIMPs). The aim of this study was to investigate the expression of MMP-1, MMP-2, TIMP-1 and TIMP-2 in cervical intraepithelial neoplasias(CINs) and

invasive squamous cell carcinomas. Paraffin-embedded tissue sections from 36 CINs (10 CIN I and 26 CIN II & III) and 60 invasive squamous cell carcinomas. We investigated the expression of MMP-1, MMP-2, TIMP-1 and TIMP-2 by using immunoperoxidase staining.MMP-1 expression rate in invasive carcinoma(66.7%) was higher than that of CIN I (10%) and CIN II & III (11.5% ($p<0.0001$). Expression rates of MMP-2 in CIN II & III and invasive carcinoma were 42.3% and 48.3%, but no MMP-2 expression was found in CIN I ($p=0.0162$). TIMP-1 expression rate in CIN I(60.0%) was higher than that of CIN II & III(34.6%) and invasive carcinoma(16.7%)($p=0.0078$). Expression rates of TIMP-2 in stromal cells of CIN II & III and invasive carcinoma were 30.8% and 46.7%, respectively. But no TIMP-2 expression was found in CIN I ($p=0.0114$). No significant correlations between MMP-1and TIMP-1, MMP-2 and TIMP-2 were found. The presence of MMP-1 in tumor cells may enhance the invasive ability, but MMP-2 expression is an early event during malignant transformation in cervical neoplasia. TIMP-1 have inhibitory activity in progression in cervical neoplasia, but TIMP-2 may enhance the progression of cervical neoplasia through activation of MMP-2.

P 753

EFFICIENCY OF IMMUNOHISTOCHEMICAL P16 EXPRESSION AND HPV TYPING IN CERVICAL SQUAMOUS INTRAEPITHELIAL LESION GRADING

YILDIZ Iþýl Z., USUBÜTÜN Alp, FIRAT Pýnar, AYHAN Ali, KÜÇÜKALÝ Türkan
Hacettepe University Medical School Departments of Pathology and Obstetrics and Gynecology

Diagnosing and grading cervical cancer precursors is challenging at some point.In search of a solution,this study detects presence of HPV and investigates the staining pattern of p16,a cyclin-dependent kinase inhibitor whose overexpression is reported to be typical for dysplastic and neoplastic epithelium of cervix,on the basis of distribution and intensity,immunohistochemically.
H&E stained slides from cervical loop excision materials formerly diagnosed as LSIL (15 cases) and HSIL (20 cases), were reviewed. An immunohistochemical panel consisting of p16,all HPV types (Viroactiv® HPV Screening Kit) and HR (high risk)-HPV types (16,18, 33, 35, 39, 45, 56, 58) (Viroactiv® HPV High Risk Kit) was applied. Nuclear staining was interpreted as positive for HPV evaluation. Both nuclear and cytoplasmic staining were accepted as positive for p16. Staining of p16 was evaluated as rare, basal and full thickness according to the distribution and the intensity was classified as weak, variable and strong. Chi-Square Test and Fisher's Exact Test were used for statistical analysis.
All HSIL cases (20/20) and % 80 of LSIL cases (12/15) were positive with p16. Of p16 (+) HSIL cases, epithelial distribution was % 50 full thickness, % 45 basal and % 5 rare. The staining intensity of the same cases were % 70 strong, % 20 variable and % 10 weak. Of p16 (+) LSIL cases, epithelial distribution was % 58.3 basal and % 41.7 rare. No cases of LSIL showed full thickness p16 positivity. The staining intensity of the same cases were , % 25 strong, % 16.7 variable and % 58.3 weak . % 48.6 of all cases (17/35) was positive with screening kit (all HPV types). % 31.4 of all cases (11/35) was positive with HR-HPV. The distribution of this positivity was as % 35 of HSIL and % 26.6 of LSIL cases. All HPV type positivity rate was % 48.6,the distribution being % 50 of HSIL and % 46.6 of LSIL cases.
P16 is a highly sensitive marker of cervical epithelial dysplasia. Strong and full thickness staining of p16 in the cervix epithelium is highly supportive of HSIL diagnosis, while weak and basal/rare staining is in the favor of LSIL.All HPV positive cases were also p16 positive but no statistically significant relationship between HPV positivity and the intensity and the distribution of p16 was found. Although HPV is very sensitive for the detection of the infection, it is not helpful in the grading of SIL since an unignorable rate of HR-HPV positivity (% 26.6) was detected in LSIL group.

P 754

THE ROLE OF CELL CYCLE REGULATORS IN THE MULTISTEP PROCESS OF HPV-ASSOCIATED CERVICAL CARCINOMA

1- Abeer A. Bahnassy: Ass. Prof. Pathology
2- Abdel-Rahman N.Zekri: Prof. Virology&Immunology
3- Hanaa M. Alam El-Din: Lecturer of virology&Immunology
4- Osama A. Shawki: Prof. Gynaecology&Obstetrics

High-risk HPV (HR-HPV) types have long been implicated in the pathogenesis of cervical carcinoma with a reported interaction between HR-HPV oncogenic proteins and cell cycle regulators. We investigated the involvement of aberrant expression and coexpression of some cell cycle related genes in the multistep process of HPV16/18- associated cervical carcinogenesis.
Forty-three invasive squamous cell carcinoma (ISCC), 38 carcinoma in situ (CIS), 11 high grade dysplasia (HGD), 18 low grade dysplasia (LGD) and 20 normal cervical tissues were evaluated for aberrations in p53, mdm2, Rb, cyclin D1, cyclin E, CDK4, p21waf, p27 KIP1, p16INK4A and SPF using immunohistochemistry, flowcytometry and molecular techniques.
There was a significant increase in the expression level of cyclin E, CDK4, Rb, SPF and a significant decrease in the expression of p27 KIP1 in the sequence from normal mucosa to ISCC. Aberration involving cyclin D1, p21waf, p53, mdm2 and p16INK4A were detected in CIS and ISCC cases only.
In conclusion, infection of normal cervical mucosa by HR-HPV types leads to dysregulation of the cell cycle control via altering the expression of some cell cycle related genes. Aberrations involving p27 KIP1, cyclin E, Rb and CDK4 are early events, whereas aberrations involving the p53f pathway, cyclin D1 and p16INK4A are late events in the genetic cascade of cervical carcinogenesis. Together, these alterations lead to acceleration of the cell cycle with an increased proliferation rate and acquisition of more genetic damage.

P 755

DETECTION OF HPV IN TISSUE BIOPSIES: A COMPARATIVE STUDY OF TWO VERSIONS OF INNO-LIPA SYSTEM AND MY09/11 PRIMERS

M.A. García-Cabezas, C. Perna, D.A. Hardisson, I. Briones, J. Jiménez-Heffernan and A. Suárez
Pathology Services from Guadalajara University Hospital and La Paz (Madrid) University Hospital, Spain

INTRODUCTION: we have detected the different HPV genital genotypes by PCR in paraffin-embedded biopsies since 1993 using the primers MY09/11, that amplify a 452-bp DNA fragment. Since 2003 we have used the INNO-LIPA system version 1 (IL-1). IL-1 amplifies a short 65-bp DNA fragment followed by reverse hybridization with type-specific probes of the 25 most relevant genotypes. Since 2004 we have used the second version of this system (IL-2).
METHODS: during 2003-4 we performed both MY and IL-1 tests in 56 biopsies. During 2004-5 we performed both MY and IL-2 tests in another 56 biopsies. All the biopsies showed pathologic findings of HPV related lesions. The presence of HPV DNA, the total number of viral genotypes and the presence of mixed infections were compared between MY and IL-1 (group 1) and MY and IL-2 (group 2).
RESULTS. GROUP 1: MY detected HPV DNA in 40 biopsies (71%) and IL-1 in 53 biopsies (94%). The total number of viral genotypes detected by MY was 42 and by IL-1 was 71. Mixed infections were detected by MY in 2

biopsies (5%) and IL-1 in 11 biopsies (20%). The viral genotypes detected by MY and IL-1 were the same in 25 biopsies. IL-1 detected more viral genotypes than MY in 20 biopsies and MY detected more than IL-1 in 2 biopsies. GROUP 2: MY detected HPV DNA in 46 biopsies (82%) and IL-2 in 49 biopsies (87%). The total number of viral genotypes detected by MY was 50 and by IL-2 was 58. Mixed infections were detected by MY in 4 biopsies (8%) and IL-2 in 7 biopsies (14%). The viral genotypes detected by MY and IL-2 were the same in 31 biopsies. IL-2 detected more viral genotypes than MY in 11 biopsies and MY detected more than IL-2 in 5 biopsies. IL-1 and 2 typified 4 cases of MY-unknown viral genotypes in both groups.
CONCLUSIONS: IL-1 was more sensible than MY in the detection of HPV DNA, several viral genotypes and mixed infections. IL-2 has reduced these differences in sensitivity. The material used in this study does not allow us to determine whether IL-1 is over-detecting HPV DNA (false positive results) or IL-2 is under-detecting HPV DNA (false negative results). However, IL-2 reveals no discordances compared with MY.

P 756
RETROSPECTIVE STUDY OF 68 PATIENTS WHO HAD COLPOSCOPY-GUIDED BIOPSY: COMPARISON OF THE CYTOLOGY RESULTS WITH HISTOLOGY

METE Ozgur (*), YAVUZ Ekrem (*), TUZLALI Sitki (*), ILHAN Ridvan (*), OZLUK Yasemin (*), TOPUZ Samet (**), IYIBOZKURT Cem (**) and IPLIKCI Altan (*)
(*) Istanbul University, Istanbul Faculty of Medicine, Department of Pathology
(**) Istanbul University, Istanbul Faculty of Medicine, Department of Obstetrics and Gynaecology

Reducing morbidity and mortality is the main aim of the health system in the world. The incidence of cervical cancer has been declining in the last decades due to the Papanicolau (PAP) smear which is the preferred screening test for cervical squamous cell carcinoma and its precursors. A zero error standard does not exist in cytopathology. The false negativity or positivity were determined by many factors. We aimed to examine the final histological findings in patients who had a cervical intraepithelial lesion (CIN/dysplasia), atypical squamous cells of undetermined significance (ASCUS) on PAP smears and underwent colposcopy-guided biopsy.
This study is a retrospective review of 68 smears obtained from patients who had colposcopy-guided biopsy between 2002 to 2004 in a single center where 10000 PAP smears have been screening annually. All cases were examined by experienced gynaecopathologists.
Of 17 patients who had CIN 1 on the PAP smear, 15 had CIN 1 or higher lesion and 2 had benign changes (inflammation, reparation) on the final histology. All of 11 patients who had CIN 2 on the PAP smear, had at least CIN 1 on the biopsy. Only in one of the 21 patients diagnosed as CIN 3 on the PAP smear, dysplasia can not be found on the final histology. We later found out that this patient has recently received chemotherapy for leukemia. Of 14 patients diagnosed as ASCUS, six had CIN 1, two had CIN 2, four had CIN 3 and two had benign changes such as reparation and inflammation. Five patients who had benign cytologic changes, had undergone colposcopic examination, which revealed CIN 1 in three and CIN 2 in two patients.
Based on the results of our study, we determined a 7.7% of false negativity rate and a 4.8% of false positivity rate for the PAP smear examination. The efficiency of the PAP smear was 88.2%.
After the reassessment of patients having benign cytologic features, we found that sampling errors, which were possibly related to small lesions or those exfoliating few cells, were practically the main reason of the false negativity in our study. It is well known that chemotherapy induces cellular atypia mimicking those of dysplasia or carcinoma, which was present in one of our cases. Even with optimal conditions, about 5-10 % of false negativity exist in cervical cytology.

P 757
STANDARDS FOR THE HISTOPATHOLOGICAL REPORTING OF UTERINE CERVICAL NEOPLASIA

PELLEGRIN de VILLENEUVE Michèle 1-2, d'ANJOU Joelle 1, MERINO Céline 1-2, MAC GROGAN Gaëtan 1-2, MERCIER Sylvaine 1-2, BELLEANNEE Geneviève 1-2, ETCHARRY Francine 1-2, MASSOT-BORDENAVE Mireille 1-2 , CARTIER Isalelle 1, PETITJEAN Alain 1, CIRILO-CASSAIGNE Isabelle 2, MATHOULIN Simone 2, VACHER-LAVENU Marie Cécile 1
1Groupe National du Compte Rendu Standardisé du Col Utérin, Service Central d'Anatomie et Cytologie Pathologiques, CHU Cochin-27 rue du Faubourg Saint Jacques-75679 Paris Cedex 14
2 Réseau de Cancérologie d'Aquitaine, 229 cours de l'Argonne - 33076 Bordeaux Cedex

Current practices in cancer pathologies has resulted in pathologists globally joining together in the elaboration of a standard histopathological report of samples for uterine cervical neoplasia. The accomplishment of this form was possible with the support of the INCa (Institut National du Cancer), the DGS (Direction Générale de la Santé), the DHOS (Direction de l'Hospitalisation et de l'Organisation des Soins) and the InVS (Institut National de Veille Sanitaire). This required the following stages. Firstly, the constitution of a multicentric work group. Secondly, the feasibility tests to use this form. Finally, its validity. A regular update is planned in accordance with the standard types of literature. This standardised report form and its handbook have been developed with the assistance of bibliographical references, actual standardised reports, publications, ANAES recommendations, WHO proposed classifications, UICC, and a consensus of experts. This document should replace the original and be part of the computerised medical records. Its intention is to be used as a shared document between the pathologists and the practioners. It will supply the practioner with appropriate datas for patient care. It takes into account or not organised screening tests. It allows a homogeneous procedure in the diagnosis of uterine cervical neoplasia. It supplies cancer registers with the necessary data for the epidemiological surveillance, and finally it facilitates the elaboration of computerised datas for the relevant pathologies.The proposed report will contain precise datas on the practioner, the pathologist, the patient and the samples. It will give the most complete macroscopic and microscopic diagnosis as possible. Thus providing the key elements to allow for an objective prognosis and a therapeutic follow up of the patient. It will be succinct, clear, homogenous and standardised. Therefore, facilitating a better understanding by all practioners and pathologists.

P 758
DETECTION OF HPV GENOTYPES IN CERVICAL LESIONS BY THE HPV DNA CHIP AND SEQUENCING

NAM Jong-Hee, CHOI Yoo-Duk, *CHOI Ho-Sun, PARK Chang-Soo
Department of Pathology, and *Obstetrics & Gynecology, Chonnam National University Medical School

Introduction: Cervical cancer is the second most common cancer in terms of both incidence and mortality worldwide. Recently, there is some agreement that the availability of high sensitive human papillomavirus (HPV) tests offers the potential for replacement of conventional cytologic screening

programs. In addition, the importance of HPV testing has been increasing because genetic typing is required to predict clinical progression. Digene hybrid-capture (HC-2) technology was widely used for it is highly sensitive, and if appropriately used, highly specific as well. A newly introduced HPV detection technique in cervical lesion, the HPV DNA chip test, contains 24 HPV probes and has the advantage of being able to detect 24 HPV types at once.
Objective: In this study, we evaluated the accuracy of HPV DNA Chip test for detection and typing of HPV in cervical lesions by comparing with result of HPV DNA sequencing of same samples. In addition, we desired to find out the types which were not detected in HPV DNA Chip test by HPV DNA sequencing of HPV-other types.
Methods: The HPV DNA sequencing was performed in samples of 282 patients, where specific HPV type had been shown in HPV DNA Chip test. The sixteen cases where multiple HPV types had been found in HPV DNA Chip test were included in 282 cases. The sequencing was also performed in HPV-other type samples of 95 patients, where positive in HPV-PCR, but specific HPV type had not been found.
Results: In 257 cases (91.1%) of 282 cases, the HPV types of the HPV DNA sequencing test was in agreement with types of the HPV DNA Chip. In 16 cases (5.7%), the sequencing types were different from the types of HPV DNA Chip. But, in nine of 16 cases, types in HPV DNA sequencing were absent types in HPV DNA Chip test. The interpretation of HPV DNA sequencing was impossible in nine cases (3.2%). The HPV DNA sequencing test of 95 cases of HPV-other type showed that the sequencing types from 94 cases (98.9%) were absent types in HPV DNA chip test. In sequencing test of HPV-other type, HPV-81 (20.0%), HPV-62 (14.7%), HPV-84 (13.7%), and HPV-61 (13.7%) were frequently detected.
Conclusion: HPV DNA chip is an accurate method for detecting the 24 HPV genotypes.

P 759
DNA VERSUS RNA BASED METHODS FOR HUMAN PAPILLOMAVIRUS DETECTION IN CERVICAL NEOPLASIA
Lie AK (1), Risberg B (1), Borge B (1), Sandstad B (2,3), Delabie J (1), Rimala R (4), Onsrud M (5), Thoresen S (6).

Background. Given the results summarized in the 2005 IARC monograph, HPV testing is likely to be implemented as the primary screening test within few years. HPV tests detecting either HPV DNA or HPV E6/E7 mRNA are now commercially available, and needs to be validated before inclusion in clinical practice. The aims of this study were to compare DNA-based and mRNA-based methods for detection of high-grade cervical neoplasia.
Methods. HPV prevalence was analyzed in 383 women with positive index cytology, selected from gynecology clinics. All patients were investigated by a new PAP smear, histology and two commercially available HPV tests: Hybrid Capture II (Digene Corporation) and the Pre Tect HPV-Proofer (NorChip AS). Cases with positive DNA test and negative mRNA test, and cases with high-grade histology and negative HPV tests were retested with PCR and sequencing. We regarded the infection as latent or transient if sequencing revealed a HPV type included in both assays.
Results. High-risk HPV was detected in 99.7% of the histological confirmed high-grade lesions (CIN2+) (290/291). The DNA test was positive in 95% (275/291), and the mRNA test was positive in 77% (225/291) of the histological confirmed high-grade lesions. All invasive carcinomas were mRNA positive. The DNA test was significantly more often positive in benign and low-grade lesions, some of which were found to be false positive due to cross-contamination with unrelated types. High-grade histology was detected in 83% of women with normal cytology and positive mRNA test. Latent or transient infections were detected in 11 low-grade and 12 high-grade preinvasive lesions. Sequencing revealed high-risk HPV types included only in the DNA test in 35 high-grade preinvasive lesions, HPV 52 and 58 were the most prevalent HPV types.
Conclusions. These HPV tests have potential to improve the detection rate of high-grade cervical neoplasia, with some limitations. The mRNA test seems to be more appropriate for risk-evaluation. Larger scale, population based studies are necessary to evaluate the predictive values of HPV testing in Norway. National monitoring of HPV testing should be obligate and incorporate cytology and histology results in order to give recommendations for follow-up.

P 760
SQUAMOUS CELL CARCINOMAS OF THE VULVA: ASSOCIATED EPITHELIAL LESIONS AND VALUE OF P16 AND P53 IMMUNOSTAINING.
S. Landolfi, M. Santos, L.M. Puig-Tintoré, B. Mellado, A. Torné, E. Campo, J. Ordi
Departments of Pathology, Oncology and Obstetrics and Gynecology, Hospital Clínic-Institut d'Investigacions Biomèdiques August Pi i Sunyer (IDIBAPS), University of Barcelona, School of Medicine, Barcelona, Spain

Introduction and aim: Two types of vulvar squamous cell carcinomas (SCC) have been delineated: human papillomavirus related (HPV+) and unrelated (HPV-) SCC. HPV+ tumors are basaloid or warty (B/W), are considered to arise in relatively young women, are frequently associated to undifferentiated vulvar intraepithelial neoplasia (VIN) and over express p16. HPV-tumors are keratinizing (KER), arise in elderly patients, are frequently associated with differentiated VIN, lichen sclerosus (LS) and squamous cell hyperplasia (SCH), and show a high proportion of p53 mutations that result in p53 immunohistochemical positivity. However, some overlap between HPV+ and HPV- tumors exist. The aim of our study was to evaluate the correlation between the two major types of SCC and concurrent epithelial lesions and determine whether p16 immunostaining could be a good discriminator between these forms.
Methods: All patients diagnosed of vulvar SCC treated in our institution with radical vulvectomy or partial resection from 1995 to March 2005 were included. 84 patients were identified. 4 to 20 slides of every case (mean 8), including tumor and non-neoplastic tissue, were reviewed focusing on histological type of tumor and concurrent epithelial changes. Immunohistochemical analysis of p16 and p53 was performed.
Results: 70 (83,3%) were KER SCC, whereas 14 (16,6%) were B/W type (9 and 5 respectively). LS and SCH were present respectively in 36 and 60% of KER and in 7 and 21% of B/W SCC ($p<0.05$). VIN was detected in 47% of KER and in 43% of B/W SCC. p53 was positive in 50 cases (67% of KER, 7% of B/W) and p16 in 18 cases (7% KER, 93% B/W). p16 and p53 positivity were almost always mutually exclusive. Interestingly, 3 out of 5 keratinizing SCC positive for p16 showed undifferentiated VIN, suggesting a relationship with HPV, and the only basaloid SCC negative for p16 was intensely positive for p53 and showed differentiated VIN and LS in the non-neoplastic skin, indicating an HPV-unrelated pathway.
Conclusion: p16 and p53 immunostaining, seem to discriminate adequately between HPV-associated and HPV-unrelated vulvar squamous cell carcinomas. A small percentage of keratinizing SCC are probably related to HPV infection, whereas a few tumors not associated to HPV may have a basaloid or warty histology.

P 761
EXTRACELLULAR SIGNAL-REGULATED KINASE 2(ERK 2) EXPRESSION IN CERVICAL

INTRAEPITHELIAL NEOPLASIA AND CARCINOMA OF THE CERVIX.

Kouneli S, Arvaniti H, Kapetanios V, Bogris P, Stylianidi A, Lazaris a, Bairaktari-Kouri E

The HPV protein E5 seems to be weakly oncogenic and has been suggested to potentiate the transforming activity of E7.The molecular mechanisms of E5-induced cell proliferation are transmitted through the activation of potent transcription factors by the ERK/MAPK signaling pathway.The key event in E5 induced cell proliferation involves the activation if the mitogen-activated protein kinases(MAPK),which include a pair of protein kinases known as ERK1 and ERK2.
The aim of this study is to investigate the usefulness of ERK2 expression in predicting the grade of CIN lesions as well as to compare the expression with that of cervical carcinoma.
Immunohistochemistry was performed on paraffin embedded sections of 76 CIN lesions(20 CIN1, 20 CIN2 and 36 CIN3)and 30 cervical carcinomas(21 squamous,9 adenocarcinomas) using standard procedures with the application of the ERK2 monoclonal antibody(Santa Cruz Biotechnology, USA 1/300 dilution).A semiquantitative scoring into 3 categories was used as follows:1.slight staining equivalent to that of normal squamous epithelium 2.moderately increased staining cytoplasmic and/or nuclear 3.intense diffuse cytoplasmic and/or nuclear staining.
Results:The frequency of strong ERK2 expression increased from 0% for CIN1 lesions to 61% for CIN3 lesions.Specifically the majority of of CIN1 lesions(60%) showed a weak cytoplasmic expression in the basal and parabasal layers equivalent to that of the normal squamous epithelium while 40% showed a moderately increased staining.In CIN2 lesions 40% of the cases displayed either a weak equivalent to normal(20%) or intense(20%) expression while the majority(60%) showed a moderately increased expression.Finally in CIN3 lesions only 11% showed weak ERK2 expression while 28% and 61% of the cases expressed ERK2 moderately and strongly respectively.In cervical squamous carcinomas moderate and strong expression was found in 91% of the cases in approximately equal percentages(48% moderate,43% strong)while in cervical adenocarcinomas all the cases showed either strong(67%) or moderate(33%) expression.
Conclusions:According to our study a direct relationship between the increasing grade of the CIN lesion and the intensity of ERK2 staining was found.Moderate and strong ERK2 expression was related to high grade lesions(CIN3 or cancer).All cervical adenocarcinomas showed either moderate or intense ERK2 expression while in 10% of squamous cee carcinomas only weak equivalent tonormal staining was found.

P 762

HUMAN PAPILLOMAVIRUS TYPES IN SQUAMOUS CELL CARCINOMAS AND ADENOCARCINOMAS OF THE UTERINE CERVIX IN REGION OF RIJEKA, CROATIA

KRAŠEVIÆ Maja, ŠIMAT Marina, GRAHOVAC Blaženka
Department of Pathology,Medical Faculty University of Rijeka, Croatia

Introduction: The association between human papillomavirus (HPV) infection and cervical cancer have been well established. The different carcinoma-associated HPV types have been reported world wide. However in Croatian population, such data have not been reported to date.
Purpose of the study: To analyse the frequency and distribution in HPV types in two different histological forms of uterine cervical carcinoma among the patients in region of Rijeka, Croatia.
Material and Methods: A retrospective analysis was undertaken on formalin fixed paraffin embedded specimens of 54 squamous cell carcinoma (SCCs) and 40 adenocarcinomas (ACs), including 15 adenocarcinoma in situ, from patients treated in Clinical Hospital Rijeka. HPV genotyping was performed by consensus and type specific primers directed PCR. The results were correlated with clinicopathologic parameters i.e.age of the patients, FIGO stage, histological subtype and grade of the lesions.
Results: Of the 94 cases examined, 87(92.5) were HPV DNA positive; 50/54 (92.6%) of SCCs and 37/40 (92.5%) ACs. Eight different HPV genotypes were detected: 6/11, 16, 18, 31, 33, 52, 74 and undetermined type X. HPV types 6/11, detectable in 9.1 % of HPV positive cases, were observed as a part of coinfection, except in one case of AC. HPV 16 was the predominant type in SCCs, detectable in 26/50 (52.0%) of cases, whereas HPV 18 was the most common type in ACs 25/37 (67.5%). HPV 31 and 33 accounted for 16.0 % and 8.0 % of HPV positive SCCs and 8.1% and 5.4 % of HPV positive ACs, respectively. In addition, multiple HPV types were found in 21/87 (24.1 %) of carcinomas, without significant correlation to the histologic type, with 19.9 % in ACCs and 29.0 % in ACs. No relationship was found between viral type and any of the clinico-pathologic parameters analysed.
Conclusion: Our results indicate that cervical carcinomas are largerly associated with HPV types 16, 18, 31 and 33 in our study group in Rijeka region, with statistically significant predominance of HPV 16 in SCCs (52.0%) and HPV 18 in ACs (67.5%).

P 763

CYTOKERATIN 17 AND P63 IN METAPLASTIC AND NEOPLASTIC CERVICAL LESIONS

VASILESCU Florina 1,2, FLOREA-GRAMADA Zenaida1, POPA Elena 3, IOSIF Cristina 1, DOBREA Camelia 1, BUTUR Georgeta, CEAUSU Mihai 1, ARDELEANU Carmen 1
1. "V.Babes" National Institute-Bucharest
2. Military Hospital Bucharest
3. "Bucur" Obstetrical Hospital Bucharest

The transformation zone of the cervix is the place where most malignancies appear. The epithelial turn over seems to differ here from that of more stable structures in the vicinity. The occurrences of squamous metaplasia makes this zone more prone to malignancies but the reason why this happens remains a matter of debate. The extension of the stem cell theory to solid tumors has prompted new insight into tumor genesis. Classically it is admitted that a bipotent stem-like cell, the subcolumnar cell, is the origin of squamous metaplasia of the cervix. In this study we identified expression of p63 , a homologue of the tumor suppressor gene p53 and cytokeratin 17(CK17) in metaplastic and neoplastic cervical lesions. Cervical tissue from archival paraffin blocks was available from 30 pacients which had variable lesions:mature squamos metaplasia, moderate and severe dysplasia and squamos invasive carcinoma . We noted p63 expression consistently in the nuclei of reserve cells, hyperplasia of the basal layer of the dysplastic and neoplastic epithelium of ectocervix , while CK17 was sporadically found in the basal layer of ectocervical epithelium and always present in the basal cells of squamos metaplastic epithelium. Also, CK17 has increased expression during progression of CIN, and diffuse stained in squamos carcinoma. Our results concluded that a considerable number of premalignant and malignant lesions of the uterine cervix express CK17 and p63 which is also found in the progenitor reserve cells.

P 764

LARGE CELL NEUROENDOCRINE CARCINOMA OF THE UTERINE CERVIX: A CLINICOPATHOLOGIC STUDY OF FIVE CASES.

Chanona Vilchis JG, Vela Chavez TA, Dominguez Malagon HR, Cantu de Leon DF, Perez Montiel MD.

Background: Cervical carcinoma in not developed countries is the first cause of death for woman's cancer, in Mexico 9,913 new cases were reported on 2000 whit 4,620 deaths in the same year. The large cell neuroendocrine carcinoma (LCNC)of the uterine cervix is a rare entity and few cases have been reported in the international literature. The LCNC have been described as aggressive tumor with "organoid" growth patterns (trabecular, insular and solid). The neoplastic cells are large whit vesicular nuclei, prominent nucleoli, atypical mitosis (3-12 per high power field) and necrosis.
Design: All the cases identified as small cell neuroendocrine or undifferentiated cervical carcinoma from a period from 1991 to 2003 were revised separately by three pathologist using the criteria described in the background. Immunohistochemical staining with cromogranin and synaptophysin were done. Clinical information was obtained from patient's charts.
Results: Five patients were selected using the previous mentioned criteria from a pool of 103 cases; the tumors where no consensus in the diagnosis were obtained were excluded. Patients age ranged in 43-61 years. One patient was stage IIA and four patients were stage IIB. Maximal dimensions were 8 cm. Two patients were treated with surgery, chemotherapy and radiotherapy, two patients with chemotherapy and radiotherapy without surgery and one patient was lost, this patient was associated whit adenocarcinoma of the colon treated whit surgery and chemotherapy. Immunohistochemestry study was done, all the cases were positive for cromogranin and synaptophysin. Disease progression was documented in three patients; two with cerebral metastasis, one with node metastasis; one patient had persistent disease. Two patients are alive whit disease 17 and 18 months after diagnosis and two die with disease 6 and 8 months after diagnosis.
Conclusions: large cell neuroendocrine carcinoma is a rare neoplasia frequently confused with small cell neuroendocrine carcinoma or undifferentiated carcinoma. The patients had a high grade tumors whit advanced disease, and despite aggressive treatment, the patients have had progression and early recurrence.

P 765

SMALL AND LARGE CELL NEUROENDOCRINE CARCINOMAS OF THE UTERINE CERVIX. A REPORT OF 10 CASES

KUBELKA-SABIT Katerina1, PLASESKA-KARANFILSKA Dijana4, PRODANOVA Irina1, YASHAR Genghis1, HADZI-NICHEVA Biljana3, VELJANOSKA Slavica2, ZOGRAFSKI Georgi1, BASHESKA Neli 1
1Department of Histopathology and Clinical Cytology, 2Institute of Radiotherapy and Oncology, 3Department of Gynecological Cytology, Clinic for Gynecology and Obstetrics, Medical Faculty, Skopje, Macedonia
4Research Center for Biotechnologic Engineering and Genetics, Macedonian Academy of Science and Arts, Skopje, Republic of Macedonia

BACKGROUND: Small (SCC) and large cell (LCC) neuroendocrine carcinomas of the uterine cervix are rare and highly aggressive neoplasms. Their association with the integration of human papilloma virus (HPV) DNA of the types 16 or 18 has been documented in many studies.
AIMS: The purpose of this study is to present the clinical, histopathological, immunohistochemical characteristics and the presence of HPV DNA in ten cases of SCCs and LCCs of the uterine cervix.
METHODS: Seven patients with primary SCCs and three patients with LCCs of the uterine cervix were diagnosed at our department between 1989 and 2004. Clinical data were retrieved from the patients' files and included age, recurrence and survival. Routinely processed operative and/or biopsy specimens were used for immunohistochemical stains and hybridization procedures. Primary antibodies against several epithelial, neuroendocrine, mesenchimal and proliferative markers were included. The presence of HPV DNA was assessed by conventional in situ hybridization (ISH) using probes for HPV 16/18 and 31/33/51 and polymerase chain reaction (PCR), using three primers (MY09/11, GP5+/GP6+, E6). Six of the patients were surgically treated. Postoperatively, four received chemo and/or radiotherapy, two rejected further treatment and one patient was lost to follow-up. The other four patients underwent conservative treatment due to advanced disease.
RESULTS: The patients' age ranged from 25 to 71 years. Histologically, the tumors showed trabecular, nesting or a sheet-like pattern, with areas of necrosis and frequent mitoses. Their neuroendocrine nature was confirmed by diffuse positive immunostaining for neuron-specific enolase and low molecular weight cytokeratins. Focal positivity for chromogranin, synaptophysin and S100, together with pancytokeratin and EMA, was evident in the majority of the tumors. Their aggressive potential was confirmed by high Ki-67 proliferative index (50-90%). HPV types 16/18 were found in 4 tumors using ISH, and HPV 16 in additional 3, using PCR (type 16). 3 of the patients developed distant metastases and died 7-48 months after receiving partial or full treatment, while 6 are alive and without evidence of disease after 4-38 months.
CONCLUSIONS: SCCs and LCCs are highly aggressive neoplasms. However, early diagnosis and combined therapy may improve survival in some patients. Although mainly a morphologic diagnosis, immunohistochemistry may help in the diagnosis of SCC and LCC.

P 766

EVALUATION OF TUMOUR NECROSIS FACTOR (TNF ALPHA_) IN EUTOPIC &ECTOPIC ENDOMETRIA OF WOMEN WITH ENDOMETRIOSIS& ENDOMETRIUM OF HEALTHY WOMEN

PROF. DR.MAGDA HASSAN,PROF.DR.M.E.AZZAM ,PROF.DR.M.H.NASR EL DIN, DR.KHAED SAIID,DR. A. M. ABDEL AZIZ.
DEPT. OF PATHOLOGY,OBSTETRICS & GYNECOLOGY.AIN SHAMS UNIVERSITY.

To achieve a successful implantation, in addition to adequate embryonic quality,an appropriate endometrium is mandatory. Some alterations have been found in the eutopic endometrium of women with endometriosis that could be responsible, at least in part,for the subfertility in these women.
The aim of this study is to compare eutopic &ectopic endometrium of women with endometriosis with that of healthy controls , regarding expression of TNF alpha using immunohistochemical staining.Also, to gain more information about the possible role of cytokine TNF alpha in autocrine & paracrine growth regulation of endometriosis.
The study included 30 patients having endometriosis & endometriotic cysts in the ovary (study group) .Those patients were subjected to laparoscopy to confirm the diagnosis & obtain a biopsy of the endometriotic cyst , besides an endometrial biopsy. The control group included 30 healthy fertile women without endometriosis ,they did laparoscopy for tubal ligation followed by endometrial biopsy.For both groups the biopsies obtained were immunohistochemically stained & examined for TNF alpha expression.

.
The results revealed higher expression of TNFalpha in eutopic endometrium of patients having endometriosis than endometrium of healthy fertile female controls,with a highly statistically significant difference .Theses results have been confirmed by using image analyzer computer system which measured TNF alpha expressed in tissues quantitatively by measuring the optical density. Optical density was then expressed in the form of sum grey & mean grey.The sum grey of TNF alpha expression in eutopic endometrium of endometriosis patients was higher than that of healthy women (control group).
This study shows that increase TNF alpha expression in eutopic endometrium & ovarian endometriosis may explain why endometriosis develop in certain females, as TNF alpha was implicated as one of the factors related to the attachment & growth of the ectopic endometrium through its angiogenic & paracrine activities ..Besides high TNF alpha expression in the endometrium of patients having endometriosis may be a cause of endometriosis- associated infertility through affecting implantation.

P 767
THE EVALUTATION OF MALIGNANCY POTENTIAL IN ENDOMETRIAL HYPERPLASIA BY USING PROLIFERATION MARKERS (PCNA AN KI-67)
Itýr GERÇEKER MD, Sema ZERGEROĐLU MD, Tuðrul AYDOĐDU MD, Ümit BÝLGE MD, Leyla MOLLAMAHMUTOĐLU MD.

Introduction and objects : Endometrial hyperplasia can be described as proliferation of endometrial glands by disordered number and shape with an increase in gland/stroma ratio. The aim of the study is, to evaluate the malignancy potential of endometrial hyperplazia by using proliferating cell nuclear antigen (PCNA)and Ki-67. Which are known as proliferation markers.
Methods : We evaluated 62 pations (20 of them control group), ages between 25-62, whom are operated or taken specimen by D&C in Zekai Tahir Burak Womens Health and Education Hospital, between years 2002-2003. After routin procedures of preparation, pathologic specimens are labeled with PCNA and Ki-67 by using immunohystochemical methods. For statiscal analyses, Anowa and Post Hoc Tukey tests were used. ($p<0,05$)
Results : In complex atypic hyperplasia, both PCNA an Ki-67 expression was higher than in control group, with a statical significance.
Discussion : We suggest that, theese proliferation markers (PCNA and Ki-67) can bu useful specially to determine the malignancy potential of complex atypic hyperplasia of endometrium.

P 768
HISTOPATHOLOGIC CHANGES AFTER UTERINE ARTERIAL EMBOLIZATION WITH TRIS-ACRYL GELATIN MICROSPHERES
WEICHERT Wilko (1), DENKERT Carsten (1), GARUDER-BURMESTER Annett (2), KURZEJA Roberto (2), HAMM Bernd (3), DIETEL Manfred (1), KRÖNCKE Thomas (3)
(1) Institute of Pathology, (2) Department of Gynecology and Obstretics, (3) Department of Radiology, Charité University Hospital, Berlin, Germany

Introduction: Uterine artery embolization (UAE) as an alternative treatment of uterine fibroids and adenomyosis uteri becomes increasingly popular. Because there is considerable uncertainty with respect to the wanted and unwanted morphological changes induced by UAE we conducted a histopatholgic study on post UAE tissue specimen. Methods: A total of 173 women were treated with UAE using tris-acryl gelatin microspheres (TGMS) for either symptomatic adenomyosis or leiomyoma. Surgical specimen of 8 women who underwent subsequent myomectomy or hysterectomy were evaluated by conventional histology and immunohistochemistry.
Results: TGMS were readily apparent in both macroscopy and routine histology. In patients with fibroids, TGMS accumulated preferably in medium size vessels in the direct tumor vicinity. In patients with adenomyosis, a random distribution of TGMS was noted throughout the outer myometrium. A granulomatous foreign body reaction occurred in the vicinity of particles, eventually followed by formation of vascular pseudoaneurysms and complete vessel destruction. Leiomyoma treated with UAE showed either fibrinoid necrosis, coagulative necrosis or no change at all. Increased mitotic activity and tumor cell polymorphism was evident in some but not all treated smooth muscle tumors. Foci of adenomyosis remained unaltered.
Conclusions: In conclusion, after UAE with TGMS, particles were identified predominately but not exclusively at the periphery of fibroids. Pathologists must be aware of the morphologic changes induced by UAE in leiomyoma, to avoid misinterpretation of induced tissue alterations as signs of malignant tumor growth.

P 769
PTEN IMMUNEXPRESSION IN RANDOMLY SELECTED ENDOMETRIAL POLYPS
EREN Funda, ERBARUT Ipek
Marmara University School of Medicine, Deaprtment of Pathology, Istanbul, Turkey

Endometrial polyps are common in women over 40 and are thought to arise due to some type of hyperplastic process. Although most of them are benign, carcinoma developing in polyps is a rare but well-known condition especially in postmenopausal women. Recently, PTEN inactivation has been shown to be a common event in endometrial carcinogenesis. Also PTEN loss has been documented in some normal-appearing endometrial glands of 43% of premenopausal women suggesting that PTEN loss might be an early step in endometrial carcinogenesis. In order to search for the PTEN expression pattern in endometrial polyps we investigated the immunhistochemical expression of PTEN in 50 randomly selected endometrial polyps. The morphology of polyps were atrophic (n:21), functional (n:17), inactive (n:12) and hyperplastic (n: 1). PTEN was lost in more than 50% of the glands in 88% (n:17) of atrophic polyps. Also in the 2 of the 3 polyps with secretory epithelium there was diffuse PTEN loss. On the contrary there was diffuse PTEN expression in 75% of proliferative glands in functional polyps . None of the glands with PTEN loss showed atypical histological findings. In polyps containing both proliferative and inactive or atrophic glands, PTEN-null glands were restricted to atrophic or inactive glands. Expression of PTEN in stromal cells also was parallel to that of the epithelia. This data shows that in polyps PTEN is expressed strongly in proliferative epithelium but it is commonly decreased or lost in any kind of nonproliferative epithelium. Although it is strongly suggested that PTEN-inactivated glands could be 'latent precancers' care should be taken in evaluating the immunexpression in the absence of morphologic evidence of atypia. In conclusion, we think that finding PTEN inactivated glands in a polyp could be valuable in proliferative type glands but in normal-appearing nonproliferative epithelium it seems like a normal event.

P 770
IMMUNOHISTOCHEMICAL EXPRESSION OF P63 IN ENDOMETRIAL POLYPS: AN EVIDENCE OF THE MAINTENANCE OF A BASAL CELL IMMUNOPHENOTYPE
Antonio A Nogueira(1), MD

Omero B Poli Neto(2), MD
Elza C S Almeida(1)
Leandra N Z Ramalho(3), MD
Júlio C Rosa e Silva(1), MD
Francisco J Candido dos Reis(1), MD
(1)Departamento de Ginecologia e Obstetrícia da Faculdade de Medicina de Ribeirão Preto da Universidade de São Paulo.
(2)Departamento de Cirurgia e Anatomia da Faculdade de Medicina de Ribeirão Preto da Universidade de São Paulo.
(3)Departamento de Patologia da Faculdade de Medicina de Ribeirão Preto da Universidade de São Paulo.

Introduction: Endometrial polyps likely originate from basal layer but their biology underlying is not fully understood. Recently, p63, an important protein in regulating epithelial proliferation and differentiation, has been described as a marker of basal/ reserve cells in female genital tract.
Objective: Our objective was to verify if p63 is expressed differently in postmenopausal endometrial polyps and adjacent endometrium.
Design: In this study we evaluated the p63 expression in 36 specimens of postmenopausal endometrial polyps, obtained by hysteroscopic polipectomy realized in a tertiary care university hospital, using a monoclonal antibody clone 4A4 (1:200), which recognizes all p63 variants.
Results: The majority of endometrial polyps (94.4%) were p63-positive. Otherwise, only 5.6% of adjacent endometrium had presented rare nuclei immunostaining for p63 ($P < 0.0001$). Endometrial polyps had presented homogeneous pattern of distribution of p63 immunostaining.
Conclusions: Our results are an evidence of the maintenance of a basal cell immunophenotype in postmenopausal endometrial polyps. Furthermore, they suggest that P63 has a role in the pathogenesis of endometrial polyps and emphasize the necessity of more studies about P63 role and its different isoforms in the biological and clinical behavior of endometrial polyps.
Key-words: endometrial polyps, menopause, basal cells, P63.

P 771
HISTOPATHOLOGIC DIAGNOSES OF THE ENDOMETRIUM OBTAINED BY CONSECUTIVE BIOPSY PROCEDURES IN 1699 FRENCH AND 2887 ISRAELI WOMEN.

Czernobilsky, Bernard1, Lifschitz-Mercer Beatriz2,Bergeron Christine3
1PATHO-LAB Laboratories, Ness Ziona, Israel
2Institute of Pathology, Tel-Aviv Medical Center, Tel-Aviv, Israel
3Laboratoire Pasteur-Cerba, France

Introduction: Histologic examination of the endometrium is a common diagnostic procedure in peri and menopausal women with abnormal bleeding and/or thickened endometrium by ultrasound (US).
Purpose: This study, performed in France and Israel, was undertaken to compare frequency of histologic diagnoses in both populations and correlate the results with clinical information.
Methods: Hematoxylin-eosin stained slides of endometrial formalin fixed, paraffin embedded tissue from 1699 French and 2887 Israeli women aged 45 and above were examined independently by pathologists in each country.
Results: Proliferative endometrium was present in 22.3% of the French and 28.3% of the Israeli cases. Secretory endometrium including menstrual was seen in 10.1% of French and in 12% of Israeli patients. Atrophic endometrium, mostly in menopausal patients was diagnosed in 48.4% of the French and 32.2% of the Israeli population. No tissue was available for histologic evaluation in 5.5% of the French and in 10% of Israelis, most of them menopausal. Chronic endometritis was diagnosed in 0.2% of Israelis but none in French patients. Thus, in 86.3% of the French and in 82.5% of the Israeli women, the histology was within normal range of the age group studied. Endometrial polyps were found in 9.4% of the French and in 9.0% of Israelis. Endometrial adenocarcinoma was diagnosed in 2.1% of French and 2% of Israeli women. The only significant discrepancy between the French and Israeli series was simple hyperplasia without atypia diagnosed in 1.7% of the French and 6% of the Israelis. Complex hyperplasia was rare in both populations (0.1%). Atypical hyperplasia was also rare (0.4% in the French and none in the Israelis). Most likely these cases were classified as well differentiated endometriod carcinoma.
Conclusion: Histopathologic diagnoses of endometrium in French and Israeli populations showed with few exceptions remarkable similarities. Thickened endometrium (measured by US) and abnormal bleeding were not restricted to women with polyps, hyperplasia or carcinoma, but were present in the entire histopathologic spectrum including in atrophy.

P 772
EXPRESSION PATTERN OF OSTEOPONTIN (OPN) IN ENDOMETRIAL CARCINOMA – CORRELATION WITH EXPRESSION OF THE ADHESION MOLECULE CEACAM1

BRIESE Juliane, SCHULTE Heinrich M., LÖNING Thomas, BAMBERGER Ana-Maria

Introduction:
OPN and CEACAM1 have diverse biological functions in the uterus throughout the estrous cycle and have been shown to interact with integrin beta3. OPN is a glycoprotein of the extracellular matrix, which has been shown to mediate cellular migration and invasion and to contribute to tumorigenesis in several types of cancers. CEACAM1 is an adhesion molecule of the carcinoembryonic antigen family which we have recently found to be expressed in endometrial cancer and which has been shown to be down-regulated in colorectal and breast cancer.
Purpose:
Endometrial carcinoma is the most frequent invasive malignancy of the female genital tract in developed countries. The present study was designed to investigate the expression pattern of OPN in the normal human endometrium and in endometrial carcinomas and to correlate it with the expression of CEACAM1.
Material and methods:
In the present study, immunohistochemistry and immunofluorescence with specific antibodies were performed on a series of 20 normal endometrial samples and 40 endometrial carcinomas to investigate the expression pattern and cell-type specific localization of OPN and to correlate it with the expression of CEACAM1. In addition, western blot was performed on normal human endometrium and endometrial neoplasia.
Results:
Strong OPN expression with a consistent cytoplasmic localization in epithelial glandular cells was observed in the normal human endometrium in 80% of the samples of the proliferative and secretory phase (score 8-12). CEACAM1 showed similar results. Strong expression of OPN could be observed in 35 (87,5%) of the 40 analyzed endometrial carcinomas. Of the 40 analyzed tumors, 19 (47,5%) were in the high score (8-12) category with a strong OPN expression level, nine tumors of 40 (22,5%) showed a moderate score (4-7) category. With increasing malignancy grade, increasing areas with low OPN expression level or complete loss of OPN expression could be observed. CEACAM1 had shown similar results and was found to be co-expressed with OPN in normal human endometrium and in endometrial neoplasia.
Conclusion:
The expression pattern of osteopontin in endometrial tissue indicates that it might play a role in the pathogenesis of

endometrial cancer (possibly as a functional complex with CEACAM1) and to be useful as an additional diagnostic marker for such lesions. The correlation between pathological stage and OPN suggests a role for OPN in tumor prognosis.

P 773
MALIGNANT LYMPHOMA OF THE UTERUS: A CLINICOPATHOLOGIC ANALYSIS OF 14 CASES
HP Chien, SM Jung, S Hsueh, WY Chuang, TT Kuo.
Department of Pathology, Chang Gung Memorial Hospital, Tao Yuan, Taiwan

Introduction: Non-Hodgkin¡¦s lymphoma involving uterus is uncommon. Most tumors arise in the cervix while those of the uterine corpus are extremely rare. We evaluate the clinicopathologic features of 14 cases in Taiwan and reclassify them using new WHO classification.
Methods: Fourteen cases of Non-Hodgkin¡¦s lymphoma involving the uterus were retrieved from the pathology file of Chang Gung Memorial Hospital from 1987 to 2004 and reclassified by new WHO classification. Pathology slides, immunochemical study, and clinical information were reviewed.
Results: Patients ranged from 20 to 78 years (mean, 51.8 years). Of fourteen cases, eleven had primary tumor involving uterus at the presentation and three were secondary cases. The most common presenting symptoms were vaginal bleeding (43%). Histologically, nine tumors were diffuse large B-cell lymphoma (DLBCL) (5 centroblastic variant, 4 immunoblastic variant), three were follicular lymphoma and two were Burkitt¡¦s lymphoma. Six cases (43%) involved cervix (5 DLBCL, 1 Follicular) and were stage IE or IIE. Three cases (21%) involved corpus (all DLBCL) only and were all stage IVE. Five cases (36%) involved both cervix and corpus (2 Burkitt¡¦s, 2 Follicular, 1 DLBCL) and were stage IIIE or IVE. Follow-up information was available for 10 cases and ranged up to 75 months (mean, 26.9 months). Two follicular lymphomas relapsed in uterus transformed to diffuse large B-cell lymphoma 2 and 26 months after the diagnosis and were both stage IV cases. All low-stage (IE or IIE) cases received chemotherapy and were all alive without recurrence for 1-75 months (mean, 29.2months). Two stage IV cases died 0.5 and 2 months after the diagnosis.
Conclusion: Our study showed that malignant lymphomas involving cervix are all low stage irrespective of histological type. However, those involving uterine corpus (with or without cervical involvement) are of high-stage disease and more aggressive tumor type. Two cases of Follicular lymphoma showed transformation to diffuse large B-cell lymphoma.

P 774
AN UTERINE PECOMA : A CASE REPORT
IRVANLOO Gity, NOZARIAN Zohre
Cancer institute, Imam Khomeini Hospital, Tehran University of Medical Sciences

Epithelioid mesenchymal tumors of the uterus were previously considered to be either from smooth muscle or endometrial stromal lineage, but recently a new family of lesion have been described including HMB45 + epitheliod cells with clear to granular cytoplasm and perivascular distribution.
We described an uterine PECOMA in a 33 years old woman that tumor cells were positive for HMB45 but negative for epithelial and smooth muscle markers.

P 775
LOW GRADE ENDOMETRIAL STROMAL SARCOMA OF THE UTERUS WITH EXTENSIVE ENDOMETRIOID GLANDULAR DIFFERENTIATION
CC Wu, SM Jung, S Hsueh, CH Lai
Department of Pathology and Department of Obstetrics and Gynecology, Chang Gung Memorial Hospital, Taoyuan, Taiwan

Introduction: Low grade endometrial stromal sarcoma (LGESS) is a rare tumor of uterus. Occasional cases may cause problems in differential diagnosis because of variable patterns: epithelioid cells, sex-cord-like differentiation, benign or malignant endometrioid glands, smooth muscle metaplasia, and myxoid areas. We reported a rare case of LGESS with extensive glandular differentiation.
Case report: A 29-year-old woman presented with a painless palpable mass in the left lower abdomen for a month. She went to local hospital and a left ovarian mass with suspect of malignancy was noted under sonography and the CA-125 was elevated. She received left salpingo-oophorectomy, and hormone therapy after surgery for four months. Then she was transferred to our hospital for further management. Hysterectomy was performed. On gross examination, an ill-defined, tan to yellowish elastic multi-nodular mass measuring 8 cm in maximal diameter was in the myometrium. Histologically, the tumor diffusely penetrated the myometrium and lymphovascular space as irregular tongues or nests. It composed of oval or spindle tumor cells with rich network of delicate small arterioles and focal myxoid and fibrous stroma. The cells exhibited mild nuclear pleomorphism and a mitotic rate of 10/10 HPF. Most of the tumor also contained diffusely benign-appearing endometrioid glands. Immunohistochemical stains showed that the tumor cells were positive for ER, PR, smooth muscle actin, and CD10, and negative for desmin.
Conclusion: The differential diagnosis of LGESS with extensive glandular differentiation includes endometriosis, adenomyosis, endometrial stromal sarcomas arising in adenomyosis or endometriosis, and adenosarcomas. It is important that LGESS with extensive glandular differentiation in myometrium not to be mistaken for adenomyosis.

P 776
DEPICTION OF ANGIOGENIC AND LYMPHANGIOGENIC FACTORS INCLUDING VASCULAR ENDOTHELIAL GROWTH FACTOR (VEGF-C), PROLACTIN (C-17), PLATELET DERIVED GROWTH FACTOR (PDFG-A), FIBROBLASTS GROWTH FACTOR –1 (FGF-1), AND THEIR EXPRESSION IN 90 CASES OF ENDOMETRIOID AD
CATALANO Edison M.D., WEIDMANN James BSCT HTL (ASCP) Cooper University Hospital, Camden, NJ USA

Introduction: PDGF-A (N-30) is a mitogen for mesenchymal cells, which plays an important role in the angiogenesis and progression of tumor. The Vascular Endothelial Growth Factor C is a member of the family of growth factors, which is an important endothelial cell mitogen and is associated with an increase in angiogenesis and lymphangiogenesis. The increase in expression of Prolactin (C-17) protein has been related to a more aggressive tumor behavior.
The fibroblastic growth factor-1 (FGF-1) is a growth factor that stimulates the proliferation of mesenchymal, epithelial and neural ectodermal cells.
Purpose: This study was to investigate the relationship of the overexpression of VEGF-C, Prolactin (C-17), PDGF-A (N-30), and FGF-1 in 90 cases of invasive endometrioid adenocarcinoma, the effects of these factors over the angio and lymphangiogenesis. Also, through the survival tables we evaluate the prognostic significance of overexpression of these factors, as well as the relationship with the staging of the tumor and degree of differentiation.
Methods: Formalin fixed and paraffin embedded sections of the endometrial tumors were obtained from 90 cases. Immunohistochemical staining was obtained for VEGF,

Prolactin (C-17), PDGF-A (N-30) and FGF-1, and the measurement of the action of these factors, over the vascular proliferation evaluated with CD-34 and the microvascular density (MVD).
Summary of Results: In the 90 cases studied there was a perfect correlation in 50% of the cases between the VEGF-C and the increase in angiogenesis. Also, Prolactin and PDGF-A (N-30) showed an excellent correlation between the antibody staining (overexpression), in relationship to the tumor differentiation, staging and survival statistics.
In general the staining of this antibody, FGF-1 (C-19), was lighter in comparison with the previous and shows a diffuse cytoplasmic staining with no nuclear staining. There were more negative cases and the only positive cases were only 2+ or 3+. The correlation; however, with the survival was excellent, as well as with the staging and degree of tumor differentiation.
Conclusion: The overexpression of the factors VEGF-C, Prolactin (C-17), PDGF-A (N-30) and FGF-1 (C-19) demonstrated a cytoplasmic overexpression of these antibodies that activates the angio and lymphangiogenesis and leads to a more rapid tumor growth, higher stage of the disease and more aggressive clinical behavior demonstrated with the statistic analysis.

P 777
ABERRANT CDX-2 EXPRESSION IN SQUAMOUS MORULES IN ENDOMETRIOID ADENOCARCINOMA AND BENIGN ENDOMETRIAL LESIONS. –IMMUNOHISTOCHEMICAL ANALYSIS OF HOMEOBOX GENE TRANSCRIPTION FACTOR CDX2 AND PDX1-
WANI Yoji, NOTOHARA Kenji, TSUKAYAMA Choutatsu

Introduction: Cdx2 protein is a intestine-specific homeobox gene transcription factor that plays an important role in the regulation of differentiation of intestinal epithelium. Only a few data exist with Cdx2 expression of endometrial lesions. Pdx1 is also a homeobox gene that plays an essential role in the development or exocrine and endocrine of pancreas. Pdx1 expression is observed not only in the pancreas but also in Brunner's glands and pyloric glands. Little is known whether Pdx1 is expressed in the endometrium.
Purpose of Study: To investigate the potential role of Cdx-2 and Pdx-1 in endometrial lesions, we performed immunostaining for Cdx-2 and Pdx-1.
Methods: We selected 17 cases of normal or benign endometrial lesions(NBEs), 20 cases of Atypical endometrial hyperplasia(AEH)/endometrioid adenocarcinoma(EAC) with Squamous metaplasia(SqM), 24 cases of AEH/EAC without SqM. We defined that SqM is consisted of morules(MOs) and/or mature squamous cells(SCs). Cdx2 and Pdx1 expression was evaluated in formalin-fixed, paraffin-embedded materials. All cases were immunostained with the Envision+ method(DAKO), using a monoclonal anti-Cdx2 antibody(CDX2-88, 1:200 BioGenex), and a polyclonal rabbit anti-Pdx1 antibody(1:50 TransGenic Inc.). We used the following scoring system for Cdx2 and Pdx1 immnostaining: 0= negative; 1=1% to 10%; 2=11% to 50%, 3=51% to 100%.
Results: Four of 13 NBE cases contained foci of MO, where intense immunoreactivity for Cdx2 was seen. All AEH/EACs cases with SqM, except one (high-grade adenosquamous carcinoma), had variably Cdx2-expressed cells. In paticular, most foci of MOs in AEH/EACs are intensely positive, while sporadic immunoreactivity for Cdx2 was seen in foci of SCs. Neoplastic glandular cells in the backgrounds of SqM were variably Cdx2 positive in itself. Glandular cells were sporadically positive in six AEH/EACs without SqM. None of NBEs and AEH/EACs revealed positive for Pdx1.
Conclusion: We should note there are aberrant and distinct Cdx2 expressions for MO foci in NBEs. In four cases with MOs, Cdx2-positive cells are sporadicaly seen in glandular epithelium. In other words, morular formation itself seems to be made by intraluminal proliferation of Cdx2-positive glandular cells. Cdx2 expressions in MOs of NBEs and AEH/EACs tend to be very similar to that of nuclear beta-catenin(data not shown). Pdx1 does not seem to be related to NBEs and AEH/EACs.

P 778
CLINICO-MORPHOLOGICAL CHARACTERISTICS OF CANCER ARISING IN ENDOMETRIAL POLYPS
DERIZHANOVA Irina, VOLOSHIN Vladimir, VOLOSHINA Nina

Aims: to study morphogenesis of the carcinoma, arising in polyps of the uterus mucous membrane (EP).

The data of the clinical observations were analyzed. Endometrium scraps and the excised uterus and appendages from 16 patients with histological proved cancer in EP were subjected to common histological and histochemical examinations, the receptors of estrogen (ER) and progesterone (PR), as well as the markers of Ki67 (MIB-1) proliferation and p53, bcl-2 àpoptosis being simultaneously clearly seen.

Endometrioid adenocarcinoma (EA) was diagnosed in 13 of these patients. The patients age averaged 52,2 years, most of whom had their menstrual cycle still alive. 84,6 % of these patients suffered adiposity, 76,9 % - had hypertension, 61,5 % - diabetes. In all 13 patients ÅÀ was accompanied with àdenomyosis, uterus leiomyoma and hyperplasia of the ovarian theca. In 10 cases ÅÀ in Ò1à stage was well differentiated (G1). In 3 patients of Ò1b stage of EA it was of grade 2 (G2). ÅÀ was found to develop in polyps with diffuse (8) or focal adenomatosis (5), epithelium metaplasia and dysplasia I - III stage. Diffuse (5) or focal (5) simple (6) and complex (4) hyperplasia was seen in surrounding endometrium. The receptors of sexual hormones in prolipherating epithelium polyps and ÅÀ were exhibited in abundance. As epithelium àtypia grew, the ER content, PR in particular, was noted to decrease. The expression of Ki67, p53 was gradually intensifying.

Serous (SA) adenocarcinoma (G2) of T1c, Ò2 stages was found in 67-75-year - old women with the episodes of bleeding during menopausa (3 cases). The tumor was embedded in adeno-fibrous polyps accompanied by endometrium cyst atrophy. No attributes àdenomatosis and epithelium metaplasia were revealed. PR in the tumor was not revealed either. Poorly positive reaction to ER was demonstrated in some single epithelium cells, SA stroma and in the surrounding polyp. Expression Ki67 and p53 in cells was positively higher, compared to that of in the polyp surrounding epithelium and in àtrophic endometrium, with bcl-2 being reduced.

Conclusion: ÅÀ (81,3 %) developed in the polyps followed by àdenomatosis, metaplasia, epithelium àtypia and corresponded to estrogen-dependent neoplasia. SA (18,7%) embedded in adenî-fibrous polyps accompanied by the atrophy of glandular epithelium and were characterized by a high proliferation activity and corresponded to estrogen-independent carcinoma.

P 779
CARCINOMA ARISING FROM ENDOMETRIOSIS OF THE ROUND LIGAMENT
YAEGASHI Hiroshi 1), HAYAKAWA Seiichiroh 2,3), Seiichiroh kyoko 3), ANZO Misturu 1), H\AKAMAZUKA Jun-ichi 1), KITAZAWA Kaori 1), AOKI Nozomu 1,4)
1) Department of pathology, Mito Kyodo General Hospital, Mito, Japan.
2) Department of Obsterics and Gynecology, Mito Kyodo General Hospital, Mito, Japan.
3) Hayakawa Clinic, Hitachinaka, Japan.

4) Department of pathology, The Institute of Chemotherapy, Ichikawa, Japan.

Introduction Endometriosis of the extraperitoneral part of the round ligament is very rare, from 0.4 to 0.6 % in the literature, mostly on the right side. Carcinoma arising from this endometriosis is an extremely rare event. Only a few cases have been reported. We present a case of endometrioid adenocarcinoma arising from endometriosis of the left round ligament.
Case report A 41-year-old woman, gravida III, para I, presented a left inguinal mass. Histerectomy with bilateral salpingo-oophorectomy and a tumorectomy ware performed under the clinical diagnosis of ovarian carcinoma and ltinguinal metastasis. The left inguinal tumor, a grey-whitish solid mass, arised from the extraperitoneal part of the round ligament. Frozen sections and imprint cytology suggested a epithelial malignant tumor. Macro- and microscopical examination revealed that uterus and bilateral adnexa were within normal limit. However the inguinal tumor was diagnosed as endometrioid adenocarcinoma(G3) associated with endometriosis. It was suggested that the tumor was arising from endometriosis of the extraperitoneal round ligament. Thereafter chemotherapy was performed. The patient is currently 2 years free of disease after operation.
Conclusion Extraperitoneal endometriosis is extremely rare moreover on the left side, malignancies arising from that should be considered in the differential diagnosis in women with an inguinal mass of reproductive age.

P 780
CELLULAR RETINOL BINDING PROTEIN-1 IS VARIABLY EXPRESSED IN ENDOMETRIAL CARCINOMA AND CORRELATES WITH HISTOLOGICAL GRADING

Augusto Orlandi1, Amedeo Ferlosio1, Arianna Francesconi1, Beatrice Lifschitz-Mercer2, Giulio Gabbiani3, Bernard Czernobilsky4, Luigi Giusto Spagnoli1
1Anatomic Pathology, Tor Vergata University of Rome, Italy
2Institute of Pathology, Tel-Aviv Medical Centre, Israel
3Institute of Pathology and Immunology, University of Geneva, Switzerland
4Patho-Lab Laboratories, Ness-Ziona, Israel

Cellular retinol binding protein-1 (CRBP-1) contributes to maintain the differentiated state of the endometrium through regulation of retinol bioavailability of endometrial epithelial cells. Purpose of the study was the determination of CRBP-1 expression by immunohistochemistry in a consecutive series of 8 atypical hyperplasias and 42 endometrial carcinomas. Methods used: 40 endometrioid (well-differentiated =14; moderately differentiated =18; poorly differentiated n=8) and two serous adenocarcinomas were stained using a polyclonal antibody to CRBP-1. Staining was graded according to the percentage of tumor cells stained: intense (>75% positive), intermediate (25-75% positive) and weak or absent (<25% positive). The slides were examined independently by two pathologists, with an intervariability of less than 5%.
Summary of the results: CRBP-1 staining was mainly cytoplasmic. A high expression of CRBP-1 was observed in atypical hyperplasia and well-differentiated adenocarcinoma, with no significant differences between these two groups. The positivity was the highest in areas of squamous differentiation. A significant decrease of CRBP-1 immunostaining was detected with the progressive increase of histological grade of endometrial carcinomas. In fact, a comparison of CRBP-1 immunodetection and the degree of tumor differentiation revealed significant statistic differences (G1 vs G2: $P<0.005$, G1 vs G3: $P<0.005$ and G2 vs G3: $P<0.005$, respectively). The decrease of CRBP-1 expression in moderately and poorly differentiated carcinomas was parallel to that of estrogen and progesteron receptor positivity. In areas of different degree of differentiation in the same tumor, a variable CRBP-1 expression was maintained. Serous carcinomas were almost CRBP-1 negative. In 39.5% of cases (75% of them well-to moderately differentiated carcinomas), nuclear staining also observed. In contrast to cytoplasmic staining, nuclear CRBP-1 positivity was focal, and positive nuclei alternated with negative nuclei even in the same neoplastic glandular structure. Conclusions: Cytoplasmic staining for CRBP-1 can be considered a reliable method to support histological grading of endometrial carcinoma. Further studies are needed to define the biological role of these different patterns of CRBP-1 expression in endometrial neoplasms.

P 781
STRONG IMPACT OF VASCULAR PROLIFERATION, VASCULAR MATURATION AND LYMPHANGIOGENESIS ON PROGRESSION OF ENDOMETRIAL CANCER

STEFANSSON Ingunn, SALVESEN Helga B., AKSLEN Lars A.
The Gade Institute, Section for Pathology;
Department of Clinical Medicine, Section for Obstetrics and Gynecology, University of Bergen, Haukeland University Hospital, Bergen, Norway

Introduction:
In endometrial carcinoma, studies have reported reduced survival in tumors with high microvessel density.However, MVD might have limitations as a prognostic factor.The biological and clinical significance of lymphangiogenesis has not been much studied, predominantly due to the lack of specific lymphatic markers. Metastatic spread to regional lymph nodes is an important prognostic indicator, but lymphangiogenesis has not been previously studied in these tumors.
Purpose of the study:
To examine the significance of other angiogenic markers in endometrial cancer, especially vascular proliferation (by Ki-67/Factor-VIII staining) and vascular maturation (by á-SMA/Factor-VIII staining), as well as lymph vessel density (LVD) in a large and population-based series of endometrial carcinoma (n=281), with long and complete follow-up.
Methods used:
Paraffin-embedded tumor tissue was examined immunohistochemically by using double staining for Ki-67/F-VIII (vascular proliferation) and SMA/F-VIII (vascular maturation). To assess lymphatic vessel density (LVD), we used the LYVE-1 antibody. Tumor sections were scanned at low magnification to identify areas with the highest amount of vessels (“hot spots”), either stained by double-staining or LYVE-1. A panel of angiogenic factors (VEGF-A, VEGF-C, VEGF-D and bFGF) was also examined in this series, by Tissue Microarray analysis. The information was related to other molecular markers, clinico-pathologic data and patient prognosis.
Summary of the results:
Median vascular proliferation index (VPI) was 3.9%, and high VPI was associated with features of aggressive tumors like presence of necrosis, high FIGO stage, and decreased survival in multivariate analysis. The prognostic impact was superior to that of microvessel density. Median vascular maturation index (VMI) was 35%, and low VMI was significantly associated with vascular invasion and poor prognosis in univariate analysis. Peri-tumoral lymphatic vessels were found in 39.5% of the cases, and high LVD-pt was significantly associated with features of aggressive tumors and decreased survival.
Conclusion:
Other tissue-based angiogenic features than microvessel density, in particular vascular proliferation, should be evaluated as a part of the angiogenic profile of human

tumors. Peri-tumoral lymphatic vessel density also seems to play a significant role in the proggression and prognosis of endometrial carcinoma.

P 782
MICROSATELLITE INSTABILITY AT TETRANUCLEOTIDE REPEAT IN TYPE I ENDOMETRIAL CARCINOMA

*CHOI Jin, *CHOI Ho-Sun, KIM Hyun-Joong, NAM Jong-Hee, PARK Chang-Soo, JHUNG Sang-Woo
Department of *Obstetrics & Gynecology and Pathology, Chonnam National University Medical School, Gwangju, South Korea

Defects in the DNA mismatch repair (MMR) system results in a mutator phenotype, which is manifested as microsatellite instability (MSI). Colon cancers exhibiting MSI could be divided into 2 forms: MSI-high(MSI-H) and MSI-low(MSI-L), based on the observed frequency of genomic mutations. Noncolonic human cancers also show two types of MSI. One group shows a high frequency of MSI at mono- and di-nucleotide repeats similar to colon MSI-H type tumors. Another group rarely exhibits MSI in the mono- and dinucleotide repeats but does often exhibits MSI in the tri- or tetranucleotide repeats. This distinctive subtype of MSI is termed 'elevated microsatellite alterations at selected tetranucleotide repeat (EMAST)'. In contrast to MSI-H tumors, the underlying molecular mechanisms for MSI in MSI-L or noncolonic EMAST tumors have not been clarified.

In order to investigate the prevalence of MSI at tetranucleotide repeat in Type I endometrial carcinoma and the correlation between MSI staus and alterations of MMR gene, such as hMLH1 and hMSH2, we examined the 3 mono-, 3 di- and 6 tetra-nucleotide repeat markers by PCR and denaturation gel electrophoresis and the expression of hMLH1 and hMSH2 protein by immunohistochemistry in 39 Type I endometrial carcinomas.

The presence of at least one new allele, consistent with MSI, was observed in 9 (23.1%) at mononucleotide repeat, in 6 (15.4%) at dinucleotide repeats, and in 23 (59.0%) at tetranucleotide repeats of 39 endometrial carcinomas. MSI was divided into high frequency of MSI (MSI-H), single EMAST and multiple EMAST by the number of affected loci. MSI-H was detected in 9 (23.1%) of 39 patients, and single EMAST and multiple EMAST were noted in 10 (25.6%) and 4 (10.3%) of 39 carcinomas, respectively. MSI status was not associated with clinicopathologic features, such as FIGO stage, histologic grade and depth of invasion. Of 39 carcinomas, 12 (30.8%) showed an absence of hMLH1 expression, 8 (20.5%) revealed an absence of hMSH2 expression, and 16 (41.0%) tumors demonstrated the absence of either hMLH1 or hMSH2 expression. Seven (77.8%) of 9 MSI-H tumors, 2 (20.0%) of 10 single EMAST tumors, and 3 (75.0%) of 4 multiple EMAST tumors revealed the absence of either hMLH1 or hMSH2 expression.

These resulsts suggest that MSI-high and multiple EMAST endometrial carcinomas are highly associated with alterations of hMLH1 or hMSH2 and single EMAST tumors may be associated with another mechanism.

P 783
THE ASSESSMENT OF THE EPITHELIOSTROMAL MICRO ANATOMICAL RELATIONS IN THE UTERUS EPITHELIUM METAPLASIA

G.S Dragoi, Galbenu M., Patrascu M., P.R. Melinte, Rodica Silca, A.F. Vreju
Academic Hospital Filantropia Craiova Romania
University of Medicine and Pharmacy from Craiova

Objectives. The transformation and evolution sometimes abnormal of the endometrium and endocervix epithelium frequently become a dilemma for the pathologist. It draws the attention to the unknown problems of the metaplasia phenomena: the determined factors of the metaplasia genesis, the morph and functional epitheliostromal relations and finally its integration in neoplazia and displasia.
Purpose of the study. We proposed ourselves to identify and evaluate the potential of phenotype transformation of the epithelial cells and metaplasic epithelial structures inside uterus glands.
Materials and methods. We studied 400 cases of metaplasia of the uterus ephitelium, investigated by histologic and histochemic visualization methods for the epithelium cells, fiber elements of the extra cellular matrix and glicosaminoglicans.
Results and conclusions. The epithelial and stromal structures of the endometrium and endocervix suffer cycle transformations that we integrated inside “uterus epithelium remodeling cycle”. The extra cellular matrix integrates itself in this cycle but also in the processes of angiogenesis and apoptosis. Ortomeplasia imposes the evaluation of the epithelial transformations in ontogenesis and during normal and pathologic hormonal cycles. We discuss the integration of mataplasia in displasia and neoplasia pathomorphogenesis.
Key words: uterus, metaplasia, displasia, epithelium

P 784
AN IMMUNOHISTOCHEMICAL COMPARISON BETWEEN LOW GRADE AND HIGH GRADE OVARIAN SEROUS CARCINOMAS: SIGNIFICANTLY HIGHER EXPRESSION OF P53, MIB1, BCL2, HER-2/NEU AND C-KIT IN HIGH GRADE NEOPLASMS

C.J. O’Neill 1, M.T. Deavers 2, A. Malpica 2, H. Foster 3, W.G. McCluggage 1
1 Department of Pathology, Royal Group of Hospitals Trust, Belfast, Northern Ireland.
2 Department of Pathology, University of Texas, M.D. Anderson Cancer Centre,
Houston, Texas, USA and 3 Department of Pathology, Belfast City Hospital Trust,
Belfast, Northern Ireland

INTRODUCTION: Recently, a dualistic pathway of ovarian serous carcinogenesis has been proposed based on morphologic observations and molecular genetic analysis. In this scheme, low grade OSC arises in a stepwise fashion from a benign serous cystadenoma through a usual serous borderline tumour through a micropapillary variant of serous borderline tumour. In contrast, the more common high grade OSC arises de novo from the ovarian surface epithelium.
PURPOSE OF STUDY: Although the division of OSC into low and high grade variants is gaining greater acceptance, and although there is accumulating molecular genetic evidence for this, there is little published information regarding a comparison of protein expression between these two types of OSC. In this study, we have investigated the immunohistochemical expression of a wide range of proteins in cases of low grade (n=22) and high grade (n=47) OSC.
METHODS: Antibodies used were p53, MIB1, BCL2, WT1, HER-2/neu, C-KIT, osteopontin and survivin. For all antibodies, except MIB1, cases were scored as 0 (negative or occasional positive cells), 1+ (<10% cells positive), 2+ (10-25% cells positive), 3+ (26-50% cells positive), 4+ (51-75% cells positive) or 5+ (>75% cells positive). For MIB1, the percentage of positive nuclei was calculated. SUMMARY OF RESULTS: There was a statistically significant higher expression of p53, MIB1, BCL2, HER-2/neu and C-KIT in high grade compared to low grade OSC ($p < 0.05$). Thirty of 47 (64%) cases of high grade OSC exhibited 5+ staining with p53 compared to 4 of 22 (18%) low grade neoplasms. Twelve of 47 (26%) high grade OSC exhibited 5+ staining with BCL2 compared to one of 22 (5%) low grade OSC. The mean MIB1 proliferative index in high grade OSC was 55.4 % compared to 23.0 % in low grade OSC. Virtually all cases

of both low grade and high grade OSC exhibited diffuse nuclear positivity with WT1 and diffuse cytoplasmic positivity with survivin. Osteopontin expression was variable with no significant difference in expression between low grade and high grade OSC. CONCLUSION: The significant differences in protein expression between low grade and high grade OSC provides further support for a different underlying pathogenesis. In particular, the differences in p53 immunoreactivity are in keeping with the observation that p53 gene mutation is more common in high grade than low grade OSC.

P 785

OVARIAN ENDOMETRIOID TUMOR WITH YOLK SAC TUMOR COMPONENT.

Alejandro Pascual+, Enrique Poblet+ and Monica Romeu*
(+)Servicio de Anatomía Patológica.
(*)Servicio de Ginecología y Obstericia.
Hospital General Universitario de Albacete (Spain)

Case Report:
A 47 year old woman was admitted to our Hospital for abdominal pain. Physical examination showed, on palpation, a painful and firm Douglas sac. Transvaginal ecography revealed a 104 x 107 mm solid and cystic mass, located on the left ovary. The wall of the cysts appeared thick and irregular.
Histologically, the mass showed endometrioid carcinoma areas intimately admixed with yolk sac tumor areas. Reticulo-microcystic, enteroid-glandular, and solid histological patterns were readily identified on the endodermal sinus component.
FIGO stage of the tumor at this time was I-A.
Five months later a metastatic liver nodule was identified, with a significant rise of the serum alfa-fetoprotein. Histological examination of the liver nodule showed metastasis of the endodermal sinus tract component of the ovarian tumor.
Discussion:
Neoplasms that reproduce extraembrionary tissues (trophoblast or endodermal sinus tissue) not always have a germinal cell origin. These neoplasms may also be derived from somatic cells, usually from endoderm or mesoderm.
A differential diagnosis between an endometriod tumor associated with a endodermal sinus tumor, and the endometrioid variant of the endodermal sinus tumor, should be establish. Features that support the diagnosis of an endometrioid tumor associated with an endodermal sinus tumour are: the older age of the patient, the presence of endometriosic focus, and the presence of a biphasic immunohistochemical staining pattern. The biphasic immunohistochemical staining pattern is characterized by the presence of areas that are positive for EMA, estrogen and progesterone receptors (that represent the endometroid component of the tumor), and areas that are positive for alfa-fetoprotein, and negative for EMA (that represent the endodermal sinus tumor component).
The response of this tumours to chemotherapy is poor and they are usually cis-platinum resistant. Poor prognostic should be expected

P 786

IMMUNOHISTOCHEMICAL DISTRIBUTION OF AN USEFUL ANTIBODIES PANEL FOR OVARIAN NEOPLASMS

Camelia-Doina Vrabie1, Aura Mihalcea2, V. Muresan2, Cristina Bordea2, C. Copaescu2, Marieta Costache2, Elena Ionica3; 1National Institute of Pathology “V. Babes”; 2Department of Surgery, Hospital “Sf. Ioan”, 3Molecular Biology Center, University of Bucharest

Introduction. Cancer of the ovary represents about 30% of all cancers of the female genital organs (WHO, 2003). In developed countries it is about as common as cancer of the corpus uteri and invasive cancer of the cervix. About 70-75% of patients with ovarian cancer have tumor spread beyond the pelvis at the time of diagnosis.
Aim. Immunohistochemical study of the main epithelial tumors of the ovary-serous and mucinous adenocarcinomas-is a valuable adjunct the trorough histologic examination. Using a wide panel of antibodies, as ER (estrogen receptor), PGR (progesterone receptor), EGFR (epidermal growth factor receptor), cerbB2 (HER2NEU protooncogene), PCNA (proliferative cellular nucleolar antigen), CA125, Ki67 ,P53 (P53 oncoprotein) and CK7 (cytokeratin 7) we have tried to find a “happy combination” for an early and precisely diagnosis of ovarian epithelial cancers.
Matherial and methods. We investigated immunohistochemical a group of 60 patients with serous (n=45, 45.75%), mucinous (n=12, 20%) adenocarcinomas and borderline tumors (n=3; 5%). We used the tristadium methods of Hsu (1981) Avidin-Biotin-Peroxidase. A number of 19 patientshave had peritoneal implants (31,6%) and tumors were bilateral in 7 cases (11,66%).
Results. The method used revealed that the ER was positive in 70% cases, PGR in 60%, PCNA in 61,66% and p53 in 63,33%, CA125 in 81,66% and the perimembrane pattern of cerbB2 in 63,33%. The majority of cases were the serous carcinomas.
Conclusions. The relevance of CA125-an useful antibody in ovarian cancer, also for metastatic disease-is limited because it is positive in many conditions (mesothelial proliferations, metastatic carcinomas, etc).
The ovarian serous carcinomas are an homogenous group from the standpoint of pathogenesis. The panel of antibodies was positive in more than 50% of serous carcinomas.
None of the antibodies or combination has a clearly established role for staging and prognosis of the tumor.
Only the three-tiered grading system has important prognostic and therapeutic implications.

P 787

DIFFERENTIAL EXPRESSION OF CADHERINS AND CATENINS ASSOCIATES WITH DISTINCT OVARIAN CANCER HISTOLOGICAL TYPES

HARDISSON David (1), SARRIO David (2), HERNANDEZ-CORTES Gines (3), SANCHEZ-ESTEVEZ Carolina (2), MORENO-BUENO Gema (2), SUAREZ Asuncion (1), PALACIOS Jose (2)
(1) Dpto. Anatomia Patologica, Hospital Universitario La Paz, Madrid, Spain
(2) Laboratorio de Cancer Ginecologico y Mamario, Centro Nacional de Investigaciones Oncologicas, Madrid, Spain
(3) S. Obstetricia y Ginecologia, Hospital Universitario La Paz, Madrid, Spain

BACKGROUND: Ovarian carcinoma (OvC) is the leading cause of death among all gynecologic malignancies. In the last years, it has been demonstrated that alterations in the cadherin-catenin adhesion complexes are involved in tumor initiation, progression and metastasis. The aim of this study was to evaluate the immunoreactivity of the cadherins and the catenins in ovarian cancer and to correlate their expression with clinicopathological features.
DESIGN: Immunohistochemical staining was performed in 85 ovarian carcinomas: clear cell (CCs), n=31; serous (SCs), n=28; endometrioid (ECs), n=13; mucinous (MCs), n=13) using a tissue microarray. Monoclonal antibodies against E-cadherin (4A2C7, Zymed), P-cadherin, N-cadherin, cadherin-11, beta-catenin, gamma-catenin, and p120ctn (Transduction Labs) were applied using the LSAB method.
RESULTS: Overall, membranous expression of E-CD, N-CD, and P-CD was observed in 96%, 29.8%, and 8.4% of the OvCs analyzed, respectively. Cadherin-11 was rarely expressed in tumor cells but frequently in the stromal cells adjacent to the tumor nests. Each of the cadherins was

differentially expressed among the histological types of OvCs: E-CD preserved expression was frequent in MCs (61.5%) but very rare in SCs (3.6%). Serous tumors showed the higher incidence of N-CD (67.9%) and P-CD (21.4%) expression compared to the other histotypes. MCs and CCs rarely expressed N-CD or P-CD. With respect to catenins, significative differences were observed among the histological types: CC tumors and SCs showed more frequently reduced or absent expression of beta-catenin, gamma-catenin and p120 than other types. MCs were characterized by the frequent preservation of the three catenins. Abnormal nucleo-cytoplasmic beta-catenin expression was clearly associated with the EC histotype, since all cases showing this pattern (12%) were endometrioid tumors ($p<0.001$). Cytoplasmic localization of gamma-catenin and p120 was observed in 4.5% and 7% of OvCs respectively, but these expression patterns were not statistically associated to any histological type.
CONCLUSIONS: Our results suggest that each of the different histological types of OvC show a distinct and characteristic cadherin and catenin expression profile that could help in the differential diagnosis of these tumors and could explain differences in biological characteristics, such as the ability to dissemination.
GRANTS: FIS PI020342 and PI020355.

P 788
STAGE I OVARIAN CARCINOMA. A DIFFERENT DISTRIBUTION OF HISTOLOGIC PATTERN
L.Deligdisch,P.Schlosshauer,D.Fatemi, F.Nezhat
The Mount Sinai School of Medicine (MSSM), New York N.Y.USA

INTRODUCTION.Only a minority of ovarian carcinomas are diagnosed in StageI. The histologic subtypes of ovarian carcinomas,despite their common epithelial origin, arise in different histogenetic settings being associated with different clinical and diagnostic implications.
PURPOSE OF STUDY is to identify histopathologic patterns of ovarian carcinoma that are likely to have an impact on early stage diagnosis.
METHODS USED. Histologic slides and clinical charts from 27 consecutive patients diagnosed from 2000 to 2004 at the MSSM with Stage I non-mucinous ovarian carcinoma were reviewed. The tumors were classified into serous papillary (OSPC),endometrioid (OEC)and clear cell (OCCC) carcinomas. Associated pathologic findings including ovarian endometriosis (OE),endometrial carcinoma (EC),endometrial hyperplastic polyps (EP) and clinical data (age of patients, history of breast cancer,presenting symptoms)were correlated with the histologic subtypes of the ovarian tumors.
SUMMSRY OF RESULTS. The histologic subtypes of the ovarian carcinomas were: 15 OEC(55%),8 OSPC (29%) and 4 OCCC (15%). In 12 patients the OEC arose in OE (44%) and their clinical presentation was pelvic mass due to endometriotic cysts. Concomitant EC was diagnosed in 7 patients (26%) and EP in two(0.07%). Four of these patients presented with vaginal bleeding. Of the patients diagnosed with OSPC three had histories of breast cancer,presenting with pelvic masses,one had concomitant EC presenting with vaginal bleeding and one was BRCA1 mutation positive, her ovarian carcinoma being diagnosed incidentally in the prophylactically removed ovaries. The remaining three presented with pelvic masses, of which one due to cystic endometriosis. The four patients with OCCC presented with pelvic masses, three arose in cystic endometriosis and one had concomitant EC with vaginal bleeding. The average age of the patients with OEC was 49,4, with OSPC 58,9 and with OCCC 67 years.
CONCLUSION. OEC and OCCC are more commonly diagnosed in StageI because of their frequent association with symptomatic OC and OE. OSPC, the most prevalent ovarian carcinoma overall, is less commonly diagnosed in StageI, more often, however, in patients with breast cancer histories who are closely followed. Our findings suggest that screening of patients with OE, endometrial pathology and history of breast cancer can contribute to diagnose ovarian cancer in earlier stages.

P 789
RELATIONSHIP BETWEEN P53-ASSOCIATED PROTEINS AND ESTROGEN RECEPTOR (ER) STATUS IN OVARIAN SEROUS NEOPLASMS
Eun Yoon Cho(a), YoonLa Choi(a), Seoung Wan Chae(b), Jin Hee Sohn(b), Geung Hwan Ahn(a)
a Department of Pathology, Samsung Medical Center, Sungkyunkwan University School of Medicine, Seoul, Korea
b Department of pathology, Kangbuk Samsung Hospital, Sungkyunkwan University School of Medicine, Seoul, Korea

Objective. This study was undertaken to evaluate the relationship between p53-associated proteins and ER status, and the methylation status of the ER CpG island in ovarian serous tumors.
Methods. We studied the immunoexpression of p14ARF, MDM2, and p53, and relationship between those protein expression and ERa in 158 cases of ovarian serous tumors, which comprised benign (n=23), borderline (n=41), and malignant tumors (n=94). We also investigated the methylation status of ER with correlation of ER status.
Results. The aberrant expression of p14ARF, MDM2, p53, and p53-associated proteins were observed in 19.6% (31/158), 47.5% (75/158), 39.9% (63/158), and 70.3% (111/158) of cases, respectively. The expression of MDM2 was significantly higher in borderline serous ovarian tumors than in benign ($P=0.04$) and malignant tumors ($P<0.01$). p53 expression in borderline tumors was not frequent and p14ARF expressional loss was mainly observed in carcinoma. Significant differences in the expressions of MDM2 ($P=0.01$), p14ARF ($P=0.04$), and p53-associated proteins ($P=0.02$) were observed between ER-positive and ER-negative cases. Methylation specific PCR for the ER CpG island revealed methylation bands in 48.3% (14/29) of borderline tumors, and in 36.4% (12/33) of malignant tumors. Methylation statuses of ER were not significantly related to ER status.
Conclusions. This study shows a significant association between ER status and p53-associated proteins, but no relationship between ER status and ER CpG island methylation. This study indicates that alteration of p53-associated proteins may affect tumor behavior in ovarian serous neoplasms, but ER methylation is probably not an important cause of ER loss.

P 790
AN IMMUNOHISTOCHEMICAL STUDY OF THE EXPRESSION OF ADHESION MOLECULES IN OVARIAN SEROUS NEOPLASMS
JiEun Kwon(1), Eun Yoon Cho(1), YoonLa Choi(1), Seoung Wan Chae(2), Jin Hee Sohn(2), Geung Hwan Ahn(1)
1Department of Pathology, Samsung Medical Center, Sungkyunkwan University School of Medicine, Seoul, Korea
2Department of Pathology, Kangbuk Samsung Hospital, Sungkyunkwan University School of Medicine, Seoul, Korea

To clarify possible roles of adhesion molecules including E-cadherin, beta, gamma-catenin, CD44s, CD44v6, CD56, and CD99 in ovarian tumor development and progression, an immunohistochemical study was undertaken for 23 cases of benign, 41 cases of borderline, and 94 cases of malignant ovarian serous neoplasms using tissue microarray (TMA). Significantly reduced expression of E-cadherin, and overexpression of CD44s, CD56, and CD99 were more frequently observed in malignant tumors than benign and borderline tumors. Reduced expression of E-cadherin was

also correlated with high tumor grade (P=0.03), presence of peritoneal seeding (P=0.03), and low overall survival rate (P=0.02). Overexpression of CD44s was significantly associated with high tumor grade (P=0.04), advanced stage (P=0.03), and low overall survival rate (P=0.02). CD56 was increasingly expressed in the case of advanced stage (P=0.008) and peritoneal seeding (P=0.002). Among all clinicopathologic factors, E-cadherin expression, CD44s expression and stage were correlated with overall survival in univariate study. The results of immunohistochemical analysis suggest that E-cadherin, CD44s, and CD56 may be useful prognostic markers for serous neoplasm of the ovary.

P 791

EARLY STAGE EPITHELIAL OVARIAN CARCINOMAS: A STUDY OF MORPHOLOGIC PROGNOSTIC FACTORS

USUBÜTÜN Alp, YILDIZ Iþýl, GÜLTEKÝN Murat, AYHAN Ali, KÜÇÜKALÝ Türkan.

There is limited experience with the early stage ovarian carcinoma. We intented to evaluate the prognostic factors that are commonly used, and reavaluated the diagnosis in the light of new knowledge especially related with borderline neoplasia.

For this purpose we examined 111 patients' slides chosen from156 clinical early stage patients from the files of gynecologic oncology between 1984-2001, we eliminated the patients if we didn't have that patients' slides in our laboratory, if no absolute data and/or microscopic features concerning that it's a primary ovarian carcinoma was present and if patients' disease was reported as higher stage after the operation. We reviewed the slides, blinded to the clinical outcome, using current diagnostic criteria and graded the neoplasm according to the system suggested by Shimizu and noted the presence or absence of endometriosis. Statistical analysis for survival was done by Kaplan Meier Analysis and group comparisons were made with Log Rank test.

86 patients were stage 1 and 25 patients were stage 2. Distrubution of histologic subtypes were as follows; 16 serous papillary carcinoma (%14.4), 14 mucinous carcinoma (%12.6), 16 endometrioid carcinoma (%14.4), 9 clear cell carcinoma (%8.1), 2 mixed carcinoma, 1 transistional carcinoma, 1 indiferantiated carcinoma, 26 serous borderline (%26), 17 mucinous borderline (%17), 3 endometrioid borderline (% 2.7), 2 serous cystadenoma, 3 mucinous cystadenoma, and 1 brenner tumor. There was statistically significant difference in survival between stage 1 and stage 2 patients (p=0.0188) and endometrioid type had a better prognosis than clear cell (p=0.0105) and mucinous type (p=0.0321). In contrast there was no statistically significant difference in survival between mitotic scores, architecture scores, cytology scores and tumor grades. Endometriosis was present in 19 (%17.1) patients and endometriosis mostly related with endometrioid and clear cell type carcinoma (p< 0.05).

As a result pathologist must be familiar with the borderline tumor when dealing with early stage ovarian carcinoma, because borderline tumors can be diagnosed as carcinoma erroneously especially by non-gynecologic pathologist. Stage is the only significant prognostic factor in the early stage ovarian carcinoma. In contrast to wide spread knowledge, "clear cell carcinoma" histologic type is not a poor prognostic factor and tumor grade has no effect on survival for early stage carcinomas.

P 792

EXPRESSION AND PROGNOSTIC VALUE OF MATRIX METALLOPROTEINASE 7 AND ITS RELATION TO BETA-CATENIN EXPRESSION IN EPITHELIAL OVARIAN CANCER

Reijo Sironen (1), Sari Sillanpää (1), Maarit Anttila (1,2), Kirsi Voutilainen (1), Kirsi Ropponen (1), Markku Tammi (3), Raija Tammi (3), Seppo Saarikoski (2), Veli-Matti Kosma (1)

1) Department of Pathology and Forensic Medicine, University of Kuopio and Kuopio University Hospital, P.O.B. 1627, FIN-70211 Kuopio, Finland. Phone: +358-500-675780, Fax: +358-17-162 753, Email: klpato@uku.fi

2) Department of Obstetrics and Gynecology, Kuopio University Hospital, P.O.B. 1777, FIN-70211 Kuopio, Finland

3) Department of Anatomy, University of Kuopio, P.O.B. 1627, FIN-70211 Kuopio, Finland

Introduction: Matrix metalloproteinase 7 (MMP-7) is a small member of MMP-family, which degrades various components of extracellular matrix. It has been shown that epithelial ovarian tumor cells produce MMP-7. Expression of MMP-7 has been shown to be regulated by beta-catenin.

Purpose of the study: To evaluate the prognostic significance of MMP-7 expression in human epithelial ovarian cancer. The relation between MMP-7 and beta-catenin expression was also studied.

Methods: Two hundred eighty four patients were diagnosed at Kuopio University Hospital and Jyväskylä Central Hospital, Finland, between 1976 and 1992. The median follow-up time was 29 months. The FIGO standards were used for staging. For histological typing and grading, the WHO classification was used. For immunohistochemical analyses, monoclonal antibodies for human MMP-7 and beta-catenin were used. Specimens were analysed by three independent observers and the intensity of staining and percentage area of positive tumor cells in the section were scored.

Results: Median percentage of MMP-7 expression was found to be 40%. A high percentage area (>40 %) of MMP-7 expression in tumor cells was significantly correlated with positive nuclear expression of beta-catenin (p=0.01). A low percentage area (< 40 %) of MMP-7 expression was correlated with high histologic grade of a tumor (p=0.003), advanced stage (p=0.002) and large primary residual tumor (p=0.005). A high percentage area of intense MMP-7 expression in tumor cells was found to be an prognostic factor predicting favorable disease related and recurrence free survival (p=0.0003 and 0.0052, respectively). Also in multivariate analysis a high percentage area of intense MMP-7 expression in tumor cells retained its prognostic power.

Conclusion: The low expression of MMP-7 in epithelial ovarian cancer cells is associated with high histologic grade, advanced stage and large residual tumor and the high MMP-7 expression with positive nuclear expression of beta-catenin. According to our results, the expression of MMP-7 seems to have prognostic significance in epithelial ovarian cancer.

P 793

CLINICOPATHOLOGICAL STUDY OF METALLOTHIONEIN IMMUNOHISTOCHEMICAL EXPRESSION, IN BENIGN, BORDERLINE AND MALIGNANT OVARIAN EPITHELIAL TUMORS.

N. Zagorianakou (1), P. Zagorianakou (1), G. Makrydimas (2), E. Briasoulis (3), V. Karavasilis (3), N J. Agnantis (1), Stefanou D. (1).

Departments of Pathology (1), Obstetrics and Gynecology (2) and Medical Oncology (3), Medical School, University of Ioannina, Greece.

Metallothioneins (MTs) are a family of cystein-rich metal-binding proteins, which are expressed in normal cells during fetal and postnatal life but also in a variety of human neoplasms. MT expression in human tumors has been linked to resistance to anticancer drugs and differentiation and progression in some types of tumors. This study examined the immunohistochemical expression of MTs in benign,

borderline and malignant tumors of ovarian surface epithelium and the possible correlations with clinicopathological parameters and survival. A total of 87 cases with diagnosis of ovarian surface epithelial tumors were included. Specifically, 21 cases of benign cystadenomas (11 serous and 10 mucinous), 14 borderline (low malignant potential tumors, 8 mucinous and 6 serous) and 52 cases of ovarian cancer were analysed.
Immunohistochemical expression of MT (cut-off level >10% of tumor cells) was clearly associated with malignancy. A statistically significant correlation was found between the expression of MT in cancer cases and benign tumors ($p<0.0001$) and cancer cases and borderline tumors $p= 0.003$. In cancer cases was observed a difference between grade I and III ($p=0.002$). There was no correlation of MT overexpression with survival in the small number of ovarian carcinoma patients where it was analysed. MT constitutes a marker that characterizes aggressiveness and a high malignant potential in ovarian epithelial tumors. In diagnostic problems MT may help distinguish between benign, borderline and malignant tumors.

P 794
INTRAOPERATIVE FROZEN SECTION DIAGNOSIS OF OVARIAN MASSES: HOW ACCURATE ARE WE?
TURAN Dilagah, YOLAC Evrim, MUEZZINOGLU Bahar
Kocaeli University Medical School Department of Pathology Kocaeli, TURKEY

In ovarian masses, intraoperative frozen section diagnosis is requested either to rule out malignancy or to verify the borderline or malignant tumor before proceeding with radical surgery.
A retrospectine study was conducted to determine the accuracy of frozen section diagnosis in ovarian masses.
We reviewed the frozen section diagnosis and permanent pathological diagnosis of 227 resected ovarian masses from May 1999 to December 2004. Frozen and permanent section diagnoses were divided into 3 groups: benign, borderline and malignant.
The accuracy, sensitivity,specificity, positive and negative predictive value of frozen section were studied.
Final histological diagnosis was benign in 173 (76.3%) cases, borderline in 8 (%3.5) cases and malignant in 46 (20.2%) cases. The sensitivity for malignant, borderline and benign cases were 93.4%, 87.5% and 99.4% respectively.There were one false positive and four false negative cases. The specificity for malignancy was 100%, for borderline 98.6% and 98% for the benign masses. The positive predictive value of a malignant frozen section diagnosis was 100%; the negative predictive value of a benign frozen section diagnosis was 98%.
Most of the false negative cases were belong to mucinous tumor group.Two mucinous adenocarcinomas were incorrectly diagnosed as borderline and a borderline mucinous tumor diagnosed as benign.False positive case was also a mucinous tumor having frozen section diagnosis of borderline mucinous tumor turned out to be a benign mucinous cystadenoma in permenant sections.
In conclusion, although we have limited number of borderline cases, the accuracy of frozen section diagnosis was high in benign, borderline and malignant cases.
Mucinous tumors constituted the main diagnostic problems in frozen section evaluation. Large masses with wide range of tissue types from benign to malignant underline the sampling errors leading to false frozen section diagnosis. Surgeons and the pathologists should be aware of the limitations of frozen section diagnosis particularly in mucinous tumors of the ovary.

P 795
OVARIAN WOLFFIAN TUMOUR: A CASE REPORT
R Sellami Dhouib, S Sassi, I Abbess, M Driss, K Mrad, K Ben Romdhane
Department of Pathology, Salah Azaiez Institute, Tunis, Tunisia.

Introduction: Ovarian wolffian tumors are defined according to OMS as tumor of presumtive wolffian origin characterized by a variety of epithelial patterns. This epithelial tumour may show diffuse solid tubular, hollow tubular and sieve-like patterns and a combination of the various patterns may occur. Altough more commun in the broad ligament, this tumour may occurs in the ovary.
Aims: To review clinical data, histologic features, immunohistochemical profile and to study the differencial of the ovarian wolffian tumor mainly from the endometroid carcinoma of the follopian tube.
Materials and methods: A 71-year-old woman presented with left ovarian tumour. Gross and microscopic finding were noted. Immunohistochemical stains for alpha inhibin was performed.
Results: Macroscopically, the tumour had 90x70x40 mm, lobulated, well circumscribed margins and was white and yellow. Histologic examination showed a well circumscribed islands or lobules of glandular and ductal epithelium in a back to back pattern. The lobules exhibited focal or extensive hyalinisation with obliteration of the epithelial component. The nuclei appeared moderately atypical and uniform. The central most part of the nodules appeared necrotic. The cells tumors were positive for alpha- inhibin.
Discussion and conclusion: The immunoreactivity of tumour cells with alpha inhibin and absence of squamous differenciation and destructive stromal invasion supported the wolffian nature of the neoplasm. Because of moderately nuclear atypia and striking mitotic activity, this tumor was considered as low grade malignancy.

P 796
THE RELATIVE FREQUENCY OF OVARIAN TUMORS AND THEIR AGE DISTRIBUTION OVER A 20 YEAR PERIOD IN SHARIATI TEACHING HOSPITAL, TEHRAN , IRAN .
- Maryam Kashanian, M.D, Assistant professor of Iran University of Medical Sciences. Department of Obstetrics and Gynecology , Tehran , Iran ,Tel : 0098217523487- Fax :0098217607016- Email : maryamkashanian@yahoo.com
- Naser Kamalian ,MD, Prof

Abstract:
Objective:
The evaluation of the relative frequency of ovarian tumors and their age distribution over a 20 year period in Shariati Teaching Hospital, Tehran, Iran.
Method:
A retrospective descriptive study was performed on all pathologic reports of ovarian tumors, from 1983 to 2003 in Shariati Teaching Hospital in Tehran, Iran. Then the relative frequency and their age distribution was evaluated .
Results:
493 ovarian neoplasia had been recruited. Surface epithelial tumors were the most frequent tumors with 283 cases (57.4%) followed by germ cell tumors with 152 cases (30.83%) and sex cord stromal tumors with 31 cases (6.28%). Metastatic tumors were present in 24 cases (4.86%) and the remaining 3 cases were 2 cases of luteoma and 1 case of chondroma. The most frequent benign neoplasia of the ovary was a dermoid cyst (mature cystic tratoma)(39.53%) followed by serocystadenoma (29.94 %) and mucinous cyst adenoma (14.82%) .
The most frequent ovarian malignancy was malignant serous tumors (53.69%) and then metastatic tumors (16.1%) and

mucinous cyst adeno carcinoma (14.09%). The most frequent age group was the 21-30 years old (111 cases).
Conclusion:
In this study the surface epithelial tumors were less than other studies, and the germ cell tumors were more so. It may have been due to the younger age of our patients or genetic factors. Metastatic tumors were more frequent probably due to the late diagnosis of malignancies.
Between sex-card stromal tumors, the most common tumor was fibrothecoma. Whereas in other studies granulosa – theca cell tumors were the most frequent. Genetic and racial factors may have played a role in this.
Key words:
Ovarian tumors, benign ovarian neoplasia, malignant ovarian neoplasia, Iran.

P 797

IMPORTANCE OF IMMUNOHISTOLOGICAL ER, PR EXPRESSION IN TUMOR FOR ENDOMETROID OVARIAN CARCINOMA HORMONOTHERAPY

E. Simonchuk, L. Zakhartseva, Y. Kokhanevich, M.Klevetenko

I. Introduction.
Endometroid ovarian carcinoma makes up 20% of ovarian carcinomas. Hormonotherapy of endometroid ovarian carcinoma equally with surgical treatment and chemotherapy improves patient's survivability and quality of their lives.
The aim of this investigation is to specify the hormonotherapeutic indications in patients with endometroid ovarian carcinoma taking into account the level of tumor's differentiation, receptors content to steroid hormones.
II. Materials and methods.
We examined 38 endometroid ovarian carcinoma patients. The immunohistochemical analysis for estrogen/progesterone receptors (ER/PR), was performed using formalin-fixed. The dependence between the level of tumor's differentiation and estrogen/progesterone receptors content in it was found.
III. Results.
Endometroid ovarian carcinoma is characterized by the high level of estrogen – 66.7% and progesterone – 98.8% in women in menopause (61-67 years old) with G I-II.
The absence of estrogen receptors expression , and the high level of progesterone receptors expression were noted in 32% of women in menopause with G I-II. The low estrogen/progesterone receptors content in women in menopause and their absence were noted in 86% of endometroid ovarian carcinoma women in childbearing age (27-42 years old) with G III-IV. Prescription of Depo-Provera 500mg once a day during 3 weeks together with single dosing of Carboplatin and Mitotaks resulted to the tumor decrease up to 2-3 sm, revealed after Second Look, comparatively with initial data of patients with III level of endometroid ovarian carcinoma with G I-II.
IV. Conclusion.
In complex treatment of endometroid ovarian carcinoma patients the hormonotherapy was used effectively in every case of finding out the high level of estrogen/progesterone receptors expression in tumor's cells.

P 798

LOCALIZATION OF ABCC2 (MRP2, CMOAT) IN NUCLEAR MEMBRANE OF OVARIAN CARCINOMA CELLS CORRELATES WITH RESISTANCE TO CISPLATIN AND CLINICAL OUTCOME

Pawel Surowiak1,2, Verena Materna2, Irina Kaplenko3, Marek Spaczynski3, Barbara Dolinska-Krajewska1, Elzbieta Gebarowska1, Manfred Dietel2, Maciej Zabel1,4, Hermann Lage2
1 Chair and Department of Histology and Embryology, University School of Medicine, Wroclaw, Poland
2 Charité Campus Mitte, Institute of Pathology, Berlin, Germany
3 Chair and Department of Obstetrics and Gynaecology, University School of Medicine, Poznan, Poland
4 Chair and Department of Histology and Embryology, University School of Medicine, Poznan, Poland

Because the majority of ovarian cancer patients are diagnosed in an advanced stage of the disease, first-line therapy commonly consists of surgical resection, followed by platinum drug-based chemotherapeutic regiments. Unfortunately, second-line chemotherapeutic treatment merely achieve response rates of about 20%. These clinical observations indicate that long-term prognosis of ovarian carcinoma depends on intrinsic and acquired drug resistance. In vitro experiments demonstrated that multidrug resistance-associated protein-2 (ABCC2) overexpression can confer resistance to platinum-containing anticancer drugs like cisplatin and carboplatin to cancer cell lines including ovarian carcinoma cells
In the present study we analyzed the expression and cellular localization of ABCC2 in ovarian carcinoma-derived cell lines exhibiting different levels of resistance against cisplatin and in a group of post-surgically platinum-containing drug treated ovarian cancer specimens taken from first-look laparotomies and from secondary cytoreductions in the same group of patients. ABCC2 expression was correlated in dependence on cellular localization with sensitivity against cisplatin or clinical outcome.
The analyses were performed on samples of ovarian cancer originating from 73 laparotomies and on 11 ovarian cancer cell lines. To check specificities of antibodies by reproducing the cellular localization of ABCC2 described in other studies, immunohistochemical reactions were performed on two tissue microarrays (TMAs).
The performed immunohistochemical reactions on the level of light and electron microscope showed, that ABCC2 expression in nuclear envelopes of studied cells significantly correlates with cisplatin resistance. In tumor samples we have shown, that nuclear ABCC2 expression is specific for cases of shorter overall- and progression-free survival.
This study for the first time demonstrates, that ABCC2 can be expressed in nuclear envelope and this localization is specific for cisplatin-resistant ovarian carcinoma cases.

P 799

GRANULOSA CELL TUMORS FREQUENTLY EXPRESS EGFR (HER-1), HER-3, AND HER-4: POTENTIAL RELEVANCE TO NOVEL ANTI-HER THERAPIES

Sebastian Leibl 1, Farid Moinfar 1, Koppany Bodo 1, Margit Gogg-Kammerer 1, Andelko Hrzenjak 1, Edgar Petru 2, Raimund Winter 2, Helmut Denk 1 .
1 Department of Pathology, Medical University of Graz, Austria
2 Department of Obstetrics and Gynaecology, Medical University of Graz, Austria

Granulosa cell tumors (GCT) of the ovary are rare sex cord-stromal tumors. Up to 50% of patients develop recurrences which sometimes occur as late as 30 years following the initial surgical treatment. Although some recurrent tumors have been treated successfully by re-operation, radiation therapy and/or chemotherapy, the prognosis is usually poor.
The aim of this study was to analyze immunohistochemically the expressions of EGFR (Her-1), Her-2, Her-3, and Her-4 in 40 tumors comprising 38 adult type GCTs (AGCT) and 2 juvenile type GCT (JGCT). Thirty one cases (77,5%) were positive for at least one of the receptors EGFR (Her-1), Her-3, and Her-4. Twenty six out of 40 (65%) GCTs showed positive reaction for EGFR (Her-1). Eight tumors (20%) were exclusively positive for EGFR (Her-1). None of 40 cases

showed a positive reaction for Her-2. Positive reactions for Her-3 and Her-4 were observed in 18 (45%) and 23 (57,5%) tumors. Only one case (2.5%) was exclusively positive for Her-4. Four tumors (10%) showed positivity for Her-3 and Her-4 but were negative for EGFR (HER-1). While one of the two JGCTs was negative for all members of the Her-family, one showed reactivity for EGFR (Her-1), Her-3, and Her-4.
These findings may provide the basis for clinical trials using monoclonal antibodies against extracellular domain of EGFR (such as cetuximab) or small molecule inhibitors of EGFR (such as gefitinib). Furthermore, the expression of Her-4 in GCTs raises the intriguing possibility of treatment with Heregulin-beta2/PE40, a ligand toxin with known anti-proliferative effects on granulosa cell lines.

P 800
GRANULOSA-CELL TUMOURS OF THE OVARY: A STUDY OF 16 CASES
ELLOUZE Sameh, MAKNI Saloua, BAHRI Ibticem, GOUIAA Naourez, AYADI Lobna, GHARIANI Mekki, SELLAMI Ahmed, BOUDAWARA SELLAMI Tahya

Introduction:
The granulosa-cell tumors of ovary (TG) are the most known malignant tumours of the mésenchyme and sexual cords; they are rare, accounting for 2 to 5% of the whole of the malignant tumours of the ovary. These tumours are of two types; the adult type and the juvenile type.
Purpose: Through our results and after a review of the literature, we reported the epidemiological, anatomoclinical and therapeutical aspects of the TG of the ovary.
Methods used:
We made a retrospective study of 16 cases of TG that were examinated at the laboratory of pathological anatomy and cytology of the CHU Habib Bourguiba of Sfax, over 10 years period (1994-2003).
Resalts : The average age of our patients was 46 years for the adult type with extremes of age of 20 and 70 years and 35 years for the juvenile type; 19% of our patients were nulliparous, 31 % were menopausal women and an inductive treatment of ovulation was reported in 19 % of the cases; clinical symptomatology was dominated by the abdomino-pelvic mass and endometrial signs related to hyperoestrinism like disturbances of the menstrual cycle and post menopausic metrorragia. The tumour was unilateral in 94 % of the cases and bilateral in 6 % of the cases. Macroscopically, the tumor size was often important varying from 6 to 27 cm with a solido-cystic aspect in 50 % of the cases; histologically, the adult type was found in 94 % of the cases and the juvenile type in 6 % of the cases. The immunostaining was positive for the mesenchymatous markers (vimentine); variable positivity for the chromogranine, the NSE and the PS100 was observed. Association with endometrial lesions was noted in 44 % of the cases with simple hyperplasia without atypia in 25 % of the cases, polyp in 12,5 % of the cases and adenocarcinoma in 6 % of the cases. The treatment was surgical in all cases; only the patient with juvenile type was treated by chemotherapy. No relapse nor recurrence was noted after a follow up of 30 months for the adult type contrary to the juvenile type who developed multilocated metastasis.
Conclusion : granulosa-cell tumors are an interesting entity witch has several epidemiological and histological characteristics and a potential to aggressive behaviour.

P 801
ADULT TYPE GRANULOSA CELL TUMOR – MORPHOLOGICAL FEATURES
AMALINEI Cornelia*, BALAN Raluca*, PRICOP Florentina**, RADULESCU Doinita*, BUTUREANU Stefan**, DUMITRACHE Florentin**, COTUTIU Coriolan*
*Department of Pathology, University of Medicine and Pharmacy Iasi, Romania
**Department of Obstetrics and Gynecology, University of Medicine and Pharmacy Iasi, Romania

Granulosa cell tumors (GCT) account for about 5% of all ovarian tumors. They are usually unilateral and variable in size. Adult granulosa cell tumors (AGCT) account for approximately 1-2% of all ovarian tumors and 95% of all GCT. They occur more often in postmenopausal women, with a peak incidence between 50 and 55 years. 6 cases of AGCT were diagnosed in the Clinical Hospital of Obstetrics and Gynecology Iasi, in a 7 years period. The age of the patients ranged between 35 and 67 years, 4 of them (66.66%) being postmenopausal. The macroscopical appearance showed that all were unilateral tumors – 4 of them (66.66%) solid and 2 cystic (33.33%). After paraffin-embedding and usual stainings, we observed the granulosa cells as small, cuboidal to polygonal cells, arranged in anastomosing cords, and gland-like structures filled with an acidophilic material recalling immature follicles (Call-Exner bodies). Two tumors presented microfollicular and macrofollicular patterns. Three tumors (50%) presented also a thecoma component formed by sheets of cuboidal to polygonal cells (specifically called granulosa-theca cell tumors). In two of them both granulosa and theca cells presented aspects of luteinization (luteinized granulosa-theca cell tumors). Only one tumor (16.66%) was associated with simple hyperplasia of the endometrium (suggesting an active endocrine tumor). 4 of them (66.66%) presented areas of malignant transformation, 3 of them being associated with tumoral necrosis, 1 with calcifications, and 2 with vascular invasion. Although considered as benign tumors, only 5-25% of them being malignant, with an indolent course and only local recurrences, in the reported cases the tumors were mainly malignant (66.66%), two of them being highly aggressive, as vascular invasion was noted, and one of them was also advanced, with histologically confirmed implants of abdominal peritoneal surfaces.

P 802
SALPINGITIS WITH CHLAMYDIA TRACHOMATIS; POSSIBLE ROLE IN SECONDARY STERILITY
DAHI Fahed 1,2, HUDITA Decebal 1, CEAUSU Iuliana 1, HALALAU Florin 2, CEAUSU Mihai 2
1 – Department of Gynecological Pathology, Cantacuzino Hospital, Bucharest, Romania
2 – "Victor Babes" National Institute of Pathology, Bucharest, Romania

In etiopathogenesis of secondary sterility, salpingitis with various etiology plays an important role. The main infections of the tube in etiopathogensis of sterility, except gonorrhea, are Chlamydia Trachomatis, Mycoplasma Hominis and in post-partum streptococci and staphylococci.

This work is to demonstrate the role of Chlamydia Trachomatis infection in this matter.

A retrospective study was performed on 450 cases (women with age between 20 and 35 years) with secondary sterility, from which 160 cases (35,5%) had positive serology for IgM and 40 cases (9%) had positive cultures for C. Trachomatis from uterine cervix. Laparoscopic examination with prelevation of biopsies in 290 cases revealed in the majority of cases (280) chronic salpingitis with important sclerosis with obstruction of the tubal lumen and adhesions between fallopian tube and ovary and pelvic peritoneum. In five cases the histopathologic examination revealed the pattern of "salpingitis isthmica nodosa".

This high incidence of infection with important process of fibrosis demonstrates the main role of Chlamydia Trachomatis in the pathogenesis of sterility with tubal origin.

P 803

ANDROGENS AND PROGESTERONE IN PREECLAMPSIA

Dabirioskoei Atousa *,Golmohammadloo Sariyeh **,Nanbakhsh Fariba **
*Department of Obstetrics and Gynecology, Zanjan University of Medical Sciences, Zanjan, Iran
**Department of Obstetrics and Gynecology, Urmia University of Medical Sciences, Urmia, Iran

Hypertensive disorders of pregnancy are from the most common ones. As the pathogenesis of this disease is not clear yet and as there are so many reasons to prove the role of sex hormones in this disease, so this study tries to investigate the change of serum progesterone, total testosterone, free testosterone and dehydroepiandrosterone sulfate (DHEAS) levels in the patients with preeclampsia. Nineteen patients with preeclampsia who were referred to Kosar hospital of Urmia were compared gestational age and body mass index. All subjects were primigravid women. They were also compared considering those four mentioned hormones. T-test was used as statistical way of analysis. $P<0.05$ was considered as significant. Progesterone and free testosterone levels were significantly lower in patients with preeclampsia than in the control group ($p<0.05$). There were no significant differences in total testosterone and DHEAS. There were also no significant differences in maternal age, gestational age and body mass index. Sex hormone binding globulin can increases in preeclampsia, so that it can decrease the amount of free testosterone in serum. On the other hand progesterone can relax smooth muscle of vessels resulting decreasing of blood pressure. So it can be said that decreasing of progesterone in preeclampsia may indicate a role fore it in the pathogenesis of preeclampsia

P 804

THE ROLE OF P63 IN HYDROPIC ABORTION, PARTIAL HYDATIDIFORM MOLE, COMPLETE HYDATIDIFORM MOLE AND CHORIOCARCINOMA

Leandra Náira Zambelli Ramalho
Alfredo Ribeiro-Silva
Mariana Spigiorin Maggiori
Luiz Cesar Peres
Department of Pathology, Faculty of Medicine of Ribeirão Preto, University of São Paulo, Brazil

Gestational trophoblastic diseases (GTD) are a group of interrelated diseases of trophoblastic tissue that include partial hydatidiform mole, complete hydatidiform mole, invasive mole, choriocarcinoma, and placental site trophoblastic tumor. Choriocarcinomas are clearly malignant neoplastic lesions but hydatidiform moles are just abnormal placental tissues with potential to malignant change. Thus, the identification of biological markers that allow differentiate these pathologies in doubtful cases are important in clinical practice. P63 is a p53 homologue that is associated to several malignancies. In normal placentas p63 is expressed in cytotrophoblast cells. The role of p63 in gestational trophoblastic diseases, however, merits further investigation. This work was carried out to study the expression of p63 in hydropic abortion (HA) and gestational trophoblastic diseases, including partial hydatidiform mole (PM), complete hydatidiform mole (CM), and choriocarcinoma (CC). Immunohistochemistry with the antibody p63 (clone 4A4) was performed in 40 formalin-fixed paraffin-embedded samples of placenta tissue. The cases were selected to represent HA (n=12), PM (n=11), CM (n=12), and CC (n=5). The distribution of p63 was quantitatively assessed in cytotrophoblast cells and recorded as: + (0-25% of cells stained by p63), ++ (26-50%), +++ (51-75%), and ++++ (75-100%). The intensity of immunostaining was also evaluated as weak, moderate, or strong. Statistical analysis was determined by the Fisher test. Contrary to the other diagnoses, none of the choriocarcinomas analyzed exhibited positive cells for p63 (CC x CM, P=0.0036; CC x PM, P=0.0002; and CC x HA, P=0.0104). There were no statistical relationship between CM x PM (P=0.5008); CM x HA (P=0.2825); and PM x HA (P=0.0444). Concerning the intensity of immunostaining, there was statistical difference only between PM and HA (P=0.0045). The lack of p63 expression in choriocarcinomas indicates that this protein may be helpful in distinguishing CC from other GTD in challenging cases. We also verified that the intensity of p63 expression was much stronger in PM than in HA. Since sometimes is difficult to differentiate an abortion from partial hydatidiform mole because villous blood vessels may be not easily identified within villous with exuberant edema, this find may have clinical importance.

P 805

EXPRESSION OF EGFR IN MOLE HYDATIDIFORMS, EXAGGARATED PLACENTAL SITES AND NORMAL PLACENTAS AND KI 67 IN MOLE HYDATIDIFORMS AND NORMAL PLACENTAS

KUPESIZ YILDIRIM Gokben*, PESTERELÝ Hadice Elif*, ERDOGAN Gulgun*, SIMSEK Mehmet**, KARAVELI Fatma Seyda*
Akdeniz University School of Medicine Departments of Pathology* and Obstetrics and Gyneacology

PURPOSE:The aim of this study is to find out differences between expression of EGFR in complete, incomplete mole hydatidiforms, exaggareted placental sites and Ki 67 labeling index (LI) in complete, incomplete mole hydatidiforms and normal placentas.
METHODS:Parafin embedded sections of 18 incomplete, 7 complete hydatidiform moles, 19 exaggareted placental sites and 10 placentas (control group) were studied immunohistochemically for EGFR and Ki 67. Statistical analysis of the results were made using student t or ANOVA with post huc Tukey test.
RESULTS:Ki 67 was detected immunohistochemically in villous cytotrophoblasts and extravillous intermediate trophoblast of complete , incomplete hydatidiform moles, and only in villous cytotrophoblasts of control group. Ki67 LI of villous cytotrophoblasts differed significantly between complete and incomplete hydatidiform moles ($p < 0.01$). Ki67 LIs of hydatidiform moles were significantly higher than control group ($p < 0.001$).
Immunostaining of Ki67 in extravillous intermediate trophoblasts were not different between complete and incomplete hydatidiform moles ($p = 0.58$).
EGFR was detected in syncytiotrophoblast and cytotrophoblasts of complete and incomplete hydatidiform moles, and control group. Staining of villous cytotrophoblasts differed significantly between complete hydatidiform moles and control group ($p < 0.001$) and incomplete hydatidiform moles and control group ($p < 0.001$) but staining of villous cytotrophoblasts was not differed significantly between complete and incomplete hydatidiform moles ($p=0.10$).
EGFR expression of syncytiotrophoblast differed significantly between complete,incomplete hydatidiform moles and control group ($p < 0.001$).However the difference of syncytotiotrophoblasts immunopositivity between complete and incomplete moles was not significant ($p > 0.05$).
EGFR immunostaining was not detected either in extravillous intermediate trophoblasts of mole hydatidiformes or exaggarated placental site.
CONCLUSION:Expression of EGFR in syncytiotrophoblast and cytotrophoblasts is important in the pathogenesis of complete and incomplete hydatidiform moles. Negative staining of EGFR in exaggareted placental sites may show us that EGFR-releated family of oncogens does not play a role in the pathogenesis of exaggarated placental site. Ki67 LI can be a useful marker in differentiating complete and incomplete moles.

P 806

EFFECT OF OBSTRUCTIVE CHOLESTASIS ON GONADOTROPINS AND GERM CELLS APOPTOSIS IN THE ADULT MALE RATS

NOORI Mugahi, Mohammad Hossein., NABAVI, Mohammad Bagher
Department of Marine Biology, Faculty of Marine Sciences, Khoramshahr University of Marine Sciences and Technology , Khoramshahr , Iran

Obstructive cholestasis is associated with overproduction of endogenous opioids (EOP) , nitric oxide (NO) and cytokins in the blood streams. These consequences can be affected sex hormones. Since proper fertility will be resulting of physiological balance of sex hormones so that we investigated the relationship between obstructive cholestasis and sex hormones and apoptotic germ cells in adult male rats.

To study this, we used three groups of animals: Control (No-surgery), Sham (surgerical control), and cholestatic (surgical ligation of the bile duct). After 3 weeks all animal were killed by ether, and serum concentrations of inhibin B , FSH and LH were determined by ELISA and Radioimmunoassay respectively, testicular germinal cells apoptosis was evaluated by DNA fragmentation detected by in situ terminal deoxynucloetidyl Transfrase-mediated dUTP nike end labeling (TUNEL).

Results: The findings of this study were shown that LH and FSH levels were significantly decreased in cholestatic compared to control and sham groups ($p<0.05$). However, inhibin B level was significantly higher in cholestasis than control and sham ($p<0.05$),On the other hand, we could not be shown any significant difference in germinal cells apoptotic index between cholestatic and other groups ($P>0.19$).

These findings have been shown which as obstructive cholestasis was although decreased the levels of serum gonadotropins but it has no significant effector testicular germinal cells apoptosis.We were speculated that testicular germinal cell apoptosis was not only dependent on gonadotropin hormones but also other factors may involved.

P 807

MULTICENTRIC FIBROADENOMA WITH FLAT EPITHELIAL ATYPIA

Simona Stolnicu1, Simona Mocan2, Florin Coros3, Doiniþa Rãdulescu4
1Department of Pathology, University of Medicine Targu Mures, Romania
2Department of Pathology, County Clinical Hospital Targu Mures, Romania
33 th Surgical Clinic, University of Medicine Targu Mures, Romania
4Department of Pathology, University of Medicine Iasi, Romania

Introduction: Fibroadenoma of the breast represents a benign biphasic tumour, wich occurs most frequently under 30 years old. The epithelial component may show a wide spectrum of typical hyperplasia but very rare, this hyperplasia presents atypia. We present the case of an 18 years old woman, with 5 fibroadenomas in the left breast, two of them presenting flat epithelial atypia.

Matherial and method: The five tumours (25, 35, 55, 40, 45 mm diameter) were evaluated on hematoxylin and eosin-stained sections. Immunohistochemical studies were performed on formalin-fixed, paraffin-embedded tissue, using Actin, p 53, ki 67, ER, PR.

Results: All the five tumours had classic fibroadenoma's pattern. Two of them presented the replacement of the normal epithelium by a single or stratified epithelium (up to 3-5 cell layers), columnar type.The epithelial cells showed mildly atypia. The acini and ducts were distended and contained an eosinophilic material. They were surrounded by myoepithelial cells, wich were Actin-positive. The epithelial cells were ki 67, p 53, ER and PR-positive.

Conclusions: The presence of multicentric fibroadenoma, two of them with flat epithelial atypia increases the risk of developing cancer in this patient. Clinical and mamographic follow-up of this patient is necessary in the future. Six month later the patient developed three more fibroadenoma in the same breast, one of them with flat epithelial atypia.

P 808

LOCALISING NYBR-1 - A LASER-CONFOCAL AND IMMUNO-ELECTRON MICROSCOPIC STUDY

B. Sasse, Institute of Clinical Pathology, University Hospital Zurich, Switzerland
C. Zuber, Division of Cellular and Molecular Pathology, University Hospital Zurich, Switzerland
J.-P. Theurillat, Institute of Clinical Pathology, University Hospital Zurich, Switzerland
Z. Varga, Institute of Clinical Pathology, University Hospital Zurich, Switzerland
D. Jäger, Department of Oncology, University Hospital Zurich, Switzerland
H. Moch, Institute of Clinical Pathology, University Hospital Zurich, Switzerland

Background: NY-BR-1 is a breast differentiation antigen recently discovered by SEREX technology in a breast cancer patient. Here we report on the localisation of this antigen in breast cancer cell lines as determined by confocal laser microscopy and immuno-electron microscopy. Methods: NY-BR-1 transfected breast cancer cell lines were cultured on glass cover slips, fixed, permeabilised and labelled with an anti-NY-BR-1 antibody. Further examinations involved confocal laser microscopy or transmission electron microscopy. Results: NY-BR-1 is associated to cytoplasmic vesicles preferentially close to the nucleus and follows the architecture of microtubules. In metaphase nuclei, NY-BR-1 co-localises with the chromosomes. Conclusions: NY-BR-1 is associated to microtubules, to vesicles and to chromatin. This suggests a function of the protein in cytoplasmic trafficking and/or chromosomal regulation in mitotic nuclei.

P 809

Introduction: Breast cancer is a significant public health problem worldwide. Plenty of mammographic screening programs resulted in the detection of breast carcinomas at early stage. The presence of microcalcifications in mammogram not only correlates with breast cancer in many cases, but also sometimes is the only early sign of this disease. Nowadays, Computer Aided Diagnosis (CAD) systems may help radiologists detecting and classifying clustered microcalcifications, which is vital for proper treatment.

Objectives: The objective of this work was to evaluate the performance of the computerized classification method for automatically detected clusters of microcalcifications.

Materials and Methods: In our research we used 106 images from Digital Database for Screening Mammography (DDSM), among which 67 presented malignant and 39 benign cases. Our experiments were carried out in two steps: automatic detection and automatic classification. For the detection, previously developed morphological method has been used. Before the classification task was conducted, the whole set of mammograms was divided into two groups: training and testing sets, including the same number of images. Only images from training set were used to train the Support Vector Machine (SVM) classifier. The performance of the classifier has been tested on images from testing set.

Results: Automatic classification of clustered microcalcifications in mammograms is a final stage of CAD

system which helps the radiologist in diagnosis. According to ROC analysis the presented algorithms yielded Az=95,23%. Conclusions: The SVM classifier used in experiments gave very good results and will be used in further research on complex CAD system.

P 810
PRODUCTION AND CHARACTERIZATION OF ANTIBODIES TO ESTROGEN RECEPTOR-BETA ISOFORMS EFFECTIVE FOR USE ON ROUTINELY-PROCESSED HUMAN TISSUES

DIMOLEA Eugene(1), TINIAKOS Dina(2), PECHTELIDOU Anastasia(1), FLORENTIN Ida(1), KITTAS Christos(2), SEKERIS Constantinos(1), ALEXIS Michail(1)
1. Molecular Endocrinology Programme, Institute of Biological Research and Biotechnology, National Hellenic Research Foundation, Athens, Greece,
2. Laboratory of Histology and Embryology, Medical School, National & Capodistrian University of Athens,Greece.

Introduction-aim: Estrogen receptor a (ERa) expression is a well established prognostic and predictive marker for breast cancer. Recent data indicate that ERß, a recently described estrogen receptor type mainly expressed through two isoforms, ERß1 and ERß2, may also play a role in human breast cancer progression. Clinical studies suggest that a correlation may exist between breast cancer responsiveness to tamoxifen and ERß1 or ERß2 expression. The lack of suitable antibodies has been a preventing factor for the elucidation of the role of ERß isoforms in breast cancer prognosis and treatment. We aimed to produce monoclonal antibodies (mAb) to ERß1 and polyclonal antisera (pAb) to ERß2 effective for the immunostaining of routinely processed human tissues.
Methods: An appropriately designed synthetic peptide (ERß1 aminoacids 517-530) and an appropriate GST-fusion protein were used as immunogens for the generation of mouse anti-ERß1 mAbs and rabbit anti-ERß2 pAbs, respectively. Following well established techniques, a number of specific ? Rß1 mAbs and ERß2 pAbs have been produced as determined by Western blotting.
Results: One anti-ERß1 mAb and one anti-ERß2 pAb proved to be effective for use on formalin-fixed, paraffin embedded human tissues. Both antibodies produced intense nuclear staining in the majority of epithelial cells in normal breast, while in archival breast carcinoma tissues the percentage of ERâ expressing neoplastic cells as well as the intensity of immunostaining varied considerably between tumours. Expression of ERß was also observed in lymphocytes, fibroblasts, endothelial cells as well as squamous cells of the nipple epidermis.
Conclusions: The newly produced anti ? Rß-antibodies may prove useful for studying the expression of ERß isoforms at the protein level in normal and malignant breast tissues in an effort to assess their significance in mammary carcinogenesis and their value as prognostic and predictive markers in human breast cancer.

P 811
FOUR SYNCHRONOUS FEMALE GENITAL MALIGNANCIES: THE OVARY, CERVIX, ENDOMETRIUM AND FALLOPIAN TUBE

SAÐLAM Arzu, BOZDAÐ Gürkan, USUBÜTÜN Alp, KUZEY Gamze Mocan, KÜÇÜKALÝ Türkan, GÜLTEKÝN Murat, AYHAN Ali
Hacettepe University Faculty of Medicine

The coexistence of multiple primary carcinomas in the female genital tract, and especially the common occurrence of synchronous ovarian and endometrial adenocarcinoma is well-known. While the etiology of this phenomenon remains unclear, it has been postulated that tissues of a common embryologic origin when simultaneously exposed to certain carcinogens may develop synchronous neoplasms.
We present the unique case of a 63 year-old woman with coexistent adenocarcinoma of the ovary, endometrium, cervix and fallopian tube; all of which we believe to be separate primaries, supported by the fact that that all four lesions are of low grade and stage and exist together with neighboring preinvasive lesions. To our knowledge, four synchronous primaries involving each aspect of the female genital tract has not previously been reported.

P 812
THE STUDY OF THE ULTRASTRUCTURE AND HORMONAL VARIATION OF CORPUS LUTEUM IN FEMALE RATS FED ANETHUM GRAVEOLENS EXTRACT

MONSEFI M, GHASEMI M, BAHAODDINI A
Biology department, School of Sciences, Shiraz university

Anethum graveolens L.(Dill) as a medicinal herb, used as a remedy for inducer of menstruation and increase mother's milk production. Using too much dill leads to sexual weaknesses and decrease spermatogenesis. This investigation was preformed on 54 Wistar female rats with regular estrous cycle divided into 6 groups: control, sham, low dose of aqueous extract (0.045 gr/kg), high dose of aqueous extract (.045 gr/kg), low dose of ethanol extract (0.5 gr/kg) and high dose of ethanol extract (5 gr/kg). The above mentioned doses of extracts were orally administrated by feeding needle for 10 days. Blood samples were taken at the following steps: 1- Blood sampling from tail vessels before the beginning of experiment, 2- Blood sampling from dorsal aorta after the end of experiment. Estrogen and progesterone hormones were measured by Elisa and RIA methods, respectively. In order to ultrastructural study of the corpus luteum , ovaries were dissected. The data was analyzed by the ANOVA test to determine the significant difference at $p<0.05$.
The results indicated no significant difference in serum estradiol concentration, but the serum concentration of progesterone hormone increased significantly in high dose of aqueous and ethanol extract groups. Ultrastructural studies showed the increase of mitochondria, SER, RER and polyribosome in granulosa lutein cells of the high dose of aqueous and ethanol extracts administrated rats.

It may be concluded that high dose of aqueous and ethanol extract of Anethum graveolens L. act as LH hormone, which induced modifications on structure and synthetic activity of the granulosa lutein cells and lead to prolongation of luteal phase and increase progesterone hormone concentrations.

P 813
ENDOMETRIAL AVB3 INTEGRIN AND OSTEOPONTIN EXPRESSION IN FERTILE WOMEN AND INFERTILE PATIENTS

Jaume Ordi, Gemma Casals, Helena Suárez, Cristina Guix, Montserrat Creus, Elias Campo and Juan Balasch
Department of Pathology, and Institut Clínic of Ginecologia, Obstetrícia and Neonatology, IDIBAPS-Hospital Clínic, University of Barcelona, School of Medicine, Barcelona, Spain

Background: Osteopontin (OPN) is a glycosilated protein originally identified as a constituent of bone matrix that mediates cell adhesion and cellular signaling by binding to integrin heterodimers. Osteopontin is the ligand of one of the putative embryo implantation factor, avb3 integrin, and recent evidence has suggested that osteopontin and its receptor avb3 integrin are coexpressed in the human endometrium around the time of the "implantation window". The aim of this study was to evaluate investigate the endometrial expression of OPN and avb3 integrin as well as its temporal relationship

throughout the luteal phase in both normal fertile women and infertile patients.
Design: We studied 10 fertile controls and 88 infertile patients. All women underwent two endometrial biopsies during a single menstrual cycle (a midluteal biopsy on postovulatory day +7 to +8 and another biopsy four days later). Biopsies were evaluated according to the criteria of Noyes et al. avb3 integrin was detected in frozen tissue and OPN in formalin-fixed, paraffin-embedded material using the EnVision system. Immunohistochemistry results were correlated with the histological dating, cause of infertility (endometriosis, unexplained infertility or male infertility) and fecundity.
Results: OPN and avb3 integrin endometrial expression followed a similar pattern, with glandular expression increasing from histological day +3, when 37.5% of endometria expressed OPN and 0% expressed avb3 integrin, to day 9, when 100% co-expressed both factors. Co-expression of OPN and avb3 integrin was less frequently observed in out-of-phase than in-phase endometria (7.4% vs. 56.5%, $p<0.05$). However, no differences in the co-expression of OPN and avb3 integrin were observed between fertile and infertile women or according to the different causes of infertility. No relationship was observed between endometrial expression of these factors and fecundity outcome for subsequently untreated infertile patients.
Conclusions: Integrin avb3 and osteopontin expression are markers of endometrial maturation but their significance in terms of endometrial receptivity for embryo implantation in the clinical setting remains to be shown.
Acknowledgements.-This work has been supported in part by grant PI020036 from the Fondo de Investigaciones Sanitarias.

P 814
ANALYSIS OF GENE EXPRESSION IN LIPOSARCOMA OF MIXED TYPE
Kyung Un Choi, Do Youn Park, Jee Yeon Kim, Chang Hun Lee, Mee Young Sol, Hyun Jeong Kang, and Dong Hun Shin.
Department of Pathology, Pusan University College of Medicine, Busan, Korea.

Abstract : Liposarcomas of mixed type are rare. We experienced a case of liposarcoma composed of pelomorphic and well differentiated components. To identify molecular alterations in this tumor, gene expression in pleomorphic liposarcoma (PL), well differentiated liposarcoma (WDL), and normal adipose tissue (NA) was examined using cDNA microarray representing 17,000 genes. The cDNA microarray analysis showed that 6 genes in WDL, not in PL, were upregulated more than 5-fold compared to NA, and 40 genes in PL, not in WD, were upregulated. Other 6 genes in both WDL and PL, were downregulated more than 5-fold compared to NA. The differentially expressed genes included those associated with signal transduction, transcription, cell cycle, enzyme, structural protein, immune system and others. Our experimental data domonstrated that multiple genes are differentially expressed in liposarcoma of mixed type. It is suggested that these genes are involved with the differences in morphological characteristics and carcinogenesis of liposarcoma.

P 815
CLINICO-MORPHOLOGICAL AND CYTOGENETIC STUDY OF SOFT TISSUE LEIOMYOSARCOMAS
WYSOCKA Joanna, ILISZKO Mariola*, WASILEWSKA Anna, LACKOWSKA Bozena, JASZCZ-GRUCHALA Agnieszka, MARKIEWICZ Dorota, KRUCZAK Anna, SZPOR Joanna, MOSKAL Julia, KOLODZIEJSKI Leszek, RYS Janusz
Cracow Center of Oncology, *Dept. Biology and Genetics Medical University of Gdansk, Poland

Introduction: Leiomyosarcomas of soft part (SPLsa) are relatively rare neoplasms which estimate less than 10% of all malignant soft tissue tumours. What is more they were a heterogeneous group of neoplasms divided according to their localization. Thus the pathologists' experience concerning these lesions is limited.
Purpose of the study: The aims of study are: morphological and cytogenetic characteristics of neoplasm and the estimation of prognostic parameters for patients treated because of separate groups of SPLsa.
Materials and methods: Clinical records of 37 patients treated for SPLsa were reviewed. Formalin-fixed, paraffin embedded material from 44 tumours was available for routine examination in light microscopy. In 7 cases we had at our disposal the primary tumours as well as recurrent or metastatic ones. Two pathologists independently analyzed the slides stained with hematoxylin-eosin, Masson's trichrome and/or stained immunohistochemically. Immuno-histochemical reactions were carried out using the avidin-biotin complex immunoperoxidase technique (LSAB2+ kit) or ultravision labeled polymer. Small fragments of fresh tumour tissue from 24 cases were taken for ultrastructural and flow cytometric studies. Additionally, in 12 cases, short- term in vitro cultures from tumour material were used to obtain metaphases for cytogenetic analysis.
Results: Patients included 21 female and 16 men. The tumours localized in soft tissues of extremities (31 cases), retroperitoneal space (4 cases), head and neck region, abdominal cavity and thoracic or abdominal wall (2 cases each) The metastatic tumours were situated in lungs and subcutaneous tissue. Histologically, all tumours consisted of long fascicles which were built of the spindle cells with cigar-shaped nuclei and deeply staining eosinophilic cytoplasm. Masson's trichrome dyed the cell cytoplasm red. In 18 cases the additional MFH-like component of tumour was observed (so-called pleomorphic leiomyosarcoma) The tumour cell were stained positively for smooth actin (29 cases), and H-caldesmon (35 cases). Additionally the positive reaction to S100-protein, CD57 and CD68 were noticed in 6, 1, and 7 cases, respectively. Mitotic activity varies from 4 to 150 figures per 10HPF. 24 patients live from 15 to 155 months after tumour resection. For 8 patients who died the mean survival reached 30 months.
Acknowledgement: Supported by Polish Ministry of Science - grant no PBZ-KBN-091/P05/2003

P 816
SMALL ROUND CELL MYOEPITHELIOMA OF SOFT TISSUE: CLINICOPATHOLOGIC STUDY OF 3 CASES EXPANDING THE MORPHOLOGICAL SPECTRUM OF MALIGNANT MYOEPITHELIOMA.
SALGADO Roberto (1), GEBHART Michael (2), SEGERS Valérie (3), DELHOVE Olivier (4), LEEMPOEL Martine (5), DE SAINT AUBAIN SOMERHAUSEN Nicolas (1).
(1) Department of Pathology, Jules Bordet Institute, Brussels/ Belgium.
(2) Department of Orthopaedic Surgery, Jules Bordet Institute, Brussels/ Belgium.
(3) Department of Pathology, Brugmann Hospital, Brussels/ Belgium.
(4) Department of Pathology, Jolimont Hospital, Brussels/ Belgium.
(5) Laboratoire d'Analyses Morphologiques, Brussels/Belgium

Background:
Myoepitheliomas and mixed tumors (« pleiomorphic adenomas ») are well-characterized in salivary glands but have only recently been recognized as primary soft tissue neoplasms. The plasticity of myoepithelial cells is responsible for a broad morphological spectrum. Tumors are usually composed of epithelioid, spindle or plasmacytoid cells,

arranged in nests or intersecting cords within an abundant chondromyxoid or hyalinized matrix.
Design:
We recently encountered a few cases of malignant myoepithelial tumors of soft tissue with an unusual small round cell component, mimicking other small round cell malignant neoplasms. We present the clinicopathologic features of 3 cases of this rare morphological variant.
Results:
There were 2 male and 1 female patients aged 4-21 years at the time of resection. Tumors were located in the mediastinum, elbow and leg (within a nerve). Histologically, 2 tumors had infiltrative margins; the intraneural tumor was well circumbscribed. All tumors were composed predominantly (60-95% of tumor tissue) of sheets of dyscohesive small round cells, with scant eosinophilic or clear cytoplasm and round hyperchromatic nuclei. All cases showed a high mitotic index (>10 mitoses / 10 high power fields). In all tumors, foci composed of epithelioid cells, arranged in a reticular growth pattern within a chondromyxoid or hyalinized matrix, were identified in the surgical resection specimen.
In all cases, tumor cells expressed at least focally cytokeratins (AE1-AE3), epithelial membran antigen, S-100 protein, smooth muscle actin, calponin, and GFAP.
Two tumors recurred locally and one metastasized in an inguinal lymph node, after 2 years.

Summary & Conclusion:
We present 3 cases of malignant myepithelioma of soft tissue showing a previously unreported small round cell appearance. All tumors affected young patients and the 2 cases with available follow-up behaved aggressively. The diagnosis was based on the identification of areas showing classical morphological features of myoepithelial differentiation, and on the co-expression of S-100, GFAP, myogenic and epithelial markers.
Our study expands the morphological spectrum of myoepithelial tumors. The differential diagnosis of small round cell myoepithelioma includes metastatic carcinoma, poorly differentiated synovial sarcoma, PNET/Ewing Sarcoma, mesenchymal chondrosarcoma and desmoplastic small round cell tumor.

P 817
MALIGNANT PERIPHERAL NEUROEPITHELIOMA 'PERIPHERAL NEUROBLASTOMA' A CASE REPORT
Al-IRHAYIM Bedoor, YOUSIF Amer A.
Departments of Pathology and Surgery
College of Medicine
Mosul, Iraq

Peripheral neuroepithelioma is a rare malignant tumour of primitive peripheral non autonomic nervous system. The tumour can occur at any age involving soft tissue mainly of lower extremities. Other sites of occurrence are the shoulder-thoracic region and the head and neck. It is a very aggressive tumour with early metastasis mainly to the lung.
We report a case of 16 years old female who was presented with rapidly enlarging soft mass of labia majora. Physical examination revealed a 15x10 cm oval lobulated firm mass covered by normal skin on the right side of labia majora. There was no lymphadenopathy. The remainder of the physical examination of the patient in general, was within normal, so were routine laboratory tests.
The mass was excised followed by administration of chemotherapy and radiotherapy. The tumour was very cellular with wide areas of necrosis and viability around vessels. The cells are small and rounded arranged all over in Homer-Wright rosettes. Vascular invasion was noticed at the periphery of the tumour with retained rosettes formation of the intravascular clumps. However, 3 months after excision, the patient developed secondaries in the lung, with pleural effusion, but no local recurrence.
This is a rare case of Peripheral neuroepithelioma. This tumour is classified under peripheral neuroectodermal tumours (PNET). Histologically, it is reminiscent to neuroblastoma, but the two tumours vary in clinical aspect, behaviour, prognosis, and response to treatment.

P 818
PLEXIFORM CELLULAR SCHWANNOMA: THE HISTOLOGICAL, IMMUNOHISTOCHEMICAL, ULTRASTRUCTURAL AND CYTOGENETIC STUDIES OF A RARE CASE WITH A LONG FOLLOW-UP.
MARKIEWICZ Dorota, DRABIK Gra¿yna*, KRUCZAK Anna, ILISZKO Mariola**, WASILEWSKA Anna, LACKOWSKA Bozena, SZPOR Joanna, WYSOCKA Joanna, MOSKAL Julia, KOLODZIEJSKI Leszek, MIERZYNSKI Wojciech*, RYS Janusz
Cracow Center of Oncology, *Polish-American Children's Hospital, Jagiellonian University, Cracow, **Dept. of Biology and Genetics Medical University of Gdansk, Poland

Introduction: Cellular variant of schwannoma is defined as the hypercellular tumor composed exclusively or predominantly of Antoni A tissue, and devoid of formed Verocay bodies. The cellular schwannomas growing in a plexiform or multinodular pattern are extremely rare and their diagnosis controversial. We found only 15 described cases of plexiform cellular schwannoma (PCS). The longest clinical observation in all those cases was about 13 years.
Aims: The aims of the study are: presentation of the case of a very rare neoplasm with very long follow-up and the analysis of criteria of malignancy in peripheral nerve tumours.
Case report: A 1-year-old girl underwent surgery in a case of a deeply localized lateral neck tumour. After 4, 18 and 20 years she developed 3 recurrences treated by incomplete excisions. Since the last one, she has been living for 3 years with loco regional, slowly growing tumour. No malignant transformation nor metastases was observed.
Materials and methods: Formalin-fixed, paraffin embedded material from primary and all recurrent tumours were available for routine examinations in light microscopy. Immunohistochemical (IHC), ultrastructural, flow cytometric and cytogenetic studies were made on the tissue samples from the third recurrent tumour.
Results: Gross examination showed tumor of 11cm in diameter, composed of multiple, variable in size nodules. The histological examination showed plexiform tumor infiltrating thyroid gland and soft tissue. At higher magnification the tumor was composed of uniform spindle cells, arranged in fascicles of high cellular density. Their nuclei were of low polymorphism. Mitotic activity was 2/10 HPF, neither atypical mitotic figures nor necrosis were found. IHC stainings for S100 and CD57 were strongly positive, and reaction to p53 was negative. MIB index reached 2.0. Evaluation in electron microscopy showed neoplasmatic well differentiated Schwann cells. The tumor cells were diploid and S phase fraction reached 2.2. The karyotype of tumour cells was normal.
Discussion: PCS is a entity that resemble MPNST. In our opinion multinodularity, infiltrative tumor borders and local tissue destruction are designative for local recurrence but not for capacity to metastases. Low or moderate polymorphism of cells, low mitotic activity and MiB-1-index, low S phase fraction, and negative reaction to p53 protein, as well as normal karyotype can prove against malignancy and metastatic potential of the tumor.

P 819
ECTOPIC MYXOPAPILLARY EPENDYMOMA: AN UNCOMMON CASE ARISING IN THE PELVIS

HARADA Hiroshi1,2, HIROSE Takanori1, KANEYUKI Utako2, ARIMA Nobuyuki2,3,
NOGAMI Sei-ichiro4, HIRAI Nobuyuki5
1Department of Pathology, Saitama Medical School, Iruma, Japan
2Department of Pathology, Kurume University School of Medicine, Kurume, Japan
3Department of Clinical Pathology, Kumamoto City Hospital, Kumamoto, Japan
4Section of Laboratory Medicine, Oita-ken Saiseikai Hita Hospital, Hita, Japan
5Department of Gynecology, Oita-ken Saiseikai Hita Hospital, Hita, Japan

Myxopapillary ependymoma is a well recognized variant of ependymoma, which usually arises from the filum terminale. However, ectopic presentation in the pevis and around male and female genital tracts is extremely rare. We recently encountered a case arising in the pelvis of an elder Japanese female without any relationship to the spine, which was diagnosed as a myxopapillary ependymoma on basis of the histological appearance. The patient was a 69-year-old female, who was referred complaining of irregular genital bleeding in September 2003. Computed tomography and MR imaging revealed a mass lesion, which was measured approximately 8cm in the largest dimension and was located between the rectum and posterior wall of the vagina, but no relationship to the spine was confirmed. Two months later from initial presentation, transvaginal biopsy was performed along with resection of the uterus and left appendages, but failed to reach any specific diagnosis. In the middle of November 2003, the tumor was surgically removed. Microscopic examination revealed a lobulated mass lesion with dense fibrous septa, in which ovoid or polyhedral neoplastic cells were arranged in trabecular and reticular patterns against the background of loose myxoid stroma. In some areas, plump spindle cells showed solid growth with poorly organized fascicles. Intra- and extracellular hyaline globules were identified. Immunohistochemically, neoplastic cells showed diffuse positive reaction for vimentin and S100 protein, and focally positive for GFAP. Actins, desmin, CD34, cytokeratins, EMA, and Glut1 were completely negative. Follow-up observation detected a recurrent lesion three months later after surgical removal. But the lesion did not show aggressive growth and the patient is alive and well for a year. Myxopapillary ependymoma is not a highly lethal tumor and is designated as WHO grade I. Post-operative course in the present case would support the diagnosis. We present its histological features in detail and the literature is briefly reviewed.

P 820

BENIGN TRITON TUMOR: ABOUT ONE CASE

FATIHA BENADRA,HICHAM EL ATTAR,HANANE RAIS,BADIA BEELABIDIA

Benign Triton tumor of the hand: about one case
Introduction: The neuromuscular hamartoma or benign triton tumor is a developmental lesion composed of mature elements of both striated muscle and nerve.
Observation: A 22 years old woman presented a nodular mass of 1.5 cm in his finger; appeared since the birth. The excision was complete. Microscopic examination showed multiples nodules of fascicles striated muscles and nerves.
Discussion:
The benign triton tumor is rare. Large nerves are the most involved. Hand's location is unfrequent. The histological diagnosis has sometimes proved to be difficult. The differential diagnosis can be made with fibromatosis and rhabdomyoma. The pathogenesis still unclear and could be the result of incorporation of mesenchymal tissue into nerve sheaths during embryogenesis.

P 821

UNUSUAL PRESENTATION OF EWING SARCOMA IN A PATIENT WITH PLEXIFORM NEUROFIBROMA

METE Ozgur (*), BILGIC Bilge (*), DEMIRYONT Misten (*), OZGER Harzem (**), AYAN Inci (***)
(*) Istanbul University, Istanbul Faculty of Medicine, Department of Pathology
(**) Istanbul University, Istanbul Faculty of Medicine, Orthopedic Surgery
(***) Istanbul University, Institute of Oncology

Plexiform neurofibromas (PNF) are benign tumours of the peripheral nerves which mostly develop in patients with neurofibromatosis type 1 (NF1). Approximately in 10 % of NF1 patients, a malignant peripheral nerve sheath tumour (MPNST) emerges from a preexisting PNF. Ewing sarcoma, which is the second most common soft tissue malignancy in children has not been described in NF1 patients.
A 4-year-old female child presented with right thigh pain, swelling and with cafe au lait spots. MRI showed a large multilobulated mass. The plexiform tumour measured 50 cm. Immunohistochemical and architectural findings supported the diagnosis of PNF. Five years later, a mass measuring 16 cm in diameter occured in the soft tissue of left shoulder. Tru-cut biopsy revealed a high-grade, primitive small round cell malignancy. The neoplastic cells were diffusely immunoreactive for MIC-2. The cells were nonreactive for S100 protein, desmin, leukocyte common antigen, and keratin. The tumour was diagnosed as Ewing sarcoma. Initial treatment consisted of 3 cycles of chemotherapy (consisting of ifosfamide-etoposide alternating with vincristine, adriamycine, actinomycin-D and cyclophosphamide) (IE/VAC) every three weeks. Thorax computerised tomography revealed small lesions in both lungs, which were disappeared after 3 cycles of chemotherapy. After 3 cycles of chemotherapy the mass, which regressed radiologically more than 50%, was resected. The histopathological examination revealed 80 % of necrosis. Although the patient is now free of disease, she is going to have chemotherapy until 18 cycles will have finished.
Ewing sarcoma has not been described in NF1 patients. The immunohistochemical findings and response to chemotherapy justified our diagnosis. The t(11;22) (q24;q12) is the most detectable genetic changes in Ewing sarcoma, whereas the inactivation of the CDKN2A (9p21)is the second most common genetic alteration. It is noteworthy that the inactivation of CDKN2A is also responsible for the malignant transformation of PNF to MPNST. But there was no preexisting PNF in the left shoulder of our patient. Therefore, we can suggest that there may be a common genetic alteration on the gene regulating CDKN2A, which may be responsible for developing both tumour in our case.

P 822

HIGH NUCLEAR SURVIVIN EXPRESSION IS ASSOCIATED WITH METASTATIC DISEASE IN EWING SARCOMA

Aubert S*, Buob D*, Gonzales S*, Fron D°, Pichon F§, Leroy X*.
*Department of Pathology,CHRU Lille France
°Department of Pediatric Surgery, CHRU Lille France
§Departement of Oncology, Centre Oscar Lambret,Lille France

Introduction: Ewing's sarcoma (ES) is a small round blue cell tumour with a high incidence of metastasis and poor survival. Metastatic disease at diagnostic is the key adverse prognostic factor with a significant influence on relapse-free survival.

Recently, the overexpression of surviving, apoptotic inhibitor, has been shown to be correlated with unfavorable clinical outcome in several types of tumours.
Purpose: to assess the prognostic value of the immunohistochemical expression of survivin in ES of bone. This is the first study to evaluate the expression of survivin on ES.
Methods: Biopsy tissues of 24 consecutive patients with ES were assessed retrospectively for the immunohistochemical expression of survivin (monoclonal D-8, SantaCruz Biotechnology) by the streptavidin-biotin peroxydase procedure. For survivin, 1000 cells were counted and the percentage of positively stained nuclei was computed. A statistical analysis using the non-parametric Mann-Withney test was performed. Clinical data and follow-up were obtained by the patient charts.
Results: the series comprised 17 males for 7 females with a mean age of 17, 4 yrs (range 1-45 yrs). Metastases were present in 11 patients at diagnosis. Treatment consisted of chemotherapy, surgery and/or radiotherapy in all the patients. 8 patients developed metastasis and/or local recurrence after treatment. 5 patients died of the disease, 4 patients were alive with disease and 15 were alive without disease at last follow-up (mean follow-up : 26,8 months). Survivin immunostaining was only nuclear. The mean expression was statistically higher in ES with metastases (range : 0-26% ; mean 14,8 %) than in ES without metastasis at diagnosis (range : 0-23,7% ; mean 6,67 %) ($p=0,023$).
Comments: This preliminary retrospective study shows that a high level of nuclear survivin expression implied a more aggressive biological behaviour of ES of bone ($p<0,05$). So, survivin seems to be involved in the critical steps of cancer onset and may be associated with unfavorable clinical outcome.

P 823
ANALYSIS OF SEQUENTIAL SECONDARY CYTOGENETIC CHANGES IN EWING'S SARCOMA: A XENOTRANSPLANTATION MODEL
FERRER Jaime, NOGUERA Rosa, RUIZ Amparo, LOPEZ-GUERRERO Jose Antonio, BALLESTER Sandra, CARDA Carmen, PELLIN Antonio, LLOMBART-BOSCH Antonio.
Department of Pathology, University of Valencia, Valencia, Spain.

Background: Ewing's sarcoma (ES) is characterized by the specific cytogenetic event t(11;22)(q21;q24) and its variants, although minor cytogenetic aberrations have also been described, the most frequent being trisomy 8, trysomy 12 and the derivative chromosome der(1;16). Their prognostic relevance in ES is still unclear.
Purpose: Our aim was to evaluate the occurrence, frecuency and changes in the pattern of secondary numerical aberrations in a dynamic model of ES.
Methods: seven tumors were transplanted into athymic nude mice and sequentially maintained through serial passages, during a period of time ranging from 18 months to 6 years. Fresh samples from original tumors and their consecutive passages were cultured and karyotyped, and analyzed by means of comparative genomic hybridization (CGH), FISH, and image analysis (cytometry and morphometry). For CGH, tumor DNA and normal DNA from healthy donors were amplified, differentially labelled and cohybridized. FISH analysis with centromere-specific probes was carried out for chromosomes 8 and 12. Image analysis was performed with Isis 2.50 software (Metasytems, Germany).
Results: a good correlation between karyotypic changes and CGH and FISH results was found in all cases. All cases harbored the specific change t(11;22). The total mean number of numerical aberrations detected by CGH in the original tumors and their subsequent passages was low (1.9). Gain of chromosome 8, whether complete or restricted to the long arm, was the most frequent numerical aberration found by CGH (4 out of 7 tumors). Its appearance ranged from 0 to 26 months. In these cases, trisomy or tetrasomy of chromosome 8 was detected by FISH analysis. In two cell lines, gain of chromosome 8 was associated with gain of chromosome 12. Gain of 1q, loss of 16q (2/7 each) and other minor events were also detected by CGH.
Conclusion: gain of chromosome 8, whether associated or not with gain of chromosome 12, is the most frequent secondary change in ES. The cytogenetic heterogeneity in the pattern of occurrence of this numerical aberration could be related to the different proliferative advantage observed in these tumors.
*Supported by grants Prothest PN-503036 (European Comission) and PI040822 (Madrid, Spain)

P 824
CD117 EXPRESSION IN MALIGNANT TUMORS, OTHER THAN GIST
ARDELEANU Carmen 1, VASILESCU Florina 1, CEAUSU Mihai 1, ANDREI Florin 1,
IOSIF Cristina 1, MIHAI Mihaela 1, DOBREA Camelia 1, FLOREA-GRAMADA Zenaida 1, TERZEA Dana 1,
POPESCU Carmen 2, BUTUR Georgeta 1, NEAGU Maria 1, HALALAU Florin 1
1. "Victor Babes" National Institute of Pathology, Bucharest, Romania
2. Clinical Hospital, Craiova, Romania

CD117, the c-kit proto-oncogene product is a transmembrane receptor for stem cell factor, normally expressed by interstitial cells of Cajal of the gastrointestinal tract and by many others cells like: mast cells, melanocytes, germ cells, subsets of hematopoietic cells; it is expressed also by their malignant tumors. The positivity for CD117 in a tumor does not necessarily indicate a mutation of the gene. The problem to be solved is if a targeted therapy against CD117, may be useful only in GIST or equally in other CD117 positive tumors; for this reason it is necessary to assess a large number of such tumors.
We performed a tristadial indirect immunohistochemical method on formalin fixed, paraffin embedded sections for detecting CD 117 (Policlonal,DAKO,Denmark), CD34 (Monoclonal, BIOGENEX, USA) and Nestin (Monoclonal, Santa Cruz, USA).
We found a IHC positivity for CD117 in cases of : malignant melanomas (MM) (10), seminomas (6), disgerminomas (3), granulosa cell tumors (GCT) (2), phyllodes tumors of breast (BPT) (5), solitary malignant fibrous tumor (SMFT)(1), gastric glomic tumor (GGT) (1). The MM and the BPT presented also a positivity for Nestin; the SMFT and GGT were positive also for CD34.
We concluded that at least a part of various tumors expressing CD117 may be considered as extra GISTs. It remain to establish if all the CD 117 positive tumors could benefit a specific therapy.

P 825
RECURRENT AMPLIFICATION WITHIN CHROMOSOME 6P DETECTED BY FISH IN OSTEOSARCOMA
Gilda da Cunha Santos
Ontario Cancer Institute, Princess Margaret Hospital, University of Toronto, Toronto, Ontario, Canada and Department of Pathology, Universidade Federal de Sao Paulo, Sao Paulo, Brazil
Paula Marrano
Ontario Cancer Institute, Princess Margaret Hospital, University of Toronto, Toronto, Ontario, Canada
Paulo Nuin
Ontario Cancer Institute, Princess Margaret Hospital, University of Toronto, Toronto, Ontario, Canada

Maria Zielenska
Laboratory Medicine and Pathobiology, University of Toronto and Dept. of Pathology and Laboratory Medicine, The Hospital for Sick Children, Toronto, Ontario, Canada
Jeremy A. Squire
Ontario Cancer Institute, Princess Margaret Hospital, University of Toronto, Toronto, Ontario, Canada

Osteosarcoma (OS) is characterized by complex karyotype, high frequency of cytogenetic aberrations and gene amplification. Chromosomal instability (CIN) provides genetic diversity for OS tumour progression, but both the mechanisms that lead to CIN and the biological basis of the conferred selective advantage of genomic aberrations in this tumour are poorly understood. CGH studies have identified frequent amplification and rearrangement involving the central genomic region of 6p. A number of genes associated with oncogenesis such as RUNX2, TNFa and VEGF cluster to this region and their increased expression by amplification would be predicted to be associated with tumor progression. Moreover, the chromosomal domain hypothesis suggests that genes with a functional relationship may be closely linked within subchromosomal regions of the nucleus. Thus the location of a gene within a chromosomal territory is thought to influence access to the proliferative machinery responsible for specific nuclear functions, such as replication, transcription, splicing and repair. Segmental duplications within this region may facilitate amplification by homologous recombination. The aim of this study was to evaluate, by FISH technique, the frequency and distribution of 6p amplification in osteosarcoma. Fluorescence in situ hybridization (FISH) was performed on a 77 core tissue microrray of primary osteosarcoma using chromosome enumeration probe (CEP) for the centromeric region of chromosome 6 (SpectrumOrange, Vysis Inc., Downers Grove, IL). Hybridization signals were scored among 100 non-overlapping tumor cell nuclei using the following scoring criteria: disomy < or = 2 chromosome copies in > 90% of the cells, low trisomy 3 copies in > 10% but < 40% of the cells, high trisomy 3 copies in > or = 40% of the cells, low polysomy > or = 4 copies in > 10% but < 40% of the cells, high polysomy > or = 4 copies in > or = 40% of the cells. Numerical aberrations of chromosome 6 were observed in 7 out of 8 tumors. Low polysomy was detected in 4 cases, low trisomy in 3 and disomy in 1 case. An increase in the number of chromosome 6 may frequently occur in osteosarcoma. Further studies at molecular and clinical level must be carried out to identify the gene alterations reflected by polysomy 6 or amplification within 6p. Such studies may facilitate the detection of specific tumours subtypes and genes directly associated with OS-tumour progression and clinical response.

P 826

THE RESULTS OF PREOPERATIVE CHEMOTHERAPY AND/OR RADIOTHERAPY IN NONMETASTATIC HIGH-GRADE OSTEOSARCOMA OF THE EXTREMITIES

ONER Dincbas Fazilet*, DERVISOGLU Sergulen**,KOCA Sedat*, MANDEL Molinas Nil***,HIZ Murat****,KESMEZACAR Hayrettin****, OKSUZ Colpan Didem *,BICAKCI Ceylaner Beyhan* ,UZEL Burak***, KANBEROGLU Kaya*****Istanbul University, Cerrahpasa Medical Faculty, Departments of Radiation Oncology*, Pathology**, Medical Oncology***, Orthopedic Surgery****, Radiology*****

Purpose: To assess the role of neadjuvant chemotherapy and adding of radiotherapy to the chemotherapy in patients with nonmetastatic high-grade osteosarcoma of the extremities and to compare the response of therapies on local control, tumor necrosis rate and overall survival rate.

Methods and materials: Between 1990 and 2002, 61 extremity-localized nonmetastatic high grade osteosarcoma patients were treated with radiotherapy in our hospital. Thirty-eight patients were male and 23 patients were female. Median age was 17 years (11-66 years). All patients were treated with neoadjuvant chemotherapy. Chemotherapy schedule that was consisted of epirubicin, cisplatin and ifosfamide ¡À high dose methotraxate was given before surgery. In order to increase the chance of limb sparing surgery, preoperative radiotherapy was added to patients who refused amputation or whose limb-sparing surgery would have been difficult because of borderline respectability. Radiotherapy was applied usually between the second and the third cycle of chemotherapy. Radiotherapy was given 35 Gy in 10 fractions to 44 patients. Remaining 2 patients were treated with 46 Gy with 2 Gy/day. Chemotherapy was given 3-6 cycles after surgery. In the radiotherapy group tumor size was between 3-32 cm (median 10 cm). In the chemotherapy group tumor size was between 4-20 cm (median 10 cm).
Results: Fourty-four patients out of 46 patients who were treated with radiotherapy, had limb-sparing surgery. Thirteen patients out of 15 patients who were treated with only chemotherapy had limb-sparing surgery and 26 patients (56.5%) in radiotherapy group, 7 patients (46.7%) in the chemotherapy group had tumor necrosis rate ¡Ý90% (p=0.05). In the radiotherapy group the 5-year local control, disease-free and actuarial survival rates were 98, 38 and 52, respectively. In chemotherapy group the 5-year local control, disease-free and actuarial survival rates were 92, 41 and 31, respectively.
Conclusion: Preoperative radiotherapy helps to increase the tumor necrosis rate and the chance of extremity sparing surgery when combined with chemotherapy. Though local control and overall survival rates were higher in patients with treated radiotherapy and chemotherapy, this difference was not statistically significant. It is difficult to make definite conclusions, because this was a nonrandomized and retrospectively analyzed study and the quality and the quantity of the patients were not the same in two groups.

P 827

EXPRESSION OF E-CADERIN, P-CADERIN, BETA-CATENIN, APC AND C-ERBB-2 IN CONVENTIONAL OSTEOSARCOMAS OF EXTREMITIES

Guimarães APG, Cunha IW, Guimarães GC, Vilela RS, Soares FA. Research and Medical Center Hospital do Cancer, São Paulo, Brazil

Background: Several series of osteosarcomas (OS) have been reported in the literature, but debate still exists regarding the clinical prognostic factors for this disease. The WNT proteins form a large family of secreted signaling proteins implicated in the proliferation and morphology of several tumors. The prognostic importance of WNT pathway and c-erbB-2 expression in OS has not been totally clarified.
Methods: The present study included 97 extremities conventional OS cases (70 osteoblastic, 20 chondroblastic and 7 fibroblastic) retrieved from our files. Cases were stained immunohistochemically using antibodies against E-cadherin, P-cadherin, beta-catenin, APC and c-erbB-2. Expression of the markers was correlated with clinical data and local recurrence, distant metastasis, free-disease survival, and overall survival.
Results: Expression of E-cadherin was not observed in all cases of OS. However, expression of P-cadherin, could be observed in 94 cases (96.9%). All the three patients with loss of P-cadherin expression had overall survival less than 8 months. Positive APC staining was observed in 65 cases (67%). APC was more expressed in patients under 18yo (p=0.025). In patients treated with chemotherapy, positive immunoexpression of APC correlated with better survival. Patients APC positive had 69% of five year survival against

APC negative patients with 34% of five year survival. Only 3 cases showed immunoexpression of beta-catenin. Expression of c-erbB-2 was observed in 16 cases and did not show any correlation with clinical parameters and tumor outcome.
Conclusion: P-cadherin is the adhesion molecule expressed in extremities OS and loss of its expression is an indicative of worse prognosis. However it is a very infrequent event and further studies should be performed to validate this finding. Downregulation of APC was an important prognostic factor in patients treated with chemotherapy. Expression of beta-catenin and c-erbB-2 are infrequent events in OS, and did not correlate with clinical behaviour.

P 828
EVIDENCE OF GENETIC ALTERATIONS IN CHROMOSOME 11, 9, AND 2 IN EMBRYONAL AND ALVEOLAR RHABDOMYOSARCOMAS
KRSKOVÁ Lenka, KALINOVÁ Markéta, KOPECKÁ Pavla, HILSKÁ Irena, KODET Roman
Department of Pathology and Molecular Medicine, 2nd Faculty of Medicine, Charles University in Prague, Czech republic

Introduction: Rhabdomyosarcomas (RMS) are most common soft-tissue sarcomas of childhood. They are subclassified into two major subtypes - embryonal RMS (E-RMS) and alveolar RMS (A-RMS). Various chromosomal alterations have been described in both subtypes. Inactivation of tumor suppressor genes frequently occurs due to loss of heterozygosity (LOH). Mutations of one allele may be followed by a loss of the remaining wild-type allele.
Purpose: To study LOH in RMS in microsatellite loci at mismatch repair genes, at loci close to the genes coding p15 and p16, and at loci at 11p with three probable suppressor gene regions which may be involved in pathogenesis of RMS.
Methods: We used microsatellite polymorphic markers from the region 9p (tumor suppressor genes p15, p16), and from mismatch repair genes hPMS1, hMSH2 and hMLH1. The main attention was paid to telomeric region on 11p. We analyzed 11 patients with E-RMS and with 17 A-RMS. In all patients the presence of LOH was studied using frozen samples from tumor tissue taken at diagnosis. Each tumor sample was compared with constitutional DNA of the same patient obtained from peripheral blood or bone marrow aspirate.
Results: In the study 6/9 (67 %) informative E-RMS patients and 8/15 (53 %) informative A-RMS patients demonstrated LOH on at least one of the microsatellite loci in 11p region. The frequency of LOH for hMSH2 was 4/6 (67%) in E-RMS, and 2/11 (18 %) of informative A-RMS. For hPMS1 the result was 1/5 (20%) and 2/6 (33 %) of informative E-RMS and A-RMS, respectively. LOH in the region 9p was not detected in any of nine informative E-RMS and it was found in 5/14 (36%) A-RMS.
Conclusion: Our study demonstrates a frequent loss of heterozygosity on the short arm of chromosome 11 in both E-RMS and A-RMS and a relatively high frequency of LOH in 9p in A-RMS. High frequency of LOH in the locus D2S123 (hMSH2) in E-RMS may be caused by a relatively high portion of non-informative (homozygous) cases. At this stage of understanding it is impossible to speculate whether the described LOH are involved at early stages of the tumor development or whether they are secondary events of the tumor progression.
The study was supported by grants from Czech Ministry of Health 00064203, Czech Ministry of Education 0021620813 and Internal grant of FNM 9746.

P 829
RHABDOMYOSARCOMA OF THE SPINAL CORD: A CASE WITH IMMUNOHISTOCHEMICAL, ULTRASTRUCTURAL AND CYTOGENETIC STUDY
HEMMINGS Chris*, HALLAM Lavinia*, MAXWELL Lesley#, JAMMU Vapinder^
Departments of Anatomic Pathology*, Ultrastructural Pathology# and Cytogenetics^, ACT Pathology, The Canberra Hospital, ACT, Australia

INTRODUCTION
Although primary Central Nervous System (CNS) rhabdomyosarcoma has been described, it is very rare and is thought most often to arise from the meninges. We report a case of a spinal cord tumour showing rhabdomyoblastic differentiation on light microscopy, immunohistochemistry and electron microscopy. Cytogenetic analysis showed an unusual karyotype, which has not previously been reported in rhabdomyosarcoma.
METHODS
Case report
RESULTS
A 14 year old boy was found to have a contrast-enhancing spinal cord tumour at the level of the conus. At surgery the tumour appeared invasive and was not attached to the dura. Microscopy revealed a malignant tumour composed of rounded and spindled cells, with widespread rhabdomyosarcomatous differentiation, including strap cells. Although entrapped nerve fibres were identified within the infiltrative tumour, no evidence of a coexistant glial or other CNS neoplasm was found. Immunophenotyping confirmed positivity for vimentin, desmin and myoglobin.
Ultrastructural examination confirmed the presence of thick and thin cytoplasmic filaments, with clear evidence of sarcomere formation in places. Z bands were readily seen. Admixed myelinated neural cells were also seen, but there was no evidence of ependymal differentiation.
Cytogenetic analysis revealed an abnormal karyotype in 19 of 20 metaphases, containing a derivative chromosome 5 resulting from a t(5;18) translocation. The karyotype was: 45,XY,der(5)t(5;18)(p?15.3,p?11.2),-18 [19]/46,XY [1].
CONCLUSION
As only a small amount of tissue was available for study, we cannot entirely discount the possibility that this tumour represents myosarcomatous differentiation within a composite mixed or multiphasic malignant tumour. However, in the absence of any other evidence to the contrary, we present this as a case of apparent primary CNS rhabdomyosarcoma, with a novel cytogenetic aberration.

P 830
RHABDOMYOSARCOMA: CLINICOPATHOLOGIC REVIEW OF 36 CASES
DERVISOGLU Sergulen*,BAGCI Pelin*,OZTURK Kilicaslan Tulin*, CELKAN Tiraje**,MANDEL Molinas Nil***,ONER Dincbas Fazilet****
Istanbul University, Cerrahpasa Medical Faculty, Departments of
Pathology*, Pediatric Oncology**,Medical Oncology***, Radiation Oncology****

INTRODUCTION:Rhabdomyosarcoma (RMS) is the most common soft tissue sarcoma of childhood and adolescent periods and can seldomly be seen adults too. Despite all research, a single prognostic classification for modelling the treatment is still needed. The clinicopathological features of our recorded rhabdomyosarcoma cases are reviewed and the major prognostic factors are discussed.
MATERIALS AND METHOD: Thirtysix RMS cases diagnosed in our department between 2000 and 2005 were reevaluated with respect to age, sex, localization, histological type, immunohistochemical stains, therapy, recurrences, metastasis, survival time and correlations between these entities were studied.
RESULTS and CONCLUSION:Eleven Percent of our total malignant tumor material in this period was diagnosed as

sarcoma, among which 1,8% was RMS. The male / female ratio was almost equal and no significant difference was observed in survival between sexes (p>0,41). Cases below 10 years of age were 57%, between 10-20 were 23% and over 20 were 20% .Embriyonel RMS was the frequent histological type and had the best prognosis (p<0,002). Thirtyseven percent were located on head and neck region, 25% were intraabdominal. Desmin, HHF35, and Myogenin positivity of different intensities were observed in all cases . Fortyeight percent of the patients were at the stage of III or IV (IRS clinical classification) at the time of diagnosis. All of the cases were treated by chemotherapy (VAC) and radiotherapy whenever was needed. Some of the cases were inoperable , resection was done pre - or posttherapeutically in most of the cases. According to the clinical follow-ups ; 31% of the cases showed relapse or metastasis. The survival time was longer in early ages (p<0,02). Most of the chilhood cases were at the head and neck localization. If it was intracranial and parameningeal the survival time gets shorter and if there was spreading to serebrospinal fluid this time was too short . Histologic type may have an influence on prognosis and in the presence of alveolar component agressive course was expected, but it may be difficult to subclassify the tumor in a small biopsy specimen due to common use of FNAB or trucut biopsies because of the sample size and mixed nature of the tumor .

P 831
SPINDLE CELL RHABDOMYOSARCOMA IN ADULTS
BRACKO Matej, FRKOVIC GRAZIO Snjezana
Institute of Oncology Ljubljana, Slovenia

Spindle cell rhabdomyosarcoma (SCRMS), a rare variant of embryonal rhabdomyosarcoma, occurs mainly in the group of pediatric patients and is characterized by a predilection to male sex and paratesticular and head and neck location as well as very favourable prognosis which is superior to that of classical embryonal rhabdomyosarcoma. SCRMS is rare in adults and, to the best of our knowledge, only seven cases have been reported to date in patients older than 18 years.
To further elucidate the features of SCRMS occurring in adults we report additional three cases of this rare entity.
The tumours were identified in a 24-year-old woman, a 35-year-old man and a 39-year-old woman, and arose in the vulva, muscles of the calf and subcutaneous fatty tissue of the leg, respectively. They were all treated by surgery and chemotherapy. The first patient developed uncontrollable local recurrence in the pelvic soft tissues and died due to metastatic disease 22 months after the first surgery; the second patient developed inguinal lymph node metastases 24 months after surgery and was then lost to follow up; the third patient is alive with no evidence of disease 12 months after surgery.
Microscopically, the tumours were composed mainly of fascicles of relatively monomorphic spindle cells with eosinophilic cytoplasm and rare rounded or strap-shaped rhabdomyoblasts. Cross-striations could be identified in one case only. Immunohistochemically, all three tumors were positive for muscle specific actin (HHF35), desmin, myoglobin and MyoD1; two tumors were focally positive for alpha smooth-muscle specific actin, and none was reactive for S-100 protein.
The analysis of the data of the ten reported cases, including the three presented here, indicates that, as opposed to the pediatric group, SCRMS in adults shows no predilection to particular anatomic site or male sex, and is not associated with favourable outcome. In fact, its prognosis in adults seems to be equally poor as that of other histologic types of rhabdomyosarcoma.

P 832
HER-2 ONCOGENE AMPLIFICATION IN SYNOVIAL SARCOMA
Zoltán Sápi MD.Ph.D1, Zsuzsa Pápai MD.Ph.D2., Anett Hruska MD3, Imre Antal MD.Ph.D4, Miklós Bodó MD.DSc1, Zsolt Orosz MD.Ph.D5
1 Department of Pathology, St John's Hospital, Budapest, Hungary
2 Department of Oncology, National Helth Institute, Budapest,
3 Institute of Morphology and Physiology, Semmelweis University, Budapest
4 Department of Orthopedics, Semmelweis University, Budapest
5 Department of Pathology, National Institute of Oncology, Budapest

Background
The treatment regimens for synovial sarcoma (SS) is very limited, though this type of sarcoma seems to be more heterogeneous as it has been traditionally considered. The present study investigates the Her-2 oncogene status of 20 cases of SSs, whether the Her-2 amplification can be considered as an independent prognostic factor.
Materials and methods
Her-2 oncogene amplification was determined on smears (in each case frozen material was used from our tumor bank) using Fluorescence in Situ Hybridization technique (dual color FISH with centromeric probe of chromosome 17 and unique specific probe for Her-2 oncogene). Beside this, the DNA ploidy status was measured using image analysis. We had 5 biphasic and 15 monophasic SSs, patient age ranged from 13 to 68 years (mean, 39.8). Tumor size was larger than 5 cm in each case. Follow up ranged from 6 to 78 months (mean, 38.5 months). For statistical analysis the chi-squared-test was used.
Results
Her-2 oncogene amplification was found in three cases (15.0%) of 20 SSs, but so called massive amplification which is characteristic of some subset of breast carcinoma, was not observed. Her-2 oncogene amplification was significantly associated with a lower risk of developing metastasis (P<0.05) (none of 3 amplified cases had metastases), while no association was found concerning recurrences (P<0.5). 6 cases proved to be aneoploid and 14 were diploid but no association was found between Her-2 amplification status and ploidy and between ploidy status and metastases or recurrences.
Conclusions
Her-2 oncogene amplification is a rare event among SSs, but this small subset of SS has a better overall prognosis. Beside this, there may be a theoretically new treatment possibility with Trastusumab for Her-2 amplified cases of SSs.

P 833
A PULMONARY METASTASIS OF SYNOVIAL SARCOMA APPEARING 18 YEARS AFTER TREATMENT OF THE PRIMARY NEOPLASM
V. Janevska, S. Banev, L. Spasevska, V. Filipovski, M. Nikolovski
Institute of Pathology, faculty of Medicine, Skopje, FYRO Macedonia

A 57 years-old woman presented with weakness and coughing. Investigations revealed a mass in the left lower pulmonary lobe, which was resected. The histological examination suggested a diagnosis of synovial sarcoma. Anamnestic data found out a primary neoplasm treated 18 years ago, only by surgery. The patient is well doing a year after operation of the lung.
Methods: Tissue was examined by routine histological slides, stained by H.E. and immunohistochemically. A revision of the primary tumor was made.

Results: The bought tumors showed biphasic pattern. The pulmonary mass showed a presence of sheets and cords of polygonal epithelial cells with quite rare split like spaces. The epithelial component was intimately intermixed with a spindle-cell component, composed of uniform spindle cells with hyper chromatic nuclei. Immunohistochemical analysis showed widespread labeling for cytokeratins and local labeling for vimentin in the epithelial component, and positive labeling for epithelial membrane antigen in the epithelial and spindle-cell components.
Conclusion: This is a rare case of synovial sarcoma treated with surgery only, metastasing in the lung, after being indolent 18 years.

P 834
MYXOID MONOPHASIC SYNOVIAL SARCOMA OF THE FOOT: A CASE REPORT
R Sellami Dhouib, M Driss, S Sassi, I Abbess, K Mrad, K Ben Romdhane
Department of Pathology, Salah Azaiez Institute, Tunis, Tunisia.

Introduction and aims: Focal myxoid change is a well recognized feature of synovial sarcoma, but the presence of a predominatly myxoid stroma is rare. We described a case of myxoid monophasic synovial sarcoma in which marked myxoid change initially obscured the diagnosis, leading confusion principally with malignant peripheral nerve sheath tumor.
Case report: A 16-year-old adolescent presented with left foot tumour. Roentgenographic studies demonstrated tumor with irregular margin and evidence of bone destruction. Histologically, the tumour had an alternating hypercellular and hypocelllar foci. The areas of hypercellularity consisted of spindle cells arranged in fascicular growth. The cells had bland round or ovoid nuclei with a slightly wavy appearance. Because of nuclear hyperchromasia, the evaluation of mitotic activity is very difficult. Areas of hypocellularity contained individual spindle cells in a myxoid stroma. Neither calcifications nor foci of glandular differentiation were noted. Immunohistochemical stains for cytokeratin, S100 protein, desmin, myogenin and CD34 were negative, while a focal positivity for epithelial membrane antigen was noted. By reverse transcriptase polymerase chain reaction, a SSX1 transcript of synovial sarcoma was found.
Discussion and conclusion: Clinical differences between myxoid synovial sarcoma and conventional synovial sarcoma can't be evaluated because of too limited cases in the literature. Recognition of this rare histological variant of synovial sarcoma is important because it can be easily mistaken for other myxoid spindle cell neoplasms, potentially resulting in suboptimal therapy.

P 835
MORTALITY OF TUBERCULOSIS IN RHEUMATOID ARTHRITIS
Miklós Bély MD, PhD, DSc1 and Ágnes Apáthy MD2
1Department of Pathology,
Policlinic of the Hospitaller Brothers of St.John of God,
Budapest, Hungary
2Department of Rheumatology,
National Institute of Rheumatology and Physiotherapy,
Budapest, Hungary

The risk of tuberculosis is higher in RA, or other autoimmune diseases, than in a normal population.
The aim of this study was to determine
1. the mortality due to tuberculosis (Tb), or miliary disseminated tuberculosis (mTb) in RA,
2. the clinicllly missed diagnosis of Tb, or mTb in RA,
3. the main complications associated with Tb, or mTb in RA
4. the link between Tb, or mTb and coexistent major complications, such as systemic vasculitis (SV), or secondary AA amyloidosis (AAa), lethal septic infection (SI), or associated diseases like malignant tumours (mTu), diabetes mellitus (DM), and atherosclerosis (Ath) in RA.
Patients and Methods
A randomized (non-selected) autopsy population of 234 in-patients with RA was studied. RA was confirmed clinically according to the criteria of the ACR.
Post-primary tuberculosis, (with, or without miliary dissemination) and the major complications of rheumatoid arthritis (SV, AAa, SI) associated to Tb, or mTb, and accompanying diseases (mTu, DM, Ath) were confirmed histologically.
A possible link between tuberculosis, or disseminated miliary tuberculosis and coexistent complications, or associated diseases was determined statistically by Chi^2-tests.
Results
1. Post-primary fibrous, or fibrocaseous tuberculosis accompanied RA in 27 (11.54 %) of 234 cases.
Eight (3.4%, 29.6 rel%) of 27 post-primary fibrous, or fibrocaseous tuberculosis cases were complicated by disseminated miliary tuberculosis.
Three patients (1.28 %) died of circulatory failure due to Tb complicated by miliary dissemination.
2. Only one case of Tb with mTb and lethal outcome was clinically recognized.
3. There was a significant and positive correlation between vasculitis and tuberculosis ($Chi^2=4.16$ $p<0.04$), or mTb ($Chi^2=3.86$ $p<0.04$); furthermore between granulomatous type of vasculitis and mTb ($Chi^2=5.55$ $p<0.01$).
Conclusions
Coexisting complications modify the basic disease (RA) and present atypical clinical manifestations. The age of the patients, the autoimmune character of the underlying disease, the steroid and/or immunosuppressive treatment may also play a role in missing the clinical diagnosis of miliary tuberculosis.
The correlation between Tb, or mTb and vasculitis may represent statistically an influence of Tb, or mTb on vasculitis.
The diagnosis of vasculitis of the granulomatous type should alert the surgical pathologist to initiate clinical exclusion of existing tuberculosis with miliary dissemination.

P 836
CHRONOLOGIC SEQUENCE OF AA AMYLOIDOSIS IN RHEUMATOID ARTHRITIS - A RETROSPECTIVE CLINICOPATHOLOGIC STUDY OF 161 AUTOPSY PATIENTS
Miklós Bély MD, PhD, DSc1 and Ágnes Apáthy MD2
1Department of Pathology,
Policlinic of the Hospitaller Brothers of St.John of God,
Budapest, Hungary
2Department of Rheumatology,
National Institute of Rheumatology and Physiotherapy,
Budapest, Hungary

Statement
AA amyloidosis (AAa) is a progressive, cumulative process, involving in its early stages only a few structures in some organs, and increasingly more in the later stages of the disease.
During the progression of systemic secondary amyloidosis, amyloid A deposition begins in the organs and tissue structures that are frequently involved and later show marked deposition of amyloid. Where amyloid deposits are infrequent or less marked, deposition starts later (1).
The aim of this study was to determine
(1) the frequency and extent of amyloid A deposits in various tissue structures,
(2) the frequency and extent of AAa in different organs,

(3) the chronologic sequence of amyloid A deposition in various organs and tissue structures.
Patients and Methods
A randomized autopsy population of 161 in-patients.
Systemic AAa was observed in 34 (21.1%) of 161 cases (1).
AAa was diagnosed histologically.
Results
Amyloid deposits were frequent and massive in the wall of blood vessels, and along collagen and reticulin fibers (or, if present, on the basal lamina), mainly in the GI tract, heart, kidney, spleen, adrenal glands, and the liver.
Amyloid deposits were less frequent and in limited amount in skeletal muscles, synovial membranes, lymph nodes, peripheral nerves, bones, or skin.
The frequently involved structures and organs showed marked deposits of amyloid. In less frequently involved tissue structures and organs the amyloid deposits were less marked at death.
Discussion
The amyloid deposition starts in the wall of blood vessels (capillaries, arterioles, small arteries), followed by deposits on collagen fibers, basal membranes, and reticulin fibers (fat tissue). Deposition in the wall of medium size vessels starts later. The involvement of venules, small and medium size veins increases in case of stasis. Amyloidosis of peripheral nerves is a late, end- stage phenomenon.
The chronology of AA amyloid deposition in various organs is as follows: GI tract, heart, kidney, spleen, adrenal gland and liver. Other organs like pancreas, lung, thyroid gland, aorta, skeletal muscle, synovial membrane, lymph nodes, peripheral nerves, bones and skin are less frequently involved, and AA deposition starts later in them.
References
Bély M: Krankheitsmodifizierende Faktoren bei chronischer Polyarthritis. D.Sc. Thesis of Hungarian Academy of Science, Budapest 1993.

P 837
FOCAL MYOSITIS OF THE TEMPORAL MUSCLE
PERKOVIC Tanja 1, BAJROVIC Fajko 2, TOMSIC Matija 3, ROTAR Ziga 3, HOCEVAR Alojzija 3, VIZJAK Alenka 1
1 Institute of Pathology Medical Faculty Ljubljana
2 Department of Neurology, University Medical Center Ljubljana
3 Department of Rheumatology, Umiversity Medical Center Ljubljana, Slovenia

Focal myositis is a rare inflammatory disease of the skeletal muscle with histopathological features of interstitial myositis. Any skeletal muscle in the body can be affected. We present a 40-year-old female, previously in good health, with headache of one year duration and the three month history of a painful pseudotumor in the right temporal region. MRI pictures showed markedly thickened right temporal muscle with focally increased signal intensity on T2-weighted scan. Muscle biopsy revealed the characteristic histological findings of polymyositis. However, immunohistochemistry revealed the predominance of CD4 positive cells. In addition, immunofluorescence showed granular deposits of IgM and C3 in the walls of small endomysial and perimysial vessels. Therapy with nonsteroidal antiinflammatory drugs as well as with metilprednisolone was not effective, but responded to radiation therapy.

P 838
MULTIPLE MICROSCOPIC RENAL ANGIOMYOLIPOMA INDICATING TUBEROUS SCLEROSIS
Augros M.(1), Denis E.(2), Touraine R.(3), Cordier M.P(4)., Bouvier R.(5)
(1)Service d'Anatomie Pathologique, Laboratoire M. Mérieux, Lyon, (2) Service de Chirurgie, Centre Hospitalier St Joseph-St Luc, Lyon, (3) Service de génétique Faculté de Médecine de StEtienne , (4) Service de génétique et (5)Service d'Anatomie Pathologique, Hôpital Edouard Herriot, Lyon

Renal manifestations are present in one half of patients with tuberous sclerosis (TS). They include angiomyolipomas, cysts, combination of both and renal cell carcinomas. They are usually detected by imaging techniques. Pure microscopic diagnosis is rather rare.
We report the case of a 36 years old patient, treated surgically for ureteropelvic junction obstruction with calyceal and pelvic dilation and atrophic renal parenchyma.
The histological pictures were unusual. The obstructive lesions were rather moderate when compared to the severity of the renal atrophy. These were associated with chronic ischemic damages, low grade papillary tumor and medial angiodysplasia of arteries. In addition, small multi-focal nodules suggested smooth muscle-cells proliferation. Immunohistochemistry screening for these clusters show positive staining for HMB45. As such, diagnosis of multiple microscopic angiomyolipomas is confirmed.
These microscopic features led to conduct a genetic survey. No cutaneous ophthalmologic or neurological tumors were detected. However, one of his daughters presented neonatal achromatic spots and hypsarythmia when she was 5 months old. The study of the two known genes (TSC1 and TSC2) is in process.
Microscopic renal angiomyolipomas are often predominantly composed of epithelioid smooth muscle cells. These could be associated with vascular affection. They must be recognised as they are highly evocative of TS. Their presence must lead to a full clinical check, complementary imaging analysis, genetic investigation and screening for TS genes mutation.

P 839
A CASE OF PRIMARY RENAL MALIGNANT FIBROUS HISTIOCYTOMA AND ANGIOMYOLIPOMA
DEMIR Dilek(*), KILICASLAN Isin(*), NANE Ismet(**), DEMIRYONT Misten(*), UYSAL Veli(*)
(*) Istanbul University, Istanbul Faculty of Medicine, Department of Pathology
(**) Istanbul University, Istanbul Faculty of Medicine, Department of Urology

Primary renal malignant fibrous histiocytoma (RMFH) is a rare tumor of the kidney. Fiftytwo cases of RMFH have been reported in the literature. It is clinically and radiologically indistinguishable from a renal cell carcinoma.
We report a case of RMFH originating in the capsule of the upper pole of right kidney which was detected incidentally on routine physical examination of a 43-year-old man. The patient underwent right radical nephrectomy with a diagnosis of renal cell carcinoma clinically. The tumor was also seen peroperatively as a bulky mass around the vena cava and could not be resected totally. Gross examination of the specimen revealed two tumoral foci, one of which was a huge, yellowish white, rubbery, nodular mass measured 9x8.5x8.5 cm. Histologically, the tumor was mainly composed of inflammatory cells including lymphocytes, plazmocytes and histiocytes. There were also areas of plump spindle-epithelioid histiocytic cells densely arranged in whorl-like pattern. Because the differential diagnosis included inflammatory pseudotumor, sarcomatoid renal cell carcinoma and RMFH, immunohistochemical analyzes were performed for antibodies pancytokeratin, smooth muscle actin (SMA), desmin, CD31, CD34, CD68 and Ki67. Immunohistochemistry revealed diffuse positivity for CD68 and focal positivity for SMA. Ki67 proliferation index was detected to be 8-10%. The tumor cells were negative for other antibodies. Therefore, the tumor was diagnosed as RMFH.

The other tumor, 1 cm in diameter displaying similar macroscopical features to RMFH, was localised in the lower pole, diagnosed as angiomyolipoma histologically.

In conclusion, RMFH is a very rare tumor and it may lead to differential diagnostic difficulties in the reassesment of renal masses. To our knowledge this case is a unique example of RMFH because of its coexistence with angiomyolipoma.

P 840

COLLECTING DUCT CARCINOMA OF THE KIDNEY: A REPORT OF FIVE CASES AND REVIEW OF THE LITERATURE

Garrido Ruiz M, Meizoso T, Enguita AB, Saiz González A, Usera G

INTRODUCTION

Collecting duct carcinoma of the kidney is a rare neoplasm centered in the renal medulla; these tumors are aggresive, often metastatic and commonly result in death. The clinicopathological features of five cases are here presented to add to the approximately 100 cases reported so far in the literature.

CASES

Clinical presentation in the majoriry of cases has been hematuria, less frecuently loin or back pain, or urinary. Upper tract imaging often suggests urothelial carcinoma of the renal palvis. We report five illustrating cases.

PATHOLOGY

Macroscopic: CDC is usually located in the central region of the kidney and often involves hiliar structures. It ranges widely in size from 0,5 to12cm. The typical CDC is firm and gray-white with irregular infiltration borders; areas of necrosis, and rarely cystic elements may be present.

Microscopic: Typical CDC has a tubular or tubulo-papillary growth pattern. Irregular and disorganised tubules or ducts within a desmoplastic stroma infiltrate and expand the interstitial tissue of both the cortex and medulla, with scattered normal tubules and glomeruli within the malignant tissue.Vascular and lymphatic space invasion is common .Tumor cells are seen both infiltrating into stroma and evoking desmoplasia. Their cytoplasm appears granular and lightly eosinophilic; nuclear grade according to the grading system of Furhman et al. is typically grade 3 or 4. Cells with a hobnail pattern are often present.

Immunohistochemical studies on these carcinomas have been variable; the expected profile would be positive for low molecular weight keratin, for EMA, Ulex europaeus agglutinin and peanut lectin.

DISCUSSION

CDC shows a male predominance (ratio of about 2:1). There is a wide age range with a mean of 55 years, and it has been noted a strong family history of cancer. CDC are the most aggressive carcinomas of the renal tubular epithelium. Approximately 35% of patients have metastases at presentation. Approximately two thirds of patients with collecting duct carcinoma have died of the cancer within two years of diagnosis.

CDC are unlikely to be confused histologically with other renal cell carcinomas (including papillary renal cell carcinoma, urothelial carcinoma with glandular differentiation, adenocarcinoma arising from the urothelium of renal pelvis, and metastatic carcinomas). Accurate classification is important because CDC has a considerably worse prognosis than other renal neoplasms.

P 841

AN UNUSUAL CASE OF UNILATERAL PYELOURETERAL IDIOPATHIC RETROPERITONEAL FIBROSIS SIMULATING RENAL MALIGNANCY

Yolanda Rodriguez Gil
Murillo Lázaro Cristina
Segovia Blazquez Beatriz
Usera Sagarra Gabriel

INTRODUCTION

Idiopathic Retroperitoneal Fibrosis (IRF) or Ormond´s disease is a relatively uncommon disorder, with a reported incidence of 1 in 200000 inhabitants,with a male: female ratio of 2-3:1. It tipically presents insidiously, in the fifth and sixth decades of life and it is rare in children. It is most commonly localized around aorta and iliac vessels, it usually spreads laterally to involve the inferior vena cava and one or both ureters which are displaced medially. It can cause obstructive uropathy and renal failure.

CASE REPORT

A 85 year old man presented with fatigue, anorexia and weight loss, lasting about three months. History was significant for diabetes mellitus type 2 and hypertension. Computerized tomography (CT) showed a deformation of the right kidney due to a low density area which involved the renal hilum and was not clearly separated from the perirenal fat. On magnetic resonance imaging (MRI) the soft tissue mass appeared isointense with muscle on T1 weighted images and hyperintense on T2 weighted images. Excretory urography revealed proximal hydronephrosis and complete obstruction of the ureter. Radiological studies suggested a malignant tumor of the renal pelvis.

RESULTS

Lumbar incision revealed a dense hard grayish-white mass encasing the upper part of the ureter and extending to the hilum of the right kidney. Right nephrectomy was performed. Microscopic examination revealed a fibrous proliferation, broad anastomosing bands of hyalinized collagen and a prominent inflammatory infiltrate composed of mainly of lymphocytes and plasma cells often containing germinal centers, there were also some macrophages and eosinophils. Multiple histological sections were performed to rule out a malignant neoplasia with desmoplastic reaction. The diagnosis of IRF was made after secondary conditions both benignant and malignan were ruled out. The postoperative course was uneventful.

DISCUSSION AND CONCLUSIONS

IRF renal involvement is generally bilateral and tipically involves the middle third of both ureters. In our case renal pelvis and proximal part of right ureter were diffusely and deeply infiltrated by an inflammatory fibrous process. Originally sarcomatous or carcinomatous neoplasia were strongly considered in the clinical differential diagnosis and treated it with nephrectomy. The correct histologic diagnosis of IRF with multiple histological sections,allows urologist to choose less aggresive options of treatment.

P 842

NEPHROGENIC ADENOMA A PITFALL DIAGNOSIS WITH AMACR (P504S) STAINING

Eva Comperat (1), Marya Skrima (2), Isabelle de Pinieux (2), Annick
Vieillefond (3), Vincent Molinie (3).

Introduction : Nephrogenic adenoma is a rare distinctive benign lesion typically found in areas of urothelial mucosa after urinary injury. Microscopically, the lesion usually confined to the urothelial mucosa, exhibits a range of patterns with variable proportions of papillary, microcystic, solid nested, or tubular patterns. The cells lining the tubules, cysts, and papillae are predominantly cuboidal to low columnar with a small amount of cytoplasm, and with sometimes prominent nucleoli. In such cases when the tubular pattern is exclusive it could mimics prostatic carcinoma. Aim of the study : To characterise the morphology and immunoprofile of nephrogenic adenoma. Materials and methods : 23 cases of NA from surgical pathological files of two institution, were selected. Immunostaining was performed with Urinary and

prostate markers CK5/6 (Dako), CK7 (Dako), 34âE12 (Dako), PSA (Dako), PSAP (Dako), P63/p504s (PIN cocktail, Menarini Dg) antibodies.
Results : Histological features displayed a papillary pattern, associated with a tubular component in most cases. The tubes are lined by one layer of small cuboids cells with nucleolar nuclei, surrounded by an inflammatory stroma. In case of exclusive tubular pattern, infiltration could mimic a small acinar proliferation suspicious of prostatic cancer. No mitosis, necrosis or cytonuclear atypia was seen except in 1 case.immunostaining study revealed a 34âE12, CK 5/6 and CK7 positivity, with a diffuse cytoplasmic positivity with P504s. Furthermore only in urethral cases a weak and focal positivity for PSA and PSAP was observed. In all cases P63 was negative.
Discussion : One must be aware of the range of appearances of nephrogenic adenoma to avoid its misinterpretation. In exclusive tubular pattern with muscular involvement nephrogenic adenoma could mimic prostate carcinoma. In such cases one must remind that the over expression of AMACR (P504s) in such small glandular tubular structure may be misinterpreted as prostatic carcinoma. The presence of inflammatory stroma surrounding the small atypical tubes, and the positivity of CK 5/6, CK7 and 34âE12 positivity would restore the true diagnosis of such benign lesion.

P 843

INTERSTITIAL KIDNEY FIBROSIS IN AN EXPERIMENTAL MODEL OF UNILATERAL URETERAL OBSTRUCTION (UUO)

ARALICA Gorana, LJUBANOVIC Danica, RADOVIC Nikola*, RACAR Arijana, MÜLLER Danko, MANOJLOVIC Spomenka, KNOTEK Mladen**.
Department of Pathology, Clinical Hospital “Dubrava”, Zagreb, Croatia
*Department of Urology, Clinical Hospital “Dubrava”, Zagreb, Croatia
**Department of Internal Medicine, Clinical Hospital “Merkur”, Zagreb, Croatia

INTRODUCTION
Interstitial fibrosis is a final outcome of many chronic renal diseases, including obstructive nephropathy. Fibrosis considers fibroblast proliferation and intercellular matrix deposition, leading to characteristic tissue changes resulting in chronic renal failure. Angiotensin II is one of the most important factors in the progression of renal diseases.
OBJECTIVE
The objective of this study is to quantify the degree of interstitial fibrosis in rat kidney after experimental UUO and administration of an angiotensin converting enzyme (ACE) inhibitor – cilazapril.
MATERIAL AND METHODS
Male Wistar rats, weigh 210-300 g, were used in this experimental model. There were 4 experimental groups, 6 rats each: 1. sham-operated (sham-UUO); 2. UUO (left ureter was ligated); 3. sham-UUO+cilazapril 10 mg/kg oraly q.d. (Cilazil, Pliva, Zagreb, Croatia); 4. UUO+cilazapril 10 mg/kg oraly. Rats were sacrificed on the 10th day after the operation. The interstitial kidney fibrosis quantification was performed on Gomory stain slides using semiquantitative scale (0- no reticulin increase; 1- rare foci of reticulin multiplication; 2- fine reticulin net around tubuls; 3- dense reticulin net around tubuls; 4- reticulin foci in more then 50% of HPF; 5- diffuse fibrosis) and morphometric system ISSA (Vamstec, Zagreb, Croatia). Morphometric quantification was performed using computer grid (13x10 fields) by counting the number of grid fields containing interstitial fibrosis. Six, randomly selected, microscopic fields (400x) were reviewed for each case.
RESULTS
Interstitial fibrosis developed in all animals after UUO. Number of grid field containing fibrosis per HPF in UUO group was significantly higher than in sham-operated group ($p<0,05$) and in sham-operated+cilazapril group ($p<0,01$). Fibrosis level obtained by semiquantitative analysis did not showed statistically significant difference between experimental groups. However, there was significant corelation between semiquantitative and morphometric method (Pearson`s coefficient $r=0,71$, $p<0,0001$).
CONCLUSION
Interstitial kidney fibrosis developed after the UUO does not decrease after the ACE-inhibitor administration. The level of interstitial fibrosis can be determined using several methods, such as semiquantitative scale and morphometric quantification. The morphometric quantification is more sensitive method than semiquantitative scale.

P 844

LYMPHOEPITHELIOMA-LIKE CARCINOMA OF THE RENAL PELVIS: A CASE REPORT AND REVIEW OF THE LITERATURE

TSAI Chien-Chen(1), YANG Ching-Hua(2)
Department of Pathology(1) and Urology(2), Far Eastern Memorial Hospital, Taipei, Taiwan

[Introduction] Lymphoepithelioma-like carcinoma (LELC) shares the same morphologic features with undifferentiated nasopharyngeal carcinoma and is very rare in the urinary tract, especially the renal pelvis. We report the third documented case of LELC of the renal pelvis and review the literature to elucidate its clinicopathologic features.
[Case report] The tumor was found in a 58-year-old woman suffered from left flank pain and gross hematuria. The ultrasound study showed left hydronephrosis with a renal pelvic tumor; therefore, left nephroureterectomy was performed. Grossly, the tumor was fungating and fragile within the dilated renal pelvis. Microscopically, it was composed of sheets or ill-defined nests of syncytial undifferentiated cells exhibiting prominent nucleoli and mixed with extensive lymphoplasmacytic infiltrations. Immunohistochemically, the tumor cells were positive for cytokeratin, but negative for leukocyte common antigen and vimentin. No Epstein-Barr viral (EBV) transcripts were detected by in-situ hybridization for EBER-1. The tumor was limited within the pelvis with no renal parenchymal invasion. No evidence of conventional transitional cell carcinoma was seen after thorough sampling, although focal dysplasia was noted in the urothelium elsewhere. The patient remains well without malignancy 2 years after surgery.
[Conclusion] Reviewing the literature, all three cases of LELC of the renal pelvis occurred in the elderly with a good prognosis. They were not associated with EBV latent infection, unlike LELCs in salivary glands, lungs, or stomach. These clinicopathologic features were almost identical to those seen in the cases of LELC of the urinary bladder. Accordingly, urothelial LELCs should be separated from high-grade urothelial carcinoma and be classified as a distinct entity with a favorable outcome, although they were composed of undifferentiated tumor cells.

P 845

MIXED EPITHELIAL AND STROMAL TUMOUR OF THE KIDNEY IN MALE-CASE REPORTMIXED EPITHELIAL AND STROMAL TUMOUR OF THE KIDNEY IN MALE-CASE REPORTMIXED EPITHELIAL AND STROMAL TUMOUR OF THE KIDNEY IN MALE-CASE REPORTMIXED EPITHELIAL AND STROMAL TUMOUR OF THE KIDNE

PETRESCU Amelia 1,ANDREI Florin 2,ARDELEANU Carmen 2,NICULESCU Liviu 3, BISCEGLIA Michele 4
1.”Prof.Dr.Th.Burghele”Clinical Hospital, Bucharest, Romania 2”Victor Babes “Institute, Bucharest, Romania 3.”Carol Davila” University of Medicine and Pharmacy

Bucharest, Romania 4."Casa Sollievo della Sofferenza"Hospital,San Giovanni Rotondo, Italy

Introduction and aim:We present the case of an 60 year old man with no history of hormonal treatment and urological diseases except renal lithiasis. He was hospitalized for left lombar pain and intermittent hematuria. Echography and NMR revealed a kidney mass. A total left nephrectomy was performed The left kidney showed a polar tumor mass. Macroscopically examination of the tumour on cut section showed a solid white tissue with numerous cystic formations of several sizes.
Material and methods: Fragments of the tumor were fixed in formalin10%, embedded in paraffin and sections were stained with HE. Immunohistochemical tests have been done: ACT, CD 34,Progesterone receptors, Estrogen receptors, CD 117,CD 56,HMB 45,Androgen receptors, NK 1
Results:The tumor was composed of a mixture of a spindle cell proliferation intermingled epithelial elements that formed microcyst and macrocystic dilatation No hemorrhages areas, necrosis ,cytologic atypia or mitotic activity were present. Immunohistochemical analyses revealed: ACT, CD 34, Progesterone receptors expression in tumoral areas were positive and CD 117, HMB 45, Androgen receptors, Estrogen receptors, CD 56, NK 1 were negatives
Conclusions: The morphological appearance and immunohistochemical results enabled us to diagnose this case as a mixed epithelial and stromal tumour of the kidney. This is a rare entity in male (few cases previously reported) but our case present the particularity of no hormonal treatment and positive Progesterone expression.

P 846
MUCINOUS TUBULAR AND SPINDLE RENAL CELL CARCINOMA :

KOURDA Nadia, CHELBI Emna, , ZERMANI Rachida, RAMMEH Soumaya, FERCHICHI Leila, KACEM Olfa, FARAH Faten, AYED Mohsen, BALTAGI Sarrah.
Department of pathology. CHARLES NICOLLE Hospital, Tunis, Tunisia.

INTRODUCTION
The mucinous tubular and spindle renal cell carcinoma (MTSCC) is a very rare neoplasm, recently described as a distinct subtype of renal cell carcinoma (RCC). This low-grade polymorphic renal epithelial neoplasm with mucinous, tubular and spindle cell features may have striking morphologic similarities to the more common papillary RCC. Herein, we report an additional case of MTSCC with immunohistochemical study and summarise the present knowledge of this newly recognised entity.
CASE REPORT
A 52-years-old woman with uncontrolled hypertension underwent a renal ultrasonography that disclosed a 6.4-cm-sized mass involving the left kidney. A radical nephrectomy was performed. The gross pathology revealed a well-circumscribed whitish solid tumour. Microscopy showed a proliferation of regular cuboidal cells often arranged in long cords and tightly packed tubules and spindle cells component forming small sheets with low grade nuclear cytology. The stroma showed focally a mucinous materiel and clumps of foamy histiocytes. The mucinous material react strongly with alcian blue. The tumour's cells exhibit positive reactions for vimentin, epithelial membrane antigen (EMA), high-molecular-weight cytokeratin (CK), CK7 and CK18 the diagnosis of mucinous tubular and spindle renal cell carcinoma was made. The patient is free of disease since more than 12 months.
DISCUSSION
Clinically, female predominance is reported with a mean age of 53 years. MTSCC often presents as asymptomatic mass.
The MTSCC have a distinctive histologic appearance composed of cuboidal and spindle cells with mucinous extracellular matrix with some degree of morphologic variability. Some authors have reported small foci of clear cells. These pathologic features may be reminiscent of papillary RCC with sarcomatoid features or metanephric adenoma. Most MTSCC are immunoreactive for vimentin, EMA, CK cocktail, CK 7 and Ulex Europeus agglutinin-1 but usually not for CD10. Ultrastructurally, focal short microvilli are generally observed with sometimes junctional complexes and basal lamina. MTSCC exhibit multiple losses of chromosomes 1, 4, 6, 8, 9, 13, 14, 15, and 22 with no VHL deletions. The prognosis is commonly Favourable. However, few cases of local recurrence or metastasis are reported. Morphologic, immunohistochemical and ultrastructure features indicate differentiation toward distal nephron segments has been suggested as the MTSCC phenotype but this view is debatable.

P 847
BILATERAL RENAL ADENOMATOSIS AND ONCOCYTOSIS WITH MIXED ONCOCYTIC AND PAPILLARY TUMOURS

Tomas Tichy, Martin Dobias, Katerina Musilova, Patrik Flodr
Institute of Pathology, Faculty of Medicine, Palacky University and Faculty Hospital, Hnevotinska 3, 775 15 Olomouc, Czech Republic

Adenomatosis and oncocytosis are rarely described in the kidney. We report a case of 66-year-old man with bilateral renal adenomatosis and oncocytosis found at authopsy. Both kidneys were occupied by innumerable tumours, the majority of them fulfilled the criteria of renal papillary adenomas. Three tumours showed mixed solid alveolar and papillary patterns composed of oncocytic cells and small cells of papillary adenoma type. Transitional features between patterns were clearly visible. Moreover, apart from dysplastic tubules and microadenomas nearly all histological sections revealed multiple foci of oncocytic transformation of tubular epithelium and microoncocytomas. Oncocytic features of cells were confirmed ultrastructurally. Results of immunohistochemical examination showed that papillary adenomas might be of distal nephron origin.
To our knowledge this is the first case of bilateral renal adenomatosis and oncocytosis described. Mixed oncocytic and papillary tumours are not considered distinct entity. In this case they probably represent collision tumours but taking into account distal nephron origin of described papillary adenomas, oncocytic transformation of papillary tumour cells cannot be excluded.

P 848
COMPARISON OF HEP PAR 1 AND MITOCHONDRIAL ANTIGEN EXPRESSION IN RENAL ONCOCYTOMAS: IS IT MITOCHONDRIA WHICH HEP PAR 1 REACTS WITH?

G.GULLUOGLU Mine (*), METE Ozgur (*), KILICASLAN Isin (*), UYSAL Veli(*)
(*) Istanbul University, Istanbul Faculty of Medicine, Department of Pathology

Introduction: Monoclonal antibody, Hep Par 1 has been used to identify tissues of hepatocytic origin and those with hepatoid differentiation. The characteristic diffuse cytoplasmic granular immunostaining pattern suggests an organelle, possibly mitochondial localisation of the antigen. We investigated Hep Par 1 immunoreactivity in the renal oncocytomas which were proved to be rich in mitochondria and compared the mitochondrial antigen (Mab-2) expression of this tumor with Hep Par 1 expression.
Material and Methods: Thirty two cases of renal oncocytoma were included in this study. Staining intensity (+, ++, +++)

and staining area (0-25%, 25-50%, 50-75%, 75-100%) were noted for Hep Par 1 and Mab-2.
Results: We detected the mitochondrial antigen in 75-100% of tumoral areas with (++) to (+++) staining intensity whereas none of the tumors showed the coarse granular staining which is characteristic to Hep Par 1 immunohistochemistry. Only two oncocytomas displayed diffuse cytoplasmic immunoreactivity which is moderately intense while eleven showed faint cytoplasmic staining in <25% of the cells. Twenty tumors showed no immunoreactivity. We did not detect any correlation between the immunoexpression profiles of Hep Par 1 and Mab-2 in renal oncocytomas.
Conclusion: These findings suggest that there is no relationship between the mitochondria and the antigen which Hep Par 1 antibody reacts with.

P 849

IMMUNOHISTOCHEMICAL EVALUATION OF CATENINS IN RENAL CELL CARCINOMA

G. Basta-Jovanovic1, S. Radojevic-Skodric1, S. Djuricic2, D. Brasanac1, R. Bogdanovic2, S. Skodric11-Institute of pathology, Medical school,University of Belgrade
2-Mother and Child Health Institute of Serbia "Dr Vukan Cupic"

SUMMARY: Catenins have prognostic value in several human tumors.
AIMS: The aim of this study was to determine the expression of catenins in Renal cell carcinoma (RCC) and their relationship with tumor morphology and TNM status. METHODS: 28 cases of RCC, 2 metastasis and 2 samples of normal kidney tissue were studied using streptavidin-biotin-complex technique.Catenins expression levels were semiquantitatively scored. RESULTS: Alpha-, beta and gamma catenin were present in most cases of RCC (43%, 64% i 50%,respectively). Sarcomatid type of RCC and T3 RCCs displayed higher beta-catenin level than T1/T2 tumours. There is no correlation between cell type and level of alpha or gamma catenin expression($p>0.05$). Beta catenin is predominantly expressed in sarcomatoid type of RCC and this correlation showed statistical significance ($p<0.05$). Tumors of grade 1 more often showed alpha and beta catenin expression (84%;100%) then tumors of grade 2/3 (46%;50%), while there was no differences between gamma catenin distribution in this two groups of tumors (G1-65%;G2/3-41%). Alpha and gamma catenin were expressed more often in tumors of stage T3(57%;71%) then in T1/T2 tumors(38% for both catenins) and that difference has statistically significant association ($p< 0.05$). On the contrary, tumors of lower stage (T1/T2) showed beta catenin expression more often then tumors of higher stage (62%:57%), but this expression did not show significant correlation ($p>0.05$) with tumor stage.CONCLUSIONS: Our results indicate that there is different expression of cell adhesion molecules (alpha, beta and gamma catenin) in RCC, which depends on histological type, tumor stage and grade.

P 850

IMMUNOHISTOCHEMICAL EXPRESSION OF EPIDERMAL GROWTH FACTOR RECEPTOR AND MICROVESSEL DENSITY IN RENAL CELL CARCINOMA: PROGNOSTIC VALUE AND RELATION TO CLINICAPATHOLOGIC PARAMETERS.

Suheyla Uyar Bozkurt*, Arman Ozdemir**, Handan Kaya*
*Department of Pathology,** Department of Urology, Marmara University School of Medicine, Ýstanbul, Turkey

INTRODUCTION AND OBJECTIVE: Epidermal growth factor receptor and tumoral angiogenesis have been proposed as potential prognostic parameters in renal cell carcinoma.The aim of this study is to detect the immunohistochemical expression of epidermal growth factor receptor(EGFR) and microvessel density(MVD) and to relate to prognosis and clinicopathologic parameters.
METHODS: Immunohistochemical stains using EGFR and CD 34 monoclonal antibodies were used in 55 renal cell carcinomas diagnosed subsequent to radical nephrectomy or nephron sparing surgery between 1987 and 2001. The MVD was detected by counting the number of microvessels stained by CD 34 in the most vascularised area of tumor.
RESULTS:Univariate analysis showed only pathological stage of tumor has highly significant association with cancer specific survival($p<0.01$). EGFR immunostaining was present in 22 of 55 (40%) RCCs and mean number of counting vessel was 53,31.EGFR immunoexpression and MVD were not exhibited prognostic significance with respect to survival and clinicopathologic parameters such as stage and grade of tumors.
CONCLUSIONS: The expression of EGFR and MVD seems not to provide additional prognostic information in RCCs. Our results show that the best predictors of cancer spesific survival is pathologic stage of tumor in RCCs.

P 851

EXPRESSION OF CLAUDIN 1,2,3,4 AND 7 IN NORMAL AND NEOPLASTIC KIDNEY

KARDOS Magdolna1, KISS András1, SZENDRÕI Attila2, RIESZ Péter2, ROMICS Imre2, SCHAFF Zs1
1: 2nd Department of Pathology, Semmelweis University, Budapest, Hungary
2: Department of Urology, Semmelweis University, Budapest, Hungary

Introduction: Claudins (CLDNs) are tight junctional (TJ) proteins expressed in epithelial and endothelial cells. They participate in the formation of barriers between different tissue compartments by regulating the efflux of molecules through TJ complexes.
Purpose: Our aim was to detect the difference between the expression of CLDNs in the embryonal and adult kidneys. Further, the expression of CLDNs in benign and malignant tumours of the kidney was also studied.
Method: CLDN 1,2,3,4,7 were studied by immunhistochemistry in formalin fixed, paraffin embedded samples of 11 normal embryonal and adult kidneys, and 18 kidney tumours [5 oncocytomas, 5 conventional renal cell carcinomas (CRCC), 5 papillary renal cell carcinomas (PRCC) and 3 chromophobe renal carcinomas (CRC)]. A semiquantitative evaluation was used.
Results: The expression of CLDNs was found to be similar in embryonal and adult kidneys. CLDN1 was expressed only in the Bowman's capsule, CLDN2 in the proximal tubules, CLDN3 in the distal tubules, CLDN4, 7 in the distal tubules, the collecting duct and the pyelon. In oncocytomas only CLDN7 showed a weak, focal, positive reaction, while the other CLDNs were negative. Similarly, CLDN7 was the only CLDN detected in CRC, though with much stronger reaction. In CRCCs intensive expression of CLDN4, 7, and a weak reaction for CLDN2 were observed, while CLDN1 and 3 were negative. In contrast, CLDN1 was expressed in PRCCs, while reaction for the other CLDNs was similar to that observed in CRCCs.
Conclusions: We described a characteristic CLDN pattern in the kidney, which is preserved through the embryonal development till the adult stage. Marked differences were noted among the tumors probably representing different cellular origin, which might be used in differential diagnosis too.
This work was supported by grants NKFP-1A/0023/2002 and ETT-077/2003

P 852

RELATIONSHIP BETWEEN VASCULAR ENDOTHELIAL GROWTH FACTOR (VEGF) IMMUNOSTAINING PATTERN, VEGF PLASMA LEVELS, TUMOR NECROSIS AND USUAL PROGNOSTIC VARIABLES IN RENAL CELL CARCINOMAS

Nathalie Rioux-Leclercq, Patricia Fergelot, Emmanuelle Leray, Karim Bensalah, Francois Guille, Bernard Lobel, Jean-Jacques Patard.
Departement d'Anatomie et Cytologie Pathologique, Service de Santé Publique, Service d'Urologie, Groupe de Génétique et du Développement UMR-CNRS 6061, CHU, Faculté de Médecine, Rennes.

Objectives: VEGF has been proposed as an important prognostic marker in RCC. However no optimal method of VEGF measurement has been defined so far. The objective of this study was to compare different VEGF measurement modalities to usual clinical and pathological variables in order to better define links between tumor aggressiveness and VEGF blood release.
Methods. 50 clear cell carcinomas were prospectively analysed for VEGF levels by enzyme-linked immunosorbent assay in peripheral blood and in renal vein during nephrectomy (VEGFrv). In addition, detection of VEGF expression was performed in tumor tissue by immunohistochemistry (VEGFt) and three different types of VEGF immunostaining were defined: membranous (type 1), cytoplasmic (type 2) or both: (type 3) . The results were correlated together as well as to the following clinical and pathological variables: TNM stage, Fuhrman grade, tumor size, ECOG performance status, presence of tumor necrosis on pathological analysis, haemoglobin, platelet and leucocyte counts. Mann-Whitney and Kruskal-Wallis tests were used for comparison.
Results : VEGF immunostaining types and tumor necrosis were both correlated to T Stage (p:0.02) and Fuhrman grade (p:0.001 and 0.002 respectively). Tumor necrosis and VEGF immunostaining type were strongly correlated together: 5.3%, 62.2% and 80% of tumors with type 1, 2 and 3 VEGF immunostaining displayed necrotic lesions respectively ($p<0.0001$). VEGFpv (p:0.003), VEGFrv (p:0.03), VEGFt ($p<0.001$), platelet count (p:0.02) and haemoglobin (p:0.01) were correlated to VEGF immunostaining type. For example median VEGFpv was 99 (12-582), 144 (20-437) and 301pg/ml (230-1087) in type 1, 2 and 3 immunostaining type respectively. Similarly the presence of tumor necrosis was associated with increased VEGFpv (p:0.03), VEGFrv (p:0.0001), VEGFt (p:0.001), and platelet count (p:0.001) as well as with decreased haemoglobin level (p:0.02). Finally both VEGF immunostaining profile and tumor necrosis were associated with early cancer recurrence (p:0.003).
Conclusion. We presented here a particular VEGF tumor immunostaining pattern which is related to high levels of circulating VEGF and higher tumor stages. Moreover relationship between tumor necrosis and VEGF both in tissue and in peripheral blood is an additional evidence of the importance of the VHL/hypoxia inducible pathway in RCC.

P 853

CORRELATION BETWEEN RENAL ARTERY CHANGES AND TUMOR NECROSIS IN PATIENTS WITH RENAL CELL CARCINOMA

Tomi; K, Mladinov D, Tomas D, Tomi&; L, Belicza M, Krušlin B.
Department of pathology, Josip Benevi General Hospital Slavonski Brod, Croatia
Ljudevit Jurak Department of Pathology, Sestre milosrdnice University Hospital Zagreb, Croatia

INTRODUCTION: Different lesions might involve main renal artery such as arteriosclerosis, fibromuscular dysplasia (FMD) and some other conditions (arteritis, radiation injury and congenital malformations). Renal cell carcinoma (RCC) represents 2% of all human malignancies and over 90% of all malignancies of the kidney. Necrosis, cysts, hemorrhage and calcification are commonly present.
PURPOSE OF THE STUDY: Aim of the study was to correlate the presence and extent of necrosis in RCC and renal artery status.
METHODS: We analyzed a consecutive series of 112 patients (M: F=71:41) with RCC who underwent nephrectomy in the period from 2003 to 2004. Patients were aging from 35-82 years (mean 60.5) and the tumor size was 2-20 cm (mean 6.1). Necrosis was found in 88 (78.6%) cases of RCC of which 63 had less than 50% necrosis and 25 tumors contained more than 50% necrotic areas. Specimens were routinely fixed, embedded in paraffin, cut and stained with hematoxylin and eosin, Mallory trichrome method and orcein.
RESULTS: Renal arteries of 50 (44.6%) patients (M: F=36:14) showed no changes (Group I). These patients were in age from 38-78 years (mean 57.8) and tumors measured from 2.5-17 cm (mean 7.4). FMD (Group II) was found in 41 (36.6%) patients (M:F=17:24) ranging in age from 35-81 years (mean 59.1), and the tumor size was 2-19 cm (mean 8.2 cm). Atherosclerotic changes of renal arteries (Group III) were observed in 21 (18.8%) patients (M:F=18:3), aged from 42-82 years (mean 67.2) with tumors from 2-20 cm (mean 6.7).
In the first group necrosis was not found in 11 (22.0%) cases, 30 (60.0%) had less than 50% necrosis and 9 (18.0%) tumors were necrotic in more than 50%. In the second group, 7 (17.1%) cases were without tumor necrosis, 24 (58.5%) had less than 50% necrosis and 10 (24.4%) tumors were more than 50% necrotic. In the third group, 6 (28.6%) tumors did not show necrosis, 10 (47.6%) were less than 50% necrotic and 5 (23.8%) had more than 50% necrosis. Within the second group RCC of patients with FMD type I, 3 cases were less than 50% necrotic, while 4 cases were more than 50% necrotic, and only one was without necrosis. In the group of patients with FMD type IIb, 5 tumors were without necrosis, 21 had less than 50% necrosis and 4 were more than 50% necrotic.
CONCLUSION: Renal artery changes are very common in patients with RCC. Necrosis of the tumor was more common in patients with associated FMD and atherosclerotic changes of renal artery. However, t

P 854

SARCOMATOID RENAL CELL CARCINOMA. REPORT OF TWO CASES WITH IMMUNOCHISTOCHEMICAL STUDY

TSOBANIDOU Chrysoula1, NIKOLAIDOU Anastasia2, HASAKIOILIS Pantelis3, KLAMBATSAS Athanasios3, SACHINIS Konstantinos3
AMANATIDOU Simela, Technisian 2
1Department of Pathology, "Theagenio" Anticancer Institute, Thessaloniki, Greece
2Department of Pathology, General Hospital of Kilkis, Kilkis, Greece
3Department of Urology, General Hospital of Kilkis, Kilkis, Greece

Introduction: Sarcomatoid Renal Cell Carcinoma (SRCC) is an uncommon subtype of Renal Cell Carcinoma (RCC) with a poor prognosis. The origin of the sarcomatoid component is controversial: some authors consider it to be a dedifferentiation of the epithelial component while others believe that this tumor is a true carcinosarcoma.

Purpose-Method: In the present report two cases of this rare entity were studied using an extensive immunohistochemical panel of antibodies: cytokeratin 7, cytokeratin 20, cytokeratin 8, cytokeratin 18, cytokeratin 19,

P53, Bcl-2, Ki-67, AFP, PLAP, EMA, CEA, Vimentin Cyclin D1 and S-100.
The expression of these antibodies was evaluated in the sarcomatoid component.

Results: The first case showed no epithelial differentiation and in the second case the epithelial component was conventional RCC.
The two cases were intense and diffusely positive against vimentin. The second case did not show any positivity for any of the cytokeratin antibodies. The first case showed positivity for cytokeratin 8, cytokeratin 19, EMA, CEA, Cyclin D1, P53 overexpression and Ki-67 high labeling index.

Conclusion: Our results suggest that SRCC includes two different entities that should be separated: a sarcomatoid carcinoma and a mixed tumor with a true sarcomatous component.

P 855
CELL CYCLE REGLATORY FACTORS IN RENAL CELL CARCINOMA

PETRUSCA Daniela1, PETRESCU Amelia2, CONSTANTIN Claudia1, JINGA Viorel2, NICULESCU Liviu3, ROMAN Viviana1, HOTNOG Dan1, BRASOVEANU Lorelei1
1. Center of Immunology "St.S. Nicolau"Institute of Virology, Bucharest Roamnia 2."Prof.Dr.Th. Burghele" Hospital, Bucharest Romania 3.University of Medicine and Pharmacy "Carol Davila", Bucharest, Romania

Introduction and aims: In this study we analysed the immunohistochemical expression of p53, Bcl-2, Rb and PCNA and the relation of this expression to apoptotic status, clinicopathological characteristics and prognosis in renal cell carcinoma specimens.
Material and methods: The expression of p53, Bcl-2, Rb and PCNA was studied by immunohistochemical methods in paraffin-embedded nephrectomy specimens from 22 patients with no history of chemotherapy, radiotherapy, or immunotherapy. The apoptotic status was determined by flow-cytometry following propidium iodide incorporation.
Results: The p53 protein expression was recognized with a very low intensity (1-8%) in most of the cases but not in those with sarcomatoid features where it was elevated (30%). The expression of Bcl-2 was recognized in only 17% of cases also with low intensity; it was associated with the high tumoral grade and medium apoptotic intensity. Half of the tumor specimens were Rb positive, it absences correlated with a high grade and a high mitotic index. PCNA was detected in 86% of cases and showed a heterogeneous expression and correlated with the high grade of tumor. In 2 cases PCNA expression was absent and was correlated with a very differentiated tumor tissue.
Conclusions: Our observations suggest that the high apoptotic intensity of these tumors seems to be not p53 dependent. Thus, the low p53 expression could sustain the high degree of resistance to chemotherapy and radiation of renal cell carcinomas. Also, our results emphasizes that high grade differentiated tumor cells induce Bcl-2 expression in order to stop apoptotic process. In renal cell carcinomas Rb protein seems to act like an antiproliferative factor but not like an antiapoptotic one. We observed that PCNA expression increase while apoptotic intensity decrease. In our study the expression of p53, bcl-2 had no independent prognostic value and suggests that they would play a minimal role in helping to further stratify patients at high risk for disease progression or recurrence. Rb and PCNA seem to be a good objective and quantitative marker of biological malignant potential in renal cell carcinoma.

P 856
CYSTIC RENAL CELL CARCINOMAS IN ADULTS: IS PREOPERATIVE RECOGNITION OF MULTILOCULAR CYSTIC RENAL CELL CARCINOMA POSSIBLE?

AUBERT S°, ZINI L*, DELOMEZ J§, BISERTE J*, LEMAITRE L§,GOSSELIN B°, LEROY X°
°Department of Pathlogy, CHRU LILLE FRANCE
*Department of Urology, CHRU LILLE FRANCE
§Department of Radiology, CHRU LILLE FRANCE

Purposes: To correlate clinicopathological and imaging features of multilocular cystic renal cell carcinomas in order to propose preoperative criteria for therapeutic modalities.
Materials and Methods: Twenty four clear renal cell carcinomas with a chiefly cystic component were identified from 1993 to 2002. For each case, histological slides and available imaging studies were retrieved. Two tumor groups were defined: multilocular cystic renal cell carcinomas (MCRCC) and clear renal cell carcinomas with cystic change (CRCC) either by intrinsic growth or necrotic degeneration. Radiological correlation using CT scan and MRI studies was performed considering criteria such as mural nodule, cyst wall thickness, septa.
Results: On imaging study, MCRCC presented as a multilocular cystic mass lacking mural nodule, with regular thin cyst wall and septa. On pathologic study, MCRCC presented as complex, multilocular cystic carcinomas with septa covered by low nuclear grade clear renal tumor cells without grossly expansible nodule. They were all staged pT1 with a free clinical course. On the opposite, CRCC were described on imaging study with a mural nodule (5 mm or higher), thick, irregular cyst wall and irregular septa. On pathologic study, CRCC were characterized by a grossly expansible nodule within the septa and/or the cyst wall. Nuclear grade and TNM stage were higher in CRCC.
Conclusions: Preoperative recognition of MCRCC is possible when using strict CT and/or MRI criteria. The current study confirms the low malignant potential of MCRCC. A nephron sparing surgery should be proposed when MCRCC is suspected.

P 857
MORPHOMETRICAL ANALYSIS OF RENAL ARTERIES IN PATIENTS WITH RENAL CELL CARCINOMA

Batelja VuleticL, Mladinov D, TomicK, VucicM, Belicza M, Krušlin B
Dpt of Pathology, School of Medicine, Ljudevit Jurak Department of Pathology, Sestre Milosrdnice University Hospital, Zagreb, General Hospital Josip Bencevic, Slavonski Brod, Croatia

Introduction: The presence of tumor necrosis in renal cell carcinoma (RCC) is very common and was correlated with different features including tumor size, cell type, nuclear grade as well as microvessel density and the expression of different markers. However, there are no data about the relationship between renal artery changes including atherosclerosis and fibromuscular dysplasia (FMD) and the extent of necrosis in RCC.
Purpose of the study: to analyze renal arteries in patients with RCC especially regarding the thickness of medial layer and circumference of the artery using image analyzer.
Methods: We analyzed a consecutive series of 57 (35 male and 22 female) patients ranging in age from 35-79 years (mean 58.9 years) who underwent nephrectomy due to RCC in the year 2003. The patients had RCC measuring from 2-16 cm (mean 7.1 cm). Renal arteries were cut during nephrectomy up to 2 cm from renal hilus. Specimens were routinely fixed, embedded in paraffin, cut and stained with hematoxylin and eosin, Mallory trichrome method and orcein.
Results: The thickness of the media of 40 patients measured from 167.86-1177.21 μm (mean 571.35). Renal arteries of 17 patients (11 male, 6 female) were not measured due to

technical problems. The mean thickness of media in patients with FMD was 567.33 μm, those with arteriosclerosis 637.18 μm and with no renal artery changes 551.11. μm). There was a difference between the thicknesses of media in different types of FMD (FMD type I = 590.83 μm, FMD type IIA was 476.92 μm). Renal arteries of patients with arteriosclerosis were larger in comparison to arteries with no changes (4.2 mm: 3.5 mm), and control arteries obtained at autopsy, however this difference was not statistically significant.
Conclusion: Renal arteries of patients with RCC and atherosclerotic changes have thicker media and larger diameter in comparison with controls, and those with FMD.
The cause of such changes and their relationship to the degree of tumor necrosis and other changes in renal arteries should be further analyzed.

P 858
RENAL SINUS INVASION IN RENAL CELL CARCINOMAS.
Pasechnik D.

The renal sinus (RS) is the fatty region located near the renal cortex and not delineated from it by a fibrous capsule. The large quantity of vessels promotes a hematogenous and lymphogenous dissemination of the cancer cells at the tumor invasion to this zone. However, the present TNM staging system for renal cell carcinomas (RCC) does not take into the RS involvement.
The aim of research was to estimate the frequency of the RS invasion in RCC and its connection with tumor stage, grade and the histological form.
118 RCC were investigated (86 clear cell carcinomas, 13 papillary carcinomas, 11 chromophobe cell carcinomas, 8 oncocytomas). The tumor size of 51 renal carcinomas did not exceed 7cm; 67 RCC were over 7cm. The RS invasion was revealed in 81 cases RCC (68,6 %): 66 (76,7 %) clear cell carcinomas, 7 (53,8 %) papillary renal carcinomas, 8 (72,7%) chromophobe cell cancer. Oncocytomas did not invade into the RS. The RS involvement correlated with a nuclear grade of RCC. The RS invasion was 10 of 30 a low nuclear grade tumours (Fuhrman's grade 1-2) (33,3%), 55 of 71 a moderate nuclear grade tumours (Fuhrman's grade 2-3) (77,5%) and all of 17 a high nuclear grade tumours (Fuhrman's grade 3-4). However, the RS invasion did not depend on the tumor size. The RS involvement was marked at 39 (33,1 %) of patients at the tumor size up to 7 cm, and in 42 (35,6 %) cases at the tumor size over 7 cm. Tumour localization was the prior feature than tumour size. Among the RCC up to 7cm, the RS involvement was 19 (65,5%) of the 29 lateral location tumours, and 20 (90,9%) of the 22 medial location tumours. Besides fatty tissue, 44 (37,3 %) RCC invaded into the RS veins and lymphatic vessels. 11 (9,3 %) kidney cancer invaded into the lumen of the main renal vein. In 25 (21,2 %) RCC, the RS invasion combined with intrarenal dissemination of tumor. At the absence of the RS invasion, metastasizes were lacking.
The RS involvement should be regarded as a risk factor of the tumor dissemination. The prognostic value of the RS invasion in RCC is necessary to take into future revision of the TNM stading system for the tumors of this localization.

P 859
INCIDENTALLY DIAGNOSED RENAL CELL CARCINOMA: CLINICOPATHOLOGICAL FEATURES.
Pasechnik D., Gusev A., Kogan M., Derizhnova I.

In the last 20 years, with the increasing use of abdominal ultrasound and CT scans, many renal tumours are being diagnosed incidentally during examinations for other conditions.
Our study aimed to compare the clinicopathological features of renal cell carcinomas (RCC) discovered incidentally with those of symptomatic tumours. We retrospectively analyzed 149 patients subjected to radical nephrectomy.
61 tumours (40,93%) were diagnosed incidentally. No significant difference was detected between both groups in regards to middle age, sex, and histological type. A greater incidence of tumours in stage T1a was found in incidental RCC (59,21% vs 12,5%), while advanced forms (stage T3) were more frequent in symptomatic RCC (24,59% vs 67,04%). 33 (54,1)% incidental RCC were a low nuclear grade (Fuhrman's grade 1 or 2) and only 3 (5%) tumours were high grade. 2 (3,3)% incidental RCC were N1, and none were M1, whereas 15 (17%) symptomatic RCC were N1-2, and 9 (10,2%) were M1. Survival after 5 years was of 69,1% for symptomatic patients in comparison to 85,7% for the incidental group, which implies high statistical signification (log rank = 0.0018).
The patients with incidentally discovered RCC had a prognostically more favorable tumour size, stage and grade.

P 860
ASSOCIATION OF CXCR4 CHEMOKINE RECEPTOR EXPRESSION WITH MMP AND TIMP MRNA TRANSCRIPTION IN CLEAR-CELL RENAL CELL CARCINOMA
K. Struckmann 1, K. Mertz 1, P. Staller 2, W. Krek 2, P. Schraml 1, and H. Moch 1
1 Institute of Clinical Pathology; University Hospital Zurich
2 Institute of Cellbiology, ETH Zurich

Introduction: CXCR4 chemokine receptor mediated signalling is of importance for the metastatic process in a variety of human cancers. We have recently found increased CXCR4 expression levels in clear-cell renal cell carcinoma (ccRCC) compared with normal renal tissue. This study also revealed an association between strong CXCR4 expression and poor tumour-specific survival indicating the importance of this chemokine receptor in renal tumour biology (ccRCC; Nature, 425, 2003). Interestingly, it has been shown in vitro that ligand stimulation of CXCR4 leads to alterations in the expression levels of certain Matrix Metalloproteinases (MMPs) and Tissue Inhibitors of Matrix Metalloproteinases (TIMPs). Since deregulated expression of MMPs and TIMPs is one of the pre-requisites for tumour growth and tissue invasion in many human cancers including ccRCC one might consequently speculate that increased CXCR4 signalling contributes to tumour progression and metastatic dissemination by influencing the expression of MMPs and TIMPs.
Aims: In order to analyse the association of CXCR4 and MMP/TIMP expression in ccRCC we have correlated the mRNA abundance of certain MMPs and TIMPs with the CXCR4 expression status in primary tumour samples.
Methods: mRNA expression levels of MMP2, MMP9, TIMP1, and TIMP2 were determined in 29 primary ccRCC and 7 normal renal tissues with known CXCR4 expression levels by RT-PCR using the LightCycler system. The abundance of MMP/TIMP transcripts were correlated with the CXCR4 mRNA expression status of the given tissue samples.
Results: Twenty-six of 29 ccRCCs showed an increase of more than 2-fold in the expression level of CXCR4. The average increase in CXCR4 expression was 7.3-fold (range 2.3-18.8-fold). Expression of TIMP1 and TIMP2 did not correlate with CXCR4 expression levels. In contrast, mRNA expression of MMP2 and MMP9 was significantly higher in tumours with strong CXCR4 expression ($p=0.04$ and $p=0.01$, respectively).
Conclusions: CXCR4 up-regulation in ccRCC is associated with increased mRNA expression levels of MMP2 and MMP9. Our results provide first evidence for the involvement

of the CXCR4-MMP/TIMP pathway in renal cancer progression.

P 861

CIGARETTE SMOKING, VON HIPPEL-LINDAU GENE MUTATIONS AND SPORADIC RENAL CELL CARCINOMA

VAN DIJK Boukje A.C. (1), SCHOUTEN Leo J. (1), OOSTERWIJK Egbert (2), HULSBERGEN-VAN DE KAA Christina A. (3), KIEMENEY Lambertus A.L.M (2,4), GOLDBOHM R. Alexandra (5), SCHALKEN Jack A. (2) and VAN DEN BRANDT Piet A.(1).
1)Department of Epidemiology, NUTRIM, Maastricht University, Maastricht, the Netherlands.
2) Department of Urology, Radboud University, Nijmegen Medical Centre , Nijmegen, the Netherlands.
3) Department of Pathology, Radboud University, Nijmegen Medical Centre, Nijmegen, the Netherlands.
4) Department of Epidemiology and Biostatistics, Radboud University, Nijmegen Medical Centre, Nijmegen, the Netherlands.
5)Department of Food and Chemical Risk Analysis, TNO Nutrition and Food Research, Zeist, the Netherlands.

INTRODUCTION
Cigarette smoking is a known risk factor for renal cell carcinoma (RCC) with a modestly increased rate ratio (RR) and a positive dose-response relation. Cigarette smoke metabolites can cause mutations in human DNA.
Von Hippel-Lindau (VHL) gene mutations are considered a primary event in the carcinogenesis of RCC.
PURPOSE
We investigated whether smoking is associated with mutations in the VHL gene in sporadic RCC.
METHODS
The Netherlands Cohort Study on diet and cancer (NLCS) includes 120,852 persons, who completed a self-administered questionnaire on smoking habits and other factors. After 11.3 years of follow-up, 337 cases and a random sample of 5,000 persons (subcohort) were used in a case-cohort approach. Collected tumor DNA (N=235) was analyzed for VHL gene mutations. RRs and corresponding 95% confidence intervals (CI) were estimated using Cox proportional hazard models, adjusting for age, sex and body mass index.
RESULTS
For men, RRs for total RCC were 1.52 (95% CI: 0.89-2.59) and 2.07 (95% CI: 1.20-3.56) for ex- and current smokers compared to never smokers, respectively. Estimates for women equaled 0.95 (95% CI: 0.57-1.59) and 1.37 (95% CI: 0.87-2.16), respectively. For men, RRs for current smokers compared to never smokers were 2.34 (0.79-6.94) and 2.95 (0.65-13.28), for VHL gene mutated and VHL wildtype tumors, respectively. For women, these estimates were 0.82 (0.35-1.93) and 2.04 (0.94-4.45), respectively. Results have to be interpreted cautiously because of small numbers.
CONCLUSION
Smoking was associated with RCC risk of men, but not specifically with VHL gene mutations, irrespective of sex, suggesting that smoking may cause RCC independent of VHL gene mutations.

P 862

C-KIT EXPRESSION IN RENAL EPITHELIAL TUMORS

ÖZAÐARI Ayþim, KABUKÇUOÐLU Fevziye, SAKIZ Damlanur, ÇAÞKURLU Turhan, KÝREMÝT Murat Can, GÜMÜÞ Eyüp
Þiþli Etfal Education and Research Hospital, Department of Pathology and Department of Urology, Ýstanbul, TURKEY

C-kit encodes the membrane-bound tyrosine kinase KIT, whose expression has been identified in several types of human neoplasms. The overexpression of c-kit in chromophobe renal cell carcinoma and oncocytoma has been proposed as a possible specific hallmark of these neoplasms. The aim of this study is to establish immunohistochemical expression of KIT in a series of renal epithelial neoplasms and the normal renal tissues.
In this study we analysed KIT expression in 45 surgical specimens of clear cell, papillary, and chromophobe renal cell carcinomas and oncocytomas with the adjacent normal renal tissue. There were focal sarcomatoid differantiation in 6 cases. The extent of immunoreactivity was categorized as focal, moderate, and diffuse. Only membranous staining was considered positive.
All cases of chromophobe renal cell carcinomas (n=6) and two of 3 cases of oncocytomas showed diffuse membranous staining. Three of 33 cases of clear cell renal cell carcinomas were focally positive for KIT. One case with sarcomatoid differantiation showed focal positivity in the sarcomatoid areas. None of 3 papillary carcinomas were positive. In non-neoplastic kidney tissue adjacent to the tumor, strong KIT expression was detected in the cytoplasm of the renal tubules. The results suggest that KIT plays a role in the tumorigenesis of chromophobe renal cell carcinoma and oncocytoma, and could be a useful marker for differential diagnosis of different renal cell carcinomas. Overexpression of KIT in some subtypes of renal tumors indicates a potential therapeutic role for tyrosine kinase inhibitors in managing patients with these tumors.

P 863

EPITHELIAL CELL ADHESION MOLECULE (EPCAM) EXPRESSION IN RENAL CELL CARCINOMAS (RCC). A TISSUE MICROARRAY (TMA) STUDY

PANIZO Angel, SOLA Jesus Javier, TOLEDO Gemma, IDOATE Miguel Angel, LOZANO Maria Dolores, PARDO Javier.
Departamento de Anatomia Patologica. Clinica Universitaria de Navarra. Pamplona. Spain

Introduction: EpCam is a widely expressed adhesion molecule in normal epithelium of different organs and in epithelial neoplasms. Due to its membrane distribution, specific immunotherapies are now being used with promising results. Advances in the treatment of patients with RCC are utmost importance to improve the prognosis. The aim of this study was to study the expression of EpCam in RCC using TMA.
Methods: We studied retrospectively EpCam expression of renal tumors and matched normal renal tissue using a TMA. Different histologic subtypes of RCC were investigated, including 109 clear cell, 38 papillary RCC, 10 papillary adenomas, 50 chromophobe, 31 oncocytomas, 2 collecting duct carcinomas, and 2 mucinous tubular-spindle cell carcinomas. Primary clear RCC and corresponding metastases (n=32) were also studied. A mouse mAb anti-EpCam (clone VU-1D9, Novocastra, dilution 1:50) was applied after trypsin pretreatment. The immunoreactivity was correlated with clinicopathological data.
Results: EpCam is expressed in the distal nephron on normal renal tissue. EpCam overexpression was found in 17.4% of clear RCC (4.6% strong, 12.8% moderate). A total of 59 cases were negative. There was significant association between EpCam overexpression and distant metastases at diagnosis (pM stage) (p=0.03), and overall stage (p=0.039). Overall, 18.8% of metastases of clear RCC did show EpCam overexpression. EpCam overexpression was a significant univariate predictor of increased survival in clear RCC (p=0.035). Twelve (31.6%) of 38 papillary RCC showed EpCam overexpression. There was no different EpCam expression in type 1 and 2 papillary RCC. Three of 10 papillary adenomas showed EpCam overexpression. Fourty-

six (92%) chromophobe RCC showed EpCam overexpression (88% strong, 4% moderate), whereas only one (3.2%) oncocytoma revealed moderate EpCam in sparsely clustered cells ($p<0.05$). All cases of collecting duct and mucinous tubular-spindle cell carcinomas were negatives.
Conclusions: In clear RCCs, EpCam overexpression could be used as a prognostic marker (associated with improved survival). EpCam represents a potential target for immunotherapy (mAbs or vaccines) in the adjuvant and palliative treatment of RCCs. EpCam immunohistochemistry proves to be a useful tool in the differential diagnosis between chromophobe RCC and oncocytoma, because of the different staining patterns of these two entities.
Funded by the Ministry of Health of Spain FIS 02/0835

P 864
GRANULOMATOUS REACTION IN PRIMARY ADULT RENAL NEOPLASMS: A CLINICOPATHOLOGICAL AND MOLECULAR STUDY OF 17 CASES
PANIZO Angel, SOLA Jesus Javier, TOLEDO Gemma, IDOATE Miguel Angel, LOZANO Maria Dolores, PARDO Javier.
Departamento de Anatomia Patologica. Clinica Universitaria de Navarra

Introduction: Granulomatous reactions (GR) within lymph nodes draining malignant neoplasms are well known. More rarely, GR may occur within the stroma of malignancies. The occurrence of GR in renal neoplasms appears to be much more rare (few cases reported).
Methods: Retrospective analysis of 488 renal cell carcinomas (RCC) and 25 renal angiomyolipomas (AML), diagnosed between 1994 and 2005, was performed. Clinicopathological data were reviewed. In selected cases, sections were stained with PAS, Grocott, and Ziehl-Neelsen. Immunohistochemical studies were performed using mAb againts CD20, CD3, CD4, CD8, and CD68. Paraffin sections and/or frozen tissue were subjected to molecular analysis: PCR method was used to detect the presence of M. tuberculosis complex DNA.
Results: Among 488 RCC studied, 16 cases (3.27%) with GR were detected. Thirteen patients were male (81.3%), and three were female, with a mean age of 60.4 yrs (range:34-77 yrs). No patient from our serie had any history of sarcoidosis or other granulomatous disease. The histological type of RCC were clear cell (n=12), papilary (n=1), chromophobe (n=1), and unclassifiable (n=2). Mean tumor size was 4.85 cm (range: 2.2-10 cm). Eleven of the 16 cases were TNM stage I or II. One case of GR was detected among 25 AML reviewed. GR was observed within the tumor stroma in all cases (focal: 7 cases, and diffuse 10 cases) and 3 cases had also GR within the normal kidney. One case demonstrated GR within lymph node metastasis. GR was characterized by groups of epithelioid cells and multinucleated giant cells (strongly positive for CD68), and small lymphocytes (predominantly CD3 althoug scattered CD20 positive were observed) without central necrosis in 14 cases (sarcoid-like). In 3 cases GR had central caseating necrosis: Mycobacteria were identified using Ziehl-Neelsen in 2 cases, and infection by M. tuberculosis complex were proved in 2 cases using PCR. Clinical follow-up was complete in 16 patients (median: 8.18 mos.; range: 1.83-109.13 mos): twelve patients were alive without clinically detectable tumor and granulomatous process.
Conclusions: The occurrence of granulomas within the stroma of renal neoplasms is extremly rare. Sarcoid-like GR in renal neoplasms could be an immunological response to tumor antigens. In patients with no previous diagnosis of tuberculosis, the discovery of caseating granulomas after nephrectomy for RCC is exceptional
Funded by the Ministry of Health of Spain FIS 02/083

P 865
STRONG COEXPRESSION OF OSTEOPONTIN AND VASCULAR ENDOTHELIAL GROWTH FACTOR CORRELATES WITH SURVIVAL IN CLEAR CELL RENAL-CELL CARCINOMA
MATUSAN Koviljka, DORDEVIC Gordana, MOZETIC Vladimir*, JONJIC Nives, LUCIN Ksenija
Department of Pathology, Rijeka University School of Medicine and Department of Urology*, Clinical Hospital Center Rijeka, Rijeka, Croatia

INTRODUCTION: Osteopontin (OPN) is a highly phosphorylated protein with numerous functions, including roles in bone remodelling, cell-adhesion, cell-mediated immunity, cell signalling, and angiogenesis. It has been recognized as a transformation-associated protein and as a potential prognostic factor for various human cancers. Several lines of experiments have implicated OPN in angiogenesis, and it has been shown that vascular endothelial growth factor may induce expression of OPN. Also, it has been shown that osteopontin overproduced by tumour cells acts as a potent angiogenic factor contributing to tumour growth.
PURPOSE OF THE STUDY: The aim of this study was to analyse the relationship between the OPN and vascular endothelial growth factor (VEGF) expression in clear cell renal-cell carcinoma. Also, we have analysed the association of VEGF and OPN coexpression with disease outcome.
METHODS: A total of 81 clear cell renal-cell carcinomas were immunohistochemically analyzed for the OPN and VEGF expression and scored in a semi-quantitative manner, by combining tumour epithelial proportion score and intensity score. Statistical analysis was performed by nonparametric Spearman's correlation coefficient method. Survival probabilities were estimated by the univariate Kaplan-Meier method and survival curves were compared by the log-rank test.
RESULTS: Renal-cell carcinomas showed heterogeneous staining pattern for both OPN and VEGF, ranging from focal expression of low intensity to strong and diffuse cytoplasmic staining of tumor cells. We found statistically significant correlation between OPN and VEGF expression at the level $p=0.0026$, ($rs=0.3304$). Also, the survival of patients with strong OPN and VEGF coexpression was significantly worse compared to those with either low or without OPN and VEGF coexpression ($p<0.003$).
CONCLUSION: Our results show the upregulation of OPN and VEGF in clear cell renal-cell carcinomas. The correlation between their expression and the association of their strong coexpression with poor disease outcome support the hypothesis that cooperation of OPN and VEGF may facilitate tumor progression in human cancer.

P 866
CD34 EXPRESSION IN RENAL CELL CARCINOMA IS EXCEPTIONAL BUT MAY BE FOUND IN HIGH GRADE TUMORS
N. Juanpere1, M. Jimeno 1, M. Iglesias 1, V. Baena1, M. Garcia1, R. Esgueva1, R. Jaramillo 1, , O. Bielsa 2, A. Gelabert 2, S. Serrano 1 and J. Lloreta 1. 1

Background:
CD34 is a transmembrane protein expressed by primitive hematopoietic and mesenchymal cells, endothelial cells, and a variety of other cell types. Its expression in epithelial cells and carcinomas is exceptional, and has never been reported in renal cell carcinoma (RCC). The observation of CD117 expression in some subtypes of RCC prompted us to investigate the expression of CD34, as both molecules are often coexpressed in other proliferations, most notably gastrointestinal stromal tumors.
Design:
A total of 138 renal epithelial tumors (104 clear cell, 17 chromophilic, and 2

chromophobe carcinomas; 1 collecting duct carcinoma; 14 oncocytomas) were used to construct two different TMA blocks with 200 cores each. Consecutive sections of both were stained with H E and with antibodies (Ab) for CD34 (QBEND, Biomeda, CA), and CD117 (DakoCytomation, Denmark). Representative sections of the positive tumors were stained with Ab for CD34, CD117, CD10, Cam 5.2, AE1-AE3, keratin 7, keratin 34 E12, vimentin, and HMB45. The immunohistochemical reaction was visualized with the Envision system (DakoCytomation, Denmark).
Results:
Only two out of 138 tumors showed intense and diffuse CD34 expression but were negative for the CD117 Ab. In standard sections, both tumors showed strong and diffuse membranous staining of epithelial cells with CD34 Ab, and were in addition positive with Ab for CD10, Cam 5.2, AE1-AE3, and vimentin. Keratins 7 and 34 E12, and HMB45 were negative. Both cases were morphologically and immunohistochemically classified as clear cell RCC. Case 1 is a 53 year-old man with a Fuhrman grade 4, stage T1 N0 M0 tumor, that subsequently developed lymph node metastases, and that is alive with residual disease 15 years after surgery. Case 2 is a 70 year-old woman with a grade 4, T3a N1 M0 tumor, and she is alive without disease 4 years after surgery.
Conclusion:
CD34, although exceptionally, may be expressed in clear cell RCC, without CD117 coexpression. The two cases in this series suggest that this feature may be observed in a subset of high grade tumors progressing to or presenting with high stage disease.
Funded in part by grant FIS 99/0736, Fondo de Investigacion Sanitaria, Spanish Government

P 867
TISSUE MICROARRAY OVEREXPRESSION OF CYCLIN D1 IN RENAL EPITHELIAL TUMORS
N. Juanpere 1, M. Jimeno 1, M. Iglesias1, V. Baena1, M. Garcia1, R. Esgueva1, R. Jaramillo 1, O. Bielsa 2, S. Hernandez 3, A. Gelabert 2,4, S. Serrano 1,4 and J. Lloreta 1,3.

ABSTRACT
Background: Cyclins have an essential role in cell cycle control. Cyclin D is involved in the G1/S transition. The prevalence, biological meaning and prognostic impact of Cyclin D1 (CyD1) expression in renal cell carcinoma (RCC) are controversial. Some studies suggest a favorable role, but other series do not support this conclusion. This is a descriptive study of the immunohistochemical (IHC) overexpression of CyD1 in a RCC/oncocytoma tissue microarray (TMA), and its related clinicopathological variables in different tumor subtypes.
Design: A total of 138 renal epithelial tumors (104 clear cell (CCRCC), 17 papillary chromophilic (PCRCC), and 2 chromophobe carcinomas; 1 collecting duct carcinoma; 14 oncocytomas) were used to construct two different TMA blocks, 200 cores each. Consecutive sections were stained with an antibody for CyD1(DSC-6, DakoCytomation, Glostrup, Denmark). The IHC reaction was visualized with the Envision system (DakoCytomation, Glostrup, Denmark). CyD1 overexpression was defined as a 3+ intensity in more than 20% of the tumor cell nuclei.
Results: We found CyD1 overexpression in 9 (65%) of 14 oncocytomas, 23 (22%) of 104 CCRCCs, and 5 (30%) of 17 PCRCCs. From the 23 CyD1 overexpressing CCRCCs, 19 (82%) were low stage (T1-2), 17 (74%) were low grade (G1-2), and 18 (78%) were alive without disease. In the overall group of CCRCCs, 68% of the tumors were low stage, 57% were low grade, and 66% were alive without tumor. From the 5 CyD1 overexpressing PCRCCs, 4 were low stage, 1 was low grade, and all were alive without disease. In comparison, 65% of all the PCRCCs were low stage and low grade, and 70% were alive without disease.
Conclusion: 1.CyD1 is not uniformly overexpressed in all oncocytomas. 2.The proportion of CCRCCs overexpressing CyD1 is slightly lower than that of PCRCCs. 3.In both tumor types, this feature seems to be associated with more favorable prognostic variables than their respective overall groups. There is a paradoxically increased proportion of high grade cases in overexpressing PCRCC, that is not associated with higher stages or more adverse outcome. 4.CyD1 overexpression is relatively uncommon in RCC, and although it is associated with better outcome, it does not appear to be a useful tool in the prognosis of these tumors.
Supported in part by grant FIS 99/0736 (Fondo de Investigacion Sanitaria, Spain)

P 868
TISSUE MICROARRAY OVEREXPRESSION OF P53 AND PAB 240 IN RENAL CELL CARCINOMA
V. Baena1, M. Iglesias 1, M. Jimeno 1, N. Juanpere1, M. Garcia1, R. Esgueva1, R. Jaramillo 1, O. Bielsa 2, J. Santos 2, S. Hernandez 3, T. Baro 1,4, A. Gelabert 2,4, S. Serrano 1,4 and J. Lloreta 1,3

Background: The prognostic impact of p53 overexpression in renal cell carcinoma (RCC) is not fully understood. In different series, with diverse immunohistochemical (IHC) and evaluation protocols, variable p53 overexpression is reported, although association with poor outcome is usually suggested. We investigated the IHC overexpression of p53 in a RCC tissue microarray (TMA), using strictly standardized methods. We also studied expression of PAb-240, an antibody (Ab) that recognizes a p53 epitope exposed in many mutant forms of this protein. Expression of this Ab in RCC has not been previously reported.
Design: 138 renal epithelial tumors (104 clear cell (CRCC), 17 papillary chromophilic (PRCC), 2 chromophobe, and 1 collecting duct carcinoma; 14 oncocytomas) were used to construct two different TMA blocks (200 cores each). Ab for p53 (DO7, Novocastra, UK), and mutated p53 (PAb 240, DakoCytomation, Denmark) were used. A standardized IHC protocol included mutated cell lines as controls. p53 overexpression was defined as a 3+ intensity in >20% of the nuclei. PAb 240 was investigated in p53+ and - cases.
Results: p53 overexpression was observed in 12% (17 of 138 tumors): 30% (5 of 17) of PRCC and 12% (12 of 104) of CRCC. From those, 2 CRCC and 2 PRCC were positive with PAb 240, and the remaining cases in the TMA were negative. From all TMA cases, CRCC were high grade in 43%, high stage in 32% and progressed in 33% of cases. In contrast, 92% (11) of the p53 overexpressing CRCCs were high grade (3 G3 and 8 G4) and 75% (9) were high stage (6 T3 and 3 T4) and died with tumor. Similarly, p53 negative PRCCs were high grade in 20%, high stage in 30% and progressed in 20% of the cases, while 80% (4) of the overexpressing PRCCs were high grade (3 G3, 1 G4) and 40% (2) were high stage (T3,T4), progressing tumors.
Conclusion: 1. In both CRCC and PRCC, p53 overexpression is associated with a marked increase in grade, stage, and tumor progression. 3. Negativity of PAb 240 does not exclude non-productive mutations, but suggests that p53 overexpression is probably not associated with mutation. 3. p53 overexpression is uncommon in RCC, and is more often observed in PRCC than in CRCC. A large number of RCCs should be examined both by IHC and molecular methods to establish the prognostic and pathogenetic role of TP53 in renal cancer. (Funded by Fondo de Investigacion Sanitaria, FIS 99/0736, Spain.)

P 869
TESTICULAR GERM CELL TUMOR PATHOLOGY REPORTING

Climent MJ, Vidal A, Lerin MA, Tascon R, Garcia del Muro X*, Germà-Lluch JR* and Condom E.
Department of Pathology. IDIBELL. Hospital Universitari de Bellvitge (HUB). *Department of Medical Oncology (ICO).IDIBELL. Institut Català d'Oncologia. L'Hospitalet de Llobregat. Spain.

Introduction.
Accurate pathology report is crucial in providing information regarding prognostic factors and possible further treatment.
Purpose of the study.
To compare the standard of pathology reporting for testicular tumors with the checklist provided by the College of American Pathologists (CAP) and to evaluate potential variation in reporting by hospital type.
Methods.
We reviewed 211 pathology reports for adherence to recommendations of the CAP and calculated the overall percentage of each item. We classified hospitals by teaching and non-teaching hospitals and used the chi-squared test to determine whether statistically significant difference existed by hospital type (teaching and non-teaching).
Results.
Adherence to CAP recommendations was 100% for description of histologic type, 87% for tumor size and 82% for laterality. All other criteria were reported in <80% of cases. Overall, teaching hospitals demonstrated greater adherence to CAP recommendations when compared with non-teaching hospitals ($p<0.05$).
Conclusions.
Pathology reports of testicular germ cell tumors omitted some critical items. The variability in reporting is based on hospital type.

P 870
MORPHOLOGICAL VARIANTS OF A V. TESTICULARIS SINISTRA FORMATION IN CHILDREN WITH VARICOCELE
Severgina E, Leonova L, Kondakov V, Godlevskyi D, Pykov M, Sporius R

There is no clear conception about the venous system, generated from pl. pampinifomis in a retroperitoneal space in patients with varicocele now. We evaluated the incision biopsies of vessels received during a high ligation from 20 boys from 8 to 15 years old. The biopsies were fixed and paraffinized. Light microscopy, immunohistochemistry was performed with labeled, specific anti-VEGF and CD 34 antibodies.
There were arterial vessels, surrounded with groups of muscular type veins and a plenty of engorged capillaries and postcapillar venules in biopsies. We found three morphological variants of the muscularis type veins. Type I was presented by veins of a large diameter with gaping lumens and thick walls composed of three layers. The most thin internal layer contained endothelial and longitudinal smooth muscle cells; a medium layer included circularly directed smooth muscle cells; and the thickest external layer was composed of smooth muscle cell bundles directed longitudinally and separated from each other by collagen fibers. This morphological variant of veins was considered as the basic trunk of v. testicularis.
Type II veins had a irregular configuration of a lumen. Their walls were thinner, than these of type I veins and were composed of three layers. The thick longitudinal external layer had fragments of collagen and elastic fibers. The flabby valves or fragments of the valves were found in some veins. Dilated vessels with fibrous walls were present.
Type III veins had a small diameter and thick walls with well defined three layers. The external muscular longitudinal layer was much thicker than the medium and internal layers both. The characteristic feature of these vessels was a present of small “pillows” generated from longitudinal smooth muscle cells of the internal layer. These “pillows” filled the lumens of some veins. This is considered to be an adaptive response to prevent a retrograde blood flow.
Engorged capillaries are most likely the newly formed vessels ensuring improved outflow of blood. This is confirmed by expression of the angiogenic factor VEGF and CD34 on endothelium cells.
The morphological analysis of vessels within the incision biopsies revealed multiple character of v. testiculatis sinistra formation in pediatric patients with varicocele, represented by three morphological variants of muscularis type veins. First of them is principal. We showed the possible variants of compensatory drainage of blood from the pl. pampinifomis system.

P 871
EXPRESSION OF KLF-6 TRANSCRIPTIONAL FACTOR IN CIS AND MALIGNANT TESTICULAR GERM CELL TUMORS.
Regadera J 1, Sanz-Rodriguez F 2, Botella ML 3, Serrano A 4, Nistal M 1,5, P. Gonzalez-Peramato 6.
1 Department of Anatomy, Histology and Neuroscience, Autonoma University of Madrid; 2 Department of Biology, Autonoma University of Madrid; 3 Centro de Investigaciones Biologicas, CSIC, Madrid; 4 Department of Urology, Guadalajara General Hospital, Guadalajara; 5 Department of Pathology, La Paz Hospital, Madrid; 6 Department of Pathology, Guadalajara General Hospital, Guadalajara and University of Alcalá, Madrid. Spain.

INTRODUCTION. KLF-6 (Kruppel-like factor 6) is a transcriptional factor that has been shown to be mutated in a significant number of prostate and colon carcinomas. KLF-6 is a candidate tumor suppressor gene.
PURPOSE OF THE STUDY. KLF-6 immunoexpression was explored in 21 seminomas, 12 embryonal carcinomas, 7 immature teratomas, 4 mature teratomas, 6 yolk sac tumors, and 27 combined tumors, including carcinoma in situ (CIS) as well as 4 normal adult testes.
METHODS. A polyclonal anti-KLF-6 antibody (Santa Cruz) was used at 1:400 dilution. Streptavidine peroxidase Zymed kit was employed. The immunoreaction was revelated with DAB. KLF-6 western blotting was done in 13 cases, including 2 normal testis.
RESULTS. Variable KLF-6 expression was observed in the cytoplasm of spermatogonia in human normal testis. However a significant increased expression was shown in the cytoplasm of CIS cells. This intense stain was constantly seen in intratubular and infiltrative seminoma. In mature teratoma, KLF-6 the expression of KLF-6 is higher in the epithelial component than in the mesenquimal tissues, although KLF-6 is always present in the immature neuroepithelial teratomatous differentiation. Interestingly, KLF-6 expression is lost in undifferentiated embryonal carcinoma, the most aggressive of the testicular cancers studied. No specific KLF-6 stain in the different patterns of yolk sac tumors was observed. KLF-6 expression is significantly higher by Western blotting and densitometric measuring in the cancer cases than in the normal cases.
CONCLUSION. The overexpression of KLF-6 in all types of testicular germ cells tumors and even in CIS cells suggests that KLF-6 is a transcriptional factor that may be implicated in the development and progression of testicular malignant tumors.

P 872
SEMINIFEROUS TUBULES WITH AN ABNORMAL CONFIGURATION: A NEW LESION OF THE TESTICULAR DYSGENESIS SYNDROME.
González-Peramato P.1, Nistal M.2,3, Regadera J.3, Jiménez-Heffernan JA 1, Serrano A 4.

1Department of Pathology, University Hospital of Guadalajara, Guadalajara and University of Alcalá, Madrid. 2 Department of Pathology, La Paz Hospital, Madrid; 3 Department of Anatomy, Histology and Neuroscience, Autonoma University of Madrid; 4 Department of Urology, University Hospital of Guadalajara; Spain.

INTRODUCTION. The entity of "Testicular dysgenesis syndrome" includes several heterogenic pathologies as undescended testis, hypospadias, testis cancer and infertility. Associations of different testicular histological lesions have been observed in the testicular dysgenesis syndrome including undifferenciated seminiferous tubules, partial Sertoli-cell-only tubules, testicular microliths, CIS cells and Leydig-cell micronodules.
MATERIAL AND METHODS. In a retrospective revision of 450 prepubertal and adult patients with infertility, crytorchidism, intersex and testicular cancer from the files of La Paz University Hospital, 15 cases with seminiferous tubules with abnormal configuration were observed.
RESULTS. In all 15 cases a spectrum of different patterns of malformative configuration of the seminiferous tubules abnormally were seen. The morphological anomalies of the seminiferous tubules included frequent ramifications, annular configuration, culde sac dichotomy ending and changes in diameter in different segments, with dilatations alternating with hypoplastic stenosed tubular segments. Different grades of impairment of the spermatogenesis was observed in this variants of abnormally configurated tubules. This new lesion was found in: 7 crytorchidic testis (5 with ambiguous external genitalia), 3 patients with descended testes that consulted on infertility, 2 patients with testicular microliths and 3 in the testicular biopsy contralateral to the testis excised by testicular cancer.
CONCLUSIONS. Seminiferous tubules with abnormal configuration was present both in infantile and adult testis which suggest a primary lesion. The lesion we describe should have been begin at that moment of the fetal development, because the abnormal tubules resemble the first stadies of the formation of sexual cords in normal fetus. However, the absence of remodelation of these sexual cords will cause the persistence of seminiferous tubules with an irregular caliber, frequent anatomosis and an irregular spermatogenesis varying from normal to completely absent. We suggest that the seminiferous tubules with abnormal configuration are characteristic lesions founded in testicular dysgenesis syndrome.

P 873
THE EFFECT OF CAFFEIC ACID PHENETHYL ESTER (CAPE) ON HISTOPATHOLOGICAL CHANGES IN TESTICULAR ISCHEMIA-REPERFUSION INJURY

* ATÝK Esin, **GÖRÜR Sadýk, **CANDAN Yaþar, **KÝPER Ahmet
(*)Department of Pathology, Mustafa Kemal University, Faculty of Medicine, Antakya-Hatay / Turkey
(**) Department of Urology, Mustafa Kemal University, Faculty of Medicine, Antakya-Hatay / Turkey

Purpose: Testicular torsion causes an enhanced formation of reactive oxygen species which contributes to the pathophysiology of ischemia-reperfusion injury in testis. We evaluated here the effect of caffeic acid phenethyl ester (CAPE), a new antioxidant and anti-inflammatory agent on histopathological changes in testicular ischemia-reperfusion injury.
Materials and Methods: Adult male Wistar rats were divided into 6 groups of 5 each: Control group1 (n=5), sham operation group2 (n=5), torsion/detorsion (T/D) group3 (n=5), T/D+Saline group4 (n=5), T/D+CAPE group5 (n=5) and T/D+CAPE group6 (n=5). One group served to determine baseline values of histopathological parameters, 1 that underwent sham operation served as a control, others were subjected to left unilateral torsion (2 h) and detorsion (4 h) periods. Rats were sacrified and unilateral orchiectomy was performed. Testis tissues were put into Bouin's solution. After routine tissue proccesing myeloperoxidase (MPO) and inducible nitric oxide synthase (iNOS) immunohistochemical methods were studied from paraffin embedded tissues.
Results: Treating rats with CAPE (applied at 10 µmol/kg, 30 min. prior to T/D) attenuated the testicular injury and as well as the tissue levels of MPO. At the same time testis tissue showed an increase in iNOS activity.
Conclusion: Our results suggest that CAPE treatment have a protective role on testicular T/D and this effect may be due to inhibiting the neutrophil mediated cellular injury.

P 874
CANCERS OF THE TESTIS: A RETROSPECTIVE STUDY OF 29 CASES

CHTOUROU Imen, GOUIAA Naourez, MAKNI Saloua, FAKHFAKH Ines, AYADI Lobna, SELLAMI Ahmed, BOUDAWARA SELLAMI Tahya

Intoduction:
Cancer of the testis (CT) is rare, accounting for about 1 % of all cancers in men; in Europe, the annual incidence rates range between 7,3 (West) and 4,6 (south) per 100.000; in Africa, the annual incidence rates are very low (less then 1 pour 100.000). It is the commenest cancer in men under 45 years old. Cryptorchidism is the only confirmed risk factor. The majority of CT are testicular germ cell tumours witch are divided into seminoma and non séminoma types for treatment planning because seminomatous testicular cancers are more sensitive to radiotherapy.
Objectives:
The purpose of this study is to discuss the clinic and pathologic characteristics, the course and the prognosis of CT.
Methods and materials:
We report a retrospective study of 29 cases of CT diagnosed in the department of pathology of the Habib Bourguiba hospital-Sfax-Tunisia over a five years period (2000-2004).
Resultats:
The mean age of our patients was 40 years (extremes 1 and 83 years). Indescended or maldescended testis are found in 80% of cases; all of CT are clinically detectable at initial presentation (diffuse pelvic mass 50%, inguinal swelling 30%; hardness scrotal mass: 20%).The chirurgical procedure to make the diagnosis was a radical orchidectomy in all cases. Pure seminoma was the most frequent histological type (30%) followed by mixed germ cell tumours (20%); 18% of patients have a testicular lymphoma and are old mens. Only four cases of paratesticular tumours are found and are a rabdomyosarcoma type in three cases. After testicular surgery, the management was depended on type and stage of disease.The mean fallow up was 47 months, 20% of patients with mixed germ cell tumours developed a pelvic recurrence versus any relapse for pure seminoma; a paratesticular rhabdomyosarcoma representthe most aggressive pathologic variant and early visceral metastases are observed in all cases.
Conclusion:
Cancer of the testis is a relatively rare disease; the majority are testicular germ cell tumours who occur most frequently in young men and have a good prognosis: it is highly treatable, often curable cancer; many germ cell tumours produce tumoral markers(AFP, HCG, LDH) who are useful in the diagnosis and staging of disease, to monitor the therapeutic reponse and to detect tumour recurrence.

P 875

CASE OF ABSOLUTE RELAPSE OF " BURNT-OUT" TESTICULAR TUMOR OF LECITHAL SAC

PAPANIKOLAOU Athanasios1,KAMPAS Lambros1,NIKOLAIDOU Anastasia2,FLARIS Nikolaos1,HATZIKALIAS Argirios1, PAPATHANASIOU Athanasios3
1Department of Pathology, Hippokration Hospital, Thessaloniki
2 Department of Pathology, General Hospital, Kilkis
3Department of Urology, Hippokration Hospital, Thessaloniki, Greece

We report the case of a 25-year- old man with testicular tumor of lecithal sac having as initial clinical indication a retroperitoneal tumor.
Macroscopically, the retroperitoneal tumor consisted of numerous grey, elastic- friable pieces of tissue. The maximum dimensions of the greatest piece were 6x4,5x3,5 cm.
Microscopically, the tumor was solid, dedifferentiated and metastatic. From the immunohistochemical examination performed with a great range of antibodies (CEA, EMA, LCA, UCHL1, CD 20, Vimentin, SMA, HMB-45, CD 56,HCG, PLAP, CD68, Ulex europaeus, CD 34, Desmin, S-100, MIC-2, pancytokeratin AE1/AE3, Synaptophysin) we concluded that the tumor cells were positive only for low grade molecular weight cytokeratin (AE1).
On ultrasonography numerous punctate ultrasonic lesions were found in the left testis. Later on, left testectomy was operated. The histological examination of the testis revealed a small scar with calcification and numerous testicular tubules with decations of intratubular neoplasia of germinal cells. Further estimation of the retroperitoneal tumor showed that the tumor cells were positive for AFP.
In conclusion, we can report that in case of a retroperitoneal metastatic tumor we should examine testis meticulously.

P 876

ADENOCARCINOMA ORIGINATING FROM A MATURE TERATOMA OF THE TESTIS; CASE REPORT

Resit Dogan Koseoglu*, Bekir Suha Parlaktas**, Nurper Onuk Filiz *, Fikret Erdemir**,
Özden Tulunay***
*Gaziosmanpasa University, School of Medicine, Department of Pathology, Tokat,
TURKEY
**Gaziosmanpasa University, School of Medicine, Department of Urology, Tokat,
TURKEY
***Ankara University, School of Medicine, Department of Pathology, Ankara, TURKEY

Malignant transformation in testicular teratomas has been reported very rarely in the literature. Although testicular teratomas in childhood are regarded as benign neoplasms, if these tumors are left untreated until advanced ages, the risk of malignant transformation may be in question.
We report a case of differentiated adenocarcinoma originated from colonic glands existing in primary testicular teratoma.

P 877

PURE SEMINOMA IN A MALE PHENOTYPE 46,XY TRUE HERMAPHRODITE

CHELBI Emna (1), RAMMEH Soumaya (1), ZERMANI Rachida (1), BEN MOUALLI Sami(2), FARAH Faten (1), KOURDA Nadia (1), FERCHICHI Leila (1), KACEM Olfa (1), ZEDDINI Abdelfateh (1), AYED Mohsen (2), BEN JILANI Sarrah (1)
(1) Departement of Pathology, Charles Nicolle Hospital, Tunis.
(2) Departement of Urology, Charles Nicolle Hospital, Tunis.

INTRODUCTION
True hermaphroditism (TH) is a rare cause of intersexuality characterized by the development of ovarian and testicular tissue in the same individual. The most frequent karyotype is 46,XX followed by various forms of mosaicism. The karyotype 46,XY is extremely rare, present in only 7% of cases. Gonadal tumours are reported in 4.6% of patients with TH, most of them are gonadoblastoma. Herein, we report a case of a pure seminoma occurring in a male phenotype 46,XY true hermaphrodite.
PATIENT AND METHODS
A 32-year-old man presented with pelvic pain, constipation and important weight loss. Physical examination revealed bilateral cryptorchidism and a firm pelvic mass, without gynecomastia. â-human chorionic gonadotropin, á-fetoprotein and carcinoembryonic antigen had normal levels in serum. The computerized tomography showed a large retrovesical tumor of unkown origin. The ultrasonography guided biopsies concluded to a pure seminoma. At surgery, an uterus, two tubes, two gonads, a prostate and two seminal vesicles were identified. The tumour (7 cm), adherent to the uterine cervix and to the prostate, was almost entirely excised.
RESULTS
The pathological examination confirmed the diagnosis of pure seminoma. The gonads were consistent with two ovotestis one of them was massively unfiltered. Cytogenetic evaluation of peripheral leukocytes revealed a 46,XY karyotype with a sex-determining region of the Y chromosome (SRY gene) detected by PCR. The patient received a complement of radiotherapy (35 Gy). He was free of disease six months later.
CONCLUSION
TH is a complex and heterogeneous condition. SRY gene seems to play a major role. Further studies are needed to better characterize its pathogenesis. Few cases of tumours occurring in the gonads of true hermaphrodites have been reported. Our report is peculiar by the arising of a pure seminoma in the ovotestis of a male phenotype 46,XY true hermaphrodite.

P 878

HISTOLOGICAL INHOMOGENEITY IN MULTIPLE TESTICULAR BIOPSIES

MAGYAR Éva, ERDEI Edit*, LELLEI Ilona
National Medical Centre, Department of Pathology and Andrology*, Budapest, Hungary

Introduction:
Histological evaluation of testicular biopsy is an important method in management of male infertility.
Materials and methods: Multiple testicular biopsies of 143 infertile men were taken using atraumatic microsurgical method. Samples were fixed for 24 hours in Bouin's fixative or buffered formaline. After paraffin embedding 3-4 um slides were cut and stained by HE. Data of histological reports were examined concerning inhomogeneity using three different methods.
Results:
1. Etiological inhomogeneity: 43 of the 86 azoospermic, 22 of the 29 OATS and 21 of the 28 oligozoospermic patient showed different etiology int he biopsies.
2. Spermatogenetic activity: 24 of the azoospermic individuals presented mature spermatozoa only in some of the samples. 13 men int he OATS group showed spermatogenesis only in some of the biopsies. 10 of the oligozoospermic patients was proven inhomogenous concerning spermatogenetic activity.
3. Statistical inhomogeneity: The number of mature spermatozoa counted in 10 round shaped tubules was evaluated. In the azoospermic group an average of 59,4 +/- 92,3 was found. Int he OATS an oligozoospermic group it was 122 +/-120,4 and 152,7 +/-130,5, respectively.
Discussion:

Our data proved that function of testicular tissue shows marked local differences in etiology and spermatogenetic activity either. Taking of single biopsy might give a false impression of spermatozoa content and alterations. Histological evaluation of multiple biopsies helps andrologist to plan further therapy.

P 879

IMMUNOHISTOCHEMICAL EVALUATION OF THE STEM CELL FACTOR RECEPTOR (SCFR, CD-117, C-KIT) EXPRESSION IN TESTICULAR GERM CELL TUMORS

Valavanis C.1a,b, Lekka J.1, Nikolaou M.2, Aravantinos G.3, Fountzilas G.4, Zizi A.5, Elemenoglou J.5, Bourli A.6 ,Kyparidou E.6, Pectasides D.2, Arapantoni-Dadioti P.1
1. a.Dept. of Pathology – b. Molecular Pathology Unit, METAXA Cancer Hospital, Piraeus, Greece, 2. 2nd Dept of Internal Medicine-Propaedeutic, Attikon Hospital, Athens University Medical School, Greece, 3. 3rd Dept. of Medical Oncology, "Ag. Anargiri" Cancer Hospital, Athens, Greece, 4. Dept of Medical Oncology, Papageorgiou Hospital, Aristotle University of Thessaloniki, School of Medicine, 5. Dept of Pathology, Tzaneio Hospital, Piraeus, Greece, 6. Department of Pathology, "Ag. Anargiri" Cancer Hospital, Athens, Greece

BACKGROUND AND OBJECTIVE : Testicular germ cell tumors consist 95% of all malignant tumors arising in the testis and most of them are sensitive to chemotherapy. However 10-20% of those develop resistance to chemotherapy. Recently, targeted therapy drugs are in use for the management of chemoresistant malignancies. Imatinib (STI571) is one of them and targets c-Kit among other molecules. Overexpression or constitutive activation of c-Kit by mutations have been associated with the development and progression of various malignancies. In this context we investigated the expression of c-Kit in testicular germ cell tumors in order to evaluate the incidence of its expression in various tumor types along with the possible use of c-Kit inhibitors as a tool for therapeutic intervention.
MATERIALS AND METHODS: In this study, 169 archival tumor samples were analyzed immunohistochemically, using a polyclonal rabbit anti-human antibody against c-Kit (DAKO). From them 61 were seminomatous (49 pure, 11 anaplastic, 1 spermocytic) and 108 non-seminomatous tumors (36 malignant teratoma undifferentiated , 15 malignant teratoma trophoblastic , 21 malignant teratoma intermediate , 32 malignant teratoma combined , 5 other). c-Kit expression was considered as positive, if >10% of tumor cells displayed membranous staining.
RESULTS: 77.5% (n=38) of pure seminoma exhibited a positive immunostaining for c-Kit, while only 18.2% (n=2) of anaplastic were identified as positive ($p<0.001$). Out of 32 cases with a combined tumor, 17 showed a positive c-Kit reactivity and 15 a negative one, while only 2 non-seminomatous tumors had a positive staining. Although c-Kit expression is strongly correlated with seminomatous histological features ($p<0.001$), there is no correlation with stage ($p=0.19$) or chemotherapy treatment response ($p=0.11$). Overall, 4 (1 seminoma, 3 combined tumors) out of 22 chemoresistant cases revealed a positive expression for c-Kit and one of them had a positive response to Imatinib treatment in combination with chemotherapy.
CONCLUSIONS: c-Kit is expressed in the majority of seminomas and in seminomatous components of the combined tumors, in a minority of anaplastic seminomas and rarely in non-seminomatous tumors. The recent development of c-Kit inhibitors may offer a possibility of cure in chemoresistant testicular germ cell tumors overexpressing this transmembrane receptor.

P 880

BLOOD VESSELS IN TESTICULAR BIOPSIES OF INFERTILE MEN

JEZEK Davor, BILIC Ernest, GRAHOVAC Gordan, KNEZEVIC Nikola
University of Zagreb, Medical School, Zagreb,Croatia

INTRODUCTION
Infertile men were shown to have reduced lumen of the testicular blood vessels. The reduced lumen is mostly due to the process called "hyalinization", pathological accumulation of glycoprotein substance within the blood vessel wall. Hyalinization could be found in the case of cryptorchidism, immune orchitis, Klinefelter's syndrome and in the significant number of patients with idiopathic infertility. Microangiographic data on the testicular arterioles in severe cases of male infertility demonstrated irregular blood flow, damage of the blood vessel wall and reduced spermatogeneis within the seminiferous tubules.
AIM
There is a lack of electron microscopic, immunohistochemical and morphometric studies dealing with the structure of testicular blood vessels in patients with the non-obstructive azoospermia. Therefore, the aim of our study was: a) to identify the most frequent blood vessel type affected in this group of infertile patients; b) to describe blood vessels changes both at light and electron microscopic level; c) to perform an immunohistochemical and morphometric (stereological) analysis of small blood vessels of the testicular biopsies of infertile men.
MATERIALS & METHODS
48 couples that consulted andrologist at the Urology Clinic (University of Zagreb, Medical School) for infertility in the period 1997-2003 were included in the current study. The infertility problem was due to the male factor. In 40 infertile men, a non-obstructive azoospermia could be diagnosed. 8 patients had obstructive azoospermia with completely preserved testicular tissue and served as controls. Whenever possible, a bilateral biopsy was performed. Testicular biopsies were examined by light and electron microscopy, immunohistochemistry (IHC) and stereology.
RESULTS
Interstitial blood vessels in the control group displayed regular architecture. In infertile group, there was a change in the morphology of some arterioles and venules. In the subendothelial layer of these vessels, an accumulation of a hyaline could be observed. Observed by the transmission electron microscope, the thickened subendothelial layer had an accumulated material of a moderate electron density. IHC and stereological analysis pointed out a significantly increased number, volume, length and curvature of capillary network in the infertile group of patients.
CONCLUSION
In the testis of infertile men, there is a pathological change of arterioles, venules and capillaries.

P 881

PRIMARY MALIGNANT LYMPHOMA OF THE TESTIS

PETRESCU Amelia 1, DOBREA Camelia 2, NICULESCU Liviu 3,.GÃLEªEANU Mihai 1, VASILICÃ Mariana 4 ANDREI Florin 2
1.Prof. Dr.Th.Burghele Hospital Bucharest, Romania 2.V Babes Institute of Pathology, Bucharest, Romania 3. Carol Davila University of Medicine and Pharmacy Bucharest Romania 4. Department of Hematology, Fundeni Clinical Institute, Bucharest Romania

Introduction and aim: Primary testicular lymphomas are rare entities representing 1-2% of non –Hodgkin lymphoma (NHML) and 1-7% of malignant testicular tumors and they are the most common testicular tumor in men older than 50 years of age. This study included 8 cases of inpatients

diagnosed by echography and NMR) with testicular tumors. The age of patients was between 46 and 81 (with a mean of 52). The tumors were unilateral, with disease limited to testicle and accompanied by pain. Orchectomy was performed as first therapeutic and diagnostic purpose. All patients were clinically staged according to the Ann Arbor criteria and received a doxorubicin based chemotherapy regimen (CHOP, MTX, CVP, and Leukeran).. A standard chemotherapy protocol has not been used because of reduced number of patients.
Material and method: Tumor fragments were fixed in 10% formallin, paraffin embedded, sectioned and standard H.E. stained. Immunohistochemistry for L26, Alphafetoprotein, NK1, CD30, and CLA was performed.
Results: Microscopy revealed in all cases a stromal proliferation with medium size cells, monomorphic shape and prominent nucleoli. Alphafetoprotein was positive in seminal tubes and negative in tumor, NK1 in small lymphocyte and negative in tumor and L26 diffuse positive in tumor. We were able to follow up only four patients.
Conclusions: The diagnosis was of NHML in 6 cases and for 2 secondary involvement of hematopoietic malignancy (myeloid sarcoma and leukemia). Lymphoma cases were typed using REAL classification as small and large B cell lymphoma. Unfavorable evolution with 6 months relapse and one death prove a more aggressive evolution of primitive testicular lymphoma.

P 882
SEMINOMA WITH A MICROCYSTIC AND TUBULAR GROWTH PATTERN
H.L. Barrett, M. Redmond, M. Leader
Royal College of Surgeons in Ireland.

A 63year old gentleman presented with a large right testicular mass, which was subsequently resected. On macroscopic examination, the testis was extensively replaced by a cream coloured tumour, which focally had a nodular appearance. On histological examination, the tumour was composed of polygonal cells with clear cytoplasm and a stippled chromatin pattern. Much of the tumour had a solid growth pattern but, in large areas, showed florid microcystic change and tubule formation. The spaces were generally small and closely packed. Granulomata were present and there was a mild lymphocytic inflammatory infiltrate. There was no evidence of intra-tubular germ cell neoplasia in the residual tubules. On immunohistochemical staining, the tumour cells were negative for PLAP. The tumour cells were immunoreactive for CD117 (c-kit).
Seminomas with microcystic and tubular growth patterns are unusual and should not be confused with a yolk sac tumour, but the cytological features are helpful in distinguishing these two entities. It is not yet known if these tumours are associated with an adverse prognosis compared to the classical seminoma.

P 883
ISOLATED POLYARTERITIS OF THE MALE REPRODUCTIVE SYSTEM COINCIDING/ASSOCIATED WITH A MALIGNANT GERM CELL TUMOUR OF THE TESTIS: A CASE REPORT
Achim Fleischmann[1], Urs E. Studer[2]
Departments of Pathology[1] and Urology[2], University of Bern, Switzerland

Polyarteritis nodosa (PAN) is a necrotizing vasculitis affecting primarily small and medium-sized arteries. PAN presents mostly as a systemic disease with poor prognosis, rarely in an isolated form with a usually favorable outcome. Both forms may affect the male reproductive system. The etiology of this inflammatory disease is still unclear. However, PAN has been described in the contexture of various diseases such as systemic lupus erythematodes, rheumatoid arthritis, hepatitis B and C, human immunodeficiency virus (HIV) infections and neoplasms. Therefore it has been speculated that triggering events may be identified in most cases in the future. We report for the first time a localized PAN of the reproductive system coinciding/associated with a mixed germ cell tumour of the testis in a 21-year-old man. One year after surgery he is without evidence of recurrence of either the tumour or PAN.

P 884
SURVEYING 177 TESTIS BIOPSIES OF INFERTILE MALES AND COMPARING THE RESULTS WITH OTHER DIAGNOSTIC MODALITIES
Mozaffari Reza*, Ensani Fereshteh** , Saremi Aboutaleb**
* Department of Pathology, Islamic Azad University, Tehran Medical Unit
** Department of Pathology, Tehran University of Medical Sciences

Background : Recently infertility becomes more common. In half of the infertile couples, men are completely or relatively responsible. Therapeutic approaches to infertile males impose great expenses on the family. Present study deals with sensitive clinical or paraclinical methods, other than testis biopsy, that could provide informative data regarding the absence or presence of sperms.
Material and Methods : Medical files of 177 infertile men were reviewed. Then findings of physical examination, hormonal studies, past medical history and testis aspiration were compared with hystopathological findings of testis biopsies. All these patients underwent testis biopsy following the initial studies. Spermatid count per tubule was considered to be the major criteria of fertility in patiants' biopsies.
Result : of 177 patients, 95 (53.5%) had no chance of fertility due to the absence of mature spermatid or spermatozoa in their biopsies. Testis aspiration has a sensitivity of 86%, specificity of 85% and positive predictive value of 93% to detect sperm.
Conclusion : Our result revealed that physical examination, serum hormone assay and testis needle aspiration can not substitute hystopathological studies of the testis biopsy to prove infertility.

P 885
CANCER OF THE PENIS.PATHOLOGICAL ASPECTS OF SEVEN CASES OBSERVED IN CAMEROON(CENTRAL AFRICA)
NKEGOUM Blaise,SOW Mamadou,FOUDA Pierre,SASTRE-GARAU Xavier,DECREMOUX Patricia,BOSMAN Fred, ESSAME OYONO J L.

BACKGROUND:Cancer of the penis is an ucommon malignancy in developed countries,but the incidence is as high as 17% of all male cancers in some undeveloped countries. The most important etiologic factor is the presence of an intact foreskin but this is still unknown.
METHODS/ We described the pathological aspects of seven cases of penile cancers observed in Cameroon, an underdeveloped country of 15000000 inhabitants situated in Central Africa, within a period of twenty years (1984-2004). Human Papilloma Virus(HPV) DNA detection and typing were carried out on paraffin-embedded specimens of our cases by Polymerase Chain Reaction.
RESULTS
The patients aged 43 to 75 years and were circumcised. Four of the seven cases were observed in 2004 an one of this four patient was HIV(Hman immunodeficient Virus) positive and another was diabetic. All patients consulted late with

metastatic disease.The pathological aspect was squamous cell carcinoma. HPV DNA was detected in four cases.
CONCLUSION/ Penile cancer is still rare in Cameroon were only 10%of cancers are confirmed histologically.The etiology is unclear. The HIV should be investigated as an etiologic cofactor.

P 886
AMYLOID TUMOR OF THE RETROPERITONEUM: REPORT OF A CASE.
GEORGIU Carmen*, FODOR Daniela**, PETRESCU Magdalena ***, IACOB Gh.****, GEORGIU A.*****, OLINICI C.D.*
* Department of Pathology – U.M.Ph. "Iuliu Hatieganu" Cluj Napoca, Romania
** Department of Internal Medicine – U.M.Ph. "Iuliu Hatieganu" Cluj Napoca, Romania
*** Department of Pathology – County Hospital Cluj, Romania
**** Department of Pathology – Renal Transplant and Urology Center Cluj, Romania
***** Individual Medical Center 81, Cluj Napoca, Romania

A case of primary localized multinodular amyloid tumor of the retroperitoneum is reported. A previously healthy 40 year old man presented with non specific symptoms of lower abdominal pain and a tumour mass in the inguinal region. The clinical diagnosis (based mainly on echography and computed tomography, the serology being normal) was that of a very large tumor mass, of 20/8/6 cm, occupying the right retroperitoneal space, from the kidney to the inguinal region. The surgical excision revealed a multilobular tumor mass with an osseous consistency, apparently well circumscribed but infiltrating the adipose tissue and pressing the ureter. The patient needed an ureterostoma. Subsequent histology showed nodular amyloid deposits associated with osseous metaplasia, giant cell reaction and an apparently normal lymphocyte and plasma cell infiltrate. Further standard tinctorial tests, like a positive dimethyl benzaldehide method for triptophan and permanganate-resistant congophilia, revealed the lesion to be a primary AL type immunoamyloid. Immunohistochemical investigations did not reveal any immunoglobulin light chain restriction, being ê and ë intense positive, at the site of plasma cells but also of the amyloid deposits. These observations indicate that the amyloid nodules are produced by the plasma cells, which are of polyclonal rather than monoclonal origin, implying an inflammatory process rather than a solitary extramedullary plasmacytoma. The patient is well two years after the surgical excision, without recurrences.

P 887
RNA QUALITY AND TISSUE PRESERVATION OF DIFFERENT FIXATIVES IN PARAFFIN EMBEDDED TISSUE
C. Páska1*, K. Bögi1, L. Szilák1, A. Tõkés1, E. Szabó1, I. Sziller2, J. Rigó Jr.2, G. Sobel3, I. Szabó3, P. Kaposi-Novák1, A. Kiss1, Z. Schaffl
1. II. Dept. of Pathology, Semmelweis University, Budapest, Hungary
2. I. Dept. of Obstetrics and Gynecology, Semmelweis University, Budapest, Hungary
3. II. Dept. of Obstetrics and Gynecology, Semmelweis University, Budapest, Hungary

Introduction Several publications reported that RNA recovered from paraffin embedded tissue could be used as a substrate for PCR. Formalin fixed, paraffin embedded histopathology archives contain an inestimable collection, which could be analyzed to investigate changes in mRNA expression in pathological processes. It would be also reasonable to decide for future tissue conservation of pathology samples which fixative to use to satisfy both histological and molecular biological needs.
Aim Three different fixation methods were compared by histology, immunohistochemistry and Real-Time RT-PCR.
Materials and Methods 24 hours' fixation with RNAlaterTM, acetone and formalin, followed by paraffin embedding, were compared on human endometrium samples. Hematoxylin-eosin staining and immunohistochemistry with mono- and polyclonal antibodies were performed. RNA was extracted and the transcription of different size amplicons (121, 225, 406 bp for GAPDH; 166, 310, 536 bp for beta globin) were compared by Real-Time RT-PCR.
Results The most adequate tissue preservation was found with formalin fixation, while there were no significant differences in the 3 fixative's yields for various size amplicons with Real-Time PCR (GAPDH 121 bp threshold cycle number for RNA later 28,4±3,3, acetone 26,9±2,7, formalin 27,8±3,0). PCR product quantity decreased with length regularly, longer than 225 bp amplicons gave poorer results.
Conclusion Acetone and formalin fixatives followed by paraffin embedding can also be used for RNA studies besides histological and immunohistochemical use, with the limitation of using short amplicons for paraffin embedded material. Longer amplicons gave less reliable results because of RNA fragmentation, while shorter amplicons can represent better real tissue composition. Our findings confirmed the importance of suitably designed primers' on the success of RNA recovery. Further investigations are necessary to define the correct use and validity of paraffin RNA for gene expression studies.
This project was supported by grants: NKFP-1/0023/2002, NKFP-1A/002/2004.

P 888
MOLECULAR ANALYSIS OF GENOMIC LOW COPY NUMBER DNA EXTRACTED FROM LASER-MICRODISSECTED CELLS
G. Giuffrè, L. Saravo*, D. Di Martino*, N. Staiti*, A. Simone, G. Sippelli, G. Tuccari.
Department of Human Pathology, University of Messina, and *Laboratory of Molecular Biology – Raggruppamento Carabinieri Investigazioni Scientifiche, Messina, Italy

INTRODUCTION. Tissue microdissection techniques, allowing a correlation between the topologic organization of the cells and the molecular analysis of nucleic acid extracted, represent a key technique in molecular pathology. In fact, the presence of a wide spectrum of cell types in tissue samples may complicate the analysis of a particular cellular population. Laser-assisted microdissection is an advanced procedure to cut small tissue fragments as well as single cells by an ultraviolet laser beam in order to select a specific cell population of interest from a heterogeneous sample, under direct microscopic visualization. In the present report we evaluate the sensitivity of this method in order to perform genomic analysis from low copy number DNA.
METHODS. Laser-microdissection was performed using a Leica AS LMD system (Leica Microsystems, Germany) on smears of aploid (spermatozoa) and diploid (lymphocytes) cells, on sections of tissues routinely formalin-fixed and paraffin-embedded, on cryostatic sections obtained at surgery and post-fixed with cold methanol. The samples were stained with specific procedures (Haematoxilin-Eosin, Giemsa, Papanicolau, Picroindigocarmine-Nuclear fast red). For each sample, an increasing number of cells from 1 to 100 was harvested in different PCR tubes. DNA extraction was performed by Chelex™ 100 (Biorad), QIAmp DNA Micro Kit (Qiagen) and DNA IQ™ System (Promega Corp.). The DNA extracted from each sample was amplified to identify a specific genetic profile by the most common microsatellite loci (BAT25, BAT26, BAT40, D2S123, D5S346, D17S250) as well as multiple Short Tandem Repeat (STR) typing

(AmpFLSTR Identifiler, PE Biosystems) of forensic interest. PCR products were separated by capillary electrophoresis with 3100 AB Prism Genetic Analyzer; and analyzed by the Genescan and Genotyper Softwares v 3.7.
RESULTS. We have obtained sufficient DNA for amplification and STR typing starting from 10 aploid cells while amplification for microsatellite loci was achieved with 5 diploid cells obtained from routinely processed tissue samples. Moreover, some differences in relation to the integrity of the extracted DNA was found with the specified staining procedures.
CONCLUSIONS. The documented possibility to perform a genomic analysis of low copy number DNA from few cells harvested by laser microdissection represents a valid aid in order to solve diagnostic and forensic problems in the medical practice.

P 889
ASPECTS OF DIGITAL MICROSCOPY IN HUNGARY
GOMBÁS Péter, MOLNÁR Béla*
MI Central Hospital, Department of Pathology;
Cellanalysis Laboratory, 2nd Department of Medicine, Semmelweis University, Budapest, Hungary

AIMS: Although telepathology techniques have been accepted as global method, there are serious doubts to implement cyber age tools in professional practice. Traditional static telepathology has proven biased due to the low explicit/implicit ratio of transmitted information; dynamic telepathology can not be automated using remote controlled conventional microscopes. Our aim is to present concept and realizations of digital
microscopy in Hungary.
METHODS: Selected histopathological samples were captured with a bright field transmitted light microscope and in house developed slide scanner. Images of biopsies have been joined in order to create digital slides using different scanning methods. Electric slides have been stored on slide server, then diagnosed at remote stations via Internet.
RESULTS: The value of bias of transferred digital information can be reduced to zero digitizing series of histopathology slides. We tested the following systems:
1. Manual digitizing of the specimen via x and y axes using RGB microscopic camera and frame grabber is extremely laborious and inappropriate in the routine practice.
2. Automatic scanning of slides applying traditional microscope, which is equipped with motorized stage digitizes the entirety of selected slides but not able for fully automated capturing of large slide series.
3. Histological slide scanner without conventional microscope but with network connected slide server, containing software controlled stage and auto-focus, enable creation and storage digital slide series and remote diagnostics on routine way.
CONCLUSION: Basic questions of digital slide's application in the routine practice are the way of slide scanning, the speed of archive's access and image quality of digital slides. Application of slide scanner, slide server accessed via TCP/IP protocol dissolves bias experienced in telepathology practice and enables a new agenda for expert discussions, consultations, archiving, education and quality assurance.

P 890
THE ADVANCES IN SCANNING FLUORESCENT MICROSCOPY, (AUTOMATED SLIDE HANDLING, METAL-HALIDE ILLUMINATION, SOFTWARE FEATURES) MEANS SIGNIFICANT ADVANTAGE FOR ROUTINE APPLICATIONS
MOLNAR Bela, VARGA Viktor, CSENDES Gabor, VIRAG Tibor *, TULASSAY Zsolt
Cell Analysis Lab, II.Dept. of Medicine, Semmelweis University
3DHISTECH ltd, Budapest, Hungary

Background: we reported recently about the application of single slide fluorescent scanning technology on a routine motorised microscopy. Several technical limitations became known as scanning speed, slide identification, scanning area determination., Internet access to fluorescent digital slides, application on histological sections.
Aims: Development and evaluation of an automated new fluorescent slide scanner (HI-Scope, 3DHISTECH Ltd, Budapest) and software enhancements for supporting high volume automated analysis.
Materials and methods: For automated slide handling slides, coverslips and slide boxes(50 slides) were developed. Hi-Scope (3DHISTECH Ltd, Budapest Hungary) features a vertical fluorescent illumination pathyway of a commercial microscope, automated slide box movement (upto 6), slide loading and barcoded identification, edge fluorescent labelled coverslip localication and laser triangulometry based focus point determination. Automated scanning software features multichannel slide digitisation depiding on the staining intensity upto 1 sec for three channels. Coverslips are fixed using Pro-long media (MolecularProbes, USA). Illumination was enhanced using a metal-halide fluorescent light source. Cytometric calibration and standardisation was done using beads Coulter beads.
Results: The Hi-scope system"s slide box and slide loading safety was proven in a three month tests. Mechanical slide loading errors were found occasionally after loading 300-400 slides. Focus determination worked without error. CV of the densitiy measurements on the calibration beads were 3.9 %. The determination of area of interest using prelabelled coverslips was automatically perforemd without failures. Resolution of the system is 0.3 um2
/ pixel. Digitisation of a field of view took upto 0.1 sec in FITC, 0.1 sec in DAPI, upto 0 sec in the Rhodamine channel. This way a cytospin area could be scanned in three channels in less then 4 minutes.
Conclusions: Hi-Scope can contribute to high volume fluorescent slide scanning. The produced image quality is acceptable for routine use. Based on these results development of routine applications can be started.

P 891
WORKING EXPERIENCE WITH DIGITAL SLIDE AND VIRTUAL MICROSCOPY-BASED ROUTINE AND TELEPATHOLOGY EVALUATION OF BIOPSY SPECIMENS
ZALATNAI Attila, SZENDE Béla, BERCZI Lajos, FÓNYAD László, KOPPER László
Semmelweis University, 1st Department of Pathology and Exp. Oncology

INTRODUCTION
Automated scanning of histological sections and visualisation of the histological image by virtual microscopy is becoming increasingly important in routine diagnostic pathology.
PURPOSE OF THE STUDY
The aim of present study is to test Zeiss Mirax slide scanner solution (Carl Zeiss, Jena) as virtual microscope system about its usability in routine diagnosis of biopsy specimens as well as in telepathology.
METHODS
Altogether 1500 biopsy sections were scanned and examined on screen until the submission of this abstract. The established diagnoses were compared to those which were given after light microscopic examination. The study was carried out by four experienced pathologists, both on site and at a remote workstation equipped with the software including the facility of remote access for digital slides.
RESULTS
Accurate diagnosis could be established in all cases using the virtual microscope, if the sections and the staining were of

good quality and 8 u thin or less, both on site and from the remote workstation. The images taken by use of 20x objective were suitable for routine diagnosis. The scanning of an average sized section took 5-7 minutes at this magnification. Three hundred sections/day can be scanned without difficulty. Further digital magnification of the images did not improve the quality of structures. A period of 3-4 weeks is needed even for experienced pathologists to get used to microscopic images on the screen. The system enables the establishment of collections and the storage of histological images, first of all for gradual and postgradual education.
CONCLUSION
The Mirax virtual microscope system is valid for use in diagnostic histopathology and telepathology.

P 892
THE EFFECT OF DIFFERENT THICKNESS OF THE SAME TISSUE SECTIONS ON THE COLORIMETRIC DETERMINATION OF COLLAGEN CONTENT
GEDIK Nursal[1],TARCIN Orhan[2]
[1]Istanbul Naval Hospital, Division of Clinical Biochemistry,
[2]Gumussuyu Military Hospital, Division of Gastroenterology, Istanbul, TURKEY

In clinical and experimental studies, it is important to measure the collagen content quantitatively in tissues for study in the development of fibrotic changes. Fibrosis has been estimated by histomorphometric or qualitative methods. Histomorphometric methods are time consuming and qualitative analysis inaccurate. A simple and reproducible method has been reported by López-de-León and Rojkind routinely to estimate collagen content in formalin-fixed paraffin-embedded sections. The method is based on the selective binding of Sirius Red and Fast Green FCF to collagen and noncollagenous proteins, respectively.In this method 15 µm thick- sections are frequently used. But studying with 15 µm thick- sections have some difficulties in process. The aim of this study is to evaluate the reliability of the colorimetric collagen measurement method with different tissue sections and staining procedures.
40 bile duct ligated-female Wistar Albino rats (200 ±30 gr) were used in this study. 3, 6, 9 and 15 µm-thick double sections were obtained for each liver section.
Collagen content was measured 320 liver-tissue sections for using two different staining procedures. First staining procedure was based on the method published by Lopez-de León and Rojkind.After the liver sections were deparaffinized, all of them covered with saturated solution of picric acid in distilled water that contained 0,1% Sirius Red and 0,1% Fast Green FCF and incubated 30 minutes in a rotary shaker. Sections were rinsed several times with distilled water until the fluid was colourless. 1 ml of 0,1 N NaOH in absolute methanol was then added and mixed until all the colour was eluted from the section. Eluted colour was read immediately in Jasco V 50 UV-VIS spectrophotometer at 540 and 605 nm, i.e.Second staining procedure was based on Gascon Barrë and et al. In this procedure, sections were first stained with 0,04% Fast Green FCF and with both dyes. Different from Lopez-de León and Rojkind's procedure 1 ml of 0,05 N NaOH in 50% aqueous methanol was added for obtaining eluted colour. Eluted colour was read immediately in Jasco V 50 UV-VIS spectrophotometer at 530 and 605 nm.
Collagen contents of four different thickness of the same tissues showed a high correlation with each other (r mean= 0, 9896, $p<0.01$). The results of the different staining procedures are highly correlated (r mean= 0, 9638, $p<0.01$).
This method is not affected by tissue thickness and different staining procedures.

P 893
LOW RESOLUTION VIRTUAL SLIDES: AN INEXPENSIVE AND SWIFT SOLUTION FOR BOTH EDUCATIONAL PURPOSES AND AUTOMATIC QUANTITATIVE PATHOLOGY
HERLIN Paulette (1,2), ELIE Nicolas (1), SIGNOLLE Nicolas (1), OGER Myriam (1), CONTREMOULINS Vincent (1), LABICHE Alexandre (1), PLANCOULAINE Benoît (1,3), BELHOMME Philippe (4), MICHELS Jean-Jacques (1,2).
(1) GRECAN, CLCC F. Baclesse, 14076 CAEN
(2) Service d'Anatomie Pathologique, CLCC F. Baclesse, 14076 CAEN
(3) IUT Mesures Physiques, Université de Caen Basse-Normandie, 14032 CAEN
(4) LUSAC, Université de Caen Basse-Normandie, 50130 CHERBOURG-OCTEVILLE

Whole histological slide digitization, allowing "virtual slide" examination and analysis, has several potential applications for pathologists.
It may be useful first for teaching purposes, using web-based interactive self-instructive methods. It is expected to provide, in the near future, adequate solutions for telepathology exchanges. It also potentially offers the best response to the difficult problem of tissue heterogeneity for quantification of prognostic markers in oncology.
Nowadays, virtual slides are obtained using costly and more or less rapid devices, yielding to images which can barely be manipulated and which cannot be automatically processed, due to their huge size. The issue of disk storage capacity will probably be solved in the near future, but the development of efficient, rapid and economic methods, for fully automatic analysis of images of more than 10 Gigabytes, will not be achieved before several years.
Purpose : In this context, we propose an inexpensive, swift and multipurpose approach, using 4,000 dpi scanned images of the whole histological slide, ranging from 15 to 70 Megabytes, which can be either stored in a database or automatically processed for tissue marker quantification.
Methods : Thanks to a simple calibrated professional slide scanner, we were able to build a user-friendly website dedicated to breast pathology, including around 250 cases (scanner image associated to relevant microscopical details). Furthermore, dedicated image analysis routines have been developed, one allowing automatic quantification of tissue markers on whole slides (cytoplasmic or nuclear immunostaining, immunolabeled blood vessels or stroma), the other performing automatic labeling and analysis of Tissue Micro Arrays. Superimposition and image matching of serial immunostained sections, as well as analysis of staining heterogeneity, are also available.
Conclusion : We herein propose to take advantage of an inexpensive and swift image acquisition device, affordable by each pathology, biology or research department, for low resolution virtual slide production, examination and analysis.

P 894
TOWARDS COHORT BASED FROZEN TISSUE BIOBANKS: LOGISTICS AND RNA QUALITY
BOTLING Johan, PONTEN Fredrik, MICKE Patrick
Department of Pathology
Uppsala University Hospital
SE-751 85 Sweden

New sophisticated tools for molecular profiling generally require collection of fresh frozen tissue as a source of high quality DNA and RNA. Unfortunately, most frozen tissue biobanks represent a selected fraction of surgically removed cancer cases. There is usually an over-representation of large, well-demarcated tumors while sampling of small, diffuse tumors is avoided due an appropriate concern about diagnostic safety. To address this issue, we have implemented a prospective biobank allowing for "clinical cohort-based" collection of cancer tissues.

Novel logistics for managing non-fixed specimens has been established. Resected tumors and biopsies are sent on ice to the Department of Pathology. Selected pieces of representative diseased and normal tissue are cut out, blocked in cryogel, and snap frozen. High quality "tape-transfer" frozen sections are produced from each case and the sections are included in the routine histopathological examination. In our experience safe evaluation of small lesions and even resection margins can be done on these slides. In this way a non-selected collection of cases can be obtained from a treated patient cohort. Digital images of the frozen sections are linked to the biobank register. Thus, the cellular composition of the tissue can be assessed before profiling experiments and microdissection.
Difficulties associated with the fragile nature of RNA prompted us to examine the effects of transport time and transport conditions. Structural RNA integrity was checked by microchip electrophoresis in a Bioanalyzer, and gene expression patterns were analysed using real-time PCR. In an experimental set-up, tonsil tissue was cut into cubes and some pieces were snap frozen immediately after surgery. The remaining pieces were left at room temperature, kept on wet ice, in normal saline or in a commercial RNA-stabilising buffer. Surprisingly, the RNA remained quite stable in the tonsil specimens under all conditions and time points tested. Even after 16 h at room temperature only slight RNA degradation was revealed by the electropherograms. However, gene expression levels at different transport time points were most stable during transport on ice.
Our study shows that non-fixed tissue from most tumors can be collected safely in a routine pathology setting and that RNA degradation is a minor problem during handling of fresh tissue before biobanking.

P 895
SOFTWARE DEVELOPMENT FOR FRACTAL ANALYSIS OF HISTOPATHOLOGIC IMAGES

PAVLOPOULOS Petros (1), KAVANTZAS Nikolaos (2), AGAPITOS Emmanouel (2), PATSOURIS Efstrastios(2).
(1) Urologic Clinic, 1st Social Security Hospital, Athens, Greece.
(2) Department of Pathology, Medical School, National University of Athens, Greece.

Aim: Considering the multiple applications of fractal analysis in the field of histopathology, we developed "Fractalyser", a specialized fractal analysis software program for Windows operating system.
Material and Methods: The application was developed in Visual Basic 6.0 (SP5) (Microsoft Corp.) environment. For user friendliness the program was designed with multiple document interface and Windows XP compatibility. "Fractalyser" can open, edit and analyze the most common image file types (bmp, jpg, gif). Images and graphs created by the program can be saved as bmp files, while numerical results can be saved in a text file. The program has some basic image processing functions such as invert, horizontal and vertical flip, grayscale conversion and crop. The user can precisely select the area of interest applying parameterized threshold or edge detection algorithms in the color image, while getting real time graphical feedback on the process. The produced binary image, which is projected as a red layer on the original image for user facilitation, can be further optimized before fractal analysis with 'dilation', 'erosion' or several noise reduction filters. The estimation of the fractal dimension of the image is carried out by using the "box-counting" algorithm. The box size range as well as the number of grid offsets are specified by the user. The program provides detailed numerical results, as well as a graphic presentation of the data and the least-squares linear regression results. The correlation coefficient and the coefficient of determination are also estimated.
Results: The accuracy of the application was assessed by analyzing images with theoretically known fractal dimension. The errors ranged from 0.0 to 5.8%, being conversely proportional to the number of grid offsets. Repeated comparisons of the statistical results of the program with the corresponding data of a commercially available statistical package (Statistica v.6.0, StatSoft Inc.) confirmed their validity and precision.
Conclusion: As it has been observed in thorough testing, the application presented here constitutes a stable, relatively fast, reliable and easy to use tool for fractal analysis. "Fractalyser" is provided as freeware to researchers after request via e-mail to pavlopoulos@medscape.com.

P 896
THE PATHOLOGIST AND THE ELECTRONIC HEALTH RECORD.THE ROLE OF THE IHE (INTEGRATING THE HEALTHCARE ENTERPRISE) INITIATIVE.

Daniel-Le Bozec Christel1, Henin D2, Hemet J3, Martin A3
1 Georges Pompidou Hospital, INSERM U729, 2 Bichat Hospital, 3 ADICAP, France

The challenging aim of the Electronic Health Record (EHR) is to gather current and previous medical data, including images, coming from several experts. In pathology, the necessary technology for digital imaging is available allowing pathologists to enrich the EHR. The challenge now is to define specific healthcare needs and workflows and to agree on technical protocols and file formats for "virtual slides" and reports exchange. The goal of the Integrating the Healthcare Enterprise (IHE) initiative is precisely to stimulate integration of healthcare information resources to improve clinical care. IHE promotes implementation and use of established data standards. Although the ADICAP (Association for the Development of Informatics in Cytology and Pathology) proposed a European de facto standard for image folders in pathology, the most used standards in medical imaging are HL7 and DICOM standards.
The objective of the presented work, done in the framework of a national IHE initiative promoted by ADICAP, consisted identifying the main integration profiles that could be addressed in pathology, taking advantage of the work done in radiology and biology, and to define the main requirements for virtual slides and reports communication according to both the principles of the ADICAP and the DICOM modes.
ADICAP, with the collaboration of the GMSIH (Group promoting the Modernization of Hospital Information Systems in France), recruited national IHE initiative participants to work on the Pathology Technical Framework: 7 pathologists and haematologists, 4 IT professionals, 2 professional associations and 12 vendors. Three working sessions were organized to define the pathologists' needs and to propose Integration Profiles. Furthermore, a DICOM module was developed to produce DICOM Visible Light objects and DICOM Structured Reports and tested at the Georges Pompidou Hospital.
The integration profiles for pathology were defined and presented at the 2005 IHE-Europe workshop in Noordwijkkerhout (Netherland). The images and reports produced by the DICOM module were stored into the Picture Archiving and Communicating System (PACS) of the Georges Pompidou Hospital and available within the EHR.
In conclusion, the national IHE initiative in pathology produced a first definition of useful integration profiles in pathology. On that basis, a first version of the Pathology Technical Framework could be proposed at an European level. Next steps are to support testing, demonstration and educational activities to promote the deployment of this framework by vendors and users.

P 897

QUALITY ASSURANCE IN PATHOLOGY : AUDITS ON LABORATORY WORKFLOW AND INDIVIDUAL PRACTICE

HENIN* Dominique, MICHIELS** Jean-François, RIOLACCI-DHOYEN*** Nathalie and the members of the Committee n°4 "Organisation et Structures", on behalf of the AFAQAP (French Association of Quality Assurance in Pathology).
*Pathology department, Bichat-Claude Bernard hospital, Paris, France; ** Pathology departmentPasteur hospital, Nice, France; ***HAS, Saint-Denis, France.

In 1998, on behalf of the AFAQAP, standards and guidelines of quality management for individual Pathologists or in Pathology department were published. AFAQAP Committees have elaborated and conducted numerous voluntary audits, mainly on diagnostic performance or technical quality in the past 10 years. In 2002 and 2004 clinical governance was introduced in France, as in other countries, to ensure that each doctor was involved in a continuing professional development (CPD) program. The pathologists always had a duty to patients but that duty now becomes a legal obligation. Clinical audit are performed against standards is the process by which pathologists can gather the evidence to improve patient care. ANAES (National Healthcare Accreditation and Evaluation Agency) /HAS (Main Healthcare Authority) has developed a strict methodology for the certification of clinical audit. To ensure high quality of clinical audit, it has to fit in the audit cycle : choose a frequent topic, identify agreed relevant standards, collect data, compare to standards, plan changes, re-evaluate. The AFAQAP intends to help pathologists (either individual or in pathology department) to meet their duty of quality by providing a selection of audits. To ensure high quality for pathologists 2 kinds of clinical audit are necessary, based either on laboratory work organization (preanalytic, analytic or postanalytic processes, risks assessment …) or on individual professional performance (applying evidence-based practice, clinical standards). In 2004, Committee 4 in relation with HAS developed 2 audits,

? "laboratory work" testing the pre-analytic process of the specimen (collection, transport, reception and registration). Are procedures written, available knowledgeable to persons involved in those activities? Is the personal safety appropriate (adequate space? formadehyde vapor …) ? Are the patient and specimen identification satisfactory?…

? "individual practice" testing histopathological reports on tissue samples. Is every specimen identity maintained at all times? Are gross examination performed in accordance with guidelines? Do gross and microscopic findings support pathological diagnosis or hypothesis? Are standards systems of grading and staging used in cancer cases?…

More than 90 voluntary pathologists underwent those 2 self auto-evaluations. Statistical analysis in on progress.

Many other countries, such as Great Britain or US, are involved in CPD program. Quality programs should be maintained under pathologists responsibility. Europe is an opportunity to exchange experiences.

P 898

THE NEW FIXATIVE RCL2, A NON TOXIC ALTERNATIVE TO CRYOPRESERVATION.

ROCHAIX Philippe*, LACROIX-TRIKI Magali*, LAMANT Laurence**, DECHA Audrey***, VOIGT Jean-Jacques*.
*Pathology department, Institut Claudius REGAUD ; ** Pathology department, CHU PURPAN ; *** Oncogenetic Laboratory Institut Claudius REGAUD, TOULOUSE, FRANCE

Introduction

Fixed specimens are suitable for most of diagnosis and immunostainings. However, identifying tumour determinants of drug efficacy looks like a new Holy Grail quest and the conservation of the cellular components becomes a key step in the specimen management.

Purpose

We present a new fixative fluid developed in our laboratory that allows extraction of RNA, DNA and proteins from paraffin embedded specimens.

Methods

The quality of tissue samples fixed and paraffin embedded according to our technique was evaluated on:

- the tissue morphology (H&E staining)
- the immunostaining results of more than 20 antibodies
- the FISH (PathVysion Vysis™) results
- the mRNA quality using a 2100 bioanalyzer (Agilent™), and quantity using RQ-PCR
- the DNA size and quality using agarose gel electrophoresis and three different long range PCR of 600bp , 800bp and 2600bp followed by DNA sequencing
- the protein quality using the bioanalyzer and by Western blotting of a nuclear protein (estrogen receptor), a cytoplasmic protein (actin F) and a mitochondrial protein (Bcl-2).

Results

The tissue morphology was very good, close to that obtained using AFA or Bouin's fluids. The immunostaining results were similar to those obtained on formalin fixed specimens. We succeeded in FISH technique (PathVysion Vysis ™) without modification of the procedure designed for formalin fixed specimens. The mRNA quality was very good with 28S/18S ratio rising above 1.5. The results of RQ-PCR were always similar to those of the frozen samples of the same specimen. The DNA extracted was of very large size (>> 10 kbp) and all the long range PCR worked without modification of the procedures designed for frozen samples. The sequencing of the amplification products was also performed easily without procedure modification. While the protein profiles were slightly different from those observed in the frozen samples of the same specimen, the Western blotting results were similar for the proteins tested.

Conclusion

This new fixative fluid allows the extraction of high quality mRNA, DNA and good quality proteins from paraffin embedded tissue samples. Furthermore, the tissue morphology and immunoreactivity are very well preserved. It can be a good alternative for tissue preservation when freezing is difficult such as for small biopsy or in private laboratory.

Moreover, it is worthy of note that this fixative fluid does not contain any toxic product.

P 899

EUROPEAN TISSUE ARRAY : A USEFUL TOOL FOR QUALITY CONTROL OF IMMUNOHISTOCHEMISTRY. A PROGRAM OF THE EORTC GI GROUP

JULIÉ Catherine, AUST Daniela, BELLUCO Claudio, NORDLINGER Bernard, KÖHNE Claus, VAN CUTSEM Eric, BRÜNNER Niels, LUTZ Manfred P., EORTC GI and RB Groups; CHU Ambroise Paré, Boulogne, France; University of Dresden, Dresden, Germany; University of Padova, Padova, Italy; Klinikum Oldenburg, Oldenburg, Germany; University Hospital Gasthuisberg, Leuven, Belgium; Royal Veterinary and Agriculture University, Frederiksberg, Denmark; Caritasklinik St. Theresia, Saarbrucken, Germany

Background: Numerous studies are based on immunohistochemistry (IHC) results, but IHC is not standardized and quality control is not yet widely established. In addition, important variability may be due to fixation time

and tissue heterogeneity. Therefore, the EORTC GI group designed a quality control tissue array (TA), in order to evaluate the suitability of a given antigen/antibody test before use in clinical trials. Here we report testing of the TA with routine antibodies.
Methods: A 216-spot-TA was designed using paraffin-embedded tissue from 14 colorectal cancers coming from 4 european centers. Immediately after surgery, specimen from tumor rim or tumor center were formalin-fixed individually overnight, for >24 h, or for >48 h, respectively. After evaluation by H&E staining, 3 cores from each specimen were assembled in a tissue array, i.e. 18 cores per tumor. Sections were distributed to 3 pathology departments for IHC, each using one or more of nuclear (p53, Ki67) or cytoplasmic antibodies (CEA, CK20, Cox2) in routine staining protocols. Blinded reading of immunoreaction was performed manually using a visual grading system based on the percentage of positively stained malignant cells.
Results: IHC was successful in the 3 laboratories. The staining pattern varied considerably between cores from individual specimen (e.g. Ki67: from 10-90% pos. nuclei; CEA: 50-100% pos. cells, CK20: 10-60% pos. cells) with moderate differences for staining intensity (variation from weak to moderate or moderate to strong). If average staining intensity or staining pattern for the 3 cores per location were calculated, there was no difference between tumor center and rim ($p = 0.62$ in paired t-tests for all comparisons). Most importantly, fixation time had no impact on the expression levels of the five antigens (p values from 0.12 to 0.93).
Conclusions: We observed a high heterogeneity in the staining from core to core for each tumor. However, we couldn't demonstrate an impact of location (rim or center) or fixation time on the expression levels for the five tested antibodies. This quality control TA is a useful tool to ensure the reliability of a given antibody and staining procedure before its use in translational research in multicenter clinical trials.

P 900
THE HOPE TECHNIQUE OFFERS A COMPLETE PANEL OF MOLECULAR APPLICATIONS IN PARAFFIN-EMBEDDED MATERIALS
T. Goldmann, D. Drömann, J. Gerdes, S. Uhlig, U. Uhlig, S. Loeschke, A Flohr, J. Bullerdiek, P. Zabel, D. Branscheid, E. Vollmer.
Research Center Borstel, Borstel, Germany
Inst. of Human Genetics, Univ. Bremen, Bremen, Germany
Hospital Großhansdorf, Großhansdorf, Germany

Introduction: Asservation of materials for pathologic diagnostics is mostly achieved by formalin-fixation and paraffin embedding. This results in good preservation of histologic details, but to a large degree prevents the application of modern molecular techniques due to the bad condition of nucleic acids and proteins if compared to fresh or frozen specimens, which show a comparably low preservation of histomorhologic details.
Purpose of the study: To establish an alternative fixation technique to overcome with these problems.
Methods used: We have shown that the novel HOPE-technique allows for both, well preserved 'formalin-like' morphology and excellent preservation of nucleic acids and proteins. In this study we present protocols for In situ hybridization, Immunohistochemistry, Western-blot, Northern-blot and Transcription-microarrays.
Summary of the results: All of these methods can be unambiguously performed with HOPE-fixed materials.
Conclusions reached: These results open up new perspectives for molecular approaches in paraffin-embedded probes providing a novel powerful tool for modern pathology.

P 901
ICON-TMA® FOR QUALITY CONTROL OF IMMUNOHISTOCHEMISTRY
IVER PETERSEN, AXEL KOEPENIK*, MANFRED DIETEL, VEIT KRENN
Institute of pathology, Charité Campus Mitte, Berlin, FRG
*Oligene GmbH, Charité Campus Mitte, Berlin, FRG

Immunohistochemistry (IHC) has become an essential adjunct in daily histopathological diagnosis. However, quality control is difficult and becoming critically important considering the need for standardization and quantification of immunoreactivity.
To help solving these problems we developed small size tissue microarrays (TMAs) with 2 to 4 punch biopsies from well characterized specimens of sizes between 0.6 and 2 mm diameter. In its simple variant these internal control (iCon) TMAs consist of 2 tissue cylinders, one being clearly positive and the other clearly negative for a specific immunohistochemical marker, e.g. cytokeratins or hormone receptors. In its more elaborate format, the iCon-TMAs carry additional tissue spots providing a scale for quantitatively assessable markers, e.g. providing examples of immunoreactivity scores 0, 1+, 2+, 3+. The specimen with the yet unknown immunoreactivity is then applied to the iCon-TMA section and both are simultaneously analyzed.
A successful IHC analysis could almost be judged by the macroscopical inspection of the two +/- spots representing the positive and negative sample of the iCon TMA. While the spot with positive control provided an internal standard for strong immunoreactivity, the negative one provided an estimate to differentiate weak positivity from unspecific background staining. The technique proved to be particularly useful for markers that were not necessarily present in the uncharacterized specimen.
iCon-TMAs provided a convenient measure for internal quality control and may become an indispensable tool for standardization and quantification of gene expression by immunohistochemistry or related techniques like mRNA in-situ hybridization.

P 902
PRESERVED COUPLING OF OXYDATIVE PHOSPHORYLATION BUT DECREASED MITOCHONDRIAL RESPIRATORY CAPACITY IN IL-1B TREATED HUMAN
Patrizia Lucia Moser1, Sylvia Stadlmann2, Kathrin Renner3, Juergen Pollheimer4, Alain Gustave Zeimet5, Felix Albert Offner6, and Erich Gnaiger7
Institute of Pathological Anatomy1, Medical University Innsbruck, Austria, Institute of Pathology2, University Hospital Basel, Switzerland, Department of Pathophysiology3, Medical University Innsbruck, Austria, Institute of Ecology and Conservation Biology4, University of Vienna, Austria, Department of Obstetrics and Gynecology5, Medical University Innsbruck, Austria, Department of Pathology6, Academic Teaching Hospital Feldkirch, Austria, Department of General and Transplant Surgery7, Daniel Swarovsky Research Laboratory, Medical University Innsbruck, Austria

The peritoneal mesothelium acts as a bioactive cellular membrane regulating serosal responses to injury, infection and neoplastic diseases. Inflammation of the serosal surfaces induces an "activated" mesothelial cell phenotype. In the present study we simulated activation of cultured human peritoneal mesothelial cells (HPMC, isolated from human omentum majus) by treatment with the pro-inflammatory cytokine interleukin-1beta (IL-1beta). Respiratory activity of suspended cells was analysed by high-resolution respirometry to assess changes in respiratory capacity and coupling of oxidative phosphorylation in activated HPMC. Citrate synthase (CS) and lactate dehydrogenase (LDH) activites

were determined by spectrophotometry. IL-1beta activation for 48 hours resulted in a significant decline of respiratory capacity ($P < 0.05$), without affecting integrity of the inner mitochondrial membrane or cell viability. Treatment of HPMC with IL-1beta resulted in a decrease of CS activity ($P < 0.05$) and an increase of LDH activity ($P < 0.05$). The present data indicate that activation of peritoneal mesothelial cells with IL-1beta is associated with a decrease of oxidative phosphorylation and mitochondrial content that appears to be compensated by an increase in glycolytic capacity.

P 903

THE IMPORTANCE OF HISTOPATHOLOGICAL/ NECROPTIC EXAMINATION IN COWDEN'S DISEASE

ZURAC Sabina*, LAVRIC Luciana*, VRABIE Alexandra*, MICU Gianina*, GRAMADA Eliza*, ZAHARIA Anca*, ANDREI Razvan*, OPRISAN Alexandra*, STANICEANU Florica*, NICA Sanda**
*Department of Pathology, Colentina Universitary Hospital
**Department of Neurology, Colentina Universitary Hospital
Bucharest, Romania

Cowden's disease (CD) is a rare autosomal dominant inherited disease characterized by multiple hamartomas with ectodermal, mesodermal and endodermal origin, the most constant features being the mucocutaneous lesions (almost pathognomonic). It associates an increased risk of malignancies (especially breast and thyroid) and, sometimes, due to the presence of multiple tumors in different organs, an overestimation of the stage is possible ("metastatic cancer")
We present the case of a 82-years-old female recently investigated for progressive alteration of the general status and loss of weight; a supposition of possible metastatic malignant melanoma was made – based on the presence of innumerable pigmented cutaneous lesions (with diffuse distribution including face and palmoplantar localization) and CT findings (many tumors in the skull, meninges, lungs and liver).
The current episode consisted in hemyplegia in right limbs; during admission, an acute ischemia of the left leg developed; considering the neurological status and the "terminal malignant disease" no surgical treatment was considered. Autopsy revealed recent left sylvian infarct, recent thrombotic occlusion of the left external iliac artery and numerous tumors (oncocytic meningioma, intraosseous cranial, pulmonary and hepatic hemangioma, pulmonary hamartoma, bilateral adrenal adenomas, gastric leiomyoma, ovarian serous papilifer cystadenofibroma, pigmented seborrheic keratosis); previous hysterectomy for leiomyomas. CD was concluded (1996 International CD Consortium criteria).
Despite the simplicity of the case, we want to emphasize the risks of clinically misinterpretation of CD as metastatic cancer (without histopathologically proven malignancy) and a subsequent therapeutical redrawn. Only histopathologic/autopsy examination establishes the correct nature of these tumors and a precise diagnosis.

P 904

PATHOGENIC CONSEQUENCES OF ALV INFECTION IN CHICKENS INOCULATED IN MID EMBRYOGENESIS

VERNEROVA Zdenka, PRUKOVA Dana, STEPANETS Volodymir, GERYK Josef, SVOBODA Jan
Department of Pathology, 3rd Faculty of Medicine, Charles University Prague, Czech Republic, Institute of Molecular Genetics, Academy of Sciences of the Czech Republic

Introduction: Avian leukosis viruses (ALV) in addition to their oncogenic potential are responsible for induction of a syndrome called wasting disease (WD). Clinical signs of WD are progressive weight loss, anaemia and occassionally diarrhoea as well. Histopathological findings include depletion of lymphoid tissue and immunosupression.
The aim of this study was to determine the rate and severity of WD induced in chickens by various ALV strains and to evaluate pathological and immunological consequences of the disease.
Material and Methods: For the experiments outbred Brown–Leghorn chickens (genotype C/E) were used. Virus was inoculated in mid embryogenesis into the chorioallantoic vein. ALV viruses of subgroups A–D were tested. Signs of the wasting were monitored during the first 2 weeks after hatching. Lymphatic organs were thoroughly examined immunohistochemically.
Results: When comparing ALVs of different subgroups for their ability to induce WD, viruses of subgroup C (namely td B77-C) were found to cause the most prominent changes. Chickens infected with viruses of subgroup A did not differ significantly from the control birds. WD can be induced only by intraembryonic inoculation of the virus and in a mild form also when inoculated on the 1st day after hatching. The lowest limit for WD induction was determined as 102 infectious units of the virus. In diseased chickens, severe B cell depletion in primary and secondary lymphatic organs was found. Thymus atrophy seems to be partially compensated by a moderate increase of the T lymphocyte number in T-dependent regions. Lymphocyte depletion is accompanied by prominent activation of the a monocyte-macrophage system. While defects of both humoral and cellular immunity were found in chickens infected by ALV-C, only the second one was injured by viruses of subgroup A. A significant increase of peripheral CD8+ T lymphocytes was produced by viruses of subgroup C.
Conclusion: These results indicate that inoculation of chicken embryos by ALVs provides a suitable experimental model for study of retroviruses-induced impairment of immunity.
This work was supported by grant No. 523/04/0489 from the Grant Agency of the Czech Republic.

P 905

MORPHOLOGICAL EVALUATION OF THE HEALING OF BONE DEFECTS IN RABBITS FILLED WITH A COMPOSITE MADE OF POLYLACTIDE/POLYGLYCOLIDE COPOLYMER AND CARBON FIBERS [P(LLA/GLA)+CF]

PROSZEK Magdalena **, SABAT Daniel *, CIESLIK Tadeusz **, ADWENT Marek **, BAJOR Grzegorz ***, SZCZUREK Zbigniew *, CHLOPEK Jan ****, ZEMBALA-NOZYNSKA Ewa *, ZAJECKI Wojciech *, CIESLIK-BIELECKA Agata **
*Chair and Department of Pathomorphology, Medical University of Silesia, Zabrze, Poland
**Chair and Clinic of Maxillo-Facial Surgery, Medical University of Silesia, Zabrze, Poland
***Chair and Clinic of Pediatric Surgery, Medical University of Silesia, Katowice, Poland
****Department of Biomaterials, Faculty of Materials Science and Technology, AGH – University of Science and Technology, Cracov, Poland

Biodegradable polylactide/polyglycolide copolymers are applied widely in medicine for joining broken bones. Their disadvantage is a small mechanical endurance. It can be increased by creating copolymer and carbon fire composite. The aim of the study was morphological evaluation of the healing process of mandibular bone defects in rabbits filled with a composite made of polylactide/polyglycolide copolymer and carbon fibers [P(LLA/GLA)+CF].
The study was performed on 30 New Zealand rabbits. After the soft tissue was prepared, the mandibular bone was exposed. The hole here a composite implant was inserted, had been drilled with a 3.2 mm bur. The wound was suture. Moreover, the composite cylinders were inserted into

subcutaneous and intramuscular pockets. The animals were divided into 7 groups, 4 rabbits in each group. The groups were euthanazied after 1, 2, 3, 6, 12, 24 and 52 weeks and bones were fixed in 10% solution of neutralized formalin. Bone tissue was decalcified in Romeis fluid with decalcifying agent PW23. After the typical procedure, the samples were emerged in paraplast. The blocks were sliced in a microtome. The 6 microtone slices were deparaffinizied and dyed routinely wit hematoxylin and eosin. The obtained preparations were evaluated in a light microscope wit magnifications from 40 to 400x. After 1 week, clearly formed canal around the implant was visible in the mandible. The features of active band of bone tissue in the form of numerous young, immature bone trabeculas surrounded by osteoblasts. Numerous, immature and mature bone trabeculas covered with osteoblasts were present after two weeks. Three weeks later and in the following periods, mature bone trabeculas without osteoblastic activity were observed. A connective tissue capsule was formed around the implant in the subcutaneous tissue. Mature, cicatrizing, fibrous connective tissue, growing among the injured bundle of muscle fibers was visible in the muscle tissue around the implant. The study showed good tolerance of the applied P(LLA/GLA)+CF composite implants in the animal body, no inflammatory reactions and an increased time of bone tissue regeneration around implants.

P 906

EVALUATION OF RATS STRIATED MUSCULAR TISSUE RESPONSE TO TINICO IMPLANTS

DROZD Aleksandra *, DRUGACZ Jan **, BIERZYNSKA-MACYSZYN Grazyna ****,
WLASZCZUK Pawel ****, WOLANSKA-KARUT Joanna ****, KWIEK Stanislaw J *** DROZD Wojciech **, LEKSTON Zdzislaw *****,
*Dental Practice, Katowice, Poland
**Department of Maxillofacial Surgery, Medical University of Silesia, Katowice , Poland
***Department of Neurosurgery, Medical University of Silesia, Katowice, Poland
****Department of Pathology, Medical University of Silesia, Katowice, Poland
*****Faculty of Computer and Material Sciences, Silesian University, Katowice, Poland

Rapid progress of medicine connected with reconstructive surgery leads us to searching for the new materials which would substitute, temporarily or permanently, harmed tissues.

The TiNiCo alloy with the shape-memory effect was taken upon the study and implanted to rats of Sprague-Dawley breed. After the implantation period lasting 12, 24 or 52 weeks the implants were removed and the surrounding tissues subjected to histopathological examination.

The morphologic features of inflammation (lymphocytic, granulocytic, eosinophilic, plasmocytic infiltrations), necrosis, fibrosis (fibrous capsulae formation), degeneration, giant cells and granulomas presence in the tissue samples were evaluated. The vascular proliferation and nuclear changes were estimated as well. The TiNiCo alloy and Titanium placed in the tissues accordingly to the ASTM F 981-99 standards cause low biologic tissue activity.

The investigated materials do not trigger any tissue response that could suggest their cytotoxicity or carcinogenic properties. The achieved results indicate high biocompatibility of TiNiCo alloys.

Key words: tissue response, rat, shape-memory effect alloy, TiNiCo implant, biocompatibility, Titanium

P 907

A HIGH AUTOPSY RATE IN A TEACHING HOSPITAL IN BRAZIL

Alfredo Ribeiro-Silva, MD, PhD
Luiz Cesar Peres, MD, PhD
Department of Pathology, Faculty of Medicine of Ribeirão Preto, University of São Paulo, Brazil

Autopsy is an invaluable diagnostic tool in medical practice since postmortem studies provide relevant information in patients with complex pathologies. In academic hospitals, autopsy also contributes to research and teaching by supplying a rich material to these purposes. In our Institution, autopsy is performed in 85% of patients that die during hospitalization (75% among adults and 90% among fetal and pediatric patients). A high autopsy rate allows accurate epidemiological studies and quality control. As a teaching Hospital, it is also important to know if death of patients varies along the year, days and months in an attempt to identify if there are medical and non-medical factors such as the activity of less trained residents and undergraduate students influencing it. We analyzed all autopsies performed in a University Teaching Hospital in Brazil during 52 consecutive weeks. The following data were retrieved from individual autopsy records: gender, age, time of death (hour of the day, day of the week and month) and the main cause of death. There were 1419 autopsies (79% adults and 21% pediatrics, 60% male and 40% female). Those performed during working days summed up to 67.5%, the remainder 32.5% were performed during weekends or holydays. They were more frequent during the nocturne than diurnal period (52.6% and 47.4%, respectively). The causes of death distributed among the ICD-10 categories were: cardiovascular diseases 21.3%, infectious diseases 19.2%, neoplasms 12.8%, perinatal conditions 10.8%, respiratory diseases 6.6%, gastrointestinal diseases 6%, congenital anomalies 4.7%, CNS diseases 3.8%, genito-urinary diseases 1.8%, and others 13%. In our Hospital a high autopsy rate is maintained due to readiness of results, performance of autopsy during the 24 hours of the day, very short interval between death and autopsy and a team composed by an experienced pathologist, a resident and a mortuary assistant. There was coexistence of diseases typical of both industrialized and developing countries, indicating the epidemiological transition in our country. The regular distribution of deaths along the day, weeks and months indicate that it is not affected by the inexperience of training students and residents probably due to adequate supervision.

P 908

UNUSUAL SITES OF FUNGAL INFECTION

Barboza-Quintana Oralia MD FIAC,Mendez-Olvera Nora MD, Ancer-Rodriguez Jesús MD, Garza-Guajardo Raquel MD FIAC Anatomic Pathology and Cytopathology Service, Universitary Hospital “Dr. José E. González”, UANL, Monterrey, México

Aspergillus is a filamentous fungus commonly isolated from soil, plant debris, and indoor air environment, includes over 185 species, and Aspergillus fumigatus is the most commonly isolated. Immunosupression is the major factor predisposing to development of opportunistic infections. There are several reported cases that describe female genital tract infections with opportunistic fungi, Candida and Aspergillus are most commonly found in fungal endometritis and are generally requering some type of predisposing condition like a use of Intrauterine Device

Coccidioidomycosis is a systemic infection caused by Coccidioides immitis, a dimorphic fungus endemic in the south of the USA and in the north of Mexico. The disease usually affects the lungs. Primary cutaneous infection is extremely rare.

Blastomycosis is a disease caused by the dimorphic fungi Blastomyces dermatitidis, and is acquired via inhalation of the conidia, which transform into the yeast form once in the lungs, however at least 50% of primary infections are

asymptomatic and most of the cases become manifest during a chronic phase that may affect the lungs, skin, bones, genitourinary tract and other reticuloendothelial organs. Involvement of genitourinary tract is seen in 10% of cases and affects the prostate and epididymis.
We present 5 cases of non-usual sites infections with this 3 fungi: 2 cases of aspergiliosis in a curettage secondary to spontaneous abortion, 2 cases of primarious cutaneous coccidioidomycosis localized in the nose and ear, and a case of blastomycosis localized on the prostate, in the 5 cases the patients did not reveal the presence of a primary infection in any other system. It is important to have in mind this unusual sites of primary infection by fungi because we can mislead the opportunity to bring the patient an opportune treatment with anti-fungal drugs.

P 909

UNKNOWN PRIMARY CANCER: IMMUNOHISTOCHEMICAL ALGORITHMIC APPROACH FOR EPITHELIAL NEOPLASMS WITH MULTIPLE METASTASES.

SAVELOV Nikita*, SHAPOVALOV Dmitry**, KOMAROV Igor** and PETROVICHEV Nikolay*.
*Department of Pathology, N.N.Blokhin Cancer Research Center, Moscow, Russia.
**Department of Diagnostic Oncology, N.N.Blokhin Cancer Research Center, Moscow, Russia.

Introduction: The exact diagnosis of unknown primary cancer (UPC) is a common problem for the surgical pathologist especially in cases with multiple metastases at different sites. The typical feature of a UPC with > 2 metastatic sites at the initial clinical presentation is a rapid progression of the disease, often less than three months. This requires rapid diagnosis in these patients. The aim of this study was to develop an optimal algorithm of immunohistochemical investigation of UPC with multiple metastatic sites.
Materials and methods: Histopathological and immunohistochemical investigations were performed in thirty two cases with UPC with > 2 metastatic sites, mainly in lymph nodes. A broad immunohistochemical panel and high sensitivity polymer detection system were performed on formalin fixed paraffin embedded tissues from each case.
Results: Because the metastatic tumors were mainly poorly differentiated carcinomas or poorly differentiated adenocarcinomas, the initial step of immunohistochemical investigation was to determine lines of cell differentiation. For this purpose we used the panel consisting of p63, CK8, HMW, CD56 (N-CAM) and calretinin. For adenocarcinomas (CK8+, HMW+/-, p63-, CD56-, calretinin-) the second step was to identify a primary site. To perform this we investigated expression of CK7 and CK20, and 'tissue specific' transcription factors - TTF1, Cdx2, WT1, ER and PR. In addition we investigated expression of some specific cell products, such as CA-125, PSA, GCDFP-15. Approximately in thirty percent of performed cases the results of histopathological and immunohistochemical investigations were the same. In seventy percent of cases the results of immunohistochemical investigations gave important additional information for further management of the patients or radically changed the interpretation of histopathological date.
Conclusion: Although the morphological examinations is the basis of diagnosis in surgical pathology, immunohistochemistry is a powerful ancillary method, particularly in cases with multiple metastases of unknown primary site.

P 910

POLY(ADP-RIBOSYLATION) MODULATES THE EXPRESSION OF TUMOR-RELATED GENES DURING CARCINOGENESIS

MARTIN-OLIVA David,MUÑOZ-GAMEZ Jose Antonio, AGUILAR-QUESADA Rocio, O'VALLE Francisco, GARCIA del MORAL Raimundo,RUIZ de ALMODOVAR Mariano, PIRIS Miguel Angel, OLIVER F Javier.
University Hospital, San Cecilio, Granada; Institute of Parasitology and Biomedicine, CSIC, Granada, Spain. Department of Pathology, University of Granada;Department of Radiology and Physical Medicine, University of Granada; Centro Nacional de Investigaciones Oncológicas (CNIO), Madrid, Spain.

PARP-1, an enzyme that catalyzes the attachment of ADP ribose units to target proteins, acts as a component of enhancer/promoter regulatory complexes. In a previous study we have shown that parp-1 knockout mice exhibit resistance to chemical carcinogenesis and this was related to a decreased NF-kB activation. Objetive: Our aim was evaluated the effect of parp-1 inhibitor on skin carcinogenesis in a model of parp-1 knockout mice. Material and Methods: We used cDNA expression arrays analyis, Real-Time PCR, image analysis and morphological conventional techniques in this study.
Results: We show that pharmacological inhibition of PARP-1 with DPQ (3,4-dihydro-5-[4-(1-piperidinyl)butoxyl]-1(2H)-isoquinolinone) results in a strong delay in tumor formation and in a dramatic reduction in tumor size and in skin morphological changes and multiplicity during DMBA+TPA-induced skin carcinogenesis. PARP inhibition also affected AP-1 activation but not NF-kB. Using cDNA expression arrays analysis, a substantial difference in key tumor-related gene expression was found between chemically-induced mice untreated or not with PARP inhibitor and also between wild type and parp-1 knockout mice. Most important differences were found in gene expression, mainly for nfkbiz, s100a9, hif1alfa and other genes all of them involved in carcinogenesis and inflammation. These results were corroborated by Real-Time PCR. In summary, this study shows that inhibition of PARP on itself is able to control tumor growth and PARP inhibition or genetic deletion of PARP-1 modulates tumor promotion through their ability to cooperate with the activation AP-1 and/or NF-kB and to regulate the expression of genes related with tumor promotion/progression.

P 911

ABSENCE OF MYCOBACTERIUM TUBERCULOSIS PCR DETECTION FROM LYMPH NODES'SARCOIDOSIS GRANULOMAS ISOLATED BY LASER CAPTURE MICRODISSECTION.

LASSALLE Sandra (1), SELVA Eric (1), HOFMAN Véronique (1), VENISSAC Nicolas (2), MOUROUX Jérome (2), DELLAMONICA Pierre (3), HOFMAN Paul (1).
(1) Laboratory of Clinical and Experimental Pathology, (2) Department of Thoracic Surgery, and (3) Department of Infectious Diseases, University of Nice, Nice, France

Previous recent works have shown the usefulness of polymerase chain reaction (PCR) performed in granulomas isolated by laser capture microdissection (LCM) for improving the detection of M. tuberculosis in formalin-fixed paraffin-embedded tissues. Some studies have demonstrated that mycobacterial DNA can been sporadically detected by means of PCR amplification performed on formalin-fixed paraffin-embedded tissues in granulomatous diseases other than tuberculosis, such as sarcoidosis and Crohn'disease. The aim of the present work was to investigate if mycobacterial DNA could be detected by PCR in granulomas isolated by LCM from lymph nodes'sarcoidosis. The PCR DNA amplification method was used to detect M. tuberculosis in granulomas microdissected from one section stained by haematoxylin and eosin from a formalin-fixed paraffin-embedded specimen. The results were compared to those obtained from PCR performed from tuberculosis granulomas

with positive Ziehl staining. Twenty-nine formalin-fixed and paraffin-embedded samples from 29 patients with sarcoidosis and 24 similar conditionned samples obtained from 24 lymph nodes'tuberculosis were investigated by this combined method. After staining with hematoxylin and eosin, granulomas were microdissected using a LCM microscope (PixCell II, Arcturus Engineering). For the PCR reaction, we used specific sequences of the 16S ribosomal RNA gene to M. tuberculosis. Results: PCR from microdissected sarcoidosis granulomas procured from one 5 mm section of each specimen was negative in the 29 studied cases, whereas PCR from microdissected tuberculosis granulomas was positve in the 24 studied cases. In conclusion, our work showed that mycobacterial DNA is not detected in lymph nodes'sarcoidosis when using PCR on laser microdissected granulomas from formalin-fixed paraffin-embedded specimen.

P 912

HYPERMETHYLATION PATTERNS IN THE FHIT REGULATORY REGION ARE TISSUE SPECIFIC

GULER G 1,2*, ILIOPOULOS D 2,5*, HAN Shuang-Yin 2, FONG Louise YY 2, LUBET Ronald A 3, GRUBBS Clinton J 4, HUEBNER K 2,5
1 Hacettepe University Department of Pathology 06100 Ankara Tukey, 2 Department of Microbiology-Immunology, Kimmel Cancer Center, Jefferson Medical College, Philadelphia, PA 19107,USA, 3 Division of Cancer Prevention and Control,
DCPC, National Cancer Institute, Bethesda, MD 20852, USA, 4 Department of Surgery, University of Alabama at Birmingham, Birmingham AL 35294,USA, 5 Current address: Comprehensive Cancer Center, Ohio State University, Columbus, Ohio,43210 USA.

DNA hypermethylation is associated with decreased gene expression of tumor suppressor genes. In a previous study we observed decreased Fhit expression and Fhit promoter region methylation in rodent tumors induced by various carcinogens and noted differential methylation patterns in DNA from tissues of different organs; i.e., the 5' regulatory regions in the promoter, exon 1 and intron 1 were differentially methylated, depending on the tissue of organ. Because different carcinogens were used for induction of tumors of the different organs, we could not conclude that the methylation patterns were tissue-specific. In order to determine if 1) rat Fhit methylation status is related with expression levels and 2) rat Fhit methylation patterns were tissue or carcinogen-specific, by examining Fhit methylation status and expression levels in DMBA and MNU-induced benign and malignant mammary tumors. Fhit intron 1 was methylated in 3/9 DMBA and all (5/5) MNU-induced benign mammary tumors in association with reduced Fhit expression levels; Fhit promoter and intron 1 were methylated in all DMBA and MNU-induced tumors in association with highly reduced Fhit expression levels. Treatment of rat cancer cells in vitro with the DNA methyltransferase inhibitor, 5'-Aza-2'deoxycytidine, for 4 days, increased Fhit expression and altered the methylation status. Before treatment both promoter and intron 1 regions were methylated; after treatment only intron 1 remained methylated. Thus there is an overall association of rat Fhit regulatory region methylation with its expression and hypermethylation patterns were tissue and not carcinogen-specific.
*These authors contributed equally to this work

P 913

HIGH MOBILITY GROUP (HMG) PROTEINS IN MALIGNANT TUMOURS - FROM DIAGNOSTIC MARKER TO INDEPENDENT PROGNOSTIC FACTOR?

IIntroduction: High mobility group proteins are structural transcription factors with further involvement in enhancosomes and hormone-receptors. Because of their ability to boost proliferation, infiltration and metastasis of tumour-cells, they are sometimes referred to as kinases. In the normal adult tissue they are either not or only very weak expressed.
Purpose: In previous publications it was shown that HMGA1 and A2 are expressed in many neoplastic tissues and mark either malignancy or bad prognosis. Because there were no data concerning Breast- and Non-Small-Cell-Lung-Carcinoma (NSCLC) we started investigations concerning these frequent tumours.
Methods: Breast- and NSCLC tissue were investigated concerning HMG expression on RNA-Level (using Real-Time PCR) and Protein level (using Immunohistochemistry). First data are compared concerning immunohistological and Real-Time PCR results. Furthermore, first data of HMGA1 and HMGA2 expression in these frequent tumours are shown.
Results and Conclusions: In breast-carcinoma HMGA1 expression is significiantly correlated with Grading, Hormone-Receptors and HER-2.
In NSCLC HMGA2 is highly expressed in appr. 50% of squamous cell carcinoma and 20% of adenocarcinoma. There seems to be no correlation with any other morphological marker, but, as first data suggest, with disease free and over-all-survival.

P 914

PILOMATRIX CARCINOMA: A CHALLENGING DIAGNOSIS OF BASALOID CELL TUMORS

Dr Homayon Moslehi, Assistant professor of dermatology Tehran university of medical science
Dr Monsour Nasiri Kashani, Assistant professor of dermatology Tehran university of medical science
Dr masoud Asgari, assistant professor of pathology Tehran university of medical science

Pilomatrix carcinoma (PC) is a rare locally aggressive tumor of hair matrix that has a predilection for head and neck. There is male to female ratio of 2:1. The mean age of affected patients is 48 with a reported range from age 2 to 88. We report a case of PC treated by Mohs surgery that initially diagnosed as basal cell carcinoma (BCC) which is the main and most challenging differential diagnosis.

A 35-years old man was evaluated of a solitary, slow growing nodule on his dorsum of the nose. The nodule has been present for a few years without any pain and tenderness. The nodule was ulcerated by patient manipulation. On physical examination a 2cm firm nodule with telangiectasia and central depression on surface was noted on the dorsum of the nose. From initial biopsy specimens, It has been reported lobulated island of basaloid cells connected to the epidermis with a final diagnosis of BCC that involve surgical margins and depth. Mohs surgery carried out for an incomplete excised and recurrent BCC of the nose. Frozen section revealed island of tumors in deep dermis without connection to epidermis. Permanent slides showed sheets and nests of neoplastic basaloid cells in deep dermis, hypodermis and between muscles with varing degree of central necrosis. The neoplastic cells had hyper chromatic nuclei, moderate pleomorphism and numerous mitosis, some of which were atypical. The mitotic rate was 75 per 10 high power fields (35/mm2). The basaloid nest went abrupt transition to central necrotic areas with pycnotic and shadow cells. Using immunohistochemical techniques, Ki-67 showed proliferation rate of 50%. Bcl-2 was expressed in 3% and P53 in 36% of the tumor cells. A large portion of neoplastic cells expressed Low molecular cytokeratin (CK19). S100 and CEA were negative, all findings confirming the diagnosis of PC.

In summery, although the histopathological diagnosis of PC is simple, in the presence of epidermal connection as our case

in first biopsies, it will be problematic. However with more careful study, numerous mitosis and central necrosis can be seen which are rare in BCC.

P 915

ROLE OF NON-HISTONE PROTEINS IN EARLY DIAGNOSIS OF NORMAL AND SKIN LESIONS

Monsef Ar, MD*- Hosseinipanah SM, Ph.D- Ebrahimi M, MD – Mahjob H, Ph.D – Eghbalian F, MD.
*Dept. of Pathology, Faculty of Medicine, Hamadan University of Medical Siences,
Hamadan, IRAN.
e-mail: monsef_ar2001@yahoo.com

Abstract:
Objective: Evaluation of the diagnostic value of silver nucleolar organizer Region assessment in skin diseases is important. According to this reason we want to study the Argyrophilic Nucleolar Organizer Region (Ag-NOR) count and Subjective Ag-NOR Pattern Assessment (SAPA) score in normal skin, Squamous Cell Carcinoma (SCC), Basal Cell Carcinoma (BCC) and Solar Keratosis (SK).
Method: The study groups considered of 69 cases (18 SCC, 18 SK, 17 BCC and 16 Normal skin) was studied by H&E staining and silver staining for Ag-NOR.
Results: The mean count was in SCC 2.92, in SK 2.29 in BCC 1.59 and 0.93 in normal skin (p value <0.001).
The SAPA score was in SCC 7.94 in SK 7.61 in BCC 6.35 and in normal skin 5.00 (p value <0.001).
Conclusion: Ag-NOR count and SAPA score in normal and pathological state of skin has positive results.
Key Words: Ag-NOR, SCC, BCC, SK, Skin.

P 916

HISTOPATHOLOGIC STUDY OF ROSACEA

A.R.Monsef Esfahani. F.Eghbalian
Dermatopathology dept. Sina Hospital. Hamedan university of medical sciences Hamedan, Iran

Bakground :
Rosacea is a common but ill-defined disease and Demodex follicularum has been reported in rosacea in a number of clinical studies. As the Demodex mite is also present in many healthy individuals, the mite may have a pathogenic role only when it is present in high densities.
In this study the possible role of demodex follicularum and the importance of mite density had investigated using an elliptical incisional skin biopsy technique.
Methods :
Thirty-nine patients with rocacea, twenty-five female, 14 male, and 41age and sex matched healthy persons entered the study. With the incisional skin biopsy of face we studied six section of each sample. We studied the number of follicles, mite dencity in them, epidermal changes, solar elastosis, inflammatory cells in the dermis and their pattern , granuloma formation and vascular changes.
Result :
Varing degree of vasodilatation, solar elastosis and in flammatory infiltrate were found in all patients. The infiltrate were lympho-histiocytic in 29 cases, lympho-plasmacytic in 6 cases and neuropilic, specially around hair follicles in 2 cases, and eosinophilic infiltration mixed with mononuclear cells in 2 cases. The number of D. follicularum was statistically significant. Between male and female there was not important difference, 0.929 to 1.200, P value 0.81; .
There was important difference in the number of mite in rosacea related to age , it was 0.545 in under 40 year group and 1.308 over 40 year age, P value 0.047. But it was not meaningful in non rosacea group 0.118 mite per follicle under 40 and 0.509 mite per follicle over 40 year, P value 0.53.
There was granuloma to appendages in 3 of cases and granuluma around hair folicole in 2 of cases. One of the later group revealed degenerated demodex demodex cuticle.
Conclusion :
Rosacea is a multifactorial disease, and high densities of demodex is important, in the form of hypersensitivity reaction to antigens or granuloma formation in response to its cuticle or destructed hair follicles. The individual properties may modify the severity of inflammatory response to demodex.

P 917

ANALYSIS OF CYCLOOXYGENASE-2 EXPRESSION AS A POSSIBLE MARKER OF VITALITY IN CUTANEOUS WOUNDS

ORTIZ-REY José Antonio, SUÁREZ-PEÑARANDA José Manuel* ,SAN MIGUEL Pilar , ÁLVAREZ Carlos, MUÑOZ José Ignacio* ,RODRÍGUEZ-CALVO María Soledad*, CONCHEIRO Luís*
Servicio de Anatomía Patológica, Hospital POVISA, Vigo.
*Instituto de Medicina Legal, Universidad de Santiago. Spain.

Introduction
The histologic differential diagnosis between vital and postmortem cutaneous wounds is difficult when the injury is inflicted close to the time of death. Ancillary techniques such as immunohistochemistry may aid to the diagnosis of vitality through the analysis of molecules implied in the initial inflammatory reaction.Cyclooxygenase-2 (COX-2), an enzyme rapidly synthesized in response to different insults to the skin, is essential for prostaglandin biosynthesis, which is an important process for cutaneous wound healing.
Purpose
Our objective has been to investigate COX-2 expression in vital and postmortem cutaneous wounds to check its possible application as a marker of vitality.
Materials and methods
41 samples from human incised cutaneous wounds were investigated comprising: 16 vital injuries aged 3 minutes to 8 hours (mean:125 minutes), 14 inflicted postmortem (collected after a period of 1-3 hours), and 11 scars from sutured surgical incisions whose age was 0.5 to 11 months. Formalin-fixed paraffin-embedded sections were immunostained through the labelled streptavidin-biotin technique using a monoclonal antibody anti COX-2 (DakoCytomation).
Results
All of the samples showed normal immunoreactivity for COX-2 in eccrine glands with faint staining in sebaceous glands and the basal layer of the epidermis. Differences in staining were not observed when comparing the injury edge with the opposite margin in every specimen, nor between vital and postmortem wounds. Scars with inflammatory reaction in the dermis (aged 0.5 to 3 months) showed overexpression of COX-2 in histiocytes and mononuclear cells.
Conclusions
Immunohistochemical analysis of COX-2 has not been useful to differentiate vital and postmortem injuries. Overexpression of COX-2 could only be detected in the histiocytic inflammatory phase of wound healing. For these reasons it is not a good marker to diagnose vitality in difficult injuries, aged just a few hours.

P 918

EXPRESSION OF E-CADHERIN AND CATENINS IN VITAL AND POSTMORTEM CUTANEOUS WOUNDS

ORTIZ-REY José Antonio, SUÁREZ-PEÑARANDA José Manuel* ,SAN MIGUEL Pilar , IGLESIAS Begoña , MUÑOZ José Ignacio* ,RODRÍGUEZ-CALVO María Soledad*, CONCHEIRO Luís*
Servicio de Anatomía Patológica, Hospital POVISA, Vigo.
*Instituto de Medicina Legal, Universidad de Santiago. Spain.

Introduction
The differential diagnosis between vital and postmortem wounds is often difficult for the pathologist, specially when the injury is produced close to time of death. Immunohistochemical detection of different molecules involved in inflammatory reaction and healing process have been proposed to aid to the diagnosis. Re-epithelialization is a key process in the wound healing and it begins early after the injury. E-cadherin and catenins, critical for adhesion between keratinocytes, play an important role in the process. The diagnostic value of their expression as markers of vitality has not been well established.
Purpose
Our objective was to analyse the expression of E-cadherin and catenins (alpha, beta and gamma) in vital and postmortem wounds as possible markers of vitality.
Materials and methods
The study comprised 42 human incised wounds (32 vital and 10 postmortem) and 3 cutaneous scars. The vital wounds were obtained from abdominal surgical incisions with post infliction intervals between 55 minutes and 8 hours. Two of the scars were 2 months old and the other was 5 months old. The postmortem specimens were obtained from autopsy abdominal incisions and were collected after a mean period of 105 minutes (range 15-180).
Formalin-fixed paraffin-embedded sections were immunostained following the labelled streptavidin-biotin technique with monoclonal antibodies against E-cadherin (BioGenex) and alpha, beta and gamma catenins (Transduction Laboratories). Staining of the wound edge was compared to that of the opposite margin of the sample.
Results
Differences in the staining between the two margins of the specimen were noted in 11 cases (9 vital and 2 postmortem). The staining was increased in the wound edge in 7 cases and in the control edge in 4. The differences corresponded to E-cadherin in 5 cases, alpha-catenin and gamma-catenin in 3. No differences were appreciated for beta-catenin.
Conclusions
Immunohistochemical analyses of E-cadherin, alpha, beta and gamma catenins are not useful for the differential diagnosis between vital and postmortem wounds. This could be related to a low sensitivity of immunohistochemical techniques to detect the subtle changes of levels of these proteins at the beginning of the inflammatory reaction.

P 919
GENERALIZED LICHEN AMYLOIDOSIS: A CASE REPORT
* ATÝK Esin, **SERARSLAN Gamze
(*)Department of Pathology, Mustafa Kemal University, Faculty of Medicine, Antakya-
Hatay / Turkey
(**)Department of Dermatology, Mustafa Kemal University, Faculty of Medicine, Antakya-Hatay / Turkey

Lichen amyloidosis is a type of cutaneous amyloidosis, caused by the extracellular deposition of amyloid composed primarily of degenerated keratin filaments. Generalized lichen amyloidosis is a rare form of the disease and characterized by pruritic discrete hyperkeratotic scaly papules. We report a case of lichen amyloidosis with extensive distribution in a 33-year-old female.

P 920
SUBACUTE RADIODERMATITIS
SIBON Claire 1, BERTOCCHI Céline 1, POUGET Florence 2, CLERICI Thierry 1, REVUZ Jean 2, FRANC Brigitte 1.
1- Department of Pathology, A. Paré Hospital (APHP), 92100 Boulogne-Billancourt, France.
2- Department of Dermatology, H. Mondor Hospital (APHP), 94010 Créteil, France.

Introduction : Radiodermatitis is a rare cutaneous disorder induced by radiation used in diagnostic and interventional procedures. The histologic characteristics of this entity have been poorly described.
Case report : A 74-year-old man with a history of coronary disease presented with a 10-centimeters, pruritic, fixed, well demarked erythematous patch of the back, which had begun four weeks after a coronary artery stenting. A skin biopsy was performed showing interface dermatitis. Given the history of radiation exposure and the clinical course of the lesion, the histological findings were felt to be consistent with subacute radiodermatitis.
Discussion : Skin damages in subacute radiodermatitis involve epidermis and dermis. The main histological findings are : interface dermatitis with keratinocyte necrosis, clefting along the dermal-epidermal junction and variable perivascular lympho-histiocytic infiltrate with no eosinophils. Key differentiating factors from graft-versus-host disease and fixed drug reaction include history, clinical morphology, type and distribution of cutaneous infiltrate.
Conclusion : With the increased use of radiation for diagnostic and interventional technique, this entity should be known and discussed by both clinicians and pathologists, when an interface dermatitis is observed.

P 921
IMMUNOHISTOCHEMICAL STUDY OF SKIN LESIONS AFTER THERAPEUTIC IRRADIATION
Monica Banita, Cătălina Pisoschi, Gh. Drăgoi
University of Medicine and Pharmacy Craiova, Romania

Introduction. We focused on skin alterations after cobalto-therapy knowing that exposure to overdoses of radiation could induce cancerous lesions.
Purpose of the study. We studied the expression of S100 protein in order to assess melanoblastic cells, dendritic cells and nervs, Vascular Endothelial Growth Factor (VEGF) for its mitogenic effects on endothelial cells and that of cytochrome c to evaluate apoptosis as a phenomenon involved in regulation of cell number using immunohistochemistry.
Materials and methods. Samples of breast integument irradiated for therapeutic reasons and control non-irradiated ones were collected after tumor excision and than processed for paraffin embedding. Serial sections were rehydrated and incubated with each required primary antibodies and then the immunoreaction was amplified using avidin – biotin or PAP (peroxidase - antiperoxidase) technique.
Results. After irradiation we noted an increased number of melanoblastic cells in the epidermal basal layer and also in the deep intermediate one revealed by the S100 immunolabeling. The same antibody marked also an increased number of Langerhans cells with the same distribution. The latest were also increased in the papillary dermis with a pericapillary disposition from the irradiated skin compared to control samples.
VEGF were found positive in few stromal cells and negative in endothelial cells from normal integument. In the irradiated dermis the number of VEGF positive fibroblast cells was increased and same the endothelial cells of capillaries from the papillary dermis. Vessel walls of arterioles and venules were entirely negative.
Epidermal germinative layer displayed few cytochrome c positive cells disposed with an insular pattern. Some cells from vessel walls were also positive for the apoptotic marker.
Conclusions. Irradiated skin has a non specific cellular reaction similar to that from the inflammatory process. The most obvious changes were found in the upper dermis layer

where mitotic effect and increase of permeability induced by VEGF seem to imbalance apoptotic post irradiated response.

P 922
CD 30 EXPRESSION IN TWO CASES OF NODULAR SCABIES
POTIER Alexandra(1), LECLECH Christian(2), VERRET Jean-Luc(2), CROUE Anne(1)
(1) Department of Pathology, University Hospital, 4 rue Larrey, 49933 Angers Cedex 09, France.
(2)Department of Dermatology , University Hospital, 4 rue Larrey, 49933 Angers Cedex 09, France.

CD30 antigen, protein of the tumor necrosis factor receptor family is a marker of lymphocyte activation. Its expression in large atypical cells has been observed in non neoplastic cutaneous inflammatory infiltrates. We report two cases of nodular scabies with CD30-positive large cells.

A 74-year-old woman presented with a nine-month history of generalized pruritus. On examination there were well demarcated papuloerythematous prurigo-like lesions on the back and the buttocks. The second patient, a-30-year old man, presented with a persistant pruritus after scabies treated six months before. Clinically, papulonodules of the external genitalia and the buttocks suggested nodular scabies. Histopathological examination of the two cutaneous biopsies revealed a prominent perivascular inflammatory infiltrate in the papillary and reticular dermis. It contained lymphocytes, histiocytes, few eosinophils and many large lymphoid cells with cleaved nuclei and one or more large nucleoli resembling Reed-Sternberg cells. Many mitoses were found in one case. Immunohistochemichal analysis revealed that most cells of the infiltrate including large cells were CD3 positive. The large cells expressed CD30 in a membranous pattern with accentuation of the Golgi apparatus. We suspected a primary cutaneous CD30-positive lymphoproliferation. Nevertheless the demonstration of Sarcoptes Scabiei after skin scraping and the improvement of cutaneous lesions with treatment for scabies led us to the diagnosis of nodular scabies.

The presence of large CD30-positive atypical cells has been reported in cutaneous inflammatory infiltrates of scabies with long standing lesions. No CD30 expression has been found in early lesions (less than two months). Atypical CD30-positive lymphoid cells have also been observed in activated lymphocytes in a variety of inflammatory reactions rich in neutrophils and eosinophils especially in insect bites, infectious conditions including bacterial, viral (herpes virus and molluscum contagiosum) and fungal, hidradenitis suppurativa, Sweet syndrome, drug eruptions…

CD30 expression in cutaneous infiltrates is not uncommon in non neoplastic inflammatory conditions and doesn't imply a diagnosis of primary cutaneous CD30-positive lymphoproliferative disorder, particularly lymphomatoid papulosis: others parameters (clinical feature, evolution) are required to establish this definitive diagnosis.

P 923
MERKEL CELL CARCINOMA – CASE REPORT
Dimov D, Mihailoviæ D, Katiæ V, Petroviæ A, Kostadinov V.
Medical faculty of Niš, University of Niš, Serbia

Introduction: Merkel cell carcinoma (MCC), first described by Tang and Toker in 1972., is a rare highly malignant skin tumour of neuroendocrine origin. Pathognomonic immunohistochemical markers for the diagnosis are epithelial (CK20), as well as neuroendocrine (chromogranine) markers.
Case report: A 69 years old woman, showed dark-red nodules, located in the lateral side of the her right leg. Although the mass was large measuring 28 cm, there was no evidence of nodal involvement. It consisted of small epithelial cells (small cell type) which formed solid cell complexes, arranged in characteristic trabecular patterns. The tumour cells were monomorphic, with oval nucleus, numerous mitotic figures, and massive necrosis. These cells infiltrated subcutaneous fat. The diagnosis MCC was confirmed through the histological and immunohistochemical analysis: Merkel cell tumour expressed epithelial (CK20) as well as neuroendocrine (chromogranine) markers.
Conclusion: In addition to histological/immunohistochemical characteristics for MCC diagnosis, the clinical data that indicate on primary skin tumour, provide a great help to pathologist in establishing the diagnosis of Merkel cell carcinoma.

P 924
ASSOCIATION OF MERKEL CELL CARCINOMA AND BOWEN´S DISEASE
Suárez-Peñaranda JM, Delgado-Gonzáles V(1), Casas Fernández L(2), Vieites B, Ortiz-Rey JA(3), Varela Durán J.
Department of Pathology. University of Santiago de Compostela Hospital and Medical School. Santiago de Compostela. Spain.
(1) Department of Surgical Pathology. Hospital Guillermo Almenara. Lima. Perú.
(2) Department of Dermatology. Fundación Hospital Barbanza. Ribeira. Spain.
(3) Department of Pathology. Centro Médico POVISA. Vigo. Spain

Introduction
Merkel cell carcinoma (MCC) is an uncommon neuroendocrine malignant neoplasm whose origin has not been well established. Little is known about its association with other malignant skin diseases, although there have been some reports associating it with basal cell carcinoma in-situ or infiltrating squamous cell carcinoma and malignan tmelanoma.
Case report
An 86-year-old woman was referred to the hospital complaining of a 10-cm tumour located in her left forearm. The tumour was completely excised.
Histopathological examination showed dermal nests of small and medium-sized, round, basophilic cells arranged in a trabecular or diffuse pattern, extending deeply through the dermis to the subcutaneous fat tissue. In some sections, the keratinocytes located in the overlying epidermis were atypical and immature in appearance, exhibiting hyperchromatic nuclei and pleomorphism. Occasionally, dyskeratotic cells and areas of pagetoid appearance were also observed.
Dermal tumour cells were positive for neuron-specific enolase, synaptophysin, chromogranin A, CK 20 and CK AE1-AE3. The neoplastic epidermal cells were negative for neuron-specific enolase, synaptophysin, chromogranin A and CK20, but strongly positive for CKAE1-3. The diagnosis of Merkel cell carcinoma associated with Bowen's disease was established. The patient died two years later of an unrelated disease.
Comments
Histopathological examination and immunohistochemistry clearly demonstrate that this patient has two different but synchronous neoplasms arising in the same place. The reason for the association of both neoplasms remains unknown. Although the induction of a second neoplasm by the first tumour cannot be excluded, the most probable explanation is that we are dealing with a collision tumour, well casual or because they share some common etiopathogenic agents or risk factors that have not yet been identified.

P 925
CYCLO-OXYGENASE 2 EXPRESSION IN MERKEL CELL CARCINOMA
JOACHIMS Zohar, FEINMESSER Raphael, PURIM Ofer, HAlPERN Marisa, BRENNER Baruch, FENIG Eyal, ROIZMAN Pepy, SULKES Jaqueline, FEINMESSER Meora.

Departments of Otolaryngology, Pathology, Oncology and Epidemiology, Rabin Medical Center and Sackler School of Medicine, Tel Aviv University

Introduction: Merkel cell carcinoma (MCC) is an aggressive neuroendocrine tumor of the skin associated with a high rate of recurrence and metastasis and only partial response to current radio- and chemotherapy regimens. The cyclo-oxygenase 2 (COX2) enzyme is involved in the development and progression of many tumors, including large bowel, breast and lung cancers. COX2 inhibitors have been shown to block tumor growth. The aim of this study was to examine COX2 expression in 26 primary MCCs and 5 of their lymph node metastases.
Materials and methods: Formalin-fixed paraffin-embedded tissues were stained immunohistochemically with monoclonal antibody directed against COX2. The percentage and intensity of staining were analyzed semiquantitatively using a three-tiered system.
Results: Immunopositivity for COX2 was found in 20 out of the 26 primary tumors (76%), including 16 (80%) with widespread positivity. Staining intensity was mostly weak (9 tumors-45%) or moderate (6 tumors-30%). Three of the 5 metastases (71%) showed similar staining. Tumors with prominent mitotic activity were associated with more widespread COX2 immunopositivity. No association was found between COX2 expression and outcome.
Conclusions: Most MCCs express COX2. Expression is related to one parameter of aggressive behavior- a high mitotic rate- but not to any others. Owing to the large number of MCCs that express COX2, the possibility of treating patients with COX2 inhibitors should be considered.

P 926
MYXOID NEUROTHEKEOMA: IMMUNOHISTOCHEMICAL ANALYSIS OF A CASE
Zioga A, Batistatou A, Bonitsis N, Agnantis NJ
Department of Pathology, University of Ioannina Medical School, Ioannina, Greece

Introduction: The myxoid variant of neurothekeoma is a benign, myxomatous neoplasm, that most probably originates from the peripheral nerve sheath. Recently it has been proposed that the so-called cellular and mixed (intermediate) variants of neurothekeomas warrant a separate classification, since they show no evidence of neurosustentacular differentiation.
Method: Herein, we describe the clinical, histopathologic and immunohistochemical features of a case of myxoid neurothekeoma, in a 53-year-old woman.
Results: The patient presented with a subcutaneous tumor, measuring 1.5 cm in maximal dimention at her lower back (sacrococcygeal area). The preoperative diagnosis was a lipoma. On macroscopic examination, a circumscribed mass with a rubbery to hard consistency and gray-white cut surface was noted. On microscopic examination, the tumor was centered to the dermis, and extended to the subcutaneous fat, without extending to the epidermis. At low-power magnification it had a multinodular architecture, with varying-sized nodules of moderate cellularity, separated by dense bands of collagen. The neoplastic cells were small, stellate- or oval-shaped, with bland nucleus, pale eosinophilic cytoplasm and very rare mitoses. They were loosely arranged within Alcian blue-positive myxomatous stroma. Upon immunohistochemical examination, the neoplastic cells showed strong nuclear and cytoplasmic staining for S100 protein. In addition they exhibited weak immunoreactivity for NSE (Neuron Specific Enolase) and CD57 (Leu-7). Based on the morphologic and immunohistochemical features the diagnosis of myxoid neurothekeoma was made. The tumor had been excised completely. The patient is well 1 year after excision, without evidence of local recurrence.
Conclusion: Myxoid neurothekeoma is a benign neoplasm of probable Schwannian origin. Dermatologists should be aware of this neoplasm, whose complete surgical excision appears to be curative.

P 927
INTRAPARENCHYMAL MELANOCYTIC NEVUS IN AXILLARY LYMPH NODE
SAN MILLÁN Beatriz1, FACHAL Carmen1, RIVAS Eloy1, TARDÍO Antoni1, ALLEGUE Francisco2
1Department of Pathology, Vigo University Hospital Trust (Meixoeiro Hospital),SPAIN
2Departament of Dermatology, Vigo University Hospital Trust (Meixoeiro Hospital),SPAIN

INTRODUCTION
Benign melanocytic cells within lymph nodes is a well-documented but unusual finding. Stewart and Copeland firstly reported it in 1931. Focal aggregates of nevocytes are occasionally found in the fibrous capsule and trabeculae of lymph nodes, whereas an intraparenchymal location is exceptional. Only 20 cases have previously been reported. Non-malignant cellular inclusions can be misinterpreted as metastases from a melanoma or carcinoma.
We report here an intraparenchymal nodal nevus within an axillary node removed from a patient with breast cancer and nodal metastases.

CASE REPORT
A 64-year-old woman underwent a left radical modified mastectomy with axillary lymphadenectomy for a 6cm breast carcinoma in the external quadrants. Tissue specimens removed were fixed in 10% buffered formalin and routinely processed for light microscopy. Histopathological examination showed a multicentric infiltrating pleomorphic lobular carcinoma with histological grade 3 and an associated in situ component. Metastases were found in 5 out of the 24 nodes identified.
Clusters of medium size cells were detected within the nodal parenchyma, as well as in the capsule and trabeculae of one of the metastases-free lymph nodes. This cells showed a pale citoplasm, with little or no melanin pigment and indistinct cell borders. Nuclei with diffuse chromatin pattern were centrally placed. Cytological atypia, mitosis, and prominent nucleoli were not observed. When we compared this aggregates with the primary carcinoma cells they showed morphological differences. The query cells were positive for S-100 but negative for CEA, Keratins, HMB-45, Ki-67 and hormone receptors.
CONCLUSION
Melanocytic nevi within lymph node parenchyma is a very unusual finding.
Nevus cell aggregates could be easily mistaken for metastatic melanoma or carcinoma. A differential diagnosis between nodal nevi and metastases requires a careful morphological examination and supportive immunohistochemical studies, mainly in patients with a primary tumor without obvious features of malignancy.
This case highlights the rarity of nevus cell aggregates within the parenchyma of lymph nodes, and alerts the pathologist to avoid a misdiagnosis of malignancy.

P 928
EZH2 EXPRESSION IS ASSOCIATED WITH INCREASED PROLIFERATION RATE AND AGGRESSIVE TUMOR SUBGROUPS IN MELANOMA AND CANCER OF THE ENDOMETRIUM, PROSTATE, AND BREAST
BACHMANN Ingeborg M .1, HALVORSEN Ole J. 1, COLLETT Karin 1, STEFANSSON Ingunn M. 1, STRAUME Oddbjørn 1, HAUKAAS Svein A. 3,

SALVESEN Helga B. 1,2, OTTE Arie P. 4, and AKSLEN Lars A. 1

Introduction:
The Enhancer of Zeste Homolog 2 (EZH2) is a member of the polycomb group of genes (PcG), which are important for transcriptional regulation through nucleosome modification, chromatin remodelling and interaction with other transcription factors. EZH2 serves as a histone methyl transferase (HMT), and disruption of EZH2 expression may lead to dysregulation of genes critical for the G2/M transition. Further, EZH2 is controlled by E2F transcription factors, which is downstream of the retinoblastoma protein (Rb), and is also involved in p53 regulated œll cycle control. EZH2 is previously shown to be overexpressed in prostate, and breast cancer, and increased expression evaluated by in situ mRNA was found in 34% of human cancers in a recent study.
Purpose:
The aim of our study was to evaluate the expression of EZH2 in a broader range of human cancers, with special attention to key features such as tumor cell proliferation, tumor extent, and patient outcome. This is especially relevant since the polycomb group proteins have recently been suggested as candidates for targeted therapy.
Patients and methods:
In our study of 696 patients, we examined EZH2 expression by immunohistochemistry using high-throughput Tissue Microarray (TMA), and its association with clinical features and other tumor markers in malignant melanoma and cancers of the endometrium, prostate and breast.
Results:
Strong EZH2 expression was significantly associated with increased tumor cell proliferation in all four cancer types. Associations were also found between EZH2 and important clinico-pathological variables, such as tumor thickness and level of invasion, histologic grade, locally invasive growth, and extent of the disease. Further, EZH2 expression showed significant prognostic impact in melanomas, prostate and endometrial carcinomas in univariate survival analyses, and revealed independent prognostic importance in carcinomas of the endometrium and prostate.
Conclusion:
Our present findings point at EZH2 as a novel prognostic marker in malignant melanoma and endometrial cancer, and extend previous findings on prostate and breast cancer. The fact that EZH2 might identify aggressive subgroups in several cancers may be of significant practical interest, since the polycomb group proteins have recently been suggested as candidates for targeted therapy.

P 929

TMA: CADHERINS & CATENINS STUDY IN DIFFERENT STAGES PROGRESSION OF CUTANEOUS MALIGNANT MELANOMA

RODRIGUEZ PERALTO Jose Luis, SAIZ Ana, ALONSO Soledad, CARRILLO Rosario*.
Staff of Pathology Hospital Universitario 12 de Octubre de Madrid.
*Staff of Pathology Hospital Universitario Ramón y Cajal de Madrid.

INTRODUCTION
Cutaneous malignant melanoma, the most agressive common skin tumor, is characterized by a multifactorial etiology. The incidence and mortality of this tumor have increased over the last several decades.
Cadherins comprise a growing family of surface membrane glycoproteins that mediate cell-cell adhesion. The extracellular domains of cadherins serve as zippers conecting neighboring cells, whereas the citoplasmic tails are linked noncovalenty to the actin cytoskeleton via catenins.
PURPOSE OF STUDY
The aim of our study is to determine the protein expression patterns of some catenins and cadherins using tissue microarrays (TMA), in 191 malignant melanomas samples from 162 patients in different histological progression phases. The study tries to identify a set of stage-specific markers, and allows a predictor model to be developed that identifies groups of patients with increased risk of death.
METHODS USED
Primary radial and vertical phases, and metastatic malignant melanoma were used to construct a TMA´s from a series of 162 patients diagnosed at Ramon y Cajal University Hospital, Madrid, between 1978 and 2002. There was no history of familial incidence. We also included normal tissues as internal controls, with a 1.5mm diameter needle.
Antibodies used for these study were E-Cadherin, N-Cadherin, Cadherin 11, ?catenin, ßcatenin and p120.
RESULTS
The serie compriseS 162 patients diagnosed of cutaneous malignant melanoma. Fourty (20.7%) radial growth phase malignant melanomas, 128 vertical ones (66.3%), and 24 (12.4%) cutaneous or ganglionar metastases. Patients with radial growth phase malignant melanomas never had metastases, and vertical growth phase malignant melanomas had metastases in 42.9% of cases.
In general, all immunostaining showed a membranous pattern, except for ßcatenin which also expressed on the nucleous. E-cadherin and ? catenin expression showed notably decreasement with melanoma progression. The expression pattern of ß;- catenin was very similar to p-120 expression. Both proteins showed moderate decreasement with tumor progression. The expression pattern of Cadherin11 was absent.
CONCLUSIONS
The current study demonstrates the suitability analysis of TMA technique in the study of a classical model of human tumor progression. This study also demonstrates qualitative changes in the expression of some catenins and cadherins in different stages of malignant melanoma progression.

P 930

THE CORRELATION OF ANGIOGENESIS WITH METASTASIS IN PRIMARY CUTANEOUS MELANOMA: A COMPARATIVE ANALYSIS OF MICROVESSEL DENSITY, EXPRESSION OF VASCULAR ENDOTHELIAL GROWTH FACTOR AND BASIC FIBROBLASTIC GROWTH FACTOR

RAMAZANOGLU Rana*,DEMIRKESEN Cuyan*,BUYUKPINARBASILI Nur*, OGUZ Oya**, MANDEL Molinas Nil***, KANER Gultekin*
*Department of Pathology,**Department of Dermatology, ***Department of Oncology, Cerrahpaþa Medical Faculty, University of Istanbul

Tumor cells supply oxygen and nutrients necessary for growth by the recruitment of new blood vessels.Angiogenesis is not only a must in tumor growth but in metastasis as well. However, the prognostic significance of angiogenesis in malignant melanoma is controversial. In order to find out the correlation of angiogenesis with metastasis in primary cutaneous melanoma (PCMM), we studied the microvessel density, the expression of vascular endothelial growth factor (VEGF) and basic fibroblastic growth factor (bFGF) in 22 cases of PCMM with metastasis at presentation (metastatic group) and 28 cases of PCMM without any metastasis for 24 months or more (nonmetastatic group). Microvessels were stained with CD31/PECAM-1 antibody and counted. Besides the proportion of VEGF expression in tumor cells, lymphocytes infiltrating the tumor (TIL) and lymphocytes at the periphery of the tumor, as well as, the proportion of bFGF expression in tumor cell cytoplasms, nuclei and intra- and peritumoral vessels were assessed. An increased microvessel density was detected in the metastatic group [15-33

(24.09±5.55) vs. 2-24 (12.96±6.02)]. Moreover, enhanced expression of VEGF in tumor cells and peritumoral lymphocytes (Chi-square p=0.038 and p=0.018) and bFGF in peritumoral vessels (Chi-square p=0.013) correlated with the simultaneous presence of melanoma metastasis in PCMM.
In conclusion microvessel density, as well as, the expression of both VEGF and bFGF might be informative concerning the progression of melanoma.

P 931
THE MITOCHONDRIAL SIGNATURE OF MELANOMAS PROVIDES A MARKER OF PROGNOSIS
CAMARASA Natalia1 ,CARRILLO Rosario1 , MARTINEZ-DIEZ Marta2, MOYA Laura3, CUEZVA Jose M2.
1Departamento de Anatomia Patologica y 3Dermatologia, Hospital Universitario Ramon y Cajal, 28034 Madrid and 2Departamento de Biologia Molecular, Centro de Biologia Molecular Severo Ochoa, Universidad Autonoma de Madrid, 28049 Madrid, Spain.

Introduction: A large body of clinical data documents that most human carcinomas contain reduced levels of the catalytic subunit of the mitochondrial H+ATP synthase (B-F1-ATPase). In colon and lung cancer this alteration correlates with a poor patient prognosis.
Purpose of the study: In this study we have investigated the mitochondrial phenotype of melanomas as a prognostic marker of disease progression.
Material and methods: A set of twenty-one nevi, forty-one melanomas and thirteen metastases were examined for quantitative differences in protein expression of the mitochondrial B-F1-ATPase and Hsp60 markers by immunohistochemical techniques. Quantification of the expression level of the markers was carried out in digital images acquired at 20x magnification with a Leica DC100 camera and processed with the Leica QWin software. Correlations of the expression level of the protein markers were established with the clinicopathological information of the melanomas and the follow-up data of the patients.
Results: The expression B-F1-ATPase and Hsp60 was significantly higher in melanomas and metastases than in nevocellular nevi. However, with advanced disease, the expression of both mitochondrial markers was significantly diminished in the melanomas. Cluster analysis by the expression level of the mitochondrial markers allowed the identification of a group of melanomas that predicted a worse prognosis for the patients. The good prognosis group had an expression level of B-F1-ATPase that was 50% higher (P<0.001) than that found in melanomas of worse prognosis. Kaplan-Meier survival analysis showed that the expression level of B-F1-ATPase significantly correlated (P=0.024) with overall survival of the patients.
Conclusion: The alteration of the mitochondrial proteome of melanomas provides a relevant marker to add in the prognosis of these patients.

P 932
IMMUNOHISTOCHEMICAL EXPRESSION OF MSH-2 AND MLH-1 EN MALIGNANT MELANOMAS:CORRELATION WITH TUMOR STAGE AND PROGNOSIS
SAN MIGUEL Pilar, ORTIZ-REY Jose Antonio, MONTEAGUDO Benigno, ALMANZA Concepción, BARBOSA Mª jose, IGLESIAS Begoña, ÁLVAREZ Carlos, ANTÓN Iosu.

Introduction: Defects in DNA mismatch-repair genes MLH-1 and MSH-2 first described in hereditary nonpolyposis colon cancer, have been postulated to be responsible for malignant transformation in many types of tumors, including malignant melanomas.
Purpose of the study: The main aim of this study was to investigate the expression of these genes in malignant melanomas in relation to tumor stage and prognosis.
Methods: We examined the protein expression pattern of MLH-1 and MSH-2 by immunohistochemistry in 20 cutaneous melanomas. Formalin-fixed paraffin-embedded sections were immunostained following the labelled streptavidin-biotin technique (LSAB2Ò, DAKO) using monoclonal antibodies against MLH-1 (1:10, clone G168-15, BD Biosciences) and MSH2 (1:200, cloneG219-1129, BD Biosciences). For epitope retrieval slides were pretreated with citrate buffer for 5 minutes in a pressure cooker.
Association of expression of MSH-2 and MLH-1 with clinical stage (pT1, pT2, pT3 and pT4) and prognosis (alive or died) was evaluated.
Results: The study cohort comprised 12 females and 8 males ranging in age from 17 to 74 years (average 55 years). The 20 patients in the study cohort had malignant melanomas with the following pT distribution: pT1:35%, pT2:20%; pT3:10% and pT4:35%.
Relation between tumor stage and detection of MLH-1 was: pT1:50%, pT2:42%, pT3:37% and pT4:48%.
Relation beween tumor stage and presence of MSH-2 was: pT1:81%, pT2: 82%, pT3: 75% and pT4:44%.
Relation between prognosis and positivity for MLH-1 was: alive: 46.6%; died:46.4%.
Relation between prognosis and detection of MSH-2 was: alive: 80%; died:45.7%.
The immunohistochemical expression of MSH-2 was significantly correlated with tumor stage (p=0.01) and prognosis (p=0.002).
Conclusions: The analysis of mismatch-repair genes MLH1 and MSH-2 can be studied by immunohistochemistry. Our study demonstrates that expression of MSH-2 has statistical correlation with tumor stage and prognosis. Further studies with larger series should be performed in order to confirm our results.

P 933
VEGF AND VEGF-C IMMUNOHISTOCHEMISTRY IN HUMAN CUTANEOUS NEVI AND MALIGNANT MELANOMAS
Michala Fiuraskova, Svetlana Brychtova, Alice Hlobilkova, Martin Tichy*, Eva Sedlakova, Tomas Brychta**
Institute of Pathology & Laboratory of Molecular Pathology, Faculty of Medicine, Palacky University and Faculty Hospital, Hnevotinska 3, 775 15 Olomouc, Czech Republic, *Department of Dermatology and Venerology, Faculty of Medicine, Palacky University and Faculty Hospital, I.P. Pavlova 6, 775 20 Olomouc, Czech Republic
**SPEA Olomouc, s.r.o., nam. Hrdinu 2, 772 00 Olomouc, Czech Republic

Vascular endothelial growth factors (VEGFs) are a family of secreted endothelial cell-specific cytokines that act as endothelial cell mitogens. They play a hierarchical role in regulating physiologic and pathologic angiogenesis. These factors are involved in vasculogenesis and vasculogenic sprouting which are crucial for tumour development and metastasis. VEGFs also act as vascular permeability factors. VEGFs are overexpressed in many skin disorders characterized by angiogenesis and increased vascular permeability. In order to determine their possible role in melanocytic tumour progression, VEGF (immunoreactive for VEGF-A and VEGF-C) immunohistochemical expression were evaluated in 107 biopsy specimens of human skin including 28 superficial spreading melanomas (SSM), 40 nodular melanomas (NM) and 39 common nevi. Primary mouse monoclonal antibody VEGF (Santa Cruz Biotechnology, clone C-1, diluted 1:50) and goat polyclonal antibody VEFG-C (Santa Cruz Biotechnology, clone N-19, diluted 1:50) were used for the analysis. VEGF was expressed

markedly not only in malignant melanoma cells but also in half the cases of common nevi. In malignant lesions staining of stromal cells - fibrocytes, endothelial and inflammatory cells predominated. VEGF-C staining was found mainly in malignant lesions but less frequently in cells of common nevi. Stromal staining in malignant lesions was significantly higher in comparison with the stroma microenvironment surrounding moles. Our results indicate that VEGFs expression may regulate skin vessel function under benign as well malignant conditions and therefore cannot be used to discriminate between malignant melanoma and benign melanocytic lesions. Nevertheless strong up-regulation of the above mentioned factors may contribute to the progression of melanoma.

The work was supported by IGA MZ CR 1A8245-3/2004 and MSM 6198959216.

P 934

IMMUNOHISTOCHEMICAL ANALYSES OF KI67, P53 AND BCL-2 EXPRESSION IN CUTANEOUS MELANOCYTIC LESIONS

G. Zamolo1, C. Štemberger1, M. Èoklo1, A. Dekaniæ1, A. Bosnar1, S. Štifter1, T. Batinac2, E. Grgurevic3.
1Department of Pathology and Forensic Medicine, Rijeka University School of Medicine, Rijeka, Croatia
2Department of Dermatovenerology, Rijeka University Hospital, Rijeka, Croatia
3Institute of Public Health, Rijeka, Croatia

INTRODUCTION: The clinical behaviour of melanoma is often unpredictable using clinical and histological criteria. Differentiation between naevi, especially dysplastic naevi and melanomas, can sometimes be difficult to assess by conventional histopathological analysis. Malignant transformation of melanocytes is a multistep process characterized by distinct histopathological stages.
AIM: To analyse the differences in proliferative activity and apoptosis between intradermal naevi (IN), dysplastic naevi (DN) and cutaneous melanoma (CM).
MATERIALS AND METHODS: 45 IN, 45 DN and 45 CM (thickness less than 1.5 mm) were immunohistochemically stained for Ki-67, which was used as a proliferative marker, p53 as an apoptotic and bcl-2 as an antiapoptotic marker. The number of positive cells was counted on 200 melanocytes.
RESULTS: The median values of Ki-67 positive cells in IN, DN and CM were 2.5, 6.0 and 12.16, respectively. Statistical analysis showed a significant difference in proliferative activity comparing IN, DN and CM group ($p=0.000$) with a significant positive correlation ($r=0.659$, $p=0.000$) between the proliferative activity and lesion malignancy. The p53 overexpression was present in 3.3 IN, 50.0 DN and 22.6 CM cells. Statistical analysis showed that the observed difference in p53 overexpression comparing IN with both DN and CM is statistically significant ($p=0.000$), but showed no significant difference between DN and CM. The median values of bcl-2 in IN, DN and CM were 49.2, 42.3 and 26.7. Statistical analysis showed a significant difference between IN and DN comparing to CM ($p=0.000$).
CONCLUSION: Our preliminary results show a progressive growth of proliferative activity from benign to malignant melanocytic lesions. The strongest expression of p53 in DN suggests that its overexpression could be the first step in the loss of cell cycle regulation and possible malignant transformation of melanocytes. Lack of bcl-2 expression correlates with progression of malignant melanoma and it could be related with poor prognosis.

P 935

CUTANEOUS B-CELL LYMPHOMA IN AN ELEVEN YEAR OLD IRANIAN GIRL

Dr.H.Mortazavi,Assistant professor of dermatology Tehran university of medical science Dr.K.Balighi,Assistant professor of dermatology Tehran university of medical science
Dr.M.Asgari,Assistant professor of pathology Tehran university of medical science
Dr A.Tavangar,Assistant professor of pathology Tehran university of medical science
Dr.y.Sedaghat Resident of dermatology
Tehran university of medical science

Primary cutaneous B-cell lymphoma (PCBCL) is an uncommon neoplasm of skin giving rise to anywhere between 4.5 to 20 percent of all primary cutaneous non-Hodgkin's lymphomas (Zackheim HS, et al. J Am Acad Dermatol 2000; 43:793-96). Although this type of lymphoma was primarily reported in older individuals, the occurrence of this neoplasm has also been observed in children. We would like to report a unique case study performed on an 11-year old Iranian female suffering from a slowly expanding round tumour on her left lower leg.

The 11-year old Iranian girl was seen in our clinic with a 2-year history of asymptomatic tumours on her left lower leg. Physical examination revealed two firm tumoral masses on her lower leg, the larger measuring 8 cm x 8 cm. No hepatosplenomegaly or lymphadenopathy was detected. The patient otherwise felt well and a review of systems was negative. Laboratory studies, X-ray of leg, CT scan of chest, abdomen and pelvic and sonography were all normal. Smear for leishmaniosis, culture for deep mycosis and atypical mycobacterium were all negative. Histopathologic examination of multiple ellipse biopsy specimens from the larger lesion demonstrated dense diffuse infiltration of small blue round cells in superficial and deep dermis in 'botton heavy' pattern with destruction of hair follicles and eccrine glands. The neoplastic cells have round hyper chromatic atypical nuclei and scant cytoplasm of small to intermediate size without any rosette formation. No differentiation is observed. Mitosis is inconspicuous. No well-formed germinal centers were evident and tingible body macrophages were not seen. Using immunohistochemical techniques, a large portion of neoplastic cells expressed common leukocyte antigen confirming the lymphoid origin of the tumour with demonstrated lambda light chain restriction. Stains with CD19 were invariably positive. Stain with HMB45, S100, cytokeratin20, CD5, CD3 were all negative; the latter excluded any T-cell lymphoma.

In summary, PCBCL is an entity that can be suspected clinically, detected and confirmed pathologically. To the best of our knowledge this is amongst the first rare reports of PCBCL without dissemination in a very young girl.

P 936

HISTOPATOLOGICAL, IMMUNOHISTOCHEMICAL AND CLINICAL CORELATIONS IN CUTANEOUS LEIOMYOSARCOMAS (CLMS)

Mariana Costache 1 , Ana Maria Ene2, Maria Sajin3, Olga Simionescu2
1-Department of Pathology , ¨Victor Babes ¨ National Institute Bucharest , Romania
2-Department of Dermathology, ¨Carol Davila ¨University of Medicine, Bucharest, Romania
3- University of Bucharest, Biology Faculty, Romania

Introduction: Cutaneous leiomyosarcomas (CLMS) is a malignant tumour who may be derived from arrector pili muscles or subcutaneous blood vessel walls and is more common in a deep location.
Materials and methods: The authors make a retrospective study of 10 parafin - embedded cases diagnosticated histopathologycal like leiomyosarcomas and confirmated by immunohistochemical reactions. The immunohistochemical tests are : Actin, Desmin, Mioglobulin, Caldesmon, Vimentin, S-100 protein, citokeratin. IHC study was carried on formalin

fixed, parafin - embedded tissue using the avidin-biotin peroxidase complex.
Discussion and conclusion: Histopathologycal (with hematoxylin and eosin stain), CLMS is composed by numerous interlacing bundles of smooth muscle cells with eosinophilic cytoplasm and large , sometimes monstruous , hyperchromatic , blunt-ended nucleus.
Their pleomorphism and presence of mitotic activity , particulary abnormal and greater , constituting an important criteria for malignancy. Sometimes areas of myxoid degenerescensy may occur.
Usually CLMS can occurs at any age but in childhood are rare ; both sexes are affected , with a slight prediction for males ; is present tendency to local recurence . Most of the tumors appear solitary (nodules ulcerated or not) and the usual site is the limbs
(especially the legs).

P 937

MALIGNANT ECCRINE SPIRADENOMA (SPIRADENOCARCINOMA) : A CASE REPORT

FERCHICHI Leila*, RAMMEH-ROMMANI Soumaya*, ZERMANI Rachida*, FAZAA Becima**, FAREH-KLIBI Faten*, KOURDA Nadia*, CHELBI Emna*, BALTAGI BEN JILANI Sarrah*
* Departement of Pathology, Charles Nicolle Hospital, Tunis Tunisia.
**Departement of Dermatology, Charles Nicolle Hospital, Tunis, Tunisia.

Introduction : Eccrine spiradenocarcinoma is a rare dermal appendage carcinoma believed to arise from transformation of a long-standing benign spiradenoma. This tumor demonstrates highly malignant biologic behavior with a high recurrence rate, frequent lymph node metastases, and overall poor survival.
Observation: We report the clinicopathologic and immunohistochemical features of a spiradenocarcinoma occurring in the forehead of a 73-year-old man. The lesion had been present for 10 years; recently, it had increased in size and had bleeded occasionally. Cervical lymph nodes were inconspicuous on palpation and full body examination was within normal ranges. Sections cut from excision specimen revealed a lobulated tumor with illdefined borders and cavity-like structures. The proliferation, located in the dermis without obvious continuity with the epidermis, consisted of multiple lobules of epithelial cells surrounded by connective tissue and contained ducts and cystic spaces. The tumor cells were polygonal in shape with scant pale cytoplasm and round slightly hyperchromatic nuclei. Mitoses were up to four per high-power field. Areas of necrosis were seen. In certain foci, especially at the periphery of lobules, sheets, nests and glandular structures were surrounded by abundant stroma and infiltrated skeletal muscle infiltration and perineural tissue. Immunohistochemical studies for markers of proliferation (Ki-67, Mib1, proliferating cell nuclear antigen: PCNA) revealed 80% of tumor cells staining positive for PCNA and 20% for Ki-67. One year after the excision of the nodule, the patient is free of signs and symptoms of recurrence or metastasis. No complementary treatment had been administered.
Conclusion: Spiradenocarcinoma is an exceedingly rare malignant neoplasm with ductal differentiation. Many authors consider it to be an eccrine neoplasm, and others favor apocrine differentiation. It originate from previous spiradenoma that remained unaltered for many years, but de novo spiradenocarcinomas had already been reported.
The authors report a new case and review the literature about spiradenocarcinoma, and discuss briefly some histogenetic concepts relevant to this neoplasm.

P 938

IMMUNOHISTOCHEMICAL STUDY OF MUC1, MUC2, AND MUC5AC EXPRESSION IN MALIGNANT SWEAT GLAND NEOPLASMS

JUNG shih-ming, CHU po-hsien, KUO tseng-tong
Department of Pathology and Department of Internal Medicine, Chang Gung Memorial Hospital and Chang Gung University, Taoyuan, Taiwan

Introduction: Malignant sweat gland neoplasms are rare skin tumors. MUCs are glycoproteins associated with carcinogenesis and cell adhesion. MUC1 is suggestive to inhibit cell to cell adhesion. In the present study, we examine the immunohistochemical expression of MUC1, MUC2, and MUC5AC in malignant sweat gland neoplasms.
Materials and Methods: Formalin fixed, paraffin embedded tissues of nineteen cases of malignant sweat gland neoplasms were immunohistochemically studied. Intensity and percentage of staining were evaluated.
Results: Patients included eleven females and eight males, mean age 60 yrs (age range: 24-84 yrs). Three cases had extramammary Paget¡¦s disease. The head and neck was involved in 6 cases, the trunk in 5 cases, the genital regions in 4 cases, the thigh in 3 cases. The histologic feature showed sweat gland adenocarcinomas (n=9), sweat duct carcinoma (n=4), porocarcinoma (n=2), microcystic adnexal carcinoma (n=3). 18 cases were immunopositive for MUC1. One porocarcinoma case was negative for MUC1. All 19 cases of malignant sweat gland neoplasms were immunonegative for MUC2 and MUC5AC. The intraepidermal component of extrammary Paget¡¦s diseases in 3 cases was positive for MUC5AC. Follow up data was available in 12 cases.
Conclusion: Malignant sweat gland neoplasms are associated with expression of MUC1 and not associated with MUC2 and MUC5AC expression. These observations suggest that MUC1 may play a role in cancer cell invasion malignant sweat gland neoplasms.

P 939

HYALINE-CELL RICH MALIGNANT CHONDROID SYRINGOMA WITH OVERT MORPHOLOCIGAL FEATURES OF MALIGNANCY. A CASE REPORT

STOJŠIÆ Zorica1, BACETIÆ Dragoljub1, JANKOVIÆ Radmila1, DRNDAREVIÆ Neda2
1Institute of Pathology Medical School, Belgrade, 2Institute for Medical Research, Belgrade

Malignant chondroid syringoma (MCS) is malignant mixed tumor of the skin. It is extremely rare neoplasm. We describe a case of MCS which was characterized by predominant hyaline-cell population and distinctive morphological signs of malignancy. A 62-year-old female presented with subcutaneous mass 5 cm in diameter on the lateral side of the left forearm. After a 15-year period of slow growth, the lump suddenly increased in size. The surgically excised neoplasm was evaluated by routine histology and immunohistochemistry. Histopathologically, the tumour consisted mainly of broad sheets of pleomorphic plasmacytoid-hyaline cells with rare mitoses. A part of the tumor showed the features of benign mixed tumor, where uniform slightly eosinophilic cells formed irregular small nests, partly with tubular and cystic lumina, in the myxoid and hyaline matrix. Large areas of necrosis were surrounded with small undifferentiated cells with high mitotic rate: 7/10HPF. Invasion of the capsule and satellite nodules in subcutaneous adipose tissue were found. The hyaline cells were strongly and diffusely immunopositive for CK, EMA, CAM 5.2, CEA, and partialy for GFAP antibody. S-100, aSMA, desmin, calponin and bcl-2 immunostaining was negative. In areas with high mitotic activity mean p53 protein index was 21%. Although the ductal differentiation was vague, we favour the diagnosis of MCS over myoepithelial

carcinoma due to the lack of immunoexpression of myogenic markers and S-100 protein.

P 940
SYRINGOID ECCRINE CARCINOMA
Alfaro Luis, Roca Mª José, Froufe Agustín, Rayón Miguel, Baena Pablo.
Hospital 9 de Octubre. Valencia. Spain

Syringoid eccrine carcinoma is a rare variant of adnexal carcinoma thought to derive from eccrine sweat glands. It's often clinically underestimate which lead to local recurrences. We received a lesion developed on the forehead of a 27 year old woman. Clinically a lipoma was suspected. The lesion measured 1'1 x 0'7 cm and was excised reaching focally the muscular layer. On microscopic examination the epidermis was unremarkable, and a proliferation of small, low density, glandular structures was seen all over the dermis. A few of them configured small keratinous cysts especially in superficial areas. The lumina were lined by two layers of cuboidal cells, and contained a granular eosinophilic material. There was a slight pleomorfism in nuclei, mainly in the inner layer, with small single nucleoli. Mitotic activity was very scant, lower than 1 per 10 high power fields. Some of the glands had a thin projection, giving a comma shaped appearance. The stroma had a fibrous configuration, with dense collagenous pseudonodular disposition centred by the glands. Perineural invasion was occasionally seen, and deep dermic infiltration, although not reaching the muscular layer.
Immunohistochemical study showed in the glandular cells expression for keratin (AE1-AE3); epithelial membrane antigen, carcinoembryonic antigen (CEA), and S-100 protein. Cytokeratin 7 was focally positive, and Cytokeratin 20 negative.
This neoplasm shares certain similitude with the more common eccrine microcystic carcinoma. In fact many reports use those terms as synonyms, but syringoid carcinoma lacks the basaloid nest differentiation of microcystic carcinoma, has the typical comma shaped tubules, and has a less prominent perineural invasion. Confusion extends when using the other synonymous term, sclerosing duct carcinoma, generally referred to microcystic carcinoma, but present also in our case with a prominent concentrically peritubular stromal reaction.

P 941
THE INTERPRETATION OF BENIGN BIOLOGIC BEHAVIOR FOR KERATOACANTHOMA VERSUS CUTANEOUS SQUAMOUS CELL CARCINOMA, USING A PANEL OF ANTIBODIES AGAINST:CYCLIND1,P53,P21RAS,EGFR
AL- SHAWAF A. Zahi MD
Prof. of Pathology
Department of pathology
Al-BAATH University

Introduction:

The keratoacanthoma (KA) is a relatively common tumor which most often occurs on the sun – exposed areas of light skinned individuals of middle age and older.

This tumor is regressing spontaneously ,so the recognition of the true nature of this tumor is of considerable practical and biological important

Its etiology is unlcear, although ultraviolet light, viruses, oncogenic chemicals, and epidermal growth factor have been considered.

- EGFR : is membrane growth factor receptor encoded by the Cerb 1 gene
- P21 ras: is a signal transducing (cytoplasmic) oncoprotein with GTP as activity. Ras mutative abolishes GTP as activity and results in constitutive stimulation of the way.
- P 53 Nuclear protein playing an important protective role in the response to DNA damage induced by ionizing radiation chemical carcinogens and viruses.
- Cyclin D 1: CDK Complex regulates the RB protein (PRB) . Mutational gene causes hyperphosphory lat of RB

protein .with consultative stimulation of the pathway

Material and methods :

- 24 cases of Keratoacanthoma
- 26 cases of SCC
- Immunostainning of EGFR, P21 ras, P53, Cyclin D 1 oncoprotein
- Scores of Positive staining : diffuse basal and suprabasal staining. Focal basal and suprabasal staining

Results

- The expression of P53 (mutant gene) showed a great difference between SCC and Keratoacanthoma (20/26 – 80% in SCC versus 4/24 – 16% in KA) (P<0.01) -2/4 of KA . Cases were reevaluated as SCC (KA –like SCC) .
- The expression of P21 ras was more evident in KA versus SCC (14/24 -58 % in KA versus 5/26- 19% in SCC (P < 0.05).
- EGFR was negative in both all cases of KA and SCC.
- Cyclin D1 showed more evident (focal expression) in SCC (10/26 -38% in SCC versus 4/24 – 16 % in KA)

Conclusions:

- - Our results refer to the decisive role of P53 mutation in the development of SCC and Its invaluable role in setting down a convincing diagnosis of SCC.
- - P21 ras was more definitive in KA
- - EGFR : is expressed more in reactive and benign epidermal growths , and has no role in both KA and SCC.
- – P53 mutation is critical and decisive in the development of cutaneous malignancy.

P 942
APOPTOSIS AND PROLIFERATION IN SQUAMOUS CELL CARCINOMA AND KERATOACANTHOMA
Batinac Tanja1, Zamolo Gordana2, Stemberger Christophe2, Zauhar Gordana3, Simat Marina2, Grahovac Blazenka2
1 Department of Dermatovenerology, Clinical Hospital Center Rijeka, Rijeka, Croatia
2 Department of Pathology, University of Rijeka, Rijeka, Croatia
3 Department of Physics, University of Rijeka, Rijeka, Croatia

BACKGROUND: The controversy of distinguishing keratoacanthomas (KAs) from a well-differentiated squamous cell carcinoma (wdSCCs) is still present. Model of cutaneous carcinogenesis focus on the regulation of keratinocyte proliferation, differentiation, apoptosis and/or inability to undergo growth arrest.
OBJECTIVE: We investigated the expression of proliferation and apoptosis markers in wdSCC, poorly differentiated squamous cell carcinoma (pdSCC), proliferating keratoacanthoma (pKA) and regressing keratoacanthoma (rKA) in order to distinguish a factors important in the progression of SCC and the regression of KA.
METHODS: 120 tumors (30 of each group) were analyzed for p53 protein, Bcl-2, Bak and Ki-67.
RESULTS: The percentage of p53 positive tumor cells was 73.20% in pKA, 46.62% in rKA, 69.32% in wdSCC and 78.96% in pdSCC. Ki67 was found in 35.13% in pKA, 30.11% in rKA, 48.57% in wdSCC, and 65,68% in pdSCC. Bcl-2 protein was found in 3.07% of cells in pKA, 13.43% in rKA, 14.97% in wdSCC, and 4.69% in pdSCC. Pro-apopotic protein Bak was expressed in 96.23% in pKA, 41.63% in rKA, 93.04% in wdSCC, and 54.69% in pdSCC.
CONCLUSION: Relatively slow proliferation rate, as compared to SCC, coupled with an intensive apoptosis seen in

pKA could lead to regression of this tumors. Growth and malignancy of pdSCC could be a result of intensive proliferation of tumor cells. Proliferation in pdSCC is mainly controlled by an intensive but still not sufficient apoptosis. This preliminary study suggest that balance in expression of proliferation and apoptosis related proteins could be important factor in determining a tumor progression or regression.

P 943

AN INCIDENTAL FINDING OF COEXISTENT, CUTANEOUS KAPOSI'S SARCOMA AND LEISHMANIASIS IN AN HIV-INFECTED PATIENT.

FFOLKES Lorrette, BHAGANI Sanjay, PATALAY Rakesh, DEROIDE Florence
Royal Free Hospital NHS Trust, Royal Free Hospital, London, UK

Cutaneous lesions in Mediterranean visceral leishmaniasis are very unusual, except for the presence of Leishmania organisms in cutaneous Kaposi's sarcoma in patients infected by the Human Immunodeficiency Virus (HIV). A 40 year old male with a 15 year history of HIV presented with a one month history of multiple purple asymptomatic papules on his left forearm, feet, penile tip, buccal mucosa and splenomegaly. His current CD4 count was 39 cells/mm3 and viral load, 10411. The patient lived in Southern Spain and had recently adopted a dog. Histological examination of one of the biopsied lesions on his forearm showed a dermal vascular proliferation suggestive of kaposi's sarcoma, with positive immunostaining for Human Herpes Virus 8 (HHV8). There was an associated peripheral infiltrate of plasma cells and histiocytes, the cytoplasm of which contained many small round Leishmania amastigotes. A large number of these Giemsa positive, PAS negative organisms were also seen extracellularly. The features of the skin biopsy were those of coexistent cutaneous leishmaniasis and Kaposi's sarcoma. The patient's splenomegaly was attributed to visceral leishmaniasis. Canines are the natural host of Leishmania donovani. Most cases of leishmaniasis in HIV-positive patients appear in the advanced stages of the disease (CD4<200mm3). Leishmania organisms are thought to reach the skin by dissemination during visceral disease, either after external infection or by reactivation of latent leishmaniasis. Kaposi's sarcoma is now classified as a low-grade malignancy but is regarded by many authours as a non-tumoural, reactive, entity. DNA sequences from HHV8 have been found in all types of Kaposi's sarcoma. The role of Leishmania in Kaposi's sarcoma remains a subject of discussion. The fact that the vascular tumour usually regresses after treatment of the parasitic infection, strengthens the proposal that it is a reactive process.

P 944

DIFFERENTIAL PROX-1 AND CD 31 EXPRESSION IN MUCOUSAE CUTANEOUS AND SOFT TISSUE VASCULAR LESIONS AND TUMOURS

Jorge S. Reis-Filho, Rui M. Reis, Adhemar Longatto Filho, Stanislav Tomarev, Paula Silva and José M. Lopes.
Life and Health Sciences Research Institute, School of Health Sciences, University of Minho, Braga, Portugal (RMR, ALF, JSRF).
Pathology Division, Adolfo Lutz Institute, São Paulo, Brazil (ALF).
Section of Molecular Mechanisms of Glaucoma, Laboratory of Molecular and Developmental Biology, National Eye Institute, Bethesda, MD, USA (ST).
The Breakthrough Toby Robins Breast Cancer Research Centre, Institute of Cancer Research, London, UK (JSRF)
Medical Faculty, Department of Pathology, University of Porto, Porto, Portugal (JML).
IPATIMUP – Institute of Molecular Pathology and Immunology, University of Porto, Porto, Portugal (PS, JML)

The study of lymphatic vessels and lymphatic tumours has been hampered with difficulty, due to the overlapping morphological features between blood and lymphatic endothelial cells, as well as to the lack of specific lymphatic endothelial markers. Over the last few years, lymphatic vessels and lymphangiogenesis have received great attention owing to their putative implications in terms of metastatic dissemination and the promise of targets for lymphangiogenic therapy. Prox-1 is a nuclear transcription factor that plays a major role during embryonic lymphangiogenesis and is deemed to be a useful marker for differentiating lymphatic endothelial cells from the other blood vessels endothelial cells. Here we describe a double-immunostaining strategy for formalin-fixed paraffin-embedded tissues aiming to evaluate the distribution of Prox-1 and CD 31 - a cytoplasmic pan-endothelial marker - in a series of twenty eight mucousae, cutaneous and soft tissue vascular lesions and tumours (haemangiomas, n=12; spindle cell haemangioma, n=1; lymphangiomas, n=10; lymphangiectasia, n=1; Kaposi's sarcoma, n=4). Our results showed that in non lesional mucousae and skin, Prox-1 decorated exclusively the nuclei of endothelial cells in vascular structures with bona fide morphological features of lymphatic vessels. CD 31 stained endothelial cells of blood vessels of superficial and deep dermal plexuses and also lymphatics. Prox-1 stained almost all the benign lymphatic vascular lesions/tumours (93%) and was absent or only focally positive in 75% of blood vascular tumours. CD 31 showed positive staining in all blood vascular lesions/tumours, being focal in two lymphatic lesions/tumours. Kaposi's sarcomas were all positive for both CD 31 and Prox-1 markers. In conclusion, whilst not utterly specific in the tumoral setting, Prox-1 may be employed as an adjunct marker of lymphatic endothelial cells in routinely processed formalin-fixed paraffin-embedded samples, namely of non-tumoral vessels.

P 945

EXPRESSION OF CYTOKERATIN SUBTYPES IN INTRAEPIDERMAL MALIGNANCIES: A GUIDE FOR DIFFERENTIATION

DEMIRKESEN Cuyan, ASLAN Figen, TUZUNER Nukhet
Department of Pathology, Cerrahpaþa Medical Faculty, University of Istanbul

Among intraepidermal malignancies of epithelial origin, Bowen's disease, bowenoid actinic keratosis (BAK), intraepidermal malignant eccrine poroma (MEP) and Paget's disease may pose diagnostic difficulties. Considering these difficulties, the localization, histologic features, and immunohistochemical profiles of 24 cases of Bowen's disease, 21 cases of BAK, 18 cases of intraepidermal MEP and 11 cases of Paget's disease were analyzed. Using multivariate logistic regression test, multinuclear giant cells and solar degeneration were found to be the only histologic parameters of diagnostic help. On the other hand, bivariate tests, performed for each pair of diseases revealed that an immunohistochemical panel composed of four different cytokeratin (CK) subtypes could be of benefit in the differential diagnosis. A widespread positive reaction for CK 5/8, CK 7, CK 19,and negative reaction for CK 10, was a helpful feature in differentiation of Paget's disease from Bowen's disease and BAK. CK 10 expression could be considered in favor of Bowen's disease, when compared to BAK. The widespread expression of CK 5/8 and CK 7 and negative reaction for CK 10, was in favor of Paget's disease, compared to intraepidermal MEP. On the other hand, widespread expression of CK 19 was a common finding in inraepidermal MEP, in contrast to Bowen's disease. In conclusion, our findings suggest that an immunohistochemical panel including certain cytokeratin subtypes such as CK 5/8, CK 7, CK 10 and CK 19, can

provide significant hints in the differentiation of common intraepidermal malignancies, Bowen's disease, BAK, MEP and Paget's disease, especially in problematic cases.

P 946

LOCALIZED AMYLOIDOSIS IN BASAL CELL CARCINOMA

CINGIL Hakan. Istanbul Naval Hospital, Istanbul, Turkey

Introduction: Amyloid can be found in some disease localized on lesion regions. One of these diseases is Basal Cell Carcinoma(BCC). The existence of amyloid deposits in basal cell carcinomas of the skin has been an established fact since 1930. Purpose: In my study I purposed to investigate the presence of amyloid in 60 BCC tissue specimen and the amyloid's relationship between BCC's histopathologic types, mitotic rate, solar elastosis, degree of apoptosis and the age of the patients.
Material and Methods: Their ages ranged from 24 years to 92 years with a mean age of 56 years. The male to female ratio was 1.14. Excisional biopsy specimens were obtained from 60 patients were fixed in 10% buffered formalin and embedded in paraffin. Five micrometer thick sections were stained with hematoxylin and eosin and Congo Red. Results: The histologic distribution of the amyloid deposits was fairly consistent. They were found in the fibrous stroma between clumps of tumor cells and in the connective tissue abutting the advancing front of the carcinoma. Amyloid was identified as amorphous, eosinophilic extracellular material which stained rose-pink with Congo Red. Conclusion: Amyloid is found on the 55% of the BCC patients. The presence of amyloid didn't change with the age of the the patients, the tumours histopathologic types and apoptosis. A relationship between solar elastosis and mitotic rate quantity and the presence of amyloid is detected.

P 947

MEASUREMENT OF TELOMERE LENGTHS IN SQUAMOUS CELL CARCINOMAS FROM BOTH RENAL TRANSPLANT RECIPIENTS AND NON-TRANSPLANT INDIVIDUALS USING AN ESTABLISHED FLUORESCENT IN SITU HYBRIDISATION METHOD FOR ARCHIVAL TUMOUR MATERIAL.

LYNCH Ailish, CONNEELY Maura, PERREM Kilian, LEADER Mary, KAY Elaine
Department of Pathology, The Royal College of Surgeons in Ireland, Beaumont Hospital, Dublin 9, Ireland.

Telomeres are specialised repeats at the extreme ends of chromosomes that prevent chromosomal instability and that shorten in most normal somatic cells at each round of cell division. This is due to the inability of the replication machinery to fully maintain the ends of linear DNA molecules. Critically shortened telomeres cause cessation of cellular proliferation and it is significant that most human cancers have reactivated the ribonucleoprotein enzyme telomerase, which compensates for telomere shortening and maintains the telomere lengths.
We have performed telomere length measurements in formalin fixed paraffin embedded tissue sections of both normal skin and squamous cell carcinoma from renal transplant recipients (SCCRTR) and non-transplant individuals (SCCN). These analyses were undertaken to determine whether telomere length maintenance via telomerase plays a role in the almost 100-fold increased incidence and more biologically aggressive nature of the SCCs that develop in immunocompromised renal transplant patients, compared with the non-transplant population. Telomere lengths were determined using a modified TELomere Fluorescence In-Situ Hybridisation (TEL-FISH) technique recently developed for archival material. We examined TEL-FISH signals in 21 SCCRTR tumours, 25 SCCN lesions and in 10 normal skin specimens from both renal transplant and non-transplant patient groups. We then established a telomere length standard curve using FISH and Southern analysis of telomere lengths from three different human cell lines. Statistical analysis subsequently revealed that both SCCRTR and SCCN tumours have shorter telomeres than their respective normal skin controls, which is consistent with the telomere length profiles of many types of carcinoma. Furthermore, there is a statistically significant trend towards longer telomeres in the SCCRTR than in the SCCN tumours. This may be indicative of a central role for telomere lengthening and maintenance in the increased incidence and aggressiveness of SCC in renal transplant recipients.

P 948

BASAL CELL CARCINOMAS OF THE SCROTUM

CINGIL H. Istanbul Naval Hospital, Istanbul, Turkey

Introduction: Basal Cell Carcinoma(BCC) is the most common human tumor. However, its appearance on scrotal skin is rare with an estimated incidence of 0.1/100.000 cases per year. These tumors must be differentiated from the more common Squamous Cell Carcinoma(SCC).
Purpose: Their etiology remains unclear compared to the occupational predisposing factors reported in the literature for SCC in the same area. Wide surgical excision is recommended and prognosis is usually good. I report the clinical and histologic features of scrotal BCC and review the literature. Methods: A 88-year-old man presented with a 6-month history of asymptomatic scrotal plaque. Physical examination lesion was 1.2cm. indiameter, erythematous and had irregular, ill defined borders. No adenopathy was present and the remainder of the skin examination was unremarkable. In case, it was no history of trauma, radiation therapy, or exposure to chemicals, or arsenic. Results: Tissue from the incisional and then excisional biopsy were fixed in formalin and embedded in paraffin. Samples were stained with hematoxylin and eosin. Biopsy specimen showed superficial BCC. The lesion was excised with a margin of 1.8cm. of normal skin. Examination of the surgical specimen revealed a superficial BCC, which was completely excised. The patient has been free of disease for 24 months. Conclusion: Scrotal carcinomas are uncommon, with an estimated annual incidence of 0.1/100.000. The majority are squamous lesions and cases of BCC of the scrotum have been documented in the world literature. In contrast to SCC, BCC is usually of low malignancy. Thorough clinical evaluation, followed by wide local excision may be most appropriate initial therapeutic approach to these lesions.

P 949

EXPRESSION PROFILES OF P53 AND KI67 IN PREINVASIVE AND INVASIVE LESIONS OF BURN SCAR

SAKIZ Damlanur, TASKIN Tugba, LIVAOGLU Ayten, KARASOY Aysin, KABUKCUOGLU Fevziye
Departments of Pathology, Plastic and Reconstructive Surgery Sisli Etfal Education and Research Hospital, Department of Pathology Erzurum State Hospital

Introduction: Burn scars with the reconstruction difficulties and developing tumor are still the lesions that cause problems. In the background of burn scars usually squamous cell carcinoma, basal cell carcinoma, malignant melanoma, skin adnexial tumors and soft tissue sarcomas can develop. In this study we investigated the presence of reactive atipia, dysplasia, melanocytic hyperplasia, melanocytic atypia in the

epidermis and the tumors that develop from burn scars and evaluated the relation of these findings with p53 and Ki67 immunohistochemically.
Materials Methods: The study subjects were 35 cases of burn scar from 1999 to 2005. Parafin blocks of all specimens were examined immunohistochemically with monoclonal antibodies p53 and Ki67.
Results: 21 cases were male and 14 female. Their ages varied from 9 to 80 years, with a mean age of 44.6 years. The causes of the initial burn injury were flame, 20; hot water, 4; lightning, 3; electrical, 1; chemical , 1; and hot milk,1. The duration of burn ranged from 10 months to 57 years with a mean of 27,3 years. The lesions were located on the limbs in 22 cases, 8 on the head and neck, and 5 on the trunk.
On the histopathological examination we described squamous cell carcinoma in 10 cases, malignant melanoma acral lentiginous type in 1 case, basosquamous cell carcinoma in 1 case and pseudosarcomatous fasciitis in 1 case. In the cases that had no tumor, showed the following changes in the epidermis: low grade and high grade dysplasia in 2 cases, low grade dysplasia in 11 cases, melanocytic hyperplasia in 10 cases, atypical melanocytic proliferation in 3 cases, reactive atypia in 5 cases, and changes indefinite for dysplasia in 2 cases. In 2 cases there were no pathological finding in the epidermis. With Ki67 proliferation marker, in the cases with dysplasia, there was a continuous nuclear staining at the basal layer of the epidermis. The tumors showed high staining ratio with Ki67. In the cases with dysplasia or tumor, we established varying staining ratios with p53.
Conclusion: In this report we found out that Ki67 proliferation marker can be helpful in the differential diagnosis of the dysplasia in burn scars. We also suggest that p53 gene mutation can play a role in some of the tumors that arise in burn scars.

P 950
MULTIPLE CONDYLOMATOUS CARCINOMA (WARTY CARCINOMA): A CASE REPORT
SAKIZ Damlanur, TASKIN Tugba, KABUKCUOGLU Fevziye, KARSIDAG HACIKERIM Semra
Departments of Pathology, Plastic and Reconstructive Surgery Sisli Etfal Education and Research Hospital

Introduction: Condylomatous carcinoma is a variant of squamous cell carcinoma that has marked condylomatous features. Unlike verrucous carcinoma, condylomatous carcinoma demonstrate features of cytoplasmic vacuolization and nuclear changes resembling koilocytic atypia. It is frequently associated with HPV infection. This tumor has been reported in various sites, such as anogenital region, oral cavity, vagina, cervix and bladder. Two condylomatous carcinomas which arise in condyloma acuminata in the same patient are introduced.
Case Report: The patient was a 66 year old, male. He referred with genital and right axillary lesions, present for 15 years. The diameters of the tumors were 15cm and 2,7cm in the genital and axillar regions respectively. On histopathological examination, there were typical features of condyloma acuminatum at the periphery of each lesion. Each tumor has multiple papillary projections with a keratinized epithelial surface. Most of the tumor cells have cytoplasmic perinuclear clearing similar to koilocytosis.
Conclusion: To our knowledge, this is the first case of multiple condylomatous carcinoma on the skin. Light microscopic, immunohistochemical features and differential diagnosis of condylomatous carcinoma are presented here.

P 951
THE FIRST REPORT ON SARCOID OCCURRENCE IN CASPIAN PONY IN IRAN
Abavisani,Abbas
Maleki,Mohsen
Adibnishabouri

INTRODUCTION:
Sarcoid as the most common skin tumor,take place in different breeds,colors,and both genders of perisodactyla(horse,donkey,mule).The most common areas of such an occurrence are those area with thin skin and less hair.Diffrent forms of sarcoi consist occult,warty,fibroblastic, and mixed types. Treatment approaches are different,but recurrent state is the most important problem in this regard.
Methods and materials:
A five-year-old Caspian pony was observed with a warty mass in axillary site and around its prepuce in rakhsh equestrian section of khorasan Jihad-e-agriculture educational complex and was examined. To confirm the diagnosis,the biopsy of the mass was conducted .
Results and conclusions:
Given the examination of the mass under study,the sarcoid warty type was identified. The histopathological examinations proved the sarcoid tumor.They include acantotic hyperplasia,prolifration of sattelite and fusiform fibroblasts,vast ground substance with collagen fibers and mitotic form of cells.
Although sarcoid has been frequently reported in horse so far,the recent article is the first report of sarcoid occurrence in Caspian pony.
Key words: sarcoid, caspian pony.

P 952
THE NATURAL COMPOUND BUTYLIDENEPHTHALIDE STRONGLY SUPPRESSES HUMAN MALIGNANT BRAIN TUMOR GROWTH IN VITRO AND IN VIVO
Nu-Man Tsai. Shinn-Zong Lin, Chau-Chin Leec, Hsuan-Chi Su, Wen-Liang Chang, Horng-Jyh Harn
Institute of Medical Sciences, Buddhist Tzu-Chi University, Hualien, Taiwan, ROCa;
Neuro-Medical Scientific Centerb and Departments of Radiologyc and Pathologyd, Buddhist Tzu Chi General Hospital, Hualien, Taiwan, R.O.C., and School of Pharmacy, National Defense Medical Center ,Taipei, Taiwan

Brain tumors are the third leading cause of cancer-related death in those aged 15-34 years old. In particular, glioblastoma multiforme (GBM) and malignant gliomas present the lowest one-year survival rates. Current anti-tumor drugs are not effective against GBM. The naturally occurring compound butylidenephthalide (BP) isolated from the chloroform extract of Angelica sinensis (AS-C) has been studied in treatment of angina. Presently, we report on the potency of BP in the growth suppression of malignant brain tumor cells without coincident fibroblast cytotocixity. BP up-regulated the expression of CKI including p16 and p21 and down-regulated the expressions of cell cycle regulators. The result was a decrease of phosphorylated Rb proteins and the cell arrest at G0/G1 phase. The expression of p53 protein was increased by BP and correlated with the activation of apoptosis-associated proteins. In vivo, BP not only suppressed growth of subcutaneous rat and human brain tumors, but also shrank the volume of GBM tumors in situ. The post-BP survival period of the rats was significantly prolonged. These in vitro and in vivo anticancer effects indicates that BP has the potential as a new anti-brain tumor drug.

P 953
AN ANALYSIS OF CENTRAL NERVOUS SYTSEM TUMORS IN RASOOL AKRAM HOSPITAL IN IRAN
SADEGHIPOOR Alireza,SABZEVARY Saeedeh
Departement of neurosurgery, Rasool Akram Hospital, Tehran, Iran

Neoplasm of the nervous system and its adjacent structures are diverse group of lesions.They can be primary neoplasm in all degrees of differentiation derived from any of the many normal cellular constituents of this organ or secondary neoplasm metastatic from a variety of primary sites.
A series of 240 pathologically verified brain and spinal cord tumors from the neurosurgical department of Rasool Akram Hospital in Tehran, Iran were analyzed for the relative incidence as well as the distribution of the age and sex.
These data were compared with series from another countries.The male/female ratio was 119/121 and the age distribution was:<4 years old(y/o)(3.7%), 4-11 y/o(8.1%), 12-18 y/o(3.6%), 19-44 y/o(45%), 45-54 y/o(16%), 55-64 y/o(12%), 65-74 y/o(9.9%) and >75 y/o(1.3%).Percentage of representative tumors were meningioma(26.25%), glioma(25.4%), pituitary adenoma(11.6%), and neurinoma(13.7%).The incidence of glioma was lower and that of neurinoma was higher in Rasool Akram Hospital than those in other reports.

P 954
PATHOLOGIC CHARACTERISTICS OF CONVENTIONAL AND ANAPLASTIC PLEOMORPHIC XANTHOASTROCYTOMAS
Takanori Hirose, MD
Department of Pathology, Saitama Medical School
Moroyama, Irumagun, Saitama 350-0495, JAPAN

Introduction: Pleomorphic xanthoastrocytoma (PXA) is an uncommon CNS tumor characterized by a relatively favorable prognosis despite of ominous pathologic features. However, PXA may occasionally undergo anaplastic transformation. The aim of this study is to clarify pathologic characteristics of conventional and anaplastic PXAs.
Cases: According to the WHO classification, 8 PXAs were divided into conventional (5) and anaplastic (3) types. The age of 8 patients (7 females and 1 male) ranged from 16 to 79 years (median 45.5, mean 42.6). All tumors were located in supratentorial regions: frontal (3), occipital (2), parietal (1), frontotemporal (1), and sellar (1). Radiologic images, available in 5 patients, exhibited contrast-enhancement in 5 and cystic changes in 3.
Results: All tumors showed typical microscopic features of PXA, that is, pleomorphic tumor cells with xanthic changes, intranuclear pseudoinclusion, marked desmoplasia, perivascular lymphoid cuff, numerous eosinophilic granular bodies, and occasional calcification. In anaplastic PXA, monotonous proliferation of atypical cells was noted and mitotic counts were 10, 11, and 15/10 HPF, respectively. Two also showed necrosis and microvascular proliferation. One was a combined tumor of conventional PXA and glioblastoma. Another PXA underwent anaplastic changes through two recurrences. PXA showed immunoreactivity for GFAP (100%), S-100 protein (100%), neurofilament proteins (88%), and synaptophysin (33%).
Conclusions: Anaplastic transformation may occur de novo or through recurrences in PXA probably more frequently than previously postulated. This anaplastic variant should be distinguished from glioblastoma by identifying areas showing conventional microscopic features. PXA often shows neuronal immunophenotype, which may arouse some controversies about its classification and histogenesis.

P 955
THE RHABDOID TUMOURS OF THE NERVE CENTRE : SEVEN CASE STUDIES
CHTOUROU Imen, MAKNI Saloua, KHABIR Abdelmajid, BAHRI Ibticem, MNIF Hela, SELLAMI Ahmed, BOUDAWARA SELLAMI Tahya

Introduction :
The rhabdoid cerebral tumours were first identified by Beckwith and Palmer in 1978.Their frequence was estimated to be 2,1% of those affecting children under eighteen. Such tumours are equally characterised by a critically and speedy mortal development. Their historical genesis is still a controversial issue.
Purpose statement:
The aim of the present study is to discuss the various anatomically clinical aspects and examine the prognosis of this rare tumours.
Methods and materials:
In the course of this study, we will observe, examine and compare seven cases hospitalised in a period of eight years (1994-1997) in the sfax laboratory of anatomy and pathological cytology.
Results:
The average age of hospitalised patients is 22 years old among whom four being under fourteen and five males. The clinical symptomatology showed a predominance of the intracranial hypertension syndrom. Radiography through magnetic resonance revelat a heterogenous tumours processus localised respectively at the level of the spine (two cases), the insula (1 case) the temporal front (three cases) and the medulla (one case). The histological examination of those tumours has also showed a proliferation of giant cells whose cytoplasmic inclusion is hyalin based. These inclusion were rather positive for the vimentine and the keratin.
A tumours rhabdoid diagnosis was made and an adjuvant X-ray treatment was prescribed for five patients. The evolution was equally marked by a recurrence of rhabdoid tumoursamong three cases. Five patients were pronounced dead with a delay range between a week to eighteen months.
Conclusion:
The cerebral rhabdoid malignant tumour constitutes one of the most aggressive intracranial tumours. Still, there is hardly any efficient therapeutic protocol.

P 956
EXPRESSION OF TTF-1, CK7, AND CK20 IN BRAIN METASTASES
JUNG shih-ming, CHU po-hsien
Department of Pathology and Internal Medicine, Chang Gung Memorial Hospital and Chang Gung University, Taoyuan, Taiwan

Introduction: Metastatic carcinoma to the brain is a common problem but complicated by the histologic similarity to determine the primary origin. Thyroid transcription factor (TTF-1) is a tissue specific transcription expressed in the thyroid cancer and lung neoplasms. In the present study, we evaluate the role of TTF-1, CK7, and CK20 in identifying the primary source.
Materials and Methods: Forty-eight consecutive cases of histological proven brain metastases cases were retrieved from a four-year period. Formalin-fixed, paraffin-embedded sections of metastatic carcinoma to the brain were immunostained with TTF-1, CK7, and CK20.
Results: There were 24 females and 24 males ranging in age from 35 to 78 years (mean 59 years). 22 cases were immunopositive for TTF-1. TTF-1 staining was present in 20 (71%) of the 28 metastatic lung carcinomas. 26 cases were negative for TTF-1 and the sites of origin included: lung (n=8), colon (n=7), breast (n=3), liver (n=2), esophagus (n=1), nasopharynx (n=1), kidney (n=1), prostate (n=1), and unknown primary (n=2). CK7 staining was present in 26 (93%) of the 28 metastatic lung carcinomas. CK20 staining was negative in 24 (86%) of the 28 metastatic lung carcinomas. 28 metastatic lung carcinomas showed CK7(+)/TTF-1(+)/CK20(-) (n=17), CK7(+)/TTF-1(+)/CK20(+) (n=3), CK7(+)/TTF-1(-)/CK20(-) (n=5), CK7(+)/TTF-1(-)/CK20(+) (n=1), CK7(-)/TTF-1(-)/CK20(-) (n=2).

Conclusion: CK 7 and TTF-1 are helpful aid in brain metastases with lung origin. Positive staining is suggestive of lung primary. However, in our study, about 30% of metastatic lung carcinomas to the brain are negative staining for TTF-1.

P 957

HAEMANGIOBLASTOMA : REPORT OF 5 CASES AND REVIEW OF THE LITERATURE

BENADRA Fatiha(1),RAIS Hanane(1), ELATTAR Hicham(1), AITBENALI Said(2),BELAABIDIA Badia(1)
(1) anatomie pathologie, (2)Neurochirurgie

Central nervous system haemangioblastoma is a histologically benign tumor that usually occurs in the cerebellum and represents 1,1 % to 2,4 % of all tumors of the central nervous system. Haemangioblastoma can present as sporadic lesions or as manifestations of Von Hippel-Lindau syndrome (VHL).
Five patients with haemangioblastoma are presented. They were 4 men and 1 woman . The age of patients at diagnosis ranged from 36 to 60 years. In 4 cases, the tumors were located in the cerebellum. One patient had intramedullary tumor. The younger patient had VHL syndrome. Histologically, the tumors were composed of small blood vessels and large vacuolated stromal cells. No deaths associated with surgery occurred.
Haemangioblastoma is a rare tumor, affects mostly young adults and has a favorable prognosis after surgery. However, patients with VHL syndrome are at risk of developing new lesions. They require lifelong follow-up

P 958

LARGE CELL/ANAPLASTIC MEDULLOBLASTOMA WITH LONG SURVIVAL - A CASE REPORT

CVETKOVIC-DOZIC Dubravka*, GOLUBICIC Ivana**, DOZIC Slobodan*, SKENDER-GAZIBARA Milica*, DOZIC Branko*
Institute of Pathology, School of Medicine* and Institute of Oncology and Radiology of Serbia**, University of Belgrade, Serbia and Montenegro

Medulloblastomas (MBs) are malignant small cell embryonal tumors of the cerebellum found predominantly in children. Modern diagnostic methods, classification and treatment of MBs contribute to the progress in five-year survival. However, the clinical outcome and response to therapy is sometimes difficult to predict although, there are some increasing evidence that clinical outcome may depend on histological type of MB. Besides the histologically “classic” MBs there are two extremes of the histological spectrum that could correlate to their survival: MBs with extensive nodularity versus large cell/anaplastic (LC/A) MBs which are associated with better and worse clinical outcome, respectively.
We present a case of LC/A MB with unusual long survival. Our patient 26 years-old male was operated on for the first time at the age of 11-years because of cerebellar tumor without CSF dissemination. The tumor was totally resected and diagnosed as MB. The combined radiation and chemotherapy for pediatric MB was performed and the patient was free of disease without cognitive and hormonal disturbances almost fifteen years. He was followed-up with serial brain CT scans and MRI. In the meantime he graduated Secondary School and University School for Agriculture. At the age of 26-years because of recurrent cerebellar tumor the patient underwent to the second operation. However he died three months later due to CSF metastases.
We analyzed histologically and immunohistochemically surgical specimens of the first and recurrent tumor. Both tumors were similar and showed the features of LC/A MB. Histologically, they were predominantly composed of large highly pleomorphic cells that wrapped around one another. Their nuclei were also large, markedly atypical with irregular shapes, often without prominent nucleoli. The mitotic and apoptotic rate were increased. There were zones of necrosis and vascular proliferation. In the vicinity of highly severe anaplastic foci of LC/A MB small zones of “classic” MB were present. Immunohistochemically, the cells expressed synaptophysin, NF and focally GFAP. The EMA, LCA, CK and SMA were negative.

The poor survival should be expected in our case with LC/A MB. However, patient age, absence of CSF metastases and total tumor resection may contribute to long survival of fifteen years. We concluded that determination of histological subtype of MBs is not sufficient for clinical outcome and that the correlation with clinical data is mandatory.

P 959

INTRACRANIAL LOW GRADE FIBROMYXOID SARCOMA (A CASE REPORT)

Mahzooni Parvin MD *, Sanei Mohammad Hossein MD *, Masih Saboori MD†
*Department of pathology, Isfahan university school of Medicin, Isfahan
†Department of neurosurgery, Isfahan university school of Medicin, Isfahan

Intracranial low grade fibromyxoid sarcoma (A case report)
We report Low grade fibromyxoid sarcoma of brain(LGFS) a very rare tumor in the twelve's years old boy with history of temporal bulging from two months ago.MRI study was shown a large extra-axial mass with wide dural base at left frontal region with compress effect on brain tissue and subfalcian herniation and thinning of bone.Resected tumor was 10*9*5 cm with firm gray cut surface.In microscopic examination ,proliferation of bland spindle cell in background of fibromyxoid stroma was seen.cellularity varied from low to high.we considered all primary or metastatic spindle cell tumor ,include: neurofibroma, schwannoma, perineurioma, fibromatosis, solitary fibrous tumor, , myxofibrosarcoma , chordoma,and mono phasic synovial sarcoma .The tumor cells were negative for pancytokeratin ,epithelial membrane antigen,S100, CD34, actin , GFAP and were reactive only for vimentin.Therfore, we have excluded all suggestive differential diagnosis and have established LGFS.In pub med we have found only one case of intracranial LGFS which was reported by paulus and colleage in1991.
Key words:Intracranial sarcoma, Low grade fibromyxoid sarcoma

P 960

EFFICACY OF NEUROENDOSCOPIC BIOPSIES IN OBTAINING MATERIAL FOR HISTOPATHOLOGICAL EXAMINATIONS OF BRAIN TUMORS IN PEDIATRIC PATIENTS.

Grajkowska W.1, Barszcz S.2, Roszkowski M.2, Daszkiewicz P.2, Gadaj P.2
1. Department of Pathology, 2. Department of Neurosurgery, Children’s Memorial Health Institute, Warsaw, Poland

Introduction
Neuroendoscopic biopsies seem to be valuable method in obtaining material for pathological examination in cases of intra- and periventricular brain tumors. The procedure is usually performed in patients in whom total microneurosurgical tumor resection is impossible or is to be delayed. In some cases neuroendoscopic technique facilitates removal of small intraventricular lesions.
Aims of the study were: 1. to evaluate the efficacy of endoscopy in obtaining representative tissue samples according to particular tumor locations; 2. to estimate the accuracy of pathological diagnosis in a subgroup of patients in whom pathology was verified by open or stereotactic

biopsies; 3. to define locations and growth characteristics of tumors where endoscopic biopsies were ineffective.
Material and methods
Between years 1996 and 2003 we performed 93 neuroendoscopic biopsies of brain tumors in children. The material was analysed according to the following locations of the lesions: tumors of the lateral ventricles, suprasellar tumors, pineal region and posterior third ventricle tumors, thalamic tumors (focal and diffuse), posterior fossa tumors and others.
Results
In 65/93 cases representative samples were obtained. In the remaining 28/93 patients the biopsies were not informative, the samples were too small or the tissue specimens were removed from the tumor margins. In 55 out of 93 patients open and/or stereotactic biopsies were also performed, moreover in 42 children we could compare the diagnoses established on the basis of neuroendoscopic biopsies with the diagnoses after open/stereotactic procedures. In 38/42 cases the diagnoses were the same. The biopsies of thalamic tumors were less reliable. Ineffective procedures in 3/8 lesions of lateral ventricles were caused by thin ependymal tumor spread, marked tissue necrosis or calcifications.
Conclusions
This study proved that neuroendoscopic biopsies were most effective in cases of suprasellar, pineal region and posterior third ventricle tumors as well as in patients with posterior fossa lesions. The biopsies of thalamic tumors were less reliable.
Stereotactic or open biopsy seem to be better method for thalamic lesions. Indications for neuroendoscopic procedures should be established on the basis of careful evaluation of neuroradiologic examinations to avoid false results.

P 961
MALIGNANT PERIPHERAL NERVE SHEATH TUMOR (MPNST) WITH GIANT ROSETTES: THE FIRST CASE ASSOCIATED WITH SPINAL NERVES IN NEUROFIBROMATOSIS (NF1).
MOLNÁR Péter Pál(1), SZILÁGYI László(2), NÉMETH Tamás(1), LAJGUT Attila(3), DOBAI József(3)
(1)University of Debrecen, Medical and Health Sciences Center, Department of Pathology; (2)Regional Hospital, Department of Pathology, Berettyóújfalu; (3)County Medical Center, Department of Neurosurgery, Miskolc, Hungary

Introduction: MPNST associated with NF1 and characterized by giant rosettes, complex immunohistochemical (IHC) profile, arising from spinal nerve-roots has not as yet been reported.
Purpose: To present the results of thorough analysis of the first case of MPNST with giant rosettes arising from spinal nerves and associated with NF1, and to discuss differential diagnostic aspects of the case.
Methods: conventional histological, IHC and electron microscopic (TEM) methods were used on formalin-fixed, paraffin embedded tissue.
Findings: The 24-y-old woman had had café-au-lait spots, several subcutaneous and one subpleural, indolent, slowly growing nodules, that did not cause clinical or cosmetic problems. She was admitted and urgently operated on because of subtotal „cauda-syndrome'. Partial resection of a necrotic, hemorrhagic, grossly encapsulated tumor, attached to a nerve root, located at the level of vertebrae ThXII-LII was accomplished. Severe, progressive caudal syndrome developed 4 months later and the patient died of ARDS. None of the neurofibromata were malignant. The caudal 18 cm long portion of the myelon was almost completely destroyed by a firm, hemorrhagic-necrotic, grayish-white neoplasm ensheathing nerve roots and the filum terminale without distant metastases. The spindle-celled tumor displyed focal regimentation and whorls. Antoni A or B areas and Verocay bodies were absent. The mitotic activity was marked (Mib-1 LI: 35-55%.) Rich vascularity with endothelial cells which strongly reacted with CD31, CD34 and FVIII was present. The vascular smooth muscle cells were SM actin positive. None of these antibodies reacted with the neoplastic elements. The latter were intensively decorated by vimentin and S100, were focally positive with NSE, NF, GFAP. Desmin, panCK, FXIIIa, CK14, CAM5.2, synaptophysin and CD57 did not react with the tumor cells. The most striking feature was the high number of S100 and NSE positive giant rosettes (diameter = 100-350 μm). Homer-Wright- or ependymal rosettes and perivascular pseudorosettes were absent. EM showed schwannian differentiation, broad processes, incomplete basal lamina plus long spacing collagen and broad amianthoid fibers in the matrix.
Differential diagnosis: giant rosettes were described in one case of „neuroblastoma-like neurilemmoma' and rarely in fibromyxoid fibrosarcoma, but our results excluded these entities. A thorough search of PubMed and Google Scholar failed to disclose a similar case.

P 962
CORRELATION OF THE HISTOLOGICAL FEATURES AND CLINICAL PICTURE IN VESTIBULAR SCHWANNOMAS
BIERZYNSKA-MACYSZYN Grazyna *, KWIEK Stanislaw J. **, WLASZCZUK Pawel *, GOLKA Dariusz *, LUSZAWSK Jerzy I**, BAZOWSKI Piotr **, WOJCIKIEWICZ Tomasz **
*Department of Pathology, and **Department of Neurosurgery in Katowice,
Medical University of Silesia, Katowice, Poland

The objective of the study was to evaluate relationships between histological features of vestibular Schwannomas and onset of early clinical symptoms.

The 125 patients, who had their first surgery for vestibular Schwannoma in the years 1988-2004, were analyzed retrospectively.

Conventional Schwannoma (including the “ancient” variety) and Cellular Schwannoma variant, according to the WHO 2000 classification, were diagnosed. The relationships of facial nerve paresis before the surgery and the histology of the tumour (including 15 morphological criteria), the tumour size and historical classification into Antoni A, B and mixed types, were statistically analysed.

· The early onset of facial nerve paresis was most frequent (50%) in patients suffering from Cellular Schwannoma variant, less frequent in connection with Conventional (ancient) Schwannoma (37%), and the least frequent in Conventional Schwannoma (26%).

· In the group of “small” tumours (up to 20mm), the incidence of facial nerve paresis was lower (25%) than in “medium sized” lesions (20-40mm), and in “large” tumours (larger than 40mm). In these two groups, the incidence of facial nerve paresis was nearly equal (36% and 38% respectively).

· Facial nerve paresis before the surgery was observed with similar frequency (33% and 38%) in cases classified as Antoni A and A/B or as in Antoni B and B/A. These relationships were representative for tumours of different diameters.

· Analysis of relationship between early onset of the facial nerve paresis and histological picture of vestibular Schwannomas revealed statistically significant correlation ($chi2=6,56$; $p<0,05$) of this symptom with low cellularity of the tumour. The paresis appeared sooner in lesions with low number of cells, rich in blood vessels, with effusions, oedema, other degenerative changes, necrosis in large tumours.

· We observed as well statistically significant coexistence ($chi2=6,63$; $p<0,05$) of early onset of the facial nerve paresis and numerous Verocay’s bodies, plexiform

structures, coiled structures and nuclear palisades in small tumours.

· Correlations of other morphological features and early onset of facial nerve paresis were not statistically significant.

P 963

P 53, KI-67 AND BAX EXPRESSION AND THEIR RELATION WITH SURVIVAL IN GRADE II AND GRADE IV ASTROCYTOMAS

GÜRER Ýnanç Elif MD., UÇAR Tanju* MD., BAÞSORGUN Ýbrahim MD., KORKMAZ Emre* MD., GÖKHAN Güzide MD. Departments of Pathology and Neurosurgery* of the University Hospital of Akdeniz, ANTALYA, TURKEY

Introduction: Diffusely infiltrating astrocytomas are the most frequent intracranial neoplasms. Patient factors influencing patient survival includes the age and the general condition, tumor location and the adequacy of the surgical resection performed prior to conditional radiotherapy and/ or chemotherapy. Mutation of tumor supressor genes, expression apopitosis related genes and Ki-67 labeling index are the markers used to predict the patient survival.

Purpose of the study: In this study, we investigated immunohistochemical expression and the correlation between proapopitotic gene bax, Ki-67 labeling index and mutant p53 in glioblastoma multiforme (GBM) and grade II astrocytoma specimens with the patients' survival.

Material and methods: The immunohistochemical expression of p53,Ki-67 and bax, in the specimens of the 9 grade II, and 40 in GBM specimens who underwent resection for glial tumors in the Department of Neurosurgery were evaluated. Histological parameters were based on WHO criteria. Grade II and IV tumors were compared by Mann-Whitney U tests. Spearmans's rho test was used to analyse the correlation between parameters.Karnovsky performance scale was used for the survival.

Results: 9 patients with grade II and 40 patients with grade IV tumors were evaluated. Median ages were 39 in grade II, 50 in grade IV tumors (p= 0.009). Median Ki-67 values were 4 in grade II and , 14.5 in grade IV tumors (p=0.001). No difference for bax, p53 or Karnovsky score was observed between groups. Correlation analysis showed no statistically significant relation between age, Karnovsky score and immunostaining parameters.

Conclusion: Value of the largely used immunohistochemical markers related with apopitosis or cell proliferation in prediction of the patient survival is controversial.It seems that adequate surgical resection is the gold standart for the patients with glial tumors. In this study we conclude that utilisation of these markers is not cost effective since we did not obtain statistically significant results.

P 964

ANALYSIS OF PROTEIN EXPRESSION REGULATING THE PI3-K/PKB/AKT SIGNALING PATHWAY IN RELATION TO ASTROCYTOMA PATHOGENESIS

HLOBILKOVA Alice, MALIKOVA Jana, SEDLAKOVA Eva, EHRMANN Jiri, SVACHOVA Michaela, STRAKOVA Nicol, FIURASKOVA Michala, BRYCHTOVA Svetlana, and KOLAR Zdenek

Laboratory of Molecular Pathology and Institute of Pathology, Faculty of Medicine, Palacky University, Hnevotinska 3, Olomouc, CZ-775 15, Czech Republic, hlob@hotmail.com

Introduction: The most frequent alterations in astrocytomas are mutations and deletions of the tumour suppressor genes PTEN, p53 and amplification of epidermal growth factor receptor (EGFR) and platelet derived growth factor receptor (PDGFR). Growth factor receptors activate phosphatidyl-inositol-3-kinase (PI3-K) in the PI3-K/protein kinase B/Akt (PI3-K/PKB/Akt) pathway. PTEN dephosporylates phosphatidyl-inositol-3 phosphate and inactivates its downstream target, PKB/Akt.

Aim: The aim of our study was to detect changes in: PTEN, the phosphorylated form of PKB/Akt and EGFR protein expression in astrocytoma tissue samples.

Material and methods: We used paraffin embedded astrocytoma tissue samples from 71 patients which were divided into low grade astrocytomas (grade I-II) 34 samples and high grade astrocytomas (grade III IV) 37 samples. Mouse monoclonal antibodies against PTEN (26H9, Cell Signaling), PKB/Akt phosphorylated on serin 473 (587F11, Cell Signalig) and EGFR (31G7, Zymed) were used, followed by standard indirect immunohistochemical method with Envision plus kit (DakoCytomation).

Results: EGFR was expressed mainly in membranes. EGFR protein expression was detected in 25 % of low grade and in 65 % of high grade astrocytomas with stronger intensity of staining in high grade compare to low grade tumours. The phosphorylated form of PKB/Akt was localised in both nucleus and cytoplasm. Protein expression of phosphorylated PKB/Akt was found in about 85 % in both groups of astrocytomas with similar intensity of staining. In the group of high grade tumours a slight increase in PKB/Akt phosphorylation in the nucleus was observed. PTEN was detected mainly in the cell cytoplasm but in a few cases it was seen in the nucleus. Generally, PTEN protein expression was lower compared to EGFR and the phosphorylated form of PKB/Akt expression. PTEN was detected in 30 % of all astrocytomas, in 20 % of high grade, and in 40 % of low grade tumours.

Conclusion: Protein expression of EGFR increases with astrocytoma grading. This may subsequently lead to activation of PI3 K/PKB/Akt survival pathway. A rather suprising finding was no difference in phoshorylation of PKB/Akt in either group of tumours. We expected high level of PKB/Akt phosphorylation in high grade astrocytomas. PTEN expression was alterated in more than half the analysed astrocytomas, more frequently in high grade tumours.

This work was supported by grant IGA MZ CR NR/7828-3 and MSM 6198959216.

P 965

GRANULAR CELL ASTROCYTOMA: A RARE MORPHOLOGIC VARIANT OF DIFFUSE ASTROCYTOMAS

YILDIRIM S, KURTKAYA YAPICIER O*, HAHOLU A, YILMAZ I, CERMÝK H, BERBER U, BALOGLU H

GATA HEH Pathology Department and *Marmara University Neurologic Sciences Instýtute ISTANBUL,TR

Aim: To present a rare morphologic variant of diffuse astrocytoma, namely granular cell asstrocytoma and to define the diagnostic criteria of this tumor.

Introduction: Granular cell astrocytoma is an infiltrative glioma consisting of astrocytes with prominent granular cytoplasm due to lyzozomal accumulation. Morphologically may be confused with demyenilating disorders, infarctus and other granular cell tumors. Although it has not been set in the recent WHO classification, it is known a granular cell variant of diffuse astrocytoma.

CASE REPORT

58 years old male aplied to our emergency room with a strong headache lasting for a month in lower stringency. In addition, tendency to sleep and walking disability were seen. Physical examination revealed only a left-sit paresis prominently. A 6x4.5X3 cm-contrast enhancing mass with an oedomatous halo was located in the cerebral right frontoparietal lob with a striking shift on his CT scans. The cerebral mass was totally removed under urgent surgical circumstances. On histologic examination of the sample submitted during the operation

were seen numerous macrophage-like cells as well as hemoragic and ischemic changes. Owing to atypical cells observed, low grade neuroglial tumors were included in the differentiel diagnosis. The microscopic examination of the permanent sections revealed the cells with abundant granular and polygonal cytoplasm, round and peripheral nuclei. Morphologically fibrilar formations were also seen in scarcely seperated spindle cells. Mitosis was observed, but there was no necrosis. The MIB-1 index was moderately high. Cytoplasms of the tumor cells showed strong PAS staining. Tumor cells were reactive for GFAP, S100, CD68 proteins immunohistochemically. The tumor was diagnosed as granular cell astrocytoma.
Conclusion: Because of the rarity and the morphologic similarity to some non-tumoral lesions of the cerebrum, practicing surgical pathologists should keep in mind this morphologic variant of diffuse astrocytoma.

P 966
EVALUATION OF HTERT IMMUNOPOSITIVITY IN THE BRAIN AND ASTROCYTIC TUMORS.
KOTOULA Vassiliki, CHEVA Angeliki, PAPADIMITRIOU Constantine, KARKAVELAS George
Dept. of Pathology, Medical School, Aristotle University, Thessaloniki, Greece

Assessing the histological grade of astrocytic tumors can be problematic because these tumors are often quite heterogeneous in terms of histology and biomarker distribution. This problem becomes more pronounced in stereotactic biopsies where limited material needs to be evaluated. In this study, we asked whether hTERT expression, which has been reported to correlate with the histological grade of astrocytic tumors, could serve as a diagnostic aid when evaluating stereotactic biopsies. For this purpose, we used 45 astrocytic tumor specimens, 31 of these from stereotactic biopsies (16 low-grade [I and II], 29 high- grade [III and IV]) and 12 normal brain specimens, 6 from patients without cancer. hTERT expression was assessed by immunohistochemistry (IHC) with the NCL-TERT antibody, in situ hybridization (ISH) and relative quantification (RQ) with real time PCR on paraffin embedded tissues. With ISH and IHC, hTERT was identified in the majority of neoplastic cells in high-grade tumors, but also in single neurons and endothelial cells. IHC further showed focal hTERT positivity in neoplastic cells of low-grade tumors that were negative with ISH. These findings corresponded to the RQ values obtained from hTERT positive microdissected specimen areas ($p < 0,001$) but not from respective whole tumor extracts. hTERT protein was specifically localized in the nucleus, in a lacy pattern with prominent nucleolar positivity (pattern A), or as dense granular staining throughout the nuclear area with or without recognizable nucleoli (pattern B). When positive, normal and neoplastic cells of all grades exhibited pattern A of hTERT protein distribution. Pattern B was observed rarely in neurons, focally in low-grade, and focally or diffuse in high-grade tumors. Rarely, cytoplasmic staining was observed. According to these data, IHC but not PCR seems to be a valuable tool for the investigation of hTERT in the brain, since astrocytic tumors heterogeneously express this protein. It will be interesting to evaluate the patterns of hTERT positivity in larger series of these tumors in order to determine the respective clinical impact. The limited but specific positivity observed in low-grade astrocytic tumors should be taken into account when assessing stereotactic biopsies with this marker. hTERT is expressed in normal neurons, a finding of potential important biological significance in the context of neuronal progenitor research.

P 967
CHONDROID METAPLASIA IN GLIOMAS - AN IMMUNOHISTOCHEMICAL STUDY
KODETOVA Daniela, ZAMECNIK Josef, SKAPA Petr, KODET Roman
Department of Pathology and Molecular Medicine, Charles University, 2nd Medical Faculty, Prague, Czech Republic

The presence of cartilage in neuroepithelial brain tumors was rarely reported in the literature and there are many controversies concerning its origin. We present an immunohistochemical study of four cases of gliomas (two ependymomas and two astrocytomas) in which foci of hyaline cartilage with a formation of metaplastic bone were found. No other tissues suggesting diagnosis of teratoma were identified. Immunohistochemistry for extracellular matrix (ECM) components (tenascin, vitronectin, fibronectin, laminin, collagen types II, IV and VI) revealed that the type II collagen, which represents one of the major structural components of a cartilage, was present in these tumors in the wall of the blood vessels as well as in the intercellular spaces. Investigation of other ECM glycoproteins, tenascin and type VI collagen, which were also reported to be structural components of human cartilage revealed a similar observation. The abundant ECM production was in these particular tumors accompanied by areas of dystrophic calcifications. The anti-GFAP immunohistochemical reaction revealed the cartilage to be GFAP-positive in the astrocytomas and in one case of ependymoma. We interpret the cartilaginous islands as having their origin from neoplastic glial cells. A rare coexistence of the specific local conditions such as calcifications and a capacity for production of cartilaginous ECM might lead in such gliomas to the formation of chondroid areas even with metaplastic ossification.
Supported by Research Project VZ FNM 00000064203.

P 968
EGFR AMPLIFICATION AND NFKB OVEREXPRESSION IN PRIMARY GLIOBLASTOMAS.
CERDA-NICOLAS Miguel(1), LOPEZ-GINES Concha(1), GIL-BENSO Rosario(1), BENITO Rafa(1),CALLAGHAN Robert(1) MATA Manolo(2), MORCILLO Esteban(2), PELLIN Antonio(1). LOPÉZ-GUERRERO Jose(1), ROLDAN Pedro(3), MARCH Guillermo(3), BARBERA Jose(3).
(1)Department of Pathology. Neuropathology. Cytogenetic. (2)Department of Pharmacology. (3)Department of Surgery. Neurosurgery. Medical School.University of Valencia. Spain.

Glioblastoma multiforme (GBM) are the most frequent and malignant tumors of the human central nervous system. Within these tumors primary glioblastomas develop rapidly, with a short clinical history de novo, a mean age at diagnosis of 55 years, and with a genetic pathway showing EGFR gene amplification/overexpression, and only in exceptional cases TP53 mutations.
EGFR, a tyrosine kinase receptor, has been implicated in tumorigenesis and neoplastic progression in many tumors. EGFR has been reported to activate NFkB, a transcription factor that regulates genes involved in cell survival and oncogenesis.

We present 16 newly diagnosed GBM with initial symptoms detected between 7 days to 4 months before diagnosis. The mean age was 58 years old (ranging from 45 to 77 years). CT scans of the brain showed mass tumors in supratentorial localization, with a size from 2,5 to 4,5 cm large. Histopathological study revealed cellular heterogeneity, anaplasia and glial astrocytic differentiation. Hyperplastic and irregular vascularization, and necrosis have been observed. Evaluation of proliferation showed a mean of 6,5 mitosis per 10 HPF (ranging from 3 to 12) and a mean of 26,6% Ki-67 (MIB-1) labelling index. Neoplastic cells were GFAP

immunoreactive. Inmunohistochemical expression of EGFR was also detected.

All cases showed trisomy/polysomy of chromosome 7 by FISH analysis. EGFR gene amplification and no mutations in TP53 gene (exons 5 to 8) were demonstrated in all cases.

Overexpresion of NFKB was detected with EMSA (electrophoretic mobility shift assay) in 11 cases of these primary glioblastomas. Neoplastic cells showed positive expression of NFkB in all cases by immunohistochemistry.

These data suggest a relationship between EGFR activation and the NFkB transduction pathway during the neoplastic progression of primary glioblastomas.

This work was supported by a grant from FISH PI020228.

The recipient of the grant was Miguel Cerdá-Nicolás (jose.m.cerda@uv.es)

P 969

HYPOXIA-INDUCIBLE FACTOR 1ALPHA (HIF-1) AND CARBONIC ANHYDRASE IX (CA 9) EXPRESSIONS IN GLIOBLASTOMA MULTIFORM ARE PREDICTIVE OF RESPONSE TO RADIATION THERAPY.

MOKHTARI Karima, SIMON J.Marc, BISSERY Anne, CAPRON Frederique, HAUW J.Jacques, JAILLON Patrice, GENESTIE Catherine.

Pitié-Salpêtrière and Saint-Antoine Hospitals, AP-HP, Paris, France.

Background: Tumor hypoxia is known to be associated with resistance to radiotherapy. Hypoxia induces the expression of hypoxia-inducible factor-1alpha (HIF-1), allowing up-regulation of the expression of downstream genes such as carbonic anhydrase IX (CA 9).

Methods: We examined the expression of HIF-1 and CA 9 by immunohistochemistry in glioblastoma multiform (GBM) biopsies, and investigated their relationship with response to radiation therapy. The response to irradiation was assessed by comparing contrast-enhanced magnetic resonance images obtained before and six weeks after the completion of radiotherapy. Assessment of odds ratio were based on the logistic regression model with stepwise adjustment. The multivariate model included HIF-1 and CA 9 coded on a semi quantitative scale according to the positive tumor cell percentage (0 = no expression; + = 1-10%; ++ = 11-50%; +++ = 51-100%), and age.

Results: Fifty six consecutive patients with inoperable glioblastoma treated with radiotherapy (59.4 Gy in 1.8 Gy/fraction) at the Pitié-Salpêtrière hospital between 1995 and 2002, were included in this study (median age: 56 years, range, 30 to 67 years). HIF-1 was expressed in 33 of 56 (59%), and CA 9 in 38 of 52 (73%) of glioblastomas. Tumor HIF-1 expression correlated significantly with that of CA 9 (Kappa = 0.23, p = 0.003). The response rate to radiotherapy for the entire population was 29%. The expressions of HIF-1 and CA 9 were correlated inversely with the rate of response to radiotherapy (univariate analysis: HIF-1 +: odds ratio 0.21, 95% CI [0.06, 0.71], p = 0.012; CA 9 +: odds ratio 0.15, 95% CI [0.04, 0.59], p = 0.0063). The multivariate analysis showed that HIF-1 + (odds ratio 0.13, 95% CI [0.03, 0.65], p = 0.013), CA 9 +++ (odds ratio 0.21, 95% CI [0.04, 0.98], p = 0.047) and age (odds ratio 0.91, 95% CI [0.82, 0.99], p = 0.046) were independent predictors of response to radiotherapy.

Conclusions: Glioblastomas with a hypoxic profile (expression of HIF-1 and/or CA 9) were associated with a significantly worse response to radiotherapy, independently of known prognostic factors.

Grant from Regional PHRC: AOR 03059, Assistance Publique - Hopitaux de Paris

P 970

MOLECULAR PROFILING IN ADULT TYPE OF GLIOBLASTOMA MULTIFORME IN POLISH PATIENTS (LOH 9, 10, 13,17, P53 MUTATIONS AND EGFR AMPLIFICATION).

JESIONEK-KUPNICKA Dorota(1), KULCZYCKA Dominika (1),SOWA Piotr (1), MUSIA£ Jacek(1), OCH Waldemar (6), RIESKE Piotr(2), JASKÓLSKI Dariusz(4), KOLASA Pawe³ (5), PAPIERZ Wielis³aw (3), LIBESRKI Pawe³ Piotr (2), KORDEK Radzis³aw (1).

1) Department of Tumour Pathology, and 2) Department of Molecular Biology and Neuropathology, Chair of Oncology, 3) Department of Pathology, Chair of Anatomopathology, 4) Department of Neurosurgery, Medical University of £ódŸ, 5) Department of Neurosurgery, "Copernicus" Hospital, £ódŸ, Poland 6) Department of Neurosurgery, Specialistic Hospital, Olsztyn, Poland

According to the classical model of carcinogenesis in glioblastoma multiforme (GM) the primary (de novo) GM is related mainly to the amplification or overexpression of EGFR and MDM2, LOH 10p and 10q, p16 deletion, PTEN mutation. The secondary GM, occurring after the progression of low-grade astrocytomas is related to the p53 mutation and loss of heterozygisity (LOH) on chromosome 17.

The aim of our study was identification of molecular markers in GM in 32 tumor tissue with GM and peripheral blood from patients. We examinated the LOH on chromosome 9, 10, 13, 17, EGFR amplification. Mutations of p53 were examinated in patients with EGFR amplification or/and LOH 10. Additionally, the immunohistochemical study was performed using antibodies against p53, Rb, EGFR, p21 and p27, Ki67.

LOH 10 was detected in 25% (8/32) cases, in one case a deletion on chromosome 10 was detected; LOH 9 in 15,5% (5/32); LOH 17 in 12,5% (4/32); LOH 13 in 9,3% (3/32); EGFR amplification was identified in 21,8% (7/32) cases.

In one of cases, p53 mutation was detected together with LOH 9,10, 13. In other unusual case, the genetic alterations were more complex, consisted in p53 mutation, LOH 10, LOH 17, and EGFR amplification.

Our study reveals, that molecular changes in GM may be complex and indicates overlapping of two main genetic pathways of primary and secondary GM.

P 971

PROGNOSTIC SIGNIFICANCE OF CELL CYCLE PROTEINS P53, P21, P27, P14, P16 AND MDM2 IN GLIOMAS.

ZOLOTA Vassiliki, TSAMANDAS Athanassios, AROUKATOS Panagiotis, FRATZOGLOY Akis*, PANAGIOTOPOULOS Vassilios*, SCOPA Chrisoula.Department of Pathology and *Neurosurgery, University of Patras, Medical School, Rion, Patras, Greece.

Background: Gliomas are among the most aggressive and treatment refractory of all human tumors and molecular pathogenesis has been under intense investigation as a part of the effort to develop more effective therapeutic strategies for these tumors. Cell cycle regulatory genes and especially CDK inhibitors have been found commonly affected in gliomas. This study investigates the immunohistochemical expression of 6 essential cell cycle proteins (p53, p21, p27, p14, p16 and mdm2) in astrocytomas and their correlation with tumor grade, proliferating index (Ki67 positivity) and patients' survival.

Material and Methods: Paraffin-embedded sections of 63 brain biopsies from equal number of patients with astrocytomas of the central nervous system divided in low grade (I and II, N=15) and high grade (III and IV, N=48) tumors, were analyzed immunohistochemically using polyclonal and monoclonal antibodies. Follow up data were available for all patients (follow-up time: 2-70 months, mean 22.2). Cases containing >5% immunostained tumor cells were

considered as positive. Tumors with high proliferating index were considered those with >10% immunostained tumor cells. Results: The number of cases in which the expression of p53, p14, p16, p21 p27 and mdm2 were detected was: 54%(34/63), 76%(48/63), 63%(40/63), 45%(28/63), 87%(55/63) and 100%(63/63) respectively. The mean index for Ki67 was 14.58. A highly significant relationship was observed between tumor grade and survival ($p<0.001$) as well as between proliferating index and survival ($p<0.001$). P53 and p21 were more frequently expressed in high grade tumors ($p<0.05$ respectively). P53 expression was associated with lower survival only in p21(+) tumors ($p<0.05$). Neither p14 nor p16 expression were associated with grade, Ki67 index or overall survival. Cox regression analysis revealed that only tumor grade and Ki67 index were independent prognostic factors (CI: 0.032-0.502, p=0.03 and CI:1.167-5.408, p=0.019).
Conclusions: The study confirms that in cases of gliomas, tumor grade and proliferating index, predict the outcome of the patients. P53 was associated with poor prognosis only in tumors overexpressing p21; that means high levels of p21 in tumor cells associated with aberrant p53 protein expression, may result in a state refractory to therapy.

P 972

ANTI-INVASIC AND ANTI-ANGIOGENIC EFFECTS OF MMI166 ON GLIOMA CELLS

Nakabayashi H, Park KC, Yamada SM, Toyonaga S, *Maki H, Shimizu K
Department of Neurosurgery, Kochi University, Medical School, Kochi, Japan and *SHIONOGI & CO., LTD., Osaka, Japan

Constitutive overexpression of matrix metallo-proteinases (MMPs) is frequently observed in malignant tumors. In particular, MMP-2 and MMP-9 are reported to be closely associated with invasion and angiogenesis in malignant gliomas. The aim of our study was to evaluate the anti-tumor effects of MMI-166, a new MMP inhibitor in three human glioma cell lines (T98G, U87MG, KNS2). The gene expression of MMP-2 and MMP-9 were analyzed by semi-quantative RT-PCR. The anti-invasive effect of MMI-166 was analyzed by in vitro invasion assay. The cytotoxicity of MMI-166 was determined by MTT assay. The gelatinase activity was analyzed by gelatin zymography. In vitro angiogenesis assay was also performed. Glioma cell lines, which produced both MMP-2 and MMP-9, showed invasive capacity in invasion assay. The invasion of glioma cells was suppressed by MMI-166. No remarkable suppression of the proliferation by MMI-166 was observed in the MTT assay. Gelatin zymography revealed complete suppression of MMP-2 and MMP-9 activity by MMI-166. Angiogenesis assay showed the suppressive effect of MMI-166 on angiogenesis induced by glioma cells. These results suggest that MMI-166 has potential suppresive effects on invasion and angiogenesis of glioma.

P 973

ESTROGEN RECEPTOR BETA (ERÂ) PROTEIN EXPRESSION CORRELATES WITH BAG-1 AND PROGNOSIS IN BRAIN GLIAL TUMOURS

Batistatou A1, Kyzas PA1, Goussia A1, Arkoumani E1, Voulgaris S2, Polyzoidis K2, Agnantis NJ1, Stefanou D2
1Department of Pathology and 2Department of Neurosurgery, University of Ioannina, Medical School, Ioannina, Greece

Introduction: Estrogen receptor â (ERâ) is an important mediator of estrogen function in a variety of tissues. Its expression declines in breast, ovarian, prostatic and colon carcinomas as well as in astrocytic tumours. BAG-1 is a multifunctional protein with anti-apoptotic action that may have an important role in neoplasia and is possibly regulated by estrogen receptors. One of the direct targets of BAG-1 is HSP70.
Aim: The purpose of this study was to analyse the expression pattern of ERâ, BAG-1 and HSP70 proteins in two distinct types of glial neoplasms (astrocytic and oligodendroglial), to investigate their possible correlation and probe their impact in prognosis.
Patients-Methods: ERâ, BAG-1 and HSP70 protein expression was monitored immunohistochemically in 66 cases of astrocytomas of all Grades (I-IV) and 20 oligodendrogliomas. Grading was performed according to the WHO grading system. Protein expression was detected by immunohistochemistry using the EnVision System (DAKO, Carpinteria, CA, USA) and the following antibodies: monospecific polyclonal antibody to Estrogen Receptor â protein (Ab No. 385P, Biogenex, San Ramon, CA, USA/ MENARINI diagnostics, Greece), monoclonal mouse antibody to BAG-1 (Mob 335, DBS, Pleasanton, CA, USA/MENARINI diagnostics, Greece) and monoclonal mouse antibody to HSP70 (clone 8B11, NOVOCASTRA Lab Ltd, Newcastle Upon Tyne, UK).
Results: In astrocytic tumours low ERâ expression correlated significantly with high grade ($p<0.001$), higher expression of cytoplasmic BAG-1 ($p<0.001$) and worse survival (log rank p=0.02). ERâ expression had an independent prognostic value for overall survival in this cohort of patients (Cox p=0.03). There was also statistically significant association of BAG-1 nuclear expression with HSP70 cytoplasmic expression. This last association was noted in oligodendrogliomas as well.
Conclusion: Our results strengthen the hypothesis that ERâ, BAG-1 and HSP70 play an important role in the pathogenesis and progression of glial neoplasms, particularly those of astrocytic origin. Moreover, ERâ expression in astrocytic tumors appears to be an important, independent prognostic factor for survival, and a possible target in therapeutic strategies.

P 974

EXPRESSION OF HISTONE GENES IN ASTROCYTIC BRAIN TUMOURS AND ITS PROGNOSTIC SIGNIFICANCE IN PATIENTS AFTER SURGICAL TREATMENT

SLOWINSKI Jerzy *, MAZUREK Urszula **, BIERZYNSKA-MACYSZYN Grazyna ***, ORCHEL Joanna **, GLOGOWSKA-LIGUS Joanna **, STOMAL Monika *, MROWKA Ryszard *
* Department of Neurosurgery and Neurotraumatology in Bytom, **Department of Molecular Biology and Genetics in Sosnowiec, ***Department of Pathology in Katowice, Medical University of Silesia, Poland

Introduction:
Expression of histone genes is known to reflect proliferative activity of normal and neoplastic cells. It is hypothesised that expression of histone genes also characterizes biological aggressiveness of astrocytic tumours (AT) and can be useful in the prediction of clinical course in patients after surgical treatment.
Purpose of the study: 1) To assess the correlation between expression of histone genes H1, H2A, H2B, H3 and H4 and histological grade as well as other proliferative indices in AT. 2) To validate the usefulness of histone genes expression in prognostication in patients with AT.
Methods:
Eighty four patients (52 men and 32 women, mean age: 50.5 years), with supratentorial astrocytic tumour grade II (n = 13), III (n = 19) and grade IV (n = 52) were studied. The expression of histone genes was analyzed semi-quantitatively by in situ hybridization (ISH) in paraffin sections and defined as histone labeling index (HLI). In 52 patients the histone genes expression was analyzed with quantitative reverse-transcriptase polymerase chain reaction (QRT-PCR). The

RNA extract served as a matrix in the QRT-PCR reaction for quantitative analysis of histone H1, H2A, H2B, H3 and H4 mRNAs, with application of sequence detector ABI Prism 7700 (TaqMan). The results of QRT-PCR reaction were calculated as a target gene mRNA copy number to the reference gene (beta-actin) mRNA copy number ratio. For ISH study a cocktail of fluorescent-labeled oligonucleotide probes, labeling histone H2B, H3 and H4 mRNAs was used. The Ki-67 labeling index was studied after immunostaining performed in paraffin sections with use of avidin-biotin complex.

Results:

The global expression of histone genes increased significantly with increasing grade of the tumour. Expression of histone H3 gene showed the highest correlation with histological grade (R=0.55), HLI (R=0.33) and Ki-67 (R=0.37) proliferative indices. Multivariate analysis using the Cox proportional hazard model showed that patient age, tumour grade, postoperative performance score and the expression of histone H3 gene are independent prognostic factors. Significantly shorter survival times were observed in patients with histone H3 mRNA levels higher than 1.26.

Conclusion:

Our results support value of the histone genes expression as a marker of biological malignancy, tumour progression and cellular proliferative activity in AT. The level of H3 mRNA is an independent molecular prognostic factor in patients

P 975

MOLECULAR INVESTIGATIONS OF GLIOMAS IN STEREOTACTIC BIOPSY MATERIAL

BIERZYNSKA-MACYSZYN G.*, MAZUREK U.**, WLASZCZUK P.*, LECH A. ***, STEPIEN T.***, GOLA J.**, KAPRAL M.**, FIJALKOWSKI M.****, BLAMEK S.****, BIALAS B.****, MAJCHRZAK H.***, WILCZOK T.**

*Departement of Pathology, Medical University of Silesia, Katowice, Poland.

**Departement of Molecular Biology and Genetics, Medical University of Silesia, Sosnowiec,

***Departement of Neurosurgery, Medical University of Silesia, Sosnowiec,

****Departement of Brachytherapy, Center of Oncology – MSC Memorial Institute, Gliwice.

The difficulties connected with diagnosing and treating of gliomas are a reason to develop new methods of precise determination of these tumours biology. The determination of the gliomas malignancy was supplemented with molecular analysis of transcriptinal activity of some proliferation and apoptosis markers in stereotactic biopsy samples of these tumours.

The objective of our study was to determine the expression profiles of genes taking part in proliferation and apoptosis in diffuse brain astrocytomas and to search for correlation between mRNA concentration profiles of these genes,the findings of the morphological examinations, the course of the disease and the response to the implemented treatment.

The biopsy samples of 232 patients who had undergone stereotactic biopsy in the last 6 years in the Department of Neurosurgery in Sosnowiec, Poland, were investigated. In most patients, radiotherapy was the only treatment or it was adjuvant to surgery. The morphological and molecular analyses were carried out on 85 gliomas (30 cases of G2 WHO diffuse astrocytomas of low malignancy and 55 cases of G3 WHO anaplastic astrocytomas), 62 of these patients underwent radiotherapy.

An analysis of full clinical data, cytological examination, routine histopathological examination, determination of malignancy grade according to the WHO criteria and immunohistochemical proliferative responses (Ki-67) and investigation of apoptosis markers (p53, BCL2, BAX, FAS, FAS-L) were performed. A pattern of material processing for the molecular analysis was developed - the markers were determined by the RT-QPCR method (Taq-Man) with application of an ABI PRISM 7700 sequence detector. The response to brachytherapy was assessed with imaging techniques (CT, MRI).

We found that fixed in pure alcohol, dry and not-stained cytological smears are enough to obtain the amounts of mRNA sufficient to carry out molecular analyses. Analysing clinical data, histological findings, and number of the mRNA molecules coding H3, p53, BCL2, BAX and FAS proteins in the investigated material, we found that molecular investigations are better correlated with the course of the disease and the response to implemented treatment than morphological examinations. Our findings enable us to claim that assessment of the genes' expression may be considered as a valuable additional marker in the diagnosis and prognosis of diffused astrocytomas.

P 976

RELATIONS OF CLINICAL AND PATHOLOGICAL CHARACTERISTICS WITH LOSS OF HETEROZYGOSITY ON CHROMOSOME 10 IN GLIOBLASTOMA.

E.Izycka-Swieszewska(1), A.Wozniak (2), J.Limon (2), W.Kloc (3), R.Rzepko (1), K.Jaskiewicz (1)

1- Dpt. of Pathomorphology, 2- Dpt. of Biology and Genetics; Medical University of Gdansk; 3- Dpt. of Neurosurgery, Province Hospital, Gdansk, Poland.

P 977

PROGNOSTIC SIGNIFICANCE OF STEROID HORMONE RECEPTORS AND DNA CONTENT IN MENINGIOMAS

Marwa A. El-Shaer
Sonia L. El-Sharkawy
Naglaa F. Abbas
Nabila S. Hassan

The possibility that meningioma growth may be related to female sex hormone levels is suggested by several lines of evidence. Meningiomas are twice as common in women as in men, have been observed to wax and wane with pregnancy, and are positively associated with breast cancer. However, unlike breast cancer, meningiomas are much more commonly positive for progesterone receptor than for estrogen receptors. Overall, 70% of meningioma specimens have been found positive for progesterone receptor while only 30% were positive for estrogen receptor. Therefore, clinically and biologically more interesting are the unexpectedly aggressive clinical course of some meningioma, is a diagnostic dilemma for routine histopathology. Comparison between hormone levels was mostly significant. Also the relationship between expression of progesterone with the ploidy determined by image cytometric measurement (Leica Quin 500 DNA Cytometry Software) has been interpreted as signs of aggressive in the tumor tissue support the possibility of their application as a test for grading and for adequate treatment choice.

Key words: Meningioma-Steroid receptors-DNA ploidy.

P 978

MULTIPLE SPINAL MENINGIOMAS WITH POSITIVE PR – CASE REPORT

MILENKOVIC Sanja,Department of Pathology Clinical Hospital Center Zemun, Zemun
BERISAVAC Iva,Department of Neurosurgery,Clinical Hospital Center Zemun, Zemun
BOJOVIC Vladimir,Department of Neurology, Clinical Hospital Center Zemun, Zemun
CVETKOVIC-DOZIC Dubravka,Institute of Pathology, Medical Faculty, University of Belgrade

SKENDER - GAZIBARA Milica,Institute of Pathology, Medical Faculty, University of Belgrade
MARKOVIC Marko,Department of Neurosurgery, Clinical Hospital Center Zemun, Zemun

Short introduction
Multiple spinal meningiomas are relatively rare neoplasma and accounting only about 3% of all spinal meningiomas. They are defined as at least two spatially separated meningiomas occurring at the same time or more than two meningiomas arising sequentially from two clearly distinct regions. We report a case of the 52-year-old woman who was admitted to Department of Neurosurgery because of a progressive motor weakness with spastic paraparesis and sensation disturbance which gradually developed in the in both legs for last 3 years. Computed tomography (CT) scan revealed clearly defined three intradural extramedullary lessions at the Th6, Th10 and Th12. After operation in which the total resected tumors were performed histopathological examination showed two psammomatous meningiomas and one menigothelial meningiomas which was progestereone receptors (PR) positive. Proliferative potential which were measured by Ki67 antibodies were lower than 1%.
Purpose of the study:
In the present case rare multiple spinal meningiomas were investigated by the presence and distribution of the PR and proliferative potential with Ki 67 antibody with aim to predict eventually recurrence.
Methods used
Tumor samples after the third operation was analyzed by standard pathohostological technics, histochemical staining and immunohistochemical methods for PR,Vimentin, EMA and Ki 67 antibodies.
Summary of the results
The two tumors specimens from the Th10 and Th 12 showed a psammomatous meningiomas with large numbers of psammoma bodies (round calcified bodies). One tumor specimen from the Th 6 showed classic meningothelial meningiomas with cellular whorls and pseudonuclear inclusion.
Samples of the meningothelial meningiomas showed exclusively nuclear PR stain in a 15% of the tumor cells. In contrast, PR was negative in other two psammomatous meningiomas. Proliferative index were measured by Ki67 antibodies and in all tumors samples was lower than 1%.
Conclusion reached
To our knowledge, this is the first report of an association between multiple (three) spinal meningiomas (three) and PR.

P 979
CASPASE-3 EXPRESSION IS AN INDEPENDENT PREDICTOR OF RECURRENCE IN PATIENTS WITH INTRACRANIAL MENINGIOMAS

KONSTANTINIDOU Anastasia Evangelia1, GIVALOS Nikolaos1, NONNI Aphrodite1, GAKIOPOULOU Hariklia1, THYMARA Irene1, KOTSIAKIS Xenophon2, PATSOURIS Efstratios1
1Department of Pathology, Medical School ,University of Athens, Greece,
2Division of Neurosurgery, General Hospital of Hania,Greece.

Caspase-3 is the ultimate executioner caspase that is essential for the nuclear changes associated with apoptosis. In this study, we investigated caspase-3 expression in relation to baseline apoptosis, in order to assess the prognostic impact of an apoptotic mode of cell death in meningiomas' recurrence.
The expression of caspase-3 was evaluated immunohistochemically in a consecutive series of 56 patients with primary intracranial, totally resected meningiomas. Caspase-3 expression was investigated in relation to baseline apoptosis -as illustrated by the expression of the ssDNA-, the apoptosis suppressor protein bcl-2, proliferation indices (Ki-67, PCNA, Topoisomerase IIa and Mitosin C), and hormonal status as expressed by estrogen, progesterone and androgen receptors. Furthermore, caspase-3 expression was correlated to standard clinicopathological parameters and patients' disease-free survival.
Immunostaining for caspase-3 was observed in 60.7% of cases demonstrating a cytoplasmic granular pattern of expression. Caspase-3 labeling index was significantly associated with ss-DNA expression (p=0.03). Moreover, significant positive correlations emerged between caspase-3 labeling index and mitotic index (p=0.002), PCNA labeling index (p=0.004), while a suggestive association was observed between caspase-3 and the proliferation associated molecule mitocinC. As far as the conventional parameters are concerned, a significant correlation was established between caspase-3 expression and histological grade of meningiomas,in that grade II and III meningiomas (atypical and malignant respectively) demonstrated a significantly increased caspase-3 labeling index ($p<0.0001$). In univariate and multivariate survival analyses caspase-3 predicted meningiomas' recurrence affecting independently disease-free survival (p=0.0297 and p=0.047 respectively).
In conclusion, caspase-3 may prove to be a useful marker of recurrence in a group of neoplasms characterized by the frequent discordance between histology and clinical behavior.

P 980
INTRACRANIAL LESIONS MIMICKING MENINGIOMAS: REPORT OF 18 CASES.

(BOUHAJEB Youssef, MIGUEL SALAS María teresa, ANEIROS FERNANDEZ José, RUÍZ BARNÉS Pedro*, SARASA CORRAL Jose luis,). Department of pathology, *Department of Neurosurgery, Hospital "Fundación Jiménez Díaz", Madrid.

OBJECTIVE:
To analize the neurosurgical cases in which both the clinical and neuroimaging features suggested intracranial meningioma but resulted in different entities from a neuropathological point of view.
PATIENTS AND METHODS:
The clinical history and histopathological reports of patients with intracranial mass lesions mimicking meningioma and operated in our hospital, were reviewed.
RESULTS:
Our analysis revealed 18 cases with different neuropathological diagnosis. They were distributed as follows: 8 cases of hemangiopericytoma, 2 cases of Rosai-Dorfman´s disease, and one case of each of the following entities: solitary fibrous tumor, medulloblastoma, cerebral lymphoma, histiocytosis X, metastasis of adenocarcinoma,oligodendroglioma, pleomorphic xanthoastrocytoma and fibrous pseudotumor.
CONCLUSIONS:
The clinical and neuroimaging features of meningiomas are mimicked by different neoplastic and nonneoplastic entities. Because these lesions can resemble a meningioma during intraoperative biopsy, they must be considered in the differential diagnosis and kept in mind by the pathologist at this moment.

P 981
PARTICULAR FORMS OF MENINGIOMA: ABOUT FOUR CASES

HICHAM ELATTAR,HIND ATAWNA,FATIHA BENADRA,HANANE RAIS,BADIA BELAABIDIA
HOPITAL IBN TOFAIL-MARRKESH-MOROCCO

Meningothelial tumors or meningioma represent between 13 and 26 % of all nervous tumors in adult. The intracerebral meningotheliomatous form is the most frequent. We report

four cases which have a particular clinical presentation and particular microscopic patterns.
The first case occurred in 39-years-old women who developed a multifocal cystic tumour. The CT scan proposed the diagnosis of glioma. Microscopic pattern and immunochemistry made the diagnosis of multifocal meningioma. The second case is about another parietal cystic tumour occurring in a 60 years old woman. The diagnosis was a microcystic meningioma.
The third case is about a sixty years old woman who developing an intraventricular atypical meningioma.
The last case is about a 40 years old woman who developing an intramedullary papillary meningioma.
Consequences of Particular clinical and histological forms of meningiomas can be their misdiagnosis. The knowledge of this entities is important for a successful therapy

P 982
CORRELATION BETWEEN VITAMIN E AND FOLIC ACID LEVELS AND THE DEVELOPMENT OF ALZHEIMERS DISEASE IN A MOUSE MODEL OF AD
NEGAR OMIDI;PARICHEHR PASBAKHSH;

Alzheimers disease(ad)is the most common type of dementia(75%),manifesting as a severe deterioration of mental functions.the brains of people with alzheimer disease exhibit deposition of amyloid beta peptid and progressive degeneration of nerve cells.scientist are studying ways that may help decrease or prevent neurodegeneration and may help injured neurons to regrow.we determined whether the antioxidant vitamin e+folic acid affected the presence of amyloid plaques in brain of aged pdapp transgenic mice.beta-amyloid precursor protein (app).is important for the pathogenesis of alzheimers disease(ad),which is characterized by progressive decline of cognitive functions,formation of a beta plaques,and neurofibrillary tangles,and loss of neurons.in the present study we have examined that treatment by vitamin e+folic acid in pdapp aged mice compare with control groups is able to decrease 20% in ab plaques levels of cerebral amyloidosis in neocortex.more over ,our results suggest that treatment by vitamins is able to prevent the disruption of basal cholinergic forebrain system and prevent of loss of cholinergic basal forebrain neurons(ms+hdb,vdb)

P 983
AN AMINO ACID MOTIF COMMON TO BETA AMYLOID PROTEIN AND TO NEURODEGENERATIVE VIRUSES MAY TRIGGER NEURONAL DESTRUCTION.
Parvaneh Rahimi-Moghaddam MD. Ph.D.
Razi Institute for Drug Research, Iran University of Medical Sciences, Tehran, Iran

Research in the field of neuroscience has provided a better understanding of the cascade of biochemical events in neurodegenerative diseases. Most neurodegenerative conditions are marked by the presence of protein aggregations, and, in many cases, increased levels of oxidative damage in post-mortem tissues. The proteins associated with the neurodegenerative conditions may cause the over-production of free radicals in the neuronal tissues of the patients. We discovered that a 5-amino-acid sequence, Gly-Ala-Ile-Ile-Gly, residues 29-to-33 of the b-amyloid protein from Alzheimer's disease, is also found in proteins from three neurodegenerative viruses: HIV-1, Newcastle disease virus, and Japanese encephalitis virus. We used PC12 cells and SH-SY5Y cells to study the toxicity of this pentapeptide, using the 3-(4,5-dimethylthiazol-2-yl)-2,5-diphenyltetrazolium (MTT) assay and the measurement of caspase-3 activity. b-Amyloid 29-to-33 produces a concentration-dependent cytotoxicity to PC12 cells and to differentiate SH-SY5Y cells, but the reverse sequence (b-amyloid 33-to-29) is not toxic. Also, b-amyloid 29-to-33, but not b-amyloid 33-to-29, increases the caspase-3 activity in PC12 cells in a dose-dependent manner, which is blocked by U-83836E, U-101033E and vitamin E. These results emphasize role of free radicals in the pathogenesis of neurodegeneration.

P 984
1H MRS COMPARATIVE STUDY OF CEREBRAL METABOLISM IN PATIENTS WITH MILD COGNITIVE IMPAIRMENT (MCI), VASCULAR DEMENTIA (VD) AND IN NORMAL ELDERLY SUBJECTS (N)
ROZHKOVA Zina, ROGOZHYN Vladimir, Bachinskaya Nataliya
Radiological Center of the Academy of Medical Sciences of Ukraine, Kiev, Ukraine

Purpose: The aim of our study is to characterize the metabolic changes in the brain of patients with MCI, VD, and normal elderly subjects on the basis of analysis of 1H MRS data.
Materials and Methods: Three groups of patients are studied by MRI and 1H MRS with 1.5T Magnetom Vision (SIEMENS). The 1st group includes 25 patients (56-84y) with MCI. The 2nd group consists of 9 patients with VD (52-73 y). The 3rd group (N) consists of 30 healthy volunteers (60-75 y). 1H spectra are recorded in hippocampus (H), amygdala (A), frontal lobes (FL) and in entothinal cortex (EC) with the SVS STEAM method: TR/TE=1500/135,30 ms, VOI = 8cm3, NS = 128.
RESULTS: In the 1H spectra the following signals are identified: N-acetylaspartic acid (NAA)-2.02 ppm, total creatine (Cr)-3.03 ppm, choline (Cho)-3.24 ppm, and myo-Inositol (mIns)-3.56 ppm. From the spectra in all sampled regions of the brain the peak areas of main metabolites: NAA, Cr, Cho and mIns, and also the metabolite ratios are obtained. For the patients of the 1st verse the 3rd group the significant decrease of NAA and Cr and the increase of Cho peak areas in all regions and also significant decrease of NAA/Cr, and Cho/Cr in H and FL are observed. In the 1st group (NAA/Cr=1.01; mIns/Cr=0.82; Cho/NAA=0.96), in the 2nd group (NAA/Cr=1.14; mIns/Cr=0.58; Cho/NAA=0.86), and in the 3rd group (NAA/Cr=1.25; mIns/Cr=0.62; Cho/NAA=0.53) are obtained. There is the significant increasing in mIns/Cr (0.69) ratios in the patients of the 1st group compared with the patients of the 2nd group (0.52). Comparison 1H data in the right and left FL and EC for the patients of the all groups a significant reduction of NAA/Cr in the left hemisphere and non-significant reduction of NAA/Cr in the right hemisphere are found. The ratios of Cho/NAA, mIns/NAA in H, FL and EC are the most accurate values for differentiation MCI, VD and N.
CONCLUSION: 1H MRS data are useful in predicting the progression of MCI and VD and also for identification of cognitively normal subjects at risk for developing MCI.

P 985
DECREASED THYMIDINE PHOSPHORYLASE EXPRESSION IN BRAINS AFFECTED BY ALZHEIMER DISEASE
SULE Norbert(1), POWELL Suzanne(2), LUPSKI R. James(3), SZIGETI Kinga(4)
(1)Departmenbt of Pathology, University of Pécs Medical School, Pécs
(2) Department of Pathology, Baylor College of Meidcine, Houston TX
(3) Department of Genetics, Baylor College of Meidcine, Houston TX
(4) Department of Neurology, Integrated Health System, Pécs

INTRODUCTION: Whether the alteration of blood-brain permeability plays a role in the pathophysiology of Alzheimer disease (AD) has long been debated and recently white matter

disturbance was implicated in AD's pathogenesis. We have recently shown, that mutations in TP present in patients with MNGIE result in loss of expression of thymidine phosphorylase in the white matter, which correlates with white matter hypointensity on MRI and albumin positive cells in the white matter suggesting increased BBB permeability. Furthermore its embryological expression reveals a maturation pattern, which coincides with the temporal and spatial maturation of the BBB.
PURPOSE: The aim of the pilot study is to test whether TP expression is altered in AD and this alteration correlate with increased BBB permeability
METHODS: We completed a pilot study on post mortem brain tissue from patients with definite AD and age and sex matched controls. Immunohistochemical stains for TP and intracellular albumin were performed and quantified by counting positive cells per 10 high-power fields.
RESULTS: The number of TP positive cells was 5.36 and 14.15 ($p<0.01$) in the parietal lobe, 5.97 and 16.22 ($p<0.01$) in the frontal lobe of Alzheimer and control brains, respectively and inversely correlated with the number of albumin positive cells (29.99 and 16.08 ($p<0.01$) in the parietal lobe, 25.94 and 12.06 ($p<0.01$) in the frontal lobe of Alzheimer and control brains, respectively). The number of TP positive cells was independent of age. Although patients with MNGIE do not develop AD, they succumb at a young age usually. Formal neuropsychological testing has not been performed on patients with MNGIE or their heterozygote family members to detect subtle cognitive impairment.
CONCLUSION: Whether loss of TP expression contributes to the pathogenesis of AD or it is a secondary phenomenon , needs further elucidation.

P 986
RETROSPECTIVE STUDY OF SKIN NEUROFIBROMATOSIS (SN) OF TWENTY YEARS PERIOD (1991 -2000) IN 4 IRANIAN PATHOLOGY CENTERS
NOORI Mugahi Seyed Mohammad Hossein,NABAVI Seyed Mohammad Bagher
Khoramshahr University of Marine Sciences and Technology

The present study was designed to assess the frequency and stage of Skin Neurofibroma in the samples of patients with age, gender and biopsy locations.
Data obtained from annual record files of four different pathology centers with considering factors of Diagnosis, Age, and Gender and Biopsy location, examined for statistical difference. Each diagnosis has been coded by ICD method. Statistical examination has been done in 4186 samples of skin related to 52907 cases. The results of this experiment showed that
1) SN distributed in 52.9% of male cases and 47.1% of female cases.
2) Among all cases, trunk was the most common site of biopsy with 691 cases (24.7%). 632 cases (22.6%) were in face & 438 cases (15.8%) were in head & neck. Three samples (5.3%) were taken from the eyelids, 9 (15.8%) were taken from the faces, 11(19.3%) were taken from the heads and necks, 9 (15.8%) were taken from the trunks, 9 (15.8%) were taken from the upper limbs, and 19 samples (28.1%) were taken from the lower limbs showed Neurofibroma.
3) Among all cases, the third decades of life was the most common time of SN appearance with 860 cases (21.7%). 648 cases (16.4%) were in 4th decade & 592 cases (14.9%) were in 5th decade. This results may indicated that we should work more about (SN) and its effects on our life story.

P 987
INTERACTION OF VESICULAR MONOAMINE TRANSPORTER2 (VMAT2)AND NEUROMELANIN PIGMENT AMONG THE MIDBRAIN DOPAMINERGIC NEURONS ,IN MAN
P.PASBAKHSH(Ph.D);D.C.GERMAN(Ph.D);N.OMIDI(M)
Neuromelanin(nm)pigment accumulates with age in catecholaminergic neurons in man,and the ventral substantia nigra dopaminergic neurons that are the most vulnerable to degeneration in parkinsons disease(pd)contain the greatest amount of this pigment.in vitro data indicate that nm pigment is formed from the excess cytosolic catecholamine that is not accumulated into synaptic vesicles via the vesicular monoamine transporter2(vmat2).using semi-quantitative immunohistochemical methods in human postmortem brain,we sought to examine the relationship between the cotents of vmat2 and nm pigment.the immunostaining intensity(isi)was measured for vmat2 in two regions of the midbrain dopaminergic cell complex. The isi of the cells was related to the density of nm pigment within the cells.we also measured the isi for tyrosine hydroxylase(th)and examined the noradrenergic neurons in the locus coeruleus(lc).in brains 22-65 years of age:1)ventral substantia nigra neurons had the lowest vmat2 isi of all neurons in the midbrain cell complex,whereas over 2-fold higher levels are found in most ventral tegmental area neurons :2)there was an inverse relationship between vmat2 isi and neuromelanin pigment in the midbrain dopaminergic neurons:3)neurons with the highest vmat2 isi resided in lc:4)neurons with high vmat2 isi also had high th isi:and 5)inthe newborn brain,which has not yet accumulated neuromelanin pigment in the aminergic neurons,the regional distribution of vmat2 and th-isi was similar to that found in the adult brain.these data support the hypothesis that among the midbrain dopaminergic neurons,the ventral substantia nigra dopamine neurons accumulate the highest levels of nm pigment because they have the lowest levels of vmat2,which thereby renders them especially vulnerable to degeneration in pd.

P 988
DENSITIES OF PARVALBUMIN-IMMUNOREACTIVE NEURONS IN CORTICAL DYSPLASIAS AND NON-MALFORMED EPILEPTIC TEMPORAL NEOCORTEX
ZAMECNIK Josef (1), KRSEK Pavel (2), DRUGA Rastislav (3), MARUSIC Petr (4), BENES Vladimir (5), TICHY Michal (6), KOMAREK Vladimir (2)
(1) Department of Pathology and Molecular Medicine, Charles University, 2nd Medical Faculty; (2) Department of Pediatric Neurology, Charles University, 2nd Medical Faculty; (3) Department of Anatomy, Charles University, 2nd Medical Faculty; (4) Department of Neurology, Charles University, 2nd Medical Faculty; (5) Department of Neurosurgery, Charles University, 1st Medical Faculty; (6) Department of Neurosurgery, Charles University, 2nd Medical Faculty; PRAGUE, Czech Republic

The changes in density of inhibitory parvalbumin-immunoreactive (PV-ir) interneurons were quantitatively studied by immunohistochemistry in series of human neocortical samples comprising a whole spectrum of malformations of cortical development (MCD) and the non-malformed epileptic temporal neocortex in patients with temporal lobe epilepsy (NET). The highest counts of PV-ir cells were obtained in the control samples ($n = 21$). The number of PV-ir neurons was significantly decreased in NET ($n = 73$, 80.5 % of control values). In a proportion of pacients with NET as well as in two control samples we observed patchy regions of absence of PV staining. The total count of PV-ir cells in categories of MCD was further decreased, representing 72.4%, 55.0% and 12.2% of control values in groups of 'mild MCD' ($n = 25$), focal cortical dysplasia (FCD) type I ($n = 16$) and type II ($n = 15$), respectively. Significantly different PV-ir cell densities were demonstrated between the FCD types IIA and IIB. In MCD, we observed the decrease of

PV-ir cells to be more pronounced in infragranular layers. No significant differences were revealed between the temporal and extratemporal examples of MCD. This study provides evidence for reduction of inhibitory PV-ir interneurons in the epileptic neocortex affected by MCD as well as in morphologically unaffected temporal neocortex representing thus a possible mechanism for their epileptogenicity.
Supported by Grants: GACR No. 309/02/D076, IGA NF 7411-3 and Research Project VZ FNM 00000064203.

P 989

1H MRS STUDY OF METABOLIC ALTERATIONS IN PATIENTS AFTER ISCHEMIC STROKE IN ACUTE AND REHABILITATION PERIODS

ROGOZHYN Vladimir, ROZHKOVA Zina, SHCHEGLOV Viktor, SHCHEGLOV Dmitrii, KUZNETSOVA Svetlana, KUZNETSOV Viktor
Radiological Center of the Academy of Medical Sciences of Ukraine, Kiev, Ukraine

Purpose: We propose the quantitative indicators for the characteristics of regional multivoxel distributions of the brain metabolites (Cho, Cr, NAA) in patients after ischemic stroke in acute and rehabilitation periods.
Materials and Methods: Two groups of subjects are examined by 1H MRS using 1.5T Magnetom Vision (SIEMENS). The 1st group (VG) consists of 75 volunteers (in the age from 18 to 73 years). The 2nd group (SG) includes 80 (60 females and 20 males) patients (in the age from 46 to 87 years) in the acute (<12 hours), subacute (<10 days) and chronic (from 10 days to 12 months) stages of ischemic stroke. In all patients 12x12 spectral matrixes in supraventricular region parallel to the canthomeatal line are obtained. 2DCSI 1H spectra are recorded with: TR/TE=1500/135 ms, VOI=8x8x2cm.
Results: In each voxel of the spectral matrix we introduce two indicators: the metabolite content AM as the peak area and the metabolite concentration CM as the ratio of the peak area to the sum of all the peak areas S: CM=AM/S. We describe the metabolic state in each voxel by the triad T* = {ACho, ACr, ANAA}, where ACho, ACr, and ANAA are the peak areas of the signals from Cho, Cr and NAA. For each of the areas we assign three values: 1, 2 and 3, to obtain six symbolic spectral configurations: 1* ={1,2,3}, 2* = {2,1,3}, 3* = {1,3,2}, 4* = {3,2,1}, 5* = {3,1,2} and 6* = {2,3,1}. We analyzed the temporal alterations of the triad distributions after ischemic stroke. In the VG triads 1* and 2* dominate in all voxels of VOI. The most frequent configurations in the acute period are 5* and 6*. The triad regional variability decreased during rehabilitation period. Triads 3* and 4* are more often in elderly subjects.
Conclusion: The triad distributions give us a quantitative way for the estimation of efficiency of stroke therapy.

P 990

REGIONAL ALTERATIONS OF CONTENT AND VALUES OF T2 RELAXATION TIME OF THE MAIN CEREBRAL METABOLITES IN PATIENTS WITH PARKINSON'S DISEASE (PD): IN VIVO 1H MRS STUDY

KARABAN' Irina, KARABAN' Nikolay, ROGOZHYN Vladimir, ROZHKOVA Zina
Radiological Center of the Academy of Madical Sciences of Ukraine, Kiev, Ukraine

PURPOSE:From the analysis of ¹H MRS data and their echo-time dependence we propose the quantitative indicators for the characteristics of the brain state in patients with PD.
MATERIALS AND METHODS:Two groups of patients are studied by ¹H MRS with 1.5T Magnetom Vision (SIEMENS). The 1st group (PG) includes 40 patients with PD (48-70 y). The 2nd group (VG) consists of 15 healthy volunteers (50-73 y). Spectra are recorded in the temporoparietal cortex (TC), lentiform nucleus (LN), putamen (P) and substantia nigra (SN) with STEAM method:TR/TE=1500/135,155,175,200,270 ms.
RESULTS:We introduce two indicators: the metabolite content A^M as the peak area and the concentration C^M=A^M/S. We describe the metabolic state in VOI by the triad T*={A^{Cho}, A^{Cr}, A^{NAA}}, where A^{Cho}, A^{Cr}, and A^{NAA} are the peak areas of the signals of metabolites. For each of the areas we assign three values:1,2,3, to obtain six symbolic spectral configurations:1* ={1,2,3}, 2* = {2,1,3}, 3* = {1,3,2}, 4* = {3,2,1}, 5* = {3,1,2}, 6* = {2,3,1}. In the VG triads 1* and 2* dominate in all VOI, 3* and 4* are often in elderly subjects. In the PG the most frequent configurations in TC are 2* and 5* and in LN, P and SN are 5* and 6*. From comparison of T₂^M values in P, LN and SN in the both groups the shortening of T₂^M in the PG are obtained. In the TC the T₂^M values are similar in PG and VG.
CONCLUSION:This study gives a new insight into brain biochemistry in patients with PD.

P 991

PERONEAL NERVE REGENERATION THROUGH A HEALTHY TIBIAL NERVE: A DETAILED MORPHOMETRIC ANALYSIS

SAKELLARIOU A1, BATISTATOU A2, LYKISSAS M3, BAI M2, BERIS A3, AGNANTIS NJ2
Departments of 1Plastic Surgery and Burns, 2Pathology and 3Orthopaedics,
University of Ioannina Medical School, Ioannina, Greece

INTRODUCTION: End-to-end nerve reconstruction is considered to be the treatment of choice, in the repair of peripheral nerve injuries. However, in cases of long nerve defects, the optimal surgical procedure has not yet been established, but the gold standard continues to be the use of autologous nerve grafts. For short nerve defects, a lot of different conduits have been studied, as well as the end-to-side nerve suture.
PURPOSE: The purpose of this study was to evaluate the regeneration of the transected peroneal nerve utilizing the tibial nerve as a conduit, with the use of proximal and distal neurorraphy.
METHODS: Forty male Wistar rats, weighing 230-300g, were included in this study. The peroneal nerve was transected and the animals were divided in five groups. Group I: End-to-end neurorraphy. Group II: The proximal stump of the peroneal nerve was sutured in an end-to-side fashion to the tibial nerve. The distal stump was sutured end-to-side 1.0 cm distally, along the tibial nerve. All coaptations were performed with epineurotomy of the tibial nerve. Group III:The proximal and distal stumps were left in situ. Group IV: Double end-to-side neurorraphy with intraperitoneal injection of valproic acid. Group V: Double end-to-side neurorraphy, plus subcutaneous injection of erythropoietin. During the waiting period, walking track analysis was performed in all animals. After 16 weeks, all rats were sacrifised. Specimens including sciatic, tibial and peroneal nerves from both sides were dissected and fixed in 2.5% Glutaraldehyde in 0.1M Cacodylate. Representative samples were taken, embedded in a resin mixture and semi-thin sections (1im) were stained with a modified solution of Toluidin blue and evaluated. A semiquantitative morphometric analysis using an image analyzer, was performed. The tibialis anterior muscle weight was recorded.
RESULTS: Axonal counting, the mean axonal diameter and area and the mean myelin thickness were estimated in all

groups, and compared to the contralateral unoperated side. The morphometric parameters of the Group II were comparable to Group I, while the preliminary data regarding Group V, suggest a further slight improvement.
CONCLUSIONS: The morphometric data presented in this study support the use of the tibial nerve as a conduit for the regeneration of the peroneal nerve, when the immediate repair is not possible

P 992
COMPARATIVE STUDY OF THE ABNORMALITIES OF CENTRAL NERVOUS SYSTEM IN CHILDREN AND ADULTS AUTOPSIED AFTER BONE MARROW TRANSPLANTATION
BENITES FILHO Paulo Roberto, TAFAREL Jean R., ZANIS NETO José, DE MEDEIROS Carlos R., PASQUINI Ricardo, BLEGGI-TORRES Luiz F.
Department of Pathology, Hospital de Clinicas, UFPR, Curitiba, Brazil
Bone Marrow Transplantation Unit, Hospital de Clinicas, UFPR, Curitiba, Brazil

Background: We compare the neuropathological abnormalities found in children and adults after bone marrow transplantation (BMT) who were autopsied in the Department of Pathology, University of Paraná, Brazil.
Methods: The autopsy reports of 180 patients were reviewed. They were divided in two groups: patients under 15 years old and those with 15 or more. Age, gender, clinical diagnosis at time of BMT, survival time, neuropathological abnormalities and cause of death were analyzed.
Results: In children (26,6% of total) and in the adult group (73.4% of total), the main clinical diagnosis prior to BMT were respectively: severe aplastic anemia (31.2%) and chronic myeloid leukemia (36.3%). The mean survival time for children was 102.6 days and for adults 185.9 days after BMT. The brain lesions were considered cause of death in 20.8% of paediatric cases and 11.3% of the adult group. The neuropathological abnormalities were morphologically similar in children and adults with the following respectively prevalence: cerebrovascular diseases in 58.3 and 56% (p=0.8655), neurotoxoplasmosis in 6.2% and 3% (p=0.3856) and infections in 27 and 25.7% (p=0.8489).
Conclusions: The paediatric patients had a shorter survival than adults with increasing prevalence of neurotoxoplasmosis and the brain lesions were considered cause of death in twice as many as compared to adult patients.

P 993
PATHOGENESIS OF HETEROTOPIC ECTOPIC GRAY MATTER IN THE BRAIN OF MOUSE PRENATALLY EXPOSED TO IRRADIATION
X.Z. SUN, S. TAKAHASHI, Y. KUBOTA, *R. ZHANG, *C. CUI, H. *Y. FUKUI, S. YOSHIDA
Environmental and Toxicological Sciences Research Group, National Institute of Radiological Sciences, Japan;
*Department of Anatomy and Developmental Neurobiology, School of Medicine, Tokushima University, Japan

The developing brain is one of the fetal structures most susceptible to irradiation. Studies of survivors exposed to atomic bombing in Hiroshima and Nagasaki or to x-rays during medical procedures indicated that mental retardation and microcephaly with heterotopic gray matter are prominent findings after in utero radiation exposure. The heterotopic gray matter could be caused by cell death and abnormal neuronal migration during a critical gestational stage of sensitivity to irradiation. However, the possible cellular and molecular mechanisms involved in the abnormal neuronal migration caused by irradiation are unknown. We have examined the pattern of brain malformations in 8-week-old mice prenatally exposed to doses of rradiation ranging from 0.5 to 2.0 Gy at different embryonic days. Brain malformations, identical to radiation-related small-sized heads with heterotopic gray matter, were reproduced in mice exposed to 1.5 Gy on embryonic day 13 (E13). In the present experiment, pathogenesis of such brain malformation was studied with immunohistochemical detection methods. Pregnant females were exposed to irradiation at a dose of 1.5 Gy on E13. Brains from fetuses and pups were obtained every day from 6 hrs after exposure to different postnatal days. Six hrs after exposure extensive dead cells appeared throughout the brain mantle. On E16 some cells came together to form rosettes. On E18 a high proportion of BrdU-labeled cells reached the superficial layers of the cortical plate with the remaining cells located in the heterotopic neuronal masses. The quantitative study showed that labeled-cells in layers II-III were fewer and those in layers IV-VI more numerous in the adult mice prenatally irradiated than controls. These results indicated the disruption of normal cell migration in the irradiated brain. The anti-GFAP immunostaining revealed that radial glial fibers were markedly straight and perpendicular to the pial surface in the controls, but disorganized after the irradiation exposure. Migration of young neurons along radial glial fibers is the prevalent mode of neuronal cell movement in the developing mammalian brain. The crumpled fibers might have presented unpassable, only partially passable, or disoriented pathway for neuronal migration. These findings suggested that the heterotopic gray matter in the brain of mice prenatally exposed to irradiation resulted from interrupted neuronal cell migration and migratory pathway.

P 994
EXPRESSION AND CELLULAR DISTRIBUTION OF MULTIDRUG RESISTANCE PROTEINS (MRP-1 AND MDR-1) IN FOCAL CORTICAL DYSPLASIA CASES
Oz Büge, AY Bahadýr, UZAN Mustafa, ÖZKARA Ciðdem, AK Halil, SAR Mehmet

PURPOSE:
Focal cortical dysplasia (FCD) is a congenital cortical developmental abnormality, which is generally characterized by drug resistant epilepsy. We aimed to investigate, multidrug resistance-associated protein 1 (MRP-1) and multidrug resistance gene-1 P glycoprotein (MDR-1) in the resection material of patients with FCD who underwent surgery.
METHODS:
Formalin-fixed parafin-embedded human brain tissues obtained from 20 patients and 10 age-match autopsy controls were studied ,. Sections of 5 µm were cut and the sections were stained with HE, Bielschowsky and Luxol-Fast-Blue. The resection materials were evaluated according to Palmini's Focal Cortical Dysplasia classification. Different type neurons, reactive astrocytes, endothelial cells within the dispastic cortex were examined for the expression MDR-1 and MRP-1 by immunocytochemistry. Immunreactivity in the cells was scored as -, - / +, + and ++.
RESULTS:
The Disstribution of cases were 2 type IA, 4 Type IB, 8 Type IIA (40%) and Type IIB (30%) FCD.
Evaluation of immunreactivity::
Neuron: MDR-1 and/or MRP1 was strogly positive in 16 cases (80%) of patients whereas in control cases MDR-1 was none or MRP-1 weakly positive in 50% of cases. Astrocytes: 10 % (2 cases) with MRD-1 ,and 55% (11 cases) with MRP-1 positivity were observed in FCD patients whereas MDR-1 was none and MRP-1 was 22% weakly positive for controls. Capillary endothelial cell: MDR-1 in 90% of controls, 50% of patients, whereas MRP-1 50% of patients, 10% of control were positive. In type IIA and type IIB FCD cases, MRP-1 positivity was detected 70 % (10/14 cases)in dysmorphic neurons and 20% (3/14 cases) giant neurons whereas MDR-1 positivity were seen only 15 % in dysmorphic neurons (2/14

cases) and 7% in giant neurons (1/14 cases). Immunreactivity for MDR-1 and MRP-1 in the balon cells of Type IIB FKD cases was observed in 4 cases (33%).

CONCLUSIONS:
The distribution of MRP-1 was more strong than MDR-1 in FCD cases.
MDR-1 and MRP-1 expression were prominent in neuronal cell were than the other cells. The overt expression of MDR proteins within the dysplastic tissue may be an evidence for the drug resistant seizures in patients with FCD comparing the control cases.

P 995
NEUROCYSTICERCOSIS: BIOPSY ANALYSIS OF FIVE YEARS PERIOD
SKENDER GAZIBARA Milica, CVETKOVIC DOZIC Dubravka, GAZIBARA Tatjana, MILENKOVIC Sanja, DOZIC Slobodan

Introduction. Neurocysticercosis (NC) is caused by larval stage of the pork tapeworm, Taenia solium. It is the most common parasitic cerebral infection encountered in worldwide neurosurgical practice. In some geographic regions it is the leading cause of space-occupying intracranial lesions.
Purpose of this study was neuropathological analyses of NC in surgical material of patients with space-occupying intracranial lesions, operated on during five years period (2000-2004).
Methods. Surgical biopsy specimens of NC were examined using standard histological and histochemical staining procedures.
Results. Of 4987 patients with intracranial lesions, NC was diagnosed in 18 cases (0,37%). The most frequent clinical manifestations included: hydrocephalus, epileptic seizures and chronic psychoorganic syndrome. The mean age of the patients was 51,66 (ranged from 40 to 68) years. Female to male ratio was 1:1. The great majority (16/18) of cases had solitary cystic lesion. In other two cases there were two parenchymal cystic lesions associated in one of them with third, solid, partly calcified suprasellar nodus. Cysticercus was located more frequently in the ventricular system (13 cases - 72%) than in brain parenchyma (5 cases – 28%). Inside of ventricular system, left lateral ventricle was the most frequently involved (7 cases).
Grossly, majority of cystic lesions were approximately 2 cm in diameter with thin, translucent membrane and water-clear fluid. Three ventricular cysts had a grapelike appearance (racemose form of cysticerci). Occasionally, single small (2-4 mm) whitish nodule was attached to the luminal surface of the wall. Microscopically, typical three-layered vesicular membrane was consisted of external wavy eosinophilic lamina, cellular layer and interior to this loose connective tissue. Rudimentary parasitic body and scolex showed different stages of involution. In some sections of viable scolex there were muscular suckers and hooklets. Around degenerated and dead parasite there was so called reactive membrane, composed of histiocytes, multinuclear giant cells, collagen fibers, prominent inflammatory cells (lymphocytes, plasmocytes and eosinophils) and layer of reactive astrogliosis.
Conclusions. According to our series of neurosurgical biopsy material, NC accounts for only 0,37% of surgically treated space-occupying intracranial lesions. This percent is significantly less than in series of NC from well known endemic regions in the world

P 996
A NEUROPATHOLOGICAL STUDY OF AUTISM
CASTAGNA Maura*, BIANCHI Francesco$, D'ALESSANDRO Delfo$, BECHERINI Francesca*, BARBOLINI Giuseppe

$Department of Human Morphology and Applied Biology University of Pisa (Italy)
*Department of Surgery University of Pisa (Italy)
Department of Morphological Sciences University of Modena (Italy)

Autism is a severe developmental disorder characterized by impairments in reciprocal social interaction and communication, restricted and stereotyped patterns of behaviour and interests, and an onset before 3 years of age (World Health Organization, 1992). Many regions of the brain have been implicated in the genesis of autism, but the neurobiological basis of the disorder remains unknown. Autism is a rare disorder which was described relatively recently and there are only a few post-mortem studies. Few data are available about molecular mechanisms of this pathology. A neuropathological study of autism was established and post-mortem brain tissue examined from one male individual.
It is known that RhoA, a small GTPase, inhibits axonal growth during early neuronal differentiation and axonal regeneration, while promotes the axonal growth during late neuronal differentiation. Infact RhoA controls a wide variety of cellular processes such as actin cytoskeleton rearrangement, microtubule dinamics, cell adhesion and polarity.
The cerebellar cortex was fixed in 10% formaldehyde, embedded in paraffin and sectioned.
Immunohistochemistry for glial fibrillary acid protein (GFAP), neurofilaments and RhoA was performed using the avidin-biotin complex method with diaminobenzidine as the chromogen.
The sections were acquired on digital support. Studied antigens distribution and expression analysis were evaluated by image analysis software Quantimet 500 plus.
Our results showed a reduced Purkinje cells number in the autistic cerebellum compared to the control one. RhoA expression was greater in Purkinje cells than other cells. GFAP and RhoA expression were reduced, while neurofilaments production was increased in the autistic cerebellum compared to the control one.
GFAP expression is mainly localized in granular layer cells both in control and autistic specimens. These data, together with the literature, suggest that an abnormal behaviour of cerebellar cells can occur, as shown by GFAP and neurofilament expression, also because of an alteration of RhoA expression.

P 997
STRUCTURAL CHANGES OF THE HUMAN PINEAL GLAND IN RELATION TO HYPOXY DURATION.
Manevska B., V. Dokov, W. Dokov?
Department of Pathology, *Department of Forensic Medicine, Medical University of Varna, Bulgaria

Introduction: Morphological data of the relation of hypoxy to the structure of the human pineal gland (PG) are very few.
The aim of this study was to investigate the morphological changes of PG in relation to acute and chronic hypoxy.
Methods: Seventy three PG's were observed – 56 male and 17 female. Length, width, weight and density of the glands were measured. To determine the duration of hypoxia, the cases were separated in three groups: 1st – 26 died of mechanical asfixia of hanging (MAH), mean age 57.24 ± 11.34; 2nd – 28 died of acute respiratory insufficience (ARI), mean age 51.5 ± 10.93; 3rd – 19 died of chronic respiratory insufficience with exacerbation (CRIE), mean age 52.33 ±13.06. Paraffin slides were stained with hematoxylin–eosine and Azan.
Results: PG's of the 1st group were significantly (t=7,3, P<0,05) heavier (168.15±42.15 mg) than 2nd (111.67±42.94 mg) and 3rd (115.61±50.58 mg). In the cases of ARI the density is significantly higher than those of MAH (2.6±1.77

kg/m3) and CRIE (3.45±1.97 kg/m3). In the cases of CRIE the stroma increases and the pseudolobs are atrophic. The frequency of well shaped pseudolobs is significantly higher in the 3rd (58.92%) than in the 1st (26.92%) and 2nd group (25%). The frequency of glial prolifration in MAH (46.15%) and ARI (64.29%) is significantly lower (t=2,39, P<0,05) than CRIE(76.47%).
Conclusions: Continuous hypoxia in the cases of CRIE developes gliosis and increases the relative share of well shaped pseudolobs of PG and proliferation of stroma and different stages of pseudolobar atrophy. The acute hypoxia of MAH and ARI does not develope structural changes of the PG.

P 998
PATHOGENESIS OF HETEROTOPIC ECTOPIC GRAY MATTER IN THE BRAIN OF MOUSE PRENATALLY EXPOSED TO IRRADIATION

X.Z. SUN, S. TAKAHASHI, Y. KUBOTA, *R. ZHANG, *C. CUI, H. *Y. FUKUI, S. YOSHIDA
Environmental and Toxicological Sciences Research Group, National Institute of Radiological Sciences, Japan;
*Department of Anatomy and Developmental Neurobiology, School of Medicine, Tokushima University, Japan

The developing brain is one of the fetal structures most susceptible to irradiation. Studies of survivors exposed to atomic bombing in Hiroshima and Nagasaki or to x-rays during medical procedures indicated that mental retardation and microcephaly with heterotopic gray matter are prominent findings after in utero radiation exposure. The heterotopic gray matter could be caused by cell death and abnormal neuronal migration during a critical gestational stage of sensitivity to irradiation. However, the possible cellular and molecular mechanisms involved in the abnormal neuronal migration caused by irradiation are unknown. We have examined the pattern of brain malformations in 8-week-old mice prenatally exposed to doses of rradiation ranging from 0.5 to 2.0 Gy at different embryonic days. Brain malformations, identical to radiation-related small-sized heads with heterotopic gray matter, were reproduced in mice exposed to 1.5 Gy on embryonic day 13 (E13). In the present experiment, pathogenesis of such brain malformation was studied with immunohistochemical detection methods. Pregnant females were exposed to irradiation at a dose of 1.5 Gy on E13. Brains from fetuses and pups were obtained every day from 6 hrs after exposure to different postnatal days. Six hrs after exposure extensive dead cells appeared throughout the brain mantle. On E16 some cells came together to form rosettes. On E18 a high proportion of BrdU-labeled cells reached the superficial layers of the cortical plate with the remaining cells located in the heterotopic neuronal masses. The quantitative study showed that labeled-cells in layers II-III were fewer and those in layers IV-VI more numerous in the adult mice prenatally irradiated than controls. These results indicated the disruption of normal cell migration in the irradiated brain. The anti-GFAP immunostaining revealed that radial glial fibers were markedly straight and perpendicular to the pial surface in the controls, but disorganized after the irradiation exposure. Migration of young neurons along radial glial fibers is the prevalent mode of neuronal cell movement in the developing mammalian brain. The crumpled fibers might have presented unpassable, only partially passable, or disoriented pathway for neuronal migration. These findings suggested that the heterotopic gray matter in the brain of mice prenatally exposed to irradiation resulted from interrupted neuronal cell migration and migratory pathway.

Author Index

The numbers are the abstract numbers; oral presentations (O), poster presentations (P)

A. Kouraklis-Symeonidis, A. P-117
Aarts, M. O-164
Abakar-Mahamat, A. O-79
Abakushin, D.N. P-606
Abavisani, A. P-951
Abbas, M. P-951
Abbas, N.F. P-977
Abbes, I. P-68, P-325, P-419, P-659, P-795, P-834
Abbey-Toby, A. P-233, P-550
Abbou, C. O-81, O-82, P-670
Abbou, C.-C. O-86
Abd El All, H. P-88
Abdel Salam, S.M. P-535
Abdel, Aziz, A.M. P-766
Abdel-Rahman, E. P-230
Abdolvahhabi, A. O-221
Abdou, M.-T. P-378
Abdulkader, I. P-64, P-588, P-591, P-597, P-682
Abdullah-Sani, M. P-567
Abedi-Ardakani, B. P-229
Abeler, V.M. O-234
Aberger, F. O-152, P-136, P-195, P-412
Aboltins, A. P-493
Abo-Shousha, T. P-366
Abou El-Ela, M. P-182
Abou-Asabeh, L. P-394
Aboulela, M. P-181
Aboutaleb, S. P-884
Abrosimov, A. P-605, P-616
Abrosimov, A.Y. P-606
Abu-Madian, A. P-223
Achach, A. P-144
Acimovic, M. P-698
Acquafreda, T. P-561, P-568
Acuña, M.J. P-168
Adam, R.L. O-57, O-94, O-100
Adamopoulou, M. P-251
Adeniran, A. O-48
Adle-Biassette, H. O-184, O-255
Adouani, A. P-655
Adwent, M. P-905
Adzic, T. P-244, P-245, P-481
Aebi, U. P-738
Affiliations:Liapis, George P-526
Agapitos, E. P-895
Agelidis, P. P-394
Agnantis, N.J. O-142, P-45, P-83, P-84, P-121, P-201, P-375, P-612, P-631, P-632, P-639, P-793, P-926, P-973, P-991
Agócs, L. P-258
Agrogiannis, G. P-251
Aguilar, M. P-457
Aguilar-Quesada, R. P-910
Ahiskali, R. P-156
Ahjfm, C. P-87
Ahmed, F. O-40
Ahn, Geung Hwan P-789, P-790
Ahn, Young-Joon P-545
Aiello, V. P-733
Aigelsreiter, A. O-188, P-103
Aiglová, K. P-208
Aikio, O. P-426
Ait, B. P-442
Aitbenali, Said P-957
Akakpo, J.-P. O-84
Akbulut, M. P-297, P-405
Akbulut, M.M. P-558
Akel, S. P-2
Akhan, S. P-11
Akhmetov, T. P-282
Akinori, I. P-153
Akkaya, B. P-469
Akkiprik, M. P-180
Akl, M. P-211, P-220, P-223, P-387
Akman, H. P-174, P-405
Akpulat, S. P-221
Akriviadis, E. O-46
Akslen, L.A. P-691, P-781, P-928
Aktepe, F. P-315, P-580
Akyildiz Igdem, A. P-692
Al Atawna, H. P-630
Al Ghuzlan, A. O-212, O-263
Alain, B. O-149
Alam El-Din, H.M. P-754
Alatawna, H. P-442
Alborghetti, M.R. O-100
Aldred, V.I. P-87
Alejo, M. P-744
Aleksandrakis, K. P-705
Aleksic, A. P-204
Aleric, I. P-473
Alexandrou, P. P-118, P-217, P-416, P-417, P-421, P-526
Alexandru, D. P-19
Alexeev, B. P-675
Alexis, M. P-810
Alexopoulou, E. P-199
Alfaro, L. P-548, P-940
Alfonsín-Barreiro, N. P-588, P-591
Alhamany, Z. P-459
Ali, H. P-748
Aligholi, S. P-635
Alinger, B. O-152, P-136, P-195, P-412, P-751
Al-Irhayim, B. P-817
Allegue, F. P-927
Allende, H. P-190
Aller, P. P-667
Allia, E. O-166
Allie, N. P-161, P-169
Allory, Y. O-81, O-82, O-86, O-138, O-204, P-670
Almanza, C. P-932
Almeida, E.C.S. P-770
Alobeid, B. O-54
Alonso, S. P-929
Alonso, V. O-139
Alos, L. O-14
Alponat, A, . P-543
Al-Salam, S. P-594
Al-Shawaf, A.Z. P-941
Altavilla, A. P-151
Altemani, A. O-172
Altinok, G. P-289, P-309
Álvarez, C. P-917, P-932
Alvarez, I. P-165
Álvarez, M. P-272, P-551, P-702
Alvarez-Iglesias, M.T. P-624
Alves, G. P-69
Álves, J. P-702
Alves, Jr., S.M. P-570
Alves, V.A.F. P-213, P-214
Amalinei, C. P-71, P-150, P-189, P-276, P-696, P-697, P-801
Amanatidou, S. P-854
Amara, K. P-349
Amaro, T. O-29
Amat, I. P-33
Ambalov, Y. P-224
Amberger, A. O-108
Ambrosetti, D. O-131
Ambrosini, S.A. P-162
Ambu, R. O-153
Amer, A. P-223
Amin, M. O-175
Amini, M. O-210, O-211, P-4, P-5
Amir, Zine-Charaf P-302
Amirmozafari, N. P-395
Amoian, S. P-229
Amsellem-Ouazana, D. O-177
Anagnostakis, D. P-184, P-341
Anagnostopoulou, H. P-475, P-476
Anastasiou, N. P-251, P-497
Ancer, J. P-492
Ancer-Rodriguez, J. P-279, P-908
Andrade, R.G. P-335
André, F. P-17
Andrea, K. O-51
Andreeva, Y. P-367, P-675
Andrei, F. P-50, P-127, P-219, P-314, P-573, P-824, P-845, P-881
Andrei, R. P-155, P-227, P-530, P-903
Andreu, J. P-510
Andriamampionona, F. O-47
Androulaki, A. P-115, P-118, P-526
Androutsopoulos, G. P-410
Androylaki, A. P-377
Aneiros, F.J. P-980
Anestakis, D. P-67
Anestiadi, V. P-716
Ángeles-Ángeles, A. P-123, P-124
Angelopoulou, R. P-25
Anlauf, M. P-619
Anlauf, Martin O-112
Ann, G. P-47
Anna, B. P-564
Antabak, A. P-643
Antal, I. P-832
Antoine, E. P-206
Anton Valenti, E. O-240
Antón, I. P-932
Antonopoulos, Z. P-324
Anurova, O.A P-576
Anwar, H. P-223
Anzo, M. P-779
Aoki, N. P-779
Apáthy, Á. O-217, O-249, P-663, P-835, P-836
Apessou, D. P-317
Apostolidou, M. P-248
Apostolikas, N. P-24
Apostolski, S. P-715
Appelman, H.D. P-152
Arakawa, H. O-87
Aralica, G. P-843
Aramburu, J.A. P-187
Arapantoni, P. P-317
Arapantoni-Dadioti, P. P-7, P-24, P-348, P-879
Araujo, V. O-172, P-560
Aravantinos, G. P-879
Arcaini, L. P-114
Arcangelli, G. P-234
Ardeleanu, C. P-50, P-127, P-219, P-314, P-430, P-433, P-534, P-573, P-628, P-763, P-824, P-845
Aretini, P. P-44
Argyrakos, T. P-443
Aribal, E. P-54
Arima, N. P-819
Ariza, A. P-129
Arkoumani, E. P-45, P-85, P-973
Arman, B. P-479
Arman, O. P-850
Armengol, C. O-71
Arnholdt, H. P-695
Arnould, L. O-30, P-173, P-409
Aroukatos, P. P-96, P-971
Arrive, L. P-533
Arrivi, A. P-380
Arsene, D. P-628
Arvaniti, H. P-24, P-761
Arzu, E. O-33, P-283
Asgari, M. P-935
Ashwal, S. O-251
Ashworth, A. O-216
Asimakh, S. P-317
Asimaki, N. O-182

Asioli, S. O-11
Aslan, F. P-945
Asoglu, O. P-11, P-65
Assaad, A. O-202
Asselah, F. P-241, P-302
Asselain, B. O-215
Assous, D. P-409
Assumpção, L.V.M. P-615
Astbury, K. O-190
Aster, J.C. O-26
Asztalos, L. P-511
Atanackovic, M. P-267, P-640
Atanackovich, M. P-587
Atanckovic, M. P-633
Atawna, H. P-981
Athanassiadou, S. P-416, P-417, P-421
Atmatzides, C. P-509
Atoum, M. P-2
Attems, J. O-254
Atýk, E. P-104, P-873, P-919
Aubert, I. O-179
Aubert, S. O-126, P-822, P-856
Aubriot-Lorton, M.-H. P-604
Audard, V. P-517
Audouin, J. O-59
Audran, M. P-642
Augros, M. P-838
Auperin, I. P-93
Auprich, M. P-671
Aurias, A. O-156
Aust, D. P-899
Autonell, J. P-744
Avancini Ferreira Alves, V. P-537
Avant, C.C. O-92
Avgoloupi, A. P-91
Avsar, E. P-221, P-284
Ayadi, A. P-484, P-485, P-486
Ayadi, L. P-100, P-393, P-423, P-554, P-800, P-874
Ayala, G. P-680
Ayala-Sanmartin, J. O-34
Ayan, I. P-821
Aydin, O. P-179, P-527
Ayed, M. P-360, P-368, P-846
Ayhan, A. P-753, P-791, P-811
Ayhan, K. O-33
Azizi, R. P-385, P-386
Azoulay, S. O-263, P-670
Azria, D. P-173
Azzam, M.E. P-766

Baba, H. A. O-224
Babiæ, D. P-750
Babic, B. P-495
Babinet, F. P-470
Baccarini, P. P-162
Bacchi, C. P-308
Bacetiæ, D. P-939
Bachinskaya, N. P-984
Bachmann, I.M. P-928
Bacq, Y. O-114
Badal, J. P-744
Badawy, A. P-212, P-366, P-389, P-390
Badea, P. P-20
Badoual, C. O-8, O-171, O-199
Baena, P. P-940
Baena, V. P-129, P-701, P-866, P-867, P-868
Bagci, P. P-830
Baglin, A. P-139
Baglin, A.-C. O-62
Bagot, M. O-136, O-137
Bahadýr, A.Y. P-994
Bahaoddini, A. P-812
Bahlmann, M. O-67
Bahloul, A. P-393
Bahmanpour, S. P-625
Bahnassy, A.A. P-754
Bahram, M. P-363
Bahri, I. P-100, P-423, P-800, P-955
Bai, M. P-83, P-84, P-85, P-121, P-201, P-375, P-991
Bairaktari, E. P-24
Bairaktari, G. P-681, P-705
Bairaktari-Kouri, E. P-761
Baixeras, E. P-222
Bajor, G. P-905
Bajrovic, F. P-837
Balabaud Antonio Sa Cunha, C. P-538
Balabaud, C. O-41, O-42, O-114
Balafrej, L. P-459
Balan, R. P-71, P-150, P-276, P-801
Balasch, J. P-813
Balasi, E. P-45, P-85
Balaton, A. O-93, O-109, O-200, P-93, P-520
Baldet, P. O-250, P-94, P-407, P-555
Baldoni, C. P-162
Baldus, S.E. O-75, O-264, P-99, P-197
Baldy-Moulinier, M. O-250
Balen, E. P-425
Bali, C. P-85
Balighi, K. P-935
Ballester, S. P-823
Ballestín, C. P-168
Balm, A. O-9
Balogh, K. P-330
Baloglu, H. P-411, P-965
Baltaci, S. P-686
Baltagi Ben Jilani, S. P-157, P-323, P-937
Baltagi, S. P-846
Baltaziak, M. P-42
Bamberger, A.-M. P-772
Banev, S. P-446, P-734, P-833
Banita, M. P-921
Banner, J. P-728
Baracat, E. P-72
Barak, A. O-243
Barakat, M. P-680
Barakauskienë, A. P-131
Baralic, I. P-449
Barange, K. P-215
Barbarestani, M. O-221
Barbatis, C. O-182, O-196, P-203, P-317, P-394, P-539
Barbato, A. O-90
Barbera, J. P-968
Barbolini, G. P-996
Barbosa, A.P. O-29
Barbosa, M.J. P-932
Barboza-Quintana, O. P-279, P-908
Barbry, P. O-148
Bardier, A. O-181, P-693
Bardier-Dupas, A. P-202
Barete, S. P-331
Baretton, G.B. O-220
Barnoud, R. O-145
Baro, T. P-868
Baron, L. P-746
Barranco, C. P-129
Barraza-Ibarra, B. P-623
Barreiro, F. P-64, P-588
Barresi, G. O-52, P-592
Barrett, H.L. P-882
Barros, F. O-252
Barszcz, S. P-960
Bart, S. P-679
Barta, N. P-197
Bartoletti, R. P-372
Bartolic, K. P-146
Baruti-Kelmendi, A. P-299
Basdra, E.K. O-142, P-632, P-639
Basheska, N. P-277, P-747, P-765
Bassarova, A. O-147, P-138
Basta-Jovanovic, G. P-449, P-849
Bastard, J.-P. O-39
Batelja Vuletic, L. P-857
Batelja, L. O-4, P-643
Baþsorgun, Ý. P-963
Batinac, T. P-934, P-942
Batistatou, A. P-45, P-201, P-612, P-631, P-926, P-973, P-991
Batmunkh, E. P-544
Battista, G. P-556
Bauersfeld, J. P-619
Bautista, D. P-222
Bayani, J. O-85
Bayati, V. O-221
Bayer, I. P-508
Baykov, V. P-95
Bayraktar, Y. P-289
Bazille, C. O-204
Bazowski, P. P-962
Beaugerie, L. O-36
Beaugrand, M. O-44
Becherini, F. P-996
Becker De Moura, H. P-60, P-61
Becker, B. O-89
Bedossa, P. O-111, O-115, O-178, P-234, P-235, P-343, P-550
Beelabidia, B. P-820
Begriche, K. P-233
Beham, A. P-103
Beham-Schmid, C. O-122, O-188, P-103
Bekir Suha, P. P-876
Beksac, M. P-97, P-98
Belaabidia, B. P-441, P-442, P-445, P-630, P-665, P-957, P-981
Belaid, L. P-143, P-144
Belaud-Rotureau, M.-A. O-63, O-65, O-134, O-135, O-241
Belghiti, J. O-111, O-115, P-235, P-550
Belhadj, K. O-62
Belhomme, P. P-893
Belichard, C. P-29
Belicza, M. P-703, P-853, P-857
Beljebbar, A. O-38
Bella, M.R. O-129, P-154, P-266
Bellan, C. P-132
Bellaud, P. O-195, P-669
Belleannee, G. O-31, P-757
Bellefqih, S. O-212, P-331, P-336
Bellier, C. P-343
Bellil, K. P-340, P-342
Bellil, S. P-340, P-342
Bellina, M. O-180
Bellocq, J.P. O-130
Belluco, C. P-899
Belosillo, B. P-129
Belov, I.U.V. P-730
Beltotti, P. P-746
Belushkina, N. P-291
Bély, M. O-217, O-249, P-663, P-835, P-836
Ben Abdelkader, A. P-143, P-144
Ben Ghorbal, I. P-340, P-342
Ben Jilani, S. P-350, P-360, P-655
Ben Jilanibaltagi, S. P-368
Ben Moualli, S. P-360, P-877
Ben Romdhane, K. P-325, P-419, P-647, P-659, P-68, P-795, P-834
Benadra, F. P-441, P-630, P-820, P-957, P-981
Benahmed, M. P-689
Bendardaf, R. P-175
Benediktsson, H. O-15
Benes, V. P-988
Benhattar, J. O-159, O-205, O-206
Benites Filho P.R. P-992
Benitez, M.d.C. P-457
Benito, R. P-968
Benizri, E. P-39
Benoît, G. O-178
Bensalah, K. O-195, P-852
Bensussan, A. O-136
Bentata, Y. P-459
Benvenga, S. P-592
Benyó, G. P-552
Berardengo, E. O-261
Berber, U. P-411, P-965
Berczi, L. P-891
Berger, F. O-62
Berger, N. O-130, P-685
Bergero, N. O-167, O-180
Bergeron, C. P-771
Bergh, A. P-668
Beris, A. P-991
Berisavac, I. P-978
Berna, S. O-33, P-283
Bernardi, A. O-261
Berndt, A. O-10
Berner, A. O-192

Berra, E. P-39
Bertagna, X. O-163
Bertheau, P. O-257, O-260
Bertherat, J. O-163
Berthold, F. O-66
Berto, F. P-326
Bertocchi, C. P-920
Bértolo, C. P-425
Bertrand, G. O-206
Bertrand, J.-C. P-331, P-336
Betka, J. P-566
Betova, T. P-171
Betta, P.-G. O-124
Bettaieb, I. P-325
Betts, C.M. P-162
Beubler, E. P-198
Beuzeboc, P. O-205
Bevilacqua, G. P-44, P-436
Beylot-Barry, M. O-134, O-135
Bhagani, S. P-943
Bhagat, G. O-54, P-128
Bialas, B. P-975
Biancalani, M. P-556
Bianchi, C. P-262
Bianchi, F. P-996
Bianchi, L. P-531
Bianchi, T. P-262
Bianchi, V. O-161
Bibeau, F. O-145, O-30, P-8, P-173, P-407
Bickels, J. P-652
Biczysko, W. P-740
Bièche, I. O-177, O-178
Bielsa, O. P-866, P-867, P-868
Bienvenu, L. P-685
Bierzynska-Macyszyn, G. P-906, P-962, P-974, P-975
Bighetti, S. P-424
Bilalovic, N. P-38
Bilde, A. O-3
Bilge, O. O-162
Bilgic, B. P-821
Bilic, E. P-880
Bioulac-Sage, P. O-41, O-42, O-47, O-70, O-114, O-179, P-134, P-218, P-538, P-547
Bir, F. P-297, P-405, P-558
Birbe, R. O-74
Birembaut, P. O-154, O-170
Birg, F. O-55
Birnbaum, D. O-55
Birtolo, C. P-33
Bisceglia, M. P-845
Bisdorff, A. P-660
Biserte, J. P-856
Bismar, T.A. O-26
Bissery, A. P-969
Bitker, M.O. O-84
Blaas, L. O-152, P-136, P-195, P-412
Blaich, S. O-25
Blamek, S. P-975
Blanc, J.-F. O-47
Blanes, A. O-165, P-373
Blaschke, S. O-21
Blaukovitsch, M. O-121
Blazicevic, V. P-146
Blechet, C. O-119
Bleggi-Torres, L.F. P-992
Bloch, B. O-179, P-134
Blokhin, N.N. P-596
Blons, H. O-120
Blot, E. O-214
Bø, T.H. P-691
Bobos, M. P-116, P-216, P-617
Boccon-Gibod, L. O-198
Bockaert, J. O-250
Böcker, W. O-208
Bocsi, J. P-328
Bode-Lesniewska, B. P-662
Bodlovic, K. P-338, P-339
Bodó, K. P-658, P-799
Bodó, M. P-832
Boëlle, P.-Y. O-34
Boerner, S. P-278
Boerrigter, L. P-513
Bogdanovic, A. O-37, P-86
Bogdanovic, R. P-849
Bögi, K. P-887
Bogoeva, B. P-622
Bogos, K. P-258
Bogris, P. P-761
Böhm, J. O-2
Bohm, J. P-477
Boileau, C. O-35
Boissiere, F. P-8, P-173
Boissin, H. P-525
Bojovic, S. P-392
Bojovic, V. P-978
Bokeria, L. O-248, P-711
Boldrini, R. O-246
Boletis, J. P-217
Bollito, E. O-180, P-382
Bollschweiler, E. O-75
Boluda, S. P-129
Bombí, J.-A. P-528, P-741
Bombonati, A. O-74
Bombonatti, F. P-69
Bonetti, F. O-199, P-268, P-275, P-357, P-400, P-401
Bongain, A. P-39
Bonikos, D.S. P-96
Bonitsis, N. P-926
Bonnetain, F. P-409
Bonte, E. O-82, P-670
Bordea, C. P-786
Borg, A. P-35
Borge, B. P-759
Boricic, I. P-307
Borisov, K. O-248, P-711
Borka, K. P-515
Borrelly, C. P-8
Borrini, F. O-145
Borza, C. P-731
Bosch, X. P-744
Boskovic, D. P-86
Bosman, F. P-885
Bosnar, A. P-934
Bossard, C. O-62
Bosset, J.F. P-312
Bossi, P. O-116
Bostad Leif, H. O-20
Boštjan, J.K. P-305
Boštjan, L. P-305
Bot, F.J. O-169
Botelho, T. O-29
Botella, M.L. P-871
Botina, A.V. P-200
Botling, J. P-894
Botto, H. O-177, P-365
Bouabdallah, K. O-63
Bouabdallah, R. O-55
Bouaziz, Y. P-423
Bouchal, J. P-408, P-677
Bouche, O. O-38
Boucher, E. P-685
Bouchet, P.-E. O-59
Boudawara Sellami, T. P-100, P-393, P-402, P-423, P-554, P-800, P-874, P-955
Boudjema, K. P-549
Bouhajeb, Y. P-980
Bouillot-Eimer, S. P-664
Bourantas, K. P-121
Bourgau, C. P-77
Bourli, A. P-879
Bourne, A. O-219
Bousoulegas, A. P-67, P-75
Bouvier, R. P-838
Bouziani, A. P-419
Bouzid-Bendisari, K. O-133
Boveri, E. P-114
Boyault, S. P-538
Bozbora, A. P-383
Bozdað, G. P-811
Bozkaya, H. P-226
Bozkurt, S. P-46, P-53, P-54
Brachkova, Y. P-304, P-306
Bracko, M. O-258, P-831
Braga, C.E.N. P-87
Braham, E. P-484, P-485
Brajuskovic, G. O-37, P-130, P-204, P-585
Bralet, M. O-30
Bralet, M.-P. P-173
Bramis, J. P-160, P-186
Branca, M. P-749
Brandão, L.F. P-69
Branquet, D. P-122
Branscheid, D. P-900
Brasanac, D. P-449, P-698, P-849
Brasch, F. O-67
Brasnu, D. O-8, O-171
Brasoveanu, L. P-855
Brcic, L. P-643
Brenner, B. P-925
Brest, P. O-148
Breviere, G.-M. O-155
Briasoulis, E. P-201, P-45, P-793
Brière, J. O-62
Briese, J. P-772
Briones, I. P-755
Brisse, H. O-242
Brito, M. P-316
Brito, M.-J. P-589
Britsou, M. P-7
Brocheriou, I. O-16, O-245
Broet, P. O-64
Broto, R. P-492
Brouquet, A. O-35
Brousse, N. O-98, P-81
Brousset, P. P-225, P-455, P-456
Brugières, L. O-71
Bruguera, M. O-43, P-546
Bruix, J. P-531
Brullet, E. P-154
Brunelli, M. O-199
Bruneval, P. O-8, O-171, O-244
Brunner, A. P-370
Brünner, N. P-899
Brychta, T. P-933
Brychtova, S. P-933, P-964
Budka, H. O-255
Buendia, M.A. O-71
Büge, O. P-994
Bui Nguyen, B.M. O-156
Bulak, J. P-672
Bulanov, D. O-147
Bulata, R. P-250
Bulbul Dogusoy, G. P-504, P-516, P-527
Bulimbasic, S. P-322
Bullerdiek, J. P-900
Bumber, Z. O-4
Bumm, K. P-559
Buob, D. O-126, P-822
Bureau, C. P-225
Bürger, H. O-208
Buriæ, N. P-359
Burkadze, G. P-408
Burke, A. P-726
Burmester, G.R. O-144
Burmistrov, M. P-282
Burnley, H. P-727
Bussolati, G. O-167
Bussone, R. O-261
Butcher, D. P-253
Butcovan, D. P-133, P-731
Butori, C. O-131, P-501
Butrón, M. P-187
Butruk, E. O-78
Buttyan, R. O-86
Butur, G. P-50, P-219, P-314, P-534, P-573, P-763, P-824
Butureanu, S. P-801
Buyukpinarbasili, N. P-930
Býcakcý, U. P-79
Býlge, Ü. P-767

Caballero, M.C. P-33
Caballero-Mendoza, E. P-492
Cabaret, V. P-409
Cai, T. P-372
Caillou, B. O-130
Cairo, S. O-71
Cajal, S.R.Y. P-492
Çakalaðaoðlu, F. P-458
Cakar, M. P-289
Cakir, C. P-263
Calabrese, F. O-90, P-454, P-541
Calabuig-Fariñas, S. P-396
Calero, F. P-51
Caligo, M.A. P-44
Calin, D.L. P-688, P-720
Callaghan, R. P-968
Callard, P. O-181, O-204
Callea, F. O-246
Callol, L. P-502
Caly, M. O-212
Camarasa, N. P-66, P-931
Cameselle-Teijeiro, J. P-64, P-588, P-591, P-597
Camilleri-Broet, S. O-64
Campani, D. O-232, P-30
Camparo, P. O-198, O-204, P-122, P-693, P-706
Campo, E. P-120, P-374, P-760, P-813
Campr, V. P-112, P-113
Canavese, G. O-261

Cancer Ersev, A. P-479
Candan, Y. P-873
Candanedo-Gonzalez, F.A. O-127, P-623
Candea, V. P-712
Candelaresi, G. O-261
Cândido dos Reis, F.J. P-424, P-770
Cangro, C. O-96
Canioni, D. O-98, P-81
Canis, M. O-235
Cantu de Leon, D.F. P-764
Cantürk, N.Z. P-621
Cantürk, Z. P-621
Capdepont, M. O-31
Capeau, J. O-39
Capela, J. O-29
Capella, C. O-161, P-36, P-521, P-627
Capelli, P. P-275
Capizzello, A. P-201
Capodanno, A. P-44
Capote, L.F. P-66
Capovilla, M. O-154
Cappia, S. O-166, P-382
Capron, F. O-16, O-84, O-178, O-245, P-202, P-241, P-331, P-336, P-586, P-604, P-679, P-969
Caramés, N. P-682
Carda, C. P-823
Cardesa, A. O-14
Cardillo, A. P-270
Carerre, N. O-63
Carles, D. O-42
Carnaille, B. O-126
Carnevali, I. P-627
Carnot, F. O-171
Carraro, U. P-468
Carrasco, H. P-733
Carrère, N. O-65
Carrillo, R. P-929, P-931
Carteyron, M. O-179
Cartier, I. P-757
Caruntu, I.-D. P-467
Caruso, G. P-151
Carvalho, I. P-34
Carvalho, L. P-69, P-70
Carvalho, S. O-213
Casadio, C. P-270
Casalots, A. O-129, P-154, P-266, P-510
Casals, G. P-813
Casas, F.L. P-924
Casiraghi, O. O-62
Casnedi, S. P-36
Cassandro, G. P-21
Castagna, M. P-996
Castagnini, M. P-745
Castaing, D. O-114
Castello, A. P-114
Castéra, L. O-70
Castiglione, F. O-106
Castillo, M. P-374, P-376
Castro, P. P-608
Catalano, E. P-776
Catalina, P. P-148
Catherine, L. P-235
Çaþkurlu, T. P-862
Cattani, M.G. P-13
Cattoretti, G. P-128
Catu, R. P-433
Caulet-Maugendre, S. P-494
Cavalcanti, V. P-351
Cavard, C. O-163
Caverivière, P. O-130
Cayre, A. O-30
Cazals-Hatem, D. O-115, P-234, P-343
Ceausu, I. P-802
Ceausu, M. P-50, P-219, P-314, P-534, P-534, P-573, P-763, P-802, P-824
Cecchetti, D. P-436
Cegielski, M. P-468
Cekin, N. P-97
Celikel Cigdem, A. P-221, P-284
Celikel, C. P-287, P-288, P-296
Celikel, C. A. P-180
Celkan, T. P-79, P-830
Cemerikic-Martinovic, V. P-86
Cerbulo-Vazquez, A. P-623
Cerda-Nicolas, M. P-968
Cerf-Bensussan, N. O-98
Cermik, H. P-411
Cermýk, H. P-965
Cerovic, S. O-37, P-130, P-585
Cerrina, J. P-709
Cerutti, R. P-627
Cervera, P. O-39
Cesar Peres, L. P-804
Çetinarslan, B. P-621
Çetinkaya, H. P-226
Ceva-Grimaldi, G. O-116, P-559
Cevýkbas, U. P-523
Chae, Seoung Wan P-789, P-790
Chalabreysse, L. P-498
Chalbos, D. P-407
Chamilos, E. P-681
Champy, O. P-29
Chandra, A. O-207
Chang, D. P-237
Chang, Hui-Mei P-120
Chang, Wen-Liang P-952
Chanona Vilchis, J.G. P-764
Chapelin, D. O-257
Chaponnier, C. O-42
Charalabopoulos, K. P-612
Charalampidis, C. P-194
Charchanti, A. P-375
Charfi, L. P-29
Charlotte, F. O-39, P-331
Charny, A. P-246
Chartier-Kasteler, E. P-679
Chase, D. P-727
Chassevent, A. P-48
Chateau, M.-C. P-8
Chays, A. O-170
Cheddadi, F. P-428
Chefani, A. P-280
Chelbi, E. P-323, P-350, P-360, P-655, P-846, P-877, P-937
Chen, Ching-Mei P-569
Chen, Min-Wei O-86
Chenard, Marie, P. P-294
Cheng, Jiin-Tsuey P-569
Cherradi, N. P-459
Cheva, A. P-966
Chevé, M.T. P-451
Cheville, J.C. O-175
Chevret, E. O-134
Chevret, L. O-67
Chi, Je Geun P-439
Chiariello, L. O-225
Chibaudel, B. P-139
Chiche, L. O-114
Chien, Chih-Yen P-569
Chien, H.P. P-773
Chilosi, M. O-58, O-199, P-111
Chinnaiyan Arul, M. O-26
Chiriva-Internati, M. O-116, P-559
Chlopek, J. P-905
Chmielik, E. P-74, P-163, P-609
Chneker, L. O-212
Cho, Chi-Yi P-120
Cho, Eun Yoon P-789, P-790
Choe, G. P-439, P-600
Choi, Chan P-269
Choi, Ho-Sun P-758, P-782
Choi, Jin P-782
Choi, Kyung Un P-814
Choi, Yoo-Duk P-269, P-758
Choi, Yoonla P-790
Chomarat, P. P-17
Chopin, D. O-81, O-82, O-86, P-670
Chorti, M. P-476
Chortis, M. P-475
Choudat, L. O-255
Christiansen, M. P-370
Christodoulou, D.K. P-201
Christoforidou, V. P-67
Christova, S. P-687
Chrysomali, E. P-341
Chtourou, I. P-554, P-874, P-955
Chu, A.P. O-35
Chu, Po-Hsien P-483, P-938, P-956
Chuang, Shih-Sung P-120
Chuang, W.Y. P-773
Chudacek, Z. P-249
Chung, Jin Haeng P-439, P-600
Ciampi, L. P-18
Ciðdem, Özkara P-994
Cieply, K. O-240
Cieslik, T. P-905
Cieslik-Bielecka, A. P-905
Cigerciogullarý, E. P-504
Cigudosa, J.C. P-404
Cimmino, A. P-21
Cingil, H. P-946, P-948
Cintra, M.L. O-100
Ciobanu, A. P-720
Ciobanu, D. P-133
Cirilo-Cassaigne, I. P-757
Citu, R. P-430
Ciubotaru, V. P-628
Ciucci, A. O-225
Claessen, S.M.H. O-160, O-164, O-169
Clarence-Ko, C.H. P-567
Clavel, C. O-170
Clerici, T. P-920
Clot, P. O-260
Cocchi, R. O-11, P-346
Cocco, M. P-132, P-745
Codorean, E. P-628
Coer, A. O-239
Coindre, J.-M. O-156, O-159, P-664
Coissard, C. O-170
Colita, A. P-127
Colita, D. P-127
Collan, Y. P-175
Collecchi, P. P-44
Collett, K. P-928
Colnot, N. O-111
Colombari, R. O-199
Colombat, M. P-247
Colombat, P. O-64
Colomer, D. P-120
Colomo, L. P-528
Colpaert, C. P-420
Comanescu, V. P-20
Combalia, N. O-129, P-266, P-744
Compérat, E. O-84, O-178, P-586, P-679, P-693, P-842
Concheiro, L. P-624, P-917, P-918
Condom, E. P-869
Conio, M. P-281
Conneely, M. P-947
Constantin, A.S. P-280
Constantin, C. P-855
Constantin, L. P-314
Conti, S. P-556
Contremoulins, V. P-893
Copaescu, C. P-786
Copie-Bergman, C. P-101
Coppola, S. P-707
Coracin, F.L. O-100
Corazza, G.R. P-505
Cordier, J.-F. P-498
Cordier, M.P. P-838
Cordoba, A. P-33
Córdoba, A. P-425
Coric, M. O-4
Cornelisse, C. O-233
Cornic, M. O-214
Coros, F. P-807
Corrêa, M.E.P. O-100
Corrêa, Z.M. O-222
Correa-Giannella, M.L. P-213
Cosic Micev, M. P-102, P-307
Cosinski Marana, H.R. P-418, P-424
Cosnes, J. O-36
Cossu Rocca, P. O-199
Costa, S. P-28
Costache, M. P-786, P-936
Costarelli, L. O-210, O-211, P-4, P-5
Costes, V. P-94, P-555
Côte, J.-F. O-120
Cotutiu, C. P-71, P-150, P-276, P-801
Coubes, P. O-250
Couce Matovelle, M.E. O-240
Couchie, D. O-45
Coudert, B. P-409
Coulet, F. O-35

Courtin, P. O-130
Couturier, J. O-198, O-242, P-336
Couvelard, A. O-111, P-101, P-517
Cozma, L.G. P-683, P-684
Cranshaw, I. O-126
Creput, C. O-97
Crespel, A. O-250
Creus, M. P-813
Cribier, B. O-137
Criniere, E. O-64
Croue, A. P-642, P-922
Cruceru, L. P-628
Csala, J. P-379
Csekeõ, A. P-499
Csendes, G. P-890
Cuatrecasas, M. P-190
Cubukluöz, F. P-695
Cuburu, N. P-326
Cucherousset, J. O-154
Cuevas Gonzalez, J. O-118
Cuezva, J.M. P-931
Cui, C. P-993, P-998
Cui, X. O-32
Cuilliere-Dartigues, P. P-101
Cukrowska, B. P-710
Cullen, K. P-30
Culubret, M. P-744
Cunha, I.W. P-827
Cupic, H. P-703
Curea, M. P-250
Cutz, J.-.C. O-85
Cuvelier, C. O-77
Cuzin, L. P-215
Cvetkovic-Dozic, D. P-125, P-959, P-978, P-995
Cvetkovski, P. P-622
Cwikla, M. O-78
Czarniecka, A. P-609
Czarnowska, E. P-427, P-710, P-719
Czerkinsky, C. P-326
Czernobilsky, B. P-771, P-780
Czyzewska, J. P-176, P-178

D'Armiento, M. O-52
da Costa Gayotto, L.C. P-537
Da Cunha Santos, G. P-825
Dahi, F. P-802
Dahse, R. O-10, P-636
Dainese, E. P-36
D'Alessandro, D. P-996
Dalfior, D. P-268, P-275, P-357, P-400, P-401
Dalton, L. P-674
Daltro, B. P-69
Damber, J.-E. P-668
Damotte, D. O-98
Danciu, M. P-133, P-185
Danel, C. O-120, P-247
Daniel-Le Bozec, C. P-896
Danilova, T. P-675
D'Anjou, J. P-757
Danjoux, M. P-215
Dannenberg, H. O-164
Danzon, A. P-312
Dargère, D. O-178
Darreye, G. P-707
Darriet, M. O-70
Dartevelle, P. P-709
Daszkiewicz, P. P-960
Datta, K. O-24
Datz, C. O-152, P-195
Dauge, M.-C. O-255
Dauplat, J. O-235
Dauplat, M.-M. O-209
Dautheribes, M. P-664
Davidson, B. O-192, O-234
Davila, S. P-643
De Armas, R. P-308
De Bock, F. O-250
De Carvalho, R.B. O-94
De Crémoux, P. O-168, O-256
De Falco, G. P-132, P-745
De Feraudy, S. O-138
De Fromont, M. O-193, P-685
De Hertogh, G. O-153
De Jong, D. O-9
De Jong, S. P-255
De Krijger, R.R. O-160, O-164, P-626
De la M. Hall, P. P-161, P-169
De la Taille, A. O-81, O-82, O-86, P-670
De Lajarte-Thirouard, A.-S. P-549
De Lédinghen, V. O-70
De Mascarel, A. O-63, O-65
De Medeiros, C.R. P-992
De Micco, C. O-130
De Oliveira, L.R. P-562
De Pinieux, G. O-156
De Pinieux, I. O-109
De Pinieux, I. O-200, O-93, P-93, P-520, P-842
De Pompa, R. P-382
De Quillacq, A. O-125
De Roquancourt, A. O-260
De Rosa, G. O-236
De Saint Aubain Somerhausen, N. P-816
De Saintmaur, P.P. O-154
De Sanjose, S. P-744
De Souza, C.A. O-100
De Stefano, N. O-52, P-746
De The, H. O-257
De Torres, I. P-190, P-492
De Winter, R. O-223
De Wolf-Peeters, C. P-131
De, Vries, E.G.E. P-255
Deau, B. P-81
Deavers, M.T. P-784
Debiec-Rychter, M. O-158
Debinska-Szymanska, T. P-710
Debré, B. O-177
Decaussin-Petrucci, M. P-689
Decha, A. P-898
Decker, T. O-208
Decremoux, P. P-885
Dehghani, F. P-452, P-453, P-514, P-625
Dekaniæ, A. P-934
Del Carmen Martín Guijarro, M. P-404
Del Moral Raimundo, M.G P-457
Delabie, J. P-138, P-759
Delarue, R. P-81
Delatour, M. O-209
Delaval, P. P-494
Delcourt, A. O-84, P-679
Deleeuw, R.J. O-164
Delektorskaya, V.V. P-177
Delfour, C. P-8
Delgado-Gonzáles, V. P-924
Delhove, O. P-816
Deligdisch, L. O-237, P-788
Delisle, M.-B. O-83
Dell'Osso, A. O-210, O-211, P-5
Delladetsima, I. P-203, P-217
Delladetsima, J. P-377
Dellamonica, P. P-911
Delomez, J. P-856
Delwail, V. O-64
Demello, D. O-89
Demetter, P. O-77
Demichelis, F. O-26
Deminiere, C. O-179
Demir, Dilek P-839
Demirkan, N. P-174, P-297, P-405, P-558
Demirkesen, C. P-651, P-930, P-945
Demiryont, M. P-821, P-839
Demonakou, M. P-317, P-654
Denis, E. P-838
Denk, H. O-104, P-799
Denkert, C. P-768
Denoux, Y. P-693
Deraedt, K. O-76
Derakhshan, M.H. P-229
Deray, G. O-16
Derchain, S.M.F. P-749
D'Eredita', G. P-18
Derekoy, S. P-580
Derin, D. P-11, P-65
Derizhanova, I. O-186, P-778, P-859
Deroide, F. P-943
Dervisoglu, S. P-356, P-651, P-826, P-830
Desangles, F. P-122
Desmoulière, A. O-42
Deutsch, A. P-103
Devez, F. O-59
Devilard, E. O-55
Devito, R. O-246
Devocelle, A O-149
Devonec, M. P-689
Devos, P. O-126
Dezfulian, R. P-453
Dhouib, R. P-325, P-419, P-68
Di Benedetto, M. O-236
Di Cristofano, C. P-44
Di Martino, D. P-888
Di Matteo, C. P-308
Di Napoli, A. O-128
Diakomanolis, E. O-102
Diamantopoulou, K. P-371
Diaz-Cano, S.J. O-165, P-373
Diebold, J. O-59
Diebold, M.D. O-38, O-170
Dienes, H.P. O-17, O-18, O-75, O-264, P-197
Dieras, V. O-212
Dietel, M. O-220, P-768, P-798, P-901
Dietmaier, W. P-662
Dietz, A. O-28
Dietze, O. O-152, P-136, P-195, P-412, P-751
Díez, A. P-168
Diez, M. P-165
Dijoud, F. P-498
Dilek, F.H. P-315
Dilek, H. P-580
Dimet, S. P-707
Dimitrakopoulos, J. P-344
Dimitrijevic, J. P-204
Dimitrios, S. P-47, P-564
Dimitropoulou, D. P-207
Dimolea, E. P-810
Dimou, S. P-375
Dimov, D. P-694, P-923
Dinares, C. P-510
Dinarés, M.C. O-129, P-154, P-266
Dinjens, W.N.M. O-164, P-626
Dinu, C. P-353, P-586
Dioguardi, N. O-116, P-559
Diomedi Camassei, F. O-246
Dirican, A. P-179
Dirks, W. O-60
Dirnhofer, S. P-77
Dizdaroglu, F. O-162
Djanic, D. O-4
Djenouni, A. P-653
Djilani, H. P-485, P-486
Djokic, M. P-204
Djordjeviæ, G. P-137
Djordjevic, B. O-189, P-435, P-694
Djurdjevic, N. P-392
Djuricic, S. P-449, P-849
Dmitrovic, B. P-146
Dobai, J. P-961
Dobias, M. P-847
Dobrea, C. P-127, P-573, P-763, P-824, P-881
Dobrescu, G. P-276, P-467
Doganavsargil, B. P-297
Doglioni, C. O-58
Dogusoy, G. P-179
Dojcinov, S. P-102
Dokov, V. P-997
Dokov, W. P-997
Dolenc-Strazar, Z. P-725
Dolinska-Krajewska, B. P-468, P-798
Dolores, B. P-422
Domagala, W. O-7
Dominguez Malagon, H.R. P-764
Dominici, R. O-52
Dominique, G. P-498
Domján, G. P-330
Dondero, F. O-115
Dong, J. O-237
Dordevic, G. P-865
Dotor de Lama, A.M. P-187
Dotor, A. O-262
Doublet, J.-D. O-181
Doucet, L. P-699
Doudnikoff, E. P-134
Douik, M. P-647
Doumbe, P. P-444
Dozic, B. P-338, P-339, P-959

Dozic, M. P-339
Dozic, S. P-959, P-995
Drabik, G. P-649
Drabik, G.Y. P-818
Drachenberg, C. O-96
Dragoi, G.S. P-148, P-149, P-471, P-645, P-783, P-921
Drak, A.K. O-93
Dralle, H. P-619
Dreher Irion, L.C. O-222, P-478
Dreux, N. P-699
Driemel, O. O-10
Drijkoningen, M. P-3
Driss, M. P-325, P-419, P-659, P-68, P-795, P-834
Drndareviæ, N. P-939
Drndarevic, N. P-244, P-481
Drömann, D. P-900
Drozd, A. P-906
Drozd, W. P-906
Druga, R. P-988
Drugacz, J. P-906
Drummond, Z. O-49
Dubin, J. P-578
Dubois, S. P-233
Dubon, E. P-414
Dubus, P. O-241, O-63, O-65
Ducruit, V. O-59
Dudu, C. P-479
Duganovska, S. P-734
Dulbecco, P. P-281
Dulmet, E. P-709
Dumitrache, F. P-801
Dumitrescu, M. P-250
Dumollard, J.M. P-598
Dumont, S. P-101
Dumpis, J. P-345
Dunant, A. P-17
Durana-Tonder, C. P-588
Durand, D. P-455, P-456
Durand, F. O-115, P-234, P-235
Durand, H. O-245
Durrbach, A. O-97
Dursun, A. P-309
Durzynska, M. P-170
Dusmet, M. P-253
Dusunceli, F. P-180
Duval, A. O-36
Duzcan Süleyman, E. P-405
Duzcan, E. P-174
Dýlek Osman, N. P-315
Dynybil, C. P-641
Dýzbay Sak, S. O-229, P-611
Dýzdaroglu, F. P-523
Dzieciol, J. P-92
Dziegiel, P. P-468
Dzikova, S. P-462

E-Abhar, H. P-236
Eber, M. P-603
Ebrahimi, M. P-915
Eccher, A. P-268, P-275, P-357, P-400, P-401
Economopoulos, T. P-126
Economou, M. P-85, P-201
Ectors, N. O-76
Efkarpidis, T. P-295
Efstratiou, I. P-438
Eftekhari, M.H. P-582
Egevad, L. P-271, P-676
Eghbalian, F. P-915, P-916
Ehrmann, J. P-208, P-964
Ehrmann, Jr., J. P-208
Eiber, M. O-175
Eimer, S. O-241
Eissa, S. P-388
Ekman, P. P-271, P-676
El Attar, H. P-630, P-820
El Bakouri, J. P-630
El Behairy, N. P-211
El Halfawy, K.A. P-535
El Hindawi, A. P-220
El Mezni, F. P-484, P-485, P-486
El Raziky, M. P-211, P-220, P-223, P-223
El Sherief, A. P-469
El, Batanouny, M.M.D. P-230
El, Behairy, N. P-220
El, Hindawi, A. P-211
Elattar, H. P-442, P-957, P-981
Elbakkouri, J. P-442, P-445
Eld, M. P-728
Elder, J. P-46, P-53
Elemenoglou, I. P-188, P-524
Elemenoglou, J. P-879
Elhafey, A. P-726
Elham, N. P-57
Elhan, A.H. O-229, P-97, P-98
El-Hasafy, M. P-535
El-Hindawy, A. P-366
Elias, S. P-72
Elie, N. P-893
Elif Pestereli, H. P-469
Eller, J. O-95
Ellouze, S. P-554, P-800
El-Mehelmy, E. P-736
El-Shaer, M.A. P-977
El-Shahat, N. P-366
El-Sharkawy, S.L. P-977
El-Shazli, E.M. P-736
El-Teraifi, H. P-594
Elzagheid, A. P-175
Emile, J. O-149
Emile, J.F. P-139
Enache, S.D. P-19, P-20
Endoh, M. P-700
Ene, A.M. P-936
Enguita, A.B. O-185, P-840
Enjolras, O. O-155, P-660
Ensari, A. P-309
Ensinger, C. P-370
Èojbašiæ, I. P-137
Eo-Jin, Kim, P-183
Èoklo, M. P-934
Eortc, G.I. P-899
Epstein, J.I. P-669
Eray, M. P-107
Erbarut, I. P-46, P-53, P-54, P-284, P-769
Erbarut, Ý. P-458
Erbil, Y. O-162
Erçin, C. P-621
Erdamar Cetin, S. P-504, P-516
Erdamar, S. P-179, P-527
Erdei, E. P-878
Erden, E. O-229, P-226, P-611
Erdoðan, þ. P-104
Erdogan, G. P-805
Erdogan, N. P-692
Eren, F. P-156, P-296, P-769
Ergun, D. O-229, P-611
Ergur, R. P-411
Ergýn, M. P-104
Eri, Z. P-495, P-565, P-583
Ernestus, K. O-66
Eržen, M. P-749
Erzin, Y. P-504
Escoda, M.R. O-129, P-154, P-266, P-510
Esgueva, R. P-129, P-701, P-866, P-867, P-868
Eshraghian, M.R. P-582
Eskandari, M. P-507
Esme, H. P-487
Espie, M. O-257, O-260
Espinoza, P. P-147, P-190
Essame Oyono, J.L. P-885
Essawy, M.M. P-230
Esslimani, M. P-403
Esslimani-Sahla, M. P-407
Esslimanisahla, M. P-8
Esterbauer, H. O-152, P-195, P-412
Estour, B. P-598
Etcharry, F. P-757
Etesam, F. O-221
Ettore, F. O-130, P-39
Evans, A.J. O-85
Evdokia, A. P-47
Evgenidis, N. P-203
Ezanee-Azlina, M.H P-567

Faa, G. O-153
Fabiani, B. P-101
Fabre, A. O-123
Fabre, M. O-71, O-93, O-114
Fachal, C. P-927
Facuri, F.O. P-615
Fahkrjou, A. P-474
Faivre-Bonhomme, L O-149
Fakhfakh, I. P-402, P-874
Fakhry, S. P-211, P-220
Falchetti, M. O-146
Falkowski, S. P-646
Fang, Xiaolei P-676
Fanourakis, G. P-613
Farah, F. P-360, P-368, P-846, P-877
Farah-Klibi, F. P-350, P-323, P-655, P-937
Farges, O. O-115, P-235
Farina, M. O-210, O-211, P-4, P-5
Farinotti, R O-149
Farkas, L. P-379
Farnedi, A. P-579
Fasli, H. P-274
Fatemeh, M. P-635
Fatemi, D. P-788
Faucon, H. O-86, P-670
Fazaa, B. P-937
Fazeli, M.S. P-1
Febbo, P.G. O-26
Fedorina, T.A. P-480
Fedorov, D.N. P-463
Feillel, V. O-209
Feinmesser, M. P-925
Feinmesser, R. P-925
Feit, J. O-132
Feldmann, G. P-234
Fend, F. P-123
Feng, K. P-542
Feng, N.H. P-301, P-737
Fenig, E. P-925
Fenwick, K. O-216
Feoli, F. O-117
Ferariu, D. P-133, P-185
Ferchichi, L. P-323, P-350, P-360, P-655, P-846, P-877, P-937
Fereshteh, E. P-884
Fergelot, P. P-852
Ferhat Çelik, A. P-504
Fericean, A. P-199
Ferjaoui, M. P-350
Ferlicot, S. O-97, O-178, O-198, P-707
Ferlosio, A. O-225, P-780
Ferluga, D. O-19
Fernandes, M.I. P-237
Fernandez Burguera, D. O-240
Fernández, C. P-667
Fernandez, P. O-203
Fernandez, S. O-129, P-154, P-265, P-510
Fernandez-Cruz, L. P-528
Fernandez-Esparrach, G. P-528
Ferran, M. P-492
Ferraz, A. P-568
Ferreira, A.P. P-615
Ferreira, M. P-43
Ferreira, S.S. P-87
Ferrell, L. P-214
Ferrer, J. P-823
Ferreres, J.C. P-147
Ferriere, J.-M. O-179
Feugeas, J.-P. O-257
Ffolkes, L. P-943
Ficsor, L. O-80, P-328, P-329
Fidan, F. P-487
Fidler, V. P-255
Fiedor, P. O-99
Fierabracci, P. O-232, P-30
Figaro Gattás, G.J. P-537
Figueiredo, P. P-399
Fijalkowski, M. P-975
Fikret, E. P-876
Filinte, D. P-621
Filipovski, V. P-734, P-833
Fillinger, J. P-238, P-499
Finokaliotis, N. P-654
Fiocca, R. P-281
Fiore, G. P-18
Fiore, M.G. O-173
Firat, P. P-753
Fitoussi, O. O-63
Fiuraskova, M. P-933, P-964
Flad, T. O-21
Flanagan, A. O-233
Flaris, N. P-875
Fleischmann, A. P-883
Flejou, J.-F. O-34, O-36, O-39, O-154, P-101, P-517, P-533, P-158
Fleuren, G.J. O-233
Fleury, C. O-125
Flodr, P. P-847
Flohr, A P-900

Florea, N. P-185
Florea-Gramada, Z. P-219, P-250, P-314, P-763, P-824
Florentin, I. P-810
Flusser, G. P-652
Fodor, D. P-886
Fokkema, E. P-255
Fondimare, A. P-685
Fong, L.Y.Y. P-912
Fontes, A. P-560, P-581
Fonti, G. P-355
Fónyad, L. P-891
Forns, X. O-43
Forteza, J. P-597
Fortunato, L. O-210, O-211, P-4, P-5
Foschini, M.P. O-11, P-162, P-333, P-346, P-579
Foster, H. P-784
Fotinou, M. P-248
Foucher, J. O-70
Fouda, P. P-885
Fouilhoux, G. O-209
Foulet, A. O-130
Foulet-Rogé, A. P-451
Fountzilas, G. P-879
Fouret, P. P-331, P-336
Fournier, G. P-699
Fournier, M. P-247
Fournier, M.-C. O-179
Fourquet, A. O-263
Fraile, B. P-55, P-56, P-666, P-667
Franc, B. O-35, O-130, P-920
Francalanci, P. O-246
Franceschini, B. O-116
Franceschini, G. P-559
Francesconi, A. P-780
Franchi, A. O-14, P-556
Francino, A. P-741
Francoz, C. O-115, P-234, P-235
Francu, L.L. P-720
Frank, G. P-675
Frank, G.A. P-367
Fransis, S. P-3
Franzi, F. P-521
Frassati-Biaggi, A. O-44
Fratzogloy, A. P-971
Freant, L.J. O-92
Frei, C. P-415
Fréneaux, P. O-168, O-215, O-242, O-256, O-263
Frezza, G.P. P-162
Fridman, W.H. O-8
Fries, J.W.U. O-17, O-18
Frigerio, S. P-135, P-378
Frincu, D.L. P-688
Frizzera, G.J. O-54
Frkoviæ-Grazio, S. P-9
Frkovic, G.S. O-258, P-831
Froment, N. O-130
Fromenty, B. P-233
Fromont, G. O-198
Fron, D. P-822
Frootan, K. P-384
Froufe, A. P-548, P-940
Fuenmayor, C.E. P-733
Führer, A. O-22
Fujarewicz, K. P-609
Fujimura, M. P-434
Fukui, H.Y. P-993, P-998
Fukushima, S. O-174
Fumey, G. O-163
Funel, N. P-436
Furák, J. P-259
Furlan, D. P-627
Furuse, C. P-351

G. Martos, M. P-66
G-Cosio, M. P-66
Gabbiani, G. P-780
Gabriela, P. P-305
Gadaj, P. P-960
Gaiba, A. P-346
Gaiger, A.M. O-222
Gajanin, R. P-495
Gajanin, V. P-495
Gakiopoulou, H. P-160, P-186, P-371, P-979
Galal, M.K. P-26
Galani, V. P-84
Galántai, I. P-552
Galbenu, M. P-783
Gale, N. O-5, O-14, P-571
Gãleeanu, M. P-881
Gallagher, G. O-159, O-205, O-206
Gallagher, P.J. P-727
Gallardo, F. P-129
Galle, J. P-500
Gallego, E. P-551
Galusca, B. P-598
Galvin, N. P-429
Gamboa-Domínguez, A. O-127, P-623
Gambotti, L. O-212
Ganne-Carrie, N. O-44
Garbini, F. O-106
Garcia del Moral, R. P-910
Garcia del Muro, X. P-869
Garcia, A. P-546
García, M. O-43, P-129, P-380, P-701, P-733, P-866, P-867, P-868
García, R. P-168
García-Cabezas, M.A. P-755
García-Fernández, E. P-437
García-González, M. P-597
García-Tuñon, I. P-55, P-56, P-666, P-667
Garcia-Valdecasas, J.-C. P-546
Gargin, V.V., P-718
Garipidou, V. P-105
Garoste, J.-C. O-65
Garrel, R. P-555
Garrido Ruiz, M. P-840
Garrido, M. O-43, O-185, P-528
Garuderburmester, A. P-768
Garza-Guajardo, R. P-279, P-908
Gaspa, A. O-203, P-374, P-376
Gasparri, G. O-167
Gastl, G. O-108
Gastrointestinal Study Group of Hellenic Society of Pathology P-317
Gaulard for the Gela, P. O-62
Gaulard, P. P-88
Gaumann, A. P-662
Gautier, C. O-215
Gavino, J. P-70
Gavrictanga, V. O-131
Gavric-Tanga, V. P-326
Gazibara, T. P-995
Gazouli, M. P-160
GCsior, M. P-721
Gebarowska, E. P-798
Gebhart, M. P-816
Geboes, K. O-76, O-153, P-131
Geddie, W. P-278
Gedik, N. P-892
Gedikoglu, G. P-289, P-309
Gedýkoðlu, G. P-657
Gehanno, P. P-353
Gelabert, A. P-701, P-866, P-867, P-868
Gelly-Marty, M. P-409
Genestie, C. P-969
Gengler, C. O-159, O-205, O-206
Georgescu, C. P-20
Georgescu, M. P-628
Georgiadou, E. P-24
Georgiu, A. P-572, P-886
Georgiu, C. P-572, P-886
Gerasimidou, D. P-509, P-617
Gerçeker, I. P-767
Gerdes, J. P-900
Germà-Lluch, J.R. P-869
German, D.C. P-987
Gerovassilis, F. P-199
Gersak, B. P-725
Geryk, J. P-904
Gerzelis, I. P-705
Gessain, A. P-444
Gesualdo, L. P-145
Geurts, T. O-9
Ghada, I. P-166
Ghaffari Novin, M. P-274, P-742
Ghaffarzadegan, K. P-172, P-229
Ghaini, M.H. P-290, P-384
Ghanad Kafi, S. P-172
Ghariani, M. P-100, P-393, P-423, P-800
Ghasemi, M. P-812
Ghavam Nadir, M. P-172
Gheghessi, F. P-653
Gheonea Dan, I. P-19
Gheorghita, V. P-150
Gherghiceanu, M. P-460, P-461
Ghevondyan, T. P-724
Ghibirsina, C.C. P-720
Ghikonti, I. P-681, P-705
Ghnassia, J.-P. P-603
Ghorbel, M. P-554
Giacometti, C. O-90, P-454, P-541
Gianginis, K. P-295
Giani, C. O-232, P-30
Giani, R. O-261
Giannella-Neto, D. P-213
Giannopoulou, I. P-417, P-421
Giardina, C. P-18, P-21
Giaslakiotis, C. P-377
Giaslakiotis, K. P-115, P-118
Giatromanolaki, A. P-194
Gicquel, C. O-163
Gierlotka, M. P-721
Gigi, E. P-216
Gigonti, I. P-317
Gil, S. O-149
Gil, Y.R. P-841
Gil-Benso, R. P-968
Gil-Diez-De-Medina, S. O-86
Giles, Y. O-162
Gillardin, J.-P. P-610
Gilusi, M. P-19
Giménez, G. P-266
Gimenez-Perez, G. O-129
Giordano, A. P-132, P-745
Giordano, M. P-4
Girardi Lucia, R. P-372
Girardi, L.R. O-146
Girre, V. O-256
Gist, Working Group O-150
Giuffrè, G. P-888
Giustarini, E. O-232, P-30
Givalos, N. P-371, P-979
Glavaè, D. O-5
Glogowska-Ligus, J. P-974
Glumac, S. O-226, P-449, P-714, P-715, P-729
Gluzman, D. P-108
Gnaiger, E. P-902
Gobbo, S. O-199
Gocener, S. P-527
Godard, C. P-538
Godlevskyi, D. P-870
Goere, D. P-550
Gogg-Kammerer, M. P-799
Gogos, C. P-207
Gökhan, G. P-963
Goksel, S. P-179, P-504, P-516, P-527
Gol, A. P-507
Gola, J. P-975
Golaszewska, J. P-42
Goldbohm, R.A. P-861
Goldmann, T. O-220, P-500, P-900
Goldstraw, P. P-253
Golitsyna, E.P. P-463
Golka, D. P-962
Golubicic, I. P-959
Goluboviæ, I. P-137
Golubovic, M. P-583
Gomba, S. P-511
Gombás, P. P-889
Gomes, A. P-316
Gomez-Morales, M. P-457
Gomez-Roman, J.J. O-118
Gomulkiewicz, A. P-468
Gong, Gyung-Yub P-269
Gontijo, R P-749
Gonzales, S. P-822
González-Obeso, E. P-272, P-437, P-489
Gonzalez-Palacios, J.F. P-66
González-Peramato, P. P-6, P-871, P-872
Goraj-Zajac, A. P-74
Gorantonakis, G. P-681, P-705
Gorbacheva, J.V. P-140
Gordillo, J. P-32
Gorissen Hanneke, J.M. O-197
Görür, S. P-873

Gosselin, B. P-856
Goudopoulou, A. P-371
Gouiaa, N. P-100, P-554, P-800, P-874
Goulet, O. O-98
Gourgou, S. P-173
Goussia, A. P-121, P-375, P-84, P-973
Goutas, N. P-25
Govedarevic, N. P-435
Govedarovic, V. P-698
Gradinac, S. O-226
Graf, A.-H. P-751
Grahovac, B. P-762, P-942
Grahovac, G. P-880
Grajkowska, W. P-710, P-719, P-960
Gramada Zenaida, F. P-534
Gramada, E. P-155, P-227, P-530, P-903
Grande, S. O-180
Granier, G. P-206
Grayson, W. P-748
Grcevska, L. P-462
Green, P. P-128
Grenier, P. O-84, P-679
Grepi, C. P-84
Gressens, P. O-255
Grgurevic, E. P-934
Griese, M. O-67
Grigoriou, M. P-509
Grimber, G. P-538
Grimelius, L. P-618
Grizzi, F. O-116, P-559
Grncharovska, Z. P-277
Grodecka, J. O-13
Grodet, A. P-234
Groen, H.J.M. P-255
Groisman, G.M. P-152
Groma, V. P-210, P-345
Grosber, M. O-138
Grosclaude, P. O-83
Gross, O. O-17
Grosser, M. O-220
Grosshans, E. O-137
Grosso, M. O-52
Groulet-Martinec, A. O-55
Groussard, O. P-247
Groussin, L. O-163
Grubb, J. P-429
Grubbs, C.J. P-912
Gruber-Mösenbacher, U. O-122, P-239
Gruel, Y. O-119
Gruetzkau, A. O-143
Gruffaz, F. P-336
Gryczynski, M. P-358, P-574
Gryko, M. P-176, P-178
Guanaes, J. P-214
Gude, A. O-240
Gudkova, A. O-248, P-711, P-713
Guenther, R. O-143
Guercio, S. O-180
Guerrero, D. P-33, P-425
Guerrieri, A. P-21
Guettier, C. O-97, O-114
Guevara, N. O-131
Guigay, J. P-257, P-472
Guillé, F. O-195, P-669, P-852
Guillemet, C. O-214
Guillot, S. P-494
Guillou, L. O-156, O-159, O-200, O-205, O-206
Guillou, P.-J. O-38, O-170
Guimarães Tiezzi, D. P-424
Guimarães Tiezzi, M. P-418
Guimarães, A.P.G. P-827
Guimarães, G.C. P-827
Guimarães, T., D. P-418
Guinebretiere, J.M. P-29
Guix, C. P-813
Güldal, Y. P-540
Gülen, A. P-540
Guler, G. P-912
Gulluoglu Mine, G. P-252, P-263, P-523
Gulluoglu, B. P-46, P-53, P-54, P-180, P-296
Gulluoglu, M.G. O-162, P-848
Gültekýn, M. P-791, P-811
Gümüþ, E. P-862
Guney, N. P-11
Gungen, Y. P-309
Gunhan, O. P-309
Gürbüz, Y. P-293, P-543, P-621
Gurel, B. P-289, P-309
Gürer Ýnanç, E. P-963
Gursan, M.S. P-298, P-522
Gursan, N P-522
Gursan, N. P-298
Gürsoy, S. P-318
Gusev, A. P-859
Gutierrez, C.M. O-53
Guyétant, S. O-119, O-130
Guziñska-Ustymowicz, K. P-14, P-176, P-178
Gvozden, R.L. P-327
Gwak, G.-Y. P-545
Gyorffy, H. O-73

H\Akamazuka, Jun-Ichi P-779
Haas, C.J. P-695
Hacke, E.M. O-251
Hadjigeorgi, C. P-443
Hadjileontis, C. P-91, P-199
Hadravska, S. P-249
Hadzi-Djokic, J. P-698
Hadzi-Nicheva, B. P-277, P-765
Haesevoets, A. O-169
Hafiza, A P-567
Hafkamp, H.C. O-169
Hagen, J. O-175
Haghazali, S. P-229
Hagnere, A.-M. O-163
Haholu, A. P-411, P-965
Hajduch, M. P-677
Hájková, P. O-227
Halalau, F. P-802, P-824
Halász, J. P-552
Halbwedl, I. O-121
Halil, A.K. P-994
Hallam, L. P-829
Haller, A. O-117
Halpern, M. P-925
Haltiti, R. P-485
Halvorsen, O.J. P-691, P-928
Hamel, N. P-241
Hamelin, R. O-34, O-36
Hamid, R. P-629
Hamilton, J. O-207
Hamm, B. P-768
Hammam, O. P-211, P-212, P-220, P-390
Hammel, P. O-111
Hammes, L. P-749
Hamzaoglu, I. P-504
Han, Bo P-73
Han, Shuang-Yin P-912
Han, Ü. O-61
Handan, K. P-850
Handra-Luca, A. O-44, P-336
Hanisch, F.-G. O-264
Hannachi, S.S. P-68, P-647
Hans, S. O-8
Hanslik, T. P-139
Haouet, S. P-340, P-342
Harach, R. O-29
Harada, H. P-243, P-482, P-819
Hardisson, D. O-262, P-6, P-51, P-404, P-787
Hardisson, D.A. P-755
Harhalakis, N. P-126
Hariri, A. P-395
Harisfazal, M.B. P-567
Harn, Horng-Jyh P-952
Harrison, S.M. P-159
Hart, A. O-9
Hart, A.A.M. P-513
Hartan, A. P-467
Hartmann, A. O-175, P-478
Hasakioilis, P. P-369, P-854
Hasegawa, T. O-141
Hassan, M. P-766
Hassan, Nabila S. P-977
Hatakeyama, K. O-32
Hatsue, I.-U. P-732
Hatzakis, A. P-217
Hatzianastassiou, D. P-377
Hatzikalias, A. P-875
Haukaas Svein, A. P-691, P-928
Haus, R. P-693
Hauser-Kronberger, C. O-152, P-136, P-195, P-412, P-751
Hauw, J.J. P-969
Havelka, M. P-267, P-583
Haverich, A. O-67
Havet, K. O-131
Hawranek, M. P-721
Hayakawa, S. P-779
Hayashi, K. O-218
Hayran, M. O-61
Hazes, T. O-227
He, Le O-26
Hebuterne, X. O-79, O-148
Heffron, C.C.B.B. O-190
Hege, S. P-261
Hegedûs, Á. P-273
Heinke, T. P-72
Heish, Pin-Pen P-120
Heiss, S. P-370
Heitz, P.U. O-112, P-619
Helin, H. P-292
Hemar, P. P-679
Hemet, J. P-896
Hemmings, C. P-319, P-829
Henin, D. O-184, O-255, P-353, P-896, P-897
Herlea, V. P-311, P-525
Herlin, P. P-893
Hermine, O. P-81
Hernández, G. P-51
Hernández, L. P-51, P-404
Hernandez, S. P-502, P-701, P-867, P-868
Hernandez-Cortes, G. P-787
Hernández-Rodríguez, N. P-414
Hero, B. O-66
Herson, S. P-247
Herva, R. P-426
Hervé, J.M. P-365
Hessler, R. O-92
Heudes, D. O-171
Hibner, U. P-206
Hibshoosh, H. O-202
Hidar, S. P-143, P-144
Hideki, K. P-347
Hierro, I. P-551
Higuchi, M.L. P-733
Hillemann, D. P-500
Hilská, I. P-110, P-828
Himmetoglu, C. P-289, P-309
Hinder, F. O-224
Hinescu, M. P-628
Hinterleitner, T.A. P-198
Hiradfar, M. P-432
Hirai, N. P-819
Hirano, S. O-32
Hirohashi, S. P-612
Hiroko, A. P-347
Hirose, T. P-819
Hiroyuki, Hao P-732
Hirsch, H. O-96
Hirvikoski, P. P-426
Hiz, M. P-826
Hlobilkova, A. P-933, P-964
Hlupic, L. O-27
Hmissa, S. P-143, P-144, P-349
Hoang, C. P-202, P-586, P-604
Hoang-Xuan, Khe O-64
Hocevar, A. P-837
Hoefler, G. O-60, P-708
Hoegenauer, C. P-198
Hofer, M.D. O-26
Hofland, L.J. O-160
Hofler, G. O-176
Hofman, P. O-131, O-148, O-79, P-326, P-501, P-911
Hofman, V. O-79, O-131, O-148, P-501, P-911
Hofstädter, F. O-175, P-662
Hogendoorn Pancras, C.W. O-158
Holczbauer, A. O-73, P-552, P-544
Holm, H. P-161, P-169
Hölscher, A.H. O-75
Homayon, M. P-914
Homsi, T. O-93, O-109, O-200, P-93, P-520
Honma, K. O-87
Honsova, E. P-231, P-465
Hood, L. P-691
Hopman, A.H.N. O-169
Horeanga, I. P-525
Horianopoulos, N. P-83
Horn, L.C. P-58

Hornychová, H. P-337
Hortopan, M. P-311
Hosseinipanah, S.M. P-915
Hostein, I. O-156
Hotnog, D. P-855
Hou, Serey Vannak P-398
Houman, M.H. P-340, P-342
Housset, C. O-39
Hoznek, A. O-82, P-670
Hruska, A. P-832
Hrvacevic, R. P-585
Hrzenjak, A. O-104, P-799
Hsi, Sheng-Chuan P-49
Hsueh, C.W. P-301, P-737
Hsueh, S. P-773, P-775
Huang, Chao-Cheng P-569
Huang, Hsuan-Ying P-321, P-648
Huang, Shih-Hung P-120
Huang, Wan-Ting P-120
Huang, Wei O-81
Huang, Wen-Wei P-321
Huber, M. O-254
Hudita, D. P-802
Huebner, K. P-912
Hughes, C. O-190
Hulsbergen van de Kaa, C.A. O-197, P-861
Hungermann, D. O-208
Hussein, E. P-230
Hwang, Chung-Feng P-569
Hye, Kyoung Yoon P-334, P-752
Hyjek, E. O-40
Hytiroglou, P. O-46
Hyun, Chang-Lim P-439

Iacob, G.H. P-886
Iaia, T.E. P-556
Iakovidou, J. P-348
Ibarrola, C. P-168
Ibrahim, R. P-211, P-220
Ichihara, Shu P-12, P-16
Idoate, M.A. P-863, P-864
Idrees, M. O-237
Iglesias, B. P-918, P-932
Iglesias, C. P-190
Iglesias, M. P-129, P-701, P-866, P-867, P-868
Ignatova, V.E. O-107
Ignjatovic, M. P-585
Igoudjil, A. P-233
Ikbal, A. P-166
Ikuko, I. P-153
Ilhan, R. P-11, P-65, P-756
Ilhem, B. P-157
Iliæ-Forko, J. P-750
Iliopoulos, D. P-912
Iliszko, M. P-649, P-650, P-815, P-818
Ilkhanizade, B. P-507
Illyes, G. P-544
Ilyin, I. P-739
Ilyina, O. P-739
Imaizumi, T. O-247
Iman, A.K. P-230
Immervoll, H. O-20
Inagaki, Y. O-247
Infante, M. P-517
Ingravallo, G. P-18, P-21
Insabato, L. O-151
Invernizzi, R. P-114
Iochmann, S. O-119
Ionescu, D. O-240
Ionescu, M. P-311
Ionica, E. P-786
Iosif, C. P-127, P-219, P-763, P-824
Iosif, Cristina, I. P-573
Iplikçi, A. P-11, P-65, P-756
Ippoliti, G. P-114
Iraj Ragerdi, K. P-635
Iraqi, A. P-82, P-89, P-109
Iraqi, W. O-64
Iravani, M. O-216
Iro, H. P-559
Irvanloo, G. P-774
Isabel, A. P-422
Isajevs, S. P-490
Isin, K. P-848
Isinsu, K. O-33
Ismail, O. P-484, P-485, P-486
Isola, P. P-44
Issakov, J. P-652
Istók, R. P-273, P-532
Iþýnsu, K. P-283
Ivan, L. P-185
Ivana, M.L.J. P-327, P-563
Ivanov, A. P-675
Ivanov, A.A. P-730
Ivanova, R. P-614
Ivanovic, M. P-146
Iványi, B. O-95
Iwata, Jun O-140
Iyibozkurt, C. P-756
Izopet, J. P-225
Izycka-Swieszewska, E. P-976
Izzedine, H. O-16

Jabri, L. P-82, P-89, P-109
Jäckel, M. P-258
Jacqmin, D. O-193
Jaegal, Young-Jong P-40
Jäger, D. P-415, P-808
Jahanzad, I. P-1
Jaillon, P. P-969
Jakic-Razumovic, J. P-473
Jakoniuk, I. O-99
Jáksó, P. P-80
Jalali, M. P-582
Jalali, N. P-364
Jammu, V. P-829
Jan, D. O-98
Janákova O-230
Jancic, A.S. P-590
Jancova, E. P-465
Jancovici, R. P-260
Janczewska-Kazek, E. P-205
Janevska, V. P-446, P-833
Janicic, D. P-565
Janicka-Jedyñska, M. P-672
Janin, A. O-257, O-260
Jankoviæ, R. P-939
Jankovic, S. P-86
Jaramillo, R. P-866, P-867, P-868
Járay, B. P-273, P-532
Jaresova, M., P-231
Jarosz, D. O-78
Jarz, B. P-609
Jarz, M. P-609
Jarzab, B. P-595
Jarzab, M. P-595
Jaskiewicz, K. P-976
Jaskólski, D. P-970
Jassar, A. P-661
Jastania, R. P-278
Jaszcz-Gruchala, A. P-815
Jaworska, M. P-163, P-74
Jeandidier, N. P-603
Jeannot, E. O-114, P-533
Jellinger, K.A. O-254
Jenni, B. O-56, P-135
Jeruc, J. O-19
Jesionek-Kupnicka, D. P-970
Jeunemaitre, X. O-244
Jezdic, Z. P-338, P-339
Jezek, D. P-880
Jhung, Sang-Woo, P-782
Jiang, Shi-Xu P-602
Jimenez, J. P-190
Jimenez-Heffernan, J.A. P-6, P-755, P-872
Jimeno, M. P-129, P-701, P-866, P-867, P-868
Jin, Hee Sohn P-183
Jin, Tai-Yi P-700
Jinga, V. P-855
Jo, Young-Suk P-601
Joachims, Z. P-925
Johansson, R. O-2, P-477
John, H. P-378
Johnen, G. O-67
Jonas, Ludwig O-22
Jonassen, I. P-691
Jones, C. O-216
Jonjic, N. P-865
Jonker, M.R. O-91
Jonkers, Y.M.H. O-160
Jonmarker, S. P-271
Jordá, E. O-139
Josselin, N. P-193, P-381, P-578, P-642
Jouan, F. O-195, P-669
Jouffroy, T. O-168
Jouian, N. P-364
Jouneau, S. P-494
Jouniaux, A.-M. O-34
Jovanovic, D. P-481
Jovanovic, R. P-446
Jozef, K. P-448
Juanpere, N. P-129, P-701, P-866, P-867, P-868
Jugie, M. O-98
Juhng, Sang-Woo P-269
Julia, M.I. P-567
Juliano, P. O-172
Julié, C. O-35, O-149, P-899
Jullian, E. O-163
Jung, S.M. P-773, P-775
Jung, Shih-Ming P-483, P-938, P-956
Juniku-Shkololli, M.I. P-299
Just, P.A. O-84, P-604

Kabukcuoglu, F. P-518, P-862, P-949, P-950
Kacem, D. P-419
Kacem, O. P-846, P-877
Kaczmarek, E. P-672
Kadi-Hanifi, A.-M. O-130
Kadin Marshall, E. O-60
Kadri, I. P-68
Kafami, L. P-229
Kafiri, C. P-317
Kahveci, O. P-580
Kaidi, C. P-78
Kailash, P. P-506
Kaiser, A. P-77
Kajdaniuk, D. P-205
Kajo, K. O-230, P-310, P-313
Kajtár, B. P-80
Kakkis, E. P-429
Kakudo, K. P-73
Kala, M. P-318
Kalantzakis, S. O-182
Kalayci, G. P-252
Kalekou, C. P-317
Kalinová, M. P-110, P-828
Kaliszky, P. P-515
Kalkandi, P. P-248
Kalland, K.-H. P-691
Kaloutsi, V. P-91
Kamar, N. P-215
Kamaras, V. O-80
Kamble, M. O-235
Kamel, N.A.F. P-535
Kamenova, M. P-285
Kamienska, E. P-119
Kamina, S. P-83, P-84, P-85
Kampas, L. P-90, P-105, P-875
Kanavaros, P. P-83, P-84
Kanczuga-Koda, L. P-42, P-575
Kaner, G. P-930
Kanev, N. P-614
Kaneyuki, U. O-247, P-243, P-819
Kang, Hyun Jeong P-814
Kanjuh, V. P-714, P-729
Kankaya, D. P-686
Kantelip, B. P-312
Kantomaa, T. P-632, P-639
Kapetanios, V. P-761
Kaplenko, I. P-798
Kaposi-Novák, P. P-887
Kapp, P. O-249
Kappas, A. P-85
Kapral, M. P-975
Kapran, Y. O-162, P-523
Kapranos, N. P-24
Karaban', I. P-990
Karaban', N. P-990
Karabina, S.-A. O-245
Karameris, A. P-377
Karanova, P. P-614
Karasoy, A. P-949
Karatapanis, S. P-184
Karatza, C. P-536
Karavasilis, V. P-201, P-793
Karaveli Fatma, S. P-805
Karayannopoulou, G. P-116, P-509, P-617
Karayigit, E. P-11, P-523
Karbalay-Doost, S. P-452, P-514
Karczmarewicz, E. O-68, P-427
Kardasi, M. P-199
Kardos, M. P-851
Karentzou, O. P-443
Karimi, A. P-191
Karimpour, M. P-625
Karita, M. O-140
Karkavelas, G. P-966

Karkouri, M. P-82, P-109
Karpov, S.Y. P-209
Karray, S. P-647
Karsidag Hacikerim, S. P-950
Karttunen, T.J. P-159
Kasai, K. P-240
Kashanian, M. P-796
Kaskenpää, N. O-227
Kassimi, N. P-445
Kast, M.W. P-559
Katarzyna, T. P-448
Katebi, M. P-76
Katiæ, K. P-359
Katiæ, V. P-137, P-359, P-923
Katic, V. P-694
Katikos, E. P-126
Kato, S. O-247
Katsamagou, E. P-188, P-524
Katsanos, K. P-85
Katsanos, K.H. P-201
Katsaraki, A. P-121
Katsifotis, C. P-394
Katsos, I. P-324
Katzenberger, T. P-111
Kavantzas, N. P-251, P-497, P-895
Kawaguchi, N. O-224
Kawahara, N. O-140
Kawakubo, Y. P-602
Kawalec, W. P-719
Kay, E. P-947
Kaya, H. P-46, P-53, P-54, P-458
Kayasut, K. O-59
Kaygusuz, G. P-97, P-98
Kchir, N. P-340, P-342
Kefala, M. O-196
Keiko, Ohta-Ogo P-732
Keller, C. O-54, P-128
Kellokoski, J. O-2
Kelten Esra, C. P-558
Kemény, É. O-95
Kemona, A. P-176, P-178
Kemp, C. O-259, P-72
Keramopoulos, A. P-416, P-417
Kerényi, A. P-238
Kerliu, A. P-299
Kern, I. P-488
Kersting, C. O-208
Keshavarz, S.A. P-582
Kesmezacar, H. P-826
Kettani, S. O-130
Khabir, A. P-393, P-423, P-554, P-955
Kharnas, S. P-291
Khashayar Varkoohi, A. P-264
Khattab, H. P-366
Khau van Kien, P. O-244
Kholová, I. O-227
Kianmanesh, R. O-111
Kido, D. O-251
Kiemeney, L.A.L.M. P-861
Kilani, T. P-484, P-486
Kilian, O. P-636
Kilicaslan, I. P-383, P-839
Kim, Hun-Taek O-253
Kim, Hyun-Joong P-40, P-269, P-782
Kim, Jee Yeon P-814
Kim, Jin-Man P-601
Kim, M. O-39
Kim, Mi-Jung Jung P-269
Kim, R. O-26
Kim, Y.-A. P-545
Kim, Young-Kun P-601
Kiral, H. P-479
Kiriakou, V. P-526
Kirichenko, Y. P-224, P-466
Kirillova, L. P-440
Kirsi, R. P-792
Kirsi, V. P-792
Kisiel, W. O-41
Kisiela, D. P-468
Kisielewski, W. P-42
Kiss, A. O-73, O-95, O-113, P-515, P-544, P-552, P-851, P-887
Kitajima, H. P-434
Kitamura, Y. O-218
Kitazawa, K. P-779
Kitis, G. P-203
Kitsoulis, P. P-83
Kittas, C. O-194, P-810
Kiyasov, A.P. P-232
Kizil, M. P-97, P-98
Klai, K. P-486
Klambatsas, A. P-369, P-854
Klatt, T. O-21
Klein, B. P-94
Klein, C. O-8
Klein, G. O-21
Kleina, R. P-493
Kleinert, R. P-708
Klem, I. P-495, P-565, P-583
KlevetenkoM. P-797
Klijanienko, J. O-242
Klimstra, D.S. P-519
Klinger, F. O-12, P-354, P-577
Klinger, M. O-12, P-354, P-577
Kloc, W. P-976
Kloczko, J. P-92
Klomp, H. O-9
Klopèiè, U. P-9
Klöppel, G. O-112, P-519, P-619
Kludák, I. P-499
Kneif, M. P-379
Kneževiæ, F. P-10
Knezevic Usaj, S. P-204, P-585
Knezevic, N. P-880
Kniepeiss, D. P-708
Knolle, J. P-261
Knotek, M. P-843
Kobos, J. O-13, P-358, P-574
Koca, S. P-826
Koch, C.A. P-619
Koch, K. O-223
Kochuyt, A.-M. O-153
Kocova, M. P-622
Koda, M. P-42, P-575
Kodet, R. P-110, P-413, P-566, P-828, P-967
Kodetova, D. P-967
Koepenik, A. O-144, P-901
Koffi, E. P-193, P-381, P-642
Kofler, A. O-56
Kogan, E. P-246, P-491
Kogan, E.A. O-88, O-107
Kogan, M. P-859
Köhne, C. P-899
Kohout, A. P-337
Kojc, N. P-722
Kojiro, M. P-243
Koken, T. P-487
Kokhanevich, Y. P-797
Kokka, H. P-24
Kokkinaki, A. P-539
Köksal, H. P-518
Kolar, Z. P-408, P-677, P-964
Kolasa, P. P-970
Koletsa, T. P-617
Kolkman-Uljee, S. O-233
Kollender, Y. P-652
Kollmann, K. O-152, P-136, P-195, P-412
Kolodziejski, L. P-650, P-815, P-818
Komarek, V. P-988
Komarov, I. P-909
Komminoth, P. O-112, O-160, P-619, P-626
Kondakov, V. P-870
Konninoth, P. P-620
Kononenko, O. P-141
Konova, M.V. P-606
Konovalov, D.M. P-431
Konstantinides, P. P-656
Konstantinidou, A.E. P-979
Konstantinovsky, S. O-192
Kontostolis, E. P-45
Kopecká, P. P-110, P-828
Kopeika, U. P-490
Kopolovic, J. O-234
Kopper, L. P-259, P-891
Korbi, S. P-143, P-144, P-349
Kordek, R. P-970
Kordela, V. P-375
Korkmaz, E. P-963
Korkolopoulou, P. P-251, P-371, P-497
Korol, D. O-56
Korpershoek, E. P-626
Kortankova, H. P-112
Kos, M. P-703
Köse, N. P-293
Kösemehmetoðlu, K. P-657
Koseoglu, R.D. P-79
Kosma, V. O-2
Kosma, V.-M. P-477
Kosmahl, M. P-519
Kosmehl, H. O-10, P-636
Kostadinov, V. P-923
Kostadinova, S. P-462
Kostakis, A. P-217
Kostolna, E. P-231
Kostopoulos, I. P-116
Kosunen, A. O-2
Kothmaier, H. O-121
Kotoula, V. O-46, P-116, P-966
Kotsev, A. P-285
Kotsiakis, X. P-979
Koukourakis, M.I. P-194
Koumoundourou, D. P-410
Kouneli, S. P-24, P-25, P-761
Kouraklis, G. P-295
Kourda, N. P-323, P-360, P-368, P-846, P-877, P-937
Kourelis, T. P-96
Kourounis, G. P-410
Koustiani, G. O-46
Koutsoubi, K. P-24
Kouvatseas, G. P-184
Kouvidou, C. P-184, P-341
Kovacheva, R. P-614
Kovács, G. P-258
Kovács, M. P-552
Kovrigina, A. P-106
Kowalska, M. P-609
Kozakewich, H. O-155
Kozelj, M. P-725
Kozlowski, W. P-15
Kra Snova, T.N. P-209
Kram, A. O-7
Kramar, A. P-407
Kraševiæ, M. P-762
Krasiæ, D. P-359
Krek, W. P-860
Krel, P.E. P-209
Kremser, M.-L. O-104
Krenács, T. P-259
Krenn, V. O-143, O-144, P-641, P-901
Krennbauer, S. P-195
Kriaka, A. P-317
Kriegsmann, J. O-144, P-641
Krishnan, B. P-391
Kristensen, I.B. P-728
Krizanac, S. P-322
Krizeck, M.-C. P-451
Kröncke, T. P-768
Krsek, P. P-988
Krsková, L. P-110, P-828
Krtolica, K. O-37
Kruczak, A. P-649, P-650, P-815, P-818
Kruse, M.L. O-112
Krušlin, B. P-519, P-703, P-853, P-857
Kryj, M. P-163
Krzakowski, M. P-170
Krzysik, M. P-254, P-256
Ku, Bon Jeong P-601
Kubelka-Sabit, K. P-277, P-747, P-765
Kubica, T. P-500
Kubota, Y. P-993, P-998
Küçükalý, T. P-753, P-791, P-811
Kuefer, R. O-26
Kujas, M. O-64
Kujundžiæ-Tiljak, M. P-31
Kukulska, A. P-609
Kulczycka, D. P-970
Kullu, S. P-288
Kumar, A. P-661
Kumar, V.K. P-661
Kume, K. O-110
Kümmer, A. O-62
Kumpulainen, E. O-2
Kuo, Tseng-Tong, P-773, P-938
Kupcsulik, P. O-73, O-113, P-515, P-544
Kupesiz, Y.G. P-805
Kupryjanczyk, J. O-78
Kursun, N. P-611
Kurtkaya Yapicier, O. P-965
Kurylak, A. P-119
Kurzeja, R. P-768
Kushlinsky, N.E., P-177

Kuten, A. O-81
Kutlesic, C. P-435
Kutok, J. O-26
Kuzey Gamze, M. P-811
Kuznetsov, V. P-989
Kuznetsova, A. P-675
Kuznetsova, I.A. P-717
Kuznetsova, S. P-989
Kuzu, I. O-229, P-52, P-97, P-98, P-611, P-686
Kviatkovská, Z. O-230, P-310, P-313
Kwiek, S.J. P-906, P-962
Kwon, J. P-790
Kwon, Ki-Hyun P-601
Kyogo, A. P-347
Kyparidou, E. P-879
Kýper, A. P-873
Kýremýt Murat, C. P-862
Kyroudi, A. O-102, O-194
Kyzas, P.A. P-973

La Choi, Y. P-789
La Rosa, S. O-161, P-627
Laberge-Le Couteulx, S. O-214
Labib, S. P-469
Labiche, A. P-893
Lacaille, F. O-98
Laccoureye, L. P-578
Laccourreye, O. O-171
Lacerda, M. P-399
Lackowska, B. P-650, P-815, P-818
Lacramioara Roznovan, S. P-683, P-684
Lacroix-Triki, M. P-898
Lacza, Á. P-80
Ladas, G. P-253
Laddeb, F. P-647
Laé, M. O-198, O-212, O-215, O-256, O-263
Lafdil, F. O-45
Lagace, R. O-156
Lagarde, N. P-699
Lage, H. P-798
Lagente, V. P-494
Lagha, M. P-485
Lahmer, A. P-143
Lai, C.H. P-775
Laios, A. O-101
Laithier, V. O-71
Laize, H. P-472
Lajgut, A. P-961
Lakhani, S.R. O-213, O-216
Laky, D. P-712
Lala, T. P-216
Lam, W.L. O-164
Lamalmi, N. P-459
Lamant, L. P-898
Lamarque, D. O-148
Lambros, M. O-216
Lamireau, T. O-70
Lamlum, H. P-175
Landolfi, S. P-546, P-760
Landsberg, S. O-264
Lang, H. O-193
Lange, D. P-74, P-163, P-529, P-595, P-609, P-721
Langner, C. O-176, P-198, P-361, P-362
Languren, M. P-124
Lankar, A. P-78, P-653
Lankar, N. P-78
Lantsov, D. P-605
Lanzer, G. P-103
Laouar, O. P-78
Laperche, Y. O-45
Lara, C. P-123, P-124
Lassalle, S. O-79, O-131, P-501, P-911
Lastic-Maletic, S. P-714, P-729
László, R. P-80
Latif, S. O-191
Latoufis, C. P-184
Launayvacher, V. O-16
Launoy, G. O-125
Laurendeau, I. O-178
Laurent, C. O-31, O-114, P-294, P-547
Laurent-Puig, P. O-114, O-120
Lavaill, R. P-8, P-407
Lavayssiere, L. P-456
Lavergne-Slove, A O-149
Lavoine, E. P-381
Lavra, L. O-52
Lavric, L. P-155, P-227, P-530, P-903
Lazar, V. P-525
Lazaris, A. P-160, P-186, P-761
Lazaroiu, A. P-280
Lazarovici, P. O-234
Lazure, T. O-93
Le Bail, B. O-41, O-47, P-218, P-547
Le Bail, B. O-70
Le Bihan, C. O-98
Le Cesne, A O-149
Le Corre, D. O-120
Le Deist, F. P-139
Le Marc Hadour, F. P-707
Le Naour, G. P-679
Le Pelletier, F. P-331
Le Tourneau, A. O-59
Leader, M. P-882, P-947
Lebouedec, G. O-209
Lebret, T. P-365
Lech, A. P-975
Leclech, C. P-922
Lee, Chang Hun P-814
Lee, Hye Seung P-439, P-600
Lee, Hyo-Jin P-601
Lee, Ji-Shin P-269
Lee, Jun-Chul P-601
Lee, Kyoung-Bun P-600
Lee, T.M. P-301, P-737
Lee, Youn Kyung P-439
Leec, Chau-Chin P-952
Leempoel, M. P-816
Leenhardt, L. P-604
Lefèvre, M. O-181, O-204
Legaki, S. P-476
Legakis, S. P-475
Leh, S. O-20
Lehy, T. O-184
Leibl, S. P-27, P-799
Leinonen, T. P-477
Leite, N.J. O-57, O-94
Lekka, J. P-7, P-879
Lekston, Z. P-906
Lellei, I. P-878
Lemaitre, L. P-856
Lemancewicz, D. P-92
Lemarie, E. O-119
Lemery, S. O-209
Lemoine, A O-149
Lemoine, M. O-39
Lenders, J.W. P-626
Lenggenhager, D. P-378
Lens Neo Xosé, M. P-597
Leoncini, L. P-132, P-745
Leonova, L. P-637, P-870
Lepage, E. O-62
Lepreux, S. O-42, O-179, P-134, P-664
Lequeux, N. P-403
Lera, J.M. P-33, P-425
Leray, E. O-195, P-669, P-852
Lerebours, F. O-260
Lerin, M.A. P-869
Lernernatoli, M. O-250
Leroy, X. O-81, O-198, P-822, P-856
Lestani, M. P-111
Leteurtre, E. O-114, O-126
Letourneux, H. O-193
Lettéron, P. P-233
Leucci, E. P-132, P-745
Leung, C. O-238
Levin, L. P-142
Levy, B. P-429
Levy, P. O-111, O-181
Li, Chien-Feng P-321, P-648
Lianou, E. P-184
Liapis, G. P-115, P-118, P-416
Liapis, H. O-23
Liard-Meillon, M.-E. P-706
Liava, A. P-207, P-503
Libener, R. O-124
Libesrki, P.P. P-970
Libório, T.N. P-561
Libório, T.N. P-568
Licht, C. O-18
Licht, Ch. O-17
Lichvansceva, V.G P-576
Lidereau, R. O-177
Lie, A.K. P-759
Liegl, B. O-105, O-187, P-58, P-658
Lifschitz-Mercer, B. P-652, P-771, P-780
Lima, J. O-29
Lima, T.P. P-749
Limaiem, F. P-485
Limon, J. P-976
Limón, M. P-32
Lin, Ching-Nan P-321, P-648
Lin, Shinn-Zong P-952
Lindner, V. O-193
Linkesch, W. P-103
Lintner, F. O-254
Lippman, M.E. O-232
Litsiou, H. P-613
Livaoglu, A. P-949
Ljubanovic, D. P-843
Llombart-Bosch, A. O-139, P-823, P-396
Lloreta, J. P-129, P-701, P-866, P-867, P-868
Lobanova, O. P-406
Lobel, B. O-195, P-669, P-852
Lodererova, A. P-465
Lodi, C. P-544
Loeschke, S. P-900
Loget, P. P-451
Logullo, Â. O-259, P-72
Loiseau, H. O-241
Loman, N. P-35
Lombardi, G. P-44
Lome-Maldonado, C. P-123, P-124
Longatto Filho, A. P-28, P-749, P-944
Löning, T. P-772
Loomis, E.D. O-92
Lopatin, A. P-637
Lopatkina, T.N. P-209
Lopes, J.M. P-944
Lopes, Tito P-420
López, J.C. P-682
Lopez-Alonso, G. P-168
Lopezbeltran, A. P-382, P-678
Lopezbrea, M. O-118
Lopez-Ferrer, P. P-6, P-272
Lopez-Gines, C. P-968
Lopéz-Guerrero, J. P-968
Lopez-Guerrero, J.A. O-139, P-396, P-823
Loqa, C. P-442
Lorand-Metze, I. O-57
Lorente, J.A. P-701
Lorenzato, M. O-170
Loutraris, C. P-497
Loutzenhiser, R. O-15
Løvø M.G.S. O-20
Lozano, M.D. P-863, P-864
Lu, Yin-Che P-120
Lubet Ronald, A. P-912
Luca, L. P-250
Lucchesi, P. P-436
Lucin, K. P-865
Luna, M. P-557
Lungu, G. O-253
Lupi, R. O-146
Luque, R.J. P-678, P-985
Lushnikov, E. P-605, P-616
Lushnikov, E.F. P-606
Lusiardi, M. P-270
Luszawsk, J.I. P-962
Luts, L. P-35
Lutz, M.P. P-899
Lyer, S. O-25
Lykaki-Karatza, E. P-410
Lykissas, M. P-991
Lynch, A. P-947
Lysenko, A.I. P-730

Maa, J. O-25
Maarit, A. P-792
Mac Grogan, G. P-757
Macarenco, C. P-560
Machado, M.C.C P-213
Machálekoká, K. P-310, P-313
Machera, E. P-317
Machera, H. P-654
Machovcova, A. P-112
Mackay, A. O-216
Madani, A. P-82, P-89
Madelenat, P. O-184

Madiha, M. P-236
Maeda, M. P-243
Maertens, G. P-214
Maes, B. O-76
Maèukanoviæ-Goluboviæ, L. P-137
Magalhães, J. O-29, P-607, P-608
Magrini, E. O-11, P-579
Magrini, U. P-114
Magyar, É. P-878
Mahjob, H. P-915
Mahzooni, P. P-242, P-958
Mainhaguiet, G. O-134, O-135
Maiorano, E. P-18
Maja, K. P-305
Maja, S. P-305
Majchrzak, H. P-975
Majo, J. P-492
Makarova, N. P-210
Maki, H. P-972
Mäkinen, M.J. P-159
Makni, S. P-402, P-554, P-800, P-874, P-955
Makos, C. P-344, P-656
Makrydimas, G. P-793
Maksymowicz, M. P-743
Malavaud, B. O-83
Malekzadeh, R. P-229
Malihy, A. P-459
Malikova, J. P-964
Malinowska, M. P-286
Mallet, L. P-520
Mallofré, C. O-203, P-374, P-376
Malpeli, G. O-58
Malpica, A. P-784
Mameri Saâdia, Z.F. O-133
Mandache, E. P-460, P-461
Mandakova, P. P-112
Mandala, E. P-90
Mandel Molinas, N. P-826, P-830, P-930
Manevska, B. P-997
Manfait, M. O-38
Manfrin, E. P-268, P-275, P-357, P-400, P-401
Manita, Isabel P-589
Manni, J.J. O-169
Mannweiler, S. P-671
Manojlovic, S. P-843
Manolia, L. P-475, P-654
Mansi, C. P-281
Mansoor, S. P-196
Mansukhani, M. O-201, O-202
Mansuy, J.-M. P-225
Mantion, G. P-312
Manunta, A. O-195
Manxhuka-Kerliu, S. P-299
Maouni, N. P-476
Maounis, N. P-475
March, G. P-968
Marchetti, C. P-333, P-579
Marchini, F. P-454
Marchiori, E. P-478
Marcon, I. O-222
Marek, B. P-205
Marenich, N.S. P-431
Margaria, E. O-261
Margery, J. P-472
Margreiter, R. O-108
Maria, M.N. P-148
Maric, L.J.I. P-590
Marietta, V. O-135
Marin, C. P-294
Mariño, A. P-308, P-437
Marino, S. O-238
Mario, P. P-305
Mariotto, R. P-268, P-400, P-401
Marit, G. O-63
Marjanoviæ, G. P-137
Marjanovic, K. P-146
Marjanovic, M. P-146
Marjanovic, S. P-130
Markaki, S. P-24, P-416, P-417
Markert, E. P-239
Markiewicz, D. P-649, P-650, P-815, P-818
Markku, T. P-792
Markova, E. P-171, P-304, P-306
Markovic, L. P-267
Markovich, L. P-587
Markovic-Lipkovski, J. O-21, P-698
Marlia, E. P-355
Marnissi, F. P-82, P-89
Marquès, G. O-129
Marquez, E. P-551
Marrano, P. P-825
Marszalek, A. P-740
Martignoni, G. O-199, P-357
Martikainen, P. P-292
Martin, A. O-64, P-896
Martin, B. O-117
Martin, C. O-190
Martin, D. P-451, P-451
Martin, N. O-45
Martin-Chouly, C. P-494
Martinelli, A. P-151
Martinelli, A.L.C. P-237
Martinez Tello, F. O-6
Martínez-Benítez, B. P-123, P-124
Martinezdiez, M. P-931
Martínez-Peñuela, J.M. P-33, P-425
Martin-Garcia, N. O-62, O-136
Martin-Negrier, M.-L. O-179, P-134
Martin-Oliva, D. P-457, P-910
Martins, A. P-28, P-34
Martins, M. P-560, P-581
Marty, M. O-260
Marty, O. O-109, P-520
Marty-Double, C. P-206
Marucci, G. P-333
Marunica, J. P-31
Marusic, P. P-988
Marzullo, A. P-145
Masaaki, S. P-347
Mascaux, C. O-117
Mascolo, M. O-151, O-236
Masih, S. P-958
Masliah, J. O-34
Masoud, A. P-914
Massarollo, P.C.B. P-213
Massei, A. P-436
Massi, D. O-14
Masson, B. P-8
Massot-Bordenave, M. P-757
Mastracci, L. P-281
Mata, M. P-968
Materna, V. P-798
Mathieu, M.C. P-17
Mathoulin, S. P-757
Matilla, A. P-551
Matizonkas-Antonio, L.F. P-561, P-568
Matjaž, H. P-305
Matos, J. P-749
Matos, P.S. P-615
Matsionis, A. P-224, P-466, P-673
Matsouka, P. P-96
Matsuo, T. P-482
Matthews-Greer, J. O-191
Mattö, M. P-107
Matusan, K. P-865
Matyja, E. O-68, P-427
Matysiak, M. P-119
Maudelonde, T. P-407
Mauduit, C. P-689
Maurice, E. P-738
Mavier, P. O-45
Maximo, V. O-29
Maxwell, L. P-829
Maza, R. P-653
Mazerolles, C. O-83
Mazurek, U. P-974, P-975
Mazzini, R. O-259
Mccarthy, E. O-140
Mccluggage, W.G. P-784
Mcfadden, K. O-240
Mckiernan, J. O-202
Mckinney, J. O-96
Mclaughlin, K. O-15
Meditzkou, K. P-317
Medvedev, V. P-673
Medvedeva, L. P-673
Mehaye, C. O-179
Mehmet, S. P-994
Mehrbod, K. P-300
Mehrenberger, M. P-455, P-456
Mehrnami, A. P-229
Meijer, C. P-255
Meirmanov, S. P-605
Meizoso, T. O-185, P-840
Mekni, A. P-340, P-342
Melachrinou, M. P-96, P-117
Melamed, J. O-201
Melcher, I. O-143
Melinte, P.R. P-471, P-783
Mellado, B. O-203, P-760
Meller, I. P-652
Mellottee, L. O-114
Melotti, F. O-128
Memeo, L. O-201, O-202
Mendez, I. P-744
Mendez-Olvera, N. P-279, P-908
Menegaux, F. P-586, P-604
Menegeaux, F. P-202
Menestrina, F. O-199, O-58, P-111, P-275
Meningaud, J.P. P-331, P-336
Mentzel, T. P-337
Mérabet, Z. O-82
Merabet, Z. P-670
Mercier, M. P-312
Mercier, S. P-757
Merimsky, O. P-652
Merino, C. P-757
Merland, J-J P-660
Merle, S. O-263
Merlio, J.-P. O-63, O-65, O-134, O-135, O-241
Merol, J.-C. O-170
Mertz, K. P-860
Mesquita, Marta P-43
Messthaler, A. P-378
Mestiri, S. P-349
Mete, O. P-756, P-821
Metze, K. O-57, O-94, O-100, O-172, P-615
Metzger, R. O-75
Meulemans, E.V. O-157
Meunier, N. O-241
Meyer, C.L. O-112
Meyer, N. O-193
Meyronet, D. P-498
Mezza, E. O-236
Mi Seon, Kang P-752
Micello, D. P-36
Micev, M. P-102, P-307
Michail, G. P-410
Michalak, S. P-193
Michalak-Provost, S. O-114
Michalk, D.V. O-17
Michaluarte, P. P-561
Michej, W. P-320
Michels, J.-J. P-893
Michenet, P. P-8
Michiels, J.-F. P-897
Michigishi, T. P-584
Michon, J. O-242
Micke, P. P-894
Micu, G. P-155, P-227, P-530, P-903
Midi, A. P-651
Mierzewska, H. P-427
Mierzynski, W. P-649, P-818
Migeon, C. P-409
Mignogna, C. O-151, O-236
Miguel Salas, M.T. P-980
Mihai, M. P-127, P-311, P-573, P-824
Mihailoviæ, D. P-923
Mihailovic, D. O-189, P-435
Mihailovici, M.-S. P-133, P-185
Mihalcea, A. P-786
Mihaljevic, B. P-86
Mihalopoulou, A. P-681, P-705
Mijovic, Z. P-435
Mikuz, G. P-370
Milan, M. P-563
Milanezi, F. O-213, P-28, P-34, P-316
Milas, I. P-31
Mildenberger, E. O-67
Milenkovic, B. P-244
Milenkovic, S. P-978, P-995
Milenoviæ, M. P-137
Milentijevic, M. O-189
Milicevic, M. P-102
Millan, A. P-222
Millon, R. P-603
Milovanova, S.Y. P-209
Milovidova, A. P-735

Milutin, D. P-167
Min, Kyung Kim P-183
Mina, M.M. O-199
Minarik, M. P-249
Minnei, F. O-153
Miquel, R. O-43, P-528, P-546
Mir, J. P-548
Miranda, C. P-33, P-425
Miroglu, C. P-383
Mi-Seon, Kang P-334
Mishellany, F. O-209, O-235
Misset, J.-L. O-257, O-260
Missoury, R. P-225
Mitani, K. O-110
Mitchell, R. O-202
Mitroo, P. O-74
Mitropoulos, D. O-194
Mitrovic, D. P-125, P-698
Mitrovic, O. P-307
Mitsiades, C. P-613
Mitsiades, N. P-613
Mizukami, Yuji. P-584
Mladinov, D. P-853, P-857
Mneimneh, W. P-343
Mnif, H. P-100, P-393, P-955
Mnif, Hela P-402
Moazezi, Z. P-265
Mocan, S. P-167, P-189, P-553, P-638, P-807
Mocanu, S. P-683, P-684
Moch, H. O-56, O-238, P-135, P-378, P-415, P-620, P-808, P-860
Modesto, A. P-455, P-456
Moeenvaziri, N. P-582
Mohamed, A. P-230
Mohammad, H. P-806
Mohammadzadeh, M. P-229
Mohsen, A. P-951
Moinfar, F. O-104, P-27, P-58, P-671, P-799
Mokhtar, M. P-144
Mokhtari, K. O-64, P-969
Mokhtari, M. P-599
Mokni, M. P-143, P-144, P-349
Moldvay, J. P-258, P-259
Molina, T. P-101
Molina, T.J. O-59
Molinié, V. O-81, O-93, O-109, O-177, O-193, O-200, O-204, P-93, P-365, P-520, P-685, P-693, P-842
Mollamahmutoðlu, L. P-767
Mollenhauer, J. O-25
Molnár, B. O-80, P-328, P-329, P-889, P-890
Molnár, P.P. P-511, P-961
Mona, M.N. P-230
Monaghan, J. P-420
Monchy, D. P-398
Monica, B. P-148
Mönig, S. O-75
Monnet, I. P-247
Monnien, F. P-312
Mons, R. O-118
Monsef, A.R. P-915
Monsef, Esfahani, A.R. P-916
Monsefi, M. P-812
Monsour Nasiri, K. P-914
Montani, M. P-620
Montazeri, V. P-474
Monteagudo, B. P-932
Monteagudo, C. O-139
Montebugnoli, L. P-333, P-579
Mora, A. P-414
Morales, C. P-437
Morand, C. P-48
Morawietz, L. O-143, O-144, P-641
Morcillo, E. P-968
Moreau, A. O-64
Moreilhon, C. O-148
Moreira de Andrade, J. P-418, P-424
Moreno, J. P-32
Moreno, S.M. O-6
Moreno-Bueno, G. P-787
Morente, M. P-187
Mori, I. P-73
Moritani, S. P-12, P-16
Moriya, T. P-700
Morozov, S. P-141, P-450, P-735
Morphopoulos, G. P-24
Mortazavi, H. P-935
Morvay, Z. O-95
Moschovi, M. P-443
Moser, G. O-60
Moser, P.L. P-902
Moskal, J. P-649, P-650, P-815, P-818
Mosnier, I. P-343
Mossafa, H. P-122
Mostafa, N. P-181
Mouchel, F. P-451
Mouchel, J. P-451
Mounier, N. O-260
Mouquet, C. P-202
Mourão, M. O-231
Mouroux, J. P-911
Mousazadeh, M. P-191
Moussa, M. P-389
Moutchou, A. P-665
Moya, L. P-931
Moyano, S. P-546
Mozer, P. O-84, P-679
Mozetic, V. P-865
Mozos, A. P-531
Mrad, K. P-325, P-419, P-659, P-68, P-795, P-834
Mrèela, M. P-750
Mrhalova, M. P-113, P-413, P-566
Mrowka, R. P-974
Mrozkowiak, A. P-22, P-23
Muawia, S. P-535
Muccioli, G. O-166
Mudraya, V. P-332
Muezzinoglu, B. P-794
Mukensnabl, P. P-249
Mukhopadhyay, D. O-24
Mularczyk, M. P-215
Müller, C. O-21
Müller, D. P-843
Müller, G. O-21
Müller, K.-M. O-67
Müller, O. O-25
Müller, R.-P. O-75
Müller-Quernheim, J. P-500
Mulliken, J. O-155
Mumba, E. P-748
Munivenkatappa, R. O-96
Munoz, A. P-502
Muñoz, J.I. P-624, P-917, P-918
Muñoz-Gamez, J.A. P-910
Munteanu, M. P-19
Murakami, H. O-140
Murat, P. P-283
Muresan, V. P-786
Murillo Lázaro, C. P-841
Murphy, N. O-190
Murty, V. O-54
Musia, J. P-970
Musilova, K. P-847
Musizzano, Y. P-281
Mustafa, G. P-751
Mustafa, L. P-751
Mustafa, U. P-994
Muti, C. O-35
Mylona, E. P-416, P-417, P-421
Mylona, S. P-539

Nabavi, M.B. P-806
Nabavi, S.M.B. P-986
Naccarato, G. P-44
Nadgornaya, V. P-108
Nadia, K. P-157
Nadji, M. P-388
Nagulic, M. P-633
Nagy, P. O-73, P-228, P-330
Nagy-Fricska, A. O-95
Naik, R. P-420
Náira Zambelli Ramalho, L. P-562
Najafi, F. P-593
Najafi, M.R. P-593
Najah, N. P-323
Nakabayashi, H. P-972
Nakajima, M. P-434
Nakamura, M. P-73
Nakamura, Y. P-73
Nakanishi, Y. P-612
Nakashima, M. P-605
Nakayama, M. P-434
Nakopoulou, L. P-416, P-417, P-421
Nam, Jong-Hee P-269, P-40, P-758, P-782
Namba, H. P-605
Nane, I. P-839
Napoli, A. P-18, P-21
Nappi, C. O-236
Naser, K. P-796
Naser, V. P-57
Nasierowska-Guttmejer, A. P-286, P-320
Nasr El Din, M.H. P-766
Nassiri, M. P-388
Nastaran, E. P-506
Naud, P. P-749
Navabakbar, F. P-303
Navarro, C. O-252
Navarro, F. P-741
Navarro, S. P-528
Navas, R. O-185
Näyhä, V. O-103
Nazmiye, K. O-33, P-283
Neagu, M. P-50, P-824
Necati, Ö. P-283
Nechitailo, T. O-186
Nedeljkov-Jancic, R. P-86
Nederlof, P. O-9
Nederlof, P.M. P-513
Negar, O. P-982
Neid, M. O-24
Nekrasova, T.P. P-209
Nemes, Z. P-511
Németh, T. P-961
Nenezic, T. P-583
Nenopoulou, E. P-317
Neofytou, A. P-438
Neradova, M. P-113, P-413
Nerlich, A. O-220
Nesi, G. O-146, P-372
Neškovic, A. O-226
Nesland, J.M. O-147, O-192, P-138
Neto, A. P-557
Neumeister, P. P-103
Neves, J.I. P-87
Nezhat, F. O-237, P-788
Ngae, Min Yi O-15
Nica, S. P-903
Nicholls, J. O-219
Nicholson, A. O-123, P-253
Nicolas, A. O-168
Niculescu, L. P-430, P-433, P-845, P-855, P-881
Nigmatjanova, F. P-210
Nikbakhtian, S. P-1
Niki, J.A. P-47, P-564
Nikiel, B. P-595, P-609
Nikolaidou, A. P-344, P-369, P-656, P-854, P-875
Nikolakaki, E. O-46
Nikolaou, I. P-416, P-417, P-421
Nikolaou, M. P-879
Nikolic, I. P-322
Nikolopoulos, G. P-217
Nikolovski, M. P-734, P-833
Nilsson, B. P-676
Ninane, V. O-117
Ninio, E. O-245
Nirkin, A. P-652
Nishikubo, T. P-434
Nishino, M. P-434
Nistal, M. P-489, P-871, P-872
Nizze, H. O-22
Nkegoum, B. P-444, P-885
Nobukawa, B. O-110
Nofroni, I. P-4
Nogami, Sei-Ichiro P-819
Nogueira, A.A. P-770
Nogueira, J. O-96
Noguera, R. P-823
Nohra, O. O-235
Nomikos, A. O-196, P-203, P-539
Nonni, A. P-160, P-186, P-979
Nonogaki, S. P-87
Noorafshan, A. P-625
Noordhoek, J.A. O-91
Noori, M. P-806
Noori, M.S.M.H. P-986
Nooshin, A. P-164
Nordlinger, B. O-35, P-899
Nosseir, M. P-223, P-223, P-387, P-389
Notohara, K. P-777

Nouri, M. P-742
Noyes, B. O-89
Nozarian, Z. P-774
Nozic, D. P-204
Nozynski, J. P-163
Nozyñski, J. P-529, P-721
Nugnes, L. O-236
Nuin, P. O-85, P-825
Nunes Fabio, D. P-568
Nunes, F.D. P-561
Nurper Onuk, F. P-876
Nuta, M.M. P-149
Nuutinen, J. O-2
Nyagol, J. P-745

O'Leary, J.J. O-190
O'Neill, C.J. P-784
O'Valle, F. P-910
Obernaus, A. O-251
Obukhova, V. P-291
Och, W. P-970
Ochs, M. O-67
Ociepa, T. P-119
Oczko, M. P-609
Oda, W. O-218
Odak, L.J. P-703
Ødegaard, E. O-234
Odenthal, M. O-17, O-18, P-197
Odintsova, A. P-232
Œnietura, M. P-529, P-721
Offerhaus, G.J.A. P-513
Offner, F. O-122
Offner, F.A. O-108, P-902
Ogahara, I. O-218
Oger, M. P-893
Ogrezean, I. P-628
Oguz, O. P-930
Ohashi, M. O-218
Ojer, A. P-425
Ok, E. P-318
Okamoto, N. O-7
Okayasu, I. P-602
Oksuz Colpan, D. P-826
Okuda, S. O-247
Oldrini, R. P-627
O'Leary, J. O-101
Olinici, C.D. P-572, P-886
Oliver, F.J. P-457, P-910
Olmedilla, G. P-165, P-690
Olsen, S. P-691
Olsson, H. P-35
Olszewski, W. P-22, P-23, P-170
Olszewski, W.T. P-743
Oltulu, T. P-52
Omidi, N. P-987
Omran, Z. P-366
Onea, A. P-294
Oner Dincbas, F. P-826, P-830
Onnis, A. P-132, P-745
Onoguchi, M. P-584
Onsrud, M. O-234, P-759
Ontiveros, P. P-124
Onuk Filiz, N. P-79
Oosterwijk, E. O-197, P-861
Oosting, J. O-233
Oprisan, A. P-903
Orban, E. O-113
Orchel, J. P-974
Ordi, J. P-760, P-813
Orecchia, S. O-124
O'Regan, E. O-101
Orellana, R. O-129, P-154, P-266, P-510
Orlandi, A. O-225, P-780
Orlowska, J. O-78
Orolicki Vukosavic, S. P-130
Orosz, Z. P-832
Orphanou, Eleni P-216
Ortiz-Rey, J.A. P-624, P-917, P-918, P-924, P-932
Ortonne, N. O-136, O-137, O-138
Oshima, C. O-259
Osman, M.A. P-535
Osório, C.A O-231
Ostalska-Nowicka, D. O-72
Ostrowska, J. O-78
Otaševic, Petar O-226
Otero, C. P-397
O'Toole, S. O-101
Ott, G. P-111
Otte, A.P. P-928
Ottini, L. O-146
Ouahioune, W. O-133
Oukid, N. P-78
Ouled, S. P-445
Ouzeddoune, N. P-459
O'Valle, F. P-457
Ovchinnikov, S. P-637
Øyan, A.M. P-691
Oz, B. P-356
Özaðari, A. P-862
Özdemýr, M.A. P-318
Ozden, I. P-523
Özden, T. P-876
Ozer, A. P-180
Ozger, H. P-821
Ozgur, M. P-848
Ozkan, M. P-37, P-318
Ozkan, N. P-156, P-284
Özlem, E. P-540
Ozluk, Y. P-65, P-252, P-756
Ozturk Kilicaslan, T. P-651, P-830
Ozturk, A.S. O-162, P-383
Ozturk, F. P-37

Pacchioni, D. P-382
Paciencia, M. O-125
Padberg, B. P-378
Pagliari, A.V. O-12, P-354, P-577
Pagoni, Niki P-536
Pahl, S. O-220
Paillocher, N. P-48
Paiva, G.R. P-335
Pajares, R. P-168
Pajor, G. P-379
Pajor, L. P-80, P-379
Paku, S. P-544
Palacin, A. O-203
Palacios, J. O-262, P-51, P-187, P-404, P-787
Palamidas, F. P-476
Palamidas, P. P-475
Palazzo, J.P. O-74
Palli, D. O-146
Pallud, C. P-29
Palmen, C. P-99
Palomba, A. P-556
Palot, J.-P. O-38
Paltsev, M. P-246, P-675
Paltsev, M.A. P-140, P-730
Paltseva, E.M. P-730
Panagiotopoulos, V. P-971
Panayiotis, A.K. P-47, P-564
Pandeleon, B. P-126
Panel, V. O-34
Panelos, I. P-201, P-375
Pang, See-Tong P-676
Paniagua, R. P-55, P-56, P-666, P-667
Panizo, A. P-863, P-864
Panizzolo, C. O-90
Panjehshahin, M.R. P-452, P-453, P-514
Panoulas, V. P-83
Panoussopoulos, D. P-186
Panteli, K. P-121
Panuncio, A. P-308
Papachristou, D.J. O-142, P-631, P-632, P-639
Papachristou, G.I. O-142
Papadimitriou, C. O-46, P-91, P-966
Papadimitriou, C.S. P-509
Papadimitriou, J.C. O-96, P-726
Papadimitriou, S.C. P-116, P-617
Papadopoulos, S. P-317
Papadopoulou, K. P-248
Papaefthimiou, O.A. O-142
Papaefthymiou, O.A. P-631
Pápai, Z. P-832
Papaioannou, M. P-91
Papaioanou, M. P-203
Papanikolaou, A. P-656, P-875
Papaspirou, I. O-102
Papaspyrou, E. P-24
Papathanasiou, A. P-875
Papathanassiou, Z. P-536
Papatheofanis, I. P-188
Papavassiliou, A.G. O-142, P-632, P-639
Pápay, J. P-259
Papierz, W. P-970
Papotti, M. O-166, O-167, P-382
Papoudou-Bai, A. P-83
Pappa, V. P-126
Paradias, I. P-90
Paradis, V. O-114, O-115, O-178, P-235, P-550
Parascan, L. P-712
Parasi, K. P-317
Paraskevi, A. P-115
Parc, R. O-36
Pardo, J. P-863, P-864
Parfenov, V. O-248, P-711
Parichehr, P. P-635, P-982
Pariente, J.-L. O-179
Parisi, F. O-246
Park So, Yeon P-439
Park, Chang-Soo P-40, P-758, P-782
Park, Do Youn P-814
Park, Jong-Moo P-545
Park, K.C. P-972
Park, Moon-Il P-512
Park, Seong Hoe P-600
Park, So Yeon P-600
Parra, T. O-129, P-154, P-510
Parrens, M. O-63, O-65
Parsons, R. O-202
Partensky, C O-114
Pasalega, M. P-20
Pasbakhsh, P. P-987
Pascazio, F. P-18
Pascual, A. P-785
Pasechnik, D. P-858, P-859
Páska, C. O-73, O-113, P-552, P-887
Paslaru, L. P-525
Pasquini, R. P-992
Passamonti, F. P-114
Patakiouta, F. P-24, P-67, P-75, P-317, P-324
Patalay, R. P-943
Patard, J.-J. O-195, P-669, P-852
Patera, J. P-15
Patereli, A. P-443
Patey, M. O-130
Patrascu, M. P-783
Patsioura, C. P-317
Patsouris, E. P-160, P-186, P-251, P-371, P-497, P-613, P-895, P-979
Pauser, U. P-519
Pauwels, P. O-157
Pavlopoulos, P. P-895
Pavlov, N. P-429
Pavlovskaya, A.I. P-596
Pawluch, L. P-119
Paye, F. P-517
Pea, M. O-199
Pechianu, C. P-311
Pechtelidou, A. P-810
Pectasides, D. P-879
Peg, V. P-147
Peiris, M. O-219
Peirovi, T. P-274
Peivareh, H. P-363
Peker, D. P-516
Pekul, M. P-646
Pelkonen, J. P-107
Pellegrin De Villeneuve, M. P-757
Pellegrino, A. O-225
Pellin, A. O-139, P-823, P-396, P-968
Pelling, N. O-123
Pelluard-Nehme, F. O-42
Peltier, E. P-685
Peña, C. P-547
Penault-Llorca, F. O-209
Penaultllorca, F. O-235, P-173, P-409
Penault-Llorca, F.M. O-30
Penescu, M. P-461
Penna, C. O-35
Penna-Renard, R. P-679
Pennesi, M.G. P-346
Peoch, K. O-255
Peoch, M. P-598
Percinel, S. P-52
Perçýnel, S. O-229, P-611, P-686
Perdomo Coral, G. P-537
Pereira, A.P. P-424
Pereira, E. P-70
Pereira, F.F. O-57

Peres, L.C. O-50, O-53, O-69, P-907
Perevoschikov, A.G. P-177
Perez Montiel, M.D. P-764
Pérez, V. P-414
Perezcampos, A. P-6
Perifanis, V. P-105
Perkovic, T. P-837
Perlemoine, K. O-163
Perna, C. P-755
Peron, J.-M. P-225
Perrem, K. P-947
Perren, A. O-112, O-160, P-619, P-620, P-626
Perret, C. O-163, P-538
Perunicic, M. P-86
Perusso, V. P-70
Pesek, M. P-249
Pesko, P. P-307
Pession, A. P-346, P-579
Pessoa, G.M. P-214
Pesterelý, H.E. P-805
Petersen, I. O-220, P-901
Petit, A. O-203, P-374, P-376, P-528, P-741
Petitjean, A. P-757
Petraki, C. P-317
Petrescu, A. P-430, P-433, P-845, P-855, P-881
Petrescu, M. P-886
Petri, B. P-626
Petridis, N. P-348
Petropoulos, A. P-438
Petrov, S. P-282
Petrov, S.B. P-232
Petroviæ, A. P-923
Petrovic, L.M. O-40
Petrovic, M. P-86
Petrovichev, N. P-909
Petrovski, P. P-622
Petru, E. P-799
Petrusca, D. P-855
Petrusevska, G. P-446, P-462, P-734
Petsas, T. P-536
Pettinato, G. O-151
Petukhova, N.S. P-606
Peyrard, S. O-8
Philippe, B. P-409
Piascik, A. P-23, P-646
Picazo, M. P-702
Pichel, J.G. P-32
Pichler, M. P-708
Pichon, F. P-822
Pickering, G. O-245
Picquenot, J.-M. O-214
Piek, J. O-223
Piekutowska-Abramczuk, D. O-68
Pierga, J.-Y. O-215
Pietruszewska, W. P-358, P-574
Pileri, S.A. O-11, P-77
Pillet, A. P-455
Pina-Neto, J.M. O-50
Pinchera, A. O-232
Pineda, K. P-557
Pinto Clóvis, A.L. P-335
Pinto Jr., D.S. O-1, P-570
Piperi, E. P-341
Piram, A. O-50
Pirinen, R. O-2, P-477
Piris, M.A. P-910
Piro, F.R. O-210, O-211, P-4, P-5
Piron, D. P-685
Pirttiniemi, P. P-632, P-639
Piscitelli, D. O-173, P-145
Pisoschi, C. P-921
Pistner, H. O-10
Pitak-Arnnop, P. P-331, P-336
Pizem, J. O-239
Pizzolo, G. P-111
Placke, J. P-519
Plamadeala, P. P-185
Plancoulaine, B. P-893
Plank, L. O-230, P-310, P-313
Plaseskakaranfilska, D. P-765
Plastira, K. P-25
Ples, R. O-97, P-707
Plesea Iancu, E. P-19
Plesea, L.E. P-20
Ploton, D. O-154
Pluot, M. O-170
Plzak, J. P-566
Poblet, E. P-785
Pocard, M. O-145
Podgórski, J. P-743
Podhorska-Okolow, M. P-468
Podpeènik, D. O-5
Poirson, H. P-225
Poizat, F. P-94, P-555
Polak-Charcon, S. P-152
Polat, N. P-518
Poli Neto, O.B. P-770
Poliaková, K. P-310
Pollán, M. P-187
Pollheimer, J. O-108, P-902
Pollina, L.E. P-436
Polyzoidis, K. P-973
Ponikiewska, D. P-74
Ponten, F. P-894
Pontisso, P. P-541
Pop, D. P-634
Pop, F. P-634
Pop, Oltin, T. P-20
Popa, E. P-763
Popescu, C. P-19, P-824
Popescu, D.I. P-628
Popescu, I. P-311, P-525
Popescu, M. P-471
Popova-Gladskikh, O. P-675
Popovic, M. O-239
Popovic, V.Z. O-226
Popovic, Z. P-714, P-729
Popovska, S. P-171
Popovska, Z. P-277
Popowska, E. O-68
Popper, H. O-121
Popper, H.H. O-122, P-239
Portela-Gomes, G.M. P-618
Portugal, J. P-589
Porubsky, C. P-239
Postiglione, M. P-746
Postma, D.S. O-91
Pothos, A. P-25
Potier, A. P-922
Pouget, F. P-920
Poulias, H. O-196, P-394
Poupon, R. O-39, P-533
Poustka, A. O-25
Pouysségur, J. P-39
Povilaitite, P. P-224, P-466
Powell, S. P-985
Prades, J.M. P-598
Prat, J. O-233
Preto, A. O-29, P-591
Prezas, L. P-497
Pricop, F. P-71, P-276, P-801
Prinseau, J. P-139
Probatova, N. P-106
Probst-Hensch, N.-M. O-56
Prochazkova, M. O-134
Prodanova, I. P-277, P-747, P-765
Prodromou, F. P-443
Prolla Joao, C. P-478
Pronicka, E. O-68, P-427
Pronicki, M. O-68, P-427, P-710, P-719
Proszek, M. P-905
Pruglo, Y. P-680
Prukova, D. P-904
Prüter, E. O-67
Pruthi, D. P-299
Psichogiou, M. P-217
Ptaszynski, K. P-646
Puig-Tintoré, L.M. P-760
Pujol, R. P-129
Pukkila, M. O-2
Pummer, K. P-671
Puñal, L. P-682
Purim, O. P-925
Pykov, M. P-870
Pyrhonen, S. P-175
Pytlik, R. P-113

Quaresma, M. P-43
Quarto, F. P-746
Queires, L. O-86
Quintanilla-Martínez, L. P-123

Raafat, A. P-181, P-182
Racar, A. P-843
Radeljak, S. O-27
Radhi, J.M. P-397
Radojevic, S. P-125
Radojevic-Skodric, S. P-449, P-714, P-849
Radojicic, J. P-244, P-481
Radosavljevic, R. P-698
Radovic, N. P-843
Raducan, E. P-628
Radulescu, D. P-71, P-167, P-189, P-276, P-553, P-638, P-683, P-684, P-688, P-696, P-697, P-801, P-807
Radvanyi, H. O-35
Rafie Alavi, E. P-264
Ragab, N.M. P-26
Raghavan, R. O-251
Rahimi-Moghaddam, P. P-983
Rahou, Hakima P-459
Raija, T. P-792
Rais, H. P-441, P-442, P-630, P-665, P-820, P-957, P-981
Rakhshani, N. P-229
Rakoèevic-Stojanovic, V. P-715
Ramadan S. P-288
Ramadan S.S. P-287
Ramaekers, F.C.S. O-160, O-169
Ramaioli, A. P-39
Ramalho, F.S. P-63, P-237
Ramalho, L.N.Z. P-237, P-770
Ramani, L. P-262
Ramazanoglu, R. P-930
Ramesar, R. P-161, P-169
Ramírez, J. P-741
Rammeh, S. P-323, P-350, P-360, P-655, P-846, P-877
Rammeh-Rommani, S. P-368, P-937
Ramon y Cajal, S. P-190
Ramos, D. O-139, P-396
Ramos, E. O-96
Ramos, P. P-165, P-690
Ramuz, O. O-55
Ranchère, D. O-205
Ranchère-V., D. O-159
Ranèiæ, G. P-137
Rapa, I. O-167
Raphael, M. O-64
Raptis, I. P-654
Raptopoulou, M. P-216
Rashed, M.M. P-26
Rasoul, S. P-196
Raspollini, M.R. O-106
Ratschek, M. P-671
Rautou, P.E. P-234
Ravazoula, P. P-410
Raymond, J. O-148
Raynaud, P. O-250, P-94, P-555
Rayón, M. P-548, P-940
Razavi, F. O-255
RB Groups P-899
Rebassa, M. P-380
Rebocho, A. P-608
Rebouissou, S. O-114
Rebouissoux, L. O-70
Redmond, M. P-882
Regadera, J. P-871, P-872
Regauer, S. O-105, O-187, O-188, P-658
Reghellin, D P-400, P-401
Reghellin, D. P-268, P-275, P-357
Regl, G. P-136
Regueiro, J.C. P-678
Reguero, M.E. P-66
Rehak, P. O-176, P-361, P-362
Reich, O. O-105, O-188
Reich, R. O-192, O-234
Reid, S. P-397
Reijo, S. P-792
Reineke, T. O-56, P-135
Reis Rui, M. P-28
Reis, M.M. P-733
Reis, R. P-34, P-316
Reis, R.M. P-944
Reis-Filho, J.S. O-213, P-944
Reis-Filho, J.S. O-216
Reisifar, M. P-593
Remo, A. P-268, P-275, P-357, P-400, P-401
Renard, C.-A. O-71
Renard-Penna, R. O-84
Renecorail, F. O-163
Renne, G. P-270
Renner, K. P-902

Reporting, C.M.J. P-869
Repše-Fokter, A. P-488
Reshetnikova, O. P-141, P-332, P-450, P-735
Resit, D.K. P-876
Resnikova, G. P-673
Resta, L. O-173, P-145, P-151
Reszec, J. P-42, P-575
Reverdiau, P. O-119
Révillon, Y. O-98
Revuz, J. P-920
Rey, M. O-129, P-154, P-266, P-510
Reyal, F. O-256
Reyes, F. O-62
Reyes, R. O-191
Reyes-Santías, R. P-64, P-591
Reza Jalali Nadoushan, M. P-363
Reza, J.N.M. P-57
Reza, M. P-364, P-884
Reznikova, G. P-466
Rha, So-Young P-601
Rhonda, W. O-74
Ribeiro, C.M.F. P-213
Ribeiro, C.N. O-69
Ribeiro, K.C.B. P-87
Ribeiro-Silva, A. P-59, P-60, P-61, P-62, P-63, P-418, P-424, P-562, P-804, P-907
Ribes, D. P-455
Riboni, R. P-114
Ricco, R. P-21
Richa, H. P-517
Richard, F. O-84, P-679
Ricote, M. P-55, P-56, P-666, P-667
Rieske, P. P-970
Riesz, P. P-851
Rigas, A. P-476
Rigau, V. O-250, P-94, P-555
Righi, A. P-333
Rigó Jr., J. P-887
Rigoli, E. O-161
Rigotti, P. P-454
Rigourd, V. O-67
Rihova, Z. P-465
Rimala, R. P-759
Rimola, A. O-43
Ring, M. O-190
Ringenbach, F. P-312
Rioja, L.A. P-701
Riolacci-Dhoyen, N. P-897
Rioux-Leclercq, N. O-195, P-669, P-852
Riquet, M. O-120
Risberg, B. O-192, P-759
Rischmann, P. O-83
Ristovski, M. P-446
Rittersma, S. O-223
Riva, A. O-26
Riva, C. P-36
Rivas, E. O-252, P-927
Rivera, M. O-40
Rivette, D. O-191
Riza, L. P-471
Rizzo, M. P-372
Rizzo, S. O-90
Ro, Heung-Kyu P-601
Roca, M. J. P-940
Rocha, B. O-127
Rochaix, P. O-30, P-173, P-898
Rochefort, H. P-407
Roderick, P. P-727
Rodica, S. P-471, P-783
Rodica, S.E.T. P-149
Rodier, J.-F. P-603
Rodolakis, A. O-102
Rodrigo, M. O-185
Rodríguez Gil, Y. P-51
Rodriguez Peralto, J.L. P-929
Rodríguez Pinilla, S.M. O-6
Rodriguez, A. O-118, O-195
Rodriguez, J. O-8, O-168
Rodríguez, J.I. P-437
Rodriguez, J.L. O-185
Rodríguez, R. P-187
Rodríguez-Calvo, M.S. P-624, P-917, P-918
Rodríguez-Gil, Y. P-404
Rodríguez-Pinilla, S.M. O-262, P-51, P-404
Roduner, S. O-238
Roemen, G. O-233
Rogounovitch, T. P-605
Rogozhyn, V. P-440, P-704, P-984, P-989, P-990
Rogozyn, V. P-464
Roig, F. P-502
Roizman, P. P-925
Rojo, F. P-190
Roldan, P. P-968
Rollin, J. O-119
Romac, S. P-130
Roman, V. P-855
Romanenko, A. O-174
Romanova, E. P-224
Romeu, M. P-785
Romics, I. P-851
Ronot, M. P-235, P-550
Rontogianni, D. P-83, P-84, P-126
Ropponen, K. O-2, P-477
Roque, L. P-608
Rosa e Silva, J.C. P-770
Rosas, R. O-166, O-167
Rosenbaum, J. O-41
Rosenberg, F. P-139
Rosenhahn, J. P-636
Roshani, S. P-264
Rosic, L.G. P-590
Rossi Degl'Innocenti, D. O-106
Rostad, K. P-691
Rostaing, L. P-455, P-456
Rosty, C. O-168, O-215, O-256, O-263
Roszkowski, M. P-960
Rotar, Z. P-837
Roteli-Martins, C. P-749
Roth, T. O-18
Rothe, B. O-75
Rothmund, J. O-122
Rotin, D.L. P-596
Rouas, L. P-459
Rougier, P. O-35
Roujeau, J.-C. O-138
Rouleau, V. O-125
Rousseau, A. O-171
Rousselet, M.-C. P-381, P-470, P-578, P-642
Rousset, M.-C. O-250
Rouxel, A. P-586
Royuela, M. P-55, P-56, P-666, P-667
Rozentale, B. P-210
Rozhkova, Z. P-440, P-464, P-704, P-984, P-989, P-990
Roznovanu Lacramioara, S. P-696, P-697
Roznovanu, S. P-688
Ruacan, þ. O-61
Rubin, M.A. O-26
Rubin, M.A. O-81
Rubini, G. P-18
Rubio, J. P-396
Ruco, Luigi O-128
Ruffion, A. P-689
Ruggeri, R.M. P-592
Ruiz de Almodovar, M. P-910
Ruiz Villaespesa, A. P-690
Ruiz, A. P-165, P-823
Ruíz, Barnés, P. P-980
Ruiz, E. P-272, P-489
Ruiz-Ponte, C. P-64, P-588
Rüland, A.M. O-157
Rullier, A. O-31, O-41, P-547
Rullier, E. O-31
Rupar, G. O-176
Ruszniewski, P. O-111
Ryan, D. O-123
Rybakova, M. O-248, P-711, P-713
Rybakova, M.G. P-200, P-717
Rybin, P.N. P-463
Rys, J. P-649, P-650, P-815, P-818
Ryška, A. P-337
Rzepko, R. P-976

Sá Couto, P. P-607
Saadat, N. P-582
Saadatnia, H. P-229
Sabahi, A. P-303
Sabat, D. P-905
Sabourin, J.-C. O-30, O-145, P-173
Sabzevary, S. P-953
Sacerdote, C. O-167
Sachinis, K. P-854
Sadeghi, M. P-599
Sadeghipoor, A. P-953
Sadeghipour, R. P-629
Saðlam, A. O-61, P-811
Saenko, V. P-605
Saetta, A. P-371
Saetta, M. O-90
Saez, M. P-502
Sagindikova, G. P-491
Sahan, E. P-692
Sahin, F. P-97
Sahin, O. P-487, P-580
Sahýn Dursun, A. P-315
Saieva, C. O-146
Saiid, K. P-766
Saint-André, J.-P. P-193, P-381, P470, P-642
Saint-Blancard, P. P-257, P-260, P-472
Sairenji, T. O-218
Saiz González, A. P-840
Saiz, A. P-929
Sajin, A.-M. P-280
Sajin, M. P-280, P-467, P-936
Sak, S.D. P-52
Sakamoto Maeda, M.Y. P-749
Sakellariou, A. P-991
Sakelliadis, E. P-443
Saki, S. P-384
Sakiz, D. P-518, P-862, P-949, P-950
Sala, M. P-531
Salamon, F. P-330
Salcedo, M.T. P-147
Salehi, M. P-191, P-303
Salehi, R. P-191, P-303
Salerno, A. P-355, P-447
Sales Katiuchia, U. P-570
Salgado, R. P-816
Salhi, A. O-155
Sallemi, R. P-659
Salles, F.T. O-1, P-570
Salmon, R. O-215, O-256, O-263
Salms, G. P-345
Salomon, L. O-81, O-82, P-670
Salowsky, R. O-25, P-197
Salvatore, G. O-236
Salvesen, H.B. P-781, P-928
Salvi, F. P-162
Salvio, M. O-124
Salwa-Zurawska, W. O-72
Samaras, V. O-182, O-196, P-394, P-539
Samira, S. P-236
Samokhvalov, A. P-291
San José, C. P-32
San Miguel, P. P-917, P-918, P-932
San Millán, B. O-252, P-927
Sánchez Céspedes, M. O-6
Sánchez Chapado, M. P-690
Sánchez Verde, L. O-6
Sanchez, M. P-528, P-546
Sanchez-Estevez, C. P-787
Sánchez-Verde, L. P-168
Sandstad, B. P-759
Sanei, B. P-242
Sanei, M.H. P-164, P-242, P-958
Sanford, I O-54
Sanguedolce, F. O-173, P-145
Sanjuán, F. P-548
Sansevero, S. P-436
Santini, J. O-131
Santon, A. P-66
Santopietro, R. P-745
Santorelli, F.M. O-246
Santos, E. P-70
Santos, J. P-868
Santos, M. P-760
Santos, O.P. P-87
Santos, S. P-589
Santucci, M. O-14
Sanz-Esponera, J. P-502
Sanz-Ortega, J. P-502
Sanz-Rodriguez, F. P-871
Sápi, Z. P-832

Saqui-Salces, M. O-127, P-623
Sar, M. P-356
Sarafoleanu, C. P-573
Saraiva, C. P-589
Sarasa Corral, J.L. P-980
Saravo, L. P-888
Sarbianova, N. P-285
Sardi, I. P-372
Šarèeviæ, B. P-31
Saremaslani, P. O-112
Sari, S. P-792
Sarian, L.O. P-749
Saric, J. O-47
Sarmento-Filho, J.M. P-418
Sarnacki, S. O-98
Sarrió, D. O-262, P-51, P-404, P-787
Sasano, H. P-700
Sasse, B. P-415, P-738, P-808
Sassi, S. P-325, P-419, P-659, P-795, P-834
Sastre-Garau, X. O-156, O-168, O-212, O-215, O-242, O-256, O-263, P-885
Sato, Yuichi P-602
Saudade, A. P-43
Sauter, G. O-175
Sautesfridman, C. O-64
Sauvanet, A. O-111
Sav, A. P-180
Savarino, V. P-281
Savas, B. P-226, P-309
Savci, D. P-284
Savelov, N. P-909
Savelov, N.A. P-596
Savjak, D. P-583
Savva, S. P-317
Saygin, T. P-692
Sblano, S. P-145
Scarpa, A. O-58, O-199, P-111
Scarpa, R.M. O-180
Scarpino, S. O-128
Schaff, Z. O-113, O-73, P-258, P-515, P-544, P-552, P-887
Schaff, Z.S. P-851
Schaider, H. P-103
Schalken, J.A. O-197, P-861
Schaser, K.-D. O-143
Schauer, S. O-60
Schelfout, K. P-420
Schepers, M. O-169
Schewe, C. O-220
Schillaci, F. O-124
Schimanski, S. O-67
Schlenger, R. P-619
Schlosshauer, P. O-237, P-788
Schlyakhto, E. O-248
Schmid, K. P-254
Schmid, K.W P-256
Schmid, S. O-112, O-160, P-619, P-620, P-626
Schmitt, A. P-620
Schmitt, F. P-34, P-316, P-399
Schmitt, F.C. O-213, P-28
Schmitt, J.P.F. O-216
Schmitz, G. O-67
Schmitz, K.J. O-224
Schneegans, O. P-603
Schneider, P.M. O-75
Schneider-Stoch, R. O-151, O-175
Schouten, L.J. O-197, P-861
Schraml, P. P-860
Schreiber, C. P-261
Schreiber, J. P-261
Schroeder, J. P-641
Schroten, H. O-67
Schulte, H.M. P-772
Schulz, S. O-74
Sciacchitano, S. O-52, P-592
Sciot, R. O-158
Scoazec, J.-Y. O-114, P-158
Scopa, C. P-503, P-536, P-971
Scopa, C.D. P-207, P-612
Sculier, J.-P. O-117
Sebastian, L. P-422
Sedaghat, Y. P-935
Sedlakova, E. P-933, P-964
Sedliarou, I. P-605
Segers, V. P-816
Segovia Blazquez, B. P-841
Segovia, B. O-185
Seiichiroh, K. P-779
Seiji, H. P-153
Seiwerth, S. O-4, O-27, P-643
Sekeris, C. P-810
Selivanova, G. O-248, P-711
Sellami Dhouib, R. P-795, P-834
Sellami, A. P-100, P-402, P-423, P-800, P-874, P-955
Selva, E. O-79, O-131, P-911
Selves, J. P-215, P-225
Semernin, E. P-711
Sen, N. P-558
Senant, N. O-41
Senaylý, A. P-79
Seo, Seung-Won P-40
Seoung, Wan Chae P-183
Seppo, S. P-792
Sera, F. O-146
Serafetinides, E. O-194
Serarslan, G. P-919
Serfaty, L. O-39
Serio, G. P-18
Serrano, A. P-871, P-872
Serrano, S. P-129, P-701, P-866, P-867, P-868
Serres, I. O-83
Sers, C. O-143
Sertçelýk, A. P-686
Servant, J.-M. O-260
Sessa, F. P-36, P-521
Setareshenas, R. P-385, P-386
Severgina, E. P-637, P-870
Severgina, L. P-637
Sevilla, I. P-551
Seyam, M. P-220
Seyasi, F. P-582
Seyed, M.O. P-300
Sezer, M. P-487
Sezer, T. P-79
Sfakianos, G. P-443
Sfaxi, M. P-368
Sfiniadakis, I. P-295
Shadman, M. P-1
Shafigh, E. P-265
Shahgoli, B. P-392
Shakeri, T. P-172
Shapovalov, D. P-909
Sharifah, N.A. P-567
Sharifi, N. P-76, P-172
Sharifi-Salamatian, V. P-403
Shawki, O.A. P-754
Shcheglov, D. P-989
Shcheglov, V. P-989
Shchepotin, I. P-406
Shegai, P. P-675
Sheils, O. O-101
Shen, S.S. P-391
Sheppard, B. O-101
Sheppard, M. P-253
Sheppard, M.N. P-723
Shestakova, L. P-246
Shimizu, K. P-972
Shin, Dong Hun P-814
Shipkova, M. O-76
Shirpoor, A. P-507
Shlyakhto, E. P-711
Shokrgozar, M.A. O-221
Shoman, S. P-181, P-182, P-388
Shong, M. P-601
Siadati, S. P-265
Sibel, P. O-33
Sibon, C. P-920
Sibony, M. O-181, O-198, O-204, P-685, P-693
Sicard, D. O-148
Sieben, N. O-233
Siemiatkowska, K. P-496
Sigal, E. P-282
Sigal-Zafrani, B. O-212, O-215, O-256, O-263
Signolle, N. P-893
Sikiriæ, P. O-27
Silva, P. P-944
Silva, P.W.T. O-94
Silva, R.C. O-57
Silva, V. P-478
Silvana, G. P-47, P-564
Silva-Valenzuela, M.d.G. P-561, P-568
Silvestre, J. P-733
Šimat, M. P-762, P-942
Simek, K. P-609
Simion, A. P-127
Simion, S. P-155
Simionescu, O. P-936
Simões da Silva, M.T. P-519
Simon, J.M. P-969
Simonchuk, E. P-797
Simone, A. P-888
Simonet, M.L. P-108
Simonetti, S. O-151
Simony-Lafontaine, J. P-403, P-407
Simoulis, A. P-348
Simpson, P.T. O-213, O-216
Simsek, M. P-805
Sinakos, E. P-216
Sinha, K.U. P-559
Sintou-Mantela, E. P-85, P-375
Sioutopoulou, D. P-90, P-105
Sipos, F. P-328
Sippelli, G. P-888
Sirbu, P. P-638
Sirinian, C. P-117
Siti-Aishah, M.A P-567
Sivridis, E. P-194
Skagers, A. P-345
Skapa, P. P-967
Skaro Milic, A. P-204
Skender-Gazibara, M. P-125, P-959, P-995
Sklyarenko, L. P-108
Skodric, S. P-849
Skommer, J. P-107
Skoulidakis, G. P-681, P-705
Skrima, M. P-842
Slavisa, J.A P-327, P-563
Slavov, C. P-687
Slodkowska, J. P-496
Slootweg, P.J. O-160
Slowinski, J. P-974
Sly, W.S. P-429
Smati, B. P-486
Smirnova, E.A. P-596
Smok-Ragankiewicz, A. P-74
Smyth, P. O-101
Snezana, J. P-563
Soares, A. O-172
Soares, F.A. P-87, P-827
Soares, N. P-351
Soares, P. O-29, P-591, P-607, P-608
Soares, R. P-607, P-608
Sobel, G. P-887
Sobhani, A. O-221
Sobrinho-Simões, M. O-29, P-64, P-588, P-591, P-607, P-608
Sobrosa De Mello, E. P-537
Socha, K. O-99, P-15
Socha, M. O-99
Socolov, R. P-150
Sohn, Jin Hee P-789, P-790
Soini, Y. P-292
Sok, Kim Eng P-398
Sokmensuer, C. P-289, P-309
Sol, Mee Young P-814
Sola, J.J. P-863, P-864
Solé, F. P-129
Solé, M. P-528, P-531
Soleimanirad, J. P-274
Soliman, H. O-257
Solovyeva, O.I. P-200
Solsona, E. P-396
Soltész, I. P-238, P-258, P-499
Somogyi, L. P-379
Song, Kyu-Sang P-512
Sonmez, O. P-180
Sonoue, H. O-110
Sopta, J. P-267, P-449, P-633, P-640
Soptamd, J. P-587
Soriano, A. P-528
Soriano, P. P-33
Sorokina, I.V. P-718
Sosa, G P-702
Sotelo, C. O-89
Sotiropoulou, M. P-24, P-317
Sotoudeh, M. P-229
Soubrier, F. O-35
Souleau, B. P-122
Soultoyannis, I. O-46
Soumakis, K. O-102

Soumaya, R. P-157
Sousa, S. P-560, P-581
Sow, M. P-885
Sowa, P. P-970
Soydan, E. P-97, P-98
Soylemezoglu, F. O-243
Soysal, M.E. P-405
Soyuer, I. P-37, P-318
Soyuer, S. P-37, P-318
Spaczynski, M. P-798
Spaggiari, P. P-281
Spagnoli, L.G. O-225, P-780
Spanos, I. P-524
Spasevska, L. P-446, P-833
Speel, E.J.M. O-157, O-160, O-164, O-169
Spener, R. P-561
Spidlen, V. P-249
Spielmann, M. P-17
Spigiorin Maggiori, M. P-804
Spiliopoulou, C. P-295
Spitz, R. O-66
Sporius, R. P-870
Spuller, E. P-658
Squire, J.A. O-85
Staber, P.B. O-60
Stadlmann, S. O-108, P-902
Staff, A.C. O-234
Staibano, S. O-236
Staiti, N. P-888
Staller, P. P-860
Stanculescu, D. P-20
Stanek, J. O-48, O-49, P-142
Staniceanu, F. P-155, P-227, P-530, P-903
Stanojevic, Z. O-189
Staroz, F. P-685
Steele, D. O-216
Stefan, M. P-103
Stefanaki, K. P-83, P-84, P-126, P-443
Stefano, J.T. P-213
Stefanou, D. P-45, P-793, P-973
Stefansson, I. P-781
Stefansson, I.M. P-928
Šteiner, I. O-227, O-228
Stelkovics, É. P-259
Štelzl, E. P-103
Štemberger, C. P-934, P-942
Stenbäck, F. O-103
Stengel, D. O-245
Stepanets, V. P-904
Stepien, T. P-975
Sterkers, O. P-343
Stern, M. P-247
Sternberg, D.W. O-60
Štifter, S. P-934
Stita, W. P-144
Stobiecka, E. P-74, P-163
Stoehr, R. O-175
Stoica, G. O-253
Stoica-Mustafa, E. P-311
Stojšiæ, Z. P-939
Stojsic, J. P-244, P-245, P-481
Stojsic, Z. P-714, P-729
Stolnicu, S. P-167, P-189, P-553, P-638, P-683, P-684, P-696, P-697, P-807
Stomal, M. P-974
Stömmer, P.E. P-508
Stordrange, L. P-691
Störkel, S. O-175
Storz, M. O-238
Straka, U. P-310
Strakova, N. P-964
Straume, O. P-928
Strazda, G. P-490
Strebel, R. P-378
Strefanou, D. P-631
Streinucercel, A. P-227, P-530
Stridsberg, M. P-618
Strohmeier, B. O-104
Stropahl, G. O-22
Stropahl, K. O-22
Struckmann, K. P-860
Stubbe, H.D. O-224
Stubbe, H.D. O-224
Student, V. P-677
Studer, U.E. P-883
Stylianidi, A. P-761
Stylianou, P. P-476
Su, Chih-Ying P-569
Su, Hsuan-Chi P-952
Suárez, A. P-755, P-787
Suárez, H. P-813
Suárez-Peñaranda, J.M. P-624, P-917, P-918, P-924
Suda, K. O-110
Sugihara, S. O-140
Suh, Kwang-Sun P-512
Suhail N Abdullah Al-Salam P-192
Suheyla, U.B. P-850
Süle, N. P-379, P-391, P-985
Sulkes, J. P-925
Sulkowska, M. P-42, P-575
Sulkowski, S. P-42, P-575
Sun, X.Z. P-993, P-998
Sungur, A. O-61
Surowiak, P. P-798
Susini, T. O-106
Susman, S. O-145
Susnik, B. O-258
Sutter, C. O-238
Suvajdzic, N. P-125
Svachova, M. P-677, P-964
Svoboda, J. P-904
Svrcek, M. O-36, P-533
Swierniak, A. P-609
Symeonidis, A. P-117
Syrjänen, K. P-175, P-749
Syrjänen, S. P-749
Sysoenko, O. P-450
Szabó, E. P-544, P-887
Szabó, I. P-273, P-887
Szabó, L.Z. P-330
Szabo, Z. O-73
Szalecki, M. P-595
Szczeniak-Klusek, B. P-74
Szczurek, Z. P-905
Szederkényi, E. O-95
Székely, E. P-273, P-532
Székely, T. P-532
Szende, B. P-891
Szendrõi, A. P-851
Szenohradszky, P. O-95
Szentirmay, Z. P-511
Szentjóbi Szabó, T. O-249
Szépe, P. P-310, P-313
Szewski, W. P-23
Szigeti, K. P-985
Szijarto, A. O-113
Szilágyi, L. P-961
Szilák, L. P-887
Sziller, I. P-887
Szpor, J. P-649, P-650, P-815, P-818
Szuhai, K. O-158

Tabatabaie Seid, A. P-242
Tabernero, J. P-190
Taddei Gian, L. O-106, P-372
Tadic Latinovic, L. P-565
Tafarel, J.R. P-992
Taffuri, M. P-4
Tagscherer, A. O-80
Taieb, J. P-525
Taivans, I. P-490
Takahashi, S. P-993, P-998
Takahashi, Y. P-434
Takamori, S. P-482
Takano, D. O-259
Takanori, H. P-954
Takashima, K. O-218
Takayama, T. P-584
Takeda, A. O-224
Takeda, N. O-224
Takemura, A. P-584
Talaei Khozani, T. P-452
Talalaev, A.G. P-431
Talebi, A. P-599
Tamási, A. P-259
Tamayo, J.C. P-690
Tamvakis, N. P-475, P-476, P-654
Tamvakos, G. P-681
Tan, Yun P-429
Tanase, C. P-628
Tancredi, M. P-44
Tang, J. O-26
Tannapfel, A. O-24, O-28
Tanoglidi, A. O-182, O-196, P-394, P-539
Tarabar, D. O-37
Tarabra, E. O-166
Tarcin, O. P-892
Tardío, A. P-927
Tarkýn, I. P-621
Tárnok, A. P-328
Tarricone, V. P-69, P-70
Tarroch, X. P-744
Tartour, E. O-8
Tascon, R. P-869
Taskin, T. P-949, P-950
Tatic, S. P-267, P-583
Tatsiou, Z.A. P-90, P-105
Tatsuru, I. P-347
Tatti, S. P-749
Taupin, P. P-81
Tavangar, A. P-935
Taveira, A. O-29
Tazir, M. P-78
Tcherveniakov, A. P-285
Tebbi, Z. P-653
Teijeira, S. O-252
Telaku, S. P-299
Teleman, S. P-133
Televantou, D. P-617
Teresinski, L. O-7
Terinte, C. P-133
Terracciano, L. O-151
Terrasa, F. P-380
Terrier, P. O-156
Terris, B. P-517
Terrone, C. O-180
Terry, S. O-86
Tertychnyy, A.S. P-431
Terzea, D. P-824
Terzi, A. O-243
Terzi, M. P-7
Terzic, T. P-86, P-125, P-449
Tessa, A. O-246
Tessaro, B. P-708
Tetik, L. P-487
Tezel, C. P-479
þahin, Ç. P-283
Thalassinos, N. P-497
Thanos, L. P-539
The Getco Group P-173
The Members of Committee N. "Digestive Tract" P-158
Thebault, S. P-215
Theobald, S. P-603
Theocharis, S. O-102, O-194, O-242, P-295
Theodoropoulos, G. P-160, P-186
Theodoropoulos, V. P-681, P-705
Theodosopoulos, N. P-681, P-705
Théou, N O-149
Therkildsen, M.H. O-3
Theurillat, J.-P. P-415, P-808
Thezenas, S. P-407
Thiefin, G. O-38
Thiele, J. O-75, P-99
Thienpont, L. P-610
Thioux, M. O-168
Thivolet-Bejui, F. P-498
Thomas De Montpréville, V. P-709
Thomas-Tsagli, E. P-371
Thomopoulou, G. P-160, P-186
Thoresen, S. P-759
Thymara, I. P-251, P-371, P-979
Tian, H.R. O-251
Tichy, M. P-933, P-988
Tichy, T. P-847
Tiensuu-Janson, E. P-618
Tiftikci, A. P-221
Tilli, C. P-132, P-745
Timens, W. O-91, P-255
Tina, M. P-305
Tinguely, M. O-56, P-135
Tiniakos, D. P-810
Tiret, E. O-36
Tischoff, I. O-28
Tisseau, L. P-706
Tissier, F. O-163, P-538
Tjalma, W. P-420
Todorovic, V. P-102, P-244, P-307, P-481
Tohru, K. P-347
Toker, A. P-252
Tõkés, A. P-887
Toledo, B. O-231
Toledo, G. P-863, P-864
Toli, A. P-369
Toliou, T. P-24, P-369
Tolovska, M. P-734
Toma, L. P-250

Tomarev, S. P-28, P-944
Tomas, D. P-703, P-853
Tomi, K. P-853
Tomi, L. P-853
Tomic, K. P-857
Tomin, D. P-86
Tomita, K. O-140
Tommola, S. P-292
Tomoyuki, O. P-347
Tomsic, M. P-837
Tomulescu, V. P-311
Tong, Guo-Xia O-201
Toprak Selami, K. P-97, P-98
Toptsis, K. P-656
Topuz, Bulent P-558
Topuz, S. P-756
Toran, N. P-147
Torné, A. P-760
Tornillo, L. O-151
Toth, L. P-511
Tötsch, M. P-254, P-256
Toublanc, M. P-353
Touraine, R. P-838
Townsend, R. O-23
Toyonaga, S. P-972
Tozlu, S. O-177
Trabelsi, A. P-144
Trakas, N. P-475, P-476
Tran van Nhieu, J. O-114
Trasca, E.T. P-471, P-645
Trasca, P.R.M. P-149
Trasca, T.E. P-148
Trastour, C. P-39
Trauner, A. P-751
Traversi, C. P-18
Trenkiæ, M. P-359
Tresallet, C. O-35, P-604
Triau, S. P-193, P-381, P-578
Trierveiler, M. P-351
Trihia, H. P-7, P-24
Triller, M. P-685
Trimarchi, F. P-592
Trimeche, M. P-349
Tringidou, R. P-248
Tripault, F. O-131, P-326
Troccaz, J. P-679
Trocoli, F. P-70
Troung, D.L. P-391
Trovato, M. O-52, P-592
Trovisco, V. P-607
Trpkov, K. O-183
Truan, D. O-203
Trugnan, G. O-34
Trunecka, P. P-231
Tsai, Chien-Chen P-844
Tsai, Nu-Man P-952
Tsai, Y.Y. P-301, P-737
Tsakistou, G. P-341
Tsamandas, A. P-117, P-503, P-536, P-971
Tsamandas, A.C. P-207
Tsamouri, M. O-196
Tsanou, E. P-84
Tsatsaroni, A. P-91
Tschernev, K. P-285
Tsekeris, P. P-201
Tseleni-Balafouta S. P-613
Tsianos, E. P-85
Tsianos, E.V. P-201
Tsigka, A. P-681, P-705
Tsikou-Papafragou, A. P-539
Tsiple, I. P-716
Tsobanidou, C. P-369, P-854
Tsolakis, A.V. P-618
Tsompanidou, C. P-75
Tsuchiya, H. O-140
Tsukayama, C. P-777
Tsybrovskyy, O. P-671
Tuccari, G. P-888
Tuðlular, S. P-458
Tulassay, Z. O-80, P-329, P-890
Tulic, G. P-633
Tuncer, Ý. P-104
Tuppurainen, K. P-159
Turan, C. P-318
Turan, D. P-794
Turan, G. P-543
Turashvili, G. P-408
Turbat-Herrera, E.A. O-191
Türemen, E. P-621
Turhal, S. P-296
Turlin, B. P-549
Turmo, M. O-135, O-241
Turpin, E. O-257
Turrin, N. P-202
Turska-Kmiec, A. P-719
Turton, D. P-748
Tuzlali, S. P-11, P-65, P-756
Tuzuner, N. P-945
Tzaida, O. P-7, P-348
Tzankov, A. P-77, P-370
Tzilves, D. P-324
Tzioufa, V. P-216
Tzirakis, M. P-115, P-118, P-526

Uçar, T. P-963
Uccella, S. O-161, P-627
Udud, K. P-499
Ueda, S. O-247
Uela, J.M. P-33
Ugnius, M. P-131
Uhlig, S. P-900
Uhlig, U. P-900
Ulivieri, A. O-52
Üner, A.H. O-61
Unlu, M. P-487
Urasinska, E. P-119
Urasinski, T. P-119
Urawski, J. P-672
Urek, S. P-479
Usaj Knezevic, S. P-130, P-583
Usaj, S. O-37
Usera Sagarra, G.. P-841
Usera, G. P-840
Us-Krašovec, M. P-9
Ustymowicz, M. P-14
Usubütün, A. P-753, P-791, P-811
Utkan, Z. P-543
Uysal, V. P-383, P-839

Vääräsmäki, M. P-426
Vacherlavenu, M.-C. O-163, P-757
Vacherot, F. O-86
Vakiani, E. O-54, P-128
Valavanis, C. P-24, P-348, P-879
Val-Bernal, J.F. O-118
Valdman, A. P-271, P-676
Valente, M. O-90, P-454, P-541
Valeri, A. P-699
Valerio, J.C. P-124
Valeyre, D. P-247
Valgeirsson, H. O-216
Valla, D. P-234
Valmary, S. P-215
Valo, I. P-48
Vamvakaris, J. P-248
Vamvouka, C. P-126
van 'T Veer, L. O-9
van Crombrugge Beatrix Cochand-Priollet, P. P-610
van Cutsem, E. P-899
van de Sompele, J. O-77
van den Bempt, I. P-3
van den Brandt, P.A. O-197, P-861
van den Brekel, M. O-9
van den Eynden, G. P-420
van der Borght, B. P-214
van der Kwast, T. O-175
van der Wal, A. O-223
van Dijk Boukje, A.C. O-197, P-861
van Eeden, S. P-513
van Eijk, R. O-233
van Engeland, M. O-233
van Eyken, P. O-153
van Houwelingen, K.P. O-197
van Marck, E. P-420
van Nederveen, F. O-164, P-626
van Oers, J. O-175
van Velthuysen, M.-L. O-9, P-513
van Vliet-Constantinidou, C. P-443
van Zandwijk, N. O-9
Varambally, S. O-26
Varela Durán, J. P-924
Varga, V. P-328, P-890
Varga, V.S. O-80
Varga, Z. P-415, P-808
Varna, M. O-257
Varshavsky, V.A. P-463
Vasilescu, C. P-311
Vasilescu, F. P-127, P-219, P-250, P-573, P-763, P-824
Vasiliadis, T. P-203
Vasilicã, M. P-881
Vasiliu, V. O-198, P-81, P-706
Vasiljevic, A. P-498
Vasiljevic, D.J. O-226, P-714, P-715, P-729
Vassalo, J. P-87
Vassilakaki, T. P-524
Vaunois, B. P-598
Vázquez Boquete, A. P-597
Vecchione, R. O-52
Vela Chavez, T.A. P-764
Vela, T. P-414
Vela-Chavez, T. P-123, P-124
Veli, U. P-848
Velickovic, L. O-189
Velickovic, L.J. P-694
Veli-Matti, K. P-792
Velimir, Vrdoljak, D. P-10
Veljanoska, S. P-765
Vendrell, T. P-147
Vendrely, V. O-31
Venissac, N. P-911
Venizelos, I.D. P-90, P-105
Venizelos, J. P-317
Verbrugghe, P. O-77
Vereschagina, M.V. P-576
Vergier, B. O-134, O-135
Verhest, A. O-117
Verhofstad, A.A. O-160, O-164, P-626
Verhulst, P. O-126
Verine, J. O-256
Vernerey, D. O-145
Vernerova, Z. P-904
Verney, C. O-255
Verret, J.-L. P-922
Verrièle, V. P-48
Vesely, P. O-60
Viacava, P. P-436
Viale, G. P-162
Vicandi, B. P-6, P-272
Vicente, F. P-33, P-425
Vicioso, L. P-551
Vidal, A. P-869
Vidaud, M. O-178
Vieillefond, A. O-177, O-178, O-198, O-204, O-205, P-685, P-693, P-706, P-707, P-842
Vieites, B. P-924
Vielh, P. O-242
Viennet, G. P-312
Viguer, J.M. P-6, P-272
Vilallonga, R. P-492
Vilana, R. P-531
Vilchez, J. P-589
Vilela Rafael, S. P-335
Vilela, R.S. O-231, P-827
Vilgrain, V. P-235, P-550
Villanacci, V. P-505
Villers, A. O-83
Vincendeau, S. O-195
Vincent-Salomon, A. O-212, O-215, O-256, O-263
Vinel, J.-P. P-225
Vintman, L. O-192
Virag, T. P-890
Vire, O. P-706
Virtaniemi, J. O-2
Vital, A. O-241
Vitarelli, E. P-592
Vitelli, C.E. O-210, O-211, P-4, P-5
Vitry, F. O-170
Vizjak, A. O-19, P-837
Vlachodimitropoulos, D. P-25
Vlachos, G. O-102
Vladika, N. P-75, P-324
Vlahova, A. P-687
Vlasova, T. O-248, P-711
Vletsi, E. P-475
Vogiatzis, G. P-203
Vogler, C. P-429
Voigt, J.-J. P-898
Voiosu, R. P-155, P-227
Volant, A. P-699
Volante, M. O-166, O-167, P-382
Volavšek, M. O-5
Vollmer, E. O-220, P-500, P-900

Voloschuk, I.N. P-140
Voloshin, V. P-778
Voloshina, N. P-778
von Buchwald, C. O-3
Voogd, A.C. O-169
Vordos, D. O-82, P-670
Vos, J.T.W.M. O-91
Vosooghynia, H. P-172
Vossoghinia, H. P-229
Voulgaris, S. P-973
Voulgaris, Z. O-102
Voutsinas, G. P-613
Vozianov, A. O-174
Vozianov, S. P-464, P-704
Vrabie, A. P-155, P-227, P-530, P-903
Vrabie, C.-D. P-786
Vranic, S. P-38
Vreju, A.F. P-645, P-783
Vretou, E. P-317
Vrettou, E. P-216
Vrettou-Aravani, V. P-184, P-341
Vucic, M. P-857
Vuckovic, L. P-583
Vukièeviæ, T. P-137
Vukmirovic, F. P-583

W'och, J. P-609
Waelput, W. O-77
Wagner, B. P-695
Wagner, T. P-695
Waisman, J. O-201
Wakai, T. O-32
Wakamatsu, A. P-214
Waldman, S.A. O-74
Wali, R. O-96
Walker, F. O-184
Wallraf, J. O-18
Walter, P. P-294
Wang, B.Y. O-92
Wang, W. P-668
Wani, Y. P-777
Ward, L.S. P-615
Wasilewska, A. P-649, P-650, P-815, P-818
Wassef, M. O-155, P-353, P-660
Watanabe, M. P-700
Weber, A. O-28
Weber, M. O-17
Wechsler, J. O-136, O-137, O-138
Weckermann, D. P-695
Weichert, W. P-768
Weidmann, J. P-776
Weihe, E. O-112, P-619
Wemeau, J.-L. O-126
Wen, S.C. P-301
Wendum, D. O-114, O-34, O-39, P-533
Weng, E. P-142
Went, P. P-77
Werner, J.P. O-264
Wessels, J. O-21
Wetzels, C. O-153
Weybora, W. P-658
Wheeler, T. P-680
Wieben, D. P-619
Wienand, J.R. O-264
Wiesli, P. P-620
Wilczok, T. P-975
Wild, P. O-175
Wiley, C. O-240
Willems, J.S. P-610
Willems, S.M. O-158
Williams, D. O-29
Wilt, M. P-603
Wincewicz, A. P-42
Winter, R. P-799
Wisniewski, P. P-15
Wittekind, C. O-24, O-28
Wittig, R. O-25
Wlaszczuk, P. P-906, P-962, P-975
Wloch, J. P-595
Wlodkowic, D. P-107
Wohlschlaeger, J. O-224
Wojciechowski, M. P-496
Wojcikiewicz, T. P-962
Wolanska-Karut, J. P-906
Woloszynska-Preidl, K. P-74, P-163
Wong, P.K.Y. O-253
Woo-Hyung, K. P-334
Working on, Behalf of Afaqap (French Association for Quality Assurance in Pathology) P-158
Woÿniak, A. P-672
Woÿniewicz, B. P-719
Wozniak, A. O-72, P-976
Wozniewicz, B. P-710
Wright, T. P-214
Wu Mark, Li-Cheng O-80
Wu, C.C. P-775
Wu, J.-D. P-120
Wycliffe, N. O-251
Wygoda, Z. P-609
Wysocka, J. P-649, P-650, P-815, P-818
Wysocki, M. P-119

Xagoraris, I. P-96
Xerri, L. O-55
Xirou, P. P-67, P-75, P-324

Yacoubi, M.T. P-143, P-144
Yaegashi, H. P-779
Yakovtsova, A.F. P-718
Yakupoglu, U. P-391
Yalcinkaya, A. P-226
Yamada, S.M. P-972
Yamagishi, Sho-Ichi O-247
Yamaguchi, T. O-141
Yamaguchi, Takehiko O-140
Yamakawa, A. P-434
Yamasaki, S. O-110
Yamashita, S. P-605
Yang, Ching-Hua P-844
Yano, H. P-482
Yashar, G. P-277, P-747, P-765
Yassi, F. P-653
Yassonov, S. P-637
Yavuz, E. P-11, P-65, P-756
Ychou, M. P-173
Yehia, H. P-211, P-220
Yiang, Yia-Tang P-49
Yildirim, S. P-411, P-965
Yildiz, I. P-791
Yildiz, I.Z. P-753
Yilmaz, A. O-183
Yilmaz, B. P-518
Yilmaz, D. P-580
Yilmaz, I. P-411, P-965
Yilmaz, S. O-15
Yilmazbayhan, D. P-252, P-263
Yiou, R. O-82, P-670
Yip, D. P-319
Ylä-Herttuala, S. O-227
Yolac, E. P-794
Yoon, Jung-Hwan P-545
Yoon, Wan-Hee P-512
Yoshida, S. P-993, P-998
Yoshimoto, M. O-85
Yoshimura, J. O-247, P-243
Young, R. O-207
Yousif, A.A. P-817
Yu, Cheng-Ping P-49
Yu, Jyh-Cherng P-49
Yugina, O.V. P-480
Yurakh, A. P-396
Yurtaydýn, C. P-226

Zabel, M. P-468, P-798
Zabel, P. P-900
Zabolinejad, N. P-432
Zaccaria, M. P-21
Zachilas, D. P-251, P-497
Zadorozhnaya, T. P-739
Zadravec-Zaletel, L. O-239
Zaeri, F. P-364
Zafrani Elie, S. O-45, O-114
Zafrani, E.-S. P-549
Zagorianakou, N. P-121, P-793
Zagorianakou, P. P-793
Zaharia, A. P-155, P-227, P-530, P-903
Zaharia, B. P-19
Zahiri, S. P-453
Zairi, A. O-83
Zairi, I. P-655
Zajaczkowska, A. P-710
Zajecki, W. P-905
Zakaria, S. P-211, P-220, P-223, P-223
Zakhartseva, L. P-406, P-797
Zalatnai, A. P-891
Zalcmane, V. P-210
Zambelli Ramalho, L.N. P-59, P-63, P-804
Zamboni, G. P-275
Zamecnik, J. P-967, P-988
Zamiati, S. P-89, P-109
Zamò, A. O-58, P-111
Zamolo, G. P-934, P-942
Zampatti, C. P-521
Zandvoort, A. O-91
Zanis Neto, J. P-992
Zanotti, R. P-111
Zaouche, A. P-323
Zatloukal, K. O-104
Zauhar, G. P-942
Zavalishina, L.E. P-367
Zavelevich, M. P-108
Zavitsanakis, A. P-438
Zavrldis, H. P-188
Zeddini, A. P-350
Zeimet, A.G. O-108, P-902
Zeinab, O. P-236
Zeinab, S.O. P-230
Zekri, A.-R.N. P-754
Zelek, L. P-17
Zeman, M. P-163
Zembala, M. P-529
Zembala-Nozynska, E. P-163, P-529, P-721, P-905
Zentilin, P. P-281
Zeppetella del Sesto F.S. O-52
Zergeroðlu, S. P-767
Zermani, R. P-157, P-323, P-350, P-360, P-368, P-655, P-846, P-877, P-937
Zervas, K. P-91
Zhang, J. P-542
Zhang, R. P-993, P-998
Zheng, Y. P-542
Zhu, L. O-244
Ziadi, S. P-349
Zidane, M. P-470
Zidar, N. O-14, P-571, P-722
Zielenska, M. O-85
Zieliñski, G. P-743
Zietara, K. P-92
Zigeuner, R. O-176, P-361, P-362
Zimmermann, D. P-378, P-662
Zimpfer, A. P-77
Zini, L. P-856
Zink, A. O-220
Zioga, A. P-121, P-375, P-926
Ziol, M. O-44
Ziotopoulos, P. P-476
Zissel, G. P-500
Zitouna, M.M. P-340, P-342
Zitvogel, L. P-17
Zivkovic, V. O-189, P-694
Zizi, A. P-879
Zizi-Serbetzoglou, A. P-188, P-524
Zografski, G. P-765
Zola, F.E. P-418
Zolota, V. P-117, P-503, P-96, P-971
Zouari, B. P-325, P-368
Zougris, S. P-475
Zoumpouli, C. P-421
Zrnic, B. P-495
Zuber, C. P-808
Zubler, P. P-135
Zucman-Rossi, J. O-114, P-533, P-538
Zucoloto, S. P-59, P-60, P-61, P-62, P-63, P-237, P-562
Zurac, S. P-155, P-227, P-530, P-903
Zurawski, J. O-72
Zwarthoff, E. O-175

Virchows Arch (2005) 447: 573–585
DOI 10.1007/s00428-005-1233-3

ORIGINAL ARTICLE

Christiane Schewe · Torsten Goldmann · Marianne Grosser · Albert Zink · Karsten Schlüns · Stefan Pahl · Timo Ulrichs · Stefan H. E. Kaufmann · Andreas Nerlich · Gustavo B. Baretton · Manfred Dietel · Ekkehard Vollmer · Iver Petersen

Inter-laboratory validation of PCR-based detection of *Mycobacterium tuberculosis* in formalin-fixed, paraffin-embedded tissues

Received: 1 November 2004 / Accepted: 15 February 2005 / Published online: 21 June 2005
© Springer-Verlag 2005

Abstract The present study is based on the initiative for quality assurance in pathology of the German Society of Pathology and the Professional Association of German Pathologists. Four panel laboratories with experience and expertise in polymerase chain reaction (PCR) detection of *Mycobacterium tuberculosis* were selected to establish the prerequisites for continuous external laboratory trials, in particular, by providing pre-tested specimens and evaluation criteria for participating institutes. In the first step, the four panel laboratories performed an internal trial to test their own reliability and reproducibility. Paraffin sections and DNA preparations from 34 tissues (25 clinical specimens and 9 controls) totalling to 66 samples were evaluated by each panel institute according to their own protocols. The methodologies differed and are described in detail. Despite these differences, a high degree of inter-laboratory reliability was achieved. In this report, we summarise our results including the correlation with the histology and provide recommendations for applying PCR-based methodology for the detection of mycobacterial DNA in surgical specimens. Supplementary data are available online at http://www.charite.de/ch/patho (rubric "Forschung"). Pre-tested specimens are now available for the external trial and can be ordered from the steering institute via Oligene (http://www.oligene.com/). All molecular pathology laboratories are invited to participate in this quality assurance initiative.

Keywords PCR · Tuberculosis · Multi-centre study · Quality assurance · Reference standards

C. Schewe (✉) · K. Schlüns · S. Pahl · M. Dietel · I. Petersen (✉)
Charité-Campus Mitte,
Institute of Pathology,
Universitätsmedizin Berlin,
Schumannstr. 20-21,
10098 Berlin, Germany
e-mail: christiane.schewe@charite.de
Tel.: +49-30-450536106
Fax: +49-30-450536916
e-mail: iver.petersen@charite.de
Tel.: +49-30-450536050
Fax: +49-30-450536902

T. Goldmann · E. Vollmer
Forschungszentrum Borstel,
Klin. & Exp. Pathologie,
23845 Borstel, Germany

M. Grosser · G. B. Baretton
Institut für Pathologie,
Technische Universität Dresden,
01307 Dresden, Germany

A. Zink · A. Nerlich
Krankenhaus München-Bogenhausen,
Institut für Pathologie,
81925 Munich, Germany

T. Ulrichs · S. H. E. Kaufmann
Max-Planck-Institut für Infektionsbiologie,
10117 Berlin, Germany

Introduction

Polymerase chain reaction (PCR)-based analytical technologies have developed to a standard methodology in nearly all disciplines of biosciences. Among others, this approach provides the option to look at targeted gene sequences and to amplify them, thus, enormously increasing sensitivity for detection. Detection and identification of disease-related genes in surgical pathology specimens, i.e. in biopsies, cytology samples, surgical resections and specimens from autopsies, have gained increasing importance in recent years and have created the discipline of molecular pathology [19]. The use of formalin fixation and paraffin embedding (FFPE) in pathology, however, implies several methodological obstacles, which need to be accounted for and cleared appropriately [13, 40, 48]. The commonly used fixation agent formalin is known to cause damage to DNA via fragmentation and/or cross-linkage. For this reason, the primer sets should be selected in such a way that specific and small, preferably multi-copy or repetitive, sequences are amplified. Additionally, reaction periods of the PCR cycles need to be sufficiently long.

In the literature, a large number of successfully applied set-ups are recommended for this purpose [2, 8, 17, 20, 26, 30, 39]. However, their reliability and reproducibility have only rarely been validated by comparative inter-laboratory trials [3, 28].

PCR-based investigation for mycobacterial DNA is an important application of molecular pathology, because granulomatous tissue responses are frequently, although not exclusively, attributed to mycobacterial infections. Detection of mycobacterial DNA is mandatory in tissues affected by granulomatous disorders, because the Ziehl–Neelsen (ZN) staining for acid-fast bacteria often fails to yield conclusive results [18, 24, 43].

Similarly, other approaches such as auramine staining or immunohistochemical identification using polyclonal antibodies against mycobacteria proved to be not sensitive enough for this purpose [29, 41]. Moreover, none of these classical techniques enables the distinction among *Mycobacterium tuberculosis*, atypical mycobacteria [also called mycobacteria other than tuberculosis complex (MOTT), or non-tuberculous mycobacteria (NTM)] and their subtyping [9, 35]. With FFPE, this task can only be solved by PCR-based methodology to date.

In addition to FFPE-related problems, mycobacteria carry a further methodological obstacle because of their thick mycolate-rich outer cell wall, which requires special measures of cell disintegration without causing further damage to DNA [14]. Thus, detection of mycobacteria in pathology samples is particularly critical and needs validation.

As part of a joint initiative of the German Society of Pathology (Deutsche Gesellschaft für Pathologie, http://www.mh-hannover.de/institute/pathologie/dgp/) and the Professional Association of German Pathologists (Berufsverband Deutscher Pathologen, http://www.bv-pathologie.de/) for quality control in pathology (QuIP), we performed an internal comparative inter-laboratory trial in the field of PCR-based detection of *M. tuberculosis*. Four institutes were selected by both societies because of their expertise and experience in this area [13, 16, 40, 47]. Our aim was to compare and to validate methodological variants employed by the four panel laboratories in order to draw general conclusions how to achieve high-level standards for PCR-based diagnostics of mycobacteria, but also to provide recommendations for nucleic acid amplification technology of surgical pathology specimens in general. This study followed the general guidelines in molecular pathology [19] and is similar to another multi-centre trial on Ki-67 labelling index [27]. General minimal demands for employing PCR and its terminology have been defined by the German Industrial Standard [7].

Despite a number of methodological variations, PCR-based diagnostics of mycobacteria proved to be reliable and reproducible. The specimens tested constitute the stock of a sample collection that is available for external molecular pathology laboratories in order to test their methodology and to increase quality assurance.

Materials and methods

Design of study

Each of the four panel groups (A–D) supplied eight cases for examination of *M. tuberculosis* by PCR including *M. tuberculosis*-positive and *M. tuberculosis*-negative samples (see below). Both DNA stock solution and the corresponding paraffin block were provided.

These materials were collected by the steering institute in Berlin, encoded and sent to the single panel laboratories. Each laboratory received a set of 66 samples consisting of 30 cases from clinical material and two experimentally infected human lung tissues for which paraffin sections and DNA stock solutions were provided as well as two paraffin samples from *M. tuberculosis*-infected mice.

The samples were provided in an anonymous fashion so that the respective investigators of the laboratories were blinded concerning the expected results.

Tissue samples

Of the 32 human samples, 25 were clinical cases that were previously investigated by one of the panel laboratories for *M. tuberculosis* because of clinical or histopathological suspicion for infection.

Negative controls consisted of three foetal lung tissues as well as two adult lung samples, one with lipoid pneumonia around a squamous cell carcinoma and one with little unspecific inflammatory reaction. Two cases of freshly operated human lung samples that were infected in tissue culture with *M. tuberculosis* BCG similarly as recently described for *Chlamydia pneumoniae* [37] acted as positive controls. Furthermore, lungs of *M. tuberculosis*-infected mice adjusted to defined colony forming units (0.7–0.8 CFU/lung) served as positive controls. These specimens originated from the Max Planck Institute for Infection Biology, Berlin [41]. Two positive and one negative control was submitted to HOPE (Hepes Glutamic Acid Buffer Mediated Organic Solvent Protection Effect) fixation instead of formalin followed by paraffin embedding [42].

For the 32 human tissues, one tube with 5 to 10 paraffin slices of 3-μm thickness as well as one tube containing 30–50 μl of DNA stock solution were assessed. For the two experimental mouse specimens, tubes with five paraffin slices of 3-μm thickness were sent to the panel laboratories. A survey of the tested specimens is provided in Table 5.

Histological evaluation

The paraffin blocks used for PCR analysis were histologically reassessed. Tissue sections were stained by hematoxylin and eosin (H&E), ZN, auramine–rhodamine and immunohistochemistry (DAKO, rabbit anti-*Mycobacteri-*

um bovis BCG), and semi-quantitatively evaluated in the following way:

- Necrosis. Extent: 0, negative; 1, minimal/punctuate; 2, low; 3, medium/confluent; 4, strong/greater than 50%. Type (predominant): 0, negative; 1, mainly caseous; 2, cellular; 3, fibrinoid
- Perinecrotic reaction. Intensity of inflammation: 0, negative; 1, little; 2, medium; 3, strong. Fibrosis: 0, negative; 1, little/focal granulation; 2, medium; 3, strong/circular sclerosis
- Granulomas. Each of the three granuloma types (caseous, pseudotuberculoid and sarcoidosis-like) were assessed as 0, absent; 1, present; 2, abundant
- Giant cells. Samples were searched for Langhans type or other (generally foreign body) types of giant cells and scored as 0, absent; 1, present; 2, abundant
- General inflammation intensity: 0, none; 1, little; 2, medium; 3, strong
- ZN, auramine and the immunohistochemical stainings were each scored as 0, negative; 1, weakly; 2, medium; 3, strongly positive

The histological parameters were statistically correlated with the PCR results using the SPSS software package (version 11.5). The detailed histological evaluation and representative microscopic images of each case are available as supplementary data at the abovementioned Charité web site.

Preparation of DNA from paraffin-embedded tissue

A survey on the experimental strategy is shown in Fig. 1. The methods for tissue preparation and DNA extraction differed slightly and are specified in Table 1.

In general, sections were cut from each tissue block and collected in 1.5 ml of Eppendorf vials. After each block, the microtome was cleaned and the knife changed. Paraffin was removed by extraction with xylene and centrifugation. This procedure was carried out either once, twice or three times; the pellet was then washed one to three times with ethanol (see Table 1). The supernatant was removed and the pellet air-dried. In parallel, blank extraction controls (dummies) containing no mycobacterial material were processed. These controls consisted of extractions containing all of the reagents without tissue and extractions of tissues ascertained to be negative for mycobacterial DNA.

All panel laboratories applied proteinase K digestion to disrupt the tissue, but the procedures to obtain the mycobacterial DNA as well as extraction and enrichment methods differed. Details of the respective protocols of the four laboratories are specified in the following.

Laboratory A

Air-dried tissue pellets were processed using the QIAamp DNA Mini tissue kit (http://www.qiagen.com/). Briefly, the pellets were suspended in lysis buffer and heated for 15–20 min at 95°C. After cooling to room temperature, the following steps were carried out according to the manufacturer's instructions with the exception that elution of DNA was performed with 50–80 µl of buffer.

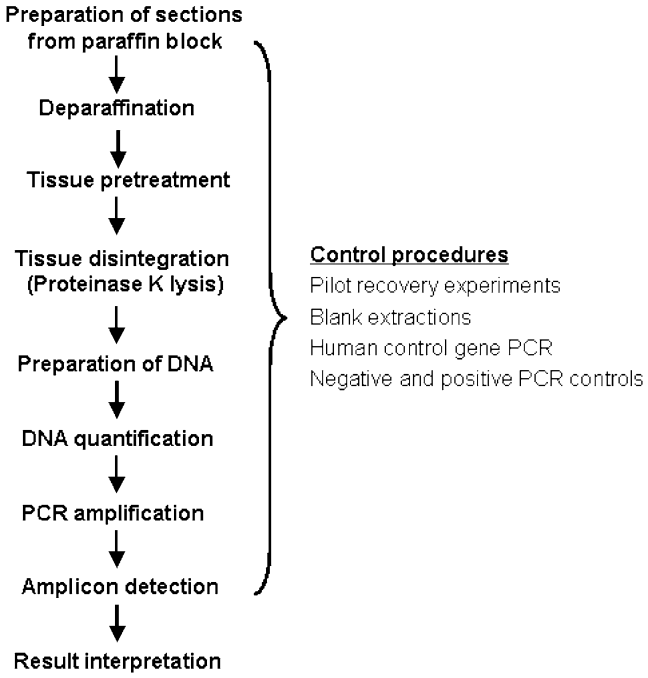


Fig. 1 Experimental steps in PCR-based detection of *M. tuberculosis* from paraffin-embedded tissue

Laboratory B

DNA preparation was performed according to the protocol by Ghossein et al. [12] and Popper et al. [31]. For digestion, the pellet was suspended in 100 µl of TEN-buffer (0.04 M Tris–HCl, 0.2 M NaCl, pH 8.0, 1 mM EDTA), 5 µl of proteinase K (Merck, Darmstadt, Germany, 20 mg/ml) and 5.25 µl of sodium dodecyl sulphate [final concentration 1% (w/w)] at 55°C for 3–4 h. To inactivate proteinase K, the solution was boiled for 10 min and centrifuged, and the DNA was precipitated with 96% ethanol (two volumes) in the presence of NaCl (final concentration 0.2 M) at room temperature for 30 min, recentrifuged at 13,000 rpm for 30 min and dissolved in 30–50 µl of ultrapure water (HPLC grade, Merck).

Laboratory C

DNA was extracted by the use of the Gen-ial First-DNA Kit (Fa. Gen-ial, Troisdorf, Germany, http://www.gen-ial.de/). Briefly, after removal of xylene, 500 µl of lysis buffer 1, 50 µl of lysis buffer 2 and 10 µl of proteinase K were added and incubated at 37°C overnight. To get access to mycobacterial DNA, the solution was heated to 90°C for 4 min and then shock-frozen in liquid nitrogen five times. After this step, 375 µl of lysis buffer 3 were added, vortexed and

Table 1 Methodological variants for tissue preparation and DNA extraction

Laboratory[a]	Sections	Deparaffinization	Tissue pre-treatment	Proteinase K lysis	Preparation of DNA	DNA amount[b] (µl, ~µg/PCR)	PCR volume (µl)
A	5–10 (3 µm)	1×xylene, 1×ethanol, air drying	Heating in lysis buffer for 15–20 min at 95°C	2–3 h at 55°C	QIAamp DNA Mini Kit	1–5 µl, 0.2–0.5 µg	25
B	5 (10 µm)	3×xylene, 3×ethanol, air drying	Nothing	3–4 h at 55°C	Precipitation with 96% ethanol	1–10 µl	50
C	2–5 (5 µm)	1×xylene	5×heating to 90°C followed by shock freezing with liquid nitrogen after proteolysis	at 37°C over-night	Gen-ial First-DNA Kit, precipitation with 96% ethanol	1–3 µl according to intensity after agarose (2%) gel electrophoresis	20
D	5 (2 µm)	2×xylene, 2×ethanol, air drying	Freeze-thawing before and after proteolysis	16 h at 55°C	QIAamp DNA Micro Kit	1–10 µl, 0.4 µg	50

[a]Laboratories: A, Berlin; B, Dresden; C, Munich; D, Borstel
[b]Extraction volume/DNA mass per reaction

cooled down for 5 min at −20°C. The samples were centrifuged at 13,000 rpm for 20 min, and the supernatant was transferred into new sterile tubes. At last, the DNA was precipitated with ethanol, and the pellet was diluted with sterile H_2O to a final volume of 50 µl.

Laboratory D

Extraction of DNA was performed by the use of QIAamp DNA Micro Kit (QIAGEN) with the following modifications: Two temperature treatments were included before and after the proteinase K incubation step (16 h at 55°C). Each of these treatments consisted of three cycles of 2-min incubation of the samples at 37°C, 30-s vortexing and 2-min incubation at −80°C in a dry ice/ethanol bath.

DNA quantification

To standardise the conditions and to estimate the amount of extracted DNA, the concentration of DNA was measured spectrophotometrically (laboratories A, B and D). In addition, the OD ratio (260 nm/280 nm) was measured to obtain information about the purity of the template DNA (laboratories B and D). The integrity and the quantity of the DNA was assessed semi-quantitatively via gel electrophoresis by laboratory C. DNA amounts and PCR reaction volumes of each laboratory are specified in Table 1. To examine whether amplifiable DNA was present in the samples, all panel laboratories assessed the quality of the prepared DNA by different control PCR to amplify an appropriate segment of a human gene (Table 2).

PCR amplification and amplicon detection

PCR of mycobacterial DNA sequences was performed employing different primer sequences for the amplification of distinct target genes of *M. tuberculosis* (Table 3). The genus-specific 16*S* rDNA and 65-kDa antigen genes harbour consensus sequences of mycobacterial organisms and thus cover the broadest detection range. The IS*6110* gene from the *M. tuberculosis* complex is suitable to detect

Table 2 Human control genes

Laboratory	Gene	Direction	Sequence 5′→3′	Amplicon (bp)	Reference
A	β-Globin	sense	GAA GAG CCA AGG ACA GGT AC	268	[15]
		antisense	CAA CTT CAT CCA CGT TCA CC		[5]
B	GAPDH	sense	CGGAGTCAACGGATTTGGTCGTAT	306	[46]
		antisense	AGCCTTCTCCATGGTGGTGAAGAC		
C	β-Actin	sense	CCT TCC TGG GCA TGG AGT CCT G	202	[12]
		antisense	GGA GCA ATG ATC TTG ATC TTC		
D	β-Actin	sense	AGC GGG AAA TCG TGC GTG	303	[33, 34]
		antisense	CAG GGT ACA TGG TGG TGC		

Table 3 Set of primers to detect mycobacterial DNA sequences

Laboratory	Target (Method No.)[a]	Direction (primer names)	Sequence 5′→3′	Amplicon (bp)	Gene	Detected *Mycobacterium* subtypes	Reference
B, D	*M. tub* complex (1)	sense (A) antisense (tb)	AGA GTT TGA TCC TGG CTC AG ACC ACA AGA CAT GCA TCC CG	193	16S rDNA	*M. tuberculosis* complex (*M. tuberculosis*, *M. bovis*, *M. bovis* BCG, *M. microti*, *M. africanum*)	[34]
A–C, A	*M. tub* complex (2)	sense antisense probe	CCT GCG AGC GTA GGC GTC GG CTC GTC CAG CGC CGC TTC GG Biotin-CAT AGG TGA GGT CTG CTA CC′	123	IS*6110*	*M. tuberculosis* complex (*M. tuberculosis*, *M. bovis*, *M. bovis BCG*, *M. microti*, *M. africanum*)	[8, 45]
D	*M.* genus	sense (A) antisense (247) primer (9)	AGA GTT TGA TCC TGG CTC AG TTT CAC GAA CAA CGC GAC AA CGT GCT TAA CAC ATG CAA GTC	590	16S rDNA	Variety of bacteria, conserved region within the mycobacterial species, sequencing of atypical mycobacteria	[1, 34, 33]
A	*M.* genus (3)	sense antisense	CTA GGT CGG GAC GGT GAG GCC AGG CAT TGC GAA GTG ATT CCT CCG GAT	125–165	65 kDa Ag	Variety of mycobacteria, conserved region of mycobacteria	[30]
A	*M.* genus (nested PCR) (4)	T1U1, T1U2, T1D T2U T2D	First round: AAG GAG ATC GAG CTG GAG GA, AGG CGT TGG TTC GCG AGG G TGA, TGA CGC CCT CGT TGC C Second round with internal primers: GTC TCA AAC GCG GCA TCG, GTC ACC GAT GGA CTG GTC	310, 231 133	65 kDa Ag	Variety of mycobacteria, conserved region of mycobacteria	[4]

[a]Method numbering corresponds to that of Tables 5 and 6

M. tuberculosis, *M. bovis*, *M. bovis* BCG, *M. africanum* and *M. microti*.

The PCR protocols, i.e. reaction conditions, cycle programmes and detection method also differed and are compiled in Tables 1 and 4. Further details are as follows.

Laboratory A

For detection of *M. tuberculosis*, the oligonucleotide primers described by Eisenach et al. [8] were used to amplify a 123-bp fragment of the IS*6110* insertion sequence. The PCR reagents were commercially available (Reddy Mix, *AB* gene, http://www.abgene.com/). The final reaction volume of 25 µl contained 75 mM Tris–HCl (pH 8.8 at 25°C), 20 mM ammonium sulphate, 1.5 mM $MgCl_2$, 0.2 mM of each deoxynucleotide trisphosphate, 0.01% (v/v) Tween 20, 1.25 units Thermoprime DNA polymerase, as well as loading buffer and dyes for electrophoresis. The twofold concentrated kit reagents were complemented by a PCR DIG labelling mix (DIG detection, Roche, http://www.roche.com/), with a final concentration of 120 µM to render possible PCR-ELISA detection. The primer concentration was adjusted to 0.1 µM. The cycle conditions are specified in Table 4. A 10-µl aliquot of the reaction mix was subjected to 3.3% agarose gel electrophoresis and ethidium bromide staining. A second 2.5-µl aliquot containing the digoxigenin-labelled PCR products was hybridised with the biotinylated probe (Table 3), immobilised onto a streptavidin-coated microtiter plate and detected as described in the instruction manual (Roche, see above).

The amplification of the consensus 65-kDa antigen gene was similarly performed by the use of Reddy Mix (*AB* gene) without labelling using a 0.125-µM primer concentration.

The nested PCR was performed according to Cook et al. [4] by the use of PCR Master Mix (Promega, http://www.promega.com/) without restriction enzyme analysis of PCR product. One microliter of the first round product was amplified in the second PCR. Again, the PCR products were detected by 3.3% agarose gel electrophoresis.

Table 4 PCR conditions and amplicon detection

Laboratory	PCR reaction mixtures	Final Concentrations	Thermocycler profile	Detection procedure
A	Reddy Mix: Thermoprime DNA polymerase (*AB* gene) PCR, Dig-labelling mix (Roche)	0.65 units enzyme, 1.5 mM $MgCl_2$, 0.1 µM primer, 0.2 mM dNTPs, 120 µM dNTPs and 6 µM DIG-dUTP	I*6110*: 94°C 5 min, 40× (94°C 1 min, 68°C 2 min, 72°C 1.5 min), 72°C 7 min	*DIG PCR/ELISA*: 2,5 µl digoxigenin labelled PCR products were hybridised with biotinylated probe, immobilised and detected on microtiter plates (Roche)
	Reddy Mix: Thermoprime DNA polymerase (*AB* gene)	0.65 units enzyme, 1.5 mM $MgCl_2$, 0.125 µM primer, 0.2 mM dNTPs	65 kDa Ag: 94°C 5 min, 40× (94°C 1 min, 60°C 1 min, 72°C 1 min), 72°C 5 min	Electrophoresis: 3.3% agarose gel, ethidium bromide staining and UV visualisation
	Promega PCR Master Mix (2×)	0.65 units enzyme, 1.5 mM $MgCl_2$, 0.3 µM primer, 0.2 mM dNTPs	Nested PCR 65 kDa Ag: 94°C 5 min, 40× [94°C 1 min, 57°C 1 min (first round), 52°C (second round), 72°C 1 min], 72°C 5 min	
B	Ampli Taq Gold (Perkin Elmer Applied Biosystems)	1 unit enzyme, 1.5 mM $MgCl_2$, 0.1 µM primer, 0.2 mM dNTPs	IS*6110*: 94°C 9 min, 35× (94°C 1 min, 68°C 1 min, 72°C 1 min), 72°C 7 min	Electrophoresis: 6% polyacrylamide gel
	Ampli Taq Gold (Perkin Elmer Applied Biosystems)	1 unit enzyme, 1.5 mM $MgCl_2$, 0.1 µM primer, 0.2 mM dNTPs	M. tub. 16S rDNA: 94°C 9 min, 40× (94°C 1 min, 57°C 1 min, 72°C 1.5 min), 72°C 15 min	
C	Ampli Taq Gold (Perkin Elmer Applied Biosystems) Nucleotides (Amersham Pharmacia)	0.025 units enzyme, 1.5 mM $MgCl_2$, 1 µM primer, 0.2 mM dNTPs	IS*6110*: 95 °C 10 min, 45× (94 °C 1 min, 66°C 1 min, 72°C 1 min) 72°C 8 min.	Electrophoresis: 4% polyacrylamide gel
D	Invitrogen	5 units enzyme, 5 mM $MgCl_2$, 0.8 µM primer, 0.2 mM dNTPs	M. tub. 16S rDNA: 94°C 5 min, 40× (94°C 1 min, 57°C 1 min, 72°C 1,5 min) 72°C 15 min	Electrophoresis: 2% agarose-gels stained with ethidium-bromide and UV visualisation. Sequencing: according (Richter 1995)

Laboratory B

For detection of *M. tuberculosis*, the IS*6110* and the 16*S* rDNA genes were amplified. All reactions were throughout performed in a volume of 50 µl using Ampli Taq Gold DNA polymerase (1U PE Applied Biosystems, http://www.appliedbiosystems.com/) and reagents according to the manufacturer's instructions. Further details are given in Tables 3 and 4. PCR products were run on 6% polyacrylamide gel and visualised by staining with SYBR Green I (Biozym FMC) and UV transillumination.

Laboratory C

Similar to laboratories A and B, the detection of *M. tuberculosis* complex DNA was performed by amplification of the IS*6110* sequence. The cycler profile is given in Table 4. The detection was performed by gel electrophoresis after cleaving the PCR product by a specific restriction endonuclease digestion with *Hae*III (Roche Diagnostics, Mannheim, Germany, http://www.roche.com/) [2]. The PCR products were separated on a 4% agarose gel and visualised on a UV screen after staining with ethidium bromide. All samples with positive amplification of IS*6110* were subjected to further analysis by spoligotyping. The method was performed as described previously [22, 32, 44]. We used a commercial Spoligotyping Kit (Isogen, Maarsen, The Netherlands, http://www.isogen.nl/). Due to differences in the presence of non-repetitive DNA spacers, the hybridisation patterns vary among *M. tuberculosis* complex strains. Due to the absence of spacers 39 to 43 in all known *M. bovis* isolates, this approach allows a clear differentiation between *M. tuberculosis* and *M. bovis* strains, as well as the identification of sub-species or defined genetically related families.

Laboratory D

Amplifications were performed by the use of oligonucleotide primer sets for a 590-bp genus-specific fragment of mycobacterial 16*S* rDNA and a 193-bp fragment of the 16*S* rDNA of *M. tuberculosis* complex, respectively (Table 3), as described previously [34]. For amplification, 400 ng DNA, 20 mM Tris–HCl (pH 8.4), 50 mM KCl, 1.5 mM

$MgCl_2$, 200 μM of each deoxynucleotide trisphosphate (Invitrogen), 5 units Taq-Polymerase (Invitrogen) and 0.8 μM of each primer were added to a final volume of 50 μl. PCR was performed in a Biometra Uno-II thermocycler with cycle conditions as specified in Table 4. The amplicons were detected by 2% agarose gel electrophoresis.

When the outcome of the 193 bp PCR was negative and the 590 bp PCR was positive, the long PCR products were subjected to sequencing by the use of primer 9 as previously described by Richter et al. [34]. Sequence analysis was carried out using an automated fluorescent DNA-sequencer (AbiPrism 377, Applied Biosystems) to determine the respective (atypical) mycobacterial species. Database comparison was done with the aid of GenBank at the NCBI applying the BLAST tool (http://www.ncbi.nlm.nih.gov/BLAST/). Because this analysis was performed only in single selected cases, it was not included in the sensitivity and specificity analysis.

Control procedures

Two different types of negative controls were included in the study to rule out contaminations: In the first one, sterilised water was used instead of the sample to check the PCR. In the second one, material from 'blank extractions' (dummies, see above) was used in order to exclude any contamination in the extraction system [14]. To examine the reliability of both reaction mixtures and reaction conditions, each analysis was combined with a positive control of mycobacterial DNA obtained from highly diluted suspensions of *M. tuberculosis* DNA or *M. szulgai* (genus PCR, laboratory D).

Results

Of the 34 cases, 25 were clinical samples that were previously investigated by one of the panel laboratories for tuberculosis because of clinical or histopathological suspicion for infection. In addition, five negative human control samples and four positive, two human and two mice, tissues were included (Table 5).

Amplification of control genes

DNA stock solutions (n=32) and paraffin sections (n=34) were sent to the four panel laboratories for PCR, thus, totalling to 264 control reactions. Only a small share of them did not supply the expected results. Thirteen were negative and six displayed only a weakly positive outcome. A higher share of negativity occurred when large target sequences were amplified (16/19, laboratories B, D) compared to small target sequences (3/19, laboratories A, C). A somewhat higher abundance of negative outcomes was observed with the DNA stock solutions (8× negative, 3× weakly positive) compared to DNA that was extracted from the paraffin sections by each laboratory (5× negative, 3× weakly positive).

PCR detection of *M. tuberculosis*

The results for PCR detection of *M. tuberculosis* genes are shown in detail in Table 5. It represents the analysis of each case using DNA solutions and DNA from paraffin sections by all four laboratories using five different detection methods. Each laboratory provided a definite final assignment (positive or negative) of the 34 specimens that was based on the investigation of the different DNA preparations and PCR approaches for detection of mycobacterial DNA (column 'laboratory score', 0 = negative, 1 = positive). These were added for the calculation of a total score ranging from 0 to 4.

For 29 out of 34 sample sets, all four laboratories achieved identical assessments. The specimens from mouse tissues with defined CFU (samples 33 and 34) were evaluated consistently positive. From these samples, it could be calculated that 5–10 copies of the bacterium per set-up were reliably detected.

In five cases, conflicting data were obtained by one of the four laboratories, i.e. three aberrant positive results (samples 7, 21, 31) and two aberrant negative ones (samples 12 and 28). Case 7 was positive with the paraffin sample, but not with the DNA solution, which was interpreted as final positive result by the panel laboratory C. Both sample types also gave a positive result in the nested PCR of laboratory A; however, it was finally interpreted as negative because the IS*6110 M. tub*. complex PCR was negative. Similarly, case 21 gave positive results in the IS*6110* complex PCR and spoligotyping analysis in both sample types. This case was consistently negative in all analyses of the other laboratories. The third case (31) was positive in the DNA preparation from the paraffin sections, but not in the conveyed solution in laboratory D. In the same case, laboratory B detected mycobacterial DNA in the IS*6110* region, which, however, was not confirmed by the 16*S* rDNA analysis (A/tb primers) leading to a final negative evaluation. In one of two cases that were aberrantly evaluated as negative (case 28), amplification of the 193 bp sequence of 16SrDNA yielded no amplicon; however, the PCR for IS*6110* was positive. In the second case (sample 12), an amplicon of wrong size was seen with the A/tb primers thus leading to the negative final interpretation.

Three aberrant results, two aberrant positive and one aberrant negative, were obtained in the two laboratories that used freeze-thawing for DNA extraction as compared to one aberrant negative result in the two laboratories that did not employ this technique.

The results of the majority of the panel laboratories were defined as PCR consensus and served for the comparison of the applied methodologies regarding sensitivity and specificity (Table 6). The highest sensitivity was achieved for the amplification of the IS*6110* gene followed by the

Table 5 Results for PCR detection of *M. tuberculosis* genes

Sample			Laboratory	A						B					C					D		
			Method No.	(2)		(4)		(3)	Laboratory score	(2)		(1)		Laboratory score	(2)		Spoligotyping (5)		Laboratory score	(1)		Laboratory score
Code	Localization	Type	Total score	DNA	P	DNA	P	P		DNA	P	DNA	P		DNA	P	DNA	P		DNA	P	
1	Lung	Clinical	4	1	1	1	1	0	1	1	1	1	1	1	1	1	1	1	1	0	1	1
2	Aorta	Clinical	4	1	1	1	1	1	1	1	1	1	1	1	0	1	0	1	1	0	1	1
3	Aorta/Lung	Clinical	4	1	1	1	1	1	1	1	1	1	1	1	1	1	1	1	1	1	1	1
4	Liver	Clinical	0	0	0	0	0	0	0	0	0	0	n.a.	0	0	0	0	0	0	0	0	0
5	Lymph node	Clinical	4	1	1	1	1	1	1	1	1	1	1	1	1	1	1	1	1	1	1	1
6	Lymph node	Clinical	0	0	0	0	0	0	0	0	1	0	0	0	1	0	1	0	0	0	0	0
7	Lymph node	Clinical	1	0	0	1	1	0	0	0	0	n.a.	n.a.	0	0	1	0	1	1	0	0	0
8	Foetal lung	n.c.	0	0	0	0	0	0	0	0	0	n.a.	n.a.	0	0	0	0	0	0	0	0	0
9	Lung	Clinical	4	1	1	n.a.	n.a.	1	1	1	1	1	1	1	1	1	1	1	1	1	1	1
10	Lung/Lymph node	Clinical	4	1	1	n.a.	n.a.	1	1	1	1	1	1	1	1	1	1	1	1	1	1	1
11	Foetal lung	n.c.	0	0	0	0	1	0	0	0	0	n.a.	n.a.	0	1	0	1	0	0	0	0	0
12	Lymph node	Clinical	3	1	1	n.a.	n.a.	1	1	1	1	1	1	1	1	1	1	1	1	0	0	0
13	Lung	Clinical	4	1	1	n.a.	n.a.	1	1	1	1	1	1	1	1	1	1	1	1	1	1	1
14	Lung/Lymph node	Clinical	4	1	1	n.a.	n.a.	1	1	1	1	1	1	1	1	1	1	1	1	1	1	1
15	Foetal lung	n.c.	0	0	0	0	0	0	0	0	1	0	0	0	0	0	0	0	0	0	0	0
16	Lung	Clinical	0	0	0	0	0	0	0	0	0	n.a.	n.a.	0	0	0	0	0	0	0	0	0
17	Lung	p.c.	4	1	1	n.a.	n.a.	1	1	1	1	1	1	1	1	1	1	1	1	1	1	1
18	Lung	p.c.	4	1	1	n.a.	n.a.	1	1	1	1	1	1	1	1	1	1	1	1	1	1	1
19	Prostate	Clinical	0	1	0	0	0	0	0	0	0	n.a.	n.a.	0	0	0	0	0	0	0	0	0
20	Lung	n.c.	0	0	0	1	0	0	0	1	0	1	0	0	1	0	1	0	0	0	0	0
21	Lung	Clinical	1	0	0	0	0	0	0	0	0	n.a.	n.a.	0	1	1	1	1	1	0	0	0
22	Lung	n.c.	0	0	0	0	1	0	0	0	0	0	0	0	0	0	0	0	0	0	0	0
23	Pleura/diaphragma	Clinical	4	1	1	1	0	0	1	1	1	1	1	1	1	0	1	0	1	1	0	1
24	Diaphragma	Clinical	4	1	1	n.a.	n.a.	0	1	1	1	1	1	1	1	1	1	1	1	1	0	1
25	Vertebra	Clinical	4	1	1	n.a.	n.a.	1	1	1	1	1	1	1	1	1	1	1	1	1	1	1
26	Soft tissue/serous cyst	Clinical	4	1	1	n.a.	n.a.	0	1	1	1	1	1	1	1	0	1	0	1	0	1	1
27	Lung	Clinical	4	1	1	n.a.	n.a.	1	1	1	1	1	1	1	1	1	1	1	1	1	1	1
28	Epididymis	Clinical	3	1	1	n.a.	n.a.	1	1	1	1	0	0	0	1	0	1	0	1	1	1	1
29	Prostate	Clinical	0	0	0	0	0	0	0	0	0	n.a.	n.a.	0	0	0	0	0	0	0	0	0

Table 5 (continued)

Sample			Laboratory	A						B				C				D		
			Method No.	(2)		(4)			(3)	Laboratory score	(2)		(1)		Laboratory score	(2)		Spoligotyping (5)	Laboratory score	(1)		Laboratory score
Code	Localization	Type	Total score	DNA	P	DNA	P	P			DNA	P	DNA	P		DNA	P	DNA		DNA	P	
30	Pleura	Clinical	0	0	0	0	0	0	0	0	0	0	n.a.	n.a.	0	0	0	0	0	0	0	0
31	Lung	Clinical	1	0	0	0	0	0	0	0	1	1	0	0	0	0	0	0	0	0	1	1
32	Epididymis	Clinical	4	1	1	n.a.	n.a.	1	1	1	0	1	0	1	1	1	0	1	0	0	1	1
33[a]	Mouse lung	p.c.	4	n.a.[a]	1	n.a.[a]	n.a.	1	1	1	n.a.[a]	1	n.a.[a]	1	1	n.a.[a]	1	n.a.[a]	1	n.a.[a]	1	1
34[a]	Mouse lung	p.c.	4	n.a.[a]	1	n.a.[a]	n.a.	1	1	1	n.a.[a]	1	n.a.[a]	1	1	n.a.[a]	1	n.a.[a]	1	n.a.[a]	1	1

Method numbering (see also Table 3 and Table 6): (1), 16SrDNA, A/tb primer; (2), IS6110/M. tub. complex; (3), 65 kDa Ag/*M.* genus; (4), 65 kDa Ag/nested PCR
p.c. Positive control, *n.c.* negative control, *DNA* results for DNA solutions, *P* results for paraffin sections, *n.a.* not analysed
[a]Only paraffin slices were shipped

16*S* rDNA of *M. tuberculosis* complex, whereas regarding specificity, the latter was superior to the IS*6110* detection.

Correlation with microscopic findings

During the course of this study, all samples were microscopically reassessed and semi-quantitatively scored for the parameters necrosis, granuloma, giant cells, inflammation/fibrosis and acid-fast bacilli. The data were statistically correlated with the PCR consensus results. The extent of necrosis was highly significantly associated with the positive PCR result (P=0.006 by Fisher's exact test). Furthermore, there was also a positive correlation with immunohistochemical detection of acid-fast bacilli (P=0.027). For the other parameters, there were no statistically significant correlations. Details of the histological evaluation together with representative histological images of each case are available as supplementary data at http://www.charite.de/ch/patho under the rubric "Forschung".

Discussion

Detection of pathogen-specific DNA or RNA by using methodology of molecular pathology is implicated in diagnostics and characterisation of infections. This task includes the choice of the suitable methodological approach, its correct handling by an expert and experienced staff as well as critical interpretation of results and their impact in the final diagnosis.

PCR is a highly sensitive procedure, which is extremely susceptible to interference by contamination [23, 36]. Moreover, particular requirements are needed as to disintegration of sample material and quality of nucleic acid preparation. Therefore, a number of preconditions should be fulfilled to prevent both false-positive and false-negative results. Some essential general preconditions for PCR analysis are provided as supplementary data to the manuscript (http://www.charite.de/ch/patho, rubric Forschung).

The present inter-laboratory trial indicated a high degree of inter-laboratory reliability of the PCR-based detection of *M. tuberculosis* genes. Importantly, all positive and negative controls were evaluated consistently. Positive controls originated from experimentally *M. tuberculosis*-infected mice and human lung tissue cultured in the presence of *M. bovis* BCG. Negative samples were from foetal and adult human lung that had no clinical or histological evidence of infection and were previously PCR negative. The majority of the samples consisted of clinical material that harboured characteristic morphological signs suggestive for mycobacterial infection, i.e. caseous necrosis, granulomas and/or giant cells. Interestingly, the extent of necrosis carried the most significant association with the detection of *M. tuberculosis* DNA. In contrast, neither the presence and type of giant cells, granuloma type, nor the staining results for ZN and auramine showed a significant correlation. The insufficient association with the conventional stainings is probably due to

Table 6 Sensitivity and specificity of the *M. tuberculosis* detection methods

No.	Method	Sensitivity[a]			Specificity[b]		
		All	*P*	DNA	All	*P*	DNA
1	*M. tub.* complex (16S rDNA)	0.87, *n*=76	0.91, *n*=40	0.84, *n*=36	0.95, *n*=39	0.95, *n*=20	0.95, *n*=19
2	*M. tub.* complex (IS*6110*)	0.95, *n*=114	0.94, *n*=60	0.96, *n*=54	0.88, *n*=84	0.89, *n*=42	0.86, *n*=42
3	*M.* genus		0.83, *n*=20			1.0, *n*=14	
4	*M.* genus nested	0.92, *n*=12			0.84, *n*=26		
5	Spoligotyping	0.88, *n*=38	0.83, *n*=20	0.95, *n*=18	0.82, *n*=28	0.88, *n*=14	0.78, *n*=14

Samples with score 0 or 1 are defined as true negative, samples with score 3 and 4 are defined as true positive. This agreement is important for the estimation of sensitivity and specificity

[1–4]Method numbering corresponds to that of Table 3

[a]Sensitivity [true positive results/(true positive plus false negative results)]

[b]Specificity [true negative results/(true negative plus false positive results)]

the preselection of cases, because generally, only the ZN-negative cases are further analysed by PCR. Auramine revealed more positive cases that, however, by PCR, turned out to be related to unspecific staining. Only immunohistochemical detection correlated significantly with the PCR results and may thus increase the armamentarium of morphology-based methods.

Except for the positive controls, no microbiological data were available. Although this may be a limitation of our study, it is representative for the inherent problem of tuberculosis detection in pathology specimens. On the one hand, clinicians and surgeons do not always pay attention to the possibility of an infection, and therefore, do not send adequate material to the microbiology department. On the other hand, the suspicion of such an infection is frequently raised only by histomorphological analysis. Thus, the available specimen is already formalin-fixed and cannot be further analysed microbiologically.

The molecular pathological analysis needs to be considered in the context of the histopathological and clinical setting. On the one hand, it may strongly enhance the sensitivity and considerably shorten the time period for achieving the specific diagnosis of an infection. On the other hand, the PCR methodology itself with all the pre-amplification, amplification and detection procedures implicates multiple obstacles that may hinder the detection of the pathogen unless appropriate conditions are maintained.

Sectioning of paraffin blocks

Paraffin blocks, usually generated after formalin fixation of the tissue, are the fundamental working material in pathological institutes. These blocks need to be cut to gain paraffin sections that are suitable for DNA extraction. To our knowledge, there are so far no general rules for tissue sectioning in molecular pathology analysis.

The panel laboratories took the following measures for paraffin block sectioning:

- Cleaning of the microtome after each tissue block from unused paraffin material by aspirator
- Cleaning of knives after each block to remove paraffin and tissue remnants
- Change of knives between each block (in particular if the same microorganism is detected)
- Precautions for contaminations during transfer of tissue sections into the tubes

Within the panel laboratories, the section thickness varied between 2 and 10 μm, the number of sections was between 2 and 10, thus giving a range of tissue thickness between 10 and 50 μm. This variation is mainly due to the area of tissue within the paraffin block and its cellular composition. The optimal amount depends largely on the experience of each laboratory and should be tested. Interestingly, one report recently described a higher sensitivity for the detection of mycobacterial DNA using thin tissue sections [25].

For this investigation, the sections were provided by one laboratory for the in-house preparations by each panel member (P). The additionally distributed DNA preparation (DNA) originated from all four laboratories that contributed DNA solutions and paraffin blocks.

DNA extraction

The use of formalin-fixed and paraffin-embedded tissue is hampered by a high degree of cross-linking, which renders its disintegration difficult. This difficulty is reinforced by the presence of a thick mycolate-rich outer cell wall in mycobacteria. Therefore, additional and even drastic methods of cell rupture were applied by the laboratories. The aim is to keep a balance between DNA recovery from the bacteria and tissue and DNA integrity for later amplification. Although the influence of the DNA extraction method was not systematically tested, our experience suggests that tissue pretreatment enhances the amount of recovered DNA whereas higher number of cycles in tissue pretreatment does not necessarily increase the sensitivity of detection. It was observed in the present study that heating prior to proteinase K digestion promotes tissue disintegration and may thus increase DNA recovery. Additional

cycles of freeze thawing were applied by two laboratories and resulted in two additional (aberrant) positive results. Whether this reflects contamination or an increase in sensitivity needs to be clarified by future studies. The optimal conditions should be examined in pilot recovery experiments by each laboratory independently.

DNA quantification

The variation of amount and composition of a tissue will greatly influence DNA recovery and purity. Differences in the preparation procedures like extraction volume, addition of proteinase K, duration of digestion, procedures for DNA concentration and others may also contribute to this variation. In daily practice, this variability is firstly accounted for by the tissue amount entering the extraction procedure and secondly by measurement and standardisation of the DNA amount for PCR. In addition to quantification, photometric measurement of the OD ratio at 260/280 nm may also provide an indication for sufficient DNA purity and is thus highly recommended.

Each laboratory should find out the optimal DNA concentration for its PCR set-up. The few discrepancies of the PCR results between the P and DNA preparations within the panel laboratories may be attributed to differences in DNA preparation and partitioning for amplification. In our experience, amounts of 100 ng for the control gene and up to 400 ng for the detection of mycobacteria, respectively, yielded best results.

PCR amplification

Formalin fixation results in cross-linking and degradation of the DNA, thus, limiting its use as template for amplification. The impact of the fragment size for the detection of the pathogen and the control gene was clearly evident from our inter-laboratory trial. Small target sequences should be applied in order to minimise the risk of false-negative results. We observed the highest frequency of positive control gene amplification for β-globin (268 bp fragment, 1 dropout) followed by β-actin (202 bp fragment, 2 dropouts).

Similarly, the 123-bp fragment of the IS*6110* gene of *M. tuberculosis* complex showed the highest sensitivity, which is additionally owed to the fact that it constitutes a repetitive genomic sequence of the bacterium. To achieve high yields of PCR products, cycle numbers between 35 and 45 as well as prolonged reaction times between 60 and 90 s were applied.

Nested PCR being additionally performed by one laboratory for amplification of the 65-kDa antigen harbours the potential of an even higher sensitivity. However, in our experience, this method should only be applied in the context of further tests due to the relatively low specificity (Table 6).

Recently, it has been shown that application of the novel *HOPE* fixation boosts the sensitivity of PCR to detect mycobacteria in paraffin-embedded samples at least 100-fold along with a well-preserved morphology [42]. The HOPE-fixed samples (code no. 17, 18, 20), including two positive and one negative control, gave highly reproducible results. The morphology was similar to the conventionally fixed specimens and can be checked on the supplementary data web site. Formalin, however, is and probably will remain for some time the standard fixative in most hospitals and pathological institutes, thus requiring accordingly optimised procedures in molecular pathology.

Amplicon detection

The most common and convenient way to confirm a successful amplification is agarose or polyacrylamide gel electrophoresis. However, an amplicon of the correct size does not necessarily represent the specific target. Therefore, further confirmative analysis is recommended. This is one reason why all panel laboratories applied different primer sets for PCR to detect mycobacterial DNA. For additional confirmation, restriction enzyme digestion, hybridisation to a specific internal probe followed by ELISA detection, DNA sequencing and spoligotyping were performed. Hybridisation techniques and restriction enzyme digestion are easier and faster than DNA sequencing followed by database comparison. Therefore, the latter approach is often restricted to the detection and subtyping of atypical mycobacteria.

Extremely high sensitivity can be achieved by the spoligotyping technique [22]. In the present study, as compared to conventional PCR, the typing was successful, providing additional information on distinct strains of the *M. tuberculosis* complex. Most of the samples exhibited a *M. tuberculosis*-specific signature. In two lung samples, *M. bovis* BCG strains were detected. A number of the *M. tuberculosis* strains revealed spoligotyping patterns, which are listed in an international database [11] and resemble common and well-characterised signatures. However, two samples provided aberrant positive spoligotyping results, which were found out by PCR to be negative as to the presence of *M. tuberculosis* DNA. Interestingly, these cases yielded only incomplete, patchy spoligotyping patterns. Further studies are needed to clarify whether these findings are due to non-specific amplification or hybridisation products or whether they indicate an extremely low level of *M. tuberculosis* DNA, whose clinical relevance has to be established. At present, this approach is not mandatory and generally recommended for diagnostic purposes, but may be used to address alternative issues, such as evolution and spread of the *M. tuberculosis* complex.

Interpretation of PCR results

The final plus/minus assignment of the PCR results for *M. tuberculosis* genes (Table 5, laboratory score) stands for a summing up of all analyses that were performed by each laboratory. Similar to the amplification of the control genes,

there were also discrepancies in single cases between the multiple approaches for *M. tuberculosis* detection (DNA solution vs new extractions from paraffin section, different PCR methods). The specifications in Table 5 may thus reflect complex considerations. The criteria that were applied by the laboratories will be discussed in the following:

Generally, a case was scored positive when the PCR and the following detection yielded a definite outcome in one of the preparations. As an exception of this rule, laboratory B required two positive parameters, i.e. either positive outcome in the PCR for IS*6110* and A/tb or positive outcome in both DNA preparations (D+P) for a definitive assessment. The backgrounds for these more stringent criteria are reports from the literature indicating that the use of the primer set for IS*6110* by Eisenach et al. [8] may identify *M. tuberculosis* in cases of sarcoidosis [6, 10, 21, 38]. Thus, the positive detection of the A/tb was scored with a higher priority than the IS*6110* fragments. From the experience of the other panel laboratories, positive outcome for IS*6110* in cases of sarcoidosis is not or only occasionally observed. However, this phenomenon was not systematically investigated in this inter-laboratory trial and merits further investigation. In general, this issue highlights the need to apply multiple approaches for the detection of mycobacterial DNA, in particular, in case of suspicion of sarcoidosis.

Similarly, the nested PCR performed by laboratory A was scored only when both preparations showed equal results in repetitive analyses, thus, considering the high frequency of false-positive results.

Discrepancies within and between the laboratories can also be due to low-copy infection and unequal distribution of the mycobacteria in the tissue. Considering the multiple difficulties in the *M. tuberculosis* detection as mentioned here, we achieved a high rate of consistent results.

Conclusions

The present inter-laboratory trial has clearly demonstrated reliability and reproducibility of PCR-based detection of *M. tuberculosis*, provided that appropriate conditions are kept. Moreover, the prerequisites are now established for a subsequent external inter-laboratory trial in which other molecular pathology laboratories are invited to participate.

Acknowledgements The authors are indebted to following persons for technical assistance, material support and web site implementation: Sabine Rüsch-Gerdes, Waltraut Martens, Elvira Richter, Sina Adrian, Stefan Niemann, Heike Kühl, Ulf Greinert and Jürgen Galle in Borstel; Mirko Rizzello, Carola Priebe, Annemarie Ehsani, Martina Eickmann, Wolfgang Trosch and Peter Seiler in Berlin, Annelie Zürich in Dresden and Stephanie Köhler in Munich.

References

1. Böddinghaus B, Rogall T, Flohr T, Blöcker H, Böttger EC (1990) Detection and identification of mycobacteria by amplification of rRNA. J Clin Microbiol 28:1751–1759
2. Bohle RM, Heidemann A, Borkhardt A, Velcovsky HG, Altmannsberger HM (1994) Detection of mycobacterial DNA from paraffin-embedded tissue with epithelioid granulomas of lung and lymph nodes. Verh Dtsch Ges Pathol 78:189–194
3. Cabras AD, Kremer M, Schulz S, Werner M, Hummel M, Komminoth P, Höfler G, Höfler H (2000) Quality assessment in diagnostic molecular pathology: experience from a German–Austrian–Swiss multicenter trial. Virchows Arch 437:46–51
4. Cook SM, Bartos RE, Pierson CL, Frank TS (1994) Detection and characterization of atypical mycobacteria by the polymerase chain reaction. Diagn Mol Pathol 3:53–58
5. Coutlee F, de Ladurantaye M, Tremblay C, Vincelette J, Labrecque L, Roger M (2000) An important proportion of genital samples submitted for *Chlamydia trachomatis* detection by PCR contain small amounts of cellular DNA as measured by beta-globin gene amplification. J Clin Microbiol 38:2512–2515
6. Degnitz K (1996) Detection of mycobacterial DNA in the skin. Arch Dermatol 132:71–75
7. DIN 58967-60: serodiagnosis of infectious diseases and diseases of immune system—Polymerase chain reaction (PCR)—Part 60: terminology, general method-specific requirements. German Institute for Standardization (Deutsches Institut für Normung e.V.), department for medical standards (Normenausschuß Medizin) 1995–01
8. Eisenach KD, Cave MD, Bates JH, Crawford JT (1990) Polymerase chain reaction amplification of a repetitive DNA sequence specific for *Mycobacterium tuberculosis*. J Infect Dis 161:977–981
9. Ergin A, Hascelik G (2004) Nontuberculous mycobacteria (NTM) in patients with underlying diseases: results obtained by using polymerase chain reaction–restriction enzyme analysis between 1997–2002. New Microbiol 27:49–53
10. Fidler HM, Rook GA, Johnson NM, McFadden J (1993) *Mycobacterium tuberculosis* DNA in tissue affected by sarcoidosis. BMJ 306:546–549
11. Filliol I, Driscoll JR, van Soolingen D, Kreiswirth BN et al (2003) Snapshot of moving and expanding clones of *Mycobacterium tuberculosis* and their global distribution assessed by spoligotyping in an international study. J Clin Microbiol 41:1963–1970
12. Ghossein RA, Ross DG, Salomon RN, Rabson AR (1994) A search for mycobacterial DNA in sarcoidosis using the polymerase chain reaction. Am J Clin Pathol 101:733–737
13. Goldmann T, Zissel G, Sen Gupta R, Schlaak M, Vollmer E, Müller-Quernheim J (2001) Formation of granulomas in the lungs of severe combined immunodeficient mice after infection with *Bacillus Calmette-Guerin*. Am J Pathol 158:1890–1891
14. Goldmann T, Vollmer E (2002) PCR-based diagnosis of mycobacteria: use and pitfalls of formalin-fixed, paraffin-embedded specimens. Eur J Pathol 8:4–03
15. Greer CE, Peterson SL, Kiviat NB, Manos MM (1991) PCR amplification from paraffin-embedded tissues. Effects of fixative and fixation time. Am J Clin Pathol 95:117–124
16. Grosser M, Luther T, Müller J, Schuppler M, Bickhardt J, Matthiessen W, Müller M (1999) Detection of *M. tuberculosis* DNA in sarcoidosis: correlation with T-cell response. Lab Invest 79:775–784
17. Hellyer TJ, DesJardin LE, Assaf MK, Bates JH, Cave MD, Eisenach KD (1996) Specificity of IS*6110*-based amplification assays for *Mycobacterium tuberculosis* complex. J Clin Microbiol 34:2843–2846
18. Hsiao PF, Tzen CY, Chen HC, Su HY (2003) Polymerase chain reaction based detection of *Mycobacterium tuberculosis* in tissues showing granulomatous inflammation without demonstrable acid-fast bacilli. Int J Dermatol 42:281–286
19. Höfler H (1999) Leitlinien der Deutschen Gesellschaft für Pathologie. Leitlinien Diagnostische Molekulare Pathologie. Pathologe 20:306–307

20. Hofman V, Selva E, Landraud L, Sicard D, Venissac N, Castillo L, Kermarec A, Mouroux J, Dellamonica P, Hofman P (2003) Value of PCR amplification from formalin-fixed paraffin-embedded tissues in the diagnosis of *Mycobacterium tuberculosis* infection. Ann Pathol 23:206–215
21. Ikonomopoulos JA, Gorgoulis VG, Zacharatos PV, Manolis EN, Kanavaros P, Rassidakis A, Kittas C (1999) Multiplex polymerase chain reaction for the detection of mycobacterial DNA in cases of tuberculosis and sarcoidosis. Mod Pathol 12: 854–862
22. Kamerbeek J, Schouls L, Kolk A, van Agterveld M, van Soolingen D, Kuijper S, Bunschoten A, Molhuizen H, Shaw R, Goyal M, van Embden J (1997) Simultaneous detection and strain differentiation of *Mycobacterium tuberculosis* for diagnosis and epidemiology. J Clin Microbiol 35:907–914
23. Küchler R, Pfyffer GE, Rüsch-Gerdes S, Beer J, Roth A, Mauch H (eds) (1998) Tuberculosis/mycobacteriosis. MiQ quality standards for microbiological diagnostic techniques for infectious diseases, vol. 5. Gustav Fischer, Stuttgart
24. Li JYW, Lo STH, Ng CS (2000) Molecular detection of *Mycobacterium tuberculosis* in tissues showing granulomatous inflammation without demonstrable acid-fast bacilli. Diagn Mol Pathol 9:67–74
25. Loeschke S, Goldmann T, Vollmer E (2005) Improved detection of mycobacterial DNA by PCR in formalin-fixed, paraffin-embedded tissues using thin sections. Pathol Res Pract 201:37–40
26. Marchetti G, Gori A, Catozzi L, Vago L, Nebuloni M, Rossi MC, Esposti D, Bandera A, Franzetti F (1998) Evaluation of PCR in detection of *Mycobacterium tuberculosis* from formalin-fixed, paraffin-embedded tissues: comparison of four amplification assays. J Clin Microbiol 36:1512–1517
27. Mengel M, von Wasielewski R, Wiese B, Rüdiger T, Müller-Hermelink HK, Kreipe H (2002) Inter-laboratory and inter-observer reproducibility of immunohistochemical assessment of the Ki-67 labelling index in a large multi-centre trial. J Pathol 198:292–299
28. Noordhoek GT, Kolk AH, Bjune G, Catty D, Dale JW, Fine PE, Godfrey-Faussett P, Cho SN, Shinnik T, Svenson SB (1994) Sensitivity and specificity of PCR for detection of *Mycobacterium tuberculosis*: a blind comparison study among seven laboratories. J Clin Microbiol 32:277–284
29. Park do Y, Kim JY, Choi KU, Lee JS, Lee CH, Sol MY, Suh KS (2003) Comparison of polymerase chain reaction with histopathologic features for diagnosis of tuberculosis in formalin-fixed, paraffin-embedded histologic specimens. Arch Pathol Lab Med 127:326–330
30. Pao CC, Yen TSB, You JB, Maa JS, Fiss EH, Chang CH (1990) Detection and identification of *Mycobacterium tuberculosis* by DNA amplification. J Clin Microbiol 28:1877–1880
31. Popper HH, Klemen H, Hoefler G, Winter E (1997) Presence of mycobacterial DNA in sarcoidosis. Human Pathol 28:796–800
32. Qian L, Van Embden JDA, Van Der Zanden AGM, Weltevreden EF, Duanmu H, Douglas JT (1999) Retrospective analysis of the Beijing family of *Mycobacterium tuberculosis* in preserved lung tissues. J Clin Microbiol 37:471–474
33. Richter E, Greinert U, Kirsten D, Rüsch-Gerdes S, Schlüter C, Duchrow M, Galle J, Magnussen H, Schlaak M, Flad HD, Gerdes J (1996) Assessment of mycobacterial DNA in cells and tissues of mycobacterial and sarcoid lesions. Am J Respir Crit Care Med 153:375–380
34. Richter E, Schlüter C, Duchrow M, Hahn M, Rüsch-Gerdes S, Galle J, Flad HD, Gerdes J (1995) An improved method for the species-specific assessment of mycobacteria in routinely formalin-fixed and paraffin-embedded tissues. J Pathol 175:85–92
35. Rogall T, Wolters J, Flohr T, Böttger EC (1990) Toward a phylogeny and definition of species at a molecular level within the genus Mycobacterium. Int J Syst Bacteriol 40:323–330
36. Roth A, Mauch H, Göbel U (eds) (1997) Nucleic acid amplification techniques. Recommendations for employing molecular methods in diagnostic routine microbiology laboratories and measures for internal quality assurance. MiQ quality standards for microbiological diagnostic techniques for infectious diseases, vol. 1. Gustav Fischer, Stuttgart
37. Rupp J, Droemann D, Goldmann T, Zabel P, Solbach W, Vollmer E, Branscheid D, Dalhoff K, Maass M (2004) Alveolar epithelial cells type II are major target cells for *C. pneumoniae* in chronic but not in acute respiratory infection. FEMS Immunol Med Microbiol 41:197–203
38. Saboor SA, Johnson NM, McFadden J (1992) Detection of mycobacterial DNA in sarcoidosis and tuberculosis with polymerase chain reaction. Lancet 339:1012–1015
39. Salian NV, Rish JA, Eisenach KD, Cave MD, Bates JH (1998) Polymerase chain reaction to detect *Mycobacterium tuberculosis* in histologic specimens. Am J Respir Crit Care Med 158: 1150–1155
40. Schewe C, Rizzello M, Dietel M, Hauptmann S (2000) PCR based diagnosis in pathology. Pathologe 21:218–228
41. Seiler P, Ulrichs T, Bandermann S, Pradl L, Jörg S, Krenn V, Morawietz L, Kaufmann SHE, Aichele P (2003) Cell-wall alterations as an attribute of *Mycobacterium tuberculosis* in latent infection. J Infect Dis 188:1326–1331
42. Sen Gupta R, Hillemann D, Kubica T, Zissel G, Müller-Quernheim J, Galle J, Vollmer E, Goldmann T (2003) HOPE-fixation enables improved PCR-based detection and differentiation of *Mycobacterium tuberculosis* complex in paraffin-embedded tissues. Pathol Res Pract 199:619–623
43. Vago L, Zerbi P, Caldarelli-Stefano R, Cannone M, D'Amico M, Bonetto S, Barberis M (2000) Polymerase chain reaction for *Mycobacterium tuberculosis* complex DNA. Use on negative archival Ziehl–Neelsen cytologic samples. Acta Cytol 44:1023–1028
44. Van der Zanden AGM, Hoentjen AH, Heilmann FGC, Weltevreden EF, Schouls LM, van Embden JDA (1998) Simultaneous detection and strain differentiation of *Mycobacterium tuberculosis* complex in paraffin wax embedded tissues and in stained microscopic preparations. J Clin Pathol: Mol Pathol 51:209–214
45. Walker DA, Taylor IK, Mitchell DM, Shaw RJ (1992) Comparison of polymerase chain reaction amplification of two mycobacterial DNA sequences, IS*6110* and the 65 kDa antigen gene, in the diagnosis of tuberculosis. Thorax 47:690–694
46. Wong H, Anderson WD, Cheng T, Riabowol KT (1994) Monitoring m RNS expression by polymerase chain reaction: the primer-dropping method. Anal Biochem 223:251–258
47. Zink AR, Sola C, Reischl U, Grabner W, Rastogi N, Wolf H, Nerlich AG (2003) Characterization of *Mycobacterium tuberculosis* complex DNAs from Egyptian mummies by spoligotyping. J Clin Microbiol 41:359–367
48. Zink AR, Nerlich AG (2004) Molecular strain identification of the *M. tuberculosis* complex in archival tissue samples. J Clin Pathol 57:1185–1192

Virchows Arch (2005) 447: 586–592
DOI 10.1007/s00428-005-1211-9

ORIGINAL ARTICLE

Ludwig Wilkens · Heidrun Gerr · Dorothea Gadzicki · Hans Kreipe · Brigitte Schlegelberger

Standardised fluorescence in situ hybridisation in cytological and histological specimens

Received: 29 November 2004 / Accepted: 7 January 2005 / Published online: 10 June 2005
© Springer-Verlag 2005

Abstract Fluorescence in situ hybridisation (FISH) has gained major impact in the detection of chromosomal aberrations. The application of FISH, however, is hampered due to complicated protocols. We therefore designed a FISH protocol that allows the fast and reliable application on cytological and histological specimens. Cytological and histological specimens of bone marrow, lymph nodes, liver and breast were analysed with 14 sets of centromere or locus-specific probes. A pretreatment of enzymatic digestion and microwave heating with the same incubation times for all specimens and probes used was performed. Hybridisation efficiency was proved by calculating the thresholds for monosomy, trisomy and translocations. Values in cytological specimens reached 9.0, 3.9 and 4.6%, respectively. In histological sections, values of 6.4% were seen for aneusomy and 3.1% for translocations. However, values for monosomy reached 20.5% in bone marrow and 61.8% in liver tissues due to cutting artifacts. In bone marrow with acute myeloid leukaemias, lymph nodes with follicular and mantle cell lymphomas, breast carcinomas and liver cell carcinomas, FISH confirmed aberrations already found using conventional cytogenetics. The protocol shown here is easy to perform and can be used with cytological and histological specimens. Moreover, with "hands on" time of less than 2 h, FISH can also be used for daily routine purposes.

Keywords Chromosome aberrations · In situ hybridisation · Cytology · Histology

L. Wilkens (✉) · H. Gerr · D. Gadzicki · B. Schlegelberger
Institute of Cell and Molecular Pathology,
Hannover Medical School,
Carl-Neuberg-Str. 1,
30625 Hannover, Germany
e-mail: wilkens.ludwig@mh-hannover.de
Tel.: +49-511-5324517
Fax: +49-511-5324521

L. Wilkens · H. Kreipe
Institute of Pathology, Hannover Medical School,
Carl-Neuberg-Str. 1,
30625 Hanover, Germany

Introduction

Chromosomal imbalances are characteristically found in most solid and haematological neoplasias [12]. For some leukaemias, such as chronic myeloid leukaemia (CML), acute myeloid leukaemia (AML) M3 and AML M4Eo, translocations t(9;22), t(15;17) and inv(16), respectively, have already been defined as specific [2, 14, 17]. Also, in solid tumours, characteristic imbalances have been found to be associated with carcinomas of the urinary tract, the lung and the liver [8, 16, 22]. Moreover, new treatment regimens focus on important genetic changes such as amplification of Her2/neu in breast carcinoma [5].

However, detection of aberrations by conventional cytogenetics, in particular in solid tumours, is impaired due to low proliferative activity and metaphase number in vitro [1, 18]. As an alternative approach, fluorescence in situ hybridisation (FISH) has been developed. FISH is based on the hybridisation of hapten or fluorescent labelled probes complementary to target DNA or RNA sequences in the nucleus and cytoplasm [15]. A major drawback of FISH, however, is the complicated and time-consuming protocols that have to be adapted to the cytological and histological specimens analysed. The effort required for these procedures seems to be high even for larger institutional laboratories.

Therefore, the aim of this study was to establish an easy-to-perform FISH protocol suitable for both cytological and histological specimens. Based on our previous experience in this field, this protocol was tested on normal and neoplastic specimens with a variety of commercially available probe sets, to ensure high quality of results.

Materials and methods

Cytological and histological specimens

Non-neoplastic bone marrow aspirates as well as trephine core biopsies were available from five different patients. Smears and bare nuclei were prepared as described else-

where [7]. Smear preparations were air dried. Bare nuclei were fixed and stored until use in a mixture of methanol and acetic acid (3:1). Trephine core biopsies were fixed for 24 h in a mixture of buffered formalin and methanol (3,200 ml methanol, 1,667 ml 37% formaldehyde, 133 ml buffer (150 ml 802.97 g $NaH_2PO_4 \cdot H_2O$ and 1,000 ml dH_2O and 650 ml 10.67 g Na_2HPO_4 and 1,000 ml dH_2O) and 6.65 g glucose adjusted to pH 7.4. Biopsies were then decalcified in a solution of 200 g Tetriplex 3 and 66 g Tris(hydroxymethyl)-aminomethane (both Merck, Darmstadt, Germany) and 2,000 ml dH_2O adjusted to pH 7.4 and paraffin embedded. Fine-needle aspirates (FNA) of livers with reactive changes of five patients were analysed as well as non-neoplastic tissues of the liver of five other patients as histological specimens.

For detection of chromosomal changes, cytological and histological samples of patients with haematological disorders were included; cytogenetic analysis of these patients was performed in parallel. This included a case of myelodysplastic syndrome (MDS) with del(5)(q14q31), an myelodysplastic syndrome (MDS) with monosomy 7, an AML with trisomy 8, and AML with a translocation t(8;21).

Additionally cytological and histological samples of neoplasms were analysed for which typical aberrations are known, but conventional cytogenetics was not performed due to the problems mentioned above and/or to the fact that only paraffin-embedded tissue was available. This group included a breast carcinoma with amplification of Her2/neu, a follicular centre lymphoma (FCL) with t(14;18), a mantle cell lymphoma with t(11;14) and hepatocellular carcinoma (HCC) with aneuploidy of chromosomes 1 and 8, and gains of 8q24.

Probes

Fourteen different probes and/or probe combinations were used. These were specific for the centromeric regions of chromosomes 1, 7, 8 and 17, for 5q31, 8q24, 13q14, 17q21, tel19q, 20q12 and 21q22, and for the detection of translocations t(8;21), t(11;14) and t(14;18) (Table 1). Probes were commercially available and supplied by Abbott Corp. (Wiesbaden, Germany).

Table 1 Fluorescence in situ hybridisation (FISH) probes used for the experiments performed in this study (all probes supplied by Abbott, Wiesbaden, Germany)

Probe	Specific for
CEP1	cen1
CEP7	cen7
CEP8	cen8
CEP17	cen17
EGR1	5q31
c-MYC	8q24
RB1	13q14
Her2/neu	17q21
tel19q	tel19q
D20S108	20q12
ETO	21q22
AML/ETO	t(8;21)(q22;q22)
IgH/CCND1	t(11;14)(q13;q32)
IgH/BCL2	t(14;18)(q32;q21)

Pretreatment

Pretreatment of bare nuclei and cytological smears started with incubation for 3 min at room temperature in 50 ml of a pepsin solution in a coplin jar. The pepsin solution was prepared from 99 ml dH_2O, 1 ml HCl 1 N and 5 mg pepsin (Sigma, Taufkirchen, Germany), and was made freshly every day. Slides were then washed for 1 min in dH_20 followed by washing for 10 min in paraformaldehyde [1.5% (v/v), Merck, Darmstadt, Germany]. A new solution was prepared every 7 days and stored at 4°C until use. After washing for 1 min in dH_2O, slides were air dried at room temperature.

Paraffin-embedded tissues (4-μm sections) were mounted on Super Frost Plus slides (Menzel, Braunschweig, Germany), dried overnight at 56°C and subsequently passed through xylol and a series of 95, 80 and 70% ethanol. To minimise the amount of probe needed to cover the tissue, the specimens were downsized with a microtome blade to a size of 0.2×0.2 cm. For this purpose, the area of interest was marked on the H&E or Giemsa-stained sections and scratched away with a scalpel on the parallel sections used for FISH. The specimens were then boiled in a microwave oven for 30 min in 6 M Na-citrate buffer (pH 6.0), cooled to room temperature and rinsed in distilled water. This was followed by incubation with the pepsin solution described above for 5 min at room temperature, washing for 1 min in dH_20, incubation for 10 min in paraformaldehyde (1.5%) and again washing for 1 min in dH_2O. The slides were then air dried.

Hybridisation and washings

Hybridisation of both cytological and histological sections was started by adding 0.5 μl of centromere or locus-specific probes to 4 μl hybridisation buffer (Abbott, Wiesbaden, Germany) and 1 μl H_2O pipetted onto the slide. A glass coverslip (Menzel, Braunschweig, Germany) was placed onto the slides and sealed with rubber cement (Fixogum, Marabu, Tamm, Germany). Specimens were heated to 80°C for 10 min to denature probe and specimen DNA and incubated overnight at 37°C in a humidified dark chamber. Afterwards, the rubber cement was stripped off and the coverslip was removed by gently washing the slides twice in 0.4×SSC/0.3% Igepal (Abbott, Wiesbaden, Germany) at 75°C for 2 min. Slides were then counterstained in a light-protected coplin jar filled with 50 ml DAPI (40 ng/ml, Qiagen, Heidelberg, Germany). Finally, a drop of Vectashield antifade (Vector, USA) was added and the slide was covered with a coverslip. Excessive fluid was removed with a Kim wipe and a drying block (Schleicher & Schuell, Dassel, Germany). The "hands-on" time for the experimen-

tal steps before hybridisation was less than 90 min and after hybridisation less than 30 min.

Evaluation of signals was carried out using an epifluorescence microscope (Axioskop 2, Zeiss, Oberkochen, Germany) equipped with a fluorescein, Cy3 and DAPI filter set and a 100-W mercury lamp. In each tumour, 50 nuclei were evaluated and documented with the ISIS software package (Metasystems, Altlußheim, Germany).

Results

Non-neoplastic samples

Bare nuclei bone marrow aspirates

The mean percentages of nuclei with one signal only for cen7, 13q14 and 20q12 were 2.90, 1.6 and 2.6%, respectively, with standard deviations (SDs) of 1.40, 1.1 and 1.5% (Table 2). According to Ward et al. [21], the thresholds were calculated by adding three SDs to the mean obtained for the particular probe. Thus, thresholds were 7.1, 4.9 and 7.10%, respectively. For defining aneusomy of cen8, tel19q and 21q22, mean values were 0.30, 1.40 and 1.2% (SD 0.33, 0.8 and 1.30%), and the depending thresholds 1.28, 3.80 and 5.10%. For the translocation probe t(8;21), the mean, SD and threshold were 1.00, 1.20 and 4.60, respectively.

Table 2 Mean values, standard deviations (SDs) and thresholds for defining monosomy, aneusomy and translocations based on the evaluation of normal specimens of bare nuclei of leucocytes, smears of bone marrow aspirates, bone marrow trephines, fine needle aspirates (FNAs) of the liver and core biopsies of the liver

	Percentage of nuclei revealing						
	Monosomy			Aneusomy			Translocation
Probe	cen7	13q14	20q12	cen8	tel19q	21q22	t(8;21)
Bare nuclei of leucocytes							
Mean	2.90	1.60	2.60	0.30	1.40	1.20	1.00
SD	1.40	1.10	1.50	0.33	0.80	1.30	1.20
Threshold	7.10	4.90	7.10	1.28	3.80	5.10	4.60
Smears of bone marrow aspirates							
Mean	1.78	2.40	1.21	2.20	2.33	2.26	0.60
SD	0.45	1.90	1.10	2.00	0.52	0.43	0.43
Threshold	3.13	8.10	3.31	8.20	3.89	3.55	1.89
Bone marrow trephines							
Mean	12.78	11.20	13.66	1.66	0.93	2.21	0.80
SD	1.96	3.10	2.00	0.90	0.68	1.14	0.78
Threshold	18.66	20.50	19.66	4.36	2.97	5.63	3.14

	Percentage of nuclei revealing					
	Monosomy			Aneusomy		
Probe	cen1	cen8	8q24	cen1	cen8	8q24
FNAs of the liver						
Mean	2.65	3.20	4.80	0.65	0.50	1.20
SD	0.86	1.55	1.40	0.14	0.18	0.80
Threshold	5.23	7.84	9.00	1.06	1.03	3.60
Core biopsies of the liver						
Mean	39.60	36.00	35.00	2.00	2.80	1.60
SD	7.40	6.78	4.00	1.41	1.10	1.60
Threshold	61.81	56.35	47.00	6.24	6.09	6.40

Smear preparations of bone marrow aspirates

Monosomy for cen7, 13q14 and 20q12 was seen with mean values of 1.78, 2.4 and 1.21% (SD 0.45, 1.90, 1.1%). Thresholds were set at 3.13, 8.10 and 3.31%. Aneusomy was seen for cen8, tel19q and 21q22 in 2.2, 2.33 and 2.26% (SD 2.0, 0.52, 0.43%) with thresholds at 8.2, 3.89 and 3.55%. For t(8;21), values were 0.6, 0.43 and 1.89%, respectively.

Histological specimens of bone marrow

The percentage values of cells bearing one signal only for cen7, 13q14 and 20q12 were 12.78, 11.2 and 13.66% (SD 1.96, 3.1 and 2.0). Accordingly, thresholds had values of 17.74, 17.30 and 18.66%. For aneusomic count, values for cen8, tel19q and 21q22 were 1.66, 0.93 and 2.21% of cells (SD 0.9, 0.68 and 1.1.4). Thresholds were set at 4.36, 2.97 and 5.63. For t(8;21), values were 0.8, 0.78 and 3.14%, respectively.

FNA of the liver

The analysis of the cytological specimens of the liver revealed mean values of one signal/cell for cen1, cen8 and 8q24 in 2.65, 3.2 and 4.8% (SD 0.86, 1.55 and 1.40%). Thresholds were set at 5.23, 7.84 and 9.00%. For aneusomic counts of these probes, mean values were 0.65, 0.50 and 1.20% (SD 0.14, 0.18 and 0.80%). Thresholds were 1.06, 1.03 and 3.60%, respectively.

Core biopsies of the liver

For these histological samples, the values for one signal/cell for cen1, cen8 and 8q24 were 39.6, 36.0 and 35.0% (SD 7.4, 6.78 4.0%), respectively. Therefore, thresholds for these probes were 61.81, 56.35 and 47.0%. For aneusomic counts, mean values were 2.00, 2.80 and 1.6% (SD 1.41, 1.1 and 1.6%). Thresholds were 6.24, 6.09 and 6.4%, respectively.

Neoplastic samples

MDS with del5q and −7

For these cases of histologically proven MDS, conventional cytogenetics revealed del(5)(q14q34) in 20 of 20

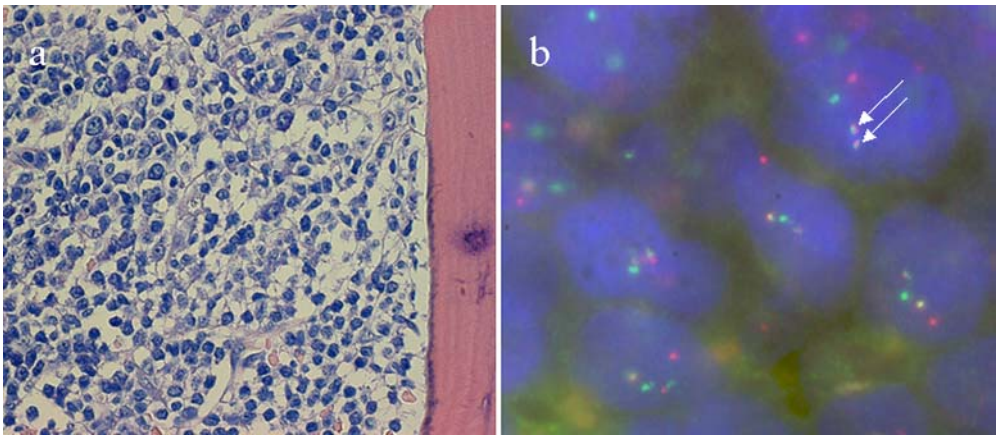


Fig. 1 Histological section of bone marrow infiltrates of a follicular cell lymphoma (**a** original magnification ×400). Fluorescence in situ hybridisation (FISH) was performed with a probe set giving two yellow fusion signals for the translocated chromosomes and one green and one red signal for the normal chromosomes. Fusion signals in the neoplastic cells are indicated by *arrows* in a cell example (**b** original magnification ×1,000). Due to cutting artifacts, not all signals expected are detectable in the nuclei

metaphases and −7 in 18 of 20 metaphases. Using FISH with the combined probes for cen5/5q31, one signal for 5q31 occurred in 78% of bare interphase nuclei. In the cytological specimens, this value was 61.5%; whereas in the bone marrow core, the percentage was 31%. In the case with monosomy 7, 78% of the bare nuclei revealed only one signal. In the cytological specimens, 60% of cells were affected, and in the trephine biopsy this value was 65.5%.

AML with trisomy 8

Again, this aberration was seen in all metaphases (15 of 15). The percentages of aberrant cells in the bare interphase nuclei, in the cytological specimens and in the core biopsy were 87, 74.5 and 68%, respectively.

AML with t(8;21)

A translocation t(8;21) was detectable in 22 of 22 metaphases. The number of aberrant bare interphase nuclei was 97%. In the cytological specimens, 88% and, in the core biopsy, 91% of the cells had the signal constellation typical for t(8;21).

Lymphomas

In a core biopsy, histological examination raised the differential diagnosis of splenic marginal zone and FCL. Using a probe set specific for t(14;18), fusion signals were detected in the neoplastic tumour cell population in 70% of the nuclei analysed, arguing the case for a FCL (Fig. 1). In a lymph node of another patient, a mantle cell lymphoma was seen. This diagnosis was confirmed using FISH with fusion signals in 80% of the lymphoma cells (Fig. 2).

Breast carcinoma

In the histological specimen of this sample, a ductal carcinoma in situ and an invasive ductal carcinoma of the breast were detected. The relationship between signals of Her2/neu and cen17, calculated from signals of 60 nuclei as recommended, was 6.7 in the DCIS, whereas this ratio was 1.4 in the invasive breast carcinoma (Fig. 3).

FNA of the liver

In a sample of low differentiated HCC, means of 4.90 signals per nucleus for #1 and 14.66 signals per nucleus for

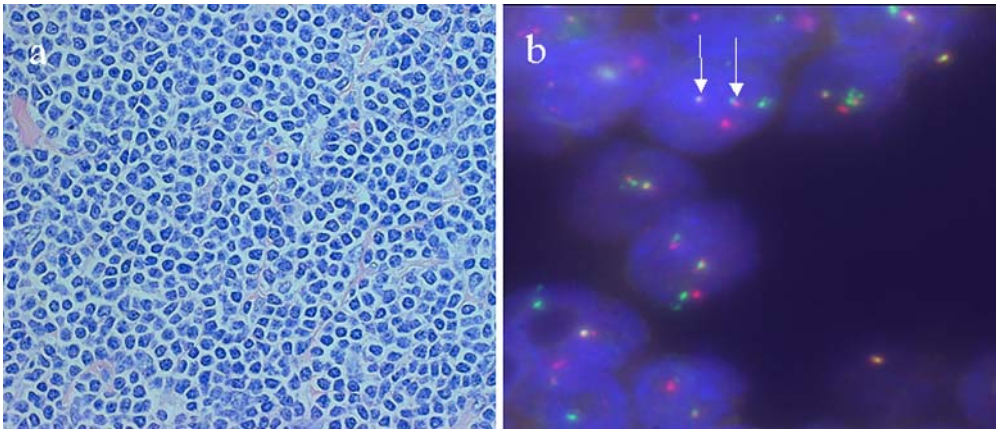


Fig. 2 Histological section of a mantle cell lymphoma in a lymph node (**a** original magnification ×400). For detection of the t(11;14), a probe set was used giving two yellow fusion signals besides the normal green and red signals of unaltered chromosomes 11 and 14, respectively (**b** original magnification ×1,000). These two fusion signals are indicated by *arrows* in a given cell

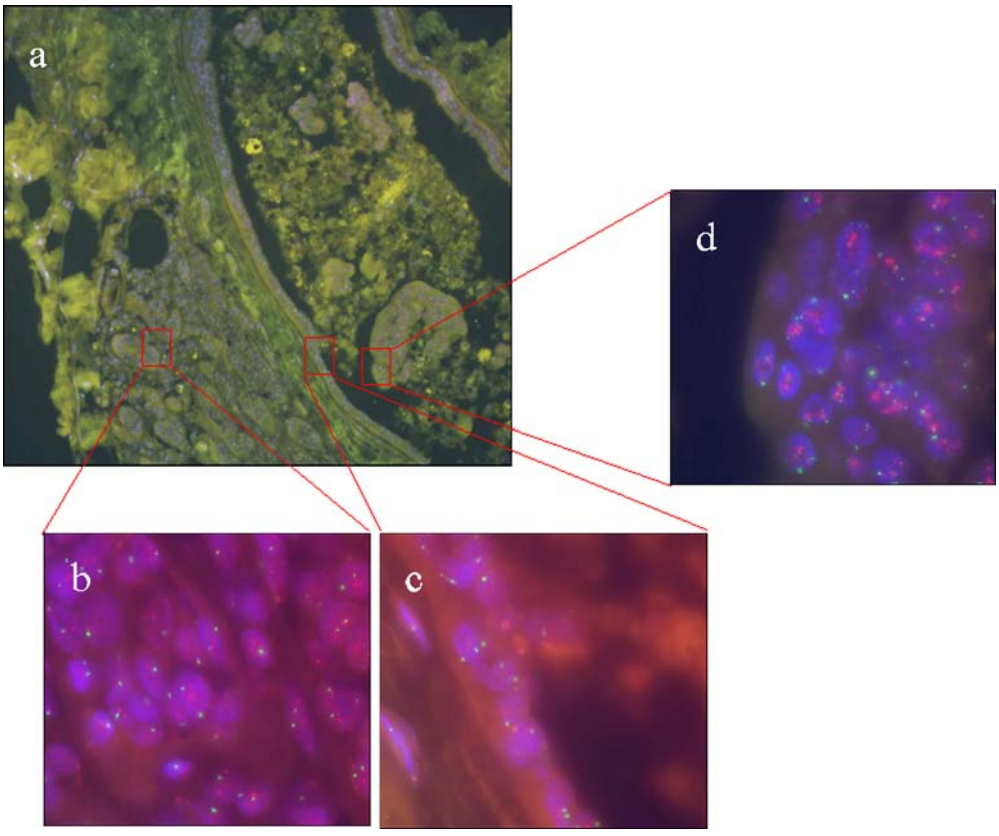


Fig. 3 **a** Fluorescence in situ hybridisation (FISH) using specific probes for Her2/neu (*red*) and cen17 (*green*) in a case of a breast carcinoma with an invasive component (**b**) and an intraductal carcinoma (DCIS) (**d**). In the invasive carcinoma and the epithelial cells covering the inner layer of the duct (**c**), an amplification of Her2/neu was not detectable, although a high amplification occurred for the DCIS (×100, ×630)

#8 with 41 different signal combinations, indicating a high chromosomal instability in this sample, were found.

Application in daily routine work

To determine the applicability of the FISH protocol for daily routine work, FISH analyses of bare nuclei, cytological specimens and histological sections were evaluated for sufficient hybridisation efficiency, i.e. more than 90% of nuclei bearing signals. By counting at least 100 nuclei, 100 cases each were analysed. The percentages of cases with sufficient hybridisation efficiency were 95% for specimens of bare nuclei, 93% for cytological specimens and 87% for histological sections.

Discussion

The definition of diagnostically and prognostically important genetic markers in neoplastic diseases implicates an increasing impact of FISH. The main advantage of this technique is found in the combination of the detection of cytogenetic aberrations in interphase nuclei with preserved morphology. This ensures that the neoplastic cells are analysed even when mixed with non-neoplastic cell populations. Here, FISH is clearly superior to other techniques such as conventional cytogenetics or polymerase chain reaction. In this study, we aimed to find an easy and fast-to-perform protocol. It is applicable to both cytological and histological specimens by standardised pretreatment and hybridisation steps. This allows a distinct analysis, not only of numerical changes but also of structural alterations of particular importance in leukaemias and lymphomas [6, 12].

The main step in the successful application of the protocol was the pretreatment of the specimens. First, enzymatic digestion was carried out by incubation of cells with a pepsin solution. In comparison with proteinase K, it was not necessary to adapt the time of digestion with regard to the type of cells treated. Three minutes of pepsin digestion allowed FISH analysis of all specimens used to be carried out with high hybridisation efficiency and well-preserved morphology. This is of particular interest when only one sample is available.

However, the single use of pepsin was not sufficient for histological sections. Microwave pretreatment was mandatory in these cases. Microwave pretreatment is a well-known technique to enhance staining intensity in immunohistochemistry [3, 19, 20]. Cross-links between proteins caused by formalin fixation and their break-up by microwave irradiation have been described as the underlying effect of staining enhancement in immunohistochemistry [19, 20]. Those cross-links can also occur after formalin fixation in nucleic acids [11]. Accordingly, a positive effect of this technique in the detection of DNA and RNA sequences has been described previously [13, 23]. Leers et al. [10] proposed that heating dewaxed tissue sections leads to a diminishing of nucleic proteins, allowing propidium iodide to get into the nuclei. This effect could

also be helpful for diffusion of probes in the nuclei. As seen for pepsin digestion in cytological specimens, an adaptation of incubation time for the different tissues is not necessary. Heating reaches a maximum effect after breaking up all proteins affectable by this harsh procedure with no further improvement by additional incubation. In our study, a standardised time of 30 min was sufficient to obtain clearly detectable signals against a low background.

In this point, our results differ from those of Chin et al. [4] who also reported a combination of microwave pretreatment and enzymatic digestion. In their study, an incubation time of 60 min was found necessary to detect both kinds of probes. This probably is due to the different temperatures during the heating process. Chin et al. [4] used 80°C whereas, in our study, the temperature was raised to the boiling point above 100°C. Moreover, our protocol also worked acceptably in liver specimens reported to give high autofluorescence by Chin et al. [4]. The protocol also gave highly adequate results in bone marrow biopsies despite decalcification steps before paraffin embedding. A further advantage of our protocol was seen in the decreased number of washing steps performed, bringing down the total "hands-on" time needed for the whole procedure to less than 2 h.

A decreased number of incubation steps is also seen in comparison with the protocol of Haralambieva et al. [9] using RNAse treatment not necessary in our protocol.

As a drawback of FISH, it has to be mentioned that assessing losses of chromosomes in histological sections is hampered by high thresholds of 20% in bone marrow sections and 60% in liver sections. This problem is due to the cutting artifacts that have an increasing influence in larger cells, as seen for the smaller cells of the bone marrow in comparison with the larger cells of the liver. As shown for the detection of chromosome gains and structural imbalances, this problem seems to be of lower impact.

A further point to be mentioned is the time of tissue fixation. Since 24 h of fixation is normally taken as a standard for routine purposes, we focused on this time here. Nevertheless, based on our own experience with tissues taken from surgical specimens of the liver after 4 days or more of fixation, FISH can be impaired (data not shown). Therefore, overfixation should be avoided.

In conclusion, the new protocol is easy and fast to perform and can be applied to both cytological and histological specimens. With this protocol, the advantages of FISH can be used not only for research but also for daily routine purposes even in smaller laboratories.

References

1. Bardi G, Johansson B, Pandis N, Heim S, Mandahl N, Andren SA, Hagerstrand I, Mitelman F (1992) Cytogenetic findings in three primary hepatocellular carcinomas. Cancer Genet Cytogenet 58:191–195
2. Campbell LJ, Challis J, Fok T, Garson OM (1991) Chromosome 16 abnormalities associated with myeloid malignancies. Genes Chromosomes Cancer 3:55–61
3. Cattoretti G, Pileri S, Parravicini C, Becker MHG, Poggi S, Bilfulco C (1993) Antigen unmasking on formalin-fixed, paraffin-embedded tissue sections. J Pathol 171:83–98
4. Chin SF, Daigo Y, Huang H, Iyer NG, Callagy G, Kranjac T, Gonzalez M, Sangan T, Earl H, Caldas C (2003) A simple and reliable pretreatment protocol facilitates fluorescent in situ hybridisation on tissue microarrays of paraffin wax embedded tumour samples. J Clin Pathol Mol Pathol 56:275–279
5. Dowsett M, Bartlett J, Ellis IO, Salter J, Hills M, Mallon E, Watters AD, Cooke T, Paish C, Wencyk PM, Pinder SE (2003) Correlation between immunohistochemistry (HercepTest) and fluorescence in situ hybridization (FISH) for HER-2 in 426 breast carcinomas from 37 centres. J Pathol 199:418–423
6. Feller A, Diebold J (2004): Histopathology of nodal and extranodal non-Hodgkin's lymphomas. Springer, New York Berlin Heidelberg
7. Gosden CM, Davidson C, Robertson M (1992) Human cytogenetics: a practical approach. Oxford University Press, Oxford
8. Gunawan B, Huber W, Holtrup M, von Heydebreck A, Efferth T, Poustka A, Ringert RH, Jakse G, Fuzesi L (2001): Prognostic impacts of cytogenetic findings in clear cell renal cell carcinoma: gain of 5q31-qter predicts a distinct clinical phenotype with favorable prognosis. Cancer Res 61:7731–7738
9. Haralambieva E, Kleiverda K, Mason DY, Schuuring E, and Kluin PM (2002) Detection of three common translocation breakpoints in non-Hodgkin's lymphomas by fluorescence in situ hybridization on routine paraffin-embedded tissue sections. J Pathol 198:163–170
10. Leers MP, Schutte B, Theunissen PH, Ramaekers FC, Nap M (1999) Heat pretreatment increases resolution in DNA flow cytometry of paraffin-embedded tumor tissue. Cytometry 35: 260–266
11. McGhee JD, von Hippel PH (1977) Formaldehyde as a probe of DNA Structure. 4. Mechanisms of the initial reaction of formaldehyde with DNA. Biochemistry 16:3276–3293
12. Mitelman F (1994) Catalog of chromosome aberrations in cancer. Wiley-Liss, New York
13. Nolte M, Werner M, Ewig M, von Wasielewski R, Wilkens L, Georgii A (1995) Demonstration of the Philadelphia translocation by fluorescence in situ hybridization (FISH) in paraffin sections and identification of aberrant cells by a combined FISH/immunophenotyping approach. Histopathology 26:433–437
14. Nowell PC, Hungerford DA (2003) A minute chromosome in human chronic granulocytic leukemia. Science 132:1497
15. Pinkel D, Straume T, Gray JW (1986) Cytogenetic analysis using quantitative, high sensitivity, fluorescence hybridization. Proc Natl Acad Sci U S A 83:2934–2938
16. Richter J, Jiang F, Gorog JP, Sartorius G, Egenter C, Gasser TC, Moch H, Mihatsch MJ, Sauter G (1997) Marked genetic differences between stage pTa and stage pT1 papillary bladder cancer detected by comparative genomic hybridization. Cancer Res 57:2860–2864
17. Rowley JD (1990) Recurring chromosome abnormalities in leukemia and lymphoma. Semin Hematol 27:122–136
18. Saito H, Morizane T, Watanabe T, Kagawa T, Iwabuchi MN, Kumagai N, Inagaki Y, Tsuchimoto K, Tsuchiya M (1989) Establishment of a human cell line (HCC-T) from a patient with hepatoma bearing no evidence of hepatitis B or A virus infection. Cancer 64:1054–1060
19. Shi SR, Key ME, Kalra KL (1991) Antigen retrieval in formalin-fixed, paraffin-embedded tissues; an enhancement method for immunohistochemical staining based on microwave oven heating of tissue sections. J Histochem Cytochem 39:741–748

20. von Wasielewski R, Werner M, Nolte M, Wilkens L, Georgii A (1994) Effects of antigen retrieval by microwave heating in formalin-fixed tissue sections on a broad panel of antibodies. Histochemistry 102:165–172
21. Ward BE, Gersen SL, Carelli MP, McGuire NM, Dackowski WR, Weinstein M, Sandlin C, Warren R, Klinger KW (1993) Rapid prenatal diagnosis of chromosomal aneuploidies by fluorescence in situ hybridization: clinical experience with 4,500 specimens. Am J Hum Genet 52:854–865
22. Wilkens L, Bredt M, Flemming P, Schwarze Y, Becker T, Mengel M, von Wasielewski R, Klempnauer J, Kreipe H (2001): Diagnostic impact of fluorescence in situ hybridization in the differentiation of hepatocellular adenoma and well-differentiated hepatocellular carcinoma. J Mol Diagnostics 3:68–73
23. Wilkens L, von Wasielewski R, Werner M, Nolte M, Georgii A (1996) Microwave pretreatment improves RNA-FISH in various formalin-fixed tissues using a uniform protocol. Pathol Res Pract 192:588–594

Virchows Arch (2005) 447: 593–596
DOI 10.1007/s00428-005-1277-4

ORIGINAL ARTICLE

DongHoon Kim · YoungHyeh Ko · Yeonlim Suh · HongHoe Koo · JooRyung Huh · WonKeun Lee

Characteristics of Epstein-Barr virus associated childhood non-Hodgkin's lymphoma in the Republic of Korea

Received: 15 February 2005 / Accepted: 21 April 2005 / Published online: 1 July 2005
© Springer-Verlag 2005

Abstract To analyze the clinicopathologic characteristics of childhood non-Hodgkin's lymphoma (NHL) associated with Epstein-Barr virus (EBV), EBER in situ hybridization was performed in 80 cases of NHLs. EBER-positive lymphomas account for 25% (20/80) and include NK/T-cell lymphoma (6/6), aggressive NK-cell leukemia (1/1), peripheral T cell lymphoma (5/11), diffuse large B-cell lymphoma (5/14), hydroa-like T-cell lymphoma (1/1), marginal zone B-cell lymphoma (1/2), and post-transplantation lymphoproliferative disorder (1/1). Other types including 19 cases of Burkitt's lymphoma were negative. For 9 EBER-positive cases, immunohistochemical staining for LMP-1, and EBNA-2 was performed to determine the EBV latency pattern. Two of nine EBER-positive cases expressed both LMP-1 and EBNA-2. Clinically, patients with EBV-positive B-cell lymphomas were cured with chemotherapy, whereas EBV-associated NK- and T cell lymphomas pursued fatal clinical course. In conclusion, EBVs infected in childhood NHLs are frequently associated not only with NK- and T- cell lymphomas but also large B-cell lymphomas.

D. Kim · Y. Ko (✉) · Y. Suh
Department of Pathology, Samsung Medical Center,
Sungkyunkwan University School of Medicine,
Kangnam-gu, Ilwon-dong 50,
135-710 Seoul, South Korea
e-mail: yhko@smc.samsung.co.kr
Tel.: +82-02-34102762
Fax: +82-02-34100025

H. Koo
Department of Pediatrics, Samsung Medical Center,
Sungkyunkwan University School of Medicine,
Kangnam-gu, Ilwon-dong 50,
135-710 Seoul, South Korea

J. Huh
Department of Pathology, Asan Medical Center,
University of Ulsan College of Medicine,
Songpa-gu, Pungnap-dong 388-1,
138-736 Seoul, South Korea

W. Lee
Department of Biological Science, Myongji University,
Yongin-si, Namdong,
449-728 Kyunggi-do, South Korea

Introduction

Epstein–Barr virus (EBV) is a well known oncogenic virus associated with various lymphoproliferative disorders. EBV is identified in endemic Burkitt's lymphoma, peripheral T-cell lymphoma, T/NK (natural killer) cell lymphoma, aggressive B cell lymphoma, human immunodeficiency virus (HIV) -associated lymphoproliferative disorder, and Hodgkin's lymphoma. In Hodgkin's lymphoma, the highest frequency (approximately 75%) is found in mixed cellularity HL, and the lowest incidence (10–40%) in nodular sclerosis Hodgkin's lymphoma [5]. According to several studies, the EBV association in T/NK cell lymphoma approaches 50–60%, while that of B cell lymphoma is only between 5–10% [11, 12, 15].

Malignant lymphomas arising in children differ in the frequency of subtype and response to chemotherapy from those of adult patients. In adult patients, EBV is strongly associated with T or NK cell lymphoma such as nasal-type NK/T cell lymphoma which commonly occurs in Far East Asia, especially Hong Kong, Japan, and Korea, suggesting racial or environmental influence. In pediatric patients, there have been few studies regarding EBV-infected non-Hodgkin's lymphomas (NHLs). Recently, Chabay et al. reported high association of EBV in NHLs in children with immune deficiency such as HIV infection or primary immune deficiency [2]. On the other hand, pediatric patients analyzed by Peh et al. showed that EBV was more strongly associated with B-lineage lymphomas than T-lineage lymphoma [12]. Korea is one of the endemic area of EBV infection. At preschool age, more than 80% of children show positive serology for EBV antigen. Considering the common occurrence of EBV-associated NK/T cell lymphoma in adult patients, high prevalence of EBV in pediatric NHLs is strongly suspected. In this study, we analyzed the distribution of EBV in NHLs of children.

Materials and methods

Cases

NHLs diagnosed in patients under the age of 18 years were retrieved from the surgical pathology files. A total of 99 cases were diagnosed in Samsung Medical Center (43 cases) from 1995 to 2003 and Asan Medical Center (56 cases) from 1991 to 2003. Among these, 80 cases for which information for EBER in situ hybridization or paraffin block for the study was available were further analyzed. Clinical information including age, sex, site of involvement, and outcome was obtained from the medical records.

EBV in situ hybridization

Paraffin-embedded tissue sections (5 μm) containing lymphoma were prepared on glass slides. The tissues were digested with proteinase K, dehydrated in 95% ethanol and dried. Hybridization was performed using FITC-labeled EBER-1 and -2 oligonuclotide probes (Novocastra). Following the incubation with anti-FITC antibody tagged with alkaline phosphatase, slides were covered with 5-bromo-4-chloro-3-indolyl phosphatase (BCIP), nitroblue-tetrazolium (NBT), and 1M levamisole. Positive reaction was regarded as such when the majority of tumor cells show nuclear signal.

Immunohistochemical staining

To determine the type of EBV latency, immunohistochemical stain for LMP-1 (Dako, 1:20) and EBNA-2 (Dako, 1:20) was performed in nine EBER-positive cases. A standard three-step immunoperoxidase staining was performed using automated stainer (Dakochemate, Dakocytomation). All cases underwent antigen retrieval with microwave treatment in citrate buffer at pH 6.0.

Results

The 99 patients comprised 30 females, and 69 males, aged 10 months to 18 years (median age 9.5 years) at diagnosis. Histologic subtypes include lymphoblastic lymphoma (13), marginal zone B-cell lymphoma (2), diffuse large B-cell lymphoma (16), mediastinal large B-cell lymphoma (1), Burkitt's lymphoma (32), anaplastic large cell lymphoma (14), NK/T-cell lymphoma (8), peripheral T-cell lymphoma, unspecified (11), hydroa-like T-cell lymphoma (1), and post-transplantation lymphoproliferative disorder (1).

Distribution of EBV in non-Hodgkin's lymphoma (Table 1)

Among 80 cases analyzed by in situ hybridization, 20 cases (25%) were EBER-positive.

Table 1 EBER positivity according to histologic subtype

Subtypes	Positive case/no. of cases examined
Marginal zone B-cell lymphoma	1/2
Diffuse large B-cell lymphoma	5/14
Peripheral T-cell lymphoma	5/11
NK/T-cell lymphoma	6/6
Aggressive NK cell leukemia	1/1
Hydroa-like T-cell lymphoma	1/1
Post-transplantation lymphoproliferative disorder	1/1
Lymphoblastic lymphoma	0/10
Mediastinal large B-cell lymphoma	0/1
Burkitt's lymphoma	0/19
Blastic NK-cell lymphoma	0/1
Anaplastic large cell lymphoma	0/13

EBV positive rate was lower in male patients (9/53) than in female patients (11/26). There was no discernible difference according to age. Five of 19 patients younger than 7 years of age were positive for EBV, four of 24 patients between 7 and 12 years, and 11 of 36 patients between 13 and 18 years. According to histologic subtypes, EBER was negative in all cases of anaplastic large cell lymphoma (0/13), Burkitt's lymphoma (0/19), lymphoblastic lymphoma (0/10), mediastinal large B-cell lymphoma (0/1) and blastic NK-cell lymphoma (0/1). EBER was positive in marginal zone B-cell lymphoma (1/2), diffuse large B-cell lymphoma (5/14), peripheral T-cell lymphoma (5/11), NK/T-cell lymphoma (6/6), aggressive NK cell leukemia (1/1), hydroa-like T-cell lymphoma (1/1), and post-transplantation lymphoproliferative disorder (1/1) (Table 1).

Determination of EBV latency (Table 2 and Fig. 1)

By immunohistochemistry, LMP-1 was detected in two of nine EBER-positive cases. Both were diffuse large B-cell lymphoma and expressed EBNA-2 as well. Clinically, those two patients had no obvious immune deficiency. The remaining seven cases were negative for both LMP-1 and EBNA-2 (Table 2 and Fig. 1).

Discussion

The predominant histologic subtypes of cases enrolled for the study were Burkitt's lymphoma (32 cases, 32%) followed by diffuse large B-cell lymphoma (16 cases, 16%) and anaplastic large cell lymphoma (14 cases, 14%). The distribution of common subtypes is similar to that of previous studies for pediatric non-Hodgkin's lymphoma [1, 12, 14]. On the other hand, the frequency of lymphoblastic lymphoma (13 cases, 13%) was relatively low. The frequency of NK/T-cell lymphoma (8 cases, 8%), and peripheral T-cell lymphoma (11 cases, 11%) was higher than

Table 2 Results of immunohistochemical study for EBER positive cases of which paraffin blocks were available for further study

No.	Age	Sex	Site	Diagnosis	LMP-1	EBNA-2	Survival (Mo.)
1	17	F	Lymph node	MZBCL	−	−	alive (53)
2	13	M	Nasopharynx	DLBCL	+	+	alive (12)
3	6	F	Small intestine	DLBCL	−	−	alive (30)
4	12	M	Bone marrow	PTCL	−	−	dead (13)
5	18	M	Bone marrow	PTCL	−	−	dead (10)
6	4	M	Tonsil	DLBCL	+	+	alive (30)
7	2	F	Lymph node	NK/T cell lymphoma	−	−	dead (2)
8	16	F	Bone marrow	Aggressive NK-cell leukemia	−	−	dead (1)
9	17	F	Supraglottis	Hydroa-like T-cell lymphoma	−	−	dead (6)

MZBCL marginal zone B-cell lymphoma, *DLBCL* diffuse large B-cell lymphoma, *PTCL* peripheral T-cell lymphoma: *NK/T* NK/T-cell lymphoma

that from different geographic location showing that peripheral T-cell lymphoma accounts for 1–10% [1, 14].

EBV is one of DNA viruses belonging to the herpes virus family, which consists of 172 kilobase double-stranded DNA [4]. Since EBV was discovered in tumor cells of Burkitt's lymphoma in 1964, the spectrum of EBV-associated human disease has been expanded and includes infectious mononucleosis, nasopharyngeal carcinoma, gastric lymphoepithelioma-like carcinoma, gastric adenocarcinoma, leiomyosarcoma, leiomyoma, and lymphoproliferative disorder of various type [10].

Regarding EBV-related pediatric lymphoid malignancy, there have been three reports so far, from Argentina, Malaysia, and Western Europe [2, 7, 12]. Overall frequency of EBER expression in the present study was similar to that from Argentina group [2], which reported EBER expression in eight out of 32 cases (25%) of pediatric non-Hodgkin's lymphoma. However, since five out of eight EBER positive patients in the study from Argentina were immunocompromised, actual EBV positivity in patients without immunodeficiency was much lower than that in the present study [2]. Compared with the result from Malaysia which showed EBV association in 21% of non-Hodgkin's lymphoma, EBV positive rate in the present series was slightly higher, which might be due to the higher number of EBV-associated malignancies such as NK/T cell lymphoma and peripheral T cell lymphoma, unspecified type, enrolled in the present study. Otherwise EBER-positive rates of each subtype, including NK/T-cell lymphoma, anaplastic large cell lymphoma, peripheral T-cell lymphoma, unspecified type, and diffuse large B-cell lymphoma, were similar [12].

All 19 Burkitt's lymphomas in this study were EBER-negative. This frequency is the lowest among those of previous studies from Pakistan (80%: 8/10), Israel (34%: 11/32), Taiwan (80%: 8/10), Malaysia (38%: 3/8), and Western Europe (11.3%: 25/222) [3, 7, 9, 12, 13]. Although sporadic Burkitt's lymphoma, which is the type of Korean Burkitt's lymphoma, generally has a low frequency of EBV infection, negativity of EBV in Burkitt's lymphoma was unexpected. It may be postulated that pathogenetic association of EBV with sporadic Burkitt's lymphoma differs

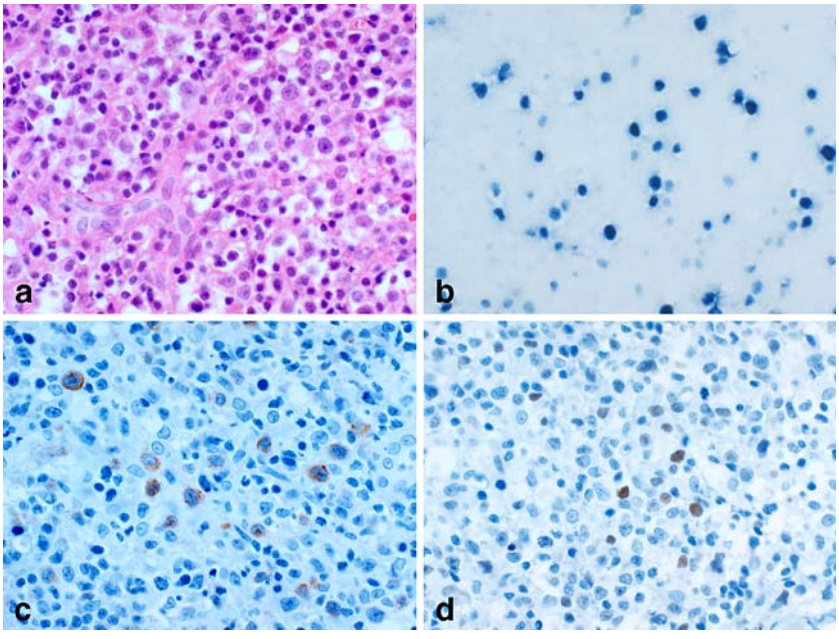


Fig. 1 Diffuse large B-cell lymphoma with expression of LMP-1 and EBNA-2 (Table 2, case 6) (**a**) Histologic finding. (**b**) EBER in situ hybridization. (**c**) Immunostain for LMP-1 protein. Some tumor cells express LMP-1. (**d**) Immunostain for EBNA-2 protein. Some tumor cells express EBNA-2

according to the ethnic group; however, further study with larger numbers of cases is required to verify this finding.

Three types of latency, types I, II, and III, have been identified in different EBV-associated malignancy. Latency I expressing EBNA-1 in the absence of other proteins such as EBNA-2, LP, LMP-1, LMP-2 is observed in Burkitt's lymphoma; latency II, coexpressing EBNA-1 and LMPs in the absence of other EBNA proteins is found in Hodgkin's lymphoma or nasopharyngeal carcinoma. Latency III, which is characterized by expression of all latent viral proteins, is found in B-lymphoblastoid cell lines and HIV-associated lymphomas [6]. The present study is limited in its ability to evaluate the latency type of EBV because the antibody panel for immunostain in this study did not include EBNA-1 and other latent infection-associated protein, except EBNA-2 and LMP-1. However, the seven cases which did not express LMP-1 gene and EBNA-2 seem to represent type I latency. Interestingly, the other two cases showed type III latency, which is usually identified in immuno-compromised patients. Clinically, those two patients had diffuse large B cell lymphoma in the nasopharynx, without obvious immune deficiency.

Generally, patients with EBV-positive T and NK cell lymphomas pursued an aggressive clinical course. In particular, patients with NK/T-cell lymphoma have a poor prognosis. Five patients with NK cell leukemia/lymphoma, peripheral T-cell lymphoma, or hydroa-like T-cell lymphoma died within 13 months after diagnosis. Three of these patients had hemophagocytic syndrome. In contrast to T and NK cell lymphoma, three patients with EBER-positive diffuse large B-cell lymphomas and one patient with marginal zone B-cell lymphoma were cured with chemotherapy and still alive. A large previous series for diffuse large B-cell lymphoma reported no significantly different clinical features between EBV-positive and EBV-negative cases [8].

In conclusion, EBV infected in pediatric non-Hodgkin's lymphomas are frequently associated with not only NK- and T- cell lymphomas but also large B-cell lymphomas.

References

1. Anderson JR, Armitage JO, Weisenburger DD(1998) Epidemiology of the non-Hodgkin's lymphomas: distributions of the major subtypes differ by geographic locations. Non-Hodgkin's lymphoma classification project. Ann Oncol 9:717–720
2. Chabay PA, De Matteo EN, Aversa L, Maglio S, Grinstein S, Preciado MV (2002) Assessment of Epstein-Barr virus association with pediatric non-Hodgkin lymphoma in immunocompetent and in immunocompromised patients in Argentina. Arch Pathol Lab Med 126:331–335
3. Chao TY, Wang TY, Lee WH (1997) Association between Epstein-Barr virus and Burkitt's lymphoma in Taiwan. Cancer 80:121–128
4. Kieff E, Rickinson AB (2001) Epstein-Barr virus and its replication. In: Knipe DM, Howley PM, Griffin DE (ed) Fundamental virology, 4th edn. Lippincott Williams and Wilkins, Philadelphia, pp 1185–1190
5. Stein H, Mann R, Delsol G, Poppema S, Pileri S, Jaffe ES, Said J, Swerdlow SH (2001) Classical Hodgkin lymphoma. In: Jaffe ES, Harris NL, Stein H, Vardiman JW (ed) World Health Organization classification of tumours. Tumours of haematopoietic and lymphoid tissues. IARC Press, Lyon, p 248
6. Joske D, Knecht H (1993) Epstein-Barr virus in lymphomas: a review. Blood Rev 7:215–222
7. Karajannis MA, Hummel M, Oschlies I, Anagnostopoulos I, Zimmermann M, Stein H, Parwaresch R, Reiter A (2003) Epstein-Barr virus infection in Western European pediatric non-Hodgkin lymphomas. Blood 102:4244
8. Kuze T, Nakamura N, Hashimoto Y, Sasaki Y, Abe M (2000) The characteristics of Epstein-Barr virus (EBV)-positive diffuse large B-cell lymphoma: comparison between EBV(+) and EBV (−) cases in Japanese population. Jpn J Cancer Res 91:1233–1240
9. Mansoor A, Stevenson MS, Li RZ, Frekko K, Weiss W, Ahmad M, Khan AH, Mushtaq S, Saleem M, Raffeld M, Kingma DW, Jaffe ES (1997) Prevalence of Epstein-Barr viral sequences and EBV LMP1 oncogene deletions in Burkitt's lymphoma from Pakistan: epidemiological correlations. Hum Pathol 28:283–288
10. Okano M, Gross TG (2001) From Burkitt's lymphoma to chronic active Epstein-Barr virus (EBV) infection: an expanding spectrum of EBV-associated diseases. Pediatr Hematol Oncol 18:427–442
11. Pallesen G, Hamilton-Dutoit SJ, Zhou X (1993) The association of Epstein-Barr virus (EBV) with T cell lymphoproliferations and Hodgkin's disease: two new developments in the EBV field. Adv Cancer Res 62:179–239
12. Peh SC, Nadarajah VS, Tai YC, Kim LH, Abdullah WA (2004) Pattern of Epstein-Barr virus association in childhood non-Hodgkin's lymphoma: experience of university of Malaya medical center. Pathol Int 54:151–157
13. Peylan-Ramu N, Diment J, Krichevsky S, Ben-Yehuda D, Bhatia K, Magrath IT (2001) Expression of EBV encoded nuclear small non-polyadenylated RNA (EBER) molecules in 32 cases of childhood Burkitt's lymphoma from Israel. Leuk Lymphoma 40:405–411
14. Wilson JF, Jenkin RD, Anderson JR, Chilcote RR, Coccia P, Exelby PR, Kersey J, Kjeldsberg CR, Kushner J, Meadows A (1984) Studies on the pathology of non-Hodgkin's lymphoma of childhood, I. The role of routine histopathology as a prognostic factor. A report from the children's cancer study group. Cancer 53:1695–1704
15. Zhou XG, Hamilton-Dutoit SJ, Yan QG, Pallesen G (1994) High frequency of Epstein-Barr virus in Chinese peripheral T-cell lymphoma. Histopathology 24:115–122

Virchows Arch (2005) 447: 597–602
DOI 10.1007/s00428-005-1226-2

ORIGINAL ARTICLE

Eui Jin Lee · Chan Choi · Cheol Keun Park · Leeso Maeng · Jehoon Lee · Anhi Lee · Kyoung-Mee Kim

Tracing origin of serrated adenomas with *BRAF* and *KRAS* mutations

Received: 14 December 2004 / Accepted: 6 February 2005 / Published online: 1 July 2005
© Springer-Verlag 2005

Abstract Serrated neoplasm of the colorectum raised many as-yet unanswered issues. To characterize serrated neoplasia pathway, we investigated *BRAF* and *KRAS* mutations in 35 traditional serrated adenomas. *BRAF* exons 11 and 15, and *KRAS* exon 2 were amplified by polymerase chain reaction and directly sequenced. *BRAF* V599E mutation was found in 27 serrated adenomas (77.1%), and *KRAS* mutations were found in 3 (8.6%) of 35 traditional serrated adenomas. In 13 cases, mixed polyps composed of traditional serrated adenomas and hyperplastic (serrated) polyps were observed, and seven of them showed the same *BRAF* mutations in both components. Somatic mutations of *BRAF* and *KRAS* genes were mutually exclusive. These findings suggest that *BRAF* mutations are early and a critical event in the serrated adenomas, and most serrated adenomas in both sides of colon may progress from microvesicular hyperplastic polyps via *BRAF* mutations, and some left-sided serrated adenomas develop via *KRAS* mutations.

Keywords Serrated adenomas · *BRAF* · *KRAS* · Mutations

Introduction

The serrated neoplasia pathway suggests that dysplasia can arise within hyperplastic colonic polyps, resulting in the formation of a traditional serrated adenoma and potentially the development of colorectal carcinoma [7, 9–13]. Although the concept of a "serrated pathway" for colorectal neoplasia is very exciting from a scientific point of view, from a practical perspective, it raised many as-yet unanswered issues (K.P. Batts, unpublished material). The consistent morphological identification of serrated adenomas is prerequisite to gaining a clearer understanding of the serrated neoplasia pathway [2]. The polyps of this pathway differ morphologically and genetically from those of traditional adenoma–carcinoma sequence. Genetically, serrated adenomas are characterized by a high frequency of low mutator phenotype, *p53* mutations, *KRAS* mutations, *BRAF* mutations, and low frequency of *APC* gene mutation than in sporadic tubular adenomas [5]. However, activation of the *RAF*/*RAS* signal transduction cascade by *RAS* mutations in serrated neoplasia is mainly concentrated on hyperplastic (serrated) polyps, and their occurrence in traditional type SA is limited to small numbers of cases, and their relation to histogenesis is not described [3, 14, 26, 27]. To explore the clinicopathological and genetic characteristics of traditional serrated adenomas during the serrated neoplasia pathway, well-recognized and reproducible pathological diagnostic criteria of serrated adenomas were adopted, and this is the first large-scale study on *BRAF* and *KRAS* mutations using traditional serrated adenomas.

E. J. Lee · L. Maeng · J. Lee · A. Lee · K.-M. Kim (✉)
Department of Pathology, Our Lady of Mercy Hospital,
The Catholic University of Korea,
665, Bupyung dong, Bupyung-gu,
Inchon, South Korea, 403-026
e-mail: kkmkys@catholic.ac.kr
Tel.: +82-32-5105538
Fax: +82-32-5105881

C. Choi
Department of Pathology, Chonnam National University,
Gwangju, South Korea

C. K. Park
Department of Pathology, Samsung Medical Center,
Sungkyunkwan University,
Seoul, South Korea

Material and methods

Material

Thirty-five traditional serrated adenomas and five hyperplastic polyps were included in this study for detection of mutations in *BRAF* and *KRAS*. Four retention polyps and 15 cases of colonic mucosa from histologically normal portion of the polypectomy specimens were selected as negative controls. All the samples were obtained from Our Lady of Mercy Hospital and Samsung Medical Center from 1998 to 2004 by computer search and review of the slides. The 35 patients included 12 women and 23 men with a

mean age of 54.2 years (range 32–73). In the present study, serrated polyps were reviewed according to the provisional classification proposed by Torlakovic et al. [24], and only traditional type serrated adenomas with pseudostratification, micropapillations of the surface epithelium with eosinophilic cytoplasm, were selected. According to the presence of hyperplastic (serrated) polyp components and epithelial dysplasia based on histological and cytological criteria, the tumors were divided into 13 mixed serrated adenomas with hyperplastic (serrated) polyp, 21 serrated adenomas with low-grade dysplasia, and one serrated adenoma with high-grade dysplasia.

Mutation of *BRAF* and *KRAS*

DNA was extracted from 0.1% methylene blue-stained 10-μm sections under microscopy using 20 gauge needles and proteinase K solution as previously described [5]. In 7 of the 13 mixed polyps composed of serrated adenomas and hyperplastic (serrated) polyps, DNAs from both serrated adenomas and hyperplastic areas were obtained by manual microdissection and examined for mutations of *BRAF* and *KRAS*. Primer pairs were used to amplify the complete coding sequences of *BRAF* exon 11 (forward TTC TGT TTG GCT TGA CTT GAC TT, reverse ACT TGT CAC AAT GTC ACC TT) and exon 15 (forward TGC TTG CTC TGA TAG GAA AAT G, reverse AGC ATC TCA GGG CCA AAA AT), and of *KRAS* exon 2 (forward CTG AAA ATG ACT GAA TAT AAA CTT GT, reverse ATA TGC ATA TTA AAA CAA GAT TTA CC). Polymerase chain reaction (PCR) was performed in a 20-μl volume containing 100 ng of template DNA, 10×PCR buffer; 0.25 mM deoxynucleoside triphosphate (dNTP), 20 pmol primers, and 1.5 U *Taq* DNA polymerase (Takara Shuzo, Kyoto, Japan). PCR products were electrophoresed on 2% agarose gels, purified, and both strands were directly sequenced using the BigDye Terminator v3.1 cycle sequencing kit, followed by analysis with an Applied Biosystems 3700 automated sequencer (Applied Biosystems, Foster City, CA, USA).

Statistics

A statistical analysis comparing clinical, histological, and mutation results was performed using χ^2 test and two-tailed Pearson correlation analysis with the statistical software SPSS (version 10.0, Chicago, IL, USA).

Results

Clinicopathological findings of traditional serrated adenomas

Of the serrated adenomas, 8 (22.9%) occurred in the right colon and 27 (77.1%) occurred in the left colon. Every traditional serrated adenoma in this study was endoscopically and grossly protruded, polypoid, and nodular in shape with a size ranging from 0.3 to 2.2 cm (mean 1.0 cm). All the serrated adenomas had serrations more than 50% of the lesion, frequent pseudostratification, nuclear atypia, and micropapillations of the surface epithelium with eosinophilic cytoplasm. In one case, high-grade dysplasia was noted in the head portion of the polyp (Fig. 1a–c). Thirteen cases of serrated adenomas showed hyperplastic (serrated) polyp areas featuring microvesicular type hyperplastic polyp described by Torlakovic et al. [24]. These hyperplastic areas were noted in the neck or mid-portion of the polyps (Fig. 2a–c).

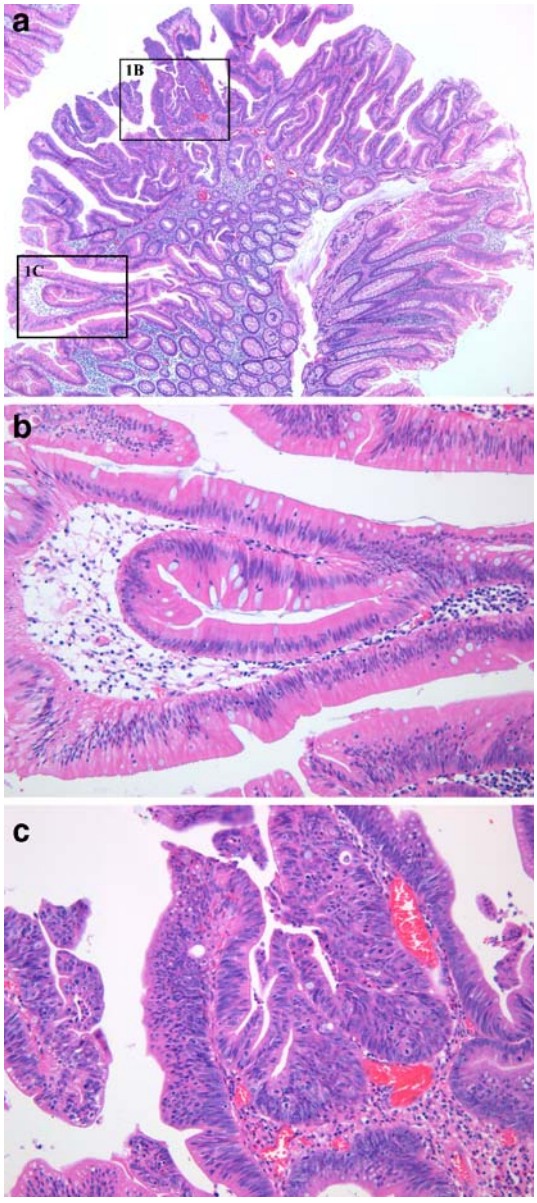


Fig. 1 **a** Representative photomicrograph of traditional serrated adenoma with low-grade and high-grade dysplasia. **b** High-power photograph of low-grade dysplasia shown in **a**. **c** High-power photograph of high-grade dysplasia localized in the head portion of the polyp shown in **a**

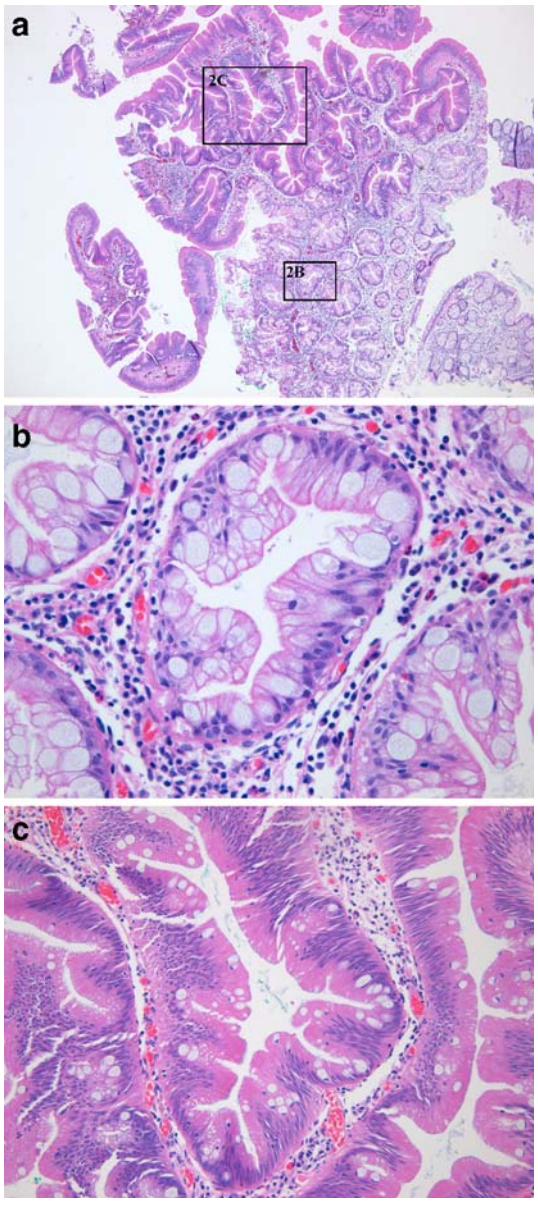


Fig. 2 **a** Representative photomicrograph of serrated adenoma with low-grade dysplasia and hyperplastic (serrated) polyp area. **b** High-power photograph of hyperplastic area observed in the neck portion of the polyp shown in **a**. **c** High-power photograph of serrated adenoma with low-grade dysplasia located in the head portion of the polyp in **a**

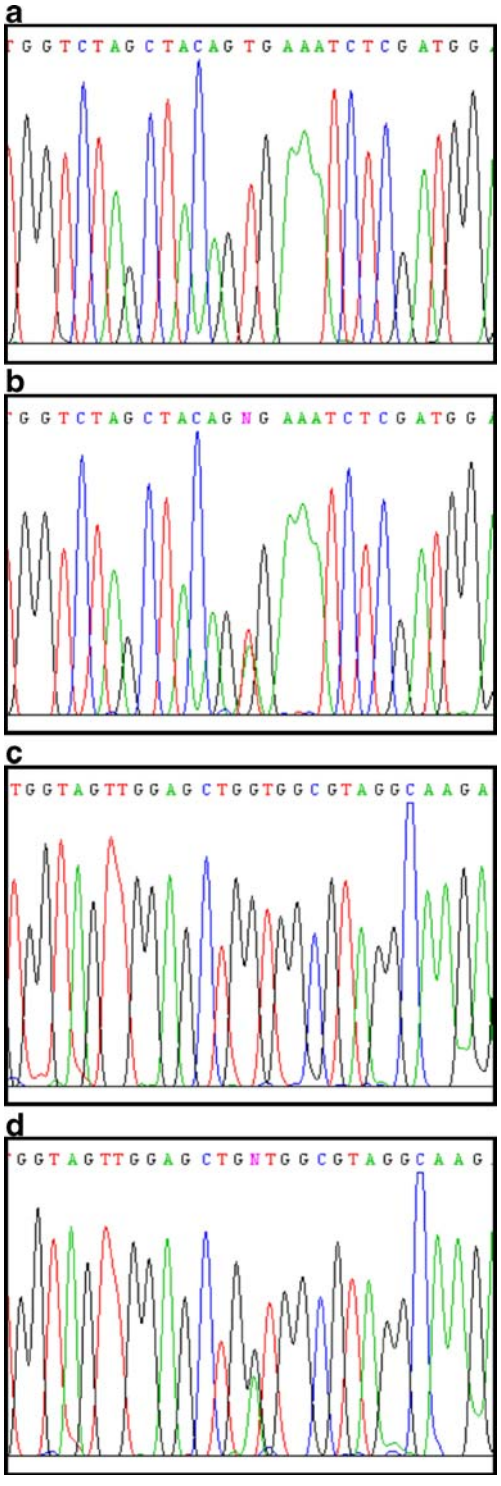


Fig. 3 Sequence chromatographs of serrated adenomas. **a** Serrated adenoma with wild-type *BRAF*. **b** A serrated adenoma with V599E mutation of *BRAF*. **c** Serrated adenoma with wild-type *KRAS*. **d** A serrated adenoma with G12D (G35A) mutation of *KRAS*

BRAF mutations in traditional serrated adenomas

BRAF mutation was found in 27 (77.1%) serrated adenomas and in 1 (20%) hyperplastic polyp, whereas 15 normal colon tissue and 4 retention polyps had wild-type *BRAF*. Mutations found in this study were a single missense mutation in codon 599 of exon 15 (V599E), an activation segment of *BRAF* (Fig. 3a,b). All 13 mixed polyps with serrated adenomas and hyperplastic areas had *BRAF* mutations. Using seven mixed polyps, DNAs from both serrated adenomas and hyperplastic (serrated) polyp areas were examined for *BRAF* mutations. Surprisingly, both of these areas in all examined cases had the same V599E mutations. In serrated adenomas displaying low-grade dysplasia (21 cases), 14 cases (66.7%) exhibited *BRAF* mutation. One serrated adenoma displaying high-grade dysplasia harbored no *BRAF* mutations. When we scrutinized the histology, all serrated adenomas without *BRAF*

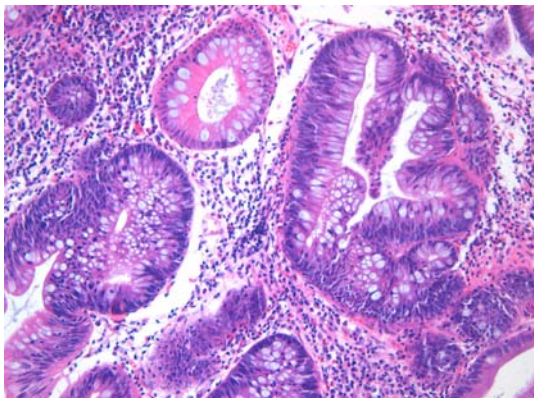


Fig. 4 Abnormal proliferations with increased dysplasia and pseudostratification, abundant dystrophic, and mature goblet cells were noted focally in traditional serrated adenomas without *BRAF* mutations

mutations had areas of abnormal proliferations, increased dysplasia, pseudostratification, and abundant dystrophic and mature goblet cells along with traditional eosinophilic cells (Fig. 4), and five of them showed tubular adenomas focally (Fig. 5). One hundred percent of serrated adenomas from the right colon had mutations of *BRAF*, whereas 70.4% of left-sided serrated adenomas had *BRAF* mutations although statistically not significant (p=0.08). The incidence of *BRAF* and *KRAS* mutations and their relationship to clinicopathological findings are depicted in Table 1.

KRAS mutation in serrated adenomas

KRAS G12D (G35A) mutations were found in 3 of 35 (8.6%) traditional serrated adenomas (Fig. 3c,d). One high-grade serrated adenoma had *KRAS* mutation. Of the seven mixed polyps with serrated adenomas and hyperplastic areas, both serrated adenomas and hyperplastic areas harbored no *KRAS* mutations. All three serrated adenomas with *KRAS* mutations occurred in the left colon and showed focal area of tubular adenoma and shared the histological features of serrated adenomas without *BRAF* mutations.

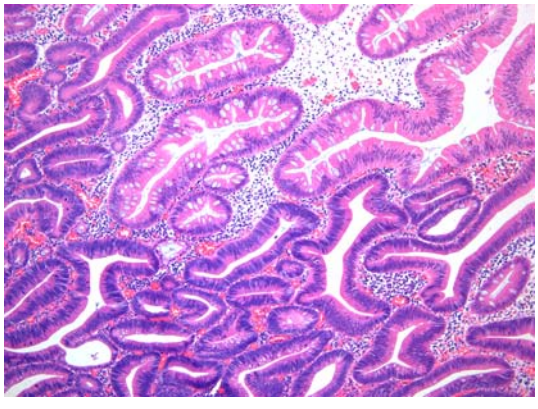


Fig. 5 Focal tubular adenoma areas were observed in serrated adenomas with *KRAS* or without *BRAF* mutations

Table 1 Mutations of *BRAF* and *KRAS* and their relationship to clinical findings of traditional serrated adenomas

	No. of *BRAF* mutation (%)	No. of *KRAS* mutation (G to A) (%)	No. of *BRAF* and *KRAS* mutations	Total no. of patients
Age				
≤55	13 (48.1)	0 (0.0)	13	16
>55	14 (51.9)	3 (100.0)	17	19
Sex				
Female	10 (63.0)	0 (0.0)	10	12
Male	17 (37.0)	3 (100.0)	20	23
Tumor site				
Right	8 (29.6)	0 (0.0)	8	8
Left	19 (70.4)	3 (100.0)	22	27
Size				
<1.0 cm	11 (40.7)	1 (33.3)	12	15
≥1.0 cm	16 (59.3)	2 (66.7)	18	20

Five hyperplastic polyps, 15 normal colon tissue, and 4 retention polyps showed no *KRAS* mutations.

Discussion

The *BRAF* gene is mutated in about 70% of malignant melanomas, 10 to 22% of colon cancers, and a smaller proportion of other cancer types. *BRAF* mutation in the active segment, a conversion of valine 599 to glutamic acid (V599E), is a hotspot for *BRAF* mutation in human cancers. All mutations identified to date are within the kinase domain, with a single missense mutation (V599E) accounting for 80% [4]. In this study, all *BRAF* mutations were found in this hotspot of *BRAF*, and we could confirm that V599E is the most common mutation found in traditional serrated adenomas. Moreover, no *BRAF* mutations in exon 15, other than the common hotspot mutation, were identified in our large series, and furthermore, we could demonstrate no mutations at all in exon 11. Previous mutation analysis of *BRAF* using colonic carcinoma samples has shown that *BRAF* mutations are more common in the earlier stages, and the subjects had long-term survival without recurrence. This suggests less invasive biological behavior for those cancers harboring *BRAF* mutations [27]. In our study, mutation of *BRAF* was frequent in traditional serrated adenomas with low histological grades. Chan et al. [3] reported a 100% frequency of *BRAF* mutations for 10 cases of serrated adenomas and 30% for 50 cases of hyperplastic polyps. We could demonstrate *BRAF* mutations in 77.1% of traditional serrated adenomas and in 20% of hyperplastic polyps, respectively, in this large-scale study. It is very interesting that *BRAF* mutations go with traditional serrated adenomas with hyperplastic (serrated) polyp components (mixed polyps). These results suggest that mutation of *BRAF* is a critical event in traditional serrated adenomas that arise from or differentiate into hyperplastic (serrated) polyps of microvesicular type during

the serrated neoplasia pathway. We found that traditional serrated adenomas with frequent serration and surface micropapillations with eosinophilic cytoplasm had a high frequency of *BRAF* mutations. All the *BRAF* mutation-negative and *KRAS* mutation-positive serrated adenomas were left-sided and showed frequent immaturity of epithelium with increased dysplasia and abundant dystrophic or mature goblet cells among eosinophilic cells, featuring the serrated polyp with abnormal proliferation or goblet cell type hyperplastic polyps. In a previous report, goblet cell type hyperplastic polyps seem to have frequent *KRAS* mutation and to be left-sided [16]. Therefore, this would explain the lack of *BRAF* mutation given the possible origin of some serrated adenomas in this variant. Along with colonic villous adenomas [27], papillary thyroid carcinomas [6], and serous papillary ovarian tumors [20–22], these findings suggest that the *BRAF* mutations may be related to the specific histological morphology of epithelial cells, i.e., the formation of papillary projections. All traditional serrated adenomas derived from the right colon had *BRAF* mutations. Right side serrated adenomas had a higher frequency of *BRAF* mutations than did the left one. *BRAF* was previously reported to be mutated in 11 to 22% of colonic carcinomas, with a strong association with the epigenetic alteration of *hMLH1* [15, 17, 25], although *BRAF* mutation was not caused by a mismatch repair deficiency [25]. Our right side predilection of *BRAF* mutation is consistent with these previous observations. A negative correlation between mutations in the *BRAF* and *KRAS* genes is also evident, which supports earlier studies that found that somatic mutations in these genes are mutually exclusive [22, 23]. *KRAS* mutations were found in three left serrated adenoma cases. In previous studies, *KRAS* mutations in serrated adenomas are heterogeneous ranging from 0 to 40.4% [1, 8, 18, 19]. In this study, *KRAS* mutations were found in 8.6% of traditional serrated adenomas in the left colon. Although *BRAF* mutations occurred in both younger and older ages (Table 1), *KRAS* mutations were exclusively found in older age. All three serrated adenomas with *KRAS* mutations occurred in the left colon, showed focal area of tubular adenoma, abnormal proliferations, and increased dysplasia with more pseudostratification. These results suggest that *KRAS* mutations involve some left-sided serrated adenomas with high-grade dysplasia occurring in older age.

Although our data on the natural history of traditional serrated adenomas need more supporting evidences, we propose that *BRAF* mutations are early and a critical event in serrated adenomas. The occurrence of the same *BRAF* mutations found in both serrated adenomas and hyperplastic areas observed in mixed polyps suggests that some of traditional serrated adenomas may progress from hyperplastic (serrated) polyps via *BRAF* mutations and some left serrated adenomas originate via *KRAS* mutations.

Acknowledgements This work was supported by a grant of the National Cancer Center R&D Program 200323301, Ministry of Health and Welfare, Republic of Korea, to K.M. Kim.

References

1. Ajioka Y, Watanabe H, Jass JR, Yokota Y, Kobayashi M, Nishikura K (1998) Infrequent K-ras codon 12 mutation in serrated adenomas of human colorectum. Gut 42:680–684
2. Bariol C, Hawkins NJ, Turner JJ, Meagher AP, Williams DB, Ward RL (2004) Histopathological and clinical evaluation of serrated adenomas of the colon and rectum. Mod Pathol 16:417–423
3. Chan TL, Zhao W, Leung SY, Yuen ST (2003) BRAF and KRAS mutations in colorectal hyperplastic polyps and serrated adenomas. Cancer Res 63:4878–4881
4. Davies H, Bignell GR, Cox C, Stephens P, Edkins S, Clegg S, Teague J, Woffendin H, Garnett MJ, Bottomley W, Davis N, Dicks E, Ewing R, Floyd Y, Gray K, Hall S, Hawes R, Hughes J, Kosmidou V, Menzies A, Mould C, Parker A, Stevens C, Watt S, Hooper S, Wilson R, Jayatilake H, Gusterson BA, Cooper C, Shipley J, Hargrave D, Pritchard-Jones K, Maitland N, Chenevix-Trench G, Riggins GJ, Bigner DD, Palmieri G, Cossu A, Flanagan A, Nicholson A, Ho JW, Leung SY, Yuen ST, Weber BL, Seigler HF, Darrow TL, Paterson H, Marais R, Marshall CJ, Wooster R, Stratton MR, Futreal PA (2002) Mutations of the BRAF gene in human cancer. Nature 417: 949–954
5. Dong SM, Lee EJ, Jeon ES, Park CK, Kim KM (2004) Progressive methylation during the serrated neoplasia pathway of the colorectum. Mod Pathol [Epub ahead of print]
6. Fukushima T, Suzuki S, Mashiko M, Ohtake T, Endo Y, Takebayashi Y, Sekikawa K, Hagiwara K, Takenoshita S (2003) BRAF mutations in papillary carcinomas of the thyroid. Oncogene 322:6455–6457
7. Hawkins NJ, Bariol C, Ward RL (2002) The serrated neoplasia pathway. Pathology 34:548–555
8. Higashidani Y, Tamura S, Morita T, Tadokoro T, Yokoyama Y, Miyazaki J, Yang Y, Takeuchi S, Taguchi H, Onishi S (2003) Analysis of K-ras codon 12 mutation in flat and nodular variants of serrated adenoma in the colon. Dis Colon Rectum 46: 327–332
9. Iino H, Jass JR, Simms LA, Young J, Leggett B, Ajioka Y, Watanabe H (1999) DNA microsatellite instability in hyperplastic polyps, serrated adenomas, and mixed polyps: a mild mutator pathway for colorectal cancer? J Clin Pathol 52:5–9
10. Jass JR (1999) Serrated adenoma and colorectal cancer. J Pathol 187:499–502
11. Jass JR, Young J, Leggett BA (2000) Hyperplastic polyps and DNA microsatellite unstable cancers of the colorectum. Histopathology 37:295–301
12. Jass JR (2001) Serrated route to colorectal cancer: back street or super highway? J Pathol 193:283–285
13. Jass JR (2002) Progress in gastrointestinal pathology in the genetic era. Pathology 34:493
14. Kambara T, Simms LA, Whitehall VL, Spring KJ, Wynter CV, Walsh MD, Barker MA, Arnold S, McGivern A, Matsubara N, Tanaka N, Higuchi T, Young J, Jass JR, Leggett BA (2004) BRAF mutation is associated with DNA methylation in serrated polyps and cancers of the colorectum. Gut 53(8):1137–1144
15. Koinuma K, Shitoh K, Miyakura Y, Furukawa T, Yamashita Y, Ota J, Ohki R, Choi YL, Wada T, Konishi F, Nagai H, Mano H (2004) Mutations of BRAF are associated with extensive hMLH1 promoter methylation in sporadic colorectal carcinomas. Int J Cancer 108:237–242
16. O'Brien MJ, Yang S, Clebanoff JL, Mulcahy E, Farraye FA, Amorosino M, Swan N (2004) Hyperplastic (serrated) polyps of the colorectum: relationship of CpG island methylator phenotype and K-ras mutation to location and histologic subtype. Am J Surg Pathol 28:423–434
17. Oliveira C, Pinto M, Duval A, Brennetot C, Domingo E, Espin E, Armengol M, Yamamoto H, Hamelin R, Seruca R, Schwartz S Jr (2003) BRAF mutations characterize colon but not gastric cancer with mismatch repair deficiency. Oncogene 22:9192–9196

18. Otori K, Oda Y, Sugiyama K, Hasebe T, Mukai K, Fujii T, Tajiri H, Yoshida S, Fukushima S, Esumi H (1997) High frequency of K-ras mutations in human colorectal hyperplastic polyps. Gut 40:660–663
19. Rashid A, Houlihan PS, Booker S, Petersen GM, Giardiello FM, Hamilton SR (2000) Phenotypic and molecular characteristics of hyperplastic polyposis. Gastroenterology 119:323–332
20. Russell SE, McCluggage WG (2004) A multistep model for ovarian tumorigenesis: the value of mutation analysis in the KRAS and BRAF genes. J Pathol 203:617–619
21. Sieben NL, Macropoulos P, Roemen GM, Kolkman-Uljee SM, Jan Fleuren G, Houmadi R, Diss T, Warren B, Al Adnani M, De Goeij AP, Krausz T, Flanagan AM (2004) In ovarian neoplasms, BRAF, but not KRAS, mutations are restricted to low-grade serous tumours. J Pathol 202:336–340
22. Singer G, Oldt R III, Cohen Y, Wang BG, Sidransky D, Kurman RJ, Shih I-M (2003) Mutations in BRAF and KRAS characterize the development of low-grade ovarian serous carcinoma. J Natl Cancer Inst 395:484–486
23. Sommerer F, Vieth M, Markwarth A, Rohrich K, Vomschloss S, May A, Ell C, Stolte M, Hengge UR, Wittekind C, Tannapfel A (2004) Mutations of BRAF and KRAS2 in the development of Barrett's adenocarcinoma. Oncogene 23:554–558
24. Torlakovic E, Skovlund E, Snover DC, Torlakovic G, Nesland JM (2003) Morphologic reappraisal of serrated colorectal polyps. Am J Surg Pathol 27:65–81
25. Wang L, Cunningham JM, Winters JL, Guenther JC, French AJ, Boardman LA, Burgart LJ, McDonnell SK, Schaid DJ, Thibodeau SN (2003) BRAF mutations in colon cancer are not likely attributable to defective DNA mismatch repair. Cancer Res 63:5209–5212
26. Yang S, Farraye FA, Mack C, Posnik O, O'Brien MJ (2004) BRAF and KRAS mutations in hyperplastic polyps and serrated adenomas of the colorectum: relationship to histology and CpG island methylation status. Am J Surg Pathol 28(11):1452–1459
27. Yuen ST, Davies H, Chan TL, Ho JW, Bignell GR, Cox C, Stephens P, Edkins S, Tsui WW, Chan AS, Futreal PA, Stratton MR, Wooster R, Leung SY (2002) Similarity of the phenotypic patterns associated with BRAF and KRAS mutations in colorectal neoplasia. Cancer Res 62:6451–6455

Virchows Arch (2005) 447: 603–609
DOI 10.1007/s00428-005-1272-9

ORIGINAL ARTICLE

Katharina Pauls · Folker E. Franke · Reinhard Büttner · Hui Zhou

Gonadoblastoma: evidence for a stepwise progression to dysgerminoma in a dysgenetic ovary

Received: 9 February 2005 / Accepted: 12 April 2005 / Published online: 21 June 2005
© Springer-Verlag 2005

Abstract Gonadoblastomas are neoplasms of dysgenetic gonads which may undergo regression or become overgrown by malignant germ cell tumors (mGCTs). Since little is known about their relationship to normal gonadal development and mGCTs, we studied the phenotype and antigenic profile of gonadoblastomas in comparison with adjacent dysgerminomas and fetal gonads. Three cases of gonadoblastomas and fetal gonads of both sexes were analyzed using oncofetal markers to M2A-antigen (M2A), germ cell alkaline phosphatase (PLAP/GCAP), receptor tyrosine kinase c-kit (c-kit), and somatic angiotensin converting enzyme (sACE) as well as the proliferation marker MIB-1. Morphologically, microfollicular pattern of gonadoblastomas showed a fetal germ cell organization reminiscent of oocytic clusters of fetal ovaries. They contained both cell types, similar to oocytes (M2A-, GCAP-, c-kit+/−, sACE-) and oogonia (M2A+, GCAP+, c-kit+, sACE+). The percentage of germ cells immunoreactive for oncofetal markers and the proliferation index increased from microfollicular over coronary patterns to adjacent dysgerminomas. Supportive cells of gonadoblastomas showed a uniform phenotype (CK18+, vimentin+, sACE+, alpha-inhibin+, M2A-) but in contrast to fetal germ cells lacked a clear equivalence to fetal tissues. Our results show that gonadoblastomas mimic female fetal ovary and exhibit a stepwise progression from follicular pattern to coronary pattern and finally to dysgerminomas.

Keywords Gonadoblastoma · Dysgerminoma · Oncofetal

K. Pauls · R. Büttner · H. Zhou
Institute of Pathology,
University of Bonn, Bonn, Germany

K. Pauls · R. Büttner
Section of Paidopathology,
University of Bonn, Bonn, Germany

F. E. Franke
Institute of Pathology,
University of Giessen, Giessen, Germany

K. Pauls (✉)
Institut für Pathologie,
Sigmund-Freud-Strasse 25,
53127 Bonn, Germany
e-mail: katharina.pauls@ukb.uni-bonn.de
Tel.: +49-228-2879245
Fax: +49-228-2875030

Introduction

Gonadoblastoma is a rare tumor which may occur in gonadal streaks, ovaries, or abdominal testes. It is composed of sex-cord derivatives and germ cells, intimately arranged in nests of two different forms, the microfollicular and coronary patterns. These peculiar nests of uncertain origin and significance are generally surrounded by dense connective tissue, similar to the ovarian cortex [18, 20, 22].

Most gonadoblastomas arise in dysgenetic gonads of XY sex-reversed individuals, who are phenotypically females due to mutations of the single sex determining region gene of the Y chromosome (*SRY*) or few other genes involved in the early sex determining pathway [1, 4, 5]. Mutation and dysfunction of *SRY* lead to impairment or absence of fetal testes, dysgenetic gonads, and partial or complete female sex development [3, 9]. Very rarely, gonadoblastomas may also occur in fertile females and in Turner patients [28]. However, probably all gonadoblastomas need fragments or still functioning genes of the Y chromosome to develop. Only Turner patients with a 45, X/46,XY mosaicism in their dysgenetic gonads are at risk to develop these lesions, in contrast to those with a pure 45,X karyotype [25].

In 50–60% of cases, gonadoblastomas are associated with malignant germ cell tumors (mGCTs), mostly presenting as a pure dysgerminoma or, less frequently, as immature teratoma, yolk sac tumor, embryonal carcinoma or choriocarcinoma. Other gonadoblastomas do not progress to invasive malignancies but regress to calcifying masses, referred to as “burned out gonadoblastoma [20]”. In general, the stromal component of gonadoblastomas is

thought to be benign, although in few cases associated Sertoli cell-like tumors have been reported [13].

In the absence of comparative studies, various practical and theoretical issues remain a matter of debate. It is still unclear whether gonadoblastomas are true neoplasms with initial characteristics of in situ-germinomas [11, 20] or rather hamartomatous lesions [6, 11, 17], what is the meaning of its two growth patterns and to what extent these patterns match with the supposed "recapitulation of gonadal development" [20]. To address these issues, we performed this study on typical gonadoblastomas using well known oncofetal antigens germ cell alkaline phosphatase (GCAP), c-kit receptor (c-kit), M2A, and sACE. Additionally, markers to ovarian stroma cells, cytokeratin 18 (CK18), vimentin and alpha-inhibin, were also studied. Histological patterns and antigenic profiles of gonadoblastomas were compared to adjacent dysgerminomas and normally developed fetal gonads of both sexes.

Materials and methods

Tissues

Tissues of gonadoblastomas in three adult patients were selected from the files of the Departments of Pathology, Universities of Bonn and Giessen. Two patients had a unilateral, one a bilateral gonadoblastoma. Two phenotypically female patients, one 19 (patient 1) and the other 18 (patient 2) years old, underwent preventive adnexectomy because of a history of XY-pure gonadal dysgenesis and high risk of developing mGCTs. The third patient, a 52-year-old, had a female phenotype and XY-genotype and underwent bilateral adnexectomy because of acute small bowel obstruction and adhesive ileus and a 9 cm sized tumor of the right ovary. The clinical data of all patients are summarized in Table 2.

Specimens of ten fetal ovaries and 16 fetal testes from fetuses of various weeks of gestation (weeks 15, 16, 19, 20, 22, 24, 25, 33 and 35) were collected during the period 1999–2004 from the tissue archives of the Department of Pathology, University of Bonn. All fetal tissues were obtained for diagnostic or documentary reasons because of legal interruptions or fetal deaths (amnion infection or premature rupture, congenital heart failure). Normal ovaries from six mature newborns removed for enlarged benign cystic lesions were also included in this study.

Tissue preparation and immunohistochemistry

Tissues were fixed by immersion in phosphate-buffered formalin (pH 7.0) and embedded in paraffin using standard techniques. Gonadal tissues from adult patients were embedded completely and 4–15 paraffin blocks were prepared. Consecutive tissue sections were mounted on superfrost slides (Menzel-Gläser, Braunschweig, Germany), dried for 12 h at 37°C, and the first section of each series was stained by hematoxylin and eosin (HE). Immunohistochemistry was performed using alkaline phosphatase anti-alkaline phosphatase (APAAP) or avidin-biotin peroxidase complex (ABC) techniques, as published before [14, 26]. Prior to incubation with the primary antibodies, the dewaxed tissue sections were microwave-pretreated for antigen retrieval. The antibodies and their working dilutions are summarized in Table 1.

Results

Clinical data and histomorphological findings

Histological examination of right ovaries of patients 1 and 2 revealed partially calcified gonadoblastoma with numerous vital gonadoblastoma nests next to a small dysgerminoma. In addition, calcified masses in the left ovary were found in patient 1, corresponding to a burned out gonadoblastoma. In the third patient, the 9 cm sized tumor of the right ovary was mainly composed of pure dysgerminoma with a minor gonadoblastoma part. In patients 2 and 3 the left ovary contained fibrous stroma without germ cells or gonadoblastoma (Table 2).

Histologically, all vital parts of the analyzed gonadoblastomas showed the arrangement of germinal structures in both microfollicular (Fig. 1a) and coronary growth patterns (Fig. 1b). In microfollicular pattern, the supportive cells were predominant and surrounded individual germ cells or laminated hyaline material. In gonadoblastoma nests of the coronary pattern, an increased number of germ cells displaced the supportive cells to the periphery. Next to coronary pattern, invasive dysgerminomas were found in all three vital gonadoblastomas, presenting either as small invasive tumor cords within the ovarian stroma or as large solid tumor masses.

Table 1 Antibodies

Antigens	Antibody	Concentration (μg/ml)	Source
Kit	Anti-CD117, pAb	5	DAKO, Hamburg, Germany
PLAP/ GCAP	PL8-F6, mAb	3	BioGenex, San Ramon, USA
	8A9, mAb	7	DAKO
	Anti-PLAP, pAb	15	DAKO
SACE	CG2, mAb	5	BMA, Augst, Schweiz
M2A	D2-40, mAb	0.1	Abcam, Cambrigde, UK
Vimentin	V9, mAb	20	DAKO
Alpha-inhibin	R1, mAb	4	DAKO
Ki-67	Mib-1, mAb	7	Dianova, Hamburg, Germany
CK 18	DC10, mAb	10	DAKO

Table 2 Clinical and morphological data of three patients with XY-gonadal dysgenesis and gonadoblastoma (GB)

	Patient 1, 19 years old		Patient 2, 18 years old		Patient 3, 52 years old	
Indication to adnexectomy	High risk of malignancy				Abdominal tumor	
Symptoms	Amenorrhea		Amenorrhea		Acute bowel obstruction	
Side	Right	Left	Right	Left	Right	Left
Size of the ovary/[cm]	11.5	5	6	4	13	5
Size of the tumor/[cm]	4	1	5		9	
Histology	GB (90%)+DG[a] (10%)	calcified GB	GB (80%)+DG[a] (20%)	atrophic ovary	GB (10%)+DG[a] (90%)	atrophic ovary
Clinico-pathological stage (pTNM)	pT1A, N0		pT1A, N0		pT1C, N0 (peritoneal metastasis)	

[a]DG: Dysgerminoma

Immunohistochemical findings

In all vital gonadoblastoma nests, germ cells were found to be selectively labeled by GCAP (with identical pattern of the two antibodies used), c-kit, and M2A, while sACE labeled both, germ cells and stromal cells. In general, percentage of germ cells positive for GCAP, c-kit and M2A was higher in the coronary than in microfollicular nests of each gonadoblastoma (Figs. 1c,d and 2). This increase could not be statistically calculated because of the small number of cases included in this study. However, the highest number of positive germ cells was counted for c-kit, which ranged from 50 to 70% in the microfollicular and from 80 to 95% in the coronary pattern of patients 2 and 1, respectively (Fig. 2). In contrast, M2A, GCAP, and sACE labeled only a small germ cell fraction within the microfollicular gonadoblastoma nests of patient 1, but showed also a marked increase of immunopositive germ cells in coronary nests and adjacent dysgerminoma (Fig. 2). The clear difference in immunoreactive germ cells among

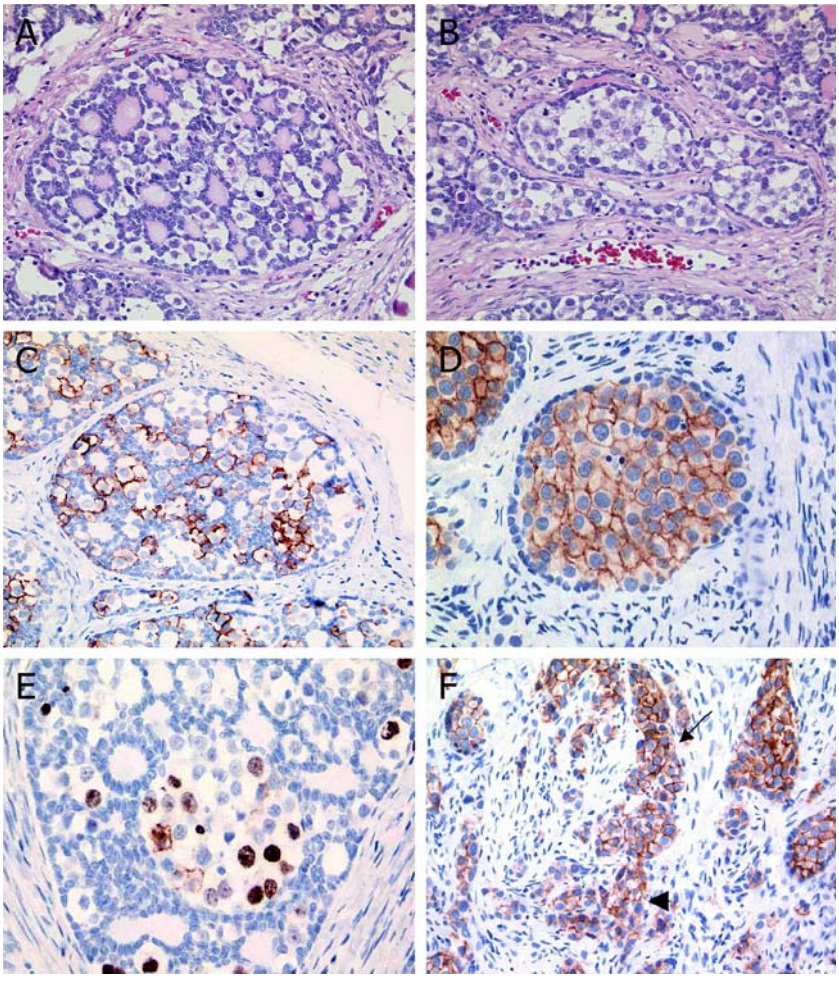


Fig. 1 In (**a**) und (**b**): microfollicular and coronary pattern of gonadoblastoma (H&E, respectively). Increasing number of c-kit positive germ cells from microfollicular (**c**) to coronary pattern (**d**) (immunohistochemistry with c-kit polyclonal antibody). **e** immunohistochemistry with Ki-67 antibody demarks clonal expansion of mitotic active cells within the microfollicular nests. **f** Coronary pattern (*arrow*) and adjacent stroma-invasive dysgerminoma (*arrowhead*) (c-kit). Original magnification ×20 **a**–**d**, **f**; ×40 **e**

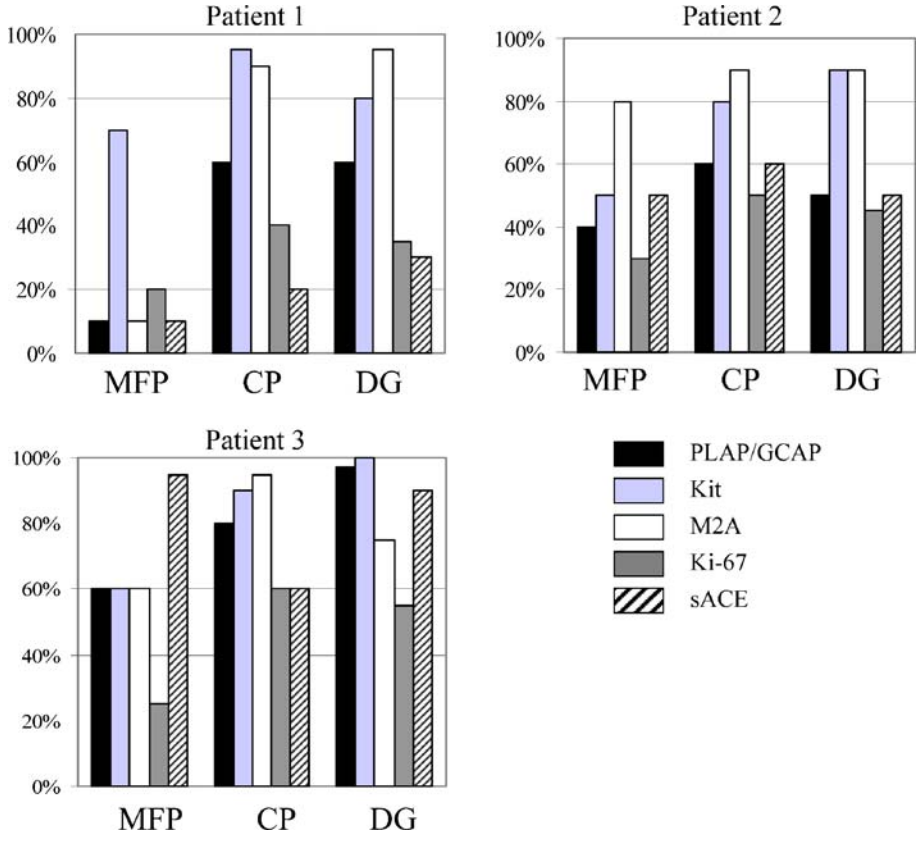


Fig. 2 Relative distribution of oncofetal markers PLAP, Kit, M2A and sACE and Ki-67 staining in gonadoblastomas of three patients (1–3), evaluated separately in follicular pattern (*MFP*), coronal pattern (*CP*), and in invasive dysgerminoma (*DG*)

the growth patterns of gonadoblastomas was also paralleled by changes in germ cell proliferation index. Similar to germ cell markers, the highest proliferation index (estimated with Mib-1 antibody) was found in the coronary pattern and in adjacent dysgerminomas (Fig. 2). Generally, germ cells in microfollicular pattern showed a lower proliferation index than in the coronary pattern. Interestingly, nest-forming clonal expansion of germ cell within microfollicular nests showed the same proliferating activity as in coronary pattern and in invasive dysgerminoma (Fig. 1e and 2). Independent of histological pattern, the supportive cells of all gonadoblastomas showed uniform immunoreactivity for CK18, vimentin, alpha-inhibin, and sACE. M2A was negative and the number of MIB-1 positive stromal cells was low and less than 5%.

Histological and immunohistochemical comparison with fetal gonads

In none of the analyzed fetal testes were any complex structures found that were morphologically identical to that of gonadoblastoma. Fetal seminiferous tubules were clearly distinguishable from the intestitial space and contained numerous c-KIT positive gonocytes (not shown). In contrast, in all ovaries obtained from mature newborns and fetuses (from weeks 15 to 35) nests similar to microfollicular pattern of gonadoblastoma were observed within the ovarian stroma (Fig. 3a–c). In all fetuses, the majority of oogonia were found in the cortical region of the ovary and were positive for M2A, GCAP, c-kit, and sACE (Fig. 4a). In the medullar region of ovaries, oocytes were closely assembled in the nest-like clusters and were negative for M2A, GCAP, and sACE but positive for c-kit (Fig. 4b). Primordial follicles in the medullary region of the ovaries were also negative for M2A, GCAP, sACE and positive for c-kit (Fig. 4c and d). Taken together, the germ cell population of microfollicular gonadoblastoma nests matched the antigenic profiles of oogonia and oocytes in fetal ovaries.

Supportive cells and surrounding stroma of gonadoblastoma diverged morphologically and immunohistochemically from their fetal counterparts. As demonstrated in Table 3, the immunophenotype of stromal sex cord of gonadoblastomas did not match with fetal testicular and ovarian counterparts at any stage (Table 3). No structural or cytological similarities have been found between gonadoblastoma and the forming seminiferous tubules of fetal male gonads including pre-Sertoli cells.

Discussion

Gonadoblastomas are tumors that are linked to gonadal development, and are reported to contain immature germ and stromal cells. Our study confirms that gonadoblastomas are populated by germ cells at a fetal stage of differentiation [11]. This is shown by the uniform expression of oncofetal markers similar to those produced by their fetal ovarian analogues, namely proliferating oogonia (M2A+, GCAP+, c-kit+, sACE+) and oocytes (M2A−, GCAP−,

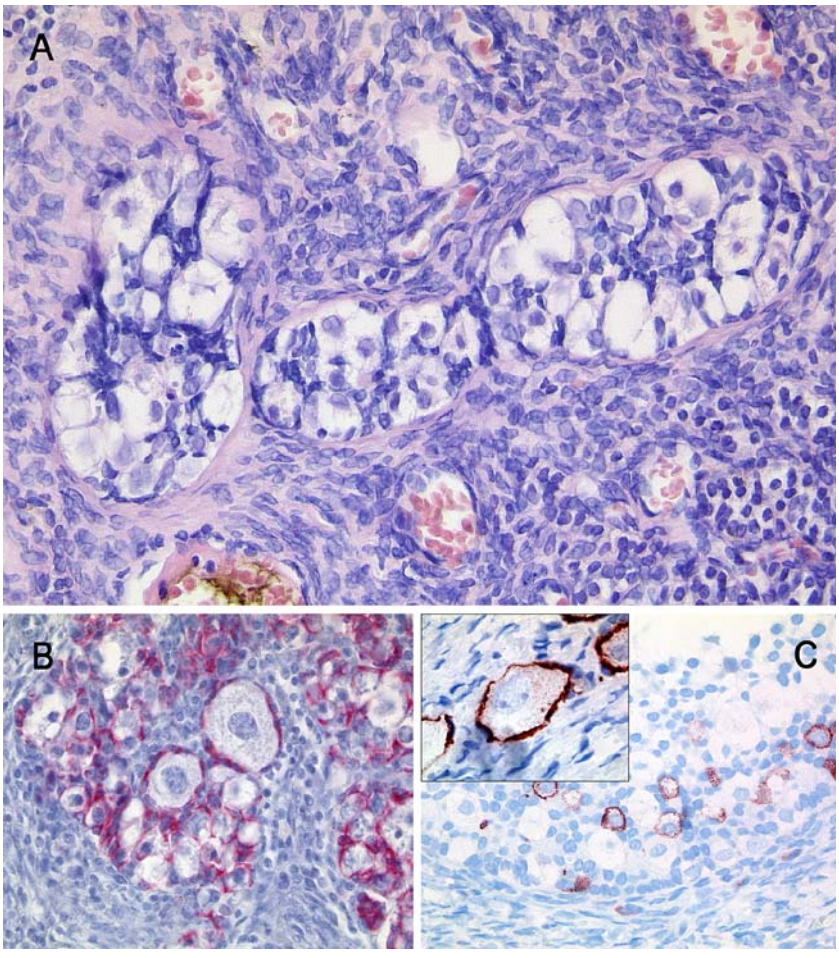


Fig. 3 Fetal organization of germ cells in oocytic clusters within the normal ovary of newborns (**a**, H&E) and in fetal ovaries (week 22 of pregnancy) (**b**, vimentin) resembling the microfollicular pattern of gonadoblastoma. Germ cells inside of oocytic clusters are partially surrounded by fetal stromal cells, which are positive for vimentin (**b**). **c** C-kit is expressed in a portion of oocytes (insert indicate membraneous staining pattern). Original magnification ×20 **a**, **c**, ×40 **b**

c-kit+/−, sACE−). We also found histological similarities between the microfollicular pattern of gonadoblastoma and the fetal ovarian organization of oocytes in nest-like structures, the so-called oocytic clusters [24]. These represent groups of germ cells entering the prophase of meiosis until primordial follicles are formed and subsequently separated

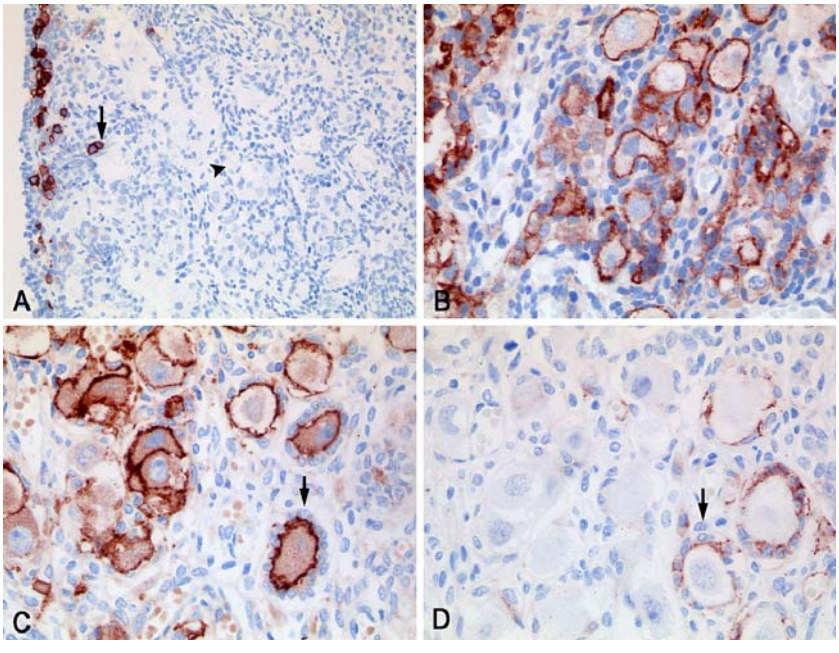


Fig. 4 Immunophenotype of fetal female germ cells. Oogonia in the cortical region of fetal ovary of 15th week of pregnancy are positive for GCAP/PLAP (**a**, arrow), whereas oocytes in the medullar region are PLAP-negative (**a**, arrowhead). Germ cells in oocytic clusters express c-kit (**b**) (week 22 of pregnancy). In week 25 of pregnancy, germ cells at the stage of primordial follicles are still c-kit positive (**c**, arrow) and are surrounded by fetal sACE-positive pre-granulosa cells (**d**, arrow; immunohistochemistry with mAb to sACE)

Table 3 Markers of sex-cord cells in gonadoblastomas (*GB*) and fetal gonads

	Stromal cells in GB	Fetal testicular pre-Sertoli cells		Fetal ovarian pre-granulosa cells	
		Mid fetal	Late fetal	Mid fetal	Late fetal
CK18	+	(+)	−	+	+
Vimentin	+	+	+	+	+
sACE	+	(+)	+	−	(+)
Inhibin	+	+	+	−	(+)
M2A	−	(+)	+	−	(+)

into the late-fetal ovarian stroma [24]. We believe that the microfollicular pattern of gonadoblastoma reflect early female germ cell differentiation blocked at the developmental cluster stage of pachytene oocytes prior to their stromal integration.

This view is in agreement with the fact that patients with loss or mutations of the single Y-chromosomal gene *SRY* or its regulatory sequences develop a female phenotype and dysgenetic gonads, and carry a high risk of developing gonadoblastomas [3, 19]. Without proper function of *SRY* or several other genes involved in the early sex-determining pathway, Sertoli-cells and testicular structures cannot be formed [2, 3]. Moreover, a recent report showed that an XY female human fetus, deficient in *SRY*, developed ovaries and a regular appearing female germ cell population, including oocytes, at least until the 14th gestational week [1]. This is definitely later than the structural sex determination in human gonads when formation of testicular cords and pre-Sertoli cells can be recognized (between the 5th and 6th gestational week) [27].

In dysgenetic ovaries, failure in meiotic pairing of different chromosomes may be followed by loss or absence of oocytes in animals and humans [5, 12, 23]. This is well documented in Turner patients, who show degeneration of meiotic oocytes, and loss of almost all oocytes in early childhood [21]. In contrast, the germ cells in dysgenetic gonads of XY females or XY mosaicisms may survive, leading to the frequent occurrence of gonadoblastoma. Since we found the phenotypes of oogonia and oocytes still present in gonadoblastoma of a 52-year-old patient (patient 3), oogonia probably gained a survival advantage similar to that of spermatogonia which are able to persist in a pre-meiotic stage during the male life-span [10]. This advantage is most likely provided by genes from the Y chromosome or its fragments *TSPY* [14, 29].

In gonadoblastomas, supportive cells appear more differentiated compared with fetal ovaries and testis. They showed a distribution still reminiscent of oocytic clusters, whereas their cytological and molecular features differed from any definable fetal stage and often resembled activated granulosa cells [6, 7, 16]. Furthermore, in this and different previous studies, fetal testes from the 8th gestational week onwards never showed structures comparable with that of gonadoblastoma [8]. The fact that Sertoli cells cannot be formed without proper function of *SRY* supports the granulosa origin of these cells [2, 3]. However, it cannot be ruled out that these granulosa-like cells imitate few morphologic and ultrastructural features of adult Sertoli-cells [17]. This may be due to Y-derived gene products from the residual Y chromosome.

Most gonadoblastomas are found incidentally during the investigation of amenorrhea and sometimes beneath a surgically removed mGCT or in the contralateral ovary of adult tumor patients [18, 20, 22]. Therefore, the reported frequencies of associated mGCTs and in situ germinomas may be biased by some selection routine, neglecting small and non-apparent lesions. In this study, we show that the percentage of proliferating germ cells with oogonial features (M2A+, GCAP+, c-kit+, sACE+) increased from the microfollicular to the coronary pattern (Figs. 1 and 2). In parallel, the number of supportive cells decreased from microfollicular to coronary patterns, where they were displaced to the periphery of the gonablastoma nests. Proliferation index and marker expression of germ cells found in the coronary nests of gonadoblastomas were almost the same as in the neighboring dysgerminomas. This suggests that particularly the coronary pattern bear a neoplastic population of oogonia-like cells, the in situ germinoma. Thus, coronary pattern obviously represents an important step in the progression of gonadoblastoma to invasive dysgerminoma. Furthermore, invasion of neoplastic germ cells into the stroma was demarked by loss of supportive cells as shown in our study.

In conclusion, our results indicate that gonadoblastoma is a true in situ neoplasm with two different histological pattern. The microfollicular pattern represents an early stage of gonadoblastoma development and recapitulates the fetal female gonadal development. Proliferation of neoplastic germ cells inside microfollicular nests give rise to the coronary pattern of gonadoblastoma. The latter results from expansion of highly proliferating neoplastic germ cells and represents an advanced stage of gonadoblastoma.

This suggests that every gonadoblastoma, especially if a coronary pattern is present, should be examined completely and carefully in order to exclude an invasive dysgerminoma component. Because early invasion may be difficult to recognize by routine histology, serial immunohistochemical examinations using antibodies to neoplastic germ cells and to sex-cord stromal cells as presented in our study may help to identify an invasive tumor.

Acknowledgements The skillful technical assistance of Barbara Reddeman, Susanne Steiner, Christiane Esch and Gerrit Klemm is gratefully acknowledged. We would like to thank Dr. Irina Fenic for a critical review of the manuscript. This study was supported from a BONFOR research grant of the Medical Faculty, University of Bonn.

References

1. Aviv H, Heller D, Fajardo A, Hoot A, Mavaro L (2001) Sex chromosome mosaicism in gonads of a fetus with cystic hygroma and deletion of the short arm of Y chromosome including loss of SRY. Am J Med Genet 102:157–160

2. Brennan J, Capel B (2004) One tissue, two fates: molecular genetic events that underlie testis versus ovary development. Nature Rev 5:509–521
3. Cameron FJ, Sinclair AH (1997) Mutations in SRY and SOX9: testis-determining genes. Hum Mutat 9:388–395
4. Carrillo AA, Berkovitz GD (2004) Genetic mechanisms that regulate testis determination. Rev Endocr Metab Disord 5:77–82
5. Cunniff C, Jones KL, Benirschle K (1992) Ovarian dysgenesis in individuals with chromosomal abnormalities. Hum Genet 86:552–556
6. Damjanov I, Klauber G (1980) Microscopic gonadoblastoma in dysgenetic gonad of an infant: an ultrastructural study. Urology 15:605–609
7. Daud AI, Bumpus FM, Husain A (1990) Characterization of angiotensin I-converting enzyme (ACE)-containing follicles in the rat ovary during the estrous cycle and effects of ACE inhibitor on ovulation. Endocrinology 126:2927–3295
8. Franke FE, Pauls K, Rey R, Marks A, Bergmann M, Steger K (2004) Differentiation markers of Sertoli cells and germ cells in fetal and early postnatal human testis. Anat Embryol 209:169–177
9. Harley VR, Layfield S, Mitchell CL, Forwood JK, John AP, Briggs LJ, McDowall SG, Jans DA (2003) Defective importin β recognition and nuclear import of the sex-determining factor SRY are associated with XY sex-reversing mutations. Proc Natl Acad Sci USA 100:7045–7050
10. Hilscher W (1991) The genetic control and germ cell kinetics of the female and male germ line in mammals including man. Hum Reprod 6:1416–1425
11. Jorgensen N, Muller J, Jaubert F, Clausen OP, Skakkebaek NE (1997) Heterogeneity of gonadoblastoma germ cells: similarities with immature germ cells, spermatogonia and testicular carcinoma in situ cells. Histopathology 30:177–186
12. Mahadevaiah SK, Lowell-Badge R, Burgoyne PS (1993) Tdy-negative XY, XXY and XYY female mice: breeding data and synaptonemal complex analysis. J Reprod Fert 97:151–160
13. Nomura K, Matsui T, Aizawa S (1999) Gonadoblastoma with proliferation resembling Sertoli cell tumor. Int J Gynecol Pathol 18:91–93
14. Page DC (1987) Hypothesis: a Y-chromosomal gene causes gonadoblastoma in dysgenetic gonads. Development 101:151–155
15. Pauls K, Fink L, Franke FE (1999) Angiotensin-converting enzyme (CD143) in neoplastic germ cells. Lab Invest 79:1425–1435
16. Rishi M, Howard LN, Bratthauer GL, Tavassoli FA (1997) Use of monoclonal antibody against human inhibin as a marker for sex cord-stromal tumors of the ovary. Am J Surg Pathol 21:583–589
17. Roth LM, Eglen DE (1989) Gonadoblastoma. Immunohistochemical and ultrastructural observations. Int J Gynecol Pathol 8:72–81
18. Russell P, Robboy S, Anderson MC (2002) Gonadoblastoma. In: Robboy S, Anderson MC, Russell P (eds) Pathology of the female reproductive tract. Churchill Livingstone, pp 682–685
19. Sahid M, Dhillion VS, Jain N, Hedau S, Diwakar S, Sachdeva P, Batra S, Das BC, Husain SA (2004) Two novel point mutations localized upstream and downstream of the HMG box region of the SRY gene in three Indian 46,XY females with sex reversal and gonadal tumour formation. Mol Hum Reprod 10: 521–526
20. Scully RE (1970) Gonadoblastoma. A review of 74 cases. Cancer 25:1340–1356
21. Singh RD, Carr DH (1966) The anatomy and histology of XO human embryos and fetuses. Anat Rec 155:369–383
22. Talerman A (2002) Germ cell tumors of the ovary. In: Kurman RJ (ed) Blaustein's pathology of the female genital tract, 5th edn. Springer, Berlin Heidelberg New York, pp 967–1034
23. Turner JM, Mahadevaiah SK, Benavente R, Offenberg HH, Heyting C, Burgoyne PS (2000) Analysis of male meiotic "sex body" proteins during XY female meiosis provides new insights into their functions. Chromosoma 109:426–432
24. van Wagenen G, Simpson ME (1965) Embryology of the ovary and testis: homo sapiens and Macaca mulatta. Yale University Press, New Haven
25. Verp MS, Simpson JL (1987) Abnormal sexual differentiation and neoplasia. Cancer Genet Cytogenet 25:191–218
26. Wardelmann E, Hrychyk A, Merkelbach-Bruse S, Pauls K et al (2004) Association of plateled-derived growth factor receptor alpha mutations with gastric primary site and epitheloid or mixed cell morphology in gastrointestinal stromal tumors. J Mol Diag 6:197–204
27. Wartenberg H (1981) Differentiation and development of the testis. In: Burger H, de Kretser D (eds) The testis. Raven Press, pp 39–80
28. Zhao S, Kato N, Endoh Y, Jin Z, Ajioka Y, Motoyama T (2000) Ovarian gonadoblastoma with mixed germ cell tumor in a woman with 46, XX karyotype and successful pregnancies. Pathol Int 50:332–335
29. Zhang JS, Yang-Feng TL, Muller U, Mohandas TK, de Jong PJ, Lau YF (1992) Molecular isolation and characterization of an expressed gene from the human Y chromosome. Hum Mol Genet 1:717–726

Virchows Arch (2005) 447: 610–625
DOI 10.1007/s00428-005-1257-8

ORIGINAL ARTICLE

Finn Edler von Eyben · Grete Krag Jacobsen · Rolf Inge Skotheim

Microinvasive germ cell tumor of the testis

Received: 20 December 2004 / Accepted: 7 March 2005 / Published online: 21 June 2005
© Springer-Verlag 2005

Abstract Microinvasive germ cell tumor (MGCT) consists of a limited number of malignant germ cells in the intertubular tissue of the testis. The cells have large nuclei, prominent nucleoli, abundant clear cytoplasm, and distinct cellular borders in hematoxylin and eosin staining. MGCT can be the first stage of malignancy in the development of testicular germ cell tumor (TGCT). Biopsies from men with maldescended testes have been reported to contain intratubular germ cell neoplasia, unclassified (IGCN) and MGCT in 1.8% of the examined cases (95% CI 0.5–4.6%). MGCT has also been found in testes of subfertile men and in the contralateral testis of patients with TGCT. MGCT is a frequent finding (19%) in the testicular tissue adjacent to an overt TGCT. Men with a high risk of TGCT may gain from screening for precursor lesions of TGCT with ultrasonography of the testes followed by a testicular biopsy if suspicious abnormalities are found: Treatment is high-voltage radiotherapy for intratubular germ cell neoplasia (IGCN), and orchidectomy for MGCT and germ cell tumor in situ, either intratubular seminoma or intratubular embryonal carcinoma. After local treatment, patients with precursor lesions can be followed with a surveillance program. The mRNA levels of invasion-related genes were evaluated based on a DNA microarray data set, and we found two gene abnormalities most relevant for the invasion of malignant germ cells: matrix metalloproteinase 9 (MMP9) and plasminogen activator, urokinase (PLAU) genes were up-regulated in a study comparing tissue samples of TGCT and IGCN.

Keywords Germ cell tumors · Precursors · Invasion · Matrix metalloproteinases · Matrix metalloproteinase inhibitors · Plasminogen activator · Urokinase

F. E. von Eyben (✉)
Center of Tobacco Control Research,
Birkevej 17,
5230 Odense, Denmark
e-mail: feve@post5.tele.dk
Tel.: +45-66145862

G. K. Jacobsen
Department of Pathology,
National University Hospital,
and the Bartholin Institute,
Copenhagen, Denmark

R. I. Skotheim
Department of Genetics,
Institute of Cancer Research,
The Norwegian Radium Hospital,
Oslo, Norway

Introduction

Macroscopically overt testicular germ cell tumors (TGCT) for adult men develop through a preclinical phase with at least one of three precursor neoplastic lesions: intratubular germ cell neoplasia non-otherwise specified (IGCN) [20, 71, 80, 99, 149], microinvasive germ cell tumor (MGCT) [180], and intratubular germ cell tumor in situ (Fig. 1) (GCTIS) [12]. The only exception is spermatocytic seminoma. Langhans described IGCN in 1887 [91], and in 1896, Wilms reported that the testicular tissue adjacent to a TGCT could have atrophic tubules containing neoplastic seminoma-like germ cells [194]. In 1972, Skakkebaek reported that untreated IGCN, denoted carcinoma in situ of the testis, could progress to MGCT or TGCT during follow-up [148].

MGCT is a secondary precursor stage of TGCT with extratubular invasion of neoplastic germ cells in the interstitial tissue of the testis. Therefore MGCT is by definition malignant. In 1977, Schulze and Holstein described MGCT as a step in the development from IGCN to seminoma [141]. Supporting MGCT as a separate precursor stage for TGCT, von Eyben and coworkers reported three patients with MGCT, but without overt TGCT, diagnosed within a decade in a limited region of Sweden [180]. Recently, Henley et al. reported 12 additional patients evaluated at two institutions in the USA [61]. Another secondary precursor lesion is GCTIS with either seminoma or embryonal carcinoma, found only intratubularly [12, 116].

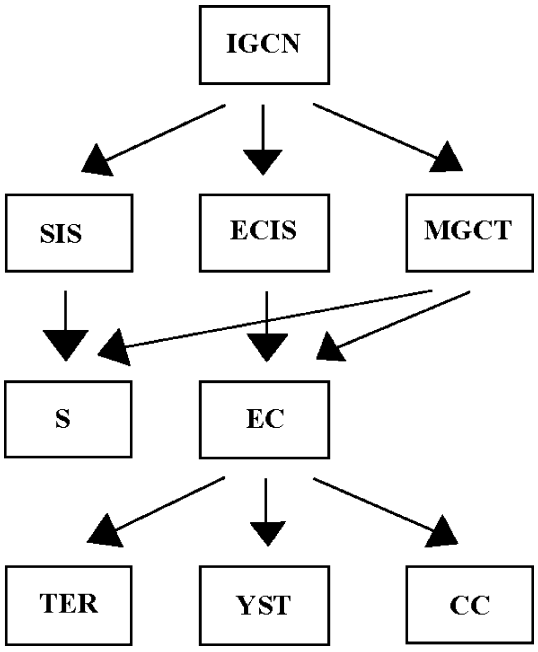


Fig. 1 Progression from IGCN through secondary precursor stages to TGCT. *EC* denotes embryonal carcinoma, *TER* teratoma, *YST* yolk sac tumor, and *CC* choriocarcinoma

Despite the expanding literature on the precursor lesions, there is no consensus about the role of MGCT in the development of TGCT or of its relevance for staging and management of patients. Authors have used 33 different terms for MGCT [4, 6, 20, 21, 24, 38, 39, 53, 61, 62, 78, 80, 94, 101, 104, 105, 109, 111, 116, 117, 125, 128, 143, 149, 171, 180, 196, 198], but most terms are questionable. A term such as "invasive carcinoma" [104, 109] does not separate MGCT from cancers of non-germ cell origin. Furthermore, IGCN and MGCT may progress to both embryonal carcinoma and TGCT with other histologic patterns. The cells of the precursor lesions have morphologic similarities with the cells of seminoma and not with the cells of embryonal carcinoma. The precursor lesions develop from germ cells and do not show epithelial features — the main criteria for carcinoma [70, 111, 141, 142]. The terms "early seminoma" [127], "interstitial seminoma" [143, 196], "intertubular seminoma" [61], and "microinvasive seminoma" [24] imply that MGCT is a small seminoma despite that fact that MGCT are found also in testes with non-seminomatous TGCT without a seminoma component. Tumor is a general term for both benign and malignant swellings, but the World Health Organization (WHO) classification of tumors of the male genital system uses the term "testicular germ cell tumors" to denote testicular germ cell malignancies [40]. The present review applies the term "microinvasive germ cell tumor" as it describes the lesion best. Men with MGCT can have germ cell tumor metastases, but the metastatic potential does not militate against MGCT being applied as the term for the primary testicular lesion.

This review summarizes the present knowledge regarding clinical aspects of MGCT such as incidence, etiology, detection, histopathology, immunohistochemistry, ultrastructure, differential diagnosis, clinical course, and treatment. For comparison, similar aspects are reported regarding IGCN, GCTIS, and TGCT. Moreover, the review describes cytogenetics, genetics, and pathogenesis of TGCT in the perspective of factors contributing to the invasion of malignant germ cells, and the development from IGCN to TGCT.

Clinical studies

Incidence

TGCT is the most frequent malignancy in young men, whereas this group have a very low incidence of precursor lesions of TGCT [48, 50]. Several subgroups of men have a high risk of TGCT. Men with intersex, gonadal dysgenesis, androgen insensitivity, and testicular feminization have a very high incidence of IGCN [130, 131, 137].

The incidence of IGCN is also increased (0.5–7%) in other groups of men [37, 134, 150]. Patients with maldescended testis have a lifetime risk of TGCT of 4%, which is 4–35 times the risk for men in general [48, 103, 191, 192], and the risk is higher for the affected testis than for the contralateral testis. Correspondingly, men with maldescended testes undergoing testicular biopsies have a 1–3% incidence of IGCN [25, 48, 90, 107, 119, 120, 134, 151]. The incidence is lower before than after puberty [41, 107], and a hypoplastic testis increases the incidence [48, 90, 107, 119]. Adult men with intra-abdominal testis, abnormal external genitalia, or abnormal constitutive karyotype have an especially increased risk of germ cell neoplasia [25]. Men treated for maldescended testis had an incidence of MGCT of 1.8% (Table 1) [120, 190, 198].

Table 1 Prevalence of IGCN and MGCT in men treated for maldescended testes. The table details three studies of men with maldescended testes that reported the prevalence of IGCN, MGCT, and TGCT

Reference	Total number of men	No. with IGCN[a]	No. with MGCT[b]	No. with TGCT
Krabbe, 1979 [90]	75	2	1	1[c]
Zwierstra, 1984 [198]	35	0	1	1
Pedersen, 1987 [120]	109	1	2	0
Total	219	3 (1.4%, CI 0.3–4.0%)	4 (1.8%, CI 0.5–4.6%)	2 (0.9%, CI 0.1–3.3%)

[a]Without MGCT and TGCT. CI denotes the 95% confidence interval
[b]All cases with MGCT also had IGCN in the testis. There was a trend towards a higher incidence of precursor lesions than of TGCT in connection with the screening (P=0.09, binomial test)
[c]The patient with a TGCT had a testicular mass that had been misdiagnosed for an inflammatory process before the screening

Table 2 Prevalence of IGCN and MGCT in subfertile men

Reference	Total number of men	No. with IGCN[a]	No. with MGCT[b]	No. with TGCT
Pryor, 1983 [125]	2043	7	1	0
Schutte, 1988 [143]	2047	6	4	5
Total	4090	17 (0.4%, CI 0.2–0.7%)	5 (0.1%, CI 0.0–0.3%)	5 (0.1%, CI 0.0–0.3%)

[a]Without MGCT and TGCT. CI denotes the 95% confidence interval
[b]All cases with MGCT also had IGCN in the testis. There was a trend towards a higher incidence of precursor lesions than of TGCT in connection with the screening

Men who are subfertile due to oligospermia or azoospermia have a 0.3% incidence of IGCN [14, 28, 112, 146] and a lower incidence of MGCT (Table 2) [125, 143]. For such men, only hypoplastic testes with a Johnson score lower than 4 contained IGCN [14]. For patients with TGCT, the contralateral testis has a 4–11% incidence of IGCN [32, 33, 57, 110, 174]. The incidence of IGCN is especially increased for those less than 30 years of age, and for those with hypoplastic testes [57]. In addition, MGCT was reported in the contralateral testis in a series of patients with TGCT (Table 3) [68]. Testes with a macroscopically overt TGCT have an especially high incidence of IGCN and MGCT in the surrounding testicular tissue [78, 87, 142, 185]. Testes of patients with metastatic germ cell tumor may contain precursor lesions in the absence of an overt testicular tumor. A study described autopsy findings for 17 men without a primary TGCT who died of widespread metastases of non-seminomatous germ cell tumor, of whom 13 men had testes with IGCN, and 4 had testes that also contained MGCT [6].

IGCN can also be found in men with extragonadal germ cell tumors [27, 43]. The incidence of IGCN is not significantly associated with the site of the extragonadal germ cell tumor. Eighteen of 53 patients with retroperitoneal germ cell tumors had IGCN as had 3 of 12 patients with mediastinal germ cell tumors (P=0.36, Fisher's exact test). Testes with a macroscopically overt TGCT have a high incidence of IGCN (77%) in the tissue adjacent to the tumor [78, 87, 99, 142, 185].

Table 3 Prevalence of IGCN and MGCT in the contralateral testis of patients with TGCT

Reference	Total number of men	No. with IGCN[a]	No. with MGCT[b]	No. with TGCT
Holm, 2003 [68]	64	7 (11%, CI 5–21%)	1 (2%, CI 0–8%)	0 (0%, CI 0–5%)

[a]Without MGCT and TGCT. CI denotes the 95% confidence interval
[b]All cases with MGCT also had IGCN in the testis

Two cases have been reported with an intratubular embryonal carcinoma without TGCT [129]. The frequency of GCTIS adjacent to TGCT remains to be determined. GCTIS was found in 0.7% and 1.0% of the patients with TGCT stage I in two series by the Danish Testis Cancer (DATECA) Study group [185], and in 36% of the patients in two other studies [12, 116].

In contrast, the testes of men with spermatocytic seminoma, and testes of prepubertal boys with TGCT seldom contained IGCN [158]. Therefore these tumors may not be associated with the secondary precursor lesions [54, 145, 152].

Most patients with testicular germ cell neoplasia are diagnosed with TGCT and only a few patients are diagnosed with precursor lesions. Nevertheless, the two types of germ cell neoplasia had the inverse pattern for the predominance in prospective screening studies of high-risk men (Table 1, 2, 3).

Etiology

Several observations suggest that an initial damage inducing a neoplastic transformation of testicular germ cells may occur during intrauterine, fetal life [84, 123, 190]. Brothers to patients with TGCT have an increased risk of TGCT in contrast to the relatively low risk for their fathers [190]. Smoking of the pregnant mother may cause an initial damage to the testis of the male fetus [84, 123] but some studies showed inconsistent results [103]. TGCT has an association with the childhood residence but not with the geographical site at diagnosis [102]. Smoking of men increased the risk of TGCT whereas smoking cessation did not mitigate the risk [160].

Detection

Precursor lesions for these high-risk men can be detected with a testicular biopsy. Therefore, it is important that physicians consider the possibility of IGCN and MGCT and offer screening in the management of these men. The precursor lesions do not cause testicular enlargement and rarely causes clinical symptoms [98, 177]. Nevertheless, screening studies of high-risk men have regularly detected the precursor lesions.

The initial screening procedure for testicular germ cell malignancy is ultrasonography (Fig. 2), because 11 of 15 testes with testicular germ cell neoplasia examined with ultrasound, contained microlithiasis [7, 28]. It is calcium deposits in the seminiferous tubules and is seen on ultrasonography as multiple, dispersed, punctuate, uniform, non-shadowing hyperechogenic foci. The examination may also reveal a very irregular pattern suggestive of IGCN, or a focal lesion [92]. A homogenous hypoechoic lesion indicates a subclinical seminoma, while a heterogeneous lesion with poorly defined margins and cystic areas indicates a subclinical non-seminomatous TGCT [54, 145]. Men may accept an ultrasonographic examination more

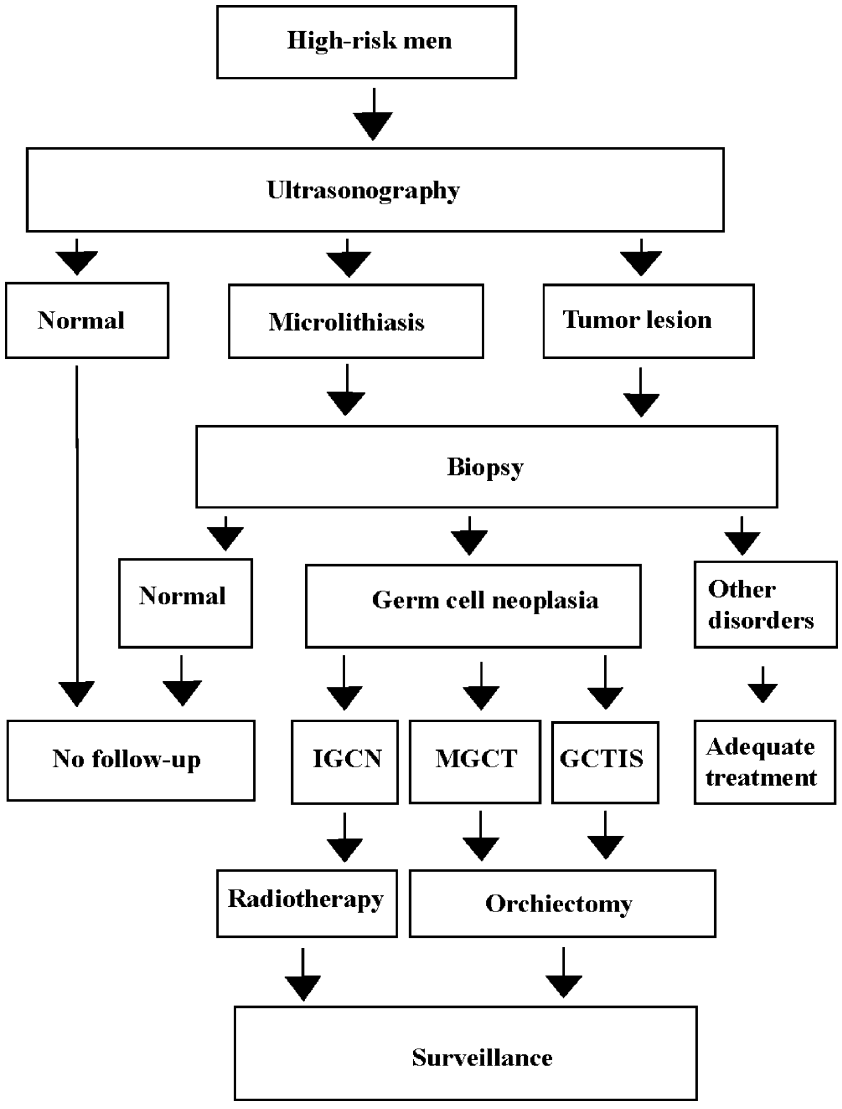


Fig. 2 Screening for testicular germ cell neoplasia and management following the examination of high-risk men without palpable testicular tumors

often than a surgical biopsy [90]. Testicular microlithiasis is found in 1% to 9% of men. In three series of high-risk men, 85 of 483 (17%) men had microlithiasis, and 18 of the 85 (21%) men with microlithiasis had testicular germ cell neoplasia [7, 28, 68].

If the testes contain testicular microlithiasis or a focal lesion, the next diagnostic step is a surgical biopsy (Fig. 2). A testicular biopsy can be obtained on an outpatient basis, and while the biopsy caused minor complications for half the examined men, none had persistent sequelae [19]. One to three tissue samples of the testis, 3 mm in diameter, are sufficient for detection of most IGCN [13, 36, 86]. Tissue specimens can be obtained from most parts of the testis. In a study of the contralateral testis for men with TGCT, one biopsy detected IGCN in 18 of 295 (6%) testes, and additional two biopsies detected IGCN in a further six testes (2%) [86]. A surgical testicular biopsy is efficient in the search for germ cell neoplasia, and adult men with a biopsy that did not reveal IGCN, have a very small risk of later developing TGCT [14, 33, 51, 112, 119]. The biopsies do not cause scrotal seeding of neoplastic germ cells [151].

A fine needle aspiration biopsy has also been used in detection of IGCN [17, 188]. A fine needle biopsy has occasionally been used in connection with surgical exploration for impalpable focal lesions demonstrated by ultrasonography [18]. The findings show good agreement with the histologic findings after orchiectomy for TGCT [10]. The fine needle biopsy may be as sensitive for detection of IGCN as a surgical biopsy [56]. Genetic analyses of ejaculates can detect genetic abnormalities in spermatozoa suggestive of IGCT [17, 76].

The European Association of Pathologists has published guidelines for the handling of testicular specimens [195]. Tissue samples must not be mechanically compressed, and the fixative should be adequate, for example, Stieve's fluid, Bouin's solution, Cleland's solution or formalin [33]. Tissue specimens should be cut and stained according to routine procedures, including staining with hematoxylin and eosin (H & E) and periodic acid-Schiff. Immunohis-

tochemical staining for placental alkaline phosphatase (PLAP) is helpful in diagnosing IGCN and MGCT.

Histopathology

The diagnosis of all precursor lesions, IGCN, MGCT, and GCTIS, depends on examination of a testicular specimen in a microscope and should be based on characteristic histologic criteria.

The first precursor lesion, IGCN, is composed of atypical germ cells in the seminiferous tubules of the testes [72, 80]. The lesion may be present widely or focally in the tubules of a testis. The cells are characteristically located side-to-side, mostly in one, or slightly more than one, layer, in the basal part of germinative cell layer, beneath or between the Sertoli cells (Fig. 3a). Tubules with IGCN rarely contain spermatocytes, spermatides, and spermatozoa. The wall of the tubules is thickened and often multilayered. IGCN may be infiltrated with lymphocytes and plasma cells [15]. Neoplastic germ cells are rather uniform, polygonal and large (20 μm in diameter) [111, 189]. The nucleus is large (10–12 μm in diameter) and rounded, with a coarse chromatin pattern and one or more large and irregular nucleoli. Mitoses are often seen and some are abnormal. The cytoplasm is abundant and usually contains large amounts of glycogen. In H & E staining, the cytoplasm appears clear, and it stains positive with periodic acid-Schiff. The cellular borders are distinct. Syncytiotrophoblastic giant cells may be found in IGCN. Many studies, reviews, and textbooks have described IGCN [40, 71, 106, 134, 171]. The sixth edition of the TNM (T for primary tumor, N for metastases in regional lymph nodes, and M for distant metastases) classification by the International Union against Cancer (UICC) from 2002 included IGCN as a precursor stage for TGCT [157], as did the WHO classification of testicular tumors from 2004 [40]. The Danish version of SNOMED includes IGCN as a separate tumor lesion.

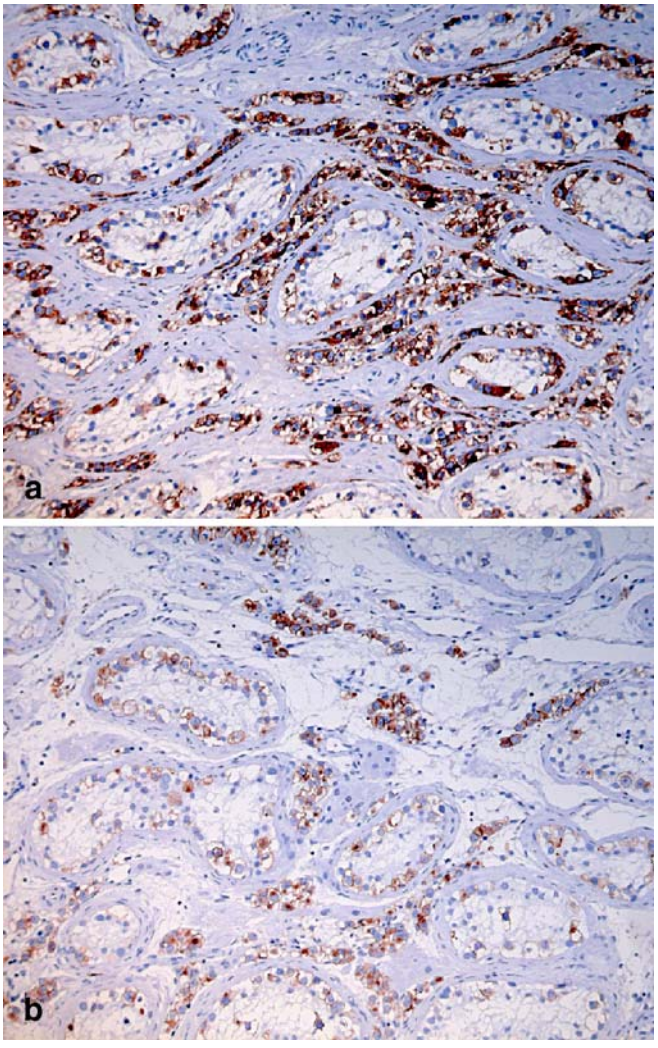


Fig. 3 Microinvasive germ cell tumor from a testis with TGCT stained for placental alkaline phosphatase (**a**), and stained for c-kit receptor (CD-117) (**b**)

MGCT is a secondary precursor stage characterized by extratubular malignant germ cells without a macroscopically overt TGCT. Testis with MGCT may exhibit gross features such as an ill-defined firm area with a pale to brown discoloration [61]. MGCT may appear as single cells or as one or more small groups of rather uniform malignant germ cells (<1 mm^3) in the testicular interstitium (Fig. 2a and b). MGCT is focally distributed in the testicular parenchyma. Tubules near MGCT have thickened and multilayered walls. Otherwise, the tubular structures and the overall architecture of the testis are preserved. MGCT can be associated with infiltration of lymphocytes [82]. Histopathologic tumor classifications by WHO mentioned MGCT [41, 109]. The Danish version of SNOMED includes MGCT as a separate tumor lesion.

GCTIS is another secondary precursor stage with intratubular differentiation of neoplastic germ cells into a seminoma or an embryonal carcinoma without extratubular invasion of the cells. The malignant germ cells fill and distend the affected tubules, and typically eradicate the Sertoli cells [12, 116]. The intratubular malignant cells of these lesions and the cells of overt seminoma and embryonal carcinoma have similar morphology. GCTIS is usually found at the margin of an overt TGCT, in contrast to MGCT [12]. Intratubular embryonal carcinoma is often very necrotic [116].

TGCT is a mass of malignant germ cells (>1 mm^3) that is immediately visible. TGCT destroys the tubules and the architecture of the interstitial tissue [40]. The tumors comprise two main groups, seminoma and non-seminomatous TGCT. Non-seminomatous TGCT consists of embryonal carcinoma and histological subtypes that are differentiated toward embryonal and extra-embryonal cellular patterns and tissues, such as teratoma, yolk sac tumor, and choriocarcinoma.

In adult testes with TGCT, IGCN, MGCT, and GCTIS may be present in the adjacent testicular tissue [5, 59, 78, 87, 99, 142, 185]. IGCN and MGCT may be found distant and separate from the TGCT, indicating that IGCN and

Table 4 Criteria for relevance of secondary precursor lesions in development of TGCT

	MGCT	GCTIS	Reference
TGCT	+	(+)	von Eyben [180]
Relative prevalence in testis with TGCT	++	+	von Eyben [185]
Lesion separate from TGCT in a testis	+	(+)	Berney [12]; Oosterhuis [116]; von Eyben [185]

MGCT are not extensions of TGCT (Table 4) [101]. IGCN is not found in the adjacent part of the testis in children with TGCT [55].

Immunohistochemistry

The cells of IGCN show a positive staining for PLAP (Fig. 3a), whereas normal germ cells have negatively staining [21, 79, 98, 128]. IGCN also stain positive for the stem cell factor receptor (*KIT*, v-kit Hardy Zuckerman 4 feline sarcoma viral oncogene homolog, CD-117, c-kit receptor) (Fig. 3b) [126], ferritin [77], and lactate dehydrogenase (LD) subunit B [22]. IGCN stained positive with a monoclonal anti-seminoma antibody M2A [8, 49]. Cancer/testis antigen 1B and the melanoma antigen family A4, MAGEA4, have also been demonstrated immunohistochemically in IGCN [5, 143]. Most neoplastic germ cells of IGCN expressed junction plakoglobin, alias γ-catenin, whereas it is rarely expressed in normal germ cells (12%) [154]. IGCN expressed growth factor receptor-bound protein 7 more often than normal germ cells. The antigens HB5, HE11, HF2, and 43-9F [49, 64], and proteinases like cathepsin D (lysosomal aspartyl protease) were also demonstrated in IGCN [59, 60]. Embryonal carcinoma expresses tumor necrosis factor receptor super family, member 8, CD30, and in testes with embryonal carcinoma, CD30 is also present in half of the IGCN [12]. IGCN adjacent to embryonal carcinoma often have positive staining with a monoclonal antibody against an embryonal carcinoma antigen, TRA-1-60, in contrast to IGCN appearing alone or adjacent to seminoma [128]. Syncytiotrophoblastic giant cells present in IGCN show a positive staining for human chorionic gonadotropin (hCG) [87].

IGCN stain negative for alpha-fetoprotein (AFP), hCG, lactate dehydrogenase subunit C (LDHC), actin, cytokeratin 18, integrin α6, laminin, and vimentin, with few exceptions [22, 38, 80, 87, 147, 158]. IGCN stain negative for protein tyrosine phosphatase, receptor type, C (CD45, leucocyte-common-antigen) and other markers of lymphoma [171].

MGCT stain positive for PLAP, cathepsin D, c-kit receptor, and LD subunit B, and stain negative for LDHC [22, 59, 60, 185]. MGCT is partly surrounded by basement membrane material showing immunoreactivity for actin, integrin α6, and laminin, like the basement membrane of seminiferous tubules [38]. MGCT and seminoma are often infiltrated by reactive, mainly T, lymphocytes that stain positive for integrin, alpha L (antigen CD11A (p180), lymphocyte function-associated antigen 1; alpha polypeptide, LFA).

Intratubular embryonal carcinoma is CD30 positive, and immunohistochemical examination for CD30 may reveal lesions of malignant germ cells in tubules not recognized in H & E staining [12]. Intratubular embryonal carcinoma may also stain positive for AE1/AE3 and p53, and stain negative for cytokeratin 20, cyclin dependent kinase inhibitor 1A, alias p21, and AFP [129].

TGCT showed a reduced expression of p21 compared with IGCN, and an increased expression of mouse double minute 2 homolog, mdm2, transformed 3T3 cell double minute 2, p53 binding protein (mouse) [26]. TGCT also had a downreglation of cyclin-dependent, kinase inhibitor 2A, $p16^{INK4A}$ [11]. TGCT did not express the NK3 transcription factor related, locus 1 (Drosophila), NKX3-1 while it was expressed in normal germ cells and IGCN [155]. The same difference was found for the expression of cancer/testis antigen 1B [140]. TGCT had an up-regulated expression of cyclin D2 gene compared with normal testicular germ cells and IGCN, whereas the fragile histidine triad gene and 0-6-methylguanine-DNA methyltransferase gene were down-regulated [154]. TGCT stain negative for epithelial membrane antigen (EMA). Seminoma stain positive for PLAP, and negative77 for CD30 and inhibin. In contrast, embryonal carcinoma stain positive for CD30. Yolk sac tumor stain positive for AFP, and choriocarcinoma stain positive for hCG.

Electron microscopy

The cells of IGCN adhere broadly to the basement membrane of the tubules [52, 69, 72, 111]. The walls of the involved tubules are 1–20 μm thick. The nuclei of the neoplastic germ cells have a homogenous and finely granular chromatin and may be eccentrically placed [52]. Nucleoli are usually placed centrally in the nuclei, and have a reticular pattern. The cytoplasm contains large mitochondria that are often clustered regionally in the cytoplasm of some cells, and may contain abundant glycogen. The cell membranes are smooth and regular, and do not have intercellular bridges [52, 72].

The cells of IGCN, MGCT and of seminoma share many ultrastructural features [52, 83, 124, 144, 161] whereas the cells of IGCN and MGCT also differ in some aspects [72, 111]. Extratubular malignant germ cells are partly surrounded by a thin layer of basement membrane material [72], and might be slightly larger than the intratubular neoplastic germ cells, and might have a higher nucleocytoplasmic ratio [111].

Seminoma cells may also be surrounded by basement membrane material [38]. Spermatocytic seminoma has a different ultrastructural pattern [135, 166]. Cells of embryonal carcinoma have mature desmosomes, junctional complexes, and prominent microvilli, and have only little glycogen in the cytoplasm [124].

Differential diagnosis

Gynecomastia can be due to endocrine disorders, but may also be due to precursor lesions in testis or TGCT.

Impalpable small, focal, centrally located lesions in the testis detected by ultrasonography may be due to fibrosis, Leydig cell tumors, Sertoli cell tumors, adenomatoid tumors, malignant lymphomas, and metastatic tumors or germ cell neoplasia [62, 156, 165]. In ultrasonograms, the benign tumors present generally as homogenous and hyperechoic lesions.

The cells of IGCN, MGCT and of seminoma have similar morphologies [4, 70, 141, 180]. In contrast, seminoma is organized in a large cluster or large masses of malignant germ cells that destroy the architecture of the interstitium and the tubules.

Malignant cells of malignant lymphomas and metastatic tumors can also be found in the interstitial testicular tissue, and these malignancies may later invade the tubules, eradicate the normal intratubular cells, and cause thickening of the tubular walls. However, malignant testicular lymphomas and metastatic lesions are diagnosed at a higher age (in men more than 50 years old) than MGCT and TGCT [42, 80]. The cells of malignant lymphomas are smaller than malignant germ cells, have scant cytoplasm without glycogen, are more irregularly shaped, have nuclei with irregular chromatin, and stain positive for various markers for lymphomas. Plasmacytoma of the testis has a positive staining for immunoglobulin. Testicular metastases of high-grade prostatic adenocarcinoma have a positive staining for prostata specific antigen (PSA) and EMA.

Serum tumor markers

The sixth edition of the TNM classification recommends that three serum tumor markers are used routinely in the staging of TGCT [157]: serum concentrations of AFP and hCG, and serum activity of LD. Patients with IGCN or MGCT have normal levels of the three serum tumor markers [24, 61, 62, 120, 167, 179, 182]. If a patient with a precursor lesion has raised levels of the serum tumor markers, a search should be undertaken for an overt TGCT [184].

Clinical findings

Most cases of IGCN without a concomitant TGCT are diagnosed in men 20–50 years old. The clinical course for men with IGCN is known from studies where treatment was postponed until tumor invasion was diagnosed [113, 149]. Up to 98% of untreated IGCN in adult men progresses to MGCT and TGCT [14, 33, 36, 146, 149, 171], whereas only 0.05% of the examined testes of adult men with a biopsy negative for IGCN developed MGCT or TGCT during follow-up. Detected in prepubertal men, IGCN rarely develop into TGCT [41, 109]. IGCN may be found in the testes of patients with extragonadal germ cell tumors, suggesting that these tumors may be metastases from IGCN [27, 110].

Previously reported patients with MGCT without concomitant TGCT were often 30 to 34 years old at diagnosis (Fig. 4a) and had often hypoplastic testes (Fig. 4b). Regarding the patients with TGCT stage I examined by the DATECA Study group, those who had both seminoma and MGCT were significantly younger at diagnosis than those who had only seminoma [185], whereas the two groups of patients had similar size of the seminoma. In patients with nonseminoma, the presence or absence of MGCT was not associated with the age at diagnosis and the size of the tumor [185]. The progression of MGCT into TGCT has been described in a few case reports [111, 113]. Patients with MGCT without an overt TGCT can have germ cell tumor metastases [4, 61].

Clinical studies of TGCT stage I followed with surveillance revealed characteristics that predict a later relapse, such as the size of the primary tumor for seminomas, and

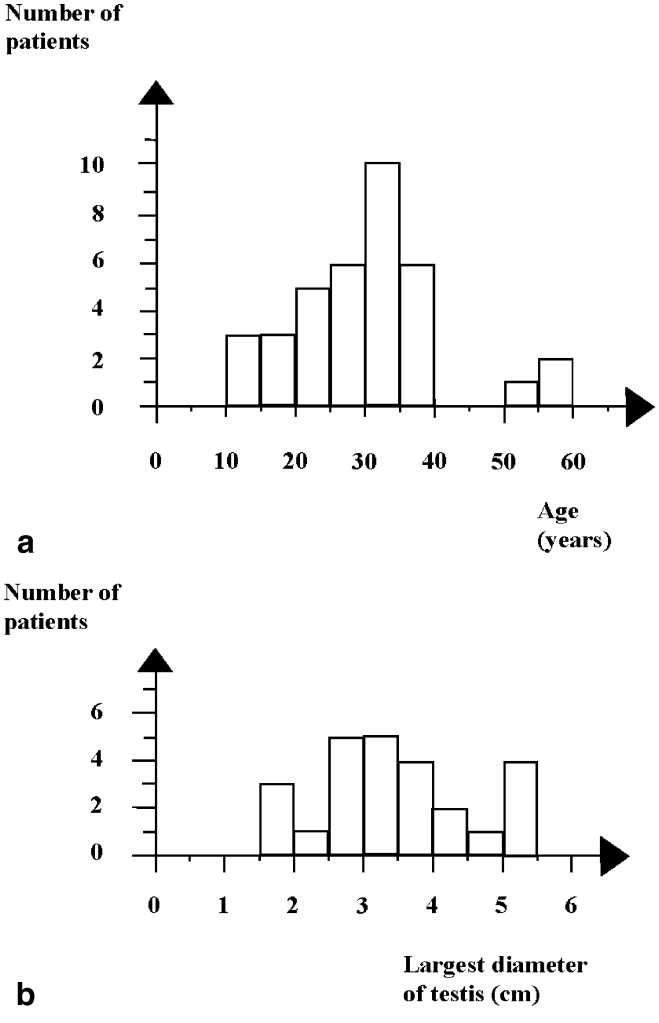


Fig. 4 Findings in previously reported patients with MGCT. Age at diagnosis (**a**), and size of largest diameter of the testis with MGCT (**b**). Smallest size for the largest diameter of the normal testis is 4 cm

presence of embryonal carcinoma for nonseminomas [81, 82, 177]. The two precursor stages, IGCN and MGCT, did not predict relapse for these patients [185].

Treatment

Patients with precursor lesions of the testis have localized disease, with few exceptions, and should be treated accordingly. Local treatment of patients with precursor lesions depends on the histologic findings (Fig. 2). IGCN is treated with radiotherapy of the testis to a total dose of 18 to 20 Gy delivered as nine to ten fractions of 2 Gy each (one fraction per day, 5 days per week) using 16 to 18 MeV electrons [23]. Radiotherapy is curative with few exceptions [35], whereas modern chemotherapy is less efficient [176]. High-voltage radiotherapy of the testis impairs the testosterone production only moderately [34, 122, 175].

Treatment of MGCT is sparsely documented. A few patients with MGCT were treated with orchiectomy and adjuvant radiotherapy [101, 180], but orchiectomy and follow-up with surveillance without adjuvant radiotherapy can be sufficient to secure long-term cure, provided that the patients adhere to a 5-year surveillance follow-up program [181, 185].

Treatment of GCTIS is not documented. If GCTIS is diagnosed without TGCT, adequate local treatment will be orchiectomy. It remains to be shown whether local irradiation of the testis can cure SIS without causing extensive damage of the normal testicular tissue.

After adequate local treatment, the follow-up for patients with precursor lesions of the testis is similar. Follow-up with surveillance is a safe and effective monitoring of the patients with precursor lesions according to the two DATECA studies of surveillance for patients with TGCT stage I (Fig. 1) [133, 177, 185].

Biological studies

Cytogenetics and genetics

IGCN is mainly hypertriploid to hypotetraploid [17, 29, 108, 115]. Two cytogenetic studies showed that IGCN adjacent to TGCT had an increased copy number of 12p material [172, 186], whereas studies of microdissected IGCN cells and investigations using comparative genomic hybridization showed a more complex, sometimes polyclonal, pattern [95, 99, 117, 118, 136, 163].

Studies using differential display polymerase chain reaction and microarrays showed that IGCN was associated with abnormal expression of genes and expressed sequence tags [3, 66, 156]. IGCN consistently expressed NANOG and POU5F1, alias OCT3/4, two transcription factors that were also expressed in the early blastocyst [3, 46, 156]. Microarray studies and a study of array comparative genomic hybridization described gene expressions associated with IGCN and TGCT [3, 100, 114, 132, 153, 156, 159, 193, 197]. These studies added valuable information to that of the previous genetic studies. One study gave information as to AP-2gamma as a biomarker of IGCN [67].

Progression from IGCN to MGCT and TGCT is associated with cytogenetic and genetic abnormalities [178]. A microspectrophotometric study of a testis with IGCN and MGCT showed that the malignant germ cells of MGCT had a higher DNA index than the neoplastic germ cells of IGCN [183]. TGCTs characteristically have an increased copy number of the short arm of chromosome 12, 12p, in part due to one, or more than one, isochromosome i (12p) [30, 31], and the increase may be associated with the extratubular invasion of malignant germ cells [97, 136]. MGCT has not been examined in studies using microarrays.

Seminoma and nonseminoma differ in abnormalities in cytogenetics compared with IGCN [29]. TGCT is associated with abnormal expressions of many genes [178]. Some abnormalities are associated with the stage of the localized TGCT, and other abnormalities are associated with differentiation into either seminoma or embryonal carcinoma [114]. TGCT may have mutations and polymorphisms of *KIT* that can contribute to the development of bilateral TGCT [85, 96, 139]. A few microarray studies described how IGCN and TGCT differ in gene expression [3, 153, 156].

Pathogenesis

Morphologic and genetic studies point to germ cells of the testis as the origin for TGCT. The tumor development in adult men reflects many histological and histochemical similarities between prepubertal prespermatogonia and cells of IGCN and MGCT [52, 73, 111, 127]. According to Gondos, neoplastic germ cells derive from prespermatogonia that remain after puberty, continue to proliferate and differentiate, and finally undergo malignant transformation [52]. Otherwise, Holstein argued that TGCT initiate from post-pubertal spermatogonia A that dedifferentiate as part of the malignant transformation and revert structurally and functionally to a fetal or pre-pubertal pattern of germ cells [69]. The neoplastic germ cells of IGCN have similarities in gene expression with gonocytes but not with spermatogonia [11, 74].

MGCT have caused two controversies. IGCN can progress through MGCT to seminoma in adult men [141], and correspondingly Mikulowski and Oldbring argued that MGCT is the first definitely malignant stage in the progression, and a starting point for differentiation into seminoma and non-seminoma [101]. Alternatively, Oosterhuis and coworkers argued that IGCN could be the starting point for the differentiation. According to this concept, IGCN differentiates intratubularly into GCTIS, either seminoma or non-seminoma, prior to the invasion into the extratubular tissue [116]. Perhaps both secondary precursor stages contribute to the development of TGCT (Fig. 1). Several criteria may be applied in judgement of the relevance of these precursor stages (Table 4). One study indicated that malignant germ cells emigrate passively out of the testicular tubules as consequence of an extensive

intratubular proliferation and accumulation of neoplastic germ cells [38]. Alternatively, the extratubular invasion of the malignant germ cells can be an active process.

Malignant cells break down extracellular matrix and move in the interstitial tissue as part of an active invasion. Several groups of proteins contribute to these processes, and the proteins have been studied in IGCN and TGCT. Cell adhesion molecules may inhibit movements of the cells. Among these proteins, cadherin type 1, E cadherin (epithelial) was not expressed in normal germ cells whereas 18% of seminomas and 62% of nonseminomas expressed the protein [59]. Catenin (cadherin-associated protein) alpha-1, 102 kDa, was not expressed in seminomas but was expressed in a quarter of nonseminomas [138]. Three quarters of seminomas and non-seminomas expressed catenin (cadherin-associated protein) beta-1, 88 kDa. The Ig supergene family of the cell adhesion molecules might also be involved in the invasion of malignant germ cells. However, seven of ten seminomas expressed low levels of intercellular adhesion molecule-1 (CD54), human rhinovirus receptor, and the expression was not associated with clinical aspects [170]. In addition, integrins may contribute to the invasiveness of the malignant cells. Integrin alpha 3 was expressed in IGCN, but not in seminoma [169]. Integrin alpha 5 (fibronectin receptor, alpha polypeptide) was not found in IGCN [159], whereas embryonal carcinoma cells expressed integrin alpha V (vitronectin receptor alpha polypeptide, CD 51) [121]. Another cell adhesion molecule, trophinin, was expressed in TGCT, and the stage correlated with the expression of the protein [58].

Proteinases that destroy basement membranes and extracellular matrix contribute to the invasion of malignant cells. Matrix metalloproteinases (zinc-dependent endopeptidases, MMPs) may interact with tissue inhibitors of matrix metalloproteinases (TIMPs) and cleave type IV collagen, the predominant protein of the basement membranes. MMP-14 forms a complex with TIMP-2 and MMP-2, and the complex activates MMP-14 and stimulates the enzymatic activity of MMP-2. Activated MMP-2 and MMP-9 cleave type IV collagen, elastin, and laminin-1.

A microarray study of seminomas showed that MMP-9 was up-regulated, and MMP-19 and TIMP-2 were down-regulated [114]. In a tumor xenograft model, MMP-2, MMP-16, vascular endothelial growth factor, VEGF, and plasminogen activator inhibitor-2 (PAI-2) were associated with development of seminoma metastases in lymph nodes [88]. Retinoic acid can induce embryonal carcinoma cells to differentiate into teratoma, and the differentiation was associated with an increased expression of MMP-2 while the expression of TIMP-1 and TIMP-2 remained unchanged [168]. Analyses of data from a recent oligo DNA microarray study allowed a comparison of the gene expression in normal germ cells, IGCN, seminoma, embryonal carcinoma, choriocarcinoma, yolk sac tumor, and teratoma [156]. The expression levels of invasion-related genes differed significantly between the various histological subgroups of TGCT (Fig. 5 and Table 5). Compared with normal germ cells, TIMP2 was down-regulated in TGCT apart from teratoma (median expression levels relative to that in normal testes 0.60, range 0.19 to 1.2 versus 0.97, range 0.81 to 1.01, P=0.018, Fisher's exact test). TIMP2 was up-regulated in teratoma compared with other testicular germ cell neoplasia (median 1.28, range 0.70–2.71, versus median 0.53, range 0.19–1.2, P=0.004, Fisher's exact test). TIMP3 was up-regulated in IGCN, yolk sac tumor, choriocarcinoma and teratoma compared with normal germ cells (median 1.80, range 0.63–15.1 versus 1.00,

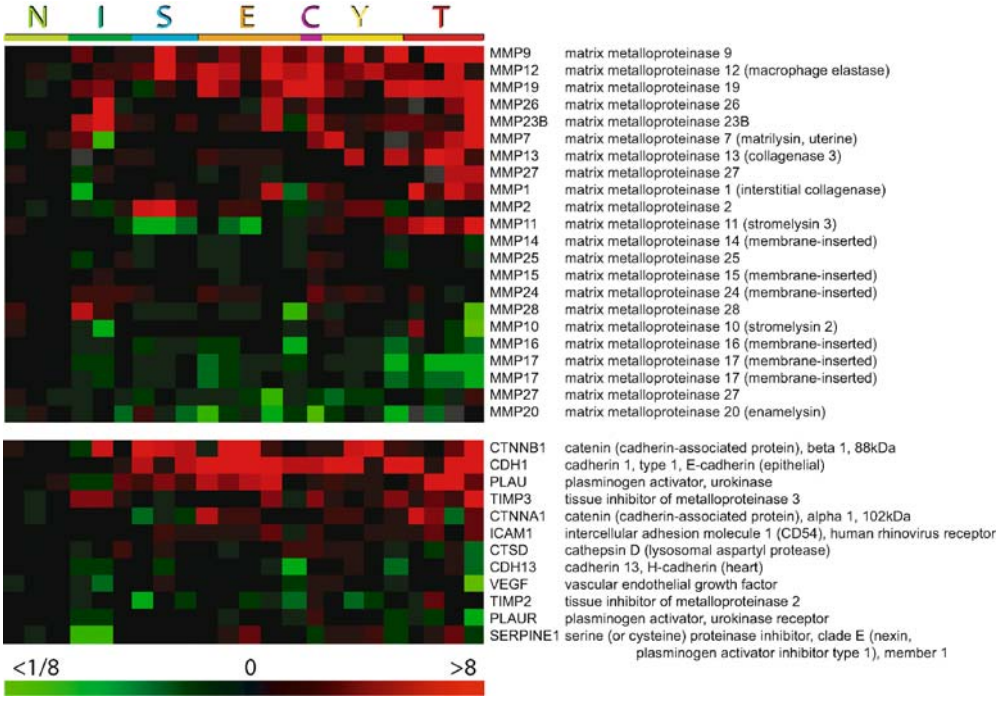


Fig. 5 Gene transcript levels of MMPs, TIMPs, and other genes encoding invasion relevant products from a recent microarray study [156]. *N* denotes normal testis, *I* IGCN, *S* seminoma, *E* embryonic carcinoma, *C* choriocarcinoma, *Y* yolk sac tumor, and *T* teratoma. Approved gene symbols and names are used

Table 5 Matrix metalloproteinases and plasminogen activator, urokinase in 1GCN and histological subgroups of TGCT

Gene symbol	Expression level of gene for histologic subgroups							*P*-value
	IGCN (*n*=3)	TGCT (*n*=17)	IGCN and NS (*n*=17)	S (*n*=3)	NS (*n*=14)	IGCN and non-Ter (*n*=16)	Ter (*n*=4)	
MMP9	1.31 (0.87–2.23)	2.58 (1.08–8.23)	-	-	-	-	-	0.046
MMP12	1.64 (1.08–1.64)	3.22 (1.09–24.52)	-	-	-	-	-	0.014
PLAU	0.63 (0.52–2.66)	1.87 (0.96–7.35)	-	-	-	-	-	0.016
SERPINE1	0.16 (0.146–0.96)	1.32 (0.37–2.78)	-	-	-	-	-	0.16
MMP2	-	-	1.07 (0.51–2.10)	4.77 (2.03–5.17)	-	-	-	0.009
MMP19	-	-	3.16 (1.23–43.99)	0.85 (0.6–1.88)	-	-	-	0.029
MMP11	-	-	-	0.38 (0.35–0.50)	1.32 (0.38–13.99)	-	-	0.014
	-	-	-			0.90 (0.35–2.01)	4.3 (2.11–13.99)	<0.0005
MMP7						1.04 (0.29–4.8)	2.61 (1.55–27.69)	0.006
MMP17	-	-	-		-	0.67 (0.38–1.05)	0.36 (0.33–0.53)	0.007

The findings derive from a recent microarray study [156]. Each row compares gene expression in two histological groups of testicular germ cell neoplasia (e.g. IGCN versus TGCT) using Fisher's exact test, without correction for multiple testing. The values indicate the genes' RNA levels relative to the median level among the normal testes samples. *S* denotes seminoma, *NS* non-seminomam, *Ter* teratoma, and *non-Ter* TGCT apart from teratoma. Approved gene symbols are used

range 0.55–1.01, *P*=0.009, Fisher's exact test). TIMP3 was also up-regulated in testicular germ cell neoplasia apart from seminoma and embryonal carcinoma compared with seminoma and embryonal carcinoma (median 3.0, range 0.64–15.1 versus 0.86, range 0.53–4.0, *P*=0.001, Fisher's exact test). Most histologic types of TGCT had a distinct pattern of expression of the MMPs, as shown in Fig. 6.

Serine proteinases form another group that can contribute to the invasiveness of malignant germ cells. The active form for plasminogen activator, urokinase, PLAU, can modify plasminogen into plasmin that activates MMPs. *PLAU* was up-regulated in TGCT compared with IGCN, while the plasminogen activator, urokinase receptor, *PLAUR*, did not change similarly. Expression of serine proteinase inhibitor, clade E, member 1 (SERINE1, alias plasminogen activator inhibitor-1, PAI-1), was downregulated in IGCN but not in TGCT (Figs. 5 and 6). Thus the proteinase may have a role in the migration of malignant germ cells (Fig. 5). Another serine protease, testitin, was shown in IGCN but not in TGCT [75]. A third group of proteinases is cysteine proteinases. Of these, cathepsin D has been demonstrated in IGCN and was up-regulated in MGCT [59].

Inducers of angiogenesis also facilitate the growth of invasive malignant germ cells. Vascular endothelial growth factor (VEGF) was up-regulated in TGCT, and the up-regulation was associated with presence of microvessels [45, 88, 89, 173]. Also the protooncogene v-ets avian erythroblastosis virus E26 oncogene like, ETS1, differed significantly between metastatic and non-metastatic TGCT [2]. Abnormalities in angiogenetic factors may be useful for the treatment of TGCT. An experimental study showed that angiostatic factors like thrombospondin or endostatin, and low dose carboplatin acted synergistically to inhibit a nonseminoma from developing metastases [1].

According to cytogenetic studies, IGCN may develop into embryonal carcinoma through a cytogenetic seminoma-like stage [30, 31]. It is likely that the morphologic equivalent to this stage in the tumor development is MGCT whereas it is unlikely that the morphologic equivalent is ECIS. The precursor lesions of TGCT progress through a seminomatous and a non-seminomatous line [44]. In the non-seminomatous line, embryonal carcinoma may be an intermediate step in the development of teratoma, yolk sac tumor, and choriocarcinoma [44, 113]. Gene abnormalities shared by seminoma and nonseminoma, but not found in precursor lesions, can be associated with invasion, whereas other gene abnormalities specific for either seminoma or embryonal carcinoma can be associated with differentiation of TGCT [63, 156, 162, 164, 178]. The genes DPPA3, DPPA4, GDF3, and POU5F1 contribute to the pluripotency of embryonal carcinoma cells [3, 9, 16, 156]. External stimuli may induce embryonal carcinoma to differentiate into teratoma, and the stimuli may be mediated by signal

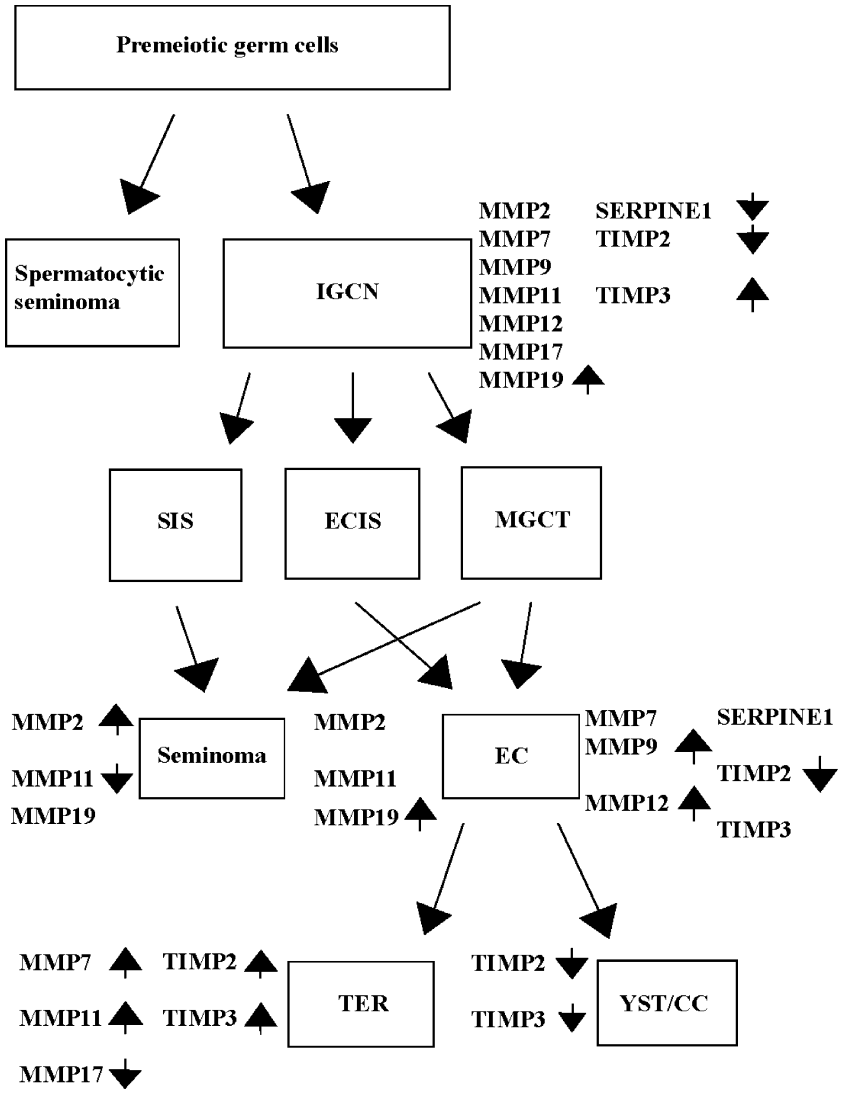


Fig. 6 Significant MMPs and TIMPs in relation to a model for development of TGCT. Abbreviations for histology as in Fig. 1, and use of approved gene symbols. The arrows besides the gene symbol denote a significant change in regulation of the biologic analytes, either up-regulation or down-regulation. Absence of an arrow besides a gene symbol indicates that the gene had no significant deviation in expression from normal testicular tissue. Gene symbols to the right of the boxes indicate gene abnormalities associated with stage of the germ cell neoplasia, and gene symbols to the left of the boxes indicate genes related to differentiation

transduction through the wingless–type MMTV integration site family, WNT, and NOTCH pathways [187, 193].

The concomitantly presence of primary and secondary precursor lesions and TGCT in a testis supports that these lesions are closely related in the tumor development. Such testes provide a platform for new studies that may evaluate the gene abnormalities associated with tumor invasion and with tumor differentiation.

Perspectives

We recommend a strict definition of MGCT and use of a single term for MGCT. If men with high-risk of testicular malignancy are adequately examined, testicular germ cell neoplasia can be detected while it is in a precursor stage such as IGCN, MGCT, or GCTIS. TGCT is associated with up-regulated MMP-9 and PLAU genes compared with IGCN. The up-regulated genes may facilitate the invasion process, and the details in the up-regulation should be studied further in relation to the development of TGCT. It remains to be shown whether the upregulation is associated with the transition from IGCN to MGCT. The abnormalities may also inspire to new forms for treatment of TGCT.

Detection of precursor lesions in the testis has implications for the management of men with high-risk for TGCT. Screening for precursor lesions should be undertaken in two steps where ultrasonography of the testes is followed by a testicular biopsy for men with findings associated with germ cell neoplasia. Local treatment for IGCN is high-voltage irradiation of the affected testis, whereas it is orchiectomy for MGCT and GCTIS. Patients with precursor lesions should be followed-up with surveillance. Thus, it is advantageous to detect precursor stages of testicular germ cell neoplasia because patients with these lesions can be cured with a less extensive and toxic treatment than that used for most TGCT. Urologists, radiologists, pathologists, and oncologists should be aware of the precursor lesions of TGCT so that they can provide an adequate counselling and management for men in whom the lesions are suspected or diagnosed.

Acknowledgements The authors thank consultant Peter Ottosen, Department of Pathology, Aarhus University Hospital, for the histologic figures.

References

1. Abraham D, Abri S, Hofmann M, Holtl W, Aharinejad S (2003) Low dose carboplatin combined with angiostatic agents prevents metastasis in human testicular germ cell tumor xenografts. J Urol 170:1388–1393
2. Adam M, Schmidt D, Wardelmann E, Wernert N, Albers P (2003) Angiogenetic protooncogene ets-1 induced neovascularization is involved in the metastatic process of testicular germ cell tumors. Eur Urol 44:329–336
3. Almstrup K, Hoei-Hansen CE, Wirkner U, Blake J, Schwager C, Ansorge W, Nielsen JE, Skakkebaek NE, Rajpert-De Meyts E, Leffers H (2004) Embryonic stem cell-like features of testicular carcinoma in situ revealed by genome-wide gene expression profiling. Cancer Res 64:4736–4743
4. Asif S, Uehling DT (1968) Microscopic tumor foci in testis. J Urol 99:776–779
5. Aubry F, Satie AP, Rioux-Leclercq N, Rajpert-De Meyts E, Spagnoli GC, Chomez P, De Backe O, Jegou B, Samson M (2001) MAGE-A4, a germ cell specific marker, is expressed differentially in testicular tumors. Cancer 92:2778–2785
6. Azzopardi JG, Mostofi FK, Theiss EA (1961) Lesions of testes observed in certain patients with widespread choriocarcinoma and related tumors. The significance and genesis of hematoxylin-staining bodies in the human testis. Am J Pathol 38:207–225
7. Bach AM, Hann LE, Shi W, Giess CS, Yoo HH, Sheinfeld J, Thaler HT (2003) Is there an increased incidence of contralateral testicular cancer in patients with intratesticular microlithiasis? Am J Roentgenol 180:497–500
8. Bailey D, Marks A, Stratis M, Baumal R (1991) Immunohistochemical staining of germ cell tumors and intratubular malignant germ cells of the testis using antibody to placental alkaline phosphatase and a monoclonal anti-seminoma antibody. Mod Path 4:167–171
9. Baldassarre G, Romano A, Armenante F, Rambaldi M, Paoletti I, Sandomenico C, Pepe S, Staibano S, Salvatore G, De Rosa G, Persico MG, Viglietto G (1997) Expression of teratocarcinoma-derived growth factor-1 (TDGF-1) in testis germ cell tumors and its effect on growth and differentiation of embryonal carcinoma cell line NTERA-2/D1. Oncogene 15:927–936
10. Balslev E, Francis D, Jacobsen GK (1990) Testicular germ cell tumours. Classification based on fine needle aspiration biopsy. Acta Cytol 34:690–694
11. Bartkova J, Rajpert-De Meyts E, Skakkebaek NE, Lukas J, Bartek J (2003) Deregulation of the G1/S-phase control in human testicular germ cell tumours. Acta Pathol Microbiol Immunol Scand 111:252–266
12. Berney DM, Lee A, Randle SJ, Jordan S, Shamash J, Oliver RT (2004) The frequency of intratubular embryonal carcinoma: implications for the pathogenesis of germ cell tumours. Histopathology 45:155–161
13. Berthelsen JG, Skakkebaek NE (1981) Distribution of carcinoma-in-situ in testes from infertile men. Int J Androl Suppl 4: 172–183
14. Bettocchi C, Coker CB, Deacon J, Parkinson C, Pryor JP (1994) A review of testicular intratubular germ cell neoplasia in infertile men. J Androl 15(Suppl):14S–16S
15. Bols B, Jensen E, Jensen A, Braendstrup O (2000) Immunopathology of in situ seminoma. Int J Exp Pathol 81:211–217
16. Bowles J, Teasdale RP, James K, Koopman P (2003) Dppa3 is a marker of pluripotency and has a human homologue that is expressed in germ cell tumours. Cytogenet Genome Res 101:261–265
17. Brackenbury ET, Hagreave TB, Howard GW, McIntyre MA (1993) Seminal fluid analysis and fine-needle aspiration cytology in the diagnosis of carcinoma in situ of the testis. Eur Urol 23:123–128
18. Browne F, Jeffers M, McDermott T, Grainger R, Mulvins D, Gibney RG,Torreggiani WC (2003) Technical report. Intraoperative ultrasound-guided needle localization for impalpable testicular lesions. Clin Radiol 68:566–569
19. Bruun E, Frimodt-Moller C, Giwercman A, Lenz S, Skakkebaek NE (1987) Testicular biopsy as an outpatient procedure in screening for carcinoma-in-situ; complications and patient's acceptance. Int J Androl 10:199–202
20. Bunge G, Bradbury JT (1965) An early seminoma. JAMA 193:960–962
21. Burke AP, Mostofi FK (1988) Placental alkaline phosphatase immunohistochemistry of intratubular malignant germ cells and associated testicular germ cell tumors. Hum Pathol 19:663–670
22. Byrialsen A, von Eyben FE, Kristiansen K (1998) Carcinoma in situ of the testis and seminoma express a high protein level of lactate dehydrogenase subunit B but no subunit C. J Tumor Marker Oncol 13:79–86
23. Classen J, Dieckmann KP, Loy V, Banberg M (1998) Testicular intraepithelial neoplasms (TIN). An indication for radiotherapy? Strahlenther Onkol 174:173–177
24. Conte A, Tremps E, Conejero J, Ruiz Marcellan FJ, Villanueva I (1980) Microinvasive seminoma in a cryptorchid testis. An incidental finding. Actas Urol Esp 4:163–166
25. Cortes D, Thorup JM, Visfelt J (2001) Cryptorchidism: aspects of fertility and neoplasm. A study including data of 1,335 consecutive boys who underwent testicular biopsy simultaneously with surgery for cryptorchidism. Horm Res 55:21–27
26. Datta MW, Maori E, Signoretti S, Renshaw AA, Loda M (2001) Transition from in situ to invasive testicular germ cell neoplasia is associated with loss of p21 and gain of mdm-2 expression. Mod Pathol 14:437442
27. Daugaard G, von der Maase H, Olsen J, Rorth M, Skakkebaek NE (1987) Carcinoma-in-situ testis in patients with assumed extragonadal germ-cell tumors. Lancet 2:528–530
28. de Gouveia Brazao CA, Pierik FH, Oosterhuis JW, Dohle GR, Looijenga LH, Weber RF (2004) Bilateral testicular microlithiasis predicts the presence of the precursor of testicular germ cell tumors in subfertile men. J Urol 171:158–160
29. de Graaff WE, Oosterhuis JW, de Jong B, Dam A, van Putten WL, Castedo SM, Sleijfer DT, Schraffordt Koops H (1992) Ploidy of testicular carcinoma in situ. Lab Invest 66:166–168
30. de Jong B, Oosterhuis JW, Castedo SM, Vos A, te Meerman GJ (1990) Pathogenesis of adult testicular germ cell tumors. A cytogenetic model. Cancer Genet Cytogenet 48:1434–1467
31. de Jong B, van Echten J, Looijenga LH, Geurt van Kessel A, Oosterhuis JW (1997) Cytogenetics of the progression of adult testicular germ cell tumors. Cancer Genet Cytogenet 95:88–95
32. Dieckmann KP, Loy V (1998) The value of the biopsy of the contralateral testis in patients with germ cell cancer: the recent German experience. APMIS 106:13–20
33. Dieckmann KP, Souchon R, Hahn E, Loy V (1999) False-negative biopsies for testicular intraepithelial neoplasia. J Urol 162:364–368
34. Dieckmann KP, Classen J, Souchon R, Loy V (2001) Management of intraepithelial neoplasia–a review based on evidence-based medicine. Wiener Klin Wochenschr 113:7–14
35. Dieckmann KP, Lauke H, Michl U, Winter E, Loy V (2002) Testicular germ cell cancer despite previous local radiotherapy to the testis. Eur Urol 41:643–650
36. Dieckmann KP, Classen J, Loy V (2003) Diagnosis and management of testicular intraepithelial neoplasia (carcinoma in situ)–surgical aspects. APMIS 111:64–69
37. Dieckmann KP, Pichlmeier U (2004) Clinical epidemiology of testicular germ cell tumors. World J Urol 22:2–14
38. Donner J, Kliesch S, Brehm R, Bergmann M (2004) From carcinoma in situ to testicular germ cell tumour. APMIS 112: 79–88

39. Dorman S, Trainer TD, Lefke D, Leadbetter G (1979) Incipient germ cell tumor in a cryptorchid testis. Cancer 44:1357–1362
40. Eble JN, Sauter G, Epstein JI, Sesterhenn IA (2004) WHO classification of tumours. Pathology and genetics of tumours of the urinary system and male genital organs. IARC, Lyon
41. Engeler DS, Hosli PO, John H, Bannwart E, Sulser T, Amin MR, Heitz PU, Hailemariam S (2000) Early orchipexy: prepubertal intratubular germ cell neoplasia and fertility outcome. Urology 56:144–148
42. Ferry JA, Harris NL, Young RH, Coen J, Zietman A, Scully RE (1994) Malignant lymphoma of the testis, epididymis, and spermatic cord. A clinicopathologic study of 69 cases with immunophenotypic analysis. Am J Surg Pathol 18:376–390
43. Fossa SD, Aass N, Heilo A, Daugaaard G, Skakkebaek NE, Stenwig AE, Nesland JM, Looijenga LH, Oosterhuis JW (2003) Testicular carcinoma in situ in patients with extragonadal germ-cell tumours: the clinical role of pretreatment biopsy. Ann Oncol 14:1412–1418
44. Friedman NB (1951) The comparative morphogenesis of extragenital and gonadal teratoid tumors. Cancer 4:265–276
45. Fukuda S, Shirahama S, Imazono Y, Tsushima T, Ohmori H, Kayajima T, Take S, Nishiyama K, Yonezawa S, Akiba S, Akiyama S, Ohi Y (1999) Expression of vascular endothelial growth factor in patients with testicular germ cell tumors as an indicator of metastatic disease. Cancer 85:1323–1330
46. Gidekel S, Pizov G, Bergman Y, Pikarsky E (2003) Oct 3/4 is a dose-dependent oncogene fate determinant. Cancer Cell 4:361–370
47. Giwercman A, Marks A, Bailey D, Baumal R, Skakkebaek NE (1988) A monoclonal antibody as a marker for carcinoma in situ germ cells of the human adult testis. Acta Pathol Microbiol Immunol Scand 96:667–670
48. Giwercman A, Bruun E, Frimodt-Moller C, Skakkebaek NE (1989) Prevalence of carcinoma-in-situ and other histopathologic abnormalities in testes of men with a history of cryptorchidism. J Urol 99:998–1002
49. Giwercman A, Lindenberg S, Kimber SJ, Andersson T, Muller J, Skakkebaek NE (1990) Monoclonal antibody 43-9F as a sensitive immunohistochemical marker of carcinoma in situ of human testis. Cancer 65:1135–1142
50. Giwercman A, Muller J, Skakkebaek NE (1991) Prevalence of carcinoma in situ and other histopathological abnormalities in testes from 399 men who died suddenly and unexpectedly. J Urol 145:77–80
51. Giwercman A, Skakkebaek NE (1991) Carcinoma-in-situ (gonocytoma-in-situ) of the testis. In: Burger H, De Kretser D (eds) The testis. Raven Press, New York, pp 475–491
52. Gondos B (1993) Ultrastructure of developing and malignant germ cells. Eur Urol 23:66–75
53. Gondos B, Migliozzi JA (1987) Intratubular germ cell neoplasia. Semin Diagn Pathol 4:292–303
54. Gronvall S, Brunner N, Jacobsen GK, Holm HH (1980) Ultrasound in the detection of testicular tumours. Int J Androl Suppl 4:185–190
55. Guinand S, Hedinger C (1981) Atypical intratubular germ cells and testicular germ cell tumors in children. Ann Pathol 1:251–257
56. Harland SJ, Cook PA, Fossa SD, Horwich A, Parkinson MC, Roberts JT, Stenning SP (1993) Risk factors for carcinoma in situ of the contralateral testis in patients with testicular cancer. An interim report. Eur Urol 23:115–118
57. Harland SJ, Cook PA, Fossa SD, Horwich A, Mead GM, Parkinson MC, Roberts JT, Stenning SP (1998) Intratubular germ cell neoplasia of the contralateral testis in testicular cancer: defining a high risk group. J Urol 160:1353–1357
58. Hatakeyama S, Ohyama C, Minagawa S, Inoue T, Kakinuma H, Kyan A, Arai Y, Suga T, Nakyama J, Kato T, Habuchi T, Fukuda MN (2004) Functional correlation of trophinin expression with the malignancy of testicular germ cell tumor. Cancer Res 64:4257–4262
59. Heidenreich A, Sesterhenn IA, Mostofi FK, Moul JW (1998) Prognostic factors that identify patients with clinical stage I non-seminomatous germ cell tumors at low and high risk for metastasis. Cancer 83:1002–1011
60. Heidenreich A, Sesterhenn IA, Mostofi FK, Moul JW, Engelmann (1999) Histopathological and biological prognostic factors of clinical stage I non-seminomatous germ cell tumors. Implications for risk adjusted therapy. Urologe A 38:168–178
61. Henley JD, Young RH, Wade CL, Ulbright TM (2004) Seminoma with exclusive intertubular growth. A report of 12 clinically and grossly inconspicuous tumors. Am J Surg Pathol 28:1163–1168
62. Hindley RG, Chandra A, Saunders A, O'Brien TS (2003) Impalpable testis cancer. BJU Int 92:572–574
63. Hirai K, Sasaki H, Sakamoto H, Takeshita F, Asano K, Kubota Y, Ochiya T, Terada M (2003) Antisense oligodeoxynucleotide against HST-1/FGF-4 suppresses tumorigenesis of an orthotopic model for human germ cell tumor in nude mice. J Gene Med 5:951–957
64. Hiraoka N, Yamada T, Abe H, Hata J (1997) Establishment of three monoclonal antibodies specific for prespermatogonia and intratubular malignant germ cells in humans. Lab Invest 76: 427–438
65. Hittmair A, Rogatsch H, Hobish A, Mihnz G, Feichfinger H (1996) CD30 expression in seminoma. Hum Pathol 27:1166–1171
66. Hoei-Hansen CE, Nielsen JE, Almstrup K, Hansen MA, Skakkebaek NE, Rajpert-De Meyts E, Leffers H (2004) Identification of genes differentially expressed in testes containing carcinoma in situ. Mol Hum Reprod 10:423–431
67. Hoei-Hansen CE, Nielsen JE, Almtrup K, Sonne SB, Graem N, Skakkebaek NE, Leffers H, Rajpert-De Meyts E (2004) Transcription factor AP-2gamma is a developmentally regulated marker of testicular carcinoma in situ and germ cell tumors. Clin Cancer Res 10:8521–8530
68. Holm M, Hoei-Hansen CE, Rajpert-De Meyts E, Skakkebaek NE (2003) Increased risk of carcinoma in situ in patients with testicular germ cell cancer with ultrasonic microlithiasis in the contralateral testicle. J Urol 170:1163–1167
69. Holstein AF (1993) Cellular components of early testicular cancer. Eur Urol 23(Suppl 2):9–18
70. Holstein AF, Korner F (1974) Light and electron microscopical analysis of cell types in human seminoma. Virchows Arch A Pathol Anat Histopathol 363:97–112
71. Holstein AF, Roosen-Runge EC, Schirren C (1988) Illustrated pathology of human spermatogenesis. Grosse Verlag, Berlin
72. Holstein AF, Schutte B, Becker H, Hartmann M (1987) Morphology of normal testis and malignant germ cells. Int J Androl 10:1–18
73. Honecker F, Kersemaeker A-M, Molier M, van Weeren PC, Stoop H, Jkrijger RR, Woplffenbuttel KP, Oosterhuis JW, Bokemeyer C, Looijenga LH (2004) Involvement of E-cadherin and beta-catenin in germ cell tumours and in normal fetal germ cell development. J Pathol 204:167–174
74. Honecker F, Stoop H, de Krijger RR, Chris Lau YF, Bokemeyer C, Looijenga LH (2004) Pathobiological implications of the expression of markers of testicular carcinoma in situ by fetal germ cells. J Pathol 203:849–857
75. Hooper JD, Nicol DL, Dickinson JL, Eyre HJ, Scarman AL, Normyle JF, Stuttgen MA, Douglas ML, Loveland KA, Sutherland GR, Antalis TM (1999) Testitin, a new human serine protease expressed by premeiotic testicular germ cells and lost in testicular germ cell tumors. Cancer Res 59:3199–3205
76. Howard GC, Hargreave TR, McIntyre (1989) Carcinoma in situ of the testis diagnosed on semen cytology. Clin Radiol 40:323–324
77. Jacobsen GK, Jacobsen M, Clausen PF (1980) Ferritin as a possible marker protein of carcinoma in situ of the testis. Lancet 2:533–534
78. Jacobsen GK, Henriksen OB, von der Maase H (1981) Carcinoma in situ of testicular tissue adjacent to malignant germ-cell tumors: a study of 105 cases. Cancer 47:2660–2662

79. Jacobsen GK, Norgaard-Pedersen B (1984) Placental alkaline phosphatase in testicular germ cell tumours and in carcinoma-in-situ of the testis: an immunohistochemical study. Acta Pathol Microbiol Immunol Scand A 92:323–329
80. Jacobsen GK, Talerman A (1989) Atlas of germ cell tumours. Munksgaard, Copenhagen
81. Jacobsen GK, Rorth M, Osterlind K, von der Maase H, Jacobsen A, Madsen EL, Schultz H (1990) Histopathological features in stage I non-seminomatous testicular germ cell tumours correlated to relapse. Danish Testicular Cancer Study Group. Acta Pathol Microbiol Immunol Scand 98:377–382
82. Jacobsen GK, von der Maase H, Specht L, Jakobsen A, Madsen EL, Pedersen M, Rorth M, Schultz H (1995) Histopathological features in stage I seminoma treated with orchidectomy only. J Urol Pathol 3:85–394
83. Janssen M, Johnston WH (1978) Anaplastic seminoma of the testis: ultrastructural analysis of three cases. Cancer 41:538–544
84. Kaijser M, Akre O, Cnattinguis S, Ekbom A (2003) Maternal lung cancer and testicular cancer risk in the offspring. Cancer Epidemiol Biomark Prev 12:643–646
85. Kemmer K, Corless CL, Fletcher JA, McGreevey L, Haley A, Griffith D, Cummings W, Wait C, Town A, Heinrich NC (2004) KIT mutations are common in testicular seminomas. Am J Pathol 164:305–313
86. Kliesch S, Thomaidis T, Schutte B, Pusche G, Kater B, Roth S, Bergmann M (2003) Update on the diagnostic safety for detection of testicular intraepithelial neoplasia (TIN). APMIS 111:70–75
87. Koide O, Iwai S, Baba K, Iri H (1987) Identification of testicular atypical germ cells by an immunohistochemical technique for placental alkaline phosphatase. Cancer 60:1325–1330
88. Konaka H, Koshida K, Endo Y, Uchibayashi T, Sasaki T, Namiki M (1999) A human seminoma xenograft model with regional lymph node metastasis. J Urol 161:342–348
89. Koshida K, Konaka H, Kato H, Miyagi T, Egawa M, Uchibayashi T Namiki M (2000) Correlation between expression of metastasis-related genes and lymph node metastasis in testicular cancer. Hinyokika Kiyo 46:775–781
90. Krabbe S, Skakkebaek NE, Berthelsen JG, Eyben FV, Volsted P, Mauritzen K, Eldrup J, Nielsen AH (1979) High incidence of undetected neoplasia in maldescended testes. Lancet 1:999–1000
91. Langhans T (1887) Carcinoma testis. In: Kocher T (ed) Disorders of the male genital organs. Enke Verlag, Stuttgart, pp 438–492
92. Lenz S, Skakkebaek NE, Hertel NT (1996) Abnormal ultrasonic pattern in contralateral testes in patients with unilateral testicular cancer. World J Urol 14(Suppl):S55–S58
93. Leroy (2002) CD30 and CD117 (ckit) used in combination are useful for distinguishing embryonal carcinoma and seminoma. J Histochem Cytochem 50:283–285
94. Levin HS (1984) Malignant intratubular and interstitial germ-cell neoplasia in bilaterally cryptorchid testes. Clevel Clin Q 51:387–394
95. Looijenga LH, Rosenberg C, van Gurp RJ, Geelen E, van Echten-Arends J, de Jong B, Mostert M, Oosterhuis JW (2000) Comparative genomic hybridization of microdissection samples from different stages in the development of a seminoma and a non-seminoma. J Pathol 191:187–192
96. Looijenga LH, de Leeuw H, van Oorschot M, van Gurp RJ, Stoop H, Gillis AJ, De Gouveia Brazao CA, Weber RF, Kirkels W, van Dijk T, von Lindern M, Valk P, Lajos G, Olah E, Nesland JM, Fossa SD, Oosterhuis JW (2003) Stem cell factor receptor (c-KIT) codon 816 mutations predict development of bilateral testicular germ-cell tumors. Cancer Res 63:7674–7678
97. Looijenga LH, Zafarana G, Grygalewicz B, Summersgill B, Debiec-Rychter M, Veltman J, Schoemakers EF, Rodriguez S, Jafer O, Clark J, van Kessel AG, Shipley J, van Gurp RJ, Gillis AJ, Oosterhuis JW (2003) Role of gain of 12p in germ cell tumour development. APMIS 111:161–173
98. Manivel JC, Jessurun J, Wick MR, Dehar LP (1987) Placental alkaline phosphatase immunoreactivity in testicular germ-cell neoplasms. Am J Surg Pathol 11:21–29
99. Mark GJ, Hedinger C (1965) Changes in the remaining tumor-free testicular tissue in cases of seminoma and teratoma. Virchows Arch Pathol Anat Physiol Klin Med 340:84–92
100. McIntyre A, Summersgill B, Jafer O, Rodriguez S, Zafrana G, Oosterhuis JW, Gillis AJ, Looijenga L, Cooper C, Huddart R (2004) Defining minimum genomic regions of imbalance involved in testicular cell tumors of adolescents and adults through genomic wide microarray analysis of cDNA clones. Oncogene 223:9142–9147
101. Mikulowski P, Oldbring J (1992) Microinvasive germ cell neoplasia of the testis. Cancer 70:659–664
102. Moller H (1997) Work in agriculture, childhood residence, nitrate exposure, and testicular cancer risk. A case control study in Denmark. Cancer Epidemiol Biomark Prev 6:141–144
103. Moller H, Skakkebaek NE (1996) Risk of testicular cancer and cryptorchidism in relation to socio-economic status and related factors: case-control studies in Denmark. Int J Cancer 66:287–293
104. Mortensen J, Krarup NB, Rasmussen A, Sogaard H (1983) Malignant degeneration in cryptorchid testes. A report of two cases. Andrologia 15:709–712
105. Mostofi FK, Price EB (1973) Tumors of the male genital system. Armed Forces Institute of Pathology, Washington
106. Mostofi FK, Sesterhenn IA, for the World Health Organisation (1998) International classification of tumours. Histological typing of testis tumours, 2nd edn. Springer, Berlin Heidelberg New York
107. Muffly KE, McWhorter CA, Bartone FF, Gardner PJ (1984) The absence of premalignant changes in the cryptorchid testis before adulthood. J Urol 131:523–525
108. Muller J, Skakkebaek NE (1981) Microspectrophotometric DNA measurements of carcinoma-in-situ germ cells in the testis. Int J Androl 4(Suppl):211–221
109. Muller J, Skakkebaek NE, Nielsen OH, Graem N (1984) Cryptorchidism and testis cancer. Atypical infantile germ cells followed by carcinoma in situ and invasive carcinoma in adulthood. Cancer 54:629–634
110. Mumperow E, Lauke H, Holstein AF, Hartmann M (1992) Further practical experiences in the recognition and management of carcinoma in situ of the testis. Urol Int 48:162–166
111. Nielsen H, Nielsen M, Skakkebaek NE (1974) The fine structure of a possible carcinoma-in-situ of the seminiferous tubules in the testis of four infertile men. Acta Pathol Microbiol Scand A 82:235–248
112. Nistal M, Codesal J, Paniagua R (1989) Carcinoma in situ of the testis in infertile men. A histological, immunocytochemical, and cytophotometric study of DNA content. J Pathol 159:205–210
113. Nuesch-Backmann I, Hedinger C (1977) Atypical spermatogonia as precursor to cancer. Schweiz Med Wochenschr 107:795–801
114. Okada K, Katgiri T, Tsunoda T, Mizutani Y, Suzuki Y, Kamada M, Fujioka T, Shuin T, Man T, Nakamura Y (2003) Analysis of gene-expression profiles in testicular seminomas using a genome-wide cDNA microarray. Int J Oncol 23:1615–1635
115. Oosterhuis JW, Looijenga LH (1993) The biology of human germ cell tumours: retrospective speculations and new prospectives. Eur Urol 23:16–22
116. Oosterhuis JW, Kersemaekers AM, Jacobsen GK, Timmer A, Steyerberg EW, Molier M, van Weeren PC, Stoop H, Looijenga LH (2003) Morphology of testicular parenchyma adjacent to germ cell tumours. An interim report. APMIS 111: 32–42
117. Ottesen AM, Larsen J, Gerdes T, Larsen JK, Lundsteen C, Skakkebaek NE, Rajpert-De Meyts E (2004) Cytogenetic investigation of testicular carcinoma in situ and early seminoma by high-resolution comparative genomic hybridization analysis of subpopulations flow sorted according to DNA content. Cancer Genet Cytogenet 149:89–97

118. Ottesen AM, Skakkebaek NE, Lundsteen C, Leffers H, Larsen J, Rajpert-De Meyts E (2004) High-resolution comparative genomic hybridization detects extra chromosome arm 12p adjacent to overt germ cell tumors, but not before the invasive tumor development. Genes Chromosomes Cancer 48:117–125
119. Parkinson MC, Swerdlow AJ, Pike MC (1994) Carcinoma in situ in boys with cryptorchidism: when can it be detected? Br J Urol 73:431–435
120. Pedersen KV, Boiesen P, Zetterlund CG (1987) Experience of screening for carcinoma-in-situ of the testis among young men with surgically corrected maldescended testes. Int J Androl 10:181–185
121. Pera M, Roach S, Ellis CJ (1990) Comparative biology of mouse and human embryonal carcinoma. Cancer Surv 9:243–262
122. Petersen PM, Giwercman A, Daugaard G, Rorth M, Petersen JH, Skakkebaek NE, Hansen SW, von der Maase H (2002) Effect of graded testicular doses of radiotherapy in patients treated for carcinoma-in-situ in the testis. J Clin Oncol 20: 1537–1543
123. Petterson A, Kaijser M, Richiardi L, Askling J, Ekbom A, Akre O (2004) Women smoking and testicular cancer: one epidemic causing the another? Int J Cancer 109:941–944
124. Pierce GB Jr (1966) Ultrastructure of human testicular tumors. Cancer 19:1963–1983
125. Pryor JP, Cameron KM, Chilton CP, Ford TE, Parkinson MC, Sinikrot J, Westwood CA (1983) Carcinoma in situ in testicular biopsies from men presenting with infertility. Br J Urol 55:780–784
126. Rajpert-De Meyts E, Skakkebaek NE (1994) Expression of the c-kit protein product in carcinoma-in-situ and invasive testicular germ cell tumours. Int J Androl 17:85–92
127. Rajpert-De Meyts E, Kvist M, Skakkebaek NE (1996) Heterogeneity of expression of immunohistochemical tumour markers in testicular carcinoma in situ: pathogenetic relevance. Virchows Arch 428:133–139
128. Rajpert-De Meyts E, Bartkova J, Samson M, Hoei-Hansen C, Frydelund-Larsen L, Bartek J, Skakkebaek NE (2003) The emerging phenotype of the testicular carcinoma in situ germ cells. APMIS 111:267–279
129. Rakheja D, Hoang MP, Sharma S, Albores-Saavedra J (2002) Intratubular embryonal carcinoma. Arch Path Lab Med 126:487–490
130. Ramani P, Yeung CK, Habeeba SS (1993) Testicular intratubular germ cell neoplasia in children and adolescents with intersex. Am J Surg Pathol 17:1124–1133
131. Reinberg Y, Manivel JC, Fraley EE (1989) Carcinoma in situ of the testis. J Urol 142:243–247
132. Rodriguez S, Jafer O, Goker H, Summersgill BM, Zafarana G, Gillis AJ, van Gurp RJ, Oosterhuis JW, Lu YJ, Huddart R, Cooper CS, Clark J, Looijenga LH, Shipley J (2003) Expression profile of genes from 12p in testicular germ cell tumors of adolescents and adults associated with i(12p) and amplification at 12p11.2-p12.1. Oncogene 22:1880–1891
133. Rorth M, Jacobsen GK, von der Maase H, Madsen EL, Nielsen OS, Pedersen M, Schultz H (1991) Surveillance alone versus radiotherapy after orchiectomy for clinical stage I non-seminomatous testicular cancer. Danish Testicular Cancer Group. J Clin Oncol 9:1543–1548
134. Rorth M, Rajpert-De Meyts E, Andersson L, Dieckmann KP, Fossa SD, Grigor KM, Hendry WF, Herr HW, Looijenga LH, Oosterhuis JW, Skakkebaek NE (2000) Carcinoma in situ in the testis. Scand J Nephrol Urol Suppl 205:166–186
135. Rosai J, Khodadoust K, Silber I (1969) Spermatocytic seminoma. II. Ultrastructural study. Cancer 23:103–116
136. Rosenberg C, van Gurp RJ, Geelen E, Oosterhuis JW, Looijenga LH (2000) Overrepresentation of the short arm of chromosome 12 is related to invasive growth of human testicular seminomas and nonseminomas. Oncogene 19:5858–5862
137. Rutgers JL, Scully RE (1991) The androgen insensitivity syndrome (testicular feminization): a clinicopathologic study of 43 cases. Int J Gynecol Pathol 10:126–144
138. Saito T, Katagiri A, Watanabe R, Tanikawa T, Kawasaki T, Tomita Y, Takahashi K (2000) Expression of E-cadherin and catenins on testis tumor. Urol Int 65:140–143
139. Sakuma Y, Sakurai S, Oguni S, Hironaka M, Saito K (2003) Alterations of the c-kit gene in testicular germ cell tumors. Cancer Sci 94:486–491
140. Satie AP, Rajpert-De Meyts E, Spagnoli GC, Henno S, Olivo L, Jacobsen GK, Rioux-Leclercq N, Jegou B, Samson M (2002) The cancer-testis gene, NY-ESO-1, is expressed in normal fetal and adult testes and in spermatocytic seminomas and testicular carcinoma in situ. Lab Invest 82:775–780
141. Schulze C, Holstein AF (1977) On the histology of human seminoma: development of the solid tumour from intratubular seminoma cells. Cancer 39:1090–1100
142. Schulze C, Holstein AF, Selberg W, Korner F (1978) Contribution to the formal pathogenesis of the classical seminoma. Early diagnosis from testicular biopsies? Schweiz Med Wochenschr 108:1119–1126
143. Schutte B, Holstein AF, Schirren C (1988) Macrophages lysing seminoma cells in patients with carcinoma-in-situ of the testis. Andrologia 20:295–303
144. Sehested M, Jacobsen GK (1987) Ultrastructure of syncytiotrophoblast-like cells in seminomas of the testis. Int J Androl 10:121–126
145. Sheynkin YR, Sukkarich T, Lipke M, Cohen HL, Schulsinger DA (2004) Management of nonpalpable testicular tumors. Urology 63:1163–1167
146. Sigg C, Hedinger C (1980) Testicular germ cell tumors and atypical germ cells. Schweiz Med Wochenschr 110:801–816
147. Sigg C, Hedinger C (1984) Atypical germ cells of testis. Comparative ultrastructural and immunochemical investigations. Virchows Arch A Pathol Anat Histopathol 402:439–450
148. Skakkebaek NE (1972) Possible carcinoma-in-situ of the testis. Lancet 2:516–517
149. Skakkebaek NE (1978) Carcinoma in situ of the testis: frequency and relationship to invasive germ cell tumours in infertile men. Histopathology 2:157–170
150. Skakkebaek NE, Berthelsen JG, Visfeldt J (1981) Clinical aspects of testicular carcinoma-in-situ. Int J Androl suppl 4: 153–162
151. Skakkebaek NE, Berthelsen JG, Muller J (1982) Carcinoma-in-situ of the undescended testis. Urol Clin N Am 9:377–385
152. Skakkebaek NE, Berthelsen JG, Giwercman A, Muller J (1987) Carcinoma-in-situ of the testis: possible origin from gonocytes and precursor of all types of germ cell tumours except spermatocytoma. Int J Androl 10:19–28
153. Skotheim RI,Monni O, Mousses S, Fossa SD, Kallioniemi O-P, Lothe RA, Kallioniemi A (2002) New insights into testicular germ cell tumorigenesis from gene expression profiling. Cancer Res 62:2359–2364
154. Skotheim RI, Abeler VM, Nesland JM, Fossa SD, Holm R, Wagner U, Florenes VA, Aass N, Kallioniemi OP, Lothe RA (2003) Candidate genes for testicular cancer evaluated by in situ protein expression analyses on tissue microarrays. Neoplasia 5:397–404
155. Skotheim RI, Korkmaz KS, Klok TI, Abeler V, Korkmaz CG, Nesland JM, Fossa SD, Lothe RA, Saatcioglu F (2003) NKX3.1 expression is lost in testicular germ cell tumors. Am J Pathol 163:2149–2154
156. Skotheim RI, Lind GE, Monni O, Nesland JM, Abeler VM, Fossa SD, Duale N, Brunborg G, Kallioniemi O-P, Andrews PW, Lothe RA (2005) Differentiation of human embryonal carcinomas, in vitro and in vivo, reveals expression profiles relevant to normal development. Cancer Res, in press
157. Sobin LH, Wittekind C (2002) TNM classification of malignant tumours, 6th edn. International Union Against Cancer. Wiley-Liss, New York

158. Soosay GN, Bobrow L, Happerfield L, Parkinson MC (1991) Morphology and immunohistochemistry of carcinoma in situ adjacent to testicular germ cell tumours in adults and children: implications for histiogenesis. Histopathology 19:537–544
159. Sperger JM, Chen X, Draper JS, Antosiewics JE, Chon CH, Jones SB, Brooks JD, Andrews PW, Brown PO, Thomson JA (2003) Gene expression patterns in human embryonic stem cells and human pluripotent germ cell tumors. Proc Natl Acad Sci USA 100:13350–13355
160. Srivastava A, Kreiger N (2004) Cigarette smoking and testicular cancer. Cancer Epidemiol Biomark Prev 13:49–54
161. Stiller D, Holzhausen HJ (1986) Ultrastructural cytology of testicular seminomas. Zentralbl Allg Pathol 131:437–449
162. Strohmeyer T, Peter S, Hartmann M, Munemitsu S, Ackermann R, Ullrich A, Slamon DJ (1991) Expression of the hst-1 and c-kit protooncogenes in human testicular germ cell tumors. Cancer Res 51:1811–1816
163. Summersgill B, Osin P, Lu YJ, Huddart R, Shipley J (2001) Chromosomal imbalances associated with carcinoma in situ and associated testicular germ cell tumours of adolescents and adults. Br J Cancer 85:213–220
164. Suzuki K, Tokue A, Kamiakito T, Kuriki K, Saito K, Tanaka A (2001) Predominant expression of fibroblast growth factor (FGF) 8, FGF4, and FGF receptor 1 in non-seminomatous and highly proliferative components of testicular germ cell tumors. Virchows Arch 439:616–621
165. Tal R, Holland R, Belensky A, Konichezky M, Baniel J (2004) Incidental testicular tumors in infertile men. Fertil Steril 82:469–471
166. Talerman A, Fu YS, Okagaki T (1984) Spermatocytic seminoma. Ultrastructural and microspectrophotometric observations. Lab Invest 51:343–349
167. Thore J, Zetterlund CG, Boiesen P (1984) Seminoma after orchiopexy. A case report. Scand J Urol Nephrol 18:357–359
168. Tienari J, Pertovaara L, Saksela O, Lehonen E, Vario T (1994) Increased expression of the matrix metalloproteinase 2 in differentiating Tera 2 human embryonal carcinoma cells. Int J Cancer 56:219–223
169. Timmer A, Oosterhuis JW, Schraffordt Koops H, Sleijfer DT, Szabo BG, Timens W (1994) The tumor microenvironment: possible role of integrins and the extracellular matrix in tumor biologic behavior of intratubular germ cell neoplasia and testicular seminomas. Am J Pathol 144:1035–1044
170. Tomita Y, Kimura M, Tanikawa T, Nishiyama T, Morishita H, Takeda M, Fujiwara M, Sato S (1993) Immunohistochemical detection of intercellular adhesion molecule-1 (ICAM-1) and major histocompatibility complex class I antigens in seminoma. J Urol 149:659–663
171. Ulbright TM, Scully RE (2001) Testis. In: Henderson DA (ed) Pathology of incipient neoplasia. Oxford University Press, Oxford, pp 570–590
172. van Echten J, van Gurp RJ, Stoepker M, Looijenga LH, de Jong B, Oosterhuis W (1995) Cytogenetic evidence that carcinoma in situ is the precursor lesion for invasive testicular germ cell tumors. Cancer Genet Cytogenet 85:133–137
173. Viglietto G, Romano A, Maglione D, Rambaldi M, Paoletti I, Lago CT, Califano D, Monaco C, Mineo A, Santelli G, Manzo G, Botti G, Chiappetta G, Persico MG (1996) Neovascularization in human germ cell tumors correlates with marked increase in the expression of the vascular endothelial growth factor but not the placenta-derived growth factor. Oncogene 13:577–587
174. von der Maase H, Rorth M, Walbom-Jorgensen S, Sorensen BL, Christophersen IS, Hald T, Jacobsen GK, Berthelsen JG (1986) Carcinoma in situ of contralateral testis in patients with testicular germ cell cancer: study of 27 cases in 500 patients. BMJ 293:1398–1401
175. von der Maase H, Giwercman A, Muller J, Skakkebaek NE (1987) Management of carcinoma-in-situ of the testis. Int J Androl 10:209–220
176. von der Maase H, Meincke R, Skakkebaek NE (1988) Residual carcinoma in situ of contralateral testis after chemotherapy. Lancet 1:477–478
177. von der Maase H, Specht L, Jacobsen GK, Jacobsen A, Madsen EL, Pedersen M, Schultz H (1993) Surveillance following orchiectomy for seminoma of the testis. Eur J Cancer 29A:1931–1934
178. von Eyben FE (2004) Chromosomes and genes and development of testicular germ cell tumors. Cancer Genet Cytogenet 151:93–138
179. von Eyben F, Krabbe S, Skakkebaek NE (1980) Alpha-foetoprotein and human chorionic gonadotropin in men with maldescended testes. Br J Cancer 42:156–157
180. von Eyben FE, Mikulowski P, Busch C (1981) Microinvasive germ cell tumors of the testis. J Urol 126:842–844
181. von Eyben FE, Mikulowski P, Krabbe S, Busch C (1981) Is treatment of regional lymph nodes necessary in microinvasive testicular germ cell tumours? In: Anderson CK, Jones WG, Ward AM (eds) Germ cell tumours. Taylor & Francis, London, pp 290–291
182. von Eyben FE, Skude G, Krabbe S (1982) Serum lactate dehydrogenase and its isoenzymes in men with maldescended testes. J Urol 128:1195–1197
183. von Eyben FE, Hoyer PE, Busch C (1986) Microspectrophotometric observations of a microinvasive testicular germ cell tumour. In: Jones WG, Ward AM, Anderson CK (eds) Germ cell tumours II. Pergamon Press, Oxford, pp 57–58
184. von Eyben FE (2003) Laboratory markers and germ cells tumors. Crit Rev Lab Med 40:377–427
185. von Eyben FE, Jacobsen GK, Rorth M, von der Maase H (2004) Microinvasive germ cell tumour (MGCT) adjacent to testicular germ cell tumours. Histopathology 44:547–554
186. Vos A, Oosterhuis JW, de Jong B, Buist J, Schraffordt Koops H (1990) Cytogenetics of carcinoma in situ of the testis. Cancer Genet Cytogenet 46:75–81
187. Walsh J, Andrews PW (2003) Expression of Wnt and Notch pathway genes in a pluripotent human embryonal carcinoma cell line and embryonic stem cells. APMIS 111:197–211
188. Waxman M (1976) Malignant germ cell in situ in a cryptorchid testis. Cancer 38:1452–1456
189. West AB, Butler MR, Fitzpatrick J, O'Brien A (1985) Testicular tumors in subfertile men: report of 4 cases with implications for management of patients presenting with infertility. J Urol 133:107–109
190. Westergaard T, Olsen JH, Frisch M, Kroman N, Nielsen JW, Melbye M (1996) Cancer risk of fathers and brothers of testicular cancer patients in Denmark. A population-based study. Int J Cancer 66:627–631
191. Whitaker RH (1970) Management of the undescended testis. Br J Hosp Med 4:25–37
192. Whitaker RH (1988) Neoplasia in cryptorchid men. Semin Urol 6:107–109
193. Willert J, Epping M, Pollack JR, Brown PO, Nusse R (2002) A transcriptional response to Wnt protein in human embryonic carcinoma cells. BMC Dev Biol 2:8
194. Wilms M (1896) Teratoid tumors of the testis with inclusion of so-called cystoids and enchromdomas. Beitr Pathol Anat 19:233–266
195. Winstanley AM, Mikuz G, Debruyne F, Schulman CC, Parkinson MC: European Association of Pathologists, Uropathology Division of Florence (2004) Handling and reporting of biopsy and surgical specimens of testicular cancer. Eur Urol 45:564–573
196. Wittekind C, Loy V (2001) Pathology and pathomorphologic diagnosis of germ cell tumors of the testis. Pathologe 22:316–325
197. Zafarana G, Grygalewicz B, Gilis AJ, Vissers LE, van de Vliet W, van Gurp RJ, Debiec-Rychter M, Oosterhuis JW, Gert van Kessel A, Schenmakers EF, Looijenga LH, Veltman JA (2003) 12p-amplicon structure analysis in testicular germ cell tumors of adolescents and adults by array CGH. Oncogene 22:7695–7701
198. Zwierstra RP, Bleichrodt RP, Suurmeyer AJ (1984) Undescended testes and puberty. Orchidopexia or orchiectomy. Z Kinderchir 39:255–258

Virchows Arch (2005) 447: 626–633
DOI 10.1007/s00428-005-1228-0

ORIGINAL ARTICLE

Paweł Surowiak · Verena Materna · Irina Kaplenko · Marek Spaczyński · Manfred Dietel · Hermann Lage · Maciej Zabel

Augmented expression of metallothionein and glutathione S-transferase pi as unfavourable prognostic factors in cisplatin-treated ovarian cancer patients

Received: 10 December 2004 / Accepted: 9 February 2005 / Published online: 21 June 2005
© Springer-Verlag 2005

Abstract Resistance to cis- or carboplatin represents the principal cause of therapeutic failures in ovarian carcinoma. The phenomenon of resistance to platinum-based drugs is partly related to expression of metallothionein (MT) and of glutathione S-transferase pi (GST-pi), but opinion on the subject is discordant. Documentation of a negative predictive effect of MT and GST-pi expression for the therapy employing platinum-based drugs would permit to select resistant cases in which other therapeutic approaches could be employed. The present study aimed at examining the relation between intensities of MT and GST-pi expressions in ovarian carcinomas and dynamics of the clinical course in the neoplastic disease in a group of cisplatin-treated patients. The analyses were performed on samples of ovarian carcinoma originating from 43 first-look laparotomies (FLLs) and, in 30 cases, from second-look laparotomies (SLL) from the same patients. Immunohistochemical reactions were performed on paraffin sections of studied tumors, using monoclonal antibodies to MT and GST-pi. The calculations showed that in cases with augmented expression of MT, mortality was higher. On the other hand, augmented expression of GST-pi predisposed to more frequent relapses, deaths and progression of the tumor. Kaplan–Meier analysis showed that a significantly shorter survival time was linked to cases of higher expression of MT at FLL and of higher expression of GST-pi at FLL, whereas a shorter progression-free time was manifested by cases with higher expression of GST-pi at FLL. The performed investigations indicate that augmented expressions of MT at FLL and GST-pi at FLL in ovarian cancer represent an unfavourable predictive factor in cisplatin-treated patients.

Keywords Ovarian cancer · Metallothionein · Glutathione S-transferase pi · Cisplatin

P. Surowiak · M. Zabel
Department of Histology and Embryology,
University School of Medicine,
ul. Chałubińskiego 6a,
50-356 Wrocław, Poland

P. Surowiak · V. Materna · M. Dietel · H. Lage (✉)
Charité Campus Mitte,
Institute of Pathology,
Schumannstr. 20/21,
10117 Berlin, Germany
e-mail: hermann.lage@charite.de
Tel.: +49-30-450536045
Fax: +49-30-450536900

P. Surowiak
Lower Silesian Centre of Oncology,
pl. Hirszfelda 12,
53-413 Wrocław, Poland

I. Kaplenko · M. Spaczyński
Department of Obstetrics and Gynaecology,
University School of Medicine,
ul. Polna 33,
60-535 Poznań, Poland

M. Zabel
Department of Histology and Embryology,
University School of Medicine,
ul. Swięcickiego 6,
60-781 Poznań, Poland

Introduction

In Western and Northern Europe, as well as in the United States, ovarian carcinoma represents the third leading cause of incidence of malignant tumors in female genital organs and the fifth leading malignancy in women. It represents also the fifth most common cause of death due to malignant tumors, next to breast carcinoma, colorectal carcinoma, lung carcinoma and gastric carcinoma. In the European Union, the incidence is appraised at 12–17 new cases per 100,000 inhabitants per year. This corresponds to 27,000–30,000 new cases per year [9]. The rising incidence of the tumor is observed worldwide. According to the data of the National Cancer Data Base in the United States, duration of 5-year survival in respective FIGO stages amounted to I (74%), II (58%), III (30%) and IV (19%) [1].

Due to their location, ovarian cancers are frequently diagnosed at an advanced stage of the disease. Therefore,

surgical procedures are accompanied by chemotherapy in a significant proportion of the cases. Most schemes of the treatment in the disease are based on cis- or carboplatin [1]. Thus, resistance of tumor cells to the platinum-based drugs involves the principal reason of therapeutic failures of the disease.

Metallothioneins (MTs) are low molecular weight proteins (6–7 kDa), whose chains are composed of 61 or 62 amino acids. Typically, they contain multiple cysteine residues and few aromatic amino acids. MTs are thought to mediate several functions, including, i.a. control of indispensable trace element levels (e.g. zinc and copper), alleviation of toxic effects of cadmium and mercury or protection of cells from oxidative stress [6, 11]. Numerous reports document MT presence in cells of various tumors, including ovarian cancer [3, 7, 17, 28].

Studies in vitro documented the strict relationship between expression of MT and resistance to cisplatin [12]. A single molecule of MT was found to be capable of binding ten molecules of cisplatin [5]. However, no relation has been discovered until now between intensity of MT expression in ovarian carcinomas and clinical response of patients treated with cisplatin [11].

Glutathione S-transferases (GSTs) catalyse conjugation of reduced glutathione with a variety of electrophilic xenobiotics and also play a role in degradation of lipid peroxidation products. A relationship has been suggested between expression of GST-pi isoform and resistance to cisplatin, adriamycin, cyclophosphamide and etoposide [23]. However, the data on relations between expression of GST-pi and clinical response to cisplatin therapy are divergent: in several studies, expression of GST-pi has been noted to correlate with less favourable response to cisplatin [2, 16], whereas no such a relationship can be detected in other investigations [10, 15, 31].

Previous studies failed to demonstrate unequivocal links between expression of MT and GST-pi, and clinical course in ovarian cancer patients treated with platinum-based drugs. On the other hand, in vitro studies suggested participation of the proteins in detoxication of the tumor cells from platinum-containing compounds [5, 12, 32]. Moreover, expression of MT and GST-pi has not been analyzed in ovarian cancer samples originating from first-look laparotomies (FLLs) and second-look laparotomies (SLLs) in the same patients. Demonstration of a link between expression of MT and GST-pi, and poor clinical response of ovarian cancer patients to therapy with the discussed compounds would facilitate prospective selection of resistant cases in whom other therapeutic approaches could be employed. Examination of the resistance to platinum-based compounds in detail is also highly significant for studies on novel therapeutic strategies.

In the present study, the expression levels of MT and GST-pi were determined by immunohistochemistry in platinum-based drug-treated ovarian cancer specimens from FLL and from second-look procedures in the same group of patients, and the expression levels were correlated with histopathological criteria and clinical outcome.

Materials and methods

Patients

Immunohistochemical examination was performed retrospectively on tissue samples taken for routine diagnostic purposes. Forty-three patients who underwent surgery in 1999–2002 due to ovarian carcinoma in the Department of Gynaecology and Obstetrics, University Medical School in Poznań, Poland, were qualified for the studies. The cases were selected based on availability of tissue and were not stratified for known preoperative or pathological prognostic factors. The study was approved by an Institutional Review Board (IRB) and the patients gave their informed consent before their inclusion into the study. Following the first surgery, all the patients were subjected to chemotherapy using cisplatin-based schemes (Table 1). Thirty-six patients from the same group were subjected also to the second-look operation. In seven cases, no second-look procedure was performed due to advancement of the disease. In six cases, no tumor cells were detected in the material originating from the second-look procedure (Table 1). The patients were monitored by periodic medical checkups, CA-125 serum levels, ultrasonographic and radiological examinations. During the follow-up period, 22 patients (51%) had a recurrent disease and 13 patients (30%) died of the disease. The mean (median) progression-free survival time was 16.9 months (range 0–52 months), whereas the mean (median) overall-free survival time was 24.6 months (range 6–52 months).

Fragments sampled from studied tumors were fixed in 10% buffered formalin and embedded in paraffin. In each case, haematoxylin-and-eosin-stained preparations were subjected to histopathological evaluation by two pathologists. The stage of the tumors was assessed according to the International Federation of Gynaecology and Obstetrics [30]. Tumors were graded according to the Silverberg grading system [24].

Immunohistochemistry

Formalin-fixed paraffin-embedded tissue was freshly cut (4 μm). The sections were mounted on Superfrost slides (Menzel Gläser, Germany), dewaxed with xylene and gradually rehydrated. Activity of endogenous peroxidase was blocked by 30-min incubation in 1% H_2O_2. Immunohistochemical reactions were performed using the monoclonal mouse antibodies (clone E9) detecting isoforms 1 and 2 of MT (DakoCytomation, Denmark) at dilution 1:100, and monoclonal mouse antibodies (clone 353-10) to GST-pi (DakoCytomation) at dilution 1:100. The antibodies were diluted in the Antibody Diluent, Background Reducing (DakoCytomation). Tested sections were incubated with the antibodies for 1 h at room temperature. Subsequently, incubations were performed with biotinylated antibodies (15 min, room temperature) and with streptavidin-biotinylated peroxidase complex (15 min, room

Table 1 Patient and tumor characteristics

Characteristics	No. (%)[a]
All patients	43 (100)
Age (mean 51.0)[b]	
≤50	20 (47)
>50–60	16 (37)
>60	7 (16)
Grade[b]	
1	7 (16)
2	18 (42)
3	18 (42)
FIGO[b]	
I	1 (2)
II	1 (2)
III	41 (95)
Histology[b]	
Serous	37 (86)
Endometrioid	3 (7)
Other	3 (7)
Clinical response	
Complete response	16 (37)
Stable disease	5 (12)
Progressive disease	22 (51)
Chemotherapy (in total)	
Cisplatin/paclitaxel	31 (72)
Cisplatin/cyclophosphamide/adriblastin	6 (14)
Cisplatin/cyclophosphamide/paclitaxel	3 (7)
Cisplatin/cyclophosphamide/paclitaxel/adriblastin	2 (5)
Carboplatin/paclitaxel	1 (2)

[a]Differences in the sum to 100% in groups are due to rounding off
[b]Data are given to the first operation/diagnosis implemented

temperature) (LSAB+, HRP, DakoCytomation). NovaRed (Vector Laboratories, UK) was used as a chromogen (10 min at room temperature). All the sections were counterstained with Meyer's haematoxylin. In every case, controls were included in which the specific antibody was substituted by the Primary Mouse Negative Control (DakoCytomation).

Intensity of the immunohistochemical reactions was appraised using the semi-quantitative ImmunoReactive Score (IRS) scale, in which intensity of the reaction and percentage of positive cells were scored (Table 2). The final result represented a product of scores given for individual traits and ranged between 0 and 12 [22]. Intensity of immunohistochemical reactions was evaluated independently by two pathologists. In cases of divergencies, the evaluation was repeated using double-headed microscope.

Statistical analysis

Statistical analysis of the results took advantage of Statistica 98 PL software (Statsoft, Poland). The employed tests included Mann–Whitney *U* test and ANOVA rank test of Kruskal–Wallis. Kaplan–Meier statistics and log-rank tests were performed using SPSS software (release 10.0; SPSS, Chicago, IL, USA) to estimate significance of differences in survival times. The length of progression-free survival was defined as the time between the primary surgical treatment and diagnosis of a recurrent tumor or death. Because univariate analysis revealed no significant relationships between studied clinicopathological parameters (age, histology, grade, CA-125 at FLL level) and overall survival and progression-free time of studied patients ($P>0.05$), we have not performed a multivariate analysis. Because 95% of the studied patients were in stage FIGO III, we have not investigated relationships between stage and survival data.

Table 2 Evaluation criteria of MT and GST-pi expression using IRS score [19]

Percentage of positive cells	Points	Intensity of reaction	Points
No positive cells	0	No reaction	0
<10% positive cells	1	Weak colour reaction	1
10–50% positive cells	2	Moderate intensity	2
51–80% positive cells	3	Intense reaction	3
>80% positive cells	4		

Results

The data obtained by clinical observation of the studied patients are included in Table 1. In the case of MT, reactions of a nuclear and a cytoplasmic localization of various intensity in individual cases were obtained (Fig. 1a). In preparations originating from the first operation (FLL), mean intensity of the reaction was 5.44±0.58 (min. 0, max. 12), whereas in the material obtained upon the second-look procedure (SLL), it amounted to 7.07±3.28 (min. 1, max. 12). In the case of GST-pi, a cytoplasmic reaction of a variable intensity in individual cases was obtained (Fig. 1b). Mean intensity of GST-pi reaction at FLL was 4.28±3.83 (min. 0, max. 12), whereas mean intensity of GST-pi reaction at SLL amounted to 5.1±3.81 (min. 0, max. 12).

At the first stage of statistical analysis, Mann–Whitney *U* test was used to compare intensity of MT expression at FLL and SLL, and intensity of GST-pi expression at FLL and SLL. Expression of MT at FLL was found to be lower compared to the expression of MT at SLL (at the verge of significance, $P=0.058$). In the case of GST-pi, the differences were far from being significant ($P=0.31$).

Using the ANOVA rank test of Kruskal–Wallis, relations were examined between intensities of MT and GST-pi expression on the one hand, and relapses, patient death, grade and response to therapy on the other. We have shown that cases with relapse of the neoplastic disease demonstrated higher expression of GST-pi at FLL ($P=0.004$) and at SLL ($P=0.02$), compared to the cases with no relapse (Table 4). No such relationship was detected in the case of MT at FLL or SLL (Table 3). In the cases terminated by death of the patient, expression of MT at FLL (Table 3), of GST-pi at FLL and at SLL (Table 4) was significantly higher ($P=0.003$, $P=0.0006$, $P=0.03$, respectively) than those in surviving patients. No such relationship could be

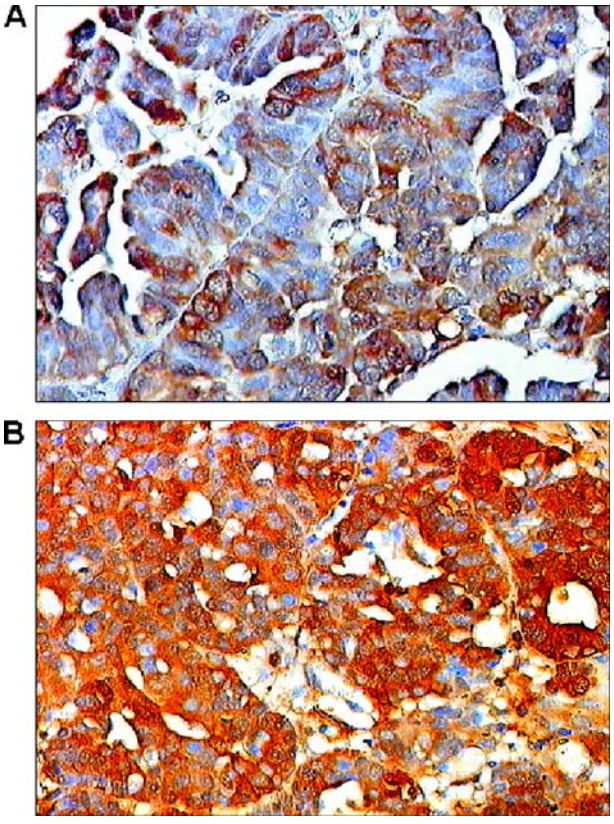


Fig. 1 Immunohistochemical localization of **a** metallothionein (MT) (×400, haematoxylin counterstaining) and **b** glutathione S-transferase pi (GST-pi) (haematoxylin counterstaining, ×200) in ovarian carcinoma. The red reaction product is located in the cytoplasm (in the case of MT, also in cell nuclei) of neoplastic cells

disclosed in the case of MT at SLL (Table 3). In the case of MT, clinical response to the therapy manifested no relationship to intensity of the protein expression (Table 3), but expression of GST-pi at FLL was the highest in cases of progressive disease (PD) (P=0.009). A similar tendency was seen in the case of GST-pi at SLL (P=0.06) (Table 4).

None of the examined variables was related to the grade of the tumor (Tables 3 and 4).

Spearman's rank correlation demonstrated a positive correlation between intensities of MT expression at FLL and GST-pi expression at FLL (P=0.008) (Fig. 2).

In the analysis of Kaplan–Meier, the cut-off value of 4 was accepted for MT at FLL, MT at SLL, GST-pi at FLL and for GST-pi at SLL to make calculations uniform in all studied groups. Accordingly, the overall survival time and the progression-free time were examined for groups manifesting expression of 0–4 (no or lower expression intensity) and those manifesting expression of 5–12 (the higher expression intensity). The calculations demonstrated that (1) cases of no/lower MT expression at FLL showed a significantly longer overall survival time (P=0.009) (Fig. 3) and (2) cases of no/lower GST-pi expression at FLL showed a significantly longer overall survival time (P=0.003) and progression-free time (P=0.002). For GST-pi expression at SLL, a marginally significant relationship was detected for the progression-free time (P=0.0500) (Fig. 4).

Discussion

Cisplatin displays clinical activity against a wide variety of solid tumors. In advanced ovarian carcinoma, cisplatin-based combination chemotherapy including paclitaxel (PC scheme) and topotecan (PT scheme) represents the main treatment option, along with debulking surgery [1]. Its cytotoxic mode of action is mediated by its interaction with DNA to form DNA adducts, primarily intrastrand cross-link adducts, which activate several signal transduction pathways, and culminate in activation of apoptosis [25]. There are several mechanisms responsible for cisplatin resistance, and they include reduced intracellular drug accumulation, increased inactivation by thiol-containing molecules (MTs and GSTs), modulation of DNA damage repair pathways, dysfunction of tumor-suppressor p53 and overexpression of apoptosis inhibitors [13].

Table 3 Analysis of a relationship between metallothionein expression and clinicopathological parameters (ANOVA rank test of Kruskal–Wallis)

Mean MT expression as detected by immunohistochemistry (IRS score)				
Characteristics	MT at FLL±SD	P value, χ^2 test	MT at SLL±SD	P value, χ^2 test
Grade		0.4295		0.4562
1	3.86±3.34		7.00±4.30	
2	6.28±4.52		6.50±3.52	
3	5.22±3.15		7.82±2.56	
Clinical response		0.1742		0.4295
Complete response	4.62±4.16		5.92±2.87	
Stable disease	3.80±3.03		7.60±2.07	
Progressive disease	6.41±3.61		7.92±3.84	
Relapse		0.0654		0.1540
Relapse	6.41±3.61		7.92±3.84	
No relapse	4.43±3.87		6.41±2.72	
Death		0.0030		0.0773
Death	8.00±3.08		8.40±4.14	
Alive	4.33±3.61		6.40±2.62	

FLL First-look laparotomy, *SLL* second-look laparotomy, *MT* metallothionein, *IRS* ImmunoReactive Score

Table 4 Analysis of a relationship between glutathione S-transferase pi expression and clinicopathological parameters (ANOVA rank test of Kruskal–Wallis)

Mean GST-pi expression as detected by immunohistochemistry (IRS score)				
Characteristics	GST-pi at FLL±SD	*P* value, χ^2 test	GST-pi at SLL±SD	*P* value, χ^2 test
Grade		0.1358		0.3246
1	2.00±2.58		3.80±4.02	
2	4.33±3.94		5.64±4.05	
3	5.11±3.92		5.00±3.61	
Clinical response		0.0096		0.0603
Complete response	3.19±3.60		4.17±4.32	
Stable disease	1.00±1.73		3.00±3.74	
Progressive disease	5.82±3.67		6.77±2.74	
Relapse		0.0045		0.0217
Relapse	5.82±3.67		6.77±2.74	
No relapse	2.67±3.35		3.82±4.08	
Death		0.0006	4.10±3.97	0.0286
Death	7.31±2.69		7.10±2.60	
Alive	2.97±3.51			

FLL First-look laparotomy, *SLL* second-look laparotomy, *GST-pi* glutathione S-transferase pi

In this study, we describe the expression of MT and GST-pi proteins detected by immunohistochemistry in the group of 43 primarily isolated samples and in the group of 36 samples originating from the second-look procedure performed in the same patients. The studied group was uniform: 95% of the patients were in FIGO stage III, 86% of the studied cases involved serous carcinoma, 98% of the patients were treated with cisplatin-based schemes and 2% or one patient with a carboplatin-based scheme. We confirm that the studied proteins are expressed in ovarian carcinomas [2, 17]. We have found that intensity of MT expression is higher in sections from second-look procedures (after chemotherapy) and that there is no difference in expression intensity of GST-pi between sections from primary laparotomies and second-look procedures. There are also no relationships between MT and GST-pi expression, and grade of studied tumors.

The data on the relationship between MT expression and resistance to cisplatin are divergent. Studies in vitro showed that cells transfected with *MT* gene demonstrated a significantly lower sensitivity to cisplatin compared to the non-transfected cells [29]. In immunohistochemical studies, cases of squamous cell carcinoma of the esophagus [8], bladder carcinoma [26] or urothelial transitional cell carcinoma [27] showing a higher MT expression reacted less favourably to treatment with cisplatin. In the case of head and neck squamous cell carcinoma, expression of MT in samples isolated following treatment with cisplatin was significantly higher than that in untreated tumors [20]. In the cases of germ cell tumors and testicular germ cell tumors, no relationship could be demonstrated between expression of MT and response to cisplatin therapy [16, 18]. Wrigley et al. [32] studied a group of 80 cases of ovarian cancer of a variable grade, stage and histology (59 cases involved primary laparotomies and 21 samples originated from second-look procedures, but not from the same patients). Forty-four patients were treated with cisplatin, and MT expression was measured by radioimmunoassay. The studies disclosed no relationships between MT expression and clinical response to cisplatin therapy. We have found that cases with relapse of the disease and cases that have been terminated by death of the patient have been characterised by a significantly higher expression of MT at FLL. The Kaplan–Meier analysis has shown that cases with higher MT expression at FLL have manifested a shorter overall survival time. Thus, we have shown that ovarian cancer cases treated with platinum-based drugs and manifesting augmented expression of MT at FLL carry less favourable prognosis, suggesting that MT participates in the mechanisms of resistance to the drugs. No such significant relationships could be noted for MT at SLL. The absence of relationship between MT expression at SLL and clinical course of the disease explains the fact that following SLL, the patients no longer received any chemotherapy. The phenomenon suggests that MT expression in ovarian cancer represents an exponent of resistance to platinum-based drugs, and not of a more dynamic course of the disease, as suggested for other tumors [3, 7]. To our knowledge, this study demonstrates for the first time significant unfavourable predictive value of MT expres-

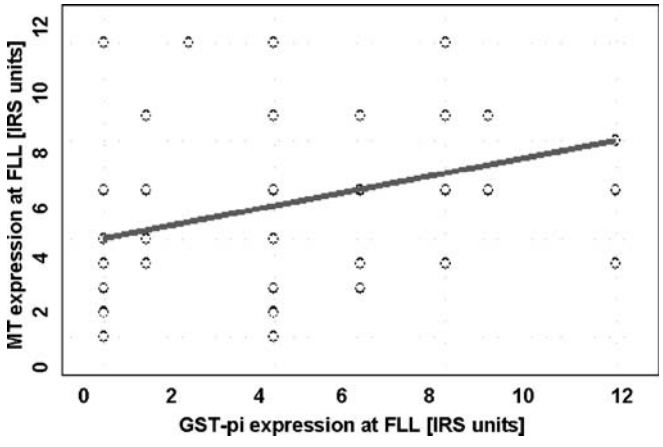


Fig. 2 Positive correlation between MT at FLL and GST-pi at FLL expression (Spearman's rank correlation, *P*=0.008). ImmunoReactive Score (IRS) (see Table 2) was used for immunohistochemical reaction evaluation

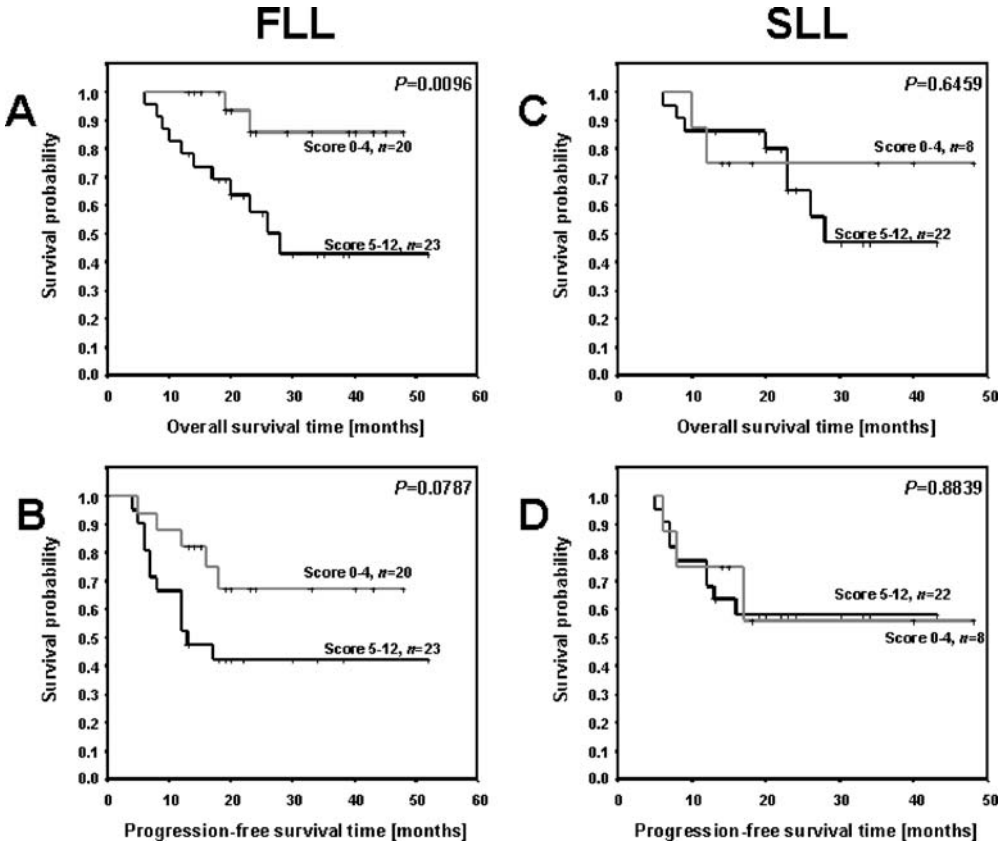


Fig. 3 Kaplan–Meier curves for survival and expression of GST-pi in the studied group of 43 ovarian cancer patients: **a** patients with lower MT at FLL expression have an increased overall survival time; **b** no significant differences in progression-free time between patients with lower and higher MT at FLL expression; **c** no significant differences in overall survival time between patients with lower and higher MT at SLL expression; **d** no significant differences in progression-free time between patients with lower and higher MT at SLL expression. Analyzed tissues were obtained during the first- and second-look operations (FLL and SLL, respectively). IRS (see Table 2) was used for dividing patients in groups with no/lower or higher expression of MT determined by immunohistochemistry. *n* number of patients

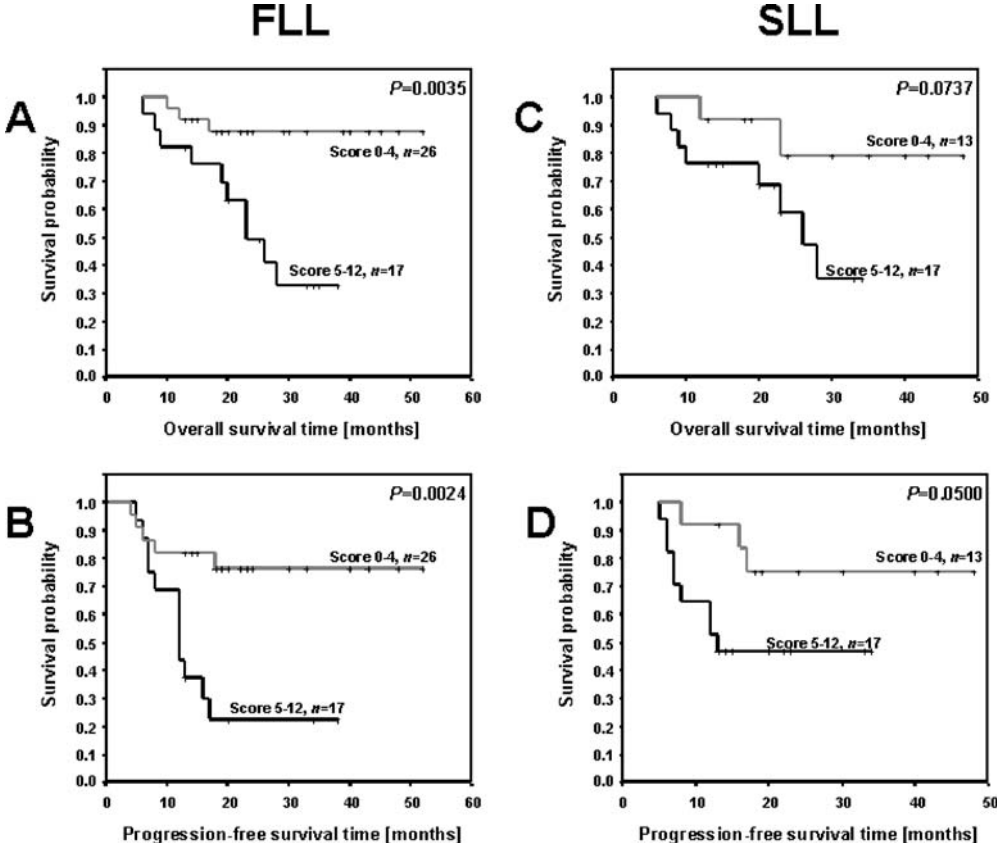


Fig. 4 Kaplan–Meier curves for survival and expression of MT in studied group of 43 ovarian cancer patients: **a** patients with lower GST-pi at FLL expression have an increased overall survival time; **b** patients with lower GST-pi at FLL expression have an increased progression-free time; **c** no significant differences in overall survival time between patients with lower and higher GST-pi at SLL expression; **d** patients with lower GST-pi at SLL expression have an increased progression-free time (marginally significant relationship, $P=0.05$). Analyzed tissues were obtained during the first- and second-look operations (FLL and SLL, respectively). IRS (see Table 2) was used for dividing patients in groups with no/lower or higher expression of GST-pi determined by immunohistochemistry. *n* number of patients

sion on platinum-based drugs therapies in human ovarian carcinomas.

The relationship between GST-pi expression and resistance to cisplatin was demonstrated in cell lines (colon adenocarcinoma, lung adenocarcinoma and glioblastoma cell lines) [4] and in clinical cases of head and neck cancers [21]. In contrast, no relationship could be documented in cases of cervical carcinoma [14] and non-small cell lung cancer [19]. In the case of ovarian carcinoma, similarly equivocal data were documented on the relationship between GST-pi and clinical response to cisplatin therapy. Mayr et al. [16] and Satoh et al. [23] documented relationship between elevated expression of GST-pi and a less favourable response to treatment with cisplatin in the heterogenous group of 213 cases and in the heterogenous group of 117 cases. On the other hand, Ikeda et al. [10] and Van der Zee et al. [31] were unable to document any dependence between expression of GST-pi in ovarian carcinomas and a resistance to cisplatin in the heterogenous group of 93 cases and in the equally heterogenous group of 127 cases, respectively. Our studies have shown that cases with relapse of the disease, terminated by death of the patient or in which progression of the disease has been noted by clinical observations, have been characterised by more pronounced expression of GST-pi at FLL and at SLL. Moreover, Kaplan–Meier analysis has shown that the cases with higher expression of GST-pi at FLL and SLL showed shorter overall survival and progression-free time. In our study, we have shown that augmented expression of GST-pi is typical for cases with less favourable response to chemotherapy with platinum-based drugs. Poor prognosis in patients manifesting augmented expression of GST-pi at SLL suggests that the protein displays a more intense expression in cases of a more aggressive clinical course.

We have also demonstrated a positive correlation between MT expression at FLL and GST-pi expression at FLL. The correlation suggests that cases resistant to cisplatin manifest higher expression of the two proteins, and therefore, MT and GST-pi have to be taken into account in the search of approaches aimed to overcome resistance to platinum-based drugs.

In summary, we found that augmented expression of MT and GST-pi in ovarian cancers characterises cases that are resistant to platinum-based drugs. In such patients, application of other therapeutic modalities should be considered.

Acknowledgements The study was supported by the grant no. 3 PO5E 064 22 from the Committee of Scientific Investigations, Poland, and by the "Berliner Krebsgesellschaft e.V.", Germany.

References

1. Averette HE, Hoskins W, Nguyen HN, Boike G, Flessa HC, Chmiel JS, Zuber K, Karnel LH, Winchester DPSO (1993) National survey of ovarian carcinoma. 1. A patient care evaluation study of the American College of Surgeons. Cancer 71:1629–1638
2. Cullen KJ, Newkirk KA, Schumaker LM, Aldosari N, Rone JD (2003) Glutathione S-transferase pi amplification is associated with cisplatin resistance in head and neck squamous cell carcinoma cell lines and primary tumors. Cancer Res 63: 8097–8102
3. Dzięgiel P, Forgacz J, Suder E, Surowiak P, Kornafel J, Zabel M (2003) Prognostic significance of metallothionein expression in correlation with Ki67 expression in adenocarcinomas of large intestine. Histol Histopathol 18:401–407
4. Goto S, Kamada K, Soh Y, Ihara Y, Kondo T (2002) Significance of nuclear glutathione S-transferase pi in resistance to anti-cancer drugs. Jpn J Cancer Res 93:1047–1056
5. Hagrman D, Goodisman J, Dabrowiak JC, Souid AK (2003) Kinetic study on the relation of cisplatin with metallothionein. Drug Metab Dispos 31:916–923
6. Hamer DH (1986) Metallothionein. Annu Rev Biochem 55:913–951
7. Hishikawa Y, Abe S, Kinugasa S, Yoshimura H, Monden N, Igarashi M, Tachibana M, Nagasue N (1997) Overexpression of metallothionein correlates with chemoresistance to cisplatin and prognosis in esophageal cancer. Lab Invest 54:342–347
8. Hishikawa Y, Koji T, Dhar DK, Kinugasa S, Yamaguchi M, Nagasue N (1999) Metallothionein expression correlates with metastatic and proliferative potential in squamous cell carcinoma of the oesophagus. Br J Cancer 81:712–720
9. Holschneider CH, Berek JS (2000) Ovarian cancer: epidemiology, biology, and prognostic factors. Sem Surg Oncol 19:3–10
10. Ikeda K, Sakai K, Yamamoto R, Hareyama H, Tsumura N, Watari H, Shimizus M, Minanami H, Sakuragi N (2003) Multivariate analysis for prognostic significance of histologic subtype, GST-pi, MDR-1, and p53 in stages II–IV ovarian cancer. Int J Gynecol Cancer 13:776–784
11. Kagi JHR (1991) Overview of metallothionein. Methods Enzymol 205:613–626
12. Kaina B, Lohrer H, Karin M, Herrlich P (1990) Overexpressed human metallothionein IIA gene protects Chinese hamster ovary from killing by alkylating agents. Proc Natl Acad Sci U S A 87:2710–2714
13. Kartalou M, Essigmann JM (2001) Mechanisms of resistance to cisplatin. Mutat Res 478:23–43
14. Konishi I, Nanbu K, Mandai M, Tsuruta Y, Kataoka N, Nagata Y (1998) Tumor response to neoadjuvant chemotherapy correlates with the expression of P-glycoprotein and PCNA but not GST-pi in the tumor cells of cervical carcinoma. Gynecol Oncol 70:365–371
15. Mayer F, Stoop H, Scheffer GL, Scheper R, Oosterhuis JW, Looijeng LH, Bokemeyer C (2003) Molecular determinants of treatment response in human germ-cell tumors. Clin Cancer Res 9:767–773
16. Mayr D, Pannekamp U, Baretton GB, Gropp M, Meier W, Flens MJ, Scheper R, Diebold J (2000) Immunohistochemical analysis of drug resistance-associated proteins in ovarian carcinomas. Pathol Res Pract 196:469–475
17. McCluggage WG, Strand K, Abdulkair A (2002) Immunohistochemical localization of metallothionein in benign and malignant epithelial ovarian tumours. Int J Gynecol Cancer 12:62–65
18. Meijer C, Timmer A, De Vries EG, Groten JP, Knol A, Zwart N, Sleijefer DT, Mulder NH (2000) Role of metallothionein in cisplatin sensitivity of germ-cell tumours. Int J Cancer 85 (6):777–781
19. Miyatake K, Gemba K, Ueoka H, Nishii K, Kiura K, Tabata M, Shibayama T, Takigawa N, Kawaraya M, Tanimoto M (2003) Prognostic significance of mutant p53 protein, P-glycoprotein and glutathione S-transferase-pi in patients with unresectable non-small cell lung cancer. Anticancer Res 23:2829–2836
20. Muramatsu Y, Hasegawa Y, Fukano H, Ogawa T, Namuba M, Mour S, Fujimoto Y, Matsuura H, Takai Y, Mori M (2000) Metallothionein immunoreactivity in head and neck carcinomas —special reference to clinical behaviors and chemotherapy responses. Anticancer Res 20:257–264

21. Nishimura T, Newkirk K, Sessions RB, Andrews PA, Trock BJ, Rasmussen AA, Montgomery EA, Bischoff EK, Cullen KJ (1996) Immunohistochemical staining for glutathione S-transferase predicts response to platinum-based chemotherapy in head and neck cancer. Clin Cancer Res 2:1859–1865
22. Remmele W, Stegner HE (1987) Recommendation for uniform definition of an ImmunoReactive Score (IRS) for immunohistochemical estrogen receptor detection (ER-ICA) in breast cancer tissue. Pathologe 8:138–140
23. Satoh T, Nishida M, Tsunoda H, Kubo T (2001) Expression of glutathione S-transferase pi (GST-pi) in human ovarian tumors. Eur J Obstet Gynecol Reprod Biol 96:202–208
24. Shimizu Y, Kamoi S, Amada S, Silverberg SG (1998) Toward the development of a universal grading system of ovarian epithelial carcinoma: testing of a proposed system in a series of 461 patients with uniform treatment and follow-up. Cancer 82: 893–901
25. Siddik ZH (2003) Cisplatin: mode of cytotoxic action and molecular basis of resistance. Oncogene 22:7265–7279
26. Siegsmund MJ, Marx C, Seeman O, Schummer B, Steidler A, Toktomambetova L, Kohrmann KU, Rassweiler J, Alken P (1999) Cisplatin-resistant bladder carcinoma cells: enhanced expression of metallothioneins. Urol Res 27:157–163
27. Siu LL, Banerjee D, Khurana RJ, Pan X, Pflueger R, Tannock IF (1998) The prognostic role of p53, metallothionein, P-glycoprotein, and MIB-1 in muscle-invasive urothelial transitional cell carcinoma. Clin Cancer Res 4:559–565
28. Surowiak P, Dzięgiel P, Matkowski R, Kornafel J, Wojnar A, Zabel M (2002) Immunohistochemical evaluation of metallothionein (MT) expression in myoepithelial cells of ductal mammary carcinoma and its relation to survival time: analysis of 7 year-course of the disease. Folia Histochem Cytobiol 40: 105–106
29. Toyoda H, Mizushima T, Satoh T, Iizuka N, Nomoto A, Chiba H, Mita M, Naganuma A, Himeno S, Imura N (2000) HeLa cell transformants overproducing mouse metallothionein show in vivo resistance to cis-platinum in nude mice. Jpn J Cancer Res 91:91–98
30. UICC (1997) TNM classification of malignant tumors. In: Sobin LH, Wittekind C (eds). Wiley-Liss, New York
31. Van der Zee AGJ, Hollema H, Suurmeijer AJH, Krans M, Sluiter WJ, Wilemse PHB, Aalders JG, Vries EGE (1995) Value of P-glycoprotein, glutathione S-transferase pi, c-*erb*B-2, and p53 as prognostic factors in ovarian carcinomas. J Clin Oncol 13:70–78
32. Wrigley E, Verpaget HW, Jayson GC, McGown AT (2000) Metallothionein expression in epithelial ovarian cancer: effect of chemotherapy and prognostic significance. J Cancer Res Clin Oncol 126:717–721

Virchows Arch (2005) 447: 634–642
DOI 10.1007/s00428-005-1262-y

ORIGINAL ARTICLE

Derek John Atkins · Christian Gingert · Christina Justenhoven · Gerd Emil Schmahl · Marcellus Stephanus Bonato · Hiltrud Brauch · Stephan Störkel

Concomitant deregulation of HIF1α and cell cycle proteins in *VHL*-mutated renal cell carcinomas

Received: 18 January 2005 / Accepted: 21 March 2005 / Published online: 1 July 2005
© Springer-Verlag 2005

Abstract Renal cell carcinomas (RCCs) of the clear cell type are associated with alteration of the von Hippel-Lindau (VHL) tumour suppressor gene as well as subsequent stabilization and over-expression of hypoxia inducible factor (HIF), which causes up-regulation of cyclin D1. On the basis of their ability to interact with cyclin D1 we investigated a number of cell cycle proteins to shed further light on the downstream effects of HIF dysregulation. Expression of HIF1α, cyclin D1, cyclin-dependent kinase 4 and cyclin-dependent kinase inhibitors p16, p21 and p27 was studied by immunohistochemistry. Since NFκB1/RelA have been shown to bind to the cyclin D1 promoter, mRNA expression of these transcription factors was further analysed by quantitative PCR. In RCCs harbouring VHL mutations/hypermethylation, over-expression of HIF1α was paralleled by up-regulation of cyclin D1 and CDK4 and down-regulation of p21 and p27. Moreover, p27 expression was inversely correlated with tumour cell differentiation. Comparison of non-tumorous autologous kidney tissues revealed a significant down-regulation of NFκB1 mRNA expression in patients harbouring RCC with *VHL* mutations/hypermethyation. Our data support the notion of a link between VHL deficiency/HIF dysfunction and disturbances of cell cycle control in the tumorigenesis of VHL-negative RCC.

Keywords Cell cycle · HIF1 · Renal cell carcinoma · Transcription factors · VHL

This work represents part of the M.D. thesis of C. Gingert

D. J. Atkins (✉) · C. Gingert · G. E. Schmahl · S. Störkel
Institute of Pathology,
Helios-Kliniken Wuppertal,
University Witten/Herdecke,
Heusnerstrasse 40,
42283 Wuppertal, Germany
e-mail: datkins@wuppertal.helios-kliniken.de
Tel.: +49-202-8962850
Fax: +49-202-8962739

C. Justenhoven · H. Brauch
Dr. Margarete Fischer-Bosch Institute
of Clinical Pharmacology,
Stuttgart, Germany

M. S. Bonato
University of Applied Sciences,
Münster, Germany

Introduction

At least 50% of renal cell carcinomas (RCCs) develop upon bi-allelic inactivation of the von Hippel-Lindau (VHL) tumour suppressor gene [3, 6, 16, 32]. The *VHL* gene product (pVHL) represents the substrate recognition site of an E3–ubiquitin–ligase complex, thereby targeting proteins for proteasomal degradation [13]. pVHL is involved in many celular processes, including cell cycle control, extracellular matrix formation and regulation of microtubule stability [2, 7, 12, 20]. Known pVHL targets are α-subunits of the hypoxia-inducible factors (HIF) 1 and HIF2 [18]. Under normoxic conditions HIFα undergoes ubiquitylation by the pVHL-E3-ligase complex for subsequent degradation [18, 24]. However, under hypoxic conditions HIF1α is stabilized and forms a dimer with the constitutive subunit HIF1β (aryl hydrocarbon nuclear translocator, ARNT) to form HIF1, which, in turn, causes the transcription of a number of hypoxia-inducible genes, including glucose transporter 1, vascular endothelial growth factor (VEGF), transforming growth factor alpha (TGFα), erythropoietin and others [9, 15, 17, 24, 30]. Loss of pVHL function interrupts the hypoxia response pathway thus mimicking hypoxic conditions. Accordingly, loss of pVHL leads to the accumulation of HIF, resulting in excessive transcription of HIF target genes [30]. This mechanism might explain why VHL-negative tumours, such as RCCs of the clear cell type, overexpress VEGF and are highly vascularized [22].

Studies on murine and human cell lines suggested that HIFα subunits might be also involved in the regulation and control of the cell cycle machinery [1, 5, 8, 21, 31]. Cyclin

D1 and cyclin-dependent kinases (CDKs) CDK4/CDK6 are important cell cycle regulators that promote G1/S progression, at least in part, by phosphorylating the retinoblastoma protein (pRb) and thereby inactivating its ability to bind to proteins of the E2F transcription factor family and to suppress their transcriptional activity [19, 25]. Relaxed control of cell cycle regulation is considered a hallmark of malignant transformation, and *Rb* has been shown to be frequently altered in human malignancies [19]. However, in RCC, mutational inactivation of *Rb* is rare [11, 29].

Thus, there is a possibility that, in RCC, the Rb pathway might be disrupted due to disturbances of crosstalk with the HIF pathway triggered by VHL deficiency. This view is supported by recent observations of cyclin D1 up-regulation in *VHL*-deficient RCC, both in cell line and sporadic tumours [1, 2]. To establish the role of *VHL* deficiency and HIF dysfunction in cell cycle regulation it is important to further explore known cell cycle regulators in *VHL*-mutated/hypermethylated and non-mutated [*VHL* wild type (wt)] clear cell RCC. Since the hypoxia-responsive transcription factors NFκB1/RelA transactivate cell cycle regulator genes such as cyclin D1, we further tested whether these factors are up-regulated in RCC with and without *VHL* alterations, using quantitative PCR. Here we report comparative analyses of cyclin D1, CDK4 and cyclin-dependant kinase inhibitors (CDKIs) p16, p21 and p27, as well as transcription factors NFκB1 and Rel A, and discuss the findings with respect to their potential meaning in the tumorigenesis of clear cell RCC.

Material and methods

Patients and tissue samples

Formalin-fixed, paraffin-embedded tissue samples and snap-frozen tissues from 56 clear cell RCCs and the autologous normal kidney tissues were obtained from patients (male to female=2:1; median age 62.5 years, range 39–83 years) who had undergone radical nephrectomy. Of these patients, 22 had somatic *VHL* mutations/hypermethylations and/or 3 p LOH as recently described by Brauch et al. (Table 1) [3]. Histopathological classification of each tumour was performed according to the criteria proposed by Thoenes and co-workers, which are in line with the recent classification of the World Health Organization [26, 28]. Tumour grading was performed according to the grading scheme of Störkel et al. [27]. After paraffin embedding, tumour specimens were cut into 5 µm sections and stained routinely with H&E to define representative tumour regions. For the preparation of tissue micro-arrays (TMAs) at least two tissue cylinders (3 mm in diameter) from each tumour and the corresponding normal kidney were punched from these regions of the donor blocks, placed on 25 mm×35 mm paraffin blocks and H&E stained for control purposes.

Monoclonal and polyclonal antibodies

Immunohistochemical (IHC) staining was performed with monoclonal mouse antibodies (mAbs) or polyclonal rabbit antibodies (rAbs) to the following antigens: cyclin D1

Table 1 Characteristics of the VHL-negative RCCs [3]

No.	pT	pN	pM	G	Nucleotide changes	Codon	Protein Change	Mutation type	LOH
01	3	1	x	2	557A→C	115	His→Pro	Missense	NA
02	3b	x	x	2	653del7nt	147	Truncation	Frameshift	Yes
03	2	x	1	2	653–657delT	147/148	Truncation	Frameshift	No
04	3	x	x	1	651 T→C	147	Pro→Pro	Silent	NI
05	2	0	1	1	664 A→T	151	Ile→Phe	Missense	N
06	3a	0	x	2	578 C→A	122	Ala→Glu	Missense	NA
07	2	x	x	1	608 delA	132	Truncation	Frameshift	NA
08	3a	x	x	1	686 T→C	158	Leu→Pro	Missense	Yes
09	2	0	x	1	416 C→A	68	Ser→Stop	Nonsense	NA
10	2	x	x	1	564 delG	117	Truncation	Frameshift	Yes
11	3b	x	x	2	679/681delTA	156	Truncation	Frameshift	Yes
12	3b	3	x	2	418 del 3nt	69	Truncation	Frameshift	Yes
13	2	x	x	2	652 del16nt	147	Truncation	Frameshift	Yes
14	2	x	x	1	863 delA	UTR	Unknown		Yes
15	2	x	x	1	385	58		Hypermethylation	Yes
16	2	x	x	3	385	58		Hypermethylation	Yes
17	2	x	x	1	385	58		Hypermethylation	No
18	3b	1	x	1	507C→A	98	Tyr→Stop	Nonsense	NA
19	3b	x	x	2	553 delG	114	Truncation	Frameshift	Yes
20	3a	x	x	2	385	58		Hypermethylation	Yes
21	2	x	x	3	559 delC	116	Truncation	Frameshift	Yes
22	1	x	x	2	686 T→C	158	Leu→Pro	Missense	NA

del deletion, *nt* nucleotides, *NA* not available, *NI* not informative

(1:25, mAb; Novo Castra Laboratories, Newcastle upon Tyne, UK); CDK4 (1:80, rAb; Santa Cruz Biotechnology, Heidelberg, Germany); $p16^{INK4A}$ (1:20, rAb) and HIF1α (1:800, mAb; both Abcam, Cambridge, UK); $p21^{WAF1/cip1}$ (1:20, mAb; Calbiochem, San Diego, Calif., USA), $p27^{Kip1}$ (1:50, mAb; DAKO, Glostrup, Denmark). The secondary biotinylated rabbit anti-mouse and goat anti-rabbit immunoglobulin antibodies (IgGs) were purchased from DAKO (Hamburg, Germany).

Immunohistochemistry

TMA blocks were serially cut into 5 μm sections. In brief, after deparaffinization, sections were microwaved for 2–7 min in citrate buffer at 750 W. Following a washing procedure with Tris-buffered saline (TBS; pH 7.4) blocking of endogenous peroxidase was done with 3% H_2O_2 for 15 min. The tissue sections were then incubated for 10 min at room temperature with normal swine serum diluted 1:10. Primary antibodies were applied and allowed to react for 1 h at room temperature. After being rinsed twice in buffer the sections were incubated with the secondary biotinylated anti-mouse/anti-rabbit antibodies. Tissue staining was detected with the Vectastain ABC-kit (Vector Laboratories, Burlingham, Calif., USA) and DAB substrate chromogen solution. Slides were counterstained with haematoxylin, dehydrated and mounted.

All slides were independently reviewed by two investigators (D.A., C.G). Only tumour cells or mesangial/epithelial cells of the normal kidney tissues displaying nuclear reactivity were considered positive. We evaluated the number of positive cells by counting at least 200 cells in randomly chosen high-power fields (HPFs; magnification ×400) and calculating the mean from the results of both investigators.

RNA isolation and real-time PCR

Total RNA from the 56 clear cell RCCs and the autologous normal kidney tissues was extracted from snap-frozen fresh material using the Rneasy Kit as described by the manufacturer (Qiagen, Hilden, Germany). The RNA was randomly primed by hexanucleotide primers and reverse transcribed with a first-strand cDNA synthesis kit (MBI Fermentas, Lithuania). RNA expression of the transcription factors NFκB1 and RelA was quantitated by real-time PCR (RT-PCR) relative to the expression level of the house-keeping gene β-actin using the ABI Prism 7,700 Sequence Detection System (Applied Biosystems, Foster City, Calif., USA). Sequences of PCR primers and the 3′-Fam/5′-BHQ probes were as follows:

NFκB1: 5′-GCACTGGAAGTACAGGTCCA-3′/5′-GTCATCACTTTTGTCACAA CCT-3′ with probe 5′-CCTGGAACTACTAAATCTAATGCTGGGATGAAGC-3′ and RelA:5′-GAAGAGTCCTTTCAGCGGAC-3′/5′-ACACCATGGTGGGAAACTCAT-3′ with probe 5′-CCAAGCCAGCACCCCAGCCC-3′.

Primer and probe for β-actin (Human ACTB Endogenous Control, cat. no. 4326315E), as well as probes for NFκB1 and RelA, were purchased from Applied Biosystems. Primers for NFκB1 and RelA were synthesized by Roth (Karlsruhe, Germany).

RT-PCR reactions were carried out in a final volume of 25 μl. The final concentration of reagents in the RT-PCR mix for NFκB1 and RelA were 1×TaqMan Universal PCR Master Mix (cat. no. 4304437, Applied Biosystems), 300 nM forward primer, 300 nM reverse primer, and 200 nM probe. RT-PCR for β-actin was performed according to the manufacturer's instructions. PCR conditions were 50°C for 2 min followed by 95°C for 10 min, followed by 45 cycles of 15 s at 92°C and 1 min at 60°C. The RT-PCR data are given in Ct values.

Statistical analysis

IHC staining results, *VHL* mutation/hypermethylation status and RT-PCR data were statistically analysed according to their scale level: data description was based on absolute and relative frequencies for binary endpoints and on medians and quartiles for continuous endpoints. Univariate significance analysis was based on the Mann–Whitney U-test for binary parameters and on the two-sample Wilcoxon's test for continuous parameters. The Kendall's tau-b correlation coefficient was used to assess the associations. Local significance was assumed for two-sided P values <0.05. All computations were performed with SPSS release 11.0 for Windows.

Table 2 Expression of cell cycle proteins in RCCs and corresponding autologous non-tumorous kidney tissues (*NK*)

Protein	RCC		NK	
	VHL altered (*n*)	VHL wt (*n*=34)	VHL altered (*n*=18)	VHL wt (*n*=28)
HIF1α	63 (4.8)	42.5** (5.5)	0	0
cyclin D1	45 (6.8)	20** (2.7)	5 (1.1)	3 (0.6)
CDK4	40 (5.6)	27 (3.5)	8 (1.5)	6 (0.9)
p16	36 (8.1)	42 (5.3)	54 (5.5)	54 (5.1)
p21	3 (0.8)	10** (1.2)	7 (1.3)	5 (0.4)
p27	35 (9.1)	19 (3.1)	67 (4.6)	59 (4.0)

Data represent median values of the percentage of stained cells; standard deviations are in parentheses
**Differences are statistically significant (P<0.05)

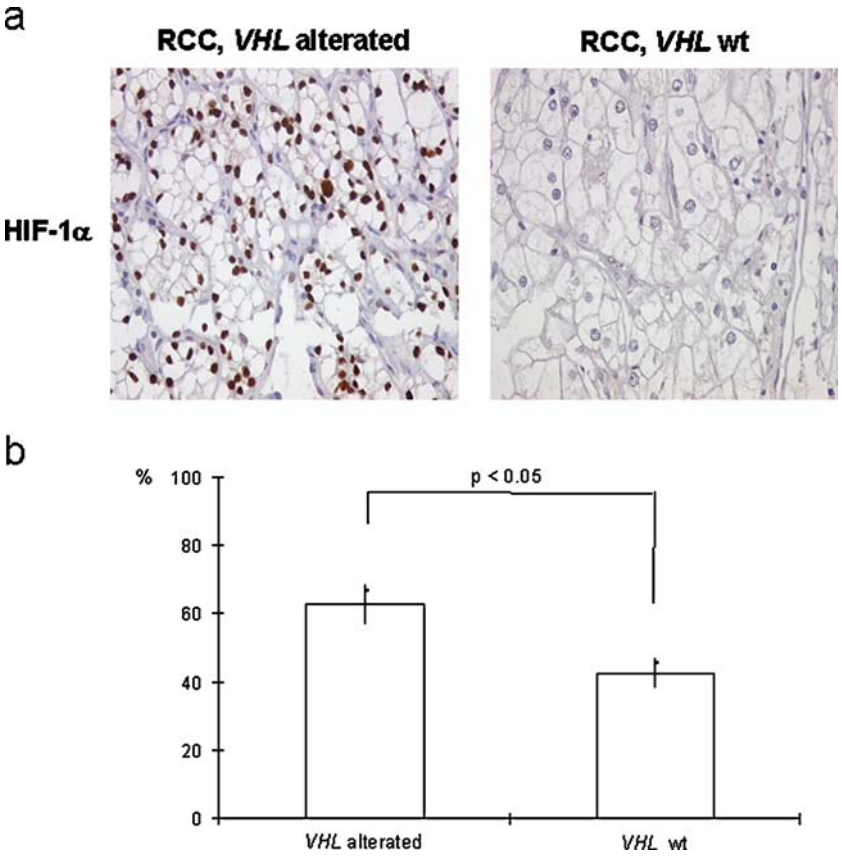


Fig. 1 **a** Immunohistochemical detection of HIF-1α protein in RCCs of the clear cell type demonstrating positive nuclear staining in a RCC bearing *VHL* alterations and mainly negative staining in a *VHL* wt RCC (×400). **b** HIF1α nuclear staining is significantly greater in RCCs harbouring *VHL* alterations than in *VHL* wt RCCs

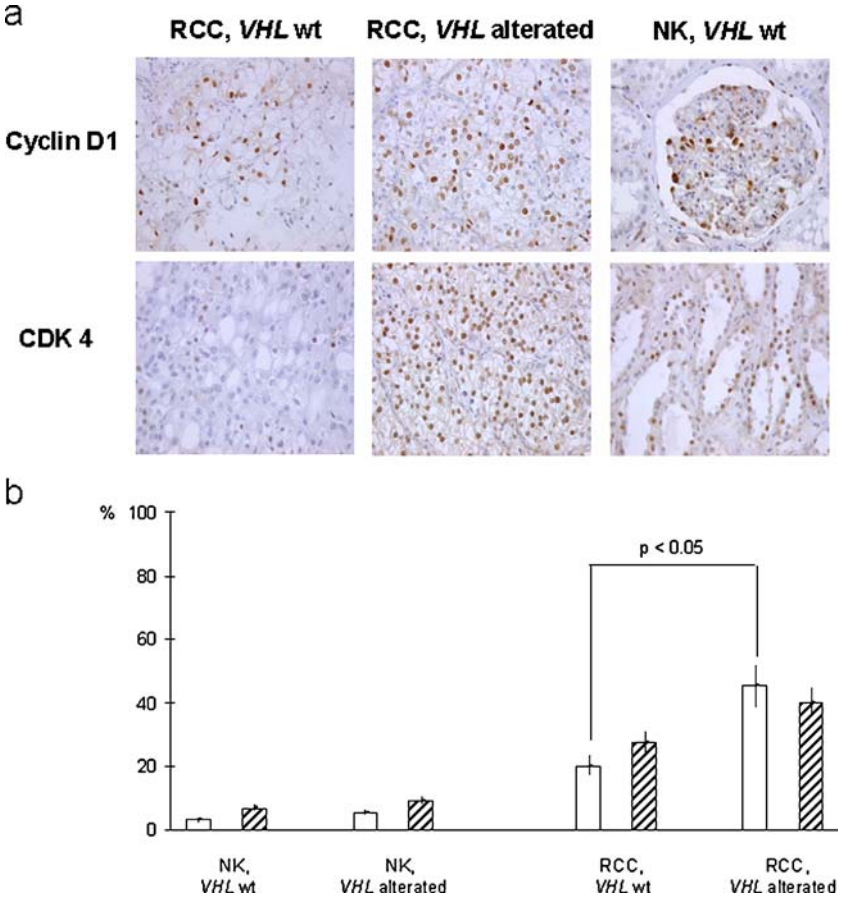


Fig. 2 **a** Immunohistochemical detection of expression levels of cyclin D1 and CDK4 in clear cell RCCs and autologous non-tumorous tissues (×400). *From left to right* RCC *VHL* wt, RCC *VHL* mutated/hypermethylated (*VHL* altered), autologous normal kidney tissue (*NK*, *VHL* wt). Nuclear staining positive for both antigens was seen in approximately 30% of all tumour cells. In contrast, less than 10% of the epithelial and mesangial cells stained positive for cyclin D1 and CDK4 in non-tumorous kidney tissue. Both antigens revealed a higher percentage of positively stained tumour cells in *VHL*-altered RCCs than in *VHL* wt RCCs. **b** Comparison of nuclear staining frequencies of cyclin D1 (*open columns*) and CDK4 (*hatched columns*) of NKs and RCCs with and without *VHL* mutations/hypermethylation. Expression of cyclin D1 and CDK4 is higher in RCCs harbouring *VHL* alterations, a difference which is significant for cyclin D1 ($P<0.05$)

Results

Up-regulation of HIF1α in RCCs bearing *VHL* alterations

RCCs were stratified according to the presence or absence of *VHL* mutations/hypermethylation and tested for differential HIF1α protein expression [3]. As expected for *VHL*-mutated/hypermethylated RCCs, IHC staining for HIF1α showed a significant up-regulation, as shown by positive nuclear staining of tumour cells. More than 60% of *VHL*-mutated/hypermethylated tumour cells, but only 42% of the *VHL* wt tumour cells, displayed staining positive for HIF1α ($P<0.05$; Table 2, Fig. 1). In contrast, nuclear staining positive for HIF1α was not detectable in epithelial or mesangial cells of non-tumorous kidney tissues (not shown).

Differential expression of cell-cycle proteins in RCCs and autologous non-tumorous kidney tissues

We determined the differential expression of the various cell cycle proteins, including cyclin D1, CDK4, p16, p21, and p27, in RCCs and matched autologous non-tumorous kidney tissues (Table 2). IHC results showed up-regulation of cyclin D1 and CDK4 in RCCs when compared with non-tumourous autologous tissues (Fig. 2). Only 4% and 7% of the epithelial and mesangial cells in non-tumorous kidney tissues expressed cyclin D1 and CDK4, respectively. In contrast, RCC cells showed nuclear staining positive for cyclin D1 and CDK4 in 30% and 32%, respectively (Table 2). The differences between RCC cells and autologous non-tumorous kidney tissues were significant for both cell cycle proteins ($P<0.001$). Moreover, the expression of both antigens was significantly correlated to each other ($P<0.05$).

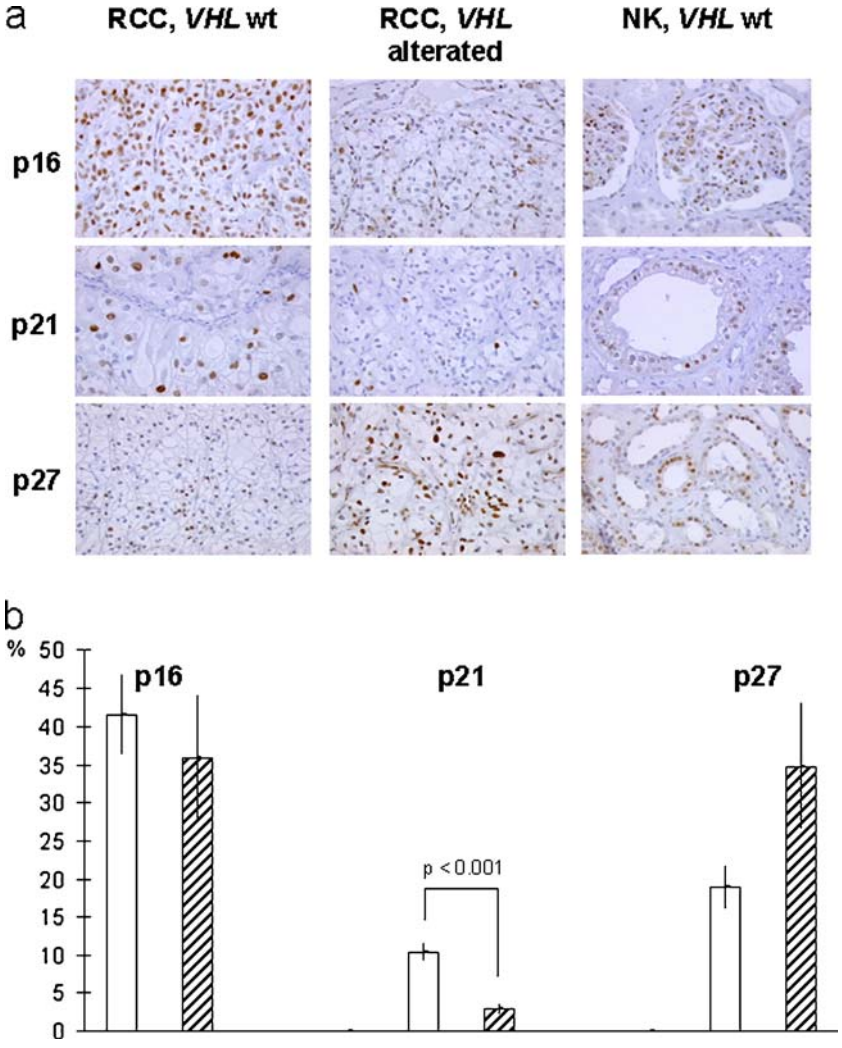


Fig. 3 **a** Immunohistochemical detection of CDKIs p16, p21 and p27 in *VHL* wt and *VHL*-altered RCCs and non-tumorous kidney tissues (NKs). (400×) p16: Only 39 % of all tumour cells (RCC, *VHL* wt and RCC, *VHL* altered), but more than 50% of normal epithelial and mesangial cells (NK, *VHL* wt), show positive staining for p16. p21: Although overall expression of p21 was low in both RCCs and matched non-tumorous kidney tissues, *VHL* wt RCCs displayed a higher percentage of stained tumour nuclei than did RCCs bearing *VHL* mutations/hypermethylation. p27: More than 30% of *VHL*-mutated/hypermethylated tumour cells, but less than 20% of *VHL* wt tumour cells, showed nuclear p27 expression. **b** Comparison of nuclear staining frequencies showed a significant difference between *VHL* wt RCCs (*open columns*) and *VHL*-mutated/hypermethylated RCCs for p21 (*hatched columns*) but not for p16 and p27

In contrast, expression levels of CDKI were lower in tumour cells than in corresponding normal epithelial and mesangial cells. In particular, p16 and p27 expression levels were 39% and 25% in tumour cells and 54% and 62% in epithelial and mesangial cells of non-tumorous kidney tissues ($P<0.02$, Table 2). Approximately 7% of the tumour cells, but only 5% of the non-tumorous epithelial and mesangial cells, displayed nuclear staining positive for p21 ($P=0.137$).

Differential expression of cell cycle proteins in RCCs with and without *VHL* alterations

Comparison of cyclin D1 expression and CDK4 expression in RCCs with and without *VHL* alterations revealed a statistically significant increase of cyclin D1 expression in *VHL*-mutated/hypermethylated tumours ($P<0.05$; Table 2, Fig. 2). In parallel, expression of CDK4 was increased in *VHL*-mutated/hypermethylated RCCs, but the difference between *VHL*-mutated/hypermethylated and *VHL* wt tumours did not reach statistical significance.

Since expression of cyclin D1 and CDK4 appears to be more frequent in RCCs harbouring *VHL* alterations (Fig. 2), we further analysed whether this was also the case for CDK inhibitors. As shown in Fig. 3, there is a differential expression of p21 and p27, but not of p16, in *VHL*-mutated/hypermethylated versus *VHL* wt RCCs. In detail, only 3% of *VHL*-mutated/hypermethylated tumour cells but 10% of the tumour cells without *VHL* alterations stained positive when the anti-p21 mAbs were used ($P<0.001$). In contrast, 35% of the *VHL*-mutated/hypermethylated tumour cells, but only 19% of the *VHL* wt tumour cells, displayed nuclear staining positive for p27. However, the difference between RCCs with and without *VHL* alterations did not reach statistical significance for p27 expression.

Correlation of VHL-deficiency, tumour grade, and expression of cyclin D1 and p27

In order to assess a possible correlation between *VHL* mutations/hypermethylation and tumour cell differentiation we grouped RCCs according to their *VHL* status and tumour grading (G1 versus G2/G3). Analysis of the IHC results revealed an inverse correlation for cyclin D1, p27 and tumour grading only in RCCs bearing *VHL* alterations. Among the latter, ten tumours were well-differentiated (G1) and 12 tumours displayed intermediate (G2; $n=10$) or low (G3; $n=2$) differentiation. Expression of cyclin D1 and p27 was detectable in 73% and 59% of well-differentiated tumour cells but only in 22% and 15% of intermediate or low differentiated tumour cells, respectively ($P<0.05$; Fig. 4). In contrast, among RCCs without *VHL* alterations, only 23% and 25% of well-differentiated tumour cells (G1; $n=17$) displayed nuclear staining positive for cyclin D1 and p27, respectively, whereas 17% and 13% of intermediate (G2; $n=15$) or low (G3; $n=2$) differentiated tumour cells stained positive for both antibodies, respectively (Fig. 4). These differences were not significant.

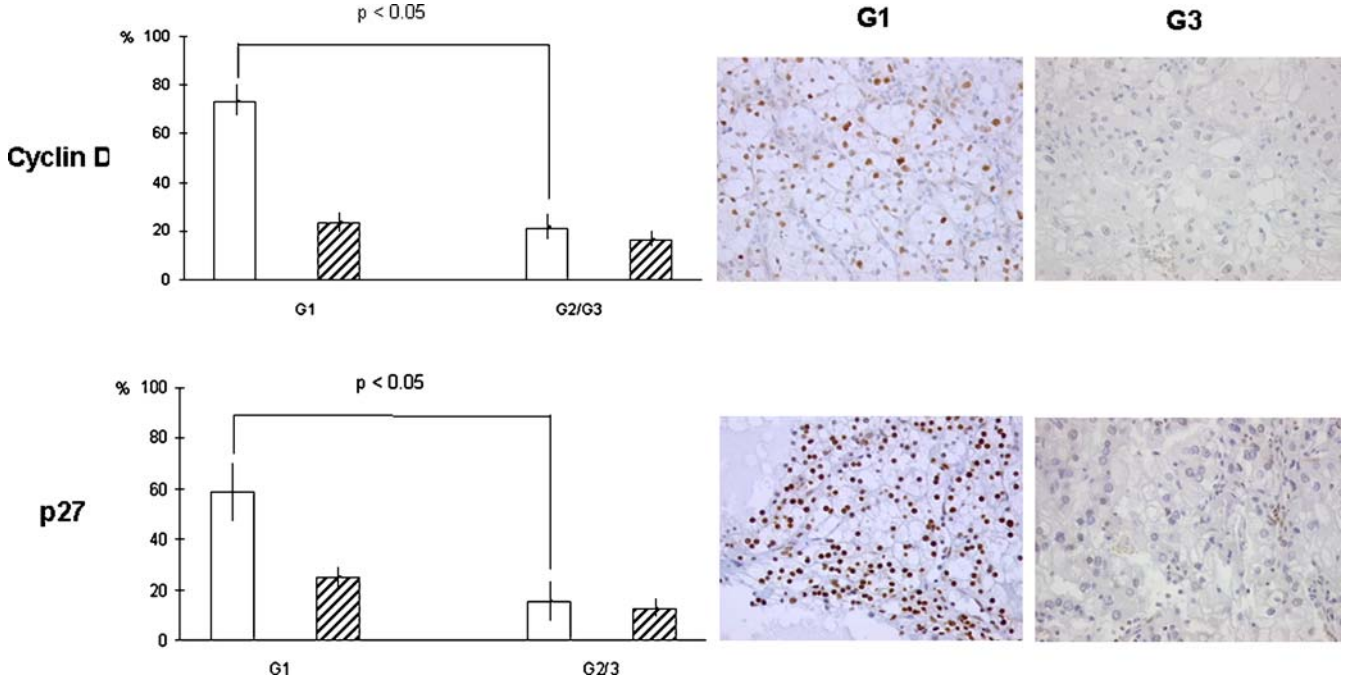


Fig. 4 Inverse correlation between cyclin D1/p27 expression and tumour grading in *VHL*-mutated/hypermethylated RCCs (×400). IHC staining for cyclin D1 and p27 demonstrated that both antigens are highly expressed in well-differentiated tumour cells (G1), whereas the majority of intermediate (G2) or low (G3) differentiated tumour cells stained negative. *Open columns* RCC, *VHL* mutated/hypermethylated, *hatched columns* RCC, *VHL* wt

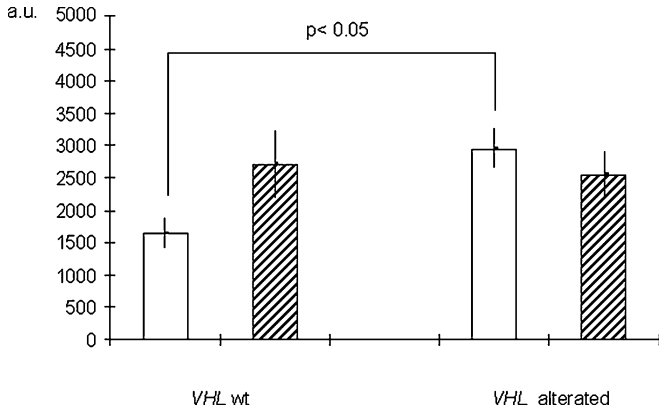


Fig. 5 mRNA expression of NFκB1 assessed by quantitative RT-PCR, which does not show significant differences in the amount of NFκB1 mRNA between matched normal kidney tissues (*open columns*) and RCCs (*hatched columns*), or between RCCs with or without *VHL* alterations. However, mRNA expression significantly differed between normal kidney tissues, depending on the *VHL* status of the corresponding tumour. Data represent means from two independent experiments

Transcriptional up-regulation of NFκB1 in RCCs bearing *VHL* alterations

Besides HIF1 there are several other well-characterized transcription factors, such as NFκB1 and RelA, that are known to regulate genes coding for cell cycle proteins. In order to assess a possible role of these transcription factors in the context of RCCs bearing *VHL* alterations, we quantified RNA expression levels by RT-PCR and correlated them with the IHC data. Comparison of *VHL* wt RCCs with RCCs bearing *VHL* alterations showed no statistically significant difference with respect to the RNA expression levels of both transcription factors. However, there was an obvious difference in the expression of NFκB1 in the corresponding non-tumorous kidney tissues, indicating that NFκB1 is up-regulated during the tumorigenic process of RCCs that acquire *VHL* mutation/hypermethylation. The different NFκB1 expression in autologous normal kidney tissues was significant ($P<0.05$; Fig. 5).

Discussion

The results from this study show that factors involved in cell cycle regulation are differentially expressed in clinical samples of clear cell RCCs and that these differences might be related to VHL deficiency and HIF pathway dysfunction. These findings are based on comparisons of protein or mRNA expression levels between normal and tumorous tissues and on comparisons between RCCs with and without *VHL* alterations.

Firstly, we stratified clear cell RCCs according to diagnostic and molecular characteristics such as grading and *VHL* mutation status previously established [3]. To explore a possible relationship between *VHL* alterations and cell cycle dysregulation we assessed protein expression of HIF1α by IHC. The rationale behind this is that VHL negativity due to *VHL* mutation/hypermethylation may interrupt the HIF pathway, which, in turn, may affect cell cycle control. As expected from previous reports, we observed a significant correlation of HIF1α up-regulation with *VHL* alterations [9, 30].

In a next step we showed that expression of cell cycle regulators cyclin D1 and CDK4 was significantly increased in RCCs when compared with normal renal epithelial and mesangial cells. These data suggest that nearly one-third of tumours were in G1/S transition. When we further stratified RCCs into *VHL* wt and *VHL*-mutated/hypermethylated tumours it became evident that cyclin D1 and CDK4 levels were more increased in RCCs with *VHL* alterations, particularly those with increased HIF1α expression. Thus, our data obtained from clinical clear cell RCCs support the notion of a regulatory role of HIF1α in the transcription of cyclin D1 and CDK4. In particular, over-expression of cyclin D1, resulting from pVHL deficiency and HIF1α dysregulation, might point to a mechanism by which the Rb pathway is deregulated in clear cell RCC, a notion that has been previously suggested on the basis of in vitro experiments [2]. A possible link between VHL deficiency, HIF dysregulation and subsequent overexpression of cyclin D1 seems plausible, since the cyclin D1 promoter contains at least two HIF-binding consensus sites (hypoxia-responsive elements, HREs) at positions -552 and -390 [23]. Thus, our data suggesting HIFα-dependent up-regulation of cyclin D1 and CDK4 expression are in line with an HIFα-mediated dysfunction of cell cycle control in clear cell RCCs harbouring *VHL* mutations/hypermethylation.

When we further extended our investigations to inhibitors of the cyclin D1/CDK4 complex we observed significant expression between autologous non-tumorous tissues and RCCs, with respect to CDKIs p16 and p27 but not p21. However, in contrast to cyclin D1 and CDK4, variation of CDKI expression resulted in a decrease rather than an increase. Further comparison of CDKI protein expression levels between RCCs with and without *VHL* alterations showed that, for p27, this decrease was less pronounced in tumours with *VHL* alterations than in VHL wt tumours. Although, there was no significant variation of p21 expression levels between non-tumorous tissues and RCCs, already mentioned above, we observed a significant difference between *VHL* wt and *VHL*-mutated/hypermethylated RCCs in that expression levels of p21 were decreased in RCCs with VHL mutations/hypermethylation but increased in *VHL* wt RCCs (Fig. 3). Interestingly, a concomitant increase of cyclin D1 expression and p27 expression in RCCs bearing *VHL* alterations was correlated with more favourable tumour cell differentiation (Fig. 4).

Cyclin D1 abundance varies with the cell cycle. In short-lived cells cyclin D1 is subject to rapid ubiquitination and proteasomal degradation [14, 25]. Since cyclin D1 abundance is largely controlled by the rate of gene transcription, we also included transcription factors NFκB1 and RelA, which are able to bind to the cyclin D1 promoter, for analysis [10, 14]. Interestingly, a significant difference in NFκB1 mRNA expression was found in autologous non-tumorous renal epithelial tissue that corresponded to tu-

mours harbouring *VHL* alterations. This raises the possibility that the tumorigenic process of clear cell RCCs harbouring *VHL* alterations might require substantial upregulation of NFκB1 prior to the initiating tumorigenic event. This interpretation is in line with recent findings of Figueroa et al., who linked NFκB with HIF-target gene expression by blocking HIF1α protein expression and subsequent erythropoietin gene expression through inhibition of NFκB under hypoxic conditions [4].

Altogether, our observations obtained from clinical RCC samples support a possible role of cell cycle proteins in the tumorigenesis of RCCs bearing *VHL* mutations/hypermethylation. In particular, CDKIs of the CIP/Kip family of proteins (p21 and p27), but not of the Ink4 family (p16), seem to be associated with the tumorigenic process of RCCs harbouring *VHL* mutations/hypermethylation. Accordingly, cell cycle dysregulation might require pVHL deficiency and HIF1α dysfunction to mediate the disruption of the control of G1/S transition on the level of cyclin–CDK complex inhibition. Although the precise mechanisms of interaction of cell cycle proteins in *VHL*-altered tumorigenesis remains elusive, our results acknowledge the prominent role of cyclin D1 and its regulatory factors within the CDK/CDKI system of cell cycle regulation.

Acknowledgements This work was, in part, supported by the Robert Bosch Foundation of Medical Research, Stuttgart, Germany. We would like to thank P. Böhmer and R. Baumann for excellent technical assistance.

References

1. Baba M, Hirai S, Yamada-Okabe H, Hamada K, Tabuchi H, Kobayashi K, Kondo K, Yoshida M, Yamashita A, Kishida T, Nakaigawa N, Nagashima Y, et al (2003) Loss of von Hippel-Lindau protein causes cell density dependent deregulation of cyclin D1 expression through hypoxia-inducible factor. Oncogene 22:2728–2738
2. Bindra RS, Vasselli JR, Stearman R, Linehan WM, Klausner RD (2002) VHL-mediated hypoxia regulation of cyclin D1 in renal carcinoma cells. Cancer Res 62:3014–3019
3. Brauch H, Weirich G, Brieger J, Glavac D, Rodl H, Eichinger M, Feurer M, Weidt E, Puranakanitstha C, Neuhaus C, Pomer S, Brenner W, et al (2000) VHL alterations in human clear-cell renal-cell carcinoma: association with advanced tumor stage and a novel hot spot mutation. Cancer Res 60:1942–1948
4. Figueroa YG, Chan AK, Ibrahim R, Tang Y, Burow ME, Alam J, Scandurro AB, Beckman BS (2002) NF-kappa B plays a key role in hypoxia-inducible factor-1- regulated erythropoietin gene expression. Exp Hematol 30:1419–1427
5. Gardner LB, Li Q, Park MS, Flanagan WM, Semenza G, Dang CV (2001) Hypoxia inhibits G_1/S transition through regulation of p27 expression. J Biol Chem 276:7919–7926
6. Gnarra JR, Tory K, Weng Y, Schmidt L, Wei MH, Li H, Latif F, Liu S, Chen F, Duh FM (1994) Mutations of the VHL tumour suppressor gene in renal carcinoma. Nat Genet 7:85–90
7. Goda N, Dozier SJ, Johnson RS (2003) HIF-1 in cell cycle regulation, apoptosis, and tumor progression. Antioxid Redox Signal 5:467–473
8. Goda N, Ryan HE, Khadivi B, McNulty W, Rickert RC, Johnson RS (2003) Hypoxia-inducible factor 1α is essential for cell cycle arrest during hypoxia. Mol Cell Biol 23:359–369
9. Gunaratnam L, Morley M, Franovic A, de Paulsen N, Mekhail K, Parolin DA, Nakamura E, Lorimer IA, Lee S (2003) Hypoxia inducible factor activates the transforming growth factor-α/epidermal growth factor receptor growth stimulatory pathway in $VHL^{-/-}$ renal cell carcinoma cells. J Biol Chem 45:44966–44974
10. Guttridge DC, Albanese C, Reuther JY, Pestell RG, Baldwin AS (1999) NF-κB controls cell growth and differentiation through the transcriptional regulation of cyclin D1. Mol Cell Biol 19: 5785–5799
11. Hedberg Y, Ljungberg B, Roos G, Landberg G (2004) Retinoblastoma protein in human renal cell carcinoma in relation to alterations in G1/S regulatory proteins. Int J Cancer 109:189–193
12. Hergovich A, Lisztwan J, Barry R, Ballschmieter P, Krek W (2003) Regulation of microtubule stability by the von Hippel-Lindau tumour suppressor protein pVHL. Nat Cell Biol 5:64–70
13. Jaakkola P, Mole DR, Tian YM, Wilson MI, Gielbert J, Gaskell SJ, Kriegsheim Av, Hebestreit HF, Mukherji M, Schofield CJ, Maxwell PH, Pugh CW, et al (2001) Targeting of HIF-alpha to the von Hippel-Lindau ubiquitylation complex by O2- regulated prolyl hydroxylation. Science 292:468–472
14. Joyce D, Albanese C, Steer J, Fu M, Bouzahzah B, Pestell RG (2001) NF-κB and cell-cycle regulation: the cyclin connection. Cytokine Growth Factor Rev 12:73–90
15. Knebelmann B, Ananth S, Cohen HT and Sukhatme VP (1998) Transforming growth factor alpha is a target for the von Hippel-Lindau tumor suppressor. Cancer Res 58:226–231
16. Latif F, Tory K, Gnarra J, Yao M, Duh FM, Orcutt ML, Stackhouse T, Kuzmin I, Modi W, Geil L, Schmidt L, Zhou F, et al (1993) Identification of the von Hippel- Lindau disease tumor suppressor gene. Science 260:1317–1320
17. Leonard MO, Cottell DC, Godson C, Brady HR, Taylor CT (2003) The role of HIF-1α in transcriptional regulation of the proximal tubular epithelial cell response to hypoxia. J Biol Chem 278:40296–40304
18. Maxwell PH, Wiesener MS, Chang GW, Clifford SC, Vaux EC, Cockman ME, Wykoff CC, Pugh CW, Maher ER, Ratcliffe PJ (1999) The tumour suppressor protein VHL targets hypoxia-inducible factors for oxygen-dependent proteolysis. Nature 399: 271–275
19. Nehvins JR (2001) The Rb/E2F pathway and cancer. Hum Mol Genet 10:699–703
20. Ohh M, Yauch RL, Lonergan KM, Whaley JM, Stemmer-Rachamimov AO, Louis DN, Gavin BJ, Kley N, Kaelin WG Jr, Iliopoulos O (1998) The von Hippel-Lindau tumor suppressor protein is required for proper assembly of an extracellular fibronectin matrix. Mol Cell 1:959–968
21. Pause A, Lee S, Lonergan KM, Klausner RD (1998) The von Hippel-Lindau tumor suppressor gene is required for cell cycle exit upon serum withdrawal. Proc Natl Acad Sci U S A 95:993–998
22. Schraml P, Struckmann K, Hatz F, Sonnet S, Kully C, Gasser T, Sauter G, Mihatsch MJ, Moch H (2002) VHL mutations and their correlation with tumour cell proliferation, microvessel density, and patient prognosis in clear-cell renal-cell carcinoma. J Pathol 196:186–193
23. Semenza GL (1998) Hypoxia-inducible factor 1 and the molecular physiology of oxygen homeostasis. J Lab Clin Med 131: 207–214
24. Semenza GL (2001) HIF-1, O(2), and the 3 PHDs: how animal cells signal hypoxia to the nucleus. Cell 107:1–3
25. Sherr CJ (2000) The Pezcoller lecture: cancer cell cycles revisited. Cancer Res 60:3689–3695

26. Störkel S (1997) Classification of renal cell carcinoma: workgroup no. 1. Union Internationale Contre le Cancer (UICC) and the American Joint Committee on Cancer (AJCC). Cancer 80: 987–989
27. Störkel S, Thoenes W, Jacobi GH, Lippold R (1989) Prognostic parameters in renal cell carcinomas: a new approach. Eur Urol 16:416–422
28. Thoenes W, Störkel S, Rumpelt HJ (1986) Histopathology and classification of renal cell tumors (adenomas, oncocytomas and carcinomas): the basic cytological and histopathological elements and their use for diagnostics. Pathol Res Pract 181:125–143
29. Walther MM, Gnarra JR, Elwood L, Xu HJ, Florence C, Anglard P, Hu SX, King C, Trahan E, Hurley K (1995) Loss of heterozygosity occurs centromeric to RB without associated abnormalities in the retinoblastoma gene in tumors from patients with metastatic renal cell carcinoma. J Urol 153:2050–2054
30. Wiesener MS, Munchenhagen PM, Berger I, Morgan NV, Roigas J, Schwiertz A, Jurgensen JS, Gruber G, Maxwell PH, Loning SA, Frei U, Maher ER, et al (2001) Constitutive activation of hypoxia-inducible genes related to overexpression of hypoxia-inducible factor-1α in clear cell renal carcinomas. Cancer Res 61:5215–5222
31. Zatyka M, da Silva NF, Clifford SC, Morris MR, Wiesener MS, Eckardt KU, Houlston RS, Richards FM, Latif F, Maher ER (2002) Identification of cyclin D1 and other novel targets for the von Hippel-Lindau tumor suppressor gene by expression array analysis and investigation of cyclin D1 genotype as a modifier in von Hippel-Lindau disease. Cancer Res 62:3803–3811
32. Zbar B, Kishida T, Chen F, Schmidt L, Maher ER, Richards FM, Crossey PA, Webster AR, Affara NA, Ferguson-Smith MA, Brauch H, Glavac D, et al (1996) Germline mutations in the von Hippel-Lindau disease (VHL) gene in families from North America, Europe, and Japan. Hum Mutat 8:348–357

Virchows Arch (2005) 447: 643–648
DOI 10.1007/s00428-004-1183-1

ORIGINAL ARTICLE

Ryosuke Watanabe · Tokuhiro Chano · Hirokazu Inoue · Takahiro Isono · Osamu Koiwai · Hidetoshi Okabe

Rb1cc1 is critical for myoblast differentiation through Rb1 regulation

Received: 18 November 2004 / Accepted: 19 November 2004 / Published online: 21 June 2005
© Springer-Verlag 2005

Abstract Rb1-inducible coiled-coil 1 (Rb1cc1) expressed at high levels is associated with the maturation of human embryonic musculoskeletal cells. To clarify the molecular role of Rb1cc1 in muscular differentiation, we investigated the expression of Rb1cc1 and other genes that regulate differentiation in murine embryonic tissues and in C2C12 myoblasts. We also evaluated the effects of RNA interference (RNAi)-mediated *Rb1cc1* knockdown on C2C12 myoblast differentiation. After Rb1cc1, Rb1 and myosin heavy chain (Myhc) were expressed in mouse embryonic muscles. The synchronous expression of *Rb1cc1* and *Rb1* predicted *Myhc* expression during C2C12 myoblast differentiation. RNAi-mediated knockdown of *Rb1cc1* led to *Rb1* suppression, and C2C12 myoblasts failed to differentiate. These results indicated that Rb1cc1 is a potent regulator of the Rb1 pathway and a novel mediator that plays a crucial role in muscular differentiation. Rb1cc1 expression is, thus, a prerequisite for myogenic differentiation.

Keywords Rb1cc1 · Rb1 · Myoblast · Differentiation

R. Watanabe · O. Koiwai
Department of Applied Biological Science,
Faculty of Science and Technology,
Science University of Tokyo,
278-0022 Chiba, Japan

T. Chano (✉) · H. Okabe
Department of Clinical Laboratory Medicine,
Shiga University of Medical Science,
Tsukinowa-cho, Seta, Otsu,
520-2192 Shiga, Japan
e-mail: chano@belle.shiga-med.ac.jp
Tel.: +81-77-5482865
Fax: +81-77-5482407

H. Inoue
Department of Microbiology,
Shiga University of Medical Science,
Tsukinowa-cho, Seta, Otsu,
520-2192 Shiga, Japan

T. Isono
Central Research Laboratory,
Shiga University of Medical Science,
Tsukinowa-cho, Seta, Otsu,
520-2192 Shiga, Japan

T. Chano
PRESTO, Japan Science and Technology Agency,
Saitama, Japan

Introduction

During differentiation, skeletal muscle undergoes terminal withdrawal from the cell cycle, the activation of coordinated gene expression, and the fusion of myoblasts into multinucleated myotubes. These events are largely dependent on muscle-specific transcription factors and the retinoblastoma 1 (Rb1) tumor suppressor. The MyoD family includes MyoD, myf5, myogenin, and MRF4 [3, 11, 22], among which MyoD plays particularly pivotal roles in the activation of muscle-specific gene expression and cell-cycle arrest [7, 19]. However, the roles of these myogenic factors apparently depend on Rb1, which might mediate both terminal withdrawal from cell cycle and the upregulation of tissue-specific genes associated with terminal differentiation [12, 23]. Myotubes deficient in *Rb1* do not differentiate and, in fact, re-enter the cell cycle in response to mitogens [21]. Moreover, introducing MyoD into *Rb1*-deficient mouse embryonic fibroblasts cannot induce late markers of myogenic differentiation and cell-cycle arrest, indicating that Rb1 is required for MyoD-mediated myogenic function [8, 18]. Although Rb1 is important to muscular differentiation, the precise mechanisms remain obscure.

We recently identified a novel molecule, Rb1-inducible coiled-coil 1 (Rb1cc1), which is expressed at high levels in human embryonic musculoskeletal and cultured osteosarcoma cells. Rb1cc1 induces Rb1 expression in a variety of cultured cells [5, 6], and the expression of both molecules is synchronous [5]. We also demonstrated that Rb1cc1 contributes to the maturation of human embryonic musculoskeletal cells [6]. These findings implied that Rb1cc1 is involved in muscular differentiation.

To define the relationship between Rb1cc1 function and muscle differentiation, we used the murine C2C12 myoblast model, which has been widely studied as an in vitro model to understand the regulation of myogenic differentiation [10, 13]. Switching C2C12 cell lines to low-serum medium induces their differentiation. This process closely resembles myogenic differentiation in vivo. The expression of both *Rb1cc1* and *Rb1* is similarly upregulated in the model. Furthermore, *Rb1cc1* knockdown led to the downregulation of *Rb1* expression, and late markers of myogenic differentiation were not expressed. The present study showed that Rb1cc1 is vitally involved in skeletal muscle differentiation.

Materials and methods

Northern blots

Mouse embryo full stage blots (Seegene, Seoul, Korea) were hybridized with gene-specific probe nucleotides (nt) 1536–3500 of *Rb1cc1* (GenBank accession number, AB070619), 336–675 of *Rb1* (GenBank accession number, NM000321), and 2695–2719 of *myosin heavy chain* (*Myhc*) (GenBank accession number, NM144961). The probes were labeled with [α-^{32}P] dCTP (3000 Ci/mmol; Amersham, Piscataway, NJ) using random priming and hybridized with the blot membrane at 42°C overnight in 50% formamide containing 1% sodium dodecyl sulfate (SDS), 1 mol/l NaCl, 200 mg/ml sonicated herring sperm DNA, and 10% dextran sulfate. The blots were then washed twice at 42°C in 2×standard saline citrate (SSC) containing 1% SDS and once with 0.2×SSC containing 1% SDS for 5 min at 65°C. Blots were visualized using autoradiography with a Kodak BioMax and intensifying screens (Kodak, New Haven, CT).

Histology and immunohistochemistry

Pregnant female C57BL6 mice were sacrificed by cervical dislocation, and embryos were transferred to 10% buffered formalin and fixed overnight. The embryos were washed several times in 70% ethanol, embedded in paraffin, and serially sliced into 4-μm sections. Deparaffinized sections were immersed in 0.3% H_20_2, autoclaved at 120°C for 1 min, and rinsed with 1×Tris-buffered saline (TBS) prior to incubation overnight at 4°C with the following primary antibodies: anti-Rb1cc1 rabbit antiserum (α-Rb1cc1–1104) [2, 5], anti-Rb1 monoclonal antibody (G3–245; PharMingen, San Diego, CA), and anti-Myhc monoclonal antibody (RNMy2/9D2; Novo Castra, Newcastle, UK). The sections were rinsed with 1×TBS and incubated with secondary antibody (Simple Stain MAX-PO; Nichirei, Japan) at room temperature for 1 h. The sections were then stained with 3,3′-diaminobenzidine tetrahydrochloride and counterstained with hematoxylin.

Cell culture

C2C12 mouse skeletal myoblasts were cultured in Dulbecco's modified Eagle's medium supplemented with 10% fetal bovine serum (growth medium). To induce muscular differentiation, the cells were rendered quiescent by serum withdrawal for 48 h and stimulated to differentiate by adding 2% horse serum [differentiation medium (DM)].

RNAi and transfection

Three kinds of small interfering RNA (siRNA) plasmid vectors (608, 1993 and 4525) corresponding to different targeting sites (nt.608–626, nt. 1993–2013 and nt. 4525–4545, respectively) of *Rb1cc1* mRNA (GenBank accession number, AB070619) were synthesized in vitro by inserting artificial oligonucleotides into pRNAT-H1.1/Hygro (GenScript, Piscataway, NJ). We introduced each siRNA or control vector into C2C12 cells using FuGENE6 according to the supplier's recommendations (Roche Applied Science).

Reverse-transcription polymerase chain reaction

Total RNA was isolated from C2C12 cells using TRIzol (Gibco-BRL), and first-strand cDNA was synthesized using Superscript III reverse transcriptase and Oligo d(T)$_{12–18}$ primer (Gibco-BRL). The gene primer sequences were as follows: murine *Rb1cc1*: forward, 5′- TGCTGCACAA GACTCTCACA and reverse, 5′- CAGCATTTCCTTCTG CTGTG; *Rb1*: forward, 5′- CACGTGTAAATTCTGCTG CAA and reverse, 5′- CCTGG TGGAGGCATACTGTAA; *Gapdh*: forward, 5′- CATGACAACTTTGGCATTGTG and reverse, 5′- GTTGAAGTCGCAGGAGACAAC; *Myhc*: forward, 5′- AAGG AACTTGAAGAAAAGATGGTG and reverse, 5′- TCAAGTTTTCTCTTG GCTCTTTCT; *cyclin D3*: forward, 5′- TAGGCGCCTGCTCTATGTCT and reverse, 5′-ATCTGTGGGAGTGCTGGTCT; *p21*: forward 5′-GTCCAATCCTGGTGATGT CC and reverse, 5′- CAG GGCAGAGGAAGTACTGG. The PCR protocols consisted of 26 cycles for *Rb1cc1*, *Rb1* and *p21*, 21 for *Gapdh*, 38 for *Myhc*, and 36 cycles for *cyclin D3* of a 20-s denaturation at 95 C, 20-s annealing at 55 C, and 30-s extension at 72°C.

Immunocytochemical analysis of C2C12 cells

The above-mentioned primary antibodies were labeled with Alexa Fluor 555 (Molecular Probes, Eugene, OR) accord-

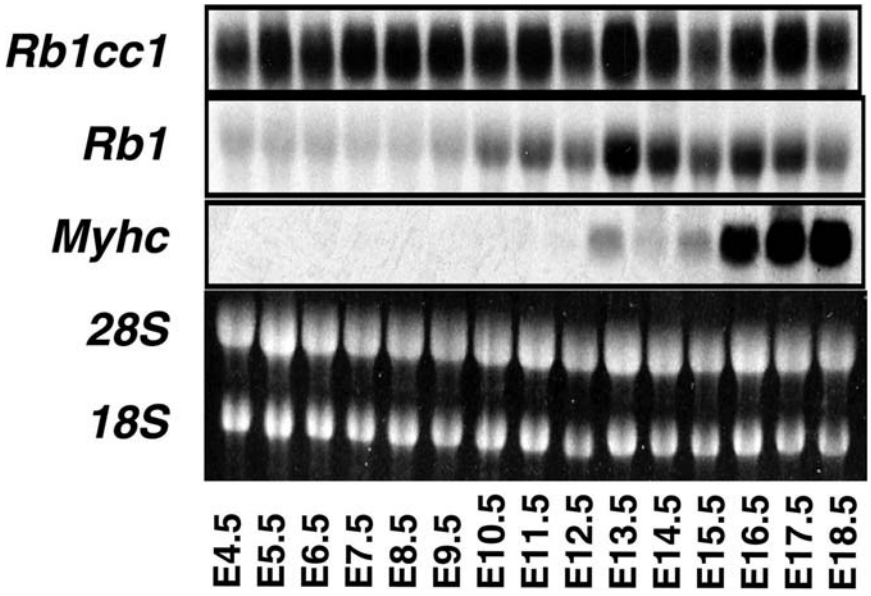


Fig. 1 Expression of mRNA during mouse embryogenesis. Membranes were hybridized with specific probes for *Rb1cc1*, *Rb1*, and myosin heavy chain (*Myhc*). Equal sample loading was conformed by ethidium bromide staining of RNAs. Rb1cc1 mRNA was constitutively expressed in embryos and predicted Rb1 and Myhc

ing to the supplier's protocol. The C2C12 cells treated with siRNA were fixed, incubated with the appropriate labeled antibody, and evaluated using fluorescent microscopy.

Results

Rb1cc1 predicts Rb1 and Myhc

To determine the importance of Rb1cc1 in muscular differentiation, we analyzed Rb1cc1 expression in murine embryos. Northern blotting showed that *Rb1cc1* mRNA was constitutively expressed in the embryos and predicted *Rb1* and *Myhc*. *Rb1* mRNA was obviously induced in E10.5 embryos and upregulated at E13.5–14.5 and E16.5–17.5. Following *Rb1cc1* and *Rb1* expression, *Myhc*, a late marker of myogenic differentiation, was expressed in E13.5 embryos and obviously induced at E16.5 (Fig. 1).

Immunohistochemical staining with Rb1cc1, Rb1, and Myhc in murine embryos also showed Rb1cc1, Rb1, and Myhc expression in developing murine muscular tissues (Fig. 2). Rb1cc1 was expressed predominantly in the cytoplasm, and Rb1 was located in the nucleus. Myhc was expressed throughout 18 dpc mouse muscles.

Expression of *Rb1cc1* and *Rb1* is associated with muscular differentiation

To investigate the Rb1cc1-mediated molecular mechanism in muscle differentiation, we used the murine C2C12 myoblast system. *Rb1cc1* and *Rb1* gene expression was induced

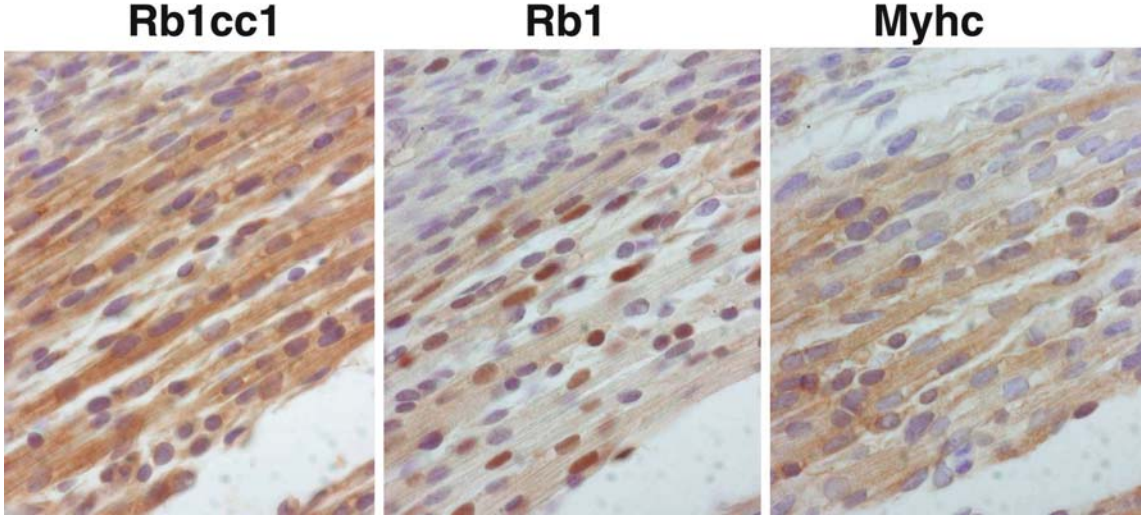


Fig. 2 Expression of Rb1cc1, Rb1, and Myhc in mouse embryos. Immunohistochemical analysis demonstrated predominant Rb1cc1 expression in cytoplasm and Rb1 in nuclei. Myhc expression is scattered throughout 18.5 days post-conception (dpc) mouse muscles

in C2C12 cells by DM. Thereafter, differentiated C2C12 cells also expressed high levels of *Myhc*, a late marker of myogenic differentiation, compared with proliferating C2C12 cells. More *p21* expression was induced in differentiating than in proliferating C2C12 cells (Fig. 3).

Rb1cc1-specific knockdown disturbs myoblast differentiation

To study the functions of endogenous Rb1cc1 during the differentiation of C2C12 myoblasts, we knocked down *Rb1cc1* expression using siRNAs. This process led to *Rb1* repression, as well as failed *Myhc* expression and myoblast differentiation. The expression of a series of genes, including *p21* and *cyclin D3*, was similar during the experimental process for the differentiation (Fig. 4). Immunocytochemically, C2C12 cells with siRNA vectors failed to synthesize Rb1cc1 and expressed low levels of Rb1 and Myhc (Fig. 5). Exposure to several siRNAs corresponding to different regions of *Rb1cc1* mRNA similarly caused C2C12 myoblast differentiation to fail (data not shown).

Discussion

Rb1cc1 is a novel gene that is associated with multidrug resistance to anti-cancer agents. The expression of both *Rb1cc1* and *Rb1* is synchronized in various cancer cell lines and in normal human tissues. Moreover, the introduction of wild-type *Rb1cc1* induces *Rb1* expression in human leukemic cells [5]. Rb1cc1 expressed at high levels contributes to the maturation of human embryonic musculoskeletal cells [6]. To our knowledge, Rb1cc1 might interact with Stathmin [17], the Listeria monocytogenesis surface protein ActA [20], or with focal adhesion kinase

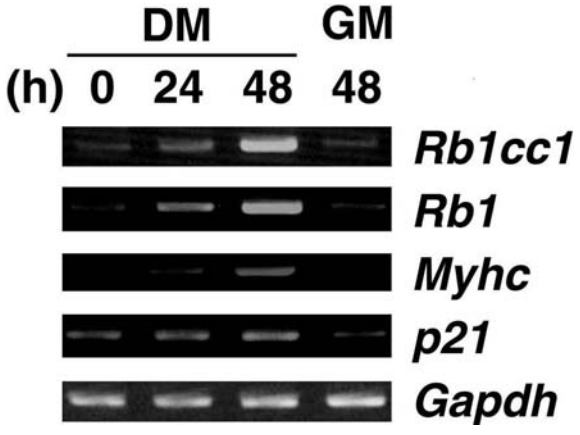


Fig. 3 Serial expressional analysis of genes regulating muscle differentiation. Expression levels of *Rb1cc1*, *Rb1*, *Myhc*, *p21*, and *Gapdh* in C2C12 cells incubated in differentiation medium (DM) for indicated periods, or maintained in growth medium (GM) were determined by semi-quantitative reverse-transcription polymerase chain reaction. More *Rb1cc1* and *Rb1* genes were induced by DM. Following expression of these genes, *Myhc* was obviously inducted in differentiated C2C12 cells

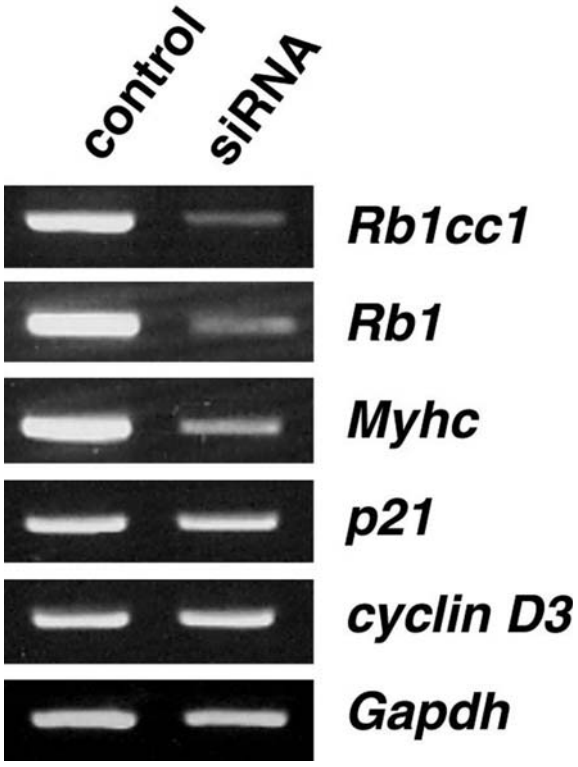


Fig. 4 Effects of *Rb1cc1* knockdown in C2C12 cells. C2C12 cells treated with siRNA vector (4525) were incubated in differentiation medium (DM). Expression levels of *Rb1cc1*, *Rb1*, *Myhc*, *p21*, *cyclin D3* and *Gapdh* were determined using semi-quantitative reverse-transcription polymerase chain reaction. *Rb1cc1* siRNA inhibited *Rb1* expression and resulted in failed *Myhc* expression. Expression of *p21* and *cyclin D3* was not affected

[1]. However, other molecules that associate with Rb1cc1 remain unknown, and the molecular mechanisms of Rb1cc1-mediated cellular functions are obscure.

To determine the function of Rb1cc1, the present study investigated the roles of Rb1cc1 on skeletal muscle differentiation. Northern and immunohistochemical analyses of mouse embryos showed that *Rb1cc1* expression predicted that of *Rb1* and *Myhc*. Although we demonstrated that the expression of Rb1cc1 and Rb1 is synchronized in musculoskeletal tissues of human embryos [6], Rb1cc1 was expressed more ubiquitously and earlier in mouse than in human embryos. Further, the intracellular localization of Rb1cc1 could change according to the developing status, and Rb1cc1 is involved in the murine developmental process [2]. More importantly, *Rb1cc1* and *Rb1* expression closely correlated and led to *Myhc* expression during C2C12 myoblast differentiation. These results suggest that Rb1cc1 is intimately involved in muscle differentiation in vivo and in vitro. Rb1 protein plays crucial roles in the induction of late markers during myogenic differentiation [8, 18]. Rb1cc1 predicted Rb1 during mouse myogenic differentiation and might play an important role in the expression of Rb1 and subsequent Myhc, a late marker of this process.

The RNAi-mediated knockdown of *Rb1cc1* reduced Rb1 expression at the transcriptional level, and Myhc was

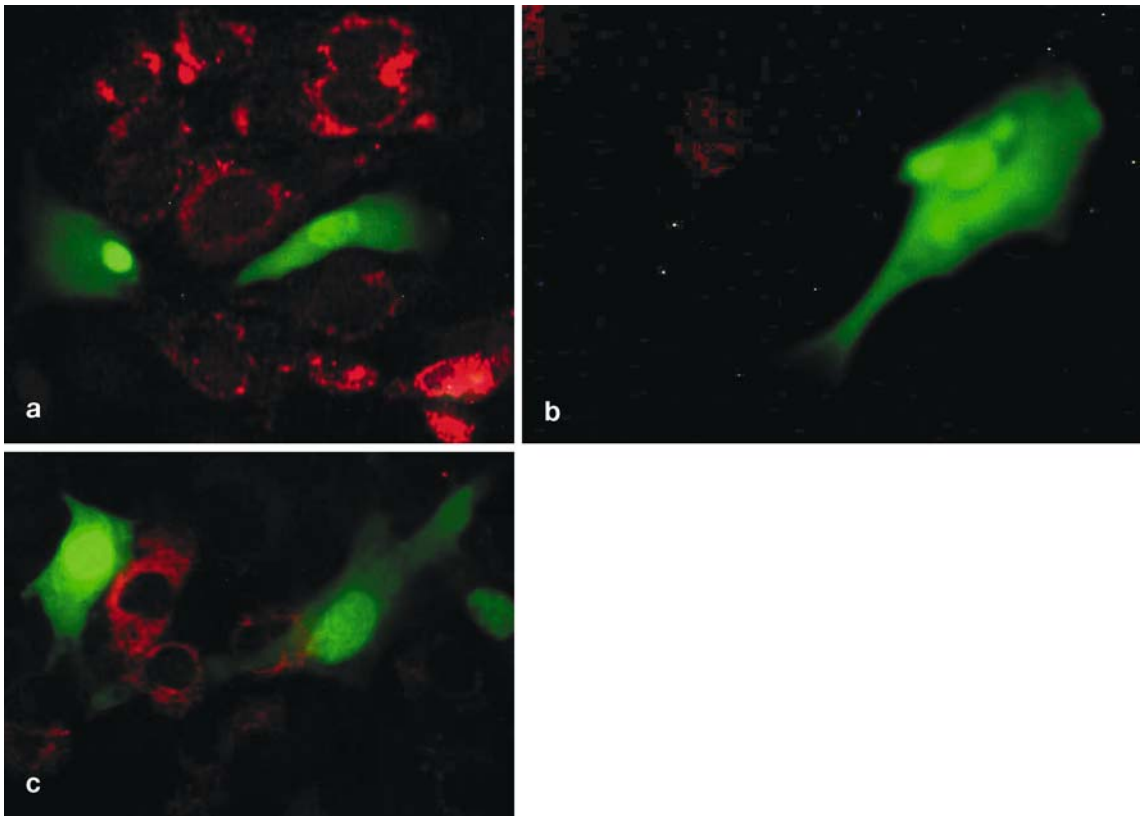


Fig. 5 Effects of Rb1cc1 knockdown on C2C12 myoblasts differentiation. C2C12 cells treated with siRNA vector (4525) were incubated in differentiation medium (DM). Fluorescent immunocytochemistry of Rb1cc1, Rb1, and Myhc demonstrated that the C2C12 cells treated with Rb1cc1 siRNA (green: GFP) failed to synthesize Rb1cc1 (Red, Alexa Fluor 555; A) in the cytoplasm, and they expressed neither Rb1 (Red, Alexa Fluor 555; B) nor Myhc (Red, Alexa Fluor 555; C)

not induced during C2C12 myoblast differentiation. The findings suggest that Rb1cc1 acts in the same pathway as Rb1 and plays a crucial role in myoblast differentiation upstream of Rb1 rather than downstream.

Although many proteins are implicated as critical modulators of myogenic differentiation, the complexity of this process suggests that more remain to be discovered. Here, we postulate that Rb1cc1 is a novel modulator of myogenic differentiation. We found that Rb1cc1 appears to be primarily required for muscular differentiation and that its suppression causes failed maturation of myoblasts largely due to the loss of Rb1 expression. Rb1cc1 is thought to induce Rb1 expression [5]. Rb1cc1 regulated Rb1 expression at the transcriptional level, although many proteins are involved in Rb1 regulation by affecting its phosphorylation status [9, 14, 21, 23]. Rb1cc1 might directly bind the *Rb1* gene promoter and induce its expression. Although Rb1cc1 predicted Rb1, such concordance was incomplete during mouse embryonic development. These findings indicate that Rb1cc1 indirectly rather than directly regulates Rb1 expression. Otherwise, Rb1cc1 might associate with Rb1. The Rb1cc1 protein contains a consensus nuclear localization signal (KPRK) [5], and the protein was localized in both the nucleus and cytoplasm. In addition, intracellular sublocalization of Rb1cc1 changes in accordance with developmental status [2]. Rb1cc1 may play functional roles by altering its intracellular sublocalization. Thus, Rb1cc1 might cooperate in nuclear Rb1 expression.

The present study demonstrated that *Rb1cc1*-siRNAs decreased the expression of *Rb1* and subsequently *Myhc* but not that of *p21* and *cyclin D3*. MyoD, a pivotal factor for myogenic differentiation, can activate muscle-specific gene expression and induce cell-cycle arrest through Rb1-dependent pathways [18, 21]. At the onset of myogenic differentiation, MyoD activates the expression of *Rb1*, *p21*, *cyclin D3* and induces cell cycle arrest, a process that is referred to as early events [4, 15, 16]. MyoD also co-operates with Rb1 to promote the expression of late markers of muscular differentiation, such as Myhc, which is referred to as a late myogenic event [4]. Therefore, the failed differentiation of myoblasts due to *Rb1cc1*-specific knockdown was largely dependent on Rb1 repression with no change in *p21* and *cyclin D3*, suggesting that Rb1cc1 is a crucial regulator of late, rather than early myogenic events.

Here, we reported that Rb1cc1 is a novel modulator of myogenic differentiation. The Rb1cc1-Rb1 pathway is primarily required for myogenic differentiation, and elucidating the components and precise mechanisms of the pathway during this process will help to clarify how Rb1cc1 functions under physiological conditions.

Acknowledgements This study was supported in part by grants-in-aid for PRESTO, JST; Scientific Research on Priority Areas (no. 16021223) and Young Scientists (A) (no. 15689008), MEXT.

References

1. Abbi S, Ueda H, Zheng C, Cooper LA, Zhao J, Christopher R, Guan JL (2002) Regulation of focal adhesion kinase by a novel protein inhibitor FIP200. Mol Biol Cell 13:3178–3191
2. Bamba N, Chano T, Taga T, Ohta S, Takeuchi Y, Okabe H (2004) Expression and regulation of RB1CC1 in developing murine and human tissues. Int J Mol Med 14:583–587
3. Blackwell TK, Weintraub H (1990) Differences and similarities in DNA-binding preferences of MyoD and E2A protein complexes revealed by binding site selection. Science 250:1104–1110
4. Cenciarelli C, De Santa F, Puri PL, Mattei E, Ricci L, Bucci F, Felsani A, Caruso M (1999) Critical role played by cyclin D3 in the MyoD-mediated arrest of cell cycle during myoblast differentiation. Mol Cell Biol 19:5203–5217
5. Chano T, Ikegawa S, Kontani K, Okabe H, Baldini N, Saeki Y (2002) Identification of RB1CC1, a novel human gene that can induce RB1 in various human cells. Oncogene 21:1295–1298
6. Chano T, Saeki Y, Serra M, Matsumoto K, Okabe H (2002) Preferential expression of RB1-inducible coiled-coil 1 in terminal differentiated musculoskeletal cells. Am J Pathol 161:359–364
7. Crescenzi M, Fleming TP, Lassar AB, Weintraub H, Aaronson SA (1990) MyoD induces growth arrest independent of differentiation in normal and transformed cells. Proc Natl Acad Sci U S A 87:8442–8446
8. Gu W, Schneider JW, Condorelli G, Kaushal S, Mahdavi V, Nadal-Ginard B (1993) Interaction of myogenic factors and the retinoblastoma protein mediates muscle cell commitment and differentiation. Cell 72:309–324
9. Halevy O, Novitch BG, Spicer DB, Skapek SX, Rhee J, Hannon GJ, Beach D, Lassar AB (1995) Correlation of terminal cell cycle arrest of skeletal muscle with induction of p21 by MyoD. Science 267:1018–1021
10. Hlaing M, Shen X, Dazin P, Bernstein HS (2002) The hypertrophic response in C2C12 myoblasts recruits the G1 cell cycle machinery. J Biol Chem 277:23794–23799
11. Lassar A, Davis R, Wright W, Kadesch T, Murre C, Voronova A, Baltimone D, Weintraub H (1991) Functional activity of myogenic HLH proteins requires hetero-oligomerization with E12/E47-like proteins in vivo. Cell 66:305–315
12. Lipinski MM, Jacks T (1999) The retinoblastoma gene family in differentiation and development. Oncogene 18:7873–7882
13. Liu CJ, Ding B, Wang H, Lengyel P (2002) The MyoD-inducible p204 protein overcomes the inhibition of myoblast differentiation by Id proteins. Mol Cell Biol 22:2893–2905
14. Lundberg AS, Weinberg RA (1998) Functional inactivation of the retinoblastoma protein requires sequential modification by at least two distinct cyclin-cdk complexes. Mol Cell Biol 18:753–761
15. Magenta A, Cenciarelli C, De Santa F, Fuschi P, Martelli F, Caruso M, Felsani A (2003) MyoD stimulates RB promoter activity via the CREB/p300 nuclear transduction pathway. Mol Cell Biol 23:2893–2906
16. Martelli F, Cenciarelli C, Santarelli G, Polikar B, Felsani A, Caruso M (1994) MyoD induces retinoblastoma gene expression during myogenic differentiation. Oncogene 9:3579–3590
17. Maucuer A, Camonis JH, Sobel A (1995) Stathmin interaction with a putative kinase and coiled-coil-forming protein domains. Proc Natl Acad Sci U S A 92:3100–3104
18. Novitch BG, Mulligan GJ, Jacks T, Lassar AB (1996) Skeletal muscle cells lacking the retinoblastoma protein display defects in muscle gene expression and accumulate in S and G2 phases of the cell cycle. J Cell Biol 135:441–456
19. Novitch BG, Spicer DB, Kim PS, Cheung WL, Lassar AB (1999) pRb is required for MEF2-dependent gene expression as well as cell-cycle arrest during skeletal muscle differentiation. Curr Biol 9:449–459
20. Pfeuffer T, Goebel W, Laubinger J, Bachmann M, Kuhn M (2000) LaXp180, a mammalian ActA-binding protein, identified with the yeast two-hybrid system, co-localizes with intracellular Listeria monocytogenes. Cell Microbiol 2:101–114
21. Schneider JW, Gu W, Zhu L, Mahdavi V, Nadal-Ginard B (1994) Reversal of terminal differentiation mediated by p107 in Rb−/− muscle cells. Science 264:1467–1471
22. Weintraub H (1993) The MyoD family and myogenesis: redundancy, networks, and thresholds. Cell 75:1241–1244
23. Wiman KG (1993) The retinoblastoma gene: role in cell cycle control and cell differentiation. FASEB J 7:841–845

Virchows Arch (2005) 447: 649–652
DOI 10.1007/s00428-005-1229-z

CASE REPORT

Paulo R. Benites Filho · Daniele Sakamoto · Tiago Noguchi Machuca · Maria José Serapião · Leo Ditzel · Luiz F. Bleggi Torres

Granular cell tumor of the neurohypophysis: report of a case with unusual age presentation

Received: 12 July 2004 / Accepted: 9 February 2005 / Published online: 18 August 2005
© Springer-Verlag 2005

Abstract Granular cell tumor (GCT) usually occurs as a solitary, small, nodular tumor and rarely grows to a sufficient size to present symptoms. The tumor is more prevalent in female adults. The authors report a case of an 8-year-old boy with GCT of the neurohypophysis presenting with central precocious puberty. Few cases of symptomatic GCT have been reported in the literature, none of them in a patient in the first decade of life. Clinical picture, histopathological features, and histogenesis of GCT of neurohypophysis are discussed.

Keywords Granular cell tumor · Neurohypophysis · Central precocious puberty

Introduction

Granular cell tumor (GCT) is a neoplasm commonly found in the head and neck; however, it may occur in different locations such as tongue, skin, gastrointestinal tract, and central nervous system [1, 7, 18, 21]. It usually occurs as a solitary, nodular, and asymptomatic mass and is most frequently diagnosed as an incidental finding at autopsy [1, 2, 6, 16, 20, 27]. The tumor is more prevalent in female adults [1, 2, 27]. Since the initial description by Boyce and Beadles in 1893, GCTs have been described under many names such as choristoma, granular cell myoblastoma, granular cell pituicytoma, and granular cell schwannoma, reflecting the ongoing controversy concerning the cells of origin of these tumors [1, 7–9, 19–23].

We report the clinical, radiological, and pathological findings of a case of GCT affecting the neurohypophysis of an 8-year-old boy.

P. R. Benites Filho · D. Sakamoto · T. N. Machuca · M. J. Serapião · L. F. Bleggi Torres (✉)
Department of Pathology,
Hospital de Clinicas,
Universidade Federal do Paraná (UFPR),
Rua General Carneiro 181,
80060-900 Curitiba, Paraná, Brazil
e-mail: lfbt@terra.com.br
Tel.: +55-41-2641304
Fax: +55-41-2641304

L. Ditzel
Department of Neurosurgery,
Hospital de Clinicas, UFPR,
Curitiba, Brazil

Clinical history

An 8-year-old boy suffering from obesity since he was 3 years old (weight 20.8 kg, height 90 cm) presented with a 2-month history of pubarche. The penis and testes were enlarged, and he also showed acne, dizziness, frontal headache, decreased visual acuity, and occasional vomiting.

Hormonal evaluation revealed a normal thyroid function. A provocative test with insulin-induced hypoglycemia was also normal for growth hormone (GH) and adrenocorticotropic hormone. A test with intravenous infusion of gonadotropin-releasing hormone rendered pubertal ranges of gonadotropic hormones, thus supporting the clinical suspicions of central precocious puberty.

Computed tomography scans revealed a round, well-delineated suprasellar mass. The tumor was solid, with calcifications, and was enhanced homogeneously after administration of contrast.

Materials and methods

The surgically resected specimen was fixed in 10% buffered formalin, embedded in paraffin, cut in 4-μm-thick sections, and stained with hematoxylin and eosin (H & E) as well as periodic acid-Schiff (PAS) stain. Immunohistochemical studies using the biotin–streptavidin peroxidase technique were performed using antibodies against cytokeratin (1:400; Dako, CA, USA), neuron-specific enolase (1:2,500; Dako), S-100 protein (1:1,500; Dako), chromo-

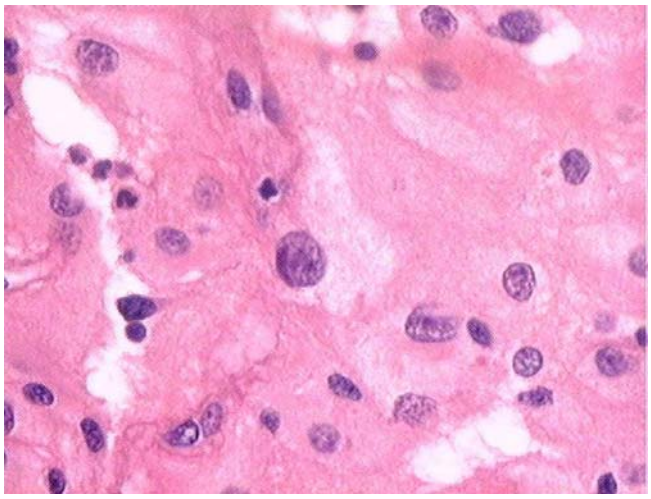


Fig. 1 Photomicrographs displaying large polygonal cells arranged in lobules separated by thin septa of tumorous cells presenting abundant eosinophilic, granular cytoplasm and nuclear polymorphism (H & E, ×100)

granin A (prediluted; Zymet, CA, USA), synaptophysin (1:200; Dako), desmin (1:800; Dako), muscle-specific actin (HHF-35) (1:500; Dako), and glial fibrillary acidic protein (GFAP) (1:500; Dako).

Results

Histological sections revealed a hypercellular tumor with large and polygonal cells arranged in lobules separated by thin septa of tumors cells presenting abundant eosinophilic and granular cytoplasm and nuclear polymorphism (Figs. 1 and 2). Cytoplasmic granules were PAS-positive and resistant to diastase digestion (Fig. 3).

Immunohistochemical analysis revealed strong positivity for neuron-specific enolase, but negative for S-100

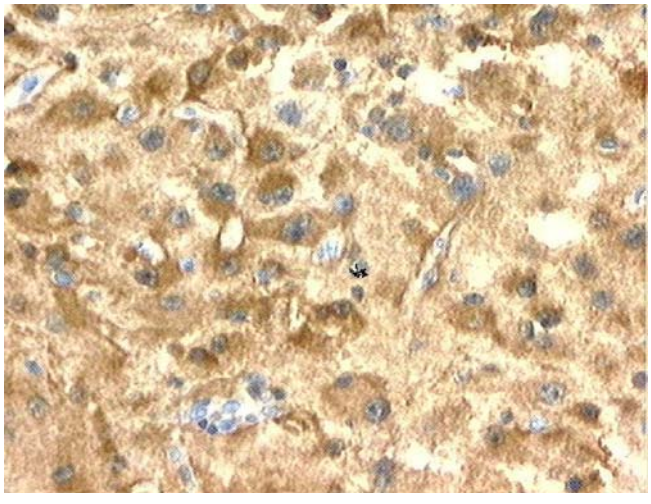


Fig. 2 Photomicrographs displaying large polygonal cells arranged in lobules separated by thin septa of tumorous cells presenting abundant eosinophilic, granular cytoplasm and nuclear polymorphism (H & E, ×400)

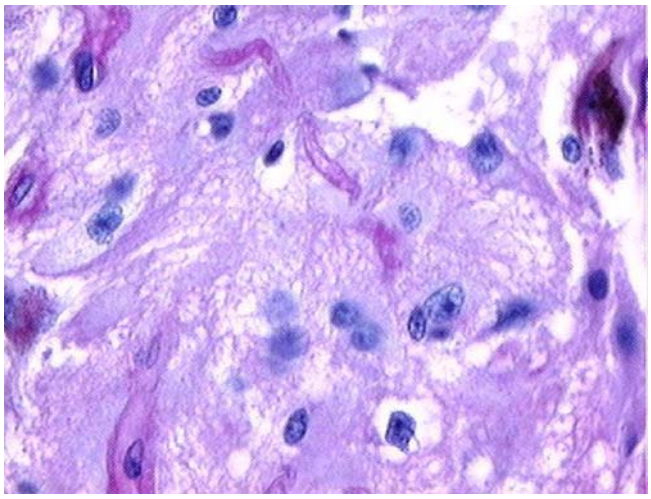


Fig. 3 Cytoplasmic granules displaying PAS-positivity resistant to diastase digestion

protein, cytokeratins, chromogranin A, synaptophysin, desmin, actin, and GFAP (Fig. 4). The histopathological diagnosis was GCT of the neurohypophysis.

Discussion

Granular cell tumors may occur in virtually any anatomic site, but they have a prediction for the head and neck. Intracranial GCTs are usually found in the posterior hypophysis and rarely in the cerebral hemispheres or leptomeninges. They are more often encountered as incidental autopsy findings in up to 17% of unselected adult autopsy cases as clusters of granular cell "tumorettes" [16, 20]. There is a 2:1 predominance in females, and despite the wide range of age distribution (30–60 years old) [1, 18], we could not find any case diagnosed in the first decade of life, like the present report. It usually occurs as a solitary, small, nodular tumor and rarely grows to a sufficient size to present symptoms [2, 3, 15, 20, 27]. To date, only 50 clinically

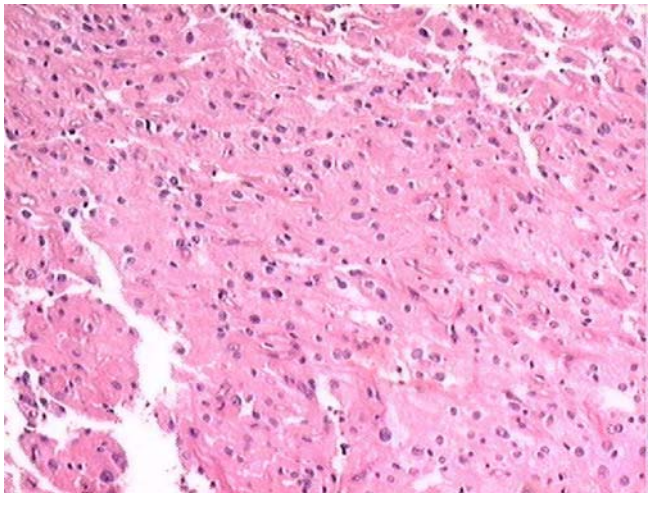


Fig. 4 Immunohistochemical staining displaying neuron-specific enolase positivity (×400)

symptomatic cases of GCT have been reported in the literature.

Symptomatic GCTs of the neurohypophysis present usually with ophthalmologic abnormalities in up to 90% of patients, which include bilateral temporal field deficit, optic nerve atrophy, and decreased visual acuity resulting from compression of the optic chiasm. Hormonal disturbance is described in 50% of patients and includes secondary amenorrhea, galactorrhea, decreased libido, infertility, and weight gain or loss. Diabetes insipidus, as well as multiple endocrine neoplasia type 1, was described in one case each [1]. Persistent headache, repeated vomiting, memory loss, and behavior disorder are rarely seen [2, 7–9, 10, 21].

In our case, ophthalmological and hormonal disturbances were found probably due to a compressive process. Hamartomas, optic nerve gliomas, and astrocytomas are frequently associated with the development of central precocious puberty, whereas craniopharyngioma, Rathke's cysts, germinomas, and Langerhans cell histiocytosis are not. One explanation would be coexistence with a pituitary adenoma, a well-known cause of precocious puberty [5, 24]. Tomita and Gates [25] studied 100 pituitary glands examined at autopsy and found that 9% harbored a GCT, and of these, a coexisting pituitary adenoma was observed in three cases. Despite that, we did not find any tumor in the adenohypophysis.

Another possible mechanism for central precocious puberty would be the secretion of a luteinizing hormone (LH)/follicle-stimulating hormone (FSH) precursor or FSH/LH per se. A similar picture was reported by Losa et al. [10] regarding GH. These authors suggested that a GCT could secrete a GH precursor, thus explaining the acromegaly presentation of their patient. However, as in our case, it was not possible to establish a scientifically proven pathogenetic pathway.

GCTs of the sellar region are morphologically similar to those tumors occurring outside the nervous system. The tumors are composed of densely packed polygonal cells with eosinophilic, granular, PAS-positive, diastase-resistant cytoplasm. Sometimes, small areas of foamy cells can be observed, as well as cytoplasm and round nuclei with delicate chromatin and uniform nucleoli. Perivascular lymphocytic aggregates are a common feature [1, 7, 9]. Despite absent mitotic activity, Kasashima et al. [7], in their literature review of GCT with histologically atypical features, found lesions that were characterized by remarkable cellular and nuclear polymorphism, nuclear hyperchromatism, large nucleoli, mitosis, and necrosis.

Although the histological appearance is remarkably characteristic, the histogenesis of GCTs is unknown [1]. The numerous denominations attributed to the tumor reflect this uncertainty [7, 17, 18, 20]. These tumors were initially believed to be an aberrant growth of embryological tissue and were called "choristomas" [11]. Later, the term "granular myoblastoma" was suggested because of the similarity to the GCTs of the tongue originally considered to be derived from embryonic muscle cells [4, 12, 13]. There is, however, no evidence that these neurohypophysial tumors originate from muscle cells [14], due to their negativity for immunoperoxidase staining for desmin and smooth muscle actin. Currently, their histogenesis is disputed to be between Schwann cell and the modified glial cell of the pituitary, the pituicyte [1, 7, 16]. Becker and Wilson [3] described strong GFAP immunoreactivity in neurohypophysial GCT. However, several other investigators have reported negative staining for GFAP in the tumor, which constitutes evidence against a pituicyte origin [9, 15, 17, 21]. A third hypothesis, which is endorsed by some authors, including us, believes that, due to the variable immunoreactivity, these tumors are biologically heterogeneous in spite of histological homogeneity [4, 26].

In summary, we have reported an additional case of symptomatic GCT, a rare condition. However, the most astonishing feature in our case is the early presenting age of a tumor, which, to the best of our knowledge, has not previously been reported to occur in the first decade. Furthermore, the present report documents the possibility of a GCT present with central precocious puberty.

References

1. Asa LS (1998) Tumors of the pituitary gland. In: Atlas of tumor pathology, fasc 22, 3rd edn. Armed Forces Institute of Pathology, Washington, D.C., pp 159–160
2. Barrande G, Kujas M, Gancel A, Turpin G, Bruckert E, Kuhn JM, Luton JP (1995) Granular cell tumors. Rare tumors of the neurohypophysis. Presse Med 24(30):1376–1380
3. Becker DH, Wilson CB (1981) Symptomatic parasellar granular cell tumors. Neurosurgery 8:173–180
4. Buley ID, Gatter KC, Kelly PMA (1988) Granular cell tumors revisited. An immunohistological and ultrastructural study. Histopathology 12:263–274
5. Chermaitilly W, Trivin C, Adan L, Gail V, Sainte-Rose C, Brauner R (2001) Central precocious puberty: clinical and laboratory features. Clin Endocrin (Oxf) 54:289–294
6. Cusick JF, Ho K, Hagern TC, Kun L (1982) Granular cell pituicytoma associated with multiple endocrine neoplasia type 2. J Neurosurg 56:594–596
7. Kasashima S, Oda Y, Nozaki J, Shirasaki M, Nakanishi I (2000) A case of atypical granular cell tumor of the neurohypophysis. Pathol Int 50:568–573
8. Lafitte C, Aesch B, Henry-Lebras F, Fetissof F, Jan M (1994) Granular cell tumor of the pituitary stalk. J Neurosurg 80:1103–1107
9. Liwnicz BH, Liwnicz RG, Huff JS, McBride BH, Tew JM (1984) Giant granular cell tumor of the suprasellar area: immunocytochemical and electron microscopy studies. Neurosurgery 15:246–251
10. Losa M, Saeger W, Mortini P, Pandolfi C, Terreni MR, Taccagni G, Giovanelli M (2000) Acromegaly associated with a granular cell tumor of the neurohypophysis: a clinical and histological study. J Neurosurg 93:121–126
11. Lüthy F, Klinger J (1951) Der Tumoretten-Tumor des Hypophysenhinterlappens. Schweiz Z Allg Pathol Bakteriol 14:721–729
12. Markesberry WR, Duffy PE, Cowen D (1973) Granular cell tumors of the central nervous system. J Neuropathol Exp Neurol 32:92–109
13. Massie AP (1979) A granular cell pituicytoma of the neurohypophysis. J Pathol 129:53–56
14. Miettinen M, Lehtonen E, Lehtola H, Ekblorm P, Lehto VP, Virtanen I (1984) Histogenesis of granular cell tumor—an immunohistochemical and ultrastructural study. J Pathol 142:221–229

15. Nathrath WBJ, Remberger K (1986) Immunohistochemical study of the granular cell tumors. Virchows Arch B 53:52–57
16. Nishio S, Takeshita I, Yoshimoto K, Yamaguchi T (1998) Granular cell tumor of the pituitary stalk. Clin Neurol Neurosurg 100:144–147
17. Nishioka H, Kunio L, Llena JF, Hirano A (1991) Immunohistochemical study of granular cell tumors of the neurohypophysis. Virchows Arch B 60:413–417
18. Rhee JS, Wackym PA, Hague K, King WA, Wolfe D (2002) Granular cell tumor of the pituitary fossa. Ann Otol Rhinol Laryngol 111:754–758
19. Sarah A, Kernohan JW (1955) Granular cell tumors of the stalk and posterior lobe of the pituitary gland. Cancer 8(3):616–622
20. Satyamurti S, Huntington HW (1972) Granular cell myoblastoma of the pituitary. J Neurosurg 37:483–486
21. Schaller B, Kirsch E, Tolnay M, Mindermann T (1998) Symptomatic granular cell tumor of the pituitary gland: case report and review of the literature. Neurosurgery 42:166–171
22. Symon L, Ganz JC, Burston J (1971) Granular cell myoblastoma of the neurohypophysis. J Neurosurg 35:82–89
23. Stanhope R (2001) Central precocious puberty and occult intracranial tumors. Clin Endocrin (Oxf) 54:287–288
24. Sterberg C (1921) Ein Choristoma der Neruohypophyse bei ausgebreiteten Oedemen. Zentralbl Pathol Anat 31:585–591
25. Tomita T, Gates E (1999) Pituitary adenomas and granular cell tumors. Incidence, cell type, and location of tumors in 100 pituitary glands at autopsy. Am J Clin Pathol 111:817–825
26. Ulrich J, Heitz PU, Fischer T, Obrist E, Gullotta F (1987) Granular cell tumors—evidence for heterogeneous tumor cell differentiation. An immunohistochemical study. Virchows Arch B 53:52–57
27. Vogelgesang S, Junge MH, Pahnke J, Gaab MR, Warzok W (2002) August 2001: Sellar/Suparasellar mass in a 59 year-old woman. Brain Pathol 12(1):135–136, 139

Virchows Arch (2005) 447: 653–659
DOI 10.1007/s00428-004-1195-x

CASE REPORT

Akira Kurose · Ryo Ichinohasama · Hiroyuki Kanno · Tetsuto Kobayashi · Motoo Ishida · Naoto Nishinari · Takashi Sawai

Lymphoepithelioma-like carcinoma of the breast. Report of a case with the first electron microscopic study and review of the literature

Received: 26 April 2004 / Accepted: 6 December 2004 / Published online: 10 June 2005
© Springer-Verlag 2005

Abstract Lymphoepithelioma-like carcinoma (LELC) is a tumor which occurs outside the nasopharynx and has morphological features identical to nasopharyngeal lymphoepithelioma. LELC of the breast (LELC-B) is uncommon, and its resemblance to medullary carcinoma of the breast (MC-B) obscures distinction between these two tumors. We report a case of LELC-B occurring in a 47-year-old woman. The tumor consisted of multinodules without circumscription. The tumor cells mainly exhibited loose clusters being permeated by numerous lymphocytes. The tumor cell clusters showed inconspicuous margins, which were far from syncytial patterns. The epithelial nature of the tumor cells was demonstrated by positivity for epithelial membrane antigen, AE1/AE3 and CAM5.2. Furthermore, glandular differentiation of the tumor cells was confirmed using electron microscopy for the first time. Epstein–Barr virus (EBV) was not detected using either in situ hybridization or polymerase chain reaction. These findings, together with former reports of LELC-B, suggest that the distinction between LELC-B and MC-B depends on whether circumscription and syncytial growth patterns exist. The other findings, including absence of EBV and immunohistochemical aspects of the tumor cells, are not considered different thus far. Although the prognosis of LELC-B is thought to be favorable, which is also similar to MC-B, distant metastasis was detected in the present case. To confirm the clinicopathological entity of these two tumors, it is important to recognize the difference between LELC-B and MC-B.

Keywords Lymphoepithelioma · Breast · Carcinoma · Medullary carcinoma

A. Kurose (✉) · H. Kanno · T. Kobayashi · T. Sawai
Department of Pathology,
Iwate Medical University, Morioka,
020-8505 Iwate, Japan
e-mail: akurose@iwate-med.ac.jp
Tel.: +81-19-6515110
Fax: +81-19-6519246

R. Ichinohasama
Department of Oral Pathology,
Tohoku University School of Dentistry,
Sendai, Japan

M. Ishida
Ishida Surgical and Gastroenterological Clinic,
Morioka, Japan

N. Nishinari
Morioka Yuai Hospital,
Morioka, Japan

Introduction

Lymphoepithelioma is a distinctive neoplasm of the nasopharynx, composed of undifferentiated malignant epithelial cells in a background of lymphocytes. The counterpart of the other sites is diagnosed lymphoepithelioma-like carcinoma (LELC), which has been seen in the major and minor salivary glands [10, 13, 17, 19, 30, 31], larynx [3], thyroid [32], thymus [21, 38], lungs [5, 12, 27], stomach [4, 16, 23, 26, 33, 39], uterine cervix [22, 35, 37], prostate [28], urinary bladder [2, 9] and skin [6, 34, 35, 36]. Including the first description of LELC of the breast (LELC-B) by Kumar et al. [18] in 1994, there have been four reports and nine cases of LELC-B. Morphological similarity of LELC-B to medullary carcinoma of the breast (MC-B) seems to make the clinicopathological entity of LELC-B obscure. It might be one reason for the rarity of LELC-B. Although the role of Epstein–Barr virus (EBV) in the pathogenesis of nasopharyngeal lymphoepithelioma is now well established, EBV has not been detected in LELCs, except for those of the lung, stomach, salivary gland and thymus [15]. All reported cases of LELC-B were negative for EBV [7, 8, 18, 24], as has been the case in MC-B. Thus far, the most conspicuous difference between LELC-B and MC-B that has been indicated in most reports [7, 8, 24] is the absence of cir-

cumscription and syncytial growth patterns of tumor cells in LELC-B. Cristina et al. emphasized that hormone and adhesion molecule status was different between LELC-B and MC-B [7], but no obvious difference except circumscription and syncytial growth patterns has been detected. Our present report, which includes the first electron microscopic study of LELC-B, must be meaningful in considering the clinicopathological entity of LELC-B.

Clinical history

A 47-year-old female noticed a palpable mass of 40 mm in diameter located between the upper outer and inner quadrants of her left breast. Since fine needle aspiration cytology proved it to be malignant, a total mastectomy with axillary node dissection and anti-estrogen therapy with tamoxifen citrate were performed. After 4 months, a parasternal mass thought to be lymph-node metastasis, detected using computed tomography scan, was confirmed to be malignant using aspiration cytology. Radiation (total 40 Gy) and CEF (cyclophosphamide, epirubicin hydrochloride and 5FU) therapy (for 2 months) was performed. Metastasis to the parasternal lymph node and the lung was detected 19 months after the therapy.

Materials and methods

The removed breast was fixed in 10% buffered formalin and routinely processed for microscopic examination. The paraffin-embedded tissues were investigated by means of histopathology using hematoxylin and eosin stain, immunohistochemistry, in situ hybridization (ISH) and polymerase chain reaction (PCR) for the EBV genome.

Immunohistochemistry

Immunohistochemical studies were performed on formalin-fixed and paraffin-embedded tissues after microwave antigen retrieval with an avidin-biotin-peroxidase complex method using monoclonal antibodies: AE1/AE3 (Nichirei, Tokyo, Japan; dilution 1:4), KL-1 (Immunotech, Marseille, France; 1:100), CAM 5.2 (BD Immunocytometry Systems, San Jose, CA, USA; 1:3), epithelial membrane antigen (EMA) (Dako, Glostrup, Denmark; 1:100), MPO (Dako; 1:3200), p80 (Dako; 1:100), CD1a (Immunotech; 1:2), CD3 (Dako; 1:800), CD4 (Novocastra, Newcastle, UK; 1:50), CD5 (Novocastra; 1:400), CD8 (Nichirei; 1:2), CD10 (Novocastra; 1:80), CD20 (Dako; 1:200), CD30 (Dako; 1:80), CD45 (Dako; 1:100), CD56 (Novocastra; 1:100), CD68 (Dako; 1:1100), CD79a (Dako; 1:100), e-cadherin (BD Pharmingen, San Jose, CA, USA; 1:100), estrogen and progesterone receptors (Dako; prediluted), c-erb-B2 (Dako; prediluted), bcl-2 (Dako; 1:50), MIB-1 (Dako; 1:50), latent membrane protein-1 (LMP-1) (Dako; 1:25) and EBV-encoded nuclear antigen-2 (EBNA2) (Dako; 1:25).

Electron microscopy

An electron microscopic study was carried out using tumor tissues from the specimen fixed in 10% buffered formalin.

In situ hybridization

ISH with EBV-encoded RNAs (EBERs) was performed on 5-μm-thick paraffin sections using Rembrandt ISH and detection kit (Pan Path, Amsterdam, Netherlands) following the manufacturer's recommendation.

PCR amplification of EBV genome

DNA was extracted from formalin-fixed, paraffin-embedded tissues using chelating resin as described previously [25]. Briefly, two 10-μm sections were transferred into sterile distilled water containing 20% (w/v) chelating resin Chelex 100 (Bio-Rad Labs, Hercules, CA) and boiled for 15 min. After centrifugation (12,000 *g* for 10 min), the supernatant was used as a DNA sample. The recovery of amplifiable DNA was verified using PCR amplification of

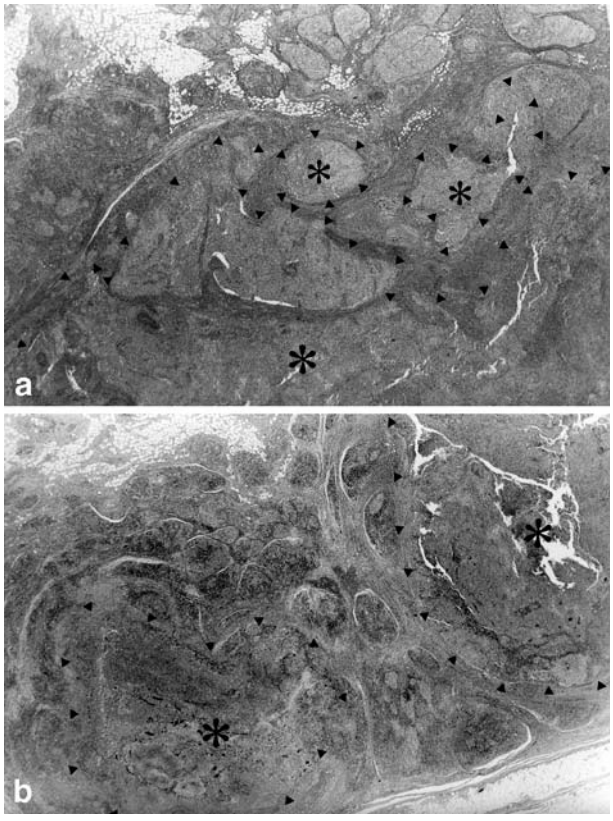


Fig. 1 The tumor shows irregular borders without circumscription. **A** Small tumorous nodules exist on the periphery of the tumor. **B** At one end of the tumor, it separates into two tumorous nodules. The breast tissue surrounding the tumor shows lobulocentric lymphocytic infiltration. *Asterisks* and *arrowheads* indicate tumor nodules and borders of them, respectively. Hematoxylin and eosin stain (**A** ×1.6, **B** ×1.4)

beta-globin gene, which produced a 123-bp fragment. A 5-μl aliquot of the DNA sample was diluted into 25 μl containing 0.2 mM dNTP, 1.5 mM $MgCl_2$, 500 nM of each primer, 0.6 U of AmpliTaq Gold DNA polymerase (Applied Biosystems, Foster City, CA) and 1× PCR reaction buffer provided by the manufacturer. Primer sequences for EBV BamHI-W fragments were 5′-CGGTCGCCCAGTC CTACCAG-3′ and 5′-CCTGGAGAGGTCAGGTTACT-3′, amplifying a 126-bp segment of EBV genome. PCR was performed (35 cycles at 95 C for 30 s, 58 C for 30 s and 72 C for 30 s), and amplified products were electrophoresed and examined in ethidium bromide-stained 3% agarose gels on an ultraviolet transilluminator.

Results

The tumor, of which the size was 28×23 mm in the greatest dimension, showed irregular borders. The cut surface had a gray-white appearance and was soft and of uniform consistency. No hemorrhagic foci existed.

Microscopically, at low magnification, the tumor existed in the breast tissue and was composed of multinodular tumorous lesions without encapsulation (Fig. 1A, B). The surrounding breast tissue showed a mild degree of fibrous proliferation. The tumor was composed of tumor cells and dense infiltrates of predominantly small lymphocytes. Occasional aggregates of plasma cells and histiocytes were also present. The tumor cells had pale eosinophilic cytoplasm with inconspicuous cell boundaries (Fig. 2A). The nuclei were round or oval in shape with single prominent nucleoli. These tumor cells formed vague small or large clusters (Fig. 2B) or were scattered in the numerous lymphoplasmacytic background (Fig. 2C). In part, sheet-like growth patterns were seen (Fig. 2D). Most of the clusters showed unclear margins because they were permeated by the lymphocytes as seen in nasopharyngeal lymphoepithelioma with the Schmincke pattern. These findings were distinct from syncytial patterns of growth observed in MC-B and lymphoepithelioma with the Regaud pattern and were hardly recognized as the epithelial nature of the tumor cells. Mitotic figures were 15 per 10 high-power fields. Small areas of necrosis were identified.

Although the breast tissue surrounding the tumor displayed marked lobulocentric lymphocytic infiltration, disruption of the lobular or duct structure by lymphocytes was not significant. Lymphoepithelial lesions were indistinct. The distant part of the breast from the tumor did not show conspicuous infiltration of lymphocytes. Neither ductal nor lobular carcinoma in situ was found in multiple sections of both tumorous and non-tumorous breast tissue. No metastases were found in the 33 isolated axillary lymph nodes.

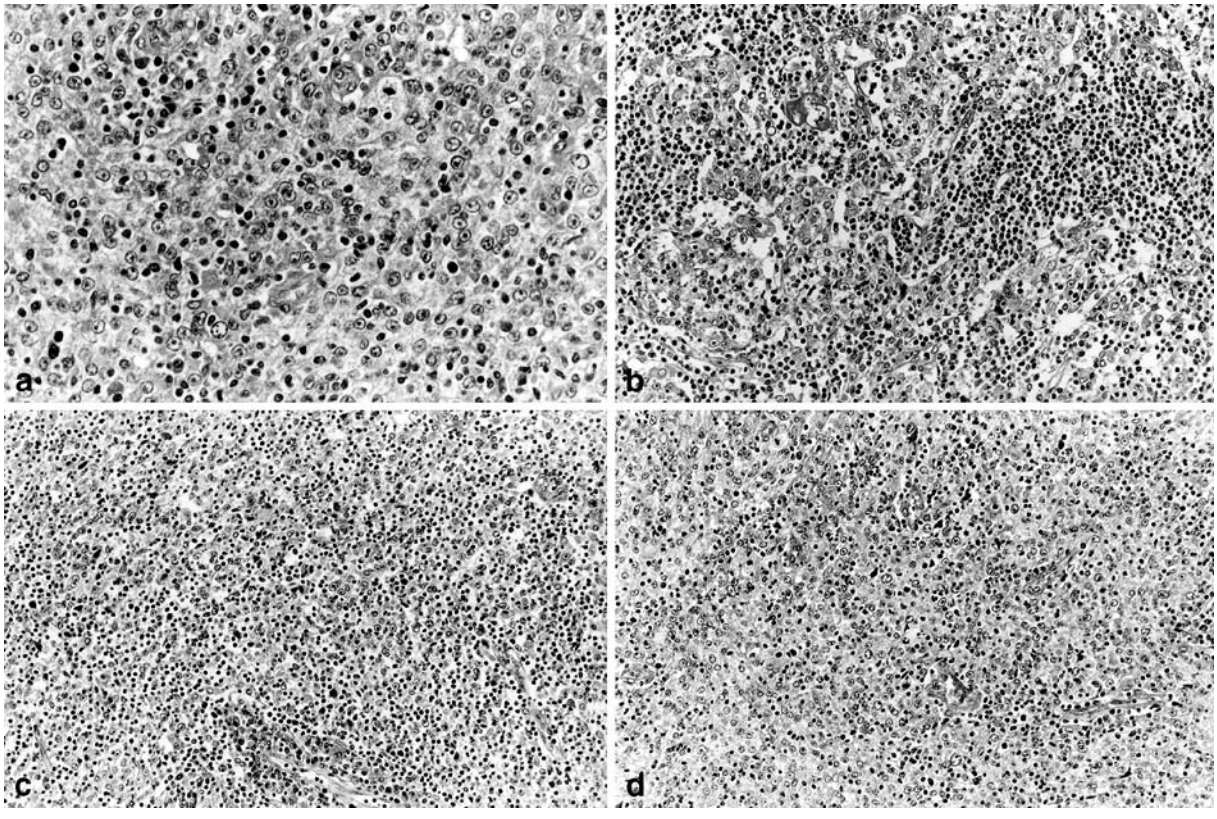


Fig. 2 **A** The tumor cells have round or oval nuclei with single prominent nucleoli. The cell boundaries are inconspicuous. **B** Although the tumor cells have a tendency to aggregate, the clusters are loose and vague. **C** In large areas, the tumor cells are scattered in the lymphoplasmacytic background without forming clusters. **D** In part, sheet-like growth patterns are present, but margins of the clusters are unclear. Hematoxylin and eosin stain (**A** ×20, **B** ×15, **C** and **D** ×13)

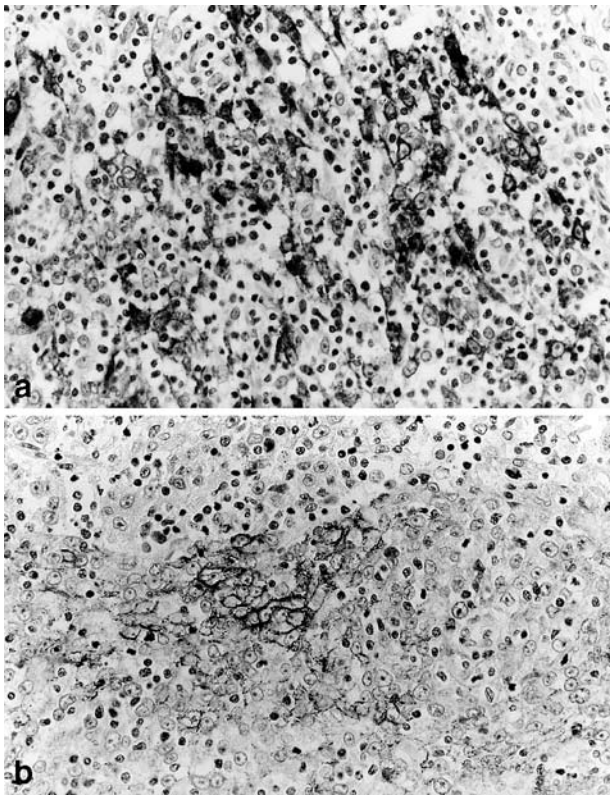


Fig. 3 **A** Most tumor cells show strong positivity for epithelial membrane antigen. **B** Approximately 70% of the tumor cells are positive for AE1/AE3. Immunoperoxidase stain, hematoxylin counterstain (**A** and **B** ×40)

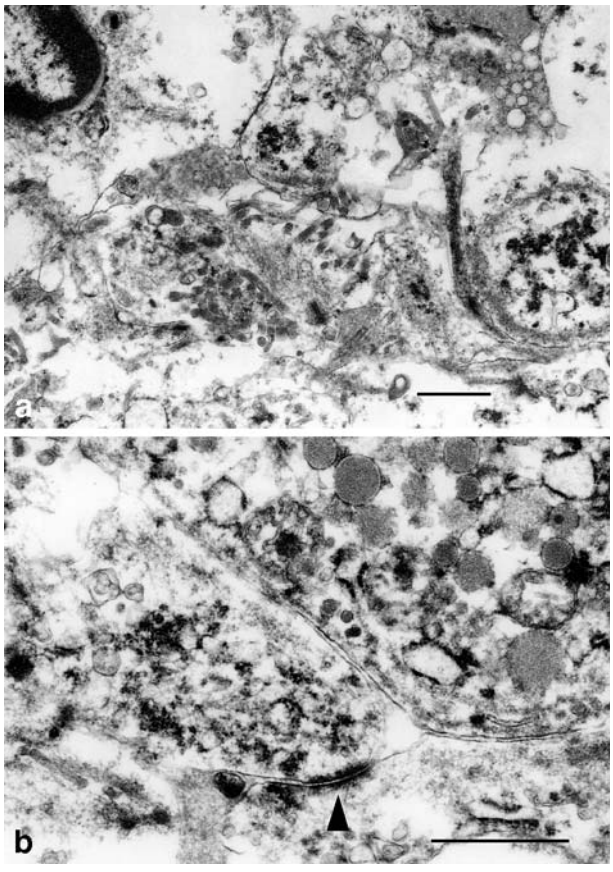


Fig. 4 An electron microscopic study. **A** Some tumor cells possess microvilli with irregular projections. *Bar*=1 μm. **B** Tumor cells having secretory granules (*right upper portion*) and a desmosome (*arrowhead*). *Bar*=1 μm

On immunostaining, nearly all of the tumor cells were strongly positive for EMA (Fig. 3A). Approximately 70% and nearly half of the tumor cells were positive for AE1/AE3 (Fig. 3B) and CAM 5.2, respectively. However, no tumor cells reacted with KL-1. Other than the epithelial markers, the tumor cells were positive for e-cadherin and c-erb-B2 and negative for MPO, p80, CD3, CD4, CD5, CD8, CD20, CD30, CD45, CD56, CD68, CD79a, p53, bcl-2 and estrogen and progesterone receptors. About half of the tumor cells were positive for CD10. Neither LMP-1 nor EBNA2 was present. The MIB-1 staining index was approximately 80%. Most lymphocytes permeating in the tumor cells were positive for CD3 and negative for CD1a, whereas lymphocytes in the surrounding breast tissue consisted of both B and T cells; the distribution of lymphocytes was the same as that seen in reactive hyperplasia of lymphatic tissues.

An electron microscope revealed aggregation of microvilli with irregular projections (Fig. 4A) and secretory granules in some tumor cells (Fig. 4B). In part, desmosomes existed between tumor cells (Fig. 4B).

ISH for detection of the EBV genome was negative in both neoplastic cells and lymphocytes. We extracted DNA from two paraffin blocks of the tumor and examined the presence of EBV genome using PCR. The 35-cycle amplification of BamHI-W fragment of EBV genome did not show any clear bands (results not shown).

Discussion

LELC describes tumors occurring outside the nasopharynx, which show similar morphological features to those of nasopharyngeal lymphoepithelioma, consisting of malignant epithelial cells and diffusely infiltrating lymphocytes. This is the tenth reported case of LELC-B.

Because of the undifferentiated appearance of neoplastic cells and presence of intensely infiltrating lymphocytes, LELC and lymphoepithelioma of the nasopharynx with the Schmincke pattern could be confused with lymphoma. The present case should also be differentiated from lymphoma, particularly anaplastic large cell lymphoma. However, neoplastic cells were positive for EMA and specific types of cytokeratin and lacked any lymphocytic markers analyzed except CD10, which is also detected on some types of epithelial cells. These immunohistochemical findings were consistent with the epithelial nature of the tumor cells. Dadmanesh et al. reported that tumor cells reacted only with low-molecular-weight cytokeratin [8]. Since tu-mor cell reactivity to cytokeratin depended on one type, caution is required when using cytokeratin as an epithelial marker.

Moreover, an electron microscopic study, which was first carried out on LELC-B, showed differentiation toward glandular epithelium as well as epithelial origin of the

Table 1 Summary of clinicalinformation of LELC-B reported in literature. *R*right, *L* left, *Quad*quadrantectomy, *Ax* axillary nodedissection, *Rx* radiotherapy, *ANED* alive with no evidence of disease, *PS* parasternal node

Report	Sex/age (years)	Tumor site	Tumor size (mm)	Lymph node metastasis	Surgical treatment	Clinical outcome
S. Kumar [18]	Female/65	R upper outer	20	0/?	Mastectomy+Ax	ANED (7 months)
S. Cristina [7]	Female/54	R upper outer	15	0/19	Quad+extensive excision+Ax+Rx	ANED (6 months)
P. Naidoo [24]	Female/50	R	25×20	2/24	Wide local excision+Ax	ANED (3 months)
F. Dadmanesh [8]						
Case 1	Female/43	L	19	1/1	Quad+Ax	ANED (60 months)
Case 2	Female/53	R	20			ANED (72 months)
Case 3	Female/49	L	10	0/19	Quad+Ax	Contralateral LEC 3 years after L quad (case 4)
Case 4	Female/52	R	27	0/20	Quad+Ax	ANED (36 months)
Case 5	Female/64	R	20	0/29	R mastectomy+Ax	ANED (60 months)
Case 6	Female/69	R	23	0/19	R mastectomy+Ax+Rx	ANED (48 months)
Present case	Female/47	L upper outer+inner	28×23	0/33	L mastectomy+Ax	PS and lung metastasis 19 months after
					Anti-estrogen+ chemotherapy+Rx	Radiation and chemotherapy

Table 2 Summary of characters oflymphoepithelioma-like carcinoma of the breast reported inliterature. *CK* cytokeratin,*ER* estrogen receptor, *PrR*progesterone receptor, *ND* not done, *LMW* low molecular weight, *EBV*Epstein–Barr virus, *PCR* polymerase chain-reaction, *ISH* in situ hybridization, *EMA* epithelial membrane antigen, *ER*estrogen receptor, *PrR* progesterone receptor

Report	Lymphocytes in the tumor	CK	EMA	ER	PrR	c-erb-B2	p53	e-cadherin	EBV ISH	EBV PCR	LMP-1 &/or EBNA2	MIB-1
S. Kumar [18]	B, T	AE1/AE3	+	+	+	ND	ND	ND	−	ND	ND	ND
S. Cristina [7]	B, T	CK*	+	+(42%)	−(<10%)	−	−	−	−	−	ND	5%
P. Naidoo [24]	T	AE1/AE3, CAM5.2	+	ND	ND	ND	ND	ND	−	ND	−	ND
F. Dadmanesh [8]												
Case 1	B>T	LMW	+	−	−	−		−	0/4**			30-60%
Case 2	B>T	LMW	+	−	−	−		+	0/4**			“
Case 3	B>T	LMW	+	−	−	−		ND	0/4**			“
Case 4	B>T	LMW	+	+	−	−		−	0/4**			“
Case 5	B>T	LMW	+	−	−	−		+	0/4**			“
Case 6	B>T	LMW	+	−	−	−		+	0/4**			“
Present case	T	AE1/AE3, CAM5.2	+	−	−	+	−	+	−	−	−	80%

*CK: Biomeda,Foster City, CA
**Negative infour cases examined

neoplastic cells. This is the first case of LELC-B with glandular differentiation. The phenotype of permeating lymphocytes in the tumor, positive for CD3 and negative for CD1a, excluded involvement of type-B2 thymoma (cortical thymoma).

All the reports stated that LELC-B seemed to behave favorably, although the follow-up period was not long [7, 8, 18, 24] (Table 1). However, prognosis of LELC-B may not be necessarily good, because distant metastasis to the lung was detected 19 months after the therapy in the present case.

The evidence of EBV infection was not detected, even using PCR, as well as ISH and immunohistochemistry, similar to reported cases of LELC-B [7, 8, 18, 24] (Table 1, Table 2).

In the discussion as to a clinicopathological entity of LELC-B, distinction from MC-B is most important. The tumor margins of MC-B are characteristically well circumscribed, with smooth round edges, and tend to push against the surrounding breast tissue without invasion. The tumor cells are sharply demarcated from the adjacent stroma, with a various amount of lymphoplasmacytic infiltrate, and form irregular interconnecting islands, resulting in a syncytial mass. Definitive histopathological features of MC-B include a prominent lymphoplasmacytic reaction, circumscription, a syncytial growth pattern, poorly differentiated nuclear grade and high mitotic rate [29]. The present case did not fulfill this criteria with respect to circumscription and a syncytial growth pattern because the tumor consisted of multinodular lesions, and there was no circumscription. Furthermore, tumor cells formed small clusters, nests or sheet-like growth patterns with unclear margins because they were permeated by numerous lymphocytes. These findings did not correspond to the syncytial growth patterns seen in MC-B. Atypical MC-B also requires a syncytial growth pattern in its pathological diagnosis. Therefore, our tumor should be distinguished from MC-B from the morphological standpoints of dissociation of tumor cells with infiltrating lymphocytes and the poorly described outer margins.

Cristina et al. described LELC-B as different from MC-B in immunoreactivity as well as the growth patterns stated above [7]. They reported that LELC-B was positive for estrogen receptor and negative for e-cadherin. However, not all reported cases demonstrated a constant result (Table 2). In our case, both estrogen and progesterone receptors were negative, and e-cadherin was positive. As far as we know, no significant differences have been recognized between LELC-B and MC-B, except for growth patterns. Glandular differentiation of tumor cells first observed by our electron microscopic study in LELC-B is also reported in MC-B [14], but ultrastructural study has not yielded consistent findings, even in MC-B [1, 14].

Iezzoni et al. summarized that EBV was associated with LELCs only in the stomach, salivary gland, lung and thymus [15]. The evidence that EBV is involved in the pathogenesis of MC-B also has not been shown [11, 20].

LELC-B and MC-B share many clinicopathological findings, including admixture of tumor cells and lymphocytes, favorable prognosis and absence of EBV. Thus far, although the difference between LELC-B and MC-B has been limited to growth patterns, i.e., whether circumscription and a syncytial growth pattern exist, these might be the significant characters that define each tumor. Therefore, LELC-B should be recognized as a distinct entity, and acquiring more cases for study is important.

Acknowledgment We thank Yuji Shibata for his excellent technical assistance.

References

1. Ahmed A (1980) The ultrastructure of medullary carcinoma of the breast. Virchows Arch 388:175–186
2. Amin MB, Ro JY, Lee KM, Ordonez NG, Dinney CP, Gulley ML, Ayala AG (1994) Lymphoepithelioma-like carcinoma of the urinary bladder. Am J Surg Pathol 18:466–473
3. Andryk J, Freije JE, Schultz CJ, Campbell BH, Komorowski RA (1996) Lymphoepithelioma of the larynx. Am J Otolaryngol 17:61–63
4. Burke AP, Yen TS, Shekitka KM, Sobin LH (1990) Lymphoepithelial carcinoma of the stomach with Epstein–Barr virus demonstrated by polymerase chain reaction. Mod Pathol 3:377–380
5. Butler AE, Colby TV, Weiss L, Lombard C (1989) Lymphoepithelioma-like carcinoma of the lung. Am J Surg Pathol 13:632–639
6. Carr KA, Bulengo-Ransby SM, Weiss LM, Nickoloff BJ, Bulengo S (1992) Lymphoepithelioma-like carcinoma of the skin: a case report with immunophenotypic analysis and in situ hybridization for Epstein–Barr viral genome. Am J Surg Pathol 16:909–913
7. Cristina S, Boldorini R, Brustia F, Monga G (2000) Lymphoepithelioma-like carcinoma of the breast: an unusual pattern of infiltrating lobular carcinoma. Virchows Arch 437:198–202
8. Dadmanesh F, Peterse JL, Sapino A, Fonelli A, Eusebi V (2001) Lymphoepithelioma-like carcinoma of the breast: lack of evidence of Epstein-Barr virus infection. Histopathology 38:54–61
9. Dinney CP, Ro JY, Babaian RJ, Johnson DE (1993) Lymphoepithelioma of the bladder: a clinicopathological study of 3 cases. J Urol 149:840–841
10. Evans AT, Guthrie W (1991) Lymphoepithelioma-like carcinoma of the uvula and soft palate: a rare lesion in an unusual site. Histopathology 19:184–186
11. Gaffey MJ, Frierson HF, Mills SE, Boyd JC, Zarbo RJ, Simpson JF, Gross LK, Weiss LM (1993) Medullary carcinoma of the breast: identification of lymphocyte subpopulations and their significance. Mod Pathol 6:721–728
12. Gal AA, Unger ER, Koss MN, Yen TS (1991) Detection of Epstein–Barr virus in lymphoepithelioma-like carcinoma of the lung. Mod Pathol 4:264–268
13. Hamilton-Dutoit SJ, Therkildsen MH, Neilsen NH, Jensen H, Hansen JP, Pallesen G (1991) Undifferentiated carcinoma of the salivary gland in Greenlandic Eskimos: demonstration of Epstein–Barr virus DNA by in situ nucleic acid hybridization. Hum Pathol 22:811–815
14. Harris M, Lessells AM (1986) The ultrastructure of medullary, atypical medullary and non-medullary carcinomas of the breast. Histopathology 10:405–414
15. Iezzoni JC, Gaffey MJ, Weiss LM (1995) The role of Epstein–Barr virus in lymphoepithelioma-like carcinomas. Am J Clin Pathol 103:308–315

16. Kijima Y, Hokita S, Takao S, Baba M, Natsugoe S, Yoshinaka H, Aridome K, Otsuji T, Itoh T, Tokunaga M, Eizuru Y, Aikou T (2001) Epstein–Barr virus involvement is mainly restricted to lymphoepithelial type of gastric carcinoma among various epithelial neoplasms. J Med Virol 64:513–518
17. Krishnamurthy S, Lanier AP, Dohan P, Lanier JF, Henle W (1987) Salivary gland cancer in Alaskan natives, 1966–1980. Hum Pathol 18:986–996
18. Kumar S, Kumar D (1994) Lymphoepithelioma-like carcinoma of the breast. Mod Pathol 7:129–131
19. Kuo T, Hsueh C (1997) Lymphoepithelioma-like salivary gland carcinoma in Taiwan: a clinicopathological study of nine cases demonstrating a strong association with Epstein–Barr virus. Histopathology 31:75–82
20. Lespagnard L, Cochaux P, Larsimont D, Degeyter M, Velu T, Heimann R (1995) Absence of Epstein–Barr virus in medullary carcinoma of the breast as demonstrated by immunophenotyping, in situ hybridization and polymerase chain reaction. Am J Clin Pathol 103:449–452
21. Leyvraz S, Henle W, Chahinian AP, Perlmann C, Klein G, Gordon RE, Rosenblum M, Holland JF (1985) Association of Epstein–Barr virus with thymic carcinoma. N Engl J Med 312:1296–1299
22. Mills SE, Austin MB, Randall ME (1985) Lymphoepithelioma-like carcinoma of the uterine cervix: a distinctive, undifferentiated carcinoma with inflammatory stroma. Am J Surg Pathol 9:883–889
23. Min KW, Holmquist S, Peiper SC, O'Leary TJ (1991) Poorly differentiated adenocarcinoma with lymphoid stroma (lymphoepithelioma-like carcinomas) of the stomach: report of three cases with Epstein–Barr virus genome demonstrated by the polymerase chain reaction. Am J Clin Pathol 96:219–227
24. Naidoo P, Chetty R (2001) Lymphoepithelioma-like carcinoma of the breast with associated sclerosing lymphocytic lobulitis. Arch Pathol Lab Med 125:669–672
25. Ohsawa M, Tomita Y, Kanno H, Iuchi K, Kawabata Y, Nakajima Y, Komatsu H, Mukai K, Shimoyama M, Aozasa K (1995) Role of Epstein–Barr virus in pleural lymphomagenesis. Mod Pathol 8:848–853
26. Pittaluga S, Loke SL, So KC, Cheung KN, Ma L (1992) Clonal Epstein–Barr virus in lymphoepithelioma-like carcinoma of the stomach: demonstration of viral genome by in situ hybridization and Southern blot analysis. Mod Pathol 5:661–664
27. Pittaluga S, Wong MP, Chung LP, Loke SL (1993) Clonal Epstein–Barr virus in lymphoepithelioma-like carcinoma of the lung. Am J Surg Pathol 17:678–682
28. Randolph TL, Amin MB, Ro JY, Ayala AG (1997) Histologic variants of adenocarcinoma and other carcinomas of prostate: pathologic criteria and clinical significance. Mod Pathol 10: 612–629
29. Rosen PP, Oberman HA (eds) (1993) Tumors of the mammary gland, 3rd Series. Armed Forces Institute of Pathology, Washington, DC
30. Saemundsen AK, Albeck H, Hansen JP, Nielsen NH, Anvret M, Henle W, Henle G, Thomsen KA, Kristensen HK, Klein G (1982) Epstein–Barr virus in nasopharyngeal and salivary gland carcinomas of Greenland Eskimos. Br J Cancer 46:721–728
31. Saw D, Lau WH, Ho JH, Chan JK, Ng CS (1986) Malignant lymphoepithelial lesion of the salivary gland. Hum Pathol 17: 914–923
32. Shek TW, Luk IS, Ng IO, Lo CY (1996) Lymphoepithelioma-like carcinoma of the thyroid gland: lack of evidence of association with Epstein–Barr virus. Hum Pathol 27:851–853
33. Shibata D, Tokunaga M, Uemura Y, Sato E, Tanaka S, Weiss LM (1991) Association of Epstein–Barr virus with undifferentiated gastric carcinomas with intense lymphoid infiltration: lymphoepithelioma-like carcinoma. Am J Pathol 139:469–474
34. Swanson SA, Cooper PH, Mills SE, Wick MR (1988) Lymphoepithelioma-like carcinoma of the skin. Mod Pathol 1:359–365
35. Tseng CJ, Pao CC, Tseng LH, Chang CT, Lai CH, Soong YK, Hsueh S, Jyu-Jen H (1997) Lymphoepithelioma-like carcinoma of the uterine cervix: association with Epstein–Barr virus and human papillomavirus. Cancer 80:91–97
36. Walker AN, Kent D, Mitchell AR (1990) Lymphoepithelioma-like carcinoma in the skin. J Am Acad Dermatol 22:691–693
37. Weinberg E, Hoisington S, Eastman AY, Rice DK, Malfetano J, Ross JS (1993) Uterine cervical lymphoepithelial-like carcinoma: absence of Epstein–Barr virus genomes. Am J Clin Pathol 99:195–199
38. Wu TC, Kuo TT (1993) Study of Epstein–Barr virus early RNA 1 (EBER1) expression by in situ hybridization in thymic epithelial tumors of Chinese patients in Taiwan. Hum Pathol 24:235–238
39. Yuen ST, Chung LP, Leung SY, Luk IS, Chan SY, Ho J (1994) In situ detection of Epstein–Barr virus in gastric and colorectal adenocarcinomas. Am J Surg Pathol 18:1158–1163

Virchows Arch (2005) 447: 660–664
DOI 10.1007/s00428-005-1206-6

CASE REPORT

Rieko Nishimura · Norihiro Teramoto · Minoru Tanada · Akira Kurita · Hiroshi Mogami

Inflammatory pseudotumor of the liver associated with malignant disease: report of two cases and a review of the literature

Received: 2 November 2004 / Accepted: 20 December 2004 / Published online: 21 June 2005
© Springer-Verlag 2005

Abstract Two cases of inflammatory pseudotumor (IPT) of the liver associated with gastrointestinal tract cancer are reported. In addition, the etiological correlation between IPT and abscesses of the liver in cancer patients is discussed. The first patient was a 63-year-old woman who underwent distal gastrectomy and partial hepatectomy under a diagnosis of stomach cancer with liver metastasis. The second patient was a 66-year-old man who had undergone surgery for rectal cancer 6 years previously and underwent partial hepatectomy under a diagnosis of metastasis of rectal cancer to the liver. The gastric cancer was a papillary adenocarcinoma limited to the mucosa, and the rectal cancer was a moderately differentiated adenocarcinoma limited to the subserosa. The resected liver tumor in the first case measured 5.5×5.0×4.0 cm and was 2.5×1.9×1.6 cm in the second. The cut surface showed that both masses were well circumscribed and divided into lobules by fibrous tissue. They were yellowish white in color and there was no evidence of necrosis or hemorrhage. Histologically the masses consisted of fibrous areas and cellular areas, and the cellular areas consisted of fascicles of plump spindle cells mingled with varying numbers of plasma cells, lymphocytes, and histiocytes. The masses were diagnosed as IPTs. Obliterating phlebitis suggesting infection via the portal vein was seen in the adjacent liver tissue in both cases. According to previous cases reported in the literature, there are three types of cancers associated with hepatic IPT: gastrointestinal tract cancer, biliary tract cancer, and cancers that need strong systemic chemotherapy. The underlying cancer types of IPT of the liver are almost similar to those associated with pyogenic liver abscesses suggesting the etiological correlation between IPT and abscesses of the liver.

Keywords Inflammatory pseudotumor · Liver · Cancer · Literature review

R. Nishimura (✉) · N. Teramoto
Department of Clinical Laboratory,
National Hospital Organization
Shikoku Cancer Center, 13 Horinouchi,
Matsuyama, Ehime 790-0007, Japan
e-mail: rnishimu@shikoku-cc.go.jp
Tel.: +81-89-9321111
Fax: +81-89-9327519

M. Tanada · A. Kurita
Department of Surgery,
National Hospital Organization
Shikoku Cancer Center,
Matsuyama, Ehime, Japan

H. Mogami
Department of Radiology,
National Hospital Organization
Shikoku Cancer Center,
Matsuyama, Ehime, Japan

Introduction

The inflammatory pseudotumor (IPT) of the liver is a rare, benign tumor-like lesion [6, 15], and about 60 cases have been reported in the English-language literature [17]. Some cases of IPT of the liver have been associated with malignant tumors [1, 7–9, 11, 13, 16]. Six such cases have been reported in the English-language literature [1, 7, 8, 11, 13, 16] and four cases in Japanese-language literature [9], but the etiological correlation between hepatic IPT and liver abscess in cancer patients has never been mentioned. In this paper, we report two cases of IPT of the liver with gastrointestinal tract cancer and discuss the etiological correlation between IPT and abscess of the liver in cancer patients.

Clinical history

Case A

A 63-year-old Japanese woman was admitted to our hospital because of epigastralgia, nausea and progressive appetite loss over 3 months. Laboratory tests on admission including serology tests for HBsAg and HBcAb were all normal except for an elevated blood glucose level. Early

gastric cancer of the protruding type was detected by gastroscopy. A post-contrast computed tomographic (CT) scan showed a large irregular-shaped mass in the left lobe of the liver. The mass showed peripheral rim-like or septal enhancement and an internal low density area. Gastric cancer and liver metastasis were diagnosed, and a distal gastrectomy and partial hepatectomy were performed. The patient is currently well, 25 months after surgery.

Case B

A 66-year-old Japanese man was referred to our hospital because of a small hepatic mass detected on a follow-up CT scan 6 years after surgery for rectal cancer at another hospital. Laboratory tests on admission, including serology tests for HBsAg and HBcAb, were all normal. No local recurrence was detected at the site of resection. A post-contrast CT scan showed a 2.5-cm mass in the right lobe of the liver. The mass showed contrast enhancement at the peripheral rim on the delayed-phase image. Rectal cancer metastasis to the liver was diagnosed, and a partial hepatectomy was performed. The patient is currently well, 25 months after the operation.

Pathological findings

Case A

The resected stomach contained a protruding tumor that was histologically diagnosed as papillary adenocarcinoma limited to the mucosa. The resected liver measured 13.0×11.0×5.0 cm in size and contained a tumor that measured 5.5×5.0×4.0 cm. The cut surface showed that the tumor was well-circumscribed and was divided into lobules by fibrous tissue. It was yellowish white in color, and there was no evidence of necrosis or hemorrhage (Fig. 1). Histologically, the mass showed lobulation into the fibrous area and cellular areas (Fig. 2a), and the cellular areas consisted of fascicles of plump spindle cells mingled with varying numbers of plasma cells, lymphocytes, and histiocytes. Residual bile ducts and hepatocytes were seen in the tumor (Fig. 2b). Immunohistochemical stains were performed on formalin-fixed, paraffin-embedded tissue. Antibodies to both kappa and lambda light chains were positive on plasma cells in normal proportions, revealing the polyclonal nature of the plasma cells. Spindle cells were all positive for vimentin, and some were weakly positive for muscle actin, but negative for CD21 and CD35. Thus, these results suggest that spindle cells are differentiated into myofibroblastic cells not into follicular dendritic reticulum cells (FDCs). Epstein–Barr virus (EBV), latent membrane protein (LMP-1) and anaplastic lymphoma kinase (ALK) protein were not expressed in spindle cells and inflammatory cells. No EBV RNA (EBER-1) transcripts were detected using in situ hybridization (ISH). No bacteria or fungi were found on histological sections. No bacterial cultures of the tumor were performed. The

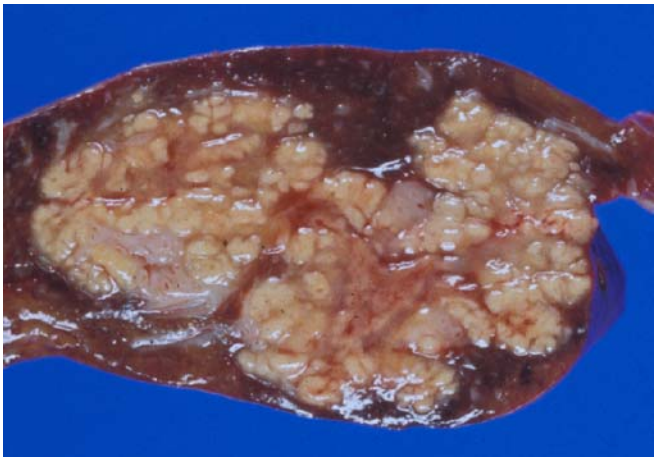


Fig. 1 Gross appearance of the hepatic tumor in case A. The size of the tumor was 5.5×5.0×4.0 cm. The mass was divided into lobules by fibrous tissue. It was *yellowish white* in color and there was no evidence of necrosis or hemorrhage

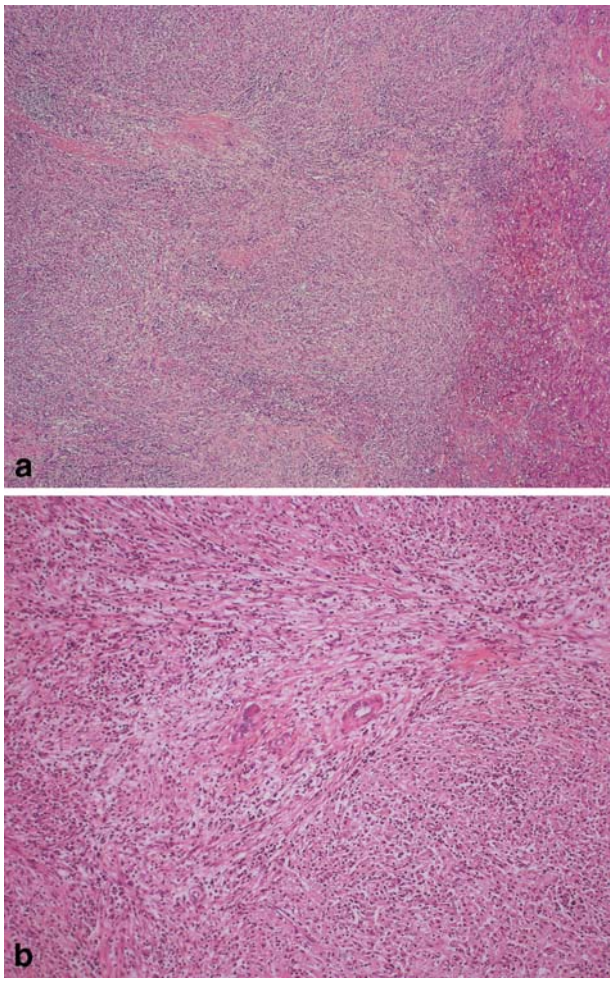


Fig. 2 Histological appearance of the hepatic tumor in case A. **a** The mass showed lobulation into fibrous areas and cellular areas (hematoxylin and eosin; H&E). **b** The cellular areas consisted of fascicles of plump spindle cells intermixed with varying numbers of plasma cells, lymphocytes, and histiocytes. Residual bile ducts were seen in the tumor (H&E)

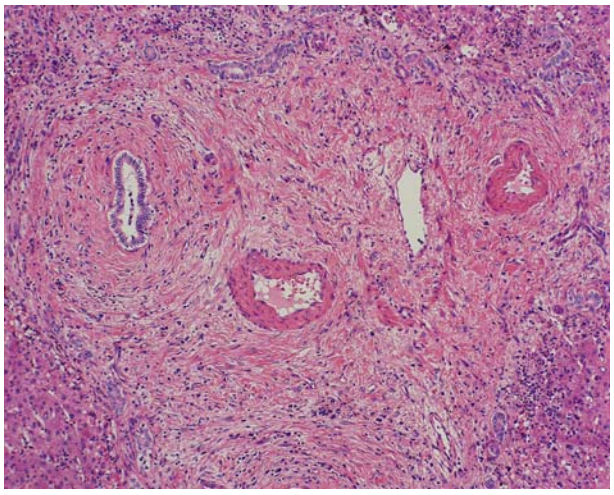


Fig. 3 Histological appearance of obliterating phlebitis in the adjacent liver in case A. A medium size portal vein was thickened by fibrosis (hematoxylin and eosin)

histological appearance of the hepatic tumor was consistent with a diagnosis of IPT. The hepatic tissue outside the tumor was non-cirrhotic. The portal veins penetrating and surrounding the tumor were thickened with fibrosis, suggesting obliterating phlebitis (Fig. 3).

Case B

The rectal cancer was ulcerated, and a review of the slides showed a histologically moderately differentiated adenocarcinoma limited to the subserosa. The hepatic tumor measured 2.5×1.9×1.6 cm. Its gross appearance, histological appearance, and the immunohistochemical and ISH results were almost the same as in case A. The non-tumorous liver tissue was non-cirrhotic, and the small portal veins surrounding the tumor were thickened by fibrosis, suggesting obliterating phlebitis.

Discussion

IPT is a relatively benign tumor-like lesion mostly occurring in the lung [12]. The liver is the second most common site of IPT, reported in about 60 cases to date [17], but the etiology of hepatic IPT in cancer patients has never been discussed.

Some IPT of the liver have been associated with malignant tumors. In the English-language literature, 6 such cases have been reported [1, 7, 8, 11, 13, 16] and 4 such cases in the Japanese-language literature [9]. The clinical findings of 10 reported cases and the present 2 cases are summarized in Table 1; 11 cases were reported from Japan and 1 from the United Kingdom. The patient population consisted of nine men and three women, ranging in age from 3 years to 66 years (average 52 years). The most common symptom was upper abdominal pain. The clinical diagnosis was metastatic liver cancer (seven cases), liver abscess (two cases) and cystadenocarcinoma (one case). Therefore, we should need a systemic liver biopsy to avoid unnecessary surgical resection, because laboratory data and imaging findings do not discriminate between metastasis and IPT. In our case A, if we had taken notice of an unusual association of early gastric cancer and a huge hepatic mass, we could have performed systemic biopsy and diagnosed the hepatic tumor as IPT before the operation. The tumor was located on the right in seven cases, on the left in four cases and bilaterally in one. The tumor was single in eight cases and multiple in four cases. The size of the tumor ranged from 1.5 cm to 12 cm (average 3.9 cm). The primary malignancy was colorectal carcinoma in four cases; leukemia in two cases; and gastric carcinoma, gallbladder carcinoma, ampula Vater carcinoma, ovarian carcinoma, breast carcinoma, and nephroblastoma in one case each. In six patients, the hepatic IPT was detected at the time of diagnosis of the malignancy, and in another six patients the hepatic IPT was detected after or during the therapy for malignant disease. The stage of the cancer was advanced in seven cases and early in two. The hepatic tumor was resected in ten cases, and followed and shrunken in two cases. The patient outcome was excellent in all cases, which the authors described in their papers.

There are three types of cancer patients associated with IPT of the liver: one is gastrointestinal tract cancer patients, the second is biliary tract cancer patients, and the third is the patients who might be receiving strong systemic chemotherapy, e.g., leukemia, nephroblastoma, ovarian, and breast cancer patients. The correlation between pyogenic liver abscesses and cancer has been reported previously, and the type of cancer in which pyogenic liver abscess and liver IPT have been reported to develop is almost similar [10, 19]. Common types of cancer associated with pyogenic liver abscesses are hematological malignancies, hepatobiliary tract cancers, and gastrointestinal tract cancers [10, 19]. Systemic chemotherapy with resultant neutropenia may be a cause of liver abscess in leukemia or lymphoma patients [10]. Hepatic artery seeding with uncertain infectious organisms following systemic chemotherapy is suggested [19]. The pathogenesis of liver abscesses in hepatobiliary tract cancer patients is mainly malignant biliary obstruction and spontaneous or iatrogenic necrosis of primary hepatic neoplasms with superimposed bacterial infection [19]. The pathogenesis of liver abscesses in gastrointestinal tract cancer patients includes portal venous suppuration secondary to colorectal cancer, and postgastrectomy for gastric cancer [19]. Obliterating phlebitis is seen in five of nine hepatic IPT patients reported by Horiuchi et al. [6]. They suggest that infection through the portal vein is one of the causal participants in hepatic IPT. In addition, some reports indicate that cholangitis may also be responsible for the development of hepatic IPT [6, 12, 15, 17]. In Table 1, there are two cases (cases 6 and 10) [1, 8] that suggest the etiological correlation between liver abscesses and liver IPT. In cases 6 and 10, a cystic space was detected in the lesions of the liver, and *Staphylococcus aureus* was cultured from the cystic fluid in both cases. Obliterating phlebitis was found

Table 1 A literature survey of inflammatory pseudotumors of the liver in cancer patients. *ND* not described

Cases	1	2	3	4	5	6	7	8	9	10	11	12
Country	Japan	Japan	Japan	Japan	Japan	Japan	Japan	Japan	Japan	Japan	Japan	U.K.
Age (years)	63	66	64	54	48	62	65	56	54	57	26	3
Sex	Female	Male	Male	Male	Male	Male	Male	Female	Female	Male	Male	Male
Presentation	Upper abdominal pain	No	Upper abdominal pain	No	Melena	Fever	Upper abdominal pain	Appetite loss	No	Upper abdominal pain	Upper abdominal pain	palpable non tender mass
Suspected disease	Cancer metastasis	Cancer metastasis	Liver abscess	Cancer metastasis	Cancer metastasis	Cystadenocarcinoma	Cancer metastasis	Cancer metastasis	Cancer metastasis	ND	Liver abscess	ND
Solitary/ multiple (The number of tumors)	Solitary	Solitary	Multiple (10)	Multiple (2)	Solitary	Solitary	Solitary	Solitary	Multiple (2)	Solitary	Multiple	Solitary
Site	Left	Right	Both	Left	Right	Right	Right	Right	Right	Left	Right	Left
Size (cm)	5.5	2.5	3.5	4.0	2.7	12.0	2.0	ND	1.5	ND	3.0	2.0
Treatment	Resection	Resection	Resection	Resection	Resection	Resection	Resection	Resection	Resection	Nothing	Nothing	Resection
Outcome	Alive 25 months after operation	Alive 25 months after operation	Alive 1 year after operation	Alive 3 years after operation	ND	ND	Alive 20 months after operation	Alive 38 days after operation	ND	ND	Alive 10 months after initial symptom	Alive 1 year after operation
Underlying cancer	Gastric cancer	Rectal cancer	Colon cancer	Colon cancer	Rectal cancer	Gallbladder cancer	Ampula Vater cancer	Ovarian cancer	Breast cancer	Leukemia	Leukemia	Nephroblastoma
Cancer stage [a]	IA	IIA	I	IIIB	ND	IIB	IIB	IIB	IIA	ND	ND	IV
Chemotherapy for cancer	No	No	No	No	ND	No	No	Yes	Yes	Yes	Yes	Yes
Correlation with underlying cancer	Synchronous	6 years after operation	Synchronous	6 months after operation	Synchronous	Synchronous	Synchronous	Synchronous	3 years after operation	During chemotherapy for cancer recurrence	Before cancer consolidation therapy	7 months after completion of cancer
Reference	Present case A	Present case B	Iguchi et al. [9]	Ishida et al. [7]	Saito et al. [13]	Akiyama et al. [1]	Kobayashi et al. [9]	Yokoyama et al. [9]	Nakamura et al. [9]	Isobe et al. [8]	Tajima et al. [16]	Newbould et al. [11]

[a]Cancer stage is classified using TNM Classification of Malignant Tumors (Sixth Edition) from the International Union Against Cancer

in case 3 [9] and our present cases (cases 1 and 2). Therefore, the etiology of hepatic IPT may be similar to that of the pyogenic liver abscess because of the similarity of associated cancer types and the etiological correlation of clinical course in some patients.

Recent studies suggest that a proportion of so-called hepatic IPT represents EBV-associated FDC proliferations [3, 14]. Therefore, these tumors are thought to become a different entity from IPT and the name IPT-like FDC tumor is recommended [3]. Hepatic tumors of both our cases did not express FDC markers, and neither contained EBV. Some cases of hepatic IPT, especially in young age, show ALK expression [2], and IPT-like FDC tumors never express ALK [3]. Neither of our cases expressed ALK in immunohistochemical study.

In cancer patients, Japanese patients were predominant even in the English-language literature [1, 7, 8, 13, 16]. It has been reported that all hepatic IPT patients are predominantly Japanese: 17 of 51 patients (33%) are Japanese [15]. Furthermore, there are some reasons why Japanese people may more prone to develop IPT of the liver than patients in other populations. EBV may be related to the development of some so-called hepatic IPTs: now they should be called IPT-like FDC tumors [3, 14] and Japan is an EBV endemic area [3]. An autoimmune reaction has also been suggested as a cause of IPT of the liver [18]. Immunological disturbances and staphylococcal infection may have been the cause of hepatic IPT in a Papillon–Lefevre syndrome patient [4]. Therefore, viral infection or the body's autoimmunity may be another basic cause for the development of IPT of the liver. It is thought to be possible that the Japanese population may have some inherent physiological factors that make them prone to develop IPT.

In summary, we have reported two cases in which IPT of the liver was associated with gastrointestinal tract cancer and discussed the etiology of hepatic IPT in cancer patients. Populations at particular risk of developing hepatic IPT may be those with cancer—especially of the gastrointestinal and hepatobiliary tracts, and patients who are undergoing strong systemic chemotherapy.

Acknowledgements We thank Professor Tadashi Yoshino of the Department of Pathology, Okayama University Graduate School of Medicine and Dentistry for detection of the Epstein–Barr virus and immunohistochemical stainings against CD21, CD35, and ALK. This study was partially supported by Grants-in-Aid for Cancer Research from the Ministry of Health, Labour and Welfare of Japan.

Note added in proof. Case A has been published recently in Japanese Journal of Clinical Oncology (2005) 35:218–220. That is a case report focussing on CT and histopathological correlation, and its discussing point is completely different from this report.

References

1. Akiyama T, Saito H, Kiriyama M, Tomita F, Kosaka T, Kita I, Takashima S, Matsunou H (1995) A case of gallbladder cancer associated with a common bile duct neuroma, and a cystic lesion of the liver with histologic findings similar to those of an inflammatory pseudotumor. J Gastroenterol 30:408–412
2. Chan JK, Cheuk W, Shimizu M (2001) Anaplastic lymphoma kinase expression in inflammatory pseudotumors. Am J Surg Pathol 25:761–768
3. Cheuk W, Chan JKC, Shek TWH, Chang JH, Tsou M, Yuen NWF, Ng W, Chan ACL, Prat J (2001) Inflammatory pseudotumor-like follicular dendritic cell tumor: a distinctive low-grade malignant intra-abdominal neoplasm with consistent Epstein–Barr virus association. Am J Surg Pathol 25:721–731
4. Czauderna P, Sznurkowska K, Korzon M, Roszkiewicz A, Stoba C (1999) Association of inflammatory pseudotumor of the liver and Papillon–Lefevre syndrome: case report. Eur J Pediatr Surg 9:343–346
5. Harada S, Kamata Y, Ishii Y, Eda H, Kitamura R, Obayashi M, Ito S, Ban F, Kuranari J, Nakajima H, Kuze T, Hayashi M, Okabe N, Senpuku H, Miyasaka N, Nakamura Y, Kanegane H, Yanagi K (2004) Maintenance of serum immunoglobulin G antibodies to Epstein Barr virus (EBV) nuclear antigen 2 in healthy individuals from different age groups in a Japanese population with a high childhood incidence of asymptomatic primary EBV infection. Clin Diagn Lab Immunol 11:123–130
6. Horiuchi R, Uchida T, Kojima T, Shikata T (1990) Inflammatory pseudotumor of the liver: clinicopathologic study and review of the literature. Cancer 65:1583–1590
7. Ishida H, Tatsuta M, Furukawa H, Ohta H, Hashimoto K, Hayashi N, Morimoto O, Ikeda M, Miya A, Masutani S, Kawasaki T, Satomi T, Yoshioka H, Nanai J (2000) Multiple inflammatory pseudotumors mimicking liver metastasis from colon cancer: report of a case. Surg Today 30:530–533
8. Isobe H, Nishi Y, Fukutomi T, Iwamoto H, Nakamuta M, Sakai H, Andoh B, Sakamoto S, Nawata H (1991) Inflammatory pseudotumor of the liver associated with acute myelomonocytic leukemia. Am J Gastroenterol 86:238–240
9. Kobayashi H, Yamazaki K, Yoshimoto K, Earashi M, Matsuki N (2001) A case of inflammatory pseudotumor of the liver associated with carcinoma of the papilla of Vater (in Japanese). Jpn J Clin Surg 62:1711–1716
10. Marcus SG, Walsh TJ, Pizzo PA, Danforth DN (1993) Hepatic abscess in cancer patients: characterization and management. Arch Surg 128:1358–1364
11. Newbould MJ, Kelsey A, Lendon M, Gururangan S (1992) Inflammatory pseudotumor of the liver masquerading as a metastasis in a child treated for nephroblastoma. Med Pediatr Oncol 20:172–175
12. Nonomura A, Minato H, Shimizu K, Kadoya M, Matsui O (1997) Hepatic hilar inflammatory pseudotumor mimicking cholangiocarcinoma with cholangitis and phlebitis: a variant of primary sclerosing cholangitis? Pathol Res Pract 193:519–525
13. Saito K, Kotake F, Ito N, Tabuchi T, Goto Y, Katano M, Hashimoto T, Abe K (2002) Inflammatory pseudotumor of the liver in a patient with rectal cancer: a case report. Eur Radiol 12:2484–2487
14. Selves J, Meggetto F, Brousset P, Voigt JJ, Pradère B, Grasset D, Icart J, Mariamé B, Knecht H, Delsol G (1996) Inflammatory pseudotumor of the liver: evidence for follicular dendritic reticulum cell proliferation associated with clonal Epstein–Barr virus. Am J Surg Pathol 20:747–753
15. Shek TWH, Ng IOL, Chan KW (1993) Inflammatory pseudotumor of the liver: report of four cases and review of the literature. Am J Surg Pathol 17:231–238
16. Tajima K, Kosugi S, Fuyama S, Maeda K, Hayashi T, Yahagi A, Akiba J, Suzuki K, Satoh S, Sasaki H (1998) Multiple inflammatory pseudotumors of the liver associated with acute myeloblastic leukemia. Intern Med 37:542–545
17. Toda K, Yasuda I, Nishigaki Y, Enya M, Yamada T, Nagura K, Sugihara J, Wakahara T, Tomita E, Moriwaki H (2000) Inflammatory pseudotumor of the liver with primary sclerosing cholangitis. J Gastroenterol 35:304–309
18. Voss SD, Kruskal JB, Kane RA (1999) Chronic inflammatory pseudotumor arising in the hepatobiliary–pancreatic system: progressive multisystemic organ involvement in four patients. Am J Roentgenol 173:1049–1054
19. Yeh TS, Jan YY, Jeng LB, Hwang TL, Chao TC, Chien RN, Chen MF (1998) Pyogenic liver abscesses in patients with malignant disease: a report of 52 cases treated at a single institution. Arch Surg 133:242–245

Virchows Arch (2005) 447: 665–668
DOI 10.1007/s00428-005-1263-x

CASE REPORT

Junji Shibahara · Masashi Fukayama

Secondary glioblastoma with advanced neuronal immunophenotype

Received: 5 January 2005 / Accepted: 21 March 2005 / Published online: 21 June 2005
© Springer-Verlag 2005

Abstract We describe an unusual progression of astrocytoma into secondary glioblastoma exhibiting advanced neuronal immunophenotype. A tumor of the left frontal lobe of a 35-year-old man was diagnosed as astrocytoma. The tumor was treated by partial removal with postoperative chemoradiotherapy, followed by extensive removal of the residual regrowing tumor 5 month later. A secondary tumor was discovered and partially resected 8 years later, but the patient died 11 months following the operation due to extensive tumor progression showing subarachnoidal and intraventricular dissemination. The secondary tumor was small cell-predominant, highly proliferative tumor with an extremely high MIB-1 labeling index (80%). Unexpectedly, most of the tumor cells were positive for neuronal markers (synaptophysin and NeuN), but not for glial fibrillary acidic protein (GFAP). Retrospective examination of the original tumor revealed not only diffuse GFAP expression, but also neuronal marker expressions in small numbers of tumor cells that were hard to discriminate from the other cells on hematoxylin-eosin (HE) stain. This way of malignant progression of astrocytoma was quite unusual. Although the secondary tumor was classified as glioblastoma according to World Health Organization (WHO) classification (2000), it might be categorized into new variants of malignant glioneuronal tumors proposed recently.

Keywords Astrocytoma · Secondary glioblastoma · Neuronal phenotype · Immunohistochemistry

J. Shibahara (✉) · M. Fukayama
Department of Pathology, Graduate School of Medicine,
University of Tokyo,
7-3-1 Hongo, Bunkyo-ku,
113-0033 Tokyo, Japan
e-mail: jshiba-tky@umin.ac.jp
Tel.: +81-3-38155411
Fax: +81-3-38158379

Introduction

Glioblastoma, the most common malignant neuroectodermal tumor of the central nervous system (CNS), can be divided into two major categories, primary and secondary [8]. These are not only clinically but also genetically distinct subsets. Primary glioblastoma is a de novo malignancy and characterized by epidermal growth factor receptor (EGFR) gene ampflication or overexpression, mouse double minute 2 homolog (MDM2) gene ampflication or overexpression, p16 deletion, or phosphatase and tensin homolog (PTEN) gene mutation. Secondary glioblastoma develops from diffuse astrocytoma (WHO grade II) or anaplastic astrocytoma (WHO grade III). Secondary glioblastoma usually retains an astrocytic nature, as evidenced by immunoreactivity to glial fibrillary acidic protein (GFAP), but its reactivity tends to be reduced, especially in undifferentiated types. Genetically, secondary glioblastoma often shows TP53 mutation, an alteration also present in the precursor lower grade tumor in most cases [11]. No histological feature precisely discriminates primary and secondary glioblastoma, but small cell architecture is implicated as a hallmark of the former [3]. We describe here an unusual progression of astrocytoma into secondary glioblastoma exhibiting an undifferentiated, small cell-predominant morphology and advanced neuronal immunophenotype.

Clinical history

A 35-year-old male presented with general tonic convulsion. Computed tomography (CT) scan revealed a mass in the left frontal lobe. The patient underwent partial removal of the tumor with postoperative irradiation (60 Gy) and chemotherapy with nimustine (ACNU), followed by extensive removal of the residual regrowing tumor 5 months later. A small enhanced nodule remained on CT, but additional interferon (IFN) therapy was discontinued because of the patient's leukocytopenia.

Eight years following the last operation, the patient presented with a headache and nausea. A huge destructive mass involving the left lateral ventricle was noted in the left frontal lobe on CT. The patient underwent 70% removal of the tumor, but died from extensive tumor progression 11 months later. Autopsy examination was performed.

Materials and methods

The tumor tissues resected in each operation and the whole brain at autopsy were fixed in 10% formalin. All the surgical materials and sufficient portions of the autopsy material were embedded in paraffin. Routine hematoxylin-eosin (HE)-stained sections were generated from 5 μm-thick sections.

All immunohistochemical examinations, including the retrospective study of the original tumor, were performed on the paraffin sections by the avidin-biotinylated immunoperoxidase method. To enhance the staining, heat-induced epitope retrieval was performed. The following antibody reagents were applied: GFAP (polyclonal, 1:100; Dako Corporation, Santa Barbara, Calif., USA), S-100 protein (polyclonal, 1:250; Dako), synaptophysin (monoclonal, 1:100; Dako), NeuN (monoclonal, 1:1000; Chemicon, Tamecula, Calif., USA), neurofilament protein (NFP) (monoclonal, 1:100; Dako), p53 (monoclonal, 1:100; Novocastra, Newcastle, UK), EGFR (monoclonal, 1:20; Zymed Laboratories, South San Francisco, Calif., USA), and MIB-1(monoclonal, 1:200; Immunotech, Marseilles, France).

Results

Findings on the original tumor

The original tumor was diffuse astrocytoma [World Health Organization (WHO) grade II]. The tumor consisted of an admixture of fibrillary, protoplasmic, and gemistocytic cells, exhibiting a relatively low cellularity and frequent microcystic change with a pooling of mucoid material (Fig. 1a,b). In accordance with the astrocytic character, an immunohistochemical examination of the tumor cells performed retrospectively indicated diffuse immunoreactivity to GFAP (Fig. 1c) and S-100 protein. Some of the tumor cells were also immunoreactive for synaptophysin with perinuclear and punctate staining pattern. In addition, occasional cells were positive for a more specific neuronal marker, NeuN (Fig. 1d). NFP-positive tumor cells were not identified. The tumor cells showing the neuronal immunophenotype were difficult to discriminate from the other tumor cells on HE stain. These cells were not considered as entrapped neurons because of the morphology and their location (deep white matter). Immunoreactivity to p53 was observed in a small number of the cells. Growth fraction was low, as estimated by an MIB-1 labeling index of 2%. At the second operation 5 months later, gemistocytic tumor cells predominated, and very few neuronal cells were recognized.

Findings on the secondary tumor

The resected specimen of the secondary tumor exhibited an extremely high cellularity that gave it the appearance of a blue cell tumor (Fig. 2a). Most of the tumor cells had small

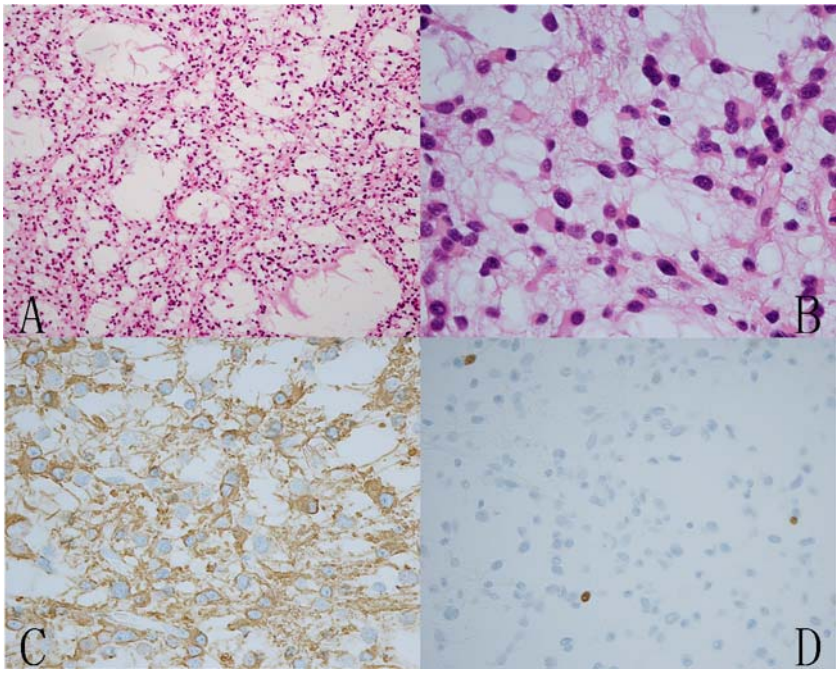


Fig. 1 (**a**) The original tumor was diffuse astrocytoma (WHO grade II), showing frequent microcystic change (hematoxylin-eosin stain; ×100). (**b**) A higher magnification view of the tumor (×400). (**c**) The tumor cells are diffusely immunoreactive for GFAP (×400). (**d**) Occasional cells are immunoreactive for NeuN (×400)

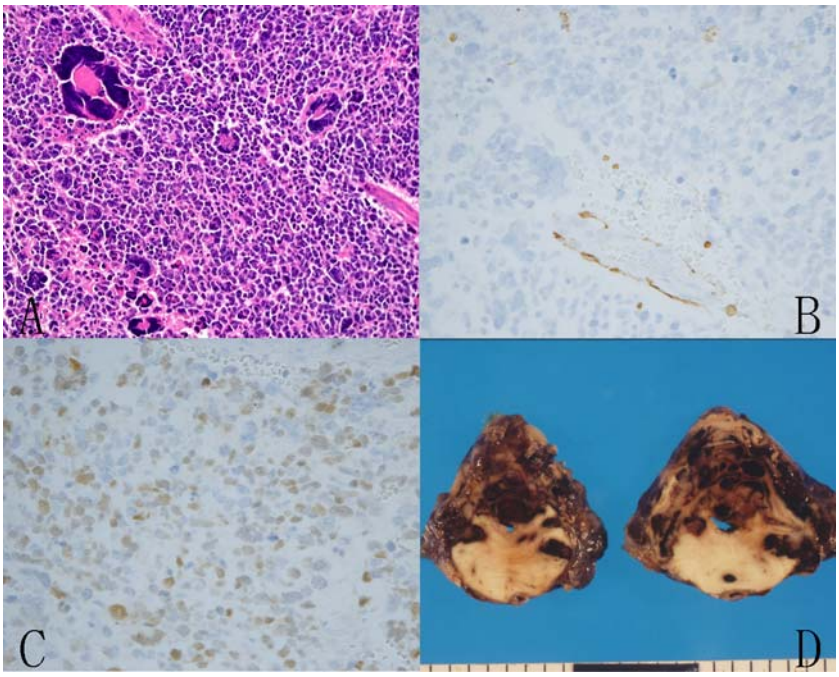


Fig. 2 (**a**) The secondary tumor was small cell-predominant glioblastoma with scattered large pleomorphic or multinucleated giant cell (hematoxylin-eosin stain; ×100). (**b**) Immunoreactivity to GFAP is obvious around the vessel, whereas tumor cells were almost non-reactive (×400). (**c**) In contrast, more than half of the tumor cells show immunoreactivity to NeuN (×400). (**d**) The tumor showed extensive subarachnoidal dissemination at autopsy

angular nuclei containing coarse, granular chromatin and scant cytoplasm without notable fibrillary process. Large pleomorphic cells bearing bizarre nuclei and multinucleated giant cells were scattered individually or in clusters. Other malignant features included frequent mitoses or atypical mitoses, high densities of microvessels with endothelial cell proliferation and geographic necrosis accompanying nuclear palisadings. This morphological appearance was consistent with undifferentiated, small cell-predominant glioblastoma. As is usually the case with this type of glioblastoma, few tumor cells were reactive to GFAP or S-100 protein on immunohistochemical examination (Fig. 2b). Unexpectedly, however, the tumor cells, including the large pleomorphic or multinucleated giant cells, were diffusely immunoreactive to synaptophysin and more than half of the cells were positive for NeuN (Fig. 2c). Expression of NFP was not detected. Immunoreactivity to p53 was observed in about 20% of the tumor cells, whereas EGFR expression was completely absent. The MIB-1 labeling index was about 80%.

At autopsy, the brain weighed 1360 g. On gross examination, local recurrence surrounding a large defect after surgical treatment was noted in the left frontal lobe as a poorly circumscribed infiltrating mass with encasement of the left lateral ventricle. In addition, subarachnoidal and intraventricular dissemination was extensive, forming numerous hemorrhagic tumor nodules in the cerebrum, cerebellum, brain stem (Fig. 2d), and spinal cord. On microscopic examination, the tumor showed almost the same histology as the last surgical specimen, namely, small cell-predominant glioblastoma showing prominent neuronal immunophenotype and a high MIB-1 labeling index. Exceptionally, part of the local recurrent lesion in the left frontal lobe contained relatively small numbers of apparently astrocytic tumor cells that exhibited immunoreactivity to GFAP and S-100 protein. The MIB-1 labeling index of these astrocytic cells was somewhat lower than that of the small cells.

Discussion

The clinical course of the present case was a typical malignant progression of diffuse astrocytoma into secondary glioblastoma. Histologically, the secondary tumor exhibited a small cell-predominant architecture with scattered large pleomorphic cells and multinucleated giant cells. Glioblastoma often contains small cell constituents as minor or predominant components, and these “undifferentiated” or “embryonal” cells often lack immunoreactivity to GFAP. In a recent report, Burger et al. concluded that the small cell-predominant glioblastoma is an important component of primary glioblastomas through observation of EGFR gene amplification at a high frequency in this type of glioblastoma [3]. The present case was inconsistent with this finding, as the small cell-predominant glioblastoma of the case was obviously a secondary tumor.

The most unusual finding was advanced neuronal immunophenotype of the secondary tumor. A considerable number of the tumor cells other than apparently astrocytic cells in the local recurrent region were positive for neuronal markers, synaptophysin and NeuN. Retrospective examination revealed that the original tumor also contained a small number of NeuN-positive neuronal cells which were hard to discriminate from the other tumor cells based on morphological appearance. The tumor was ordinal diffuse astrocytoma, except that it contained such neuronal cells, and there was no finding indicating that it was a specific

type of glioneuronal tumor such as papillary glioneruonal tumor, glioneuronal tumor with neuropil-like islands and several other new entities [4].

Recently, Varlet et al. proposed new variants of malignant glioneuronal tumors (MGNTs) [10]. The tumors had histopathological features indistinguishable from conventional malignant gliomas, but all coexpressed GFAP and NFP by definition. Other neuronal markers (NeuN, synaptophysin and chromogranin A) were expressed inconstantly. Neuronal phenotype of malignant glioma was not a new finding, as was described in earlier literatures that showed NFP-positive tumor cells in 20–33% of malignant glioma [5, 7]. In their series, however, MGNTs had a marked tendency to metastasis, an infrequent event in malignant glioma [2], and that gross total resection was curative in some cases. The latter finding indicated that distinction of MGNT from malignant glioma is of clinical importance. Two cases in the series were secondary MGNT. The retrospective examination of the initial tumors, which had been diagnosed as pleomorphic xanthoastrocytoma and pilocytic astrocytoma respectively, revealed NFP-positive tumor cells in both cases. As for the present case, we could not detect NFP expression in either the initial or secondary tumor even with epitope retrieval procedure. However, we consider that expression of synaptophysin and NeuN is sufficient evidence for the neuronal phenotype and NFP expression is not requisite, as central neurocytoma, a representative neuronal tumor, generally lacks NFP expression [6]. Extensive subarachnoidal and intraventricular dissemination of the secondary tumor is consistent with the characteristic feature of MGNTs by Varlet et al. Thus, this unusual secondary tumor might be classified into the similar category.

Advances in embryology have revealed that both the neuronal and glial cells of CNS develop from the common multipotential stem cell previously referred to as the radial glia [1]. Moreover, Singh et al. recently isolated brain tumor stem cell expressing the neural stem cell surface marker CD133 and nestin from several human gliomas [9]. These findings form a basis to explain the possibility that CNS neuroectodermal tumors could contain both neuronal and glial neoplastic cells originating from the common precursor.

At present, we do not know the meanings or significance of neuronal cells in an otherwise ordinary astrocytoma. Their presence might indicate possible progression into the unusual glioblastoma (or MGNT) characterized by diffuse neuronal immunophenotype as well as a highly proliferative state and extensive dissemination. Accumulation of similar cases will be required before we can resolve this issue and clarify the genetic alterations in this type of glioma progression.

References

1. Alvarez-Buylla A, Garcia-Verdugo JM, Tramontin AD (2001) A unified hypothesis on the lineage of neural stem cells. Nat Rev Neurosci 2:287–293
2. Arita N, Taneda M, Hayakawa T (1994) Leptomeningeal dissemination of malignant gliomas. Incidence, diagnosis and outcome. Acta Neurochir (Wien) 126:84–92
3. Burger PC, Pearl DK, Aldape K, Yates AJ, Scheithauer BW, Passe SM, Jenkins RB, James CD (2001) Small cell architecture-a histological equivalent of EGFR amplification in glioblastoma multiforme? J Neuropathol Exp Neurol 60:1099–1104
4. Cenacchi G, Giangaspero F (2004) Emerning tumor entities and variants of CNS neoplasms. J Neuropathol Exp Neurol 63:185–192
5. Franke FE, Schachenmayr W, Osborn M, Altmannsberger M (1991) Unexpected immunoreactivities of intermediate filament antibodies in human brain and brain tumors. Am J Pathol 139:67–79
6. Hassoun J, Soylemezoglu F, Gambarelli D, Figarella-Branger D, von Ammon K, Kleihues P (1993) Central neurocytoma: a synopsis of clinical and histological features. Brain Pathol 3:297–306
7. Hirato J, Nakazato Y, Ogawa A (1994) Expression of non-glial intermediate filament proteins in gliomas. Clin Neuropathol 13:1–11
8. Kleihues P, Burger PC, Collins VP, Newcomb EW, Ohgaki H, Cavenee WK (2000) Glioblastoma. In: Kleihues P, Cavenee WK (ed) Pathology & genetics. Tumours of the nervous system. World Health Organization classification of tumours. IARC Press, Lyon, pp 29–39
9. Singh SK, Clarke ID, Terasaki M, Bonn VE, Hawkins C, Squire J, Dirks PB (2003) Identification of a cancer stem cell in human brain tumors. Cancer Res 63:5821–5828
10. Varlet P, Soni D, Miquel C, Roux FX, Meder JF, Chneiweiss H, Daumas-Duport C (2004) New variants of malignant glioneuronal tumors: a clinicopathological study of 40 cases. Neurosurgery 55:1377–1392
11. Watanabe K, Sato K, Biernat W, Tachibana O, von Ammon K, Ogata N, Yonekawa Y, Kleihues P, Ohgaki H (1997) Incidence and timing of p53 mutations during astrocytoma progression in patients with multiple biopsies. Clin Cancer Res 3:523–530

Virchows Arch (2005) 447: 669–671
DOI 10.1007/s00428-005-1269-4

LETTER TO THE EDITOR

Yu Yang · Hes Ondrej · Lanjing Zhang · Jian Lu · Min Lu · Hua Wang · Jie Zheng · Michal Michal

Mixed epithelial and stromal tumor of the kidney with cervical and intestinal differentiation

Received: 20 February 2005 / Accepted: 3 April 2005 / Published online: 16 July 2005
© Springer-Verlag 2005

Dear Editors:
Mixed epithelial and stromal tumor of the kidney (MESTK) has only recently been recognized as a rare benign tumor of the kidney which has distinct clinical and morphological characteristics. The name MESTK was first used by Michal and Syrucek in 1998 [1], and was newly recognized in the recent WHO classification of the urinary system as a distinct entity [2].

We report a unique case of MESTK which showed cervical and intestinal epithelial differentiation. To the best of our knowledge, no such differentiation within MESTK has ever been described in the literature [3, 4]. A 50-year-old woman presented with hematuria associated with pain in the left flank. The patient had a 20-year history of taking oral contraceptives. Computed tomography revealed a 7 cm solid and cystic mass at the upper poles of the left kidney. On thorough clinical check-up, no other tumor was found in the patient. Under the diagnosis of renal tumor, the patient underwent total nephrectomy and adrenalectomy. After surgery, no additional treatment was given. Seven months after excision of the tumor, the patient is without signs of recurrence and metastasis. Macroscopically, the tumor was localized in the upper part of the kidney. The tumor was 7 cm in diameter, well-circumscribed, and composed of irregular mixtures of solid and cystic areas. The solid areas of the tumor were firm and gray-white on gross section. The cysts varied in size ranging from 0.5 to 2 cm in diameter. There were no signs of infiltrative growth into the surrounding renal parenchyma and the adjacent calyceal system.

Histologically, the tumor was composed of a mixture of epithelial elements that formed glands and cysts and stromal component formed mainly by spindle cells. The epithelial component had a characteristic appearance both

Y. Yang · M. Lu · H. Wang · J. Zheng (✉)
Department of Pathology,
Health Science Center,
Peking University,
38 Xue-yuan Road,
100083 Beijing, China
e-mail: zhengjie@bjmu.edu.cn
Tel.: +86-010-82801731
Fax: +86-010-82801731

H. Ondrej · M. Michal
Sikl's Department of Pathology,
Charles University Hospital,
Pilsen, Czech Republic

L. Zhang
Department of Internal Medicine,
University of Michigan
Medical School,
Ann Arbor, MI, USA

J. Lu
Department of Urology,
3rd Hospital,
Peking University,
Beijing, China

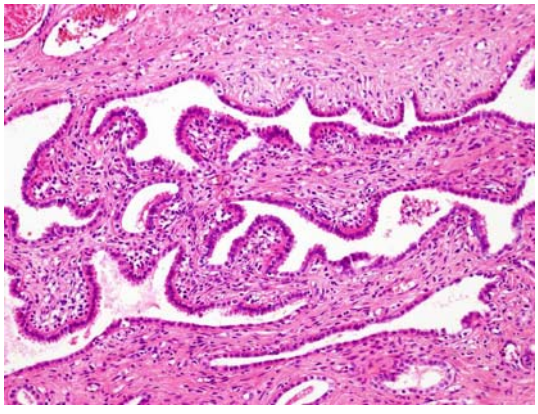


Fig. 1 Glandular epithelium formed serous tubules and multilocular cysts lined by cells with ciliated brush border and peg cells typical of Fallopian tubes. The stroma has bland looking spindle cell appearance, typical of MESTKs

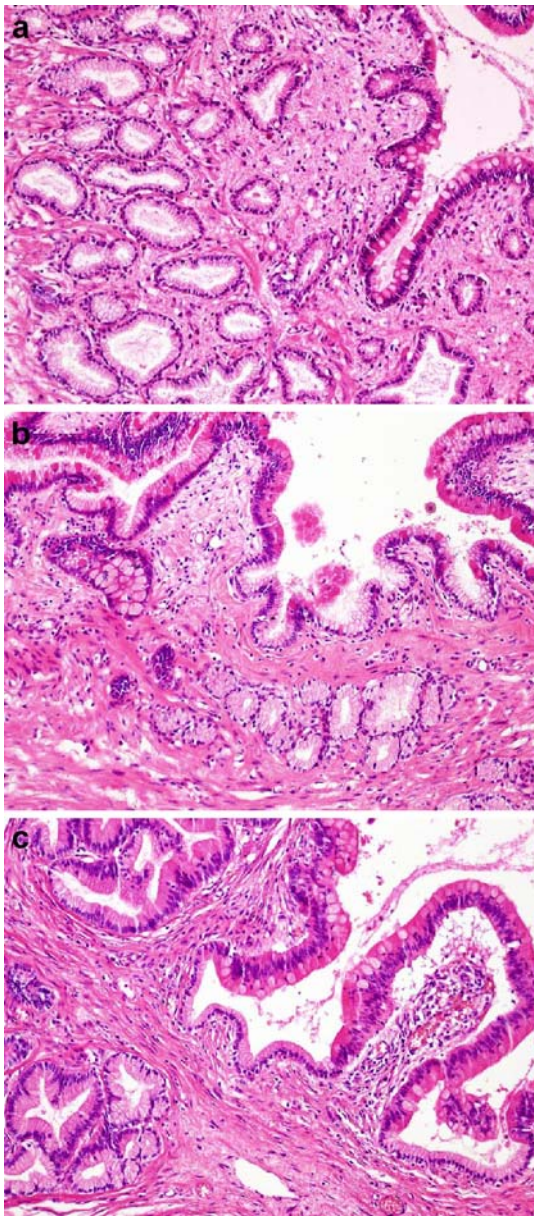


Fig. 2 In some places, the adenomatous structures had the appearance of cervical glands (left side) and intestinal (right side) (**a**). Focally Paneth cell differentiation was seen in the epithelium of the MESTK (**b**). The border between the intestinal and pyloric epithelium was often sharp (**c**)

in architecture and cell type. In some places, glandular epithelium formed serous tubules and multilocular cysts lined by ciliated brush border and peg cells typical of Fallopian tubes (Fig. 1). In other places, the adenomatous structures had the appearance of cervical glands (Fig. 2a) and still other areas revealed typical intestinal epithelium (Fig. 2a) containing Paneth (Fig. 2b) and goblet cells. The border between the intestinal and cervical epithelium was often sharp (Fig. 2c). No cytological atypia or mitotic figures were observed in the epithelial component. The excised adrenal gland was normal without signs of tumor. Immunohistochemically, the epithelial elements expressed cytokeratin (dilution 1:50; Dako, Denmark) and were immunonegative for ER (dilution 1:50; Dako), PR (dilution 1:50; Dako). The stromal elements were focally ER (Fig. 3) , PR and smooth muscle actin (SMA) (dilution 1:50; Dako) positive. Both the epithelial and stromal elements failed to react with S-100 (dilution 1:50; Dako, Denmark), CD34 (dilution 1:50; Dako), HMB-45 (dilution 1:50; Dako) antibodies. Considering the clinicopathological features, a diagnosis of MESTK was easily established in our case [3, 4].

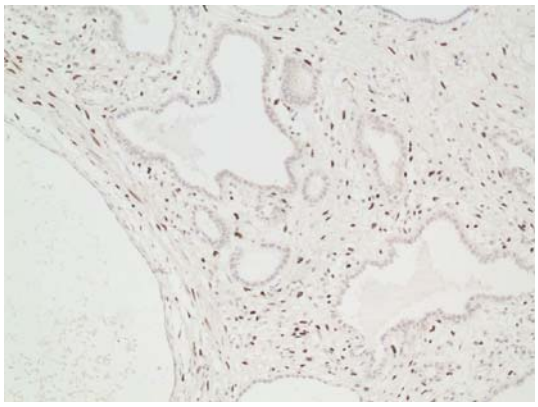


Fig. 3 The stromal elements were immunoreactive to ER

While our case demonstrated morphological features typical for MESTKs, it also showed unique glandular structures represented by cervical and intestinal mucinous epithelium containing goblet and Paneth cells, which is a hitherto undescribed differentiation in MESTK. The presence of cervical and intestinal mucinous epithelia in MESTK is a hitherto undescribed feature of MESTK. The cervical and intestinal mucinous cystic tumors belong to the most common types of epithelial neoplasms occurring in the ovary. In addition, transition between cervical and intestinal epithelium containing goblet cells within single glandular structures is a well known phenomenon described in ovarian tumors [5]. Since MESKT is a tumor displaying a wide range of epithelia and the stroma are often indistinguishable from that of the ovary, it is not surprising that the same transitions between cervical and intestinal epithelium containing goblet cells within single glandular structures were observed in our case. The description of intestinal epithelium in MSTK is important, because it must be differentiated from metastatic mucinous well-differentiated cystadenocarcinomas originating in intestinal tract, gallbladder and pancreas to kidney. This differentiation is easy, because metastatic adenocarcinomas with intestinal differentiation do not reveal other types of epithelium as cervical or that of Fallopian tubes and spindle cell stroma as seen in our case.

References

1. Michal M, Syrucek M (1998) Benign mixed epithelial and stromal tumour of the kidney. Pathol Res Pract 194:445–448
2. Eble JN, Sauter G, Epstein JI, Sesterhenn IA (2004) World health organization classification of tumors. Pathology and genetics of tumors of the urinary system and male genital organs. IARC Press, Lyon
3. Michal M, Hes O, Bisceglia M, Simpson RHW, Spagnolo DV, Parma A, Boudova L, Hora M, Zachoval R, Suster S (2004) Mixed epithelial and stromal tumors of the kidney. A report of 22 cases. Virchows Arch 445:359–367
4. Adsay NV, Eble JN, Srigley JR, Jones EC, Grignon DJ (2000) Mixed epithelial and stromal tumor of the kidney. Am J Surg Pathol 24:958–970
5. Scully RE, Young RH, Clement PB (1996) Atlas of tumor pathology. Tumors of the ovary, maldeveloped gonads, fallopian tube and broad ligament. Armed Forces Institute of Pathology, Washington, D.C.

Virchows Arch (2005) 447: 672–674
DOI 10.1007/s00428-005-1232-4

LETTER TO THE EDITOR

Zbigniew Rudzki · Wacław Wilk · Michał Śmigielski

Splenic tumors in an adult with tuberous sclerosis: the giant "histiocytoid" cells are dysplastic histiocytes

Received: 15 December 2004 / Accepted: 11 February 2005 / Published online: 25 August 2005
© Springer-Verlag 2005

Dear Editor,

Tuberous sclerosis (TS) patients suffer from a wide constellation of lesions, including hamartomatous tumors affecting virtually every major organ system and renal carcinomas [5]. A recently developed set of criteria has facilitated and standardized the diagnostic process in the setting of the individually variable disease phenotype [2]. Splenic lesions are rare in TS and, by these criteria, are not considered diagnostic. A few reports summarized by Bender and Yunis [1] described three cases of large-cell nodular lesions in neonates. These authors added five additional neonate autopsy cases of diffuse splenic lesions composed of very large cells with eosinophilic cytoplasm. On the basis of morphological features and the presence of lysosome-like ultrastructures, they called these cells "histiocytoid." No such lesions have been reported in adults.

In our case, a 21-year-old female underwent splenectomy due to remittent anemia of unknown origin since the age of 16 years (hemoglobin ranging from 6 to 11.4 g/dL, red blood cell packed volume 19–35.5%) and the presence of several splenic tumors. The splenic tumors were hypoechogenic on the ultrasound. Their sizes ranged from 11 to 57 mm on the computerized tomography scan. The patient had a documented personal and familial history of TS. At the age of 3 months, she started to suffer from seizures, which were later associated with the presence of numerous subependymal calcifying tumors in close proximity to the lateral ventricles and/or a large tumor at the frontal horn of her right lateral ventricle. An unspecified retinal tumor was photocoagulated in her childhood. She manifests subungual fibromas and facial angiofibromas. Her kidneys are currently extremely enlarged (beyond the ultrasound measurement capacity), with their appearance consisting of numerous angiomyolipomas in the computerized tomography. Psychological evaluation done at the age of 20 years demonstrated mild mental retardation. The patient's father died at the age of 34 shortly after emergency surgery due to massive intra-abdominal bleeding from his "polycystic" kidneys (an autopsy was not performed). His charts did not mention splenomegaly.

Grossly, the formaldehyde-fixed spleen measured 18×11×5.5 cm and weighed 420 g. Cross sections revealed several rather sharply circumscribed, lobulated gray-brown tumors measuring up to 37 mm [Fig 1]. One small tumor was reddish and was microscopically proven to be necrotic. The remaining tumors consisted of fibrovascular proliferations containing locally variable numbers of very large cells. The large cells displayed ample cytoplasm with individually varying characteristics: deeply or faintly uniformly eosinophilic, clear, delicately granular, or even foamy, but with transitional forms indicating that they all belong to the same population [Fig 2]. The cytoplasm was faintly periodic acid-Schiff stain (PAS) positive and bluish in the Giemsa stain. Some cells contained a granular yellow-brown birefringent pigment consistent with hemosiderin. The nuclei of the large cells were usually oval and regular, sporadically double, and occasionally with prominent nucleoli. The most spectacular nucleoli were reminiscent of viral inclusions or even imparted some similarity to the RS cells. Immunohistochemically, most of the large cells were positive for CD68–KP1, and some for CD68–PGM1 [Fig 3], S100, CD4, and vimentin. There was no correlation between the immunopositivity of the markers and the nuances of the morphologic features in the large

Z. Rudzki (✉)
Department of Pathomorphology,
Collegium Medicum,
Jagiellonian University,
Grzegórzecka 16,
Kraków, 31-531, Poland
e-mail: mprudzki@cyf-kr.edu.pl
Tel.: +48-12-4215210
Fax: +48-12-4119725

W. Wilk
Department of Pathomorphology,
Ludwik Rydygier Memorial Hospital,
Kraków, Poland

M. Śmigielski
Department of Nephrology and Dialysis,
Ludwik Rydygier Memorial Hospital,
Kraków, Poland



Fig. 1 The largest nodule on a cross section of the fixed spleen

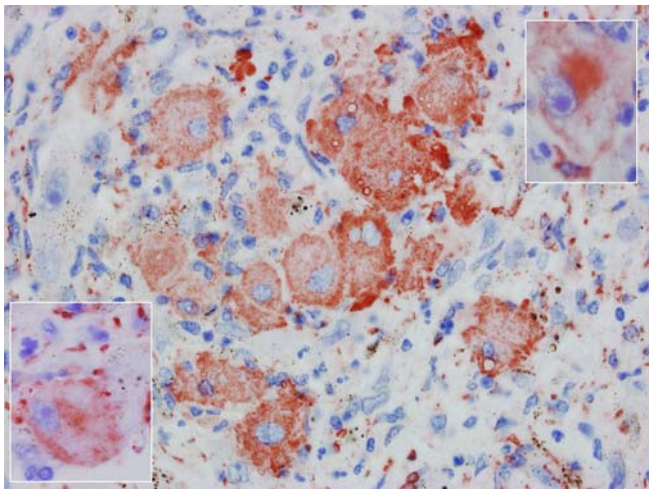


Fig. 3 Strong expression of CD68–PGM1 in a cluster of large cells. A cell with a prominent inclusion-like nucleolus to the *left* of the cluster is immunonegative. The *insets* show various cytoplasmic patterns of CD68–PGM1 expression in similar cells (APAAP technique, lens ×60)

cells, although CD68–PGM1- and S100-positive cells tended to cluster, the latter ones close to fibrous bands, partially delineating the tumors. Clustering was also observed for most CD4-positive large cells. The large cells were negative for other immunomarkers: desmin; smooth muscle actin (SMA); muscle-specific actin (MSA); CD31; CD34; FVIIIR; epithelium membrane antigen (EMA); polyclonal cytokeratins; CK7; CK19; CK20; CD45-leukocyte common antigen (LCA); CD20; CD79a; CD138; CD43; CD3; CD45RO; CD1a; CD35; CD23; placental alkaline phosphatase (PLAP); mast cell tryptase; CD117; myeloperoxidase; lysozyme; CD30; glial fibrillary acidic protein (GFAP); neurofilaments; chromogranin; synaptophysin; HMB45; cytomegalovirus (CMV); and p53. Remarkably, they did not show any mitotic activity nor Ki67 expression. The tumor background contained numerous typical histiocytes, frequently interspersed between the large cells, some granulocytes, and small regular lymphocytes, almost exclusively of the T lineage. The number of interspersed mast cells was striking (up to 30/high-power field), which contrasted with their rare occurrence in the adjacent unaffected spleen. The mast cells were dispersed and cytologically typical, oval in shape, and with no signs of degranulation. Several clusters of disorganized vessels were located at the tumor periphery, usually close to the hyaline fibrous bands partially ramifying the lesions [Fig 4]. These bands contained few smooth muscle cells as documented by immunohistochemistry (SMA, MSA, and desmin).

Aside from the tumors and small accessory spleen, the spleen histology was unremarkable. Two small hilar lymph nodes presented with nonspecific reactive changes, including sinus histiocytosis, but without an accumulation of the characteristic large cells. A trephine bone marrow biopsy

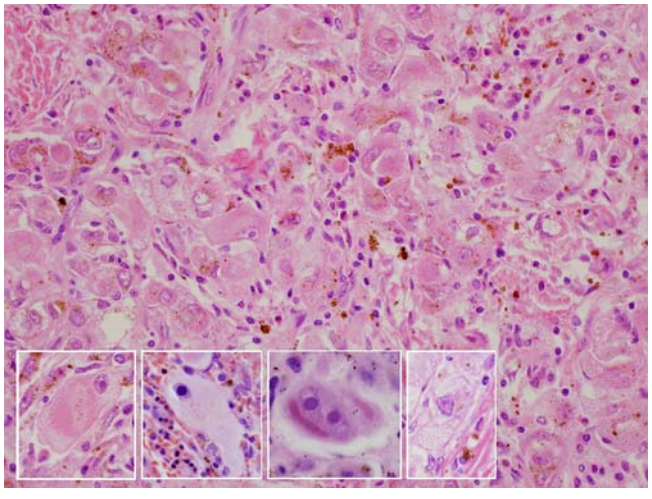


Fig. 2 Large cells composing the nodules show eosinophilic cytoplasm, hemosiderin pigment, and, occasionally, prominent nucleoli (H & E, lens ×40). *Inset*: morphological variability of the giant cells (lens ×60)

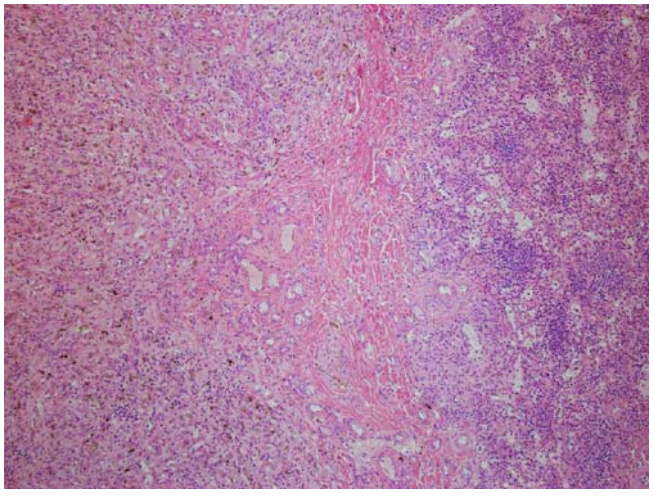


Fig. 4 Fibrous connective tissue strand containing an angiomatoid structure which separates the tumor (*left*) from the normal spleen (*right*) (H & E, lens ×10)

submitted shortly prior to the splenectomy specimen also demonstrated mild reactive changes and lacked the large cells.

The features of the large cells in our case are comparable to the histiocytoid cells reported by Bender and Yunis [1]. Inferring from the apparent lack of analogous lesions in adults, these authors supposed that the presence of histiocytoid cells could have been a transient phenomenon limited to the neonatal period. Our case clearly shows that the tumors composed of histiocytoid cells may belong to the permanent clinicopathologic spectrum of TS, although these probably constitute a great rarity.

Medline-indexed literature contains only nine papers on TS-associated splenic pathology, with one report of a neonatal histiocytoid cell lesion, and the remaining reports describing splenic hemorrhages or vascular tumors, including angiosarcomas in a rat model of TS.

The vascular origin of the histiocytoid cells may be excluded by our immunomarker panel (CD31, CD34, FVIIIR). Emerging from our study, the most likely phenotype of the histiocytoid cells is actually the true histiocyte, with the strongest argument being the positivity for the PGM1 epitope of CD68, a very sensitive and specific marker of histiocytes [4]. Positive immunoreaction with CD68–PGM1 can only be found in synovial cells, neoplastic mast cells, and occasionally in specialized antigen-presenting cells [3, 4]. The synovial origin of the large cells can be excluded on the basis of the histological and topographic context of the lesions. Other features of immunophenotype (negativity for CD1a, CD23, CD35, CD117, and mast cell tryptase) are inconsistent with the antigen-presenting cell or mast cell origin. Expression of CD4 in the absence of other T-cell markers is typical for histiocytes [4]. A nearly "null" phenotype, with only a focal expression of CD68–PGM1, S100, and CD4, and a notable absence of LCA, is a perplexing phenomenon for which we have no explanation. We can only speculate that the silencing of some genes may contribute to the functional inertia of the large histiocytes, possibly resulting in their accumulation. A lack of lysozyme and no Ki67 expression indirectly corroborate this hypothesis.

Most probably, the splenic tumors containing dysplastic histiocytes have little or no direct clinical significance. They grow very slowly, as they were present in our patient 3 years ago, and on the computerized tomography scans, their size seemed to be stable. The large cells and other tumor components showed no appreciable proliferative activity. Upon splenectomy, the patient's anemia did not improve, so it seems highly unlikely that these tumors contribute to the increased erythrocyte consumption. However, in TS patients with a proven or suspected renal carcinoma, these tumors can pose a significant problem in differential diagnosis with splenic metastases. We did not have an occasion to examine the cytological specimen of such a tumor, so we may only speculate that fine-needle aspiration could be helpful in solving this dilemma.

The fibrovascular tumors with large dysplastic histiocytes were confined to the spleen. Their absence in other histiocyte-rich organs, like the accessory spleen, perisplenic lymph nodes, and bone marrow, argues against any fundamental defect in histiocytic maturation or the sequel of storage of unknown substance and supports the hypothesis of the hamartomatous origin of these lesions. It is likely that the dysplastic histiocytes are responsible for the abnormal local milieu attracting the reactive T cells and mast cells, whereas the pathogenetic relation of histiocytes to adjacent fibromuscular and vascular hamartomatous structures remains enigmatic.

To summarize, the fibrovascular tumors with giant dysplastic histiocytes may occur in adult patients with TS. Most probably, they are clinically irrelevant and belong to the spectrum of the hamartomatous lesions of TS.

Acknowledgements We thank Miss Hillary Lowenstein B.A. for the English language revision of the text.

References

1. Bender BL, Yunis EJ (1981) Splenic involvement in tuberous sclerosis. Report of three cases. Virchows Arch [Pathol Anat] 391:363–369
2. Hyman MH, Whittemore VH (2000) National Institutes of Health consensus conference: tuberous sclerosis complex. Arch Neurol 57:662–665
3. Jaffe ES (2001) Histiocytic and dendritic cell neoplasms. In: Jaffe ES, Harris NL, Stein H, Vardiman JW (eds) World Health Organization classification of tumours. Pathology and genetics of tumours of haematopoietic and lymphoid tissues. IARC, Lyon, pp 274–289
4. Knowles DM (2001) Immunophenotypic markers useful in the diagnosis and classification of hematopoietic neoplasms. In: Knowles DM (ed) Neoplastic hematopathology, 2nd edn. Lippincott Williams & Wilkins, Philadelphia, pp 142, 159–160
5. Online Mendelian Inheritance in Man, OMIM (TM) (2005) Johns Hopkins University, Baltimore, MD. MIM number: 191100:2004-09-07.http://www.ncbi.nlm.nih.gov/omim/

Virchows Arch (2005) 447: 675
DOI 10.1007/s00428-005-1297-0
© Springer-Verlag 2005

ANNOUNCEMENTS

1–2 December 2005
International Symposium on "Salivary Gland Tumours; Present Concepts of Diagnosis and Management"
Amsterdam, The Netherlands

For further information please contact congress secretariat
Mrs. D. Chavalking
Vrije Universiteit Medical Center (Vumc)
Department of Oral and Maxillofacial Surgery/Oral Pathology
PO Box 7057
1007 MB Amsterdam
The Netherlands
Tel.: +31-20-444-4039
Fax: +31-20-444-4046
E-mail: d.chevalking@vumc.nl
Internet: www.vumc.nl

Virchows Arch (2005) 447: 677–682
DOI 10.1007/s00428-005-0057-5

REVIEW ARTICLE

Thomas Mentzel · Heinz Kutzner

Reticular and plexiform perineurioma: clinicopathological and immunohistochemical analysis of two cases and review of perineurial neoplasms of skin and soft tissues

Received: 24 May 2005 / Accepted: 31 July 2005 / Published online: 27 August 2005
© Springer-Verlag 2005

Abstract Perineurioma represents a recently described and relatively rare neoplasm in the spectrum of benign peripheral nerve sheath tumours composed of perineurial cells staining immunohistochemically positive for epithelial membrane antigen (EMA). In addition to intraneural, extraneural and sclerosing perineurioma, rare variants of perineurioma may occur, and their knowledge is important in the differential diagnosis of mesenchymal tumours of different lines of differentiation and clinically more aggressive neoplasms. We present a case of deep-seated reticular perineurioma arising on the upper arm of a 34-year-old female and a case of a dermal plexiform perineurioma arising on the lower lip of a 60-year-old female. The diagnosis was confirmed in both cases immunohistochemically; neoplastic cells stained positively for EMA and for the newly described perineurial markers, claudin-1 and glut-1. The morphological spectrum and the differential diagnosis of perineurial neoplasms of skin and soft tissues are discussed.

Keywords Nerve sheath neoplasms · Perineurioma · Epithelial membrane antigen · Claudin-1 · Human erythrocyte glucose transporter (glut-1)

Introduction

Peripheral nerve sheath tumours, both benign and malignant, are composed of one or several cellular components including S-100-positive Schwann cells, CD34-positive or negative fibroblasts and perineurial cells in varying proportions. In addition to neurofibromas, schwannomas, different forms of neuromas and malignant peripheral nerve sheath tumours, neoplasms consisting predominantly or exclusively of perineurial cells, have been described and characterised as perineuriomas in the last years. Perineuriomas arise in dermal, subcutaneous and deep soft tissues and only rarely in visceral location [12, 17, 29]. Although perineurioma has been first described in 1978 [19], it still represents a poorly recognised neoplasm in the spectrum of peripheral nerve sheath tumours [25], and, especially, examples of unusual histological variants cause considerable diagnostic problems and may be mistaken for different or more aggressive soft tissue tumours. Interestingly, rare examples of benign peripheral nerve sheath tumours showing a combination of perineurioma and schwannoma as well as of perineurioma and neurofibroma have been reported most recently [18, 23]. In this review one case each of reticular and plexiform perineurioma is reported, and a review of perineurial neoplasms of skin and soft tissues is given.

T. Mentzel (✉) · H. Kutzner
Dermatopathologische Gemeinschaftspraxis,
Siemensstrasse 6/1,
88048 Friedrichshafen, Germany
e-mail: tmentzel@w-4.de
Tel.: +49-7541-604431
Fax: +49-7541-604410

Materials and methods

The cases were retrieved from the routine files of the Dermatopathologische Gemeinschaftspraxis in Friedrichshafen, Germany, and from the consultation files of one of the authors (T.M.; see acknowledgment). The specimens were obtained by surgical excision, fixed in 10% buffered formalin and processed routinely for paraffin embedding. Four micrometer-thick sections were stained with haematoxylin and eosin. In addition, sections were stained immunohistochemically by the labelled Streptavidin Biotin (LSAB) technique using commercially available antibodies; appropriate positive and negative controls were used in each case. The used antibodies, their sources and dilutions are summarised in Table 1. The clinical and follow-up informations were obtained from the referring clinicians and pathologists.

Table 1 Immunohistochemical reagents used

Antibody	Clone	Dilution	Source
EMA	Mc5	1:400	Biogenex, CA, USA
Glut-1	Polyklonal	1:200	DAKO, Glostrup, Denmark
Claudin-1	Polyklonal	1:600	Zymed, CA, USA
Pancytokeratin	MNF116	1:100	DAKO
Desmin	D33	1:200	DAKO
ASMA	1A4	1:300	DAKO
S-100 protein	Polyklonal	1:4000	DAKO
CD31	JC70A	1:100	DAKO
CD34	HPCA-1	1:100	Becton & Dickinson, CA, USA

Results

Case 1

A 34-year-old lady developed a deep-seated soft tissue neoplasm on her right upper arm. The patient complained about a slowly growing mass that was not painful, and, clinically, a lipoma was suspected. The intramuscular neoplasm was completely excised and measured 8×5×3 cm. There is no sign of recurrence at 18 months. Grossly, a circumscribed mass with soft and yellow-white cut surfaces was described, areas of haemorrhage or tumour necrosis were not evident. Microscopically, the paucicellular neoplasm was partly circumscribed but unencapsulated. Focally, a superficial infiltration into the skeletal muscle was noted. On low-power view, the neoplasm was characterised by a reticular pattern of anastomosing spindled cells set in a prominent myxoid matrix with microcystic changes (Fig. 1). Cytologically, the neoplastic cells contained a pale eosinophilic cytoplasm and ovoid to fusiform nuclei with mild nuclear pleomorphism, nucleoli were not seen or inconspicuous and no increased proliferative activity was noted. Characteristically, neoplastic cells had elongated and very thin cytoplasmic processes, which appeared to interconnect in many areas (Fig. 2). Focally, a slightly increased cellularity with a rather lamellar growth pattern of elongated tumour cells was identified (Fig. 3). The intercellular matrix contained abundant myxoid/mucoid material, and numerous capillary sized blood vessels with focal hyalinisations of their walls were present. Immunohistochemically, neoplastic cells stained strongly and homogenously positive for claudin and glut-1, whereas epithelial membrane antigen (EMA) was expressed only focally (Fig. 4). The remaining immunohistochemical markers (S-100 protein, CD34, alpha-smooth muscle actin, desmin, CD31 and pancytokeratin) were all negative.

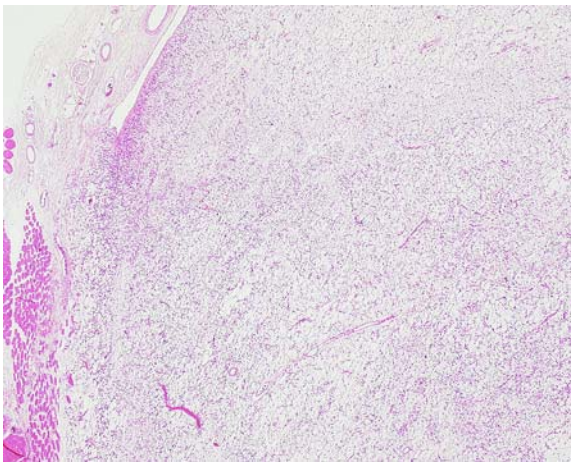


Fig. 1 Low-power view of case 1 shows a deep-seated, well-circumscribed, but focally infiltrating hypocellular neoplasm

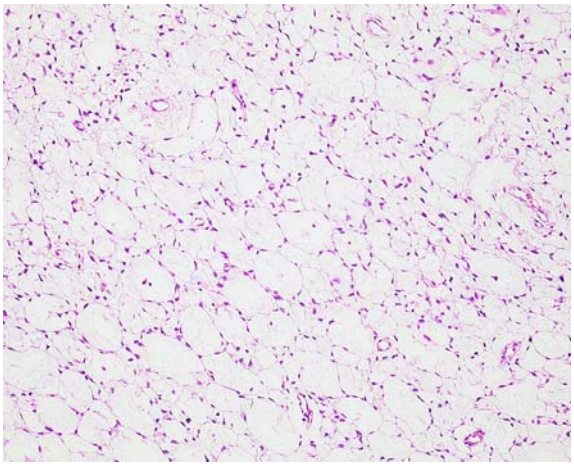


Fig. 2 The neoplasm is composed of spindle-shaped cells containing elongated cell processes, anastomosing in a lace-like pattern. Note slightly enlarged hyperchromatic nuclei

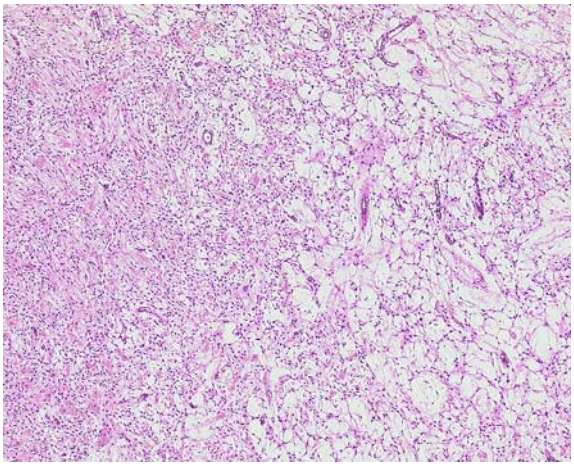


Fig. 3 Focally, a transition to more cellular tumour areas was present

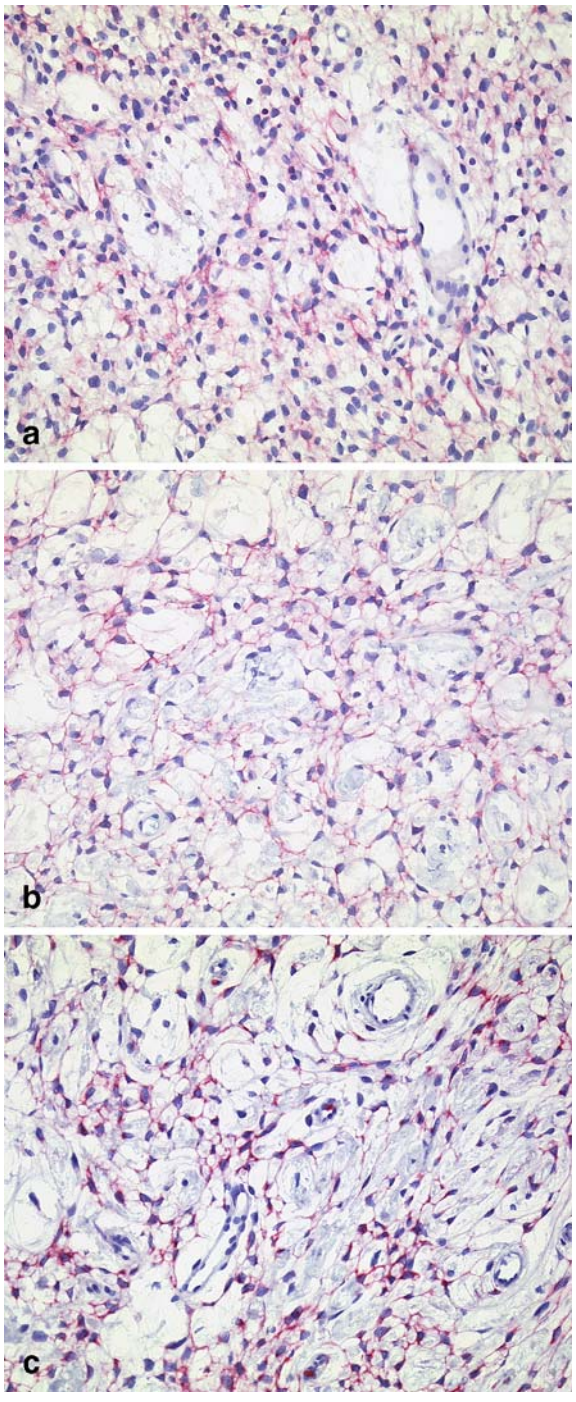


Fig. 4 Immunohistochemically, tumour cells stained positively for EMA (**a**), claudin-1 (**b**) and glut-1 (**c**)

Case 2

A 60-year-old female patient complained about a papular lesion on the lower lip present since childhood. Clinically, a soft and yellowish lesion was described. The neoplasm was marginally excised, and there was no sign of recurrence at 21 months. Grossly, a spindled skin specimen with an indurated dermal nodule measuring 0.4 cm in largest diameter was described. Histologically, a plexiform mesenchymal neoplasm composed of plump spindle-shaped tumour

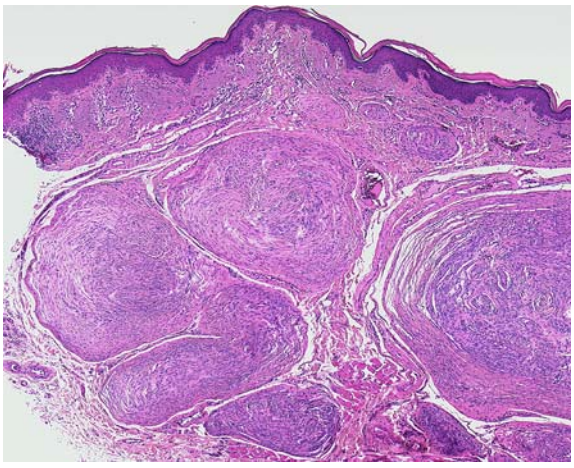


Fig. 5 In case 2 a plexiform, dermal neoplasm is seen

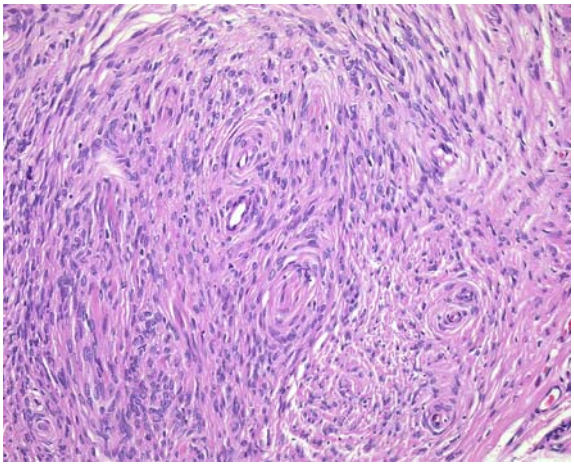


Fig. 6 The neoplasm is composed of plump spindled tumour cells set in a collagenous stroma with thin-walled blood vessels

cells with an ill-defined, pale eosinophilic cytoplasm and spindled or round nuclei was noted (Fig. 5). Neoplastic cells were arranged in nodular formations of different size and set in a collagenous matrix with thin-walled blood vessels (Fig. 6). Tumour cells stained positively for EMA, claudin and glut-1 (Fig. 7), whereas S-100 protein and CD34 were negative.

Discussion

Perineurial cells, both non-neoplastic and neoplastic, are usually spindle-shaped with bipolar, palely eosinophilic cytoplasm and fusiform nuclei with a finely distributed chromatin, which are variably tapering or plump; typically long and very thin cell processes are evident. Ultrastructurally, these bipolar cell processes are surrounded incompletely by an external lamina, and numerous pinocytic vesicles as well as well-formed tight junctions are noted [8, 19]. Immunohistochemically, perineurial cells stain positively for EMA [27, 28]. Whereas CD34 is expressed in

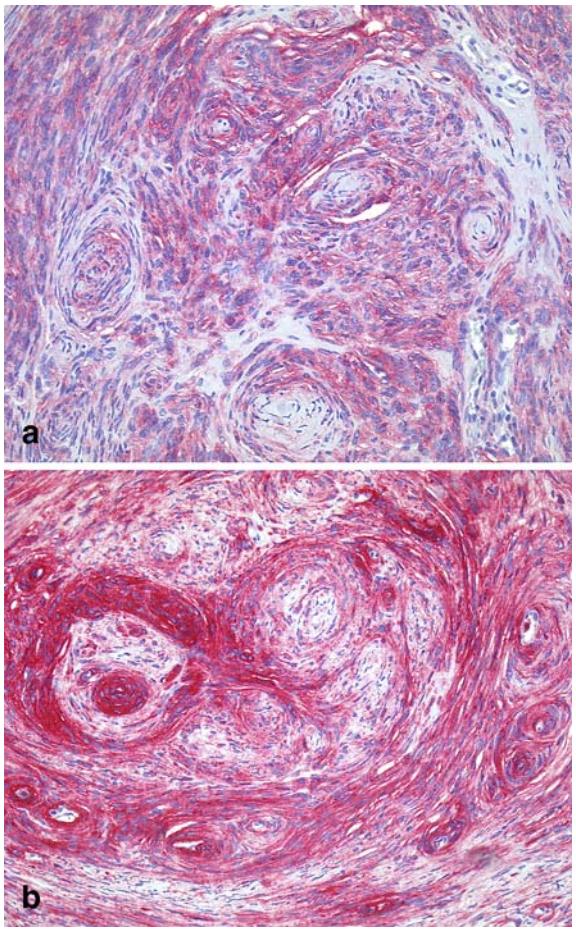


Fig. 7 Neoplastic cells stained positively for EMA (**a**) and glut-1 (**b**)

several perineuriomas [13, 16], S-100 protein and myogenic markers are negative by definition. Unfortunately, there are as well limitations in the use of EMA as a perineurial marker. Firstly, EMA is expressed in several spindled mesenchymal neoplasms showing a fibroblastic line of differentiation (i.e. solitary fibrous tumour). In addition, EMA expression in classical cases of perineurioma may be only focal and weak, given the presence of elongated and very thin cell processes with a small amount of cytoplasm. In the last years, claudin-1 [10] and glut-1 [30] have been described as new perineurial markers. Claudin-1 belongs to a family of integral transmembrane proteins with structural and functional role in tight junctions and has been found in non-neoplastic and neoplastic perineurial cells, whereas tested fibro- and myofibroblastic neoplasms did not show an expression of this marker [10]. Human erythrocyte glucose transporter glut-1 is normally expressed in erythrocytes, perineurial cells, renal tubules, germinal centres of lymphoid tissue and in several carcinomas [31]. Whereas cases of schwannoma and neurofibroma are negative for glut-1, this marker is strongly expressed in cases of perineurioma [30]. In addition, it has been mentioned that soft tissue meningioma, which resembles perineurioma histologically and immunohistochemically [21], is consistently negative for glut-1 [30]. Although not specific, claudin-1 and glut-1 are quite sensitive perineurial markers and should be included in the immunohistochemical panel for the diagnosis of perineurial neoplasms.

Perineurial-differentiated neoplasms of skin and soft tissues composed predominantly of neoplastic perineurial cells are rare and represent less than 1% of nerve sheath and soft tissue neoplasms, respectively [26]. After the delineation of perineurioma in 1978 [19], several clinical and morphological variants have been described in the last years, and their knowledge is important to avoid misdiagnosis of different or more aggressive mesenchymal neoplasms.

Intraneural perineurioma, also known formerly as localised hypertrophic neuropathy of the limbs [3, 7], is characterised clinically by a fusiform swelling with progressive muscle weakness and/or sensory disturbances. Histologically, residual S-100-positive nerve fibres are surrounded concentrically by EMA-positive perineurial cells forming concentric layers around nerve fibres and characteristic pseudo-onion bulbs. No prominent atypia and no increased proliferative activity of neoplastic perineurial cells are seen. Although some authors still regard this condition not as a form of perineurioma, cytogenetic findings add strong support to the interpretation of these lesions as an intraneural form of perineurioma [7].

Extraneural spindle cell perineurioma arises often on the trunk and the extremities of middle-aged adults and is not associated with neurofibromatosis; only rarely perineurioma occurs in children [2]. These neoplasms are seen frequently in subcutaneous tissue, whereas deep soft tissues and the dermis are more rarely affected. Perineuriomas of soft tissues are usually well circumscribed but unencapsulated; however, rarely and focally an infiltration into surrounding structures may be present [16]. Histologically, extraneural perineurioma is characterised by a variable cellularity and different growth patterns (storiform, whorled, lamellar, fascicular) of spindled tumour cells showing features as described above. The collagenous stroma often shows focal hyalinisations. It has been shown convincingly that the presence of focal infiltration and of cytological atypia does not affect the benign biological behaviour of perineurioma [16]. Cytological features and the immunophenotype of neoplastic perineurial cells allow distinction from benign and malignant spindle cell neoplasms of skin and soft tissues (i.e. dermatofibroma, superficial acral fibromyxoma, dermatofibrosarcoma protuberans, neurofibroma, schwannoma, solitary fibrous tumour, low-grade fibromyxoid sarcoma). The evidence of identical cytogenetic changes in intra- and extraneural perineuriomas, monosomy of chromosome 22, supports the view that both forms are part of a clinicopathological spectrum of a single entity [7, 11].

Sclerosing perineurioma tends to occur in superficial tissue of the hands of young adults and is composed of plump spindled and epithelioid tumour cells set in a hyalinised stroma containing numerous thin-walled blood vessels. Often a perivascular and lace-like arrangement of neoplastic cells is noted [9]. The differential diagnosis of

sclerosing perineurioma comprises epithelioid dermatofibroma, sclerosing dermal fibroma in acral location, superfical epithelioid haemangioendothelioma and sclerosing melanocytic and epithelial neoplasms; however, the characteristic immunoprofile of sclerosing perineurioma is of help in the distinction of these entities. Interestingly, in superficial location, neoplasms showing a combination of features of spindle extraneural cell perineurioma and sclerosing perineurioma have been reported [25].

Reticular perineurioma, first reported as retiform perineurioma [22], represents a recently described rare subset of perineurioma that is easily admixed with several mesenchymal neoplasms [13]. Most cases of reticular perineurioma occurred in soft tissues, whereas a single case of intraneural reticular perineurioma has been reported [5]. Reticular perineurioma is characterised by the presence of prominent degenerative myxoid or edematous stromal changes sometimes with the formation of pseudocystic spaces. The neoplastic cells contain very thin and elongated cell processes anastomosing in a lace-like, reticular pattern. Occasionally, degenerative nuclear atypia is noted [13]. Especially in deep-seated, intramuscular examples of reticular perineurioma, intramuscular myxoma represents the most important differential diagnosis. Tumour cells in intramuscular myxoma do not contain very thin and elongated cell processes anastomosing in a lace-like pattern and are usually negative for perineurial markers. However, as said before, a focal staining for EMA may be seen in intramuscular myxoma as well, but claudin and glut-1 are not expressed. Myxoid solitary fibrous tumour is composed of plumper fibroblastic cells staining positively for CD34 and often for CD99 and bcl-2, whereas EMA is negative or only focally positive. Myxoid monophasic fibrous synovial sarcoma may also closely resemble reticular perineurioma; however, tumour cells in synovial sarcoma are plumper and stain only focally positive for EMA. In addition, often pancytokeratin is focally expressed, and frequently, positivity of CD99 and bcl-2 is observed. Rare myxoid dermatofibrosarcoma protuberans is composed of CD34-positive, EMA-negative tumour cells arranged predominantly in a storiform pattern and characterised by a diffuse infiltration of subcutaneous tissue. Myoepithelioma of soft tissues may show a reticular growth pattern, but neoplastic cells are variably positive for S-100 protein, pancytokeratin, actins, glial fibrillary acidic protein, desmin and p63 [15]. In several cases of extraskeletal myxoid chondrosarcoma, a focal expression of EMA has been reported [20], but tumour cells in extraskeletal myxoid chondrosarcoma tend to be larger and contain more eosinophilic cytoplasm with PAS-positive material.

Plexiform perineurioma seems an extremely rare variant of perineurioma with only one case reported so far [34], and several neoplasms showing a plexiform architecture have to be distinguished. Plexiform neurofibroma, plexiform schwannoma and rare plexiform (solitary) circumscribed neuroma [1] are predominantly composed of S-100-positive Schwann cells, and in neurofibromas, scattered EMA-positive perineurial cells are noted only. Plexiform fibrohistiocytic tumour is composed of spindled fibro- and myofibroblasts associated with CD68-positive histiocytoid cells including osteoclast-like giant cells, whereas EMA-positive perineurial cells are not present.

Rare sclerosing pacinian-like perineurioma, lipomatous perineurioma, perineurioma with granular cells and ossifying perineurioma have been reported in the last years [4, 6, 24, 33].

Malignant perineuriomas, also known as malignant peripheral nerve sheath neoplasms showing a perineurial differentiation, represent exceedingly rare malignant neoplasms, and are characterised morphologically by an infiltrative growth, prominent cytological atypia and increased proliferative activity [14]. So-called atypical cellular perineurioma may be regarded as a lesion intermediate between benign and obvious malignant perineurioma, and among four lesions reported so far, two neoplasms recurred locally, but none metastasized [32].

In summary, perineurial neoplasms of skin and soft tissues represent a heterogeneous group of mesenchymal neoplasms composed of spindle shaped and/or epithelioid tumour cells showing histological, immunohistochemical, ultrastructural and molecular features of perineurial-differentiated cells. Reticular and plexiform perineurioma represent rare and recently delineated morphological variants of benign perineurioma of skin and soft tissues. Although not specific, claudin-1 and glut-1 are quite sensitive perineurial markers and should be included in the immunohistochemical panel for the diagnosis of perineurial neoplasms.

Acknowledgements The authors are grateful to Dr. Outrata, Stuttgart, Germany, for kindly providing case material and clinical follow-up for case 1.

References

1. Argenyi ZB, Cooper PH, Santa Cruz D (1993) Plexiform and other unusual variants of palisaded encapsulated neuroma. J Cutan Pathol 20:34–39
2. Balarezo FS, Muller RC, Weiss RG, Brown T, Knibbs D, Joshi VV (2003) Soft tissue perineurioma in children: report of three cases and review of the literature. Pediatr Dev Pathol 6:137–141
3. Bilbao JM, Khoury NJ, Hudson AR, Briggs SJ (1984) Perineurioma (localized hypertrophic neuropathy). Arch Pathol Lab Med 108:557–560
4. Burgues O, Monteagudo C, Noguera R, Revert A, Molina I, Llombart-Bosch A (2001) Cutaneous sclerosing pacinian-like perineurioma. Histopathology 39:498–502
5. de La Jarte-Thirouard AS, Jacquier I, de Saint-Maur PP (2003) Intraneural reticular perineurioma of the neck. Ann Diagn Pathol 7:120–123
6. Diaz-Flores L, Alvarez-Argüelles H, Madrid JF, Varela H, Gonzalez MP, Guitierrez R (1997) Perineurial cell tumor (perineurioma) with granular cells. J Cutan Pathol 24:575–579
7. Emory TS, Scheithauer BW, Hirose T, Wood M, Onofrio BM, Jenkins RB (1995) Intraneural perineurioma. A clonal neoplasm associated with abnormalities of chromosome 22. Am J Clin Pathol 103:696–704
8. Erlandson RA (1991) The enigmatic perineurial cell and its participation in tumors and tumor-like entities. Ultrastruct Pathol 15:335–351

9. Fetsch JF, Miettinen M (1997) Sclerosing perineurioma. A clinicopathologic study of 19 cases of a distinctive soft tissue lesion with a predilection for the fingers and palms of young adults. Am J Surg Pathol 21:1433–1442
10. Folpe AL, Billings SD, McKenney JK, Walsh SV, Nusrat A, Weiss SW (2002) Expression of claudin-1, a recently described tight junction-associated protein, distinguishes soft tissue perineurioma from potential mimics. Am J Surg Pathol 26: 1620–1626
11. Giannini C, Scheithauer BW, Jenkins RB, Erlandson RA, Perry A, Borell TJ, Hoda RS, Woodruff JM (1997) Soft-tissue perineurioma. Evidence for an abnormality of chromosome 22, criteria for diagnosis, and review of the literature. Am J Surg Pathol 21:164–173
12. Giannini C, Scheithauer BW, Stenberg J, Cosgrove TJ (1998) Intraventricular perineurioma: case report. Neurosurgery 43: 1478–1481
13. Graadt van Roggen JF, McMenamin ME, Belchis DA, Nielsen GP, Rosenberg AE, Fletcher CDM (2001) Reticular perineurioma. A distinctive variant of soft tissue perineurioma. Am J Surg Pathol 25:485–493
14. Hirose T, Scheithauer BW, Sano T (1998) Perineurial malignant peripheral nerve sheath tumor (MPNST). A clinicopathologic, immunohistochemical, and ultrastructural study of seven cases. Am J Surg Pathol 22:1368–1378
15. Hornick JL, Fletcher CDM (2003) Myoepithelial tumors of soft tissue: a clinicopathologic and immunohistochemical study of 101 cases with evaluation of prognostic parameters. Am J Surg Pathol 27:1183–1196
16. Hornick JL, Fletcher CDM (2005) Soft tissue perineurioma: clinicopathologic analysis of 81 cases including those with atypical histologic features. Am J Surg Pathol 29:845–858
17. Hornick JL, Fletcher CDM (2005) Intestinal perineurioma: clinicopathologic definition of a new anatomic subset in a series of 10 cases. Am J Surg Pathol 29:859–865
18. Kazakov DV, Pitha J, Sima R, Vanecek T, Shelekhova K, Mukensnabl P, Michal M (2005) Hybrid peripheral nerve sheath tumors: schwannoma–perineurioma and neurofibroma–perineurioma. A report of three cases in extradigital locations. Ann Diagn Pathol 9:16–23
19. Lazarus SS, Trombetta LD (1978) Ultrastructural identification of a benign perineurial cell tumor. Cancer 41:1823–1829
20. Meis-Kindblom JM, Bergh P, Gunterberg G, Kindblom LG (1999) Extraskeletal myxoid chondrosarcoma: a reappraisal of its morphologic spectrum and prognostic factors based on 117 cases. Am J Surg Pathol 23:636–650
21. Mentzel T, Dei Tos AP, Fletcher CDM (1994) Perineurioma (storiform perineurial fibroma): clinicopathological analysis of four cases. Histopathology 25:261–267
22. Michal M (1999) Extraneural retiform perineurioma. A report of four cases. Pathol Res Pract 195:759–763
23. Michal M, Kazakov DV, Belousova I, Bisceglia M, Zamecnik M, Mukensnabl P (2004) A benign neoplasm with histopathological features of both schwannoma and retiform perineurioma (benign schwannoma–perineurioma): a report of six cases of a distinctive soft tissue tumor with a predilection for the fingers. Virchows Arch 445:347–353
24. Rank JP, Rostad SW (1998) Perineurioma with ossification. A case report with immunohistochemical and ultrastructural studies. Arch Pathol Lab Med 122:366–370
25. Robson AM, Calonje E (2000) Cutaneous perineurioma: a poorly recognized tumour often misdiagnosed as epithelioid histiocytoma. Histopathology 37:332–339
26. Scheithauer BW, Giannini C, Woodruff JM (2000) Perineurioma. In: Kleihues P, Cavenee WK (eds) WHO-classification. Tumours of the nervous system. IARC Press, Lyon
27. Theaker JM, Gatter KC, Puddle J (1988) Epithelial membrane antigen expression by the perineurium of peripheral nerve and in peripheral nerve tumours. Histopathology 13:171–179
28. Theaker JM, Fletcher CDM (1989) Epithelial membrane antigen expression by the perineurial cell: further studies of peripheral nerve lesions. Histopathology 14:581–592
29. Val-Bernal JF, Hernando M, Gariji MF, Villa P (1997) Renal perineurioma in childhood. Gen Diagn Pathol 143:75–81
30. Yamaguchi U, Hasegawa T, Hirose T, Fugo K, Mitsuhashi T, Shimizu M, Kawai A, Ito Y, Chuman H, Beppu Y (2003) Sclerosing perineurioma: a clinicopathological study of five cases and diagnostic utility of immunohistochemical staining for glut-1. Virchows Arch 443:159–163
31. Younes M, Lechago LV, Somoano JR, Mosharaf M, Lechago J (1996) Wide expression of the human erythrocyte glucose transporter Glut 1 in human cancers. Cancer Res 56:1164–1167
32. Zamecnik M, Koys F, Gomolcak P (2002) Atypical cellular perineurioma. Histopathology 40:296–298
33. Zamecnik M (2003) Perineurioma with adipocytes (lipomatous perineurioma). Am J Dermatopathol 25:171–173
34. Zelger BG, Weinlich G, Zelger B (2000) Perineuroma. A frequently unrecognized entity with emphasis on a plexiform variant. Adv Clin Pathol 4:25–33

Virchows Arch (2005) 447: 683–687
DOI 10.1007/s00428-005-0018-z

ORIGINAL ARTICLE

Sergio Fernández-Aguilar · Philippe Simon · Frédéric Buxant · Thierry Simonart · Jean-Christophe Noël

Tubular carcinoma of the breast and associated intra-epithelial lesions: a comparative study with invasive low-grade ductal carcinomas

Received: 14 February 2005 / Accepted: 2 June 2005 / Published online: 10 August 2005
© Springer-Verlag 2005

Abstract Ductal intra-epithelial lesions of the breast are associated with invasive neoplasms and comprise a large spectrum of histological patterns. We have examined 23 cases of pure tubular carcinomas (TCs) of the breast and 53 cases of invasive ductal low-grade carcinomas to determine the relationship and distribution of intra-epithelial lesions, mainly of ductal in situ carcinoma type, but including also lobular intra-epithelial neoplasia (LIN) in both entities. Eleven cases of TC showed flat epithelial atypia (FEA) (47.8%), and, in 14 and 6 cases, micropapillary and cribriform low-grade ductal carcinoma in situ (DCIS) were present (60.7 and 26.1%, respectively). On the opposite, in ductal grade I invasive carcinomas, the most frequent architectural pattern was low-grade DCIS growing in arcades in 26 cases (49%). While absent in TCs, low-grade DCIS of solid type was found in five (9.4%) cases of ductal invasive carcinomas, where FEA were present in seven (13.2%) cases. LIN lesions were present in four (17.4%) cases of TC, whereas they represented 7.5%, as reported by Carstens et al. (Am J Clin Pathol 58:231–238, 1972), of cases of low-grade carcinomas. These results suggest that invasive pure TC and low-grade ductal carcinomas of the breast are different lesions, and support the fact that TC, of low histopathological grade, is a particular distinct tumoural entity.

Keywords Breast · Tubular carcinoma · Ductal intra-epithelial neoplasia · Ductal carcinoma in situ · Flat epithelial atypia

S. Fernández-Aguilar (✉) · T. Simonart · J.-C. Noël
Department of Senology and Gynecopathology,
Erasmus University Hospital,
808 Route de Lennik,
1070 Brussels, Belgium
e-mail: sergiofa75@yahoo.com

P. Simon · F. Buxant
Department of Obstetrics and Gynecology,
Erasmus University Hospital,
Brussels, Belgium

Introduction

Tubular carcinoma (TC) of the breast is a distinct low-grade ductal neoplasm characterized by well-differentiated tubular structures, typically one layer thick, and surrounded by abundant stroma (Fig. 1) [5, 11, 15]. It is an uncommon entity, as it represents less than 2% of all breast carcinomas. However, with the advent of mammographic screening, this proportion is increasing [14].

The majority of ductal invasive breast carcinomas are considered to develop from premalignant lesions [1], mostly atypical duct hyperplasia (ADH), and ductal carcinoma in situ (DCIS). In the majority of cases, the grade of the intra-epithelial lesions is highly correlated with the grade of their invasive counterpart.

Different studies have found an association of TC with low-grade DCIS of cribriform and micropapillary type [7, 9], and also with flat epithelial atypia (FEA) [9]. However, to date, there are no studies comparing a larger spectrum of low-grade DCIS lesions and lobular intra-epithelial neoplasia (LIN) found in TCs with those encountered in well-differentiated low-grade invasive ductal carcinomas of the breast of no specific type. This investigation was undertaken to assess the different types and grades of in situ carcinoma lesions accompanying TCs and to compare them with the intra-epithelial lesions associated with grade I, not otherwise specified and not mixed, invasive ductal neoplasms.

Material and methods

The analysed surgical specimens were obtained from the surgical pathology data base of the Department of Pathology of the Erasmus University Hospital, Brussels, Belgium, from 1988 to 2004. Twenty-three cases of TCs were retrieved. Afterwards, the rest of the invasive carcinomas were evaluated, and the ductal grade I neoplasms were selected. Therefore, 53 cases of well-differentiated invasive ductal carcinoma of not otherwise specified (NOS) type were examined. The histological diagnosis was reviewed

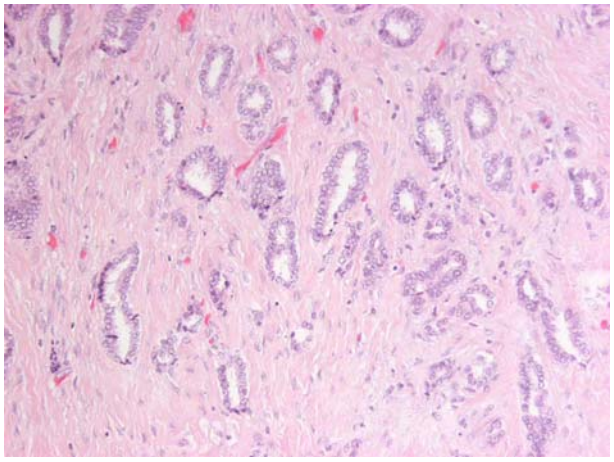


Fig. 1 Tubular carcinoma. Invasive haphazardly distributed round to oval and focally angulated glands in a fibrous stroma (×100)

independently by two pathologists on routine hematoxylin and eosin sections. Strict diagnostic criteria were used to select TCs. Indeed, following the 2003 World Health Organization (WHO) classification of breast tumours [19] and recent refined morphologic criteria [8], the lesions should be composed of at least 70% well-differentiated tubular structures, with the open lumina lined by a single layer of epithelial cells with grade I nuclei and few or no mitoses (Fig. 1). As for the NOS well-differentiated invasive ductal carcinomas, mixed, pleomorphic, osteoclastic giant cells, choriocarcinomatous and melanotic neoplasms were excluded. The histopathological low grade was evaluated according to the semi-quantitative method from Elston and Ellis [5, 6], which takes into account tubular formation, nuclear pleomorphism and mitotic index.

Afterwards, associated intra-epithelial lesions were assessed according to the 2003 WHO classification of breast tumours [19]. Therefore, we divided intra-epithelial breast proliferative lesions into FEA (DIN1a), ADH (DIN1b) and ductal intra-epithelial neoplasia with its different grades (DIN1c, DIN2 and DIN3). Low-grade in situ carcinoma (DIN1c) lesions were subdivided following the 2003 WHO classification into cribriform, solid, micropapillary, papillary and arcade patterns. Cribriform-type lesions were characterized by multiple adjacent ducts distended by a sieve-like proliferation of monotonous, uniform cells with homogeneous, regular and organized lumens. In solid DIN1c lesions no lumens were present. Arcade pattern lesions showed a principally roman bridge architecture, and the ductal spaces within these lesions were not regular, as was the case of cribriform lesions. We also took into consideration the minimum size criterium of 2 mm to establish the diagnosis of DIN1c [18]. Concerning LIN, only low-grade (LIN1) lesions were evidenced in the cases analysed, with no distended acini or necrosis. Histopathological lesions were confirmed by means of immunohistochemistry techniques. For this purpose, high-molecular-weight keratines (Dako, clones 34BE12 and D5/14B4, 1/100 and 1/50 dilutions, respectively, citrate pH 6.00), and E-cadherin (Novocastra, clone 36B5, 1/25 dilution, citrate pH 6.00) antibodies were used. Statistical analyses were made using the Fisher's Exact Test (two-tailed).

Results

The results and patients' characteristics are summarized in Table 1. The mean age of patients was 51.7 (34–73) years for TCs and 54.8 (36–78) years for ductal low-grade carcinomas. Mean tumour size was 9.2 (4–27) and 10.9 (6–19) mm in TC and ductal low-grade neoplasms, respectively.

In 22 of 23 patients with TC no lymph node metastases were found, and the tumour size was less than 2 cm. Therefore, they were staged as T1N0 according to the 2003 WHO classification. The remaining case was represented by a 27-mm tumour with four lymph node metastases. Regarding low-grade ductal carcinomas (LGDCs), the 53 cases analysed corresponded to T1 lesions measuring less than 2 cm. Seven cases showed positive axillary lymph nodes (13.2%).

For practical reasons, we did not take into account atypical hyperplasia lesions (DIN1b) because they are morphologically similar to low-grade ductal in situ carcinoma lesions, and the only valid criterium nowadays for the differential diagnosis is size (2 mm) [18]. These lesions were included within the DCIS group. Eleven cases of TC contained FEA (47.8%) (Fig. 2). These lesions were characterized by cuboidal to columnar cells showing mild atypia and indistinguishable in most cases from TC cells. Apical cytoplasmic eosinophilic snouts were focally prominent. When present, these lesions were often located right next to invasive glands and adjacent to DCIS lesions. In situ carcinoma of micropapillary type was frequently encountered next to TCs (60.9% of cases), whereas their presence in invasive grade I ductal carcinoma was more rare (17% of cases, P=0.0012). The percentage of in situ carcinoma le-

Table 1 Distribution of intra-epithelial lesions in tubular carcinomas (TCs) and grade I ductal carcinomas (GI DCs)

	No. of cases	Age (years)	Size (mm)	FEA	DCIS MP	DCIS CRIB	DCIS SOL	DCIS ARC	DCIS GII	DCIS GIII	LIN
TC	23	51.7 (34–73)	9.2 (4–27)	11	14	6	0	2	0	0	4
GI DC	53	54.8 (36–78)	10.9 (6–19)	7	11	3	5	26	2	0	4
P				0.032	0.0012	0.0192	0.03146	0.0007	1	NS	0.2344

FEA Flat epithelial atypia; *DCIS MP* ductal carcinoma in situ of micropapillary type; *DCIS CRIB* DCIS of cribriform type; *DCIS SOL* DCIS of solid type; *DCIS ARC* DCIS, arcade pattern; *DCIS GII* DCIS, grade II; *DCIS GIII* DCIS, grade III; *LIN* lobular intra-epithelial neoplasia; *TC* tubular carcinoma; *GI DC* low-grade invasive duct carcinoma; *NS* not significant

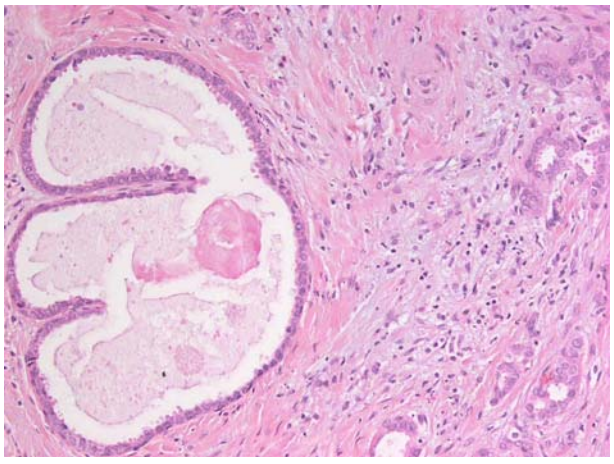


Fig. 2 Flat epithelial atypia associated with tubular carcinoma. Glandular structures are lined by mono to paucistratified mildly atypical cuboidal to cylindrical cells with focal apical secretions (×100)

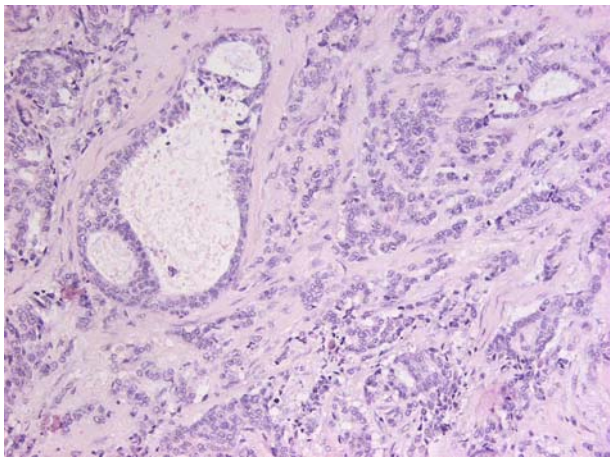


Fig. 4 Focus of DCIS of arcade pattern found in a low-grade invasive duct carcinoma, with variable, rigid lumens in the shape of a "roman bridge" (×100)

sions with a cribriform pattern was also greater in TCs than in invasive low-grade carcinomas of ductal type (26.1 vs 5.7% of cases, respectively, P=0.0192) (Fig. 3).

Interestingly, FEA, although not so frequent as in TCs, were evidenced in seven cases (13.2%) in association with invasive grade I ductal carcinomas, where the predominant in situ lesions were of arcade pattern (49% of cases) (Fig. 4) in contrast with TCs, in which they were only encountered in two cases (10%) (P=0.0007). Finally, in situ ductal carcinoma of solid type was observed adjacent to grade I ductal invasive neoplasms in five cases (9.4%), while it was absent in TCs (P=0.3146). No higher grade intra-epithelial (DIN2 and DIN3) lesions were observed in TCs, whereas DIN2 was evidenced in two cases of invasive duct carcinoma (3.8%) (P=1).

Lobular intra-epithelial neoplasia lesions were observed in 4 (17.4%) of the 23 TC cases. They were seen in 100% (4 of 4) of cases associated with FEA (DIN1a) lesions and in 50% (2 of 4) accompanying DCIS of micropapillary type. In one case (25%) they were also associated with DCIS of arcade and solid type. From the four cases of LGDC showing LIN (7.5%), two cases were associated with DCIS of arcade and solid type, and in one case, with DCIS of micropapillary type. Interestingly, in one case, LIN was the only intra-epithelial lesion encountered in LGDC.

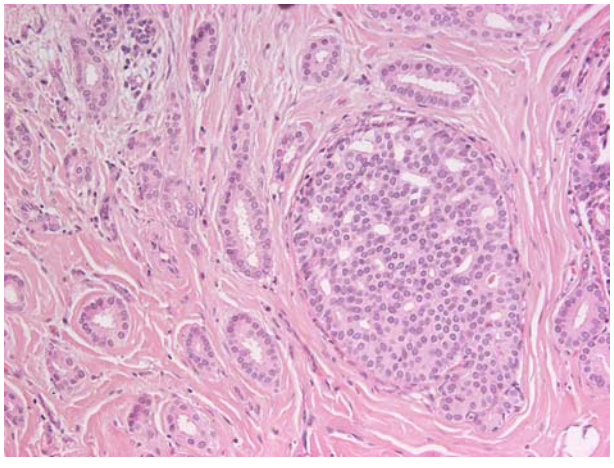


Fig. 3 Intraductal carcinoma of cribriform type in association with tubular carcinoma. Note the sieve-like architecture with homogeneous round and rigid lumens (×100)

Discussion

As recently stated by Goldstein et al. [8], there has been a lack of standardized definitions for TCs of the breast. These limitations mostly concern the percentage of tubularity.

These authors have therefore refined the histopathologic criteria and claim neoplasms with at least 70% tubularity, grade I nuclei and rare mitoses to have an excellent prognosis. In this study we have compared a wide spectrum of different intra-epithelial mammary lesions associated with invasive TCs and those encountered in low-grade ductal invasive breast carcinomas of no specific type. Patients with TCs and ductal low-grade carcinomas had similar demographic and neoplasm characteristics, including age and tumour dimensions. For so doing, we have used the last standardized 2003 WHO classification of breast tumours featuring the DIN concept [17–19]. To date, there are a few studies that have analysed the association of some intra-epithelial ductal neoplasia and TCs [7, 9]. These studies mostly concern on one hand, "ductal carcinoma in situ cells with apocrine snouts", a term that corresponds now to FEA, and on the other hand, ductal intra-epithelial neoplasia of micropapillary and, to a lesser degree, cribriform type [11, 12]. However, to the best of our knowledge, the former is the only article comparing TCs and grade I invasive ductal carcinoma associated lesions, which are limited to FEA. Indeed, the authors demonstrated a higher prevalence of these lesions in TCs, which were present in 43.7% of cases, than in invasive grade I carcinomas, where the proportion only attained 3.7% of cases. Our data are in ac-

cordance with those ones (47.8 vs 13.2%, respectively). We should point out that the slightly higher rate of FEA encountered in our 53 grade I invasive carcinomas in relation to previous studies can be explained by the fact that four out of the seven carcinomas displaying these lesions (57%) showed tubular features (Fig. 4), that is to say, neoplastic areas with regular, opened and tubular structures whose proportion was not sufficient to establish a diagnosis of TC (to strictly diagnose TC as such, a minimum 70% proportion of invasive tubular structures, according to recent criteria with grade I nuclei, and few or no mitoses is required [8]). In these cases, as stated above for TC, flat lesions were mostly evidenced next to infiltrative tubular structures.

But no specific comparative analysis seem to have been performed to establish if there is really a difference between TCs and grade I invasive ductal neoplasm intra-epithelial associated lesions if we exclude the study by Goldstein and O'Malley [9], in which FEA are more frequently encountered in TCs than in LGDCs.

Previous studies have shown an overall increased frequency of ductal intra-epithelial lesions concurrent with ductal invasive neoplasms [2], with a good correlation between the histological grade of ductal intra-epithelial neoplasia and the grade of the infiltrative component. Our results also concur with previously reported data stating a close relationship of micropapillary in situ carcinoma and TCs as well as a higher frequency of FEA in these particular tumours. Interestingly, a clear relationship between low-grade DCIS, with an arcade growing pattern, and low-grade invasive ductal carcinoma emerged from this study with respect to TCs. Low-grade DCIS of solid type, although not so frequent, was also distinctively observed in association with low-grade invasive ductal carcinomas. However, the results were not statistically significant (P= 0.3146), perhaps partly due to the small number of cases examined. Another important issue is the higher frequency of LIN in TC, and also their close association with FEA, and in a lesser degree, with low-grade DCIS of micropapillary type. Indeed, FEA lesions and fully established micropapillary DCIS have been reported together in the same surgical specimen in a high proportion of cases [3, 13] as well as in coexistence with LIN. Our results seem to be in accordance with these data and we put them together in the context of TC. The small number of TC cases assessed, however, does not show a statistically significant difference (P=0.2344).

The difference in the lesions observed, together with the results of some genetic studies, give further evidence that TC and invasive grade I ductal carcinoma are different entities. Genetic alterations in TCs have proven to be less frequent than in other breast neoplasms [10, 16, 20]. The nature of these mutations is also different, with a predominance of 16q loss [20]. However, to date, there are no genetic studies comparing the different morphological patterns of (low-, intermediate- or high-grade) DCIS lesions classified within the same differentiation grade. This issue can be interesting, as genetic alterations seem to be different from a quantitative and qualitative point of view when comparing tubular and other (including grade I) ductal carcinomas and, perhaps, genetic abnormalities may vary according to the architectural type of lesion. Unfortunately, the number of genetic studies is scarce and hampered by the paucity of cases analysed.

In summary, our study shows a different profile and distribution of intra-epithelial lesions in TC and ductal low-grade invasive carcinomas. These data, put together with the results of previous histopathologic and genetic studies, support TC of the breast as a clear distinctive entity.

References

1. Allred DC, Mohsin SK, Fuqua SA (2001) Histological and biological evolution of human premalignant breast disease. Endocr Relat Cancer 8:47–61
2. Bratthauer GL, Tavassoli FA (2004) Assessment of lesions coexisting with various grades of intraepithelial neoplasia of the breast. Virchows Arch 444:340–344
3. Brogi E, Oyama T, Koerner FC (2001) Atypical cystic lobules in patients with lobular neoplasia. Int J Surg Pathol 9:201–206
4. Carstens PH, Huvos AG, Foote FW Jr, Ashikari R (1972) Tubular carcinoma of the breast: a clinicopathologic study of 35 cases. Am J Clin Pathol 58:231–238
5. Ellis IO et al (2003) Invasive breast carcinoma. In: World Health Organization classification of tumors. Tumors of the breast and female genital organs. Fascicle 5. International Agency for Research on Cancer, Lyon, pp 13–59
6. Elston CW, Ellis IO (1991) Pathological prognostic factors in breast cancer. The value of histological grade in breast cancer: experience from a large study with long-term follow-up. Histopathology 19:403–410
7. Fraser JL, Plaza S, Chorny K, Connolly JL, Schnitt SJ (1998) Columnar alteration with prominent apical snouts and secretions: a spectrum of changes frequently present in breast biopsies performed for microcalcifications. Am J Surg Pathol 22: 1521–1527
8. Goldstein NS, Kestin LL, Vicini FA (2004) Refined morphologic criteria for tubular carcinoma to retain its favorable outcome in contemporary breast carcinoma patients. Am J Clin Pathol 122: 728–739
9. Goldstein NS, O'Malley BA (1997) Cancerization of small ecstatic ducts of the breast by ductal carcinoma in situ cells with apocrine snouts: a lesion associated with tubular carcinoma. Am J Clin Pathol 107:561–566
10. Martinez A, Walker RA, Shaw JA, Dearing SJ, Maher ER, Latif F (2001) Chromosome 3p allele loss in early invasive breast cancer: detailed mapping and association with clinicopathological features. Mol Pathol 54:300–306
11. McDivitt RW, Boyce W, Gersell D (1982) Tubular carcinoma of the breast. Clinical and pathological observations concerning 135 cases. Am J Surg Pathol 6:401–410
12. McDivitt RW, Stewart FW, Berg JW (1968) Tumors of the breast. In: Atlas of tumor pathology, series 2, fascicle 2. Armed Forces Institute of Pathology, Washington, DC, pp 69–90
13. Oyama T, Maluf H, Koerner F (1999) Atypical cystic lobules: an early stage in the formation of low-grade ductal carcinoma in situ. Virchows Arch 435:413–421

14. Papadatos G, Rangan AM, Psarianos T, Ung O, Taylor R, Boyages J (2001) Probability of axillary lymph node involvement in patients with tubular carcinoma of the breast. Br J Surg 88:860–864
15. Rosen PP (2001) Tubular carcinoma. In: Rosen's breast pathology. Lippincott, Philadelphia, pp 365–380
16. Roylance R et al (1999) Comparative genomic hybridization of breast tumors stratified by histological grade reveals new insights into the biological progression of breast cancer. Cancer Res 59:1433–1436
17. Tavassoli FA (1998) Ductal carcinoma in situ: introduction of the concept of ductal intraepithelial neoplasia. Mod Pathol 11: 140–154
18. Tavassoli FA (2001) Ductal intraepithelial neoplasia of the breast. Virchows Arch 438:221–227
19. Tavassoli FA et al (2003) Intraductal proliferative lesions. In: World Health Organization classification of tumors. Tumors of the breast and female genital organs, fascicle 5. International Agency for Research of Cancer, Lyon, pp 63–73
20. Waldman FM et al (2001) Genomic alterations in tubular breast carcinomas. Hum Pathol 32:222–226

Virchows Arch (2005) 447: 688–694
DOI 10.1007/s00428-005-0010-7

ORIGINAL ARTICLE

Irina Matos · Rozany Dufloth · Marcelo Alvarenga · Luiz Carlos Zeferino · Fernando Schmitt

p63, cytokeratin 5, and P-cadherin: three molecular markers to distinguish basal phenotype in breast carcinomas

Received: 30 November 2004 / Accepted: 17 May 2005 / Published online: 13 July 2005
© Springer-Verlag 2005

Abstract Human breast carcinomas represent a heterogeneous group of tumors diverse in behavior, outcome, and response to therapy. However, the current system of pathological classification does not take into account biologic determinants of prognosis. The purpose of this study was to classify and characterize breast carcinomas based on variations in protein expression patterns derived from immunohistochemical analyses on tissue microarrays (TMAs). Therefore, 11 TMAs representing 168 invasive breast carcinomas were constructed. Breast tumors were classified into four different subtypes depending on estrogen receptor (ER) and HER2 expression. Basal-type tumors expressed neither of these proteins and represented 7.6% of our series; basal-like HER2-overexpressing tumors did not express ER and represented 17.7%; luminal-type tumors expressed ER and represented 72.8% of this series (luminal A 56.3%, luminal B 16.5%). Moreover, we characterized each subtype based on P-cadherin (P-CD), p63, cytokeratin (CK) 5, BCL2, and Ki67 expression. Basal-type tumors were mostly grade III, more frequently P-CD-, p63-, and CK5-positive, and had a high proliferation rate. Conversely, luminal-type tumors rarely expressed basal markers and had a low grade and proliferation rate. Basal-like HER2-overexpressing tumors showed a basal-type profile similar with a high grade and up-regulation of P-CD and CK5. With this study, we show that P-CD, p63, and CK5 are important molecular markers that can be used to distinguish a basal phenotype. In addition, we also demonstrate the usefulness of TMAs in breast carcinoma immunoprofiling.

Keywords Breast cancer · Basal marker · Tissue microarray · Expression profile

I. Matos · R. Dufloth · F. Schmitt (✉)
Institute of Molecular Pathology and Immunology of the University of Porto (IPATIMUP),
Rua Dr. Roberto Frias, s/n,
4200-465 Porto, Portugal
e-mail: fschmitt@ipatimup.pt
Tel.: +35-122-5570700
Fax: +35-122-5570799

R. Dufloth · M. Alvarenga · L. C. Zeferino
Centro de Atenção Integral à Saúde da Mulher (CAISM),
Faculty of Medical Sciences, State University of Campinas,
Av. Alexander Fleming 101,
13084-971 Campinas, Sao Paolo, Brazil

F. Schmitt
Medical Faculty, University of Porto,
Porto, Portugal

Introduction

Human breast carcinomas represent a heterogeneous group of tumors with a diverse biologic behavior, outcome, and response to therapy. An important challenge to the study and treatment of breast cancer relies on the resolution of molecular heterogeneity that is not apparent by morphological evaluation. Recent cDNA microarray profiling studies on breast tumors have identified distinct subtypes of breast carcinomas that are associated with different clinical outcomes [21, 22]. Sorlie et al. analyzed the expression profiles of 115 sporadic breast tumor samples and categorized them into five main groups: one basal-like, one HER2-overexpressing, two luminal-like (luminal A and luminal B), and one normal breast-tissue-like. When tumors from *BRCA1*-mutated carriers were similarly analyzed, it was found that this genotype strongly predisposes to the basal-like tumor subtype [22, 25]. The so-called basal tumors expressed cytokeratin (CK)5 and CK17 mRNAs, resembling the pattern found in the basal epithelial cells of the normal breast, whereas the luminal phenotype was based on the expression of CK8/18 and CK19 mRNAs similar to those of luminal epithelial cells [2]. The expression of HER1 and P-cadherin (P-CD) was later associated to the basal subtype [15, 16].

Breast cancer treatments evolved and directed target therapies against the estrogen receptor (ER) and HER2 oncogene. However, these therapies would not be expected to be effective against basal breast carcinomas because these tumors express neither of these proteins [15]. The characterization of this subtype assumes a major importance, leading to a more focused investigation on putative

therapeutic targets. Therefore, in the present study, we confirmed by immunohistochemistry (IHC) on tissue microarrays (TMAs) the association of high levels of P-CD and CK5 expression to the basal subtype. Moreover, we show that p63 is also up-regulated in this subgroup and can help distinguish basal breast carcinomas. p63 is a p53 homolog crucial for the maintenance of a stem cell population in several epithelial tissues and is necessary for the normal development of the human mammary gland [9, 13, 14, 26]. According to previous studies from our group, approximately 9% of the invasive ductal carcinomas of the breast are positive for p63 [18].

In this report, the existence of four different subtypes of breast cancer was confirmed by protein expression patterns assessed by IHC on 11 TMAs containing 168 independent breast carcinoma cases. The definition and characterization of the different subtypes were based on the expression of seven molecular markers (ER, HER2, P-CD, p63, CK5, Ki67, and BCL2).

Materials and methods

Patients' selection

One hundred sixty eight tumor samples were obtained from patients treated at the State University of Campinas (UNICAMP), Sao Paulo, Brazil, and at Hospital Sao Joao, Porto, Portugal. Of these, 50 tumors presented clinical features of familial breast cancer according to the Breast Cancer Linkage Consortium [5, 6]: early onset, bilaterality, and multiple cases of breast and ovarian cancer in the family (more than two first-degree relatives involved). The remaining 118 cases were from patients without any clinical familial feature (sporadic). All sporadic cases had ER IHC information available for whole tissue sections. From these, 62 tumors also had previous information for P-CD expression, and 73, for fluorescence in situ hybridization (FISH) analysis.

Tissue microarray construction

Representative areas of different lesions were carefully selected on hematoxylin and eosin (H & E)-stained sections and marked on individual paraffin blocks. Two tissue cores (2 mm in diameter) were obtained from each selected specimen and precisely deposited into a recipient paraffin block using a TMA workstation (TMA builder ab1802, Abcam, Cambridge, UK). Eleven TMA blocks were constructed, each containing 24 tissue cores, arranged in a 4×6 sector. In each TMA block, nonneoplastic breast tissue cores were also included as controls. After construction, 2-μm tissue sections were cut and adhered to Superfrost Plus glass slides. An H & E-stained 4-μm section from each block was reviewed to confirm the presence of morphological representative areas of the original lesions.

Immunohistochemistry

Immunohistochemical staining was performed using the streptavidin–biotin–peroxidase technique (Lab Vision Corporation, Fremont, CA, USA) in each set of 11 glass slides comprising the TMAs. Antigen retrieval was done by incubating TMA sections in an antigen-unmasking solution, pH 6.0 (Vector Laboratories Inc., Burlingame, CA, USA), or in ethylenediaminetetraacetic acid (EDTA), pH 8 (Lab Vision) at 98°C. The antigen retrieval times, antibodies, dilutions, and suppliers are listed in Table 1. After washes in a phosphate buffer solution (PBS), endogenous peroxidase activity was blocked by incubation of the slides in a 3% hydrogen peroxide solution in methanol (Merck, Germany). The slides were incubated with a blocking serum (Lab Vision) for 10 min and then incubated with the specific antibody. Immunostaining was performed overnight at 4°C (P-CD and CK5) or for 1 h at room temperature (HER2, ER, p63, BCL2, and Ki67). After washes, the slides were incubated with biotinylated secondary antibody, followed by streptavidin-conjugated peroxidase (Lab Vision). Diaminobenzidine was used as a chromogen. Tissues were then counterstained with hematoxylin and coverslipped using a permanent mounting solution (Zymed, San Francisco, CA, USA).

Immunoreactivities were classified by estimating the percentage of tumor cells showing characteristic staining. In nonneoplastic breast tissues, p63 showed nuclear positivity in myoepithelial cells. P-CD presented a distinctive membranous and occasionally cytoplasmic immunoreactivity in nonneoplastic myoepithelial cells. CK5 stained the myoepithelial cells of breast lobules and ducts. Two pathologists (F.S. and R.D.) evaluated the IHC staining. Because nonneoplastic mammary secretory cells do not express P-CD, either membranous or cytoplasmic immu-

Table 1 Antibodies used in the IHC study

Molecular marker	Antibody	Origin	Clone	Dilution	Antigenic retrieval (min)
BCL2	Mmab	Novocastra, UK	NCL-L-Bcl2	1:10	30
CK5	Mmab	Neomarkers, USA	XM26	1:80	20
ERα	Rmab	Neomarkers, USA	SP-1	1:20	30
HER2	Mmab	Novocastra, UK	NCL-L-CB11	1:60	30
Ki67	Rmab	Neomarkers, USA	SP6	1:300	20
P-CD	Mmab	BD Transduction, KY, USA	56	1:50	20
p63	Mmab	Neomarkers, USA	4A4	1:150	30

Mmab Mouse monoclonal antibody, *Rmab* rabbit monoclonal antibody

noreactivity was considered positive when more than 10% of the neoplastic cells expressed this marker [19]. Similarly, we adopted the same cutoff value for nuclear p63 and ER reactivity and for cytoplasmic CK5 and BCL2 reactivity. Four categories were defined for Ki67: 0, 0–5%, 5–25%, and >25% of stained nuclei. To evaluate HER2, the percentage of cells with membranous staining and intensity was assessed. HER2 was evaluated according to the four-category system (0–3+) and considered positive when 3+ was attributed. We compared our HER2 results with previously obtained FISH information. Of 73 tumor cases, 27 were simultaneously positive, and 39 were simultaneously negative. Only seven tumors presented discordant information: five were HER2-positive and FISH-negative, while the remaining two cases were HER2-negative and HER2-positive for the FISH analysis. For those discordant cases, we assumed FISH results.

Statistical analysis

The χ^2 contingency test was used for categorical variables to determine differences between phenotypes. A p value of <0.05 was considered to reflect a significant association. The StatView 5.0 (SAS Institute Inc., Cary, NC, USA) program was used for this analysis.

Results

Tissue microarray analysis and validation data

To validate the use of TMA for immunoprofiling, we compared, from whole tissue sections, available information on protein expression levels of ER and P-CD with those obtained by IHC on TMA. Of 118 breast carcinomas, 88 were simultaneously ER-positive, whereas 25 were simultaneously negative. Only three cases presented divergent information, and four were not interpretable. Overall, the concordance was 97.4%. In the same way, P-CD expression was also validated. Of 62 sporadic tumors, 12 were simultaneously positive and 48 were simultaneously negative, whereas only 2 cases were discordant. For this basal marker, we observed an overall concordance of 96.8%. This high concordance between IHC on whole tissue sections and on TMAs justified the further use of TMAs.

Immunohistochemistry profiles in breast tumors

We performed IHC on each set of 11 TMA slides for ERα, HER2, P-CD, p63, CK5, Ki67, and BCL2. The results are shown in Table 2 and Fig. 1. Cases positive for ER, p63, and Ki67 showed the characteristic nuclear staining, whereas BCL2 and CK5 showed a cytoplasmic pattern on neoplastic cells. HER2- and P-CD-positive tumors showed a membranous staining. We observed that 72.9% of breast carcinomas in our series were ER-positive, whereas 34.5% were HER2-positive (3+). Less than 31.7% of the tumors analyzed presented expression of a basal marker (P-CD, p63, and CK5).

Like Nielsen et al. [15], we also classified each tumor in a practical way based on its ER and HER2 expression. A total of 158 cases were immunohistochemically interpretable to allow sample characterization into one of five groups (Table 3). If a tumor was ER-positive, it would be classified as luminal; however, we distinguish luminals A and B on the basis of HER2 overexpression. If a tumor was ER-positive and HER2-negative (0, 1, or 2+), it would be classified as luminal A (ER+/HER2−); however, if it was ER- and HER2-positive, it would be classified as luminal B (ER+/HER2+). If a tumor was ER-negative and HER2-positive (ER−/HER2+), it would be classified as basal-like HER2-overexpressing, and if it was both ER- and HER2-negative but positive for at least one basal marker (P-CD and/or p63 and/or CK5), it would be classified as basal (ER−/HER2−). If a tumor did not show expression for any of these markers, it would be classified as negative and would not be considered in the remaining analyses. Using this definition, we observed that basal type comprised 7.6% of all tumors, whereas luminals A and B comprised 56.3 and 16.5%, respectively. Basal-like HER2-overexpressing tumors represented 17.7% of the series, and null phenotype, 1.9% (Table 3). When these immunoprofiles were compared in relation to familial and sporadic origin (Table 4), we observed that basal tumors were mostly associated to familial cases (83.3%), whereas luminal and basal-like HER2-overexpressing cases were more frequently sporadic (69.7% of luminal A, 92.3% of luminal B, and 71.4% of basal-like HER2-overexpressing tumors; $p<0.0001$).

The protein expression profiles clearly differed in luminal A, luminal B, basal, and basal-like HER2-overexpressing tumors concerning P-CD, p63, CK5, Ki67, and BCL2 (Table 4). Statistically strong significant differences between the four groups were observed in this study. Basal and basal-like HER2-overexpressing tumors presented a high histological grade (75 and 81.5% grade III, respectively, $p=0.0001$), had a higher proliferative rate, and demonstrated a clearly higher frequency of P-CD (83.3 and 60.9%, $p<0.0001$) and CK5 (66.7 and 37%, $p<0.0001$) expression (Table 4). Luminal pattern was associated with an increasing frequency of tumors expressing BCL2 (69.1% luminal A and 56.5% luminal B, $p=0.0006$) and with a lower expression of basal markers. Actually, less than 20%

Table 2 Results of IHC stainings on TMA

Molecular marker	Interpretable cores	Positive staining (%)[a]	Negative staining (%)
ER	166	121 (72.9)	45 (27.1)
HER2	162	56 (34.5)	106 (65.5)
P-CD	145	46 (31.7)	99 (68.3)
p63	154	31 (20.1)	123 (79.9)
CK5	149	33 (22.1)	116 (77.9)
BCL2	138	78 (56.5)	60 (43.5)
Ki67	138	33 (23.9)	105 (76.1)

[a]Ki67 positives include all positive categories defined

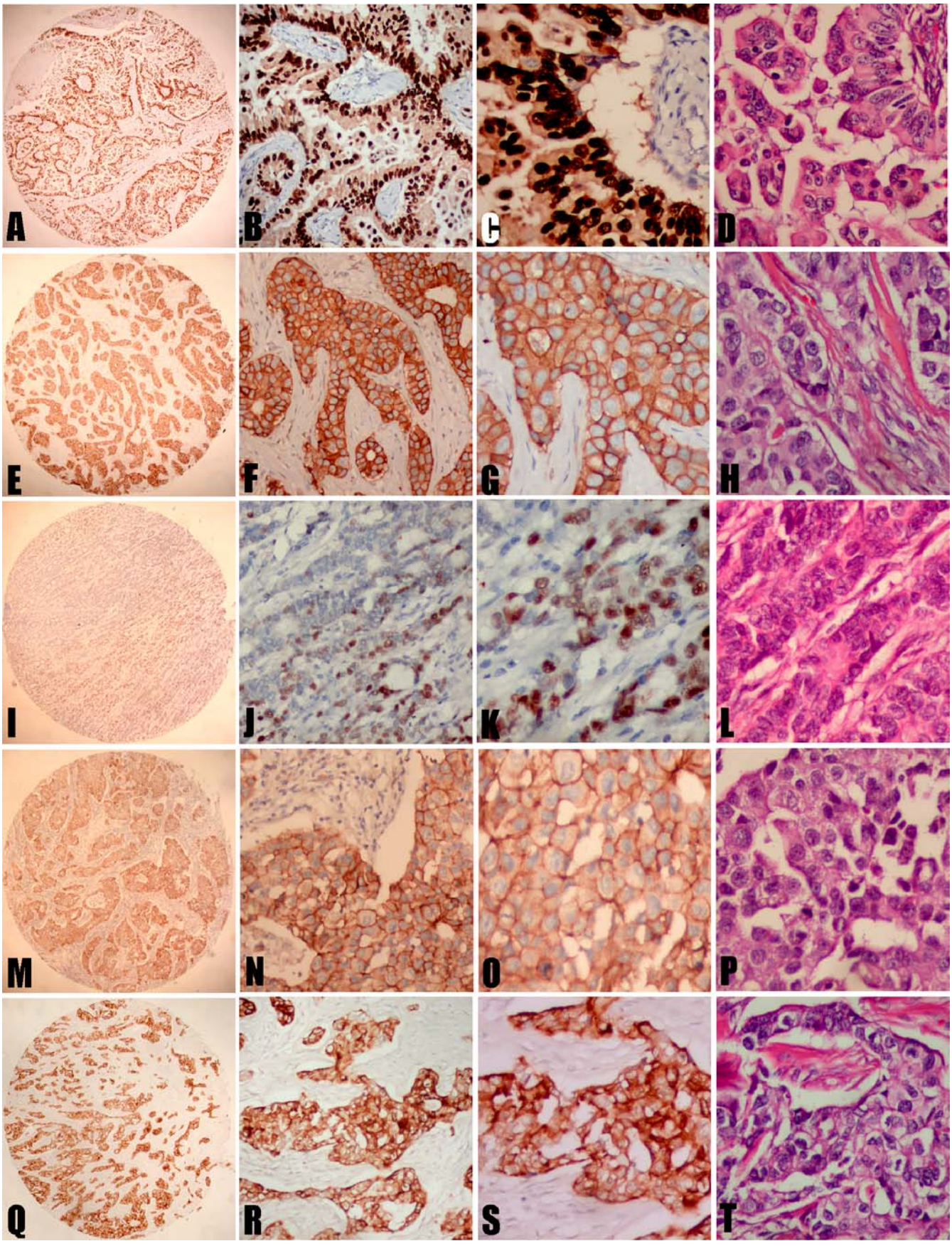


Fig. 1 Expression of proteins studied by IHC on TMAs. **a**–**c** ER staining. **e**–**g** HER2 staining. **i**–**k** p63 staining. **m**–**o** P-CD staining. **q**–**s** CK5 staining. All TMA cores represent neoplastic tissue with a strong staining pattern. **d**, **h**, **l**, **p**, **t** H & E staining of the core represented in each line [original magnification×50 (**a**, **e**, **i**, **m**, **q**), ×200 (**b**, **f**, **j**, **n**, **r**), and ×400 (**c**, **d**, **g**, **h**, **k**, **l**, **o**, **p**, **s**, **t**)]

Table 3 Frequencies of immunohistochemically defined subtypes of breast carcinomas in 158 informative tumors for the tested markers using TMA

Subtype	ER	HER2	P-CD and/or p63 and/or CK5	Frequency (%)
Luminal A	Positive	Negative	Positive/negative	89 (56.3)
Luminal B	Positive	Positive	Positive/negative	26 (16.5)
Basal	Negative	Negative	Positive	12 (7.6)
Basal-like	Negative	Positive	Positive/negative	28 (17.7)
HER2-overexpressing				
Negative	Negative	Negative	Negative	3 (1.9)

of luminal tumors presented a basal marker expression (Table 4). p63 expression was strongly associated to basal tumors (55.5%, p=0.0255).

Finally, we analyzed whether each basal marker was expressed exclusively by the tumors or if its expression was associated with another basal marker (Table 5). We observed that the majority of the luminal tumors (60.3% luminal A and 73.8% luminal B) were simultaneously negative to P-CD, CK5, and p63. This percentage was much lower for basal-like HER2-overexpressing tumors (36.4%) and absent for basal ones. Within basal and basal-like HER2-overexpressing subtypes, p63 was only positive when coexpressed with other basal markers. The same occurred for CK5 within a basal subtype. Simultaneous expression of P-CD, p63, and CK5 was rare in luminal A tumors (4.1%), being completely absent within the luminal B subtype. Interestingly, we observed that 18.2% of basal tumors and 13.7% of basal-like HER2-overexpressing tumors were simultaneously positive for all basal markers (p=0.0016).

Discussion

Gene expression profiling has refined the classification of sporadic breast tumors into distinct subtypes [17, 21, 22, 25]. Basal breast tumors represent one of the most important subtypes since there is no efficient therapy against it, and it is often associated with a poor prognosis [1, 21, 22, 24, 25]. Gene expression profiling approaches have also allowed the observation that familial *BRCA1* mutant tumors segregate strongly with basal-type sporadic cancers, which indicate that basal-type sporadic tumors and familial *BRCA1* tumors can have similar etiologies [23]. *BRCA1* tumors commonly express basal cytokeratins, but not ER, and are of a higher histological grade, indicating a

Table 4 IHC profiles in relation to pathological and clinical variables

	Luminal A [*n* (%)]	Luminal B [*n* (%)]	Basal [*n* (%)]	Basal-like HER2-overexpressing [*n* (%)]	*p*
Clustering					
Familial	27 (30.3)	2 (7.7)	10 (83.3)	8 (28.6)	<0.0001
Sporadic	62 (69.7)	24 (92.3)	2 (16.7)	20 (71.4)	
Grade					
I	18 (21.2)	5 (20)	0	2 (7.4)	0.0001
II	42 (49.4)	11 (44)	2 (25)	3 (11.1)	
III	25 (29.4)	9 (36)	6 (75)	22 (81.5)	
P-CD					
Negative	64 (80)	21 (84)	2 (16.7)	9 (39.1)	<0.0001
Positive	16 (20)	4 (16)	10 (83.3)	14 (60.9)	
p63					
Negative	70 (80.5)	21 (87.5)	5 (45.5)	22 (84.6)	0.0255
Positive	17 (19.5)	3 (12.5)	6 (55.5)	4 (15.4)	
CK5					
Negative	69 (84.1)	22 (91.7)	4 (33.3)	17 (63)	<0.0001
Positive	13 (15.9)	2 (8.3)	8 (66.7)	10 (37)	
Ki67					
0	67 (83.8)	16 (69.6)	5 (45.5)	15 (68.2)	0.0230
>0–5%	5 (6.2)	3 (13)	2 (18.1)	2 (9.1)	
>5–25%	8 (10)	4 (17.4)	3 (27.3)	5 (22.7)	
>25%	0	0	1 (9.1)	0	
BCL2					
Negative	25 (30.9)	10 (43.5)	7 (63.6)	17 (77.3)	0.0006
Positive	56 (69.1)	13 (56.5)	4 (36.4)	5 (22.7)	

Table 5 Basal marker expression in relation to different subtypes

	Luminal A (*n*=73) (%)	Luminal B (*n*=23) (%)	Basal (*n*=11) (%)	Basal-like HER2-overexpressing (*n*=22) (%)	*p*
Simultaneously negative	44 (60.3)	17 (73.8)	0	8 (36.4)	0.0016
Exclusively P-CD+	7 (9.6)	1 (4.4)	2 (18.2)	5 (22.7)	
Exclusively p63+	7 (9.6)	2 (8.6)	0	0	
Exclusively CK5+	4 (5.5)	1 (4.4)	0	1 (4.5)	
P-CD+ and p63+	2 (2.7)	1 (4.4)	2 (18.2)	1 (4.5)	
P-CD+ and CK5+	3 (4.1)	1 (4.4)	3 (27.2)	4 (18.2)	
CK5+ and p63+	3 (4.1)	0	2 (18.2)	0	
P-CD+ and p63+ and CK5+	3 (4.1)	0	2 (18.2)	3 (13.7)	

more rapidly dividing tumor [10, 16]. In the present study, we observed that the majority of basal tumors had a familial clustering, were the most proliferative ones, and were more frequently grade III. Foulkes et al. [10] associated CK5 expression to *BRCA1*-derived tumors. In their study, 40% of CK5-positive tumors were from *BRCA1*-mutated carriers. Palacios et al. [16] have also demonstrated a strong correlation between P-CD- and *BRCA1*-derived tumors. In the present study, we show that P-CD and CK5 were up-regulated in the basal subtype. This evidence suggests that these patients are at a high risk of having *BRCA1* mutations; however, additional studies are needed to investigate this issue further. Basal tumors were also characterized by p63 overexpression. This molecular marker, expressed in the basal cell layer, is thought to play an essential role in the differentiation and growth control in stratified epithelia [13].

Besides the identification of a basal-like subtype, we also distinguish luminal A, luminal B, and basal-like HER2-overexpressing subtypes. For this purpose, we used TMA technology since it allows the screening of a large series of samples at the same time without losing tumor representativity [7, 11, 12, 20].

The basal-like HER2-overexpressing subtype was characterized by a high grade and up-regulation of P-CD and CK5. In fact, Birnbaum et al. [2] have recently suggested that HER2-overexpressing tumors should be included in a bona fide basal-like subclass. Luminal-like tumors were distinguished on the basis of HER2 expression. The luminal A subtype did not express HER2 and was strongly associated with low proliferation and with high levels of BCL2 expression. This is not surprising since it is well known that BCL2 is up-regulated by ER [7]. The luminal B subtype was characterized by HER2 overexpression. These tumors were mostly sporadic and rarely expressed a basal marker.

Finally, we studied whether each basal marker was expressed exclusively by the tumors, or if its expression was associated with another basal marker. p63, P-CD, and CK5 are proteins that are expressed early in epithelial differentiation and may contribute to a committed stem cell and/or progenitor phenotype [3, 4, 9]. In this study, we thus confirmed the existence of heterogeneity among breast tumor cells since we observed different patterns of basal marker expression within luminal A, luminal B, basal-like HER2-overexpressing, and basal subtypes. Luminal A and luminal B subtypes were characterized by tumors that expressed exclusively one or two molecular markers, the majority being simultaneously negative. In contrast, the basal subtype rarely expressed just one basal marker but frequently expressed them simultaneously, which suggests a more undifferentiated profile. These pieces of evidence are in accordance with a hierarchy model of breast cancer oncogenesis that predicts functional heterogeneity among the cells that comprise the tumor [2, 8]. Malignant cells may have been derived from stem cells that were either able to differentiate to a mature estrogen-responsive stage (luminal tumors) or, due to a block in differentiation, stopped earlier in an immature stage (basal tumors). A basal-like HER2-overexpressing profile may represent an intermediary phenotype which failed the terminal differentiation of cells toward the luminal lineage due to a constitutive activation of HER2, an epidermal growth factor receptor (EGFR) family member [2].

With this work, we demonstrated that TMAs are an efficient and reliable platform for subclassifying breast cancers into relevant subtypes, using only a limited number of markers. Moreover, we showed that ER, HER2, P-CD, p63, and CK5 were important to characterize and distinguish basal-like breast tumors.

Acknowledgements This work was partially supported by grants from CAPES-Ministério da Educação-Brasil, BEX2448/02–5; Fundo de Apoio ao Ensino e Pesquisa (FAEP) da UNICAMP, 1294/02 and 238/04; and Fundação Luso Americana para o Desenvolvimento (FLAD), ref L-V-172/2002.

References

1. Abd El-Rehim DM, Pinder SE, Paish CE, Bell J, Blamey RW, Robertson JF, Nicholson RI, Ellis IO (2004) Expression of luminal and basal cytokeratins in human breast carcinoma. J Pathol 203:661–671
2. Birnbaum D, Bertucci F, Ginestier C, Tagett R, Jacquemier J, Charafe-Jauffret E (2004) Basal and luminal breast cancers: basic or luminous? Int J Oncol 25:249–258

3. Boecker W, Moll R, Poremba C, Holland R, Van Diest PJ, Dervan P, Burger H, Wai D, Ina DR, Brandt B, Herbst H, Schmidt A, Lerch MM, Buchwallow IB (2002) Common adult stem cells in the human breast give rise to glandular and myoepithelial cell lineages: a new cell biological concept. Lab Invest 82:737–746
4. Boecker W, Buerger H (2003) Evidence of progenitor cells of glandular and myoepithelial cell lineages in the human adult female breast epithelium: a new progenitor (adult stem) cell concept. Cell Prolif 36(Suppl 1):73–84
5. Breast Cancer Linkage Consortium (1997) Pathology of familial breast cancer: differences between breast cancers in carriers of BRCA1 or BRCA2 mutations and sporadic cases. Lancet 349:1505–1509
6. Breast Cancer Linkage Consortium (1998) Genetic heterogeneity and penetrance analysis of the BRCA1 and BRCA2 genes in breast cancer families. Am J Hum Genet 62:676–689
7. Callagy G, Cattaneo E, Daigo Y, Happerfield L, Bobrow LG, Pharoah PDP, Caldas C (2003) Molecular classification of breast carcinomas using tissue microarrays. Diagn Mol Pathol 12:27–34
8. Dick JE (2003) Breast cancer stem cells revealed. Proc Natl Acad Sci U S A 100:3547–3549
9. DiRenzo J, Signoretti S, Nakamura N, Rivera-Gonzalez R, Sellers W, Loda M, Brown M (2002) Growth factor requirements and basal phenotype of an immortalized mammary epithelial cell line. Cancer Res 62:89–98
10. Foulkes WD, Ingunn M, Stefansson S, Chappuis PO, Bégin LR, Goffin JR, Wong N, Trudel M, Asklen LA (2003) Germline BRCA1 mutations and a basal epithelial phenotype in breast cancer. J Natl Cancer Inst 95:1482–1485
11. Hoos A, Cordon-Cardo C (2001) Tissue microarray profiling of cancer specimens and cell lines: opportunities and limitations. Lab Invest 10:1331–1338
12. Kononem J, Bubendorf L, Kallioniemi A, Barlund M, Schraml P, Leighton S, Torhorst J, Mihatsch MJ, Sauter G, Kallioniemi OP (1998) Tissue microarrays for high-throughput molecular profiling of tumor specimens. Nat Med 4:844–847
13. Koster MI, Kim S, Mills AA, DeMayo FJ, Roop DR (2004) p63 is the molecular switch for initiation of an epithelial stratification program. Genes Dev 18:126–131
14. McKeon F (2004) p63 and the epithelial stem cell: more than status quo? Genes Dev 18:465–469
15. Nielsen TO, Hsu FD, Jensen K, Hu Z, Hernandez-Boussard T, Livasy C, Cowan D, Dressler L, Akslen LA, Regaz J, Gown AM, Gilks CB, van de Rijn M, Perou CM (2004) Immunohistochemical and clinical characterization of the basal-like subtype of invasive breast carcinoma. Clin Cancer Res 10: 5367–5374
16. Palacios J, Honrado E, Osorio A, Cazorla A, Sarrio D, Barroso A, Rodriguez S, Cigudosa JC, Diez O, Alonso C, Lerma E, Sanchez L, Rivas C, Benitez J (2003) Immunohistochemical characteristics defined by tissue microarray of hereditary breast cancer not attributable to BRCA1 or BRCA2 mutations: differences from breast carcinomas arising in BRCA1 and BRCA2 mutation carriers. Clin Cancer Res 9:3606–3614
17. Perou CM, Sorlie T, Eisen MB, van de Rijn M, Jeffrey SS, Rees CA, Pollack JR, Ross DT, Johnsen H, Akslen LA, Fluge O, Pergamenschikov A, Williams C, Zhu SX, Lonning PE, Borresen-Dale AL, Brown PO, Botstein D (2000) Molecular portraits of human breast tumours. Nature 406:747–752
18. Reis-Filho JS, Simpson PT, Martins A, Preto A, Gártner F, Schmitt FC (2003) Distribution of p63, cytokeratins 5/6 and 14 in 51 normal and 400 neoplastic human tissue samples using TARP-4 multi-tumor tissue microarray. Virchows Arch 443: 122–132
19. Reis-Filho JS, Milanezi F, Paredes J, Silva P, Pereira EM, Maeda SA, Carvalho LV, Schmitt FC (2003) Novel and classic myoepithelial/stem cell markers in metaplastic carcinomas of the breast. Appl Immunohistochem Mol Morphol 11:1–8
20. Skacel M, Skilton B, Pettay JD, Tubbs RR (2002) Tissue microarrays: a powerful tool for high-throughput analysis of clinical specimens. Appl Immunohistochem Mol Morphol 10: 1–6
21. Sorlie T, Perou CM, Tibshirani R, Aas T, Geisler S, Johnsen H, Hastie T, Eisen MB, Rijn MV, Jeffrey SS, Thorsen T, Quist H, Matese JC, Brown PO, Botstein D, Lonning PE, Borresen-Dale AL (2001) Gene expression patterns of breast carcinomas distinguish tumor subclasses with clinical implications. Proc Natl Acad Sci U S A 98:10859–10874
22. Sorlie T, Tibshirani R, Parker J, Hastie T, Marron JS, Nobel A, Deng S, Johnsen H, Pesich R, Geisler S, Demeter J, Perou CM, Lonning PE, Brown PO, Borresen-Dale AL, Botstein D (2003) Repeated observation of breast tumor subtypes in independent gene expression data sets. Proc Natl Acad Sci U S A 100:8418–8423
23. Turner N, Tutt A, Ashworth A (2004) Hallmarks of "BRCA-ness" in sporadic cancers. Nat Rev Cancer 4:1–6
24. van de Rijn M, Perou CM, Tibshirani R, Haas P, Kallioniemi O, Kononen J, Torhorst J, Sauter G, Zuber M, Köchli OR, Mross F, Dieterich H, Seitz R, Ross D, Botstein D, Brown P (2002) Expression of cytokeratins 17 and 5 identifies a group of breast carcinomas with poor clinical outcome. Am J Pathol 161:1991–1996
25. van 't Veer LJ, Dai H, van de Vijver MJ, He YD, Hart AA, Mao M, Peterse HL, van der Kooy K, Marton MJ, Witteveen AT, Schreiber GJ, Kerkhoven RM, Roberts C, Linsley PS, Bernards R, Friend SH (2002) Gene expression profiling predicts clinical outcome of breast cancer. Nature 415:530–536
26. Westfall MD, Pietenpol J (2004) p63: molecular complexity in development and cancer. Carcinogenesis 25:857–864

Virchows Arch (2005) 447: 695–700
DOI 10.1007/s00428-005-0003-6

ORIGINAL ARTICLE

Cristina Riva · Emanuele Dainese · Giacomo Caprara · Paolo Cossu Rocca · Giovanni Massarelli · Tibor Tot · Carlo Capella · Vincenzo Eusebi

Immunohistochemical study of androgen receptors in breast carcinoma. Evidence of their frequent expression in lobular carcinoma

Received: 14 March 2005 / Accepted: 16 May 2005 / Published online: 2 August 2005
© Springer-Verlag 2005

Abstract Androgens and androgen receptors (AR) are involved in the pathogenesis of breast cancer. Epidemiological studies have shown a significant association between the risk of breast cancer and androgens. However, the functional role and clinical value of AR expression in breast carcinoma have still not been clearly defined. The present study was set up to investigate the prevalence of ARs in a series of consecutive invasive breast carcinomas (IBCs) and to evaluate the patterns of AR phenotypes in a series of selected invasive lobular carcinomas (ILCs). Among the 250 consecutive IBCs (consisting of 212 ductal and 38 lobular neoplasms), AR immunoreactivity was observed in 151/250 (60.4%) cases, being expressed in 118/212 (56%) ductal and 33/38 (87%) lobular carcinomas (a statistically significant difference, χ^2=11.82). AR expression was frequently associated with ER (65.2%, χ^2=14.33) and PR positivity (66.9%, χ^2=7.36). Most AR positive cases showed a low proliferative index (63.7%) and a low or intermediate histological grade (G1–G2, 63.9%). Among the 80 selected ILCs, AR expression was observed in 64/80 (80%) cases. Our results confirm that ARs are expressed in most breast cancers. Moreover, we demonstrated that AR positivity is particularly marked in lobular neoplasms. In addition, AR positive carcinomas are frequently characterized by a low or intermediate grade, a low proliferative index and ER and/or PR co-expression.

Keywords Breast carcinoma · Lobular carcinoma · Androgen receptors

C. Riva (✉) · E. Dainese · C. Capella
Department of Human Morphology, Section of Pathology,
University of Insubria,
Varese, Italy
e-mail: cristina.riva@uninsubria.it
Tel.: +39-033-2264557
Fax: +39-033-2262313

G. Caprara · V. Eusebi
Section of Pathology M. Malpighi at Bellaria Hospital,
University of Bologna,
Bologna, Italy

P. C. Rocca · G. Massarelli
Institute of Pathology, University of Sassari,
Sassari, Italy

T. Tot
Department of Pathology and Clinical Cytology,
Central Hospital,
Falun, Sweden

Introduction

In the last two decades the molecular mechanisms related to the hormone dependence of breast tumours have been extensively investigated and the role of estrogen and progesterone receptors (ERs and PRs) in promoting breast cancer has been well documented [28]. It has been demonstrated that these hormone receptors are present in a large proportion of breast cancers, ranging from 50 to 80% of cases [30, 36, 39]. The prognostic value of ER and PR status in breast carcinoma in predicting a good response rate to hormone treatment has been well established [14, 28, 35]. In contrast, the clinical value and functional role of both androgen levels in circulating blood and AR expression in breast carcinomas are less well defined.

Epidemiological evidence of an association between breast cancer risk and androgens has been documented [8, 17, 27]. In particular, it has been observed that high serum testosterone levels can precede the occurrence of breast cancer in both premenopausal [27] and postmenopausal women [3]. However, the role played by androgens in the pathogenesis of breast cancer is not well understood; in particular, the mechanism by which testosterone exerts its proliferative or anti-proliferative effects on breast carcinomatous cells remains unclear [25].

Recent biochemical and immunohistochemical studies indicate that ARs are expressed in a considerable proportion of breast carcinomas, ranging from 35 to 90% of cases [9, 11, 19–22, 32]; in addition, a consistent co-expression of ARs, ERs and PRs has been demonstrated in the same breast cancers [19, 21]. In about 25% of breast cancer metastases, ARs are the sole sex steroid receptors observed

Table 1 Antibodies, methods and dilutions used in the current study

Antigen	Antibody	Autostainer	Dilution	Incubation time (min)	Antigen retrieval (min)
AR	AR27 (Novocastra)	Streptoavidin-DAB (Ventana)	1/20	32	24
ER	6F11 (Ventana)	Streptoavidin-DAB (Ventana)	Ready to use	28	16
PR	16 (Ventana)	Streptoavidin-DAB (Ventana)	Ready to use	24	16
Ki-67	MIB-1 (Dako)	Streptoavidin-DAB (Ventana)	1/100	32	16
E-cadherin	ECH-6 (Ventana)	Streptoavidin-DAB (Ventana)	Ready to use	32	16

AR Androgen receptor, *ER* estrogen receptor, *PR* progesterone receptor, *DAB* diaminobenzidine

in neoplastic cells [22]. ARs have also been detected in the majority of breast carcinomas in situ [28, 31], and their expression appeared to be unrelated to the degree of differentiation in ductal carcinomas in situ (DCIS) [31].

Some studies have focused on the pattern of AR expression in different histological subtypes of breast cancer but the majority of data refer only to ductal carcinomas [7, 28]. A strong, consistent AR positivity has been described both in in situ and in invasive apocrine carcinomas as well as in apocrine metaplasia and the intense expression of ARs was often accompanied by a lack of ER and PR immunoreactivity; AR positivity was therefore proposed as a specific marker of apocrine differentiation [15].In one series of invasive breast carcinomas [21], in which ARs were examined, only 14 lobular carcinomas were included; most of these showed an intense AR immunoreactivity.

The aim of the present study was to conduct an immunohistochemical investigation of the prevalence of ARs in a large series of consecutive breast carcinomas. In addition the patterns of AR phenotypes in a series of selected lobular carcinomas were evaluated. Finally, the AR status was matched with the following clinicopathological parameters: histological type, grade, proliferative index, ER and PR expression and stage of the tumours.

Materials and methods

A total of 330 cases of breast carcinomas were retrieved from the files of the pathology departments at the universities of Bologna, Sassari, Insubria-Varese (Italy) and Falun (Sweden).

This series included two subgroups:

1. Two hundred fifty invasive breast carcinomas (IBCs) consecutively collected during 2003;
2. Eighty selected invasive lobular carcinomas (ILCs).

Among the 250 consecutive IBCs, 28 cases (11.2%) were associated with an extensive carcinoma in situ component, represented by DCIS in 27 cases and lobular neoplasia (LN) in one case. Clinicopathological information about patient age, tumour site, size and local extension was obtained from patient records. The tumour stage was assessed according to the TNM sixth edition recommendations [37].

Formalin-fixed paraffin-embedded sections of tissues obtained from surgical samples were stained routinely with hematoxylin and eosin (H&E). Microscopic slides of all 330 cases were reviewed by two senior pathologists in order to assess histological type, according to the WHO criteria [33], and the grade, applying the Elston–Ellis score system [12]. Lobular carcinomas were graded G2 when classical and G3 when pleomorphic in type [13].Immunohistochemical stains for ARs, ERs, PRs and MIB-1 were applied in all cases; a stain for E-cadherin was applied to all lobular carcinomas (Table 1). Serial, 4-μm-thick, paraffin sections mounted on precoated slides were deparaffinized, hydrated in a graded alcohol series and incubated with primary antibodies using standardized automated procedures (Ventana).

Immunoreactivity was evaluated semiquantitatively as the percentage of positive cells in all the cases. Samples were considered positive for ARs, ERs and PRs when at least 10% of nuclei were immunoreactive, independently of the intensity of the immunostain; For ARs, we considered nuclear labeling in ≥10% neoplastic cells as the cut-off point for positivity, similar to standardized criteria used for other steroid hormone receptors [28]. The MIB-1 labeling index (LI) was calculated as a percentage of positive cells in at least 1,000 tumour cells and was scored as 'high' when the MIB-1 LI was ≥30% and 'low' when the MIB-1 LI was <30%. E-cadherin negativity reinforced the diagnosis of lobular carcinoma.

Table 2 Anatomo-clinical correlation

Series	Histotype	No. of cases	Age (mean)	T1	T2	T3	T4
Consecutive series	IDC	212 (84.8%)	65	116 (54.7%)	51 (24%)	23 (10.8%)	22 (10.3%)
	ILC	38 (15.2%)	64.7	16 (42.1%)	13 (34.2%)	7 (18.4%)	2 (5.2%)
	Total	250		132	64	30	24
Selected series	ILC	80	63.5	41 (51.2%)	28 (35%)	9 (11.2%)	2 (2.5%)

IDC Invasive duct carcinoma, *ILC* invasive lobular carcinoma

Positive controls included normal breast tissue that surrounded the neoplastic lesion (for all antibodies) and normal prostatic tissue (for ARs). Negative controls included the omission of primary antibodies.

All the immunoreactions were separately evaluated by two senior pathologists.

The statistical significance of the results was tested using the chi-square and the Fisher exact tests.

Results

Clinicopathological results

The consecutive series of 250 IBCs included 249 female patients and one male patient. There were 212 invasive ductal carcinomas (IDCs) (84.8%) and 38 invasive lobular carcinoma (ILCs) (15.2%). The age of the patients ranged from 34 to 96 years (mean age 64.9) (Table 2). Among the IDCs, 21 (10%) were well-differentiated (G1), 123 (58%) moderately differentiated (G2) and 68 (32%) poorly differentiated (G3) tumors. Among the ILCs, 27 were G2 (71%) and 11 G3 (29%) neoplasms.

The selected series of 80 ILCs included only female patients whose age ranged from 37 to 86 years (mean age 63.5). Among these cases, 60 (75%) were G2 and 20 (25%) G3 tumors. All relevant clinicopathological data are reported in Tables 2 and 3.

Immunohistochemical results

The immunohistochemical analysis of the consecutive IBCs revealed AR positivity in 151 out of 250 cases (60.4%). The data are reported in Table 3. AR immunoreactivity was observed more frequently in grade 1 and 2 carcinomas (110/172, 63.9%) than in grade 3 carcinomas (41/78, 52.5%). Looking at the tumour stage, ARs were observed in 78/132 (59%) T1 tumors and in 73/128 (61.8%) T2–T3–T4 tumors. AR positivity was observed in 121/190 cases (63.7%) in association with a low MIB-1 LI, whereas half of the cases with a high MIB-1 LI (30/60, 50%) were AR negative. AR immunoreactivity was expressed in 118/212 cases (56%) of IDCs and in 33/38 cases (87%) of ICLs (Table 2). The number of AR positive cells ranged from 10 to 100%, with a mean of 50.2%, in IDCs, and from 30 to 90%, with a mean of 62.4%, in ILCs. The intensity of AR immunoreactivity was generally proportionate to the percentage of positive cells.

There were 216 ER positive cases (86.4%), 141 of which (65.2%) were also AR immunoreactive. Ten ER negative carcinomas (29.4%) showed AR expression. In addition, 109 out of 163 PR positive carcinomas (66.9%) also displayed AR positivity, while 42 out of 87 PR negative carcinomas (48.2%) showed AR immunoreactivity.

Table 3 Grade and immunohistochemistry in 250 consecutive ductal (IDC) and lobular (ILC) carcinomas

	IDC (212 cases)	ILC (38 cases)
G1	21 (10%)	0
G2	124 (58%)	27 (71%)
G3	67 (32%)	11 (29%)
AR+	118 (56%)	33 (87%)
AR−	94 (44%)	5 (13%)
ER+	180 (85%)	36 (95%)
ER−	32 (15%)	2 (5%)
PR+	137 (65%)	26 (68%)
PR−	75 (35%)	12 (32%)
MIB-1+	56 (26%)	4 (11%)
MIB-1−	156 (74%)	34 (89%)

AR Androgen receptor, *ER* estrogen receptor, *PR* progesterone receptor; *G1*, *G2*, *G3* grade of tumour differentiation

Table 4 Number of ductal (IDC) and lobular (ILC) carcinomas among consecutive series of 250 IBCs with androgen receptor (AR) positivity and lack of immunoreactivity for estrogen receptor (ER) and progesterone receptor (PR) according to degree of differentiation (G2, G3)

	ER−/PR−
AR+IDC G2	4/12 (33.3%)
AR+IDC G3	3/18 (16.6%)
AR+ILC G2	3/3 (100%)
AR+ILC G3	2/3 (66.6%)

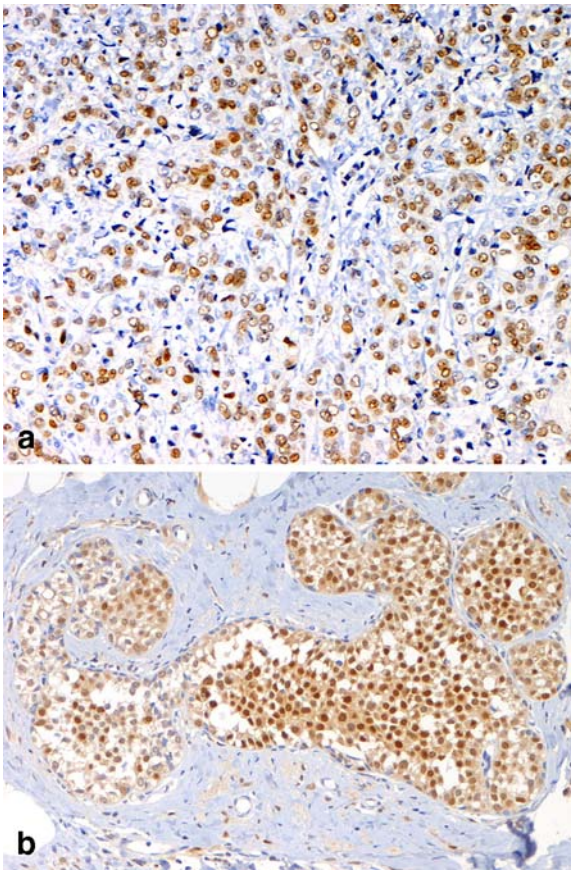


Fig. 1 Lobular carcinoma showing intense AR immunoreactivity both in invasive (**a**) and in situ component (**b**) (DAB-H, 200×)

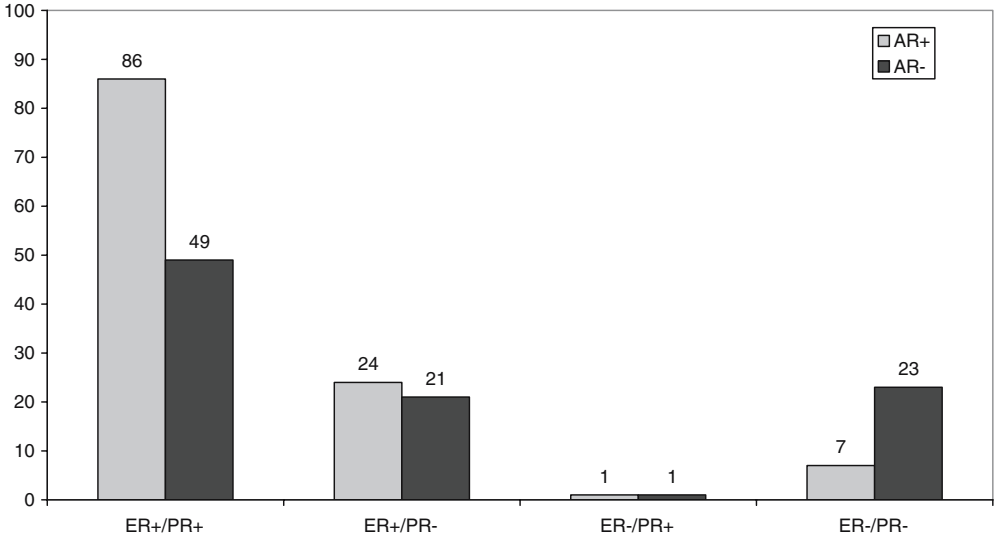


Fig. 2 Comparison of androgen receptor (*AR*) expression and simultaneous estrogen receptor (*ER*) and progesterone receptor (*PR*) immunoreactivity in 212 invasive ductal carcinomas (IDC) consecutively collected

Twelve out of 36 (33.3%) tumors, negative for both ER and PR, were AR-immunoreactive; in these cases, the number of AR positive cells ranged from 15 to 90% with a mean of 60.4%. The distribution of grade in AR+/ER−PR− is shown in Table 4. Twenty-three cases (9.2%) were negative for all hormone receptors tested; all these negative cases were IDCs.

The IDC cases showing a DCIS component revealed AR positivity in both the invasive and in the in situ components in 18 out of 27 (66.6%) cases. In such cases the proportion of AR positive tumor cells in DCIS was usually lower than that observed in invasive areas. Six out of 27 (22.2%) carcinomas expressed ARs in only the invasive component, whereas three cases were negative in both the in situ and in the invasive areas. The only case with lobular neoplasia associated with ILC showed strong AR positivity in both components (Fig. 1a,b).

In the selected series of ILCs, AR immunoreactivity was observed in 64 out of 80 cases (80%). AR expression was present in 51 (85%) cases of classical ILC (G2) and in 12 (65%) pleomorphic ILC (G3). AR immunoreactivity was detected in 34/41 (83%) T1 ILC and in 30/39 (77%) T2–T3–T4 ILC.

ERs and PRs were expressed in 56/64 (87.5%) and 48/64 (75%) of AR positive ILCs, respectively; only one case (1.2%) was negative for AR, ER and PR.

Statistical analysis of all the data showed a significant association between:

1. AR expression and lobular histotype in the series of 250 consecutive IBCs (χ^2=11.82).
2. ER and AR positive status (χ^2=14.33) in the consecutive series.
3. PR and AR positive status (χ^2=7.36) in the consecutive series.

None of the other parameters considered, including grade (χ^2=3.55), stage (χ^2=0.09) and proliferative index

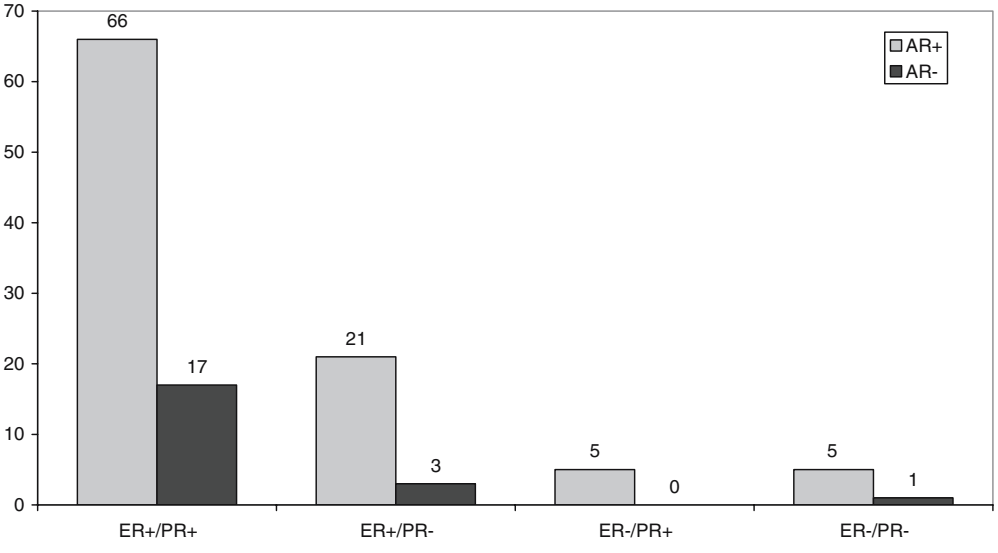


Fig. 3 Comparison of androgen receptor (*AR*) expression and simultaneous estrogen receptor (*ER*) and progesterone receptor (*PR*) immunoreactivity in 118 invasive lobular carcinomas (80 selected and 38 consecutive ILC)

(χ^2=3.02), showed a significant correlation with AR immunoreactivity.

In the series of 80 selected ILCs, no significant association was found between AR expression and other parameters such as hormonal status, proliferative index, grade, stage and age.

Discussion

Numerous studies have demonstrated the role of estrogen (ER) and/or progesterone (PR) receptors as strong predictors of a good response rate to hormone therapy and chemotherapy in the management of patients with breast carcinoma [2, 18]. However, the clinical significance and functional role of androgen levels and of androgen receptor (AR) expression in breast cancer has not been well defined.

There is evidence that androgens can directly stimulate the growth of human breast cancer cell lines [26]. Various studies that were conducted to establish the levels of adrenal and ovarian androgens in breast cancer patients have led to conflicting data [4, 41]. An Italian perspective investigation enrolling a large cohort of premenopausal and postmenopausal women from the province of Varese demonstrated the relationship between invasive breast cancer and preoperative high serum androgen levels in both premenopausal [27] and postmenopausal women [3].

AR is a member of the larger nuclear receptor family that mediates the biological functions of androgens [6]. Some biochemical and immunohistochemical data have indicated the presence of AR in breast cancer tissue. In particular, recent studies show that AR is expressed in a considerable proportion of breast cancers, ranging from 35 to 70% of cases [5, 19, 20, 28, 32]. The results of our study appear support these findings; in fact, we found AR expression in a high percentage (60.4%) of a large series of 250 consecutive IBCs. These data suggest that ARs are involved in the pathogenesis of at least a subset of breast carcinomas.

Moreover, our study showed a strong widespread AR positivity in the majority of lobular carcinomas (87%) and the difference of expression between lobular and ductal carcinomas was statistically significant.

Similar results were obtained in the series of selected lobular carcinomas that showed AR immunoreactivity in 80% of the cases, confirming that a frequent, widespread, intense AR expression seems to be a distinctive feature of invasive lobular carcinomas.

The present immunohistochemical analysis of the hormone status of 250 IBCs indicated a statistically significant positive correlation between AR and ER expression (χ^2= 14.33) as well as a statistically significant co-expression of AR and PR (χ^2=7.36). These data concur fully with those reported in previous studies [11, 19, 21].

Most AR positive carcinomas in our series were associated with a low or intermediate histological grade (G1–G2, 66%) and a low proliferative index (80%); this association reflects that of the majority of ER and PR positive IBCs [29].

Furthermore, our study demonstrated that most ILCs are characterized by a generally low proliferative index and high ER, PR and AR expression. This steroid receptor pattern clearly suggests a hormonal involvement in the pathogenesis of ILCs [10, 23, 24, 38].

An interesting result obtained in our study was the isolated AR positivity found in a subset of ER and PR negative IDCs (7/30 cases) (Fig. 2) and ILCs (5/6 cases) (Fig. 3). This hormonal pattern (ER−, PR−, AR+) did not show any correlation with tumor grade (Table 3), in either ductal or lobular histotypes. This is in contrast with the results reported in recent studies [1, 28] in which AR expression was detected in a subset of G3 ER/PR negative IBCs.

The efficacy of response to endocrine treatment is generally correlated with ER and PR positivity of tumors, but not with AR expression [40]. In this context, it must be recalled that a previous study [16] has shown that medroxyprogesterone acetate (MPA), a synthetic progestin, inhibits the proliferation of ER and PR negative cancer cell lines via androgen receptors. Moreover, in a group of women with metastatic breast cancer, a good response determined by the AR, but not PR levels was seen after a high dose treatment using megestrol acetate, another synthetic progestin [34]. Thus, the detection of AR in a small subset of ER and PR negative tumors, especially in infiltrating lobular carcinomas may indicate new endocrine therapeutic strategies in women who would not fully benefit from conventional, mainly anti-estrogen based, hormonal treatment.

In conclusion, our study confirms that ARs are expressed in most breast cancers. In addition, we demonstrated that AR positivity is a common feature of invasive lobular carcinomas. AR positive tumors are frequently characterized by ER and/or PR co-expression and by a low grade and a low proliferative index.

The potential role and the impact of ARs in breast carcinoma needs further study; however, ARs are a potential new target for hormonal therapies and they may be clinically useful predictors.

Acknowledgements This work was supported by grant no. 2002064975 (COFIN 2002) from the Ministry of University and Research (MIUR).

References

1. Agoff SN, Swanson PE, Linden H, Hawes SE, Lawton TJ (2003) Androgen receptor expression in estrogen receptor-negative breast cancer. Immunohistochemical, clinical, and prognostic associations. Am J Clin Pathol 120:725–731
2. Barnes DM, Hanby AM (2001) Oestrogen and progesterone receptors in breast cancer: past, present and future. Histopathology 38:271–274
3. Berrino F, Muti P, Micheli A, Bolelli G, Krogh V, Sciajno R, Pisani P, Panico S, Secreto G (1996) Serum sex hormone levels after menopause and subsequent breast cancer. J Natl Cancer Inst 88:291–296
4. Berstein L, Ross RK (1993) Endogenous hormones and breast cancer risk. Epidemiol Rev 15:48–65

5. Birrell SN, Hall RE, Tilley WD (1998) Role of the androgen receptor in human breast cancer. J Mammary Biol Neoplasia 3:95–103
6. Brinkmann AO, Blok LJ, de Ruiter PE, Doesburg P, Steketee K, Berrevoets CA, Trapman J (1999) Mechanism of androgen receptor activation and function. J Steroid Biochem Mol Biol 69:307–313
7. Brys M, Wojcik M, Romanowicz-Makowska H, Krajewska WM (2002) Androgen receptor status in female breast cancer: RT-PCR and Western blot studies. J Cancer Res Clin Oncol 128:85–90
8. Cauley JA, Lucas FL, Kuller LH, Stone K, Browner W, Cummings SR (1999) Elevated serum estradiol and testosterone concentrations are associated with a high risk for breast cancer. Ann Intern Med 130:270–277
9. Collett K, Maehle BO, Skjarven R (1996) Prognostic role of oestrogen, progesterone and androgen receptor in relation to patient age in patients with breast cancer. Breast 5:123–126
10. Daling JR, Malone KE, Doody DR, Voigt LF, Bernstein L, Coates RJ, Marchbanks PA, Norman SA, Weiss LK, Ursin G, Berlin JA, Burkman RT, Deapen D, Folger SG, McDonald JA, Simon MS, Strom BL, Wingo PA, Spirtas R (2002) Relation of regimens of combined hormone replacement therapy to lobular, ductal, and other histologic types of breast carcinoma. Cancer 95:2455–2464
11. Ellis LM, Wittliff L, Bryant MS (1989) Correlation of estrogen, progesterone and androgen receptors in breast cancer. Am J Surg 157:577–581
12. Elston CW, Ellis IO (1991) Pathological prognostic factors in breast cancer. I. The value of histological grade in breast cancer: experience from a large study with long-term follow-up. Histopathology 19:403–410
13. Eusebi V, Magalhaes F, Azzopardi JG (1992) Pleomorphic lobular carcinoma of the breast: an aggressive tumor showing apocrine differentiation. Human Pathol 23:655–662
14. Foekens JA, Portensen H, Van Putten WLJ (1989) Prognostic value of estrogen and progesterone receptors measured by enzyme immunoassay in human breast tumor cytosols. Cancer Res 49:5823–5828
15. Gatalica Z (1997) Immunohistochemical analysis of apocrine breast lesions. Consistent over-expression of androgen receptor accompanied by the loss of estrogen and progesterone receptors in apocrine metaplasia and apocrine carcinoma in situ. Pathol Res Pract 193:753–758
16. Hackenberg R, Hawighorst T, Filmer A, Nia AH, Schulz KD (1993) Medroxyprogesterone acetate inhibits the proliferation of estrogen- and progesterone-receptor negative MFM-223 human mammary cancer cells via androgen receptor. Breast Cancer Res Treat 25:217–224
17. Hankinson SE, Willett WC, Manson JE, Colditz GA, Hunter DJ, Spiegelman D, Barbieri RL, Speizer FE (1998) Plasma sex steroid hormone levels and risk of breast cancer in postmenopausal women. J Natl Cancer Inst 90:1292–1299
18. Hawkins RA, Roberts MM, Forrest AP (1980) Oestrogen receptors and breast cancer: current status. Br J Surg 67:162–165
19. Isola JJ (1993) Immunohistochemical demonstration of androgen receptor in breast cancer and its relationship to other prognostic factors. J Pathol 170:31–35
20. Kimura N, Mizokami A, Oonuma T, Sasano H, Natura H (1993) Immunocytochemical localization of androgen receptor with polyclonal antibody in paraffin-embedded human tissue. J Histochem Cytochem 41:671–678
21. Kuenen-Boumeester V, Vanderkwast TH, Van Putten WLJ, Claassen C, Vanooijen B, Henzenlogmans SC (1992) Immunohistochemical determination of androgen receptors in relation to oestrogen and progesterone receptors in female breast cancer. Int J Cancer 52:581–584
22. Lea OA, Kvinnsland S, Thorsen T (1989) Improved measurement of androgen receptors in human breast cancer. Cancer Res 49:7162–7167
23. Li CI, Malone KE, Porter PL, Weiss NS, Tang MT, Cushing-Haugen KL, Daling JR (2003) Relationship between long durations and different regimens of hormone therapy and risk of breast cancer. JAMA 289:3254–3263
24. Li CI, Weiss NS, Stanford JL, Daling JR (2000) Hormone replacement therapy in relation to risk of lobular and ductal breast carcinoma in middle-aged women. Cancer 88:2570–2577
25. Lillie E, Bernstein L, Ursin G (2003) The role of androgens and polymorphisms in the androgen receptor in the epidemiology of breast cancer. Breast Cancer Res 5:164–173
26. Lippman M, Bolan G, Huff K (1976) The effects of androgens and antiandrogens on hormone-responsive human breast cancer in long-term tissue culture. Cancer Res 36:4610–4618
27. Micheli A, Muti P, Secreto G, Krogh V, Meneghini E, Venturelli E, Sieri S, Pala V, Berrino F (2004) Endogenous sex hormones and subsequent breast cancer in premenopausal women. Int J Cancer 112:312–318
28. Moinfar F, Okcu M, Tsybrovskyy O, Regitnig P, Lax SF, Weybora W, Ratschek M, Tavassoli FA, Denk H (2003) Androgen receptors frequently are expressed in breast carcinomas. Cancer 98:703–711
29. Nishizaki T, Chew K, Chu L, Isola J, Kallioniemi A, Weidner N, Waldman FM (1997) Genetic alterations in lobular breast cancer by comparative genomic hybridization. Int J Cancer 74:513–517
30. Pichon MF, Broet P, Magdelenat H, Delarue JC, Spyratos F, Basuyan JP, Saez S, Rallet A, Courriere P, Millon R, Asselain B (1996) Prognostic value of steroid receptors after long term follow-up of 2257 operable breast cancers. Br J Cancer 73: 1545–1551
31. Selim A, El-Ayat G, Wells A (2002) Androgen receptor expression in ductal carcinoma in situ of the breast: relation to oestrogen and progesterone receptors. J Clin Pathol 55:14–16
32. Soreide JA, Lea OA, Varhaug JE, Skarstein A, Kvinnsland S (1992) Androgen receptors in operable breast cancer: relation to other steroid hormone receptors, correlation to prognostic factors and predictive value for effect of adjuvant tamoxifen treatment. Eur J Surg Oncol 18:112–118
33. Tavassoli FA, Devilee P (eds) (2003) Pathology and genetics of tumours of the breast and female genital organs. World Health Organization Classification of Tumors. IARC Press, Lyon
34. Teulings FA, van Gilse HA, Henkelman MS, Portensen H, Alexieva-Figusch J (1980) Estrogen, androgen, glucocorticoid, and progesterone receptors in progestin-induced regression of human breast cancer. Cancer Res 40:2557–2561
35. Thorpe SM (1988) Estrogen and progesterone receptor determinations in breast cancer. Acta Oncol 27:1–18
36. Thorpe SM, Rose C (1986) Oestrogen and progesterone receptor determination in breast cancer; technology and biology. Cancer Surv 5:505–525
37. TNM Classification of Malignant Tumours, Sixth Edition (2002)
38. Verkooijen HM, Fioretta G, Vlastos G, Morabia A, Schubert H, Sappino AP, Pelte MF, Schafer P, Kurtz J, Bouchardy C (2003) Important increase of invasive lobular breast cancer incidence in Geneva, Switzerland. Int J Cancer 104:778–781
39. Wenger CR, Beardslee S, Owens MA, Pounds G, Oldaker T, Vendely P, Pandian MR, Harrington D, Clark GM, Mc Guire WL (1993) DNA-ploidy, S-phase, and steroid receptors in more than 127,000 breast cancer patients. Breast Cancer Res Treat 28:9–26
40. Wittliff JL (1984) Steroid-hormone receptors in breast cancer. Cancer 53:630–643
41. Zumoff B, Levin J, Rosenfeld RS, Markham M, Strain GW, Fukushima DK (1981) Abnormal 24-h mean plasma concentrations of dehydroisoandrosterone and dehydroisoandrosterone sulfate in women with primary operable breast cancer. Cancer Res 41:3360–3363

Virchows Arch (2005) 447: 701–709
DOI 10.1007/s00428-005-0002-7

ORIGINAL ARTICLE

Wafaey Gomaa · Youqiang Ke · Hiroshi Fujii · Timothy Helliwell

Tissue microarray of head and neck squamous carcinoma: validation of the methodology for the study of cutaneous fatty acid-binding protein, vascular endothelial growth factor, involucrin and Ki-67

Received: 20 January 2005 / Accepted: 16 May 2005 / Published online: 13 July 2005
© Springer-Verlag 2005

Abstract Tissue microarrays allow the simultaneous analysis of many tumours using small-diameter cores sampled from larger blocks of tissue, but may be limited by tumour heterogeneity. This study considers the validation of tissue microarray for the study of four molecules of interest as prognostic factors in head and neck squamous carcinoma, including a consideration of methods for assessing immunocytochemical scoring of microarrays. Tissue microarray blocks were constructed from 100 cases of head and neck squamous carcinoma, taking four cores from different areas of each tumour. Immunocytochemical labelling was performed for cutaneous fatty acid binding protein, involucrin, vascular endothelial growth factor and Ki-67. The extent and intensity of scoring was determined for each core and the degree of agreement determined for results from the assessment of two, three or four cores for each carcinoma. In a subset of 30 representative cases, the labelling in the tissue microarrays was compared with that in whole-tissue sections of the same carcinomas. An adequate sample of carcinoma was achieved in more than 90% of the 400 cores; unsuccessful results were attributed to uneven core alignment or to poor targeting of the tumour tissue in the donor blocks. The degree of agreement in the assessment of extent and intensity of labelling was moderate to good (weighted kappa, range 0.479–0.902) between whole-tissue sections and microarray sections depending on the antigen and the scoring system. Tissue microarray is a reliable tool to demonstrate cellular and molecular alterations in head and neck squamous carcinomas. We recommend using the mean results from four cores for biological studies, with analysis of categorical data based on quartile groups. Concordance with whole-tissue section data is reassuring, but data from microarrays need to be validated against clinical outcomes.

Keywords Head and neck squamous carcinoma · Tissue microarray · Validation · Immunocytochemistry · Cutaneous fatty acid binding protein · Proliferation

W. Gomaa · Y. Ke · H. Fujii · T. Helliwell (✉)
Department of Pathology,
University of Liverpool,
Duncan Building, Daulby Street,
Liverpool, L69 3GA, UK
e-mail: trh@liv.ac.uk
Tel.: +44-151-7064492
Fax: +44-151-7065859

H. Fujii
Department of Biochemistry,
University of Niigata Medical School,
Niigata, 951, Japan

Introduction

Tissue microarray (TMA) technology has been developed to address the limitations of conventional histopathological techniques and to facilitate genome-scale molecular pathology studies linking novel genes with clinical end points [20, 26]. TMA is a purely mechanical technique, which involves taking tissue cores from multiple donor blocks with precise insertion (arraying) into an empty 'recipient' block [13]. Each core provides two to three high-power microscopic fields for assessment, approximately 0.05% of the area of a section from a conventional wax block of tissue [3, 32]. Potential problems with the use of TMAs in molecular pathological studies include technical aspects of TMA preparation, targeting of tumour tissue and the extent to which TMA cores are representative of a whole tumour because of tissue heterogeneity, particularly in epithelial tumours [1]. Discrepancies between data from arrays and full sections may bias clinicopathological correlations [15], although it is uncertain which method is more appropriate, and this may be a minor concern if the focus of the study is the expression profiles of tumour populations under standardized experimental conditions rather than individual cases [23, 34, 37].

Validation studies have compared TMA discs and whole-tissue sections to consider the number of cores required to adequately represent the expression of the antigen [17,

19]. Sampling typical and representative regions of each tumour is the key step in TMA construction [41], and punching multiple sites from each original block is recommended to compensate for tumour heterogeneity [30]. In breast carcinomas, two 0.6-mm-diameter cores accurately represent 95% of whole-tissue section specimens [3], although one core may be sufficient to derive most of the information on oestrogen receptor expression [20]. A high concordance between whole-tissue sections and TMA sections when using three cores was achieved in immunocytochemical studies on fibroblastic tumours [17].

Head and neck carcinomas are relatively uncommon, although oral carcinomas account for 2.6% of all malignancies worldwide and, like carcinoma of the larynx, are particularly common in Europe and south and west Asia [27]. In England, head and neck carcinomas are most common in the northwest of the country, with a prevalence of 13.7 per 100,000 [2]. Heterogeneous protein expression in head and neck squamous carcinomas has been described [36], but the optimal strategy to describe this phenomenon and its clinical significance are uncertain. Few studies describe the validation of the technical aspects of TMAs in head and neck squamous carcinomas [5, 12], and some studies have validated against clinical outcomes rather than whole-tissue sections data [9, 10].

As part of a study of mechanisms involved in cell proliferation and angiogenesis in head and neck squamous carcinomas, we have constructed TMAs to investigate the expression of a range of molecules. Cutaneous fatty acid binding protein (C-FABP) is one of the family of small intracellular fatty acid-binding proteins that bind growth regulatory ligands and modulate cellular differentiation, growth and metabolic pathways [6, 42]. C-FABP is associated with differentiating keratinocytes and is strongly expressed in cutaneous squamous carcinomas but not in basal cell carcinomas [38]. C-FABP expression is associated with metastatic behaviour and expression of vascular endothelial growth factor (VEGF) in prostatic adenocarcinomas [18]. VEGF is also closely associated with angiogenesis in head and neck squamous carcinomas [31].

This paper describes the validation of TMA data on the immunocytochemical expression in squamous carcinomas of C-FABP, VEGF and Ki-67, as a marker of proliferation, and involucrin, as a marker of squamous differentiation [39]. Issues related to the number of cores that are needed to minimise problems of heterogeneity and the scoring of results are considered.

Materials and methods

Paraffin wax blocks from 100 cases of head and neck squamous carcinomas were retrieved from the archives in the Department of Pathology at the University of Liverpool, UK. The cases were received between 1993 and 2000 and all patients gave consent for the storage and use of their tissue for research as part of the Cancer Tissue Bank Research Centre. The study was approved by the Liverpool Research Ethics Committee. The mean age of the patients at surgery was 60 years (range 32–88) and 91 patients were male. The primary sites of the carcinomas were oral cavity (n=27), pharynx (n=30), and larynx (n=43). Tumour size according to the TNM classification [35] was T1 (n=10), T2 (n=23), T3 (n=12) and T4 (n=55). Ninety-one percent of the carcinomas were keratinizing, with a range of grades: grade I (n=24), grade II (n=36) and grade III (n=40).

Whole-tissue sections from tumour blocks of a subset of 30 cases were compared with the corresponding TMA discs. The cases were selected to include 10 cases of each grade. The clinicopathological data of these cases were very similar to those of the whole series (not shown).

Tissue microarray construction

Haematoxylin and eosin-stained sections of primary tumours were reviewed, and areas of tumour and normal tissue were marked on the slides, avoiding areas of necrosis and keratin pools. Where possible (63% of the cases), two donor blocks of each carcinoma were used, but for the other cases, only one donor block was available. Two tissue cores, each 0.6 mm in diameter, were placed into each of two recipient paraffin blocks using a manual tissue microarrayer (Beecher Instruments, Silver Spring, MD, USA). Normal liver, kidney, intestine and pancreas were used for orientation. Cores were spaced at intervals of 1 mm in the x- and y-axes. Sections (5 μm thick) were placed on precoated adhesive slides, left to dry at 37°C overnight, immersed in molten paraffin and stored in the dark to protect from oxidation. One section from each TMA block was

Table 1 Antibodies used

Antibody	Source	Clone and code	Dilution	Pretreatment	Positive control
C-FABP	Iwaki Glass Corporation, Japan	Polyclonal	1:1,000	None	Normal tongue squamous epithelium
Involucrin	Santa Cruz Biotechnology	Monoclonal involucrin (SY5): sc-21748	1:400	None	Normal squamous epithelium adjacent to carcinoma
VEGF	Santa Cruz Biotechnology	Monoclonal VEGF (C-1): sc-7269	1:100	None	Normal kidney and breast carcinoma
Ki-67	Novocastra	Monoclonal NCL-Ki-67-MM1	1:200	Pressure cooker with EDTA (pH 7.0)	Palatine tonsil

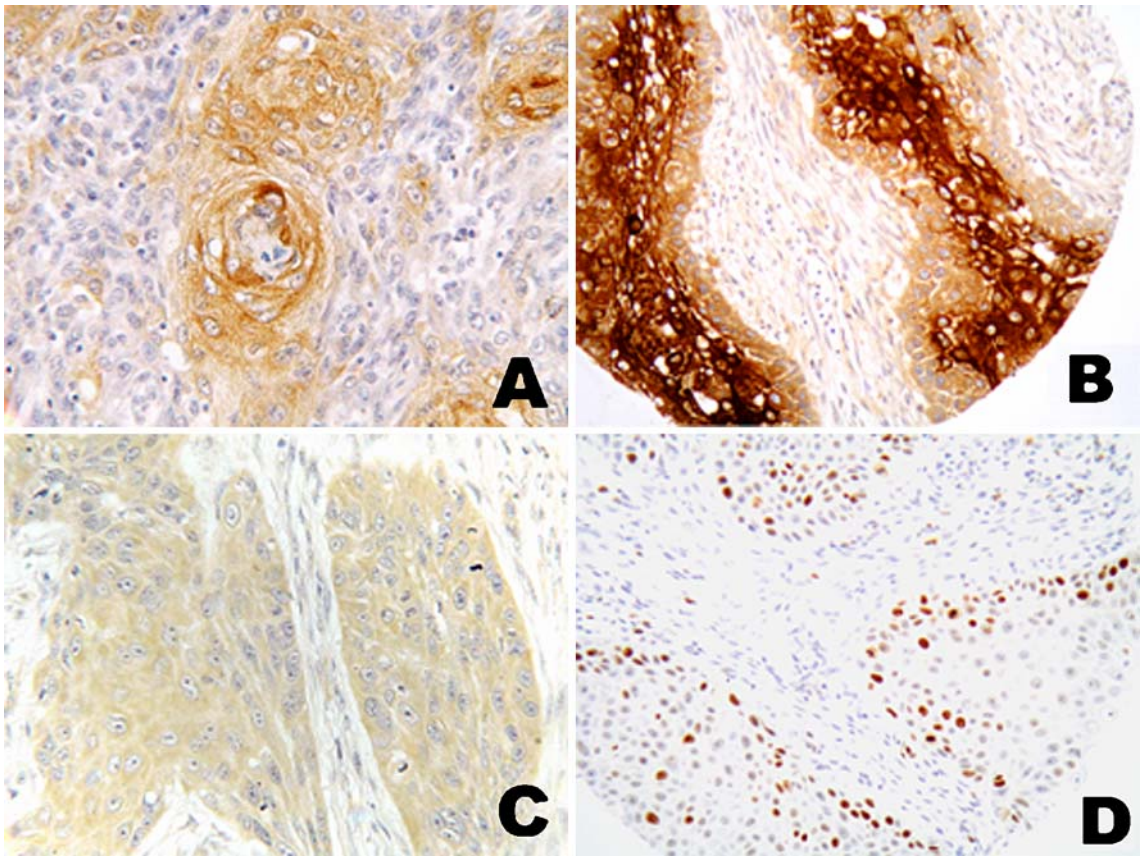


Fig. 1 **a** Cytoplasmic expression of C-FABP is stronger in keratinizing cells. **b** Strong cytoplasmic expression of involucrin is present in most cells in a well-differentiated carcinoma. **c** Cytoplasmic expression of VEGF in carcinoma cells. **d** Nuclear expression with Ki-67 is more frequent in cells at the edges of the islands of carcinoma cells. Immunocytochemical labelling using the primary antibodies stated, with diaminobenzidine as the chromogen and haematoxylin counterstain

stained with haematoxylin and eosin for morphological assessment.

Immunocytochemistry

Immunocytochemistry was performed using antibodies to C-FABP, involucrin, Ki-67 and VEGF (Table 1) and the Dako ChemMate Envision HRP detection Kit (code no. K5007). This is a two-step immunocytochemical staining technique using a polymeric horseradish peroxidase-labelled conjugate. TMA sections on slides previously immersed in molten paraffin were placed in xylene for 1 h. Thereafter, whole-tissue sections and TMA sections were treated identically. Sections were deparaffinized in xylene and rehydrated in industrial methylated spirits, and endogenous peroxidase activity was blocked with H_2O_2/methanol. Sections were pre-treated as indicated (Table 1) and incubated on a Dako autostainer with the primary antibody for 40 min, followed by the labelled polymer for 30 min and ChemMate DAB+ chromogen for 20 min. Slides were washed and counterstained with Mayer's haematoxylin. Negative control slides were prepared by substituting Dako ChemMate antibody diluent for primary antibody. Positive control sections were included (Table 1).

Table 2 Percentage cells showing immunocytochemical labelling for each antibody

	C-FABP		Involucrin		VEGF		Ki-67	
	W	T	W	T	W	T	W	T
Mean	15.7	17.6	46.2	45.3	24.2	22.2	15.5	19.3
SEM	3.5	3.4	5.5	5.8	3.9	2.6	1.9	1.8
SD	19.3	18.4	30.1	31.7	21.7	14.3	10.6	10.3
Percentiles								
25	0.5	5.5	18.9	18.9	5.4	12.1	7.6	12.3
50	8.4	14.1	41.0	33.1	18.0	21.4	13.3	19.7
75	26.6	21.3	75.0	70.4	38.3	32.2	19.4	23.7

W whole-tissue section data, *T* TMA section data

Table 3 Number of cases falling into specified assessment groups for 30 cases assessed by both whole-tissue sections and TMA

Category	C-FABP		Involucrin		VEGF		Ki-67	
	T	W	T	W	T	W	T	W
5-Point scale of extent (% cells) of expression (see text for details)								
1	15	10	2	2	10	6	8	6
2	7	13	7	8	9	12	16	18
3	6	5	9	7	8	11	6	6
4	1	1	7	7	3	1	0	0
5	1	1	5	6	0	0	0	0
Quartile scale of extent (%) of expression (see text for details)								
1	7	8	7	7	7	7	7	7
2	8	7	8	8	9	8	8	8
3	8	8	10	8	7	8	8	8
4	7	7	5	7	7	7	7	7
4-Point scale of staining intensity								
0	6	1	0	0	2	1	0	0
1	8	10	0	1	11	7	9	4
2	12	16	6	6	17	22	14	17
3	4	3	24	23	0	0	7	9

T Results from TMA sections, *W* results from whole-tissue section analysis

Scoring of immunocytochemistry

A disc was considered unsuccessful for analysis if it was completely absent, it contained no tumour tissue at all (sampling error), or it contained too few tumour cells (<10%) for analysis (uninformative). One observer (W.G.) scored all of the sections on two separate occasions. The percentage of tumour cells that were positive for each antibody was assessed at ×200 magnification, guided by a square lattice, eyepiece graticule. Intensity of labelling was categorized as negative (0), weak (1), moderate (2), and strong (3), where strong intensity was seen at ×40, moderate when staining is evident at ×200 and weak staining is evident only at ×400. Each informative disc from each tumour was scored and the mean values calculated. Ten fields (×200 magnification) were randomly selected from each of the whole-tissue sections and assessed as above.

Statistical analysis

Non-parametric correlation (Spearman's rho coefficient; SPSS Release 12.0.1) was used to compare data from whole-tissue sections and discs and to relate the mean scores obtained from four discs to the scores obtained from individual discs, the mean scores of two discs and the mean scores of three discs.

For categorical analysis, the data on percent labelling were grouped in two ways: an arbitrary 5-point scale where 0–10%=1, 10–25%=2, 25–50%=3, 50–75%=4, and 75–100%=5; and an unbiased, 4-point quartile scale where the groups were separated at the 25th, 50th and 75th centiles. The degree of agreement between data from whole-tissue sections and the mean of four discs was assessed using weighted Cohen's kappa coefficient (SAS for Windows, release 8.02). For descriptive purposes, kappa <0.4 represents poor-to-fair agreement, 0.4–0.6 moderate agreement, 0.6–0.8 substantial agreement, and >0.8 almost perfect agreement [21].

Results

Cutaneous fatty acid binding protein is expressed in the cytoplasm and/or the nuclei of carcinoma cells with stronger and more extensive expression in the more differentiated and keratinized carcinomas (Fig. 1a). Nuclear expression was observed in a small number of cases and was not included in this study. Cytoplasmic expression occurred in 86% of the cases included in TMA. In the validation study, C-FABP was expressed in 29 (96.7%) of 30 TMA cases and in 24 (80%) of 30 whole-tissue sections. Involucrin was expressed in the cytoplasm of carcinoma cells (Fig. 1b) in 94% of all cases and in 100% of the cases

Table 4 Spearman's correlation coefficients for the scores for extent of labelling on individual discs and the average of four discs

	Disc 1	Disc 2	Disc 3	Disc 4
C-FABP				
Correlation	0.882	0.843	0.786	0.836
No. of cases	84	94	93	93
Involucrin				
Correlation	0.872	0.848	0.870	0.851
No. of cases	84	95	93	93
VEGF				
Correlation	0.881	0.871	0.723	0.852
No. of cases	82	95	93	91
Ki-67				
Correlation	0.703	0.807	0.805	0.809
No. of cases	85	94	92	92

$p<0.001$ for all values of the correlation coefficient

Table 5 Spearman's correlation coefficients for the scores for the extent of labelling on different disc combinations and the average of four discs

	Average score of			
	First 3 discs	Last 3 discs	First 2 discs	Last 2 discs
C-FABP (n=74)	0.973	0.957	0.950	0.883
Involucrin (n=76)	0.974	0.974	0.898	0.892
VEGF (n=72)	0.982	0.973	0.934	0.842
Ki-67 (n=74)	0.965	0.970	0.810	0.879

p<0.001 for all values of the correlation coefficient

used in the validation study. VEGF expression is cytoplasmic and was seen in 95% of all TMA cases (Fig. 1c). In the validation study, VEGF was expressed in 100% of the TMA sections and in 28 (93.3%) of the whole-tissue sections. Nuclear expression of Ki-67 was present in all cases (Fig. 1d). The median, interquartile ranges, mean and standard deviation of each assessment are shown in Table 2. Table 3 indicates the numbers of cases falling into each scoring category.

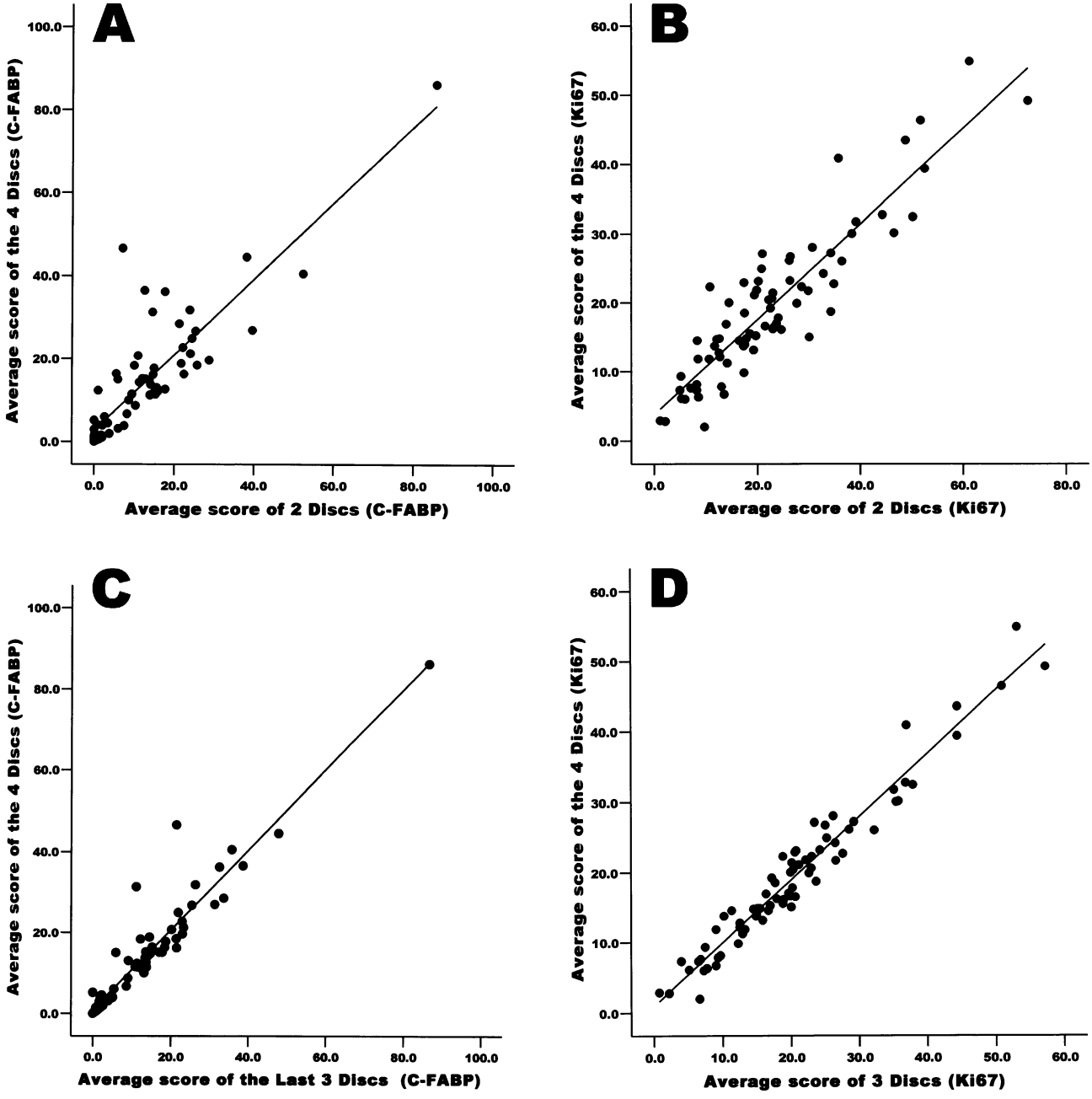


Fig. 2 Scatter plots show a tighter grouping of points when the mean of four discs is plotted against the mean of three discs (*lower plots*) than when plotted against the mean of two discs for both C-FABP and Ki-67 (*upper plots*). The *added lines* are the lines of best fit

Technical validation

Overall, 8.75–9.5% of the discs were unsuccessful. Absent discs on sections were attributable in two instances to absence of the whole core and in seven cases to uneven tissue representation in the cores. Five slides had absent discs due to part of the section being lost during staining. Pressure cooker pretreatment of sections for Ki-67 labelling did not affect the number of lost discs. When two donor blocks were used, the proportion of unsuccessful discs was lower (mean 8.4%) than when one donor block was used (mean 10.1%). Sampling errors were seen throughout the cores in 28 instances, including cores composed mainly of stromal tissue and mucosal glands, or necrotic tissue (one case). Only two cores had uninformative discs (<10% tumour). The 30 cases used in the validation study had 6.6–9.2% unsuccessful cores for individual antibodies.

Overall, 362–365 cores (depending on the antibody) were assessable. Seventy-five percent (range 73–80%) of the cases had four discs available for evaluation. Sixteen percent of the cases had three evaluable discs and 8% of the cases had two evaluable discs. Only two cases had a single

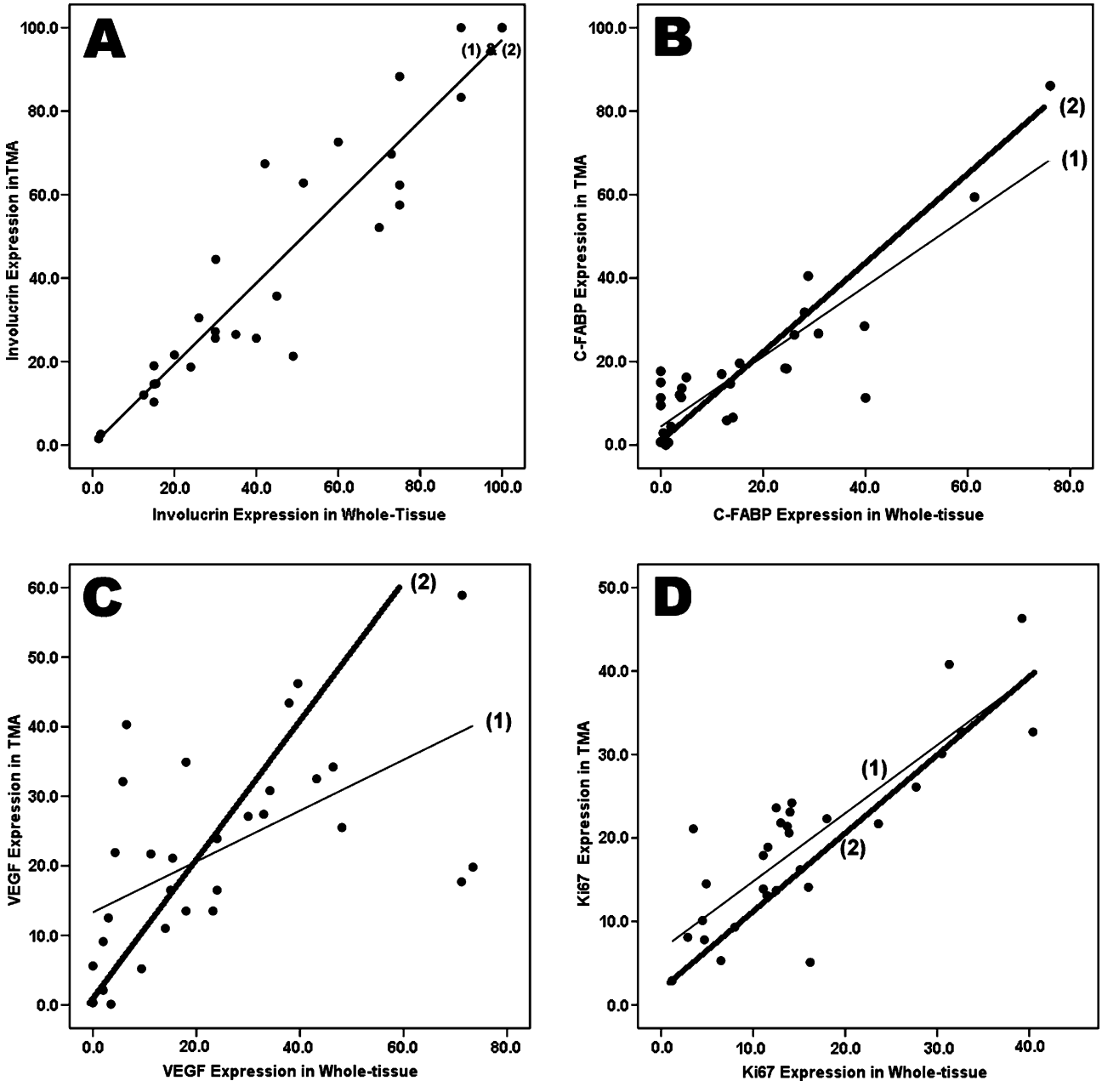


Fig. 3 Comparison of the percent labelled cells on TMA sections and whole-tissue sections for the four antibodies. *Line (1)* indicates line of best fit for the data, whereas *line (2)* is the line of equivalent labelling if both methods gave the same result. For involucrin, the two lines overlap, whereas for the other markers there is a tendency for C-FABP and VEGF to show more extensive labelling in TMA sections and for Ki-67 to be more extensive in whole-tissue sections

Table 6 Weighted kappa scores and Spearman's correlation coefficients for the agreement between values for the scoring of extent (% cells) of labelling of TMA sections and whole-tissue sections

*$p<0.001$

Antibody	Quartile scale		5-Point scale		Correlation coefficient
	k value	95% CI	*k* value	95% CI	
C-FABP	0.5946	0.3861–0.8031	0.6868	0.4828–0.8908	0.724*
Involucrin	0.7495	0.5832–0.9159	0.9211	0.8341–1.0081	0.936*
VEGF	0.4790	0.2388–0.7192	0.6333	0.3929–0.8737	0.635*
Ki-67	0.6709	0.4767–0.8652	0.8039	0.6198–0.9880	0.760*

successful disc. In the 30 cases used for the validation study, 77, 13 and 10% of the cases had four, three or two discs containing adequate carcinoma for evaluation.

Validation of immunocytochemical scoring

All TMA cases

On continuous data, highly significant ($p>0.001$) correlations were found in all comparisons between four discs and smaller numbers of discs (Table 4). The values of Spearman's correlation coefficient are higher (Table 5), and there is less scatter of data points (Fig. 2) when comparing the means of three discs to the means of four discs than when comparing two discs to four discs.

Selected 30 cases

For percentage positivity, analysis of continuous data shows a highly significant ($p<0.001$) correlation between whole-tissue section and TMA data for each antibody (Fig. 3). For C-FABP and VEGF, the percent labelled cells tends to be greater in TMA sections than in whole-tissue sections. For involucrin, there is no difference between the section types, and for Ki-67, the percent labelled cells tends to be higher in whole-tissue sections. For categorical data (Table 6), the weighted kappa values for most antibodies indicate mod erate or substantial agreement between TMA and whole-tissue section data, with higher kappa scores for the 5-point scale than the quartile scale. For involucrin, the level of agreement was almost perfect on the 5-point scale.

For intensity of staining, categorical data (Table 7) show substantial agreement between TMA sections and whole-tissue sections for C-FABP and Ki-67 (*k* values 0.6005 and 0.6699, respectively). For involucrin, the agreement was almost perfect (*k* value 0.9020), whereas for VEGF, agreement was moderate (*k* value 0.5207).

Table 7 Weighted kappa scores for the agreement between the scoring of intensity of labelling of TMA sections and whole-tissue sections

Antibody	*k* value	95% CI
C-FABP	0.6005	0.3860–0.8149
Involucrin	0.9020	0.7139–1.0900
VEGF	0.5207	0.3080–0.7333
Ki-67	0.6699	0.4571–0.8827

Discussion

This study has demonstrated that for the selected antigens, TMAs can provide a realistic and reliable estimate of the extent of antigen expression in head and neck squamous carcinomas. These results support the findings of other groups who have considered the validity and technical issues of using TMAs to study p53, cyclin D1, retinoblastoma (Rb) and epidermal growth factor receptor (EGFR) [5, 12]. Other papers confirm the prognostic significance of results derived from TMA [9, 10].

The techniques of TMA are well established, and most authors indicate that validation studies to consider technical, biological and statistical issues are necessary to establish the optimal number of cores for each molecular marker and tumour type. Some loss of discs is inevitable due to technical issues of poor core location, sections floating and variations in tumour content of cores at different depths in the recipient block. In our microarrays, 8.75–9.50% of the discs were unsuccessful in producing stained tumour tissue. Discs that were completely absent (1.25–2% of all discs) may be due to poor tissue fixation and processing or poor punching technique leading to tissue loss from the block or to tissue loss during sectioning or staining. Our percentage disc loss is similar to that of Griffin et al. [12] and is lower than the figures reported in most other studies [7, 11, 17, 19, 22, 37, 41], particularly those that have used high-density TMAs [4]. We used a relatively low-density array to facilitate screening of the slides, and this may have helped to reduce disc loss. Others have reported that disc loss was higher when heat-facilitated antigen retrieval was used [37], although this was not our experience.

Uninformative discs with 0–10% tumour tissue result from errors in sampling the donor blocks and comprise the majority of unsuccessful discs (7.5%). This compares favourably with other studies [5, 7, 12, 17, 22, 29, 41] and may reflect the careful comparison with haematoxylin and eosin-stained sections at the time of donor site selection and the avoidance of necrotic areas and keratinous debris. When possible, the use of two donor blocks also reduces the number of unsuccessful discs.

Whether or not TMAs allow adequate representation of the range of antigen expression in a particular tumour is fundamentally no different from considering how many whole-tissue sections might be representative of a tumour, or how to assess an adequate number of fields in one large section [3, 29, 37], and ultimately will reflect whether one is trying to assess the 'average' characteristics of the neoplastic cells or trying to detect more aggressive subclones within a tumour. Heterogeneous protein expression has

been described in squamous carcinomas [36], but studies of TMA in squamous carcinomas, as well as the present study, suggest that this is not a major problem.

Most authors view the whole-tissue section as the 'gold standard' against which microarrays are judged. This approach has its limitations as a single 3-μm-thick tissue section of 3×2 cm represents only 1/19,000 of the volume of a tumour with diameter of 4 cm [33] and may in itself not be representative of the whole tumour. A single TMA disc has an area that is approximately 0.05% of that of a whole-tissue section, although this may underestimate its value when whole-tissue sections contain significant stromal or normal tissue. However, validation against whole-tissue sections provides a pragmatic way forward and some reassurance that microarrays provide data comparable with whole-tissue section analyses. The taking of cores from more than one donor block achieves better representation than more restricted sampling.

Using continuous data, the present study found a good correlation between the results from TMA sections and whole-tissue sections for the extent and intensity of expression of all of the antigens studied. Using categorical data, the kappa statistics indicate substantial or almost perfect agreement between TMA and whole-tissue sections for all antigens. An important issue to be considered is whether the scoring categories should be assigned arbitrarily (e.g., as our 5-point scale) or in an unbiased manner (e.g., using quartile values). Our data indicate that the cut-off points between categories can influence the degree of statistical agreement, particularly where the cut-off values are close to the median or where most data points fall into one category. The 5-point scale used in the present study is similar to that used by many groups and has the merit of being simple to apply and easily transferred to the clinical/diagnostic setting. However, arbitrary cut-off points may obscure potentially interesting biological differences between tumours [14]. Despite these difficulties, our observations are similar to those of other groups for Ki-67 [15, 28, 29] and for VEGF [24], indicating that the technique is robust across tumour and tissue types and different antibodies. Data on intensity of immunocytochemical labelling need to be viewed with some caution due to variations in fixation and tissue processing when cases are collected over a period of several years.

Heterogeneity of antigen expression is difficult to quantify in whole-tissue sections requiring statistically rigorous random selection of microscopic fields for assessment. Depending on the antigen of interest, point counting or 'hot spot' counts may be used, with the potential for bias in the selection of areas for assessment. The relatively unbiased selection of cores for microarrays provides an easy method to define and quantify heterogeneity of expression by comparing the results of one core with those in other cores [24]. Either the mean value or the highest value from a set of cores could be used depending on the biological relevance of the marker being studied.

We have shown that as more discs (one to three) are evaluated, the closer is the level of agreement with the mean of four discs. Others have noted similar findings [3, 7, 8, 16, 17, 25, 29] and that using more than four cores does not improve tissue loss or the degree of agreement [30, 40]. We agree that selecting four cores is optimal to allow for the inevitable loss of informative cores due to technical and sampling issues and to assess tumour heterogeneity [8, 30].

A novel observation is that for some antigens there appears to be a trend for TMA-labelled sections to show slightly more or less extensive labelling than whole-tissue sections. The reason for this is not obvious but may relate to TMA sections having a lower proportion of the section containing tissue-binding sites for antibodies (due to the spaces between the cores) compared with whole-tissue sections or to different rates of oxidation of antigens after cutting sections. This observation followed the realisation that the arbitrary selection of categories for kappa analysis may not be appropriate and indicates that it may not be appropriate to try to validate TMAs against whole-tissue sections. Correlation between microarray data and clinical outcomes may be more relevant [33].

In summary, our results show that the use of three cores will produce a mean value for antigen expression (extent or intensity) similar to that of four cores or whole-tissue sections. We suggest that four cores be taken from each tumour to allow for unavoidable unsuccessful cores due to disc loss or sampling of uninformative tissue. TMA is most valuable for high-throughput analysis of many tumours and, although the use of multiple cores provides some information on tumour heterogeneity, the technique is not ideally suited to the detailed investigation of the microanatomical distribution of antigens within a tumour. This study expands the range of antigens studied by TMA in squamous carcinomas and reinforces the view that TMA is a reliable tool to demonstrate cellular and molecular alterations in these tumours. There are unresolved issues on how TMA data should be expressed, although we would advocate unbiased description of molecular data (using median and quartile values) as a first stage. The nature of the antigens and the genetic mechanisms underlying under- or over-expression may then suggest other options for biologically meaningful categorisation of data.

Acknowledgements This work forms part of the Ph.D. thesis of Dr. Gomaa, who is sponsored by the Ministry of Higher Education, Egypt. The authors would like to express their thanks to Mrs. Wendy Prime for her kind guidance during construction of the TMA and Mr. Andy Dodson for his support while performing the immunocytochemistry.

References

1. Baisse B, Bouzourene H, Saraga EP et al (2001) Intratumor genetic heterogeneity in advanced human colorectal adenocarcinoma. Int J Cancer 93:346–352
2. Bradley P, Morgan D, Slevin N et al (2001) Practice care guidance for clinicians participating in the management of head and neck cancer patients in the UK. Eur J Surg Oncol 27(Suppl A):S1–S17

3. Camp RL, Charette LA, Rimm DL (2000) Validation of tissue microarray technology in breast carcinoma. Lab Invest 80: 1943–1949
4. Chang BW, Kim DH, Kowalski DP et al (2004) Prognostic significance of cyclooxygenase-2 in oropharyngeal squamous cell carcinoma. Clin Cancer Res 10:1678–1684
5. Chen B, van den Brekel MW, Buschers W et al (2003) Validation of tissue array technology in head and neck squamous cell carcinoma. Head Neck 25:922–930
6. Ek BA, Cistola DP, Hamilton JA et al (1997) Fatty acid binding proteins reduce 15-lipoxygenase-induced oxygenation of linoleic acid and arachidonic acid. Biochim Biophys Acta 1346: 75–85
7. Engellau J, Akerman M, Anderson H et al (2001) Tissue microarray technique in soft tissue sarcoma: immunohistochemical Ki-67 expression in malignant fibrous histiocytoma. Appl Immunohistochem Mol Morphol 9:358–363
8. Fernebro E, Dictor M, Bendahl PO et al (2002) Evaluation of the tissue microarray technique for immunohistochemical analysis in rectal cancer. Arch Pathol Lab Med 126:702–705
9. Freier K, Bosch FX, Flechtenmacher C et al (2003) Distinct site-specific oncoprotein overexpression in head and neck squamous cell carcinoma: a tissue microarray analysis. Anticancer Res 23:3971–3977
10. Freier K, Joos S, Flechtenmacher C et al (2003) Tissue microarray analysis reveals site-specific prevalence of oncogene amplifications in head and neck squamous cell carcinoma. Cancer Res 63:1179–1182
11. Gillett CE, Springall RJ, Barnes DM et al (2000) Multiple tissue core arrays in histopathology research: a validation study. J Pathol 192:549–553
12. Griffin MC, Robinson RA, Trask DK (2003) Validation of tissue microarrays using p53 immunohistochemical studies of squamous cell carcinoma of the larynx. Mod Pathol 16:1181–1188
13. Gulmann C, O'Grady A (2003) Tissue microarrays: an overview. Curr Diagn Pathol 9:149–154
14. Helliwell TR (2001) Molecular markers of metastasis in squamous carcinomas. J Pathol 194:289–293
15. Hoos A, Cordon-Cardo C (2001) Tissue microarray profiling of cancer specimens and cell lines: opportunities and limitations. Lab Invest 81:1331–1338
16. Hoos A, Nissan A, Stojadinovic A et al (2002) Tissue microarray molecular profiling of early, node-negative adenocarcinoma of the rectum: a comprehensive analysis. Clin Cancer Res 8:3841–3849
17. Hoos A, Urist MJ, Stojadinovic A et al (2001) Validation of tissue microarrays for immunohistochemical profiling of cancer specimens using the example of human fibroblastic tumors. Am J Pathol 158:1245–1251
18. Jing C, Beesley C, Foster CS et al (2001) Human cutaneous fatty acid-binding protein induces metastasis by up-regulating the expression of vascular endothelial growth factor gene in rat Rama 37 model cells. Cancer Res 61:4357–4364
19. Jourdan F, Sebbagh N, Comperat E et al (2003) Tissue microarray technology: validation in colorectal carcinoma and analysis of p53, hMLH1, and hMSH2 immunohistochemical expression. Virchows Arch 443:115–121
20. Kononen J, Bubendorf L, Kallioniemi A et al (1998) Tissue microarrays for high-throughput molecular profiling of tumor specimens. Nat Med 4:844–847
21. Landis JR, Koch GG (1977) The measurement of observer agreement for categorical data. Biometrics 33:159–174
22. Leversha MA, Fielding P, Watson S et al (2003) Expression of p53, pRB, and p16 in lung tumours: a validation study on tissue microarrays. J Pathol 200:610–619
23. Moch H, Kononen T, Kallioniemi OP et al (2001) Tissue microarrays: what will they bring to molecular and anatomic pathology? Adv Anat Pathol 8:14–20
24. Mucci NR, Akdas G, Manely S et al (2000) Neuroendocrine expression in metastatic prostate cancer: evaluation of high throughput tissue microarrays to detect heterogeneous protein expression. Hum Pathol 31:406–414
25. Nilbert M, Engellau J (2004) Experiences from tissue microarray in soft tissue sarcomas. Acta Orthop Scand Suppl 75: 29–34
26. Nocito A, Kononen J, Kallioniemi OP et al (2001) Tissue microarrays (TMAs) for high-throughput molecular pathology research. Int J Cancer 94:1–5
27. Parkin DM, Pisani P, Ferlay J (1999) Estimates of the worldwide incidence of 25 major cancers in 1990. Int J Cancer 80: 827–841
28. Peters S, Hambek M, Gstottner W et al (2004) Tissue microarrays. Value of immunohistochemical proliferation markers for serial investigations of head and neck cancer. HNO 52:409–412
29. Rosen DG, Huang X, Deavers MT et al (2004) Validation of tissue microarray technology in ovarian carcinoma. Mod Pathol 17:790–797
30. Rubin MA, Dunn R, Strawderman M et al (2002) Tissue microarray sampling strategy for prostate cancer biomarker analysis. Am J Surg Pathol 26:312–319
31. Sauter ER, Nesbit M, Watson JC et al (1999) Vascular endothelial growth factor is a marker of tumor invasion and metastasis in squamous cell carcinomas of the head and neck. Clin Cancer Res 5:775–782
32. Sauter G, Mirlacher M (2002) Tissue microarrays for predictive molecular pathology. J Clin Pathol 55:575–576
33. Simon R, Mirlacher M, Sauter G (2003) Tissue microarrays in cancer diagnosis. Expert Rev Mol Diagn 3:421–430
34. Skacel M, Skilton B, Pettay JD et al (2002) Tissue microarrays: a powerful tool for high-throughput analysis of clinical specimens: a review of the method with validation data. Appl Immunohistochem Mol Morphol 10:1–6
35. Sobin LH, Wittekind C (eds) (2002) TNM classification of malignant tumours, 6th edn. Wiley-Liss, New York
36. Takes RP, Baatenburg de Jong RJ, Schuuring E et al (1998) Differences in expression of oncogenes and tumor suppressor genes in different sites of head and neck squamous cell carcinoma. Anticancer Res 18:4793–4800
37. Van den Eynden GG, Van der Auwera I, Van Laere S et al (2004) Validation of a tissue microarray to study differential protein expression in inflammatory and non-inflammatory breast cancer. Breast Cancer Res Treat 85:13–22
38. Watanabe R, Fujii H, Yamamoto A et al (1997) Immunohistochemical distribution of cutaneous fatty acid-binding protein in human skin. J Dermatol Sci 16:17–22
39. Watt FM (1983) Involucrin and other markers of keratinocyte terminal differentiation. J Invest Dermatol 81:100s–103s
40. Zettl A, Meister S, Katzenberger T et al (2003) Immunohistochemical analysis of B-cell lymphoma using tissue microarrays identifies particular phenotypic profiles of B-cell lymphomas. Histopathology 43:209–219
41. Zhang D, Salto-Tellez M, Putti TC et al (2003) Reliability of tissue microarrays in detecting protein expression and gene amplification in breast cancer. Mod Pathol 16:79–85
42. Zimmerman AW, Veerkamp JH (2002) New insights into the structure and function of fatty acid-binding proteins. Cell Mol Life Sci 59:1096–1116

Virchows Arch (2005) 447: 710–716
DOI 10.1007/s00428-005-0016-1

ORIGINAL ARTICLE

Hitoshi Nagatsuka · Rosario Santos Rivera · Mehmet Gunduz · You-Jin Lee · Ryo Tamamura · Esra Gunduz · Ichiro Naito · Yoshikazu Sado · Noriyuki Nagai

Immunolocalization and distribution patterns of type IV collagen alpha chains in oral mucosal melanoma

Received: 11 January 2005 / Accepted: 27 April 2005 / Published online: 27 July 2005
© Springer-Verlag 2005

Abstract The basement membrane (BM) is mainly composed of type IV collagen, which is composed of triple combinations of six distinct alpha (α) chains in a tissue-specific manner. The six collagen chain-specific antibodies (α1–α6) were used to examine the BMs of the oral epithelium (OE) and tumor clusters in oral mucosal melanoma (OMM). Eight OMM cases were examined. Results showed that the α1 and α2 chains were constantly detected at the BM of the normal OE as well as at the OE with atypical melanocytic proliferation and in invasive melanoma with nodular nests. The α1 and α2 chains were intermittently detected in in situ OMM, early invasive OMM and advanced invasive OMM with sheet-like nests. Gradual loss of α5 and α6 from the OE with atypical melanocyte through in situ OMM and early invasive OMM was observed. These findings suggest that changes in the immunolocalization and distribution patterns of type IV collagen α chains are associated with the progression of OMM. The distribution pattern of type IV collagen α chain varies depending on the architecture of the nest.

Keywords Oral mucosal melanoma · Basement membrane · Type IV collagen alpha chains · Immunohistochemistry

H. Nagatsuka (✉) · R. Santos Rivera · M. Gunduz · Y.-J. Lee · R. Tamamura · E. Gunduz · N. Nagai
Department of Oral Pathology and Medicine,
Graduate School of Medicine and Dentistry,
Okayama University,
2-5-1 Shikata-cho,
Okayama, 700-8525, Japan
e-mail: jin@md.okayama-u.ac.jp
Tel.: +81-862-356652
Fax: +81-862-356654

R. Santos Rivera
College of Dentistry, University of the East,
Manila, Philippines

I. Naito · Y. Sado
Ultrastructural Biology and Division of Immunology,
Shigei Medical Research Institute,
Yamada, Okayama, Japan

Introduction

The basement membrane (BM) is a specialized form of extracellular matrix (ECM) that not only lines the epithelial sheets and blood vessels but also exists in other cell types that come in contact with the connective tissue. The BM is essential in normal biological functions such as cell adhesion, growth and differentiation [3]. It provides a barrier that limits or regulates the exchanges of macromolecules between connective tissue and other tissue types [10]. It has also been regarded as the site of tumor invasion and metastasis by associating the loss of its components during tumor progression [3]. Type IV collagen is the main component of the BM. Other components are laminin, nidogen/entactin and heparan sulfate proteoglycans.

Type IV collagen molecule is composed of a triple helix structure consisting of three polypeptides called alpha (α) chains [10].

Six α chains have been identified based on their amino acid sequence differences [11]. α1 and α2 are called "classic chains" and are widely distributed in tissues [11]. On the other hand, α3, α4, α5 and α6 are called "novel chains" and are selectively distributed in human tissues [11]. Random combinations of the six (α) chains assemble into triple helical protromers which further associate with other protomers forming multiple networks [4]. The three common and distinct networks are composed of α1, α2 found in human BMs [28]; α3, α4, α5 in the alveolar BM of the lung, glomerulus and some parts of the tubular BM of the kidney [22, 28]; and α5, α6 in the BM of the mammary duct and lobule, epidermis, smooth muscle and prostate gland [5, 21, 29, 30, 32]. Additional distinct type IV collagen network consisting of α1, α2, α5 and α6 have been detected in BMs of bladder, uterus, stomach, small intestine, Bowman's capsule and that of the oral epithelium (OE) [19, 22, 29, 30, 35].

Various studies have been focused on the distribution of these α chains in breast [21], skin [32], prostate [5], lung [20], pancreas [11], colorectal tumors [8, 23] as well as odontogenic [19] and salivary gland tumors [17], but so far the immunolocalization and distribution of type IV colla-

gen α chains in OMM has not been reported. The objectives of the study were to determine the distribution patterns of type IV collagen α chains at the BM of OMM and to determine the variations in the distribution of these α chains in different types of OMM, employing immunohistochemical procedures.

Materials and methods

Paraffin sections

The paraffin sections used were obtained from biopsy and surgical tissues examined at the Department of Oral Pathology and Medicine, Graduate School of Medicine and Dentistry, Okayama University. The study protocol was approved by the Experimental Ethics Review Committee of Our Institution. The cases were categorized using the Western Society of Teachers in Oral Pathology (WESTOP) system of nomenclature [1]. Microscopically, two major patterns have been identified. These are in situ pattern in which the neoplasm is limited to both the epithelium and epithelium-connective tissue interface, and invasive pattern in which the neoplasm is found within the supporting connective tissue only. Invasive OMM with in situ component was also included in the study. Invasive OMM and invasive OMM with in situ component that depicted the invasion of the melanoma cells from the epithelium into the connective tissue were specifically referred to as early invasive OMM, whereas the tumor clusters deeply localized within the connective tissue were referred as advanced invasive OMM. Atypical melanocytic proliferation was designated as part of oral mucosal lesions with equivocal histopathologic features, such as hyperchromatic and angulated nuclei with very infrequent mitotic activity as described previously [1]. A total of eight cases were examined: one case of in situ OMM, one case of invasive OMM and six cases of invasive OMM with in situ component. The specimens were stained using routine hematoxylin and eosin, and malignant melanoma markers such as S-100, HMB-45, Vimentin and Melan-A. Other markers such as Masson-Fontana, CD34, Actin, Leucocyte Common Antigen and Cytokeratins were used for differential diagnoses (data not included).

Table 1 Type IV collagen alpha chain antibodies

Specificity	Clone	Dilution
α1	H11	1:400
α2	H22	1:400
α3	H31	1:100
α4	H43	1:10
α5	H53	1:100
α6	H63	1:20

Immunohistochemistry

Deparaffinized tissue sections of 3-μm thickness were blocked for endogenous peroxidase activity using 3% hydrogen peroxide in methanol for 30 min and then washed in Tris-buffered saline (TBS) three times for 5 min each. Heat pressure antigen retrieval was the pretreatment done by immersing in a citrate buffer with a pH of 3.5 for 5 min at

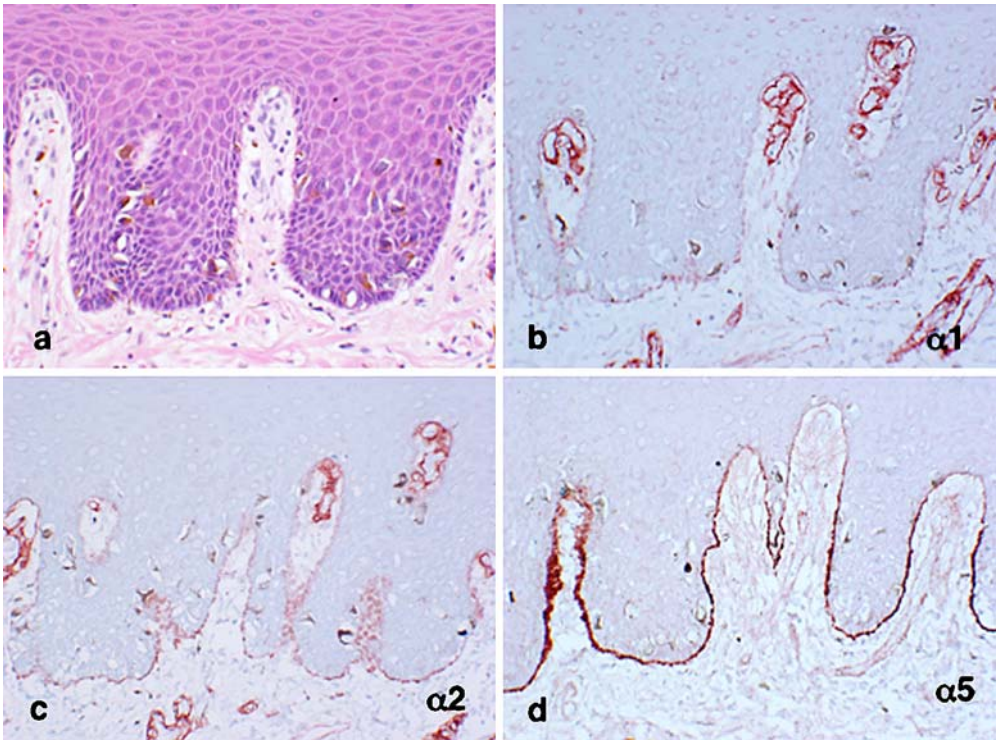


Fig. 1 Oral epithelium with atypical melanocytes. Immunostaining for α1 (**b**) and α2 (**c**) were constant, whereas that for α5 (**d**) chain was intermittent (×400)

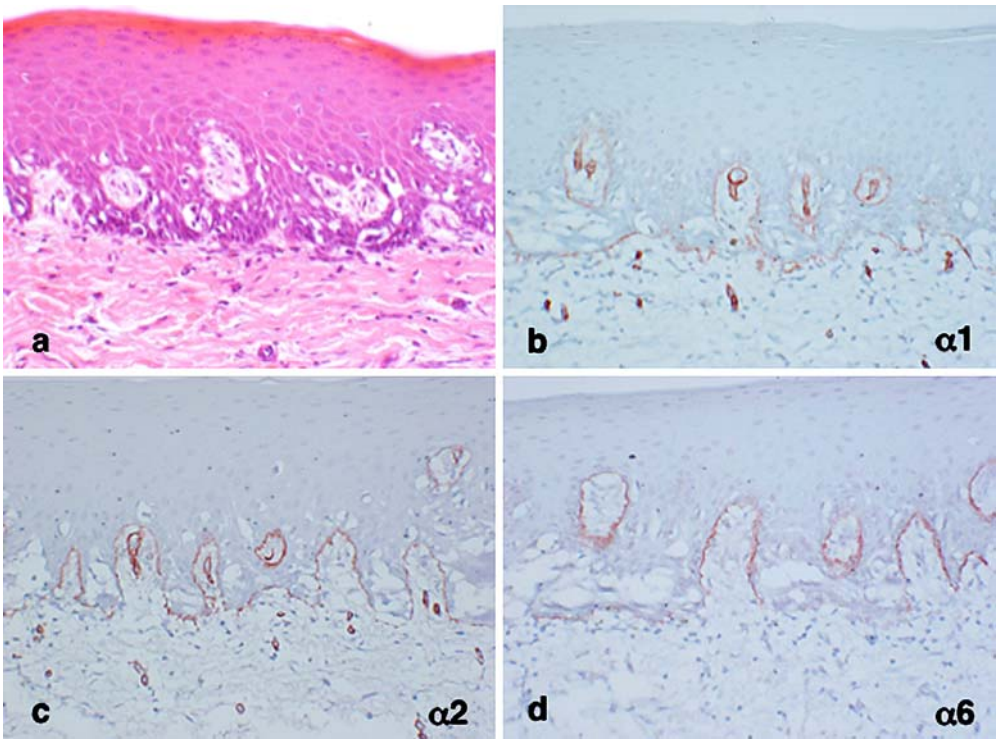


Fig. 2 In situ oral mucosal melanoma. Intermittent immunostainings for α1 (**b**), α2 (**c**), and α6 (**d**) chains at the basement membranes of the oral epithelium (×400)

121°C. The slides were then immersed in 5% normal rat serum blocking solution for 15 min, covered with each of the type IV collagen α chain antibodies and incubated overnight at 4°C. The specificity of rat monoclonal antibodies recognizing type IV collagen α chains was previously reported via ELISA and immunoblotting, and epitopes were determined by multipin-peptide scanning [12, 27]. The clones and dilutions of each type IV collagen α chain-specific antibody are shown in Table 1. Immunoreactions were performed using Vectastain peroxidase ABC Kit (Vector Laboratories, Burlingame, CA, USA). The antigenic sites were disclosed using 3-amino-9-ethylcarbazole (AEC) substrate chromogen (Dako, Carpinteria, CA, USA) and counterstained with Mayer's hematoxylin.

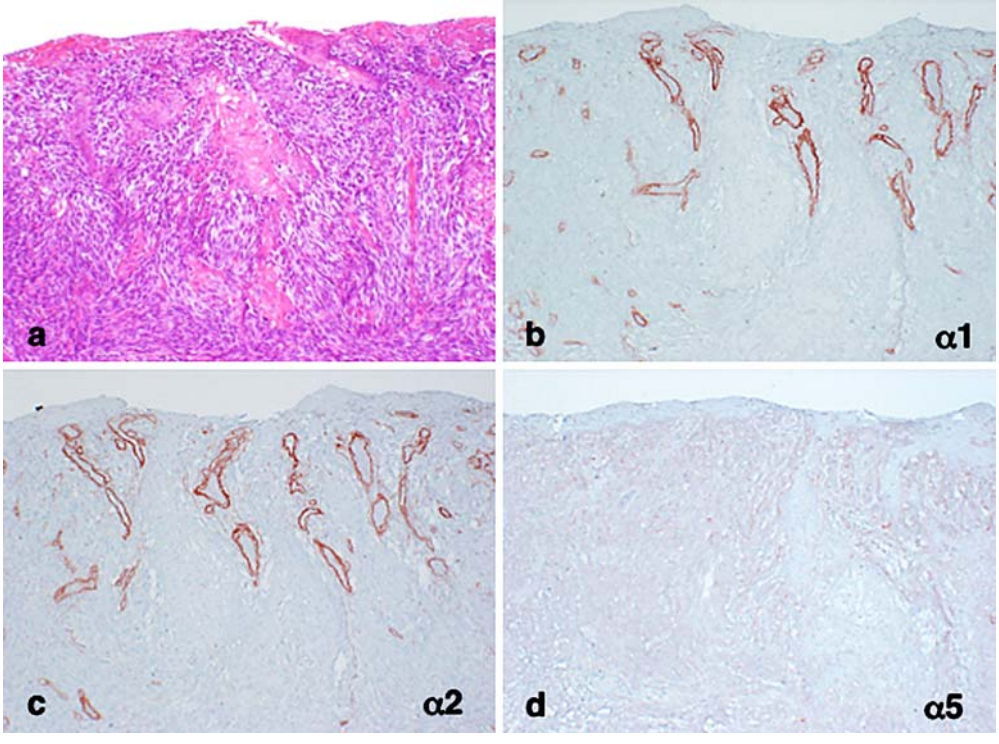


Fig. 3 Early invasive oral mucosal melanoma. Immunostainings for α1 (**b**) and α2 (**c**) chains were intermittent at the basement membrane of the oral epithelium, while that for α5 (**d**) chain was negative (×200)

Results

The BMs of the normal OE as well as those surrounding the melanoma nests were examined for the immunolocalization and distribution of type IV collagen α chains. Qualitative analysis of the BM immunoreactivity was microscopically examined and categorized into three patterns: (1) constant, in which the immunostaining can be seen without a disruption on its continuity; (2) intermittent, in which the pattern is discontinuous; and (3) negative, in which no immunostaining was detected.

α1, α2, α5 and α6 chains were detected at the BM of the normal OE (figure not shown). They were also detected at the BM of the OE with atypical melanocytic proliferation (Fig. 1). Immunostainings for α1 and α2 were both constant (Fig. 1b,c), while those for α5 (Fig. 1d) and α6 (figure not shown) were intermittent although the α5 immunoreaction was more intense compared to α1, α2 and α6 chains. α1, α2, α5 and α6 chains were intermittently detected at the BM of the OE in in situ OMM (Fig. 2). α1 (Fig. 3b) and α2 (Fig. 3c) chains were intermittently detected at the BM of the OE in early invasive OMM, while immunostainings for α5 (Fig. 3d) and α6 (figure not shown) were negative.

Tumor clusters in invasive OMM were surrounded by BMs. α1 (Fig. 4b) and α2 (Fig. 4c) chains were constantly detected at the BM of nests with nodular architecture, while they were intermittently detected at the BM of the nests with sheet-like architecture (Fig. 5b,c). Most of these nests that were constantly positive for α1 and α2 chains were detected at the center of the tumor mass. α5 and α6 chains were both negative in nodular (Fig. 4d) and sheet-like nests (Fig. 5d). In all of the cases, α3 and α4 chains were not detected (figure not shown) at the BMs of the OE and melanoma nests. Table 2 summarizes the results of the immunohistochemistry.

Discussion

In the head and neck region, OMM is an extremely rare neoplasm representing 0.5% of oral malignancies [6]. The most common sites are the hard palate and the gingiva [1], although it may also occur in other areas of the oral cavity. It has a poor prognosis with a 5–20% survival rate [25]. Although researches have been conducted, the classification of OMM is still not settled. Some studies reported similarities between OMM and acral lentiginous melanoma (ALM) with a radial growth phase both clinically and histologically [26, 34]. Others regarded OMM separately from cutaneous melanoma because of the difference in the prognosis [13]. Nevertheless, WESTOP has stated that OMM appeared similar to ALM and less frequently to nodular melanoma when no in situ component was evident [1].

Melanocytes are specialized melanin-producing cells that developed embryonically from the neural crest and migrated to the skin, hair follicle and retina. The presence of melanocytes in these structures is necessary and known, but their existence and function in the oral mucosa are not known for certain [7]. Melanocytes in the oral mucosa may transform into atypical melanocytes and tumor cells. These tumor cells may either be confined within the OE or within the connective tissue, or may be found both in the OE and the connective tissue at the same time.

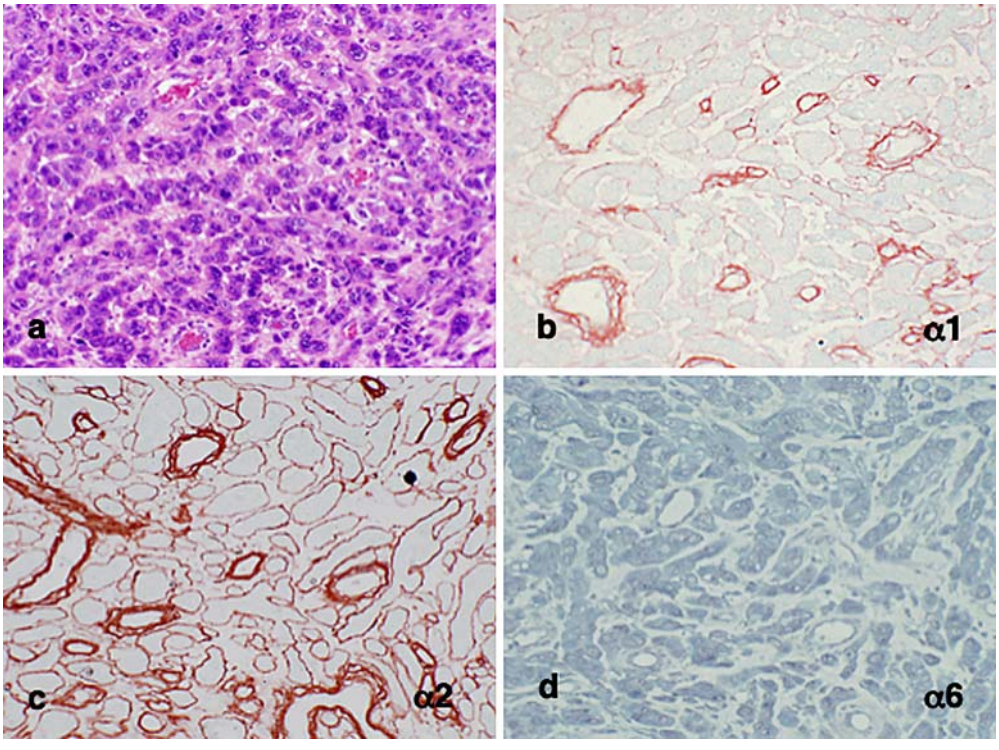


Fig. 4 Advanced invasive melanoma nodular architecture. Immunostainings for α1 (**b**) and α2 (**c**) chains were both constant, while that for α6 (**d**) chain was negative (×400)

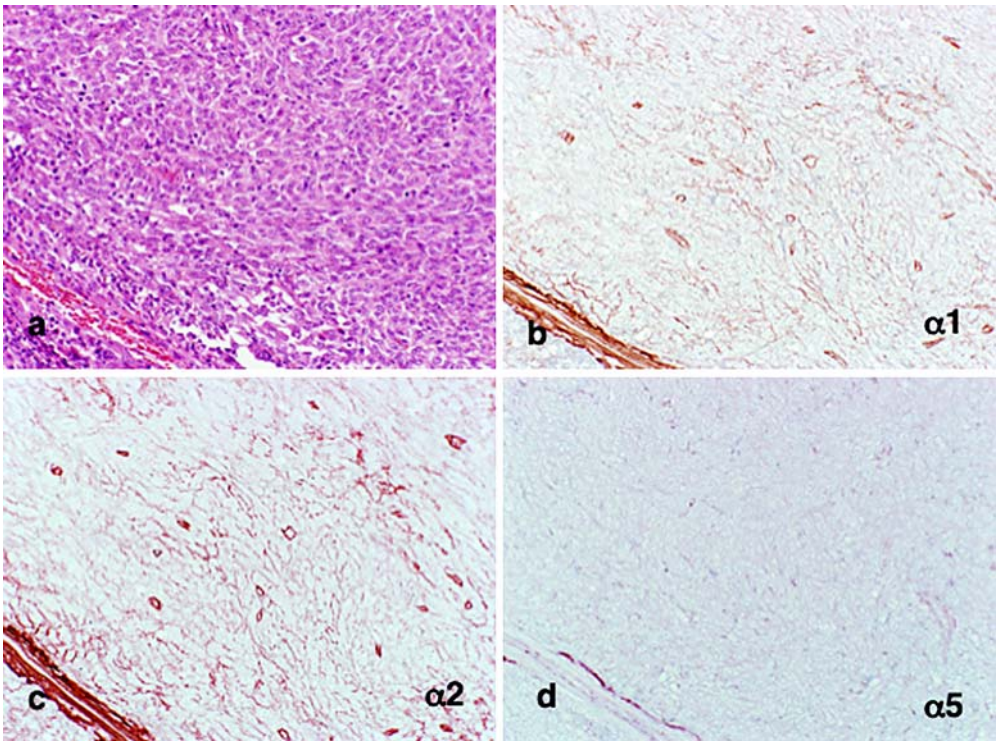


Fig. 5 Advanced invasive melanoma sheet-like architecture. Immunostaining for α1 (**b**) and α2 (**c**) chains were intermittent, while that for α5 (**d**) chain was negative (×400)

Melanoma cells may either be epithelioid or spindle in shape. Both cell types can be found in a single tumor. When these tumor cells invade the connective tissue, they tend to organize and form tumor clusters surrounded by BMs. Various architectures have been described, ranging from sheet-like, organoid, alveolar, neurotropic and desmoplastic [7]. The BM was either produced by the tumor cells or stromal cells or by both [31].

The study illustrated, for the first time, the gradual modifications in the immunolocalization of type IV collagen α chains at the BM of the OE during the carcinogenic progression of OMM. The BM of the OE is composed of the combined supramolecular network of α1, α2 and α5, α6. However, the BM of OE with atypical melanocytes was intermittently stained for α5 and α6 chains, suggesting a possible malignant change. The presence of atypical melanocytes at the BM of the OE might have caused the change in the pattern since no inflammatory reaction was observed. Atypical melanocytic proliferation is used for lesions with equivocal histologic features and is sometimes difficult to differentiate from in situ melanoma. Nevertheless, the condition may exemplify an undetermined to premalignant melanocytic lesion similar to cutaneous atypical mole (dysplastic nevus) as described previously [7]. Atypical melanocytic proliferation in the oral mucosa may represent a precursor lesion to melanoma or an indication of increased risk for developing mucosal melanoma at other sites [7]. Taken together, the changes in the type IV collagen α chains may suggest the possibility of progress to OMM.

Table 2 Summary of the immunolocalization of type IV collagen alpha chains in the basement membranes of normal oral mucosa and melanoma[a]

	α1	α2	α5	α6
Normal oral epithelium	+	+	+	+
With atypical melanocytes	+	+	±	±
In situ OMM	±	±	±	±
Early invasive OMM	±	±	−	−
Advanced invasive OMM (nodular architecture)	+	+	−	−
Advanced invasive OMM (sheet-like architecture)	±	±	−	−

+ Constant, ± intermittent, − negative; *OMM* oral mucosal melanoma
[a]Eight cases as well as their normal margins were studied, including one in situ, one invasive, six invasive with in situ OMM

In situ OMM is characterized by the transformation of atypical melanocytes into melanoma cells. Melanoma cells retain some features of the atypical melanocytes but they possess considerable pleomorphism with large, irregular, hyperchromatic nuclei and prominent nucleoli, and have readily detectable mitotic activity [7]. Our results showed that a more dramatic change was observed in in situ OMM by the interruption of the continuity of each α1, α2, α5 and α6 chains, suggesting the further modification of the α chain component during carcinogenic progression.

Degradation of the oral epithelial BM is necessary for invasion to the surrounding tissues prior to metastasis. The action of proteases particularly matrix metalloproteinases (MMP) family and plasminogen activation system are also involved in the degradation of the BM [24]. It has been shown that MMP-2 and MMP-9, both of which can degrade BM components such as type IV collagen, were highly expressed in melanoma cells or by stromal cells in the case of MMP-9 [9]. Furthermore, plasmin can either directly degrade extracellular macromolecules or activate pro-MMPs [18]. In this study, the degradation of the BM

was accompanied by the change in its type IV collagen α chain specific composition. Initially, the BM of the OE was composed of type IV collagen α1, α2, α5 and α6 chains and followed by intermittency in α5 and α6 chains, although α1 and α2 chains remained constant. Further invasion resulted in the intermittency of α1 and α2 chains and the total loss of α5 and α6 chains, suggesting that α1 and α2 chains were more stable against degradation compared to α5 and α6 chains.

Melanoma cells that invaded the connective tissue synthesized BMs [31]. Our results confirmed previous findings that melanoma cell clusters were surrounded by BMs [31, 33]. Invasive tumor clusters formed two types of architecture. The first architecture was characterized by nodular nests, which included epithelioid cells resembling melanocytes that are highly differentiated. These were constant to α1 and α2 immunostainings. The second architecture was characterized by sheet-like nests consisting of spindle cells that are diffusely arranged and less-differentiated. These were intermittent to α1 and α2 immunostainings. Both architectures were negative to α5 and α6 stainings. The production of ECM, including BM mostly, is advantageous for the melanomas since growth factors can be stored in it [31]. This may be the rationale for the production of BM around tumor clusters. However, the variation in the type IV collagen α chain distribution in relation to metastasis was not considered due to the paucity of cases.

Studies regarding the concepts of vasculogenesis of melanoma have been reported including endothelium-lined tumor vessels, tumor cell-lined matrix and matrix-rich vascular channels [14, 16, 33]. Type IV collagen has the capacity to promote and modulate angiogenic response [2]. Type IV collagen also has an important role in promoting the adhesion and motility of various cell types to include endothelial cells [15]. The BM molecules and interstitial collagen may also provide a scaffold for the neovessels [2]. Altogether, it may be speculated that the presence of BM type IV collagen may enhance the formation of the heterogenous tumor microvasculature in OMM necessary for its progression.

In conclusion, the study suggests that the change in the immunolocalization of type IV collagen α chains is associated with the progression of OMM. BMs are dynamic structures that are not only degraded in the process of invasion but are also deposited around melanoma cell clusters and the distribution pattern varies depending on the architecture of the nest.

Acknowledgements The authors would like to thank Ms. Yoshiko Kurashige and Ms. Reiko Kirino for their technical expertise.

This work was supported by grant-in-aid for scientific research A from the Ministry of Education, Culture, Sports, Science and Technology to N Nagai (#15209060).

References

1. Barker BF, Carpenter WM, Daniels TE, Kahn MA, Leider AS, Lozada-Nur F, Lynch DP, Melrose R, Merrell P, Morton T, Peters E, Regezi JA, Richards SD, Rick GM, Rohrer MD, Slater L, Stewart JC, Tomich CE, Vickers RA, Wood NK, Young SK (1997) Oral mucosal melanomas: the WESTOP Banff workshop proceedings. Western Society of Teachers of Oral Pathology. Oral Surg Oral Med Oral Pathol Oral Radiol Endo 83:672–679
2. Bonanno E, Iurlaro M, Madri JA, Nicosia RF (2000) Type IV collagen modulates angiogenesis and neovessel survival in rat aorta model. In Vitro Cell Dev Biol Anim 5:336–340
3. Borza DB, Bondar O, Ninomiya Y, Sado Y, Naito I, Todd P, Hudson BG (2001) The NC1 domain of collagen IV encodes a novel network composed of the alpha 1, alpha 2, alpha 5, and alpha 6 chains in smooth muscle basement membranes. J Biol Chem 276:28532–28540
4. Boutad A, Borza DB, Bondar O, Gunwar S, Netzer KO, Singh N, Ninomiya Y, Sado Y, Noelken ME, Hudson BG (2000) Type IV collagen of the glomerular basement membrane. Evidence that the chain specificity of network assembly is encoded by the noncollagenous NC1 domains. J Biol Chem 275:30716–30724
5. Dehan P, Waltregny D, Beschin A, Noel A, Castronovo V, Trygvason K, De Leval J, Foidart JM (1997) Loss of type IV collagen alpha 5 and alpha 6 chains in human invasive prostate carcinomas. Am J Pathol 151:1097–10104
6. Garzino-Demo P, Fasolis M, Maggiore GM, Pagano M, Berrone S (2004) Oral mucosal melanoma: a series of case reports. J Craniomaxillofac Surg 32:251–257
7. Hicks MJ, Flaitz CM (2000) Oral mucosal melanoma: epidemiology and pathobiology. Oral Oncol 36:152–169
8. Hiki Y, Iyama K, Tsuruta J, Egami H, Kamio T, Suko S, Naito I, Sado Y, Ninomiya Y, Ogawa M (2002) Differential distribution of basement membrane type IV collagen alpha1(IV), alpha2(IV), alpha5(IV) and alpha6(IV) chains in colorectal epithelial tumors. Pathol Int 52:224–233
9. Hofmann UB, Westphal JR, Van Muijen GN, Ruiter DJ (2000) Matrix metalloproteinases in human melanoma. J Invest Dermatol 115:337–344
10. Hudson BG, Reeders ST, Tryggvason K (1993) Type IV collagen: structure, gene organization, and role in human diseases. Molecular basis of Goodpasture and Alport syndromes and diffuse leiomyomatosis. J Biol Chem 268:26033–26036
11. Kadono G, Ishihara T, Yamaguchi T, Kato K, Kondo F, Naito I, Sado Y, Saisho H (2004) Immunohistochemical localization of type IV collagen alpha chains in the basement membrane of the pancreatic duct in human normal pancreas and pancreatic diseases. Pancreas 29:61–66
12. Kagawa M, Kishiro Y, Naito I, Nemoto T, Nakanishi H, Ninomiya Y, Sado Y (1997) Epitope-defined monoclonal antibodies against type-IV collagen for diagnosis of Alport's syndrome. Nephrol Dial Transplant 12:1238–1241
13. Kato T, Takematsu H, Tomita Y, Takahashi M, Abe R (1987) Malignant melanoma of mucous membranes. A clinicopathologic study of 13 cases in Japanese patients. Arch Dermatol 123: 216–220
14. Lee YJ, Nagai N, Siar CH, Nakano K, Nagatsuka H, Tsujigiwa H, Roan CH, Gunduz M (2002) Angioarchitecture of primary oral malignant melanomas. J Histochem Cytochem 50:1555–1562
15. Marneros AG, Olsen BR (2001) The role of collagen-derived proteolytic fragments in angiogenesis. Matrix Biol 5–6:337–345
16. Maniotis AJ, Folberg R, Hess A, Seftor EA, Gardner LM, Pe'er J, Trent JM, Meltzer PS, Hendrix MJ (1999) Vascular channel formation by human melanoma cells in vivo and in vitro: vasculogenic mimicry. Am J Pathol 155:739–752

17. Misumi S, Iyama K, Honda Y, Kitano T, Sado Y, Ninomiya Y, Shinohara M (2004) Differential expression of basement membrane type-IV collagen alpha1, alpha2, alpha5 and alpha6 chains among the histological subtypes of adenoid cystic carcinoma. Virchows Arch 445:54–462
18. Nagase H, Woessner JF (1999) Matrix metalloproteinases. J Biol Chem 274:21491–21494
19. Nagatsuka H, Siar CH, Nakano K, Tsujigiwa H, Gunduz M, Choufuku H, Lee YJ, Naito I, Sado Y, Nagai N (2002) Differential expression of collagen IV alpha1 to alpha6 chains in basement membranes of benign and malignant odontogenic tumors. Virchows Arch 441:392–399
20. Nakano KY, Iyama KI, Mori T, Yoshioka M, Hiraoka T, Sado Y, Ninomiya Y (2001) Loss of alveolar basement membrane type IV collagen alpha3, alpha4, and alpha5 chains in bronchioloalveolar carcinoma of the lung. J Pathol 194:420–427
21. Nakano S, Iyama K, Ogawa M, Yoshioka H, Sado Y, Oohashi T, Ninomiya Y (1999) Differential tissular expression and localization of type IV collagen alpha1(IV), alpha2(IV), alpha5(IV), and alpha6(IV) chains and their mRNA in normal breast and in benign and malignant breast tumors. Lab Invest 79:281–292
22. Ninomiya Y, Kagawa M, Iyama K, Naito I, Kishiro Y, Seyer JM, Sugimoto M, Oohashi T, Sado Y (1995) Differential expression of two basement membrane collagen genes, COL4A6 and COL4A5, demonstrated by immunofluorescence staining using peptide-specific monoclonal antibodies. J Cell Biol 5:1219–1229
23. Oka Y, Naito I, Manabe K, Sado Y, Matsushima H, Ninomiya Y, Mizuno M, Tsuji T (2002) Distribution of collagen type IV alpha1-6 chains in human normal colorectum and colorectal cancer demonstrated by immunofluorescence staining using chain-specific epitope-defined monoclonal antibodies. J Gastroenterol Hepatol 9:980–986
24. Pasco S, Ramont L, Maquart FX, Monboisse JC (2004) Control of melanoma progression by various matrikines from basement membrane macromolecules. Crit Rev Oncol Hematol 49:221–233
25. Rapidis AD, Apostolidis C, Vilos G, Valsamis S (2003) Primary malignant melanoma of the oral mucosa. J Oral Maxillofac Surg 61:1132–1139
26. Regezi JA, Hayward JR, Pickens TN (1978) Superficial melanomas of oral mucous membranes. Oral Surg Oral Med Oral Pathol 5:730–740
27. Sado Y, Kagawa M, Kishiro Y, Sugihara K, Naito I, Seyer JM, Sugimoto M, Oohashi T, Ninomiya Y (1995) Establishment by the rat lymph node method of epitope-defined monoclonal antibodies recognizing the six different α chains of human type IV collagen. Histochem Cell Biol 104:267–275
28. Sado Y, Kagawa M, Naito I, Ueki Y, Seki T, Momota R, Oohashi T, Ninomya Y (1998) Organization and expression of basement membrane collagen IV genes and their roles in human disorders. J Biochem (Tokyo) 15:767–776
29. Saito K, Naito I, Seki T, Oohashi T, Kimura E, Momota R, Kishiro Y, Sado Y, Yoshioka H, Ninomiya Y (2000) Differential expression of mouse alpha5(IV) and alpha6(IV) collagen genes in epithelial basement membranes. J Biochem (Tokyo) 3:427–434
30. Seki T, Naito I, Oohashi T, Sado Y, Ninomiya Y (1998) Differential expression of type IV collagen isoforms, alpha5(IV) and alpha6(IV) chains, in basement membranes surrounding smooth muscle cells. Histochem Cell Biol 4:359–366
31. Schaumburg-Lever G, Lever I, Fehrenbacher B, Moller H, Bischof B, Kaiserling E, Garbe C, Rassner G (2000) Melanocytes in nevi and melanomas synthesize basement membrane and basement membrane-like material. An immunohistochemical and electron microscopic study including immunoelectron microscopy. J Cutan Pathol 27:67–75
32. Tanaka K, Iyama K, Kitaoka M, Ninomiya Y, Oohashi T, Sado Y, Ono T (1997) Differential expression of alpha 1(IV), alpha 2 (IV), alpha 5(IV) and alpha 6(IV) collagen chains in the basement membrane of basal cell carcinoma. Histochem J 29:563–570
33. Timar J, Toth J (2000) Tumor sinuses-vascular channels. Pathol Oncol Res 6:83–85
34. Umeda M, Komatsubara H, Shibuya Y, Yokoo S, Komori T (2002) Premalignant melanocytic dysplasia and malignant melanoma of the oral mucosa. Oral Oncol 7:714–722
35. Zheng K, Harvey S, Sado Y, Naito I, Ninomiya Y, Jacobs R, Thorner PS (1999) Absence of the alpha6(IV) chain of collagen type IV in Alport syndrome is related to a failure at the protein assembly level and does not result in diffuse leiomyomatosis. Am J Pathol 6:1883–1891

Virchows Arch (2005) 447: 717–722
DOI 10.1007/s00428-005-0015-2

ORIGINAL ARTICLE

Reiko Ito · Naohide Oue · Kazuhiro Yoshida · Kyoko Kunimitsu · Hirofumi Nakayama · Kei Nakachi · Wataru Yasui

Clinicopathological significant and prognostic influence of cadherin-17 expression in gastric cancer

Received: 15 March 2005 / Accepted: 17 May 2005 / Published online: 26 July 2005
© Springer-Verlag 2005

Abstract Cadherin-17 (CDH17), also called liver–intestine cadherin, is a structurally unique member of the cadherin superfamily. Our serial analysis of gene expression demonstrated that CDH17 was one of the most up-regulated genes in advanced gastric carcinomas. CDH17 expression is known to be regulated by Cdx2. In the present study, we examined the expression of CDH17 in primary gastric carcinoma tissues by immunohistochemistry, and analyzed the correlation of CDH17 expression with clinicopathological characteristics and patients prognosis. CDH17 expression was detected in 63/94 (67%) of gastric adenocarcinomas in addition to intestinal metaplasia. The expression of CDH17 tended to be associated with intestinal type carcinoma, and carcinomas with CDH17 expression was significantly more frequent in advanced stage cases (80%) than in early stage (53%). The prognosis of patients with positive CDH17 expression was significantly poorer than that of the negative cases (P=0.0314). However, multivariate analysis revealed that CDH17 was not an independent prognostic factor. Six of seven cases that showed positive expression of Cdx2 simultaneously expressed CDH17 protein. These results suggested that the expression of CDH17 was characteristic of the advanced gastric carcinoma that is associated with poor prognosis.

Keywords CDH17 · Gastric carcinoma · Prognosis · Immunohistochemistry

R. Ito · K. Nakachi
Department of Radiobiology/Molecular Epidemiology,
Radiation Effect Research Foundation,
5-2 Hijiyama Park, Minami-ku,
Hiroshima, Japan

N. Oue · K. Kunimitsu · H. Nakayama · W. Yasui (✉)
Department of Molecular Pathology,
Hiroshima University Graduate School of Biomedical Sciences,
Minami-ku,
Hiroshima, Japan
e-mail: wyasui@hiroshima-u.ac.jp
Tel.: +81-82-2575147
Fax: +81-82-2575149

K. Yoshida
Department of Surgical Oncology,
Research Institute for Radiation Biology and Medicine,
Hiroshima University,
1-2-3 Kasumi, Minami-ku,
Hiroshima, 734-8551, Japan

Introduction

Cadherin-17 (CDH17), which is also called liver–intestine (LI) cadherin or human peptide transporter-1 (HPT-1), is a structurally unique member of the cadherin superfamily [2, 4]. Whereas the so-called classic cadherins, such as E-, N- and P-cadherin, have five cadherin repeats within the extracellular domain, CDH17 consists of seven cadherin repeats. Moreover, CDH17 has only 20 amino acids in the cytoplasmic domain, whereas classic cadherins have a highly conserved cytoplasmic domain consisting of 150–160 amino acids. CDH17 is expressed in mice and humans almost exclusively in epithelial cells of both embryonic and adult small intestine and colon, with no detectable expression in the liver [1, 5]. It has been reported that transcription factor Cdx2 regulates CDH17 gene expression in the gastrointestinal tract [6]. Cdx2 gene is quite broadly expressed during the early stages of embryonic development; however, in later stages of development and in normal adult tissues, expression of the genes is restricted to epithelium of the small intestine and colon [15]. Cdx2 has been reported as a tumor suppressive factor in colon cancer. It has been reported that CDH17 is overexpressed in hepatocellular carcinoma [18], and the expression of CDH17 could be useful as a marker for predicting the outcome of patients with pancreas cancers [17].

We examined the gene expression profiles of gastric cancer by serial analysis of gene expression (SAGE) and found that CDH17 was one of the most up-regulated genes in the advanced cases [20]. Quantitative RT-PCR analysis had confirmed that over 70% of gastric carcinoma overexpressed CDH17 and the expression levels was significantly associated with depth of tumor invasion [20]. Recent

reports indicated that the expression of CDH17 was correlated with lymph node metastasis [8, 9]. Therefore, CDH17 could be a novel prognostic factor of gastric carcinoma. However, no study has demonstrated the prognostic impact of CDH17 in gastric carcinoma. In the present study, we examined the expression of CDH17 protein in primary gastric carcinoma tissues and corresponding non-neoplastic mucosa by immunohistochemistry, and analyzed the correlation of CDH17 expression with clinicopathological characteristics and patient's prognosis. We also compared CDH17 expression with Cdx2 in gastric carcinoma tissue.

Materials and methods

Tissue samples

We used a total of 94 gastric adenocarcinoma cases. Tumor tissues and corresponding non-neoplastic gastric mucosa were obtained by surgery at the Hiroshima University Hospital and its affiliated hospitals. For immunohistochemistry, tissues were fixed in 10% buffered formalin and embedded in paraffin.

Histological classification of gastric cancer was done according to the Lauren classification system [11]. Staging of gastric carcinoma was done according to the Tumor-Node-Metastasis Stage Grouping [16]. Classification of the quantity of stroma was made according to the criteria of the Japanese Classification of Gastric Cancer [7] as follows: scirrhous type (sci), stroma is abundant and fibrous; medullary type (med), stroma is scanty; intermediate type (int), the quantity of stroma is intermediate between sci and med.

Western blotting and immunohistochemistry

To confirm the specificity of the anti-CDH17 antibody, Western blotting was carried out as described [14]. Human gastric carcinoma cell line, HSC39, was used. The cells were lysed in lysis buffer [50 mM Tris–HCL pH 7.4, 125 mM NaCl, 0.1% (v/v) NP-40, 5 mM ethylene diamine tetraacetic acid (EDTA), 50 mM NaF, 50 μg/ml phenylmethylsulfonyl fluoride (PMSF), 10 μg/ml leupeptin, 10 μg/ml soybean trypsin inhibitor, and 1 μg/ml aprotinin]. Protein (50 μg) was subjected to Western blot analysis. Anti-CDH17 polyclonal antibody (C-17, sc-6978; Santa Cruz Biotechnology, USA) at a 1:100 dilution was used in primary reaction. As expected, a single band of 120 kDa was detected (Fig. 1).

Consecutive 4-μm tissue sections were prepared from paraffin blocks and immunostained for CDH17 and Cdx2. Each section was mounted on a MAS-coated glass slide, deparaffinized, and soaked for 15 min at room temperature in 3% H_2O_2/methanol to block endogenous peroxidase. Anti-CDH17 polyclonal antibody at a 1:200 dilution and anti-Cdx2 monoclonal antibody (CDX2-88, BioGenex, USA) at a 1:100 dilution were used as primary antibody and was applied for overnight at 4°C. The primary antibody was visualized using the Histofine Simple Stain MAX-PO (MULTI) kit (Nichirei, Tokyo, Japan) according to the instruction manual. The slide was counterstained with hematoxylin. Negative control staining was done using non-specific IgG in the primary reaction. The stained slides were observed without clinicopathological information. Reproducibility of staining was confirmed by re-immunostaining via the same method in multiple, randomly selected specimens. To determine the definition of CDH17 expression, we counted the number of positive cells that showed immunoreactivity on the cell membrane among tumor cells in the representative ten microscopic fields, and calculated the percentage of positive cells. The definition of staining was as follows: positive, more than 40% of tumor cells showed immunoreactivity; weak, 5–40% of tumor cells showed immunoreactivity; negative, from 0% to less than 5% of tumor cells showed immunoreactivity. To define Cdx2 expression, we counted the number of nuclear stained cells. Definition of staining was as follows: positive, over 40% of tumor cells showed immunoreactivity; negative, from 0% to less than 40% of tumor cells showed immunoreactivity.

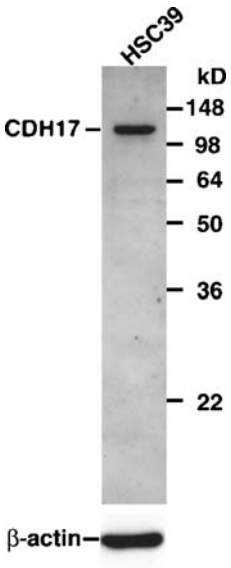


Fig. 1 The specificity of CDH17 antibody. Western blot analysis was performed as described in Materials and methods. A single band of 120 kDa was detected in HSC-39 gastric carcinoma cell lines

Statistical analysis

Statistical analyses were performed with non-parametric test and *P* values were shown. If the P value is less than 0.05, it means that each parameter has a significant correlation with the level of CDH17 expression. Survival rates were calculated via the Kaplan–Meier method. The difference between the survival curves was analyzed by means of log-rank test.

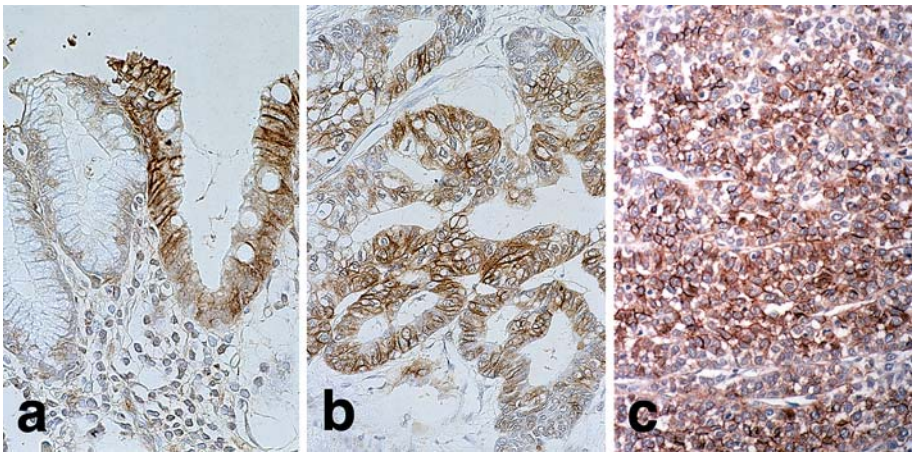


Fig. 2 Expression of CDH17 protein in gastric carcinoma tissues and non-neoplastic mucosa. CDH17 immunohistochemical staining: **a** non-neoplastic mucosa with intestinal metaplasia, **b** intestinal-type carcinoma, **c** diffuse-type carcinoma. CDH17 expression was found in cell membrane and cytoplasm at various levels in gastric carcinoma tissues. In non-neoplastic mucosa, the expression of CDH17 was not recognized in normal foveolar epithelia, while intestinal metaplasia revealed expression of CDH17

Results

Immunohistochemical detection of CDH17 in gastric carcinoma tissues and non-neoplastic mucosa

We immunohistochemically examined the expression and localization of CDH17 protein in 94 cases of gastric carcinoma and non-neoplastic mucosa. Representative stainings of CDH17 are shown in Fig. 2, and the results are summarized in Table 1. CDH17 was expressed in 67% (63/94) of gastric carcinomas at various levels (Fig. 2b, c and Table 1). CDH17 expression was mainly localized in cell membrane and cytoplasm. In non-neoplastic gastric mucosa, CDH17 was also detected in the cell membrane of epithelial cells with intestinal metaplasia (Fig. 2a).

Correlation between CDH17 expression and clinicopathological characteristics of gastric carcinoma

We next analyzed the relationship between the expression of CDH17 and the clinicopathological parameters of gastric carcinoma. As shown in Table 1, the expression of CDH17 tended to be associated with intestinal histology. The incidence of cases with positive expression of CDH17 was significantly higher in medullary type (37/47, 79%),

Table 1 Expression of CDH17 in gastric carcinomas and its correlation with clinicopathological parameters

	Case no.	CDH17 expression[a]		*P* value
		Positive	Weak and negative	
Gastric carcinomas	94	63 (67%)	31 (33%)	
Histology[b]				
Intestinal type	53	39 (74%)	14 (26%)	
Diffuse type	41	24 (59%)	17 (41%)	0.0621
Quantity of stroma[c]				
med	47	37 (79%)	10 (21%)	
sci and int	47	26 (55%)	21 (45%)	0.01581
Depth of invasion[d]				
t1	47	26 (55%)	21 (45%)	
t2–4	47	37 (79%)	10 (21%)	0.01581
Lymph node metastasis				
n0	47	31 (66%)	16 (34%)	
n1–4	47	32 (68%)	15 (32%)	0.08263
Stage[e]				
I	45	24 (53%)	21 (47%)	
II–IV	49	39 (80%)	10 (20%)	0.0683

[a]Grades of CDH17 expression were classified as "positive" and "weak and negative", as described in Materials and methods
[b]Histological classification of gastric carcinoma was done according to the Laure classification system [11]
[c]According to the criteria of the Japanese Classification of Gastric Cancer [7]
[d]Tumor staging of gastric carcinoma was done according to be Tumor-Node-Metastasis Stage Grouping [16]
[e]Correlation was analyzed by non-parametric test and *P* values are shown. *P* values less than 0.05 were regarded as statistically significant

than in scirrhous and intermediate type (26/47, 55%). Positive expression of CDH17 was significantly associated with deep invasion of tumor cells in gastric wall (P=0.01581). The incidence of positive expression of CDH17 tended to be higher in carcinomas with lymph node metastasis. Further more, cases with positive CDH17 expression were significantly more frequent in carcinomas of stages II–IV than stage I (P=0.00683).

Prognosis of gastric carcinoma cases with or without CDH17 expression

We studied the survival rate of gastric carcinoma patients after surgery. If all patients with carcinoma of different stages were included, the cases with positive expression of CDH17 showed worse prognosis than the cases with negative expression of CDH17 (P=0.0314) (Fig. 3). However, we did not find any significant correlation between CDH17 expression and the prognosis of the patients with "stage I and II" carcinoma (P>0.5) or "stage III and IV" carcinoma (P=0.1072). With multivariate survival analysis, the factor that gave the strongest influence was not CDH17 expression, but tumor stage (data not shown). Thus CDH17 expression must be one of the effective factors for gastric cancer prognosis.

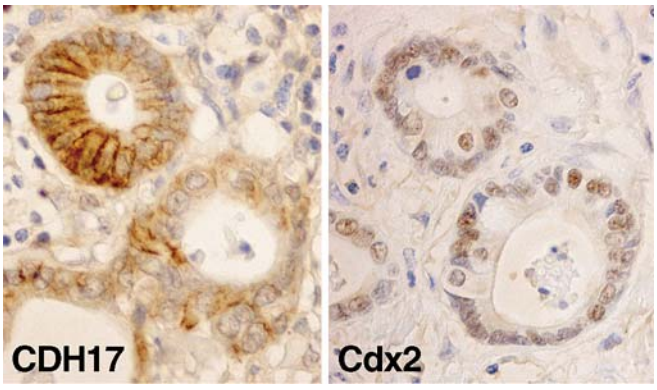


Fig. 4 Relationship of the expression of CDH17 and Cdx2. Synchronous expression of CDH17 and Cdx2 was detected in intestinal type gastric carcinoma

Comparison of the Cdx2 expression with CDH17 expression

We finally compared CDH17 expression with Cdx2 protein expression. Cdx2 immunohistochemical staining was performed in 52 gastric cancer cases extracted from cases that had been investigated with CDH17 immunohistochemical staining. Representative stainings are shown in Fig. 4. Seven

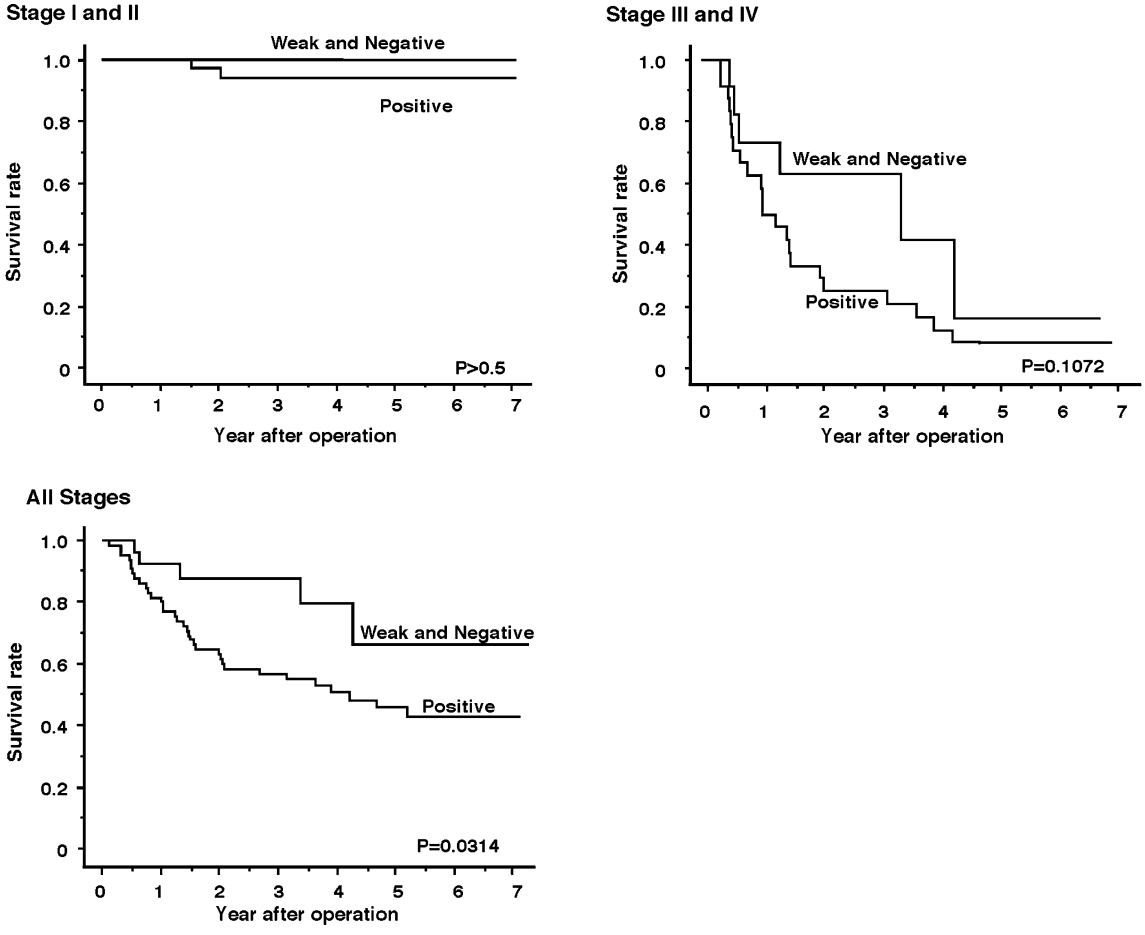


Fig. 3 Comparison of survival rates in patients between CDH17 positive cases, and weak and negative cases. The prognosis of patients with CDH17 positive cases was significantly poorer than that of the patients weak and negative for CDH17, whereas there is no significance between survival rate and CDH17 expression when divided the cases into "stage I and II" and "stage III and IV"

Cdx2 positive cases (7/52, 13%) were found in 52 gastric cancer cases, and all of them were intestinal-type gastric carcinoma. Six of the seven cases (86%) expressed CDH17 simultaneously, and five of these six cases were stage I (data not shown).

Discussion

In the present study, we examined the expression of CDH17 in human gastric carcinoma and compared it with clinicopathological parameters, prognosis and Cdx2 expression. The expression of CDH17 protein was detected in 67% of gastric carcinomas that were correlated with depth of tumor invasion, tumor stage and amount of stromal tissue. It was recently reported that CDH17 mRNA expression is an independent factor associated with lymph node metastasis [8, 9]. Furthermore, our study demonstrated an association between CDH17 expression and poor prognosis. Although CDH17 was not an independent prognostic factor by multivariate analysis, CDH17 expression may be associated with aggressiveness of gastric carcinoma and can be a good marker for high-grade malignancy. On the other hand, in pancreas carcinoma, the survival prognosis was significantly poorer in CDH17 negative tumors compared with CDH17 positive tumors, and CDH17 might participate in the early stage through interaction with galectin-3 [17]. CDH17 may have a distinct organ-specific distribution and the role of CDH17 may be different through distinct intracellular interacting molecules.

Dysregulation of the classical cadherin–catenin adhesion network has been implicated in the progression of gastrointestinal tract cancer [3]. CDH17 is structurally distinct from its E-cadherin counterpart, and there is no direct association with the β-catenin network [10]. According to a previous report, tumor aggressiveness is associated with changes in cadherin expression. For example, P-cadherin, one of the classical cadherins, is highly expressed in well-differentiated adenocarcinoma, and its expression decreased in the advanced stage [19]. E-cadherin expression is also down-regulated in advanced gastric carcinoma cases [12]. LI cadherin is capable of mediating Ca^{2+}-dependent homophilic cell–cell adhesion independent of interactions with the cytoskeleton, indicating that the adhesive function of CDH17 may be complementary to that of E-cadherin. At present, while the role of CDH17 in tumor progression remains unknown, overexpression of CDH17 might be complementary to the co-expressed classical cadherins that are down-regulated in advanced gastric carcinoma.

Cdx2 is one of the transcription factors regulating CDH17 gene expression in normal, metaplastic and neoplastic tissues of the gastrointestinal tract via binding to elements in the 5′-flanking region of the gene [6]. In gastric carcinoma, Cdx2 gene is known to be methylated [21], and therefore epigenetic alteration of CDH17 may be one of the important steps in gastric carcinogenesis. In our study, most of the gastric carcinomas with simultaneous expression of Cdx2 and CDH17 were in the early stage (stage I). All the seven Cdx2 positive cases showed intestinal phenotype and CDH17 positive expression. Moreover, six of seven cases were early stage. Mizoshita et al. [13] examined Cdx2 protein expression with T1 (intramucosal and submucosal invasion) gastric carcinoma cases and the data suggest that Cdx2 is expressed in the very early stage of gastric carcinogenesis in association with the shift from gastric to intestinal phenotypic expression. Because our samples were constructed from all stages of gastric carcinomas, the number of Cdx2 positive cases is lower in our study. Alternatively, CDH17 may regulate not only Cdx2 but also other transcriptional factors.

Our results suggest that CDH17 may participate not only in stomach carcinogenesis, but also in tumor progression which is associated with poor prognosis. CDH17 and Cdx2 may serve as molecular targets for gastric carcinoma treatment.

Acknowledgements This work was supported in part by Grants-in-Aid from the Ministry of Education, Culture, Sports, and Technology of Japan, and the Ministry of Health, Labor, and Welfare of Japan. The authors thank Masayoshi Takatani and Mutsumi Ueda for their skillful technical assistance.

References

1. Angres B, Kim L, Jung R, Gessner R, Tauber R (2001) LI-cadherin gene expression during mouse intestinal development. Dev Dyn 221:182–193
2. Berndorff D, Gessner R, Kreft B, Schnoy N, Lajous-Petter A, Loch N, Reutter W, Hortsch M, Tauber R (1994) Liver–intestine cadherin: molecular cloning and characterization of a novel Ca(2+)-dependent cell adhesion molecule expressed in liver and intestine. J Cell Biol 125:1353–1369
3. Conacci-Sorrell M, Zhuringky J, Ben-Ze'ev A (2002) The cadherin-catenin adhesion system in signaling and cancer. J Clin Invest 109:987–991
4. Dantzig A, Hoskins J, Tabas L, Bright S, Shepard R, Jenkins I, Duckworth D, Sportsman J, Mackensen D, Paul R Jr (1994) Association of intestinal peptide transport with a protein related to the cadherin superfamily. Science 264:430–433
5. Gessner R, Tauber R (2000) Intestinal cell adhesion molecules. Liver–intestine cadherin. Ann NY Acad Sci 915:136–143
6. Hinoi T, Lucas PC, Kuick R, Hanash S, Cho KR, Fearon ER (2002) CDX2 regulates liver intestine-cadherin expression in normal and malignant colon epithelium and intestinal metaplasia. Gastroenterology 123:1565–1577
7. Japanese Classification of Gastric Carcinoma, 1st English edn. Kanehara, Tokyo, pp 38–65
8. Ko S, Chu K, Luk J, Wong B, Yuen S, Leung S, Wong J (2004) Overexpression of LI-cadherin in gastric cancer is associated with lymph node metastasis. Biochem Biophys Res Commun 319:562–568
9. Ko S, Chu K-M, Luk JM-C, Wong BW-Y, Yuen S-T, Leung S-Y, Wong J (2005) CDX2 co-localized with liver–intestine cadherin in intestinal metaplasia and adenocarcinoma of the stomach. J Pathol 205:615–622
10. Kreft B, Berndorff D, Bottinger A, Finnemann S, Wedlich D, Hortsch M, Tauber R, Gessner R (1997) LI-cadherin-mediated cell–cell adhesion does not require sytoplasmic interactions. J Cell Biol 136:1109–1121
11. Lauren P (1965) The two histological main types of gastric carcinoma. Diffuse and so-called intestinal type carcinoma: an attempt at histological classification. Acta Pathol Microbiol Scand 64:31–49

12. Mayer B, Johnson J, Leitl F, Jauch K, Heiss M, Schildberg F, Birchmeier W, Funke I (1993) E-cadherin expression in primary and metastatic gastric cancer: down-regulation correlates with cellular dedifferentiation and glandular disintegration. Cancer Res 53:1690–1695
13. Mizoshita T, Tsukamoto T, Inada K, Ogasawara N, Hirata A, Kato S, Joh T, Itoh M, Yamamura Y, Tatematsu M (2004) Immunohistochemically detectable Cdx2 is present in intestinal phenotypic elements in early gastric cancers of both differentiated and undifferentiated types, with no correlation to non-neoplastic surrounding mucosa. Pathol Int 54:392–400
14. Oue N, Shigeishi H, Kuniyasu H, Yokozaki H, Kuraoka K, Ito R, Yasui W (2001) Promoter hypermethylation of MGMT is associated with protein loss in gastric carcinoma. Int J Cancer 93:805–809
15. Silberg D, Swain G, Suh E, Traber P (2000) Cdx1 and Cdx2 expression during intestinal development. Gastroenterology 119:661–671
16. Sobin L, Wittekind C (1997) TNM classification of malignant tumors, 5th edn. Wiley-Liss, New York, pp 59–62
17. Takamura M, Sakamoto M, Ino Y, Shimamura T, Ichida T, Asakura H, Hirohashi S (2003) Expression of liver–intestine cadherin and its possible interaction with galectin-3 in ductal adenocarcinoma of the pancreas. Cancer Sci 94:425–430
18. Wong BW, Luk JM, Ng IO, Hu MY, Liu KD, Fan ST (2003) Identification of liver-intestine cadherin in hepatocellular carcinoma—a potential disease marker. Biochem Biophys Res Commun 311:618–624
19. Yasui W, Sano T, Nishimura K, Kitadai Y, Ji ZQ, Yokozaki H, Ito H, Tahara E (1993) Expression of P-cadherin in gastric carcinomas and its reduction in tumor progression. Int J Cancer 54:49–52
20. Yasui W, Oue N, Ito R, Kuraoka K, Nakayama H (2004) Search for new biomarkers of gastric cancer through serial analysis of gene expression and its clinical implication. Cancer Sci 95:385–392
21. Yuasa Y, Nagasaki H, Akiyama Y, Sakai H, Nakajima T, Ohkura Y, Takizawa T, Koike M, Tani M, Iwai T, Sugihara K, Imai K, Nakachi K (2005) Relationship between Cdx2 gene methylation aid dietary factors in gastric cancer patients. Carcinogenesis 26:193–200

Virchows Arch (2005) 447: 723–730
DOI 10.1007/s00428-005-0014-3

ORIGINAL ARTICLE

Ryouta Hori · Yoshihiro Murai · Kouichi Tsuneyama · Hekmat Osman Abdel-Aziz · Kazuhiro Nomoto · Hiroyuki Takahashi · Chun-mei Cheng · Tomohiko Kuchina · Brian V. Harman · Yasuo Takano

Detection of JC virus DNA sequences in colorectal cancers in Japan

Received: 13 November 2004 / Accepted: 21 April 2005 / Published online: 14 July 2005
© Springer-Verlag 2005

Abstract JC virus (JCV), a ubiquitous polyoma virus that commonly infects humans, was first identified as the etiologic agent for the fetal demyelinating disease, progressive multifocal leukoencephalopathy. Recently, a number of reports have documented detection of JCV in samples derived from several types of neural as well as non-neural human tumors. It has been suggested that oncogenicity of JCV depends on a T antigen having a strict structural homology to the T antigen of simian virus 40. To clarify whether JCV might have a potential role with regard to colorectal cancers, we investigated the presence of its genome in a series of cases along with colorectal adenomas and normal colonic mucosa, targeting T antigen, VP and agnoprotein by nested polymerase chain reaction and Southern blotting and T antigen by immunohistochemistry. While VP and agnoprotein were not found in any of the samples examined, T antigen was detected in 6 of 23 colorectal cancers (26.1%) and 1 of 21 adenomas (4.8%), but none of 20 samples of normal colonic mucosa. No clear and diffuse staining with anti-T-antigen antibodies (1:100) could be detected, and there was no correlation with CD20-positive cells, which might have indicated JCV latent infection of B lymphocytes. Presence of T antigen did not influence clinicopathological variables, including survival. In one colonic cancer case positive for T antigen together with lymph node metastasis, DNA extracted from cancer cells in the lymph node revealed no detection of T antigen. Our results are in the intermediate position between the high T antigen rate (81%) in one report and the lack of it (0%) in another focused on colon cancers. It was concluded that T antigen might be integrated in cancer cells in approximately one fourth of Japanese colon cancer cases without clear and diffuse expression of the protein, suggesting a possible role in oncogenesis which might involve a hit-and-run mechanism.

Keywords JC virus · Colon cancer · T antigen · Carcinogenesis

R. Hori · Y. Murai · K. Tsuneyama · H. O. Abdel-Aziz · K. Nomoto · H. Takahashi · C.-m. Cheng · T. Kuchina · Y. Takano (✉)
First Department of Pathology, Faculty of Medicine, Toyama Medical and Pharmaceutical University, 2630 Sugitani, Toyama, 930-0152, Japan
e-mail: ytakano@ms.toyama-mpu.ac.jp
Tel.: +81-76-4347236
Fax: +81-76-4345016

B. V. Harman
School of Life Science, Queensland University of Technology, Brisbane, 4000, Australia

Introduction

Recently, a number of authors have reported detection of the JC virus (JCV) genome in colorectal cancers [3, 6]. Normally, JCV is thought of as a neurotropic virus which can cause the fatal demyelinating disease, progressive multifocal leukoencephalopathy (PML), and usually occurs in individuals with cell-mediated immunity, including AIDS [24]. However, its genome has also been detected at high rates in neurogenic tumors, such as astrocytomas, oligoastrocytomas, glioblastomas and ependymomas [6, 7, 25], and there is mounting evidence of oncogenic potential for the T antigen viral regulatory protein [16].

JCV, identified as a member of the polyoma virus group, was first isolated from the brain of a patient suffering from PML [23]. It is a non-enveloped DNA virus with icosahedral capsids containing small, circular, double-stranded DNA and has a limited host range, not usually causing productive infections in other species [13]. Its circular genome contains two major regions known as the early region and late transcription units, and the primary transcript from the early region is alternatively spliced to give two mRNAs that encode T antigen (large T antigen) and t antigen (small T antigen). T antigen is a large nuclear phosphoprotein and is an essential factor for viral DNA replication. It binds to the viral origin of replication region (ori) where it promotes the unwinding of the double helix

and recruitment of cellular proteins that are required for DNA synthesis [5, 8, 19]. The late region encodes the capsid structural proteins VP1, VP2 and VP3 due to alternative spliced mRNAs derived from the same primary late transcript and a small regulatory protein known as agnoprotein [13]. It has been reported that JCV binds specifically to certain cell types such as glial cells, tonsillar stromal cells and B lymphocytes but not T lymphocytes [20, 28]. The virus can also infect cells in the kidney, which is a major organ for JCV persistence during latency [4].

After binding to the cell surface, JCV capsids undergo endocytosis and are transported to the nucleus where the viral DNA is uncoated and transcription of the early region begins by a clathrin-dependent mechanism that is blocked by tyrosine-specific protein kinase inhibition [22]. JCV can become integrated into the chromosomal DNA of the cell, especially upon non-permissive infection, the location being random both in terms of sites in the cellular genome and the point in the viral genome where recombination occurs [11, 18]. There are two possible outcomes to infection of a cell by JCV. Permissive cells are able to replicate viral DNA, and the result of JCV entry is lytic infection (PML) with viral amplification. Non-permissive cells do not support viral DNA replication, and the result of viral entry is an abortive infection or cell transformation (oncogenesis).

T antigen is considered to play the most important role in JCV oncogenesis [17] since it interferes with two tumor suppressor proteins, pRb and p53, that regulate cell cycle progression. T antigen binds to pRb and displaces E2F, thereby promoting cell cycle progression and the inappropriate cell proliferation characteristic of oncogenically transformed cells [17]. The release of E2F from Rb normally activates p14ARF expression that leads to stabilization of p53. However, T antigen binds to and inactivates p53 and thus prevents inhibition of the cell cycle, providing an optimal cell environment for viral replication and packaging during JCV lytic infection and facilitating transformation in non-permissive cells [11]. The T antigen also directly binds to β-catenin, increasing protein stability and causing accumulation, the protein then translocating to the nucleus where it enhances expression of genes such as c-myc and cyclin D1, typical of deregulation of the Wnt pathway [10].

The present study was conducted to assess possible involvement of JCV in colon cancer, using a combined immunohistochemical, nested polymerase chain reaction (PCR) and Southern blotting approach, comparing expression of viral components in normal, benign and malignant tissue.

Materials and methods

Cases

Thirty-five cases of surgically resected colorectal adenocarcinomas, 21 endoscopically resected colorectal adenomas (not including high-grade dysplasia, such as non-invasive carcinoma) and 27 cases of normal colonic mucosa biopsies without cancerous lesions were selected from the pathology archives of Toyama Medical and Pharmaceutical University from 1999 to 2000. All patients were immunocompetent and none showed signs or symptoms of PML. All adenocarcinoma cases underwent the TNM system of UICC and Dukes classification. After glyceraldehydes phosphate dehydrogenase (GAPDH) checking, as described below, final entry cases were 64 in total (64/83, 77.1%): 23 adenocarcinomas (23/30, 76.7%; m/f 13:10, 40–85 years), 21 adenomas (21/21, 100%; m/f 18:3, 41–88 years) and 20 samples of normal mucosa (20/27, 74.1%; m/f 7:13, 17–80 years), the last being obtained from non-cancer and non-severe inflammatory disease patients through colonic endoscopy. Clinicopathological details for the colorectal cancer cases are summarized in Table 1. The patients were 13 females and 10 males, with an average age of 66.3 years. Ten cases were complicated by regional lymph node metastasis, and three had distant metastases. All cases were followed up from 0.1 to 5.3 years (mean 3.4 years); three patients died of the disease, and three patients were alive with persistent tumors.

DNA extraction

A dedicated microtome was used to cut the paraffin blocks. Furthermore, the block and blade holder were periodically autoclaved, and a new disposable blade was used for each specimen. The sections were handled with a disposable, one-time use applicator to prevent contamination. Samples from eight to ten sections were employed for DNA extraction using a QIAamp DNA mini kit according to the manufacturer's instructions (Qiagen, Maryland, USA).

Quality of sample DNA

Before JCV genome PCR, we checked the quality of samples by PCR for the housekeeping gene, GAPDH. Extracted DNA was amplified with GAPDH primers (Table 2, 199 bp) in 25-μl reaction mixtures containing 0.12 μl Takara Ex Taq HS (Takara Bio Inc., Siga, Japan) with 2.0 mM $MgCl_2$, 2.5 μl×10 PCR buffer (Takara Bio Inc.), 2.5 μl dNTP mixture (Takara Bio Inc.), 5-μl sample DNA and 0.7 μl (100 μM) of each primer set. The PCR consisted of denaturation pretreatment at 95°C for 7 min and 35 cycles of denaturation at 95°C for 60 s, annealing at 53°C for 60 s and extension at 72°C for 60 s followed by an additional 7 min at 72°C. All reactions were regulated using the Gene Amp 9700 PCR System (Applied Biosystems, Foster City, USA). Ten-microliter aliquots of each PCR product were examined by electrophoresis on 8% polyacrylamide gels. After loading, the gels were stained with ethidium bromide and photographed under ultraviolet light. The positive control was DNA extracted from the paraffin block of colorectal cancer tissue fixed in 10% formalin.

Table 1 Clinicopathological variables for colorectal cancer patients and JCV genome results

Case	Sex	Age	Site	T	N	M	Follow-up	Year	PCR/Southern blot		
									T antigen	VP	Agnoprotein
1	m	52	S	3	0	0	AAW	5.2	+	−	−
2	m	47	S	1	0	0	AAW	5.1	−	−	−
3	m	61	S	4	1	1	AWD	5.2	−	−	−
4	f	77	R	3	0	0	UK	2.7	−	−	−
5	m	85	C	3	0	0	UK	0.5	+	−	−
6	m	71	C	0	0	0	AAW	5.3	+	−	−
7	f	71	A	3	2	0	UK	1.1	−	−	−
8	f	58	R	3	2	0	AAW	5	−	−	−
9	m	71	S	2	0	0	UK	0.1	−	−	−
10	m	68	S	1	0	0	AAW	4.8	+	−	−
11	f	67	T	4	1	0	AWD	4.9	−	−	−
12	f	83	S	1	1	0	UK	0.3	−	−	−
13	f	55	C	3	1	1	DOD	3.2	−	−	−
14	f	69	R	4	1	0	DOD	3.4	−	−	−
15	m	62	R	3	2	0	UK	1.1	−	−	−
16	m	70	C	4	1	0	UK	1.7	+	−	−
17	f	73	S	1	1	0	AAW	4.6	−	−	−
18	m	40	T	4	x	1	DOD	0.8	−	−	−
19	f	65	S	3	0	0	AWD	4.7	−	−	−
20	m	82	A	3	x	0	AAW	4.6	+	−	−
21	m	59	A	0	0	0	AWW	4.6	−	−	−
22	f	65	R	0	0	0	AAW	4.7	−	−	−
23	m	71	R	3	0	0	AAW	4.6	−	−	−

f Female, *m* male, *c* cecum, *A* ascending colon, *T* transverse colon, *S* sigmoid colon, *R* rectum, *x* no lymph node dissection, *AAW* alive and well, *DOD* died of disease, *AWD* alive with disease, *UK* unknown

Nested PCR for the JCV genome

PCR amplification was performed using three individual sets of primers for T antigen, agnoprotein and VP. Some of the primers were used in previous reports [3] (Table 2). Reaction mixtures (25 μl) contained 0.125 μl Takara Ex Taq HS with 2.0 mM $MgCl_2$ 2.5 μl×10 PCR buffer, 2.5 μl dNTP mixture, 1 μmol/l of each primer set (primers 1 and 2) and 2 ml of sample DNA. PCR conditions were denatured at 95°C for 10 min, followed by 30 cycles of denaturation at 95°C for 15 s, annealing for 30 s and extension at 72°C for 30 s. The annealing steps were performed at temperatures of 55°C for the T antigen primers, 57°C for the agnoprotein primers and 54°C for the VP primers. As a termination step, the extension time of the last cycle was increased to 7 min. DNA extracted from JCI cells (JCV cultured neuroblastoma cell line), kindly provided by Associate Professor Sawa (Department of

Table 2 Primer sets and probes used and the PCR procedure

Primers and probes		
T antigen		55°C
Primer 1 (both)	5′-AGT CTT TAG GGT CTT CTA-3′	4255–4272
Primer 2 (first PCR)	5′-GGT GCC AAC CTA TGG AAC AG-3′	4427–4408
Primer 3 (second PCR)	5′-TGA AGA CCT GTT TTG CCA TG-3′	4364–4345
Probe	5′-GTT GGG ATC CTG TGT TTT CAT CAT C-3′	4303–4327
VP		54°C
Primer 1 (both)	5′-TGT GCA CTC TAA TGG GCA AGC-3′	1828–1848
Primer 2 (first PCR)	5′-CTA GGT ACG CCT TGT GCT CTG-3′	2039–2019
Primer 3 (second PCR)	5′-GAT TGC ACT GTG GCA TTC TTT GG-3′	2004–1982
Probe	5′-AGC CAG TGC AGG GCA CCA GC-3′	1872–1891
Agnoprotein		57°C
Primer 1 (both)	5′-GTC TGC TCA GTC AAA CCA CTG-3′	458–438
Primer 2 (first PCR)	5′-GTT CTT CGC CAG CTG TCA C-3′	280–298
Primer 3 (second PCR)	5′-GCA CAG GTG AAG ACA GTG TAG-3′	395–415
Probe	5′-AAA GAC AGA GAC ACA GTG GTT-3′	425–445
GAPDH		53°C
Sense primer	5′-ACA TCA AGA AGG TGG TGA GC-3′	
Antisense primer	5′-CTG TTG CTG TAG CCA AAT TCG T-3′	

Neuropathology, Graduate School of Medicine, Hokkaido University), served as a positive control. Samples amplified in the absence of template DNA were employed as negative controls. Nested PCR was carried out as for the first PCR cycles, using 0.08% (volume) of the first PCR product with primer 1 and primer 3 in each case.

Southern blotting

The nested PCR products were electrophoresed through 2% agarose gels containing ethidium bromide and photographed under ultraviolet light. After gels were denatured, neutralized and Southern blot transferred onto nylon membranes (Roche Diagnostics GmbH, Mannheim, Germany), hybridization was performed using 10 pmol/ml of digoxygenin-labeled oligonucleotide probe (Table 2) at 48°C for 3 h. After washing the membranes with 2×SSC, 0.1% sodium dodecyl sulfate (SDS) and 0.1×SSC, 0.1% SDS at the same temperature as the hybrid temperature, luminescence was detected with X-ray film (Fuji RX-U, Minamiashigara, Japan) using a DIG luminescent detection kit for nucleic acids (Roche Diagnostics GmbH).

Immunohistochemistry

For the immunohistochemical procedure, 4-μm-thick sections were deparaffinized with xylene and rehydrated through an alcohol gradient. The sections were then immersed in TBS-Tween buffer and autoclaved at 120°C for 15 min. The primary antibodies used were clone PAb416 (1:100 dilution, Oncogene Research Products, San Diego, CA, USA) that reacts with the simian virus 40 (SV40) large T antigen, cross-reacting with JCV T antigen as described in previous reports [3] and CD20 (Dako Cytomation, Inc., Carpinteria, CA, USA) for B lymphocytes to inspect the possibility of JCV latent infection. Incubation was with the primary antibodies for overnight, followed by exposure to DAKO EnVision-labeled polymer (Dako Cytomation, Inc.) for 30 min. Staining was developed by reaction with diaminobenzidine chromogen, and counterstaining for 1 min with haematoylin was then performed.

JCI cells, tightened with fibrin clots, fixed with 10% formalin overnight and embedded in paraffin, were cut at 4 μm thick and used as a positive control for clone Pab416.

Statistical analysis

Differences in clinicopathological factors were evaluated by the chi-square test and Student's *t*-test as appropriate. Survival curves were plotted using the Kaplan–Meier method, and *P* values were calculated using the log-rank test. In all analyses, $P<0.05$ was considered to indicate statistical significance.

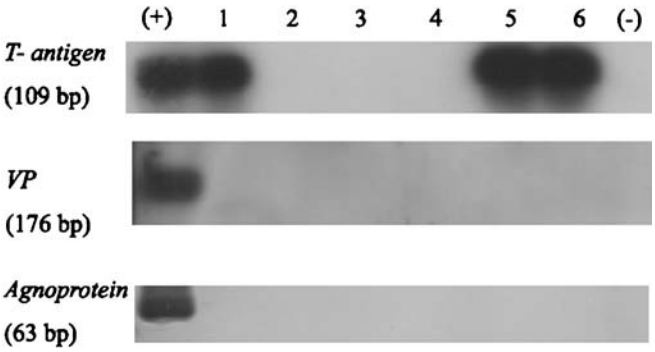


Fig. 1 The *left side* shows the positive control (JCI cells). T antigen, VP and agnoprotein bands are evident in the Southern blot. Cases 1, 5 and 6 of colorectal cancer also show clear single bands for T antigen. VP and agnoprotein bands are only apparent in the positive control. On the *right* is the negative control

Results

Detection of the JCV genome

Figure 1 showed the results of nested PCR/Southern blotting for the T antigen, VP and agnoprotein in some cases (Fig. 1). With regard to T antigen, clear and strong bands were visible in cases 1, 5, 6, 10, 16 and 20 of colorectal cancer (6/23, 26.1%). One adenoma demonstrated the T antigen (1/21, 4.8%) but none of the normal colonic mucosa samples were positive (0/20, 0%). These types of tissue were significantly associated with the presence of T antigen (Table 3; adenoma vs. normal, $P=0.2432$; carcinoma vs. adenoma, $P=0.0425$; carcinoma vs. normal, $P=0.0039$). However, we could not detect VP and agnoprotein in any of the samples, including cancer and adenoma cases and normal mucosa (Table 3). In addition, the one case with lymph node metastasis in six T-antigen-positive cases did not have T antigen present in the metastatic deposits (data not shown).

Correlation between the presence of T antigen and clinicopathological variables and survival in colorectal cancer cases

Since T antigen was only detected in colorectal cancer and adenoma cases, the correlation with clinicopathological variables was investigated. There was no statistically significant links between the presence of T antigen and pT, pN, pM, Dukes classification or histological type (Table 4).

Table 3 Detection rate of T antigen, VP and agnoprotein between colorectal cancer, adenoma and normal mucosa

PCR/Southern blot				
	Number	T antigen	VP	Agnoprotein
Normal mucosa	20	0 (0.0%)	0	0
Adenoma	21	1 (4.8%)	0	0
Adenocarcinoma	23	6 (26.1%)	0	0
		$P=0.0077$	–	–

Table 4 Correlation between clinicopathological variables of colorectal cancer patients and T antigen presence

	T antigen			
	Number	(−)	(+)	
pT				*P*=0.9298
pT0	3	2	1	
pT1	4	3	1	
pT2	1	1	0	
pT3	10	7	3	
pT4	5	4	1	
pN				*P*=0.2357
pN0	11	7	4	
pN1	7	6	1	
pN2	3	3	0	
pM				*P*=0.1607
pM0	20	14	6	
pM1	3	3	0	
Dukes				*P*=0.3654
A	6	4	2	
B	7	4	3	
C	8	7	1	
D	2	2	0	
Type				*P*=0.1642
Well	20	16	4	
Moderate	2	1	1	
Mucinous	1	0	1	

Well Well differentiated adenocarcinoma, *Moderate* moderately differentiated adenocarcinoma, *Mucinous* mucinous adenocarcinoma

As for survival, although a good prognosis was evident for T-antigen-positive cases, statistical significance was not attained (Fig. 2).

Immunohistochemistry

Immunohistochemistry demonstrated no positive staining for T antigen in any of the cases. However, the antibody reacted well with the positive control (Fig. 3a), with cy-

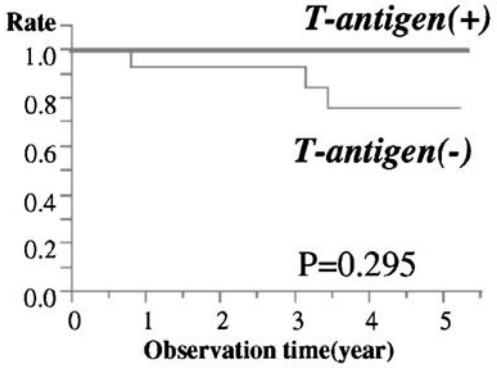


Fig. 2 Survival curves using the Kaplan–Meier method for the T-antigen-positive and negative groups. No statistically significant difference is apparent

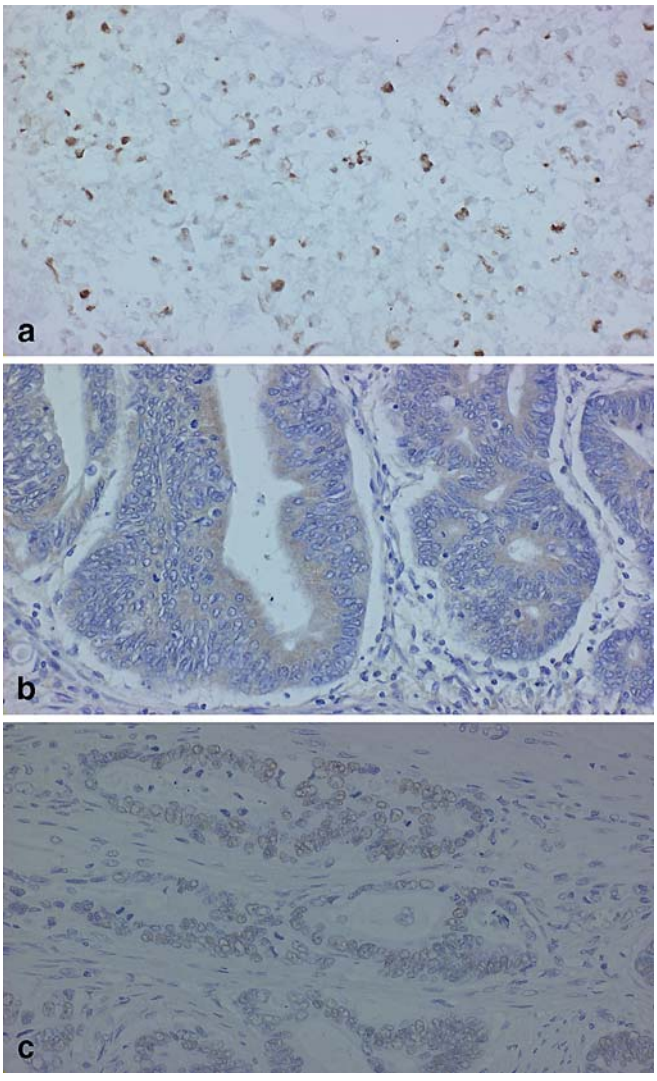


Fig. 3 **a** 10% formalin-fixed and paraffin-embedded JCI cells. About 30% of nuclei of JCI cells bind the PAb146 antibody (1:1,000 titer). **b** A colorectal cancer case reacts for the T antigen(1:100 titer). Cytoplasmic staining is visible weakly. However, this case was judged negative for T antigen (case 15). **c** Another colorectal cancer case reacts for the T antigen (1:100 titer). While a moderate degree of nuclear staining is evident, positive cells were less than 5% and the case was also judged negative (case 23)

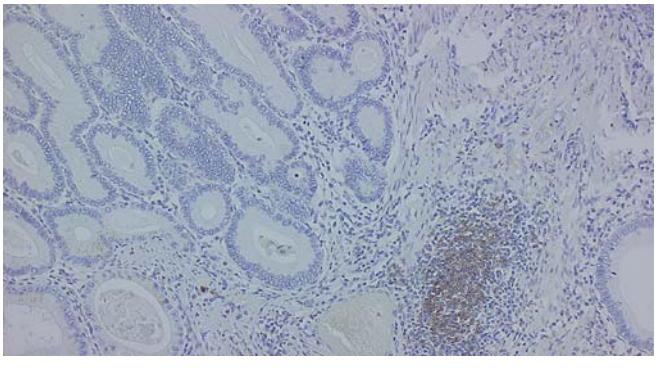


Fig. 4 Aggregates of CD20-positive cells in adenoma tissue

toplasmic staining and limited nuclear staining in less than 10% of cells (Fig. 3b, c).

CD20-positive aggregations consisting of over 30 CD20-positive lymphocytes were counted in each cancer case (Fig. 4). No correlation was evident between the number of CD20-positive aggregations and T antigen presence (Student's *t*-test P=0.64, data not shown).

Discussion

In the present study, JCV T antigen was detected in about 25% of colon cancers, one colon adenoma (5%) and no normal colon samples, whereas agnoprotein and VP were absent in all cases. These results are in contrast to the extremely high rate of 81% in colon cancers reported by Enam et al. [9]. At first, we applied a PCR system for identifying T antigen, agnoprotein and VP in accordance with their approach, although they employed γ32P and we used chemiluminescence. Since obtained bands were actually weak in some cases, the results were not convincing. However, nested PCR succeeded in obtaining clear and strong bands. If JCV integration was a cause of colonic cancer, one could expect to find approximately one virus genome/human genome in cancer tissue [17]. For this reason, weak or faint bands should not be counted as unequivocal positives. Opposite to the results of Enam et al., a recent study reported no evidence of any association of JCV with 233 American cases of invasive colorectal cancer on comparison of matched colorectal tumor/normal tissue samples. They found evidence of the JCV genome only in one normal tissue in spite of usage of a quite sensitive PCR assay [22].

For estimating quality of DNA extracted from paraffin-embedded blocks, it is essential to evaluate PCR products since DNA is easily degraded by formalin fixation. Inoue et al. [14] found fixation in unbuffered 10% formalin to give samples (100% eligible samples) fixed for 1 day, 44% with 2–3 days and only 14% with 4–6 days using PCR amplification with primers producing a 190-bps targeted DNA segment p53 exon 5. Actually, we here first entered over 35 cases of colon carcinomas, but only 23 passed the DNA qualification using primers for the GAPDH housekeeping gene 199 bps in length. However, with fixation in formalin for only 2 days, about 90% of cases complied with the criterion. In the two reports showing completely opposite data (81 vs. 0% in T antigen), where formalin-fixed and paraffin-embedded tissues were employed, there was no mention of the quality of extracted DNA in detail [3, 22]. Another report concerning colonic biopsy samples found a high rate of JCV T antigen detection (81.2%). The assay included treatment with topoisomerase I, which enhanced the sensitivity of JCV T antigen detection [25]. We did not include such topoisomerase I treatment, which may have been a cause of the relatively lower rate for T antigen. However, PCR is a powerful tool for detection of DNA sequences of interest, and problems can arise if there is the possibility of carry-over of amplified DNA into genomic DNA. This is true with screening for virus infection, and therefore, it is necessary to include both positive and negative controls [22]. Even when precautions are taken, contamination may still be a problem. We here performed triplicate experiments for detecting the JCV genome with enough negative controls in each experiment. Results were completely identical in all cases, and no contamination might be evident.

It is essential for evaluating differences to know the background of JCV infection in the general population. JCV is a ubiquitous human polyoma virus which can be detected in raw sewage of urban areas [3]. Infection rates vary among populations and range from 20 to 80% on the basis of urine examination [2]. In one report, 40% of American Caucasians were infected with JCV on inspection of urine samples targeting VP region, but a higher rate was noted for native Americans (from 56 to 69%) [1]. Another report documented a rate of 71% from a similar study [22]. A figure of 40% has been described for Korean people infected with two distinct subtypes of JCV, CY and type 2A [15]. An earlier Japanese study found almost all JCV-infected Japanese to be also subdivided into CY or type 2A, although the infection rate was not determined [12]. Since Japanese and Korean are racially related, a similar incidence of JCV infection might be expected. Enam et al. [9] used 17 Mexican cases out of total 27 cases, and racial variation could clearly be a factor leading to differences.

The detection rates for agnoprotein and VP were lower than that of T antigen in an earlier report [3] and neither could be identified in the present study. JCV may be integrated into the chromosomal DNA of the cell on non-permissive infection, where it occurs at random like SV40 [11, 18]. In laboratory animal studies, when examined by immunohistochemical analysis, JCV-related tumor tissues showed the T antigen in the nuclei of tumor cells. However, attempts to detect VP by immunohistochemistry or virion formation by electron microscopy were unsuccessful [16] in line with our results. The antibody we used has frequently been employed to demonstrate the presence of JCV T antigen [3, 26]. Generally, half-lives of key molecules linked to cell proliferation are very short [27] and hard to detect by immunohistochemistry because these expressions are usually very low, and fixation would be expected to have a major influence. Actually, Shollar et al. [26] employed fresh animal tumor samples for investigating T antigen immunohistochemically. However, immunohistochemistry here precluded the possibility that background JCV latent infection in B lymphocytes could have influenced the detection rate of JCV in colorectal cancer samples.

It remains to be stringently proven that JCV has a causal role in human neoplasia. The incubation period between infection and appearance is long and the initial viral infection is usually subclinical, making it difficult to establish when it may have occurred. Environmental co-factors, such as carcinogens, or host factors, such as immune status, modulate pathogenesis [29] so that Koch's postulates cannot be simply applied in the JCV case. Alternative criteria have been proposed for defining a

causal role for an infection in cancer by zur Hausen [30]: first, epidemiological plausibility and evidence that a virus infection represents a risk factor for the development of a specific tumor; second, regular presence and persistence of the nucleic acid of the respective agent in the specific tumor; third, simulation of cell proliferation upon transfection of the respective genome or parts therefrom in corresponding culture cells; fourth, demonstration that induction of proliferation and the malignant phenotype of specific tumor cells depend on functions exerted by the persisting nucleic acid of the respective agents. Evidence has been described in the present study and earlier reviews [4, 16, 29] that JCV fulfills at least three of these criteria. It seems likely that JCV may perform some role, although possibly limited, in the genesis of colon cancers.

One of our cases positive for T antigen demonstrated lymph node metastasis, but DNA extracted from cancer cells in the lymph node demonstrated no presence of T antigen. A similar phenomenon has been noted in one of cell cultures derived from primitive neuroectodermal tumors (PNETs). After several passages, T-antigen-positive cells lose their expression of T antigen, yet retain their transforming phenotype [16]. It is well established that the adenovirus E1A and E1B gene products can cooperatively transform primary human and rodent cells to a tumorigenic phenotype. Recent studies discovered that oncoproteins E4orf6 and E4orf3 encoded by adenovirus E4 region cooperate with viral E1A proteins to transform primary rat cells in an E1B-like fashion. However, cells transformed by E1A and either E4orf6 or E4orf3 failed to express the viral E4 gene products, and only a subset contained E1A protein. The majority of the cells lack E4- and E1A-specific sequences, indicating that transformation occurs through a hit-and-run mechanism [21]. The same may explain our one case.

In conclusion, T antigen of JCV might be integrated into cancer cells in approximately one fourth of colorectal carcinoma cases, but no clear and diffuse expression of the protein was observed by immunohistochemistry. These results suggested that a hit-and-run mechanism of JCV may be important for the carcinogenesis of human colorectal cancers.

Acknowledgements We thank Tokimasa Kumada, Hideki Hatta, Kanako Yasuyoshi, Nobuhide Hata and Hiroyo Ueda for expert technical support and Yukari Inoue for her secretarial assistance. This investigation was financially supported by a Grant-in-Aid for Basic Scientific Research from the Ministry of Education, Culture, Sports, Science and Technology of Japan.

References

1. Agostini HT, Yanagihara R, Davis V, Ryschkewitsch CF, Stoner GL (1997) Asian genotypes of JC virus in native Americans and in a Pacific Island population: markers of viral evolution and human migration. Proc Natl Acad Sci U S A 94:14542–14546
2. Agostini HT, Jobes DV, Stoner GL (2001) In: Khalili K, Stoner GD (eds) Molecular evolution and epidemiology of JC virus: molecular and clinical perspectives. Wiley-Liss, New York, pp 491–526
3. Bofill-Mas S, Formiga-Cruz M, Clemente-Casares P, Calafell F, Girones R (2001) Potential transmission of human polyomaviruses through the gastrointestinal tract after exposure to virions or viral DNA. J Virol 75:10290–10299
4. Chesters PM, Heritage J, McCance DJ (1983) Persistence of DNA sequences of BK virus and JC virus in normal human tissues and in diseased tissues. J Infect Dis 147:676–684
5. Dean FB, Bullock P, Murakami Y, Wobbe CR, Weissbach L, Hurwitz J (1987) Simian virus 40 (SV40) DNA replication: SV40 large T antigen unwinds DNA containing the SV40 origin of replication. Proc Natl Acad Sci U S A 84:16–20
6. Del Valle L, Delbue S, Gordon J, Enam S, Croul S, Ferrante P, Khalili K (2002) Expression of JC virus T-antigen in a patient with MS and glioblastoma multiforme. Neurology 58:895–900
7. Del Valle L, Gordon J, Enam S, Delbue S, Croul S, Abraham S, Radhakrishnan S, Assimakopoulou M, Katsetos CD, Khalili K (2002) Expression of human neurotropic polyomavirus JCV late gene product agnoprotein in human medulloblastoma. J Natl Cancer Inst 94:267–273
8. Dornreiter I, Hoss A, Arthur AK, Fanning E (1990) SV40 T antigen binds directly to the large subunit of purified DNA polymerase alpha. EMBO J 9:3329–3336
9. Enam S, Del Valle L, Lara C, Gan DD, Ortiz-Hidalgo C, Palazzo JP, Khalili K (2002) Association of human polyomavirus JCV with colon cancer: evidence for interaction of viral T-antigen and beta-catenin. Cancer Res 62:7093–7101
10. Gan DD, Reiss K, Carrill T, Del Valle L, Croul S, Giordano A, Fishman P, Khalili K (2001) Involvement of Wnt signaling pathway in murine medulloblastoma induced by human neurotropic JC virus. Oncogene 20:4864–4870
11. Hara H, Kaji H (1987) Random integration of SV40 in SV40-transformed, immortalized human fibroblasts. Exp Cell Res 168:531–538
12. Ikegaya H, Iwase H (2004) Trial for the geographical identification using JC viral genotyping in Japan. Forensic Sci Int 139:169–172
13. Imperiale M (2001) In: Khalili K, Stoner GL (eds) The human polyoma viruses: molecular and clinical perspective. Wiley-Liss, New York, pp 53–71
14. Inoue T, Nabeshima K, Kataoka H, Koono M (1996) Feasibility of archival non-buffered formalin-fixed and paraffin-embedded tissues for PCR amplification: an analysis of resected gastric carcinoma. Pathol Int 46:997–1004
15. Jeong BH, Lee KH, Choi EK, Kim K, Kim YS (2004) Genotyping of the JC virus in urine samples of healthy Korean individuals. J Med Virol 72:281–289
16. Khalili K, Del Valle L, Otte J, Weaver M, Gordon J (2003) Human neurotropic polyomavirus, JCV, and its role in carcinogenesis. Oncogene 22:5181–5191
17. Krynska B, Gordon J, Otte J, Franks R, Knobler R, DeLuca A, Giordano A, Khalili K (1997) Role of cell cycle regulators in tumor formation in transgenic mice expressing the human neurotropic virus, JCV, early protein. J Cell Biochem 67:223–230
18. Mandl CW, Frisque RJ (1986) Characterization of cells transformed by the human polyomavirus JC virus. J Gen Virol 67(Pt 8):1733–1739
19. Melendy T, Stillman B (1993) An interaction between replication protein A and SV40 T antigen appears essential for primosome assembly during SV40 DNA replication. J Biol Chem 268:3389–3395
20. Monaco MC, Jensen PN, Hou J, Durham LC, Major EO (1998) Detection of JC virus DNA in human tonsil tissue: evidence for site of initial viral infection. J Virol 72:9918–9923
21. Nevels M, Tauber B, Spruss T, Wolf H, Dobner T (2001) "Hit-and-run" transformation by adenovirus oncogenes. J Virol 75:3089–3094

22. Newcomb PA, Bush AC, Stoner GL, Lampe JW, Potter JD, Bigler J (2004) No evidence of an association of JC virus and colon neoplasia. Cancer Epidemiol Biomark Prev 13:662–666
23. Padgett BL, Walker DL (1973) Prevalence of antibodies in human sera against JC virus, an isolate from a case of progressive multifocal leukoencephalopathy. J Infect Dis 127:467–470
24. Price RW (1996) Neurological complications of HIV infection. Lancet 348:445–452
25. Rencic A, Gordon J, Otte J, Curtis M, Kovatich A, Zoltick P, Khalili K, Andrews D (1996) Detection of JC virus DNA sequence and expression of the viral oncoprotein, tumor antigen, in brain of immunocompetent patient with oligoastrocytoma. Proc Natl Acad Sci U S A 93:7352–7357
26. Shollar D, Del Valle L, Khalili K, Otte J, Gordon J (2004) JCV T-antigen interacts with the neurofibromatosis type 2 gene product in a transgenic mouse model of malignant peripheral nerve sheath tumors. Oncogene 23:5459–5467
27. Takano Y, Kato Y, van Diest PJ, Masuda M, Mitomi H, Okayasu I (2000) Cyclin D2 overexpression and lack of p27 correlate positively and cyclin E inversely with a poor prognosis in gastric cancer cases. Am J Pathol 156:585–594
28. Wei G, Liu CK, Atwood WJ (2000) JC virus binds to primary human glial cells, tonsillar stromal cells, and B-lymphocytes, but not to T lymphocytes. J Neurovirol 6:127–136
29. White MK, Khalili K (2004) Polyomaviruses and human cancer: molecular mechanisms underlying patterns of tumorigenesis. Virology 324:1–16
30. zur Hausen H (1999) Viruses in human cancers. Eur J Cancer 35:1878–1885

Virchows Arch (2005) 447: 731–741
DOI 10.1007/s00428-005-0006-3

ORIGINAL ARTICLE

Daniel Palmes · Evgeny Minin · Tymoteusz Budny · Dirk Uhlmann · Barbara Armann · Udo Stratmann · Hermann Herbst · Hans-Ullrich Spiegel

The endothelin/nitric oxide balance determines small-for-size liver injury after reduced-size rat liver transplantation

Received: 5 January 2005 / Accepted: 10 May 2005 / Published online: 13 July 2005
© Springer-Verlag 2005

Abstract Small-for-size (SFS) liver graft injury is probably related to microcirculatory disorders due to an imbalance of vasoconstricting, e.g. endothelin (ET)-1, and vasorelaxing mediators, e.g. nitric oxide (NO). We studied the role of ET-1/NO balance and the effect of an endothelin A receptor (ETAR) antagonist on SFS injury after liver resection and reduced-size liver transplantation (RSLT). One hundred twenty-six Lewis rats were divided into five groups: (I) 70% liver resection, (II) 70% liver resection treated with the ETAR antagonist LU 135252 (1 mg/kg b. w. i.v.), (III) RSLT (30% residual liver volume), (IV) RSLT treated with the ETAR antagonist, (V) sham operation. Liver microcirculation was measured by intravital microscopy. ET-1, ETAR, endothelial NO-synthase (eNOS), activation of Kupffer cells (KCs) and parenchymal injury were studied by immunohistology. Survival and liver function were followed up to 14 days. RSLT led to increased ET-1, ETAR and decreased eNOS protein expression, accompanied by activation of KC, reduced perfusion rate, vasoconstriction and elevated sinusoidal blood flow, as well as hepatocellular damage, impaired liver function and impaired survival. ETAR blockade (groups II + IV) improved the ET-1/NO balance, attenuated microcirculatory disorders and improved hepatocellular apoptosis and liver function. Microcirculatory disorders related to an ET-1/NO imbalance may contribute to SFS liver injury. Maintenance of ET-1/NO balance by blocking ETAR reduces SFS injury by protecting liver microcirculation, thus reducing hepatocellular damage.

Keywords Small-for-size syndrome · Liver transplantation · Endothelin · Endothelin A receptor · Nitric oxide

D. Palmes · T. Budny · H.-U. Spiegel (✉)
Surgical Research, Department of General Surgery,
Muenster University Hospital,
Waldeyer Str. 1,
48149 Muenster, Germany
e-mail: spiegeh@uni-muenster.de
Tel.: +49-251-8356338
Fax: +49-251-8356366

E. Minin · H. Herbst
Institute of Pathology, Muenster University Hospital,
Domagkstr. 17,
48149 Muenster, Germany

D. Uhlmann · B. Armann
Department of Surgery, University of Leipzig,
Leipzig, Germany

U. Stratmann
Department of Anatomy, Muenster University Hospital,
Vesaliusweg 1,
48149 Muenster, Germany

Introduction

Reduced-size liver transplantation (RSLT) in adults, e.g. by living donation, is an accepted alternative used to overcome the increasing demand for donor organs [12]. However, after living graft donation and RSLT, a certain minimal residual liver size in the donor and graft size in the recipient are required to allow rapid liver regeneration and maintenance of liver function. Whereas after standard liver resection, 25% of residual normal liver parenchyma is sufficient; more than 40% residual liver parenchyma is necessary after RSLT to allow liver regeneration without profound impairment of liver function [8, 11, 12]. Indeed, to ensure adequate liver function and regeneration after RSLT, it is recommended that the graft weight to recipient body weight ratio (GRBWR) should be close to 1% [8, 11, 12]. If the GRBWR is less than 0.8%, the residual liver function and regeneration will be impaired, leading to a small-for-size (SFS) syndrome [8, 11, 12].

The mechanism of SFS injury is currently under investigation. Irrespective of individual donor and recipient factors, the SFS injury seems to be primarily linked to graft over-perfusion [7]. It has been shown that portal decompression and improvement of hepatic vein drainage of reduced-size liver grafts might improve liver function [4, 12]. We thought that the same effect could be obtained by optimizing the sinusoidal diameter in reduced-size liver grafts by an administration of a selective endothelin A

receptor (ETAR) antagonist. Endothelin (ET)-1 is a potent vasoconstrictor that is synthesized in sinusoidal endothelial cells (SECs) and generates its effects via the endothelin A receptor, largely on hepatic stellate cells (HSCs) [10, 23]. Under physiological conditions, the ET-1 effects are counterbalanced by vasorelaxing agents such as nitric oxide (NO). In the injured liver, ET-1 production is increased, whereas NO release from SEC is reduced, leading to a reduced perfusion rate, reduced sinusoidal diameter and increased leukocyte–endothelial interaction [13, 18]. Here we investigated the potential role of ET-1/NO balance and the effect of ETAR blockade on the SFS injury after liver resection (simulating the donor after living graft donation) and RSLT (simulating the recipient after RSLT).

Materials and methods

Animals and study design

All operations and handling procedures were in accordance with local animal welfare regulations and approved by the veterinary district administration of Muenster. One hundred and twenty-six isogeneic male Lewis rats (238.8± 40.9 g, Charles River, Germany) were divided into five experimental groups. In group I (RES), a two-thirds hepatectomy was performed (Fig. 1). In group II (RES-ETA), a two-thirds hepatectomy was performed just as in group I, but with treatment of the reduced-size liver with Darusentan (LU 135252, Knoll, Ludwigshafen, Germany, 1 mg/kg b.w. i.v.), immediately before liver resection. In group III (RSLT), an RSLT was performed. For this purpose the donor operation comprised a size reduction of the transplant by a two-thirds hepatectomy. The reduced-size liver transplant (30% of the original liver volume) was then orthotopically transplanted with portal venous reperfusion and transplant arterialisation according to the model of Engemann [19]. In group IV (RSLT-ETA), an RSLT was performed just as in group III, but with ETAR blockade of the reduced-size liver transplants, immediately before reperfusion as in group II. In group V (SHAM), the liver was mobilized by dividing the hepatic ligaments. In groups I, III and V, saline solution was given as vehicle.

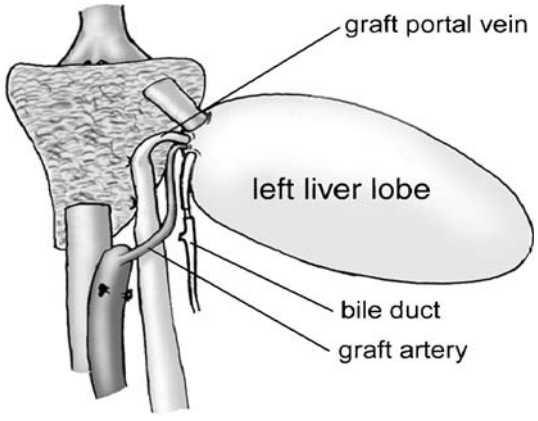


Fig. 1 Surgical technique. RSLT was performed (group III+IV) using a reduced-size liver transplant represented by the left liver lobe (approximately 30% of the original liver volume). The portal vein, supra-, and infrahepatic vena cava were sutured, transplant rearterialisation was carried out using a donor aortic segment and the bile duct was reconstructed by the splint technique according to the model of Engemann [19]

All procedures were carried out under nitrous oxide/isoflurane anaesthesia (N_2O/O_2=2:1+1.5% isoflurane). All animals were assigned to short-term experiments (n=7 per group), in which hepatic microcirculation was assessed by intravital microscopy, or to long-term experiments (resection groups I + II, n=7; transplantation groups III+IV, n=14), in which the rats were kept under observation up to the 14th postoperative day. Preoperatively, the rats were fasted for 24 h, but had free access to water. Postoperatively, animals received water and fed ad libitum.

Liver weight to body weight ratio

In groups I, II and V, the remnant liver weight was determined relative to the liver weight of the remnant liver in untreated Lewis rats (150–250 g, n=10) which had been killed in preliminary experiments. In groups III and IV, the weight of the reduced-size liver graft was determined prior to the recipient operation. Liver weight to body weight ratio (LWBWR) was assessed following the assessment of GRBWR after clinical RSLT using the following formula: liver weight×100/body weight (%) [12]. In this study, an LWBWR of less than 1% was claimed to investigate SFS liver injury.

Serum parameters

Preoperatively, and again 90 min after reperfusion and 1, 2, 7 and 14 days after operation, ammonia (NH_3), bilirubin, albumin and alanine-aminotransferase (ALT) were determined at 25°C by standard enzymatic techniques (micromethod, Ektachem-Kodak, Germany).

Intravital microscopy

Intravital microscopy was performed under constant conditions of anaesthesia and temperature by an adjustable heating system integrated into the table. A polyethylene catheter was inserted into the carotid artery for measurement of arterial blood pressure. Contrast medium was injected via the central venous catheter.

The hepatic microcirculation was studied on the lower surface of the left liver lobe (penetration depth approximately 300 μm) 60 min after liver resection and reperfusion, by intravital fluorescence microscopy [12]. Sodium fluorescein (2 μmol/kg b.w. i.v.; Sigma, Germany) was used to enhance contrast for assessing sinusoidal perfusion, whereas rhodamine 6G (0.2 μmol/kg b.w. i.v., Sigma) was used for vital staining of leukocytes. Microcirculatory parameters were quantified offline by frame-to-frame analysis of video-recorded microscopic images via the

computer-assisted image analysis system AnalySIS (SIS, Muenster, Germany). A final magnification of ×750 was employed for measurement of the microcirculation. Acini (10–12) and post-sinusoidal venules (10–12) were randomly selected and observed for 30 s in each experiment. The following parameters were analysed: sinusoidal perfusion rate [perfused sinusoids/total number of sinusoids observed (%)], sinusoidal diameters [measured in 100 sinusoids per liver both in the periportal and pericentral zones (μm)] and diameters of post-sinusoidal venules (μm); number of sticking leukocytes in sinusoids [stagnant leukocytes not moving during a period of 20 s (n/mm^2)] and sticking leukocytes in post-sinusoidal venules (stagnant leukocytes not moving during a period of 20 s (n/mm^2)]; number of rolling leukocytes in sinusoids [temporarily stagnant leukocytes with adhesion times between 0.2 and 20 s (n/mm^2)] and number of rolling leukocytes in post-sinusoidal venules [leukocytes rolling along the endothelial lining of post-sinusoidal venules (n/mm^2)], as well as the velocity of free-flowing leukocytes in sinusoids and post-sinusoidal venules (μm/s) [21].

Immunohistochemistry

For histological evaluation, all liver specimens were fixed by immersion for at least 2 days in 4% formaldehyde solution and were subsequently dehydrated and embedded in paraffin wax to cut sections at a thickness of 5 μm. Morphologic parameters were recorded by routine histology (hematoxylin and eosin stain). From all sections, photomicrographs were taken off the periportal and pericentral zones of the liver lobule and from the corresponding regions of the control livers in group IV (sham operation). Sections were evaluated for proliferation, atrophy and necrosis of the hepatic parenchyma.

Ultrastructural parameters were recorded by scanning electron microscopy. Liver specimens were cut into 2×2×5 mm blocks, ethanol-dehydrated, freeze-fractured in liquid nitrogen, prepared critical point-dried, ion-sputtered, coated with platinum and viewed with a high-resolution scanning electron microscope (1530 VP, LEO, Germany). Photographs were taken at a magnification of ×20,000.

Immunostaining for activation of Kupffer cells (KCs) (ED-1) and sinusoidal endothelium reactivity detection of the rat endothelial cell antigen (RECA) by His 52 was performed on cryostat sections using the immuno-alkaline phosphatase (APAAP) method, with fuchsin as chromogen. Immunostaining on paraffin sections for ET-1, ETAR, endothelial NO-synthase (eNOS), apoptosis (ssDNA) and nitrotyrosine was performed as follows. After antigen retrieval (Revial, Biocarta, Hamburg, Germany) for 5 min in a domestic pressure cooker as described earlier [15] and after blocking non-specific binding sites with BSA-c basic blocking solution (1:10 in PBS, Aurion, Wageningen, the Netherlands), the sections were immunoreacted with primary antibodies (See Table 1) overnight at 4°C and, after washing in PBS, the sections were treated for 10 min with methanol containing 0.6% H_2O_2 to quench endogenous peroxidase. For fluorescent visualization of bound primary rabbit antibodies, sections were further treated for 1 h at room temperature with DAKO anti-rabbit EnVision-HRP. The HRP label was amplified with FITC-conjugated tyramine at a dilution of 1:300 in PBS in the presence of 0.02% H_20_2 for 10 min. Finally, samples were counterstained for 15 sec with DAPI (5 μg ml^{-1} PBS, Sigma) and mounted with Vectashield (Vector Laboratories, Burlingame, CA, USA). For bright-field microscopy, bound

Table 1 Antibodies and conditions used in this study

Parameter	Primary antibodies	Secondary systems	Analysis
Endothelin-1 (ET-1)	Endothelin-1 (1:50, rabbit polyclonal, DPC Biermann, Bad Nauheim, Germany)	Goat anti-rabbit biotinilated AB (1:20, BiGenex, Hamburg, Germany)	Semi-quantitative score (0–4) [20]
Endothelin A receptor (ETAR)	Endothelin A receptor (1:10, rabbit polyclonal, DPC Biermann)	Goat anti-rabbit biotinilated AB (1:20, BiGenex)	Semi-quantitative score (0–4) [20]
Kupffer cells (KCs)	CD-68 (ED-1) (1:400, mouse monoclonal, Serotec, Oxford, UK)	Goat anti-mouse EnVision-HRP (DAKO Corporation, Hamburg, Germany)	*n* (KC)/100 cells
Apoptosis	ssDNA (1:1,500, rabbit polyclonal, IBL, Gunma, Japan)	Goat anti-rabbit biotinilated AB (1:300, Vector)	*n* (apoptotic HEP)/100 HEP *n* (apoptotic NPC)/100 NPC
Endothelial nitric oxide synthase (eNOS)	eNOS (1 :100, rabbit polyclonal, Transduction Lab., Lexington, KY, USA)	Goat anti-rabbit EnVision-HRP (DAKO)	Semi-quantitative score (0–3)
Nitrotyrosine	Nitrotyrosine (1:20, mouse monoclonal, Zymed, San Francisco, USA)	Goat anti-mouse EnVision-HRP (DAKO)	Semi-quantitative score (0–3)
Rat endothelial cell antigen (RECA)	His 52 (1:40, mouse monoclonal, Serotec)	Goat anti-mouse EnVision-HRP (DAKO)	Semi-quantitative score (0–3)

primary antibodies were detected using DAKO EnVision-HRP and DAB substrate kit (Vector Laboratories), counterstained with Ehrlich hematoxylin for 30 s and mounted with an aqueous mounting medium GelTol (Immunotech, Marseilles, France).

Images shown are representative of at least five independent experiments which gave similar results. The number of KC per 100 hepatocytes (HEPs) was assessed by counting approximately 1,000 HEPs and non-parenchymal cells (NPCs). The apoptosis index, i.e. the proportion of ssDNA decorated nuclei per 100 hepatocellular nuclei, was semi-quantitated by counting approximately 1,000 HEPs and NPCs each. The immunostaining intensity of eNOS, RECA and nitrotyrosine was evaluated by a four-grade score: 0=negative, 1=partially (<25%) weak positive-stained cells, 2=partially (<25%) moderate or diffuse (>75%) weak positive cells, 3=diffuse (>75%) moderate or strong positive cells, 4=diffuse (>75%) strong positive cells. The intensity of cytoplasmic ET-1 and ETAR immunostaining was graded from 0 (no staining) to 3 (maximal intensity of staining). The number of labelled cells was counted and scored semi-quantitatively from 0 to 4 (0=0, 1=1–30, 2=31–60, 3=61–90, 4=>90 stained cells in 1 of 10 observed areas per section; Fig. 5) [20].

Statistics

All data are presented as means±SD. Statistical analysis was performed by the Kruskal–Wallis test using SPSS software. Survival rates were assessed by the Kaplan–Meier method. The log-rank test was used to compare significance. A level of significance of $p<0.05$ was considered as sufficient in all experimental groups.

Results

Survival

After liver resection (group I) six of seven rats survived until their sacrifice at the 14th day (Fig. 2). One rat died on the first postoperative day, showing a macroscopically pale liver. All animals, after liver resection, which were treated with the ETAR antagonist (group II), survived up to the 14th day. After RSLT (group III), the survival rate was significantly reduced compared with that of after liver resection (groups I + II). Three and four rats died on the first or second postoperative day, respectively, displaying pallor and discoloration of the liver in the presence of intact vascular anastomoses. ETAR blockade before RSLT (group IV) led to a survival of 9 of 14 rats. One rat died on the first postoperative day, two rats on the third day and another two on the fourth day (Fig. 2).

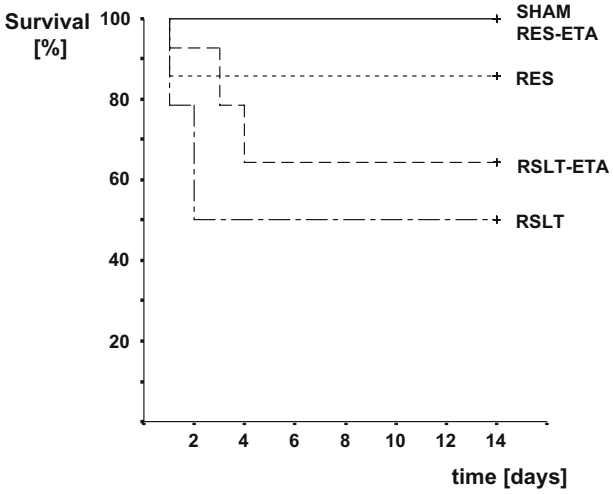


Fig. 2 Survival rates. After RSLT (group III), the survival rate was significantly impaired compared with that of after liver resection (groups I+II), whereas ETAR blockade before RSLT (group IV) led to a survival of 9 of 14 rats. *RES*-Liver resection (group I), *RES-ETA*-liver resection treated by the ETAR antagonist (group II), *RSLT*-reduced-size liver transplantation (group III), *RSLT-ETA*-reduced-size liver transplantation treated by the ETAR antagonist (group IV), *SHAM*-sham operation (group V)

Liver weight body weight ratio

LWBWR was 0.8±0.0% (groups II + III) or 0.8±0.1% (groups I+IV), respectively, and did not differ among groups I–IV, but was significantly lower than in the sham-operation group (Table 2).

Serum parameters

Preoperatively, all serum parameters were within the normal range and did not significantly differ among the groups (Table 3). Liver resection (group I) led to a maximum of ALT release of 912.2±502.1 U/l and an NH_3 level of 199±65.3 μg/dl on the first day, but that was significantly reduced by ETAR blockade (group II). Albumin levels dropped on the first day to 2,285.7±211.6 mg/dl after liver resection (group I) and 1,900±152.8 mg/dl in group II, but normalised by the 14th day. In both groups (I+II), bilirubin levels were within the normal range during the whole postoperative course. RSLT (group III) led to a maximum ALT release of 1,144.1±435.2 U/l on the first day and a maximum NH_3 level of 399.8±141.3 μg/dl 90 min postoperatively, which differed significantly from the liver resection groups (groups I + II). ETAR blockade of reduced-size liver grafts significantly reduced ALT levels at the first, second and seventh day and NH_3 levels 90 min and 1 day after surgery. Albumin levels after RSLT (group III) dropped significantly after surgery compared to the

Table 2 Liver weight body weight ratio (LWBWR)

	RES	RES-ETA	RSLT	RSLT-ETA	SHAM
Rat body weight (g)	232±20.3[a]	178.9±10.3[b,c,d]	244.2±35.9	271.8±36.9	244.4± 21.8
Liver weight (g)	2.0±0.2[a]	1.5±0.1[b,c,d]	2.0±0.2	2.3±0.3	7.5±0.3
LWBWR (%)	0.8±0.1[e]	0.8±0.0[d]	0.8±0.0[f]	0.8±0.1[g]	3.1±0.2

[a]$p<0.05$ RES (I) vs RES-ETA (II), [b]$p<0.05$ RES-ETA (II) vs RSLT (III),
[c]$p<0.05$ RES-ETA (II) vs RSLT-ETA (IV), [d]$p<0.05$ RES-ETA (II) vs SHAM (V),
[e]$p<0.05$ RES (I) vs SHAM (V), [f]$p<0.05$ RSLT (III) vs SHAM (V),
[g]$p<0.05$ RSLT-ETA (IV) vs SHAM (V)
RES-Liver resection (group I), *RES-ETA*-liver resection treated by the ETAR antagonist (group II), *RSLT*-reduced-size liver transplantation (group III), *RSLT-ETA*-reduced-size liver transplantation treated by the ETAR antagonist (group IV), *SHAM*-sham operation (group V)

sham group (group V), but did not differ significantly between both RSLT groups (groups III + IV). Bilirubin levels after RSLT (group III) were significantly increased on the 7th and 14th day and could be reduced by ETAR blockade (group IV).

Intravital microscopy

Arterial blood pressure (mean, 86±12 mm Hg), heart rate (mean, 398±12/min) and body temperature (37.0±0.4°C) showed no significant differences among all groups. Sixty minutes after liver resection (group I), all animals showed microcirculatory disorders with a significantly reduced perfusion rate of 94±1.1%, a reduced periportal sinusoidal diameter of 4.9±0.1 μm and increased numbers of sinusoidal and venular stagnant leukocytes compared to sham-operated animals (group V, Fig. 3). The leukocyte velocity within the liver acini and in the post-sinusoidal veins was increased to 615.7±84.9 μm/s and 1,434.9±176.9 μm/s, respectively, and almost twice as compared to sham-operated animals (group V). ETAR blockade before liver resection (group II) significantly increased the sinusoidal diameter as well as decreased the leukocyte velocity.

Table 3 Serum parameters

Parameter	Group	Preoperatively	90 min after surgery	1st postoperative day	2nd postoperative day	7th postoperative day	14th postoperative day
ALT	RES	17.4±3.2	46.6±15.4[a,b,c]	912.2±502.1[d,b,c]	333.6±213.4[d,a,b,c]	36.1±4.4[a]	33.0±6.5
(<40 U/l)	RES-ETA	21.4±2.1	49.7±10[e,f,g]	700.4±105.3[e,g]	232±79.5[e,g]	27.6±4.9[e]	32.4±7.8
	RSLT	34.3±16.2	289.7±108.3[h]	1,144.1±435.2[i,h]	668.6±333.4[i,h]	294.6±396.1[i,h]	59.5±20.2
	RSLT-ETA	27.0±0.0	236.4±100.8[j]	611.6±59.7	322.7±74.4[j]	74.3±56.8[g]	47±28.6
	SHAM	21.9±1.9	28.3±4.3	44.7±8.8[j]	33.0±5.8	29.9±3.6	27.3±3.9
NH_3	RES	79.3±25.0	127.6±19.8[a,b,c]	199.0±65.3[b,c,d]	112±33.9[c,d]	102.16±23.9[c]	82.4±81.5
(<85 μg/dl)	RES-ETA	66.9±22	126.6±97.1[e,f,g]	87.1±60[e,f,g]	69.1±46[e,g]	81.6±21[g]	85.1±56.9
	RSLT	69.7±17.2	399.8±141.3[h,i]	195.3±16.9[h,i]	103.6±58.2[h]	136.3±79.1[h]	118.4±38.3
	RSLT-ETA	59.0±0.0	229.6±39.6[j]	138.3±28.0[j]	101.4±52.3	95.3±51.6[g]	108.4±86.5
	SHAM	68.7±12.7	86.6±22.5	39.7±21.0	40.6±24.2[i]	58.7±13.9	51.7±18.5
Albumin	RES	2,928.6±243.0	2871.4±298.4[a,b,d]	2285.7±211.6[a,b,c,d]	2,200±216[a,b,c,d]	2,185.7±134.5[a,b,c]	2,600±260.8
(2700–	RES-ETA	2,728.6±95.1	1,928.6±205.9[g]	1,900±152.8[g]	1,900±141.4[g]	2,157.1±214.9[e,f,g]	2,500±238
3000	RSLT	2,750±0.0	2,106.7±90.2[h]	1,828.6±111.3[h]	1,957.1±171.8[h]	2,466.7±196.6[h]	2,683.3±160.2
mg/dl)	RSLT-ETA	2,800±0.0	1,950±251.7[g]	1,757.1±113.4[j]	1,942.9±127.2[j]	2,442.9±335.9[j]	2,542.9±345.7
	SHAM	2,714.3±90.0	2,628.6±95.1	2,771.4±96.2	2,727.6±95.0	2,700±129.1	2,885.7±90.1
Bilirubin	RES	0.2±0.1	0.1±0.1	0.4±0.3	0.2±0.1	0.2±0.1[a]	0.2±0.1
(<1.0	RES-ETA	0.1±0.1	0.1±0.0	0.2±0.2	0.2±0.1	0.1±0.0[b,e]	0.1±0.0
mg/dl)	RSLT	0.2±0.1	0.2±0.1	0.2±0.1	0.4±0.4[h]	2.0±2.1[h]	0.8±3.2[h]
	RSLT-ETA	0.1±0.0	0.1±0.0	0.2±0.1	0.3±0.2[j]	1.8±3.6[g]	0.3±0.2
	SHAM	0.1±0.1	0.1±0.1	0.1±0.0	0.1±0.0	0.1±0.0	0.1±0.0

[a]$p<0.05$ RES (I) vs RSLT (III), [b]$p<0.05$ RES (I) vs RSLT-ETA (IV),
[c]$p<0.05$ RES (I) vs SHAM (V), [d]$p<0.05$ RES (I) vs RES-ETA (II),
[e]$p<0.05$ RES-ETA (II) vs RSLT (III), [f]$p<0.05$ RES-ETA (II) vs RSLT-ETA (IV),
[g]$p<0.05$ RES-ETA (II) vs SHAM (V), [h]$p<0.05$ RSLT (III) vs SHAM (V),
[i]$p<0.05$ RSLT (III) vs RSLT-ETA (IV) [j]$p<0.05$ RSLT-ETA (IV) vs SHAM (V)
RES-Liver resection (group I), *RES-ETA*-liver resection treated by the ETAR antagonist (group II), *RSLT*-reduced-size liver transplantation (group III), *RSLT-ETA*-reduced-size liver transplantation treated by the ETAR antagonist (group IV), *SHAM*-sham operation (group V)

RSLT (group III) led to a significantly decreased perfusion rate of 81.2±1.4%, a sinusoidal diameter of 3.9±0.1 μm and constriction of post-sinusoidal venules, as well as increased counts of sinusoidal and venular stagnant leukocytes, compared to the liver resection (groups I + II) and sham group (group V). The leukocyte velocity within the liver sinusoids and post-sinusoidal veins was increased to 516.5±92.7 and 926.3±239.2 μm/s, respectively. ETAR blockade of reduced-size liver grafts (group IV) significantly reduced microcirculatory disturbances by increasing the perfusion rate, sinusoidal diameter and reducing the sinusoidal leukocyte velocity as well as the numbers of sinusoidal and venular stagnant leukocytes.

Morphology and ultrastructure

After 120 min, all rats which had undergone RES (group I; Fig. 4a,b) and RSLT (group III; Fig. 4e,f) showed a characteristic pattern of damage in the HEPs by cytoplasmic vacuolization and a definite thickening of the endothelium, combined with patchy desquamation of endothelial cells, occasionally resulting in a total loss of endothelium. ETAR blockade in these rats (groups II + IV; Fig. 4c,d,g,h) restored the liver architecture without causing any conspicuous features of cellular damage or destruction in the HEPs and NPCs and preserved the continuity of the endothelium except for some cellular edema and defenestration.

After 14 days, normal liver architecture, without any conspicuous features of cellular damage or destruction among the HEPs and NPCs, was seen in all groups.

Endothelin-1, endothelin A receptor and eNOS

Sham-operated animals (group V) showed no immunoreactivity or only a focal presence of ET-1 (1.0±0.0 pts.) and ETAR (0.3±0.6 pts.) and a strong eNOS protein expression (1.5±0.9 pts.) (Figs. 5i,j and 6). All rats displayed a significantly increased immunoreactivity of ET-1 (3.3±1.2 pts.) and ETAR (2.5±2.1 pts.) 120 min after liver resection (group I), whereas the eNOS protein expression (0.7±1.0 pts.) was reduced (Figs. 5a,b and 6). ETAR blockade before liver resection (group II) significantly

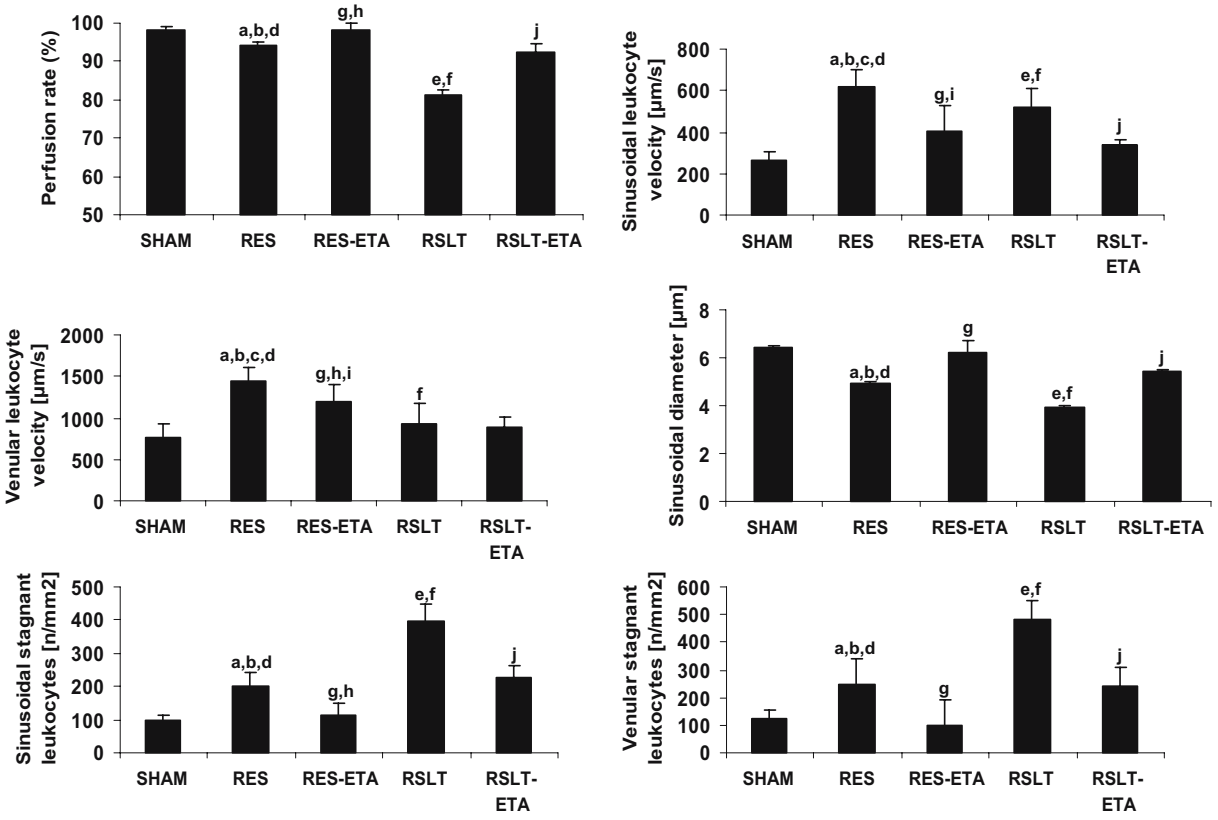


Fig. 3 Results of intravital microscopy. Sixty minutes after surgery, RES and RSLT (groups I+III) had a reduced perfusion rate, vasoconstriction, and elevated leukocyte velocity and leukocyte–endothelial interaction compared to sham-operated animals (group V). ETAR blockade (groups II+IV) reduced these microcirculatory disorders. *RES* Liver resection (group I), *RES-ETA* liver resection treated by the ETAR antagonist (group II), *RSLT* reduced-size liver transplantation (group III), *RSLT-ETA* reduced-size liver transplantation treated by the ETAR antagonist (group IV), *SHAM* sham operation (group V). [a]$p<0.05$ RES (I) vs RES-ETA (II), [b]$p<0.05$, RES (I) vs RSLT (III), [c]$p<0.05$ RES (I) vs RSLT-ETA (IV), [d]$p<0.05$ RES (I) vs SHAM (V), [e]$p<0.05$ RSLT (III) vs RSLT-ETA (IV), [f]$p<0.05$ RSLT (III) vs SHAM (V), [g]$p<0.05$ RES-ETA (II) vs RSLT (III), [h]$p<0.05$ RES-ETA (II) vs RSLT-ETA (IV), [i]$p<0.05$ RES-ETA (II) vs SHAM (V), [j]$p<0.05$ RSLT-ETA (IV) vs SHAM (V)

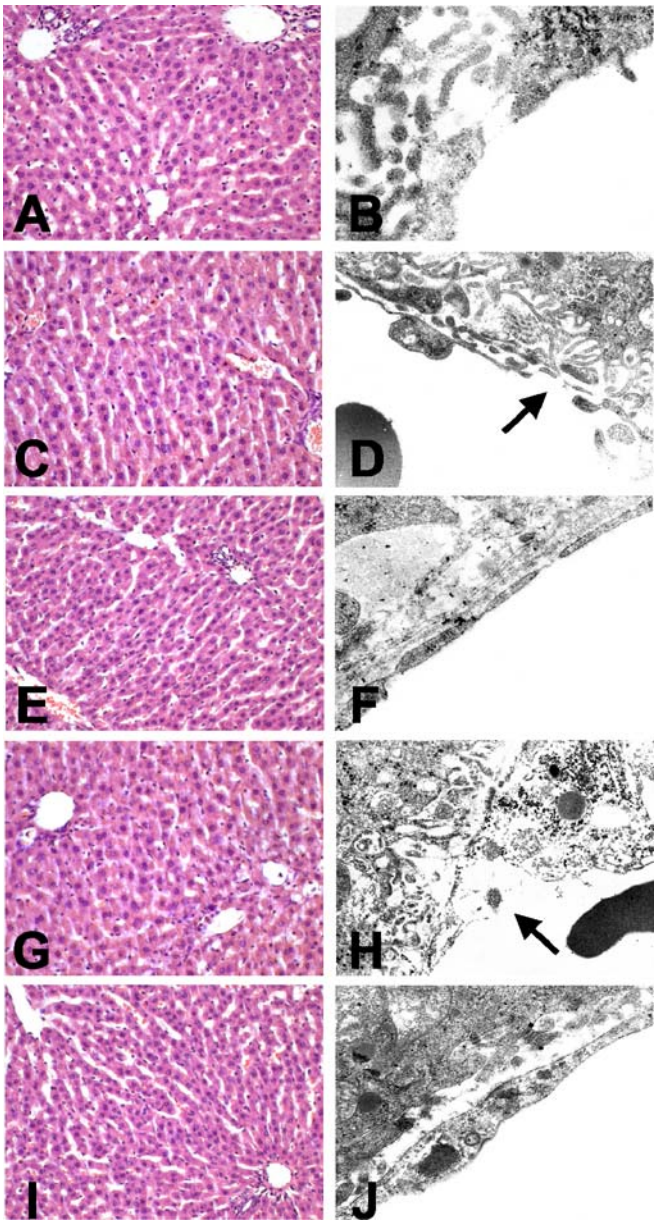


Fig. 4 Morphologic and ultrastructural results. One hundred twenty minutes after RES and RSLT (groups I+III), a characteristic pattern of damage in the hepatocytes, characterised by cytoplasmic vacuolization and definite thickening of the endothelium, combined with patchy desquamation of endothelial cells occurred, occasionally resulting in a total loss of endothelium (*arrow*). ETAR blockade in these groups (II+IV) preserved the continuity of the endothelium with some cellular edema and defenestration (groups II+IV). HE-staining (*left column*) magnification ×120, electron microscopy (*right column*) magnification ×20,000, SHAM (group V, **a**+**b**), RES (group I, **c**+**d**), RES-ETA (group II, **e**+**f**), RSLT (group III, **g**+**h**), RSLT-ETA (group IV, **i**+**j**)

reduced the ET-1 (1.0±0.8 pts.) and ETAR immunoreactivity (1.0±0.0 pts.) and led to moderate eNOS protein expression (3.0±1.0 pts.) (Figs. 5c,d and 6). Just as in the liver resection groups (groups I + II), all animals after RSLT (group III) showed a significantly increased ET-1 (4.0±0.0 pts.) and ETAR protein expression (3.0±2.6 pts.) and decreased eNOS expression (1.1±1.1 pts.) (Figs. 5g,h and 6). Reduced-size liver grafts treated with the ETAR antagonist (group IV) displayed significantly lower ET-1 (3.0±1.7 pts.) and ETAR levels (2.5±1 pts.) as well as moderate eNOS protein expression (2.5±1.2 pts.) (Figs. 5g,h and 6).

After 14 days, the immunoreactivity of ET-1 and ETAR after RES, RSLT and RSLT-ETA and eNOS after RES-ETA and RSLT-ETA were significantly decreased compared to day 0. Furthermore, at this time, differences in the immu-

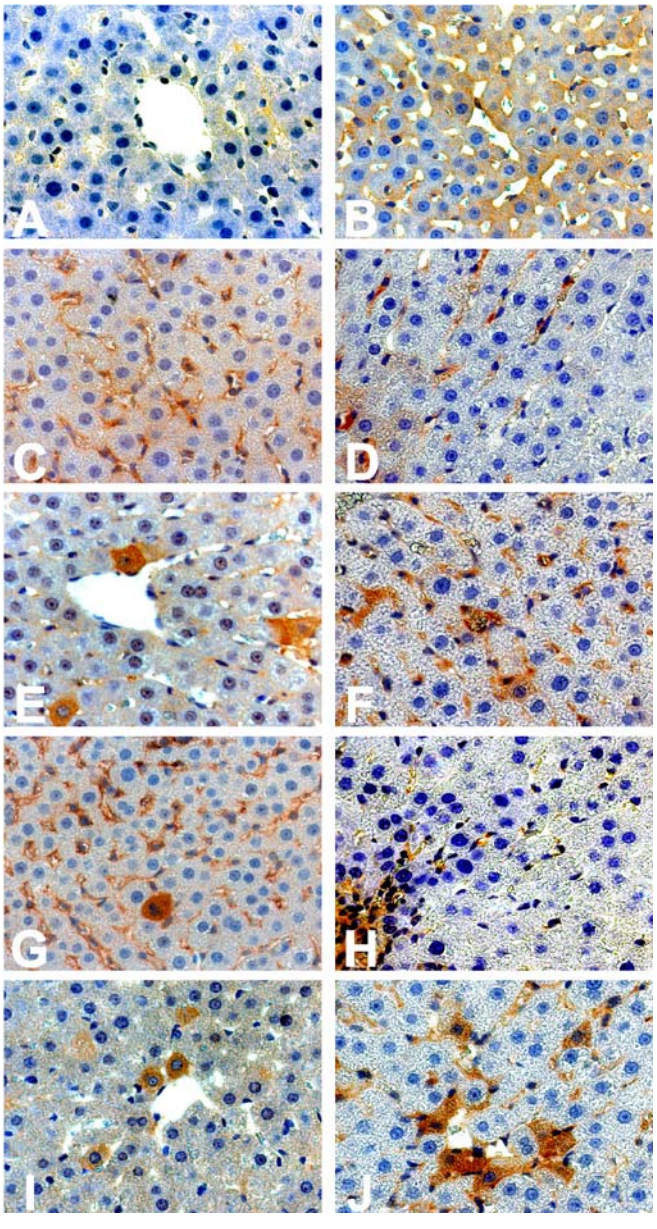


Fig. 5 Intracellular protein expression of ET-1 and eNOS 120 min after surgery. All rats displayed a significantly increased immunoreactivity of ET-1 and ETAR 120 min after RES and RSLT (group I +III), whereas the eNOS protein expression was reduced. ETAR blockade in these groups (II + IV) significantly reduced the ET-1 and ETAR immunoreactivity and led to moderate eNOS protein expression. ET-1 (*left column*), eNOS (*right column*), SHAM (group V, **a**+**b**), RES (group I, **c**+**d**), RES-ETA (group II, **e**+**f**), RSLT (group III, **g**+**h**), RSLT-ETA (group IV, **i**+**j**), magnification ×120

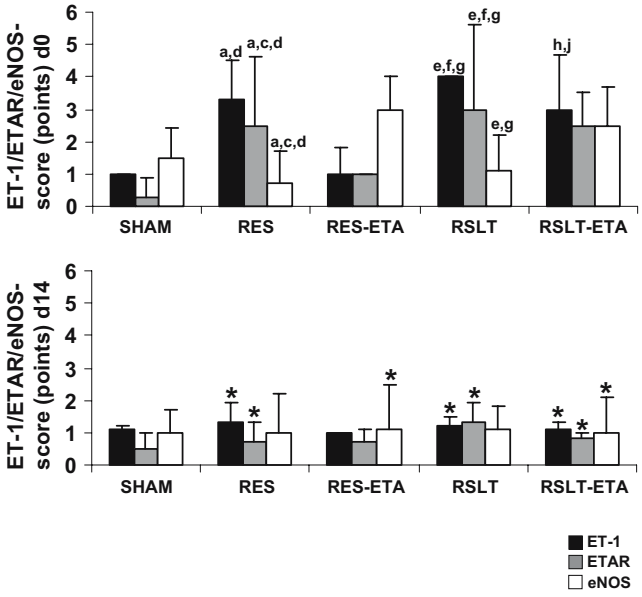


Fig. 6 Semi-quantitative ET-1, ETAR, and eNOS score 120 min and 14 days after surgery (see text for details). [a]$p<0.05$ RES (I) vs RES-ETA (II), [b]$p<0.05$, RES (I) vs RSLT (III), [c]$p<0.05$ RES (I) vs RSLT-ETA (IV), [d]$p<0.05$ RES (I) vs SHAM (V), [e]$p<0.05$ RSLT (III) vs RSLT-ETA (IV), [f]$p<0.05$ RSLT (III) vs SHAM (V), [g]$p<0.05$ RES-ETA (II) vs RSLT (III), [h]$p<0.05$ RES-ETA (II) vs RSLT-ETA (IV), [i]$p<0.05$ RES-ETA (II) vs SHAM (V), [j]$p<0.05$ RSLT-ETA (IV) vs SHAM (V), *$p<0.05$ day 0 vs day 14

noreactivity of ET-1, ETAR and eNOS between all groups were no longer evident (Fig. 6).

Kupffer cells and rat endothelial cell antigen

Sham-operated animals (group V) showed a weakly expression of RECA and numbers of immunostained KC in the sinusoids (Figs. 7a,b and 8). Liver resection (group I, Fig. 7c) and, particularly, RSLT (group III, Fig. 7g) led to an activation of KC up to 9.6±2.4/100 cells and 14.3±3.6/100 cells, respectively, showing a distribution gradient increasing from the periportal tracts towards the central vein (Fig. 8). In addition, these animals showed strong expression of RECA (RES, 3.3±0.5 pts.; RSLT, 3.9±0.3 pts.; Figs. 7d,h and 8). ETAR blockade significantly reduced the number of immunostained KC (RES-ETA, 4.4±3/100 cells; RSLT-ETA, 6.8±2.9/100 cells; Figs. 7e,i and 8) and lowered the expression of RECA after liver resection (group II: 1.4±0.5 pts.; Figs. 7f, and 8) and RSLT (group IV: 1.7±0.5 pts.; Figs. 7j, and 8).

After 14 days, the number of immunostained KC and the expression of RECA were significantly decreased in groups I–IV compared to day 0, and there were no differences between the groups (Fig. 8).

Apoptosis index and nitrotyrosine

After sham operation (group V), no nitrotyrosine and only a few apoptotic cells could be detected (Fig. 9a,b and 10).

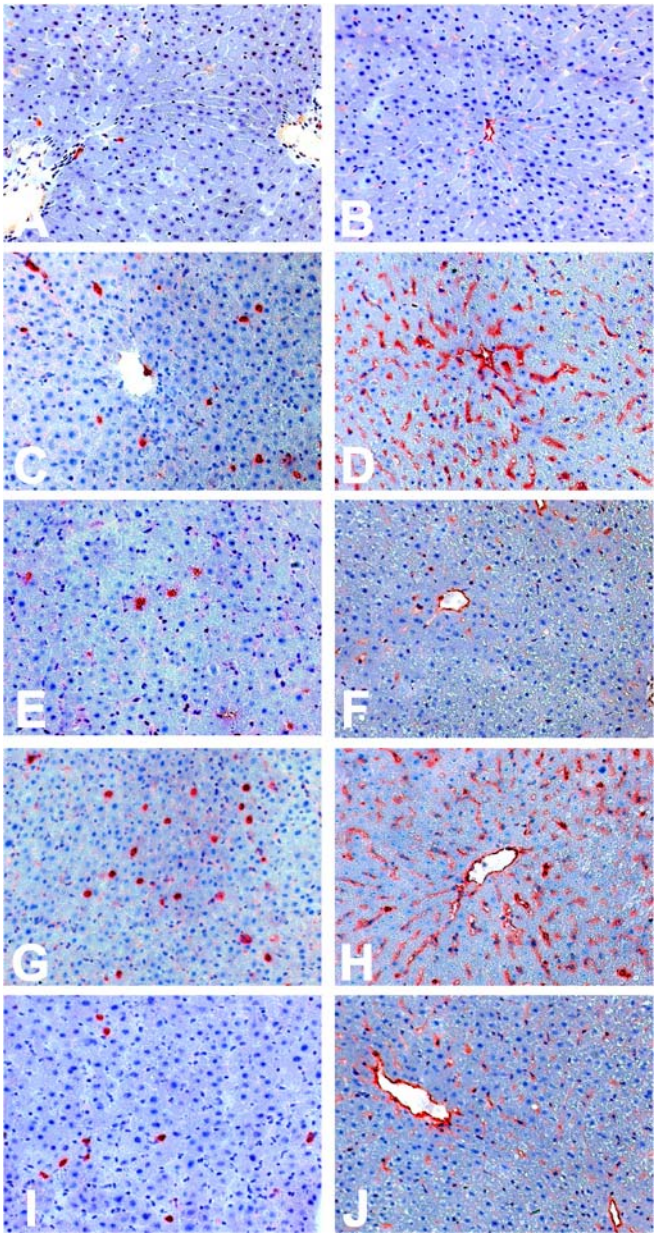


Fig. 7 Kupffer cell and rat endothelial cell antigen staining 120 min after surgery. Sham-operated animals revealed a weak expression of RECA and low number of immunostained KC in the sinusoids, whereas RES and RSLT led to a significant activation of KC and strong expression of RECA. ETAR blockade in these groups reduced the number of immunostained KC and lowered endothelial cell reactivity. Kupffer cell (ED-1)-staining (*left column*), RECA (*right column*), SHAM (group V, **a**+**b**), RES (group I, **c**+**d**), RES-ETA (group II, **e**+**f**), RSLT (group III, **g**+**h**), RSLT-ETA (group IV, **i**+**j**), magnification ×120

After 120 min, the apoptosis index of HEPs and, in particular, of NPCs was significantly increased after RES (group I: 1.7±1.8/100 HEP; 3.8±2.8/100 NPC; Figs. 9c and 10) and RSLT (group III: 3.3±2.5/100 HEP; 4.1±2.3/100 NPC; Figs. 9g and 10). These animals simultaneously showed strong nitrotyrosine immunoreactivity of the endothelial cells in particular (RES, 3.4±0.9 pts.; RSLT, 3.7±0.8 pts.; Figs. 9d,h and 10). ETAR blockade significantly

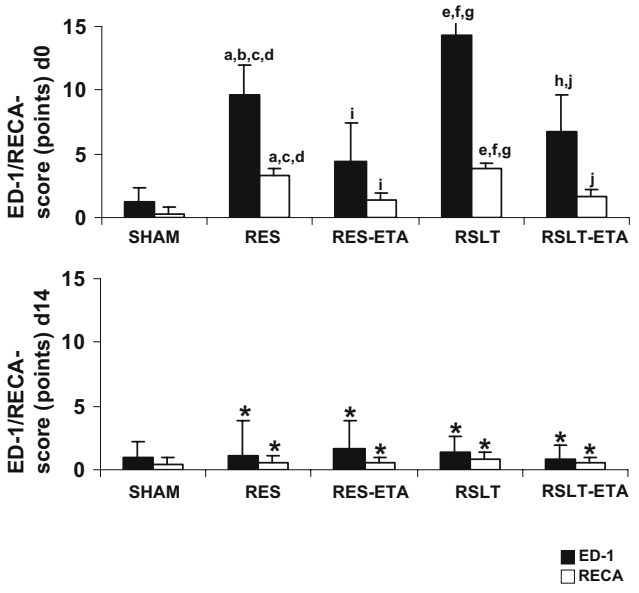


Fig. 8 Semi-quantitative ED-1 and RECA score 120 min and 14 days after surgery (see text for details). [a]$p<0.05$ RES (I) vs RES-ETA (II), [b]$p<0.05$, RES (I) vs RSLT (III), [c]$p<0.05$ RES (I) vs RSLT-ETA (IV), [d]$p<0.05$ RES (I) vs SHAM (V), [e]$p<0.05$ RSLT (III) vs RSLT-ETA (IV), [f]$p<0.05$ RSLT (III) vs SHAM (V), [g]$p<0.05$ RES-ETA (II) vs RSLT (III), [h]$p<0.05$ RES-ETA (II) vs RSLT-ETA (IV), [i]$p<0.05$ RES-ETA (II) vs SHAM (V), [j]$p<0.05$ RSLT-ETA (IV) vs SHAM (V), *$p<0.05$ day 0 vs day 14

reduced the apoptosis index in groups II (1.0±0.8/100 HEP; 1.2±1.1/100 NPC; Figs. 9e and 10) and IV (1.9±1.2/100 HEP; 2.5±2.3/100 NPC; Figs. 9i, 10) as well as reduced nitrotyrosine expression (RES, 1.1±0.7 pts.; RSLT, 1.5±0.8 pts.; Fig. 9f,j).

After 14 days, the apoptotic index of HEP and NPC and nitrotyrosine immunoreactivity were significantly decreased compared to day 0, and there were no differences between the groups (Fig. 10).

Discussion

Microcirculatory disorders correlate with SFS injury after liver resection and RSLT. In this study, rats with a LWBWR of 0.8% displayed characteristic microcirculatory damage with decreased sinusoidal perfusion rates, vasoconstriction and over-proportional sinusoidal blood flow. These microcirculatory changes were accompanied by increased hepatocellular apoptosis, activation of KC and, in particular, damage to SEC with thickening, patchy desquamation and strong expression of RECA leading to impaired liver function and increased mortality. Resection of two-thirds of the liver resection without transplantation—this is a model of the remnant donor liver after living graft donation—led to impaired liver microcirculation and function, but did not affect survival. However, transplantation of a liver graft having the same size—this is a model of the recipient after living graft donation—significantly impairs liver function and survival rate because of the additional ischemia/reperfusion injury [6].

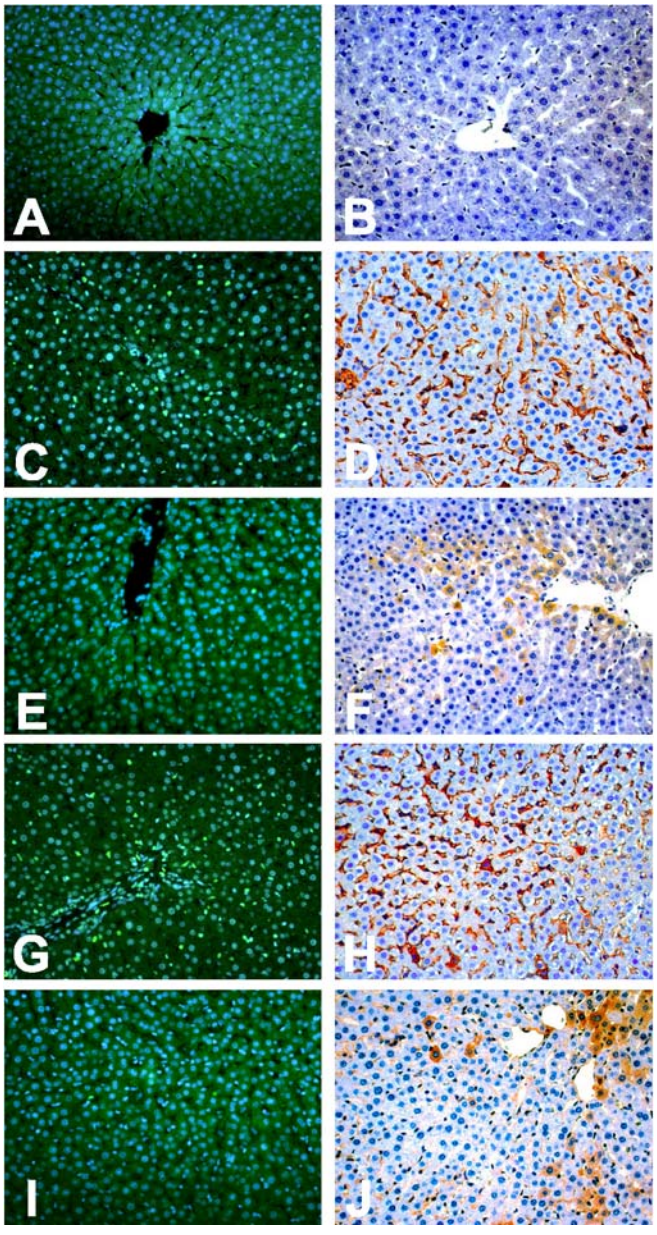


Fig. 9 Apoptosis and nitrotyrosine labelling 120 min after surgery. After sham operation, no nitrotyrosine and only a few apoptotic cells could be detected. The apoptosis index of hepatocytes (HEPs) and non-parenchymal cells (NPCs) and the nitrotyrosine immunoreactivity was significantly increased after RES and RSLT and could be significantly lowered by ETAR blockade. After 14 days, no differences between all groups occurred concerning the apoptosis index and nitrotyrosine immunoreactivity. Apoptosis (*left column*), Nitrotyrosine (*right column*), SHAM (group V, **a**+**b**), RES (group I, **c**+**d**), RES-ETA (group II, **e**+**f**), RSLT (group III, **g**+**h**), RSLT-ETA (group IV, **i**+**j**), magnification ×120

ET-1 and NO seem to play a key role in the pathogenesis of SFS liver injury. NO has vasorelaxing effects and is produced from L-arginine, e.g. by the constitutive eNOS [14]. Whereas under physiological conditions, the sinusoidal diameters are regulated by a balance between ET-1 and NO, liver resection and RSLT lead to a significant increase of ET-1 and ETAR protein expression and, in parallel, to a reduced eNOS expression [15]. It might be postulated that

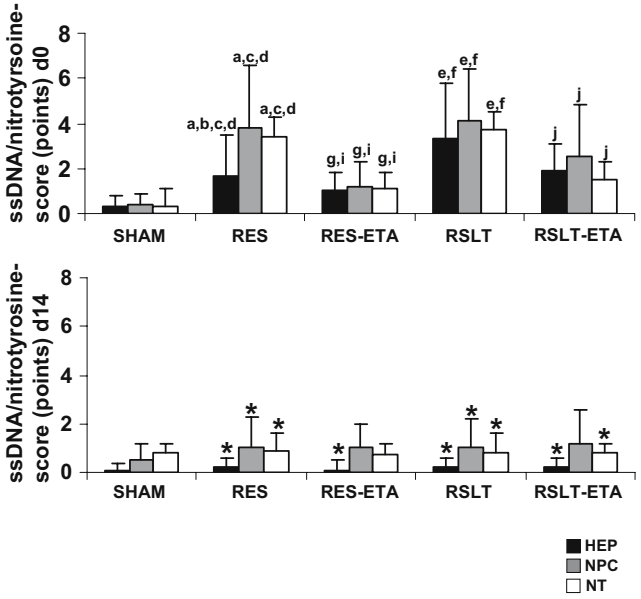


Fig. 10 Apoptosis and nitrotyrosine score 120 min and 14 days after surgery (see text for details). [a]$p<0.05$ RES (I) vs RES-ETA (II), [b]$p<0.05$, RES (I) vs RSLT (III), [c]$p<0.05$ RES (I) vs RSLT-ETA (IV), [d]$p<0.05$ RES (I) vs SHAM (V), [e]$p<0.05$ RSLT (III) vs RSLT-ETA (IV), [f]$p<0.05$ RSLT (III) vs SHAM (V), [g]$p<0.05$ RES-ETA (II) vs RSLT (III), [h]$p<0.05$ RES-ETA (II) vs RSLT-ETA (IV), [i]$p<0.05$ RES-ETA (II) vs SHAM (V), [j]$p<0.05$ RSLT-ETA (IV) vs SHAM (V), *$p<0.05$ day 0 vs day 14

the increased sinusoidal blood flow in the residual livers and the activation of KC would lead to an "endotheliopathy", with increased ET-1 release and up-regulation of ETAR on HSC as well as impaired SEC eNOS activity [10, 14, 16]. KCs are capable of releasing cytokines such as IL-1 or TNF-α, which are known to be potent stimulators of ET-1 release, as well as causing endothelial shear stress and anoxia [2, 9]. The rapid onset of ET-1 and ETAR synthesis, which follows liver damage in this study, is consistent with the kinetics of ET-1 and ETAR–mRNA and protein expression in reperfused pancreas transplants [9, 22]. Increased ET-1 promotes the ETAR-mediated HSC contractility, which is followed by sinusoidal vasoconstriction and the leukocyte–endothelium interaction, as well as the ETBR-mediated constriction of post-sinusoidal venules [19, 21, 22, 24]. Because NO antagonises the effect of ET-1, the reduced production of NO additionally contributes to sinusoidal constriction by HSC and hepatic vascular smooth muscle cells, respectively [14].

Although many vasoactive compounds are likely to play a role in the imbalance of vasoconstrictors and vasodilators leading to an "endotheliopathy" after SFS injury, ET-1 and NO cause the highest magnitude of sinusoidal constriction and relaxation, respectively. To reduce the transient ET-1-mediated sinusoidal constriction and over-perfusion relative to the small size of the remnant liver, a selective ETAR antagonist seemed to be a promising treatment for the acute phase after reperfusion. Selective ETB- and mixed ETA/B-receptor antagonists were rejected because of the absence of any hepatoprotective effect and their narrow therapeutic margin, respectively [3, 24]. ETAR antagonists have been shown to ameliorate toxin- and ischemia-reperfusion-induced hepatic injury as well as portal hypertension and to reduce liver fibrosis [1, 5, 9, 17]. The rationale for administration of the ETAR antagonist immediately before liver resection (group II) or reperfusion (group IV) was the concept that the first few minutes of microcirculatory disturbances seem to be crucially important for the manifestation of SFS liver injury. In view of the transient SFS injury that decreases with progressive regeneration of the liver and the rapid metabolism of the rat, we considered that a single dose of the ETAR antagonist Darusentan—with a half life of 24 h—would be sufficient in this study.

ETAR blockade balanced out the ET-1 and NO levels after liver resection and RSLT with significantly reduced ET-1 and ETAR protein expression and elevated eNOS protein expression, resulting in increased sinusoidal diameter and reduced flow velocity. The reduced number of KC in the treatment groups (groups II + IV) might have additionally contributed to the reduced ET-1 levels by a decreased release of pro-inflammatory mediators [9, 10]. The improved microcirculatory parameters were also reflected in reduced hepatocellular damage, especially SEC apoptosis, and improved serum parameters. However, ETAR blockade did not significantly improve survival after RSLT in this study, probably because the single dose was not sufficient to bridge-over the transient SFS injury that decreases as liver regeneration progresses. Further investigations will be necessary to ascertain whether repeated administration of the ETAR antagonist might significantly improve survival after RSLT.

In summary, it seems possible that the microcirculatory disorders related to ET-1/NO imbalance may have contributed to SFS liver injury. This study has furnished evidence to show that ETAR blockade attenuates microcirculatory disorders and their morphologic sequelae by correcting the ET-1/NO balance and displayed its potential clinical application for the prevention of SFS liver injury in recipients after RSLT, as well as in donors after living graft donation.

Acknowledgements Dr. Daniel Palmes was supported by a grant from the Else Kröner-Fresenius-Stiftung. Evgeny Minin was supported by a Dame Sheila Sherlock Award of the EASL. The authors wish to thank Mrs. K. Cebulla and G. Krull for technical assistance and M. Bühner, Department of Physics, for help with the electron microscopy.

References

1. Anselmi K, Subbotin VM, Nemoto E, Gandhi CR (2002) Accelerated reversal of carbon tetrachloride-induced cirrhosis in rats by the endothelin receptor antagonist TAK-044. J Gastroenterol Hepatol 17:589–597
2. Battistini B, Forget MA, Laight D (1996) Potential roles for endothelins in systemic inflammatory response syndrome with a particular relationship to cytokines. Shock 5:167–183

3. Bauer M, Bauer I, Sonin NV, Kresge N, Baveja R, Yokoyama Y, Harding D, Zhang JX, Clemens MG (2000) Functional significance of endothelin B receptors in mediating sinusoidal and extrasinusoidal effects of endothelins in the intact rat liver. Hepatology 31:937–947
4. Boillot O, Delafosse B, Mechet I, Boucaud C, Pouyet M (2002) Small-for-size reduced-size liver graft in an adult recipient: a new transplant technique. Lancet 359:406
5. Cho JJ, Hocher B, Herbst H, Jia JD, Ruehl M, Hahn EG, Riecken EO, Schuppan D (2000) An oral endothelin-A receptor antagonist blocks collagen synthesis and deposition in advanced rat liver fibrosis. Gastroenterology 118:1179–1186
6. Clavien PA (1998) Sinusoidal endothelial cell injury during hepatic preservation and reperfusion. Hepatology 28:281–285
7. Emond JC, Renz JF, Ferrell LD, Rosenthal P, Lim RC, Roberts JP, Lake JR, Ascher NL (1996) Functional analysis of transplants from living donors. Implications for the treatment of older recipients. Ann Surg 224:544–552
8. Furukawa H, Kishida A, Omura T, Kamiyama T, Suzuki T, Matsushita M, Nakajima Y, Todo S (1999) Indication and strategy for adult living related liver transplantation. Transplant Proc 31:1952
9. Goto M, Takei Y, Kawano S, Nagano K, Tsuji S, Masuda E, Nishimura Y et al (1994) Endothelin-1 is involved in the pathogenesis of ischemia/reperfusion liver injury by hepatic microcirculatory disturbances. Hepatology 19:675–681
10. Housset C, Rockey DC, Bissell DM (1993) Endothelin receptors in rat liver: lipocytes as a contractile target for endothelin 1. Proc Natl Acad Sci U S A 90:9266–9270
11. Kiuchi T, Kasahara M, Uryuhara K, Inomata Y, Uemoto S, Asonuma K, Egawa H, Fujita S, Hayashi M, Tanaka K (1999) Impact of graft size mismatching on graft prognosis in liver transplantation from living donors. Transplantation 67:321–327
12. Kiuchi T, Tanaka K, Ito T, Oike F, Ogura Y, Fujimoto Y, Ogawa K (2003) Small-for-size graft in living donor liver transplantation: how far should we go? Liver Transplant 9:S29–S35
13. Leivas A, Jimenez W, Bruix J, Boix L, Bosch J, Arroyo V, Rivera F, Rodes J (1998) Gene expression of endothelin-1 and ET(A) and ET(B) receptors in human cirrhosis: relationship with hepatic hemodynamics. J Vasc Res 35:186–193
14. Moncada S, Higgs A (1993) The L-arginine-nitric oxide pathway. N Engl J Med 329:2002–2012
15. Rockey DC (2003) Vascular mediators in the injured liver. Hepatology 37:4–12
16. Rockey DC, Chung JJ (1998) Reduced nitric oxide production by endothelial cells in cirrhotic rat liver: endothelial dysfunction in portal hypertension. Gastroenterology 114:344–351
17. Rockey DC, Weisiger RA (1996) Endothelin induced contractility of stellate cells from normal and cirrhotic rat liver: implications for regulation of portal pressure and resistance. Hepatology 24:233–240
18. Shao R, Yan W, Rockey DC (1999) Regulation of endothelin-1 synthesis by endothelin-converting enzyme-1 during wound healing. J Biol Chem 274:3228–3234
19. Spiegel HU, Palmes D (1998) Surgical techniques of orthotopic rat liver transplantation. Invited review. J Invest Surg 11:83–96
20. Uhlmann D, Armann B, Gaebel G, Ludwig S, Hess J, Pietsch UC, Escher E, Fiedler M, Tannapfel A, Hauss J, Witzigmann H (2003) Endothelin a receptor blockade reduces hepatic ischemia/reperfusion injury after warm ischemia in a pig model. J Gastrointest Surg 7:331–339
21. Uhlmann S, Uhlmann D, Spiegel HU (1999) Evaluation of hepatic microcirculation by in vivo microscopy. J Invest Surg 12:179–193
22. Witzigmann H, Ludwig S, Armann B, Gabel G, Teupser D, Kratzsch J, Pietsch UC, Tannapfel A, Geissler F, Hauss J, Uhlmann D (2003) Endothelin (A) receptor blockade reduces ischemia/reperfusion injury in pig pancreas transplantation. Ann Surg 238:264–274
23. Zhang JX, Pegoli W Jr, Clemens MG (1994) Endothelin-1 induces direct constriction of hepatic sinusoids. Am J Physiol 266:G624–G632
24. Zhang XY, Francis RJ, Sun CK, Wheatley AM (2002) Endothelin receptor A blockade ameliorates hypothermic ischemia-reperfusion-related microhemodynamic disturbances during liver transplantation in the rat. J Surg Res 102:63–70

Virchows Arch (2005) 447: 742–746
DOI 10.1007/s00428-005-0017-0

ORIGINAL ARTICLE

Naoki Nishida · Takashi Chiba · Maki Ohtani · Naofumi Yoshioka

Two adult cases of congenital atresia of the left coronary ostium—comparison of a sudden death case with a long-term survival case

Received: 24 February 2005 / Accepted: 16 May 2005 / Published online: 13 July 2005
© Springer-Verlag 2005

Abstract We present two extremely rare autopsy cases with atresia of the left coronary ostium. Case 1 was a 34-year-old man who died of sudden cardiac causes with localized acute subendocardial infarction and Case 2 was an 82-year-old woman who died from non-cardiac causes. In both cases, a string-like small left main trunk that was located in its normal position was found; however, the orifice of the left coronary artery was absent in both cases. The collateral artery (CA), whose caliber was smaller than that of the proximal left descending artery (LAD), arose from the right coronary sinus and was anastomosed with the distal LAD. However, it was only in Case 1 that the CA showed an acute angle of take-off from the aorta, subsequently coursing between the root of the aorta and the pulmonary trunk, with possible mechanical compression by these two arteries. These two cases suggest that atresia of the left coronary ostium is developmentally and anatomically different from single coronary artery or left coronary artery arising from the opposite sinus of valsalva. Atresia of the left coronary ostium is considered to be an important differential diagnosis as a cause of sudden death, not only in the pediatric population but also in adults. The caliber and/or other anatomical features of the CA may predominantly dictate the clinical course of patients with atresia of the left coronary ostium.

Keywords Atresia of left coronary ostium · Collateral artery · Autopsy · Sudden death · Coronary artery anomaly

N. Nishida (✉) · T. Chiba · M. Ohtani · N. Yoshioka
Department of Forensic Science,
Akita University School of Medicine,
Hondo 1-1-1,
Akita, 010-8543, Japan
e-mail: nishida@med.akita-u.ac.jp
Tel.: +81-18-8348712
Fax: +81-18-8362610

Introduction

Congenital atresia of the left coronary ostium is a very rare anomaly of the coronary artery. In a recent publication, the incidence in a continuous series of 1,950 angiograms was 0.67% [1]. Many of the patients whose cases have been previously reported were symptomatic, demonstrating angina, acute myocardial infarction, dyspnea, syncope, and sudden death [8]. Nevertheless, in many of the patients with atresia of the left main coronary ostium, one or more collateral arteries (CA) from the right coronary artery to the left coronary artery were present [8], and the amount of blood flow in the left coronary artery was probably inadequate in almost all of the cases. Here we show the detailed anatomical and pathological findings of two considerably rare adult cases of atresia of the left coronary ostium. One case was found following sudden cardiac death, while the other case was found following non-cardiac death of an aged woman. We compare the anatomical features of the coronary arteries of these two cases with those of other coronary artery anomalies which possibly have identical hemodynamics. In addition, we attempt to compare the anatomical and pathological findings between these two cases with a view to discussing the factors that gave rise to their different outcomes.

Case histories

Case 1 was a 34-year-old man (office worker) who was found dead in the bedroom of his home by one of his office colleagues. He was a single man who had been absent from work for 3 days due to his poor physical condition. He had spoken with the same colleague 2 days before his death. At that time, he had said that he had a cold, but he had not complained of any symptoms that suggested the presence of heart disease. He did not have any apparent medical history, but had not received a medical check-up for at least the past 10 years. He had no problems with his usual daily activities, and he had no history of playing sports of any kind. At autopsy, no traumatic injuries were found on

his body, and alcohol and toxicological examination were negative.

Case 2 was an 82-year-old woman (housewife) who was dead in a severely burned home. Since the level of carbon monoxide in her blood was found to be 70%, the direct cause of death was determined to have been the fire. No other traumatic injuries were found on her body, and alcohol and toxicological examinations were negative. Based on investigations at the scene, we assumed that the cause of the fire had been mismanagement of a wood-burning stove. On the other hand, the woman had a history of mild hypertension and angina pectoris of about 10 years' duration, and oral calcium antagonists had been regularly administered. Since more serious complications had not appeared during those 10 years, and since her age was relatively high, further investigations by invasive procedures had not been performed. She was physically active, and she had no trouble with her daily life. On an electrocardiogram that had been taken the previous year, slight ST segment depression was found on the lead AVF, and a negative T-wave was found on leads I and V4.

Materials and methods

The heart was excised and dissected free from the great vessels. Heart weight, including epicardial coronary arteries and epicardial fat, was measured to the nearest gram. The right and left ventricles were cut at 1-cm intervals parallel to the level of the papillary muscle from the apex. The heart was then opened along the direction of blood flow, and any abnormality in the myocardium, endocardium, or valves was noted. After being fixed with 20% buffered formaldehyde, sections at the level of the papillary muscle and the apex were thoroughly examined histologically. The bilateral atria were also sectioned. The major epicardial coronary arteries, left main trunk, left anterior descending artery (LAD), left circumflex artery, right coronary artery, and their major branches were cut transversely at 5-mm intervals and decalcified as required.

Results

Case 1

The deceased was 170 cm tall and weighed 59 kg. The heart weighed 530 g. On examination of the epicardial coronary arteries, the left main trunk could be discerned as having a string-like appearance and superficially it looked as if it arose from the aorta, but the orifice of the left main trunk was not opened in the left coronary sinus. The LAD and left circumflex artery ended blindly and were located at their normal position with a normal caliber. The CA arose from the right coronary sinus, and the orifice was independent from the right coronary artery. The take-off of the CA demonstrated an acute angle, and the CA finally terminated in the distal LAD after coursing between the root of the aorta and the pulmonary trunk (Fig. 1a, b). While passing between the two large arteries, the surface of the CA was covered by a thin layer of atrial muscle. Horizontal sections of both ventricles showed concentric hypertrophy of the left ventricle and discoloration with softening of the subendocardium of the lateral wall of the left ventricle. No discoloration was found in other regions of the left ventricle or the right ventricle (Fig. 1c). The thickness of the wall was 2.0 cm in the case of the anterior and posterior walls, 2.3 cm in the lateral wall, 1.8 cm in the ventricular septum, and 0.3 cm in the right ventricle. Valvular deformity was not found in any of the valves. As for important gross findings of other organs, polycystic kidney was noted.

On microscopic examination, the heart muscle in the area that was discolored on gross examination revealed focal coagulative necrosis with localized infiltration of neutrophils, these being the findings of acute myocardial infarction (Fig. 2a). The left main trunk demonstrated an arterial appearance, but was completely occluded by non-atherosclerotic intimal hyperplasia. The caliber of the CA was smaller than that of the left-sided coronary artery where it was anastomosed with the CA. The right coronary

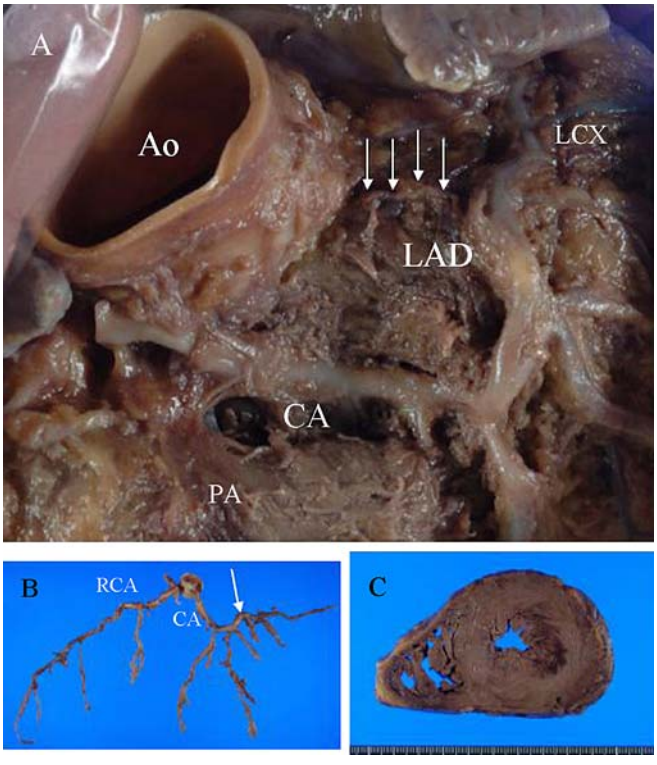


Fig. 1 Gross findings of the heart in Case 1. **a** Gross anatomy of the coronary artery. The pulmonary artery (*PA*) is strongly pulled forward. A string-like left main trunk is indicated by *arrows*. The collateral artery (*CA*) shows an acute angle of take-off from the aorta (*Ao*) and courses between the Ao and the PA. *LAD* Left descending artery, *LCX* left circumflex artery. **b** Coronary artery tree. The left main trunk is already extirpated. Instead, bifurcation of the left descending artery and left circumflex artery is indicated by an *arrow*. The collateral artery (*CA*) is anastomosed with the distal left descending artery. The right coronary artery (*RCA*) is well developed. **c** Horizontal section of the ventricles in Case 1. Discoloration is evident in the subendocardial layer of the lateral wall of the left ventricle

artery was well developed, and atherosclerosis was not found in any artery (Fig. 2b, c).

Case 2

The subject's heart weighed 334 g. The left main trunk showed almost the same appearance as that in Case 1 (Fig. 3a), and the orifice of the left coronary artery was absent (Fig. 3b). A relatively large CA arose from the right coronary sinus with an independent orifice, and then anastomosed with the LAD (Fig. 3a). The CA did not course between the aorta and the pulmonary trunk, but ran through the anterior aspect of the pulmonary trunk before reaching the LAD (Fig. 3c). The right coronary artery was dominant. Serial sectioning of almost the entire epicardial coronary artery revealed diffuse and marked atherosclerosis of both the LAD and the CA. The cut surface of the horizontal sections of both ventricles showed mild symmetric hypertrophy; however, no old or fresh ischemic foci were visible. The thickness of the wall was 1.4 cm in the case of the anterior, lateral, and posterior walls, 1.5 cm in the ventricular septum, and 0.2 cm in the right ventricle. No deformity was found in any of the valves. As for other important findings, severe benign nephrosclerosis, and fusiform atherosclerotic aneurysm of the distal aortic arch (ca. 5 cm) was found.

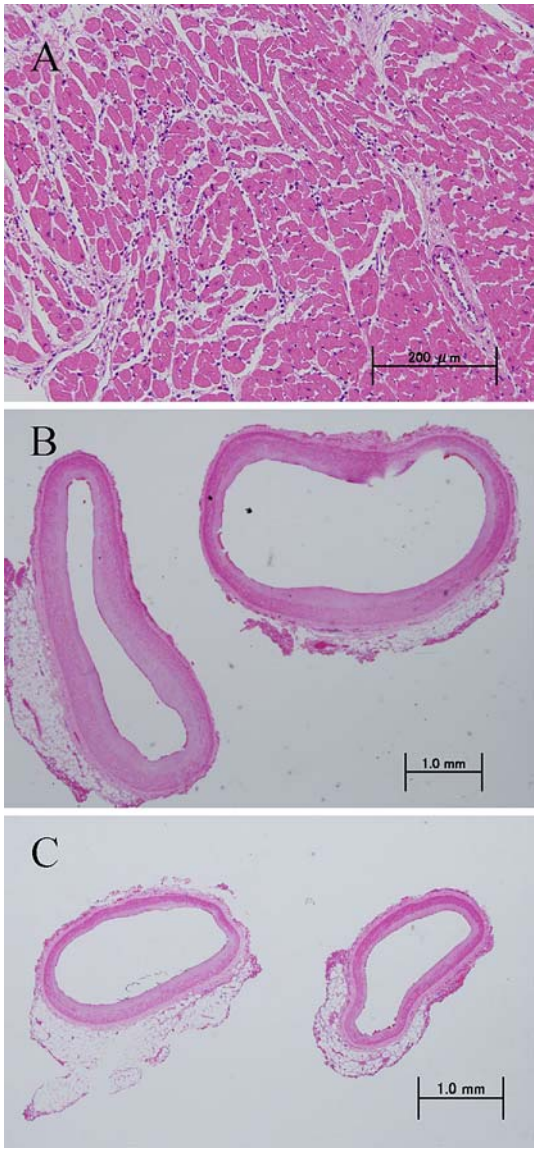


Fig. 2 Histological findings of the heart in Case 1. **a** Histological appearance of the left lateral wall. Eosinophilic degeneration of myocytes with loss of nucleus and infiltration of granulocytes. These findings show evidence of acute myocardial infarction (hematoxylin and eosin stain, 400×). Histological appearance of the **b** left descending artery and **c** collateral artery. The caliber of the collateral artery is thinner than that in the left descending artery (hematoxylin and eosin stain, 4×)

On microscopic examination, small scars whose diameter was not greater than 1.0 cm were found at the posterior papillary muscle (Fig. 4a) and the basal third of the septum. Acute ischemic foci were not visible in either of the ventricles. In the left ventricle, diffuse and severe interstitial fibrosis and focal hypertrophy of myocytes was seen. The left main trunk demonstrated an arterial appearance, but was completely occluded by non-atherosclerotic intimal hyperplasia, as in Case 1 (Fig. 4b). The caliber of the CA was smaller than that of the LAD, where it was anastomosed with the CA, as in Case 1. However, the LAD and CA showed marked stenosis (>95%) due to the progression of atherosclerosis (Fig. 4c). The right coronary artery was well developed and focal mild atherosclerosis was found (Fig. 4d).

Discussion

Referring to previous literature, atresia of the left coronary ostium seems to be synonymous with atresia of the left main trunk [2–9]. In the current report, the left coronary orifice of both cases was absent, but the left main trunk was anatomically present in a rudimentary form. Histologically, two different sets of findings of the left main trunk in the case of atresia of the left coronary ostium have been reported. In one case reported by Leivo and Laurila [7], the left main trunk showed a fibrous string-like structure without any vascular component, whereas in another case reported by Goormaghtigh et al. [6], the left main trunk had a vascular structure but showed severe narrowing of the lumen [9]. In the present two cases, the arterial structure was found in the left main trunks of both cases; however, the lumens were severely obstructed by non-atherosclerotic intimal hyperplasia. We consider that atresia of the left coronary ostium may be a more appropriate anatomical diagnosis for such cases rather than atresia of the left main coronary artery. Moreover, this diagnostic term can be used whether the left main trunk is present in a rudimentary form or is completely absent, since the presence or absence of the left main trunk should be of no clinical significance when the ostium is absent.

Atresia of the left coronary ostium has recently been considered as a different entity from single coronary artery [9] or anomalous orifice of the left coronary artery [2, 11].

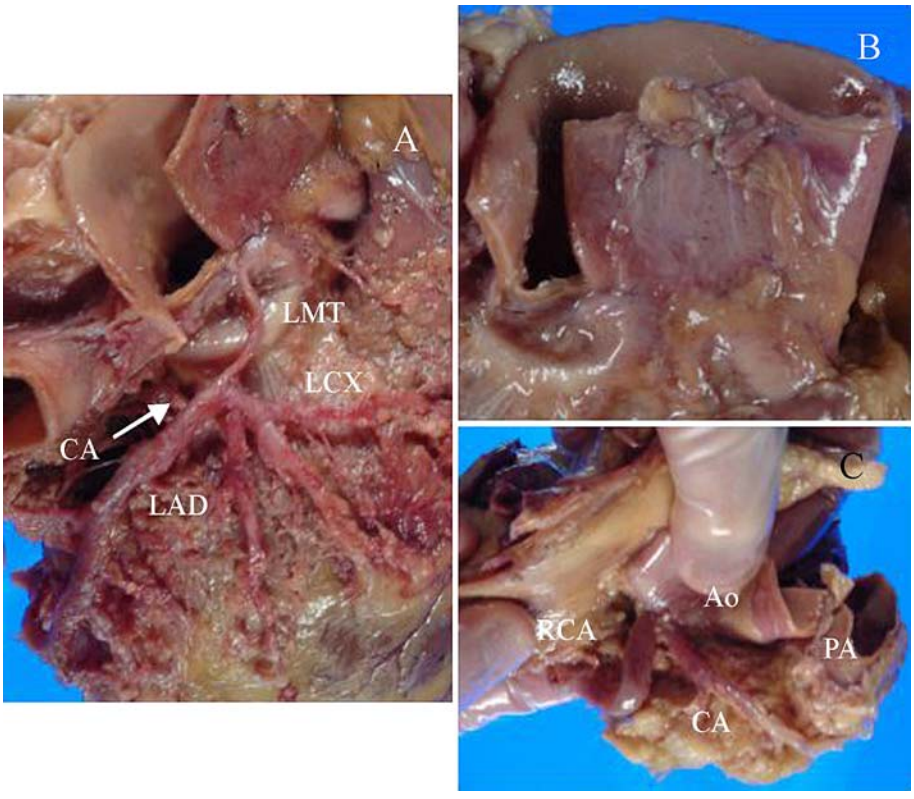


Fig. 3 Gross findings of the heart in Case 2. **a** Gross anatomy of the left coronary artery. A string-like left main trunk (*LMT*) can be seen. Other arteries have a normal caliber. *CA* Collateral artery, *LAD* left descending artery, *LCX* left circumflex artery. **b** After removal of the coronary tree, the orifice of the left main trunk (*LMT*) is not evident. **c** Proximal region of the collateral artery (*CA*). The CA courses in the anterior aspect of the pulmonary artery (*PA*). *RCA* Right coronary artery, *Ao* aorta

In the former cases, the myocardial blood supply is derived from coronary arteries of the opposite side, which run a normal course and ramify extensively [3]. On the other hand, in the latter cases, the left coronary artery arises from the right aortic sinus, whereas the right coronary artery originates normally and runs a normal course [10]. In atresia of the left coronary ostium, the blood flows from the right to the left coronary artery via one or more collateral arteries whose caliber is smaller than that of the target left-sided vessels, as in the present cases. Therefore, the flow is

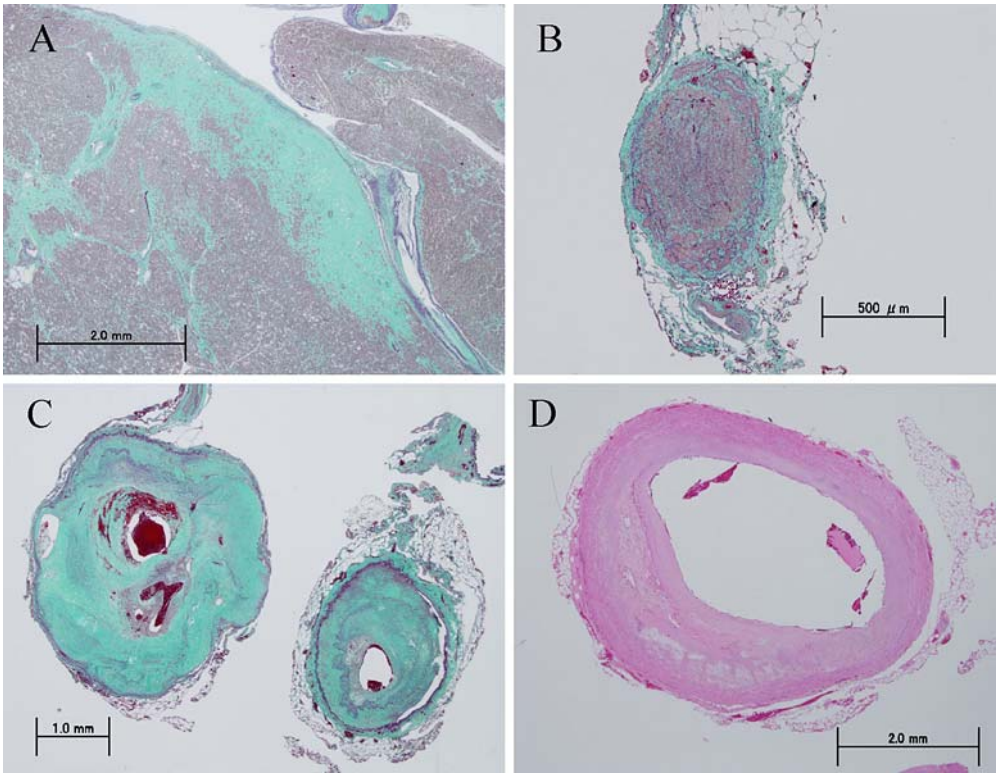


Fig. 4 Histological findings of the hearts in Case 2. **a** Histological appearance of the posterior papillary muscle of the left ventricle. A small scar can be seen in the subendocardial region (Elastica–Masson stain, 4×). **b** Histological appearance of the left main trunk. No significant lumen can be seen. Internal elastic lamina and medial smooth muscle is evident (Elastica–Masson stain, 4×). **c** Histological appearance of the collateral artery. Severe atherosclerosis with stenosis is evident. (Elastica–Masson stain, 4×). **d** Histological appearance of the right coronary artery. The artery shows a large caliber with mild atherosclerosis (hematoxylin and eosin stain, 4×)

in part centripetal, because it flows retrogradely (from the periphery to the center). Under normal conditions, such as with a single coronary artery, or anomalous orifice of the left coronary artery, the blood flow is always centrifugal, flowing from bigger to small arteries [5]. Embriologically, segmental atresia of the left main trunk may suggest that regression of the left main trunk has taken place after elongation of the coronary artery anlage has started, and the mechanism may be different from cases where the left coronary artery arises from the right aortic sinus, which may reflect displacement of the left main trunk anlage during rotation of the trunchus arteriosus [7].

In the case of atresia of the left coronary ostium, many patients die in infancy or childhood after a relatively short interval of cardiac symptoms; however, manifestation of the symptoms that occur with ischemia is not necessarily limited to childhood [7]. Referring to our two cases, the caliber of each of the CAs may have been relatively large, and therefore the timing of the appearance of the symptoms might have been delayed. Nevertheless, atherosclerosis was severe in the CA and the LAD of Case 2, where the cause of death was non-cardiac and where the patient would seem to have been older than any of the previously reported patients with atresia of the left coronary ostium [7], although the mild angina experienced by Case 2 may have been caused by progression of the atherosclerosis of the CA and LAD, rather than by the anomaly of the coronary artery.

One of the striking features of the CA of Case 1 in comparison to Case 2 was the course of the CA. In Case 1, the CA coursed between the aortic and pulmonary root and was sandwiched between these two large vessels. Dymond et al. speculated that mechanical compression of the CA by two large arteries was an accelerating factor of myocardial ischemia in atresia of the left coronary ostium since it diminished the blood flow within the CA [4]. Chronic or transient mechanical compression of the CA could cause a delay in the delivery of blood to the left-sided artery, having blood arrive during systole rather than diastole [3, 4]. Mechanical compression of the CA may become more severe following exercise or emotional stress which are already known to be important risk factors of sudden death in cases where the left main coronary artery originates from the right aortic sinus [2, 11]. We believe that the course of the CA may be one of the important factors for the long survival of Case 2, even though atresia of the left coronary ostium and severe atherosclerosis were present.

An acute angle of take-off from the coronary artery, as in Case 1, and a slit-like appearance of the orifice have also been considered to be risk factors for diminishing the blood flow in the coronary artery based on mechanisms similar to mechanical compression of the CA [3, 4]. Our Case 1 would seem to suggest that the angle of take-off of the CA is also a possible anatomical abnormality in atresia of the left coronary ostium. The presence of a significant anatomical correlation between the angle of take-off and the course of CA has not yet been fully established; however, the CA of Case 1 headed for the LAD more linearly between the aorta and the pulmonary trunk after deriving from the aorta, whereas the CA of Case 2, whose angle of take-off was not acute, ran in a semicircle through the anterior aspect of the right ventricular outflow tract before reaching the LAD.

In summary, atresia of the left coronary ostium should be a developmentally and anatomically different entity from the single coronary artery or a left coronary artery which arises from the right coronary sinus. In the present cases, although a developed CA may delay the appearance of clinical symptoms in atresia of the left coronary ostium, the gradual progression of an insufficient blood supply in the CA due to mechanical or pathological obstruction will eventually cause the development of ischemic complications in the heart and sudden death, even if the patients can survive ordinary life until adulthood. Our Case 2 was considered to be an extremely rare case where the patient had experienced long-term survival due to the overlap of various fortunate factors, which may have comprised some anatomical features, especially with regard to the course of the CA, together with that individual's own personal lifestyle.

Acknowledgements The authors wish to express their special gratitude to Miss. K. Miller (Royal English Language Centre, Fukuoka, Japan) for revising the English used in this manuscript. This report was supported by a Grant-in-Aid for Scientific Research (C) from the Japan Society for the Promotion of Science (JSPS).

References

1. Angelini P, Velasco JA, Flamm S (2002) Coronary anomalies. Incidence, pathophysiology, and clinical relevance. Circulation 105:2449–2454
2. Basso C, Maron BJ, Corrado D, Thiene G (2000) Clinical profile of congenital coronary artery anomalies with origin from the wrong sinus leading to sudden death in young competitive athletes. J Am Coll Cardiol 35:1493–1501
3. Beretta L, Lemma M, Santoli C (1990) Isolated atresia of the left main coronary artery in an adult. Eur J Cardio-Thorac Surg 4:169–170
4. Dymond D, Camm J, Stone D, Rees S, Rees G, Sprurrell R (1980) Dual isotope stress testing in congenital atresia of left main coronary ostium. Application before and after treatment. Br Heart J 43:270–275
5. Ghosh PK, Friedman M, Vidne BA (1993) Isolated congenital atresia of the left main coronary artery and atherosclerosis. Ann Thorac Surg 55:1564–1565
6. Goormaghtigh N, De Vos L, Blancquaert A (1955) Ostial stenosis of the coronary arteries in a 9-year-old girl. Arch Intern Med 95:341–348
7. Leivo IV, Laurila PK (1987) Atresia of left coronary ostium and left main coronary artery. Arch Pathol Lab Med 111:1173–1175
8. Musiani A, Cernigliaro C, Sensa M, Maselli D, De Gasperis C (1997) Left main coronary atresia: literature review and therapeutical considerations. Eur J Cardiovasc Surg 11:505–514
9. Sharbaugh AH, White RS (1974) Single coronary artery. JAMA 230:243–246
10. Smith JC (1950) Review of single coronary artery with report of two cases. Circulation 1:1168–1175
11. Taylor AJ, Rogan KM, Virmani R (1992) Sudden cardiac death associated with isolated congenital coronary artery anomalies. J Am Coll Cardiol 20:640–647

Virchows Arch (2005) 447: 747–755
DOI 10.1007/s00428-005-0012-5

ORIGINAL ARTICLE

Lei Shi · Shigeyuki Tsurusaki · Noriko Futa · Tamami Sakamoto · Tomoko Matsuda · Norikazu Nishino · Ryuji Kunitomo · Michio Kawasuji · Kazutaka Tokita · Tetsuro Yamamoto

Monocyte chemotactic S19 ribosomal protein dimer in atherosclerotic vascular lesion

Received: 17 September 2004 / Accepted: 27 April 2005 / Published online: 13 July 2005
© Springer-Verlag 2005

Abstract To elucidate the molecular mechanism inducing monocyte/macrophage infiltration in the atherosclerotic lesion, we measured the monocyte chemotactic capacity in the extracts of aortic lesions. Five out of seven extracts exhibited significant chemotactic activities. Immunohistochemical examination with an anti-CD68 monoclonal antibody demonstrated that the five positive lesions possessed obvious monocyte/macrophage infiltrations at the intima, whereas the two negative lesions did so at significantly lower intensities. We subjected the chemotactic extracts to immunological analyses to identify the monocyte chemoattractant in them. The monocyte chemotactic capacities of all positive extracts were removed with anti-S19 ribosomal protein (RP S19) antibody beads and antimonocyte chemoattractant protein-1 (MCP-1) antibody beads. In three of the five extracts, the anti-RP S19 antibody beads were more effective than the anti-MCP-1 antibody beads for removal, while in the remaining two extracts, the opposite was observed. A combined immunoabsorption with these beads depleted the monocyte chemotactic capacity of a representative sample of each group. Consistently, the chemotactic capacity of an apparently RP S19 dimer-predominant extract was strongly inhibited by the presence of a C5a receptor antagonist. These results suggest that the RP S19 dimer and MCP-1 play a major role in the monocyte/macrophage infiltration of the atherosclerotic vascular lesion.

Keywords S19 ribosomal protein · Monocyte chemoattractant protein-1 · Leukocyte chemoattraction · C5a receptor · Atherosclerosis

L. Shi and S. Tsurusaki contributed equally to this work.

L. Shi · K. Tokita (✉) · T. Yamamoto
Department of Molecular Pathology, Faculty of Medical and Pharmaceutical Sciences, Kumamoto University,
2-2-1 Honjo, Kumamoto,
860-0811, Japan
e-mail: ktokita@kaiju.medic.kumamoto-u.ac.jp
Fax: +81-96-3735308

S. Tsurusaki · R. Kunitomo · M. Kawasuji
Department of Cardiovascular Surgery, Faculty of Medical and Pharmaceutical Sciences, Kumamoto University,
2-2-1 Honjo, Kumamoto,
860-0811, Japan

N. Futa · T. Sakamoto · T. Matsuda
Trans Genic Incorporation,
Kumamoto, Japan

N. Nishino
Department of Biological Functions and Engineering, Graduate School of Life Science and Systems Engineering,
Kyushu Institute of Technology,
Kitakyushu, Japan

Introduction

S19 ribosomal protein (RP S19), a component of the small subunit of ribosome, is intermolecularly cross-linked by a transglutaminase-catalyzed reaction during the apoptotic process [5, 10], and acquires the monocyte-selective leukocyte chemotactic capacity [10]. The RP S19 dimer is then extracellularly released and plays an essential role in the phagocytic clearance of apoptotic cells that have liberated the dimer by recruiting circulating monocytes to the extravascular apoptotic lesion [21]. The phagocytic clearance of the apoptotic cells would then be followed by an acquired immune response to the apoptotic cells when the apoptotic cells possessed not-self antigens [15].

We initially discovered the RP S19 dimer in the extract of synovial lesion of rheumatoid arthritis as the major monocyte chemotactic factor in it [10]. The RP S19 dimer has a dual effect to the chemotactic C5a receptor of phagocytic leukocytes: an agonist effect on the monocyte receptor and an antagonist effect on the polymorphonuclear (PMN) leukocyte receptor [12, 14, 17]. Thus the RP S19 dimer induces monocyte predominant infiltration in vivo. Therefore, the RP S19 dimer is assumed to be a chemical mediator of monocyte predominant infiltration in chronic inflammation, such as rheumatoid arthritis.

Monocyte/macrophage predominant infiltration is also observed in atherosclerotic lesion, which is usually clas-

sified into metabolic disorders. In this lesion, macrophages phagocytically clear lipoprotein complexes exuded and deposited, and become foam cells. It was immunohistochemically demonstrated that the majority of the lipid-engulfed macrophages originated from circulating monocytes [1, 20]. Regarding the molecular mechanism that causes monocyte-predominant infiltration, the presence of monocyte chemoattractant protein-1 (MCP-1) in the atherosclerotic lesion was immunohistochemically demonstrated [18, 22]. On the other hand, the presence of apoptotic cells in the atherosclerotic lesion has been histochemically shown [6, 13], suggesting the presence of RP S19 dimer as a monocyte chemoattracting factor in this lesion.

In the current study, we examined whether the RP S19 dimer is really present in the atherosclerotic lesion with the active monocyte chemoattracting capacity by analyzing the extract of the clinical lesion. Furthermore, we functionally evaluated the contribution of MCP-1 and the RP S19 dimer in the monocyte/macrophage recruitment to the atheromatous lesion.

To perform these studies, we needed antibodies against RP S19 with high affinity and high specificity. Because the amino acid sequence of RP S19 is conserved among mammalian species [19], it was not easy to prepare the antibodies against human RP S19. We used a synthetic peptide fragment of RP S19 with 14 amino acid residues, which were conjugated to a carrier protein, to produce anti-RP S19 antibodies in a rabbit.

Materials and methods

Animal

A New Zealand White male rabbit (2.5 kg body weight) was used to produce antibodies.

Reagents and other compounds

RPMI 1640 medium and Hank's balanced salt solution (HBSS) were purchased from Nissui Pharmaceutical (Tokyo, Japan). We obtained fetal bovine serum (FBS) from Gibco BRC (Paisley, Scotland) and Mono–Poly Resolving MediumR from Flow Laboratory (Hertsfordshire, UK). An anti-CD68 monoclonal antibody, KP-1, an anti-MCP-1 monoclonal antibody, and an immunoperoxidase staining kit, Envision/horseradish peroxidase (HRP) were obtained from DAKO (Carpinteria, CA, USA). We also acquired HRP-labeled antirabbit IgG (H+L) goat IgG from Bio-Rad Japan (Tokyo, Japan), and a recombinant MCP-1 from Pepro Tech (London, UK). All other chemicals were obtained from Nacalai Tesque (Kyoto, Japan) or from Wako Pure Chemicals (Osaka, Japan), unless otherwise specified. NMePhe-Lys-Pro-dCha-dCha-dArg was synthesized as described previously [7].

Preparation of RP S19 dimer

A recombinant RP S19 was prepared in an *E. coli* transgene expression system as described previously [11]. RP S19 was dimerized via treatment with type II transglutaminase, after which the RP S19 dimer was separated by immunoaffinity column chromatography with anti-isopeptide bond monoclonal antibody beads as described previously [9].

Preparations of rabbit anti-RP S19 IgG antibodies

A peptide having 15 amino acid residues, Arg-Lys-Leu-Thr-Pro-Gln-Gly-Gln-Arg-Asp-Leu-Asp-Arg-Ile-Cys, with the same sequence as a part of RP S19 from Arg121 to Ile134, except for the C-terminal Cys, was synthesized. This peptide was covalently coupled at the C-terminal Cys residue to keyhole limpet hemocyanin (KLH) with *m*-maleimidobenzoyl-*N*-hydroxysuccinimide ester as described previously [3]. Antiserum to the RP S19 peptide–KLH was grown in a rabbit via multiple intradermal injections of the peptide–KLH emulsified with Freund's complete adjuvant (at first sensitization) or with incomplete adjuvant (at the booster injections) four times at weekly intervals. During the initial sensitization and booster injections, 500 and 250 μg of the peptide–carrier conjugate, respectively, were administered. One week after the fourth inoculation, the antiserum was obtained from the rabbit. Next, we analyzed the binding capacities of the antiserum to the peptide–carrier antigen, to the carrier protein, and to RP S19. The IgG fraction was prepared from the antiserum by an affinity column chromatography with a protein G column in the usual way. The purified IgG was used as anti-RP S19 rabbit IgG for the antibody beads preparation.

Enzyme-linked immunosorbent assay

The surface of the 96-well microchamber was coated with a protein solution of the RP S19 peptide–KLH, KLH, or recombinant RP S19 at a concentration of 5 μg/ml. After blocking with phosphate-buffered saline containing 0.5% gelatin and 0.05% Tween 20, the adsorbed proteins were reacted with serially diluted anti-RP S19 peptide–KLH antiserum or preimmune serum. The antigen–first antibody complex on the surface was then reacted with the HRP-labeled antirabbit IgG goat IgG, and the HRP on the surface was reacted with an *o*-phenylenediamine solution (Wako Pure Chemicals). After a 10-min incubation, the enzyme reaction was stopped with 2 M H_2SO_4, and the absorbance at 490 nm was measured using a microplate reader (Ultra Microplate Reader, Bio-Tek Instruments, Winooski, VT, USA).

Preparation of antibody beads

The anti-RP S19 rabbit IgG as well as the anti-MCP-1 monoclonal antibody were covalently coupled by succinylation to NHS-activated Sepharose 4 Fast Flow (Amersham Pharmacia Biotech, Piscataway, NJ, USA) in a 0.2 M $NaHCO_3$ buffer containing 0.5 M NaCl (pH 8.3). The remaining uncoupled *N*-hydroxisuccinimide ester groups on the gel beads were blocked with monoethanolamine as previously described [3]. Control rabbit IgG beads were prepared in the same process. These IgG beads were used for the immunoabsorption experiments.

Immunoabsorption with antibody beads

For immunoabsorption experiments with the anti-RP S19 rabbit IgG beads, with the anti-MCP-1 monoclonal antibody beads, or with the normal rabbit IgG beads, we used the batch-wise method as previously described [17]. Briefly, the sample was mixed with one-fourth volume of the antibody beads and incubated for 60 min at 4°C with continuous shaking. After centrifugation at 10,000×*g* for 20 min at 4°C, the supernatant was recovered and the monocyte polarization capacity remaining in it was measured as described below.

Morphologic polarization assay to measure leukocyte chemoattracting capacity

Mononuclear cells and PMNs were isolated from heparinized human venous blood of healthy donors according to the method of Fernandez et al. [4] as described previously [8]. The mononuclear cell fraction contained monocytes at a ratio of about 20%, and the PMN fraction was composed of over 95% PMNs. Mononuclear cells and PMNs were suspended at a cell density of 1×10^6 cells/ml in RPMI 1640 containing 10% FBS, and in HBSS containing 2% bovine serum albumin, respectively, for the morphologic polarization assay.

The morphologic polarization assay was performed according to the method of Cianciolo and Snyderman [2], as described previously [8]. Briefly, the mononuclear cell suspension was incubated with each sample for 10 min at 37°C in a polypropylene tube. Immediately after the incubation, 1 ml of cold parafolmaldehyde (8% w/v) buffered with 100 mM phosphate (pH 7.2) was added to fix the cells. The fixed cells were washed twice with phosphate-buffered saline and were stained cytochemically for nonspecific esterase with α-naphthylacetate as the substrate for 50 min at 37°C to identify monocytes in the mononuclear cells. The number of polarized and nonpolarized cells of monocytes was counted to at least 100 using an inverted microscope (IMT-2, Olympus Optical Co., Tokyo, Japan). The activity of the sample was expressed as the percentage of the monocyte number with polarized morphology against the total number of monocytes counted. When the effect of the C5a receptor antagonist was examined, the indicator monocytes were pretreated with various concentrations of the antagonist for 10 min at 37°C just before the chemoattractant was added.

Preparation of intimal extract

Small pieces of aortic tissue with atheromatous lesion were obtained from patients undergoing aorta replacement therapy, and those of apparently normal tissue were obtained during autopsy, with the permission of IRB of Kumamoto University Hospital. Shortly after, a part of the aortic tissue was resected and used for the histological examination, and the remainder was used for the preparation of intimal extract.

The intima was separated from the aortic tissue with a sterilized razor blade, weighted, dissected, and stored at −80°C until use. After thawing, the dissected intima was mixed with a cold extraction buffer at a volume of 2.5 ml per g weight of the intimal tissue, homogenized using a polytron homogenizer for 1 min on ice, and extracted for 4 h at 4°C. The extraction buffer used was 10 mM phosphate buffer (pH 7.4) containing 500 mM NaCl, 5 mM EDTA, 20 mM pepstatin A, 0.5 mM *N*-ethylmaleimide, and 1 mM diisopropylfluorophosphate. The supernatant of the extract was obtained by centrifugation at 10,000×*g* for 10 min at 4°C, and used for the experiments.

Immunohistochemistry

For histological examination, aorta specimens were fixed in 10% formalin. Paraffin sections of 4-μm thickness were prepared in the usual way. A section was stained with hematoxylin and eosin; other sections were used for the indirect immunoperoxidase staining.

In immunoperoxidase staining, sections were treated with drops of the anti-CD68 monoclonal antibody solution or of normal mouse IgG solution overnight at 4°C. Mouse IgG was visualized with dextrose-conjugated horseradish peroxidase-labeled antimouse IgG rabbit IgG and diaminobenzidine by using the immunoperoxidase staining kit, Envision/HRP, according to the manufacturer's instructions. The microscopical pictures were prepared using an automatic microscope, Provis AX (Olympus, Tokyo, Japan) and a digital camera, Penguin 600CL (Pixera, Los Gatos, CA, USA).

Results

Monocyte chemotactic capacities of intimal extracts of aortic atherosclerotic lesion

To assess the leukocyte chemotactic capacity in the intimal extracts of atherosclerotic lesions, we used the morphologic polarization assay. Because the incubation period required in the polarization assay (10 min) is much shorter than that in the multiwell chamber assay (90 min), the odds

for undesirable secondary chemical reactions during the incubation period in crude samples must be substantially less in the former.

The chemotaxis assay was performed at various concentrations for each sample, because the dose–response curve in the chemotaxis assay usually forms a bell shape with an optimal concentration of the assay sample. Because all of the samples exhibited the strongest chemoattracting activity at 100-fold dilution (see Fig. 6 as representatives), the polarized ratios of monocytes responded to the 100-fold diluted samples are comparatively shown in Fig. 1. When compared to the chemoattracting capacity of the extracts of apparently normal intima, five out of seven atherosclerotic intimal extracts showed significant chemoattractant capacities to monocytes.

We also examined the chemoattracting capacity of the intimal extracts to PMNs. The capacities were low and the optimum concentrations were varied, from undiluted to 100-fold diluted concentrations, among the intimal extracts (data not shown). Therefore, in the following sections, we only describe the study on monocyte chemoattraction in the atherosclerotic intima.

Immunohistochemical observation of monocyte/macrophage infiltration with anti-CD68 monoclonal antibody

The intensity of monocyte/macrophage infiltration at the atherosclerotic lesion was immunohistochemically observed by using the anti-CD68 monoclonal antibody, KP-1, to detect the infiltrated monocytes/macrophages. The immunoperoxidase method with this antibody visualized two different types of substances. One type was morphologically identified as infiltrating monocytes/macrophages by their size, their shapes, from round to spindle, and their nuclei that had been counterstained. The other type seemed to be degenerated foam cells or their fragments, because their sizes were big, the border was unclear, and many of them did not possess a nucleus. Because a negative control staining with normal mouse IgG as the first antibody instead of the anti-CD68 monoclonal antibody demonstrated no immunopositive signal (data not shown), we neglected the possibility that the immunoreactivity of the latter substance was a nonspecific reaction.

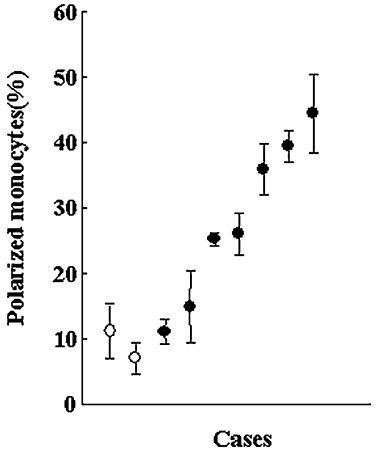


Fig. 1 Monocyte chemotactic capacities of atherosclerotic intimal extracts. Aortic tissues with atheromatous lesion were obtained from seven patients (*closed circles*) during the aorta replacement therapy, and apparently normal tissues (*open circles*) were obtained from two autopsy cases. Their intimas were homogenized and extracted. Monocyte chemoattracting capacities of the intimal extracts were measured using the morphological polarization assay at various concentrations. Because the optimal concentration of the intimal extracts according to the chemoattracting capacity was observed at the 100-fold dilution (see Fig. 6 as representatives), only the polarized ratios at this dilution are shown. The experiments were carried out in triplicate samples. The polarized ratio (percent) of monocytes is expressed as mean±SD

Histological specimens of the two lesions whose extracts exhibited negligible monocyte chemotactic capacity demonstrated severe atheromatous change of the intima containing abundant lipid crystals. However, the cell numbers of infiltrating monocytes/macrophages were very limited, although the immunopositive cell fragments were observed to some extent, as shown in Fig. 2b. In these cases, the biological response seemed very weak compared to the intensities of the intimal alteration.

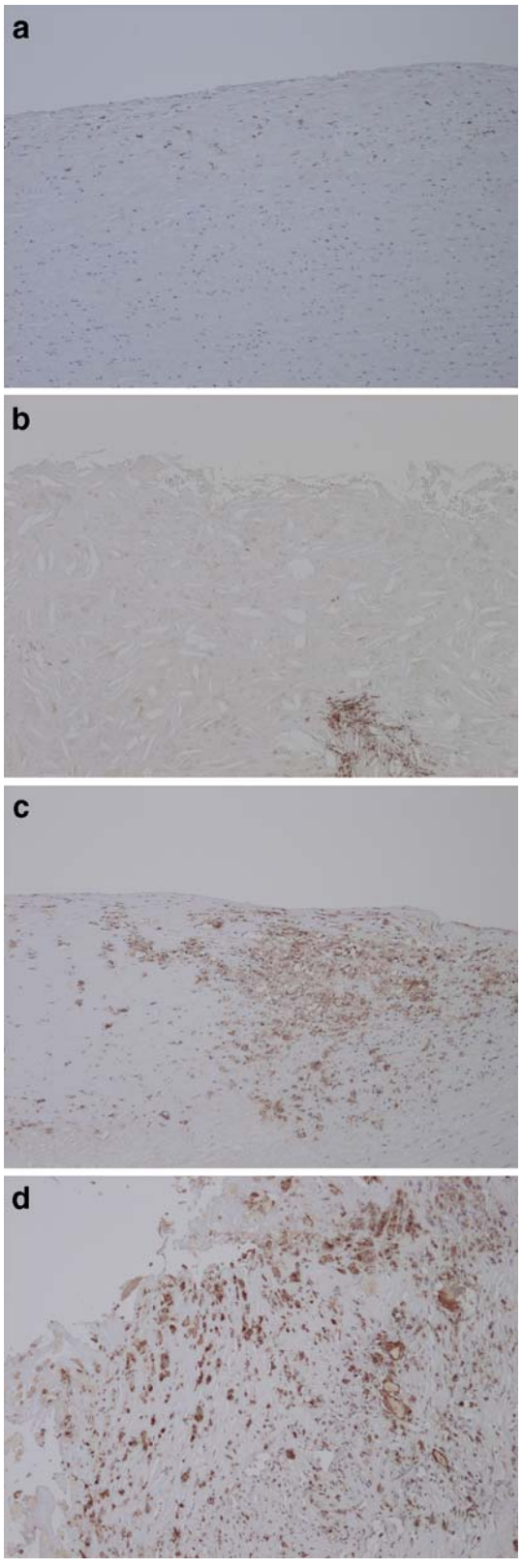
In a striking contrast, the specimens of the five lesions whose extracts exhibited significant monocyte attracting capacities all demonstrated obvious monocyte/macrophage infiltration, as shown in Fig. 2c. The specimen whose extract exhibited the strongest monocyte attraction capacity demonstrated a severe monocyte/macrophage infiltration, as shown in Fig. 2d. A macroscopically normal aortic tissue, which had been obtained from a 70-year-old man and used as a normal sample for the chemotaxis assay, demonstrated a minor alteration of endothelial cells and a sparse subendothelial monocyte/macrophage infiltration with a weak atheromatous change as seen in Fig. 2a. These changes were similarly seen in the other normal control sample. This would be an age-related phenomenon.

The intensities of intimal monocyte/macrophage infiltration observed via immunohistochemical means fairly corresponded to the functionally measured monocyte chemoattracting capacities of the intimal extracts obtained. This consistency strongly suggested that the monocyte chemoattractant(s) in the chemotactic intimal extracts would be the chemical mediator working to induce the monocyte/macrophage infiltration at the intimal lesion.

Immunoreactivity of anti-RP S19 peptide–KLH antiserum

We initially examined the binding capacity of the anti-RP S19 peptide–KLH antiserum to RP S19 by using a simple enzyme-linked immunosorbent assay (ELISA) method. The surface of the 96-well microchamber was coated with the recombinant human RP S19, RP S19 peptide–KLH, or carrier KLH, and the relative binding affinities of the antiserum to them were examined with serially diluted antiserum.

As shown in Fig. 3, the relative binding affinities of the antiserum to RP S19 peptide–KLH, RP S19, and KLH



◀ **Fig. 2** Immunohistochemical examination of atherosclerotic lesions with anti-CD 68 monoclonal antibody. Usual paraffin sections of formalin-fixed aortic tissues were stained by an indirect immunoperoxidase method with anti-CD 68 monoclonal antibody, KP-1, and dextrose-conjugated horseradish peroxidase-labeled antimouse IgG rabbit antibodies. The microscopical pictures were prepared using an automatic microscope and a digital camera. **a** A macroscopically normal aorta used in the experiments shown in Fig. 1. **b** A monocyte chemotactic capacity-negative aorta. **c** A monocyte chemotactic capacity-positive aorta. **d** The aorta with the strongest monocyte chemotactic capacity

were observed, in this order. Because a significant immunoperoxidase activity in the interaction between RP S19 and the antiserum was observed even when the antiserum was diluted 243,000-fold, we recognized that the binding affinity of the anti-RP S19 peptide antibodies to RP S19 was high enough to be used in the immunoabsorption experiment with the antibody beads. ELISA with the preimmune serum exhibited a weak peroxidase activity only to KLH when the serum was used at a 1,000-fold dilution (data not shown).

Specific absorptions of monocyte chemoattractant with two kinds of antibody beads

In the immunologic analysis of monocyte chemoattractants, we next examined the absorption capacities and the specificities of the anti-RP S19 antibody beads and the anti-MCP-1 antibody beads. As shown in Fig. 4a, the anti-RP S19 antibody beads removed the chemoattracting capacity of the RP S19 dimer but not that of MCP-1. Inversely, the anti-MCP-1 antibody beads removed the capacity of MCP-1 but not that of the RP S19 dimer (Fig. 4b).

C5a is the complement-derived leukocyte chemotactic factor, attracting monocytes as well as PMNs. C5a and the RP S19 dimer share the C5a receptor, although the latter functions as an antagonist to the C5a receptor on PMNs [12, 14, 16]. Concerning receptor sharing, we thought it would be necessary to neglect the cross-immunoreaction

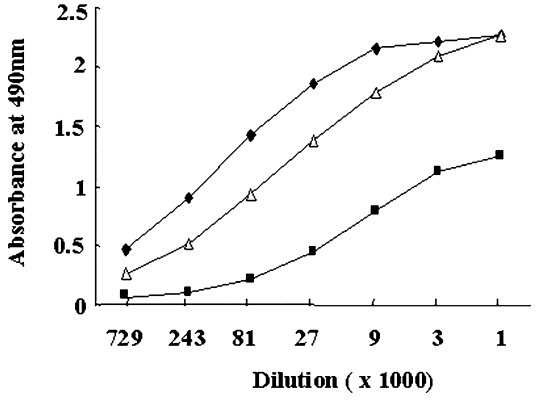


Fig. 3 Relative binding affinity of anti-RP S19 peptide antiserum to RP S19. The surface of the 96-well microchamber was coated with the RP S19 peptide–KLH (antigen, *closed diamonds*), with KLH (antigen carrier, *closed squares*), or with the recombinant RP S19 (*open triangles*). The protein-coated surface was reacted with serially diluted antiserum, and the amounts of rabbit IgG bound to these peptides were respectively measured by the immunoperoxidase method. The relative peroxidase activity is expressed as the absorbance unit at a wavelength of 490 nm on the *y*-axis

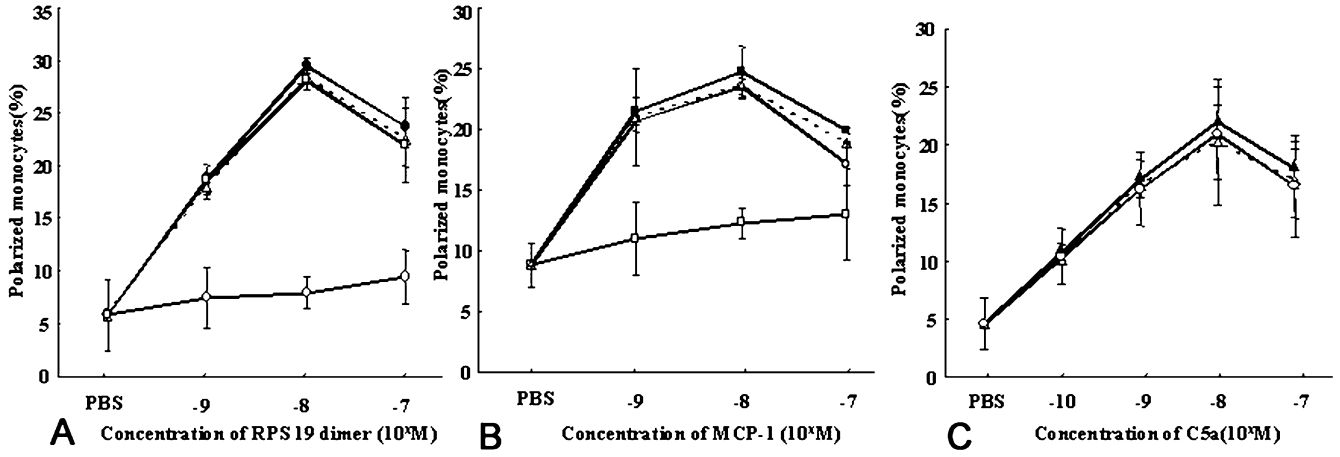


Fig. 4 Chemoattractant-specific immunoabsorption with anti-S19 ribosomal protein (RP S19) antibody beads, or with anti-monocyte chemoattractant protein-1 (MCP-1) antibody beads. Fifty microliters of 10^{-7} M RP S19 dimer (**a**), 10^{-7} M MCP-1 (**b**), or 10^{-7} M C5a (**c**) was treated with 10 μl of anti-RP S19 IgG beads (*open circles*), of anti-MCP-1 IgG beads (*open squares*), or of normal rabbit IgG beads (*open triangles*) for 60 min at 4°C; the supernatants were recovered. The remaining monocyte polarization capacities in the supernatants were measured with serially diluted samples. The *closed symbols* denote the polarization activities of the original samples before treatment with the antibody beads. The experiments were carried out in triplicate samples. The polarized ratio (percent) of monocytes is expressed as mean±SD

of C5a to the anti-RP S19 antibody beads. As shown in Fig. 4c, the anti-RP S19 antibody beads did not absorb the recombinant human C5a. We also confirmed that the anti-MCP-1 antibody beads did not absorb C5a (data not shown).

The control IgG beads did not affect the capacities of these chemoattractant except for exhibiting a dilution effect of the beads added. From the theoretical point of view, we should use the normal rabbit IgG beads and mouse monoclonal IgG beads in the negative control experiments for the absorption experiments with the anti-RP S19 rabbit IgG beads and with the anti-MCP-1 IgG beads, respectively. However, we only used the normal rabbit IgG beads, not the mouse monoclonal IgG beads, because we have never observed any difference between these two IgG beads when they were used in the negative control experiment.

These results indicated the chemoattractant-specific absorption capacities of the antibody beads without any cross-reactivity among these chemoattractants and the antibody beads.

Immunoabsorptions of monocyte chemotactic capacities of intimal extracts with antibody beads

We then subjected five intimal extracts that had exhibited the significant monocyte chemotactic capacities to the immunoabsorption experiments. In all of the cases, dec-

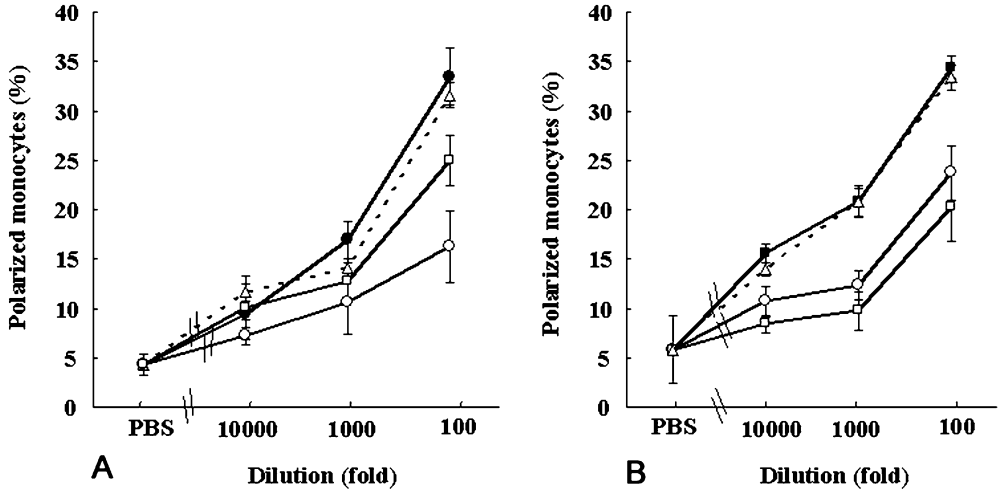


Fig. 5 Immunoabsorption of monocyte polarization capacities of two representative intimal extracts (**a**, **b**) with antibody beads. Eighty microliters of two chemoattractive extracts (*closed circles* or *closed squares*) was treated with 20 μl of the anti-RP S19 IgG beads (*open circles*), of the anti-MCP-1 IgG beads (*open squares*), or of the normal IgG beads (*open triangles*), and the supernatants were recovered. The remaining monocyte polarization capacities in the supernatants were measured with serially diluted supernatants from 100- to 10,000-fold. The experiments were carried out in triplicate samples. The polarized ratio (percent) of monocytes is expressed as mean±SD

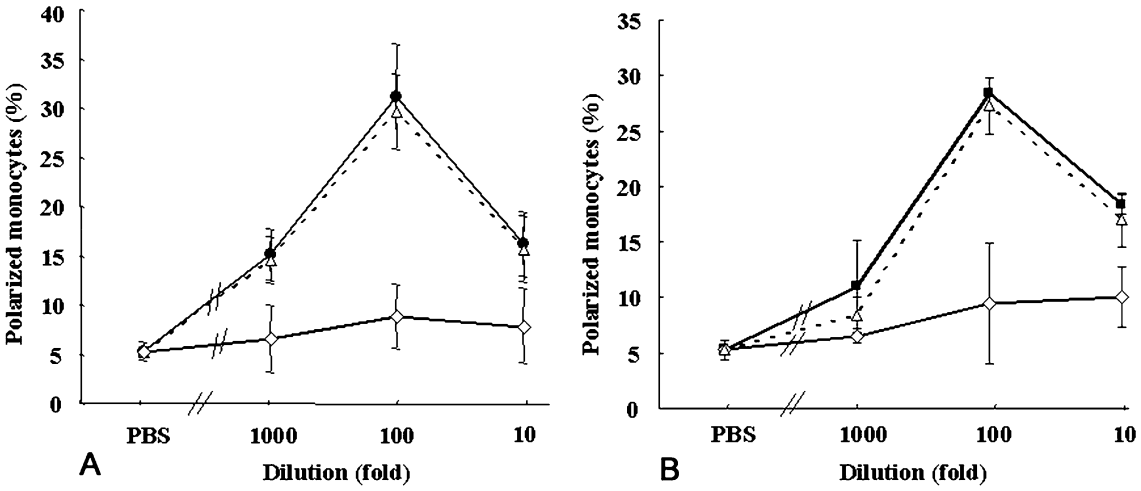


Fig. 6 Combination immunoabsorption of monocyte polarization capacities of two intimal extracts (**a**, **b**) with mixture of antibody beads. The anti-RP S19 IgG beads and the anti-MCP-1 IgG beads were mixed at an equal volume. The same experiment as in Fig. 4 was performed except for using the antibody beads mixture (*open diamonds*). In the control experiment, the normal IgG beads were used (*open triangles*). The remaining polarization capacities were measure with serially diluted supernatants from 10- to 1,000-fold. The experiments were carried out in triplicate samples. The polarized ratio (percent) of monocytes is expressed as mean±SD

rements of the chemotactic capacities after the treatment with anti-RP S19 antibody beads and with anti-MCP-1 antibody beads were observed. In three cases out of five, stronger effects of the anti-RP S19 antibody beads on absorption were observed than those of the anti-MCP-1 antibody beads. In the remaining two cases, inverse phenomena were observed. A representative result of each case is respectively shown in Fig. 5.

We then subjected these representative samples to a combination of immunoabsorption experiments. In this experiment, we used a mixture of an equal volume of the anti-RP S19 antibody beads and the anti-MCP-1 antibody beads for the absorption experiment in the same way as when using the single kinds of immunobeads. As shown in Fig. 6, the combination beads absorbed almost all of the chemotactic capacities of these extracts.

Inhibition of monocyte chemotactic capacities of intimal extracts with C5a receptor antagonist

The RP S19 dimer and MCP-1 induce the chemotactic response of monocytes via the C5a receptor and the C–C chemokine receptor 2, respectively. An authentic C5a re-

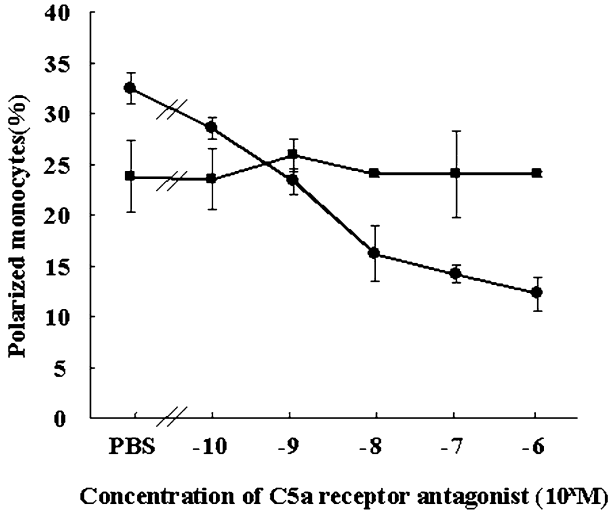


Fig. 7 RP S19 dimer-selective inhibition with C5a receptor antagonist. The indicator monocytes were pretreated with various concentrations of an authentic C5a receptor antagonist (NMePhe-Lys-Pro-dCha-dCha-dArg) for 10 min at 37°C, and used for the polarization assay with the RP S19 dimer (*closed circles*) or with MCP-1 (*closed squares*) as the chemoattractant at a final concentration of 10^{-8} M. The experiments were carried out in triplicate samples. The polarized ratio (percent) of monocytes is expressed as mean±SD

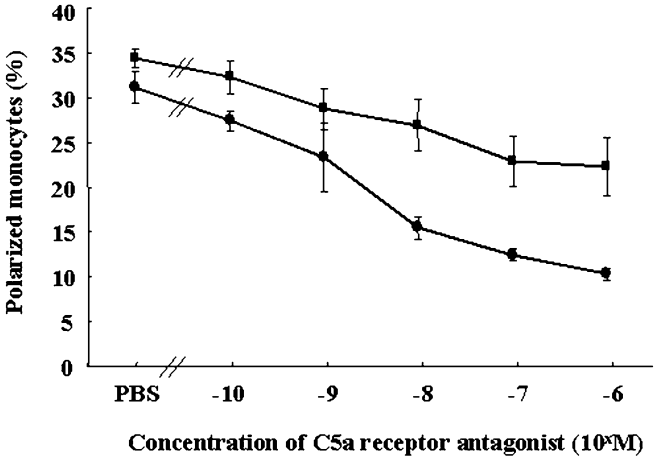


Fig. 8 Inhibition of monocyte chemotactic activity of intimal extracts with C5a receptor antagonist. The RP S19 dimer-predominant (*closed circles*) and the MCP-1-predominant (*closed squares*) intimal extracts, which had been used for the experiments shown in Fig. 4, were subjected to the experiments with the C5a receptor antagonist in the same way as in Fig. 6. The experiments were carried out in triplicate samples. The polarized ratio (percent) of monocytes is expressed as mean±SD

ceptor antagonist, NMePhe-Lys-Pro-dCha-dArg, must be useful in confirming the presence of the RP S19 dimer in the monocyte chemotactic intimal extracts, whereas an available antagonist of the C–C chemokine receptor 2 is not present.

Before the experiment with the intimal extract, we confirmed the inhibition capacity and the specificity of the receptor antagonist using the RP S19 dimer and MCP-1. As shown in Fig. 7, the C5a receptor antagonist inhibited the chemotactic response of monocytes to the RP S19 dimer in a dose-dependent manner but not to MCP-1.

In the next experiment, we selected a representative sample of the RP S19 dimer predominant extracts or of the MCP-1 predominant extracts. As shown in Fig. 8, the chemotactic response was inhibited by the pretreatment of the indicator monocytes in both cases. The intensity of the inhibition was stronger in the case of the RP S19 dimer predominant extract.

In the final experiment, we confirmed that the monocyte chemoattracting capacity suppressed by the C5a receptor antagonist in the intimal extracts was attributable to the RP S19 dimer. We initially treated the MCP-1-predominant extracts with the anti-RP S19 antibody beads, and we then examined the sensitivity of the remaining chemotactic activity to the C5a receptor antagonist. As shown in Fig. 9, the remaining chemotactic activities in the two cases were resistant to the C5a receptor antagonist. These results indicated that the chemotactic activities that were removed by the anti-RP S19 antibody bead treatment and inhibited by the C5a receptor antagonist treatment were attributable to the single monocyte chemotactic factor—the RP S19 dimer.

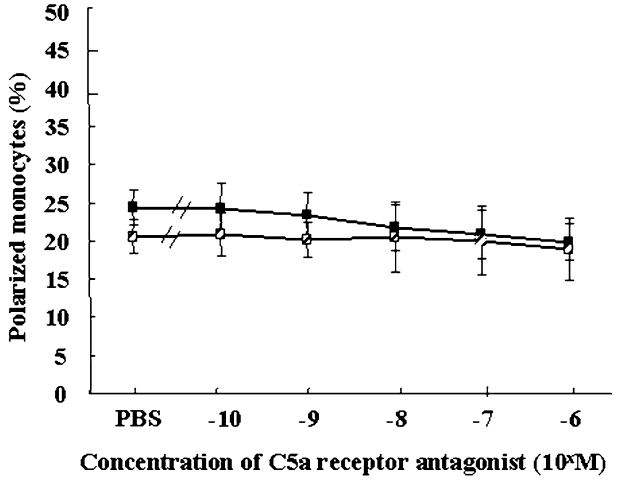


Fig. 9 Insensitivity to C5a receptor antagonist of monocyte chemotactic activity in intimal extracts after absorption with anti-RP S19 antibody beads. The two MCP-1 predominant intimal extracts were initially treated with the anti-RP S19 antibody beads in the same way as in Fig. 5, and the supernatants (*closed squares* and *slashed squares*) were subjected to the polarization assay using the indicator monocytes pretreated with the C5a receptor antagonist in the same way as in Fig. 8. The experiments were carried out in triplicate samples. The polarized ratio (percent) of monocytes is expressed as mean±SD

Discussion

In the present study, we used the anti-RP S19 peptide rabbit antibodies and the anti-MCP-1 monoclonal antibody. Although the latter was an authorized antibody, the former was only prepared for this study. To support the immunochemical identification of the RP S19 dimer, we performed the experiments with the C5a receptor antagonist. By combining the immunochemical data with the results using the C5a receptor antagonist, we were able to conclude that the monocyte chemoattractant capacity that was removed by the anti-RP S19 antibody beads in the intimal extracts was attributable to the RP S19 dimer.

Therefore, the totality of the results described above indicated that the monocyte chemotactic intimal extracts of atherosclerotic lesion contained both the RP S19 dimer and MCP-1, and that these chemoattractant molecules encompassed the whole monocyte chemotactic capacity in the intimal extracts. The contributions of these molecules to the whole monocyte chemotactic capacity varied among the intimal extracts. From the present functional and immunochemical analyses of the intimal extract, we assume that the RP S19 dimer and MCP-1 would recruit circulating monocytes to the atherosclerotic lesion as the major monocyte chemoattractant factors.

The aortic tissue specimens used as normal control samples were obtained from two fresh autopsy cases, whereas the atherosclerotic lesions were obtained during surgical operation. This development ensued because a specimen of a normal region of the aorta could not be resected in the operation due to technical and ethical reasons. We did not macroscopically notice any abnormality in the control specimens; however, histological observation demonstrated minor degenerative changes in endothelial cells with very weak atheromatous sign. The subendothelial monocyte infiltration was already observed immunohistochemically, even though the infiltration was sparse. Extracts of the control intima exhibited weak monocyte chemoattraction capacities. Therefore, there is a possibility that the normal control samples used in the present study might be at an early phase of atherosclerosis.

In the present study, two atherosclerotic lesions possessed very low biological responses in terms of the monocyte/macrophage infiltration despite the presence of severe atheromatous changes with the atheromatous plaque. This is consistent with previous reports that the monocyte/macrophage recruitment, concomitant with the MCP-1 production, was observed most prominently in the developing lesions such as the intimal thickening and the fatty streak, but less prominently in the mature lesion such as the atheromatous plaque [18, 22].

MCP-1-producing cells were immunohistochemically identified to be endothelial cells and subendothelial monocytes/macrophages in human and rabbit atherosclerotic lesions [18, 22]. On the other hand, we are unable to identify the cells producing the RP S19 dimer in this lesion by immunohistochemical means at this time. It is because the anti-RP S19 antibodies are not capable of distinguishing between the monomer form and the dimer form of RP

S19, and because the RP S19 monomer is ubiquitously present as a component of the ribosome. We only speculate that the cells' ongoing apoptosis produces and releases the RP S19 dimer according to our previous in vitro studies [5, 10]. Therefore, we tried to histologically compare the apoptotic cell number between the RP S19 dimer predominant specimens and the MCP-1 predominant specimens with the terminal deoxynucleotidyltransferase-mediated dUTP- digoxigenin nicked end labeling (TUNEL), which we had previously used to detect cultured apoptotic cells [8]. However, the TUNEL method demonstrated the presence of the highest positive cell number in the control specimens, which were obtained at autopsy, and many of the positive cells were morphologically nonapoptotic. We do not know whether the DNA fragmentation would start rapidly after the resection of the tissue or in the postmortem period. For this reason, we could not compare the apoptotic cell number among the specimens.

Acknowledgements The authors are grateful to Prof. M. Takeya and Miss T. Kubo of Faculty of Medical and Pharmaceutical Sciences, Kumamoto University for helpful suggestions and technical advice, respectively.

References

1. Aquel NM, Ball RY, Waldman H, Mitchinson MJ (1985) Identification of macrophages and smooth muscle cells in human atherosclerosis using monoclonal amtibodies. J Pathol 146: 197–204
2. Cianciolo GJ, Snyderman R (1981) Monocyte responsiveness to chemotactic stimuli in a property of subpopulation of cells that can respond to multiple chemoattractants. J Clin Invest 67:60–68
3. Edwards RJ, Singleton AM, Boobis AR, Davies DS (1989) Cross-reaction of antibodies to coupling groups used in the production of anti-peptide antibodies. J Immunol Methods 117: 215–220
4. Fernandez HN, Henson PM, Otani A, Hugli TE (1978) Chemotactic response to human C3a and C5a anaphylatoxins. I. Evaluation of C3a and C5a leukotaxis in vitro and under stimulated in vivo conditions. J Immunol 120:109–115
5. Horino K, Nishiura H, Ohsako T, Shibuya Y, Hiraoka T, Kitamura N, Yamamoto T (1998) A monocyte chemotactic factor, S19 ribosomal protein dimer, in phagocytic clearance of apoptotic cells. Lab Invest 78:603–617
6. Kockx MM, Herman AG (1998) Apoptosis in atherogenesis: implications for plaque destabilization (review). Eur Heart J 19 (Suppl G):G23–G28
7. Kondoh N, Schweinfest CW, Henderson KW, Papas TS (1992) Differential expression of S19 ribosomal protein, laminin-binding protein, and human lymphocyte antigen class I messenger RNAs associated with colon carcinoma progression and differentiation. Cancer Res 52:791–796
8. Matsubara S, Yamamoto T, Tsuruta T, Takagi K, Kambara T (1991) Complement C4-derived monocyte-directed chemotaxis-inhibitory factor: a molecular mechanism to cause polymorphonuclear leukocyte-predominant infiltration in rheumatoid arthritis synovial cavities. Am J Pathol 138:1279–1291
9. Nishimura T, Horino K, Nishiura H, Shibuya Y, Hiraoka T, Tanase S, Yamamoto T (2001) Apoptotic cells of an epithelial cell line, AsPC-1, release monocyte chemotactic S19 ribosomal protein dimer. J Biochem 129:445–454
10. Nishiura H, Shibuya Y, Matsubara S, Tanase S, Kambara T, Yamamoto T (1996) Monocyte chemotactic factor in rheumatoid arthritis synovial tissue: probably a cross-linked derivative of S19 ribosomal protein. J Biol Chem 271:878–882
11. Nishiura H, Shibuya Y, Yamamoto T (1998) S19 ribosomal protein cross-linked dimer causes monocyte-predominant infiltration by means of molecular mimicry to complement C5a. Lab Invest 78:1615–1623
12. Nishiura H, Tanase S, Shibuya Y, Nishimura T, Yamamoto T (1999) Determination of the cross-linked residues in homodimerization of S19 ribosomal protein concomitant with exhibition of monocyte chemotactic activity. Lab Invest 79:915–923
13. Okura Y, Brink M, Itabe H, Scheidegger KJ, Kalangos A, Delafontaine P (2000) Oxidized low-density lipoprotein is associated with apoptosis of vascular smooth muscle cells in human atherosclerotic plaques. Circulation 102:2680–2686
14. Shibuya Y, Shiokawa M, Nishiura H, Nishimura T, Nishimura T, Nishino N, Okabe H, Takagi K, Yamamoto T (2001) Identification of receptor binding sites of monocyte chemotactic S19 ribosomal protein dimer. Am J Pathol 159:2293–2301
15. Shrestha A, Horino K, Nishiura H, Yamamoto T (1999) Acquired immune response as a consequence of the macrophage-dependent apoptotic cell clearance and role of the monocyte chemotactic S19 ribosomal protein dimer in this connection. Lab Invest 79:1629–1642
16. Shrestha A, Shiokawa M, Nishimura T, Nishiura H, Tanaka Y, Nishino N, Shibuya Y, Yamamoto T (2003) Switch moiety in agonist/antagonist dual effect of S19 ribosomal protein dimer on leukocyte chemotactic C5a receptor. Am J Pathol 162:1381–1388
17. Shrestha A, Shi L, Tanase S, Tsukamoto M, Nishino N, Tokita K, Yamamoto T (2004) Bacterial chaperon protein, Skp, induces leukocyte chemotaxis via C5a receptor. Am J Pathol 164:763–772
18. Takeya M, Yoshimura T, Leonard EJ, Takahashi K (1993) Detection of monocyte chemoattractant protein-1 in human atherosclerotic lesions by an anti-monocyte chemoattractant protein-1 monoclonal antibody. Human Pathol 24:534–539
19. Umeda Y, Shibuya Y, Semba U, Tokita K, Nishino N, Yamamoto T (2004) Guinea pig ribosomal protein as precursor of C5a receptor-directed monocyte-selected leukocyte chemotactic factor. Inflam Res 53:623–630
20. Watanabe T, Hirata M, Yoshikawa Y, Nagafuchi Y, Toyoshima H, Watanabe T (1985) Role of macrophages in atherosclerosis. Sequential observation of cholesterol-induced rabbit aortic lesions by the immunoperoxidase technique using monoclonal anti-macrophage antibody. Lab Invest 53:80–90
21. Yamamoto T (2000) Molecular mechanism of monocyte predominant infiltration in chronic inflammation: mediation by a novel monocyte chemotactic factor, S19 ribosomal protein dimer. Pathol Int 50:863–871
22. Ylä-Herttura S, Lipton BA, Rosenfeld ME, Särkioja T, Yoshimura T, Leonard EJ, Witztum JL, Steinberg D (1991) Expression of monocyte chemoattractant protein 1 in macrophage-rich areas of human and rabbit atherosclerotic lesions. Proc Natl Acad Sci U S A 88:5252–5256

Virchows Arch (2005) 447: 756–761
DOI 10.1007/s00428-005-0009-0

ORIGINAL ARTICLE

Batia Kaplan · Brian M. Martin · Olga Boykov · Rivka Gal · Mordechai Pras · Itzhak Shechtman · Milton Saute · Mordechai R. Kramer

Co-deposition of amyloidogenic immunoglobulin light and heavy chains in localized pulmonary amyloidosis

Received: 16 January 2005 / Accepted: 27 April 2005 / Published online: 14 July 2005
© Springer-Verlag 2005

Abstract Localized pulmonary amyloidosis is a rare condition whose pathogenesis is insufficiently understood. In the present study, we report a case of localized pulmonary amyloidosis associated with lung-restricted lymphoplasmacytoid lymphoma, monoclonal for immunoglobulin (Ig) G lambda (λ). Biochemical microtechniques have been applied for extraction, purification, and characterization of amyloid proteins. Surprisingly, chemical analysis of these proteins revealed a not-previously-described case of combined deposits containing Ig fragments of gamma heavy chain (variable domain) and λ light chain (constant domain). In view of the absence of circulating monoclonal Ig, this case supports the hypothesis that localized amyloid is formed by local plasmacytoid cells.

Keywords Amyloid · Pulmonary amyloidosis · Immunoglobulin light and heavy chains · Microtechniques

B. Kaplan (✉) · M. Pras
Heller Institute of Medical Research, Sheba Medical Center,
Tel Hashomer, 52621, Israel
e-mail: kaplanb@sheba.health.gov.il
Tel.: +972-3-5303363
Fax: +972-3-7377002

B. Kaplan · R. Gal · M. Pras
Sackler School of Medicine, Tel-Aviv University,
Tel Hashomer, Israel

B. M. Martin
Laboratory of Neurotoxicology,
National Institute of Mental Health,
Bethesda, MD, USA

O. Boykov · I. Shechtman
Department of Pathology, Rabin Medical Center,
Beilinson Campus,
Petah Tiqva, Israel

R. Gal
Department of Pathology, Rabin Medical Center,
Golda Campus,
Petah Tiqva, Israel

M. Saute
Department of Thoracic Surgery, Rabin Medical Center,
Beilinson Campus,
Petah Tiqva, Israel

M. R. Kramer
Pulmonary Institute, Rabin Medical Center,
Beilinson Campus,
Petah Tiqva, Israel

Introduction

Localized pulmonary amyloidosis is a rare condition usually characterized by a local deposition of immunoglobulin (Ig) light chain-derived amyloid. In addition to the cases with a benign course [9, 10], some studies have demonstrated the coexistence of nodular pulmonary amyloidosis with low-grade pulmonary lymphomas: marginal zone lymphoma of mucosa-associated lymphoid tissue (MALT) [18, 35], small-cell non-Hodgkin's lymphoma [4], and lymphoplasmacytoid lymphoma [11]. Clinically, in these cases of localized pulmonary amyloidosis, the lymphomas were restricted to the lung alone, at least in the early stages when amyloid disease was discovered. Nodular pulmonary Ig light chain deposits having amyloid and nonamyloid features were revealed in one HIV-infected patient [32]. Two cases of localized pulmonary nonamyloid light chain deposition (LCDD) accompanied by low-grade lymphoplasmacytic lymphoma limited to the lung have been recently described [17, 27].

The pathogenesis of localized, organ-restricted amyloidosis is not fully understood. In localized pulmonary amyloidosis, the presence of lymphocytes and plasma cells in the vicinity of amyloid deposits, as well as within them, has been described as an invariable feature of the lesion [1–3, 10]. It has been proposed that the localized amyloid deposits arise from a local monoclonal proliferation of immunocytes [25]. Other authors, however, demonstrated that in most cases of localized pulmonary amyloidosis, these plasma cells are polyclonal rather than monoclonal and are therefore unlikely to be the source of monoclonal Ig [9, 10]. Thus, according to the alternative hypothesis, the Ig light chain precursor protein in localized amyloidosis is syn-

thesized by circulating plasma cells, with targeting of the amyloid formation to a specific organ. This hypothesis was supported by the findings of circulating monoclonal Ig in several patients with localized pulmonary amyloidosis [9, 10, 22]. Whether or not the affinity to a specific organ depends on the primary structure of the amyloidogenic protein, and how, is a question also being raised. However, only a few reported data are based on a direct chemical analysis of amyloid deposits localized in the lung [21]. In this respect, a detailed chemical analysis of such amyloid deposits, together with careful clonal evaluation of the adjacent immunocytes, will aid in understanding the mechanisms of organ-specific amyloid deposition [8].

In the present study, we report a case of localized pulmonary amyloidosis associated with lung-restricted lymphoplasmacytoid lymphoma, monoclonal for IgG lambda (IgG-λ). Surprisingly, chemical analysis of the amyloid proteins revealed a not-previously-described case of amyloid deposits containing fragments of IgG heavy chain (variable region) and λ light chain (constant region), in contrast to the expected λ light chain variable region fragments. In view of the absence of circulating monoclonal Ig, this case supports the hypothesis that in localized amyloidosis, the amyloid is formed entirely by the local plasma cells.

Patient and methods

Patient

A 69-year-old man with a past history of pneumonia 5 years ago was followed by chest x-ray every 6 months, which showed a small mass in the left upper lobe. Following a recurrent pneumonia recently, the chest x-ray and computed tomography (CT) scan showed large consolidation and mass involving the whole left upper lobe. Fluorodeoxyglucose positron emission tomography (FDG-PET) scan showed marked uptake of the same area. Bronchoscopy revealed irregular mucosa, whereas the Congo-red-stained biopsy material was positive for amyloid. There were no clinical or laboratory findings indicating amyloid involvement of other organs such as heart, liver, kidneys, peripheral nerves, intestine, or skin. Due to the unresolved consolidation in the left upper lobe, the patient underwent thoractomy and left upper lobe resection. Bone marrow biopsy showed normal differentiation of the hematopoietic cell lines. Mild increase in plasma cells was noted with polyclonal stain for both kappa (κ) and λ light chains. Using protein electrophoresis and immunofixation electrophoresis, no monoclonal protein was detected on the patient's serum and urine. The patient recovered from surgery and is alive and well.

Pathological studies

Formalin-fixed, paraffin-embedded tissue specimens obtained following lobectomy were subjected to histological and immunohistochemical examination. Sections were stained with hematoxylin and eosin (H & E) and Congo red according to standard methods. Immunostaining was performed with rabbit antihuman antibodies to κ and λ light chains, as well as to IgG, IgM, and IgA heavy chains (Dako, Carpenteria, CA, USA), and visualized by the immunoperoxidase method according to the established protocols. Immunophenotyping of B (CD20) and T (CD3) cells was performed on paraffin sections with a standard avidin–biotin–peroxidase complex (ABC) method.

Isolation of amyloid material

For the biochemical characterization of amyloid proteins, the part of the excised lung tissue was immediately frozen and stored at −70°C until used. Extraction of amyloid proteins was performed by the microtechnique described earlier [13]. Briefly, tissue specimen (about 50 mg wet weight) was homogenized with phosphate-buffered saline (PBS) pH 7.4, followed by centrifugation at 14,000×*g* for 10 min. The obtained pellet was repeatedly homogenized in PBS, and the mixture was centrifuged. The resulting pellet was again washed with deionized water and extracted with aqueous 20% acetonitrile containing 0.1% trifluoroacetic acid (TFA) solution. The extracted material was lyophilized.

Sodium dodecyl sulfate polyacrylamide gel electrophoresis

Electrophoresis was performed in a Novex gel running apparatus (Novex, San Diego, CA, USA) using the precast 20–25% polyacrylamide LongLife microgels, ten wells (Gradipore, Frenchs Forest, NSW, Australia). The extracted material was dissolved in sodium dodecyl sulfate–polycrylamide gel electrophoresis (SDS-PAGE) sample buffer (10 μg/μl) applied to gel (5–8 μl per well). Rainbow-colored molecular mass markers ranging in M_r from 3 to 45 kDa (Amersham, Buckinghamshire, England, UK) were used. Samples were run with Tris SDS HEPES Long Life Running Buffer (Gradipore).

Western blotting

Samples were run by SDS-PAGE and electrotransferred onto nitrocellulose (Schleicher and Schuell, Dassel, Germany) with a Gradipore LongLife Transfer Buffer. The immunostaining was performed by using rabbit antibodies to human Ig κ and λ light chains (Dako) as described earlier [12, 16]. Proteins were visualized using SuperSignal West Pico Chemiluminescent Substrate (Pierce, Rockford, IL, USA).

Micropreparative purification of amyloid proteins

For concentration and micropreparative purification of amyloid proteins, the extracted sample (10 μg/μl) was applied to nine wells of the microgel and run by SDS-PAGE together with the molecular mass markers applied to the remaining well. The electrophoresed proteins were electrotransferred onto Sequi-Blot polyvinylidene difluoride (PVDF) membranes (Bio-Rad, Hercules, CA, USA) with a Gradipore LongLife Transfer Buffer and stained with Coomassie blue R-250. The protein bands of interest were excised, and the bands with the same M_r from different lanes were pooled and eluted with TFA/acetonitrile/water (3:4:3) as described [14]. The eluted material containing protein and Coomassie blue stain was dried (in Speed Vac apparatus). To separate the proteins from the stain, the obtained material was rerun on SDS-PAGE and blotted onto PVDF. One lane of the blot was stained to locate the position of the unstained proteins, which were subsequently recovered from PVDF as indicated above.

N-terminal amino acid sequence analysis (Edman degradation)

The electrophoresed proteins were electrotransferred onto Sequi-Blot PVDF membranes and stained with Coomassie blue R-250. Protein bands were excised and subjected to amino acid sequence analysis as described [16].

Results

The excised left upper lobe specimen (490 g, 6×13×21 cm) was covered by the focal irregular pleura (Fig. 1). The cutting showed extensive exchange of the lung parenchyma by a firm gray tumoral mass. Histopathological examination of the excised lung tissue demonstrated a large infiltrate of small round lymphoid cell with focal plasmacytoid differentiation (Fig. 2a). In and around this lymphoid infiltrate, large amounts of eosinophilic amorphous material were seen. These were Congo-red-positive and showed apple green birefringence under polarized light (Fig. 2b). Immunohistochemical staining of the lymphocyte cells using a panel of antibodies to Ig heavy and light chains showed cytoplasmatic staining with antibodies to γ heavy chains (Fig. 3a) and λ light chains (Fig. 3b). Lymphocytic cells were positive for CD20. Ki-67 proliferative index was positive in 15% of cells. The obtained morphological and immunohistochemical data were typical of a lymphoid neoplasm, whereas the presence of small round lymphocytes expressing CD20 and showing plasmacytoid differentiation was indicative of lymphoplasmacytoid lymphoma. The low proliferative index (ki-67) supports the diagnosis of low-grade lymphoma. Together with clinical and laboratory data, the histopathological findings were consistent with a localized pulmonary lymphoplasmacytoid lymphoma, monoclonal for IgG-λ, with heavy amyloid deposition.

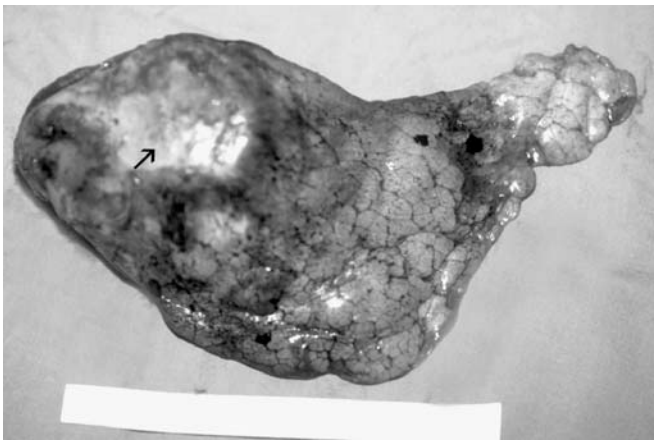


Fig. 1 Macroscopic examination of left upper lobectomy specimen demonstrates irregular mass (indicated by *arrow*) adjacent to pleural surface

For biochemical examination of the amyloid deposits, proteins were extracted from the excised lung tissue specimen according to the procedure described above. By this

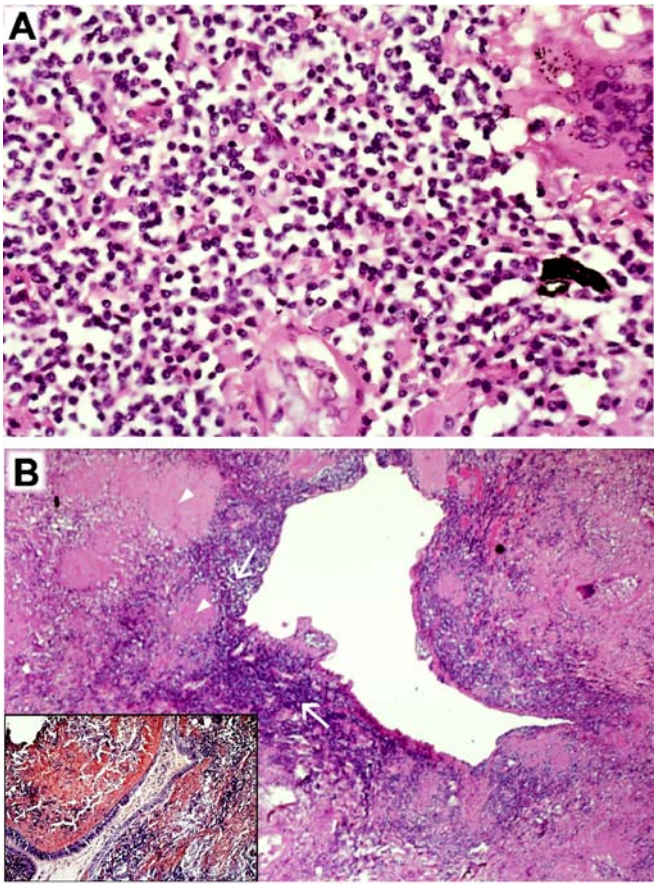


Fig. 2 Histological sections of the lung tissue showing peribronchial lung parenchyma. **a** Small round lymphoid cells with focal plasmacytoid differentiation and reactive foreign body giant cell. H & E, × 400. **b** Lymphoid infiltrates (*arrows*) intermixed with deposits of pink amorphous material of amyloid (*triangles*). H&E, ×100. Congo red staining of amyloid is demonstrated in the *left lower corner* (×200)

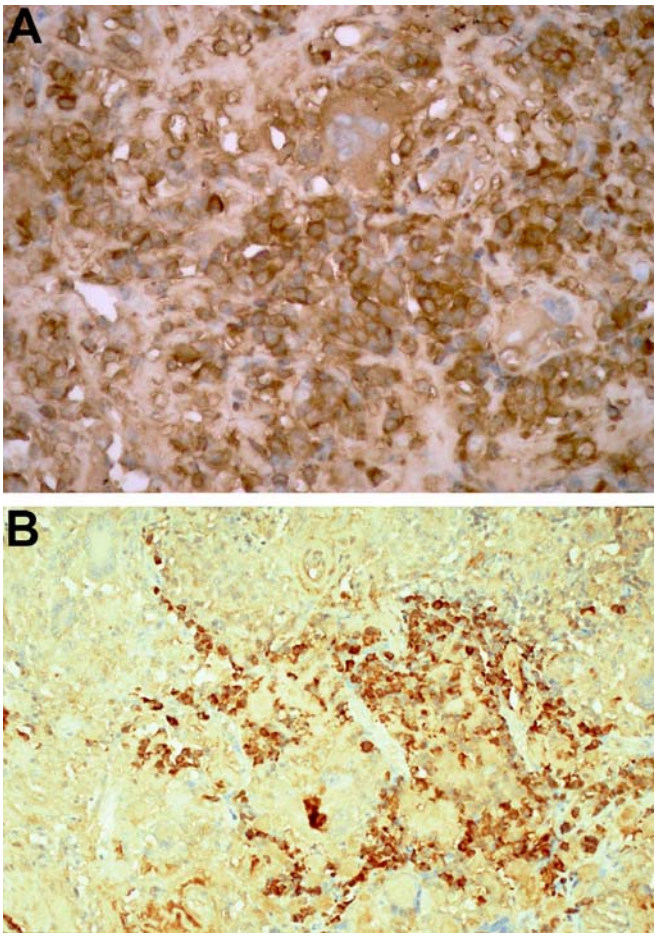


Fig. 3 Immunohistochemical analysis of tumoral lymphoid cells shows positive cytoplasmatic staining for **a** Ig γ heavy chains (×400) and **b** λ light chains (×200)

procedure, tissue sample was first homogenized and washed with PBS to remove soluble tissue components. Because the disruption of cells is a necessary condition for the removal of soluble cytoplasmatic proteins, including monoclonal Ig of lymphoplasmacytoid cells and mature plasma cells, the samples of the obtained washed tissue homogenate were stained with H & E and examined microscopically. Both the tissue smears and the paraffin block material showed no presence of intact cells. The obtained tissue homogenate was then extracted with acetonitrile/TFA solution. The electrophoretic analysis of the extracted material demonstrated multiple protein bands from about 5 to more than 45 kDa. Inasmuch as the major amyloid components represent the relatively small molecular mass proteins ranging from 3 to less than 30 kDa, the following proteins detected within this molecular weight (MW) range were of major interest: the 12- and 18-kDa protein bands strongly stained with Coomassie blue and two weaker bands with MWs of about 5 and 8 kDa (Fig. 4, track 2). Because the immunohistochemical findings indicated the presence of lymphoid cells monoclonal for IgG-λ, the lung tissue of the patient was presumed to contain amyloid deposits of the AL-λ type. However, in Western blotting, the 8-, 12- and 18-kDa bands revealed no specific immunoreactivity with antibodies to Ig κ and λ light chains; only the 5-kDa protein band showed specific immunostaining for Ig λ light chains. Therefore, for elucidation of the chemical nature of these proteins, they were further analyzed by automated Edman degradation. For this purpose, proteins were concentrated and purified by the micropreparative SDS-PAGE procedure described above (Fig. 4, tracks 3–6). N-terminal amino acid sequence analysis of the purified 5-kDa protein band allowed identification of an Ig λ light chain constant region fragment; this band showed ATLV*LISDF sequence (from position 153 to 163), where the missing amino acid marked with * (blank cycle) was consistent with the presence of cysteine. Analysis of the 12- and 18-kDa bands revealed VQMTRDKT sequences matching a fragment of IgG heavy chain variable region (starting at position 87) [5].

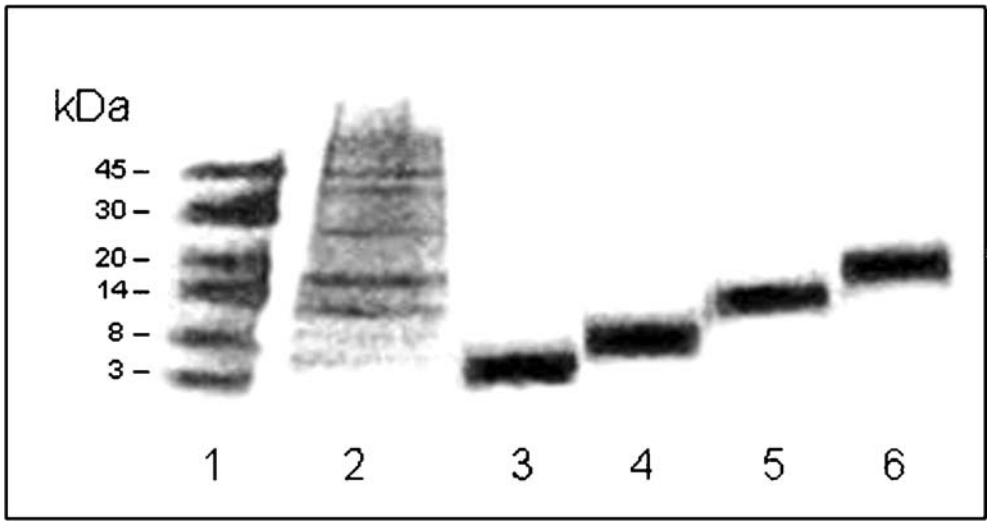


Fig. 4 Electrophoretic analysis of amyloid proteins extracted and purified from a lung tissue in a case of localized pulmonary amyloidosis associated with lymphoplasmacytoid lymphoma. *1* Molecular weight markers, *2* tissue extract, *3–6* purified proteins of 5, 8, 12 and 18 kDa, respectively

Table 1 Cases with Ig heavy chain amyloidosis

Reference	Diagnosis	Deposits	Structural features based on amino acid sequencing
[3]	Renal amyloidosis and LCDD	LCDD-λ and IgG heavy chain amyloid	–
[7]	Primary systemic amyloidosis	IgG heavy chain amyloid	Intact IgG1 constant domain
[20]	Renal amyloidosis	IgM heavy chain amyloid	–
[30]	Renal amyloidosis	IgG heavy chain amyloid	IgG heavy chain variable domain fragment
[33]	Primary localized orbital amyloidosis	IgG heavy chain amyloid	IgG heavy chain constant domain fragment
[36]	Renal amyloidosis	IgG heavy chain amyloid	IgG heavy chain variable domain fragment
Present study	Localized pulmonary lymphoplasmacytoid lymphoma and amyloidosis	λ light chain and IgG heavy chain amyloid	λ light chain constant domain fragment; IgG heavy chain variable domain fragment

Discussion

In the present case of localized pulmonary amyloidosis, the deposited amyloid proteins were composed of Ig fragments derived from both the IgG heavy chain variable region and the Ig light chain λ constant region. This case is unusual, first, because heavy chain amyloidosis is a rare condition, not yet described in localized pulmonary amyloidosis [7, 20, 23, 30, 33, 36]. Second, to the best of our knowledge, there are no reports on co-deposition of amyloidogenic Ig heavy and light chains in the same patient (Table 1), although it is possible that some of the smaller-molecular-weight proteins that are found in almost every immunocyte-related amyloid material and are not routinely examined contained proteins derived from either light or heavy Ig chains. Deposition of light and heavy chain fragments found in the same patient may probably be explained by the aberrant biosynthesis of these Ig chains in the monoclonal population of B cells, as it was demonstrated in a case of nonamyloidogenic, monoclonal light and heavy chain deposition disease [2]. On the other hand, the abnormal biclonality of B lymphocytes has been observed in several patients with plasma cell disorders [1, 28, 29], monoclonal gammopathy of unknown significance (MGUS) [19] and combined amyloid and LCDD [3, 26]. Therefore, it is also possible that in some cases, the co-deposited light and heavy chain fragments might originate from different clones. The third uncommon feature of our case is that amyloid deposits contained protein originating from constant, but not variable, Ig light chain domain. In fact, it is commonly accepted that the fragments of variable domains of monoclonal Ig light chains play a major role in fibril formation. In this respect, our findings support some recent studies suggesting that the presence of constant region fragments in amyloid deposits may be more common than formerly held and their role in fibril formation was underestimated [6, 16, 24, 31, 34].

The biochemical micromethods of extraction and characterization of amyloid fibrils applied here were used by us previously and were found to be helpful when revealing rare amyloid types or when the immunohistochemical findings were either unexpected or questionable [13, 15, 16]. In the present case, these techniques aided in achieving a precise diagnosis of the disorder. The lung-restricted amyloid proteins presently identified appear to share the same isotypic Ig determinants as those found in monoclonal lymphoid cell population within amyloid deposits (IgG-λ). In light of the absence of circulating monoclonal Ig protein, these data support the view that organ-restricted amyloid formation may occur as a result of a local monoclonal proliferation of immunocytes.

References

1. Brohee D, Cauchie P, Delval L, Govaerts D, Neve P, Piro P (2002) Frequent discordance of the light-chain isotypes expressed by serum monoclonal components and leukaemic B-cells. Clin Lab Haematol 24:151–154
2. Buxbaum JN (2001) Abnormal immunoglobulin synthesis in monoclonal light chain and light and heavy chain deposition disease. Amyloid 8:84–93
3. Copeland JN, Kouides PA, Grieff M, Nadasdy T (2003) Metachronous development of nonamyloidogenic λ light chain deposition disease and IgG heavy chain amyloidosis. Am J Surg Pathol 27:1477–1482
4. Davis CJ, Butchart, Gibbs AR (1991) Nodular pulmonary amyloidosis occurring in association with pulmonary lymphoma. Thorax 46:217–218
5. Ditzel HJ, Barbas SM, Barbas CF III, Burton DR (1994) The nature of the autoimmune antibody repertoire in human immunodeficiency virus type λ infection. Proc Natl Acad Sci U S A 91:3710–3714
6. Envig JP, Olsen KE, Gislefoss RE, Sletten K, Wahlstrom O, Westermark P (1998) Constant region of a κIII immunoglobulin light chain as a major AL-amyloid protein. Scand J Immunol 48:92–98
7. Eulitz M, Weiss DT, Solomon A (1990) Immunoglobulin heavy-chain-associated amyloidosis. Proc Natl Acad Sci U S A 87: 6542–6546
8. Hamidi Asl K, Liepnieks JJ, Nakamura M, Benson MD (1999) Organ-specific (localized) synthesis of Ig light chain amyloid. J Immunol 162:5556–5560
9. Howard ME, Ireton J, Daniels F, Langton D, Manolitsas ND, Fogarty P, McDonald CE (2001) Pulmonary presentations of amyloidosis. Respirology 6:61–64
10. Hui AN, Koss MN, Hochholzer L, Wehunt WD (1986) Amyloidosis presenting in the lower respiratory tract. Arch Pathol Lab Med 110:212–218
11. Ihling C, Weirich G, Gaa A, Schaefer HE (1996) Amyloid tumors of the lung—an immunocytoma? Pathol Res Pract 192: 446–452
12. Kaplan B, Yakar S, Kumar A, Pras M, Gallo G (1997) Immunochemical characterization of amyloid in diagnostic biopsy tissues. Amyloid 4:80–86

13. Kaplan B, Hrncic R, Murphy CL, Gallo G, Weiss DT, Solomon A (1999) Microextraction and purification techniques applicable to the characterization of amyloid proteins in minute amounts of tissue. Methods Enzymol 309:67–81
14. Kaplan B, Murphy CL, Ratner V, Pras M, Weiss D, Solomon A (2001) Micro-method to isolate and purify amyloid proteins for chemical characterization. Amyloid 8:22–29
15. Kaplan B, Shtrasburg S, Pras M (2003) Micropurification techniques in analysis of amyloid proteins. J Clin Pathol 56:86–90
16. Kaplan B, Martin BM, Livneh A, Pras M, Gallo G (2004) Biochemical subtyping of amyloid in formalin-fixed tissue samples confirms and supplements immunohistochemical data. Am J Clin Pathol 121:794–800
17. Khoor A, Myers JL, Tazelaar HD, Kurtin PJ (2004) Amyloid-like pulmonary nodules, including localized light-chain deposition. Am J Clin Pathol 121:200–204
18. Lim JK, Lacy MQ, Kyle RA, Gertz MA (2001) Pulmonary marginal zone lymphoma of MALT type as a cause of localized pulmonary amyloidosis. J Clin Pathol 54:642–646
19. Lolin YI, Chow J, Wickman NW (1996) Monoclonal gammopathy of unknown significance and malignant paraproteinemia in Hong Kong. Am J Clin Pathol 106:449–456
20. Mai HL, Sheikh-Hamad D, Herrera GA, Gu X, Truong LD (2003) Immunoglobulin heavy chain can be amyloidogenic: morphological characterization including immunoelectron microscopy. Am J Surg Pathol 27:541–545
21. Miura K, Shirasawa H (1993) Lambda III subgroup immunoglobulin light chains are precursor proteins of nodular pulmonary amyloidosis. Am J Clin Pathol 100:561–566
22. Moriyama E, Yokose T, Kodama T, Matsuno Y, Hojo F, Takahasshi K, Nagai K, Nishiwaki Y, Ochiai A (2000) Low-grade B-cell lymphoma of mucosa-associated lymphoid tissue in the thymus of a patient with pulmonary amyloid nodules. Jpn J Clin Oncol 30:349–353
23. Murphy CL, Eulitz M, Hrncic R, Sletten K, Westermark P, Williams T, Macy SD, Wooliver C, Wall J, Weiss DT, Solomon DT, Solomon A (2001) Chemical typing of amyloid proteins contained in formalin-fixed paraffin-embedded biopsy specimens. Am J Clin Pathol 116:135–142
24. Olsen KR, Sletten K, Westermark P (1998) Fragments of the constant region of immunoglobulin light chains are constituents of AL-amyloid proteins. Biochem Biophys Res Commun 251: 642–647
25. Page DL, Isersky CH, Harada M, Glenner GG (1972) Immunoglobulin origin of localized nodular pulmonary amyloidosis. Res Exp Med 159:75–86
26. Rodilla Sala R, Kratzin HD, Pick AI, Hilschmann N (1991) Biclonality in amyloidosis patient MAL: one clone producing an amyloidogenic, the other a non-amyloidogenic kappa λ-chain. In: Natvig JB, Forre O, Husby G, Husebekk A, Skogen B, Sletten K, Westermark P (eds) Amyloid and amyloidosis 1990. Kluwer, Dordrecht, pp 161–164
27. Rostango A, Frizzera G, Ylagan L, Kumar A, Ghiso J, Gallo G (2002) Tumoral non-amyloidotic monoclonal immunoglobulin light chain deposits ("aggregoma"): presenting feature of B-cell dyscrasia in three cases with immunohistochemical and biochemical analyses. Br J Haematol 119:62–69
28. Sahota SS, Garand R, Bataille R, Smith AJ, Stevenson FK (1998) V_H gene analysis of clonality related IgM and IgG from human lymphoplasmacytoid B-cell tumors with chronic lymphocytic leukemia features and high serum monoclonal IgG. Blood 91:238–243
29. Sklar J, Cleary ML, Thielemans K, Gralow J, Warnke R, Levy R (1984) Biclonal B-cell lymphoma. N Engl J Med 311:20–27
30. Solomon A, Weiss DT, Murphy C (1994) Primary amyloidosis associated with a novel heavy-chain fragment (AH amyloidosis). Am J Hematol 45:171–176
31. Solomon A, Weiss D, Murphy CL, Hrncic R, Wall JS, Schell M (1998) Light chain-associated amyloid deposits comprised of a novel κ constant domain. Proc Natl Acad Sci U S A 95:9547–9551
32. Stokes MB, Jagirdar J, Burshstin O, Kornacki S, Kumar A, Gallo G (1997) Nodular pulmonary immunoglobulin light chain deposits with coexistent amyloid and nonamyloid features in an HIV-infected patient. Mod Path 10:1059–1065
33. Tan SY, Murdoch IE, Sullivan TJ, Wright JE, Truong O, Hsuan JJ, Hawkins PN, Pepys MB (1994) Primary localized orbital amyloidosis composed of the immunoglobulin γ heavy chain CH3 domain. Clin Sci 87:487–491
34. Wally J, Kica G, Zhang Y, Ericsson T, Benson MD, Liepnieks JJ, Murray J, Skinner M, Comenzo RL (1999) Identification of a novel substitution in the constant region of a gene coding for an amyloidogenic κ_1 light chain. Biochim Biophys Acta 1454:49–56
35. Wieker K, Rocken C, Koenigsmann M, Roessner A, Franke A (2002) Pulmonary low-grade MALT-lymphoma associated with localized pulmonary amyloidosis. Amyloid 9:190–193
36. Yazaki M, Fushimi T, Tokuda T, Kametani F, Yamamoto K, Matsuda M, Shimojo H, Hosshii Y, Higuchi K, Ikeda S (2004) A patient with severe renal amyloidosis associated with an immunoglobulin γ-heavy chain fragment. Am J Kidney Dis 43: E23–E28

Virchows Arch (2005) 447: 762–767
DOI 10.1007/s00428-005-0005-4

CASE REPORT

Frank Simon · Georg Johnen · Michael Krismann · Klaus-Michael Müller

Chromosomal alterations in early stages of malignant mesotheliomas

Received: 17 February 2005 / Accepted: 30 April 2005 / Published online: 13 July 2005
© Springer-Verlag 2005

Abstract In a case of a 67-year-old man with two different early stages of a predominantly epithelioid mesothelioma ("mesothelioma in situ", "early-stage mesothelioma"), chromosomal imbalances were determined by comparative genomic hybridisation (CGH), a molecular cytogenetic technique to detect chromosomal gains and losses in tumour cells. In the case of the mesothelioma in situ cells, nine different chromosomal alterations could be detected (losses on 3p, 5q, 6q, 8p, 9p, 15q, 22q, Y; gain on 7q), whereas the early-stage mesothelioma showed the same defects except for the gain on 7q. The simultaneous losses of 6q, 9p and 22q, as well as other chromosomal regions, correlate well with the most common defects previously found in 90 cases of more-advanced-stage mesotheliomas using CGH. These data demonstrate that initial chromosomal defects in early stages of mesotheliomas can be detected by conventional CGH in combination with laser microdissection. The molecular cytogenetic findings support the histological diagnosis of a pleural mesothelioma. The surprisingly high number and extent of genomic alterations found in the examined case probably reflects the genomic instability in the tumour cells and indicates a "genetic chaos" even in earlier stages of malignant mesotheliomas.

Keywords Malignant mesothelioma · Genomic alterations · CGH · Laser microdissection · Chromosomal defects

F. Simon (✉) · G. Johnen · M. Krismann · K.-M. Müller
Institut für Pathologie der Ruhr-Universität Bochum an den Berufsgenossenschaftlichen Kliniken Bergmannsheil,
Bürkle-de-la-Camp-Platz 1,
44789 Bochum, Germany
e-mail: simon-franky@t-online.de
Tel.: +49-234-3024987
Fax: +49-234-3024819

G. Johnen
Berufsgenossenschaftliches Forschungsinstitut für Arbeitsmedizin (BGFA), Institut der Ruhr-Universität Bochum,
Bürkle-de-la-Camp-Platz 1,
44789 Bochum, Germany

Introduction

Malignant mesothelioma (MM) is an asbestos-associated tumour of the serous membranes. Pleural manifestation of a diffuse MM is much more common than peritoneal mesothelioma, mesothelioma of the pericardium or the tunica vaginalis testis. Tumour manifestation is mainly in the sixth decade of life. Pleural mesothelioma is a tumour with a poor prognosis. MMs are relatively resistant to radiotherapy and chemotherapy [13]. MMs have a broad histomorphological spectrum that includes predominantly epithelioid, predominantly sarcomatoid and biphasic subtypes as well as some rare subtypes, which are associated with different survival times [4]. The long latency (20≥40 years from initial exposure) suggests that multiple somatic genetic events are involved, which is supported by the detection of numerous chromosomal aberrations in late-stage mesotheliomas. Advanced stages of mesotheliomas have been examined by Bjorkqvist and co-workers and by our group using the comparative genomic hybridisation (CGH) method [1, 8, 10]. Chromosomal defects of two different earlier stages of an MM were analysed in this report using conventional CGH in combination with laser-assisted microdissection, a method to isolate tumour cell populations free of surrounding normal tissue by an ultraviolet (UV) laser. The interesting biological question behind this study is whether even in early tumour stages there are gross genomic alterations (e.g. loss or gain of chromosome arms). The initial defects were studied in early-stage mesotheliomas and compared to the alterations in manifest mesotheliomas.

Clinical history

A 67-year-old quarry worker with recurrent pleural effusions showed signs of a malignant epithelial tumour in a cytological sample. Tissue samples of the right costal pleura and the right pulmonary lobe were taken. The visceral pleura showed focal structures of an epithelioid neoplasia with pseudo-polypoid histology. Two histologically

different early tumour stages of an MM could be detected in the pleural tissue (mesothelioma in situ, early-stage mesothelioma).

Materials and methods

We have investigated two samples of pleural MM in early stages of tumour development in a 67-year-old patient by immunohistochemistry and CGH in combination with laser microdissection. CGH is a well-established method to screen tumour tissues for chromosomal alterations [3, 5, 7]. A mesothelioma in situ is characterised either by a monolayer of atypically proliferating mesothelial cells (cytokeratin 5/6, pancytokeratin, calretinin positive) with beginning branching to the pleural cavity or by a multilayered solid atypical mesothelial proliferation with branching and/or formation of stromal papillae, but without invasive growth. Similar lesions have been described in a paper by the Australian group of Whitaker and co-workers in 1992 [19]. In contrast, early mesothelioma is defined by beginning infiltrative growth into the adjacent pleural connective tissue as stage pT1 according to the tumour–node–metastasis (TNM) classification [15].

Immunohistochemistry for calretinin, human epithelial antigen, cytokeratin 5/6, epithelial membrane antigen, thyroid transcription factor 1, MiB1 and keratin

Immunohistochemistry was performed on archival formalin-fixed and paraffin-embedded tissue sections using a streptavidin-biotin peroxidase complex technique (LSAB2 System, DAKO, Hamburg, Germany). To distinguish between a secondary pleural carcinosis of adenocarcinoma and epithelioid mesothelioma, periodic acid-Schiff (PAS) staining and an immunohistochemical marker panel including cytokeratin (MNF116, CK5/6), calretinin, human epithelial antigen (HEA) , epithelial membrane antigen (EMA), thyroid transcription factor 1 (TTF-1) and MiB1 (proliferation marker) were used. All used antibodies were acquired from DAKO.

Laser microdissection

Laser microdissection was used to isolate pure tumour cell populations without surrounding normal tissue [16, 17]. Prior to laser microdissection, four sequential 3-μm sections were cut from archival tissue blocks using a microtome with a disposable blade. Three tissue sections were mounted onto 2-μm-thick sterile polyester membranes [Molecular Machines & Industries AG (MMI), Glattbrugg, Switzerland] followed by deparaffination (1 hr at 65°C, 2×10 min xylene at room temperature), rehydration (100, 96 and 70% ethanol; 1 min each) and staining with 1% methylene green/eosin. The fourth tissue section was stained with hematoxylin and eosin (H&E) for a better detection of the tumour cell populations. Dissection of the few mesothelioma cells (100–300 cells) was carried out with a microscopic UV laser system (MMI). The UV laser microdissection system (UV CUT) consists of an inverted research microscope (Axiovert S100, Carl Zeiss, Jena, Germany) with motorised scanning stage, a UV laser unit (connected through the epifluorescence entrance of the microscope), a digital camera and a Pentium computer with control software. The microscopic image of the tissue is displayed on the computer monitor, and the area of interest is marked on the screen. The computer-controlled laser cuts around the area of interest and the dissectate is removed by an adherent lid of a special reaction tube. The selected microdissected areas (tumour and normal DNA) were documented with a digital camera and then transferred to a reaction tube. Handling and digestion of the isolated cells have been described before [6, 16].

Degenerate oligonucleotide-primed polymerase chain reaction

After digestion of the tumour cells, a whole genome amplification was performed by degenerate oligonucleotide-primed polymerase chain reaction (DOP-PCR) to obtain sufficient DNA quantities for subsequent CGH studies [18]. DOP-PCR was performed according to a modified standard protocol [11, 16]. Tests confirmed that amplification of DNA by DOP-PCR did not generate amplification imbalances visible by chromosomal CGH (G. Johnen and M. Jaworska, unpublished data).

Comparative genomic hybridisation analysis

For CGH analysis, we used a slightly modified standard protocol [9, 14]. Reference DNA (extracted from blood lymphocytes of a healthy male donor or normal microdissected tissue of the patient) and tumour DNA were both amplified by DOP-PCR. Reference and tumour DNA were labelled with tetramethylrhodamine isothiocyanate (TRITC) and fluorescein isothiocyanate (FITC), respectively, by random primed labelling. The two DNA samples were simultaneously hybridised to normal metaphase chromosomes (Abbott, Wiesbaden, Germany) in the presence of high concentrations of unlabelled Cot-1 DNA (30 μg), which blocks repetitive DNA sequences. After hybridisation, the fluorescence ratio was measured along the axis of each chromosome using fluorescence microscopy and digital image processing. Fluorescence images were evaluated with the program Quips (Applied Imaging, Sandhausen, Germany). For each tumour sample, 10–11 metaphases were analysed and the results were averaged. A 95% confidence interval and the average profile for each chromosome were calculated. As positive control, we used a tumour cell line with known defects (MPE 600, Abbott), and tissue from a healthy person without a tumour served as a negative control. The DNA of both controls was amplified by DOP-PCR.

Results

Histochemistry and immunohistochemical profile

The immunohistochemical examinations give valuable information for the diagnosis of a malignant pleural mesothelioma and its differential diagnosis (pleural metastases of other primary neoplasia). Benign reactive mesothelial hyperplasia shows monolayered enlarged, partially cuboid and columnar mesothelial cells without atypical mitoses and without papillary structures. In mesothelioma in situ, there is a beginning formation of pseudo-papillary branching (Fig. 1a, upper left), partly with stromal connective tissue, but without infiltration into the connective tissue. Cell proliferation in reactive mesothelial hyperplasia is usually very low in contrast to mesothelioma in situ. Cells of early-stage mesothelioma show invasive growth, as illustrated in Fig. 1b. An infiltration of lung tissue or chest wall as well as pericardium and mediastinal tissues is a sign of more advanced stages. As described in the paper by Whitaker and co-workers [19], we have also immunohistochemically demonstrated a positive membraneous staining for the EMA in mesothelioma in situ (Fig. 1c), and early mesotheliomas in contrast to negative staining results in reactive mesothelial hyperplasia. Adenocarcinomas show a more cytoplasmic-located positive EMA staining in most cases. MiB1 expression is markedly increased in mesothelioma in situ cells in contrast to reactive mesothelial hyperplasia (Fig. 1d)

Co-expression of the mesothelial markers keratin 5/6 and calretinin in the tumour cells with simultaneous negative staining of HEA and PAS leads to the diagnosis of a predominantly epithelioid pleural mesothelioma. The tumour cells did not express the marker for adenocarcinomas of the lung and the thyroid, TTF-1.

Comparative genomic hybridisation results

Detailed results of the CGH analysis are depicted in Fig. 2 and Table 1. In the case of mesothelioma in situ cells, nine different chromosomal aberrations could be detected (losses on 3p21, 5q, 6q, 8p, 9p13–21, 15q11.2–13, 22q, Y and a gain on 7q22), whereas in the early-stage mesothelioma, eight defects could be found (losses on 3p21, 5q, 6q, 8p, 9p13–21, 15q12–14, 22q, Y). The chromosomal losses

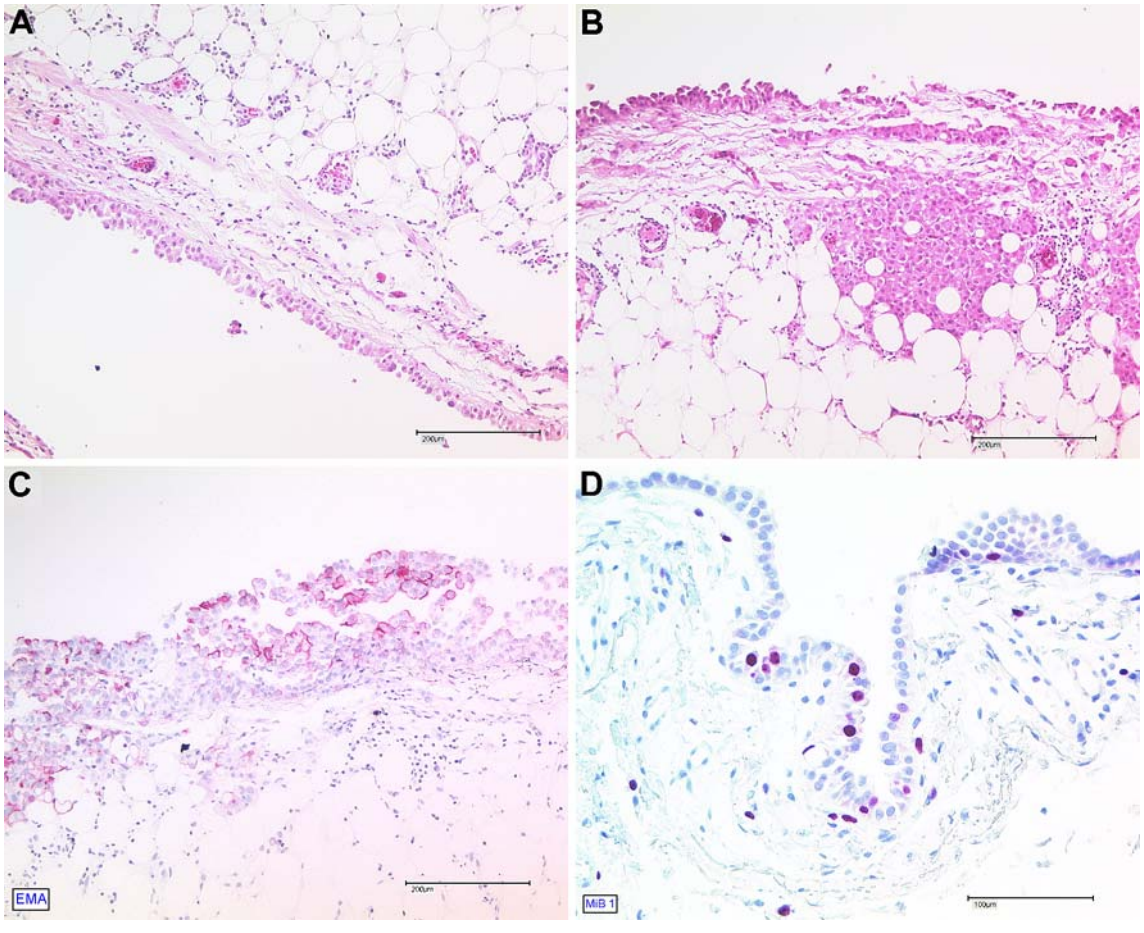


Fig. 1 **a** Light microscopy of mesothelioma in situ cells, showing a pseudo-papillary growth pattern in the *upper left side*. Tumour invasion is not detectable. H&E staining. **b** In contrast to **a**, early-stage mesothelioma cells show an infiltration into the main layer of the pleura and the fat tissue. H&E staining. **c** Membrane-associated EMA expression of early-stage mesothelioma cells. **d** MiB1 expression in mesothelioma in situ cells. Proliferative activity is markedly increased in contrast to reactive mesothelial hyperplasia

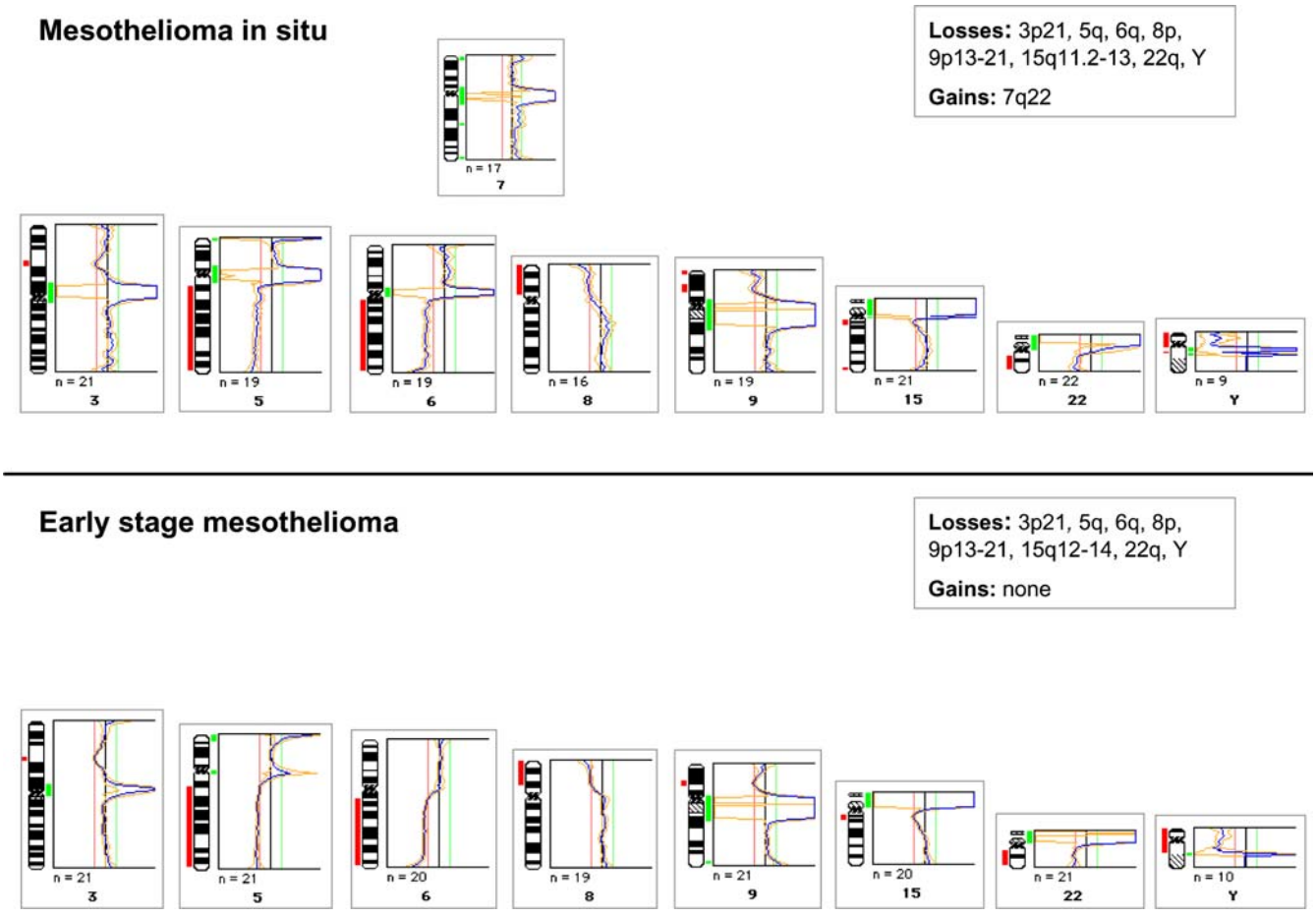


Fig. 2 CGH results of two histologically different early growth stages of an MM from a 67-year-old man. Chromosomal losses are represented as *red bars* on the *left side* of each chromosome ideogram; gains are represented as *green bars* on the *right side*. Only the fluorescence ratio profiles of chromosomes with detectable defects are shown. For each sample, 11 metaphases were analysed and averaged

found in this study were also detected in more-advanced-stage mesotheliomas in former studies [10]. Especially the simultaneous loss of 6q, 9p and 22q was often found in advanced-stage mesotheliomas. To validate the chromosomal defects found by using normal DNA extracted from blood lymphocytes from a healthy male donor, CGH was also performed with normal DNA from the fat tissue of the tumour patient. In the case of early-stage mesothelioma, CGH with normal DNA from the patient showed basically the same defects (losses on 3p21, 5q, 6q, 8p, 9p13-21, 15q11.2-14, 22q, Y). In the case of mesothelioma in situ cells, two more gains on chromosomes 4q (4q21, 4q28) and 5p could be detected with normal DNA from the tumour patient.

Table 1 Detailed CGH results in comparison to common defects in advanced-stage MMs

Case	Losses	Gains	∑ Defects
Mesothelioma in situ	3p21, 5q, **6q**, 8p, **9p**13–21, **15q**11.2–13, **22q**, Y	**7q**22	9
Early-stage mesothelioma	3p21, 5q, **6q**, 8p, **9p**13–21, **15q**12–14, **22q**, Y	none	8
Advanced-stage MM	1p, 4pq, **6q**, **9p**, 13q, 14q, **22q**	1q, **7pq**, 15q	6.2 (average)

Chromosomal aberrations that are in good agreement with common defects found in advanced-stage MMs are printed in bold-type

Discussion

The diagnosis of an early-stage epithelioid MM in the presented case is based on conventional light microscopical examination in combination with immunohistochemical findings. While the cytogenetic analysis is in agreement with the MM diagnosis, it was somewhat unexpected that the chromosomal defect patterns in both tumour stages were almost identical and very similar to those frequently found in late-stage MMs [1, 10]. Within the large pleural surfaces, it is not possible to determine the exact region of development of the first neoplastic lesion by means of macroscopical examination. It may be that mesothelial cells undergo a multifocal neoplastic transformation or a discontinuous synchronous growth by spread via effusion, which is usually the first clinical manifestation of the neo-

plasia. Our CGH results favour the second hypothesis with nearly identical chromosomal defects in different manifestations of one tumour. We can not clearly state the significance of the gain on chromosome 7q22. Most probably, this lesion accumulated in the primary lesion after the postulated multifocal tumour cell dissemination with implantation and early invasive growth at another site. On the other hand, it can not be completely excluded that this lesion in the early mesothelioma or the missing of this lesion in the mesothelioma in situ is an artefact during the process of formalin fixation, amplification and the complex process of CGH.

Most cancers show abnormalities in chromosome number and structure (aneuploidy). It has been postulated that chromosomal instability is the cause of aneuploidy and necessary to drive the development of cancer by increased mutation rates. A question is whether this genomic instability is an early event in carcinogenesis or just a side-effect of late-stage cancer [12]. If it is a late event, it would be more likely that normal mutation rates are sufficient and cancer cells accumulate genomic defects in the form of point mutations and other small lesions first. Nevertheless, it is not unlikely that even in cases with an early appearance of chromosomal imbalances, some smaller defects might have occurred initially, e.g. mutations in genes that control and maintain chromosome segregation. To find an answer to the question what kind of alterations can be found in different early stages of pleural MM cells, we used conventional chromosomal CGH in combination with laser microdissection and DOP-PCR amplification. Though the resolution of CGH is not very high (defects in the range of 10–20 Mb can be detected), we found a high number of chromosomal defects. We did not see any signs of DOP-PCR-generated amplification bias between chromosomal regions in the control experiments. These large defects (e.g. losses of chromosome arms 5q, 6q, 8p and 22q) do not rule out the presence of additional smaller defects. The high number of aberrations detected in early stages of MMs would be in accordance with the notion that chromosomal instability contributes to early events in cancer development. A recent publication supports the possibility that at least some cancers start with an early development of aneuploidy [2]. It has to be noted, however, that, considering the age of our patient, “early stage” is a relative term. The development of the MM might have started decades ago, and it is known that MM can progress rapidly at their late stages. Therefore, the examination of more cases, preferably of younger patients, is absolutely necessary. Because most of these very rare cases are discovered by chance, a prospective screening study with former asbestos workers would be a promising approach. The results of the present case report will be a basis for further studies of early stages of MMs with classical CGH and high-resolution methods like array CGH. CGH analysis on cytological specimen may in some cases also be possible if there is a high number of neoplastic and a low number of inflammatory cells. Otherwise, there is a high probability of dilution artefacts with finding too few chromosomal imbalances. The presented method of laser microdissection of fixed and paraffin-embedded tissue provides a pure DNA of only the cells of interest. At the present time, it is too early to draw clinical and therapeutical consequences from the results, but if further CGH results on larger collectives of preneoplastic and early neoplastic mesothelial lesions provide information that helps classify the dignity, the method could gain a clinical relevance in mesothelioma diagnosis.

References

1. Bjorkqvist AM, Tammilehto L, Nordling S, Nurminen M, Anttila S, Mattson K, Knuutila S (1998) Comparison of DNA copy number changes in malignant mesothelioma, adenocarcinoma and large-cell anaplastic carcinoma of the lung. Br J Cancer 77:260–269
2. Hanks S, Coleman K, Reid S, Plaja A, Firth H, Fitzpatrick D, Kidd A, Mehes K, Nash R, Robin N, Shannon N, Tolmie J, Swansbury J, Irrthum A, Douglas J, Rahman N (2004) Constitutional aneuploidy and cancer predisposition caused by biallelic mutations in BUB1B. Nat Genet 36:1159–1161
3. Hermsen MAJA, Meijer GA, Baak JPA, Joenje H, Waldbloomers JJM (1996) Comparative genomic hybridization: a new tool in cancer pathology. Human Pathol 27:342–349
4. Johannson L, Linden CJ (1996) Aspects of histopathologic subtype as a prognostic factor in 85 pleural mesotheliomas. Chest 109:109–114
5. Kallioniemi A, Kallioniemi OP, Sudar D, Rutovitz D, Gray JW, Waldman F et al (1992) Comparative genomic hybridization for molecular cytogenetic analysis of solid tumors. Science 258: 818–821
6. Klein CA, Schmidt-Kittler O, Schardt JA, Pantel K, Speicher MR, Riethmüller G (1999) Comparative genomic hybridization, loss of heterozygosity, and DNA sequence analysis of single cells. Proc Natl Acad Sci U S A 96:4494–4499
7. Knuutila S, Aalto Y, Autio K, Björkqvist AM, El-Rifai W, Hemmer S, Huhta T, Kettunen E, Kiuru-Kuhlefelt S, Larramendy ML, Lushnikowa T, Monni O, Pere H, Tapper J, Tarkkanen M, Varis A, Wasenius VM, Wolf M, Zhu Y (1999) DNA copy number losses in human neoplasms. Am J Pathol 155:683–694
8. Krismann M, Jaworska M, Müller KM, Johnen G (2000) Severe chromosomal aberrations in pleural mesotheliomas with unusual mesodermal features —CGH evidence for a mesothelioma subgroup. J Mol Diagn 2:209–216
9. Krismann M, Adams H, Jaworska M, Müller KM, Johnen G (2000) Patterns of chromosomal imbalances in benign solitary fibrous tumours of the pleura. Virchows Arch 437:248–255
10. Krismann M, Müller KM, Jaworska M, Johnen G (2002) Molecular cytogenetic differences between histological subtypes of malignant mesotheliomas: DNA cytometry and comparative genomic hybridization of 90 cases. J Pathol 197:363–371
11. Kuukasjärvi T, Tanner M, Pennanen S, Karhu R, Visakorpi T, Isola J (1997) Optimizing DOP-PCR for universal amplification of small DNA samples in comparative genomic hybridization. Genes Chromosomes Cancer 18:94–101
12. Lengauer C, Kinzler KW, Vogelstein B (1998) Genetic instabilities in human cancers. Nature 396:643–649
13. Nowak AK, Lake RA, Kindler HL, Robinson BWS (2002) New approaches for mesothelioma: biologics, vaccines, gene therapy, and other novel agents. Semin Oncol 29:82–96
14. Petersen I, Langreck H, Wolf G, Schwendel A, Psille R, Vogt P, Reichel MB, Ried T, Dietel M (1997) Small-cell lung cancer is characterized by a high incidence of deletions on chromosomes 3p, 4q, 5q, 10q, 13q and 17p. Br J Cancer 75:79–86
15. Rusch VW (1995) A proposed new international TNM staging system for malignant pleural mesothelioma. From the International Mesothelioma Interest Group. Chest 108:1122–1128

16. Schipper H, Papp T, Johnen G, Pemsel H, Bastrop R, Müller KM, Wiethege T, Jaworska M, Krismann M, Schiffmann D, Rahman Q (2003) Mutational analysis of the nf2 tumour suppressor gene in three subtypes of primary human malignant mesotheliomas. Int J Oncol 22:1009–1018
17. Sirivatanauksorn Y, Drury R, Crnogorac-Jurcevic C, Sirivatanauksorn V, Lemoine NR (1999) Laser-assisted microdissection: applications in molecular pathology. J Pathol 189: 150–154
18. Telenius H, Carter NP, Bebb CE, Nordenskjold M, Ponder BA, Tunnacliffe A (1992) Degenerate oligonucleotide-primed PCR: general amplification of target DNA by a single degenerate primer. Genomics 13:718–725
19. Whitaker D, Henderson DW, Shilkin KB (1992) The concept of mesothelioma in situ: implications for diagnosis and histogenesis. Sem Diagn Pathol 9:151–161

Virchows Arch (2005) 447: 768–771
DOI 10.1007/s00428-005-0021-4

CASE REPORT

Eduard Fridman · Josef Skarda · Efrat Ofek-Moravsky · Mario Cordoba

Complex multilocular cystic lesion of rete testis, accompanied by smooth muscle hyperplasia, mimicking intratesticular Leydig cell neoplasm

Received: 30 March 2005 / Accepted: 23 May 2005 / Published online: 13 July 2005
© Springer-Verlag 2005

Abstract Non-neoplastic smooth muscle cell proliferation occurs under a variety of circumstances in many body organs. These abnormalities have been described as hypertrophy, hyperplasia or hamartomatous proliferations. In the male genital system, the excessive growth of smooth muscle in spermatic cord or paratesticular tissue is rare. In previously described cases, these lesions presented as masses but lacked the microscopic features of a neoplasm. We describe a complex multilocular cystic lesion composed of cystic transformation of the rete testis associated with smooth muscle proliferation mimicking intratesticular Leydig cell neoplasm. The lesion consists of three separate components: (1) cystic dilatation of the rete testis; (2) diffuse, interstitial smooth muscle proliferation with intraseptal expansion; and (3) extensive stroma with myxoid areas and scattered interstitial Leydig cells. These morphological findings, supported by a wide immunohistochemical panel, are consistent with cystic dilatation of the rete testis associated with smooth muscle hyperplasia, most probably of myoid origin. To the best of our knowledge, no similar complex lesion of the rete testis has yet been reported.

Keywords Smooth muscle hyperplasia · Cystic transformation · Rete testis · Hamartoma

E. Fridman (✉) · E. Ofek-Moravsky
Department of Pathology, Sheba Medical Center,
Sackler School of Medicine, Tel-Aviv University,
Tel-Hashomer, 52621 Israel
e-mail: ef@sheba.health.gov.il
Tel.: +972-3-5302354
Fax: +972-3-5302381

J. Skarda
Department of Pathology, Medical Faculty, Palacky University,
Olomouc, Czech Republic

M. Cordoba
Department of Pathology, Meir Medical Center,
Kfar-Sava, Israel

Introduction

Non-neoplastic smooth muscle proliferation occurs under a variety of circumstances in many body organs, including the skin, breast, oral cavity, trachea and lungs, vascular system, gastrointestinal tract, kidney and bladder [7, 11]. Excessive smooth muscle proliferation occurring in the spermatic cord or rete testis has received relatively little attention.

Intratesticular leiomyoma was first described by Honore and Sullivan [5], who suggested that the tumor arose from myoid cells of the tunica propria of the seminiferous tubules. Barton et al. [2] later reviewed 16 cases of smooth muscle cell hyperplasia of the testicular adnexa clinically mimicking neoplasm. Out of the 16, 14 were located either in the epididymis or the spermatic cord or both, and two others involved the tunica vaginalis and the tunica albuginea. Microscopic examination in all cases showed an increase in smooth muscle fascicles arranged in a periductal, perivascular or interstitial pattern and lacking the cohesion and well-circumscribed proliferation typical of leiomyoma. No significant inflammation or mitotic activity was seen in any case. Another myxoid gonadal stromal tumor with epithelial differentiation was described by Weidner [10]. Tumor cells, in that case, were immunoreactive for vimentin and S-100 protein, but negative for cytokeratin and desmin and appeared to show bidirectional differentiation, mimicking both peritubular myoid spindle cells and epithelial-like cells.

Cystic testicular dysplasia is a rare disorder affecting the testis of infants and children typically within the first decade of life [6, 8]. In a case of cystic dysplasia of the rete testis, reported in a 22-year-old man, the lesion consisted of a grossly visible, 3.5 cm, multilobulated cystic mass in the upper pole of the left testis. Microscopic examination revealed cystic dilatation of rete channels with a normal branching configuration, lined predominantly by flat cells, although occasional cuboidal cells could be observed. There was no atypia [8].

In the following report, we present a complex multilocular cystic lesion consistent with cystic dilatation of the rete

testis associated with smooth muscle hyperplasia. To the best of our knowledge, no similar complex lesion of the rete testis has yet been described.

Case report

A 26-year-old, previously healthy man presented with a 4.5-cm cystic, probably intraparenchymal, lesion of the testis, detected by manual and ultrasonographic examination. The patient underwent simple orchiectomy without complications or further complaints.

Materials and methods

The surgical specimen, consisting of testis and paratesticular structures, was received in 10% buffered formalin and processed for histological evaluation. Sections were stained with hematoxylin and eosin, phosphotungstic acid–hematoxylin (PTAH), Alcian Blue, PAS and mucicarmine, and immunohistochemical stains included Cam-5.2, AE-3, MNF-116, CK-7, CK-20, CA-125, CEA, EMA, CD-31, EMA, α_1-antitrypsin, CK-20, GFAP, NSE, S-100, MELAN-A, chromogranin, ACTH, β-HCG, α-inhibin, Calretinin, α-fetoprotein and CD-34.

Immunostaining incorporated the streptavidin–biotin–peroxidase method after overnight incubation at 4°C. A microwave antigen retrieval method was used with all antibodies. Slides were immersed in 200 ml of microwave buffer and heated in 800-W microwave oven using a high setting for 5 min. Fifty milliliters of deionized water was added to replace evaporated water from heating, and slides were microwaved for an additional 5 min before automated immunostaining in the Ventana Nexes (Ventana Corp.). Internal and external control tissues with established reactivity were stained concomitantly.

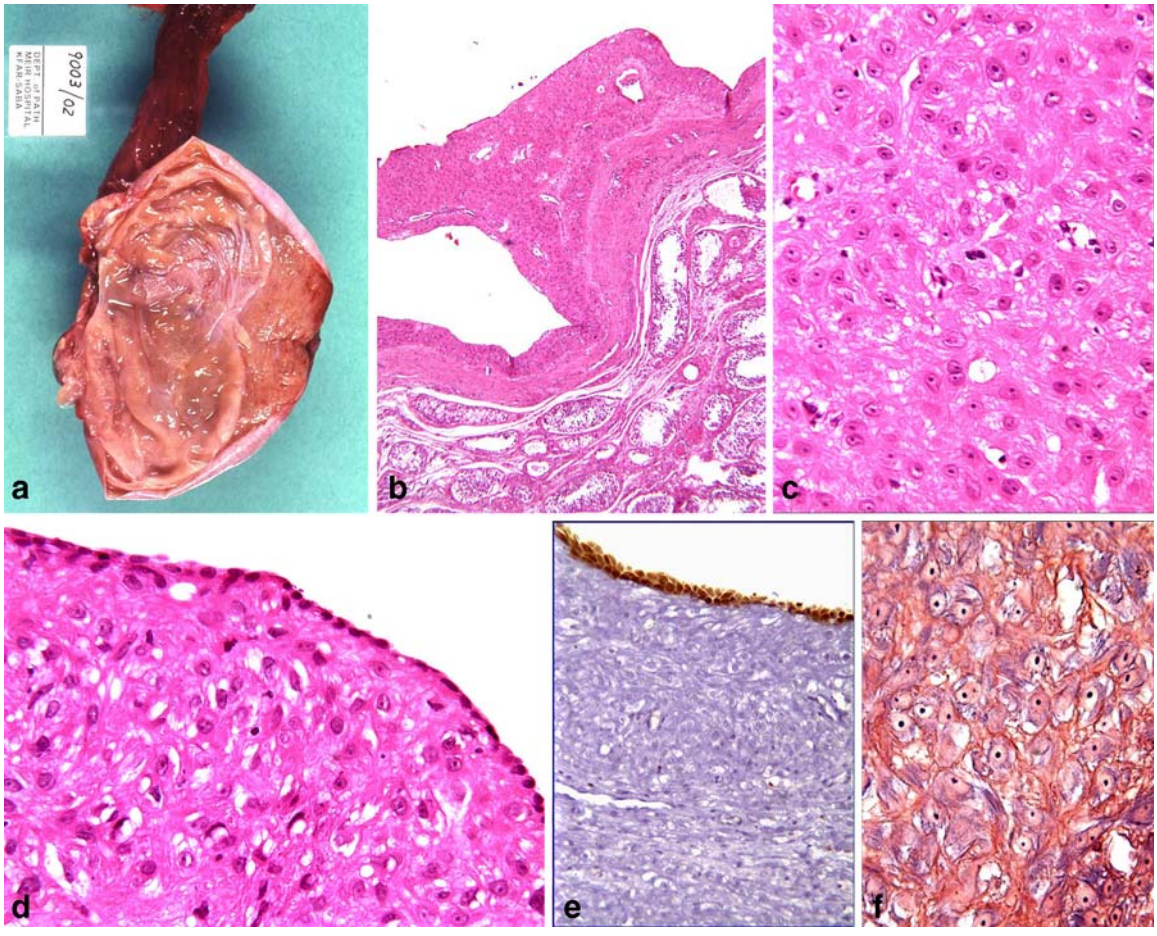


Fig. 1 **a** Macroscopic view of the specimen with multilocular "intratesticular" cystic mass. **b** H&E stain, original magnification ×100. Septal formation composed of large "tumoral" cells and cuboidal epithelial lining. Note distinct border between mass and surrounding testicular parenchyma. **c** H&E stain, original magnification ×400. Center of the mass showing monomorphous large epithelioid cells with centered round nucleus containing prominent nucleolus (Leydig-like cells). Note only one typical mitotic figure (*arrow*). **d**, **e** H&E and Calretinin stains, original magnification ×400. Cystic septa lined by normal mesothelial cells, highlighted by Calretinin immunohistochemical stain. No reactivity for Calretinin is present in large epithelioid cells. **f** PTAH stain, original magnification ×400. Intracellular fibers (*arrow*) are seen in a few epithelioid cells

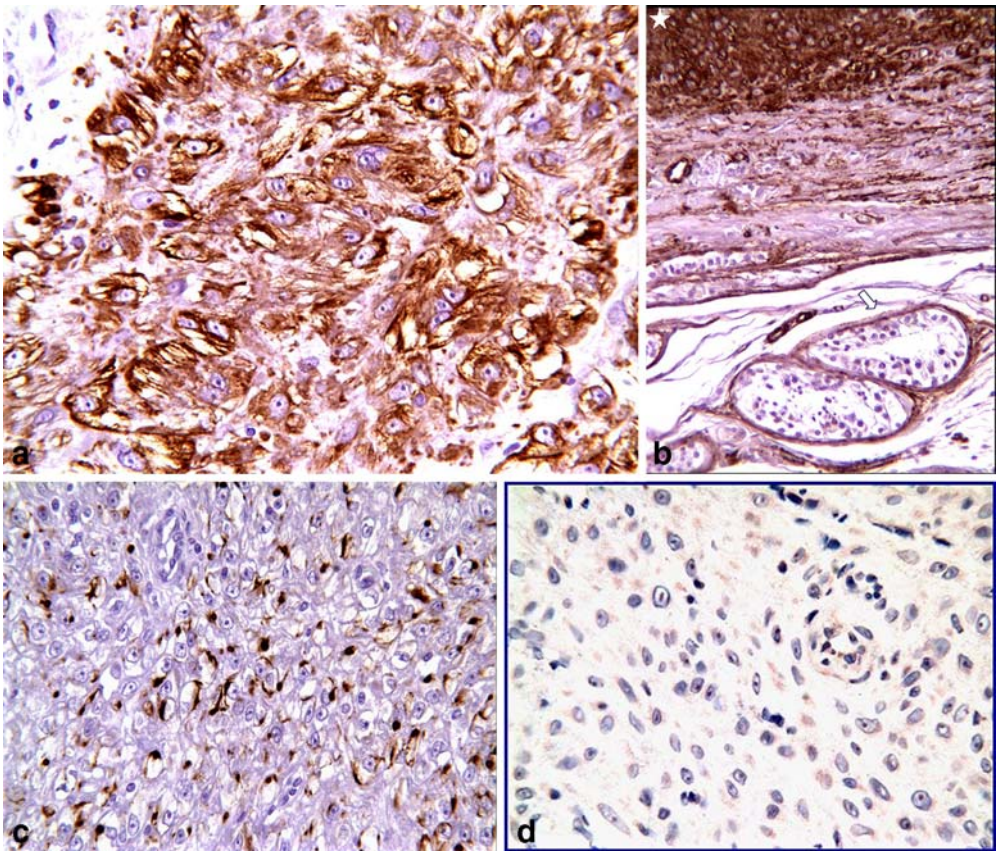


Fig. 2 **a** Desmin stain, original magnification ×400. Diffuse strong cytoplasmic positivity in the large epithelioid cells. **b** α-Smooth muscle actin stain, original magnification ×100. Diffuse strong cytoplasmic positivity in the large epithelioid cells (*asterisk*) and only focal positivity in the periacinar myoid cells in the surrounding normal testicular parenchyma (*arrow*). **c** Cam 5.2 stain, original magnification ×400. Diffuse perinuclear pattern of stain in the large epithelioid cells. **d** α-Inhibin stain, original magnification ×400. No reactivity is seen in large epithelioid cells, but single residual Leydig cells are positive

Results

Macroscopical examination showed a multilocular cystic lesion, 4.5 cm in diameter, separated from residual testicular tissue by a fibrous septum (Fig. 1a). The spermatic cord and adjacent structures were of normal appearance.

Histological examination revealed a complex cystic lesion composed of three different components. The first component consisted of a cystic dilatation of rete testicular channels lined by normal-looking flat cells (Fig. 1b–d). Immunohistochemical stains of these cells were positive for Calretinin, Cam-5.2, MNF-116, AE-3 and CK-7 (Fig. 1e) and non-reactive for CK-20, CA-125, CEA and EMA. This staining pattern supports a mesothelial origin for these cells. The second component consisted of a diffuse proliferation of large eosinophilic epithelioid cells with an interstitial pattern of growth and intraseptal expansion. No cytological atypia was observed, and only rare typical mitotic figures were identified (Fig. 1c, d). PTAH staining highlighted the intracellular myofibrillar bundles (Fig. 1f). These cells also showed diffuse cytoplasmic positivity for α-smooth muscle actin (SMA) and desmin and a perinuclear ("dot-like") pattern of staining for MNF-116, AE-3 and CAM-5.2 (Fig. 2a–c). They were negative for Alcian Blue, mucicarmine and PAS and non-reactive for Calretinin (Fig. 1e), α-inhibin (Fig. 2d), α-fetoprotein, CD-34, CD-31, CA-125, CEA, EMA, α_1-antitrypsin, CK-20, GFAP, NSE, S-100, Melan-A, chromogranin, ACTH and β-HCG [4, 9]. This staining pattern supports a smooth muscle, most probably myoid, origin for these epithelioid cells. Finally, the third component was composed of extensive stroma with myxoid areas and sparse interstitial Leydig cells (Table 1).

Table 1 Comparison of immunophenotypes of the three lesion components

Lesion component	Immunohistochemical stains						
	Cal	MNF-116	AE-3	CAM-5.2	α-Inhibin	SMA	Desmin
Cystic mesothelial lining	pos	pos	pos	pos (cyt)	neg	neg	neg
Large epithelioid cell component	neg	pos (perinuclear pattern)	pos (perinuclear pattern)	pos (perinuclear pattern)	neg	pos (cyt)	pos (cyt)
Residual Leydig cells (in lesion and normal testis)	pos	neg	neg	neg	pos	neg	neg

pos Positive; *neg* negative; *cyt* cytoplasmic; *Cal* Calretinin; *SMA* α-smooth muscle actin

Discussion

Smooth muscle hyperplasia of the rete testis is uncommon even in a consultant practice in genitourinary pathology. A large proportion of palpable masses in this location prove to be malignant, notably liposarcomas, leiomyosarcomas, malignant fibrous histiocytomas and, less often, mesotheliomas and metastatic carcinomas [11]. Determining the type of non-neoplastic smooth muscle cell growth occurring in the rete testis may be difficult. In previous studies, a total of 20 cases of benign smooth muscle proliferation of the rete testis have been described [2, 6]. In addition to epididymal lesions and cysts, most of the benign lesions are adenomatoid tumors, nodular periorchitis (fibrous pseudotumor), leiomyomas and lipomas [2]. Extratesticular lesions closely adherent to the tunica albuginea may not be ultrasonographically distinguishable from intratesticular lesions in some cases. These cases are usually composed of a non-neoplastic excess of smooth muscle bundles growing around and/or between normal paratesticular structures, rather than forming a well-defined tumor nodule.

While a chapter on spermatic cord and testicular adnexa in a recently published urologic pathology textbook [2] reviews and briefly discusses three types of hamartomas arising from smooth muscle, rete testis and fibrous tissue, and a recent case report and review of epididymal leiomyomas describes two lesions as diffuse smooth muscle cell proliferation in and around epididymal structures, a careful literature search indicates that these unique lesions have never really been the object of any focused study or investigation [2, 4–7, 9, 11]. Until now, only one case of rete testis containing smooth muscle proliferation with an extensive stromal myxoid component has been described [5].

Histological examination of our surgical specimen in comparison with previously described cases revealed a complex cystic lesion of the rete testis associated with smooth muscle proliferation, ultrasonographically and macroscopically mimicking intratesticular Leydig cell tumor. The major component of this lesion was the cystic dilatation of rete testis, which has been called cystic transformation of the rete testis and can occur at any age [6, 8]. The second major component was a diffuse smooth muscle proliferation, most probably of myoid cell origin, with intraseptal expansion, which has also been described as a separate entity: “myoid gonadal stromal tumor with epithelial differentiation” [10]. The third component consisted of extensive stroma with myxoid areas and scattered interstitial Leydig cells. This component has also been observed separately as mentioned above [2].

Unlike the cases described in previous studies, our morphological and histochemical findings are consistent with cystic transformation of the rete testis associated with smooth muscle hyperplasia, most probably of myoid origin. To the best of our knowledge, no similar complex cystic lesion of the rete testis has yet been reported with complete immunophenotypic characterization. The wide immunohistochemical panel applied enabled a precise determination of the histogenetic origin of individual cellular components of the lesion [1, 3]. Based on the three admixed components, the diagnostic options for this entity include: (1) epithelioid leiomyoma of myoid origin (leiomyoblastoma) associated with cystic transformation of the rete testis or (2) cystic hamartoma of rete testis associated with smooth muscle cell hyperplasia. In any case, this is an extremely rare, complex, benign lesion located in the testicular adnexa and simulating intratesticular neoplasia. A detailed description and characterization of this unique entity may help in difficult differential diagnoses between benign and malignant testicular lesions.

References

1. Augusto D, Leteurtre E, De La Taille A, Gosselin B, Leroy X (2002) Calretinin: a valuable marker of normal and neoplastic Leydig cells of the testis. Appl Immunohistochem Mol Morphol 10:116–159
2. Barton JH, Davis CJ Jr, Sesterhenn IA, Mostofi FK (1999) Smooth muscle hyperplasia of the testicular adnexa clinically mimicking neoplasia: clinicopathologic study of sixteen cases. Am J Surg Pathol 23:903–909
3. Cao QJ, Jones JG, Li M (2001) Expression of Calretinin in human ovary, testis, and ovarian sex cord-stromal tumors. Int J Gynecol Pathol 20:346–352
4. Fisher C, Goldblum JR, Epstein JI, Montgomery E (2001) Leiomyosarcoma of the paratesticular region: a clinicopathologic study. Am J Surg Pathol 25:1143–1149
5. Honore LH, Sullivan LD (1975) Intratesticular leiomyoma: a case report with discussion of differential diagnosis and histogenesis. J Urol 114:631–635
6. Jones EC, Murray SK, Young RH (2000) Cysts and epithelial proliferations of the testicular collecting system (including rete testis) review. Sem Diagn Pathol 17:270–293
7. Nappi O, Ferrara G, Wick MR (1999) Neoplasms composed of eosinophilic polygonal cells: an overview with consideration of different cytomorphologic patterns. Sem Diagn Pathol 16:82–90
8. Nistal M, Mate A, Paniagua R (1996) Cystic transformation of the rete testis. Am J Surg Pathol 20:1231–1239
9. Tokunaka S, Taniguchi N, Hashimoto H, Yachiku S, Fujita M (1990) Leiomyoblastoma of the epididymis in a child. J Urol 143:991–993
10. Weidner N (1991) Myoid gonadal stromal tumor with epithelial differentiation (testicular myoepithelioma?). Ultrastruct Pathol 15:409–416
11. Young RH, Scully RE (1999) Oxyphilic tumors of the female and male genital tracts. Sem Diagn Pathol 16:146–161

Virchows Arch (2005) 447: 772–777
DOI 10.1007/s00428-005-0019-y

CASE REPORT

Lorenzo Taminelli · Khalil Zaman · Carole Gengler · Nicolas Peloponissios · Hanifa Bouzourene · Jean-Michel Coindre · Isabelle Hostein · Louis Guillou

Primary clear cell sarcoma of the ileum: an uncommon and misleading site

Received: 27 February 2005 / Accepted: 23 May 2005 / Published online: 14 July 2005
© Springer-Verlag 2005

Abstract A clear cell sarcoma, arising primarily in the ileum of a 35-year-old man, is reported. Histologically, the neoplasm infiltrated the full thickness of the intestinal wall. It consisted of strands and sheets of round to spindle-shaped cells with clear to eosinophilic cytoplasm, vesicular nuclei and prominent nucleoli. Vascular invasion was present at diagnosis. Tumour cells expressed S-100 protein, melan-A and tyrosinase. They were negative for HMB45, CD117, cytokeratins, epithelial membrane antigen, smooth muscle actin, desmin, CD31, CD34, chromogranin and synaptophysin. Reverse transcription–polymerase chain reaction analysis performed on paraffin-embedded tissue showed EWS–ATF1 fusion transcripts representative of the t(12;22) (q13;q12) clear cell sarcoma reciprocal translocation. The patient, who developed liver metastases 2 months after diagnosis, died of disease at 15 months. This case demonstrates that the gastrointestinal tract is a potential site for primary clear cell sarcoma of soft tissues, and, furthermore, that cytogenetics and/or molecular techniques play a central role in the diagnosis.

L. Taminelli · C. Gengler · H. Bouzourene · L. Guillou
Department of Pathology, University Hospital,
Lausanne, Switzerland

K. Zaman
Department of Oncology, University Hospital,
Lausanne, Switzerland

N. Peloponissios
Department of Surgery, University Hospital,
Lausanne, Switzerland

J.-M. Coindre · I. Hostein
Department of Pathology, Bergonié Institute,
Bordeaux, France

L. Guillou (✉)
Institut Universitaire de Pathologie,
Rue du Bugnon 25,
1011 Lausanne, Switzerland
e-mail: louis.guillou@chuv.hospvd.ch
Tel.: +41-21-3147216
Fax: +41-21-3147207

Keywords Clear cell sarcoma · Ileum · Immunohistochemistry · RT-PCR · t(12;22) (q13;q12)

Introduction

Clear cell sarcoma (also known as malignant melanoma of soft tissues) is a rare tumour that typically occurs in the tendon sheaths and aponeuroses of distal extremities of adolescents and young adults [3, 6, 10, 11]. Involvement of the gastrointestinal tract is exceedingly rare and, frequently, a source of diagnostic problems. Six cases of digestive tract clear cell sarcoma were heretofore reported in the literature, most of them very recently [1, 4, 5, 7, 13, 15], including one in the ileum [4]. A second ileal case is described below. It occurred in a 35-year-old man and caused the death of the patient 15 months after diagnosis.

Clinical history

A 35-year-old, HIV-negative man without any previous significant medical history was admitted in March 2003 for a 15-kg weight loss over a few months and symptoms of intestinal obstruction (i.e. colic pain, vomiting) without fever. CT scans showed a segmental thickening of the ileum, situated 80 cm above the ileo–caecal valve. Preoperative diagnoses included Meckel diverticulum, polyps and a malignant neoplasm. At laparotomy, a single circumferential, stenotic lesion of the ileum was found. There was neither other detectable tumour in the abdominal cavity nor any liver metastases. The ileal mass was resected along with 20 cm of ileum and one regional mesenteric lymph node. A pathologic diagnosis of unclassified non-epithelial malignant neoplasm was rendered. The mesenteric lymph node was devoid of tumour deposits, but the ascitic fluid, sampled at the time of surgery, contained clusters of malignant cells. A lymphoma, a GIST, a neuroendocrine neoplasm were excluded on the basis of immunohistochemical results. A melanoma (primary or metastatic) was strongly suspected owing to tumour cell reactivity for S-100 protein.

Careful examination of the patient, including extensive examination of skin, eyes, nasosinusal cavities, throat, testes and soft tissues failed to detect any other potential primary tumour. The metastatic work-up was negative, as was the PET scan. A colonoscopy showed several polyps in the ascending and sigmoid colon, which turned out to be adenomatous polyps with low-grade dysplasia at microscopic examination.

Two months post-operatively, several metastases were detected in the liver, along with multiple peritoneal implants and a malignant ascitis. The tumour regressed dramatically after six courses of a platinum-based chemotherapy, but a second look, performed in November 2003, showed that the malignant process extended microscopically to the whole peritoneal subserosa and to the omentum. Lymph node and liver biopsy specimens, taken during the second surgical procedure, were tumour-free. From then on, and despite various treatments, the tumour gradually progressed in the abdomen, leading to several episodes of intestinal obstruction. Patient's death occurred 15 months after disease onset, as a result of *Candida albicans* septicemia. No autopsy was performed.

Materials and methods

Tumour samples were fixed in 4% buffered formalin, embedded in paraffin and stained with hematoxylin and eosin and Fontana–Masson stains. Additional sections were studied with the following antibodies: S-100 protein (Dakopatts, Glostrup, Denmark, pre-diluted), melan-A (Dako, diluted 1:50), HMB45 (Dako, diluted 1:50), tyrosinase (Ludwig Institute, Lausanne, Switzerland, diluted 1:50, gift from Dr. D. Rimoldi), cytokeratins (clone C-11, diluted 1:40 and clone AE1/AE3, diluted 1:200, Novocastra Laboratories Inc., Newcastle upon Tyne, UK), CD31 (Dako, diluted 1:40), CD34 (Immunotech Beckam Coulter, Inc., Fullerton, CA, USA, diluted 1:160), CD45 (Dako, diluted 1:50), CD3 (Novocastra, pre-diluted), CD20 (clone L26, Dako, pre-diluted), CD56 (clone 1B6, Novocastra, diluted 1:50), smooth muscle actin (clone 1A4, Sigma Aldrich, St Louis, MI, USA, diluted 1:20,000), myeloperoxidase (Dako, diluted 1:2,000), synaptophysin (Dako, diluted 1:25), chromogranin-A (Dako, diluted 1:1,000), somatostatin (Bachem Peninsula Laboratories, Inc., San Carlos, CA, USA, diluted 1:800), serotonin (clone 5HT-H209, Dako, diluted 1:50) and CD117 (c-kit, Dako, polyclonal diluted 1:200). Immunostaining was performed according to the avidin biotin complex (ABC) method. Tissue sections were submitted to microwave oven heating prior to staining, except for CD117 staining. All steps were performed at room temperature, and diaminobenzidine was used as chromogen. Appropriate positive and negative controls were employed throughout.

Reverse transcription–polymerase chain reaction (RT-PCR) was used to detect the presence of EWS–ATF1 transcripts in paraffin-embedded tumour samples. RNA extraction and RT-PCR reaction were performed as previously described [9]. Briefly, PCR amplification was performed in duplicate using a 96-well plate (Applied Biosystems, Foster City, CA, USA) with a 50 μl final reaction mixture containing 300 nM each primer; 200 nM probe ATF1 or 50 nM probe beta2-microglobulin; 200 μM of an equal concentration of dATP, dCTP, dGTP, dTTP, dUTP; MgCl2 4 mM; 1.25 U Taq polymerase and 0.25 U Amperase UNG in a 1X Real-Time PCR Buffer containing a passive reference (Rox fluorochrome). Thermal cycling conditions were 2 min at 50°C for amperase activation, 10 min at 95°C for Taq polymerase activation, then 50 cycles of two PCR steps consisting of 15 s at 95°C and 60°C for 1 min. All reactions were performed in the ABI Prism 5700 Sequence Detection System (Applied Biosystems).

Primers and probe sequences were chosen with Primer Express software (Applied Biosystems). Primers were purchased from Eurobio (Les Ulis, France) and probes and QPCR Core kit containing Real-Time PCR Buffer, dNTP, MgCl2, amperase UNG and Taq polymerase were purchased from Eurogentec (Herstal, Belgium). Probes and primer sequences were as follows: forward primer EWS, 5′-CAT GAG CAG AGG TGG GCG-3′; reverse primer ATF1, 5′-CCC CGT GTA TCT TCA GAA GAT AAG TC-3′; probe ATF1, 5′-6-FAM-AGG AGG ACG CGG TGG AAT GGG-TAMRA-3′; forward primer beta2-microglobulin, 5′-TGA CTT TGT CAC AGC CCA AGA TA-3′; reverse primer beta 2-microglobulin, 5′-AAT CCA AAT GCG GCA TCT TC-3′; probe beta 2-microglobulin, 5′-6-FAM-TGA TGC TGC TTA CAT GTC TCG ATC CCA-TAMRA-3′.

Results

A 20-cm segment of ileum was resected, centered by a well-defined firm, circumferential mass, measuring 1.8 cm in maximal diameter. Cut section showed a whitish neoplasm that ulcerated the overlying mucosa and infiltrated the whole thickness of the intestinal wall, extending into the subserosa (Fig. 1.). The tumour cells, arranged in sheets and nests separated by fibrous septa of varying thickness, were polygonal, with a clear to eosinophilic cytoplasm. Tumour cell nuclei were oval, often vesicular with a single central prominent nucleolus (Fig. 2.). Neither multinucleate giant cells nor melanin pigment were observed. Mitoses were numerous (up to 32 mitoses per ten high-power fields; one high-power field, 0.174 mm^2). There was no necrosis, but vascular invasion was present. The mesenteric lymph node sampled was devoid of metastatic deposits. The peritoneal and omental biopsies taken in November 2003 showed the same neoplastic proliferation, although tumour cells were very scarce, embedded in an abundant collagenous matrix. These tumour cells could easily be overlooked in some samples.

Immunohistochemically, the tumour cells were diffusely positive for S-100 protein (Fig. 3.) and, focally, for tyrosinase and melan-A. They were negative for HMB45, keratins, EMA, smooth muscle actin, desmin, chromogranin-A, synaptophysin, CD117, CD31, CD34, CD45, CD20, CD3 and myeloperoxidase. Ultrastructurally, the tumour

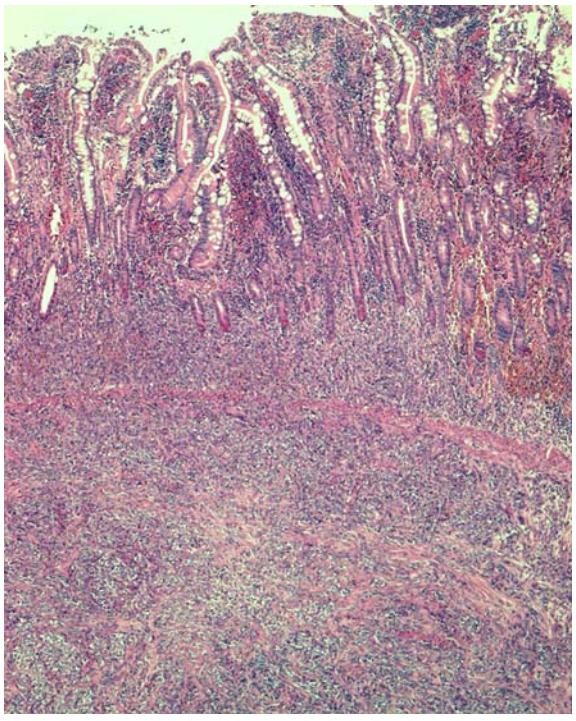


Fig. 1 Diffuse infiltration of the mucosa and submucosa of the ileum by tumour cells. Hematoxylin and eosin stain ×50

cells showed rounded to oval nuclei with smooth or indented contours, open chromatin and one or two prominent nucleoli. The cytoplasm was moderately abundant and contained few organelles as well as immature melanosomes. EWS–ATF1 fusion transcripts representative of the t(12;22) (q13;q12) clear cell sarcoma translocation were detected using real-time RT-PCR (Fig. 4.). The fusion occurred between the exon 8 of EWS gene and the exon 4 of the ATF-1 gene. SYT-SSX1/2 fusion transcripts, representative of the t(X;18) synovial sarcoma translocation, were not detected.

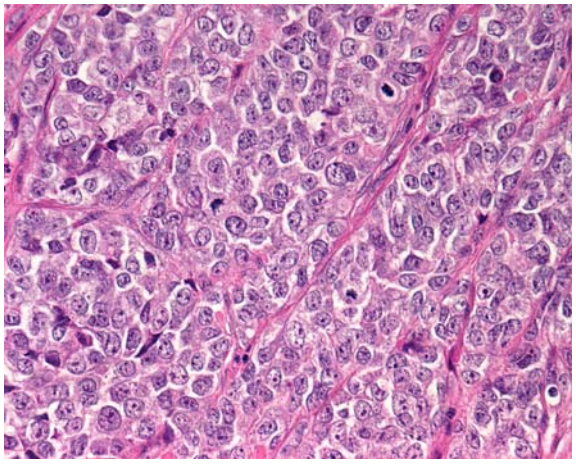


Fig. 2 Tumour cells are arranged in nests and fascicles separated by collagenous septa. Nuclei are round to oval, vesicular, with prominent nucleoli. Mitotic figures are numerous. Hematoxylin and eosin stain ×400

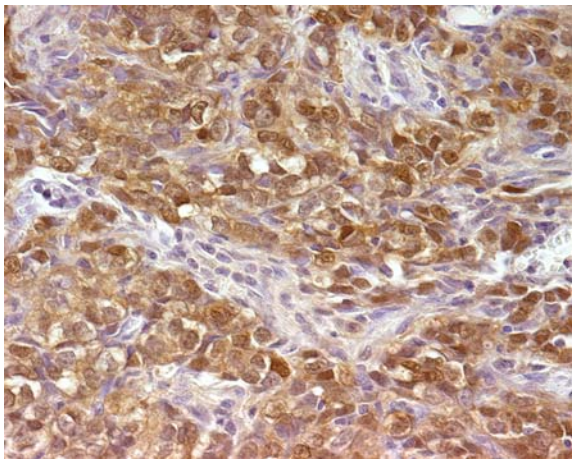


Fig. 3 Strong reactivity of clear cell sarcoma cells for S-100 protein ×400

Discussion

Described in 1965 by FM Enzinger [6], clear cell sarcoma of tendons and aponeuroses is a peculiar type of sarcoma which shows features of melanocytic differentiation. Clinically, it presents as a slow-growing tumour (median size, 2–5 cm) that mainly affects young adults (20–40 years). These tumours may be present for years before coming to clinical attention. The distal extremities, particularly the feet, ankles, knees, wrists and hands are the most common sites of tumour development [3, 6, 10, 11]. The lesions are almost always deep seated and intimately associated with tendons, aponeuroses and fascia.

Clear cell sarcoma is infrequent outside the limbs. Heretofore, six cases of clear cell sarcoma of the digestive tract have been reported [1, 4, 5, 7, 13, 15]. The salient clinicopathologic features of those cases, and the case under discussion, are summarized in Table 1. Males seem to be predominantly affected, in contrast to soft tissue lesions, which are divided equally between the sexes. Median age is 37 years (mean, 40 years), and median tumour size is 4 cm. Clear cell sarcoma of soft tissue has a poor prognosis, despite various treatment regimens [3, 6, 10, 11]. The tumour tends to metastasize to lungs but also to regional lymph nodes and bone. The 5-year survival rate is about 50–60%. Long term follow-up is mandatory because metastases can develop late in the course of the disease (10 years or more after diagnosis). Of the seven patients with a clear cell sarcoma of the gastrointestinal tract, two had metastatic disease at the time of diagnosis [13, 15], and an additional four developed liver metastases 2 (current case) to 24 [4] months post-operatively. Only two patients were disease-free at last follow-up, 11 [1] and 18 [5] months after diagnosis. Follow-up of patients 4 and 6 of Table 1 have been updated recently (see Acknowledgements).

In the digestive tract, clear cell sarcoma has the same histology and immunoprofile as in the soft tissues. The tumour presents as bundles or nests of pale staining to eosinophilic spindle cells separated by dense fibrous tissue septa. Tumour cells have prominent vesicular nuclei with

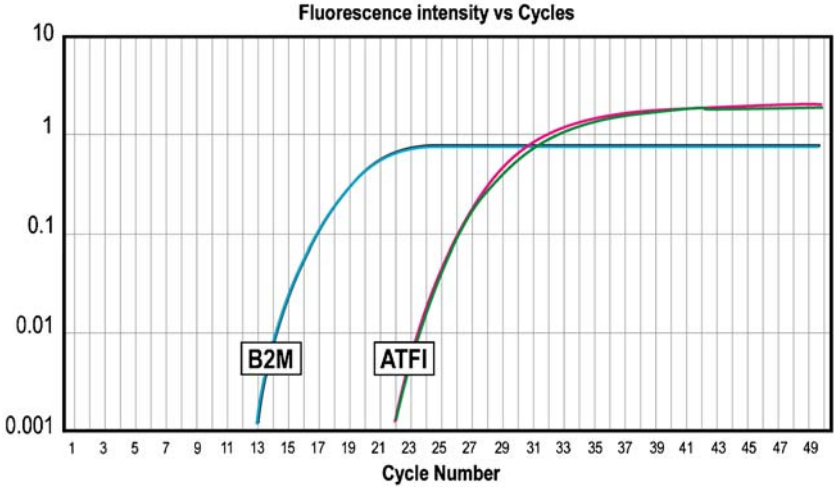


Fig. 4 Real-time PCR assay demonstrating the presence of EWS–ATF1 transcripts. *Graphs* show fluorescence emission data during each PCR cycle. This fluorescence is directly related to the quantity of PCR products. ATF1, graph of amplification of EWS–ATF1 transcripts. B2M, graph of amplification of beta-2-microglobulin transcripts, used as internal control

mostly a large, central, single nucleolus. Multinucleate giant tumour cells, a relatively common feature of clear cell sarcoma of soft tissues, seem to be rarer in the gastrointestinal tract (one of seven cases). Intracellular melanin accumulation is reported in half of the cases.

The tumour cells in clear cell sarcoma of soft tissues usually express melanocytic makers, including S-100 protein,

Table 1 Clear cell sarcoma of the gastrointestinal tract

Case	Author (reference)	Age (years)	Sex	Site	Size (cm)	Metastases at diagnosis	Molecular confirmation	Treatment	Adequacy of surgical resection	Outcome
1	Ekfors et al. [5]	38	M	Duodenum	3	No	No	Truncal vagotomy, pancreatico-duodenectomy, cholecystectomy	Complete	AWNED at 18 months
2	Donner et al. [4]	37	M	Ileum	6.5	No	Yes (karyotype)	Intestinal resection, along with tumour	Complete	Liver mets at 24 and 46 months, AWD at 46 months
3	Fukuda et al. [7]	74	M	Transverse colon	2	No	Yes (RT–PCR on liver met)	Partial colectomy+ regional lymphadenectomy	Complete	Single liver met at 9 months (resected), AWD at 15 months
4	Pauwels et al. [13]	30	M	Stomach	4	Yes (peritoneum, regional lymph nodes)	Yes (karyotype and FISH)	Palliative partial gastric resection	Complete	Pancreatic, liver and Douglas cul-de-sac mets at 4 months, AWD at 18 months
5	Zambrano et al. [15]	15	F	Jejunum	5	Yes (mesenteric lymph nodes)	Yes (karyotype)	Intestinal resection, along with tumour and enlarged lymph nodes + CT	Incomplete	Tumour progression at 12 months, DOD at 16 months
6	Achten et al. [1]	57	M	Jejunum	6.5	No	Yes (FISH)	Intestinal resection, along with tumour	Complete	AWNED at 11 months
7	Current case	35	M	Ileum	1.8	No	Yes (RT-PCR)	Intestinal resection, along with tumour	Complete	Liver mets at 2 months, DOD at 15 months

DOD Dead of disease, *AWD* Alive with disease, *AWNED* Alive with no evidence of disease, *mets* metastases, *CT* Chemotherapy, *RT–PCR* Reverse transcriptase–polymerase chain reaction, *FISH* Fluorescence in situ hybridization

HMB45, melan-A and the melanoma isoform of microphthalmia transcription factor (MITF-M) [2]. In the gastrointestinal tract, clear cell sarcoma cells consistently expressed vimentin and S-100 protein. HMB45 was expressed in three of seven cases only, and melan-A in two of four cases with available data. They were consistently negative for EMA, cytokeratins, muscle-specific actin, smooth muscle actin, desmin, CD34, chromogranin, synaptophysin, CD45 and CD117. Melanosomes at varying stages of development were visible ultrastructurally in all (6/6) cases with available data.

The diagnosis of clear cell sarcoma is a challenging one, especially if the tumour occurs in an unexpected site such as the gastrointestinal tract. In our case, the diagnosis was considered only at the time of the peritoneal tumour regrowth 8 months after the primary tumour had been removed. A metastatic melanoma was initially suspected, but an extensive work-up failed to find any primary elsewhere. The other differential diagnoses, successively contemplated and ruled out on the basis of tumour immunoprofile, included a poorly-differentiated neuroendocrine carcinoma (tumour cells were negative for keratins, EMA, chromogranin and synaptophysin), a malignant gastrointestinal stromal tumour (negativity for CD117 and CD34), a clear cell myomelanocytic tumour/PEComa (negativity for smooth muscle actin, strong positivity for S-100 protein), a paraganglioma (negativity for chromogranin and synaptophysin, diffuse positivity for S-100 protein), some sort of germ cell neoplasia (negativity for epithelial markers and placental alkaline phosphatase), a synovial sarcoma (negativity for epithelial markers, absence of detectable SYT-SSX fusion transcripts), a leiomyosarcoma (negativity for muscle markers) and a lymphoma (negativity for lymphoid markers). Although initially considered as improbable, the other diagnostic hypotheses that could not be definitely ruled out included epithelioid malignant peripheral nerve sheath tumour, sclerosing epithelioid fibrosarcoma and clear cell sarcoma. Ruling out the diagnosis of malignant peripheral nerve sheath tumour was effectively difficult on account of the negativity of the HMB45 marker. Nevertheless, the focal positivity of the melan-A marker was a helpful indication of the melanocytic differentiation of the tumour. The detection of EWS–ATF1 fusion transcripts by RT-PCR finally demonstrated that this lesion was a clear cell sarcoma. The lack of primary tumour elsewhere strongly suggests that this tumour arose primarily in the ileum and was not a metastatic deposit from a soft tissue tumour, as has sometimes been reported [12].

The relationship between clear cell sarcoma and melanoma has been controversial for a long time. Both neoplasms show morphologic features of melanocytic differentiation (melanin pigment), as well as immunohistochemical and ultrastructural features (melanosomes), and some authors refer to clear cell sarcoma as malignant melanoma of soft parts [3, 5]. Clear cell sarcoma differs, however, from cutaneous melanoma in several respects: it is almost always deep-seated, associated with tendons, tendon sheaths and aponeuroses, seldom involves the epidermis and behaves differently, metastasizing predominantly to the lungs. In addition, clear cell sarcoma bears the t(12;22) (q13;q12) translocation which is specific for this tumour type and had never been identified in cutaneous melanoma [2, 8]. This translocation, present in 75 to 90% of cases, fuses the activating transcription factor 1 (ATF1) gene on chromosome 12 with the EWS gene on chromosome 22 [2, 8].

Based on these differences, clear cell sarcoma was considered heretofore as a clinicopathologic entity distinct from melanoma. However, recent gene expression profiling data would suggest that this is not really the case. While examining a series of sarcomas including clear cell sarcomas, Segal et al. [14] found that clear cell sarcomas do not 'cluster' with other soft tissue sarcomas and may rather represent a distinct genomic subtype of melanoma. In addition to genes of melanocytic differentiation, this tumour was also shown to express fibroblast growth factor receptor 1 (FGFR1), a tyrosine kinase receptor involved in angiogenesis and tumour cell growth and migration, suggesting that the use of tyrosine kinase inhibitors might have some value in the treatment of patients with uncontrolled disease.

In conclusion, this case shows that clear cell sarcoma of soft tissues may occur as a primary neoplasm of the gastrointestinal tract. It also underlines the pivotal role of molecular techniques in the diagnostic approach when dealing with 'unusual' locations.

Acknowledgements The authors thank Dr. P. Pauwels and Dr. R. Sciot for updating the follow-up of patients 4 and 6, respectively, and Dr S.Taylor for proofreading.

References

1. Achten R, Debiec-Rychter M, de Wever I, Sciot R (2005) An unusual case of clear cell sarcoma arising in the jejunum highlights the diagnostic value of molecular genetic techniques in establishing a correct diagnosis. Histopathology 46:472–474
2. Antonescu CR, Tschernyavsky SJ, Woodruff JM, Jungbluth AA, Brennan MF, Ladanyi M (2002) Molecular diagnosis of clear cell sarcoma. Detection of EWS–ATF1 and MITF-M transcripts and histopathological and ultrastructural analysis of 12 cases. J Mol Diagn 4:44–52
3. Deenik W, Mooi WJ, Rutgers EJ, Peterse JL, Hart AA, Kroon BB (1999) Clear cell sarcoma (malignant melanoma) of soft parts. A clinicopathologic study of 30 cases. Cancer 86:969–975
4. Donner LR, Trompler RA, Dobin S (1998) Clear cell sarcoma of the ileum: the crucial role of cytogenetics for the diagnosis. Am J Surg Pathol 22:121–124
5. Ekfors TO, Kujari H, Isomaki M (1993) Clear cell sarcoma of tendons and aponeurosis (malignant melanoma of soft parts) in the duodenum: the first visceral case. Histopathology 22:255–259
6. Enzinger FM (1965) Clear cell sarcoma of tendons and aponeuroses. An analysis of 21 cases. Cancer 18:1163–1174
7. Fukuda T, Kakihara T, Baba K, Yamaki T, Yamaguchi T, Susuki T (2000) Clear cell sarcoma arising in the transverse colon. Pathol Int 50:412–416

8. Graadt van Roggen JF, Mooi WJ, Hogendoorn PCW (1998) Clear cell sarcoma of tendons and aponeuroses (malignant melanoma of soft parts) and cutaneous melanoma: exploring the histogenetic relationship between these two clinicopathological entities. J Pathol 186:3–7
9. Hostein I, Andraud-Fregeville M, Guillou L, Terrier-Lacombe MJ, Deminiere C, Ranchere D, Lussan C, Longavenne E, Bui NB, Delattre O, Coindre JM (2004) Rhabdomyosarcoma: value of myogenin expression analysis and molecular testing in diagnosing the alveolar subtype: an analysis of 109 paraffin-embedded specimens. Cancer 101:2817–2824
10. Lucas DR, Nascimento AG, Sim FH (1992) Clear cell sarcoma of soft tissues. Mayo Clinic experience with 35 cases. Am J Surg Pathol 16:1197–1204
11. Montgomery EA, Meis JM, Ramos AG, Martz KL (1993) Clear cell sarcoma of tendons and aponeuroses. A clinicopathologic study of 58 cases with analysis of prognostic factors. Int J Surg Pathol 1:89–100
12. Ohba Y, Suzuki H, Hiraga H, Ito T, Sawa H, Nagai M, Satoh SI, Iwaki H, Nagashima K (1999) Melanotic peritoneal sarcomatosis originating from clear cell sarcoma. Pathol Int 49: 653–657
13. Pauwels P, Debiec-Rychter, Sciot R, Vlasveld T, Den Butter B, Hagenmeijer A, Hogendoorn PCW (2002) Clear cell sarcoma of the stomach. Histopathology 41:526–530
14. Segal NH, Pavlidis P, Noble WS, Antonescu CR, Viale A, Wesley UV, Busam K, Gallardo H, DeSantis D, Brennan MF, Cordon-Cardo C, Wolchok JD, Houghton AN (2003) Classification of clear-cell sarcoma as a subtype of melanoma by genomic profiling. J Clin Oncol 21:1775–1781
15. Zambrano E, Reyes-Mugica M, Franchi A, Rosai J (2003) An osteoclast-rich tumour of the gastrointestinal tract with features resembling clear cell sarcoma of soft parts: reports of 6 cases of a GIST simulator. Int J Surg Pathol 11:75–81

Virchows Arch (2005) 447: 778–780
DOI 10.1007/s00428-005-0008-1

LETTER TO THE EDITOR

Jean-Louis Dargent · Laurence Lespagnard · Isabelle Meiers · Christophe Bradstreet · Pierre Heimann · Christiane De Wolf-Peeters

Composite follicular lymphoma and nodular lymphocyte predominance Hodgkin's disease

Received: 17 April 2005 / Accepted: 17 May 2005 / Published online: 28 June 2005
© Springer-Verlag 2005

Dear Editor:

Composite lymphoma (CL) is a lymphoid neoplasm in which two (or more) distinct lymphoma subtypes involve the same lymph node or extranodal site [9]. This condition is relatively rare and raises interesting questions about the pathogenesis as well as the relationship that might exist between the various neoplastic components. Recently, we observed the case of a 29-year-old male who developed a distinctive CL consisting of follicular lymphoma (FL) and nodular lymphocyte predominance Hodgkin's disease (NLPHD) within the same lymph node.

The patient was admitted in our hospital because of a slow-growing lymphadenopathy localized in the left inguinal area. This lymphadenopathy spontaneously appeared and progressively increased in size to reach a diameter of almost 4 cm. There was no history of fever or deterioration in the patient's general condition. Clinical examination did not reveal any other abnormality and peripheral blood analysis was within normal limits. Serum investigations for human immunodeficiency virus, hepatitis B and C viruses, Epstein–Barr virus (EBV), cytomegalovirus, and syphilis were negative. In contrast, the patient demonstrated acquired immunity for toxoplasmosis and hepatitis A virus. A surgical excision of the abnormal lymph node was performed for diagnostic purposes.

Microscopically, the nodal architecture was effaced by numerous uniformly sized follicles (Fig. 1). These follicles were closely packed together and lacked mantle zones. They were mostly composed of small centrocytes mixed up with few centroblasts. Tangible body macrophages as well as mitotic figures were almost completely absent. In a small area of the lymph node, we noted several large lymphoid nodules composed of small lymphocytes mixed up with some large atypical cells (Fig. 2). The latter featured the characteristics of "pop corn" cells, indicative of NLPHD (Fig. 3). Both lymphomatous proliferations were relatively well delineated from each other. On immunohistochemical analysis, the lymphoid cells inside the follicles were found to express CD20, CD79a, and CD10. These cells also expressed the bcl-2 and bcl-6 proteins. Small clusters of CD20- and CD10-positive cells were found in the interfollicular areas. "Pop corn" cells showed immunoreactivity with antibodies directed against CD45, CD20, CD79a, and bcl-6 protein. Although some of these cells were weakly CD30-positive, they did not express CD10, CD15, or bcl-2 protein. "Pop corn" cells were found between CD20-, CD79a-, bcl-2 protein-, and CD10-positive centrocytes, CD23-positive follicular dendritic cells, and CD57-positive T lymphocytes. These CD57-positive T lymphocytes often formed rosettes around the "pop corn" cells (Fig. 4). Polymerase chain reaction (PCR) analysis of DNA extracted from the paraffin embedded sections demonstrated a bcl-2 gene rearrangement resulting from a t(14;18) chromosomal translocation in the major breakpoint region. However, no clonal rearrangement of the genes coding for the immunoglobulin (Ig) heavy (IgH) chain or EBV genomic sequences could be evidenced, using the same method of molecular investigation.

Based on these data, a diagnosis of CL consisting of FL and NLPHD was made. Additional investigations revealed the involvement of several lymph nodes located in the left inguinal area, the retroperitoneal and mesenteric regions, and the right axillary area, respectively. No infiltration of

J.-L. Dargent (✉) · L. Lespagnard · I. Meiers
Service d'Anatomie Pathologique, Institut Jules Bordet,
1 rue Héger-Bordet,
1000 Brussels, Belgium
e-mail: jl.dargent@skynet.be
Tel.: +32-2-5413124
Fax: +32-2-5413281

C. Bradstreet
Service de Médecine Interne, C. H. U. Saint-Pierre,
322 rue Haute,
1000 Brussels, Belgium

P. Heimann
Laboratoire de Cytogénétique, Institut Jules Bordet,
1 rue Héger-Bordet,
1000 Brussels, Belgium

C. De Wolf-Peeters
Pathologische Ontleedkunde, K. U. Leuven,
Minderbroedersstraat 12,
3000 Louvain, Belgium

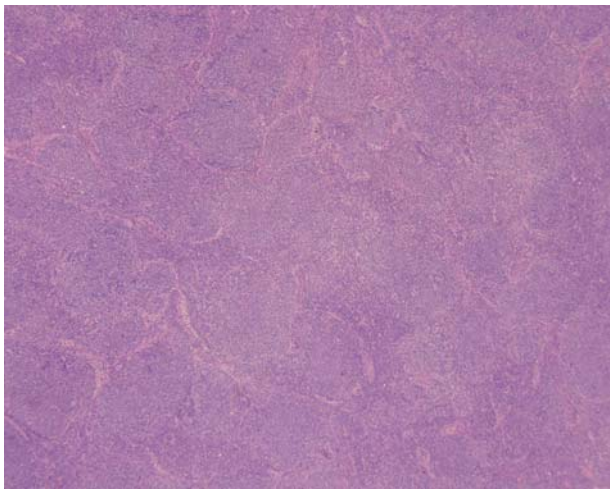


Fig. 1 The nodal architecture is effaced by numerous uniformly sized follicles that are closely packed together. These follicles lack mantle zones and are mostly composed of centrocytes

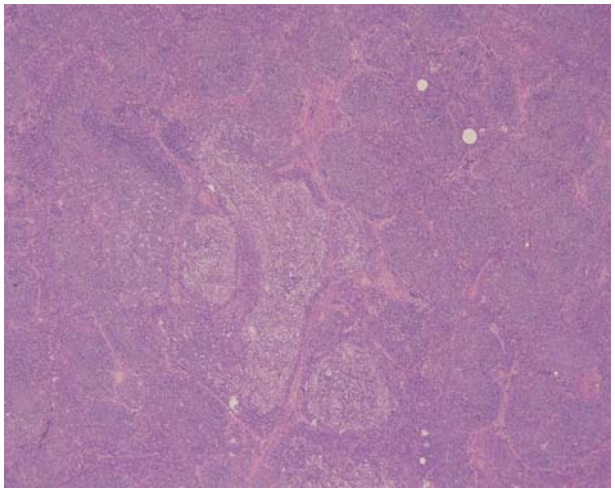


Fig. 2 Several nodules of larger size and featuring large atypical cells were found in a small area of the lymph node

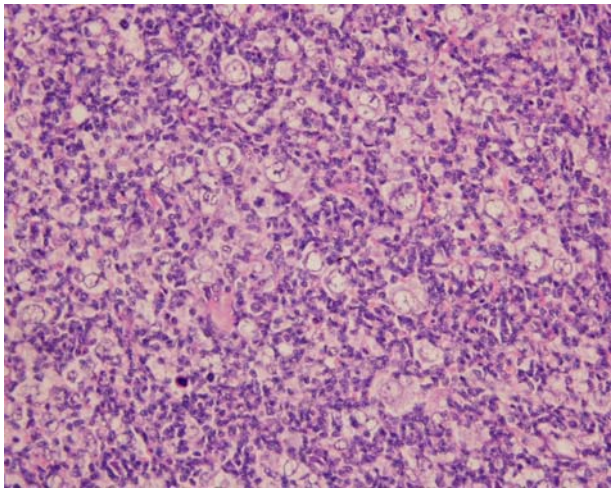


Fig. 3 The large atypical cells look like "pop corn" cells

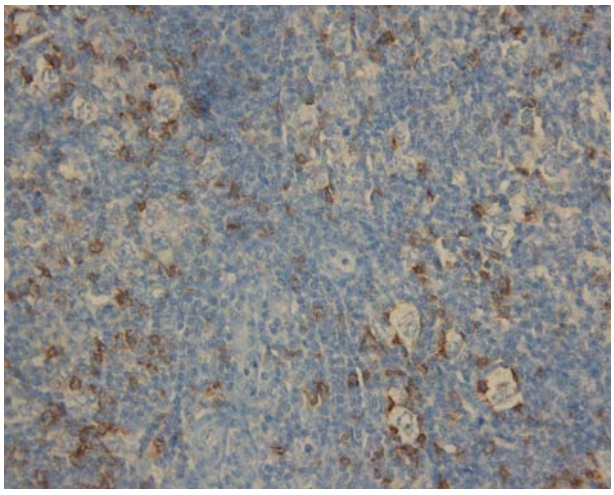


Fig. 4 Immunostaining with antibody directed against CD57. "Pop corn" cells are surrounded by CD57-positive lymphocytes

the bone marrow could be demonstrated. Six courses of R-CHOP (rituximab, cyclophosphamide, doxorubicin, vincristine, and prednisone) chemotherapy were therefore given. The patient is in complete remission, 3 months after the end of therapy.

On rare occasions, CLs consisting of FL and classic Hodgkin's disease (HD) have been reported in the literature [4, 6–8, 10–12, 15, 16]. Using laser capture microdissection, PCR analysis, and sequencing of IgH gene rearrangements, a clonal relationship between the FL and HD has been demonstrated in some of these cases [4, 10, 12]. Interestingly, RS cells often express the bcl-2 protein or carry the t(14;18) translocation in these CLs [11, 12, 16]. To our knowledge, however, there has been no case report documenting the occurrence of FL and NLPHD within a single lymph node. Progression of NLPHD to diffuse large B cell lymphoma is a relatively well-known phenomenon [8], but the association with other B-cell lymphoproliferative disorders, in contrast with classic HD [5], is definitely unusual. Therefore, the present observation raises interesting questions about the relationship that might exist between FL and NLPHD. Unfortunately, we could not perform further molecular investigations in order to determine whether a clonal link between the "pop corn" cells and the FL cells does exist in our patient. Thus, we can only offer speculations on this issue. Nevertheless, two main possibilities may be considered, as follows.

At first, the NLPHD and FL components are totally unrelated and their occurrence together within the same lymph node simply represents a coincidental occurrence. In this regard, the absence of clonal relationship between the neoplastic components in some CL, like those involving HD and mantle cell lymphoma for instance [5], may support such a model of pathogenesis.

Second, both NLPHD and FL originate from a common precursor B cell, that is, the same abnormal B cell gives rise to the two neoplastic disorders through distinct maturation pathways in the germinal center (GC). In such a situation, the timing of t(14;18) translocation is of paramount im-

portance because this chromosomal anomaly is classically not involved in the pathogenesis of NLPHD [1]. Also, it was generally acknowledged that t(14;18) translocation takes place at the pre-B ontogenetic stage, during the initial phase of the IgH V region recombination process [13, 14]. However, recent studies have demonstrated that this chromosomal anomaly may arise at a later stage of B cell development, during receptor revision in the GC [13, 14]. Therefore, the possibility that a common precursor B cell first gives rise to NLPHD and thereafter to FL may be not so unreasonable. Moreover, the numerous similarities that exist between "pop corn" cells in NLPHD and GC B cells at the centroblastic stage of differentiation and the knowledge that FL cells may correspond to late centroblast or centrocyte GC B cells also are consistent with such a hypothesis [12, 14].

Due to differences in terms of prognosis, our case should be distinguished from FL showing progression to CD30-positive large cell lymphoma and from FL featuring numerous RS-like cells [2, 3]. In our patient, the phenotype of the "pop corn" cells as well as the presence of numerous CD57-positive T lymphocytes, notably around these cells, make such a progression unlikely and rather favor a diagnosis of CL featuring FL and NLPHD components. Interestingly, numerous small B lymphocytes in the large follicles harboring the "pop corn" cells were bcl-2 protein- and CD10-positive centrocytes, a finding that can be interpreted as colonization of these follicles by FL cells.

Whatever the precise pathogenesis may be, this intriguing observation further expands the spectrum of CL.

References

1. Algara P, Martinez P, Sanchez L, Villuendas R, Orradre JL, Oliva H, Piris MA (1991) Lymphocyte predominance Hodgkin's disease (nodular paragranuloma): a bcl-2 negative germinal centre lymphoma. Histopathology 19:69–75
2. Alsabeh R, Medeiros LJ, Glackin C, Weiss LM (1997) Transformation of follicular lymphoma into CD30-large cell lymphoma with anaplastic cytologic features. Am J Surg Pathol 21: 528–536
3. Bayerl MG, Bentley G, Bellan C, Leoncini L, Ehmann WC, Palutke M (2004) Lacunar and Reed–Sternberg-like cells in follicular lymphomas are clonally related to the centrocytic and centroblastic cells as demonstrated by laser capture microdissection. Am J Clin Pathol 122:858–864
4. Bräuninger A, Hansmann ML, Strickler JG, Dummer R, Burg G, Rajewsky K, Küppers R (1999) Identification of common germinal-center B-cell precursors in two patients with both Hodgkin's disease and non-Hodgkin's lymphoma. N Engl J Med 340:1239–1247
5. Caleo A, Sanchez-Aguilera A, Rodriguez S, Dotor AM, Beltran L, de Larrinoa AF, Menarguez FJ, Piris MA, Garcia JF (2003) Composite Hodgkin lymphoma and mantle cell lymphoma. Two clonally unrelated tumors. Am J Surg Pathol 27:1577–1580
6. Gonzalez CL, Medeiros LJ, Jaffe ES (1991) Composite lymphoma. A clinicopathologic analysis of nine patients with Hodgkin's disease and B-cell non-Hodgkin's lymphoma. Am J Clin Pathol 96:81–89
7. Hansmann ML, Fellbaum C, Hui PK, Lennert K (1989) Morphological and immunohistochemical investigation of non-Hodgkin's lymphoma combined with Hodgkin's disease. Histopathology 15:35–48
8. Jaffe ES, Zarate-Osorno A, Kingma DW, Raffeld M, Medeiros LJ (1994) The interrelationship between Hodgkin's disease and non-Hodgkin's lymphomas. Ann Oncol 5(suppl 1):7–11
9. Kim H (1993) Composite lymphoma and related disorders. Am J Clin Pathol 99:445–451
10. Küppers R, Sousa AB, Baur AS, Strickler JG, Rajewsky K, Hansmann ML (2001) Common germinal-center B-cell origin of the malignant cells in two composite lymphomas, involving classical Hodgkin's disease and either follicular lymphoma or B-CLL. Mol Med 7:285–292
11. Le Brun DP, Ngan BY, Weiss LM, Huie P, Warnke RA, Cleary ML (1994) The bcl-2 oncogene in Hodgkin's disease arising in the setting of follicular non-Hodgkin's lymphoma. Blood 83: 223–230
12. Marafioti T, Hummel M, Anagnostopoulos I, Foss HD, Huhn D, Stein H (1999) Classical Hodgkin's disease and follicular lymphoma originating from the same germinal center B cell. J Clin Oncol 17:3804–3809
13. Nadel B, Marculescu R, Le T, Rudnicki M, Böcskör S, Jäger U (2001) Novel insights into the mechanism of t(14;18)(q32;q21) translocation in follicular lymphoma. Leuk Lymphoma 42: 1181–1194
14. Stamatopoulos K, Kosmas C, Belessi C, Stavroyianni N, Kyriazopoulos P, Papadaki T (2000) Molecular insights into the immunopathogenesis of follicular lymphoma. Immunol Today 21:298–305
15. Thirumala S, Esposito M, Fuchs A (2000) An unusual variant of composite lymphoma. A short case report and review of the literature. Arch Pathol Lab Med 124:1376–1378
16. Urano M, Mizoguchi Y, Nishio T, Abe M, Kuroda M, Saito S, Sakurai K (2004) Composite lymphoma arising in the parotid gland: a case report. Auris Nasus Larynx 31:89–93

Virchows Arch (2005) 447: 781–783
DOI 10.1007/s00428-005-0007-2

LETTER TO THE EDITOR

M. Zamecnik

Pseudoangiomatous spindle cell lipoma with "true" angiomatous features

Received: 10 April 2005 / Accepted: 7 May 2005 / Published online: 13 July 2005
© Springer-Verlag 2005

Keywords Pseudoangiomatous · Sex steroid receptor · Spindle cell lipoma · CD31 · F-VIII

Sir,

The pseudoangiomatous variant of spindle cell lipoma (PASCL) is a rare tumor of which only six cases were reported to date [4, 7]. The tumor differs from common spindle cell lipoma [2] by distinctive irregular branching spaces and pseudopapillary projections into these spaces. The spaces were labeled as pseudovascular because their lining cells lacked immunohistochemical reactivity for endothelial markers. Recently, I have seen a further case of this rare lesion. Clinical and morphological features of the tumor were similar to those reported previously, but immunohistochemical results indicated that distinctive spaces in this tumor were true vascular. In addition, the tumor expressed sex steroid receptors, which had not been described in spindle cell lipoma until now.

A 74-year-old male patient presented with superficial subcutaneous lesion in the nuchal region. The tumor grew slowly for 8 years. The clinician suggested an enlarged lymph node, and performed a marginal tumor excision. The lesion was ovoid and well circumscribed, and measured 2 cm in maximum diameter. Histologically, the tumor showed patterns of spindle cell lipoma with mixture of mature fat and short spindle cells, and with abundant small capillary vessels (Fig. 1). The nuclei of spindle cells were regular and bland appearing, but very few of them showed slight pleomorphism similar to that observed in pleomorphic lipoma. Mitotic figures and significant atypia were not found. The intercellular space was slightly mucoid and contained very rare refractile, wavy collagen bundles. Scattered mast cells were identified. A prominent feature of the lesion was the presence of branching cleft-like spaces and villiform tumor tissue projections into these spaces. The spaces and the surface of tissue projections were lined by flat cells, which in hematoxylin and eosin stained sections suggested an endothelial nature of the spaces.

Immunohistochemically, CD34 (QBEnd/10, 1:800, Neomarkers, Westinghouse) was strongly positive in the spindle stromal cells, endothelium of the vessels, and in surface cells of the villous projections and clefted spaces (Fig. 2a). Endothelial markers F-VIII (F8/86, MW, 1:100; Dako, Carpenteria, CA, USA) and CD31 (JC70A, 1:50, MW; Dako) stained endothelium of the vessels and in addition they were positive in many surface cells of villous projections and tissue clefts (Fig. 2b, c). Alpha smooth muscle actin (1A4, 1:1,000; Dako) stained pericytes and rare cells on the surface of the villous projections. Actin was also focally positive in rare spindle cells that were immediately beneath the surface cells (Fig. 2d), thus resembling an "organoid" pericytic positivity. Calponin reactivity (CALP, 1:1,000, MW; Dako) was limited to the smooth muscle cells in larger vessels and to very rare spindle cells, and was negative in pericytes of small vessels. Estrogen receptor (ER) (ER1D5, Immunotech), progesterone receptor (PR) (1A6, Immunotech), and androgen receptor (AR) (AR441, Dako) were positive in 50, 70, and 40% of the tumor cells, respectively (Fig. 2e). S100 protein (S1/61/69, 1:50; Novocastra, Newcastle) reactivity highlighted the adipocytes. EMA, cytokeratin AE1–AE3, and CD10 gave negative results.

M. Zamecnik
Sikl's Department of Pathology,
Medical Faculty,
Charles University,
Pilsen, Czech Republic

M. Zamecnik (✉)
Biopticka Laboratory,
Mikulasske Nam. 4,
326 00 Pilsen, Czech Republic
e-mail: zamecnik@medima.cz
Fax: +420-19-377440539

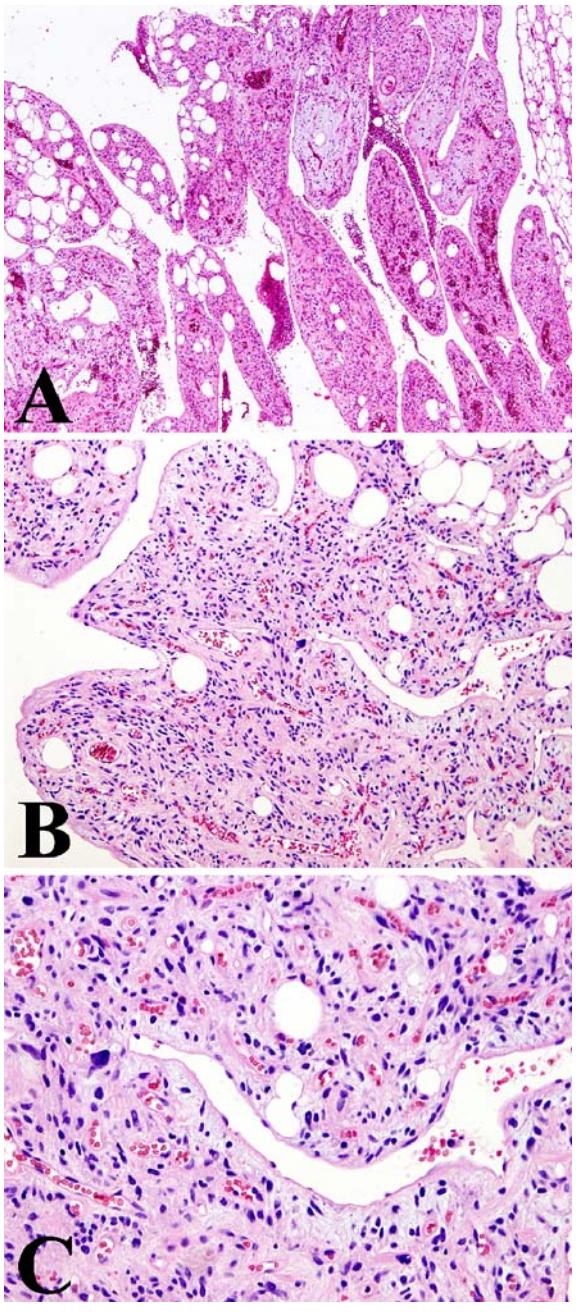


Fig. 1 **a** Low-power view of a villous architecture of the tumor. **b** Medium-power view shows an arrangement of spindle cells and adipocytes in the villous projection. **c** Rare nuclear pseudoatypia of stromal cells and flat cells on the surface of the villous projection are shown

The present tumor shows histological features of PASCL as described by Hawley et al. [4] in 1994. Like common spindle cell lipoma, PASL occurs mostly in the shoulder and neck regions of adult males. Thus, in this case, the patient's gender, age, and location are in keeping with previous observations of PASCL (and of spindle cell lipoma in general) [2, 4, 7].

Our case differs from previously published ones [4, 7] in that immunohistochemical results suggested the true vascular nature of the distinctive spaces inside the tumor. These spaces are lined by flattened and relatively inconspicuous cells. In both previous studies the lining cells were negative for endothelial markers CD31, CD34, F-VIII, *Ulex europaeus* I, and type IV collagen, and therefore the spaces were not regarded as true vascular (hence the adjective *pseudoangiomatous* in the name of the lesion). In contrast, a majority of the lining cells in the present case showed strong positivity for endothelial markers F-VIII, CD31, and CD34. In addition, some actin+ cells resembling pericytes were seen focally beneath the lining cells. The finding of unquestionable endothelial features and possible pericytic nature of rare associated actin+ spindle cells indicates that the spaces represent dilated vessels, and that at least the present case should be labeled as angiomatous spindle cell lipoma. The difference between the present and the previously reported findings is difficult to explain. I suppose that the antibodies and techniques used in both previous studies [4, 7] 10 and 11 years ago, respectively, were less sensitive (e.g., CD34 in the original study was negative in the spindle cells in all cases, which contrasts with almost consistent CD34 positivity in spindle cell lipomas reported in recent years) [8]. The exact cause of dilatation of small vessels in the present tumor remains unknown. It can be hypothesized that such dilatation is a consequence of microcirculation disturbance within a lesion containing abundant abnormal vessels. Of interest, all reported cases of PASCL appear to contain higher number of vessels [4, 7] in comparison with common spindle cell lipomas [2]. Some space-lining cells in the present lesion were positive for actin and CD34, and lacked reactivity for endothelial markers. One can speculate that these spaces may represent immature vascular channels with "incomplete" endothelial cell differentiation and with myoid features of some lining cells, since they resemble similar primitive channels and tissue clefts already described in connective tissue of the skin and mammary stroma [1, 3, 5]. Perhaps such "hidden" channels can distend and their lining cells can differentiate toward more mature (CD31- and F-VIII-positive) endothelial cells. However, a study on additional cases is certainly needed for a more exact characterization of the spaces in PASCL.

Expression of ER, PR, and AR, as seen in our case, was not previously described in spindle cell lipoma. However, to the best of my knowledge, sex steroid receptors were not studied in these tumors as well as in lipomatous tumors in general. The presence of ER, PR, and AR was described in normal adipose tissue (although in quantity lower than in mullerian-derived tissues) [6], and this observation can explain the positivity for these receptors also in some lipomatous tumors.

In sum, a further case of PASCL was reported. The lesion showed clinical and histological features similar to those described previously. In contrast, however, immunohistochemical results indicated that the distinctive intratumoral spaces (having pseudovascular features in the previous reports) in fact possessed a true vascular nature. In addition, a hitherto undescribed positivity for sex steroid hormone receptors was found in the tumor.

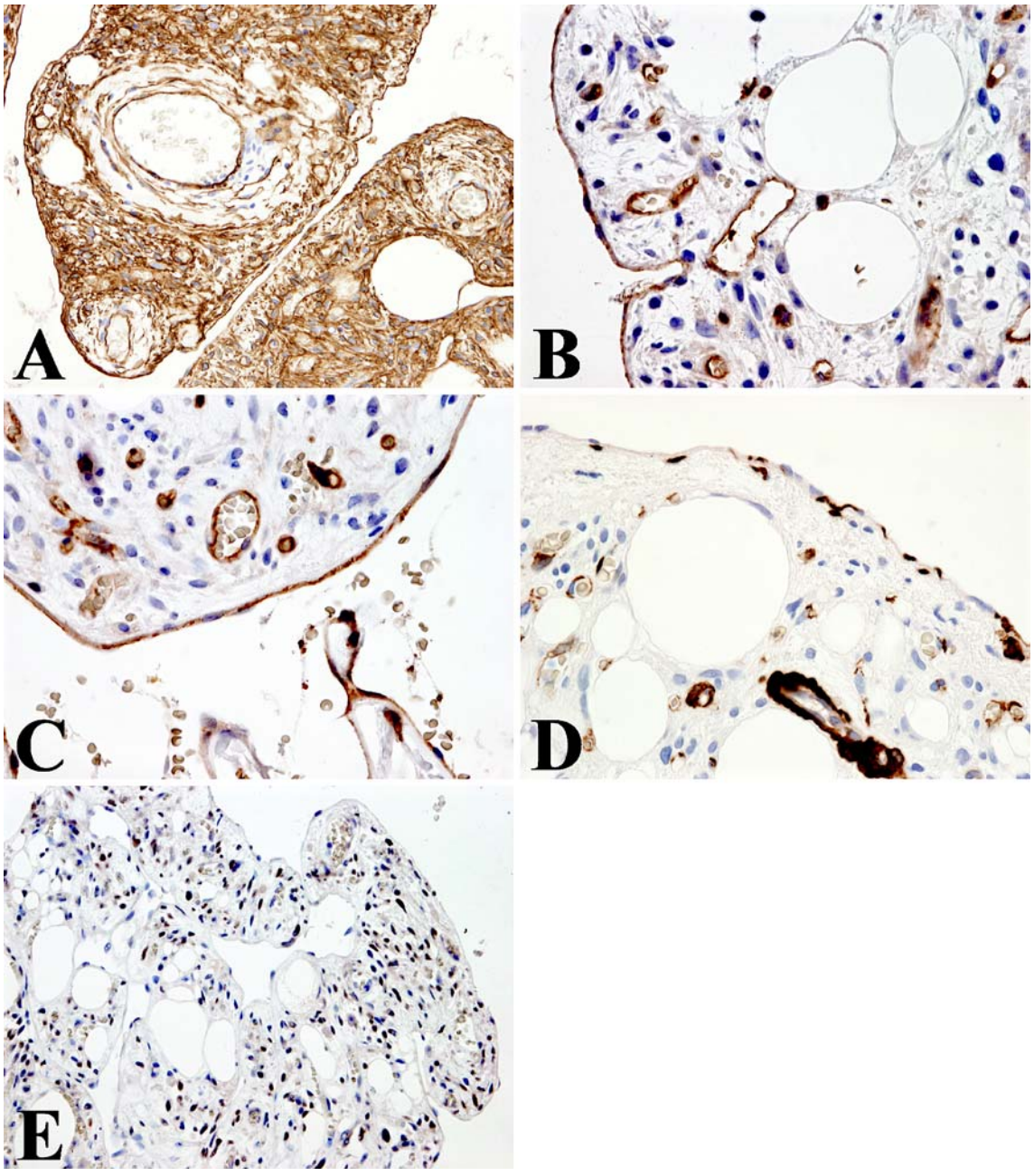


Fig. 2 Immunohistochemical results. **a** Diffuse CD34 positivity. Immunoreactivity for **b** F-VIII and **c** CD31. In addition to the endothelium of small vessels, both antibodies also strongly stain surface cells of the villous projections. **d** Pericytic-like actin positivity of some cells near the surface of the projection, and a typical pericytic positivity of small vessels. **e** Estrogen receptor is positive in numerous stromal cells

References

1. Damiani S, Eusebi V, Peterse JL (2002) Malignant neoplasms infiltrating pseudoangiomatous' stromal hyperplasia of the breast: an unrecognized pathway of tumour spread. Histopathology 41:208–215
2. Enzinger FM, Harvey DA (1975) Spindle cell lipoma. Cancer 36:1852–1859
3. Hartveit F (1990) Attenuated cells in breast stroma: the missing lymphatic system of the breast. Histopathology 16:533–543
4. Hawley IC, Krausz T, Evans DJ, Fletcher CD (1994) Spindle cell lipoma—a pseudoangiomatous variant. Histopathology 24:565–569
5. Leak LV (1970) Electron microscopic observations on lymphatic capillaries and the structural components of the connective tissue–lymph interface. Microvasc Res 2:361–391
6. Pedersen SB, Fuglsig S, Sjogren P, Richelsen B (1996) Identification of steroid receptors in human adipose tissue. Eur J Clin Investig 26:1051–1056
7. Richmond I, Banerjee SS (1995) Spindle cell lipoma—a pseudoangiomatous variant. Histopathology 27:201(L)
8. Templeton SF, Solomon AR Jr (1996) Spindle cell lipoma is strongly CD34 positive. An immunohistochemical study. J Cutan Pathol 23:546–550

Virchows Arch (2005) 447: 784
DOI 10.1007/s00428-005-0097-x
© Springer-Verlag 2005

ANNOUNCEMENTS

1–2 December 2005
International Symposium on "Salivary Gland Tumors; present concepts of diagnosis and management"
Amsterdam, The Netherlands

For further information please contact congress secretariat
D. Chavalking
Department of Oral and Maxillofacial Surgery/Oral Pathology
Vrije Universiteit Medical Center (Vumc)
P.O. Box 7057
1007 MB Amsterdam
The Netherlands
E-mail: d.chevalking@vumc.nl
Tel: +31-20-4444039
Fax: +31-20-4444046
Internet: www.vumc.nl

Virchows Arch (2005) 447: 785–786
DOI 10.1007/s00428-005-0004-5

EDITORIAL

Anna Kádár · Zsuzsa Schaff · Tibor Kerényi

In memoriam: Professor Harry Jellinek, M.D. (1924–2005)

Received: 29 April 2005 / Accepted: 29 April 2005 / Published online: 3 September 2005
© Springer-Verlag 2005



Dr. Harry Jellinek, emeritus professor of the Semmelweis University, former director of the 2nd Department of Pathology (1968–1993), died on 6 January 2005 after a prolonged illness, which was little noticed by his environment. He celebrated his 80th birthday in September 2004 at the plenary session of the annual meeting of the Hungarian Society of Pathologists. It was attended by many of his colleagues, students and friends from home and abroad, and Professor Jellinek himself delivered a well-acclaimed lecture.

Professor Harry Jellinek was born in Rimaszombat (Slovakia) on 25 November 1924. He obtained his M.D. degree "summa cum laude" from the Budapest University in 1950. In 1952, he joined the 2nd Department of Pathology of Semmelweis University (Budapest, Hungary) as an assistant to Professor L. Haranghy (head of the department, 1952–1967). Later he served as head of the 2nd Department of Pathology for 25 years (1968–1993). He remained active in the department until his death.

A. Kádár (✉) · Z. Schaff · T. Kerényi
2nd Department of Pathology, Semmelweis University,
Üllői út 93,
1091 Budapest, Hungary
e-mail: kadann@korb2.sote.hu

Dr. Jellinek obtained his Ph.D. degree (1959) and later D.Sc. degree (1965) based on his studies on the pathomorphology, regeneration and alterations of the arteries. His continuous interest in research stayed within the arterial structure and permeability changes associated with atherosclerosis.

Throughout his career Dr. Jellinek distinguished himself as an outstanding teacher, academician, investigator and an expert in the practice of pathology. One of his main goals when he was appointed as the deputy dean of medicine was to improve and modernize the medical education of the undergraduate, postgraduate, graduate and faculty levels. He himself was an enthusiastic teacher. His lectures in pathology were always interesting, stressing the clinicopathologic approach to diseases. These activities laid the foundation in Hungary for research in pathology of the arteries and earned an international reputation for the Hungarian pathologist. His close to 300 publications with his co-workers cover a wide spectrum of angiopathology; his university handbooks went through many editions, and he was the editor, co-editor or author/co-author of several books in English.

Dr. Jellinek was well aware that productive research requires not only collaborations but financial support, both lacking in Hungary at that time. Given the possibilities of the period and making use of his foreign-language skills, he developed contacts with the German-speaking and later with the English-speaking scientific communities.

Dr. Jellinek forged formal collaboration agreements between Semmelweis University and other universities (Heidelberg, 1981; Freiburg, 1982; Padova, 1984 and the Freie Universität Berlin, 1988). In appreciation of these achievements, Professor Jellinek was appointed Honorary Consul of the Semmelweis Medical University of Budapest in 1995 and earned the distinction of Honorary Senator of the University of Freiburg (Germany) in 2004.

Generations of Hungarian pathologists were able to benefit from the knowledge and guidance of Professor Jellinek. His attitude towards pathology made it possible for his students and colleagues to gain insight into the

beauty of diagnostic pathology. A number of his former co-workers and students have become directors of institutes and clinics or professors and head physicians in several reputable Hungarian and foreign institutions.

Striving for acknowledgement and promotion of his fellow pathologists, Professor Jellinek attempted to augment his efforts at the university level by other activities and avenues: as a director of the National Institute of Pathology (1984–2001) and as the president of the Hungarian College of Pathologists (1984–1992) and of the Hungarian Society of Pathologists (1981–1994).

Dr. Jellinek was a member, or an honorary member, of several foreign scientific societies; he was the founder of the Hungarian Division of the International Academy of Pathology (IAP) and its chairman since its foundation (1972) until 1995, the deputy chairman of the European Society of Pathology (1971–1979) and the European vice president of the IAP (1974–1980). In acknowledgement of his many fruitful activities for the IAP, Professor Jellinek received a letter of recognition from the then president of the IAP (1996).

Dr. Jellinek's outstanding achievements in pathology and in education were acknowledged by several prestigious national and international awards, such as the Jozsef Baló Prize (Hungarian Society of Pathology), Linser Prize (German Society of Arteriosclerosis) and Ratschow Preis und Medal (Freiburg University, Germany). The most honorable was the last, i.e. that of the Hungarian Republic Decoration of the Civil Servants Cross awarded to Professor Jellinek in 2004 by the President of the Hungarian Republic.

The above summary of Dr. Jellinek's life would be incomplete without even a brief reference to the person himself. His commitment to science and higher education, selfless devotion, his charming personality, legendary hospitality, and a limitless benevolence towards his colleagues and co-workers do explain the respect and affection for, and the long-lasting friendships with, Professor Jellinek.

Professor Jellinek's departure appears to have come too early for all of us. The Medical Faculty of the Semmelweis University, all Hungarian pathologists, and in a broader sense the world community of pathologists his, former students and colleagues, together with his family, wife and children, mourn the loss of the scholar, the committed mentor, the outstanding pathologist and the gentle humane "Boss".

Acknowledgements We are indebted to Professor M. Daria Haust of The University of Western Ontario, London, Canada for her input into this account as an old friend of Professor Harry Jellinek, and as a supporter of Pathology and Atherosclerosis Research of Hungary.

Virchows Arch (2005) 447: 787–793
DOI 10.1007/s00428-005-0065-5

REVIEW ARTICLE

Manuel Sobrinho-Simões · Ana Preto · Ana Sofia Rocha · Patrícia Castro · Valdemar Máximo · Elsa Fonseca · Paula Soares

Molecular pathology of well-differentiated thyroid carcinomas

Received: 28 July 2005 / Accepted: 15 August 2005 / Published online: 28 September 2005
© Springer-Verlag 2005

Abstract The newly discovered molecular features of well-differentiated thyroid carcinomas derived from follicular cells are reviewed, within the frame of the 2004 WHO classification of thyroid tumours, under the following headings: "Follicular carcinoma", "Papillary carcinoma", "Follicular variant of papillary carcinoma" and "Hürthle cell tumours". A particular emphasis is put on the meaning of *PAX8–PPARγ* rearrangements, *RAS* and *BRAF* mutations, and deletions and mutations of mitochondrial genes and of nuclear genes encoding for mitochondrial enzymes, for thyroid tumorigenesis.

Keywords Thyroid · Follicular carcinoma · Papillary carcinoma · Follicular variant of papillary carcinoma · Hürthle cell tumours · *RET/PTC* rearrangements · *BRAF* mutations · *RAS* mutations

Introduction

The last 5 years has witnessed some major advances in the molecular characterisation of the well-differentiated carcinomas of the thyroid derived from follicular cells. The most important findings were the following:

(a) Detection of *PAX8–PPARγ* rearrangements in follicular carcinomas [28], follicular adenomas [32, 42] and follicular variant of papillary carcinoma [6].
(b) Identification of point mutations and large deletions of mitochondrial DNA (mtDNA) [34] and of mutations of *GRIM-19*, a nuclear gene involved in the mitochondrial respiratory chain (MRC) and cell death [33], which appear to be specific for oncocytic (Hürthle cell) tumours regardless of their histotype (follicular adenoma, follicular carcinoma or papillary carcinoma).
(c) Detection of an extremely high prevalence of *BRAF* mutations in papillary thyroid carcinoma (PTC) [12, 27, 59], namely in PTCs displaying a conventional (papillary or mixed follicular–papillary) growth pattern [65, 67].

In the present article, we have summarised the pathogenic, diagnostic and prognostic meaning of the aforementioned molecular features, together with the available evidence on some other genetic alterations, using as a classificative frame the recently published WHO book on endocrine tumours [14].

For the sake of simplicity, four tumour types will be addressed: follicular carcinoma, papillary carcinoma, follicular variant of papillary carcinoma and oncocytic (Hürthle cell) tumours.

Follicular carcinoma

The most distinctive molecular features of follicular carcinoma are the prominence of aneuploidy and the high prevalence of *RAS* mutations and *PAX8–PPARγ* rearrangements (as the result of a 2;3 translocation).

Aneuploidy is thought to indicate chromosomal instability (CIN) [53] and is frequently observed both in follicular adenomas, namely in those displaying a foetal/embryonal growth pattern, and in follicular carcinomas [4, 7].

Follicular adenomas with a foetal/embryonal growth pattern and follicular carcinomas, besides being aneuploid,

M. Sobrinho-Simões (✉) · A. Preto · A. S. Rocha · P. Castro · V. Máximo · E. Fonseca · P. Soares
Institute of Molecular Pathology and Immunology of the University of Porto (IPATIMUP),
R. Roberto Frias s/n,
4200 Porto, Portugal
e-mail: ssimoes@ipatimup.pt
Tel.: +351-22-5570700
Fax: +351-22-5570799

M. Sobrinho-Simões · P. Castro · E. Fonseca · P. Soares
Department of Pathology,
Medical Faculty of the University of Porto,
Porto, Portugal

M. Sobrinho-Simões · E. Fonseca
Department of Pathology, University Hospital of S. João,
Porto, Portugal

present, in about 60% of the cases, a DNA content which falls within the triploid range [7]. We have found evidence indicating that this DNA pattern is probably attained after a preliminary state of tetraploidisation, which is followed by a consistent loss of some chromosomes [4].

Giaretti et al. [20–22] showed that activating mutations of K-*RAS* were involved in the control of chromosome stability in aneuploidy in colorectal tumours. Fagin [18] advanced that a similar mechanism, also involving *RAS*, might cause aneuploidy in follicular thyroid tumours. This possibility has been recently supported by the finding of a significant relationship between H-*RAS* 81T→C polymorphism, together with increased amount of p21 (which is the active form of *RAS*), and the occurrence of aneuploidy in follicular adenomas and follicular carcinomas (P. Castro et al., unpublished data).

The available evidence suggests there are at least two main pathways for thyroid follicular carcinogenesis: one, characterised by gross aneuploidy and a foetal-like growth pattern, displaying prominent chromosomal gains, and the other, occurring in lesions with a "common" follicular growth pattern and a diploid or near-diploid DNA content, displaying frequent chromosomal losses [4].

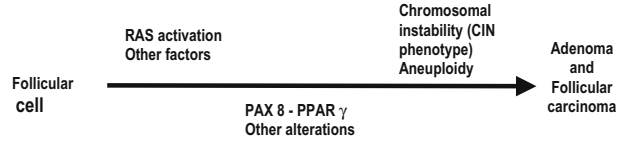
The aneuploid pattern and the various molecular alterations detected in follicular adenomas and follicular carcinomas support the assumption that the development of such tumours is the end product of multiple oncogenic steps, thus justifying their usual appearance as single (unicentric) neoplasms.

RAS mutations are frequently detected in follicular adenomas and follicular carcinomas and do not provide any useful information from the diagnostic standpoint [40]. In most cases, N-*RAS* and, less often, H-*RAS* are mutated in codon 61 (and less often in codons 12 and 13) [23, 45]. In some studies, it was advanced that *RAS* mutations carried a guarded prognosis, but such results have not been confirmed in most series, namely when the analyses were restricted to well-differentiated carcinomas, with the exclusion of poorly differentiated and undifferentiated carcinomas [23, 44].

In 2000, Kroll et al. [28] reported the frequent occurrence in follicular carcinomas of the *PAX8–PPARγ* rearrangement, thus creating a sort of mirror image for follicular tumours of the well-known *RET/PTC* and *TRK* rearrangements of papillary carcinomas [19].

Initially, it was claimed that the *PAX8–PPARγ* translocation was exclusively detected in follicular carcinoma and thus could be considered as a sign of malignancy [28]. This concept was disproved in several studies that showed the presence of the translocation in a number of follicular adenomas [10, 15, 32, 42].

The most important molecular features of follicular cell tumorigenesis (follicular adenoma and follicular carcinoma) are summarised in the following scheme:



Regardless of the advances at the molecular level, the diagnosis of follicular carcinomas rests on the identification of signs of invasion, namely of vascular invasion at the tumour capsule [14, 49]. Besides the classic categories of minimally invasive and widely invasive follicular carcinoma, it is crucial to identify the vascular invasive tumours and, whenever possible, to quantify the type and number of vessels invaded [14, 49].

Papillary carcinoma

At variance with follicular carcinoma, almost every PTC is diploid or quasi-diploid [24, 25]. Furthermore, PTCs display microsatellite stability [56]. Taking these facts together with the tendency of PTC to occur as multicentric neoplasms, which are clonally independent from each other [37, 54], it is tempting to advance that PTC tumorigenesis reflects the end product of (very) few oncogenic steps.

The major role played by *RET/PTC* and *TRK* rearrangements in the etiopathogenesis of PTC has been known for a while (for a thorough review, see Santoro et al. [51]). The prevalence of the different types of *RET/PTC* rearrangements is not the same in the different variants of PTC—e.g. *RET/PTC1* is particularly prevalent in conventional PTC and in some prominent papillary PTC variants, whereas *RET/PTC3* is more prevalent in the follicular/solid variant of PTC [41]. The overall prevalence of *RET/PTC* rearrangement varies greatly from series to series, depending on geographic factors and radiation exposure [41, 51]. Three other genetic and/or epigenetic alterations play a role in PTC pathogenesis: activating mutation of *RAS* genes, despite its much lower frequency than in follicular tumours [40, 44, 59], c-met overexpression [52] and downregulation of E-cadherin in PTC [47, 57].

Recently, another major player in PTC etiopathogenesis has been reported: the *BRAF* gene. The results on record show that, after melanoma, PTC is the human cancer displaying the highest prevalence of *BRAF* mutations, which occur almost always in the same hot spot (V600E) [12, 27, 59]. This mutation consists in a transversion from thymine to adenine in position 1799, leading to the substitution of a valine by a glutamate in codon 600. The V600E mutation is quasi-restricted to PTC with a conventional (papillary or mixed follicular–papillary) growth pattern and is particularly prevalent in PTCs with a prominent papillary structure, as is the case for tall cell variant and Warthin-like PTC [65, 67]. The prevalence of the *BRAF* mutation is also strongly associated with age, being rarely detected in young patients both in the post-Chernobyl setting and in sporadic cases occurring in western Europe [30].

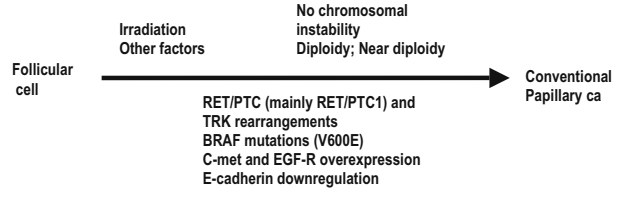
The finding of a high prevalence of *BRAF* mutations, together with the involvement of *RAS* mutations and *RET/PTC* rearrangements in the majority of PTCs, points to the crucial role played by alterations at the RET/RAS/BRAF/MAPK signal transduction pathway in the etiopathogenesis of PTC. The three mutation groups (*RET*, *RAS* and *BRAF*) appear to be functionally similar and mutually exclusive [27, 59]. Despite the large amount of new molecular data,

the etiology of PTC remains to be fully clarified (for example, there is evidence to support that *RET/PTC* rearrangements are among the earliest initiating events in PTC, but one still ignores the timing of *BRAF* mutations in PTC oncogenesis) [30].

The prognostic significance of $BRAF^{V600E}$ mutation remains controversial. Some groups claimed mutated cases carry a worse prognosis [39], whereas in our hands, mutated *BRAF* PTCs do not display worse pathologic features than wild-type *BRAF* PTC [65]. As a matter of fact, PTCs with $BRAF^{V600E}$ mutation were less often multicentric and less vascular invasive than non-mutated PTCs [65]. Large series with longer follow-up are necessary to clarify the putative prognostic meaning of the $BRAF^{V600E}$ mutation in PTC.

At variance with *RET/PTC*, which is not detected in poorly differentiated and undifferentiated carcinomas [51, 57, 64], $BRAF^{V600E}$ mutation is detected in about one third of poorly differentiated carcinomas and undifferentiated (anaplastic) carcinomas, mainly in those tumours that appear to have arisen from pre-existing PTCs [43, 58].

The most important molecular features of PTC tumorigenesis are summarised in the following scheme:



Despite all these molecular data, the diagnosis of PTC still depends on the identification of the typical nuclei: large, irregular, clear, grooved, occasionally displaying pseudoinclusions. The differential diagnosis is particularly difficult in the field of encapsulated follicular patterned lesions that may correspond to follicular adenoma, follicular carcinoma or follicular variant of PTC (FVPTC; see below) [31].

Follicular variant of papillary carcinoma

In contrast to the high prevalence of the V600E mutation in conventional PTC, a distinct *BRAF* mutation (K601E) has been detected in 9% of cases of FVPTC [67]. The $BRAF^{K601E}$ mutation has also been detected in two follicular adenomas of the thyroid [30, 59], but one cannot exclude the possibility that such $BRAF^{K601E}$ mutated lesions might represent misdiagnosed cases of FVPTC. Leaving this controversy aside, we think we have obtained enough evidence, after having searched for *BRAF* mutations in several hundreds of thyroid tumours and tumour-like lesions, to conclude that the $BRAF^{K601E}$ mutation is typical of FVPTC although much less frequent (about 7%) than the $BRAF^{V600E}$ in conventional PTC (46–75%) [65].

The 1802A–G transition leading to the substitution of a lysine by a glutamate in codon 601 ($BRAF^{K601E}$) that is detected in the FVPTC mimics the $BRAF^{V600E}$ mutation found in conventional PTC. Both types of mutation affect the activation segment of the protein, particularly the two adjacent residues (V600 and K601) that are localised between two major phosphoregulatory residues (T599 and S602) [11]. It was shown that the two mutations have high kinase activity in vitro [13, 68] and that the $BRAF^{V600E}$ has about 2.5× the kinase activity of $BRAF^{K601E}$ [68]. $BRAF^{V600E}$ and $BRAF^{K601E}$ mutations incorporate a negatively charged amino acid (glutamate) into the activation segment of *BRAF*; it was advanced that such glutamate may mimic the activating phosphorylation of T599 and/or S602 [13]. With so many similarities, the apparent specificity of the mutations vis-à-vis the PTC histotypes remains unexplained. Interestingly, in a microfollicular/solid variant of PTC, we have recently described [66], there was an in-frame triplet deletion of *BRAF* leading, again, to the replacement of a valine and a lysine by a glutamate in the same *BRAF* activation segment (*BRAF VK600-601E*) [66].

Besides the type of *BRAF* mutation, there are other molecular features of FVPTC that differ from those of conventional PTC. Some of those features resemble the molecular alterations that are thought to be characteristic of follicular carcinoma.

E-cadherin immunoexpression in FVPTC resembles that of follicular carcinoma (and normal thyroid) rather than that of conventional PTC [47, 55]. The same holds true regarding some cytogenetic alterations, namely gains at chromosome arms 2q, 4q, 5q, 6q, 8q and 13q and deletions at 1p, 9q, 16q, 17q, 19q and 22q and the 2;3 translocation [5, 48, 69, P. Castro et al., unpublished data].

The frequency of *RAS* mutations is much higher in FVPTC than in conventional PTC [70], thus contributing to approach the FVPTC to follicular carcinoma. We have recently confirmed the results of Zhu et al. with regard to the high prevalence of *RAS* mutations in FVPTC (P. Castro et al., unpublished data). We have found, furthermore, similar prevalence of *RAS* mutations [in most cases, in codon 61 of N-*RAS*] in follicular adenoma (33%), follicular carcinoma (22%) and FVPTC (25%) (P. Castro et al., unpublished data).

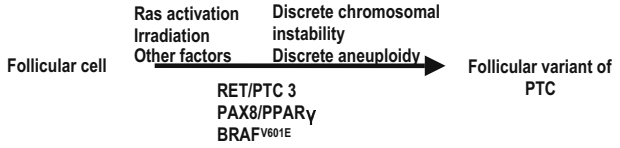
Finally, Roque et al. described in 2001, using conventional cytogenetics, the t(2;3)(q12;p25) in one case of FVPTC [48], and Wreesmann et al. [69], using immunohistochemistry, demonstrated in 2004 the overexpression of PPARγ in three cases; in one of these cases, the presence of rearranged *PPARγ* was detected by Southern blot [69]. After having detected in a small preliminary study the presence of the *PAX8–PPARγ* rearrangement in some cases of FVPTC [6], we confirmed such findings in a large series: the *PAX8–PPARγ* rearrangement was detected in 38% of the cases of FVPTC, in 33% of follicular adenomas, in 45% of follicular carcinomas and in no case of conventional PTC (P. Castro et al., unpublished data).

At variance with the rarity of the coexistence of *RAS* mutations and *PAX8–PPARγ* rearrangement in follicular tumours reported by Nikiforova et al. [44], we detected both alterations in 13% of the cases of FVPTC, as well as in 14% of follicular carcinomas and in 8% of follicular adenomas (P. Castro et al., unpublished data). The presence of both alterations was significantly associated with the younger

age of the patients, favouring the concept that such coexistence may lead to more rapidly growing tumours.

Taken together, all the aforementioned data support the conclusion that FVPTC shows genetic differences from conventional PTC and suggest that at least a subset of FVPTC shares some of the molecular features of follicular carcinomas.

The most important molecular features of FVPTC are summarised in the following scheme:



FVPTC cases, like most conventional PTCs, are slowly growing neoplasms that tend to give rise to lymph node metastases [3, 8, 50]. In 1985, Carcangiu et al. [3] pointed out that, differently from conventional PTC, some FVPTC cases were prone to give rise to lung metastases. It was observed, moreover, that the growth pattern of the encapsulated form of FVPTC mimicked that of follicular carcinomas, pushing borders and signs of capsular and/or vascular invasion [4, 8, 50]. Baloch and LiVolsi [2] showed that these encapsulated FVPTCs may give rise to blood-borne metastases in the absence of lymph node metastases.

We still ignore the putative prognostic meaning of the molecular alterations detected in FVPTC (*BRAF*^{K601E} mutation, *RAS* mutations and *PAX8–PPARγ* rearrangements). It remains also to be seen if the subset of FVPTC displaying genetic alterations of the follicular carcinoma-type encompasses cases particularly prone to give rise to lung and/or bone metastases.

Oncocytic (Hürthle cell) tumours

Tumours with oncocytic (Hürthle cell) features may be benign (oncocytic variant of follicular adenoma) or malignant (oncocytic variant of papillary carcinoma and oncocytic variant of follicular carcinoma). Medullary and poorly differentiated carcinomas may also display oncocytic features [14, 35, 46, 60].

It is also well established that oncocytes (Hürthle cells) occur frequently in non-neoplastic conditions such as Hashimoto thyroiditis, nodular goiters and atrophic glands of old individuals [35, 60]. The same holds true for oncocytic transformation in tumours and non-neoplastic conditions of other organs such as the salivary glands, parathyroids, pituitary and kidneys.

Hürthle cells are stuffed with mitochondria with morphologic, functional and genetic abnormalities [35, 60, 61]. The accumulation of the mitochondria may be due to a primary alteration of the mitochondrial DNA (mtDNA) or of the nuclear DNA (nDNA) that encodes mitochondrial enzymes [33, 34, 38]. The most typical mtDNA alteration in oncocytic cells is the presence of a large deletion (about 5 kb, which corresponds to one third of the total DNA in each mitochondrial chromosome) [38]. This large deletion is usually designated by "common deletion" and has been detected in oncocytic cells of Hashimoto thyroiditis and all sorts of oncocytic tumours of the thyroid, as well as in Warthin tumour of the salivary glands [29, 34, 38]. Point mutations in the mitochondrial genes encoding for enzymes of the complexes I, III, IV and V of the mitochondrial respiratory chain (MRC) have also been reported in oncocytic tumours of the thyroid [34]. The mitochondria containing deleted and/or mutated mtDNA proliferate more than "normal" mitochondria, thus leading to a progressive increase in the percentage of abnormal mitochondria [35]. The mechanism of tumour formation under these circumstances is not yet well understood; however, several possibilities have been advanced: (a) The mitochondrial abnormalities block the apoptotic process, increasing the survival of the cells [29]. (b) The deficient mitochondrial function is sensed as a hypoxic stimulus leading to increased levels of the inducible form of the hypoxia inducible factor-1 (HIF-1), which triggers some pro-angiogenesis pathways (and also proliferation?). (For a review on these two possibilities, see Ref. [16].)

Regardless of the mechanism(s) involved in the process, a deficient mitochondrial function leads to an increased number of mitochondria through the stimulation of mitochondrial proliferation [16, 34–36, 60].

The oncocytic variant of PTC has papillary carcinomas that have *RET/PTC* rearrangements and *BRAF* mutations with similar frequency as the non-oncocytic PTC [9, 65, 67]. With regard to the oncocytic variant of follicular tumours, it remains controversial whether or not such Hürthle cell tumours have similar prevalences of *RAS* mutations and *PAX8–PPARγ* rearrangements as their non-Hürthle cell counterparts [62, 63].

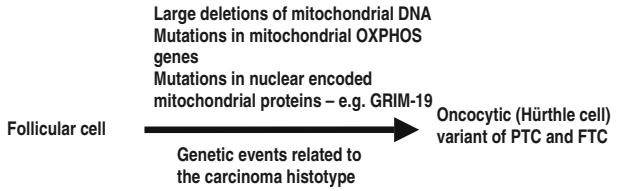
The molecular features of the oncocytic tumours of the thyroid are thus associated for one side with the mitochondrial abnormalities that are their hallmarks and, for the other, with the oncogenic alterations that are associated with the carcinoma histotype (e.g. *RET/PTC* rearrangements and *BRAF* mutations in PTC) [9, 33, 67].

The presence of abundant (and abnormal) mitochondria in the cytoplasm of the neoplastic cells may be seen throughout the entire tumour ("primary" oxyphilia, indicating that the carcinogenic hit has occurred in cells with abnormalities of the mtDNA or mitochondrial abnormalities resulting from the nDNA encoding mitochondrial enzymes) or just in some parts of the tumour ("secondary" oxyphilia, indicating that the mitochondrial abnormalities have occurred after tumour development) [1, 34, 35].

The familial forms of benign and malignant Hürthle cell tumours [26] may be due to a germline mutation in *GRIM-19*, a dual-function nuclear gene involved in mitochondrial metabolism and cell death. Downregulation of *GRIM-19* has been shown to confer a growth advantage on cells and to reduce the likelihood that they will enter apoptosis [1]. The detection of a *RET/PTC1* rearrangement in one case of the oncocytic variant of PTC in which there was also a *GRIM-19* mutation suggests that the latter mutation may serve as a predisposing alteration for the occurrence of

tumours with cell oxyphilia; other alterations such as *RET/PTC* rearrangement or *BRAF* mutation may be necessary for the acquisition of the malignant phenotype (for a thorough review, see Ref. [33]).

The most important molecular features of oncocytic (Hürthle cell) tumours are summarised in the following scheme:



The criteria used in the diagnosis of the oncocytic variants of papillary carcinoma and follicular carcinoma are those used in the diagnosis of conventional tumours, i.e. mainly the nuclear characteristics in PTC and the signs of capsular and/or vascular invasion in follicular carcinoma. In other words, the presence of oncocytic cells should not interfere with the diagnostic criteria in any of the thyroid tumour settings. The prognosis of patients with the oncocytic variant of PTC is similar to that of patients with conventional PTC (and the same holds true regarding follicular carcinomas) provided the age of the patients and the staging of the tumours are comparable [17, 60]. From a clinical standpoint, the only negative aspect of oncocytic carcinomas of the thyroid is their lesser ability to trap iodine, thus rendering them less responsive to radioactive iodine [35, 60].

Acknowledgements We are grateful to Fundação para a Ciência e Tecnologia for grant support to Ana Preto, Ana Sofia Rocha, Patrícia Castro and Valdemar Máximo. This study was supported by Fundação para a Ciência e Tecnologia POCTI/FEDER (POCTI/NSE/48171/2002).

References

1. Angell J, Lindner D, Shapiro P, Hofmann E, Kalvakolanu D (2000) Identification of GRIM-19, a novel cell death-regulatory gene induced by the interferon- and retinoic acid combination, using a genetic approach. J Biol Chem 275:33416–33426
2. Baloch ZW, LiVolsi VA (2000) Encapsulated follicular variant of papillary thyroid carcinoma with bone metastases. Mod Pathol 13:861–865
3. Carcangiu M, Zampi G, Pupi A, Castagnoli A, Rosai J (1985) Papillary carcinoma of the thyroid. A clinicopathologic study of 241 cases treated at the University of Florence, Italy. Cancer 55:805–828
4. Castro P, Eknaes M, Teixeira MR, Danielsen HE, Soares P, Lothe RA, Sobrinho-Simoes M (2005) Adenomas and follicular carcinomas of the thyroid display two major patterns of chromosomal changes. J Pathol 206:305–311
5. Castro P, Fonseca E, Magalhaes J, Sobrinho-Simoes M (2002) Follicular, papillary, and "hybrid" carcinomas of the thyroid. Endocr Pathol 13:313–320
6. Castro P, Roque L, Magalhães J, Sobrinho-Simoes M (2005) A subset of follicular variant of papillary carcinoma harbors PAX8–PPARγ translocation. Int J Surg Pathol 206:305–311
7. Castro P, Sansonetty F, Soares P, Dias A, Sobrinho-Simoes M (2001) Fetal adenomas and minimally invasive follicular carcinomas of the thyroid frequently display a triploid or near triploid DNA pattern. Virchows Arch 438:336–342
8. Chem KY, Rosai J (1977) Follicular variant of thyroid papillary carcinoma: a clinicopathologic study of six cases. Am J Surg Pathol 1:123–130
9. Cheung CC, Ezzat S, Ramyar L, Freeman JL, Asa SL (2000) Molecular basis off Hurthle cell papillary thyroid carcinoma. J Clin Endocrinol Metab 85:878–882
10. Cheung L, Messina M, Gill A, Clarkson A, Learoyd D, Delbridge L, Wentworth J, Philips J, Clifton-Bligh R, Robinson BG (2003) Detection of the PAX8–PPAR gamma fusion oncogene in both follicular thyroid carcinomas and adenomas. J Clin Endocrinol Metab 88:354–357
11. Chong H, Lee J, Guan KL (2001) Positive and negative regulation of Raf kinase activity and function by phosphorylation. EMBO J 20:3716–3727
12. Cohen Y, Xing M, Mambo E, Guo Z, Wu G, Trink B, Beller U, Westra WH, Ladenson PW, Sidransky D (2003) BRAF mutation in papillary thyroid carcinoma. J Natl Cancer Inst 95:625–627
13. Davies H, Bignell GR, Cox C, Stephens P, Edkins S, Clegg S, Teague J, Woffendin H, Garnett MJ, Bottomley W, Davis N, Dicks E, Ewing R, Floyd Y, Gray K, Hall S, Hawes R, Hughes J, Kosmidou V, Menzies A, Mould C, Parker A, Stevens C, Watt S, Hooper S, Wilson R, Jayatilake H, Gusterson BA, Cooper C, Shipley J, Hargrave D, Pritchard-Jones K, Maitland N, Chenevix-Trench G, Riggins GJ, Bigner DD, Palmieri G, Cossu A, Flanagan A, Nicholson A, Ho JW, Leung SY, Yuen ST, Weber BL, Seigler HF, Darrow TL, Paterson H, Marais R, Marshall CJ, Wooster R, Stratton M, Futreal PA (2002) Mutations of the BRAF gene in human cancer. Nature 417:949–954
14. DeLellis RA, Lloyd RV, Heitz PU, Eng C (eds) (2004) World Health Organization classification of tumors. Pathology and genetics of tumours of endocrine organs. IARC Press, Lyon
15. Dwight T, Thoppe SR, Foukakis T, Lui WO, Wallin G, Hoog A, Frisk T, Larsson C, Zedenius J (2003) Involvement of the PAX8/peroxisome proliferator-activated receptor gamma rearrangement in follicular thyroid tumors. J Clin Endocrinol Metab 8:4440–4445
16. Eng C, Kiuru M, Fernandez MJ, Aaltonen LA (2003) A role for mitochondrial enzymes in inherited neoplasia and beyond. Nat Rev Cancer 3:193–202
17. Evans HL, Vassilopoulou-Sellin R (1998) Follicular and Hurthle cell carcinomas of the thyroid: a comparative study. Am J Surg Pathol 22:1512–1520
18. Fagin JA (2002) Minireview: branded from the start-distinct oncogenic initiating events may determine tumor fate in the thyroid. Mol Endocrinol 16:903–911
19. Frattini M, Ferrario C, Bressan P, Balestra D, De Cecco L, Mondellini P, Bongarzone I, Collini P, Gariboldi M, Pilotti S, Pierotti MA, Greco A (2004) Alternative mutations of BRAF, RET and NTRK1 are associated with similar but distinct gene expression patterns in papillary thyroid cancer. Oncogene 23:7436–7440
20. Giaretti W, Molinu S, Ceccarelli J, Prevosto C (2004) Chromosomal instability, aneuploidy, and gene mutations in human sporadic colorectal adenomas. Cell Oncol 26:301–305
21. Giaretti W, Pujic N, Rapallo A, Nigro S, Di Vinci A, Geido E, Risio M (1995) K-ras-2 G–C and G–T transversions correlate with DNA aneuploidy in colorectal adenomas. Gastroenterology 108:1040–1047
22. Giaretti W, Rapallo A, Geido E, Sciutto A, Merlo F, Risio M, Rossini FP (1998) Specific K-ras2 mutations in human sporadic colorectal adenomas are associated with DNA near-diploid aneuploidy and inhibition of proliferation. Am J Pathol 153:1201–1209
23. Hara H, Fulton N, Yashiro T, Ito K, DeGroot LJ, Kaplan EL (1994) N-ras mutation: an independent prognostic factor for aggressiveness of papillary thyroid carcinoma. Surgery 116:1010–1016

24. Johannessen JV, Sobrinho-Simões M, Tangen KO (1982) The diagnostic value of flow cytometric DNA measurements in selected disorders of the human thyroid. Am J Clin Pathol 77:20–25
25. Johannessen JV, Sobrinho-Simoes M, Tangen KO, Lindmo T (1981) A flow cytometric deoxyribonucleic acid analysis of papillary thyroid carcinoma. Lab Invest 45:336–341
26. Katoh R, Harach HR, Williams ED (1998) Solitary, multiple, and familial oxyphil tumours of the thyroid gland. J Pathol 186:292–299
27. Kimura ET, Nikiforova MN, Zhu Z, Knauf JA, Nikiforov YE, Fagin JA (2003) High prevalence of BRAF mutations in thyroid cancer: genetic evidence for constitutive activation of the RET/PTC–RAS–BRAF signaling pathway in papillary thyroid carcinoma. Cancer Res 63:1454–1457
28. Kroll TG, Sarraf P, Pecciarini L, Chen CJ, Mueller E, Spiegelman BM, Fletcher JA (2000) PAX8–PPARgamma1 fusion oncogene in human thyroid carcinoma. Science 289:1357–1360
29. Lewis PD, Baxter P, Griffiths AP, Parry JM, Skibinski DOF (2000) Detection of damage to the mitochondrial genome in the oncocytic cells of Warthins tumour. J Pathol 191:274–281
30. Lima J, Trovisco V, Soares P, Maximo V, Magalhaes J, Salvatore G, Santoro M, Bogdanova T, Tronko M, Abrosimov A, Jeremiah S, Thomas G, Williams D, Sobrinho-Simoes M (2004) BRAF mutations are not a major event in post-Chernobyl childhood thyroid carcinomas. J Clin Endocrinol Metab 89:4267–4271
31. Lloyd RV, Erickson LA, Casey MB, Lam KY, Lohse CM, Asa SL, Chan JK, DeLellis RA, Harach HR, Kakudo K, LiVolsi VA, Rosai J, Sebo TJ, Sobrinho-Simoes M, Wenig BM, Lae ME (2004) Observer variation in the diagnosis of follicular variant of papillary thyroid carcinoma. Am J Surg Pathol 28:1336–1340
32. Marques AR, Espadinha C, Catarino AL, Moniz S, Pereira T, Sobrinho LG, Leite V (2002) Expression of PAX8–PPAR gamma 1 rearrangements in both follicular thyroid carcinomas and adenomas. J Clin Endocrinol Metab 87:3947–3952
33. Máximo V, Botelho T, Capela J, Soares P, Lima J, Taveira A, Amaro T, Barbosa A, Preto A, Harach H, Williams D, Sobrinho-Simões M (2005) Somatic and germline mutation in GRIM-19, a dual function gene involved in mitochondrial metabolism and cell death, is linked to mitochondrion-rich (Hürthle cell) tumours of the thyroid. Br J Cancer 92:1892–1898
34. Máximo V, Soares P, Lima J, Cameselle-Teijeiro J, Sobrinho-Simões M (2002) Mitochondrial DNA somatic mutations (point mutations and large deletions) and mitochondrial DNA variants in human thyroid pathology. A study with emphasis on Hürthle cell tumors. Am J Pathol 160:1857–1865
35. Máximo V, Sobrinho-Simões M (2000) Hürthle cell tumours of the thyroid. A review with emphasis on mitochondrial abnormalities with clinical relevance. Virchows Arch 437:107–115
36. Maximo V, Sobrinho-Simoes M (2000) Mitochondrial DNA 'common' deletion in Hürthle cell lesions of the thyroid. J Pathol 192:561–562
37. Moniz S, Catarino AL, Marques AR, Cavaco B, Sobrinho L, Leite V (2002) Clonal origin of non-medullary thyroid tumours assessed by non-random X-chromosome inactivation. Eur J Endocrinol 146:27–33
38. Muller-Hocker J, Jacob U, Seibel P (1998) Hashimoto thyroiditis is associated with defects of cytochrome-c oxidase in oxyphil Askanazy cells and with the common deletion (4,977) of mitochondrial DNA. Ultrastruct Pathol 22:91–100
39. Namba H, Nakashima M, Hayashi T, Hayashida N, Maeda S, Rogounovitch TI, Ohtsuru A, Saenko VA, Kanematsu T, Yamashita S (2003) Clinical implication of hot spot BRAF mutation, V599E, in papillary thyroid cancers. J Clin Endocrinol Metab 88:4393–4397
40. Namba H, Rubin SA, Fagin JA (1990) Point mutations of ras oncogenes are an early event in thyroid tumorigenesis. Mol Endocrinol 4:1474–1479
41. Nikiforov YE (2002) RET/PTC rearrangement in thyroid tumors. Endocr Pathol 13:3–16
42. Nikiforova MN, Biddinger PW, Caudill CM, Kroll TG, Nikiforov YE (2002) PAX8–PPARgamma rearrangement in thyroid tumors: RT-PCR and immunohistochemical analyses. Am J Surg Pathol 26:1016–1023
43. Nikiforova MN, Kimura ET, Gandhi M, Biddinger PW, Knauf JA, Basolo F, Zhu Z, Giannini R, Salvatore G, Fusco A, Santoro M, Fagin JA, Nikiforov YE (2003) BRAF mutations in thyroid tumors are restricted to papillary carcinomas and anaplastic or poorly differentiated carcinomas arising from papillary carcinomas. J Clin Endocrinol Metab 88:5399–53404
44. Nikiforova MN, Lynch RA, Biddinger PW, Alexander EK, Dorn GW II, Tallini G, Kroll TG, Nikiforov YE (2003) RAS point mutations and PAX8–PPAR gamma rearrangement in thyroid tumors: evidence for distinct molecular pathways in thyroid follicular carcinoma. J Clin Endocrinol Metab 88:2318–2326
45. Oyama T, Suzuki T, Hara F, Iino Y, Ishida T, Sakamoto A, Nakajima T (1995) N-ras mutation of thyroid tumor with special reference to the follicular type. Pathol Int 45:45–50
46. Papotti M, Botto Micca F, Favero A, Palestini N, Bussolati G (1993) Poorly differentiated thyroid carcinomas with primordial cell component. A group of aggressive lesions sharing insular, trabecular, and solid patterns. Am J Surg Pathol 17:291–301
47. Rocha AS, Soares P, Seruca R, Máximo V, Matias-Guiu X, Cameselle-Teijero J, Sobrinho-Simões M (2001) Abnormalities of E-cadherin/catenin complex in classical papillary thyroid carcinoma and its diffuse sclerosing variant. J Pathol 194:358–366
48. Roque L, Nunes VM, Ribeiro C, Martins C, Soares J (2001) Karyotypic characterization of papillary thyroid carcinomas. Cancer 92:2529–2538
49. Rosai J, Carcangiu ML, DeLellis RA (1993) Tumors of the thyroid gland. Atlas of tumor pathology, 3rd series, fascicle 5. Armed Forces Institute of Pathology, Washington, DC
50. Rosai J, Zampi G, Carcangiu ML (1983) Papillary carcinoma of the thyroid A discussion of its several morphologic expressions, with particular emphasis on the follicular variant. Am J Surg Pathol 7:809–817
51. Santoro M, Carlomagno F, Hay ID, Herrmann MA, Grieco M, Melillo R, Pierotti MA, Bongarzone I, Della Porta G, Berger N (1992) Ret oncogene activation in human thyroid neoplasms is restricted to the papillary cancer subtype. J Clin Invest 89:1517–1522
52. Scarpino S, Cancellario d'Alena F, Di Napoli A, Pasquini A, Marzullo A, Ruco LP (2004) Increased expression of Met protein is associated with up-regulation of hypoxia inducible factor-1 (HIF-1) in tumour cells in papillary carcinoma of the thyroid. J Pathol 202:352–358
53. Schelfhout LJ, Cornelisse CJ, Goslings BM, Hamming JF, Kuipers-Dijkshoorn NJ, van de Velde CJ, Leuren GJ (1990) Frequency and degree of aneuploidy in benign and malignant thyroid neoplasms. Int J Cancer 45:16–20
54. Shattuck TM, Westra WH, Ladenson PW, Arnold A (2005) Independent clonal origins of distinct tumor foci in multifocal papillary thyroid carcinoma. N Engl J Med 352:2406–2412
55. Soares P, Berx G, van Roy F, Sobrinho-Simoes M (1997) E-cadherin gene alterations are rare events in thyroid tumors. Int J Cancer 70:32–38
56. Soares P, dos Santos NR, Seruca R, Lothe RA, Sobrinho-Simoes M (1997) Benign and malignant thyroid lesions show instability at microsatellite loci. Eur J Cancer 33:293–296
57. Soares P, Fonseca E, Wynford-Thomas D, Sobrinho-Simoes M (1998) Sporadic ret-rearranged papillary carcinoma of the thyroid: a subset of slow growing, less aggressive thyroid neoplasms? J Pathol 185:71–78
58. Soares P, Trovisco V, Rocha AS, Feijao T, Rebocho AP, Fonseca E, Vieira De Castro I, Cameselle-Teijeiro J, Cardoso-Oliveira M, Sobrinho-Simoes M (2004) BRAF mutations typical of papillary thyroid carcinoma are more frequently detected in undifferentiated than in insular and insular-like poorly differentiated carcinomas. Virchows Arch 44:572–576

59. Soares P, Trovisco V, Rocha AS, Lima J, Castro P, Preto A, Maximo V, Botelho T, Seruca R, Sobrinho-Simoes M (2003) BRAF mutations and RET/PTC rearrangements are alternative events in the etiopathogenesis of PTC. Oncogene 22:4578–4580
60. Sobrinho-Simoes M, Maximo V, Vieira de Castro I, Fonseca E, Soares P, Garcia-Rostan G, Cardoso de Oliveira M (2005) Hurthle (oncocytic) cell tumors of thyroid: etiopathogenesis, diagnosis and clinical significance. Int J Surg Pathol 13:29–35
61. Sobrinho-Simoes MA, Nesland JM, Holm R, Sambade MC, Johannessen JV (1985) Hurthle cell and mitochondrion-rich papillary carcinomas of the thyroid gland: an ultrastructural and immunocytochemical study. Ultrastruct Pathol 8:131–142
62. Tallini G, Hsueh A, Liu S, Garcia-Rostan G, Speicher MR, Ward DC (1999) Frequent chromosomal DNA unbalance in thyroid oncocytic (Hurthle cell) neoplasms detected by comparative genomic hybridization. Lab Invest 79:547–555
63. Tallini G, Ladanyi M, Rosai J, Jhanwar SC (1994) Analysis of nuclear and mitochondrial DNA alterations in thyroid and renal oncocytic tumors. Cytogenet Cell Genet 66:253–259
64. Tallini G, Santoro M, Helie M, Carlomagno F, Salvatore G, Chiappetta G, Carcangiu ML, Fusco A (1998) RET/PTC oncogene activation defines a subset of papillary thyroid carcinomas lacking evidence of progression to poorly differentiated or undifferentiated tumor phenotypes. Clin Cancer Res 4:287–294
65. Trovisco V, Soares P, Preto A, Vieira de Castro I, Lima J, Castro P, Máximo V, Botelho T, Moreira S, Meireles AM, Magalhães J, Abrosimov A, Cameselle-Teijeiro J, Sobrinho-Simões M (2005) Type and prevalence of BRAF mutations are closely associated to papillary thyroid carcinoma histotype and patients' age but not with tumour aggressiveness. Virchows Arch 446:589–595
66. Trovisco V, Soares P, Soares R, Magalhães J, Sá-Couto P, Sobrinho-Simões M (2005) A new BRAF gene mutation detected in a case of a solid variant of papillary thyroid carcinoma. Hum Pathol 36:694–697
67. Trovisco V, Vieira de Castro I, Soares P, Maximo V, Silva P, Magalhaes J, Abrosimov A, Guiu XM, Sobrinho-Simoes M (2004) BRAF mutations are associated with some histological types of papillary thyroid carcinoma. J Pathol 202:247–251
68. Wan PT, Garnett MJ, Roe SM, Lee S, Niculescu-Duvaz D, Good VM, Jones CM, Marshall CJ, Springer CJ, Barford D, Marais R (2004) Mechanism of activation of the RAF–ERK signaling pathway by oncogenic mutations of B-RAF. Cell 116:855–867
69. Wreesmann VB, Ghossein RA, Hezel M, Banerjee D, Shaha AR, Tuttle RM, Shah JP, Rao PH, Singh B (2004) Follicular variant of papillary thyroid carcinoma: genome-wide appraisal of a controversial entity. Genes Chromosomes Cancer 40:355–364
70. Zhu Z, Gandhi M, Nikiforova MN, Fischer AH, Nikiforov YE (2003) Molecular profile and clinical–pathologic features of the follicular variant of papillary thyroid carcinoma. An unusually high prevalence of ras mutations. Am J Clin Pathol 120:71–77

Virchows Arch (2005) 447: 794–799
DOI 10.1007/s00428-005-0039-7

ORIGINAL ARTICLE

Toru Furukawa · Günter Klöppel · N. Volkan Adsay · Jorge Albores-Saavedra · Noriyoshi Fukushima · Akira Horii · Ralph H. Hruban · Yo Kato · David S. Klimstra · Daniel S. Longnecker · Jutta Lüttges · G. Johan A. Offerhaus · Michio Shimizu · Makoto Sunamura · Arief Suriawinata · Kyoichi Takaori · Suguru Yonezawa

Classification of types of intraductal papillary-mucinous neoplasm of the pancreas: a consensus study

Received: 17 May 2005 / Accepted: 24 June 2005 / Published online: 9 August 2005
© Springer-Verlag 2005

Abstract Now that more than two decades have passed since the first reports of intraductal papillary-mucinous neoplasms (IPMNs), it has become clear that IPMN consists of a spectrum of neoplasms with both morphological and immunohistochemical variations. At a meeting of international experts on pancreatic precursor lesions held in 2003, it was agreed that a consensus classification of IPMN subtypes should be established to enable a more detailed analysis of the clinicopathological significance of the variations. Based on our experience and on information from the literature, we selected representative histological examples of IPMNs and defined a consensus nomenclature and criteria for classifying variants as distinctive IPMN subtypes including gastric type, intestinal type, pancreato-

This work was supported in part by a Grant-in-Aid from the Ministry of Education, Culture, Sports, Science and Technology of Japan, the Pancreas Research Foundation of Japan, the Gonryo Medical Foundation, and NIH SPORE (Specialized Programs of Research Excellence) in Gastrointestinal Cancer Grant CA62924.

T. Furukawa (✉) · A. Horii
Department of Molecular Pathology,
Tohoku University School of Medicine,
2-1 Seiryomachi, Aoba-ku,
Sendai, 980-8575, Japan
e-mail: furukawa@mail.tains.tohoku.ac.jp
Tel.: +81-22-7178043
Fax: +81-22-7178047

G. Klöppel · J. Lüttges
Department of Pathology, University of Kiel,
Kiel, Germany

N. Volkan Adsay
Department of Pathology, Wayne State University,
Detroit, MI, USA

J. Albores-Saavedra
Department of Pathology, LSU Health Sciences Center,
Shreveport, LA, USA

N. Fukushima
Department of Pathology, Tokyo Medical College,
Tokyo, Japan

R. H. Hruban
Departments of Pathology and Oncology,
The Sol Goldman Pancreatic Cancer Research Center,
The Johns Hopkins Medical Institutions,
Baltimore, MD, USA

Y. Kato
Department of Pathology, Cancer Institute,
Japanese Foundation for Cancer Research,
Tokyo, Japan

D. S. Klimstra
Department of Pathology,
Memorial Sloan-Kettering Cancer Center,
New York, NY, USA

D. S. Longnecker · A. Suriawinata
Department of Pathology,
Dartmouth-Hitchcock Medical Center,
Lebanon, NH, USA

G. J. A. Offerhaus
Department of Pathology,
Academic Medical Center,
Amsterdam, The Netherlands

M. Shimizu
Department of Pathology,
Saitama Medical School,
Saitama, Japan

M. Sunamura
Department of Gastroenterological Surgery,
Tohoku University School of Medicine,
Sendai, Japan

K. Takaori
Department of General and Gastroenterological Surgery,
Osaka Medical College,
Osaka, Japan

S. Yonezawa
Department of Human Pathology, Field of Oncology,
Kagoshima University Graduate School of
Medical and Dental Sciences,
Kagoshima, Japan

biliary type, and oncocytic type. These definitions can be used for further analyses of the clinicopathological significance of the variations of IPMN.

Keywords Pancreatic tumor · Intraductal papillary-mucinous neoplasm · Classification · MUC

Introduction

The first cases of intraductal papillary-mucinous neoplasm (IPMN) were reported in the 1970s and 1980s [17, 23]. In the 1990s, the term IPMN was coined, and the tumor was established as a special entity among the pancreatic neoplasms [25]. It was also found that IPMN is related to invasive pancreatic adenocarcinoma because one third of IPMNs have an associated invasive adenocarcinoma and some patients with a noninvasive IPMN subsequently develop either invasive colloid (mucinous noncystic) carcinoma or invasive ductal adenocarcinoma [5, 9, 10]. During the more than two decades that have passed since its first description, a number of reports have been published, and it has become clear that IPMNs include a spectrum of neoplasms with both morphological and immunohistochemical variations. These variations include neoplasms with tall columnar cells arranged in relatively short papillae without significant atypia, those with villous projections lined by cells with significant atypia, those with complex branching papillae containing cells with marked atypia, and those with oncocytic cells with complex papillae [2, 4, 8, 22, 30]. Several authors have proposed classification systems for the spectrum of morphologies seen in IPMNs [4, 8, 22, 30]. One such system divides IPMNs into clear-, dark-, and compact-cell types according to the density of the cytoplasm, shapes of the epithelial cells, and expression patterns of glycoproteins contained in mucin (MUCs), while another system separates IPMNs into intestinal, pancreatobiliary, and oncocytic subtypes primarily based on their architecture and cytology [4, 22, 30].

At a meeting of international experts on pancreatic precursor lesions held at the Johns Hopkins Hospital from August 18 to 19, 2003, a basic definition of an IPMN that is employed in the current study (Table 1) was worked out, and it was agreed that a consensus classification of IPMN subtypes should be established to make it easier to compare studies from different institutions and to improve patient care [14]. The purpose of this report is to establish consensus criteria for the classification of IPMN subtypes based on histological features and immunohistochemical reactivities with antibodies to specific types of mucin (MUCs).

Table 1 Definition of intraductal papillary-mucinous neoplasm of the pancreas [14]

Intraductal papillary mucinous neoplasm is a grossly visible, noninvasive, mucin-producing, predominantly papillary or rarely flat epithelial neoplasm arising from the main pancreatic duct or branch ducts, with varying degrees of duct dilatation. IPMNs usually produce a lesion greater than 1 cm in diameter and include a variety of cell types with a spectrum of cytologic and architectural atypia.

Materials and methods

Review of slides

Representative slides of candidate subtypes of IPMNs were selected from the pathology files of Tohoku University Hospital. They were chosen so as to represent a broad spectrum of the morphological variations of IPMN, based on discussions at the Baltimore meeting and including information from the literature and personal communications. The slide set consisted of ten cases. Each case consisted of four slides, one stained with hematoxylin and eosin and one each labeled for MUC1, MUC2, and MUC5AC. The slides were reviewed by the authors independently and subsequently discussed at an international meeting in Sendai, Japan (July 2004). The goal of this meeting was to establish an international consensus on the classification of IPMNs.

Immunohistochemistry

The primary antibodies employed were a monoclonal antibody to MUC1-core (clone Ma552, Novocastra Laboratories Ltd., Newcastle upon Tyne, UK, 1:100), a monoclonal antibody to MUC2 (clone Ccp58, Santa Cruz Biotechnology Inc., Santa Cruz, CA, USA, 1:600), and a monoclonal antibody to MUC5AC (clone CLH2, Chemicon International Inc., Temecula, CA, USA, 1:1000). Paraffin sections cut at 4 μm were dewaxed with xylene and hydrated with serial immersing in 100, 90, 70, and 50% ethanol solutions and distilled water. Antigen retrieval was performed by incubating slides in boiled citric acid buffer (0.18 mM citric acid, 0.82 mM sodium citrate) for 15 min in a microwave oven. Indirect immunohistochemical labeling was performed as follows: The slides were incubated with PBS containing 0.3% hydrogen peroxide for 30 min to block the endogenous peroxidase activity. After washing with PBS, the slides were incubated with the primary antibody diluted in PBS containing 10% rabbit serum at 4°C overnight. After washing with PBS, the slides were incubated with the biotinylated rabbit anti-mouse IgG antibody solution (Nichirei, Tokyo, Japan) for 30 min at room temperature. The slides were then washed with PBS and incubated with streptavidin-horseradish peroxidase solution (Nichirei) for 30 min at room temperature. After washing with PBS, the slides were incubated with 3, 3′-diaminobenzidine tetrahydrochloride (DAB) diluted in PBS containing 0.05% hydrogen peroxide at a final concentration in 0.2 mg/ml. The slides were washed with running tap water and counterstained with hematoxylin.

Table 2 Consensus nomenclature and criteria for classification of features of four types of intraductal papillary-mucinous neoplasm of the pancreas

Type	Mimicker	Criteria	Atypia	MUC1	MUC2	MUC5AC
Gastric	Gastric foveolae	Thick finger-like papillae, eosinophilic > basophilic cytoplasm, basally located nuclei. This type may have abundant flat areas	Mild/ low-grade	−	−	+
Intestinal	Intestinal villous neoplasm	Villous papillae, basophilic > eosinophilic cytoplasm, enlarged oval and hyperchromatic nuclei with pseudostratification. This type may show low papillae consisting of cells with amphophilic cytoplasm	Moderate or severe/ high-grade	−	+	+
Pancreatobiliary	Cholangiopapillary neoplasm	Thin branching complex papillae, moderate amphophilic cytoplasm, enlarged hyperchromatic nuclei	Severe/ high-grade	+	−	+
Oncocytic	Oncocytic neoplasm	Thick branching complex papillae with intracellular and intraepithelial lumina, abundant eosinophilic (oncocytic) cytoplasm, large round nuclei with prominent nucleoli	Severe/ high-grade	+	−	+

Results

All participants agreed that the IPMN cases provided covered representative histological variations of IPMN and that they can be subclassified into four types. In the following, the consensus criteria for the classification of IPMN subtypes based on morphological features and the immunohistochemical reactivity for MUCs (Table 2) are presented.

The gastric-type IPMN consisted of cells resembling gastric foveolae and usually showed low-grade atypia corresponding to a diagnosis of intraductal papillary-mucin-

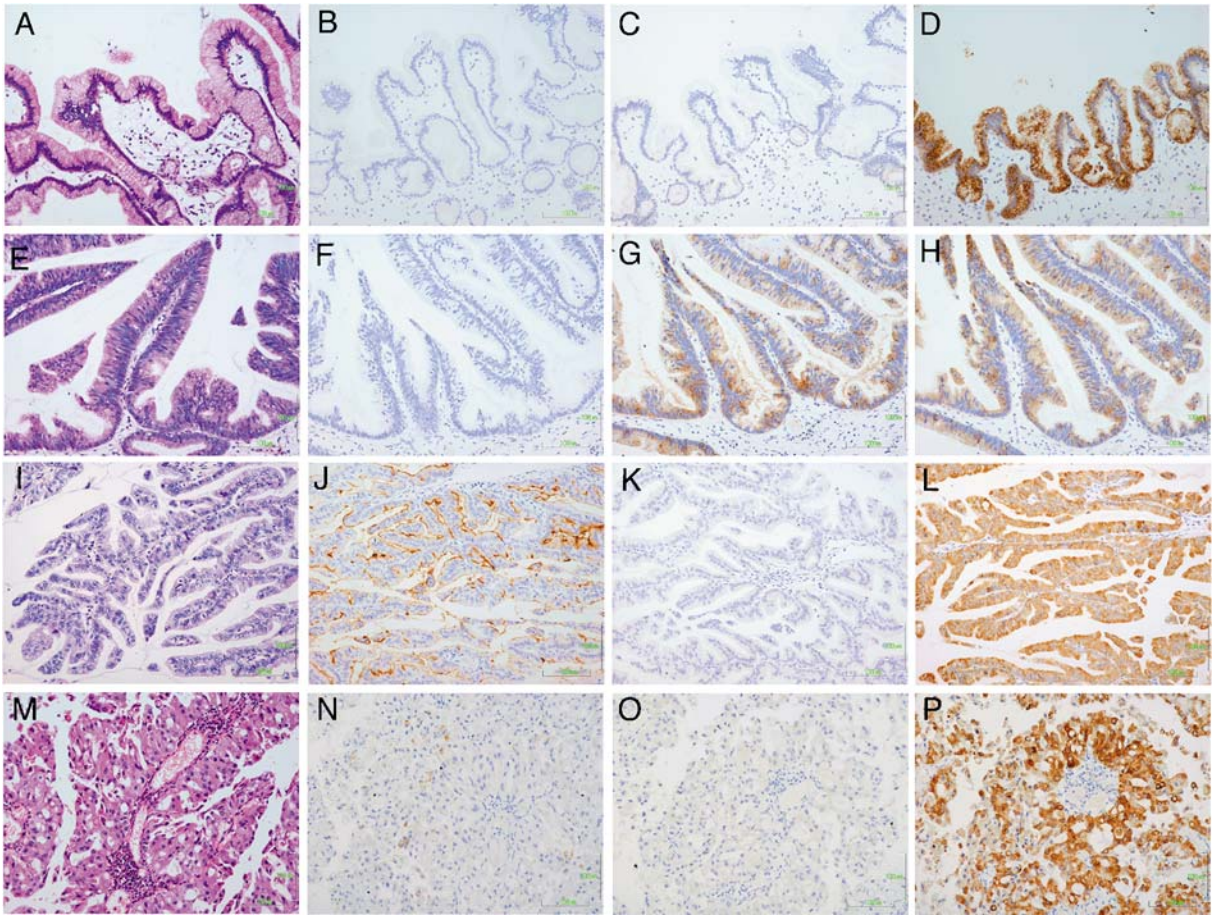


Fig. 1 Representative images of the subtypes of intraductal papillary-mucinous neoplasm of the pancreas. **a–d** The gastric type; **e–h** the intestinal type; **i–l** the pancreatobiliary type; **m–p** the oncocytic type. Hematoxylin and eosin staining (**a**, **e**, **i**, **m**) and immunohistochemical stainings of MUC1 (**b**, **f**, **j**, **n**), MUC2 (**c**, **g**, **k**, **o**), and MUC5AC (**d**, **h**, **l**, **p**)

ous adenoma (Fig. 1a). They expressed MUC5AC but were negative for MUC1 and for MUC2 (Fig. 1b–d). The gastric-type IPMN corresponded to the previously reported null type or the clear-cell type of IPMN [6, 22, 30]. The gastric-type IPMN often presented as a small cystic lesion involving branch ducts of the pancreas. This type of IPMN sometimes merged with other subtypes of IPMNs (Fig. 2c,d).

The intestinal-type IPMN resembled intestinal villous neoplasms with tall columnar epithelial cells that usually showed moderate- or severe/high-grade atypia corresponding to borderline or in situ carcinoma (Fig. 1e). It corresponded to the previously reported dark-cell type of IPMN [22, 30]. The intestinal-type IPMN usually showed large cystic lesions involving the main duct and several branch ducts. Occasionally, there were small papillae with goblet-cell-like appearance with low-grade atypia (Fig. 2a,b). The neoplastic cells consistently expressed MUC2 and MUC 5AC but were negative for MUC1 (Fig. 1f–h).

The pancreatobiliary type of IPMN consisted of cells resembling cholangiopapillary neoplasms and showed complex, thin, branching papillae with severe/high-grade atypia corresponding to carcinoma in situ (Fig. 1i). The lesion was at least focally positive for MUC1 and consistently expressed MUC5AC but not MUC2 (Fig. 1j–l).

The oncocytic type of IPMN consisted of cells with abundant, intensely eosinophilic cytoplasm and showed complex thick papillae with intraepithelial lumina and severe/high-grade atypia corresponding to carcinoma in situ (Fig. 1m). The oncocytic type of IPMN corresponded to the previously reported compact-cell type IPMN [22]. This IPMN subtype expressed MUC5AC consistently and MUC1 focally but was negative for MUC2 (Fig. 1n–p).

While it was the consensus of the group that the classification of IPMNs into these well-defined subtypes will help standardize the reporting of IPMNs, it was recognized that IPMNs often are composed of a combination of more than one cell type. The group therefore proposed that each IPMN should be subclassified by the dominant component and that any other significant subtypes present should be documented. In case of an invasive carcinoma associated with IPMN, the subtypes of the intraductal component should be evaluated and noted, especially in areas associated with the invasive component.

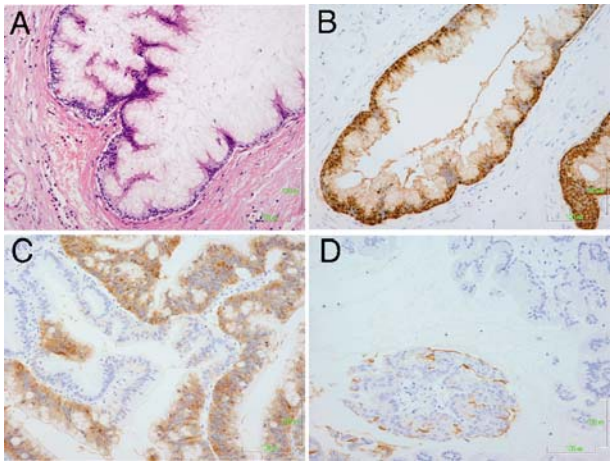


Fig. 2 Variation of the intestinal type mimicking goblet cells (hematoxylin and eosin) (**a**) and its immunohistochemical staining of MUC2 (**b**). Examples of mixed areas combining the gastric type and the intestinal type (**c**) and the gastric type and the pancreatobiliary type (**d**). Images show immunohistochemical stainings of MUC2 (**c**) and MUC1 (**d**)

Discussion

The diagnostic term IPMN encompasses a spectrum of intraductal mucin-producing neoplasms composed of a variety of cell types showing distinctive architectural and histochemical features [19, 25]. An international panel of experts was assembled to establish a nomenclature for classifying the subtypes of IPMNs. Based on the experience of the panel, information from the literature, and a review of a selected series of IPMNs, consensus criteria for the classification of subtypes of IPMNs were agreed upon. These definitions should facilitate further analyses of the clinicopathological significance of the variations of IPMN.

The panel of experts agreed unanimously that four types of IPMN can be distinguished among the series of cases that had been studied. These IPMN types were classified as gastric, intestinal, pancreatobiliary, or oncocytic type.

According to the currently available data, the gastric-type IPMN usually presents as relatively small cystic lesions in peripheral branch ducts with low-grade atypia, mostly corresponding to intraductal papillary-mucinous adenoma, while the other subtypes of IPMN usually present as large lesions involving the main duct and connecting branch ducts with marked atypia, mostly corresponding to intraductal papillary-mucinous neoplasm in the borderline category or intraductal papillary-mucinous carcinoma [4, 28]. These latter types of IPMN are often associated with an invasive adenocarcinoma [10, 18, 28].

We present this subclassification of IPMN to aid in the comparison of studies from different institutions. One interpretation of our findings is that the types of IPMN described here may simply be a manifestation of a spectrum in the differentiation and progression of a single lineage of IPMN and that these morphologies may, in part, reflect the degree of dysplasia. IPMN may be a progressive neoplastic lesion, in which a small cystic lesion with low-grade atypia may progress to large multicystic ductal lesions with severe atypia and complex histological architecture and, eventually, to invasive cancer. Areas with gastric-type epithelium can be associated with the other subtypes, implying that the gastric type might be a common precursor of the other types [6], although we feel that such a conclusion is premature. Whether the IPMN types we defined are truly distinctive lineages or variations of a single progressive neoplastic lineage should be further clarified by clinicopathological and molecular studies based on the definitions provided. One study on 51 pancreata with IPMNs that compared the various subtypes of IPMN and aberrations of tumor suppressor genes, includ-

ing CDKN2A, TP53, SMAD4, and DUSP6, revealed no significant association [11]. It is hoped that such studies will lead to an understanding of the mechanisms by which IPMNs develop and progress.

Pancreatic intraductal neoplasms consisting mainly of tubular glands of pyloric-gland type have been reported and designated as "intraductal tubular adenoma" [7, 15]. We did not include examples with predominantly tubular growth in the current study. However, because focal tubule formation is often observed in IPMNs, especially those of the gastric type or the pancreatobiliary type, the authors would assume that tubular growth may occur in IPMNs and that neoplasms with a predominantly tubular pattern may correspond to intraductal tubular adenoma, pyloric-gland type. The coexistence of papillae and tubules in both IPMNs and intraductal tubular adenoma suggests that they may be closely related, albeit distinctive, morphological features.

MUCs are useful markers for evaluating subtypes of IPMN [13, 20–22, 29, 30]. MUC1 is a component of the membrane-bound type of mucin and is usually detected in intralobular ductal lumina in the normal pancreas [1]. MUC1 is expressed in invasive ductal adenocarcinoma of the pancreas, often showing extensive positivity [24]. Among the IPMN subtypes, the pancreatobiliary type usually shows positivity for MUC1, which parallels its association with invasive ductal adenocarcinoma of the conventional tubular type [6]. The oncocytic type expresses MUC1 focally, and while it has been reported to be associated with invasive oncocytic carcinoma, its association with invasive ductal carcinoma is unknown [2]. MUC2 consists of secreted mucin usually observed in intestinal glands and is considered to be a marker of intestinal differentiation [12]. The intestinal type of IPMN, of both villous and goblet-cell features, strongly expresses MUC2 [6, 13, 21, 22, 24, 30]. The intestinal differentiation of this subtype of IPMN was supported by the demonstration that they also express CDX2, a homeobox gene involved in intestinal development [6]. MUC5AC is expressed by mucous surface cells of the stomach. MUC 5AC is not detected in the normal pancreas but is consistently detected by immunohistochemistry in all types of IPMN [13, 30]. It is also known that pancreatic intraepithelial neoplasia (PanIN), precursor lesions associated with invasive ductal adenocarcinoma, also consistently express MUC5AC [16, 21]. PanINs are usually negative for MUC2 but often express MUC1, especially in high-grade atypical lesions [5]. The differential diagnosis between PanIN and IPMN was discussed in detail in a previous publication [14].

The prognosis of patients with an IPMN has been shown to depend on the presence or absence of an associated invasive carcinoma and, if an invasive carcinoma is present, on the histological type of the associated invasive carcinoma [26]. Invasive carcinomas associated with IPMN largely consist of two distinct types, invasive carcinoma mimicking usual invasive ductal adenocarcinoma and invasive colloid (mucinous noncystic) carcinoma [5, 21]. Patients with an IPMN associated with an invasive colloid (mucinous noncystic) carcinoma usually have a better prognosis than do those with an associated invasive ductal adenocarcinoma [3, 5].

The classification proposed is based primarily on morphological features. The immunolabeling for MUCs may serve as a confirmatory marker for the classification. We believe our definitions may contribute to an understanding of the biologic behavior of IPMN and to better clinical management. For example, it would be valuable to determine whether a particular type of noninvasive IPMN is associated with a particular type of invasive adenocarcinoma. It will be also of interest to clarify the relationship of the intraductal tubular neoplasm of the pancreas [27] with the types of IPMN described herein.

Acknowledgements We thank Ms. Naomi Kanai for technical assistance and Ms. Kay Dege for editing the manuscript.

References

1. Abe M, Kufe D (1993) Characterization of cis-acting elements regulating transcription of the human DF3 breast carcinoma-associated antigen (MUC1) gene. Proc Natl Acad Sci U S A 90:282–286
2. Adsay NV, Adair CF, Heffess CS, Klimstra DS (1996) Intraductal oncocytic papillary neoplasms of the pancreas. Am J Surg Pathol 20:980–994
3. Adsay NV, Pierson C, Sarkar F, Abrams J, Weaver D, Conlon KC, Brennan MF, Klimstra DS (2001) Colloid (mucinous noncystic) carcinoma of the pancreas. Am J Surg Pathol 25: 26–42
4. Adsay NV, Conlon KC, Zee SY, Brennan MF, Klimstra DS (2002) Intraductal papillary-mucinous neoplasms of the pancreas: an analysis of in situ and invasive carcinomas in 28 patients. Cancer 94:62–77
5. Adsay NV, Merati K, Andea A, Sarkar F, Hruban RH, Wilentz RE, Goggins M, Iocobuzio-Donahue C, Longnecker DS, Klimstra DS (2002) The dichotomy in the preinvasive neoplasia to invasive carcinoma sequence in the pancreas: differential expression of MUC1 and MUC2 supports the existence of two separate pathways of carcinogenesis. Mod Pathol 15: 1087–1095
6. Adsay NV, Merati K, Basturk O, Iacobuzio-Donahue C, Levi E, Cheng JD, Sarkar FH, Hruban RH, Klimstra DS (2004) Pathologically and biologically distinct types of epithelium in intraductal papillary mucinous neoplasms: delineation of an "intestinal" pathway of carcinogenesis in the pancreas. Am J Surg Pathol 28:839–848
7. Albores-Saavedra J, Sheahan K, O'Riain C, Shukla D (2004) Intraductal tubular adenoma, pyloric type, of the pancreas: additional observations on a new type of pancreatic neoplasm. Am J Surg Pathol 28:233–238
8. Fukushima N, Mukai K, Kanai Y, Hasebe T, Shimada K, Ozaki H, Kinoshita T, Kosuge T (1997) Intraductal papillary tumors and mucinous cystic tumors of the pancreas: clinicopathologic study of 38 cases. Hum Pathol 28:1010–1017

9. Fukushima N, Mukai K, Sakamoto M, Hasebe T, Shimada K, Kosuge T, Kinoshita T, Hirohashi S (2001) Invasive carcinoma derived from intraductal papillary-mucinous carcinoma of the pancreas: clinicopathologic and immunohistochemical study of eight cases. Virchows Arch 439:6–13
10. Furukawa T, Takahashi T, Kobari M, Matsuno S (1992) The mucus-hypersecreting tumor of the pancreas. Development and extension visualized by three-dimensional computerized mapping. Cancer 70:1505–1513
11. Furukawa T, Fujisaki R, Yoshida Y, Kanai N, Sunamura M, Abe T, Takeda K, Matsuno S, Horii A (2005) Distinct progression pathways involving the dysfunction of DUSP6/MKP-3 in pancreatic intraepithelial neoplasia and intraductal papillary-mucinous neoplasms of the pancreas. Mod Pathol 18:1034–1042
12. Gum JR, Byrd JC, Hicks JW, Toribara NW, Lamport DT, Kim YS (1989) Molecular cloning of human intestinal mucin cDNAs. Sequence analysis and evidence for genetic polymorphism. J Biol Chem 264:6480–6487
13. Horinouchi M, Nagata K, Nakamura A, Goto M, Takao S, Sakamoto M, Fukushima N, Miwa A, Irimura T, Imai K, Sato E, Yonezawa S (2003) Expression of different glycoforms of membrane mucin (MUC1) and secretory mucin (MUC2, MUC5AC and MUC6) in pancreatic neoplasms. Acta Histochem Cytochem 36:443–453
14. Hruban RH, Takaori K, Klimstra DS, Adsay NV, Albores-Saavedra J, Biankin AV, Biankin SA, Compton C, Fukushima N, Furukawa T, Goggins M, Kato Y, Klöppel G, Longnecker DS, Lüttges J, Maitra A, Offerhaus GJ, Shimizu M, Yonezawa S (2004) An illustrated consensus on the classification of pancreatic intraepithelial neoplasia and intraductal papillary mucinous neoplasms. Am J Surg Pathol 28:977–987
15. Kato N, Akiyama S, Motoyama T (2002) Pyloric gland-type tubular adenoma superimposed on intraductal papillary mucinous tumor of the pancreas. Pyloric gland adenoma of the pancreas. Virchows Arch 440:205–208
16. Kim GE, Bae HI, Park HU, Kuan SF, Crawley SC, Ho JJ, Kim YS (2002) Aberrant expression of MUC5AC and MUC6 gastric mucins and sialyl Tn antigen in intraepithelial neoplasms of the pancreas. Gastroenterology 123:1052–1060
17. Klöppel G (1998) Clinicopathologic view of intraductal papillary-mucinous tumor of the pancreas. Hepatogastroenterology 45:1981–1985
18. Kobari M, Egawa S, Shibuya K, Shimamura H, Sunamura M, Takeda K, Matsuno S, Furukawa T (1999) Intraductal papillary mucinous tumors of the pancreas comprise 2 clinical subtypes: differences in clinical characteristics and surgical management. Arch Surg 134:1131–1136
19. Kosmahl M, Pauser U, Peters K, Sipos B, Lüttges J, Kremer B, Klöppel G (2004) Cystic neoplasms of the pancreas and tumor-like lesions with cystic features: a review of 418 cases and a classification proposal. Virchows Arch 445:168–178
20. Levi E, Klimstra DS, Andea A, Basturk O, Adsay NV (2004) MUC1 and MUC2 in pancreatic neoplasia. J Clin Pathol 57: 456–462
21. Lüttges J, Zamboni G, Longnecker D, Klöppel G (2001) The immunohistochemical mucin expression pattern distinguishes different types of intraductal papillary mucinous neoplasms of the pancreas and determines their relationship to mucinous noncystic carcinoma and ductal adenocarcinoma. Am J Surg Pathol 25:942–948
22. Nakamura A, Horinouchi M, Goto M, Nagata K, Sakoda K, Takao S, Imai K, Kim YS, Sato E, Yonezawa S (2002) New classification of pancreatic intraductal papillary-mucinous tumour by mucin expression: its relationship with potential for malignancy. J Pathol 197:201–210
23. Ohhashi K, Murakami Y, Maruyama M, Takekoshi T, Ohta H, Ohhashi I, Takagi K, Kato Y (1982) Four cases of mucous secreting pancreatic cancer. (in Japanese, with English abstract). Prog Digest Endosc 20:348–351
24. Osako M, Yonezawa S, Siddiki B, Huang J, Ho JJ, Kim YS, Sato E (1993) Immunohistochemical study of mucin carbohydrates and core proteins in human pancreatic tumors. Cancer 71:2191–2199
25. Sessa F, Solcia E, Capella C, Bonato M, Scarpa A, Zamboni G, Pellegata NS, Ranzani GN, Rickaert F, Klöppel G (1994) Intraductal papillary-mucinous tumours represent a distinct group of pancreatic neoplasms: an investigation of tumour cell differentiation and K-ras, p53 and c-erbB-2 abnormalities in 26 patients. Virchows Arch 425:357–367
26. Suzuki Y, Atomi Y, Sugiyama M, Isaji S, Inui K, Kimura W, Sunamura M, Furukawa T, Yanagisawa A, Ariyama J, Takada T, Watanabe H, Suda K (2004) Cystic neoplasm of the pancreas: a Japanese multiinstitutional study of intraductal papillary mucinous tumor and mucinous cystic tumor. Pancreas 28:241–246
27. Tajiri T, Tate G, Inagaki T, Kunimura T, Inoue K, Mitsuya T, Yoshiba M, Morohoshi T (2005) Intraductal tubular neoplasms of the pancreas: histogenesis and differentiation. Pancreas 30: 115–121
28. Terris B, Ponsot P, Paye F, Hammel P, Sauvanet A, Molas G, Bernades P, Belghiti J, Ruszniewski P, Flejou JF (2000) Intraductal papillary mucinous tumors of the pancreas confined to secondary ducts show less aggressive pathologic features as compared with those involving the main pancreatic duct. Am J Surg Pathol 24:1372–1377
29. Terris B, Dubois S, Buisine MP, Sauvanet A, Ruszniewski P, Aubert JP, Porchet N, Couvelard A, Degott C, Flejou JF (2002) Mucin gene expression in intraductal papillary-mucinous pancreatic tumours and related lesions. J Pathol 197:632–637
30. Yonezawa S, Horinouchi M, Osako M, Kubo M, Takao S, Arimura Y, Nagata K, Tanaka S, Sakoda K, Aikou T, Sato E (1999) Gene expression of gastric type mucin (MUC5AC) in pancreatic tumors: its relationship with the biological behavior of the tumor. Pathol Int 49:45–54

Virchows Arch (2005) 447: 800–805
DOI 10.1007/s00428-005-0032-1

ORIGINAL ARTICLE

Sönke Detlefsen · Bence Sipos · Bernd Feyerabend · Günter Klöppel

Pancreatic fibrosis associated with age and ductal papillary hyperplasia

Received: 17 May 2005 / Accepted: 15 June 2005 / Published online: 14 July 2005
© Springer-Verlag 2005

Abstract Little is known about the frequency, type and pathogenesis of fibrotic changes that may occur in the pancreas of persons without any clinically apparent or macroscopically visible pancreatic disease. We screened pancreas specimens for the presence and pattern of fibrosis, determined the relationship between fibrosis, age, and duct lesions, and studied the fibrogenic mechanisms. In 89 postmortem specimens from persons without any known pancreatic disease (age range 20–86 years), fibrosis was recorded and graded and the patients were divided into two age classes (younger or older than 60 years). In addition, we analyzed the association between ductal papillary hyperplasia [i.e., pancreatic intraepithelial neoplasia type 1B (PanIN-1B)] and fibrotic foci in the pancreatic tissue to determine the potential impact of obliterating duct lesions on pancreatic fibrosis. Finally, we studied the occurrence in the pancreas of myofibroblasts, identified on the basis of their α-SMA and desmin positivity, and determined their relationship to the fibrotic foci. Thirty-eight (44%) of 89 pancreata showed scattered foci of lobular fibrosis affecting peripheral lobuli. Fibrotic changes were significantly more common in individuals older than 60 years. Fibrotic foci were commonly associated ($p<0.05$) with ductal papillary hyperplasia in ducts draining fibrotic lobuli. Myofibroblasts were detected in the fibrotic foci. The "normal" pancreas develops a specific type of focally accentuated fibrosis that is highly age related. This patchy lobular fibrosis in the elderly (PLFE) was closely associated with PanIN-1B lesions in the ducts, suggesting that the narrowing of a duct due to papillary hyperplasia of the epithelium may hamper secretion and cause fibrosis of the drained lobule. The presence of myofibroblasts in association with the fibrotic foci indicates an ongoing fibrogenic process.

S. Detlefsen · B. Sipos · B. Feyerabend · G. Klöppel (✉)
Department of Pathology, University of Kiel,
Michaelisstrasse 11,
24105 Kiel, Germany
e-mail: gkloeppel@path.uni-kiel.de
Tel.: +49-431-5973400
Fax: +49-431-5973462

Keywords Normal pancreas · Pancreatic fibrosis · Age relationship · PanIN

Introduction

Fibrotic changes are the hallmark of chronic pancreatitis (CP) [3, 15, 16], but may also be observed in the "normal pancreas," i.e., the pancreas of persons without any known or macroscopically visible pancreatic disease. The first indications of an association between fibrosis and age came from a study by Pitchumoni et al. [22]. The patients examined were divided into two groups, alcoholics and nonalcoholics. Diffuse fibrosis was found in the alcoholics, which contrasted with the patchy type of fibrosis seen in the aged nonalcoholics, but the authors did not analyze the pathomechanisms of fibrosis in the aged nonalcoholics and no clear typing of the fibrotic changes was attempted. Fibrotic changes were also described by Stamm [27] and Shimizu et al. [25] in normal pancreatic specimens, but only in Stamm's study were they related to age. Both authors observed an association between fibrosis and ductal papillary hyperplasia. In another study that used photometric measurements to determine the collagen content of histologic sections from the pancreas of patients with CP or subjects with pancreatic disease, no information was given on the distribution of fibrotic foci or the relationship between fibrosis and age [29].

The aim of our study was to gain insights into the pathogenesis of pancreatitic fibrosis that is not associated with the clinical symptoms of CP. We therefore examined the type and extent of pancreatic fibrosis in humans without any known pancreatic disease and related the data to age. In addition, we focused on changes in the ducts draining the fibrotic lobules. These duct changes have become known as "ductal papillary hyperplasia" [18] and were recently classified among the precursor lesions of pancreatic ductal adenocarcinoma as pancreatic intraepithelial neoplasia type 1B (PanIN-1B) [8]. We show here that the fibrosis in the normal pancreas has a patchy distribution with a lobular pattern and a clear relationship to age and to duct

narrowing due to epithelial hyperplasia. Finally, we studied the occurrence of myofibroblasts, identified by their α-SMA and desmin positivity, and identified these cells in association with fibrotic foci.

Materials and methods

Tissue

Paraffin-embedded postmortem specimens were obtained from 89 patients. All cases derived from persons without clinically recognized or macroscopically evident pancreatic disease and were fixed in 10% buffered formalin. The specimens came from three different institutions, the Departments of Pathology of the University of Kiel, Germany, the Kaiser-Franz-Josef-Hospital, Vienna, Austria, and the Semmelweiss University, Budapest, Hungary. All patients had died of nonpancreatic disease, most frequently of cardiovascular, neoplastic, or respiratory disease.

The persons were between 20 and 86 years old. They were divided into two groups based on age, one from 20 to 59 years old (n=39, mean age 46.8 years, 8 women and 31 men), the other 60 years or older (n=50, mean age 72.4 years, 11 women and 39 men). From each pancreatic specimen, eight paraffin-embedded sections deriving from different regions in the pancreas were examined as described by Lüttges et al. [21]: two blocks were taken from the upper part of the head, including the main pancreatic duct (region A), and two further blocks from the lower part of the head with the accessory duct (region B). Two blocks each were taken from the body (region C) and the tail (region D). Three-micrometer-thick sections were stained with hematoxylin and eosin (H & E).

In addition, we examined 59 cases of alcoholic chronic pancreatitis (ACP) to compare the extent and pattern of pancreatic fibrosis in the normal pancreata with that in ACP patients. In these cases, two to three paraffin-embedded tissue blocks from pancreatic resection specimens of 44 men and 15 women with ACP, mean age 47.6 years, age range 31 to 86 (42 Whipple resections, 17 left-sided pancreatic resections), were available. The patients suffered from symptoms of CP (intractable pain, pseudocyst, jaundice).

Histological evaluation

The extent and intensity of pancreatic fibrosis were determined using a scoring system based on the pattern of fibrosis [focal vs diffuse, perilobular (interlobular) vs intralobular] [3]. Intralobular and perilobular fibrosis were scored on a scale from 1 to 6, with 1 (focal, weak), 2 (focal, moderate), 3 (focal, strong), 4 (diffuse, weak), 5 (diffuse, moderate), or 6 (diffuse, strong). In addition, the number of PanIN-1B lesions and their association with fibrotic foci were recorded in each pancreas. We assigned to each case only one PanIN-1B lesion, regardless of how many PanIN-1B lesions were found in an individual pancreas. A spatial association between a PanIN-1B lesion and fibrotic changes was assumed when a PanIN-1B lesion was found in close vicinity to or in direct connection with a fibrotic focus. Only one fibrotic focus connected with a PanIN-1B lesion was assigned to each case.

Immunohistology

Myofibroblasts were identified in the "normal pancreas" by immunohistological labeling with alpha smooth muscle actin (α-SMA, DAKO, Glostrup, Denmark, 1:20) and desmin (DAKO, 1:20).

Statistics

The χ^2 test (SPSS for Windows, version 10.1) was used to compare (1) the number of 20- to 59-year-old subjects with pancreatic fibrosis with that of the 60- to 86-year-old subjects showing the same change in the pancreas and (2) the number of subjects with fibrotic foci and associated PanIN-1B lesion with the number of subjects who had PanIN-1B lesions that lay between normal lobuli.

Results

Persons whose age ranged from 20 to 59 only rarely exhibited pancreatic fibrosis. In most cases, the lobular arrangement of the parenchyma was preserved and the ducts it contained were surrounded by a fibrotic band (Fig. 1). In a few cases (6/39, 15.4%) there were single foci of perilobular and intralobular fibrosis (Fig. 2 and Table 1). The person with the lowest age presenting a fibrotic focus was 40 years old. In contrast, normal pancreata from 60- to 86-year-old subjects commonly showed focal lobular fibrosis, usually affecting peripheral lobes and often containing remnants of acini, small ducts, some islets and small lymphocytic aggregates (Fig. 2). Some ducts contained eosin-

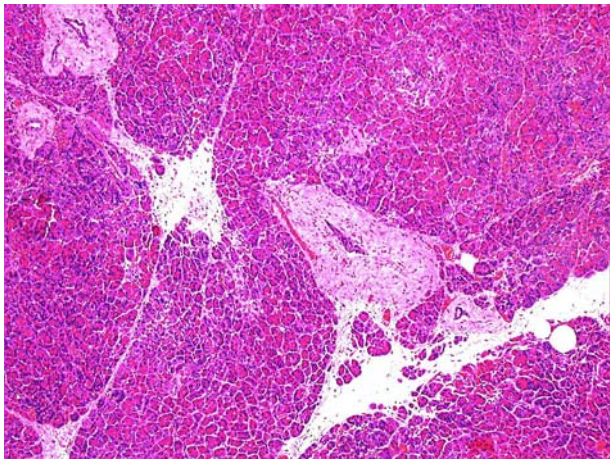


Fig. 1 Normal pancreatic tissue from an individual older than 60 years. H & E

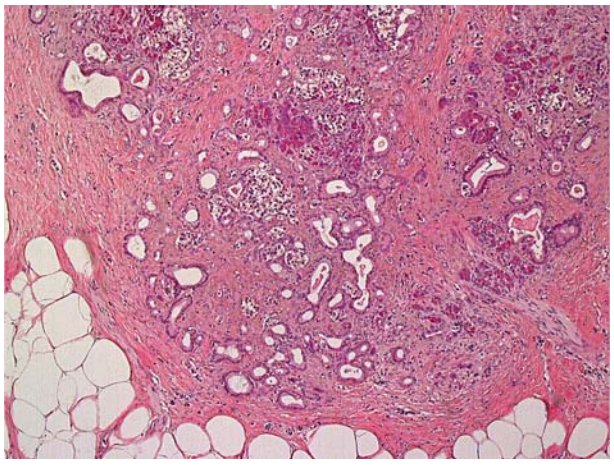


Fig. 2 Pancreatic tissue from an individual older than 60 years showing lobular fibrosis. H & E

ophilic secretions. Islet amyloidosis was detected in two pancreata and was not associated with fibrosis. The fibrotic changes were found in 32 (64.0%) of 50 cases (Table 1). The average fibrosis score was 0.9 for intralobular fibrosis and 0.7 for perilobular fibrosis. The number of fibrotic foci that were observed in the eight sections obtained from one pancreatic specimen ranged from one to seven, with an average of three. The fibrotic foci were randomly distributed in the pancreas. The number of pancreata affected by fibrosis and the grade of fibrosis in the individual pancreata increased with age, as demonstrated in Table 1 ($p<0.001$). Fibrosis was much more intense in ACP cases than in the "normal" pancreata. Whereas in the "normal" pancreata intra- or perilobular fibrosis never exceeded grade 3 (Table 1), it reached grade 5 and 6 in almost 70% of the resection specimens from patients with ACP. Moreover, a comparison of the patterns of fibrosis revealed that in ACP perilobular fibrosis was much more prominent than in the normal pancreas.

Pancreatic duct lesions of PanIN type 1A and 1B were found in a frequency similar to that previously reported [4, 21, 27]. Here we recorded only the PanIN-1B lesions and their spatial association with fibrotic foci in the pancreas. Persons whose age ranged from 20 to 59 only rarely exhibited PanIN-1B lesions (4/39, 10.3%) and there was only one case in which a PanIN-1B lesion was associated with fibrosis (Table 2). In contrast, normal pancreata from

Table 1 Grade of fibrosis in persons without any clinically known pancreatic disease, related to two age classes (50 subjects older and 39 subjects younger than 60 years)

Grade	Age 20–59		Age 60–84	
	Perilobular	Intralobular	Perilobular	Intralobular
0	34/39	33/39	22/50	18/50
1	5/39	5/39	24/50	25/50
2	–	1/39	3/50	3/50
3	–	–	1/50	4/50
4–6	–	–	–	–

Table 2 Spatial association of PanIN-1B (ductal papillary hyperplasia) with fibrosis in persons without any known pancreatic disease, related to two age classes (older and younger than 60 years)

Age	No. of examined cases	No. of cases with PanIN-1B	No. of cases with PanIN-1B and associated focal fibrosis
20–59	39	4/39	1/4
60–84	50	31/50	25/31

60- to 86-year-old subjects commonly showed PanIN-1B lesions (31/50, 62.0%). In these persons, the PanIN-1B lesions were more common in or near to fibrotic lobuli (25/31, 80.6%) (Fig. 3, Table 2) than in pancreatic lobuli unaffected by fibrosis. Table 3 shows the total number of fibrotic foci, of PanIN-1B lesions, and of fibrotic foci associated with PanIN-1B lesions identified in the eight sections (covering four different pancreatic regions) available from each patient. The association between PanIN-1B and fibrosis was statistically significant ($p<0.002$). The PanIN-1B lesions found in ACP were randomly distributed in the tissue and did not show any increased association with foci of fibrosis.

Most fibrotic foci that were found in "normal" pancreata showed myofibroblasts, which were recognizable by their expression of α-SMA (Fig. 4), and occasionally also desmin. The myofibroblasts were often seen in a perilobular position. In the pancreata without fibrosis, some scattered myofibroblasts were often detected around large ducts.

Discussion

Textbooks on anatomy and histology mention that the pancreas is surrounded by a thin, fibrous capsule and that the pancreatic ducts are surrounded by thin cords of connective tissue [11, 13], but mention nothing about pancreatic fibrosis developing in elderly patients. This is because so far only few studies have described fibrosis in pancre-

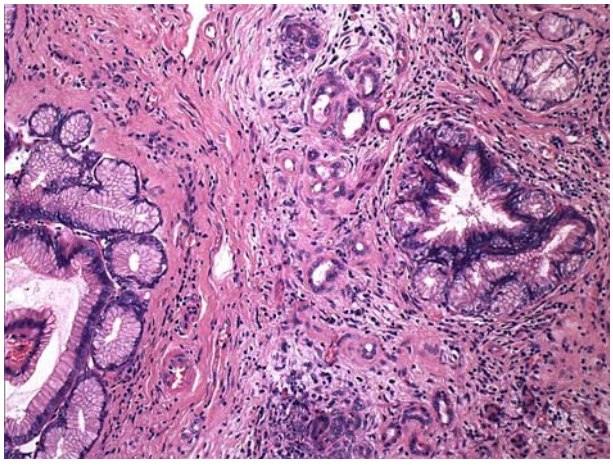


Fig. 3 Pancreatic tissue from an individual older than 60 years showing ductal papillary hyperplasia (PanIN-1B lesion) in association with fibrosis. H & E

Table 3 Association between lobular fibrosis and PanIN-1B lesions in persons older than 60 years without any known pancreatic disease

Case no.	No. of fibrotic foci	No. of PanIN-1B lesions	No. of fibrotic foci associated with a PanIN-1B lesion
1	–	–	–
2	–	1	–
3	–	–	–
4	7	1	1
5	4	1	1
6	–	2	–
7	2	–	–
8	4	1	1
9	5	4	4
10	4	–	–
11	–	–	–
12	4	4	3
13	–	–	–
14	4	2	2
15	–	–	–
16	3	2	1
17	5	–	–
18	–	–	–
19	2	2	2
20	–	–	–
21	–	3	–
22	4	2	2
23	7	8	7
24	2	4	2
25	1	1	1
26	–	–	–
27	3	3	3
28	2	1	1
29	6	8	6
30	–	–	–
31	–	–	–
32	–	4	–
33	4	2	2
34	2	2	–
35	1	2	1
36	3	3	2
37	3	1	1
38	–	–	–
39	–	–	–
40	4	–	–
41	1	1	1
42	6	4	4
43	2	3	2
44	–	–	–
45	6	–	–
46	1	1	1
47	–	–	–
48	4	2	2
49	1	1	–
50	1	1	1

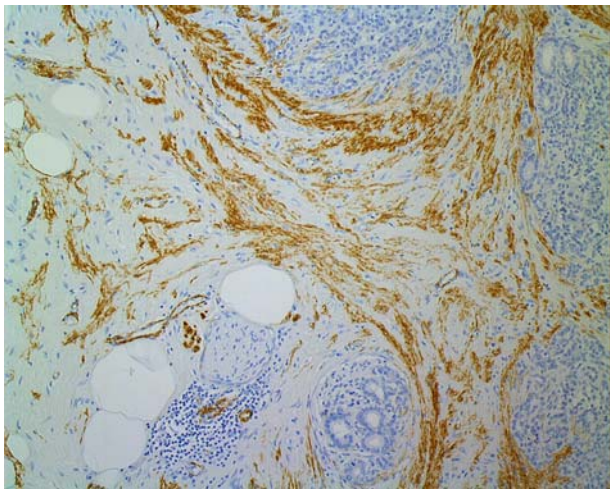


Fig. 4 Pancreatic fibrosis in an individual older than 60 years associated with myofibroblasts showing α-SMA immunoreactivity. ×50

ata that were regarded as normal, i.e., that were not affected by any clinically obvious disease known to lead to fibrotic changes in the pancreas. Pitchumoni et al. [22], Shimizu et al. [25], and Stamm [27] reported age-related fibrotic changes in the normal pancreas, without typing or grading the fibrosis or discussing its pathogenesis. One study quantified fibrosis in the normal pancreas, compared to that in CP [29] and two other studies focused on ectatic changes in the pancreatic duct system and noted in these areas periductal fibrosis that increased with age [2, 23].

We examined 89 postmortem specimens and determined the distribution of fibrosis, graded it, and related it to two age classes (younger or older than 60 years). We found an age-dependent development of fibrosis in the pancreas of persons who had no clinically apparent pancreatic disease and whose pancreas showed no macroscopic changes. Our evaluation of sections from eight different regions of the pancreatic head, body, and tail revealed fibrotic foci with increasing frequency in persons older than 60 years. Before the age of 60, these fibrotic foci were very rare. Fibrotic foci occurred in the periphery of the glands and involved one or two lobuli where the acinar cells were replaced by connective tissue. The resulting pattern of fibrosis may be described as a predominantly intralobular fibrosis since the fibrotic changes appeared to start within the lobule and not in the perilobular space, as has been suggested for ACP [3, 15], and was also seen in our series of pancreatic specimens from patients with ACP. Furthermore, because most pancreata contained more than one fibrotic focus, the pattern of fibrosis was that of multifocal intralobular fibrosis which we termed "patchy lobular fibrosis in the elderly" (PLFE).

In the subjects whose pancreatic specimens were analyzed there was no evidence of CP. This implies that the development of PLFE is most likely not mediated by a process triggered by any of the known factors that may cause CP [17]. That PLFE was age-related and usually in-

volved single peripheral lobuli suggested a causative factor that is focally active and needs time to exert its effect. From tumors such as ductal adenocarcinomas affecting the head of the pancreas and obstructing the main pancreatic duct it is known that this obstruction may lead to a replacement of the acinar tissue by fibrosis, a change called obstructive CP. The experimental model of this disease is the duct ligation procedure, which results in similar alterations in the pancreas upstream of the ligation [9, 10, 30]. As the fibrotic changes resembled obstructive CP as seen in experimental duct ligation, we searched for obliterating changes in the ducts draining the lobules affected by fibrosis. Narrowing of the duct lumen can be caused by papillary proliferations of hypertrophic duct epithelium, formerly described as "ductal papillary hyperplasia" [6, 14, 18, 19, 26]. This change in the duct epithelium has recently been classified among the precursor lesions of pancreatic ductal adenocarcinoma as pancreatic intraepithelial neoplasia type 1B (PanIN-1B) [8]. It occurs not only in association with pancreatic cancer, but also in the nonneoplastic pancreas [4, 14, 20, 21, 27]. When we analyzed this duct lesion in our pancreatic specimens, we found a close association between PanIN-1B lesions and lobular fibrotic foci. This suggests that PanIN-1B lesions may cause partial obstruction of the respective duct and thus a decrease in the flow of pancreatic fluid, promoting apoptosis of acinar cells, followed by their replacement by fibrosis.

Myofibroblasts (that are also regarded activated pancreatic stellate cells) are known to play a pivotal role in fibrogenesis in the pancreas (for a review see [15]) and have been described in the human pancreas [5]. We therefore studied the occurrence of myofibroblasts, identified by their α-SMA and desmin immunoreactivity [5], in the normal pancreata and found them in association with many of the fibrotic foci. This implies that there is an ongoing process of fibrogenesis in these areas, probably triggered by the hampered flow of secretions in the narrowed draining ducts. Experimental work has shown that the cytokines platelet-derived growth factor B and transforming growth factor β cause activation and proliferation of the resident fibroblasts, inducing them to transform into myofibroblast cells, which are capable of producing extracellular matrix [7, 15, 24]. Our data indicate that PanIN-1B lesions in the normal pancreas of elderly persons may provoke such damage to acinar cells due to decreased flow of pancreatic fluid in the ducts, followed by phagocytosis of acinar cells. Afterwards these cells appear to be replaced by connective tissue synthesized by myofibroblasts.

In summary, our study shows that focal lobular fibrosis in the normal pancreas commonly occurs in subjects who are older than 60 and is most likely caused by duct-obstructing PanIN-1B lesions. It will be interesting to clarify whether the peripheral PanIN-1B lesions are also connected with the peripheral cystic changes in the pancreas described by Kimura et al. [12] and the intraductal papillary mucinous neoplasms that occur in the periphery of the pancreas, show gastric foveolar type epithelium and stain for MUC5AC [1, 28].

Acknowledgements This work was part of the doctoral thesis of Sönke Detlefsen.

References

1. Adsay NV, Merati K, Basturk O, Iacobuzio-Donahue C, Levi E, Cheng JD, Sarkar FH, Hruban RH, Klimstra DS (2004) Pathologically and biologically distinct types of epithelium in intraductal papillary mucinous neoplasms. Delineation of an "intestinal" pathway of carcinogenesis in the pancreas. Am J Surg Pathol 28:839–848
2. Allen-Mersh TG (1985) What is the significance of pancreatic ductal mucinous hyperplasia? Gut 26:825–833
3. Ammann RW, Heitz PU, Klöppel G (1996) Course of alcoholic chronic pancreatitis: a prospective clinicomorphological long-term study. Gastroenterology 111:224–231
4. Andea A, Sarkar F, Adsay NV (2003) Clinicopathological correlates of pancreatic intraepithelial neoplasia: a comparative analysis of 82 cases with and 152 cases without pancreatic ductal adenocarcinoma. Mod Path 16:996–1006
5. Barth PJ, Ebrahimsade S, Hellinger A, Moll R, Ramaswamy A (2002) CD34+ fibrocytes in neoplastic and inflammatory pancreatic lesions. Virchows Arch 440:128–133
6. Cubilla AL, Fitzgerald PJ (1976) Morphological lesions associated with human primary invasive nonendocrine pancreas cancer. Cancer Res 36:2690–2698
7. Haber PS, Keogh GW, Apte MV, Moran CS, Stewart NL, Crawford DHG, Pirola RC, McCaughan GW, Ramm GA, Wilson JS (1999) Activation of pancreatic stellate cells in human and experimental pancreatic fibrosis. Am J Pathol 155: 1087–1095
8. Hruban RH, Adsay NV, Albores-Saavedra J, Compton C, Garrett ES, Goodman SN, Kern SE, Klimstra DS, Klöppel G, Longnecker DS, Lüttges J, Offerhaus GJA (2001) Pancreatic intraepithelial neoplasia. A new nomenclature and classification system for pancreatic duct lesions. Am J Surg Pathol 25:579–586
9. Hultquist GT, Jönsson LE (1965) Ligation of the pancreatic duct in rats. Acta Soc Med Ups 70:82–88
10. Isaksson G, Ihse I, Lundquist I (1983) Influence of pancreatic duct ligation on endocrine and exocrine rat pancreas. Acta Physiol Scand 117:281–286
11. Junqueira LC, Carneiro J (1995) Pancreas. In: LC Junqueira, J Carneiro (eds) Basic histology, 8th edn. Lange Medical Publications, Los Altos
12. Kimura W, Nagai H, Kuroda A, Muto T, Esaki Y (1995) Analysis of small cystic lesions of the pancreas. Int J Pancreatol 18:197–206
13. Klimstra DS (1997) Pancreas. In: SS Sternberg (ed) Histology for pathologists, 2nd edn. Lippincott-Raven, Philadelphia, pp 613–647
14. Klöppel G, Bommer G, Rückert K, Seifert G (1980) Intraductal proliferation in the pancreas and its relationship to human and experimental carcinogenesis. Virchows Arch, A Pathol Anat 387:221–233
15. Klöppel G, Detlefsen S, Feyerabend B (2004) Fibrosis of the pancreas: the initial tissue damage and the resulting pattern. Virchows Arch 445:1–8
16. Klöppel G, Maillet B (1993) Pathology of acute and chronic pancreatitis. Pancreas 8:659–670
17. Klöppel G, Maillet B (1998) Pathology of chronic pancreatitis. In: Beger H, Warshaw AL, Büchler M, Carr-Locke DL, Neoptolemos JP, Russell C, Sarr MG (eds) The pancreas, vol 1. Blackwell, Oxford, pp 720–723
18. Klöppel G, Solcia E, Longnecker DS, Capella C, Sobin LH (1996) Histological typing of tumours of the exocrine pancreas, 2nd edn. WHO International histological classification of tumours. Springer, Berlin Heidelberg New York

19. Kozuka S, Sassa R, Taki T, Masamoto K, Nagasawa S, Saga S, Hasegawa K, Takeuchi M (1979) Relation of pancreatic duct hyperplasia to carcinoma. Cancer 43:1418–1428
20. Lüttges J, Klöppel G (2000) Precancerous conditions of pancreatic carcinoma. J Hepatobiliary Pancreat Surg 7:568–574
21. Lüttges J, Reinecke-Lüthge A, Möllmann B, Menke MAOH, Clemens A, Klimpfinger M, Sipos B, Klöppel G (1999) Duct changes and K-*ras* mutations in the disease-free pancreas: analysis of type, age relation and spatial distribution. Virchows Arch 435:461–468
22. Pitchumoni CS, Glasser M, Saran RM, Panchacharam P, Thelmo W (1984) Pancreatic fibrosis in chronic alcoholics and nonalcoholics without clinical pancreatitis. Am J Gastroenterol 79:382–388
23. Schmitz-Moormann P, Hein J (1976) Changes of the pancreatic duct system associated with aging: their relations to parenchyma (Article in German). Virchows Arch, A Pathol Anat 371: 145–152
24. Shek FWT, Benyon RC, Walker FM, McCrudden PR, Pender SLF, Williams EJ, Johnson PA, Johnson CD, Bateman AC, Fine DR, Iredale JP (2002) Expression of transforming growth factor-β1 by pancreatic stellate cells and its implications for matrix secretion and turnover in chronic pancreatitis. Am J Pathol 160:1787–1798
25. Shimizu M, Hayashi T, Saitoh Y, Itoh H (1989) Interstitial fibrosis in the pancreas. Am J Clin Pathol 91:531–534
26. Sommers SC, Murphy SA, Warren S (1954) Pancreatic duct hyperplasia and cancer. Gastroenterology 27:629–640
27. Stamm BH (1984) Incidence and diagnostic significance of minor pathologic changes in the adult pancreas at autopsy: a systematic study of 112 autopsies in patients without known pancreatic disease. Human Pathol 15:677–683
28. Terris B, Ponsot T, Paye F, Hammel P, Sauvanet A, Molas G, Bernades P, Belghiti J, Ruszniewski P, Fléjou JF (2000) Intraductal papillary mucinous tumors of the pancreas confined to secondary ducts show less aggressive pathologic features as compared with those involving the main pancreatic duct. Am J Surg Pathol 24:1372–1377
29. Valderrama R, Navarro S, Campo E, Camps J, Gimenez A, Pares A, Caballeria J (1991) Quantitative measurement of fibrosis in pancreatic tissue. Evaluation of a colorimetric method. Int J Pancreatol 10:23–29
30. Wang RN, Klöppel G, Bouwens L (1995) Duct-to islet-cell differentiation and islet growth in the pancreas of duct-ligated adult rats. Diabetologia 38:1405–1411

Virchows Arch (2005) 447: 806–815
DOI 10.1007/s00428-005-0040-1

ORIGINAL ARTICLE

Harunari Tanaka · Tetsuya Tsukamoto · Tsutomu Mizoshita · Ken-ichi Inada · Naotaka Ogasawara · Xueyuan Cao · Sosuke Kato · Takashi Joh · Masae Tatematsu

Expression of small intestinal and colonic phenotypes in complete intestinal metaplasia of the human stomach

Received: 9 February 2005 / Accepted: 26 June 2005 / Published online: 9 August 2005
© Springer-Verlag 2005

Abstract The incomplete intestinal metaplasia (IM) that is reported to be a risk factor for gastric carcinogenesis in man usually features sulfomucin production and thus is considered of colonic type. To cast light on the underlying mechanisms, we here examined the proportions of colonic and small intestinal phenotypes in IM by immunohistochemistry and real-time reverse transcription–polymerase chain reaction at the single isolated gland level. Carbonic anhydrase 1 (CA1) is a specific marker of colonic epithelial cells, whereas sucrase is specific to absorptive cells of the small intestine. Totals of 139 (23.5%) and 452 (76.5%) IM glands were judged to be CA1 positive and CA1 negative, respectively, in resected pyloric mucosa from cancer patients. The average score for MUC5AC in CA1-positive IMs was significantly lower than in CA1-negative counterpart tissue ($P<0.0001$), whereas the opposite was the case for sucrase ($P<0.0001$). High iron diamine–Alcian blue staining revealed CA1 expression to coincide with type I complete IM. The expression of CA1 mRNA strongly correlated with that of sucrase–isomaltase, and inversely with that of MUC5AC in isolated IM glands. In conclusion, CA1 could be colocalized with small intestinal proteins such as sucrase, but only rarely with the gastric mucin, MUC5AC. Its expression warrants further study, with the focus on stimulation and/or suppression mechanisms by gastric and intestinal transcription factors.

H. Tanaka · T. Tsukamoto (✉) · T. Mizoshita · K.-i. Inada · N. Ogasawara · X. Cao · S. Kato · M. Tatematsu
Division of Oncological Pathology,
Aichi Cancer Center Research Institute,
1-1 Kanokoden, Chikusa-ku,
Nagoya, 464-8681, Japan
e-mail: ttsukamt@aichi-cc.jp
Tel.: +81-52-7626111
Fax: +81-52-7642972

T. Joh
Department of Internal Medicine and Bioregulation,
Nagoya City University Medical School,
Nagoya, Japan

Keywords Intestinal metaplasia · Carbonic anhydrase 1 · Sucrase · Stomach · Gland isolation

Introduction

Intestinal metaplasia (IM) has been extensively studied as a possible premalignant condition in the human stomach [2, 24, 36, 52, 55]. However, many questions remain regarding its pathogenesis as well as the actual relationship to gastric cancers. Several classifications of IM have been suggested by pathologists. Kawachi et al. [16] first proposed division into complete and incomplete types on the basis of morphology. Jass and Filipe [14] described three grades of IM with classical mucin staining. These classifications are generally accepted, but are only based on intestinal properties and do not take into account the gastric properties that are still preserved in association [45]. We have therefore previously proposed a new IM classification based upon the cell differentiation status using both gastric and intestinal epithelial cell markers, such as MUC5AC, MUC6, MUC2, and villin [13, 45, 49]. Division is into two major types: a gastric-and-intestinal-mixed type (GI-IM) and a solely intestinal type (I-IM). Thus, it is important to analyze not only intestinal phenotypic expression but also the contribution of gastric elements within IM glands.

Several studies have provided evidence that type III intestinal metaplasia (incomplete sulphomucin-secreting intestinal metaplasia) may be a risk factor for gastric carcinogenesis [10, 12], although this remains controversial [6]. Classification based upon mucin secretion patterns as well as morphology has allowed division into a “small intestine type” and a “colonic type” [32, 46], although this has hitherto not been confirmed with small intestinal and colonic specific markers. With regard to the distribution of intestinal epithelial cell markers such as villin and MUC2 in the normal human alimentary tract, most are present in both the colon and the small intestine. However, carbonic anhydrase 1 (CA1) is found only in epithelial cells located on the luminal side of colonic mucosa, and not in the small

intestine [29, 35]. Conversely, sucrase is detectable on the luminal surfaces of mature small intestinal absorptive cells, but only rarely in colon [51]. Therefore, regarding intestinal phenotypic expression, CA1 can be used to indicate the colonic phenotype, whereas sucrase is representative of a small intestinal phenotype. The clinicopathologic significance of colonic and small intestinal phenotypes has yet to be clarified in detail for IM. Indeed, to our knowledge, there have been no reports of expression of CA1 in IM.

Most studies for gene expression for IM have been performed using whole tissue [7, 19]. However, it is impossible to avoid contamination of epithelial cell elements with stromal or inflammatory cells using this approach. We have previously established a novel "gland isolation technique" for the isolation of pyloric and IM glands and performance of relative quantitative real-time reverse transcription–polymerase chain reaction (RT-PCR) analysis of gastric and intestinal transcription factors as well as differentiation marker genes [49]. This technique made it possible to analyze gene expression separately in each isolated gland without contamination [20]. In isolated GI-IM glands, we confirmed the expression of both gastric and intestinal transcription factors as well as differentiation markers [49].

In the present study, we evaluated the transcription of CA1, sucrase–isomaltase, and MUC5AC by relative quantitative real-time RT-PCR in individual isolated glands and analyzed the interrelationships among the markers. We also examined the expression of these markers in IMs by immunohistochemistry, with reference to histological and phenotypic classification using other epithelial cell markers.

Materials and methods

Human tissue

A total of 15 stomachs, resected because of gastric cancer at Aichi Cancer Center Hospital, were investigated. This study using human tissue was conducted with approval from the Ethical Review Board of Aichi Cancer Center and after obtaining informed consent from the patients. Non-neoplastic pyloric mucosa distant from carcinomas, at least 10 cm from the tumor margins, was collected and used for RNA analysis after gland isolation as previously described [49]. After surgery, samples were fixed in 10% buffered formalin and embedded in paraffin. Serial sections were cut at 4 μm, one being stained with hematoxylin and eosin (H&E) for routine histological and others for immunohistochemical assessments as previously described [23]. Fresh normal mucosal samples of gastrointestinal tract (antrum of the stomach, jejunum, sigmoid colon) and specimens from each IM region in the pyloric mucosa with chronic gastritis were also obtained with informed consent from other patients and stored at −80°C as previously described [19].

Mucin histochemistry and immunohistochemistry

For mucin histochemistry, Alcian blue (AB) (pH 2.5) staining was performed as described [49]. Immunohistochemical staining was carried out with antibodies against the following antigens: CA1 (Chemicon International, Temecula, CA, USA), Cdx2 (BioGenex, CA, USA), MUC5AC (Novocastra Laboratories, Newcastle upon Tyne, UK), MUC2 (Novocastra), and villin (BD Transduction Laboratories, Lexington, KY, USA). The polyclonal rabbit anti-sucrase antibody was kindly provided by Dr. Kazuyuki Hirano, Department of Pharmaceutics, Gifu Pharmaceutical University, Gifu, Japan. The precise procedures for immunohistochemical techniques were as previously described [21–23, 49–51]. Two independent pathologists (T. T. and K. I.) judged the histology, mucin histochemistry, and immunohistochemical staining of epithelial cell markers, including Cdx2. Reactivity for CA1, MUC5AC, and sucrase was scored according to the rate of mucous cells above the proliferative cell zone in each gland of the pyloric areas on a 3-point scale: score 0, no positive mucous cells; score 1, 0%<positive cells≤35%; score 2, 35%<positive cells≤70%; score 3, 70%<positive cells. Results for CA1 or MUC5AC were considered positive with a score 1 or more. Using the scoring criteria, we evaluated 850 glands, 259 pyloric and 591 IM, in the pyloric region of 10 CA1-positive surgically resected IM cases. Similarly, 444 IM glands were judged for high iron diamine (HID)-AB staining patterns and classified into three subtypes as detailed by Jass and Filipe [14]. The data were analyzed by the Mann–Whitney's U test or the Fisher's exact test for differences between the groups. P values <0.05 were considered statistically significant.

Double immunohistochemical staining of CA1 and sucrase

Double staining of CA1 and sucrase was achieved basically as we previously described [28, 44]. Sections were deparaffinized, hydrated with ethanol, and autoclaved at 121°C in water for 10 min. They were then incubated with goat polyclonal anti-CA1 antibodies at 4°C overnight. Sections were then exposed to biotin-labeled anti-goat IgG and avidin–biotin peroxidase complex (Vector), and binding sites were visualized with DAB as the chromogen. Then, the antibody complex was removed with autoclaving, and the slides were thoroughly washed with Tris-buffered saline (TBS), then incubated with rabbit polyclonal anti-sucrase antibody at 4°C overnight, followed by alkaline phosphatase-labeled chicken anti-rabbit IgG (Chemicon). Color was developed using the DAKO fast red substrate system (DakoCytomation, Glostrup, Denmark) in the presence of levamisole (Sigma Chemical Co., St. Louis, MO, USA), and sections were counter-stained with hematoxylin. By the double staining, CA1-positive cells were stained brown, and sucrase-positive cells red.

Gland isolation

Gland isolation was performed as previously described [20, 49]. Remaining portions of resected epithelium were injected with calcium- and magnesium-free Hanks' balanced salt solution containing 30 mM ethylenediaminetetraacetic acid (EDTA-HBSS) submucosally, incubated in EDTA-HBSS, and shaken for 15 min at 37°C. Then the mucosa was scraped off with a scalpel. Isolated glands were washed in phosphate buffered saline, fixed in 70% ethanol for a few hours, dehydrated with 95% ethanol, and stored at −20°C until use.

Mucin cytochemistry and classification of isolated glands

The phenotypic classification of isolated glands was performed with AB staining as described earlier, based on the presence of goblet cells and pyloric glands, instead of with detailed immunohistochemical analyses to avoid degradation of RNA [45, 49]. Glands exhibiting AB-positive goblet cells in the upper part and an AB-negative bottom region (pyloric gland) were judged as GI-IM. Examples with many AB-positive goblet cells throughout and loss of AB-negative pyloric glands were classified as I-IM. Typical glands as shown in Fig. 6 were used in this study, and transient types were discarded to avoid confusion. This simple method for the classification of isolated glands were found to fit well with histological and immunohistochemical analyses [49].

Total RNA isolation from normal gastrointestinal whole tissues and isolated glands

Total RNAs from frozen tissues were extracted with TRIzol total RNA isolation reagent (Invitrogen, Carlsbad, CA, USA) according to the manufacturer's instructions [19, 22, 47]. For the stomach, neighboring tissues were evaluated for their histology either of the presence or absence of IM irrespective of the presence of gastric component. Individual ethanol-fixed isolated classified glands were transferred to 0.5-ml microfuge tubes under an inverted microscope and subjected to total RNA isolation as described [48, 49]. A total of 12 isolated classified glands were analyzed separately.

Relative quantitative analysis for isolated glands

First strand cDNAs were synthesized as previously reported [48, 49] using the Thermoscript RT-PCR System (Invitrogen) according to the manufacturer's instructions. Relative quantitative PCR for CA1, sucrase–isomaltase, and MUC5AC was performed with the LightCycler system (Roche Diagnostics, Mannheim, Germany), using β-actin as an internal control [49]. The 5′ and 3′ primer sequences are listed in Table 1. PCR was performed basically as described [48, 49] using a SYBR Green PCR Core Reagents kit (Perkin-Elmer Applied Biosystems, Foster City, CA, USA). Quantification was performed as earlier established using β-actin as an internal control. The values for corrected crossing points were calculated by subtraction of the crossing points of the gene of interest from that of β-actin, then used for statistical analyses applying the Mann–Whitney *U* test as earlier described [48, 49]. Specificity of the PCR reaction was confirmed using the melting program provided with the LightCycler software. To further confirm that there was no obvious primer dimer formation or amplification of any extra bands, samples were electrophoresed in 2.5% agarose gels and visualized with ethidium bromide after the LightCycler reaction. Total RNA samples without RT provided a control for PCR amplification (data not shown). The sample correlation coefficient was used for comparisons. A correlation between two factors with relative quantitative real-time RT-PCR was evaluated using Spearman's nonparametric correlation coefficient by rank. *P* values <0.05 were considered statistically significant.

Results

The expression of CA1, sucrase, and MUC5AC in normal gastrointestinal mucosa, and in pyloric mucosa having IM glands, associated with chronic gastritis.

Figure 1 shows double staining of CA1 and sucrase in normal colon (Fig. 1a), jejunum (Fig. 1b), and pyloric mucosa (Fig. 1c). Expression of CA1 was detected in cy-

Table 1 Primer sequences for real-time RT-PCR

Target genes	Orientation	Sequence	Product length (bp)	GeneBank accession nos.
Carbonic anhydrase 1	Upper	TGACCCCTCTACTCTCCTTCCT	187	NM_001738
	Lower	CATGGGGACAGCGTTATCAC		
Sucrase–isomaltase	Upper	CAAATATCGACTCGCCTGCCATCAG	193	XM_010952
	Lower	CACCATGAGCATTGCCCTCCTCTT		
MUC5AC	Upper	CAGAAATCCAGGACAACCAC	192	AJ298317
	Lower	AACAGGGCTCGGAGTAGTTTTA		
Beta-actin	Upper	TGGCACCCAGCACAATGAAG	142	M10277
	Lower	GATGGAGGGGCCGGACTC		

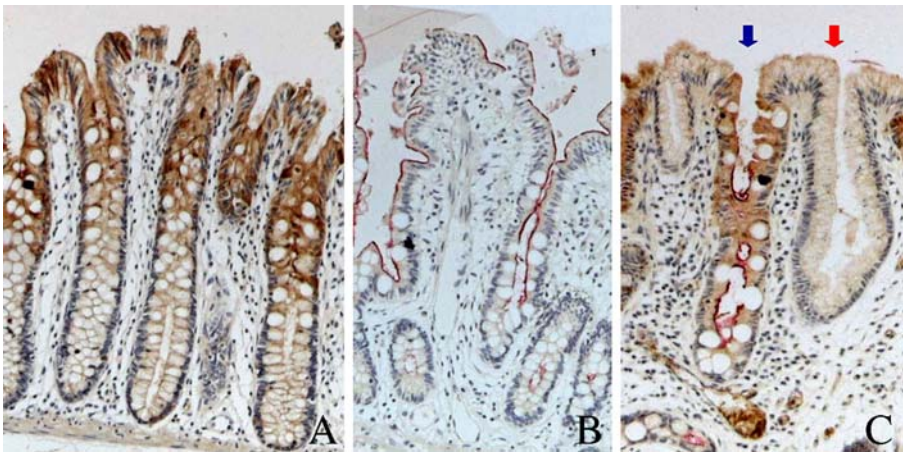


Fig. 1 Double staining of CA1 and sucrase in normal colon, jejunum, and stomach with IM. **a** Expression of CA1 is clearly evident in epithelial cells located on the luminal side of colonic mucosa, but not in the jejunum. **b** Sucrase, on the other hand, is present on the luminal surfaces of mature small intestinal absorptive cells, but not in the colon. **c** In the pyloric region with chronic gastritis, gastric foveolar cells of pyloric glands have neither CA1 nor sucrase expression (*red arrow*), whereas IM glands demonstrate both CA1 cytoplasmic staining and sucrase expression at their luminal surfaces (*blue arrow*). Original magnification, ×200. *CA1*, carbonic anhydrase 1; *IM*, intestinal metaplasia

toplasm of colon epithelial cells, especially on the luminal side of colonic mucosa, but not in the jejunum. Sucrase, on the other hand, was present on the luminal surfaces of mature small intestinal absorptive cells, but not in the colon. Neither CA1 nor sucrase expression was detected in the gastric foveolar cells of pyloric glands (Fig. 1c, red arrow). However, in the pyloric region with chronic gastritis, some IM glands had both CA1 cytoplasmic staining and sucrase expression at their luminal surfaces (Fig. 1c, blue arrow). Erythrocytes in blood vessels beneath the glands cross-reacted with the anti-CA1 antibody (Fig. 1c). Figure 2 shows results of RT-PCR analyses of CA1, sucrase–isomaltase, and MUC5AC in the normal alimentary tract including the colon, jejunum, and antrum of the stomach, with or without IM. Products of β-actin detected as a 142-bp band were used as an internal and sample quality control. CA1 RT-PCR products were detected as a 187-bp band in the colon, but not the antrum or jejunum, whereas RT-PCR products of sucrase–isomaltase were detected as a 193-bp band in the jejunum, but not the antrum or colon, compatible with the immunohistochemistry results. MUC5AC RT-PCR products were detected as a 192-bp band in the normal antrum of stomach, but not in the colon or jejunum. In pyloric mucosa having IM glands, PCR products of all of the abovementioned epithelial cell markers proved detectable (Fig. 2).

The expression of MUC5AC and sucrase in both CA1-positive and CA1-negative IM glands

Next, we evaluated the expression of gastrointestinal differentiation markers in IM at the gland level in serial sections. Figure 3 illustrates immunoreactivitiy of MUC5AC, CA1, sucrase, MUC2, villin, and Cdx2 in IM glands. Elevated MUC5AC expression was observed in CA1-negative mucous cells of GI-IM glands (Fig. 3b and c, red arrow), compared with the CA1-positive I-IM (Fig. 3b and c, blue arrow). The expression of sucrase was more strongly detected on the luminal surfaces of CA1-positive IM gland cells than in CA1-negative IM glands (Fig. 3d). MUC2, villin, and Cdx2 expression was observed in intestinal metaplastic cells irrespective of CA1 expression (Fig. 3e–g, respectively).

To quantitatively clarify the relation of CA1, MUC5AC, and sucrase, 850 glands, comprising 259 pyloric and 591 IM glands, were immunohistochemically evaluated in the pyloric regions of 10 CA1 positive surgically resected cases among a total of 15 cases. In the pyloric glands, all mucous cells demonstrated MUC5AC staining, whereas neither CA1 nor sucrase-positive cells were observed. Among 591 IM glands, totals of 139 (23.5%) and 452 (76.5%) were judged to be CA1 positive and CA1 negative, respectively. The average score for MUC5AC in CA1-positive IM was lower than that in CA1-negative IM with statistical significance ($P<0.0001$) (Fig. 4a). On the other

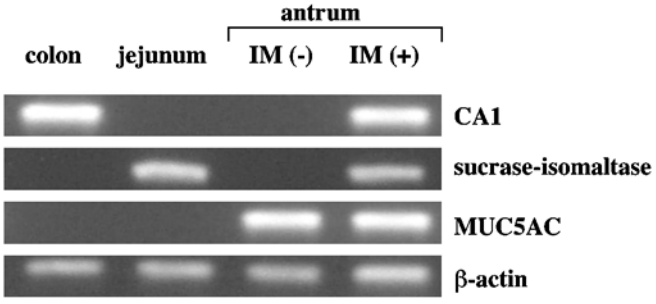


Fig. 2 CA1, sucrase–isomaltase, MUC5AC, and β-actin mRNA expression in colon, jejunum, and antrum of the stomach, with or without IM. CA1 is expressed only in colon, and sucrase–isomaltase only in jejunum. Antral mucosa possesses MUC5AC mRNA and ectopically expresses CA1 and sucrase–isomaltase with occurrence of IM. Products of β-actin detected as a 142-bp band were used as an internal control. *CA1*, carbonic anhydrase 1; *IM*, intestinal metaplasia

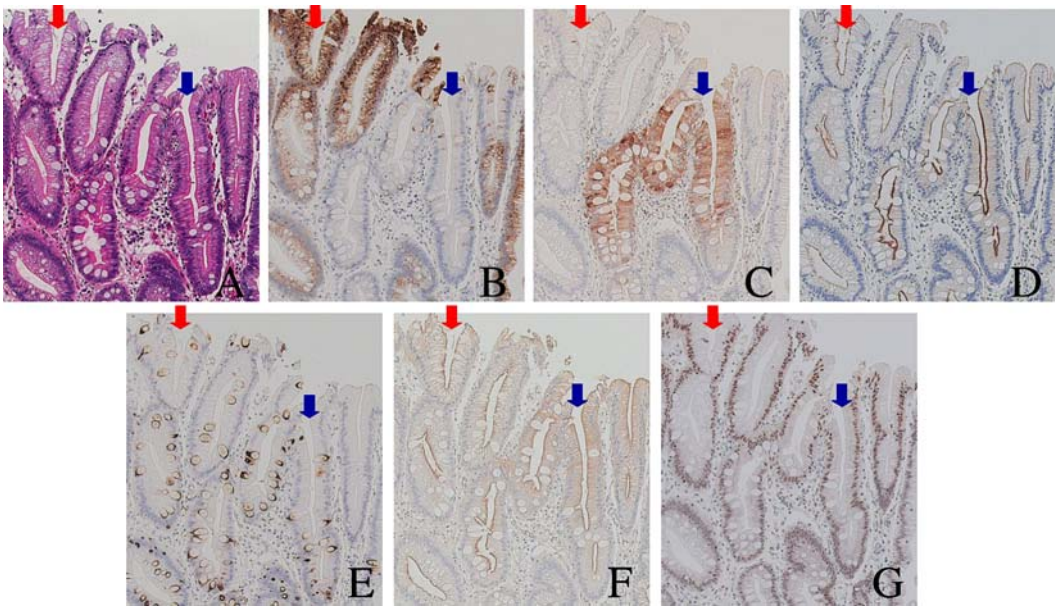


Fig. 3 Histology of IM and expression of gastric and intestinal markers. **a** H&E staining; **b** MUC5AC is apparent in the cytoplasm of CA1-negative (*red arrow*) IM glands, with little expression detected in CA1-positive (*blue arrow*) IM glands; **c** CA1 cytoplasmic staining is observed in the mucous cells of some IM glands (*blue arrow*), but not in others (*red arrow*); **d** Sucrase is apparent at the luminal surfaces of IM glands; **e** MUC2 is detectable in the cytoplasm of IM glands; **f** Villin is positive at the luminal surfaces of IM glands; **g** Cdx2 nuclear staining is apparent in IM glands. Original magnification, ×200. *CA1*, carbonic anhydrase 1; *IM*, intestinal metaplasia

hand, the average score for sucrase in CA1-positive IM was significantly higher than that in CA1-negative tissue (P<0.0001) (Fig. 4b). Considering sucrase expression, many of IM glands (80.4%=475/591) possessed sucrase on the luminal surface. Sucrase-negative IM glands in turn had high level of MUC5AC, 115 IM glands showing score 3 of MUC5AC and only 1 gland having score 2. Thus, sucrase preferred to express more strongly in I-IM than in GI-IM.

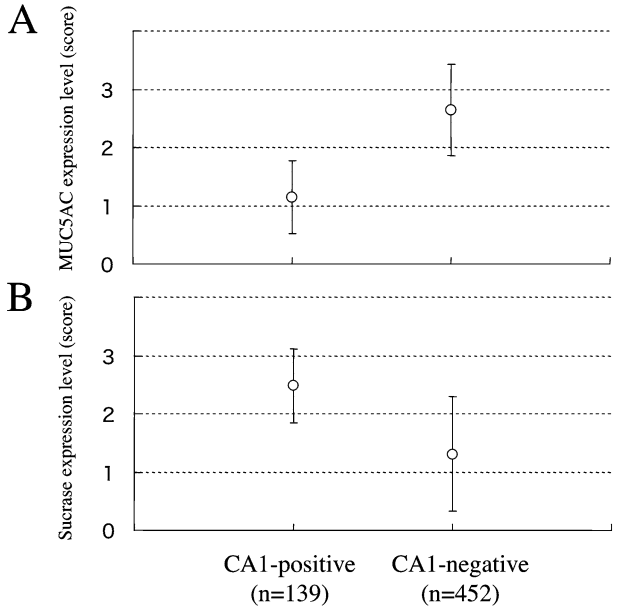


Fig. 4 Relations among MUC5AC, sucrase, and CA1 expression in IM glands by immunohistochemistry. **a** The scores for MUC5AC expression in CA1-positive and CA1-negative IMs are 1.15±0.63 and 2.64±0.78 (average±SD) (P<0.0001). **b** The scores for sucrase expression in CA1-positive and CA1-negative IMs are 2.48±0.63 and 1.31±0.98 (P<0.0001). *CA1*, carbonic anhydrase 1; *IM*, intestinal metaplasia

Comparison of HID-AB staining based IM subtypes with CA1/MUC5AC expression

Inasmuch as HID-AB staining has been widely used for classification of IM in terms of small intestinal sialomucin and colonic sulfomucin expression, we compared the localization of these mucins and the presence of CA1 and MUC5AC proteins. A total of 444 IM glands were evaluated for mucin expression and were classified into 256 type I glands having no mucins in columnar cells but with goblet cells, 104 type II glands with blue-stained columnar cells possessing sialomucins, and 84 type III glands with brown-stained columnar cells producing sulphomucins. Then, serial sections were assessed for expression of a colonic marker, CA1, and also a gastric marker, MUC5AC, for each subtype (Fig. 5 and Table 2). The number of glands with CA1 expression proved higher in type I complete IM compared to types II and III incomplete IM (P<0.005). Furthermore, there turned out to be no differences between the types II and III in terms of CA1 expression, and no correlation with colonic sulfomucin expression was apparent. Considering the gastric marker, type I glands possess less MUC5AC core protein than types II and III (P<0.0001), the last demonstrating the most MUC5AC-positive glands (79.8 and 90.5%, respectively), although this was not statistically significant (P=0.066).

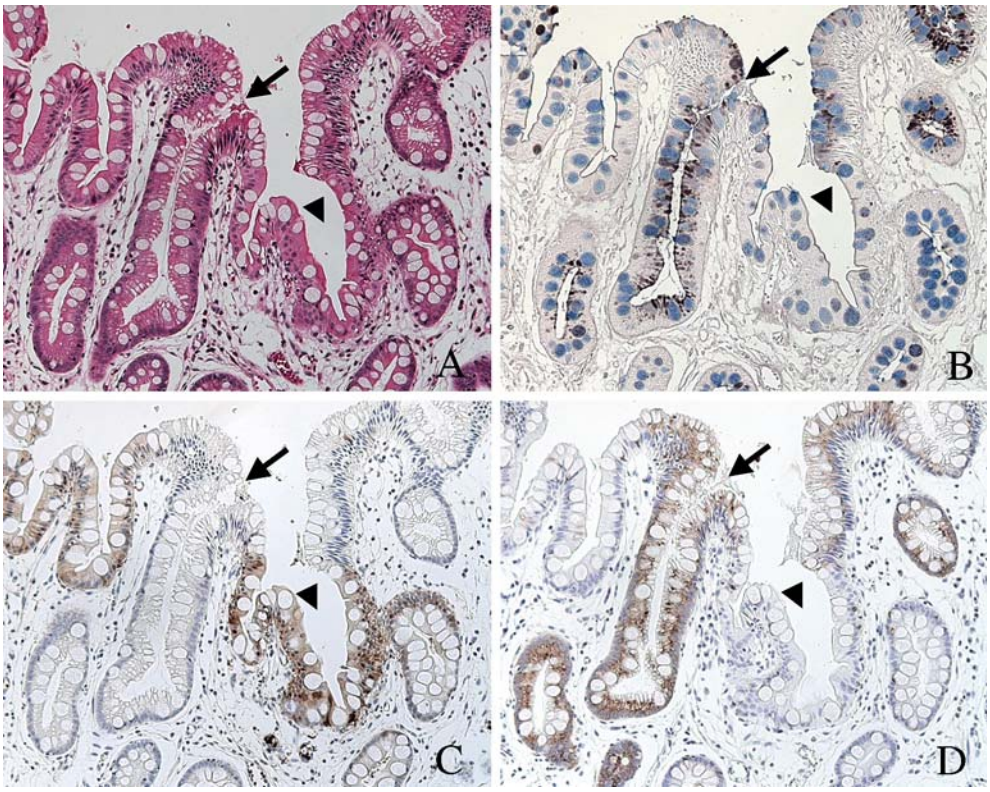


Fig. 5 HID-AB staining patterns and expression of CA1 and MUC5AC in IM glands. **a** H&E staining; **b** HID-AB staining showing subtype III (*arrow*) and subtype I (*arrowhead*) IM glands; **c** CA1 cytoplasmic staining in the columnar cells in one type I IM gland (*arrowhead*), but not in another (*arrow*); **d** MUC5AC is apparent in the cytoplasm of type III gland (*arrow*) IM glands, but expression is limited in type I (*arrowhead*) IM glands. Original magnification, ×125

Relative mRNA expression of CA1, sucrase–isomaltase, and MUC5AC in isolated GI-IM and I-IM glands by real-time RT-PCR

To determine the reliability of the data from the immunohistochemical analyses, we evaluated the relative mRNA levels for CA1, sucrase–isomaltase, and MUC5AC by real-time PCR in the isolated IM glands. Twelve isolated IM glands were stained with AB and phenotypically divided into seven GI-IMs and five I-IMs, as shown in Fig. 6. RNA extraction was performed separately for each gland, and real-time RT-PCR analysis of CA1, sucrase–isomaltase, and MUC5AC was carried out at the single gland level. Average (±SE) normalized cycle numbers for MUC5AC, sucrase–isomaltase, and CA1 in GI-IM and I-IM are described in Table 3. The level of MUC5AC mRNA was drastically lower in I-IM compared to GI-IM ($P<0.005$). Inversely, expression of sucrase–isomaltase and CA1 mRNAs was increased from GI-IM to I-IM ($P<0.05$ and $P<0.005$, respectively). Figure 7a shows the relation between CA1 and MUC5AC in the 12 isolated IM glands. The relative MUC5AC mRNA expression was inversely correlated with that of CA1 ($P<0.05$). Figure 7b shows the positive link between CA1 and sucrase–isomaltase in the isolated IM glands ($P<0.05$).

Discussion

The present data provide clear evidence that CA1 expression correlates with sucrase expression in IM glands of pyloric mucosa, and inversely with MUC5AC expression, as assessed by immunohistochemistry and relative quantitative real-time RT-PCR. Some MUC5AC expression was observed in the cytoplasm of CA1-negative mucous cells in areas of IM, and the data from real-time RT-PCR at the single isolated gland level support the results of immunohistochemical analysis. We have previously suggested that intestinalization of gastric mucosa may represent a kind of homeotic transformation [45, 49]. Cdx2, an intestinal homeobox gene, is an important factor for the development of IM [7, 19], its gastric expression alone being sufficient to induce intestinal metaplasia in mice [25, 33]. Cdx2 mRNAs are widely present in the human intestinal

Table 2 Correlation of HID-AB staining and expression of CA1 and MUC5AC

	HID-AB		
	Type I	Type II	Type III
No. of glands (%)	256	104	84
CA1 (+)	35 (13.7)*	3 (2.9)	2 (2.4)
(−)	221 (86.3)	101 (97.1)	82 (97.6)
MUC5AC (+)	97 (37.9)**	83 (79.8)	76 (90.5)
(−)	159 (62.1)	21 (20.2)	8 (9.5)

*$P<0.005$ vs. type II, $P<0.005$ vs. type III
**$P<0.0001$ vs. type II, $P<0.0001$ vs. type III

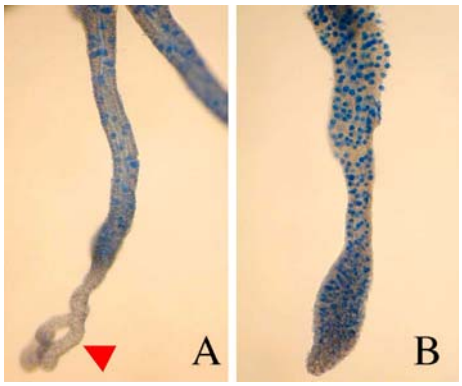


Fig. 6 Isolated IM glands from pyloric mucosa. **a** Isolated GI-IM gland with the presence of pyloric cells (*arrowhead*); **b** isolated I-IM gland with more Alcian blue-positive goblet cells. Alcian blue staining. *GI-IM*, gastric-and-intestinal mixed type intestinal metaplasia; *I-IM*, solely intestinal type intestinal metaplasia

and colonic mucosa, but not in the gastric mucosa [19]. However, the balance of gastric and intestinal specific transcription factors may be the determinant of phenotypes of IM glands, as well as the normal alimentary tract [49]. Intestinal metaplastic cells having CA1 expression exhibit Cdx2 nuclear staining, in line with the finding by Drummond et al. [4] that Cdx2 plays an important role in the intestine-specific expression of CA1. In vitro in HeLa cells, Cdx2 exerts a positive regulatory effect by binding to a motif 87-bp upstream of the CA1 TATA box [5]. Intestinal metaplastic cells having sucrase expression also exhibit Cdx2 nuclear staining, and Suh et al. [37] have shown that intestine-specific transcription of sucrase–isomaltase, a gene that is expressed exclusively in differentiated enterocytes, is dependent on binding of Cdx2 to an evolutionarily conserved promoter element.

Several subtypes of GI-IM and I-IM can be observed in the stomachs of patients suffering from chronic gastritis [13, 26, 45, 49], and these may be considered not as independent entities, but rather as a sequence of pathological states with gradual change from stomach to intestinal character [45]. In fact, experimentally, shift from GI-IM to I-IM can be observed on sequential observation in X-ray-treated rats [54] and *Helicobacter pylori*-infected gerbils [27]. In the present study, we demonstrated decrease of MUC5AC mRNAs and increase of sucrase–isomaltase mRNAs according to the shift from isolated GI-IM to isolated I-IM by relative quantitative real-time RT-PCR at the single gland level, compatible with our previous report [49]. CA1 mRNAs also increased in line with this shift. In the pyloric mucosa, GI-IM predominates over I-IM [13, 28]. In our previous study, a total of 2,004 glandular ducts were divided phenotypically into 569 (28.4%) pyloric, 1,290 (64.4%) GI-IM, and 145 (7.2%) I-IM glands, respectively, in pyloric areas with chronic gastritis

Table 3 List of IM glands for relative quantitative RT-PCR analysis

IM types	No.	β-actin	MUC5AC	Sucrase–isomaltase	Carbonic anhydrase 1
GI	1	0	−5.87	−14.71	−9.13
	2	0	−7.62	−10.49	−8.92
	3	0	−6.88	−10.43	−7.47
	4	0	−7.46	−9.03	−6.51
	5	0	−5.8	−8.19	−5.43
	6	0	−21.71	−13.07	−4.73
	7	0	−4.83	−13.42	−3.41
	Average± SE	0	−8.60± 2.22*	−11.33± 0.92**	−6.51± 0.81***
I	1	0	−69.95	−8.78	−3.12
	2	0	−71.56	−6.96	−1.01
	3	0	−67.87	−7.16	−0.41
	4	0	−65.55	−9.03	0.58
	5	0	−65.31	−7.1	1.16
	Average± SE	0	−68.05± 1.22	−7.81± 0.45	−0.56± 0.74

Relative PCR cycle numbers shown as β-actin as an internal control
*P<0.005 vs. I-IM
**P<0.05 vs. I-IM
***P<0.005 vs. I-IM

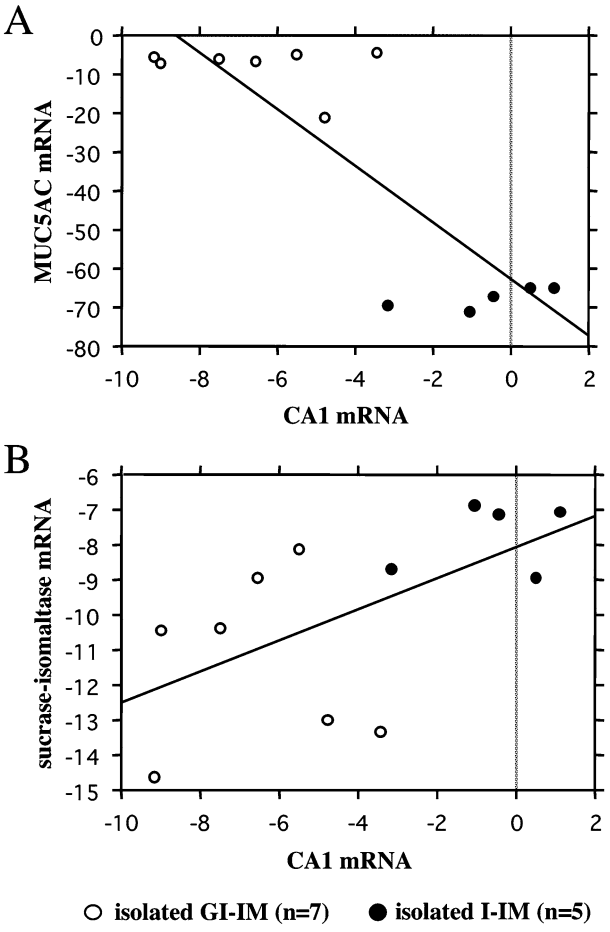


Fig. 7 Relative quantitative analysis correlation of MUC5AC, sucrase–isomaltase, and CA1 mRNAs. **a** Inverse correlation between the relative mRNA expression of CA1 and MUC5AC in isolated IM glands. y=−62.861−7.313×, r=0.720, P<0.05. **b** Correlation between the relative mRNA expression of CA1 and sucrase–isomaltase in isolated IM glands. y=−8.072+0.444×, r=0.369, P<0.05

[28]. Thus, from our present and previous data, we consider that CA1-positive IM glands may be more prone to alteration from GI-IM to I-IM compared with their CA1-negative counterparts in the pyloric region.

IM has been classified according to HID-AB staining [14], type I being considered to be virtually identical to the morphology of small intestine consisting of mucin-producing goblet cells and absorptive cells without mucin expression. Glands of types II and III are lined by goblet and columnar cells showing mild architectural distortion, respectively, with sialomucins/neutral mucins and sulphomucins in their columnar cells. Reis et al. [30] and Silva et al. [34] have analyzed expression of mucin patterns including MUC1, MUC2, MUC5AC, and MUC6 in IM glands and revealed the type I complete form to have little expression of MUC 1, MUC5AC, and MUC6 in any epithelial components, but strong expression of MUC2 in the goblet cells. In contrast, the incomplete forms of types II and III were found to express gastric markers, MUC1, MUC5AC, and MUC6, together with intestinal MUC2. Our data suggest that expression of CA1, a colonic marker, is not correlated with sulfomucin expression in type III IM, but rather is inversely related to incomplete IM expressing gastric mucins. Furthermore, CA1 was found to be more frequent in type I complete IM. On the other hand, small intestinal markers like sucrase may colocalize with gastric protein, MUC5AC, as noted with the gastric-and-intestinal-mixed phenotype.

IM is widely thought to be a precancerous lesion for differentiated type gastric cancers [1–3, 24, 36, 52, 55]. The hypothesis is based on morphological similarities between cancers and IM and on the results of comparisons of carcinomas and surrounding mucosa. However, previous studies on clonality of gastric cancers and phenotypic expression of each intestinal metaplastic or stomach cancer cells have pointed to several contradictions [8, 11, 15, 17, 23, 31, 40–44]. In addition, using microsatellite instability analysis, Tamura et al. [38] have provided evidence that the majority of differentiated adenocarcinomas of the stomach may develop through a de novo pathway. Endoh et al. [9] also made it clear that the genetic background of differentiated type tumors may differ among cellular phenotypes. In the present study, CA1 expression was observed in approximately one fourth of IM glands in the pyloric region by immunohistochemistry. We have previously shown that early stage gastric cancers, independent of the histological type, mainly consist of gastric phenotypic cancer cells, and a shift from gastric to intestinal phenotypic expression is observed with progression in experimental animal models [23, 39, 40, 41, 51, 53]. More than half of early differentiated gastric cancers have MUC5AC expression in humans [23]. However, the expression of CA1 inversely correlates with that of MUC5AC in IMs, suggesting that IM is important not as a precancerous lesion but rather as a paracancerous phenomenon [8, 18, 43]. Needless to say, many questions remain regarding the pathogenesis of IM as well as the actual relationship to gastric cancers.

In short, expression of gastric and colonic markers may be regulated in different manners, although both can be colocalized with a small intestinal marker. Although the regulatory mechanisms remain unclear, further study of stimulation and/or suppression by gastric and intestinal transcription factors appears warranted [49].

Acknowledgements This study was supported in part by a Grant-in-Aid for the Third-term Comprehensive 10-year Strategy for Cancer Control and a Grant-in-Aid for Cancer Research from the Ministry of Health, Labour and Welfare, Japan, and a Grant-in-Aid from the Ministry of Education, Culture, Sports, Science and Technology of Japan. The authors thank Dr. Malcolm A. Moore for revision of the scientific English language and Ms. Hisayo Ban for expert technical assistance. The anti-sucrase antibody was a generous gift from Dr. Kazuyuki Hirano, Department of Pharmaceutics, Gifu Pharmaceutical University, Gifu, Japan.

References

1. Correa P (1988) A human model of gastric carcinogenesis. Cancer Res 48:3554–3560
2. Correa P (1992) Human gastric carcinogenesis: a multistep and multifactorial process—First American Cancer Society Award Lecture on Cancer Epidemiology and Prevention. Cancer Res 52:6735–6740
3. Correa P (1995) *Helicobacter pylori* and gastric carcinogenesis. Am J Surg Pathol 19(Suppl 1):S37–S43
4. Drummond F, Sowden J, Morrison K, Edwards YH (1996) The caudal-type homeobox protein Cdx-2 binds to the colon promoter of the carbonic anhydrase 1 gene. Eur J Biochem 236:670–681
5. Drummond FJ, Sowden J, Morrison K, Edwards YH (1998) Colon carbonic anhydrase 1: transactivation of gene expression by the homeodomain protein Cdx2. FEBS Lett 423:218–222
6. Ectors N, Dixon MF (1986) The prognostic value of sulphomucin positive intestinal metaplasia in the development of gastric cancer. Histopathology 10:1271–1277
7. Eda A, Osawa H, Yanaka I, Satoh K, Mutoh H, Kihira K, Sugano K (2002) Expression of homeobox gene CDX2 precedes that of CDX1 during the progression of intestinal metaplasia. J Gastroenterol 37:94–100
8. Egashira Y, Shimoda T, Ikegami M (1999) Mucin histochemical analysis of minute gastric differentiated adenocarcinoma. Pathol Int 49:55–61
9. Endoh Y, Sakata K, Tamura G, Ohmura K, Ajioka Y, Watanabe H, Motoyama T (2000) Cellular phenotypes of differentiated-type adenocarcinomas and precancerous lesions of the stomach are dependent on the genetic pathways. J Pathol 191:257–263
10. Filipe MI, Potet F, Bogomoletz WV, Dawson PA, Fabiani B, Chauveinc P, Fenzy A, Gazzard B, Goldfain D, Zeegen R (1985) Incomplete sulphomucin-secreting intestinal metaplasia for gastric cancer. Preliminary data from a prospective study from three centres. Gut 26:1319–1326
11. Hattori T (1986) Development of adenocarcinomas in the stomach. Cancer 57:1528–1534
12. Huang CB, Xu J, Huang JF, Meng XY (1986) Sulphomucin colonic type intestinal metaplasia and carcinoma in the stomach. A histochemical study of 115 cases obtained by biopsy. Cancer 57:1370–1375
13. Inada K, Nakanishi H, Fujimitsu Y, Shimizu N, Ichinose M, Miki K, Nakamura S, Tatematsu M (1997) Gastric and intestinal mixed and solely intestinal types of intestinal metaplasia in the human stomach. Pathol Int 47:831–841
14. Jass JR, Filipe MI (1979) A variant of intestinal metaplasia associated with gastric carcinoma: a histochemical study. Histopathology 3:191–199

15. Kawachi H, Takizawa T, Eishi Y, Shimizu S, Kumagai J, Funata N, Koike M (2003) Absence of either gastric or intestinal phenotype in microscopic differentiated gastric carcinomas. J Pathol 199:436–446
16. Kawachi T, Kogure K, Tanaka N, Tokunaga A, Sugimura T (1974) Studies of intestinal metaplasia in the gastric mucosa by detection of disaccharidases with "Tes-Tape". J Natl Cancer Inst 53:19–30
17. Kushima R, Hattori T (1993) Histogenesis and characteristics of gastric-type adenocarcinomas in the stomach. J Cancer Res Clin Oncol 120:103–111
18. Matsukuma A, Mori M, Enjoji M (1990) Sulphomucin-secreting intestinal metaplasia in the human gastric mucosa. An association with intestinal-type gastric carcinoma. Cancer 66:689–694
19. Mizoshita T, Inada K, Tsukamoto T, Kodera Y, Yamamura Y, Hirai T, Kato T, Joh T, Itoh M, Tatematsu M (2001) Expression of Cdx1 and Cdx2 mRNAs and relevance of this expression to differentiation in human gastrointestinal mucosa—with special emphasis on participation in intestinal metaplasia of the human stomach. Gastric Cancer 4:185–191
20. Mizoshita T, Joh T, Oshima T, Yamada T, Ohara H, Nomura T, Okada N, Itoh M (2002) Differential expression of decay-accelerating factor isoforms in the digestive tract of guinea pig. Life Sci 70:867–876
21. Mizoshita T, Tsukamoto T, Nakanishi H, Inada K, Ogasawara N, Joh T, Itoh M, Yamamura Y, Tatematsu M (2003) Expression of Cdx2 and the phenotype of advanced gastric cancers: relationship with prognosis. J Cancer Res Clin Oncol 129:727–734
22. Mizoshita T, Inada K, Tsukamoto T, Nozaki K, Joh T, Itoh M, Yamamura Y, Ushijima T, Nakamura S, Tatematsu M (2004a) Expression of the intestine-specific transcription factors, Cdx1 and Cdx2, correlates shift to an intestinal phenotype in gastric cancer cells. J Cancer Res Clin Oncol 130:29–36
23. Mizoshita T, Tsukamoto T, Inada K, Ogasawara N, Hirata A, Kato S, Joh T, Itoh M, Yamamura Y, Tatematsu M (2004b) Immunohistochemically detectable Cdx2 is present in intestinal phenotypic elements in early gastric cancers of both differentiated and undifferentiated types, with no correlation to non-neoplastic surrounding mucosa. Pathol Int 54:392–400
24. Morson BC (1955) Carcinoma arising from areas of intestinal metaplasia in the gastric mucosa. Br J Cancer 9:377–385
25. Mutoh H, Hakamata Y, Sato K, Eda A, Yanaka I, Honda S, Osawa H, Kaneko Y, Sugano K (2002) Conversion of gastric mucosa to intestinal metaplasia in Cdx2-expressing transgenic mice. Biochem Biophys Res Commun 294:470–479
26. Niwa T, Ikehara Y, Nakanishi H, Tanaka H, Inada K, Tsukamoto T, Ichinose M, Tatematsu M (2005) Mixed gastric- and intestinal-type Metaplasia is formed by cells with dual intestinal and gastric differentiation. J Histochem Cytochem 53:75–85
27. Nozaki K, Shimizu N, Tsukamoto T, Inada K, Cao X, Ikehara Y, Kaminishi M, Sugiyama A, Tatematsu M (2002b) Reversibility of heterotopic proliferative glands in glandular stomach of *Helicobacter pylori*-infected Mongolian Gerbils on eradication. Jpn J Cancer Res 93:374–381
28. Otsuka T, Tsukamoto T, Mizoshita T, Inada K, Takenaka Y, Kato S, Yamamura Y, Miki K, Tatematsu M (2005) Co-existence of gastric and intestinal type endocrine cells in gastric-and-intestinal mixed intestinal metaplasia of the human stomach. Pathol Int (in press)
29. Parkkila S, Parkkila AK, Juvonen T, Rajaniemi H (1994) Distribution of the carbonic anhydrase isoenzymes I, II, and VI in the human alimentary tract. Gut 35:646–650
30. Reis CA, David L, Correa P, Carneiro F, de Bolos C, Garcia E, Mandel U, Clausen H, Sobrinho-Simoes M (1999) Intestinal metaplasia of human stomach displays distinct patterns of mucin (MUC1, MUC2, MUC5AC, and MUC6) expression. Cancer Res 59:1003–1007
31. Saito A, Shimoda T, Nakanishi Y, Ochiai A, Toda G (2001) Histologic heterogeneity and mucin phenotypic expression in early gastric cancer. Pathol Int 51:165–171
32. Segura DI, Montero C (1983) Histochemical characterization of different types of intestinal metaplasia in gastric mucosa. Cancer 52:498–503
33. Silberg DG, Sullivan J, Kang E, Swain GP, Moffett J, Sund NJ, Sackett SD, Kaestner KH (2002) Cdx2 ectopic expression induces gastric intestinal metaplasia in transgenic mice. Gastroenterology 122:689–696
34. Silva E, Teixeira A, David L, Carneiro F, Reis CA, Sobrinho-Simoes J, Serpa J, Veerman E, Bolscher J, Sobrinho-Simoes M (2002) Mucins as key molecules for the classification of intestinal metaplasia of the stomach. Virchows Arch 440:311–317
35. Sowden J, Leigh S, Talbot I, Delhanty J, Edwards Y (1993) Expression from the proximal promoter of the carbonic anhydrase 1 gene as a marker for differentiation in colon epithelia. Differentiation 53:67–74
36. Stemmermann GN, Hayashi T (1968) Intestinal metaplasia of the gastric mucosa: a gross and microscopic study of its distribution in various disease states. J Natl Cancer Inst 41:627–634
37. Suh E, Chen L, Taylor J, Traber PG (1994) A homeodomain protein related to caudal regulates intestine-specific gene transcription. Mol Cell Biol 14:7340–7351
38. Tamura G, Sakata K, Maesawa C, Suzuki Y, Terashima M, Satoh K, Sekiyama S, Suzuki A, Eda Y, Satodate R (1995) Microsatellite alterations in adenoma and differentiated adenocarcinoma of the stomach. Cancer Res 55:1933–1936
39. Tatematsu M, Katsuyama T, Fukushima S, Takahashi M, Shirai T, Ito N, Nasu T (1980) Mucin histochemistry by paradoxical concanavalin A staining in experimental gastric cancers induced in Wistar rats by *N*-methyl-*N*-nitro-*N*-nitrosoguanidine or 4-nitroquinoline 1-oxide. J Natl Cancer Inst 64:835–843
40. Tatematsu M, Furihata C, Katsuyama T, Hasegawa R, Nakanowatari J, Saito D, Takahashi M, Matsushima T, Ito N (1983) Independent induction of intestinal metaplasia and gastric cancer in rats treated with *N*-methyl-*N*′-nitro-*N*-nitrosoguanidine. Cancer Res 43:1335–1341
41. Tatematsu M, Katsuyama T, Furihata C, Tsuda H, Ito N (1984) Stable intestinal phenotypic expression of gastric and small intestinal tumor cells induced by *N*-methyl-*N*′-nitro-*N*-nitrosoguanidine or methylnitrosourea in rats. Gann 75:957–965
42. Tatematsu M, Furihata C, Katsuyama T, Miki K, Honda H, Konishi Y, Ito N (1986) Gastric and intestinal phenotypic expressions of human signet ring cell carcinomas revealed by their biochemistry, mucin histochemistry, and ultrastructure. Cancer Res 46:4866–4872
43. Tatematsu M, Ichinose M, Miki K, Hasegawa R, Kato T, Ito N (1990a) Gastric and intestinal phenotypic expression of human stomach cancers as revealed by pepsinogen immunohistochemistry and mucin histochemistry. Acta Pathol Jpn 40:494–504
44. Tatematsu M, Fukami H, Yamamoto M, Nakanishi H, Masui T, Kusakabe N, Sakakura T (1994) Clonal analysis of glandular stomach carcinogenesis in C3H/HeN⇔BALB/c chimeric mice treated with *N*-methyl-*N*-nitrosourea. Cancer Lett 83:37–42
45. Tatematsu M, Tsukamoto T, Inada K (2003) Stem cells and gastric cancer—role of gastric and intestinal mixed intestinal metaplasia. Cancer Sci 94:135–141
46. Teglbjaerg PS, Nielsen HO (1978) "Small intestinal type" and "colonic type" intestinal metaplasia of the human stomach, and their relationship to the histogenetic types of gastric adenocarcinoma. Acta Pathol Microbiol Scand, A 86A:351–355
47. Tsukamoto T, Yoo J, Hwang SI, Guzman RC, Hirokawa Y, Chou YC, Olatunde S, Huang T, Bera TK, Yang J, Nandi S (2000) Expression of MAT1/PEA-15 mRNA isoforms during physiological and neoplastic changes in the mouse mammary gland. Cancer Lett 149:105–113

48. Tsukamoto T, Fukami H, Yamanaka S, Yamaguchi A, Nakanishi H, Sakai H, Aoki I, Tatematsu M (2001) Hexosaminidase-altered aberrant crypts, carrying decreased hexosaminidase alpha and beta subunit mRNAs, in colon of 1,2-dimethylhydrazine-treated rats. Jpn J Cancer Res 92:109–118
49. Tsukamoto T, Inada K, Tanaka H, Mizoshita T, Mihara M, Ushijima T, Yamamura Y, Nakamura S, Tatematsu M (2004) Down regulation of a gastric transcription factor, Sox2, and ectopic expression of intestinal homeobox genes, Cdx1 and Cdx2: inverse correlation during progression from gastric/intestinal-mixed to complete intestinal metaplasia. J Cancer Res Clin Oncol 130:135–145
50. Tsukamoto T, Mizoshita T, Mihara M, Tanaka H, Takenaka Y, Yamamura Y, Nakamura S, Ushijima T, Tatematsu M (2005) Sox2 expression in human stomach adenocarcinomas with gastric and gastric-and-intestinal-mixed phenotypes. Histopathology (in press)
51. Yoshikawa A, Inada Ki K, Yamachika T, Shimizu N, Kaminishi M, Tatematsu M (1998) Phenotypic shift in human differentiated gastric cancers from gastric to intestinal epithelial cell type during disease progression. Gastric Cancer 1:134–141
52. You WC, Blot WJ, Li JY, Chang YS, Jin ML, Kneller R, Zhang L, Han ZX, Zeng XR, Liu WD et al (1993) Precancerous gastric lesions in a population at high risk of stomach cancer. Cancer Res 53:1317–1321
53. Yuasa H, Hirano K, Kodama H, Nakanishi H, Imai T, Tsuda H, Imaida K, Tatematsu M (1994) Immunohistochemical demonstration of intestinal-type alkaline phosphatase in stomach tumors induced by *N*-methyl-*N*′-nitro-*N*-nitrosoguanidine in rats. Jpn J Cancer Res 85:897–903
54. Yuasa H, Inada K, Watanabe H, Tatematsu M (2002) A phenotypic shift from gastric-intestinal to solely intestinal cell types in intestinal metaplasia in rat stomach following treatment with X-rays. J Toxicol Pathol 15:85–93
55. Yuasa Y (2003) Control of gut differentiation and intestinal-type gastric carcinogenesis. Nat Rev Cancer 3:592–600

Virchows Arch (2005) 447: 816–822
DOI 10.1007/s00428-005-0029-9

ORIGINAL ARTICLE

Yu-Zhen Feng · Tanri Shiozawa · Akiko Horiuchi · Hsien-Chang Shih · Tsutomu Miyamoto · Hiroyasu Kashima · Akihisa Suzuki · Toshio Nikaido · Ikuo Konishi

Intratumoral heterogeneous expression of p53 correlates with p53 mutation, Ki-67, and cyclin A expression in endometrioid-type endometrial adenocarcinomas

Received: 19 February 2005 / Accepted: 10 June 2005 / Published online: 14 July 2005
© Springer-Verlag 2005

Abstract To further elucidate the significance of p53 mutation in endometrial carcinoma, we investigated it in endometrioid-type endometrial carcinomas showing intratumoral heterogeneous p53 expression. In addition, we also examined the correlation of p53 mutation and cyclin A expression, because we previously reported a topological correlation between the expression of p53 and cyclin A. The p53 mutation in exons 5–8 in 54 cases of endometrial carcinoma showing immunohistochemical expression of p53 was examined using microdissected tissue DNAs. Of the 54 p53-positive endometrial carcinomas, 23 (43%) had p53 mutation with a tendency in histologically higher grade tumors. Ten of the 54 showed a heterogeneous p53 expression, and in 9 of the 10 cases, p53 mutation was present only in p53-positive sites, which were often found in histologically less differentiated areas with elevated Ki-67 in the same tumor. Cyclin A expression was topologically observed in p53-positive areas; however, it was noted in both tumors with (12/23, 52%) and without (18/31, 58%) p53 mutation. These results suggest that p53 mutation is a late event and plays an important role in the acquisition of malignant potentials in endometrioid-type endometrial adenocarcinomas. Unexpectedly, accumulation of the p53 protein itself may be important in cyclin A overexpression.

Y.-Z. Feng · T. Shiozawa (✉) · A. Horiuchi · H.-C. Shih · T. Miyamoto · H. Kashima · A. Suzuki · I. Konishi
Department of Obstetrics and Gynecology,
Shinshu University School of Medicine,
3-1-1 Asahi, Matsumoto,
390-8621, Japan
e-mail: tanri@hsp.md.shinshu-u.ac.jp
Tel.: +81-263-372719
Fax: +81-263-340944

T. Nikaido
Department of Organ Regeneration,
Shinshu University Graduate School of Medicine,
3-1-1 Asahi, Matsumoto,
390-8621, Japan

Keywords Endometrial carcinoma · p53 mutation · Heterogeneity · Cyclin A · Ki-67

Introduction

Endometrial carcinoma is one of the most common malignancies in the female genital tract [15] and accounts for approximately 25% of all cancer-related deaths from gynecological malignancies in developed countries [2]. Recent studies revealed that several genetic and epigenetic changes including alterations to the tumor suppressor p53 gene have occurred in endometrial carcinomas [16]. Endometrial carcinomas are now classified into two histological subtypes, endometrioid type and nonendometrioid-type carcinomas [15], and the molecular genetic changes differ between the two types [3, 13, 16]. In the representative nonendometrioid-type carcinoma, i.e., serous papillary adenocarcinoma, p53 mutation is reportedly present in approximately 90% of cases as well as frequently found in its putative precursor, endometrial intraepithelial carcinoma, suggesting that p53 mutation is an early event. In contrast, the significance of p53 gene abnormalities in endometrioid-type adenocarcinomas has been less elucidated. Previous studies showed that p53 gene mutation or overexpression is present in 10–20% of cases and mostly in histologically high-grade tumors [3, 13, 16]. Our previous studies demonstrated that p53 protein expression is inversely correlated with the expression of estrogen receptors in endometrioid-type adenocarcinomas [17]. It is therefore hypothesized that p53 abnormalities may be involved in tumor progression via transformation into higher grade tumors with loss of hormone dependence.

Our previous studies also showed that p53 expression is topologically correlated with overexpression of cyclin A. Cell growth is known to be controlled by interactions of cell cycle-related molecules, such as cyclins and cyclin-dependent kinases (cdks) [21, 22], and abnormalities of these molecules have been reported in various human malignancies [4–6]. In endometrial carcinomas, we reported

that various cyclins and cdks are overexpressed [24, 25], and that overexpression of cyclin A was more frequently found in histologically high-grade tumors and could be an independent prognostic factor for patient survival [23]. Thus, coexpression of p53 protein and cyclin A in endometrial carcinomas suggests that p53 mutation affects cyclin A expression, resulting in a transformation into a more aggressive phenotype via the acquisition of higher proliferative activity.

To address the above hypotheses, we analyzed the presence or absence of p53 gene mutations in endometrial carcinomas, especially of endometrioid type, showing immunoreactivity for p53 protein. Then, we examined the correlation of p53 mutation with histological grade and the expression of cyclin A and the proliferation marker Ki-67. Cases showing heterogeneity of p53 protein expression in the same tumor may be suitable model for an analysis on the functional role of p53 mutation in tumor progression. In these tumors, we examined the possible genetic heterogeneity of p53 mutation using the respective tissues obtained by microdissection and also analyzed the topological correlation with the expression of cyclin A and Ki-67.

Materials and methods

Case selection and DNA extraction

One hundred and thirty-five cases of endometrioid-type endometrial carcinoma were collected from our pathology files for the screening of immunohistochemical expression of p53 using formalin-fixed, paraffin-embedded tissue sections. Clinicopathological characteristics of the patients used for the screening were summarized in Table 1. Consequently, 54 (40%) of the 135 endometrial carcinomas were shown to be positive for p53 protein and were subject to the current study. The age of the 54 patients ranged from 30 to 76 years. Clinicopathological feature of the 54 patients were was also summarized in Table 1. Each tissue sample was used with the approval of the Ethics Committee of Shinshu University after obtaining written consent from the patients.

DNA extraction was performed as previously described [30]. In brief, four or five 8-μm-thick tissue sections of endometrial carcinoma which showed positive staining for p53 were prepared from the paraffin-embedded blocks. The sections were deparaffinized in xylene and rehydrated through graded alcohol. Tumor tissues corresponding to the p53 area were scraped with a razor from consecutive tissue sections avoiding areas of normal tissue using hematoxylin/eosin-stained slides as a template under the observation using stereomicroscope. In cases which showed a heterogeneous p53 immunostaining pattern, i.e., tumors that contained both p53-positive and p53-negative sites irrespective of the positive ratio, and the p53-positive sites are clearly demarcated by the negative sites, which can avoid the contamination of both sites during microdissection, the tissue DNA was scraped from both sites using a microdissection technique. For DNA extraction, the tissues were digested for 16–24 h at 55°C in a digestion buffer (2 mg/ml proteinase K and 0.5% Tween 20), then treated with phenol–chloroform.

Mutational analysis

Because 98% of p53 gene mutations in human cancers have been found in exons 5–8 [8], we also focused on these exons. The polymerase chain reaction–single strand conformational polymorphism (PCR-SSCP) method was used to detect the presence and pattern of p53 gene mutation, as described previously [10]. The oligonucleotide primers were designed based on a published sequence as follows [19]:

Exon 5	5′GGAATTCCTCTTCCTGCAGTAC3′
	5′GGAATTCGCCCCAGCTGCTCACCATCG3′
Exon 6	5′GGAATTCGATGGTGAGCAGCTGG3′
	5′GGAATCAGTTGCAAACCAGACCTCAGG3′
Exon 7	5′GGAATTCTCCTAGGTTGGCTCTGAC3′
	5′GGAATTCCAAGTGGCTCCTGACCTGGA3′
Exon 8	5′GGAATTCCCTATCCTGAGTAGTGGTAA3′
	5′GGAATTCCTGCTTGCTTACCTCG3′

Each exon was amplified by PCR using 0.5 μg of template DNA, sense and anti-sense primers, and an Ampli Taq Gold PCR kit (Applied Biosystems, Foster city, CA, USA). A total of 50 μl of reaction mixture was made according to the manufacturer's instructions, and PCR was commenced at 94°C for 3 min, followed by 35 cycles consisting of 94°C for 30 s, 55°C for 30 s, and 72°C for 1 min, with a final extension for 5 min. The PCR products was denatured at 80°C for 5 min, and 1.5 μl of the products was applied to a 5% polyacrylamide neutral gel containing 5% glycerol. The samples were run at 600 V for 7 h with fan cooling to both sides of the gel plate. After the electrophoresis, the gel was stained with SYBR Green II (Molecular Probes, Inc.,

Table 1 Summary of clinicopathological characteristics of the patients and the results of p53 mutation

	Stage		Grade			Total
	I+II	III+IV	1	2	3	
Patients screened for p53 expression	107	28	74	34	27	135
Patients with p53 expression	37 (35%)	18 (64%)[a]	27 (36%)	10 (29%)	17 (63%)	54 (40%)
Patients with p53 mutation	15 (14%)	8 (28%)	9 (12%)	6 (17%)	8 (30%)	23 (17%)

[a]Significantly different from that of stage I+II

Eugene, OR, USA) for 30 min, and the stained bands were analyzed with a FMBIO II Multi-View system (Hitachi, Tokyo, Japan).

When the SSCP band was suggestive of abnormality, the remaining PCR products was purified using an UltraClean PCR Clean-up kit (MO BIO Laboratories, Solana Beach, CA, USA) and subjected to direct sequencing. The direct sequencing was performed using purified products and the same sets of primers in a capillary automatic sequencer (ABI PRISM 3100 Genetic Analyzer, Applied Biosystems) at Shinshu University. Sequence data were analyzed using the Basic Local Alignment Search Tool (BLAST) software located at the National Center for Biotechnology Information (NCBI) web site: http://www.ncbi.nlm.nih.gov.

Immunohistochemistry

Immunostaining was performed using specific antibodies against p53 (DO-1, Immunotech, Marseille, France), Ki-67 (Immunotech), and cyclin A (BF683, Santa Cruz Biotechnology, Santa Cruz, CA, USA). Indirect immunohistochemical staining was performed by the avidin–biotin–peroxidase complex method using a Histofine SAB-PO detector kit (Nichirei, Tokyo, Japan) with microwave pretreatment as described previously [23].

The specific staining of each antibody was identified in the nucleus with/without cytoplasm. Immunoreactivity was evaluated as the percentage of nuclear-positive cells in 500 arbitrarily selected cells in five high power fields and described as a positivity index (PI). With regard to the expression of p53 and cyclin A, when the PI of a tumor was more than 1%, the case was regarded as an "overexpression" or "positive" case, because the PI of these molecules in normal endometrial glandular cells was less than 1% [23]. Cases with a PI of 1–5% were defined as focally positive (+), those with a PI of 6–50% as regionally positive (++), and those with a PI of >50% as diffusely positive (+++).

Statistical analysis

The difference in the p53 mutation ratio among the degree of p53 immunostaining, clinical stages and histological grades was examined using Mann–Whitney's *U* test (Sidak method). The difference in the PI of each immunostaining among the degree of p53 immunostaining, clinical stages, and histological grades was examined with the Kruskal–Wallis test. $p<0.05$ was considered significant.

Results

p53 expression and p53 gene mutation

Of the 54 cases positive for p53 protein, the immunostaining was focal in 14, regional in 18, and diffuse in 22 cases. Those 54 cases were subjected to a PCR-SSCP analysis of the p53 gene, and 26 showed SSCP abnormality (Fig. 1). Direct sequencing was then performed in the 26 cases with abnormal SSCP, and a total of 23 (43%) of the 54 cases were revealed to have p53 mutation. The 23 cases had a total of 26 mutation sites. The number of cases mutated in exon 5, 6, 7, and 8 was 4, 5, 14 and 3, respectively (Table 2, Fig. 2). The 26 mutations consisted of 22 missense and 4 silent mutations.

According to the immunostaining, p53 mutation was present in 8 (57%) of the 14 cases with focal staining, 4 (21%) of the 19 with regional staining, and 11 (50%) of the 22 with diffuse immunostaining (Fig. 3). There was no significant difference of the positive ratio among staining intensities. According to FIGO stage, the 23 cases with p53 mutation consisted of 15 stage I+II and 8 stage III+IV tumors (Table 1). There was no significant difference between the two stage groups. With regard to histological grade, nine were of grade 1, six were of grade 2, and eight were of grade 3 (Table 1). The grade 3 patients had the highest mutation ratio (30%) compared to other grades; however, the difference was not significant.

Correlation among the expression of p53, cyclin A, and Ki-67

Of the 54 cases with p53 expression, 30 (56%) showed cyclin A overexpression (Fig. 3). According to the p53 immunostaining, cyclin A positivity was present in 3 (21%) of the 14 with focal p53 staining, 10 (56%) of the 18 with regional staining, and 17 (77%) of the 22 with diffuse staining, with a significant difference of the positive ratio among three groups ($p<0.0001$). Topologically, the cyclin A-positive cells were frequently observed in p53-positive

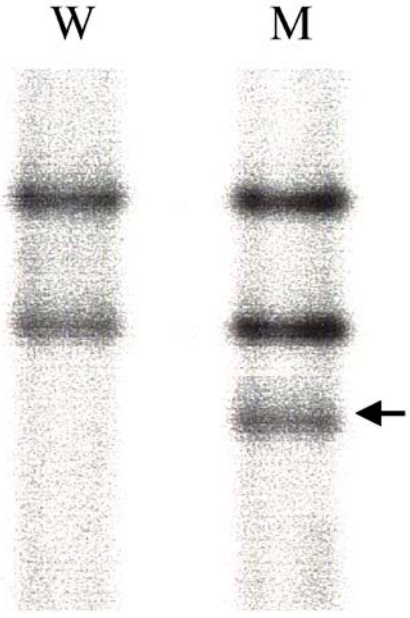


Fig. 1 A representative result of PCR-SSCP in exon 7. A tumor (*M*) showed an abnormal band (*arrow*), suggesting mutations. (*W* Wild type, *M* mutant type)

Table 2 Result of p53 mutation and p53 and cyclin A immunostainings

Number	Age	Histology	Stage	Grade	p53 staining	Cyclin A staining	Ki-67	p53 mutation		
								Exon	Nucleotide	Amino acid change
1	50	E	I	1	++	+	48	7	ATC→GTC	Ile→Val (251)
2	59	E	I	1	+	–	8	6	GAG→GAA	Silent (204)
3	51	E	I	2	+++	+	13	6	GAG→GCG	Glu→Ala (204)
4	53	E	I	2	+	+	50	7	CAC→CGC	His→Arg (233)
5	59	E	I	2	+	–	9	6	CGT→CAT	Arg→His (202)
6	65	E	I	3	+++	+	7	7	GAC→TAC	Asp→Thr (259)
7	52	E	I	3	+++	+	33	7	GAC→TAC	Asp→Thr (259)
8	43	E	I	3	++	+	38	7	GAC→AAC	Asp→Asn(259)
9	50	E	III	2	+++	–	4	7	GAC→TAC	Asp→Thr (259)
10	76	E	III	3	+++	+	21	7	GAC→TAC	Asp→Thr (259)
11	61	E	III	3	+++	–	45	7	ATC→ACC	Ile→Thr (255)
12	62	E	III	3	+	–	40	5	ACC→ACT	Silent (155)
13	74	E	IV	3	+++	++	25	7	AGG→AGC	Arg→Ser (249)
14	73	E	IV	3	+++	–	20	6	GAG→GCG	Glu→Ala (204)
Cases showing heterogeneous p53 staining										
15a	66	E	I	1(w)	+++	+	33	7	GAC→TAC	Asp→Thr (259)
								8	CTG→CTT	Silent (299)
b		E		w	–	–	2	–	–	–
16a	57	E	I	1(m)	+++	+	9	5	GTT→TTT	Val→Phe (147)
								7	ATC→GTC	Ile→Val (251)
b		E		w	–	–	7	–	–	–
17a	44	E	I	1(w)	+	–	25	6	AGT→AAT	Ser→Asn (215)
								7	AGC→GTC	Ile→Val (251)
b		E		w	–	–	8	–	–	–
18a	45	E	I	1(w)	+	–	28	5	AAG→AAC	Lys→Asn (164)
b		E		w	–	–	1	–	–	–
19a	74	E	I	2(m)	+	+	63	8	CAC→GAC	His→Asp (296)
b		E		w	–	–	51	–	–	–
20a	56	E	II	1(w)	++	+	21	7	GAC→TAC	Asp→Thr (259)
b		E		w	–	–	0	–	–	–
21a	59	E	III	2(p)	+	+	28	8	CGT→TGT	Arg→Cys (273)
b		E		w	–	–	10	–	–	–
22a	30	E	III	2(m)	+	–	26	–	–	–
b		E		w	–	–	1	–	–	–
23a	49	E	II	1(w)	+	–	27	5	ACC→ACT	Silent (155)
b		E		w	–	–	2	–	–	–
Cer		E		w	+	–	12	5	ACC→ACT	Silent (155)
24a	64	E	III	1(m)	+++	+	32	7	AAC→AGC	Asn→Ser (235)
b		E		w	–	–	5	–	–	–
Ly1		E		m	+	+	48	7	AAC→AGC	Asn→Ser (235)
Ly2		E		m	++	+	45	7	AAC→AGC	Asn→Ser (235)
Ly3		E		m	+	+	36	7	AAC→AGC	Asn→Ser (235)

E Endometrioid, *SP* serous papillary, *SQ* squamous cell carcinoma, *a* p53-positive site, *b* p53-negative site, *w* well differentiated, *m* moderately differentiated, *p* poorly differentiated, *Cer* invasion site in the cervix, *Ly* metastatic site in the lymph node

sites (Fig. 3). With regard to Ki-67 immunostaining, the PI for Ki-67 was 28.2±14.2 (M±SD) in cases with focal p53 staining, 41.0±16.4 in cases with regional staining, and 28.6±19.3 in cases with diffuse staining. There was no significant difference of the PI among three groups. With regard to the relationship between the expression of cyclin A and Ki-67, the PI for Ki-67 was 19.8±17.4 in cases negative for cyclin A, 28.6±14.9 in cases with focal staining, 47.5±16.9 in cases with regional staining, and 58.0±9.9 in cases with diffuse staining for cyclin A, with a significant difference of the PI among four groups (p=0.0001).

However, there was no significant correlation between p53 mutation and cyclin A expression; cyclin A expression was observed in 12 (52%) of the 23 cases with p53 mutation, but was also present in 18 (58%) of the 31 cases

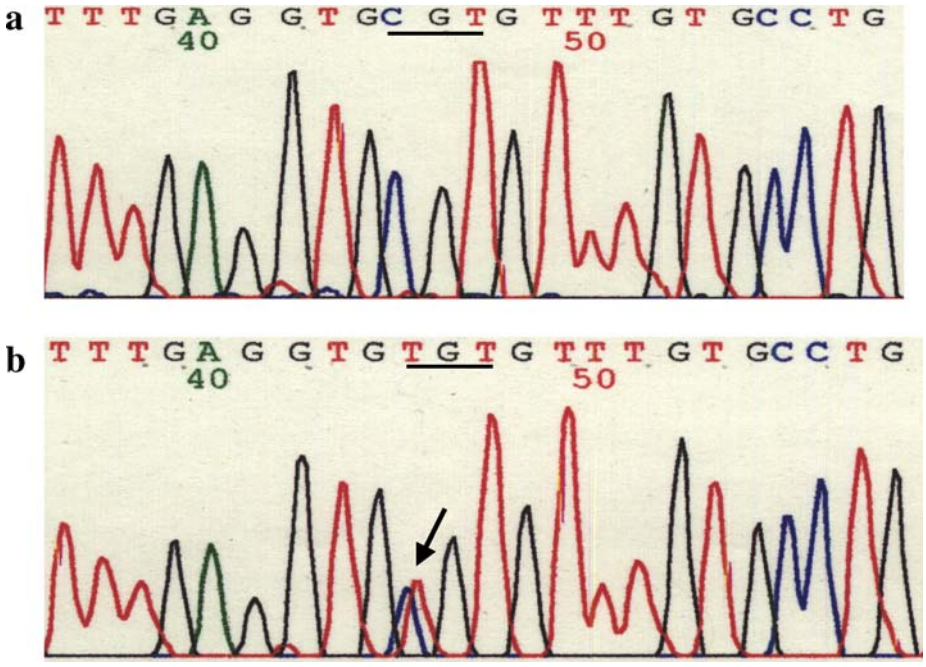


Fig. 2 Result of a direct sequencing in exon 8. **a** wild type, **b** mutated type. *CGT* in wild type (*underlined*) was changed to *TGT* in mutated type (*arrow*, *underlined*)

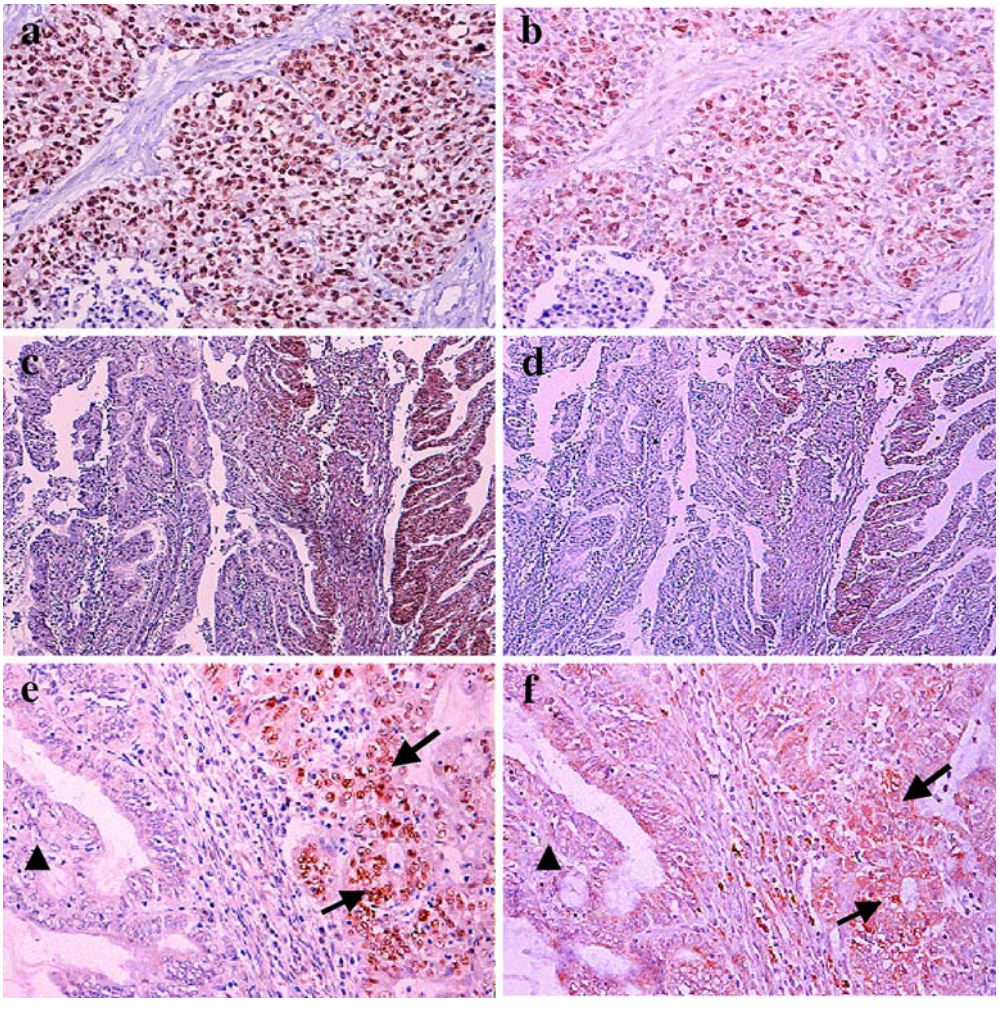


Fig. 3 Result of immunostaining for p53 (**a**, **c**, **e**) and cyclin A (**b**, **d**, **f**). **a** and **b**, **c** and **d**, **e** and **f** are serial sections. The distribution of cyclin A-positive cells (**b**) is similar with that of p53-positive cells (**a**) (×100). The p53-positive cells (**c**, case No. 6 in Table 2) and cyclin A-positive cells (**d**) were intermingled with negative cells. However, the cyclin A-positive sites correlated with the p53-positive sites. p53 mutation was detected in DNA samples obtained from the areas with p53-positive staining (**c**, *right side*) (×40). The p53-positive sites (**e**, *arrow*) locates adjacent to the negative sites (**e**, *arrowhead*) in case No. 24 in Table 2. The nuclear cyclin A-positive sites (**f**, *arrows*) are observed in the p53-positive sites, and cyclin A-negative sites (**f**, *arrowheads*) are negative for p53. p53 mutation was detected in DNA samples obtained from the areas with p53-positive staining (**e**, *right side*) (×100)

with no apparent p53 mutation. The PI for Ki-67 did not differ significantly according to the p53 mutation status (data not shown).

p53 mutation and expression of cyclin A and Ki-67 in cases with heterogeneity in p53 expression

Of the 54 p53-positive cases, 10 showed a heterogeneous pattern of p53 immunostaining and were available for p53 mutational analysis using microdissection for both p53-positive and negative areas in the same tumor (Fig. 1e). There was no apparent tendency in the topological distribution of p53-positive sites in tissue sections. In nine of the ten cases, DNA obtained from p53-positive cells had p53 mutation, whereas that from p53-negative cells had no p53 mutation (Table 2). In the remaining one case, neither of the tumor cells had mutations.

In addition, in four cases (No. 16, 19, 21, and 24), the histological grade of the p53-mutated tumor cells was higher than that of cells with wild-type p53. In the remaining five cases, there was no apparent difference in histological grade between p53-positive and negative cells.

Mutational analysis for the tumor cells invading the adjacent tissue or metastatic to lymph nodes was conducted in two cases (No. 23, 24). In case No. 23, the tumor cells invading the cervical stroma had the same p53 mutation as the tumor cells in p53-positive sites of the primary lesion. In case No. 24, all of the three metastatic nodes showed tumor cells with the same p53 mutation as the primary tumor cells.

With regard to the expression of cyclin A, p53-mutated cells were positive for cyclin A, and vice versa, in five of the nine cases, and both were negative in the remaining four cases. Regarding Ki-67 expression, the PI for Ki-67 was increased in the p53-mutated tumor cells as compared with cells with wild-type p53 in eight of the nine cases, and similar in the remaining case.

Discussion

Our study showed that 54 (40%) of the 135 endometrioid-type endometrial carcinomas were immunohistochemically positive for p53 protein, and that p53 gene mutation was present in 23 (43%) of the 54 cases found to be immunopositive for p53 protein by the PCR-SSCP method followed by direct sequencing. This is consistent with previous studies reporting that the percentage of tumors with p53 mutation among endometrial carcinomas positive for p53 immunostaining ranged 30–60% [1, 9, 27]. It had been believed that the positive p53 immunostaining represents the presence of p53 mutation [12, 20]; however, recent studies demonstrated that p53 immunoreactivity originates from both the mutated and wild-type p53 gene [1, 9, 27]. With regard to the mutation site and amino acid change, the present study showed that the mutations had occurred most frequently in exon 7, and 85% of them were missense mutations. This is also in agreement with previous reports [1, 10, 26].

The most interesting result from our study is the heterogeneous distribution of p53-mutated epithelia in the same tumor of endometrioid-type adenocarcinomas. Ten out of the 54 cases showed both p53-positive and negative areas in the primary lesion, and were available for the analysis of the mutational status of the two sites using a microdissection technique. The results indicated that, in nine of the ten cases, the gene mutation was identified in the p53-positive carcinoma cells, but not in the p53-negative cells. In eight of the nine cases, the PI for Ki-67 was increased in p53-mutated tumor cells compared to those without p53 mutation. In four of the nine cases, p53-mutated carcinoma cells showed a histology of less differentiation than those without the mutation. In a case of stage II carcinoma, the cells invading the cervical stroma had the same p53 mutation as those in the primary lesion. In another stage III case with lymph node metastasis, the tumor cells in all of the three metastatic nodes showed the same p53 mutation as demonstrated in the primary lesion. All of these findings suggest that p53 gene mutation occurred after the development of well-differentiated, endometrioid-type adenocarcinoma, and then the p53-mutated, less-differentiated tumor cell subpopulation acquired higher proliferative activity and metastatic potential. Previous studies reported that the p53 mutation was present more frequently in advanced staged and/or high grade tumors of endometrioid-type carcinomas, presenting the concept that p53 mutation is a late event in this tumor [3, 13, 16]. The current study supports this idea, and it is likely that p53 mutation plays an important role in the transformation of the tumor cells into the invasive phenotype. To our knowledge, this is the first report on a heterogeneous pattern of p53 immunostaining actually associated with p53 genetic heterogeneity in endometrial endometrioid-type adenocarcinoma.

The present study demonstrated that the distribution of cyclin A-positive cells is correlated well with that of p53 expression, especially in tumors showing a heterogeneous p53 staining pattern. This was consistent with our previous reports [23, 24], and suggested possible molecular correlations between p53 protein accumulation and cyclin A expression. Yamamoto et al. reported that wild-type p53 protein can bind the promoter region of the cyclin A gene and suppress the transcription of cyclin A mRNA in leukemic cell lines [29]. This prompted us to analyze the p53 gene mutation with relevance to cyclin A expression. Contrary to expectation, the results indicated that cyclin A positivity was present not only in 52% of p53-mutated carcinomas but also in 58% of carcinomas without p53 mutation. These findings suggest that the accumulation of the p53 protein itself, either mutated or of wild- type, may be important in overexpression of cyclin A. There may be some unknown sites in p53 protein that are involved in the expression of cyclin A protein. Recently, cyclin A-docking sites have been identified on the C-terminus of p53 protein [18]. In addition, because inasmuch as (since) the amount of wild-type p53 protein is reportedly controlled by mul-

tiple double minute two 2 (MDM2) protein which is a ubiquitin ligase acting to degenerate the p53 protein [7, 14], accumulation of wild-type p53 protein may be considered in relevance to insufficient MDM2 functions [7, 14]. It has been reported that expression of MDM2 is reduced in p53-positive areas without p53 mutation in lung adenocarcinoma [11]. Such an inverse relationship between the expression of p53 and MDM2 has also been reported in endometrial carcinomas [28]. Accordingly, the abnormal MDM2 expression may be in part involved in the accumulation of wild-type p53 protein.

In summary, the present study demonstrated that p53 mutation occurs as a late event in endometrial endometrioid-type adenocarcinoma, and may be important to the change of morphology and cell behavior. In addition, overexpression of cyclin A is associated with the accumulation of p53 protein along with higher proliferative activity. Further studies are needed to clarify the molecular interaction between p53 and cyclin A in endometrial carcinomas.

Acknowledgements This work was supported in part by a Grant-in-aid for Scientific Research from the Ministry of Education and Culture (No. 06454468 and No. 09671670), Japan.

References

1. Ambros RA, Ross JS, Kallakury BV, Malfetano J, Kim Y, Hwang J, Breese K, Figge J (1995) p53 gene status in endometrial carcinomas showing diffuse positivity for p53 protein by immunohistochemical analysis. Mod Path 8:441–445
2. Barakat RR, Grisby PW, Sabbatini P (2000) Corpus: epithelial tumors. In: Hoskins WJ, Perez CA, Young RC (eds) Principles and practice of gynecologic oncology, 3rd edn. Lippincott Williams & Wilkins, Philadelphia, pp 919–959
3. Berchuck A, Boyd J (1995) Molecular basis of endometrial cancer. Cancer 76:2034–2040
4. Crompton NE, Saydan N (1999) Control of the cell cycle. J Neuro-Oncol 22:255–259
5. Dictor M, Ehinger M, Mertens F, Akervall J, Wennerberg J (1999) Abnormal cell cycle regulation in malignancy. Am J Clin Pathol 112:40–52
6. Hartwell LH, Kasten MB (1994) Cell cycle control and cancer. Science 266:1821–1828
7. Haupt Y, Maya R, Kazaz A, Oren M (1997) Mdm2 promotes the rapid degradation of p53. Nature 387:296–299
8. Hollstein M, Sidransky D, Vogelstein B, Harris CC (1991) p53 mutations in human cancers. Science 253:49–53
9. Ito K, Sasano H, Matsunaga G, Sato S, Yajima A, Nasim S, Garret CT (1997) Correlations between p21 expression and clinicopathological findings, p53 gene and protein alterations, and survival in patients with endometrial carcinoma. J Pathol 183:318–324
10. Kihana T, Hamada K, Inoue Y, Yano N, Iketani H, Murao S, Ukita M, Matsuura S (1995) Mutation and allelic loss of the p53 gene in endometrial carcinoma. Incidence and outcome in 92 surgical patients. Cancer 76:72–78
11. Koga T, Hashimoto S, Sugio K, Yoshino I, Nakagawa K, Yonemitsu Y, Sugimachi K, Sueishi K (2001) Heterogeneous distribution of P53 immunoreactivity in human lung adenocarcinoma correlates with MDM2 protein expression, rather than with P53 gene mutation. Int J Cancer 95:232–239
12. Kohler MF, Berchuck A, Davidoff AM, Humphrey PA, Dodge RK, Iglehart JD, Soper JT, Clarke-Pearson DL, Bast RC Jr, Marks JR (1992) Overexpression and mutation of p53 in endometrial carcinoma. Cancer Res 52:1622–1627
13. Koshiyama M, Konishi I, Fujii S (1998) Pathology, hormonal aspects, and molecular genetics of the two types of endometrial cancer. Cancer J 11:277–283
14. Kubbutat MH, Jones SN, Vousden KH (1997) Regulation of p53 stability by Mdm2. Nature 387:299–303
15. Ronnett BM, Zaino RJ, Ellenson H, Kurman RJ (2002) Endometrial carcinoma. In: Kurmann RJ (ed) Blaustein's pathology of the female genital tract, 5th edn. Springer, Berlin Heidelberg New York, pp 501–559
16. Lax SF (2004) Molecular genetic pathways in various types of endometrial carcinoma: from a phenotypical to a molecular-based classification. Virchows Arch 444:213–223
17. Li SF, Shiozawa T, Nakayama K, Nikaido T, Fujii S (1996) Stepwise abnormality of sex steroid hormone receptors, tumor suppressor gene products (p53 and Rb), and cyclin E in uterine endometrioid carcinoma. Cancer 77:321–329
18. Luciani MG, Hutchins JR, Zheleva D, Hupp TR (2000) The C-terminal regulatory domain of p53 contains a functional docking site for cyclin A. J Mol Biol 300:503–518
19. Oda T, Tsuda H, Scarpa A, Sakamoto M, Hirohashi S (1992) Mutation pattern of the p53 gene as a diagnostic marker for multiple hepatocellular carcinoma. Cancer Res 52:3674–3678
20. Schneider J, Rubio MP, Rodriguez-Escudero FJ, Seizinger BR, Castresana JS (1994) Identification of p53 mutations by means of single strand conformation polymorphism analysis in gynaecological tumours: comparison with the results of immunohistochemistry. Eur J Cancer 30:504–508
21. Sherr CJ (1994) G1 phase progression: cyclin on cue. Cell 79:551–555
22. Sherr CJ, Roberts JM (1995) Inhibitors of mammalian G1 cyclin-dependent kinases. Genes Dev 9:1149–1163
23. Shih HC, Shiozawa T, Kato K, Imai T, Miyamoto T, Uchikawa J, Nikaido T, Konishi I (2003) Immunohistochemical expression of cyclins, cyclin-dependent kinases, tumor suppressor gene products, Ki-67 and sex steroid receptors in endometrial carcinoma: positive staining for cyclin A as poor prognostic indicator. Human Pathol 34:471–478
24. Shiozawa T, Xin L, Nikaido T, Fujii S (1997) Immunohistochemical detection of cyclin A with reference to p53 expression in human endometrial endometrioid carcinoma. Int J Gynecol Pathol 16:348–353
25. Shiozawa T, Nikaido T, Shimizu M, Zhai Y, Fujii S (1997) Immunohistochemical analysis of the expression of cdk4 and p16INK4 in human endometrioid-type endometrial carcinoma. Cancer 80:2250–2256
26. Soong R, Knowles S, Williams KE, Hammond IG, Wysocki SJ, Iacopetta BJ (1996) Overexpression of p53 protein is an independent prognostic indicator in human endometrial carcinoma. Br J Cancer 74:562–567
27. Soong R, Robbins PD, Dix BR, Grieu F, Lim B, Knowles S, Williams KE, Turbett GR, House AK, Iacopetta BJ (1996) Concordance between p53 protein overexpression and gene mutation in a large series of common human carcinomas. Human Pathol 27:1050–1055
28. Soslow RA, Shen PU, Chung MH, Isacson C (1998) Distinctive p53 and mdm2 immunohistochemical expression profiles suggest different pathogenetic pathways in poorly differentiated endometrial carcinoma. Int J Gynecol Pathol 17:129–134
29. Yamamoto M, Yoshida M, Ono K, Fujita T, Ohtani-Fujita N, Sakai T, Nikaido T (1994) Effect of tumor suppressors on cell cycle-regulatory genes: RB suppresses p34cdc2 expression and normal p53 suppresses cyclin A expression. Exp Cell Res 210: 94–101
30. Zhai YL, Nikaido T, Orii A, Horiuchi A, Toki T, Fujii S (1999) Frequent occurrence of loss of heterozygosity among tumor suppressor genes in uterine leiomyosarcoma. Gynecol Oncol 75:453–459

Virchows Arch (2005) 447: 823–827
DOI 10.1007/s00428-005-0023-2

ORIGINAL ARTICLE

Nelson G. Ordóñez

Clear cell mesothelioma presenting as an incarcerated abdominal hernia

Received: 4 April 2005 / Accepted: 7 June 2005 / Published online: 14 July 2005
© Springer-Verlag 2005

Abstract A clear cell mesothelioma presenting as an incarcerated ventral abdominal hernia in a 67-year-old man who had no history of asbestos exposure is described. The cause of the cytoplasmic clearing was the presence of large amounts of glycogen. Although uncommon, this variant of mesothelioma is important to recognize because it can be easily confused with other clear cell tumors involving the serosal membranes. Significant recent advances in the immunohistochemistry of epithelioid mesothelioma are briefly reviewed because immunohistochemical studies can be helpful in establishing the correct diagnosis.

Keywords Clear cell mesothelioma · Hernia · Immunohistochemistry · D2-40 · Podoplanin

Introduction

An important characteristic of tumors arising from the serosal membranes is their ability to grow in a wide variety of histologic patterns. Based on their light microscopic features, mesotheliomas have been subdivided into epithelioid (also referred to as epithelial), sarcomatoid, mixed epithelioid and sarcomatoid (biphasic), and desmoplastic types. Although epithelioid mesotheliomas more often present a tubulopapillary or solid pattern, on occasion, they may present other unusual histologic patterns, including adenomatoid, deciduoid, small cell, signet ring, rhabdoid, and pleomorphic. Mesotheliomas presenting a clear cell morphology are rare and only a few individual case reports have been published [6, 9, 24]. The purpose of this article is to report a case of a clear cell mesothelioma that was unusual in that it originated in the peritoneum and presented as an incarcerated ventral abdominal hernia. Pathologists need to be aware that mesotheliomas can present this uncommon morphology and, therefore, should be included in the differential diagnosis of those tumors that can display similar morphologic features and can metastasize to the serosal membranes.

N. G. Ordóñez (✉)
M.D. Anderson Cancer Center,
1515 Holcombe Boulevard,
Houston, TX, 77030, USA
e-mail: nordonez@mdanderson.org
Tel.: +1-713-7923167
Fax: +1-713-7923696

Clinical history

A 67-year-old black man sought medical attention for an incarcerated ventral abdominal hernia that had developed a year earlier. He had a history of diverticulitis, and prostate cancer which had been treated with a radical prostatectomy and radiation therapy 7 years previously. The patient also had a history of smoking, but not of asbestos exposure. He underwent hernial repair and resection of the hernial sac. Pathology examination of the resected specimen revealed a malignant epithelial clear cell tumor. A CT scan was performed and showed extensive omental "caking" and ascites.

Material and methods

Tissue samples of the resected specimen were fixed in 10% buffered formalin and processed for light microscopy. Sections were stained with hematoxylin-and-eosin, Mayers's mucicarmine, and periodic acid-Schiff (PAS) with and without diastase digestion. Immunohistochemical studies were performed using the avidin–biotin–peroxidase complex (ABC) method in a Dako Autostainer (Carpinteria, CA). The primary antibodies used are listed in Table 1. Immunoperoxidase staining was done using the LSAB2 peroxidase kit (Dako). To enhance the immunostaining, a heat epitope retrieval procedure was performed using a Black-and-Decker vegetable steamer (Shelton, CT) as previously described [19]. The antigen–antibody reaction was visualized using either 3-amino-9-ethylcarbazole or 3′,3-diaminobenzidine tetrahydrochloride as chromogen. To evaluate the specificity of the antibody, known positive and negative tissues were used as controls. For electron

Table 1 Antibodies used in this study

Marker	Source	Type	Dilution	Antigen retrieval
Calretinin	Zymed (South San Francisco, CA)	PAb (rabbit)	1:20	Yes (citrate)
CEA	NeoMarkers (Fremont, CA)	PAb (rabbit)	1:175	No
D2-40	Signet Laboratories (Dedham, MA)	MAb	1:25	Yes (Tris–EDTA)
Keratin 5/6	Dako Corporation (Carpinteria, CA)	D5/16B4 MAb	1:100	Yes (citrate)
MOC-31	Dako Corporation	MAb	1:50	Yes (citrate)
p63	Santa Cruz Biotechnology (Santa Cruz, CA)	4A4 MAb	1:200	Yes (Tris–EDTA)
Podoplanin	AngioBio Company (Del Mar, CA)	MAb	1:40	Yes (citrate)
PSA	Dako Corporation	PAb (rabbit)	1:3,000	No
RCC Ma	Novocastra (Newcastle-Upon-Tyne, UK)	MAb	1:40	Yes (enzymatic digestion)
TAG-72	BioGenex (San Ramon, CA)	B72.3 MAb	1:300	No
TTF-1	Dako Corporation	8G7G3/1 MAb	1:25	Yes (citrate)
WT1	Dako Corporation	6F-H2 MAb	1:40	Yes (Tris–EDTA)

CEA Carcinoembryonic antigen, *RCC Ma* renal cell carcinoma marker, *TTF-1* thyroid transcription factor-1, *WT1* Wilm's tumor protein-1, *PSA* prostate-specific antigen, *PAb* polyclonal antibody, *MAb* monoclonal antibody

microscopy studies, portions of the tumor from the paraffin blocks were deparaffinized with xylene, postfixed in 1% osmium tetroxide in S-collidine buffer, and embedded in Epon epoxy resin. Ultrathin sections were stained with uranyl acetate and lead citrate.

Results

Histologically, the tumor appeared to be made of solid clusters of uniform, polygonal cells with strikingly clear cytoplasm (Fig. 1a). Periodic acid-Schiff stain demonstrated the presence of large amounts of glycogen (Fig. 1b). Mayer's mucicarmine stain was negative for mucin. Immunohistochemical studies showed strong reactivity for calretinin, keratin 5/6, WT1 protein, D2-40, and podoplanin (Fig. 1c–f). All of the other investigated markers were negative. Ultrastructural examination of paraffin-embedded material demonstrated the presence of numerous, long branching microvilli on the apical surface of the cells.

Discussion

Tumors composed entirely or partially of cells with optically clear cytoplasm have been documented in virtually every organ, including the serosal membranes. Mesotheliomas with clear cell morphology are uncommon and only a few cases have been reported under a variety of descriptive terms, including clear cell mesothelioma [9, 24], glycogen-rich mesothelioma [23], lipid-rich mesothelioma [7], and foamy cell mesothelioma [6]. In the present case, the cytoplasmic clearing was caused by the accumulation of large amounts of glycogen, but this change has also been attributed to other factors, such as the presence of large amounts of lipid [7], or numerous cytoplasmic vesicles [24].

The clinical presentation of abdominal mesotheliomas is usually that of abdominal pain, weight loss, and abdominal distention caused by ascites. About 5–10% of the patients may develop hernias, most often inguinal or umbilical, as a result of the increase in abdominal pressure caused by the ascites [1, 18]. In many of these patients, the diagnosis of mesothelioma is established only after they seek medical attention due to discomfort resulting from the accumulation of ascites fluid in the hernial sac. Although, in most instances, the resected hernial sac only contains ascites fluid, on rare occasions, it can be involved by either an extension of or a metastasis from a peritoneal mesothelioma that has spread into the preestablished hernial sac [2, 3, 10, 11, 27]. The present case is unusual not only in that the abdominal ventral hernia was the presenting symptom of the mesothelioma, but also because of the unusual clear cell morphology of the tumor.

The diagnosis of epithelioid mesothelioma with clear cell morphology can be difficult, especially on biopsy specimens where areas showing more conventional mesothelioma features are not included. In the present case, this diagnosis was confirmed by immunohistochemical studies, in which strong reactivity was demonstrated for calretinin, keratin 5/6, and WT1 protein, and negative staining for CEA, MOC-31, and B72.3, an immunohistochemical pattern that is considered characteristic of mesothelioma [19]. It was further confirmed by the demonstration of strong positivity for D2-40 and podoplanin, two novel markers that, according to recent investigations [9, 22], could assist in the diagnosis of mesothelioma. Even though the tissue specimen used for electron microscopy was poorly preserved, this procedure clearly demonstrated the presence of ultrastructural features supporting the diagnosis of mesothelioma.

D2-40 is a recently developed monoclonal antibody that reacts with a 40-kDa surface sialoglycoprotein known as the M2A antigen that was originally detected in fetal germ cells and germ cell tumors [16]. Subsequent investigations have demonstrated that because this antibody reacts selectively with lymphatic endothelium, it could be very helpful in both the diagnosis of lymphatic-derived tumors,

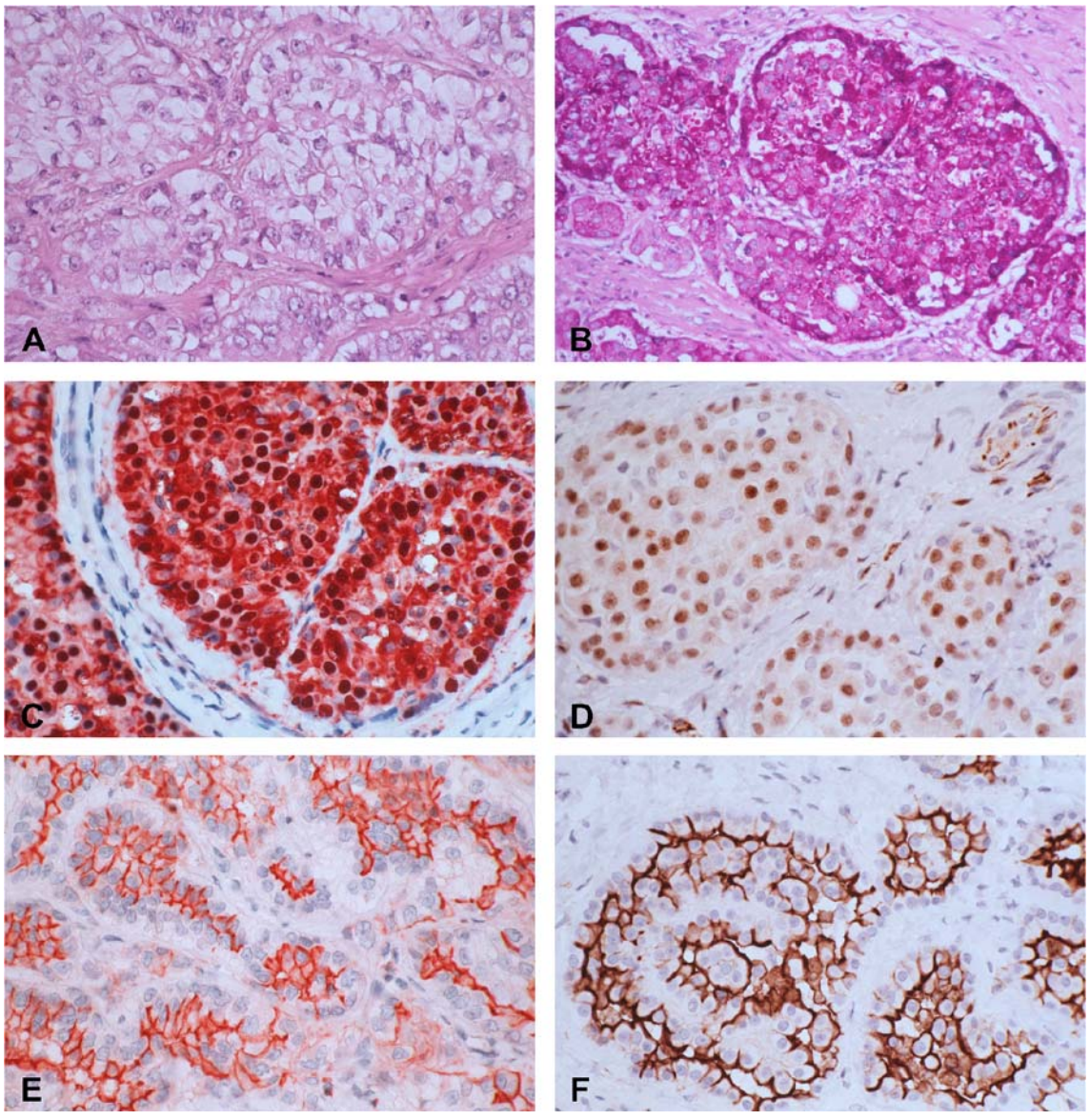


Fig. 1 **a** General appearance of the tumor demonstrating that it is composed exclusively of clear cells (H&E, ×200). **b** PAS stained section showing that the clearing seen on the H&E stained section is caused by the accumulation of large amounts of intracytoplasmic glycogen. **c** Immunohistochemical preparation showing strong nuclear and cytoplasmic reactivity for calretinin. **d** Immunohistochemical preparation demonstrating nuclear reactivity for WT1 protein. **e** Immunostain with the D2-40 antibody showing strong reactivity along the apical cell membrane. **f** Immunohistochemical preparation showing membranous positivity for podoplanin

and in determining lymphatic invasion by tumors [12, 13]. Recent investigations [8, 21] have also shown that, because this antibody usually reacts with epithelioid mesotheliomas, but not with carcinomas, it could be useful in discriminating between these malignancies. Chu et al.'s study [8] on the value of D2-40 as a mesothelioma marker reported strong membranous reactivity in all 33 (100%) epithelioid mesotheliomas and in the epithelioid component of 15 (94%) of 16 biphasic mesotheliomas. Focal, weak, membranous positivity was observed in 17 (65%) of 26 serous carcinomas, but no membranous staining was seen in any of the other carcinomas investigated. A minority of the renal cell carcinomas (5/34), breast carcinomas (3/16), and lung adenocarcinomas (2/31), however, showed weak, cytoplasmic staining. In two separate investigations using different cohorts of mesothelioma and carcinoma cases, I observed D2-40 membranous positivity in 25 (86%) of 29 and in 37 (93%) of 40 epithelioid mesotheliomas, respectively [21, 22]. Among the different types of carcinomas investigated, only about 15% of the serous carcinomas exhibited focal membranous reactivity with this antibody. None of the other carcinomas, including those of the kidney, lung, and prostate, stained with the D2-40 antibody. These findings indicate that D2-40 is one of the most specific and sensitive markers currently available for the diagnosis of epithelioid mesothelioma.

Podoplanin is a 38-kDa mucoprotein first identified in rat glomerular epithelial cells (podocytes) which was found

to be linked to the flattening of the epithelial foot processes in puromycin induced nephrosis [4]. Podoplanin, like D2-40, was found to be expressed in the lymphatic endothelium, but not in the blood vasculature. Subsequent investigations have reported podoplanin positivity in lymphangiomas, Kaposi's sarcomas, and in a subgroup of angiosarcomas [5]. Recently, Kimura and Kimura [15] reported podoplanin expression in five (100%) of five epithelioid mesotheliomas, but in none of 93 adenocarcinomas of various origins, and suggested that podoplanin could serve as a useful immunohistochemical marker for distinguishing between these malignancies. In two comparative studies, I found that podoplanin had a similar sensitivity and specificity in the diagnosis of mesotheliomas to that of D2-40 [21, 22].

The differential diagnosis of clear cell mesothelioma includes a wide variety of carcinomas with similar morphologic features. In my experience, the tumors that are most likely to be confused with clear cell mesotheliomas are renal cell carcinomas, and both adenocarcinomas and squamous cell carcinomas of the lung with clear cell morphology. Because of the high sensitivity and specificity of D2-40 and podoplanin for epithelioid mesotheliomas, immunostaining for either of these two markers can be used in combination with the renal cell carcinoma marker (RCC Ma) to distinguish between epithelioid mesotheliomas and renal cell carcinomas, or thyroid transcription factor-1 (TTF-1) to discriminate between epithelioid mesotheliomas and lung adenocarcinomas. RCC Ma is a recently commercially available monoclonal antibody that was generated using the microsomal fraction of human renal cortical tissue as immunogen and which reacts with a 200-kDa glycoprotein present in normal tubule epithelial cells. This antibody has proved to be highly specific for renal cell carcinomas and it has been reported to react with 75–85% of the clear cell carcinomas of the kidney [17, 20]. Because calretinin and keratin 5/6 are not expressed in carcinomas of the kidney, these markers may also be useful in distinguishing these tumors from epithelioid mesotheliomas. It should be mentioned, however, that because they are expressed in both epithelioid mesotheliomas and squamous cell carcinomas, neither calretinin nor keratin 5/6 is useful in discriminating between these malignancies. This differential diagnosis, however, can be facilitated by the use of p63 immunostaining because this marker is strongly and almost invariably expressed in squamous carcinomas [14, 26, 28], but not in epithelioid mesotheliomas [14, 25].

References

1. Acherman YIZ, Welch LS, Bromley CM, Sugarbaker PH (2003) Clinical presentation of peritoneal mesothelioma. Tumori 89: 269–273
2. Aggarwal M, Lakhar B, Shetty D, Ullal S (2000) Malignant peritoneal mesothelioma in an inguinal hernial sac: an unusual presentation. Indian J Cancer 37:91–94
3. Bethwaite PB, Evans R, Naik DK, Delahunt B, Teague CA (1996) Diffuse malignant mesothelioma arising in a paracolostomy hernial sac. Histopathology 29:282–284
4. Breiteneder-Geleff S, Matsui K, Soleiman A, Meraner P, Poczewski H, Kalt R, Schaffner G, Kerjaschki D (1997) Podoplanin, novel 43-kd membrane protein of glomerular epithelial cells, is down-regulated in puromycin nephrosis. Am J Pathol 151:1141–1152
5. Breiteneder-Geleff S, Soleiman A, Kowalski H, Horvat R, Amann G, Kriehuber E, Diem K, Weninger W, Tschachler E, Alitalo K, Kerjaschki D (1999) Angiosarcomas express mixed endothelial phenotypes of blood and lymphatic capillaries: podoplanin as a specific marker for lymphatic endothelium. Am J Pathol 154:385–394
6. Cavazza A, Pasquinelli G, Agostini L, Leslie KO, Colby TV (2002) Foamy cell mesothelioma (Letter). Histopathology 41: 369–371
7. Chang HT, Yantiss RK, Nielsen GP, McKee GT, Mark EJ (2000) Lipid-rich diffuse malignant mesothelioma: a case report. Hum Pathol 31:876–879
8. Chu AY, Litzky LA, Pasha TL, Acs G, Zhang PJ (2005) Utility of D2-40, a novel mesothelial marker, in the diagnosis of malignant mesothelioma. Mod Pathol 18:105–110
9. Dessy E, Falleni M, Braidotti P, Del Curto B, Panigalli T, Pietra GG (2001) Unusual clear cell variant of epithelioid mesothelioma. Arch Pathol Lab Med 125:1588–1590
10. Grove A, Jensen ML, Donna A (1989) Mesotheliomas of the tunica vaginalis testis and hernial sacs. Virchows Archiv A Pathol Anat 415:283–292
11. Kerrigan SAJ, Cagle P, Churg A (2003) Malignant mesothelioma of the peritoneum presenting as an inflammatory lesion. Am J Surg Pathol 27:248–253
12. Kahn HJ, Bailey D, Marks A (2002) Monoclonal antibody D2-40, a new marker of lymphatic endothelium, reacts with Kaposi's sarcoma and a subset of angiosarcomas. Mod Pathol 15:434–440
13. Kahn HJ, Marks A (2002) A new monoclonal antibody, D2-40, for detection of lymphatic invasion in primary tumors. Lab Invest 82:1255–1257
14. Kaufmann O, Fietze E, Mengs J, Dietel M (2001) Value of p63 and cytokeratin 5/6 as immunohistochemical markers for the differential diagnosis of poorly differentiated and undifferentiated carcinomas. Am J Clin Pathol 116:823–830
15. Kimura N, Kimura I (2005) Podoplanin as a marker for mesothelioma. Pathol Int 55:83–86
16. Marks A, Sutherland DR, Bailey D, Iglesias J, Law J, Lei M, Yeger H, Banerjee D, Baumal R (1999) Characterization and distribution of an oncofetal antigen (M2A antigen) expressed on testicular germ cell tumours. Br J Cancer 80:569–578
17. McGregor DK, Khurana KK, Cao C, Tsao CC, Ayala G, Krishnan B, Ro JY, Lechago J, Truong LD (2001) Diagnosing primary and metastatic renal cell carcinoma: The use of the monoclonal antibody "Renal Cell Carcinoma Marker". Am J Surg Pathol 25:1485–1492
18. Mirabella F (1996) Peritoneal mesothelioma and abdominal hernias. Minerva Med 87:21–24
19. Ordóñez NG (2003) The immunohistochemical diagnosis of mesothelioma: a comparative study of epithelioid mesothelioma and lung adenocarcinoma. Am J Surg Pathol 27:1031–1051
20. Ordóñez NG (2004) The diagnostic utility of immunohistochemistry in distinguishing between mesothelioma and renal cell carcinoma: a comparative study. Hum Pathol 35:697–710
21. Ordóñez NG (2005) D2-40 and podoplanin are highly specific and sensitive immunohistochemical markers of epithelioid malignant mesothelioma. Hum Pathol 36:372–380
22. Ordóñez NG (2005) The diagnostic utility of immunohistochemistry and electron microscopy in distinguishing between peritoneal mesotheliomas and serous carcinomas: a comparative study. Mod Pathol (in press)
23. Ordóñez NG, Mackay B (1999) Glycogen-rich mesothelioma. Ultrastruct Pathol 23:401–406
24. Ordóñez NG, Myhre M, Mackay B (1996) Clear cell mesothelioma. Ultrastruct Pathol 20:331–336

25. Pan C-C, Chen PC-H, Chou T-Y, Chiang H (2003) Expression of calretinin and other mesothelioma-related markers in thymic carcinoma and thymoma. Hum Pathol 34:1155–1162
26. Reis-Filho JS, Simpson PT, Martins A, Preto A, Gärtner F, Schmitt FC (2003) Distribution of p63, cytokeratins 5/6 and cytokeratin 14 in 51 normal and 400 neoplastic human tissue samples using TARP-4 multi-tumor tissue microarray. Virchows Arch 443:122–132
27. Tang CK, Gray GF, Keuhnelian JG (1976) Malignant peritoneal mesothelioma in an inguinal hernia sac. Cancer 37:1887–1890
28. Wu M, Wang B, Gil J, Sabo E, Miller L, Gan L, Burstein DE (2003) p63 and TTF-1 immunostaining. A useful marker panel for distinguishing small cell carcinoma of lung from poorly differentiated squamous cell carcinoma of lung. Am J Clin Pathol 119:696–702

Virchows Arch (2005) 447: 828–834
DOI 10.1007/s00428-005-0035-y

ORIGINAL ARTICLE

Jinru Shia · Jing Qin · Robert A. Erlandson · Roy King · Peter Illei · Jennifer Nobrega · Davis Yao · David S. Klimstra

Malignant mesothelioma with a pronounced myxoid stroma: a clinical and pathological evaluation of 19 cases

Received: 21 May 2005 / Accepted: 19 June 2005 / Published online: 14 July 2005
© Springer-Verlag 2005

Abstract Mesothelioma with a pronounced myxoid stroma has been identified as a morphological pattern that might portend a better prognosis. Reports on this type of cases are few. Its clinical and pathological features are not defined. In this study, we identified 19 such cases from a series of 234 pleural mesotheliomas and performed a comprehensive clinical and pathological analysis. The inclusion criteria were mesotheliomas with at least 50% of the tumor exhibiting a pronounced myxoid stroma that occupied more than 50% of the tumor volume (designated as myxoid mesothelioma). There were ten males and nine females, with a median age of 58 years. Forty seven percent of the patients had probable or definite asbestos exposure. Patients presented at various stages [International Mesothelioma Interest Group (IMIG) stage II, 4; stage III, 9; and stage IV, 6]. Most (16/19) patients were treated by extrapleural pneumonectomy with adjuvant radiation or chemotherapy or both. Overall, the median survival rate was 36 months (median follow-up time, 17 months), and the 2-year survival rate was 79%. Histologically, the tumor cell component was entirely epithelioid without significant cytologic atypia. The myxoid material stained positive for Alcian blue, and the staining diminished after treatment with hyaluronidase in 12 of 12 cases. The tumor cells showed a typical mesothelial immunophenotype. Ultrastructurally, all six tumors examined had typical mesothelial-type surface microvilli and a moderately electron-dense extracellular amorphous material that often formed a haze enmeshing the surface microvilli. Hyaluronic acid-type, fern-like crystals were noted in all cases. These findings show that myxoid mesotheliomas represent a group of epithelioid mesotheliomas that have retained the secretory activity of normal mesothelium. Patients may present at different stages, but survival appears to be superior to that of epithelioid mesotheliomas in general. Our study emphasizes the need for better attention to histologic subtypes, particularly in the context of prognostically or therapeutically oriented investigations of this lethal disease.

Keywords Myxoid mesothelioma · Epithelioid mesothelioma · Survival · Immunohistochemistry · Electron microscopy

Presented in part at the 93rd annual meeting of the United States and Canadian Academy of Pathology, Vancouver, British Columbia, Canada, 6–12 March, 2004

J. Shia · R. A. Erlandson · J. Nobrega · D. Yao · D. S. Klimstra (✉)
Department of Pathology,
Memorial Sloan-Kettering Cancer Center,
1275 York Avenue,
New York, NY 10021, USA
e-mail: klimstrd@mskcc.org
Tel.: +1-212-6392410
Fax: +1-212-7173203

J. Qin
Biostatistics Research Branch,
National Institute of Allergy and
Infectious Disease, NIH,
Bethsheda, MD, USA

R. King
Knoxville Dermatology Laboratory,
Knoxville, TN, USA

P. Illei
Department of Pathology,
New York University Medical Center,
New York, NY, USA

Introduction

Malignant mesotheliomas exhibit a broad histologic spectrum. Recognition of the various histologic types not only facilitates accurate diagnosis, it may also identify clinically and/or pathologically significant subsets [18]. For example, recent studies of lymphohistiocytoid mesotheliomas have demonstrated them to have a prognosis similar to sarcomatoid mesotheliomas [20], and an analysis of deciduoid mesothelioma has clarified the clinical features and anatomic distribution of this variant [19]. Malignant mesotheliomas with a pronounced myxoid stroma (myxoid mesothelioma) have been reported, but only in small series [3, 13] or single case reports [5]. This histologic pattern has

been suggested to be associated with a better outcome [3, 13]. Its clinical and pathological characteristics, however, are still to be defined.

Materials and methods

Patient data

All pleural mesothelioma cases treated at Memorial Sloan-Kettering Cancer Center between 1993 and 2001 were retrieved from the pathology database. The pathology materials were reviewed to identify mesotheliomas with extensive myxoid changes. Only those cases with hematoxylin and eosin (H & E) slides or tissue blocks available were included in the study. Clinical data were retrieved from a computer-based disease management data system. Clinicopathological staging was based on the surgical and pathological findings using the tumor-node-metastasis (TNM)-based IMIG staging system[15].

Histologic review

At least three H & E sections were reviewed in each case. Study cases designated as "myxoid mesothelioma" were defined as having at least 50% of the tumor containing a pronounced myxoid stroma that occupied more than 50% of the tumor volume in those regions.

Immunohistochemical and histochemical studies

Immunohistochemical stains were performed on 4-μ-thick, formalin-fixed, and paraffin-embedded sections using the streptavidin–biotin–peroxidase complex method. A panel of ten antibodies was applied, including AE1/AE3 (monoclonal, 1:1,000, Boehringer-Mannheim, Indianapolis, IN), CAM5.2 (monoclonal, 1:1,000, Becton Dickinson, Franklin Lakes, NJ), 34BE12 (monoclonal, 1:50, Enzo, Farmingdale, NY), Vimentin (monoclonal, Ventana, Tucson, AZ), calretinin (polyclonal, Chemicon International, Temecula, CA), WT-1 (monoclonal, 1:40, DAKO), Ber-EP4 (monoclonal, 1:1,000, DAKO), LeuM1 (CD15) (monoclonal, 1:1,000, Becton Dickinson), CEA (monoclonal, Ventana), and Ki-67 (monoclonal, 1:500, clone MIB1, Immunotech, Westbrook, ME). Antigen retrieval was performed for all antibodies (citrate buffer, microwaving at pH 7.2–7.5) Appropriate positive and negative controls were used for each antibody. Histochemical stains for Alcian blue with and without hyaluronidase pretreatment were also performed on all available cases.

Ultrastructural studies

All tissue samples were fixed in 2% glutaraldehyde, post-fixed in 1% osmium tetroxide, and embedded in epoxy resin using standard techniques. In each study case with epoxy resin blocks available, thick sections were cut and stained with toluidine blue to select suitable tissue samples. Ultrathin sections from two selected blocks were stained

Table 1 The clinical characteristics of patients with myxoid mesothelioma

Patient no.	Age/sex	Site	Asbestos	Treatment	Stage[a]	F/u time (months)	F/u status
1	72/M	R PL	Yes	Pleurodesis	IV	9	NED
2	55/M	R PL	Possible	EPP+CHEMO	IV	9	AWD
3	56/M	L PL	No	EPP+RT	IV	4	DOD
4	67/M	L PL	No	EPP	III	1	DOC (MI)
5	75/M	L PL	Yes	EPP+RT	III	27	DOD
6	69/F	R PL	Unknown	EPP+RT	IV	36	DOC (sepsis)
7	54/F	R PL	Possible	EPP+RT	III	31	NED
8	50/F	R PL	No	EPP+RT	II	75	NED
9	75/M	R PL	Yes	EPP	II	3	NED
10	53/M	R PL	No	EPP	III	1	DOC (MI)
11	40/M	R PL	No	EPP+RT	III	6	AWD
12	47/M	R PL	Yes	EPP+RT+CHEMO	III	65	DOD
13	44/F	L PL	No	EPP	III	26	AWD
14	58/M	R PL	Possible	CHEMO+EPP+CHEMO	III	20	AWD
15	48/F	L PL	No	EPP	II	2	DOD
16	74/F	R PL	No	OBSERVE	IV	17	AWD
17	66/F	R PL	No	CHEMO	IV	31	DOD
18	62/F	R PL	Yes	EPP	III	15	DOD
19	71/F	R PL	Yes	EPP+RT	II	12	NED

F/u Follow-up, *R* right, *PL* pleura, *NED* no evidence of disease, *EPP* extrapleural pneumonectomy, *CHEMO* chemotherapy, *AWD* alive with disease, *RT* radiation therapy, *L* left, *DOD* died of disease, *DOC* died of other causes, *MI* myocardial infarction

[a]Staging is according to the TNM-based IMIG system

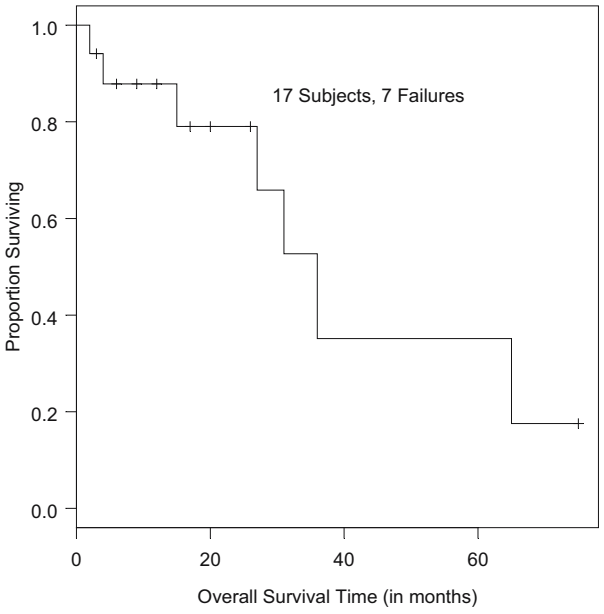


Fig. 1 Overall survival of patients with myxoid mesothelioma

with uranyl acetate and lead citrate, and examined with a Zeiss 906 transmission electron microscope.

Statistical analysis

Survival analyses were based on the patients' status at last follow-up. Survival curves were generated using the method of Kaplan and Meier [9].

Results

Patient data

A total of 234 pleural mesothelioma cases were identified from the database that had tissue slides or blocks available for review. Histologic review of the pathological material revealed 19 cases with a pronounced myxoid stroma fulfilling the inclusion criteria (8% of the 234 patients).

Clinical characteristics are summarized in Table 1. There were nine females and ten males. The age range was 40–75 years, with a median of 58 years and a mean of 59.8 years. Fourteen of the 19 patients involved the right pleura, and five involved the left pleura (right to left ratio, 2.8:1). A history of asbestos exposure was confirmed in six (32%) patients and suggested in three (16%). No asbestos exposure was identified in nine patients. In one patient, this information was not available. Sixteen patients underwent an extrapleural pneumonectomy, seven followed by radiation therapy, one by chemotherapy alone, one by combined chemotherapy and radiation, and one patient had neoadjuvant chemotherapy followed by surgery and postoperative chemotherapy. One patient had pleurodesis only, one had chemotherapy only, and one, whose medical condition prevented any surgical or cytotoxic treatment, received only supportive care. In these three cases, the biopsy specimens were available for review. Six patients presented with IMIG stage IV disease, nine patients presented with stage III, and four patients presented with stage II. Follow-up time ranged from 1 to 75 months (median 15 months). At last follow-up, six patients had died of disease at 4–65 months after initial diagnosis (median survival time, 21 months), three died of other causes (two died of myocardial infarction within 1 month of surgical intervention, and one died of sepsis 36 months after diagnosis), five were alive with disease at 9–26 months (median, 17 months), and five had no evidence of residual mesothelioma at 3–75 months (median, 12 months). The two patients who died of myocardial infarction within 1 month of surgery were excluded from survival analysis. With those two patients excluded, the overall median survival was 36 months (median follow up time, 17 months); the estimated 2-year overall survival rate was 79% (95% CI, 0.601–1.00), and the 3-year overall survival rate was 35% (95% CI 0.127–0.972) (Fig. 1).

Histologic review

As defined by the inclusion criteria, all study cases had voluminous myxoid stroma. At low power, this stroma constituted the dominant component of the tumor and imparted a bluish hue to the H & E stained sections under the light microscope. It might form pools with scattered cells floating within, or it might be intermixed with a prominent fibrous component (Fig. 2). An amorphous or granular quality and a bluish tinge were appreciated in this stroma at higher magnification (Fig. 3a). The malignant mesothelial cells were always of epithelioid type and without significant cytologic atypia. They had an eosinophilic cytoplasm. Although enlarged nuclei with prominent nucleoli could be seen, mitoses were not common. These cells formed cords or irregular tubules or clusters, sparsely embedded in the stroma (Fig. 3b). The tumors showed focal areas where the cellularity was high; however, even in

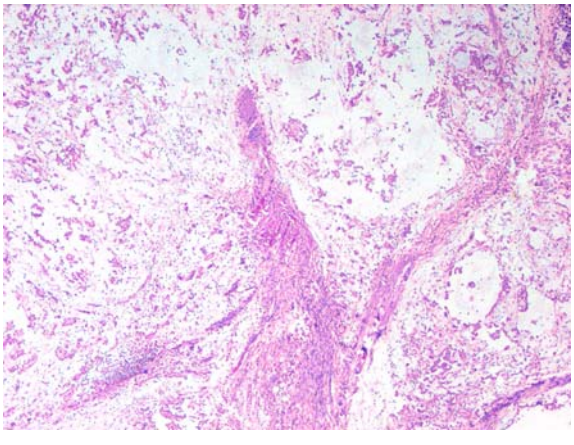


Fig. 2 Low-power view of a myxoid mesothelioma showing pools of myxoid material containing free-floating cell clusters, admixed with fibrous tissue. Note the presence of a bluish tinge imparted by this myxoid stroma

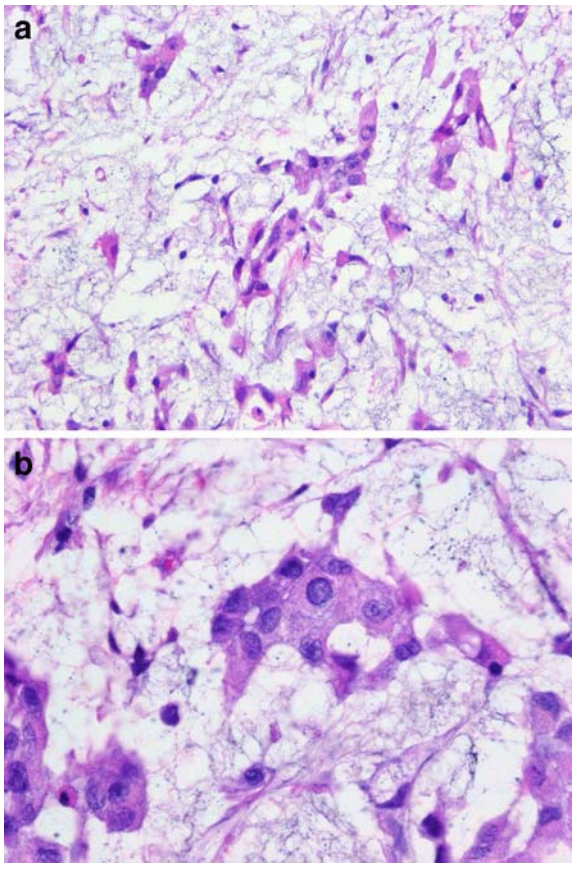


Fig. 3 Higher power view of a myxoid mesothelioma showing a granular quality of the myxoid stroma (**a**) and the tumor cells with eosinophilic cytoplasm and somewhat irregular nuclei. No mitosis is present (**b**)

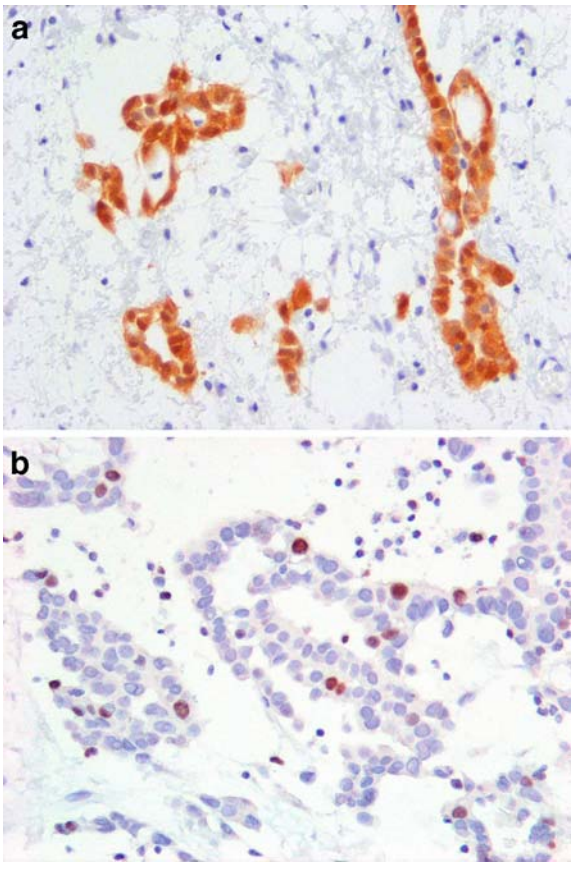


Fig. 4 Immunohistochemically, the tumor cells are strongly positive for calretinin (**a**). A Ki-67 staining demonstrating a low proliferation index (**b**)

these areas, the myxoid nature of the associated stroma could still be appreciated. No necrosis was identified in any of the cases. None of the cases showed sarcomatoid features.

Immunohistochemical and histochemical studies

Immunohistochemical studies were performed on 12 cases whose tissue blocks were available. All tumors tested were positive for calretinin (diffuse and strong in 12/12 cases) (Fig. 4a), WT-1 (diffuse and strong in 8/12, focal and weak in 4/12), AE1/AE3 (12/12), cam 5.2 (12/12), and 34BE12 (diffusely positive in 10/12, focally positive in 2/12). All tumors were negative for monoclonal CEA, Leu-M1 (CD15), and Ber-EP4. Nine tumors were diffusely positive for vimentin, one was focally positive, and one was negative. Ki-67 staining showed a proliferation index of less than 5% in seven cases and 10–30% in five (Fig. 4b).

Histochemically, the myxoid stroma in all 12 cases was diffusely positive with Alcian blue at pH 2.5 (Fig. 5a). The positivity was neutralized in every case by pretreatment with hyaluronidase (Fig. 5b).

Ultrastructural studies

Electron microscopy was performed in six cases. All six demonstrated conspicuous long and slender mesothelial-type surface microvilli. Well-formed cell junctions were present in all six cases, and a distinct basement membrane was seen in two. Duplication of the basement membrane was not observed. The cells often contained prominent intermediate filaments, focally forming tonofilaments. In all six cases, an extracellular, mildly to moderately electron-dense amorphous or slightly granular material was noted. This material was denser or more evident immediately adjacent to the tumor cells (Fig. 6a), and often formed a haze in which the surface microvilli were meshed (Fig. 6b). This diffuse haze coating the microvilli lacked the branching filaments seen in the glycocalyceal material associated with intestinal-type microvilli, and it did not form glycocalyceal body-like granules. However, electron-dense, branched fern-like material, similar in appearance to hyaluronic acid crystals, was present in all cases. These "crystals" were often seen in the extracellular spaces adjacent to surface microvilli (Fig. 6c).

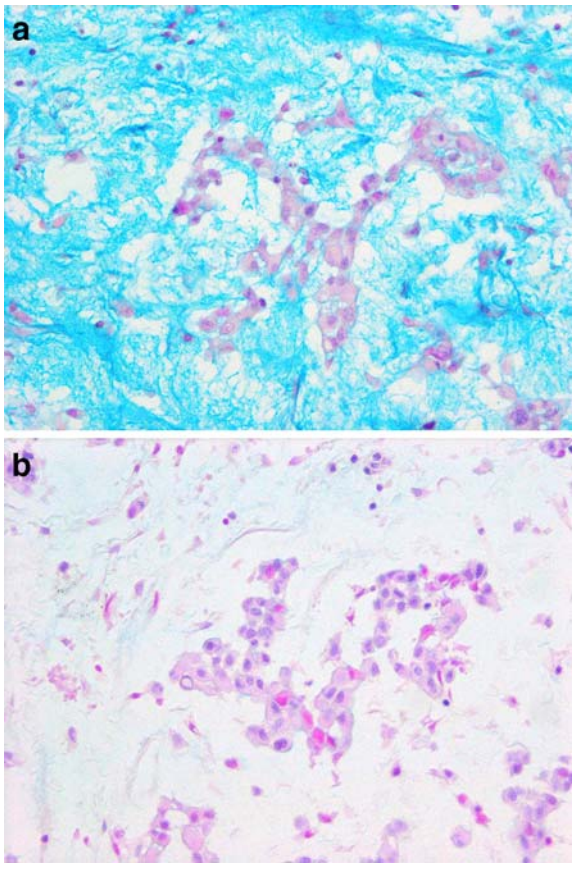


Fig. 5 Histochemically, the myxoid stroma is diffusely positive with Alcian blue at pH 2.5 (**a**). The positivity is neutralized by pretreatment with hyaluronidase (**b**)

Discussion

Histologic subtypes have long been recognized as prognostically significant in malignant mesothelioma [2]. The conventional classification separates mesotheliomas into three major types, the epithelioid type (also referred to as epithelial type), the sarcomatous (or sarcomatoid) type, and the biphasic (mixed) type. The epithelioid type has been shown to have a clear survival advantage over the other two types [1, 2]. More recently, additional subtypes in the epithelioid category have been described. Some have been shown to be associated with a longer survival such as the tubulo-papillary variant [8]; others were thought to be important both in the differential diagnosis with other morphological mimics and in carrying possible prognostic implications such as the deciduoid variant [19, 20].

The occasional presence of a pronounced myxoid stroma in some epithelioid mesotheliomas has been noted. Butchart et al. in 1976 identified three cases, from a series of 29 malignant mesotheliomas, that were characterized histologically by "abundant oedematous mucoid stroma with loosely arranged tumor cells" [3]. These three cases had a more favorable clinical outcome. Later, Mark et al. [13] reported that a prominent myxoid stroma and the formation of tubules and micropapillae were the morphological patterns shared by tumors in six patients with a

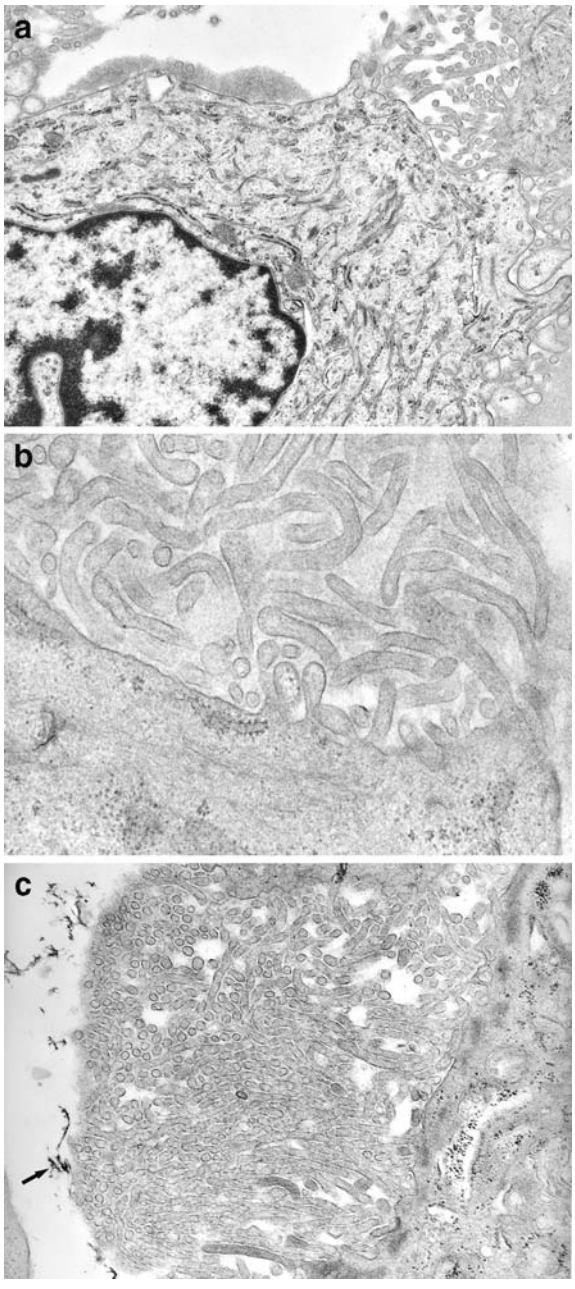


Fig. 6 Ultrastructural features of mesothelioma with a pronounced myxoid stroma. An extracellular moderately electron-dense amorphous material is present, more condensed on the cell surfaces (**a**, magnification ×27,670) and enmeshes the mesothelial-type surface microvilli (**b**, magnification ×66,836). Note the presence of electron-dense, fern-like crystalline material adjacent to the surface microvilli (**c**, magnification ×40,083. *Arrow* indicates crystalline material)

prolonged symptom-free interval or extended survival after biopsy, again suggesting a correlation between this morphological pattern and a relatively favorable prognosis. More recently, Diaz et al. [5] reported a well-differentiated papillary mesothelioma of the pelvic peritoneum that contained extensive areas of myxoid stroma, resulting in a morphology that might be misinterpreted as a soft tissue neoplasm with myxoid stroma or pseudomyxoma perito-

nei. Overall, however, information about this morphological pattern is scarce in literature. The purpose of this study was, therefore, to perform a systematic clinical and pathological assessment of a series of myxoid methotheliomas that we collected from our files.

Our study demonstrates that myxoid mesotheliomas are not rare, as they represented 8% of our series of 234 cases. When compared to a series of consecutive cases that was also treated at our institution [18], patients with myxoid mesotheliomas seem to have less of a male dominance (male to female ratio, 10:9 vs 5:1 in the general group [18]). They, however, share other epidemiological features with mesothelioma patients in general. These features include median age at diagnosis (57 vs 62 years in pleural mesothelioma in general [18]) and history of asbestos exposure (probable or definite exposure in 47 vs 62% in pleural mesothelioma in general [18]). The right-side predominance noted in myxoid mesotheliomas has also been reported in pleural mesotheliomas in general (right to left ratio, 2.8:1 vs 1.6:1 in mesotheliomas of all types [21]) and is thus not a feature unique to myxoid mesothelioma. The explanations suggested for the right-side predominance in pleural mesotheliomas include differences in asbestos fiber deposition between the two lungs, the larger pleural surface area of the right lung, or differences in lymphatic drainage [21].

Overall, patients with myxoid mesotheliomas seem to have a somewhat more favorable outcome than patients with other types of mesothelioma or mesothelioma patients in general. With disease stage varying from IMIG stages II–IV, and the majority of cases being treated with radical extrapleural pneumonectomy with or without adjuvant radiation or chemotherapy, these patients had a median overall survival rate of 36 months, and an estimated 2-year overall survival rate of 79%. When compared to data obtained from our own institution [16, 17], this survival rate is superior to the 15.1-month median survival time in patients with epithelioid meostheliomas [17] and is comparable to the 33.8-month median survival seen in early stage (stages I and II) cases that are treated similarly (i.e., mostly with radical surgery) [16]. Although limited by the small case number and lack of proper controls for stage and treatment modalities, our findings seem to at least suggest a survival advantage in patients with myxoid mesotheliomas and are in agreement with the few reports available in literature [3, 13].

The fact that myxoid mesotheliomas produce a voluminous myxoid stroma that, as demonstrated by our histochemical staining, is mainly composed of hyaluronidase-sensitive material suggests perfect tumor recapitulation of the secretory activity of its normal counterpart. Indeed, normal mesothelial cells secrete glycosaminoglycans, particularly hyaluronic acid, which act as a lubricant, facilitating the motion of the viscera within their respective cavities. Therefore, it is not surprising that these tumors are always associated with epithelioid morphology without significant atypia. Consequently, the tumor cells show a typical mesothelial immunophenotype and ultrastructural characteristics, as has been well demonstrated by this study.

Indeed, the immunohistochemical staining pattern of these tumors is classic for mesothelioma. They show positive staining for keratins, vimentin, and mesothelial markers, and negative staining for the various glycoproteins (monoclonal CEA, Leu-M1, and Ber-EP4). Ki-67 has been reported to show a significant correlation with survival in patients with mesotheliomas [10]. In our study, more than half of the cases had minimal (<5%) nuclear labeling for Ki-67, and the remaining had a labeling index of less than 30%, thus demonstrating an overall low proliferation rate. However, owing to the small sample size, a meaningful comparison of outcome between those with less than 5% Ki-67 labeling and those with more is not possible.

The ultrastructural findings of epithelioid mesotheliomas are characteristic, owing mainly to the presence of abundant long and slender surface microvilli. As expected, all tumors in this series examined ultrastructurally showed typical mesothelial-type microvilli along with other commonly seen features such as well-formed cell junctions, basement membrane, and intermediate filaments. The myxoid stroma corresponds to an extracellular, mildly to moderately electron-dense amorphous or slightly granular material. This material tends to condense around cell surfaces and enmesh the surface microvilli, and is associated with the formation of electron-dense, fern-like bodies, which are considered to represent crystalline forms of hyaluronic acid [4]. This material needs to be distinguished from the glycocalyx material seen in some adenocarcinomas. The latter usually has a filamentous and hairy quality. In contrast to fern-like crystals, it is often associated with spherical glycocalyceal bodies coating the microvilli. The associated microvilli have a filamentous core that extends into the cell cytoplasm as a rootlet. Although glycocalyceal material is most apparent on the apical surface of intestinal epithelial cells and their neoplastic equivalents, it may also be present in tumors of other organ epithelia such as pulmonary adenocarcinoma, pancreatic ductal adenocarcinoma, and urothelial carcinoma [12]. It is therefore important for electron microscopists to distinguish the hyaluronic-acid-type mucous material of myxoid mesothelioma from the glycocalyceal material of adenocarcinomas.

The presence of a voluminous hyaluronidase-sensitive stroma in this group of tumors seems to be a different phenomenon from the intracellular mucin seen in the so-called “mucin-positive mesothelioma” reported by others [4, 7, 11]. In the latter group of tumors, it is believed that the mucin is also of hyaluronic acid type, as demonstrated by its sensitivity to digestion with hyaluronidase [7], and by the presence of electron-dense intracytoplasmic “fern-like” hyaluronic acid crystals [4]. The mucin in the latter group, however, is confined to the cells, and the tumors do not have a voluminous myxoid stroma [4, 7, 11]. The aberrant immunophenotypes, including positive immunoreactivity with a number of adenocarcinoma markers (most notably CEA and Leu M1) reported in mucin-positive mesotheliomas [7, 14], have not been observed in myxoid mesotheliomas. Available data are insufficient for an accurate comparison of these two groups of tumors with regard to their clinical and biological characteristics.

Myxoid stroma is a feature common to many types of tumors, and therefore may cause diagnostic confusion [5, 6], particularly when dealing with cytologic materials or small biopsies. Entities that can be confused for myxoid mesothelioma include mucinous adenocarcinomas, myxoid chondrosarcoma, and chordoma. In myxoid mesotheliomas, the typical mesothelial appearance of the tumor cells should enable correct distinction from other myxoid entities. When in doubt, a multimodality diagnostic approach including immunohistochemical and ultrastructural studies is suggested.

In summary, myxoid mesotheliomas are a group of epithelioid mesothelioma that has retained the secretory activity of normal mesothelium. The tumor cells exhibit immunohistochemical and ultrastructural features characteristic of epithelioid mesothelioma. Patients with myxoid mesothelioma may present at different stages of the disease; however, they seem to have a better overall survival when compared to patients with epithelioid mesotheliomas in general. Obviously, additional studies are needed to confirm the survival advantage. Our study calls for attention to histologic subtypes of malignant mesothelioma, particularly in the context of prognostically and therapeutically oriented investigations of this lethal disease.

Acknowledgements The authors thank Ms. Irina Linkov and Ms. Marina Asherova of the Immunohistochemistry Core Facility, Ms. Ann Baren and Ms. Elizabeth Weiss of the Electron Microscopy Laboratory, and Mr. Kin C. Kong and Ms. Allyne Manzo of the Photography Laboratory at Memorial Sloan-Kettering Cancer Center for their technical support.

References

1. Baas P (2003) Predictive and prognostic factors in malignant pleural mesothelioma. Curr Opin Oncol 15:127–130
2. Butchart EG (1999) Contemporary management of malignant pleural mesothelioma. Oncologist 4:488–500
3. Butchart EG, Ashcroft T, Barnsley WC, Holden MP (1976) Pleuropneumonectomy in the management of diffuse malignant mesothelioma of the pleura. Experience with 29 patients. Thorax 31:15–24
4. Cook DS, Attanoos RL, Jalloh SS, Gibbs AR (2000) "Mucin-positive" epithelial mesothelioma of the peritoneum: an unusual diagnostic pitfall. Histopathology 37:33–36
5. Diaz LK, Okonkwo A, Solans EP, Bedrossian C, Rao MS (2002) Extensive myxoid change in well-differentiated papillary mesothelioma of the pelvic peritoneum. Ann Diagn Pathol 6:164–167
6. Goetz SP, Robinson RA, Landas SK (1992) Extraskeletal myxoid chondrosarcoma of the pleura. Report of a case clinically simulating mesothelioma. Am J Clin Pathol 97:498–502
7. Hammar SP, Bockus DE, Remington FL, Rohrbach KA (1996) Mucin-positive epithelial mesotheliomas: a histochemical, immunohistochemical, and ultrastructural comparison with mucin-producing pulmonary adenocarcinomas. Ultrastruct Pathol 20: 293–325
8. Johansson L, Linden CJ (1996) Aspects of histopathologic subtype as a prognostic factor in 85 pleural mesotheliomas. Chest 109:109–114
9. Kaplan EL, Meier P (1958) Nonparametric estimation from incomplete observations. J Am Stat Assoc 53:457–481
10. Leonardo E, Zanconati F, Bonifacio D, Bonito LD (2001) Immunohistochemical MIB-1 and p27kip1 as prognostic factors in pleural mesothelioma. Pathol Res Pract 197:253–256
11. MacDougall DB, Wang SE, Zidar BL (1992) Mucin-positive epithelial mesothelioma. Arch Pathol Lab Med 116:874–880
12. Marcus PB (1981) Glycocalyceal bodies and their role in tumor typing. J Submicrosc Cytol 13:483–500
13. Mark EJ, Shin DH (1993) Diffuse malignant mesothelioma of the pleura: a clinicopathological study of six patients with a prolonged symptom-free interval or extended survival after biopsy and a review of the literature of long-term survival. Virchows Arch, A Pathol Anat Histopathol 422:445–451
14. Robb JA (1989) Mesothelioma versus adenocarcinoma: false-positive CEA and Leu-M1 staining due to hyaluronic acid. Hum Pathol 20:400
15. Rusch VW (1996) A proposed new international TNM staging system for malignant pleural mesothelioma from the International Mesothelioma Interest Group. Lung Cancer 14:1–12
16. Rusch VW, Rosenzweig K, Venkatraman E, Leon L, Raben A, Harrison L, Bains MS, Downey RJ, Ginsberg RJ (2001) A phase II trial of surgical resection and adjuvant high-dose hemithoracic radiation for malignant pleural mesothelioma. J Thorac Cardiovasc Surg 122:788–795
17. Rusch VW, Venkatraman E (1996) The importance of surgical staging in the treatment of malignant pleural mesothelioma. J Thorac Cardiovasc Surg 111:815–825 (discussion 825–826)
18. Rusch VW, Venkatraman ES (1999) Important prognostic factors in patients with malignant pleural mesothelioma, managed surgically. Ann Thorac Surg 68:1799–1804
19. Shia J, Erlandson RA, Klimstra DS (2002) Deciduoid mesothelioma: a report of 5 cases and literature review. Ultrastruct Pathol 26:355–363
20. Yao DX, Shia J, Erlandson RA, Klimstra DS (2004) Lymphohistiocytoid mesothelioma: a clinical, immunohistochemical and ultrastructural study of four cases and literature review. Ultrastruct Pathol 28:213–228
21. Yates DH, Corrin B, Stidolph PN, Browne K (1997) Malignant mesothelioma in south east England: clinicopathological experience of 272 cases. Thorax 52:507–512

Virchows Arch (2005) 447: 835–841
DOI 10.1007/s00428-005-0025-0

ORIGINAL ARTICLE

Shio Shimada · Takashi Ishizawa · Keisuke Ishizawa · Kouichi Kamada · Takanori Hirose

Dedifferentiated liposarcoma with rhabdomyoblastic differentiation

Received: 5 April 2005 / Accepted: 30 May 2005 / Published online: 13 July 2005
© Springer-Verlag 2005

Abstract Dedifferentiated areas of dedifferentiated liposarcoma (DDL) usually show malignant fibrous histiocytoma (MFH)- or fibrosarcoma-like features and lack any histologic signs of specific differentiation. However, some reports have demonstrated specific differentiation in these areas, with histologic features resembling those of rhabdomyosarcoma, leiomyosarcoma, and osteosarcoma. We report here a pathologic and genetic analysis of three cases of DDLs with rhabdomyosarcomatous areas. MFH- or fibrosarcoma-like areas of one primary DDL and two recurrent DDLs contained various amounts of rhabdomyoblasts, which were immunoreactive for desmin, myoglobin, muscle actin (HHF-35), and myogenin. An ultrastructural examination demonstrated rhabdomyoblasts with abundant cytoplasm containing thin and thick filaments and Z-bands. By real-time PCR, amplification of *mdm2* and *cdk4* was confirmed in both well-differentiated and dedifferentiated areas with rhabdomyoblasts of all cases. To our knowledge, only seven cases of DDLs with rhabdomyosarcomatous components have been reported, and furthermore, the genetic profiles of the rhabdomyosarcomatous components in DDLs have not been investigated. This study demonstrates that DDLs with rhabdomyosarcomatous areas have genetic alterations that are common to well-differentiated/dedifferentiated liposarcomas.

Keywords Dedifferentiated liposarcoma · Retroperitoneum · Rhabdomyoblast · *mdm2* · *cdk4*

S. Shimada (✉) · T. Ishizawa · K. Ishizawa · K. Kamada · T. Hirose
Department of Pathology, Saitama Medical School, Morohongo 38, Moroyama, Iruma-gun, Saitama, 350-0495, Japan
e-mail: shio@saitama-med.ac.jp
Tel.: +81-49-2761164
Fax: +81-49-2761583

Introduction

Dedifferentiated liposarcoma (DDL), which was first introduced by Evans [3] in 1979, belongs to the same category as well-differentiated liposarcoma (WDL). DDL occurs most commonly in the retroperitoneum in middle-aged adults. Other locations include the extremity, the spermatic cord, and, less frequently, the head, neck, and trunk. No sex predilection is observed. About 90% of DDLs arise de novo, while 10% occur in recurrences [18].

Dedifferentiated areas of DDL usually consisted of nonspecific, undifferentiated sarcoma, such as malignant fibrous histiocytoma (MFH) and fibrosarcoma, although 10% of DDLs are known to show some specific differentiation including rhabdomyosarcoma, leiomyosarcoma, osteosarcoma, and angiosarcoma [4, 5]. In addition, dedifferentiated areas may show inflammatory MFH-like features, whorl structures, and palisaded myofibroblastoma-like structures. Among these, rhabdomyoblastic differentiation is one of the most uncommon forms of heterologous differentiation in DDLs [5]. Only seven cases of DDLs with rhabdomyoblastic differentiation have been reported in the literature so far to our knowledge [4, 5, 7, 14, 17].

Recently, it was demonstrated that WDLs and DDLs share common molecular cytogenetic abnormalities, that is, the ring or large-marker chromosome [9, 10, 13] and amplification of human homologue of the murine double-minute type 2 (*mdm2*) and cyclin-dependent kinase 4 (*cdk4*) gene [1, 2, 6, 11, 12, 15]. Alterations in *mdm2* and *cdk4* are recognized as major events in the tumorigenesis of liposarcomas. Overexpression of *mdm2* appears to act as an alternative to direct p53 mutation for inactivation of the p53-mediated pathway for cell growth suppression. Overexpression of *cdk4* interferes with the retinoblastoma (pRb)-mediated pathway through phosphorylation of pRb and inactivation of its cell growth-suppressive effect [20].

In the present study, we report three additional DDLs with rhabdomyoblastic differentiation and demonstrate for the first time the amplification of *mdm2* and *cdk4* genes in the dedifferentiated areas with heterologous elements.

Case histories

Case 1

A large retroperitoneal mass was detected in a 57-year-old man during a health checkup. The retroperitoneal tumor, which was 16×9 cm in size, and an abdominal tumor, which was found simultaneously and was 18.5×13.5 cm in size, were resected surgically. Macroscopically, the retroperitoneal tumor was hard and gray, and the abdominal tumor was soft and yellowish. They were diagnosed as DDL. Four years later, an 18×10 cm retroperitoneal tumor was found and removed again and diagnosed as DDL with rhabdomyosarcomatous components (Fig. 1a).

Case 2

A retroperitoneal mass was removed from a 53-year-old man. The tumor was diagnosed as WDL. Seven years later, a 17×17 cm abdominal mass involving the descending colon and the tail of the pancreas was resected and diagnosed as DDL. Three years after the second operation, a 6.8×6.8 cm abdominal mass was removed. The third tumor was diagnosed as WDL. One year after the third operation, a multinodular abdominal mass that involved the stomach, small intestine, and colon was resected. The fourth tumor was diagnosed as DDL with rhabdomyosarcomatous components. One year after the fourth operation,

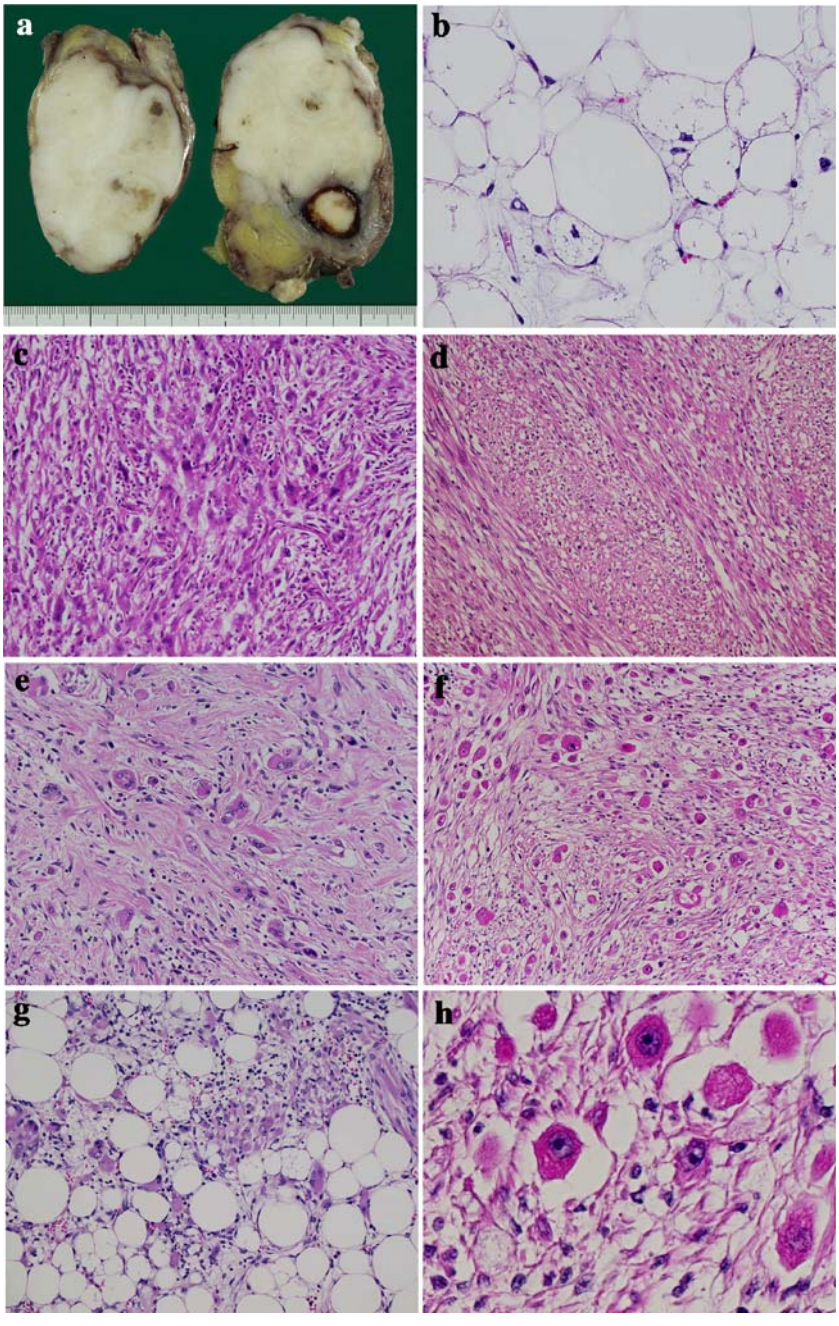


Fig. 1 Macroscopical and histological findings of dedifferentiated liposarcoma with rhabdomyoblastic differentiation. **a** The macroscopic feature of the recurrent tumor of case 1, composed of two different components, that is, gray and yellow areas. **b** The well-differentiated area of case 2, showing multivacuolated lipoblasts. **c** The dedifferentiated area of case 1, which shows MFH-like features. **d** The dedifferentiated area of case 3, which shows fibrosarcoma-like features. **e** The dedifferentiated area of case 1, showing rhabdomyoblasts which are diffusely found among spindle cells. **f** The dedifferentiated area of case 3, showing rhabdomyoblasts which are diffusely found among spindle cells. **g** The dedifferentiated area of case 2, showing rhabdomyoblasts which are sparsely found in the well-differentiated area. **h** Rhabdomyoblasts of case 3, which have an atypical nucleus with a prominent nucleolus

Table 1 Primers and probes of target genes

mdm2	
Forward primer	5′-GCATTATTTATAGCAGCC-3′
Reverse primer	5′-CAACCATTTTTAGGTCGA-3′
Fluorescence probe	5′-GGAAGGAAGAAAAGCTGCCATTTCCC-Flu-3′
LCRed probe	5′-LCRed640-ACACTCTCTTCTTTGTCTTGGGTTTCTTCC-3′
cdk4	
Forward primer	5′-GCTGACTTTTAACCCACACA-3′
Reverse primer	5′-AAAGATTGCCCTCTCAGTGT-3′
Fluorescence probe	5′-GAGTGAGCAATGGAGTGGCTGCCA-Flu-3′
LCRed probe	5′-LCRed-GGAAGGAAGAAAAGCTGCCATTTCCC-3′

a retroperitoneal tumor was resected and was diagnosed as DDL.

Case 3

A 35×24 cm retroperitoneal tumor was removed from a 69-year-old man. Macroscopically, the tumor was lipomatous in most parts and contained an 8-cm firm tan-gray mass. It was diagnosed as DDL with rhabdomyosarcomatous components. The patient died of sepsis 4 months after the operation. An autopsy was not allowed.

Materials and methods

Light microscopy

Primary and recurrent tumors of all cases were analyzed. The specimens were fixed in 10% formalin and were processed for paraffin embedding. In addition to hematoxylin-eosin (HE) stain, Masson-trichrome stain and reticulin preparation were applied.

Immunohistochemistry

Sections from all cases were immunostained with the following 14 antibodies. Antibodies were directed against myoglobin (lot 127; 1:500, DakoCytomation, Carpinteria, CA, USA), desmin (clone 33; 1:50, DakoCytomation), muscle actin (clone HHF35; 1:50, DakoCytomation), myogenin (clone F5d; 1:25, DakoCytomation), smooth muscle actin (clone 1A4; 1:50, DakoCytomation), vimentin (clone V9; 1:200, DakoCytomation), CD34 (clone My10; 1:30, BD Transduction Laboratory, San Jose, CA, USA), CD56 (clone 1B6; 1:50, Novocastra, Newcastle, English), CD99 (clone O13; 1:100, SIGNET Lab, Dedham, MA, USA), S100 protein (lot 017; 1:300, DakoCytomation), epithelial membrane antigen (clone E29; 1:100, DakoCytomation), cytokeratin (clone CAM 5.2; 1:1, BD Transduction Laboratory), and Ki-67 (clone MIB-1; 1:100, DakoCytomation). Ventana autostainer (Ventana HX system, Benchmark, Tucson, AZ, USA) was employed for the detection of the primary antibodies with diaminobenzidine as the chromogen.

Electron microscopy

Small specimens of case 3 sampled from formalin-fixed material were processed for ultrastructural study. A few 1-mm cubes were fixed in 1% glutaraldehyde in 0.1 M cacodylate buffer, postfixed in 2% osmium tetroxide, and dehydrated through graded alcohols for Epon embedding. Subsequently, the sections were prepared for electron microscopy in a standard routine.

Real-time PCR

DNA samples taken from rhabdomyosarcomatous components and WDL areas were a target for this analysis. Normal intra-abdominal fat tissues from 28 surgical materials of colonic and ovarian cancers were used as the control. All DNA samples were prepared from formalin-fixed, paraffin-embedded sections. Total DNA was isolated with DNeasy Kit (Qiagen, Hilden, Germany) according to the manufacturer's instructions. Real-time PCR was performed using

Table 2 Program for real-time PCR

Cycle program data	Denature	Amplification			Cooling
Cycles	1	45			1
Analysis mode	None	Quantification			None
Temperature targets	Segment 1	Segment 1	Segment 2	Segment 3	Segment 1
Target temperature (°C)	95	95	60	72	40
Incubation time (h:min:s)	0:10:00	00:00:10	00:00:15	00:00:6	0:00:30
Temperature transition rate(°C/s)	20/0	20	20	20	20.0
Second target temperature(°C)	0	0	0	0	0
Step size (°C)	0.0	0.0	0.0	0.0	0.0
Step delay (cycles)	0	0	0	0	0
Acquisition mode	None	None	None	None	None

Table 3 Immunohistochemical study of the DDLs with rhabdomyosarcomatous component

Antigen	Case 1		Case 2		Case 3	
	Rhabdomyoblast	Spindle cell	Rhabdomyoblast	Spindle cell	Rhabdomyoblast	Spindle cell
Myoglobin	+	+ (a few)	+	−	+	−
Desmin	+	+	+	−	+	+
Muscle actin	+	−	+	−	+	−
Myogenin	+	−	+	−	+	−
Smooth muscle actin	−	−	−	−	−	−
Vimentin	+	+	+	+	+	+
CD34	−	−	−	−	−	−
CD56	+	+	+	+	+	+
CD99	+	+	+ (a few)	−	+ (a few)	−
S100	+	−	−	−	−	−
EMA	−	−	−	−	−	−
Cytokeratin	+ (a few)	−	−	−	+	−
Ki-67	29.0%		6.6%		17.1%	

EMA Epithelial membrane antigen

LightCycler 1.2 System (Roche Diagnostics GmbH, Mannheim, Germany). Primers and probes for target genes (*mdm2* and *cdk4*) listed in Table 1 were designed and made by Nihon Gene Research Laboratories Inc., Sendai, Japan, on the basis of the sequences registered with GenBank (*mdm2*: AF527840; *cdk4*: NM000075). Human beta-globin LightCycler (Nihon Gene Research Laboratories Inc.) was selected as the reference gene. Real-time PCR was

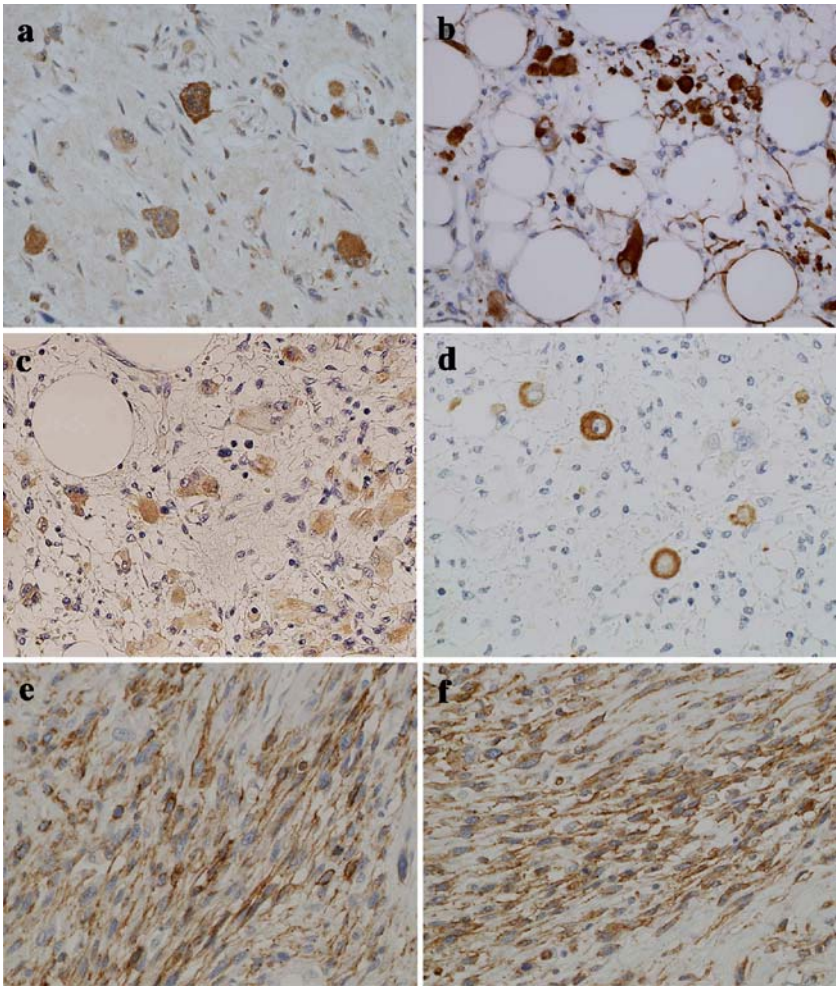


Fig. 2 Immunohistochemical findings of dedifferentiated liposarcoma with rhabdomyoblastic differentiation. Rhabdomyoblasts are immunoreactive for myoglobin (**a**), desmin (**b**), muscle actin (**c**), and cytokeratin (**d**). Spindle cells are positive for CD56 (**e**) and CD99 (**f**)

performed with 20-μl final mixture containing 50 pmol sample DNA, 10 pmol of each primer, 2 pmol of fluorescence probe, 4 pmol of LCRed probe, 2.4 μl $MgCl_2$, and 10 μl LightCycler Fast Start DNA Master Hybridization Probes (Roche Applied Science, Penzberg, Germany) according to the protocol shown in Table 2. The gene copy numbers of *mdm2* and *cdk4* were calculated from a standard curve that was constructed using a plasmid (Nihon Gene Research Laboratories Inc.), the gene number of which is already known. The level of amplification for the target gene was calculated as a ratio of the copy number of the target gene (*mdm2*, *cdk4*) to that of the reference gene (beta-globin). The cut-off value for assessment of the gene amplification level was determined based on that of normal fat tissues by creating a 99th percentile confidence interval, and individual measurements were considered as being amplified when they were beyond the above limit.

Results

Microscopic findings

In one case (case 2), the initial tumor was diagnosed as WDL and the recurrent tumors had dedifferentiated areas. In two cases (cases 1 and 3), the initial tumors were diagnosed as DDL. In all cases, WDL areas showed an atypical lipomatous neoplasm that contained lipoblasts, atypical mesenchymal cells, and mature lipomatous cells (Fig. 1b). In two cases (cases 1 and 2), dedifferentiated areas showed MFH-like features (Fig. 1c), and in one case (case 3), the dedifferentiated area showed fibrosarcoma-like structures (Fig. 1d). In two cases (cases 1 and 3), the border of WDL and DDL was clear, and many rhabdomyoblasts were diffusely seen in the DDL area, being located among bizarre and spindle cells (Fig. 1e,f). In case 2, the tumor had a well-demarcated DDL area, but the area did not contain rhabdomyoblasts. Alternatively, the tumor had a few rhabdomyoblasts scattered among spindle cells in the WDL area (Fig. 1g). The rhabdomyoblasts had atypical nuclei with prominent nucleoli (Fig. 1h) and eosinophilic cytoplasm, which contained filamentous structures.

Immunohistochemical findings

Immunohistochemical results of the cases were summarized in Table 3. The rhabdomyoblasts were immunoreactive for myoglobin (Fig. 2a), desmin (Fig. 2b), muscle actin (HHF-35) (Fig. 2c), myogenin, vimentin, CD56, and CD99 in all cases. A small number of rhabdomyoblasts were also positive for cytokeratin (CAM 5.2) in two cases (Fig. 2d). In one case, S-100 protein was expressed in rhabdomyoblasts.

The dedifferentiated components without rhabdomyoblasts were diffusely immunoreactive for vimentin, CD56 (Fig. 2e), and CD99 (Fig. 2f) in all cases. Desmin was focally expressed in cases 1 and 3. A few spindle cells in case 3 were also positive for smooth muscle actin. Myoglobin, muscle actin (HHF-35), myogenin, S-100 protein, and cytokeratin were not detected in any of these areas.

Electron microscopic findings

Ultrastructurally, rhabdomyoblastic cells had an atypical nucleus and abundant cytoplasm containing thin and thick filaments (Fig. 3a). Z-bands were focally found in the cytoplasm (Fig. 3b). Their ovoid nuclei, irregular in shape, contained euchromatin and a prominent nucleolus.

Real-time PCR

Copy number ratios for the *mdm2*, *cdk4*, and beta-globin were calculated in normal fat tissues. The mean of the copy number ratio was 1.12 for *mdm2* (range 0.12–1.67) and 1.05 for *cdk4* (range 0.52–1.58). The cut-off value (99th percentile) was 1.34 for *mdm2* and 1.20 for *cdk4*. Amplification was found in all samples of well-differentiated areas and dedifferentiated areas of liposarcomas, and the level of amplification was very high. The result of the

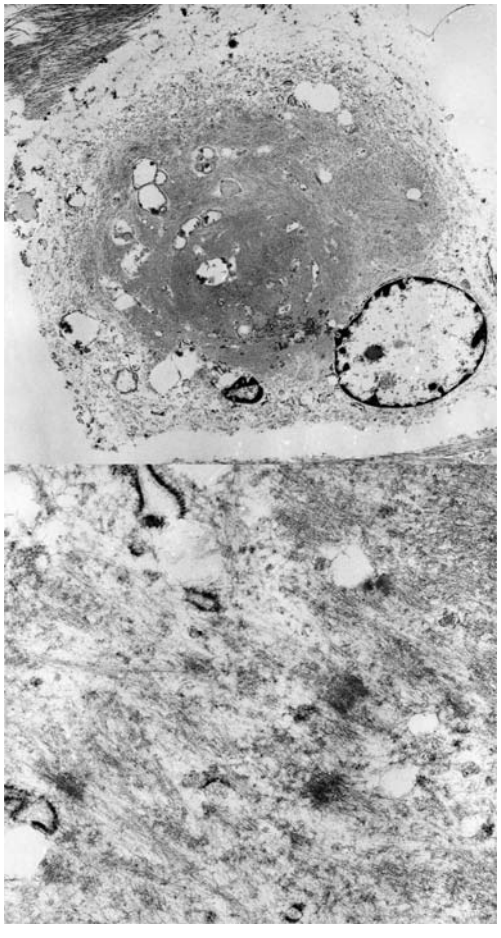


Fig. 3 Electron microscopic findings of rhabdomyoblasts. The rhabdomyoblast has an atypical nucleus and abundant cytoplasm filled with myofilaments (**a**). Z-bands are focally found with myofilaments (**b**)

Table 4 Amplification of target genes revealed by real-time PCR

Sample	Copy number ratio of *mdm2*/beta-globin	Copy number ratio of *cdk4*/beta-globin
Case 1		
WDL area	116.6	31.5
DDL area	35.9	35.3
Case 2		
WDL area	39	19.1
DDL area	59.3	66.7
Case 3		
WDL area	21.4	23.8
DDL area	30.0	10.2
Cut-off value	1.34	1.2

WDL Well-differentiated liposarcoma, *DDL* dedifferentiated liposarcoma

amplification status of the cases of liposarcomas is shown in Table 4. Amplification levels between WDL areas and dedifferentiated areas were not statistically significant (Mann–Whitney *U*-test).

Discussion

According to Henrichs et al. [5], DDLs with rhabdomyosarcomatous components account only for 1.3% of the DDLs, and to our knowledge, there have been only seven cases reported in the English literature so far [4, 5, 7, 14, 17]. The clinicopathological summary of ten cases combining seven reported cases and our three is presented in Table 5. They range from 47 to 72 years (mean age 57.4) in age and show a predilection for occurrence in men (men/women 8:2), whereas no sexual predominance is noted in DDL. All cases were located in the retroperitoneum or mesenteries. In the primary tumors, seven cases were diagnosed as WDLs, and the dedifferentiated areas with rhabdomyoblasts appeared in the recurrent tumors. The primary tumors of the remaining three cases were diagnosed as DDLs. The histology of the dedifferentiated areas was MFH in six cases, fibrosarcoma in two cases, and MFH and fibrosarcoma in two cases. Each case contained various amounts of rhabdomyoblasts, and, in addition, one case contained a leiomyosarcomatous component [17]. Follow-up data were available in nine cases. Eight cases underwent recurrences and metastasis [4] (Table 5). Taken together, the DDLs with rhabdomyosarcomatous components likely behave in a malignant fashion equivalent to the usual DDLs.

In our cases 1 and 2, the rhabdomyosarcomatous areas were not noted in the primary tumors; however, these areas were found in the recurrent tumors. In cases 1 and 3, the distribution of rhabdomyoblasts was diffuse in most of the dedifferentiated areas, but in case 2, a few rhabdomyoblasts appeared amongst some spindle cells in the well-differentiated area. The transition between the well-differentiated and dedifferentiated zones has been classified into three types [5]. In most cases, an abrupt transition is noted in such a manner that the two zones are starkly juxtaposed to one another, like in our cases 1 and 3. Less frequently, there is a gradual transition located between the two zones. The least common pattern is that of intricate commingling of dedifferentiated elements among the well-differentiated elements, giving the impression of mosaicism. The rhabdomyoblasts in case 2 were intermixed with well-differentiated areas, thus making it quite unusual in terms of the distribution of dedifferentiated components.

DDL with rhabdomyoblastic differentiation should be differentiated from malignant mesenchymoma, pleomorphic rhabdomyosarcoma, malignant Triton tumor, and malignant mixed mullarian tumor. It was previously proposed that malignant mesenchymoma is a non-epithelial malignant tumor showing two or more unrelated, differentiated tissue types in addition to the fibrosarcomatous elements [16]. In 1991, Newman and Fletcher [8] attempted to refine the criteria for this entity by excluding a variety of morphologic patterns that show no specific differentiation, such as fibrosarcoma, hemangiopericytoma, myxofibrosarcoma, and pleomorphic MFH. In addition, they reported a group of the malignant mesenchymoma with a low-grade behavior, in which six cases that contained liposarcoma and rhabdomyosarcoma were included. Since the concept of malignant mesenchymoma is now becoming less accepted,

Table 5 Review of literature of DDLs with rhabdomyosarcomatous components

Authors	Age	Sex	Site	Primary	Recurrence	Metastasis
Salzano et al. [14]	60	M	mes	WDL	4	–
Tallini et al. [17]	48	W	ret	WDL	1	–
	47	M	ret	WDL	2	–
	72	M	ret	DDL	1	–
McCormick et al. [7]	48	W	ret	DDL	recent case	–
Evans et al. [4]	54	M	ret	ALT with cartilaginous and osseous metaplasia	3	–
	66	M	mes	ALT	1	liver
Present study	57	M	ret + mes	WDL	1	–
	53	M	ret	WDL	3	–
	69	M	ret	DDL	–	–

M Men, *W* women, *ret* retroperitoneum, *mes* mesenterium, *WDL* well-differentiated liposarcoma, *DDL* dedifferentiated liposarcoma, *ALT* atypical lipomatous tumor

some authors suggest the label "malignant mesenchymoma" be deleted from classification schemes, and sarcomas displaying two or more lines of differentiation would best be diagnosed by identifying the lines of differentiation, their approximate amounts, and the grade of the most aggressive component [19]. Some cases that were diagnosed as malignant mesenchymoma may be actually dedifferentiated liposarcoma with specific differentiation.

Pleomorphic rhabdomyosarcoma is a high-grade malignant tumor that may cause an early metastasis. It is important to find a well-differentiated liposarcomatous element, and to distinguish liposarcoma from non-neoplastic fat tissues is important for the differential diagnosis for these tumors.

Recently, amplification of *mdm2* and *cdk4* was reported in WDL and DDL, and these abnormalities were helpful when a histological diagnosis was difficult [2, 6]. WDLs and DDLs belong to the same category as liposarcomas and are characterized by ring or large-marker chromosomes [9, 10, 13]. Hostein et al. [6] showed the amplification of *mdm2* and *cdk4* in WDL and DDL by FISH and quantitative PCR. In the present study, we confirmed the amplification of *mdm2* and *cdk4* in dedifferentiated components with rhabdomyoblasts, as well as the conventional well-differentiated areas by real-time PCR. This result indicates that, regardless of the differences in histologic patterns, the dedifferentiated areas with rhabdomyosarcomatous components, which have rarely been documented in DDLs, have the same genetic alterations as the WDL areas.

In conclusion, we have reported three cases of DDL with rhabdomyosarcomatous differentiation. The dedifferentiated areas with rhabdomyoblastic differentiation showed the amplification of *mdm2* and *cdk4*, which is known to be common to WDLs and DDLs.

References

1. Dei Tos AP, Doglioni C, Piccinin S, Maestro R, Mentzel T, Barbareschi M et al (1997) Molecular abnormalities of the p53 pathway in dedifferentiated liposarcoma. J Pathol 181:8–13
2. Dei Tos AP, Doglioni C, Piccinin S, Sciot R, Furlanetto A, Boiocchi M et al (2000) Coordinated expression and amplification of the MDM2, CDK4, and HMGI-C genes in atypical lipomatous tumours [comment]. J Pathol 190:531–536
3. Evans HL (1979) Liposarcoma: a study of 55 cases with reassessment of its classification. Am J Surg Pathol 3:507–523
4. Evans HL, Khurana KK, Kemp BL, Ayala AG (1994) Heterologous elements in the dedifferentiated component of dedifferentiated liposarcoma. Am J Surg Pathol 18:1150–1157
5. Henrichs WH, Chu YC, Goldblum JR, Weiss SW (1997) Dedifferentiated liposarcoma. A clinicopathological analysis of 155 cases with a proposal for an expanded definition of dedifferentiation. Am J Surg Pathol 21:271–281
6. Hostein I, Pelmus M, Aurias A, Pedeutour F, Mathoulin-Pelissier S, Coindre JM (2004) Evaluation of MDM2 and CDK4 amplification by real-time PCR on paraffin-embedded material: a potential tool for the diagnosis of atypical lipomatous tumours/well differentiated liposarcomas. J Pathol 202:95–102
7. McCormick D, Metzel T, Beham A, Fletcher C (1994) Dedifferentiated liposarcoma: clinicopathologic analysis of 32 cases suggesting a better prognostic group among pleomorphic sarcomas. Am J Surg Pathol 18:1213–1223
8. Newman PL, Fletcher CD (1991) Malignant mesenchymoma. Clinicopathologic analysis of a series with evidence of low-grade behaviour. Am J Surg Pathol 15:607–614
9. Pedeutour F, Forus A, Coindre JM, Berner JM, Nicolo G, Michiels JF et al (1999) Structure of the supernumerary ring and giant rod chromosomes in adipose tissue tumors. Genes Chromosomes Cancer 24:30–41
10. Pedeutour F, Suijkerbuijk RF, Forus A, Van Gaal J, Van de Klundert W, Coindre JM et al (1994) Complex composition and co-amplification of SAS and MDM2 in ring and giant rod marker chromosomes in well-differentiated liposarcoma. Genes Chromosomes Cancer 10:85–94
11. Pilotti S, Della Torre G, Lavarino C, Di Palma S, Sozzi G, Minoletti F et al (1997) Distinct mdm2/p53 expression patterns in liposarcoma subgroups: implications for different pathogenetic mechanisms. J Pathol 181:14–24
12. Pilotti S, Della Torre G, Mezzelani A, Tamborini E, Azzarelli A, Sozzi G et al (2000) The expression of MDM2/CDK4 gene product in the differential diagnosis of well differentiated liposarcoma and large deep-seated lipoma. Br J Cancer 82:1271–1275
13. Rosai J, Akerman M, Dal Cin P, DeWever I, Fletcher CD, Mandahl N et al (1996) Combined morphologic and karyotypic study of 59 atypical lipomatous tumors. Evaluation of their relationship and differential diagnosis with other adipose tissue tumors (a report of the CHAMP Study Group). Am J Surg Pathol 20:1182–1189
14. Salzano RP, Tomkiewicz Z, Africano WA (1991) Dedifferentiated liposarcoma with features of rhabdomyosarcoma. Conn Med 55:200–202
15. Schneider-Stock R, Walter H, Radig K, Rys J, Bosse A, Kuhnen C et al (1998) MDM2 amplification and loss of heterozygosity at Rb and p53 genes: no simultaneous alterations in the oncogenesis of liposarcomas. J Cancer Res Clin Oncol 124:532–540
16. Stout A (1948) Mesenchymoma, the mixed tumor of mesenchymal derivatives. Ann Surg 127:278–290
17. Tallini G, Erlandson R, Brennan M, Woodruff J (1993) Divergent myosarcomatous differentiation in retroperitoneal liposarcoma. Am J Surg Pathol 17:546–556
18. Tos APD, Pedeutour F (2002) Dedifferentiated liposarcoma. Pathology and genetics of tumours of soft tissue and bone. IARC Press, Lyon
19. Weiss SWW, Goldblum JR (2001) Enzinger and Weiss's soft tissue tumors, 4th edn. Mosby, St. Louis
20. Yoo J, Park SY, Kang SJ, Shim SI, Kim BK (2002) Altered expression of G1 regulatory proteins in human soft tissue sarcomas. Arch Pathol Lab Med 126:567–573

Virchows Arch (2005) 447: 842–848
DOI 10.1007/s00428-005-0024-1

ORIGINAL ARTICLE

Muna Sabah · Robert Cummins · Mary Leader · Elaine Kay

Loss of *p16^{INK4A}* expression is associated with allelic imbalance/loss of heterozygosity of chromosome 9p21 in microdissected synovial sarcomas

Received: 24 March 2005 / Accepted: 30 May 2005 / Published online: 5 August 2005
© Springer-Verlag 2005

Abstract Deletions of the short arm of chromosome 9 have been observed in many tumours and cell lines. This chromosomal region is frequently targeted during malignant transformation because it contains at least two known tumour suppressor genes: *p16^{INK4}* and *p15^{INK4B}*. *p16^{INK4A}* acts as a negative cell cycle regulator by inhibiting G_1 cyclin-dependent kinases that phosphorylate the retinoblastoma protein and therefore block the progression of the cell cycle from G_1 to S phase. The role of *p16^{INK4A}* in the development of synovial sarcoma has not been comprehensively investigated. Ten samples of synovial sarcomas were examined for allelic imbalance/loss of heterozygosity (AI/LOH) of the 9p region and p16 protein expression. DNA was isolated from microdissected sections of normal and tumour cells, amplified by polymerase chain reaction and analysed for AI/LOH by using six microsatellite markers that map to the 9p region. Immunohistochemistry for p16 expression was done. AI/LOH with at least one microsatellite marker on 9p21 was detected in six of ten samples. The most frequent allelic deletions were observed within the coding sequence of *p16^{INK4A}*. Loss of p16 immunoreactivity was detected in eight samples, six of which showed evidence of alterations at 9p21 region. These findings suggest a possible role of loss of *p16^{INK4A}* in the development of synovial sarcoma.

Keywords Synovial sarcoma · AI/LOH · 9p21 · *p16^{INK4A}* (*CDK2A*)

Abbreviations AI: allelic imbalance · LOH: loss of heterozygosity

M. Sabah (✉) · R. Cummins · M. Leader · E. Kay
Department of Histopathology, Education and Research Centre, The Royal College of Surgeons in Ireland, Beaumont Hospital, Dublin 9, Ireland
e-mail: munasabah@eircom.net
Tel.: +353-1-8092541
Fax: +353-1-8093720

Introduction

Synovial sarcoma is a soft tissue tumour of unknown histogenesis, occurring most frequently in adolescents and young adults. Most synovial sarcomas are characterised by a recurrent non-random chromosomal translocation, t(X;18)(p11.2;q11.2) [8].

Alterations affecting cell cycle regulators acting at the G_1–S checkpoint represent one of the most frequent targets in molecular tumourigenesis [6, 25] and have been implicated in the pathogenesis and progression of sarcomas [7]. Nonetheless, little is known about the role of cell cycle regulator proteins in the tumourigenesis of synovial sarcomas.

Chromosomal loss of 9p21 has been implicated in the genesis of several different tumours and cell lines [12, 14]. This chromosomal region contains at least two known tumour suppressor genes, *p16^{INK4A}* [12, 24] and *p15^{INK4B}* [11, 14]. Both encode nuclear proteins that have been shown to block cell cycle progression at the G_1–S transition by their ability to interfere with the catalytic activity of cyclin D/CDK4 complexes [24]. Active cyclin D/CDK4 complexes are necessary for the phosphorylation of Rb protein and the subsequent release of critical transcription factors such as E2F, that are required for progression into S phase.

The aim of the study was to assess the frequency of allelic imbalance at different loci of chromosome 9 and to correlate it with loss of p16 immunoexpression in synovial sarcoma.

Materials and methods

Tissue samples

Ten cases of formalin-fixed paraffin-embedded synovial sarcoma were analysed for allelic imbalance/loss of heterozygosity (AI/LOH) of chromosome 9 and examined for

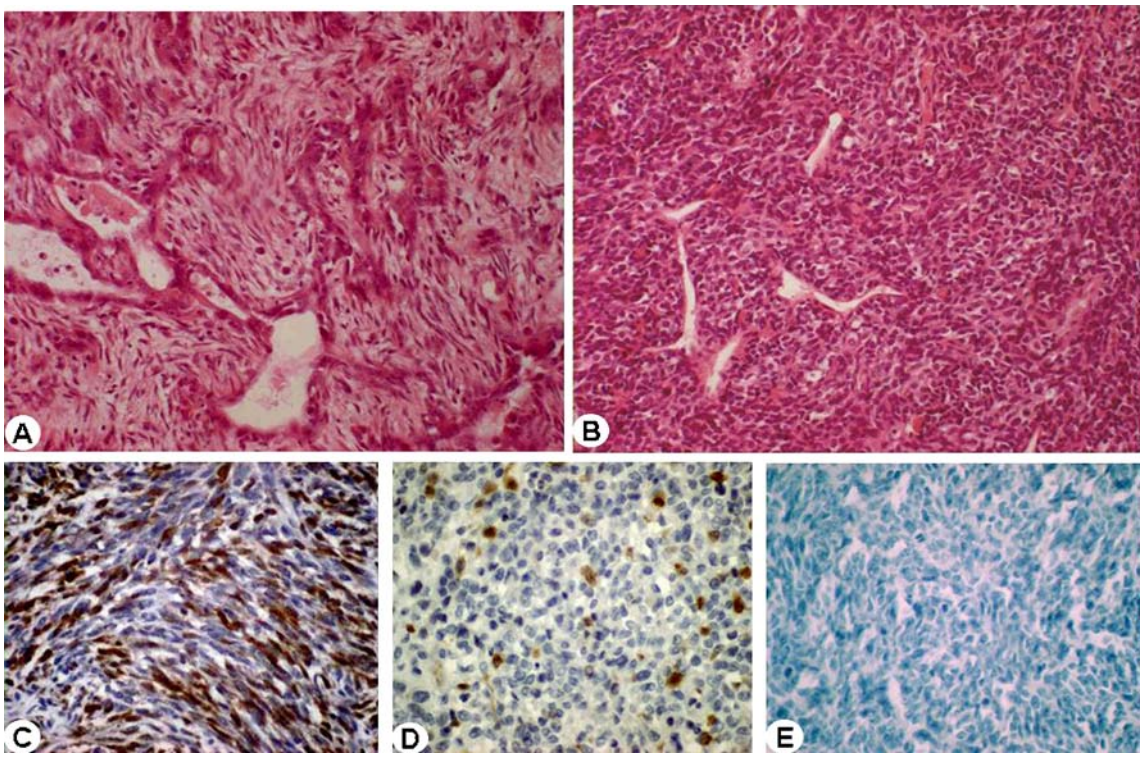


Fig. 1 Haematoxylin and eosin stain: **a** synovial sarcoma with a biphasic morphology, **b** spindle cell sarcoma (original magnification ×200). Positive p16 immunostaining (**c**). Heterogeneous staining (**d**). Negative p16 immunostaining (**e**). Original magnification ×400

p16 immunoreactivity. The diagnosis in each case was based on histologic and immunohistochemical features and was reviewed by the Dublin Soft Tissue Tumour Panel. The cases were graded according to the Fédération Nationale des Centres de Lutte Contre le Cancer (FNCLCC) scoring system [10, 28].

A single case had a biphasic morphology (Fig. 1a) and nine cases were of spindle type (Fig. 1b). Four cases were grade 2 sarcomas and six cases were grade 3 sarcomas. A summary of histologic type and tumour grade is outlined in Table 1.

Table 1 A summary of tumour grade and p16 immunostaining

Case no.	Morphology	Grade	Percentage of cells expressing p16
1	Spindle	High grade	30 (heterogeneous)
2	Spindle	High grade	100 (+)
3	Spindle	High grade	0 (−)
4	Spindle	High grade	0 (−)
5	Biphasic	Intermediate grade	0 (−)
6	Spindle	Intermediate grade	0 (−)
7	Spindle	Intermediate grade	100 (+)
8	Spindle	High grade	5 (−)
9	Spindle	High grade	0 (−)
10	Spindle	Intermediate grade	5 (−)

Immunohistochemistry

Four-micrometer-thick sections were cut and dried overnight at 55°C. Deparaffinization, rehydration and antigen retrieval was performed by using 1× Trilogy (Cell Marque, Hot Springs, AR, USA). The endogenous peroxidase activity was blocked by immersing the sections in 0.9% hydrogen peroxidase for 10 min at room temperature. The sections were incubated at room temperature for 30 min with 200 μl of primary p16 monoclonal antibody (16^{INK4A} Ab-7, clone 16P07, NewMarkers, Fremont, CA, USA), 1/100 dilution. The epitope for this antibody is aa1-32. Antibody detection was then done using Vectastain Elite Universal ABC kit (Vector Labs, Burlingame, CA, USA). Diaminobenzidine with haematoxylin counterstaining was used to develop the colour. Cervical tissue with high-grade dysplasia was used as a positive control. The antibody was omitted for negative control.

Sections were examined for nuclear staining and immunoreactivities were classified into three categories, defined as follows: negative (−), less than 20% of cells were immunoreactive; heterogeneous, 20 to 80% were immunoreactive; positive (+), greater than 80% were immunoreactive. Samples showing either negative or heterogeneous staining were considered abnormal, whereas those with positive staining were interpreted as normal [30].

DNA microdissection

Ten cases were microdissected (Table 1). For each sample, normal and tumour tissue were first identified on routinely stained sections under light microscopy. Two parallel 8-μm-thick sections were dewaxed in xylene, rehydrated through various alcohol grades, rinsed well in distilled water and finally stained with haematoxylin.

Using the original sections as a template, neoplastic and non-neoplastic tissues were microdissected under a stereomicroscope. Non-neoplastic tissue submitted as resection margins was first identified on haematoxylin and eosin sections and then microdissected from haematoxylin sections by a pathologist. The DNA obtained from non-neoplastic tissue was considered as normal DNA. Multiple areas of the tumour were sampled.

Genomic DNA extraction

DNA was isolated from microdissected tumour and normal cells using 60 μl of proteinase K solution [20 mg/ml proteinase K (Roche Diagnostics, Mannheim, Germany) in 50 mM Tris–HCl (pH 7.4), 0.1 mM EDTA, 1% Tween] at 55°C for 72 h. After digestion the proteinase K was inactivated by heating to 94°C for 10 min. The samples were then ready for polymerase chain reaction (PCR) amplifications.

PCR amplifications

Six fluorescent Cy5 end-labelled microsatellite markers were used. Four markers map to 9p21: D9S916, D9S1814, D9S974 and D9S942. The latter two are within the coding sequence of $p16^{INK4A}$. D9S916 is telomeric to $p16^{INK4A}$ and 15^{INK4B}, whereas D9S1814 is centromeric to $p15^{INK4B}$. D9S171 is on 9p13 (proximal to $p16^{INK4A}$ and $p15^{INK4B}$). D9S230 is on 9p24.

PCR amplifications were performed in a final volume of 20 μl and consisted of 1× PCR buffer, 200 μM deoxynucleotide triphosphate, 1.25 mM $MgCl_2$ (Promega, Madison, WI), 2 pmol of forward and reverse primers (TAGN, Newcastle, UK) and 1 μl of sample DNA digest. After denaturation at 95°C for 5 min, 2 μl of Taq (1 U/μl) (Promega) were added at 80°C. A touchdown PCR was then done consisting of two cycles of 95°C for 1 min, 1 min at an initial annealing temperature (Table 2) and extension at 72°C for 1 min. Subsequent steps consisted of two cycles each with annealing temperature reduced by 2°C until 30 cycles were done at the final annealing temperature. A final extension step at 72°C for 10 min completed the reactions. After PCR, 5 μl PCR products mixed with loading dye were electrophoresed through 12% polyacrylamide minigels. The DNA fragments were visualised by ethidium bromide staining under ultraviolet light.

AI/LOH assay

The PCR products were diluted in distilled water and were then mixed with Cy5.5-labelled DNA size ladder and denatured at 94°C for 10 min. Normal and tumour samples were loaded side by side on a Microcel in the OpenGene System (Visible Genetics, Toronto, Ontario, Canada). Run parameters of the OpenGene System were 1,300 V for 30 min at a plate temperature of 54°C. Data were processed and analysed using the GeneObjects Fragment Analysis Tool (Visible Genetics). For each heterozygous locus, the area under each peak representing each allele in the microsatellite pair was obtained using the GeneObjects Fragment Analysis Tool. The area of the first allele was divided by the area of the second allele in each of the normal and tumour DNA samples. A ratio of ratios between the normal and tumour PCR products was calculated to give an overall allele ratio. The cut-off allele ration value for chromosomal loss was 0.74 as was published from studies from our laboratory [2, 18–20]. This figure was obtained from evaluating normal tissue from 13 patients by triplicate PCR. It was calculated that 99.5% of the cases have an allele ratio of greater than 0.74. Furthermore, the distinction be-

Table 2 Primer sequence and annealing temperatures used in touchdown PCR

Marker	Primer sequence	Initial annealing temperature (°C)	Final annealing temperature (°C)
D9S230	Forward 5′-acaggtcaccacccttcaac-3′ Reverse 5′-acaggagaagagctgaggca-3′	65	59
D9S916	Forward 5′-gatgtccagttgtcccttcataa-3′ Reverse 5′-atagactgccaaatttttggacc-3′	61	55
D9S974	Forward 5′-cctggtctggatcataaaatgaa-3′ Reverse 5′-tgtggaaattttctgtctggttc-3′	61	55
D9S942	Forward 5′-aagcaagattccaaacagtaaaca-3′ Reverse 5′-ttcgtttcacttttgagttttcc-3′	59	53
D9S1814	Forward 5′-tgtcagtggtatttacctttttgg-3′ Reverse 5′-cagaaggtcagtaggttcacagg-3′	61	55
D9S171	Forward 5′-agctaagtgaacctcatctctg-3′ Reverse 5′-tgattgttaataaagtagcccc-3′	59	53

tween AI and LOH was made using a cut-off value of 0.30. This was in accordance with a previously published study that compared radioactive and fluorescence-based AI/LOH methods and demonstrated that the value 0.30 separated AI from LOH [26].

Therefore, the value 0.74 was used to separate AI from retention of heterozygosity and the value 0.30 was used to separate AI from LOH. Microsatellite instability (MSI) was defined as the presence of novel alleles or extra peaks in the tumour DNA sample not seen in the normal DNA. The PCR amplification and AI/LOH analysis were done twice to ensure consistency in the results.

Results

Immunohistochemical analysis

The results for p16 immunostaining are presented in Table 1. Two of ten cases showed diffuse positive nuclear staining (+) (Fig. 1c). One case showed heterogeneity in the staining pattern and was regarded as abnormal expression of p16 (Fig. 1d) and seven cases were negative (−) (Fig. 1e).

AI/LOH analysis

A summary of AI/LOH of chromosome 9p and allele ratios are given in (Fig. 2).

Of the ten samples that were analysed for AI/LOH, the average informative rate per marker was 70% (range from 60% to 80%).

Six of ten samples exhibited AI/LOH at one or more loci in the 9p region (Fig. 3). AI/LOH loss was most frequent at D9S942 locus (75% of informative cases), followed by D9S974 (62.5% of informative cases). These two microsatellite markers are located within the coding sequence of $p16^{INK4A}$. D9S916 revealed allelic loss in 50% of informative cases. Both D9S1814 and D9S171 showed AI/

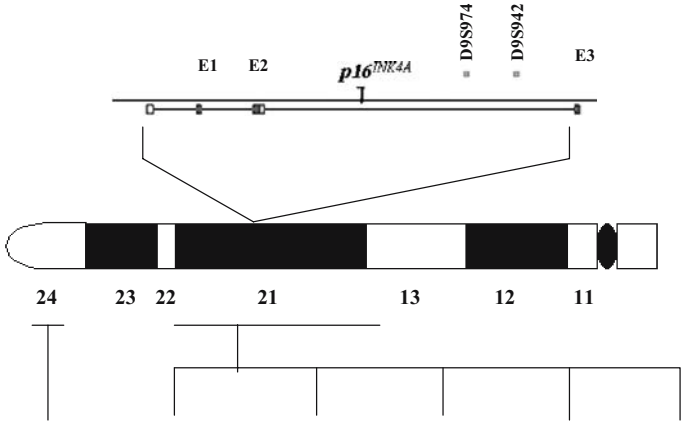


Fig. 2 Microsatellite map of AI/LOH on chromosome 9. The approximate position of each microsatellite marker from 9pter is displayed in the *marker box*. The location of $p16^{INK4A}$, D9S974 and D9S942 is presented according to NCBI map Viewer. The allele ratio is displayed in the corresponding box. *Filled circle* indicates AI/LOH, *open circle* indicates retention of heterozygosity, and *strike through circle* indicates homozygosity (uninformative)

	D9S230 (3,808Kbp)	D9S916 (21,806Kbp)	D9S974 (21,977Kbp)	D9S942 (22,980Kbp)	D9S1814 (22,078Kbp)	D9S171 (24,524Kbp)
Case 1	⊘	○ (0.98)	○ (0.77)	⊘	⊘	⊘
Case 2	○ (0.88)	○ (0.92)	⊘	○ (0.94)	○ (0.98)	○ (0.82)
Case 3	● (0.42)	● (0.57)	● (0.1)	● (0)	● (0.58)	● (0.5)
Case 4	○ (0.99)	○ (0.82)	● (0.70)	● (0.71)	⊘	⊘
Case 5	○ (0.97)	⊘	⊘MSI	● (0.66)	○ (0.91)	○ (0.98)
Case 6	⊘	● (0.45)	● (0.12)	● (0.48)	⊘	● (0.72)
Case 7	○ (0.89)	○ (0.92)	○ (0.95)	○ (0.85)	○ (0.90)	○ (0.96)
Case 8	○ (0.91)	● (0)	● (0.15)	● (0.68)	● (0.51)	⊘
Case 9	⊘	⊘	○ (0.97)	⊘	○ (0.95)	○ (0.96)
Case 10	⊘	● (0.7)	● (0.57)	● (0.44)	⊘	⊘

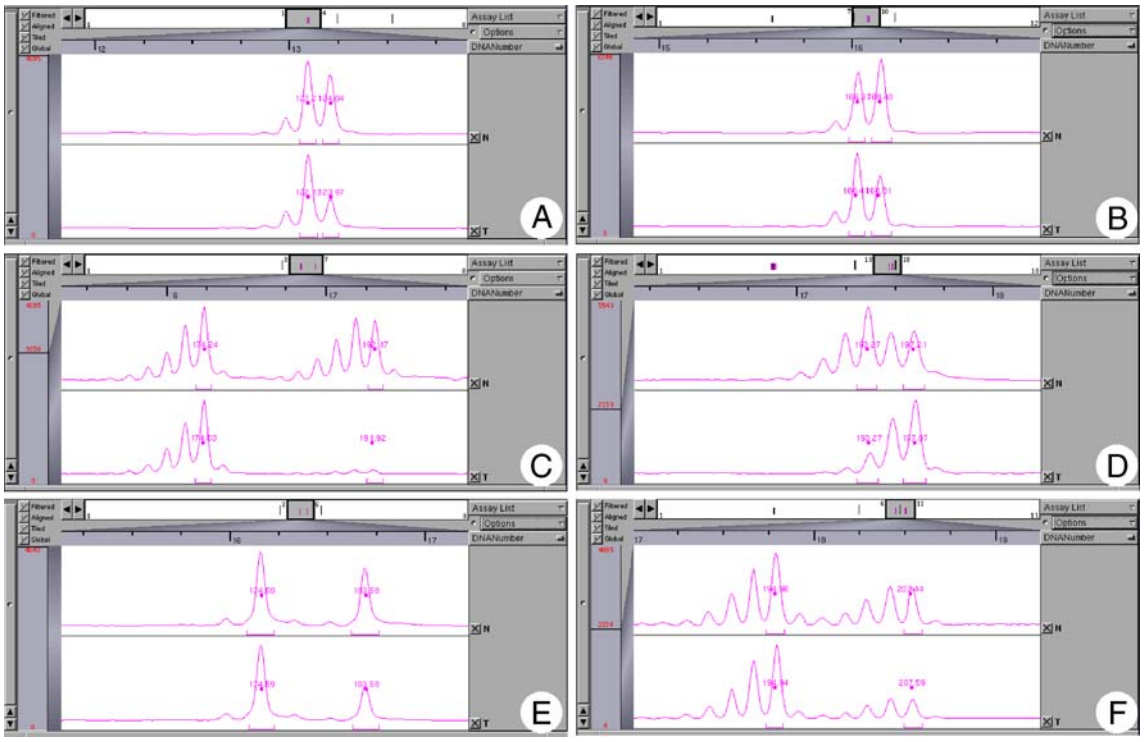


Fig. 3 Sample 3 showing AI/LOH with six microsatellite markers. AI at D9S171 (**a**), AI at D9S1814 (**b**), LOH at D9S942 (**c**), LOH at D9S974 (**d**), AI at D9S916 (**e**), AI at D9S230 (**f**). N in the *upper lane* indicates DNA from normal tissue and T in the *lower lane* indicates DNA from tumour tissue

LOH in 33.3% of informative cases. D9S230 locus on 9p24 revealed AI/LOH in 16.7% of informative cases.

Only a single case revealed evidence of MSI at D9S974 locus. AI/LOH was observed in intermediate and high-grade tumours.

Correlation between p16 protein expression and AI/LOH results

All cases with AI/LOH at 9p (cases 3, 4, 5, 6, 8 and 10) were negative for p16 immunostaining. One case showed no evidence of allelic alteration (case 1) but was heterogeneous for p16 immunostaining. This case was uninformative for four microsatellite markers including D9S942.

Two cases (cases 2 and 7) were diffusely positive for p16 immunostaining. Neither of these cases showed allelic alteration with any markers studied. The two cases were informative with retention of heterozygosity for D9S974 and D9S942 markers that are present within the coding sequence of $p16^{INK4A}$.

Discussion

Alterations of chromosomal band 9p21 have been reported in different types of human tumours and cell lines [12, 14]. Moving from the centromere to the telomere, this complex region encodes the tumour suppressor genes $p15^{INK4B}$ [11, 14], $p16^{INK4A}$ [12, 24] and the housekeeping gene methylthioadenosine phosphorylase (*MTAP*) [15]. $p16^{INK4A}$ encodes two proteins p16 and $p14^{ARF}$. p16 is a nuclear protein that blocks cellular proliferation at the G_1–S phase. It binds to the cyclin-dependent kinases CDK4 and CDK6 and inhibits phosphorylation of Rb and subsequent release of critical transcription factors such as E2F that are required for progression from G_1 into S phase [24, 25]. $p14^{ARF}$-protein blocks Mdm2-induced degradation of p53 [17]. Consequently, alteration of $p16^{INK4A}$ impairs both the Rb and p53 tumour suppressor pathways. $p15^{INK4B}$ encodes a nuclear protein, which, in addition to being an inhibitor of CDK4 and CDK6, has also been implicated in the TGF-β pathway leading to cell growth arrest [11]. Inactivation of $p16^{INK4A}$ has been described as the consequence of homozygous deletion, rearrangement, hypermethylation or point mutation [3, 4, 13].

In this study, we examined LOH of chromosome 9p using PCR-based microsatellite analysis in ten cases of microdissected synovial sarcoma. We detected AI/LOH of 9p in 60% of synovial sarcoma cases. AI/LOH at 9p21 region was a consistent finding in these cases. AI/LOH was most frequent at D9S942 locus (75% of informative cases), followed by D9S974 (62.5% of informative cases). These two microsatellite markers are located within the coding sequence of $p16^{INK4A}$. AI/LOH at D9S171 locus on 9p13 band adjacent to 9p21 was observed in 33.3% and at D9S230 locus on 9p24 was identified in 16.7% of informative cases. These findings may point to the existence of tumour suppressor genes at these two loci as was previously suggested for D9S171 [23]. Alternatively, be-

cause alterations at these two loci were associated with alterations on 9p21, they may reflect chromosomal instability secondary to deletions at 9p21.

Immunohistochemistry revealed normal expression of p16 in two of ten samples (cases 2 and 7). These two samples showed no evidence of allelic deletion with any marker examined including the two microsatellite markers that are present within the coding sequence of $p16^{INK4A}$ (D9S974 and D9S942). Loss of p16 expression was identified in eight of ten samples examined. Six of these samples showed AI/LOH at 9p21. In two cases (1 and 9), loss of p16 immunoreactivity was not associated with alterations at 9p21. There are three possible explanations: (1) Technical flaw in LOH study. (2) p16 immunoreactivity is a reflection of other genetic or epigenetic changes including DNA methylation and posttranslational modification that are not detectable by LOH. (3) The two cases were homozygous for either D9S942 or D9S974 marker and therefore were not informative. In this study, the most frequent allelic alterations were observed at these two markers. Given the uniformity of the result, the last explanation seems most likely.

Alterations of $p16^{INK4A}$ have not been comprehensively studied in synovial sarcoma. Antonescu et al. [1] examined the expression of different cell cycle regulators in synovial sarcoma by immunohistochemistry. The authors reported that aberrant expression of different molecules that are involved in regulating the cell cycle was a common event in synovial sarcoma. However, p16 protein was not among the cell cycle regulators examined.

Golouh et al. investigated the role of altered p16 and nm23 mRNA expression as prognostic factors in synovial sarcoma. The authors reported that whereas increased level of nm23 mRNA is associated with poor survival, there was no correlation between survival rate and p16 mRNA expression [9].

$p16^{INK4A}$ has been investigated in mesenchymal neoplasms, but with varying conclusions. Some studies have reported that $p16^{INK4A}$ alterations are infrequent in soft tissue sarcomas [5, 21, 22, 29], whereas others have shown that alteration of $p16^{INK4A}$ is a common event in soft tissue sarcomas. Furthermore, it has been shown that $p16^{INK4A}$ knockout mice frequently develop sarcomas [27]. Orlow et al. reported that coincident homozygous deletion of $p16^{INK4A}$ and $p15^{INK4B}$ occurs frequently in soft tissue sarcomas [16]. Cohen and Geradts reported that aberrant expression of p16 is one of the most common molecular derangements in sarcomagenesis [5]. Similarly, Yoo et al. identified altered expression of p16 protein in 94% of sarcoma cases [30].

The discrepancy in these reports can be explained by methodological factors; for example, the low frequency of genetic alteration of $p16^{INK4A}$ may be due to contamination with normal cells. Microdissection allows one to enrich for tumour cells and, thereby, more accurately analyse tumour samples. Similarly, the discordance in immunohistochemical studies can be explained by the use of different commercially available antibodies, technical variability in immunohistochemistry or differences in the criteria for interpreting the results. Alternatively, these differences can be explained by differences in tumour type, histologic grade or clinical stage of the cases studied.

Although the number of cases in this study is low, it is clear from AI/LOH and immunohistochemical findings that alterations of $p16^{INK4A}$ are common findings in synovial sarcomas. Additional studies are required to determine whether genetic alterations of $p16^{INK4A}$ are an important step in the pathogenesis of synovial sarcomas or whether they represent an epiphenomenon common in this tumour. Identifying various molecular changes in this type of sarcoma is a key to our improved understanding of the biological behaviour of this disease.

References

1. Antonescu CR, Leung DH, Dudas M, Ladanyi M, Brennan M, Woodruff JM, Cordon-Cardo C (2000) Alterations of cell cycle regulators in localized synovial sarcoma: a multifactorial study with prognostic implications. Am J Pathol 156:977–983
2. Butler D, Collins C, Mabruk M, Barry Walsh C, Leader MB, Kay EW (2000) Deletion of the FHIT gene in neoplastic and invasive cervical lesions is related to high-risk HPV infection but is independent of histopathological features. J Pathol 192:502–510
3. Cairns P, Mao L, Merlo A, Lee DJ, Schwab D, Eby Y, Tokino K, van der Riet P, Blaugrund JE, Sidransky D (1994) Rates of p16 (MTS1) mutations in primary tumors with 9p loss. Science 265:415–417
4. Cairns P, Polascik TJ, Eby Y, Tokino K, Califano J, Merlo A, Mao L, Herath J, Jenkins R, Westra W (1995) Frequency of homozygous deletion at p16/CDKN2 in primary human tumours. Nat Genet 11:210–212
5. Cohen JA, Geradts J (1997) Loss of RB and MTS1/CDKN2 (p16) expression in human sarcomas. Human Pathol 28:893–898
6. Cordon-Cardo C (1995) Mutations of cell cycle regulators. Biological and clinical implications for human neoplasia. Am J Pathol 147:545–560
7. Cordon-Cardo C (1997) Molecular biology of sarcomas. In: De Vita VT, Hellman S, Rosenberg SA (eds) Principles and practice of oncology. Lippincott, Philadelphia, pp 1731–1738
8. dos Santos NR, de Bruijn DR, van Kessel AG (2001) Molecular mechanisms underlying human synovial sarcoma development. Genes Chromosomes Cancer 30:1–14
9. Golouh R, Stanta G, Bracko M, Bonin S (2001) Correlation of MTS1/p16 and nm23 mRNA expression with survival in patients with peripheral synovial sarcoma. J Surg Oncol 76:83–88
10. Guillou L, Coindre JM, Bonichon F, Nguyen BB, Terrier P, Collin F, Vilain MO, Mandard AM, Le Doussal V, Leroux A, Jacquemier J, Duplay H, Sastre-Garau X, Costa J (1997) Comparative study of the National Cancer Institute and French Federation of Cancer Centers Sarcoma Group grading systems in a population of 410 adult patients with soft tissue sarcoma. J Clin Oncol 15:350–362
11. Hannon GJ, Beach D (1994) p15INK4B is a potential effector of TGF-beta-induced cell cycle arrest. Nature 371:257–261
12. Kamb A, Gruis NA, Weaver-Feldhaus J, Liu Q, Harshman K, Tavtigian SV, Stockert E, Day RS III, Johnson BE, Skolnick MH (1994) A cell cycle regulator potentially involved in genesis of many tumor types. Science 264:436–440

13. Merlo A, Herman JG, Mao L, Lee DJ, Gabrielson E, Burger PC, Baylin SB, Sidransky D (1995) 5′ CpG island methylation is associated with transcriptional silencing of the tumour suppressor p16/CDKN2/MTS1 in human cancers. Nat Med 1:686–692
14. Nobori T, Miura K, Wu DJ, Lois A, Takabayashi K, Carson DA (1994) Deletions of the cyclin-dependent kinase-4 inhibitor gene in multiple human cancers. Nature 368:753–756
15. Nobori T, Takabayashi K, Tran P, Orvis L, Batova A, Yu AL, Carson DA (1996) Genomic cloning of methylthioadenosine phosphorylase: a purine metabolic enzyme deficient in multiple different cancers. Proc Natl Acad Sci U S A 93:6203–6208
16. Orlow I, Drobnjak M, Zhang ZF, Lewis J, Woodruff JM, Brennan MF, Cordon-Cardo C (1999) Alterations of INK4A and INK4B genes in adult soft tissue sarcomas: effect on survival. J Natl Cancer Inst 91:73–79
17. Pomerantz J, Schreiber-Agus N, Liegeois NJ, Silverman A, Alland L, Chin L, Potes J, Chen K, Orlow I, Lee HW, Cordon-Cardo C, DePinho RA (1998) The Ink4a tumor suppressor gene product, p19Arf, interacts with MDM2 and neutralizes MDM2's inhibition of p53. Cell 92:713–723
18. Sabah M, Cummins R, Leader M, Kay E (2004) Loss of heterozygosity of chromosome 9p and loss of p16(INK4A) expression are associated with malignant gastrointestinal stromal tumors. Mod Path 17:1364–1371
19. Sabah M, Cummins R, Leader M, Kay E (2005) Leiomyosarcoma and malignant fibrous histiocytoma share similar allelic imbalance pattern at 9p. Virchows Arch 446:251–258
20. Sabah M, Cummins R, Leader M, Kay E (2005) Loss of p16INK4A expression is associated with allelic imbalance/loss of heterozygosity in microdissected malignant peripheral nerve sheath tumors. Appl Immunohistochem Mol Morphol (in press)
21. Schneider-Stock R, Radig K, Roessner A (1997) Loss of heterozygosity on chromosome 9q21 (p16 gene) uncommon in soft-tissue sarcomas. Mol Carcinog 18:63–65
22. Schneider-Stock R, Walter H, Haeckel C, Radig K, Rys J, Roessner A (1998) Gene alterations at the CDKN2A (p16/MTS1) locus in soft tissue tumors. Int J Oncol 13:325–329
23. Schraml P, Muller D, Bednar R, Gasser T, Sauter G, Mihatsch MJ, Moch H (2000) Allelic loss at the D9S171 locus on chromosome 9p13 is associated with progression of papillary renal cell carcinoma. J Pathol 190:457–461
24. Serrano M, Hannon GJ, Beach D (1993) A new regulatory motif in cell-cycle control causing specific inhibition of cyclin D/CDK4. Nature 366:704–707
25. Sherr CJ (1996) Cancer cell cycles. Science 274:1672–1677
26. Skotheim RI, Diep CB, Kraggerud SM, Jakobsen KS, Lothe RA (2001) Evaluation of loss of heterozygosity/allelic imbalance scoring in tumor DNA. Cancer Genet Cytogenet 127:64–70
27. Sotillo R, Dubus P, Martin J, de la Cueva E, Ortega S, Malumbres M, Barbacid M (2001) Wide spectrum of tumors in knock-in mice carrying a Cdk4 protein insensitive to INK4 inhibitors. EMBO J 20:6637–6647
28. Trojani M, Contesso G, Coindre JM, Rouesse J, Bui NB, De Mascarel A, Goussot JF, David M, Bonichon F, Lagarde C (1984) Soft-tissue sarcomas of adults; study of pathological prognostic variables and definition of a histopathological grading system. Int J Cancer 33:37–42
29. Yao J, Pollock RE, Lang A, Tan M, Pisters PW, Goodrich D, El Naggar A, Yu D (1998) Infrequent mutation of the p16/MTS1 gene and overexpression of cyclin-dependent kinase 4 in human primary soft-tissue sarcoma. Clin Cancer Res 4:1065–1070
30. Yoo J, Park SY, Kang SJ, Shim SI, Kim BK (2002) Altered expression of G1 regulatory proteins in human soft tissue sarcomas. Arch Pathol Lab Med 126:567–573

Virchows Arch (2005) 447: 849–854
DOI 10.1007/s00428-005-0038-8

ORIGINAL ARTICLE

Torsten Hansen · Detlef Katenkamp

Rhabdomyoma of the head and neck: morphology and differential diagnosis

Received: 16 March 2005 / Accepted: 23 June 2005 / Published online: 18 August 2005
© Springer-Verlag 2005

Abstract Rhabdomyomas of the head and neck are exceptionally rare benign mesenchymal tumors. Although histology is very characteristic, several differential diagnoses have to be considered. We investigated five patients with extracardiac rhabdomyoma of the head and neck (median age 65.9 years), four of them presenting with adult rhabdomyoma (AR) and one with fetal rhabdomyoma (FR). We analyzed the histological findings, with special regard to separation from hibernoma (two patients) and granular cell tumor (GCT; six patients, median age 31 years). Both FR and AR showed polygonal eosinophilic cells with peripherally or centrally localized nuclei and cross striations, while in hibernoma, multivacuolated cells with centrally localized nuclei were detected. In GCT, polygonal eosinophilic cells with granular periodic-acid-Schiff-positive cytoplasm were found; in one case, atypical GCT with increased pleomorphism and mitotic rate was observed. Pseudoepitheliomatous hyperplasia occurred both in FR and GCT. Immunohistochemically, rhabdomyomas were strongly positive for myogenic markers (desmin, actin, and myoglobin) but negative for S-100, while hibernoma and GCT strongly expressed S-100. Concerning the differential diagnosis of rhabdomyoma, GCT has to be especially considered since this tumor can undergo malignant transformation.

Keywords Rhabdomyoma · Head and neck · Hibernoma · Granular cell tumor · Immunohistochemistry · Pseudoepitheliomatous hyperplasia

T. Hansen (✉) · D. Katenkamp
Institute of Pathology,
Friedrich Schiller University of Jena,
Ziegelmühlenweg 1,
07743 Jena, Germany
e-mail: TORSTEN.HANSEN@med.uni-jena.de
Tel.: +49-3641-933627
Fax: +49-3641-933111

T. Hansen
Institute of Pathology,
Johannes Gutenberg University of Mainz,
Mainz, Germany

Introduction

Rhabdomyoma is a benign mesenchymal tumor with skeletal muscle differentiation. Topographically, cardiac and extracardiac types can be distinguished. The cardiac rhabdomyoma almost exclusively occurs in the hearts of young children and is often associated with congenital abnormalities like tuberous sclerosis. Extracardiac rhabdomyomas consist of four clinically and morphologically different types, i.e., the adult, the fetal, and the genital type, and rhabdomyomatous mesenchymal hamartoma [6, 19].

Adult rhabdomyoma (AR) predominantly occurs in elderly persons (median age about 60 years) with a male predilection (3:1 male to female ratio). The head and neck area is by far the most common site. AR grows most frequently as a solitary mass (about 70%), but may be multinodular with discrete nodules in the same area (about 25%) or, rarely, even multicentric (about 5%) [6, 19]. Due to high local recurrence rate (up to 42%), complete excision is recommended [6, 15, 18–21]. By contrast, malignant transformation has not been described. Etiology and pathogenesis of AR are poorly understood. Due to its typical localization in the neck, it has been suggested that this tumor arises from the branchial musculature [6, 19]. Concerning the cytogenetic characteristics, Gibas and Miettinen [8] reported on a case of a pharyngeal recurrent AR, with a reciprocal translocation of chromosomes 15 and 17 and abnormalities of chromosome 10 supporting a neoplastic rather than hamartomatous nature.

Fetal rhabdomyoma (FR) is even rarer than AR. Two forms exist: the myxoid type, which typically affects young boys, and the intermediate type, which is more common in adults. Both forms are predominantly in the head and neck area, with a favorite site in the submucosa and subcutis. While the myxoid type is histologically mainly composed of primitive oval or spindle-shaped cells in a myxoid stroma, the intermediate type generally consists of differentiated muscle fibers with frequent cross striations. However, transitional forms also exist [6, 19].

In the present study, we examined five patients with rhabdomyomas of the head and neck area (four cases with

Table 1 Patients' characteristics

Patient no.	Diagnosis	Age	Sex	Localization
1	AR	79	M	Neck
2	AR	82	F	Oral floor
3	AR	59	M	Parapharyngeal
4[a]	AR	73	M	Neck
5	FR	55	F	Larynx
6	Hibernoma	36	F	Neck
7	Hibernoma	66	M	Neck
8	GCT	53	M	Neck
9	GCT	44	M	Neck
10	GCT	41	M	Tongue
11	GCT	15	F	Tongue
12	GCT	21	F	Tongue
13	Atypical GCT	12	F	Neck

AR adult rhabdomyoma; *F* female; *FR* fetal rhabdomyoma; *GCT* granular cell tumor; *M* male

[a]Data of this patient have already been published as a case report [9]

AR and one case with FR), with special regard to the histological findings. Since granular cell tumor (GCT) and hibernoma are described as most relevant differential diagnoses, we included tissue specimens of the respective diseases in this study.

Materials and methods

The records from the Soft Tissue Registry of the Institute of Pathology in Jena were searched for cases coded as rhabdomyoma, hibernoma, and GCT of the head and neck area from 1995 to the present. The patients' characteristics are summarized in Table 1. In brief, we found five cases of extracardiac rhabdomyoma (four patients with AR and one patient with FR; female to male ratio, 2:3; median age 65.9 years); two patients suffered from hibernoma (among a total number of 31 hibernomas; female is equal to male; median age 56 years), and six patients presented with GCT (among a total number of 52 GCTs). One case presented as atypical GCT. The female to male ratio was 1:1, and the median age of the patients was 31 years. From all cases, available slides were reviewed. Immunohistochemical staining was performed according to previous protocols [11]. The primary antibodies applied for the immunohistochemical analysis are summarized in Table 2.

Table 2 Data on the antibodies used for this study

	Marker[a]	Dilution
1	Desmin (clone D33)	1:400
2	Muscle-specific actin (clone HHF-35)	1:500
3	Myoglobin (polyclonal rabbit antihuman)	1:400
4	Myogenin F5D	1:300
5	S-100 (polyclonal rabbit antihuman)	1:20,000
6	Ki-67 (clone KiS5)	1:300

[a]Antibodies 1–3, 5, and 6 were manufactured by DAKO (DAKO, Hamburg, Germany), while antibody 4 was manufactured by Pharmingen (Pharmingen, San Diego, CA, USA)

Results

Rhabdomyoma

Light microscopy revealed nonencapsulated tumors, which were composed of tightly packed polygonal cells. The cells were most frequently eosinophilic and contained a granular cytoplasm. Sometimes, cross striations were seen. Besides, vacuolated cells with centrally stellate-shaped eosinophilic cytoplasm were found that were regarded as the so-called spider cells (Fig. 1). The nuclei were localized either centrally or peripherally with some multinucleated cells. Immunohistochemistry with antibodies against muscle-specific actin, desmin, myoglobin (Fig. 2), and myogenin demonstrated strong immunostaining, confirming the diagnosis of AR.

In one case (patient no. 5), the cells showed less cytoplasm and were sometimes spindle-shaped. They obtained intracytoplasmic cross striations. Furthermore, glycogen content of cytoplasm can be confirmed by periodic acid-Schiff (PAS) staining. Nuclei were mainly peripherally

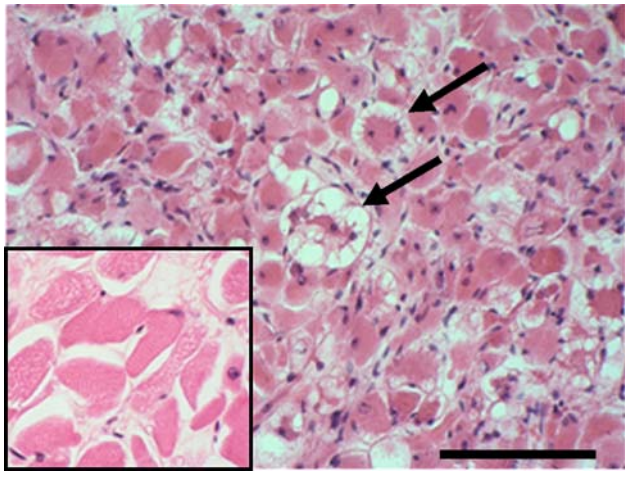


Fig. 1 AR with polygonal eosinophilic cells and some spider cells (*arrows*). *Inset*, AR cells with cross striations (hematoxylin and eosin, original magnification ×200, *bar*=100 μm; *inset*, ×400)

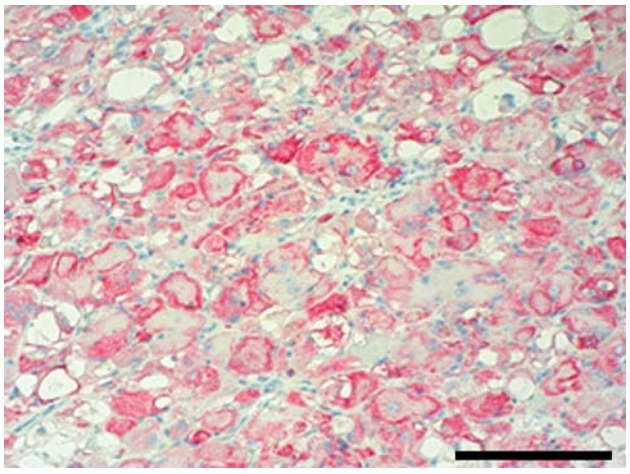


Fig. 2 Expression of myoglobin (*red*) in AR (original magnification ×200, *bar*=200 μm)

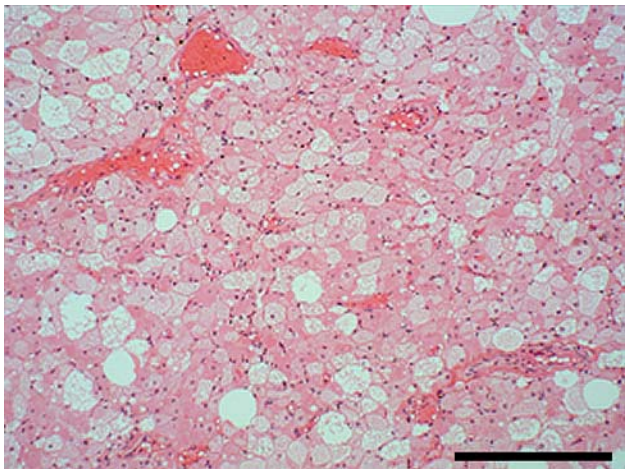


Fig. 5 Hibernoma with numerous multivacuolated and some univacuolated cells. Note that nuclei are predominantly centrally localized (hematoxylin and eosin, original magnification ×200, *bar*=100 μm)

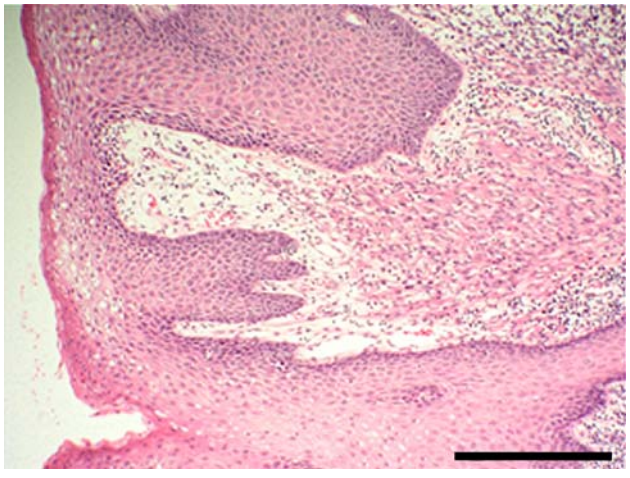


Fig. 3 Tissue specimen of patient no. 5 shows pseudoepitheliomatous hyperplasia and FR on the *right side* (hematoxylin and eosin, original magnification ×100, *bar*=200 μm)

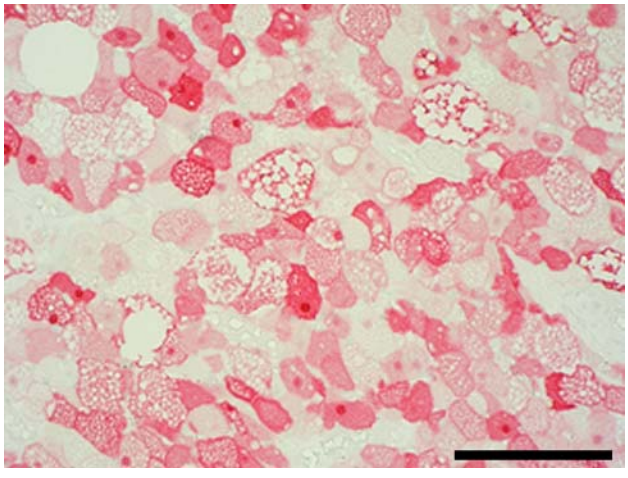


Fig. 6 Immunohistochemistry shows strong expression of S-100 (*red*) in hibernoma cells (original magnification ×400, *bar*=50 μm)

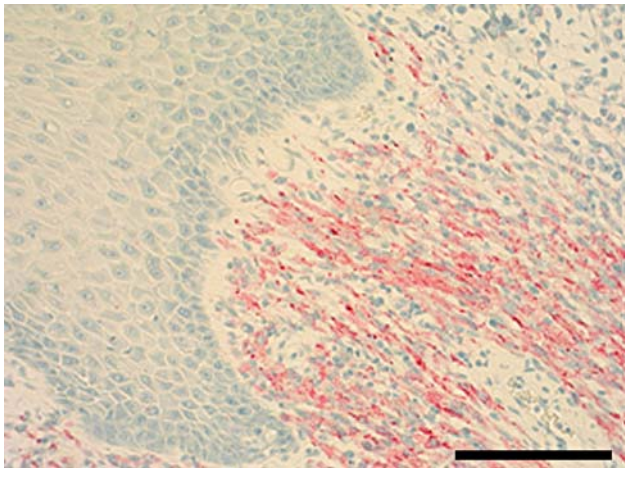


Fig. 4 Same tissue as in Fig. 3, with strong expression of desmin (*red*) in the FR cells (original magnification ×200, *bar*=100 μm)

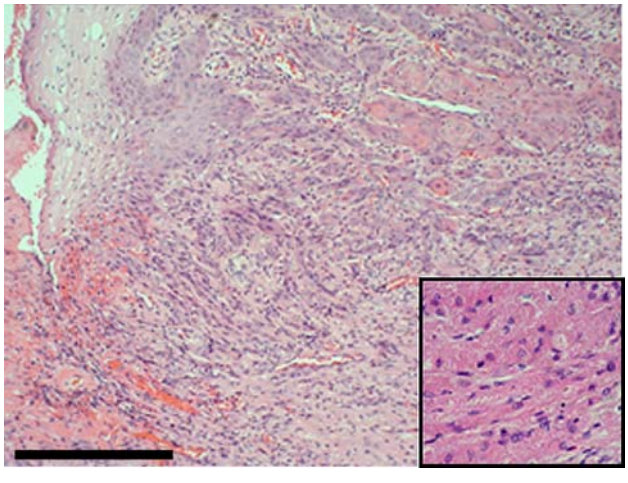


Fig. 7 GCT with considerable pseudoepitheliomatous hyperplasia of the mucosa in the *upper part*. *Inset*, GCT cells with granular eosinophilic cytoplasm and dense chromatin of the nuclei (hematoxylin and eosin, original magnification ×100, *bar*=200 μm; *inset* ×400)

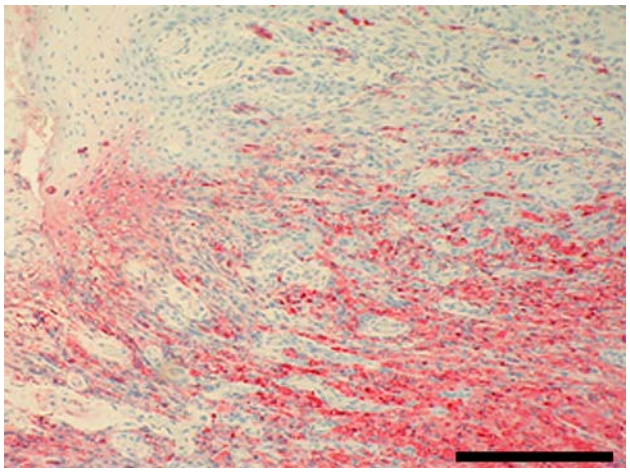


Fig. 8 Same tissue as in Fig. 7, with strong expression of S-100 (*red*) in cells of GCT (original magnification ×100, *bar*=200 μm)

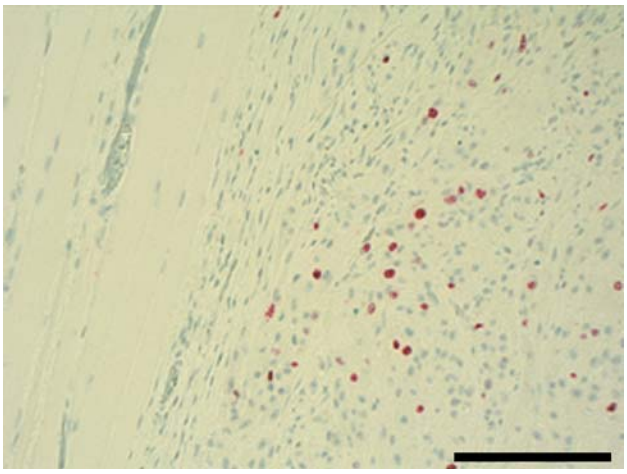


Fig. 10 Immunohistochemistry in the same tissue as in Fig. 8, with numerous ki67-positive cells (*red*; original magnification ×200, *bar*=200 μm)

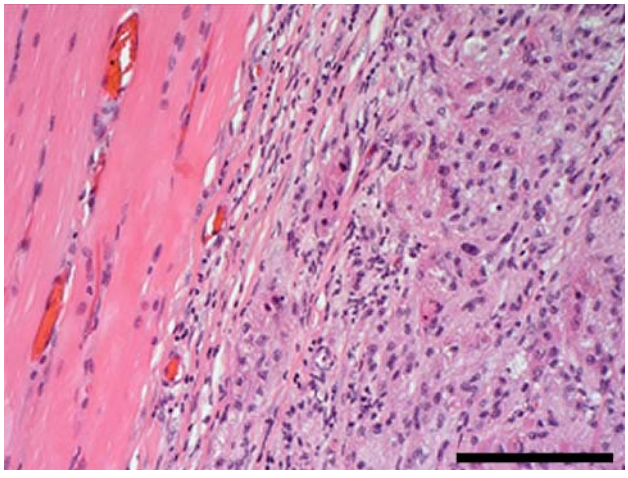


Fig. 9 Atypical GCT with nuclear pleomorphism. On the *left side*, parts of regional skeletal muscle (hematoxylin and eosin, original magnification ×200, *bar*=200 μm). Immunohistochemistry in the same tissue as in Fig. 8, with numerous ki67-positive cells (*red*; original magnification ×200, *bar*=200 μm)

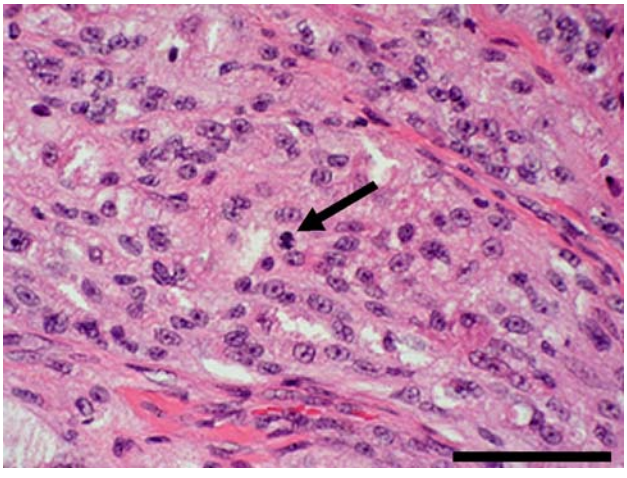


Fig. 11 Same patient as in Figs. 9 and 10 with a detailed view of nuclear pleomorphism. Note prominent nucleoli, mitosis (*arrow*), and granular eosinophilic cytoplasm of the cells (hematoxylin and eosin, original magnification ×400, *bar*=50 μm)

localized. Interestingly, the epithelium in the neighborhood of this tumor showed acanthosis, as well as parakeratosis and some nuclear pleomorphisms, without invasion of the stroma as a sign of pseudoepitheliomatous hyperplasia (Fig. 3). The myogenic nature of the cells was confirmed by immunohistochemical analysis, leading to the diagnosis of an FR (Fig. 4).

Hibernoma

Histologically, the tumors consisted of tightly packed round or oval cells. These cells showed a variable degree of vacuolization, with a few, but distinct, univacuolated cells (Fig. 5). The cytoplasm of multivacuolated cells varied from pale staining to eosinophilic and granular. In particular, nuclei were almost always localized centrally. Sometimes, they contained prominent nucleoli.

Immunohistochemically, cells displayed strong cytoplasmic positivity for S-100 (Fig. 6).

Granular cell tumor

Microscopically, the tumors were nodular but ill-defined. They were composed of polygonal, sometimes spindle-shaped cells, which throughout showed a granular eosinophilic cytoplasm (Fig. 7). Commonly, the intracytoplasmic granules can be stained by PAS reaction. The cells were tightly packed in some tumors, while in others, they were arranged as clusters dispersed between collagen fibers. The nuclei were peripherally localized and showed a dense chromatin; nucleoli were rarely seen. Particularly, two cases (patient nos. 9 and 10) showed remarkable pseudoepitheliomatous hyperplasia of the epithelial lining (Fig. 7). Strong immunoreactivity was obtained with anti-S-100

(Fig. 8) A further case (patient no. 12) focally displayed enhanced nucleocytoplasmic ratio, prominent nucleoli, and an enhanced mitotic rate [3–4 mitoses/10 high-power fields (HPF)], indicating atypical GCT (Figs. 9, 10, and 11).

Discussion

Extracardiac rhabdomyomas of the head and neck area include adult rhabdomyoma (AR) and the less common fetal rhabdomyomas (FR). Both lesions are fairly rare, with only about 150 published reports, mostly in the form of case studies. We present five patients with extracardiac rhabdomyomas of the head and neck region and discuss the relevant differential diagnoses with special regard to soft tissue tumors.

The histological findings of AR are very characteristic, and, in addition, reveal expression of myogenic markers, including desmin, muscle-specific actin, myoglobin, MyoD1, and myogenin[4, 6, 10, 19]. The typical morphology of this tumor should argue against the view that problems in diagnosis might occur at all. However, one needs to be familiar with this rare entity to exclude other diseases. Numerous diseases have been mentioned with the differential diagnosis of AR such as hibernoma, GCT, oncocytoma, paraganglioma, reticulohistiocytoma, lymphoma, rhabdomyosarcoma, and crystal-storing histiocytosis. Among these, GCT and hibernoma are the most relevant soft tissue lesions and, therefore, are especially considered (synopsis is given in Table 3).

Hibernoma is an unusual tumor which mimicks the differentiation of brown fat [2, 13]. In the largest series from Furlong et al. [7], 170 patients were examined. In contrast to the previous opinion that this tumor is mostly localized in areas of residual brown fat, namely, the neck, axilla, and back, Furlong et al. [7] found tumors more often localized in the lower and upper extremity (32 and 22%, respectively) than in the head and neck region (14%). These data are in line with the findings of our report. Of a total number of 31 hibernomas in the Soft Tissue Registry of the Institute of Pathology (Jena), we only found two cases located in the head and neck area (i.e., 6.5%).

In contrast to AR, patients are younger (median age about 40 years), and there is no obvious sex predilection. Since hibernoma cells might show a dense eosinophilic cytoplasm composed of numerous small vacuoles, they can appear granularly shaped. As they additionally can obtain prominent nucleoli, distinction between hibernoma and AR might be difficult. However, less vacuolated or even univacuolated adipocytes are generally found in hibernoma but not in AR. Furthermore, the adipocytic origin of hibernoma can be confirmed immunohistochemically by S-100. However, focal positivity for this marker has also been described in AR [10]. In these cases, distinction can be clarified by using additional myogenic markers. Recently, positivity of desmin was described in spindle cell lipomas [17]. Since a spindle cell variant of hibernoma has been described [7], and similarities of the origin of both hibernoma and spindle cell lipoma are discussed [7, 17], the use of desmin alone might not be sufficient for a clear separation from rhabdomyoma. We therefore recommend a panel of myogenic markers consisting of at least two further muscle-specific antibodies such as muscle-specific actin and/or myoglobin and, in particular, myogenin.

Granular cell tumor, formerly called Abrikossoff's tumor [1] or granular cell myoblastoma [14], has a well-known predilection for the head and neck area, especially for the tongue [14, 16]. The prevailing theory supports that GCT is a true neoplasm, which is of neural origin, and is most probably derived from the Schwann cell. In particular, the consistent positivity for S-100 separates this tumor from neoplasms of histiocytic, fibroblastic, or smooth-muscle derivation [5, 13, 16]. In contrast to AR, FR, and hibernoma, GCT can undergo malignant transformation [2, 3].

Table 3 Synopsis of histological differential diagnosis between adult rhabdomyoma, hibernoma, and granular cell tumor

Tumor	Cells/cytoplasm	Nuclei	Nucleoli	IHC
AR	Polygonal cells, eosinophilic granular cytoplasm, cross striations, spider cells	Peripherally > centrally; vesicular chromatin	Yes	⊕ desmin, muscle-specific actin, myoglobin, and myogenin; ∅ S-100[a]
FR	Small eosinophilic cells, sometimes with cross striations	Peripherally > centrally	Rarely	⊕ desmin, muscle-specific actin, myoglobin, and myogenin; ∅ S-100
Hibernoma	Oval to round cells, variable degrees of vacuolization, eosinophilic granular cytoplasm	Centrally > peripherally; vesicular chromatin	Yes	⊕ S-100; ∅ muscle-specific actin, myoglobin, and myogenin
GCT	Cells variably shaped, eosinophilic granular cytoplasm	Peripherally; dense chromatin	Rarely	⊕ S-100; ∅ desmin, muscle-specific actin, myoglobin, and myogenin
Atypical GCT	Pleomorphic cells, eosinophilic granular cytoplasm, and multinucleated cells occur	Peripherally; vesicular chromatin; increased mitotic rate	Yes	⊕ S-100[b] ∅ desmin, muscle-specific actin, myoglobin, and myogenin

[a]Positivity in a few cases is reported [10]
[b]Negativity is reported [3, 12]

Fetal rhabdomyoma may not easily be separated from GCT. Histologically, both tumors are composed of relatively small eosinophilic cells with peripherally localized nuclei. Pseudoepitheliomatous hyperplasia has been described as a typical feature of GCT [13, 14]. However, as presented in this study, this can also be found in the vicinity of FR and is thus not helpful for exclusion. Immunohistochemistry, using a panel of S-100 and myogenic markers, may help to confirm the diagnosis of either FR or GCT. Particularly, in the case of atypical or malignant GCT, negativity for S-100 has been found [19, 20]. By contrast, expression of myogenic markers has not been demonstrated in GCT so far [3, 12, 16].

In summary, although the histological findings of AR and FR are very characteristic, one needs to be familiar with these rarities. Among the soft tissue tumors, hibernoma and GCT should be especially excluded. In contrast to hibernoma, which is not frequent in the head and neck area, and which is always of a benign nature, GCT should be particularly considered since this tumor can undergo malignant transformation.

Acknowledgements We wish to thank the following colleagues for kindly providing of the cases: Dr. Boenigk (Remscheid, Germany), Prof. Bültmann (Tübingen, Germany), Dr. Hallermann (Münster, Germany), Prof. Kriegsmann (Trier, Germany), Dr. Markmann (Stuttgart, Germany), Dr. May (Berlin, Germany), Dr. Peters (Lüneburg, Germany), Dr. Rotter (Straubing, Germany), Dr. Schütze (Suhl, Germany), Dr. Sonntag (Ravensburg, Germany), and Dr. Tchiba (Hilden, Germany).

References

1. Abrikossoff A (1926) Über Myome, ausgehend von der quergestreiften willkürlichen Muskulatur. Virchows Arch 260:215
2. Brandwein M, LeBenger J, Strauchen J, Biller H (1990) Atypical granular cell tumor of the larynx: an unusually aggressive tumor clinically and microscopically. Head Neck 12:154–159
3. Fanburg-Smith JC, Meis-Kindblom JM, Fante R, Kindblom LG (1998) Malignant granular cell tumor of soft tissue: diagnostic criteria and clinicopathologic correlation. Am J Surg Pathol 22:779–794
4. Favia G, Lo Muzio L, Serpico R, Maiorano E (2003) Rhabdomyoma of the head and neck: clinicopathologic features of two cases. Head Neck 25:700–704
5. Filie AC, Lage JM, Azumi N (1996) Immunoreactivity of S100 protein, alpha-1-antitrypsin, and CD68 in adult and congenital granular cell tumors. Mod Pathol 9:888–892
6. Fletcher DM, Unni K, Mertens F (eds) (2002) World Health Organization classification of tumours. Tumours of Soft Tissue and Bone. IARC, Lyon
7. Furlong MA, Fanburg-Smith JC, Miettinen M (2001) The morphologic spectrum of hibernoma. A clinicopathologic study of 170 cases. Am J Surg Pathol 25:809–814
8. Gibas Z, Miettinen M (1992) Recurrent parapharyngeal rhabdomyoma. Evidence of neoplastic nature of the tumor from cytogenetic study. Am J Surg Pathol 16:721–728
9. Hansen T, Burg JE, Koutsimpelas D, Mann WJ, Kirkpatrick CJ (2005) Cervical adult rhabdomyoma presenting as a rapidly growing mass in a patient with diffuse large B-cell non-Hodgkin lymphoma. Mund Kiefer Gesichtschir 9:184–187
10. Kapadia SB, Meis JM, Frisman DM, Ellis GL, Heffner DK, Hyams VJ (1993) Adult rhabdomyoma of the head and neck: a clinicopathologic and immunophenotypic study. Human Pathol 24:608–617
11. Katenkamp K, Katenkamp D (2005) Low-malignant peripheral nerve sheath tumors of nasal and sinonasal mucous membranes. Pathologe 26:90–95
12. Lee MW, Chang SE, Song KY, Choi JH, Sung KJ, Moon KC, Koh JK (2002) S-100-negative atypical granular cell tumor: report of a case. Int J Dermatol 41:168–170
13. Miettinen M (ed) (2003) Diagnostic Soft Tissue Pathology. Churchill Livingstone, Philadelphia
14. Nolte E, Kleinsasser O (1982) Granular cell tumors of the larynx. HNO 30:333–339
15. Scrivner D, Meyer JS (1980) Multifocal recurrent adult rhabdomyoma. Cancer 46:790–795
16. Stewart CM, Watson RE, Eversole LR, Fischlschweiger W, Leider AS (1988) Oral granular cell tumors: a clinicopathologic and immunocytochemical study. Oral Surg Oral Med Oral Pathol Oral Radiol Endod 65:427–435
17. Tardio JC, Aramburu JA, Santonja C (2004) Desmin expression in spindle cell lipomas: a potential diagnostic pitfall. Virchows Arch 445:354–358
18. Vermeersch H, van Vugt P, Lemmerling M, Moerman M, De Potter (2000) Bilateral recurrent adult rhabdomyomas of the pharyngeal wall. Eur Arch Otorhinolaryngol 257:24–26
19. Weiss SW, Goldblum JR (eds) (2001) Soft Tissue Tumors, 4th edn. Mosby, St. Louis, pp 769–783
20. Welzel C, Gajda M, Jamali Y, Schrom T, Berghaus A, Holzhausen HJ (2001) Adult multilocular rhabdomyoma as a cause of a space-occupying lesion in the neck region. HNO 49:553–556
21. Willis J, Abdul-Karim FW, di Sant'Agnese PA (1994) Extracardiac rhabdomyomas. Semin Diagn Pathol 11:15–25

Virchows Arch (2005) 447: 855–858
DOI 10.1007/s00428-005-0037-9

ORIGINAL ARTICLE

M. Nilsson · I. Panagopoulos · F. Mertens · N. Mandahl

Fusion of the *HMGA2* and *NFIB* genes in lipoma

Received: 20 May 2005 / Accepted: 21 June 2005 / Published online: 17 August 2005
© Springer-Verlag 2005

Abstract The major cytogenetic subgroup of lipomas is characterized by aberrations of chromosome segment 12q13–15, which recombines with a large number of other chromosomal regions. The gene *HMGA2* is the main target in these aberrations. For some recurrent rearrangements, chimeric transcripts, including the 5′ part of *HMGA2*, have been described. The 3′ partners identified are *LPP*, *LHFP*, *CMKOR1*, and *EBF*. In addition, subsets of other benign solid tumors show aberrations of 12q13–15. Among pleomorphic adenomas of the salivary glands, where the preferred recombination partner with 12q13–15 is 9p22–24, an *HMGA2*/*NFIB* fusion gene has been reported. In the present study, two cases of lipoma with rearrangements of 9p22–24 and 12q15 were analyzed by reverse transcription polymerase chain reaction to find out if *HMGA2*/*NFIB* was also present in lipoma. An in-frame fusion transcript, combining the four first exons of *HMGA2* with exon 8 of *NFIB*, was detected in one case. It was identical to a transcript that was previously described in salivary gland adenoma and contained a stop codon shortly 3′ of the fusion point. The finding of the same fusion gene in different tumors is not unique. For example, *HMGA2*/*LPP* has been reported in lipoma, pulmonary chondroid hamartoma, and soft tissue chondroma. Since similar 9;12 translocations have been described also in rare cases of hamartoma and uterine leiomyoma, the occurrence of *HMGA2*/*NFIB* could be postulated in these tumors as well.

Keywords Lipoma · *HMGA2* · *NFIB* · Fusion gene

M. Nilsson · I. Panagopoulos · F. Mertens · N. Mandahl (✉)
Department of Clinical Genetics, University Hospital,
221 85 Lund, Sweden
e-mail: nils.mandahl@med.lu.se
Tel.: +46-46-173364
Fax: +46-46-131061

Introduction

Several benign solid tumor entities are characterized cytogenetically by rearrangements of the chromosome segment 12q13–15 (e.g., [3, 7–9, 11, 17]). The fraction of tumors displaying aberrations of this segment ranges from about 60% among lipomas and chondroid hamartomas of the lung, to 30–35% of uterine leiomyomas and hemangiopericytomas and 20–25% of pleomorphic adenomas of the salivary glands and chondromas [13]. Typically, 12q13–15 recombines with a large variety of other chromosome bands through translocations, insertions, and inversions. Although almost any band may be involved, there are some cytogenetically identical changes that have been detected in several cases. These recurrent aberrations may vary from one tumor type to another. Among lipomas, the preferred rearrangement t(3;12) (q27–28;q13–15) is present in every fifth tumor, with the involvement of 12q14–15 [14].

The gene *HMGA2* (previously *HMGIC*), located in 12q14–15, is the central molecular target of these chromosomal aberrations and plays an essential role in the tumorigenesis of these lesions [1, 4]. The break points related to structural chromosome aberrations may be located within the gene or at megabase distances outside of the gene, and the effects may be dysregulation of gene expression, truncation of the gene, or formation of a fusion gene encoding a chimeric transcript. Among lipomas, *HMGA2* has been reported to form fusion genes with *CMKOR1* (in 2q35–37), *LPP* (in 3q27–28), *EBF* (in 5q33), and *LHFP* (in 13q12) [2, 15, 18, 19]. The *HMGA2*/*LPP* chimera has also been described in chondroid hamartomas [20] and in one case of soft tissue chondroma [3].

Among pleomorphic adenomas of the salivary gland, the major cytogenetic subgroup is characterized by aberrations of 8q12, whereas a minor subgroup shows rearrangements of 12q13–15. The dominating aberration is t(3;8), but both 8q12 and 12q13–15 have been found to recombine with

9p22–24 in several cases. In two tumors, the recombination between 9p and 12q segments is demonstrated to result in the formation of an *HMGA2*/*NFIB* fusion gene [5].

In the present study, two cases of lipoma with a recombination between 9p and 12q were investigated by reverse transcription polymerase chain reaction (RT-PCR) to find out whether an *HMGA2*/*NFIB* chimera may be present also in this tumor type.

Materials and methods

Two cases of lipoma with rearrangements affecting 9p22–24 and 12q15, as determined by G-band karyotyping, were available for RT-PCR analyses (Table 1).

Culturing, harvesting, and chromosome banding of the tumor cells were as previously described [9, 10]. In brief, the tumor tissue was disaggregated mechanically and then enzymatically by 3–5 h of treatment with collagenase II. The resulting cell suspension was rinsed with a medium to remove released fats and was distributed to glass chamber slides and flasks. The RPMI 1640 medium with HEPES buffer, supplemented with 17% fetal bovine serum, L-glutamine, penicillin, and streptomycin, was then added to the cell suspension. The G-banding of the chromosomes was obtained using Wright's stain solution. Karyotypic descriptions were in accordance to "ISCN (1995). An International System for Human Cytogenetic Nomenclature" [12].

Total ribonucleic acid (RNA) from frozen lipoma tissues kept at −80°C was isolated using the RNeasy Lipid Tissue Mini Kit (Qiagen) according to the manufacturer's instructions. From 5 μg of total RNA, complementary deoxyribonucleic acid (cDNA) was synthesized by reverse transcription in a 20-μl reaction, containing 50 mM Tris–HCl (pH 8.3), 75 mM KCl, 3 mM $MgCl_2$, 10 mM dithiothreitol, 1 mM of each dNTP, 0.5 pM random hexamers, 28 U of RNase inhibitor (RNA guard; Amersham), and 400 U of Moloney Murine Leukemia Virus reverse transcriptase (Invitrogen). The reaction mix was incubated at 37°C for 1 h, followed by 5 min at 65°C. From each case, 1 μl of cDNA was amplified by PCR. *ABL1*-specific primers were used as quality control [16].

All RT-PCR reactions were carried out in final volumes of 50 μl containing 20 mM Tris–HCl (pH 8.3), 50 mM KCl, 1.25 mM $MgCl_2$, 0.2 mM of each dNTP, 1 U of PlatinumTaq polymerase (Invitrogen), 0.5 μM of each of the forward and reverse primers for *HMGA2* and *NFIB* (Table 2), and 1 μl of single-stranded cDNA as a template. In a second PCR with inner primers, 2 μl of the PCR product was reamplified. The PCR was run on a PCT-200 DNA Engine (MJ Research). After an initial denaturation for 5 min at 95°C, 30 amplification cycles were performed, each consisting of denaturation for 1 min at 95°C, annealing for 1 min at 60°C, and extension for 1 min at 72°C. The PCR was completed by a final extension at 72°C for 5 min.

Table 2 Primers used for RT-PCR

Name[a]	Sequence (5′–3′)
NF41475-001	GCATCTCCCGGAAAGTGCGTT
NF41475-005	TGGCCGGTAAGATGGGTGTCCT
NF41475-006	TGGACATTGGCGGGTAAGATGG
HMG846 F	CCACTTCAGCCCAGGGACAACC
HMG876 F	CAGCGCCTCAGAAGAGAGGACG
HMG902 F	GCCCCAGGAAGCAGCAGCAAG
HMG1037 R	CCATTTCCTAGGTCTGCCTCTTGGC
HMG1144 R	AGGTAGAAATCGAACGTTGCGCC

[a]Primer orientation, where F denotes forward and R denotes reverse

The PCR products were analyzed on a 1.3% agarose gel, purified using the Qiagen gel extraction kit, and directly sequenced using the ABI Prism BigDye terminator version 1.1 cycle sequencing kit (Applied Biosystems) on the Applied Biosystems Model 3100-Avant DNA sequencing system. Primers used for sequencing are listed in Table 2. For computer analyses of sequence data, the BLAST software http://www.ncbi.nlm.nih.gov/BLAST/) was used.

Results

G-banding revealed that case 1 had chromosome 12 material inserted into chromosome 9 as the sole anomaly in one clone, whereas the dominating clone had an additional copy of the derivative chromosome 9 (Table 1). All three samples of the lobulated tumor of case 2 had a balanced translocation between chromosomes 9 and 12. The break points in chromosome 9 were interpreted as 9p24 and 9p22, respectively, whereas both cases had a break in 12q15.

RT-PCR products obtained with forward primers for *HMGA2* (HMG846 and HMG876) and reverse primers for *NFIB* (NF41475-006 and NF41475-005) revealed the presence of an *HMGA2*/*NFIB* gene fusion in case 2. The size of the *HMGA2*/*NFIB* product was approximately 400 bp. Its reciprocal counterpart, *NFIB*/*HMGA2*, was not detected.

Table 1 Clinical and cytogenetic data

Case number	Age/sex	Size[a] (cm)	Site/depth	Karyotype[b]
1	41/M	20	Arm/deep	46,XY,ins(9;12)(p24;q15q23)/47,idem,+der(9)ins(9;12)
2	37/M	23	Thigh/deep	46,XY,t(9;12)(p22;q15)

[a]The largest diameter
[b]The karyotype of case 2 has been published [9]

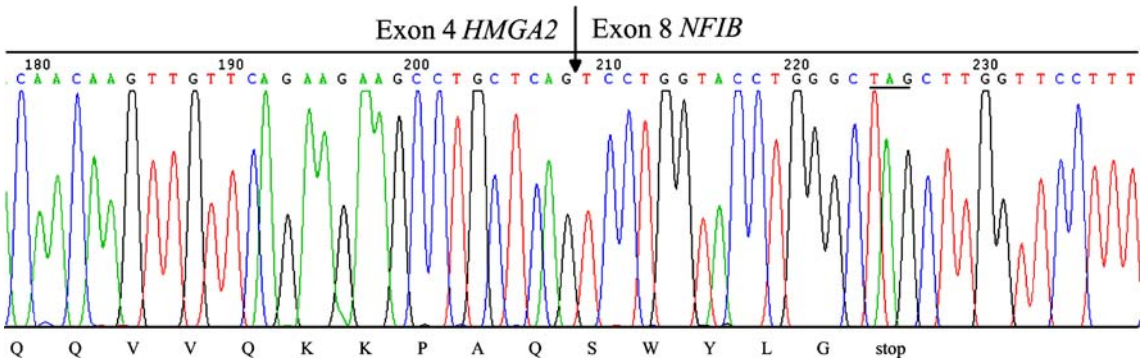


Fig. 1 Sequencing of the PCR product from case 2 showing the in-frame fusion transcript between *HMGA2* and *NFIB*. The fusion point is indicated by an arrow, and the stop codon is underlined

The amplified products were analyzed by direct sequencing (Fig. 1). Computer analyses of the sequence data, using the BLAST software, showed that the fusion of *HMGA2*/*NFIB* chimeric sequences was in frame and contained the first four exons of *HMGA2* located 5′ to exon 8, the last coding exon of *NFIB*. The sixth codon of *NFIB* was a stop codon.

Expression of *NFIB* was detected in both cases, using the forward primer NF41475-001 with reverse primers NF41475-006 and NF41475-005 (Table 2). In addition, *HMGA2* was expressed in both cases, as shown by the forward primer HMG902 combined with reverse primers HMG1037 and HMG1144, to detect transcripts from exons 1–3 and 1–5, respectively.

Discussion

In one of the two presently investigated lipomas, it was possible to demonstrate the presence of an *HMGA2*/*NFIB* fusion gene. Sequencing revealed that the resulting chimeric transcript was identical to that described previously in a case of salivary gland pleomorphic adenoma [5] (i.e., a combination of the four first exons of *HMGA2* with exon 8 of *NFIB*). Although the fusion gene was in frame, the presence of a stop codon shortly 3′ after the fusion point was compatible with the suggestion that the important outcome of the aberration was the deregulation of the expression of the DNA-binding 5′ element of *HMGA2* [1, 4, 5].

t(9;12)(p22–24;q13–15) has been reported not only in pleomorphic adenoma and lipoma but also in uterine leiomyoma and pulmonary chondroid hamartoma [6–8]. Aberrations involving 9p22–24, including t(9;12), are more common among adenomas and appear in about 9% of reported cases with chromosome aberrations, compared to <2% in the three other tumor types [13]. The fraction of tumors with t(9;12) differs less and ranges from below 1.5% among adenomas to less than 0.5% among leiomyomas. These four benign tumor types all include a cytogenetic subgroup characterized by rearrangements involving 12q13–15. Among these tumors, t(9;12)(p22–24;q13–15) has been observed in about 1% of lipomas and hamartomas, 4% of leiomyomas, and 10% of adenomas (Table 3). Several other aberrations, including 12q13–15, are shared by two or more tumor types, but the frequencies may differ distinctly. Apart from the intrachromosomal rearrangements of chromosome 12, which are common among all four tumor types, only two segments, 9p22–24 and 14q22–24, have been involved in all of them, whereas several other rearrangements are shared by only two tumor types. With respect to the low-resolution power of chromosome banding, similar cytogenetic rearrangements need not necessarily have the same consequences at the molecular level. However, the present findings, as well as previous findings of the presence of *HMGA2*/*LPP* fusion genes in lipoma, hamartoma, and chondroma, demonstrate that at least some of these shared cytogenetic aberrations are actually identical also at the molecular level. Since one and the same fusion gene may be associated with distinctly different tumor phenotypes, it seems reasonable to suggest that the aberrant gene might affect cell proliferation in an unspecific way, rather than being a determinant of tumor cell differentiation. The differences in frequencies of certain rearrangements among tumor types could then reflect the probability of a certain aberration to occur in a certain cell type. The mechanisms behind this remain unknown.

The present study provides yet another example of genetic aberrations that are shared by different tumor types. Based on these observations and available cytogenetic data, it seems reasonable to suggest that there are more

Table 3 Frequencies of the most common chromosome segments recombining with 12q13–15 in lipomas, pleomorphic adenomas, lung hamartomas, and uterine leiomyomas

Segment	Lipoma (%)	Adenoma (%)	Hamartoma (%)	Leiomyoma (%)
1p32–34	8	0	0	<1
2p22–24	5	0	1	0
2q35–37	6	0	0	3
3q27–29	20	0	8	0
5q33	6	2	0	0
9p22–24	1	10	1	4
10q22	2	0	0	4
13q12–14	4	0	3	0
14q22–24	1	2	18	61

shared aberrations to be found among benign solid tumors. More specifically, an *HMGA2*/*NFIB* fusion gene might be expected to occur also among leiomyomas and hamartomas.

Acknowledgements This work was supported by the Swedish Cancer Society.

Reference

1. Ashar HR, Tkachenko A, Shah P, Chada K (2003) HMGA2 is expressed in an allele-specific manner in human lipomas. Cancer Genet Cytogenet 143:160–168
2. Broberg K, Zhang M, Strömbeck B, Isaksson M, Nilsson M, Mertens F, Mandahl N, Panagopoulos I (2002) Fusion of *RDC1* with *HMGA2* in lipomas as the result of chromosome aberrations involving 2q35–37 and 12q13–15. Int J Oncol 21:321–326
3. Dahlén A, Mertens F, Rydholm A, Brosjö O, Wejde J, Mandahl N, Panagopoulos I (2003) Fusion, disruption and expression of *HMGA2* in bone and soft tissue chondromas. Mod Pathol 16:1132–1140
4. Fedele M, Battista S, Manfioletti G, Croce CM, Giancotti V, Fusco A (2001) Role of the high mobility group A protein in human lipomas. Carcinogenesis 22:1583–1591
5. Geurts JMW, Schoenmakers EFPM, Röijer E, Aström A-K, Stenman G, van de Ven WJM (1998) Identification of *NFIB* as recurrent translocation partner gene of *HMGIC* in pleomorphic adenomas. Oncogene 16:865–872
6. Kataoka Yamada H, Hoshi N, Kudo M, Hareyama H, Sakuragi N, Fujimoto S (2003) Cytogenetic analysis of uterine leiomyoma: the size, histopathology and GnRHa-response in relation to chromosome karyotype. Eur J Obstet Gynecol Reprod Biol 110:58–62
7. Kazmierczak B, Meyer-Bolte K, Tran KH, Wockel W, Breightman I, Rosigkeit J, Bartnitzke S, Bullerdiek J (1999) A high frequency of tumors with rearrangements of genes of the HMGI(Y) family in a series of 191 pulmonary chondroid hamartomas. Genes Chromosomes Cancer 26:125–133
8. Kiechle-Schwarz M, Sreekantaiah C, Berger CS, Pedron S, Medchill MT, Surti U, Sandberg AA (1991) Nonrandom cytogenetic changes in leiomyomas of the female genitourinary tract. A report of 35 cases. Cancer Genet Cytogenet 53:125–136
9. Mandahl N, Höglund M, Mertens F, Rydholm A, Willén H, Brosjö O, Mitelman F (1994) Cytogenetic aberrations in 188 benign and borderline adipose tissue tumors. Genes Chromosomes Cancer 9:207–215
10. Mandahl N (2001) Methods in solid tumor cytogenetics. In: Rooney DE (ed) Human cytogenetics: malignancy and acquired abnormalities, 3rd edn. Oxford University Press, New York, pp 165–203
11. Mark J, Dahlenfors R, Wedell B (1997) Impact of the in vitro technique used on the cytogenetic patterns in pleomorphic adenomas. Cancer Genet Cytogenet 95:9–15
12. Mitelman F (1995) ISCN (1995). An international system for human cytogenetic nomenclature. Karger, Basel, Switzerland
13. Mitelman Database of Chromosome Aberrations in Cancer. In: Mitelman F, Johansson B, Mertens F (eds). http://cgap.nci.nih.gov/Chromosomes/Mitelman
14. Nielsen GP, Mandahl N (2002) Lipoma. In: Fletcher CDM, Unni KK, Mertens F (eds) World Health Organization classification of tumours. Pathology and genetics of tumours of soft tissue and bone. IARC Press, Lyon, pp 19–46
15. Nilsson M, Mertens F, Höglund M, Mandahl N, Panagopoulos I (2005) Truncation and fusion of *HMGA2* in lipomas with rearrangements of 5q32–33 and 12q14–15. Cytogenet Genome Res (in press)
16. Panagopoulos I, Mertens F, Domanski HA, Isaksson M, Brosjö O, Gustafson P, Mandahl N (2001) No *EWS*/*FLI1* fusion transcripts in giant-cell tumors of bone. Int J Cancer 93:769–772
17. Pandis N, Heim S, Bardi G, Flodérus UM, Willén H, Mandahl N, Mitelman F (1991) Chromosome analysis of 96 uterine leiomyomas. Cancer Genet Cytogenet 55:11–18
18. Petit MMR, Mols R, Schoenmakers EFPM, Mandahl N, Van de Ven WJM (1996) *LPP*, the preferred fusion partner gene of *HMGIC* in lipomas, is a novel member of the LIM protein gene family. Genomics 36:118–129
19. Petit MMR, Schoenmakers EFPM, Huysman C, Geurts JMW, Mandahl N, Van de Ven WJM (1999) *LHFP*, a novel translocation partner gene of *HMGIC* in a lipoma, is a member of a new family of *LHFP*-like genes. Genomics 57:438–441
20. Rogalla P, Lemke I, Kazmierczak B, Bullerdiek J (2000) An identical *HMGIC–LPP* fusion transcript is consistently expressed in pulmonary chondroid hamartoma with t(3;12)(q27–28;q14–15). Genes Chromosomes Cancer 29:363–366

Virchows Arch (2005) 447: 859–868
DOI 10.1007/s00428-005-0001-8

ORIGINAL ARTICLE

Yasufumi Goto · Kozue Uchio-Yamada · Sayuri Anan · Yoshie Yamamoto · Atsuo Ogura · Noboru Manabe

Transforming growth factor-β1 mediated up-regulation of lysyl oxidase in the kidneys of hereditary nephrotic mouse with chronic renal fibrosis

Received: 7 March 2005 / Accepted: 16 May 2005 / Published online: 5 August 2005
© Springer-Verlag 2005

Abstract Lysyl oxidase (LOX), an extracellular emzyme, plays a key role in the post-translational modification of collagens and elastin, catalyzing inter- and intra-crosslinking reactions. Because the crosslinked extracellular matrices (ECMs) are highly resistant to degradative enzymes, it is considered that the over-expression of LOX may cause severe fibrotic degeneration. In the present study, we addressed the role of LOX-mediated crosslinking in chronic renal tubulointerstitial fibrosis using an animal model of hereditary nephrotic syndrome, the Institute of Cancer Research (ICR)-derived glomerulonephritis (ICGN) mouse. Ribonuclease protection assay (RPA) revealed that LOX mRNA expression was up-regulated in the kidneys of ICGN mice as compared with control ICR mice. High-level expression of LOX and transforming growth factor (TGF)-β1 (an up-regulator of LOX) mRNA was detected in tubular epithelial cells of ICGN mouse kidneys by in situ hybridization. Type-I and -III collagens, major substrates for LOX, were accumulated in tubulointerstitium of ICGN mouse kidneys. The present findings imply that TGF-β1 up-regulates the production of LOX in tubular epithelial cells of ICGN mouse kidneys, and the excessive LOX acts on interstitial collagens and catalyzes crosslinking reactions. As a result, the highly crosslinked collagens induce an irreversible progression of chronic renal tubulointerstitial fibrosis in the kidneys of ICGN mice.

Keywords Extracellular matrix · Lysyl oxidase · Renal tubulointerstitial fibrosis · Transforming growth factor-β1

Y. Goto · S. Anan · N. Manabe (✉)
Research Unit for Animal Life Sciences,
Animal Resource Science Center,
The University of Tokyo, 3145 Ago,
Ibaraki-Iwama, 319-0206, Japan
e-mail: amanabe@mail.ecc.u-tokyo.ac.jp
Tel.: +81-29-9458952
Fax: +81-29-9455950

Y. Goto · S. Anan
Unit of Anatomy and Cell Biology,
Department of Animal Sciences, Kyoto University,
Kyoto, 606-8502, Japan

K. Uchio-Yamada · Y. Yamamoto
Department of Veterinary Sciences,
National Institute of Infectious Diseases,
Tokyo, 162-8640, Japan

A. Ogura
Bioresource Center, RIKEN,
Tsukuba, 305-0074, Japan

Introduction

The Institute of Cancer Research (ICR)-derived glomerulonephritis (ICGN) mouse, an inbred strain of mouse with a hereditary nephrotic syndrome of unknown etiology, is considered to be a good model for human idiopathic nephrotic syndrome. ICGN mice are categorized into two groups, heterozygous and homozygous, based on outward appearance and clinical and histopathological findings [25–27, 29, 30]. Aged homozygous ICGN mice, more than 26 weeks old, have severe glomerulonephritis, showing serious proteinuria, hypoproteinemia, hypoalbuminemia, hyperlipidemia, anemia, systemic edema and glomerular and tubulointerstitial chronic fibrosis characterized by the hyper-accumulation of extracellular matrix (ECM) components. Among these pathological events, it is considered that hypertrophy of glomerular basement membrane is the earliest event of renal failure in the kidneys of ICGN mice, but detailed mechanism of this event is still unknown [30]. On the other hand, during renal failure progression, tubulointerstitial fibrosis develops in the kidney of ICGN mice. We consider that the ICGN mouse is a good model for a spontaneous progressive chronic renal tubulointerstitial fibrosis [11]. Previously, we reported the excessive accumulation of both interstitial components (type I and III collagens, fibronectin and tenascin) and basement membrane (type IV collagen and laminin), in glomeruli and the tubulointerstitial area of ICGN mice as compared with ICR mice, which were used as healthy normal controls [39–42]. However, the mechanisms responsible for the excessive accumulation of ECM components in the kidneys of ICGN mice have not been fully elucidated.

Crosslinking of ECM molecules is an initial and important step for the matrix maturation and stabilization mediated by extracellular enzymes, including lysyl oxidases (LOXs) and transglutaminases [1, 23]. The abnormality of this step disrupts the balance of ECM synthesis and degradation, and causes many kinds of fibrogenic diseases [5, 12, 13, 17, 22]. Among these extracellular enzymes, LOX performs the post-translational modification of ECMs, and catalyzes the crosslinking reaction for interstitial collagens and elastin molecules [21]. The catalytic activity of LOX is critical not only in adult and developing normal connective tissues [20, 24], but also in many organs with fibrotic degeneration including hepatic and pulmonary fibrosis and many cancer tissues [22, 33, 38]. In many cases of such pathological fibrotic processes, increased expression of LOX was noted. The excessively high activity of LOX to catalyze the crosslinking reaction in the ECMs results in abnormally high stability of the crosslinked ECMs against degradative enzymes, and thus ECM metabolism is disrupted. More interestingly, a recent study showed that lysyl oxidase activates the transcriptional activity of collagen III α1 promoter [10]. In many pathological fibrotic situations, the expression of LOX and its enzymatic activity are controlled by transforming growth factor (TGF)-β1 [9, 14, 36], which is the most potent fibrogenic cytokine [2, 4, 18, 44]. Moreover, decreased activities of matrix metalloproteinase (MMP)-1, -2 and -9, which are the major matrix degradative enzymes in normal kidneys [16], were demonstrated in ICGN mouse kidneys with renal fibrosis [40].

Based on these observations, we hypothesized that abnormally expressed LOX inhibits the degradation of the ECM in the kidneys of ICGN mice, and examined the changes in the expression levels and localization of LOX mRNA, major LOX substrates (type I and III collagens) and an LOX up-regulator (TGF-β1) to determine the progression mechanism of the chronic renal tubulointerstitial fibrosis in the kidneys of ICGN mice.

Materials and methods

Animals, tissue preparation and blood biochemistry

As previously reported [28–30], ICGN mice were prepared by mating homozygous males (*nep*/*nep*) with heterozygous females (*nep*/−) at the laboratory of the National Institute of Infectious Diseases (NIID; Tokyo, Japan). Aged male homozygous ICGN mice (26 weeks old) and age- and sex-matched ICR mice, which were purchased from Clea Japan (Tokyo, Japan) and used as normal healthy controls, were housed in autoclaved metal cages and given a standard cubed diet (MF; Oriental Yeast, Tokyo, Japan) and tap water ad libitum in an air-conditioned room (23±1°C), under controlled lighting conditions (12/12 h light/dark). All animals received humane treatment as outlined in the Guide for the Care and Use of Animals (The University of Tokyo Animal Care Committee). Under light ether anesthesia, blood was collected from the cervical vein for analyses of clinical biochemistry. The animals were killed under deep ether anesthesia, and then the kidneys were rapidly removed. One kidney was used for biochemical analyses for LOX and TGF-β1. The other kidney was fixed with 4% (w/v) formaldehyde in 0.5 M phosphate buffer, pH 7.4 (Wako, Osaka, Japan), dehydrated through a graded ethanol series, and embedded in paraffin (Histosec; Merck, Darmstadt, Germany) according to routine histopathological methods. To evaluate the nephrotic state and loss of renal function, serum samples were separated by centrifugation (3,000 *g* for 15 min), and then serum albumin (sAlb), serum creatinine (sCr), blood urea nitrogen (BUN) and serum total cholesterol (sTC) levels were measured with an automatic clinical analyzer (Dri-Chem 3500U; Fuji Film, Tokyo, Japan). All procedures were performed according to the manufacturers' recommendation.

Cell culture

Primary normal human renal proximal tubule epithelial cells (RPTECs) were purchased from Clonetics (Walkersville, MD, USA). RPTECs were grown in renal epithelial cell growth medium (REBM; Clonetics) containing 10 ng/ml of human epidermal growth factor (Clonetics), 5 μg/ml of insulin (Clonetics), 500 ng/ml of hydrocortisone (Clonetics), 500 ng/ml of epinephrine (Clonetics), 6.5 ng/ml of triiodothyronine (Clonetics), 10 μg/ml of transferring (Clonetics), 0.1% (v/v) GA-1000 (Clonetics) and 0.5% (v/v) fetal bovine serum (FBS; Sigma Aldrich, St. Louis, MO, USA) at 37°C in a 5% CO_2 air incubator (Sanyo, Osaka, Japan). Then RPTECs (at passage 2) were preincubated in REBM containing 0.5% (v/v) FBS, 100 U/ml penicillin (Sigma) and 100 mg/ml streptomycin (Sigma) for 24 h at 37°C. After removal of the culture medium, the cells were incubated in REBM medium containing 0.5% (w/v) bovine serum albumin (BSA; Sigma) with 1 or 5 ng/ml of human recombinant TGF-β1 (rTGF-β1; R&D systems, Oxon, UK), an activated form of TGF-β1, for 24 h at 37°C. As a vehicle control, the cells were incubated in REBM medium containing only 0.5% (w/v) BSA.

Extraction of total RNA, synthesis of cRNA probes and non-RI labeling

Total RNA was extracted from fresh kidney samples and RPTECs using an RNeasy mini kit (Qiagen, Chatsworth, CA, USA), and then treated with an RNase-free DNase kit (Qiagen).

To generate templates for cRNA probes, partial sequences of murine TGF-β1 (mTGF-β1), murine LOX (mLOX) and human LOX (hLOX) were amplified from mouse and human cDNA libraries by polymerase chain reaction (PCR). Primer pairs were as follows—mTGF-β1 forward: 5′-TGACG TCACT GGAGT TGTAC GG-3′ and reverse: 5′-AGACA GAAGT TGGCA TGGTA GCC-3′, product size: 375 bp; mLOX-372 forward: 5′-GGTGC

CCGAC CCCTA CTACA TCC-3′ and reverse: 5′-GCAAA GCGCC TGTGG TACCC ATAGT C-3′, product size: 372 bp; mLOX-571 forward: 5′-TGGCC AGTTC AGCAT ATAGG G-3′ and reverse: 5′-TATGT CCAAA CACCA GGTAC GG-3′, product size: 571 bp; and hLOX-583 forward: 5′-TGGCC AGTAC AGCAT ACAGG G-3′ and reverse: 5′-TATTT TTTCC CACTT CAGAA C-3′, product size: 583 bp.

Templates for mTGF-β1 and mLOX-372 cRNA probes, which were used for in situ hybridization, were synthesized using a Lig'n scribe kit (Ambion, Austin, TX, USA). Briefly, PCR products were ligated with the T7 phage RNA polymerase promoter. To generate templates for antisense cRNA probes, PCR was performed by using a T7 promoter-specific primer and target gene-specific 5′ (upstream end) primer. To generate templates for sense cRNA probes used as a negative control, a 3′ (down-stream end) primer was used instead of the 5′ primer in the PCR. For in situ hybridization, both the antisense and sense probe templates were transcribed in vitro and labeled with digoxigenin (DIG) using a DIG-RNA labeling kit (Roche Diagnostics, Rotkreuz, Switzerland). All procedures were performed according to the manufacturer's instructions.

For the quantitative ribonuclease protection assay (RPA), mLOX-571 and hLOX-583 were TA-cloned using pGEM-T easy vector system I (Promega, Madison, WI, USA). The accuracy of the PCR was confirmed by sequencing. Templates for the mLOX-571 and hLOX-583 cRNA probes and a commercial murine β-actin (mβ-actin: 245 bp) and human β-actin (hβ-actin: 245 bp) cRNA probe (Wako) were transcribed and labeled with DIG using a DIG-RNA labeling kit. Sizes of transcribed probes were as follows: mLOX-571, 630 bp; hLOX-583, 642 bp; mβ-actin, 334; hβ-actin, 334 bp. All procedures were performed according to the manufacturer's instructions.

Quantitative RPA for LOX and β-actin mRNAs

RPA was performed using an RNase protection kit (Roche) according to the manufacturer's directions. Briefly, 40 μg of total RNA prepared from kidney tissue or REPTCs, or yeast tRNA (as a negative control) was hybridized with 1 ng each of DIG-labeled mLOX-571 and mβ-actin cRNA probe mixture or hLOX-585 and hβ-actin cRNA probe mixture for 18 h at 45°C. Then, each sample was treated with RNase-T1 (Roche) for 30 min at 30°C to digest the non-hybridized, single-strand RNA. Each digested sample was electrophoresed in a 6% (w/v) denatured polyacrylamide gel, and capillary blotted on a Hybond-N^+ membrane (Amersham Pharmacia Biotech, Piscataway, NJ, USA). After ultraviolet fixation with a UVC 500 UV crosslinker (Amersham Pharmacia), each membrane was incubated with alkaline phosphatase (AP)-conjugated sheep anti-DIG antibody (diluted 1:10000 with blocking solution) for 1 h at RT (22–25°C). After washing, chemiluminescence was visualized using the CDP-star system (Amersham Pharmacia), and then chemiluminescence was recorded with a digital luminoimage analyzer (LAS-1000; Fuji Film). The intensity of chemiluminescence was quantified using Image-Gauge software (Fuji Film) on a Machintosh computer.

Assay of the catalytic activity of LOX

The catalytic activity of LOX was measured with a fluorometric assay according to the method described by Palamakumbura and Trackman [31]. Briefly, fresh kidney was washed in 0.1 M sodium phosphate buffer (pH 7.4), minced using surgical scissors, and homogenized for 10 min at 4°C. After centrifugation at 3,000 *g* for 5 min to remove debris, the supernatant was collected, and the protein concentration of the supernatant was determined with a Bradford assay kit (Bio-Rad Laboratories, Melville, NY, USA) according to the manufacturer's directions. Then, 100 μl of supernatant was mixed with 400 μl of reaction buffer [1.2 M urea (Wako), 50 mM sodium borate (pH 8.2; Wako) with 1 unit/ml horseradish peroxidase (Sigma), 10 μM Amplex Red (Molecular Probes Europe, PoortGebouw, the Netherlands), and 10 μM 1,5-diaminopentane (Wako)] and incubated for 30 min at 37°C. For inhibitory control, the reaction mixture containing a specific inhibitor of lysyl oxidase activity [500 μM β-aminopropionitrile (BAPN) Sigma] was used. After incubation, each mixture was placed on ice to stop the reaction, and the fluorescence intensity (excitation wavelength 560 nm, emission wavelength 590 nm) was measured by using a fluorescence spectrophotometer (VersaFluor; Bio-Rad Laboratories). The difference in fluorescence intensity between samples with and without BAPN was calculated to assess the LOX activity, and each result was normalized with each protein concentration.

Enzyme-linked immunosorbent assay for TGF-β1

Kidney tissue levels of TGF-β1 were determined by enzyme-linked immunosorbent assay (ELISA). Briefly, kidney was homogenized in the lysis buffer [20 mM Tris–HCl, pH 7.4, containing 2 M NaCl, 0.1% (v/v) Tween 80, 1 mM phenylmethylsulfonyl fluoride (PMSF) and 1 mM ethylenediaminetetraacetic acid (EDTA); Sigma]. Each lysate was centrifuged at 19,000 *g* for 20 min at 4°C, and the supernatant was collected. Levels of active form TGF-β1 were measured using a TGF-β1 Emax immunoassay kit (Promega), according to the manufacturer's direction. The optical density at 450 nm was measured with a microplate reader (Model 450; Bio-Rad), and the amount of active TGF-β1 in each kidney sample was expressed in pg/mg of total protein.

Immunohistochemistry

Type I and III collagens in the kidney sections were detected by a conventional indirect immunofluorescence method. Briefly, 2-μm-thick paraffin sections were depar-

affinized, rehydrated and washed with phosphate-buffered saline (PBS; pH 7.4). They were preincubated with normal goat serum [diluted 1:100 with PBS containing 5% BSA (w/v); PBS–BSA] for 20 min at room temperature, and then incubated with each diluted primary antibody for 18 h at 4°C. Primary antibodies used were as follows: rabbit anti-mouse type I collagen antibody (diluted 1:200 PBS–BSA; Calbiochem, La Jolla, CA, USA) and rabbit anti-mouse type III collagen antibody (diluted 1:200 with PBS–BSA; LSL, Nagoya, Japan). After being washed with PBS, the sections were incubated with Alexa Fluor 488-conjugated goat anti-rabbit IgG (diluted 1:300 with PBS–BSA; Molecular Probes) for 90 min at RT, and counterstained with 20 μg/ml of propidium iodide solution (PI; Sigma) for 30 s. After a wash with PBS, they were mounted with glycerol and examined with a confocal laser scanning microscope (Fluoview FV300; Olympus, Tokyo, Japan).

The active form of TGF-β1 protein in the kidney sections was detected by a conventional indirect immunoperoxidase method. Briefly, after rehydration, the paraffin sections (2 μm thick) were pretreated with 0.3% (v/v) H_2O_2 in absolute methanol for 10 min at room temperature, washed with PBS–BSA and incubated with rabbit anti-human active TGF-β1 antibody (diluted 1:100 with PBS–BSA; Promega) for 2 h at room temperature, and then incubated with biotinylated secondary antibody (goat anti-rabbit IgG, antibody, diluted 1:300 with PBS–BSA; Vector, Burlingame, CA, USA) for 1 h at room temperature. They were incubated with avidin biotin complex (ABC kit; Vector), colorized with the 3,3′-diaminobenzidine tetrahydrochloride (DAB) liquid system (Dako, Glostrup, Denmark), and counterstained with Mayer's hematoxylin. After dehydration, they were mounted in Eukitt (Kindler, Freiburg, Germany), and examined with a light microscope.

In situ hybridization for LOX and TGFβ1 mRNAs

LOX and TGF-β1 mRNAs in kidney sections were detected by the in situ hybridization method. Briefly, 4-μm-thick paraffin sections were mounted on silane-precoated slide glasses (Matsunami Glass, Tokyo, Japan), deparaffinized and rehydrated. After a wash with PBS, they were treated with 0.2 N HCl for 10 min at room temperature, washed with PBS and digested with 1 μg/ml proteinase-K (Sigma) in PBS for 25 min at 37°C. They were post-fixed with 4% (w/v) paraformaldehyde (PFA)–PBS, immersed with 2 mg/ml glycine–PBS, washed in PBS and prehybridized with hybridization cocktails 50% formamide (Amresco, Solon, OH, USA) for 1 h at 25°C. They were then hybridized with the antisense DIG-mTGF-β1 or -mLOX-372 cRNA probe for 18 h at 45°C. As a negative control, each serial section was hybridized with each DIG labeled sense cRNA probe. Each probe was diluted with hybridization cocktails 50% formamide at a concentration of 1 μg/ml. After a thorough washing with 2×SSC for 2 hr, with 0.5×SSC for 2 h and with 0.2×SSC for 1 h at 45°C, they were equilibrated with 100 mM Tris–HCl, pH 7.5, containing 150 mM NaCl (THS), blocked with commercial blocking reagent (Roche) for 1 h at RT, and then incubated with AP-conjugated sheep anti-DIG antibody (diluted 1:500 with blocking solution; Roche) for 18 h at 4°C. After a wash with THS, they were equilibrated with 100 mM Tris–HCl (pH 9.5), 100 mM NaCl and 100 mM $MgCl_2$ (THSM) and incubated with THSM containing 0.4 mM nitroblue tetrazolium chloride (Sigma), 0.4 mM 5-bromo-4-chloro-3-indolylphosphate-4-toluidine salt (Roche) and 1 mM levamisole (Roche) at 4°C. The appropriate reaction was verified by microscopy. Finally, they were washed with PBS, mounted with Histofine (Nichirei, Tokyo, Japan), and examined with a microscope. The specificity of the in situ hybridization signal was confirmed by parallel incubation with antisense and sense cRNA probes. As further negative controls, serial sections were hybridized without any probes or processed without the anti-DIG antibody. All negative controls yielded completely negative results.

Statistical analysis

Results are shown as mean±SE. The experiments were repeated independently at least twice, and every experiment was performed in triplicate. Differences in mean values were analyzed with unpaired Student's *t* test and ANOVA using Stat-View 4.5 program m (Abacus Concepts, Berkely, CA) on a Machintosh computer. Differences at $P<0.05$ were considered significant.

Results

Clinical blood biochemistry

Aged (26 weeks old) ICGN mice manifested clinical abnormalities such as exercise intolerance, pale ears and weight loss. Blood biochemical parameters showed that ICGN mice had hypoalbuminemia (mean values of sAlb in ICR and ICGN mice were 3.41±0.15 and 1.92±0.13 g/dl, respectively, a 0.56-fold decrease compared with age-matched ICR mice; $P<0.001$). Marked increases were observed in sCr (0.14±0.03 and 0.62±0.05 g/dl, respectively, 4.43-fold; $P<0.01$) and BUN (40.6±2.0 and 130.0±6.2 g/dl, respectively, 3.20-fold; $P<0.001$) in ICGN mice, indicating a loss of renal function. Increased sTC (107.4±5.9 and 233±19.4 g/dl, respectively, 2.17-fold; $P<0.01$) suggested hypercholesterolemia in ICGN mice. Thus, the aged ICGN mice used in this study were in a nephrotic state.

Expression level and localization of LOX mRNA in the kidneys of ICR and ICGN mice

To compare LOX mRNA expression levels between the kidneys of ICR and ICGN mice, we performed quantitative RPA for LOX mRNA. LOX mRNA expression was increased about 3.46-fold in the homogenated samples of

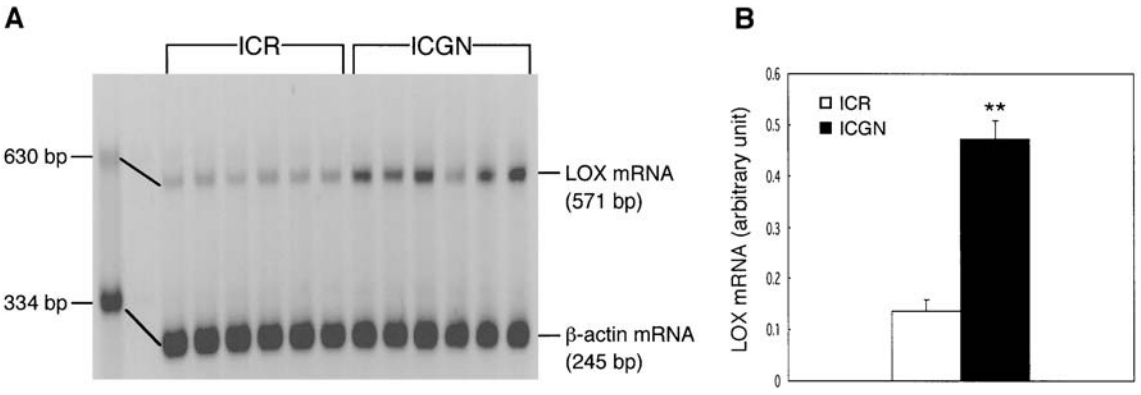


Fig. 1 Lysyl oxidase (LOX) mRNA expression levels were measured by ribonuclease protection assay (RPA) in the kidneys of ICR and ICGN mice (**a**, *lane 1*: full-length probes, *lane 2*: tRNA as negative control, *lanes 3–8*: ICR mice, *lanes 9–14*: ICGN mice). LOX mRNA chemiluminescence signals were normalized to signals of β-actin mRNA and expressed as arbitrary units (**b**). *Empty* and *filled columns* represent the data for ICR and ICGN mice, respectively. $^{**}P<0.01$, compared to control ICR mice

ICGN mouse kidneys as compared with those of ICR mouse kidneys (Fig. 1a,b).

Moreover, we performed in situ hybridization on paraffin-embedded kidney sections to visualize the localization of LOX mRNA. In the kidney sections of ICR mice, trace or low levels of LOX mRNA were detected in the vascular endothelial cells (Fig. 2a). However, in the kidney sections of ICGN mice, a strong reaction for LOX mRNA was observed in the tubular epithelial cells (Fig. 2b). These findings indicated that the synthesis of LOX was up-regulated in the tubular epithelial cells of ICGN mouse kidneys.

Enzymatic activity of LOX in the kidneys of ICR and ICGN mice

To assess the catalytic activity of LOX, whose production was up-regulated in ICGN mouse kidneys as described above, we performed the fluorometric assay based on measurements of hydrogen peroxide, which is a product of the oxidative deamination of alkyl monoamines and diamines (see the following reaction formula). The enzymatic activity of LOX was significantly stronger (2.63-fold) in the kidneys of ICGN mice than those of control ICR mice (Fig. 3).

$$RCH_2NH_2 + O_2 + H_2O \rightarrow RCHO + NH_3 + H_2O_2$$

Expression of TGF-β1 in the kidneys of ICR and ICGN mice

To reveal the factor which up-regulates the expression of LOX in tubular epithelial cells of ICGN mouse kidneys with fibrosis, we compared the expression levels of the active TGF-β1, a candidate up-regulator of LOX, in the kidneys of ICR and ICGN mice using the ELISA method. The levels of active form TGF-β1 protein was increased 8.71-fold in the kidneys of ICGN mice compared to those of normal ICR mice (Fig. 4a). Moreover, the results of in situ hybridization for TGF-β1 mRNA revealed that renal tubular epithelial cells of ICGN mice, but not ICR mice, produced high levels of TGF-β1 mRNA (Fig. 4b and c, respectively), and immunohistochemical staining for the active form of TGF-β1 protein demonstrated that the excessively produced TGF-β1 dominantly localized in the renal tubular epithelial cells (Fig. 4d,e).

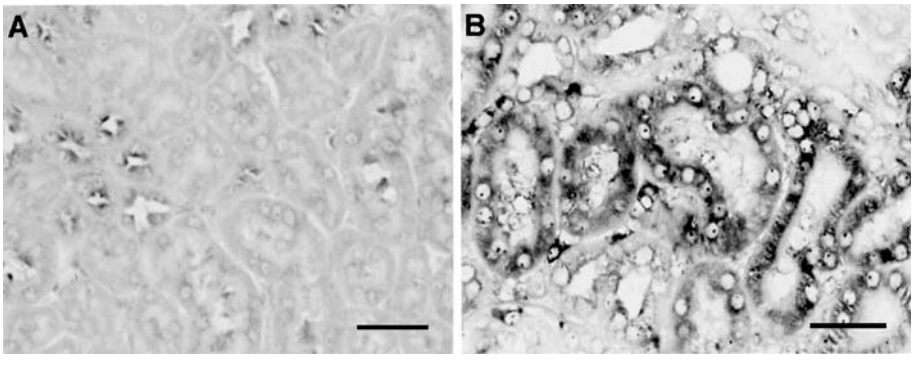


Fig. 2 Representative photographs for in situ hybridization for LOX mRNA in the kidney sections of ICR and ICGN mice (**a** and **b**, respectively). *Scale bar* 20 μm

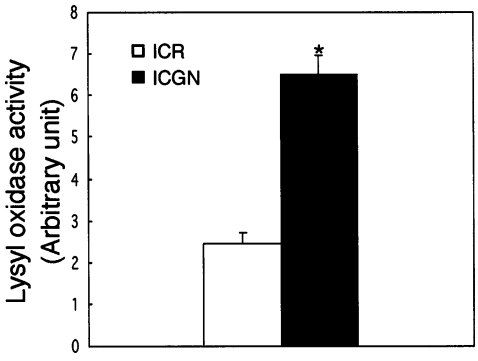


Fig. 3 LOX enzyme activity was biochemically compared by fluorometric assay in the kidneys of ICR and ICGN mice. The difference in fluorescence intensity between samples incubated with and without 500 μM β-aminopropionitrile (BAPN) was calculated, and then the result was normalized to each protein concentration. *Empty* and *filled columns* represent the data for ICR and ICGN mouse kidneys, respectively (n=6 per group). *P<0.05, compared to control ICR mice

Effect of TGF-β1 on LOX mRNA in vitro

To demonstrate the direct relationship between the up-regulated production of the active form of TGF-β1 protein and the expression of LOX mRNA in renal tubular epithelial cells, we examined the effect of TGF-β1 on LOX mRNA levels in cultured RPTECs. Quantitative RPA showed that TGF-β1 (1 or 5 ng/ml rTGF-β1) significantly up-regulated the expression of LOX mRNA in RPTECs (Fig. 5a,b).

Localization of type I and III collagens

In the kidneys of normal ICR mice, trace of type I or III collagen was detected immunohistochemically in tubulointerstitial and tubuloepithelial areas (Fig. 6a and c, respectively). On the other hand, abnormally high levels of type I and III collagens were observed in the tubulointerstitial area of ICGN mouse kidneys (Fig. 6b and d, respectively).

Discussion

It is believed that excessive accumulation of ECM components in fibrotic organs is a consequence of two parallel processes: hyper-increased synthesis and decreased degradation [7]. In normal kidneys, matrix proteases [matrix metallo-proteinases (MMPs), serine proteinases, lysosomal

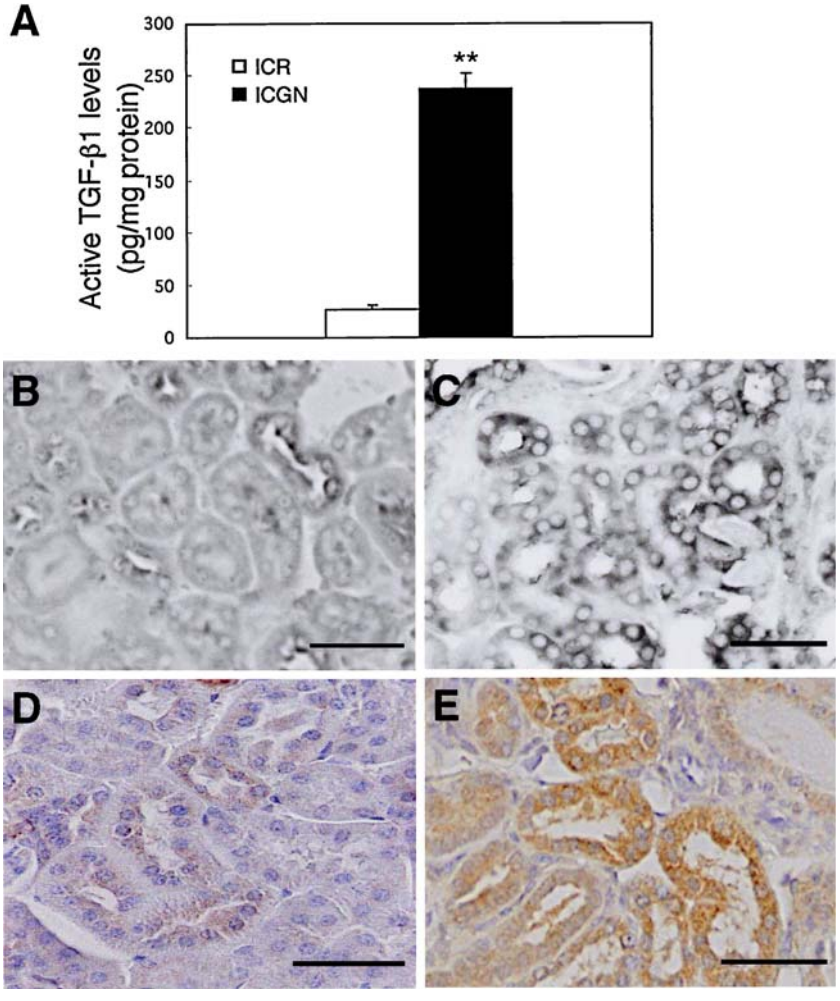


Fig. 4 Active form TGF-β1 protein levels in the kidneys of ICR and ICGN mice measured by ELISA are shown in **a**. The concentration of active form TGF-β1 in kidneys was expressed in pg/mg of total protein. *Empty* and *filled columns* represent the data for ICR and ICGN mouse kidneys, respectively. **P<0.01, compared to control ICR mice. Representative photographs for in situ hybridization for TGF-β1 mRNA in the kidney sections of ICR and ICGN mice are shown in **b** and **c**, respectively. Representative photographs for immunohistochemistry for TGF-β1 protein in the kidney sections of ICR and ICGN mice are shown in **d** and **e**, respectively. *Scale bar* 20 μm

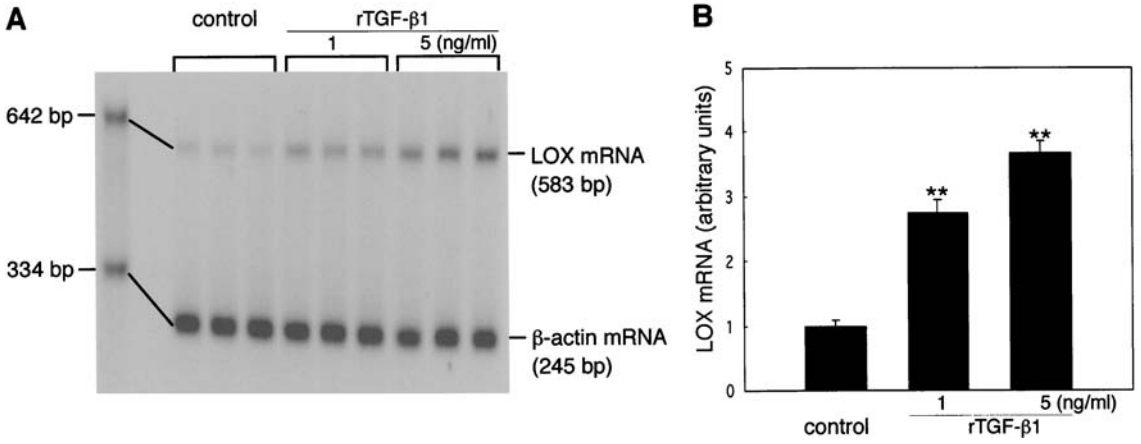


Fig. 5 Effect of active form of TGF-β1 protein on expression levels of LOX mRNA in normal human renal proximal tubule epithelial cells (RPTECs) were determined by RPA (**a**, *lane 1*: full-length probes, *lane 2*: tRNA as negative control, *lanes 3–5*: 0 ng/ml of rTGF-β1, *lanes 6–8*: 1 ng/ml of rTGF-β1, *lanes 9–11*: 5 ng/ml of rTGF-β1). Each signal for LOX mRNA chemiluminescence was normalized to signals of β-actin mRNA, and expressed as arbitrary units (**b**). $^{**}P<0.01$, compared to vehicle control

cysteine proteinases and so on] are produced and activated via physiologically sophisticated controls [16]. In ICGN mouse kidneys with fibrosis, however, increased production of ECM and decreased protease activities (MMP-1, -2 and -9 activities) were noted [40]. When interstitial collagens were crosslinked by LOX, they showed greater resistance against MMPs, which led to a severe disruption of the balance between the synthesis and degradation of ECMs. [43]. Based on these findings, we hypothesized that the type I and III collagens accumulated in ICGN mouse kidneys were overly crosslinked by LOX. In various organs with fibrosis, the earliest process in the development of fibrotic degeneration is the cell differentiation to fibrogenic cells, activated myofibroblasts [34, 35]. During fibrotic degeneration, LOX is produced by the activated myofibroblasts [19, 33, 37]. Previously, we demonstrated that many activated myofibroblasts localized in the renal tubulointerstitium of ICGN mouse kidneys with fibrosis [11]. In the present study, we showed that levels of LOX mRNA were increased in kidneys of ICGN mice compared with those of ICR mice. However, in situ hybridization indicated that the LOX was mainly produced by renal tubular epithelial cells, not myofibroblasts, in the fibrotic kidneys of aged ICGN mice. Such a tubular epithelial cell-specific hyper-induction of LOX mRNA expression was consistent with a previous report on rat kidneys with adriamycin-induced nephropathy [6]. On the other hand, trace levels of LOX mRNA expressed in the glomeruli of ICGN mouse kidneys, but it seemed to be the same expression level with those of ICR mice (data not shown). Because the development of glomerular lesion is earlier than tubulointerstitial fibrotic degeneration in the ICGN

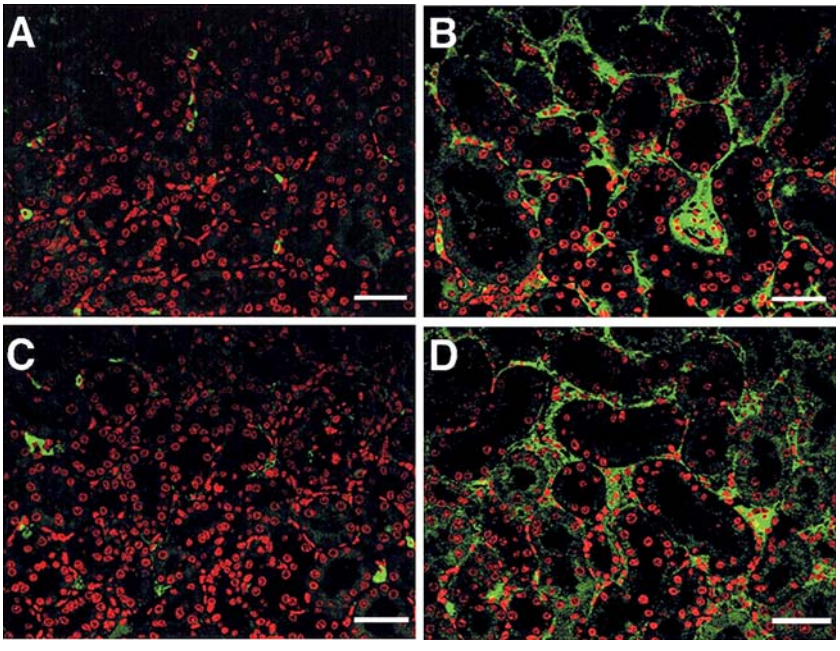


Fig. 6 Representative photographs for immunohistochemical staining for type I and III collagens in the kidney sections of ICR (**a** and **c**) and ICGN mice (**b** and **d**). Nuclei were stained with propidium iodide. *Scale bar* 20 μm

mouse kidneys [11, 30], tubulointerstitial fibrosis is mainly progressing in the kidneys of older ICGN mice (26 weeks old) used in this study. Thus, it seems appropriate that LOX is produced by tubular areas in the kidneys of 26-week-old ICGN mice. The roles and involvement of LOX and other collagen crosslinking enzymes, such as trasnsglutaminases, in the formation of earlier glomerular lesion remain unclear. Moreover, we also confirmed the augmentation of enzymatic activity of LOX in ICGN mouse kidneys. These findings indicate that the excessively produced LOX is biologically active in the kidneys of ICGN mice.

To identify the kinds of factor(s) causing the hyperproduction of LOX in the kidneys of ICGN mice, we focused on TGF-β1, which is known as a fibrogenic cytokine and an up-regulator of LOX biosynthesis [3, 36], and examined the changes in the production and localization of TGF-β1 in mouse kidneys during fibrotic degeneration. Abnormal hyper-expression of TGF-β1 has been reported in many animal models of renal fibrosis, and the sources of TGF-β1 in fibrotic kidneys have been discussed. For example, in diabetic animals with renal fibrosis, both glomerular epithelial cells and renal tubulointerstitial cells produce TGF-β1 [15, 32]. In unilateral ureteral obstruction model animals, increased expression of TGF-β1 mRNA was observed in tubular epithelial cells [8]. In the kidneys of ICGN mice, levels of active form of TGF-β1 were significantly increased, and the tubular epithelial cells dominantly produced TGF-β1. The TGF-β1 protein was activated and localized in renal tubular epithelial cell area. Previously, we investigated the mechanism of myofibroblastic differentiation in the kidneys of ICGN mice and demonstrated that abnormal over-expression of Smad4 protein in tubulointerstitial cells causes hyper-sensitivity to TGF-β1, and that such hyper-sensitivity induces the differentiation of tubulointerstitial cells to fibrogenic activated myofibroblasts [11]. However, the tubulointerstitial cells did not produce high levels of TGF-β1 by themselves. These previous findings were consistent with the present observation of TGF-β1 mRNA localization in ICGN mouse kidneys. Moreover, to confirm the relationship between the increased production of TGF-β1 and up-regulation of LOX expression in tubular epithelial cells, we performed an experiment in vitro. Stimulation with the active form TGF-β1 dose-dependently up-regulated the LOX mRNA expression in REPTCs. Interestingly, Shanley et al. [36] reported that TGF-β1 could increase the enzymatic activity of LOX. So, we consider that tubular epithelial cells of ICGN mouse kidneys with fibrosis excessively produce TGF-β1, and then TGF-β1 is activated, and that activated TGF-β1 stimulates the tubular epithelial cells in an autocrine and/or paracrine manner and up-regulates LOX production and enzymatic activity in the kidneys of ICGN mice. Moreover, in the kidneys of ICGN mice, hyperdeposition of interstitial type I and III collagens in the tubulointerstitial area was confirmed immunohistochemically. However, excessive accumulation of elastin, another substrate for LOX, was not observed in ICGN mouse kidneys (data not shown). As we demonstrated previously [11], the interstitial collagens were mainly produced by activated myofibroblasts located in the renal tubulointerstitial area of ICGN mouse kidneys. Moreover, Giampuzzi et al. [10] showed that LOX can activate the transcription activity of type III collagen promoter. This phenomenon is very interesting and may involve the excessive production of type III collagen in the tubulointerstitium of ICGN mouse kidneys. Therefore, it is suggested that the LOX excessively produced by tubular epithelial cells of ICGN mouse kidneys is secreted into the tubulointerstitial area from the basolateral side of these cells and catalyzes the crosslink reaction of type I and III collagens located in this area.

We conclude that the fibrotic process occurs in the kidneys of ICGN mice, as outlined in Fig. 7. The excessive level of TGF-β1 produced by tubular epithelial cells acts on the TGF-β1-sensitive tubulointerstitial cells (paracrine manner) and the tubulointerstitial cells are transformed to myofibroblasts [11]. Simultaneously, activated TGF-β1 stimulates tubular epithelial cells (autocrine and/or paracrine manner) and up-regulates the production of LOX in the cells. The up-regulated LOX catalyzes the crosslinking formation on the type I and III collagens, which are produced by the activated myofibroblasts located in the tubulointerstitial space. The crosslinked interstitial collagens resist degradation by proteolytic enzymes, and accumulate around the renal tubules. Thus, we propose a relationship between the TGF-β1-mediated up-regulation of LOX production and the progression of chronic renal fibrosis. To emphasize the relationship between LOX and the progression of chronic renal fibrosis and formulate an anti-fibrotic therapeutic approach, we need to examine the effect of LOX down-regulation in vivo, and we are de-

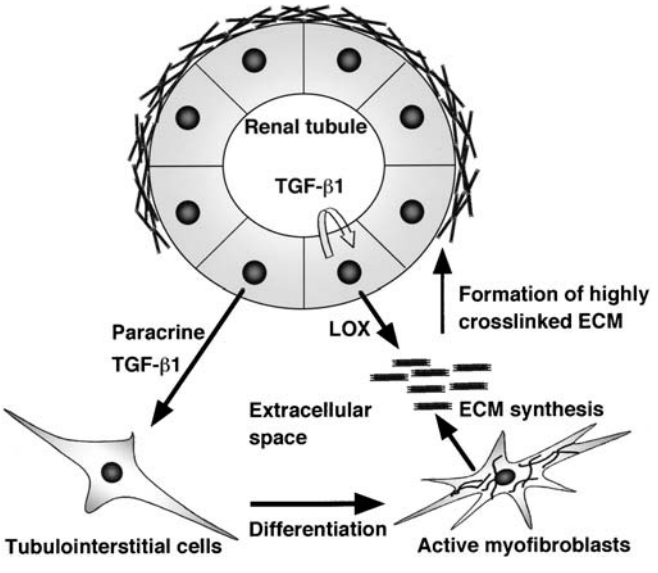


Fig. 7 Schematic illustration of the molecular mechanism of LOX-mediated hyper-crosslinking of collagens in the ICGN mouse kidneys. TGF-β1 excessively produced by renal tubular epithelial cells induces the differentiation of tubulointerestitial cells to fibrogenic activated myofibroblasts. TGF-β1 also promotes hyper synthesis of LOX in the tubular epithelial cells. The activated myofibroblasts produce much collagen and other ECM components, and the secreted LOX acts on the collagens to form hyper-crosslinked collagens, which resists degradative enzymes

veloping a novel renal-specific, long-term gene down-regulation system. Further research on the regulatory mechanism of TGF-β1, which directly affects the production, degradation and maturation of ECM, is necessary to fully understand the pathogenic mechanism of chronic renal tubulointerstitial fibrosis. Moreover, it is also important to identify other factor(s) influencing the balance of ECM metabolism. The ICGN mouse should be a useful model with which to identify novel pathogenic factor(s) and elucidate the molecular regulatory mechanism of chronic renal fibrosis.

Acknowledgements This work was supported by a Grant-in-Aid for Creative Scientific Research (13GS0008) to N.M. from the Ministry of Education, Culture, Sports, Science and Technology in Japan and by a Grant-in-Aid for Scientific Research (S) (16108003) to N.M. from the Japan Society for the Promotion of Science.

References

1. Aeschlimann D, Thomazy V (2000) Protein crosslinking in assembly and remodelling of extracellular matrices: the role of transglutaminases. Connect Tissue Res 41:1–27
2. Blobe GC, Schiemann WP, Lodish HF (2000) Role of transforming growth factor β in human disease. N Engl J Med 342:1350–1358
3. Boak AM, Roy R, Berk J, Taylor L, Polgar P, Goldstein RH, Kagan HM (1994) Regulation of lysyl oxidase expression in lung fibroblasts by transforming growth factor-beta 1 and prostaglandin E2. Am J Respir Cell Mol Biol 11:751–755
4. Border WA, Ruoslahti E (1992) Transforming growth factor-β in disease: the dark side of tissue repair. J Clin Invest 90:1–7
5. Desmouliere A, Darby I, Costa AM, Raccurt M, Tuchweber B, Sommer P, Gabbiani G (1997) Extracellular matrix deposition, lysyl oxidase expression, and myofibroblastic differentiation during the initial stages of cholestatic fibrosis in the rat. Lab Invest 76:765–778
6. Di Donato A, Ghiggeri GM, Di Duca M, Jivotenko E, Acinni R, Campolo J, Ginevri F, Gusmano R (1997) Lysyl oxidase expression and collagen cross-linking during chronic adriamycin nephropathy. Nephron 76:192–200
7. Eddy AA (2000) Molecular basis of renal fibrosis. Pediatr Nephrol 15:290–301
8. Fukuda K, Yoshitomi K, Yanagida T, Tokumoto M, Hirakata H (2001) Quantification of TGF-β1 mRNA along rat nephron in obstructive nephropathy. Am J Physiol Renal Physiol 281: F513–F521
9. Gacheru SN, Thomas KM, Murray SA, Csiszar K, Smith-Mungo LI, Kagan HM (1997) Transcriptional and post-transcriptional control of lysyl oxidase expression in vascular smooth muscle cells: effects of TGF-beta 1 and serum deprivation. J Cell Biochem 65:395–407
10. Giampuzzi M, Botti G, Di Duca M, Arata L, Ghiggeri G, Gusmano R, Ravazzolo R, Di Donato A (2000) Lysyl oxidase activates the transcription activity of human collagene III promoter. Possible involvement of Ku antigen. J Biol Chem 275: 36341–36349
11. Goto Y, Manabe N, Uchio-Yamada K, Yamaguchi-Yamada M, Inoue N, Yamamoto Y, Ogura A, Nagano N, Miyamoto H (2004) Augmented cytoplasmic Smad4 induces acceleration of TGF-beta1 signaling in renal tubulointerstitial cells of hereditary nephrotic ICGN mice with chronic renal fibrosis; possible role for myofibroblastic differentiation. Cell Tissue Res 315: 209–221
12. Grenard P, Bresson-Hadni S, El Alaoui S, Chevallier M, Vuitton DA, Ricard-Blum S (2001) Transglutaminase-mediated cross-linking is involved in the stabilization of extracellular matrix in human liver fibrosis. J Hepatol 35:367–375
13. Griffin M, Smith LL, Wynne J (1979) Changes in transglutaminase activity in an experimental model of pulmonary fibrosis induced by paraquat. Br J Exp Pathol 60:653–661
14. Hong HH, Uzel MI, Duan C, Sheff MC, Trackman PC (1999) Regulation of lysyl oxidase, collagen, and connective tissue growth factor by TGF-beta1 and detection in human gingiva. Lab Invest 79:1655–1667
15. Hong SW, Isono M, Chen S, Iglesias-De La Cruz MC, Han DC, Ziyadeh FN (2001) Increased glomerular and tubular expression of transforming growth factor-β1, its type II receptor, and activation of the Smad signaling pathway in the db/db mouse. Am J Pathol 158:1653–1663
16. Jernigan SM, Eddy AA (2000) Experimental insights into the mechanisms of tubulo-interstitial scarring. In: El Nahas M, Harris K, Anderson S (eds) Mechanism and clinical management of chronic renal failure. Oxford University Press, Oxford, pp 104–145
17. Johnson TS, Griffin M, Thomas GL, Skill J, Cox A, Yang B, Nicholas B, Birckbichler PJ, Muchaneta-Kubara C, Meguid El Nahas A (1997) The role of transglutaminase in the rat subtotal nephrectomy model of renal fibrosis. J Clin Invest 99:2950–2960
18. Jones CL, Buch S, Post M, McCulloch L, Liu E, Eddy AA (1991) Pathogenesis of interstitial fibrosis in chronic purine aminonucleoside nephrosis. Kidney Int 40:1020–1031
19. Jourdan-Le Saux C, Gleyzal C, Garnier JM, Peraldi M, Sommer P, Grimaud JA (1994) Lysyl oxidase cDNA of myofibroblast from mouse fibrotic liver. Biochem Biophys Res Commun 199:587–592
20. Kagan HM, Vaccaro CA, Bronson RE, Tang SS, Brody JS (1986) Ultrastructural immunolocalization of lysyl oxidase in vascular connective tissue. J Cell Biol 103:1121–1128
21. Kagan HM, Trackman PC (1991) Properties and function of lysyl oxidase. Am J Respir Cell Mol Biol 5:206–210
22. Kagan HM (1994) Lysyl oxidase: mechanism, regulation and relationship to liver fibrosis. Pathol Res Pract 190:910–919
23. Kagan HM, Li W (2003) Lysyl oxidase: properties, specificity, and biological roles inside and outside of the cell. J Cell Biochem 88:660–672
24. Krawerz SA (1994) The origin of Lysyl oxidase. Comp Biochem Physiol Biochem Mol Biol 108:117–119
25. Ogura A, Asano T, Matsuda J, Noguchi Y, Yamamoto Y, Takano K, Nakagawa M (1989) Development of nephrotic ICGN mice—the origin, reprodution ability, and incidence of glomerulonephritis. Exp Anim 38:349–352
26. Ogura A, Asano T, Matsuda J, Takano K, Nakagawa M, Fukui M (1989) Characteristics of mutant mice (ICGN) with spontaneous renal lesion: a new model for human nephrotic syndrome. Lab Anim 23:169–174
27. Ogura A, Asano T, Matsuda J, Takano K, Koura M, Nakagawa M, Kawaguchi H, Yamaguchi Y (1990) An electron microscopic study of glomerular lesions in hereditary nephrotic mice (ICGN strain). Virchows Arch A Pathol Anat 417:223–228
28. Ogura A, Asano T, Matsuda J, Fujimura H (1991) Evolution of glomerular lesions in nephrootic ICGN mice: serial biopsy study with electron microscopy. J Vet Med Sci 53:513–515
29. Ogura A, Asano T, Suzuki O, Yamamoto Y, Noguchi Y, Kawaguchi H, Yamaguchi Y (1994) Hereditary nephrotic syndrome with progression to renal failure in a mouse model (ICGN strain): clinical study. Nephron 68:239–244
30. Ogura A, Fujimura H, Asano T, Koura M, Naito I, Kobayashi Y (1995) Early ultrastructural glomerular alterations of neonatal nephritic mice (ICGN strain). Vet Pathol 32:321–323

31. Palamakumbura AH, Trackman PC (2002) A fluorometric assay for detection of lysyl oxidase enzyme activity in biological samples. Anal Biochem 300:245–251
32. Park IS, Kiyomoto H, Abboud SL, Abboud HE (1997) Expression of transforming growth factor-β and type IV collagen in early streptozotocin-induced diabetes. Diabetes 46: 473–480
33. Peyrol S, Raccurt M, Gerard F, Gleyzal C, Grimaud JA, Sommer P (1997) Lysyl oxidase gene expression in the stromal reaction to in situ and invasive ductal breast carcinoma. Am J Pathol 150:497–507
34. Powell DW, Mifflin RC, Valentich JD, Crowe SE, Saada JI, West AB (1999) Myofibroblasts. I. paracrine cells important in health and disease. Am J Physiol 277:C1–C9
35. Serini G, Gabbiani G (1999) Mechanisms of myofibroblast activity and phenotypic modulation. Exp Cell Res 250:273–283
36. Shanley CJ, Gharaee-Kermani M, Sarkar R, Welling TH, Kriegel A, Ford JW, Stanley JC, Phan SH (1997) Transforming growth factor-beta 1 increases lysyl oxidase enzyme activity and mRNA in rat aortic smooth muscle cells. J Vasc Surg 25: 446–452
37. Sommer P, Gleyzal C, Raccurt M, Delbourg M, Serrar M, Joazeiro P, Peyrol S, Kagan H, Trackman PC, Grimaud JA (1993) Transient expression of lysyl oxidase by liver myofibroblasts in murine schistosomiasis. Lab Invest 69:460–470
38. Streichenberger N, Peyrol S, Philit F, Loire R, Sommer P, Cordier JF (2001) Constrictive bronchiolitis obliterans. Characterisation of fibrogenesis and lysyl oxidase expression patterns. Virchows Arch 439:78–84
39. Uchio K, Manabe N, Kinoshita A, Tamura K, Miyamoto M, Ogura A, Yamamoto Y, Miyamoto H (1999) Abnormalities of extracellular matrices and transforming growth factor beta1 localization in the kidney of the hereditary nephrotic mice (ICGN strain). J Vet Med Sci 61: 769–776
40. Uchio K, Manabe N, Tamura K, Miyamoto M, Yamaguchi M, Ogura A, Yamamoto Y, Miyamoto H (2000) Decreased matrix metalloproteinase activity in the kidneys of hereditary nephrotic mice (ICGN strain). Nephron 86:145–151
41. Uchio-Yamada K, Manabe N, Yamaguchi M, Akashi N, Goto Y, Yamamoto Y, Ogura A, Miyamoto H (2001) Localization of extracellular matrix receptors in ICGN mice, a strain of mice with hereditary nephrotic syndrome. J Vet Med Sci 63:1171–1178
42. Uchio-Yamada K, Manabe N, Goto Y, Anan S, Yamamoto Y, Takano K, Ogura A, Matsuda J (2005) Decreased expression of matrix metalloproteinase and tissue inhibitor of metalloproteinase in the kidneys of hereditary nephritic (ICGN) mice. J Vet Med Sci 67:35–41
43. Vater CA, Harris ED Jr, Siegel RC (1979) Native cross-links in collagen fibrils induce resistance to human synovial collagenase. Biochem J 181:639–645
44. Westergren-Thorsson G, Hernnas J, Sarnstrand B, Oldberg A, Heinegard D, Malmstrom A (1993) Altered expression of small proteoglycans, collagen, and transforming growth factor-β1 in developing bleomycin-induced pulmonary fibrosis in rats. J Clin Invest 92:632–637

Virchows Arch (2005) 447: 869–874
DOI 10.1007/s00428-005-0041-0

CASE REPORT

Cecilia Surace · Clelia Tiziana Storlazzi · Jacob Engellau · Henryk A. Domanski · Pelle Gustafson · Ioannis Panagopoulos · Pietro D'Addabbo · Mariano Rocchi · Nils Mandahl · Fredrik Mertens

Molecular cytogenetic characterization of an ins(4;X) occurring as the sole abnormality in an aggressive, poorly differentiated soft tissue sarcoma

Received: 14 March 2005 / Accepted: 29 June 2005 / Published online: 26 August 2005
© Springer-Verlag 2005

Abstract Cytogenetic and fluorescence in situ hybridization (FISH) analysis of an aggressive undifferentiated soft tissue sarcoma diagnosed as primitive neuroectodermal tumor (PNET) revealed an insertion ins(4;X)(q31–32;p11p22) as the sole aberration. To identify the molecular genetic consequences, contigs of bacterial artificial chromosomes (BACs) covering Xp11–p22 and 4q31–32 were constructed. The breakpoint in Xp22 was considered unlikely to be of pathogenetic significance, as it was very close to the Xp telomere, a region devoid of known or predicted genes. The breakpoint in Xp11 was mapped within a BAC clone containing *BCOR*, encoding a BCL6 (B-cell lymphoma 6)-interacting protein that may influence apoptosis, as the only known gene. FISH analysis with three overlapping clones on normal chromosomes 4 disclosed that the insertion of Xp11 material in der(4) was accompanied by a deletion of chromosome 4 material. Only a predicted gene (XM_094074) was shown to be partially included in the deletion. This gene displays a high similarity with the gene encoding the embryonic blastocoelar extracellular matrix (ECM) protein in sea urchin, which is involved in the migration of the primary mesenchyme cells during embryogenesis. Our results suggest that BCOR and/or an ECM-like protein could be involved in the pathogenesis of a subgroup of PNET or PNET-like sarcomas.

Keywords Cytogenetics · In situ hybridization · Sarcomas · Cancer

C. Surace · I. Panagopoulos · N. Mandahl · F. Mertens (✉)
Department of Clinical Genetics,
Lund University Hospital,
SE-221 85 Lund, Sweden
e-mail: fredrik.mertens@klingen.lu.se
Tel.: +46-46-173387
Fax: +46-46-131061

C. Surace · C. T. Storlazzi · P. D'Addabbo · M. Rocchi
Department of Genetics and Microbiology
University of Bari,
Bari, Italy

J. Engellau
Department of Oncology,
University Hospital,
Lund, Sweden

H. A. Domanski
Department of Pathology,
University Hospital,
Lund, Sweden

P. Gustafson
Department of Orthopedics,
University Hospital,
Lund, Sweden

Introduction

Cytogenetic analyses of soft tissue tumors have disclosed several chromosomal translocations, often seen as the sole karyotypic aberration, that are strongly associated with the morphology of the tumor cells [10]. At the molecular level, these translocations often result in the creation of fusion genes, which seem to be equally strongly associated with histologic tumor type. Cytogenetic or molecular genetic information may thus provide diagnostically valuable information. This is especially true for poorly differentiated sarcomas occurring in children and adolescents, where it sometimes may be difficult to differentiate between, for example, synovial sarcoma, rhabdomyosarcoma, and primitive neuroectodermal tumor (PNET) on the basis of morphologic, ultrastructural, and immunohistochemical features alone. It is, however, vital to reach a correct diagnosis, as the different tumor types carry different prognoses and require different treatment strategies.

In the present study, we report the detailed molecular cytogenetic characterization of a previously unreported recombination between chromosomes X and 4, seen as the only cytogenetic aberration in short-term cultured cells from an aggressive undifferentiated soft tissue sarcoma occurring in an 18-year-old boy.

Clinical history

A previously healthy 18-year-old boy had for 3 months noticed increasing pain from a growing mass in his right elbow. A radiograph showed a 6-cm periosteal reaction of the proximal ulnar bone with possible cortical resorption, and MRI displayed a 10×7×3-cm tumor in the proximal ulnar diaphysis and infiltration of adjacent soft tissues. There were no signs of engagement of the bone marrow or of metastasis to the lymph nodes in the axilla. A pulmonary CT showed multiple nodules up to 0.5 cm in diameter in both lungs, but there were no signs of metastases to the mediastinal lymph nodes. A total-body radionuclear bone scan revealed increased activity only in the right elbow. A fine-needle aspiration biopsy (FNA) showed round-to-oval, often dissociated cells, a high mitotic index, and focal areas of necrosis. The tumor cells stained positive for CD99 and vimentin. Electron microscopy showed that the tumor cells displayed sparse, often extended cytoplasm, abundant mitochondria, and small organelles containing glycogen and fat. Based on these findings, the patient was diagnosed with a primitive neuroectodermal tumor (PNET). Neoadjuvant chemotherapy was initiated with vincristin (1.5 mg/m^2), doxorubicin (30 mg/m^2), ifosfamide (1,000 mg/m^2), and cisplatinum (90 mg/m^2) according to the Scandinavian Sarcoma Group protocol IX for soft tissue sarcomas. The chemotherapy was administered without significant subjective toxicity. After four cycles of treatment, a pulmonary CT showed only a minimal mass remaining in the right apical lobe, and MRI of the extremity revealed a marked regression of the primary tumor. The patient underwent surgery with en bloc resection with surgically wide margins of the primary tumor. Both lungs were explored, and the solitary remaining mass in the upper right lobe was excised. Histological examination of the primary tumor showed large areas of fibrosis and small foci of necrosis, probably due to the preoperative chemotherapy. A few small, scattered areas of viable tumor cells were found. Immunostaining showed focal positivity for CD99, while keratins and EMA were both negative. The response to the preoperative chemotherapy was classified as poor (Huvos grade III). No viable tumor cells were found in the resected lung metastasis. Treatment was then continued with one more cycle of chemotherapy, after which stem cell mobilization was intended, followed by myeloablative treatment with high-dose busulphan-melphalan. However, the patient refused further chemotherapy. Instead, the patient received total lung irradiation, with 15 Gy to both lungs (1.25 Gy per daily fraction with 6 MV photon energy).

On a pulmonary CT in October 1999, 17 months after diagnosis, metastases to the lungs were suspected, but the patient refused further examination until January 2000, when metastasectomy of all evident pulmonary metastases was performed. In sections from the lung metastases, the morphology of the tumor tissue was better preserved than in the primary tumor, and diffusely infiltrating tumor cells, having sparse-to-moderate cytoplasm and rounded-to-oval nuclei with finely granular, clumped chromatin, somewhat irregular nuclear membrane, and inconspicuous nucleoli, were seen. Numerous mitoses were seen, as well as small foci of apoptotic cells (Fig. 1). In addition, there were areas where cellular pleomorphism was more marked, with larger cells and more prominent anisokaryosis, irregular cell membranes and coarser nuclear chromatin (Fig. 2). Rosettes, perivascular pseudorosettes, or cytoplasmic glycogen were not seen. Tumor cells were negative for CD99, keratins, and EMA.

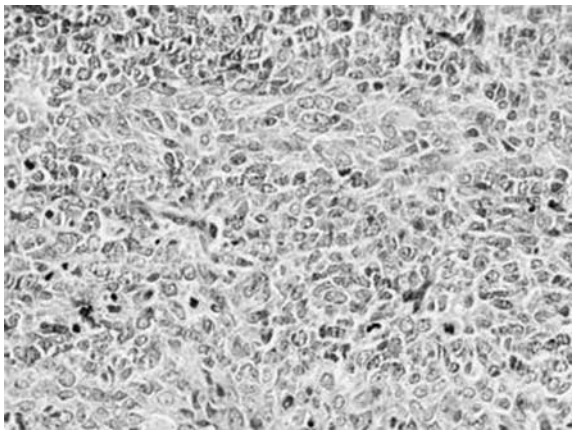


Fig. 1 Histologic section from lung metastasis showing diffusely infiltrating, relatively uniform, or moderately pleomorphic tumor cells with an admixture of apoptotic cells (H & E, ×50)

At this time, the patient refused chemotherapy. New lung metastases were detected 3 months later, and after an additional 2 months, four cycles of high-dose ifosfamide (2,000 mg/m^2) were given. No signs of tumor response were seen, and the patient was subsequently treated from September 2000–May 2001 with oral trofosfamide-etoposide. Radiotherapy to the mediastinum (30 Gy in ten fractions) and apical thoracic cavity (20 Gy in five fractions) was given, but in November 2001, the patient died of respiratory insufficiency due to massive intrathoracic tumor growth.

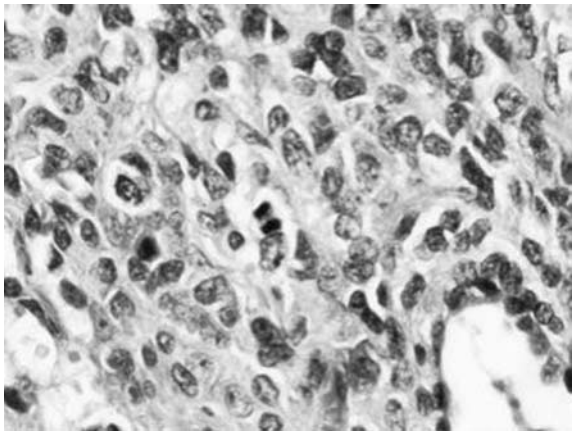


Fig. 2 High-power view from areas with more pleomorphic tumor cells showing prominent anisokaryosis and coarse nuclear chromatin (H & E, ×100)

Materials and methods

Cell culturing, harvesting, and G-banding were performed as previously reported [8]. The karyotype was described according to the International System for Human Cytogenetic Nomenclature [7].

The following bacterial artificial chromosome (BAC) clones were used as probes for fluorescence in situ hybridization (FISH) analysis in order to reveal the exact location of the breakpoints on the X chromosome (the first ten clones) and chromosome 4 (the remaining 15 clones): RP11-552J9 (accession no. AL450023); RP11-344N17 (AL606490); RP11-552E4 (AL683817); RP11-38O23 (AL356464); RP11-386N14 (AL133545); RP11-291H16 (clone placed on cytogenetic map using the STS marker RH63518); RP11-429N5 (genomic survey sequence gi|11995676|gb| AZ254511.2); RP11-495K15 (genomic survey sequence gi|11500710|gb|AZ303207.2); RP11-87M18 (AL606516); RP11-215A12 (AC084716); RP11-196J14 (AC024032); RP11-83A24 (AC097376); RP11-364L4 (AC097658); RP11-58H15 (AC104685); RP11-481K16 (AC139713); RP11-10M9 (AC018535); RP11-424A19 (genomic survey sequence gi|21955327|gb|BH861015.1); RP11-780M14 (AC104090); RP11-673E1 (AC093890); RP11-291L15 (AC098588); RP11-543H9 (AC096757); RP11-552I10 (AC093863); RP11-667D12 (AC093887); RP11-461L13 (AC080078); RP11-458C23 (genomic survey sequence gi|5009527|gb|AQ582417.1). For each chromosome, the BACs are listed according to their map position, starting with the most proximal one. Their location was defined according to the UCSC database (University of California Santa Cruz, http://genome.ucsc.edu/index.html, May 2004 release). The clones belong to the RPCI library (http://www.chori.org/bacpac/) and were obtained from Resources for Molecular Cytogenetics (http://www.biologia.uniba.it/rmc/). Whole chromosome painting (WCP) probes for the X chromosome and chromosome 4 were obtained from Vysis (Downers Grove, IL, USA) and Cambio (Cambridge, UK). Probes were directly labeled with Cy3-dUTP (Amersham Biosciences, Little Chalfont, UK) and Fluor-X-dCTP (Amersham Biosciences) and indirectly labeled with biotin-dUTP (Roche, Penzberg, Germany) and detected with streptavidin-diethylaminocoumarin (Roche and Molecular Probes, Leiden, The Netherlands). The labeling of all the clones was performed by use of Amersham's Mega Prime kit (Amersham Biosciences). FISH was carried out as described elsewhere [5]. The hybridizations were analyzed with the aid of the Chromofluor System (Applied Imaging, Newcastle, UK). The BLAST software (http://www.ncbi.nlm.nih.gov/BLAST/) was used for computer analysis of nucleotide and protein sequence data, in order to look for candidate genes potentially involved in the breakpoints of the chromosome rearrangement.

In order to exclude cryptic rearrangement of the *EWSR1* gene, metaphase-FISH was performed with BACs flanking

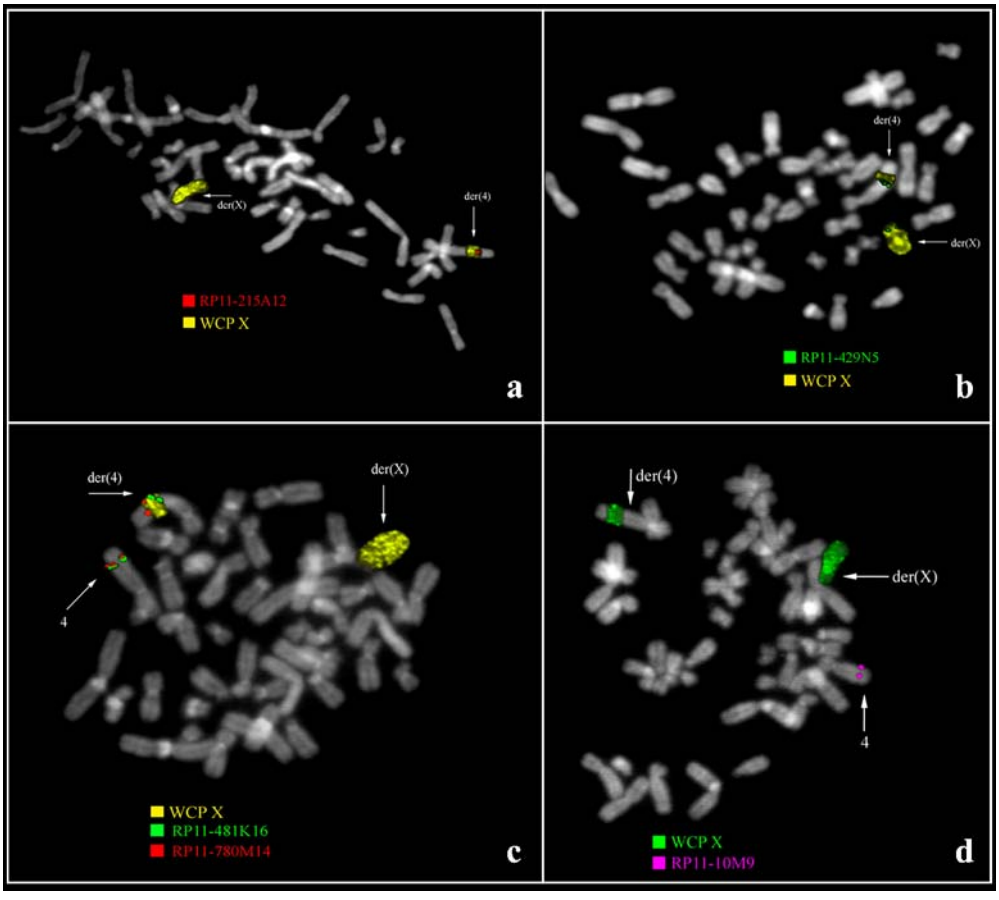


Fig. 3 Results of FISH experiments. The WCP probe for the X chromosome was cohybridized with the following probes: subtelomeric BAC specific for Xp (RP11-215A12) (**a**); BAC RP11-429N5, containing the breakpoint on the X chromosome (**b**); and RP11-481K16 (**c**), RP11-780M14 (**c**), and RP11-10M9 (**d**), covering the region containing the putative breakpoint on the chromosome 4

the *EWSR1* locus (data not shown). The presence of a cryptic *SS18/SSX* fusion gene was excluded through RT-PCR analysis as described [12].

Results

G-banding analysis of metaphase spreads from short-term cultured cells from a fine-needle aspiration biopsy obtained before treatment, as well as from the excised primary tumor obtained after chemotherapy, revealed the following karyotype: 46,Y,t(X;4)(p11;q31)/46,XY. Cytogenetic analysis of peripheral blood lymphocytes showed a normal male chromosome complement. RT-PCR did not reveal any *SS18/SSX* fusion transcript, and FISH for *EWSR1*-rearrangement was negative (data not shown). Preliminary FISH experiments using the WCP probes for X and 4 showed that the chromosomal rearrangement was an inser-

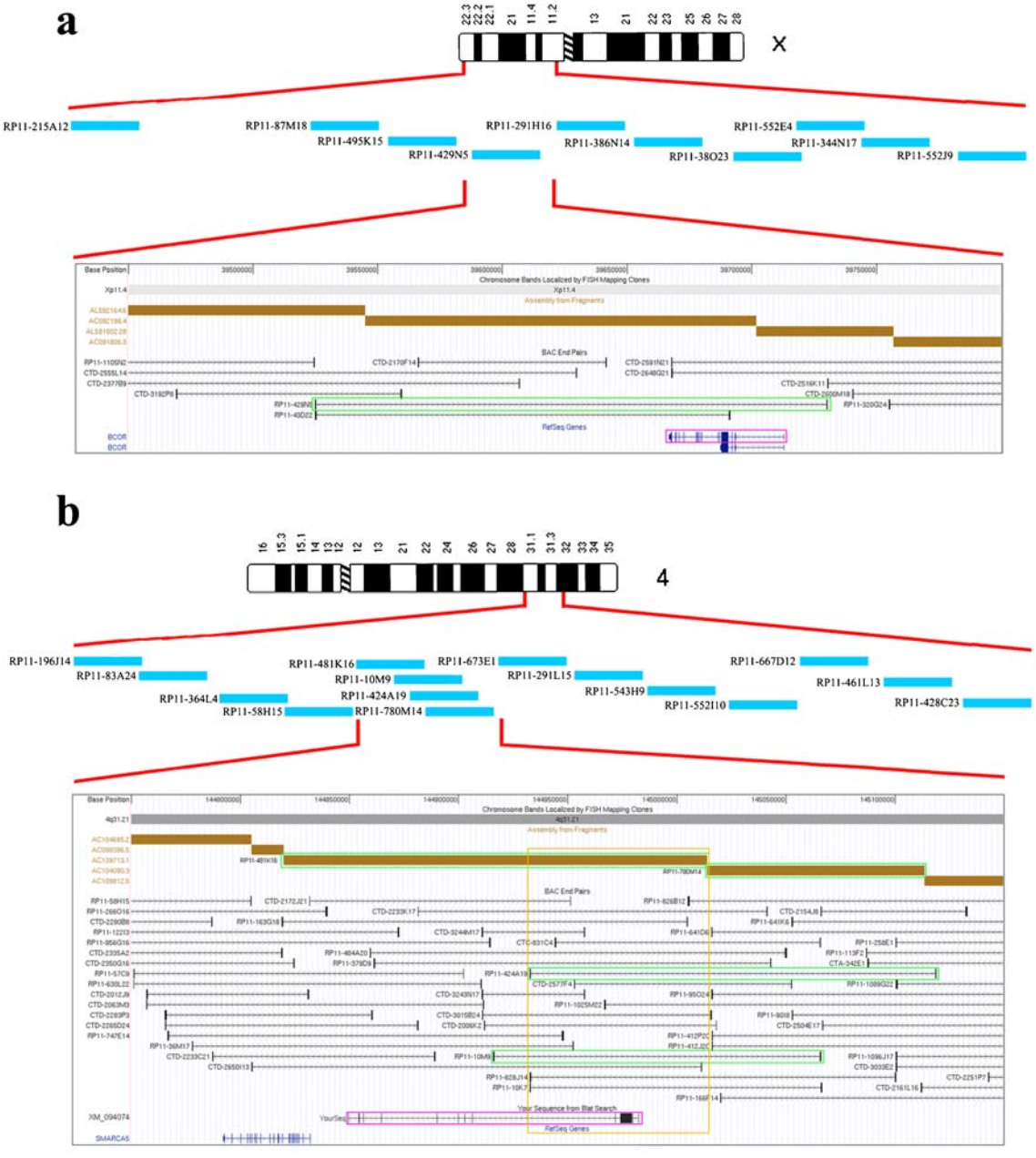


Fig. 4 Location of the clones used in FISH experiments. BACs included in the studied regions (*red intervals* starting from chromosomes) were represented as *light blue boxes*. Regions containing the breakpoints (*red intervals* starting from BACs) were enlarged, and UCSC database web pages were reported (University of California Santa Cruz, http://genome.ucsc.edu/index.html, May 2004 release). The clone RP11-429N5, containing the breakpoint on the X chromosome, was surrounded by *green frame*, and the sole gene included in this area (*BCOR*) was enclosed in a *purple rectangle* (**a**). The BACs covering the breakpoint region on the chromosome 4, RP11-481K16, RP11-10M9, RP11-424A19, RP11-780M14, were displayed surrounded by *green borders*, and the predicted gene (XM_094074) included in this region was enclosed in a *purple frame*. The deleted area was bounded by a *yellow rectangle* (**b**)

tion of Xp into 4q, rather than a translocation. Further FISH analysis revealed that the part of the X chromosome inserted into chromosome 4 spanned from Xp11 to Xpter because the signal for the Xp subtelomeric probe RP11-215A12 was seen on the der(4) (Fig. 3a). Based on these findings, the revised abnormal karyotype was 46,Y, ins(4;X)(q31–32;p11p22).

Contigs of BACs spanning chromosome bands Xp11–Xp21.1 and 4q31–4q32.1 were constructed as described in Materials and methods. The salient findings were as follows: FISH with the X-chromosome-specific clone RP11-429N5 gave a split signal on the derivative chromosomes X and 4 (Fig. 3b). Hence, the breakpoint on X could be mapped to sub-band Xp11.4, between the base positions identified by the ends of the BAC clone. None of the BACs selected for chromosome 4 resulted in a split signal, but the clones RP11-481K16 and RP11-780M14, which are adjacent on normal chromosomes 4, were separated on the der(4) because of the insertion of Xp-material (Fig. 3c). Moreover, FISH with the clone RP11-424A19, which partially overlaps both these clones, resulted in a single signal on the der(4), on the same, telomeric side of the insertion as RP11-780M14. Based on these results, the breakpoint could be mapped to the region between the centromeric end of RP11-424A19 and the telomeric end of RP11-481K16. The fact that we did not observe any splitting of signals using these clones suggested that a segment of that region was deleted. Indeed, FISH analysis with the clone RP11-10M9 did not give any detectable signal on the der(4) (Fig. 3d).

Discussion

In the present study, we report the molecular cytogenetic characterization of an aggressive undifferentiated soft tissue sarcoma diagnosed as PNET. The sole cytogenetic change detected at G-banding analysis, interpreted as a t(X;4), could after FISH analysis be shown to represent an insertion of Xp-material into the long arm of chromosome 4: ins(4;X)(q31–32;p11p22). Neither an ins(4;X) nor a t(X;4) with these or similar breakpoints has previously been reported in soft tissue tumors [10]. However, since this insertion was the sole cytogenetic abnormality, it is reasonable to assume that it was pathogenetically important, and we thus decided to investigate its molecular genetic consequences in more detail.

The X chromosome had two breakpoints, both of which potentially could have harbored genes of importance for tumor development. However, the breakpoint in Xp22 could be shown to be distal to the subtelomeric region recognized by BAC RP11-215A12, making it highly unlikely that the Xp22 breakpoint was of pathogenetic significance. The breakpoint in Xp11 was defined by BAC clone RP11-429N5, showing split signals on the derivative chromosomes X and 4. In the UCSC (May 2004 release) and Ensembl (http://www.ensembl.org/; April 2004 release) databases, there is only one known gene, *BCOR*, mapped to the region covered by this clone (Fig. 4a). *BCOR* encodes a BCL6 (B-cell lymphoma 6)-interacting corepressor that may influence apoptosis. Aberrant expression of *BCL6* due to chromosomal translocations is seen in a subset of non-Hodgkin's lymphoma [6], and BCOR binds AF9, which is a common *MLL* fusion gene partner in acute myeloid leukemia, suppressing AF9 transcriptional activity [13]. *BCOR* mutations have also been implicated in two human syndromes (oculofaciocardiodental syndrome and Lenz microphthalmia), and knock-out experiments performed on the zebrafish ortholog of *BCOR* showed developmental perturbations consistent with the human syndromes, confirming that BCOR is a key transcriptional regulator during early embryogenesis [11]. Based on this previous information, and the fact that there are no other known or predicted genes in the region covered by RP11-429N5, *BCOR* comes forth as a good candidate target gene on the X chromosome.

Regarding the characterization of the breakpoint on chromosome 4, the results suggested that the insertion was accompanied by a deletion of chromosome 4 material. We investigated this region in order to check for putative target genes. No known gene was found, but a gene predicted by Genescan (accession XM_094074.7) was partially included in the deleted region (Fig. 4b). The protein encoded by this predicted gene belongs to a family of proteins conserved from invertebrates to man, whose only member already studied is the embryonic blastocoelar extracellular matrix protein 3 (ECM3, 47% identity with the human protein) of sea urchin (*Lytechinus variegatus*), a protein that is involved in the migration of the primary mesenchyme cells during sea urchin embryogenesis [4]. Furthermore, the ECM3 protein has a large N-terminal NG2-like domain that is related to NG2, a mammalian chondroitin sulfate proteoglycan core protein, which can induce the spreading and migration of other cell types and has been found overexpressed in many human melanomas [1–3]. In addition, the BLASTP analysis of the predicted protein disclosed a 29% identity with the protein encoded by the human *FRAS1* gene that belongs to a family of proteins related to the ECM protein in sea urchin [9].

Unfortunately, lack of material precluded any attempt to investigate the involvement of any of the candidate target genes at the molecular level. However, our results strongly suggest that a subset of undifferentiated, PNET-like soft tissue sarcomas develop through aberrant expression of the *BCOR* gene on chromosome X and/or a gene encoding an ECM-like protein on chromosome 4, and rearrangements of these genes should be searched for in PNET or undifferentiated sarcomas that do not express any of the known fusion genes associated with PNET, synovial sarcoma, or alveolar rhabdomyosarcoma.

Acknowledgements This work was supported by the Swedish Cancer Society, the Swedish Children's Cancer Foundation, Associazione Italiana per la Ricerca sul Cancro (AIRC), and Centro di Eccellenza Geni in campo Biosanitario e Agroalimentare (CEGBA). Cecilia Surace was supported by a Fondazione Italiana per la Ricerca sul Cancro (FIRC) fellowship. The experiments performed comply with the Swedish and Italian laws.

References

1. Burg MA, Nishiyama A, Stallcup WB (1997) A central segment of the NG2 proteoglycan is critical for the ability of glioma cells to bind and migrate toward type VI collagen. Exp Cell Res 235:254–264
2. Burg MA, Grako KA, Stallcup WB (1998) Expression of the NG2 proteoglycan enhances the growth and metastatic properties of melanoma cells. J Cell Physiol 177:299–312
3. Burg MA, Pasqualini R, Arap W, Ruoslahti E, Stallcup WB (1999) NG2 proteoglycan-binding peptides target tumor neovasculature. Cancer Res 59:2869–2874
4. Hodor PG, Illies MR, Broadley S, Ettensohn CA (2000) Cell-substrate interactions during sea urchin gastrulation: migrating primary mesenchyme cells interact with and align extracellular matrix fibers that contain ECM3, a molecule with NG2-like and multiple calcium-binding domains. Dev Biol 222:181–194
5. Höglund M, Johansson B, Pedersen-Bjergaard J, Marynen P, Mitelman F (1996) Molecular characterization of 12p abnormalities in hematologic malignancies: deletion of KIP1, rearrangement of TEL, and amplification of CCND2. Blood 87:324–330
6. Huynh KD, Fischle W, Verdin E, Bardwell VJ (2000) BCoR, a novel corepressor involved in BCL-6 repression. Genes Dev 14:1810–18233
7. ISCN (1995) An international system for human cytogenetic nomenclature. Mitelman F (ed). Karger, Basel
8. Mandahl N, Heim S, Arheden K, Rydholm A, Willen H, Mitelman F (1988) Three major cytogenetic subgroups can be identified among chromosomally abnormal solitary lipomas. Hum Genet 79:203–208
9. McGregor L, Makela V, Darling SM, Vrontou S, Chalepakis G, Roberts C, Smart N, Rutland P, Prescott N, Hopkins J, Bentley E, Shaw A, Roberts E, Mueller R, Jadeja S, Philip N, Nelson J, Francannet C, Perez-Aytes A, Megarbane A, Kerr B, Wainwright B, Woolf AS, Winter RM, Scambler PJ (2003) Fraser syndrome and mouse blebbed phenotype caused by mutations in FRAS1/Fras1 encoding a putative extracellular matrix protein. Nat Genet 34:203–208
10. Mitelman F, Johansson B, Mertens F (eds) (2001) Mitelman database of chromosome aberrations in cancer. http://cgap.nci.nih.gov/Chromosomes/Mitelman
11. Ng D, Thakker N, Corcoran CM, Donnai D, Perveen R, Schneider A, Hadley DW, Tifft C, Zhang L, Wilkie AO, van der Smagt JJ, Gorlin RJ, Burgess SM, Bardwell VJ, Black GC, Biesecker LG (2004) Oculofaciocardiodental and Lenz microphthalmia syndromes result from distinct classes of mutations in BCOR. Nat Genet 36:411–416
12. Panagopoulos I, Mertens F, Isaksson M, Limon J, Gustafson P, Skytting B, Akerman M, Sciot R, Dal Cin P, Samson I, Iliszko M, Ryoe J, Debiec-Rychter M, Szadowska A, Brosjo O, Larsson O, Rydholm A, Mandahl N (2001) Clinical impact of molecular and cytogenetic findings in synovial sarcoma. Genes Chromosomes Cancer 31:362–372
13. Srinivasan RS, de Erkenez AC, Hemenway CS (2003) The mixed lineage leukemia fusion partner AF9 binds specific isoforms of the BCL-6 corepressor. Oncogene 22:3395–3406

Virchows Arch (2005) 447: 875–878
DOI 10.1007/s00428-005-0022-3

CASE REPORT

I. Sinicina · E. Matevossian · F. Fischer · G. Mall · M. Graw

The petrified heart in sepsis

Received: 13 February 2005 / Accepted: 25 May 2005 / Published online: 13 July 2005
© Springer-Verlag 2005

Abstract We report the case of a 33-year-old transsexual man who developed severe sepsis after an accidental intravenous injection of urine (3–5 ml) instead of methadone. He died unexpectedly 28 days after the onset of sepsis. On postmortem examination, the outstanding findings were restricted to the heart with an unusual macroscopic presentation. On histological examination extensive calcifications of the heart muscle, particularly of the left ventricle were found. The pattern of calcifications on the right ventricle was also striking. In contrast, the entire cardial conduction system was unaffected. Furthermore, there were no calcium deposits in other organs and tissues. The advanced widespread cardial calcifications in the present case can be attributed to endotoxin-related myocarditis in severe long-term sepsis. The only treatment would have been an urgent heart transplantation. Without prior knowledge of such a condition, it is impossible for clinicians to correctly recognize, diagnose and treat or prevent in due time such a complication.

Keywords Intravenous injection of urine · Sepsis · Myocardial calcification

I. Sinicina (✉) · F. Fischer · M. Graw
Department of Forensic Medicine,
Ludwig Maximilians University Munich,
Frauenlobstr. 7 a,
80337 Munich, Germany
e-mail: inga.sinicina@med.uni-muenchen.de
Tel.: +49-89-51605111
Fax: +49-89-51605144

E. Matevossian
Department of Surgery, Klinikum Rechts der Isar,
Technical University,
Munich, Germany

G. Mall
Department of Forensic Medicine,
Johannes Gutenberg University,
Mainz, Germany

Introduction

The "classic" cardiovascular signs seen with severe sepsis due to gram-negative bacteremia were first described by Waisbren in 1951 [8]. In a study with fully resuscitated young patients with septic shock, Parker at al. [5] demonstrated significant reductions in both stroke volume and ejection fraction compared with non-septic control patients from the intensive care unit. This myocardial depression was not due to myocardial ischemia, as coronary blood flow and coronary sinus lactate levels were normal in patients with septic shock. In most sepsis-related deaths, a histologic examination of heart samples usually does not reveal any pathologic findings. Sometimes single foci of infectious myocarditis can be found, making the pathological confirmation of the diagnosis easier. The myocardial damage with widespread calcifications in association with severe long-term sepsis is an extremely rare phenomenon despite the high incidence of severe sepsis. In the English literature, only a single report was found regarding cardiovascular signs and severe sepsis: that of Rossi and Santos, who described a myocardial damage with giant cell inflammation and calcifications in a young male. Unfortunately, the authors neglected to provide exact descriptions of the extent and the distribution of calcifications. However, Rossi and Santos attributed their findings to a sepsis-related microvascular myocardial damage [7].

Case report

A 33-year-old transsexual man was admitted to the university hospital 4 h after an accidental injection of urine (3–5 ml), instead of methadone, into a femoral vein. The non-sterile, "clean" urine was kept for a long period of time in a refrigerator, in order to pass monitoring tests at a narcotics out-patient clinic. The misadventure was detected immediately after the injection. Some hours passed before the patient suffered two cerebral seizures, and consequently developed fever and somnolence.

On admission the physical examination revealed an exsiccated and disoriented patient. His temperature was 40°C, pulse 140/min, and respiration 24/min. Blood pressure was 90 mmHg systolic and 40 mmHg diastolic. Laboratory findings were as follows: white blood cell count 1.43 g/l, platelet count 102 g/l, C-reactive protein 3.8 mg/ml (normal range, below 0.5), hemoglobin 12.3 g/dl, creatinine 2.1 mg/dl (normal range, 0.5–1.1 mg/dl). Serum calcium concentrations and phosphate activities were normal. The blood culture was positive for gram-negative bacteria. X-rays of the chest showed a normal-sized heart and inconspicuous lungs. The patient was placed on intensive cardiopulmonary support, and subsequently developed acute renal failure. Some days later, the patient developed an acute liver dysfunction (bilirubin 20 mg/dl) and a respiratory distress syndrome. The day following admission, an increased level of troponine T (0.29 ng/ml, normal range: <0.03 ng/ml) was measured. On the third day the troponin T concentration increased further to 3.54 ng/ml. However, the echo- and electrocardiographic examination revealed no functional or structural abnormalities. The troponin T level had slowly decreased during the first 10 days but did not reach the normal range (1.02 ng/ml). The patient's condition gradually improved and his release from hospital had been planned. However, on the 26th hospital day, 2 days before his death the patient required catecholamines. The echocardiographic examination performed on this day showed an increased density of the entire septal myocardium. His death was attributed to pulmonary embolism and/or an abscess in the septal myocardium.

One week before the incidental injection of methadone a rupture of the right silicon breast implant was diagnosed. The intended surgical replacement of the implant required an examination of the patient (cardiac auscultation, electrocardiography, laboratory tests), which revealed no pathological findings.



Fig. 1 Gross appearance of the heart. Note green discoloration of the endothelium and of the heart muscle



Fig. 2 The anterior wall of the left ventricle showing sharply demarcated, green areas with whitish foci

Autopsy findings

On postmortem examination, the significant findings were restricted to the heart, which weighed 380 g. The endocardium, in particular of the left ventricle, showed multiple, sharply demarcated areas of green discoloration (Fig. 1). The muscle in corresponding areas was very hard. The cut surface of the myocardium was green, dry and sandy, appearing almost crystalline (Fig. 2). Almost the entire septum and left papillar muscles were affected. In the subepicardial areas of the right ventricular free wall green, hard narrow-banded streaks were noted. The atria were not affected. The coronary arteries were widely patent and the cardiac valves were normal. There was no evidence of myocardial infarction.

The histological examination of the heart samples displayed widespread intra- and extracellular calcium deposits, multiple small foci of ossification, interstitial perimysial fibrosis and myocytolytic myocytes associated with inflammatory cells such as lymphocytes, granulocytes, macrophages and monocytes (Fig. 3). The von Kossa stain confirmed calcium deposits in the hematoxyphilic material (Figs. 4, 5). Many mononuclear cells reacted with antibody against CD45RO, demonstrating that the lymphocytes of the inflammatory infiltrate were predominantly

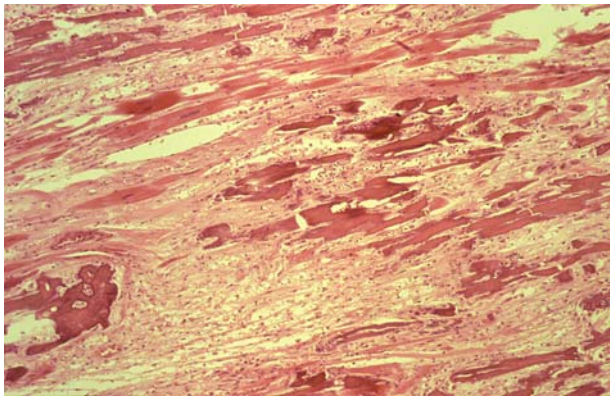


Fig. 3 Typical myocardial lesion showing fibrosis, infammatory infiltration and widespread calcifications. Only a few myocardiocytes are apparently not affected (H&E, ×100)

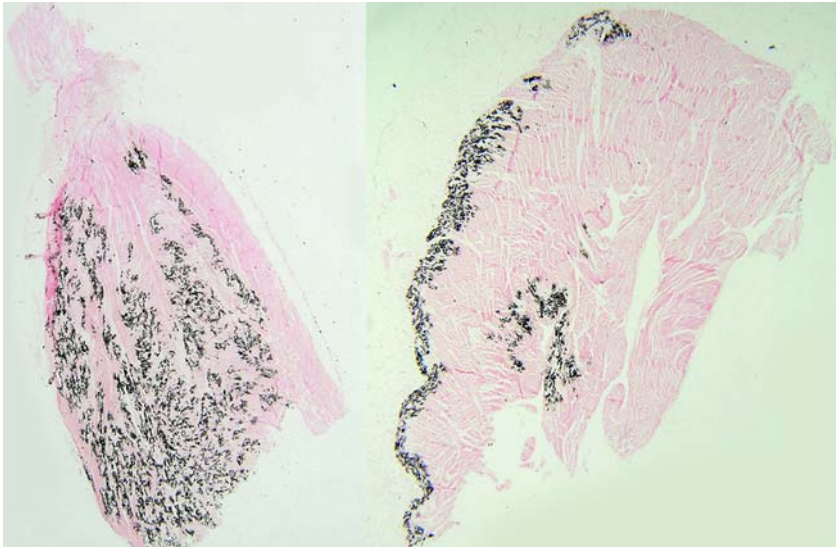


Fig. 4 Right ventricular wall with narrow-banded streaky calcifications in the outer and partially in the subendocardial layer as well as homogeneously calcified myocardial septum (von Kossa stain, whole-mount sections)

T cells. Foci of almost completely calcified embedded myocardiocytes were found in areas of apparently unaffected heart muscle of the left, but not of the right ventricle. Here, signs of inflammation, such as mononuclear cell infiltration or non-calcified fibrotic lesions, were not evident. The myocytolytic cells displayed more intense desmin expression compared to unchanged or only partially calcified myocardiocytes. In contrast, the sinus node, the atrioventricular node and the His bundle were free from inflammation and calcification. Giant cells or granulomas were absent. There were no calcium deposits noted in the other organs, including the kidneys. On postmortem examination of the femoral blood, the patient was negative for HIV.

Discussion

The fact that intensive care unit patients without coronary artery disease have an unexpectedly high percentage of elevated levels of troponin T and I has led to the suggestion of the existence of myocardial cell injury in sepsis and systemic inflammatory response syndrome. Typically, left ventricular myocardial dysfunction is detectable within the first 24 h of the development of septic shock and is completely reversible in survivors within 7–10 days [6]. The pathogenesis of depressed myocardial dysfunction is incompletely understood; however, global ischemia does not seem to be the major mechanism mediating cardiac dysfunction during sepsis. Hematogenic inflammatory foci could explain the altered cardial function only in a small group of patients. Currently, there is a consensus that myocardial dysfunction seems to result from myocardial depressant factors. Candidate mediators for myocardial depressant factor include NO as well as a series of other factors (such as endotoxin, cytokines, platelet-activating factor, reactive oxygen molecules) [2]. Thus, it should be first clarified, whether the unusual myocardial insult in our patient is a result of an endotoxin-induced myocarditis or of a common infectious myocarditis.

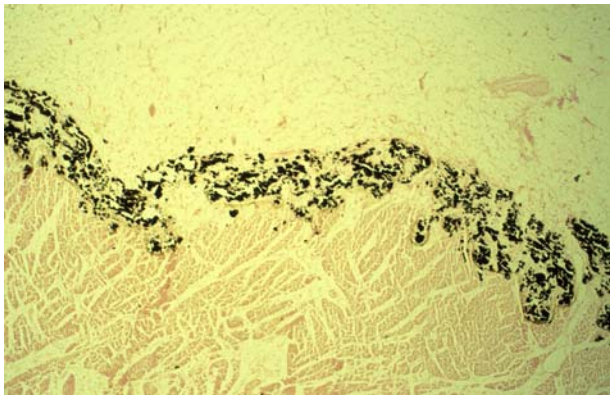


Fig. 5 Right ventricular free wall (von Kossa stain, ×25)

The macroscopic appearance of the heart with its subepicardial narrow-banded deposition of calcium in the right ventricular free wall and the homogenous involvement of the left ventricle, except for structures of the conduction system, has not been described in association with a "classic" infectious myocarditis. Furthermore, the multiple foci of intracellular granular calcifications without concomitant inflammatory signs are not typical for infectious myocarditis. The unusual pattern of the cardiac damage could be explained by regional differences of the myocardium in blood flow, blood volume, metabolism and sensitivity to an ischemic injury, once endotoxin entered the circulation directly in a high dosage [1, 4]. For example, the coronary flow is reported to be lower in the right, rather than in the left ventricle. The regional blood flow is also distributed more randomly and heterogeneously in the right ventricle [3]. Moreover, in an in vivo study, Wong et al. [9] proved spatial and temporary heterogeneity of myocardial responses in endotoxin-induced myocarditis after intravenous application of endotoxin. They also found a gene expression of nitric oxide synthase type 2 in neutrophils, endothelial cell and myocardiocytes located predominantly in the epicardium and endocardium.

The examination of the patient 1 week before the accidental injection of urine showed a healthy man with a normal cardiac function, making a previous cardiac illness appear improbable. The normal echo- and electrocardiographic findings, in association with a dramatic increase in troponin T during the first 3 days, suggest the onset of myocardial inflammation simultaneously with the onset of the sepsis. The subsequent calcifications would explain the rapidly progressing heart failure and the echocardiographic appearance of the septum. Thus, an application of endotoxin in a high dosage directly into the blood circulation followed by an immediate distribution to the heart muscle and subsequent cardiac involvement following blood flow and metabolism patterns, would explain the phenomenon of cardiac inflammation and calcification in the affected myocardial sectors of our case.

In our patient the clinicians diagnosed an increase in the myocardial septal density by echocardiography. However, unaware of such a rare complication of sepsis, they mistook the calcifications for an abscess formation.

The only possible treatment of an almost entirely calcified heart in our young patient would have been a high-urgency heart transplant. Thus, it is important to know about the existence of this unusual condition and to recognize it in due time.

References

1. Allard MF, Kamimura CT, English DR et al (1993) Regional myocardial capillary erythrocyte transit time in the normal resting heart. Circ Res 72:187–193
2. Grocott-Mason RM, Shah AM (1998) Cardiac dysfunction in sepsis: new theories and clinical implications. Intensive Care Med 24:286–295
3. Hoffman JI (1995) Heterogeneity of myocardial blood flow. Basic Res Cardiol 90:103–111
4. Matsumoto T, Ebata J, Tachibana H et al (1999) Transmural microcirculatory blood flow distribution in right and left ventricular free walls of rabbits. Am J Physiol 277:H183–H191
5. Parker MM, Shelhamer JH, Bacharach SL et al (1984) Profound but reversible myocardial depression in patients with septic shock. Ann Intern Med 100:483–490
6. Parker MM, Shelhamer JH, Natanson C et al (1987) Serial cardiovascular variables in survivors and nonsurvivors of human septic shock: heart rate as an early predictor of prognosis. Crit Care Med 15:923–929
7. Rossi MA, Santos CS (2003) Sepsis-related microvascular myocardial damage with giant cell inflammation and calcification. Virchows Arch 443:87–92
8. Waisbren BA (1951) Bacteremia due to gram-negative bacilli other than the Salmonella; a clinical and therapeutic study. AMA Arch Inter Med 88:467–488
9. Wong ML, O'Kirwan F, Khan N et al (2003) Identification, characterization, and gene expression profiling of endotoxin-induced myocarditis. Proc Natl Acad Sci U S A 100:14241–14246

Virchows Arch (2005) 447: 879–882
DOI 10.1007/s00428-005-0027-y

CASE REPORT

E. Arzu Saglam · Alp Usubütün · Cavit Kart ·
Ali Ayhan · Türkan Küçükali

Reactive nodular fibrous pseudotumor involving the pelvic and abdominal cavity: a case report and review of literature

Received: 24 April 2005 / Accepted: 10 June 2005 / Published online: 14 July 2005
© Springer-Verlag 2005

Abstract There are several entities that can present with multiple nodular lesions within the peritoneal cavity, such as "disseminated peritoneal leiomyomatosis," "peritoneal fibrosis," "calcifying fibrous pseudotumor," and the recently described lesion of "reactive nodular fibrous pseudotumor of the gastrointestinal tract and mesentery." Here we present one such lesion in a 28-year-old woman with a history of dysmenorrhea and ergotamine use for migraine attacks. Intraoperative exploration of our patient disclosed numerous nodules located throughout the pelvic and abdominal peritoneum. Histopathologically, these lesions were fibrocollagenous nodules composed of sparse wavy spindle cells within hyalinized "keloid-like" collagen surrounded by an inflammatory infiltrate. Some of the nodules were associated with small foci of endometriosis. We believe this lesion is best described by the term "reactive nodular fibrous pseudotumor" and that endometriosis and the use of ergotamine derivatives may be contributing factors.

Keywords Reactive nodular fibrous pseudotumor · Peritonitis · Endometriosis · Ergotamine · Disseminated peritoneal leiomyomatosis

Introduction

An incidental finding of multiple nodular lesions within the peritoneal cavity can be alarming. There are several entities that can present with this appearance, and it is reassuring to know that some are benign and indolent. Here we present one such lesion in a young woman, which we believe is of a reactive nature and best described by the term "reactive nodular fibrous pseudotumor" used by Yantiss et al. [9].

E. A. Saglam · A. Usubütün (✉) · T. Küçükali
Department of Pathology,
Hacettepe University Medical School, Sihhiye,
Ankara, 06100, Turkey
e-mail: usubutun@ato.org.tr
Tel.: +90-312-3051563

C. Kart · A. Ayhan
Department of Gynaecology and Obstetrics,
Division of Gynaecologic Oncology,
Hacettepe University Medical School, Sihhiye,
Ankara, 06100, Turkey

Clinical history

A 28-year-old woman presented with a gradual onset of abdominal pain that had been present for 3 months. Preoperative examination revealed bilateral cystic lesions in the ovaries, which were thought to be consistent with endometrioma on pelvic ultrasonography. Her previous medical history was significant for severe dysmenorrhea that accompanied every cycle ever since her teens and migraine attacks for which she has occasionally been using ergotamine as well as paroxetine and betahystine derivatives.

Intraoperative exploration disclosed numerous firm, tan-to-white, circumscribed nodules ranging from a few millimeters to 6 cm in diameter. These nodules were present on the surface of the ovaries and appendix, the bowel mesentery, the abdominal peritoneal wall, and the omentum. Frozen section analysis was performed and reported as being consistent with disseminated peritoneal leiomyomatosis (DPL). Debulking of the nodules followed.

Materials and methods

Specimens were fixed in 10% formalin, sectioned, and stained with routine hematoxylin and eosin (H&E). Immunohistochemistry was carried out against cytokeratin (CK- 1/100 Novacastra, Newcastle, UK), smooth muscle actin (1/1000, Neomarkers, Fremont, CA), S100 (1/1000 Neomarkers), CD34 (1/1000 Neomarkers), vimentin (1/5000 Neomarkers), desmin (1/150 Neomarkers), H-caldesmon (1/250 Neomarkers), estrogen receptor (1/100 Neomarkers), and progesterone receptor (1/450 Neomarkers) using the avidin–biotin peroxidase method.



Fig. 1 Macroscopy of the surgical specimen demonstrating numerous tan-to-white nodules of varying sizes within fibroadipose tissue

Results

The surgical specimen consisted of an omental segment, the appendix, and cystectomy specimen from the ovaries and several independent adipose tissue fragments containing circumscribed, lobulated, rubbery-to-hard, white-to-tan nodules ranging from 0.6 to 6 cm (Fig. 1). The cut surface of the nodular lesions was solid and homogeneous. The typical whorled cut surface of a leiomyoma could not be discerned. Similar nodular masses were removed from the ovary and surrounded the tip of the appendectomy specimen.

Histopathological examination largely demonstrated fibrocollagenous nodules composed of sparse wavy spindle cells within hyalinized keloid-like collagen (Fig. 2). Interestingly some of these nodules contained a somewhat-more-cellular peripheral zone composed of active fibroblasts. Most of the nodules were surrounded by an inflammatory infiltrate with abundant mononuclear lymphoid cells and scattered foreign-body giant cells. In addition to these changes, the omentum displayed signs of peritonitis. The

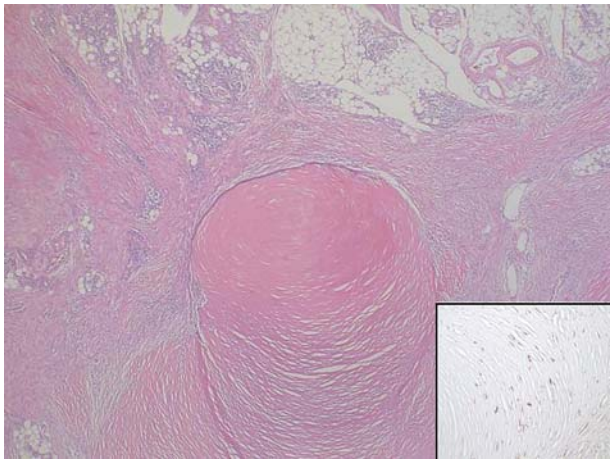


Fig. 2 Fibrous nodule with keloid-like central collagen composed of sparse spindle cells surrounded by a mononuclear inflammatory infiltrate at the very edge (H & E stain). *Inset* shows cytokeratin positivity

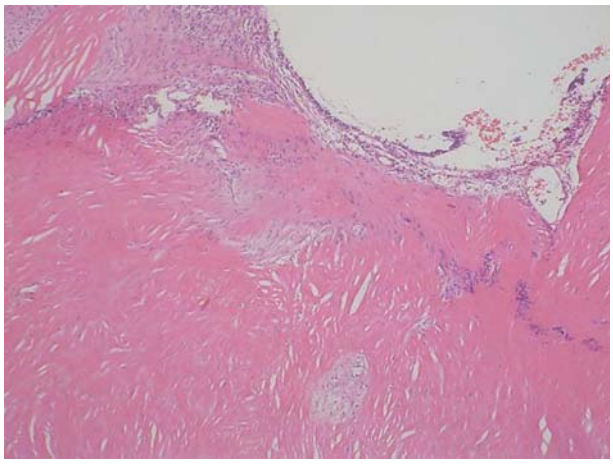


Fig. 3 Foci of endometriosis (*top left*), neighboring one of the fibrous nodules (H & E stain)

cystectomy specimen from the ovary showed endometriosis, and sparse foci of endometriosis were identified within the nodular mass removed from the contralateral ovary (Fig. 3). A nodular fibrous lesion surrounded the appendix, encased its tip, and infiltrated the appendiceal wall, almost to the mucosa in one of the sections (Fig. 4).

Immunohistochemically, the sparse spindle cells composing these nodules were positive with vimentin, CD34, CK (Fig. 2, inset), and smooth muscle actin and, focally, with estrogen and progesterone receptors. They were negative for S100, desmin, and H-caldesmon.

Discussion

The lesion presented, with its low cellularity, prominent hyalinization and lack of atypia and mitoses, and accompanying peritonitis, which we believe is of a reactive nature. Its macroscopical appearance is similar to the benign entity of disseminated peritoneal leiomyomatosis, which is commonly associated with an altered hormonal milieu such

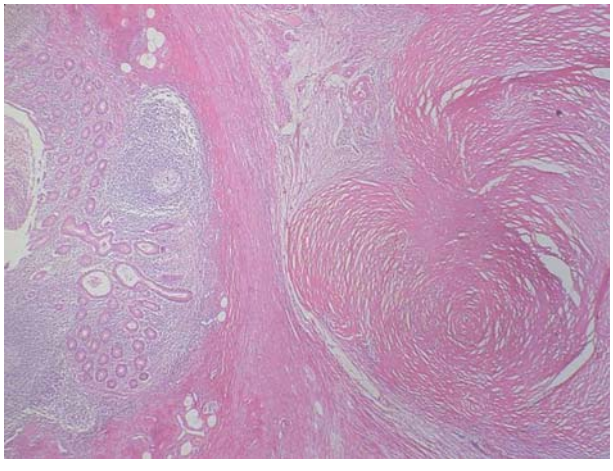


Fig. 4 Fibrous nodules within the appendix wall, close to the mucosa (H & E stain)

as pregnancy [10]. The microscopic characteristics and the size of the nodules in our case argue against DPL but do not exclude it, considering that there are reports of DPL with larger nodules and that leiomyomas can show extreme hyalinization.

If not for the mass lesions, our findings would have been consistent with sclerosing peritonitis, which is a reactive fibrous proliferation resulting in diffuse fibrous thickening of the peritoneum [4]. This lesion can be seen in patients with ascites, cirrhosis, peritoneal dialysis, familial Mediterranean fever, peritoneovenous shunts, and endometriosis [4] and is thought to be associated with chronic irritation of the peritoneum. It is also reported to occur in association with luteinized thecomas, which was not the case with our patient [2]. Nodular lesions referred to as "peritoneal fibrous nodules" by Clement are also characterized by spindle cells believed to derive from the metaplasia of multipotential subserosal cells and are associated with pelvic inflammatory disease and surgical procedures [3]. Desmoid tumor, a myofibroblastic neoplasm of the abdominal wall, also enters the differential diagnosis; however, these lesions are usually ill defined and not nodular, and the accompanying inflammatory infiltrate is not that prominent.

One other similar lesion is the recently described entity of "reactive nodular fibrous pseudotumor (RNFP) of the gastrointestinal tract and mesentery." This entity was first described in a series by Yantiss et al. [9], which was followed by two other case reports by Zardawi et al. [11] and Chatelain et al. [1] and a series of eight cases by Daum et al. [5]. This lesion, like those in our case, is characterized by nodular fibrous pseudotumors composed of scattered fibroblastic spindle cells with a hyalinized collagenous background. The lesions are believed to be reactive and are associated with previous surgery. Immunohistochemically the spindle cells can express vimentin, smooth muscle actin, CD117, and CK. The spindle cells have recently been suggested to be derived from multipotential subserosal cells based on their CK expression [5].

"Calcifying fibrous pseudotumor," a benign soft tissue lesion that is also known to present in similar locations, can also be considered in the differential diagnosis [7]. It is also characterized by a hypocellular spindle cell proliferation (displaying CD34 positivity) within dense collagen, accompanied by dystrophic calcification. Our case could be a noncalcifying variant of this entity or one that has not calcified just yet.

We believe the macroscopic and histopathologic features of our case most closely resemble the RNFP. Indeed, involvement of the mesentery, appendix, and the rest of the gastrointestinal tract represented only a small component of the lesion, and thus it is conceivable that RNFP is not limited to the mesentery. All the differential diagnostic lesions we have discussed are similar in nature and represent reactive fibrous proliferations, most probably in response to various conditions that irritate the peritoneum, and seem to be derived from multipotential subserosal cells. Our case likely represents a variant of the RNFP with more extensive involvement of the peritoneal cavity.

Our patient does not have any of the predisposing conditions described for the cases of RNFP such as previous surgery or inflammatory disorders. However, she did have accompanying endometriosis, which considering her long history of dysmenorrhea probably has been present for quite some time and is a predisposing factor for the other similar entities that we have discussed. It is known that endometriotic foci can be associated with severe fibrosis and end-stage endometriotic lesions can be predominantly composed of fibromuscular tissue rather than endometriotic tissue [6]. Her previous history is also significant for migraine therapy with ergotamine. Ergot derivatives are known to induce fibrosis, most commonly retroperitoneal fibrosis, but are also associated with pleuropulmonary and pericardial fibrosis and cardiac valve damage [8]. The association of our findings with ergotamine use is therefore also a possibility, either on its own or as a contributory factor.

We have described a case characterized by numerous fibrocollagenous nodules, involving the peritoneum of the abdominal and pelvic cavities. Similar lesions have previously been described with names such as "peritoneal fibrous nodules," "calcifying fibrous pseudotumor," and "reactive nodular fibrous pseudotumor of the gastrointestinal tract and mesentery," all of which seem to represent reactive lesions possibly derived from multipotential subserosal cells. Although initially described involving the gastrointestinal tract, we believe the term "reactive nodular fibrous pseudotumor" best characterizes our case, a reactive lesion possibly secondary to endometriosis and/or ergotamine use.

References

1. Chatelain D, Manaouil D, Levy P, Joly JP, Sevestre H, Regimbeau JM (2004) Reactive nodular fibrous pseudotumor of the gastrointestinal tract and mesentery. Am J Surg Pathol 28:416
2. Clement PB, Young RH, Hanna W, Scully RE (1994) Sclerosing peritonitis associated with luteinized thecomas of the ovary. A clinicopathological analysis of six cases. Am J Surg Pathol 18:1–13
3. Clement PB (1995) Reactive tumor-like lesions of the peritoneum. Am J Clin Pathol 103:673–676
4. Clement PB (2002) Diseases of the peritoneum. In: Kurman RJ (ed) Blaustein's pathology of the female genital tract. Springer, Berlin Heidelberg New York, pp 731–732
5. Daum O, Vanecek T, Sima R, Curik R, Zamecnik M, Yamanaka S, Mukensnabl P, Benes Z, Michal M (2004) Reactive nodular fibrous pseudotumors of the gastrointestinal tract: a report of 8 cases. Int J Surg Pathol 12:365–374
6. Itoga T, Matsumoto T, Takeuchi H, Yamasaki S, Sasahara N, Hoshi T, Kinoshita K (2003) Fibrosis and smooth muscle metaplasia in rectovaginal endometriosis. Pathol Int 53:371–375
7. Nascimento AF, Ruiz R, Hornick JL, Fletcher CD (2002) Calcifying fibrous "pseudotumor": clinicopathologic study of 15 cases and analysis of its relationship to inflammatory myofibroblastic tumor. Int J Surg Pathol 10:189–196

8. Robert M, Derbaudrenghien JP, Blampain JP, Lamy F, Meyer P (1984) Fibrotic processes associated with long-term ergotamine therapy. N Engl J Med 311:601–602
9. Yantiss RK, Nielsen GP, Lauwers GY, Rosenberg AE (2003) Reactive nodular fibrous pseudotumor of the gastrointestinal tract and mesentery: a clinicopathologic study of five cases. Am J Surg Pathol 27:532–540
10. Zaloudek C, Hendrickson MR (2002) Mesenchymal tumors of the uterus. In: Kurman RJ (ed) Blaustein's pathology of the female genital tract. Springer, Berlin Heidelberg New York, pp 577–578
11. Zardawi IM, Catterall N, Cox SA (2004) Reactive nodular fibrous pseudotumor of the gastrointestinal tract and mesentery. Am J Surg Pathol 28:276–277

Virchows Arch (2005) 447: 883–887
DOI 10.1007/s00428-005-0030-3

CASE REPORT

Oluwole Fadare · Wenxin Zheng

Well-differentiated papillary villoglandular adenocarcinoma of the uterine cervix with a focal high-grade component: is there a need for reassessment?

Received: 10 March 2005 / Accepted: 10 June 2005 / Published online: 9 August 2005
© Springer-Verlag 2005

Abstract Well-differentiated villoglandular adenocarcinoma of the uterine cervix is characterized by an exophytic growth pattern with variably sized papillae that are lined by stratified columnar cells with no more than moderate cytologic atypia. Based on the favorable outcomes in most of the previously reported cases, it has been suggested that some patients with this subtype may be managed conservatively. The case described herein is an otherwise prototypical well-differentiated villoglandular adenocarcinoma but which was associated with a 4.9-mm focus of poorly differentiated carcinoma at its invasive edge. A review of the literature revealed a variety of findings that suggests a need to reassess the potential morphologic and biologic spectrum of this group of tumors. Five of the approximately 89 reported cases were associated with a higher-grade component of the same or a different histologic subtype. At least one patient with apparently stage 1A1 disease was found to have a positive lymph node. Another patient with stage 1B1 disease but no stromal invasion died of her disease following multiple recurrences. Finally, the frequency of lymphovascular invasion and/or lymph node involvement in recent series far exceeds what was found in the two original series. Our case suggests that well-differentiated villoglandular adenocarcinoma is not a diagnosis that should be unequivocally rendered on a small biopsy since other components may be present and the patients may be undertreated. We urge caution when conservative management (cone biopsy alone when margins are negative and there is no lymphovascular invasion) is offered to patients with this tumor since knowledge about its true biologic spectrum appears to still be in evolution.

Keywords Villoglandular · Cervix · Adenocarcinoma

O. Fadare · W. Zheng
Department of Pathology,
Yale University School of Medicine,
New Haven, CT 06504, USA

O. Fadare (✉)
Women's Health Program,
Department of Pathology, EP 2-631,
Yale University School of Medicine
and Yale-New Haven Hospital,
20 York Street,
New Haven, CT 06504, USA
e-mail: oluwolefadare@yahoo.com
Tel.: +1-203-7852788
Fax: +1-203-7857146

Introduction

Although cases fitting its basic description had undoubtedly been described previously, well-differentiated villoglandular adenocarcinoma of the uterine cervix (WDVGA) attained widespread acceptance as a distinct clinicopathologic entity following a report of 13 cases by Young and Scully [15] in 1989. Compared to other types of cervical adenocarcinoma, WDVGA is most prevalent at a younger age group, with an average age of 33–37 years in two series [8, 15]. Characteristic morphologic features include an exophytic surface villoglandular papillary component that is usually thin but which may be broad, stromal cores in papillae, and a lining by endocervical, endometrioid, or intestinal-type cells showing no more than mild to moderate cytologic atypia [2–5, 7–10, 12–15]. The underlying etiopathogenesis of this tumor remains to be elucidated. A disproportionately high proportion of patients in whom this tumor was diagnosed were noted to have previously been taking oral contraceptives [8], although the precise nature of this association is currently unclear. Human papillomavirus (HPV), especially type 16, also appears to be directly involved in the pathogenesis of WDVGA [1]. WDVGA generally has an excellent prognosis, and conservative management for selected patients has been suggested [1, 2]. We describe herein a case of WDVGA, which may have important implications both for pathologists making this diagnosis and clinicians managing patients with this tumor.

Clinical history

A 47-year-old gravida 2 para 2 underwent an endometrial biopsy for persistent menorrhagia. Her past medical history was significant for use of oral contraceptives for approximately a 5-year period in her third decade. The biopsy showed an adenocarcinoma with a prominent villoglandular pattern (see below for description). However, due to the prominent endocervical type differentiation, we raised the possibility of a cervical primary tumor. The patient subsequently underwent a radical hysterectomy with bilateral salpingo-oophorectomy and pelvic/periaortic lymphadenectomies. The patient has no evidence of tumor recurrence or metastases 4.5 months after her surgery.

Pathologic findings

Within the uppermost portion of the endocervix and focally extending into the lower uterine segment, a tan-gray, mucoid, and friable mass which measured 3.5×3.0 cm was identified. The microscopic appearance of 95% of the tumor and the biopsy were identical: thin, slender papillae with stromal cores lined by endocervical-type epithelium with moderate nuclear stratification and only mild cytologic atypia (Figs. 1, 2). Some cells showed overt mucinous differentiation, whereas others showed abundant eosinophilic cytoplasmic as typically seen in endocervical adenocarcinoma of the usual type (Fig. 3). Mitotic figures were sparse (three mitoses/10 high-power fields), and stromal invasion was a maximum of 20% of the cervical wall thickness in these regions (2 mm/10 mm). However, in one section, the tumor had a distinctly different appearance: this focus measured 4.9 mm in diameter and was at the advancing edge of invasion in this region (Fig. 4). Effectively, this area showed the highest area of stromal invasion (60% of the cervical wall thickness). This focus was characterized by highly pleomorphic tumoral cells showing a high nuclear/cytoplasmic ratio, nucleomegaly, and multinucleation (Fig. 5). Scattered cells in this nodule also showed cytoplasmic mucin. Mitotic activity was high (26/10 high-power field). Papillary formations were not present. Within this area was a 0.4-mm solid aggregate of cells, which, upon closer inspection, were composed of cells distended by cytoplasmic mucin, resulting in a signet-ring-like appearance (Fig. 6). No lymphovascular or perineural invasion was present, and the lymph nodes showed no tumor involvement. Overall, the tumor was assigned an International Federation of Gynecology and Obstetrics (FIGO) stage of 1B1.

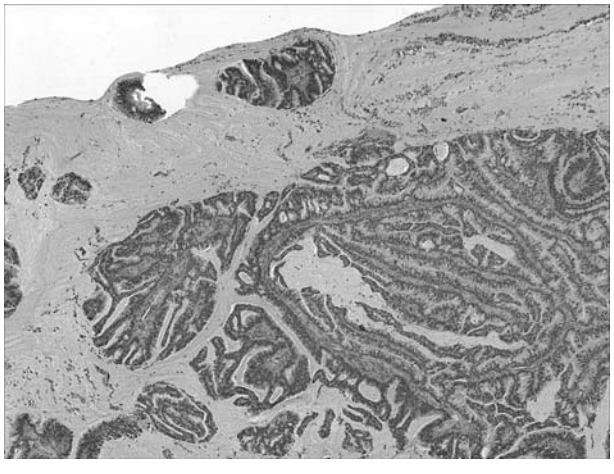


Fig. 1 Well-differentiated villoglandular adenocarcinoma with long slender papillae. Cytoplasmic differences between some of the cells in this figure and in Fig. 2 are evident even at low magnification (hematoxylin and eosin, original magnification, 60×)

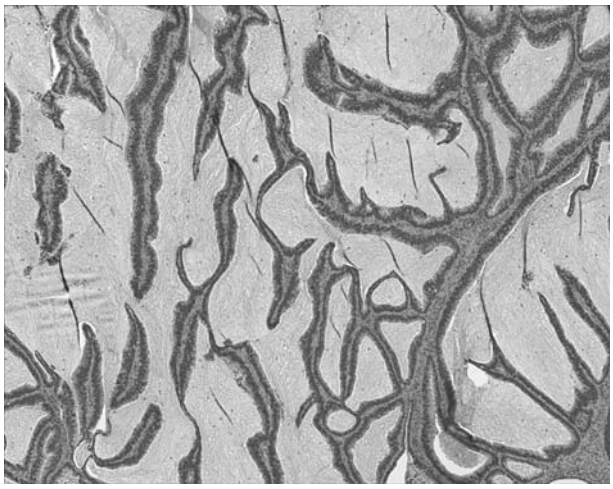


Fig. 2 Well-differentiated villoglandular adenocarcinoma with long slender papillae. Cytoplasmic differences between some of the cells in this figure and in Fig. 1 are evident even at low magnification (hematoxylin and eosin, original magnification, 60×)

Discussion

In the two original series of WDVGA, none of a total of 37 patients experienced any disease progression following their primary treatments, with follow-up ranging from 7 months to 14 years [8, 15]. For comparison, recent data from the Surveillance, Epidemiology, and End Results program (1976–1995) indicated that the 5-year survival rates for American whites <50 years old with cervical adenocarcinoma ranged from 82.5 to 88% [11]. These two series included six patients who were treated by cone biopsy alone [8, 15]. This favorable prognosis, in conjunction with the young ages of the patients in which these tumors are typically diagnosed, caused the authors of both series to suggest that carefully chosen patients wishing to preserve their fertility may be managed by cone biopsy alone [8, 15]. Young and Scully [15] outlined strict criteria that defined the clinicopathologic circumstances under which conservative management may be considered: (1) the tumor has to be superficial; (2) margins of the excision are negative for tumor; (3) there is no vascular space invasion; and (4) close follow-up examination is feasible. Since those two original reports, at least 52 additional cases have been reported, some with a variety of clinicopathologic findings that suggest a need to reassess the potential

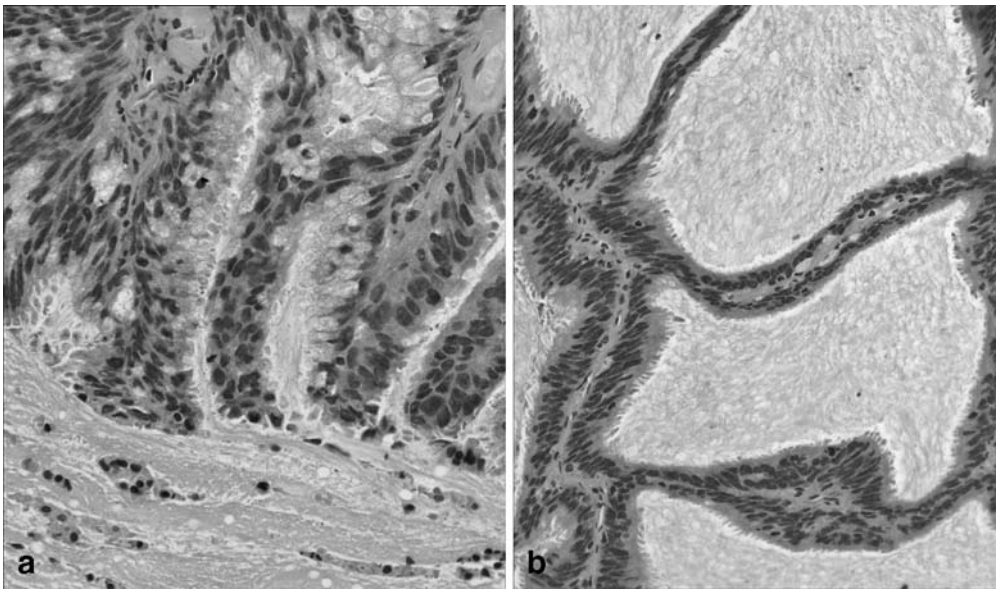


Fig. 3 Higher-power view of Fig. 1 (**a**, *left panel*) and Fig. 2 (**b**, *right panel*). In some areas of the tumor, the cells showed overt mucinous differentiation (**a**), whereas others showed abundant eosinophilic cytoplasmic as typically seen in endocervical adenocarcinoma of the usual type (**b**) (hematoxylin and eosin, original magnification, 200×)

morphologic and biologic spectrum of this group of tumors. It should be noted that the vast majority of these reported patients, irrespective of these findings, have had a favorable outcome. However, whether this is because the tumors are well differentiated and/or that approximately 94% of the tumors [5] are present at stage I (perhaps related to their being exophytic masses that are most likely detected on screening modalities or cause symptomatology) is unclear.

The current case as well as 5 of the other 89 reported cases revealed in the resection specimens histologic findings that were distinct from the main WDVGA. These cases suggest that WDVGA is not a diagnosis that should be unequivocally rendered on a small biopsy since other components may be present and the patients may be undermanaged [14]. Stanley-Christian et al. [12] described a patient in which the biopsy showed WDVGA, but the hysterectomy specimen showed moderately differentiated endocervical adenocarcinoma. Similarly, Bouman et al. [2] described a patient in which the biopsy showed WDVGA, but the hysterectomy specimen showed, in addition to the WDVGA, an infiltrating moderately differentiated papillary adenocarcinoma. Those authors also described a case in which the hysterectomy specimen showed a "well-differentiated infiltrating component with a rather abundant squamous component" [2]. WDVGA was found in coexistence with an invasive squamous cell carcinoma in a cone biopsy in another case [3]. Finally, Kaku et al. [9], in one of their series of seven cases, described a patient with a tumor, 90% of which was a WDVGA and the residual of which was a small cell nonkeratinizing squamous cell carcinoma. Interestingly, another case of a predominantly papillary serous adenocarcinoma of the cervix, which was admixed with a minor component of WDVGA, has also been described [6]. In our opinion, these cases, in addition to the present case, in which a high-grade component was

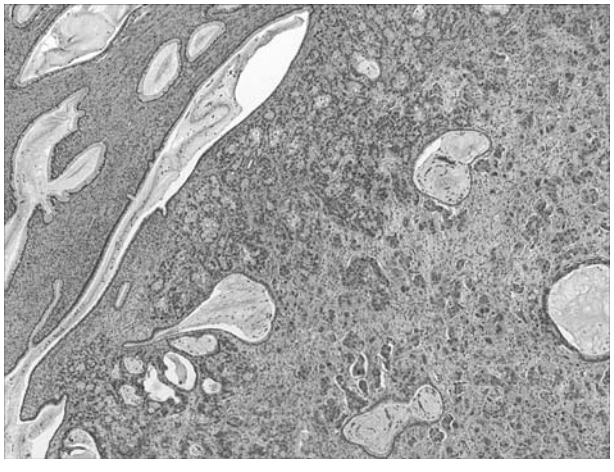


Fig. 4 The high-grade component was at the advancing edge of invasion and was not present in the biopsy. Note the benign glands in the area beneath the invasive edge (hematoxylin and eosin, original magnification, 100×)

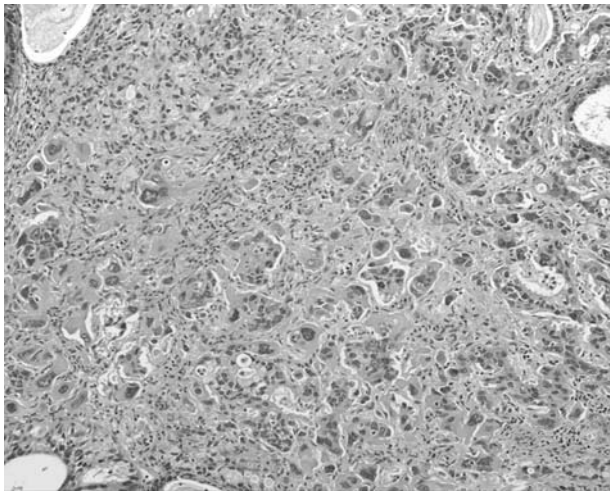


Fig. 5 The high-grade component is shown. Mitotic activity and cytologic pleomorphism is evident (hematoxylin and eosin, original magnification, 160×)

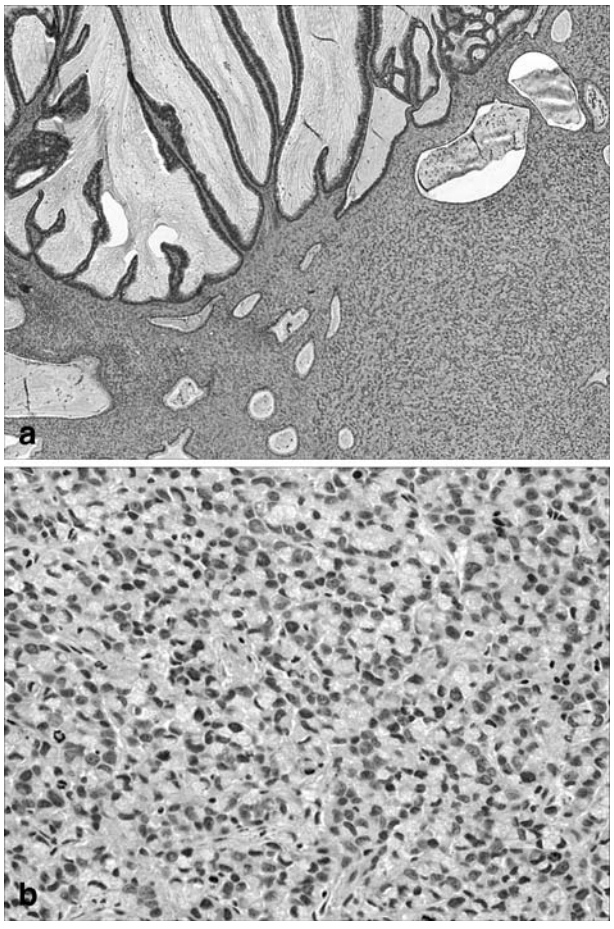


Fig. 6 A nodule of cells with a signet-ring-like appearance was also present within the high-grade nodule (hematoxylin and eosin, original magnification, 100×; *inset*, 200×)

identified at the base (advancing, invasive edge) of an otherwise prototypical WDVGA, bolster the aforementioned argument that WDVGA is not a diagnosis that should be rendered without equivocation on a small biopsy since other components may be present and the patients may be undermanaged. Young and Clement [14] have also expressed some concern about the potential undertreatment of these patients, and those authors have suggested that WDVGA should only be suggested on small biopsy material. Our case strongly bolsters that argument.

In the two original series on WDVGA, lymphovascular or lymph node involvement was not seen in all 37 cases [8, 15]. Recent reports [9, 10, 13], however, suggest a frequency of lymphovascular invasion and lymph node involvement which is not inconsequential. In the series of Khunamornpong et al. [10], lymphovascular invasion was present in 3 (20%) of 15 cases, 2 of which showed lymph node involvement. Kaku et al. [9] reported lymphovascular invasion in two (29%) of seven cases, both of which were associated with lymph node metastases and one of which was eventually fatal. In the recent report of Utsugi et al. [13], lymphovascular invasion was seen in 4 (31%) of 13 cases, one of which also had abundant lymph node metastases.

Parenthetically, it is perhaps prudent to reassess whether conservative management should be considered for WDVGA any more often that it is considered for other well-differentiated adenocarcinomas with the same histopathological parameters. As noted above, the vast majority of the reported cases of WDVGA have had favorable outcomes, although whether this is related to the early stage in which these tumors often present or the intrinsic biologic properties of these tumors is unclear. Using the criteria outlined above as a justification for conservative management, at least one patient with obturator lymph node metastases would have been missed [5]. Additionally, Dede et al. [4] recently described another patient with stage 1B1 WDVGA who was initially managed with a radical hysterectomy. There was no lymphovascular invasion and apparently no stromal invasion ("no invasion focus of atypical small gland in the wall of the cervix was noticed"). This patient would experience multiple pelvic recurrences over the ensuing 5 years and eventually died of her disease [4]. This is another patient who could have been managed with conservative treatment alone based on the above criteria.

The principal differential consideration for WDVGA is endocervical adenocarcinoma of the usual (i.e. endocervical) type, especially since the latter may show a prominent papillary pattern. Young and Clement [14] have recently reemphasized that tumors being designated WDVGA should have "no more than mild to moderate nuclear atypicality and scattered mitotic figures." Whether some of the cases being reported as WDVGA are better considered as other lesions is a matter of opinion. For example, in a recent report, the mean mitotic account in areas of typical WDVGA was reported as 43/10 high-power fields [13]. We concur with Young and Clement [14] that the term WDVGA should only be used for pure lesions, and the descriptive term used in the heading of the current case is being used only for the purposes of this report.

In summary, we have described herein an otherwise prototypical WDVGA but which was associated with a 4.9-mm focus of poorly differentiated carcinoma at its invasive edge. Our case, and others in the literature, suggests that WDVGA is not a diagnosis that should be unequivocally rendered on a small biopsy since other components may be present and the patients may be managed too conservatively. Additionally, the possibility of the coexistence of a high-grade component in WDVGA highlights the importance of adequate tumor sampling in these cases. Finally, caution is urged when conservative management is offered to patients with this tumor since knowledge about its true biologic spectrum appears to still be in evolution.

References

1. An HJ, Kim KR, Kim IS, Kim DW, Park MH, Park IA, Suh KS, Seo EJ, Sung SH, Sohn JH, Yoon HK, Chang ED, Cho HI, Han JY, Hong SR, Ahn GH (2005) Prevalence of human papillomavirus DNA in various histological subtypes of cervical adenocarcinoma: a population-based study. Mod Path 18: 528–534

2. Bouman A, Oosterhuis GJ, Naudin ten Cate L, van Doorn GA (1999) Villoglandular papillary adenocarcinoma of the cervix. Beware of a wolf in sheep's clothing. Eur J Obstet Gynecol Reprod Biol 87(2):183–189
3. Collinet P, Prolongeau JF, Vaneecloo S (1999) Villoglandular papillary adenocarcinoma of the uterine cervix. Eur J Obstet Gynecol Reprod Biol 86:101–103
4. Dede M, Deveci G, Deveci MS, Yenen MC, Goktolga U, Dilek S, Gunhan O (2004) Villoglandular papillary adenocarcinoma of the uterine cervix in a pregnant woman: a case report and review of literature. Tohoku J Exp Med 202:305–310
5. Garcea A, Nunns D, Ireland D, Brown L (2003) A case of villoglandular papillary adenocarcinoma of the cervix with lymph node metastasis. BJOG 110:627–629
6. Gilks CB, Clement PB (1992) Papillary serous adenocarcinoma of the uterine cervix: a report of three cases. Mod Path 5:426–431
7. Hopson L, Jones MA, Boyce CR, Tarraza HM Jr (1990) Papillary villoglandular carcinoma of the cervix. Gynecol Oncol 39:221–224
8. Jones MW, Silverberg SG, Kurman RJ (1993) Well-differentiated villoglandular adenocarcinoma of the uterine cervix: a clinicopathological study of 24 cases. Int J Gynecol Pathol 12:1–7
9. Kaku T, Kamura T, Shigematsu T, Sakai K, Nakanami N, Uehira K, Amada S, Kobayashi H, Saito T, Nakano H (1997) Adenocarcinoma of the uterine cervix with predominantly villoglandular papillary growth pattern. Gynecol Oncol 64:147–152
10. Khunamornpong S, Maleemonkol S, Siriaunkgul S, Pantusart A (2001) Well-differentiated villoglandular adenocarcinoma of the uterine cervix: a report of 15 cases including two with lymph node metastasis. J Med Assoc Thail 84:882–888
11. Sherman ME, Wang SS, Carreon J, Devesa SS (2005) Mortality trends for cervical squamous and adenocarcinoma in the United States. Cancer 3(103):1258–1264
12. Stanley-Christian H, Heim BK, Hines JF, Hall KL, Willett GD, Barnes WA (1997) Villoglandular adenocarcinoma of the cervix: a report of three cases and review of the literature. Gynecol Oncol 66:327–330
13. Utsugi K, Shimizu Y, Akiyama F, Umezawa S, Hasumi K (2004) Clinicopathologic features of villoglandular papillary adenocarcinoma of the uterine cervix. Gynecol Oncol 92:64–70
14. Young RH, Clement PB (2002) Endocervical adenocarcinoma and its variants: their morphology and differential diagnosis. Histopathology 41:185–207
15. Young RH, Scully RE (1989) Villoglandular papillary adenocarcinoma of the uterine cervix. A clinicopathologic analysis of 13 cases. Cancer 63:1773–1779

Virchows Arch (2005) 447: 888–891
DOI 10.1007/s00428-005-0034-z

CASE REPORT

Itsuko Nakamichi · Tetsuya Takakuwa · Yoshiro Tanio · Keiji Iuchi · Katsuyuki Aozasa

Pyothorax-associated lymphoma: an unusual case with both T- and B-cell genotypes

Received: 13 March 2005 / Accepted: 19 June 2005 / Published online: 14 July 2005
© Springer-Verlag 2005

Abstract Pyothorax-associated lymphoma (PAL) is a B-cell lymphoma which develops in the pleural cavity of patients with an over-20-year history of pyothorax. Aberrant expression of surface antigens is occassional in PAL, although genotype is not fully investigated. We report here a PAL with dual genotype, i.e., simultaneous immunoglobin (Ig) and T-cell receptor (TcR) gene rearrangement. An 82-year-old woman with pain on the left side of the chest was admitted. She had been suffering from pyothorax after artificial pneumothorax for treatment of tuberculosis of the pulmonary when she was 18 years old. The mass that was confined to the left pleural cavity affected by pyothorax was biopsied and histologically diagnosed as diffuse large cell lymphoma. The tumor cells were positive for CD20, CD16, and TIA-1 but negative for CD79a, CD45RO, CD43, CD3, and CD56. Surface antigen expression was further investigated in cultured cells, showing that the cultured cells did not express representative B-cell markers, except for CD20, as well as T-cell markers, but were positive for CD16, CD30, and CD103. Southern blotting revealed the monoclonally rearranged bands of both Ig heavy chain and TcR gene. The patients died of tumors 14 months after admission. Aberrant genotype and immunophenotype of PAL cells is discussed in reviewing the pertinent literature.

I. Nakamichi · T. Takakuwa (✉) · K. Aozasa
Department of Pathology (C3),
Osaka University Medical School,
2-2 Yamada-oka,
Suita, Osaka, 565-0871, Japan
e-mail: takakuwa@molpath.med.osaka-u.ac.jp
Tel.: +81-6-68793711
Fax: +81-6-68793719

Y. Tanio
Osaka General Medical Center,
Osaka, 558-8558, Japan

K. Iuchi
Department of Surgery,
National Kinki-Chuo Hospital,
Sakai, 591-8025, Japan

Keywords Pyothorax-associated lymphoma · Epstein–Barr virus · Immunophenotype · Immunogenotype

Introduction

Malignant lymphoma frequently develops in the pleural cavity of patients with an over-20-year history of pyothorax [5]. The term pyothorax-associated lymphoma (PAL) has been proposed by Dr. Aozasa for this type of tumor, and it is now listed as a distinct disease entity in the recent World Health Organization Classification of tumors [2]. Recent large-scale study on PAL showed that patients have an over-20-year history of pyothorax resulting from artificial pneumothorax for treatment of pulmonary tuberculosis or tuberculosis pleuritis and frequently present with chest and/or back pain and fever [7]. PAL histologically shows a diffuse proliferation of large-size B cells [diffuse large B-cell lymphoma (DLBCL)] with a strong association with Epstein–Barr virus (EBV) infection. PAL is unique not only in its clinical presentation but also in its gene expression profile, i.e., distinct from DLBCL of nodal origin [8].

Lymphomatous presentation in the pleural cavity fall into two subtypes; PAL showing mass formation in the pleural cavities and is human herpes virus 8 (HHV-8)-negative, and primary effusion lymphoma (PEL) showing pleural effusion without identifiable mass formation and is HHV-8-positive. Both types of lymphomas are usually EBV-positive. PEL is also a neoplasm of large B cells, usually occurring in the setting of immunodeficiency caused by human immunodeficiency virus (HIV) infection. Most PEL patients are young-to-middle-aged homosexual males.

Expression pattern of cell surface marker in PAL is unique. Typically, lymphoma cells are positive for CD79a and CD20. A number of cases may express at least one T-cell marker (CD2, CD3, CD4, and/or CD7), most frequently with B/T phenotype aberrant dual B/T phenotype in clinical cases [8]. Simultaneous expression of CD2 and CD20 in the cell lines derived from PAL were also

reported [3, 9]. We describe here a first case of PAL showing dual lineage at the genetic level.

Case report

An 82-year-old woman was admitted to Osaka General Medical Center with pain on the left side of the chest. She had suffered from pulmonary tuberculosis in the left lung and received an artificial pneumothorax when she was 18 years old. Computed tomographic (CT) scan revealed the mass to be confined to the left pleural cavity affected by pyothorax. Aspiration biopsy was performed, and it was diagnosed as malignant lymphoma, with no other specifications. Radiographic examination including abdominal CT, brain magnetic resonance imaging, and Gallium scintigraphy, together with bone marrow biopsy, did not reveal any metastatic lesions, whereas bone scintigraphy demonstrated increased uptake in the eighth to tenth left ribs, which was regarded as the secondary involvement of PAL because of the absence of osteoclastic and/or osteoplastic changes as revealed by CT scan. In addition, the previous study shows that lymphomas usually develop in the pleural tissue but not the bone tissue.

The patient was treated with two courses of chemotherapy (cyclophosphamide, doxorubicin, vincristine, and prednisolone) combined with 50 Gy of radiation therapy. Because the combined therapy was not effective, additional radiation therapy of 40 Gy was added. However, metastatic tumors appeared in the right lung. She suffered from nausea. Then endoscopic examination of upper digestive tracts was performed, revealing well-differentiated adenocarcinoma in the stomach. The patient died 14 months after admission. Autopsy was not performed.

Methods

Small specimens obtained from the PAL lesions by aspiration biopsy were subjected to immunohistochemistry as well as primary cultures. Culture (5×10^6 cells/ml) was started in RPMI 1640 supplemented with 20% heat-inactivated FCS at 37°C in 5% CO_2 in air. Growing cells were collected and subjected to morphological analysis, immunohistochemistry, in situ hybridization for detection of EBER-1 transcript of EBV, flow cytometric analysis, and rearrangement of immunoglobulin heavy chain (IgH) and T-cell receptor gene (TcR).

Immunohistochemistry and in situ hybridization using histologic specimen

Immunophenotyping of the proliferating cells with B-, T-, and NK-cell differentiation antigens and EBV antigens was performed on the paraffin-embedded sections from the original tumor specimens using avidin–biotin–peroxidase complex method. The antibodies used were anti-CD20 (Kyowa Medex, Tokyo, Japan), CD79a, CD3 epsilon, CD45RO (UCHL-1), latent membrane protein (LMP)-1 (CS1-4), EB nuclear antigen (EBNA)-2 (PE2) (Dakopatts, Glostrup, Denmark), CD43 (MT-1)(Bioscience, Emmenbrucke, Switzerland), and CD56 (Novocastra, Newcastle, UK).

RNA in situ hybridization using EBER-1 probe was performed as previously described, with some modification. Briefly, 30-base oligonucleotide probes which were sense and anti-sense for a portion of the EBER-1 gene, a region of the EBV genome that is actively transcribed in latently infected cells, were synthesized using a DNA synthesizer. As a positive control, the Raji cell line was used. As negative controls, the hybridizing mixture containing sense probe or antisense probe after RNase treatment was used.

Flow cytometric analysis using cultured cells

The cultured cells were analyzed by two-color immunofluorescence with a flow cytometer (EPICS XL, Beckman Coulter, Hialeah, FL, USA). Antibodies conjugated with fluorescein isothiocyanate (FITC) or phycoerythrin (PE) (Becton Dickinson, Franklin Lakes, NJ,USA) were used: they included anti-CD2, CD3, CD4, CD5, CD7, CD8, CD10, CD11c, CD15, CD16, CD19, CD20, CD21, CD23, CD24, CD25, CD30, CD34, CD38, CD56, CD103, surface

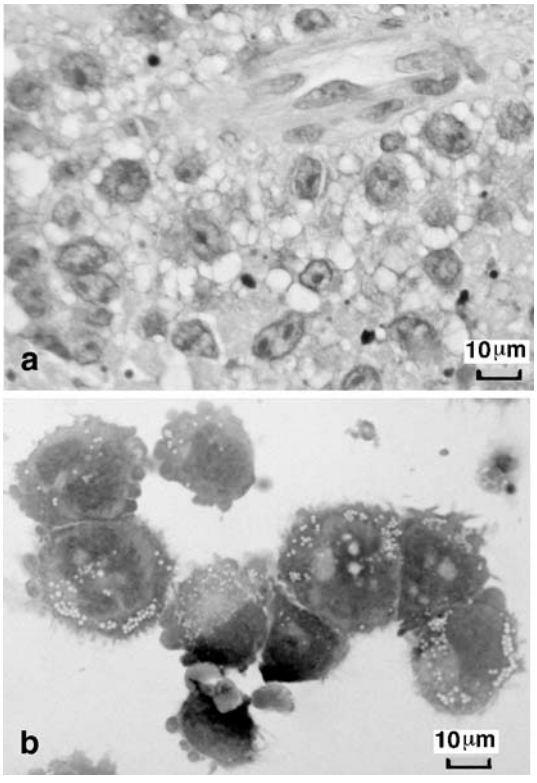


Fig. 1 **a** Microphotograph of biopsy specimen. There was a monomorphous proliferation of large lymphoid cells with one to two distinct nucleoli and massive necrotic areas. **b** Cultured cells were large round cells with occasional bizarre cells and proliferated as aggregates

Table 1 Surface markers of cultured cell

Marker	Percent	Marker	Percent
CD2	0.3	CD24	10.5
CD3	0.4	CD25	0.0
CD4	0.0	CD30	39.2
CD5	0.0	CD34	9.8
CD7	0.3	CD38	0.0
CD8	0.3	CD56	0.0
CD10	0.0	CD103	41.9
CD11c	9.1	SmIgM	0.0
CD15	0.2	SmIgD	25.4
CD16	73.4	SmIgK	0.3
CD19	0.0	SmIgL	0.3
CD20	71.4	CyIgL	1.5
CD21	0.0	CyIgK	1.2
CD23	7.3	HLA-DR	18.8

IgM (SmIgM), surface IgD (SmIgD), surface IgG kappa chain (SmIgK), surface IgG lambda chain (SmIgL), cytoplasmic IgG kappa chain (CyIgK), cytoplasmic IgG lambda chain (CyIgL), and HLA-DR.

Immunoglobulin heavy chain and T-cell receptor gene rearrangement analysis using cultures cell

Rearrangement of the IgH and TcR Cb1 and Jb1 genes was analyzed by Southern blotting. Ten micrograms of DNA were digested with appropriate restriction enzyme, electrophoresed in 0.7% agarose gels, and Southern blotted. The filters were hybridized with JH probe, CTb, and Jb1 probe, respectively. Hybridizations were visualized by a Fluorescein Gene Image System (Amersham, Buckinghamshire, UK) according to the manufacturer's instruction.

Results

The biopsy specimen contained a monomorphous proliferation of large lymphoid cells and massive necrotic areas (Fig. 1a). The large lymphoid cells had a round to oval nucleus, in which one to two nucleoli were evident. Mitotic figures were frequent. Immunohistochemical study (ABC method) on the paraffin sections revealed that the tumor cells were weakly positive for CD20 and CD16 but negative for CD79a, CD45RO (UCHL-1), CD43 (MT-1), CD3 epsilon, and CD56. Staining with TIA-1 antibody revealed numerous cytotoxic granules. In situ hybridization using EBER-1 probe revealed positive signals in the nucleus of tumor cells.

Biopsy samples contained inflammatory cells and necrotic areas. (Fig. 1a). Therefore, phenotyping was performed on the cultured PAL cells together with biopsy materials. At the culture, large round cells similar to the original tumors, with occasional bizarre forms, proliferated as clusters (Fig. 1b). Flow cytometric analysis revealed that the cultured cells did not express representative B-cell markers except for CD20 as well as T-cell markers, but positive for CD16, CD30, and CD103 (Table 1). Surface Ig expression was not detected. Southern blotting with the use of JH DNA probe and TcRJb1 probe demonstrated the monoclonally rearranged bands of IgH and TcR gene (Fig. 2).

In situ hybridization using EBER1 probe revealed positive signals in the nuclei of numerous cells (data not shown). LMP-1 and EBNA-2 expression was not detected in these cells by immunohistochemistry (data not shown).

Discussion

Previous gene rearrangement analysis on leukemia and lymphoma cases expressing dual-lineage antigens demon-

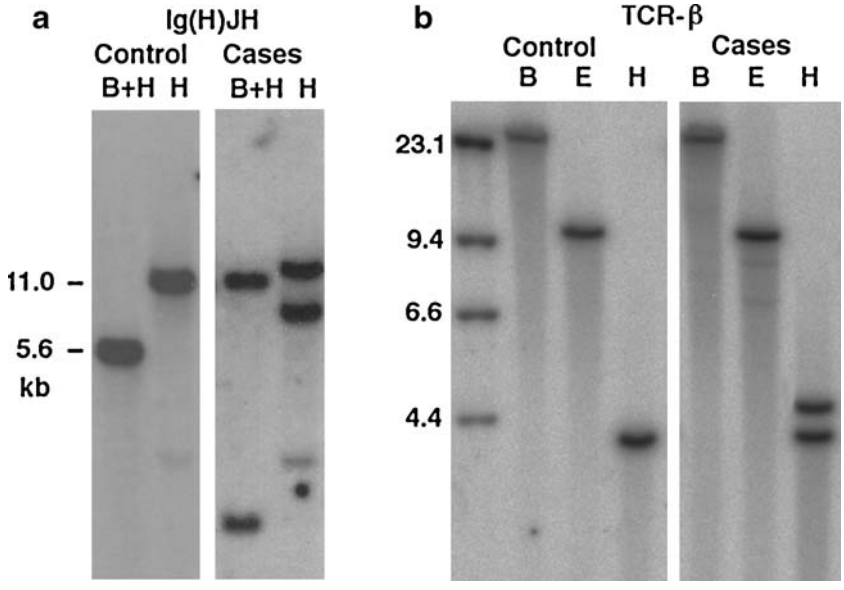


Fig. 2 Southern blot analysis of **a** IgH and **b** TcRJb1. Ten micrograms of DNA were digested with *Bam*HI+*Hin*dIII (*B*+*H*) and *Hin*dIII (*H*) or *Bam*HI (*B*) *Eco*RI (*E*), and *Hin*dIII (*H*), electrophoresed in 0.7% agarose gel, transferred to the nylon membrane, and hybridized with JH DNA probe or TcRJb1 DNA probe. Monoclonally rearranged bands for IgH and TcR were demonstrated in cultured cells

strated either B-cell or T-cell receptor rearrangement, germline configuration of both genes (null cell), or much less frequently, simultaneous Ig and TcR gene rearrangement (dual genotypes). Dual genotype has been described in up to 30% of cases of precursor lymphoid neoplasms, but this phenomenon occurs rarely in lymphomas with a mature phenotype [10]. Previously proposed explanation for dual-lineage antigen expression by leukemia/lymphoma cells are (1) derepression of masked genetic expression during neoplastic transformation, (2) transformation of stem cells committed to different pathways, and (3) neoplastic expansion of a population of normal cells that express both markers. Our previous study on hypermutation of IgH gene indicated that PAL is derived from B lymphocytes at the differentiation stage of the post germinal center [6]. Therefore, derepression of masked genetic expression during neoplastic transformation is likely in the present case.

Hollingsworth et al. [4] reported three lymphoma cases with dual phenotype arising in immunocompromised hosts and suggested that lymphomas arising in such a setting might more frequently show a deregulated differentiation than those arising in immunocompetent hosts. PAL develops mostly in patients with chronic pyothorax that resulted from lung tuberculosis. There might be some immune-deficient condition at the time of lung tuberculosis, but any findings indicative of presence of immune deficiency are not found in patients with pyothorax and PAL. Alternatively, PAL develops in the specific circumstance, i.e., an over-20-year history of chronic inflammation, where reactive oxygen species and cytokines are abundantly produced [7].

Expression pattern of cell surface markers in PAL is unique. CD79a is usually detected in a wider range of B-cell maturation than CD20. Therefore, lack of CD79a expression in the present PAL cells expressing CD20 is conspicuous. The tumor cells express CD20 but lack CD79a, whereas the opposite may be found in immature B-cell proliferations. A number of cases may express at least one T-cell marker (CD2, CD3, CD4, and/or CD7), most frequently with B/T phenotype [2]. Simultaneous expression of CD2 and CD20 in the cell lines derived from PAL was reported [3, 9]. The present case showed the dual rearrangement of both IgH and TcR genes and unusual immunophenotypes. Al Saati et al. [1] also reported a similar case with dual rearrangement, although they did not diagnose the case as PAL and sufficient clinical and pathologic data were not provided. Another interesting point in the present case is that the tumor cells expressed CD16 and contained cytotoxic granules in the cytoplasm. The CD16 is a 50- to 80-kDa glycoprotein that is expressed in two different isoforms. The transmembrane form is found on NK cells, macrophages, and mast cells. The transmembrane form plays a role in signal transduction, activation, and antibody-dependent cellular cytotoxicity. Taken together, dual rearrangement of both IgH and TcR gene and aberrant antigen expression are not uncommon in PAL.

Acknowledgements Supported by grants from the Ministry of Education, Science, Culture and Sports, Japan (14031213, 15026209, 15406013, 15590340, 16390105).

References

1. Al Saati T, Delecluze HJ, Chittal S, Brousset P, Magaud JP, Dastugue N, Cohen KE, Laurent G, Rubin B, Delsol G (1992) A novel human lymphoma cell line (Deglis) with dual B/T phenotype and gene rearrangements and containing Epstein–Barr virus genomes. Blood 80:209–216
2. Banks PM, Harris NL, Warnke RA, Gaulard P (2004) Lymphomas. In: Travis WD, Brambilla E, Mueller-Hermelink HK, Harris CC (eds) World Health Organization Classification of Tumors: pathology and genetics of tumors of the lung, pleura, thymus and heart. IARC, Lyon, pp 137–140
3. Daibata M, Taguchi T, Nemoto Y, Saito T, Machida H, Imai S, Miyoshi I, Taguchi H (2003) Epstein–Barr virus (EBV)-positive pyothorax-associated lymphoma (PAL): chromosomal integration of EBV in a novel CD2-positive PAL B-cell line. Br J Haematol 117:546–557
4. Hollingsworth HC, Stetler SM, Gagneten D, Kingma DW, Raffeld M, Jaffe ES (1994) Immunodeficiency-associated malignant lymphoma. Three cases showing genotypic evidence of both T- and B-cell lineages. Am J Surg Pathol 18:1092–1101
5. Iuchi K, Aozasa K, Yamamoto S, Mori T, Tajima K, Minato K, Mukai K, Komatsu H, Tagaki T, Kobashi Y et al (1989) Non-Hodgkin's lymphoma of the pleural cavity developing from long-standing pyothorax. Summary of clinical and pathological findings in thirty-seven cases. Jpn J Clin Oncol 19:249–257
6. Miwa H, Takakuwa T, Nakatsuka S, Tomita Y, Iuchi K, Aozasa K (2002) DNA sequences of the immunoglobulin heavy chain variable region gene in pyothorax-associated lymphoma. Oncology 62:241–250
7. Nakatsuka S, Yao M, Hoshida Y, Yamamoto S, Iuchi K, Aozasa K (2003) Pyothorax-associated lymphoma: a review of 106 cases. J Clin Oncol 20:4255–4260
8. Nishiu M, Yanagawa R, Nakatsuka S, Yao M, Tsunoda T, Nakamura Y, Aozasa K (2004) Microarray analysis of gene-expression profiles in diffuse large B-cell lymphoma: identification of genes related to disease progression. Jpn J Cancer Res 93:894–901
9. Takakuwa T, Luo WJ, Ham MF, Mizuki M, Iuchi K, Aozasa K (2003) Establishment and characterization of unique cell lines derived from pyothorax-associated lymphoma which develops in long-standing pyothorax and is strongly associated with Epstein–Barr virus infection. Cancer Sci 94:858–863
10. Williams ME, Innes DJ, Borowitz MJ, Lovell MA, Swerdlow SH, Hurtubise PE, Brynes RK, Chan WC, Byrne GJ, Whitcomb CC (1987) Immunoglobulin and T cell receptor gene rearrangements in human lymphoma and leukemia. Blood 69:79–86

Virchows Arch (2005) 447: 892–893
DOI 10.1007/s00428-005-0020-5

LETTER TO THE EDITOR

Ali Harb · Jameson Forster · Ivan Damjanov

Gastrointestinal autonomic nerve tumor secreting catecholamines

Received: 14 April 2005 / Accepted: 2 June 2005 / Published online: 14 July 2005
© Springer-Verlag 2005

Dear Editors:
Gastrointestinal autonomic nerve tumors (GANTs) form a subset of gastrointestinal stromal tumors (GISTs) [4]. In contrast to classical GISTs, GANTs have ultrastructurally a distinct neuroendocrine phenotype [1, 4]. The nature of these ultrastructural neuroendocrine granules remains enigmatic. With the exception of a single GANT, which was described as secreting vascular endothelial growth factor and endostatin [3], there are no published reports that these tumors secrete polypeptide hormones, growth factors, or biogenic amines.

In the present paper, we report a GANT found to secrete catecholamines. We are submitting this case for publication to indicate that GANTs can be functionally active.

A 49-year-old man visited his primary care physician complaining of lower quadrant pain that began following a minor work-related injury of the abdomen. During the initial examination, an abdominal mass was palpated, and a subsequent computerized tomographic examination revealed a 15-cm lower abdominal mass. He was obese and had been treated for elevated blood pressure, which fluctuated between 150/105 and 163/93 mm Hg, even though he was taking antihypertensive drugs. Because of the suspicion that the tumor might be secreting catecholamines, several laboratory tests were performed, and the following abnormalities were found: urinary 5-hydroxyindolacetic acid (5-HIAA) was elevated 13.7 mg/24 h (normal, <6 mg/24 h), homovalinic acid 10.7 mg/24 (normal, <8 mg/24 h), fractionated metanephrine 281 μg/24 h (normal,<180 μg/24 h; hypertensive range, >400 μg/24 h), normetanephrine 610 μg/24 h (normal, 451 μg/24 h), and total metanephrines 891 μg/24 h (normal, 680 μg/24 h). The tumor was located in the mesentery of the small intestine and was resected in toto with a segment of the small intestine. The patient recovered completely.

The tumor was multilobular and solid and measured 15×14×13 cm (Fig. 1a). Histologically, it was composed of elongated spindle cells showing moderate nuclear pleomorphism and hyperchomasia (Fig. 1b). There was an average of eight mitotic figures per ten high-power fields. Immunohistochemical stains showed that the tumor was positive for CD117, CD 34, and vimentin (Fig. 1c). Other immunohistochemical tests, including the staining with antibodies to S100, smooth muscle actin, desmin, cytokeratins, chromogranin, and synaptophysin gave negative results. Electron microscopy revealed that many cells have elongated or rounded-up filopodia-like processes containing neurosecretory granules (Fig. 1d). There were also prominent interdigitating cytoplasmic processes and rudimentary intercellular junctions. There was no evidence of smooth muscle or Schwann cell differentiation. On the basis of these morphologic data, the diagnosis of a malignant GANT was rendered. On the basis of the size (more than 10 cm in diameter) and the number of mitoses, the tumor was designated as high risk, as defined at the National Institutes of Health Consensus Conference [2]. The patient was treated with Gleevac, which he tolerated well. Within 18 months, he had recurrent tumor in the abdominal cavity, which was resected at another hospital. Two and half years after surgery, he is still alive and apparently free of tumor.

According to the best of our knowledge, this is the first GANT reported to secrete catecholamines. This secretory activity was discovered by accident because we thought that the tumor might be a catecholamine secreting paraganglioma/pheochromocytoma. The huge size of the tumor also played an important role; even if the tumor cells were

A. Harb · I. Damjanov
Department of Pathology,
The University of Kansas School of Medicine,
Kansas City, KS, USA

J. Forster
Department of Surgery,
The University of Kansas School of Medicine,
Kansas City, KS, USA

I. Damjanov (✉)
Department of Pathology, KUMC,
3901 Rainbow Blvd.,
Kansas City, KS, 66160, USA
e-mail: idamjano@kumc.edu
Tel.: +1-913-5887090
Fax: +1-913-5888780

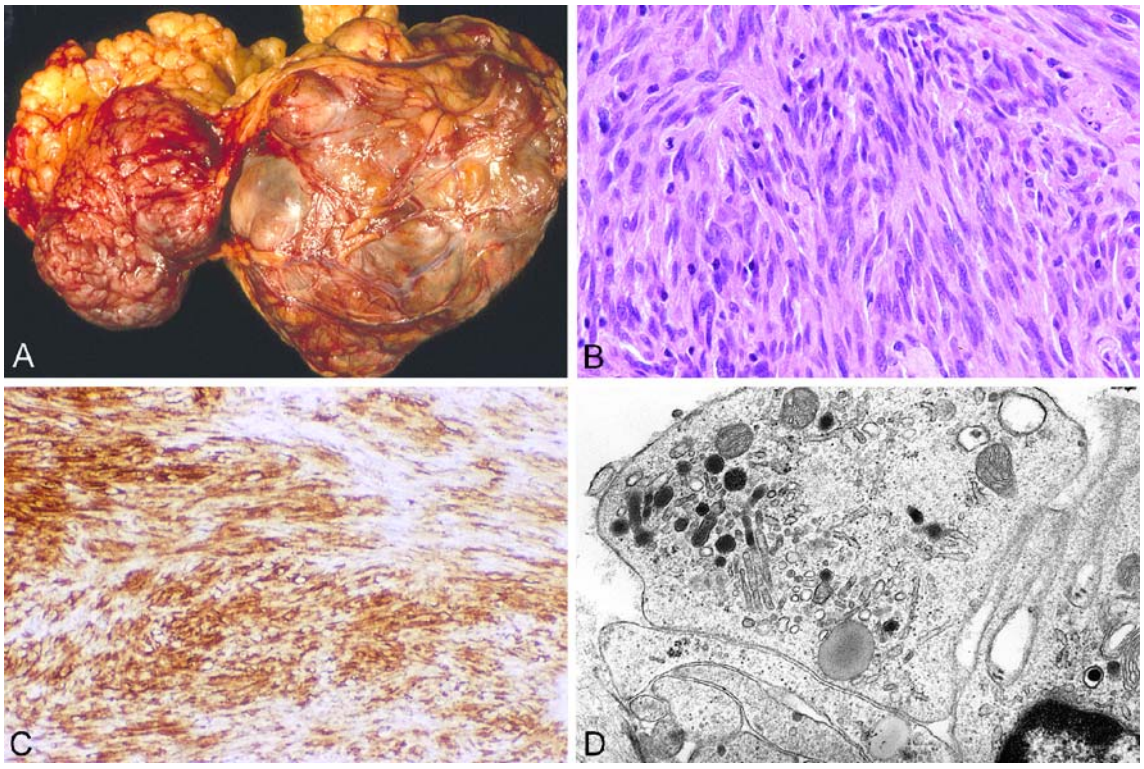


Fig. 1 Gastrointestinal autonomic nerve tumor removed in toto. **a** Macroscopically, the tumor is bulky and appears multinodular. **b** Microscopically, the tumor is composed of spindle-shaped cells. Hematoxylin and eosin, ×160. **c** Immunohistochemically, the tumor reacts with the antibodies to CD117. Immunoperoxidase staining, ×220. **d** Ultrastructurally, the tumor has cytoplasmic processes that contain neuroendocrine granules ×6,200

only weakly secretory, a large number of such cells probably contributed to the rise of catecholamines in the body. A future preoperative search for catecholamines performed prospectively on patients, suspected of having GISTs, might be warranted. Such a study could discover more secretory GANTs and thus help us define their true secretory potential.

References

1. Eyden B, Chorneyko KA, Shanks JH, Menasce LP, Banerjee SS (2002) Contribution of electron microscopy to understanding cellular differentiation in mesenchymal tumors of the gastrointestinal tract: a study of 82 tumors. Ultrastruct Pathol 26:269–285
2. Fletcher CD, Berman JJ, Corless C, Gorstein F, Lasota J, Longley BJ, Miettinen M, O'Leary TJ, Remotti H, Rubin BP, Shmookler B, Sobin LH, Weiss SW (2002) Diagnosis of gastrointestinal stromal tumors: a consensus approach. Hum Pathol 33:459–465
3. Hansma AH, van Hensbergen Y, Kuenen BC, van Diest PJ, Hanemaaijer R, Meijer S, Pinedo HM, Hoekman K (2004) A patient with a VEGF and endostatin producing gastrointestinal autonomic nerve tumour. J Clin Pathol 57:536–538
4. Lee JR, Joshi V, Griffin JW Jr, Lasota J, Miettinen M (2001) Gastrointestinal autonomic nerve tumor: immunohistochemical and molecular identity with gastrointestinal stromal tumor. Am J Surg Pathol 25:979–987

Virchows Arch (2005) 447: 894–896
DOI 10.1007/s00428-005-0026-z

LETTER TO THE EDITOR

Gaetano Magro · Maria Lopes · Paolo Amico · Lidia Puzzo

Chromophobe renal cell carcinoma with extensive rhabdomyosarcomatous component

Received: 15 April 2005 / Accepted: 10 June 2005 / Published online: 14 July 2005
© Springer-Verlag 2005

Keywords Chromophobe cell carcinoma · Rhabdomyosarcoma · Sarcomatoid carcinoma · Kidney

Sir,

Sarcomatoid changes may occur in all subtypes of renal cell carcinoma [1], especially in chromophobe cell carcinoma [3, 6], and are invariably associated with a poorer prognosis. It is likely that the sarcomatoid component arises from a metaplastic transformation of carcinomatous cells that may acquire a spindle cell morphology with a growth pattern, usually resembling that observed in malignant fibrous histiocytomatous, fibrosarcoma or unclassified high-grade spindle cell sarcoma [1, 2]. Although a focal rhabdomyosarcomatous differentiation has been rarely reported [2], we are not aware of any published renal cell carcinoma composed predominantly of a rhabdomyosarcomatous component. We report a rare case of chromophobe renal cell carcinoma with a dominating rhabdomyosarcomatous component accounting for 70% of the entire tumour. A 61-year-old man presented with abdominal and left flank pain. Ultrasonography and computerized tomography examination revealed a tumour mass in the left kidney. Radical nephrectomy with abdominal lymph node dissection was performed. Grossly, a tumour mass measuring 16 cm in its greatest dimension and whitish in colour was located in the upper pole of the kidney. Histologically, tumour was mainly composed of spindle- and large round-shaped cells with deep eosinophilic cytoplasm, frequently containing cross-striations consistent with rhabdomyoblasts (Fig. 1a). This rhabdomyosarcomatous component represented about 70% of the entire tumour. Immunohistochemical analyses, which revealed a strong and diffuse immunoreactivity for vimentin, desmin, myogenin (MyF4) and sarcomeric actin in these cells, confirmed their skeletal muscle differentiation (Fig. 1b). Focally, rhabdomyoblasts were closely intermingling with residual nests of chromophobe renal cell carcinoma (Fig. 1c), which were better highlighted by pancytokeratin immunostaining (Fig. 1d). Carcinomatous cells were also reactive to cytokeratin 7 and EMA.

The remaining tumour was composed of pure chromophobe cell carcinoma (10%) and high-grade spindle cell sarcoma NOS. (20%). The latter component was immunoreactive for vimentin and, focally, for pancytokeratins. Diffuse areas of necrosis and numerous mitotic figures were observed throughout the tumour. Perirenal and renal sinus adipose tissue was infiltrated by tumour, and iliar lymph nodes were metastatic (pTNM, T3 N1 Mx).

Differential diagnosis mainly revolved around primary renal rhabdomyosarcoma. Even if the possibility of the existence of this entity in adults cannot be completely excluded [4, 5], we suspect that at least some of the reported cases may represent renal cell carcinoma undergoing extensive rhabdomyosarcomatous differentiation. Accordingly, we recommend that an extensive tumour sampling be performed to rule out the existence of small carcinomatous areas in an otherwise typical rhabdomyosarcoma. However, we admit that a precise distinction between a

G. Magro (✉) · P. Amico · L. Puzzo
Dipartimento G.F. Ingrassia,
Anatomia Patologica,
Università di Catania,
Via S. Sofia 87,
95123 Catania, Italy
e-mail: g.magro@unict.it
Tel.: +39-95-3782024
Fax: +39-95-3782023

M. Lopes
Unità Operativa di Urologia,
Ospedale Vittorio Emanuele di Gela,
Caltanissetta, Italy

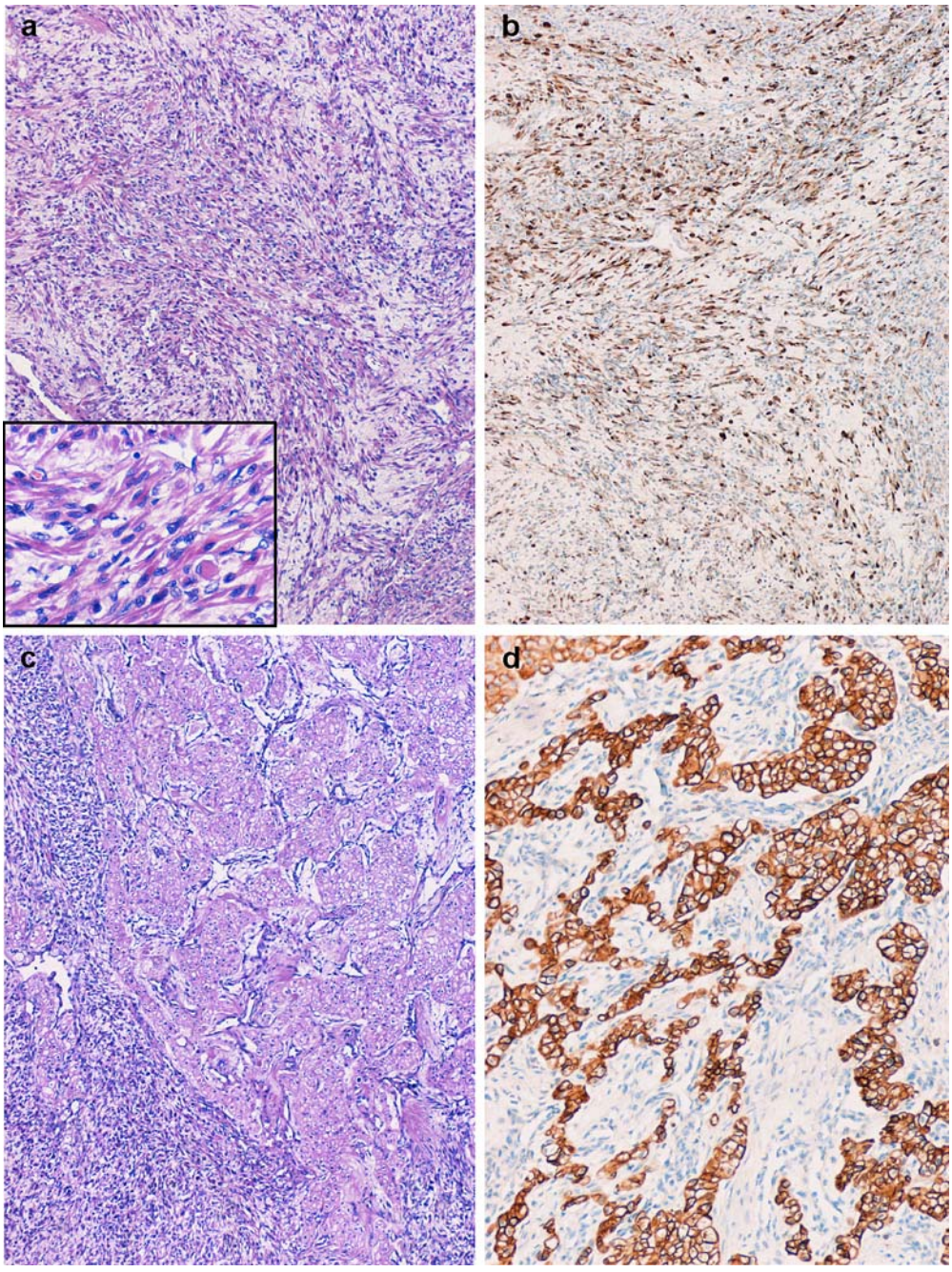


Fig. 1 **a** Tumour was mainly composed of spindled and large rounded cells with deep eosinophilic cytoplasm, sometimes exhibiting cross-striations (*inset*) consistent with rhabdomyoblasts. **b** Tumour immunostained with desmin. **c** Transition between chromophobe cell carcinoma and rhabdomyosarcomatous component was focally observed. **d** Carcinomatous cells were strongly immunostained with pancytokeratins

primary renal rhabdomyosarcoma and a sarcomatoid carcinoma with extensive rhabdomyosarcomatous differentiation appears to be rather academic, as both tumours share a high-stage disease at presentation and a poor prognosis.

Acknowledgements The authors wish to thank Mrs. Rosaria Gambino and Mrs. Falsaperna Lucia for their excellent technical support.

References

1. Cheville JC, Lohse CM, Zincke H, Weaver AL, Leibovich BC, Frank I, Blute ML (2004) Sarcomatoid renal cell carcinoma: an examination of underlying histologic subtype and an analysis of associations with patient outcome. Am J Surg Pathol 28:435–441
2. de Peralta-Venturina M, Moch H, Amin M, Tamboli P, Hailemariam S, Mihatsch M, Javidan J, Stricker H, Ro JY, Amin MB (2001) Sarcomatoid differentiation in renal cell carcinoma: a study of 101 cases. Am J Surg Pathol 25:275–284

3. Gong Y, Sun X, Haines GK III, Pins MR (2003) Renal cell carcinoma, chromophobe type, with collecting duct carcinoma and sarcomatoid components. Arch Pathol Lab Med 127:38–40
4. Grignon DJ, McIsaac GP, Armstrong RF, Wyatt JK (1988) Primary rhabdomyosarcoma of the kidney. A light microscopic, immunohistochemical, and electron microscopic study. Cancer 62:2027–2032
5. Mainguene C, Choquenet C, Cucchi JM, Dupre F, Monticelli I, Michiels JF, de Pinieux G, Vieillefond A (2003) Primary pleomorphic rhabdomyosarcoma of the kidney in adults: unusual tumor. Prog Urol 13:679–682
6. Nagashima Y, Okudela K, Osawa A, Nakamura N, Kawasaki C, Moriyama M, Nakamura N, Nakatani Y, Kitamura H, Aoki I (2000) Chromophobe renal cell carcinoma with sarcomatoid change. A case report. Pathol Res Pract 196:647–651

Virchows Arch (2005) 447: 897
DOI 10.1007/s00428-005-0033-0

BOOKREVIEW

H. Kalthoff

Apoptosis methods and protocols edited by Hugh J. M. Brady, Humana Press, Totowa, New Jersey 2004

Published online: 13 July 2005
© Springer-Verlag 2005

Major insights as well as enormous progress in understanding the role and mechanisms of apoptosis, programmed cell death, could be achieved within the last 15 years. Since apoptosis is assumed to have not only influence on cancer development within mammalian organisms, a large number of research groups focuses on this physiological process in a different context. As a matter of fact, apoptosis plays a central role in the physiology of all multi-cellular organisms studied so far. Disturbances in apoptosis, e.g. inhibition, underlie several pathological states such as cancer or auto-immunological diseases. On the other hand, excessive apoptosis may result, for example, in neurodegenerative disorders or ischemic damage.

The impact of apoptosis is still not fully determined during the above-mentioned timeframe since it proved to be of complex functions. It still requires further intense investigation to fully understand the mechanisms of regulation of apoptosis to gain tools to achieve a better control of apoptosis. Thousands of research articles about apoptosis and the surrounding mechanisms are published every year, but standard protocols to analyze apoptotic cell death are still largely missing from laboratory methods and text books.

This book offers a comprehensive overview about numerous methods to study the complex mechanisms of apoptosis. The particular chapters have been written by experts in this field and represent the achieved experiences in years of the research.

Chapters are clearly structured and therefore provide an easy access to the provided information. Each chapter starts with a short but clear introduction, giving enough background information not only for researchers working with apoptosis but also for less-experienced students and/or technical assistants. Methods to be applied are introduced with listing of the required materials like buffers, chemicals and the laboratory equipment. The very clearly written and sufficiently explained methods are supplemented by practical comments like (a) stability of chemicals or (b) some useful controls as well as (c) figures analyzing the typical results achieved. With these clear and complex instructions, a very supportive tool is provided to perform the desired experiments. Furthermore, a support for evaluation and critical examination of the gathered data is given.

In conclusion, the presented book shows the qualities to be regarded as standard manual for apoptosis research within the near future. It can be fully recommended for all scientists and for those establishing standard operation procedures to support research in this area of cutting edge technologies.

H. Kalthoff (✉)
Department of General Surgery,
Research Group of Molecular Oncology,
Arnold-Heller-Str. 7,
24105 Kiel, Germany
e-mail: hkalthoff@email.uni-kiel.de
Tel.: +49-431-5971938
Fax: +49-431-5971939

Virchows Arch (2005) 447: 898
DOI 10.1007/s00428-005-0101-5
© Springer-Verlag 2005

ANNOUNCEMENTS

15–16 June 2006
Thyroid Pathology for the Practicing Pathologist
15 rue de l'Ecole de Médecine, Paris,France

A 2-day course will take place in Paris again under the auspices of the French Division of the I.A.P.

This course will be given in English by Prof.M.Sobrinho-Simões (Porto) and Prof.R.Heimann (Brussels).

It will consist of lectures alternating with slide reviews and a slide seminar over a multihead microscope. The cases of this seminar will be sent (on CD)before the meeting.

The audience will be limited to 22 participants.
Course fees: 390 euros (320 euros for members of any I.A.P. division).
The fees include registration,hand-out, CD of the slide seminar and coffee breaks.

For further information please contact
Mrs. M. Fontanière
Administrative Secretary
French Division of the I.A.P.
32 Cours Albert Thomas
69008, Lyon, France
Fax: 33 4 78754311
e-mail: academie.pathologie@wanadoo.fr

Virchows Arch (2005) 447: 899–905
DOI 10.1007/s00428-005-0100-6

EUROPATH NEWS 4/2005



European Society
of
Pathology

Editors
Dr. Grete Krag Jacobsen
University Department of Pathology,
Teilumbuilding Rigshospitalet
Blegdamsvej 9,
DK-2100 Copenhagen Ø, Denmark
Tel.: +45 3545 5450
Fax: +45 3545 5414
e-mail: grete.krag.jacobsen@rh.hosp.dk

Dr. Bjørn Risberg
Department of Pathology
The Norwegian Radium Hospital
0310 Oslo, Norway
Tel.: +47-22934174
Fax: +47-22508554
e-mail: brisberg@labmed.uio.no
For further information look at the ESP
home page: http://129.240.38.9/espl

Newsletter of the European Society of Pathology

Dear Members,

In this newsletter you have the Presidential Address from the new President of the Society given at the Closing Ceremony at the 20th European Congress of Pathology which was a very successful congress with a huge program of very high quality, scientifically as well as socially, attended by more than 2000 participants.

The Minutes of the General Assembly, which took place at Palais des Congrès, Paris, September 7th 2005, are published in details along with the list of members of the new Executive Committee.

Notice that a new contract with Springer has been approved. This implies that the EUOPATH NEWS will appear once a month in 2006. All ESP members are invited to use the possibility to publish information in the newsletter and also on the website of the society.

For futher information look at the ESP home page: http://129.240.38.9/espl

Sincerely yours,
Grete Krag Jacobsen

Presidential Address

Dear Members,

I am proud and honoured to have been elected President of our Society. The European Society of Pathology is now 42 years old and has been developing continuously since its foundation in 1963. I am a member since 1975 and the last 25 years I have been actively involved in several administrative and/or scientific positions.

I always enjoyed the cooperative and friendly, family-like atmosphere that characterizes our Society. In the Xth ECP in Athens (Sept.1985) I was appointed to serve as the Secretary General of the local Organising Committee. By that time, I could never imagine that 20 years later you would elect me to serve our Society as its President. I am thanking you all for this great honour from the bottom of my heart.

In starting my 2 year term as President, I would like to thank all the Officers (A. Cardesa, G. Bussolati, R.R.W.Simpson and H.van Krieken) and all the Members of the Executive Committee (Fr. Capron, F. Carneiro, Ch.De Wolf-Peeters, R. Golouh, Gr. Krag Jacobsen, V.P. Lehto, M. Wells and D. Yilmazbayhan) for everything they have done for the benefit of ESP. Then, it is my privilege to welcome the new President-Elect, Fr. Bosman, ex-Member of the Executive Committee and Chairman of the Eurocell Path, and the new Members of the Executive Committee (N. Gale, Th. Kirchner, M. Marichal and F. Schmitt). I am wishing to the new comers all the best and I am sure that all together we will try to contribute for the further development of ESP.

Furthermore, I am extending my sincere thanks to each and everyone of the 17 Past Presidents, who have all served our ESP extremely well and led it to its present high standards. Due to their skills and initiatives, a lot of progress has been achieved, however, much more remains to be done. Among them, the only other woman was the late A. Piringer-Kuchinka, who served as President from 1975 to 1977 and has been a great personality in the family of European Pathologists. Therefore, as a matter of respect, I am dedicating my two-year Presidency in her memory.

My vision for the next two years is focused on the following:

1. Development of the European Institute for Continuing Medical Education in Pathology (EICME-Path).

The EICME-Path must be further developed and the best way is to make the Presidents' office responsible, while having a running Committee, chaired by the President-Elect, to devise ways and means, like the Examination Committee of UEMS. Additionally, the President, along with the Past-President, would be responsible to motivate the working groups for the expansion of Continuing Education, independently of the Intercongresses' Meetings and the ESP Congresses. I believe that this would be an immense contribution, especially to the Eastern European Countries.

The European School of Pathology with its extensions to different European cities, as well as the Eurocell Path are increasingly well regarded at a time when University investment in Academic Pathology is falling in some European Countries. The Society should strengthen its Academic Meetings as well as the main Congresses. The existing Montebello, IUCP and other well-known Postgraduate Courses in the UK are not enough for the number of young European Pathologists and/or residents. Therefore, the motivation of the working groups with didactic lectures, symposia, panel discussions and slide seminars will be very beneficial for small groups in remote Universities or State Hospitals in Eastern Europe and in the Balkans

1a. Courses for technicians

I strongly believe that the task of our Institute should be also extended towards

the continuing education of the technicians from Eastern European Countries and from Balkans. Senior Technicians should be invited to Postgraduate ESP Courses in order to see how these might be done. To my knowledge, the UK has well established University based courses in which after basic training, the technicians learn how to proceed with special techniques.

2. Links between the ESP and the UEMS.

The links between the ESP and the UEMS should be encouraged, so that the regulation of Pathology moves along with its science. The cross-border training should be advanced and if the local situation of the Country permits, on a reciprocal basis. The latter would be beneficial for both sides and will lead to the creation of common research projects. Furthermore, this training will increase the personal skills of young residents, who might try to obtain the UEMS examination, as a way of demonstrating competence and mobility in the profession.

3. Links with Forensic Societies.

I think that science is moving on fast and we should build more links with Forensic Societies. To my knowledge, there are some places lacking appropriate facilities and human resources, therefore I believe that collaboration with ESP might be sensible. Our Laboratories should offer cooperation in such forensic labs.

4. Virchows Archiv.

All Senior European Pathologists should be encouraged to contribute with editorials and/or reviews, as well as young researchers of our Specialty should be motivated by their Directors to send manuscripts, in order to maintain the quality and further increase the Impact Factor of our official Journal for the next ten years.

Last, but not least, I would like to congratulate heartly the President of the 20th ECP P. Bedossa and his brilliant Stuff for the great success (at all levels) of this major scientific event. Furthermore, the highest number of registrations ever achieved (up to 2200!!) gives us the strength to try hard to recruit new members among them.

Ending my address I am asking you, the members of our Society, to support all these initiatives and I am thanking you for the honour to elect me as President of our Society.

I am looking forward to seeing you not only in Ioannina (May 2006), but also in our 21st ECP in Istanbul (September 2007).



Prof. Dr. Niki J. Agnantis,
President of ESP

Minutes of the General Assembly, European Society of Pathology; Hall Bleu, Palais des Congrès, Paris, France; September 7th 2005, from 12.00 to 13.30hrs.

1. Welcome.

The President, Prof. Antonio Cardesa welcomed approximately 170 ESP members.

2. Approval of agenda.

Item 8 to be considered after item 5. Approved.

3. Approval of Minutes from the Extraordinary General Assembly in Paris, 7th February 2004.

These had previously been published, and copies were circulated at the start of the meeting. These were approved as a true and accurate record, and signed by the President and Secretary.

4. Report of the President.

Between 1964 and 2003, the ESP had evolved to meet great changes, and the scientific structures were satisfactory for the time being. In contrast, the administrative aspects of the ESP remained as they were in 1964, and it was agreed that major changes were needed.

In 2003, a ballot of members approved by more than 70% the decision of the Executive Committee to elect Prof. Niki Agnantis as President-elect. This was ratified by the General Assembly in Paris on 7th February 2004, which also elected Dr. Roderick Simpson to complete the term of Secretary of Prof. Jahn Nesland, who had resigned.

New Statutes were approved, and have since been accepted under Belgian law. Under the new statutes, the ESP is officially a non-profit society, with appropriate legal and financial protection. New rules for election of officers were drawn up by Prof. Michael Wells and have subsequently been approved by the Executive Committee at its meeting in Barcelona in November 2004. The meeting in Porto in April 2005 made recommendations for new officers in accordance with the new rules.

As agreed at the General Assembly in 2004, a Constitutional Sub-Committee was set up to update the By-Laws. These have been published in the 2005 Members' handbook, and will be presented in Item 5.

The biennial congresses of the ESP continue to be successful. This is especially so with the current Paris one which has more than 2000 participants, making the ESP congresses the second largest in the World. The President expressed his great thanks on behalf of the ESP to Prof. Pierre Bedossa and the French Society of Pathology.

A successful Intercontinental Congress was held in 2004 in Iguaçu, Brazil involving the ESP, Sociedad Latinamericana de Patología (SLAP) and Sociedade Brasileira Patologia. In future intercontinental congresses, it is hoped to involve additional continents.

The Inter-Congress meeting in Ioannina, Greece in May 2006 is well advanced, and progress will be reported in Item 14.

As there are now more and larger congresses, the Executive Committee has decided that a Congress Coordinator will be needed.

The Advisory Council provides a link between the ESP and the national societies of pathology, and the President expressed his thanks to the chairman, Prof. Günter Klöppel.

The Newsletter and website are in the process of being updated, and the President expressed his appreciation to the respective editors, Drs. Grete Jacobsen and Bjørn Risberg.

The European School of Pathology continues to thrive under the direction of Prof. Gianni Bussolati. In addition to courses in Turin, Italy, they are also given in Kraków, Poland, Kraiova, Romania and Ankara, Turkey. Similar courses are also sponsored by the ESP in Ioannina, Greece under the direction of Prof. Niki Agnantis.

Eurocellpath under the chairmanship of Prof. Fred Bosman has run excellent courses in Girona, Spain in 2004 and in Montebello, Norway in 2005.

The Working Groups remain the backbone of the ESP, and are doing extremely well, particularly in linking applied and basic research.

The official journal of the ESP is Virchows Archiv and its impact factor has considerably increased over the last few years. The new editor-in-chief is Prof. Heinz Höfler. A new contract has been negotiated, which is economically beneficial for the ESP. See Item 6.

It is considered that the ESP needs a strategically located permanent address. See Item 7.

The President thanked the immediate Past President, Gianni Bussolati and the departing members of the Executive Committee for their support and contribution to the Society.

The President noted that his term will finish at the end of this congress, and he expressed his best wishes to Prof. Niki Agnantis who will lead the Society to its next congress in Istanbul. He thanked all members of the ESP who will ensure that the Society continues to thrive.

Finally, the President announced with regret the death of Prof. Julius Plank, Martín, Slovakia in January 2004. The General Assembly stood silently in respect.

5. Statutes and By-Laws.

New statutes were approved by the General Assembly in Paris in 2004. A Sub-Committee chaired by Prof. Mia Marichal was set up to update the By-Laws, in particular the rules for election of officers and regulations of the Working Groups. The President expressed his thanks to the Committee comprising Profs. Michael Wells, Manuel Sobrinho-Simões, Frédérique Capron and Urbain Van Haelst.

The President added that By-Laws were relatively easy to change if necessary.

The General Assembly approved the new By-Laws unanimously.

6. Contract with Virchows Archiv.

The President reported a good interaction between the Executive Committee, the Editor-in-Chief and with Springer, and that an offer beneficial to the ESP had been made. Under the new contract, the ESP receives 50% of the net profit of the journal. On present figures, this is likely to be about €50,000. The Executive Committee (in particular, the Treasurer) support this proposal.

The Editor-in-Chief believed that the new contract was advantageous for both the ESP and Virchows Archiv. In addition, there were other benefits for the ESP. Prof. Höfler added that he believed that there was still room to increase the Impact Factor of the Journal.

The General Assembly approved the new contract with Springer unanimously.

7. Permanent office for the European Society of Pathology.

The ESP is a society registered in Belgium, at present at Prof. Mia Marichal's private address. Therefore, it needs a permanent address, as well as an office, a store for documents, and possibly a meeting room. The Executive Committee had discussed this extensively at four recent meetings, where it was felt essential that the office should be in Belgium, probably in Brussels. The Treasurer reported that the ESP could afford to spend up to €250,000. It was also felt necessary that the ESP should employ a managing assistant, probably on a part-time basis.

The President asked the General Assembly to approve the principle and allow the Executive Committee to develop the details. Open questions remain on the exact location and size of any property, whether to buy or not (based on a sum of approximately €250,000) and on the level of expertise of the society employee.

The General Assembly agreed unanimously:

a). that the ESP should have a registered permanent address in Belgium.
b). to mandate the Executive Committee to buy a property up to a maximum value of approximately €250,000.
c). to the employment of one appropriate person.

8. Report of the Treasurer.

a). Prof. Han van Krieken presented his report, which will be published in detail on the website.
b). The Treasurer thanked Christine van Haelst for her help in the transition. He noted that at present, the financial year ends on Aug 1st, which leaves too little time to collate the figures and contact the financial committee. He requested a change to 1st January, and the General Assembly approved this unanimously.
c). Total assets in 2005 are €435,684-06 (2003 - €383,686-44). A considerable sum had been changed from long term investments to interest-bearing bank accounts. The income from 2003-05 was €214,584-25 (2001-03 - €159,247) mostly from subscriptions, investments and profits from the Ljubljana congress. It will not be possible to recoup the loan of €10,000 to the Intercontinental Congress in Iguaçu. Overall expenses were €159,286-63, the largest part being the €90,320-15 paid to Virchows Archiv. There was a substantial increase in Executive Committee expenses, due to there being several meetings. The total surplus of income over expenditure was €55, 297-62.
d). The General Assembly is required to approve new members. Rather than reading out all their names, it was agreed that publication of the list of members in the Handbook was sufficient.

The General Assembly unanimously approved the Treasurer's report.

9. Report of the Chairman of the Advisory Council.

Prof. Günter Klöppel presented his report. The Advisory Council met on Saturday, 3rd September. 19 of 29 possible members attended. Amongst items discussed were:

a). It was emphasised that the AC is the link between the national societies of pathology and the Executive Committee. Under the new By-Laws, each member must be approved by his/her national society, and the representative should preferably be the secretary or president.
b). A request that each national society should have a member in each Working Group.
c). The AC should advise in the planning of the congresses, such as in Istanbul.
d). The AC would be a good forum to receive information about pathology from most countries of Europe.
e). The ESP newsletter and website should be used as a link between the national societies and the ESP.
f). Pathologists should be involved in the planning of EORTC trials.
g). A request was made by the Czech representative for the European School of Pathology to hold courses in the Czech Republic.
h). The next meeting of the Advisory Council will be held in May 2006 in Ioannina.

The General Assembly approved this report unanimously.

10. Rules for election of new officers, additional members of the Executive Committee.

New rules had been drawn up by committee led by Prof. Michael Wells. These are published on pages 21-22 of the Members' Handbook and were read out by the President.

The General Assembly approved them unanimously.

11. New Officers and members of the Executive Committee.

In accordance with the new rules for election, the following candidates for officers were proposed by the Executive Committee. No other nominations were received.

President-elect:	Fred Bosman.
Secretary:	Roderick Simpson.

Both were approved by the General Assembly, and thus duly elected.

The Executive Committee proposed as members of the Executive Committee: Nina Gale, Thomas Kirchner, Mia Marichal, Fernando Schmitt. They were approved by the General Assembly and thus duly elected.

The President noted that there were several other good potential candidates for the Executive Committee, who should not be discouraged from putting themselves forward for consideration in the future.

12. Honorary memberships.

The President proposed two outstanding members of ESP for Honorary Membership:

a). Antonio Llombart-Bosch for his great contribution to pathology and the ESP as Past President, President of the Advisory Council and for his general wisdom.

b). Paul Kleihaus for being an outstanding morphologist, cancer researcher and for coordinating the publication of the new series of WHO tumour "blue" books.

13. 21st ESP Congress, Istanbul 2007. Report of the Chairman of the Organising Committee.

Prof. Sitki Tuzlali presented the outline for the Congress scheduled for September 2007. The opening ceremony will take place on 8th September, the General Assembly on the 12th and the Congress will close on 13th September.

The site will be the Istanbul Convention and Exhibition Centre, which has 21 rooms, the largest having 2000 seats. There will be 4 keynote lectures plus many slide seminars, symposia, short courses, free paper and poster sessions. The programme would be formulated in consultation with the Advisory Council and Working Groups. There will be an active social programme, and opportunities for tourism afterwards. The second announcement will appear in Autumn 2006.

The Congress website is: www.ecp2007istanbul.org

Prof. Tuzlali invited all to attend what will be an excellent congress in an unique city.

14. ESP Inter-Congress, Ioannina, May 2006. Report of the Congress President.

Niki Agnantis presented the programme. It will be based primarily around the Working Groups and associated societies, and there will be a guest lecturer. It will last 2½ days, and will be preceded by the annual meeting of the Greek Society of Pathology. There will be an active social programme, including excursions, as well as an opportunity to visit an interesting area of Greece. The site will be the Hotel du Lac, and there are plenty of hotels of different costs. There are flights from Athens and other cities, as well as travel by sea and overland.

The congress website is: www.triaenatours.gr

15. Approval of the site of the 3rd Intercontinental Congress 2008.

The Executive Committee in 2004 approved Barcelona as the site of next Intercontinental Congress scheduled for May 2008, and to be organised by Prof. JA Bombí.

The General Assembly unanimously approved this proposal.

16. Approval of the site of the 22nd ESP congress 2009.

In 2004, the Executive Committee approved Florence as the site for the congress scheduled for September 2009, and to be organised by Prof. Marco Santucci.

The General Assembly unanimously approved this proposal.

17. Frequency of General Assemblies.

The Executive Committee believes that biennial General Assemblies are unlikely to be sufficient to deal with the increased complexity of the Society. As the Statutes state that "the General Assembly meets at each biennial congress", any additional meetings will have to be Extraordinary General Assemblies (EGAs). The President asked this General Assembly for a free hand to be given to the Executive Committee to call EGAs if required. The first would be held in Ioannina during the Intercongress meeting in May 2006.

This was approved unanimously.

18. Any other business.

The Congress Awards were presented by Prof. Pierre Bedossa. He acknowledged that due to many excellent papers, it had been a very difficult task, but the following were chosen.

a). Best oral presentation (prize of €1500): Chromosomal instability predicts the malignant phenotype in sporadic insulinomas. Speel EJM, Jonkers YMH, Claessen SMH, Perren A, Schmid S, Komminoth P, Verhofstad AA, Hofland LJ, de Krijger RR, Slootweg PJ, Ramaekers FCS - Maastricht, Nijmegen, Rotterdam (Netherlands), Zürich, Baden (Switzerland).

b). Best poster presentation (prize of €1000): Head and neck squamous cell carcinomas: epidermal growth factor receptor (EGFR) protein expression and EGFR gene copy numbers. Mrhalová M, Plzak J, Betka J, Kodet R - Czech Republic.

c). George Tiniakos award for the best presentation in gastrointestinal, liver and pancreas pathology (prize of €1000): Endocrine precursor lesions are associated with duodenal gastrinomas in patients suffering from multiple endocrine neoplasia type 1. Anlauf AM, Perren A, Meyer C, Schmid S, Saremaslani P, Kruse MI, Weihe E, Komminoth P, Heitz PU, Klöppel G - Kiel, Marburg (Germany), Zürich (Switzerland).

19. Date and place of next meeting.

An Extraordinary General Assembly will take place in Ioannina, Greece in May 2006.

The next (regular) General Assembly will take place in Istanbul on 12th September 2007.

Signed:

Professor Antonio Cardesa, President of the ESP.

Dr. Roderick HW Simpson, Secretary of the ESP.
26th September 2005.

Members of the Executive Committee of the European Society of Pathology

September 2005

President.
Prof. Niki Agnantis.
Department of Pathology, University of Ioannina Medical School, PO Box 1186, GR-451 10 IOANNINA, Greece.
Tel: +30-2651-097792.
Fax: +30-26510-72473.
E-mail: nagnanti@cc.uoi.gr

President-elect.
Prof. Fred T Bosman.
Dept. of Pathology, University of Lausanne, Rue du Bugnon 25, CH-1011, LAUSANNE. Switzerland.
Tel: +41-21-314-7202.
Fax: +41-21-314-7205.
E-mail: fred.bosman@chuv.ch

Secretary.
Dr. Roderick HW Simpson.
Department of Pathology, Church Lane, Heavitree, EXETER Devon, EX2 5DY, UK.
Tel: +44-1392-402941.
Fax: +44-1392-402964.
E-mail: roderick.simpson@virgin.net
roderick_simpson@yahoo.com

Treasurer.
Prof. J Han JM van Krieken.
Department of Pathology, 437 PAUMC St. Radboud, PO Box 9101, NL-6500HB, NIJMEGEN, The Netherlands.
Tel: +31-24-361-4352.
Fax: +31-24-354-0520.
E-mail: J.vanKrieken@pathol.umcn.nl

Ordinary Committee Members.
(elected in 2003).
Dr. Frédérique Capron.
Service d'Anatomie et Cytologie Pathologiques 1, G. H. Pitié-Salpétrière, Boulevard de l'Hôpital 47-83, FR-75651 PARIS Cédex 13, France.
Tel: +33-1-42-17-84-50.
Fax: +33-1-42-17-77-77.
E-mail: frederique.capron@psl.ap-hop-paris.fr

Prof. Yilmazbayhan Dilek.
Department of Pathology, Medical Faculty of Istanbul, 34390 Topkapi, ISTANBUL, Turkey.
Tel: +90-212-414-2400.
Fax: +90-212-631-1367.
E-mail: bayhand@superonline.com

Prof. Veli-Pekka Lehto.
Department of Pathology,University of Helsinki, Haartmaninkatu 3, PO Box 21, FI-HELSINKI, Finland.
Tel: +358-9-191-26412.
Fax: +358-9-191-26700.
E-mail: veli-pekka.lehto@helsinki.fi

Prof. Michael Wells.
Academic Unit of Pathology, University of Sheffield Medical School, Beech Hill Road, SHEFFIELD, West Riding, Yorkshire, S10 2RX. UK.
Tel: +44-114-271-2397.
Fax: +44-114-226-1464.
Cell: +44-797-342-6554.
E-mail: m.wells@sheffield.ac.uk

(elected in 2005).

Prof. Nina Gale.
Insitute of Pathology, Faculty of Medicine, Korytkova 2, 61105, LJUBLJANA, Slovenia.
Tel: +386-1-543-7103.
Fax: +386-1-543-7104.
E-mail: NINA.GALE@MF.UNI-LJ.SI

Prof. Thomas Kirchner
Institute of Pathology
University of Erlangen-Nuremberg, Krankenhausstr. 8-10, 91054 Erlangen, Germany
Tel: +49-9131-852-2286.
Fax:+ 49-9131-852-4745.
E-mail: thomas.kirchner@patho.imed.uni-erlangen.de

Prof. Miriam Marichal.
Department of Pathology, Academic Hospital, Vrije Universiteit Brussel, Laarbeeklaan 101, 1090 BRUSSELS, Belgium.
Tel: +32-2-477-5083.
+32-2-477-5080.
+32-2-477-5099.
Fax: +32-2-477-5085.
E-mail: miriam.marichal@az.vub.ac.be
miriam.marichal@vub.ac.be

Prof. Fernando Schmitt
IPATIMUP, Rua Roberto Frias s/n
P-4200-465, PORTO, Portugal.
Tel: +351-22-557-0700.
Fax: +351-22-557-0799.
E-mail: fschmitt@ipatimup.pt

Ex officio.

Past president.
Prof. Antonio Cardesa.
Dept. Anatomia Patologica, Hospital Clinic, Villaroel 170, E-08036, BARCELONA, Spain.
Tel: +34-932-27-5456.
Fax: +34-932-27-5717.
E-mail: ACARDESA@clinic.ub.es

President of the Advisory Council.
Prof. Günter Klöppel.
Department of Pathology
University of Kiel.
Michaelisstraße 11, D-24105, KIEL, Germany.
Tel: +49-431-597-3400.
Fax: +49-431-597-3462.
E-mail: gkloeppel@path.uni-kiel.de

Editor of Europath News.
Dr. Grete Krag Jacobsen,
Patologiafdelingen /Bartholin Instituttet, Teilumbygningen, Rigshospitalet, Blegdamsvej 9
DK-2100 Copenhagen Ø, Denmark.
Tel: +45-3-545-5450 or
+45-3-545-0670.
Fax: +45-3-545-5414.
e-mail: grete.krag.jacobsen@rh.hosp.dk

Editor of Virchows Archives.
Prof. Heinz Höfler.
Inst für Pathologie der TUM, Ismaningerstraße 22, D-81675 MÜNCHEN, Germany.
Tel: +49-89-4140-4160.
Fax: +49-89-4140-4865.
E-mail: hoefler@lrz.tum.de

Editorial Office.
Prof. Dr. G. Kloeppel.
Inst. of Pathology
University of Kiel
Michaelisstr. 11
24105 Kiel, Germany
Phone: +49-431-597-3400
Fax: +49-431-597-3430
e-mail: Virchows.Archiv@path.uni-kiel.de

Monika Weisleder.
Societies Liaison Manager,
Springer-Verlag, Haberstr. 7, 69126 Heidelberg,Germany.
Tel. +49-6221-487-8316.
Fax +49-6221-487-8131.
e-mail: weisleder@springer.de

Editor of the ESP website.
Dr. Bjørn Risberg.
Department of Pathology
The Norwegian Radium Hospital
Montebello, N-0310 Oslo, Norway.
Tel: +47-229-34174.
Fax: +47-225-08554.
E-mail: brisberg@labmed.uio.no

Director of the European School of Pathology.
Prof. Gianni Bussolati.
Dept. Med Sci. and Human Oncol, Sect. Pathol. Anat. - Univ. Torino, Via Santena 7, IT-10126, TORINO, Italy.
Tel: +39-011-670-6505.
Fax: +39-011-663-5267.
E-mail: gianni.bussolati@unito.it

Financial Committee.
Prof. Manuel Sobrinho Simões.
Department of Pathology, IPATIMUP, Rua Roberto Frias S/N, 4200-465 PORTO, Portugal.
Tel: +351 225570700
Fax: +351 225570799
+351 225503940
E-mail: sobrinho.simoes@ipatimup.pt

Prof. Urbain van Haelst.
van Cranenborchstraat 6, NL-6525 BN. NIJMEGEN. The Netherlands.
Tel: +31-24-323-1950.
Fax: +31-24-323-1950 (same as phone number).
E-mail: u.vanhaelst@inter.nl.net
hael.cham@inter.nl.net

Erratum

Please notice that in the Abstracts from the 20th European Congress of Pathology in Paris printed in the August 2005 issue of Virchows Archiv vol 447, number 2, page 436, the authors of P 644 are missing and should be : P644. Repair of bone defects by anionic collagen matrices. **Lenaldo B Rocha (1), Randall L Adam (2), Neucimar J Leite (3), Konradin Metze (2), and Marcos A Rossi (1).** 1. Department of Pathology, Faculty of Medicine of Riberão Preto, University of São Paulo, Brazil. 2. Department of Pathology, Faculty of Medicin, and 3. Institute of Computing, State of University of Campinas Brazil.

The European Society of Pathology

Dear Colleague,

It will surely not have escaped your attention that *Virchows Archiv* is now the Official Journal of the European Society of Pathology.

But did you realise what benefits membership in the society offer you?

- A subscription to the journal *Virchows Archiv* at no extra charge – this is automatically sent to every member every month.
- Access to the journal online (take a look at http://link.springer.de). If you are already a member of ESP but have not yet registered for your free electronic access, you will find the necessary form to complete online here too.
- A discount of 20% on most titles published by Springer. To take advantage of this, simply send your order directly to the publisher, with details of your membership.
- Attendance at the Society's conferences at a reduced fee.

If you have not yet joined the European Society of Pathology, why not do so now?
Simply complete and return the form enclosed.

We look forward to welcoming you as a member.

Yours sincerely

N. Agnantis	H. van Krieken	H. Höfler
President European Society of Pathology	Treasurer European Society of Pathology	Managing Editor Virchows Archiv

Application for Membership of the EUROPEAN SOCIETY OF PATHOLOGY



This application can also be downloaded from our website:
http://www.Europathology.org

Please complete the following form (block capitals please) and return it to the Office of the Treasurer

FAMILY NAME: .....

First Name(s): .....

Male ❑ Female ❑

Place and date of birth: .....

Title/Present Position: Prof. ❑ Dr. ❑ Resident ❑

Other: .....

Please clearly indicate which one of the following addresses should be used for subsequent correspondence, mailings, and listing in the Members Handbook:

❑ PRIVATE ADDRESS:

Name: .....

Street: .....

Postcode .....

City: .....

Country: .....

❑ INSTITUTE / OFFICE ADDRESS:

Name Institute: .....

Department: .....

Street: .....

Postcode: .....

City: .....

Country: .....

Telephone: .....

Telefax: .....

E-mail: .....

FIELDS OF INTEREST: .....

Date: ..... Signature of Applicant: .....

Please mail or fax the completed application form to:

ESP – OFFICE OF THE TREASURER,
Prof. Dr. H. VAN KRIEKEN,
University Medical Center Nijmegen
Dept. of Pathology / 437 PA
P.O.Box 9101
6500 HB NIJMEGEN, The Netherlands

Tel.: +31-24-3614352
Fax: +31-24-3540520
e-mail: j.vankrieken@pathol.umcn.nl

Your acceptance as a member of E.S.P. will be confirmed in due course.

Virchows Arch (2005) 447: 907–908
DOI 10.1007/s00428-005-0083-3

EDITORIAL

Gianni Bussolati

Of GISTs and EGISTs, ICCs and ICs

Received: 25 August 2005 / Accepted: 25 August 2005 / Published online: 21 September 2005
© Springer-Verlag 2005

Interest in the structural and biological features of cells originally described by Cajal in muscle layer of the gastrointestinal tract has recently been enhanced by demonstration of their histogenetic link with gastrointestinal stromal tumors (GISTs) and sensibility of the latter to STI-571 (imatinib mesylate) treatment. Since tumor growth is dependent from the tyrosine-kinase c-KIT product (CD117), its demonstration by immunohistochemistry has acquired diagnostic interest and is a prerequisite for the related treatment.

Immunohistochemical staining with anti-CD117 antibodies is not specific for Cajal's interstitial cells (ICCs), nor for GISTs. However, such staining is highly sensitive, being reportedly positive in the vast majority of GISTs [6], displaying diffuse or membranous and a perinuclear dot-like pattern of distribution. Another marker of interest is CD34 (positive in approximately 80% of cases), while staining for contractile proteins, such as actin and desmin, is uncommon and focal. Mutations of *c-KIT* and *PD-GFRA* genes have also been described in GISTs and carry diagnostic and therapeutic impact.

Besides the gastrointestinal tract, similar tumors, defined as extra-gastrointestinal stromal tumors (EGISTs) [13], have been described in locations such as urinary bladder, gallbladder, omentum, and mesentery [3, 5].

Most recently, rare cases of spindle cell tumors morphologically and immunohistochemically similar to GISTs have been described in the pancreas. The first observation of a single case of a pancreatic tumor histologically reminiscent of GIST, composed of spindle-shaped cells and immunohistochemically positive for vimentin, CD34 and c-KIT protein was made in 2004 by Yamaura et al. [14]. A similar case was described, in the same year, by Neto et al. [7]. Such observations were soon followed by the description of two similar cases by Pauser et al. [9]. In April 2005, Daum et al. [2] reported on a GIST of the pancreas, defined on the base of morphological, of immunohistochemical and, for the first time, of genetic data (mutation of *c-KIT* gene by deletion of six base pairs in exon 11).

Interestingly, Yamaura et al. [14] noted the presence, in the normal pancreas surrounding the tumor, of c-KIT positive cells, surrounding the intercalated ducts and the acini, and suggested that such cells might be the origin to the stromal tumor they described. These authors relied only on the relatively unspecific immunohistochemical staining for CD117 and did not go as far as defining the presence of interstitial cells (ICs) in the pancreas. This was recently achieved by Popescu et al. [12] on the base of cultural, electron-microscopical as well as immunohistochemical data. In striking similarity, Ortiz-Hidalgo et al. [8] reported a c-KIT positive stromal tumor in the gallbladder and linked such finding to the presence of numerous c-KIT expressing ICs in the gallbladder wall.

These reports just underline how much normal histology and pathological observations are mutually interconnected. Several examples of pathological observation of lesions to be regarded as an "experiment of nature" suggest properly addressed histological investigation, and vice versa.

The relatively recent burst in discoveries of ICs in several tissues outside the gastrointestinal tract such as the fallopian tubes and the myometrium, the portal vein and the stroma of the breast and of the pancreas [1, 4, 10, 11] led new light to the histology and physiology of these fascinating and still mysterious cells, which might have additional significance besides a "pacemaker" activity. We can easily predict that an origin from ICs will soon be acknowledged for a number of extra-gastrointestinal spindle cell tumors, which are presently hidden under uncommitted definitions.

In the past, tumors now unanimously recognized as GISTs were variously defined as leiomyomas, leiomyoblastoma, schwannomas, or other rather vague definitions. The possible responsiveness to appropriate treatment of tumors to be included under the generic definition of EGISTs would add impact to the biologic interest of their histogenetic definition.

G. Bussolati (✉)
Department of Biomedical Sciences and Oncology,
University of Turin,
Turin, Italy
e-mail: gianni.bussolati@unito.it

References

1. Ciontea SM, Radu E, Regalia T, Ceafalan L, Cretoiu D, Gherghiceanu M, Braga RI, Malincenco M, Zagrean L, Hinescu ME, Popescu LM (2005) C-kit immunopositive interstitial cells (Cajal-type) in human myometrium. J Cell Mol Med 9:407–420
2. Daum O, Klecka J, Ferda J, Treska V, Vanecek T, Sima R, Mukensnabl P, Michal M (2005) Gastrointestinal stromal tumor of the pancreas: case report with documentation of KIT gene mutation. Virchows Arch 446:470–472
3. Dei Tos AP (2003) The reappraisal of gastrointestinal stromal tumors: from Stout to the KIT revolution. Virchows Arch 442:421–428
4. Harhun MI, Pucovsky V, Povstyan OV, Gordienko DV, Bolton TB (2005) Interstitial cells in the vasculature. J Cell Mol Med 9:232–243
5. Miettinen M, Monihan JM, Sarlomo-Rikala M, Kovatich AJ, Carr NJ, Emory TS, Sobin LH (1999) Gastrointestinal stromal tumors/smooth muscle tumors (GISTs) primary in the omentum and mesentery: clinicopathologic and immunohistochemical study of 26 cases. Am J Surg Pathol 23:1109–1118
6. Miettinen M, Sobin LH, Lasota J (2005) Gastrointestinal stromal tumors of the stomach: a clinicopathologic, immunohistochemical, and molecular genetic study of 1765 cases with long-term follow-up. Am J Surg Pathol 29:52–68
7. Neto MR, Machuca TN, Pinho RV, Yuasa LD, Bleggi-Torres LF (2004) Gastrointestinal stromal tumor: report of two unusual cases. Virchows Arch 444:594–596
8. Ortiz-Hidalgo C, de Leon Bojorge B, Albores-Saavedra J (2000) Stromal tumor of the gallbladder with phenotype of interstitial cells of Cajal: a previously unrecognized neoplasm. Am J Surg Pathol 24:1420–1423
9. Pauser U, da Silva MT, Placke J, Klimstra DS, Kloppel G (2005) Cellular hamartoma resembling gastrointestinal stromal tumor: a solid tumor of the pancreas expressing c-kit (CD117). Mod Pathol 18(9):1211–1216
10. Popescu LM, Andrei F, Hinescu ME (2005) Snapshots of mammary gland interstitial cells: methylene-blue vital staining and c-kit immunopositivity. J Cell Mol Med 9:476–477
11. Popescu LM, Ciontea SM, Cretoiu D, Hinescu ME, Radu E, Ionescu N, Ceausu M, Gherghiceanu M, Braga RI, Vasilescu F, Zagrean L, Ardeleanu C (2005) Novel type of interstitial cell (Cajal-like) in human fallopian tube. J Cell Mol Med 9: 479–523
12. Popescu LM, Hinescu ME, Ionescu N, Ciontea SM, Cretoiu D, Ardeleanu C (2005) Interstitial cells of Cajal in pancreas. J Cell Mol Med 9:169–190
13. Yamamoto H, Oda Y, Kawaguchi K, Nakamura N, Takahira T, Tamiya S, Saito T, Oshiro Y, Ohta M, Yao T, Tsuneyoshi M (2004) c-kit and PDGFRA mutations in extragastrointestinal stromal tumor (gastrointestinal stromal tumor of the soft tissue). Am J Surg Pathol 28:479–488
14. Yamaura K, Kato K, Miyazawa M, Haba Y, Muramatsu A, Miyata K, Koide N (2004) Stromal tumor of the pancreas with expression of c-kit protein: report of a case. J Gastroenterol Hepatol 19:467–470

Virchows Arch (2005) 447: 909–919
DOI 10.1007/s00428-005-0069-1

REVIEW ARTICLE

Falko Fend · Oliver Bock · Markus Kremer · Katja Specht · Leticia Quintanilla-Martinez

Ancillary techniques in bone marrow pathology: molecular diagnostics on bone marrow trephine biopsies

Received: 18 May 2005 / Accepted: 11 July 2005 / Published online: 18 October 2005
© Springer-Verlag 2005

Abstract Pathologic examination of trephine bone marrow (BM) biopsies plays a central role in the diagnosis and staging of haematological neoplasms and other disorders affecting haematopoiesis. Haematopathology has been profoundly influenced by the advent of molecular genetic techniques suitable for paraffin-embedded tissues, and certain applications, such as the determination of B- and T-cell clonality, belong to its standard diagnostic repertoire. Many of these molecular tests can be performed successfully with nucleic acids extracted from BM trephine biopsies, if some technical aspects specific to this template source such as various fixation and decalcification procedures are taken into consideration. The current indications for molecular BM diagnostics range from the confirmation of lymphoma involvement with gene rearrangement analysis, demonstration of tumor-specific translocations in lymphoid and chronic myeloproliferative disorders along to the detection of microorganisms or marrow involvement by soft tissue sarcomas. The availability of quantitative polymerase chain reaction techniques for the investigation of allelic imbalances and gene expression levels in paraffin-embedded material also open new avenues for research and advanced diagnostics. The molecular detection of minimal residual disease in haematological neoplasms, especially in the context of new treatment strategies, will provide future challenges. This article summarizes the current state of the art in molecular diagnostics applied to paraffin-embedded BM biopsies.

Keywords Bone marrow biopsy · Molecular analysis · Clonality · Gene expression · Lymphoma · Haematological neoplasms

F. Fend (✉) · M. Kremer · K. Specht
Institute of Pathology, Technical University Munich,
Ismaningerstrasse 22,
81675 Munich, Germany
e-mail: fend@lrz.tum.de
Tel.: +49-89-41404162
Fax: +49-89-41404865

O. Bock
Institute of Pathology, Hannover Medical School,
Hannover, Germany

L. Quintanilla-Martinez
Institute of Pathology,
GSF Research Center for Environment and Health,
Neuherberg, Oberschleissheim, Germany

Introduction

Examination of the bone marrow (BM) is of central importance for the diagnosis and staging of haematological disorders. Conventional aspiration cytology, flow cytometric immunophenotyping, cytogenetics and the histopathological examination of trephine BM biopsies, usually obtained from the posterior iliac crest, are currently the standard examination techniques [4, 15, 80]. Traditional indications for a trephine biopsy include all disorders in which marrow aspiration alone is considered unreliable or insufficient, such as staging of malignant lymphoma, chronic myeloproliferative disorders, metastatic disease and any disorder accompanied by marrow fibrosis [21, 68]. However, in many centres, trephine biopsy is considered an integral part of BM examination and is taken in most instances when an aspirate is performed, irrespective of the indication. Traditionally, the examination of BM biopsies was limited to conventional histological and histochemical stains, such as hematoxylin and eosin, Giemsa, NASD-chloroacetate-esterase, as well as iron and reticulin stains. The availability of a broad range of antibodies suitable for paraffin sections as well as the development of molecular techniques applicable to fixed tissues have significantly broadened the possibilities for the examination of trephine biopsy samples. Although an excellent morphology undoubtedly remains the mainstay and basis for the diagnosis of haematological disorders, the thoughtful application of these ancillary methods can improve diagnostic accuracy, can help to obtain a better subclassification of neoplastic disorders and may increase sensitivity for the detection of residual disease. This review focuses on the methodical

possibilities and limits as well as the diagnostic applications of molecular in vitro techniques for the examination of BM trephines. The role of immunohistochemistry in BM diagnostics is addressed in a separate paper.

Relevance of BM fixation and processing for molecular studies

The presence of bone trabecules and the necessity for preservation of the subtle cytological features of haematopoietic cells poses special problems with regard to specimen fixation, decalcification and processing. To obtain optimal morphology, a variety of fixatives, including buffered formalin, Bouin's, mercury-containing solutions such as Zenker's fixative and B5 or a combination of formalin and glutaraldehyde (Schäfer's solution), are used, followed by brief acid-based or EDTA decalcification [62]. However, several of these fixatives have a detrimental influence on the immunoreactivity and/or the preservation of nucleic acids and therefore limit the application of ancillary techniques [74, 77]. In addition to paraffin embedding, plastic embedding of biopsies is still used. Extraction of DNA and even RNA suitable for molecular studies such as polymerase chain reaction (PCR)-based determination of B-cell clonality or detection of fusion transcripts is possible from plastic-embedded BM samples [6, 27]. However, due to the decreasing role of plastic embedding, the techniques described in this review are based on the use of conventional formalin-fixed, EDTA-decalcified, paraffin-embedded BM specimens, but can be equally applied to non-decalcified material such as BM clot preparations. Samples briefly decalcified with acid-based agents can also be used for DNA-based PCR assays [8, 30]. Fixation in buffered neutral formalin for 24 h followed by EDTA decalcification renders both satisfactory morphology as well as good antigen, DNA and even RNA preservation and therefore can be regarded as a good compromise between optimal morphological detail and the availability of the full spectrum of ancillary techniques. Although decalcification with EDTA is more time-consuming than treatment with acid-based agents, application of an ultrasonication bath allows decalcification within 8 to 12 h.

Similar to conventional paraffin tissues, DNA and RNA extracted from BM biopsies is significantly degraded, and the prevalent fragment size for DNA is below 500 bp. Decalcification procedures, prolonged fixation in comparison to surgical specimens and additives such as glutaraldehyde may further reduce the yield of amplifiable DNA. Nevertheless, we and others have demonstrated that DNA from trephine biopsies can be used for a broad range of PCR assays, and amplification products of more than 500 bp can be achieved [6, 43, 59, 64, 81, 83]. A large number of extraction protocols have been published for paraffin-embedded tissues. In our experience, such standard protocols can also be applied to BM trephines, as long as column-based kits designed for fresh tissue are used with caution, since they may lead to the exclusion of small DNA and RNA fragments. Common to all these procedures, proper digestion with Proteinase K (best performed at elevated temperature overnight) is mandatory to release the maximum amount of DNA from the tissue, whereas purification of DNA extracts is not necessary on a routine basis. Irrespective of the procedure used, control amplification of single copy gene fragment(s) of adequate size—usually in the range of 250–400 bp—is mandatory to check DNA quality, since some tests such as clonality analyses may render false positive results with highly degraded DNA. Control PCRs for amplificates of increasing size in a multiplex format, such as designed by the BIOMED-2 group, may help to get a better estimate of DNA quality [79].

If available, archival, air-dried BM smears can be used as an additional source for DNA and RNA of excellent quality, since they have not been subjected to cross-linking fixatives. Air-dried slides, which are received at many pathology laboratories in addition to trephine biopsies, can even be used for Southern blot analysis, which requires high molecular weight DNA [34].

Although the majority of applications of molecular diagnostics on BM biopsies still use DNA as template source, recent studies have described RNA-based analyses from paraffin-embedded BM samples for a variety of purposes, especially in combination with quantitative techniques such as real-time reverse transcriptase (RT)-PCR (Table 1). The negative effects of fixation, embedding and extraction procedures on RNA integrity, which is less resistant than DNA, have been elucidated [51]. Parameters such as tissue fixation (i.e. type of fixation reagent, duration of fixation) and RNA extraction (i.e. concentration of Proteinase K, duration of sample digestion) have different effects on RNA integrity [40, 41, 55, 73]. However, the mechanisms which lead to cross-linkage between RNA and proteins and to the addition of monomethylol ($-CH_2OH$) groups to all four bases by formalin is largely unknown [51]. The decalcification procedure applied on BM trephines also exhibits a negative effect on RNA integrity [7]. Preferably, the fixed BM trephine should be decalcified in a solution displaying a neutral pH such as EDTA, because an acidic environment augments the process of RNA fragmentation. The degree of RNA fragmentation is variable within different tissues, but the average length of RNA from archival tissues such as BM trephines can be estimated rarely to exceed 200 bp. PCR products which are 100 bp in size or less are amplified more efficiently and thus highly recommended [32, 46, 73].

Indications for molecular examination of BM biopsies

Determination of clonality in the diagnosis of lymphoproliferative disorders

The differential diagnosis of lymphoid infiltrates in the BM is one of the most frequent problems in haematopathology. Although the majority of lymphoid infiltrates can safely be diagnosed as either reactive or neoplastic based on the

Table 1 Common applications of molecular diagnostics on trephine bone marrow biopsies

Diagnostic application	Method	References
B-cell clonality	IgH PCR	[8, 9, 22, 27, 59, 61, 77]
	Microdissection and IgH PCR	[43–45]
	Quantitative RT-PCR for κ and λ light chains	[48]
T-cell clonality	TCR gamma PCR	[30, 81, 82]
	TCR gamma PCR with RNase protection assay	[35]
Cyclin D1 overexpression in B-NHL	Quantitative RT-PCR	[71, 72]
BCR–ABL fusion transcripts in CML	Quantitative RT-PCR	[3, 6, 7, 40, 41]
C-kit mutations in systemic mastocytosis	Sequencing, allele-specific probes, microdissection	[70, 76]
Mycobacterial infection	PCR	[1, 69]
General methodical studies	DNA PCR	[34, 46, 64, 74, 83]
	RT-PCR	[32, 40, 41, 49, 55]

IgH Immunoglobulin heavy chain gene, *TCR* T-cell receptor gene

extent of involvement, distribution, cytology and immunophenotype, a significant minority of cases cannot be classified with certainty [43, 78]. For some low-grade lymphoma entities such as follicular and marginal zone B-cell lymphoma, the detection of an aberrant immunophenotype may be difficult or impossible in small BM infiltrates. Even flow cytometric immunophenotyping as complementary technique may fail to detect a proportion of cases with BM infiltration, mainly due to sampling error in the presence of focal fibrosis [36, 75]. However, the presence of limited vs disseminated disease—as characterized by the presence of BM involvement—is of crucial importance as prognostic information and for therapeutic decision making.

Detection of B-cell clonality

A variety of approaches have been used for the molecular detection of B-cell clonality in BM specimens. For paraffin-embedded tissues in general, the use of consensus primers against the framework 3 (FR3) or framework 2 (FR2) regions of the immunoglobulin (Ig) heavy chain variable genes in conjunction with primers against the joining region (JH or FR4) [2, 18, 20, 56, 79] is the most frequently chosen approach and will pick up clonality in 50–90% of B-cell non-Hodgkin's lymphoma (B-NHL) cases with a significant BM infiltrate, depending on the type of lymphoma and the method used for the analysis of amplicons [8, 9, 14, 27, 61, 63, 81]. Whereas B-cell chronic lymphocytic leukemia (B-CLL) and mantle cell lymphoma show a clonal product in nearly 100% of cases with these primer sets; other entities, especially follicular lymphoma, will show much lower clonality rates. This is due to point mutations and other events during ongoing somatic hypermutation, which alter or abolish primer binding sites. This relatively high false negative rate has to be kept in mind when evaluating molecular results in the setting of suspicious lymphoid BM infiltrates. Acute lymphoid leukemias may show false negative results due to incomplete VDJ rearrangements [79].

Other primer combinations, such as the recently published BIOMED-2 primer sets, which give a much higher pick-up rate of more than 90% irrespective of lymphoma type, have not been tested sufficiently on BM samples to allow for definitive conclusions [79]. However, primer sets rendering amplicons in excess of 300 base pairs such as the family-specific framework 1 (FR1) region primers should be used with caution on fixed BM samples, because poor DNA quality may result in detection of pseudoclonality due to preferential amplification of rare B cells. The same problem may occur, if semi-nested or nested protocols are used which can give oligoclonal or pseudoclonal results with poor template quality [37, 43]. To avoid false positive results, stringent control of DNA quality and reproducibility of PCR results are mandatory. Repetition of the same PCR reaction with different template concentrations, or repeat extractions, are ways to confirm clonal results [25, 38].

To increase the sensitivity for the detection of small clonal populations in nodular lymphoid infiltrates, we have successfully used microdissection to enrich the target cell population [43–45]. Although this increases the pick-up rate through reduction of the polyclonal background population, it also increases the risk of pseudoclonality due to the small amount of template, and only clearly reproducible bands of identical size should be regarded as evidence for clonality [43, 85]. Since the most frequent diagnostic question is the presence of BM involvement by a malignant lymphoma diagnosed at another site, DNA from the primary tumor can be used for comparative purposes, and clonal products of the same size and sequence will confirm the presence of BM infiltration. However, one has to keep in mind that lymphoid infiltrates in the marrow may be the result of another clonal process, rather than dissemination of an extramedullary lymphoma. This is especially the case in so-called discordant lymphoma, where a BM infiltrate composed of small lymphocytes is found in the setting of nodal or extranodal large cell lymphoma. In a recent study, we were able to show that one third of the cases of discordant lymphoma actually represented two different clonal processes, rather than morphological progression of the same clone (Fig. 1) [45].

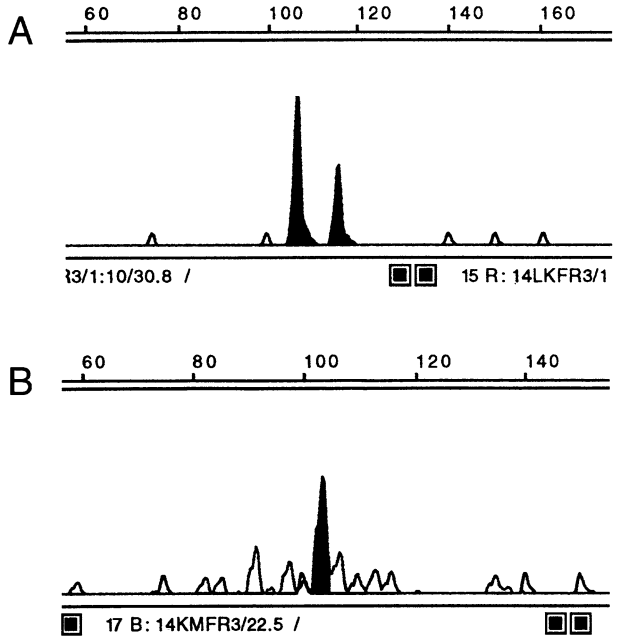


Fig. 1 Genescan analysis of immunoglobulin heavy chain gene PCR products with framework 3 (*FR3*) primers in a patient with diffuse large B-cell lymphoma and so-called discordant bone marrow involvement by small lymphocytes. **a** Lymph node biopsy. **b** Microdissected lymphoid infiltrates from the BM trephine. Genescan analysis shows two clonal products of different size. A distinct clonal origin was confirmed by sequencing

Another application of microdissection in BM biopsies is the clonal analysis of two neoplastic processes with divergent phenotype, such as composite NHL or combinations of Hodgkin's and non-Hodgkin's lymphoma [28, 29, 45]. In addition to nodular infiltrates necessitating discrimination from reactive lymphoid aggregates, some lymphoma subtypes with occasionally very subtle patterns of infiltration such as splenic marginal zone lymphoma or intravascular large B-cell lymphoma may require molecular studies for diagnostic confirmation [22].

There are very few data available concerning the sensitivity of molecular techniques in BM trephines, but it can be assumed from mixing experiments and other data that the sensitivity is the range of 2–10% clonal cells with conventional consensus primers, if sensitive detection methods such as the Genescan technique with fluorescently labelled primers, heteroduplex analysis or high resolution polyacrylamide gels are used. BM trephines may be more representative samples for molecular studies than simultaneously obtained aspirates, since the aspirate is frequently significantly diluted by peripheral blood lymphocytes, a phenomenon similarly observed in flow cytometric immunophenotyping [14, 36].

The detection rate can be increased by addition of primers for common translocations, namely the t(14;18)(q32;q21) involving the bcl-2 locus in follicular lymphoma and the t(11;14)(q13;q32) involving the bcl-1/CCND1 locus in mantle cell lymphoma. However, extremely sensitive tests such as nested PCR, which can pick up rare cells carrying the translocation, should be avoided in the diagnostic setting. A detection of the t(14;18) without morphological correlate is not sufficient for a diagnosis of malignancy on its own, since rare benign B cells carrying this translocation are a frequent finding in elderly patients [52, 53]. Positive results, especially for bcl-2 rearrangements, obtained in BM samples should always be compared to the primary diagnostic tissue by appropriate techniques such as sequencing to confirm the clonal identity of the detected translocation.

Alternative methods for detection of B-cell clonality such as the use of primers against the kappa light chains can be employed analogously to the common Ig heavy chain assays [33]. More recently, a promising technique for BM biopsies based on the quantitative detection of kappa and lambda mRNA transcript ratio has been described [48].

Detection of T-cell clonality

Since BM involvement by T-cell NHL (T-NHL) is distinctly less frequent compared to B-cell lymphoma, only a limited number of studies have dealt with the molecular detection of T-cell clonality in BM trephines [30, 35, 44, 81, 82]. Nevertheless, molecular studies may provide significant help in certain diagnostic settings. The higher number of reactive T-cells in normal BM, the frequent difficulty to identify an abnormal immunophenotype in T-cell neoplasms and the subtle pattern of infiltration characteristic for certain T-NHL such as T-cell proliferations of large granular lymphocytes (T-LGL) or hepatosplenic T-cell lymphoma are potential reasons to study T-cell clonality in BM trephines [30, 82]. The most frequently used strategy for detection of T-cell clonality in paraffin-embedded tissues are various primer combinations directed at the T-cell receptor gamma locus (TCRγ), less commonly against the TCRβ genes, since the latter locus is more complex and requires a large number of primers [2, 57, 79]. The vast majority of T-cell neoplasms of both α/β, as well as γ/δ, phenotype show TCRγ rearrangements. Since somatic hypermutation of rearranged TCR genes does not occur, mispriming is less of a problem than in B-cell lymphomas. However, due to the restricted repertoire of germline genes, pseudoclonality due to diverse rearrangements of identical length may cause false positive results, especially with a limited number of target cells. Therefore, analysis of PCR products by either Genescan or heteroduplex analysis is mandatory, and each reaction should be run at least in duplicate [79].

General issues of clonality determination

One needs to point out that demonstration of B- or T-cell clonality in the BM should not be equated with malignancy. Leaving the technical problem of pseudoclonality aside, true lymphocyte clones may be detected in a variety of fairly common benign or premalignant disorders, such as monoclonal gammopathy of unknown significance (MGUS), in patients with subclinical clonal B-cell populations with a B-

CLL phenotype or occasionally in patients with nodular lymphoid infiltrates [26, 43]. This underlines that a diagnosis of malignancy should only be made if appropriate clinical, morphological and phenotypical findings are present.

The identification of a clonal population in the presence of a morphologically suspicious lymphoid infiltrate with standard molecular techniques has to be discerned from the detection of minimal (residual) disease for staging or follow-up purposes. The presence of minimal numbers of clonal cells in morphologically negative BM samples of lymphoma patients, identified through highly sensitive techniques such as nested PCR or with clone-specific primer sets, usually does not carry the same impact on patient management as overt BM involvement, but may help to identify patients at higher risk for relapse or progression. For a more detailed review of the topic of minimal residual disease, especially in the context of new treatment options and the technical issues involved such as tumor-specific primers and quantitative PCR, the extensive haematological literature should be consulted [11, 17, 23].

Practical issues of DNA studies in trephine BM biopsies

DNA is extracted either from serial paraffin sections or microdissected tissue fragments with xylene followed by a graded alcohol series. The resulting pellet is digested overnight with Proteinase K in an adequate amount (25–200 μl) of buffer at 55°C and continuous shaking. If the supernatant is clear, Proteinase K is inactivated by boiling, and the resulting crude extract is used directly as template for PCR. Since quantitation of DNA by photometric measurement is of limited usefulness, it can be helpful to perform two PCR reactions in parallel, using two different DNA concentrations (e.g. 1–2 μl undiluted and diluted 1:10). As mentioned above, DNA extracted from trephine BM biopsies may show increased degradation, and it is crucial to check amplification efficiency with a control primer set. The size of the control product should be larger than the fragment size achieved with primer sets routinely used for clonality determination, e.g. at least 250–270 bp. Most diagnostic DNA PCR assays in our laboratory are carried out as single-step PCR with 40 cycles of amplification. For clonality determination, AmpliTaq Gold (Perkin Elmer) has shown better amplification efficiency. Separation of fluorescently labelled PCR products for clonality determination is performed in our laboratories by automated fragment length analysis using an ABI 3130 capillary sequencer (Applied Biosystems, Foster City, CA). Alternatively, polyacrylamide gels (with or without heteroduplex analysis) may be used, but agarose gel electrophoresis alone is clearly insufficient for product analysis. Currently used primer sets are listed in Table 2. Although the clonality pick-up rate in NHL varies with different primer sets, a fairly good concordance between different laboratories has been reached in multi-centre trials, if stringent quality controls are performed and more than one primer set is used [12].

Quantitation of gene expression

In addition to using the ratio of Ig light chain mRNAs as a surrogate marker for B-cell clonality [48], the recent advent of real-time RT-PCR for the precise quantitation of mRNA transcripts holds significant promise for BM diagnostics.

Table 2 Sequences of primers commonly used in our laboratories

Primer	Sequence 5′–3′	Product size
B-cell clonality		
FR3, forward	ACACGGCYSTGTATTACTGT[a]	~70–130 bp[b]
FR2a, forward	TGGRTCCGMCAGSCYYCNGG[a]	~230–270 bp[b]
Bcl2 (MBR), forward	TTAGAGAGTTGCTTTACGTGGCCTG	~100–250 bp
JHa, reverse[c]	ACCTGAGGAGACGGTCACC	–
T-cell clonality		
Vγ11, forward	TCTGGRGTCTATTACTGTG[a]	–
Vγ101, forward	CTCACACTCYCACTTC[a]	–
Jg11, reverse	CAAGTGTTGTTCCACTGCC	~60–80 bp (Vγ11 + Vγ101)[b]
Jp11, reverse	GTTACTATGAGCYTAGTCC[a]	~70–90 bp (Vγ11 + Vγ101)[b]
BCR–ABL		
b2, forward	ATCCGTGGAGCTGCAGATG	b2a2 (111 bp), b2a3 (118 bp)
b3, forward	GAGTCTCCGGGGCTCTATGG	b3a2 (98 bp), b3a3 (103 bp)
e1, forward	AGATCTGGCCCAACGATGGCGA	e1a2 (73 bp), e1a3 (79 bp)
a2, reverse	TCAGATGCTACTGGCCGCTGA	–
a3, reverse	TGTGATTATAGCCTAAGACC	–

MBR Major breakpoint region of bcl-2 in follicular lymphoma
[a]These primers contain sites with multiple ("degenerate") nucleotides to allow annealing to different VH (or TCR J) genes
[b]Gives the approximate size range for a product derived from a normal polyclonal population
[c]Alternatively, a mix of multiple JH primers (JH 1-2-4-5 and JH3 and JH6) can be employed

By using microdissected cells from paraffin sections including decalcified BM biopsies, we could show that determination of cyclin D1 levels with real-time PCR, using intron-spanning primers (exon 1/2) amplifying a 70-bp mRNA fragment and a corresponding specific TaqMan probe (Perkin Elmer) is an excellent tool for the differential diagnosis of small B-cell neoplasms [71]. Mantle cell lymphomas could be reliably discerned from other lymphoma subtypes by virtue of their constantly high cyclin D1 levels caused by the t(11;14)(q13;q32) translocation (Fig. 2). Hairy cell leukemia, which shows up-regulation of cyclin D1 by another, so far unknown mechanism, showed cyclin D1 levels intermediate between mantle cell lymphoma and other B-NHL. In multiple myeloma, real time RT-PCR was able to discriminate three groups with high, intermediate and low to negative cyclin D1 levels. All cases with high mRNA levels showed the presence of a t(11;14) by fluorescence in situ hybridization (FISH), whereas most cases with intermediate values contained a trisomy 11, pointing to a role of gene dosage for cyclin D1 levels. Cases with low to negative cyclin D1 did not show alterations of the CCND1 (cyclin D1) locus on 11q13 by FISH [72]. This example demonstrates the enormous potential of quantitative gene expression analysis in archival tissues. However, the pitfalls as well as the biological and technical limitations of these techniques have to be kept in mind if they are applied for diagnostic purposes [32, 49, 51, 73, 74]. The problem of normalization has not been solved satisfactorily to date, since many so-called "housekeeping" genes can show some variation in expression levels depending on cell type and conditions. In addition, the normalization against multiple housekeeping genes recommended by some investigators may be impractical in the diagnostic setting with sometimes very limited archival material. Furthermore, quantitative RT-PCR assays may show variable sensitivity to fixation-mediated degradation or alterations of secondary RNA structure, which necessitates stringent controls for comparisons among different mRNA species. Nevertheless, the investigation of differential expression ratios using the delta/delta Ct method is feasible in paraffin-embedded BM biopsies if results are rigorously controlled, and the expression levels of the target genes are within the linear range of the standard curve.

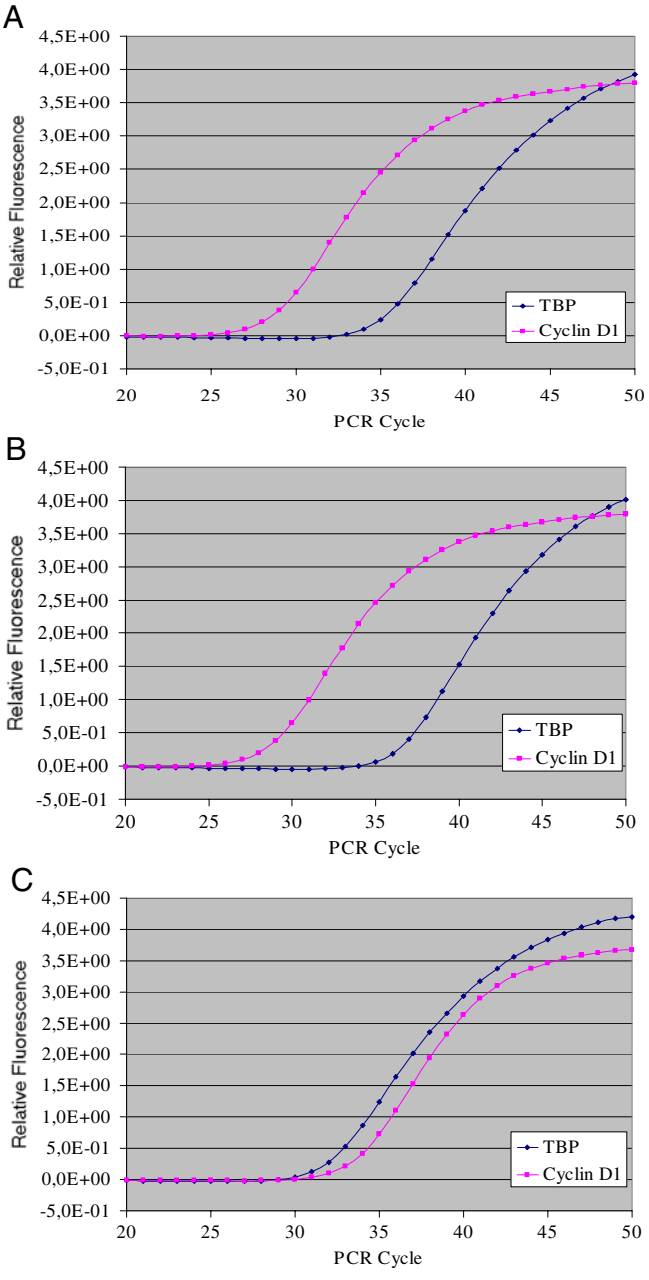


Fig. 2 Amplification plots of cyclin D1 and housekeeping gene TBP of microdissected tumor cells from a patient with mantle cell lymphoma. **a** Lymph node biopsy. **b** BM biopsy involved by lymphoma. **c** Reactive control lymph node. Whereas the curves for cyclin D1 and TBP are almost superimposed in the control tissue, both lymph node and BM biopsy show an identical left shift of the cyclin D1 curve with significantly lowered Ct, indicating significant overexpression of cyclin D1 mRNA

Molecular diagnostics in myeloproliferative disorders

The rapidly expanding knowledge of the molecular alterations in myeloproliferative diseases and their importance for patient management have resulted in an increasing amount of work aimed at identifying these genetic alterations in trephine biopsy samples. A model disease where molecular studies are of significant practical relevance is chronic myelogenous leukemia (CML), which is characterized by the hallmark Philadelphia chromosome caused by the t(9;22) translocation resulting in a breakpoint cluster region–Abelson (BCR–ABL) fusion. Already more than 10 years ago, up to two-decade-old archival tissues were demonstrated to be suitable for detection of BCR–ABL hybrid genes and fusion transcripts [3]. In accordance with these data, the successful detection of BCR–ABL transcripts also has been shown in other reports [40, 41]. Predominantly, these studies were conducted to confirm that these molecular techniques are applicable to archival tissues, i.e. proof of principle. The transfer of these techniques to the daily routine, however, represents a challenging step.

Histomorphological evaluation of the patients' BM trephine in synopsis with clinical data usually enables the diagnosis of CML. In CML, the initial diagnostic workup is often accompanied by application of metaphase cytogenetics or FISH analysis performed on BM aspirates, i.e. fresh specimens. In more than 95% of typical CML as well as in up to 30% of adult and 5% of childhood acute lymphoblastic leukemia (ALL), a reciprocal chromosomal translocation t(9;22), can be detected [13, 19]. This translocation exhibits an underlying molecular anatomy with either a major BCR (M-BCR), a minor BCR (m-BCR) or rarely a micro BCR (μ-BCR). In CML, the M-BCR typically encodes for the fusion transcript b2a2 or b3a2, whereas in ALL, the m-BCR mainly encodes for e1a2 [19]. In some cases of chronic neutrophilic leukemia, e19a2 fusion transcripts were detected as the result of a breakpoint in the μ-BCR [19]. Although several rare types of fusion transcripts have been described (e.g. b2a3, e1a3) [47], the most frequently detected types are indeed b2a2, b3a2 and e1a2 (Fig. 3). However, there is no complete concordance between the type of BCR–ABL fusion transcript and the disease type, either CML or ALL. Rare cases of typical CML can exhibit transcripts derived from the m-BCR [66]; conversely, some ALL cases contain M-BCR fusions [31]. The fusion transcripts of the M-BCR and m-BCR encode for chimeric proteins, the $p210^{BCR–ABL}$ and the $p190^{BCR–ABL}$ protein, respectively. This causes aberrant expression and constitutive activation of the ABL tyrosine kinase with uncontrolled proliferation of the affected neoplastic cells [19]. In cases of ALL, the detection of BCR–ABL fusion transcripts is associated with an aggressive course and poor survival [13].

Although CML and ALL typically can be diagnosed by histomorphological evaluation and in ALL additional immunohistochemistry, pathologists may be confronted with the need to investigate the BCR–ABL rearrangement in patients presenting with myeloproliferative disorders in case of (1) small BM biopsies with haematopoiesis that is not representative (2) leukemic infiltrates without available metaphase cytogenetics and (3) the existence of cryptic translocations that cannot be detected by conventional cytogenetics [10]. In addition, the embedded BM trephine may be the only available material when cytogenetics has not been conducted initially. Especially since the introduction of a specific tyrosine kinase inhibitor against the BCR–ABL protein (imatinib mesylate, formerly STI 571), which has shown marked activity in patients with CML and Ph1+ ALL, the detection of a BCR–ABL transcript and its type should accompany both initial diagnosis and the monitoring of tyrosine kinase inhibitor-based therapies [13, 24].

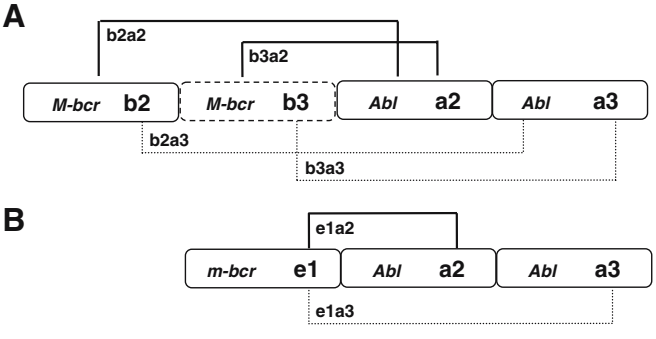


Fig. 3 Schematic illustration of the BCR and ABL hybrid genes fused in the M-BCR (**a**) and m-BCR (**b**). *Drawn lines* in the M-BCR (b2a2, b3a2) and m-BCR (e1a2) represent the most common fusion transcripts derived from the BCR–ABL hybrid genes. *Dotted lines* indicate rare but optional detectable fusion transcripts (b2a3, b3a3, e1a3)

Given the considerable extent of RNA degradation in paraffin-embedded tissues, the detection of BCR–ABL transcripts is more efficient when the product amplified by RT-PCR is less than 100 bp. In addition, for the specific detection of a particular BCR–ABL transcript, one primer should be placed directly into the fusion region. Primers suitable for RT-PCR for amplification of either b2a2 or b3a2 fusion transcripts have been previously described [16]. Although not particularly designed for the application in archival tissues, the accuracy of these assays has been successfully reproduced in our hands in archival BM trephines of patients with proven Ph-chromosome positive CML and ALL.

RT-PCR assays should be able to detect the three most common BCR–ABL transcripts. For the daily routine in a diagnostic molecular pathology laboratory, at least three RT-PCR reactions per case (+RT in duplicate, single −RT reaction as the case-specific control) per given BCR–ABL fusion type as well as adequate positive control reactions for all types have to be performed, giving a total of at least 12 RT-PCR reactions for one case. However, rare BCR–ABL fusion transcripts will not be detectable by such an approach. Multiplex RT-PCR approaches could reduce time and costs by enabling the detection of several potential BCR–ABL fusion types in a single reaction. A variety of multiplex RT-PCR assays including commercially available kits have been described by different laboratories [54, 67, 84]. However, their usefulness is restricted to fresh, unfixed samples such as peripheral blood or BM mononuclear cells because of the large amplicons generated by these assays. Unfortunately, a multiplex PCR approach often leads to a reduced sensitivity due to primer interference along with suboptimal PCR reaction conditions [60]. We have recently described a simple, robust and reliable multiplex RT-PCR, the usefulness of which for daily routine has been extensively demonstrated (Fig. 4) [7]. In addition, the detection of rare transcripts such as e1a3 is enabled by using the same forward primers and placing an additional reverse primer in ABL exon a3 (see Table 2). However, for diagnostic purposes it is highly recommended to initially establish BCR–ABL fusion type-specific RT-PCR assays separately and only consecutively design a multiplex RT-PCR along with optimization of reaction conditions.

The quantification of BCR–ABL fusion transcripts in peripheral blood mononuclear cells (PBMC) and BM aspirates of patients with CML and ALL using real-time RT-PCR has been shown to be important for monitoring the response to therapeutical intervention such as BM transplantation, peripheral blood stem cell tranplantation

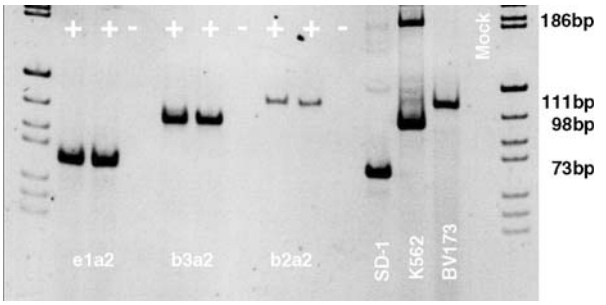


Fig. 4 Representative gel-electropheresis demonstrating BCR–ABL positivity in bone marrow trephines of patients with Ph+ CML (b3a2, b2a2) and Ph+ ALL (e1a2). Each case was analysed in duplicate by a multiplex RT-PCR along with a negative control. BCR–ABL positive cell lines (SD-1, K562, BV173) serve as positive control. Note that these primer design and primer mix respect the inevitable fragmentation of RNA in archival tissues by generating PCR products that are as small as required for an efficient RT-PCR approach. The two PCR products obtained in the K562 cell line derived from the exon-specific binding of the forward primers (b3–a2=98 bp, b2–[b3]–a2=186 bp, respectively). DNA marker, pBR322/Bsu RI. Note that it is digitally inverted

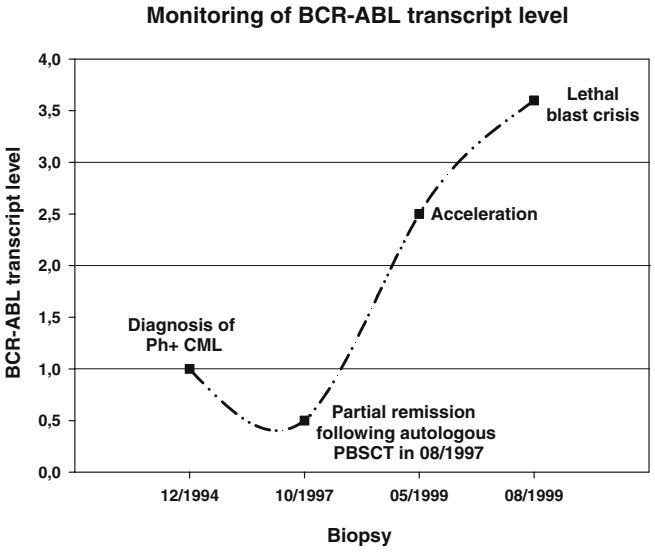


Fig. 5 Retrospective monitoring of BCR–ABL transcript levels in archival bone marrow trephines of a patient with Ph+ CML initially diagnosed in 1994. Declining levels could be correlated to a histopathologically demonstrable partial remission in 10/1997 after an autologous PBSCT in 08/1997. The phase of acceleration diagnosed in 05/1998 was accompanied with a 3.0-fold increase of BCR–ABL transcripts. The patient died in the blast crisis 3 months later after another increase of the BCR–ABL transcript level

(PBSCT), interferons and tyrosine kinase inhibitors [19]. Furthermore, the levels of BCR–ABL transcripts prior, during and after therapeutic intervention seem to predict the clinical outcome of the patients, and thus qualitative and quantitative detection of these transcripts from PBMC became a standard in clinical studies [65]. To transfer our knowledge from qualitative detection to quantitative monitoring of BCR–ABL transcripts, we investigated whether archival BM trephines of patients with proven CML are suitable for determination of the BCR–ABL transcript level at a given time point of the disease [6]. Retrospectively, we retrieved sequential BM trephines that have been taken from ten patients during the course of the disease, including more than 10-year-old plastic-embedded specimens. We were able to demonstrate that monitoring of BCR–ABL transcript levels in both plastic- and paraffin-embedded BM trephines is feasible in an accurate and sensitive manner. Moreover, the intra-individual BCR–ABL transcript level could be properly correlated with the histomorphological features at a given time point during the course of the disease. One representative time course of a CML is shown to demonstrate the BCR–ABL transcript levels in good correlation with therapeutic interventions and histopathological findings (Fig. 5).

Although the detection of BCR–ABL fusion transcripts currently is the most relevant molecular diagnostic assay in myeloproliferative disorders, several other applications have been described in the last years, e.g. suppressor gene methylation in myelodysplastic syndromes and expression of aberrant transcripts in chronic myeloproliferative disorders based on DNA and RNA extracted from paraffin-embedded trephines. Using either laser capture microdissection of immunostained BM sections or special PCR techniques for enrichment of the mutated allele, several groups demonstrated the occurrence of the activating c-kit mutation D816V in mast cells and lymphoid aggregates of patients with systemic mastocytosis [70, 76].

Another potential application of molecular diagnostics on BM trephines is the detection of the recently described activating point mutation V617F in the JAK2 gene, which is found in a high percentage of chronic myeloproliferative disorders other than CML [5, 39, 42, 50].

Other applications of molecular tests in BM pathology

Several other applications for molecular testing on BM biopsies have been described, and many assays performed on aspirates can be adapted to trephine biopsies. For example, the detection of tumor-specific fusion transcripts can also be applied to recurrent translocations of soft tissue tumors involving the BM, such as the t(11;22)(q24;q12) EWS/FLI-1 and t(21;22)(q22;q12) EWS/ERG translocations of Ewing sarcoma. In the future, minimal residual disease quantitation by real-time RT-PCR will play an increasing role for monitoring these patients under therapy [86]. In non-neoplastic disorders, detection of infectious agents such as *Mycobacteria* spp., especially in immunosuppressed patients, can be facilitated by molecular testing [1, 69].

Conclusions

In conjunction with other techniques such as immunohistochemistry and FISH [58, 72], the application of molecular genetics to paraffin-embedded BM trephines has significantly expanded the scope of histopathologic bone marrow examination. Some tests, such as PCR-based determination

of clonality, can help to resolve common diagnostic problems such as the nature of nodular lymphoid BM infiltrates in the setting of NHL. If the technical aspects of BM fixation and processing are observed and common pitfalls such as poor template quality avoided, the success rates for molecular studies in BM trephines are equal to other routinely fixed, archival tissues. The combination of excellent morphological detail and preservation of marrow architecture with the phenotypical and genetic information obtained from ancillary techniques makes the BM trephine biopsy a valuable resource for modern diagnostics and research in haematopathology.

Acknowledgements We thank Mrs. Birgit Geist for her excellent technical support. This study was supported in part by the Deutsche Forschungsgemeinschaft (DFG), grant FE 597/1 to FF, LQ-M and MK.

References

1. Akcan Y, Tuncer S, Hayran M, Sungur A, Unal S (1997) PCR on disseminated tuberculosis in bone marrow and liver biopsy specimens: correlation to histopathological and clinical diagnosis. Scand J Infect Dis 29:271–274
2. Arber DA (2000) Molecular diagnostic approach to non-Hodgkin's lymphoma. J Mol Diagn 2:178–190
3. Aurer I, Juhbashi T, Sekine I, Tomonaga M, Gale RP (1993) Analysis of BCR/ABL abnormalities in mRNA from 20-year-old paraffin-embedded tissue for BCR/ABL rearrangement by polymerase chain reaction. Acta Haematol 90:5–7
4. Bain BJ (2001) Bone marrow trephine biopsy. J Clin Pathol 54:737–742
5. Baxter EJ, Scott LM, Campbell PJ, East C, Fourouclas N, Swanton S, Vassiliou GS, Bench AJ, Boyd EM, Curtin N, Scott MA, Erber WN, Green AR (2005) Acquired mutation of the tyrosine kinase JAK2 in human myeloproliferative disorders. Lancet 365:1054–1061
6. Bock O, Lehmann U, Kreipe H (2003) Quantitative intra-individual monitoring of BCR–ABL transcript levels in archival bone marrow trephines of patients with chronic myeloid leukemia. J Mol Diagn 5:54–60
7. Bock O, Reising D, Kreipe H (2003) Multiplex RT-PCR for the detection of common BCR–ABL fusion transcripts in paraffin-embedded tissues from patients with chronic myeloid leukemia and acute lymphoblastic leukemia. Diagn Mol Pathol 12:119–123
8. Braunschweig R, Baur AS, Delacretaz F, Bricod C, Benhattar J (2003) Contribution of IgH–PCR to the evaluation of B-cell lymphoma involvement in paraffin-embedded bone marrow biopsy specimens. Am J Clin Pathol 119:634–642
9. Brinckmann R, Kaufmann O, Reinartz B, Dietel M (2000) Specificity of PCR-based clonality analysis of immunoglobulin heavy chain gene rearrangements for the detection of bone marrow involvement by low-grade B-cell lymphomas. J Pathol 190:55–60
10. Browett PJ, Cooke HM, Secker-Walker LM, Norton JD (1989) Chromosome 22 breakpoints in variant Philadelphia translocations and Philadelphia-negative chronic myeloid leukemia. Cancer Genet Cytogenet 37:169–177
11. Bruggemann M, Pott C, Ritgen M, Kneba M (2004) Significance of minimal residual disease in lymphoid malignancies. Acta Haematol 112:111–119
12. Cabras AD, Kremer M, Schulz S, Werner M, Hummel M, Komminoth P, Höfler G, Höfler H (2000) Quality assessment in diagnostic molecular pathology: experience from a German–Austrian–Swiss multicenter trial. Virchows Arch 437:46
13. Cilloni D, Guerrasio A, Giugliano E, Scaravaglio P, Volpe G, Rege-Cambrin G, Saglio G (2002) From genes to therapy: the case of Philadelphia chromosome-positive leukemias. Ann N Y Acad Sci 963:306–312
14. Coad JE, Olson DJ, Christensen DR, Lander TA, Chibbar R, McGlennen RC, Brunning RD (1997) Correlation of PCR-detected clonal gene rearrangements with bone marrow morphology in patients with B-lineage lymphomas. Am J Surg Pathol 21:1047–1056
15. Cotelingam JD (2003) Bone marrow biopsy: interpretive guidelines for the surgical pathologist. Adv Anat Pathol 10:8–26
16. Cross NC, Melo JV, Feng L, Goldman JM (1994) An optimized multiplex polymerase chain reaction (PCR) for detection of BCR–ABL fusion mRNAs in haematological disorders. Leukemia 8:186–189
17. Darby AJ, Johnson PW (2002) Molecular remission and non-Hodgkin's lymphoma. Best Pract Res Clin Haematol 15:549–562
18. Deane M, McCarthy KP, Wiedemann LM, Norton JD (1991) An improved method for detection of B-lymphoid clonality by polymerase chain reaction. Leukemia 5:726–730
19. Deininger MW, Goldman JM, Melo JV (2000) The molecular biology of chronic myeloid leukemia. Blood 96:3343–3356
20. Derksen PW, Langerak AW, Kerkhof E, Wolvers-Tettero IL, Boor PP, Mulder AH, Vrints LW, Coebergh JW, van Krieken JH, Schuuring E, Kluin PM, van Dongen JJ (1999) Comparison of different polymerase chain reaction-based approaches for clonality assessment of immunoglobulin heavy-chain gene rearrangements in B-cell neoplasia. Mod Pathol 12:794–805
21. Diebold J, Molina T, Camilleri-Broet S, Le Tourneau A, Audouin J (2000) Bone marrow manifestations of infections and systemic diseases observed in bone marrow trephine biopsy review. Histopathology 37:199–211
22. DiGiuseppe JA, Hartmann DP, Freter C, Cossman J, Mann RB (1997) Molecular detection of bone marrow involvement in intravascular lymphomatosis. Mod Pathol 10:33–37
23. Dolken G (2001) Detection of minimal residual disease. Adv Cancer Res 82:133–185
24. Druker BJ, Sawyers CL, Kantarjian H, Resta DJ, Reese SF, Ford JM, Capdeville R, Talpaz M (2001) Activity of a specific inhibitor of the BCR–ABL tyrosine kinase in the blast crisis of chronic myeloid leukemia and acute lymphoblastic leukemia with the Philadelphia chromosome. N Engl J Med 344:1038–1042
25. Elenitoba-Johnson KS, Bohling SD, Mitchell RS, Brown MS, Robetorye RS (2000) PCR analysis of the immunoglobulin heavy chain gene in polyclonal processes can yield pseudoclonal bands as an artifact of low B cell number. J Mol Diagn 2:92–96
26. Fend F, Weyrer K, Drach J, Schwaiger A, Umlauft F, Grunewald K (1993) Immunoglobulin gene rearrangement in plasma cell dyscrasias: detection of small clonal cell populations in peripheral blood and bone marrow. Leuk Lymphoma 10:223–229
27. Fend F, Gschwendtner A, Gredler E, Thaler J, Dietze O (1994) Detection of monoclonal B-cell populations in decalcified, plastic-embedded bone marrow biopsies with the polymerase chain reaction. Am J Clin Pathol 102:850–855
28. Fend F, Quintanilla-Martinez L, Kumar S, Beaty MW, Blum L, Sorbara L, Jaffe ES, Raffeld M (1999) Composite low grade B-cell lymphomas with two immunophenotypically distinct cell populations are true biclonal lymphomas. A molecular analysis using laser capture microdissection. Am J Pathol 154:1857–1866
29. Fend F, Kremer M, Specht K, Quintanilla-Martinez L (2003) Laser microdissection in hematopathology. Pathol Res Pract 199:425–430
30. Gebhard S, Benhattar J, Bricod C, Meuge-Moraw C, Delacretaz F (2001) Polymerase chain reaction in the diagnosis of T-cell lymphoma in paraffin-embedded bone marrow biopsies: a comparative study. Histopathology 38:37–44

31. Gleissner B, Gokbuget N, Bartram CR, Janssen B, Rieder H, Janssen JW, Fonatsch C, Heyll A, Voliotis D, Beck J, Lipp T, Munzert G, Maurer J, Hoelzer D, Thiel E (2002) Leading prognostic relevance of the BCR–ABL translocation in adult acute B-lineage lymphoblastic leukemia: a prospective study of the German multicenter trial group and confirmed polymerase chain reaction analysis. Blood 99:1536–1543
32. Godfrey TE, Kim SH, Chavira M, Ruff DW, Warren RS, Gray JW, Jensen RH (2000) Quantitative mRNA expression analysis from formalin-fixed, paraffin-embedded tissues using 5′ nuclease quantitative reverse transcription–polymerase chain reaction. J Mol Diagn 2:84–91
33. Gong JZ, Zheng S, Chiarle R, De Wolf-Peeters C, Palestro G, Frizzera G, Inghirami G (1999) Detection of immunoglobulin kappa light chain rearrangements by polymerase chain reaction. An improved method for detecting clonal B-cell lymphoproliferative disorders. Am J Pathol 155:355–363
34. Grunewald K, Lyons J, Hansen-Hagge TE, Janssen JW, Feichtinger H, Bartram CR (1991) Molecular genetic analysis of DNA obtained from fixed, air dried or paraffin embedded sources. Ann Hematol 62:108–114
35. Hanamura A, Kinoshita T, Kurokawa T, Nagai H, Murate T, Nagasaka T, Mori H, Saito H (1999) Molecular evaluation of bone marrow involvement in peripheral T-cell lymphoma with a PCR-mediated RNase protection assay. Int J Hematol 70:283–289
36. Hanson CA, Kurtin PJ, Katzmann JA, Hoyer JD, Li CY, Hodnefield JM, Meyers CH, Habermann TM, Witzig TE (1999) Immunophenotypic analysis of peripheral blood and bone marrow in the staging of B-cell malignant lymphoma. Blood 94:3889–3896
37. Heinmoller E, Renke B, Beyser K, Dietmaier W, Langner C, Ruschoff J (2001) Piffalls in diagnostic molecular pathology-significance of sampling error. Virchows Arch 439:504–511
38. Hoeve MA, Krol AD, Philippo K, Derksen PW, Veenendaal RA, Schuuring E, Kluin PM, van Krieken JH (2000) Limitations of clonality analysis of B cell proliferations using CDR3 polymerase chain reaction. Mol Pathol 53:194–200
39. James C, Ugo V, Le Couedic JP, Staerk J, Delhommeau F, Lacout C, Garcon L, Raslova H, Berger R, Bennaceur-Griscelli A, Villeval JL, Constantinescu SN, Casadevall N, Vainchenker W (2005) A unique clonal JAK2 mutation leading to constitutive signalling causes polycythaemia vera. Nature 434:1144–1148
40. Koopmans M, Monroe SS, Coffield LM, Zaki SR (1993) Optimization of extraction and PCR amplification of RNA extracts from paraffin-embedded tissue in different fixatives. J Virol Methods 43:189–204
41. Krafft AE, Duncan BW, Bijwaard KE, Taubenberger JK, Lichy JH (1997) Optimization of the isolation and amplification of RNA from formalin-fixed, paraffin-embedded tissue: the Armed Forces Institute of Pathology experience and literature review. Mol Diagn 2:217–230
42. Kralovics R, Passamonti F, Buser AS, Teo SS, Tiedt R, Passweg JR, Tichelli A, Cazzola M, Skoda RC (2005) A gain-of-function mutation of JAK2 in myeloproliferative disorders. N Engl J Med 352:1779–1790
43. Kremer M, Cabras AD, Fend F, Schulz S, Schwarz K, Hoefler H, Werner M (2000) PCR analysis of IgH-gene rearrangements in small lymphoid infiltrates microdissected from sections of paraffin-embedded bone marrow biopsy specimens. Hum Pathol 31:847–853
44. Kremer M, Sandherr M, Geist B, Cabras AD, Hofler H, Fend F (2001) Epstein–Barr virus-negative Hodgkin's lymphoma after mycosis fungoides: molecular evidence for distinct clonal origin. Mod Pathol 14:91–97
45. Kremer M, Spitzer M, Mandl-Weber S, Stecker K, Schmidt B, Hofler H, Quintanilla-Martinez L, Fend F (2003) Discordant bone marrow involvement in diffuse large B-cell lymphoma: comparative molecular analysis reveals a heterogeneous group of disorders. Lab Invest 83:107–114
46. Kreuzer KA, Lass U, Nagel S, Ellerbrok H, Pauli G, Pawlaczyk-Peter B, Siegert W, Huhn D, Schmidt CA (2000) Applicability of an absolute quantitative procedure to monitor intra-individual bcr/abl transcript kinetics in clinical samples from chronic myelogenous leukemia patients. Int J Cancer 86:741–746
47. Laurent E, Talpaz M, Kantarjian H, Kurzrock R (2001) The BCR gene and philadelphia chromosome-positive leukemogenesis. Cancer Res 61:2343–2355
48. Lehmann U, Bock O, Langer F, Kreipe H (2001) Demonstration of light chain restricted clonal B-lymphoid infiltrates in archival bone marrow trephines by quantitative real-time polymerase chain reaction. Am J Pathol 159:2023–2029
49. Lehmann U, Kreipe H (2001) Real-time PCR analysis of DNA and RNA extracted from formalin-fixed and paraffin-embedded biopsies. Methods 25:409–418
50. Levine RL, Wadleigh M, Cools J, Ebert BL, Wernig G, Huntly BJ, Boggon TJ, Wlodarska I, Clark JJ, Moore S, Adelsperger J, Koo S, Lee JC, Gabriel S, Mercher T, D'Andrea A, Frohling S, Dohner K, Marynen P, Vandenberghe P, Mesa RA, Tefferi A, Griffin JD, Eck MJ, Sellers WR, Meyerson M, Golub TR, Lee SJ, Gilliland DG (2005) Activating mutation in the tyrosine kinase JAK2 in polycythemia vera, essential thrombocythemia, and myeloid metaplasia with myelofibrosis. Cancer Cell 7:387–397
51. Lewis F, Maughan NJ, Smith V, Hillan K, Quirke P (2001) Unlocking the archive-gene expression in paraffin-embedded tissue. J Pathol 195:66–71
52. Limpens J, de Jong D, van Krieken JH, Price CG, Young BD, van Ommen GJ, Kluin PM (1991) Bcl-2/JH rearrangements in benign lymphoid tissues with follicular hyperplasia. Oncogene 6:2271–2276
53. Limpens J, Stad R, Vos C, de Vlaam C, de Jong D, van Ommen GJ, Schuuring E, Kluin PM (1995) Lymphoma-associated translocation t(14;18) in blood B cells of normal individuals. Blood 85:2528–2536
54. Markoulatos P, Siafakas N, Moncany M (2002) Multiplex polymerase chain reaction: a practical approach. J Clin Lab Anal 16:47–51
55. Masuda N, Ohnishi T, Kawamoto S, Monden M, Okubo K (1999) Analysis of chemical modification of RNA from formalin-fixed samples and optimization of molecular biology applications for such samples. Nucleic Acids Res 27:4436–4443
56. McCarthy KP, Sloane JP, Wiedemann LM (1990) Rapid method for distinguishing clonal from polyclonal B cell populations in surgical biopsy specimens. J Clin Pathol 43: 429–432
57. McCarthy KP, Sloane JP, Kabarowski JH, Matutes E, Wiedemann LM (1992) A simplified method of detection of clonal rearrangements of the T-cell receptor-gamma chain gene. Diagn Mol Pathol 1:173–179
58. Miranda RN, Mark HF, Medeiros LJ (1994) Fluorescent in situ hybridization in routinely processed bone marrow aspirate clot and core biopsy sections. Am J Pathol 145:1309–1314
59. Nagasaka T, Lai R, Chen YY, Chen W, Arber DA, Chang KL, Weiss LM (2000) The use of archival bone marrow specimens in detecting B-cell non-Hodgkin's lymphomas using polymerase chain reaction methods. Leuk Lymphoma 36:347–352
60. Olavarria E, Kanfer E, Szydlo R, Kaeda J, Rezvani K, Cwynarski K, Pocock C, Dazzi F, Craddock C, Apperley JF, Cross NC, Goldman JM (2001) Early detection of BCR–ABL transcripts by quantitative reverse transcriptase-polymerase chain reaction predicts outcome after allogeneic stem cell transplantation for chronic myeloid leukemia. Blood 97:1560–1565
61. Pajor L, Lacza A, Kereskai L, Jakso P, Egyed M, Ivanyi JL, Radvanyi G, Dombi P, Pal K, Losonczy H (2004) Increased incidence of monoclonal B-cell infiltrate in chronic myeloproliferative disorders. Mod Pathol 12:1521–1530

62. Peterson LA, Brunning RD (2001) Bone marrow specimen processing. In: Knowles DM (ed) Neoplastic hematopathology. Lippincott Williams & Wilkins, Philadelphia, pp 1391–1406
63. Pittaluga S, Tierens A, Dodoo YL, Delabie J, De Wolf-Peeters C (1999) How reliable is histologic examination of bone marrow trephine biopsy specimens for the staging of non-Hodgkin lymphoma? A study of hairy cell leukemia and mantle cell lymphoma involvement of the bone marrow trephine specimen by histologic, immunohistochemical, and polymerase chain reaction techniques. Am J Clin Pathol 111:179–184
64. Provan AB, Hodges E, Smith AG, Smith JL (1992) Use of paraffin wax embedded bone marrow trephine biopsy specimens as a source of archival DNA. J Clin Pathol 45:763–765
65. Radich JP, Gooley T, Bryant E, Chauncey T, Clift R, Beppu L, Edmands S, Flowers ME, Kerkof K, Nelson R, Appelbaum FR (2001) The significance of bcr–abl molecular detection in chronic myeloid leukemia patients "late," 18 months or more after transplantation. Blood 98:1701–1707
66. Ravandi F, Cortes J, Albitar M, Arlinghaus R, Qiang Guo J, Talpaz M, Kantarjian HM (1999) Chronic myelogenous leukaemia with p185(BCR/ABL) expression: characteristics and clinical significance. Br J Haematol 107:581–586
67. Salto-Tellez M, Shelat SG, Benoit B, Rennert H, Carroll M, Leonard DG, Nowell P, Bagg A (2003) Multiplex RT-PCR for the detection of leukemia-associated translocations: validation and application to routine molecular diagnostic practice. J Mol Diagn 5:231–236
68. Schmid C, Isaacson PG (1992) Bone marrow trephine biopsy in lymphoproliferative disease. J Clin Pathol 45:745–750
69. Schulz S, Cabras AD, Kremer M, Weirich G, Miethke T, Bosmuller HC, Hofler H, Werner M, Fend F (2005) Species identification of mycobacteria in paraffin-embedded tissues: frequent detection of nontuberculous mycobacteria. Mod Pathol 18(2):274–282
70. Sotlar K, Escribano L, Landt O, Mohrle S, Herrero S, Torrelo A, Lass U, Horny HP, Bultmann B (2003) One-step detection of c-kit point mutations using peptide nucleic acid-mediated polymerase chain reaction clamping and hybridization probes. Am J Pathol 162:737–746
71. Specht K, Kremer M, Muller U, Dirnhofer S, Rosemann M, Hofler H, Quintanilla-Martinez L, Fend F (2002) Identification of cyclin D1 mRNA overexpression in B-cell neoplasias by real-time reverse transcription-PCR of microdissected paraffin sections. Clin Cancer Res 8:2902–2911
72. Specht K, Haralambieva E, Bink K, Kremer M, Mandl-Weber S, Koch I, Tomer R, Hofler H, Schuuring E, Kluin PM, Fend F, Quintanilla-Martinez L (2004) Different mechanisms of cyclin D1 overexpression in multiple myeloma revealed by fluorescence in situ hybridization and quantitative analysis of mRNA levels. Blood 104:1120–1126
73. Specht K, Richter T, Müller U, Walch A, Werner M, Höfler H (2001) Quantitative gene expression analysis in microdissected archival formalin-fixed, paraffin-embedded tumor tissue. Am J Pathol 158:419–429
74. Srinivasan M, Sedmak D, Jewell S (2002) Effect of fixatives and tissue processing on the content and integrity of nucleic acids. Am J Pathol 161:1961–1971
75. Stacchini A, Demurtas A, Godio L, Martini G, Antinoro V, Palestro G (2003) Flow cytometry in the bone marrow staging of mature B-cell neoplasms. Cytometry B Clin Cytom 54:10–18
76. Taylor ML, Sehgal D, Raffeld M, Obiakor H, Akin C, Mage RG, Metcalfe DD (2004) Demonstration that mast cells, T cells, and B cells bearing the activating kit mutation D816V occur in clusters within the marrow of patients with mastocytosis. J Mol Diagn 6:335–342
77. Tbakhi A, Totos G, Pettay JD, Myles J, Tubbs RR (1999) The effect of fixation on detection of B-cell clonality by polymerase chain reaction. Mod Pathol 12:272–278
78. Thiele J, Zirbes TK, Kvasnicka HM, Fischer R (1999) Focal lymphoid aggregates (nodules) in bone marrow biopsies: differentiation between benign hyperplasia and malignant lymphoma—a practical guideline. J Clin Pathol 52:294–300
79. van Dongen JJ, Langerak AW, Bruggemann M, Evans PA, Hummel M, Lavender FL, Delabesse E, Davi F, Schuuring E, Garcia-Sanz R, van Krieken JH, Droese J, Gonzalez D, Bastard C, White HE, Spaargaren M, Gonzalez M, Parreira A, Smith JL, Morgan GJ, Kneba M, Macintyre EA (2003) Design and standardization of PCR primers and protocols for detection of clonal immunoglobulin and T-cell receptor gene recombinations in suspect lymphoproliferations: report of the BIOMED-2 concerted action BMH4-CT98-3936. Leukemia 17:2257–2317
80. Viswanatha D, Foucar K (2003) Hodgkin and non-Hodgkin lymphoma involving bone marrow. Semin Diagn Pathol 20:196–210
81. Weirich G, Funk A, Hoepner I, Heider U, Noll S, Putz B, Fellbaum C, Hofler H (1995) PCR-based assays for the detection of monoclonality in non-Hodgkin's lymphoma: application to formalin-fixed, paraffin-embedded tissue and decalcified bone marrow samples. J Mol Med 73:235–241
82. Weirich G, Sandherr M, Fellbaum C, Richter T, Schmidt L, Kinjerski T, Dietzfelbinger H, Rastetter J, Hofler H (1998) Molecular evidence of bone marrow involvement in advanced case of Tgammadelta lymphoma with secondary myelofibrosis. Hum Pathol 29:761–765
83. Wickham CL, Boyce M, Joyner MV, Sarsfield P, Wilkins BS, Jones DB, Ellard S (2000) Amplification of PCR products in excess of 600 base pairs using DNA extracted from decalcified, paraffin wax embedded bone marrow trephine biopsies. Mol Pathol 53:19–23
84. Wilson GA, Vandenberghe EA, Pollitt RC, Rees DC, Goodeve AC, Peake IR, Reilly JT (2000) Are aberrant BCR–ABL transcripts more common than previously thought? Br J Haematol 111:1109–1111
85. Zhou XG, Sandvej K, Gregersen N, Hamilton-Dutoit SJ (1999) Detection of clonal B cells in microdissected reactive lymphoproliferations: possible diagnostic pitfalls in PCR analysis of immunoglobulin heavy chain gene rearrangement. Mol Pathol 52:104–110
86. Zoubek A, Ladenstein R, Windhager R, Amann G, Fischmeister G, Kager L, Jugovic D, Ambros PF, Gadner H, Kovar H (1998) Predictive potential of testing for bone marrow involvement in Ewing tumor patients by RT-PCR: a preliminary evaluation. Int J Cancer 79:56–60

Virchows Arch (2005) 447: 920–937
DOI 10.1007/s00428-005-0070-8

REVIEW ARTICLE

Marcus Kremer · Leticia Quintanilla-Martínez · Jörg Nährig · Christoph von Schilling · Falko Fend

Immunohistochemistry in bone marrow pathology: a useful adjunct for morphologic diagnosis

Received: 13 June 2005 / Accepted: 23 August 2005 / Published online: 18 October 2005
© Springer-Verlag 2005

Abstract Pathomorphological examination of trephine biopsies of the bone marrow (BM) represents a standard method for the diagnosis and staging of hematologic neoplasms and other disorders involving the BM. The increasing knowledge about the genetic basis and biology of hematologic neoplasms, as well as the recently proposed WHO classification system, provide the framework for an accurate diagnosis. Although conventional morphology remains the gold standard for paraffin-embedded BM trephines, immunohistochemical stainings have become an integral part of the diagnostic workup. Antibodies suitable for paraffin sections are generally applicable to BM trephines, but modifications of staining protocols may be necessary due to the alternative fixatives and decalcification procedures used for BM biopsies. The indications for immunostainings range from confirmation and classification of lymphoma involvement, subclassification of acute leukemias, and estimating blast counts in myelodysplastic and myeloproliferative syndromes to characterization of BM involvement in nonhematologic neoplasms. Although subtyping of NHL in the BM is more difficult from the point of morphology, classification of the entities that frequently involve the BM, especially the small B-cell lymphomas, can easily be achieved with the help of immunohistochemistry. In this review, we try to summarize the current state of the art in BM immunohistochemistry for the diagnosis of hematologic disorders. Moreover, diagnostic algorithms and useful antibody panels are proposed for a rational and cost-effective approach.

Keywords Trephine biopsies · Hematologic disorders · Immunohistochemistry · Diagnostic algorithms

M. Kremer · J. Nährig · F. Fend (✉)
Institute of Pathology, Technical University Munich,
Ismaningerstrasse 22,
81675 Munich, Germany
e-mail: fend@lrz.tum.de
Tel.: +49-89-41404162
Fax: +49-89-41406106

L. Quintanilla-Martínez
GSF Research Center for Environment and Health,
Neuherberg, Oberschleissheim, Germany

C. von Schilling
III Department of Internal Medicine, Klinikum rechts der Isar,
Technical University,
Munich, Germany

Introduction

Morphological examination of trephine biopsies of the bone marrow (BM) is a standard method for diagnosis and staging of patients with malignant lymphoma (ML), plasma cell dyscrasias, chronic myeloproliferative syndrome (MPS) and myelodysplastic syndrome (MDS), acute leukemia, and metastatic tumors. Occasionally, the diagnosis of nonneoplastic conditions such as infectious diseases or, to a lesser extent, anemias also require examination of a BM trephine [10]. In addition, determination of BM cellularity following BM transplantation or administration of chemotherapeutic agents is most reliably established by trephine biopsies. Ideally, trephine biopsy, aspirate smears, and flow cytometry should be viewed as integral parts of a combined diagnostic approach. In some instances, e.g., myelofibrosis, the trephine biopsy will be the only specimen available for examination. Due to both technical and historical reasons, the use of immunohistochemistry for BM diagnostics has lagged behind other applications. On one hand, the availability of antibodies suitable for paraffin was limited for a long time, and flow cytometry was (and for many indications it still is) the primary technique for immunophenotyping of hematologic neoplasms. On the other hand, the aim of alternative fixation, decalcification, and embedding techniques at optimizing morphology frequently proved detrimental for the preservation of antigens. However, recent years have seen an exponential increase in antibodies suitable for paraffin-embedded tissues, plus improvements in antigen retrieval, leading to a rapid integration of immunohistochemistry into BM diagnostics. Of note, the necessity for immunohistochemical studies on trephine biopsies is greater in countries like

Germany, where the biopsy is signed out by the pathologist, whereas flow cytometry and, frequently, also cytology is seen by the hematologist, making an integrated diagnostic approach more difficult.

Since diagnosis and staging of ML are among the most frequent clinical indications for trephine biopsies, this review provides a detailed description of the morphological and immunophenotypical criteria for making the diagnosis of ML in the BM.

The role of immunohistochemistry in the classification of myeloproliferative disorders, MDSs, acute leukemias, and nonneoplastic BM changes comprises the second part of this review.

Technical issues of BM immunohistochemistry

A variety of fixatives and decalcification procedures are routinely used for BM trephines in different parts of the world. Many, but not all of them, are well suited for immunohistochemical stains. In our opinion, fixation in buffered formalin, decalcification in EDTA, and embedding in paraffin is a good compromise, because it not only provides good morphology and excellent conditions for immunohistochemistry but also allows DNA- and RNA-based molecular studies. Acceleration of the decalcifying process can be achieved by using ultrasound energization, which reduces the decalcification time to approximately 6–12 h. (Medite, Burgdorf, Germany) [106, 119]. In addition, formalin fixation allows routine processing of BM sections on automated immunostainers, which improves reproducibility and reliability of immunostaining [21, 32, 42, 161]. However, certain recommendations should be considered for obtaining optimal staining results. The fixation time should not exceed 24 h, since staining intensity decreases with prolonged fixation time. In our experience, staining results are not significantly affected by the duration of EDTA decalcification. Nevertheless, staining protocols and especially antigen retrieval used for other paraffin tissues such as lymph nodes may have to be adjusted for BM trephines to avoid inadequate staining or tissue damage due to overly strong antigen retrieval.

Schaefer's fixative (0.4% glutaraldehyde/10% formalin), a fixative solution widely used in Germany, and methacrylate embedding are two techniques that offer some advantages over conventional formalin fixation, such as excellent morphological detail and the ability to perform numerous histochemical reactions, but both techniques severely limit immunohistochemical studies [18, 60, 133]. Fixation with B5 or Zenker fixative for up to 2.5 h, frequently used in the USA, renders good staining results, but prolonged fixation of the specimen may abolish immunoreactivity. An important drawback of these fixatives, despite the good morphology achieved, is that molecular analysis, in general, cannot be performed.

Currently, a wide array of antibodies is available for BM diagnostics. Table 1 shows a list of primary antibodies used in our institution. Obviously, this selection represents the personal choice of the authors and is by no means complete. Of note, some standard antibodies for lymphoma subtyping such as CD15, CD43, or CD68 (KP1) show broad reactivity with myeloid cells and, therefore, are less suited for BM trephines than for lymph nodes. The choice of antibodies and the amount of stains necessary depend on the type of the disease and the clinical question. For instance, the primary classification of neoplasms in the BM usually requires a larger panel of antibodies, whereas confirmation of BM infiltration by lymphoma diagnosed at another site, assessment of treatment response, or detection of minimal residual disease or relapse is usually possible with a few selected stains.

Malignant lymphoma

Peripheral B-cell lymphomas

Non-Hodgkin lymphomas (NHL) composed of small B lymphocytes comprise the majority of lymphoma infiltrates in the BM. Bone marrow involvement is seen in virtually 100% of B-cell chronic lymphocytic leukemia (B-CLL)/small lymphocytic lymphoma (SLL), in almost all cases of lymphoplasmacytic lymphoma (LPL) and hairy cell leukemia (HCL), in 55–93% of mantle cell lymphoma (MCL), in 50–60% of follicular lymphoma (FL), and invariably, in splenic marginal zone B-cell lymphoma (SMZL). The only notable exception within these groups is nodal and extranodal marginal zone B-cell lymphoma, which involves the marrow in approximately 10–30% of cases [34, 37, 51, 57, 82, 83, 95, 103, 120, 121, 135, 149, 164]. Distinction of the most common types of B-NHL in the trephine biopsy can be difficult on morphological grounds alone due to overlapping cytological features and distribution patterns, and therefore, requires integration of immunophenotypic and occasionally molecular data for primary diagnosis. Nevertheless, the morphology of an infiltrate gives important clues for subclassification and should guide the selection of antibodies. The pattern of BM involvement is one of the most important hints for diagnosis. Five main patterns of BM infiltration by NHLs are recognized, namely, paratrabecular, randomly focal intertrabecular, interstitial, diffuse, and sinusoidal/intravascular [37, 72, 82, 135]. In some cases, multiple or mixed patterns are present in the same specimen. Although most infiltrates are easily recognizable in standard stains, sparse interstitial and sinusoidal involvement can be practically undetectable by conventional morphology and requires immunohistochemistry to highlight the neoplastic population.

Immunohistochemical classification of small B-cell lymphomas in the BM

A practical approach to the primary diagnosis of small B-cell lymphomas involving the BM is based on (1) infiltration pattern and cytology and (2) immunohistochemistry with a limited panel of antibodies based on morphological findings. This strategy, which is directed at reducing

Table 1 Primary antibodies employed for BM diagnostics in our institution

Antigen	Clone	Company	Main cellular expression
CD1a	MTB-1	Novocastra	T cell (thymic)
CD2	AB75	Novocastra	T cell (thymic, NK)
CD3	F7.2.38	DAKO	T cell (mature)
CD4	IF6	Ventana	T cell (helper)
CD5	4C7	Novocastra	T cell (mature)
CD7	272	Novocastra	T cell (thymic)
CD8	C8/144B	DAKO	T cell (cytotoxic)
CD10	56C6	Novocastra	LPC, GC B cell
CD15	MMA	BD	Granulocytes, monocytes
CD20	L26	DAKO	Pan B cell (except PC)
CD21	1F8	DAKO	B cell (subset), FDC
CD23	IB12	Novocastra	B cell (subset), FDC, LC
CD30	BerH2	DAKO	Activated B/T cell, HC
CD31	JC/70A	DAKO	EC, Platelets
CD34	QB-END/10	BMA	Hemopoietic SC, EC
CD43	MT1	Novocastra	T cell, myeloid cells
CD45 LCA	X16/99	Novocastra	Panleukocyte
CD56	IB6	Novocastra	T cell (NK, MM)
CD61	Y2/51	DAKO	Platelets, Megakaryocytes, EC
CD68	PGM-1	DAKO	Monocytes, LC, Macrophages
CD68	KP1	DAKO	Monocytes, Macrophages, myeloid cells
CD79a	HM57	DAKO	B cell, PC
CD117	c-kit	DAKO	SC, mast cells, Melanoc
CD138	MI15(4)	DAKO	Plasma cells
ALK 1	ALK1(2)	DAKO	Anaplastic lymphoma kinase (ALCL)
BCL-2	124(3)	DAKO	Lymphocytes (subset)
BCL-6	P1F6	Novocastra	GC, activated B cells
Cyclin D1	SP4	DC Systems	Cell cycle (MCL, MM)
DBA.44	DBA.44	DAKO	Hairy cells, B cell
Granzyme B	GrB-7	DAKO	T cell (cytotoxic)
Glycophorin C	Ret40f	DAKO	Erythroblasts, erythrocytes
Lysozyme	Polyclonal	DAKO	Monocytes
Mast cell tryptase	AA1	DAKO	Mast cells
MUM-1	MUM-1p	DAKO	PC, post-GC B cells
Myeloperoxidase	MPO-7	DAKO	Myeloid cells
PAX5	Polyclonal	BD	HC, B-cell transcription factor
p27	F8	Santa Cruz	Cell cycle
TDT	polyclonal	Zytomed	Immature B/T cells
TIA-1	2G9	Immunotech	T cell (cytotoxic)
VS38c	VS38c	DAKO	Plasma cells
kappa	R10-21-F3	DAKO	Light chain
lambda	N10/2	DAKO	Light chain
IgG	7701	BioGenex	Immunoglobulin class G
IgA	NIF2	BioGenex	Immunoglobulin class A
IgM	R1/69	DAKO	Immunoglobulin class M
IgD	Polyclonal	DAKO	Immunoglobulin class D

The most frequently used antibodies are highlighted
Abbreviations: *NK* Natural killer, *LPC* lymphoid progenitor cells, *GC* germinal center cells, *PC* plasma cells, *FDC* follicular dendritic cells, *LC* Langerhans cells, *HC* Hodgkin cells, *EC* endothelial cells, *SC* stem cells, *MM* multiple myeloma, *ALCL* anaplastic large-cell lymphoma, *MCL* mantle cell lymphoma

unnecessary stains and misinterpretations, is outlined in a flow chart (Fig. 1).

In cases with nodular or interstitial centrally located lymphoid infiltrates composed of small cells, the differential diagnoses mainly encompass B-CLL/SLL, MCL, and

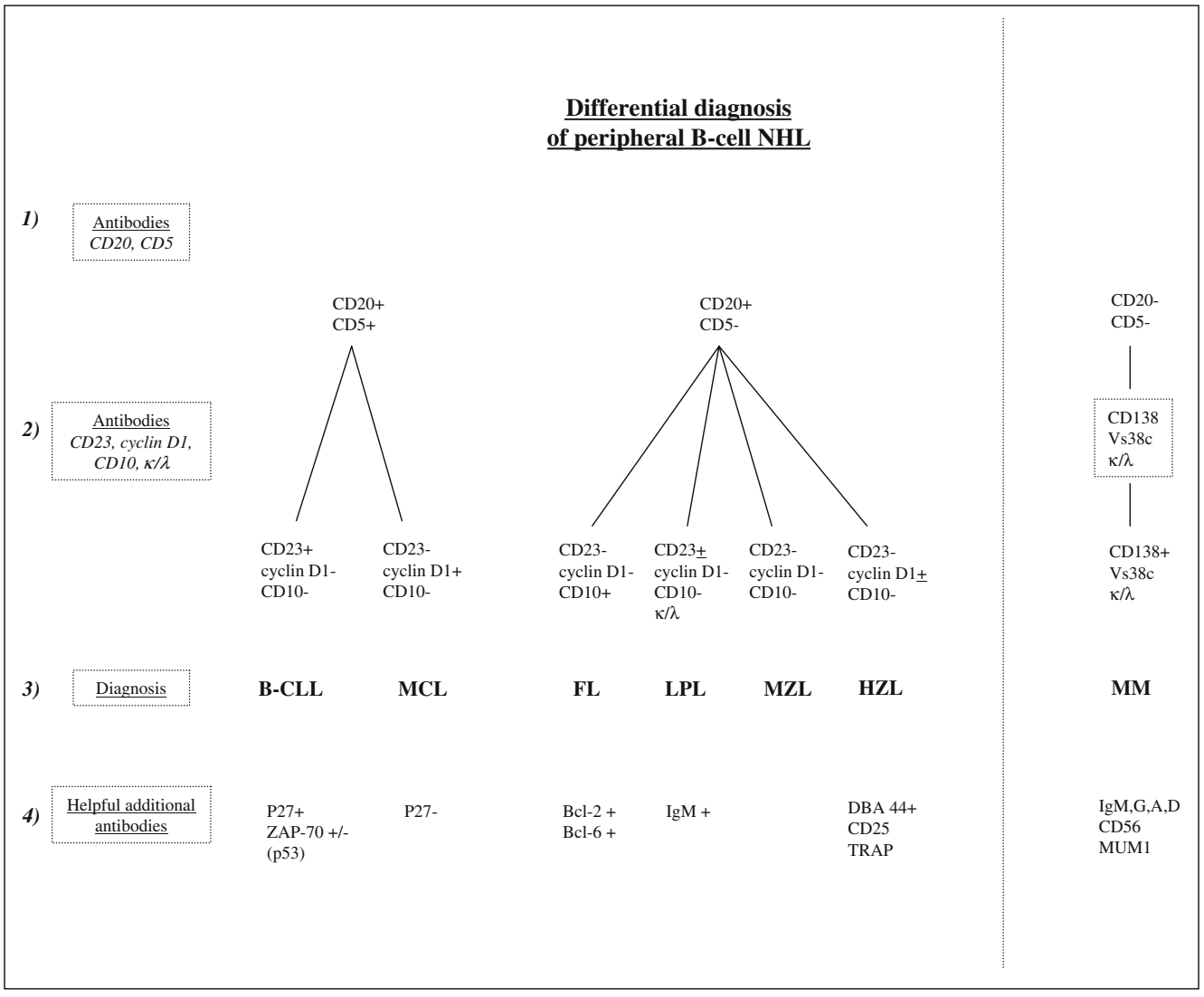


Fig. 1 Flow chart for the differential diagnosis of mature B-cell non-Hodgkin's lymphoma. If a low-grade B-cell NHL or an MM is suspected, we recommend a "first-line" staining with two basic antibodies, CD20 and CD5 (*1*). In cases of CD20-positive infiltrates, an array of antibodies consisting of CD23, cyclin D1, CD10, and possibly light chains, kappa, and lambda is required for further analysis (*2*). In most cases, these stains will lead to identification of the most frequent B-cell NHL, affecting the BM (*3*). Additional stainings for each entity, including optional prognostic markers such as ZAP-70 or p53 as shown at the baseline (*4*), conclude the immunohistochemical analysis of mature B-cell NHL. If MM is suspected, or the "first-line" immunostaining results lead to a CD20- and CD5-negative cell population; CD138, Vs38c, and light chains should be added in a second step for the diagnosis of MM. Further stains with antibodies against IgM, G, A, D, CD56, and MUM1 may help in ambiguous cases. Note the exception of cyclin D1- and CD20-positive lymhoplasmacytic MM as shown in Fig. 3D,E

MZL. In these cases, CD20 or CD5 are the most informative markers. The simultaneous expression of CD5 and CD20 helps to narrow down the differential diagnosis to mainly B-CLL and MCL, since both lymphomas express CD5 in more than 90% of cases [22, 45, 145, 157]. The choice of further antibodies depends on the main differential diagnoses and the need for additional prognostic information. Of practical importance in patients with B-NHL is the downregulation of CD20 antigen expression occasionally observed after treatment with anti CD20 antibodies (rituximab) [81]. In doubtful cases with nodular lymphoid aggregates after therapy, other B-cell antigens such as CD79a can serve to discriminate residual B-cell infiltrates from CD3+ reactive T-cell infiltrates.

B-cell chronic lymphocytic leukemia/small lymphocytic lymphoma

B-cell chronic lymphocytic leukemia/small lymphocytic lymphoma is one of the most frequently encountered B-cell neoplasms in BM trephines. The phenotype of B-CLL is characterized by coexpression of CD5, CD20, and CD23, and these three markers are usually sufficient for diagnosis (Fig. 2A,B). Of note, the staining intensity of CD20 is almost

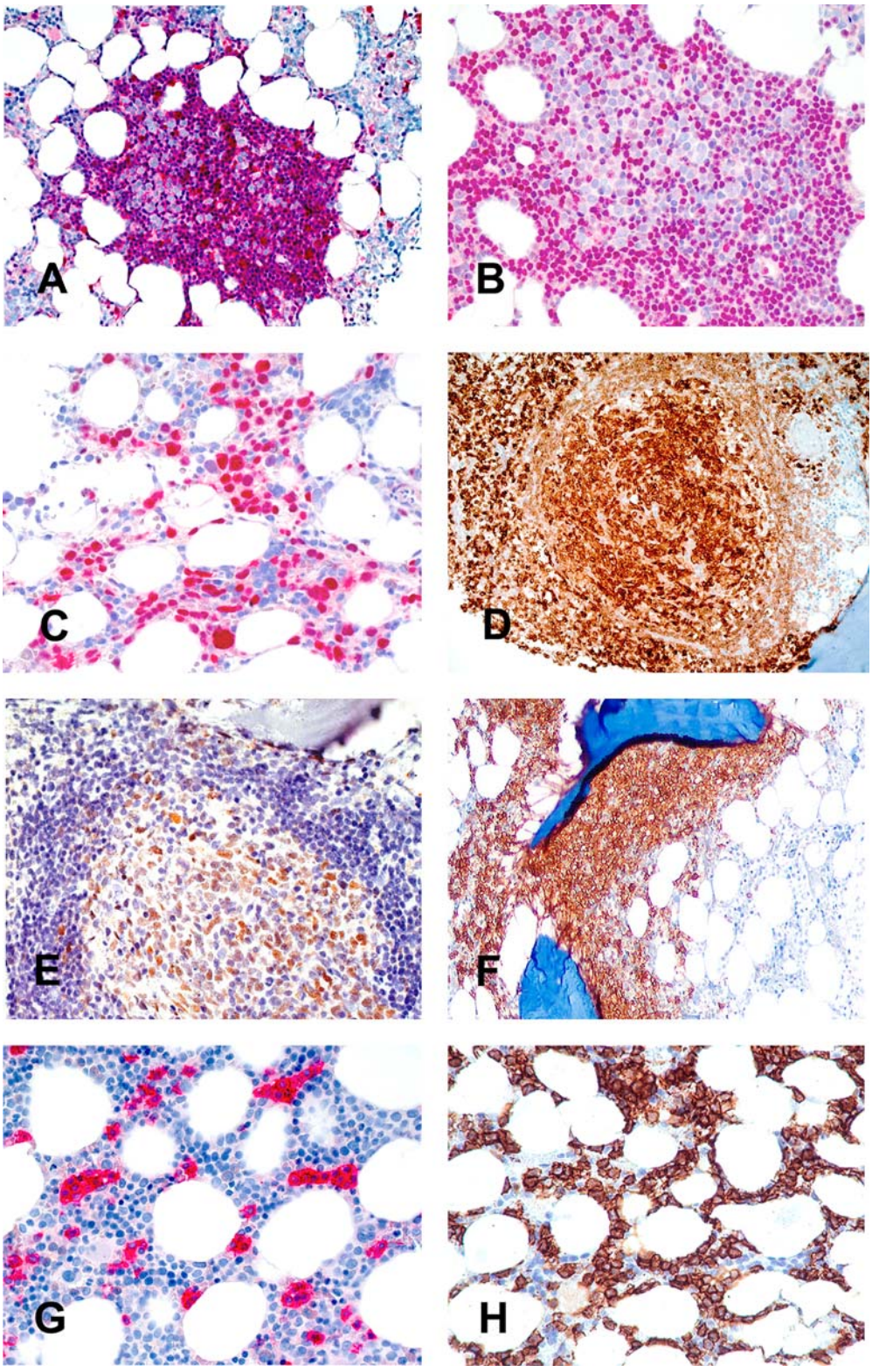


Fig. 2 Immunostainings of small B-cell NHL in the BM. **A** CD5 staining of a characteristic nodular B-CLL infiltrate. The neoplastic cells exhibit a relatively faint staining, whereas the "reactive" intermingled T cells show a strong immunostaining with CD5. Of note is the sharp border between unaffected BM cells and the neoplastic infiltrate (×200 ABC-AP). **B** $P27^{Kip1}$ staining of the same B-CLL case, with a strong immunoreactivity of the small lymphocytes. The intermingled "paraimmunoblasts" are negative for p27 (×300, ABC-AP). **C** Cyclin D1 reactivity of a MCL, pleomorphic variant. Note the interstitial infiltration pattern in this case (×400 ABC-AP). **D**, **E** These microphotographs represent an exceptional case of an FL with true neoplastic germinal centers. The tumor cells are positive for Bcl-2 (**D**) and Bcl-6 (**E**) (×200 ABC-POX, ×300 ABC-AP). Microphotograph (**F**) shows the more common peritrabecular infiltration pattern of an FL (CD20+) (×300, ABC-POX). **G** SMZL with characteristic intrasinusoidal infiltration stained for CD20. This pattern of infiltration is easily overlooked in routine stains (×200, ABC-AP). **H** HCL with characteristically strong membranous CD20 staining. (×400 ABC-POX)

always weaker than in other B-NHL [117]. The expression of CD23 in most cases is helpful, especially to rule out the diagnosis of MCL [90]. The coexpression of CD20 and CD5 is a universal finding in B-CLL. Still, there are cases of small infiltrates with large numbers of reactive T cells where comparison of CD3 and CD5 staining may be necessary to determine the presence or absence of CD5 coexpression by the B-cell population. A feature that can be very helpful is the double intensity of positivity of CD5. Reactive T cells are strongly positive for CD5, whereas the neoplastic B lymphocytes show a weaker reactivity (Fig. 2A).

In the last few years, the systematic analysis of gene expression profiling have led to the discovery of new diagnostic and prognostic markers. One of these markers is the zeta-chain-associated protein 70 (ZAP-70), which is normally expressed in T cells and was found to be highly expressed in a subgroup of B-CLL cases [165]. This finding was confirmed by flow cytometry, where the expression of ZAP-70 was found in almost 100% of patients with nonmutated immunoglobulin heavy chain (IgH) genes and only in 10% of patients with mutated IgH genes. The mutational status of the IgH gene is a strong predictor of survival in B-CLL [136]. Of interest, ZAP-70 is not only a surrogate marker for the mutational status but also seems to have independent predictive value and may provide a cheaper and easier way to obtain prognostic information [27, 136, 165]. ZAP-70 can also be detected by paraffin section immunohistochemistry, thus potentially making it an excellent prognostic marker for routine diagnostics. P53 protein and CD38 represent two other prognostic markers which can be assessed by immunostaining [102, 136]. Whether immunohistochemical demonstration of ZAP-70 and CD38 in BM biopsies renders equal prognostic information as their determination by flow cytometry remains to be shown. Worth mentioning in this context is the so-called secretory B-CLL with a detectable monoclonal paraprotein in the serum and cytoplasmic light chain expression, which is found in approximately 5% of otherwise typical cases. These cases also express CD5 and CD23, distinguishing them from LPL (see below).

B-prolymphocytic leukemia

B-prolymphocytic leukemia (B-PLL) is a rare disease defined mainly by clinical and laboratory features and shows high lymphocyte counts in the peripheral blood with more than 55% prolymphocytes, splenomegaly, and BM infiltration. The neoplastic cells are larger than lymphocytes of classical B-CLL. They typically lack CD23 and show CD5 only in a minority of cases. Cases of B-PLL carrying a t(11;14)(q13;q32) translocation as described in the earlier literature will nowadays be regarded as leukemic MCL by most investigators [128]. Further investigations will have to demonstrate whether the remaining cases of B-PLL represent a true entity or just variants of other leukemic B-NHLs.

Mantle cell lymphoma

The main differential diagnosis of CLL/SLL in the BM is MCL. MCL is characterized by the t(11;14)(q13;q32) translocation, resulting in aberrant expression of cyclin D1, which is the hallmark of the diagnosis [19, 25, 115]. MCL have a very characteristic phenotype, cyclin D1+, CD20+, CD5+, CD10−, and CD23−. Nevertheless, in the past, the inconsistency of the cyclin D1 staining in BM biopsies often precluded an accurate diagnosis. This problem seems to have been overcome with the introduction of the new monoclonal rabbit antibody against cyclin D1 (clone SP4, DC System, Germany), which gives a reliable and strong staining. Another useful marker for the diagnosis of MCL is the anti-$p27^{Kip1}$ antibody [147]. The lack of $p27^{Kip1}$ protein expression is a characteristic feature of MCL, which is not found in other small B-cell NHL. The lack of p27 staining in a small B-cell infiltrate in the BM is highly suspicious of the diagnosis of MCL [86, 123, 132]. A word of caution, since T cells are strongly positive for p27, the parallel assessment of the number of reactive T cells within the neoplastic infiltrate is important to avoid misinterpretation of staining results. As mentioned above, CD23 is very helpful in distinguishing MCL from B-CLL, although one has to keep in mind that rare cases of bona fide MCL have been reported to express CD23. Another potential problem in the differential diagnosis of MCL is the more aggressive blastic and pleomorphic variants. Aggressive MCLs show a spectrum of cytological appearances ranging from lymphoblast-like cells to large pleomorphic cells mimicking large-cell lymphomas (Fig. 2C). Similar to the classic variant of MCL, the blastic variant shows focal infiltration in the BM, a useful feature in the differential diagnosis of lymphoblastic leukemia/lymphoma that tends to infiltrate in a diffuse pattern. Immunohistochemically, blastic variants of MCL can be separated from lymphoblastic leukemia/lymphoma by their strong staining for CD20 and cyclin D1 and the lack of terminal desoxyribonucleotidyl transferase (TdT) and/or CD3. P53 overexpression and high proliferation rate in MCL are associated with the cytologically more aggressive blastic and pleomorphic variants of MCL and a worse outcome [25, 64, 66, 71, 73, 114, 123, 146].

Follicular lymphoma

Follicular lymphoma shows a characteristic infiltration pattern in the BM with peritrabecular rather than centrally located infiltrates with significant lesional fibrosis. This allows a definite diagnosis of FL by morphology in many instances. Immunostainings are useful in the presence of extensive diffuse infiltrates and in minimal paratrabecular lesions, which are hard to spot in routine stains. The phenotype of FL in the BM is virtually identical to its nodal counterpart. The tumor cells express antigens of germinal center cells, including CD10, Bcl-6, and Bcl-2. Rare cases express CD43, and even less commonly, CD5 [44]. CD10 also marks BM stromal cells and immature B cells and may be difficult to interpret in small infiltrates. A meshwork of follicular dendritic cells can be demonstrated in larger infiltrates with stains against CD21 and CD23. Rare cases of FL show centrally located neoplastic follicles with mantle zones, imitating reactive follicles [151]. In these cases, demonstration of bcl-2 positivity in the follicle centers is necessary to confirm malignancy even in patients with known FL, since most true BM follicles are of a reactive nature (Fig. 2D–F). Similar to FL in lymph nodes, BM infiltrates of FL frequently contain high numbers of intermingled “reactive” T cells within the neoplastic in-

filtrate, which should not discourage from a diagnosis of lymphoma, if the other diagnostic criteria are met.

In contrast to nodal FL, grading of FL in the BM has not been studied systematically to date. However, many cases of FL grade 3a/3b and even diffuse large-cell lymphoma show a predominance of small lymphoid cells in the BM, frequently with typical paratrabecular infiltration, also referred to as discordant BM infiltration. This phenomenon seems to be associated with a better clinical outcome than concordant infiltration by large-cell lymphoma. Discordant BM infiltration should not be confused with those cases where the large B-cell component is obscured by small reactive T cells. In these cases, immunostaining highlights the presence of malignant large B cells immersed in a sea of reactive T lymphocytes [88]. Approximately one to two thirds of patients with FL transform into large B-cell lymphoma during the course of their illness [38, 104, 105, 168].

Lymphoplasmacytic lymphoma

Lymphoplasmacytic lymphoma is a rare disease, infiltrating the BM in approximately 80% of patients at presentation and virtually all patients during the clinical course, usually with an interstitial and diffuse pattern [4, 69]. LPL in the WHO classification is a diagnosis of exclusion and is, in most cases, associated with the clinical syndrome of Waldenstrom's macroglobulinemia. Immunohistochemically, CD20 and CD79a are strongly positive, with an occasionally observed coexpression of CD43 in 20% of the cases [3, 92]. Immunoglobulin heavy (typically IgM, sometimes IgG, and rarely IgA) and light chains are virtually always demonstrable as cytoplasmic staining in paraffin sections [22, 45, 69, 70, 145, 157]. By definition, CD5 is negative. Most cases of the so-called lymphoplasmacytoid variant of immunocytoma recognized in the Kiel classification, which frequently expressed CD5, are regarded as variants of B-CLL/SLL with cytoplasmic immunoglobulin in the new WHO classification. The plasmacytoid differentiation of LPL can be easily confused with other ML showing lymphoplasmacytic or plasmacytic differentiation such as MZL, B-CLL, and multiple myeloma (MM) with lymphoplasmacytic morphology. The lymphoplasmacytic or small-cell variant of MM is frequently CD20+, adding to the potential for misdiagnosis (see below).

Nodal and extranodal (MALT-type) marginal zone B-cell lymphoma

Marginal zone B-cell lymphoma has to be considered in the differential diagnosis of CD20+ and CD5− nodular BM infiltrates [26, 51, 70]. The incidence of BM involvement in extranodal MZL is lower (~20%) than in other low-grade B-NHL, albeit recent studies described BM infiltration in up to 44% of cases [51, 83, 94, 120, 124, 149]. For nodal MZL, the available data are sparse and contradictory, with the incidence of BM infiltration ranging from 35 to 77% [11, 17, 83]. The tumor cells of both nodal and extranodal MZL express CD20, CD79a, and, in a subset of cases, CD43 [24, 92]. They are usually CD5- and CD23-negative, although rare CD5-positive MZL have been reported, potentially complicating the differential diagnosis with MCL and CLL/SLL [11, 12, 51].

Splenic marginal zone lymphoma

In contrast to nodal and extranodal MZL, BM involvement in SMZL is frequent and often shows a characteristic distribution pattern which is of great help in establishing the diagnosis. A significant percentage of SMZL show circulating B cells with small cytoplasmic projections, reflected in their previous designation as splenic lymphoma with villous lymphocytes [8, 57]. Although different patterns of infiltration can occur, the presence of intrasinusoidal tumor cells is highly characteristic for this entity. Intrasinusoidal spread may be found in the absence of obvious lymphoid nodules and can be so subtle that it is frequently overlooked in conventional stains [56, 57, 91]. Therefore, immunostainings are mandatory if SMZL is suspected (Fig. 2G). The neoplastic cells show positivity for CD20, CD79a, PAX5, Bcl-2, and express surface IgM and IgD. They are consistently negative for CD23, CD10, Bcl-6, cyclin D1, and CD43 [41, 56, 57, 108, 155]. The clinical course of SMZL is relatively indolent. A recent study documented clinical progression in 13% of cases, histologically accompanied by an increased number of blasts in the BM. Transformation usually correlates with a higher proliferation index and p53 overexpression [24, 41, 98].

An important diagnostic pitfall is persistent polyclonal B lymphocytosis with binucleated lymphocytes, a benign lymphoproliferation almost exclusively observed in female smokers, which shows an increase in intravascular B cells in the BM closely resembling the highly characteristic intrasinusoidal infiltration pattern by SMZL. Correlation with clinicopathologic findings, careful cytologic examination, and even molecular analysis may be required to avoid overdiagnosis of ML in these cases [39, 52, 154].

Hairy cell leukemia

Hairy cell leukemia involves the BM in almost all patients at the time of diagnosis. The morphology is highly characteristic, showing a patchy infiltration of widely spaced cells with oval nuclei and ample, clear cytoplasm, with progressive replacement of normal hematopoetic cells and increased reticulin fibers [137, 150]. HCL shows very strong staining for CD20, and staining of the cytoplasmic processes of the neoplastic cells may give them a "hairy" appearance (Fig. 2H). In contrast to other small-cell NHL, the combined positivity of DBA44 and tartrate-resistant acid phosphatase (TRAP) is highly suggestive for HCL. Another useful HCL marker is CD25, the interleukin (IL)-2 receptor. Very recently, Falini and coworkers described a promising new HCL-specific antibody against annexin 1

(ANXA1) suitable for paraffin [50, 163]. SMZL represents the main differential diagnosis for HCL. SMZL may also express DBA44 and TRAP, albeit the staining intensity in SMZL is generally weak [68, 78, 127, 131]. In contrast to SMZL, a significant subset of HCL shows staining for cyclin D1 in variable intensity accompanied by a reduction in p27 staining, which should not pose any problem with the differential diagnosis of MCL [86]. An important role of immunohistochemistry in HCL is the detection and quantification of residual disease. With the availability of highly efficient drugs such as 2-CDA, complete remission is frequently obtained, and histological and immunohistochemical criteria for response evaluation in the BM trephine have been defined [67].

Immunosecretory disorders: monoclonal gammopathy of undetermined significance and multiple myeloma

Immunosecretory disorders such as monoclonal gammopathy of undetermined significance (MGUS), MM, and Waldenstrom's macroglobulinemia represent a frequent indication for BM trephine examination. MM is the second most frequent B-cell tumor in Western countries and accounts for approximately 10% of all hematologic neoplasms [74, 139]. In most cases with significant infiltration, MM is a straightforward diagnosis. BM infiltration in MM is highly variable and can range from randomly distributed sheets or clusters of abnormal plasma cells to large nodules or complete obliteration of the marrow space. Immunohistochemistry is of importance for the diagnostic workup of MM in several settings, namely, (1) discrimination from MGUS, (2) identification of small numbers of tumor cells after therapy, (3) distinction from other neoplasms in morphologically unusual cases, and (4) for the identification of prognostic markers. Given the close biological relatedness of MGUS and MM, a distinction of these two disorders is somehow arbitrary in the presence of a non-tumor-forming plasmacytosis without cytologic atypia, but the presence of a clear-cut light chain restriction with a kappa/lambda ratio of more than 16:1 or the reverse and more than 10% plasma cells are suspicious for a diagnosis of MM (Fig. 3A–C) [54]. Since well-differentiated plasmacytomas can be cytologically indistinguishable from normal plasma cells, the finding of plasma cells in sheets or clusters without association with vascular structures is another important criterion for the diagnosis of MM. Immunophenotypically, neoplastic plasma cells lack in most cases the pan-B-cell antigen CD 20, whereas CD38, CD79a, the collagen-1 binding proteoglycan, syndecan (CD138), and VS38c are usually strongly expressed. The latter two markers are well suited for plasma cell enumeration in trephine biopsies. The neural adhesion molecule CD56 is abnormally expressed in approximately 75% of cases of MM and is frequently associated with lytic bone lesions. In contrast, CD56 is absent both from polyclonal plasma cells and other mature B-NHL with plasmacytic differentiation [46, 65, 87]. Together with CD138, CD56 is thought to be important for plasma-cell anchoring in the BM. Immunoglobulin heavy chains are frequently expressed, with IgG more common than IgA. IgM expression is rare in MM and usually indicates LPL. Occasionally, MM expresses aberrant antigens such as CD10 or even myeloid markers, but their importance in terms of prognosis remains unclear [47, 107]. Although currently not specified in the WHO classification, the lymphoplasmacytic or small-cell variant of MM mentioned above has some specific features such as more frequent secretion of rare Ig isotypes (IgE and IgM), common CD20 positivity, and a high frequency of the t(11;14) translocation associated with strong nuclear cyclin D1 protein expression (Fig. 3D,E). These cases represent a potential diagnostic pitfall because MCL may be suspected based on morphological and phenotypical findings. Prognostically, this MM variant seems to have a better prognosis, possibly due to a paradoxically low proliferation rate [9, 53, 122, 126, 142, 166]. Another subset of MM shows weaker, heterogeneous cyclin D1 expression frequently associated with trisomy 11.

High-grade B-cell lymphomas

Diffuse large B-cell lymphoma

Diffuse large B-cell lymphoma has a relatively low incidence of BM involvement at time of diagnosis (20%) [2, 35, 82, 109, 111, 116, 156]. Apart from discordant involvement (see above), large-cell BM infiltrates in DLBCL are highly variable, ranging from minimal small foci rarely observed intrasinusoidal involvement to subtotal replacement of the BM [111]. In cases of a minimal infiltration, immunostainings facilitate the search for tumor cells, which express CD20 and CD79a in most cases, and in up to 50% CD10, Bcl-2, and Bcl-6. Primary DLBCL expressing CD5 have to be distinguished from the blastic variant of MCL as well as Richter's transformation of B-CLL/SLL [167]. Whereas cyclin D1 positivity helps to distinguish blastic MCL, separation of secondary de novo DLBCL from clonally related Richter's transformation in patients with B-CLL may be impossible by immunohistochemistry. AML M6 is another, albeit rather infrequent differential diagnosis of DLBCL. Stainings for gylocphorin A or hemoglobin A are helpful in these cases, but immature erythroblasts can fail to show immunoreactivity for glycophorin A, whereas myeloid markers such as CD117 and MPO are variably expressed [59, 96].

Bone marrow involvement by the T-cell/histiocyte-rich variant of DLBCL requires special attention, since it resembles BM involvement by Hodgkin's lymphoma (HL) morphologically, due to its high number of reactive T cells and histiocytes and the resemblance of the rare neoplastic cells to L&H or Reed–Sternberg (RS) cells [30]. The tumor cells are usually CD20- and epithelial membrane antigen (EMA)-positive but lack CD30 and CD15. Nodular lymphocyte-predominant HL (nodular paragranuloma)

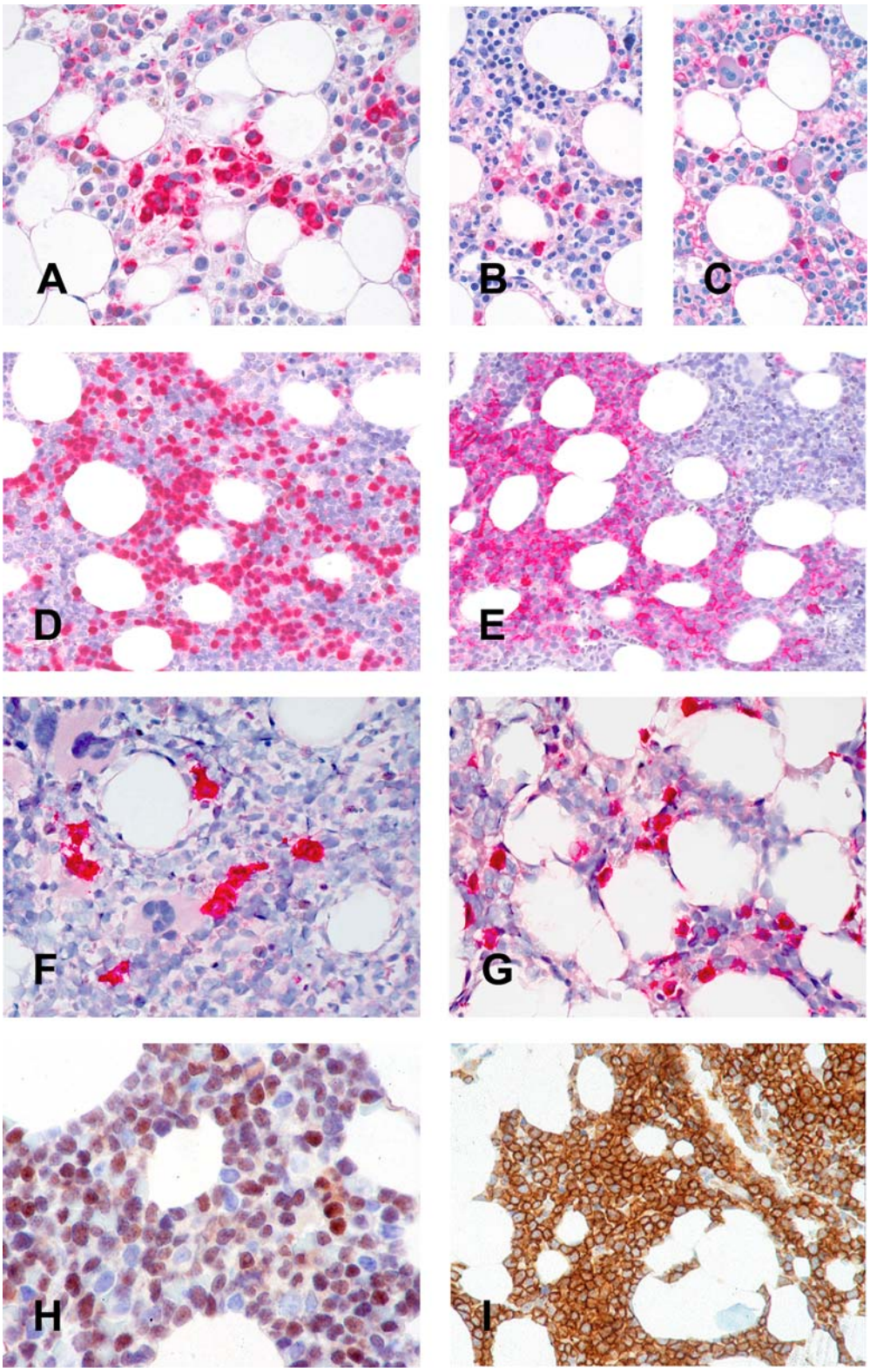


Fig. 3 Immunostainings of immunosecretory disorders, T-cell NHL, and acute lymphoblastic leukemia/lymphoblastic lymphoma. **A**–**C** Microphotographs showing a case with marked reactive BM plasmacytosis without evidence of light chain restriction. Staining for Vs38c (**A**) demonstrate the mainly perivascularly located clusters of plasma cells. There is a polyclonal distribution of immunoglobulin light-chains kappa (**B**) and lambda (**C**) (×300, ×200 ABC-AP). **D**, **E** t(11;14) positive MM with characteristic lymphoplasmacytic morphology. Note the strong cyclin D1 staining intensity with the recently introduced antibody (clone SP4, DC System, Germany) in **D**. The tumor cells in this MM subtype are regularly CD20-positive (**E**) (×300 ABC-AP). **F** BM involvement by ALCL with scattered strongly CD30-positive tumor cells. (×300 ABC-AP). **G** T-LGL with a morphologically inconspicuous interstitial infiltrate of CD8-positive T lymphocytes (×300 ABC-AP). **H**, **I** T-ALL/T-LBL. TdT shows strong homogeneous nuclear reactivity (**H**; ×400 ABC-POX). The tumor cells express the pan-T-cell marker CD7 (**I**) (×400 ABC-POX)

shows an immunophenotype similar to T-cell/histiocyte-rich DLBCL, but BM involvement, especially at primary presentation, is rare [84].

Burkitt's lymphoma

Burkitt's lymphoma (BL) involves the BM in up to 60% of cases. The pattern is nearly always diffuse or interstitial, and the extent of involvement varies from occasional

scattered lymphoma cells to complete replacement of the marrow [23, 144]. Areas of necrosis are observed frequently. Immunohistochemically, BL cells have a germinal center cell phenotype with expression of CD20, CD79a, CD10, Bcl-6, and CD43 but with constant absence of bcl-2. The proliferative activity, assessed with MIB1, should be virtually 100%. In contrast to lymphoblastic lymphoma (LBL)/acute lymphoblastic leukemia (ALL), BL lacks TdT [16, 20, 33].

Peripheral T-cell non-Hodgkin lymphoma

General considerations

The histopathology of BM involvement by T-cell non-Hodgkin lymphoma (T-NHL) has recently been reviewed comprehensively by Dogan and Morice [43]. T-NHL are rare diseases accounting for approximately 15% of all lymphoproliferative disorders in the Western world, with peripheral T-cell lymphoma (PTCL) unspecified, angioimmunoblastic T-cell lymphoma (AITL), cutaneous T-cell lymphomas, and anaplastic large-cell lymphoma (ALCL) representing the most common entities [129]. The frequency and the histology of BM involvement vary greatly between the different entities. Diagnosis of BM infiltration is hampered by frequent secondary changes in the BM microenvironment induced directly or indirectly by the lymphoma cells [49]. Some PTCL such as AITL show a vaguely nodular or interstitial infiltration pattern, whereas others, like large granular lymphocyte leukemia and hepatosplenic T-cell lymphoma (HSTCL), are characterized by a predominantly intrasinusoidal involvement [29, 31, 58, 61, 63, 99]. Immunophenotyping reveals an aberrant T-cell phenotype with considerable variations, mostly with the absence of one or more pan T-cell antigens. In T-cell NHL, in general, immunostainings are helpful in identifying the frequently subtle infiltrates and should be performed whenever possible.

Anaplastic large-cell lymphoma

Bone marrow involvement in ALCL is seen in about one quarter of the systemic cases but, as a rule, is absent in the cutaneous form. Most systemic cases have translocations involving the ALCL kinase-1 (ALK-1) gene, resulting in nuclear and/or cytoplasmic staining for ALK-1 protein [93, 143]. BM infiltration is usually interstitial and often too subtle to be recognized in routinely stained sections. This is particularly the case for the small-cell variant of ALCL, in which the neoplastic cells can easily be confused with immature megakaryocytes [14, 55]. For this reason, immunostainings for CD30 and/or ALK-1 are mandatory to identify a minimal infiltration in BM biopsies (Fig. 3F). The great majority of ALCL express one or more T-cell antigens; however, some cases may have an apparent "null cell" phenotype but, nevertheless, show evidence for T-cell lineage at the genetic level [55, 143]. Classic HL is the main differential diagnosis of ALCL, although this issue will rarely be raised in a BM biopsy.

Angioimmunoblastic T-cell lymphoma

Bone marrow involvement is seen in the majority of the cases (50–80%) and often mimics the features seen in peripheral lymph nodes [61, 62]. The infiltration pattern may be focal (paratrabecular) or diffuse and is characterized by a patchy polymorphic infiltrate often accompanied by a proliferation of arborizing vessels and fibrosis. Immunophenotypically, the phenotype of the neoplastic cells is very difficult to define, similar to the situation in involved lymph nodes. AITL cells express CD3 and CD4, whereas cytotoxic markers are negative. Interestingly, the recently described CD10 reactivity of the neoplastic cells observable in peripheral lymph nodes is often absent in the tumor cells infiltrating the BM [6, 7]. The frequent presence of large, Epstein–Barr virus (EBV)-positive B cells in AITL, which occasionally can show the morphology of Hodgkin and RS cells, may lead to confusion with either large B-cell lymphoma or HL. Another important differential diagnosis of BM involvement by AITL are reactive infiltrates with granulomas.

T-cell granular lymphocytic leukemia and hepatosplenic T-cell lymphoma

T-cell granular lymphocytic leukemia (T-LGL) is an indolent lymphoproliferative disorder, characterized by a distinct clonal cytotoxic T-cell population in the peripheral blood, which is easily identified by flow cytometric immunophenotyping. However, in BM trephines, the neoplastic cells of T-LGL cannot be reliably identified by morphological assessment alone. Immunostainings with antibodies against CD3, CD8, TIA-1, and granzyme B reveal the neoplastic infiltrate present as small interstitial infiltrates or typically in marrow sinusoids (Fig. 3G).

An important differential diagnosis is a reactive increase in cytotoxic T cells, which usually lacks the relatively distinct intrasinusoidal and intravascular pattern observed in T-LGL [110]. Like T-LGL, HSTCL shows an intrasinusoidal and subtle interstitial infiltration pattern, which is difficult to recognize by morphology alone. HSTCL is usually positive for CD3 and TIA-1 and frequently expresses CD56, whereas CD4, CD8, granzyme B, and perforin are negative [15, 36, 162].

Hodgkin's lymphoma

The incidence of BM involvement in HL ranged between 5 and 30% according to older studies, but was found in only 5.2% of patients in a recent large series of HL [77]. The lowest incidence was reported in lymphocyte-predominant HL (<5–10%), and the highest incidence was reported in HL with lymphocyte depletion (50–75%). Of note, BM

infiltration is frequent in HIV-associated HL and may be the site of primary diagnosis [80]. The infiltration pattern may be diffuse or focal, occasionally occupying the entire trephine volume. The infiltrate consists of a polymorphous inflammatory background with histiocytes, eosinophils, lymphocytes, and plasma cells with an accompanying dense collagen fibrosis. Diagnostic RS cells and variants are rare and difficult to identify even if immunohistochemistry for CD15 and CD30 is employed. However, the presence of a polymorphous lymphohistiocytic infiltrate with fibrosis, without diagnostic cells, can be regarded as sufficient evidence for BM infiltration if a diagnosis of classical HL has been established at a nodal site. ALCL, PTCL, T-cell-rich B-cell lymphoma, mast cell diseases, granulomatous or histiocyte disorders, or even metastatic carcinoma are among the differential diagnoses. If encountered as primary diagnosis in the BM, an extended panel of antibodies, including CD20, PAX5, OCT2, BOB1, CD3, granzyme B, EMA, ALK-1, and pancytokeratin may be necessary. In contrast, the neoplastic cells in nodular lymphocyte-predominant HL are characteristically positive for CD20, raising the differential diagnosis of T-cell/histiocyte-rich DLBCL.

Lymphoblastic lymphoma/acute lymphoblastic leukemia

In BM biopsies, lymphoblasts are relatively uniform in appearance with round to oval nuclei. Nucleoli are generally inconspicuous, and the chromatin is typically finely dispersed. The infiltration pattern is almost always interstitial or diffuse. Characterization of LBL/ALL is best performed using flow cytometry and cytogenetics, but a number of markers suitable for trephines have become available recently. The most constant and reliable marker for LBL/ALL of both lineages is TdT, which is expressed in almost all cases of ALL (Fig. 3H). TdT usually shows strong nuclear staining of virtually all cells. TdT expression also occurs in a significant subset of acute myeloid leukemia (AML) but is usually less intense and not as uniform as in ALL/LBL. In most cases of ALL/LBL, assignment to either B- or T-cell lineage is possible. The most reliable marker for B-LBL/ALL is the B-cell transcription factor PAX5 followed by CD10 and CD79a, whereas CD20 is variably expressed [152]. Of note, CD79a is not absolutely lineage-specific in this context and may be present both in rare cases of T-ALL and in AML [5]. T-LBL/ALL can usually be confirmed by staining for a variety of T-cell antigens, including CD1a, CD3, CD4, CD5, CD7, and CD8, with CD7 being the earliest T-cell marker to appear (Fig. 3I). Coexpression of CD4 and CD8 can be found frequently and is diagnostic for T-LBL/ALL. The number and sequence of T-cell antigens present may be used for stratification according to maturation stage. Both B- and T-ALL/LBL can show an expression of CD34 and, less frequently, CD117. In rare biphenotypic acute leukemias, an aberrant coexpression of myeloid markers is observed [13, 89, 118, 153]. The differential diagnosis of ALL/LBL includes such diverse entities as AML, BL, blastoid MCL, reactive BM with increased CD10+ hematogones, and even nonhematopoietic tumors such as Ewing sarcoma or rhabdomyosarcoma. Of practical importance is the immunoreactivity of LBL for CD99 (MIC-2), which may lead to confusion with Ewing sarcoma [100, 169].

Myeloid disorders

Myelodysplastic syndromes/acute myeloid leukemias

The diagnosis of MDS rests largely on clinicopathologic and morphological (cytological) findings complemented by cytogenetics. However, immunohistochemistry provides a useful tool for accurate classification of MDS in BM trephines. The identification of abnormally located precursors for a diagnosis of refractory anemia with excess of blasts (RAEB) type 1 or 2 is easily achieved with antibodies against the hematopoietic stem cell antigen CD34 (Fig. 4A) [76, 112]. Several studies investigated CD117 (c-kit) as an additional marker for the characterization of blasts in MDS. However, in our experience, the application of CD117 is problematic, since this marker is also expressed on immature erythroid cells [79, 101, 112]. For the differentiation between hypoplastic MDS and aplastic anemia, CD34 staining can be helpful to identify small numbers of immature precursors, which are a strong indicator for hypoplastic MDS [113].

In AML, a panel of antibodies, including CD34, TdT, myeloperoxidase, CD68 (KP-1 and PG-M1), glycophorin A, CD61, CD20, CD79a, CD3, and CD1a, is a useful adjunct for the differentiation between AML and ALL and for a tentative subgrouping of AML according to the French–American–British Group (FAB) criteria as illustrated by Pileri and coworkers [118]. CD34, TdT, and lymphoid markers are necessary for discrimination of AML M0 (Fig. 4B,C) and ALL (B/T). AML M2 and M4 can be separated by the use of two CD68 clones: PG-M1 is restricted to AML with monocytic/monoblastic differentiation (M4 and M5), whereas KP-1 is additionally positive in myeloblasts (M2). The sometimes difficult distinction between promyelocytic leukemia (AML M3) and a reactive increase in promyelocytes can be resolved by staining for CD117, which is aberrantly expressed in malignant promyelocytes of AML M3 [28, 125]. CD61 and glycophorin A are helpful markers for the identification of acute megakaryoblastic leukemia (M7) or acute erythroid leukemia (M6) (Fig. 4D,E).

The very recently described mutations in the nucleophosmin (NPM) gene, leading to abnormal cytoplasmatic protein expression in karyotypically normal AML, can be demonstrated with anti-NPM antibodies. Nevertheless, the importance of this observation in terms of prognosis has to be elucidated [1, 48].

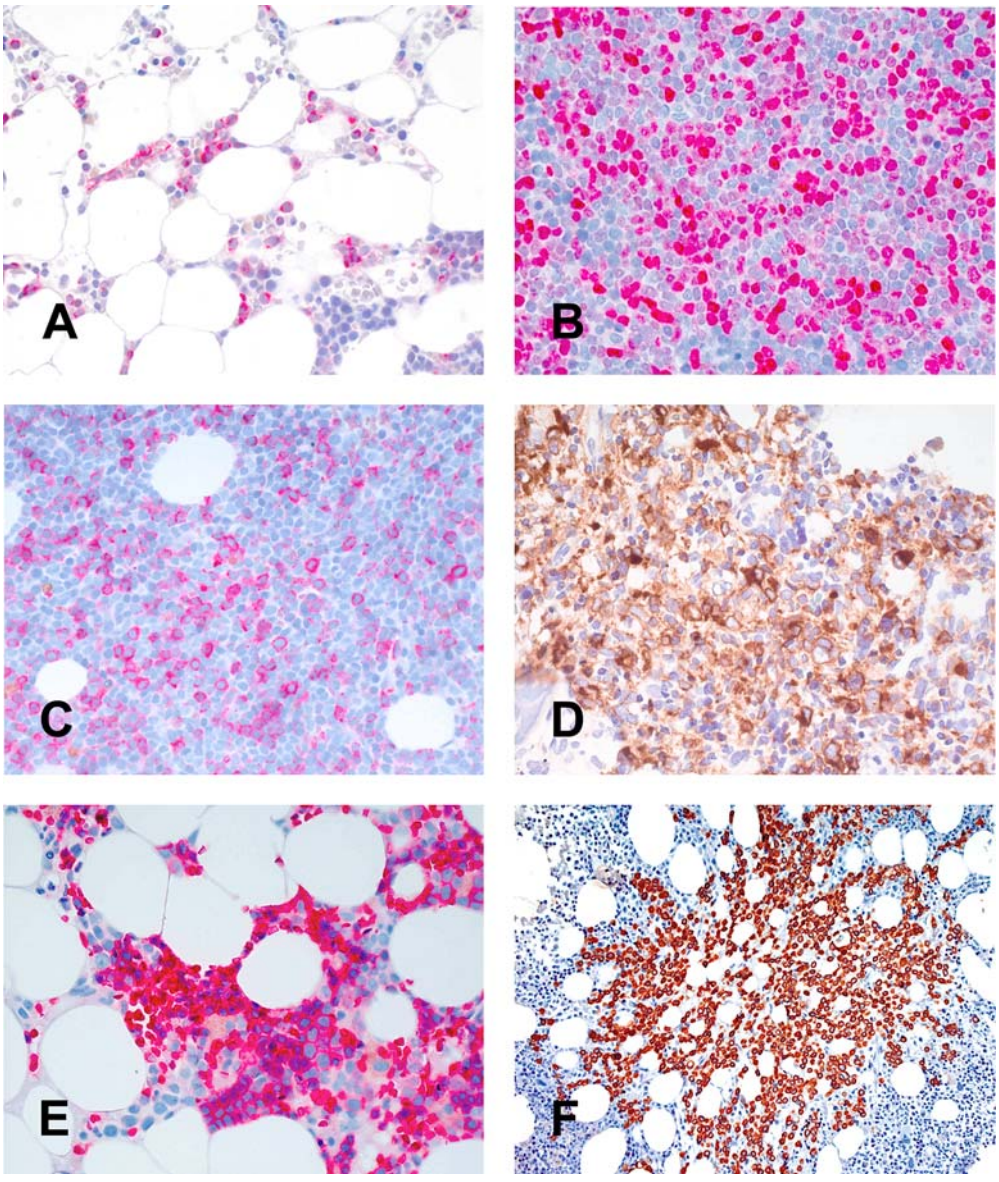


Fig. 4 Immunostainings of acute myeloid leukemias, myelodysplastic syndromes, and metastatic bone marrow disease. **A** Hypocellular MDS (RAEB-1 WHO). CD34 highlights the small interstitial aggregates of myeloblasts. The corresponding aspirate contained 9% blasts (×300 ABC-AP). **B**, **C** AML M0 (FAB) TdT (**A**) and CD34 staining (**B**) of a "packed marrow." Note the heterogeneous expression of TdT in the AML blasts in contrast to ALL (×300 ABC-AP). **D** AML M7 (acute megakaryoblastic leukemia) CD61 shows a strong cytoplasmic and membrane staining of cells of the megakaryocytic lineage. Note the mixture of small mononuclear megakaryoblasts and more differentiated cells (×300 ABC-POX). **E** Marked erythroid hyperplasia in a patient with a secondary erythrocytosis stained for glycophorin C. Maturation from erythroblasts to normoblasts is easily recognized (×300 ABC-AP). **F** BM infiltration by a lobular breast carcinoma. The infiltration by neoplastic epithelial cells is highlighted by pancytokeratin staining (×200 ABC-POX)

Chronic myeloproliferative syndromes

The diagnosis of chronic myeloproliferative syndromes such as chronic myeloid leukemia (CML), polycythemia vera (PV), essential thrombocythemia (ET), and idiopathic myelofibrosis (IMF) is generally based on a synopsis of clinical, morphological, and molecular data. However, immunostainings, including glycophorin A or C, hemoglobin, MPO, or CD61, are undoubtedly helpful for assessing the distribution and quantities of the different cell types and to identify morphologically abnormal forms such as micromegakaryocytes. In addition, CD34 is useful for determining the number of blasts present in the BM if an accelerated phase or acute transformation is suspected. Interestingly, mature megakaryocytes of MPS frequently show an aberrant cytoplasmatic CD34 expression, which can aid in the distinction from reactive processes.

Systemic mastocytosis

The BM is one of the major sites of involvement of systemic mastocytosis. The most common form of systemic mast cell disease is indolent systemic mastocytosis usually associated with cutaneous lesions. Due to the generally pronounced concomitant fibrosis in mast cell infiltrates, a BM trephine should always be performed. Although mast cells usually are easily demonstrated with 3-hydroxy-4′-nitro-2-naphthanilide chloroacetate (NASD) esterase or Giemsa stains, neoplastic mast cells may be poorly granulated, and occasionally, immunostains are required for their identification. They stain strongly for CD117 and mast cell tryptase [159, 160]. In addition, mast cells in systemic mastocytosis have been reported to aberrantly express CD2 and CD25 [141].

Metastatic disease

Bone marrow trephines generally exhibit the highest yield for detecting metastatic disease because neoplastic cells are frequently inaspirable due to concomitant fibrosis. Although metastatic solid tumors are rarely confused with hematopoetic neoplasms, immunostainings may be required for identification of the putative primary site. A diagnostic challenge, especially if minor involvement is suspected, are infiltrates of small blue round cell tumors, e.g., Ewing's sarcoma, or small-cell carcinoma. The primary antibody panel for these cases should at least contain anticytokeratin, CD99, CD56, and TdT.

The role of immunohistochemistry in reactive BM changes

In healthy adults, the mature lymphocyte compartment in the BM comprises less than 10% of nucleated cells and consist mainly of T lymphocytes (CD 3+ and CD5+) and, to a lesser extent, B lymphocytes (CD20+) [148]. However, lymphoid aggregates are commonly seen especially in the elderly or in patients with autoimmune disease. Distinction between benign nodular lymphoid aggregates and infiltrates of ML remains a difficult problem in BM histology and has been the subject of a number of studies [72, 85, 130, 134]. Benign nodules tend to have well-defined borders, are distributed at random in the marrow spaces, and have a more polymorphic cellular composition. True germinal centers can be seen occasionally. Although intralesional fibrosis, a typical feature of neoplastic infiltrates, is usually absent or mild in reactive lymphoid nodules, this feature lacks specificity. Immunohistochemically, benign lymphoid infiltrates show a polytypic staining pattern with a mixed population of B and T cells, with the latter predominating. An analysis of a light chain restriction is useful in cases with increased plasma cells. As outlined above, identification of an aberrant immunophenotype such as CD5 coexpression allows identification of early nodular involvement by B-CLL or MCL, but this feature is not present in other subtypes of B-NHL. Although most cases will be resolved by morphological and immunohistochemical studies, ambiguous cases may require molecular analysis [85]. Another important reactive condition, which may require immunostaining for its identification as mentioned above, are increased numbers of hematogones. Hematogones are immature B-cell precursors at various stages of maturation and may cause diagnostic problems when present in great numbers such as in regenerative marrow postchemotherapy or in children. In contrast to LBL/ALL, they show a range of maturation with variable expression of TdT, CD34, CD10, CD20, and/or CD79 and lack clonal antigen receptor gene rearrangements. Usually, mature forms already lacking TdT expression predominate [140].

Immunohistochemistry may also aid in the identification of infectious agents especially in immunosuppressed hosts. One of the agents worth mentioning in this context is human Parvovirus B19, which causes aplastic crisis and also the failure of nonerythroid lineages. Although B19 infections exhibit a typical morphology, with giant erythroblasts containing viral inclusions and arrest of erythroid maturation, immunostainings using a monoclonal antibody against the virus capsid protein (R92F6) can facilitate the detection [97].

Acute hemophagocytic syndrome is an important and distinctive manifestation of acute viral/bacterial infections (i.e., EBV, Parvovirus B19, hepatitis virus, and mycobacteria) especially in immunocompromised patients. The BM is characterized by an overall hematopoietic hypocellularity, variable reticulin fibrosis, and pronounced histiocytic hyperplasia, which can be highlighted by immunostainings with CD68. Highly characteristic are ingested mature and immature BM cells in the cytoplasm of histiocytes, giving them a "sack-like" appearance. The differential diagnosis includes acute monocytic leukemia and a paraneoplastic hemophagocytic syndrome in patients with peripheral T-cell NHL [75, 138, 158].

Bone marrow granulomas are encountered in both infectious and noninfectious conditions. They consist of cohesive clusters of histiocytes, lymphocytes, and occasionally, eosinophils. Immunohistochemistry can aid in the identification of microorganisms and in differentiating granulomas in the setting of ML, mastoocytosis, or reactive disorders [40].

Conclusion

Immunohistochemistry is a powerful auxiliary technique for the diagnosis of hematologic disorders in BM trephine biopsies. If standard fixation and decalcification procedures are employed, primary antibodies suitable for paraffin-embedded tissues can be applied to BM trephines without restrictions. An accurate characterization and primary classification of lymphoid neoplasms is possible in the majority of cases and expands the diagnostic scope of BM histology. Moreover, diagnostic algorithms provide a rational, fast, and cost-effective diagnostic approach.

Acknowledgements The authors are indebted to Jaqueline Müller, Sandra Rath, Nadine Kink, Birgit Geist, and in particular, Carmen Hartmann for their excellent technical assistance. Supported in part by the Deutsche Forschungsgemeinschaft (DFG), grant FE 597/1 to FF, L.Q.-M. and M.K.

References

1. Alcalay M, Tiacci E, Bergomas R, Bigerna B, Venturini E, Minardi SP, Meani N, Diverio D, Bernard L, Tizzoni L, Volorio S, Luzi L, Colombo E, Lo Coco F, Mecucci C, Falini B, Pelicci PG (2005) Acute myeloid leukemia bearing cytoplasmic nucleophosmin (NPMc+ AML) shows a distinct gene expression profile characterized by up-regulation of genes involved in stem-cell maintenance. Blood 106:899–902

2. Alvares CL, Matutes E, Scully MA, Swansbury J, Min T, Gruszka-Westwood AM, Atkinson S, Hilditch B, Morilla R, Wotherspoon AC, Catovsky D (2004) Isolated bone marrow involvement in diffuse large B cell lymphoma: a report of three cases with review of morphological, immunophenotypic and cytogenetic findings. Leuk Lymphoma 45:769–775
3. Andriko JW, Swerdlow SH, Aguilera NI, Abbondanzo SL (2001) Is lymphoplasmacytic lymphoma/immunocytoma a distinct entity? A clinicopathologic study of 20 cases. Am J Surg Pathol 25:742–751
4. The Non-Hodgkin's Lymphoma Classification Project (1997) A clinical evaluation of the international lymphoma study group classification of non-Hodgkin's lymphoma. Blood 89:3909–3918
5. Arber DA, Jenkins KA, Slovak ML (1996) CD79 alpha expression in acute myeloid leukemia. High frequency of expression in acute promyelocytic leukemia. Am J Pathol 149: 1105–1110
6. Attygalle AD, Diss TC, Munson P, Isaacson PG, Du MQ, Dogan A (2004) CD10 expression in extranodal dissemination of angioimmunoblastic T-cell lymphoma. Am J Surg Pathol 28:54–61
7. Attygalle AD, Liu H, Shirali S, Diss TC, Loddenkemper C, Stein H, Dogan A, Du MQ, Isaacson PG (2004) Atypical marginal zone hyperplasia of mucosa-associated lymphoid tissue: a reactive condition of childhood showing immunoglobulin lambda light-chain restriction. Blood 104:3343–3348
8. Audouin J, Le Tourneau A, Molina T, Camilleri-Broet S, Adida C, Comperat E, Benattar L, Delmer A, Devidas A, Rio B, Diebold J (2003) Patterns of bone marrow involvement in 58 patients presenting primary splenic marginal zone lymphoma with or without circulating villous lymphocytes. Br J Haematol 122:404–412
9. Avet-Loiseau H, Garand R, Lode L, Harousseau JL, Bataille R (2003) Translocation t(11;14)(q13;q32) is the hallmark of IgM, IgE, and nonsecretory multiple myeloma variants. Blood 101: 1570–1571
10. Bain BJ (2001) Bone marrow trephine biopsy. J Clin Pathol 54:737–742
11. Ballesteros E, Osborne BM, Matsushima AY (1998) CD5+ low-grade marginal zone B-cell lymphomas with localized presentation. Am J Surg Pathol 22:201–207
12. Batstone P, Forsyth L, Goodlad JR (2003) Cytogenetic evidence for the origin of neoplastic cells in CD5-positive marginal zone B-cell lymphoma. Hum Pathol 34:1065–1067
13. Bavikatty NR, Ross CW, Finn WG, Schnitzer B, Singleton TP (2000) Anti-CD10 immunoperoxidase staining of paraffin-embedded acute leukemias: comparison with flow cytometric immunophenotyping. Hum Pathol 31:1051–1054
14. Bayle C, Charpentier A, Duchayne E, Manel AM, Pages MP, Robert A, Lamant L, Dastugue N, Bertrand Y, Dijoud F, Emile JF, Machover D, Brugieres L, Delsol G (1999) Leukaemic presentation of small cell variant anaplastic large cell lymphoma: report of four cases. Br J Haematol 104:680–688
15. Belhadj K, Reyes F, Farcet JP, Tilly H, Bastard C, Angonin R, Deconinck E, Charlotte F, Leblond V, Labouyrie E, Lederlin P, Emile JF, Delmas-Marsalet B, Arnulf B, Zafrani ES, Gaulard P (2003) Hepatosplenic gammadelta T-cell lymphoma is a rare clinicopathologic entity with poor outcome: report on a series of 21 patients. Blood 102:4261–4269
16. Bellan C, Lazzi S, De Falco G, Nyongo A, Giordano A, Leoncini L (2003) Burkitt's lymphoma: new insights into molecular pathogenesis. J Clin Pathol 56:188–192
17. Berger F, Felman P, Thieblemont C, Pradier T, Baseggio L, Bryon PA, Salles G, Callet-Bauchu E, Coiffier B (2000) Non-MALT marginal zone B-cell lymphomas: a description of clinical presentation and outcome in 124 patients. Blood 95: 1950–1956
18. Bernhards J, Weitzel B, Werner M, Rimpler M, Georgii A (1992) A new histological embedding method by low-temperature polymerisation of methyl methacrylate allowing immuno- and enzyme histochemical studies on semi-thin sections of undecalcified bone marrow biopsies. Histochemistry 98(3): 145–154
19. Bertoni F, Zucca E, Cotter FE (2004) Molecular basis of mantle cell lymphoma. Br J Haematol 124:130–140
20. Blum KA, Lozanski G, Byrd JC (2004) Adult Burkitt leukemia and lymphoma. Blood 104:3009–3020
21. Buhr T, Laenger F, Schlué J, von Wasielewski R, Lehmann U, Braumann D, Kreipe H (2002) Reliability of lymphoma classification in bone marrow trephines. Br J Haematol 118: 470–476
22. Butmarc J, Kourea HP, Kadin ME (1997) CD5 immunostaining of lymphoid neoplasms in paraffin sections. Am J Clin Pathol 107:496–497
23. Cairo MS, Sposto R, Perkins SL, Meadows AT, Hoover-Regan ML, Anderson JR, Siegel SE, Lones MA, Tedeschi-Blok N, Kadin ME, Kjeldsberg CR, Wilson JF, Sanger W, Morris E, Krailo MD, Finlay JL (2003) Burkitt's and Burkitt-like lymphoma in children and adolescents: a review of the Children's Cancer Group experience. Br J Haematol 120 (4):660–670
24. Camacho FI, Algara P, Mollejo M, Garcia JF, Montalban C, Martinez N, Sanchez-Beato M, Piris MA (2003) Nodal marginal zone lymphoma: a heterogeneous tumor: a comprehensive analysis of a series of 27 cases. Am J Surg Pathol 27:762–771
25. Campo E (2003) Genetic and molecular genetic studies in the diagnosis of B-cell lymphomas I: mantle cell lymphoma, follicular lymphoma, and Burkitt's lymphoma. Hum Pathol 34: 330–335
26. Campo E, Miquel R, Krenacs L, Sorbara L, Raffeld M, Jaffe ES (1999) Primary nodal marginal zone lymphomas of splenic and MALT type. Am J Surg Pathol 23(1):59–68
27. Carreras J, Villamor N, Colomo L, Moreno C, Cajal SR, Crespo M, Tort F, Bosch F, Lopez-Guillermo A, Colomer D, Montserrat E, Campo E (2005) Immunohistochemical analysis of ZAP-70 expression in B-cell lymphoid neoplasms. J Pathol 205:507–513
28. Cascavilla N, Musto P, D'Arena G, Melillo L, Carella AM, Petrilli MP, Sanpaolo G, Carotenuto M (1998) CD117 (c-kit) is a restricted antigen of acute myeloid leukemia and characterizes early differentiative levels of M5 FAB subtype. Haematologica 83:392–397
29. Caulet S, Delmer A, Audouin J, Le Tourneau A, Bernadou A, Zittoun R, Diebold J (1990) Histopathological study of bone marrow biopsies in 30 cases of T-cell lymphoma with clinical, biological and survival correlations. Hematol Oncol 8:155–168
30. Chittal SM, Brousset P, Voigt JJ, Delsol G (1991) Large B-cell lymphoma rich in T-cells and simulating Hodgkin's disease. Histopathology 19:211–220
31. Chott A, Augustin I, Wrba F, Hanak H, Ohlinger W, Radaszkiewicz T (1990) Peripheral T-cell lymphomas: a clinicopathologic study of 75 cases. Hum Pathol 21(11):1117–1125
32. Chu PG, Chang KL, Arber DA, Weiss LM (1999) Practical applications of immunohistochemistry in hematolymphoid neoplasms. Ann Diagn Pathol 3:104–133
33. Cohen JI (2003) Benign and malignant Epstein–Barr virus-associated B-cell lymphoproliferative diseases. Semin Hematol 40:116–123
34. Cohen PL, Kurtin PJ, Donovan KA, Hanson CA (1998) Bone marrow and peripheral blood involvement in mantle cell lymphoma. Br J Haematol 101:302–310
35. Conlan MG, Bast M, Armitage JO, Weisenburger DD (1990) Bone marrow involvement by non-Hodgkin's lymphoma: the clinical significance of morphologic discordance between the lymph node and bone marrow. Nebraska Lymphoma Study Group. J Clin Oncol 8:1163–1172
36. Cooke CB, Krenacs L, Stetler-Stevenson M, Greiner TC, Raffeld M, Kingma DW, Abruzzo L, Frantz C, Kaviani M, Jaffe ES (1996) Hepatosplenic T-cell lymphoma: a distinct clinicopathologic entity of cytotoxic gamma delta T-cell origin. Blood 88:4265–4274
37. Crotty PL, Smith BR, Tallini G (1998) Morphologic, immunophenotypic, and molecular evaluation of bone marrow involvement in non-Hodgkin's lymphoma. Diagn Mol Pathol 7:90–95

38. deJong D, Voetdijk BMH, van Ommen GJB, Kluin PM (1989) Alterations in immunoglobulin genes reveal the origin and evolution of monotypic and bitypic B cell lymphomas. Am J Pathol 134:1233–1242
39. Delage R, Jacques L, Massinga-Loembe M, Poulin J, Bilodeau D, Mignault C, Leblond PF, Darveau A (2001) Persistent polyclonal B-cell lymphocytosis: further evidence for a genetic disorder associated with B-cell abnormalities. Br J Haematol 114(3):666–670
40. Diebold J, Molina T, Camilleri-Broet S, le Tourneau A, Audouin J (2000) Bone marrow manifestations of infections and systemic diseases observed in bone marrow trephine biopsy. Histopathology 37:199–211
41. Dierlamm J, Pittaluga S, Wlodarska I, Stul M, Thomas J, Boogaerts M, Michaux L, Driessen A, Mecucci C, Cassiman JJ (1996) Marginal zone B-cell lymphomas of different sites share similar cytogenetic and morphologic features. Blood 87:299–307
42. Dogan A, Morice WG (2004) Bone marrow histopathology in peripheral T-cell lymphomas. Br J Haematol 127:140–154
43. Dong HY, Gorczyca W, Liu Z, Tsang P, Wu CD, Cohen P, Weisberger J (2003) B-cell lymphomas with coexpression of CD5 and CD10. Am J Clin Pathol 119(2):218–230
44. Dorfman DM, Shahsafaei A (1997) Usefulness of a new CD5 antibody for the diagnosis of T-cell and B-cell lymphoproliferative disorders in paraffin sections. Mod Pathol 10:859–863
45. Ely SA, Knowles DM (2002) Expression of CD56/neural cell adhesion molecule correlates with the presence of lytic bone lesions in multiple myeloma and distinguishes myeloma from monoclonal gammopathy of undetermined significance and lymphomas with plasmocytoid differentiation. Am J Pathol 160: 1293–1299
46. Epstein J, Xiao HQ, He XY (1990) Markers of multiple hematopoietic-cell lineages in multiple myeloma. N Engl J Med 322:664–668
47. Falini B, Mecucci C, Tiacci E, Alcalay M, Rosati R, Pasqualucci L, La Starza R, Diverio D, Colombo E, Santucci A, Bigerna B, Pacini R, Pucciarini A, Liso A, Vignetti M, Fazi P, Meani N, Pettirossi V, Saglio G, Mandelli F, Lo-Coco F, Pelicci PG, Martelli MF (2005) Cytoplasmic nucleophosmin in acute myelogenous leukemia with a normal karyotype. N Engl J Med 352:254–266
48. Falini B, Pileri S, De Solas I, Martelli MF, Mason DY, Delsol G, Gatter KC, Fagioli M (1990) Peripheral T-cell lymphoma associated with hemophagocytic syndrome. Blood 75:434–444
49. Falini B, Tiacci E, Liso A, Basso K, Sabattini E, Pacini R, Foa R, Pulsoni A, Dalla Favera R, Pileri S (2004) Simple diagnostic assay for hairy cell leukaemia by immunocytochemical detection of annexin A1 (ANXA1). Lancet 363:1869–1870
50. Ferry JA, Yang WI, Zukerberg LR, Wotherspoon AC, Arnold A, Harris NL (1996) CD5+ extranodal marginal zone B-cell (MALT) lymphoma. A low grade neoplasm with a propensity for bone marrow involvement and relapse. Am J Clin Pathol 105:31–37
51. Feugier P, De March AK, Lesesve JF, Monhoven N, Dorvaux V, Braun F, Gregoire MJ, Jonveaux P, Lederlin P, Bene MC, Labouyrie E (2004) Intravascular bone marrow accumulation in persistent polyclonal lymphocytosis: a misleading feature for B-cell neoplasm. Mod Pathol 17:1087–1096
52. Fonseca R, Blood EA, Oken MM, Kyle RA, Dewald GW, Bailey RJ, Van Wier SA, Henderson KJ, Hoyer JD, Harrington D, Kay NE, Van Ness B, Greipp PR (2002) Myeloma and the t(11;14)(q13;q32); evidence for a biologically defined unique subset of patients. Blood 99:3735–3741
53. Foucar K (1995) Bone marrow pathology. ASCP, Chicago, p 320
54. Fraga M, Brousset P, Schlaifer D, Payen C, Robert A, Rubie H, Huguet-Rigal F, Delsol G (1995) Bone marrow involvement in anaplastic large cell lymphoma. Immunohistochemical detection of minimal disease and its prognostic significance. Am J Clin Pathol 103:82–89
55. Franco V, Florena AM, Campesi G (1996) Intrasinusoidal bone marrow infiltration: a possible hallmark of splenic lymphoma. Histopathology 29:571–575
56. Franco V, Florena AM, Iannitto E (2003) Splenic marginal zone lymphoma. Blood 101:2464–2472
57. Gallamini A, Stelitano C, Calvi R, Bellei M, Mattei D, Vitolo U, Morabito F, Martelli M, Brusamolino E, Iannitto E, Zaja F, Cortelazzo S, Rigacci L, Devizzi L, Todeschini G, Santini G, Brugiatelli M, Federico M (2004) Peripheral T-cell lymphoma unspecified (PTCL-U): a new prognostic model from a retrospective multicentric clinical study. Blood 103:2474–2479
58. Garand R, Duchayne E, Blanchard D, Robillard N, Kuhlein E, Fenneteau O, Salomon-Nguyen F, Grange MJ, Rousselot P, Demur C (1995) Minimally differentiated erythroleukaemia (AML M6 'variant'): a rare subset of AML distinct from AML M6. Groupe Francais d'Hematologie Cellulaire. Br J Haematol 90:868–875
59. Gatter KC, Heryet A, Brown DC, Mason DY (1987) Is it necessary to embed bone marrow biopsies in plastic for haematological diagnosis? Histopathology 11:1–7
60. Gaulard P, Kanavaros P, Farcet JP, Rocha FD, Haioun C, Divine M, Reyes F, Zafrani ES (1991) Bone marrow histologic and immunohistochemical findings in peripheral. T-cell lymphoma: a study of 38 cases. Hum Pathol 22:331–338
61. Ghani AM, Krause JR (1985) Bone marrow biopsy findings in angioimmunoblastic lymphadenopathy. Br J Haematol 61:203–213
62. Gisselbrecht C, Gaulard P, Lepage E, Coiffier B, Briere J, Haioun C, Cazals-Hatem D, Bosly A, Xerri L, Tilly H, Berger F, Bouhabdallah R, Diebold J (1998) Prognostic significance of T-cell phenotype in aggressive non-Hodgkin's lymphomas. Groupe d'Etudes des Lymphomes de l'Adulte (GELA). Blood 92:76–82
63. Greiner TC, Moynihan MJ, Chan WC, Lytle DM, Pedersen A, Anderson JR, Weisenburger DD (1996) p53 mutations in mantle cell lymphoma are associated with variant cytology and predict a poor prognosis. Blood 87:4302–4310
64. Grogan TM (2003) Plasma cell myeloma marrow diagnosis including morphologic and phenotypic features. Semin Diagn Pathol 20:211–225
65. Gronbaek K, Nedergaard T, Andersen MK, thor Straten P, Guldberg P, Moller P, Zeuthen J, Ebbe Hansen N, Hou-Jensen K, Ralfkiaer E (1998) Concurrent disruption of cell cycle associated genes in mantle cell lymphoma: a genotypic and phenotypic study of cyclin D1, p16, p15, p53 and pRb. Leukemia 12(8):1266–1271
66. Hakimian D, Tallman MS, Kiley C, Peterson L (1993) Detection of minimal residual disease by immunostaining of bone marrow biopsies after 2-chlorodeoxyadenosine for hairy cell leukemia. Blood 82:1798–1802
67. Hammer RD, Glick AD, Greer JP, Collins RD, Cousar JB (1996) Splenic marginal zone lymphoma. A distinct B-cell neoplasm. Am J Surg Pathol 20(5):613–626
68. Harris NL, Bhan AK (1985) B-cell neoplasms of the lymphocytic, lymphoplasmacytoid, and plasma cell types: immunohistologic analysis and clinical correlation. Hum Pathol 16: 829–837
69. Harris NL, Jaffe ES, Stein H, Banks PM, Chan JK, Cleary ML, Delsol G, De Wolf-Peeters C, Falini B, Gatter KC (1994) A revised European–American classification of lymphoid neoplasms: a proposal from the International Lymphoma Study Group. Blood 84:1361–1392
70. Hedvat CV, Hegde A, Chaganti RS, Chen B, Qin J, Filippa DA, Nimer SD, Teruya-Feldstein J (2002) Application of tissue microarray technology to the study of non-Hodgkin's and Hodgkin's lymphoma. Hum Pathol 33(10):968–974
71. Henrique R, Achten R, Maes B, Verhoef G, De Wolf-Peeters C (1999) Guidelines for subtyping small B-cell lymphomas in bone marrow biopsies. Virchows Arch 435:549–558
72. Hernandez L, Fest T, Cazorla M, Teruya-Feldstein J, Bosch F, Peinado MA, Piris MA, Montserrat E, Cardesa A, Jaffe ES, Campo E, Raffeld M (1996) p53 gene mutations and protein overexpression are associated with aggressive variants of mantle cell lymphomas. Blood 87(8):3351–3359

73. Hideshima T, Bergsagel PL, Kuehl WM, Anderson KC (2004) Advances in biology of multiple myeloma: clinical applications. Blood 104:607–618
74. Hirst WJ, Layton DM, Singh S, Mieli-Vergani G, Chessells JM, Strobel S, Pritchard J (1994) Haemophagocytic lymphohistiocytosis: experience at two UK centres. Br J Haematol 88:731–739
75. Horny HP, Wehrmann M, Schlicker HU, Eichstaedt A, Clemens MR, Kaiserling E (1995) QBEND10 for the diagnosis of myelodysplastic syndromes in routinely processed bone marrow biopsy specimens. J Clin Pathol 48:291–294
76. Howell SJ, Grey M, Chang J, Morgenstern GR, Cowan RA, Deakin DP, Radford JA (2002) The value of bone marrow examination in the staging of Hodgkin's lymphoma: a review of 955 cases seen in a regional cancer centre. Br J Haematol 119:408–411
77. Hoyer JD, Li CY, Yam LT, Hanson CA, Kurtin PJ (1997) Immunohistochemical demonstration of acid phosphatase isoenzyme 5 (tartrate-resistant) in paraffin sections of hairy cell leukemia and other hematologic disorders. Am J Clin Pathol 108:308–315
78. Huss R, Moosmann S (2002) The co-expression of CD117 (c-kit) and osteocalcin in activated bone marrow stem cells in different diseases. Br J Haematol 118:305–312
79. Ioachim HL, Dorsett B, Cronin W, Maya M, Wahl S (1991) Acquired immunodeficiency syndrome-associated lymphomas: clinical, pathologic, immunologic, and viral characteristics of 111 cases. Hum Pathol 22:659–673
80. Jilani I, O'Brien S, Manshuri T, Thomas DA, Thomazy VA, Imam M, Naeem S, Verstovsek S, Kantarjian H, Giles F, Keating M, Albitar M (2003) Transient down-modulation of CD20 by rituximab in patients with chronic lymphocytic leukemia. Blood 102:3514–3520
81. Juneja SK, Wolf MM, Cooper IA (1990) Value of bilateral bone marrow biopsy specimens in non-Hodgkin's lymphoma. J Clin Pathol 43:630–632
82. Kent SA, Variakojis D, Peterson LC (2002) Comparative study of marginal zone lymphoma involving bone marrow. Am J Clin Pathol 117:698–708
83. Khoury JD, Jones D, Yared MA, Manning JT Jr, Abruzzo LV, Hagemeister FB, Medeiros LJ (2004) Bone marrow involvement in patients with nodular lymphocyte predominant Hodgkin lymphoma. Am J Surg Pathol 28:489–495
84. Kremer M, Cabras AD, Fend F, Schulz S, Schwarz K, Hoefler H, Werner M (2000) PCR analysis of IgH-gene rearrangements in small lymphoid infiltrates microdissected from sections of paraffin-embedded bone marrow biopsy specimens. Hum Pathol 31:847–853
85. Kremer M, Dirnhofer S, Nickl A, Hoefler H, Quintanilla-Martinez L, Fend F (2001) p27(Kip1) immunostaining for the differential diagnosis of small b-cell neoplasms in trephine bone marrow biopsies. Mod Pathol 14:1022–1029
86. Kremer M, Ott G, Nathrath M, Specht K, Stecker K, Alexiou C, Quintanilla-Martinez L, Fend F (2005) Primary extramedullary plasmacytoma and multiple myeloma: phenotypic differences revealed by immunohistochemical analysis. J Pathol 205:92–101
87. Kremer M, Spitzer M, Mandl-Weber S, Stecker K, Schmidt B, Hofler H, Quintanilla-Martinez L, Fend F (2003) Discordant bone marrow involvement in diffuse large B-cell lymphoma: comparative molecular analysis reveals a heterogeneous group of disorders. Lab Invest 83(1):107–114
88. Krober SM, Greschniok A, Kaiserling E, Horny HP (2000) Acute lymphoblastic leukaemia: correlation between morphological/immunohistochemical and molecular biological findings in bone marrow biopsy specimens. Mol Pathol 53:83–87
89. Kumar S, Green GA, Teruya-Feldstein J, Raffeld M, Jaffe ES (1996) Use of CD23 (BU38) on paraffin sections in the diagnosis of small lymphocytic lymphoma and mantle cell lymphoma. Mod Pathol 9:925–929
90. Labouyrie E, Marit G, Vial JP, Lacombe F, Fialon P, Bernard P, de Mascarel A, Merlio JP (1997) Intrasinusoidal bone marrow involvement by splenic lymphoma with villous lymphocytes: a helpful immunohistologic feature. Mod Pathol 10:1015–1020
91. Lai R, Weiss LM, Chang KL, Arber DA (1999) Frequency of CD43 expression in non-Hodgkin lymphoma. A survey of 742 cases and further characterization of rare CD43+ follicular lymphomas. Am J Clin Pathol 111:488–494
92. Lamant L, Meggetto F, al Saati T, Brugieres L, de Paillerets BB, Dastugue N, Bernheim A, Rubie H, Terrier-Lacombe MJ, Robert A, Rigal F, Schlaifer D, Shiuta M, Mori S, Delsol G (1996) High incidence of the t(2;5)(p23;q35) translocation in anaplastic large cell lymphoma and its lack of detection in Hodgkin's disease. Comparison of cytogenetic analysis, reverse transcriptase–polymerase chain reaction, and P-80 immunostaining. Blood 87:284–291
93. Liang R, Chan VV, Chan TK, Todd D, Ho F (1990) Immunoglobulin gene rearrangement in the peripheral blood and bone marrow of patients with lymphomas of the mucosa-associated lymphoid tissues. Acta Haematol 84:19–23
94. Lim EJ, Peh SC (2000) Bone marrow and peripheral blood changes in non-Hodgkin's lymphoma. Singapore Med J 41: 279–285
95. Liu Q, Ohshima K, Sumie A, Suzushima H, Iwasaki H, Kikuchi M (2001) Nasal CD56 positive small round cell tumors. Differential diagnosis of hematological, neurogenic, and myogenic neoplasms. Virchows Arch 438:271–279
96. Liu W, Ittmann M, Liu J, Schoentag R, Tierno P, Greco MA, Sidhu G, Nierodzik M, Wieczorek R (1997) Human parvovirus B19 in bone marrows from adults with acquired immunodeficiency syndrome: a comparative study using in situ hybridization and immunohistochemistry. Hum Pathol 28:760–766
97. Lloret E, Mollejo M, Mateo MS, Villuendas R, Algara P, Martinez P, Piris MA (1999) Splenic marginal zone lymphoma with increased number of blasts: an aggressive variant? Hum Pathol 30(10):1153–1160
98. Lopez-Guillermo A, Cid J, Salar A, Lopez A, Montalban C, Castrillo JM, Gonzalez M, Ribera JM, Brunet S, Garcia-Conde J, Fernandez de Sevilla A, Bosch F, Montserrat E (1998) Peripheral T-cell lymphomas: initial features, natural history, and prognostic factors in a series of 174 patients diagnosed according to the R.E.A.L. classification. Ann Oncol 9:849–855
99. Lucas DR, Bentley G, Dan ME, Tabaczka P, Poulik JM, Mott MP (2001) Ewing sarcoma vs lymphoblastic lymphoma. A comparative immunohistochemical study. Am J Clin Pathol 115:11–17
100. Lyman SD, Jacobsen SE (1998) c-kit ligand and Flt3 ligand: stem/progenitor cell factors with overlapping yet distinct activities. Blood 15:1101–1134
101. Mainou-Fowler T, Dignum HM, Proctor SJ, Summerfield GP (2004) The prognostic value of CD38 expression and its quantification in B cell chronic lymphocytic leukemia (B-CLL). Leuk Lymphoma 45:455–462
102. Majlis A, Pugh WC, Rodriguez MA, Benedict WF, Cabanillas F (1997) Mantle cell lymphoma: correlation of clinical outcome and biologic features with three histologic variants. J Clin Oncol 15:1664–1671
103. Matolcsy A (1999) High-grade transformation of low-grade non-Hodgkin's lymphomas: mechanisms of tumor progression. Leuk Lymphoma 34:251–259
104. Matolcsy A, Schattner EJ, Knowles DM, Casali P (1999) Clonal evolution of B-cells in transformation from low- to high-grade lymphoma. Eur J Immunol 29:1253–1264
105. Milan L, Trachtenberg MC (1981) Ultrasonic decalcification of bone. Am J Surg Pathol 5:573–579
106. Mitterer M, Oduncu F, Lanthaler AJ, Drexler E, Amaddii G, Fabris P, Emmerich B, Coser P, Straka C (1999) The relationship between monoclonal myeloma precursor B cells in the peripheral blood stem cell harvests and the clinical response of multiple myeloma patients. Br J Haematol 106: 737–743

107. Mollejo M, Menarguez J, Lloret E, Sanchez A, Campo E, Algara P, Cristobal E, Sanchez E, Piris MA (1995) Splenic marginal zone lymphoma: a distinctive type of low-grade B-cell lymphoma. A clinicopathological study of 13 cases. Am J Surg Pathol 19:1146–1157
108. Morabito F, Gallamini A, Stelitano C, Callea V, Guglielmi C, Neri S, Lazzaro A, Orsucci L, Ilariucci F, Sacchi S, Vitolo U, Federico M (2004) Clinical relevance of immunophenotype in a retrospective comparative study of 297 peripheral T-cell lymphomas, unspecified, and 496 diffuse large B-cell lymphomas: experience of the Intergruppo Italiano Linformi. Cancer 101:1601–1608
109. Morice WG, Kurtin PJ, Tefferi A, Hanson CA (2002) Distinct bone marrow findings in T-cell granular lymphocytic leukemia revealed by paraffin section immunoperoxidase stains for CD8, TIA-1, and granzyme B. Blood 99:268–274
110. Morice WG, Rodriguez FJ, Hoyer JD, Kurtin PJ (2005) Diffuse large B-cell lymphoma with distinctive patterns of splenic and bone marrow involvement: clinicopathologic features of two cases. Mod Pathol 18:495–502
111. Ogata K, Nakamura K, Yokose N, Tamura H, Tachibana M, Taniguchi O, Iwakiri R, Hayashi T, Sakamaki H, Murai Y, Tohyama K, Tomoyasu S, Nonaka Y, Mori M, Dan K, Yoshida Y (2002) Clinical significance of phenotypic features of blasts in patients with myelodysplastic syndrome. Blood 100:3887–3896
112. Orazi A, Albitar M, Heerema NA, Haskins S, Neiman RS (1997) Hypoplastic myelodysplastic syndromes can be distinguished from acquired aplastic anemia by CD34 and PCNA immunostaining of bone marrow biopsy specimens. Am J Clin Pathol 107:268–274
113. Ott G, Kalla J, Hanke A, Muller JG, Rosenwald A, Katzenberger T, Kretschmar R, Kreipe H, Muller-Hermelink HK (1998) The cytomorphological spectrum of mantle cell lymphoma is reflected by distinct biological features. Leuk Lymphoma 32: 55–63
114. Ott G, Ott MM, Kalla J, Helbing A, Schryen B, Katzenberger T, Bartek J, Durr A, Muller JG, Kreipe H, Muller-Hermelink HK (1997) Genetic lesions in mantle cell lymphoma. Recent Results Cancer Res 143:307–319
115. Palacio C, Acebedo G, Navarrete M, Ruiz-Marcellan C, Sanchez C, Blanco A, Lopez A (2001) Flow cytometry in the bone marrow evaluation of follicular and diffuse large B-cell lymphomas. Haematologica 86:934–940
116. Perz J, Topaly J, Fruehauf S, Hensel M, Ho AD (2002) Level of CD 20-expression and efficacy of rituximab treatment in patients with resistant or relapsing B-cell prolymphocytic leukemia and B-cell chronic lymphocytic leukemia. Leuk Lymphoma 43:149–151
117. Pileri SA, Ascani S, Milani M, Visani G, Piccioli M, Orcioni GF, Poggi S, Sabattini E, Santini D, Falini B (1999) Acute leukemia immunophenotyping in bone-marrow routine sections. Br J Haematol 105:394–401
118. Pileri SA, Roncador G, Ceccarelli C, Piccioli M, Briskomatis A, Sabattini E, Ascani S, Santini D, Piccaluga PP, Leone O, Damiani S, Ercolessi C, Sandri F, Pieri F, Leoncini L, Falini B (1997) Antigen retrieval techniques in immunohistochemistry: comparison of different methods. J Pathol 183:116–123
119. Pinotti G, Zucca E, Roggero E, Pascarella A, Bertoni F, Savio A, Savio E, Capella C, Pedrinis E, Saletti P, Morandi E, Santandrea G, Cavalli F (1997) Clinical features, treatment and outcome in a series of 93 patients with low-grade gastric MALT lymphoma. Leuk Lymphoma 26:527–537
120. Pittaluga S, Verhoef G, Criel A, Maes A, Nuyts J, Boogaerts M, De Wolf Peeters C (1996) Prognostic significance of bone marrow trephine and peripheral blood smears in 55 patients with mantle cell lymphoma. Leuk Lymphoma 21:115–125
121. Quintanilla-Martinez L, Kremer M, Specht K, Calzada-Wack J, Nathrath M, Schaich R, Hofler H, Fend F (2003) Analysis of signal transducer and activator of transcription 3 (Stat 3) pathway in multiple myeloma: stat 3 activation and cyclin D1 dysregulation are mutually exclusive events. Am J Pathol 162: 1449–1461
122. Quintanilla-Martínez L, Thieblemont C, Fend F, Kumar S, Pinyol M, Campo E, Jaffe ES, Raffeld M (1998) Mantle cell lymphomas lack expression of p27/kip1, a cyclin-dependent kinase inhibitor. Am J Pathol 153:175–182
123. Raderer M, Vorbeck F, Formanek M, Osterreicher C, Valencak J, Penz M, Kornek G, Hamilton G, Dragosics B, Chott A (2000) Importance of extensive staging in patients with mucosa-associated lymphoid tissue (MALT)-type lymphoma. Br J Cancer 83(4):454–457
124. Rizzatti EG, Garcia AB, Portieres FL, Silva DE, Martins SL, Falcao RP (2002) Expression of CD117 and CD11b in bone marrow can differentiate acute promyelocytic leukemia from recovering benign myeloid proliferation. Am J Clin Pathol 118:31–37
125. Robillard N, Avet-Loiseau H, Garand R, Moreau P, Pineau D, Rapp MJ, Harousseau JL, Bataille R (2003) CD20 is associated with a small mature plasma cell morphology and t(11;14) in multiple myeloma. Blood 102:1070–1071
126. Rosso R, Neiman RS, Paulli M, Boveri E, Kindl S, Magrini U, Barosi G (1995) Splenic marginal zone cell lymphoma: report of an indolent variant without massive splenomegaly presumably representing an early phase of the disease. Hum Pathol 26:39–46
127. Ruchlemer R, Parry-Jones N, Brito-Babapulle V, Attolico I, Wotherspoon AC, Matutes E, Catovsky D (2004) B-prolymphocytic leukaemia with t(11;14) revisited: a splenomegalic form of mantle cell lymphoma evolving with leukaemia. Br J Haematol 125:330–336
128. Rudiger T, Gascoyne RD, Jaffe ES, de Jong D, Delabie J, De Wolf-Peeters C, Poppema S, Xerri L, Gisselbrecht C, Wiedenmann S, Muller-Hermelink HK (2002) Workshop on the relationship between nodular lymphocyte predominant Hodgkin's lymphoma and T cell/histiocyte-rich B cell lymphoma. Ann Oncol 13:44–51
129. Salisbury JR, Deverell MH, Seaton JM, Cookson MJ (1997) Three-dimensional reconstruction of non-Hodgkin's lymphoma in bone marrow trephines. J Pathol 181:451–454
130. Salomon-Nguyen F, Valensi F, Troussard X, Flandrin G (1996) The value of the monoclonal antibody, DBA44, in the diagnosis of B-lymphoid disorders. Leuk Res 20:909–913
131. Sanchez-Beato M, Saez AI, Martinez-Montero JC, Mateo MS, Sanchez-Verde L, Villuendas R, Piris MA (1997) Cyclin-dependent kinase inhibitor p27kip1 in lymphoid tissue: p27 kip1 expression is inversely proportional to the proliferative index. Am J Pathol 151:151–160
132. Schaefer HE (1995) Histological processing of iliac crest biopsies based on decalcification and paraffin embedding with reference to osteolytic and hematologic diagnosis. Pathologe 16:11–27
133. Schmid C, Isaacson PG (1992) Bone marrow trephine biopsy in lymphoproliferative disease. J Clin Pathol 45:745–750
134. Schmid G, Isaacson PG (1992) Bone marrow trephine biopsy in lymphoproliferative disease. J Clin Pathol 45:745–750
135. Shanafelt TD, Geyer SM, Kay NE (2004) Prognosis at diagnosis: integrating molecular biologic insights into clinical practice for patients with CLL Blood 103:1202–1210
136. Shehata M, Schwarzmeier JD, Hilgarth M, Hubmann R, Duechler M, Gisslinger H (2004) TGF-beta1 induces bone marrow reticulin fibrosis in hairy cell leukemia. J Clin Invest 113:676–685
137. Sibaud V, Beylot-Barry M, Thiebaut R, Parrens M, Vergier B, Delaunay M, Beylot C, Chene G, Ferrer J, de Mascarel A, Dubus P, Merlio JP (2003) Bone marrow histopathologic and molecular staging in epidermotropic T-cell lymphomas. Am J Clin Pathol 119:414–423
138. Sirohi B, Powles R (2004) Multiple myeloma. Lancet 363:875–887
139. Soslow RA, Bhargava V, Warnke RA (1997) MIC2, TdT, bcl-2, and CD34 expression in paraffin-embedded high-grade lymphoma/acute lymphoblastic leukemia distinguishes between distinct clinicopathologic entities. Hum Pathol 28:1158–1165

140. Sotlar K, Horny HP, Simonitsch I, Krokowski M, Aichberger KJ, Mayerhofer M, Printz D, Fritsch G, Valent P (2004) CD25 indicates the neoplastic phenotype of mast cells: a novel immunohistochemical marker for the diagnosis of systemic mastocytosis (SM) in routinely processed bone marrow biopsy specimens. Am J Surg Pathol 28:1319–1325
141. Specht K, Haralambieva E, Bink K, Kremer M, Mandl-Weber S, Koch I, Tomer R, Hofler H, Schuuring E, Kluin PM, Fend F, Quintanilla-Martinez L (2004) Different mechanisms of cyclin D1 overexpression in multiple myeloma revealed by fluorescence in situ hybridization and quantitative analysis of mRNA levels. Blood 15:1120–1126
142. Stein H, Foss HD, Durkop H, Marafioti T, Delsol G, Pulford K, Pileri S, Falini B (2000) CD30(+) anaplastic large cell lymphoma: a review of its histopathologic, genetic, and clinical features. Blood 96:3681–3695
143. Subira M, Domingo A, Santamaria A, Bordes R, Romagosa V, Soler J (1997) Bone marrow involvement in lymphoblastic lymphoma and small non-cleaved cell lymphoma: the role of trephine biopsy. Haematologica 82:594–595
144. Sundeen JT, Longo DL, Jaffe ES (1992) CD5 expression in B-cell small lymphocytic malignancies. Correlations with clinical presentation and sites of disease. Am J Surg Pathol 16:130–137
145. Swerdlow SH, Williams ME (2002) From centrocytic to mantle cell lymphoma: a clinicopathologic and molecular review of 3 decades. Hum Pathol 33:7–20
146. Taniguchi T, Endo H, Chikatsu N, Uchimaru K, Asano S, Fujita T, Nakahata T, Motukura T (1999) Expression of p21/cip1/waf1/sdi1 and p27/kip1 cyclin-dependent kinase inhibitors during human hematopoiesis. Blood 93:4167–4178
147. Thaler J, Greil R, Dietze O, Huber H (1989) Immunohistology for quantification of normal bone marrow lymphocyte subsets. Br J Haematol 73:576–577
148. Thieblemont C, Berger F, Dumontet C, Moullet I, Bouafia F, Felman P, Salles G, Coiffier B (2000) Mucosa-associated lymphoid tissue lymphoma is a disseminated disease in one third of 158 patients analyzed. Blood 95:802–806
149. Thiele J, Langohr J, Skorupka M, Fischer R (1990) Reticulin fibre content of bone marrow infiltrates of malignant non-Hodgkin's lymphomas (B-cell type, low malignancy)—a morphometric evaluation before and after therapy. Virchows Arch 417:485–492
150. Torlakovic E, Torlakovic G, Brunning RD (2002) Follicular pattern of bone marrow involvement by follicular lymphoma. Am J Clin Pathol 118:780–786
151. Torlakovic E, Torlakovic G, Nguyen PL, Brunning RD, Delabie J (2002) The value of anti-pax-5 immunostaining in routinely fixed and paraffin-embedded sections: a novel pan pre-B and B-cell marker. Am J Surg Pathol 26:1343–1350
152. Toth B, Wehrmann M, Kaiserling E, Horny HP (1999) Immunophenotyping of acute lymphoblastic leukaemia in routinely processed bone marrow biopsy specimens. J Clin Pathol 52:688–692
153. Troussard X, Flandrin G (1996) Chronic B-cell lymphocytosis with binucleated lymphocytes (LWBL): a review of 38 cases. Leuk Lymphoma 20:275–279
154. Troussard X, Valensi F, Duchayne E, Garand R, Felman P, Tulliez M, Henry-Amar M, Bryon PA, Flandrin G (1996) Splenic lymphoma with villous lymphocytes: clinical presentation, biology and prognostic factors in a series of 100 patients. Groupe Francais d'Hematologie Cellulaire (GFHC). Br J Haematol 93(3):731–736
155. Tsirigotis P, Economopoulos T, Rontogianni D, Dervenoulas J, Papageorgiou E, Bollas G, Mantzios G, Kalantzis D, Koumarianou A, Raptis S (2001) T-cell-rich B-cell lymphoma. Analysis of clinical features, response to treatment, survival and comparison with diffuse large B-cell lymphoma. Oncology 61:257–264
156. Tworek JA, Singleton TP, Schnitzer B, Hsi ED, Ross CW (1998) Flow cytometric and immunohistochemical analysis of small lymphocytic lymphoma, mantle cell lymphoma, and plasmacytoid small lymphocytic lymphoma. Am J Clin Pathol 110:582–589
157. Undar L, Karpuzoglu G, Karadogan I, Gelen T, Artvinli M (1996) Tuberculosis-associated haemophagocytic syndrome: a report of two cases and a review of the literature. Acta Haematol 96:73–78
158. Valent P, Akin C, Sperr WR, Horny HP, Arock M, Lechner K, Bennett JM, Metcalfe DD (2003) Diagnosis and treatment of systemic mastocytosis: state of the art. Br J Haematol 122:695–717
159. Valent P, Horny HP, Escribano L, Longley BJ, Li CY, Schwartz LB, Marone G, Nunez R, Akin C, Sotlar K, Sperr WR, Wolff K, Brunning RD, Parwaresch RM, Austen KF, Lennert K, Metcalfe DD, Vardiman JW, Bennett JM (2001) Diagnostic criteria and classification of mastocytosis: a consensus proposal. Leuk Res 25:603–625
160. Vardiman JW, Harris NL, Brunning RD (2002) The World Health Organization (WHO) classification of the myeloid neoplasms. Blood 100:2292–2302
161. Vega F, Medeiros LJ, Bueso-Ramos C, Jones D, Lai R, Luthra R, Abruzzo LV (2001) Hepatosplenic gamma/delta T-cell lymphoma in bone marrow. A sinusoidal neoplasm with blastic cytologic features. Am J Clin Pathol 116(3):410–409
162. Went PT, Zimpfer A, Pehrs AC, Sabattini E, Pileri SA, Maurer R, Terracciano L, Tzankov A, Sauter G, Dirnhofer S (2005) High specificity of combined TRAP and DBA44 expression for hairy cell leukemia. Am J Surg Pathol 29:474–478
163. Westbrook CA, Groopman JE, Golde DW (1984) Hairy cell leukemia. Disease pattern and prognosis. Cancer 54:500–506
164. Wiestner A, Rosenwald A, Barry TS, Wright G, Davis RE, Henrickson SE, Zhao H, Ibbotson RE, Orchard JA, Davis Z, Stetler-Stevenson M, Raffeld M, Arthur DC, Marti GE, Wilson WH, Hamblin TJ, Oscier DG, Staudt LM (2003) ZAP-70 expression identifies a chronic lymphocytic leukemia subtype with unmutated immunoglobulin genes, inferior clinical outcome, and distinct gene expression profile. Blood 101:4944–4951
165. Wilson CS, Butch AW, Lai R, Medeiros LJ, Sawyer JR, Barlogie B, McCourty A, Kelly K, Brynes RK (2001) Cyclin D1 and E2F-1 immunoreactivity in bone marrow biopsy specimens of multiple myeloma: relationship to proliferative activity, cytogenetic abnormalities and DNA ploidy. Br J Haematol 112:776–782
166. Yamaguchi M, Seto M, Okamoto M, Ichinohasama R, Nakamura N, Yoshino T, Suzumiya J, Murase T, Miura I, Akasaka T, Tamaru J, Suzuki R, Kagami Y, Hirano M, Morishima Y, Ueda R, Shiku H, Nakamura S (2002) De novo CD5+diffuse large B-cell lymphoma: a clinicopathologic study of 109 patients. Blood 99:815–821
167. Zelenetz AD, Chen TT, Levy R (1991) Histologic transformation of follicular lymphoma to diffuse lymphoma represents tumor progression by a single malignant cell. J Exp Med 173:197–207
168. Zhang PJ, Barcos M, Stewart CC, Block AW, Sait S, Brooks JJ (2000) Immunoreactivity of MIC2 (CD99) in acute myelogenous leukemia and related diseases. Mod Pathol 13:452–458

Virchows Arch (2005) 447: 938–946
DOI 10.1007/s00428-005-0048-6

ORIGINAL ARTICLE

Ozgur Mete · Isin Kilicaslan · Mine G. Gulluoglu · Veli Uysal

Can renal oncocytoma be differentiated from its renal mimics? The utility of anti-mitochondrial, caveolin 1, CD63 and cytokeratin 14 antibodies in the differential diagnosis

Received: 17 February 2005 / Accepted: 14 July 2005 / Published online: 17 August 2005
© Springer-Verlag 2005

Abstract Among the epithelial renal tumours with eosinophilic cytoplasm, the main differential diagnostic problem arises between renal oncocytomas (ROs) and eosinophilic variants of chromophobe renal cell carcinomas (RCCs). We investigated the possible role of anti-mitochondrial (AMA), anti-caveolin 1 (CAV1), anti-CD63 (CD63) and anti-cytokeratin 14 (CK14) antibodies in the differential diagnosis of eosinophilic epithelial tumours and applied the Muller and Mowry modification of Hale's colloidal iron stain (HCI). Thirty-five ROs and 77 eosinophilic RCCs (27 chromophobe, 28 clear cell and 22 papillary RCCs) were included in this study. Apical and/or polar CD63 immunostaining (94%) and diffuse AMA (91%) and CAV1 (88%) immunostainings were the characteristics of ROs, whereas diffuse CD63 immunostaining (96%) and diffuse-peripheral AMA (96%) and CAV1 (92%) immunostainings were characteristic immunohistochemical features of eosinophilic chromophobe RCCs. We showed CK14 antibody not to be useful in the differential diagnosis of the eosinophilic epithelial renal tumours. The staining localisations with AMA, CAV1 and CD63 antibodies were significantly different between tumour groups. AMA had 96% sensitivity and 94% specificity, whereas CAV1 had 92% sensitivity and 97% specificity in diagnosing chromophobe RCCs. With HCI staining, ROs, showing apical and/or polar staining, could be differentiated from chromophobe RCCs, showing diffuse cytoplasmic staining. HCI had fairly low (69%) sensitivity and 100% specificity, whereas CD63 had 95% sensitivity and 100% specificity to diagnose ROs. We recommend using CD63 as the best marker of choice for distinguishing ROs from eosinophilic chromophobe RCCs when standard diagnostic criteria are not helpful.

Keywords Oncocytoma · Renal cell carcinoma · Immunohistochemistry · CD63 · Caveolin 1

O. Mete (✉) · I. Kilicaslan · M. G. Gulluoglu · V. Uysal
Department of Pathology,
Istanbul Faculty of Medicine, Istanbul University,
Temel Bilimler Binasi, 2.Bodrum, Capa,
Istanbul, Turkey
e-mail: ozgurmete77@hotmail.com
Tel.: +90-212-4142400
Fax: +90-216-4852407
e-mail: ikaslan@istanbul.edu.tr
e-mail: mggullu@istanbul.edu.tr
e-mail: vuysal@istanbul.edu.tr

Introduction

Epithelial renal tumours with eosinophilic cells include renal oncocytomas (ROs), eosinophilic variants of chromophobe and clear cell and papillary renal cell carcinomas (RCCs). The main problem in the differential diagnosis arises between ROs and eosinophilic variants of chromophobe RCC. RO is a benign neoplasm, while chromophobe RCC is a malignant tumour [1, 3, 12, 39, 49, 50]. ROs should be separated from eosinophilic variants of RCCs. Some ROs and eosinophilic variants of RCCs have several common macroscopic and microscopic features such as cellular pleomorphism and focal perinephritic adipose tissue invasion as well as microvascular invasion [4, 35, 37].

Nowadays, more renal tumours are detected incidentally due to the improvement in radiological modalities, and more are sampled preoperatively [38, 41, 45]. The differential diagnosis between ROs and eosinophilic variants of RCCs, which is sometimes difficult in resection materials, becomes more problematic in core biopsies [1, 24].

In recent years, although many markers such as cytokeratin (CK) 7, CK14 and CK20, epithelial membrane antigen (EMA), CD10 and parvalbumin have been studied for the differential diagnosis between chromophobe RCCs and ROs, the results are still unsatisfactory [1, 5, 23–25, 30, 31, 58]. However, diffuse staining with Hale's colloidal iron (HCI) stain and ultrastructural demonstration of chromophobe-type micro-vesicles in the cytoplasm of the tumoural cells are still accepted as the most important criteria for the diagnosis of chromophobe RCCs [2, 10, 24, 28, 47, 49, 50, 58].

Ultrastructural and immunohistochemical studies showed that the cytoplasmic distribution pattern of mitochondria in the eosinophilic epithelial renal tumours could be different from each other [19, 51, 53, 57]. For this reason, we used anti-mitochondrial antibody (AMA) to identify the mitochondrial distribution pattern of ROs and subtypes of RCCs.

Recently, the increased expression of CAV1 has been reported in ROs [11]. CAV1 is the major functional and structural protein component of vesicular invaginations of the plasma membrane called caveolae [26, 42]. Three proteins (caveolin 1, caveolin 2, caveolin 3) were identified in the caveolin family. CAV1 plays a key role in the membrane traffic, signal transduction and carcinogenesis [22, 26, 42, 56]. Caveolins are found in many cells, but mainly in mesenchymal tissues [26, 42].

Chu and Weiss presented CK14 as a marker of ROs [14]. However, contradictory results have been reported [24]. CK14 expression is also described in squamous cell carcinoma, thymoma, pleomorphic adenoma, Hürthle cell lesions of the thyroid and Warthin's tumour [13, 15].

CD63 is a lysosomal membrane glycoprotein translocated to plasma membrane after platelet activation [32, 43]. Anti-CD63 antibody (CD63) reacts with nevi, melanomas and alveolar soft part sarcoma [21, 29, 33, 36, 54]. CD63 has not been investigated in eosinophilic epithelial renal tumours previously, but its immunoreactivity has been reported in epithelioid angiomyolipomas of the kidney [17, 46].

HCI stain detects polyanionic acid mucopolysaccharides in tissues [52]. It has some technical difficulties, and its interpretation may be challenging. For this reason, modifications of this staining technique have been studied in the past. The Muller and Mowry modification of HCI is accepted to have the superior results due to the maintenance of pH at 1.1 to 1.3 [6, 52, 55].

The purpose of this study is to perform a detailed histopathological examination on ROs and eosinophilic variant of chromophobe RCCs on resection specimens and to investigate the possible role of AMA, CAV1, CK14 and CD63 in the differential diagnosis between them. We also applied the Muller and Mowry modification of HCI staining to compare its usefulness with those of the immunohistochemical markers.

Materials and methods

Tissue samples

A total of 112 resected eosinophilic epithelial renal tumours (35 ROs, 27 eosinophilic variants of chromophobe, 28 eosinophilic variants of clear cell and 22 eosinophilic variants of papillary RCCs) which were diagnosed in the Department of Pathology, Istanbul Faculty of Medicine, Istanbul University, were included in this study. All cases were classified according to the standard diagnostic criteria and HCI staining results [18, 34]. We reviewed our archive files for patients' age and gender information, as well as the gross pathologic features (size, presence of macroscopic necrosis, haemorrhage and scar formation) of the tumours.

Histopathological methods

The archive slides were reviewed, and a detailed histopathological examination was done in ROs and eosinophilic variants of chromophobe RCCs. We re-examined the H & E stained slides for cellular, nuclear, cytoplasmic, stromal and vascular network features of the tumours.

Immunohistochemistry

One paraffin block having the most representative tumoural area was selected for the immunohistochemical studies of each tumour. Routine immunohistochemical staining was performed on formalin-fixed, paraffin-embedded tissues using the streptavidin-biotin-complex method (Lab Vision Corp., Fremont, CA, USA) after pretreatment with heat-induced antigen unmasking by incubating the sections in 10 Mmol/l citrate buffer solution (pH 6) using a domestic pressure cooker (25 min, 1 atm). The entire procedure was carried out in room temperature. The following primary antibodies were applied: anti-mitochondrial Ab-2 (Monoclonal, mouse anti-human, Clone: MTCO2, 1:100, 60 min, Code: MS-1372-P, NeoMarkers, Fremont, CA, USA), anti-caveolin 1 (Polyclonal, rabbit anti-human, Clone: N-20, 1:50, 60 min, Code: SC-894, Santa Cruz Biotechnology Inc., USA), anti-CD63 (Monoclonal, mouse anti-human, Clone: NKI/C3, 1:100, 60 min, Code: MS-1118-P, NeoMarkers), anti-keratin 14 (Monoclonal, mouse anti-human, Clone: LL002, 1:100, 60 min, Code: MS-115-P, NeoMarkers). Blood vessels and mesenchymal tissue of the intestine and non-neoplastic tissue adjacent to the tumour for CAV1, intradermal naevus for CD63, squamous cell carcinoma for CK14 and proximal renal tubular epithelium for AMA were used as the positive controls. Staining localisations (cytoplasmic diffuse, cytoplasmic diffuse-peripheral, cytoplasmic polar and/or apical, cytoplasmic irregular-disperse) were assessed for each immunohistochemical reaction.

Histochemistry

Representative sections from each tumour were stained with HCI as modified by Muller and Mowry [6, 52, 55]. Non-neoplastic kidney parenchyma adjacent to the tumour was used as internal positive control. The tumours showing a positive blue-purple staining were documented for the staining localisation.

Photography

Photographs were taken by an Olympus BX50 microscope equipped with a Nikon E4500 digital camera (1024×768 pixel, high-resolution mode).

Statistical analysis

Kruskal–Wallis and Mann–Whitney *U* tests were used to evaluate the statistical correlations between the groups and variables. All data were analysed utilising SPSS 10.0 for Windows.

Results

Clinical findings

The main clinical findings are summarized in Table 1. A male predominance was observed in chromophobe, papillary and clear cell RCCs. ROs showed a slight female predominance (male to female ratio 16:19).

Gross pathological findings

The main gross pathological findings are summarized in Table 1. The mean size of the ROs (5.1±3 cm) was found to be significantly lower than that of the eosinophilic variants of clear cell RCCs (7. 9±4.9 cm) (p=0.024). The eosinophilic papillary RCCs were found to be the most necrotic (63%) and haemorrhagic (86%) tumour group. No necrotic area was observed in ROs. Haemorrhage was generally minimal in ROs and eosinophilic chromophobe RCCs. Scar formation was observed in ROs (80%), eosinophilic chromophobe (17%) and clear cell (21%) RCCs.

Histopathological findings

The results of histopathological examination are summarized in Table 2. Two types of eosinophilic cells were observed in varying proportions in ROs and chromophobe RCCs. A delicate vasculature separating tumoural cell groups in solid sheets was seen in 26 eosinophilic variants of chromophobe RCCs (96%). This kind of typical vascular network was totally absent in ROs. We also observed entrapped normal tubules in the central and/or peripheral parts of the tumour in 25 ROs (71%). This feature was totally absent in the eosinophilic chromophobe RCCs. Microscopic necrosis was found in only one RO (2%) which measured 15 cm in diameter.

Table 2 Histopathological findings of ROs and eosinophilic variants of chromophobe RCCs

Parameters	ROs, *n* (%)	Eosinophilic variant of chromophobe RCCs, *n* (%)
Total	35 (100)	27 (100)
Nuclear features		
Intranuclear inclusion	10 (28)	16 (59)
Nucleolar prominence	11 (31)	15 (57)
Nuclear atypia	15 (42)	13 (48)
Irregularity of nuclear membrane	2 (6)	27 (100)
Binucleation	14 (40)	14 (52)
Bi-multinucleation	18 (51)	8 (30)
Perinuclear clearing (Halo)	9 (25)	27 (100)
Fibrohyalinous scar	28 (80)	7 (25)
Stromal oedema	29 (82)	4 (14)
Haemorrhage	26 (74)	24 (88)
Stromal hyalinisation	15 (42)	3 (11)
Calcification, ossification	8 (22)	11 (40)
Psammoma bodies	5/8 (62)	6/11 (54)
Coarse calcification	1/8 (12)	4/11 (36)
Ossification	2/8 (25)	1/11 (9)
Microscopic necrosis	1 (2)	11 (40)
Delicate vascular network	0 (0)	26 (96)
Entrapped tubules	25 (71)	0 (0)
Peripheral	17/25 (68)	0 (0)
Peripheral and central	8/25 (32)	0 (0)

ROs renal oncocytomas, *RCCs* renal cell carcinomas

Table 1 Clinical and gross findings of eosinophilic epithelial renal tumours

Parameters	ROs	Chromophobe RCCs	Clear cell RCCs	Papillary RCCs
Total, *n* (%)	35 (100)	27 (100)	28 (100)	22 (100)
Female, *n* (%)	19 (54)	11 (41)	10 (36)	4 (18)
Male, *n* (%)	16 (46)	16 (59)	18 (64)	18 (82)
Age, (mean±sd) (years)	58.3±12	55±13.7	61.3±9.8	62.1±0.4
Available gross details, *n* (%)	30 (85)	23 (85)	28 (100)	22 (100)
Size, (mean±sd) (cm)	5.1±3	7.1±3.1	7.9±4.9	6.9±3.3
Macroscopic necrosis, *n* (%)	0 (0)	7 (30)	15 (53)	14 (63)
Scar, *n* (%)	24 (80)	4 (17)	6 (21)	0 (0)
Haemorrhage, *n* (%)	13 (43)	17 (73)	20 (71)	19 (86)

sd standard deviation, *ROs* renal oncocytomas, *RCCs* renal cell carcinomas

Table 3 Cytoplasmic distribution of the immunoreactivities in eosinophilic epithelial renal tumours

	ROs, *n* (%)	Chromophobe RCCs, *n* (%)	Clear cell RCCs, *n* (%)	Papillary RCCs, *n* (%)
Total	35 (100)	27 (100)	28 (100)	22 (100)
AMA[a]	35 (100)	27 (100)	28 (100)	22 (100)
No staining	0 (0)	0 (0)	0 (0)	0 (0)
Diffuse	32 (91)	1 (4)	5 (18)	12 (55)
Apical and/or polar	0 (0)	0 (0)	0 (0)	0 (0)
Disperse-irregular	1 (3)	0 (0)	23 (82)	10 (45)
Diffuse and peripheral	2 (6)	26 (96)	0 (0)	0 (0)
CAV1[a]	34 (97)	27 (100)	28 (100)	22 (100)
No staining	1 (3)	0 (0)	0 (0)	0 (0)
Diffuse	31 (88)	1 (4)	8 (29)	13 (59)
Apical and/or polar	0 (0)	0 (0)	0 (0)	0 (0)
Disperse-irregular	2 (6)	1 (4)	20 (71)	9 (41)
Diffuse and peripheral	1 (3)	25 (92)	0 (0)	0 (0)
CD63[a]	35 (100)	27 (100)	19 (68)	14 (64)
No staining	0 (0)	0 (0)	9 (32)	8 (36)
Diffuse	1 (3)	26 (96)	2 (7)	1 (5)
Apical and/or polar	33 (94)	0 (0)	2 (7)	7 (32)
Disperse-irregular	1 (3)	1 (4)	15 (54)	6 (27)
Diffuse and peripheral	0 (0)	0 (0)	0 (0)	0 (0)
CK14[a]	9 (26)	5 (18.5)	0 (0)	3 (14)
No staining	26 (74)	22 (81.5)	28 (100)	19 (86)
Diffuse	9 (26)	1 (3.7)	0 (0)	2 (9)
Apical and/or polar	0 (0)	0 (0)	0 (0)	0 (0)
Disperse-irregular	0 (0)	4 (14.8)	0 (0)	1 (5)
Diffuse and peripheral	0 (0)	0 (0)	0 (0)	0 (0)
HCI[a]	25 (71)	27 (100)	6 (21.4)	0 (0)
No staining	10 (29)	0 (0)	22 (78.6)	22 (100)
Diffuse	1 (3)	27 (100)	0 (0)	0 (0)
Apical and/or polar	24 (68)	0 (0)	1 (3.5)	0 (0)
Disperse-irregular	0 (0)	0 (0)	5 (17.9)	0 (0)
Diffuse and peripheral	0 (0)	0 (0)	0 (0)	0 (0)

ROs renal oncocytomas, *RCCs* renal cell carcinomas
[a]Number of cases which were positive out of total

Table 4 Statistical results of Mann–Witney *U* test

Localisation	ROs–eosinophilic variants of chromophobe RCCs, *z*;*p*	ROs–eosinophilic variants of clear cell RCCs, *z*;*p*	ROs–eosinophilic variants of papillary RCCs, *z*;*p*
AMA	*z*=6.97; *p*=0.0005	*z*=5.41; *p*=0.0005	*z*=2.96; *p*=0.003
CAV1	*z*=7.01; *p*=0.0005	*z*=4.84; *p*=0.0005	*z*=2.72; *p*=0.007
CD63	*z*=6.89; *p*=0.0005	*z*=4.77; *p*=0.0005	*z*=2.79; *p*=0.005
CK14	Not significant	[a]	Not significant
HCI	*z*=6.87; *p*=0.0005	*z*=4.58; *p*=0.001	[a]

ROs renal oncocytomas, *RCCs* renal cell carcinomas
[a]Test could not be performed because at least one group was not stained

Immunohistochemical findings

Staining localisation details and statistical results are summarized in Tables 3 and 4.

Anti-mitochondrial antibody

A positive weak cytoplasmic immunostaining was seen in the non-neoplastic kidney tubules. All tumour groups were positive with AMA (Table 3). A diffuse cytoplasmic immunostaining in 32 ROs (91%) (Fig. 1a), a diffuse and peripheral immunostaining in 26 eosinophilic chromophobe RCCs (96%) (Fig. 1b) and an irregular-disperse cytoplasmic immunostaining in 23 eosinophilic clear cell RCCs (82%) were observed. Twelve papillary RCCs showed diffuse cytoplasmic (55%), and ten cases showed irregular-disperse cytoplasmic (45%) immunoreactivity. The difference in the staining patterns of the ROs and the

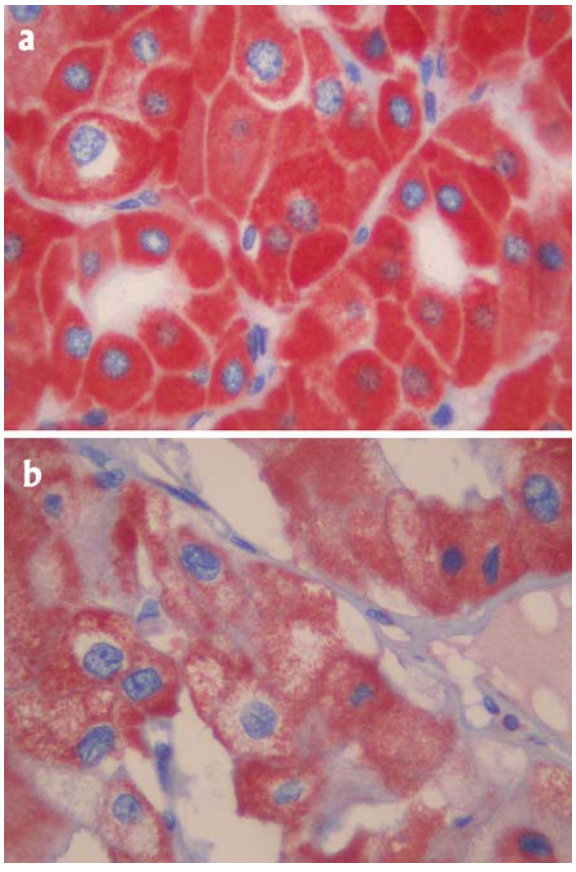


Fig. 1 **a** Diffuse cytoplasmic immunostaining with anti-mitochondrial antibody (AMA) in renal oncocytoma (original magnification ×400). **b** Diffuse and peripheral cytoplasmic immunostaining with AMA in chromophobe renal cell carcinoma (original magnification ×400)

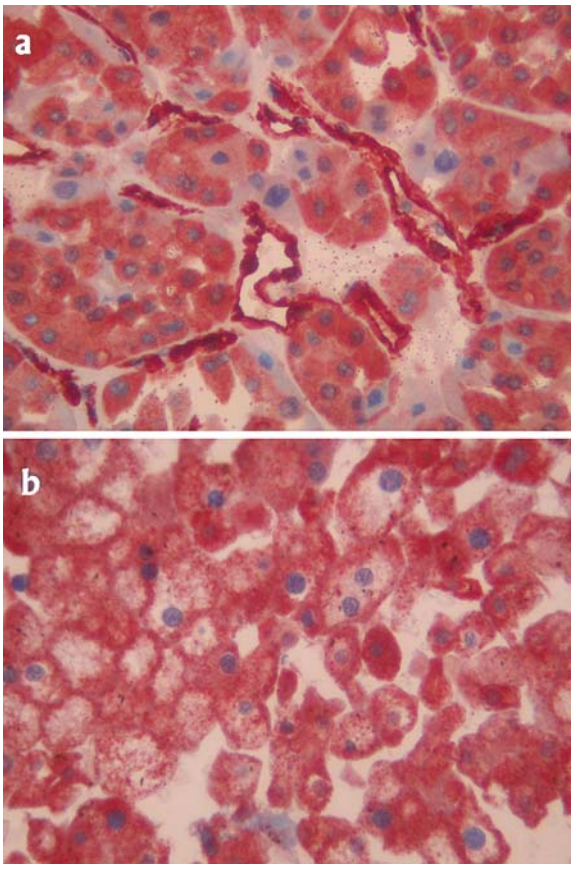


Fig. 2 **a** Diffuse cytoplasmic immunostaining with anti-caveolin 1 antibody (CAV1) in renal oncocytoma and positive cytoplasmic immunostaining in endothelial cells (original magnification ×200). **b** Diffuse and peripheral cytoplasmic immunostaining with CAV1 in chromophobe renal cell carcinoma (original magnification ×400)

subtypes of RCCs was found to be statistically significant (Tables 3, 4).

Anti-caveolin 1 antibody

A weak positive diffuse cytoplasmic staining in the tubular epithelium and a moderate-to-strong staining in the Bowman's parietal cells and visceral epithelium of the glomerulus were seen in the non-neoplastic tissue. Vascular endothelial cells in the non-neoplastic tissues showed strong immunoreaction. Cytoplasm was the main staining area in all tumour groups. In addition to the cytoplasmic staining, focal membranous staining was present in one (3%) RO and four (14%) eosinophilic chromophobe RCCs. A diffuse cytoplasmic staining in 31 ROs (88%) (Fig. 2a), a diffuse and peripheral cytoplasmic staining in 25 eosinophilic variants of chromophobe RCCs (93%) (Fig. 2b) and an irregular-disperse staining in 20 eosinophilic variants of clear RCCs (71%) were observed. Thirteen eosinophilic papillary RCCs (59%) showed a diffuse cytoplasmic staining predominantly and nine (41%) cases showed an irregular-disperse cytoplasmic staining. The difference in the staining patterns of the ROs and the subtypes of RCCs was found to be statistically significant (Tables 3, 4).

Anti-CD63 antibody

Non-neoplastic tubular epithelium showed focal apical and weak staining. All of the ROs (35/35) and all of the eosinophilic chromophobe RCCs, 19 (68%) eosinophilic variants of clear cell RCCs and 14 (64%) eosinophilic variants of papillary RCCs were positive for CD63 (Table 3). Positive staining in the apical part of the cytoplasm and/or in one pole was observed in 33 ROs (94%) (Fig. 3a). Diffuse cytoplasmic staining was seen in 26 (96%) eosinophilic variants of chromophobe RCCs (Fig. 3b). Fifteen (54%) eosinophilic variants of clear cell RCCs showed an irregular-disperse staining. Seven (32%) eosinophilic variants of papillary RCCs showed apical cytoplasmic, and six cases (27%) showed irregular-disperse staining. The differences between ROs and eosinophilic variants of chromophobe, clear cell and papillary RCCs were found to be statistically significant (Tables 3, 4).

Anti-cytokeratin 14 antibody

A non-specific weak staining was observed in the tubular epithelium of the non-neoplastic kidney tissue. All the eosinophilic clear cell RCCs were negative for CK14. Only

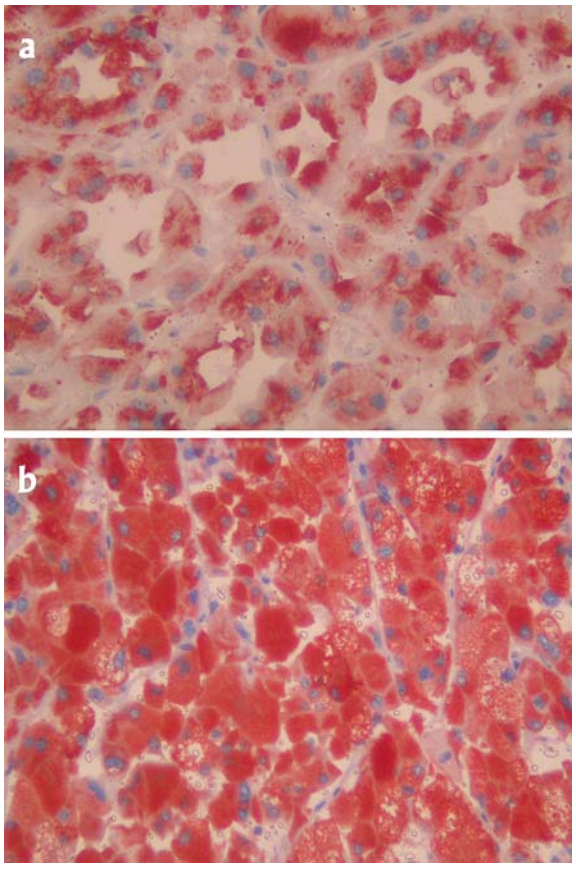


Fig. 3 **a** Apical and/or polar cytoplasmic immunostaining with anti-CD63 antibody (CD63) in renal oncocytoma (original magnification ×200). **b** Diffuse cytoplasmic immunostaining with CD63 in chromophobe renal cell carcinoma (original magnification ×200)

nine (26%) of the ROs, five (18,5%) of the eosinophilic variants of chromophobe RCCs and three (14%) of the eosinophilic variants of papillary RCCs were immunopositive with mild staining intensity and small stained area. No significant difference was found between the groups (Tables 3, 4).

Histochemical findings

Focal weak cytoplasmic HCI staining in the apical part of renal tubular cells was observed. Areas of haemorrhage showed strongly positive staining. Twenty-five (71%) of the ROs, all of the eosinophilic variants of chromophobe RCCs (100%) and six (21.4%) of the eosinophilic variants of clear cell RCCs showed positive reaction for HCI (Table 3). Eosinophilic variants of papillary RCCs did not show any positivity related to the tumour cells. Only frequent areas of haemorrhage at the apical part of the cell cytoplasm and the histiocytes in the cores of the papilla showed strong-to-moderate positivity. Apical cytoplasmic staining associated with weak-to-moderate staining intensity was observed focally in 24 (68%) ROs (Fig. 4a), whereas all of the eosinophilic variants of chromophobe RCCs showed diffuse cytoplasmic staining (Fig. 4b). In five (17.9%) of the eosinophilic variants of clear cell RCCs, irregular-disperse and weak positivity was observed and was associated with a small percentage of stained cells. The staining intensity was mild or very mild (almost negative) in eosinophilic cells without clearing.

According to the staining results, HCI distinguished ROs significantly from eosinophilic variants of chromophobe RCCs and from eosinophilic variants of clear cell RCCs by their different staining localisations (Tables 3, 4).

Sensitivity and specificity of anti-mitochondrial, anti-caveolin 1, anti-CD63 and Hale's colloidal iron stain

We differentiated chromophobe RCCs from ROs by way of diffuse-peripheral AMA staining, with a sensitivity of 96% and a specificity of 94%. The differentiation of chromophobe RCC by way of diffuse-peripheral CAV1 staining was done with a sensitivity of 92% and a specificity of 97%.

CD63 immunohistochemistry distinguished ROs, with apical and/or polar staining, from eosinophilic chromophobe RCCs with 95% sensitivity and 100% specificity.

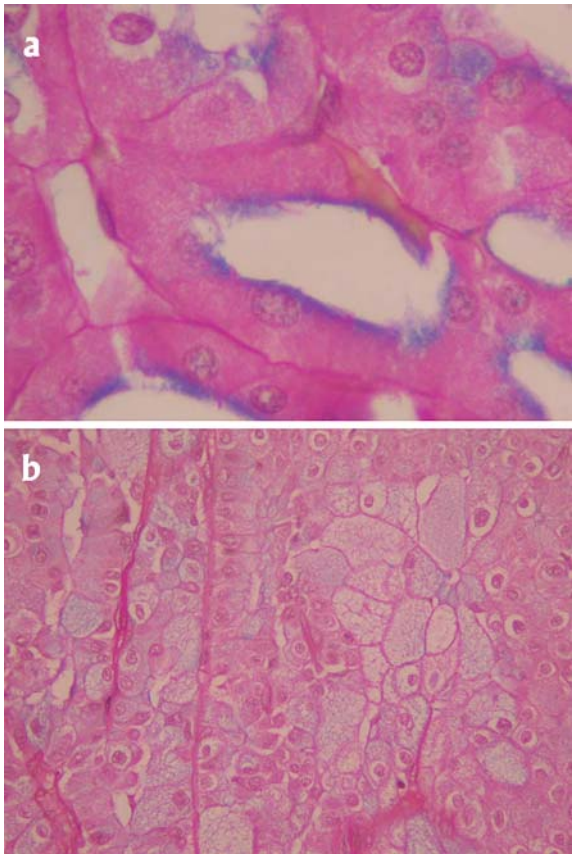


Fig. 4 **a** Apical cytoplasmic staining with Hale's colloidal iron (HCI) in RO (original magnification ×400). **b** Diffuse reticular cytoplasmic staining with HCI in chromophobe renal cell carcinoma (original magnification ×200)

The sensitivity and specificity of apical and/or polar HCI staining for diagnosing ROs from eosinophilic variants of chromophobe RCCs were 69% and 100%, respectively. The sensitivity of apical and/or polar CD63 staining in the HCI false-negative group (11 of 35 ROs) for diagnosing ROs was 82%.

Discussion

Histopathological examination should be the first and the most important step in the diagnostic approach to eosinophilic epithelial renal tumours. Based on our histopathological examination results, entrapped normal-appearing tubules and absence of delicate vascular network are important factors for differentiating ROs from eosinophilic variant of chromophobe RCCs in routine sections, but the interpretation of these two parameters could be difficult in their absence in core biopsies. Thus, additional criteria are required.

It has been shown in some previous ultrastructural studies that the distribution of mitochondria varies among eosinophilic epithelial renal tumour groups [19, 51, 53]. Our results showed that AMA immunostaining could be used to distinguish ROs from eosinophilic variants of chromophobe RCCs. ROs showed predominantly diffuse immunostaining, whereas the eosinophilic variants of chromophobe RCCs showed both peripheral and diffuse immunostaining. The distinctive peripheral immunostaining could be explained by the peripheral distribution of the mitochondria within the cells. In fact, the peripheral immunostaining is related to the cells exhibiting perinuclear clearing and peripheral eosinophilia seen in H & E stained slides. The absence or scarcity of the perinuclear clearing in chromophobe RCCs causes the major limitation of AMA immunostaining, which has a 96% sensitivity and 94% specificity in distinguishing them from ROs. Furthermore, this limitation could be more pronounced in core biopsies. Although the difference between the AMA staining patterns of the ROs and the eosinophilic variants of papillary RCCs was found to be statistically significant, the presence of diffuse cytoplasmic immunostaining in papillary RCCs causes the second limitation of AMA in the differential diagnosis of ROs.

Carrion et al. have recently investigated the CAV1 expression in adult renal tumours including ROs and reported an increased expression of CAV1 in ROs and a decreased expression level among RCC subtypes [11]. They have suggested that ROs could be differentiated from malignant renal tumours by their high CAV1 expression levels [11]. In contrast to their result, we observed increased expression levels of CAV1 in all eosinophilic variants of RCCs. According to our study results, the dominant diffuse immunostaining for ROs and the diffuse and peripheral immunostaining for chromophobe RCCs made the differentiation possible. Our results showed that CAV1 immunostaining localisations could be used to differentiate ROs from eosinophilic variants of RCCs. In addition to the diffuse cytoplasmic CAV1 immunostaining in the eosinophilic variants of chromophobe RCCs, the peripheral cytoplasmic CAV1 immunostaining was also observed in our study. It is this staining localisation that proved useful in differentiating them from ROs. It is interesting to note that the distribution of CAV1 and AMA immunostainings were nearly identical in the tumour groups. With these findings, we suggest that CAV1, which has a 92% sensitivity and a 97% specificity for differentiating chromophobe RCCs from ROs, reacts as a mitochondrial marker and that it has the same diagnostic benefits and limitations of AMA in the differentiation of eosinophilic epithelial renal tumours. These findings could also explain why Carrion et al. [11] observed a decreased expression in the non-eosinophilic variants of RCCs where mitochondria were scanty. The data supporting our results are few, but the accumulation of CAV1 in the modified mitochondria of airway epithelial cells has been reported before and this finding could suggest one of the possible mechanisms of CAV1 for regulating intracellular traffic between mitochondria and cell membrane [27, 40].

Based on our study results, CK14 immunohistochemistry cannot be used in the differential diagnosis of eosinophilic epithelial renal tumours due to small number of tumours showing positive immunoreactivity associated with a mild staining intensity and small stained area. Chu and Weiss studied and reviewed keratin expression in human tissues and neoplasms, and they observed CK14 positivity in many oncocytic tumours [13–15]. They have found that CK14 immunoreactivity could distinguish ROs from its renal mimics [14]. In contrast, Langner et al. have recently reported diffuse weak cytoplasmic staining, and they regarded this reaction as non-specific since they observed a similar reaction with nuclear antigens and other cytokeratins. For this reason, they used the biotin-free EnVision+System, and no immunostaining was observed. They suggested that this staining pattern was due to the presence of endogenous mitochondrial biotin in ROs [24].

We suggest that CD63 can be used in the differential diagnosis of eosinophilic epithelial renal tumours. ROs, by their dominantly apical and/or polar immunostaining, could be differentiated from eosinophilic variants of chromophobe RCCs showing cytoplasmic diffuse immunostaining. Papillary RCCs with an apical and/or polar immunostaining determine the limitation of CD63 in differentiating ROs from eosinophilic variants of papillary RCCs; however, a statistically significant difference was found regarding their cytoplasmic immunostaining localisations. Disperse-irregular cytoplasmic immunostaining of clear cell RCCs could be useful in the differential diagnosis of ROs and clear cell RCCs.

The typical HCI staining is believed to be due to the intracytoplasmic micro-vesicles in chromophobe RCCs [8, 10]. Although ROs were previously found to be negative for HCI, Skinnider and Jones reported the ultrastructural presence of micro-vesicles in ROs showing focal cytoplasmic distribution [44]. However, focal cytoplasmic HCI stainings such as apical, perinuclear and perimembranous localisations have been shown in various studies [16, 44, 52]. In our case, apical and/or polar cytoplasm was the

dominant (68%) HCI staining localisation of ROs. Similarly, Cochand-Priollet et al. reported an apical HCI staining in 89% of ROs [16]. We did not observe any perinuclear HCI staining and perimembranous staining as reported in other previous reports [16, 44, 52].

As mentioned before, HCI staining is related to the presence of micro-vesicles, and it detects polyanionic acid mucopolysaccharide context of these micro-vesicles [8, 9]. The nature of micro-vesicles is still unknown. The correlation of micro-vesicles with endoplasmic reticulum, lysosomes and mitochondria has been questioned, and the mitochondrial origin is mostly suspected [2, 48, 49]. It is noteworthy that CD63 staining localisations were similar to those seen in HCI staining. Our observation may suggest the lysosomal nature of micro-vesicles or a cross-reaction between the mucopolysaccharide content of micro-vesicles and anti-CD63 antibody, which is targeted to lysosomal membrane glycoprotein [32, 43]. However, it is known that acid mucopolysaccharides are degraded in lysosomal vacuoles [20].

In the present study, diffuse cytoplasmic staining of HCI and CD63 is found to be useful in distinguishing chromophobe RCCs from ROs showing an apical and/or polar staining. All apically stained ROs with HCI were also stained apically with CD63. Only nine HCI-negative ROs were CD63-positive with respect to apical staining. Similarly, Skinnider and Jones reported that three HCI-negative ROs contained ultrastructurally intracytoplasmic micro-vesicles [44]. In our opinion, anti-CD63 antibody might detect a small amount of micro-vesicles which were not detected by HCI stain. This could be related to HCI staining, which is known to have some technical difficulties arising from unbalanced pH level in the study solution [52, 55]. Due to the technical problems, a negative HCI result is not reliable, and as it is shown in our study, anti-CD63 antibody sensitivity (95%) is higher than HCI sensitivity (69%). The sensitivity of apical and/or polar CD63 staining in the HCI false-negative group for diagnosing ROs was 82%. Therefore, we recommend CD63 immunochemistry in HCI-negative cases in the differential diagnosis of ROs.

In spite of their high sensitivity and specificity rates, AMA (96 and 94%, respectively) and CAV1 (92 and 97%, respectively), which react as a mitochondrial marker, are not the first markers of choice due to their limitations in the differential diagnosis between ROs and chromophobe RCCs. HCI, with a 69% sensitivity and a 100% specificity, still plays an important role in the absence of some technical problems, but it lacks sensitivity. We advocate that the diagnostic dilemmas arising from these two entities will decrease in many cases by using CD63 alone, which was found to be the marker of choice with a high sensitivity (95%) and specificity (100%).

Acknowledgements This work was supported by the Research Fund of Istanbul University (Project number: T-332/03112003). The authors would also to thank Dr. N. Büyükbabani (Department of Pathology, Istanbul Faculty of Medicine, Istanbul University) for his observations about CD63.

References

1. Abrahams NA, MacLennan GT, Khoury JD et al (2004) Chromophobe renal cell carcinoma: a comparative study of histological, immunohistochemical and ultrastructural features using high throughput tissue microarray. Histopathology 45: 593–602
2. Akhtar M, Kardar H, Linjawi T et al (1995) Chromophobe cell carcinoma of the kidney: a clinicopathologic study of 21 cases. Am J Surg Pathol 19:1245–1256
3. Amin MB, Amin MB, Tamboli P et al (2002) Prognostic impact of histologic subtyping of adult renal epithelial neoplasms: an experience of 405 cases. Am J Surg Pathol 26:281–291
4. Amin MB, Crotty TB, Tickoo SK et al (1997) Renal oncocytoma: a reappraisal of morphologic features with clinicopathologic findings in 80 cases. Am J Surg Pathol 21:1–12
5. Avery AK, Beckstead J, Renshaw AA et al (2000) Use of antibodies to RCC and CD10 in the differential diagnosis of renal neoplasms. Am J Surg Pathol 24:203–210
6. Bancroft JD, Gamble M (eds) (2002) Theory and practice of histological techniques, 5th edn. Churchill Livingstone, Edinburgh
7. Barnes CA, Beckman EN (1983) Renal oncocytoma and its congeners. Am J Clin Pathol 79:312–318
8. Bonsib SM (1996) Renal chromophobe cell carcinoma: the relationship between cytoplasmic vesicles and colloidal iron stain. J Urol Pathol 4:9–14
9. Bonsib SM, Bray C, Timmerman TG (1993) Renal chromophobe cell carcinoma: limitations of paraffin-embedded tissue. Ultrastruct Pathol 17:529–536
10. Bonsib SM, Larger D (1990) Chromophobe cell carcinoma: analysis of five cases. Am J Surg Pathol 14:260–267
11. Carrion R, Morgan BE, Tannenbaum M et al (2003) Caveolin expression in adult renal tumors. Urol Oncol 21:191–196
12. Cheville JC, Lohse CM, Zincke H et al (2003) Comparisons of outcome and prognostic features among histologic subtypes of renal cell carcinoma. Am J Surg Pathol 27:612–624
13. Chu PG, Lyda MH, Weiss LM (2001) Cytokeratin 14 expression in epithelial neoplasms: a survey of 435 cases with emphasis on its value in differentiating squamous cell carcinomas from other epithelial tumours. Histopathology 39:9–16
14. Chu PG, Weiss LM (2001) Cytokeratin 14 immunoreactivity distinguishes oncocytic tumour from its renal mimics: an immunohistochemical study of 63 cases. Histopathology 39:455–462
15. Chu PG, Weiss LM (2002) Keratin expression in human tissues and neoplasms. Histopathology 40:403–439
16. Cochand-Priollet B, Molinie V, Bougaran J et al (1997) Renal chromophobe cell carcinoma and oncocytoma. A comparative morphologic, histochemical, and immunohistochemical study of 124 cases. Arch Pathol Lab Med 121:1081–1086
17. Eble JN, Amin MB, Young RH (1997) Epithelioid angiomyolipoma of the kidney: a report of five cases with a prominent and diagnostically confusing epithelioid smooth muscle component. Am J Surg Pathol 21:1123–1130
18. Eble JN, Sauter G, Epstein JI, Sesterhenn IA (eds) (2004) World Health Organization classification of tumours. Pathology and genetics of the urinary system and male genital organs. IARC, Lyon
19. Erlandson RA, Shek TWH, Reuter VE (1997) Diagnostic significance of mitochondria in four types of renal epithelial neoplasms: an ultrastructural study of 60 tumors. Ultrastruct Pathol 21:409–417
20. Gartner LP, Hiatt JL (eds) (2001) Color textbook of histology, 2nd edn. WB Saunders, Philadelphia

21. Hagen EC, Vennegoor C, Schlingemann RO et al (1986) Correlation of histopathological characteristics with staining patterns in human melanoma assessed by (monoclonal) antibodies reactive on paraffin sections. Histopathology 10:689–700
22. Juhasz M, Chen J, Tulassay Z et al (2003) Expression of caveolin-1 in gastrointestinal and extraintestinal cancers. J Cancer Res Clin Oncol 129:493–497
23. Khoury JD, Abrahams NA, Levin HS et al (2002) The utility of epithelial membrane antigen and vimentin in the diagnosis of chromophobe renal cell carcinoma. Ann Diagn Pathol 6:154–158
24. Langner C, Wegscheider BJ, Ratschek M et al (2004) Keratin immunohistochemistry in renal cell carcinoma subtypes and renal oncocytomas: a systematic analysis of 233 tumors. Virchows Arch 444:127–134
25. Leroy X, Mouskassa D, Copin MC et al (2000) Utility of cytokeratin 7 for distinguishing chromophobe renal cell carcinoma from renal cell carcinoma. Eur Urol 37:484–487
26. Li S, Couet J, Lisanti MP (1996) Src tyrosine kinases, G alpha subunits, and H-ras share a common membrane-anchored scaffolding protein caveolin: caveolin binding negatively regulates the auto-activation of Src tyrosine kinases. J Biol Chem 271:29182–29190
27. Li WP, Liu P, Anderson RG (2001) Cell-specific targeting of caveolin-1 to caveolae, secretory vesicles, cytoplasm or mitochondria. J Cell Sci 114:1397–1408
28. Liu J, Fanning CV (2001) Can renal oncocytomas be distinguished from renal cell carcinoma on fine-needle aspiration specimens? Cancer 93:390–397
29. Mackie RM, Campbell I, Turbitt ML (1984) Use of NK1 C3 monoclonal antibody in the assessment of benign and malignant melanocytic lesions. J Clin Pathol 37:367–372
30. Martignoni G, Pea M, Chilosi M et al (2001) Parvalbumin is constantly expressed in chromophobe renal carcinoma. Mod Pathol 14:760–767
31. Mathers ME, Pollock AM, Marsh C et al (2002) Cytokeratin 7: a useful adjunct in the diagnosis of chromophobe renal cell carcinoma. Histopathology 563–567
32. Metzelaar MJ, Wijngaard PL, Peters PJ et al (1991) A novel lysosomal membrane glycoprotein, cloned by a screening procedure for intracellular antigens in eukaryotic cells. J Biol Chem 266:3239–3245
33. Miettinen M, Ekfors T (1990) Alveolar soft part sarcoma. Immunohistochemical evidence for muscle cell differentiation. Am J Clin Pathol 93:32–38
34. Murphy WM, Beckwith JB, Farrow GM (1994) Tumors of the kidney, bladder and related urinary structures. In: Rosai J (ed) Atlas of Tumor Pathology, 3rd series, fascicle 11. Armed Forces Institute of Pathology, Washington, DC
35. Ordonez NG, Rosai J (2004) Urinary tract: kidney, renal pelvis and ureter. In: Rosai J (ed) Rosai and Ackerman's surgical pathology, vol 1, 9th edn. Mosby, Edinburgh, pp 1163–1316
36. Palmer AA, Hall BE, Lew M (1985) A comparison of some methods for identifying melanotic and amelanotic melanoma metastases in paraffin sections. Pathology 17:335–339
37. Perez-Ordonez B, Hamed G, Campbell S et al (1997) Renal oncocytoma: a clinicopathologic study of 70 cases. Am J Surg Pathol 21:871–883
38. Porena M, Vespasiani G, Rosi P et al (1992) Incidentally detected renal cell carcinoma: role of ultrasonography. J Clin Ultrasound 20:395–400
39. Renshaw AA (2002) Subclassification of renal cell neoplasms: an update for practising pathologist. Histopathology 41:283–300
40. Robenek MJ, Schlattmann K, Zimmer KP et al (2003) Cholesterol transporter caveolin-1 transits the lipid bilayer during intracellular cycling. FASEB J 17:1940–1942
41. Romis L, Cindolo L, Patard JJ et al (2004) Frequency, clinical presentation and evolution of renal oncocytomas: multicentric experience from a European database. Eur Urol 45:53–57
42. Rothberg KG, Heuser JE, Donzell WC et al (1992) Caveolin, a protein component of caveolae membrane coats. Cell 68:673–682
43. Rous BA, Reaves BJ, Ihrke G et al (2002) Role of adaptor complex AP-3 in targeting wild type and mutated CD63 to lysosomes. Mol Biol Cell 13:1071–1082
44. Skinnider BF, Jones EC (1999) Renal oncocytoma and chromophobe renal cell carcinoma. A comparison of colloidal iron staining and electron microscopy. Am J Clin Pathol 111:796–803
45. Stoller ML, Carroll PR (2003) Urology. In: Tierney LM, McPhee SJ, Papadakis MA (eds) Current medical diagnosis & treatment 2003, 42nd edn. Lange Medical Books/McGraw-Hill, New York, pp 903–945
46. Stone CH, Lee MW, Amin MB et al (2001) Renal angiomyolipoma: further immunophenotypic characterization of an expanding morphologic spectrum. Arch Pathol Lab Med 125:751–758
47. Störkel S, Steart PV, Drenckhahn D et al (1989) The human chromophobe cell renal cell carcinoma: its probable relation to intercalated cells of the collecting duct. Virchows Arch B Cell Pathol Incl Mol Pathol 56:237–245
48. Thoenes W, Baum HP, Störkel S et al (1987) Cytoplasmic microvesicles in chromophobe cell renal carcinoma demonstrated by freeze fracture. Short communication. Virchows Arch B Cell Pathol Incl Mol Pathol 54:127–130
49. Thoenes W, Störkel S, Rumpelt HJ (1985) Human chromophobe cell renal carcinoma. Virchows Arch B Pathol 48:207–217
50. Thoenes W, Störkel S, Rumpelt HJ et al (1988) Chromophobe cell renal carcinoma and its variants: a report on 32 cases. J Pathol 155:277–287
51. Tickoo SK, Amin MB, Linden MD et al (1997) Antimitochondrial antibody (113-1) in the differential diagnosis of granular renal cell tumors. Am J Surg Pathol 21:922–930
52. Tickoo SK, Amin MB, Zarbo RJ (1998) Colloidal iron staining in renal epithelial neoplasms, including chromophobe renal cell carcinoma. Emphasis on technique and patterns of staining. Am J Surg Pathol 22:419–424
53. Tickoo SK, Lee MW, Eble JN et al (2000) Ultrastructural observations on mitochondria and microvesicles in renal oncocytoma, chromophobe renal cell carcinoma and eosinophilic variant of conventional (clear cell) renal cell carcinoma. Am J Surg Pathol 24:1247–1256
54. Vennegoor C, Calafat J, Hageman P et al (1985) Biochemical characterization and cellular localization of a formalin-resistant melanoma-associated antigen reacting with monoclonal antibody NKI/C3. Int J Cancer 35:287–295
55. Vieillefond A, Paradis V, Bouvier GR et al (1992) Est-il utile d'isoler parmi les carcinomes du rein, une variante a cellules chromophobes? Arch Anat Cytol Pathol 40:250–254
56. Wanaski SP, Glaser BK, Glaser M (2003) Caveolin scaffolding region and the membrane binding region of Src form lateral membrane domains. Biochemistry 42:42–56
57. Weiss LM, Gaffey MJ, Warhol MJ (1991) Immunohistochemical characterization of a monoclonal antibody directed against mitochondria reactive in paraffin-embedded sections. Mod Pathol 4:596–601
58. Wu SL, Kothari P, Wheeler TM et al (2002) Cytokeratins 7 and 20 immunoreactivity in chromophobe renal cell carcinomas and oncocytomas. Mod Pathol 15:712–717

Virchows Arch (2005) 447: 947–953
DOI 10.1007/s00428-005-0047-7

ORIGINAL ARTICLE

Udo Siebolts · Murat Ates · Rüdiger Spitz · Jürgen Thiele · Claudia Wickenhauser

Quantification of clonal hematopoiesis in polycythemia vera

Received: 23 June 2005 / Accepted: 3 July 2005 / Published online: 19 August 2005
© Springer-Verlag 2005

Abstract Polycythemia vera (PV) is believed to represent a clonal trilineage myeloaccumulative hematopoietic disorder. This study was undertaken to estimate for the first time the proportion not only of the neoplastic clone but also of clonal and residual nonneoplastic $CD34^+$ progenitor cells. Chromosomal abnormalities, including trisomy 8 or 9, are phenomena associated in about 20% of PV patients. Therefore, we screened peripheral blood (PB) mononuclear cells of PV patients in the chronic phase of the disease and looked for chromosomal abnormalities performing comparative genomic hybridization. Two of the ten patients revealed cytogenetic changes, including trisomy 8 or 9. To quantify the proportion of cytogenetic abnormal cells in these patients, we applied fluorescence in situ hybridization (FISH) technique on immunomagnetically enriched cell fractions. Ninety percent of the mononuclear cells and up to 79% of PB-derived $CD34^+$ progenitor cells presented three signals for chromosome 8 or 9. The diagnostic value of FISH to detect trisomies in trephine biopsies was then tested in all patients under study. Although the probability to detect FISH signals in a certain section plane is reduced, constantly 10–15% of the cells revealed three signals. Concerning the $CD34^+$ progenitor cell pool, a distinct nonclonal population exists in these patients. Our data underline the stem cell character of PV and additionally quantify the proportion of clonal $CD34^+$ progenitor cells for the first time. The finding of a distinct, not aberrant, $CD34^+$ progenitor cell population in chronic phase PV may offer perspectives in treatment of the disease. Finally, FISH analysis of bone marrow biopsies can be helpful to consolidate diagnosis of early PV.

Keywords Polycythemia vera · Chromosomal aberrations · $CD34^+$ · FISH · CGH

U. Siebolts · M. Ates · J. Thiele · C. Wickenhauser (✉)
Institute of Pathology, University of Cologne,
Joseph-Stelzmannstr. 9,
50924 Cologne, Germany
e-mail: c.wickenhauser@uni-koeln.de
Tel.: +49-221-4786368
Fax: +49-221-4786360

R. Spitz
Children's Hospital, Pediatric Oncology,
University of Cologne,
Cologne, Germany

Introduction

Polycythemia vera (PV) is believed to be a clonal disorder arising in a multipotent hematopoietic progenitor cell that causes the accumulation of morphologically normal red cells, white cells, platelets, and their precursors in the absence of a definable stimulus [26]. However, the molecular basis of PV remains elusive. The hallmark of the disease is trilineage hematopoietic proliferation (panmyelosis) dominated by erythropoiesis [26]. Therefore, most investigations on the pathogenesis of PV have focused on the red cell lineage. Indeed, a peculiarity of PV patients is the reduced serum erythropoietin (Epo) level [6]. The results concerning functional aspects of the erythropoiesis in PV, however, are contradictory. PV erythroid progenitor cells are able to proliferate in vitro in the absence of Epo, but this does not define the limits of the abnormal clone since not all PV erythroid progenitor cells exhibit Epo independence [7]. The existence of several hematologic subpopulations in PV may therefore be speculated, and a quiescent significant proportion of nonneoplastic cells in blood and bone marrow of PV patients cannot be excluded. In several recently published studies, the hypersensitivity of PV progenitors to several growth factors was explained by a point mutation of Janus kinase 2 gene (JAK2), leading to a constitutive activation of this downstream transductor of growth-factor-induced signaling [2, 14, 21]. This point mutation, however, was also seen in other chronic myeloproliferative disorders and, therefore, is not specific for PV.

Although there is no pathognomonic chromosomal abnormality defining PV, consistent, acquired cytogenetic changes, including del(20q), del(13q), trisomies 8 and 9 as well as duplication of 1q, have been observed at diagnosis

[1, 5, 24, 29]. Analysis of genomic abnormalities in individual cells of PV hematopoiesis, therefore, might elucidate the proportion of the neoplastic clone in this disease. In addition, fluorescence in situ hybridization (FISH) analysis on bone marrow trephine biopsies can be helpful for the diagnosis of early PV.

Materials and methods

Patients

Following informed consent, bone marrow trephine biopsies and peripheral blood (PB) derived samples from ten patients with histopathologically determined chronic phase PV (seven males and three females) were gained for diagnostic or therapeutical purpose (phlebotomy). The age of the patients ranged from 42 to 86 years (mean 64). According to the relevant clinical records, the duration of the disease ranged from 0.5 to 10 months. No additional myelosuppressive regimens were administered. The diagnosis of PV was ascertained according to the criteria of the WHO classification. At initial diagnosis, all patients presented hemoglobin values of >18.5 g/dl (in men) and >16.5 g/dl (in women), a thrombocytosis of $>400\times10^9$/l, and low Epo levels. Ten trephine biopsies from patients with lymphoproliferative disorders (without bone marrow involvement) and ten healthy blood donors served as controls.

Blood cell preparation

For FISH analysis, blood samples underwent centrifugation over Ficoll-Paque (Pharmacia, Uppsala, Sweden) to obtain a mononuclear cell concentrate. Selection of $CD34^+$ progenitor cells was performed by immunoaffinity selection, employing an immunomagnetic separation kit (Miltenyi Biotec, Bergisch Gladbach, Germany) as described before [30]. The purified cells were washed three times in phosphate-buffered saline (PBS), swollen in 75 mmol/l KCl at 37°C for 45 min, and then resuspended in ice-cold acetic methanol (1:3) fixative. The nuclei were then washed twice and stored in fixative at −20°C before FISH analysis.

Fixed nuclei were dried onto glass slides and sequentially incubated in solutions of ribonuclease A (Sigma, Dreisenhofen, Germany) at 37°C for 60 min, saline sodium citrate (SSC) for 5 min, pepsin (100 μg/ml, pH 2.0, 37°C; Sigma) for 10 min, PBS (room temperature) for 10 min, and 2× SSC (37°C) for 30 min. The slides were then dehydrated through ethanol solutions (70, 90, and 100%) and dried before denaturing in formamide (70% in 2× SSC and sodium phosphate buffer, 50 mmol/l, pH 7.0; Fluka) under coverslips on a hot plate at 73°C for 1 min. The slides were washed in 2× SSC, dehydrated through the ethanol solutions, and dried.

Preparation of the bone marrow biopsies

Bone marrow biopsies were transferred in buffered fixative (pH 7.4) containing 0.5% glutaraldehyde and decalcificated overnight in ethylenediaminetetraacetic acid (EDTA; 10% w/v in Tris pH 7.4). For phenotypic evaluation, 4-μm paraffin-embedded sections of trephine biopsies were dewaxed through xylene, air-dried, microwave-heated in appropriate buffer (100 mM Tris/50 mM EDTA, pH 7.0) for 12 min, cooled, and rinsed twice in Tris–HCl/0.05% Tween 20 buffer (pH 7.6) at 4°C. Subsequently, immunostaining with CD34 (QBEND10, Dako, Hamburg, Germany) or glycophorin C (Dako) monoclonal antibodies was performed by the alkaline phosphatase–antialkaline phosphatase method. Bromochloroindolylphosphate and nitro blue tetrazolium (Sigma) were used as chromogenic substances. Following preparation for FISH was performed as described before [31]. Briefly, samples were dehydrated through graded ethanol solutions, air-dried, and permeabilized by microwave treatment, followed by enzymatic digestion (proteinase K, Sigma). After this procedure, slides were quickly dehydrated and air-dried.

Fluorescence in situ hybridization

Fluorophore-labeled alpha-satellite DNA probes specific for the centromere of chromosomes 8 or 9 (Abbott-Vysis, Bergisch Gladbach, Germany) from all patients under study as well as the controls were placed on the coverslips. In case of the trephine biopsies, slides were incubated at 94°C for 3 min on a hot plate. After denaturation, the slides were quickly brought to 37°C, sealed with rubber cement, and then placed in a humified box for 16 h at 42°C. Coverslips were removed, and slides were placed in 0.4× SSC at 73°C for 2 min, immersed in 2× SSC/0.01% NP40 at room temperature for 1 min, and then air-dried before mounting in 0.125 μg of 4′-6′-diamidine-2-phenylindole dihydrochloride (DAPI)/ml antifade (DAPI II, Vysis). Slides were evaluated with an Aristoplan microscope (Leitz, Wetzlar, Germany), equipped with an optimized triple-bandpass filter, and imaged by digital camera (Photometrics, SenSys, Tucson, AZ, USA) and appropriate software (IPLab Spectrum P, Vienna, VA, USA).

Specimens were evaluated using fluorescence microscopy by two observers independently of each other. The percentage of nuclei bearing one, two, or three signals for each probe was determined from counts of 200 nuclei concerning the mononuclear cells and the immunomagnetic enriched $CD34^+$ progenitor cells and all cells bearing signals concerning the bone marrow slides.

Comparative genomic hybridization

DNA of mononuclear cells was extracted by standard methods. Samples of DNA were subsequently labeled using

digoxigenin-11-dUTP (normal DNA) or biotin-16-dUTP (test DNA) by nick-translation, according to the supplier's protocol (Roche, Mannheim, Germany). Comparative genomic hybridization (CGH) probes were prepared by co-precipitating gender-matched digoxigenin-1-dUTP normal DNA (1 μg), biotin-16-dUTP test DNA (1 μg), cot-1-DNA (100 μg, Gibco Life Technologies, Paisley, Scotland, UK), and salmon sperm DNA (11 μg, Roche) using 0.1- and 2.5-fold volumes, respectively, of sodium acetate and ethanol at −80°C followed by centrifugation at 4°C. The DNA pellets were dried, dissolved in 10 μl of hybridization buffer (50% v/v formamide, Fluka; 10% w/v dextran sulfate, Sigma, in 4× SSC), denaturized at 73°C for 5 min, and preannealed at 37°C for 60 to 120 min. CGH target metaphase slides, prepared using acetic acid methanol (1:3) fixed phytohemagglutinin-stimulated normal male lymphocytes, were denaturized in formamide (70% v/v in 2× SSC) at 75°C. The CGH probe was applied to the CGH target slide, sealed under a coverslip and the slide incubated at 37°C for 72 h. Posthybridization washes consisted of 0.3% v/v NP40 (Merck) in 0.4× SSC at 74°C for 2 min followed by 0.1% v/v NP40 in 2× SSC at room temperature for 1 min. For the signal detection, probes were incubated with 30 μl fluorescein isothiocyanate (FITC) conjugated avidin and TRIC-conjugated anti-digoxigenin for 30 min and 37°C (both from Oncor, Gaithersburg, MD, USA). The slides were then mounted under a DAPI-containing medium (Vector Laboratories) and subsequently analyzed using a Power Macintosh G3 and the Quips Genetics Workstation (IPLab Spectrum Imaging Software). Fluorescence and DAPI images were captured from as many as 19 meta-

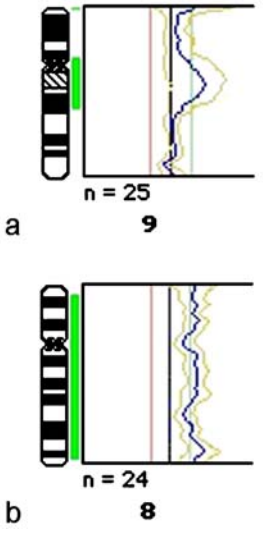


Fig. 1 CGH data of two PV cases: The *vertical black line* represents the mean green/red fluorescence ratio (1.0) of 24 (**a**) and 25 (**b**) captured chromosomes hybridized with CGH probes containing FITC-labeled DNA from the PV patient. The *magenta line* represents the 0.8, and the *green line* represents the 1.2 green/red fluorescence ratio **a** CGH data from a patient (case 1) with gain of material from chromosome 9. **b** CGH data from a patient (case 2) with gain in material from the whole of chromosome 8 pointing at a trisomy of this chromosome

Table 1 Selected data from FISH assays with probes for centromere of chromosome 8 and 9

		PB mononuclear cells			PB $CD34^+$ cells			BM hematopoiesis			BM erythropoiesis			BM $CD34^+$ cells		
Case no.	Probe	One signal (%)	Two signals (%)	Three signals (%)	One signal (%)	Two signals (%)	Three signals (%)	One signal (%)	Two signals (%)	Three signals (%)	One signal (%)	Two signals (%)	Three signals (%)	One signal (%)	Two signals (%)	Three signals (%)
1	Centromere 9	0	9	91	4	17	79	35	54	12	41	49	10	49	43	8
9	Centromere 9	5	95	0	7	93	0	60	40	0	55	45	0	57	43	0
2	Centromere 8	2	12	86	2	36	62	30	52	18	47	45	8	54	40	6
6	Centromere 8	10	90	0	7	93	0	51	49	0	65	35	0	61	39	0

Cases 6 and 9 represent normal karyotype according to CGH data. Two hundred cells with at least one signal were counted concerning the PB-derived cell fractions; concerning the bone marrow slides, all cells with at least one signal were counted (18 to 210 cells)
BM Bone marrow

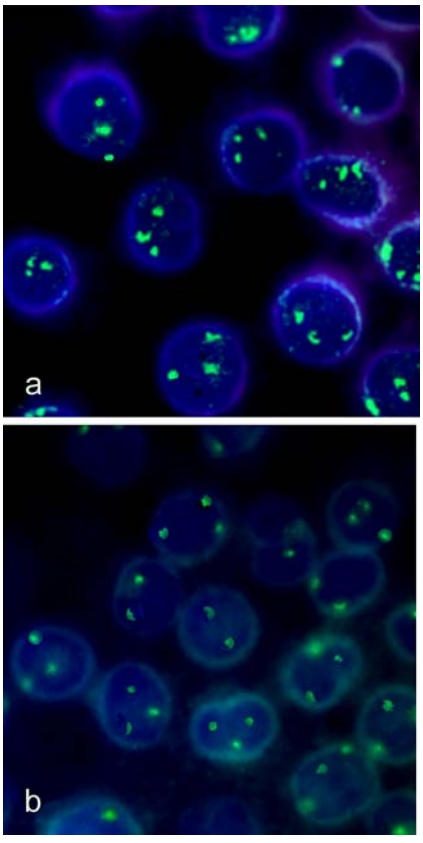


Fig. 2 FISH assays for centromeres 9 (**a**) and 8 (**b**). Alpha-satellite DNA probes for centromeres 8 and 9 were hybridized to fixed PB mononuclear cells (case 1) (**a**) and immunomagnetically enriched PB CD34$^+$progenitor cells (case 2) (**b**)

phases per slide for the generation of composite CGH profiles. Chromosome classification was validated by two authors. Deletions and amplifications were suspected when the slide average green/red fluorescence ratio for a given chromosomal region lay outside the range 0.7 to 1.2. Telomer regions, X and Y chromosomes, were excluded from analysis.

Results

Comparative genomic hybridization analysis of peripheral blood mononuclear cells

PB mononuclear cells from ten PV patients and the controls were tested for chromosomal aberrations. Evaluation of 15 to 19 metaphases per slide for fluorescence and DAPI images and generation of composite CGH profiles revealed abnormal pictures in CGH analysis in two of ten patients (cases 1 and 2) and in none of the controls. Both cases presented complex chromosomal aberrations, including gain of material from the centromere region and the q arm of chromosome 9 (Fig. 1a; case 1) or gain of material from the whole of chromosome 8 (Fig. 1b; case 2). Concerning the other eight patients, no chromosomal aberrations were observable. The CGH data were then compared with FISH analysis for centromere region of chromosomes 8 and 9.

Fluorescence in situ hybridization analysis of peripheral blood mononuclear cells

FISH analysis from the PB mononuclear cells from the same ten patients and the controls were undertaken to prove CGH results. As summarized in Table 1, PB mononuclear cells of both CGH-positive cases revealed 91% (case 1) and 86% (case 2) triple FISH signals for centromeres 9 and 8, respectively (Fig. 2a). Concerning the CGH-negative patients and the healthy controls, no triple but 90 to 95% double signals were observed. These findings underline the excellent specificity and good sensitivity of the tests. When analyzing the CD34$^+$ progenitor cells of the above-mentioned cases, the fraction of triple FISH signals was diminished with 79% (case 1) and 62% (case 2), compared to the findings in mononuclear cells (Fig 2b). The CGH-

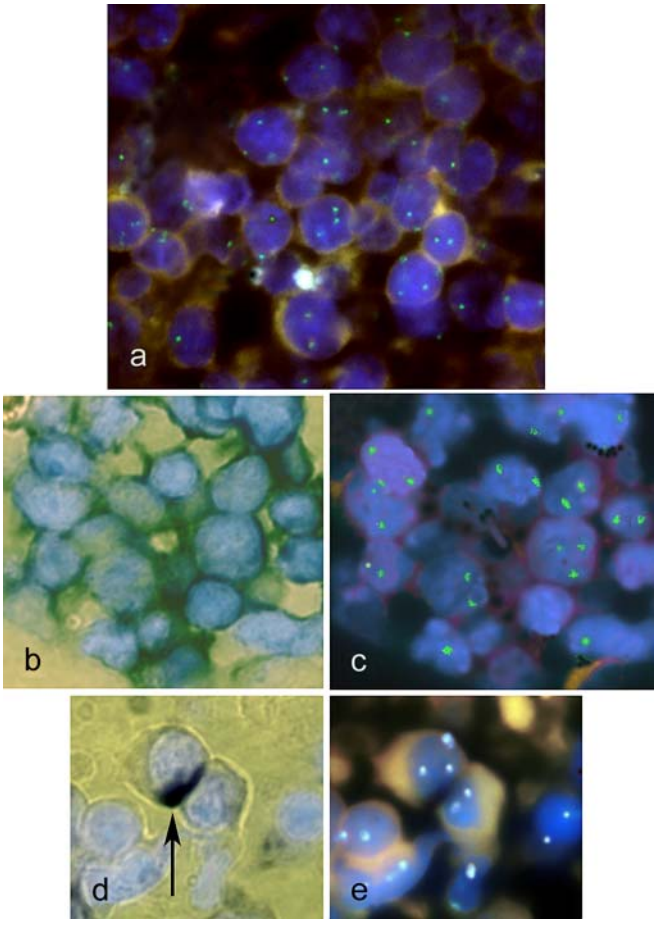


Fig. 3 Representative areas from bone marrow trephine biopsies. **a** and **e** FISH assays for centromere 8 (case 2). **d** Same area of case 2 with one CD34$^+$progenitor cell (*arrow*), CD34 immunostaining. **c** FISH assay for centromere 9 (case 1) of a selected erythrone. **b** Same area of case 1 with strong glycophorin C immunostaining of the erythropoietic precursor cells

negative cases presented the same distribution of FISH signals for $CD34^+$ progenitor cells as for mononuclear cells.

Fluorescence in situ hybridization analysis of bone marrow trephine biopsies

Of the above-mentioned ten patients and the controls, FISH analysis from 4-μm-thick bone marrow slides were performed to test the probability for triple signals in individual hematopoietic cells. Corresponding to the results of the mononuclear cell fractions, none of the CGH-negative cases presented FISH data indicating trisomy 8 or 9. However, in cases 1 and 2, a small but distinct cellular subgroup (12 and 18%; Fig. 3a) bared three signals for chromosome 9 or 8, respectively. In addition, the proportion of two signals per cell was higher in this group, compared with the CGH-negative fraction.

In a second approach, immunohistochemistry was followed by FISH analysis (Fig. 3b–e). Assisted by photographic documentation of the same area of the biopsy in different types of light, phenotype and genotype of individual cells were ascertained. In this experiment, three signals in glycophorin-C-positive erythropoietic cells as well as in $CD34^+$ progenitor cells could be demonstrated. Again, in the CGH-positive cases, $CD34^+$ progenitor cells presented lower levels of triple signaling (6–8%), compared to the overall hematopoiesis (12–18%), and, con cerning the erythropoiesis as well, slightly reduced levels of triple signaling were found (Table 1).

Discussion

When clinical features are suggestive for PV, assays for Epo and erythroid colony-forming cells, bone marrow trephine biopsies, and clonality assays can strongly support the diagnosis [9, 18, 26]. Analysis of X chromosome inactivation patterns, however, is reserved to female patients and may lead to false positive results because some normal elderly women present X chromosome inactivation patterns indistinguishable from those seen in patients with clonal myeloproliferative disorders [8, 10, 11]. Acquired karyotypic abnormalities, being direct markers of clonally transformed cells, are potentially more reliable for diagnostic purposes, but only 34% of PV patients have an abnormal karyotype revealed by conventional cytogenetic techniques [3, 13]. Among them, trisomies 8 and 9 or deletion of chromosome 20 represent the most frequent aberrations [5, 24, 29]. Although not specific for PV, cytogenetic conversion in one case treated with interferon alpha and clinical remission of the disease [23] indicates that the neoplastic cell fraction comprises the karyotypic abnormal cell clone. In this situation, analysis of frequent chromosomal aberrations might help to quantify the neoplastic clone proportion in PV hematopoiesis, even if above-mentioned aberrations in PV are characterized as secondary genetic changes [20].

CGH technique is a cytogenetic screening method with moderate sensitivity and excellent specificity (25% abnormal cells are necessary for correct diagnosis); it requires interphase cells and, therefore, can be applied on viable cells as well as fixed material [17, 22]. The diagnostic utility of this method applied to PV blood granulocytes has already been tested [28]. FISH analysis requires preknowledge of the abnormality to select the appropriate probes. Combined with immunohistochemical analysis, FISH technology allows the identification of single neoplastic cells and, therefore, the proper affiliation to a certain cell fraction. Altogether, this methodological approach is able to answer the question whether and to which extent clonal hematopoiesis in PV dominates residual reactive hematopoiesis and whether there are differences between the certain cell lineages.

The two cases presenting gain of material in CGH concerning chromosome 8 or 9 offered three signals in most PB mononuclear cells performing FISH. This finding as well as the result of 90–95% cells baring two signals in the CGH-negative patients indicates the high sensitivity of FISH. Further, the lack of triple signals in the CGH-negative cases demonstrates the high specificity of this method.

In detail, our data demonstrate a proportion of 86–91% clonal PB-derived mononuclear cells in contrast to 62–79% PB-derived $CD34^+$ cells. In this context, it is necessary to mention that the possibility that $CD34^+$ endothelial cells were taken into account, despite the different morphology of both cell types, cannot be ruled out. However, this difference might also be due to the fact that nonneoplastic primitive $CD34^+$ progenitor cells survive by being quiescent and not proliferating. Probably depending on an ill-defined effect already described in chronic myelogeneous leukemia (CML) [4], the microenvironment in the bone marrow seems to support neoplastic hematopoiesis, thus leading to a dominance of the clonally transformed cell fraction in the more differentiated hematopoietic cell pool of PV. Our data for the first time prove considerable contribution of $CD34^+$ progenitor cells in the neoplastic cell clone in PV. In view of the fact that until now many investigations on PV were undertaken on granulocytes [25, 27], these results indicate that further investigations on molecular pathogenesis of this disease should focus on this $CD34^+$ progenitor cell fraction. The detailed quantification of the $CD34^+$ progenitor cell fraction might further offer important data for potential further therapy strategies in PV.

To analyze the value of FISH technique for diagnosis of early PV examination of bone marrow, biopsies from CGH-tested patients was undertaken to find out whether chromosomal aberrations, especially gain of chromosomal material in the centromere region 8 or 9, could be detected. In this context, it is noteworthy to emphasize that the probability to identify three signals per cell is much lower in the 4-μm-thick sections than in cell smears. The excellent specificity of the test and the finding of 10% genotypic aberrant cells in all CGH-positive cases demonstrate that FISH indeed may facilitate PV diagnosis in chromosomal aberrant cases. Our results further indicate

the affiliation of the erythropoiesis and the $CD34^+$ progenitor cell pool to the neoplastic cell fraction.

A point mutation of JAK2 leading to a constitutive activation was recently described for a certain proportion of PV patients as well as for other Philadelphia chromosome negative chronic myeloproliferative disorders [2, 14, 15, 19, 21]. However, according to the most recently published results, the incidence of JAK2 mutations reveals a significant range of about 65 to 97% in PV. Taking this genomic aberration into account, more detailed information about the distribution of the neoplastic cell clone as well as the dynamics following cytoreductive therapy will now be available and will give more insights in the biology of PV and further provides a means for molecularly targeted therapeutic strategies [12, 16].

Acknowledgements Supported by the Cologne Fortune Foundation and by the Center for Molecular Medicine, University of Cologne (CMMC).

Declaration: all experiments comply with the laws of the Federal Republic of Germany and the European Union.

References

1. Amiel A, Gaber E, Manor Y, Fejgin M, Joseph-Lerner N, Ravid M, Lishner M (1995) Fluorescence in situ hybridization for the detection of trisomies 8 and 9 in polycythemia vera. Cancer Genet Cytogenet 79:153–156
2. Baxter EJ, Scott LM, Campbell PJ, East C, Fourouclas N, Swanton S, Vassiliou GS, Bench AJ, Boyd EM, Curtin N, Scott MA, Erber WN, Green AR (2005) Acquired mutation of the tyrosine kinase JAK2 in human myeloproliferative disorders. Lancet 365:1054–1061
3. Bench AJ, Nacheva EP, Champion KM, Green AR (1998) Molecular genetics and cytogenetics of myeloproliferative disorders. Bailliere's Clin Haematol 11:819–848
4. Bhatia R, McGlave PB, Dewald GW, Blazar BR, Verfaillie CM (1995) Abnormal function of the bone marrow microenvironment in chronic myelogenous leukemia: role of malignant stromal macrophages. Blood 85:3636–3645
5. Busson M, Romana S, Khac FN, Bernard O, Berger R (2004) Cryptic translocations involving chromosome 20 in polycythemia vera. Ann Genet 47:365–371
6. Carneskog J, Kutti J, Wadenvik H, Lundberg PA, Lindstedt G (1998) Plasma erythropoietin by high-detectability immunoradiometric assay in untreated and treated patients with polycythaemia vera and essential thrombocythaemia. Eur J Haematol 60:278–282
7. Cashman J, Henkelman D, Humphries K, Eaves C, Eaves A (1983) Individual BFU-E in polycythemia vera produce both erythropoietin dependent and independent progeny. Blood 61: 876–884
8. Champion KM, Gilbert JG, Asimakopoulos FA, Hinshelwood S, Green AR (1997) Clonal haemopoiesis in normal elderly women: implications for the myeloproliferative disorders and myelodysplastic syndromes. Br J Haematol 97:920–926
9. Florensa L, Besses C, Zamora L, Bellosillo B, Espinet B, Serrano S, Woessner S, Sole F (2004) Endogenous erythroid and megakaryocytic circulating progenitors, HUMARA clonality assay, and PRV-1 expression are useful tools for diagnosis of polycythemia vera and essential thrombocythemia. Blood 103:2427–2428
10. Gale RE, Fielding AK, Harrison CN, Linch DC (1997) Acquired skewing of X-chromosome inactivation patterns in myeloid cells of the elderly suggests stochastic clonal loss with age. Br J Haematol 98:512–519
11. Gilbert HL, Acharya J, Pearson TC (1998) Implications for the use of X-chromosome inactivation patterns and their relevance to the myeloproliferative disorders. Eur J Haematol 61:282–283
12. Goldman JM (2005) A unifying mutation in chronic myeloproliferative disorders. N Engl J Med 352:1744–1746
13. Herishanu Y, Lishner M, Bomstein Y, Kitay-Cohen Y, Fejgin MD, Gaber E, Amiel A (2001) Comparative genomic hybridization in polycythemia vera and essential thrombocytosis patients. Cancer Genet Cytogenet 128:154–157
14. James C, Ugo V, Le Couedic JP, Staerk J, Delhommeau F, Lacout C, Garcon L, Raslova H, Berger R, Bennaceur-Griscelli A, Villeval JL, Constantinescu SN, Casadevall N, Vainchenker W (2005) A unique clonal JAK2 mutation leading to constitutive signalling causes polycythaemia vera. Nature 434:1144–1148
15. Jones AV, Kreil S, Zoi K, Waghorn K, Curtis C, Zhang L, Score J, Seear R, Chase AJ, Grand FH, White H, Zoi C, Loukopoulos D, Terpos E, Vervessou EC, Schultheis B, Emig M, Ernst T, Lengfelder E, Hehlmann R, Hochhaus A, Oscier D, Silver RT, Reiter A, Cross NC (2005) Widespread occurrence of the JAK2 V617F mutation in chronic myeloproliferative disorders. Blood [Epub ahead of print]
16. Kaushansky K (2005) On the molecular origins of the chronic myeloproliferative disorders: it all makes sense. Blood 105: 4187–4190
17. Knuutila S, Armengol G, Bjorkqvist AM, el-Rifai W, Larramendy ML, Monni O, Szymanska J (1998) Comparative genomic hybridization study on pooled DNAs from tumors of one clinical–pathological entity. Cancer Genet Cytogenet 100:25–30
18. Kralovics R, Buser AS, Teo SS, Coers J, Tichelli A, van der Maas AP, Skoda RC (2003) Comparison of molecular markers in a cohort of patients with chronic myeloproliferative disorders. Blood 102:1869–1871
19. Kralovics R, Passamonti F, Buser AS, Teo SS, Tiedt R, Passweg JR, Tichelli A, Cazzola M, Skoda RC (2005) A gain-of-function mutation of JAK2 in myeloproliferative disorders. N Engl J Med 352:1779–1790
20. Kralovics R, Stockton DW, Prchal JT (2003) Clonal hematopoiesis in familial polycythemia vera suggests the involvement of multiple mutational events in the early pathogenesis of the disease. Blood 102:3793–3796
21. Levine RL, Wadleigh M, Cools J, Ebert BL, Wernig G, Huntly BJ, Boggon TJ, Wlodarska I, Clark JJ, Moore S, Adelsperger J, Koo S, Lee JC, Gabriel S, Mercher T, D'Andrea A, Frohling S, Dohner K, Marynen P, Vandenberghe P, Mesa RA, Tefferi A, Griffin JD, Eck MJ, Sellers WR, Meyerson M, Golub TR, Lee SJ, Gilliland DG (2005) Activating mutation in the tyrosine kinase JAK2 in polycythemia vera, essential thrombocythemia, and myeloid metaplasia with myelofibrosis. Cancer Cell 7:387–397
22. Lichter P, Joos S, Bentz M, Lampel S (2000) Comparative genomic hybridization: uses and limitations. Semin Hematol 37:348–357
23. Messora C, Bensi L, Vecchi A, Longo R, Giacobbi F, Temperani P, Bevini M, Emilia G, Sacchi S (1994) Cytogenetic conversion in a case of polycythaemia vera treated with interferon-alpha. Br J Haematol 86:402–404
24. Najfeld V, Montella L, Scalise A, Fruchtman S (2002) Exploring polycythaemia vera with fluorescence in situ hybridization: additional cryptic 9p is the most frequent abnormality detected. Br J Haematol 119:558–566
25. Pellagatti A, Vetrie D, Langford CF, Gama S, Eagleton H, Wainscoat JS, Boultwood J (2003) Gene expression profiling in polycythemia vera using cDNA microarray technology. Cancer Res 63:3940–3944
26. Spivak JL (2002) Polycythemia vera: myths, mechanisms, and management. Blood 100:4272–4290

27. Temerinac S, Klippel S, Strunck E, Roder S, Lubbert M, Lange W, Azemar M, Meinhardt G, Schaefer HE, Pahl HL (2000) Cloning of PRV-1, a novel member of the uPAR receptor superfamily, which is overexpressed in polycythemia rubra vera. Blood 95:2569–2576
28. Westwood NB, Gruszka-Westwood AM, Atkinson S, Pearson TC (2001) Polycythemia vera: analysis of DNA from blood granulocytes using comparative genomic hybridization. Haematologica 86:464–469
29. Westwood NB, Gruszka-Westwood AM, Pearson CE, Delord CF, Green AR, Huntly BJ, Lakhani A, McMullin MF, Pearson TC (2000) The incidences of trisomy 8, trisomy 9 and D20S108 deletion in polycythaemia vera: an analysis of blood granulocytes using interphase fluorescence in situ hybridization. Br J Haematol 110:839–846
30. Wickenhauser C, Perez F, Siebolts U, Lorenzen J, Varus E, Frimpong S, Thiele J (2003) Structural, antigenetic and transcriptional characteristics in peripheral blood CD34+ progenitor cells from polycythemia vera patients: evidence for delayed determination. Int J Oncol 23:437–443
31. Wickenhauser C, Thiele J, Perez F, Varus E, Stoffel MS, Kvasnicka HM, Beelen DW, Schaefer UW (2002) Mixed chimerism of the resident macrophage population after allogeneic bone marrow transplantation for chronic myeloid leukemia. Transplantation 73:104–111

Virchows Arch (2005) 447: 954–960
DOI 10.1007/s00428-005-0046-8

ORIGINAL ARTICLE

Tiina Kuivanen · Katja Ahokas · Susanna Virolainen · Tiina Jahkola · Erkki Hölttä · Olli Saksela · Ulpu Saarialho-Kere

MMP-21 is upregulated at early stages of melanoma progression but disappears with more aggressive phenotype

Received: 17 February 2005 / Accepted: 18 July 2005 / Published online: 20 August 2005
© Springer-Verlag 2005

Abstract The expression of matrix metalloproteinases (MMPs) is frequently altered during malignant transformation. We examined the profile of three recently cloned MMPs, MMP-21, MMP-26, and MMP-28, in melanomas in vivo and in culture. Immunohistochemistry for MMPs-21, -26, -28, and -13 in melanoma specimens (27 non-metastatic, 26 with nodal micrometastases, and 10 in situ melanomas) from 63 patients was performed. MMP-21 was expressed in melanoma cells in 29/53 cases, being more frequent in melanoma samples without micrometastases. Six out of ten in situ melanomas were positive, while five nevus samples were negative. MMP-26 and -28 were not generally expressed in melanoma cells. MMP-13 was detected in melanoma cells in 36/53 samples. MMP-21 was not found in sentinel nodes with metastases, while MMP-13 was seen in all of them. MMP-21 messenger RNA was variably expressed in all five melanoma cell lines investigated using reverse transcriptase–polymerase chain reaction. Our results suggest that expression of MMP-21 may serve as a marker of malignant transformation of melanocytes and does not associate with the presence of micrometastases.

Keywords Sentinel node · MMP-13 · Immunohistochemistry · RT-PCR

Abbreviations BM: basement membrane

This study was supported by the Academy of Finland, the Sigrid Juselius Foundation, Finska Läkaresällskapet, the Finnish Cancer Foundation, Helsinki University Central Hospital Research Funds (EVO) and National Graduate School of Clinical Investigation

T. Kuivanen · K. Ahokas · O. Saksela · U. Saarialho-Kere
Department of Dermatology, Helsinki University Central Hospital and Biomedicum Helsinki, Helsinki, Finland

S. Virolainen · E. Hölttä
Department of Pathology, Helsinki University Central Hospital and Biomedicum Helsinki, Helsinki, Finland

T. Jahkola
Department of Plastic Surgery, Helsinki University Central Hospital and Biomedicum Helsinki, Helsinki, Finland

U. Saarialho-Kere (✉)
Department of Dermatology, Karolinska Institutet at Stockholm Soder Hospital, Plan 5, Södersjukhuset, SE-11883 Stockholm, Sweden
e-mail: ulpu.saarialho-kere@helsinki.fi
Fax: +46-8-6162588

Introduction

Cutaneous melanoma is a tumor with significant metastatic potential, the incidence of which has increased significantly over the last two decades. The prognosis of melanoma has historically been based on histological criteria, mainly tumor thickness [7] and the level of invasion [9]. Other prognostic factors include mitotic rate, increased nuclear volume, satellite deposits, and hemangiolymphatic invasion [31]. These criteria have been further supplemented by tumor ulceration and sentinel lymphadenectomy to gain a new, more accurate staging system. According to the recent staging recommendations by the American Joint Committee on Cancer (AJCC), tumor status in melanoma is based on thickness, ulceration, and the number of metastatic lymph nodes [5]. Lymphatic mapping and sentinel lymphadenectomy were created as minimally invasive techniques to provide regional lymph node staging information for patients at high risk for metastatic melanoma. Sentinel lymph node status has become the most significant prognostic factor for patients with melanoma [27].

The invasion of melanomas from the epidermis to the dermis requires degradation of several basement membrane (BM) components. Matrix metalloproteinases (MMPs), a family of 23 human structurally related zinc-dependent endopeptidases, are collectively capable of degrading all extracellular matrix and BM proteins [23]. However, MMPs also regulate angiogenesis and apoptosis as well as cleave growth factors, cytokines, chemokines, and their receptors

and therefore regulate growth factor response and inflammation [10]. We and others have previously shown that several MMPs are overexpressed in melanoma cells in vitro and in vivo [4, 12]. MMP-2 and MT1-MMP have a prominent role in melanoma progression [12, 16]. Induction of MMP-1 and -13 messenger RNA (mRNA) expressions is a late event in melanocytic tumor progression and correlates with the level of invasion [4], while MMP-9 is involved in the early steps of metastasis formation [11]. Furthermore, MMP-1 and MMP-2 have been shown to be prognostic markers in melanoma [24, 30]. Synthetic MMP inhibitors and adenoviral therapy using them have been demonstrated to inhibit the metastatic spread and growth of melanoma in mice [3, 8]. Analogously, new therapies designed to interfere with specific MMP actions may be useful in the treatment of melanoma.

We have recently studied the role of several novel MMPs, such as MMP-19, -26 (matrilysin-2), and -28 (epilysin), in skin cancer [13, 28]. Unlike most classical MMPs, they seem to be downregulated in poorly-differentiated tumors. Furthermore, our group has recently cloned a novel MMP, MMP-21, from placental complementary DNA (cDNA) library [2]. It is expressed in a variety of normal, malignant, and fetal epithelial tissues and might play a role in human embryogenesis and tumor progression [1]. Its physiologic activators or substrates are not yet known. The objective of this study was to examine the expression profiles of three recently cloned MMPs, MMP-21, MMP-26, and MMP-28, in melanomas in vivo and in culture, correlating the findings with lymph node status as determined by sentinel node biopsies. MMP-13 was studied based on previous reports on its expression and prognostic significance in melanoma.

Materials and methods

Tissue samples

The melanoma specimens were routinely formalin-fixed, paraffin-embedded histological material from 63 cases (10 in situ melanomas and 53 invasive melanomas), of which all invasive melanoma patients had undergone lymphatic mapping and sentinel node biopsies at the Helsinki University Central Hospital, during the years 2001 to 2003 (Table 1). Five additional benign nevi and seven sentinel node positive and 12 sentinel node negative lymph nodes obtained from these 63 patients were also analyzed. The study was approved by the corresponding Hospital Ethical Committee. Lymph node micrometastases were detected by hematoxylin–eosin, MART-1, and tyrosinase immunostainings. There were 21 females and 32 males in the invasive melanoma study group, and their average age at diagnosis was 65 years (range 36–87) (Table 1). Invasion levels of the melanomas were determined by Clark's classification [9], and node classification was performed according to Balch et al. [5]. Tumor thickness was measured according to Breslow [7]. The samples included 2 Clark's grade II, 14 grade III, 34 grade IV and 2 grade V malignant melanomas. Mean Clark value was 3.7 and mean Breslow was value 3.1. Twenty-seven samples were from nonmetastatic melanoma, and 26 were from melanomas with nodal micrometastasis (Table 1).

Immunohistochemistry

Immunohistochemical stainings were performed using the Streptavidin–biotin–peroxidase complex technique (DAKO StreptABComplex/HRP Duet, Mouse/Rabbit, Glostrup, Denmark). The following antibodies were used: MMP-13 (1:10, Clone VIIIA2, Labvision Corporation, Fremont, CA, USA), MMP-21 (1:300, RP3MMP-21, Triple Point Biologics, Forest Grove, OR, USA) [1], MMP-26 (1:150, kindly provided by Keiichi Isaka, Tokyo Medical University, Tokyo, Japan) [14], and MMP-28 (1:800, kindly provided by Dr. Jouko Lohi) [18]. Pretreatment included incubation in a +95°C water bath for MMP-13 and MMP-26 and microwaving in citrate buffer for MMP-28. Aminoethylcarbazole (AEC) was used as chromogenic substrate, and tissues were counterstained with hematoxylin. The slides were analyzed by two investigators (SV, US-K) experienced in dermatopathology, and positive immunostaining was scored semiquantitatively (0=under 10 positive cells, 1=10–100 positive cells, 2=over 100 positive cells) (Table 1).

Cell cultures

Melanoma cell lines Bowes, G361, WM852, WM164, and WM165 were cultivated in Dulbecco's modified Eagle's medium/F-12 (D-MEM/F-12) (Gibco BRL, Gaithersburg, MD, USA), containing 10% heat-activated fetal bovine serum (FBS), 2 mM L-glutamine, 100 IU ml^{-1} penicillin, 50 mg ml^{-1} streptomycin, 0.1 μg ml^{-1} cholera toxin, and 3 ng ml^{-1} fibroblast growth factor-2 (FGF-2) at 37°C in humified atmosphere of 5% CO_2 and 95% air. The medium was changed twice a week.

Polymerase chain reaction and RNA analysis

Total cellular RNA from cultured cells was extracted using Rneasy Miniprep-kit (Qiagen, Chasworth, CA, USA) according to manufacturer's instructions. RNA was then reverse-transcribed to cDNA with Taqman Reverse Transcription reagents (Applied Biosystems) with random hexamers and used in a 1:5 dilution as a template for reverse transcriptase–polymerase chain reaction (RT-PCR). As primers, we used T21F (forward nucleotides) and T21R (reverse nucleotides) for human MMP-21 (Sigma Genosys, Cambridge, UK) [1]. TaqMan PCR primers and probes for human MMP-26 were purchased as a ready-to-use 20× reaction mix, and the sequences are property of the vendor (Applied Biosystems). MMP-28 primers (Sigma Genosys) and probes (PE Biosystems, Warrington, UK), described in more detail in our previous work [28], were designed using

Table 1 Clinical information on melanoma patients and expression of MMP proteins in tumor samples

Sentinel node	Clark	Breslow (mm)	Sex	Ulceration	MMP-21	MMP-13
−	III	1.3	M	0	1	1
−	III	2.5	F	0	2	2
−	III	2.5	M	0	2	0
−	III	1.1	M	0	1	0
−	III	0.8	M	0	1	1
−	III	0.7	F	0	0	0
−	III	1.3	M	0	1	0
−	III	2.0	M	0	1	1
−	IV	2.0	M	1	2	0
−	IV	1.9	M	0	1	0
−	IV	3.0	M	0	1	1
−	IV	3.5	F	1	1	2
−	IV	2.5	F	0	2	0
−	IV	0.95	M	0	0	1
−	IV	1.9	F	0	1	1
−	IV	3.2	F	0	1	2
−	Nd	Nd	F	0	0	1
−	IV	1.5	F	1	1	2
−	IV	1.2	M	0	1	1
−	IV	1.95	M	0	0	1
−	IV	0.85	F	0	0	0
−	IV	1.5	M	0	0	0
−	IV	2.4	F	0	0	1
−	IV	1.6	M	1	0	0
−	IV	1.0	F	0	1	1
−	IV	2.6	M	1	1	1
−	V	6.5	F	1	0	0
+	II	0.3	F	0	2	0
+	II	2.8	M	0	2	2
+	III	1.2	M	0	1	1
+	III	2.3	M	0	0	1
+	III	2.5	M	0	1	2
+	III	6.0	M	0	0	2
+	III	0.95	M	0	0	1
+	III	2.0	M	1	1	0
+	IV	2.5	F	1	0	2
+	IV	1.2	M	0	1	1
+	IV	3.3	F	1	0	1
+	IV	1.4	F	0	0	0
+	IV	3.0	M	0	0	1
+	IV	1.35	M	0	1	1
+	IV	12.0	M	1	0	1
+	IV	6.0	F	0	1	2
+	IV	3.2	F	1	0	1
+	IV	6.0	F	1	0	1
+	IV	2.5	M	1	2	2
+	IV	1.15	M	0	1	0
+	IV	1.6	M	0	0	1
+	IV	2.25	M	0	0	1
+	IV	1.0	M	0	0	0
+	IV	2.1	F	1	0	0
+	IV	1.7	F	0	0	1
+	V	6.0	M	1	2	2

Immunohistochemical positivity for MMPs was evaluated under bright-field microscopy
The number of AEC positive cells was assessed as follows: 0= under 10 positive cells, 1=10–100 positive cells, 2=over 100 positive cells
Nd Not determined

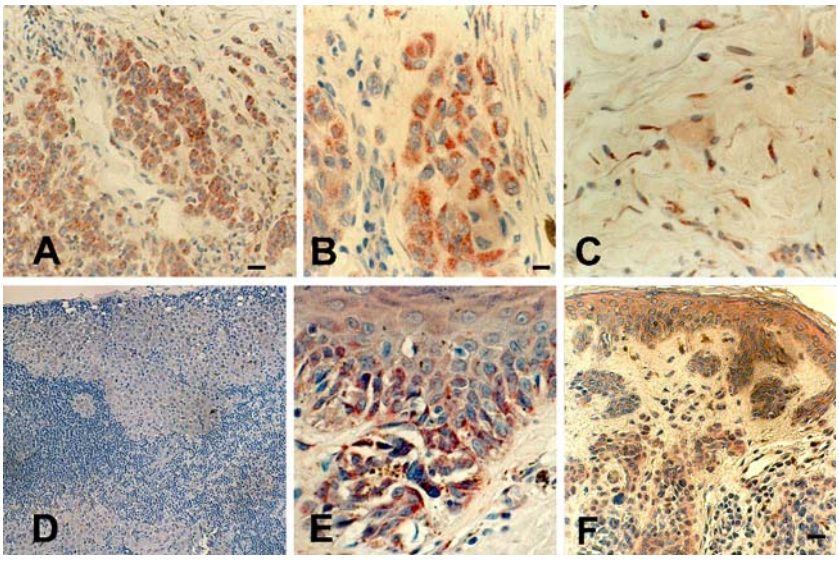


Fig. 1 MMP-21 in melanoma. **a** MMP-21 protein is expressed in melanoma cells of a node negative tumor. **b** Higher magnification of MMP-21 positive melanoma cells. **c** MMP-21 protein was also detected in a subset of melanomas in fibroblasts surrounding melanoma islands. **d** No staining for MMP-21 is detected in a positive sentinel node. **e** MMP-21 was also detected in melanoma cells of in situ melanomas. **f** Nevus samples did not express MMP-21. *Scale bars*: 50 μm (**a** and **f**), 12.5 μm (**b**, **c**, and **e**), 125 μm (**d**)

computer program Primer Express (PE Biosystems). Human glyceraldehyde-3-phosphate dehydrogenase (GAPDH) was used as an endogenous control. The PCR for MMPs-21, -26, and -28 was performed by conventional PCR in separate reactions. The primers were used in a final concentration of 200 nM each (T21F, T21R, GAPDH forward, and GAPDH reverse), 400 μM of each nucleotide, 0.5 μl Advantage-2, 5.5 mM $MgCl_2$, and 3 μl of cDNA-template in a 75-μl reaction. The PCR was started with an initial denaturation of 3 min at 94°C, followed by a total of 40 cycles of 30-s denaturation at 94°C and 30 s of annealing at 60°C, and 30 s of elongation at 72°C followed by 10-min final elongation at 72°C. Finally, PCR products were analyzed in 2.5% agarose gel and stained with 5 ng/ml of ethidium bromide and visualized under ultraviolet light.

Statistical analysis

Chi-square test was performed to compare the number of MMP-21 and -13 positive and negative samples in sentinel node negative and positive patients. The medians of Breslow values of MMP-21 positive and negative melanoma patients as well as the medians of numeric ratings of positivity for MMP-21 and -13 in the sentinel node positive vs negative groups were compared using unpaired two-tailed *t* test. *P* value under 0.05 was considered as significant.

Results

Immunohistochemistry MMP-21 protein was expressed in invasive melanoma cells in 29/53 of the cases (Fig. 1a,b) and in 6/10 in situ melanomas (Fig. 1e). Its expression was more frequent in melanoma samples without nodal invasion (Table 1): 18/27 of the cases without micrometastases and 11/26 with micrometastases in invasive melanoma were positive for MMP-21. No correlation of MMP-21 expression to the presence of ulceration was detected (Table 1). MMP-21 was also expressed by fibroblasts surrounding the melanoma islands in some samples but not by keratinocytes or endothelial cells (Fig. 1c). None of the 19 metastatic or nonmetastatic sentinel nodes examined expressed MMP-21 (Fig. 1d). Five compound nevi samples were immunostained for MMP-21, and they were all negative (Fig. 1f).

Twenty-one melanoma samples and five nevus samples were immunostained for MMP-26. They all turned out to be negative except for fibroblasts surrounding the tumor in a few specimens (Fig. 2a) and for occasional basal keratinocytes bordering ulcerations (data not shown).

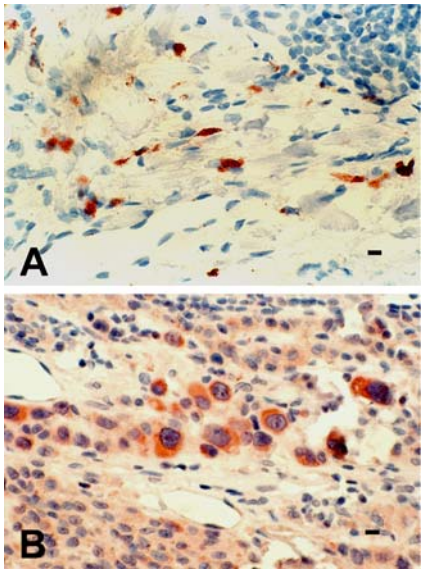


Fig. 2 MMP-26 and MMP-28 in melanoma. **a** MMP-26 was not detected in melanoma cells but occasionally in fibroblasts surrounding the tumor. **b** Staining for MMP-28 in melanoma cells. *Scale bars*: 25 μm (**a** and **b**)

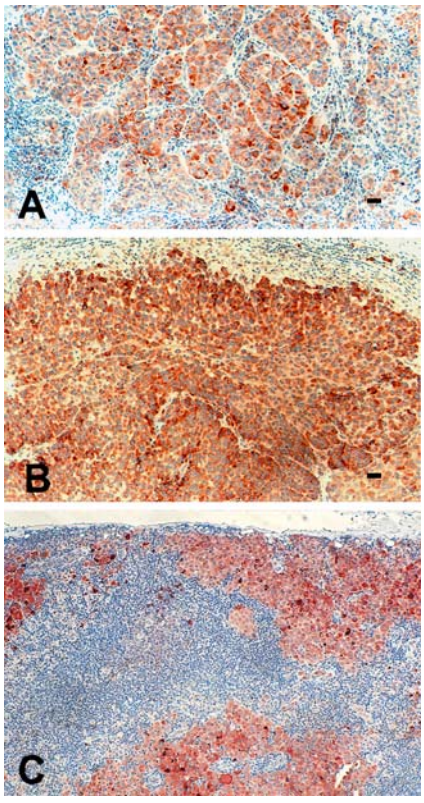


Fig. 3 MMP-13 in melanoma cells. **a**, **b** Immunostaining for MMP-13 in melanomas without (**a**) and with (**b**) micrometastasis. **c** Staining for MMP-13 in a positive sentinel node. *Scale bars*: 50 μm (**a** and **b**), 125 μm (**c**)

Thirty-six invasive melanomas and ten in situ melanomas were immunostained for MMP-28, and expression in melanoma cells was found in only five of them (Fig. 2b). Micrometastases were detected in 2/5 MMP-28 positive melanoma samples. All of the seven positive melanoma metastases were immunostained with MMP-28, and two of them showed a small number of positive melanoma cells. All five compound nevi were devoid of MMP-28 protein. Keratinocytes, endothelial, or macrophages did not express MMP-28.

MMP-13 was detected in melanoma cells in 39/53 samples in invasive melanoma (Fig. 3a,b). Nineteen out of twenty-seven of the cases without micrometastases and 20/26 with micrometastases were positive for MMP-13. There were no statistically significant differences between MMP-21 and MMP-13 positive and negative groups when their Breslow values were compared, respectively. All metastatic sentinel lymph nodes expressed MMP-13 (Fig. 3c), whereas none of the 12 nonmetastatic sentinel lymph nodes expressed MMP-13.

Cell cultures To study whether melanoma cells are able to express any of the three novel MMPs in culture, five melanoma cell lines were studied. MMP-21 was clearly expressed by RT-PCR in Bowes and ML852 melanoma lines, while lower levels were apparent in WM164, WM165, and G361 cells (data not shown). MMP-26 mRNA was detected only at low levels in ML852 and WM165 cells (data not shown). A very low level of MMP-28 was detected in WM165 cells, while all other cell lines turned out negative (data not shown).

Discussion

To our knowledge, this is the first report examining the correlation of expression of several MMPs to sentinel node status of melanoma patients and particularly the expression of MMPs-21, -26, and -28 in melanoma in vivo. Here, we demonstrate that MMP-21 can be expressed by melanoma cells in tissue and in vitro. Expression was more frequent in nonmetastatic melanoma samples, suggesting that MMP-21 is upregulated at early stages of melanoma progression. This is further supported by our negative findings in metastatic sentinel nodes. MMP-21 was present already in in situ melanomas but not in nevus cells. Thus, MMP-21 could possibly serve as a marker of malignant transformation in melanocytes. However, a larger sample set of various stages of melanoma would be required to finally confirm this. Furthermore, our immunohistochemical approach cannot differentiate between latent and active MMP-21 which would require conventional or in situ zymography but would lead to difficulties in determining the cells of origin of MMP-21 on tissue level.

Human MMP-21 is expressed in developing but not in normal adult skin [1]. Furthermore, its expression has previously been associated with aggressive dedifferentiated subtypes of squamous cell cancer, but it is not upregulated by mere keratinocyte hyperproliferation or wound repair [1]. MMP-21 is upregulated at least in keratinocytes by transforming growth factor beta 1 (TGF-β1) [1]. Interestingly, TGF-β1 is also known to modulate melanoma growth and survival [6] and may thus be a potential candidate to upregulate MMP-21 in melanomas in vivo as well. Based on its promoter analysis, MMP-21 is a direct target of beta-catenin transactivation [19]. Indeed, alterations of beta-catenin pathway have been reported in melanoma [15].

MMP-26 (endometase or matrilysin-2) is a rather novel MMP originally found in normal placenta and endometrium [17, 26, 29] but is also widely expressed in malignant tumors, such as endometrial, prostate, breast, and oral squamous cell cancers, and tumor cell lines [14, 21, 32]. We did not detect MMP-26 in melanoma cells in vivo. However, in vitro, two metastatic melanoma cell lines (WM165, ML852) expressed MMP-26. This discrepancy is often seen in the context of MMPs, which are generally expressed by cancer cell lines in vitro, but are not detected necessarily in corresponding tissue in vivo. While this study was in progress, Li et al. [17] reported the expression of MMP-26 by several melanoma cell lines in culture using immunohistochemistry and its correlation with estrogen dependency. We also detected MMP-26 occasionally in fibroblasts surrounding melanoma cell islands. This is in agreement with a recent report demonstrating MMP-

26 in corneal fibroblasts [20] and may be related to contribution of host-derived proteases to tumor progression.

Epilysin (MMP-28) was first cloned from human keratinocyte and testis cDNA libraries [18] and a lung cDNA library [22]. MMP-28 is expressed in various carcinomas, including ovarian, colon, and pancreatic adenocarcinoma [22], and also by proliferative keratinocytes during wound repair [18, 28]. Since 41/46 melanomas were negative in vivo for MMP-28 and the cell lines in culture turned out almost negative by RT-PCR, we conclude that this protease does not play an important role in the biology of melanoma. Our results on negative MMP-26 and -28 expressions in G631 melanoma cells agree with those recently published by Nuttall et al. [25].

Our earlier investigations suggest that MMP-13 expression is induced during melanoma progression [4]. This agrees with the current results showing that MMP-13 is generally present in metastatic melanoma cells of positive sentinel nodes. High expression of MMP-13, unlike that of MMP-1, in melanomas does not, however, correlate with survival parameters but is associated with the presence of visceral metastases [24].

In conclusion, our results show that upregulation of MMP-21 may serve as a marker of malignant transformation of melanocytes and is associated with initial stages of tumorigenesis rather than with micrometastases and poor outcome. While MMPs-26 and -28 are not generally expressed in melanomas in vivo, the presence of MMP-13 positive cells may correlate to more aggressive disease.

Acknowledgements We thank Dr. Jouko Lohi, University of Helsinki, for MMP-28 and Prof. Keichi Isaka, Tokyo Medical University, for MMP-26 reagents and Mr. Sakari Maatta and Ms. Alli Tallqvist for skillful technical assistance.

References

1. Ahokas K, Lohi J, Illman SA, Llano E, Elomaa O, Impola U, Karjalainen-Lindsberg ML, Saarialho-Kere U (2003) Matrix metalloproteinase-21 is expressed epithelially during development and in cancer and is upregulated by transforming growth factor-beta1 in keratinocytes. Lab Invest 83:1887–1899
2. Ahokas K, Lohi J, Lohi H, Elomaa O, Karjalainen-Lindsberg ML, Kere J, Saarialho-Kere U (2002) Matrix metalloproteinase-21, the human orthologue for XMMP, is expressed during fetal development and in cancer. Gene 301:31–41
3. Ahonen M, Poukkula M, Baker AH, Kashiwagi M, Nagase H, Eriksson JE, Kahari VM (2003) Tissue inhibitor of metalloproteinases-3 induces apoptosis in melanoma cells by stabilization of death receptors. Oncogene 22:2121–2134
4. Airola K, Karonen T, Vaalamo M, Lehti K, Lohi J, Kariniemi AL, Keski-Oja J, Saarialho-Kere U (1999) Expression of collagenases-1 and -3 and their inhibitors TIMP-1 and TIMP-3 correlates with the level of invasion in malignant melanomas. Br J Cancer 80:733–743
5. Balch CM, Soong S-J, Gershenwald JE, Thompson JF, Reintgen DS, Cascinelli N, Urist M, McMasters KM, Ross MI, Kirkwood JM, Atkins MB, Thompson JA, Coit DG, Byrd D, Desmond R, Zhang Y, Liu PY, Lyman GH, Morabito A (2001) Prognostic factors analysis of 17,600 melanoma patients: validation of the American Joint Committee on Cancer melanoma staging system. J Clin Oncol 19:3622–3634
6. Berking C, Takemoto R, Schaider H, Showe L, Satyamoorthy K, Robbins P, Herlyn M (2001) Transforming growth factor beta-1 increases survival of human melanoma through stroma remodelling. Cancer Res 61:8306–8316
7. Breslow A (1970) Thickness, cross-sectional areas and depth of invasion in the prognosis of cutaneous melanoma. Ann Surg 172:902–908
8. Chirivi RG, Garofalo A, Crimmin MJ, Bawden LJ, Stoppacciaro A, Brown PD, Giavazzi R (1994) Inhibition of the metastatic spread and growth of B16-B16 murine melanoma by a synthetic matrix metalloproteinase inhibitor. Int J Cancer 58:460–464
9. Clark WH Jr, From L, Bernardino EH (1969) Histogenesis and biologic behavior of primary human malignant melanoma of the skin. Cancer Res 29:705–727
10. Egeblad M, Werb Z (2002) New functions for the matrix metalloproteinases in cancer progression. Nat Rev Cancer 2: 161–174
11. Hofmann UB, Eggert AOA, Blass K, Bröcker E-B, Becker JC (2003) Expression of matrix metalloproteinases in the microenvironment of spontaneous and experimental melanoma metastases reflects the requirements for tumor formation. Cancer Res 63:8221–8225
12. Hofmann UB, Westphal JR, Van Muijen GN, Ruiter DJ (2000) Matrix metalloproteinases in human melanoma. J Invest Dermatol 115:337–344
13. Impola U, Toriseva M, Suomela S, Jeskanen L, Hieta N, Jahkola T, Grenman R, Kahari VM, Saarialho-Kere U (2003) Matrix metalloproteinase-19 is expressed by proliferating epithelium but disappears with neoplastic dedifferentiation. Int J Cancer 103:709–716
14. Impola U, Uitto VJ, Hietanen J, Hakkinen L, Zhang L, Larjava H, Isaka K, Saarialho-Kere U (2004) Differential expression of matrilysin-1 (MMP-7), 92 kD gelatinase (MMP-9), and metalloelastase (MMP-12) in oral and verrucous and squamous cell cancer. J Pathol 202:14–21
15. Kielhorn E, Provost E, Olsen D, D'Aquila TG, Smith BL, Camp RL, Rimm DL (2003) Tissue microarray-based analysis shows phosphor beta-catenin expression in malignant melanoma is associated with poor outcome. Int J Cancer 103:652–656
16. Krengel S, Alexander M, Brinckmann J, Tronnier M (2002) MMP-2, TIMP-2 and MT1-MMP are differentially expressed in lesional skin of melanocytic nevi and their expression is modulated by UV light. J Cutan Pathol 29:390–396
17. Li W, Savinov AY, Rozanov DV, Golubkov VS, Hedavat H, Postnova TI, Golubkova NV, Linli Y, Krajewski S, Strongin AY (2004) Matrix metalloproteinase-26 is associated with estrogen-dependent malignancies and targets alpha1-antitrypsinserpin. Cancer Res 64:8657–8665
18. Lohi J, Wilson CL, Roby JD, Parks WC (2001) Epilysin, a novel human matrix metalloproteinase (MMP-28) expressed in testis and in keratinocytes and in response to injury. J Biol Chem 30:10134–10144
19. Marchenko GN, Marchenko ND, Strongin AY (2003) The structure and regulation of the human and mouse matrix metalloproteinase-21 gene and protein. Biochem J 372:503
20. Marchenko ND, Marchenko GN, Weinreb RN, Lindsey JD, Kyshtoobayeva A, Crawford HC, Strongin AY (2004) Beta-catenin regulates the gene of MMP-26, a novel matrix metalloproteinase expressed both in carcinomas and normal epithelial cells. Int J Biochem Cell Biol 36:942–956
21. Marchenko GN, Ratnikov BI, Rozanov DV, Godzik A, Deryugina EI, Strongin AY (2001) Characterization of matrix metalloproteinase-26, a novel metalloproteinase widely expressed in cancer cells of epithelial origin. Biochem J 356:705–718
22. Marchenko GN, Strongin AY (2001) MMP-28, a new human matrix metalloproteinase with an unusual cysteine-switch sequence is widely expressed in tumors. Gene 265:87–93

23. Nagase H, Woessner JF (1999) Matrix metalloproteinases. J Biol Chem 274:21491–21494
24. Nikkola J, Vihinen P, Vlaykova T, Hahka-Kemppinen M, Kahari VM, Pyrhonen S (2002) High expression levels of collagenase-1 and stromelysin-1 correlate with shorter disease-free survival in human metastatic melanoma. Int J Cancer 97: 432–438
25. Nuttall RK, Pennington CJ, Taplin J, Wheal A, Yong VW, Forsyth PA, Edwards DR (2003) Elevated membrane-type matrix metalloproteinases in gliomas revealed by profiling proteases and inhibitors in human cancer cells. Mol Cancer Res 1:333–345
26. Park HI, Ni J, Gerkema FE, Liu D, Belozerov VE, Sang QX (2000) Identification and characterization of human endometase (matrix metalloproteinase-26) from endometrial tumor. J Biol Chem 275:20540-20544
27. Perrott RE, Glass LF, Reintgen DS, Fenske NA (2003) Reassessing the role of lymphatic mapping and sentinel lymphadenectomy in the management of cutaneous malignant melanoma. J Am Acad Dermatol 49:567–588
28. Saarialho-Kere U, Kerkela E, Jahkola T, Suomela S, Keski-Oja J, Lohi J (2002) Epilysin (MMP-28) expression is associated with cell proliferation during epithelial repair. J Invest Dermatol 119:14–21
29. Uria JA, Lopez-Otin C (2000) Matrilysin-2, a new matrix metalloproteinase expressed in human tumors and showing the minimal domain organization required for secretion, latency, and activity. Cancer Res 60:4745–4751
30. Väisänen A, Kallioinen M, Taskinen PJ, Turpeenniemi-Hujanen T (1998) Prognostic value of MMP-2 immunoreactive protein (72 kD type IV collagenase) in primary skin melanoma. J Pathol 186:51–58
31. Weedon D (2002) Tumors of the epidermis. In: skin pathology. Churchill Livingstone, London 753–802
32. Zhao YG, Xiao AZ, Newcomer RG, Park HI, Kang T, Chung LW, Swanson MG, Zhau HE, Kurhanewicz J, Sang QX (2003) Activation of pro-gelatinase B by endometase/matrilysin-2 promotes invasion of human prostate cancer cells. J Biol Chem 278:15056–15064

Virchows Arch (2005) 447: 961–968
DOI 10.1007/s00428-005-0045-9

ORIGINAL ARTICLE

Hajnalka Győrffy · Ágnes Holczbauer · Pál Nagy · Zsuzsa Szabó · Péter Kupcsulik · Csilla Páska · János Papp · Zsuzsa Schaff · András Kiss

Claudin expression in Barrett's esophagus and adenocarcinoma

Received: 26 May 2005 / Accepted: 18 July 2005 / Published online: 30 August 2005
© Springer-Verlag 2005

Abstract Claudins (CLDNs) are key molecules in cell adhesion, polarity, and control of paracellular solute transport. Several studies suggested that changes in claudin pattern have a role in cancer development. This study aimed to detect alterations in CLDN 1, 2, 3, 4, and 7 expression patterns in Barrett's esophagus (BE) and adenocarcinoma (ACC) compared with that in foveolar epithelium (FOV), normal squamous epithelium (SQ), and squamous cell carcinoma (SQCC). One hundred twenty five surgically or endoscopically removed, paraffin-embedded cases were studied by immunohistochemistry and analyzed statistically. BE, ACC, and FOV were dissected from 30 paraffin-embedded samples for further mRNA expression analysis. CLDN 7 was the dominating type in all epithelia and carcinomas, but its expression did not differ in normal and altered tissues. CLDN 1 expression was significantly increased in SQCC compared with that in SQ. CLDNs 3 and 4 were significantly elevated both in BE and ACC compared with that in FOV. CLDN 2 expression increased significantly in ACCs compared with that in BE. This is the first report proving similarities and differences regarding claudin expression pattern in BE and ACC compared with that in FOV and SQ. Our data prove a close link in CLDN pattern between BE and ACC, adding further evidence that BE is an alteration preceding esophageal ACC.

Keywords Barrett's esophagus · Adenocarcinoma · Claudin · Tight junction · Immunohistochemistry

H. Győrffy and Á. Holczbauer have equally contributed to this study

H. Győrffy · Á. Holczbauer · C. Páska · Z. Schaff (✉) · A. Kiss
2nd Department of Pathology, Semmelweis Medical University,
Üllői út 93,
1091 Budapest, Hungary
e-mail: schaff@korb2.sote.hu
Tel.: +36-1-2156921
Fax: +36-1-2156921

P. Nagy
Department of Pathology, National Medical Centre,
Szabolcs u. 35,
1135 Budapest, Hungary

Z. Szabó
Municipal Saint László Hospital,
Gyáli út 5-7,
1097 Budapest, Hungary

P. Kupcsulik
1st Department of Surgery, Semmelweis University,
Üllői út 78,
1082 Budapest, Hungary

J. Papp
1st Department of Internal Medicine, Semmelweis University,
Korányi Sándor u. 2/a,
1083 Budapest, Hungary

Introduction

The incidence of adenocarcinoma (ACC) of the esophagus has shown a rapid increase in the past few decades with a rate of 5–10% per year in the industrialized Western world [3, 5, 18, 25]. Since these tumors have poor prognosis, early detection and treatment are of special importance [25]. It has been proven that ACC of the distal esophagus almost always originates from epithelium that has undergone glandular metaplasia, the so-called Barrett's esophagus (BE) [10, 25].

A number of studies have characterized the biology and carcinogenetic pathways in BE using immunohistochemical and molecular biological methods [2, 9, 17, 18, 32, 36, 39–41], and there are also data related to cancer progression and survival [17].

The definition of BE has changed in the past 50 years from the macroscopically defined lesion to the present criteria [25]. It is now accepted by most authors that BE denotes a precancerous lesion where the normal squamous epithelial lining of the distal esophagus is replaced by specialized intestinal metaplasia (SIM) [25]. ACC develops in BE through a multistep sequence of molecular alterations [18], the understanding of which might allow improvement of diagnosis and better management of the disease [2]. It has been shown that altered cadherin and

catenin complexes correlate with disease progression and differentiation in the BE–dysplasia–ACC sequence [2].

Cell adhesion plays an important role in cancer development and progression [12, 15, 27]. Claudins (CLDNs), the recently identified multigene transmembrane protein family, are thought to be the major constituents of tight junctions (TJ), the most apical components of cell sealing complexes responsible for cell–cell adhesion, cell polarity, and control of paracellular ion transport [7, 22, 33]. Several recent studies have detected changes in claudin expression during carcinogenesis, as in cervical neoplasia [35], breast [16, 38], ovarian [11], pancreatic [23, 26], colorectal [24, 31], prostate [21], and other cancers. TJ proteins have even been suggested as potential antibody targets for pancarcinoma therapy [27].

The aim of the present study was to characterize the expression pattern and changes of different claudins in BE and ACC as well as to draw comparison with the foveolar epithelium (FOV; cardiac type) and with normal and neoplastic squamous epithelia. Based on our previous studies on other tissues and tumors [35, 38], it is likely that certain claudin patterns characterize the different types of glandular/columnar epithelia. Specific changes in claudin expression are anticipated during tumorous transformation. Progression through the metaplasia–carcinoma sequence may well be reflected in the changes in cell–cell contacts influenced and characterized by the TJ proteins.

Materials and methods

Tissue blocks of 125 cases were taken from surgically removed tissues and biopsies including esophageal squamous cell carcinoma (SQCC) (25 cases), BE (25 cases), and ACC (25 cases), with the permission of the Regional Ethical Committee of the Semmelweis University of Budapest (#172/2003). Twenty-five cases of normal esophageal squamous epithelia (SQ) from the distal third of the esophagus obtained from individuals who died unrelated to esophageal or gastrointestinal diseases were used for comparison. The interval between death and tissue fixation was 6 to 12 h. Further 25 biopsy specimens were also included in the study, diagnosed as FOV of the cardiac type without intestinal metaplasia, sampled by endoscopy due to macroscopic alterations. Thirty paraffin-embedded samples were chosen for further molecular biological analysis and dissected for specialized intestinal metaplastic areas of BE, ACC, and FOV components (10–10 cases from each group) then followed by total RNA isolation and mRNA expression analysis.

The age range of the SQCC cases was 48–75 years (mean 60.6), 46–63 years for the ACC (mean 52.0), 58–67 years for the BE (mean 63.2 years), and 16–75 years for the control cases (mean 55.4), respectively. The male/female ratio was equal in every group involved in the study.

The removed tissues were fixed in 4% buffered formalin for 24 h, dehydrated, and embedded in paraffin. The 3–4 μm thick sections were stained by hematoxylin–eosin (HE) and alcian blue–PAS reaction.

Paraffin sections were used for immunohistochemistry studies. The anti-CLDNs 2 and 4 antibodies were monoclonal, anti-CLDNs 1, 3 and 7 antibodies were polyclonal purified from rabbit antiserum (Zymed, San Francisco, CA, USA). First, the slides were treated for 30 min in a target retrieval solution (Dako, Glostrup, Denmark) in a microwave oven, followed by incubation with the primary antibody at a 1:80 dilution at room temperature for 1 h. For visualization, a standard avidin–biotin peroxidase technique (ABC system, Dako) was used with diaminobenzidine as chromogen. The sections were counterstained with hematoxylin. For each CLDN, a negative control with omission of the primary antibody was included. Colon carcinoma and endometrial tissue samples previously shown to express different CLDNs [28] served as positive controls. The reactions were carried out in a Ventana ES automatic immunostainer (Ventana Medical Systems Inc., Tucson, AZ, USA) using the reagents provided by the manufacturer.

The number of positive cells was calculated as follows: 10 randomly selected areas per slide were analyzed using ×20 objective with 100 cells counted in each field. The scoring standardized for each group was as follows: 5=80 to 100%, 4=60 to 80%, 3=40 to 60%, 2=20 to 40%, 1=5 to 20% and 0≤5% of the cells showed positive reactions.

For *statistical analysis*, the Mann–Whitney *U* test was used to compare the expression of individual CLDNs in the different groups.

Real-time RT-PCR for CLDN 2, CLDN 3, CLDN 4, and GAPDH mRNA detection

Tissue specimens

The sample set consisted of ten formalin-fixed, paraffin-embedded ACCs, ten cases of BE and ten foveolar glandular epithelial tissues.

RNA isolation

Total RNA from formalin-fixed paraffin, embedded-tissues was isolated with High Pure RNA Paraffin Kit (Roche, Indianapolis, IN, USA). Depending on the size of the dissected area, two to eight 5-μm-thick sections were cut from each tissue block. Samples from the Barrett's and foveolar epithelia were microdissected to select the areas of SIM of BE and the columnar epithelial cells without goblet cells. Proteinase K digestion time was 16 h for each sample. All purifications were performed in accordance with the manufacturer's protocol. After total RNA isolation, samples were kept at −80°C until use. Total RNA integrity was verified as described previously [28].

Reverse transcription of RNA

Total RNA (500 ng) was reverse transcribed for 50 min at 42°C in 30 μl with MulV reverse transcriptase (Applied

Biosystems, Foster City, CA, USA) in the presence of RNAse inhibitor (Applied Biosystems), using Random Hexamers (Applied Biosystems).

Real-time quantitative RT-PCR

Real-time PCR reaction was performed with 2 μl cDNA template in a total volume of 25 μl, using the ABI Prism 7000 sequence detection system (Applied Biosystems). Each PCR was conducted in 25 μl volume of SYBR Green Supermix (Bio-Rad, Hercules, CA, USA, 1708851). Primer sequences were as follows: CLDN 2 (GI: 9966780), forward 5′-CTCCCTGGCCTGCATTATCTC-3′ (273–293), reverse 5′-ACCTGCTACCGCCACTCTGT-3′ (344–363); CLDN 3 (GI: 21536298), forward 5′-CTGCTCTGCTGCTCGTGTCC-3′ (732–751), reverse 5′-TTAGACGTAGTCCTTGCGGTCGTAG-3′ (836–860); CLDN 4 (GI: 14790131), forward 5′-GGCTGCTTTGCTGCAACTGTC-3′ (741–761), reverse 5′-GAGCCGTGGCACCTTACACG-3′ (829–848) [36]; GAPDH (GI: 7669491), forward 5′-CATTGACCTCAACTACATGG-3′ (186–205), reverse 5′-GAAGATGGTGATGGGATTTC-3′ (287–306) and β-actin (GI:15928802) forward 5′-CCTGGCACCCAGCACAAT-3′ (1031–1048), reverse 5′-GGGCCGGACTCGTCATAC-3′ (1157–1174).

PCR was done in duplicates in 96-well plates, for 2 min at 95°C for initial denaturing, then 40 cycles at 95°C for 20 s, at 63°C for 30 s and 72°C for 1 min. Data analysis and statistical evaluation were performed by REST (expression software tool, http://www.wzw.tum.de/gene-quantification)

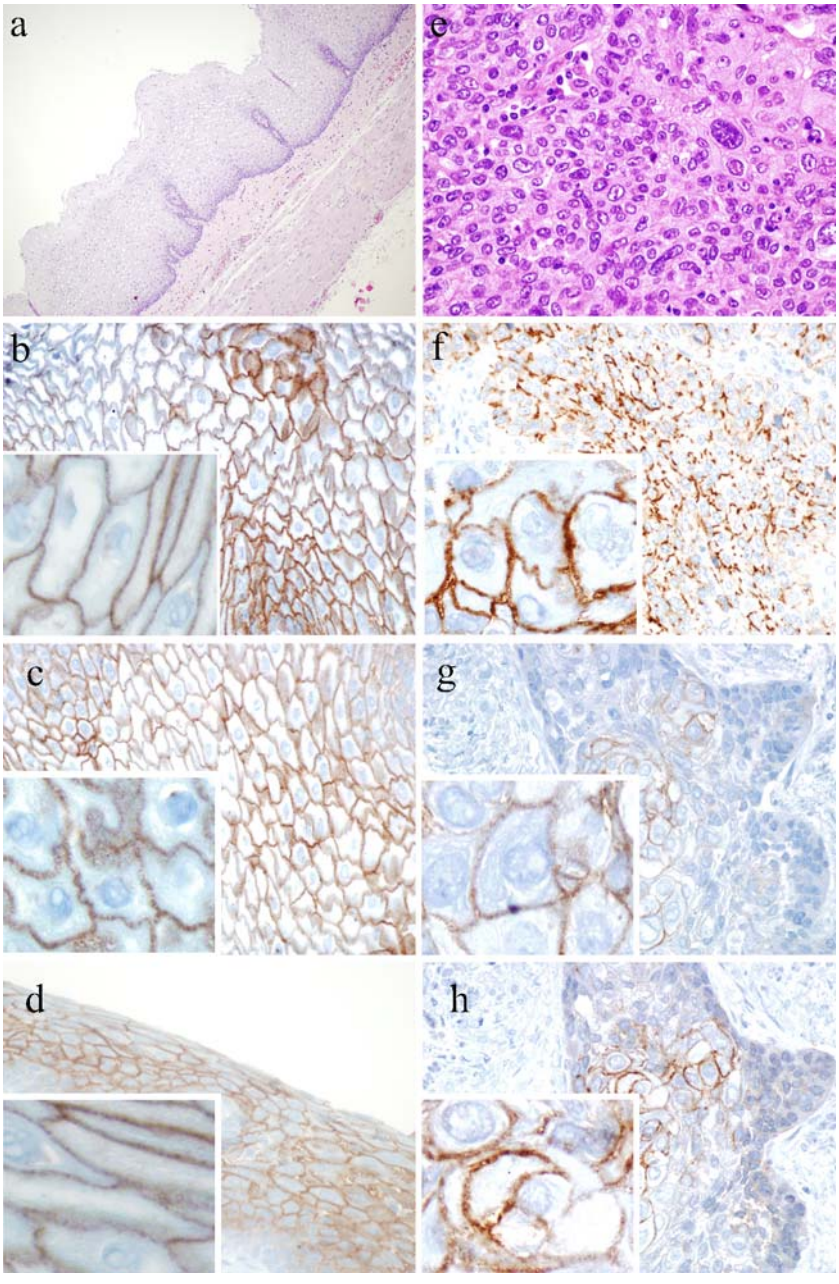


Fig. 1 Normal stratified squamous epithelium (**a**–**d**) and squamous cell carcinoma (**e**–**h**). Immunohistochemical detection of CLDN 1 (**b**, **f**), CLDN 4 (**c**, **g**), and CLDN 7 (**d**, **h**). "Typical" membranous stainings. HE (**a**, **e**), ×150, ×250; hematoxylin counterstain (**b**–**h**), ×250; insets, ×750

[29], using the average of GAPDH and β-actin as reference genes.

Results

Immunohistochemistry

Normal stratified squamous epithelium (Fig. 1a–d) CLDNs 1, 4, and 7 gave a membranous reaction in the suprabasal layer of the epithelium showing a honeycomb appearance. The strongest, most extended reaction was seen with CLDN 7 (Fig. 1d). CLDN 2 reacted in a granular pattern, outlining the cell membrane and sometimes found localized intracytoplasmatically. No CLDN 3 could be detected. The number of cells reacting with the individual CLDN antibodies was variable (Fig. 3). The highest number of positive cells was seen with CLDN 7, followed, in order, by CLDNs 4, 2, and 1 (Fig. 3; Table 1).

Squamous cell carcinoma (Fig. 1e–h) The pattern and staining intensity in SQCC did not change in comparison with that in SQ. The "honeycomb" membraneous staining of the cancer cells for CLDNs 1, 4, and 7 (Fig. 1f–h) was similar to that of the normal cells. The number of positive cells, however, increased significantly in case of CLDN 1 (Fig. 3; Table 1); it was higher, though not significant for CLDN 4, and was equally high for CLDN 7 (Fig. 3; Table 1).

Foveolar epithelium (Fig. 2a–f) The strongest reactions were detected for CLDNs 1 and 7, while CLDNs 2 and 3 were negative. CLDN 4 was positive in only a low percentage of the cells (Figs. 2e and 3).

Barrett's esophagus (Fig. 2g–l) A significant increase in staining intensity and number of positive cells was seen for CLDNs 3 and 4 (Fig. 2j–k), as compared with the FOV (Fig. 3; Table 1). Strong reactions were detected for CLDNs 1 and 7 (Fig. 2h,l) too, but the number of positive cells did not significantly differ from that observed in the FOV, where it was already highly expressed. CLDN 2 reaction was detected in a small percentage of the cells (Fig. 3).

Adenocarcinoma (Fig. 2m–s) In the ACCs, the pattern of CLDN expression was similar to that in BE for CLDNs 3 and 4 (Fig. 2p–r), with a significant increase in CLDN expression noticeable when compared with that in the FOV (Fig. 3; Table 1). Interestingly, CLDN 2 showed a considerable increase (Fig. 2o; Table 1), which was significantly higher in comparison with both BE and FOV.

Both similarities and differences could be noted when comparing CLDN expression in the squamous and foveolar epithelia, BE and carcinomas (Fig. 3; Table 1). CLDN 7 was the dominating type in all epithelia and carcinomas studied in the esophagus, without significant changes in the normal and altered epithelia and tumors. In SQCC, CLDN 1 showed considerable increase as compared with that in SQ. CLDNs 3 and 4 were the prominently elevated types both in BE and ACC when compared with that in FOV. CLDN 2 increased significantly in the ACCs as compared with that in BE.

mRNA expression of CLDNs 2, 3, and 4 detected by real-time RT-PCR The CLDNs which showed significant, characteristic differences at the protein level between BE and ACCs were further studied. mRNA expression analysis of representative and dissected samples comparing FOV with BE and ACC showed that mRNA expression of certain CLDNs reflected parallel changes that were found with the protein production of these dissected tissue components. Increased CLDN 3 and 4 expressions were detected at the mRNA level both in BE and in ACC, in contrast to FOV. Real-time RT-PCR analysis revealed CLDN 2 mRNA expression to be higher in ACC than in FOV, coinciding with the immunohistochemical results. The significantly increased CLDN 2 mRNA expression, however, was not found to be parallel with the slightly increased protein expression noted in BE as compared with that in FOV (Figs. 4 and 5; Table 2).

Table 1 Results of the immunostaining for claudins in different esophageal epithelia and carcinomas*

	CLDN 1	CLDN 2	CLDN 3	CLDN 4	CLDN 7
FOV–BE	3.8–3.0	0.0–0.22	0.0–3.4	0.8–4.4	4.8–5.0
	NS	NS	p=0.0025	p=0.0012	NS
FOV–ACC	3.8–2.45	0.0–3.8	0.0–3.9	0.8–3.6	4.8–4.9
	NS	p=0.0022	p=0.0064	p=0.0107	NS
BE–ACC	3.0–2.45	0.22–3.8	3.4–3.9	4.4–3.6	5.0–4.9
	NS	p=0.0001	NS	NS	NS
SQ–SQCC	0.53–3.5	1.13–0.3	0.0–0.2	1.73–3.3	4.6–4.8
	p=0.0161	NS	NS	NS	NS

$p<0.05$

*Means and probability values by Mann–Whitney U test for pairwise comparison of claudins

p significance, *NS* not significant, *CLDN* claudin, *FOV* foveolar epithelium, *BE* Barrett's esophagus, *SQ* squamous epithelium, *ACC* adenocarcinoma, *SQCC* squamous cell carcinoma

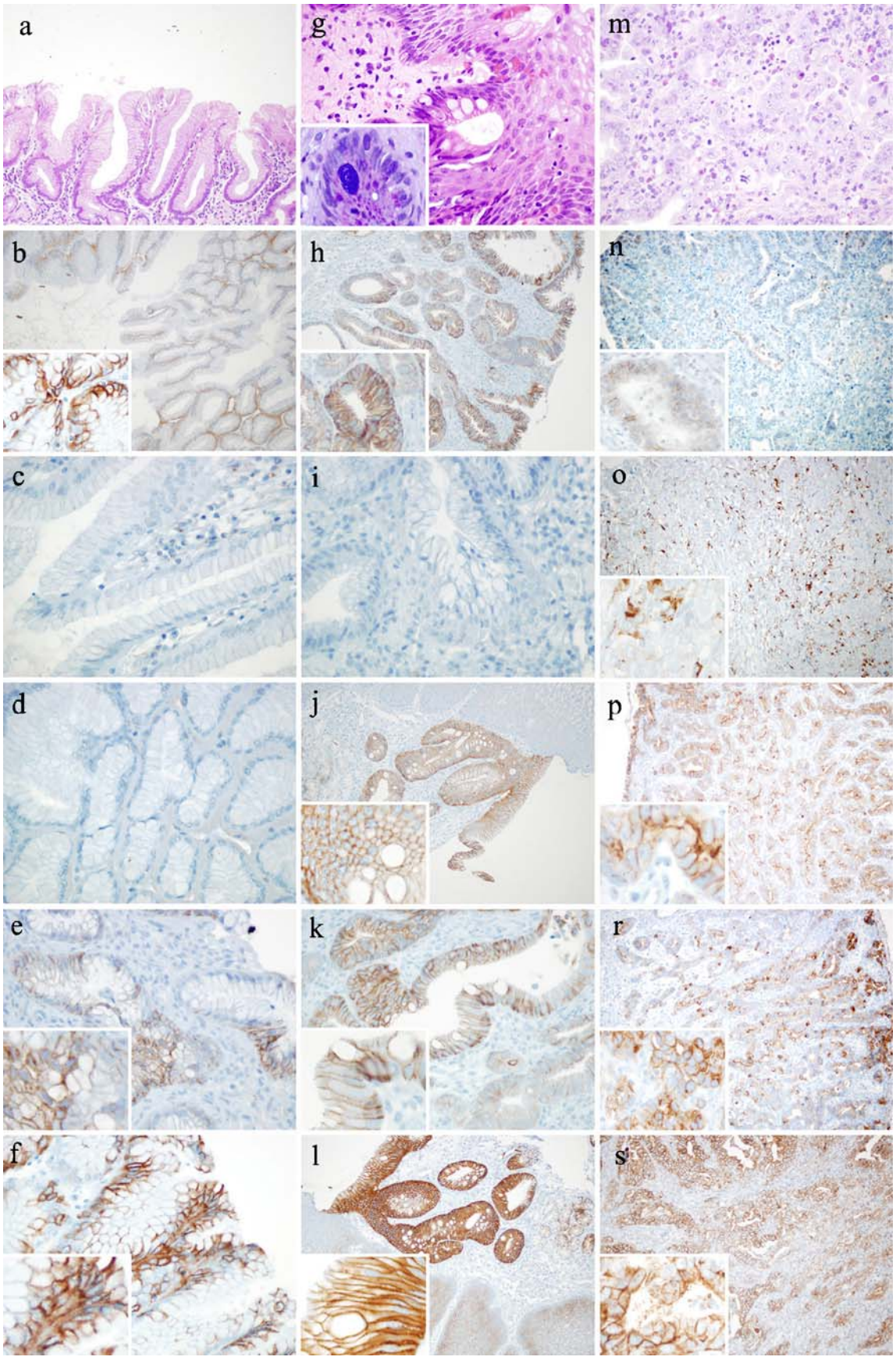


Fig. 2 Foveolar epithelium (**a**–**f**), Barrett's esophagus (**g**–**l**) and adenocarcinoma (**m**–**s**). Immunohistochemical detection of CLDN 1 (**b**, **h**, **n**), CLDN 2 (**c**, **i**, **o**), CLDN 3 (**d**, **j**, **p**), CLDN 4 (**e**, **k**, **r**), and CLDN 7 (**f**, **l**, **s**). Linear membranous and granular (for CLDN 2) stainings. HE (**a**, **g**, **m**), ×150; alcian blue-PAS (**g**, inset), ×750; hematoxylin counterstain (**b**–**s**), ×250; inset, ×750

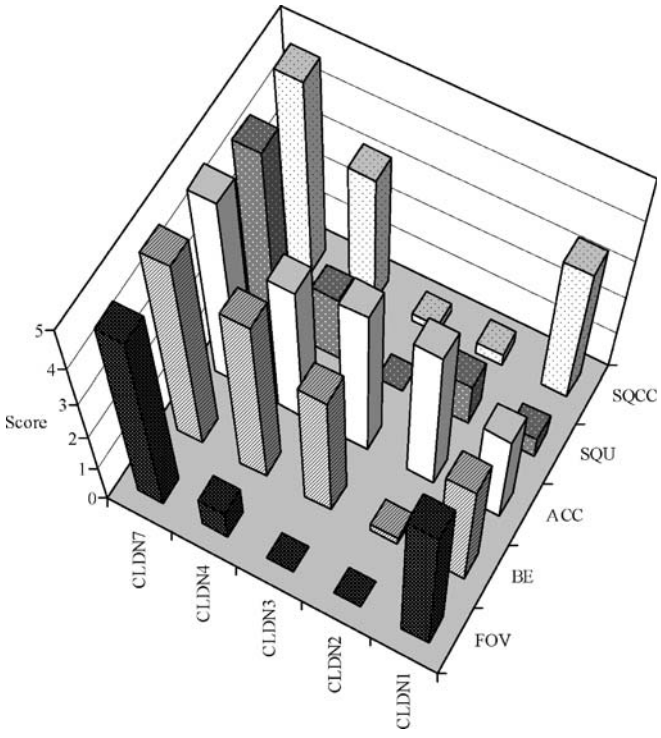


Fig. 3 Bar diagrams illustrating the difference in CLDN expression detected by immunohistochemistry and evaluated by semiquantitative scoring. *BE* Barrett's esophagus, *ACC* adenocarcinoma, *FOV* foveolar epithelium, *SQ* normal squamous epithelium, *SQCC* squamous cell carcinoma

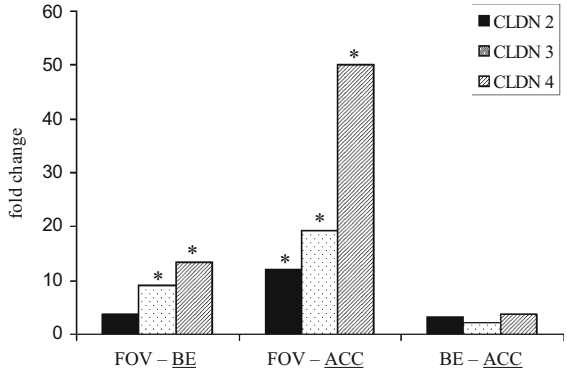


Fig. 4 mRNA expression analysis of foveolar epithelium, Barrett's esophagus, and adenocarcinoma (data shown in Table 2). Data indicate the fold change differences in the expression of claudins in the underlined group compared with the other group. *Significant difference, *CLDN* claudin, *FOV* foveolar epithelium, *BE* Barrett's esophagus, *ACC* adenocarcinoma

Discussion

Our study has shown that besides CLDNs 1 and 7, CLDNs 3 and 4 are the main characteristic types of claudins both in BE and in ACC. The expressions of CLDNs 3 and 4 in BE and ACC differ considerably from both the unaltered squamous and foveolar epithelium. These findings associate the SIM of the BE and ACC, clearly distinguishing them from FOV, showing no sign of intestinal metaplasia. The presented data demonstrate that BE differs from FOV even in such a basic characteristic feature as the molecular composition of the main sealing complex—the TJs.

Several studies have described the specific molecular changes that are likely to progress to carcinoma in the esophagus, as changes in protein expression [2], genomic, and chromosomal alterations [39, 41], etc. The best predictor, however, is still the histologic identification of dysplasia [25].

Previously, three types of glandular epithelia were accepted as being a characteristic of BE [25]. More recently, however, the SIM located in the distal esophagus was found to be associated with increased risk to develop ACC [25] and was established as a precancerous lesion. The detection of CLDNs 3 and 4 further helps the definition of "specialized intestinal" epithelium. The increased CLDN 3 and 4 expressions in BE and ACC in contrast to FOV could be demonstrated both at protein and mRNA levels. These data implicate that the expression of these adhesion molecules is regulated at the mRNA transcription level. BE and ACC can therefore be grouped together based on the claudin expression changes, which might further strengthen the link between these two entities in the carcinogenesis sequence.

Other cell adhesion molecules have also been studied in esophageal carcinomas and BE, in relation to prognosis and tumor behavior. Downregulation of CD44s and CD44v4 was described to result in a significantly poorer prognosis for patients with esophageal ACC; expression of CD44v4 proved to be an independent factor in prognosis [4]. Overexpression of alpha-6 integrin was found in 87% of esophageal ACC cases investigated [37] further; cDNA microarray experiments revealed that the expression of alpha-3 and alpha-6 integrins was upregulated in the tumor tissue. This result, however, did not correlate with the clinicopathological features [13].

The transmembrane protein family of claudins is the main component of TJs responsible for maintaining cell polarity, cellular arrangement, adhesion, and paracellular fluid transport. At least two transmembrane CLDN molecules (generally more) characterize each cell and tissue type [7]. This is partly due to the different function of the epithelium: "leaky" or more resistant type [42]. The heterogeneous claudin types are copolymerized to form individual TJs [7]. Homophylic and heterophylic interactions with other claudins as well as with other TJ-related proteins, as occludin, JAM, and ZO1, define the characteristics and function of TJs [19, 34]. The epithelia in different organs and even within the same organ differ qualitatively in their overall ability to regulate paracellular solute and ion movement, and this difference is defined by the quality and complexity of the TJs [34]. Disruption of the TJs due to the change in correlation between the individual CLDNs might lead to the reduction of TJ function [34].

Glandular epithelia have been proven to show a characteristic pattern of CLDNs, including breast [16, 38], pancreas [26], prostate [21], etc., which might be conserved during carcinogenesis, at least qualitatively. Several reports, however, detected increased expression of TJ proteins in carcinomas as in bile duct [20], or pancreatic

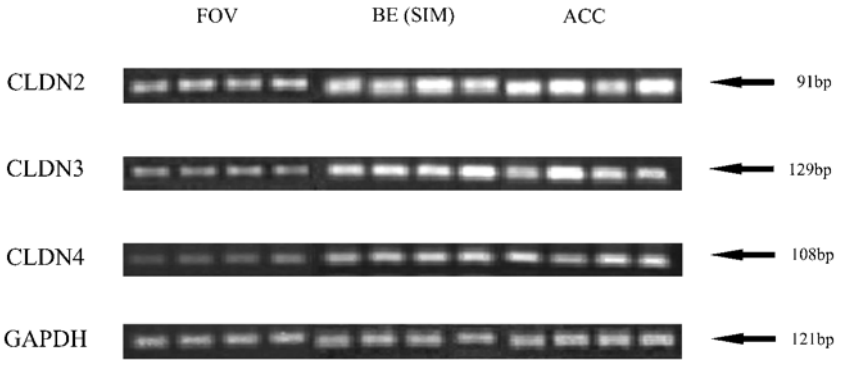


Fig. 5 Electrophoresis of RT-PCR products on 2% agarose gel. *CLDN* claudin, *GAPDH* glyceraldehyde-3-phosphate dehydrogenase, *FOV* foveolar epithelium, *BE (SIM)* Barrett's esophagus (specialized intestinal metaplasia), *ACC* adenocarcinoma, *bp* base pairs

Table 2 Fold change differences in the expression of claudins based on the real-time RT-PCR reactions

	CLDN 2 GAPDH–β-actin	CLDN 3 GAPDH–β-actin	CLDN 4 GAPDH–β-actin
FOV–BE	U 3.735	U 9.085*	U 13.366*
	NS	p=0.032	p=0.001
BE–ACC	U 3.237	U 2.129	U 3.744
	NS	NS	NS
FOV–ACC	U 12.087*	U 19.338*	U 50.047*
	p=0.0095	p=0.0035	p=0.001

Relative quantification was carried out using the mean of GAPDH and β-actin as reference genes. The underlined group is compared to the other group

$p<0.05$

*Significant difference

p significance, *U* upregulated, *NS* not significant, *CLDN* claudin, *GAPDH* glyceraldehyde-3-phosphate dehydrogenase, *FOV* foveolar epithelium, *BE* Barrett's esophagus, *ACC* adenocarcinoma

cancers [26]. CLDN 4 protein was significantly higher in BE and esophageal ACCs than in the foveolar glandular or squamous epithelia in our study too.

The increased expressions of CLDNs 3 and 4 are of specific interest since these CLDNs have been known as receptors for the cytotoxic *Clostridium perfringens* enterotoxin (CPE) [14]. CPE treatment might cause cell death by increasing membrane permeability, and, more recently, CLDN 4 has been suggested as a future target for adjuvant therapy in tumors expressing this TJ protein, namely cancers of the breast [16], prostate [21], pancreas [23, 26], ovary [11], and bile ducts [20]. From this point of view, our findings that both BE and ACC highly express CLDN 4 might be of further specific interest.

In addition to CLDNs 3 and 4, significant increase in CLDN 2 expression was detected in ACCs as compared with that in BE and FOV in our study at the protein expression level. This, however, was not shown regarding mRNA expression when comparing BE and ACC. Recent observations have suggested that optimal CLDN 2 expression in the gut is required for regulation of the intestinal barrier function and plays a role in enterocyte differentiation [6]. The significant increase in CLDN 2 expression in the esophageal adenocarcinomas in our study might suggest a sign of perturbation during carcinogenesis, being the type of claudin associated with intestinal differentiation. CLDN 2 is considered to form ion-selective channels in TJs of epithelial cells [1, 8, 30], functions as a measure of integrity of TJs [34], and is inversely proportional to transepithelial resistance. Therefore, in the present study, the increase of this protein in esophageal ACCs might suggest a "functional decrease" of TJ integrity.

The increased CLDN 2 expression in ACC at protein level might further help to define the multistep process of esophageal carcinogenesis. Moreover, our data exhibit the characteristic upregulation of CLDNs 3 and 4 in both BE and ACC and add evidence to the link between these two entities, possibly also advocating the use of these two TJ proteins as differentiation markers.

Acknowledgements This work was supported by grants NKFP-1A/0023/2002 from the Hungarian Ministry of Health, National Research Development Projects; OTKA T 049559 from the National Science Research Foundation; and ETT-077/2003 from the Hungarian Ministry of Health.

References

1. Amasheh S, Meiri N, Gitter AH, Schoneberg T, Mankertz J, Schulzke JD, Fromm M (2002) Claudin-2 expression induces cation-selective channels in tight junctions of epithelial cells. J Cell Sci 115:4969–4976
2. Bailey T, Biddlestone L, Shepher N, Barr H, Warner P, Jankowski J (1998) Altered cadherin and catenin complexes in the Barrett's esophagus–dysplasia–adenocarcinoma sequence. Correlation with disease progression and dedifferentiation. Am J Pathol 152:135–144
3. Blot WJ, Devesa SS, Kneller RW, Fraumeni JF Jr (1991) Rising incidence of adeno-carcinoma of the esophagus and gastric cardia. JAMA 265:1287–1289
4. Bottger TC, Youssef V, Dutkowski P, Maschek H, Brenner W, Junginger T (1998) Expression of CD44 variant proteins in adenocarcinoma of Barrett's esophagus and its relation to prognosis. Cancer 83:1074–1080
5. Cameron AJ (2002) Epidemiology of Barrett's esophagus and adenocarcinoma. Dis Esophagus 15:106–108
6. Escaffit F, Boudreau F, Beaulieu JF (2005) Differential expression of claudin-2 along the human intestine: implication of GATA-4 in the maintenance of claudin-2 in differentiating cells. J Cell Physiol 203:15–26
7. Furuse M, Sasaki H, Tsukita S (1999) Manner of interaction of heterogeneous claudin species within and between tight junction strands. J Cell Biol 147:891–903
8. Furuse M, Furuse K, Sasaki H, Tsukita S (2001) Conversion of zonulae occludentes from tight to leaky strand type by introducing claudin-2 into Madin-Darby canine kidney I cells. J Cell Biol 153:263–272

9. Hamelin R, Flejou JF, Muzeau F, Potet F, Laurent-Puig P, Fekete F, Thomas G (1994) TP53 gene mutations and p53 protein immunoreactivity in malignant and premalignant Barrett's esophagus. Gastroenterology 107:1012–1018
10. Hamilton SR, Smith RR (1987) The relationship between columnar epithelial dysplasia and invasive adenocarcinoma arising in Barrett's esophagus. Am J Clin Pathol 87:301–312
11. Heinzelmann-Schwarz VA, Gardiner-Garden M, Henshall SM, Scurry J, Scolyer RA, Davies MJ (2004) Overexpression of the cell adhesion molecules DDR1, Claudin 3, and Ep-CAM in metaplastic ovarian epithelium and ovarian cancer. Clin Cancer Res 10:4427–4436
12. Hirohashi S, Kanal Y (2003) Cell adhesion system and human cancer morphogenesis. Cancer Sci 94:575–581
13. Hourihan RN, O'Sullivan GC, Morgan JG (2003) Transcriptional gene expression profiles of oesophageal adenocarcinoma and normal oesophageal tissues. Anticancer Res 23:161–165
14. Katahira J, Inoue N, Horiguchi Y, Matsuda M, Sugimoto N (1997) Molecular cloning and functional characterization of the receptor for *Clostridium perfringens* enterotoxin. J Cell Biol 136:1239–1247
15. Kimura Y, Shiozaki H, Hirao M, Maeno Y, Doki Y, Inoue M, Monden T Ando-Akatsuka Y, Furuse M, Tsukita S, Monden M (1997) Expression of occludin, tight-junction-associated protein, in human digestive tract. Am J Pathol 151:45–54
16. Kominsky SL, Argani P, Korz D, Evron E, Raman V, Garrett E, Rein A, Sauter G, Kallioniemi O-P, Sukumar S (2003) Loss of the tight junction protein claudin-7 correlates with histological grade in both ductal carcinoma in situ and invasive ductal carcinoma of the breast. Oncogene 22:2021–2033
17. Krishnadath KK, Tilanus HW, van Blankenstein M, Hop WCJ, Kremers ED, Dinjens WNM, Bosman FT (1997) Reduced expression of the cadherin–catenin complex in oesophageal adenocarcinoma correlates with poor prognosis. J Pathol 182:331–338
18. Lagorce-Pagès C, Paraf F, Wendum D, Martin A, Fléjou J-F (2004) Expression of inflammatory secretory phospholipase A2 and cytosolic phospholipase A2 in premalignant and malignant Barrett's oesophagus. Virchows Arch 444:426–435
19. Langbein L, Grund C, Kuhn C, Praetzel S, Kartenbeck J, Brandner JM, Moll I, Franke WW (2002) Tight junctions and compositionally related junctional structures in mammalian stratified epithelia and cell cultures derived therefrom. Eur J Cell Biol 81:419–435
20. Lódi C, Kiss A, Holczbauer Á, Batmunkh E, Paku S, Illyés G, Kupcsulik P, Schaff Z (2004) High expression of claudin 4 in human cholangiocellular carcinomas. Gastroenterology Week Freiburg 2004: Gastroenterology yesterday–today–tomorrow: a review and preview. FALK symposium no. 144, Freiburg, Germany, October 16–17
21. Long H, Crean CD, Lee WH, Cummings OW, Gabig TG (2001) Expression of *Clostridium perfringens* enterotoxin receptors claudin-3 and claudin-4 in prostate cancer epithelium. Cancer Res 61:7878–7881
22. Matsuda M, Kubo A, Furuse M, Tsukita S (2004) A peculiar internalization of claudins, tight junction-specific adhesion molecules, during the intercellular movement of epithelial cells. J Cell Sci 117:1247–1257
23. Michl P, Buchholz M, Rolke M, Kunsch S, Lohr M, McClane B, Tsukita S, Leder G, Adler G, Gress TM (2001) Claudin-4: a new target for pancreatic cancer treatment using *Clostridium perfringens* enterotoxin. Gastroenterology 121:678–684
24. Miwa N, Furuse M, Tsukita S, Niikawa N, Nakamura Y, Furukawa Y (2001) Involvement of claudin-1 in the β-catenin/Tcf signaling pathway and its frequent upregulation in human colorectal cancers. Oncol Res 12:469–476
25. Mueller J, Werner M, Stolte M (2004) Barrett's esophagus: histopathologic definitions and diagnostic criteria. World J Surg 28:148–154
26. Nichols LS, Ashfaq R, Iacobuzio-Donahue CA (2004) Claudin 4 protein expression in primary and metastatic pancreatic cancer: support for use as a therapeutic target. Am J Clin Pathol 121:226–230
27. Offner S, Hekele A, Teichmann U, Weinberger S, Gross S, Kufer P, Itin C, Baeuerle PA, Kohleisen B (2004) Epithelial tight junction proteins as potential antibody targets for pancarcinoma therapy. Cancer Immunol Immunother 54:431–445
28. Páska C, Bögi K, Szilák L, Tőkés AM, Szabó E, Sziller I, Rigó J, Sobel G, Szabó I, Kaposi-Novák P, Kiss A, Schaff Z (2004) Effect of formalin, acetone and RNAlater fixatives on tissue preservation and different size amplicons by real-time PCR from paraffin-embedded tissue. Diagn Mol Pathol 13:234–240
29. Pfaffl MW, Horgan GW, Dempfle L (2002) Relative expression software tool (REST) for group-wise comparison and statistical analysis of relative expression results in real-time PCR. Nucleic Acids Res 30:e36
30. Rahner C, Mitic LL, Anderson JM (2002) Heterogeneity in expression and subcellular localization of claudins 2, 3, 4 and 5 in the rat liver, pancreas, and gut. Gastroenterology 120: 411–422
31. Resnick MB, Konkin T, Routhier J, Sabo E, Pricolo VE (2005) Claudin-1 is a strong prognostic indicator in stage II colonic cancer: a tissue microarray study. Mod Pathol 18:511–518
32. Sarbia M, Donner A, Franke C, Gabbert HE (2004) Distinction between intestinal metaplasia in the cardia and in Barrett's esophagus: the role of histology and immunohistochemistry. Human Pathol 35:371–376
33. Sawada N, Murata M, Kikuchi K, Osanai M, Tobioka H, Kojima T, Chiba H (2003) Tight junctions and human diseases. Med Electron Microsc 36:147–156
34. Singh AB, Harris RC (2004) Epidermal growth factor receptor activation differentially regulates claudin expression and enhances transepithelial resistance in Madin-Darby canine kidney cells. J Biol Chem 279:3543–3552
35. Sobel G, Páska C, Szabó I, Kiss A, Kádár A, Schaff Z (2005) Increased expression of claudins in cervical squamous intraepithelial neoplasia and invasive carcinoma. Human Pathol 36: 162–169
36. Swami S, Kumble S, Triadafilopoulos G (1995) E-cadherin expression in gastro-esophageal reflux disease, Barrett's esophagus, and esophageal adenocarcinoma: an immunohistochemical and immunoblot study. Am J Gastroenterol 90:1808–1813
37. Tanaka Y, Mimori K, Shiraishi T, Okhura Y, Takubo K, Mafune K, Barnard GF, Mori M (2000) Alpha 6 integrin expression in esophageal carcinoma. Int J Oncol 16:725–729
38. Tőkés AM, Kulka J, Paku S, Szik Á, Páska Cs, Kaposi Novák P, Szilák L, Kiss A, Bögi K, Schaff Zs (2005) Claudin 1, 3 and 4 and proteins and mRNA expression in benign and malignant breast lesions: a research study. Breast Cancer Res 7:R296–R305
39. van Dekken H, Geelen E, Dinjens WN Wijnhoven BP, Tilanus HW, Tanke HJ, Rosenberg C (1999) Comparative genomic hybridization of cancer of the gastro-esophageal (Barrett's) and gastric cardia adenocarcinomas. Cancer Res 59:748–752
40. Vieth M, Schneider-Stock R, Röhrich K, May A, Ell C, Markwarth A, Roessner A, Stolte M, Tannapfel A (2004) INK4a-ARF alterations in Barrett's epithelium, intraepithelial neoplasia and Barrett's adenocarcinoma. Virchows Arch 445: 135–141
41. Walch A, Specht K, Bink K, Zitzelbarger H, Braselmann H, Bauer M, Aubele M, Stein H, Siewert JR, Hofler H, Werner M (2001) Her-2/neu gene amplification, elevated mRNA expression and protein overexpression in the metaplasia–dysplasia–adenocarcinoma sequence of Barrett's esophagus. Lab Invest 81:791–801
42. Weng XH, Beyenbach KW, Quaroni A (2005) Cultured monolayers of the dog jejunum with the structural and functional properties resembling the normal epithelium. Am J Physiol Gastrointest Liver Physiol 288:G705–G717

Virchows Arch (2005) 447: 969–977
DOI 10.1007/s00428-005-0044-x

ORIGINAL ARTICLE

**Giuseppe Pelosi · Aldo Scarpa · Giulia Veronesi
Lorenzo Spaggiari · Barbara Del Curto · Patrick S. Moore
Patrick Maisonneuve · Angelica Sonzogni · Michele Masullo
Giuseppe Viale**

A subset of high-grade pulmonary neuroendocrine carcinomas shows up-regulation of matrix metalloproteinase-7 associated with nuclear β-catenin immunoreactivity, independent of EGFR and HER-2 gene amplification or expression

Received: 18 May 2005 / Accepted: 4 July 2005 / Published online: 13 September 2005
© Springer-Verlag 2005

Abstract Nuclear translocation of β-catenin has been correlated with epidermal growth factor receptor (EGFR) overexpression/activation in nonsmall cell lung cancer. Less is known on β-catenin transactivation in high-grade pulmonary neuroendocrine tumors and on the status of β-catenin activating EGFR and human epidermal growth factor receptor 2 (HER-2) or β-catenin target genes cyclin D1 and matrix metalloproteinase-7 (MMP-7). β-catenin immunoreactivity was evaluated in 51 large-cell neuroendocrine carcinomas (LCNEC) and 45 small-cell lung carcinomas (SCLC). Nineteen cases were assessed for *β-catenin* gene exon 3 mutations, expression of MMP-7, and expression/gene amplification of EGFR, HER-2, and cyclin D1. β-catenin was expressed in all 96 high-grade neuroendocrine tumors, the vast majority (94%) showing >50% immunopositive cells. A disarrayed immunoreactivity, however, was commonly encountered consisting in variably altered membrane-associated patterns of staining along with progressive accumulation of cytoplasmic immunoreactivity. In LCNEC, but not in SCLC, the disarrayed patterns correlated with EGFR and HER-2 protein expression. β-catenin nuclear accumulation was found in nine tumors, including seven LCNEC and two SCLC, and was always associated with disarrayed immunoreactivity and increased MMP-7, but not cyclin D1 expression. These cases, however, did not show *β-catenin* gene mutations or EGFR and HER-2 gene amplification or expression. No association was found between nuclear β-catenin and any clinicopathological variable including patients' survival. The subcellular compartmentalization of β-catenin is profoundly altered in high-grade pulmonary neuroendocrine tumors. A minor subset of these tumors shows β-catenin nuclear accumulation in association with increased expression of MMP-7, but not of cyclin D1, independent of EGFR and HER-2 gene amplification or expression.

Keywords Lung · Neuroendocrine carcinoma · β-catenin · EGFR · MMP-7

The authors have no significant financial or other relationship with the manufacturers of any commercial products or commercial services presented in this paper

G. Pelosi · B. Del Curto · A. Sonzogni · M. Masullo · G. Viale
Division of Pathology and Laboratory Medicine,
European Institute of Oncology
and University of Milan School of Medicine,
Milan, Italy

A. Scarpa · P. S. Moore
Department of Pathology
University of Verona,
Verona, Italy

G. Veronesi · L. Spaggiari
Division of Thoracic Surgery
European Institute of Oncology,
Milan, Italy

P. Maisonneuve
Division of Epidemiology and Biostatistics,
European Institute of Oncology,
Milan, Italy

G. Pelosi (✉)
Divisione di Anatomia Patologica
e Medicina di Laboratorio, Istituto Europeo di Oncologia,
Via G. Ripamonti, 435,
I-20141 Milano, Italy
e-mail: giuseppe.pelosi@ieo.it
Tel.: +39-02-57489414
Fax: +39-02-57489417

Introduction

A family of closely related structural cytoplasmic proteins, namely, α-, β-, γ-catenin, tightly connects the transmembrane glycoprotein E-cadherin to the underlying

cytoskeleton network [13, 58] to form a highly effective Ca^{2+}-dependent epithelial cell-cell homophylic adhesion complex at the adherens junctions [17, 53], essential for maintaining normal tissue architecture and morphogenesis [16]. In particular, β-catenin interacts directly with the intracellular domain of E-cadherin, connecting it to the actin cytoskeleton via another actin-binding protein, α-catenin, which in turn binds to vinculin, α-actinin, and zonula occludens-1 [33]. At variance with this spatially segregated and stable pool at the cell membrane, freely-soluble cytoplasmic β-catenin is usually phosphorylated by binding to axin/conductin, glycogen synthase kinase-3β (GSK-3β), and the adenomatous polyposis coli protein (APC) [18, 45, 51] and rapidly degraded via the ubiquitin/proteasome pathway [1]. This mechanism prevents an inappropriate cytoplasmic accumulation of stabilized, hypophosphorylated β-catenin that, after translocation to the nucleus, might be responsible for several biological effects, including increased expression of target genes, such as cyclin D1 [54] and matrix metalloproteinase-7 (MMP-7)/matrilysin [6, 10], augmentation of ligand-dependent activity of androgen receptor [60], or enhancement of vitamin D receptor activity [36]. In general, nuclear accumulation of hypophosphorylated β-catenin may derive from inhibition of the GSK-3β-dependent β-catenin phosphorylation via activation of Wnt/Wingless signal transduction cascade, loss-of-function mutations of *APC*, *AXIN* or *CTNNB1* (encoding for β-catenin), or overexpression/activation of growth factors, such as epidermal growth factor receptor (EGFR), causing β-catenin to dissociate from the membrane E-cadherin complex [27, 28]. Therefore, it is not surprising that dysregulation of β-catenin by a variety of different molecular mechanisms may play major role in several human diseases, including certain types of cancer [43].

Dysregulation of the E-cadherin/β-catenin-dependent adhesion complex has been associated with the development and progression of endocrine-related tumors, whereby either down-regulation or an altered subcellular compartmentalization of these proteins has been documented [2, 8, 15, 20, 23–25, 41, 49, 50, 52, 55]. In particular, nuclear accumulation of β-catenin has been reported in carcinoids of the gastrointestinal tract [25, 49] and of the pancreas [49] and in pituitary adenomas [48], whereas mutations in exon 3 of the *CTNNB1* gene, encoding serine/threonine-rich phosphorylation site for GSK-3β, or *APC* gene, are consistently uncommon [15, 43, 48–50]. Nuclear accumulation of β-catenin has been detected in a subset of pulmonary high-grade neuroendocrine carcinomas [9, 41, 47] in the absence of loss-of-function mutations or polymorphisms of either *CTNNB1* or *APC* [9]. However, insights into target gene expression resulting from β-catenin transactivation activity or mechanisms underlying β-catenin nuclear accumulation in pulmonary neuroendocrine tumor cells are still lacking.

Herein, we demonstrate that nuclear redistribution of β-catenin in a subset of pulmonary high-grade pulmonary neuroendocrine tumors is associated with up-regulation of MMP-7, but not of cyclin D1, and it is independent of EGFR and human epidermal growth factor receptor 2 (HER-2) gene amplification or expression.

Materials and methods

Patients

Ninety-six consecutive patients (82 men and 14 women) with stage I–III high-grade neuroendocrine tumors of the lung, including 51 large-cell neuroendocrine carcinomas (LCNEC) and 45 small-cell carcinomas (SCLC), that were radically resected at the participating Institutions between 1985 and 2004, have been evaluated. Relevant clinicopathological data of the entire cohort of patients is summarized in Table 1. All patients had been studied by total body CT scan and had undergone extensive mediastinal lymph node dissection (median value, nine excised lymph nodes per patient) to ensure accurate staging. The diagnosis of neuroendocrine tumor was based on either morphological features [56] or on previously refined immunohistochemical criteria (i.e., immunoreactivity for synaptophysin, chromogranin A, and a variety of respiratory tract-related

Table 1 Clinicopathological characteristics of 96 high-grade neuroendocrine tumors

Variable	Category	LCNEC (n=51)	SCLC (n=45)	p value
Age (years)	≤49	6	2	NS
	50–59	11	11	
	60–69	19	17	
	≥70	15	15	
Sex	male	47	34	0.046
	female	4	11	
Stage	I	26	13	0.039
	II–III	25	32	
pT	1	12	19	0.024
	2	30	23	
	3–4	9	3	
pN	N0	29	14	0.011
	N1	14	17	
	N2	8	14	
LN metastasis	No	29	14	0.014
	Yes	22	31	
No. of positive lymph nodes	Median	0	2	0.022
Tumor size	<2 cm	5	9	0.025
	2–4 cm	19	22	
	>4 cm	27	14	
Vital status	Alive	34	26	NS
	Dead	17	19	
Recurrences	No	29	22	NS
	Yes	22	23	
Ki-67 index	≤50%	28	9	0.0007
	>50%	23	36	

NS not significant

hormones, including gastrin-related peptide, calcitonin, adrenocorticotropic hormone, serotonin and alpha-subunit of human chorionic gonadotropin) [38, 41].

Accurate follow-up information was available for 86 patients: 45 (47%) patients had recurrent disease and 36 (37%) died of disease. Follow-up time was 29±39 months (median 12) for LCNEC and 20±21 months (median 15) for SCLC patients. No patient presented with symptoms due to hormone hyperproduction. Detailed information on cigarette smoking history was unavailable at the time of the present study, although most patients were known to be heavy smokers. Ten LCNEC and 17 SCLC patients underwent neoadjuvant combination chemotherapy using the CAVE protocol (cyclophosphamide, doxorubicin, vincristine and etoposide).

Immunohistochemistry

Paraffin-embedded tumor samples were investigated using the antibodies listed in Table 2, according to staining protocols previously reported [38]. Samples of normal lung from 10 patients with nonmalignant lung diseases and 10 pulmonary neuroendocrine tumorlets were used as control groups. Tumorlets and normal neuroendocrine cells were highlighted by chromogranin A immunostaining as previously detailed [39]. All immunostains were evaluated in a blinded fashion. Immunoreactivity for β-catenin, EGFR, and Her-2 was assessed as reported [12, 37, 41]. Proliferative activity of neuroendocrine tumors was assessed by Ki-67 immunolabeling [40]. For all other markers, the percentage of immunoreactive tumor cells was evaluated scanning at least 2,000 neoplastic cells in randomly selected fields. Tumors were scored as negative if staining was either absent or identified in less than 5% of tumor cells. In particular, nuclear immunoreactivity was defined as the nuclear accumulation of immunostaining product in at least 5% tumor cells, independent of the distribution of any additional staining. The specificity of immunoreactions was assessed substituting the primary antibody with a nonrelated isotypic mouse immunoglobulin or normal rabbit serum.

Dual-color FISH

Commercially available dual-color fluorescence in situ hybridization (FISH) assays [LSI EGFR/CEP7 (code 32-191053) and LSI Cyclin D1 11q13/CEP11 (code 32-191039), both from Abbott-Vysis Inc., IL, USA] were employed using 4-μm-thick paraffin-embedded sections according to the manufacturer's instructions to evaluate the status of the EGFR and cyclin D1 genes, respectively. Briefly, the locus-specific identifier EGFR or cyclin D1 DNA probe is a 300 kb SpectrumOrange (Abbott-Vysis, Inc.) fluorescent DNA probe specific for the EGFR (7p12) or cyclin D1 (11q13) gene locus. The chromosome 7 or 11 enumeration DNA probe is a SpectrumGreen (Abbott-Vysis, Inc.) labeled DNA probe specific for the alpha satellite DNA sequence at the centromeric region of chromosome 7 (7p11.1-q11.1) or 11 (11p11.11-q11), respectively. At least 100 neoplastic cells were evaluated for gene amplification as previously described [37]. Digital images were obtained using a Leica DMRB epifluorescence microscope equipped with a Leica digital camera DC250 (Leica Imaging Systems Ltd., Cambridge, UK). FITC, Cy3, and DAPI fluorescent signals were detected using specific filters. The images were recorded, pseudo-colored, and merged using the QFluoro software (Leica).

Table 2 Antibody panel used

Antibodies	m/p[a]	Clone	Source	Dilution	Pretreatment[b]
β-catenin	m	E-5	Santa Cruz Biotechnology, Santa Cruz, CA, USA	1:100	MWO-EDTA
E-cadherin	m	4A2C7	Zymed, San Francisco, CA, USA	1:400	MWO-EDTA
EGFR/HER-1	m	31G7	DBA, Milan, Italy	1:20	Pronase
Phospho-EGFR (Tyr 992)	p	–	Cell Signaling Technology, Beverly, MA, USA	1:400	MWO-EDTA
Phospho-EGFR (Tyr 1068)	p	–	Cell Signaling Technology	1:25	MWO-EDTA
HER-2/neu	p	–	DAKO, Glostrup, Denmark	1:1600	MWO-EDTA
Phospho-HER-2 (Tyr 877)	p	–	Cell Signaling Technology	1:200	MWO-EDTA
Phospho-HER-2 (Tyr 1221/1222)	p	–	Cell Signaling Technology	1:25	MWO-EDTA
Phospho-p38 MAPK (Tyr 180/182)	p	–	Cell Signaling Technology	1:100	MWO-CB
Phospho-p42/44 MAPK (Tyr 202/204)	p	–	Cell Signaling Technology	1:100	MWO-CB
Amphiregulin	p	–	Santa Cruz Biotechnology	1:20	–
TGF-alpha	m	p/T1	Abcam, Cambridge, UK	1:50	–
EGF	m	EGF-10	Abcam	1:10	–
Cyclin D1	p	–	Lab Vision Corporation, Fremont, CA, USA	1:50	MWO-EDTA
Matrix metalloproteinase 7 (matrilysin)	p	–	Lab Vision Corporation	1:200	–
Ki-67 antigen	m	MIB-1	Immunotech, Marseille, France	1:400	MWO-EDTA

[a] *m* Monoclonal antibody, *p* polyclonal antibody
[b] MWO-EDTA, microwave 750W for 12 min in EDTA 0.1 M pH 8; MWO-CB, microwave 750W for 10 min in citrate buffer 0.01 M pH 6; 0,1% pronase solution in PBS 0.01 M pH 7.4

DNA extraction and mutational analysis

Tumor cells from nuclearly immunoreactive high-grade neuroendocrine neoplasms were microdissected from 5-μm-thick sections of formalin-fixed paraffin-embedded tissue, and DNA was extracted by digesting the tissues in lysis buffer [100 mM Tris–HCl (pH 8.0), 500 mM KCl, 0.01% Tween 20, and 200 μg/ml proteinase K]. Exon 3 of β-catenin was amplified by polymerase chain reaction (PCR) using the following primer pair: forward, 59-GAA CCA GAC AG AAA AGC GGC TG-39 and reverse, 59-ACT CAT ACA GGA CTT GGG AGG-39 (nucleotides 257–278 and 410–390 respectively; GenBank NM001904). Each PCR reaction was performed in a 20-μl reaction mixture containing 0.5 units of Taq polymerase, 0.25 μM of each primer, 0.2 μM deoxynucleotide triphosphates, 2.5 mM $MgCl_2$, and PCR buffer containing 100 mM Tris–HCl (pH 8.0), 500 mM KCl, and 0.01% Tween 20. Reaction conditions were as follows: 94°C for 5 min and then 35 cycles of 94°C for 1 min, 55°C for 1 min, 72°C for 1 min followed by a final extension of 70°C for 10 min. Products were purified and then sequenced in both directions using Big Dye Terminator Cycle Sequencing kit (Applied Biosystems, Foster City, CA, USA). The sequence reactions were run and analyzed on an ABI 3,100 Genetic Analyzer (Applied Biosystems).

Statistical analysis

Associations of categorical or ordinal variables were evaluated by the Fisher exact test or the Mantel–Haenszel chi-square test for trends (with 1 DF), respectively. Survival curves were assessed according to the Kaplan–Meier method and compared with log-rank. All estimates were performed using the SAS statistical software package (SAS Institute, Inc., Cary, NC, USA). All p values were based on two-sided testing and were considered significant when ≤0.05.

Results

Disarrayed β-catenin immunoreactivity is common in LCNEC and SCLC and is associated with EGFR and HER2 expression in LCNEC

Normal cells from bronchial mucosa and lung tissue from both neoplastic and nonneoplastic patient groups, as well as scattered bronchial neuroendocrine cells and all neuroendocrine tumorlets, showed exclusively a membrane-associated immunoreactivity for β-catenin, characterized by linear decoration of the entire cell membrane without any cytoplasmic or nuclear immunostaining.

β-catenin was expressed in all the 96 high-grade neuroendocrine tumors, with 20 to 100% immunoreactive tumor cells in LCNEC and 50 to 100% in SCLC (Table 3). The two tumor groups did not differ significantly with regard to the β-catenin labeling index, and the vast majority showed more than 50% immunoreactive cells. Only four (8%) LCNEC and one (2%) SCLC showed 50% or less immunoreactive cells.

Significant differences were instead observed in the staining patterns of these two tumor groups that persisted even after adjustment for confounding factors such as age, gender, and tumor size (Table 3). Indeed, a disarrayed β-catenin immunoreactivity was seen in both groups, consisting in a variably retained membrane-associated pattern along with progressive increase of cytoplasmic staining. A membrane-linear/cytoplasmic pattern prevailed in LCNEC, showing preservation of the membrane-linear signal along with variable degrees of cytoplasmic staining. Conversely, a membrane-disrupted pattern was more prevalent in SCLC exhibiting irregularly wrinkled staining of the cell membrane along with more prominent cytoplasmic staining.

In LCNEC, an inverse relationship was found between β-catenin labeling index and pT class (p=0.014) and as a trend with more advanced tumor stage (p=0.091) or size (p=0.087), but not with the other demographic (age, gender) or clinicopathological (recurrence rate, survival) variables under evaluation. As far as the β-catenin immunostaining pattern is concerned, a nonmembrane-linear staining was associated with complete and intense membrane immunoreactivity for EGFR (p=0.017) and as a trend with HER-2 expression tumors (p=0.080). At variance, LCNEC with cyclin D1-immunoreactive tumor cells showed a retained membrane-linear signal (p=0.009). No other significant associations between the immunostaining pattern of β-catenin and any other parameter were observed.

In SCLC, reduced expression of β-catenin was associated with tumor recurrence (p=0.043), death for tumor (p=0.015), and Ki-67 labeling index ≥50% (p=0.004), but not with age, gender, tumor stage, and EGFR and HER-2 or cyclin D1 expression. No relationship was found between β-catenin immunostaining patterns and the different clinicopathological variables investigated.

Table 3 Prevalence of β-catenin immunoreactivity according to histology

Variable	Category	LCNEC	SCLC	p
β-catenin labeling index	Mean±SD	90.4±18.9	94.4±10.9	NS
	Median	100	100	
	Range	20–100	50–100	
β-catenin pattern	Membrane linear	10 (91%)	1 (9%)	<0.0001*
	Membrane cytoplasmic	12 (86%)	2 (14%)	
	Membrane disrupted	29 (41%)	42 (59%)	

NS not significant
*These differences remained significant even after adjusting for confounding factors such as patients' age and gender and tumor size

β-catenin nuclear immunoreactivity is detected only in a subset of LCNEC and SCLC

Nuclear accumulation was observed in a subset of high-grade neuroendocrine tumors, including 7/51 (14%) LCNEC and 2/45 (4%) SCLC, where positive tumor cells ranged from 10 to 95% (mean±SD, 45±26%; median 45), with either diffuse (three cases) or patchy (six cases) distribution pattern within individual tumors, the latter being characterized by irregular clustering of positive tumor cells (Fig. 1). Nuclear immunostaining was always associated with a disarrayed, nonmembrane/linear immunoreactivity for β-catenin, including either membrane-linear/cytoplasmic or membrane-disrupted pattern. Specifically, four of seven LCNEC and the two SCLC with nuclear staining presented a simultaneous membrane-linear/cytoplasmic pattern, whereas the remaining three LCNEC were associated with a membrane-disrupted pattern ($p<0.001$). Nuclear immunoreactivity for β-catenin was also associated as a trend with either absent (one LCNEC) or variably misplaced E-cadherin immunoreactivity, the latter consisting in wrinkled staining of the cell membrane along with prominent cytoplasmic accumulation (six LCNEC and two SCLC) ($p=0.053$).

No association was found between nuclear accumulation of β-catenin and any parameters.

β-catenin nuclear accumulation correlates with increased MMP-7 but is independent of EGFR/HER-2 or cyclin D1 expression/activation or gene amplification

The nine tumors showing nuclear immunoreactivity for β-catenin were compared for immunohistochemical expression of target genes such as MMP-7 and cyclin D1 and growth factor membrane receptors responsible for nuclear accumulation of β-catenin upon activation using a control group of 10 randomly selected, consecutive, nuclear-unreactive high-grade neuroendocrine carcinomas, including LCNEC and SCLC, randomly chosen among those exhibiting the same β-catenin membrane/cytoplasmic pattern of immunoreactivity. We found matrilysin (MMP-7) immunoreactivity in four of nine tumors (three LCNEC and one SCLC) showing nuclear staining of β-catenin vs none of the 10 control tumors ($p=0.070$), with a mean percentage (±sd) of immunoreactive cells being 18.8% (±8.5; median 17.5%, range 10–30) ($p=0.033$). Conversely,

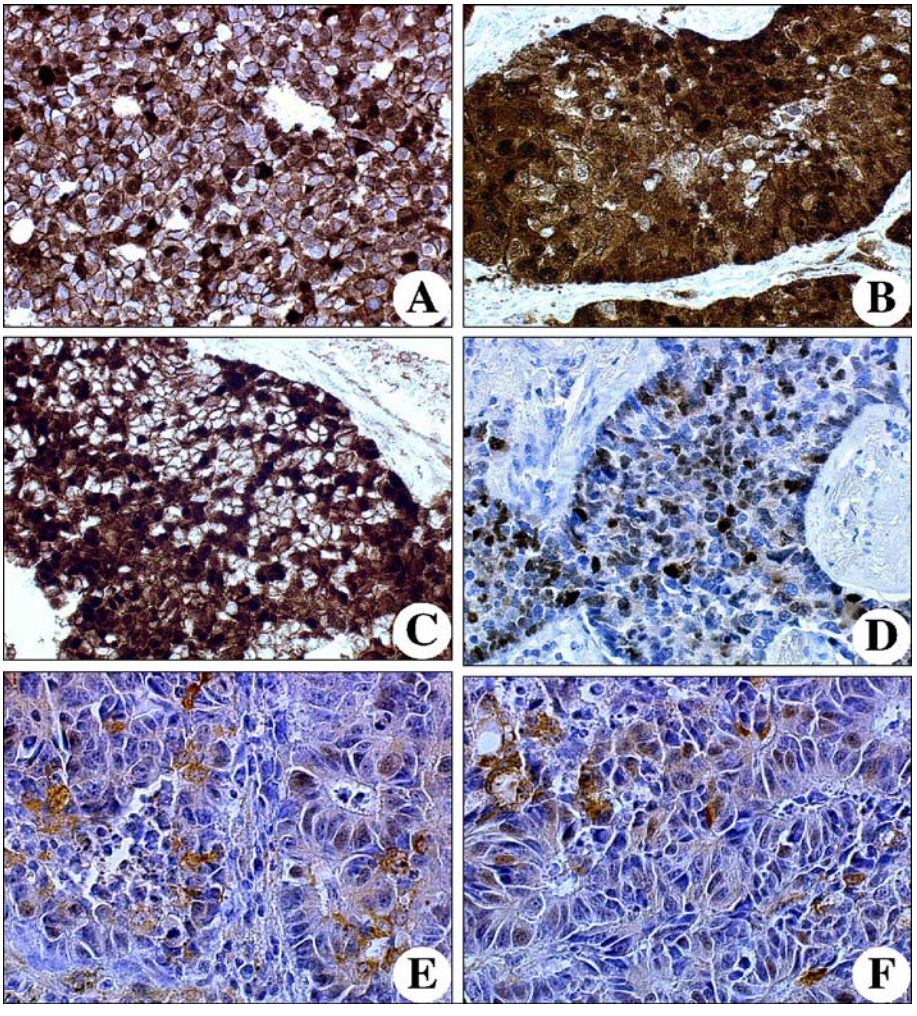


Fig. 1 Representative immunoreactivity patterns for β-catenin (**a**–**c**), cyclin D1 (**d**), and matrix metalloproteinase-7 (**e**, **f**) in high-grade neuroendocrine tumors of the lung. A membrane-linear pattern for β-catenin with scattered nuclearly immunoreactive tumor cells is shown in two different cases of LCNEC along with variable degrees of cytoplasmic staining (**a**, **b**), whereas a more evident cytoplasmic pattern with some membrane disruption and consistent nuclear immunoreactivity is seen in another case of LCNEC (**c**). Nuclear accumulation of cyclin D1 by tumor cells is virtually confined to LCNEC although it is not differentially expressed by β-catenin nuclearly immunoreactive tumors (**d**). The cytoplasmic immunolabeling pattern for matrix metalloproteinase-7 is shown in two different cases of β-catenin nuclearly accumulating LCNEC (**e**, **f**)

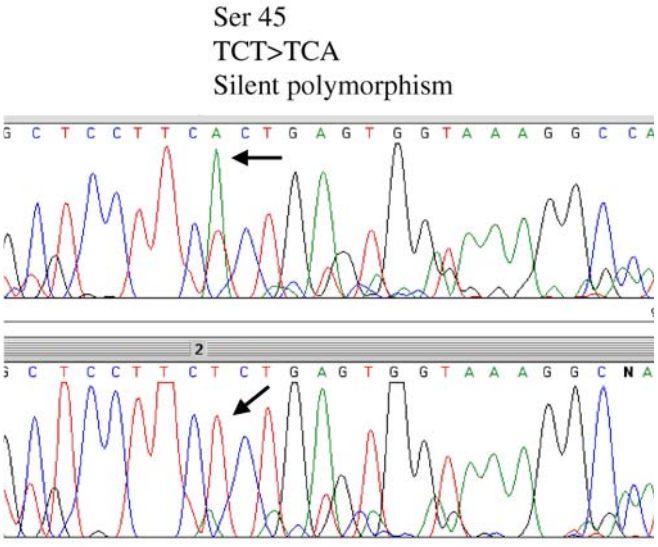


Fig. 2 Sequence analysis of β-catenin exon 3 in a case of LCNEC showing a silent polymorphism at the codon Ser 45 with TCT→TCA transversion

no differences were found between the two tumor groups for all the other markers evaluated, including phosphorylated and unphosphorylated EGFR or HER-2, p38 and p42/44 MAPK, amphiregulin, TGF-α, and EGF. Finally, FISH analysis did not show any gene amplification for HER-1/EGFR or HER-2/Neu genes in either tumor group, and direct sequencing of exon 3 of the *CTNNB1* gene encoding β-catenin did not show any mutation, apart from a silent polymorphism in one LCNEC (Fig. 2). Cyclin D1 immunoreactivity was confined to LCNEC (mean±sd, 13± 18%; median 5), but was not differentially expressed between the two tumor groups, and FISH analysis did not reveal any specific gene amplification.

Discussion

In this study, we demonstrate that (1) disarrayed β-catenin immunoreactivity is common in high-grade neuroendocrine tumors, whereas normal and hyperplastic (tumorlets) bronchial-associated neuroendocrine cells express only membrane-bound β-catenin; (2) nuclear β-catenin immunoreactivity is present in a minor subset of high-grade neuroendocrine tumors, where it correlates with matrilysin, but not with cyclin D1 expression. Nuclear immunoreactivity is independent of either mutations in exon 3 of β-catenin or expression/activation or gene amplification of members of the HER membrane receptor gene family.

The genotypic and phenotypic relationships between LCNEC and SCLC are still a matter of debate. Similarities have been suggested by experiments with gene expression profiling [19] or morphometry [30], whereas comparative genomic hybridization [57] and immunohistochemistry [7, 14] have suggested that the opposite is true. Our data are based upon the largest series of LCNEC and SCLC analyzed to date for β-catenin immunoreactivity and suggest that this protein is likely to play a different role in these tumors. Overall, the expression of β-catenin is highly conserved in high-grade pulmonary neuroendocrine tumors, inasmuch as their labeling indexes do not differ significantly. However, what is dramatically subverted is the subcellular distribution of β-catenin, as argued by the differential distribution between LCNEC and SCLC of the diverse immunoreactivity patterns. In fact, a retained membrane-linear decoration prevails in the former along with variable cytoplasmic accentuation of immunostaining, whereas a more disarrayed pattern is common to the latter with irregularly wrinkled membrane immunoreactivity and a more accentuated cytoplasmic reinforcement of immunostaining. The close positive relationship between β-catenin and E-cadherin immunoreactivity patterns we have recently documented in LCNEC, but not in SCLC [41], was confirmed in the current investigation (data not shown), indicating that the majority of β-catenin molecules is tightly connected to E-cadherin, not only when localized at the cell membrane but also when they are displaced into the cytoplasm. This colocalization is partially lost only when β-catenin is translocated into the nucleus, as E-cadherin has never been found in the nuclei of pulmonary neuroendocrine tumors [9, 41].

In LCNEC, down-regulation of β-catenin correlates with pathological indicators of tumor growth, such as pT and tumor stage or size, and in SCLC with tumor recurrence rate, cancer-related deaths, and increased proliferative activity, indicating a critical role of reduced β-catenin for impaired cell-cell adhesion responsible for local tumor development and progression. Moreover, in LCNEC, a nonmembrane-linear immunoreactivity pattern is associated with the expression/overexpression of two important members of HER family in lung cancer, namely, EGFR and HER-2, but not with cyclin D1, one of the target genes transactivated by nuclear β-catenin [54]. This indicates on one hand that overexpression/activation of these growth factors may favor the cytoplasmic accumulation of β-catenin, causing it to dissociate from the membrane E-cadherin complex [27, 28], on the other hand that modulation of cyclin D1 expression, a protein reportedly overexpressed in LCNEC [3, 14], is independent of either β-catenin nuclear activation or cyclin D1 gene amplification. As a matter of fact, in such tumors, cyclin D1 immunoreactivity is significantly associated with a distinct membrane-linear signal of tumor cells and the absence of cyclin D1 gene amplification.

The nuclear accumulation of β-catenin in a minor subset of high-grade neuroendocrine tumors is always associated with disarrayed distribution of the E-cadherin/β-catenin complex, evoking a profoundly altered function of this cell-to-cell adhesion complex in such subset of tumors. Moreover, we first get new insights into the gene activation occurring in nuclearly immunoreactive high-grade pulmonary neuroendocrine tumors, reporting that matrilysin (MMP-7), but not cyclin D1 immunoreactivity, is significantly increased in this subset of tumors as compared with the nuclearly unreactive control arm. This overlap between MMP-7 and β-catenin nuclear immunoreactivity

we documented in a subset of high-grade pulmonary neuroendocrine carcinomas has also been reported in other human cancers, including colorectal [35], endometrial [29], esophageal [46], and pancreatic [26] carcinomas, at variance with breast [32] or liver [44] cancer where β-catenin nuclear accumulation does not correlate with MMP-7 immunoreactivity. These findings emphasize once again the complex multifunctional role of β-catenin in the activation process of reporter genes in human cancers where diverse mechanisms are likely to be responsible for the final tumor development. Our findings of 9% high-grade pulmonary neuroendocrine carcinomas being nuclearly immunoreactive for β-catenin, of an inverse relationship between membrane/linear and nuclear localization, and of the absence of mutations in exon 3 of the *CTNNB1* gene, are also in keeping with recent data obtained on nonsmall cell lung cancer [22, 42]. This suggests that common carcinogenetic events may cause different subtypes of lung cancer to develop, and that the destruction mechanisms of the E-cadherin/β-catenin system may be functional in neuroendocrine tumors of the lung.

In addition to Wnt pathway, it has been proposed that β-catenin nuclear accumulation may also result from EGFR activation in A431 squamous carcinoma cell line [28], but this mechanism is unlikely to play a role in our series of high-grade pulmonary neuroendocrine tumors, because either EGFR and HER-2 expression or up-/down-stream signals of the corresponding pathways, such as p38 and p42/44 MAPK, amphiregulin, TGF-α, and EGF, do not differ between the two tumor control arms under evaluation. On the contrary, we found that EGFR or HER-2 expression is associated with a nonmembrane-linear immunoreactivity pattern of β-catenin in LCNEC, but not in SCLC, indicating that the same receptor(s) may account for subcellular redistribution of the protein with detachment from cell membrane and cytoplasmic accumulation. This mechanism is different from that proposed in human esophageal squamous cell carcinoma lines where EGF activation signaling pathway plays an active role in MMP-7 production of tumor cells [59]. FISH analysis of *EGFR* or *HER-2* gene copy number status excludes that gene amplification may account for the nuclear accumulation of β-catenin in high-grade pulmonary neuroendocrine tumors. Our results on direct sequencing of exon 3 of the *CTNNB1* gene confirm previous studies failing to detect any mutation in the β-catenin gene in pulmonary endocrine tumors [9], at variance with the reported occurrence of such mutations in gastrointestinal carcinoids [15]. On the other hand, loss-of-function mutations or deletions of key regulators of the Wnt pathway, such as APC gene, have not been detected in neuroendocrine tumors of the lung [9], and mutations or deletions of other important regulatory genes, such as GSK-3β, are unlikely to be found in tumors probably because its overall ablation is incompatible with cell viability [43].

Matrilysin has been found in neuroendocrine carcinomas of the lung up to 20% of tumors with a prevalence of LCNEC over SCLC [4], and our findings of 4/19 (21%) immunoreactive tumors (three LCNEC and one SCLC) for MMP-7 are in full agreement with these results. Although the expression of several matrix metalloproteinases has been linked to the invasive phenotype of lung cancer [4], we failed to find any relationship between matrilysin expression and indicators of tumor aggressiveness probably because of the little number of cases being reactive rather than to the lack of biopathological meaning in these neuroendocrine tumors of the lung that are known to be highly aggressive tumors. The same explanation could hold true for the lack of any correlation between β-catenin nuclear occurrence and indicators of tumor growth or progression. Besides its function in the degradation of extracellular matrix, it has also been reported that MMP-7 is able to mediate E-cadherin ectodomain shedding in either injured lung epithelium [31] or human cancer cells [11, 34], resulting in a soluble E-cadherin fragment that in turn inhibits the E-cadherin/β-catenin system functions via a paracrine mechanism and accelerates cell migration required for either epithelial repair or tumor invasiveness. Moreover, the levels of MMP-7—an enzyme able to efficiently bind to cell surface and produce homotypic loose cell aggregates [21]—may also be regulated in human cancers by the degree of E-cadherin-mediated cell-cell connections [5], making the functional relationships among these molecules complex and intriguing. Therefore, further studies on a larger number of β-catenin nuclearly immunoreactive high-grade neuroendocrine tumors of the lung are warranted to elucidate these challenging aspects.

Acknowledgements This study was supported by Associazione Italiana Ricerca Cancro (AIRC), Fondazione Cassa di Risparmio di Verona (Bando 2001), CNR "Diagnostica molecolare in oncologia" and MIUR, Rome, Italy.

References

1. Aberle H, Bauer A, Stappert J, Kispert A, Kemler R (1997) b-catenin is a target for the ubiquitin-proteasome pathway. EMBO J 16:3797–3804
2. Barshack I, Goldberg I, Chowers Y, Horowitz A, Kopolovic J (2002) Different beta-catenin immunoexpression in carcinoid tumors of the appendix in comparison to other gastrointestinal carcinoid tumors. Pathol Res Pract 198:531–536
3. Beasley MB, Lantuejoul S, Abbondanzo S, Chu WS, Hasleton PS, Travis WD, Brambilla E (2003) The P16/cyclin D1/Rb pathway in neuroendocrine tumors of the lung. Human Pathol 34:136–142
4. Bolon I, Devouassoux M, Roberft C, Moro D, Brambilla C, Brambilla E (1997) Expression of urokinase-type plasminogen activator, stromelysin 1, stromelysin 3, and matrilysin genes in lung carcinomas. Am J Pathol 150:1619–1629
5. Borchers AH, Sanders LA, Bowden GT (1997) Regulation of matrilysin expression in cells of squamous cell carcinoma by E-cadherin-mediated cell-cell contact. J Cancer Res Clin Oncol 123:13–20
6. Brabletz T, Jung A, Dag S, Hlubek F, Kirchner T (1999) b-catenin regulates the expression of the matrix metalloproteinase-7 in human colorectal cancer. Am J Pathol 155:1033–1038
7. Brambilla E, Negoescu A, Gazzeri S, Lantuejoul S, Moro D, Brambilla C, Coll JL (1996) Apoptosis-related factors p53, Bcl2, and Bax in neuroendocrine lung tumors. Am J Pathol 149:1941–1452

8. Chan AO, Kim SG, Bedeir A, Issak JP, Hamilton SR, Rashid A (2003) CpG island methylation in carcinoid and pancreatic endocrine tumors. Oncogene 22:924–934
9. Clavel CE, Nollet F, Berx G, Tejpar S, Nawrocki-Raby B, Kaplan HH, van Roy FM, Birembaut PL (2001) Expression of the E-cadherin–catenin complex in lung neuroendocrine tumours. J Pathol 194:20–26
10. Crawford HC, Fingleton BM, Rudolph-Owen LA, Goss KJ, Rubinfeld B, Polakis P, Matrisian LM (1999) The metalloproteinase matrilysin is a target of beta-catenin transactivation in intestinal tumors. Oncogene 18:2883–2891
11. Davies G, Jiang WG, Mason MD (2001) Matrilysin mediates extracellular cleavage of E-cadherin from prostate cancer cells: a key mechanism in hepatocyte growth factor/scatter factor-induced cell-cell dissociation and in vitro invasion. Clin Cancer Res 7:3289–3297
12. De Pas T, Pelosi G, de Braud F, Veronesi G, Curigliano G, Leon ME, Danesi R, Noberasco C, d'Aiuto M, Catalano G, Viale G, Spaggiari L (2004) Modulation of epidermal growth factor receptor status by chemotherapy in patients with locally advanced non-small-cell lung cancer is rare. J Clin Oncol 22: 4966–4970
13. Dorudi S, Hanby AM, Poulsom R, Northover J, Hart IR (1995) Level of expression of E-cadherin mRNA in colorectal cancer correlates with clinical outcome. Br J Cancer 71:614–616
14. Dosaka-Akita H, Cagle PT, Hiroumi H, Fujita M, Yamashita M, Sharma A, Kawakami Y, Benedict WF (2000) Differential retinoblastoma and p16(INK4A) protein expression in neuroendocrine tumors of the lung. Cancer 88:550–556
15. Fujimori M, Ikeda S, Shimizu Y, Okajima M, Asahara T (2001) Accumulation of beta-catenin protein and mutations in exon 3 of beta-catenin gene in gastrointestinal carcinoid tumor. Cancer Res 61:6656–6659
16. Gumbinber BM (2000) Regulation of cadherin adhesive activity. J Cell Biol 148:399–404
17. Huber AH, Weis WI (2001) The structure of the b-catenin/E-cadherin complex and the molecular basis of diverse ligand recognition by b-catenin. Cell 105:391–402
18. Ikeda S, Kishida S, Yamamoto H, Murai H, Koyama S, Kikuchi A (1998) Axin, a negative regulator of the Wnt signaling pathway, forms a complex with GSK-3b and b-catenin and promotes GSK-3b-dependent phospholylation of b-catenin. EMBO J 17:1371–1384
19. Jones MH, Virtanen C, Honjoh D, Miyoshi T, Satoh Y, Okumura S, Nakagawa K, Nomura H, Ishikawa Y (2004) Two prognostically significant subtypes of high-grade lung neuroendocrine tumours independent of small-cell and large-cell neuroendocrine carcinomas identified by gene expression profiles. Lancet 363:775–781
20. Kawahara M, Kammori M, Kanauchi H, Noguchi C, Kuramoto S, Kaminishi M, Endo H, Takubo K (2002) Immunohistochemical prognostic indicators of gastrointestinal carcinoid tumours. Eur J Surg Oncol 28:140–146
21. Kioi M, Yamamoto K, Higashi S, Koshikawa N, Fujita K, Miyazaki K (2003) Matrilysin (MMP-7) induces homotypic adhesion of human colon cancer cells and enhances their metastatic potential in nude mouse model. Oncogene 22:8662–8670
22. Kotsinas A, Evangelou K, Zacharatos P, Kittas C, Gorgoulis VG (2002) Proliferation, but not apoptosis, is associated with distinct beta-catenin expression patterns in non-small-cell lung carcinomas: relationship with adenomatous polyposis coli and G(1)-to S-phase cell-cycle regulators. Am J Pathol 161:1619–1634
23. Kuroda N, Mizushima S, Guo L, Jin Y, Tao L, Miyazaki E, Toi M, Naruse K, Hiroi M, Enzan H (2001) Goblet cell carcinoid of the appendix: investigation of the expression of beta-catenin and E-cadherin. Pathol Int 51:283–287
24. Leotlela PD, Jauch A, Holtgreve-Grez H, Thakker RV (2003) Genetics of neuroendocrine and carcinoid tumours. Endocr Relat Cancer 10:437–450
25. Li CC, Hirowaka M, Qian ZR, Xu B, Sano T (2002) Expression of E-cadherin, b-catenin, and Ki-67 in goblet cell carcinoids of the appendix: an immunohistochemical study with clinical correlation. Endocr Pathol 13:47–58
26. Li YJ, Wei ZM, Meng YX, Ji XR (2005) Beta-catenin up-regulates the expression of cyclinD1, c-myc and MMP-7 in human pancreatic cancer: relationships with carcinogenesis and metastasis. World J Gastroenterol 11:2117–2123
27. Lu Z, Ghosh S, Wang Z, Hunter T (2003) Downregulation of caveolin-1 function by EGF leads to the loss of E-cadherin, increased transcriptional activity of beta-catenin, and enhanced tumor cell invasion. Cancer Cell 4:499–515
28. Lu Z, Hunter T (2004) Wnt-independent β-catenin transactivation in tumor development. Cell Cycle 3:571–573
29. Machin P, Catasus L, Pons C, Munoz J, Matias-Guiu X, Prat J (2002) CTNNB1 mutations and beta-catenin expression in endometrial carcinomas. Human Pathol 33:206–212
30. Marchevsky AM, Gal AA, Shah S, Koss MN (2001) Morphometry confirms the presence of considerable nuclear size overlap between "small cells" and "large cells" in high-grade pulmonary neuroendocrine neoplasms. Am J Clin Pathol 116:466–472
31. McGuire JK, Li Q, Parks WC (2003) Matrilysin (matrix metalloproteinase-7) mediates E-cadherin ectodomain shedding in injured lung epithelium. Am J Pathol 162:1831–1843
32. Mylona E, Kapranou A, Mavrommatis J, Markaki S, Keramopoulos A, Nakopoulou L (2005) The multifunctional role of the immunohistochemical expression of MMP-7 in invasive breast cancer. Acta Pathol Microbiol Immunol Scand 113: 246–255
33. Nagafuchi A (2001) Molecular architecture of the adherens junctions. Curr Opin Cell Biol 13:600–603
34. Noe V, Fingleton B, Jacobs K, Crawford HC, Vermeulen S, Steelant W, Bruyneel E, Matrisian LM, Mareel M (2001) Release of an invasion promoter E-cadherin fragment by matrilysin and stromelysin-1. J Cell Sci 114:111–118
35. Ougolkov AV, Yamashita K, Mai M, Minamoto T (2002) Oncogenic beta-catenin and MMP-7 (matrilysin) cosegregate in late-stage clinical colon cancer. Gastroenterology 122:60–71
36. Palmer H, Gonzales-Sancho JM, Espada J, Berciano MT, Puig I, Baulida J, Quintanilla M, Cano A, Garcia de Herreros A, Lafarga M, Munoz A (2001) Vitamin D_3 promotes the differentiation of colon carcinoma cells by the induction of E-cadherin and the inhibition of b-catenin signaling. J Cell Biol 154:369–387
37. Pelosi G, Del Curto B, Dell'Orto P, Pasini F, Veronesi G, Spaggiari L, Maisonneuve P, Iannucci A, Terzi A, Lonardoni A, Viale G (2005) Lack of prognostic implications of HER-2/neu abnormalities in 345 stage I non-small cell carcinomas (NSCLC) and 207 stage I–III neuroendocrine tumours (NET) of the lung. Int J Cancer 113:101–108
38. Pelosi G, Pasini F, Fraggetta F, Pastorino U, Iannucci A, Maisonneuve P, Arrigoni G, De Manzoni G, Bresaola E, Viale G (2003) Independent value of fascin immunoreactivity for predicting lymph node metastases in typical and atypical pulmonary carcinoids. Lung Cancer J IASLC 42:203–213
39. Pelosi G, Pasini F, Olsen Stenholm C, Pastorino U, Maisonneuve P, Sonzogni A, Maffini F, Pruneri G, Fraggetta F, Cavallon A, Roz E, Iannucci A, Bresaola E, Viale G (2002) p63 immunoreactivity in lung cancer: yet another player in the development of squamous cell carcinomas? J Pathol 198:100–109
40. Pelosi G, Rodriguez J, Viale G, Rosai J (2005) Pulmonary carcinoid tumor overdiagnosed as small-cell carcinoma on biopsy specimens: a major pitfall in the management of lung cancer patients. Am J Surg Pathol 29:179–187
41. Pelosi G, Scarpa A, Puppa G, Veronesi G, Spaggiari L, Pasini F, Maisonneuve P, Iannucci A, Arrigoni GL, Viale G (2005) Alteration of the E-cadherin/b-catenin cell adhesion system is common in pulmonary neuroendocrine tumors and is an independent predictor of lymph node metastasis in atypical carcinoid. Cancer 103:1154–1164

42. Pirinen RT, Hirvikoski P, Johansson RT, Hollmen S, Kosma VM (2001) Reduced expression of alpha-catenin, beta-catenin, and gamma-catenin is associated with high cell proliferative activity and poor differentiation in non-small cell lung cancer. J Clin Pathol 54:391–395
43. Polakis P (2000) Wnt signaling and cancer. Genes Dev 14:1837–1851
44. Prange W, Breuhahn K, Fischer F, Zilkens C, Pietsch T, Petmecky K, Eilers R, Dienes HP, Schirmacher P (2003) Beta-catenin accumulation in the progression of human hepatocarcinogenesis correlates with loss of E-cadherin and accumulation of p53, but not with expression of conventional WNT-1 target genes. J Pathol 201:250–259
45. Rubinfeld B, Albert I, Porfiri E, Fiol C, Munemitsu S, Polakis P (1996) Binding of GSK3b to the APC-b-catenin complex and regulation of complex assembly. Science 272:1023–1026
46. Saeki H, Tanaka S, Sugimachi K, Kimura Y, Miyazaki M, Ohga T, Sugimachi K (2002) Interrelation between expression of matrix metalloproteinase 7 and beta-catenin in esophageal cancer. Dig Dis Sci 47:2738–2742
47. Salon C, Moro D, Lantuejoul S, Brichon PY, Drabkin H, Brambilla C, Brambilla E (2004) E-cadherin–b-catenin adhesion complex in neuroendocrine tumors of the lung: a suggested role upon local invasion and metastasis. Human Pathol 35: 1148–1155
48. Semba S, Han S-Y, Ikeda H, Akira H (2001) Frequent nuclear accumulation of b-catenin in pituitary adenoma. Cancer 91:42–48
49. Semba S, Kusumi R, Moriya T, Sasano H (2000) Nuclear accumulation of B-Catenin in human endocrine tumors: association with Ki-67 (MIB-1) proliferative activity. Endocr Pathol 11:243–250
50. Stancu M, Wu TT, Wallace C, Houlihan PS, Hamilton SR, Rashid A (2003) Genetic alterations in goblet cell carcinoids of the vermiform appendix and comparison with gastrointestinal carcinoid tumors. Mod Pathol 16:1189–1198
51. Su LK, Vogelstein B, Kinzler KW (1993) Association of APC tumor suppressor protein with catenins. Science 262:1734–1737
52. Sun X, Gong Y, Talamont MS, Rao MS (2002) Expression of cell adhesion molecules, CD44s and E-cadherin, and microvessel density in carcinoid tumors. Mod Pathol 15:1333–1338
53. Takeichi M (1991) Cadherin cell adhesion receptors as a morphogenetic regulator. Science 251:1451–1455
54. Tetsu O, McCormick F (1999) b-catenin regulates expression of cyclin D1 in colon carcinoma cells. Nature 398:422–426
55. Toyooka S, Toyooka KO, Maruyama R, Virmani AK, Girard L, Miyajima K, Harada K, Ariyoshi Y, Takahashi T, Sugio K, Brambilla E, Gilcrease M, Minna JD, Gazdar AF (2001) DNA methylation profiles of lung tumors. Mol Cancer Ther 1:61–67
56. Travis WD, Brambilla E, Muller-Hermelink HK, Harris CC (2004) Tumours of the lung, pleura, thymus and heart. IARC Press, Lyon
57. Ullmann R, Petzmann S, Sharma A, Cagle PT, Popper HH (2001) Chromosomal aberrations in a series of large-cell neuroendocrine carcinomas: unexpected divergence from small-cell carcinoma of the lung. Human Pathol 32:1059–1063
58. Watabe M, Nagafuchi A, Tsukita S, Takeichi M (1994) Induction of polarized cell-cell association and retardation of growth by activation of the E-cadherin–catenin adhesion system in a dispersed carcinoma line. J Cell Biol 127:247–256
59. Xu H, Tanimoto A, Murata Y, Kimura S, Wang KY, Sasaguri Y (2003) Difference in responsiveness of human esophageal squamous cell carcinoma lines to epidermal growth factor for MMP-7 expression. Int J Oncol 23:469–476
60. Yang F, Li X, Sharma M, Sasaki CY, Longo DL, Lim B, Sun Z (2002) Linking b-catenin to androgen-signaling pathway. J Biol Chem 277:11336–11344

Virchows Arch (2005) 447: 978–983
DOI 10.1007/s00428-005-0036-x

ORIGINAL ARTICLE

Sophie Ferlicot · Yves Allory · Eva Compérat · Florence Mege-Lechevalier · Stéphanie Dimet · Mathilde Sibony · Jérome Couturier · Annick Vieillefond

Mucinous tubular and spindle cell carcinoma: a report of 15 cases and a review of the literature

Received: 31 January 2005 / Revised: 25 May 2005 / Accepted: 29 June 2005 / Published online: 18 October 2005
© Springer-Verlag 2005

Abstract Mucinous tubular and spindle cell carcinomas are low-grade renal epithelial neoplasms, which were first recognized as a specific entity in the World Health Organization 2004 classification. Forty-five documented cases have been reported. We present 15 additional cases that were incidentally discovered in ten women and five men, with a mean age of 53 years. The tumor is characteristically made up of large eosinophilic regular spindle cells separated by a myxoid stroma with intercellular alcian-blue-positive clear droplets. In peripheral areas, elongated tubules and papillae covered by cubic cells are found. Until this entity had been defined, pathologists used to classify these tumors as variants of solid papillary carcinomas with compressed and elongated papillae, metanephric adenomas, and sarcomatoid carcinomas. In the literature, cytogenetic data indicate various chromosomal losses and gains, but no loss of 3p or trisomy 7 and/or trisomy 17. In two cases, we demonstrate chromosomal loss involving chromosomes 1, 4, 6, 11, 8, 13, 14, 15, 18, and 22. In our 15 cases, immunohistochemistry favored a distal tubule origin (EMA$^+$, AE1/AE3$^+$, CK7$^+$, CK19$^+$, E-cadherin$^+$, AMACR$^+$, and CD10$^-$). Prognosis was favorable in our cases, while in the literature, two metastatic cases were reported. Further investigations are required to determine the frequency and true prognosis of these tumors, which are easily identifiable morphologically.

Keywords Spindle cells · Mucinous stroma · Low grade · Tubular renal carcinoma

S. Ferlicot (✉) · S. Dimet
Service d'Anatomie Pathologique, Hôpital de Bicêtre,
Paris, France
e-mail: sophie.ferlicot@bct.ap-hop-paris.fr
Tel.: +33-1-45212441
Fax: +33-1-45213281

Y. Allory
Service d'Anatomie Pathologique, Hôpital Henri Mondor,
Créteil, France

E. Compérat
Service d'Anatomie Pathologique, Hôpital La Pitié Salpêtrière,
Paris, France

F. Mege-Lechevalier
Service d'Anatomie Pathologique, Hôpital Edouard Herriot,
Lyon, France

M. Sibony
Service d'Anatomie Pathologique, Hôpital Tenon,
Paris, France

J. Couturier
Département de Génétique, Section Médicale, Institut Curie,
Paris, France

A. Vieillefond
Service d'Anatomie Pathologique, Hôpital Cochin,
Paris, France

Introduction

A novel entity among low-grade renal epithelial neoplasms has recently been identified under the denomination "mucinous tubular and spindle cell carcinoma", which was adopted at the World Health Organization consensus conference on the classification of renal neoplasms in December 2002 [11]. The histological profile of this tumor is well-established, and pathologists easily recognize it on routine hematoxylin–eosin staining (HES) [1]. We report our clinical, histological, and immunohistochemical experiences with 15 such cases.

Materials and methods

Case selection

Fifteen cases of renal tumors, which were originally seen by one of the authors (A.V.) in consultations between 1995 and 2003 and were initially considered as a "compact variant of papillary carcinoma without papillae", corresponded to the new entity. One of the cases had been previously reported [2]. Macroscopic descriptions and follow-up were obtained by communications with referring pathologists.

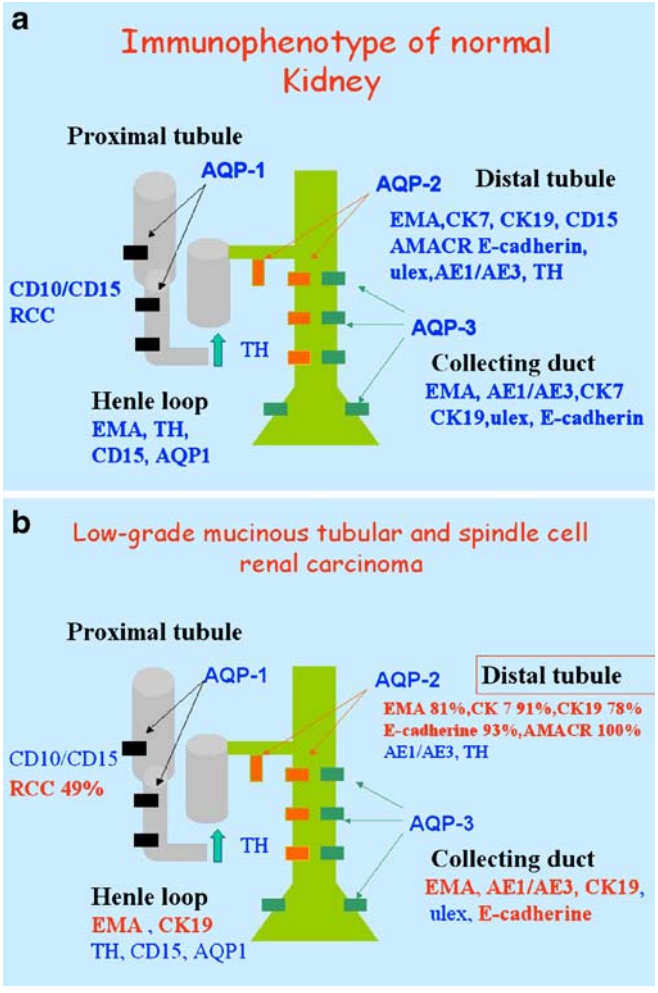


Fig. 1 **a** Immunophenotype of normal kidney. **b** Immunophenotype of low-grade mucinous tubular and spindle cell carcinoma. Results of literature and personal experience

Table 1 Sources and dilutions of the antibodies used in immunohistochemistry

RCC	Monoclonal, clone 66.4.C2, 1/20 (Novocastra, Newcastle upon Tyne, UK)
CD10	Monoclonal, clone 56C6, 1/10 (Novocastra)
CD15	Monoclonal, clone C3D-1, 1/100 (Dako, Denmark)
Aquaporin 1	Polyclonal, 1/50 (Alomone Laboratories, Israel)
EMA	Monoclonal, E29, 1/200 (Dako)
Tamm–Horsfall	Monoclonal, clone THP-1, 1/50 (Cedarlane, California, USA)
AE1/AE3	Monoclonal, clone AE1/AE3, PCK16, 1/100 (Dako)
CK19	Monoclonal, RCK 108, 1/25 (Dako)
E-cadherin	Monoclonal, A42-C7, 1/100 (Zymed, Invitrogen, France)
Aquaporin 3	Polyclonal, 1/100 (Alomone Laboratories)
Ulex	Monoclonal, UEA-1, 1/100 (Vector, Burlingame, CA, USA)
AMACR	Monoclonal, clone RP134, 1/100 (Dako)
Vimentin	Monoclonal, clone Vim3B4, 1/20 (Dako)
Smooth muscle actin	Monoclonal, clone 1A4, 1/500 (Dako)

Immunohistochemistry

Immunohistochemistry stains were performed on paraffin-embedded tissues, with antibodies representing different parts of the nephron (Fig. 1a), to determine the histogenesis of these tumors. We analyzed antibodies for the proximal tubule (RCC, CD10, CD15, and aquaporin 1), the loop of Henle (EMA, Tamm–Horsfall, and CD15), the distal tubule (EMA, Tamm–Horsfall, CD15, AE1/AE3, CK19, E-cadherin, and aquaporin 2), and the collecting duct (EMA, AE1/AE3, CK19, E-cadherin, Ulex, and aquaporin 3). Racemase (AMACR), vimentin, and smooth muscle actin were also explored. Immunohistochemical data are summarized in Table 1.

Results

Clinical data

Clinicopathological data are summarized in Table 2.

Patients' age ranged from 21 to 81 years (mean, 53 years), with a male/female ratio of 1:2. All tumors were solitary, and all had been treated with total nephrectomy. Clinical follow-up, which ranged from 1 to 6 years (mean, 3 years), was available for ten patients. One patient died with lymph node metastasis, but she had also been treated for breast carcinoma. No autopsy was performed, and the origin of lymph node metastasis remained undetermined.

Rough features

The rough aspects of these tumors were highly stereotypical and differed from the usual macroscopic aspects seen in renal carcinomas. The tumors were well-defined and had a firm, smooth consistency. They consistently

Table 2 Clinicopathological data in our 15 personal cases

Case	Sex	Age (years)	Size	Follow-up
1	F	41	11	NED, 4 years
2	F	44	6	Death from unknown causes
3	M	58	3.8	NA
4	F	81	8	NA
5	F	81	10	NED, 4 years
6	F	75	3	NED, 4 years
7	F	27	6	NED, 2 years
8	M	62	4	NA
9	M	27	10	NA
10	M	54	4	NED, 6 years
11	F	68	3	NA
12	F	46	9	NED, 2 years
13	M	65	3.5	NED, 1 year
14	F	44	4.5	NED, 1 year
15	F	21	4.5	NED, 1 year

M Male, *F* female, *NED* no evidence of disease, *NA* not available



Fig. 2 Mucinous tubular and spindle cell carcinoma rough features. Well-defined whitish tumor

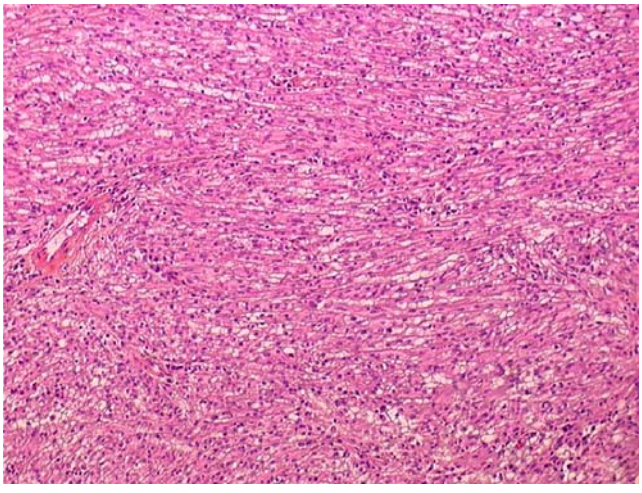


Fig. 3 Mucinous tubular and spindle cell carcinoma histology. Sheets of regular spindle cells separated by mucinous stromas that are made up of clear droplets (HES, ×10)

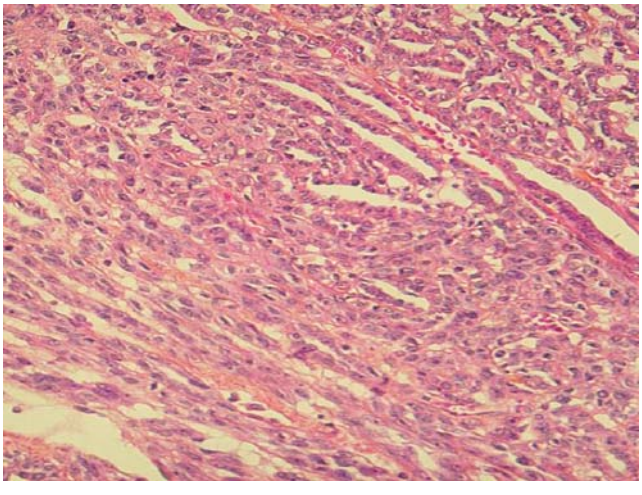


Fig. 4 Mucinous tubular and spindle cell carcinoma histology. Fusiform cells and peripheral elongated papillae (HES, ×20)

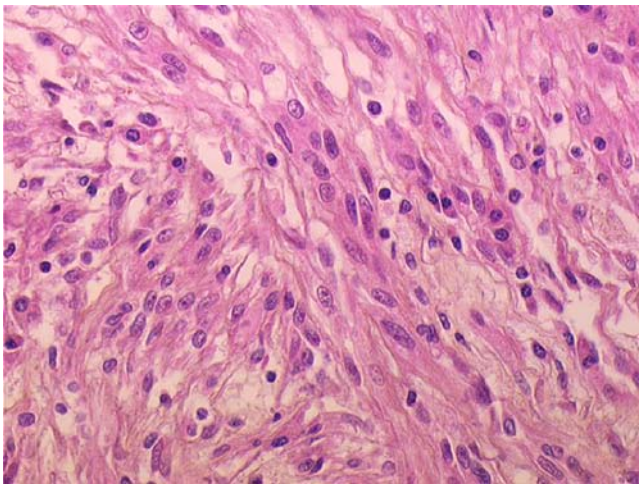


Fig. 5 Mucinous tubular and spindle cell carcinoma histology. Fuiform cells with regular nuclear features and eosinophilic cytoplasm (HES, ×40)

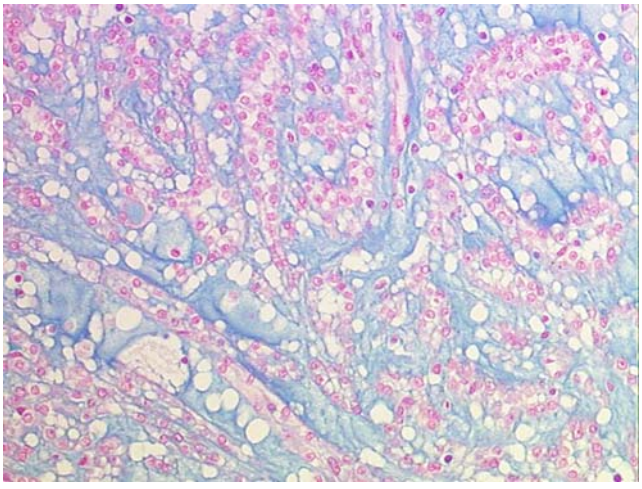


Fig. 6 Mucinous tubular and spindle cell carcinoma histology. Alcian blue staining of mucinous stroma (HES, ×40)

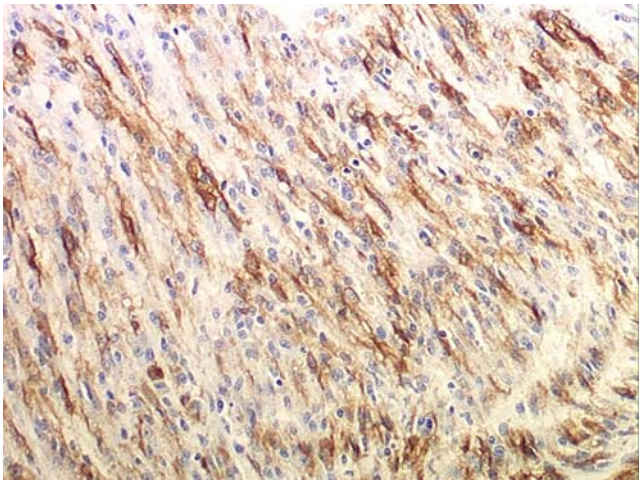


Fig. 7 Mucinous tubular and spindle cell carcinoma immunohistochemistry. CK19 positivity of spindle cells

Table 3 Immunohistochemical data: 45 literature cases and 15 personal cases

Antibodies	References							Our series	Total (%)
	[3]	[4]	[5]	[7]	[8]	[9]	[13]		
Vimentin	+	8+/11	2+/2	+	4+/4	2+/5	NA	2+/14	55
Smooth muscle actin	−	−	NA	NA	NA	NA	NA	−	
EMA	+	4+/11	2+/2	+	4+/4	5+/5	NA	14+/14	81
AE1/AE3	+	6+/11	2+/2	+	4+/4	NA	NA	13+/13	83
CK7	NA	6+/9	2+/2	NA	4+/4	NA	NA	14+/14	91
CK19	NA	NA	NA	NA	NA	4+/5	14+/21	13+/13	78
CK903	NA	NA	2+/2	−	4+/4	NA	NA	2+/14	32
CD10	NA	NA	NA	−	NA	NA	1+/21	3+/14	9
CD15	−	−	2−/2	+	4−/4	NA	NA	4+/14	16
RCC	NA	NA	NA	NA	NA	5−/5	13+/21	5+/11	49
Tamm–Horsfall	NA	NA	NA	NA	NA	NA	1+/21	11−/11	0
Ulex	NA	NA	2−/2	+	1+/4	5−/5	21−/21	6+/14	16
Bnh9	NA	NA	NA	NA	NA	NA	NA	1+/14	8
Aquaporin 1	NA	NA	NA	NA	NA	NA	NA	2+/11	18
Aquaporin 3	NA	NA	NA	NA	NA	NA	NA	2+/11	18
E-cadherin	NA	NA	NA	+	NA	NA	NA	10+/11	93
AMACR	NA	NA	NA	NA	NA	NA	NA	12+/12	100

NA Not Available

displayed a whitish aspect with grayish sectors. Necroses and hemorrhages were rare (Fig. 2). Their diameter varied between 3 and 11 cm (mean diameter, 6 cm).

Microscopic findings

On microscopic examination, a predominant pattern of regular spindle cells arranged in sheets (Fig. 3) and some peripheral areas with cuboidal regular cells arranged in cord tubules and papillae (Fig. 4) consistently existed. Spindle cell areas consisted of monotonous sheets of fairly uniform cells with large eosinophilic cytoplasms. The tubular papillary pattern was made up of cuboidal cells with eosinophilic cytoplasm. Tumor cells always displayed a low nuclear grade (Fig. 5), while the interstitium appeared clear. Numerous small intercellular droplets locally formed an abundant myxoid stroma. The stroma reacted characteristically with alcian blue (Fig. 6). Clusters of foamy cells were present in papillae and also among fusiform cells. No vascular or sinus invasion or lymph node metastases were observed.

Immunohistochemistry

In all our cases, immunophenotype was epithelial, with an expression of a panel of epithelial markers in most cells: EMA, AE1/AE3, CK7, and CK19 (Fig. 7). E-cadherin expression was observed in 90% of cases, and AMACR (racemase) was strongly expressed in 100% of them. RCC was expressed in 45% of cases.

A few cases displayed an expression of vimentin, CD10, CD15, aquaporin 1, aquaporin 3, Tamm–Horsfall protein, or Ulex.

Table 3 and Fig. 1b summarize immunohistochemical findings in 45 cases from the literature and in our personal series of 15 cases.

Cytogenetic analysis

Two cases were selected for cytogenetic analysis. For one tumor, comparative genomic hybridization showed chromosomal losses involving chromosomes 1, 4, 6, 8, 13, 14, 15, and 18. For the second tumor, the karyotype was hypodiploid (42, XX), with chromosomal losses involving chromosomes 1, 6, 11, 14, and 22 and with a gain on chromosome 15.

Discussion

Low-grade mucinous tubular and spindle cell carcinomas can easily be identified and separated from other primitive renal malignancies. Since 1998, single cases and small series have been reported [3–5, 7–10, 13]. They are preferentially observed in adults, with female predominance. These tumors constitute firm, compact, whitish, well-defined masses [9]. Microscopically, they have the same typical features as those described in our series, including an interconnecting tubular and spindled architecture within myxoid stromas and low-grade nuclei.

As seen in Table 2, our results are similar to those found in the literature, except for vimentin staining, which was expressed in only a few of our cases in contrast to half of the cases in the literature.

For the first time, we have explored two additional markers AMACR and aquaporin 3. Our study demonstrates the

positivity of AMACR in 100% of cases and the expression of aquaporin 3 in a few cases.

Immunohistochemical data do not enable the elucidation of the exact histogenenesis of these tumors. Epithelial markers, especially CK7, CK19, EMA, E-cadherin, and AMACR, have been shown to be positive in 80–100% of cases both in the literature and in our series. Although these markers are not specific to the distal tubule, their positivity lends support to the hypothesis of a distal tubule origin. The rest of the markers, which are more specific to the proximal tubules (CD10 and aquaporin 1), the loop of Henle (Tamm–Horsfall, CD15, and Ulex), and the collecting duct (aquaporin 3), are expressed in only a few cases. As in our series, Weber et al. [13] eliminated the hypothesis of proximal tubular origin, as they found only 1 of 21 cases to be weakly marked by CD10. However, they described positivity for RCC but excluded a proximal origin, as RCC remains a new marker that does not seem to be very reliable. They also found very weak Tamm–Horsfall protein staining, which tends to refute the hypothesis of a loop-of-Henle origin, which had previously fueled controversy [10]. Moreover, AMACR expression rendered a distal tubular origin more likely [12]. Rakozy et al. [9] observed a weak expression of vimentin in the periphery in two of five cases. These results complemented our series, with positivity in 2 of 14 cases (14%).

Cytogenetic studies demonstrate that mucinous tubular and spindle cell carcinoma seems to have very high genomic instability [13]. In the cases explored in the literature and in two personal cases, karyotyping, comparative genomic hybridization, and fluorescent in situ hybridization demonstrate complex genomic aberrations, with losses (on chromosomes 1, 4, 6, 8, 13, and 14) and gains (on chromosomes 7, 11, 16, and 17). Although these abnormalities are varied and nonspecific, loss of chromosome 3p, trisomy 7, and/or trisomy 17 has never been encountered. This is a strong argument for the hypothesis that mucinous tubular and spindle cell carcinoma is a distinctively new entity [6].

Differential diagnosis with other renal tumors presented a problem prior to the definition of this entity.

Pathologists might tend to classify this tumor as a variant of solid papillary carcinoma with compressed and elongated papillae, metanephric adenoma, collecting duct carcinoma, or fusiform sarcomatoid carcinoma [11].

The most accurate diagnosis would be that of a solid variant of type 1 papillary carcinoma. Macroscopically, papillary carcinomas are quite different—often not very firm, but necrotic; not whitish, but yellowish. However, a solid variant has been described. Papillary carcinomas have a predominantly tubulopapillary pattern, but compression of elongated tubules and papillae can create a fusiform pattern. The hypothesis that there exists a continuum between the fusiform areas observed in mucinous tubular and spindle cell carcinomas and tubulopapillary structures is reinforced by the presence of lipophage nests within tumor cells. However, mucinous stroma is never observed in papillary carcinomas. Moreover, genomic profile without trisomy 7 and/or trisomy 17 has eliminated the diagnosis of solid papillary carcinoma. Metanephric adenoma has a different pattern: cells are small, cuboidal, and embryonic in appearance, with a very scant cytoplasm and a hyperchromatic oval nucleus. There is no myxoid stroma, but psammoma bodies may be present. Immunohistochemical profile is not discriminative: keratins and vimentin can be expressed by both tumors. However, negativity for CK7 is usually found in metanephric adenomas. Collecting duct carcinomas may have a papillary compact growth pattern, but they have larger eosinophilic cells with marked atypia. The stroma is often fibrous with necrosis. Ulex, the emblematic marker of collecting duct carcinomas, is expressed only in rare cases. The diagnosis of sarcomatoid carcinoma can be evoked. In some areas, sarcomatoid carcinomas display monotonous fusiform cells without atypia, but in other areas, they are obviously high-grade tumors with marked nuclear atypia and numerous mitoses.

In our series, prognosis seems to be favorable based on low histological grade, with a follow-up of between 1 and 6 years. In the literature, two cases with lymph node metastasis have been reported [4, 13]. In conclusion, we feel that the true frequency of this entity is probably underestimated. It is essential to report new cases to determine the frequency and prognosis of low-grade mucinous tubular carcinomas.

Acknowledgements We thank Dr. Bergemere-Fouquet (Tours), Dr. Billey Kijner (Villennes-sur-Seine), Dr. Bourdier (Brest), Dr. Bouvier (Lyon), Dr. Chanoz-Poulard (Roanne), Dr. Douchet (Saint-Etienne), Dr. Hibon (Reims), Dr. Jouannelle (Fort de France), Dr. Kaffe (Paris), Dr. Kapfer (Orléans), Dr. Krzisch (Colmar), Prof. Lhuintre (Tours), Dr. Loridon (Paris), Dr. Mirica (Paris), Dr. Tricot (St. Germain-en-Laye), and Dr. Vuong (Bièvres) for kindly providing the cases and the illustrations.

References

1. Eble JN (2003) Mucinous tubular and spindle cell carcinoma and post-neuroblastoma carcinoma: newly recognised entities in the renal cell carcinoma family. Pathology 35:499–504
2. Ferlicot S, Lupo A, Lazure T, Bedossa P, Vieillefond A (2005) A novel entity: low grade mucinous tubular renal carcinoma. Histopathology 47:218–219
3. He Q, Ohaki Y, Mori O, Asano G, Tuboi N (1998) A case report of renal cell tumor in a 45-year-old female mimicking lower portion nephrogenesis. Pathol Int 48:416–420
4. Hes O, Hora M, Perez-Montiel DM, Suster S, Curik R, Sokol L, Ondic O, Mikulastik J, Betlach J, Peychl L, Hrabal P, Kodet R, Straka L, Ferak I, Vrabec V, Michal M (2002) Spindle and cuboidal renal cell carcinoma, a tumor having frequent association with nephrolithiasis: report of 11 cases including a case with hybrid conventional renal cell carcinoma/spindle and cuboidal renal cell carcinoma components. Histopathology 4:549–555
5. Leroy X, Aubert S, Gosselin B (2002) Low-grade myxoid renal epithelial neoplasms with distal nephron differentiation: a distinct clinicopathologic entity? Human Pathol 33:574–575
6. Meloni-Ehrig AM (2002) Renal cancer: cytogenetic and molecular genetic aspects. Am J Med Genet 115(3):164–172
7. Otani M, Shimizu T, Serizawa H, Ebihara Y, Nagashima Y (2001) Low-grade renal cell carcinoma arising from the lower nephron: a case report with immunohistochemical, histochemical and ultrastructural studies. Pathol Int 51:954–960

8. Parwani AV, Husain AN, Epstein JI, Beckwith JB, Argani P (2001) Low-grade myxoid renal epithelial neoplasms with distal nephron differentiation. Human Pathol 32:506–512
9. Rakozy C, Schmahl GE, Bogner S, Störkel S (2002) Low-grade tubular–mucinous renal neoplasms: morphologic, immunohistochemical, and genetic features. Mod Pathol 15:1162–1171
10. Srigley JR, Eble JN, Grignon DJ, Hartwick RWJ (1999) Unusual renal cell carcinoma (RCC) with prominent spindle cell change possibly related to the loop of Henle. Mod Pathol 12:107A
11. Srigley JR (2004) Mucinous tubular and spindle cell carcinoma. WHO classification of tumors In: Eble JN, Sauter G, Epstein JI, Sesterhenn IA (eds) Tumors of the genito-urinary and male genital organs. IARC, Washington, DC, USA
12. Tretiakova MS, Sahoo S, Takahashi M, Turkyilmaz M, Vogelzang NJ, Lin F, Krausz T, Teh BT, Yang XJ (2004) Expression of alpha-methylacyl-CoA racemase in papillary renal cell carcinoma. Am J Surg Pathol 28:69–76
13. Weber A, Srigley J, Moch H (2003) Mucinous spindle cell carcinoma of the kidney. A molecular analysis. Pathologe 24: 453–459

Virchows Arch (2005) 447: 984–989
DOI 10.1007/s00428-005-0031-2

ORIGINAL ARTICLE

Yukitoshi Satoh · Yuichi Ishikawa · Kentaro Inamura · Sakae Okumura · Ken Nakagawa · Eiju Tsuchiya

Classification of parietal pleural invasion at adhesion sites with surgical specimens of lung cancer and implications for prognosis

Received: 8 February 2005 / Accepted: 15 June 2005 / Published online: 21 September 2005
© Springer-Verlag 2005

Abstract Parietal pleural invasion of non-small cell lung cancer (NSCLC) is a factor for poor prognosis, and a tumor of any size that invades the parietal pleura is classified as T3. However, with microscopic invasion beyond elastic fibers of the visceral pleura but no penetration to the parietal pleura at tight adhesion sites (we term this p1–3), classification as to the T factor is unclear. Among 1,179 consecutive patients with NSCLCs who underwent curative surgery between 1980 and 2002, 20 were in this category. Here, a comparison was made with subgroups of p stages IB, II, and IIIA with regard to histology, pleural invasion, and survival rates. To maximize the power of assessing prognostic potential, we set the significance level at 0.10, one-sided. The p1–3 condition sites of the 20 cases were the parietal pleura for 17 cases and the pericardium, diaphragm, and chest wall for one each of the remainder. The 5-year survival rate for these p1–3 patients was 71.6%. Significant differences were observed between p1–3 and IIIA groups. Although the 5-year survival rates did not significantly differ between p1–3 and T3N0 or unequivocal T3 subgroups, the prognosis of p1–3 patients was rather better than that of T3 and identical to T2. It was demonstrated that p1–3 status is not a factor warranting T3 classification for NSCLCs. Considering the prognosis, pathologic p1–3 tumors should be managed as a T2 disease for the present.

Keywords Lung cancer · Surgery · Pathology · Pleural invasion · Prognosis · Staging

Y. Satoh · Y. Ishikawa · K. Inamura
Department of Pathology, The Cancer Institute,
The Japanese Foundation for Cancer Research,
Koto-ku,
Tokyo, 135-8550, Japan

Y. Satoh (✉) · S. Okumura · K. Nakagawa
Department of Chest Surgery, The Cancer Institute Hospital,
The Japanese Foundation for Cancer Research,
Koto-ku,
Tokyo, 135-8550, Japan
e-mail: ysatoh@jfcr.or.jp
Tel.: +81-3-3520-0111
Fax: +81-3-3570-0343

E. Tsuchiya
Research Institute, Kanagawa Cancer Center,
Nakao, Asahi-ku, Yokohama,
Kanagawa, 241-0815, Japan

Introduction

Pleural invasion of lung cancers is recognized as an important poor prognostic factor [1–3]. Visceral pleural invasion has been adopted as a specific parameter in the current Tumor–Node–Metastasis (TNM) classification of the International Union Against Cancer (UICC) staging system [4, 5]: a lung cancer tumor of any size that invades the visceral pleura is classified as T2, and it is classified as T3 when it directly invades the chest wall including the parietal pleura, diaphragm, mediastinal pleura, or parietal pericardium [4, 5] (Fig. 1).

The UICC TNM classification includes little detail on histological pleural invasion in its definitions. In contrast, the Japan Lung Cancer Society (JLCS) classifies visceral pleural invasion based upon histological examinations as follows: p0, tumor with no pleural involvement beyond its elastic layer; p1, tumor extension beyond the elastic layer of the visceral pleura but with no exposure on the pleural surface; p2, tumor exposure on the pleural surface but no involvement of adjacent anatomic structures; and p3, tumor that involves adjacent anatomic structures [6] (Fig. 1). The Society classifies a p2 tumor of any size as T2 and a p1 tumor of 3 cm or less as T1.

However, there is no clear definition as to the T factor when a tumor shows invasion extending beyond the visceral pleura but with no clear adjacent parietal pleural invasion despite tight adhesion between visceral and parietal pleurae histologically (we term this p1–3; Figs. 1, 2). From a practical matter, this pathologic issue poses a potential staging problem in spite of a small subset of the total number of patients with this status. The current TNM classification does not take this condition into account [4, 5].

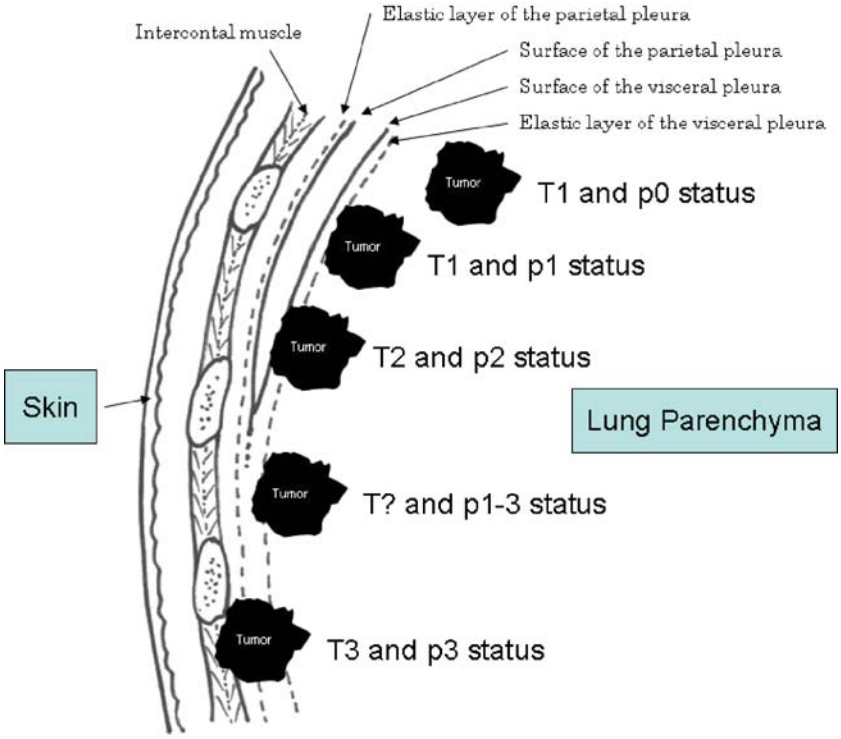


Fig. 1 Schematic illustration of the T factor and the histological pleural invasion grades. The current TNM classifications of the UICC staging system are as follows: T1 disease is defined as a tumor 3 cm or less in greatest dimension, surrounded by lung or visceral pleura; T2 disease involves tumors more than 3 cm in greatest dimension and/or invasion of the visceral pleura; and T3 disease is a tumor of any size that directly invades the chest wall, including the parietal pleura. On the other hand, the JLCS classifications of visceral pleural invasion based upon histological examinations are as follows: p0, tumor with no pleural involvement beyond its elastic layer; p1, a tumor that extends beyond the elastic layer of the visceral pleura but with no exposure on the pleural surface; p2, a tumor with exposure on the visceral pleural surface but no involvement of adjacent anatomic structures; and p3, a tumor that involves adjacent anatomic structures. However, there is no clear definition as to the p factor when a tumor extends beyond the visceral pleura but has no clear adjacent parietal pleural invasion in cases with tight adhesion between visceral and parietal pleurae histologically (we term this condition p1–3)

Since unequivocal parietal pleural invasion is diagnosed as T3, the question arises as to whether invasion beyond the visceral pleura at tight adhesion sites (excluding interlobar invasion) should also be considered in the same way. To clarify this point, a series of resected non-small cell lung cancers (NSCLCs) with invasion histologically demonstrated beyond the visceral pleura at adhesion sites were studied here.

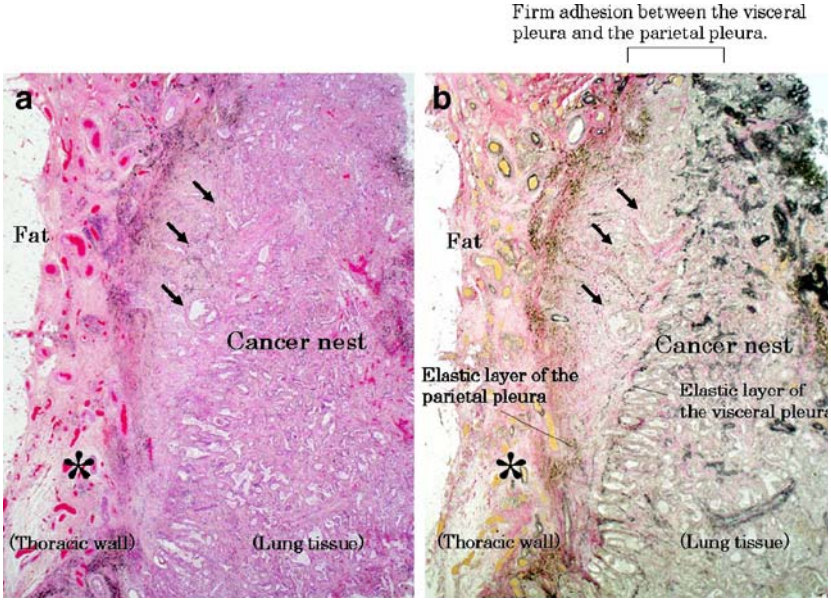


Fig. 2 Histologic features of a p1–3 case. Note cancer invasion extending beyond the visceral pleura with firm adhesion between visceral and parietal pleurae (*arrows*). However, destruction of parietal elastic fibers and chest wall invasion are not apparent. (**a** Hematoxylin and eosin stain, ×4; **b** elastica van Gieson stain, ×4; *asterisks* indicate the endothoracic fascia.)

Materials and methods

Between 1980 and 2002, 1,179 consecutive patients with NSCLCs underwent curative surgical resection at the Cancer Institute Hospital. Staging definitions for T (primary tumor), N (regional lymph nodes), and M (distant metastasis) components were according to the International Staging System for Lung Cancer [4, 5]. Twenty lung cancer patients (1.7%) with p1–3 pleural invasion were included. These patients were studied clinically and pathologically in comparison with cases having stage IB (T2N0), IIA (T1N1), IIB (T2N1 or T3N0), or IIIA (N2 disease) treated during the same period.

Histologically, pleural invasion was evaluated by elastic fiber staining and subdivided into four pleural invasion grades according to the JLCS criteria [6], as follows: p0, tumor with no pleural involvement beyond its elastic layer; p1, tumor that extends beyond the elastic layer of the visceral pleura but is not exposed on the pleural surface; p2, tumor that is exposed on the pleural surface but does not involve adjacent anatomic structures; and p3, tumor that involves adjacent anatomic structures with destruction of parietal pleural elastic fibers (Fig. 1). Briefly, p0 and p1 diseases belong to T1, p2 to T2, and p3 to T3 disease. Further, the p1–3 status was identified as follows: invasion extending beyond the visceral pleura but showing unclear parietal pleural invasion (excluding interlobar invasion) in cases with firm adhesion between the tumor and parietal pleura (Fig. 2). In this condition, parietal pleural invasion was hard to evaluate due to destruction of parietal pleural elastic fibers as a result of inflammatory process. When the elastic layer of the visceral pleura was not sufficiently well developed, we turned the existence of fat layer to account as an auxiliary pointer for parietal pleura.

Table 1 Clinicopathologic status of the examined p1–3 patients (n=20)

No. of patients	
Men	19
Woman	1
Age (years)	
Mean	68.9
Tumor location	
Right	7
Left	13
No. of smokers	19
Histologic type	
Adenocarcinoma	9
Squamous cell carcinoma	7
Large cell carcinoma	4
Tumor diameter (mm)	
Range	20–95
Type of operation	
Segmentectomy	1
Lobectomy	17
Bilobectomy	1
Pneumonectomy	1

Table 2 Preoperative and postoperative T and N status for the p1–3 group (n=20)

	Preoperative	Postoperative[a]
T status		
T1	5	–
T2	12	–
T3	3	–
N status		
N0	15	14
N1	3	1
N2	1	5
N3	1	0

[a]All cases were diagnosed as p1–3 on postoperative pathological examination

The 20 patients with p1–3 were 19 men and one woman with an age distribution of 44–80 years. The tumors comprised nine adenocarcinomas, seven squamous cell carcinomas, and four large cell carcinomas (Table 1). There were 14 N0, one N1, and five N2 cases (Table 2). Lobectomy and parietal resection with a sufficient safety margin was performed for 18 patients, bilobectomy for one, and pneumonectomy for the remaining one. Parietal resection included the parietal pleura in 17 cases, and the pericardium, diaphragm, and chest wall in one case each. En bloc mediastinal lymph node dissection was performed for all patients, and lymph nodes were carefully examined for pathological staging. Five suffered relapses and died of lung cancer (one with locoregional recurrence, two with distant metastases, and two for which precise data were not available). One patient died of pneumonia. Fourteen patients are alive and disease-free 5 years after surgery.

Survival curves were plotted using the Kaplan–Meier method, and p values were calculated using the log-rank test, $p<0.1$ being considered statistically significant. To maximize the power to detect a potential of p1–3 as a prognostic marker, we set the significance level at 0.10, one-sided, in accordance with common statistical practice and the proposal by Makuch and Simon [7].

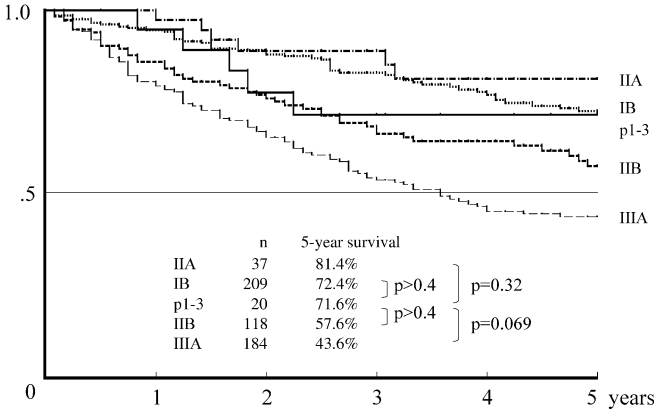


Fig. 3 The 5-year survival rates for patients with p1–3 or stage IB, IIA, IIB, or IIIA disease

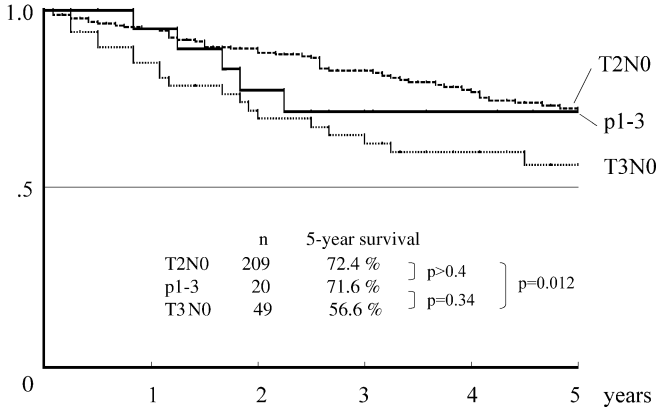


Fig. 4 The 5-year survival rates for patients of the p1–3, T2N0, and T3N0 subgroups

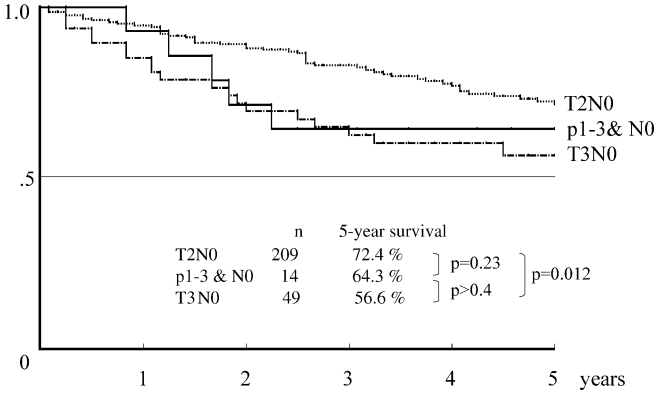


Fig. 6 The 5-year survival rates for patients of the p1–3 and N0, T2N0, and T3N0 groups

The operative technique was as follows: the chest cavity of each patient was entered posterolaterally. Within the pleural cavity, the limits of chest wall invasion and the state of the mediastinal lymph nodes were explored to ascertain operability. To define the disease-free margins of resection for the parietal pleura, diaphragm, rib and pericardium, the tumor was palpated and the boundaries were grossly assessed. Thus, a free margin was estimated, and en bloc resection of the chest wall with lungs was performed. When obvious chest wall invasion was not found but tight adhesion between visceral and parietal pleurae near the tumors was apparent, extrapleural resection was performed. Areas suspected of neoplastic involvement at the margin were sent for immediate histologic analysis of frozen sections.

Results

First, the p1–3 group was compared with those with stage IB (n=209), IIA (n=37), IIB (n=118), and IIIA (n=184) diseases regarding survival. The 5-year survival rates were 71.6, 72.4, 81.4, 57.6, and 43.6%, respectively, with significant intergroup differences for IB and IIIA, IIA and IIIA, IIB and IIA (p<0.05), and p1–3 and IIIA (p=0.069) (Fig. 3).

Then, 5-year survival rates were compared between p1–3 and stage IB (T2N0), and IIB (T3N0 and T2N1) subgroups with regard to status of pleural invasion and lymph node metastasis. When disease was subclassified into T2N0 (n=209), T3N0 (n=49) and p1–3, the values were 72.4, 56.6, and 71.6%, respectively. Those for T3N0 and T2N1 were 56.6 and 58%, respectively. No significant differences in prognosis were evident between p1–3 patients and T3N0 or T2N1 subgroups (Fig. 4). Among the N0 and pm0 (no intrapulmonary metastasis) patients, the 5-year survival rates for p0 (n=401), p1 (n=74), p2 (n=39), p3 (n=51), and p1–3 groups were 87.2, 74.4, 54.6, 50.4, and 71.6%, respectively, being statistically significant between p0 and p1–3 (p=0.006) and p0 and p1 subgroups (p=0.003) (Fig. 5). Although no significant difference in survival rates was found between p1–3 and p2 or p3 subgroups, the 5-year survival rate of the p3 subgroup was poorer than those of p1–3 (Fig. 4). The 5-year survival rates of patients with T2N0 (n=209), T3N0 (n=49), and p1–3 with N0 (n=14) were 72.4, 56.6, and 64.3%, respectively, the differences between p1–3 and T2N0 or T3N0 subgroups not being statistically significant (p values were

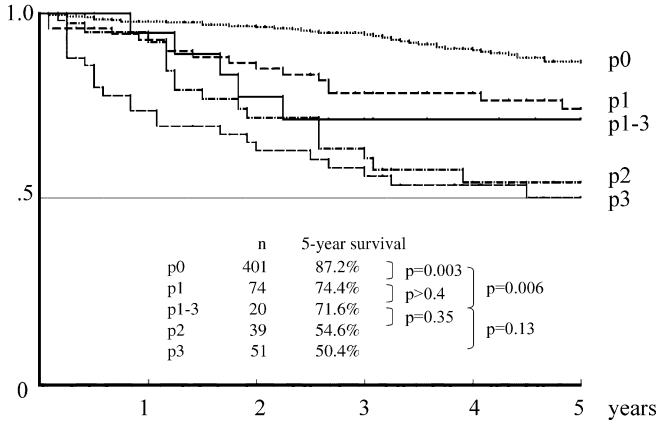


Fig. 5 The 5-year survival rates for patients with different p factor grades

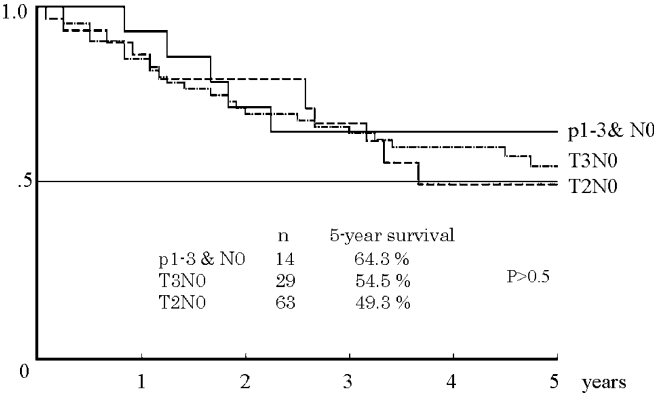


Fig. 7 The 5-year survival rates for patients of the p1–3 and N0, T2N0, and T3N0 groups of cases undergoing pulmonary with chest wall resection

0.23 and >0.4; Fig. 6). Moreover, the 5-year survival rates of patients with T2N0 (n=63), T3N0 (n=29), and p1–3 with N0 (n=14), a series of cases undergoing pulmonary resection with chest wall resection, were 49.3, 54.5, and 64.3%, respectively, the differences not being statistically significant (p values >0.5; Fig. 7).

Among five cases with N2 disease in the p1–3 group, two remain alive without evidence of disease, one alive with disease, and two died of other diseases, which suggest a relatively good prognosis.

Although chest wall invasion was assessed preoperatively in three cases (15%), no patient had symptoms of chest pain (Table 2).

Postoperative radiotherapy was carried out for two (10%) patients in the p1–3 group. Preoperative systemic chemotherapy was also administered in only one case, but none received such drugs postoperatively.

Discussion

It was reported that elastic fiber stains provide prognostically important information for diagnosis of pleural invasion [8, 9]. However, it is difficult to determine the accurate pleural invasion factor histologically when a cancer shows the p1–3 status, extending beyond elastic fibers of visceral pleura but not reaching those of the parietal pleura at tight adhesion sites. We therefore performed the present comparative study, which indicated that classification as a T2 disease may be most appropriate. Thus, the outcome was better than that of patients with T3 invasion, although without statistical significance because of the small numbers. The outcome of five cases with N2 disease indicates that complete resection is a more influential positive factor for prognosis than the degree of pleural invasion [10]. Our results therefore agree with the currently prevailing notion that long-term survival is related to the extent of nodal involvement and completeness of resection in lung cancer with chest wall invasion [11–13].

Preoperative diagnosis of chest wall invasion is still a matter of debate [5]. Modalities such as chest X-rays, ultrasounds, CT, and magnetic resonance imaging lack specificity and sensitivity, except in the presence of extensive bone destruction [14, 15]. In our series, invasion beyond visceral pleura was not evident in CT scans of 17 patients (85%), and this approach may be inaccurate for assessing the p1–3 status.

Visceral pleural invasion, which is frequently associated with extensive N2 involvement of lung cancer, is a factor of poor prognosis [3, 16]. In our p1–3 group, nodal involvement was very few, and the presence of lymph node metastases did not reduce survival time. We did not use N factor in the current study for survival analysis because there was no significant difference in preoperative and postoperative N status in our series (Table 2).

A number of investigators have reported that patients with chest wall invasion show different prognoses depending on the site, i.e., whether it be the parietal pleura, intercostal muscle layer, or ribs [17, 18]. When a lung cancer invades beyond the parietal pleura (T3 status), en bloc resection of both lung and chest wall resection should be performed. As a surgical procedure, Akay et al. have argued that an extrapleural resection provides adequate tumor clearance of firm adhesion between the tumor and only the parietal pleura of the chest wall [19]. However, in a series reported by Albertucci et al., the rate of local recurrence was significantly lower in patients undergoing en bloc chest wall resection than their counterparts receiving extrapleural resection [20]. When comparing the stages and p factors, we found similar survival times between the p1–3 group and stage IB and p1 subgroups (Figs. 2, 3, 4). We conclude, therefore, that extrapleural resection is appropriate for NSCLCs with p1–3 status.

In conclusion, our results indicate that p1–3 patients should be managed as having a T2 disease for the present, and that in such cases, complete tumor removal improves the long-term survival. Because of the small number of patients available for this analysis, additional studies are warranted for validation of p1–3 status as a T2 disease for NSCLCs.

Acknowledgements This study was supported by Grants-in-aid from the Ministry of Education, Sports, Culture, Science and Technology, as well as grants from the Ministry of Health, Labour and Welfare, the Smoking Research Foundation, and the Vehicle Racing Commemorative Foundation. We thank Ms. Miyuki Kogure, Kazuko Yokokawa, and Mr. Motoyoshi Iwakoshi for their technical assistance. We also thank Mr. Hiroyuki Kubonoya for his artistic assistance.

References

1. Brewer LA, Bai AF, Little JN, Pardo GR (1958) Carcinoma of the lung: practical classification of early diagnosis and survival treatment. JAMA 166:1149–1154
2. Ichinose Y, Yano T, Asoh H, Yokoyama H, Yoshino I, Katsuda Y (1995) Prognostic factors obtained by a pathologic examination in completely resected non-small-cell lung cancer. An analysis in each pathologic stage. J Thorac Cardiovasc Surg 110:601–605
3. Manac'h D, Riquet M, Medioni J, Le Pimpec-Barthes F, Dujon A, Danel C (2001) Visceral pleura invasion by non-small cell lung cancer: an underrated bad prognostic factor. Ann Thorac Surg 71:1088–1093
4. Mountain CF (1997) Revisions in the international system for staging lung cancer. Chest 111:1710–1717
5. International Union Against Cancer (2002) TNM classification of malignant tumours, 6th edn. Wiley-Liss, New York, pp 97–103
6. Japan Lung Cancer Society (2003) General rule for clinical and pathologic record of lung cancer [in Japanese], 6th edn. Kanehara, Tokyo
7. Makuch R, Simon R (1978) Sample size requirements for evaluating a conservative therapy. Cancer Treat Rep 62:1037–1040
8. Bunker ML, Raab SS, Landreneau RJ, Silverman JF (1999) The diagnosis and significance of visceral pleural invasion in lung carcinoma. Histologic predictors and the role of elastic stains. Am J Clin Pathol 112:777–783
9. Gallagher B, Urbanski SJ (1990) The significance of pleural elastica invasion by lung carcinomas. Hum Pathol 21:512–517

10. Miura H, Taira O, Uchida O, Kato H (1998) Invasion beyond interlobar pleura in non-small cell lung cancer. Chest 114: 1301–1304
11. Magdeleinat P, Alifano M, Benbrahem C, Spaggiari L, Porrello C, Puyo P, Levasseur P, Regnard JF (2001) Surgical treatment of lung cancer invading the chest wall: results and prognostic factors. Ann Thorac Surg 71:1094–1099
12. Miller JD, Gorenstein LA, Patterson GA (1992) Staging: the key to rational management of lung cancer. Ann Thorac Surg 53:170–178
13. Facciolo F, Cardillo G, Lopergolo M, Pallone G, Sera F, Martelli M (2001) Chest wall invasion in non-small cell lung carcinoma: a rationale for en bloc resection. J Thorac Cardiovasc Surg 121:649–656
14. Nakano N, Yasumitsu T, Kotake Y, Morino H, Ikezoe J (1994) Preoperative histologic diagnosis of chest wall invasion by lung cancer using ultrasonically guided biopsy. J Thorac Cardiovasc Surg 107:891–895
15. Albain KS, Hoffman PC, Little AG, Bitran JD, Golomb HM, DeMeester TR, Griem ML, Blough RR, Skosey C (1986) Pleural involvement in stage IIIM0 non-small-cell bronchogenic carcinoma. A need to differentiate subtypes. Am J Clin Oncol 9:255–261
16. Kang JH, Kim KD, Chung KY (2003) Prognostic value of visceral pleura invasion in non-small cell lung cancer. Eur J Cardiothorac Surg 23:865–869
17. McCaughan BC, Martini N, Bains MS, McCormack PM (1985) Chest wall invasion in carcinoma of the lung. Therapeutic and prognostic implications. J Thorac Cardiovasc Surg 89:836–841
18. Ratto GB, Piacenza G, Frola C, Musante F, Serrano I, Giua R, Salio M, Jacovoni P, Rovida S (1991) Chest wall involvement by lung cancer: computed tomographic detection and results of operation. Ann Thorac Surg 51:182–188
19. Akay H, Cangir AK, Kutlay H, Kavukcu S, Okten I, Yavuzer S (2002) Surgical treatment of peripheral lung cancer adherent to the parietal pleura. Eur J Cardiothorac Surg 22:615–620
20. Albertucci M, DeMeester TR, Rothberg M, Hagen JA, Santoscoy R, Smyrk TC (1992) Surgery and the management of peripheral lung tumors adherent to the parietal pleura. J Thorac Cardiovasc Surg 103:8–12

Virchows Arch (2005) 447: 990–995
DOI 10.1007/s00428-005-0043-y

CASE REPORT

Lars Morawietz · Cornelius Kuhnen · Detlef Katenkamp · Philipp Le Coutre · Axel Ladhoff · Iver Petersen

Unusual sarcomatoid neoplasm of the lung suggesting a myofibrosarcoma

Received: 15 April 2005 / Accepted: 7 July 2005 / Published online: 13 September 2005
© Springer-Verlag 2005

Abstract Myofibrosarcoma is a rare neoplasm that occurs mainly in the head and neck region and extremities of middle-aged patients. It often appears as a low-grade sarcoma and rarely metastasizes. We report the case of a 47-year-old male patient with a malignant mesenchymal pulmonary tumor affecting almost the entire lower left lobe. Clinically suggestive for a lung carcinoma, the tumor showed typical features of a myofibrosarcoma. A major spindle cell component was observed being positive for smooth-muscle actin, calponin, and vimentin, while stainings for desmin, h-caldesmon, alkaline phosphatase (ALK), and extensively studied cytokeratins were negative. Striking was a strong infiltrate with neutrophilic and eosinophilic granulocytes. DNA cytometry revealed aneuploidy with a peak in the near triploid range. Comparative genomic hybridization demonstrated multiple DNA gains and losses correlating with an aggressive clinical course. Shortly after resection of the primary tumor, the patient showed multiple distant metastases in the contralateral lung, the mediastinal lymph nodes, the left adrenal gland, and the pectoral and deltoid muscle, which responded well to chemotherapy. The case report will discuss the evidence for the final diagnosis of a primary pulmonary myofibrosarcoma and the differential diagnosis of sarcomatoid tumors of the lung.

Keywords Myofibrosarcoma · Lung · Carcinoma · CGH · DNA cytometry

L. Morawietz · A. Ladhoff · I. Petersen
Institut für Pathologie,
Charité Universitätsmedizin Berlin,
Schumannstrasse 20/21,
10117 Berlin, Germany

C. Kuhnen
Institut für Pathologie,
Berufsgenossenschaftliche Kliniken Bergmannsheil,
Buerkle-de-la-Camp-Platz 1,
44789 Bochum, Germany

D. Katenkamp
Institut für Pathologie,
Universität Jena,
Ziegelmühlenweg 1,
07740 Jena, Germany

P. Le Coutre
Medizinische Klinik mit Schwerpunkt
Hämatologie und Onkologie,
Charité Universitätsmedizin Berlin,
Augustenburger Platz 1,
13353 Berlin, Germany

I. Petersen (✉)
Institute of Pathology-Rudolf-Virchow Haus,
Charité Medical School-Campus Mitte,
Schumannstrasse 20/21,
10117 Berlin, Germany
e-mail: iver.petersen@charite.de
Tel.: +49-30-450536050
Fax: +49-30-450536110

Introduction

The concept of myofibroblastic sarcoma, also known as myofibrosarcoma, has been the subject of controversial discussions [7, 16, 20]. The cell type of a myofibroblast was described only 30 years ago, primarily based on ultrastructural criteria, i.e., the coexistence of features of fibroblasts and smooth muscle cells as well as the finding of so-called fibronexus [7, 9, 14, 16, 22]. Meanwhile, myofibroblasts are regarded as distinct cell types, and a variety of myofibroblastic tumors has been defined. The myofibrosarcoma, which has now also been generally accepted as an entity by the World Health Organization (WHO) [8, 15, 16], is diagnosed by its histomorphological appearance and its immunohistochemical phenotype with expression of smooth-muscle actin and/or desmin [16, 17].

Myofibrosarcoma is a rare neoplasm, which is possibly underdiagnosed due to a lack of consensus on diagnostic criteria and pathological variability. Our knowledge about this entity comes from various case reports and two larger studies, describing 15 and 18 cases, respectively [16, 17]. Mostly, the tumor is located in the head and neck region (tongue, neck, and face) or in the extremities [4, 8, 15, 16, 17]. Montgomery et al. described 15 cases, 5 of which

involved the head and neck region, 5 the extremities, 3 the trunk, and 1 each the abdominal cavity and the breast [17]. Mentzel et al. reported 18 cases, 5 of which arose in the oral cavity, 7 in the extremities, 4 in the abdominal/pelvic cavity, and 2 in the trunk [16]. Intraosseous tumors have also been observed [24]. The lung has not yet been described as a site of primary myofibrosarcoma. The tumor occurs predominantly in adults rather than children; the patients' age ranged from 33 to 73 years (median 52 years) in the study of Montgomery et al. and from 19 to 72 years (median 42 years) in the study of Mentzel et al. It showed a slight male predominance [8, 16, 17].

Most tumors present as low-grade sarcomas and exhibit a rather benign behavior, with a local recurrence rate of 27% [8]. They rarely metastasize; however, both Mentzel and Montgomery each described one case with distant metastases in their studies [8, 16, 17]. Although the general term "low-grade myofibrosarcoma" is often used [15], intermediate-grade tumors have also been described when grading the tumor according to the French Federation Nationale des Centres de Lutte Contre le Cancer (FNCLCC) system [8, 11]. These are associated with a worse outcome [8, 12, 17].

Clinical history

The 47-year-old male patient presented with clinical signs of pneumonia and was hospitalized for diagnostics and therapy. The patient had been smoking for 30 years, and the family anamnesis for cancer or lung disease was blank. Computer tomography (CT) demonstrated a solid mass of 103×89 mm in the lower lobe of the left lung with a poststenotic pneumonia, impression, but not infiltration of the diaphragm and no significant effusion. Three small lesions, with diameters up to 20 mm, were demonstrated in the upper left and the lower right lobe. Positron electron tomography (PET) demonstrated a metabolically active tumor with a necrotic center; the smaller lesions described in the CT were not detected by PET. The scintigraphy of the bone revealed no uptake. Taken together, there was strong evidence for a large primary lung tumor, with metastatic dissemination into both lungs.

The resection of the lower left lobe was executed shortly after the detection of the tumor. Preoperative biopsies had only shown necrotic material or chronic and florid inflammation and had not led to a tumor diagnosis. The postoperative course was uneventful, and the patient can be dismissed into ambulant aftercare. One month after the primary surgery, the control CT revealed a new tumor nodule 4 mm in size in the upper left lobe and progression of the contralateral foci, the largest now being 26 mm in diameter. New findings were multiple mediastinal lymph nodes of up to 12 mm and a node in the left adrenal gland with a size of 17×12 mm.

The patient was hospitalized again 3 weeks later with new foci, this time in the left deltoid and pectoral muscle and the left axilla, all being around 20 mm in diameter. One lesion was sampled, showing the same histomorphology as the primary. Assessment of the renal function revealed a decreased creatinine clearance of 48 ml/min. Therefore, as systemic chemotherapy, a combination of dimetyl-triazeno-imidasole-carboxamide (DTIC) and doxorubicin was chosen instead of an ifosfamide-containing regimen. Within the following 6 weeks, the patient received three cycles of DTIC 300 mg/m^2 (d1-3) and doxorubicine 75 mg/m^2 (d1). Chemotherapy was well tolerated, but fever due to neutropenia occurred after the second cycle and was successfully treated with piperacillin–tazobactam. Clinical observation after the third cycle of chemotherapy showed regression of the subcutaneous lesions. Likewise, abdominal ultrasound at this time showed regression of the adrenal gland metastasis, confirming partial remission.

Materials and methods

The pneumonectomy specimen was fixed in 4% buffered formalin. After fixation, the larger bronchi were opened lengthwise, and the parenchyma was laminated into slices of 5 mm. Thirty specimens, representative of the tumor, including bronchial and vascular invasion sites, tumor center, and tumor margin, were paraffin-embedded for routine histology and immunohistochemistry. Hematoxylin and eosin (H & E) staining was performed on 5-μm sections according to standard procedures.

Immunohistochemistry was carried out using antibodies for BerEP 4, pancytokeratin, CK7, CK18, EMA, TTF-1, surfactant A, calretinin, vimentin, desmin, alpha-smooth-muscle actin (BioGenex) and myosin, h-caldesmon (Bio Genex), calponin, alkaline phosphatase (ALK), factor VIII, CD34, MIB-1, CD117, melan A, S-100, synaptophysin, chromogranin, CD56, CD3, CD20, CD30, and CD68. Antibodies and detection system were purchased from DAKO if not otherwise indicated and were applied according to the manufacturer's recommendations.

For static DNA cytometry, a tumor slide of 15 μm was deparaffinized and digested with trypsin. After Feulgen staining was carried out using Merck reagents, the DNA content of 308 selected tumor cells was measured on a Leica microscope and analyzed using AutoCyte software (AutoCyte, Burlington, NC, USA) [2]. For calibration, 28 normal fibroblasts from cell cultures were used.

Comparative genomic hybridization (CGH) was performed as previously described [19]. Digital image analysis with karyotyping and calculation of the CGH ratio was performed using the computer program Karyomed, available through Karyomedics (http://www.KaryoMedics.de).

Results

The majority of the resected lung lobe was affected by a solid tumor with mainly well-defined margins (Fig. 1a). The tumor cambered but did not penetrate the pleura. Its cut surface was firm, rather homogeneous grayish white, with some areas of gelatinous necrosis, each about 10–20 mm in diameter. The tumor infiltrated large and small bronchi and

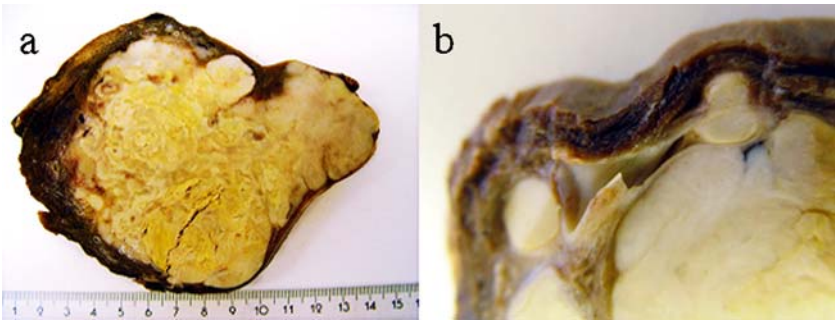


Fig. 1 **a** Cross section through the resected lung lobe showing a large tumor with rather well-defined margins and a nodular, white cut surface. **b** Close-up view of the tumor periphery demonstrating nodular margins and tumor invasion into a large blood vessel

one large blood vessel (Fig. 1b). The rest of the lung showed a slight mucus retention. One separate subpleural, circumscribed tumor nodule of 5-mm size, with a firm white cut surface, was additionally detected.

Histopathological examination demonstrated a spindle cell neoplasm with a strong inflammatory superposition. The tumor showed marked heterogeneity. Fasciculated areas alternated with solid ones. In some parts, an almost netlike vascularization was found. Focally, a pale eosinophilic extracellular matrix was present, which passed into hyalinized areas. Several central areas of about 10–20 mm diameter were necrotic, constituting less than 50% of the entire tumor (score 1 according to FNCLCC grading [11, 15]). In large parts, the picture was dominated by neutrophilic and eosinophilic granulocytes; additionally, lymphocytes and plasma cells were present in smaller numbers (Fig. 2a). The tumor infiltrated diffusely into the surrounding lung tissue, filling the alveoli rather than infiltrating the septa; no pushing borders were seen. The tumor cells themselves were basically spindle-shaped and displayed a remarkable heterogeneity. The cytoplasm was blurred and pale eosinophilic. No perinuclear vacuoles could be found. Some tumor cells had medium-sized, cigar-shaped nuclei, others had elongated and undulated nuclei, while others had markedly enlarged, plump, oval, or bizarre nuclei with indentations (score 2; Fig. 2b,c).

Prominent nucleoli were sometimes present. Up to three mitoses per ten high-power fields (HPF) (0.196 mm^2) were counted (score 1); the proliferation index (MIB-1 immunohistochemistry) was approximately 20%.

The tumor cells were immunohistochemically positive for smooth-muscle actin (Fig. 2d), calponin, and vimentin. No expression was detectable for desmin, h-caldesmon, pancytokeratin, CK7, CK18, (five samples for each antibody), ALK, BerEP4, EMA, CD117, melan A, S-100, synaptophysin, chromogranin, CD56, calretinin, TTF-1, surfactant A, CD3, CD20, CD30, and CD68 (one sample for each antibody).

The separate subpleural tumor nodule and the subsequently sampled subcutaneous metastasis exhibited a similar histomorphology as the large tumor of the lung. The remote lung tissue showed no pneumonia. The bronchial

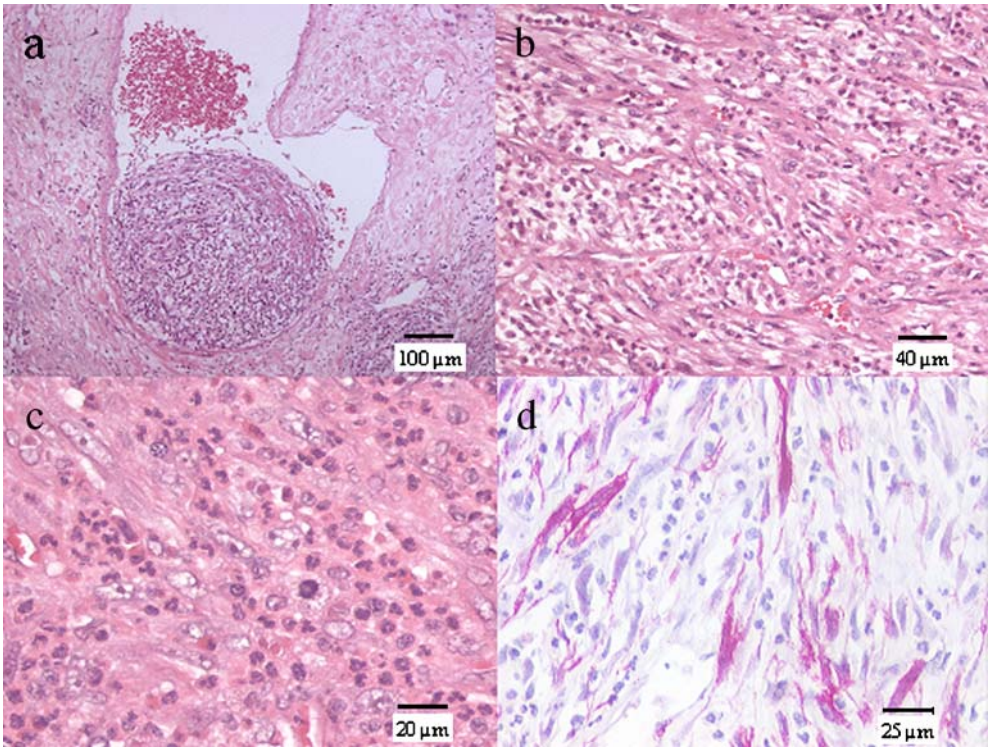


Fig. 2 Histomorphology of the tumor. **a** Example of vascular tumor invasion (H & E, original magnification 100×). **b** The tumor shows a fascicular, in parts storiform pattern, and the spindle-shaped tumor cells are accompanied by numerous neutrophilic and eosinophilic granulocytes (H & E, original magnification 200×). **c** Polymorphic tumor cells with medium- and large-sized, elongated, indented, or plump nuclei as well as a single mitotic figure (H & E, original magnification 400×). **d** Strong cytoplasmic expression of smooth-muscle actin in tumor cells (immunohistochemistry, original magnification 400×)

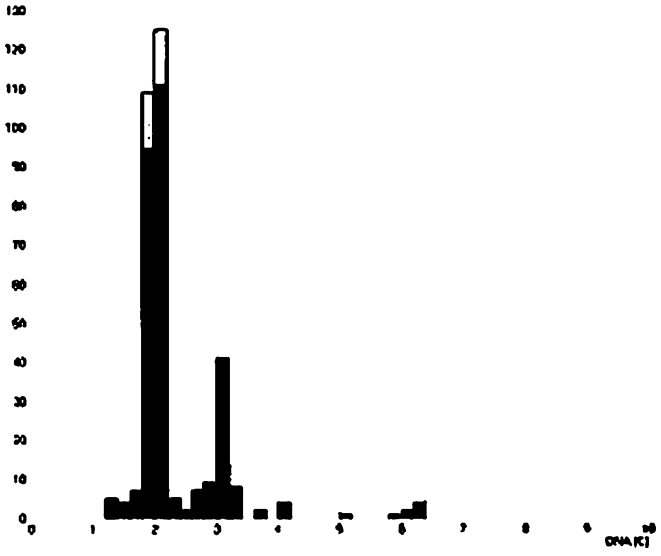


Fig. 3 Histogram of the DNA cytometry measurement demonstrating an aneuploid tumor stemline at 3.1c and a doubling line at 6.2c in addition to peak at 2c, which might be due to normal cell contamination or near diploid tumor cells (*dark*, tumor cells; *light*, reference cells)

epithelium displayed no squamous metaplasia, and, in particular, no dysplasia.

Electron microscopy was carried out on samples from five different tumor sites. However, due to fixation in formalin for some days, the membrane integrity was destroyed, and neither features of epithelia nor of myofibroblasts could clearly be detected. Therefore, electron microscopy was not contributory to the diagnosis.

DNA cytometry demonstrated an aneuploid tumor (Fig. 3) with an abnormal stemline at 3.1c and the appropriate doubling peak at 6.2c.

Comparative genomic hybridization was carried out twice. In a first evaluation of a tumor area with the typical pronounced granulocytic infiltration, no DNA gain or loss could be unequivocally detected. In a second analysis of another tumor area with less inflammation and almost pure spindle cell differentiation, numerous chromosomal imbalances became visible, correlating with the aneuploidy detected by DNA cytometry. Prominent DNA overrepresentations (ratio>1.25) were detected at 1p34.1–p36.2, 11q12, 16p12–p13, 17p12–p13, 17q12–q25, 19p + q, 20q12–q13, and 22q12–q13, while a clear deletion (ratio< 0.75) was seen at 13q13–q34 (Fig. 4).

Based on the histopathological evaluation and the immunohistochemical expression profile, we diagnosed a primary myofibrosarcoma of the lung. According to the FNCL CC grading system, a total score of 4 leads to the diagnosis of an intermediate-grade tumor (grade 2) [11].

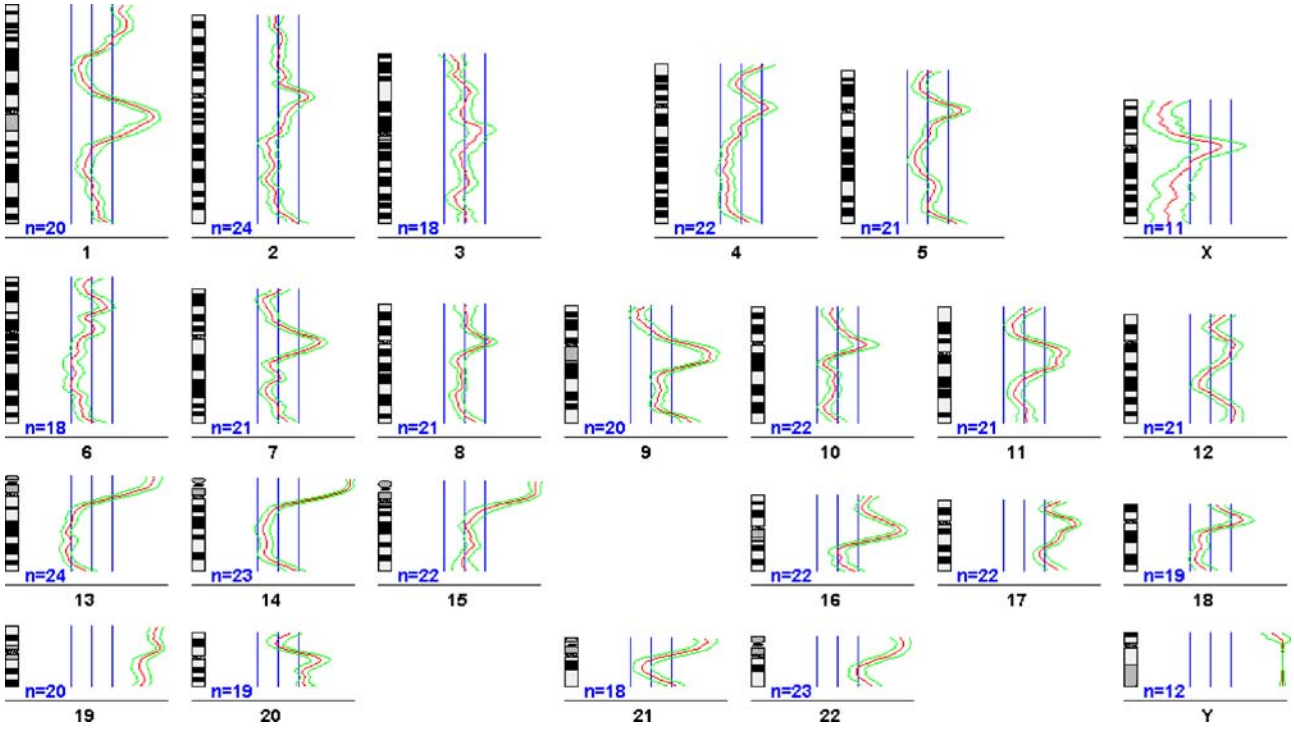


Fig. 4 Results of the CGH demonstrating multiple DNA gains and losses. Deviation of the ratio profile together with its 95% confidence interval to the *left side* from the mean *vertical line* representing the normal ratio 1.0 was scored as deletion, deviation to the *right* was scored as overrepresentation. The *left* and *right* vertical lines represent the ratio values *0.75* and *1.25*, respectively. Pronounced DNA gains and losses, potentially representing high-copy amplifications or multi-copy deletions, were defined by regions in which the ratio profile exceeded the values *1.5* or *0.5*. The tumor DNA of the male patient was hybridized together with female reference DNA, leading to the deviations of ratio profiles of Y and X chromosomes which served as internal control

Discussion

The myofibrosarcoma, or myofibroblastic sarcoma, is a rare tumor that rarely metastasizes. We report the first example of such a tumor occurring in the lung [8, 16, 17].

Our diagnosis was based on the typical light microscopic picture of the tumor cells with blurred cytoplasm and heterogeneous, partly spindle or cigar-shaped, sometimes undulated, sometimes plump nuclei with indentations. The immunohistochemical demonstration of smooth-muscle actin and calponin in the absence of cytokeratins, ALK, and h-caldesmon especially led to the diagnosis of a myofibrosarcoma. Electron microscopy was not contributory due to membrane degradation. A variety of differential diagnoses (DD), however, needs to be considered, i.e., inflammatory myofibroblastic tumor (IMT, also known as inflammatory pseudotumor), sarcomatoid mesothelioma, spindle cell melanoma, lymphoma, leiomyosarcoma, fibrosarcoma, and, in particular, lung carcinoma.

From tumor morphology, particularly the pronounced inflammatory cell infiltrate, IMT was the most imminent DD. This entity typically shows a mixture of histiocytes, lymphocytes, fibroblasts, and, in particular, plasma cells, with the fibroblasts showing expression of ALK [1, 12, 13]. Plasma cells were also present in our case but not as the predominant population. The major distinction, however, was the infiltrative growth pattern, the absence of ALK-positive cells, and finally, the presence of distance metastases in our case. Due to the morphological similarity, it might be hypothesized that the tumor originated as an IMT since Donner described a case in which an IMT progressed into a spindle cell sarcoma after several recurrences and a 12-year course [5]. However, such a long preclinical development was not evident in our case.

Apart from the untypical morphology, melanoma and malignant lymphoma can be excluded by the negative immunostains for protein S-100, melan A, as well as CD3, CD20, and CD30. Similarly, other sarcomatous lesions, especially leiomyosarcoma and fibrosarcoma, were excluded by histology and immunohistochemistry [8, 12, 23]. Sarcomatoid mesothelioma was excluded because of lack of calretinin and cytokeratin expression. Furthermore, the tumor exhibited a predominant intrapulmonary growth pattern, with only secondary involvement of the pleura.

The DD of a synovial sarcoma and spindle cell carcinomas was essentially excluded by the negativity of the tumor cells for cytokeratin expression, which was tested by investigating a panel of cytokeratins on different tissue blocks. High-grade synovial sarcoma may occur in the lung [6]; however, the tumor cells rather have a scanty cytoplasm, and the nuclei, which are tightly seated and often overlapping, are oval, with finely dispersed chromatin [3]. Furthermore, glandular elements typical for biphasic synovial sarcoma were not detectable.

Spindle cell carcinoma is another important and critical DD. Clinical and pathological parameters were suspicious, i.e., the clinical history of long-time cigarette smoking, the pattern of metastasis formation, the good response to chemotherapy, and the association with the bronchial airways. Spindle cell carcinomas have been reported to lose their cytokeratin expression while acquiring mesenchymal markers, like desmin, actin, or vimentin [18]. However, spindle cell carcinomas are described as rather homogeneous with plump cytoplasm and prominent nucleoli [3], which was not evident in the present case.

By cDNA microarray analysis, we had demonstrated that large cell lung carcinomas acquire an expression profile indicative of an epithelial–mesenchymal transition [10]. Large cell cancer may show a prominent inflammatory infiltrate with eosinophilia, which might be related to the expression of granulocyte colony-stimulating factors by the tumor cells [21]. Additionally, the DNA histogram of the present tumor showed a peak at the near triploid range, clearly indicating an aneuploid tumor, with many tumor cells having a chromosome complement in the near trisomic range similar to many nonsmall cell lung carcinomas [19]. Furthermore, the complexity of the chromosomal imbalance pattern detected by CGH, which, when applying more sensitive criteria for scoring DNA gains and losses, suggested even more alterations, including interstitial deletions on chromosome 3p, is also reminiscent of lung cancer. However, no precursor lesions of lung carcinoma, like dysplasia or squamous metaplasia, were detectable. Similarly, not even small areas with clear epithelioid tumor differentiation or cytokeratin expression were seen. Finally, neither DNA measurement nor extensive chromosomal studies have yet been performed on myofibrosarcomas that provide further criteria for establishing or disproving the diagnosis. In summary, the evidence prevailed for the final diagnosis of a primary myofibrosarcoma of the lung.

Acknowledgements The technical assistance of Manuela Pacyna-Gengelbach and Karl-Heinz Friedrich is gratefully acknowledged. Martina Eickmann provided excellent secretarial help in preparing the manuscript. We thank Christa Scholz for the macroscopic photographs.

References

1. Bahadori M, Liebow AA (1973) Plasma cell granulomas of the lung. Cancer 31:191–208
2. Bocking A, Nguyen VQ (2004) Diagnostic and prognostic use of DNA image cytometry in cervical squamous intraepithelial lesions and invasive carcinoma. Cancer 102:41–54
3. Brooks JSJ (2004) Disorders of soft tissue. In: Mills SE (ed) Sternberg's diagnostic surgical pathology. Lippincott, Philadelphia, p139
4. Chang SE, Choi JH, Sung KJ et al (2001) A case of cutaneous low-grade myofibroblastic sarcoma. J Dermatol 28:383–387
5. Donner LR, Trompler RA, White RR IV (1996) Progression of inflammatory myofibroblastic tumor (inflammatory pseudotumor) of soft tissue into sarcoma after several recurrences. Human Pathol 27:1095–1098
6. Essary LR, Vargas SO, Fletcher CD (2002) Primary pleuropulmonary synovial sarcoma: reappraisal of a recently described anatomic subset. Cancer 94:459–469
7. Eyden BD (1993) Brief review of the fibronexus and its significance for myofibroblastic differentiation and tumor diagnosis. Ultrastruct Pathol 17:611–622

8. Fisher C (2004) Myofibrosarcoma. Virchows Arch 445:215–223
9. Fletcher CD (1998) Myofibroblastic tumours: an update. Verh Dtsch Ges Pathol 82:75–82
10. Garber ME, Troyanskaya OG, Schluens K et al (2001) Diversity of gene expression in adenocarcinoma of the lung. Proc Natl Acad Sci U S A 98:13784–13789
11. Guillou L, Coindre JM, Bonichon F et al (1997) Comparative study of the National Cancer Institute and French Federation of Cancer Centers Sarcoma Group grading systems in a population of 410 adult patients with soft tissue sarcoma. J Clin Oncol 15:350–362
12. Kuhnen C, Homann HH, Mentzel T (2003) Myofibroblastic sarcoma of the thoracic wall. Change in appearance in tumor recurrence. Pathologe 24:128–135
13. Li XQ, Hisaoka M, Shi DR, Zhu XZ, Hashimoto H (2004) Expression of anaplastic lymphoma kinase in soft tissue tumors: an immunohistochemical and molecular study of 249 cases. Human Pathol 35:711–721
14. Majno G (1997) The story of the myofibroblast. Am J Surg Pathol 3:535–542
15. Mentzel T, Fletcher JA (2002) Low grade myofibroblastic sarcoma. In: Fletcher CDM, Unni KK, Mertens F (eds) World Health Organization classification of tumours. Pathology and genetics. Tumours of soft tissue and bone. IARC, Lyon, pp 94–95
16. Mentzel T, Dry S, Katenkamp D et al (1998) Low-grade myofibroblastic sarcoma: analysis of 18 cases in the spectrum of myofibroblastic tumors. Am J Surg Pathol 22:1228–1238
17. Montgomery E, Goldblum JR, Fisher C (2001) Myofibrosarcoma: a clinicopathologic study. Am J Surg Pathol 25:219–228
18. Nappi O, Glasner SD, Swanson PE et al (1994) Biphasic and monophasic sarcomatoid carcinomas of the lung. A reappraisal of ‘carcinosarcomas’ and ‘spindle-cell carcinomas'. Am J Clin Pathol 102:331–340
19. Petersen I, Langreck H, Wolf G et al (1997) Small-cell lung cancer is characterized by a high incidence of deletions on chromosomes 3p, 4q, 5q, 10q, 13q and 17p. Br J Cancer 75:79–86
20. Schurch W, Seemayer TA, Gabbiani G (1998) The myofibroblast: a quarter century after its discovery. Am J Surg Pathol 22:141–147
21. Taccagni G, Rovere E, Masullo M et al (1997) Myofibrosarcoma of the breast: review of the literature on myofibroblastic tumors and criteria for defining myofibroblastic differentiation. Am J Surg Pathol 21:489–496
22. Sekido Y, Sato M, Usami N et al (2002) Establishment of a large cell lung cancer cell line (Y-ML-1B) producing granulocyte colony-stimulating factor. Cancer Genet Cytogenet 137: 33–42
23. Watanabe K (2002) Leiomyosarcoma versus myofibrosarcoma. Am J Surg Pathol 26:393–394
24. Watanabe K, Ogura G, Tajino T et al (2001) Myofibrosarcoma of the bone: a clinicopathologic study. Am J Surg Pathol 25:1501–1507

Virchows Arch (2005) 447: 996–999
DOI 10.1007/s00428-005-0042-z

CASE REPORT

Katsuaki Sato · Yoshimichi Ueda · Keiichi Ueno · Kazuya Okamoto · Hideaki Iizuka · Shogo Katsuda

Hepatocellular carcinoma and nonalcoholic steatohepatitis developing during long-term administration of valproic acid

Received: 25 February 2005 / Accepted: 6 July 2005 / Published online: 17 August 2005
© Springer-Verlag 2005

Abstract We report a case of hepatocellular carcinoma (HCC) arising in nonalcoholic steatohepatitis (NASH). The patient, a 64-year-old man, was incidentally found to have multiple tumors in the liver when admitted for pneumonia. He had been obese, had been receiving a standard dose of valproic acid since clipping surgery for subarachnoid hemorrhage 17 years previously, and had not consumed any alcohol since the surgery. Laboratory data revealed moderate hyperlipidemia and no evidence of diabetes mellitus, hepatitis B or C infection. The patient died of hepatic insufficiency, and an autopsy was performed. A tumor, a maximum of 13 cm in diameter, grossly occupied the entire left lobe and one third of the right lobe of the liver. Histologically, moderately differentiated HCC was found with foci of poorly differentiated HCC. The non-tumorous area showed NASH with moderate bridging fibrosis, without interface hepatitis, hemochromatosis, or copper accumulation. In this patient, obesity, hyperlipidemia, and long-term treatment with valproic acid could have all been associated with induction of NASH. The present case suggests that HCC could develop in non-cirrhotic NASH liver, and that chronic inflammation in itself could be an important risk factor in the development of HCC.

K. Sato (✉) · Y. Ueda · S. Katsuda
Department of Pathophysiological and Experimental Pathology,
Kanazawa Medical University,
1-1 Daigaku, Uchinada, Kahoku,
Ishikawa, 920-0293, Japan
e-mail: sato-k@kanazawa-med.ac.jp
Tel.: +81-76-2188119
Fax: +81-76-2862484

K. Ueno
Department of Surgical Oncology,
Kanazawa Medical University,
Ishikawa, Japan

K. Okamoto · H. Iizuka
Department of Neurosurgery,
Kanazawa Medical University,
Ishikawa, Japan

Keywords Hepatocellular carcinoma · Nonalcoholic steatohepatitis · Nonalcoholic fatty liver disease · Valproic acid

Introduction

Nonalcoholic steatohepatitis (NASH) is part of the spectrum of nonalcoholic fatty liver disease (NAFLD), clinically related with metabolic syndrome [3], and is histologically indistinguishable from alcoholic hepatitis [1]. Although the natural history of NASH has yet to be fully clarified, simple hepatic steatosis is nonprogressive, whereas nearly 20% of NASH cases may slowly progress to cirrhosis [8], and distinctive cases with hepatocellular carcinoma (HCC) arising in NASH have recently been reported [6, 13, 16, 17, 19, 23]. Valproic acid (VPA) is a worldwide antiepileptic drug, which occasionally causes idiosyncratic hepatotoxicity, but the association of VPA with steatohepatitis and HCC has not been determined [1]. This is the first report of HCC arising in moderately fibrosing NASH liver in a patient receiving long-term VPA administration.

Clinical history

A 64-year-old man was admitted to hospital with a diagnosis of pneumonia. CT scans of the lower chest incidentally detected multiple tumors in the liver. The patient had received VPA (800 mg per day, standard dose) since clipping surgery for subarachnoid hemorrhage 17 years previously. He had been a chance drinker but had consumed no alcohol since the surgery 17 years previously. His family history was unremarkable. Laboratory data had irregularly shown slightly elevated liver enzymes. At the time of admission, total cholesterol (261 mg/dl) and triglyceride (175 mg/dl) levels were moderately increased, and the serum levels of α-fetoprotein (18,270 ng/ml) and PIVKA-II (487 AU/ml) were highly elevated. The HbA_{1C} value was within the normal range. Hepatitis B surface



Fig. 1 Macroscopic appearance of the cut surface of the autopsied liver. The main tumor occupies the entire left lobe and approximately one third of the right lobe of the liver. There are also multiple nodules in the right lobe

antigen and anti-hepatitis C virus antibody in the serum were negative. Neither liver biopsy nor chemotherapy was performed. The patient died of hepatic insufficiency 1 year after admission, and an autopsy was performed 2 h after death.

Materials and methods

The autopsy specimens were fixed in 10% formalin and embedded in paraffin. Tissue sections of 4 μm in thickness were stained for hematoxylin and eosin as well as the Azan-Mallory method.

Results

At autopsy; the patient was obese, 82 kg in weight (BMI 34.1 kg/m^2), and 155 cm in height. The skin showed an icteric discoloration. Massive ascitic fluid (6,000 ml) was observed. The liver weighed 1,500 g, and the gross appearance showed that the tumor measured a maximum of 13 cm in diameter. The tumor occupied the entire left lobe and one third of the right lobe of the liver (Fig. 1). Histologic examination revealed that the tumor consisted mainly of moderately differentiated HCC, with a focal pseudoglandular pattern (Fig. 2a). A poorly differentiated HCC component was also observed in some parts of the tumor. HCC cells with marked fatty deposition were also observed focally (Fig. 2b). In the background of the tumor, both micro- and macrovesicular steatosis was apparent, especially in the centrilobular area. Ballooned liver cells with Mallory bodies and infiltrates of neutrophilic cells were commonly observed around the central veins (Fig. 2c). Spotty necrosis was scattered throughout the lobules. Perivenular and pericellular fibroses were also manifested. Bridging fibrosis between the central veins and portal tracts was evident, but regenerative nodules had not formed (Fig. 2d). There was no evidence of interface hepatitis, hemochromatosis, or copper accumulation.

Discussion

This case is interesting as HCC developed in a non-cirrhotic NASH liver, and the patient had received long-term VPA therapy. The liver, in the presence of NASH, may have the potential to progress to cirrhosis and liver

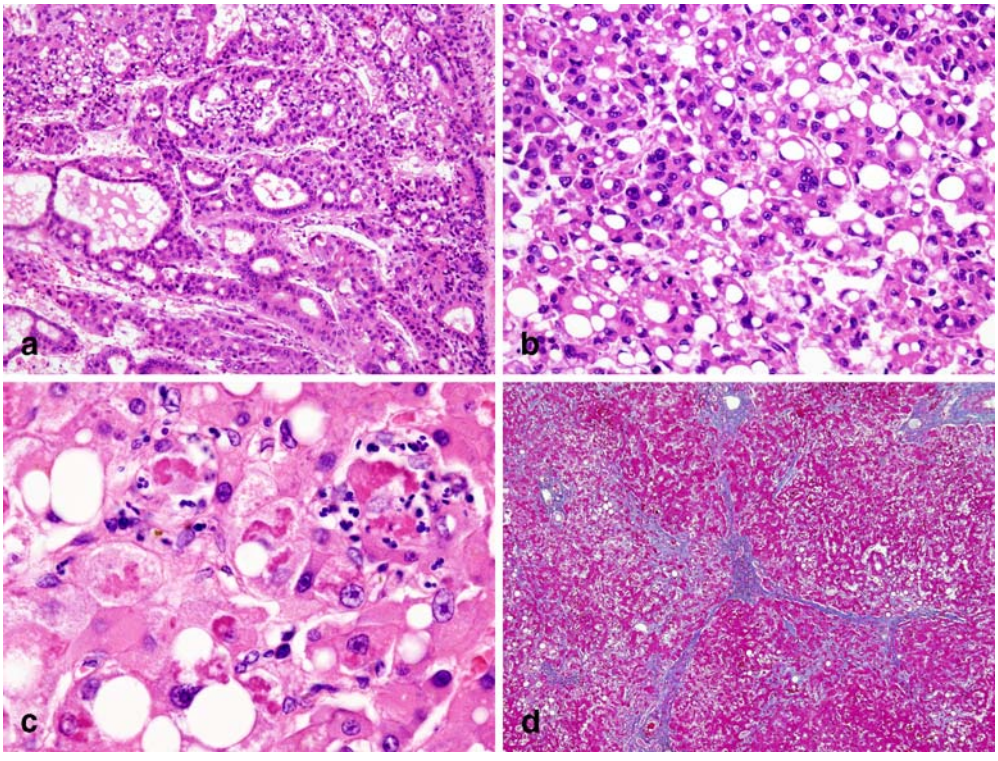


Fig. 2 Histologic features of the tumor. **a** The tumor consists mainly of moderately differentiated hepatocellular carcinoma with a focal pseudoglandular pattern. Hematoxylin and eosin, ×100. **b** There are hepatocellular carcinoma cells with marked fatty depositions. Hematoxylin and eosin, ×200. **c** Ballooned liver cells with Mallory bodies and infiltrates of neutrophilic cells are frequently observed around the central vein. Hematoxylin and eosin, ×400. **d** Bridging, perivenular, and pericellular fibrosis are diffusely observed in the non-tumorous area, but regenerative nodules are not visible. Azan-Mallory, ×40

Table 1 Clinicopathologic features of cases with hepatocellular carcinoma and nonalcoholic steatohepatitis

Case	Author [reference]	Age/Sex	Background disease	HCC histology	Tumor size (cm)	Liver histology
1	Powell et al. [17]	57/F	DM	ND	ND	Cirrhosis
2	Cotrim et al. [6]	62/M	DM, OB	ND	3	Cirrhosis
3	Zen et al. [23]	72/F	DM	Mod	1.3	Cirrhosis
				Wel	1.0	
				Dys	1.4	
4	Orikasa et al. [16]	67/F	DM	Clear-cell	2.6	Pre-cirrhosis
5	Shimada et al. [19]	66/F	DM	Mod	1.5	Cirrhosis
6	Shimada et al. [19]	69/F	ND	Wel	1.5×2	Cirrhosis
7	Shimada et al. [19]	69/F	DM, OB	ND	2.5	Cirrhosis
8	Shimada et al. [19]	72/M	OB	Wel	3	Cirrhosis
9	Shimada et al. [19]	63/M	HL, OB	Wel	2	Cirrhosis
10	Shimada et al. [19]	56/M	DM	Mod	1–6, M	Cirrhosis
11	Mori et al. [13]	76/M	DM, OB	Wel	1.9	Cirrhosis
12	Present case	64/M	OB, HL, Drug	Mod	13, M	Fibrosis

F female, *M* male, *DM* diabetes mellitus, *OB* obesity, *HL* hyperlipidemia, *HCC* hepatocellular carcinoma, *ND* not described, *Mod* moderately differentiated, *Wel* well differentiated, *Dys* dysplasia, *M* multiple

failure, thereby promoting the development of HCC [17]. Although a large number of HCCs have been reported to arise in cryptogenic cirrhosis in patients with risk factors for NAFLD [4], the accurate incidence of HCC in NASH remains undetermined [3]. Half of the patients with cryptogenic cirrhosis have pathological and clinical characteristics consistent with NAFLD and account for 13% of HCC cases [12]. Some cases of cryptogenic cirrhosis have histologic features of burned-out NASH [15]. Cases of HCC that developed in NASH are not uncommon; however, to our knowledge, there have been only 11 well-documented cases reported in the literature [6, 13, 16, 17, 19, 23].

Table 1 summarizes the clinicopathologic features of the cases of HCC developing in NASH, including the present case. The histology of the background liver was cirrhosis in ten cases, and pre-cirrhosis in only one case. The present case is unique in that the tumor developed in a non-cirrhotic liver. More than 80% of patients with HCC have underlying cirrhosis [18], and cirrhosis itself is recognized as a common factor promoting HCC. However, the remaining cases of HCC, approximately 20%, can develop in a non-cirrhotic liver. There is a report of an animal study in which a new inbred mouse strain, fatty liver Shionogi, spontaneously developed fatty liver and HCC in the non-cirrhotic liver [21]. Although it remains uncertain whether cirrhosis is required for the development of HCC, at least, this case indicates that HCC can arise in a non-cirrhotic NASH liver.

Reactive oxygen species (ROS), products due to oxidative stress, activate lipid peroxidation, and TGF-β induction, can stimulate fibrosis [1]. On the other hand, the major products of lipid peroxidation, malondialdehyde, and 4-hydroxynonenal, act as DNA mutagens [11], which might be associated with the initiation of HCC [5]. Because inflammation is a principal source of ROS, chronic inflammation can be a risk factor for various carcinomas [7]. Recently, mice with somatic inactivation of the *nrf1* gene in the liver have been reported to spontaneously develop HCC in a background of non-cirrhotic liver, and oxidative injury had been present before tumor development [22]. These results suggest that ROS overproduced in NASH liver could trigger carcinogenesis as well as fibrosis, and that cirrhosis is not essential for the development of HCC.

Major risk factors for primary NASH are: obesity, type 2 (non-insulin-dependent) diabetes mellitus, and hyperlipidemia [1]. Hyperinsulinemia is an underlying factor in these conditions. NAFLD was found to be present in almost 90% of patients with obesity; approximately 25% of whom had NASH [14]. About 50% of patients treated with VPA, which is speculated to modulate insulin secretion and systemic metabolism, experienced weight gain [2]. The present patient was obese and presented moderate hyperlipidemia, without evidence of diabetes mellitus. Obesity might be influenced by VPA and be indirectly associated with the development of HCC through the induction of NASH.

Causes of secondary NASH include: drugs, nutritional factors, and metabolic or genetic disorders [1]. VPA, a short fatty acid derivative, can cause hepatic microvesicular steatosis, which is related to insulin resistance [1]. VPA also impairs mitochondrial β-oxidation, a frequent mechanism underlying drug-induced steatohepatitis [9]. Derangements of mitochondrial β-oxidation generate an overproduction of ROS, leading to enhanced lipid peroxidation and cytokine production similar to primary (obesity-related) NASH [1]. These pathogenetic factors may act as an enhancement of HCC development. Contrarily, VPA has shown anticancer activity mediating inhibition of histone deacetylases and an induction of carcinoma cell differentiation [10, 20]. However, the antiproliferative effect on carcinoma cells of VPA and the relationship between VPA treatment and HCC development are not evident.

References

1. Angulo P (2002) Nonalcoholic fatty liver disease. N Engl J Med 346:1221–1231
2. Biton V, Mirza W, Montouris G, Vuong A, Hammer AE, Barrett PS (2001) Weight change associated with valproate and lamotrigine monotherapy in patients with epilepsy. Neurology 56:172–177
3. Brunt EM (2004) Nonalcoholic steatohepatitis. Semin Liver Dis 24:3–20
4. Bugianesi E, Leone N, Vanni E, Marchesini G, Brunello F, Carucci P, Musso A, De Paolis P, Capussotti L, Salizzoni M, Rizzetto M (2002) Expanding the natural history of nonalcoholic steatohepatitis: from cryptogenic cirrhosis to hepatocellular carcinoma. Gastroenterology 123:134–140
5. Caldwell SH, Crespo DM, Kang HS, Al-Osaimi AM (2004) Obesity and hepatocellular carcinoma. Gastroenterology 127: S97–S103
6. Cotrim HP, Parana R, Braga E, Lyra L (2000) Nonalcoholic steatohepatitis and hepatocellular carcinoma: natural history? Am J Gastroenterol 95:3018–3019
7. Coussens LM, Werb Z (2002) Inflammation and cancer. Nature 420:860–867
8. Falck-Ytter Y, Younossi ZM, Marchesini G, McCullough AJ (2001) Clinical features and natural history of nonalcoholic steatosis syndromes. Semin Liver Dis 21:17–26
9. Farrell GC (2002) Drugs and steatohepatitis. Semin Liver Dis 22:185–194
10. Göttlicher M, Minucci S, Zhu P, Krämer OH, Schimpf A, Giavara S, Sleeman JP, Lo Coco F, Nervi C, Pelicci PG, Heinzel T (2001) Valproic acid defines a novel class of HDAC inhibitors inducing differentiation of transformed cells. EMBO J 20:6969–6978
11. Marnett LJ (2000) Oxyradicals and DNA damage. Carcinogenesis 21:361–370
12. Marrero JA, Fontana RJ, Su GL, Conjeevaram HS, Emick DM, Lok AS (2002) NAFLD may be a common underlying liver disease in patients with hepatocellular carcinoma in the United States. Hepatology 36:1349–1354
13. Mori S, Yamasaki T, Sakaida I, Takami T, Sakaguchi E, Kimura T, Kurokawa F, Maeyama S, Okita K (2004) Hepatocellular carcinoma with nonalcoholic steatohepatitis. J Gastroenterol 39:391–396
14. Neuschwander-Tetri BA, Caldwell SH (2003) Nonalcoholic steatohepatitis: summary of an AASLD single topic conference. Hepatology 37:1202–1219 (Erratum in: Hepatology 2003; 38:536)
15. Ong J, Younossi ZM, Reddy V, Price LL, Gramlich T, Mayes J, Boparai N (2001) Cryptogenic cirrhosis and posttransplantation nonalcoholic fatty liver disease. Liver Transpl 7:797–801
16. Orikasa H, Ohyama R, Tsuka N, Eyden BP, Yamazaki K (2001) Lipid-rich clear-cell hepatocellular carcinoma arising in nonalcoholic steatohepatitis in a patient with diabetes mellitus. J Submicrosc Cytol Pathol 33:195–200
17. Powell EE, Cooksley WG, Hanson R, Searle J, Halliday JW, Powell LW (1990) The natural history of nonalcoholic steatohepatitis: a follow-up study of forty-two patients for up to 21 years. Hepatology 11:74–80
18. Schafer DF, Sorrell MF (1999) Hepatocellular carcinoma. Lancet 353:1253–1257
19. Shimada M, Hashimoto E, Taniai M, Hasegawa K, Okuda H, Hayashi N, Takasaki K, Ludwig J (2002) Hepatocellular carcinoma in patients with non-alcoholic steatohepatitis. J Hepatol 37:154–160
20. Singh G, Driever PH, Sander JW (2005) Cancer risk in people with epilepsy: the role of antiepileptic drugs. Brain 128:7–17
21. Soga M, Kishimoto Y, Kawamura Y, Inagaki S, Makino S, Saibara T (2003) Spontaneous development of hepatocellular carcinomas in the FLS mice with hereditary fatty liver. Cancer Lett 196:43–48
22. Xu Z, Chen L, Leung L, Yen TS, Lee C, Chan JY (2005) Liver-specific inactivation of the Nrf1 gene in adult mouse leads to nonalcoholic steatohepatitis and hepatic neoplasia. Proc Natl Acad Sci U S A 102:4120–4125
23. Zen Y, Katayanagi K, Tsuneyama K, Harada K, Araki I, Nakanuma Y (2001) Hepatocellular carcinoma arising in nonalcoholic steatohepatitis. Pathol Int 51:127–131

Virchows Arch (2005) 447: 1000–1006
DOI 10.1007/s00428-005-0080-6

CASE REPORT

Emiko Takahashi · Kazuyoshi Kajimoto · Toshiaki Fukatsu · Megumi Yoshida · Tadaaki Eimoto · Shigeo Nakamura

Intravascular large T-cell lymphoma: a case report of CD30-positive and ALK-negative anaplastic type with cytotoxic molecule expression

Received: 15 June 2005 / Accepted: 25 August 2005 / Published online: 28 September 2005
© Springer-Verlag 2005

Abstract We reported a case of intravascular T-cell lymphoma (T-IVL) with anaplastic large cell morphology, the hemophagocytic syndrome, and an aggressive clinical course. Phenotypic analysis of the tumor cells revealed CD2+, CD3−, CD4+, CD5−, CD8−, CD30+, CD56−, T-cell receptor alpha/beta−, ALK−, TIA1+, granzyme B+, and perforin+. No association with Epstein–Barr virus was found by in situ hybridization. A review revealed that 25 cases of T-IVL have been reported in the available literature, only two of which were of CD30+ anaplastic large cell or cytotoxic T-cell type. The findings in the present case may highlight the unique clinicopathologic aspects of a subset of CD30-positive T-IVLs with an ALK-negative cytotoxic phenotype.

Keywords Intravascular lymphoma · Cytotoxic T cell · Anaplastic large cell morphology · Hemophagocytic syndrome · Immunohistochemistry

E. Takahashi (✉)
Department of Pathology, Aichi Cancer Center,
1-1 Kanokoden, Chikusa-ku,
Nagoya, 464-8681, Japan
e-mail: etakahashi@aichi-cc.jp
Tel.: +81-52-7626111
Fax: +81-52-7635233

K. Kajimoto
Department of Pathology, Hyogo Medical Center for Adults,
Akashi, Japan

T. Fukatsu
Clinical Laboratories,
Nagoya Ekisaikai Hospital,
Nagoya, Japan

M. Yoshida · T. Eimoto
Department of Pathology,
Nagoya City University School of Medicine,
Nagoya, Japan

S. Nakamura
Department of Pathology and Clinical Laboratories,
Nagoya University Hospital,
Nagoya, Japan

Introduction

Intravascular lymphoma (IVL) is a rare malignancy characterized by a proliferation of lymphoma cells only within the blood vessels. This disease was originally described in 1959 as "angioendotheliomatosis proliferans systemisata" when it was regarded as an endothelial neoplasm by Pfeger and Tappeiner [19]. However, in mid-1980s, immunohistochemical investigation and gene rearrangement studies demonstrated the neoplastic cells to be of lymphoid origin [21, 23].

An increasing number of IVL cases have been documented, most of which have provided evidence of derivation from B cells. The recent World Health Organization (WHO) classification defined intravascular B-cell lymphoma (B-IVL) as a rare subtype of extranodal diffuse large B-cell lymphoma [9]. A recent nationwide study of 3,194 Japanese patients with malignant lymphoma classified according to the new WHO classification showed a very low incidence (0.09%, three cases) of B-IVL and none of IVLs of T-cell type (T-IVL) [15]. On the other hand, 25 cases of T-IVL have hitherto been reported in the English literature [3–5, 7, 10–14, 16, 17, 20–23, 25–28, 30]. Among them, only one case was described as CD30+ anaplastic large cell type [12], whereas another CD30− case in a HIV-positive patient showed TIA1+ cytotoxic T-cell phenotype in association with Epstein–Barr virus (EBV) infection [17].

We herein report a case of T-IVL, which was unique in having a constellation of anaplastic large cell morphology, CD30+ALK−TIA1+granzyme B+perforin+ phenotype, the hemophagocytic syndrome (HPS), and an aggressive clinical course.

Case history

A 72-year-old Japanese man presented with a 7-day history of worsening flu-like syndrome. On admission, physical examination revealed hypotension, fever, and breathlessness. Lymphadenopathy or skin nodules were

not found. There were no risk factors for HIV infection in his lifestyle analysis. Two days after admission, the patient rapidly developed multiorgan failure. Laboratory examination revealed pancytopenia with a white blood cell count of 3.6×10^9/l, a hemoglobin level of 10.7 g/dl, and a platelet count of 17×10^9/l. Examination of bone marrow smears revealed many atypical large lymphoid cells and hemophagocytic macrophages, compatible with a clinical diagnosis of malignant lymphoma associated with HPS. The patient died within a week of admission despite CHOP (cyclophosphamide, doxorubicin, vincristine, and prednisone) chemotherapy. An autopsy was performed, and a systemic gross examination showed no lymphadenopathy, hepatosplenomegaly, or tumor mass formation.

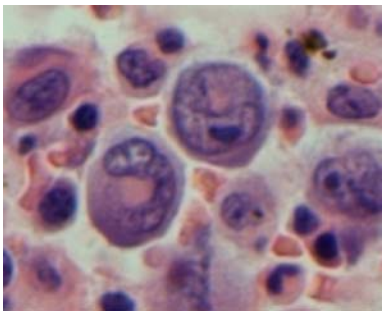


Fig. 2 Bone marrow section with tumor cells showing eccentric horseshoe-like nuclei with an adjacent eosinophilic region. These cells resemble "hallmark" cells in anaplastic large cell lymphoma (hematoxylin and eosin; original magnification ×400)

Materials and methods

Histologic and immunohistochemical staining

Formalin-fixed paraffin-embedded tissue blocks were available from all organs at autopsy. Immunoperoxidase studies were performed on formalin-fixed paraffin sections from autopsy specimens of bone marrow, lung, and lymph nodes using an avidin–biotin peroxidase complex method.

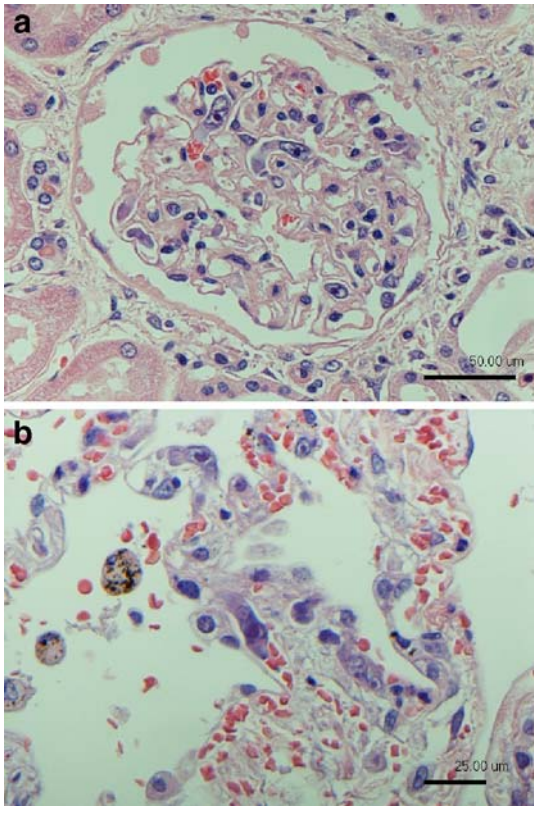


Fig. 1 **a** Autopsy kidney tissue shows single tumor cells in the capillaries of the glomeruli (hematoxylin and eosin; original magnification ×300). **b** Lung section exhibiting single tumor cells in the capillaries of alveolar septa (hematoxylin and eosin; original magnification ×400)

A panel of monoclonal antibodies against CD1a (O10, dilution 1:10; Immunotech), CD2 (AB75, dilution 1:40; Novocastra), CD3 (F7.2.38, dilution 1:25, Dako), CD4 (1F6, dilution 1:40; Novocastra), CD5 (4C7, dilution 1:40; Novocastra), CD8 (C8/144B, dilution 1:25; Dako), CD10 (NCL-CD10, dilution 1:40; Novocastra), CD15 (MMA, dilution 1:80; Becton-Dickinson), CD20 (L26, dilution 1:300; Dako), CD21 (1F8, dilution 1:20; Dako), CD23 (1B12, dilution 1:30; Novocastra), CD27 (137B4, dilution 1:50; Novocastra), CD30 (Ber-H2, dilution 1:15; Dako), CD43 (MT1, dilution 1:40; BioScience), CD45RA (4KB5, dilution 1:80; Dako), CD45RO (UCHL1, dilution 1:80; Dako), CD56 (1B6, dilution 1:50, Novocastra), CD57 (Leu7, dilution 1:50; Becton-Dickinson), CD68 (KP1, dilution 1:50; Dako), CD79a (JCB117, dilution 1:80; Dako), ALK (ALK1, dilution 1:25; Dako), EMA (E29, dilution 1:50; Dako), bcl-2 (124, dilution 1:80; Dako), βF1 (8A3, dilution 1:10; Endogen), granzyme B (GrB-7, dilution 1:80; Monosan), TIA1 (TIA-1, dilution 1:80; Immunotech), and perforin (5B10, dilution 1:20; Novocastra) were applied. For all antibodies except CD4, CD15, CD20, CD43, CD57, CD68, and EMA, the slides were pretreated with a microwave procedure for antigen retrieval.

In situ hybridization study

Assessment of the presence or the absence of EBV small ribonucleic acids (RNAs) by in situ hybridization using EBV-encoded small nuclear early region (EBER) oligonucleotides was performed on formalin-fixed paraffin-embedded sections. Briefly, a Dako hybridization kit was used with a cocktail of fluorescein isothiocyanate (FITC)-labeled EBER oligonucleotides (one oligonucleotide corresponding to EBER1 and one to EBER2, both 30 bases long; Dako A/S code Y017). Hybridization products were detected using a mouse monoclonal anti-FITC (M878) and a Vectastain ABC Kit (Vector, Burlingame, CA). RNase A or DNase I pretreatment was applied as negative controls and EBER-positive Hodgkin lymphoma specimens as positive controls.

Results

Histopathology

Tumor cells were seen within vascular spaces of many extranodal sites, such as the liver, spleen, kidney, lung, and bone marrow. The tumor cells were primarily scattered in the hepatic sinusoids, the splenic sinusoids, and the renal capillaries, especially those of the glomeruli (Fig. 1a). In both lungs, single or small clusters of tumor cells were found mainly in the capillaries of alveolar septa (Fig. 1b). The bone marrow showed small foci of aggregated tumor cells and scattered single tumor cells intermingled with normal trilineage hematopoietic marrow tissue. Hemophagocytic macrophages were indistinct in the bone marrow sections at autopsy; this may have been due to chemotherapy. Some lymph nodes adjacent to trachea also showed infiltration of tumor cells mainly in the sinuses, although the nodal architecture was preserved.

Lymphoma cells were large-sized with irregular nuclei containing one or two conspicuous nucleoli and abundant amphophilic cytoplasm. Some appeared to bear the cytomorphologic features of "hallmark" anaplastic large cell lymphoma (ALCL) cells, having horseshoe/kidney-shaped nuclei often with an eosinophilic region in the adjacent abundant cytoplasm, although they were scattered in distribution (Fig. 2). The involved blood vessels showed no occlusion or fibrin thrombi.

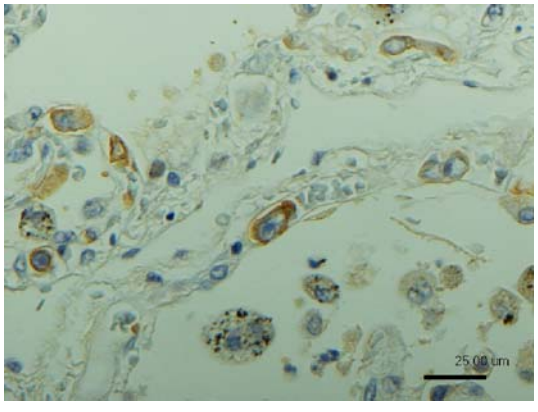


Fig. 3 Tumor cells are positive for CD30 on the cell membrane and in the Golgi region (original magnification ×400)

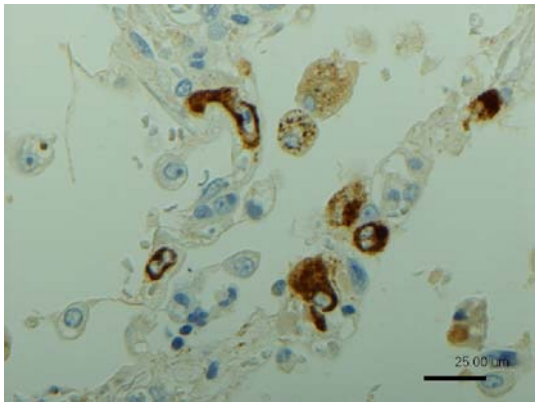


Fig. 4 Tumor cells show strong granular staining for granzyme B (original magnification ×400)

Immunohistochemistry and in situ hybridization

The tumor cells were positive for CD2, CD4, CD30 (Fig. 3), CD43, CD45RO, granzyme B (Fig. 4), TIA-1, and perforin and were negative for CD1a, CD3, CD5, CD8, CD10, CD15, CD20, CD21, CD23, CD27, CD45RA, CD56, CD57, CD68, CD79a, ALK, EMA, Bcl-2, and TCRβF1. No positive signals for nuclear EBV-encoded RNA transcripts were evident on in situ hybridization.

Discussion

In this article, we document a unique CD30-positive case of IVL featuring anaplastic large cell morphology and an ALK-negative T-cytotoxic phenotype, with the HPS and an aggressive clinical course. Based on the cytopathologic features of the tumor cells, the present case could be diagnosed as T-IVL within the ALK-negative ALCLs, a heterogeneous or undefined category in the WHO classification [6] whose diagnostic implications remain controversial among pathologists. The ALCL is a T-cell lymphoma usually with large tumor cells having pleomorphic, often horseshoe-shaped nuclei [6] as seen in the present case. Most cases of ALCL express cytotoxic granule-associated antigens, such as TIA1, granzyme B, and perforin [6], and predominantly show a CD2+, CD3−, and CD4+ T-cell phenotype, again as in the present case [6].

Details for the 25 cases of T-IVL documented in the English literature are listed in Table 1. These include only one case of CD30+ anaplastic large cell type, reported by Ko et al. [12]. That patient was a 55-year-old male who died within 3 months of the diagnosis, having an aggressive clinical profile similar to our case. Another case associated with EBV infection in a HIV-positive patient showed a TIA1+ cytotoxic T-cell phenotype, but was negative for CD30 [17]. In case 3 of Table 1, only a few cells were positive for CD30 and CD8, and the expression of cytotoxic molecules was not investigated, providing no definite evidence of ALCL [21]. Thus, our case may be only the second reported case of CD30+ anaplastic large cell type and also only the second case with a cytotoxic T-cell phenotype. Although Ko et al.'s [12] case, with the expression of CD30 and anaplastic large cell morphology, belongs to ALCL T-IVL, the expression of ALK was not analyzed. Our case is thus the first for which tumor cells could be shown to be ALK-negative but cytotoxic-molecules-positive. However, it is possible that some of the other reported T-IVL cases lacking immunophenotypic evaluation of CD30, ALK, or cytotoxic molecules might also have been intravascular ALCLs or cytotoxic T-IVLs.

One stillborn [28], one renal allograft recipient [10], and two HIV-positive cases with acquired immunodeficiency syndrome [16, 17] are included among the 25 cases of

Table 1 Intravascular T-cell lymphoma reported in English literature (including present case)

Case no.	Age/sex	Outcome	CD2	CD3	CD4	CD8	CD20	CD30	CD45	CD45RO	TIA1	ALK	EMA	EBV	Gene rearrangement analysis	Involved organ		Other Findings	Reference
1	84/F	Complete resolution for 9 months	+	ND	+	+	−	ND	−	ND	ND	ND	ND	ND	ND	Skin	Biopsy		Sheibani [23]
2	81/F	Died at 6 months	ND	+	+	+	ND	ND	+	ND	ND	ND	ND	ND	ND	Skin	Biopsy		Sepp [21]
3	75/F	Died at 18 months	+	ND	+	A few +	ND	A few +	+	ND	ND	ND	ND	ND	+	Skin	Biopsy		Sepp [21]
4	73/M	ND	ND	ND	ND	ND	−	ND	+	+	ND	ND	ND	ND	ND	Skin	Biopsy		Stroup [26]
5	75/M	Died at 17 months	ND	ND	ND	ND	ND	ND	ND	+	ND	ND	−	ND	ND	Skin	Biopsy		Shimokawa [25]
6	Stillborn	Stillbirth	ND	ND	ND	ND	−	ND	±	±	ND	ND	ND	ND	ND	Bone marrow, lymph node, thymus, spleen, liver, and placenta	Autopsy		Tateyama [28]
7[a]	36/M	Died at 4 months	ND	ND	ND	ND	ND	ND	ND	ND	ND	ND	ND	ND	ND	Brain	Autopsy		Clark [5]
8	63/M	Died at 6 months	ND	ND	ND	ND	−	−	+	+	ND	ND	−	ND	ND	Skin	Biopsy		Lopez-Gil [14]
9	59/F	Died at 1 month after chemotherapy	ND	+	−	ND	−	−	+	+	ND	ND	−	ND	ND	Skin	Biopsy		Setoyama [22]
10	17/M	Died at 3 months	ND	−	ND	ND	−	−	+	+	ND	ND	ND	ND	ND	Skin and liver	Biopsy		Sangueza [20]
11[b]	75/M	Died at 12 months	ND	ND	ND	ND	ND	ND	ND	ND	ND	ND	ND	ND	ND	Cerebrum, cerebellum, midbrain, pons, spinal cord, peripheral nerve, muscle, and liver	Autopsy		Glass [11]
12	55/F	Died soon	ND	+	ND	ND	−	ND	+	+	ND	ND	ND	ND	+	Ovary, lung, brain, spleen, and vulva	Autopsy		Lakhani [13]
13	71/F	Died at 2 months	ND	ND	ND	ND	−	ND	ND	+	ND	ND	ND	ND	ND	Every organ system	Autopsy		DiGiuseppe [7]
14	38/M	Died at 6 months	ND	ND	ND	ND	−	ND	+	+	ND	ND	ND	ND	ND	Kidney and cerebrum	Autopsy	Renal allograft recipient	Ghorbani [10]
15	56/M	Died at 11 months	ND	+	ND	ND	−	ND	+	+	ND	ND	ND	+	ND	Lung, pleura, spleen, and epididymis	Autopsy		Au [3]

Table 1 (continued)

Case no.	Age/sex	Outcome	CD2	CD3	CD4	CD8	CD20	CD30	CD45	CD45RO	TIA1	ALK	EMA	EBV	Gene rearrangement analysis	Involved organ		Other Findings	Reference
16	54/M	Died at 3 months	ND	+	ND	ND	ND	ND	+	+	ND	ND	ND	ND	ND	Lung	Biopsy		Suh [27]
17	55/M	Died at 3 months	ND	+	ND	ND	−	+	ND	ND	ND	ND	−	ND	+	Lung	Biopsy		Ko [12]
18	53/M	Died at 3 months	ND	ND	ND	ND	−	ND	+	+	ND	ND	ND	ND	ND	Skin	Biopsy		Chen [4]
19	24/F	Died at 4 months	ND	ND	ND	ND	ND	ND	+	+	ND	ND	ND	ND	ND	Skin	Biopsy		Chen [4]
20	33/M	Alive at 1 year	ND	ND	ND	ND	−	ND	+	+	ND	ND	ND	ND	ND	Skin	Biopsy		Chen [4]
21	32/M	Alive at 14 months	ND	+	ND	ND	ND	ND	+	+	ND	ND	ND	−	ND	Appendix	Appendectomy	HIV(+)	Malicki [16]
22	37/M	Died at 2 months	ND	+	−	+	−	−	ND	ND	+	−	ND	+	+	Kidney, brain, liver, lung, and adrenal gland	Autopsy	HIV(+)	Merchant [17]
23	23/M	In remission for >100 weeks	ND	+	ND	ND	ND	ND	ND	ND	ND	ND	ND	ND	−	Colon	Subtotal colectomy with ileostomy		Williams [30]
24	62/ND	Postmortem diagnosis	ND	+	ND	ND	ND	ND	ND	ND	ND	ND	ND	ND	ND	Multiorgan involvement with sparing of bone marrow, spleen, and lymph node	Autopsy		Williams [30]
25	73/ND	Died at 8 months	ND	+	ND	ND	ND	ND	ND	ND	ND	ND	ND	ND	ND	ND	ND		Williams [30]
26	72/M	Died at 1 week	+	−	+	−	−	+	ND	+	+	−	−	−	ND	Liver, lung, spleen, kidney, bone marrow, and lymph node	Autopsy		Present case

ND Not described
[a]Scattered tumor cells stained strongly for the T-cell antigen
[b]Positive for T-cell markers, not otherwise specified, negative for B-cell markers

reported T-IVL (Table 1). The latter three cases were males in their third decade of life [10, 16, 17]. The remaining 21 of the T-IVL cases, as well as the present case, were mainly elderly with a mean age of 58 years, median age of 61 years, and ranging from 17 to 84 years old, with a male predominance (male-to-female ratio of 13:7), no age being given for two cases. The patients generally exhibited an aggressive clinical course, and the longest duration of survival was 18 months after the diagnosis, except in one patient demonstrating complete resolution and two others. Regarding the affecting organs, only one location was involved in 14 cases: the skin in 10 [4, 14, 21–23, 25, 26], the lung in 2 [12, 27], the colon in 1 [30], and the brain in 1 [5]. Multiple organ involvement was observed in seven cases, as well as ours [3, 7, 11, 13, 20, 30]. In a recent study, 38 IVLs, all except one T-IVL being of B-cell type, also were found in elderly patients (median age 70 years, range 34–90; male-to-female ratio 0.9) and resulted in a poor prognosis (3-year overall survival 25±7%) [8]. T-IVL seems to slightly differ from B-IVL regarding occurrence in younger individuals with a male predilection. However, the prognosis is essentially the same. Although the CD30+ ALCL tends to show a relatively better prognosis compared to other high-grade lymphomas, its IVL form may follow a poor clinical course as in our case and as suggested by Ko et al. [12].

The present case was clinically accompanied by HPS, a feature frequently reported in B-IVL patients especially in Asian populations [18, 24, 29]. Allory et al. [1] recently described a high number of reactive T cells of predominantly CD8+/TIA1+ cytotoxic phenotype to possibly play a role in the pathogenesis of HPS in diffuse large B-cell lymphomas. In a separate study in our laboratory, lymphoma-associated HPS was also observed in 20% of peripheral T-cell lymphomas of cytotoxic phenotype during their clinical course [2].

In conclusion, we here have documented a rare case of intravascular T-cell lymphoma with anaplastic large cell morphology and a CD30+ALK−TIA1+granzyme B+perforin+ phenotype, indicating the presence of heterogeneity in T-IVLs. In the WHO classification, the more common B-IVLs have been categorized into a single entity [9]. Accumulation of more cases of rare T-IVLs is now needed to allow subtyping.

References

1. Allory Y, Challine D, Haioun C, Copie-Bergman C, Delfau-Larue MH, Boucher E, Charlotte F, Fabre M, Michel M, Gaulard P (2001) Bone marrow involvement in lymphomas with hemophagocytic syndrome at presentation: a clinicopathologic study of 11 patients in a Western institution. Am J Surg Pathol 25:865–874
2. Asano N, Suzuki R, Kagami Y, Ishida F, Kitamura K, Fukutani H, Morishima Y, Takeuchi K, Nakamura S (2005) Clinicopathologic and prognostic significance of cytotoxic molecule expression in nodal peripheral T-cell lymphoma, unspecified. Am J Surg Pathol 29:1284–1293
3. Au WY, Shek WH, Nicholls J, Tse KM, Todd D, Kwong YL (1997) T cell intravascular lymphomatosis (angiotropic large cell lymphoma): association with Epstein–Barr viral infection. Histopathology 31:563–567
4. Chen M, Qiu B, Kong J, Chen J (1998) Angiotropic T cell lymphoma. Chin Med J 111:762–764
5. Clark WC, Dohan FC Jr, Moss T, Schweitzer JB (1991) Immunocytochemical evidence of lymphocytic derivation of neoplastic cells in malignant angioendotheliomatosis. J Neurosurg 74:757–762
6. Delsol G, Ralfkiaer E, Stein H, Wright D, Jaffe ES (2001) Anaplastic large cell lymphoma. In: Jaffe ES, Harris NL, Stein H, Vardiman JW (eds) World Health Organization classification of tumors. Pathology and genetics of tumours of haematopoietic and lymphoid tissues. IARC Press, Lyon, France, pp 230–235
7. DiGiuseppe JA, Nelson WG, Seifter EJ, Boitnott JK, Mann RB (1994) Intravascular lymphomatosis: a clinicopathologic study of 10 cases and assessment of response to chemotherapy. J Clin Oncol 12:2573–2579
8. Ferreri AJ, Campo E, Seymour JF, Willemze R, Ilariucci F, Ambrosetti A, Zucca E, Rossi G, Lopez-Guillermo A, Pavlovsky MA, Geerts ML, Candoni A, Lestani M, Asioli S, Milani M, Piris MA, Pileri S, Facchetti F, Cavalli F, Ponzoni M, International Extranodal Lymphoma Study Group (IELSG) (2004) Intravascular lymphoma: clinical presentation, natural history, management and prognostic factors in a series of 38 cases, with special emphasis on the 'cutaneous variant'. Br J Haematol 127:173–183
9. Gatter KC, Warnke RA (2001) Intravascular large B-cell lymphoma. In: Jaffe ES, Harris NL, Stein H, Vardiman JW (eds) World Health Organization classification of tumors. Pathology and genetics of tumours of haematopoietic and lymphoid tissues. IARC Press, Lyon, France, pp 177–178
10. Ghorbani RP, Shokouh-Amiri H, Gaber LW (1996) Intragraft angiotropic large-cell lymphoma of T cell-type in a long-term renal allograft recipient. Mod Pathol 9:671–676
11. Glass J, Hochberg FH, Miller DC (1993) Intravascular lymphomatosis. A systemic disease with neurologic manifestations. Cancer 71:3156–3164
12. Ko YH, Han JH, Go JH, Kim DS, Kwon OJ, Yang WI, Shin DH, Ree HJ (1997) Intravascular lymphomatosis: a clinicopathological study of two cases presenting as an interstitial lung disease. Histopathology 31:555–562
13. Lakhani SR, Hulman G, Hall JM, Slack DN, Sloane JP (1994) Intravascular malignant lymphomatosis (angiotropic large-cell lymphoma). A case report with evidence for T-cell lineage with polymerase chain reaction analysis. Histopathology 25:283–286
14. Lopez-Gil F, Roura M, Umbert I, Umbert P (1992) Malignant proliferative angioendotheliomatosis or angiotropic lymphoma associated with a soft-tissue lymphoma. J Am Acad Dermatol 26:101–104
15. Lymphoma Study Group of Japanese Pathologists (2000) The World Health Organization classification of malignant lymphomas in Japan: incidence of recently recognized entities. Pathol Int 50:696–702
16. Malicki DM, Suh YK, Fuller GN, Shin SS (1999) Angiotropic (intravascular) large cell lymphoma of T-cell phenotype presenting as acute appendicitis in a patient with acquired immunodeficiency syndrome. Arch Pathol Lab Med 123:335–337
17. Merchant SH, Viswanatha DS, Zumwalt RE, Foucar K (2003) Epstein–Barr virus-associated intravascular large T-cell lymphoma presenting as acute renal failure in a patient with acquired immune deficiency syndrome. Human Pathol 34:950–954

18. Murase T, Nakamura S, Kawauchi K, Matsuzaki H, Sakai C, Inaba T, Nasu K, Tashiro K, Suchi T, Saito H (2000) An Asian variant of intravascular large B-cell lymphoma: clinical, pathological and cytogenetic approaches to diffuse large B-cell lymphoma associated with haemophagocytic syndrome. Br J Haematol 111:826–834
19. Pfeger L, Tappeiner J (1959) Zur Kenntnis der Systemisierten Endotheliomatose der cuanen Blutegefasse (Reticulo-endotheilose?). Hautarzt 10:359–363
20. Sangueza O, Hyder DM, Sangueza P (1992) Intravascular lymphomatosis: report of an unusual case with T cell phenotype occurring in an adolescent male. Cutan Pathol 19:226–231
21. Sepp N, Schuler G, Romani N, Geissler D, Gattringer C, Burg G, Bartram CR, Fritsch P (1990) "Intravascular lymphomatosis" (angioendotheliomatosis): evidence for a T-cell origin in two cases. Human Pathol 21:1051–1058
22. Setoyama M, Mizoguchi S, Orikawa T, Tashiro M (1992) A case of intravascular malignant lymphomatosis (angiotropic large-cell lymphoma) presenting memory T cell phenotype and its expression of adhesion molecules. J Dermatol 19:263–269
23. Sheibani K, Battifora H, Winberg CD, Burke JS, Ben-Ezra J, Ellinger GM, Quigley NJ, Fernandez BB, Morrow D, Rappaport H (1986) Further evidence that "malignant angioendotheliomatosis" is an angiotropic large-cell lymphoma. N Engl J Med 614:943–948
24. Shimazaki C, Inaba T, Nakagawa M (2000) B-cell lymphoma-associated hemophagocytic syndrome. Leuk Lymphoma 38:121–130
25. Shimokawa I, Higami Y, Sakai H, Moriuchi Y, Murase K, Ikeda T (1991) Intravascular malignant lymphomatosis: a case of T-cell lymphoma probably associated with human T-cell lymphotropic virus. Human Pathol 22:200–202
26. Stroup RM, Sheibani K, Moncada A, Purdy LJ, Battifora H (1990) Angiotropic (intravascular) large cell lymphoma. A clinicopathologic study of seven cases with unique clinical presentations. Cancer 66:1781–1788
27. Suh CH, Kim SK, Shin DH, Chung KY, Kim SK (1997) Intravascular lymphomatosis of the T cell type presenting as interstitial lung disease–a case report. J Korean Med Sci 12: 457–460
28. Tateyama H, Eimoto T, Tada T, Kamiya M, Fujiyoshi Y, Kajiura S (1991) Congenital angiotropic lymphoma (intravascular lymphomatosis) of the T-cell type. Cancer 67:2131–2136
29. Watabe R, Shibata K, Hirase N, Kodera T, Muta K, Nishimura J, Nawata H (2000) Angiotropic B-cell lymphoma with hemophagocytic syndrome associated with syndrome of inappropriate secretion of antidiuretic hormone. Ann Hematol 79:581–584
30. Williams G, Foyle A, White D, Greer W, Burrell S, Couban S (2005) Intravascular T-cell lymphoma with bowel involvement: case report and literature review. Am J Hematol 78:207–211

Virchows Arch (2005) 447: 1007–1008
DOI 10.1007/s00428-005-0074-4

LETTER TO THE EDITOR

Kunimitsu Kawahara · Motoaki Yasukawa · Katsuhiro Nakagawa · Hiroshi Katsura · Teruaki Nagano · Teruo Iwasaki

Multiple calcifying fibrous tumor of the pleura

Received: 6 June 2005 / Accepted: 19 August 2005 / Published online: 21 September 2005
© Springer-Verlag 2005

Dear Sir,

The article by Mito et al. [4] concerning multiple calcifying fibrous tumor of the pleura (CFTP) is a great contribution to the subject of respiratory pathology, as only eight cases of CFTP have been reported [2–4], and multiple CFTP has been poorly documented. In our opinion, pathologists and surgeons should be made aware of multiple CFTP since it is possible to confuse CFTP macroscopically with disseminated metastatic sarcoma or diffuse malignant mesothelioma during surgery. We would like to add one additional case of multiple CFTP that was pathologically diagnosed on intraoperative frozen section slides.

Case report

A 35-year-old Japanese woman, who had smoked about 20 cigarettes per day for 15 years, consulted our hospital complaining of right chest pain that had occurred for the past 2 years. Occupational exposure to asbestos was probable. Computed tomographic scan of the chest showed remarkable thickening of the parietal pleurae of the right hemithorax. A tentative diagnosis of diffuse malignant mesothelioma was made. Family history and past medical history were unremarkable. Video-assisted thoracoscopic surgery was performed for histological examination. Thoracoscopic examination demonstrated a large arborized nodule, 5 cm in diameter on the diaphragmatic pleura (Fig. 1a), and other miliary dome-shaped nodules at the costal and mediastinal pleurae as well as visceral pleura mainly in the lower lobe (Fig. 1b). There was a small amount of serous pleural effusion. In the pleural fluid, no cytological abnormalities were observed. Pleural plaques were present at the fourth, fifth, and sixth costal pleura. The surgeons thoracoscopically diagnosed eccentric disseminated metastatic sarcoma or diffuse malignant mesothelioma at resection of the largest nodule. Intraoperative frozen section slide showed hyalinized fibrosclerotic nodular lesions with microcalcifications, which highly supported the pathological diagnosis of multiple CFTP. Thoracotomy was performed, and all remaining nodules were extirpated. On postoperative gross examination, all nodules were well circumscribed, solid, or firm with a uniform gray-white fibrous cut appearance without any hemorrhage or necrosis (Fig. 1c). All nodules were pleural-based. Histologically, the nodules were circumscribed, nonencapsulated, and composed chiefly of hypocellular hyalinized fibrosclerotic tissue with scattered cytologically bland spindle cells, scant lymphoplasmacytic infiltrate, and small calcifications. The calcifications had a laminated appearance showing typical psammoma bodies (Fig. 2a). The surface of the nodules was occasionally covered by a single layer of mesothelial cells. Asbestos bodies were not detected in or around the nodules. Immunohistochemical studies showed that most spindle cells were positive for vimentin and factor XIIIa (Fig. 2b) but negative for epithelial membrane antigen (EMA), keratin (AE1/3), desmin, α-smooth muscle actin, S-100, anaplastic lymphoma kinase, and CD34. Taken together, a pathological diagnosis of multiple CFTP was made.

Recognition of this extremely rare miliary type of CFTP is important because of the possibility of confusing it intraoperatively with malignant fibrous neoplasms including desmoplastic mesothelioma or disseminated metastatic sarcoma [2–4]. Desmoplastic mesothelioma shows a storiform collagen pattern, collagen necrosis, bland acellular collagen, and focal cytologic features of malignancy [5]. Moreover, desmoplastic mesothelioma stains for cytokeratins, but our case was negative for AE1/3. In disseminated metastatic fibrous sarcoma with pleural

K. Kawahara (✉) · T. Nagano
Department of Pathology, Osaka Prefectural Medical Center for Respiratory and Allergic Diseases,
3-7-1 Habikino,
Habikino, Osaka, 583-8588, Japan
e-mail: kawahara@hbk.pref.osaka.jp
Tel.: +81-729-572121
Fax: +81-729-583291

M. Yasukawa · K. Nakagawa · H. Katsura · T. Iwasaki
Department of Thoracic Surgery, Osaka Prefectural Medical Center for Respiratory and Allergic Diseases,
Habikino, Japan

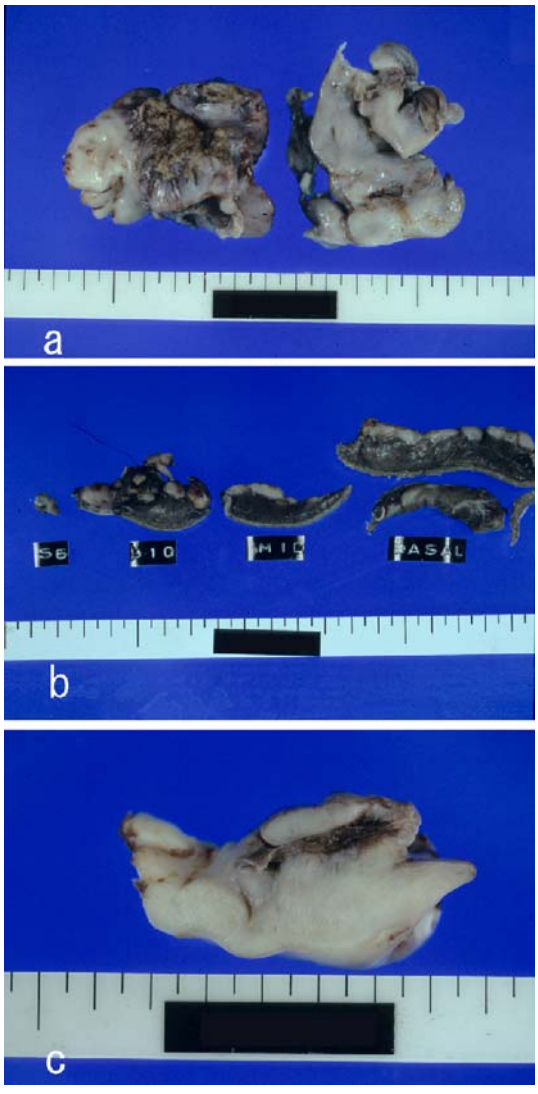


Fig. 1 **a** A large arborized nodule measuring 5 cm in diameter was present on the diaphragmatic pleura. **b** Miliary dome-shaped nodules were also present at the visceral pleura of the right lower lobe. **c** The cut surface of the largest nodule showed a uniform fibrous appearance

calcification, monophasic synovial sarcoma (MSS) should be considered. MSS is usually a localized pleural-based mass [1]. MSS is composed of nearly uniform spindle fibroblast-like cells that are arranged in dense cellular sheets or vague fascicles. Hyalinization and calcification are occasionally seen. In our case, dense cellular areas composed of fibroblast-like cells were absent. Immunohistochemically, cytokeratin and/or EMA is positive in MSS, but this finding was negative in our patient.

In this case, we made a diagnosis of multiple CFTP based on intraoperative frozen section slides. The keys to accurate diagnosis were as follows: (1) recognition of submesothelial origin; (2) hypocellular hyalinized fibrosclerotic tumor with psammoma bodies; and (3) knowledge about multiple CFTP obtained from the article by Mito et al. [4].

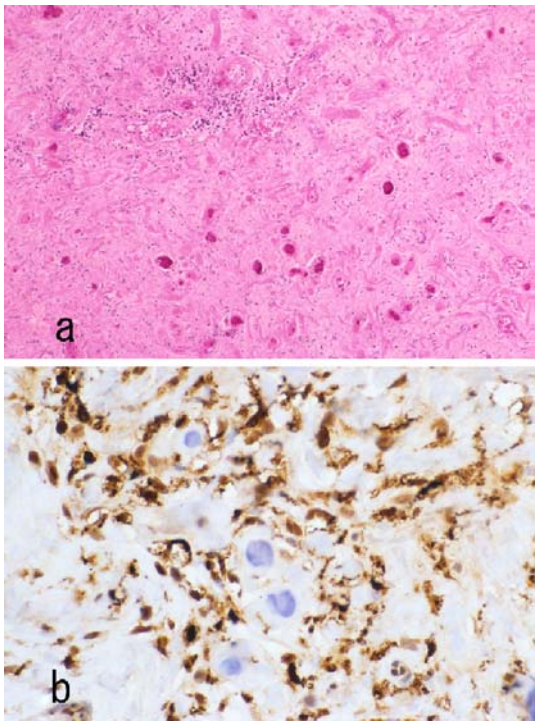


Fig. 2 **a** Histologically, the tumor was predominantly composed of hypocellular hyalinized fibrosclerotic tissue with psammoma bodies and scant lymphoplasmacytic infiltrate (×50). **b** The spindle cells showed positive staining for factor XIIIa immunohistochemically (×100)

References

1. Aubry MC, Bridge JA, Wickert R, Tazelaar HD (2001) Primary monophasic synovial sarcoma of the pleura: five cases confirmed by the presence of SYT–SSX fusion transcript. Am J Surg Pathol 25:776–781
2. Cavazza A, Gelli MC, Agostini L, Sgarbi G, De Marco L, Gardini G (2002) Calcified pseudotumor of the pleura: description of a case. Pathologica 94:201–205
3. Jang KS, Oh YH, Han HX, Chon SH, Chung WS, Park CK, Paik SS (2004) Calcifying fibrous pseudotumor of the pleura. Ann Thorac Surg 78:e87–e88
4. Mito K, Kashima K, Daa T, Kondoh Y, Miura T, Kawahara K, Nakayama I, Yokoyama S (2005) Multiple calcifying fibrous tumors of the pleura. Virchows Arch 446:78–81
5. Wilson GE, Hasleton PS, Chatterjee AK (1992) Desmoplastic malignant mesothelioma: a review of 17 cases. J Clin Pathol 45:295–298

Virchows Arch (2005) 447: 1009
DOI 10.1007/s00428-005-0121-1
© Springer-Verlag 2005

ANNOUNCEMENTS

6 May 2006
Problems in Breast Pathology
Malta College of Pathologists
Malta

Course Director
Professor J.G. Azzopardi

Scientific Secretariat
J. De Gaetano and V. Eusebi

9.00 Registration

Chair: J.G. Azzopardi (London/Malta) & Rosemary Millis (London)
9.30–10.00 Ian Ellis (Nottingham) : Prognostic factors: old versus new.
10.00–10.30 Gianni Bussolati (Torino) : The contribution of 3D models to the understanding of breast pathology.
10.30–11.00 Tibor Tot (Falun) : The theory of the sick lobe and the possible consequences.
11.00–11.30 Frederick Koerner (Boston) : The histogenesis of early breast carcinoma.
11.30–12.00 Tanya Tavassoli (New Haven) : To DIN or not to DIN, that is the question.
12.00–12.30 Discussion

Chair: J. Rosai (Milano) & G. Stamp (London)
14.30–15.00: James Connolly (Boston) : Present findings from the benign breast project of the nurses health study.
15.00–15.30: Stuart Schnitt (Boston) : Columnar cell lesions and flat epithelial atypia.
15.30–16.00 Hans Peterse (Amsterdam) : Ring carcinomas: the phenomenon of shift of cell polarization.
16.00–16.30: Thomas Krausz (Chicago) : Breast tumours. Race, loneliness and the pathologist.
16.30–17.00 : Werner Boecker (Muenster): The progenitor cell concept of breast epithelium and how it changes our understanding of proliferative breast disease.
17.00–17.30 : Sunil Lakhani (Brisbane): Myoepithelial cell and breast cancer.
17.30–18.00 : Vincenzo Eusebi (Bologna) : Salivary-like tumours of the breast.
18.00–18.30 : Juan Rosai (Milano) : The vascular lobule. A pitfall on the interpretation of vascular skin lesions following irradiation for breast carcinoma.

S.G. Silveberg (Baltimore) & Jane Dahlstrom
(Camberra) : Conclusive remarks

The congress fee is 30 ∈, that includes light lunch payable on the spot.

Scientific Organizer:
Dr. James De Gaetano
Pathology Department
St. Luke's Hospital
Gwardamangia
Malta
tel.n. xx356 25951117
e-mail james.degaetano@gov.mt

Venue and Hotel accomodation:
Hilton Hotel
Portomaso
St. Julians
Malta PTM01
Tel.n. XX 356 21383383
www.hilton.com.mt

15–16 June 2006
Thyroid Pathology for the Practicing Pathologist
15 rue de l'Ecole de Médecine, Paris,France

A 2-day course will take place in Paris again under the auspices of the French Division of the I.A.P.

This course will be given in English by Prof. M. Sobrinho-Simões (Porto) and Prof. R. Heimann (Brussels).

It will consist of lectures alternating with slide reviews and a slide seminar over a multihead microscope. The cases of this seminar will be sent (on CD) before the meeting.

The audience will be limited to 22 participants.
Course fees: 390 euros (320 euros for members of any I.A.P. division). The fees include registration, hand-out, CD of the slide seminar and coffee breaks.

For further information please contact
Mrs. M. Fontaniére
Administrative Secretary
French Division of the I.A.P.
32 Cours Albert Thomas
69008, Lyon, France
Fax: 33 4 78754311
e-mail: academie.pathologie@wanadoo.fr